ENGINEERING-TRANSPORTATION
LIBRARY

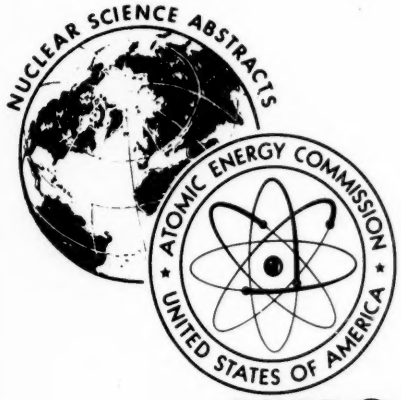

THE UNIVERSITY
OF MICHIGAN
JUL 2 1966
ENGINEERING
LIBRARY

NUCLEAR SCIENCE ABSTRACTS

Volume 20 Number 12

Abstracts 20368–22529

June 30, 1966

UNITED STATES ATOMIC ENERGY COMMISSION
Division of Technical Information

DEPOSITED BY THE
UNITED STATES OF AMERICA

USAEC DEPOSITORY LIBRARIES

Collections of USAEC reports are maintained in the libraries of the organizations listed below for reference use by the general public. Facilities for making photocopies are available. The USAEC also makes available through these libraries atomic energy reports of countries other than the U. S. that are abstracted in *Nuclear Science Abstracts*.

ALABAMA
Auburn, Auburn University
ALASKA
College, University of Alaska
ARIZONA
Tucson, University of Arizona
ARKANSAS
Fayetteville, University of Arkansas
CALIFORNIA
Berkeley, University of California
Davis, University of California
Los Angeles, University of California
San Diego, Public Library
Stanford, Stanford University
COLORADO
Boulder, University of Colorado
Denver, Public Library
CONNECTICUT
New Haven, Yale University
DELAWARE
Newark, University of Delaware
DISTRICT OF COLUMBIA
Washington, Library of Congress
FLORIDA
Coral Gables, University of Miami
Gainesville, University of Florida
Tallahassee, The Florida State University
GEORGIA
Atlanta, Georgia Institute of Technology
HAWAII
Honolulu, University of Hawaii
ILLINOIS
Chicago, John Crerar Library
Chicago, University of Chicago
Evanston, Northwestern University
Urbana, University of Illinois
INDIANA
Bloomington, Indiana University
Lafayette, Purdue University
IOWA
Ames, Iowa State University
KANSAS
Manhattan, Kansas State University
KENTUCKY
Lexington, University of Kentucky
Louisville, University of Louisville
LOUISIANA
Baton Rouge, Louisiana State University
New Orleans, Tulane University
MARYLAND
Baltimore, Johns Hopkins University
College Park, University of Maryland
MASSACHUSETTS
Cambridge, Harvard University
Cambridge, Massachusetts Institute of Technology
MICHIGAN
Ann Arbor, University of Michigan
Detroit, Public Library
East Lansing, Michigan State University
MINNESOTA
Minneapolis, University of Minnesota
MISSISSIPPI
State College, Mississippi State University
MISSOURI
Kansas City, Linda Hall Library
Rolla, University of Missouri School of Mines and Metallurgy
St. Louis, Washington University
MONTANA
Bozeman, Montana State College
NEVADA
Las Vegas, Nevada Southern University
Reno, University of Nevada
NEW JERSEY
Princeton, Princeton University
Teaneck, Fairleigh Dickinson University
NEW MEXICO
Albuquerque, University of New Mexico
NEW YORK
Albany, The University of the State of New York
Buffalo, State University of New York at Buffalo
Ithaca, Cornell University
New York, Atomic Industrial Forum, Inc.
New York, Columbia University
New York, New York University
Rochester, University of Rochester
Schenectady, Union College
Syracuse, Syracuse University
Troy, Rensselaer Polytechnic Institute
NORTH CAROLINA
Charlotte, Public Library of Charlotte and Mecklenburg County
Durham, Duke University
Raleigh, North Carolina State College
NORTH DAKOTA
Grand Forks, University of North Dakota
OHIO
Cincinnati, University of Cincinnati
Cleveland, Public Library
OHIO (CONT.)
Columbus, Ohio State University
Toledo, University of Toledo
Youngstown, Youngstown University
OKLAHOMA
Norman, University of Oklahoma
Stillwater, Oklahoma State University
OREGON
Corvallis, Oregon State University
Portland, Reed College
PENNSYLVANIA
Philadelphia, University of Pennsylvania
Pittsburgh, Carnegie Library
University Park, Pennsylvania State University
PUERTO RICO
Rio Piedras, University of Puerto Rico
RHODE ISLAND
Providence, Brown University
SOUTH CAROLINA
Columbia, University of South Carolina
TENNESSEE
Knoxville, University of Tennessee
Memphis, Public Library
Nashville, Joint University Libraries
Oak Ridge, Oak Ridge Associated Universities
TEXAS
Austin, University of Texas
College Station, Texas A & M University
Dallas, Southern Methodist University
Houston, Rice University
Lubbock, Texas Technological College
San Antonio, Public Library
UTAH
Salt Lake City, University of Utah
VIRGINIA
Blacksburg, Virginia Polytechnic Institute
Charlottesville, University of Virginia
Norfolk, Old Dominion College
WASHINGTON
Pullman, Washington State University
Seattle, University of Washington
WEST VIRGINIA
Morgantown, West Virginia University
WISCONSIN
Madison, University of Wisconsin
Milwaukee, Public Library
WYOMING
Laramie, University of Wyoming

EPOSITED BY THE
D STATES OF AMERICA

NOTICE

A title page for Volume 20, Numbers 7–12, is included at the back of this issue for use in binding the second quarter of this volume.

CORRECTIONS

NSA Vol. 18, No. 9, p. 1912, Abst. No. 14188, line 3 . . . Should read . . . 34 p. (CONF-63111-1).

NSA Vol. 20, No. 2, p. 371, Abst. No. 2944, line 4 . . . Should read . . . kernenergie, 10: 239-42(July-Aug. 1965). (In German).

NSA Vol. 20, No. 2, p. 375, Abst. No. 3005, line 3 . . . Should read . . . search Lab., Baldock, Eng.). 12p. (CONF-650405-20).

A semi
Publis

Nuclea
nology
mation
Atomi
cies a
patents
appear
Numbe
the U.
62, Oa

Abstra
Definit
item i
abstra

Corpor
and ar
issued
issued
to incl
item a
beginni

A

The pu
port n
availab

Disser
Univer

Most
Associ
throug
volume

Volume 20, Number 12, June 30, 1966

NUCLEAR SCIENCE ABSTRACTS

A semimonthly publication of the USAEC Division of Technical Information, Edward J. Brunenkant, Director. Published by the USAEC Division of Technical Information Extension, Robert L. Shannon, Extension Manager.

Nuclear Science Abstracts covers the international literature on nuclear science and technology and provides the only comprehensive abstracting and indexing of this body of information. Published twice each month since 1947, *NSA* covers technical reports of the U. S. Atomic Energy Commission and its contractors, technical reports of U. S. Government agencies and other governments, universities, industrial and research organizations, as well as patents, books, and journal literature on a world-wide basis. Nearly 350,000 abstracts have appeared in *NSA* through Volume 19. The subject matter covered in *NSA* is described in issue Number 1 and in TID-4552, *Subject Scope of Nuclear Science Abstracts*, available free from the U. S. Atomic Energy Commission, Division of Technical Information Extension, P. O. Box 62, Oak Ridge, Tennessee 37830.

Abstracts are arranged according to a number of subject categories and subcategories. Definitions of categories appear in issues Number 1 and 13. If the language of the original item is not English, the language will be indicated. Translations are not abstracted where an abstract of the original item has appeared in *NSA*.

INDEXES TO NSA

Corporate author, personal author, subject, and report number indexes appear in each issue and are cumulated quarterly, semiannually, and annually. Multi-volume cumulations have been issued as indicated on the following page. Report number indexes for all volumes (1–18) were issued at the end of Vol. 18. At the end of Vol. 19, the indexes for Vols. 1–15 were reissued to include additional public availability information. This cumulation will be a permanent shelf item and will not be reissued. Report number indexes for Vol. 19 are included as a cumulation beginning with Vol. 16.

AVAILABILITY OF PUBLICATIONS ABSTRACTED

The public availability of all U. S. Atomic Energy Commission reports is indicated in the report number indexes. The availability of other reports, when known, is also indicated. The availability of some unnumbered reports is given in the abstract.

Dissertations abstracted in *Dissertation Abstracts* and included in *NSA* are available from University Microfilms, Inc., 315 N. First Street, Ann Arbor, Michigan 48103.

Most of the published literature abstracted in *NSA* is on deposit at the Library, Oak Ridge Associated Universities, Oak Ridge, Tennessee, (a USAEC depository library) and is available through interlibrary loan. When requesting papers from this source, it is important that *NSA* volume and abstract number be cited.

HOW TO OBTAIN NUCLEAR SCIENCE ABSTRACTS

NSA is available on an exchange basis to universities, research institutions, industrial firms, and publishers of scientific information. Inquiries should be directed to the U. S. Atomic Energy Commission, Division of Technical Information Extension, P. O. Box 62, Oak Ridge, Tennessee 37830.

Government agencies may obtain *NSA* free of charge.

NSA is available to the general public on a subscription basis from the Superintendent of Documents, U. S. Government Printing Office, Washington, D. C. 20402, as follows:

For the 24 regular issues, $30.00 domestic, $37.00 foreign. A single issue costs $1.75, plus 25 per cent for foreign mailing. Domestic rates apply to the United States, Canada, Mexico, and Central and South American countries except Argentina, Brazil, British and French Guiana, Surinam, and British Honduras. Foreign rates apply to the countries excepted above and to all other countries throughout the world.

For the quarterly, semiannual, and annual indexes, $22.00 domestic, $25.00 foreign.

Multivolume subject and author indexes are available as follows:

Vols. 1–4 (1948–1950) Johnson Reprint Corporation, 111 Fifth Avenue, New York, N. Y. 10003, $30.00.

Vols. 5–10 (1951–1956) Superintendent of Documents, U. S. Government Printing Office, Washington, D. C. 20402, $5.25.

Vols. 11–15, Subjects, Superintendent of Documents, U. S. Government Printing Office, Washington, D. C. 20402, $19.00.

Vols. 11–15, Personal Authors, Superintendent of Documents, U. S. Government Printing Office, Washington, D. C. 20402, $14.25.

Vols. 11–15, Corporate Authors, Superintendent of Documents, U. S. Government Printing Office, Washington, D. C. 20402, $2.50.

Cumulative Report Number Index, Vols. 1–15, Revised, is available from the Superintendent of Documents, U. S. Government Printing Office, Washington, D. C. 20402, $4.00.

Cumulative Report Number Index, Vols. 16–19, is available from the Superintendent of Documents, U. S. Government Printing Office, Washington, D. C. 20402, $2.50.

Annual Indexes are available separately from the U. S. Government Printing Office as follows:

Vol. 16, Subject and Authors, $9.75.
Vol. 17, Subject and Authors, $12.25.
Vol. 18, Subject and Authors, $12.50.
Vol. 19, Subject and Authors, $12.50.

ACKNOWLEDGMENTS

Agreements between the United States Atomic Energy Commission and the following organizations with regard to providing continuing services and specific literature coverage for *Nuclear Science Abstracts* are gratefully acknowledged:

American Institute of Physics; Atomic Energy of Canada Limited; Atomic Energy Research Establishment, United Kingdom; European Atomic Energy Community (EURATOM); Gmelin Institute; International Atomic Energy Agency; Japan Atomic Energy Bureau—Japan Atomic Energy Research Institute; Netherlands Patent Office; Reactor Centrum Nederland.

TABLE OF CONTENTS

Volume 20, Number 12, June 30, 1966

Category	*Page*
BIOLOGY AND MEDICINE	2481
General	2481
Ecology	2483
Metabolism, Tissue Distribution, and Toxicology	2483
Radiation Effects on Biochemicals	2486
Radiation Effects on Tissues	2490
Radiation Effects Therapy and Countermeasures	2500
Radiation Hazards and Protection	2502
Radiotherapy and Radiodiagnosis	2502
CHEMISTRY	2507
General	2507
Analytical Procedures	2507
Inorganic and Physical Chemistry	2519
Organic Chemistry	2527
Radiation Chemistry	2528
Radiochemistry	2538
Separation Processes and Procedures	2539
ENGINEERING	2545
General	2545
Applications of Nuclear Explosions	2545
Facilities and Equipment	2545
Heat Transfer and Fluid Flow	2547
Materials Testing	2548
Protective Structures	2549
Space Propulsion	2549
GEOLOGY, METEOROLOGY, AND MINERALOGY	2551
General	2551
Natural Radioactivity and Fallout	2551
Site Survey and Selection	2554
Techniques and Equipment	2554
Thorium and Uranium Minerals	2557
HEALTH AND SAFETY	2558
INSTRUMENTATION	2567
General	2567
Radiation Detection	2570
Radiation Effects	2583
ISOTOPE TECHNOLOGY	2587
General	2587
Industrial Applications	2587
Power Application	2591
Separation and Production	2591
MATHEMATICS AND COMPUTERS	2593
METALS, CERAMICS, AND OTHER MATERIALS	2594
General	2594
Corrosion	2597
Fabrication	2601
Properties and Structure	2605
Radiation Effects	2619
PHYSICS	2624
General	2624
Accelerators	2625
Astrophysics and Cosmology	2628
Atomic Physics	2631
Cosmic Radiation	2634
Direct Energy Conversion	2637
Elementary Particles and Radiations	2640
Field Theory, Scattering Theory, and Symmetries	2651
Fluid Physics and Thermodynamics	2658
Geophysics	2663
Gravitation, Quantum Mechanics, and Relativity Theory	2666
Low Temperature Physics	2670
Neutron Physics	2675
Nuclear Properties and Reactions	2679
Plasma Physics and Thermonuclear Processes	2700
Shielding	2719
Solid State Physics	2720
REACTOR TECHNOLOGY	2724
General	2724
Auxiliaries and Components	2724
Criticality Studies	2726
Design and Feasibility	2730
Fuels	2730
Power and Power-Breeder Reactors	2731
Process Heat Reactors	2737
Production Reactors	2737
Propulsion and Space	2738
Research and Test Reactors	2740
WASTE DISPOSAL AND PROCESSING	2743
GENERAL AND MISCELLANEOUS	2745
CORPORATE AUTHOR INDEX	INDEX-1
PERSONAL AUTHOR INDEX	INDEX-13
SUBJECT INDEX	INDEX-59
REPORT NUMBER INDEX	INDEX-147

STAFF OF NUCLEAR SCIENCE ABSTRACTS

MANAGING EDITOR

John W. Norris

ASSISTANT MANAGING EDITOR

Donald D. Davis

ASSOCIATE EDITORS

Lawrence T. Whitehead
David E. Bost
Robert C. Kelly
Lee M. Thompson

SUBJECT INDEX EDITOR

Everett J. Hoffman

EVALUATORS

William D. Matheny
John H. Mitchell
Mary H. Newman

ABSTRACTORS

F. S. Armstrong (AECL)
Jane G. Buchanan
D. Lamar Cason
Bennie G. Di Bona
Helen G. Donald
James R. Dulaney
Wells L. Green
Mary Catherine Grissom
Fernando J. Hamilton
Phyllis C. Hansen
Carolyn D. Houston
Rose V. Jermain
Betty L. McDowell
Jean F. Peckham
Mona H. Raridon
Julia Redford
Francis L. Sachs
Lila B. Smith
Charles E. Stuber
Martha J. Thomas
Anne G. Ward
David C. West
Milton O. Whitson
Gabriel O. Ycaza

SUBJECT HEADING SPECIALIST

Robert E. Upchurch

CORPORATE AUTHOR SPECIALIST

Clara L. Fox

DESCRIPTIVE CATALOGING SPECIALIST

J. Paul Meredith

SCHEDULING AND PUBLISHING COORDINATOR

Brainard L. Patton

Communication concerning the editorial policy and content of *NSA* should be addressed to the Managing Editor, *Nuclear Science Abstracts*, AEC Division of Technical Information Extension, P. O. Box 62, Oak Ridge, Tennessee 37830.

Use of funds for printing this publication approved by the Director of the Bureau of the Budget, May 20, 1963

Volume 20, Number 12 June 30, 1966

NUCLEAR SCIENCE ABSTRACTS

BIOLOGY AND MEDICINE

General

Refer also to abstract 21224.

20368 (CONF-640309-1) MICROBIOLOGICAL ASSAYS OF SEAWATER USING RADIOISOTOPES. Gold, Kenneth (Columbia Univ., Palisades, N. Y. Lamont Geological Observatory). [1964]. Contract AT(30-1)-3233. 19p. Dep. mn. CFSTI $1.00 cy, $0.50 mn.
From Conference on Estuaries, Jekyll Island, Ga.

Research was conducted to determine whether microbiological assays of seawater for growth-promoting/inhibiting substances are possible using sensitive marine organisms and incorporation of radioisotopes through physiological processes. Heterotrophic and photosynthetic organisms are being screened for selectivity and sensitivity, and several isotopes are being compared for their usefulness in bioassays. Initial work using incorporation of ^{14}C through photosynthesis to measure algal responses to different nutrients at varying concentrations, indicates that bioassays of this kind will be extremely sensitive and very rapid. Extensive experimentation with the marine diatom Cyclotella nana Hustedt has resulted in a rapid and sensitive bioassay for vitamin B_{12} in seawater using radiocarbon. Linear responses in the range $<0.3-6$ $\mu\mu g$ B_{12}/ml were obtained within a 24 hr period. In this same period cell density may have increased 2–3 fold with added B_{12}, but the ratio of assimilated ^{14}C in cultures incubated with B_{12} compared with B_{12}-free controls was usually 10:1 or greater. The increased sensitivity is gained from the combination of differences in cell density, cell size, and metabolic rate. (auth)

20369 (NASA-SP-7011(22)) AEROSPACE MEDICINE AND BIOLOGY. A Continuing Bibliography with Indexes. (National Aeronautics and Space Administration, Washington, D. C. Scientific and Technical Information Div.). Mar. 1966. 174p. CFSTI $1.00 cy, $1.00 mn.

References (497) are given to reports and journals published from 1964 through Jan. 1966. Emphasis is given to references on biological, physiological, psychological, and environmental effects to which man is subjected during and following simulated or actual flight in the earth's atmosphere or in interplanetary space. References describing similar effects on biological organisms of lower order are also included, along with related topics on sanitary problems, pharmacology, toxicology, safety and survival, life support systems, exobiology, and personnel factors. Separate author, corporate author, and subject indexes are included. (P.C.H.)

20370 (UCRL-14658) ISCHEMIC HEART DISEASE, ATHEROSCLEROSIS, AND LONGEVITY. Gofman, John W.; Young, Wei; Tandy, Robert (Lawrence Radiation Lab., Univ. of California, Livermore). Feb. 1, 1966. Contract W-7405-eng-48. 37p. Dep. mn. CFSTI $2.00 cy, $0.50 mn.

Results are reviewed from studies on the relationship of serum lipids and lipoproteins to the incidence of overt clinical ischemic heart disease and atherosclerosis in human populations. Data are presented from a 12-year study that showed that serum lipoproteins, serum cholesterol, A.I. function, the systolic and diastolic blood pressures, and relative weight were all elevated in individuals destined to develop ischemic heart disease. The results of statistical analysis of data on 221 cases of de novo ischemic heart disease in men and 98 cases in women are discussed in relation to age of the individuals. Data are also included from a study of atherosclerosis in autopsy material from subjects whose blood lipid and lipoprotein parameters had been determined during life. The results of the study showed no evidence of a relationship between blood lipid parameters and atherogenesis in men 60 to 69 years of age. The interpretation of data from studies of de novo ischemic heart disease and coronary atherosclerosis is discussed. (35 references.) (C.H.)

20371 THE IMPORTANCE OF NONSPECIFIC RESISTANCE AND ITS INCREASE IN THE ETIOLOGY OF ACUTE HEMATOGENIC OSTEOMYELITIS. Huener, H. (Staatliches Luitpold Krankenhaus, Wurzburg, Ger.). Arch. Klin. Chir., 309: 383-400(Mar. 5, 1965). (In German).

The prevailing view of the etiology of acute hematogenic osteomyelitis is that allergization or the conversion of the reactability of the organism is with some anatomical conditioning factor the leading factor for the unilocular manifestation of the disease process in the metaphyses of growing bones. In this reaction there is increased reactability of the organism to the disease manifestation, and the irritation of the circulatory system in the metaphysis leads to extravasation of the irritant. Sensitization to a reduced dose of staphylococci appears to increase resistance of individuals to what otherwise later would be fatal doses. Animals exposed to x irradiation may die, although antibody formation is not entirely prevented. Their increased susceptibility to infection is due to depression of cellular and humoral defense mechanisms by the irradiation. The presence of an irritant and the reactability of the organism are both important for induction of a characteristic, unilocular, acute hematogenic osteomyelitis. Extravasation of the irritant by an injurious agent such as radiation thus may lead to production of osteomyelitis. (BBB)

20372 EFFECTS OF A RADIOMIMETIC SUBSTANCE, NITROGENOUS YPERITE, ON THE MORPHOLOGY AND OXYGEN CONSUMPTION OF AN EMBRYONIC ORGAN CULTIVATED IN VITRO. Kirrmann, Jean-Michel; Cuminge, Danielle (College de France, Paris. CNRS, Paris). Compt. Rend., 261: 5211-14(Dec. 8, 1965). (In French).

Nitrogenous yperite (mustard gas) applied in aqueous solution on the embryonic intestine of the chicken culti-

vated in vitro caused an inhibition of the respiration of this organ. The percentage of the respiratory inhibition was a linear function of the logarithm of the yperite concentration beginning at a dose of 1mM. The principal structures altered by this substance were the nucleus and the adhesivity of cellular membranes. (tr-auth)

20373 NUCLEAR MEDICINE IN THE SERVICE OF AFRICA. Dumont, Jacques E. (EURATOM, Brussels); Ermans, Andre M.; Vis, Henri L. Euratom Bull., 5: 8-15(Mar. 1966).

Studies on endemic goiter, cretinism, and deficiency diseases in the Congo (Leopoldville) are reported. Two radioisotopes of iodine were used for biochemical, kinetic, and anatomical studies of endemic goiter. It was found that the process of adaptation to an iodine deficiency was accompanied by radical alteration in the thyroid machinery, which ultimately lead to a substantial drop in its efficiency. All cretins examined suffered from hypothyroidism. A correlation between mental development of adult cretins and their size or bone age was found. Tracer studies indicated that an insufficiency of thyroid tissue during infancy was the cause of endemic cretinism in the Congo. Investigations of disorders in protein and salt metabolisms were made using isotopic dilution techniques. The main isotopes employed were ^{3}H, ^{22}Na, ^{40}K, and ^{14}C- or ^{35}S-labeled amino acids. (M.C.G.)

20374 PHYSIOLOGICAL NORMS IN INDIAN ADULTS. STATISTICAL ANALYSES OF DATA ON ORGAN WEIGHTS. Venkataraman, K.; Raghunath, V. M.; Santhanam, K.; Somasundaram, S. (Atomic Energy Establishment, Bombay). Health Phys., 12: 572-4(Apr. 1966).

The Health Physics Division of the Atomic Energy Establishment at Bombay, India, studied physiological norms in Indian adults to derive a basis on which to recommend values for maximum permissible body burdens and maximum permissible concentrations of radionuclides. Data on total body weight and weight of adrenals, brain, heart, kidneys, liver, lungs, pancreas, prostate, spleen, stomach, testes, and thyroid were compared to those of the same organs in the ICRP standard man. Correlation ratios of organ weight are tabulated by sex and age group. (H.G.D.)

20375 DEPHOSPHORYLATION OF SOME COFERMENTS WITH THORIUM AND ZIRCONIUM IONS. Trapmann, H.; Devani, M. (Univ., Munich). Indian J. Pharm., 27: 72-5(1965).

Thorium and zirconium ions are shown to catalyze the removal of phosphate groups from cocarboxylase (thiamin pyrophosphate), riboflavin-5'-phosphate, and pyridoxal phosphate under physiological conditions. The initial rapid dephosphorylation of the first substrate in the presence of thorium ions showed that the terminal phosphate group in thiamin pyrophosphate splits easier than that bound directly to the alcoholic group in the substrate. With increasing concentrations of the ions there was a considerable increase in substrate turnover. In alkaline as well as in acidic medium thorium ions possessed better catalytic activity than zirconium; both catalysts were more active in acidic medium than in alkaline medium. It was inferred that these metal ions, when used in therapy, may cause a profound effect on biological systems so that normal metabolism may be stopped altogether or may be directed in abnormal directions. In acid medium, in the absence of catalyst, the terminal phosphate group in thiamin pyrophosphate is hydrolyzed easily. Acid phosphatases from prostate gland dephosphorylate both the phosphate groups in the substrate, whereas alkaline phosphatases from kidney hydrolyze only the terminal phosphate group. The experiments showed that the terminal phosphate group in thiamin pyrophosphate is hydrolyzed rapidly in presence of thorium ions in acidic as well as in alkaline medium, whereas the remaining phosphate group is removed comparatively slowly. Thiamin pyrophosphate is hydrolyzed ~6 times more rapidly with Ce(3+) (at pH 8.6; 37°C) than the corresponding monophosphate. Pyridoxal phosphate is hydrolyzed with phosphatases as well as with Ce(3+), Ce(4+), La(3+), and Mn(2+). These ions are active only in alkaline medium (pH = 8.6). (BBB)

20376 SYNTHESIS OF THE ENZYMES OF THE MANDELATE PATHWAY BY PSEUDOMONAS PUTIDA. III. ISOLATION AND PROPERTIES OF CONSTITUTIVE MUTANTS. Hegeman, G. D. (Univ. of California, Berkeley). J. Bacteriol., 91: 1161-7(Mar. 1966).

Mutants of Pseudomonas putida constitutive for the synthesis of L(+)-mandelate dehydrogenase were obtained after mandelate- or benzoylformate-limited growth in a chemostat. When grown in media noninducing for the wild type, the mutants are capable of coordinate, constitutive synthesis of the first five enzymes of the mandelate pathway. Later enzymes of the pathway that were examined are normally repressed. The constitutive mutants have two other noteworthy properties: they are superinducible by some compounds which induce the mandelate group enzymes in the wild type, or as a result of exhaustion of the carbon and energy source of the medium in which they are grown; and they exhibit a decreased specificity of induction, being inducible by a wide range of compounds devoid of inductive function for the wild type. These results, together with other evidence indicating that the five mandelate group enzymes comprise a regulatory unit, are discussed and evaluated in the context of the general problem of the regulation of complex dissimilatory pathways. (auth)

20377 CYTOPATHIC EFFECTS OF TUMOR VIRUSES IN HUMAN DIPLOID CELLS. SIMILARITY WITH LESIONS OF IRRADIATED CELLS. De Fabritiis, Adriana; Balducci, D. D. (Laboratoire di Microbiologia, Rome). Oncologia, 19: 391-400(1965).

Human diploid cells are the best models at present available for studying the characteristic morphological alterations occurring in a normal human cell populations exposed to tumor viruses. The cytopathology of these cells infected by two animal viruses, Mixoma and Simian Virus 40, and one human, Adenovirus type 12 has been compared. Some of the lesions found in cultures infected by Simian Virus 40 and Adenovirus type 12 are very similar to those found in irradiated cell cultures. (auth)

20378 OTHER BIOLOGICAL EFFECTS OF THE NOBLE GASES. Schreiner, H. R. (Linde Co., Tonawanda, N. Y.). pp 535-8 of Proceedings of International Union Physiology Science, 22nd International Congress, Leiden, 1962.

The growth rates of Neurospora crassa were determined in gaseous environments of air, He, Ne, Ar, Kr, Xe, and N_2. The nature of the gaseous environment was found to have a highly significant effect on the growth rate of N. crassa, but no significant trends attributable to the nature of the gaseous environment could be shown for the lag period. This indicates that germination of the mold spores is not affected by these gases. The rate of oxygen uptake paralleled the growth rate of the mold in all experiments. Sporulation of the mold was diminished in the presence of krypton and completely inhibited by xenon. Molecular weight per se was not responsible for these effects, as is seen by observing the action of sulfur hexafluoride, a gas which is usually unreactive under conditions of cellular metabolism. The partial pressures of inert gases required, when added to 1 atm of air, to halve the oxygen-dependent radiosensitivity of bean roots are shown. These observations indicate that inert gases are capable of displacing oxygen from specific lipid-water interfaces or lipid structures of the cell nucleus. On the basis of this concept, it is reasonable to expect an over-all retardation of hyphae growth and sporulation if a condition of subcellular hypoxia exists which interferes with nuclear division. The results presented here indicate that helium enhances the growth rate of N. crassa relative to a nitrogen–oxygen atmosphere at low but not at high oxygen tensions or a partial pressure of helium greater than 0.5 atm partial pressure. This is explained by the fact that xenon generally exhibits stronger binding forces (Van der Waals forces) than the other inert gases. (TCO)

Ecology

Refer also to abstracts 20879 and 20884.

20379 (COO–1191-10) RADIOECOLOGY OF THE COLORADO FRONT RANGE. Terminal Report. Osburn, W. S. Jr. (Colorado Univ., Boulder). [1964]. Contract AT(11-1)-1191. 173p. Dep. mn. CFSTI $5.00 cy, $1.00 mn.

Results are reported from a study of patterns and processes involved in the distribution of fallout in an alpine watershed. The area selected for study was the Boulder City watershed, Boulder Co., Colo. The characteristics, location, topography, and physiography of the 11 sq. mile area are described and the typical animal activities and plant responses usually associated with the general climatic sequence are outlined for an entire year. Data are included on the soil characteristics; precipitation including snow; population of small animals; and ground surface gross β radioactivity. (C.H.)

20380 (TID–22499) DEVELOPMENT OF A ^{137}Cs FACILITY FOR ECOLOGICAL RESEARCH. Golley, Frank B.; McCormick, J. Frank (Savannah River Ecology Lab., Aiken, S. C. North Carolina Univ., Chapel Hill. Dept. of Botany). Jan. 1966. 27p. Dep. mn. CFSTI $2.00 cy, $0.50 mn.

The criteria, construction, and subsequent testing and operation of a 9200 curie 137-cesium source for ecological studies are described. The source was designed to be used as both a fixed radiation source and a portable facility. The cask and stand is approximately 47 inches high and 55 inches wide and weighs 1500 pounds. The cesium is exposed by opening two doors with handles attached to flexible shafts. These shafts extend through a concrete wall shield. The cask can be lifted onto a truck and transported to the field for in situ exposure of ecosystems. Safety precautions, shielding requirements, and examples of dosimetry are also discussed. (auth)

20381 INFLUENCE OF APPLICATION OF STABLE STRONTIUM TO THE SOIL ON THE ^{90}Sr CONTAMINATION OF CULTIVATED PLANTS: RYE GRASS AND CLOVER. Kirchmann, R. (Centre d'Etude de l'Energie Nucleaire, Mol, France). Physiol. Plant., 18: 885-90(1965). (In French).

Field experiments were carried out in 1960, 1961, and 1962 on the effect of adding stable Sr to soil on the ^{90}Sr content of various parts of Lolium italicum and Trifolium pratense. A low-Ca soil was used, and stable Sr was added at levels of 3 or 7.5 g/m^2. The ^{90}Sr and Ca concentrations of the roots and foliage was measured in each of the three years. Statistical analysis of results showed that the treatments had no significant effect, at the $p = 0.05$ level, on the ^{90}Sr content of the foliage or the roots. However, the differences in ^{90}Sr content of the two species were significant at the $p = 0.01$ level; the content of rye grass was lower than that of clover. It was also observed that the addition of stable Sr to soil modified strongly the $^{90}Sr/Sr$ ratio in the plant. It is concluded that application of stable Sr to soil is not of practical value in attempting to reduce the animal and human ingestion of radiostrontium originating from fallout. (BBB)

Metabolism, Tissue Distribution, and Toxicology

Refer also to abstract 20712.

20382 (BNWL-SA-623) ACCUMULATION AND TRANSPORT OF RADIONUCLIDES BY COLUMBIA RIVER BIOTA. Cushing, C. E.; Watson, D. G. (Battelle-Northwest, Richland, Wash. Pacific Northwest Lab.). Mar. 31, 1966. Contract AT(45-1)-1830. 24p. (CONF-660507–5). Dep. mn. CFSTI $1.00 cy, $0.50 mn.

From Symposium for the Disposal of Radioactive Wastes into Sea, Oceans, and Surface Waters, Vienna.

Data from investigation of the uptake and transport of radionuclides by periphyton, plankton, fish, and selected invertebrates in the Columbia River are presented. A preliminary study of the periphyton was made to determine which biological and environmental factors are most influential in governing the accumulation of ^{32}P and ^{65}Zn from the river and to investigate the relationships between some commonly used indices of production and certain environmental factors. Phosphorus-32 concentrations in Stigeoclonium fluctuated markedly with no apparent trend. Solar radiation had a high correlation with net production rate (NPR) and chlorophyll a. It is suggested that the high correlation between NPR and chlorophyll is consistent with the fact that closest relationships between pigment content and productivity are usually found only during periods of rapid growth. Accumulation and transport of ^{32}P and ^{65}Zn by net plankton was determined in the Columbia River below the Hanford reactors. Reactor effluent contribution to the river remained relatively constant. In general, despite lesser concentrations of radionuclides per unit weight in spring and late summer, more ^{32}P and ^{65}Zn are transported by the plankton at those times due to the increased biomass. In late fall of 1964 and 1965 a wide variety of invertebrates were collected and analyzed for 18 different radioisotopes by multidimensional gamma-ray spectrometry. Samples were collected for the purpose of evaluating the effect of shutting down three production reactors during the first half of 1965. Except for October levels of ^{32}P, ^{51}Cr, and ^{65}Zn (representing 90% of the total gamma activity) were present in lower quantities in 1965. Zinc-65 measurements in whitefish were used to define the extent and time of resident fish movement upstream from the Hanford reactor effluent outfalls and in a tributary stream. (H.G.D.)

20383 (CNEA–185) MARCACION DE INSULINA CON ^{131}I Y SU USO EN TECNICA "IN-VIVO E IN-VITRO". (Insulin Labeling With ^{131}I and its Uses in In Vivo and In Vitro Techniques). Mitta, Aldo E. A.; Penalva, Hernan Juarez (Comision Nacional de Energia Atomica, Buenos Aires (Argentina)). 1965. 10p. Dep. mn.

The technique used for the preparation of ^{131}I-insulin is described. The results obtained with its use in the study of in vivo hepatic turn-over in non-diabetic and in diabetic patients are reported. In vitro studies were also made of the binding capacity of serum fractions with labeled insulin. The results are reported graphically. (J.S.R.)

20384 (COO–1156-13) CONCENTRATION PATTERNS OF ^{90}Sr, ^{137}Cs, AND ^{131}I IN A WILD DEER POPULATION AND ENVIRONMENT. Whicker, F. W.; Farris, G. C.; Dahl, A. H. (Colorado State Univ., Fort Collins. Dept. of Radiology and Radiation Biology). 1966. Contract AT(11-1)-1156. 30p. (CONF-660405–2). Dep. mn. CFSTI $2.00 cy, $0.50 mn.

From Symposium on Radioecological Concentration Processes, Stockholm.

The content of ^{137}Cs, ^{131}I, and ^{90}Sr from fallout in wild mule deer, Odocoileus hemionus hemionus, that inhabit the mountainous region of north-central Colorado was determined. A wide variability in the radionuclide burdens among individual deer was found and the factors responsible for producing the variations were studied. These factors included age, food habits, elevation of residence and associated climatic and vegetative differences and the structure of the population sampled. Simple concentration factors for predicting average tissue levels and doses from vegetative concentrations were calculated for ^{90}Sr and ^{137}Cs and compared to the observed values. (C.H.)

20385 (COO–1184-3) DISTRIBUTION OF AND DISCRIMINATION AGAINST NATURALLY OCCURRING ^{226}Ra IN SWINE. Nelson, Neal S.; Rust, John H. (Chicago Univ., Ill. Dept. of Pharmacology). [1965]. Contract AT(11-1)-1184. 43p. (CONF-660405–5). Dep. mn. CFSTI $2.00 cy, $0.50 mn.

From Symposium on Radioecological Concentration Processes, Stockholm.

Physiological similarities between swine and humans suggest that information on the metabolism and discrimination against ^{226}Ra in swine may have a correlation with human data. Results are reported from a study of the distribution and discrimination against naturally occurring ^{226}Ra in swine on various diets. Samples of food and water ingested by the swine were analyzed for ^{226}Ra content, and the content of ^{226}Ra in soft tissues, bones, blood, fetuses, and milk of swine was determined. The Ca and P content of all samples were also determined. Results indicate that the distribution of ^{226}Ra in the porcine skeleton is relatively uniform while the distribution in soft tissues is extremely variable. The existence of selective barriers for ^{226}Ra was demonstrated. A power function model for the retention of ^{226}Ra by swine was developed. (64 references). (C.H.)

20386 (NP-15916) ANNUAL REPORT ON RESEARCH CONTRACT No. 201/R1/RB, JULY 1964–JUNE 1965. (Institut "Rudjer Boskovic," Zagreb (Yugoslavia)). 104p. Dep. mn.

Progress is reported in investigations on the radioecology of the Bay of Venice. Field observations on several permanent hydrographic stations were made. Besides the common meteorological, physical, and chemical parameters for the whole vertical column of water and above it, investigations concerning the quality and quantity of the phytoplankton were made. These results were completed with the in situ and laboratory determination of the photosynthetic rate for phytoplankton samples. The physico-chemical behavior of some microconstituents in sea water was investigated using electromigration techniques and studying precipitation phenomena. The bioaccumulation of various radioelements in some characteristic animals and natural populations of phytoplankton was studied in laboratory experiments. In these experiments some radionuclides which can play a certain role as potential hazard in controlled and uncontrolled waste discharge from nuclear plants or weapons were used, including $^{56,57,58}Co$, ^{54}Mn, ^{65}Zn, ^{106}Ru. Shrimps (Leander sp.) and mussels (Mytilus galloprovincialis Lam.) were chosen as experimental animals because they can serve as an ideal indicator for the contamination of coastal waters. Besides the uptake and loss rate under more or less natural conditions, the mechanism of the exchange was studied using EDTA as modifier. Some interesting results were obtained when the influence of the increased iron, cobalt, and zinc concentration on the uptake of radiozinc and radiocobalt was followed. (C.H.)

20387 (NYO-2181-3) EPIDEMIOLOGICAL FOLLOW-UP OF THE NEW JERSEY RADIUM CASES. I. REPORT OF THE EPIDEMIOLOGICAL AND MEDICAL STUDY GROUP AND THE PROJECT SUBCONTRACTORS. II. RESUME OF COOPERATIVE LABORATORY STUDIES ON PROJECT CASES AND SPECIMENS. III. RESUMES OF FINDINGS FROM INDIVIDUAL CASE STUDIES. Progress Report to September 1, 1965. (New Jersey State Dept. of Health, West Orange. Radium Research Project). Contract AT(30-1)-2181. 136p. Dep. mn. CFSTI $4.00 cy, $1.00 mn.

A brief résumé of the goals and organization of the project is given along with: a summary of clinical, laboratory, and statistical studies conducted during the reporting period; supportive tabulations and other pertinent exhibits, including a schema for coding x-ray bone lesions; and résumés of findings from twenty-three cases not previously published. (auth)

20388 (SAN-34-2) COMPARISON OF THE ENVIRONMENTAL AND BIOLOGICAL FACTORS AFFECTING THE ACCUMULATION OF ^{90}Sr AND ^{137}Cs IN DEER AND SHEEP. Longhurst, W. M.; Goldman, M.; Della Rosa, R. J. (California Univ., Davis). [1966]. Contract AT(11-1)-34. 30p. (CONF-660405-4). Dep. mn. CFSTI $2.00 cy, $0.50 mn.

From Symposium on Radioecological Concentration Processes, Stockholm.

Factors affecting the accumulation of ^{90}Sr and ^{137}Cs in deer and sheep, on contrasting natural diets, were investigated as an important phase of a continuing study of the comparative biology of these two species of ruminants. The species studied were the native Columbia black-tailed deer (Odocoiles hemionus columbianus) and the domestic sheep (Ovis aries), which forage together over the 5000 acres of range land of the Hopland Field Station, California. Studies encompassing several hundred of these two ruminants have shown that although they occupy the same areas, they are separated ecologically by their food preference. Examination of ruminal contents throughout the year has indicated that deer are primarily browsers while the diet of sheep is approximately 80% grass. Although deer eat some grass (18%), and sheep consume a certain amount of browse (7%), their intake of fallout radionuclides is derived largely from the dominant forage species in their diets. Related factors which affect the accumulation of ^{90}Sr and ^{137}Cs in deer and sheep are considered. (C.H.)

20389 (STI-PUB-108) ISOTOPES AND RADIATION IN SOIL-PLANT NUTRITION STUDIES. Proceeding Series. Proceedings of the Symposium held in Ankara, June 28–July 2, 1965. (International Atomic Energy Agency, Vienna (Austria)). 1965. 612p. (CONF-650614). IAEA: $12.00; Sch 252,-; £ 3.12.0; F Fr 48,-; DM 42,-.

The 45 papers presented at this symposium included discussions on applications of radioisotopes and radiation in studies of the soil chemistry of inorganic ions, soil organic matter, the measurement and movement of soil water, ion uptake and translocation, and the reactions and interactions of fertilizer nutrients in soils and their distribution and use by plants. (681 references.) (C.H.)

20390 (TID-22767) THE PRE-NATAL AND POST-NATAL SEQUELLAE OF THE INTRAUTERINE ADMINISTRATION OF ^{131}I IN THE RAT. Final Technical Report, June 1, 1963–February 28, 1965. Sikov, Melvin R. (Wayne State Univ., Detroit, Mich. Dept. of Radiology). Contract AT(11-1)-1306. 35p. Dep. mn. CFSTI $2.00 cy, $0.50 mn.

Extensive experiments were performed in which ^{131}I was administered to the pregnant female rat twice daily by gavage, either for the first sixteen days of gestation or for the last six. These animals were sacrificed at intervals during the period of administration and thereafter, and the distribution of radioiodine quantitated in the fetal tissues. From these concentration values and from known physical factors the radiation dose to the fetal tissues was calculated, making correction for the organ sizes, which were small relative to the path length of the beta particles. This was done using a model of the fetus which was developed during the course of these studies. This same pattern of administration was used at several high dose levels and a number of animals were studied both prenatally and postnatally. A number of morphologic effects, primarily of the thyroid, were seen. Studies on the physiology of the thyroid were also performed postnatally: it was determined that alterations in thyroid physiology (notably a low thyroid reserve) had been induced in animals after administration of iodine at dose levels which produced little or no morphologic change. It was concluded that it would be of value to perform more intensive studies on the postnatal effects of prenatal radioiodine administration. (auth)

20391 (TID-22825) AUTORADIOGRAPHIC INVESTIGATION OF BRAIN METABOLISM UNDER NORMAL, EXPERIMENTAL, AND PATHOLOGICAL CONDITIONS. Annual Progress Report, June 1965–March 1966. Altman, Joseph (Massachusetts Inst. of Tech., Cambridge). Contract AT(30-1)-3045. 23p. Dep. mn. CFSTI $1.00 cy, $0.50 mn.

Progress is reported in studies of postnatal neurogenesis in rats in which ^{3}H-thymidine was used as a tracer for autoradiographic studies. A generalization concerning the development of the central nervous system in rats is presented according to which the bulk of microneurons forming discrete granular layers in various brain structures are of postnatal origin. Autoradiographic technique was

also used to study alterations in the uptake of labeled amino acids by single nerve cells as a function of behavioral activation. (C.H.)

20392 THE ACTION OF URANYL SALTS ON THE STRUCTURE OF THE BACTERIAL NUCLEOID. I. COMMUNICATION ON THE NUCLEOID. **Fuhs, G. Wolfgang (Univ., Bonn). Arch. Mikrobiol., 49: 383-404 (Nov. 19, 1964). (In German).**

Use of uranyl salts to demonstrate the nucleus (nucleoid) or DNA components is reported in three bacterial species: Bacillus subtilus, Escherichia coli, and Rhodospirillum rubrum. Cells of these bacteria appear to have their nuclear regions filled with fibrous DNA-containing material, instead of dense irregular masses, when treated with aqueous solutions of uranyl acetate after osmic fixation, prior to dehydration and embedding for ultrathin sectioning. The conditions for the occurrence of this effect were studied in detail. The phenomenon occurs in an all-or-none fashion and is dependent on the presence of sufficient free uranyl ions in solution. It is concluded that the formation of a well-defined uranyl complex of DNA is necessary for the induction of the structure effect. Complex formation induces the structure effect by preventing the nucleoid from contraction during subsequent dehydration in organic solvents. This was demonstrated by use of sufficiently concentrated solutions of uranyl nitrate in 70% ethanol after partial dehydration of the bacteria. Besides their action on nuclear structures uranyl ions reduce shrinking of the cells as a whole, presumably by forming complexes with cytoplasmic RNA. These and earlier results are interpreted as evidence that there are no condensed states of DNA material in normally developing bacterial cells. (TCO)

20393 ANALYSIS OF TRACER EXPERIMENTS. V. INTEGRAL EQUATIONS OF PERTURBATION-TRACER ANALYSIS. **Hart, H. E. (City Coll., New York). Bull. Math. Biophys., 27: 417-29(Dec. 1965).**

An integral equation approach to perturbation-tracer analysis in steady-state multi-compartment systems is formulated. The theory is developed for function perturbation and tracer inputs and extended to the case of continuous small perturbations and continuous tracer inputs. Under general conditions, knowledge of the initial entry functions between various pairs of accessible compartments in an otherwise inaccessible and complex system is sufficient to determine fundamental steady-state transport rates between the accessible compartments. The initial entry function approach is therefore particularly useful for studying physiological systems when only a subgroup of compartments is available for injection and tracer measurement. (BBB)

20394 ANALYSIS OF TRACER EXPERIMENTS. VI. DETERMINATION OF PARTITIONED INITIAL ENTRY FUNCTIONS. **Hart, H. E. (City Coll, New York). Bull. Math. Biophys., 27: Suppl. 1, 329-32(1965).**

It is shown that the partitioned initial entry functions in multicompartment analysis can be directly and uniquely determined from the experimental data. A general solution for noncontiguous multicompartment systems is possible. In the solution, initial entry and partitioned initial entry functions play a prominent role. While the initial entry functions are directly determined from the experimental data, the partitioned initial entry functions are evaluated in turn from the initial entry functions. This second, indirect evaluation, though correct, is somewhat cumbersome for numerical and algebraic analysis. The present report indicates that the partitioned initial entry functions can, in fact, also be directly and uniquely determined from the experimental results. (BBB)

20395 THE INCORPORATION OF TRITIATED THYMIDINE BY THE GERMINAL CELLS OF THE EMBRYONIC OVARY OF THE CHICKEN CULTIVATED IN VITRO. **Callebaut, Marc; Dubois, Regis (College de France, Paris). Compt. Rend., 261: 5215-18(Dec. 8, 1965). (In French).**

Fragments of embryonic ovaries of the chicken were cultivated in vitro in the presence of tritiated thymidine. The synthesis of DNA, revealed by autoradiography, showed the homogeneity of the germinal cells of the ovary. The cortex on the 14th day of incubation was an exception: The oögonia with reticulated nucleus did not incorporate thymidine. Graphic representations of the variation of the rate of incorporation of thymidine at different stages of development showed two peaks. The first corresponded to the phase of intense multiplication of the oögonia. The significance of the second peak was not determined. (tr-auth)

20396 INVESTIGATION OF THE METABOLISM OF CARRIER-FREE $^{106}RuCl_3$ AFTER INTRATRACHEAL APPLICATION. **Pleskova, A.; Trnovec, T.; Beno, M. (Ustav Hygieny Prace a Chorob z Povolania, Bratislava). Bratisl. Lek. Listy, 44: 719-24(Dec. 31, 1964). (In Czech).**

The resorption and organ distribution of carrier-free $^{106}RuCl_3$ (0.4 ml, 50 μC/ml, pH 3–4) after intratracheal application was studied in the rat. Various organs were examined 1, 7, 15, 21, and 30 days after administration. The isotope was distributed fairly evenly over the entire body, but the lungs and kidneys showed higher concentrations (4% and 26%, respectively, one day after administration; 2% and 6% 30 days afterwards). Administration of butylene-2,3-diaminetetraacetic acid (DBTA) in 100 μmole dose 2, 4, 6, 8, and 10 days after application of $^{106}RuCl_3$ did not show appreciable protection in animals sacrificed on the fifteenth and thirtieth days. (BBB)

20397 EFFECT OF CHELATING AGENTS ON THE REMOVAL OF ^{65}Zn IN MAN. **Spencer, Herta; Rosoff, Betty (Veterans Administration Hospital, Hines, Ill.). Health Phys., 12: 475-80(Apr. 1966).**

The chelating agents ethylenediaminetetraacetic acid (EDTA) and diethylenetriaminepentaacetic acid (DTPA) were both effective in removing zinc-65 from man and, in most instances, DTPA appeared to be more effective than EDTA. Considerable enhancement in urinary ^{65}Zn excretion could be induced by both these chelating agents at relatively long time intervals following the intravenous administration of tracer doses of $^{65}ZnCl_2$. Also, the chelating agents, bis 2-aminoethylethertetraacetic acid (BAETA) and ethylenediamine di-orthohydroxyphenyl acetic acid (EDDHA) were effective in increasing ^{65}Zn excretion after prolonged time intervals following the injection of $^{65}ZnCl_2$. (auth)

20398 ESTIMATION OF INTERNAL RADIATION DOSE FROM METABOLIC AND URINARY EXCRETION DATA FOR A NUMBER OF IMPORTANT RADIONUCLIDES. **Jackson, S.; Dolphin, G. W. (United Kingdom Atomic Energy Authority, Harwell, Eng.). Health Phys., 12: 481-500(Apr. 1966). (AHSB(RP)–R-51).**

A review is presented of the human data available on the metabolism and excretion of cesium, phosphorus, polonium, plutonium, radium, strontium, sulfur, tritium and uranium, and values of investigation level are suggested for these radionuclides. Use of the data to determine internal radiation dose is discussed. (H.G.D.)

20399 A COMPARATIVE STUDY OF UPTAKE OF ^{32}P BY DIFFERENT ROUTES IN THE NUCLEIC ACIDS OF DEVELOPING CHICK EMBRYO. **Chowdhury, Jayasree Roy; Neogy, Rajat Kumar (Chittaranjan National Cancer research Center, Calcutta). Indian J. Cancer, 2: 118-21 (June 1965).**

Effectiveness of different routes of introduction of radiophosphorus on the incorporation of the isotope into RNA and DNA was investigated. Four sets of eggs 11 days old were injected with ^{32}P through the air sac, yolk sac, amniotic cavity, or allantoic cavity. At different time intervals, ranging from one to 48 hr, four eggs from each set were studied. The embryo tissues were fractionated into nucleus and cytoplasm and each fraction was extracted for nucleic acids. The activities of DNA and RNA were measured and expressed as per cent per g of embryo and nucleus or cytoplasm. The results showed the very slow absorption rate from allantoic cavity. The yolk sac method

was faster but the rate of absorption was not as high as that from air sac or amniotic cavity. As the method of inoculation into the amniotic cavity was rather complicated, the air sac method was considered the best route for max ^{32}P uptake by nucleic acids. Qualitatively, the ^{32}P uptake remained more or less the same with all four routes, when incorporation per g of embryo was considered; cytoplasmic RNA had the max uptake followed by nuclear RNA and DNA. The metabolic activity of RNA in cytoplasm is not greater than that of nucleus. The ^{32}P incorporation in RNA per g of nucleus or cytoplasm was comparable but sometimes greater in nucleus than cytoplasm (weight basis). This is in accord with the findings of others that RNA of the cell nucleus in all tissues becomes labeled much more rapidly and more extensively than RNA in cytoplasm. (BBB)

20400 STRONTIUM AND CALCIUM SKELETAL DISCRIMINATION DETERMINED BY COMPARTMENTAL ANALYSIS. Cohn, S. H.; Bozzo, S. R.; Jesseph, J. E.; Constantinides, C.; Gusmano, E. A.; Robertson, J. S. (Brookhaven National Lab., Upton, N. Y.). J. Appl. Physiol., 21: 67-72(Jan. 1966). (BNL-9089).

Data obtained with ^{85}Sr and ^{47}Ca simultaneously administered to seven human subjects were analyzed according to a compartmental model and an IBM-7094 program. A whole-body counter was employed to obtain data beyond 10 days, and a collimated detector was used to measure the activity in a bone compartment (knee). The results demonstrated that while the absolute values of the parameters obtained with Sr differ from those obtained with Ca, the differences are small and the Sr-derived values do reflect Ca metabolism quite well in terms of the model derived from the 10-day data. With the inclusion of the longer term data, it should be possible to improve the model and permit the quantification of the differences in the physiological parameters of resorption, slow exchange, and bone turnover as measured by Ca and Sr. (TCO)

20401 ON THE DETERMINATION OF INORGANIC IODINE IN HUMAN SERUM. Fitting, W. (Evangelisches Krankenhaus, Cologne). Klin. Wochschr., 42: 744-8(Aug. 1, 1964). (In German).

Under physiological conditions the concentration of inorganic serum I in fasting patients is too small for direct microchemical determination. The exact separation of inorganic from organic I is particularly difficult. Direct determinations usually lead only to very inexact and mostly too large values. The indirect calculation of serum I concentration from the sp act. of the serum I and the urinary I generally gives more accurate values but ones that are still too high. The principal error here is the assumption that the radioactivity of the blood reflects the inorganic serum ^{131}I. This is true only for a short interval after intravenous injection. After this time some of the ^{131}I is organically bound, especially in hyperthyroid patients. In addition, some of the organically bound ^{131}I is excreted by the kidneys. Although the serum I sp act. falls exponentially, the measured sp act. of the urine represents only an average value. Neutron activation of urinary I on an ion exchange column is also used for estimation of serum I. Calculation of serum I concentration by comparison to sp act. of ^{127}I in salivary I gives the most exact values so far. Results have shown that the true serum I concentration is ~0.1 μg I/100 ml serum. This is much smaller than has been assumed heretofore. The accuracy of this method permits accurate quantitative calculations of I metabolism in humans to be made. (BBB)

20402 SELECTIVE INHIBITION OF CATION ABSORPTION BY URANYL. Mason, Benjamin J.; Moore, David P.; Maas, Eugene V. (Oregon State Univ., Corvallis). Nature, 209: 318-19(Jan. 15, 1966).

Detailed experiments were carried out to evaluate the effect of UO_2^{2+} on the metabolic absorption of Li^+, Na^+, K^+, Mg^{2+}, and Mn^{2+} by excised barley roots. From the results, which are shown, it was found that UO_2^{2+} had considerably different effects on the cations studied. The effects of pretreating the barley roots with UO_2^{2+} instead of placing the uranyl in the solution to be absorbed was also investigated and found to be not as pronounced. These results suggest that UO_2^{2+} may be a means of separating and characterizing various cation transport sites. (J.F.P.)

20403 RATE CONSTANTS OF HYDRATED ELECTRON REACTIONS WITH AMINO ACIDS. Braams, Reinier (Argonne National Lab., Ill.). Radiat. Res., 27: 319-29 (Mar. 1966).

The rate constants for reactions between the hydrated electron and amino acids were measured in aqueous deaerated solutions at different pH's. Cystine, cysteine, and the positive histidine ion were very reactive at neutral pH. Asparagine, arginine, and the three aromatic amino acids; phenylalanine, tryptophan, and tyrosine, were found to be moderately active. The other common amino acids were unreactive. With increasing pH the reactivity always decreased. Compounds effective as chemical protecting agents with sulfhydryl or disulfide groups showed high reactivity at neutral pH. (auth)

20404 A COMPARISON OF THE BINDING OF RADIO-CALCIUM ^{47}Ca AND RADIO-STRONTIUM ^{85}Sr WITH THE PLASMA PROTEINS IN DISEASE. Guerin, Marie-Therese (Institut National de Sante et de la Recherche Medicale, Paris). Rev. Franc. Etud. Clin. Biol., 10: 1097-1101(Dec. 1965). (In French).

Binding of ^{47}Ca and ^{85}Sr by plasma proteins was studied in patients with bone metastases. Strontium-85 was recovered entirely in the plasma filtrate, whereas ^{47}Ca was fixed on β globulins. (H.G.D.)

20405 STUDIES ON THE CALCIUM UPTAKE BY TELEOST FISHES. I. ^{45}Ca UPTAKE BY THE CRUCIAN CARP. Mashiko, Kikuya; Jozuka, Kenji (Univ. of Kanazawa, Japan). Sci. Rep. Kanazawa Univ., 8: 107-26(Dec. 1962).

Accumulation of ^{45}Ca by the crucian carp, Carassium carassius, including the pathways of ^{45}Ca exchange, was studied. The ^{45}Ca uptake from the environmental medium by various tissues was measured 12 hr to 30 days after exposure to the isotope. The ^{45}Ca taken up was rapidly accumulated by osseous tissues such as scales, gills, and fins, but the accumulation by bones such as rib, vertebra, and operculum was relatively low initially, followed by increase to a higher rate compared with that of the osseous tissues. This is explained by the fact that the ^{45}Ca supplied by the blood system to these bones is not as great as in the osseous tissues, but the total capacity of ^{45}Ca accumulation is greater. The ^{45}Ca injected into the abdominal cavity was found to be transported by the blood system and mainly distributed in osseous tissues in a similar manner to that when it is taken up from the external medium. Incorporation of ^{45}Ca into the osseous tissues decreased with increase in concentration of stable calcium in the external medium. On the other hand, incorporation of total calcium (isotopic and stable Ca) was constant and independent of the total concentration in the external medium when the latter became more than 20 mg/l. Most of the body surface of the fish, excluding the gills and fins, was practically impermeable to the ^{45}Ca ions. A considerable amount of the ^{45}Ca, about half of the total excretion, is excreted through the anterior part of the fish body. Ion exchange uptake seems generally to occur most actively during the first five days. Both ion exchange and growth accumulation uptake took place more readily in younger than in older fish. (TCO)

Radiation Effects on Biochemicals

See *also* CHEMISTRY — Radiation Chemistry

20406 (N-65-27062) A STUDY OF THE ROLE OF RADIOACTIVITY AND HYDROTHERMAL PROCESSES IN PROTOBIOCHEMISTRY. Bogner, R. L.; Hood, S. L.; White, E. R.; Somani, S. (Nuclear Science and Engineering Corp., Pittsburgh, Pa.). June 1965. Contract NASw-

989. 70p. (NASA-CR-63560; NSEC-118). CFSTI $3.00 cy, $0.75 mn.

The initial phases of a study designed to test the novel and unique hypothesis that organic synthesis and chemical evolution in primitive planetary environments may have proceeded in radioactive hydrothermal systems are described. It was demonstrated that an abundance of biochemically significant organic compounds can be formed from the simplest chemical resources in hot, aqueous environments under the influence of ionizing radiation. Furthermore, it was found that high-molecular weight peptides and proteinoids can be produced in the same unique model system thus providing mechanisms for the generation of macromolecules, an essential development for the evolutionary progression from chemical simplicity to prebiotic molecular complexity. This experimental verification of the possible geological origin of biochemical substances (chemical abiogenesis) suggests that spontaneous primordial chemical reactions might well have led to the production and proliferation of organic molecules in favorable local environments, e.g., hot springs, early in the history of the planet Earth. These ground-based studies assume an immediate significance for lunar and planetary exploration in view of the fact that propitious geochemical events and conditions on the moon and Mars, similar to those present earlier in the history of the Earth, may provide primitive hydrothermal radioactive systems in which abiogenic formation of extraterrestrial organic compounds proceeds at present. (auth)

20407 (ORNL-P-1118) CHANGE IN THE PARTITION OF TOTAL-BODY NITROGEN IN RADIATION CHIMERAS. Kretchmar, A. L.; McArthur, W. H.; Congdon, C. C. (Oak Ridge National Lab., Tenn.). [1964]. Contract W-7405-eng-26. 12p. Dep. mn. CFSTI $1.00 cy, $0.50 mn.

X-irradiated mice treated with homologous bone marrow cells showed decreased fraction of total-body nitrogen in the carcass and an increased fraction in skin. The shift in nitrogen distribution is detectable as early as 4 days after irradiation and marrow treatment, but more definite at 25 days. The results are biochemical evidence that some integumentary structure or structures may be a major target of the graft-versus-host reaction in radiation chimeras. (auth)

20408 INFLUENCE OF IRRADIATED NITROGEN ON THE NITROGEN-FIXING ACTIVITY OF BLUE-GREEN ALGAE. Balloni, W.; Florenzano, G.; Materassi, R. (Univ., Florence). Ann. Inst. Pasteur, 109: Suppl., 62-7 (Sept. 1965). (In French).

Four species (Nostoc muscorum, Anabaena cylindrica, A. variabilis, and Tolypothrix tenuis) of nitrogen-fixing blue-green algae showed, when grown in the presence of uv-irradiated nitrogen, an increase of growth in comparison with the cultures grown in the presence of nonirradiated nitrogen. Irradiation of the gas was carried out with a TUV-6W germicidal lamp (maximum emission at 254 mμ). Moreover, uv-irradiated nitrogen stimulated the nitrogen-fixing activity of algae, as attested by the higher percentage of nitrogen in the dry matter of algae grown in the presence of nitrogen. (BBB)

20409 THE PHOTOCHEMICAL SYNTHESIS OF NOREPINEPHRINE FROM TYRAMINE. Ferrari, R. A.; Luduena, F. P. (Sterling-Winthrop Research Inst., Rensselaer, N. Y.). Arch. Int. Pharmacodyn., 156: 405-13 (Aug. 1965).

The effects of uv radiation on tyramine were investigated by exposing aqueous solutions of tyramine-^{14}C to a Hanovia lamp and examining the products at various intervals by paper chromatography. During uv irradiation tyramine concentration in the reaction system was reduced with time following the second order rate equation. The rate constant was found to be 12 liters per mole-min and the half life was 91 min. Dopamine synthesis took place at the greatest rate. Norepinephrine synthesis took place linearly for the first 60 min of irradiation before the rate fell off at later times. Octopamine formation occurred at the slowest rate. This was about one-third of the rate of norepinephrine synthesis. A sequence of reactions leading from tyramine to norepinephrine is proposed. The rate of introduction of an oxygen atom into the phenolic ring of tyramine to form dopamine was rapid, which showed that dopamine synthesis takes place at the fastest rate. Octopamine synthesis from tyramine was a slow step in the sequence. Tyramine must be oxidized to both dopamine and octopamine simultaneously, but at rates corresponding to the relative ease of oxidation at each of the two sites on the tyramine molecule. Norepinephrine synthesis from dopamine is presumed to be slow by analogy to the rate of side chain oxidation of tyramine to give octopamine. Likewise, norepinephrine synthesis from octopamine is presumed to be more rapid by analogy to the rapid rate of dopamine formation from tyramine. Since norepinephrine formation is shown to be initially zero order or pseudo zero order, it was assumed that most of the norepinephrine arises from the large amount of dopamine synthesized at early times. Therefore, the major route of norepinephrine synthesis from tyramine under these conditions is from tyramine to dopamine to norepinephrine. The oxidation reactions leading from tyramine to norepinephrine probably involve free radical mechanisms. (BBB)

20410 UTILIZATION OF SODIUM SULFATE-^{35}S BY HEPATIC TISSUE OF THE NORMAL AND IRRADIATED RAT. Santagati, G.; Slaviero, G. E.; Cultrera, G.; Bosco, G. (Istituto di Clinica Medica Generale, Pavia). Arch. Sci. Med., 119: 48-56(Feb. 1965). (In Italian).

The effect of whole-body ionizing irradiation on the synthesis by liver of sulfur-containing amino acids was studied in adult Wistar rats. The rats were exposed to 500- or 1000-R doses of 120-kv x rays, and five days later were injected intravenously with 20 μC of $Na_2{}^{35}SO_4$. After one hr the animals were sacrificed and ^{35}S content of various liver fractions was determined on homogenates. In the liver protein fraction, the specific activity was reduced to a similar extent after both doses, to ~500 cpm/g dry tissue compared with ~700 cpm/g in unirradiated controls. In liver polypeptides, specific activity was slightly reduced after 500 R doses but increased more than two-fold after 1000 R. The organic fraction (mainly amino acids) of liver homogenate, obtained after precipitating proteins and peptides by reprecipitation with 50% alcohol, showed a marked reduction of ^{35}S uptake after both doses of radiation. Plasma protein and polypeptide fractions, but not the organic fraction, also showed lower incorporation of ^{35}S following irradiation. The results demonstrate the inhibitory effect of ionizing irradiation on liver protein synthesis. (BBB)

20411 EFFECTS OF γ RAYS ON POLYRIBOADENYLIC AND POLYRIBOURIDYLIC ACIDS AND THEIR TWO- AND THREE-CHAIN ASSOCIATIONS. Ekert, B.; Tisne, M. R. (Univ., Paris). Biochim. Biophys. Acta, 114: 481-90 (March. 21, 1966). (In French).

Using the melting curve technique, the partial denaturation of the secondary structure of irradiated poly-(A + U): γ rays, 3.5×10^{-4} M nucleotides was demonstrated. The T_m decreased rapidly as the dose of radiation increased. The radiochemical yields (G) for the destruction of the bases in the presence of oxygen were, respectively: G(−A) = 1.11; G(−U) = 1.11; the G value (number of breakages of phosphodiester bonds) was 0.19. However, this denatured poly-(A + U) structure was still able to form a triple helix with another chain of unirradiated poly-U. It was shown that a single strand of irradiated poly-A or poly-U can easily combine with the complementary unirradiated chain. As the oxygen renders the bases more sensitive to radiation, the recombination is more efficient when the irradiation has been carried out in the absence of oxygen. Moreover, the association of two complementary irradiated chains seems quite difficult. The G values for bases destroyed within the irradiated polymer (when the irradiation is done in twice-distilled water at pH 7) were, for poly-A: G (in the presence of oxygen), 1; G (in the absence of oxygen), 0.47; for poly-U: G (in the presence of oxygen), 2.1; G (in the absence of oxygen), 1. (auth)

20412 THE KINETICS OF DNA DENATURATION UNDER ULTRAVIOLET RADIATION. Zhil'tsova, V. M.;

Kruglyakova, K. E.; Ulanov, B. P.; Gindin, L. G. (All-Union Correspondence Polytechnic Inst., USSR. Inst. of Chemical Physics, Academy of Sciences, USSR). Dokl. Akad. Nauk SSSR, 164: 198-200 (Sept. 1, 1965). (In Russian).

In order to establish whether ultraviolet radiation exerts a destructive effect on DNA, similar to those caused by x radiation, in vitro studies were carried out with DNA prepared from calf's thymus and rat's spleen. The denaturation of the DNA and the effect of radioprotective agents were followed by means of physico-chemical measurements, including viscosity and spectrophotometric measurements and electron microscopic examinations. The kinetic studies were carried out with solutions containing 20 to 1000 μg/ml of DNA, irradiated with a mercury resonance lamp at 5.7×10^{13} quanta/mm^2 at 22.5 ± 0.2°C. A stepwise decrease of the viscosity was noted; this was attributed to the aggregation of the DNA molecules. The microphotographs confirmed the denaturation of DNA. The radioprotecting agents tested included propyl gallate, hydroquinone, phenol, thymine, and 3-pyridinol; their effects were compared with those of glutathione and cysteine. These free-radical reaction inhibitors, added before exposure, were found to provide better protection than glutathione and cysteine. The protective action is based on the shielding of the DNA molecule, as these compounds absorb the ultraviolet radiation in the 254 mμ range. No free-radical reactions are involved in the denaturation process of DNA. (TTT)

20413 CYTOMORPHOLOGIC AND CYTOCHEMICAL STUDY OF THE CYTOLYSOMES OF THE DUODENAL CRYPTS OF X-IRRADIATED MICE. Hugon, Jean; Borgers, Marcel (Centre d'Etude de l'Energie Nucleaire, Mol, Belg.). J. Microscop., 4: 643-56 (Oct. 1965). (In French).

Electron microscope studies were conducted on intracellular organelles of 12-week-old male mice of the BALB/C strain 30 minutes to 72 hr after 200-kv x irradiation at a dose rate of 100 R/min. A large number of cytolysomes were prominent in the stem cells of the epithelium of the duodenal crypts a few hours after a whole-body irradiation with 1350 R doses. At different time periods after irradiation, the development of these organelles was followed. It seemed that smooth endoplasmic reticulum and golgi vesicles took part in the formation of the triple-layered membrane enclosing this structure. Localization of acid phosphatase in it was demonstrated, and an increased enzyme action was found in the golgi zone and in numerous small vesicles soon after irradiation. Lead salt deposits were prominent in cytolysomes, first confined to the enclosed granules and, at a later stage, dispersed in the cytoplasm. The morphological aspects and relation between lysosomes and cytolysomes and also the transformation of the latter into residual bodies are discussed. It is concluded that acute radiation stress does not prevent the formation of cytolysomes in undifferentiated cells of the duodenal crypts. (BBB)

20414 EFFECT OF ULTRAVIOLET RAYS ON GASTRIC TRANSIT IN THE RAT. Peres, G.; Dumas, J. (Faculte des Sciences, Lyon). J. Physiol. (Paris), 57: 674-5 (Sept.-Oct. 1965). (In French).

Gastric transit of 1.5 ml of a 5.4% glucose solution was studied in rats subjected to a double vagotomy at the level of the cardia, and compared with rats that were subjected to laparotomy. No differences in gastric transit times were observed when the animals were exposed to daylight and free to move. When the animals' movements were restricted, gastric transit in the vagotomized animals exposed to daylight was reduced by ~20%. When restricted animals were exposed to uv light of 1580 and 2500 Å, gastric transit in the laparotomized animals was reduced ~20%, but in the vagotomized animals it was reduced by ~35%. Gastric transit was not as greatly reduced in either group when restricted animals were exposed to incandescent light. The results suggested that vagotomy did not suppress the decreased gastric transit produced by exposure to uv, under the experimental conditions used. The results seemed to indicate that splanchnectomy produces a slightly favorable effect. (BBB)

20415 UTILIZATION OF CERTAIN BIOCHEMICAL INDICES FOR ASSESSING EFFECTS OF IONIZING RADIATION ON THE ORGANISM. Sviderskaya, T. A. (Inst. for Research in Radiation Protection, Leningrad). Med. Radiol., 10: No. 12, 51-7 (Dec. 1965). (In Russian).

The effects of x-irradiation (450- to 500-R doses) on the sulfhydryl content and the alkaline phosphastase activity in the blood were studied clinically and experimentally during the course of acute radiation sickness. Latent effects of gamma irradiation in small doses on these parameters were also investigated. (H.G.D.)

20416 MECHANISMS OF NECROSIS AND PREPARATION OF CELLS DAMAGED BY IONIZING RADIATION. de Waard, R. H. Ned. Tijdschr. Geneesk., 109: 1187-8 (June 19, 1965). (In Dutch).

The injury which leads to the death of irradiated tumor cells appears to affect vital organelles of these cells. Damage in normal, nonmalignant tissues is repaired by regeneration so that vital organs are maintained. Fractionated administration of the total radiation dose causes more damage to normally growing cells than a single dose. Cellular injury may be produced chemically, by combination of two radiation-produced OH radicals. The quantity of H_2O_2 produced may be calculated; kinetic behavior is in agreement with observations on fractionated irradiation. Likewise, the removal of H_2O_2-damaged cellular materials as metabolites may explain the ability of normal cells to maintain themselves postirradiation. Consideration of the rate of replication of tumor cells leads to formulation of the replication period of the cell as a fraction of its lifetime, 0.03, the same order of magnitude as for normal cells. Other calculations which are provided relate the radiation dose and volume of the tumor to the chance of destroying the tumor; the smaller the tumor, the smaller the dose necessary to nearly ensure destruction. (BBB)

20417 BIOCHEMICAL LESIONS INDUCED IN SUBCELLULAR STRUCTURES BY IONIZING RADIATION. III. CYTOCHROME C OXIDASE AND GLUCOSE-6-PHOSPHATASE ACTIVITY OF RAT LIVER. Dancewicz, Antoni M.; Mazanowska, Anna; Panfil, Barbara (Inst. of Nuclear Research, Warsaw). Nukleonika, 10: 783-9 (1965).

Cytochrome c oxidase and glucose-6-phosphatase activity of subcellular fractions isolated from rat liver were assayed at 0.2 or 24 hours after whole-body irradiation of rats with a dose of 750 R. No definite changes in activity of cytochrome oxidase were found, whereas an increase in glucose-6-phosphatase activity in nuclear (at 0, 2 and 24 hr) mitochondrial (at 2 and 24 hr) and in microsomal (at 2 hr) fractions were clearly demonstrated. (auth)

20418 ASSAY FOR ADENOSINE TRIPHOSPHATE IN X-IRRADIATED TRADESCANTIA ANTHERS. Beatty, Alvin V.; Beatty, Jeanne W. (Emory Univ., Atlanta). Contract AT-(40-1)-2669. Radiat. Res., 27: 347-54 (Mar. 1966).

Recovery from radiation damage in Tradescantia was brought about only be treatment with ATP, not with such constituents as ADP, AMP, adenine, and sodium pyrophosphate. As determined by luciferin–luciferinase assay, the ATP content of the anthers of x irradiated Tradescantia was doubled after treatment for 1½ hours in an ATP solution. The ATP content of the microspore protoplasm remained relatively constant. Periods of anoxia from 16 minutes to 400 minutes were accompanied by a corresponding decrease in ATP content in the anthers and an increase in chromosomal aberrations in the microspores. When inflorescences were placed in ATP solutions during this 400-minute period of anoxia, the ATP levels in the anthers remained high, and the aberration frequency in the microspores was lowered almost to the control value. When inflorescences were treated with ATP^{32}, radioactivity was demonstrated in the microspore protoplasm. Twice as much radioactivity was found in the microspores of irradiated inflorescences as in nonirradiated, indicating that under stress of radiation more ATP is used. (auth)

20419 DOSE-DEPENDENT GAMMA IRRADIATION EFFECTS ON THE RESTING POTENTIAL OF NITELLA FLEXILIS. Esch, Harald E. (Univ. of Notre Dame, Ind.). Radiat. Res., 27: 355-62(Mar. 1966). (COO-205-57).

The dose dependency of changes in the resting potential of Nitella flexilis induced by cobalt-60 γ rays at a dose rate of approximately 6 kR/min in the dose range from 1 to 800 kR is described. The drop in resting potential, which begins immediately at the start of irradiation, increases up to approximately 20 mv by 50 kR. With doses from 50 to 200 kR there is no further drop. With doses from 200 up to 800 kR the potential decreases faster and faster and drops suddenly to zero. The bath solution in which the cell is irradiated influences the magnitude of the observed effect in the range from 1 to 30 kR. The time required to reach the peak also increases with increasing doses. A hypothesis for the reason for the difference in effects in the ranges from 1 to 50 kR and from 200 to 800 kR is given. (auth)

20420 TRIGLYCERIDE BIOSYNTHESIS IN IRRADIATED BONE MARROW. Snyder, Fred (Oak Ridge Associated Universities, Tenn.). Radiat. Res., 27: 375-83 (Mar. 1966).

A study of the effect of γ irradiation on the lipids of rat marrow showed that a fat cell fraction of marrow contained only triglycerides, with incorporation of fatty acids limited to this class of lipids in both control and irradiated rats. In control rats only a small quantity of the ^{14}C-labeled fatty acid (<12%) was incorporated into the triglycerides of the sedimented fraction consisting principally of hemopoietic cells, but after irradiation this fraction incorporated palmitic-1-^{14}C (60%) and stearic-1-^{14}C (79%) acids at a high rate. The data demonstrate that total-body irradiation stimulates the esterification of saturated fatty acids in the marrow into triglycerides and that this stimulation occurs in the sedimented hemopoietic fraction separated by centrifugation of a marrow suspension, rather than in the floating fraction of mature fat cells. (auth)

20421 THE ACTION OF IONIZING RADIATION ON POSTIRRADIATION SYNTHESIS AND DEGRADATION OF DNA IN ESCHERICHIA COLI 15 T^-L^-. Pollard, Ernest C.; Achey, Phillip M. (Pennsylvania State Univ., University Park). Contract AT(30-1)-2804. Radiat. Res., 27: 419-33(Mar. 1966).

The effect of γ radiation on the synthesis and degradation of DNA in E. coli 15 T^-L^- has been studied. Synthesis continues for low doses for about a division time, but the greater the dose is, the lower the rate. There is a dose-reduction factor of 2 for the action on synthesis between oxygenated and nitrogenated medium. Degradation of DNA is observed in E. coli 15 T^-L^-, WWU, B, and B/r strains. The dose-effect relationship for degradation has been established for normal cells, both oxygenated and nitrogenated, and for cells with 5-BU in the DNA. In the latter case degradation occurs at smaller doses than for normal DNA. DNA synthesized after irradiation does not degrade as readily as normal DNA. Cells heated to 70°C for 10 minutes show no DNA degradation after irradiation. No evidence of cell lysis was found. (auth)

20422 SODIUM AND POTASSIUM BINDING IN X-IRRADIATED NUCLEI. Jackson, Kenneth L.; Christensen, Gerald M. (Univ. of Washington, Seattle). Radiat. Res., 27: 434-44(Mar. 1966).

Rat spleen nuclei were subjected to in vitro x irradiation over a dose range from 25 R to 2000 R. No effect of these doses on the levels of bound nuclear sodium or potassium could be detected within 5 to 10 minutes after exposure. Increasing the time to 2 hours after in vitro exposure with 1000 R also failed to show a radiation-induced loss of sodium or potassium. Similarly, in vivo irradiation of rats with 1000 R did not result in lowered levels of sodium or potassium in spleen nuclei isolated 1 hour after exposure. The response of lymphoid cell nuclei from calf thymus glands was also investigated. In vitro x irradiation of isolated calf thymus nuclei with doses of 100 R and 1000 R did not cause a loss of bound nuclear sodium or potassium 5 to 10 minutes post-exposure. It is concluded that, under the conditions employed in these experiments, sodium and potassium binding by lymphoid cell nuclei is not a radiosensitive process. (auth)

20423 THE EFFECTS OF RADICAL SCAVENGERS ON THE RADIOSENSITIVITY OF LYSOZYME IN DILUTE AQUEOUS SOLUTIONS OF VARYING pH. Brustad, Tor (Norsk Hydro's Inst. for Cancer Research, Montebello, Norway). Radiat. Res., 27: 456-73(Mar. 1966).

X radiation inactivation of lysozyme dissolved in a buffer containing citric acid and sodium phosphate was studied in the pH range from 2.5 to about 11. The radiosensitivity was determined under conditions where the enzyme solution was bubbled with O_2 or N_2 during irradiation. The relationship between α and pH has thus been established for the present experimental conditions within this wide pH range. Changes in the radiosensitivity of lysozyme, caused by the presence of specific radical scavengers during the exposure, were studied. Taking into account reactions between the radical scavengers and the primary radiolysis products of water, we have arrived at rough estimates of the contributions to the enzyme inactivation from hydroxyl radicals, atomic hydrogen, and hydrated electrons within the pH range from 2.5 to about 9.0. (auth)

20424 THE MECHANISM OF ACTION OF AET. VI. THE PROTECTION OF PROTEINS AGAINST IONIZING RADIATION BY GED. Kollmann, George; Shapiro, Bernard (Albert Einstein Medical Center, Philadelphia). Radiat. Res., 27: 474-86(Mar. 1966).

The mechanism of action of the radiation-protective agent GED was studied in protein solutions. In 1% solutions of trypsin, lysozyme, and aldolase, GED (5×10^{-4}M) provided significant protection against inactivation and solubility changes. This protection was not the result of scavenging of radicals from the radiolysis of water. Such scavenging appeared to occur only in solutions containing less than 1% protein. The only change in GED during irradiation of solutions containing 1% or more protein was protein binding. This binding was always by mixed disulfide formation in proteins containing sulfhydryl or disulfide groups. The mechanism of protection by radiation-induced mixed disulfide formation between GED and protein sulfur groups is postulated, and it is suggested that this may be a mechanism of protection in the living animal. (auth)

20425 THE ACTION OF X RAYS ON BLOOD TYPING SERA. Schildt, Evert E. son; Gullbring, Bengt (Karolinska Sjukhuset, Stockholm). Rev. Int. Serv. Sante Armees Terre Mer Air, 36: 379-80(June 1963). (In French).

To investigate the possibility that blood typing sera might be inactivated by irradiation, the action of ionizing radiation on hemagglutinins was evaluated. Thus, anti-A and anti-B typing sera were irradiated with 100-, 1000-, and 10,000-R doses (air) of 260-kv x rays at a dose-rate of 96.5 R/min. In the first experiment, the irradiated hemagglutinin was tested against fresh, nonirradiated erythrocytes. In the second, irradiated red cells were used. Tests with irradiated hemagglutinin showed no variation in titers attributable to irradiation. Likewise, irradiation of erythrocytes did not cause qualitative or quantitative alterations in hemagglutination reactivity. (BBB)

20426 A RADIATION-GENETIC METHOD TO DECIDE WHETHER ONE OR BOTH OF THE DNA STRANDS INJECTED BY A VIRUS INTO ITS HOST TRANSMIT THE HEREDITARY INFORMATION TO THE PROGENY. Barricelli, Nils Aall; Womack, Frances (Vanderbilt Univ., Nashville). Virology, 27: 589-99(Dec. 1965).

A method employing uv radiation was devised to investigate whether only one or both of the DNA strands injected by an infecting virus into a cell transmit genetic information to other DNA strands. By the same procedure it was also possible to assess some of the functions of the two DNA strands. The method is based on a classification of the various types of function which are possible in the two cases: duplication of both or only one of the injected DNA strands. These two cases are referred to as duplex

hypothesis and simplex hypothesis, respectively. The types of function possible in the two cases presented differences which could be tested by appropriate experiments. In the case of the simplex hypothesis, it was also possible to decide whether the strand transmitting the hereditary information is always the same (simplex-D hypothesis) or whether it is randomly selected in each particular phage or each particular cell (simplex-R hypothesis). To decide among the simplex D, simplex R, and duplex hypotheses, an investigation was made of the survival of phenotypes (SP) and the survival of genotypes (SG) of uv-irradiated phages in a number of T4 cistrons. Both SP and SG were determined by infecting a nonpermissive host bacterium with a mutant phage unable to perform a function necessary for phage growth and an irradiated wild-type phage which can supply the function needed if a section of its genetic material essential for the function has not been hit by a photon of radiation. (BBB)

20427 RADIATION-GENETIC EVIDENCE THAT ONLY ONE OF THE TWO DNA STRANDS INJECTED BY PHAGE T4 TRANSMITS THE GENETIC INFORMATION TO THE PROGENY. **Womack, Frances; Barricelli, Nils Aall (Vanderbilt Univ., Nashville). Virology, 27: 600-13 (Dec. 1965).**

A technique using uv radiation was used to investigate whether only one or both of the DNA strands injected by phage T4 into its host transmit hereditary information to the progeny. An experimental identification of the uv responses of 16 functions of phage T4D (two rII functions and 14 amber functions) was carried out. The results are inconsistent with the theoretical predictions that would be obtained by this procedure if the information of both injected DNA strands was transmitted to the progeny. Of the 16 functions investigated, 11 fit (often with high precision in spite of the possible causes of error) the predictions obtained on the hypothesis that only one injected DNA strand (hereafter called genetic strand) transmits its information to the progeny, while the other injected strand (hereafter called associated strand) does not. The fit was obtained without use of any free parameter. Evidence is also presented to the effect that the genetic strands are all identical with respect to base sequence (except for mutant loci). Associated strands are also identical to one another and complementary to the genetic strands except for possible mutant loci. About 50% of the functions investigated was found to be of a type (called macrotarget functions) that is performed by the associated strands in the early stages of the infectious process and by copies of the genetic strand later on. (TCO)

20428 INFLUENCE OF X RADIATION ON THE HILL REACTION AND PHOTOSYNTHESIS PHOSPHORYLATION FOR ISOLATED AND FRAGMENTED CHLOROPLASTS IN VARIOUS PRESERVATIVES. **Perner, E.; von Falck, S.; Jacobi, G. (Tieraerztliche Hochschule, Hannover). Z. Naturforsch., 20b: 1077-85 (Nov. 1965). (In German).**

Isolated chloroplasts and chloroplast fragments of different structural states characterized by electron microscopy were irradiated with x rays. The resistance of Hill activity and phosphorylation coupled with ferricyanide was strongly dependent on the structural state of chloroplasts and thylakoids influenced by isolation media or by treatment with hypotonic media or digitonin. Whole chloroplasts were more resistant than free membrane systems without stroma and envelope. If free membrane systems were suspended in media of low salinity (broken chloroplasts) the rate of oxygen evolution and of phosphorylation decreased by a factor of 3.8 or 3.0 respectively after irradiation. The Hill reaction and phosphorylation were suppressed successively by washing the particles in hypotonic media or by treatment with digitonin. However, the sensitivity of oxygen evolution against x rays remained constant in the washed particles whereas the rate of ATP formation decreased. As demonstrated by dose effect curves, low intensities of x rays activated the Hill activity for all fractions. The results are discussed in relation to the integrity of chloroplasts and the state of membrane (thylakoids) as carrier for the systems of Hill reaction and phosphorylation. (auth)

Radiation Effects on Tissues

Refer also to abstract 20726.

20429 (AD-629311, pp 15-25) STUDIES ON THE EFFECT OF X-RADIATION ON THE HEXOBARBITAL METABOLIZING SYSTEM OF LIVER MICROSOMES. **Yam, Kei-ming; DuBois, Kenneth P. (USAF Radiation Lab., Univ. of Chicago, Ill.).**

Studies on the process of resynthesis of the hexobarbital metabolizing enzyme system in the regenerating liver of the hepatectomized rats showed that complete resynthesis of this enzyme system occurs within 22 days after partial hepatectomy. The process is, therefore, reversibly inhibited by x radiation. It was found that the extent of x radiation inhibition of the resynthesis process for the hexobarbital metabolizing system is somewhat dependent on the time of administration of x radiation in most instances. Thus a greater degree of inhibition of enzyme resynthesis was obtained when x ray was given at 11 to 13 hours after hepatectomy than when x ray was given at 40 to 45 hours after hepatectomy. (auth)

20430 (AD-629311, pp 26-32) HYPOBARIC OXYGEN EXPOSURE AND ACUTE RADIATION LETHALITY IN MICE. **Doull, J.; Plzak, V. (USAF Radiation Lab., Univ. of Chicago, Ill.).**

Adult, male Carworth Farms CF_1 mice were exposed to acute whole-body x irradiation in the dose range of 400 through 700 R under environmental conditions of hypobaric oxygen (100% O_2 at 5 psia) and air to determine whether this environmental situation alters acute radiation lethality in this species. There was no significant difference in the 30-day LD_{50} obtained for groups of animals irradiated in the hypobaric oxygen environment (LD_{50} = 534 ± 17 R) when compared to that of animals irradiated in air (LD_{50} = 551 ± 25 R). The mice irradiated under hypobaric oxygen conditions exhibited, however, a slightly shortened median survival time (particularly in the mid-lethal x-ray dosage range). (auth)

20431 (AD-630323) RESPONSES OF SINGLE NEURONS IN THE OLFACTORY BULBS OF RABBITS, DOGS, AND CATS TO X RAYS. **Cooper, G. P.; Kimeldorf, D. J. (Naval Radiological Defense Lab., San Francisco, Calif.). Jan. 26, 1966. 19p. (USNRDL-TR-969).**

Extracellular microelectrode recordings were made of the activity of single neurons in the olfactory bulbs of anesthetized cats, rabbits, and dogs. In all three species, brief exposure to x rays (250 kvp; exposure rate, 1 R per second) produced an alteration in firing rate in some olfactory bulb neurons. The response to irradiation was usually an increase in firing rate, but in a few cases a depression in firing rate was observed. (auth)

20432 (AD-630332) COMPARISON OF DOSE PATTERNS IN A DOG EXPOSED TO NEUTRONS AND TO X RAYS. **Wingate, C. L.; Page, N. P.; Ainsworth, E. J. (Naval Radiological Defense Lab., San Francisco, Calif.). Feb. 7, 1966. 32p. (USNRDL-TR-974).**

Dose distributions with depth in a dog cadaver and in a cylindrical phantom were obtained for 1 mvp transmitted x rays and for mixed neutron and gamma radiation from a reactor. The ratio of neutron to gamma dose was 4:1 at the surface of the dog. Measurement of the gamma or x ray dose was made using LiF thermoluminescence dosimeters, while neutron dose was obtained from the activation of small sulfur pellets, with suitable calibrations. Placement of dosimeters was verified by roentgenography. Penetration of the 1 mvp x rays is considerably higher than that of the reactor neutrons, whose effective energy is about 1 Mev, and does not appear to differ significantly in various cross sections of the body as was found for 250 kvp x rays by others. For the reactor beam administered unilaterally the energy deposition in the dog is strongly asymmetric as

shown by isodose configurations for the neutron and gamma components. However, only minor variations were found in the depth dose curves for the phantom and different sections through the dog cadaver, namely, head, chest, and abdomen, in spite of the differences in composition and density. (auth)

20433 (AD-630390) THE EFFECT IN STOMACH OF IONIZING RADIATION ON ACID SECRETION, POTENTIAL, ADENOSINE TRIPHOSPHATE AND PHOSPHOCREATINE IN COMPARISON TO SPLEEN. Cummins, J. T.; Kohl, H. H.; Vaughan, B. E. (Naval Radiological Defense Lab., San Francisco, Calif.). Feb. 21, 1966. 28p. (USNRDL-TR-980).

Results using an in vitro rat stomach preparation indicate that gastric acid secretion is stimulated through neurological pathways and induced by both handling and x irradiation. The changes in acid secretion occurred independently of alterations in the sodium-potassium dependent potential across the stomach. Despite the two functional radiation effects, there were no gross changes in phosphorylative metabolism in rat stomach, otherwise adenosinetriphosphate and phosphocreatine would have been affected. At the same time, there was the expected irradiation change in spleen ATP, but the spleen phosphocreatine remained unchanged. The latter is a new observation which puts in question some aspects of the current cellular theory of splenic irradiation effects. (auth)

20434 (AD-630870) AN ULTRASTRUCTURAL STUDY OF THE DEVELOPMENT OF RADIATION INJURY IN THE LUNG. Phillips, T. L. (Naval Radiological Defense Lab., San Francisco, Calif.). Feb. 1, 1966. 19p. (USNRDL-TR-973). CFSTI $1.00 cy, $0.50 mn.

X-radiation doses of 2000 R were given to the left hemithorax of a group of 25 rats. At intervals of from one hour to one year following irradiation, sections of the lung were examined with the electron microscope. The initial site of radiation damage appeared to lie chiefly in the endothelium. The endothelium was sloughed and the original endothelial space was replaced by collagen and mast cell infiltrates. Some capillaries were recanalized by new endothelial cells. Eventually these capillaries attained an appearance similar to that of the original capillary but with a slightly thickened endothelium and basement membrane. If the original capillary architecture was not maintained, massive fibrosis resulted. The mast cell participates extensively in the repair of the radiation damage and is closely associated with collagen and new capillary formation. It is stressed that the degree of damage occurring after a given dose of irradiation varies widely and that these observations were made on only small samples of lungs. (auth)

20435 (CONF-650560-15) BIOCHEMICAL ASPECTS OF RADIATION INJURY AND RECOVERY. Michaelson, Sol M.; Angel, Charles R.; Woodward, Kent T.; Howland, Joe W. (Rochester Univ., N. Y. Dept. of Radiation Biology. Walter Reed Army Inst. of Research, Washington, D. C. Dept. of Radiobiology). [nd]. Contract AT(30-1)-1286. 9p. Dep. mn. CFSTI $1.00 cy, $0.50 mn.

From 13th Annual Meeting of the Radiation Research Society, Philadelphia.

Principles of physiology and biochemistry were utilized in studies to assess late manifestations of ionizing radiation. Biochemical indices among beagles that survived whole- and partial-body exposure to 1 Mev x rays were correlated for comparison of relative sensitivities of vital processes in various portions of the animal's body. Altered biochemical activity in relation to diminished physiologic reserve capacity are of significance in delineating radiation injury and repair processes and the animal's ability to respond to superimposed and interposed stresses. (auth)

20436 (CONF-650560-17) OXYGEN UPTAKE IN RAT BRAIN TISSUES X-IRRADIATED IN VITRO. Lott, James R.; Hines, John F. (North Texas State Univ., Denton. Dept. of Biology). [1965]. Contract AT(40-1)-3270. 24p. Dep. mn. CFSTI $1.00 cy, $0.50 mn.

From 13th Annual Meeting of the Radiation Research Society, Philadelphia.

The changes in oxygen uptake in various brain tissues in rats x irradiated in vitro was determined manometrically. The specific areas studied were: the cerebral cortex, the thalamus, mid-brain, and pons-medulla. The doses of x irradiation used were 10 and 20 kR. The important findings were that the Qo_2 values of isolated brain tissues show a decreasing metabolic gradient from cortex to brain stem that can be altered with x irradiation; respiration of the cortex and pons-medullary tissues were inhibited during the second hour post-irradiation following 20 kR, whereas, the thalamic and mid-brain tissue slices exhibited little change to these doses; and the changes observed occurred in the absence of circulating humoral agents indicating a localized effect of the ionizing radiation. The results were discussed in terms of changes in biochemical integrity, permeability, and on the basis of differences in cellular morphology of the tissues studied. (C.H.)

20437 (CONF-650560-18) CHANGES IN 5-OH TRYPTAMINE CONTENT IN RAT BRAIN TISSUES X-IRRADIATED IN VITRO. Lott, James R.; Hines, John F. (North Texas State Univ., Denton. Dept. of Biology). [1965]. Contract AT(40-1)-3270. 22p. Dep. mn. CFSTI $1.00 cy, $0.50 mn.

From 13th Annual Meeting of the Radiation Research Society, Philadelphia.

The changes in 5-OH tryptamine (5-HT) content of various rat brain tissues x irradiated in vitro at 10 and 20 kR were determined fluorimetrically. The tissue slices were taken from the cortex, thalamus, mid-brain, pons-medulla, and cerebellum. It was found that following 10 kR all of the tissues except the pons-medulla showed slight (10 to 28%) decreases in 5-HT content, whereas, at 20 kR, all but the thalamus and the cerebellum exhibited marked increases in 5-HT content (31 to 42%). The changes observed occurred in isolated slices and in the absence of any circulating humoral agents indicating localized action of the x irradiation. There was no gradient of radiosensitivity from cortex to brain stem in regard to changes in 5-HT levels. The thalamic and cerebellar areas exhibited the least sensitivity. The results indicate a two-phase radiation effect; the first occurring at a lower dose level resulting in a net decrease in 5-HT content while the second phase occurred at the higher dose resulting in a net increase in 5-HT levels. The results are discussed on the basis of changes in 5-HT formation, degradation, binding, and membrane permeability. (22 references.) (auth)

20438 (EUR-2518.f) EFFETS DES MICRO-IRRADIATIONS DE SEGMENTS CHROMOSOMIQUES. CONSEQUENCES MORPHOLOGIQUES, BIOCHIMIQUES ET GENETIQUES. Rapport Final. (Effects of Micro-Irradiations of Chromosome Segments. Morphological, Biochemical and Genetic Consequences. Final Report). (Louvain Univ. (Belgium). Laboratoire de Cytogenetique). June 22, 1965. 44p. Dep. mn.

The experimental procedures are described that were developed for the micro irradiation of chromosomes with ultraviolet, x rays, and alpha particles. Results obtained in studies on the effects of radiation on chromosomes in developing pollen grains in culture are reported. (C.H.)

20439 (EUR-2628.i) EFFETTO DELLE RADIAZIONI SULLA DETOSSICAZIONE DELL' α-METILNAFTALENE. (Effect of Radiations on the Detoxification of α-Methylnaphthalene). Scoppa, P.; Gerbaulet, K. (European Atomic Energy Community, Ispra (Italy). Joint Nuclear Research Center). Nov. 11, 1965. 12p. (CONF-650967-2). Dep. mn.

From Italian Society of Experimental Biology, 34th General Assembly, Sorrento, Italy.

The increase in the excretion of glucuronides induced in rats by the oral administration of α-methylnaphthalene was found to be reduced by half if the animal were previously x irradiated. Some of the possible causes are examined and discussed. (auth)

20440 (EUR-2643.f) ETUDE DE L'EFFET DES RAYONNEMENTS SUR L'EMBRYON ET SES ORGANES IN VIVO ET IN VITRO. Rapport sur les Recherches Effectuees an Cours de la Periode du 1 October 1964 au

30 September 1965. (Study of Radiation Effects on the Embryo and Its Organs In Vivo and In Vitro. Report on Research Performed, October 1, 1964–September 30, 1965). (Institut d'Embryologie Experimentale, Nogent-sur-Marne (France)). Nov. 9, 1965. 14p. Dep. mn.

The effects of x rays on germ-cells, the migratory power of these cells, and DNA synthesis in gonocytes in chickens were studied by means of labelling with tritiated thymidine. The effects of x rays on the physiology and respiratory metabolism of the chick embryo intestine and heart was investigated extensively. Certain biochemical effects of x rays on coenzyme I and its glycohydrolase are reported. The mode of action of chemical and radioprotective agents, such as cysteamine, was studied in an embryonic organ cultivated in vitro. Certain early radiation lesions were detected by electron microscopy. The radiosensivitity of the natural inductor in amphibians was measured, as also was the teratogenesis action of radiomimetic substances such as nitrogenated mustard gas. Irradiation experiments were carried out on cancerous nodules cultivated in vitro and a number of regeneration problems were solved with the aid of x irradiations. (auth)

20441 (ORNL-P-1173) LATE SOMATIC EFFECTS OF RADIATION EXPOSURE IN LABORATORY MICE. Cosgrove, G. E. (Oak Ridge National Lab., Tenn.). [1964]. Contract W-7405-eng-26. 21p. Dep. mn. CFSTI $1.00 cy, $0.50 mn.

Mice exposed to sub-lethal, mid-lethal, or supra-lethal doses of x-rays show group survival and disease incidence that are different from that seen in unirradiated controls. Mean survival time of irradiated groups is shortened in proportion to radiation dose. Thymic lymphoma, myeloid leukemia, ovarian, breast and certain other tumors appear in greater incidence and at an earlier mean age in irradiated groups. Degenerative diseases such as glomerulosclerosis, ocular lens cataract, and greying of the hair are likewise radiation induced. These late changes are manifestations of the irreparable component of radiation injury. (auth)

20442 (ORNL-P-2053) COMPARATIVE OBSERVATIONS ON RADIATION CARCINOGENESIS IN MAN AND ANIMALS. Upton, Arthur C. (Oak Ridge National Lab., Tenn.). [1965]. Contract W-7405-eng-26. 78p. (CONF-660314-1). Dep. mn. CFSTI $3.00 cy, $0.75 mn.

From 20th Annual Symposium on Fundamental Cancer Research, Houston, Tex.

Developments in epidemiological studies in man directed toward radiation dose-effect relationships and in mechanisms of radiation carcinogenesis in animals are surveyed. Epidemiological studies in human populations on leukemia, prenatal irradiation, bone neoplasms, thyroid tumors, carcinomas of the respiratory tract, skin cancer, and other neoplasms are reviewed. Studies of experimental carcinogenesis in animals are included on: leukemia, osterosarcomas, and tumors of breasts, pituitary glands, thyroid, lungs, liver, kidneys, and gastrointestinal tract. (H.G.D.)

20443 (PB-181506, pp 143-54) RADIATION IN BIOLOGICAL SYSTEMS. Pollard, Ernest C. (Pennsylvania State Univ., University Park).

An analysis was made on the effects of radiation on molecules of importance in biology. This type analysis, in terms of known molecular effects of radiation, proved to be of real interest for microorganisms. Although it was not successful for mammalian cells, it failed in a way that suggests that the study of macromolecular organization, in its relation to its constitutive parts, might reveal the action of molecular damage. (P.C.H.)

20444 (TID-22820) EFFECT OF RADIATION ON A NATURAL POPULATION OF LIZARDS. Final Report. Tinkle, Donald W. (Texas Technological Coll., Lubbock). [1965]. Contract AT(40-1)-2673. 7p. Dep. mn. CFSTI $1.00 cy, $0.50 mn.

Studies were made on lizard populations exposed to whole-body x irradiation. The major results thus far are the laboratory measurement of the LD-50/30 and of the effects of radiation on the male spermatogenic cycle. The major results in the field were the demonstration of lowered natality following radiation with subsequent lowering of the density the following season. It has also been suggested that the breeding structure of the population was adversely affected by radiation. Data are available for determining what, if any, effects radiation had on growth rates, rates of tail regeneration and skin shedding, on activity and movements, and on mortality and longevity. (P.C.H.)

20445 (TRG-Inf. Ser.-166) ACTION OF ^{90}Sr–^{90}Y ON DEVELOPING KHAMSA SPAWN. Polikarpov, G. G.; Ivanov, V. N. Translated by G. R. Taylor (Reactor Group, United Kingdom Atomic Energy Authority, Sellafield, Eng.), from Vop. Ikhtiol., 1: 583-9(1961). 12p. Dep. mn. BIS $0.40. HMSO 2s.

Results of experiments on the effects of various amounts of $^{90}Sr-^{90}Y$ in seawater on the development of the spawn of the Black Sea fish Engraulis encrasicholus and of rock bass Serranus scriba showed that harmful effects were produced by concentrations of 10^{-10} c/l seawater and higher. It was concluded that there is potential danger to the reproduction of marine fish in further increases in the existing content of $^{90}Sr-^{90}Y$ in seawater. The effects of fallout from the detonation of nuclear weapons and the disposal of liquid radioactive wastes in the sea are discussed. (C.H.)

20446 ANEMIA IN MICE INFECTED WITH GAMMA-IRRADIATED OR NONIRRADIATED SCHISTOSOMA MANSONI. Erickson, Duane G. (Walter Reed Army Medical Center, Washington, D. C.). Amer. J. Trop. Med. Hyg., 14: 996-1002(Nov. 1965).

Mice were exposed to: infection with γ-irradiated schistosomes in which oviposition was either absent or greatly diminished; a nonirradiated bisexual infection; or a unisexual infection with nonirradiated male schistosomes. Anemia, evaluated in terms of microhematocrit and hemoglobin values, was the single pathological index. Group 1 mice were each exposed to 1554 cercariae of both sexes irradiated with 3000 R of ^{60}Co γ rays. Mice infected with nonirradiated schistosomes of both sexes demonstrated decreased hemoglobin and hematocrit values by 8 weeks after exposure. This anemia was severe by 12 weeks and was characterized by a depressed mean corpuscular hemoglobin concentration. Mice harboring a greater number of schistosomes of only the male sex demonstrated only a slight anemia by 16 weeks after exposure. Similarly, mice infected with both sexes of schistosomes, which had been irradiated with 3000 R so that oviposition was greatly diminished, demonstrated only slight anemia after 16 weeks of infection. (TCO)

20447 CHROMOSOME STUDIES ON A RADIOGRAPHER AND HER FAMILY: REPORT OF ONE CASE OF LEUKEMIA AND TWO CASES OF DOWN'S SYNDROME. Conen, Patrick E.; Erkman, Bayzar; Laski, Bernard (Hospital for Sick Children, Toronto). Arch. Internal Med., 117: 125-32(Jan. 1966).

A family with two mongols and a leukemic child in the same sibship is described. The role of radiation in leukemia and chromosomal trisomy is considered because the mother was a radiographer for 5½ years. As a technician she carried out standard x-ray procedures including fluoroscopy, and an average of 3500 patients were examined per year (1950 to 1955). A Landsvert pocket protection tube was worn but a protective apron was worn only by the radiologist during fluoroscopy. No reliable estimate of radiation exposure could be obtained. Chromosomal studies made on this family showed that blood and marrow cells from the leukemic child had normal chromosomes and both mongols had trisomy 21. Normal chromosome patterns were found in leukocyte cultures from both parents and from skin cultures from the mother. The relation between x-ray exposure of the mother and leukemia and mongolism in her children was uncertain, since radiation dosage received by the mother was probably not great and abnormalities were not found in offspring of other radiographers with similar exposure. (TCO)

20448 INDUCTION OF BENIGN AND MALIGNANT THYROID NEOPLASMS IN THE RAT. INDUCTION OF THYROID NEOPLASMS BY INJECTION OF ^{131}I WITH OR WITHOUT THE FEEDING OF DIETS CONTAINING PROPYLTHIOURACIL AND/OR DESICCATED THYROID. Lindsay, Stuart; Nichols, C. W. Jr.; Chaikoff, I. L. (Univ. of California, Berkeley. Univ. of California, San Francisco). Arch. Pathol., 81: 308-16(Apr. 1966).

The development of benign and malignant thyroid neoplasms was studied in Long-Evans rats one year after they were injected with 25 μc of ^{131}I and fed diets containing propylthiouracil or desiccated thyroid powder or both. Thyroid malignancies that developed were of three types: papillary carcinomas that were probably malignant from their inception; papillary carcinomas that arose from preexisting follicular adenomas; and follicular carcinomas that developed from preexisting follicular adenomas. The ^{131}I injection and the feedings of propylthiouracil and the desiccated thyroid powder all seemed to play a part in the initiation and promotion of the benign and malignant neoplasms. That their effects are additive was indicated by the findings that the incidence of benign and malignant thyroid neoplasms was higher in rats treated with all three agents than in those treated with one or two. The potentiation of the effects of propylthiouracil by the feeding of the desiccated thyroid powder seems to apply in the development of benign and malignant thyroid neoplasms as well as to the accentuation of goitrogenesis. (C.H.)

20449 RADIATION INJURIES OF THE NERVOUS SYSTEM. Zeman, Wolfgang (Indiana Univ. Medical Center, Indianapolis). Arch. Psychiat. Nervenkrankh., 206: 185-98(Nov. 19, 1964). (In German).

Cytological, biochemical, and genetic injuries induced in the central nervous system by irradiation are reviewed. Absorbed dose, dose rate, and linear energy transfer are discussed in relation to their role as physical parameters that affect cellular reactions in radiation. (H.G.D.)

20450 STUDIES OF CHLOROPLAST DEVELOPMENT IN EUGLENA. XIII. VARIATION OF ULTRAVIOLET SENSITIVITY WITH EXTENT OF CHLOROPLAST DEVELOPMENT. Hill, Helen Z.; Schiff, Jerome A.; Epstein, H. T. (Brandeis Univ., Waltham, Mass.). Biophys. J., 6: 125-33(Mar. 1966).

Ultraviolet inactivation of green colony-forming ability of several different types of Euglena gracilis var. bacillaris was studied. The observed target numbers are not widely different, while the doses required to produce a single inactivation event (D_0) vary with the type of cell used. In dark-grown cells adapting to the light in resting medium and in an x-ray-induced mutant D_0 is proportional to the chlorophyll content of the cells. However, in hyperdeveloped cells which contain abnormally high amounts of chlorophyll, the correlation does not hold, suggesting that it is not chlorophyll per se which is responsible for the differences observed. D_0's of colony-forming ability (viability) of light-grown and dark-grown cells are found to differ by the same factor as those of green-colony-forming ability. Stationary phase and exponential phase cells show a small difference in D_0 with no obvious difference in target multiplicity. The multiplicity of the various target curves has been re-evaluated by computer and found to be between 30 and 40. (auth)

20451 THE AMOUNT OF CATECHOLAMINES IN THE AURICLES OF IRRADIATED RABBITS AND THEIR RESPONSE TO QUINIDINE. Varagic, Vladislav; Stepanovic, Stepan; Svecenski, Nadezda; Hajdukovic, Srdjan. Bull. Boris Kidrich Inst. Nucl. Sci., 16: 173-83(July 1965).

Isolated auricles of rabbits irradiated with 1000 R were investigated in periods from 24 hr to 12 days after irradiation with regard to their capacity to follow various frequencies of exogenous pulses, their response to quinidine, and their spontaneous frequency. In the period between the 3rd and 10th day after irradiation the response to quinidine increased. The maximum frequencies of exogenous pulses, which the untreated auricles of irradiated animals could follow were similar from 24 hr to 12 days after irradiation, and did not differ much from those of control, nonirradiated animals. The spontaneous frequency of auricles isolated from irradiated animals was significantly smaller than that of control animals. The quantity of catecholamines in auricles of irradiated animals was significantly reduced 24 hr after irradiation. It was concluded that tissue catecholamines present in the auricles may play some role in the genesis of pulses on which the spontaneous action of the auricles depends, but they are of no significance regarding the response to quinidine and the capacity to follow exogenous pulses. (auth)

20452 PROLIFERATIVE ACTIVITY OF BONE MARROW CELLS IN MICE BLED IMMEDIATELY AFTER IRRADIATION WITH 600 r. INVESTIGATION WITH ^{3}H-THYMIDINE. Karanovic, Dobrila; Karanovic, Jovo; Hajdukovic, Srdjan. Bull. Boris Kidrich Inst. Nucl. Sci., 16: 185-9(July 1965).

Investigations on mice showed that bleeding immediately after irradiation with 600 R intensifies proliferative activity of bone marrow cells in the regeneration phase. Compared with non-bled irradiated controls there were also some indications of earlier regeneration. (auth)

20453 THE EFFECT OF GAMMA AND NEUTRON IRRADIATION ON LITTER SIZE IN THE MOUSE. Carmon, J. L.; Williams, R. G. (Univ. of Georgia, Athens). Bull. Georgia Acad. Sci., 23: 79-88(Sept. 1965).

Fertility data were collected on 1396 litters over four generations of BALB/C mice to study the effects of pure and mixed doses of ^{60}Co γ and of neutron radiation. Litters conceived within eight days after the males were treated were smaller than litters sired by males 43 days after treatment, indicating recovery from initial partial sterility effects. Treatment differences were found in first litters, but not in second litters. In the first litters, pure neutrons and pure γ irradiation produced similar results. No differences were observed between these pure doses. Males treated with pure doses produced significantly smaller litters than did the males treated with the mixed doses. This effect was probably due to a 12-hr time lapse between doses in the mixed treatments. High levels in both γ and neutron pure doses significantly decreased litter size when compared to low doses. This difference between the high and low level was not present in the mixed doses. The reduced fertility was not permanent in that no treatment differences were observed in the litters from the second matings. The treatment-by-generation interaction was insignificant. The finding that litter size in all treatments was larger in the second matings than in the first matings was explained as a function of age of females. It was shown that litter size increases with age of female and/or number of litters and that this increase is present up to the fifth litter. (BBB)

20454 RADIATION EXPOSURE IN PARENTS OF CHILDREN WITH MONGOLISM (DOWN'S SYNDROME). Sigler, Arnold T.; Lillienfeld, Abraham M.; Cohen, Bernice H.; Westlake, Jeannette E. (Johns Hopkins Univ., Baltimore). Bull. Johns Hopkins Hospital, 117: 374-99 (Dec. 1965).

As part of an epidemiologic investigation utilizing interview technique and medical record analysis, parents of children with Mongolism and control subjects were evaluated for exposure to various types of radiation. All 288 cases were matched with controls of identical sex, race, and hospital of birth. The history of irradiation as summarized from the interview and medical records was divided into the following categories: diagnostic radiation excluding fluoroscopy, fluoroscopic exposure, radiation for therapy, and occupational contact. A larger, but insignificant, number of abdominal and/or pelvic exposures were reported on interview for both parents of Mongols as compared with control parents. The total maternal fluoroscopic exposures reported on interview showed that 17.7% of the Mongol mothers had one or more fluoroscopic examinations prior to birth of the index case, as compared to only 8.1% of the controls, a difference significant at less than the 1%

level. Of the mothers of Mongols, 14.5% reported one or more therapeutic exposures as compared to only 5.1% of the control mothers—a three-fold increase. A history of radar exposure showed a significantly increased amount of radar exposure among fathers of Mongols. The results suggest that maternal ionizing radiation exposure may be one etiological factor responsible for some cases of Mongolism. It is emphasized, however, that ionizing radiation may be only one of several important factors in the pathogenesis of the condition. (TCO)

20455 PROGRESSIVE MYELOPATHY IN A DOG CAUSED BY THORIUM DIOXIDE. Lord, L. H. (McGill Univ., Montreal).; Robinson, G. A. Can. J. Comp. Med. Vet. Sci., 29: 306-11(Dec. 1965).

Hazards and tissue response to Thorotrast are described with reference to its use in dogs. Pathogenesis of Thorotrast-induced myelopathy is described in an 11-month-old boxer examined for suspected cerebrospinal disease by myelography, during which 2 ml of cerebrospinal fluid was replaced with 2 ml of Thorotrast introduced into the cisterna magna. Histological examination of the spinal cord confirmed the diagnosis. Findings at autopsy showed that the entire original dose could be accounted for in the spinal cord tissue and meninges. (H.G.D.)

20456 CONCERNING THE MECHANISM BY WHICH HADACIDIN POTENTIATES THE DAMAGING ACTION OF IONIZING IRRADIATION ON BACTERIA. Pittillo, Robert F.; Bannister, Edward R.; Johnson, Elwanda P. (Southern Research Inst., Birmingham, Ala.). Can. J. Microbiol., 12: 17-23(1966).

The potentiation of radiation damage by hadacidin in proliferating E. coli was investigated. Apparently this effect of hadacidin may be due to an effect in previously described mechanisms of inhibition by hadacidin: inhibition of adenylosuccinate synthetase and undefined inhibition of energy production. E. coli cells grown in the presence of adenylic acid, adenine, oxalacetic acid, or anthranilic acid for 4 hr before exposure to radiation were insensitive to the hadacidin radiation effect. (auth)

20457 EVALUATION OF ACRIDINE ORANGE FLUORESCENCE TEST IN VIABILITY STUDIES ON ESCHERICHIA COLI. Korgaonkar, K. S.; Ranade, S. S. (Indian Cancer Research Centre, Bombay). Can. J. Microbiol., 12: 185-90(1966).

Cultures of Escherichia coli subjected to various treatments were studied for their viability loss, as well as for the changes in fluorescent response on staining with the fluorochrome acridine orange. The treatments employed were irradiation with gamma rays (two different dose rates), beta rays, and ultraviolet rays; thermal shock; thymine starvation; and streptomycin inhibition. Marked deviations from the Strugger effect were seen. The differences in response observed at different dose rates of irradiation are discussed. (auth)

20458 PATTERNS OF CUTANEOUS PIGMENTATION FOLLOWING SUNLIGHT IRRADIATION. Becker, Sam W. Jr. (Whiting Clinic, Ind.); Freeman, Robert G.; Knox, John M. Dermatol. Trop., 3: 234-7(Oct.-Dec. 1964).

The effects of chronic exposure to sunlight on the pattern on melanin granules were studied in samples of irradiated and unirradiated skin from Caucasians representing various complexion types and from Negroes. Findings supported the concept of accelerated melanin production and distribution from melanocytes to malpighian cells and stratum corneum during response to sunlight. (H.G.D.)

20459 EXPERIMENTAL INFLAMMATION AND FIBROSIS OF LUNG STROMA BY IONIZING RADIATION. LIGHT- AND ELECTRON-MICROSCOPIC INVESTIGATIONS. Baessler, R.; Buchwald, W. (Univ., Mainz). Fortschr. Geb. Roentgenstr. Nuklearmed , 104: 192-206(Feb. 1966). (In German).

The development, extent and form of experimental radiation injury in the lungs of rats was studied by subjecting sixty animals to a single dose of 2,000 R to one half of the body. The animals were sacrificed at times varying from two hours to 174 days. Light and electron microscopic examination showed gradual development of radiation damage in the lungs. Exudation of plasma into connective tissue is accompanied by interstitial inflammation that gradually develops into progressive fibrosis. Observations of the early stages following irradiation point to the importance of increased capillary permeability in the radiation pathology of the lung. (auth)

20460 NONMALIGNANT NEW GROWTH IN IRRADIATED GROWING BONES. Kolar, J.; Bek, V. (Charles Univ., Prague). Fortschr. Geb. Roentgenstr. Nuklearmed., 105: 226-30(Feb. 1966). (In German).

Eight cases of osteochondromas in children occurring approximately ten years after irradiation of a zone of growth are reported. The most important data are presented in tabular form. Although these have so far all been benign lesions, care and further observation are advisable in order to exclude malignant change and early treatment should this occur. (auth)

20461 MUTATION RATES AT A NEW SET OF SPECIFIC LOCI IN THE MOUSE. Lyon, Mary F.; Morris, T. (M.R.C. Radiobiological Research Unit, Harwell, Eng.). Genet. Res., 7: 12-17(Feb. 1966).

Previous measurements of specific locus mutation rates in mice had all involved the seven loci, a, b, c, d, p, s and se. An experiment was performed with the same mouse stock (C3H × 101) and the same radiation dose (600 rad) to spermatogonia as had been used previously, but employing a new group of six loci, a, bp, fz, ln, pa and pe. The observed mutation rate, 5.0×10^{-3} per locus per rad, was significantly lower than that for the original seven loci, but was three to four times higher than the corresponding mutation rate in Drosophila melanogaster. (auth)

20462 GLUTAMIC DEHYDROGENASE IN REVERTANTS OF AM MUTANTS IN NEUROSPORA. Stadler, David R. (Univ. of Washington, Seattle). Genet. Res., 7: 18-31(Feb. 1966).

Five allelic mutants of Neurospora that lack glutamic dehydrogenase (am mutants) were induced to revert with ultraviolet. The glutamic dehydrogenase produced by the revertants was compared to that of wild-type. Several distinct classes of revertants could be distinguished by these tests. However, genetic analysis showed that all the reversions resulted from events at or near the site of the original am mutation. The spectrum of reversion types depended on the nature of the am mutant employed. One mutant, which produces an am protein believed to be altered in its active site, yielded revertants which were all indistinguishable from wild-type. Another mutant, which produces a protein with a functional active site but altered folding properties, gave at least six classes of revertants which were different from wild-type. (auth)

20463 INDUCTION OF MUTATIONS BY UV RADIATION AND NITROUS ACID IN EXTRACELLULAR PHAGE ϕX174. Chernik, T. P.; Krivitskii, A. S. (Inst. of Radiation and Physico-Chemical Biology, Moscow). Genetika, No. 2, 39-46(Aug. 1965). (In Russian).

Ultraviolet-induced inactivation and mutagenesis was studied in the extracellular phage ϕX174. Inactivation was exponential with dose in the survival range of 10^{-4} to 10^{-5}. An insignificant but statistically valid increase of the h-mutant was found at different doses. Spontaneous mutagenesis in regard to h-mutant development showed an inverse relation to phage density when plated on a mixed bacterial layer consisting of sensitive and resistant cultures. (H.G.D.)

20464 STUDY OF MUTABILITY IN THE WASP MORMONIELLA VITRIPENNIS WLK. Gershenson, S. M. (Inst. of Microbiology and Virology, Kiev). Genetika, No. 2, 95-101(Aug. 1965). (In Russian).

A study of dominant lethals induced by x irradition of Mormoniella vitripennis males (dosages 4500 and 3500 R) showed that dominant lethals arise with about the same

frequency as in Drosophila and Habrobracon. In recombinant males obtained by intercrossing two stocks of different geographical origin the frequency of induced dominant lethals was somewhat higher than in males of the parental stocks. A study of recessive lethals induced by x rays in males of M. vitripennis (dosage 3500 R) showed that recessive lethals arise here also with about the same frequency as in Drosophila and again their frequency was higher in recombinant males than in males of the parental stocks. The significance of the above results is discussed in relation to the mechanism of intraspecific differentiation and the influence of hybridization on mutability. (auth)

20465 THE ROLE OF NORMAL EPIDERMIS IN RECOVERY OF REGENERATIVE ABILITY IN X-RAYED LIMBS OF TRITURUS. **Rose, Florence C.; Rose, S. Meryl (Tulane Univ., New Orleans). Growth, 29: 361-93 (Dec, 1965).**

A study was made of promotion of regeneration in x-irradiated limbs of adult Triturus viridescens by normal epidermis. Comparisons were made between regeneration in unirradiated limbs, irradiated limbs, and irradiated limbs provided with a normal epidermis. In some cases both epidermis and blood cells were labeled with tritiated thymidine. In others, either the epidermis or the blood was labeled. Totally irradiated limbs in contrast to normal limbs failed to dedifferentiate appreciably, but epidermis in both continued to produce DNA and cells divided. Along with the failure of dedifferentiation there was a failure of internal cells to divide. Labeled normal epidermis both on normal limbs and irradiated limbs could be traced until basal layers of the apical cap transformed to mesenchyme. On normal limbs the transformed labeled cells could be traced until some were transformed to chondrocytes. In addition to providing cells for regeneration, normal epidermis of irradiated limbs also enabled the tissues to dedifferentiate and, at least, begin to participate in regeneration. (BBB)

20466 CONSEQUENCES OF INGESTION BY MAN OF REAL AND SIMULATED FALLOUT. **LeRoy, George V.; Rust, John H.; Hasterlik, Robert J. (Univ. of Chicago. Argonne Cancer Research Hospital, Chicago). Contract OCD-OS-62-214. Health Phys., 12: 449-73(Apr. 1966).**

Real and simulated particulate fallout and solutions of $^{85}SrCl_2$ and $^{134}CsCl$ were fed to 102 healthy volunteers. Absorption and retention of ingested radioactivity was measured by whole-body counting using the gamma-ray spectrometer at the Argonne Cancer Research Hospital. An average of 3 per cent of the radioactivity of week-old local fallout was absorbed: the range was 0 to 9 per cent. Strontium and cesium leached or dissolved from simulated fallout behaved in the same way, metabolically, after absorption as they did when the tracer was swallowed in a solution or injected intravenously. The large number of subjects studied provided additional information on the range of variation of intestinal motility, biological availability of strontium, cesium and barium following ingestion of fallout, and retention of the radionuclides of these elements. (auth)

20467 THE EFFECT OF WHOLE BODY IRRADIATION (300 R) ON EXPERIMENTAL BLADDER CALCULUS FORMATION IN RATS. **Cockett, A. T. K.; Nakamura, R. M.; Fingerhut, A. G.; Roberts, A. P. (Univ. of California, Los Angeles). Invest. Urol., 1: 552-4(May 1964).**

In a systemic evaluation of urologic factors which may be encountered in space travel, studies were directed to an evaluation of potential hazards on experimental bladder calculus formation from ionizing irradiation. The effect of whole-body x irradiation on experimental bladder calculus formation was examined in male Sprague-Dawley rats. The animals received a 300 R air dose ten days after implantation of the magnesium metal discs into the urinary bladder. Eight weeks post-irradiation all rats were sacrificed and plasma was obtained for calcium and phosphorus determinations. Bladder calculi were found in both groups that had a disc previously implanted. The weight of calculi in the disc-bearing, nonirradiated group ranged from 31 to 186 mg (mean 71 mg). In the disc-bearing, irradiated group the calculi weighed 7.8 to 103 mg (mean 37.5 mg). Phosphorus determinations in plasma showed significant differences in mean plasma phosphorus levels between the control group and the disc-nonirradiated group and between the disc-nonirradiated group and disc-irradiated group. Plasma calcium values were not significantly different between the control and experimental groups. (TCO)

20468 MYOCARDIAL INFARCTION DUE TO POST-IRRADIATION FIBROSIS OF THE CORONARY ARTERIES: CASE OF SUCCESSFULLY TREATED HODGKIN'S DISEASE WITH LOWER ESOPHAGEAL INVOLVEMENT. **Dollinger, Malin R. (Memorial Hospital for Cancer and Allied Diseases, New York); Lavine, Daniel M.; Foye, Laurance V. Jr. J. Amer. Med. Ass., 195: 316-19(Jan. 24, 1966).**

Complications following radiotherapy for Hodgkin's disease were observed in a male patient. The major disability was due to postirradiation fibrosis, resulting in elephantiasis of the legs, coronary artery occlusions, and acute myocardial infarction. At autopsy, the right coronary artery showed fibromuscular hyperplasia inferior to the internal elastic membrane, and it was concluded that the fibro-muscular proliferation of the right coronary artery was due to irradiation. (H.G.D.)

20469 CHARACTERIZATION OF MYCOPLASMA AEROSOLS AS TO VIABILITY, PARTICLE SIZE, AND LETHALITY OF ULTRAVIOLET IRRADIATION. **Kundsin, Ruth B. (Peter Bent Brigham Hospital, Boston. Harvard Medical School, Boston). J. Bacteriol., 91: 942-4(Mar. 1966).**

Viable aerosols of four strains of Mycoplasma: M. hominis II, M. pharyngis, M. pneumoniae, and an undetermined strain recovered from a lung at autopsy were dispersed, and the particle size was determined. The median diameter of the droplet nuclei ranged from 1.5 to 3.1 μ. M. pharyngis had a dieaway constant k of 0.008, indicating a survival potential of 6 hr from 10,000 colony-forming units at 23% relative humidity. Ultraviolet irradiation destroyed over 99% of the aerosols of all four strains concurrently with spraying. The particle size and viability of the droplet nuclei carrying Mycoplasma were consistent with the theory of airborne transmission of lower respiratory-track infection. (auth)

20470 SYNTHESIS OF THE ENZYMES OF THE MANDELATE PATHWAY BY PSEUDOMONAS PUTIDA. II. ISOLATION AND PROPERTIES OF BLOCKED MUTANTS. **Hegeman, G. D. (Univ. of California, Berkeley). J. Bacteriol., 91: 1155-60(Mar. 1966).**

Mutants of Pseudomonas putida, induced by uv exposure, blocked in early reactions of the pathway for oxidation of D-mandelate were isolated and partially characterized. The specific genetic lesions in these mutants made normal inducer-metabolites of the pathway nonmetabolizable. Under the conditions of gratuitous enzyme synthesis so obtained, it could be shown that the D and L isomers of mandelate are equipotent inducers, and that the synthesis of the first five enzymes of the mandelate pathway is coordinate. Further experiments with the blocked mutants showed that benzoylformate, the third intermediate of the pathway, acts as an inducer without prior conversion to mandelate, and that there is no inducible, concentrating permease for mandelate. (auth)

20471 EFFECT OF DARK REPAIR ON ULTRAVIOLET SENSITIVITY OF BACTERIOPHAGE-INFECTED BACTERIA. **Feiner, R. R.; Hill, R. F. (Columbia Univ., New York). J. Bacteriol., 91: 1239-47(Mar. 1966).**

Changes in ultraviolet (UV) sensitivity of phage-host complexes during phage development were studied for the following systems: T1 and Escherichia coli B, T1 and E. coli K-12S, λ and E. coli K-12S. Complexes were formed with bacterial strains differing in ability to dark-repair UV damage to deoxyribonucleic acid and, after irradiation, were plated on bacteria differing similarly. In the first half of the latent period, the resistance of complexes formed with nonrepairing bacteria increased considerably;

with Tl and E. coli B hcr⁻, in 4 min the resistance became the same as that of complexes formed with repairing bacteria. The repair ability of plating bacteria affected survival curves only upon irradiation in the second half of the latent period after mature phages were present in the initial complex. Use of nonrepairing bacteria both for initial infection and for plating of late complexes resulted in a series of survival curves showing for all three systems the same pattern of change originally reported for T2-E. coli B complexes. Thus, a hitherto unexplained difference between radiation survival curves for T-even and T-odd phages seems due to repair of T-odd phages by the host. (auth)

20472 MORTALITY OF RADIATION CHIMERAS IN RELATION TO THE NUMBER OF TRANSPLANTED BONE MARROW AND LYMPH NODE CELLS. Vos, O. (TNO, Rijswijk, Netherlands). J. Nat. Cancer Inst., 36: 431-43 (Mar. 1966).

Injection of lymph node cells along with therapeutic doses of bone marrow cells into x irradiated mice can cause death if the lymphoid cells are capable of reacting against the host animal. The mortality and time of death are proportional to the number of lymphoid cells injected. Death can be as late as 70 days after irradiation. Injection of bone marrow cells alone can cause death but only when very large numbers of cells are given and only in certain donor-host combinations. Great numbers of bone marrow cells raise the death rate after injection of lymph node cells in certain donor-host combinations but counteract this killing effect in other combinations. The number of immunologically competent cells in bone marrow from both CBA and C57BL mice is small. In CBA mice an equivalent number of immunologically competent cells was estimated in 20×10^6 bone marrow and in 0.05 to 0.1×10^6 lymph node cells; for C57BL mice these figures were 50×10^6 bone marrow and 0.4×10^6 lymph node cells. To explain why bone marrow can apparently offset the killing effect of lymphoid cells, it is postulated that immunologically tolerant cells developing from pluripotent stem cells in bone marrow compete with immunologically competent lymphatic cells. (auth)

20473 CHANGES IN THE ULTRA-VIOLET ABSORBENCY OF CULTURED CELLS DURING INTERPHASE AS ESTIMATED BY FLYING-SPOT MICROSCOPY. Freed, J. J.; Benner, J. A. Jr. (Inst. for Cancer Research, Philadelphia). Contract AT(30-1)-2356. J. Roy. Microscopy. Soc., 83: 79-82(June 1964). (TID-19077).

Studies are described in which a vibrating-mirror flying-spot microscope was used to follow changes in the uv absorbency of individual living cells, as well as uv-induced injury of the cells. The measurements were made using radiation at 280 mμ, and thus reflect changes in cellular protein and nucleic acids. Results of the experiments suggest that synthesis of these materials can continue in spite of the irradiation required for measurement. The construction of the vibrating-mirror flying-spot microscope, and its use in making absorption measurements are described. Measurements were made on cells of a Chinese hamster line C14 FAF28 (Yerganian) inoculated into perfusion chambers three hours prior to the beginning of measurement. Findings suggest that measurement of uv absorbency in the microscope requires doses of radiation that approach the threshold of sensitivity of the cells. In some cases, a period of normal growth is observed, but is finally terminated either by the cumulative effect of all radiation applied, or by the entry of the cell into a sensitive part of the cell cycle, e.g., prophase. (TCO)

20474 STUDY OF BIOLOGICAL EFFECTS OF X IRRADIATION ON THE HEART. (THIRD REPORT)— ON ELECTROCARDIOGRAPHIC CHANGES DURING DEEP X-RAY THERAPY. Kurata, N. (Coll. of Medicine, Sanchoh County Univ., Japan). Jap. Circ. J. (Full Ed.), 25: 916-23(Sept. 1961). (In Japanese).

Early changes in the electrocardiogram (EKG) following x irradiation were observed in three patients receiving precordial cardiac irradiation and in three cases of noncardiac region irradiation. In direct cardiac exposed cases the T wave showed early depression and PR interval prolongation in 3 to 7 min following irradiation. After 45 min, the T wave was either elongated, depressed, or unchanged, T, PR, and RR intervals were shortened, prolonged, or unchanged with no difference in cardiac irradiated and nonexposed groups. Thereafter, EKG parameters returned to the normal values. EKG changes after fractionated large-dose irradiation in the cardiac region group showed an increase in T waveheight; an increase in QT interval; and a decrease in PR interval. EKG changes after irradiation with fractionated large doses in the noncardiac region failed to show significant damage of the cardiac muscle during radiotherapy at the usual dose, as seen by bioelectric activity of heart muscle. (TCO)

20475 PECULIAR FEATURES IN RADIATION SICKNESS INDUCED BY SOFT X RAYS. Liberman, A. N.; Vainshtein, P. R.; Krisyuk, E. M.; Tikhomirova, M. D. (Inst. for Research in Radiation Protection, Leningrad). Med. Radiol., 10: No. 12, 30-4(Dec. 1965). (In Russian).

In experiments on albino mice the influence of a single total dose 4,130 R of soft x rays (10 kev) on the development of skin lesions, alteration of the body weight and leukocyte count in the peripheral blood was studied. The skin is viewed as one of the critical organs during the action of this kind of radiation on the organism. It is suggested that the sharp decrease of the body weight and increase of the leukocyte count observed on the fourth week of the disease are associated with the development of marked changes in the skin. (auth)

20476 INFLUENCE OF URETHAN ON CHANGES IN THE SKIN OF MICE CAUSED BY X IRRADIATION. Turgunov, M. B. (Inst. of Experimental and Clinical Oncology, Academy of Medical Sciences, USSR). Med. Radiol., 10: No. 12, 35-8(Dec. 1965). (In Russian).

The skin of urethan-treated mice was not noticeably affected by x irradiation (150-R doses). However, whole-body x irradiation with the same dose following urethan treatment caused temporary epilation. (H.G.D.)

20477 COMPARATIVE ASSESSMENT OF THE GROWTH OF SKIN GRAFTS IN COMBINED RADIATION-BURN INJURY OF THE MAXILLARY REGION AT DIFFERENT PERIODS OF RADIATION SICKNESS. Zalyalyutdinova, S. Z. Med. Radiol., 10: No. 12, 38-41(Dec. 1965). (In Russian).

Data are presented showing that germinal skin epithelium and skin transplants in rabbits are not affected morphologically and functionally by irradiation. When transplantation was done at the zenith of radiation sickness, proliferative and inflammatory processes were inhibited, thus leading to the death of the implant. (H.G.D.)

20478 INFLUENCE OF IONIZING RADIATION ON THE OUTCOME OF AUTO- AND HOMOVENOUS PLASTIC REPAIR OF ARTERIES. Shimanko, I. I. (Sklifosovskii Inst. of First Aid, USSR). Med. Radiol., 10: No. 12, 57-62 (Dec. 1965). (In Russian).

For the purpose of studying the influence of radiation sickness on the auto- and homovenous plastic repair of injured arteries, two series of experiments were performed on the iliac arteries of dogs with the aid of a vessel-stitching apparatus. Radiation sickness was caused by a single whole-body x-irradiation in a dose of 500 R. The results of the experiments showed that the growth of transplants (arterialization) occurred at the expense of fibrosis of the external regions. During the repair of arteries with homovenous transplants in nonirradiated animals, the majority of grafts were occluded. Histological investigation of the transplants revealed structural changes testifying to the organism's reaction to a heterogenous tissue. In the group involving the use of homovenous transplants in irradiated animals, the greater part of grafts proved to be patent. (TCO)

20479 EFFECTS OF IONIZING RADIATIONS ON SOME IMMUNOLOGIC PHENOMENA IN EHRLICH'S ASCITES TUMOR. Juliani, G.; Piccotti, F.; Isoardi Pons, A. (Univ., Turin). Minerva Radiol. Fisioterap. Radiobiol., 11: 74-7(Jan.-Feb. 1966). (In Italian).

In a series of experiments in 230 Swiss mice with Ehrlich's ascites tumor it was shown that the TD_{50} (i.e., the number of cells required to ensure grafting of the tumor in 50% of the inoculated animals) corresponds, for the strain of animals used, to 700 cells. This number drops to 400 if total-body irradiation with ^{60}Co (500 rads) is given 12 hours before inoculation. In animals which survived the inoculation of a sub-lethal dose of neoplastic cells, resistance to a subsequent inoculation is greater. This immunity is greater the higher the number of cells transplanted with the first inoculation, and is lacking in irradiated animals. It is therefore confirmed that total-body irradiation inhibits the occurrence of certain anti-neoplastic immunologic processes. (auth)

20480 RESULTS OF PHYSICAL EXAMINATION OF ATOMIC BOMB CASUALTIES. **Kuramoto, Kiyoshi (Hiroshima Red Cross Hospital); Fuzinaga, Utaka; Fuzimoto, Ukio; Isida, Kitamu Nagasaki Igakkai Zasshi, 38: Suppl.,70-80(Dec. 1963). (In Japanese).**

To study the aging process as affected by atomic bomb irradiation, 73 casualties and 475 controls were selected from patients seen over the last five years at the Hiroshima Red Cross Hospital. There was no difference in sex and age classes between casualties and controls. Incidence of hypertension and hypotension was higher in casualties aged 40 years and older. Electrocardiograms showed a high incidence, in casualties over 50 years of age, of ST and T wave abnormalities as well as right bundle branch block. Kieth-Wagner grading of arteriosclerosis for eye fundus examination revealed a high incidence in casualties of Grade I vascular abnormalities after 40 years of age. Serum cholesterol determinations failed to reveal differences between casualties and controls. Phenolsulfonphthalein tests of renal function showed lower values of dye excretion by casualties at 15 min and two hr as compared with controls. Mean and mode values both indicated relative impairment of renal function in the casualties of all age groups, but it was more pronounced in the 40-yr and higher age groups. Glucose tolerance tests failed to show differences in incidence of diabetes between casualties and controls. Various serum protein lability tests and Bromsulphalein excretion failed to demonstrate significant difference. In view of the previously demonstrated premature aging irradiation effects in mice, the possibility of irradiation causing capillary injury and renal cell damage in the human casualties can not be excluded as a factor accelerating the natural aging process. (TCO)

20481 TEMPORAL OBSERVATIONS ON PERIPHERAL HEMOGRAMS OF ATOMIC BOMB CASUALTIES AS COMPANY EMPLOYEES. III. **Casazima, Siroh; Omoki, Yosinoki; Ikeda, Yasuaki; Baba, Kozi (Nagasaki Univ.). Nagasaki Igakkai Zasshi, 38: Suppl., 81-3(Dec. 1963). (In Japanese).**

To study the latent effect of exposure to the atomic bombing on hematopoietic tissue, company employees who had been casualties were observed for five years starting in 1958. Data were collected from: subjects exposed at less than 2000 m from the hypocenter; those exposed beyond 2000 m; and those who entered the devastated city (Nagasaki) within 2 weeks postattack. Eight successive blood examinations were made. Hemograms failed to show significant differences with respect to the distance to hypocenter of the survivors. (BBB)

20482 BONE TISSUE STERILIZATION USING REACTOR FUEL GAMMA RADIATION. **Czerniewski, Michal; Panta, Przemyslaw; Zielczynski, Mieczyslaw; Zak, Wieslaw; Zarnowiecki, Krzyztof (Inst of Nuclear Research, Warsaw). Nukleonika, 10: 791-806(1965).**

An absolute ionization method of measurements of doses absorbed in bone tissue, and additional methods were developed. Measurements of spatial dose distribution in grafts were performed. From the detailed analysis it follows that each point of the graft absorbs in sterilization a dose of 3.3 Mrad, with an accuracy of 20%. In the two years of its application the sterilization method developed has proved satisfactory. This was evidenced in sterilization of more than one hundred lyophilized human bone grafts successfully used for therapeutical purposes. (auth)

20483 A METHOD OF ASSAYING IN VIVO THE SURVIVAL OF ULTRAVIOLET-IRRADIATED TUMOR CELLS. **Stevens, G. H.; Roe, E. M. F. (Royal Cancer Hospital, London). Photochem. Photobiol., 4: 749-57(Sept. 1965).**

Growth of uv-irradiated ascites tumor cells in adult animals that had received a total-body dose of x radiation was used as a method to obtain data on the survival of the treated tumor cells. If the dose of total-body radiation and its time before tumor cell inoculation are chosen correctly, the method appears to be valid. In assessing tumor cell survival, the analysis of the time of appearance of the resulting solid tumors, using the linear relation between the reciprocal of this time and the logarithm of the number of cells injected, is preferred to probit or to Reed-Muench analysis of the number of tumor takes. The 1/T method of analysis yields more precise estimates of the survival ratios and greater economy in the use of host animals without a disproportionate increase in the labor involved in obtaining the data. An application of this method to the determination of survival ratios of uv-irradiated Landschuetz ascites tumor cells is described. (TCO)

20484 THE EFFECTS OF ULTRAVIOLET AND VISIBLE RADIATION ON MOUSE ASCITES TUMOR CELLS. **Roe, E. M. F.; Stevens, G. H. (Royal Cancer Hospital, London). Photochem. Photobiol., 4: 759-67(Sept. 1965).**

Effects of uv and visible radiation on the viability of Landschuetz ascites tumor cells were tested by growing control and treated tumor samples in adult mice. The tumor cells were irradiated as a dilute suspension in isotonic buffered salt solution, and were equilibrated at 0°C with oxygen or with nitrogen before irradiation. Tumor cell proliferation was measured by a variety of techniques, but the preferred assay method was the growth of solid tumors in the axillae and groins of mice after subcutaneous inoculation of varying dilutions of treated or control ascites tumor cells. The immune response of the mice to the injected cells was reduced by whole-body 300 R doses of x rays two days before inoculation. Results were calculated from parallel line assays using the reciprocal of the delay in appearance of the solid tumors up to 30 days postinoculation. This reciprocal (1/T) was linearly related to the logarithm of the number of cells inoculated. Photoreactivation was demonstrated for this system, in which both uv and visible radiations were absorbed by the same cells. Light delivered alone in oxygen or in nitrogen was without effect on cell viability, but it increased cell-survival after uv irradiation in nitrogen and decreased survival after uv irradiation in oxygen. Ultraviolet radiation alone was not significantly more lethal in oxygen than in nitrogen. A further observation in this work was an interaction between irradiated and control tumor cells injected into the same animal. It is suggested that the radiation used may affect the antigenic character of the tumor cells as well as their reproductive capacity. (BBB)

20485 INFLUENCE OF EXTRACORPOREAL IRRADIATION OF THE BLOOD AND LYMPH ON SKIN HOMOGRAFT REJECTION. **Chanana, A. D.; Brecher, G.; Cronkite, E. P.; Joel, D.; Schnappauf, Hp. (Brookhaven National Lab., Upton, N. Y.). Radiat. Res., 27: 330-46(Mar. 1966). (BNL-9362).**

The effect of extracorporeal γ irradiation (ECI) of the circulating blood before and after skin homografting in calves on graft survival has been described in thirteen calves. In all the ECI-treated calves the normal acute and violent skin homograft rejection process occurring at 9 to 10 days was modified to a mild and slow process with an increase in rejection time by 1 to 11 days. In one calf, where thoracic duct lymph was drained for 8 days and cell-free lymph was returned to the animal followed by 4 days of ECI of the lymph, the skin graft rejection time was 40 days. Lymph drainage from the thoracic duct for 24 days and return of cell-free lymph to the animal prolonged the homograft rejection time to 18 days, and ECI

of thoracic duct lymph for 22 days prolonged graft rejection time to 17 days. In one animal no prolongation of homograft rejection was obtained with lymph drainage for 10 days and return of cell-free lymph to the animal. In two animals where ECI of the lymph was continued after skin grafting, the homografts on that part of the body not solely drained by thoracic duct were rejected at 22 and 27 days, whereas the homografts on that part of the body which is drained solely by the thoracic duct were not rejected for as long as ECI of the lymph was continued (day 29 and day 61). (auth)

20486 AGE AND DOSE DEPENDENCE OF BONE GROWTH RETARDATION INDUCED BY X-IRRADIATION. Phillips, Richard D.; Kimeldorf, Donald J. (Naval Radiological Defense Lab., San Francisco). Radiat. Res., 27: 384-96(Mar. 1966).

The quantitative aspects of bone growth retardation in rats at 60 days after x irradiation were determined with respect to radiation dose and age at exposure. It was found that the decrement in bone growth increased exponentially with a linear increase in dose within the range of 100 to 680 rads. The bone growth decrement was also a function of the age of the animal at the time of exposure; the logarithm of the decrement was a linear function of the reciprocal of age for animals exposed during the rapid phase of growth. The information obtained from the dose-response and age-response relationships was used to derive an equation which could be used to predict the bone growth decrement occurring 60 days after x irradiation on the basis of the age at exposure and the dose administered. The general equation was: Bone growth retardation = $k \times 10^{m(dose)+n(1/age)}$. Values for k, m, and n determined for the femur and tibia were found to give a good estimation of effect within the dose range of 100 to 680 rads for exposure ages of 24 to 58 days. (auth)

20487 ACUTE MORTALITY AND RECOVERY STUDIES IN SHEEP IRRADIATED WITH ^{60}Co GAMMA RAYS OR 1-Mvp X-RAYS. Hanks, G. E.; Page, N. P.; Ainsworth, E. J.; Leong, G. F.; Menkes, C. K.; Alpen, E. L. (Naval Radiological Defense Lab., San Francisco). Radiat. Res., 27: 397-405(Mar. 1966).

The $LD_{50(60)}$'s for sheep irradiated with ^{60}Co γ rays or 1-Mvp x rays are 237 R and 252 R, respectively. These midline air doses correspond to midline tissue doses of approximately 145 rads. Systematic recovery studies show that 30 days after an acutely administered two-thirds $LD_{50(30)}$ dose there has been recovery from 60 to 70% of the initial radiation injury. At least 10% of radiation deaths in sheep occur after 30 days. This indicates that the $LD_{50(60)}$ is a more satisfactory end point than the $LD_{50(30)}$ for evaluating the acute mortality response of the domestic sheep. (auth)

20488 EFFECT OF GAMMA IRRADIATION ON THE CARDIOVASCULAR SYSTEM OF THE RHESUS MONKEY. Kundel, Harold L. (School of Aerospace Medicine, Brooks Air Force Base, Tex.). Radiat. Res., 27: 406-18(Mar. 1966).

A dose-dependent decrease in blood pressure has been demonstrated in the rhesus monkey, Macaca mulatta, after total-body irradiation with ^{60}Co γ rays at doses of 1950, 3900, and 6600 rads. During the first hour after irradiation, the cardiac output was maintained at normal levels in all the dose groups. It decreased by 18 hours in the animals of the 6600-rad group. Immediately after irradiation there was a diminished response of the mean arterial pressure to norepinephrine. The response returned to normal by 24 hours in all groups except the 6600-rad group, in which it remained depressed. (auth)

20489 OBSERVATIONS COMPARING THE EFFECTS OF NEUTRON IRRADIATION ON THE BLOOD-CEREBRAL SPINAL FLUID BARRIER OF THE SHEEP AND BURRO. Wykoff, M. H. (Univ. of Tennessee, Oak Ridge). Contract AT-40-1-GEN-242. Radiat. Res., 27: 445-55(Mar. 1966).

Sheep and burros received 700 rads of fast neutrons at the rate of 40 rads/min. Clinical behavior of both species was noted. The sheep showed no active manifestation of central nervous system (CNS) involvment, in contrast to the burro, which exhibited obvious functional disturbance of the CNS. Blood plasma and cerebral spinal fluid (CSF) were examined for glucose, inorganic phosphate, sodium, and potassium levels. In addition, the CSF protein content was assayed. In the sheep, hyperglycemia was observed. Blood sodium, potassium, and inorganic phosphate were unchanged. The only change in CSF content was a significant increase in inorganic phosphate. In the burro, hyperglycemia was noted; the inorganic phosphate showed a tendency to decrease. Blood sodium and potassium were unchanged. CSF protein increased greatly. CSF glucose showed an initial increase, then a decrease. Sodium was below normal levels in CSF. Potassium showed no significant change in this medium. These results offer possible bases for hypotheses in respect to the presence or absence of CNS symptoms after exposure to ionizing irradiation. (auth)

20490 THE INFLUENCE OF GAMMA AND X RAYS ON COAGULABILITY OF BLOOD AND QUALITATIVE CHANGES OF FIBRINOGENS IN ANIMALS. Ponomarev, J. T. (Institut fuer Medizinische Radiologie der AMN, Obninsk, USSR). Radiobiol.-Radiotherap., 7: 37-45(1966), (In German).

In acute radiation disease of dogs and rats an increased coagulability of blood one to two days after irradiation and an increased fibrinolysis after 1 to 5 days were observed. The coagulability of blood and, less marked, fibrinolytic activity decreased from the 3rd to 7th day after irradiation compared with the values of animals before irradiation. Moreover, the physiological correlation of activity of the coagulative and fibrinolytic system of blood was disturbed and there was an increased fibrinolytic activity of blood with decreased coagulability. From the first day after irradiation the concentration of fibrinogen was increased. There were qualitative changes that increased with the development of acute radiation sickness. The structure of fibrin arising from fibrinogen was disturbed by the qualitative changes of fibrinogen which could be demonstrated by the method of orientation of fibrin structures. (auth)

20491 THE PROBLEM OF IMPORTANCE OF DISTURBANCES OF COAGULATION AND FIBRINOLYSIS SYSTEM OF BLOOD IN PATHOGENESIS OF PREDISPOSITION FOR BLEEDING IN ACUTE RADIATION SICKNESS. Ponomarev, J. T. (Institut fuer Medizinische Radiologie der AMN, Obninsk, USSR). Radiobiol.-Radiotherap., 7: 47-54 (1966). (In German).

Changes of coagulation and the fibrinolysis system of blood observed after whole-body x irradiation of dogs with a dose of 800 R included acceleration of blood-coagulation during the first three days after irradiation and decrease of coagulability of blood from the fourth day progressively to the death of animals. In severe cases of radiation sickness fibrinolytic activity of blood was increased in the dogs during the first five days after irradiation, then decreased, beginning with the sixth day, progressively up to the death of animals. At the acme of the radiation disease, on the fourth and fifth day after irradiation, fibrinolytic activity of the blood was increased with decreased coagulability. This obviously favors the appearance of hemorrhagical symptoms. (auth)

20492 THE DYNAMICS OF CONDITIONED REFLEXES IN STEREOTYPE DURING THE WHOLE LIFE IN RATS AFTER REPEATED PRENATAL IRRADIATION WITH SMALL DOSES. Semagin, V. N. (Institut fuer Hoehere Nerventaetigkeit und Neurophysiologie, Moscow). Radiobiol.-Radiotherap., 7: 55-62(1966). (In German).

The conditioned reflexes were examined in a group of rats prenatally x irradiated for 20 days with a daily dose of 1 R as well as in a group of control animals 2 to 29 months of age. The changes of latent periods and extents of conditioned reflexes of the irradiated animals occurring with age differ statistically from those of control animals. The changes give evidence of a diminution of excitatory and inhibitory processes progressive in the course of life in repeatedly prenatally irradiated rats. (auth)

20493 THE PROBLEM OF SEASONAL FLUCTUATIONS IN THE RADIOSENSITIVITY OF RABBITS. **Pravdina, G. M.; Zagorskaja, I. B. (Biophysikalisches Institut des Ministeriums fuer Gesundheitswesen, Moscow). Radiobiol.-Radiotherap., 7: 63-8(1966). (In German).**

From examinations of 280 rabbits a quantitative assessment of the seasonal influence on the radiosensitivity of the animals is given. The rabbits were irradiated by means of a telecobalt unit with doses of 400 to 900 R in different months of a year. The criterion was a dose causing the 50 percent mortality of the animals (LD_{50}) which had been calculated according to maximum likelihood-estimation. The dependence of the value of LD_{50} on season was found to be sinusoidal. The differences in the value of LD_{50} in January (maximum value) and in July (minimum value) are of the order of 175 R. (auth)

20494 PECULIARITIES DUE TO AGE IN THE COURSE OF ACUTE RADIATION SICKNESS IN MICE. **Cholin, V. V. Radiobiol.-Radiotherap., 7: 69-74(1966). (In German).**

The peculiarities in the course of acute radiation sickness dependent on age of animals were experimentally investigated in 1205 mice exposed to doses of 200 to 2000 R x radiation. Under the same conditions otherwise and with the same dose the age of mice was found to be the factor which determines the nature and the final picture of the radiation injury. According to the criterion of $LD_{50/30}$ radiosensitivity of newborn mice is relatively low, increasing considerably until the 9th to 10th day after birth. Radiosensitivity decreases with further maturation, being least marked in puberty. These results were compared with those of corresponding experiments which had been performed on rats. Very considerable differences of species were found in the reaction of animals to irradiation. Young growing mice proved in all groups of age more resistant to irradiation than rats. (auth)

20495 THE BEHAVIOR OF LIVING ORGANISMS IN RADIATION FIELDS. **Darenskaja, N. G.; Pravdina, G. M.; Chruscev, V. G. (Biophysikalischen Institut des Ministeriums fuer Gesundheitswesen, Moscow). Radiobiol.-Radiotherap., 7: 81-93(1966). (In German).**

The behavior of mice, rats, guinea pigs, and monkeys in gamma fields was studied. For this purpose a method was elaborated in which the intake of water and food either with simultaneous action of radiation or in a protective area is left to the animals. Mice, rats, guinea pigs, and monkeys are able to determine the position of the radiation source and to avoid a water-container in the area of radiation. The animals respond to gamma doses of the order of 1 to 2 R when head or abdomen are irradiated and of 0.01 and 0.05 R in whole-body irradiation. (auth)

20496 EXAMINATIONS ON THE EFFECTS OF IONIZING RADIATION ON $NADH_2$ OXIDATION IN PREPARATION OF MITOCHONDRIA. **Magdon, E.; Cziharz, H. (Robert-Roessle-Klinik, Berlin). Radiobiol.-Radiotherap., 7: 95-8 (1966). (In German).**

It was demonstrated that ($NADH_2$) oxidation of fractions of cattle heart mitochondria is inhibited by x radiation. Catalase reduced nicotinamide adenine dinucleotide activity of cattle-heart mitochondria as well as the addition of catalase to the suspension of mitochondria had no perceptible influence on the extent of radiation-induced inhibition of $NADH_2$-oxidation. (auth)

20497 RADIATION-INDUCED VARIEGATIONS IN EINKORN WHEAT AND THEIR INHERITANCE. **Matsumura, Seiji (National Inst. of Genetics, Mishima, Japan). Seiken Jiho, 13: 75-88(Oct. 1965). (In Japanese).**

Wheat seeds (Triticum monococcum var. flavescens) were exposed to x and to γ rays from ^{60}Co, thermal and fast neutrons (14 Mev), and β rays by ^{32}P and ^{131}I solutions. In the treated X_1 and later generations white and/or yellow stripes were often observed, their mode of inheritance was studied. The striping patterns were divided into the following types. Most of white or yellow striping found in X_1 was maternally or cytoplasmically inherited and was due to plastid mutation. The first appearance of this type occurred in the X_2 generation. In the X_2 head progeny segregating albina in a simple Mendelian ratio, white-striped leaves were often observed in a few plants. They might be due to a somatic mutation in a heterozygous plant concerning albina. Some white stripes which could be distinguished from others by the fine nature of striping occurring in all leaves of a plant (striata) were controlled by a mutated recessive gene. Special variegation was found in three X_1 plants. Their progeny contained some white seedlings. The basi-viridis (or virido-albina) seedlings, other than albina, invariably grew to be variegated; they were controlled by a mutated recessive gene. Evidence indicated that the recessive basi-viridis gene for variegation, which was stable, stimulated plastids to mutate (irreversibly) from green to white. Plastid exomutation or mutation from green to white was affected by environmental factors, such as temperature. (BBB)

20498 THE ACTION OF RADIUM EMANATION ON THE EAR. (EXPERIMENTAL STUDY). **Zlotnikov, S. A. Vestn. Otorino-Laringol., 24: 57-62(Nov.-Dec. 1962). (In Russian).**

Experiments were conducted on rabbits 6 to 10 weeks old. Sources containing 11.7 to 25 mC Ra were introduced into the left tympanum through an opening made for this purpose. Control animals received the same type ampules without Ra, after which all incisions were closed. The animals were observed for several weeks, during which the following observations were made: suppurative inflammation of the middle ear, hyperemia, and degenerative changes in the sacculus, semicircular canals, and the vestibular nerve. Studies of electric potentials in the cochlea disclosed that the ear of the irradiated animals did not respond when subjected to various auditory stimuli (tuning forks and a whistle), while in a control animal these sounds elicited a change of the potential difference. Irrespective of the severity of morphological changes in the cochlea, spiral ganglion, and nuclei of the auditory nerve, deafness occurred in all animals in the ear that had been exposed to radiation. These experiments confirm the view that the central nervous system, as highly differentiated structure, is very sensitive to ionizing radiation. (BBB)

20499 CONCERNING THE INFLUENCE OF X RADIATION ON POSTNATAL TESTICULAR DEVELOPMENT AND GERM CELL MATURATION IN THE MOUSE. **Widmaier, R. (Martin-Luther-Univ., Halle/Saale, Ger.). Z. Mikroskop. Anat. Forsch., 71: 229-55(1964). (In German).**

Newborn mice (12 hr old) were given a whole-body dose of from 570 to 800 R of x irradiation. The animals were studied from one to 90 days after irradiation. Irradiation inhibited the growth of the testes. The fertile tubuli contorti almost reached the width of the normal tubules. The growth in length of the canaliculi was markedly reduced. The fractions of fertile and sterile tubules obtained from a cross-section of the testes varied greatly. In each section ~$\frac{1}{2}$ to $\frac{3}{4}$ of the canaliculi were fertile. The first spermatogenesis cycle in the mouse, which begins right after birth was delayed ~5 days by irradiation. In addition, the degeneration of the primitive spermatoblasts took place ~5 days later than normal, and some of these cells persisted for long periods. After the irradiation spermatocyte formation and maturation division were the development stages where most of the spermatogenic cells died. The formation of Sertoli cells was delayed less than 5 days. Opening of the lumen of the canaliculi started with a delay of more than 5 days. The irradiation damage of the testes of the newborn animals was more severe than when grown mice were irradiated. Close to 90% of the surviving irradiated animals were fertile. (BBB)

20500 INACTIVATION OF VACCINIA VIRUS BY GAMMA RADIATION. **Jimenez, Rosa; Ohlbaum, Adela (Univ. Chile, Santiago). Z. Naturforsch, 21b: 52-5(Jan. 1966).**

The influence of purification on the inactivation of Vaccinia Virus (VV) by gamma radiation was studied. Differential centrifugation and sucrose density gradient centrifuga-

tion were used. Purification modified the VV compound survival curve previously published. The possibility that multiple reactivation might be the reason for the compound survival curve when crude virus preparations were irradiated was also studied, but the experiments gave negative results. Even with the best method of purification applied, the target volume of about 10^{-17} cm^3 for VV calculated from the irradiation experiments was very small compared to the volume of the virus obtained with the sedimentation methods. (auth)

20501 USE OF RADIATION APPLIED TO SEEDS TO INDUCE NEW GENETIC VARIATION FOR QUANTITATIVE TRAITS IN DURUM WHEAT. Scossiroli, R. E.; Pellegrini-Scossiroli, S. (Univ., Pavia, Italy). pp 231-6 of Symposium on Genetics and Wheat Breeding, June 12-14, Martonvasar, Hungary, 1962. Budapest, Agricultural Research Inst. of the Hungarian Academy of Sciences, 1962.

Wheat seeds at 14–16% relative humidity were exposed to 10,000 or 20,000 R doses of x rays at a dose rate of 464 R/min. The highest dose resulted in lethality at the seedling stage. A direct comparison between the genetic portion of variation for the different levels of classification obtained for the control and for the irradiated groups provided a demonstration of the effect of irradiation on the genetic variability for different quantitative traits in the population used for this experiment. Heritability estimates, given as ratio between the genetic portion of variation and the total phenotypic variance, are summarized for the R_2 and R_3 generations. These preliminary data demonstrated an increase of genetic variability in the irradiated group when compared to the controls. The increase was larger for the R_3 generation. Irradiation of seeds was thus found to be efficient in increasing the genetic variability available to the breeder of crop plants because radiation applied to plateaued populations can provide new genetic variation for further or better responses to artificial selection. (TCO)

20502 ATTEMPTS TO PRODUCE PRENEOPLASTIC AND NEOPLASTIC CHANGES IN THE MAMMARY GLAND OF THE BALB/c MOUSE BY MEANS OF X-RAY AND CHEMICAL CARCINOGEN [Thesis]. Faulkin, Leslie John Jr. Berkeley, Calif., Univ. of California, 1964. 141p.

Several parameters of the experimental procedure were investigated. The chemical carcinogens, 20-methylcholanthrene (MC) or dimethylbenzanthracene (DMBA), were fed to or painted on BALB/c female mice in combination with the hormonal stimulation of either a transplanted pituitary, a vasectomized male, or nothing additional in order to provide 9 treatment groups. The treated animals were the source of tissue transplanted into non-treated host animals. Two conclusions were derived from the data: the effect of the hormonal stimulation was to increase the number of HAN that appeared rather than the production of a change in the tumor potential of the nodules; the chemical carcinogen produced a change in the tumor potential of the nodules, thus, more of the nodules from carcinogen treated animals produced mammary tumors. The greatest number of nodules and tumors were seen when hormonal stimulation and chemical carcinogen are used together. Serial transplantation of carcinogen induced lesions showed them to be highly unstable in the types of outgrowth that they produced. It was concluded that chemically induced lesions were more varied in morphology and unstable than those resulting from MTV. (TCO)

Radiation Effects Therapy and Countermeasures

20503 (AD-629311, pp 1-14) FURTHER STUDIES ON THE EFFECTS OF VARIOUS DRUGS ON THE ADENOSINE TRIPHOSPHATASE ACTIVITY OF THE HEMATOPOIETIC TISSUES OF RATS EXPOSED REPEATEDLY TO ^{60}Co GAMMA RADIATION. Tardiff, Robert G.; DuBois, Kenneth P. (USAF Radiation Lab., Univ. of Chicago, Ill.).

Adult, female Sprague-Dawley rats were exposed to cobalt-60 gamma radiation at dose levels of 46 to 54 R per day. They were also treated daily with yeast extract, liver fraction S, liver fraction L, liver concentrate, aqueous liver fraction (Armour), liver fraction I (Armour), desiccated liver, or acridine orange at various doses administered either intraperitoneally or orally. Groups, each containing four animals, were sacrificed after 4 days of radiation and drug treatment and adenosine triphosphatase assays were performed on the spleens. When given intraperitoneally, several substances provided some protection against the enzyme change. The greatest protection was obtained with yeast extract, liver fraction S, and liver fraction L. Oral administration of these and other substances was generally ineffective. Thyroxin, thyroid stimulating hormone, adrenocorticotrophic hormone, and adrenal cortex injection were re-tested for their radioprotective effect against chronic gamma radiation injury. The degree of protection was similar to that reported previously, and thyroxin was the most effective radioprotective agent. The response of females and males to chronic gamma radiation was similar with males being slightly more resistant. The drugs produced a similar response in males and females. Substances which proved effective in reducing hematopoietic injury to the spleens of rats exposed to gamma radiation at the rate of 50 R during a 10-hour period were ineffective against x ray given at the same daily dose but at the much more rapid dose rate of 38 to 40 R per minute. (auth)

20504 NATULAN (PROCARBAZINE) COMBINED WITH RADIOTHERAPY IN MANAGEMENT OF INOPERABLE MALIGNANT MELANOMA. Falkson, Geoffrey; de Villiers, P. D.; Falkson, H. C.; Fichardt, T. (Pretoria General Hospital). Brit. Med. J., 2: 1473-4(Dec. 18, 1965).

Attempts were made to detect a tumor-radiosensitizing action of Natulan (N-isopropyl-α-(2-methylhydrazino)-p-toluamide hydrochloride) (procarbazine), which is a benzylmethyl hydrazine derivative with cytotoxic effects. The combined action of Natulan and ionizing radiation was studied in patients with malignant tumors resistant to radiation therapy. Objective improvement was seen in six out of ten cases of inoperable malignant melanoma treated with combined Natulan and radiotherapy. Doses of Natulan varied from 3350 mg in 20 days to 90,100 in 556 days. Telecobalt (^{60}Co) or deep x-ray therapy was given in doses up to 4800 R. It is felt that the results support the contention that Natulan can sensitize tumor tissue to the damaging effects of ionizing radiations. It is believed that the response as well as the quality and duration of improvement is significant. (TCO)

20505 AN ENZYMATIC EVALUATION OF THIOL RADIOPROTECTORS. Scaife, J. F. (Department of National Defence, Ottawa). Can. J. Biochem., 44: 319-30(Mar. 1966).

A number of thiol and disulfide compounds were tested for their ability to inhibit the oxidation of α-ketoglutarate by rat-liver homogenates. The inhibition involves oxidation of the thiol, and the disulfides were found to be more potent inhibitors than the thiols. There was no change in the ATP level of normal tissues after the in vivo administration of AET, and the protective ability of this compound was not considered to be related to any interference with mitochondrial oxidative phosphorylation. Mitochondrial respiration is, however, inhibited. The results support the mixed disulfide protection theory of Eldjarn and Pihl, and provide a physiologically significant test system for this hypothesis. (TCO)

20506 RELATION BETWEEN RADIOPROTECTIVE AND ANTINEOPLASTIC EFFECTS OF ANTIOXIDANT-INHIBITORS. Burlakova, E. B.; Gaintseva, V. D.; Slepukhina, L. B.; Khrapova, N. G.; Emanuel', N. M. (Leningrad Inst. of Toxicology). Dokl. Akad. Nauk SSSR, 164: 934-6(Oct. 1, 1965). (In Russian).

Experiments were carried out for the purpose of determining the properties of antioxidant-type inhibitors involved in the slowing-down of tumor-forming processes.

Mice exposed to the absolute lethal dose of 550 R of x radiation were administered various amounts of 2-methyl-2,6-di-tert-butyl phenol. It was found that the radioprotective action reaches a maximum at a dose rate of 50 mg/kg; this effect decreases with increasing amount administered, reaching the zero survival rate at 100 mg/kg body weight. Larger amounts had a negative effect, decreasing the survival period, and are considered as radiosensitizing. Similar results were obtained with a number of other inhibitors, such as polyphenols, substituted oxypyridines, stable radicals, and aminophenols. The correlation between the antitumoral activities of the inhibitors and concentration was examined by estimating the slowing down of development of leucosis in animals injected intraperitoneally with the substance under study. It was found that the antitumoral action increases with increasing C_{ther}/C_{neg} ratio, where C_{ther} designates the therapeutic dose and C_{neg} designates the zero-survival rate. This makes it possible to select a specific inhibitor. (TTT)

20507 PATHOGENESIS OF IODACETATE CATARACT AND ITS SIMILARITY TO RADIATION CATARACT. Vsevolodov, E. B. Golichenkov, V. A.; Popov, V. V. Federation Proc., Transl. Suppl., 25: T111-T117(Jan.-Feb. 1966).

Translated from Vestn. Moskov. Univ. Ser. VI: Biol. Pochvoved., 19: 3(1964).

The radiomimetic properties of iodoacetate were studied in the eyes of rabbits into which sodium monoiodoacetate was injected. Development of iodoacetate cataract was observed with the slit lamp in 20 animals. Cataract development is described. Three degrees of retinal involvement were distinguished in the experimental animals: retinas in which the outer nuclear layer contained from two to five rows of nuclei instead of the normal five; retinas in which the outer nuclear layer had disappeared completely at some points but retained from one to five rows of nuclei elsewhere; and retinas with practically no visual epithelium, except for small areas in the region of the ora serrata. Results of these experiments together with those in the literature indicate that, in all its features, iodoacetate cataract is very similar to radiation cataract. (H.G.D.)

20508 EFFECT OF LOW-PROTEIN DIET ON THE ABILITY OF THE ADULT RAT TO RECOVER FROM A SUBLETHAL DOSE OF IRRADIATION. Hopper, Arthur F.; Yatvin, Milton B.; Wannemacher, Robert W. Jr. (Rutgers State Univ., New Brunswick, N. J.). J. Nutr., 88: 202-8 (Feb. 1966).

Various biochemical parameters were investigated in an attempt to elucidate the interaction between nutritional state of an animal and its response to a sublethal dose of irradiation. Male rats of the Wistar strain received a total γ dose of 350 R from a ^{60}Co source. Prior to, during, and after irradiation the rats were fed an agar-gel diet containing 15% protein. A nonirradiated control group received the same diet. A third group was fed a 15% protein agar-gel diet prior to irradiation, but was given an agar-gel basal diet with a 5% protein content during and after irradiation. At 3, 14, and 28 days after irradiation, animals from each group were sacrificed. All rats were injected with 5 μC of ^{35}S-DL-methionine one hour before autopsy, and at necropsy blood and liver samples were taken for biochemical analysis. The results showed that a low protein diet fed to adult rats after a sublethal dose of irradiation did not affect repair processes. Irradiation appeared to stimulate maintenance of liver protein metabolism immediately after irradiation at a level higher than that of the nonirradiated 5% casein-fed controls and equal to that of nonirradiated controls fed 15% casein. (H.G.D.)

20509 SPERMATOGENESIS IN IRRADIATED RATS DURING THE PROPHYLACTIC ADMINISTRATION OF β-MERCAPTOETHYLAMINE. Fedorov, B. A. (Inst. of Experimental Pathology and Therapy, Academy of Medical Sciences, USSR). Med. Radiol., 10: No. 12, 42-3 (Dec. 1965). (In Russian).

β-Mercaptoethylamine was given to male rats x irradiated with 600-R doses. Histological examination of the testes revealed greater damage in the irradiated controls than in animals treated with MEA. Further, death was prevented in the latter group. (H.G.D.)

20510 INFLUENCE OF PROPHYLACTIC ADMINISTRATION OF A MUCOPOLYSACCHARIDE PREPARATION ON THE HEMATOPOIESIS AND SURVIVAL OF ANIMALS AFTER IRRADIATION. Shitikova, A. S. (Inst. for Research in Blood Transfusions, Leningrad). Med. Radiol., 10: No. 12, 44-6(Dec. 1965). (In Russian).

A mucopolysaccharide preparation from the spleen of cattle enhanced recovery of hematopoiesis in x irradiated mice and rabbits. (H.G.D.)

20511 ESTIMATION OF RADIATION DOSE-REDUCTION FACTOR FOR β-MERCAPTOETHYLAMINE BY ENDOGENOUS SPLEEN COLONY COUNTS. Smith, Willie W.; Budd, Roger A.; Cornfield, Jerome (National Institutes of Health, Bethesda, Md.). Radiat. Res., 27: 363-8(Mar. 1966).

A radiation dose-reduction factor (DRF) for the protective agent β-mercaptoethylamine is estimated from counts of the colonies grossly visible on the spleen of mice 10 days after γ irradiation. A logarithmic transformation would be appropriate but is precluded by the existence of zero counts. A modification is described which yields values regressing linearly with dose, the lines for control and treated groups having a common intercept at zero dose. The DRF estimated as the ratio of these slopes, 1.6 (1.5 to 1.7), is in agreement with the DRF values obtained with other response metameters. The value of the intercept, 3.4 (3.0 to 3.8) × 10^4 colony-forming units per spleen, agrees with the number obtained by direct experimentation. (auth)

20512 EFFECTS OF BACTERIAL ENDOTOXIN ON THE OCCURRENCE OF SPLEEN COLONIES IN IRRADIATED MICE. Smith, Willie W.; Brecher, George; Budd, Roger A.; Fred, Sallie (National Institutes of Health, Bethesda, Md.). Radiat. Res., 27: 369-74(Mar. 1966).

In mice given a single injection of bacterial endotoxin either before or shortly after γ irradiation, splenic nodules, as well as bone marrow cellularity and survival, were increased over the irradiated controls. The maximum effect was seen with 25 μg given 1 day before irradiation. In mice given a series of injections before irradiation there was a dissociation between the number of splenic nodules, which was increased, and bone marrow recovery and survival, which were essentially the same as in the controls. (auth)

20513 MORPHINE, CODEINE, NALORPHINE AND SURVIVAL TEST OF THE PAN-IRRADIATED MOUSE. EXPERIMENTAL CONTRIBUTION TO THE STUDY OF MORPHINE'S RADIOPROTECTIVE ACTION. Stuart, Carlo; Cittadini, Giorgio (Univ., Siena, Italy). Radiol. Med., 51: 1204-18(Nov. 1965). (In Italian).

Morphine, nalorphine, and codeine showed radioprotective properties when administered to mice prior to pan-irradiation (600, 700, and 800 R doses). However, no significant differences were found in the protective actions exerted by the three drugs. (H.G.D.)

20514 SUBSTRATE PROTECTION OF ENZYMES AGAINST IONIZING RADIATION. Winstead, Jack A.; Gass, Arthur E.; Hidgon, John P. Res. Technol. Briefs, 3: 19(Dec. 1965).

The radioprotective effects of various substrates were tested on rabbit muscle enolase and beef heart lactic dehydrogenase (LDH). The protection of enolase against gamma radiation by 2-phosphoglyceric acid depended on the buffer system. Results suggested that the protection is not specific but due to the presence of solute molecules to absorb the energy of ionization. Solutions of LDH were irradiated in the presence of nicotinamide adenine dinucleotide (NAD). NAD gave 35% protection. The protective substrates of one enzyme were found to protect other enzymes. (M.C.G.)

20515 ON THE RADIOPROTECTIVE POWER OF SOME ORGANOPHOSPHORUS COMPOUNDS. Adolphe, M.;

Cheymol, J.; Deysson, G.; Chabrier, P.; Heitz, F. Roentgen Europe., 8: 53-5(Dec. 1964). (In French).

Mice were given whole-body x-ray doses of 750 or 800 R after intraperitoneal injection of organic derivatives of hypophosphoric, pyrophosphoric, and orthophosphoric acid. Radioprotective effects of the compounds, containing various amounts of anticholinesterase activity were measured by the survival of the irradiated mice. In tests performed in vitro on HeLa cells, protective effects were measured in terms of the reduction of chromatin anomalies at various stages of mitosis. From among the many substances tested, only four had a slight radioprotective effect, two of which demonstrated effects both in vivo and in vitro. A correlation between the anticholinesterase activity and radioprotective action was not found. (H.G.D.)

Radiation Hazards and Protection

See also HEALTH AND SAFETY

20516 (AD-629311) QUARTERLY PROGRESS REPORT NO. 58. (USAF Radiation Lab., Univ. of Chicago, Ill.). Jan. 15, 1966. Contracts AF41(609)-1693 and AF41(609)-2977. 34p. CFSTI $2.00 cy, $0.50 mn.

Separate abstracts were prepared on three sections of this report. (C.H.)

For abstracts of individual sections see: 20429, 20430, and 20503.

20517 (NP-15925) RADIOSCHUTZ EFFEKT DES GLYCINS WAEHREND DER ROENTGENBESTRAHLUNG. 2. MITTEILUNG. ABHAENGIGKEIT DES RADIOSCHUTZES VON DER VERABFOLGTEN GLYCINMENGE. (Radioprotective Effect of Glycine During X Irradiation. Part II. Dependence of the Radioprotection on the Glycine Mass Injected). Capalna, S.; Stefan, Maria; Ghizari, Eugenia [1965]. 5p. Dep. mn.

White mice were injected with doses of 266, 520, and 780 μM/kg of glycine before x irradiation with 700 R. One, 24, and 48 hrs after the irradiation the ATP-ase and pyrophosphatase activities of tissues were determined. The ATP-ase, which in the non-irradiated animals had a value of 5.78 μM/g/min had in the irradiated and non-protected animals a value of 2.43 μM/g/min. After injection of 266 μM of glycine, the value rose to 426 μM/g/min and after 520 to 548 μM/g/min. In the case of pyrophosphatase, its activity of 1.09 μM/g/min in the unirradiated animals increased in the animals receiving 780 μM of glycine to 138 μM/g/min. The significance of these results is discussed. (J.S.R.)

20518 (RT-PROT-(65)41) OROLOGI RADIOLUMINESCENTI: ORIENTAMENTI INTERNAZIONALI DI RADIOPROTEZIONE. (Radioluminescent Watches: International Trends of Radioprotection). Cagnetti, P. (Comitato Nazionale per l'Energia Nucleare, Rome (Italy)). Dec. 1965. 13p. Dep. mn.

After a reference to some fundamental concepts concerning the distribution, among various exposure groups, of the maximum permissible genetic dose to the whole population, some statistical information is given, regarding the contribution to the population's genetic dose, due to the use of radioluminescent watches. Problems of health protection arising from this are then laid out, hence the necessity that the manufacturing of such watches comes under law. Some conclusions are made concerning the position of the individual who utilizes luminescent watches, with regard to the relevant Italian law; the possibility of making use of the radionuclides and limits of radioactivity previously recommended in the drawing up of future national regulations is pointed out. (auth)

20519 RADIATION HYGIENE. J. Amer. Dent. Ass., 72: 24(Jan. 1966).

A resolution adopted by the American Dental Association concerning radiation hygiene in dental offices is discussed. Education of members of the dental profession on principles of protection from unnecessary ionizing radiation is urged. It is concluded that dental x rays are relatively nonhazardous. (H.G.D.)

20520 THE INFLUENCE OF POLYOLS ON THE COURSE OF EXPERIMENTAL RADIATION DISEASE. Sonka, J.; Dienstbier, Z.; Pospisil, J. (Charles Univ., Prague). Radiobiol.-Radiotherap., 7: 75-80(1966).

Fifteen polyhydroxyl alcohols derived from sugars with 4, 5, 6, and 7 carbons, were synthesized and administered to groups of mice in a single intraperitoneal dose (0.2 ml in a 10 per cent solution) up to 4 hours after a single exposure to x rays of 600 R and 750 R. Ribilol (adonit) elicited a retardation of mortality at the 7th to 10th day by about three days and in most experiments this difference in the rate of mortality between the treated and untreated mice persisted to the 30th day following irradiation. Only an unreliable delay in the mortality was elicited by D-talitol. Following volemitol, erythritol and pentaerythritol, the manifestations of the radiation disease became worse while the other polyols did not influence the course of the illness. The therapeutic effect of ribitol is assumed to be in connection with its products of catabolism (D-ribose and reduced pyridine nucleotides) which may enhance regeneration in irradiated tissues. (auth)

20521 EXPERIMENTS ON THE POSSIBILITIES OF INFLUENCING RADIATION-INDUCED CEREBELLAR DEFECTS OF THE DOMESTIC MOUSE (MUS MUSCULUS DOMESTICUS RUTTY 1772) BY CHEMICAL RADIOPROTECTIVE AGENTS. Schmidt, R. (Martin-Luther-Univ., Halle-Wittenberg, Ger.). Radiobiol.-Radiotherap., 7: 99-109(1966). (In German).

New-born mice of the AB/Jena strain were intraperitoneally injected with AET or potassium cyanide 10 and 30 minutes before one whole-body x irradiation with 800 and 400 R in order to test the possibility of influencing radiation injuries of the cerebellum by chemical radioprotective substances. Examinations did not yield any radioprotective effect either in series pretreated with AET or in those pretreated with potassium cyanide. The protective substances were not able to reduce the primary radiation reactions in the cerebellar tissue nor could reliable symptoms of an effective reparation of radiation injuries be demonstrated. (auth)

Radiotherapy and Radiodiagnosis

Refer also to abstracts 20404 and 21082.

20522 (CNEA-167) CENTELLOGRAMA HEPATICO. (Hepatic Scintigram). Seeber, Jose Martinez; Pangaro, Juan Ceriani; Chwojnik, Abraham; Olivari, Americo; Degrossi, Osvaldo; Pecorini, Victorio (Comision Nacional de Energia Atomica, Buenos Aires (Argentina)). 1965. 12p. Dep. mn.

The experience obtained in hepatic scintillography using Bengal rose and colloidal albumin labeled with ^{131}I are reported. The utility of the method in the detection of benign or malignant tumors is emphasized. It is concluded that the correlation of the clinical, laboratory, and hepatic biopsy data would make it possible to solve the problem of the etiology of these lesions. (tr-auth)

20523 (NYO-1726-15) DEVELOPMENT OF SMALL IN VIVO β-RAY DETECTORS AND THEIR DIAGNOSTIC APPLICATIONS. EVALUATION PROGRAM AT NEUROSURGICAL CENTERS OF BRAIN TUMOR LOCALIZATION UNITS USED AT OPERATION WITH ^{32}P. Progress Report, May 15, 1965-May 14, 1966. Selverstone, Bertram (New England Medical Center Hospitals, Boston, Mass.). Contract AT(30-1)-1726. 13p. Dep. mn. CFSTI $1.00 cy, $0.50 mn.

The performance of small β-ray proportional detectors used as brain probes for use with stereotoxic technique for the location or demarcation of subcortical brain tumors is

discussed. Good results were reported when the proportional probe counter technique was used after the administration of ^{32}P. A list is included of 47 publications reporting research performed under this contract. (C.H.)

20524 (RT-PROT-(65)32) FLUX DE NEUTRONS LENTS ET DE RAYONS GAMMA A L'INTERIEUR D'UN MODERATEUR DE PARAFFINE. (Flux of Slow Neutrons and Gamma Rays in the Interior of a Paraffin Moderator). Trochev, T. (Comitato Nazionale per l'Energia Nucleare, Rome (Italy)). Oct. 1965. 11p. Dep. mn.

The evolution of the slow neutron and γ-ray flux during its passage through a phantom constituted by a block of paraffin was studied. The measurements made for the different forms of cavities indicate a larger dose than a moderator gives in other conditions. The evolution of the flux was characterized by a maximum at a depth of 2 cm. The flux maximum was always found at 2 cm of distance between two walls equivalent to the human tissue. (tr-auth)

20525 INVESTIGATION OF NEGATIVE π MESONS WITH REFERENCE TO THEIR APPLICABILITY IN RADIOTHERAPY. Tisljar-Lentulis, Georg M. (Brookhaven National Lab., Upton, N. Y.). Acta Phys. Austr., 21: 204-17(1966). (In German). (BNL-8924).

For the measurement of the Bragg ionization curve in polyethylene absorber, 150-Mev protons and 70-Mev negative π mesons with a range of approximately 15 cm in water were investigated in a parasite pulse-analyzed beam of the cosmotron with a counting telescope. For the determination of the energy given up by the beam, a 0.93 g/cm^2 sodium iodide crystal was used whose pulse spectra represented on a multichannel device made it possible with the help of an electronic and a computer method to measure the value of the energy transfer and therefore the dose in rads. The pulse spectrum showed with increasing absorber layer density characteristic variations that made it possible to determine the pattern of the ionization curve and therefore the height of the Bragg peak. For protons the relative height of the peak was established at 3.4 and, for a measurement without absorber, a dose of 1.38×10^{-7} rad/proton/cm was established. The results for π mesons were influenced by a strong background of μ mesons and electrons and necessitate further investigations. (tr-auth)

20526 TREATMENT OF CARCINOMA OF THE CERVIX WITH COMBINED RADIATION AND EXTENSIVE SURGERY. Sweeney III, William J.; Douglas, R. Gordon (Cornell Univ. Medical Coll, New York). Amer. J. Obstet. Gynecol., 84: 981-91(Oct. 15, 1962).

Doses used, clinical results, and complications are reported for 102 patients treated with combined radiation and radical surgery for cervical carcinoma. Included were 39 cases in Stage I, 54 in Stage II, and 9 in Stage III. The plan of therapy was 6 weeks of external radiation interspersed with two applications of radium at two-week intervals. An average of 13,534 R was delivered to the cervix. Complications ranged from minor ileus (3 cases) to fistulas (15 cases). The operative mortality was 2.9%. In 60 patients or 58.8% there was no residual carcinoma in the surgical specimen and the nodes were negative. It is concluded that this combined method of therapy increased the percentage of 5-yr survivals. (TCO)

20527 A MODIFIED METHOD OF RADIOISOTOPIC PLACENTAL LOCALIZATION: FOLLOW-UP REPORT. Wheeler, Paul C.; Stevens, Edward M.; Reeves, Lane (Univ. of Missouri Medical Center, Columbia). Amer. J. Obstet. Gynecol., 93: 961-4(Dec. 1, 1965).

Experience during the past year with a modified dual probe isotopic technique is examined in an attempt to verify two hypotheses: isotopic methods are superior to and may replace radiographic localization studies; and the radioisotopic modifications using a dual probe scintillation counter are superior to the single probe methods. A Picker Model 5846 dual ratemeter commonly used for renal examinations was used. One ratemeter probe was centered over the heart and was left in place during the entire examination. The second ratemeter probe was placed below the right costal margin. Ten μC of radioiodinated serum albumin (RISA) was injected intravenously while the recorder was advanced at slow speed (12 in./hr). Placenta previa was excluded in 19 of the 20 cases by the dual probe radioisotopic method (95%) and in 18 by radiographic examination (90%). Exact placental location was determined in 81% by x-ray (9 of the 11 in which the actual implantation site was verified) and in 90% by isotope technique. Although two cases of placenta previa were missed by x-ray studies and one by radioisotope, no case was missed when both methods were used simultaneously. Retrospective checking of the isotope tracing in which a placenta previa was originally missed revealed an error in interpretation rather than technique. There were no false positive reports. (TCO)

20528 AN ANALYSIS OF THE SPATIAL DISTRIBUTION OF RADIOACTIVE IODINE IN THE THYROID BY THE METHOD OF LEVEL DIAGRAMS. Albarede, P.; Di Paola, R.; Di Paola, M.; Tubiana, M. (Institut Gustave-Roussy, Villejuif, France). Ann. Radiol., 8: 829-50(1965). (In French).

A description is given of an examination method complementary to scintigraphy: the technique of the level diagram using ^{131}I as tracer. A study made on phantoms revealed that this method is useful in the case of hyper- and hypoactive thyroid nodules, and also in the case of hypoactive nodules situated at various depths in thick organs. It appeared that the nodules are often found more easily in the diagrams than in the scintigrams. Furthermore, the quantitative nature of the data obtained allows a calculation of relative activities, and statistical study of the comparative fixations of heterogeneous zones. With this method a more accurate assessment can be made of the dimensions of a radioactive area. The clinical application of the method is described on the basis of three illustrative cases. (auth)

20529 THE DIAGNOSIS OF SPACE-OCCUPYING PROCESSES IN THE SKULL WITH A COMBINATION OF GAMMA-ENCEPHALOGRAPHY AND ECHO ENCEPHALOGRAPHY (A STATISTICAL STUDY OF 650 CASES). Akerman, M.; Guiot, G. (Hopital Foch, Surenes, France). Ann. Radiol., 8: 851-79(1965). (In French).

A description and an analysis of the results of two recent methods of physical exploration that are particularly effective in the diagnosis of intracranial mass are presented. Human serum albumin labeled with ^{131}I was used as the tracer. Results are reported from a study of 650 patients of whom 178 had a verified space-occupying lesion. The results are analyzed, taking into account the localizations and the histological nature of the lesions. Attention is also given to the false-positive findings in cases in which no space occupying lesions were present. (auth)

20530 THE RESULTS OF POST-OPERATIVE IRRADIATION OF PATIENTS WITH TUMORS OF THE BRAIN, CONSIDERED IN RELATION TO THE NATURE OF THE IRRADIATION, THE IRRADIATED VOLUME AND THE DOSE. A STUDY OF 236 CASES. Legre, J.; Amalric, R.; Piratoni, A. Ann. Radiol., 8: 881-7(1965). (In French).

From a study of the results of post-operative irradiation in 236 cases of brain tumors of varying histological structure using x or γ radiation, the following conclusions could be drawn: As regards the survival after the treatment considered in relation to the nature of the radiations, it was found that where the malignant tumors are concerned, the results of conventional radiotherapy and gamma therapy are largely the same; in the cases of benign tumors, on the other hand, it seems that better results are obtained by conventional radiotherapy. The tumor dose is a very important consideration: it must range from 5,000 to 7,000 rad, because beyond 7,000 rad the periods of survival after the treatment are distinctly shorter. The irradiated volume is also an important consideration: a study of the survival figures shows that it is necessary to irradiate the entire affected hemisphere, because the periods of survival after treatment are considerably longer than after localized irradiation of the tumor. (auth)

20531 MEDICAL RADIOISOTOPE VISUALIZATION (A REVIEW OF "SCANNING"). Mallard, J. R. (St. Thomas's Hospital Medical School, London). Int. J. Appl. Radiat. Isotop., 17: 205-49(Apr. 1966).

Medical scanning is reviewed with emphasis on: techniques, moving and stationary scanners, clinical applications, and evaluation. It is concluded that scanning is a rapidly evolving technique that is moving away from empirical procedures towards physically-based quantitative ones. Perhaps one of the most significant developments in scintigraphy is the parallel hole multichannel collimator for the stationary machines, a device that threatens to replace moving detector scanners. (H.G.D.)

20532 LUNG SCANNING FOLLOWING RADIOAEROSOL INHALATION. Taplin, G. V. (Los Angeles County Olive View Hospital, Olive View, Calif. Univ. of California, Los Angeles); Poe, N. D.; Greenberg, A. Contract AT(04-1)-GEN-12. J. Nucl. Med., 7: 77-87(Feb. 1966).

The development of a safe techniques for visualizing the lower respiratory tract by chest scanning following inhalation of suitable radioaerosols is described. The aerosolization equipment and test agents are readily available. Filtration of the exhaled air and channeling it to a vented hood or to the outside atmosphere prevents contamination of the examining room and personnel. Aerosol deposition is related to factors other than diffusion, such as particle size, sedimentation, impaction, concentration of aerosol, and the rate of air movement. When inhalation is performed with the subject in the lateral position, greater amounts of aerosol are deposited in the superior lung, where ventilation and perfusion are reduced. With partial bronchial obstruction, increased deposition of radioaerosol may occur at the obstruction site and the region beyond usually shows reduced levels of radioactivity. Complete bronchial obstruction is readily detectable in the inhalation scan as an area devoid of radioactivity. A normal lung image indicates patency of the lower respiratory passages. The radioaerosol inhalation scanning procedure is a useful adjunct to bronchography in the assesment of airway patency. It may be employed safely when bronchography is contraindicated as in patients with impaired pulmonary function. Additional applications of the inhalation scanning procedure are mentioned. (auth)

20533 A COMPARISON OF ^{125}I AND ^{131}I AS TRACERS IN THE DIAGNOSIS OF THYROID DISEASE. I. PHYSICAL ASPECTS. Ben-Porath, M.; Hochman, A.; Gross, J. (Hebrew Univ., Jerusalem). J. Nucl. Med., 7: 88-98 (Feb. 1966).

The physical aspects of the use of ^{125}I for thyroid diagnosis were studied. It was shown that for in vitro studies (urine and plasma) the effect of density on assay is negligible. Using a 32.5 ml water standard and a five-inch, lucite neck phantom, thyroid uptakes may be measured with an accuracy of ±10% for thyroids in the 20 to 55 gm weight range, and ±20% for 15 to 75 gm range. The scanning resolution is improved by 20% for ^{125}I in comparison with ^{131}I. The possibility of estimating the depths of sources is indicated. Iodine-125 and ^{131}I easily may be used for double-tracer techniques. The tracer dose of ^{125}I may be reduced by a factor of six, compared to ^{131}I, without altering counting statistics. For thyroid studies, the radiation dose to the thyroid may be reduced by a factor of ten. (auth)

20534 A COMPARISON OF ^{125}I AND ^{131}I AS TRACERS IN THE DIAGNOSIS OF THYROID DISEASE. II. CLINICAL ASPECTS. Ben-Porath, M.; Hochman, A.; Gross, J. (Hebrew Univ., Jerusalem). J. Nucl. Med., 7: 99-106 (Feb. 1966).

Results of 229 tracer studies with ^{125}I were compared with the results of the same number of studies with iodine-131. Twenty patients were given a mixed dose of $^{125}I + ^{131}I$. There was no significant difference in the results, providing appropriate standards are used. (auth)

20535 HYBRID RADIOISOTOPE SCANNER. Davis, Thomas P.; Martone, Ronald J. (Univ. of Rochester, N. Y.). J. Nucl. Med., 7: 114-27(Feb. 1966).

A radioisotope mapping system intermediate in speed and complexity between a standard mechanical rectilinear scanner and a stationary camera-type device was developed. In this instrument, a scintillation position sensing system is used for the determination of activity distribution in one direction, while the complete area map is produced by a mechanical motion at right angles to this direction. Because of the combination of an electronically sensed transverse scan with a mechanical longitudinal scan, the instrument has been termed the hybrid scanner. The operating principle and design of the hybrid scanner are described, and performance characteristics of the instrument are discussed. Several clinical scans using ^{131}I-labeled compounds are presented, including brain and liver scans. The advantages and disadvantages of the present version of this instrument are discussed, and areas of potential improvement noted. (auth)

20536 THE TEN-YEAR RESULTS OF INDIVIDUALIZED TREATMENT OF CARCINOMA OF THE CERVIX BASED ON THE ANALYSIS OF SERIAL BIOPSIES. Glucksmann, Alfred; Way, Stanley; Cherry, Cora P. (Strangeways Research Lab., Cambridge, Eng.). J. Obstet. Gynecol. Brit. Commonwealth, 71: 198-201(Apr. 1964).

Cytological changes seen in serial biopsies taken from the tumor immediately before and at suitable intervals (usually on the 7th and 14th day) during therapy of cervical cancer cases were made to determine what, if any, salvage could be obtained by performing radical hysterectomy and lymph node dissection on patients in whom the histological response of the carcinoma to irradiation as seen in serial biopsies was deemed to be unfavorable. Results in 400 cases showed that where surgery was added to preliminary irradiation the cure rate was increased by about 30% for clinical stages 1 and 2 as compared with radium treatment alone. Thus in stage 1 the ten-year survival rate for cases treated by radium only was 12% while additional surgery raised it to 47%, a difference of 35%, which shows a high degree of statistical significance. In stage 2 the corresponding figures are 7 and 36%, a significant increase in cure rate of 29%. The study shows that surgery additional to radiotherapy benefits appreciably those patients whose tumors have been found by the serial biopsy technique to respond unfavorably to radium treatment. (TCO)

20537 ON THE PROBLEM OF FETAL RADIATION BURDEN IN ISOTOPIC PLACENTOGRAPHY USING HUMAN SERUM ALBUMINE LABELED WITH ^{131}I OR ^{132}I. Tautz, M. (Radiologische Klinik des Staedtische Klinkums, Berlin). Kernenergie, 8: 645-50(Nov. 1965). (In German).

The probable body burden to fetuses in isotopic placentography using human serum albumin labeled with ^{131}I or ^{132}I was investigated. The gonad doses were calculated in a geometric approximation of the anatomic conditions and compared to those quoted in the literature. The influence of the degree of geometric approximation as well as the difficulties of interpreting the dose values calculated are pointed out. (auth)

20538 RADIOACTIVE RENOGRAPHY IN DIAGNOSIS AND TREATMENT OF ACUTE OBSTRUCTIVE RENAL FAILURE. Joekes, A. M. (Inst. of Urology, London); Rellan, D. R. Lancet, 2: 96-9(July 17, 1965).

The effectiveness and safety of renal scanning technics are discussed, and reasons for using the method employing ^{131}I-Hippuran in patients with acute renal failure are presented. The value of radioactive renography in diagnosis and treatment is illustrated in 3 patients with acute renal failure. The radioactive renogram was shown to offer the following advantages: it establishes the presence of obstruction if good function still persists; it can determine the relative function of the two kidneys; and it can demonstrate whether an obstruction has been effectively removed. (TCO)

20539 TOXICITY AND PYROGENICITY OF COLLOIDAL PREPARATIONS OF ^{198}Au AND $Cr^{32}PO_4$ IN NEURO-ONCOLOGICAL PRACTICE. Volkov, A. A. Med. Radiol., 10: No. 11, 27-30(Nov. 1965). (In Russian).

Colloidal preparations of ^{198}Au and $Cr^{32}PO_4$ were used for intratissular and intracavitary irradiation in 60 patients suffering from brain tumors. A marked difference in the early reaction of the patients to the administration of these preparations was noted, especially in their intraventricular and subarachnoidal introduction. Colloidal $Cr^{32}PO_4$ proved to be much more toxic. However, upon the adminstration into closed cystic cavities of cerebral tumors the difference in reactions is less significant. Gold-198 is recommended for the intraventricular and subarachnoidal route of administration. For the irradiation of cystic tumors (craniopharyngoma in particular) it is better to use $Cr^{32}PO_4$. (H.G.D.)

20540 ASSESSMENT OF THE METHOD OF RECORDING RADIOPHOSPHORUS BREMSSTRAHLUNG FOR THE DIAGNOSIS OF MILK-DUCT CARCINOMA. Melenchuk, I. P.; Tatsievskii, V. A. Med. Radiol., 10: No. 11, 39-45 (Nov. 1965). (In Russian).

Diagnosis of mammary cancer using bremsstrahlung from the interaction of radiophosphorus with paraffin was assessed in a tissue-equivalent phantom. By using computers, bremsstrahlung was recorded in 24 μC of radiophosphorus. However, this concentration of the isotope could not be achieved in the tumors. (H.G.D.)

20541 EXPERIMENTAL DATA ON THE DOSE ASSESSMENT DURING REMOTE-CONTROL γ THERAPY. Aliev, B. M.; Misyunas, I. I.; Kaveshnikova, S. V.; Sizov, P. P. (Inst. of Experimental and Clinical Oncology, Academy of Medical Sciences, USSR. Moscow Hospital of Clinical Oncology). Med. Radiol., 10: No. 12, 13-21(Dec. 1965). (In Russian).

A method for rapidly determining optimal conditions for irradiation and for elaborating dosimetric characteristics of the individual patient is presented. Based on calculation of field dose, the required dosimetric data may be obtained for each patient in from 1 to 1½ hrs. (H.G.D.)

20542 ^{103}Pd AS A THERAPEUTIC RADIATION SOURCE. Harper, P. V.; Lathrop, Katherine (Univ. of Chicago). Nucl.-Med., Suppl. 3, 411-18(1965).

Palladium-103 was tested for prophylactic treatment in the parametrium or the internal mammary nodes. The only serious objection to its use appears to be economic. (H.G.D.)

20543 THE DANGERS OF RADIATION IN CEPHALOMETRIC RADIOGRAPHY. Franklin, J. B. Orthodont. Franc., 35: 42-4(Nov. 23, 1964). (In French).

In patients irradiated during orthodontic treatment the average dose absorbed by a patient in a normal series of 3 cephalometric radiographs, using an x-ray voltage of 90 kv at 20 ma for 0.4 sec is ~240 mrem, if an Al filter is not used. A 1.5- or 2-mm thick Al disk is usually sufficient to provide adequate filtration for this type of beam. The greater the beam dispersion, the better is the % of filtration provided by the first mm of Al. Additional Al filtration tends to promote dispersion of the radiation. If more than 2 mm of Al are used in the filter, the diagnostic quality of the radiograph is altered without reducing materially the danger of irradiation of the patient and operator. Exposure to radiation, whether primary or secondary is dangerous at any time because its effects are cumulative and irreversible. For this reason, exposure to radiation is more dangerous to the operator than to the patient since he is cumulatively exposed to dispersed x irradiation. (BBB)

20544 X RAYS, RADIATION INJURY, AND RADIATION PROTECTION. A REVIEW OF THE FUNDAMENTALS AND REQUISITES FOR RADIOGRAPHY IN TUBERCULOSIS CLINICS. Kurz, Ernst (Staatliches Gesundheitsamt, Kempten, Ger.). Praxis Pneumol., 18: 581-604(Sept. 1964). (In German).

The risks involved in x-ray examination and measures required to prevent or reduce radiation damage in patients are reviewed. The benefits that result from strictly supervised diagnostic radiology are considered to outweigh by far the dangers arising from such examinations, provided that due care is taken to prevent prolonged and unnecessary exposure to x rays. (TCO)

20545 RADIATION NECROSIS OF THE CERVICAL SPINAL CORD IMITATING METASTASES OF CARCINOMA. Raskind, R.; Bagshaw, M. A. (Kaiser Foundation Hospital, Oakland, Calif. Stanford Univ., Palo Alto, Calif.). Radiobiol.-Radiotherap., 7: 31-5(1966). (In German).

Although the neoplasm was apparently eradicated by supervoltage x irradiation, the patient succumbed to myelitis which was believed secondary to the therapy. When signs of neurologic involvement first appeared, a year and a half after radiation had been given for the nasopharyngeal tumor, the initial impression was that of a metastatic lesion in the upper portion of the cervical cord. The cerebrospinal fluid, however, contained no cells and its protein content was only slightly elevated. Myelography revealed no evidence of such involvement, and post-mortem study proved the absence of metastases. The possibility of radiation necrosis of the spinal cord, as well as that of a metastatic lesion, must be considered when neurologic signs follow radiation therapy in that region. (auth)

20546 RECORDING RESPIRATORY FUNCTION BY X RAYS: BASIC PRINCIPLES. Kourilsky, Raoul; Marchal, Maurice; Marchal, Marie-Therese (Hopital Saint-Antoine, Paris). Thorax, 20: 428-34(Sept. 1965).

New techniques for the exploration of respiratory function, using x rays, are described. The methods are based on the measurement of the flux of x rays leaving the lungs after irradiation and transformation into optical waves by a fluoroscopic screen or a scintillator, and electronic pulsations through a photomultiplier. They are amplified and recorded by an electromagnetic galvanometer. Continuous photographic records of the spontaneous respiration of each lung are obtained simultaneously. Local ventilation is recorded likewise on selected areas of each lung in the same individual. It is possible to obtain simultaneous recordings of pulsatility and ventilation of the same region of the lung. The dose of x rays needed for this method is one-tenth of the dose required for standard fluoroscopy. The pulsatility of the peripheral arterioles of the lung can also be recorded by the difference in density of the vessels in systole and diastole, and checked on the same graph with the electrocardiogram. The form and timing of aortic and cardiac transferred pulsations are different from those of the pulmonary vessels. An index of pulsatility can be calculated. Accurate adjustment of the dose of x rays falling on the photomultiplier was obtained by special calibration, ensuring true comparisons. It is emphasized that these methods do not measure the volume of ventilation but the ratios between inspiration and expiration volumes. Similarly, the pulsatility of the vessels is measured but neither the volume nor the speed of the circulation. Within these limits the techniques are quick, accurate, and reliable. (BBB)

20547 BEAM FOCUS RADIOGRAPHY FOR TAKING THE RADIOGRAM OF THE AXIAL TRANSVERSE CROSS SECTION OF THE TREATED REGION IN HIGH DENSITY OF DOSE. Sakuma, Sadayuki; Takahashi, Shinji (Nagoya Univ., Japan). Tohoku J. Exp. Med., 87: 244-8(Dec. 1965).

The principle and procedure for imaging the beam focus of a ^{60}Co rotation unit on film are described. Three components in the system, the radiation source, the rotation table A on which a patient is placed, and the rotation table B on which an x-ray film is placed, are arranged so that the radiation source and the axis of the tables A and B are in a vertical plane. When the two rotation tables are rotated synchronously during irradiation, the axial transverse cross section of the beam focus is imaged on the film on table B. In practice the patient is kept stationary on the therapy table with the radiation source rotating around the patient. The construction of the attachment for beam focus radiography is described in detail. (BBB)

20548 CASSETTE AND INTERSPACER IN BEAM FOCUS RADIOGRAPHY. Sakuma, Sadayuki (Nagoya Univ., Japan). Tohoku J. Exp. Med., 87: 281-91(Dec. 1965).

Auxiliary equipment used in radiographic visualization of beam focus for a ^{60}Co rotating unit is described, with details of its construction and operation. After an evaluation of the cassette, interspacer, and film to be used for beam focus radiography, it was decided that industrial x-ray film (Fuji type 80) is most suitable because of the adequate density obtainable during the course of therapy with 200–250 R. The edge of the cassette made of aluminum 1 mm thick and the interspacer of mortopren are adequate for routine use, though a slight increase of scattering reduces the contrast of the radiogram. Film dosimetry is applicable in supervoltage radiotherapy, including ^{60}Co γ radiation, for obtaining isodose charts or evaluating the loss of homogeneity in beam focus due to penumbra, since the radiation dose and the density of film bear a close relation to one another. However, it is pointed out that for film dosimetry, error due to unevenness of emulsion reaches 3.5% at the highest and 1.5% at mean value. In beam focus radiography the deviation of density is acceptable up to an error of 10%, so that the deviation will be negligible in practice. When the temperature of developer changes ~0.5°C, the density of the film changes ~2–5%. An automatic film processing machine was used which gives an error of less than 5%. The automatic processing machine used here has the capacity of processing 2000 sheets of film without any change of gamma of the films. (BBB)

20549 BEAM FOCUS AND ITS IMAGE ON BEAM FOCUS RADIOGRAM. Sakuma, Sadayuki (Nagoya Univ., Japan). Tohoku J. Exp. Med., 87: 306-21(Dec. 1965).

The actual dose distribution of the beam in the body with a ^{60}Co rotation unit as compared with the results obtained by densitometry of the beam focus image at the position of the turntable was studied. When fixed-field therapy was conducted with the same arrangement of the phantom and film as beam focus radiography, the patterns of the isodose curves in the phantom and at the position of the turntable were different from each other. However, the edges of the beam in the body as well as at the turntable diverged continuously. In full rotation therapy with coincidence of the rotation center of the source with center of the phantom, the beam focus image showed nearly the same figure of the actual beam focus delineated by the 80% curve of the isodose curves. When the rotation center was eccentric with the center of the phantom, the dose distribution at the turntable became less homogeneous than that in the phantom. But the loss of homogeneity was a max of 10% when the rotation center shifted up to 4 cm from the center of the axial transverse cross section of a normal-sized human body. Beam focus image increased in size with the increase of the exposure dose. It was concluded that it is best to employ an exposure dose of from 6 to 12 R to evaluate the actual beam focus from the beam focus image. (BBB)

20550 NIERENDIAGNOSTIK MIT RADIOISOTOPEN. FUNKTIONELLE UND MORPHOLOGISCHE ERGEBNISSE IN EXPERIMENT UND KLINIK. (KIDNEY DIAGNOSIS WITH RADIOISOTOPES. FUNCTIONAL AND MORPHOLOGICAL RESULTS IN EXPERIMENT AND CLINIC). zum Winkel, Karl. Stuttgart, Georg Thieme Verlag. 1964. 160p. DM 57.60.

The author describes the physical properties of synthetic radioisotopes used for measurement of kidney function and methods used for measurement of their radiation. The physiological characteristics of renal excretion, the radioactive substances used, and the results obtained in the past are reviewed. Problems and methods of study of kidney function in experimental animals are reviewed in the field of isotope nephrography, autoradiography, and estimation of organ activities. The excretion of substances with renal affinity is reviewed. Renal incubation studies in animals, with unilateral circulatory derangement and experimental analysis of the isotope nephrogram are discussed. Kidney function is discussed in connection with experimental nephrosis and artificially induced hydronephrosis. Renal excretion in man is discussed. Techniques, evaluation, and clinical findings in isotope nephrography are discussed. Advantages of and indications for, as well as modified techniques of isotope nephrography are reviewed in detail. Technique, methods of evaluation, clinical findings, and results of kidney scintigraphy are discussed briefly. (BBB)

20551 GERMAN X RAY CONGRESS OF 1964. REPORT ON THE 45th SESSION OF THE GERMAN X RAY SOCIETY FROM APRIL 9–13, 1964, IN WIESEBADEN. PART B. RADIOTHERAPY AND RADIOBIOLOGY. Strahlentherapie, Sonderbaende, 61: 1-432(1965). (In German). (CONF-640414(Pt. B)).

The 50 papers presented at the 45th session of the German X-Ray Congress in 1964 are compiled together with the discussions and comments following the various papers. The topics discussed are: clinical experiments and delayed results in tumor treatment with megavolt beams, clinical radiation biology; whole-body radioactivity measurement; and physics and technology of x-ray therapy and diagnosis. (J.S.R.)

CHEMISTRY

General

Refer also to abstract 21224.

20552 (CONF-650723(Absts.)) ABSTRACTS OF SCIENTIFIC PAPERS PRESENTED AT THE XXth INTERNATIONAL CONGRESS OF PURE AND APPLIED CHEMISTRY, MOSCOW, U.S.S.R., JULY 12–18, 1965. (Division of Isotopes Development (AEC), Washington, D. C.). 197p. CFSTI $2.00 cy, $1.00 mn.

Abstracts of 602 papers on physical chemistry of surface phenomena and disperse systems, radiation chemistry, cosmic chemistry, inorganic chemistry, analytical chemistry, and principles of chemical technology are presented. An author index is included. (P.C.H.)

20553 (MLM–1142) MOUND LABORATORY PROGRESS REPORT FOR SEPTEMBER 1962. Grove, G. R.; Jones, L. V.; Eichelberger, J. F.; Rembold, E. A. (Mound Lab., Miamisburg, Ohio). Sept. 28, 1962. Contract AT-33-1-GEN-53. 27p. Dep. mn. CFSTI $2.00 cy, $0.50 mn.

Infrared spectra techniques were evaluated to determine the molecular weight variations in plastic extruded from an experimental rheometer. Thirteen adhesives formulations were tested after being subjected to various temperature environments for 26 weeks. At room temperature, the Oxiron adhesives varied from moderate to high tensile strength with moderate to low flexibility. The Adiprene adhesives had low tensile strength but had high flexibility. At −65°F, the flexible Oxiron adhesives had an average elongation of 1.8%. At this temperature, the Adiprene adhesives had a tensile strength of over 9,000 psi with greater than 200% elongation. At 160°F most of the adhesive formulations had tensile strengths below 500 psi. Separation of ^{234}U from aged ^{238}Pu was demonstrated. Previous results indicated that an anion exchange process is advantageous over a solvent extraction system for the initial separation. It was found that the amount of Pu absorption on the anion exchange resin is dependent upon the age and condition of the resin. Data show that ^{210}Po undergoes (n,xn) reaction with high energy neutrons to form ^{209}Po and ^{208}Po. ^{13}C in CH_4 and CO is being separated and purified. Theoretical studies on the separation are being continued. The scintillation counter to detect trace quantities of ^{85}Kr in fission product Xe was assembled. Experiments with solid state alpha detectors and the 256 multichannel pulse height analyzer showed that high alpha resolution can be obtained. The viscosity of liquid Pr was determined at 15 different temperatures from 936°C to 1009°C. The activation energy for viscous flow is 1100 calories/gram-atom. The measurements of the heats of transformation for the various phase transformations in unalloyed Pu were completed. The measured values, 2540 ± 20 calories/gram-atom for Bi and 1490 ± 10 calories/gram-atom for Cd, lie within the reported accuracy of literature values. Phase equilibria studies continued in the Pu–Ce–Cu ternary system by differential thermal analysis and metallography. Microspheres were produced in the induction coupled plasma torch of an 80 wt% PuO_2–20 wt% UO_2 composition. Analysis by x-ray diffraction showed the material to be a single-phase solid solution. The microspheres exhibited the same wipe-free characteristics of pure PuO_2 microspheres. (J.R.D.)

Analytical Procedures

See also Separation Processes and Procedures

Refer also to abstracts 20738, 20963, 20976–20978, 21040, and 22039.

20554 (AD–621017) PRELIMINARY STUDY OF NEUTRON ACTIVATION ANALYSIS SERVICE: GAMMA-RAY SCINTILLATION SPECTROMETRY AND SPECTRUM ANALYSIS [Thesis]. Burns, Richard S. (Air Force Inst. of Tech., Wright-Patterson AFB, Ohio. School of Engineering). Aug. 1965. 100p. (GNE/PH–65-1). CFSTI $3.00 cy, $0.75 mn.

Studies were made on: general considerations of neutron activation analysis; instrumental approach to gamma spectrum analysis including the assembly of a scintillation spectrometer based on Heath's layout and comparison of data with his spectrum data; and comparative least-squares gamma spectrum analysis of a composite spectrum using an IBM-7094 II Computer was developed. (TAB)

20555 (AD–622200) UNFOLDING OF GAMMA-RAY SPECTRA BY STEPWISE STATISTICAL METHOD. Technical Report, September 1964–January 1965. Young, Myron H.; Singhal, Narayan S. (Louisiana State Univ., Baton Rouge). July 1965. 25p. (FDL-TR–65-86). CFSTI $1.00 cy, $0.50 mn.

The principle of the stepwise statistical method is applied to gamma-ray spectral analysis of an unknown mixture of many radionuclides. During the multiple regression procedure the F-level tests are given sequentially for entering and removing the nuclides from a set of library spectra. The unknown spectrum is unfolded when a best fit is obtained. The computer program for IBM 7040 has the capacity to resolve a mixture containing up to 99 nuclides. Various gain settings can be used for the multichannel analyzer, and the channel drift is corrected at each run by the standard sources. The flexibility of data gathering and the advantages of the stepwise principle make this method suitable for practical analysis of mixed gamma spectra. (auth)

20556 (AD–626987) PREPARATION OF STANDARD SAMPLES AND DEVELOPMENT OF ANALYTICAL TECHNIQUES FOR CARBON AND NITROGEN IN HIGH-PURITY BERYLLIUM. Final Report. Aronin, L. R.; Bauman, F. A.; Wolff, A. K. (Nuclear Metals, West Concord, Mass.). Oct. 1965. Contract AF33(615)-1692. 50p. (AFML-TR–65-195). CFSTI $2.00 cy, $0.50 mn.

Analytical techniques were developed for the determination of carbon in high-purity beryllium. The method, a modification of the combustion-conductometric technique, permits an increase in the sample size of about four times, thereby achieving a fourfold reduction in the lower limit of useful analytical results. Sensitivity was demonstrated for carbon contents as low as 25 ppM. The accuracy of a solution distillation technique for determination of nitrogen in high-purity beryllium was established. A modified micro-Kjeldahl still was employed. Nitrogen contents less than 10 ppM can be accurately determined. Three batches of beryllium weighing roughly 5 pounds each were prepared. Each batch was attritioned, sized, and blended to provide a homogeneous material for analytical standards. These standards, in the form of coarse chips, have the following carbon and nitrogen contents for the 3 standards in parts per million, respectively: carbon, 25, 101, and 120 and nitrogen, 11, 55, and 56. (TAB)

20557 (AERE-R–5129) THE ANALYSIS OF URANIUM SILICIDES. Milner, G. W. C.; Rowe, D. H.; Phillips, G. (Atomic Energy Research Establishment, Harwell (England)). Jan. 1966. 14p. Dep. BIS $0.50. HMSO 2s. 6d.

A procedure is described for the chemical analysis of uranium silicides varying in composition from the monosilicide to the disilicide. Dissolution of samples is achieved by pre-igniting at 850°C and then fusing with Na_2CO_3 in a nickel crucible. After extracting the melt with water, the silicon is converted to its silicomolybdate complex between pH 1.5 and 1.7. Excess of molybdate in solution is inactivated by the addition of concentrated hydrochloric acid, and then quinoline is added to precipitate

quinoline silicomolybdate. The precipitate is filtered onto a sintered glass filter, dried at 150°C, and then weighed. The silicon content is determined from the weight of precipitate, the precision of a determination being better than ±0.5%. For the determination of uranium, a separate sample is taken and dissolved in HNO_3 + HF. The determination is completed by controlled-potential coulometry on a sulfuric acid solution of the sample. The suitability of these procedures was confirmed by employing them for the complete analysis of typical uranium mono- and disilicide samples. (auth)

20558 (CEA-R-2863) METHODES PHYSIQUES D'ANALYSE DE L'HEXAFLUORURE D'URANIUM [THESE]. (Physical Methods of Analysis of Uranium Hexafluoride [Thesis]). Vandenbussche, Gerard (Commissariat a l'Energie Atomique, Fontenay-aux-Roses (France). Centre d'Etudes Nucleaires). Dec. 1965. 31p. Dep. mn.

Submitted to Paris Univ., France.

Physical methods used for the analysis for uranium hexafluoride were reviewed with respect to the principle of the method, its applicability, and its precision and sensitivity. The methods studied were measurement of the velocity of sound in the mixture, methods based on equilibrium diagrams, chromatography in the gaseous phase, absorption spectrometry, Hertzian spectrometry, and mass spectrometry. (83 references.) (J.S.R.)

20559 (EUR-2626.f) METHOD D'ANALYSE DU PROFIL D'ACTIVITE D'UN RADIOCHROMATOGRAMME. (Method of Analyzing the Activity Profile of a Radiochromatograph). Apelgot, S.; Duquesne, M. (Paris Univ. (France). Laboratoire Curie). Nov. 9, 1965. 28p. Dep. mn.

A study of the activity profile of a radioactive solute at various stages of chromatography shows, with a pure substance, a Gaussian distribution and makes it possible to determine a law, governing the standard deviation broadening in that distribution. In a mixture, each constituent has a Gaussian activity curve, and a complex profile can be broken down into a sum of Gaussian curves. (auth)

20560 (EUR-2753.f) DETERMINATION PAR ACTIVATION AUX NEUTRONS D'IMPURETES DANS QUELQUES MATERIAUX S'ACTIVANT FORTEMENT AU COURS DE L'IRRADIATION. (Neutron Activation Determination of Impurities in Some Materials Strongly Activated Upon Irradiation). Pietra, R.; Sabbioni, S.; Pauly, J. (European Atomic Energy Community, Ispra (Italy). Joint Nuclear Research Center). Mar. 1966. 30p. Dep. mn.

Three analyses are described. Determination of rubidium in minerals: the ^{86}Rb isotope is separated from the other activities by means of the adsorption on ammonium-phosphomolybdate. Analysis of monocrystals of potassium halogenides: Na and Br were determined after the elimination of the excess activity of ^{42}K. Therefore potassium was precipitated as KCl using gaseous HCl. The effect of the incorporation of Br in the KCl lattice was studied. The chlorine in KBr was analyzed, thus eliminating the bromine before irradiation. The yield of the separation was followed using the ^{38}Cl isotope as tracer. Analysis of impurities in semiconductor materials: lithium was determined in silicon crystals. The sample is dissolved and the solution irradiated in order to produce the ^{18}F isotope. The effect of the purity of the reagents was examined. Phosphorus was determined in germanium by eliminating the strongly activated isotopes of Ge and As by distillation. (auth)

20561 (JAERI-1099) RADIOCHEMICAL STUDIES OF NEPTUNIUM. Akatsu, Eiko (Japan Atomic Energy Research Inst., Tokyo). Sept. 1965. 56p. Dep. mn.

Solvent extraction, coprecipitation, complex formation, and reactor chemical studies on neptunium were investigated. In the study of solvent extraction of neptunium, the phosphorylated reagents, dodecylbenzenesulfonic acid and the high-molecular-weight alkylamines were taken as the organic phase, whereas nitric, hydrochloric, sulfuric, or perchloric acid were used as the aqueous. The acidity dependence curves of distribution ratios of neptunium in most of the extraction systems normally used are given. The complex formation of neptunium with oxalic, mandelic, phenylarsonic, and ethylenediaminetetraacetic acid was studied by the use of solvent extraction technique. In the study of coprecipitation, it is shown that neptunium(V) is carried with lanthanum fluoride. ^{237}Np in JRR-1 fuel solution was found. ^{238}Np and ^{238}Pu were detected in neutron irradiated ^{237}Np. 144 references are cited. (auth)

20562 (LYCEN-6538) ANALYSE PAR ACTIVATION D'UN MELANGE DE TERRES RARES [These]. (Activation Analysis of a Mixture of Rare Earths [Thesis]). Sautin, Andre (Lyon Univ. (France). Institut de Physique Nucleaire). Dec. 1965. 84p. Dep. mn.

The determination of rare earths by activation analysis when they form the major constituent of the sample is reported. In the samples used, the proportion of each rare earth varied considerably from one element to the other—from at least 40% to less than 1%. Two types of samples were used. The first was a mixture used as a primary catalytic material under the name of didymium oxide or didymium and consists of a mixture of rare earth oxides with the approximate concentration neodymium oxide 50 to 55%, praseodymium oxide 12 to 15%, and traces of lanthanum and cerium. The second sample was a catalyst of silica or alumina support impregnated by a solution of didymium and other elements among which were copper and potassium. The results of determinations made on didymium by the irradiation of deposits on paper or of solid samples are given. Spectrum of the ensemble of radioisotopes formed during irradiation was obtained by γ spectrometry. Direct analysis was used to determine lanthanum and neodymium. The results showed that thermal neutron activation can be used for the identification and determination of rare earth elements present at very different ratios as in the mixture used. A precision of 3% could easily be attained. (P.C.H.)

20563 (NP-15918) BIBLIOGRAPHY ON ATOMIC ABSORPTION. (Aztec Instruments, Inc., Westport, Conn.). [nd]. 63p.

References (422) on determination of elements by atomic absorption are given to books, journals, and reports published from 1947 through Feb. 1966. Subjects covered include: agriculture and food; biological chemistry; petroleum and petroleum products; metallurgy and mining; industry and geology; isotopes; and instrumentation, techniques, and theory. An element index is included. (P.C.H.)

20564 (NYO-10740) GAMMA SPECTROMETRIC MEASUREMENT OF ^{235}U IN 24-in. x 24-in. x 12-in. ABSOLUTE AIR FILTERS AND ASSOCIATED ECONOMICS OF URANIUM RECOVERY. Fishman, Alan M.; Cohen, Ira; Durkan, Frances K. (New York Operations Office (AEC), N. Y.). Dec. 15, 1965. 27p. Dep. mn. CFSTI $2.00 cy, $0.50 mn.

A non-destructive, gamma spectrometric procedure is described to determine the ^{235}U contained in 24 × 24 × 12 in. absolute air filters. Data obtained at two nuclear facilities using the technique are discussed. Either a prepared standard filter or a small number of filters from a contaminated filter inventory can be used to assign ^{235}U values to an entire filter inventory. Statistical tests comparing ^{235}U determined by gamma spectrometry against chemical analyses showed no significant difference. A computational method is presented, utilizing a digital computer, which provides a method for determining the number of filters that can be sent for uranium recovery to yield the greatest economic advantage. (auth)

20565 (ORNL-P-1216) ^{3}He ACTIVATION ANALYSIS. Ricci, E.; Hahn, R. L.; Strain, J. E.; Dyer, F. F. (Oak Ridge National Lab., Tenn.). [1964]. Contract W-7405-eng-26. 20p. (CONF-650405-25). Dep. mn. CFSTI $1.00 cy, $0.50 mn.

From International Conference on Modern Trends in Activation Analysis, College Station, Tex.

Studies were made on: radioactivation of oxygen leading to short-lived nuclides, as well as to 1.8 hr ^{18}F; activation

analysis for other light elements, such as Be, C, N, and F; determination of neutron yields for light elements (Li, Be, B, C, and O) exposed to ^{3}He irradiation, to investigate the applicability of the small ^{3}He cyclotron as a neutron source. Data are tabulated. (P.C.H.)

20566 (ORNL-TM-1468) THE EVALUATION OF THE HYDROUS ZIRCONIUM OXIDE/NITRIC ACID SYSTEM FOR USE IN A ^{99}Mo-^{99m}Tc GENERATOR. Pinajian, J. J. (Oak Ridge National Lab., Tenn.). Apr. 1966. Contract W-7405-eng-26. 6p. Dep. mn. CFSTI $1.00 cy, $0.50 mn.

The use of the hydrous zirconium oxide/nitric acid system for the elution of 6.0-hr ^{99m}Tc from 66-hr ^{99}Mo was examined for 1 and 2M HNO_3. Approximately 40 mg Zr per elution volume was found in each case. The presence of 0.027 and 0.5% ^{99}Mo in the 1 and 2M HNO_3, respectively, limits its use for medical applications. (auth)

20567 (UJV-1418/65) K EKSTRAKTSIONNOMU RADIOMETRIKHESKOMU TITROVANIYU. (A Contribution to the Extraction Radiometric Titrations). Kukula, F.; Krivanek, M. (Ustav Jaderneho Vyzkumu, Ceskoslovenska Akademie Ved, Rez). [1965]. 13p. Dep. mn.

A new simplified method for extraction radiometric titration, which is described, is applicable for the determination of the carrier quantity in radioisotopes and their mixtures. Single elements (Cu, Hg, Ag, Fe) as well as the combinations Hg–Cu and Ag–Cu were estimated in the particular sample. The combination of this method with double-isotopic-dilution makes it possible to carry out experiments with reagents of low stability and/or of insufficient purity. Three different ways for evaluating the titration curves and the applicability of a multichannel analyzer for studying the titration curve for radioisotope mixtures are discussed. (auth)

20568 INVESTIGATIONS IN CONNECTION WITH THE SPECTROPHOTOMETRIC DETERMINATION OF NEODYMIUM IN THE PRESENCE OF PRASEODYMIUM. Auer-Welsbach, Helga (Univ., Vienna). Acta Phys. Austr., 21: 4-9(1966). (In German).

The effect of the background in the photometric determination of neodymium in praseodymium can be considered by the correction factor $E_{obs} - E^0 = k \times cp_r$. A differential method was investigated by which it was established that deviations from a rigid concentration equality of the Pr (basic element) in the sample and comparison solutions on the order of magnitude of the Nd total concentration are possible for the validity of the Lambert-Beer law in pure Nd systems without significant impairment of the accuracy. (tr-auth)

20569 DETERMINATION OF COPPER CONTENT IN o-DIPHENOL OXIDASE BY NEUTRON ACTIVATION ANALYSIS. Hyodo, Hiroshi; Bando, Shoji (Nagoya Univ., Japan). Agr. Biol. Chem. (Tokyo), 29: 763-8(Aug. 1965).

Determination of the Cu content of enzyme preparations by neutron activation methods is described. (BBB)

20570 SIMPLIFICATION OF OXYGEN-FLASK COMBUSTION PROCEDURE FOR PREPARATION OF SAMPLES FOR LIQUID SCINTILLATION COUNTING. Conway, W. D.; Grace, A. J.; Rogers, J. E. (Sterling Winthrop Research Inst., Rensselaer, N. Y.). Anal. Biochem., 14: 491-4(Mar. 1966).

A comparison of the analytical results from the combustion of tissues containing ^{3}H and ^{14}C using Nichrome and platinum baskets is presented. The Nichrome baskets were fashioned from 8 × 8 mesh Nichrome wire (18-gage). Recoveries of ^{3}H and ^{14}C using Nichrome combustion baskets and the modified procedure are described. The results were comparable with previous recoveries of the isotopes from biological samples using platinum baskets. There was no interactions between the isotopes and the basket material during the combustion of biological samples. The analysis disclosed no significant differences between the results obtained with Nichrome as compared with platinum baskets. The Nichrome baskets are more rigid than those made of platinum. (F.J.H.)

20571 NEW CONCEPT IN PRECISION PHOTOMETRIC ANALYSIS USING A RADIOISOTOPIC LIGHT SOURCE. Ross, Harley H. (Oak Ridge National Lab., Tenn.). Anal. Chem., 38: 414-20(Mar. 1966). (ORNL-P-1694).

An experimental approach is presented for making high-precision photometric measurements. The theoretical interpretation of the proposed system is based on the unusual properties of a beta-activated radioisotopic light source. In addition to high precision, other advantages of the technique include increased stability, controlled sensitivity, simplicity, low power requirements, and direct digital results. Five colorimetric systems were investigated and the results are shown to agree with a simple mathematical model. The available high precision of the system enables absorption photometry to be effectively extended to the analysis of large amounts of material. (auth)

20572 A CRITICAL STUDY OF CARBON-REDUCTION TECHNIQUES FOR THE DETERMINATION OF OXYGEN IN THORIUM AND YTTRIUM METALS. Fassel, Velmer A.; Dallmann, Wayne E.; Hill, C. Clifton (Iowa State Univ., Ames). Anal. Chem., 38: 421-5(Mar. 1966).

The determination of the oxygen content in thorium and yttrium metals by carrier-gas fusion, vacuum fusion, and d-c carbon-arc extraction methods and the experimental conditions under which quantitative accuracy can be achieved are described. Synthetic metal–oxygen standards were employed to validate the absolute accuracy. (auth)

20573 THREE-WAVELENGTH X-RAY ABSORPTION EDGE METHOD FOR DETERMINATION OF PLUTONIUM IN NITRATE MEDIA. Hakkila, E. A.; Hurley, R. G.; Waterbury, G. R. (Los Alomos Scientific Lab., N. Mex.). Anal. Chem., 38: 425-7(Mar. 1966).

An x-ray absorption edge method was developed for determining plutonium in nitrate solutions. In this method the transmitted x-ray intensities at three wavelengths are measured. The Kβ x ray for niobium and the Kα x rays for molybdenum and niobium are produced by irradiating a niobium–molybdenum secondary target with x rays from a tungsten-target x-ray tube, and the intensities of these x rays are measured after passing through an absorption cell filled successively with water and a solution of known plutonium content. Then the reduction in the transmitted intensities of the Kβ x ray for niobium and the Kα x ray for molybdenum, which bracket the L III absorption edge for plutonium, are measured through the same cell filled with the sample solution. The absorption of these x rays is related to plutonium concentration using accepted absorption principles. The method is applicable to the determination of plutonium concentrations of 10 to 25 mg per ml with a relative standard deviation of approximately 0.6%. (auth)

20574 DETERMINATION OF SILVER IN MINERALS AND ORES BY NEUTRON ACTIVATION ANALYSIS AND HIGH-RESOLUTION GAMMA SPECTROMETRY. Schroeder, Gerald L.; Evans, Robley D.; Ragaini, Richard C. (Massachusetts Inst. of Tech., Cambridge). Anal. Chem., 38: 432-4(Mar. 1966).

A procedure is described for quantitative determination of silver in natural minerals. Analysis is based on the use of a lithium-drifted germanium detector for high-resolution spectrometry of gamma activity induced by a 5-second thermal-neutron irradiation in a reactor core. Intensities of the 660-kev gamma ray from 24-second ^{110}Ag measured in sample and standard are compared. The limit of detectability of Ag in minerals rich in Mg (~50% MgO by weight), an interfering element, is about 15 ppM. Confidence limits are calculated directly from counting data. No chemical processing is required. No spectrum peeling is required. Samples may be reanalyzed for silver following a cooling period. Sample sizes from milligrams to greater than 10 g can be analyzed by this method. (auth)

20575 TRITIATED ALUMINA AS A REAGENT FOR SELF-LABELING CHROMATOGRAPHIC ANALYSES. Klein, Peter D.; Erenrich, Eric H. (Argonne National Lab., Ill.). Anal. Chem., 38: 480-4(Mar. 1966).

Tritiated alumina prepared by exchange of the surface hydroxyl groups with tritiated water is a suitable reagent for self-labeling chromatographic analysis of appropriate classes of molecules. The absorbent can be prepared, assayed for surface specific activity, and diluted to a suitable activity with excellent reproducibility and stoichiometry. Model compounds show incorporation of activity proportionate to sample size over a range from 3 μg to 10 mg; tritium incorporation also shows a good correlation with the structural features and the number of enolic hydrogens in the compounds tested. The radiochemical visualization and separation of a mixture of three ketosteroids by a chromatographic column of tritiated alumina is presented as an illustration. (auth)

20576 EXTRACTION AND SPECTROPHOTOMETRIC DETERMINATION OF THORIUM WITH 8-QUINOLINOL. Goto, Katsumi; Russell, D. S.; Berman, S. S. (National Research Council, Ottawa). Anal. Chem., 38: 493-5(Mar. 1966).

The procedures for extraction and spectrophotometric determination of thorium using 8-quinolinol are given. The effects of pH on the extraction of 8-quinolinolates from acetate medium and the absorption spectra of Ce and Th 8-quinolinolates are presented. A comparison was made of the results obtained in the determination of thorium in monazite sand using gravimetry and the proposed method. (F.J.H.)

20577 DETERMINATION OF SODIUM, ARSENIC, COPPER, AND GALLIUM IN TIN OXIDE BY NEUTRON ACTIVATION. Rauscher, H. E. (Corning Glass Works, N. Y.). Anal. Chem., 38: 519-20(Mar. 1966).

The method for determination of arsenic, copper, and gallium in tin oxide by neutron activation is presented. The samples were irradiated and then fused with sodium peroxide. Sodium was separated by ion exchange using Dowex-1 (Cl^-), arsenic by sulfide precipitation, copper by thiocyanate precipitation, and gallium by ether extraction. The results of the determinations are shown. (F.J.H.)

20578 NUCLEAR QUADRUPOLE RESONANCE. Drago, Russell S. (Univ. of Illinois, Urbana). Anal. Chem., 38: 31A-8A(Apr. 1966).

The application of nuclear quadrupole resonance in analytical chemistry is discussed in terms of its development and future use. The fundamentals of the method, limitations, and a description of instrumentation are presented. (F.J.H.)

20579 TITRIMETRIC DETERMINATION OF PRIMARY AND SECONDARY ALCOHOLS BY XENON TRIOXIDE OXIDATION. Jaselskis, Bruno; Warriner, J. P. (Loyola Univ., Chicago). Anal. Chem., 38: 563-4(Apr. 1966).

A precise titrimetric method, employing xenon trioxide, for determination of primary and secondary alcohols in aqueous solutions is described. The solution of xenon trioxide is added to the aqueous alcohol and the reaction, whose products are carbon dioxide and xenon gas, is allowed to proceed for 2 hr at room temperature, and the excess xenon trioxide is tritrated iodometrically. The range of hydroxyl concentrations over which this method can be applied includes both the macro- and semimicro-analytical regions. Methanol, ethanol, and 2-propanol can be determined in amounts as low as 30, 25, and 25 μg with a relative standard deviation of 4%; at the 100-μg level, the relative standard deviation falls below 1%. (auth)

20580 LEAST SQUARES ANALYSIS AND SIMPLIFICATION OF MULTI-ISOTOPE MASS SPECTRA. Brauman, John I. (Stanford Univ., Calif.). Anal. Chem., 38: 607-10(Apr. 1966).

The mass spectra of molecules containing elements with many isotopes can be simplified and presented in terms of one isotope if the relative isotopic abundances are known. Use of the least squares technique permits the problem to be formulated so that it can easily be solved with a digital computer. (auth)

20581 CONTINUOUS MOISTURE ANALYZER FOR GASES CONTAINING HYDROGEN FLUORIDE. Pappas, W. S. (Oak Ridge Gaseous Diffusion Plant, Tenn.). Anal. Chem., 38: 615-18(Apr. 1966). (K-L-6059; CONF-651004-3).

A continuous analyzer was developed for determining water in gas streams containing hydrogen fluoride. The instrument withdraws a metered sample, dilutes it with a carrier gas, and removes hydrogen fluoride by selective absorption prior to moisture measurement. A moisture spiking technique ensures quantitative moisture passage and minimizes lag and memory effects of the trapping system. A compensating system uses two moisture monitors to provide a signal readout responsive only to the moisture content of the sample. A prototype analyzer was successfully applied to the off-gas stream of the MSRE chemical processing plant during an oxide removal run. With electrolytic hygrometers used as moisture monitors, the relative standard deviation is better than ±5% in the range of 0 to 5% water. (auth)

20582 SIMPLE TECHNIQUE FOR RAPID ANALYSIS OF RADIOACTIVE GASES BY LIQUID SCINTILLATION COUNTING. Curtis, Mary L.; Ness, Sandra L.; Bentz, L. L. (Monsanto Research Corp., Miamisburg, Ohio). Contract AT-33-1-GEN-53. Anal. Chem., 38: 636-7 (Apr. 1966). (MLM-1305J; CONF-651004-8).

The technique for rapid determination of ^3H in ^3He and ^{85}Kr in xenon in the concentration range from 10^{-2} to 10^{-9} mole % by liquid scintillation counting is described. In determining the efficiency factor for ^3H, 38 samples were counted in duplicate. The probable error per pair was ±5.8%. This included errors in Geiger counting as well as in liquid scintillation counting. With additional practice the precision per pair for ^3H samples was reduced to ±4.2%. The probable error in nine determinations on a single sample of ^{85}Kr was ±2.2%. The lower limit of detectability with reliable results for both ^3H and ^{85}Kr is about 5×10^9 mole %. Samples of greater concentrations than 10^{-4} mole % must be diluted. (F.J.H.)

20583 DETERMINATION OF ^{90}Sr IN URINE BY ANION EXCHANGE. Cahill, Daniel F.; Lindsey, Georgia I. (Department of Health, Education, and Welfare, Montgomery, Ala.). Anal. Chem., 38: 639-40(Apr. 1966).

The procedure for determining ^{90}Sr in human urine by ion exchange is described. The accuracy, precision, and sensitivity of the method were determined by analyzing samples spiked with known amounts of $^{90}Sr-^{90}Y$ activity. A comparison was made using the established method and the anion exchange method. The results from the analysis using one liter each of the urine were 21.0 dpm for the established method and 21.7 and 24.5 dpm for the ion exchange method. Using the intake value and time factor and integrating Fujito's empirical equation the theoretical amount of ^{90}Sr activity expected in the urine was ~4 pC/day and a range of 3 to 5 pC/day was determined. (F.J.H.)

20584 COMPARISON OF DIFFERENT PROCEDURES TO MEASURE SIMULTANEOUSLY ^{32}P AND ^{45}Ca IN INORGANIC SALTS BY LIQUID SCINTILLATION COUNTING. Lerch, P.; Cosandey, M. (Univ., Lausanne, Switzerland). Atomlight, No. 52, 1-8(Mar. 1966).

Procedures for simultaneously measuring ^{45}Ca and ^{32}P in inorganic salts by liquid scintillation counting are considered. The best method is one that gives maximum values of the ratio of the square of the ^{45}Ca efficiency to the ^{32}P efficiency. Values for seven different methods are given. The method found to be most suitable is deposition on paper, which is then soaked in the scintillating solution. This method may only be used for quantities less than 0.2 g. When larger quantities are used, gel suspension was found to be the most suitable method. Good reproducibility was obtained for quantities up to 4.0 g. (F.J.H.)

20585 ON THE DETERMINATION OF POLONIUM IN NEUTRON-IRRADIATED BISMUTH. Kamemoto, Yuichiro; Tanifuji, Takaaki (Japan Atomic Energy Research Inst., Tokyo). Bunseki Kagaku, 15: 62-4(Jan. 1966). (In Japanese).

^{210}Po can be obtained easily by separating it from neutron-irradiated bismuth. A method for separating polo-

nium from bismuth by spontaneous deposition was studied. It was found that ^{210}Po is quantitatively deposited on a silver plate, when 0.1 ml of a 0.1 to 1.2N HNO_3 solution containing bismuth and polonium is in contact with a silver plate for 1 hr or more. If the amount of bismuth is more than 1 gm in 25 ml of polonium solution, the deposition rate of polonium decreases. (auth)

20586 DETERMINATION OF ^{90}Sr BY YTTRIUM METHOD. **Godek, Jerzy (Dept. of Agricultural Chemistry, Krakow). Chem. Anal. (Warsaw), 11: 115-20(1966). (In Polish).**

Conditions of determination of ^{90}Sr by the yttrium method were studied. It was found that the quantitative precipitation of $^{90}Y(OH)_3$ on $Fe(OH)_3$ carrier occurs at pH = 8.0. The volume of solution and concentration of Ca^{2+} have little effect on the ^{90}Sr determination. The yield of ^{90}Sr in the presence of alkaline earth metals (without Ra), after sulfate → carbonate → nitrate conversion, was close to 100%. In presence of radionuclides of the natural series, the yttrium method may be applied after removal of radium isotopes from the solution. (auth)

20587 FRACTION COLLECTOR FOR MICROCHROMATOGRAPHY OF RADIOACTIVE SUBSTANCES. **Kokes, Antonin (Inst. for Nuclear Research, Czechoslovak Academy of Sciences, Rez). Chem. Listy, 59: 1232-5(1965). (In Czech).**

A device is described for the collection of fractions in column microchromatography of radioactive materials. At the microchemical level, fractions usually consist of individual drops. This apparatus dries the individual drop on a glass surface, measures its activity, registers the result graphically, and places the glass in a storage container. The fraction collector is constructed as a miniature device and may be set up in the necessary location. The whole surface of the fraction collector is made of stainless steel and plastic. The housing of the collector weighs about 600 g. A block diagram of the device is given, and the collector, detector, and device for moving samples to storage are illustrated schematically. The recorder electronics are illustrated, and a sample curve obtained on microchromatography of a mixture of La, Ce, Pr, Nd, Pm, and Sm is shown. (BBB)

20588 MASS SPECTROMETER FOR THE ISOTOPIC ANALYSIS OF URANIUM HEXAFLUORIDE. **Vastel, J.; Coulon, M. Energ. Nucl., 8: 33-9(Jan.-Feb. 1966). (In French).**

The conditions encountered in the isotope analysis of uranium hexafluoride (to carry out measurements precisely on very small samples of a highly corrosive product) present design problems, the solutions of which are discussed. The mass spectrometer can be considered as a control apparatus in the industrial field. (auth)

20589 PRESENT STATE OF THE ANALYSES OF NUCLEAR FUELS AND REACTOR MATERIALS. **Hattori, Tadao (Furukawa Electric Co., Ltd., Japan). FAPIG (Tokyo), No, 35, 312-16(Jan. 1965). (In Japanese).**

Many analytical methods for the determination of impurities in the ppM range have been developed for nuclear fuels and cladding materials through the cooperative efforts of the following committees: Uranium Analysis Committee, Advisory Committee on Analytical Chemistry of Nuclear Fuels and Reactor Materials, Thorium Analysis Committee of Japan Society of Newer Metals, Zirconium Analysis Committee of Japan Titanium Society, and Aluminum Analysis Committee of Japan Institute of Light Metals. The activities of these various committees are described. The most frequently used analytical methods, absorptiometry, polarography, and emission spectroscopy are discussed. In connection with the development of new analytical methods, the importance of the preparation of standard samples of nuclear fuel elements is emphasized. (TCO)

20590 A RAPID AND QUANTITATIVE METHOD FOR THE DETECTION OF PLUTONIUM IN URINE. **Valentin, N.; Weyers, C.; Luysterborg, J. (Centre d'Etude de l'Energie Nucleaire, Mol-Donk, Belgium). Health Phys., 12: 577-8(Apr. 1966).**

A method for plutonium determination in urine is described in which a chemisorption procedure for the concentration of Pu from natural waters on a suspension of calcium fluoride is preceded by a strong oxidation of the urine. Efficiency of the method was tested in 26 urines spiked with 1.17 cpm of Pu. Recovery was 0.96 ± 0.02 or 82 ± 2% with 95.46 per cent confidence. (H.G.D.)

20591 DETECTION OF LANTHANUM WITH HYDROQUINONE. **Alsina, J.; Buscarons, F. (Univ. of Barcelona). Inform. Quim. Anal. (Madrid), 19: 22(1965). (In Spanish).**

To 2 ml of the solution to be tested were added two drops of 1% aqueous hydroquinone and then one drop of 15N NH_4OH. A blue-green turbidity at the top of the test tube indicated a reaction of La(III); below this is a yellow-orange ring, from the reaction of hydroquinone with NH_4OH. The reaction was specific for the detection of La in the oxalate precipitate of the third group of the classical analytical scheme, and other ions which were precipitated at the same time did not interfere (Th, Ce, etc.). The procedure allowed detection of one part in 4000; semimicro technique raised the sensitivity to one part in 10,000. Thus each procedure was superior to the technique currently employed, absorption of I_2 by the basic acetate of La, whose sensitivity is one part in 1500. Other reactions of mercaptodiphenols were also studied, as well as other reactions of the diphenols themselves. (BBB)

20592 CONDUCTOMETRIC STUDY ON THE QUANTITATIVE ESTIMATION OF THORIUM AS TUNGSTATE. **Prasad, Sarju; Devi, K. Shyamala (Banaras Hindu Univ., Varanasi, India). J. Indian Chem. Soc., 42: 859-62(Dec. 1965).**

Conductometric titrations of thorium nitrate against sodium tungstate were carried out at 30 ± 0.5°C and the effect of the addition of ethanol on the results was studied. The results obtained showed that thorium was quantitatively precipitated as normal tungstate. Reverse titrations, however, did not provide satisfactory results. (auth)

20593 MICROANALYSIS BY X-RAY EMISSION IN AN ELECTRON MICROSCOPE. **Giraud-Heraud, Francois; Sifferlen, Raymond; Saulnier, Adrien (Laboratoires de Veurey, Veurey, France). J. Microscop., 4: 587-94 (Oct. 1965). (In French).**

A microanalyzer of the x-ray spectra emitted by metallic preparations examined by electron microscopy is described; it is adaptable to the Elmiskop I microscope. A qualitative microanalysis on a sample a few microns in dia may be obtained with the device at the same time microscopic examination is made. An analysis of the inclusions or of precipitates is possible in the case of inhomogeneous alloys or multiple phases. Bonding variation with respect to the matrix may be determined at relatively low concentrations. Several applications of the technique are illustrated: the AU2GN alloy (Mn, Cu, Zr), with Fe and Ni inclusions; and a Zr–Mg alloy with 0.06% Mn with inclusions of Fe and Ni. Illustrations of the spectra of matrices and inclusions and the microphotographs recorded on the same samples are given. (BBB)

20594 FLUORINE MICRODETERMINATION BY NEUTRON ACTIVATION ANALYSIS, APPLICATION TO BACTERIOLOGICAL MEDIA. **Feldman, Milton H.; Battistone, Gino C. (Army Inst. of Dental Research, Washington, D. C.). J. Nucl. Med., 7: 140-9(Feb. 1966).**

A rapid repetitive instrumental method for the microdetermination of fluorine in a complex organic matrix was developed. The method is independent of the type of fluorine bonding and is applicable to bacteriological media without prior sample preparation. Under the conditions used, the method is applicable to fluorine concentrations about 5 μg/ml. The method is amenable to automation and electronic data processing. (auth)

20595 POLAROGRAPHIC DETERMINATION OF URANIUM IN BINARY CHROMIUM–URANIUM ALLOYS. **Wilson,**

L.; Ducksbury, N. A. (Australian Defence Science Service, Melbourne). J. Polarog. Soc., 10: 37-40(1964).

The method described involves the dissociation of the chromium–uranium alloys in 50% H_2SO_4, with subsequent oxidation (with HNO_3) of any U(IV) produced by the action of nascent hydrogen. Oxalic acid (0.5M) is used as basal electrolyte. The effects of various electrolytes on the determination of uranium and experimental details are given. (Analytical Abstr.)

20596 RADIOACTIVATION ANALYSIS OF NITROGEN AND PHOSPHORUS WITH 14 Mev NEUTRONS. Tsuji, Haruo (Konan University, Kobe-shi, Japan). Jap. Anal., 263-8(1966). (In Japanese).

Nitrogen and phosphorus contents in various compounds were determined by means of ^{13}N [$^{14}N(n,2n)$, $T_{\frac{1}{2}}$ = 10 min] and ^{28}Al[$^{31}P(n,\alpha)$, $T_{\frac{1}{2}}$ = 2.3 min] radioactivities produced by 14-Mev neutron irradiation. The sample was packed in a polyethylene rabbit capsule and an inner standard (copper plate for nitrogen analysis and quartz for phosphorus analysis) was attached on the cup of the rabbit capsule. It was irradiated with 14-Mev neutrons by T-d reactions with a Cockcroft–Walton type accelerator, and then the radioactivity was measured by a well-type NaI scintillation detector connected with a single-channel pulse-height analyzer. Five minutes of irradiation and 0.51-Mev photopeak counting was adopted for the nitrogen analysis. And 2.5-min irradiation and total gammas higher than 1.40 Mev were adopted for phosphorus analysis. The radioactivity produced in each sample was normalized with an inner standard. By this method, nitrogen, and phosphorus content in various compounds, particularly organic compounds can be determined rapidly and nondestructively with an error of less than 5%. When the neutron flux could be elevated to 1.0×10^7 n per cm^2 per sec the limit of detection may be about 10 mg for nitrogen and 7 mg for phosphorus, equivalent to 0.2% N and 0.15% P in a 5 g sample. (auth)

20597 DETERMINATION OF TRACES OF FLUORINE IN URANIUM OXIDES BY PYROLYSIS-ALIZARIN COMPLEXONE PHOTOMETRIC METHOD. Hashitani, Hiroshi; Muto, Hiroshi (Japan Atomic Energy Research Inst., Tokyo). Jap. Anal., 14: 1114-19(Dec. 1965). (In Japanese).

A simple method for determining traces of fluorine in uranium oxides using pyrolytic separation technique and the alizarin complexone (ALC) photometric method is reported. A sample of uranium oxide weighing up to 10 g and containing 3 to 30 μg of fluorine is ground with 3 g powdered tungstic oxide and packed in a platinum boat. The mixture is then pyrolyzed for 15 minutes under a stream of moist oxygen (1.6 l/min) in a fused silica reactor tube (850°C). The volatilized fluorine is absorbed in 15 ml of a dilute alkaline solution without increasing the volume of the solution. The solution is then transferred into a 25 ml volumetric flask and treated with 8 ml of a La-ALC composite reagent solution. Fluorine is determined by measuring the absorbance of the La-ALC-F complex at 620 mμ using a reagent blank (La-ALC chelate). The pyrolytic separation method is rapid and simple, and does not need the dissolution of the sample. Excessive dilution of the released fluoride by condensate, which occurs if pyrohydrolytic or distillation techniques are used, is avoided with the method. (TCO)

20598 SEPARATION OF URANIUM FROM THORIUM BY TRI-ISO-OCTYLAMINE EXTRACTION AND PHOTOMETRIC DETERMINATION OF URANIUM WITH ARSENAZO III. Onishi, Hiroshi; Toita, Yukio (Japan Atomic Energy Research Inst., Tokyo). Jap. Anal., 14: 1141-6 (Dec. 1965). (In Japanese).

A colorimetric method has been developed for the determination of uranium with the colorimetric reagent Arsenazo III in the presence of the interfering elements, Th and Zr. Uranium(VI) is extracted with 5 wt/vol % tri-iso-octylamine in xylene from 5M hydrochloric acid solution. Uranium is back-extracted with 0.5M hydrochloric acid. The extraction and back-extraction of uranium are repeated. The second back-extract containing uranium is evaporated to dryness, and the residue is treated with nitric and perchloric acids. The residue is dissolved in hydrochloric acid, and uranium is reduced to the quadrivalent state with zinc. Oxalic acid is added to mask a small amount before the U-Arsenazo III color is developed in a 25 ml volume. The absorbance of the complex is measured in a 1 cm cell at 665 mμ. By this method 20 μg of uranium can be determined in the presence of 10 mg of thorium or 10 mg of zirconium. The effect of diverse ions has been studied. (TCO)

20599 ANALYSIS OF RADIOACTIVE IODINE IN ISOTOPIC TRACERS BY PAPER ELECTROPHORESIS. Nagy, G. Agnes. Magyar Tud. Akad. Kozp. Fiz. Kut. Int. Kozlem., 14: 113-18(1966). (In Hungarian).

A method based on paper electrophoresis was developed for the determination of chemical forms of carrier-free iodine isotopes. The method and the identification of the chemical forms of iodine are described in detail. (auth)

20600 SPECTROPHOTOMETRY OF AQUEOUS HOMOGENEOUS REACTOR FUEL SOLUTIONS FROM 4 TO 280 DEG C AND 0 TO 930 PSI(ABS.). Waggener, W. C.; Weinberger, A. J.; Stoughton, R. W. Nucl. Sci. Eng., 24: 336-43(1966). (ORNL-P-1599).

Aqueous homogeneous reactor fuel solutions were examined spectrophotometrically in the wavelength range 0.3 to 1.2 μ as a function of time, temperature, and overpressures of hydrogen and/or oxygen. Using a cell that was designed for liquid-gas equilibration, and which was slightly catalytic for the recombination of hydrogen and oxygen, the course of reactions (reduction, hydrolysis, precipitation, oxidation, and re-solution) of uranium and copper were followed concomitantly. Degassed solutions of the UO_2SO_4–$CuSO_4$–D_2SO_4–D_2O–H_2O system lost uranium and copper very slowly above 200°C. In the presence of hydrogen, Cu(II) and U(VI) were reduced consecutively to Cu (metal) and to U(IV) species that were partially soluble at 25°C, but insoluble above 150 to 200°C. The changing spectrum was generally uncomplicated by turbidity, since reduction of Cu(II), as well as aggregation of U(IV) hydrolytic species, occurred at the cell wall. Hydrolysis of U(IV) was slowly reversible with decreasing temperature. Reoxidation of reduced solution with oxygen was comparatively rapid and complete at all temperatures. (auth)

20601 DETERMINATION OF TRACE ZINC IN THORIUM. Kawase, Akira (Tokyo Univ.). Rep. Nat. Res. Inst. Met. (Tokyo), 8: 52-7(Apr. 1965). (In Japanese).

In the method for the determination of trace amounts of Zn in Th, the Zn is first separated from the Th by solvent extraction with dithizone-benzene or by ion exchange, and then determined by photometry or polarography. In the solvent extraction method of separation, NH_4-citrate and $NH_2OH \cdot HCl$ are added to the Th and Zn containing solution (pH 8.3), and the solution is extracted with dithizone-benzene in a solvent. The Zn is then back-extracted with HCl. In the ion-exchange separation, a 2M–HCl solution of Th and Zn is passed through a Dowex 1 × 8 mm, 100–200 mesh column and the Zn is adsorbed. The Zn is then eluted with 1M–HNO_3. For the polarographic determination of the Zn either of two kinds of electrolytic solutions were used: H_3PO_4 (5.95) or 1M–NH_4OH–1M–NH_4Cl–0.05M–Na_2SO_3. Prior to the determination by photometry, NH_4-citrate and Na-OAc are added to the test solution to adjust the pH to 5.0–5.5, KCN and Na_2SO_3 are added, then, the pH is finally adjusted to 5.2 ± 0.1. The extraction is done with dithizone-benzene, the free dithizone is removed with Na_2S, and the absorbancy is measured at 535 mμ. When determining the Zn by polarography, using phosphate solution, the residual acids or salts must be eliminated as completely as possible. In the photometric method, the pH adjustment is important when Zn is extracted. To determine extremely small amounts of Zn, the ion-exchange-polarographic method is the best, and for several ppM of Zn, the solvent extraction-polarography. (TCO)

20602 RAPID DETERMINATION OF OXYGEN IN METALS BY RADIOACTIVATION. Perdijon, J. (S. A.

de Machines Electrostatiques (SAMES), Grenoble, France). Rev. Met. (Paris), 63: 27-32(Jan. 1966). (In French).

The principle of radioactivation and its application to the determination of oxygen in metals is discussed. A description of the equipment developed and specially adapted to hydrogen determination in metals includes the neutron source, protection system, transfer system, and gamma spectrometer. The sensitivity of the method and the reproducibility of the results are reported. (auth)

20603 ^{51}Cr IN SEA WATER: CHEMISTRY. Cutshall, Norman; Johnson, Vernon; Osterberg, Charles (Oregon State Univ., Corvallis). Science, 152: 202-3(Apr. 8, 1966). (RLO-1750-1).

^{51}Cr introduced into the Pacific Ocean from the Columbia River remains in the hexavalent state. Determination of this radionuclide in sea water by hydroxide coprecipitation with iron was best accomplished if the ^{51}Cr was first reduced to the trivalent state. (auth)

20604 IODOINSULIN USED TO DETERMINE SPECIFIC ACTIVITY OF ^{131}I. Berson, Solomon A.; Yalow, Rosalyn S. (Veterans Administration Hospital, New York). Science, 152: 205-7(Apr. 8, 1966).

Anodal mobility of iodoinsulin on starch-gel electrophoresis increased progressively as the number of iodine atoms substituted in the molecule increased. The iodine content of ^{131}I solutions was determined by comparison of autoradiographic patterns of insulin heavily labeled with ^{131}I and of insulins lightly labeled with ^{131}I and known quantities of ^{127}I. (auth)

20605 AUTORADIOGRAPHIC DIFFERENTIATION OF TRITIUM AND ANOTHER β-EMITTER BY A COMBINED COLOUR-COUPLING AND DOUBLE STRIPPING-FILM TECHNIQUE. Field, E. O.; Dawson, K. B.; Gibbs, J. E. (Royal Marsden Hospital, Sutton, Eng.). Stain Technol., 40: 295-300(1965).

A technique is described that distinguishes cells labeled with ^{3}H, with ^{14}C, or with both isotopes together, in the same histological preparation. The technique depends on the application of two layers of autoradiographic stripping film, separated by a thin layer of celloidin. The first layer (in contact with the tissue) records predominantly the distribution of ^{3}H in the sample, the second exclusively that of ^{14}C. The silver grains in one layer are colored by dye coupling, which enables the grains in the two layers to be differentiated without the need for separate focusing. The merits of stripping film over liquid emulsion are given. The scatter of grains, or loss of resolution, produced in the second layer of emulsion depends on the separation between this layer and the source of β emission. To ensure that this separation is minimal and yet sufficient to absorb all tritium β particles requires rigid control of thickness and uniformity in the first emulsion layer. Coating samples by dipping in liquid emulsion was found to be unsatisfactory for various reasons. The advantages of the described technique are that three classes of labeled cells can be distinguished: those labeled with ^{3}H or with ^{14}C alone and those labeled with both isotopes together. Moreover, differential counts can be rapidly carried out with a high dry objective since coloring the grains in one layer of emulsion not only aids discrimination but also eliminates the need for focusing separately on the two layers. (BBB)

20606 AUTOMATIC SCANNING OF CHROMATOPLATES BY MULTI-SCALING USING A GAMMA-RAY SPECTROMETER. Muzzarelli, R. A. A. (Univ. of Sherbrooke, Can.). Talanta, 13: 639-40(Apr. 1966).

The location of radioactive tracers on chromatographic thin layers or papers, together with the qualitative and quantitative analysis, using a gamma spectrometer is described. (auth)

20607 ANALYSIS OF ZINC AND LEAD FOR RARE-EARTH METALS. Bayanov, A. P.; Serebrennikov, V. V. Tr. Tomsk. Gos. Univ., Ser. Khim., 170: 173-5(1964).

Zinc metal is dissolved in HCl and rare earths precipitated as hydroxides by aqueous ammonia solution. The precipitate is dissolved in HCl and the total rare earths titrated with 0.025M EDTA in the presence of Eriochrome black T. Lead and lead alloys are analyzed similarly except that HNO_3 is used to dissolve the samples and NaOH to precipitate the hydroxides. The method can be used to determine ≤0.05% of rare earths with an absolute error of 0.02%. (M.C.G.)

20608 SPECTROGRAPHIC ANALYSIS OF HIGH-PURITY TANTALUM BY THE d-c ARC METHOD. Oda, Nakaaki; Idohara, Mitsuru (Nippon Soda Co., Takaoka, Japan). Trans. Jap. Inst. Metals, 6: 247-51(Oct. 1965).

Development of tantalum refining industry made it necessary to determine the trace impurities in high-purity tantalum products. To meet the requirements of increasing the analytical sensitivity in available methods, a spectrographic d-c arc method was studied with a medium type quartz spectrograph, Zeiss Qu-24. Experiments were carried out to establish optimum conditions in regard to the various factors, such as carrier, arc current, exposure time, internal standard, and analytical line pairs. As a result, a simple and rapid method was developed for practical use. The method includes the following procedures: converting the sample to an oxide, mixing with carbon powder, which contains two internal standard materials (GeO_2, BeO), arcing in a d-c arc, and photographing spectra with a medium type quartz spectrograph. The method can be applied to the analysis of high-purity tantalum products of various forms, which are convertible to a tantalum oxide. The method can be used for quantitative determination of the fourteen elements in the tantalum products at concentrations of more than 0.01% Nb and W, 0.003% Mo, 0.001% Ti, 0.0005% Fe and Ca, 0.0003% Si, Cr, V, Ni, and Al, 0.0001% Mn and Cu, and 0.00003% Mg, within an error of about 10% in terms of the variation coefficient. (auth)

20609 STUDY OF THE WATER CONTENT IN URANIUM TETRAFLUORIDE BY THE GAS VOLUMETRIC METHOD WITH CALCIUM HYDRIDE. Kao, Li.; Chang, Shu-sen; Ch'en, Yu-te. Yuan Tzu Neng, No. 4, 320-8 (1965).

An experiment in which the water content in UF_4 was accurately determined by the volumetric method with CaH_2 at the hydrolysis temperature of $Ca(OH)_2$ is described. The temperature range necessary for the reaction between CaH_2 and H_2O was 400 to 580°C. At such high temperatures, where the temperature and the rate of dehydration of UF_4 are both optimal, the hydrolysis was extremely slight. It was therefore not necessary to add PbO_2, MgO_2, or other oxides to bind fluorine during the determination of water content in UF_4 by the volumetric method. When the amount of water added was within the range from 0.1 to 6.0 ml, the average rate of water recovery by this method was 99 ± 1%. It was also determined that, when the water content of UF_4 fell within 0.1 to 12.5%, the relative error of the gas volumetric method was 2 to 8%. About 50 min was required for each experimental run. (CFSTI)

20610 INTENSITY CALCULATIONS OF ISOTOPIC PEAKS IN MASS SPECTROGRAMS. Riedel, Oswald (Badische Anilin- and Sodafabrik AG, Ludwigshafen, Ger.). Z. Anal. Chem., 217: 1-6(1966). (In German).

A method for the calculation of isotopic peak heights in a mass spectrogram of any compound was derived and applied to examples. The method permits qualitative conclusions of the compound in question, an information that is not obtainable merely from the molecular weight. (auth)

20611 ON THE EVALUATION OF AUTORADIOGRAMS ON THE BASIS OF A LINEAR RELATION BETWEEN ACTIVITY AND BLACKENING AS A METHOD FOR MICROANALYTICAL DETERMINATION OF LONG-LIVED β-γ ACTIVITIES. Ottendorfer, Lambert J. (Technische Hochschule, Vienna). Z. Anal. Chem., 217: 81-99(1966). (In German).

It is shown that spot rings can be used for standards with known specific activity, (activity per unit area) on account of their constant surface area. The D/E function is obtained by subjecting the data obtained by density

measurements on chronoautoradiograms to regression analysis. The connection between optical density D and specific dose E = I·t is expressed by the formula D = K·E$^{\gamma}$. A straight line is obtained by using the logarithmic form log D = γ·log E + log K. The slope γ depends on the phototechnical conditions; the nuclide constant K depends on the properties of the nuclide and the carrier material. After determination of the numerical values for the parameters γ and K, autoradiograms of two-dimensional samples like spots, spot rings, chromatograms etc. can be evaluated by applying the inverse form of the D/E-function log E = 1/γ·log D + log C. (auth)

20612 INTERFERENCE COEFFICIENT FOR CHARACTERIZATION OF INTERFERING REACTIONS IN ACTIVATION ANALYSIS. Pfrepper, G. (Deutsche Akademie der Wissenschaften, Berlin). Z. Anal. Chem., 217: 99-102(1966). (In German).

Side reactions in neutron activation analysis cause especially high errors if the interfering elements are the main components of the sample. Therefore, an interference coefficient was derived, which characterizes the interfering reaction and permits an estimation of the extent of interference. (auth)

20613 DETERMINATION OF URANIUM AND THORIUM IN SEDIMENTARY CARBONIFEROUS DEPOSITS. Siemens, H.; Schwarz, E. (Technische Hochschule, Aachen). Z. Erzbergbau Metallhuettenw., 17: 233-8(1964).

A vacuum goniometer, with scintillation counting, and tungsten or molybdenum radiation, was used for the x-ray fluorescence determination of thorium and uranium. The limits of detection were 13 to 17 and 10 to 11 ppm, respectively, for a counting time of 4 min. Increasing the counting time to 10 min doubled the sensitivity. A NaI scintillation counter, together with a single-channel pulse-height analyzer, was also used for determining potassium, thorium, and uranium in concentration down to 1 ppm. At sufficiently high levels, both methods were equally suitable; the second required less apparatus, but longer counting times. (Analytical Abstr.)

20614 DETERMINATION OF URANIUM, THORIUM, AND ZIRCONIUM BY ARSENAZO III WITHOUT CHEMICAL SEPARATION. Trofimova, L. A.; Syromyatnikov, N. G. (Inst. of Geological Sciences, Academy of Sciences, Kazakh SSR). Zavodsk. Lab., 31: 1325-6(1965). (In Russian).

A 0.1 to 0.5 g sample was dissolved in HCl; the metal hydroxides were precipitated with NH_4OH at a pH of ~8; the precipitate was dissolved in HCl, and three 10-ml aliquots were taken for analysis. One mg of ascorbic acid was added to each aliquot in order to reduce iron. One ml of a 0.05% Arsenazo-III solution was added to all three aliquots. The volume was adjusted to 25 ml, and the optical density was measured on a photocolorimeter. Thorium was determined in one aliquot by adding 1 ml of a saturated oxalic acid solution to complex Zr. In another aliquot uranium was reduced by adding zinc metal to determine Th + U(IV). Th + Zr were determined in the third aliquot. The content of each element was found from a series of calibrated curves. (TTT)

20615 A RADIOMETRIC METHOD OF DETERMINING SULFUR IN NAPHTHALENE. Maklakov, V. N.; Gorelov, P. N.; Rogovoi, A. G.; Zborovskii, A. G. Zavodsk. Lab., 31: 1365-6(1965). (In Russian).

A radiometric method for determining sulfur in naphthalene from the absorption of the characteristic manganese x rays (λ = 2.05 Å, E = 5.9 kev) was worked out with the use of a radioactive ^{55}Fe source. The naphthalene sample (850 ± 1 mg) was compressed at a hydraulic pressure of 150 kg/cm^2 to give a briquette 20 mm in diameter and 2.0 mm thick. The briquette was mounted in a special holder, and the count rate of the transmitted x rays was determined. The results showed that the count rate decreased linearly with increasing sulfur content in the naphthalene. Phenol (up to 1 to 1.5%) did not interfere with the sulfur determination. The ash content should be held at <0.2%. The divergence of the radiometric results from the chemical results was 0.02% at sulfur contents from zero to 0.6%. (TTT)

20616 DETERMINATION OF SMALL QUANTITIES OF RADIOACTIVE SUBSTANCES IN THE ENVIRONMENT. INVESTIGATION USING SMALL AMOUNTS OF RADIOACTIVE SUBSTANCES. Gedeonov, L. I. pp 5-16 of Radiokhimicheskie Metody Opredeleniya Mikroelementov. Moscow-Leningrad, Izdatel'stvo Nauka, 1965. (In Russian).

A survey is given of the development of methods of radiochemical and radiometric determination of small quantities of radioisotopes in the environment. Results are reviewed on the abundance and properties of natural and artificial radionuclides, giving tables of the activities, half lives, and world accumulations of radionuclides occurring naturally, found in cosmic radiation, and produced in nuclear explosions. (M.J.T.)

20617 MEASUREMENTS OF AMOUNTS OF RADIOACTIVE TRACE ELEMENT ADSORPTION FROM SOLUTIONS. Kokotov, Yu. A. pp 54-9 of Radiokhimicheskie Metody Opredeleniya Mikroelementov. Moscow-Leningrad, Izdatel'stvo Nauka, 1965. (In Russian).

An examination is made of the effect of the container walls on the results of computing the adsorption of trace amounts of materials by a sorbent from solutions according to the decrease of the concentration of the initial solution. A formula is proposed, allowing the adsorption of radioactive material by the container walls to be taken into account, using the results of a control experiment. (tr-auth)

20618 POSSIBILITY OF USING THE SUCCESSIVE DESORPTION METHOD IN STUDIES OF ION ADSORPTION FROM SOLUTIONS. Kokotov, Yu. A.; Popova, R. F. pp 59-69 of Radiokhimicheskie Metody Opredeleniya Mikroelementov. Moscow-Leningrad, Izdatel'stvo Nauka, 1965. (In Russian).

A mathematical analysis of the accuracy of the method of successive desorption for simultaneous equilibrium and pseudoequilibrium parallel adsorption processes is carried out. This method allows the number of ions sorbed and their distribution coefficients to be found. Adsorption of microquantities of ^{137}Cs by the zeolites A and X and by clay, mica, and soil is studied using the successive desorption method; the relative selectivity of the adsorbing materials and mechanisms involved is discussed. (M.J.T.)

20619 DETERMINATION OF THE AMOUNTS OF TRACE COMPONENTS CAPTURED BY A MACROCOMPONENT PRECIPITATE. Nikolaev, A. V.; Grigor'ev, V. A.; Kuznetsova, A. K. pp 70-2 of Radiokhimicheskie Metody Opredeleniya Mikroelementov. Moscow-Leningrad, Izdatel'stvo Nauka, 1965. (In Russian).

Insufficiencies of the washing method for determining the amount of capture of a microcomponent by the precipitate of a macrocomponent during precipitation from aqueous solutions are pointed out. The method of using indicators for determining the fraction of captured microcomponent is described. The first indicator is the radioactive microcomponent; the second is an impurity nonisomorphic ion contained in a small quantity of salt added before the formation of the precipitate. The activity of the microcomponent, A, is determined by $A = A_1 - A_2$, where A_1 is the activity of the mother solution plus precipitate and A_2 is the activity of the separated precipitate. A_2 is found from $A_2 = aQ/q$, where a is the specific activity of the mother solution, q is the amount of second indicator added per gram of the mother, and Q is the amount of second indicator in the precipitate. The fraction of captured microcomponent is then A/A^0, where A^0 is the initial activity. Data on the determination of microquantities of ^{144}Ce, ^{89}Sr, and ^{137}Cs captured by the precipitate $Zn[Hg(SCN)_4]$ by means of the methods of washing and of two indicators are shown. (M.J.T.)

20620 EXTRACTION-RADIOMETRIC DETERMINATION OF MICROGRAM AMOUNTS OF LEAD BY ISOTOPIC DILUTION METHOD. Grashchenko, S. M.; Sobotovich, E. V.

pp 73-5 of Radiokhimicheskie Metody Opredeleniya Mikroelementov. Moscow-Leningrad, Izdatel'stvo Nauka, 1965. (In Russian).

The method of isotopic dilution for determining microquantities and the accuracy achieved using it are discussed. A variant of the extraction-radiometric method of isotopic dilution developed for determining microgram quantities of Pb is described. Results of determining the Pb content of two granite samples are shown. (M.J.T.)

20621 PARTITION CHROMATOGRAPHY ON POLYTETRAFLUOROETHYLENE. PART 1. SEPARATION OF LIGHT RARE EARTH ELEMENTS BY GRADIENT ELUTION. Moskvin, L. N.; Preobrazhenskii, B. K. pp 85-93 of Radiokhimicheskie Metody Opredeleniya Mikroelementov. Moscow-Leningrad, Izdatel'stvo Nauka, 1965. (In Russian).

A technique for separating light lanthanides by means of reversed-phase partition chromatography on polytetrafluoroethylene was developed. The latter was successfully used to stabilize the extracting agent, bis(2-ethylhexyl)-orthophosphoric acid (B2EHPA), in the form of a stationary organic phase in the chromatographic column. A procedure for purifying B2EHPA with ethylene glycol directly on the column to remove mono(2-ethylhexyl)-orthophosphoric acid (M2EHPA) is described; it is convenient, yields good results, and may be used for the separation of these acids. The behavior of the elements studied was followed by means of the radioisotopes ^{140}La, ^{144}Ce, ^{147}Pm, and $^{152-154}$Eu. A method proposed for calculating the concentrations of the eluent in the gradient elution of rare earths enables the position where the element will be obtained to be predetermined. When three consecutive mixing vessels are employed, there is good agreement between the calculated and observed positions of the elution peaks. Calculations and experiments showed that use of one or two mixing vessels does not produce the desired results. (CFSTI)

20622 PARTITION CHROMATOGRAPHY ON POLYTETRAFLUOROETHYLENE. PART 2. SEPARATION OF TRACE AMOUNTS OF Eu FROM A TERBIUM TRIOXIDE TARGET BOMBARDED WITH FAST PROTONS. Moskvin, L. N.; Tomilov, S. B. pp 93-5 of Radiokhimicheskie Metody Opredeleniya Mikroelementov. Moscow-Leningrad, Izdatel'stvo Nauka, 1965. (In Russian).

Bombardment of a Tb_2O_3 target with 660 Mev protons produced europium together with isotopes of other rare earths lighter than terbium. To prevent the oxidation of europium in the course of its subsequent separation, use was made of a closed system including a Jones reductor and a chromatographic column filled with polytetrafluoroethylene carrying di-n-octylphosphoric acid, and europium in the divalent state was stabilized by introducing the oxidant buffer $CrCl_3$, the reduction potential of Cr^{2+}, Cr^{3+} (−0.41 v) being very close to that of Eu^{2+}, Eu^{3+} (−0.44 v). The europium and chromium reduced in the Jones reductor pass through the chromatographic column without being adsorbed, whereas the other rare earths are adsorbed and are then eluted with hydrochloric acid. The separated Eu^{2+} and Cr^{2+} are oxidized to Eu^{3+} and CrO_4^- with ammonium persulfate, and Eu is concentrated by coprecipitation on ferric hydroxide. The hydroxide precipitate is dissolved in concentrated HCl, 1−2 mg of lanthanum salt is introduced, and europium coprecipitates on lanthanum fluoride. After dissolving the fluoride in a saturated solution of H_3BO_3 in 0.2N HCl, the separation of lanthanum and europium is performed on a small column filled with polytetrafluoroethylene carrying bis(2-ethylhexyl) orthophosphoric acid. The yield of europium is 90−95%. The europium preparation thus obtained was used to study the Mössbauer effect on ^{149}Sm. (CFSTI)

20623 PARTITION CHROMATOGRAPHY ON POLYTETRAFLUOROETHYLENE. PART 3. RAPID METHOD FOR SEPARATING LANTHANUM FROM CERIUM. Moskvin, L. N.; Novikov, V. T. pp 95-6 of Radiokhimicheskie Metody Opredeleniya Mikroelementov. Moscow-Leningrad, Izdatel'stvo Nauka, 1965. (In Russian).

A method proposed for the rapid and quantitative separation of trace amounts of lanthanum and cerium is based on the different extractability of tri- and tetravalent cations by bis(2-ethylhexyl) orthophosphoric acid (BEHPA). Partition chromatography on polytetrafluoroethylene was used. La and Ce were applied to the chromatographic column in 0.01 N HNO_3. La was eluted with a solution of 0.5 M HNO_3 + 0.4 M $(NH_4)_2S_2O_8$ + 0.1 M $AgNO_3$. At this acidity, La has a partition coefficient of less than unity and is eluted in the first fraction. Under these conditions, Ce is oxidized to the tetravalent state and is firmly held on the column. To remove the oxidizing solution, the column was washed with 0.01 N HNO_3, and cerium was eluted with 6 N HCl, which simultaneously reduced it to the tetravalent state. This procedure permitted a rapid and quantitative separation of lanthanum and cerium, and proved particularly useful in the separation of ^{134}La (T = 6.5 min) from ^{134}Ce, when it was necessary to reduce the time of the separation as much as possible. (CFSTI)

20624 STUDY OF THE SEPARATION OF THORIUM FROM IONS OF CERTAIN METALS ON THE ANION EXCHANGER AV-17 FROM NITRIC ACID SOLUTIONS. Kazantsev, E. I.; Kudusov, V. A.; Korobeinikov, V. L.; Lyashenko, V. A. pp 96-103 of Radiokhimicheskie Metody Opredeleniya Mikroelementov. Moscow-Leningrad, Izdatel'stvo Nauka, 1965. (In Russian).

The separation of gravimetric amounts of a series of di- and trivalent ions from thorium in nitric acid solutions on the strongly basic anion exchanger AV-17 × 6 is reported. The adsorbability of Th was found to depend strongly on the HNO_3 concentration. The dynamic capacity of the column for thorium was studied as a function of HNO_3 concentration, temperature, amount of anion exchanger, and presence of certain reagents. All the ions studied were divided into three groups according to their capacity for being adsorbed and eluted: thorium ions, which are adsorbed in considerable quantities and are not eluted to any appreciable extent by 7 N HNO_3; ions of La, Ce(III), Bi, Pb, Co, Ni, Cu, U(VI), and Al, which are adsorbed in small quantities; and ions of Fe(III), Cr(III), Zn, Cd, Mg, Mn(II), and Ca, which are not adsorbed by the resin. Ions of metals of groups 2 and 3, with the exception of U(VI), are quantitatively eluted from the resin by 7 N HNO_3. Thus, the results show that Th can be separated from metals of groups 2 and 3. It was found that U could be separated from Th most effectively on the KU-2 resin from HNO_3 solutions less than 2.5 N, and on the AV-17 × 6 resin from HNO_3 solutions more than 2.5 N. A simple procedure is proposed for the separation of ^{234}Th from uranium solutions. (CFSTI)

20625 ^{137}Cs BEHAVIOR DURING THE ANALYSIS OF ATMOSPHERIC PRECIPITATION SPECIMENS. Shvedov, V. P.; Zhilkina, M. I.; Gritchenko, Z. G.; Gedeonov, L. I. pp 108-13 of Radiokhimicheskie Metody Opredeleniya Mikroelementov. Moscow-Leningrad, Izdatel'stvo Nauka, 1965. (In Russian).

The method of gamma-spectrometric control was used to study the distribution of ^{137}Cs during reduction of atmospheric precipitation samples by various concentrations of the mineral acids HCl, HNO_3, HCl + HF, and HNO_3 + HF. The ^{137}Cs distribution during subsequent treatments of the sample by aqua regia and HCl was clarified. More complete dissolution of sample macroimpurities and of ^{137}Cs present as a component of radioactive fallout was observed during reduction by the concentrated mixtures HCl + HF and HNO_3 + HF. Incomplete extraction of ^{137}Cs during the reduction of dry residues from the evaporation of atmospheric precipitates by HNO_3, HCl, or aqua regia can be a source of error in its radiochemical determination. (tr-auth)

20626 ZIRCONIUM AND YTTRIUM CUPFERRONATES AND A METHOD FOR SEPARATING ^{89}Zr FROM IRRADIATED CARRIER FREE YTTRIUM. Rudenko, N. P.; Kuznetsov, V. I. pp 113-18 of Radiokhimicheskie Metody Opredeleniya Mikroelementov. Moscow-Leningrad, Izdatel'stvo Nauka, 1965. (In Russian).

A simple and rapid technique for obtaining zirconium-89

preparations without a carrier in a radiochemically pure state was developed. After calculating the stability constants of the complexes of Zr and Y with cupferron and using these constants to calculate the relative concentrations of the various forms of Zr and Y cupferronates versus the concentration of the cupferron anion, the optimum conditions for the extraction of zirconium were determined: a freshly prepared chloroform solution of cupferron is used to extract Zr from an aqueous solution containing 0.1–2N HCl, then the organic phase is washed once with a KCl + HCl buffer solution at pH ≃ 1. In the experiments, yttrium oxide irradiated with deuterons was dissolved in HCl with heating, the solution was evaporated, and the residue was dissolved in 1N HCl. Zr was extracted with a 0.005M solution of cupferron, and the organic phase was washed with the above-mentioned buffer. The first wash water contained a negligible amount of Y-90 formed by the reaction $^{89}Y(d,p)^{90}Y$, and the second one was completely free of this isotope. Zr was reextracted with 10N HNO_3. The degree of Zr extraction and the purity of the isotopes obtained were determined by measuring the half life and recording β and γ spectra. (CFSTI)

20627 ION-EXCHANGE CONCENTRATION AND SEPARATE ISOLATION OF CESIUM, STRONTIUM, AND CERIUM FROM FRESH WATER. Senyavin, M. M.; Nikitina, N. G. pp 118-24 of Radiokhimicheskie Metody Opredeleniya Mikroelementov. Moscow-Leningrad, Izdatel'stvo Nauka, 1965. (In Russian).

After calculating the optimum concentration of the HCl eluent for each element and the volume of eluent of a given concentration corresponding to the peak on the elution curve (V_{max}), a procedure for separating a mixture of ^{137}Cs, ^{90}Sr, and ^{144}Ce from fresh water was developed. The KU-2 cation-exchange resin in a hydrogenated form was employed. The activity of the filtrates was measured with a β counter. Tap water to which the three isotopes had been added was passed through a column filled with KU-2, then the following amounts of acid were successively poured through the column: 100 ml 0.05 N HCl, 230 ml 0.5 N HCl, and 200 ml 2 N HCl, to remove ^{137}Cs, ^{90}Sr, and ^{144}Ce, respectively. The data indicate that the proposed ion-exchange method permits the separation and a sufficiently accurate determination of the content of cesium, strontium, and cerium in solutions with compositions similar to those of natural waters. (CFSTI)

20628 CONCENTRATION OF RADIOACTIVE ISOTOPES WITH COLLOIDAL MANGANESE DIOXIDE BY FOAMING. Pushkarev, V. V. pp 124-9 of Radiokhimicheskie Metody Opredeleniya Mikroelementov. Moscow-Leningrad, Izdatel'stvo Nauka, 1965. (In Russian).

The radioactive isotopes ^{89}Sr, ^{90}Sr, ^{90}Y, ^{91}Y, ^{95}Zr, ^{95}Nb, ^{106}Ru, ^{106}Rh, ^{137}Cs, ^{144}Ce, and ^{144}Pr were separated and concentrated from aqueous solutions by foam chromatography, colloidal manganese dioxide being used as the carrier and gelatin as the foaming agent. The optimum amounts of gelatin at various pH values were determined. An attempt was made to obtain a precipitate with the lowest possible moisture content (1.5–2.0% of the volume of the initial solution). It was found that this content is substantially affected by the pH of the solution, amount of gelatin, rate of blowing air through the column of liquid, and difference in the levels of the liquid surface and height at which the foam fraction is poured off. It was found that from 97.0 to 99.0% yttrium at pH ≥ 6.0, zirconium with niobium at pH ≥ 2.0, and cerium at pH ≥ 3.0 are recovered from the solution with the foam product. When the foaming is repeated, these isotopes are recovered from the solution to the extent of over 99.9%. The maximum recovery of ruthenium (pH = 4.0–5.0) and cesium (pH > 6.0) is 55.0–65.0%, and that of strontium (pH = 10.0), 86.0%. (CFSTI)

20629 CHROMATOGRAPHIC SEPARATION OF TECHNETIUM AND RHENIUM. Pozdnyakov, A. A.; Ryabchikov, D. I. pp 130-3 of Radiokhimicheskie Metody Opredeleniya Mikroelementov. Moscow-Leningrad, Izdatel'stvo Nauka, 1965. (In Russian).

The possibility of separating Tc and Re ions in concentrated HCl solutions, in which these ions are present in the form of $TcCl_6^{2-}$ and ReO_4^- was investigated. A study of the partition coefficients of Tc and Re ions of various oxidation states on the anion exchangers AV-17 and Dowex 1 × 4 in HCl solutions showed the presence of a strong adsorption of the complex anions $TcCl_6^-$ ($Tc^{(IV)}$) on AV-17. It was found that the most pronounced differences in the partition coefficients of $TcCl_6^-$ and ReO_4^- occurred in ~10 M HCl solutions: the separation factors were 50 for the AV-17 resin and 17 for Dowex 1 × 4. An efficient method of chromatographic separation of Tc and Re ions was developed, based on a selective reduction of Tc ions to the tetravalent state by hydrochloric acid, and an adsorption of the $TcCl_6^-$ ions formed that was very different from the adsorption of ReO_4^- in 10 M HCl. The eluents were 10 M HCl for the elution of rhenium and 4 N NH_4OH for the recovery of technetium. (CFSTI)

20630 POLAROGRAPHIC DETERMINATION OF URANIUM IN NITRIC ACID MEDIA CONTAINING TRI-N-BUTYL PHOSPHATE. I. POLAROGRAPHY IN WEAKLY ACIDIC SOLUTIONS. Gusev, N. I.; Sklyarenko, I. S.; Chubukova, T. M. pp 147-52 of Radiokhimicheskie Metody Opredeleniya Mikroelementov. Moscow-Leningrad, Izdatel'stvo Nauka, 1965. (In Russian).

The influence of tributyl phosphate (TBP) on the polarographic reduction of U(VI) was determined so that optimum conditions for determining U(VI) could be selected. A dropping mercury electrode and an LP-55A polarograph were used. The uranyl ion was analyzed polarographically in HNO_3 solutions with and without TBP. The latter was found to have surface-active properties which complicate the quantitative determination of uranium. The interference of TBP can be eliminated by introducing a gelatin solution, which acts as a competing surfactant. The proposed method of determining U(VI) consists of diluting the HNO_3–TBP solution with water or acid (so that the acidity of the final solution is about 0.3N in HNO_3) and the polarographic analysis of U(VI) on a dropping mercury electrode at a gelatin concentration of 0.01%. HNO_3–TBP solutions with concentrations of 1.5N HNO_3, 0.5–0.8N NH_4NO_3, and 4×10^{-4}–5×10^{-3}M $UO_2(NO_3)_2$ were thus analyzed. The average relative error of 40 determinations in the range of 7×10^{-5}–1×10^{-3}M was ±3.1%. The maximum error (for the minimum uranium content) did not exceed ±8%. (ATD)

20631 POLAROGRAPHIC DETERMINATION OF URANIUM IN NITRIC ACID MEDIA CONTAINING TRI-n-BUTYL PHOSPHATE. II. POLAROGRAPHY IN MODERATELY ACIDIC SOLUTIONS. Palei, P. N.; Gusev, N. I.; Sklyarenko, I. S.; Chubukova, T. M. pp 153-6 of Radiokhimicheskie Metody Opredeleniya Mikroelementov. Moscow-Leningrad, Izdatel'stvo Nauka, 1965. (In Russian).

The advantages of the polarographic determination of U(VI) in moderately concentrated (2.0N) nitric acid solutions as compared to weakly acidic media (~0.3N HNO_3) are indicated. The presence of 0.02–0.035% gelatin eliminates the influence of TBP on the wave of U(VI) and raises the permissible concentration of Fe(III) to Fe : U = 5 : 1. When there is a considerable fluctuation of acidity (from 1.5 to 2.0N HNO_3), the determination should be carried out after diluting TBP with a three- or five-fold volume of 1.75N HNO_3. Moderately concentrated HNO_3 solutions are more convenient than dilute ones because the height of the polarographic wave obtained is nearly twice as great, and uranium can be determined in the presence of higher concentrations of impurities. The study indicates that the use of complex-forming media (e.g., oxalic acid, acetic acid, etc.) in the polarography of TBP solutions of U(VI) for the purpose of eliminating the interference of certain cations is greatly hindered by the pronounced influence of TBP in weakly acidic solutions (pH 2–5). Apparently, only those reagents can be used which react with U(VI) in acid solutions. (ATD)

20632 RADIOACTIVATION ANALYSIS OF SILICON DIOXIDE USING ION EXCHANGE CHROMATOGRAPHY. I. GROUP SEPARATION OF TRACE IMPURITIES FOL-

LOWED BY γ-SPECTROMETRIC DETERMINATION. Kalinin, A. I.; Kuzhetsov, R. A.; Moiseev, V. V.; Tsepurnek, V. E. pp 161-7 of Radiokhimicheskie Metody Opredeleniya Microelementov. Moscow-Leningrad, Izdatel'stvo Nauka, 1965. (In Russian).

A method is proposed for the rapid chromatographic separation of elements produced in activation into groups; this is followed by a γ-spectrometric analysis of the isolated fractions. The method was applied to the radioactivation determination of trace impurities in silicon dioxide. Resins AV-17 and KU-2 were used for the separation. The following elements were determined: K, Na, Rb, Cs, Ca, Sr, Ba, Cu, Co, Ga, Zn, In, Cd, Sb, Ta, Mo, Sn, As, P, W, Ni, Cr, and Au. The method has several advantages: (1) the separation is made in small volumes (0.1–0.5 ml) and with small chromatographic columns, so that the duration of the analysis is considerably reduced; (2) since the final determination is γ-spectrometric, no thorough radiochemical purification of the separated fractions is required; (3) the method permits the determination of a large number of elements as compared to the γ-spectrometric method involving no decomposition of the sample; the elements in the separated groups are selected in such a way that the interfering influence of some radioisotopes on others is eliminated during the recording of the γ spectra; (4) the group chromatographic separation permits the separation of elements which, upon irradiation, yield isotopes with pure β-radiation or isotopes having a low determination sensitivity when a γ spectrometer is used, so that the radioactivity of such isotopes can then be measured with a β-counter. A description of the entire analytical procedure is given. (ATD)

20633 RADIOACTIVATION ANALYSIS OF SILICON DIOXIDE BY MEANS OF ION EXCHANGE CHROMATOGRAPHY. PART 2. SEPARATION AND DETERMINATION OF ALKALI METALS. Zasukhin, E. N.; Kalinin, A. E.; Kuznetsov, R. A.; Moiseev, V. V. pp 168-71 of Radiokhimicheskie Metody Opredeleniya Mikroelementov. Moscow-Leningrad, Izdatel'stvo Nauka, 1965. (In Russian).

A procedure was developed for the separation of sodium, potassium, rubidium, and cesium on zirconium tungstate sorbent involving an activation determination of the impurities in silicon dioxide of high purity. Radioactive tracers were used to determine the partition coefficients of alkali metal ions for the sorbent in ammonium chloride solutions of various concentrations; from these values, the separation factors of alkali metals were calculated. It was found that alkali metals are separated much better on zirconium tungstate than on organic ion exchange resins. The yield of alkali metals, measured with tracers, was 97–98%. The purification factor for the removal of sodium from potassium was 10^5. Since the separation factors of the other elements have higher values than in the case of sodium–potassium, the purification factors for these elements are also higher. (CFSTI)

20634 RADIOACTIVATION ANALYSIS OF SILICON DIOXIDE BY MEANS OF ION EXCHANGE CHROMATOGRAPHY. PART 3. SEPARATION OF ELEMENTS ON AN ANION EXCHANGER IN THE Cl^- AND OH^- FORMS. Kalinin, A. I.; Kuznetsov, R. A.; Moiseev, V. V. pp 171-6 of Radiokhimicheskie Metody Opredeleniya Mikroelementov. Moscow-Leningrad, Izdatel'stvo Nauka, 1965. (In Russian).

Considering the limitations of a final γ spectrophotometric determination, a procedure for the chromatographic separation of two groups of elements into the individual elements, followed by measurement of the activity of these elements with an end-window counter is proposed. The two groups include: Co, Cu, In, Fe, Ga, Zn, Cd, and Mn, Ag, Ni, Cr, and the rare earths. The separation is performed in the same columns which were used previously to separate these groups of elements in the course of the group separation of trace impurities. Sensitivity of the determination is approximately one degree of magnitude higher than in the case of a final γ-spectrometric determination. The degree of separation of the elements was measured on artificial mixtures with radioactive tracers. The metals Cu, Co, Cd, Zn, In, Ga, and Fe were separated on the AV-17 × 8 resin in the Cl^- form, and Mn, Ag, Ni, Cr and the rare earths were separated on the hydroxylated form of this resin. The procedures described are convenient for a rapid separation of elements during the radioactivation determination of trace impurities in silicon dioxide. (CFSTI)

20635 RADIOACTIVATION ANALYSIS OF SILICON DIOXIDE BY MEANS OF ION EXCHANGE CHROMATOGRAPHY. PART 4. SEPARATION OF ELEMENTS ON AN ANION EXCHANGER FROM SOLUTION OF HYDROFLUORIC ACID AND A MIXTURE OF HYDROFLUORIC AND HYDROCHLORIC ACID. Kalinin, A. I.; Kuznetsov, R. A.; Moiseev, V. V. pp 176-9 of Radiokhimicheskie Metody Opredeleniya Mikroelementov. Moscow-Leningrad, Izdatel'stvo Nauka, 1965. (In Russian).

The salts of As, P, W, Sb, Mo, Sn, and Ta are characterized by a complex chromatographic behavior due to their tendency to hydrolyze and to the existence of these ions in several stable oxidation states. In order to minimize the hydrolysis, solutions of HF and HF–HCl mixtures were used for the ion exchange separation on the AV-17 resin. The procedure employed is described. To determine the extent of separation of the elements, radioactive tracers in artificial mixtures were employed. A complete separation was achieved if the activity of the separated fractions did not exceed 10^5 counts per min. The time required for the separation of P, As, W, Sb, Sn, Mo, and Ta was 1.5 to 2 hours. (CFSTI)

20636 RADIOACTIVATION ANALYSIS OF SILICON DIOXIDE BY MEANS OF ION-EXCHANGE CHROMATOGRAPHY. PART 5. SEPARATION AND DETERMINATION OF ALKALINE EARTH METALS. Kalinin, A. I.; Kuznetsov, R. A.; Moiseev, V. V.; Sokolova, M. N. pp 180-1 of Radiokhimicheskie Metody Opredeleniya Mikroelementov. Moscow-Leningrad, Izdatel'stvo Nauka, 1965. (In Russian).

A chromatographic method was used to separate calcium, strontium, and barium isolated from samples of silica bombarded with neutrons. The procedure involved the successive elution of the elements adsorbed on a KU-2 cation exchanger (in the NH_4^+ form) with solutions of trilon B of various pH values. The degree of separation was checked on artificial mixtures containing radioactive tracers. A practically complete separation of Ca, Sr, and Ba from a large amount of sodium was achieved. The sensitivity of the radio-activation determination of Ca, Sr, and Ba (involving the use of an end-window counter) is: 10^{-7} g for Ca, 9×10^{-8} g for Sr, and 2×10^{-8} for Ba (the samples had been subjected to a flux of 10^{14} neutrons/cm^2 sec for 24 hrs.). (CFSTI)

20637 RADIOCHEMICAL ANALYSIS USING TWO GAMMA-RADIOACTIVE ISOTOPES. Glazov, V. M. pp 193-7 of Radiokhimicheskie Metody Opredeleniya Mikroelementov. Moscow-Leningrad, Izdatel'stvo Nauka, 1965. (In Russian).

A method of radiometric analysis, using simultaneously two radioisotopes differing in the energy of their gamma quanta on the basis of a single-channel scintillation spectrometer, is proposed, which permits the activity of each radioisotope in the analyzed chemical compound to be determined without recourse to their separation. This method gives the possibility of carrying out studies of diverse chemical phenomena and in some cases is the only possible method of investigation. The error in the proposed radiometric analysis is ±2%. The proposed method of resolution of a complex pulse spectrum on a single-channel scintillation spectrometer can be carried over to gamma sources containing more than two isotopes in a single chemical compound. (tr-auth)

20638 USE OF SEVERAL GAMMA-RADIOACTIVE ISOTOPES IN RADIOCHEMICAL ANALYSIS. Glazov, V. M. pp 197-200 of Radiokhimicheskie Metody Opredeleniya Mikroelementov. Moscow-Leningrad, Izdatel'stvo Nauka, 1965. (In Russian).

A method of radiochemical analysis employing several gamma-active radioisotopes on the basis of several refer-

ence sources with a single-channel gamma scintillation spectrometer is described. Experimental results of the use of mixtures of ^{137}Cs, ^{65}Zn, and ^{60}Co sources on thin organic backings are discussed, and the accuracy of the method of radiometric analysis is considered. (M.J.T.)

20639 MEASUREMENT OF ACTIVITY OF COMPONENTS IN ORGANIC MIXTURES CONTAINING ^{14}C. Kirin, I. S.; Grachev, S. A.; Gusev, Yu. K.; Leonov, V. V. pp 200-2 of Radiokhimicheskie Metody Opredeleniya Mikroelementov. Moscow-Leningrad, Izdatel'stvo Nauka, 1965. (In Russian).

A method for determining the activity of components of mixtures of organic compounds containing ^{14}C is described. The separation of the labeled compounds is carried out by chromatography, using He or N as gaseous carrier, and the activity of the components is measured on a beta scintillation counter. The results of separation of mixtures of hydrocarbons and pyridine and of aromatic hydrocarbons are shown. (M.J.T.)

20640 THE ANALYSIS OF TIN AND COPPER ORES USING A PORTABLE RADIOISOTOPE X-RAY FLUORESCENCE ANALYSER. Darnley, A. G.; Leamy, C. C. (Geological Survey of Great Britain, London). Vienna, International Atomic Energy Agency, 1965, Preprint No. SM-68/11, 24p. (CONF-651023-7). ORINS.

From Symposium on Radioisotope Instruments in Industry and Geophysics, Warsaw.

An instrument was developed, which is an x-ray fluorescence analyzer using a radioisotope source for excitation and balanced filters for energy selection. The instrument weighs less than 8 kg and is transistorized, sealed, and completely self-contained. It can be used in the full range of conditions likely to be encountered in metalliferous mining or exploration. The principle of operation and method of use are described. The results obtained from a series of measurements on all types of tin samples from Southwest England; ore pulps, concentrates, heavy mineral sediments, and drill hole cores, are presented. The value of rock face measurements was assessed. As far as possible results were compared against those obtained by normal chemical procedures. The considerations to be taken into account when drawing up calibration curves for different applications are discussed in detail. Errors due to grain size and matrix variations could be significantly reduced either by careful choice of standard samples, or by comminuting samples so that the bulk of the cassiterite was <50 microns and by using the total count rate to select an appropriate calibration curve. The second group of results concerns Zambian Copperbelt material. Samples were obtained from three mines, which exhibit a variety of matrix and ore mineralogy problems, and include oxidized and unoxidized ores. The considerations relating to selection of calibration curves are discussed. (auth)

20641 HYDROGEN ANALYSIS BY SLOW NEUTRON TRANSMISSION. Mott, W. E.; Rhodes, D. F. (Gulf Research and Development Co., Pittsburgh). Vienna, International Atomic Energy Agency, 1965, Preprint No. SM-68/20, 21p. (CONF-651023-10). ORINS.

From Symposium on Radioisotope Instruments in Industry and Geophysics, Warsaw.

Instruments and procedures were developed and refined for routinely determining in the laboratory and on-stream the hydrogen content of hydrocarbons by slow neutron transmission. A basic instrument consisted of a Pu–Be neutron source that emits about 1.9×10^7 neutrons per second, a sample cell through which a beam of slow neutrons is directed, and a BF_3 or ^3He end-window proportional counter for measuring the neutron transmission. The apparatus was operated submerged in oil, which acts as a neutron moderator and constant temperature bath. The fundamental constants for an instrument; the hydrogen scattering cross section (σ_H), the carbon scattering cross section (σ_C), and a factor (α) that takes into account the effects of background, multiple scattering, and solid angle, were calculated by a least squares procedure from transmission and density data for a series of pure compounds using the equation $\mathrm{Ln}\,(I - \alpha/I_0 - \alpha) = -\rho t N_0\,[(W_H\sigma_H/A_H) + (W_C\sigma_C/A_C)]$, where I is the neutron transmission of the sample; I_0, the transmission of an empty sample cell or of a reference sample; t, the thickness of the sample; N_0, Avogadro's number; ρ, the density; W_H, W_C, the weight fractions of hydrogen and carbon; and A_H, A_C, the atomic weights of hydrogen and carbon. Experimentally determined values for σ_H, σ_C, and α for a typical instrument are 26.8 barns, 4.7 barns, and 10,000 counts/min, respectively. Hydrogen concentrations, W_H, were calculated from the transmission equation using 5-min neutron transmission measurements and densities determined at the neutron transmission cell temperature by means of a pycnometer or a low energy gamma transmission gage. Precision and accuracy were in excellent agreement with values expected from counting statistics (experimental standard deviations were approximately 0.02 wt % hydrogen) and comparable to those obtained by the longer β transmission method. (auth)

20642 RAPID ANALYSIS OF COPPER ALLOYS AND STEELS USING A RADIOISOTOPE PORTABLE ANALYZER. Rhodes, J. R.; Packer, T. W.; Boyce, I. S. (Atomic Energy Research Establishment, Wantage, Eng.). Vienna, International Atomic Energy Agency, 1965, Preprint No. SM-68/7, 28p. (CONF-651023-15). ORINS.

From Symposium on Radioisotope Instruments in Industry and Geophysics, Warsaw.

A portable analyzer consisting essentially of a radioisotope source, scintillation counter, and transistorized count ratemeter was used for rapid analysis of copper alloys and steels. The scintillation counter measuring head utilizes central source backscattering geometry and incorporates interchangeable filters for energy selection. The instrument can be adapted for x-ray fluorescence, beta backscatter, and x-ray backscatter by suitably choosing the source, phosphor, and filters. The portable instrument is used for sorting scrap before reformation of stock alloys, sorting stocks in the form of ingots, sheets, rods, tubes, and bars and recognition of components during manufacturing processes, such as extrusion and forging where ordinary markings are obliterated. The performance of the instrument using x-ray fluorescence techniques to measure flat material is typified by the following results. The Mo content of steels can be measured to ±0.03% Mo in the range from 0.03 to 5% without reference to other alloying constituents such as Cr, Ni, and Nb. The difference between a leaded steel containing 0.25% Pb and a steel with no lead can be measured with 99.9% confidence. The Cu content of brasses can be measured to ±0.5% Cu in the range from 50 to 100% and the zinc content to ±0.5% Zn in the range from 0.5 to 50%. In all cases the measurement time constant was 4 seconds. (auth)

20643 A RAPID METHOD FOR DETERMINING ^{210}Pb AND ^{210}Po IN ENVIRONMENTAL SAMPLES. Blanchard, Richard L. (Robert A. Taft Sanitary Engineering Center, Cincinnati). 22p. (CONF-650616-9). ORINS. Gmelin, AED-CONF-65-153-3.

From Health Physics Society Annual Meeting, Los Angeles.

A procedure for determining ^{210}Po and ^{210}Pb simultaneously in environmental samples was developed by determining the optimum conditions for the spontaneous deposition of ^{210}Po and ^{210}Bi on nickel from an HCl solution. The effects of HCl concentration, hydrazine concentration, temperature, time of deposition, surface area of the planchet, and the presence of the $HClO_4$ used to ensure oxidation of environmental samples, were studied. The recoveries of ^{210}Po, ^{210}Bi, and ^{210}Pb were determined for various environmental samples spiked with a ^{210}Pb–^{210}Bi–^{210}Po standard. The average efficiencies for the deposition of ^{210}Po and ^{210}Bi were 96 ± 4 and 94 ± 3%. The average efficiency for the deposition of ^{210}Pb, determined by decay measurement, was 13 ± 2%. The ^{210}Po concentrations were determined by alpha counting. The ^{210}Pb concentrations were determined by beta counting the ^{210}Bi daughter. An aluminum absorber was used to eliminate the ^{210}Po alpha and ^{210}Pb beta particles. (auth)

20644 X-RAY FLUORESCENT DETERMINATION OF MAJOR CONSTITUENTS IN MULTI-ELEMENT MATRICES BY THE USE OF COHERENT TO INCOHERENT SCATTERING RATIOS. Carman, Charles J. (B. F. Goodrich Co., Brecksville, Ohio). 23p. (CONF-650634-3). ORINS. Gmelin, AED-CONF-65-155-1.

From 16th Annual Mid-America Symposium on Spectroscopy, Chicago.

A technique using the ratio of coherent to incoherent scattering of x rays from a sample to correct for matrix effects in light atomic number matrices was reported by Ryland. This work was extended to provide elemental analyses for major constituents in multielement systems comprised of light and heavy atomic number elements. The technique involves dilution of multielement mixtures in polyethylene and using the ratio of coherent to incoherent scattering of the exciting x rays, to provide a linear working curve when concentration is plotted versus the intensity of the element being analyzed. The method provides a permanent set of standards, which require no previous knowledge of the matrix of the sample being analyzed, and which are essentially independent of any chemical changes occurring within the sample. Determinations of molybdenum, tellurium, manganese, and phosphorus in mixtures provided results slightly less accurate than by chemical methods, but in much less time. (auth)

20645 PHOTON ACTIVATION ANALYSIS OF CESIUM. Spira, Jacob (Boston Univ.). 18p. (CONF-651004-9). ORINS.

From 9th Conference on Analytical Chemistry in Nuclear Technology, Gatlinburg, Tenn.

Photon activation analysis for the determination of oxygen and other nonmetallic impurities in cesium is reported. Cesium samples were prepared in a vacuum dry box under an atmosphere of purified helium because of cesium's extreme reactivity with the atmosphere. The samples were irradiated with an x-ray beam between 20 to 30 Mev. For carbon, nitrogen, and oxygen, and for a photon energy between 20 to 30 Mev, the (γ,n) reaction was predominant. Deviation from the calculated decay curve is shown. The oxygen concentration in an unknown sample of cesium is found by normalizing for differences in weight, density, and bombarding intensity between the standard and the unknown. A similar procedure is used for carbon. The reduced-flux oxygen determination in cesium was carried out below 100 ppm. The results compared favorably with other methods. (F.J.H.)

20646 THE APPLICATION OF NEUTRON ACTIVATION ANALYSIS FOR THE INVESTIGATION OF MANGANESIAN ROCKS. Beress, M. (Roland Eoetvoes State Geophysical Inst., Budapest). Vienna, International Atomic Energy Agency, 1965, Preprint No. SM-68/21, 24p. (CONF-651023-3). ORINS.

From Symposium on Radioisotope Instruments in Industry and Geophysics, Warsaw.

Using the method of neutron activation analysis a procedure was created with an accuracy meeting industrial requirements for the simultaneous determination of manganese, aluminum, and silicon in rocks without their destruction. In a portable activation unit including a polonium-beryllium neutron source with a strength of 7 C powdered 38-g rock samples were irradiated by slow and fast neutrons simultaneously for 4.6 min. The concentrations were computed from the number of counts measured in intervals of 0.4 to 5.4 and 60 to 65 minutes after the irradiation was finished. The results of reproduction tests for MnO_2 were +0.05% average with ±1.21% standard deviation, for SiO_2 −0.11% ± 0.56%, and for Al_2O_3 +0.25% ± 1.80%. A subsequent increase of stability of the instrument and automatization of the procedure indicated that the method can attain the accuracy of chemical analysis and that its time requirement will decrease. In a series of samples representing industrial concentrates of manganesian ore a −0.90 correlation coefficient was obtained between MnO_2% and SiO_2%. The method is also suitable for determining the content of manganese with a greater accuracy. A more accurate determination of manganese requires a longer irradiation time and in this case the number of counts from the isotope ^{56}Mn dominates. The increase in accuracy by prolongation of irradiation time can be expressed in terms of MnO_2% equivalent to the statistical error, equaling ±0.11% at an irradiation time of 78 min, ±0.095% at 156 min and ±0.077% at 312 min. The practical applicability of this activation method is demonstrated on a log obtained by the activation of a complete series of samples from a borehole. The geological log must be subjected to certain corrections as indicated by the activation log. At an irradiation time of 4.6 min the manganesian bed appears clearly on the log, even the little change in manganese concentration between limestones and igneous rocks can be detected. (auth)

20647 ECONOMIC CONSIDERATIONS IN THE MEASUREMENT OF NUCLEAR MATERIALS. Tingey, F. H. (Philips Petroleum Co., Idaho Falls, Idaho). Vienna, International Atomic Energy Agency, 1965, Preprint No. SM-67/24, 11p. (CONF-650803-48). ORINS.

From IAEA Symposium on Nuclear Materials Management, Vienna.

A fundamental problem in the determination of the total quantity of a given constituent contained in several batches of material is the analytical and sampling effort to be applied to the determination. In some applications, each of several batches could be transferred to a single container to make a composite batch in order to reduce the overall effort. Often, however, the case is such that physical considerations, such as limitations imposed by process equipment, or nuclear criticality considerations as in nuclear fuel reprocessing, for example, preclude combining several batches. Thus any reduction in total analytical effort over that entailed in analyzing a sample or samples from each batch requires compositing aliquots from the batches. It is shown that the volumes of the aliquots should be in the same proportion as the volumes of the corresponding batches. Equations are presented for determining how many samples from each batch, how many analyses should be made on the composite, the method of analysis, and sensitivity. (F.J.H.)

Inorganic and Physical Chemistry

Refer also to abstracts 20375 and 20870.

20648 (AD-621029) INTERCALATION OF RARE EARTH ELEMENTS INTO GRAPHITE AND DICHALCOGENIDES [Thesis]. Craven, William Ernest (Air Force Inst. of Tech., Wright-Patterson AFB, Ohio. School of Engineering). Aug. 1965. 74p. (GNE/PH-65-02). CFSTI $3.00 cy, $0.75 mn.

The graphite intercalation compounds of Ce, Sm, Er, Tm, Dy, Ho, Gd, Tb, and Yb were prepared by reacting powdered graphite with the solution of the metal in liquid ammonia. Electrolysis was necessary to dissolve all but ytterbium. Intercalation compounds of ytterbium and samarium with the dichalcogenides: WS_2, WSe_2 and MoS_2 were prepared by the same process. The x-ray diffraction patterns showed that mixtures of several stages were present in the graphite compounds. Magnetic susceptibility measurements indicated that most of the rare earths intercalate in the trivalent state, the exception being divalent samarium. Apparently ytterbium exists in both divalent and trivalent states in the compound. (auth)

20649 (AEET-CD-24) ROLE OF SUBSTRATE SYMMETRY IN GAS-SOLID REACTIONS. PART I. REACTIONS OF GASEOUS URANIUM OXIDE WITH DIFFERENT OXIDES. PART II. STRUCTURAL INTERPRETATION OF THE REACTIONS OF GASEOUS URANIUM OXIDE. Karkhanavala, M. D.; Damani, V. D. (Atomic Energy Establishment, Trombay (India)). 1964. 12p. Dep. mn.

Studies were made on reactions between gaseous U_3O_8 (UO_3) and other oxides in order to study the effects of crystal symmetry of the substrate. Mainly, group IV oxides (SiO_2, ThO_2 stabilized ZrO_2, ZrO_2, and HfO_2) were used; CaO and CdO were also studied to ascertain the effect of polarizability in case of compounds with identical crystal structure and containing ions of similar radius.

Al_2O_3 was used as a representative of the non-polarizable trivalent oxide group. From preliminary results certain generalizations were made. The gaseous UO_3 reacts strongly with oxides of cubic fluorite symmetry forming a solid solution; reacts with oxides of rocksalt type forming compounds; reacts weakly with oxides of nearly cubic symmetry; does not react with oxides of non-cubic symmetry. It was concluded that it may be possible to take advantage of the gaseous UO_3 formation and its ready reaction with cubic substrates to obtain urania solid solutions of other oxides with which pure solid state reactions are not possible or are sluggish. (P.C.H.)

20650 (ANL–7055, pp 167-76) CALORIMETRY. Hubbard, W. N.; Feder, H. M. (Argonne National Lab., Ill.).

Work devoted to obtaining thermochemical data on compounds of interest in high-temperature chemistry is reported. Procurement of well-characterized samples and development of adequate experimental techniques are emphasized. Data are included on the hexafluorides of S, Se, and Te. Data are also included on the trifluorides of Al, Y, Gd, and Ho. Combination data are given on Si–F, and B–F reactions. Development of calorimeters is discussed. (J.R.D.)

20651 (CU–2660-26) HIGH TEMPERATURE THERMAL PROPERTIES OF GASES AND VAPORS DURING THE YEAR 1965/66. Progress Report. Bonilla, Charles F. (Columbia Univ., New York. Dept. of Chemical Engineering). Feb. 1966. Contract AT(30-1)-2660. 14p. Dep. mn. CFSTI $1.00 cy, $0.50 mn.

The principal new final experimental results obtained during the last year include data on the viscosity of cesium vapor at atmospheric pressure, and on the surface tension of potassium at high temperatures. The principal theoretical result is the calculation of errors in long sheathed thermocouples at high temperatures due to leakage currents among the thermocouple wires and the sheath, and the resulting IR drops along the wires. Results of studies on thermal conductivity of alkali metal vapors, high-temperature vapor pressure and critical point of alkali metals, near-critical saturated liquid and vapor phase densities and the critical point of alkali metals, and high-temperature thermodynamics of the K–Hg system are also reported. (P.C.H.)

20652 (IS-T–67) FLASH DESORPTION AND ISOTOPIC MIXING OF SIMPLE DIATOMIC GASES ON TUNGSTEN, IRIDIUM AND RHODIUM [Thesis]. Mimeault, Victor Joseph (Ames Lab., Iowa State Univ. of Science and Tech.). Feb. 1966. Contract W-7405-eng-82. 204p. Dep. mn. CFSTI $6.00 cy, $1.25 mn.

Flash desorption of H_2, N_2, and CO from W, Ir, and Rh dosed at 100 and 300°K was investigated together with isotope mixing in co-adsorbed mixtures of H_2-D_2 and $^{14}N_2-{}^{15}N_2$. The desorption spectrometer was constructed so that the ultimate pressure was less than 5×10^{-10} torr, the pressure and temperature could be measured simultaneously during an experiment and the desorption products identified mass spectrometrically. The desorption of H_2 from W, Ir, and Rh dosed at 300°K proceeds by a second order process with an activation energy of desorption which has the form, $\Delta H = \Delta H_0 - \alpha n$. At low surface coverages, a value of 35, 24, and 18 kcal/mole respectively was obtained for ΔH_0; the parameter α was determined from desorption curves at higher initial surface coverages and was found to be 28 ± 2, 14 ± 1, and 24 ± 2 cal/mole/10^{12} molecules/cm^2 respectively. The isotopes in the desorbed phase formed from dosing these metals at 300°K with a mixture of H_2 and D_2 are statistically distributed, whereas the ambient distribution is clearly nonstatistical. The desorption spectrum of H_2 from these metals dosed at 100°K contains two peaks, α and β. The distribution of the isotopes in the desorbed phase formed from co-adsorbing H_2 and D_2 indicates that the α-peak is due to an atomic species in the case of Ir and Rh and a molecular species in the case of W. Desorption of N_2 from W dosed at 300°K, contains two peaks, α and β. The α-peak was kinetically first order and the β, second order with activation energies of 20 and 75 kcal/mole respectively. When W was dosed with a mixture of $^{14}N_2$ and $^{15}N_2$, the α-peak was devoid of $^{14}N^{15}N$ whereas the β-peak was completely isotopically mixed on desorption. The amount of N_2 adsorbed on Ir and Rh was a function of the temperature of the filament in the ion gauge. A model is presented to account for the observed adsorption of N_2 on Ir and Rh. The desorption spectrum of CO from Ir and Rh contains only one peak which desorbs over the range 450–750°K. From the equal amounts of CO and H_2 adsorbed, it is inferred that the desorption peak is due to the bridged-bonded form of CO. (auth)

20653 (JINR–P-2558) O VOZMOZHNOSTI PRIMENENIYA ODNOI YADERNOI REAKTSII V KHIMICHESKIKH ISSLEDOVANIYAKH. (On a Possible Application of a Nuclear Reaction in Chemical Research). Petrukhin, V. I.; Ponomarev, L. I.; Prokoshkin, Yu. D. (Joint Inst. for Nuclear Research, Dubna (USSR)). 1966. 6p. Dep. mn.

The possibility of distinguishing between chemically bound and free hydrogen by using nuclear charge exchange of the stopping negative pion on the proton is reported. (auth)

20654 (LA-DC–7784) THE HIGH-TEMPERATURE CHEMISTRY OF NON-FISSIONABLE CERAMICS. Bowman, Melvin G. (Los Alamos Scientific Lab., Univ. of California, N. Mex.). [1966]. Contract W-7405-eng-36. 17p. (CONF-660505–2). Dep. mn. CFSTI $1.00 cy, $0.50 mn.

From American Ceramic Society, Washington, D. C.

The high temperature chemical properties of typical refractory compounds are discussed in the framework of the performance that might be expected under the extreme conditions of environment and temperature which will be experienced by components of different types of space vehicles. A brief review is given of some of the newer techniques for determining high temperature phase relationships and thermochemical parameters, particularly partial molal quantities. (auth)

20655 (ORNL–P–1260) THE DECOMPOSITION RATES OF CERIA IN VACUUM BETWEEN 1100 AND 1700 DEG C. Inouye, Henry (Oak Ridge National Lab., Tenn.). [1964]. Contract W-7405-eng-26. 7p. Dep. mn. CFSTI $1.00 cy, $0.50 mn.

The decomposition rates of cerium oxide between 1100 and 1200°C at pressures of approximately 10^{-10} atm were measured and the results were used to estimate the rates for temperatures as high as 1700°C. It was found that the decomposition rates of ceria in vacuums are proportional to $t^{\frac{1}{2}}$ and increase exponentially with temperature. (P.C.H.)

20656 (UCRL–11930) THE VISCOSITY OF LIQUID METALS. Chapman, Thomas W. (Lawrence Radiation Lab., Univ. of California, Berkeley). Feb. 15, 1965. Contract W-7405-eng-48. 29p. Dep. mn. CFSTI $2.00 cy, $0.50 mn.

An approximate form is suggested for the perturbation of the radial distribution function of a monatomic liquid by a nonuniform flow field. Substitution of this form into the microscopic expression for the pressure tensor yields an equation for liquid viscosity in terms of the equilibrium distribution function and the interatomic potential energy function. This equation establishes the basis for a corresponding states correlation of the viscosity of liquid metals based on atomic parameters. The viscosity data for twenty-one molten metals are made to fall on a single curve by the adjustment of one microscopic parameter. It was found that this empirically determined parameter apparently has the proper fundamental significance. Therefore, it is possible to estimate it independently and to use the general correlation for estimating the viscosity of a metal for which data are not available. It is also suggested that the atomic parameters determined might be used to correlate other properties of the liquid metals. (auth)

20657 (UCRL–11931) THE HEAT CAPACITY OF LIQUID METALS. Chapman, Thomas W. (Lawrence Radiation Lab., Univ. of California, Berkeley). Feb. 15,

1965. Contract W-7405-eng-48. 19p. CFSTI $1.00 cy, $0.50 mn.

The theory of the radial distribution function was used to establish a corresponding states correlation of the configurational heat capacities of six low-melting metals. It is suggested that this correlation may be used to estimate the configurational contribution to the specific heats of other liquid metals. The theory was also used to explain the observed temperature dependence of liquid metal heat capacities. (P.C.H.)

20658 ADVANCES IN INORGANIC CHEMISTRY AND RADIOCHEMISTRY. VOLUME 7. Emeleus, H. J.; Sharpe, A. G. (eds.) (Cambridge Univ., Eng.). Advances Inorg. Chem. Radiochem., 7: 1-449(1965).

The following topics are considered: halides of antimony, arsenic, bismuth, and phosphorus; the phthalocyanines; hydride complexes of the transition metals; reactions of chelated organic ligands; organoaluminum compounds; and carbosilanes. (F.J.H.)

20659 CHEMISTRY OF THE NOBLE GASES. Guillem Monzonis, D. Claudio (Univ., Valencia). Afinidad, 22: 17-26(Jan.-Feb. 1965). (In Spanish).

The history of the discovery of the rare gases is recounted. A table of known compounds is given, with methods of synthesis and methods of analysis outlined. A table lists appearance, mp, and vapor pressures of xenon fluorides at 25°C. The thermodynamic properties of the compounds are discussed, with tables of heats of crystallization and sublimation, and bond energies. Values for the bond energy are compared with other X–F bonds. The fluoroplatinates of xenon and the fluoroxenates are discussed. Preparation of oxyfluorides and the hydrolysis of fluorides are considered. A discussion of oxygen compounds includes descriptions of structures, kinetics of decomposition, and redox potentials. The crystal structures of the fluorides are illustrated, and a theoretical treatment of the bond energy patterns is outlined. The fluorides of krypton and radon are mentioned. (67 references). (BBB)

20660 INVESTIGATIONS ON THE FORMATION EQUILIBRIUM OF AMMONIAS AND TRIDEUTEROAMMONIAS. Schulz, G.; Schaeffer, H. (Max-Planck-Gesellschaft, Berlin). Ber. Bunsenges. Physik. Chem., 70: 21-7(1966). (In German).

The experimental determination of the equilibrium constants for formation of NH_3 and ND_3 at normal pressure and at temperatures in the range from 294 to 400 and 386 to 461°C, respectively, is described. With the aid of known thermodynamic quantities for the reaction partners the data were extrapolated beyond the range of the measurements. Comparisons were made with earlier extrapolations. The formation equilibrium for NT_3 is also discussed. (auth)

20661 THE INHIBITED ENERGY EXCHANGE BETWEEN PLATINUM AND ADSORBED ORTHO-DEUTERIUM AND PARA-DEUTERIUM. Schaefer, Klaus; Schuller, Dieter (Univ., Heidelberg). Ber. Bunsenges. Physik. Chem., 70: 27-33(1966). (In German).

The average thermal accommodation coefficient, which is an experimentally determinable quantity of the degree of energy exchange between a solid surface and adsorbed gas molecules, can be divided among the various degrees of freedom if it is examined side by side with the accommodation for single and multiple collisions of the gas molecules with the surface. For ranges of temperature in which the gas does not show an appreciable excitation of vibration, the direct measurement of the accommodation coefficients for translation and rotation is possible by determination for one- and two-fold collisions of gas molecules with the surface. At 78°K distinctly different values for the partial accommodation coefficients of ortho- and para-deuterium on platinum were obtained. The translation was accommodated better by para-deuterium than by the ortho-modification, but the reverse was true for rotation. At 275°K no differences between the respective partial accommodation coefficients of the two modifications could be established. The results are discussed in terms of the magnitude of the heat of adsorption and the rotational quanta of the two modifications. (auth)

20662 NEW VERY PRECISE METHOD FOR STANDARDIZATION OF RECORDED SPECTRA USING A FABRY-PEROT PHOTOELECTRIC SPECTROMETER. Gange, Jean-Marie (Ecole Polytechnique, Montreal). Can. J. Phys., 44: 681-92(Apr. 1966). (In French).

One of the chief experimental difficulties in measuring the isotopic shift with a precision of the order of 1% using a recording Fabry-Pérot photoelectric spectrometer of high resolution is caused by the scanning device in the spectrometer. Moreover, the study of isotopic shift of elements having odd isotopes poses a particular problem. In such a case a line with a broad and poorly resolved hyperfine structure superimposed on lines corresponding to the adjacent isotopes is usually obtained. By joining a Köster interferometer to the analyzing spectrometer, an agreement of better than one part in a thousand between intervals measured in successive orders was obtained. This method of calibration offers many advantages, which are described in detail. The experimental difficulties for uneven isotopes were overcome by using a hollow quadrupole cathode. The apparatus was used for the study of isotopic shift of the isotopes 238, 235, and 233 of uranium and to measure the intrinsic quadrupole moments of ^{238}U and ^{236}U. (auth)

20663 ON THE ABSORPTION AND FLUORESCENCE SPECTRA OF PRASEODYMIUM-DOPED KCl SINGLE CRYSTAL. Asundi, R. K.; Naik, R. C. (Atomic Energy Establishment, Trombay, Bombay). Current Sci. (India). 34: 550-2(Oct. 5, 1965).

Single crystals of KCl doped with praseodymium were grown as follows. Praseodymium oxide was treated with HCl and the chloride solution thus obtained was added to KCl solution to obtain 1% concentration of Pr ions in the mixture. The mixture was evaporated to dryness under an infrared lamp. The dry residue was then transferred to a distillation tube, which was heated under vacuum to 120 to 130°C for 72 hr to remove all water. Then the tube was heated to about 900°C. The distillate was collected under vacuum into a crystal-growing tube, filled with dry helium to a pressure of a few cm of Hg, and sealed. The tube was then placed in the temperature gradient furnace for growing the crystal. Absorption and fluorescence spectra of the crystal at liquid nitrogen temperature were determined. The spectra consisted of groups of fairly sharp and in some cases broad and diffuse lines, which lie near the same positions as in the spectra of the Pr^{3+} ion in $PrCl_3$ and (Pr + La)Cl_3 crystals. The wavelengths of the spectral lines were measured and relative intensities estimated. A comparison of these data with those known for the Pr^{3+} ion showed that praseodymium is in the triply ionized state in the KCl matrix. In some terms, viz, $^3F_2$, $^3F_4$, $^1D_2$, and $^3P_2$ the degeneracy was either completely or almost completely removed. This indicated that the Pr^{3+} ion has only a low site symmetry in the KCl matrix. Single crystals of NaCl and KBr doped with Pr were grown by the same method. The absorption and fluorescence spectra of Pr in the KBr matrix were similar in their structure to those in the KCl matrix; the line groups are in general displaced to the longer wavelength side. The spectra of Pr in the NaCl matrix were very diffuse. (BBB)

20664 STUDIES ON THE COMPOSITION OF LANTHANUM CARBONATE AND CERIUM CARBONATE. Xie, Guang-hua; Jiang, Zuo-yi. Hua Hsueh Tung Pao, No. 8, 45-52(1965). (In Chinese).

Compositions of $Ce(NO_3)_3$–K_2CO_3–H_2O and $La(NO_3)_3$–K_2CO_3–H_2O systems were studied. Methods involving solubility, pH, electrolysis, and volumetric precipitation were used to determine composition ratios with different reactant concentrations. Analysis of the $Ca(NO_3)_3$–K_2CO_3–H_2O system showed that if the value of a ($[K_2CO_3]/[La(NO_3)_3]$ value in the original solution) is less than 3.5, only $La_2(CO_3)_3$ is formed; beyond that value, $K[La(CO_3)_2]$, measured by the presence of $[CO_3^{2-}]/[La^{3+}] = 1:2$ in the solid phase, forms. Even in as low a concentration of $La(NO_3)_3$

as 0.00895M, if a is large (e.g., a = 18), this 1:2 compound still forms. Excess K_2CO_3 can increase formation of the 1:2 compound if a > 1.5, and virtually stabilize this compound. Analysis of the $Ce(NO_3)_3-K_2CO_3-H_2O$ system revealed the formation of 1:2 compound $K[Ce(CO_3)_2]$ in addition to $Ce_2(CO_3)_3$. If a = 10, at $Ce(NO_3)_3$ concentration as low as 0.01422M, $K[Ce(CO_3)_2]$ forms. The a value is higher in the $La(NO_3)_3-K_2CO_3-H_2O$ system; this is due to the larger radius of La^{3+} ion than that of Ce^{3+}. The compounds of La^{3+} are more unstable that require excess amounts of K_2CO_3 or higher values of a to form 1:2 compounds. As the $La(NO_3)_3$ concentration increases, the required level of the a value subsequently decreases. (BBB)

20665 THE PREPARATION AND SOME THERMAL PROPERTIES OF PURE XENON HEXAFLUORIDE. Malm, John G.; Schreiner, Felix; Osborne, Darrell W. (Argonne National Lab., Ill.). Inorg. Nucl. Chem. Lett., 1: 97-100 (Dec. 1965).

Results of calorimetric investigations of xenon hexafluoride are presented. A preparative method, based on the formation of a complex salt of xenon hexafluoride and sodium fluoride, was developed. Sodium fluoride was placed in a nickel reaction vessel, xenon and fluorine gases added, and the vessel heated at 250 ± 10°C for 150 hr. The compound prepared by this method could easily be freed from the most likely contaminants. Two regions were found in which the heat capacity of solid xenon hexafluoride is anomalously high, one extending approximately from 241 to 261°K and the other approximately from 288 to 297°K. There was some evidence from visual observations that these high heat capacity values are associated with a structural change. A preliminary value for the enthalpy change when the sample was heated from 232 to 270°K in excess of that given by the estimated normal heat capacity curve was 876 J/mole. A similar value for the range 286 to 310°K was 1224 J/mole. The enthalpy of fusion was found to be 5745 J/mole. The melting point of the sample was 322.38°K. (M.C.G.)

20666 VAPORIZATION BEHAVIOR OF EUROPIUM DICARBIDE. Gebelt, Robert E.; Eick, Harry A. (Michigan State Univ., East Lansing). J. Chem. Phys., 44: 2872-6 (Apr. 15, 1966). (COO-716-0014).

The temperature dependence of the vapor pressure of europium in equilibrium with solid europium dicarbide ($EuC_{1.87\pm0.07}$) and graphite was measured over the temperature range 1130° to 1600°K by both time-of-flight mass spectrometric and target collection techniques. From the vapor-pressure equation, the enthalpy of disproportionation of europium dicarbide is calculated to be 51.06 ± 1.25 kcal/gfw by a second-law treatment of the data, and 51.24 ± 2.0 kcal/gfw by the third-law method. The entropy of dissociation is calculated to be 18.43 ± 1.70 eu/gfw. Combination of these data with the reported enthalpy and entropy of vaporization of elemental europium gives −9.17 ± 1.15 kcal/gfw as the standard heat of formation and −7.47 ± 1.87 kcal/gfw as the standard free energy of formation of europium dicarbide. (auth)

20667 CONCENTRATION BROADENING AND OSCILLATOR STRENGTHS IN Pr:$LaCl_3$. Dorman, E. (Johns Hopkins Univ., Baltimore). J. Chem. Phys., 44: 2910-16(Apr. 15, 1966).

The absorption and fluorescence spectra of Pr^{3+} in $LaCl_3$ were examined for molar concentrations of 0.26%, 2%, 15%, 50%, 85%, and 100%, and were used to determine the effect of concentration on the energy levels and transitions of the ion. A model is advanced to explain the concentration broadening of spectral lines in crystals as due to heterogeneity of the lattice and resonance interaction between the spectroscopically active ions. Oscillator strengths were measured for the dilute crystal and the ratio of the strength of the ion-pair absorption $^3P_0 + {}^3F_2$ ($\mu = 2$) to that of $^3P_0$, in $PrCl_3$, was found to be 1.3×10^{-5}. (auth)

20668 ELECTRON PARAMAGNETIC RESONANCE STUDY OF SOLUTIONS OF EUROPIUM IN LIQUID AMMONIA. Thompson, D. S.; Hazen, E. E.; Waugh, J. S. (Massachusetts Inst. of Tech., Cambridge). Contract DA-36-039-AMC-03200(E). J. Chem. Phys., 44: 2954-8 (Apr. 15, 1966).

The electron spin resonance spectrum of a solution of Eu in liquid ammonia consists of a single line characteristic of the solvated electron and a complex hyperfine pattern which is shown to arise from Eu^{2+}, $^8S_{7/2}$ with a small admixture of excited states. T_2 for the electron decreases sharply with increasing concentration in contrast with other metal−ammonia solutions, whereas the change in T_2 for the Eu^{2+} is slight. The solutions decompose by a heterogeneous mechanism that involves strong adsorption on the walls of the container. (auth)

20669 URANIUM MONOSULFIDE. III. THERMOCHEMISTRY, PARTIAL PRESSURES, AND DISSOCIATION ENERGIES OF US AND US_2. Cater, E. David (Univ. of Iowa, Iowa City); Rauh, E. G.; Thorn, R. J. Contract AT(11-1)-1182. J. Chem. Phys., 44: 3106-11(Apr. 15, 1966).

A mass-spectrometric study of the sublimation of uranium monosulfide was performed over the temperature range 1825° to 2400°K. The data are combined with the previous measurements of absolute rate of effusion by means of a new method of calculation which effects an absolute pressure calibration of the spectrometer and allows a determination of the partial pressures of U, US, US_2 in the vapor, the enthalpies and entropies of sublimation to atoms and molecules, and the dissociation energies of US and US_2. The partial pressures of U, US, and US_2 at 2020°K are in the ratios 1/0.27/0.001. The data for the several sublimation processes are presented. The dissociation energies for US and US_2 and the estimated uncertainties are $D_0(US)$ = 133.8 ± 2.3 kcal/mole or 5.80 ± 0.10 ev, $D_0(US_2)$ = 252 ± 4 kcal/mole or 10.9 ± 0.2 ev. (auth)

20670 ELECTRONIC CONDUCTIVITY OF DEFECTIVE ANODIC TANTALUM OXIDE FILMS. Klein, Gerhart P. (P. R. Mallory and Co. Inc., Burlington, Mass.). J. Electrochem. Soc., 113: 348-57(Apr. 1966).

The conditions under which anodic oxide films on tantalum showed electronic conductivity were studied using an electrochemical printing-out technique with starch-iodide as the redox indicator. The sensitivity for the detection of electronic charge was approximately 1 millicoulomb/cm^2. The effect of alloying (contamination), thermal oxidation, plastic deformation, and surface topography were investigated with regard to their contribution to the electronic conductivity of anodic oxide films on mechanically treated ("rough") tantalum surfaces. It was concluded that impurities alone were responsible for the electronic conductivity even in cases where supposedly clean tantalum was abraded with tantalum. Roughness by itself was not a sufficient condition for electronic conductivity. (auth)

20671 REACTION OF TANTALUM WITH MOLTEN CERIUM−COBALT ALLOYS. Litton, Felix B.; Biery, John C. (Univ. of California, Los Alamos, N. Mex.). J. Electrochem. Soc., 113: 371-6(Apr. 1966). (LA-DC-6431).

The reaction of tantalum with molten cerium−cobalt was investigated by heating alloys containing from 6 to 18 wt % cobalt in sealed tantalum capsules at temperatures from 600 to 800°C and at times from 4 to 2069 hr. At 800°C, with 18 wt % cobalt−cerium alloy, reaction layers formed, which varied in thickness with time from 5 to 16μ. The reaction layer consisted of two separate zones. The inner diffusion zone contained discrete particles of cerium distributed in a tantalum−cobalt alloy, TaCo or Ta_2CO. The composition of the molten cerium−cobalt alloy, temperature, and reaction time controlled the composition and growth of the reaction layer. The tantalum−cobalt phase identified as Ta_2Co was predominant in layers formed from cerium−cobalt containing 12 wt % cobalt, while either TaCo or Ta_6Co_7 was predominant in the layer formed from cerium−cobalt containing 18 wt % cobalt. The sequential steps in the formation of the reaction layer are as follows: dissolution of tantalum, precipitation of Ta−Co crystals on the Ta surface, diffusion of Co into and Ta out from an

inner diffusion zone, and continued precipitation of a tantalum–cobalt alloy from the liquid cerium–cobalt melt onto the outer layer. The growth rate at long times was controlled by diffusion of tantalum and cobalt through the outer precipitation layer. (auth)

20672 STANDARD MOLAR FREE ENERGY OF FORMATION OF URANIUM DICARBIDE AND URANIUM SESQUICARBIDE BY ELECTROMOTIVE FORCE MEASUREMENTS. Behl, W. K.; Egan, J. J. (Brookhaven National Lab., Upton, N. Y.). J. Electrochem. Soc., 113: 376-8(Apr. 1966). (BNL-9710).

The free energies of formation of UC_2 and U_2C_3 were determined by means of the following solid state galvanic cells operated between 700 and 900°C $U,UF_3(s)|CaF_2(s)|UF_3,UC_2,C$ [A] and $U,UF_3(s)|CaF_2(s)|UF_3,U_2C_3,C$ [B]. Although UC_2 is in metastable equilibrium with carbon in cell A, results are significant. Experimental details are presented and results are compared with values obtained by other techniques. (auth)

20673 STUDIES IN COMPLEX FORMATION OF METAL IONS WITH TROPOLONES. PART II. DISSOCIATION CONSTANTS OF SOME TROPOLONES AND COMPOSITION AND STABILITY OF URANYL COMPLEXES. Dutt, Yag; Singh, R. P. (Univ. of Delhi). J. Indian Chem. Soc., 42: 767-72(Nov. 1965).

Dissociation constants of β-methyl-, α-carboxy-β-methyl-, and β-isopropyl-tropolones were determined potentiometrically in 0.5M KNO_3 and 50% ethanolic medium. The stability constants, log K_1 and log K_2, of the uranyl complexes with the above reagents were determined potentiometrically and spectrophotometrically. (auth)

20674 THORIUM AND MOLYBDENUM COMPLEXES WITH MYRICETIN. Gupta, B. P.; Katyal, Mohan; Singh, R. P. (Univ. of Delhi). J. Indian Chem. Soc., 42: 811-13(Nov. 1965).

The molybdenum and thorium complexes with myricetin were deep yellow in color. The absorption spectra were measured at different pHs. The composition of both complexes was found to have a molecular ratio of 1:1 by Job's method. The stability constants of molybdenum and thorium calculated from Job's curves at pH 2.0 for Mo and at pH 2.0 and at 420 mμ for Th were 4.2×10^4 (at 20°C) and 3.58×10^4 (at 20°C), respectively. (F.J.H.)

20675 THE CHEMISTRY OF URANIUM(IV). I. URANIUM-OXYGEN BONDS IN SOME PRODUCTS DERIVED FROM THE HYDROLYSIS OF UCl_4. Selbin, J.; Schober, M. (Louisiana State Univ., Baton Rouge). J. Inorg. Nucl. Chem., 28: 817-23(Mar. 1966).

In an attempt to find evidence for or against the existence of a UO^{2+} entity, infrared spectra of some U(IV) compounds were examined. UCl_4 dissolved in H_2O (or D_2O) yielded a product believed to be primarily a mixture of $[U(H_2O)_6OH]_2Cl_6$ and $[U(H_2O)_6(OH)_xCl_{1-x}]_2Cl_6$. DTA curves showed endothermic peaks at 80, 120, 154, and 190°C (with jagged shoulders at 170, 192, and 196°C) and so four products (and the four corresponding deuterium analogs) were obtained on a preparative scale: $UCl_3(OH)\cdot 3H_2O$, $UCl_3(OH)\cdot 1.5H_2O$, $UCl_{2.5}(OH)_{1.5}$, and $UO_{1.15}Cl_{2.1}$. These were examined by infrared in the 4000 to 250 cm^{-1} region. Bands at about 735 and 720 cm^{-1} are probably due to antisymmetric and symmetric stretching vibrations of a unit (O–U–O) in a chain or large ring polymeric structure and the uranium–oxygen bonds are undoubtedly of order greater than one, but less than two. Lower frequency bands at about 560, 500, and 430 cm^{-1} appeared to be ν(U–O) modes arising from bridging and terminal OH^- groups and H_2O. Absent from the spectra were strong, sharp bands in the metal–oxygen multiple-bond region although weak bands at about 965 and 930 cm^{-1} cannot be unambiguously assigned. (auth)

20676 PREPARATION OF THE SULFIDES AND PHOSPHIDES OF PLUTONIUM. Kruger, O. L.; Moser, J. B. (Argonne National Lab., Ill.). J. Inorg. Nucl. Chem., 28: 825-32(Mar. 1966).

The sulfides and phosphides of plutonium were synthesized by reaction of high-purity metal with gases. A fine powder of reduced plutonium hydride was reacted with hydrogen sulfide or phosphine over the temperature ranged from 400 to 600°C. The reaction products were characterized by means of chemical analysis, metallographic examination and lattice constant measurements. The melting point of plutonium monosulfide was 2350°C. Plutonium monophosphide melted and decomposed at 2600°C. (auth)

20677 POLAROGRAPHY OF URANYL-SEMICARBAZIDE HYDROCHLORIDE COMPLEXES. Lai, Tsai-Teh; Wu, Che-Kuang (Cheng Kung Univ., Tainan, Taiwan). J. Inorg. Nucl. Chem., 28: 869-73(Mar. 1966).

The complex formation of uranyl ion with semicarbazide hydrochloride was studied polarographically. The concentration dissociation constant of the semicarbazidonium ion, 2.0×10^{-4}, for ionic strength 0.60 to 0.80, obtained from potentiometric titration was in excellent agreement with the polarographically determined value. The complex was proved to involve one chloride as the complexing species. This behavior was distinctly different from the previous report, which showed that two chlorides existed as simple anions. (auth)

20678 ON THE PREPARATION OF XeF_2. Groz, P.; Kiss, I.; Revesz, A.; Sipos, T. (Central Research Inst. for Physics, Budapest). J. Inorg. Nucl. Chem., 28: 909-10(Mar. 1966).

A mixture of F_2 and Xe gas both of 99.9% purity was used to prepare XeF_2. The gases were heated in a reactor that was filled with small nickel plates that could be heated by a resistance furnace to 600°C. The gas was circulated under pressure by means of a teflon fan, and the product was frozen out in a trap kept below 0°C. The product consisted of well-shaped colorless crystals of the monoclinic system that melted at 130 ± 0.6°C. The product was analyzed by different methods. The mass spectra of the unrefined crystals and a sublimated product are shown. The results seemed to confirm the assumption of Malm et al. in that some of the chemical properties previously described are more characteristic of XeF_2 than of XeF_4. The chemical and physical properties in various solutions at low temperatures, and radiation effects on the xenon fluorides were determined. The gases evolved on irradiation in a quartz tube were mainly D_2, Xe, and SiF_4. (F.J.H.)

20679 SUPPOSED COMPLEXES OF URANIUM(VI) AND URANIUM(IV) WITH TRIPHENYLPHOSPHINE. Fitzsimmons, B. W.; Gans, P.; Hayton, B.; Smith, B. C. (Univ. of London). J. Inorg. Nucl. Chem., 28: 915(Mar. 1966).

The reaction between uranyl chloride and triphenylphosphine in boiling n-butyl alcohol was previously reported to give a complex, $UO_2Cl_2\cdot 2Ph_3P$, Mp 288°C. It was found that the reaction did not occur except in the presence of air, yielding a complex of triphenylphosphine oxide, $UO_2Cl_2\ 2Ph_3PO$, Mp 295°C, that showed a P=O stretching bond at 1070 cm^{-1}. No reaction was observed between triphenylphosphine and uranyl bromide or uranyl nitrate in cyclohexanol or uranyl iodide in diethyl ether, except in the presence of air. The products and melting points are given. The P=O stretching bond in the compounds appeared at 1080, 1060, and 1060 cm^{-1}, respectively. The effects of hydrochloric acid and zinc on the reaction of uranyl chloride with triphenylphosphine in cyclohexanol are given. (F.J.H.)

20680 PRODUCTION AND PROPERTIES OF CERIUM AND LANTHANUM OXYCHLORIDES. Matthes, F.; Haeseler, G.; Poeschl, R. (Technische Hochschule fuer Chemie Carl Schorlemmer, Leuna-Merseburg, Ger.). J. Less-Common Metals, 10: 344-7(May 1966). (In German).

The oxychlorides of cerium and lanthanum were prepared in a KCl-melt and their properties investigated. (auth)

20681 THIN LAYERS OF LANTHANUM FLUORIDE STUDIED BY ELECTRON MICROSCOPY. Bourg, Antoin-

ette (Faculte des Sciences, Marseille). J. Microscop., 4: 313-8(June 1965). (In French).

Thin layers of LaF_3 were prepared by thermal evaporation in a vacuum of 10^{-5} torr. Amorphous silica, fluorite, and C were used as supports. These materials were examined by shadowing with Pt, by electron microscopy, or by x-ray diffraction. They were maintained at 25, 100, 200, 300, and 500°C during the various projections. Thin layers on silica of less than 1000 Å thickness were nearly circular globules 2500 Å in diameter. Between 1000 and 5000 Å they appeared granular, and with greater than 5000 Å thickness linear boundaries were noted. Surface irregularities were about 100 Å high. Thin layers on C had a uniform, granular appearance, and crystallized without preferential orientation. On fluorite the layers had a striated appearance, with valleys, and were very poorly crystallized. Data taken at higher temperatures were similar to that at 25°C. Data for silica supports differed by the absence of linear boundaries until 12,000 to 13,000 Å, and an increase in height of surface irregularities with temperature. No great changes were noted for C supports; once again the crystallites were relatively large and had no preferential orientation. Deposits on fluorite were better crystallized at higher temperatures and at 500°C showed orientation. (BBB)

20682 STUDIES ON THE FORMATION OF COMPLEX COMPOUNDS BETWEEN RARE EARTH NITRATE AND URANYL NITRATE. THE SYSTEM: $Ce(NO_3)_3$–$UO_2(NO_3)_2$–H_2O (CONDUCTANCE, pH, SPECTROPHOTOMETRY, REFRACTIVE-INDEX). Gupta, S. S.; Marwah, S. D. (Lucknow Univ., India). J. Prakt. Chem., 29: 1-7(July 1965).

Data collected on conductance, pH, spectrophotometry, and refractive index of a series of mixed solutions of uranyl nitrate and cerous nitrate indicated the existence of the following compounds: $Ce(NO_3)_3 \cdot UO_2(NO_3)_2$ and $2Ce(NO_3)_3 \cdot UO_2(NO_3)_2$. A set of 22 mixed solutions was prepared by the monovariation method. In all the solutions the concentration of uranyl nitrate was kept constant (at 0.01M) while that of cerous nitrate was varied systematically (from 0.0 to 0.042M). When the data were plotted against the varying concentration of cerous nitrate, two breaks were obtained in the regular curves at concentrations corresponding to the compound having the above formulas. The results obtained in all these physicochemical studies were in good agreement thus leading to the same conclusions. (BBB)

20683 DETERMINATION OF THE ION ADSORPTION BY THE RADIOACTIVE TRACER TECHNIQUE. Herak, M. J.; Mirnik, M. (Inst. Rudjer Boskovic, Zagreb). Kolloid-Z., 205: 129-34(Oct. 1965).

Studies using radioisotopes to examine the adsorption of counter ions in the region of coagulating concentrations are described. When two counter ions were present in the system, it was possible to demonstrate that silver iodide is an ideal ion exchanger for which the classical thermodynamic principles in ion exchange are valid. It was also demonstrated that the same principles may be valid in the vicinity of the coagulation value, when the total concentration of the counter ions present is less than that value. Experiments with Co^{2+}, Eu^{3+}, and Na^+ were extended to the region of concentrations lower than the coagulation value of a single counter ion present, and the influence of the stable and coagulated form of AgI on the plot of absorbed quantity vs counter ion concentration was established. The adsorbed amount of a dried AgI was about ten times lower than that of fresh coagulated AgI. At pH 6.2, 100% of $Eu(OH)_3$, from a 2×10^{-4} solution was precipitated while the amount precipitated increased slowly from 1 to several percent in the region of pH 3 to 5. Similarly, the amount adsorbed increased up to about 4 mg equivalents per g-mole of AgI in the region of pH 3 to 6 where a steep increase could be observed indicating the onset of the precipitation of $Eu(OH)_3$. (TCO)

20684 MOESSBAUER SPECTROSCOPY: SOME RECENT APPLICATIONS TO CHEMICAL PROBLEMS. Herber, Rolfe H. (Rutgers, State Univ., New Brunswick, N. J.). pp 3-12 of Moessbauer Effect Methodology. Vol. 1. Gruverman, Irwin J. (ed.). New York, Plenum Press, 1965.

Standards in chemical Mössbauer spectroscopy are discussed briefly. Characteristics of sodium nitroprusside that make it the recommended standard absorber for ^{57}Fe Mössbauer work are listed. Mössbauer studies of the molecular structure of ^{119}Sn compounds, particularly SnH_4, are reviewed. Tables show isomer shifts for several source matrices and reference absorbers from the nitroprusside standard and Mössbauer data for five- and six-coordinate organotin compounds. (29 references) (A.G.W.)

20685 NEW BORIDES WITH THE $Cr_{23}C_6$ STRUCTURE. Ganglberger, E.; Nowotny, H.; Benesovsky, F. (Univ., Vienna). Monatsh. Chem., 96: 1144-6(1965). (In German).

The existence of several τ phases in the systems $Ni_{23-x}T_xB_6$ and $Co_{23-x}T_xB_6$, where T may be U, Ti, Zr, Hf, or V, is reported. These phases have the $Cr_{23}C_6$ structure, possess a relatively broad homogeneous region, and are in equilibrium with the corresponding binary systems. They are prepared by cold pressing of powder mixtures of high purity, followed by reaction in a quartz vessel at 1000 to 1100°C for 10 to 20 hr. There was very slight attack of the quartz vessel under these conditions. Samples were taken from the centers of the preparations for roentgenographic study. Lattice constants found by evaluation of the CrKα and CuKα patterns are as follows: $Co_{21}U_2B_6$, 10.62Å; $Ni_{21}U_2B_6$, 10.65; $Co_{20}Ti_3B_6$, 10.54; $Ni_{20}Ti_3B_6$, 10.58; $Co_{21}Zr_2B_6$, 10.58; $Ni_{20}Zr_3B_6$, 10.59; $Co_{21}Hf_2B_6$, 10.57; $Ni_{20}Hf_3B_6$, 10.65; $Co_{21}V_2B_6$, 1049; $Ni_{21}V_2B_6$, 10.48; $Co_{21}Nb_2B_6$, 10.52; $Co_{21}Mo_2B_6$, 10.50; $Co_{21}W_2B_6$, 10.51; $Ni_{21}Mn_2B_6$, 10.50; $Co_{21}In_2B_6$, 10.58; $Ni_{21}Sb_2B_6$, 10.60; and $Co_{21}Sb_2B_6$, 10.60. The $Ni_{21}U_2B_6$ and $Co_{21}Nb_2B_6$ preparations contained a second phase as well. (BBB)

20686 THE DISSOLUTION OF RARE EARTH METALS IN METHANOLIC SOLUTIONS OF AMMONIUM ACETATE AND THE PREPARATION OF COMPOUNDS OF THE TYPES $Ln(OAc)_3.3\ NH_4OAc.1\ H_2O$, AND $Ln(OAc)_3.1\ NH_4OAc.1\ H_2O$. Mikler, J.; Auer-Welsbach, Helga (Univ., Vienna). Monatsh. Chem., 96: 2019-24(1965). (In German).

The solubility of rare earth oxides in alcohols (methyl, ethyl, propyl, isopropyl) in the presence of ammonia was investigated. The oxides of the lanthanides and yttrium were dissolved by heating (110 to 120°C) in methanolic ammonium acetate solutions. From the solutions obtained, compounds of the type $Ln(OAc)_3 \cdot 3\ NH_4OAc \cdot 1\ H_2O$ (Ln = La, Ce, Pr, Nd, Sm, Eu, Gd, Tb, Dy, Ho) and $Ln(OAc)_3 \cdot 1\ NH_4OAc \cdot 1\ H_2O$ (Ln = E, Yb, Y), respectively, could be isolated. The higher oxides $PrO_{1.83}$ and $TbO_{1.75}$ reacted incompletely and disproportionation of valence was observed. The residues consisted of PrO_2 and TbO_2, respectively. Possible ways of formulating the compounds in question are proposed and reasons for favoring certain forms are considered. (BBB)

20687 MELTING POINT DETERMINATION OF URANIUM MONOPHOSPHIDE. Baskin, Y. Nucl. Sci. Eng., 24: 332-5(1966).

The melting point of stoichiometric uranium monophosphide (UP) was found to be 2610 ± 20°C. The pellet was sealed in a tungsten crucible and gamma radiography was used to determine when the sample had filled the lower crucible cavity. The UP was stoichiometric before and after melting and was presumed to be in equilibrium with its vapor at elevated temperatures. Composition of the melted material and the reaction between UP and tungsten were examined using x-ray diffraction, metallographic and chemical analysis. (auth)

20688 CLATHRATE COMPOUNDS OF p-CRESOL WITH RARE GASES. PART 1. COMPOUND OF p-CRESOL WITH XENON. Trofimov, A. M.; Kazankin, Yu. N. Radiokhimiya, 7: 288-92(1965). (In Russian).

Xenon was reacted with p-cresol, and the formula of the clathrate formed was calculated by analyzing curves of the

vapor pressure over the solid phase and over the region where both the solid and the liquid phase are present. The compound was assigned the formula $Xe \cdot 6C_7H_8O$. A gravimetric analysis of the compound confirmed this formula. The dissociation pressure of the compound at 25 to 35°C was determined, and from these data, the heat of formation of $Xe \cdot 6C_7H_8O$ from solid and liquid p-cresol was calculated to be 6100 and 23000 cal/mole, respectively. The apparatus used in the synthesis and in the measurements of the vapor pressure is described. (CFSTI)

20689 RATE OF OXIDATION OF TETRAVALENT URANIUM IONS WITH MOLECULAR OXYGEN. Sobkowski, Jerzy (Univ., Warsaw). Rocz. Chem., 40: 271-80 (1966).

The oxidation reaction of U(IV) ions with molecular oxygen was investigated in relation to hydrogen ion concentration, presence of sulfate ions, illumination, and temperature. (auth)

20690 PRECIPITATE FORMATION IN THE STRONTIUM–PHOSPHATE SYSTEM. Collin, Robert L. (New England Deaconess Hospital, Boston). Science, 151: 1386-8(Mar. 18, 1966).

Study of the precipitation process in the aqueous $Sr(OH)_2$–H_3PO_4 system, in order to elucidate the phase transformations and the nature of the final solid phases, shows that over much of the range of compositions studied the initial precipitate is poorly crystalline; the x-ray pattern resembles that of strontium hydroxyapatite but has a strontium : phosphorus molar ratio close to 1.3. Within 1 hour the initial precipitate changes to a stable crystalline phase (or phases), with corresponding change, either up or down, in the strontium : phosphorus ratio. At high ratios of $Sr(OH)_2$ to H_3PO_4 the initial precipitate is $Sr_3(PO_4)_2 \cdot 4H_2O$, which then converts to a phase having the x-ray diffraction pattern of strontium hydroxyapatite, but having a strontium : phosphorus ratio that depends somewhat on the initial ratio of $Sr(OH)_2$ to H_3PO_4 used in the precipitation. (auth)

20691 OXYGEN ISOTOPE FRACTIONATION IN THE SYSTEM DOLOMITE–CALCITE–CARBON DIOXIDE. O'Neil, James R.; Epstein, Samuel (California Inst. of Tech., Pasadena). Science, 152: 198-200(Apr. 8, 1966).

Oxygen isotopes were equilibrated between carbon dioxide and calcite at four temperatures in the range from 350 to 610°C and between carbon dioxide and dolomite at 350 and 400°C. Carbon of unusual isotopic composition was used as a tracer to demonstrate the nature and extent of the exchange process. Extrapolation of these data at lower temperatures indicated that at 25°C dolomite is enriched in ^{18}O by 6.8 per mil with respect to calcite. This result indicated that those natural dolomite-calcite assemblages that show very small fractionations were not formed in isotopic equilibrium. (auth)

20692 STUDY ON THE DEOXIDATION AND DESULFURIZATION OF LIQUID IRON BY URANIUM. Narita, Kiichi; Koyama, Shinji (Kobe Steel Works, Ltd., Japan). Trans. Jap. Inst. Metals, 6: 197-202(Oct, 1965).

Uranium oxide and sulfide formed in iron and steel were examined by optical microscopy, electron microscopy, electron diffraction, and x-ray diffraction. From the results, it was concluded that various molecular species of uranium oxide, oxysulfide, and sulfide, such as UO_2, UOS, and US, are formed, depending on the relative ratio of the oxygen and sulfur contents in iron and steel. In a common steelmaking condition, however, chemical reactions in liquid steel result mainly in formation of UO_2 and US as the deoxidation and desulfurization products. Since uranium has a very large affinity to such elements as oxygen and sulfur, it is difficult to determine the equilibrium constants of the deoxidation reaction $\underline{U} + 2\underline{O} = UO_2$ and the desulfurization reaction $\underline{U} + \underline{S} = US$. Therefore, from calculations of the thermodynamic data using some simple assumptions, the deoxidizing and desulfurizing powers of uranium in liquid iron can be expressed by the following formulas: $\log [a_O] = -0.5 \log [a_U] - 6.06$; and $\log [a_S] = -\log [a_U] - 4.33$ (at 1600°C). (auth)

20693 CHELATES OF β-DIKETONE DERIVATIVES. II. STABILITY INVESTIGATIONS ON METAL COMPLEXES OF THIODIBENZOYLMETHANE. Uhlemann, E.; Suchan, W. W. (Karl-Marx-Univ., Leipzig). Z. Anorg. Allg. Chem., 342: 41-5(Jan. 1966). (In German).

As a measure of the stability of the chelate ring of β-diketone derivatives, the enol dissociation constant and the stability constants of the Zn, Cd, Pb(II), Mn(II), U(VI), and Be complexes of thiodibenzoylmethane were determined potentiometrically in dioxane–water (75% dioxane) and compared with the constants for the corresponding chelates of dibenzoylmethane. In continuation of former work, the chelates of Cd, U(VI), Ag(I), and Tl(I) were isolated in the solid state. A yellow compound of the same analytical composition as thiodibenzoylmethane, easily obtainable from the latter, was shown, by potentiometric, polarographic and NMR methods, to be the corresponding disulfide. (auth)

20694 LATTICE CONSTANTS AND SPACE GROUPS OF THE ISOTYPE COMPOUNDS $Eu(OH)_2.H_2O$, $Sr(OH)_2.H_2O$, AND $Ba(OH)_2.H_2O$. Baernighausen, H. (Univ., Freiburg i. B.). Z. Anorg. Allg. Chem., 342: 233-9(Feb. 1966). (In German).

The decomposition of Eu_3O_4 in a normal atmosphere yields, in addition to $Eu(OH)_3$, the compound $Eu(OH)_2 \cdot H_2O$ for which the preparation and properties are described. According to Guinier photographs, $Eu(OH)_2 \cdot H_2O$ crystallizes in the orthorhombic space group $C_{2v}^2 - P2_1am$ and is isostructural with both $Sr(OH)_2 \cdot H_2O$ and $Ba(OH)_2 \cdot H_2O$. The lattice constants of the three compounds and the interplanar spacings d(hkl) are given. (auth)

20695 ON THE MOBILITY OF LITHIUM ISOTOPES IN MOLTEN ^6LiCl AND ^7LiCl. Lenke, R.; Klemm, A. (Max-Planck-Institut fuer Chemie, Mainz). Z. Naturforsch., 20a: 1723-4(Dec. 1965). (In German).

The conductivity ratio of fused isotopically pure ^6LiCl and ^7LiCl was determined at 680°C as 1.050 ± 0.002. That the quotient of the self-mobilities of the lithium isotopes relative to chlorine was only 1.05 indicated that the mass of the chlorine ion enters into these mobilities. From the difference between the self-mobilities of the lithium isotopes relative to chlorine, the existence of interactions of lithium ions with each other was indicated. The mass effects for the self-mobilities and the mixed mobilities of the cations are defined and discussed. (J.S.R.)

20696 RADIOCHROMATOGRAPHIC DETERMINATION OF MICROQUANTITIES OF ^{137}Cs SORPTION BY SOIL, CLAY, AND MICA. Kokotov, Yu. A.; Popova, R. F. pp 76-9 of Radiokhimicheskie Metody Opredeleniya Mikroelementov. Moscow-Leningrad, Izdatel'stvo Nauka, 1965. (In Russian).

Radiochromatographic experiments were carried out on the desorption of cesium-137 in order to shed some light on the mechanism of sorption of this isotope by soils and clays. An analysis of chromatograms showed that ^{137}Cs is sorbed simultaneously by ion exchange (with a relatively high selectivity of sorption) and fixation. The fraction of ^{137}Cs fixed during sorption by various clays, clay minerals, micas, and soils was determined. It was found that ^{137}Cs is fixed most extensively on vermiculites (particularly on hydrobiotite) and black earth. The lowest fixation was observed on kaolinite and red earth. The ability of soils to fix trace amounts of ^{137}Cs is not a function of the mechanical composition of the soil alone, since it is also a function of the mineralogical composition. It is suggested that the differences in the degree of fixation of trace amounts of ^{137}Cs are one of the reasons for differences in the assimilation of this isotope by plants on these soils. (ATD)

20697 CHEMISTRY OF TECHNETIUM AND RHENIUM. Peacock, R. D. Topics in Inorganic and General Chemistry. Monograph 6. New York, Elsevier Publishing Company, 1966. 144p. $10.00.

The chemistry of rhenium and technetium is discussed as follows: discovery and isolation of rhenium and technetium; general and elementary properties; oxides; oxoacids and

oxosalts; halides and oxide halides; complex halides, complex oxide halides and complex hydrides; chalcogenides and compounds with nonmetal and metalloids alloys; complex cyanides and related compounds; carbonyls and organometallic derivatives; compounds with group V and VI ligands; and analysis. (F.J.H.)

20698 ADVANCES IN QUANTUM CHEMISTRY. VOLUME 2. Loewdin, Per-Olov (ed.). New York, Academic Press, 1965. 380p.

Advances in quantum chemistry are discussed as follows: quantum calculations, which are accumulative in accuracy, unrestricted in expansion functions, and economical in computation; zero differential overlap in π-electron theories; theory of atomic hyperfine structure; theory of pair-correlated wave functions; quantum chemistry and crystal physics, stability of crystals of rare gas atoms and alkali halides in terms of three-atom and three-ion exchange interactions; charge fluctuation interactions in molecular biophysics; and quantum genetics and the aperiodic solid. Some aspects of the biological problems of heredity, mutations, aging, and tumors are considered in view of the quantum theory of the DNA molecule. (F.J.H.)

20699 LA RESONANCE QUADRIPOLAIRE NUCLEAIRE ET SES APPLICATIONS A LA CHIMIE. (Nuclear Quadrupole Resonance and its Applications in Chemistry). Dereppe, Jean Marie; Gobillon, Yves; Lobo, Pedro W. Publication No. 36. Tucuman, Universidad Nacional, 1964. 47p.

A review is given of nuclear quadrupole resonance and its applications in chemistry. The theory and experimental techniques are described. Examples are given. It is shown that nuclear quadrupole resonance makes it possible to obtain semiquantitative results on chemical bonds and with it the charge distributions predicted by other methods can be easily verified. It is a method for investigating various phenomena such as the effects of pressure, temperature, impurities, and radiations. It is effective in the determination of crystalline structures. (J.S.R.)

20700 ACETYLACETONATES OF TRANSITION METALS AND RARE EARTH METALS. Sjoblom, J. J. (TRG, Inc., Melville, N. Y.). 8p. (CONF-650804–15). ORINS. Gmelin, AED-CONF-65-208-14.

From 5th Rare Earth Research Conference, Ames, Iowa.

Crystalline metal acetylacetonates were investigated to find experimental media containing spectral lime emitters such as chromic ions and europium or dysprosium ions. Procedures were worked out for the preparation of pure crystalline acetylacetonates of aluminum, chromium, yttrium, europium, and dysprosium with the aluminum and yttrium chelates to serve as host crystals. A method was devised for growing crystals of aluminum acetylacetonate doped with chromic acetylacetonate. In addition, molecular metal chelates were believed capable of existence in solid solution with a dissimilar diluent. However, theoretical and experimental tests of this solid solution type have brought out its limitations. (auth)

20701 ISOTOPIC EXCHANGE REACTIONS OF TRANS-HYDRIDOCHLOROBIS(TRIETHYLPHOSPHINE) PLATINUM(II). Halpern, J.; Falk, C. D. (Univ. of Chicago). Vienna, International Atomic Energy Agency, 1965, Preprint No. SM-64/23, 16p. (CONF-650549–15). ORINS.

From IAEA Symposium on Exchange Reactions, Upton, N. Y.

The kinetics of the isotopic substitution reaction, (where Et = C_2H_5), trans-$HPtCl(PEt_3)_2 + D_2O \rightarrow$ trans-$DPtCl(PEt_3)_2 +$ HDO, in aqueous acetone solution were studied. The decrease in the intensity of the Pt–H infrared band at 2196 cm^{-1} was used to follow the reaction. The reaction was found to be catalyzed by D^+ and Cl^- according to a rate-law approximate to: $-d[HPtCl(PEt_3)_2]/dt = (k_1 + k_2[Cl^-])[D^+][HPtCl(PEt_3)_2]$ where $k_1 = 4.1 \times 10^{-2} M^{-1}sec^{-1}$ and $k_2 = 6.0 M^{-2}sec^{-1}$ at 30°C in 75% acetone–25% D_2O by volume. Both k_1 and k_2 exhibited an inverse dependence on the D_2O content of the solvent. The Cl^--catalyzed exchange path, corresponding to the k_2 term in the rate-law was interpreted in terms of a mechanism involving reversible addition of DCl to the coordination shell of the platinum complex to give a hexacoordinated Pt(IV) intermediate. An analogous mechanism in which a solvent molecule replaces the entering Cl^- ion is invoked to account for the Cl^--independent (i.e., k_1) path. This interpretation predicts that the Cl^--catalyzed substitution of H by D should be accompanied by exchange of the Cl ligand of the complex with isotopically-labeled Cl^- in the solution. Experiments to test this are in progress. (auth)

20702 THE STUDY OF COMPOUNDS FORMED AT TEMPERATURES ABOVE 600 deg C BY THE ACTION OF CARBON DIOXIDE ON GRAPHITE. Lang, F. M.; May, S.; Goenvec, H.; de Noblet, M.; Chenion, J. 7p. (CONF-650632–8). ORINS. Gmelin, AED-CONF-65-149-3.

From 7th Biennial Conference on Carbon, Cleveland.

The formation of compounds at temperatures above 600°C by the action of carbon dioxide on graphite was studied. The three methods used for the study consisted of using ^{14}C-labeled carbon dioxide, thermal degassing under vacuum, and using ^{18}O-enriched carbon dioxide. The coverage of the BET surface was found to be less than 0.5%. (F.J.H.)

20703 2,2'-DIPYRIDYL COMPLEXES OF RARE EARTHS. III. CHANGE IN FLUORESCENCE INTENSITIES OF EUROPIUM AND TERBIUM CHELATES ON LIGAND SUBSTITUTION. Sinha, S. P. (Cyanamid European Research Inst., Cologny, Switzerland). 12p. (CONF-650804–18). ORINS. Gmelin, AED-CONF-65-208-5.

From 5th Rare Earth Research Conference, Ames, Iowa.

A semiquantitative comparison of fluorescence intensities of unsubstituted and para-dimethyl-substituted dipyridyl chelates of trivalent europium and terbium is presented. The electron-donating methyl groups increased the overall intensity for both europium and terbium chelates. However, in case of europium the intensity ratio for the two transitions from $^5D_0$ to $^7F_1$ and $^7F_2$ levels were not of the same order of magnitude. The values for all transitions of terbium were roughly the same. (auth)

20704 PROCEEDINGS OF THE FOURTH CONFERENCE ON RARE EARTH RESEARCH, APRIL 22–25, 1964 HELD AT PHOENIX, ARIZONA. Eyring, LeRoy (ed.). New York, Gordon and Breach Science Publishers, 1965. 765p. (CONF-405).

Formalized papers of presentations made at the Fourth Rare Earth Research Conference are given. Topics covered by the 46 papers include: magnetic and electrical properties of rare earth compounds, properties of rare earth metals and alloys, optical properties and solution chemistry of rare earth materials and solid-state chemistry of rare earth materials. For abstract numbers of individual papers see CONF-405 in the Report Number Index. (M.C.G.)

20705 MECHANISM OF THE REDUCTION OF ADSORBED OXYGEN ON ZIRCONIUM DIOXIDE WITH HYDROGEN. Smith, Tennyson. 26p. (CONF-651017–6). ORAU. Gmelin, AED-CONF-65-289-5.

From Electrochemical Society Meeting, Buffalo.

Using experimental results obtained from the reduction of adsorbed O_2 on nuclear grade ZrO_2 with H_2, four possible reaction mechanisms are proposed. It is concluded that the hydrogen adsorbs on patches of adsorbed oxygen. The adsorbed hydrogen diffuses to the edge of the patch where an oxygen atom is less strongly bonded to the surface, and the oxygen atom and hydrogen molecule then desorb as a water molecule from the edge of the patch. Values are given for the heat of adsorption of hydrogen and for the activation energy of desorption of the hydrogen-oxygen complex. (B.L.M.)

20706 ISOTOPIC LIGAND EXCHANGE OF SOME SIX CO-ORDINATED INORGANIC COMPLEXES WITH HALIDE IONS IN SOLUTION AND IN CRYSTALS. Schmidt, G. B. (Universitaet, Cologne). Vienna, International Atomic Energy Agency, 1965, Preprint No. SM-64/4, 31p. (CONF-650549–1). ORINS.

From IAEA Symposium on Exchange Reactions, Upton, N. Y.

The exchange of ^{82}Br labeled $[Rh(NH_3)_5Br]^{2+}$ and $[Ir(NH_3)_5Br]^{2+}$ complexes with Br^- ions, of trans-$[Rh(en)_2Cl_2]^+$ with Cl^- ions, and of $[OsCl_6]^{--}$ and $[OsI_6]^{--}$ with Cl^- and I^- ions, respectively, was investigated in acid solutions. The iridium pentamminebromo complex exchanges about 60 times slower than the corresponding rhodium pentamminebromo complex. The rate constant for the Rh complex was found to be $k = (1.03 \pm 0.02) \times 10^{-2}$ min^{-1} at 100°C, for the Ir complex $k_{100°C} = 1.7 \times 10^{-4}$ min^{-1}. For both complexes the exchange rate R is first order in the complex concentration; in acid solution R is nearly independent of the bromide and hydrogen concentration as well as of the ionic strength. This indicates that the exchange takes place by a dissociation mechanism. Activation energies of 24 and 23 kcal/mole for the Rh and Ir complexes, respectively, were calculated. Rate constants of the ^{36}Cl isotopic exchange between 60 and 100°C were measured for the trans-$[Rh(en)_2Cl_2]^+$ complex and an Arrhenius activation energy of 25 kcal/mole determined. The increase of the exchange rate R is first order in the complex concentration; but it is only slightly dependent on the hydrogen and chloride concentration. The exchange seems to occur by aquation. In methanolic HCl the exchange rate of this complex is immeasurably slow at 60°C. The halide exchange of $[OsCl_6]^{--}$ and $[OsI_6]^{--}$ was investigated in hydrochloric acid and hydroiodic acid, respectively, in methanolic acid, and in ethanolic acid solution. The rates measured were compared with earlier results of the isotopic exchange of the corresponding hexabromo complex. Displacement reactions of labeled cis- and trans-$[Co(en)_2Cl^*_2]$ Cl and trans-$[Rh(en)_2Cl^*_2]Cl$ in the lattice were studied. The half time of the exchange for both solid isomeric Co complexes is about 4 hr at 140°C. For the Rh complex a half time of about 26 hr was found at 225°C. Activation energies of 30 to 35 kcal/mole were calculated. Exchange increased with the dose in x-ray irradiation. In addition, the thermal exchange of the irradiated crystals was accelerated. In contrast to the ethylendiamine complexes, the solid Rh and Ir pentammine-bromo bromides or chlorides exchange only very slowly by raising the temperature to 210°C. But in the solid complexes "activated" exchange reactions take place if the complex receives excitation energy from a nuclear process such as the $^{80m}Br \rightarrow {}^{80}Br$ isomeric transition. The phenomenon was investigated in some detail. (auth)

20707 FLUORINATION WITH URANIUM HEXAFLUORIDE. Gibbs, Hugh Harper (to E. I. du Pont de Nemours and Co.). U. S. Patent 3,235,608. Feb. 15, 1966. Filed Mar. 19, 1962.

Fluorinated organic compounds selected from the group consisting of 1-12 carbon hydrocarbons, chloro, and chlorofluoro derivatives of 1-12 carbon hydrocarbons can be prepared by contacting a feed mixture of UF_6 and the vapor of the hydrocarbon to be fluorinated with a solid fluoride selected from the group consisting of Na, K, and Ca fluorides at a temperature of 70-600°C and then collecting the fluorinated organic compound. (B.L.M.)

Organic Chemistry

20708 (AEET-213) STUDIES ON THE STABILITIES AND ALLIED PROPERTIES OF ORGANIC COOLANTS. Rao, K. Narayana; Iyer, R. Mahadeva; Rao, K. V. S. Rama; Iyer, Meena; Dayal, S. K.; Panajkar, M. S.; Bhide, K. N. (Atomic Energy Establishment, Trombay (India)). 1965. 20p. Dep. mn.

The thermal stabilities of pure o-terphenyl and m-terphenyl as well as the results of experiments carried out to study the effects of added substances to Santowax-OMI on its stability to reactor radiations are presented. Experiments were also carried out to find a coolant mixture that would be a liquid at room temperature. The solubilities of H, N, and CH_4 in Santowax-OMI at several temperatures up to 350°C were determined. A method for the determination of viscosity of Santowax up to 200°C was standarized. Several polyphenyls required for the identification of the high boiling fractions obtained during the radiolysis of terphenyls were synthesized. (P.C.H.)

20709 (EUR-2442.f) PROPRIETES THERMIQUES DES POLYPHENYLES—DETERMINATION DU DEBUT DE L'EBULLITION NUCLEEE DU TERPHENYLE OM2 EN CONVECTION FORCEE. (Thermal Properties of Polyphenyls—Determination of Inception of Nucleate Boiling in the Terphenyl OM2 in Conditions of Forced Convection). Fiore, A.; Ricque, R. (Commissariat a l'Energie Atomique, Grenoble (France). Centre d'Etudes Nucleaires). Oct. 1965. Contract 162-64-1 ORGF. 26p. Dep. mn.

Description is given of a theoretical method for determining the inception of nucleate boiling in forced convection. The method was applied to the terphenyl used in the loop LO 50 P, in the operating conditions of this loop. A comparison was then made between the theoretical and experimental results. (auth)

20710 (MIT-334-23) FRICTION FACTOR AND HEAT TRANSFER CORRELATION FOR IRRADIATED ORGANIC COOLANTS. Swan, A. H.; Mason, E. A. (Massachusetts Inst. of Tech., Cambridge. Dept. of Nuclear Engineering). Sept. 1965. Contract AT(38-1)-334. 165p. Dep. mn. CFSTI $5.00 cy, $1.00 mn.

Heat transfer and friction factor data were taken on Santowax WR over the Reynolds Number range of $10^4 < Re < 10^5$ and it was found to fit the usual correlations, within an uncertainty of ±10%. A comparison was made of other data by others to try and resolve why some of the data show a Reynolds Number exponent greater than 0.8. The Dittus-Boelter type equation $Nu_B = 0.023\ Re_B^{0.8}\ Pr_B^{0.4}$ or a Colburn-type equation $j^* \equiv St\ Pr_B^{0.6} = 0.023\ Re_B^{-0.2} = f/8$ is recommended to calculate heat transfer factors or friction factors for irradiated organic coolants. (auth)

20711 PROCEDURE FOR ELIMINATING TEMPERATURE-SENSITIVE IMPURITIES IN TOLUENE-METHYL-^3H USED FOR HYDROGEN ABSTRACTION REACTIONS. Eachus, Alan C.; Meyer, J. A. (Syracuse Univ., N. Y.). Atomlight, No. 52, 9-11(Mar. 1966).

A known amount of the aromatic hydrocarbon under study was mixed with a known amount of toluene, some of which contained tritium in its methyl side chain. After the removal of dissolved air by degassing and the addition of azomethane, the solution was sealed in an ampoule and subjected to ultraviolet photolysis in a constant temperature bath. The specific activity of the resulting methane was determined. It was higher than expected and seemed to increase with temperature. When ampoules of tritiated toluene with methane blankets were irradiated by ultraviolet light at different temperatures it was found that at 50°C and lower the amount of radioactivity in the blankets was roughly the same. At temperatures above 50°C the amount of radioactivity was higher, increasing with increasing temperature. Nitrogen was bubbled through tritiated toluene for 2 hr at room temperature. The toluene was then refluxed for 24 hr and distilled at atmospheric pressure. After this treatment no appreciable radioactivity was transferred to a methane blanket even at 95°C. (F.J.H.)

20712 ON THE TECHNIQUE OF LABELING HUMAN SERUM ALBUMIN WITH ^{99m}Tc. Herzmann, H.; Herzmann, A. (Institut fuer Angewandte Isotopenforschung, Berlin). Isotopenpraxis, 1: 130(Dec. 1965). (In German).

A technique for labeling human serum albumin with ^{99m}Tc is proposed based on the preliminary coupling of iron with technetium before the albumin is reacted with the labeling compound. (J.S.R.)

20713 ARRHENIUS PARAMETERS FOR ELEMENTARY COMBUSTION REACTIONS: H-ATOM ABSTRACTION FROM N-H BONDS. Gray, Peter (Univ. of Leeds, Eng.); Thynne, J. C. J. Symp. Combust., 10th, 435-43(1965).

The kinetics of hydrogen-atom abstraction by methyl radicals from substrates containing nitrogen-hydrogen bonds, viz, ammonia, trideuteroammonia, hydrazine, unsymmetrical dimethylhydrazine, methylamine, trideutero-

methylamine, and methylamine-d_2, were studied. The results are tabulated, giving the values of Arrhenius parameters for the hydrogen abstraction reactions. The implications of these results are discussed. Primary isotope effects, i.e., the relative reactivities of H and D, are in accord with expectations based on zero-point energy differences for a single X–H bond-stretching frequency. Secondary isotope effects are insignificant. Hydrazine is attacked much more readily than ammonia (300-fold ratio of reactivities at 150°C) and this is a consequence of a lowered activation energy with both A-factors near normal. When methylamine is attacked, both N and C sites are reactive; at 150°C, 4 out of every 7 H atoms come from the amine group and 3 from the methyl group. Dimethyl hydrazine is more reactive than methylamine, though the reactivity of different sites is not yet established. Also discussed is the interpretation of these results in terms of H–N bond dissociation energies, especially in hydrazine and the isoelectronic pairs CH_4 and C_2H_6; NH_3 and N_2H_4; H_2O and H_2O_2. (BBB)

20714 A NOVEL APPROACH TO THE C-TERMINAL DETERMINATION OF PEPTIDES: SELECTIVE ^2H- AND ^3H-LABELING REACTION OF C-TERMINAL AMINO ACIDS THROUGH OXAZOLONE. Matsuo, Hisayuki; Fujimoto, Yasuo; Tatsuno, Takashi (Inst. of Physical and Chemical Research, Tokyo). Tetrahedron Lett., No. 39, 3465-72(Oct. 1965).

In the course of a study on the racemization of amino acids and peptides in deuterium-containing media, it was found that hydrogen-deuterium exchange occurs on the asymmetric carbon of amino acids under racemization conditions involving carbanion formation. This deuteration reaction can be followed readily and precisely by the nuclear magnetic resonance method. On this basis, selective deuteration of the asymmetric carbon of C-terminal amino acids in several N-acetylpeptides was conducted through the racemization reaction, involving the corresponding oxazolone formation, followed by the base-catalyzed hydrolytic ring opening in deuterium oxide. It was thus possible to discriminate chemically the C-terminal from the others in the peptide chain. Deuterated products were characterized unambiguously by NMR spectra. This reaction was further extended to tritium exchange, using T_2O in place of D_2O, and this method is shown to be applicable to the C-terminal determination of peptides by a simple manipulation and on a microscale. The α-proton signals of the starting materials disappeared and the coupling mode of β-proton signals changed on completion of the deuterium exchange on their asymmetric α-carbon, while intensities of all other proton signals than α-proton did not decrease. The results showed that the procedure is capable of discriminating the C-terminal amino acid from the others in a peptide chain. (BBB)

20715 STEREO-SPECIFIC HYDROGEN EXCHANGE ACCOMPANYING CATALYTIC HYDROGENATION OF METHYL β,β-DIMETHYLACRYLATE. Battig, F.; Jordan, P.; Seibl, J.; Serdarevic, B. (Ecole Polytechnique Federale, Zurich). Vienna, International Atomic Energy Agency, 1965, Preprint No. SM-64/5, 10p. (In French). (CONF-650549-2). ORINS.

From IAEA Symposium on Exchange Reactions, Upton, N. Y.

During platinum or palladium-catalyzed hydrogenation in which, in solution, methyl β,β-dimethylacrylate is converted into the corresponding ester of isovaleric acid, an isotopic exchange of hydrogen between the gas and the solvent on the one hand and the substrate on the other is superposed upon the process of saturation of the double bond. This was studied by carrying out, at 20°C, hydrogenations that were interrupted after saturation of half the starting product and by employing D_2 or esters deuterated either totally or at specific positions, different positions being used from experiment to experiment. The isotopic composition of the hydrogen at each of the positions of the molecules, both saturated and nonsaturated, was determined, after separation of the molecules by chromatography in the gaseous phase, by combined mass spectrometry and nuclear magnetic resonance. A separate study was made of behavior in respect of exchange of substrate in the nonsaturated and saturated state, in the absence of hydrogen or the catalyst or both. Among the factors examined were, in particular, the effects of the solvent and the catalyst, which were very pronounced, on all the phenomena observed. Molecules of the substrate no longer exchanged once they were saturated. In the case of saturated molecules, restricted exchange took place in which only the β-methyls were involved. This exchange was stereo-specific, on an average 2.2 times greater in the cis group than in the trans group, which excluded the hypothesis of double bond migration from the α-β position to the β-γ position as an exchange mechanism; this point was confirmed by the absence of exchange at the α position. All the isotopic varieties from $-d_0$ to $-d_6$ or $-d_8$ were present in the substrate; the methyl of the ester function did not exchange. The double bond saturation process was not accompanied by intramolecular exchange. (auth)

Radiation Chemistry

See also BIOLOGY AND MEDICINE — Radiation Effects on Biochemicals Radiation Effects on Tissues

Refer also to abstracts 20406, 20658, 20708, and 21180.

20716 (AD–621022) RADIOLYSIS OF SOLID ETHYL IODIDE [Thesis]. Hermann, Gordon L. (Air Force Inst. of Tech., Wright-Patterson AFB, Ohio. School of Engineering). Aug. 1965. 71p. (GNE/PH–65-9). CFSTI $3.00 cy, $0.75 mn.

A study was made of the interaction of cobalt-60 radiation with frozen ethyl iodide in both the glass and polycrystalline states. The final reaction products of the radiolysis were measured and compared with the intermediate reaction species that were observed with an electron spin resonance spectrometer. (auth)

20717 (AD–621719) THE RADIATION CHEMISTRY OF ACETYLENIC COMPOUNDS. Final Report, December 1, 1961–May 1, 1965. Rondeau, R. E. (American Oil Co., Whiting, Ind.). July 1965. Contract AF33(616)-8247. 35p. (ML-TR-65-236). CFSTI $2.00 cy, $0.50 mn.

G-values for radiolysis products were determined for propyne and butyne-1 in the vapor phase and for butyne-1, butyne-2, pentyne-1, pentyne-2, hexyne-3, acetonitrile, and propionitrile in the liquid phase. The rupture of a C–H bond probably from a carbon beta to the triple bond resulted in H_2, coupling products, and H atom addition. H atom addition led to mono and poly olefins. The rupture of a C–C bond resulted in fragmentation in the vapor phase but recombination to form 1,2-diolefins in liquid phase. Both alpha and beta C–C bond rupture occurred. Alkyl benzene (alkyne trimers) form, probably by excitation. Analogous C_3N_3 ring compounds may form but were not detected. Gas chromatography techniques for alkyne and nitrile analyses are described. (auth)

20718 (AD–623307) LOW-TEMPERATURE POLYMERIZATION STUDIES. Progress Report No. 7, July 1-September 30, 1965. Morton, Maurice (Akron Univ., Ohio. Inst. of Rubber Research). Oct. 27, 1965. Contract AF04(611)-9694. 52p. CFSTI $3.00 cy, $0.50 mn.

Investigation of the radiation polymerization of fluoral in methylene chloride confirmed that a rate relation of the form $Rp = kp((M)(M)/S)$, (where M = monomer, and S = solvent) can be applied over a range of monomer concentration from 1 to 6 molar. This can be taken as evidence for termination by reaction with the methylene chloride. The results were consistent with a preferred anionic mode of polymerization of this monomer. Other experiments showed that fluoral is very readily polymerized by bases, even by such weakly basic compounds

as dimethylformamide. Polymerization of the fluorovinyl monomers was probably caused by the high energy radical-cation formed as a result of primary radiolysis, i.e., (using VF as an example): $CH_2 = CH_2$ + photon → $\cdot CH_2CHF$ (+) + e·(−). This species can polymerize as a cation or as a radical; however, at low temperature the cation reaction is the more vigorous: $\cdot CH_2CHF$ (+) + VF → $\cdot (CH_2CHF)mCH_2CHF$ (+). (TAB)

20719 (AD-624657) THE MECHANISM OF THE TRITIUM BETA-RAY INDUCED EXCHANGE REACTIONS OF DEUTERIUM WITH METHANE AND ETHANE IN THE GAS PHASE [Thesis]. Lawrence, Robert Henry Jr. (Ohio State Univ., Columbus). 1965. Contract AF33 (608)-1262. 111p. CFSTI $4.00 cy, $0.75 mn.

A study was made of the mechanism responsible for the exchange reactions occurring at pressures ranging from 0.85 to 0.98 atmospheres in the deuterium: methane system composed of 98.5% TD/D_2 (1:100) and 1.5% CH_4 between 77 and 500°K. The significance of this system lies in the abundance of kinetic data potentially available regarding atomic reactions induced by hydrogen atoms and ionic reactions involving proton transfer. It is shown that the application of this method to the hydrogen: methane and hydrogen: ethane systems investigated made possible a complete determination of the mechanism and evaluation of the corresponding kinetic parameters. (TAB)

20720 (AD-630891) A STUDY OF THE FAST NEUTRON-INDUCED GELATION OF TRIETHYLENE GLYCOL DIMETHACRYLATE USING 14-Mev NEUTRONS. Devanney, John A. (Ballistic Research Labs., Aberdeen Proving Ground, Md.). June 1965. 34p. (BRL-M-1686). CFSTI $2.00 cy, $0.50 mn.

The vinyl monomer investigated (triethylene glycol dimethacrylate) polymerized via a free radical mechanism. A comparison of the effects of neutrons and x rays was performed on the basis of radioinduced cross-linking on monomer molecules as exhibited by the production of a gel as an index. Neutron fluxes were measured using threshold foils and absorbed doses calculated using first collision approximations. (auth)

20721 (EUR-2295.f) ETUDE TECHNOLOGIQUE DES POLYPHENYLES. I. EXPLOITATION DE LA BOUCLE BLO 3. II. ETUDES DE DOSIMETRIE EN PILE. III. RADIOLYSE DU TERPHENYLE OM_2 SOUS ELECTRONS. (Technological Study of Polyphenyls. I. Operation of BLO 3. II. In-pile Dosimetry Studies. III. Radiolysis of Terphenyl OM_2 under Electron Bombardment). (Commissariat a l'Energie Atomique, Grenoble (France). Centre d'Etudes Nucleaires. Commissariat a l'Energie Atomique, Saclay (France). Centre d'Etudes Nucleaires). Oct. 9, 1964. 100p. Dep. mn.

The radiolysis of terphenyls in the No. 3 organic-liquid loop (BLO 3) installed in the Mélusine reactor was studied. Development of the core and activities of Société PROGIL's Analysis Laboratory at C.E.N., Grenoble, are also discussed. The construction and development of a microcalorimeter for in-pile dosimetry measurements, namely the Calvet microcalorimeter is reported. The results of the measurements carried out with the C.E.A.'s gamma source and Triton reactor are given. Experiments were also made on the radiolysis of OM_2 terphenyl under electron bombardment in a loop (SR 2) which was specially built and is operated in conjunction with the C.E.A.'s Massiot linear accelerator. The irradiation temperatures range from 250 to 450°C. (P.C.H.)

20722 (EUR-2401.f) ETUDE TECHNOLOGIQUE DES POLYPHENYLES. (Technological Study on Polyphenyls). Puig, J. R.; Houillier, A.; Rosier, D.; Romano, F. (Commissariat a l'Energie Atomique, Saclay (France). Centre d'Etudes Nucleaires). 1965. 174p. Dep. mn.

The results of thermal and radiolytic decomposition studies of terphenyls obtained in ampoules are reported. Pyrolysis was studied at temperatures between 416 and 530°C and radiolysis at temperatures around 350°C. The calorimetric dosimetry of the mixed radiations was investigated and a description is given of the construction of a dosimeter derived from the Calvet microcalorimeter. Finally, the average unit-volume gamma-ray and fast-neutron fluxes in the irradiation volume of an in-pile loop (BLO 3) were determined on a mock-up by means of graphite isothermal calorimeters and activation detectors. (auth)

20723 (MIT-334-33) IN-PILE LOOP IRRADIATION STUDIES OF ORGANIC COOLANT MATERIALS. Progress Report, January 1, 1965–September 30, 1965. Morgan, D. T. (Massachusetts Inst. of Tech., Cambridge. Dept. of Nuclear Engineering). Nov. 1, 1965. Contract AT(38-1)-334. 35p. Dep. mn. CFSTI $2.00 cy, $0.50 mn.

Irradiation of Santowax WR in the MITR in a new fuel position with a fast neutron fraction of 0.05–0.06 was initiated on May 10, 1965, as Transient Run 13. This run was continued until July 19, 1965, when the terphenyl concentration had decreased from 92% to a level of 84% as desired for Run 14. Steady-state Run 14 was started on July 19 and continued to September 27, 1965, with distillation processing and recycle of the coolant. The operating conditions and the preliminary G*(-omp) values from these runs are summarized. At the end of Run 14, a tritium dilution for the circulating organic mass was carried out. A reevaluation of previous loop data was carried out and G values calculated for individual terphenyl isomers as well as the total terphenyl and high boiler. Heat transfer and friction factor measurements using a new test heater were performed. All previous data as well as the new data were compared with the Dittus-Boelter and Colburn relations. The heat transfer data agreed with either correlation within ±10%; the friction factor data agreed with the Colburn relation within ±10%. Calorimeter and foil activation measurements were carried out in the new experimental facility to establish the dose rate. (P.C.H.)

20724 (NYO-2978-44) BETA RADIATION-INDUCED TELOMERIZATION OF METHANOL WITH ETHYLENE. Final Report, November 1, 1964–April 30, 1965. Yavorsky, P. M.; Mazzocco, N. J.; Gorin, E. (Consolidation Coal Co., Library, Pa. Research Div.). Sept. 10, 1965. Contract AT(30-1)-2978. 54p. Dep. mn. CFSTI $3.00 cy, $0.50 mn.

Using a strontium-90 beta irradiator in a continuous vapor phase processing unit at elevated temperatures and pressures, a study of controllable variables was made to optimize production of $+C_{11}$ alcohols from radioinduced telomerization of methanol with ethylene. The long-chain aliphatic alcohols produced by radiation are primarily desired as intermediates for sulfation to biodegradable detergents. Detailed results of 24 variable runs with radiation are reported, for which the dose rate was 1.69×10^6 rad/hr. G-values for the overall radiation-telomerization reaction were as high as 14,700, but for runs with the more favorable, selective yields of $+C_{11}$ alcohols, G-value for the reaction ranged between 5,000 and 10,000. Optimum operating conditions for maximum $+C_{11}$ alcohol yield, within those tested, were 4500 psi, 300°C, 2:1 methanol:ethylene feed ratio, and a 5 minute irradiation or reaction residence time. Good radiation yields also were obtained at 2500 psi, but increasing pressure had many favorable effects. Without radiation there was practically no telomerization yield at these conditions. In addition to alcohols, the radiation products contained ethers, minor amounts of hydrocarbons, some unsaturation (olefins), and had molecular branching when produced at 2500 psi. Branching disappeared for 4500 psi products. Hydrogen migration in radicals involved in the telomerization reaction can explain the array of products. (auth)

20725 (NYO-3570-2) RADIATION CHEMISTRY STUDIES OF SILANE. Annual Progress Report. Lampe, F. W.; Hess, G. G.; Schmidt, J. F. (Pennsylvania State Univ., University Park. Dept. of Chemistry). Apr. 5, 1966. Contract AT(30-1)-3570. 25p. Dep. mn. CFSTI $1.00 cy, $0.50 mn.

Ion-molecule reactions and radiolysis reactions in silane were studied. Pressure and delay-time dependencies of the intensities of ions present in silane, (ionized by 50-ev electrons) were examined over the ranges of 3 to 12×10^{-3} torr and 0 to 1 μsec. Appearance-potential studies of the $Si_2D_3^+$ ion were conducted using the retarding potential-difference method. Data on secondary ions of monosilane, ionic reactions, and mass spectra of Si_2H_6 are tabulated. Silane was exposed to gamma radiation from a 25,000 C ^{60}Co source at a dose rate of 1.50×10^{12} ev/cm^3-sec. The products were analyzed quantitatively by gas chromatography and qualitatively by mass spectrometry. Three products were found: H_2, Si_2H_6, and SiH_4. It is believed that the key to the polymerization and hydrogen production lies in the ion-molecule reactions. (P.C.H.)

20726 (PB–181506) RADIATION RESEARCH. Proceedings of an International Conference, Natick, Massachusetts, January 14–16, 1963. Fisher, Frank R. (ed.) (Army Natick Labs., Mass. Army Materiel Command, Washington, D. C. National Academy of Sciences–National Research Council, Washington, D. C. Advisory Board on Military Personnel Supplies). 195p. (CONF-27). CFSTI $3.00 cy, $1.00 mn.

Fifteen articles are included; separate abstracts were prepared for 10. Five articles on: uses of radioisotopes; chemical dosimetry at high dose rates; pulse radiolysis; radiation chemistry of gases; and wholesomeness of irradiated food were previously abstracted in NSA as 17: 14319, 16378, 18109, 30792, and 34037. (P.C.H.)

For abstracts of individual papers see: 20443, 20727–20731, 21192–21194, and 21470.

20727 (PB–181506, pp 9-18) RADIATION RESEARCH IN JAPAN. Shinohara, Kenichi (Institute of Physical and Chemical Research, Tokyo (Japan)).

Some of the research on radiation effects in Japan are discussed. These include mainly radiation chemistry and radiation preservation of food. Studies on ESR spectra of irradiated polymers are also discussed. (P.C.H.)

20728 (PB–181506, pp 49-58) SOME ASPECTS OF THE RADIATION CHEMISTRY OF ORGANIC COMPOUNDS. Swallow, A. J. (Imperial Coll. of Science and Tech., London (England)).

The irradiation of selected organic compounds in aqueous solution is discussed, along with the special phenomena that are present when organic compounds are irradiated in a concentrated solution as opposed to dilute solutions or the pure state. The organic compounds include: amino acids; cysteine; proteins; and organic redox systems. (P.C.H.)

20729 (PB–181506, pp 85-103) RADIATION CHEMISTRY IN THE SOLID STATE AS STUDIED WITH ELECTRON PARAMAGNETIC RESONANCE. Gordy, Walter (Duke Univ., Durham, N. C.).

A few specialized applications that demonstrate the use of ESR in radiation chemistry in the solid state are reviewed. These include: ESR patterns of some common free radicals; radiation effects on polypeptides; oxygen effect in radiation damage; and chemical protection from radiations. (49 references). (P.C.H.)

20730 (PB–181506, pp 104-15) RADIOCHEMISTRY IN FRANCE. Leveque, Pierre (Commissariat a l'Energie Atomique, Saclay (France). Centre d'Etudes Nucleaires).

A survey of radio- and radiation chemistry research in France is presented according to the laboratory or industry involved and its various activities. (66 references). (P.C.H.)

20731 (PB–181506, pp 133-42) THE MECHANISM OF ULTRAVIOLET AND HIGH ENERGY RADIATION DAMAGE. Reid, Cyril (British Columbia Univ., Vancouver).

The difference between radiation and thermal damage in biological materials and pure biological molecules, and the specificity of the damage are discussed. Energy redistribution via excited states is considered, with regard to the last excited species, often triplet states, and in their ultimate fate. Exciton migration is also discussed. (P.C.H.)

20732 (SGAE–CH–21/1965) ^{60}Co-GAMMA RAYS INDUCED CARBOXYLATION OF METHYLAMINE. de la Paz, L. R.; Getoff, N. (Oesterreichische Studiengesellschaft fuer Atomenergie G.m.b.H., Seibersdorf. Institut fuer Chemie). [1965]. 15p. Dep. mn.

The carboxylation of methylamine in aqueous solutions containing CO_2, bicarbonate, or carbonate was studied as a function of radiation dose, pH-value, and concentration of methylamine. Besides glycine, the main carboxylation product, some other amino acids, such as proline, alanine, and small amounts of α and γ-aminobutyric acid, were formed. The initial G-value of glycine increased from 0.24 at pH 3 to 0.8 at pH 9 and dropped to 0.2 at pH 12. To distinguish between the amino acids and other products formed, $^{14}CO_2$ was used as radioindicator. Probable reaction mechanisms are proposed for the explanation of the experimental results. (auth)

20733 (TID–22796) THE RADIOLYSIS OF LITHIUM NITRATE [Thesis]. Ward, Thomas G. Jr. (Princeton Univ., N. J.). Mar. 1966. Contract AT(30-1)-238. 193p. Dep. mn. CFSTI $5.00 cy, $1.00 mn.

The radiolysis of both molten and crystalline lithium nitrate was investigated under experimental conditions that differed widely in dose rate, linear energy transfer (LET), and temperature. Radiolysis of the crystalline salt was effected by the energetic recoil particles of the ^{6}Li(n,a)^{3}H reaction. Samples of molten $LiNO_3$ were irradiated in a reactor at 270°C and by ^{60}Co γ rays at dose rates that varied by a factor of 60. In every case, nitrite ion and molecular oxygen were the only significant decomposition products; they appeared approximately in the ratio of 2 to 1 as implied by the stoichiometry of the reaction $LiNO_3 \rightarrow LiNO_2 + \frac{1}{2}O_2$. In the solid, the decomposition was linear with an initial 100-ev yield, $G_0(NO_2^-)$, of 0.22 ± .01. For the melt irradiated by the ^{6}Li recoil particles at 5.2×10^{21} ev/mole-min, $G_0(NO_2^-) = 5.5 \pm .5$, and a steady-state nitrite ion concentration was indicated at about 3.1 mole % nitrite. Similar observations were made in the γ irradiations with $G_0(NO_2^-) = 3.73 \pm .05$ and steady states falling between 0.02 and 0.23 mole percent nitrite. There were indications that nitrite ion itself was not appreciably radiolyzed. A 3-fold variation in the dose rate had no effect on the ^{6}Li recoil irradiation of the solid; the dose rate of the corresponding molten salt irradiations was constant. In the γ exposures, however, the steady-state nitrite levels passed through a maximum as the dose rate increased from 8.9×10^{18} to 5.6×10^{20} ev/mole-min. The 10-fold increase in $G_0(NO_2^-)$ between radiolysis by ^{60}Co γ rays and ^{6}Li recoil particles in the solid (γ-ray data taken from the literature) was attributed exclusively to the large increase in LET; the 50% increase in $G_0(NO_2^-)$ and the marked increase in the steady state for the molten salt were also attributed to this factor. The primary effect of the solid-liquid phase transition was the 25-fold increase in $G_0(NO_2^-)$ for ^{6}Li recoil radiolysis and the nearly 200-fold increase for ^{60}Co γ rays. Mechanisms for the reactions are discussed. (76 references.) (P.C.H.)

20734 ION MOBILITY IN HIGHER SATURATED HYDROCARBONS. Jachym, B. (Technical Univ., Gdansk, Poland). Acta Phys. Pol., 29: 21-7(Jan. 1966).

The mobility of ions produced by x rays in liquid n-dodecane, n-tetradecane, and n-hexadecane was investigated. The activation energy for the processes involved was determined from the temperature-dependence of the ion mobility and viscosity. The results were compared with Walden's law as derived from Eyring's theory. For the liquids investigated, because of the different activation energies from ion mobility and viscosity, Walden's law as expressed by S. Glasstone, K. Laidler, and H. Eyring in terms of the charge e and the distance between two neighboring equilibrium positions of the ion λ ($u \cdot \eta = e/\lambda$ = const) had to be slightly modified to take account of that divergence. I. Adamczewski's expression, which gives a qualitatively correct description of the experimental results, agreed in numerical values only with regard to positive ions. (auth)

20735 STUDIES OF CHEMICAL REACTIONS BY PULSE RADIOLYSIS: FREE ELECTRONS AND FREE RADICALS IN AQUEOUS SOLUTION. Henglein, A. Angew. Chem. Int. Ed. Engl., 5: 256(Feb. 1966).

Reactions of OH radicals and hydrated electrons produced by decomposition of water were followed by pulse radiolysis (pulses of about 10^{-6} sec duration). Hydrated electrons reacted with tetranitromethane in a bimolecular process with the rate constant (at 20°C) 6.0×10^{10} liter/mole, with nitromethate to yield the anion $CH_3NO_2^-$, and with hydrogen sulfide in aqueous solution by a diffusion-controlled process. The rapidity of the reaction in the hydrogen sulfide solution was considered due to solvation effects. The reaction of catalase with the OH radical is diffusion controlled, as shown by a comparison of the measured rate constant of 8.3×10^{10} liter/mole sec with that calculated from the Smoluckowski equation. From the kinetic results it was concluded that values below 2.0 ev are commonest in the distribution of solvation energy of the hydrated electron, which agreed with calculations from the absorption spectrum of the hydrated electron. (F.J.H.)

20736 THE REACTION OF WHITE PHOSPHORUS WITH FREE RADICALS FROM γ-RADIOLYSED ORGANIC LIQUIDS. Henglein, A. Angew. Chem. Intern. Ed. Engl., 3: 709(Oct. 1964).

Irradiation of solutions of white phosphorus in CCl_4 using γ-rays produced trichloromethylphosphorus dichloride, phosphorus trichloride, red phosphorus, hexachloroethane, and a polymer $(CCl_2)_n$. At room temperature the main product was red P to which one trichloromethyl group (from radiolysis of the solvent) per 7 P atoms was chemically attached. Above 80°C, the low-molecular-weight P compounds were formed almost exclusively via a chain reaction. A mechanism is indicated whereby free radicals from the solvent add onto the P_4 molecules and the resultant RP_4 units either form red P or react with the solvent with abstraction of chlorine. Abstraction of a chlorine atom requires an activation energy of 8.2 kcal/mole and is therefore favored by high temperatures during the irradiation. In cyclohexane, free cyclohexyl radicals (from radiolysis of the solvent) reacted with dissolved P to form red P containing one C_6H_{11} group per 4 P atoms. About 30% of the P added appeared in the form of soluble organophosphorus compounds containing several P atoms per molecule. The radical attack in cyclohexane led neither to the scission of all the P–P bonds of the P_4 molecules nor to a chain reaction. If CCl_4 was added, however, at higher temperatures, three simultaneous chain reactions appeared, which led to: chloroform and cyclohexyl chloride, trichloromethylphosphorus dichloride, and cyclohexylphosphorus dichloride. The trichloromethyl radical is thus a common intermediate in the three chain reactions, which are linked with one another. White P participated in the polymerization of styrene induced by γ-rays. The rate of polymerization was slightly increased, but the average molecular weight was greatly lowered. In addition, P was incorporated into the polymer (one atom/100 molecules of monomer). These results indicated that P_4 molecules intercept growing styrene chains, thereby initiating more than one new chain per interception, and that breakdown of the kinetic chain by mutual deactivation follows. It was concluded from the transfer constant found that white P is a relatively poor trap for free carbon radicals and does not react with them at each encounter. Pulse radiolysis experiments with solutions of white P in cyclohexane and CCl_4 produced a short-lived intermediate, which had an absorption maximum at 650 mμ and which disappeared by reactions of first or second order, depending on the P_4 concentration, to give a stable entity, which absorbs at 350 mμ. The short-lived species is either the $C_6H_{11}P_4$ or the CCl_3P_4 radical. (BBB)

20737 A CONTRIBUTION TO THE STUDY OF THE ACTION OF IONIZING RADIATIONS ON STARCH: THE EFFECTS OF γ RADIATIONS ON POTATO STARCH AS A FUNCTION OF ITS WATER CONTENT. Reuschl, H.; Guilbot, A. (Institut National de la Recherche Agronomique, Massy, France). Ann. Technol. Agr., 13: 399-448 (1964). (In French).

The action of 30-mR doses of ^{60}Co γ radiations on potato starch was studied by observation of the degradation of polysaccharide chains and the formation of oxidation and dehydration products. The formation of glucose in dry starch and the presence of hydroxymethylfurfural implied that hydrolytic splitting took place through an intramolecular elimination reaction. Water interfered with starch radiolytic reactions in three ways. First, water acted as a radioprotector for oxidation reactions. Second, water acted as a radioprotector for chain-splitting reactions in concentrations greater than 21%. Third, water interfered chemically in glucose formation in proportion to the amount of hydration. Studies of the radiolytic reactions of hydrated starch made it possible to obtain information on its supramolecular structure. (BBB)

20738 OXIDATION PRODUCTS OF ERGOSTEROL. I. CHROMATOGRAPHIC SEPARATION OF THE OXIDATION PRODUCTS, ISOLATION OF NEW IRRADIATION PRODUCTS OF ERGOSTEROL IN THE PRESENCE OF OXYGEN. Fuerst, W. (Friedrich-Schiller-Univ., Jena, Ger.). Arch. Pharm., 298: 795-804(Nov. 1965). (In German).

A method of separation of the previously recognized oxidation products of ergosterol, based on thin-layer chromatography, was developed. In the irradiation of ergosterol in the presence of different sensitizers (methylene blue, eosin, Sudan red, dimethyl yellow, rhodamine B) three new substances were detected by thin-layer chromatography. Solvents tested were n-propanol and chloroform. One substance is believed to be 3β,5α-dihydroxy-6,7α-epoxy-8,22-ergostadiene. Another substance was obtained pure by the action of HCl on ergosterintriol I and is believed to be 3β,5α-dihydroxy-6,14,22-ergostatriene. Other substances obtained by the influence of HCl on ergosterintriol I are 3β,5α,6β-trihydroxy-7,22-ergostadiene and a material of hydrocarbon character. (BBB)

20739 PILE RADIOLYSIS OF TERPHENYLS. Proksch, E. (Oesterreichische Studiengesellschaft fuer Atomenergie GmbH, Seibersdorf, Austria). Atomkernenergie, 11: 163-6(Mar.-Apr. 1966). (In German).

The radiolytic decomposition of an isomeric terphenyl mixture was measured using two different positions of the pool-type reactor ASTRA (fast neutron dose fraction 50.4% and abt. 23%, resp.). The measured values were used to evaluate by extrapolation the radiolytic action of both, pure gamma radiation and fast neutrons. For the temperature range of 275–350°C average values were found as follows (initial G-values using first and second order kinetics, respectively): $G_\gamma^0(\rightarrow HB) = 0.158$ or 0.151; $G_n^0(\rightarrow HB) = 0.278$ or 0.333; $G_\gamma^0(gas) = 0.0139$ or 0.0112; $G_n^0(gas) = 0.096$ or 0.104. Accuracy and significance of these values are discussed. Furthermore, radiolytic gas compositions and the influence upon radiolysis of oxygen present were determined. (auth)

20740 REACTIONS OF HYDROCARBONS AS FOAMS UNDER THE INFLUENCE OF GAS DISCHARGES. IV. COMPARATIVE CONSIDERATION OF THE EFFECT OF GAS DISCHARGES AND HIGH ENERGY RADIATION ON THE CONVERSION OF SIMPLE HYDROCARBONS. Pasman, H. J.; Vlugter, J. C.; Breukink, C. J. (Technische Hochschule, Delft, Netherlands). Brennstoff-Chem., 46: 358-61(Nov. 1965). (In German).

Cracking products of saturated hydrocarbons as foams by discharges and as gas or liquid by high-energy radiation were compared. The temperature during irradiation, mode of irradiation, and relative amounts of cracking product, dehydrogenated starting material, dimer, and intermediate products were respectively as follows: n-butane, −120°C, gas discharge, 1.00, 0.06, 0.06, 0.09; n-butane, −30°C, irradiation 1.00, 0.24, 0.18, 0.17; isobutane, −120°C, gas discharge, 1.00, 0.01, 0.04, 0.13; isobutane, −30°C, irradiation, 1.00, 0.24, 0.04, 0.17. The composition of cracking products in mole percent for treatment of butane by discharge in foam, gas phase irra-

diation, and liquid phase irradiation at −120, 25, and −30°C, respectively was: methane, 66, 42, 4; ethane, 14, 28, 44; ethylene, 0, 0, 12; acetylene, 4, -, -; propane, 15, 30, 28; propylene, 1, 0, 12. Comparative studies of irradiation and gas discharge on polymerization of isobutylene indicated similar molecular weight as a function of percent conversion of olefin in the absence of decomposition; at the same molecular weight, the yield of polymer by the gas discharge technique was lower. (BBB)

20741 RADIOLYSIS OF ETHANOL–BENZENE SYSTEMS UNDER THE INFLUENCE OF ^{60}Co γ RADIATION. Kroh, J.; Mayer, J. (Technical Univ., Lodz, Poland). Bull. Acad. Pol. Sci., Ser. Sci. Chim., 14: 47-50(1966).

Results obtained in the gamma radiolysis of the benzene–ethanol system at 20 and −196°C are given. The $G(H_2)$ and $G(CH_3CHO)$ values obtained were, respectively, 4.87 and 2.18 at 20°C and 4.35 and 3.10 at −196°C. The value of $G(H_2)$ decreased on solidification of ethanol and that of $G(CH_3CHO)$ increased. Curves for the values of $G(H_2)$ and $G(CH_3CHO)$ against the electron fraction of benzene (ϵ) at 20 and −196°C are shown. For both curves the plateau appeared in the range of $\epsilon = 0.15$ to 0.40. (F.J.H.)

20742 EPR STUDIES OF γ-IRRADIATED ETHANOL–BENZENE SYSTEM AT −196°C. Kroh, J.; Mayer, J. (Technical Univ., Lodz, Poland). Bull. Acad. Pol. Sci., Ser. Sci. Chim., 14: 51-4(1966).

The EPR spectra of ethanol radicals produced in radiolysis of solid ethanol–benzene systems were studied. The radiation yield of radicals, G_R, for pure ethanol irradiated at −196°C is 7.3. No qualitative differences were observed between the spectra of pure ethanol and its mixtures with benzene in the benzene concentration range from 1×10^{-3} to 6.9×10^{-2}M/liter, but the presence of about 10^{-2}M/liter of benzene decreased the number of ethanol radicals by ~15%. The concentration of C_6H_7 radical vs benzene electron fraction in the benzene–ethanol mixtures is shown. The results are consistent with previous data. At benzene concentration higher than $\epsilon_{benzene} = 0.03$ the value of $[C_6H_7]$ decreased indicating energy transfer processes. The relation between $[C_6H_7]$ and the composition became linear for benzene fractions higher than 0.5. (F.J.H.)

20743 INFLUENCE OF CRYSTAL SIZE ON THE YIELD OF N-VINYLCARBAZOLE POLYMERIZATION. Kroh, J.; Pekala, W. (Technical Univ., Lodz, Poland). Bull. Acad. Pol. Sci., Ser. Sci. Chim., 14: 55-8(1966).

Possible relations between direction of the growth of polymer chains and the geometry of monomer crystals were investigated in the radioinduced solid-state polymerization of N-vinylcarbazole (NVC). It was found that the initial rate of reaction does not depend on the crystal size. However, the polymer yield was greater for large crystals. The polymer chain grew mainly during the post-irradiation period and the length of the polymer chain increased with the size of the crystals. (M.C.G.)

20744 HYDROLYSIS OF SALICYL PHOSPHATE AND EFFECT OF RADIATION ENERGY. Chang, Shuh-Ming; Wai, Nganshou. Bull. Inst. Chem., Acad. Sinica, No. 11, 1-8(Dec. 1965).

The effects of background radiation energy on the rate of hydrolysis of salicyl phosphate was studied. Within a heavily shielded lead box, with background radiation lowered to 40% of its ordinary value, hydrolysis of salicyl phosphate was allowed to take place. Effects of x rays were also studied. It was found that radiation, both the background and x, decreased the rate of hydrolysis. (F.J.H.)

20745 AQUEOUS TEREPHTHALIC ACID AS A SENSITIVE DOSIMETER FOR IONIZING RADIATIONS. Wai, Nganshou; Hung, Tsu-Chang. Bull. Inst. Chem., Acad. Sinica, No. 11, 9-16(Dec. 1965).

In studies of terephthalic acid for use as a dosimeter, evidences for hydroxylation of the acid by ionizing radiation were sought. The ultraviolet spectrophotometric method was used for determination of hydroxylation. The ideal concentration of the dosimeter solution was found to be 10^{-4}M terephthalic acid in 4×10^{-4}M sodium hydroxide, which was in agreement with Armstrong. The yield of hydroxyterephthalic acid was 1.07 ± 0.05 molecules per 100 ev. The degree of hydroxylation was linear with doses as low as 0.5 rad. The competitory reaction between terephthalic acid and hydrogen radicals was observed during gamma irradiation on low concentration of 5×10^{-5}M terephthalic acid in 4×10^{-4}M sodium hydroxide. The G value of the product was decreased, when the H radicals increased in the high dose irradiations. It was difficult to detect background radiation energy as low as 0.1 r/year by terephthalic acid dosimeter. Nevertheless, the hydroxylation reaction by the background radiations was still observed. (auth)

20746 RADIOLYSIS OF ETHANOL IN LIQUID PHASE. Hung, Tsu-Chang; Ou, Li-Tse; Yang, Chi-Chuen. Bull. Inst. Chem., Acad. Sinica, No. 11, 61-71(Dec. 1965).

Gamma radiolysis of air-saturated absolute ethanol in liquid phase at 29 ± 4°C was investigated. A ^{60}Co gamma source was used, acetaldehyde, formaldehyde, hydrogen peroxide, isopropanol, and water were found in the products. The G value of each product was calculated. The yield of formaldehyde was found to be a function of dose absorbed: concentration (formaldehyde) = $(0.139 \pm 0.008) \times 10^{-4} + (0.365 \pm 0.022) \times 10^{-23}$ XD. The yield of acetaldehyde was found to be dependent on the dose absorbed and isopropanol gave a large scatter of results. This was caused by an induction effect. The value for $G(H_2O_2)$ was estimated at about 4.1 ± 0.6 molecules per 100 ev. Diols including 1,2-propanediol and 2,3-butanediol were not detected. Various possible decomposition mechanisms are suggested. (auth)

20747 RADIATION INDUCED POLYMERIZATION OF ISOCYANIC ACID. Hamada, Hakuo (Ube Industrial, Ltd., Japan); Hayashi, Koichiro. Chem. High Polymers (Tokyo), 22: 639-45(Oct. 1965). (In Japanese).

It is possible to prepare 1-nylon having the structure of $[-(NHCO)_n-]$ by polymerizing isocyanic acid. In this paper, radiation induced polymerization and copolymerization of iso-cyanic acid at lower temperatures are reported. The polymers obtained have low molecular weights and no suitable solvent. They decomposed above 300°C. The rate of polymerization is small below −78°C, but considerably larger at −40°C. The copolymers were obtained with formaldehyde, ketene, acrylonitrile and methacrylic acid. However, only oily low molecular weight compounds were obtained with butadiene, ethylene, and styrene. (auth)

20748 RADIATION-INDUCED EFFECTS ON WATER-SOLUBLE POLYMERS IN AQUEOUS SOLUTIONS. III. GLUCOSE, SUCROSE, AND STARCH. Lin, Chen-Chong. Chemistry (Taipei), No. 4, 176-82(1963). (In Chinese).

The effects of 60-kv x rays on various sugars at dose rates up to 3000 R/hr were examined, using paper chromatography to separate the radiation-produced compounds. The study includes an analysis of the products formed by the action of x rays on glucose, sucrose, and amylose in aqueous solutions. Acids were formed when these carbohydrates are irradiated. The quantity of acid produced was independent of the concentration of sugars, indicating indirect action, and was also independent of the intensity of the x rays. The reducing power of the glucose solution was decreased after irradiation, as measured by copper reduction, but in both sucrose and amylose solutions there was an increase in reducing power. It is shown by paper chromatography that the products formed were glucuronic acid in glucose solution, glucose and fructose in sucrose solution, and maltose and glucose in amylose solutions. The visible absorption peak (blue) of iodine complexes of irradiated amylose solution shifted to a shorter wavelength, which was indicative of degradation. The action of radiation on water-soluble natural polymers, such as amylose, includes both oxidation and hydrolytic scission. The G values for the various products are given, and a free-radical mechanism explaining formation of the products from the different sugars is proposed. (BBB)

20749 RECOMBINATION OF HYDROGEN AND OXYGEN IN THE PRESENCE OF WATER VAPOR UNDER THE INFLUENCE OF RADIATION. Benjamin, B. M.; Isbin, H. S.

(Univ. of Minnesota, Minneapolis). Energ. Nucl. (Milan), 13: 165-72(Apr. 1966).

The recombination rates of hydrogen and oxygen are of interest in the design of boiling water reactors. The experimental results of some preliminary studies are presented. With the systems noted, the rate of recombination of hydrogen and oxygen to form water was found to be first order in the hydrogen concentration, increase with oxygen concentration though at a decreasing rate, and to be linear with the water vapor concentration at low vapor concentration. At higher concentrations (>0.3 g/l or 400 mm Hg pressure), the rate becomes almost constant, decreasing only slightly with water vapor concentrations. Increasing dose rates cause the reaction rate to increase, though at a decreasing rate. The rate is independent of temperature up to 138°C but appears to increase with temperature above this value. The results can be expressed in either of two empirical rate expressions. The initial yields $G^0(H_2O) = G^0(-H_2)$ range from 3.0 to 6.0 for most of the runs. (auth)

20750 REACTIVITY OF ELECTRONS PRODUCED IN THE γ-RADIOLYSIS OF ALIPHATIC ALCOHOLS. Sherman, Warren V. (Soreq Nuclear Research Centre, Yavne, Israel). J. Amer. Chem. Soc., 88: 1567-8(Apr. 5, 1966).

The use of nitrous oxide as a specific scavenger for solvated electrons produced in the radiolysis of 2-propanol solutions as a method for determining the reactivity of solute substrates was suggested. The method involves measurement of the yield of molecular nitrogen, $G(N_2)$. The ρ values for the reaction in 2-propanol and methanol are 3.1 and 4.7, respectively. The static dielectric constants at room temperature of 2-propanol and methanol are 19 and 33, respectively, and the hypsochromic shift observed for the optical absorption maxima of the electron in the solvents reflects an increasing stabilization of the electron by solvation. The sequence of increasing dielectric constants is paralleled by increasing ρ values for the reaction. The correlation between the optical transition energy of the solvated electron and dielectric constant observed in aliphatic alcohols was also found to break down when extended to the hydrated electron. (F.J.H.)

20751 ISOTOPIC AND PHASE EFFECTS IN NEUTRON-IRRADIATED ETHYL BROMIDE. Milman, Miriam (CEA, Saclay, France). J. Amer. Chem. Soc., 88: 1578-9(Apr. 5, 1966).

A sample of purified ethyl bromide containing a 10^{-3} M fraction of bromine scavenger was irradiated for 1 to 3 sec with a neutron flux of $\sim 10^{12}$ neutrons/cm^2/sec. The samples were irradiated at 25 and −196°C. Fifty minutes after irradiation the samples were extracted with a reducing wash. After gas chromatographic separation, the fractions were collected and counted three times; 4 hr after extraction, 20 hr later, and 48 hr after extraction, when the remaining activity was due to ^{82}Br, only. Results indicated that the products resulting from H-atom substitution should show an isotope effect favoring ^{82}Br (yield for ^{80m}Br/yield for ^{82}Br < 1) and an important phase effect, whereas those resulting from the scission of a C−C bond as well as the substitution of a Br atom present an isotope effect favoring ^{80m}Br (yield for ^{80m}Br/yield for ^{82}Br > 1), and show little or no difference in yield in the two phases. It was suggested that the formation of activated products arose mainly from the consequences of internal conversion and subsequent Auger electron emission. (F.J.H.)

20752 ION-MOLECULE REACTIONS IN THE LIQUID AND SOLID PHASE RADIOLYSIS OF HYDROCARBON MIXTURES. Ausloos, P.; Scala, A. A.; Lias, S. G. (National Bureau of Standards, Washington, D. C.). J. Amer. Chem. Soc., 88: 1583-4(Apr. 5, 1966).

The ion-molecule reactions occurring in the liquid and solid phase radiolysis of hydrocarbon mixtures are considered. The addition of 5 mole % of cyclo-C_3D_6 to protonated n-hexane, isopentane, n-pentane, or 3-methylpentane resulted in the formation of $CD_2HCD_2CD_2H$ as a major product [G(molecules per 100 ev) = 0.5 to 1.0] with the exclusion of any significant amount of other deuterated propanes. The value of $G(CD_2HCD_2CD_2H)$ did not vary by more than 20% when the temperature was varied from 77 to 300°K, unless the concentration of cyclo-C_3D_6 was increased. The addition of 1 mole % CCl_4 increased the value of $G(CD_2HCD_2CD_2H)$ to 2.5, both at 77 and 300°K. When propylene−d_6, instead of cyclopropane−d_6, was added to n−C_5H_{12} or i−C_5H_{12}, propane−d_6 appeared as the major product. Mass spectrophotometric analysis of the propane fraction (C_3D_8, 45%; C_3D_7H, 10%; CD_3CDHCD_2H, 45%) formed in the radiolysis of a n−C_5H_{12}−C_5D_{12}−CD_3CDCD_2−CCl_4 (1 : 1 : 0.01 : 0.01) mixture at 193°K indicated that the majority of the propane must be produced by an H-transfer reaction. The H-transfer reactions for unsaturated C_2D_2, C_2D_4, and $CD_3CD_2CDCD_2$ were noted to occur with high efficiency. The isotopic composition of the ethane fracture [G(ethane) = 1.5] produced in the radiolysis of a i−C_5H_{12}−i−C_5D_{12}−C_2D_4−CCl_4 (1 : 1 : 0.03 : 0.03) mixture, in the presence of oxygen at 193°K, is as follows: C_2D_6, 43%; C_2D_5H, 2%; CD_2HCD_2H, 48%; and C_2H_6, 7%. (F.J.H.)

20753 EFFECTS OF NUCLEAR RADIATIONS ON STRUCTURE AND MOLECULAR MOTIONS IN SOME CRYSTALLINE STEREOREGULAR POLYMERS. Baccaredda, Mario; Butta, Enzo; Frosini, Vittorio (Univ. of Pisa, Italy). J. Appl. Polymer Sci., 10: 399-419(Mar. 1966).

Young's modulus and the mechanical damping factor were determined between −180 and +280°C (at a frequency of several kilocycles), in samples of isotactic polypropylene, isotactic polystyrene, and trans-1,4-polybutadiene, subjected to pile irradiation (γ rays and neutrons) at γ doses from 90 to 4000 Mrad. In isotactic polypropylene no important structural changes were produced by the irradiation, except for a partial destruction of crystallinity. The samples receiving high radiation doses exhibited a low temperature loss region, which was attributed to the formation of a certain number of branches. Isotactic polystyrene showed very slight modifications of the dynamic mechanical properties at room temperature. At low temperature an increase of intensity of the δ relaxation phenomenon (probably due to oscillations of phenyl rings) with increasing radiation dose was observed. Important structural modifications produced by the radiation, destruction of crystallinity accompanied by crosslinking, which transformed the material into a crosslinked rubber, were observed in trans-1-4-polybutadiene. Unlike conventional (sulfur) vulcanization, crosslinking by radiation did not cause a marked shift of the glass transition point. A secondary low-temperature relaxation effect, not existing in the unirradiated material, appeared in the mechanical loss curves of the irradiated samples; it was attributed to the formation of $-CH_2-$ sequences in the main chains through saturation of C=C bonds. The mechanical spectrum of irradiated polybutadiene was very similar to those shown by crosslinked ethylene−butadiene copolymers. (auth)

20754 EFFECT OF γ RADIATION ON THE DYNAMIC MECHANICAL PROPERTIES OF STYRENEBUTADIENE RUBBERS. Traeger, R. K. (Sandia Corp., Albuquerque, N. Mex.); Castonguay, T. T. J. Appl. Polymer Sci., 10: 491-509(Mar. 1966).

Three different styrene−butadiene, gum rubbers were exposed to gamma doses ranging from 0 to 200 Mrad. The crosslink densities, hardness and the dynamic mechanical properties were evaluated. All specimens increased in hardness and crosslink density during radiation. This was reflected in an increased storage modulus, broadened loss tangent maximum, and increased relaxation spectrum. The dynamic data are presented in master curves that were developed using the WLF equation. (auth)

20755 TRAPPED ELECTRONS IN γ-IRRADIATED 3-METHYLPENTANE AT −196°. Skelly, David W.; Hamill, William H. (Univ. of Notre Dame, Ind.). J. Chem. Phys., 44: 2891-4(Apr. 15, 1966).

The yield of solvent-trapped electrons in γ-irradiated 3-methylpentane at −196° was 0.75 per 100 ev when measured within a few seconds, and diminished to ~0.6 after 3 min. The quantum yield for bleaching at 950 mμ de-

creased from 0.8 toward zero with progressive bleaching. Addition of 0.05% biphenyl maintained the quantum yield at >0.8 until more than 90% of the solvent trapped electrons had bleached. The initial quantum yield at $\lambda > 1.7\mu$ was ~0.01, both with and without added biphenyl. There is qualitative correlation between photobleaching and the rate of spontaneous decay. (auth)

20756 ELECTRON SPIN RESONANCE OF A γ-IRRADIATED SINGLE CRYSTAL OF A HYDROGEN PEROXIDE-UREA ADDITION COMPOUND AT 77°K. Ichikawa, Takahisa (Government Industrial Research Inst., Nagoya, Japan); Iwasaki, Machio; Kuwata, Keiji. J. Chem. Phys., 44: 2979-80(Apr. 15, 1966).

The γ-irradiated single crystal of an addition compound $H_2O_2 \cdot CO(NH_2)_2$ at 77°K exhibited ESR spectra which were attributed to an O_2^- ion radical and an $HO_2\cdot$ free radical. The measurements were made at 9.21 and 22.4 kMc/sec for various orientations of the crystal in the magnetic field. For most orientations, the spectra of O_2^- and $HO_2\cdot$ were singlet and doublet, respectively. An isotropic component of the doublet was approximately 11 G. The g values were found to be anisotropic with the principal values: $g_1 = 2.088_6$, $g_2 = 2.008_4$, and $g_3 = 2.000_9$ for O_2^-; while $g_1 = 2.049_5$, $g_2 = 2.008_1$, and $g_3 = 2.001_8$ for $HO_2\cdot$. There seems to be no report about O_2^- trapped in a molecular crystal so far, and the results were compared with O_2^- in ionic crystal. (auth)

20757 REACTION OF ETHYLENE WITH METHYLENE CHLORIDE INDUCED BY GAMMA-RADIATION. Takehisa, Masaaki; Yasumoto, Masahiko (Government Chemical Industrial Research Inst., Tokyo). J. Chem. Soc. Jap., Ind. Chem. Sect., 68: 968-71(May 1965). (In Japanese).

A series of 1,1-dichloroalkanes accompanied with a series of 1-chloroalkanes were obtained by the gamma induced reaction of ethylene with methylene chloride in the pressure range of 10 to 40 kg/cm². The result seems to be consistent with the following free radical telomerization mechanism: (1) $CH_2Cl_2 + \gamma \rightarrow \cdot Cl + \cdot CH_2Cl$, (2) $\cdot Cl + C_2H_4 \rightarrow ClC_2H_4^{\cdot}$, (3) $\cdot CH_2Cl + n(C_2H_4) \rightarrow ClCH_2(C_2H_4)_n^{\cdot}$, (4) $ClCH_2^{\cdot} + n(C_2H_4) \rightarrow Cl(C_2H_4)_{n+1}^{\cdot}$, (5) $Cl(CH_2)_{2n+1 \text{ or } 2n+2}^{\cdot} + CH_2Cl_2 \rightarrow Cl(CH_2)_{2n+1 \text{ or } 2n+2}H + \cdot CHCl_2$, (6) $\cdot CHCl_2 + n(C_2H_4) \rightarrow Cl_2CH(C_2H_4)_n^{\cdot}$, and (7) $Cl_2CH(C_2H_4)_n^{\cdot} + CH_2Cl \rightarrow Cl_2CH(C_2H_4)_nH + CHCl_2^{\cdot}$. Chain transfer constants, as for the reaction $Cl_2CH(C_2H_4)_n^{\cdot} + C_2H_4$, CH_2Cl_2 were increased 3 to 5 fold. The degree of polymerization of the radical $Cl_2CH(C_2H_4)_n^{\cdot}$ was increased from 1 to 4 and then became constant at a value of 0.14 for the radical of greater lengths in the temperature range 20 to 80°C. (TCO)

20758 RADIOLYSIS OF METHYLAL AND ETHYLENE GLYCOL DIMETHYL ETHER. Takezaki, Junichi; Hirota, Kozo. J. Chem. Soc. Jap., Pure Chem. Sect., 86: 302-6 (Mar. 1965). (In Japanese).

Radiolysis of methylal and ethylene glycol dimethyl ether (EGDE), both having a two ether group was studied at room temperature. The results on methylal and EGDE were compared with those of monoethers, polymers, ethylene glycol and dioxane. The radiolysis of methylal was different from that of EGDE in dose rate and total dose dependence of the products. The C–O bond adjacent to methoxy group of methylal was most susceptible to scission whereas the scission occurred at the central C–C bond in EGDE. Esters, ketones, olefins (except for CH_4), paraffins, and acids which were products of radiolysis of monoethers, polymers, ethylene glycol and dioxane were not detected in the products resulting from radiolysis of methylal and EGDE. Methylal and EGDE were more stable to radiation than monoethers, polymers, and dioxane. The above conclusions were based on data obtained by the gas chromatographic and mass spectroscopic data and were found to be plausible by comparison with the ESR spectra obtained. (auth)

20759 EFFECT OF γ RADIATION. PART X. ACTION OF γ RADIATION ON OXYGENATED SOLUTIONS OF DL-MANDELIC ACID. Barker, S. A.; Brimacombe, J. S.; Milner, D. J. (Univ. of Birmingham, Eng.). J. Chem. Soc., Sect. C., No. 5, 511-14(1966).

The nonvolatile products formed by γ irradiation of DL-mandelic acid in 0.1% oxygenated, aqueous solution were determined quantitatively by isotope dilution analysis. The initial products of irradiation were carbon dioxide, phenylglyoxylic acid, and benzaldehyde, part of which is converted by autoxidation to benzoic acid. Phenols resulting from hydroxylation of the aromatic nucleus were also observed but the principal abstractions occurred in the side-chain. Mechanisms to account for these products are suggested. (auth)

20760 SULFUR DIOXIDE ELIMINATION IN THE RADIOLYTIC DECOMPOSITION OF SOLID DIARYL SULFONES. Kevan, Larry; Hall, P. L.; Kaiser, E. T. (Univ. of Chicago). J. Phys. Chem., 70: 853-5(Mar. 1966).

Gamma radiolysis of solid p,p′-ditolyl sulfone resulted, almost exclusively, in simple SO_2 elimination with the production of an equivalent yield of p,p′-bitolyl. $G(SO_2) = G(p,p'\text{-bitolyl}) = 0.05$. Diphenyl sulfone and dibenzothiophene sulfone also showed simple SO_2 elimination. However, the latter cyclic sulfone only gave $G(SO_2) = 0.002$ and is therefore 25 times more stable to radiation decomposition. (auth)

20761 PRODUCTION OF POLYMER GEL WITH LEAST RADIATION DOSE. Saito, Osamu; Takahashi, Tsuneto (Chuo Univ., Tokyo). J. Phys. Soc. Jap., 21: 206(Jan. 1966).

A theoretical investigation is made of methods by which polymer gel can be produced with the least radiation dose, in which polymer sol is uniformly mixed with gel. The maximum efficiency of gel production is found for two methods of irradiation. (L.B.S.)

20762 IRRADIATION CHANGES IN ORGANIC POLYMERS AT VARIOUS ACCELERATING VOLTAGES. Kobayashi, K.; Sakaoku, K. (Kyoto Univ.). Lab. Invest., 14: 1097-1114(June 1965).

Various aspects of radiation chemistry are reviewed in relation to changes caused by electron radiation in samples examined by electron microscopy. Data are reported on the effects of 300-kv electrons on such specimens. The spectra of energy loss of electrons passing through organic polymer membranes reveal that the ionization of carbon atoms is the dominant feature in the inelastic collisions of fast electrons and organic molecules. The ionization of carbon atoms is succeeded by secondary chemical reactions, such as cross-linking between neighboring molecular chains, scission of chains, double bonding between carbon atoms, extrusion of hydrogen atoms, and radical formation. The rate of inelastic collision of incident electrons with carbon atoms and ionization of carbon atoms is not dependent on the temperature of the specimens. Only the rate of secondary chemical reactions depends on the temperature. By measuring the secondary effects, it is shown to be possible to estimate the number of primary processes caused by electron irradiation of organic specimens. The effective elastic and inelastic cross sections are reduced by accelerating electrons to high velocities, this effect is influential up to around 500 kv. Thus the effects of electron irradiation on organic specimens in the electron microscope were studied by comparing the rate of damage at various accelerating voltages up to 300 kv. High-voltage electron microscopy was found to be superior to the conventional method for observing organic specimens highly sensitive to electron irradiation. Results of damage to single crystals of linear polyethylene, polyethylene oxide of high molecular weight, and Nylon 6, precipitated from their dilute solutions, are reported. (BBB)

20763 INVESTIGATIONS IN THE FIELD OF RADIATION-INDUCED SOLID-STATE POLYMERIZATION. XII. THE γ-RAY-INITIATED COPOLYMERIZATION OF ACRYLIC ACID AND ACRYLAMIDE IN THE SOLID, LIQUID, AND SUPERCOOLED LIQUID STATES. Hardy, Gyula; Nagy, Lajos. Magyar Kem. Foly., 72: 71-4(Feb. 1966). (In Hungarian).

The solid system of acrylic acid and acrylamide has a phase diagram with two eutectic points, and a molecular compound of 2:1 molar ratio, which has the highest melting

point, is present. The rate of copolymerization is the greatest at the eutectic compositions, and goes through a minimum at the point corresponding to the molecular compound. The composition of the copolymer obtained in the solid state reflects the structure of the solid phase and differs from the composition determined by the relative reactivity constants. In the supercooled liquid phase the rate of copolymerization is higher than in the solid state, and the process probably has an ionic mechanism. (auth)

20764 THE INFLUENCE OF SPECIFIC ENERGY LOSS ON THE RADIATION REACTION OF POLYVINYLCHLORIDE, POLYDIMETHYLSILOXANE, AND POLYMETHACRYLIC ACID METHYL ESTERS IN SOLUTION. Schnabel, Wolfram (Hahn-Meitner-Institut fuer Kernforschung, Berlin). Makromol. Chem., 86: 9-19(1965). (In German).

Changes in structure of the polymers in various organic solvents, assessed by light scattering and viscosity measurements, after irradiation with ^{60}Co γ rays and with thermal neutrons were investigated. The nuclear reaction $^{10}B(n,d)^7Li$ was used as a source of $^4He/^7Li$ radiation. Polyvinylchloride was crosslinked in solution by both γ rays and $^4He/^7Li$ particles. In dilute solution, polyvinylchloride formed a microgel. Polydimethylsiloxane was crosslinked in concentrated solution and degraded in the main chain in dilute solution. Polymethyl methacrylate was degraded at all concentrations. In all these reactions, $^4He/^7Li$ particles were less efficient than γ rays. The results were compared with earlier investigations on the effect of the specific energy loss (LET) of the radiation. It is shown that a radiation-sensitive polymer is degraded more effectively by γ rays than by $^4He/^7Li$ particles, whereas a radiation-resistant polymer is more readily attacked by the densely ionizing radiation. An explanation of this is based on the previously developed theory of multiple ionization and excitation. Thus, in the radiosensitive polymers, each ionization by γ radiation causes a break in the main chain, while part of the more densely ionizing radiation is dissipated and not available for main-chain splitting. (BBB)

20765 LIGHT-SCATTERING AND VISCOSITY MEASUREMENTS ON THE DEGRADATION OF POLYMERS IN SOLUTION UNDER THE INFLUENCE OF ^{60}Co γ RADIATION. Ikada, Yoshito; Schnabel, Wolfram (Hahn-Meitner-Institut fuer Kernforschung, Berlin). Makromol. Chem., 86: 20-32(1965). (In German).

The following polymers were γ irradiated in the solvents indicated at dose rates varying from 0.34 to 0.96 Mrad/hr: polyvinylpyrrolidone (methanol), polyvinylacetate (acetone), polystyrene (benzene), and polydimethylsiloxane (benzene). Light scattering and viscosity measurements were carried out on the polymers in solutions below the critical concentration to determine whether the polymers undergo intramolecular crosslinking in dilute solutions or are predominantly degraded in the main chain. In all the cases investigated, degradation was found to occur. Polyvinylpyrrolidone showed practically no branching after irradiation below the critical concentration. Above this concentration, branching increased with radiation dose according to a relation given by Kilb (J. Polymer Sci., 38: 403(1959)). The degree of branching of a polyvinylacetate sample, which originally was strongly branched, decreased during irradiation in dilute acetone solution. Polystyrene was found to undergo practically only degradation along the main chain, in benzene at low concentration. Similar results were found for polydimethylsiloxane in benzene. The results are discussed in terms of Henglein's theory (J. Phys. Chem., 63: 1852(1959)) relating to degradation and crosslinking of polymers in organic solvents. The intramolecular interaction between polymer molecules, which occurred with a polymer such as polyvinylchloride, which undergoes association even in dilute solution, had an important effect on the radioinduced changes of the polymers in solution. (BBB)

20766 RADIATION-INDUCED REACTION IN POLYETHYLENE OXIDE. Fischer, H.; Hellwege, K.-H.; Johnsen, U.; Langbein, W. (Deutsches Kunststoff-Institut, Darmstadt, Ger.). Makromol. Chem., 91: 107-20(1966). (In German).

Gel-sol measurements, viscosity determinations, ir spectroscopy, bromination, and gas chromatography were performed in attempts to elucidate reactions involved in degradation reaction induced by irradiation. Polyethylene oxides $[HO(-CH_2-CH_2-O-)_nH]$ of molecular weights 2000, 4000, and 20,000 were irradiated in vacuo at 14°C by 1-Mev electrons. Studies revealed two reactions that corresponded to the radioinduced reactions of polyethylene, and two additional degradation reactions that occur in the oxide. The degradation reactions thus show the influence of oxygen in the molecular chain of polyethylene oxide, and are compared with the degradation under an external oxygen atmosphere. The G values for various reactions in polyethylene oxide were calculated to be as follows (in events/100 ev): chain formation 3.3, chain splitting 3.9, OH end group addition 3.6, RCH = O end group formation 0.40, C = C group formation 4.0 to 4.2, CH_3 end group formation ~0, H_2 formation 4.7, CH_4 formation 0.015, and CO formation 0.062. (BBB)

20767 SOME PROPERTIES OF γ-IRRADIATED STARCH AND GRAFT COPOLYMERS AS ADHESIVES AND DYEING MORDANTS. Mishina, Akira; Yoshimoto, Yukiko; Nikuni, Ziro (Osaka Univ.). Nippon Nogei Kagaku Kaishi, 37: 43-5(1963). (In Japanese).

For studying the putrefaction of γ-irradiated starch and graft copolymers, synthesized by irradiation of amylose-acrylamide, the multiplication of some microörganisms in the materials was tested, e.g., Aspergillus oryzae, Penicillium notatum, Rhizopus stolonifer, Mucor hiemalis, and Bacillus subtilis. The following samples were examined: nonirradiated potato starch, 1.25×10^6 R γ-irradiated potato starch, 1×10^8 R γ-irradiated potato starch, and graft copolymers synthesized from amylose-acrylamide (42.5% polyacrylamide). The samples were incubated with the microörganisms at 30°C for one week. At the end of incubation, acid production and weight of microörganisms which had grown on the samples were measured. The graft copolymers from amylose-acrylamide showed the greatest resistance to growth of microörganisms and were found to be the least degraded. The 10^8-R γ-irradiated potato starch showed no differences when compared with the nonirradiated starch on incubation with molds; however, it had some resistance to the growth of B. subtilis. In an adhesiveness test, 200 cm of cotton thread was soaked in 1% sample solution at 30°C for 60 min and then centrifuged. The residual samples were separated and their weight measured. The adhesiveness of potato starch was decreased by the γ irradiation, and that of the graft copolymer was also decreased compared with the nonirradiated potato starch. The capillary ascent test was performed on 2%, 1%, 0.5%, and 0.25% sample solutions. The ascending distance of graft copolymer solutions was not related to concentration. Moreover, the whiteness and luster values of graft copolymer were greater than that of nonirradiated and irradiated potato starch. (BBB)

20768 RADIOLYSIS OF AQUEOUS BENZENE SOLUTIONS IN THE PRESENCE OF INORGANIC OXIDES. Christensen, Hilbert C. (Aktiebolaget Atomenergie, Studsvik, Sweden). Nukleonika, 8: 121-3(Mar. 1966).

Aqueous 0.1 N alkaline solutions of benzene were irradiated with ^{60}Co γ rays in the presence of various inorganic oxides. The addition to the solution of silica gel, copper(II) oxide, and chromium(III) oxide did not increase the yield of phenol. When chromium(III) oxide gel, zinc oxide, or titanium dioxide were added, a 9 to 13% increase was obtained and the addition of uranium dioxide and thorium dioxide caused a 31 and 39% increase, respectively. The increase of the phenol yield was related to the energy absorbed by the solid, and G_{ox} values defined in this way were calculated as follows: $G_{ZnO} = 4.0$; $G_{TiO_2} = 3.7$; $G_{UO_2} = 6.4$ and $G_{ThO_2} = 8.0$. The specific surface areas of the oxides were determined and the possibility that the increase of the phenol yield may be dependent on this quantity is discussed. (auth)

20769 SUITABILITY OF ELECTRON POSTEMISSION OF $CaSO_4$ FOR DOSIMETRY. Hanle, W.; Scharmann, A.; Seibert, G.; Seibert, J. (Univ., Giessen, Ger.). Nukleonika, 8: 129-32(Mar. 1966). (In German).

The thermo-electron post emission and the photostimulated electron postemission (exoelectronemission) of $CaSO_4$ was investigated after irradiation with x, α and β rays. The results are discussed with respect to an application in the dosimetry of ionizing radiation. (auth)

20770 RADIATION CARBONYLATION OF PARAFFINIC HYDROCARBONS WITH CARBON MONOXIDE. Kalyazin, E. P.; Baranova, N. M. (Moscow State Univ.). Petrol. Chem. (USSR) (English Transl.), 4: 66-72(1965).

It is shown that carbonyl compounds are formed when mixtures of normal alkanes and carbon monoxide are γ irradiated (^{60}Co); their composition was established; and the influence on the reaction of dose, dose rate, and temperature was studied. When mixtures of heptane and CO were irradiated, carbonyl compounds were formed, and the yield was 0.44 molecules/100 ev. Under the given conditions, the stationary concentration of carbonyl compounds was 3.5×10^{-3} mole/1, which corresponds to the fixation of about 30% of the dissolved CO. The yield did not depend on the dose. By chromatography it was established that in the heptane-CO system, C_3, C_4, C_5, C_6, and C_8 aldehydes and a C_8 ketone were formed after irradiation. There were no C_1, C_2, and C_7 aldehydes. In the hexane-CO and octane-CO systems, there were no C_6 and C_8 aldehydes, respectively. Study of the change in the yield of total carbonyl compounds as a function of the pressure of CO in the sample showed that a rise in the pressure led to an increase in the yield, which reached a value of about 1 molecule/100 ev. Under these conditions, the relative contents of the components also changed; while for heptane at atmospheric pressure the C_8 fraction amounted to 60%, at 40 atm it amounted to 86%. Yield and composition of carbonyl compounds varied as functions of the temperature and the state of aggregation of the hydrocarbon. At –196°C, fragmentary aldehydes were completely absent and only the C_8 aldehyde and ketone remained. At +300°, conversely, the intensities of all the spots on the chromatograms became similar and formaldehyde and acetaldehyde appeared in addition to the products mentioned above. Some reaction mechanisms are proposed. (BBB)

20771 PHOTOCHEMISTRY OF THYMINE IN AQUEOUS SOLUTION. Alcantara, Raul; Wang, Shih Yi (Johns Hopkins Univ., Baltimore). Contract AT(30-1)-2798. Photochem. Photobiol., 4: 473-6(June 1965).

The photooxidation of the 5-methyl group of 1,3-dimethylthymine was previously demonstrated by the identification of 5-formyl-1,3-dimethyluracil and 5-carboxyl-1,3-dimethyluracil among the products. Since this reaction could be of significance in biological systems, a similar study was carried out using the DNA base component, thymine, to observe whether or not the same oxidation occurred. An aqueous solution of thymine was irradiated with uv light and the photoproducts from this irradiation were separated by paper chromatography. The results confirmed the expected photooxidation products. Thus, uracil, 5-hydroxymethyluracil, and 5-formyluracil were identified as the photooxidation products from an aqueous solution of thymine irradiated with germicidal lamps. For comparison, 5-formyluracil, 5-carboxyuracil, and 5-hydroxymethyluracil were prepared, and an improved procedure for the synthesis of 5-formyluracil is reported. A reaction mechanism is proposed to account for the formation of these products. (BBB)

20772 RADIATION-INDUCED ADDITION REACTION OF DIALKYL PHOSPHONATES TO FLUORINE-CONTAINING OLEFINS. Ueda, Teruo; Inukai, Kan (Government Industrial Research Inst., Nagoya, Japan). Rep. Gov. Ind. Res. Inst., Nagoya, 14: 280-5(July 1965). (In Japanese).

The radioinduced addition reactions of dialkyl phosphonates (methyl, ethyl, and n-propyl) to chlorofluoroölefins such as 1,2,2-trichloro-1-fluoroethylene, 1,2-dichloro-1,2-difluoroethylene, and 1,1-dichloro-2,2-difluoroethylene were made to give the corresponding dialkyl chlorofluoroethyl phosphonates. These phosphonates were hydrolyzed to the chlorofluoroethylphosphonic acids and then converted to the chlorofluoroethylphosphonic dichlorides. The obtained chlorofluoroethylphosphonic acids have an acidity similar to that of ω-hydroperfluoroalkylphosphonic acids and perfluoroalkylphosphonic acids. (auth)

20773 RADIATION-INDUCED ADDITION REACTION OF ETHERS TO 1,2-DICHLOROTETRAFLUOROCYCLOBUTENE AND 1,2-DICHLOROHEXAFLUOROCYCLOPENTENE. Muramatsu, Hiroshige; Inukai, Kan (Government Industrial Research Inst., Nagoya, Japan). Rep. Gov. Ind. Res. Inst., Nagoya, 14: 299-304(Aug. 1965). (In Japanese).

The addition reaction of tetrahydrofuran, dioxane, and diethyl ether to 1,2-dichlorotetrafluorocyclobutene and 1,2-dichlorohexafluorocyclopentene were carried out under γ-ray irradiation. The addition of tetrahydrofuran to 1,2-dichlorotetrafluorocyclobutene gave only the 1 : 1 adduct in an excellent yield, while the addition of dioxane yielded mainly the dehydrochlorinated 1 : 1 adduct, 2-(2-chlorotetrafluoro-1-cyclobutenyl)-dioxane, along with the 1 : 1 adduct. In the case of diethyl ether, both the dehydrochlorinated 1 : 1 and 1 : 2 adducts, namely α-(2-chlorotetrafluoro-1-cyclobutenyl) diethyl ether and α-(1,2-dichlorotetrafluorocyclobutyl)-α'-(2-chlorotetrafluoro-1-cyclobutenyl) diethyl ether, were formed along with the 1 : 1 and 1 : 2 adducts. In the addition of the ethers to 1,2-dichlorohexafluorocyclopentene, only the corresponding dehydrochlorinated 1 : 1 adducts were obtained. (auth)

20774 EFFECT OF GAMMA RADIATION ON α, β, γ, δ-TETRAPHENYLPORPHINE AND ITS COPPER AND COBALT CHELATES. Araki, Chiroru; Yamamoto, Kiyoko; Tonomura, Shizu (Inst. of Physical and Chemical Research, Tokyo). Rika Gaku Kenkyusho Hokoku, 39: 156-61(1963). (In Japanese).

The γ-induced radiolysis of α, β, γ, δ-tetraphenylporphine (TPP) and its copper and cobalt chelates (Cu-TPP, Co-TPP) in dioxane (10^{-4} mole/l) was studied spectrophotometrically in the visible region of the spectrum. These porphines were readily reduced by atomic hydrogen generated from dioxane by γ radiation. In the case of TPP, which has no metal-nitrogen bond, one product (α, β, γ, δ-tetraphenylchlorin (TPC)) was obtained. However, with the metal chelates, products of two sorts were observed, i.e., metal chelates of TPC and those of TPC derivatives in which the Cl ring was substituted. A comparison of the decomposition rates for TPP and its metal chelates showed that TPP was more readily broken down than the chelates. Minimum doses of γ radiation to open the ring of TPP, Cu-TPP, and Co-TPP were ~0.4, 1.8, and 2.0 MR, respectively. TPP was completely degraded by doses of 1 MR and the metal chelates by 8 MR. The metal-nitrogen bonds in metal chelates were not broken before the rupture of the porphyrin ring. (BBB)

20775 γ-RADIATION-INDUCED CHEMICAL CHANGES IN POLYVINYL BUTYRAL. Jedlinski, Zbigniew; Hippe, Zdzislaw (Gliwice Paint Research Inst., Poland). Rocz. Chem., 40: 257-64(1966).

Samples of thin polyvinvl butyral films were irradiated in air with γ rays. It was found that irradiation led to oxidation of the polymer and a change in unsaturation and in the initial molecular weight. A radical mechanism of oxidative radiolysis of polyvinyl butyral is suggested. (auth)

20776 EFFECT OF HYDROGEN ATOM AND ELECTRON SCAVENGERS ON THE RADIOLYSIS OF METHANOL VAPOR. Meaburn, Malcolm; Mellows, Frank W. (Centre d'Etudes Nucleaires, Saclay, France). Trans. Faraday Soc., 61: 1701-8(Aug. 1965).

In the radiolysis of liquid methanol the role of the two scavengeable precursors of hydrogen, previously identified as the hydrogen atom and solvated electron, in the production of hydrogen in vapor-phase radiolysis was investigated. The ^{60}Co γ radiolysis of the vapor was studied at 87 mm pressure and 20°C in the presence of various addi-

tives. The yields from pure methanol, $G(H_2) = 11.1 \pm 0.6$, $G(CO) = 1.18 \pm 0.06$, and $G(CH_4) = 0.35 \pm 0.05$, agreed with previously published values. The additives CCl_4, CH_3Br, and O_2 were found to be efficient electron scavengers and the electron yield, $G_{e^-} = 4.1 \pm 0.7$ was determined. Electron scavenging, but not hydrogen atom scavenging, was dose-rate dependent, a finding, which was consistent with the concept that the electron reacts with the acid species CH_3OH^+ and not with neutral methanol. Thus, in pulsed radiolysis experiments, addition of up to 3% methyl bromide had no effect on either the hydrogen or methane yields; i.e., the scavenging ability of methyl bromide was intensity dependent. This suggested that electrons led to the formation of hydrogen atoms by neutralization of $CH_3OH_2^+$ rather than by reaction with methanol; competition for electrons between methyl bromide and methanol would be unaffected by changes in radiation intensity. It was suggested previously that thermal hydrogen atoms do not play an important role in the radiolysis of methanol vapor and that consideration should be given to scavenging by charge transfer processes; however, the results obtained do not support these ideas. (BBB)

20777 THE EFFECT OF THE RADIATION OF ULTRAVIOLET RAY OR γ-RAY ON LUMINOL. Miyake, Takeo (Tokyo Univ.). Vaccum Chem. (Tokyo), 13: 198-200 (Oct. 1965). (In Japanese).

It has been found that luminol changes its fluorescence spectrum during the measurement in dimethyl formamide solution, while crystalline luminol has been proved to be stable in vacuo for irradiation with ultraviolet (high-pressure mercury lamp) or γ rays (total dose 5×10^7 R, dose rate 1.5×10^5 R/hr). Luminol is also found to be stable under the sunlight for three months in vacuo. (auth)

20778 RADIATION-INDUCED METHYLMETHACRYLATE AND STYRENE POLYMERIZATION IN PRESENCE OF MINERAL FILLERS. Uskov, I. A.; Tertykh, L. I.; Solomko, V. P.; Polyshchuk, Yu. N. (Kiev State Univ. Inst. of Physical Chemistry, Academy of Sciences, Ukrainian SSR). Vysokomol. Soedin., 8: 26-30(Jan. 1966). (In Russian).

The effects of mineral fillers in liquid-phase polymerization of vinyl monomers and radioinduced grafting of polymers to solid surface were studied at 20 and 70°C. In the presence of fillers the homopolymer yield and molecular weight increased. On irradiation for grafting of polymers to solid surfaces, it was found that the less-porous filters with low specific surface were more active. Increases in the temperature were accompanied by high polymer yields and better grafting, which pointed to a radical mechanism for the process. Additional irradiation of the fillers with grafted polymethylmethacrylate in styrene resulted in two-layer grafting, which can proceed to a higher degree than monolayer grafting. The less grafted polymethylmethacrylate on the filler, the higher the yield of grafted polystyrene achieved. (auth)

20779 STRUCTURE OF POLYPROPYLENE CHLORINATED BY RADIATION AND SULFOCHLORINATED. Dzhagatspanyan, R. V.; Bardenshtein, S. B.; Kolbasov, V. I.; Korolev, B. M. Vysokomol. Soedin., 8: 125-30 (Jan. 1966). (In Russian).

The infrared spectra of polypropylene (PP) chlorinated and sulfochlorinated by irradiation in the solid state with chlorine contents up to 45% and sulfur contents up to 5.8% were studied. There was a decrease in crystallinity with PP chlorination and sulfochlorination. The crystallinity of PP chlorinated in the solid state was one-third that of PP and it had a substantially lower intensity of the 685 sm^{-1} hand, a more intense 763 sm^{-1} hand, and a shift of the 762 sm^{-1} hand to 735 sm^{-1}. (auth)

20780 ACHIEVEMENTS OF THE POLISH RADIATION CHEMISTRY AND THE PERSPECTIVES OF THE DEVELOPMENT. Kroh, Jerzy; Sugier, Henryk. Wiad. Chem., 20: 85-98(Feb. 1966). (In Polish).

A survey of important publications and achievements in the field of radiation chemistry in Poland is given. Main directions of further investigations are outlined. (auth)

20781 FORMATION OF ALKALI METALS FROM ALKALI HALIDES BY IRRADIATION WITH 50-kev ELECTRONS. Creuzburg, M. (Univ., Hamburg). Z. Naturforsch., 20a: 1732-3(Dec. 1965). (In German).

The energy loss spectrum of thin layers of NaI was determined at room temperature immediately after vapor deposition of the layer and after 15 min irradiation with 50-kev electrons. The changes caused in the energy loss spectrum were attributed to the formation of sodium inclusions. (J.S.R.)

20782 ISOTOPE EFFECTS IN THE PHOTOCHEMICAL TRANSFORMATION OF TRITIUM-LABELED URACIL. Wacker, Adolf; Kornhauser, Andrija; Traeger, Lothar (Univ., Frankfurt am Main). Z. Naturforsch., 20b: 1043-7(Nov. 1965). (In German).

In the uv irradiation of uracil-(5,6-^{3}H), dimers of uracil and uracil-water addition products (5,6-dihydro-6-hydroxyuracil) are formed as radioactive photoproducts according to the irradiation energy. In the synthesis of water-addition products a considerable secondary isotope effect was evident, but the radioactivity of the uracil dimer scarcely changed with respect to the initial uracil. If the water-addition product was retransformed by heating to uracil, the molecule was also dehydrated with the appearance of an isotopic effect. If the uracil dimer was retransformed to uracil, no isotopic effect was observed. In the irradiation of uracil in tritium-containing water only very low radioactivities were introduced into the photoproduct. The isotopic effect amounted to about 8. By synthesis of the photoproduct from specific uracil tritium-labeled on the C-5 or C-6 or by bromination of 5,6-tritium-labeled uracil or its photoproducts to the 5-bromo-derivatives, indications were obtained that the velocity-determining step of the water addition proceeds on the C-6 of the uracil. The inverse secondary isotopic effect amounted to approximately 0.65 on C-6 for tritium and 0.95 for tritium on C-5. (tr-auth)

20783 USE OF GAS-LIQUID CHROMATOGRAPHY FOR DETERMINING SPECIFIC ACTIVITY AND SURVIVAL OF MOTHER COMPOUNDS LABELED WITH RECOIL ATOMS. Firsova, L. P.; Reinkhardt, M.; Barakat, M. F. pp 103-8 of Radiokhimicheskie Metody Opredeleniya Mikroelementov. Moscow-Leningrad, Izdatel'stvo Nauka, 1965. (In Russian).

Data are presented on the degree of survival and specific activity of ^{14}C-labeled heterocyclic compounds irradiated for 100 to 200 hr with 2 to 8.7×10^{12} n/cm^2 sec. The radiation stability of the heterocyclics is estimated. Materials studied are pyridine, piperidine, pyrrole, 2-methylpyrrole, and α-, β-, and γ-picoline. The scheme of the apparatus and the experimental method using gas-liquid chromatography are described. (M.J.T.)

20784 REACTIONS OF HOT SULFUR ATOMS. I. PRODUCTION OF LABELED POLYMER PRODUCTS. Dzantiev, B. G.; Stukan, R. A.; Shvedchikov, A. P. pp 181-5 of Radiokhimicheskie Metody Opredeleniya Mikroelementov. Moscow-Leningrad, Izdatel'stvo Nauka, 1965. (In Russian).

Mixtures of CCl_4 and C_6H_{12} were irradiated in a reactor, causing radioactive ^{35}S atoms to be produced according to the reaction $^{35}Cl(n,p)^{35}S$. The irradiated mixture was allowed to decay for about 1 month and then dissolved in toluene; bicyclohexyl was added as a carrier, and the volatile products were distilled in vacuum at room temperature. The polymer residue after distillation was studied. The composition of the polymer was analyzed by paper chromatography and diffusion from a capillary. The chromatogram of the polymer showed that two types of compound were formed. Results are shown of the variation of yield of polymer with composition of the irradiated mixture and of the kinetics of diffusion from the capillary for polymers of both types, obtained from various compositions of the irradiated mixture. The mechanism of formation and the properties of the polymer are discussed. (M.J.T.)

20785 METHODS FOR HOT SYNTHESIS OF ^{35}S-LABELED BIOLOGICALLY ACTIVE SUBSTANCES. I.

REACTIONS OF ^{35}S ATOMS WITH 4-METHYL-5β-OXY-ETHYLTHIAZOLE. Dzantiev, B. G.; Shishkov, A. V. pp 185-7 of Radiokhimicheskie Metody Opredeleniya Mikroelementov. Moscow-Leningrad, Izdatel'stvo Nauka, 1965. (In Russian).

The possibility is shown of obtaining ^{35}S-labeled 4-methyl-5β-oxyethylthiazole (an intermediate product in the synthesis of vitamin B_1) by the method of hot synthesis. The dependence of the yield of labeled product on the composition of the system is studied, and optimum conditions of synthesis are established. (tr-auth)

20786 METHODS FOR HOT SYNTHESIS OF ^{35}S LABELED BIOLOGICALLY ACTIVE SUBSTANCES. II. REACTIONS OF ^{35}S RECOIL ATOMS WITH CERTAIN AMINO ACIDS. Dzantiev, B. G.; Shishkov, A. V. pp 187-93 of Radiokhimicheskie Metody Opredeleniya Mikroelementov. Moscow-Leningrad, Izdatel'stvo Nauka, 1965. (In Russian).

The interaction of hot ^{35}S atoms with the amino acids methionine, norvaline, and norleucine was studied. At the same time, the radiolysis of methionine during irradiation in a reactor was investigated. The formation of labeled methionine by the replacement of the sulfur in methionine and the CH_2 group in norleucine by a hot ^{35}S atom and also by imbedding at the C—C bond in the norvaline molecule was established. The investigated processes can be used for obtaining ^{35}S-labeled methionine with high specific activity. (tr-auth)

20787 IMPROVEMENTS IN OR RELATING TO LUMINOUS COMPOSITIONS. Evans, Charles Charlton; Maynard, John Charles (to United Kingdom Atomic Energy Authority). British Patent 1,020,752. Feb. 23, 1966. Filed Mar. 12, 1962.

A luminous composition is described that consists of an intimate mixture of phosphor particles and a tritiated silicone polymer. The method of producing the composition comprises exposing the phosphor particles to the vapor or solution of a tritiated organic-substituted halogenosilane, containing more than one halogen atom per Si atom, and water vapor so that an intimate mixture of the phosphor particles and a low molecular weight tritiated silicone polymer is formed by the hydrolysis of the halogenosilane and heating the composition to cure the silicone polymer. (B.L.M.)

20788 POLYMERIZATION OF n-BUTYRALDEHYDE BY IONIZING RADIATION. Oya, Shinzo (to Teijin Ltd.). Japanese Patent 1964-545. Jan. 13, 1965. Filed Dec. 1, 1961.

A high polymer of n-butyraldehyde is easily obtained by irradiating the monomer with high-energy ionizing radiation under the defined conditions of temperature, phase, and radiation dose. Polyethertype polymer with high-degree polymerization is obtained by irradiating n-butyraldehyde with ionizing radiation at total doses of 10^3-10^9 rad in the temperature range of –200°C to the melting point of the monomer in the atmosphere of air or inert gas or under vacuum. (NSA of Japan)

Radiochemistry

See also Separation Processes and Procedures

Refer also to abstracts 20730, 21218, and 22405.

20789 (CNEA–182) METODO SIMPLIFICADO PARA LA MARCACION DE LIPIDOS CON ^{131}YODO. (A Simple Method for Labeling Lipids with ^{131}I). Mitta, Aldo E.; Dankert, Marcelo A. (Comision Nacional de Energia Atomica, Buenos Aires (Argentina)). 1965. 5p. (CONF-641126–3). Dep. mn.

From 1st Symposium on Nuclear Medicine, Mendoza, Argentina.

A procedure for the labeling of triolein, oleic acid, and other lipids with ^{131}I is described. The method is based on the preparation of iodine chloride and subsequent labeling of this compound by exchange with radioactive iodine. The labeled iodine chloride is then reacted with the lipids to produce the labeled lipids. Radioactive yields of the order from 90 to 95% were obtained. (J.S.R.)

20790 (CONF-651069–1) THE RADIOACTIVITY OF THOROTRAST AND ITS IN-VITRO DISTRIBUTION BETWEEN THE VARIOUS PHYSICAL PHASES. Parr, Robert M. (International Atomic Energy Agency, Vienna (Austria)). [1965]. Contract AT(30-1)-2819. 22p. Dep. mn. CFSTI $1.00 cy, $0.50 mn.

From IAEA Meeting on Dosimetry and Toxicity of Thorotrast, Vienna.

Work on Thorotrast is reviewed and the mechanisms that determine the distribution of thorium daughter activities among the different physical phases of Thorotrast are discussed. It is concluded that: the total in vitro activity of Thorotrast varies significantly with time, but in an accurately predictable matter for the first 50 years after manufacture; three physical phases can be distinguished in Thorotrast—particles, solution, and walls of the container; the escape of activities in vitro from the particulate phase of Thorotrast is probably due to high energy recoils; approximately 80% of the total in vitro activity of ^{228}Ra (and ^{228}Ac) is located outside the particulate phase; and significant proportions of the total in vitro activities of Thorotrast are sometimes bound to the walls of the ampoule. (H.G.D.)

20791 ON A NEW TECHNIQUE RELATING THE EFFECT OF INTENSE RADIATION FIELDS ON ELECTRODE PROCESSES. INFLUENCE OF ALIPHATIC ALCOHOLS ON THE OXIDATION OF Fe(II). Busulini, Loris; Cescon, Paolo. (Centro Nazionale di Chimica della Radiazioni e dei Radioelementi, Bologna). Ann. Chim. (Rome), 54: 1308-15(Dec. 1964). (In Italian).

Electrode potentials were measured for a radioactive (^{210}Po) electrode relative to calomel; another electrode similar in geometry but not activated was used for comparison. The solutions were 0.8M in H_2SO_4 and 10^{-3}M in $Fe_2(SO_4)_3$ and were deoxygenated. The effects of alcohols on the currents at the radioactive and normal electrodes for the reduction of Fe(III) to Fe(II) as a function of concentration were studied. Concentrations ranged up to 90% for alcohols miscible in all proportions with water, and up to the limit of solubility for others. A diminution in the height of the peak for the radioactive electrode relative to the normal one was observed to be a function of the nature of the alcohol and the concentration. The diminution became less severe with longer-chain alcohols and also less severe with increased branching of the alcohols. A scale of reactivity is diagrammed in which change in inhibiting power on the reaction (log $\Delta i/m$) is plotted vs the number of C atoms for C_1 to C_8 alcohols. (BBB)

20792 RADIOCHEMICAL STABILITY OF HIGH-BOILING HYDROCARBONS IN REACTOR. Kish, I.; Kosha-Shamodi, I.; Kulesh, I.; Roder, M.; Shiller, R. (Central Inst. of Physics, Budapest). At. Energ. (USSR), 20: 35-40(Jan. 1966). (In Russian).

The possibility of the utilization of organic materials as heat transfer agents was investigated. The radiochemical conversions of alkylbiphenyls, the radiochemical processes and thermodynamics of the equilibrium in mixtures of biphenyl and its alkyl derivatives, and the radiothermal stability of eutectic mixtures of biphenyl–diphenyl methane in reactor loops were studied. (tr-auth)

20793 INDUSTRIAL APPLICATION OF RADIOCHEMISTRY. Puig, J. R. Energ. Nucl., 8: 23-32(Jan.-Feb. 1966). (In French).

Radiochemical methods have some technical and economic advantages over classical methods. They can be applied to chain reactions (graft polymerization and graft copolymerization) and provide a means of obtaining cross linkings in the case of macromolecular systems. The possibilities provided by radiochemistry are examined. Some examples of experimental and industrial applications are given. (auth)

20794 THE PREPARATION OF POTASSIUM HEXACYANOCOBALTATE(III) LABELED WITH ^{58}Co AND ^{60}Co FOR HYDROLOGICAL STUDIES. Peisach, M. (Southern Universities Nuclear Inst., Faure, S. Africa). J. S. African Chem. Inst., 18: 1-5(Apr. 1965).

Procedural details are given for the preparation of reactor-produced ^{58}Co, by the reaction $^{58}Ni(n,p)^{58}Co$, and ^{60}Co, by $^{59}Co(n,\gamma)^{60}Co$, which were used to prepare tracer solutions of $K_3Co(CN)_6$ for hydrological studies. Preparation and irradiation of nickel, as a target material for ^{58}Co activation low in iron and cobalt, are described. Nickel carbonate was dissolved in 9N HCl, and a small amount of ^{60}Co solution was added as tracer and the solution passed through a column of Amberlite IRA-400, 30 cm in length and 2.5 cm in diameter, where all the cobalt activity was retained in the top centimeter. Nickel, free from Co, was precipitated from the eluate as the carbonate. The nickel carbonate target was irradiated in the IRR-1 reactor and left for about a week to allow short-lived products to decay. Radiocobalt was separated from the irradiated nickel in two stages, the solution was passed through the same column, where most of the nickel was recovered. Second, the radiocobalt, with some nickel eluted from the first column, was passed through a smaller column of Amberlite IRA-400 to remove all remaining nickel salts. The yield of ^{58}Co so obtained corresponded to a saturation activity of 103 mC per g of nickel at a flux of 10^{13} neutrons/cm^2 sec. Cobalt chloride was used as a target for ^{60}Co preparation. For preparation of potassium hexacyanocobaltate(III), the solution of radiocobalt, as ^{58}Co or ^{60}Co, was treated with a slight excess of potassium cyanide solution and the resulting precipitate of cobaltous cyanide was filtered off and thoroughly washed with water. It was then stirred with a 10% excess of 37% w/v aqueous potassium cyanide, and the greenish precipitate formed was converted to $K_3Co(CN)_6$ by the addition of hydrogen peroxide. Gamma measurements showed that the ^{58}Co contained less than 0.1% ^{60}Co, while no impurity could be detected in the ^{60}Co. (BBB)

20795 ELECTRODEPOSITION METHOD FOR COUNTING ALPHA AND BETA EMITTERS. Kim, Stephen M.; Noakes, John E.; Miller, W. W. (Oak Ridge Inst. of Nuclear Studies, Tenn.). Nucleonics, 24: 66-7(Mar. 1966).

A study was made of the optimum conditions for electroplating thorium, uranium, and protactinium. Such thin film preparation prevents self-absorption and increases the spectrum resolution of beta and alpha emitters. The ethanol solvent system used for electrodeposition of the samples on platinum disks gives yields approaching 100%. This method is also used to deposit lanthanide elements on platinum disks for counting. (J.F.P.)

20796 THE ARTIFICIAL ELEMENTS. Rodriquez, Dominguez (Univ., Madrid). Rev. Univ. Madrid, 12: 479-515(1963). (In Spanish).

Historical aspects and recent developments in the production and separation of artificial elements are reviewed. Technics for preparation of the following are described: Tc, Pm, Np, Pu, Am, Cm, Bk, Cf, Es, Fm, Md, No, and Lw. Steps and products of fission of ^{238}U are outlined. Various reactors being used to produce transuranium elements are discussed, along with future possibilities of production of some of the heaviest elements with very short half lives. Principal isotopes of the artificial elements are considered, and various steps in their isolation and purification are examined. (BBB)

20797 HOT ATOM CHEMISTRY OF ^{76}As USING ZIRCONIUM BENZENEARSONATE AS TARGET. Suzuki, Shin; Saito, Makoto; Inoue, Yasushi. Sci. Rept. Res. Inst., Tohoku Univ., Ser. A, 17: 267-76(Nov. 1965).

The enrichment of ^{76}As by means of hot atom effects of the (n, γ) reaction was investigated by using zirconium benzenearsonate as a target. This compound is insoluble in dilute hydrochloric acid and it is assumed that the recoil fragments can be separated from the target by extracting it with dilute hydrochloric acid. By this principle, the enrichment of ^{76}As was accomplished with an enrichment factor of 1.2×10^4. Its radiochemical purity was 99.88 to 99.98% on the basis of β counting and the main impurity was assumed to be ^{97}Zr and the chemical impurity was not detected. Although its oxidation state varied with time, 55.5 to 70% of total activity was As (III). This method of enrichment of ^{76}As has the merits of rapidity and simplicity in procedure, especially in the production of radioactive isotopes of short life. (auth)

20798 RADIOCARBON SAMPLES: CHEMICAL REMOVAL OF PLANT CONTAMINANTS. Haynes, C. Vance Jr. (Univ. of Arizona, Tucson). Science, 151: 1391-2 (Mar. 18, 1966).

Roots and similar plant matter can be efficiently removed from charcoal samples by nitration and acetone leaching after preliminary removal of humic acids and lignin by standard procedures. (auth)

20799 SPECIFIC DEUTERATION β TO A KETO GROUP: REDUCTION OF α,β-ETHYLENIC KETONES WITH LITHIUM AND DEUTERATED PROPYLAMINE. Fetizon, Marcel; Gore, Jacques (Faculte des Sciences, Orsay, France). Tetrahedron Lett., No. 5, 471-5(Feb. 1966).

For the introduction of a deuterium atom β to a keto group in steroids the reduction of the α,β ethylenic ketones by lithium in deuterated liquid ammonia has been described previously, but this procedure is not entirely satisfactory for several reasons. Deuterated liquid ammonia is difficult to prepare, to handle, and to store. Also, it is difficult to avoid the presence of some residual heavy water (used in the preparation of ND_3), so that the Li/ND_3 reduction generally proceeds further to the alcohol. Oxidation is then necessary to obtain the required ketone. It is proposed that low molecular weight amines such as propylamine (E_{760} = 48°) or isopropylamine (E_{760} = 33°) can be used to avoid these drawbacks of liquid ammonia. Initially, the scope of the reaction with undeuterated propylamine was investigated. The reduction of the various conjugated ethylenic ketones examined proceeded much more rapidly in propylamine, probably due to its superior dissolving power for lithium. Good yields were obtained with all seven of the conjugated ketones investigated. (TCO)

20800 COHERENT GAMMA RADIATION. Senett, William P. (to Leesona Corp.). U. S. Patent 3,233,107. Feb. 1, 1966. Filed June 25, 1962.

A coherent gamma radiation source includes a neutron excitation source, a container comprising a single crystal having opposed flat parallel walls, and a material disposed between the walls that can be excited in the nucleus. The material may be a gas, liquid, or solid. The container is positioned to receive energy from the source, and the material in the container is positioned so that the gamma radiation produced between the opposing walls is coherent. (B.L.M.)

Separation Processes and Procedures

See also **Analytical Procedures**
ISOTOPE TECHNOLOGY — Separation and Production

Refer also to abstracts 20969, and 20971–20974.

20801 (ANL-6830) ENGINEERING DEVELOPMENT OF FLUID-BED FLUORIDE VOLATILITY PROCESSES. PART 2. BENCH-SCALE INVESTIGATION OF A PROCESS FOR ALUMINUM–URANIUM ALLOY AND STAINLESS STEEL-CERMET FUELS. Ramaswami, D.; Levitz, N. M.; Jonke, A. A. (Argonne National Lab., Ill.). Dec. 1965. Contract W-31-109-eng-38. 48p. Dep. mn. CFSTI $3.00 cy, $0.50 mn.

Methods were developed for reprocessing highly enriched uranium–aluminum alloy and uranium dioxide–stainless steel cermet fuels. These methods involve two basic gas-solid reaction steps: a separation step, in which the cladding, the bulk constituent of the fuel, is separated from the uranium, a minor (<10 wt %) constituent of the fuel; and a fluorination step, in which the uranium is recovered through the production of the volatile hexafluoride. The reactions are conducted in a fluid bed of high-fired alumina, which serves as a heat-transfer medium. Processing of these two types of fuels differs mainly in the initial separation step: hydrogen chloride is used to remove the aluminum as the volatile chloride; the hydrogen fluoride-oxygen mixture is employed to destroy the stainless-steel matrix by producing an oxide mixture which remains with the alumina. Process studies were conducted in a $1\frac{1}{2}$-in.-dia nickel fluid-bed reactor with miniature nonirradiated fuel subassemblies. More than 99% of the uranium in the fuel charge was recovered over a range of processing conditions. (P.C.H.)

20802 (ANL–7055, pp 21-98) COMPACT PYROCHEMICAL PROCESSES. (Argonne National Lab., Ill.).

Research and development progress is reported on melt refining, liquid metal and fused salt processes, process facilities and equipment for EBR-II, fuel cycle facility operations for EBR-II, chemistry of liquid metals, and fuel preparation for fast reactors. (J.R.D.)

20803 (ANL–7055, pp 99-162) FUEL CYCLE APPLICATIONS OF VOLATILITY AND FLUIDIZATION TECHNIQUES. Jonke, A. A. (Argonne National Lab., Ill.).

Research directed toward development of all-volatility processing plant for spent fuels is summarized. Results of investigations concerning fluorination of U_3O_8, fluorination of UO_2–PuO_2, reactions of BrF_5, reactions of NpF_6, and solid-liquid equilibria are presented along with results of engineering-scale investigations on fluid-bed volatility processes. (J.R.D.)

20804 (EUR–2754.f) RECUPERATION PAR PRECIPITATION OXALIQUE DU ^{90}Sr ET DU ^{144}Ce A PARTIR DE SOLUTIONS CONCENTREES DE PRODUITS DE FISSION. (Recovery of ^{90}Sr and ^{144}Ce From Concentrated Fission-Product Solutions by Means of Oxalic-Acid Precipitation). Klose, A.; Brohee, H. (European Atomic Energy Community); Lefevre, J. (Commissariat a l'Energie Atomique, Saclay (France). Centre d'Etudes Nucleaires). Mar. 1966. 32p. Dep. mn.

With the aim of evaluating the savings that could be effected on the installation cost of a strontium recovery unit, consideration was given to the separation of strontium by means of oxalic acid precipitation in a plant envisaged for cesium recovery. A detailed study of the process showed that its selectivity and yield are too low to enable a saving to be achieved under the conditions applied, namely production of purified ^{90}Sr sources and decontamination of the fission product solutions. (auth)

20805 (IS–1329) SEPARATION OF CADMIUM FROM THE LEAD–BISMUTH EUTECTIC BY HIGH VACUUM SINGLE-STAGE DISTILLATIONS: CHAMBER DESIGN AND DISTILLATE PURITY. Murdoch, Lawrence B.; Burnet, George (Ames Lab., Iowa State Univ. of Science and Tech.). Mar. 1966. Contract W-7405-eng-82. 28p. Dep. mn. CFSTI $2.00 cy, $0.50 mn.

A distillation chamber was evaluated to determine its effectiveness for separating liquid metals by a continuous high vacuum distillation process. The chamber had an integral condenser which was cooled by a sodium-potassium eutectic. The metal to be separated flowed down an inclined distribution plate, opposite the condenser. Partial separation of cadmium from the lead-bismuth eutectic was achieved, however distillate purity was found to be low. The cause of the low purity was investigated and found to be short-circuiting of liquid metal from the distribution plate to the distillate receiver. Chamber design changes are recommended. (auth)

20806 (MLM–1274) MOUND LABORATORY PROGRESS REPORT FOR JULY 1965. Eichelberger, J. F.; Grove, G. R.; Jones, L. V. (Mound Lab., Miamisburg, Ohio). July 21, 1965. Contract AT(33-1)-Gen-53. 26p. Dep. mn. CFSTI $2.00 cy, $0.50 mn.

The swing system in the lower (^{13}C product) stages of the methane thermal diffusion cascade was removed and interstage circulation pumps were installed. The pumps for the lowermost stages were miniature canned pumps of a new design. The low-temperature fractional distillation column for enriching CO in ^{13}C was delivered and installed. In pilot experiments with material of 4.5% ^{13}C enrichment, high-purity elemental C was produced from CO_2. Experimental work to determine the effect of varying the amine solution flow rate on ^{13}C separation factor was continued. After lowering the ^{38}Ar peak into the third stage, over one liter of 17.8% ^{38}Ar was withdrawn. The third pass for enriching ^{86}Kr was started. Over 70% ^{86}Kr is being accumulated. A second run on a six-stage cascaded system with a modified gas circulating system enriched ^{131}Xe to 18%. Cascade calculations were made for separation of ^{124}Xe from natural Xe (natural abundance = 0.096%) in the 24-column tube bundle system. The heats of adsorption of Kr and Xe on Linde's Molecular Sieve 5A, 50/60 mesh were calculated to be −3091 cal/mole and −5127 cal/mole, respectively, based on separations made using He carrier gas. A complete set of experimental thermal diffusion column transport coefficients was obtained for ^{20}Ne and ^{22}Ne in one of the 12-foot experimental columns. The theoretical expressions for the transport properties of gases are used as relations between measurable quantities. Values of the diffusion coefficient and thermal diffusion factor for ^3He and ^4He mixtures were calculated and the thermal conductivity of ^3He was calculated from its viscosity. A computer program was written to calculate collision integrals for an arbitrary intermolecular potential function. Collision integrals for the modified Buckingham ($\alpha = 14$) potential were calculated. A flip coil for measuring small magnetic fields was built to measure the residual field of superconducting solenoids. The metal constituents in metal-organo compounds were determined by neutron activation analysis. (J.R.D.)

20807 (MLM–1287) MOUND LABORATORY PROGRESS REPORT FOR AUGUST 1965. Eichelberger, J. F.; Grove, G. R.; Jones, L. V. (Mound Lab., Miamisburg, Ohio). Aug. 20, 1965. Contract AT(33-1)-Gen-53. 27p. Dep. mn. CFSTI $2.00 cy, $0.50 mn.

X-ray diffraction patterns of an eight-month old sample of an isotopic mixture of $^{208}Po/^{209}Po$ were identical to the alpha phase of ^{210}Po metal. Apparently, the face-centered cubic PbPo which grows acts as a seed for the growth of the alpha phase. Material of molecular mass 18 has steadily accumulated in the 12-column, 8-stage methane thermal diffusion system. Infrared analysis showed conclusively that this material was $^{13}CH_3D$. It appears that the $^{13}CH_3D$ forms in the thermal diffusion system by an exchange reaction between $^{13}CH_4$ and $^{12}CH_3D$. Two CO_2-carbamate exchange-reaction runs were carried out using mixed amine solutions. The results were inconclusive because the carbamate did not dissociate completely. A 12-in. cylindrical charcoal trap reduced the tritium level of product ^3He from 2.5×10^{-9}% to 6.4×10^{-11}%. The new three-column neon tube bundle is being checked in preparation for start-up. It should enrich 10% intermediate ^{21}Ne to above 70%. The five-stage Ar cascade has built up an ^{38}Ar peak of approximately 28%. The fourth pass for enriching ^{86}Kr was made. Over 89% ^{86}Kr was accumulated. The new 24-column six-stage thermal diffusion cascade system constructed in two tube bundles (water jackets) was started using natural Xe as feed. The heats of adsorption of Kr and Xe on Linde Molecular Sieve 5A, 50/60 mesh were calculated to be −1208 and −1901 cal/mole, respectively, based on separations using N as the carrier gas. Discrepancies between theory and experiment for recent thermal diffusion column experiments with Ne can be explained by a stagnant gas barrier in the column. The accuracy of molecular collision integrals for gases was investigated. The possibility of

maintaining a relatively constant level of liquid He in a pumped bath for use in the distillation separation of ^3He and ^4He was investigated. Research is in progress to determine the reason for differences in measured thermomolecular pressure in He by different investigators. A direct reader procedure was developed for the determination of Be in air. A direct reader procedure was developed which could detect impurities in Au at levels below 6×10^{-5} mg. The total shrinkage of Eastman 910 adhesive (methyl 2-cyano-acrylate) was determined using thermal, free-radical and anionic polymerization conditions. (J.R.D.)

20808 (ORNL–3916) UNIT OPERATIONS SECTION QUARTERLY PROGRESS REPORT, JULY–SEPTEMBER 1965. Whatley, M. E.; Haas, P. A.; Horton, R. W.; Ryon, A. D.; Suddath, J. C.; Watson, C. D. (Oak Ridge National Lab., Tenn.). Mar. 1966. Contract W-7405-eng-26. 78p. Dep. mn. CFSTI $3.00 cy, $0.75 mn.

The flow capacity of the stacked-clone contactor is greater using hexone than Amsco; substitution of mineral oil has little effect on capacity. The average stage efficiency for U transfer in the hexone-aluminum nitrate system was 69%. In close-coupled processing of molten-salt reactor fuels, CrF_3 can be sorbed on NaF at 400°C with U loss of less than 0.01%. The capacity of low-surface-area NaF pellets is 20 g of Cr per 100 g NaF. Mechanical shearing of unirradiated Consolidated Edison and Elk River fuel assemblies was successfully demonstrated. Vapor-liquid equilibrium data for UF_6-NbF_5 are being measured to aid in design of distillation equipment for their separation. Thoria microsphere preparation and continuous calcination of thoria gels were studied. Both rotary and shear-nozzle dispersers produced satisfactory microspheres in a continuous drying column. A vertical tube furnace was demonstrated for continuous calcination of thoria-urania gel. Operating procedures were developed to avoid bridging and consequent breakage of the tube during calcination. Natural, depleted, and enriched UO_2 microspheres were prepared in a continuous drying column. The laboratory process for extracting mixed t-RNA from E. coli cells was modified and scaled up to the production of 1 kg. An outline of the purification procedure is presented. Continuous operation of the fermenter was demonstrated for 80 hr and was stopped after 300 kg of cells had been produced. Continued screening of paints has discovered three that can tolerate up to 8×10^9 R of gamma radiation when exposed in deionized water. This is 60% more than for any coating previously tested. The retention of radionuclides after exposure to conditions simulating release of radioactivity from a reactor excursion was measured. The vinyl coatings show less retention than other generic types. (J.R.D.)

20809 (ORNL–3925) CRITICAL-PATH METHOD FOR SCHEDULING THE TRANSURANIUM PROCESSING PLANT: AN APPRAISAL. Burch, W. D.; LaMaster, C. H. (Oak Ridge National Lab., Tenn.). Mar. 1966. Contract W-7405-eng-26. 44p. Dep. mn. CFSTI $2.00 cy, $0.50 mn.

At the direction of the Atomic Energy Commission, the construction of the Transuranium Processing Plant was scheduled by the critical-path method (CPM) as a test of its usefulness in coordinating and expediting all phases of a major construction project. The use of CPM for the ORNL phases of the project is summarized, along with techniques used and major problems and advantages of this method in scheduling the design, procurement, fabrication, and installation of equipment. Coordination and scheduling of associated research and development programs were attempted with only limited success. To the members of the project, CPM appeared to have outstanding advantages over previous scheduling systems for a construction project. The fact that the basic project was completed very nearly on schedule (12/31/65) and well within the originally allotted funds can be at least partially attributed to the exacting scheduling required by CPM. The cost attributed directly to scheduling represented 1.3% of total funds expended on the project by the Laboratory. Specific methods used, and discussions of day-to-day management and supervisory uses of the technique are reported. Examples are given to show advantages in developing such schedules, their usefulness in alerting management to trouble spots, and the actions taken by management. Examples of failure to meet expectations are also cited. (auth)

20810 (ANL-Trans–250) DESIGN PROBLEMS OF PILOT PLANTS FOR VOLATILIZATION RECYCLING. Schmets, J.; Heremans, R.; Pierini, G. (Centre d'Etude de l'Energie Nucleaire, Brussels (Belgium)). Translated for Argonne National Lab., Ill., from paper Presented at the Symposium on Design and Construction Problems of Pilot Plants for Recycling Irradiated Fuels, Turin, September 23–24, 1965. 27p. (CONF-650964–1). Dep. mn. JCL $2.60 fs, $1.01 mf.

Problems involved in the design of pilot plants for recycling irradiated fuel by fluoride volatilization are evaluated. Critical control of materials movement, plant capacity, equipment, residues, remote manipulation, shielding, and safety are discussed. In some cases, appropriate solutions have been found. In others, unit operations procedures developed for hot or cold work in other laboratories have been employed. Research on fluoride chemistry is also discussed. (auth)

20811 SEPARATION OF URANIUM BY COMBINED ION EXCHANGE AND SOLVENT EXTRACTION. Korkisch, Johann; Ahluwalia, S. S. (Univ. of Vienna). Anal. Chem., 38: 497-500 (Mar. 1966).

The effects of nitric acid concentration on the adsorption of uranium from 90% tetrahydrofuran(THF)-nitric acid mixtures showed that the adsorption decreases rather strongly with increasing concentrations of nitric acid. When 10% 0.6N HNO_3 is present, the Kd of uranium is $>10^3$. Increasing the concentration of nitric acid to 6N decreases the Kd of uranium, while the Kd for other metal ions increases from $>10^3$ to 10^4. Results from ion-exchange separation of uranium from other metal ions in 90% THF–10% 6N HNO_3 are given along with those for the 90% THF–10% 0.6N HNO_3 medium. The distribution coefficients of uranium in various organic solvent-water mixture containing 10% 6N HNO_3 are also given. The greatest advantage of combined ion exchange-solvent extraction (CIESE) is that immediately after removal of the extractable species (uranium), a further fractionation of the adsorbed metal ions can be achieved on the resin. (F.J.H.)

20812 IMPROVED EXTRACTION METHOD FOR ISOLATION OF TRIVALENT ACTINIDE-LANTHANIDE ELEMENTS FROM NITRATE SOLUTIONS. Moore, F. L. (Oak Ridge National Lab., Tenn.). Anal. Chem., 38: 510-11 (Mar. 1966).

The method for liquid-liquid extraction of trivalent actinide-lanthanide elements from relatively dilute solutions of aluminum nitrate-nitric acid with a quaternary ammonium salt, tricaprylmethylammonium nitrate (Aliquat 336–S–NO_3) is presented. The effects of the nitric acid concentration on the extraction efficiency are considered. Extractability of all elements decreases with increasing nitric acid concentration. The order of decreasing extractability is Ce > Am > Pm > Cf > Bk > Cm > Eu > Tm > Y. The trivalent actinide-lanthanum elements are easily stripped from the 30% Aliquat 336–S–NO_3–xylene solution into mineral acid or water. (F.J.H.)

20813 ION-EXCHANGE SEPARATION OF URANIUM AND RARE-EARTH ELEMENTS. Nikashina, V. A.; Senyavin, M. M.; Sorochan, A. M.; Alekseenko, V. A. At. Energ. (USSR), 20: 40-6 (Jan. 1966). (In Russian).

With the purpose of determining the optimum conditions for the ion exchange separation of uranium and rare earth elements, calculations were made on their sorption from mixtures onto cationite KU-2 from acid solutions of different concentrations. The experimental data agree well with the theoretical data. On the basis of the calculations, chromatographic tests were made on the separation of uranium and the rare earth elements from solutions of hydrochloric, nitric, perchloric, sulfuric, and hydrofluoric acids. The optimum conditions for their separation were found. (tr-auth)

20814 SEPARATION OF BINARY MIXTURES OF SOME LANTHANOIDS (LANTHANUM, CERIUM, PRASEODYMIUM AND NEODYMIUM) BY PAPER PRECIPITATION CHROMATOGRAPHY WITH 8-QUINOLINOL. Nagai, Hideo (Kumamoto Univ., Japan). Bunseki Kagaku, 15: 50-5(Jan. 1966). (In Japanese).

The first condition for smooth development in precipitation chromatography is that the free osmosis of the developer should not be hindered by the appearing precipitate. This condition was fulfilled over a range of developer-oxine compositions in the development of a mixture of several rare-earth nitrates on a sheet of filter paper containing oxine. The role of acid in the developer and organic solvent used was investigated. The distribution of Ce(III), La, Nd, and Pr on chromatograms was predicted and the optimum conditions for separating the elements and the mutual separation of binary mixtures with possible purification of the components. The predictions were ascertained experimentally. (auth)

20815 EUREX PLANT. Calleri, G.; Fiorelli, M.; Rolandi, G. Comit. Naz. Energ. Nucl., Notiz., 12: No. 3, 33-8(Mar. 1966). (In Italian).

The Eurex Pilot Plant for the reprocessing of irradiated nuclear fuels, under construction at Saluggia, Italy, was designed and optimized for the reprocessing of highly-enriched MTR uranium fuels, with a maximum daily capacity of 31 kg of alloy. This plant is considered to be sufficiently flexible to be used for plant-scale research on the reprocessing of fuel elements of natural uranium or uranium enriched up to 5%, with Al, Zr, or steel cladding. (auth)

20816 SOLVENT EXTRACTION SEPARATION OF PROTACTINIUM FROM ELEMENTS OF THE IVa AND Va GROUPS. Barbano, P. G.; Rigali, L. (CAMEN, Pisa, Italy). Energ. Nucl. (Milan), 13: 194-6(Apr. 1966).

The extraction of protactinium, zirconium, niobium, hafnium, uranium, thorium, and titanium from hydrochloric acid solutions into xylene solutions of two substituted high molecular weight quaternary ammonium chlorides was investigated and optimum separation conditions of protactinium from the other elements are reported. (auth)

20817 STUDY ON URANIUM REFINING. EXPERIMENTS ON THE PRODUCTION OF URANIUM BY THE SOLVENT EXTRACTION METHOD. Kinoshita, Hideo; Nishikawa, Kazuyuki (Furukawa Electric Co. Ltd., Japan). Furukawa Denko Jiho, No. 37, 40-4(Feb. 1965). (In Japanese).

Uranium ore is first infused with bicarbonate, extracted with a solvent, and then back extracted with an acid. The extracted uranium is treated with SO_2 and HCOOH at 90°C in the presence of NH_4F to precipitate $UF_4 \cdot NH_4F$. The uranium complex salt is thermally decomposed to UF_4 in an inert atmosphere, followed by the reduction with metallic Mg. The reductive fluorination is carried out at pH 1, 90°C, for 1 hour, with a slight excess of NH_4F, and 2–5 times the theoretical concentration of HCOOH. The sizes of the precipitated uranium complex particles are sufficiently large to be easily filtered. The precipitated uranium complex, desiccated in air at 110°C, is $UF_4 \cdot NH_4F$; and UF_4 is formed by sublimating NH_4F from the $UF_4 \cdot NH_4F$ at 390°C for 2 to 3 hours in a hydrogen atmosphere. The reduction of UF_4 with Mg is better done at the furnace temperature of 750°C with 20% excess Mg. The UF_4 obtained is comparable to that obtained by the dry method. The UF_4 and the uranium metal produced are both of the reactor grade with very low impurity content. (TCO)

20818 SEPARATION OF CESIUM FROM FISSION-PRODUCT WASTES BY ION EXCHANGE ON AMMONIUM MOLYBDOPHOSPHATE. Smit, J. Van R.; Jacobs, J. J. (National Chemical Research Lab., Pretoria). Ind. Eng. Chem., Process Design Develop., 5: 117-22(Apr. 1966).

A process is described for the large-scale recovery of ^{137}Cs from acid fission product solutions by selective adsorption on columns of the crystalline inorganic ion exchanger ammonium 12-molybdophosphate (AMP). Specially prepared coarse AMP was used, which allowed suitably high flow rates. At a linear flow rate of 2.5 cm per min with Butex 150-fold waste concentrate, relatively shallow beds of AMP showed a saturation capacity of about 0.65 equivalents of cesium per liter. Cesium was recovered from the column, after washing out impurities with dilute nitric acid, by stripping with hot concentrated ammonium nitrate solution, followed by chloride-catalyzed destruction of ammonium nitrate in nitric acid solution. Principal advantages of the process are small size of equipment, the small quantities of active waste produced, and applicability to virtually any nonalkaline waste, including those of very high acid or salt content. (auth)

20819 HEAVY CONCRETE USED FOR CONSTRUCTION OF PILOT PLUTONIUM PLANT AT TROMBAY. Dahanukar, S. M. Indian Concrete J., 39: No. 1, 13-14(1965).

Heavy concrete, using hematite iron ore as coarse and fine aggregate, was used in the construction of 9 cells for processing waste fuel elements from atomic reactors in the pilot plutonium plant recently completed at Trombay. The unit weight of the concrete was specified at 210 lb/ft^3. (Indian Sci. Abstr.)

20820 SEPARATION OF AIR FROM ISOTOPIC NOBLE-GAS MIXTURES. Klemm, Th. (Institut fuer Stabile Isotope, Leipzig). Isotopenpraxis, 1: 131(Dec. 1965). (In German).

In isotope production by thermodiffusion in the gaseous phase, impurities such as air enrich the primary gases. It is therefore necessary to remove the air from the rare gases. A gas purification apparatus using molten lithium for nitrogen removal is described. With this device argon gas with an air admixture of 70% can be purified within 30 to 40 min. The residual nitrogen concentration amounts to only 0.5%, and the oxygen constituents are under spectrometric detection limits. (J.S.R.)

20821 SEPARATION OF SCANDIUM BY CATION EXCHANGE IN ACID AMMONIUM SULFATE MEDIA. Kuroda, Rokuro; Nakagomi, Yoshihito; Ishida, Koji (Univ. of Chiba, Japan). J. Chromatog., 22: 143-8(Apr. 1966).

The adsorption of metal ions, in acid sulfate media, on a strong-acid type cation exchange resin, Dowex 50W-X8, indicated that the difference between the distribution coefficients of Sc(III) and many other ions is sufficiently large for good separation. This made it possible to develop a cation exchange chromatographic procedure for the separation of Sc(III) from other ions. Sc(III) can be eluted with 0.3M $(NH_4)_2SO_4$–0.025M H_2SO_4, while Al(III), Ca(II), Cd(II), Co(II), Cr(III), Cu(II), Ga(III), In(III), Mg(II), Mn(II), Ni(II), Y(III), the rare earths, and Zn(II) remain adsorbed on the column. Ions forming stable sulfatocomplexes or other types of complex are eluted earlier in the effluent from the sample solution. Suitable elution systems for these ions are given. Separation of Sc(III) from 23 metal ions is reported. (auth)

20822 SEPARATION OF LANTHANIDES AND ACTINIDES BY HYDROXYETHYLENEDIAMINETRIACETIC ACID. I. STUDY OF THE EFFECT OF SALT ON THE EFFICIENCY OF A COLUMN. Merciny, E.; Duyckaerts, G. (Univ., Liege). J. Chromatog., 22: 164-74(Apr. 1966). (In French).

To improve chromatographic separation on ion-exchange resins, the effects of different grain sizes and cross linking on the kinetics of exchange of different salts and resins were studied. The experiments were carried out with hydroxyethylenediaminetriacetic acid and a mixture of labeled rare earths. (auth)

20823 ADSORPTION OF METAL IONS ON EXCHANGERS WITH PHOSPHORIC GROUPS FROM PERCHLORIC ACID SOLUTIONS. Lederer, M.; Ossicini, L. (CNR, Rome). J. Chromatog., 22: 200-3(Apr. 1966).

The effects of $HClO_4$ concentrations on the adsorption of metal ions on the ion exchangers cellulose phosphate and zirconium phosphate are discussed. The Rf values of metal ions plotted against the $HClO_4$ concentration are

shown for Fe^{3+}, UO_2^{2+}, Ni^{2+}, Co^{3+}, Tl^{+}, Bi^{3+}, Pb^{2+}, Be, Mg, Ca, Sc, Ti, Sr, Y, Zr, Ba, La, Th, Ce, Pr, Nd, Sm, Eu, Gd, Tb, Dy, Ho, Er, Tm, Yb, Lu, Al, Cu, Zn, Ag, Cd, and Hg^{2+}. (F.J.H.)

20824 STUDY ON THE EXTRACTION OF RARE EARTHS WITH TRIBUTYLPHOSPHATE. I. THE EXTRACTION FROM CALCIUM PHOSPHATE SOLUTIONS. Werner, G.; Pritzkow, J.; Wildner, O.; Holzapfel, H. (Karl-Marx-Univ., Leipzig). J. Less-Common Metals, 10: 323-7(May 1966). (In German).

Rare earths can be extracted by tributylphosphate from nitric acid solutions even in the presence of large amounts of calcium phosphate. Calcium ions have a salting-out effect, whilst phosphate ions decrease the extraction. The calcium phosphate content is almost without influence on the distribution coefficients of neodymium, which was chosen as being typical of the rare earths. At low nitric acid concentrations, addition of calcium phosphate even brings about an improvement of the extraction. (auth)

20825 SEPARATION OF THE RARE EARTHS BY LIQUID ION EXCHANGE. II. SEPARATION OF THORIUM, RARE EARTHS, AND SCANDIUM BY PAPER CHROMATOGRAPHY WITH REVERSED PHASES. Werner, G. (Univ., Leipzig). Z. Chem., 5: 311-2(Aug. 1965). (In German).

The rare earths cannot be separated by paper chromatography using paper impregnated with dinonylnaphthalenesulfonic acid using reversed phases and elution with HCl. The R_f values indicated that no complex formation with the acid occurred; this corresponded to the adsorption of the rare earths on sulfonic acid exchange resin. This hypothesis was confirmed by the behavior of Sc; it was possible to separate Th, Sc, and the rare earths as a group using this method. Data are presented for the dependence of the R_f values of Sc, Yb, La, and Th on the concentration of HCl. Separation was achieved with HCl in the concentration range of 0.7 to 1.1N. The amount of Sc cannot exceed 10 μg; otherwise the separation will be incomplete because of tailing. Weaker retention for Sc relative to the rare earths was found; this contrasts with the behavior of di-2-ethylhexylphosphoric acid, in which complex formation plays a role. Data for R_M on paper chromatography and separation coefficients on sulfonic acid resins were compared and showed a general analogy for the rare earths, Th, and Y. (BBB)

20826 RAPID SEPARATION METHODS FOR RADIOACTIVE ELEMENTS (REVIEW). Zaitseva, N. G. pp 16-43 of Radiokhimicheskie Metody Opredeleniya Mikroelementov. Moscow-Leningrad, Izdatel'stvo Nauka, 1965. (In Russian).

Modifications of ordinary analytic methods and methods specially developed for fast radiochemistry, permitting radioisotopes with $T \leq 10$ min to be identified, are surveyed. The extraction and precipitation methods for fast separation of short-lived products of nuclear reactions and radioactive decay are described. Methods for fast extraction of gaseous and volatile radioactive elements, including gas chromatography, fractional absorption, indirect determination, and distillation methods, are discussed. Ion exchange, isotope exchange (isotope exchange on amalgam), and electrochemical methods (polarography, reduction on Hg cathode, electromigration, recoil method) are considered. A table of practical examples of the use of these methods for specific isotopes is given. 113 references. (M.J.T.)

20827 URANYL ION-EXCHANGE BEHAVIOR IN HYDROCHLORIC ACID MEDIA. SEPARATION OF URANIUM, SULFATE, AND PHOSPHATE IN THE PROCESS OF DESORPTION. Laskorin, B. N.; Slesareva, D. D.; Semenikhina, L. A. pp 80-5 of Radiokhimicheskie Metody Opredeleniya Mikroelementov. Moscow-Leningrad, Izdatel'stvo Nauka, 1965. (In Russian).

A study was made of the influence of HCl concentration on the sorption of hexavalent uranium by anion exchangers of different basicities containing amino and pyridinium groups, under static conditions. The results obtained were used in the separation of uranium, phosphate, and sulfate ions in the process of desorption. As the HCl concentration increases (up to 6-8 M), the capacity to adsorb uranium increases, the adsorption of strongly basic exchangers being more effective than that of weakly or moderately basic ones. The sorption of uranium is explained by the formation, in concentrated HCl media, of anionic chloride complexes which have a great affinity for the anion exchangers. For this reason, treatment with concentrated HCl of an anion exchanger saturated with uranium from sulfate solutions converts the sorbed sulfate complex to a chloride complex, this conversion being gradual. Subsequent desorption of uranium with water or a weak HCl solution (1–2%) makes it possible to achieve a 90–95% separation of uranium from sulfate and phosphate ions. The incomplete separation of uranium from ferric ions is explained by the sorption of anionic chloride complexes of iron, which are stable in concentrated HCl media. (ATD)

20828 CHROMATOGRAPHIC SEPARATION OF UX_1 AND U_1. Afanas'ev, Yu. A.; Ryabinin, A. I. pp 129-30 of Radiokhimicheskie Metody Opredeleniya Mikroelementov. Moscow-Leningrad, Izdatel'stvo Nauka, 1965. (In Russian).

The separation of UX_1 (^{234}Th) and U_1 (^{238}U) from uranyl nitrate solutions using the anion exchange resin AV-17 was studied, and results are shown. A fast, simple method for obtaining radiochemically pure ^{234}Th using AV-17 and HCl is described. (M.J.T.)

20829 CALCIUM AND STRONTIUM PARTITION BY EXCHANGE IN AMALGAM–SOLUTION SYSTEM. Balashov, V. L. pp 134-7 of Radiokhimicheskie Metody Opredeleniya Mikroelementov. Moscow-Leningrad, Izdatel'stvo Nauka, 1965. (In Russian).

The equilibrium coefficient of separation by exchange in a Ca amalgam–$SrCl_2$ aqueous solution system is equal to 30 ± 6 at a temperature of 20°C. The dependence of the equilibrium coefficient of separation on the temperature was studied in the temperature range from 5 to 50°C. The separation coefficient decreases with increasing temperature. The thermal effect of the exchange reaction is 3.2 ± 1.2 kcal/mole. The exchange current density at 4500 rpm of the mixer turns out to be 1.2 to 1.4 kamp/m^2. (tr-auth)

20830 PLANT MEASUREMENT, SAMPLING AND ANALYSIS FOR ACCOUNTANCY PURPOSES WITH PARTICULAR REFERENCE TO SEPARATION PLANTS AT WINDSCALE. Davidson, A. S.; Elliott, F.; Powell, R.; Swinburn, K. A. (United Kingdom Atomic Energy Authority, Sellafield, Eng.). Vienna, International Atomic Energy Agency, 1965, Preprint No. SM-67/53, 19p. (CONF-650803-17). ORINS.

From IAEA Symposium on Nuclear Materials Management, Vienna.

All figures for special materials accountancy purposes contain one or more of three parameters: plant measurement, sampling, and analysis. For plant measurements it is best to use weighings wherever possible, e.g., the plutonium in the feed to the New Separation Plant was based on the weight of uranium rods fed. Methods for measuring volumes are discussed in detail, e.g., by dipping a tank, using pneumercator or rotameter, electrical sensing of height of liquid phases, and tracer method using radioactive cesium. Judged accuracies and precisions of each method are given. Sampling of solutions in a batch process is done by using evacuated tubes after thorough homogenization of the solution. For continuous streams, where high accuracy is required, a continuous sampler was devised and is used on the feed to the New Separation Plant. Drilling of metal ingots is the normal sampling method at Windscale, whereas for other solids the method is to homogenize as far as possible and then sample. In chemical analysis the precision required of the method depends on the number of determinations in each accounting period. Methods for determining plutonium are discussed in detail, e.g., radiochemistry, colorimetrically using thoronol, plutonium separation, followed by complexing with EDTA and back titration of the excess EDTA, titrimetry, and isotope dilution followed by mass spectrometry.

Methods for determining uranium are also discussed in detail, e.g., gravimetry as U_3O_8, ether extraction followed by gravimetry or colorimetry, titrimetry, coulometry, isotope dilution followed by mass spectrometry, and enrichment determination by mass spectrometry or line shift emission spectrography. With all accounting methods standards are used to give quality control and to show any inaccuracy that must be corrected. Precisions of all the methods are given and the methods actually used for the New Separation Plant are indicated. (auth)

20831 THE SYSTEM FOR CONTROL OF SOURCE AND SPECIAL NUCLEAR MATERIAL AT THE EUROCHEMIC REPROCESSING PLANT. Frenzel, W.; Schueller, W. (Eurochemic, Mol, Belg.). Vienna, International Atomic Energy Agency, 1965, Preprint No. SM-67/3, 14p. (CONF-650803-19). ORINS.

From IAEA Symposium on Nuclear Materials Management, Vienna.

In order to maintain proper control of source and special nuclear material, the fuel reprocessing facilities of Eurochemic are divided in 9 material balance areas. The main stream of natural or slightly enriched uranium through the plant will be measured four times: after fuel element dissolution, before feeding to the extraction cycles, before transfer from the process tanks to the product storage, and before product shipment. For plutonium and highly enriched uranium an additional determination is made for the transfer between the first and second extraction cycles. All transfers to and from each material balance area will be balanced monthly. Depending on the significance of an SS-material transfer for the overall material balance, different precisions are required for the determinations. A calculated inventory time schedule, derived from operation data and balancing requirements, is discussed. This schedule will be used as a guide to establish the frequency of physical inventories. As a processing campaign may last longer than periods between successive inventories, it was planned to perform some physical inventories during a short stop of operations without complete shutdown and washout of process equipment. The international character of the company requires, at least during the initial period of operation, a communication in writing of all information regarding analytical determinations. To permit quick communication of data, a pneumatic post system was installed connecting important locations of the reprocessing plant and the analytical laboratory. Information to the Accountability Office will be communicated by special post. Bookkeeping will be performed by a double entry system. SS-material balances will be performed by aid of four books, two transfer journals and two summary ledgers. (auth)

20832 MATERIALS CONTROL SYSTEM FOR ENRICHED URANIUM CHEMICAL PROCESSING FACILITY FOR IRRADIATED NUCLEAR MATERIALS. Tingey, F. H.; Lewis, B. S. (Phillips Petroleum Co., Idaho Falls, Idaho). Vienna, International Atomic Energy Agency, 1965, Preprint No. SM-67/23, 22p. (CONF-650803-47). ORINS.

From IAEA Symposium on Nuclear Materials Management, Vienna.

Areas of consideration in the development of an effective nuclear materials management system based on experience gained at the Idaho Chemical Processing Plant include: organizational structure, accounting system, measurement system, implementation and integration of system, records and reports, internal audit, and inventory management. (M.C.G.)

20833 ECONOMIC MANAGEMENT OF A CENTER FOR PROCESSING RADIOACTIVE RESIDUES. Van Lint, J. (Societe Belge pour l'Industrie Nucleaire, S. A., Brussels). Vienna, International Atomic Energy Agency, 1965, Preprint No. SM-67/58, 15p. (In French). (CONF-650803-49). ORINS.

From IAEA Symposium on Nuclear Materials Management, Vienna.

The differences between the operations of an industrial undertaking and an installation for residue processing and the auditing system of an industry concerned with various phases of processing are described. The auditing program is shown to be necessarily and intimately connected with the general organization of the entire undertaking and to be a useful tool of economic management. The auditing principles used in arriving at the over-all cost of the final product and the specific cost of each processing phase are considered. (auth)

ENGINEERING

General

20834 JOINT AMERICAN SOCIETY OF MECHANICAL ENGINEERS [AND] AMERICAN SOCIETY OF LUBRICATION ENGINEERS INTERNATIONAL LUBRICATION CONFERENCE, 1964. ASLE (Amer. Soc. Lub. Eng.) Trans., 8: 1-777(1965).

Proceedings of the Joint American Society of Mechanical Engineers and American Society of Lubrication Engineers International Lubrication Conference, 1964, are presented. For abstract numbers of individual papers see CONF-641007 in the Report Number Index. (M.C.G.)

For abstracts of individual papers see: 21365 and 21366.

Applications of Nuclear Explosions

20835 RECOVERING OIL FROM SHALE WITH NUCLEAR EXPLOSIVES. Lombard, D. G. (Univ. of California, Livermore). J. Petrol. Technol., 17: 877-82 (Aug. 1965).

Technical aspects of the proposed use of underground nuclear explosions for recovery of oil from oil shale are discussed. Nuclear explosives can be used to break large volumes of oil shale in place at depth, where deposits are thick. The diameter of the region (chimney) of shale broken by a nuclear explosion can be as much as hundreds of feet with a height at least double the diameter. For example, a 20-kt detonation at a depth of 2000 ft will break about 800,000 t. Problems associated with the radioactivity generated by a nuclear explosion in oil shale are expected to be manageable. The probable size distribution of fragments of this broken shale was estimated. Calculations based on the theory of particle statistics led to an estimated permeability of 3×10^{-5} to 3×10^{-4} ft^2, within the broken zone. The cost of breaking the shale with nuclear explosives would range from less than $0.35 to more than $1.20/barrel of oil for recovery of 25 gal/t, according to calculations for 100- and 20-kt explosions, respectively. Other costs, including mining or in situ retorting, and refining, are not included. Basic features of a plan for in situ retorting are discussed. A relatively small-scale nonnuclear in situ retorting experiment is recommended. If successful, it would be followed by a nuclear explosion pilot experiment, from which detailed engineering criteria could be developed for using the nuclear techniques on a production basis. (BBB)

20836 ECONOMICS OF CONTAINED NUCLEAR EXPLOSIONS APPLIED TO PETROLEUM RESERVOIR STIMULATION. Bray, Bruce G.; Knutson, Carroll F.; Wahl, Harry A.; Dew, John N. (Continental Oil Co., Ponca City, Okla.). J. Petrol. Technol., 17: 1145-52 (Oct. 1965).

The major effect of a nuclear explosion in a hydrocarbon reservoir is to increase the apparent wellbore diameter by creating a cavity, chimney, and an associated annular fractured zone. This geometry results in a complex flow regime yielding increased productivity of the reservoir fluids. This flow regime and the economics of utilizing nuclear stimulation for low-productivity oil- and gas-bearing reservoirs are discussed. Gross permeability increases due to fracturing beyond the chimney-cavity rubble zone were observed in many underground shots. This geometry of a post-shot nuclear environment for a petroleum reservoir can be simulated on a computer by assigning concentric annular configurations to the cavity-chimney and surrounding fractured zones with the producing wellbore in the center. Production and economic analyses are made for both shallow and gas reservoirs. Because nuclear device cost per unit of explosion energy decreases with increasing device size, deeper reservoirs may provide more economic incentive. A 1-Mt device located at a depth of 10,000 ft would produce the following results: scaled depth of burial, 1000 ft: cavity radius, 233 ft; most probable permeable zone radius, 564 ft (maximum permeable zone radius is 810 ft); and most probable permeable zone height, 1320 ft (maximum permeable zone height is 1900 ft). Economic calculations were made using the production and economic data given. Total investment costs of $1,250,000 include the device charge of $570,000, and the post-shot production well cost of $350,000. The results showed that a deep, thick, low-productivity gas reservoir is a good nuclear stimulation prospect when compared to existing completion techniques. An analysis of oil reservoir situations indicated that multiple, thin, low-productivity reservoirs are amenable to nuclear stimulation if the zones can be stimulated by a single large device. (BBB)

20837 PROJECT GASBUGGY—A NUCLEAR FRACTURING EXPERIMENT. Ward, D. C.; Atkinson, C. H.; Watkins, J. W. (Bureau of Mines, Bartlesville, Okla.). J. Petrol. Technol., 18: 139-45(Feb. 1966).

Project Gasbuggy is an experiment designed for the detonation of a 10-kt fission explosive at a depth of 4150 ft to evaluate the stimulative effect on gas production from the Pictured Cliffs formation in the San Juan Basin, N. M. Preliminary analysis has shown that nuclear-explosive stimulation of natural gas reservoirs is technically feasible; but only from analysis of production data can the economics be determined. Favorable results from Project Gasbuggy could pave the way for substantially increased recovery from many known but low-productivity hydrocarbon reservoirs. Primary objectives of the experiment are to determine: change in productivity of existing wells within effective range of the shock effect; extent of effective range of the shock effect; productivity of a post-shot well drilled into the chimney; increase in ultimate recovery; and degree to which radioactive contamination of gas will be a production problem. The experimental design for Project Gasbuggy was made with full consideration of all safety factors, including the possibility of venting radioactive contaminants to the atmosphere, damage resulting from ground shock, and contamination of produced gas and ground water. (TCO)

Facilities and Equipment

Refer also to abstract 21215.

20838 (AD-624019) PULSED X-RAY PROMPT GAMMA SIMULATOR. Final Report. Ford, Franklin C.; Martin, Donald; Bernstein, Bernard (Physics International Co., San Leandro, Calif.). Nov. 29, 1965. Contract AF04(694)-496. 64p. CFSTI $3.00 cy, $0.75 mn.

Nuclear explosions are accompanied by the sudden release of large amounts of energy and highly penetrating nuclear radiation. Protection of a missile system or defense system against the nuclear environment of an enemy nuclear counterburst requires evaluation of the vulnerability to determine possible preventive methods. A pulsed x-ray system was selected as preferable for prompt-gamma simulation. The entire pulsed x-ray complex integrates the functions of the x-ray pulser, radiation shielding, r-f shield structures, control and diagnostic systems, and dosimetry, providing a convenient transient radiation effects test facility. The specifications and other data pertinent to the major components and subsystems of the pulsed x-ray facility, as well as to the dosimetry systems, are discussed. (auth)

20839 (AEET-ED-SG/14) FORCE REFLECTING SERVOS IN ELECTRICAL MASTER SLAVE MANIPULATORS. Abhyankar, S. S. (Atomic Energy Establishment,

Trombay (India). Electronics Div.). Sept. 10, 1962. 9p. Dep. mn.

Certain aspects that are of immediate interest in connection with a rational program for development of electronically controlled master-slave manipulators are discussed. Desirable features of a general purpose manipulator are listed, along with limitations in the use of mechanical master slave and electrically operated manipulators. It was concluded that the possibility exists of adopting mechanical M/S manipulators for operation through bi-directional force reflecting servo drives. In this device the mechanical linkages would be sectioned in the middle and each half of the manipulator would be coupled to appropriate servo drives. (P.C.H.)

20840 (BNWL-193, pp 57-67) NEUTRON INTERACTION BETWEEN MULTIPLYING MEDIA SEPARATED BY VARIOUS MATERIALS. White, J. D.; Richey, C. R. (Battelle-Northwest, Richland, Wash. Pacific Northwest Lab.).

The quantity of material necessary to effectively isolate a multiplying media is of primary concern to the design of shipping containers and formulation of storage regulations for fissionable materials. The results are given of a series of critical experiments in which the isolating properties of various materials were investigated. Those materials tested were placed at the interface between two arrays of multiplying media that comprised the core of a critical assembly. The critical length of the fuel core was then determined as a function of the test material thickness; the effective isolation thickness of a material was taken to be that thickness for which the fuel core critical length approached an asymptotic value. Comparative data were also obtained on the reflector savings associated with the various test materials, where the reflector savings is defined as the decrease in critical length due to the presence of the reflector. (M.O.W.)

20841 (NYO-3237-5) EXPERIMENTAL TEST AND EVALUATION OF A GAS-BEARING BRAYTON CYCLE TURBOCOMPRESSOR. Quarterly Progress Report, December 1, 1965-February 28, 1966. Curwen, P. W. (Mechanical Technology Inc., Latham, N. Y.). Mar. 4, 1966. Contract AT(30-1)-3237. 59p. (MTI-66TR14). Dep. mn. CFSTI $3.00 cy, $0.75 mn.

A Brayton cycle gas generator (turbocompressor) utilizing self-acting gas bearings was designed, built, and is now under test. Self-sustained closed-loop operation of the turbocompressor, using its own cycle gas as the bearing lubricant, was achieved in November 21, 1964. Through February, 1966, the turbocompressor has been successfully operated with nitrogen. The turbocompressor was also operated under "no-load" and "load" conditions in argon at turbine inlet temperatures up to 1323°F. A second failure of an electrical resistance element in the test-loop heater occurred during one of the argon tests. In order to obtain some insight into the reasons for these failures, the heater was completely disassembled, examined, repaired, and reinstalled during January and February of 1966. The turbocompressor, which is now equipped with a chrome-oxide surfaced thrust bearing, is presently being reinstalled in the loop. Additional loop testing should commence early in March. (auth)

20842 (ORNL-TM-1410) DESIGN OF A HIGH-TEMPERATURE FURNACE (3,000 DEGREES C) [Thesis]. Golson, T. J. (Oak Ridge National Lab., Tenn.). Mar. 1966. Contract W-7405-eng-26. 98p. Dep. mn. CFSTI $3.00 cy, $0.75 mn.

Submitted to Tennessee Univ., Knoxville.

The methods of designing and testing a particular high-temperature furnace are given, and some of the more important problems associated with the design for high-temperature equipment are pointed out. Some of the problems discussed are the advantages and disadvantages of both resistance and induction heating, the selection of a gas for use as an inert atmosphere and the possibilities of generating a plasma, the design for a pressure vessel to contain the inert atmosphere, the design for an induction feed-through into the pressure vessel, and establishing a heat balance. The problem of a water leak inside a pressure vessel being operated at a high temperature is also considered. (auth)

20843 HITACHI POWER MANIPULATOR. Miyazawa, Kiyoshi; Wase, Keizo (Hitachi Ltd., Japan). Hitachi Hyoron, 47: 694-9(Apr. 1965). (In Japanese).

The HITACHI power manipulator PE-1 with a 500 ton hooking capacity and 50 ton holding capacity was installed in Atomic Reactor Laboratory of Kyoto University. This manipulator consists of a tong head; an elbow pivot; a shoulder pivot; an over-head crane, moving in the three dimensions; a vertical tube to rotate the shoulder part freely; an auxiliary hoist; and a percipience detector. This percipience detector, which informs the operator of the position and behavior of the tong head, is important for the precise remote handling of radioactive materials and other equipment. The operator can control electrically the manipulator by means of the switches on the panel while watching the movement of the tong head through a radiation shielding window. (tr-auth)

20844 TELESENSORS, TELEOPERATORS, AND TELECONTROLS FOR REMOTE OPERATIONS. Johnsen, Edwin G. IEEE (Inst. Elec. Electron. Eng.), Trans. Nucl. Sci., NS-13: No. 1, 14-21(Feb. 1966).

The status of the technology of telesensors, teleoperators, and telecontrols is summarized; and some advanced concepts in the design of remotely operated equipment are discussed. (D.C.W.)

20845 DETECTING LEAKS BY SNIFFING. Chatel, J.-L. (SOGEV, Seine, France). Ind. At., 10: 69-76 (1966). (In French).

The design of a sniffer for detecting leaks is given. This is one of the methods for leak detection using a helium mass spectrometer. A diagram of this mechanical sniffer is given, and its sensitivity is calculated. The response time of the sniffer system is also determined. (J.F.P.)

20846 A SAMPLE HOLDER FOR ELECTRON SPIN RESONANCE STUDIES ON X-IRRADIATED FIBRES. Elliott, J. P. (Guy's Hospital Medical School, London). J. Sci. Instrum., 43: 55(Jan. 1966).

A sample holder and quartz tube enables oriented fibers to be irradiated and subsequently examined by electron spin resonance spectroscopy in a microwave cavity. The atmosphere, including the relative humidity, surrounding the sample can be varied. (auth)

20847 ON A ^{60}Co γ-RAY IRRADIATION LABORATORY OF KYUSHU UNIVERSITY. II. OUTLINE OF THE IRRADIATION LABORATORY. Sonoda, Masateru; Takayanagi, M. (Kyushu Univ., Japan). Kyushu Daigaku Kogaku Shuho, 38: 53-60(Mar. 1965). (In Japanese).

The ^{60}Co γ-ray Irradiation Laboratory of Kyushu University was designed and constructed, incorporating various characteristic features. Special effort was made by use of shielding walls and labyrinth to protect the personnel from gamma rays. Provisions are made for observing sample materials during the irradiation with a shielding window and periscope, for manipulating samples and other equipment, and for easily introducing or removing sample materials without interrupting the irradiation. The irradiation laboratory is a one-story building of about 100 m^2 floor space, and it consists of an irradiation room (3 × 3 × 3 m) and two front and side operation rooms (7 × 4 × 3.5 m and 6 × 2.5 × 3.5 m, respectively). Radiation sources are stored in the basement and raised into the irradiation room when irradiation is carried out. (TCO)

20848 MANIPULATOR WITH BALL AND SOCKET JOINT. Csoke, Antal. Magyar Tud. Akad. Kozp. Fiz. Kut. Int. Kozlem., 13: 407-11(1965). (In Hungarian).

A manipulator with ball and socket joint which can be built into 50- or 100-mm thick lead shield is described. (auth)

20849 MULTI-CURIE ^{60}Co IRRADIATION UNIT. Tsuda, Eiichi; Shikata, Sanji (Mitsubishi Electric Manu-

facturing Co. Ltd., Japan). Mitsubishi Denki Giho, 39: 1382-7(Nov. 1965). (In Japanese).

A multi-curie Co-60 irradiation unit was delivered to Takasaki Laboratory of the Japanese Atomic Energy Research Institute in March 1964. The device is to handle Co-60 of 300,000–500,000 curies as an irradiation source and is armed at the industrialization of radiation chemistry and the development of radiation engineering and irradiation sources. The irradiation unit is provided with a source, shielded and stowed at the bottom of a pool 6 meter deep. The facility is so constructed that the source can be moved through an underground canal to permit irradiation in any of three different cells. This is a large scale installation unprecedented in this country and well comparable to any other facilities in the world. (TCO)

20850 HIGH-PRESSURE TECHNIQUES. Ingalls, R. (Univ. of Illinois, Urbana). Contracts 1834(05); AT(11-1)-1198. pp 185-91 of Moessbauer Effect Methodology. Vol. 1. Gruverman, Irwin J. (ed.). New York, Plenum Press, 1965.

A cell is described in which pressures of 0-300 kb may be applied to Mössbauer sources. Machined pellets of pyrophyllite fit the tapered parts of two work-hardened sintered tungsten carbide pistons that ride in a hardened steel cylinder containing a window slot. Between the two pellets is a thin wafer of LiH of the same diameter, containing the Mössbauer source at its center. Pressure is applied to the entire piston and cylinder assembly by means of a hydraulic press. Radiation emitted from the cell is analyzed with a large moving absorber and detected with a proportional counter containing a large window. The LiH wafer, the calibration of the cell, problems, and applications are discussed. (A.G.W.)

20851 EQUIPEMENT DES LABORATOIRES DE RECHERCHE. (Equipment of Research Laboratories). Lapadu-Hargues, Philippe. Collection de l'A.N.R.T. Travaux de la Commission No. 23. Construction et Equipement des Laboratoires. Paris, Eyrolles. Paris, Gauthier-Villars, 1965. 100p.

Actual concepts controlling the construction of French Industrial Laboratories for research and control were previously defined. Laboratories using the new scientific concepts are considered. Standardization of the laboratories and the work plan for physical and chemical operations is described. The processing and handling of fluids are considered. The laboratory furniture is discussed and the annexes to the laboratory proper are described. It was emphasized that the design and equipment of such laboratories is still in a state of change. (J.S.R.)

20852 IMPROVEMENTS IN OR RELATING TO IRRADIATION APPARATUS. Rogers, Frank (to United Kingdom Atomic Energy Authority). British Patent 1,019,440. Feb. 9, 1966. Filed Aug. 6, 1963.

An apparatus is provided for the irradiation of granular materials with gamma radiation whereby all the material receives a substantially uniform dose while efficiently utilizing most of the radiation from the source. The apparatus includes a series of plate like sources of gamma radiation and a series of ducts spaced from and extending across each face of the sources in a vertical bank. Means are located in the vertical plane for interconnecting the ducts and for passing the granular material along the ducts in succession while imparting a helical motion to the granules relative to the axes of the ducts. The materials may be moved along and continuously stirred by a helical stirrer and may be transferred from duct to duct by a centrifugal impeller located at the end of each tube. Preferably, the stirrer is formed by a number of paddles mounted on a central shaft in the duct and having their peripheries joined by light wires or strips. (B.L.M.)

20853 ELECTRON IRRADIATION APPARATUS. Komai, Kenichiro (to Hitachi, Ltd.). Japanese Patent 1964-4163. Mar. 5, 1965. Filed Oct. 1, 1962.

In an electron irradiation apparatus for films in vacuum, provision is made for rapidly attaining a vacuum, and eliminating the gas contained in the film that produces an unfavorable effect on the electron gun. The vacuum system is divided in two parts, the higher and lower vacuums. These two parts are connected by a small hole through which the film can just pass. The film passes through this hole from the lower vacuum into the higher vacuum and the electron irradiation is carried out in the latter vacuum. (TCO)

Heat Transfer and Fluid Flow

See also PHYSICS — Fluid Physics and Thermodynamics

Refer also to abstracts 20709, 21793, and 22473.

20854 (AD-621523) THERMAL STABILITY OF COMPLETELY CONFINED FLUIDS INCLUDING MAGNETOHYDRODYNAMIC EFFECTS. Sherman, Michael; Ostrach, Simon (Case Inst. of Tech., Cleveland, Ohio). June 1965. Contract AF-AFOSR-194-65. 293p. CFSTI $6.00 cy, $1.50 mn.

The current research concerns the determination of the conditions needed to induce a state of convective motion in a fluid where a constant temperature gradient is directed parallel to a body force. The fluid is contained in a rather arbitrary region bounded by rigid walls. The principle of exchange of stability is established for arbitrary regions with a generalized thermal boundary condition on the bounding walls. The thermal stability problem is reduced to an eigenvalue problem for the critical Rayleigh number (the stability criterion) and then is reformulated as a variational principle. A method is developed for estimating upper and lower bounds to the critical Rayleigh number for regions in which the critical Rayleigh number cannot be calculated exactly. An extension of the thermal stability problem to include magnetohydrodynamic effects is presented. Here the fluid and the bounding walls are electrical conductors. A constant magnetic field is applied to the configuration. (auth)

20855 (CLM-R-54) A MONTE CARLO COMPUTER PROGRAMME FOR ANALYSIS OF MOLECULAR GAS FLOW. Chubb, J. N. (Culham Lab., United Kingdom Atomic Energy Authority, Abingdon (England)). Dec. 1965. 48p. Dep. mn. BIS $1.20. HMSO 6s. 0d.

Molecular gas flows cannot be studied analytically within vacuum systems in which a pumping orifice or surface forms an appreciable fraction of the total internal surface area of the system. Such systems may be studied successfully by the Monte Carlo method in which an average picture of the molecular flow is by mathematical simulation of the course of a large number of individual molecular histories within a mathematical representation of the vacuum system. A description is given of a Monte Carlo computer program which was developed for analysis of molecular gas flow, with emphasis placed on the ease of use and on the practical application of the information which may be extracted. The application of this program is illustrated by examples of calculations which were performed on experimental apparatus for the measurement of sticking coefficients, and on test domes for measuring the performance of diffusion pumps. (auth)

20856 (GEAP-4976) TURBULENT FLOW IN AN ANNULUS. Levy, S. (General Electric Co., San Jose, Calif. Atomic Power Equipment Dept.). Oct. 1965. Contract AT(04-3)-189. 20p. Dep. mn. CFSTI $1.00 cy, $0.50 mn.

Equations describing fully developed turbulent flow in an annulus are derived. They are based upon Reichardt's expression for the eddy diffusivity of momentum, and they assume that the velocity profiles starting from the core tube wall and the outer tube wall have the same velocity and eddy diffusivity at the plane of zero shear. The predicted location of the plane of zero shear, mixing length, eddy dif-

fusivity, velocity distribution, and friction factor are compared to available data and are found to give good agreement with the test results. Potential extension of the proposed method to more complex geometries is illustrated by considering the case of flow in an annulus with one artificially roughened surface. (auth)

20857 (SC-DC-65-1907) HEAT TRANSFER AND FLOW VISUALIZATION ON 1/2-INCH-DIAMETER CYLINDERS IN LAMINAR HYPERSONIC FLOW. (Rhodes and Bloxsom, Canoga Park, Calif.). Jan. 1966. Contracts AT(29-1)-789; 48-2672. 56p. Dep. mn. CFSTI $3.00 cy, $0.50 mn.

For Sandia Corp., Albuquerque, N. Mex.

Aeroheating rates were measured on cylinders with length-to-diameter ratios of 1, 4.5, 8, and 15 and ratios of corner radii to cylinder radii of 0, 0.2, 0.4, 0.6, 0.8, and 1.0. Angles of attack ranged from 0 to 90°. The test facility was the Rhodes and Bloxsom 60-inch hot-shot tunnel. Shock wave locations were also obtained from luminosity photographs. Tunnel conditions resulted in hypersonic laminar continuum flow with negligible radiant heating. (auth)

20858 (UCRL-14620) EFFECTIVENESS NTU RELATIONS FOR ONE-, TWO-, AND THREE-PASS CROSS COUNTERFLOW HEAT EXCHANGERS TO NTU OF 40. Cornwell, Roy S. (Lawrence Radiation Lab., Univ. of California, Livermore). Feb. 2, 1966. Contract W-7405-eng-48. 14p. Dep. mn. CFSTI $1.00 cy, $0.50 mn.

Calculations of effectiveness for one-, two-, and three-pass cross counterflow heat exchangers were made for NTU (Number of Transfer Units) up to 40 and capacity rate ratios of 0.1 to 1.0. A 20 × 20 matrix was used in each crossflow cell and the results fed into the next cell or mixed to get a final temperature. A Fortran code for the CDC-3600 is also included. (auth)

20859 (UJV-1421/65) DALSI EXPERIMENTALNI VYSLEDKY O VLIVU ELEKTRICKYCH POLI NA PRESTUP TEPLA DO CASTECNE IONIZOVANEHO CO_2. (Experimental Data on Influence of Electric Fields on Heat Transfer to Partially Ionized CO_2). Berger, Fr.; Derian, L. (Ustav Jaderneho Vyzkumu, Ceskoslovenska Akademie Ved, Rez). 1965. 43p. Dep. mn.

Experiments concerning the influence of electric fields on the heat transfer from a fuel element to partially ionized carbon dioxide in a nuclear reactor are discussed. The possibility of achieving an increase or decrease in heat transfer by the application of a direct electric field between the fuel element and the channel wall was demonstrated at gas pressures up to 40 kp/cm². Curves showing the dependency of the effect on the polarity of the heat-exchanging element and on the gas and field parameters are given. Measurements were also carried out with alternating fields with frequencies up to 250 Hz. It was established that at identical conditions the values of the effect of alternating fields or heat transfer lie between the values achieved by a direct field with positive and negative polarity of the fuel element. (auth)

20860 HEAT-SHIELD ABLATION AND SUBLIMATION DETERMINATIONS THROUGH RADIOISOTOPE TECHNIQUES. Brandon, George W. Jr.; Davis, William G. (Manned Spacecraft Center, Houston, Tex.). 7p. (CONF-650655-2). ORINS. Gmelin, AED-CONF-65-159-6.

From Aerospace Technical Conference and Exhibit, Houston, Tex.

A technique was developed for determination of heat-shield sublimation (char) and surface recession (ablation) during an atmospheric reentry. A radioactive "line" source embedded in the heat-shield material sublimes and ablates at the same rate as the heat shield. Decreases in source activity are monitored by miniaturized nuclear counters. Accuracies exceeding 90% are obtainable. The technique provides a continuous indication of char and ablation rates. (auth)

Materials Testing

Refer also to abstracts 21146 and 21477.

20861 (EUR-2443.f) PROCEDES DE RADIOGRAPHIE MECANIQUE APPLIQUES AU CONTROLE DE QUALITE DE TUBES A PAROIS MINCES EN SAP. (Mechanical Radiography Techniques for the Quality Control of Thin Walled SAP Tubes). Bonnet, P.; Jansen, J. (European Atomic Energy Community, Ispra (Italy). Joint Nuclear Research Center). 1965. 39p. Dep. mn.

For the control of light tubes intended for nuclear application, radiography may be quite useful if precautionary measures are taken as to the contrast. Furthermore one-wall techniques avoid the superimposition of images as observed in conventional radiography. Two one-wall techniques were analyzed: the so-called rotative method and the rolling method. In the rotative method the film is rolled up on an expansible mandrel introduced into the tube by a special tool. The assemblage is then primed by a uniform rotative movement and exposed to x rays collimated by a slit of adjustable width. Analysis of the method suggests that the focal distance may be short. By contrast, the slit must be small which leads to rather long, but not prohibitive, exposition periods. According to the rolling method a film carriage rolls at a velocity that approaches the peripherical velocity of the tube. The image of the wall becomes very fuzzy whereas that of the back wall rests sufficiently clear. The more intricate mathematical relations between the parameters necessitated digital computation. Greater widths of slit are acceptable in this case without impairing the quality of the image. (auth)

20862 (WAPD-TM-555) DUZ-1—A PROGRAM FOR SOLVING AXISYMMETRIC AND PLANE ELASTICITY PROBLEMS ON THE PHILCO-2000. Griffin, D. S.; Kellogg, R. B.; Peterson, W. D.; Sumner, A. E. Jr. (Bettis Atomic Power Lab., Pittsburgh, Pa.). Nov. 1965. Contract AT-11-1-GEN-14. 111p. Dep. mn. CFSTI $4.00 cy, $0.75 mn.

DUZ-1 is a digital computer program to solve two-dimensional planar and axially symmetric elasticity problems. Loading conditions may arise from nonuniform temperatures, body forces, and boundary displacements or forces. Up to 5000 points are allowed, with variable mesh and diagonal boundaries. (auth)

20863 COLOR RADIOGRAPHY—THE PHOTOGRAPHIC CONSIDERATIONS. Wise, L. K. (Hawker Siddeley Aviation, Hatfield, Eng.). Brit. J. Non-Destruct. Test., 8: 2-5(Mar. 1966).

The photographic aspects of color radiography are discussed. The process produces a radiograph presenting the various thicknesses of the subject in terms of different colors rather than in variations of density. The film has 3 emulsion layers in successive coatings, each of which is sensitive to one of the 3 primary colors that make up white light. (M.C.G.)

20864 APPLICATION OF RADIOGRAPHY TO THE INSPECTION OF FUEL PINS. Rooney, J.; Armstrong, G. A. Brit. J. Non-Destruct. Test., 8: 11-16(Mar. 1966).

Two radiographic examinations to inspect fuel pins, which consist of a stack of uranium dioxide pellets clad in a stainless steel sheath, are described. The inspection of the internal arrangement of the fuel pin is achieved using a panoramic shot. The x-ray beam must penetrate both walls of the can with a voltage sufficient to show inner detail. It need not penetrate the fuel pellets but must be perpendicular to the axis of the fuel pin to indicate gaps between pellets. The effects of contrast, unsharpness, and graininess on sensitivity are considered. Inspection of the weld between end plug and can requires a series of tangential shots. (M.C.G.)

20865 NONDESTRUCTIVE TESTING OF NUCLEAR FUEL ELEMENTS. I. Manabe, Katsumi. FAPIG (Tokyo), No. 36, 38-42(Apr. 1965). (In Japanese).

The fabrication processes and the testing specifications for the fuel elements used in JRR-2, JRR-3, JPDR, and Tokai Power Reactor are described. The principle of the x-ray examination is explained. For the metallic-uranium elements used in JRR-3 and Tokai Power Reactor a betatron was used for obtaining the x rays. In the x-ray examination of the welds of the cladding, a means must be provided for preventing the overlapping, etc. (tr-auth)

20866 IMAGE ANALYSIS OF THERMAL NEUTRON RADIOGRAPH. Inouye, Tamon; Ogawa, Kazuyuki (Tokyo Shibaura Electric Co., Ltd.). Oyo Butsuri, 34: 801-6(Nov. 1965). (In Japanese).

Images obtained in thermal neutron radiography by the use of a small nuclear reactor are analyzed by the technique of Fourier analysis. The optical transfer functions unparallel neutron beam and for the process image transfer from an activated In film to an x-ray film are derived and compared with experiment. The spurious resolution of image expected from the shape of the optical transfer function is observed. (auth)

20867 PROGRESS OF RADIATION NONDESTRUCTIVE TESTING EQUIPMENT. Toriyama, Hideaki (Shimazu Seisahusho Co. Ltd., Japan). San'yo Gijutsu Zasshi, 19: 33-8(May 1965). (In Japanese).

The progress made on the non-destructive testing equipment and techniques, light weight portable x-ray apparatus, fluoroscopic technique, and new high energy radiographic techniques, is discussed. The new 160 Kv x-ray apparatus weighs only 23 Kg. This improvement was made possible by the improvements in materials, circuits, and high insulation. The scope of the fluoroscopic method was increased by the introduction of large image intensifiers, which reduce the adaptation requirements and assist the observer to extract the maximum amount of information from the observed scene. A typical application of the fluoroscopic technique is to the inspection of welds of spiral steel pipe with a 2% sensitivity under optimum thickness. With the improvements in radiographic techniques, a considerable gain of image quality was achieved. This gain has been evaluated quantitatively by image quality indicators and densitometric measurements. Some examples of the new practical radiographic work are given. (TCO)

Protective Structures

20868 (AD-626770) AN INVESTIGATION OF SCHOOL DESIGNS TO RESIST INTEGRATED NUCLEAR WEAPONS EFFECTS. Final Technical Report. Bruce, Robert N. Jr.; Branch, James E.; Gronbeck, Marius P.; Hanley, John T.; McCahill, Dennis F. (Tulane Univ., New Orleans, La. Dept. of Civil Engineering). 1965. Contract OCD-PS-64-215. 214p. (TR-100). CFSTI $6.00 cy, $1.25 mn.

A comprehensive study was made on the capabilities of the award winning entries of the National School Fallout Shelter Design Competition, TR-19, to provide protection against effects of nuclear weapons other than those that are associated with fallout. Specific areas of investigation included: an examination and evaluation of the winning designs to ascertain their bonus protection and inherent resistance to withstand thermal radiation, overpressure, and dynamic pressure; a tabulation of advantages and disadvantages of each design, as applicable; recommendations for appropriate design modifications; and a tabulation of costs for the recommended modifications. (auth)

20869 LOW ACTIVATION MATERIALS FOR NUCLEAR TEST VAULT CONSTRUCTION. Bingham, William G. Jr.; Fernandez, H. G. (Bechtel Corp., Los Angeles). New York, American Society of Civil Engineers, 1965, Preprint No. 254, 23p., $0.50. (CONF-651036-3). ORINS.

From American Society of Civil Engineers, Environmental Engineering Conference and Annual Convention, Kansas City, Kan.

A study was conducted to find low activation materials for use in constructing nuclear test vaults. It was assumed that the space nuclear power plant endurance test is to be conducted for 10,000 hr, with the vault inner surfaces exposed to a neutron flux of 2×10^{18} neutrons/cm^2 and that unrestricted entry into the test vault (after removal of test equipment and decontamination) is required for operating personnel on an 8-hr shift basis, 45 days after endurance test completion. A structural grade aluminum alloy was developed to meet the low-activation construction materials guidelines. It was determined that special concrete constituents of limestone aggregate and white cement can be obtained at a reasonable cost. The addition of boron frit to the levels required to meet the low-activation construction materials guidelines was found to be feasible and not to significantly affect the strength or set properties of the special concrete. (M.C.G.)

Space Propulsion

See also ISOTOPE TECHNOLOGY — Power Application
REACTOR TECHNOLOGY — Propulsion and Space

20870 (LA-DC-7703) ADVANCED CONCEPTS FOR NUCLEAR PROPULSION AND RELATED PROBLEMS IN HIGH TEMPERATURE CHEMISTRY. Bowman, Melvin G. (Los Alamos Scientific Lab., Univ. of California, N. Mex.). [nd]. Contract W-7405-eng-36. 7p. (CONF-660106-1). Dep. mn. CFSTI $1.00 cy, $0.50 mn.

From Meeting on Current and Future Problems in High Temperature Chemistry, Houston, Tex.

Various concepts proposed for nuclear propulsion and related problems in high-temperature chemistry are discussed. These include: rocket engines; heat exchanger reactors; use of nuclear reactors for production of electrical power; and chemical rocket engines. (P.C.H.)

20871 (N-65-29443) NON-CHEMICAL PROPULSION. Evvard, John C. (National Aeronautics and Space Administration, Cleveland, Ohio. Lewis Research Center). [1964]. 68p. (NASA-TM-X-31993). CFSTI $3.00 cy, $0.75 mn.

The performance of nuclear and chemical rockets is compared, and an evaluation is made of such nonchemical space propulsion sources as the nuclear and the solar-heated hydrogen rockets; electric propulsion; and the gaseous core nuclear, the thermonuclear, and the photon rockets. It was pointed out that although nuclear engines are feasible to safely boost space payloads into orbit, probable political repercussions may retard their use. The problems associated with electric propulsion systems are discussed, with the major hurdle being the development of systems that can provide power with low specific weights and high reliability for manned interplanetary flights. The possibilities offered by the solar-heated hydrogen, gaseous core nuclear, thermonuclear, and photon rockets are mentioned, with the need of further research stressed. The ORION concept is discussed; however, its use would be restricted to large payloads involving requirements for substantial velocity increments. The feasibility of a radioisotope photon rocket, and an antigravity propulsion device are also mentioned. (TAB)

20872 ENERGY EFFICIENCY TRENDS IN A COAXIAL GUN PLASMA ENGINE SYSTEM. Gloersen, P. (General Electric Space Sciences Lab., Philadelphia); Gorowitz, B.; Kenney, J. T. AIAA (Amer. Inst. Aeron. Astronaut.) J., 4: 436-41(Mar. 1966).

The efficiency of converting capacitor stored energy into energy in the exhaust stream of a repetitively pulsed two-stage coaxial plasma engine has been determined calorimetrically for various capacitances, voltages, gas densities and density profiles, and gun geometries. Observed efficiency trends have led to empirically determined optimum gun lengths, electrode radius ratios, and energy storage voltages. Energy efficiencies of 63% have been measured so

far, without having reached a leveling off of the efficiency increase trend. The largest gains in efficiency have been realized by a new approach to gas pulse injection, which provides more complete filling of the gun barrel with propellant by axial rather than radial injection prior to discharge. The most efficient gun configuration resulting from the calorimetric studies was placed on a thrust balance along with its associated capacitor energy storage system, and thrust data were obtained. Propellant mass flow rate also was measured, and the results were combined with the thrust data to determine over-all efficiencies ($\eta_0 = T^2/2\dot{m}P$) and specific impulses ($I_{sp} = T/\dot{m}g$). The over-all efficiencies, so measured, were typically significantly lower than the energy efficiencies measured calorimetrically, since a large fraction of the injected propellant was not utilized in the discharge. Adjustment of η_0 and I_{sp}, taking into account the unused mass, gave rise to significantly higher η_0 but at undesirably high I_{sp}. Additional steps taken to improve the engine system performance are discussed. (auth)

20873 SIGNIFICANCE OF NONEQUILIBRIUM CONDUCTIVITY ON PLASMA ENGINE PERFORMANCE. Levoy, M. M.; Dimmock, T. H. (Thiokol Chemical Corp., Denville, N. J.). AIAA (Amer. Inst. Aeron. Astronaut.) J., 4: 553-5(Mar. 1666).

An analysis of an MHD plasma engine was conducted with the aid of a digital computer to determine the significance of nonequilibrium conductivity in relation to over-all engine performance. A potassium-seeded cross field accelerator with constant cross-sectional area and complete suppression of axial Hall currents was assumed. The accelerator was designed for maximum Mach number via appropriate electric field tailoring, and nonequilibrium conductivities were computed from Kerrebrock's two-temperature conduction equation. Three propellants were examined as typically covering a range from monatomic-high molecular weight to diatomic-low molecular weight: argon, helium, and hydrogen. (B.G.D.)

20874 PLASMA GENERATOR AND PROPULSION EXHAUST SYSTEM. Meyer, Rudolf X. (to Aerospace Corp.). U. S. Patent 3,232,046. Feb. 1, 1966. Filed June 6, 1962.

A high specific-impulse space engine comprises an inner housing having a restricted aperture only at one end, a field winding surrounding the inner housing and arranged to provide a substantially uniform magnetic field throughout a major portion of the housing and an increased magnetic mirror field coplanar with the aperture of one end of the housing and having an escape cone that enhances ion flow through the aperture. A free electron flow is provided within the magnetic field. An annular anode is positioned around the uniform magnetic field and is arranged eventually to receive substantially all of the electrons admitted to the magnetic fields. Means are provided for reflecting the electrons towards the magnetic mirrow, and the reflection means, the anode, and the magnetic mirror cooperate to entrap substantially all of the electrons that follow a gyrating path within the uniform field. Ionizable particles are introduced into the entrapment region to be bombarded and energized by the entrapped electrons. The electrons have sufficient energy to ionize the particles so that at least a portion of the resulting ions will gyrate around the lines of magnetic force throughout the engine to egress through the escape cone and the restricted aperture and escape from the rear of the engine. (B.L.M.)

GEOLOGY, METEOROLOGY, AND MINERALOGY

General

Refer also to abstract 20794.

20875 (EUR–2481.f) MIGRATION DE RADIO-ELEMENTS DANS LE SOL. Rapport Final. (Migration of Radio Elements in Soil. Final Report). Baetsle, L.; Maes, W. F.; Souffriau, J.; Staner, P. I. (Centre d'Etude de l'Energie Nucleaire, Mol (Belgium)). Mar. 1966. 66p. Dep. mn.

Meteorologic and hydrologic observations at the Mol site were studied and led to a correlation between both phenomena. From these data the recharge rate of the aquifer and the real infiltration velocities were computed. A new device called Multicounter was developed for the in situ measurement of ground water velocity and direction in non-consolidated media. The apparatus is made of a stainless steel cylinder with four counter tubes piercing the bottom and one injection needle at the center of the bottom plate. The activities of the four counters are recorded simultaneously and provide Activity-Time plots which characterize the movement. Fundamental studies on the nature of the dispersion phenomena showed the existence of two distinct mechanisms being mainly influenced by the molecular diffusion. The dispersion coefficients vary between 10^{-3} and 10^{-5} cm^2/sec for velocities ranging from 10^{-2} to 10^{-4} cm/sec. Two techniques were developed in order to increase the soil's retention capacity for ^{90}Sr. The first one is based on the introduction of lignite treated with $K_4Fe(CN)_6$ + $FeCl_3$, and the other consists of a treatment with HF followed by $K_2H_2Sb_2O_7$. Both "chemical barriers" catch all the ^{90}Sr found in 200 and 60 volumes, respectively flowing through the barrier. (auth)

20876 (NP–15949) YUBA. Long Range Seismic Measurements [of] VELA UNIFORM Project. (UED Earth Sciences Div., Teledyne, Inc., Alexandria, Va.). Mar. 17, 1966. 22p.

A long range seismic measurements (LRSM) program was established under Vela Uniform to record and analyze short-period and long-period data from a planned series of U. S. underground nuclear tests. These, and other data, will be used by Vela Uniform participants for studying and developing methods for distinguishing between explosive and earthquake sources. An analysis of data resulting from the Yuba event from the LRSM film seismograms from operating mobile field teams is reported. A table of travel-times and amplitudes of P, Pg, Lg, and surface waves is included along with other unidentified phases. (P.C.H.)

20877 DISTRIBUTION PATTERNS OF RARE EARTH ELEMENTS IN TERRESTRIAL ROCKS. Jensen, Brenda B.; Brunfelt, Arild O. (Univ. of Oslo). Norsk Geol. Tidsskr., 45: 249-83(1965).

Data on the distribution of REE in the earth's crust are discussed in terms of its formation. Methods of plotting and comparing results are considered, as well as the comparability of data obtained by neutron activation analysis and x-ray spectrographic techniques. A large number of analyses were replotted by a new method, and several conclusions concerning differentiation in terrestrial rocks were made from the results. The groupings and ranges of REE distributions which can be recognized in igneous rocks are outlined. Sediments do not show a uniform degree of differentiation of REE. Detrital sediments from a particular area and period of time appear to show a fairly close grouping, which possibly gives some indication of the average degree of REE differentiation in the land mass surrounding the basin at the time of deposition. Very little is known of REE distributions in metamorphic rocks, but there are indications that even very highly metamorphosed rocks can retain the REE distribution of their parent material. (TCO)

Natural Radioactivity and Fallout

See also HEALTH AND SAFETY

Refer also to abstracts 20384, 20603, 20616, and 20928.

20878 (AD–612030) GAMMA-RAY ENERGY AND ANGULAR DISTRIBUTIONS ABOVE AN INFINITE FALLOUT FIELD. French, R. L. (Radiation Research Associates, Inc., Fort Worth, Tex.). Nov. 1965. Contract DA-49-146-XZ-254. 100p. (AFRRI-CR-65-3).

Monte Carlo techniques were applied in a detailed study of the gamma radiation environment produced in air three feet above fallout uniformly distributed on a smooth ground surface. The basic computations included the energy and angular distributions of the scattered photon flux above monoenergetic plane isotropic gamma-ray sources for ten different source energies from 0.10 to 3.5 Mev. For each source energy, the flux arriving at the receiver in each of ten energy intervals between 0.04 and 3.5 Mev and eighteen equal receiver angle intervals between 0° (nadir) and 180° (zenith) was calculated. Separate calculations were performed for the uncollided fluxes from the infinite plane isotropic source. In addition to the fluxes, the dose arriving through each ten degree interval of receiver angle was also computed. The results of the monoenergetic calculations were combined to obtain energy and angular distributions of the photon flux from fallout of four different ages: 1.12 hours, 23.8 hours, 4.57 days, and 9.82 days. Comparisons with measured and previously calculated data, both for actual fallout fields and for simulated infinite plane sources, show favorable agreement. (auth)

20879 (BNWL-SA-530) ACCUMULATION OF ^{137}Cs IN LITTER AND UNDERSTORY PLANTS OF FOREST STANDS FROM VARIOUS CLIMATIC ZONES OF WASHINGTON. Rickard, W. H. (Battelle-Northwest, Richland, Wash. Pacific Northwest Lab.). Feb. 8, 1966. Contract AT(45-1)-1830. 11p. (CONF-660405-1). Dep. mn. CFSTI $1.00 cy, $0.50 mn.

From Symposium on Radioecological Concentration Processes, Stockholm.

Estimates of the entire amount of ^{137}Cs present in Pacific Northwest conifer forest stands are difficult to obtain because of the difficulties of obtaining samples from tall trees. However, a sampling of forest floor plants and litter indicates that gross differences in ^{137}Cs accumulations can occur in forest habitats characteristic of contrasting climatic zones of the same latitude. Cesium-137 tends to accumulate in carpets of forest moss or in litter. There is little movement of ^{137}Cs into the mineral soil of the forest floor. (auth)

20880 (CEX–62.6.5) CINCINNATI AREA (ARMS-II). Guillou, R. B. (Edgerton, Germeshausen and Grier, Inc., Santa Barbara, Calif.). Apr. 1964. Contract AT(29-1)-1183. 19p. Dep. mn. CFSTI $1.00 cy, $0.50 mn.

An Aerial Radiological Measuring Survey (ARMS) was made of the Cincinnati area between Nov. 3, and Nov. 24, 1962. The survey was part of a nationwide program to measure the present environmental levels of gamma radiation. Approximately 7600 traverse miles were flown, at an altitude of about 500 ft above the ground, in the area that consists of a 100-mile square which is centered on Fernald, Ohio. The northeast quadrant, previously surveyed by the U. S. Geological Survey, was not resurveyed. The EG&G ARMS-II instrumentation was used in the survey. The data are presented as aeroradioactivity units, or areas with similar gamma-radiation counting rates at 500 ft, at two map scales: generalized at about 1:1,000,000; and detailed at 1:250,000. The maximum aeroradioactivity in most of the area is less than 800 counts/sec. Maximum counting rates of more than 800 but less than 1200 counts/sec occur

in about one-eighth of the area. Aerial measurements of ground radioactivity in the ARMS-II Cincinnati area were consistent with expectations, considering the geology of the area. The glaciated part of the area north of the Ohio River was generally less radioactive than the area south of the river. Artificial radionuclides were probably present in only small quantities, for background gamma radioactivity was less than 200 counts/sec in several places. (auth)

20881 (DASA–1704) DEVELOPMENT OF AIRBORNE SURVEILLANCE INSTRUMENTATION. Technical Report No. S-283-R. Hand, J. E.; Lamonds, H. A. (Edgerton, Germeshausen and Grier, Inc., Santa Barbara, Calif.). Feb. 1966. 174p.

A gamma ray detector was constructed using an inorganic scintillator. The unit is a CsI(Tl) crystal, 4 inches thick and 5 inches in diameter; it is viewed by three 2-inch-diameter photomultiplier (PM) tubes. The CsI(Tl) phosphor is encased in a $\frac{3}{16}$-inch-thick NE-102 plastic fluor in such a manner that the PM tube array also detects scintillations in the fluor. The detector forms a phoswich assembly, permitting pulse shape discrimination of the interactions occurring within the detector. The external circuitry rejects single signals from the fluor, and fluor-phosphor coincident signals. The unit approaches 100 percent rejection effectiveness in preventing charged-particle reactions in the detector from introducing signals into the measurement circuitry. Gamma ray losses resulting from gamma-fluor reactions are less than 9 percent of the total recorded gamma activity in the main CsI(Tl) detector for energies below 1.4 Mev. The detector incorporates a small inset-well crystal lying on the central axis; this crystal is optically separated from the CsI. The ratio of inset-well counting rate to big-crystal counting rate provides a directionality parameter defining source position with respect to the crystal axis. A front-to-back response ratio of a factor of 2 was obtained with ^{60}Co gamma rays and about 4.5 with ^{137}Cs gammas. The detector shows an energy response linearity within the response limitations of the analyzer used in the measurements, ~5 percent. The resolution for ^{137}Cs gamma rays exhibited by the assembly is 15.4 percent. Gamma ray spectral data can be collected with the charged-particle rejection feature in operation. The CsI(Tl) phosphor contains a built-in source of ^{138}La. As ~ ...d (only 1% emitted during ... which considerably ... source calibration check ...

Data are presented on radioactivity due to fallout in samples of air particulates, precipitation, milk, water, soil, wheat, and human bone collected in Canada in Nov. 1965. Data are included on total β activity and content of ^{89}Sr, ^{90}Sr, and ^{137}Cs in fallout and milk samples. Data are included on the environmental radioactivity in the environs of Canadian reactors during Nov. 1965. (C.H.)

20884 (TID–22815) A RADIOECOLOGICAL STUDY OF THE BIOTA OF DOE RUN, MEADE COUNTY, KENTUCKY. Final Report. Krumholz, Louis A. (Louisville Univ., Ky. Dept. of Biology). 1965. Contract AT(40-1)-2595. 92p. Dep. mn. CFSTI $3.00 cy, $0.75 mn.

The contamination of man's environment by radioactive wastes, whether from nuclear detonations or from the peaceful uses of atomic energy, has been a constant cause for concern since man first demonstrated the control of nuclear fission and a great deal of research has been done both in the laboratory and in the field on the accumulation and effects of certain radionuclides on selected organisms. Results are reported from a study made between May 1959 and October 1964 on the general ecology of Doe Run, Meade County, Kentucky. The data demonstrate the overall accumulation of radioactivity from fallout by various components of the ecological system. A marked increase in the amount of radionuclides accumulated by all organisms was observed following initiation of the Russian nuclear tests in Sept. 1961. Measurements were made of gross β radioactivity, ^{137}Cs, and ^{90}Sr in samples of animals, plants and water. (C.H.)

20885 GRAIN SIZE DISTRIBUTION OF NATURAL RADIOACTIVE AEROSOLS. Sedlacek, Martin (Univ., Vienna). Acta Phys. Austr., 21: 178–81(1966). (In German).

The α activity of grain size fractions of atmospheric aerosols obtained by means of cascade impactors was determined by autoradiography. From the results of these measurements, grain size distributions can be derived for the natural radioactive aerosols on the basis of the deposition law derived by Lassen – the deposited activity is proportional to $R^2/(1 + hR)$ with $h = 1 \times 10^4$ cm^{-1}. Their maxima are between 0.2 and 0.3 μm. (tr. auth)

20886 RADIOACTIVITY IN PHOSPHATE ROCK ...

20888 RECONNAISSANCE RUBIDIUM–STRONTIUM GEOCHRONOLOGY OF NEW ZEALAND PLUTONIC AND METAMORPHIC ROCKS. Aronson, James L. (California Inst. of Tech., Pasadena). N. Zealand J. Geol. Geophys., 8: 401–23(June 1965).

The $^{87}Rb/^{86}Sr$ and $^{87}Sr/^{86}Sr$ ratios were determined in a geochronological study of the plutonic and metamorphic rocks of the South Island and Stewart Island, New Zealand. The results showed that many of these deep-seated rocks have mineral ages that fall within the limits of 98 to 119 Myr. In this grouping are rocks associated with the Separation Point Granite, the Charleston Gneiss, the Fiordland–southern Stewart Island Complex, and the Otago Schists. The metamorphism of the Otago Schists was previously related to the Rangitata Orogeny on geological grounds; the results suggest that this orogeny is of mid-Cretaceous age and associated with the production of plutonic rocks over a wide area of the South Island. Only two of the samples measured in this study showed evidence of Paleozoic orogenic activity. A schist in south Westland had an early Carboniferous age of metamorphism. A pegmatite sample associated with the basic and ultrabasic intrusives in Southland was Permian. No rocks were found with Precambrian mineral ages, not even the Charleston Gneiss, which was previously mapped as Precambrian. However, whole-rock ages on the south Westland schist suggested that the pre-metamorphic sedimentary rock possibly was deposited as long ago as the late Precambrian. Minerals from a pegmatite in the Alpine Schists gave discordant ages, supporting the complex history of these schists already deduced by previous workers. (BBB)

20889 A PEAK IN THE TRITIUM CONTENT OF ATMOSPHERIC HYDROGEN FOLLOWING THE ACCIDENT AT WINDSCALE. Ehhalt, D. H.; Heimbridge, A. E. (National Center for Atmospheric Research, Boulder, Colo.). Nature, 209: 903–4(Feb. 26, 1966).

A strong peak in the tritium content of molecular hydrogen from air samples taken at Hamburg, Germany in October 1957 is attributed to the reactor accident at Windscale on October 10 and 11, 1957. The increase began either on October 11 or 12 and the final rise to full maximum occurred [illegible] October 14 and 16. Thereafter the tritium content [illegible]

one another. These types of fossils indicated previous existence of regions of fresh to brackish water. (BBB)

20891 EXCESS RADIOGENIC ARGON IN PYROXENES AND ISOTOPIC AGES ON MINERALS FROM NORWEGIAN ECLOGITES. McGougall, Ian; Green, D. H. (Australian National Univ., Canberra). Norsk Geol. Tidsskr., 44: 183–96(June 1964).

Potassium and Ar contents of pyroxenes and associated minerals from some Norwegian eclogites are reported, as well as Rb–Sr ages measured on two micas. This study was undertaken to examine the apparent ages of pyroxenes affected by metamorphism. Determination of potassium in the pyroxenes was made by isotope dilution. A sample was digested in HF and $HClO_4$ and after addition of ^{41}K tracer the potassium was concentrated by ion exchange. Rubidium and strontium were determined by isotope dilution. The ages on the two phlogopites determined by this method were calculated by assuming an initial $^{87}Sr/^{86}Sr$ ratio of 0.71, but because of the degree of enrichment in radiogenic Sr in these micas, a higher initial ratio would have a relatively small effect on the calculated age and would decrease the age. Potassium-Argon measurements on eclogites enclosed in gneisses of the Nordfiord area, Norway, showed that the pyroxenes contain excess radiogenic argon, indicating the presence of a high partial pressure of Ar at one or more periods during the history of these rocks. Potassium-Argon determinations on secondary hornblende suggested that the eclogites are as old as 1800 Myr; dates on phlogopite and hornblende in the range 950 to 1600 Myr were interpreted as indicating a metamorphism during this period. Micas from an altered eclogite and a country rock gneiss yielded K-Ar ages of about 400 Myr, and Rb-Sr ages on two micas from altered eclogites also gave dates of about 400 Myr, showing that the area was affected by the Caledonian orogeny. (BBB)

20893 THE DISTRIBUTION OF TRITIUM IN PRECIPITATION OVER CONTINENTS AND ITS SIGNIFICANCE TO GROUND-WATER DATING. Thatcher, L. L.; Payne, B. R. (International Atomic Energy Agency, Vienna). 24p. (CONF-650651-10). ORAU, Gmelin, AED-CONF-65-150-10.

From International ^{14}C and ^{3}H Dating Conference, Pullman, Wash.

The d[illegible]tion of tritium [illegible] is significant to ground-

far, without having reached a leveling off of the efficiency increase trend. The largest gains in efficiency have been realized by a new approach to gas pulse injection, which provides more complete filling of the gun barrel with propellant by axial rather than radial injection prior to discharge. The most efficient gun configuration resulting from the calorimetric studies was placed on a thrust balance along with its associated capacitor energy storage system, and thrust data were obtained. Propellant mass flow rate also was measured, and the results were combined with the thrust data to determine over-all efficiencies ($\eta_0 = T^2/2\dot{m}P$) and specific impulses ($I_{sp} = T/\dot{m}g$). The over-all efficiencies, so measured, were typically significantly lower than the energy efficiencies measured calorimetrically, since a large fraction of the injected propellant was not utilized in the discharge. Adjustment of η_0 and I_{sp}, taking into account the unused mass, gave rise to significantly higher η_0 but at undesirably high I_{sp}. Additional steps taken to improve the engine system performance are discussed. (auth)

20873 SIGNIFICANCE OF NONEQUILIBRIUM CONDUCTIVITY ON PLASMA ENGINE PERFORMANCE. Levoy, M. M.; Dimmock, T. H. (Thiokol Chemical Corp., Denville, N. J.). AIAA (Amer. Inst. Aeron. Astronaut.) J., 4: 553-5(Mar. 1666).

An analysis of an MHD plasma engine was conducted with the aid of a digital computer to determine the significance of nonequilibrium conductivity in relation to over-all engine performance. A potassium-seeded cross field accelerator with constant cross-sectional area and complete suppression of axial Hall currents was assumed. The accelerator was designed for maximum Mach number via appropriate electric field tailoring, and nonequilibrium conductivities were computed from Kerrebrock's two-temperature conduction equation. Three propellants were examined as typically covering a range from monatomic-high molecular weight to diatomic-low molecular weight: argon, helium, and hydrogen. (B.G.D.)

20874 PLASMA GENERATOR AND PROPULSION EXHAUST SYSTEM. Meyer, Rudolf X. (to Aerospace Corp.). U. S. Patent 3,232,046. Feb. 1, 1966. Filed June 6, 1962.

A high specific-impulse space engine comprises an inner housing having a restricted aperture only at one end, a field winding surrounding the inner housing and arranged to provide a substantially uniform magnetic field throughout a major portion of the housing and an increased magnetic mirror field coplanar with the aperture of one end of the housing and having an escape cone that enhances ion flow through the aperture. A free electron flow is provided within the magnetic field. An annular anode is positioned around the uniform magnetic field and is arranged eventually to receive substantially all of the electrons admitted to the magnetic fields. Means are provided for reflecting the electrons towards the magnetic mirrow, and the reflection means, the anode, and the magnetic mirror cooperate to entrap substantially all of the electrons that follow a gyrating path within the uniform field. Ionizable particles are introduced into the entrapment region to be bombarded and energized by the entrapped electrons. The electrons have sufficient energy to ionize the particles so that at least a portion of the resulting ions will gyrate around the lines of magnetic force throughout the engine to egress through the escape cone and the restricted aperture and escape from the rear of the engine. (B.L.M.)

GEOLOGY, METEOROLOGY, AND MINERALOGY

General

Refer also to abstract 20794.

20875 (EUR-2481.f) MIGRATION DE RADIO-ELEMENTS DANS LE SOL. Rapport Final. (Migration of Radio Elements in Soil. Final Report). Baetsle, L.; Maes, W. F.; Souffriau, J.; Staner, P. I. (Centre d'Etude de l'Energie Nucleaire, Mol (Belgium)). Mar. 1966. 66p. Dep. mn.

Meteorologic and hydrologic observations at the Mol site were studied and led to a correlation between both phenomena. From these data the recharge rate of the aquifer and the real infiltration velocities were computed. A new device called Multicounter was developed for the in situ measurement of ground water velocity and direction in non-consolidated media. The apparatus is made of a stainless steel cylinder with four counter tubes piercing the bottom and one injection needle at the center of the bottom plate. The activities of the four counters are recorded simultaneously and provide Activity-Time plots which characterize the movement. Fundamental studies on the nature of the dispersion phenomena showed the existence of two distinct mechanisms being mainly influenced by the molecular diffusion. The dispersion coefficients vary between 10^{-3} and 10^{-5} cm^2/sec for velocities ranging from 10^{-2} to 10^{-4} cm/sec. Two techniques were developed in order to increase the soil's retention capacity for ^{90}Sr. The first one is based on the introduction of lignite treated with $K_4Fe(CN)_6$ + $FeCl_3$, and the other consists of a treatment with HF followed by $K_2H_2Sb_2O_7$. Both "chemical barriers" catch all the ^{90}Sr found in 200 and 60 volumes, respectively flowing through the barrier. (auth)

20876 (NP-15949) YUBA, Long Range Seismic Measurements [of] VELA UNIFORM Project. (UED Earth Sciences Div., Teledyne, Inc., Alexandria, Va.). Mar. 17, 1966. 22p.

A long range seismic measurements (LRSM) program was established under Vela Uniform to record and analyze short-period and long-period data from a planned series of U. S. underground nuclear tests. These, and other data, will be used by Vela Uniform participants for studying and developing methods for distinguishing between explosive and earthquake sources. An analysis of data resulting from the Yuba event from the LRSM film seismograms from operating mobile field teams is reported. A table of travel-times and amplitudes of P, Pg, Lg, and surface waves is included along with other unidentified phases. (P.C.H.)

20877 DISTRIBUTION PATTERNS OF RARE EARTH ELEMENTS IN TERRESTRIAL ROCKS. Jensen, Brenda B.; Brunfelt, Arild O. (Univ. of Oslo). Norsk Geol. Tidsskr., 45: 249-83(1965).

Data on the distribution of REE in the earth's crust are discussed in terms of its formation. Methods of plotting and comparing results are considered, as well as the comparability of data obtained by neutron activation analysis and x-ray spectrographic techniques. A large number of analyses were replotted by a new method, and several conclusions concerning differentiation in terrestrial rocks were made from the results. The groupings and ranges of REE distributions which can be recognized in igneous rocks are outlined. Sediments do not show a uniform degree of differentiation of REE. Detrital sediments from a particular area and period of time appear to show a fairly close grouping, which possibly gives some indication of the average degree of REE differentiation in the land mass surrounding the basin at the time of deposition. Very little is known of REE distributions in metamorphic rocks, but there are indications that even very highly metamorphosed rocks can retain the REE distribution of their parent material. (TCO)

Natural Radioactivity and Fallout

See also HEALTH AND SAFETY

Refer also to abstracts 20384, 20603, 20616, and 20928.

20878 (AD-612030) GAMMA-RAY ENERGY AND ANGULAR DISTRIBUTIONS ABOVE AN INFINITE FALLOUT FIELD. French, R. L. (Radiation Research Associates, Inc., Fort Worth, Tex.). Nov. 1965. Contract DA-49-146-XZ-254. 100p. (AFRRI-CR-65-3).

Monte Carlo techniques were applied in a detailed study of the gamma radiation environment produced in air three feet above fallout uniformly distributed on a smooth ground surface. The basic computations included the energy and angular distributions of the scattered photon flux above monoenergetic plane isotropic gamma-ray sources for ten different source energies from 0.10 to 3.5 Mev. For each source energy, the flux arriving at the receiver in each of ten energy intervals between 0.04 and 3.5 Mev and eighteen equal receiver angle intervals between 0° (nadir) and 180° (zenith) was calculated. Separate calculations were performed for the uncollided fluxes from the infinite plane isotropic source. In addition to the fluxes, the dose arriving through each ten degree interval of receiver angle was also computed. The results of the monoenergetic calculations were combined to obtain energy and angular distributions of the photon flux from fallout of four different ages: 1.12 hours, 23.8 hours, 4.57 days, and 9.82 days. Comparisons with measured and previously calculated data, both for actual fallout fields and for simulated infinite plane sources, show favorable agreement. (auth)

20879 (BNWL-SA-530) ACCUMULATION OF ^{137}Cs IN LITTER AND UNDERSTORY PLANTS OF FOREST STANDS FROM VARIOUS CLIMATIC ZONES OF WASHINGTON. Rickard, W. H. (Battelle-Northwest, Richland, Wash. Pacific Northwest Lab.). Feb. 8, 1966. Contract AT(45-1)-1830. 11p. (CONF-660405-1). Dep. mn. CFSTI $1.00 cy, $0.50 mn.

From Symposium on Radioecological Concentration Processes, Stockholm.

Estimates of the entire amount of ^{137}Cs present in Pacific Northwest conifer forest stands are difficult to obtain because of the difficulties of obtaining samples from tall trees. However, a sampling of forest floor plants and litter indicates that gross differences in ^{137}Cs accumulations can occur in forest habitats characteristic of contrasting climatic zones of the same latitude. Cesium-137 tends to accumulate in carpets of forest moss or in litter. There is little movement of ^{137}Cs into the mineral soil of the forest floor. (auth)

20880 (CEX-62.6.5) CINCINNATI AREA (ARMS-II). Guillou, R. B. (Edgerton, Germeshausen and Grier, Inc., Santa Barbara, Calif.). Apr. 1964. Contract AT(29-1)-1183. 19p. Dep. mn. CFSTI $1.00 cy, $0.50 mn.

An Aerial Radiological Measuring Survey (ARMS) was made of the Cincinnati area between Nov. 3, and Nov. 24, 1962. The survey was part of a nationwide program to measure the present environmental levels of gamma radiation. Approximately 7600 traverse miles were flown, at an altitude of about 500 ft above the ground, in the area that consists of a 100-mile square which is centered on Fernald, Ohio. The northeast quadrant, previously surveyed by the U. S. Geological Survey, was not resurveyed. The EG&G ARMS-II instrumentation was used in the survey. The data are presented as aeroradioactivity units, or areas with similar gamma-radiation counting rates at 500 ft, at two map scales: generalized at about 1 : 1,000,000; and detailed at 1 : 250,000. The maximum aeroradioactivity in most of the area is less than 800 counts/sec. Maximum counting rates of more than 800 but less than 1200 counts/sec occur

in about one-eighth of the area. Aerial measurements of ground radioactivity in the ARMS-II Cincinnati area were consistent with expectations, considering the geology of the area. The glaciated part of the area north of the Ohio River was generally less radioactive than the area south of the river. Artificial radionuclides were probably present in only small quantities, for background gamma radioactivity was less than 200 counts/sec in several places. (auth)

20881 (DASA–1704) DEVELOPMENT OF AIRBORNE SURVEILLANCE INSTRUMENTATION. Technical Report No. S-283-R. Hand, J. E.; Lamonds, H. A. (Edgerton, Germeshausen and Grier, Inc., Santa Barbara, Calif.). Feb. 1966. 174p.

A gamma ray detector was constructed using an inorganic scintillator. The unit is a CsI(Tl) crystal, 4 inches thick and 5 inches in diameter; it is viewed by three 2-inch-diameter photomultiplier (PM) tubes. The CsI(Tl) phosphor is encased in a $^3/_{16}$-inch-thick NE-102 plastic fluor in such a manner that the PM tube array also detects scintillations in the fluor. The detector forms a phoswich assembly, permitting pulse shape discrimination of the interactions occurring within the detector. The external circuitry rejects single signals from the fluor, and fluor-phosphor coincident signals. The unit approaches 100 percent rejection effectiveness in preventing charged-particle reactions in the detector from introducing signals into the measurement circuitry. Gamma ray losses resulting from gamma-fluor reactions are less than 9 percent of the total recorded gamma activity in the main CsI(Tl) detector for energies below 1.4 Mev. The detector incorporates a small inset-well crystal lying on the central axis; this crystal is optically separated from the CsI. The ratio of inset-well counting rate to big-crystal counting rate provides a directionality parameter defining source position with respect to the crystal axis. A front-to-back response ratio of a factor of 2 was obtained with ^{60}Co gamma rays and about 4.5 with ^{137}Cs gammas. The detector shows an energy response linearity within the response limitations of the analyzer used in the measurements, $\pm^1/_2$ percent. The resolution for ^{137}Cs gamma rays exhibited by the assembly is 15.4 percent. Gamma ray spectral data can be collected with the charged particle rejection feature in operation. The CsI(Tl) phosphor contains a built-in source of ^{241}Am. An α-particle is emitted during decay, which provides an energy calibration peak at an equivalent gamma energy of 4.05 Mev. Since the peak is far removed from gamma energies found in nuclear debris, it causes no interference in the spectral measurements. The α-particle peak is viewed by a single channel analyzer window, which generates a reference voltage to the power supply for stabilization of the high voltage on the detector tubes. (auth)

20882 (HASL–171) FALLOUT PROGRAM QUARTERLY SUMMARY REPORT, DECEMBER 1, 1965–MARCH 1, 1966. Hardy, Edward P. Jr.; Rivera, Joseph (Health and Safety Lab., New York Operations Office (AEC), N. Y.). Apr. 1, 1966. 430p. Dep. mn. CFSTI $7.30 cy, $2.00 mn.

Current data on fallout are presented that were obtained during 1965 from the HASL Fallout Program, the New Zealand Department of Scientific and Industrial Research, the New Zealand National Radiation Laboratory, Argonne National Laboratory, U. S. Naval Radiological Defense Laboratory and the USDA Soil Conservation Service. Data from previous studies are included for comparison. Radionuclide levels in fallout, milk, tap water, diet, and surface and high altitude air are given in tabular form. Also included are interpretive reports and notes dealing with fallout in the Pacific Ocean, depth distribution of ^{90}Sr in soil, development of a method for ^{90}Sr extraction from soil, ^{90}Sr contamination of reagents used in sea water analyses, and the transfer of ^{90}Sr fallout to cows' milk. (100 references.) (C.H.)

20883 (NP–15914) DATA FROM RADIATION PROTECTION PROGRAMS. Volume 3, Number 12. (Department of National Health and Welfare, Ottawa (Ontario). Radiation Protection Div.). Dec. 1965. 30p. Dep. mn.

Data are presented on radioactivity due to fallout in samples of air particulates, precipitation, milk, water, soil, wheat, and human bone collected in Canada in Nov. 1965. Data are included on total β activity and content of ^{89}Sr, ^{90}Sr, and ^{137}Cs in fallout and milk samples. Data are included on the environmental radioactivity in the environs of Canadian reactors during Nov. 1965. (C.H.)

20884 (TID–22815) A RADIOECOLOGICAL STUDY OF THE BIOTA OF DOE RUN, MEADE COUNTY, KENTUCKY. Final Report. Krumholz, Louis A. (Louisville Univ., Ky. Dept. of Biology). 1965. Contract AT(40-1)-2595. 92p. Dep. mn. CFSTI $3.00 cy, $0.75 mn.

The contamination of man's environment by radioactive wastes, whether from nuclear detonations or from the peaceful uses of atomic energy, has been a constant cause for concern since man first demonstrated the control of nuclear fission and a great deal of research has been done both in the laboratory and in the field on the accumulation and effects of certain radionuclides on selected organisms. Results are reported from a study made between May 1959 and October 1964 on the general ecology of Doe Run, Meade County, Kentucky. The data demonstrate the overall accumulation of radioactivity from fallout by various components of the ecological system. A marked increase in the amount of radionuclides accumulated by all organisms was observed following initiation of the Russian nuclear tests in Sept. 1961. Measurements were made of gross β radioactivity, ^{137}Cs, and ^{90}Sr in samples of animals, plants, and water. (C.H.)

20885 GRAIN SIZE DISTRIBUTION OF NATURAL RADIOACTIVE AEROSOLS. Sedlacek, Martin (Univ., Vienna). Acta Phys. Austr., 21: 178-81(1966). (In German).

The α activity of grain size fractions of atmospheric aerosols obtained by means of cascade impactors was determined by autoradiography. From the results of these measurements, grain size distributions can be derived for the natural radioactive aerosols on the basis of the deposition law derived by Lassen–the deposited activity is proportional to $R^2/(1 + hR)$ with $h = 7 \times 10^4$ cm^{-1}. Their maxima are between 0.3 and 0.4 μm. (tr-auth)

20886 RADIOACTIVITY IN PHOSPHATE ROCK. Habashi, Fathi (Montana Coll. of Mineral Science and Tech., Butte). Econ. Geol., 61: 402-5(Mar.-Apr. 1966).

The radioactivity in phosphate rock from different localities was studied by means of gamma scintillation spectrometry. Typical gamma spectra are shown. Two peaks are clearly defined, one at 180 kev due to ^{226}Ra and the other at 600 kev due to ^{214}Bi. Both are decay products of uranium. No peaks due to thorium or its decay products could be detected. It was found that in sedimentary phosphates, uranium exists in radioactive equilibrium with its decay products, and therefore the total gamma activity of a sample may be taken as a direct measure of its uranium content. (M.C.G.)

20887 NON-EQUILIBRIUM URANIUM IN CARBONATE DEPOSITS AND THEIR AGE DETERMINATION. Cherdyntsev, V. V.; Kazachevskii, I. V.; Kislitsina, G. I.; Kuz'mina, E. A.; Kind, N. V. (Geological Inst., Moscow). Geokhimiya, No. 2, 139-45(Feb. 1966). (In Russian).

Data on the isotopic composition of thorium and uranium in 57 natural objects are given. Particular attention was paid to the question of the absolute age determination according to nonequilibrium uranium (using the relation between the isotopes ^{234}U, ^{238}U, ^{234}Th, ^{230}Th, and ^{227}Th). Attempts to determine the age in marine carbonates were unsuccessful. The suitability of tufas for geochronological purposes was confirmed. The determination of the lower age limit of the Mindel–Rissian glaciation (280 thousand years) according to travertines of the mountain Mashuk was of importance. A high RdTh/Th ratio reaching up to 53 (in activity units) was noted in some lake waters in the northern part of the Russian plain as well as in young travertines. Material on the radiochemistry of carbonate formations in natural waters is discussed. (auth)

20888 RECONNAISSANCE RUBIDIUM–STRONTIUM GEOCHRONOLOGY OF NEW ZEALAND PLUTONIC AND METAMORPHIC ROCKS. Aronson, James L. (California Inst. of Tech., Pasadena). N. Zealand J. Geol. Geophys., 8: 401-23(June 1965).

The $^{87}Rb/^{86}Sr$ and $^{87}Sr/^{86}Sr$ ratios were determined in a geochronological study of the plutonic and metamorphic rocks of the South Island and Stewart Island, New Zealand. The results showed that many of these deep-seated rocks have mineral ages that fall within the limits of 98 to 119 Myr. In this grouping are rocks associated with the Separation Point Granite, the Charleston Gneiss, the Fiordland–southern Stewart Island Complex, and the Otago Schists. The metamorphism of the Otago Schists was previously related to the Rangitata Orogeny on geological grounds; the results suggest that this orogeny is of mid-Cretaceous age and associated with the production of plutonic rocks over a wide area of the South Island. Only two of the samples measured in this study showed evidence of Paleozoic orogenic activity. A schist in south Westland had an early Carboniferous age of metamorphism. A pegmatite sample associated with the basic and ultrabasic intrusives in Southland was Permian. No rocks were found with Precambrian mineral ages, not even the Charleston Gneiss, which was previously mapped as Precambrian. However, whole-rock ages on the south Westland schist suggested that the pre-metamorphic sedimentary rock possibly was deposited as long ago as the late Precambrian. Minerals from a pegmatite in the Alpine Schists gave discordant ages, supporting the complex history of these schists already deduced by previous workers. (BBB)

20889 A PEAK IN THE TRITIUM CONTENT OF ATMOSPHERIC HYDROGEN FOLLOWING THE ACCIDENT AT WINDSCALE. Ehhalt, D. H.; Bainbridge, A. E. (National Center for Atmospheric Research, Boulder, Colo.). Nature, 209: 903-4(Feb. 26, 1966).

A strong peak in the tritium content of molecular hydrogen from air samples taken at Hamburg, Germany in October 1957 is attributed to the reactor accident at Windscale on October 10 and 11, 1957. The increase began either on October 11 or 12 and the final rise to full maximum occurred between October 14 and 16. Thereafter the tritium content dropped steadily to its former value, which was reached about October 23. Sources of the tritium were ternary fission and the $^{6}Li(n,\alpha)T$ reaction due to irradiation of cartridges containing Li–Mg alloy, which were present in the pile. (M.C.G.)

20890 OBSERVATIONS ON RADIOACTIVITY AND FOSSIL CONTENT AT THE CORE OF NEW RED SANDSTONE SOUTHWEST OF BRAUNSCHWEIG. Herrmann, Friedbert (Technische Hochschule, Brunswick, Ger.). Neues Jahrb. Geol. Palaeontol., Monatsh., 1: 26-31(Jan. 1963). (In German).

Radioactivity measurements were made in Hardegsen clay of the Salzgitter and Lichtenberg mountains. In a brook fissure southwest of Osterlinde values of 15 μR/hr were observed in grey clay, and 42 μR/hr was recorded in red clay 14 m above the grey clay base. The highest value in the grey clay base was 16 μR/hr, but it was 25 μR/hr at the border of the bed above the horizontal stratum. The average intensity of the rest of the profile sections of the grey clay in both profiles was from 11 to 13 μR/hr. In the Osterlinde red clay the values were 8 to 10, and in the region of the grey-green clay stone they were 13 to 14 μR/hr. In Gebhardshagen red clay the values were from 8 to 9 μR/hr. The radiation-emitting substance was concentrated in dark grey green dolomitic argillaceous rocks a few cm thick. It consisted of U, as in Lower Savony and the Goldenstedt borehold T2. Ostracods were found in surface outcroppings, in red clay, in new red sandstone, and in the clay boundary layer. At a level of 11 m above the base of Osterlinder profile, ostracods and charophytes-gyrogonites were found. These were also discovered in other layers. Ganoid fish teeth and bone detritus were found in other strata. Many of the shells were nested within one another. These types of fossils indicated previous existence of regions of fresh to brackish water. (BBB)

20891 EXCESS RADIOGENIC ARGON IN PYROXENES AND ISOTOPIC AGES ON MINERALS FROM NORWEGIAN ECLOGITES. McGougall, Ian; Green, D. H. (Australian National Univ., Canberra). Norsk Geol. Tidsskr., 44: 183-96(June 1964).

Potassium and Ar contents of pyroxenes and associated minerals from some Norwegian eclogites are reported, as well as Rb–Sr ages measured on two micas. This study was undertaken to examine the apparent ages of pyroxenes affected by metamorphism. Determination of potassium in the pyroxenes was made by isotope dilution. A sample was digested in HF and $HClO_4$ and after addition of ^{41}K tracer the potassium was concentrated by ion exchange. Rubidium and strontium were determined by isotope dilution. The ages on the two phlogopites determined by this method were calculated by assuming an initial $^{87}Sr/^{86}Sr$ ratio of 0.71, but because of the degree of enrichment in radiogenic Sr in these micas, a higher initial ratio would have a relatively small effect on the calculated age and would decrease the age. Potassium-Argon measurements on eclogites enclosed in gneisses of the Nordfiord area, Norway, showed that the pyroxenes contain excess radiogenic argon, indicating the presence of a high partial pressure of Ar at one or more periods during the history of these rocks. Potassium-Argon determinations on secondary hornblende suggested that the eclogites are as old as 1800 Myr; dates on phlogopite and hornblende in the range 950 to 1600 Myr were interpreted as indicating a metamorphism during this period. Micas from an altered eclogite and a country rock gneiss yielded K-Ar ages of about 400 Myr, and Rb-Sr ages on two micas from altered eclogites also gave dates of about 400 Myr, showing that the area was affected by the Caledonian orogeny. (BBB)

20892 THE DISTRIBUTION OF TRITIUM IN PRECIPITATION OVER CONTINENTS AND ITS SIGNIFICANCE TO GROUND-WATER DATING. Thatcher, L. L.; Payne, B. R. (International Atomic Energy Agency, Vienna). 24p. (CONF-650652–10). ORAU. Gmelin, AED-CONF-65-158-10.

From International ^{14}C and ^{3}H Dating Conference, Pullman, Wash.

The distribution of tritium fallout is significant to groundwater dating for two reasons, the information that it provides on input of tritium into ground-water systems during the high fallout years, and the information that it provides by analogy on the relative distribution of natural tritium in time and area. The first consideration applies to future dating based on the down-gradient movement of the integrated fallout peaks and the latter applies to dating based on tritium recharge prior to the early 1950's. Current tritium fallout at a given site can usually be estimated by interpolation from the published data of the IAEA-WMO networks. The estimation of the tritium concentration in recharge at this site is more difficult since it involves considerations of the local precipitation and evaporation cycle. These are discussed using the Washington, D. C., area as an example. Information on tritium fallout in the southern hemisphere is limited. The use of ^{90}Sr fallout to estimate the tritium fallout is discussed. Tritium dating is usually relative because of the complexities involved in the estimation of tritium recharge and underground mixing. (auth)

20893 PROBLEMS IN THE ESTABLISHMENT OF A ^{14}C AND TRITIUM LABORATORY. Rafter, T. A. 14p. (CONF-650652–7). ORAU. Gmelin, AED-CONF-65-158-5.

From International ^{14}C and ^{3}H Dating Conference, Pullman, Wash.

The problems in the establishment of ^{14}C and tritium laboratory in New Zealand are discussed. Development of a method for dating volcanic ash showers by means of the radioactive carbon method is discussed. Measurements of tritium concentration in water and the variations in tritium concentrations in rainwater at Wairakei are discussed. (F.J.H.)

20894 THE DETERMINATION OF CHARACTERISTICS OF WATER-BODIES WITH THE AID OF BOMB PRODUCED TRITIUM PULSES. Gat, Joel R. (Univ. of California, San Diego, La Jolla). 13p. (CONF-650652-13). ORINS. Gmelin, AED-CONF-65-158-20.

From International ^{14}C and ^{3}H Dating Conference, Pullman, Wash.

The tritium concentration variations in water bodies can be used to determine the characteristics of water bodies exposed to the atmosphere. The formation of the pulse tracing method, analytical accuracy and representativeness of the rain data, modification of rain composition during input into reservoirs, distortion of the input data by rain selection processes, isotope fractionation during recharge, effects of molecular exchange on the tritium balance of open water bodies, and limitation of the pulse tracing method for reservoirs with exponentially decreasing transit time distribution are discussed. (F.J.H.)

Site Survey and Selection

20895 (AD-626899) ENGINEERING PROPERTIES OF NUCLEAR CRATERS. REPORT 1. SITE SELECTION INVESTIGATIONS, WET MEDIUM CRATERING EXPERIMENTS. Saucier, R. T.; Banks, D. C. (Army Engineer Waterways Experiment Station, Vicksburg, Miss.). Oct. 1965. 85p. (TR-3-699). CFSTI $3.00 cy, $0.75 mn.

Investigations were made to select a site suitable for producing craters in a saturated cohesive medium by small-scale high-energy detonations. According to prescribed criteria, the ideal site would be a large (200 acres or more), cleared, moderately flat tract of Federally owned land characterized by soft, homogeneous clays to a minimum depth of 40 feet. An evaluation of the U. S. by physical divisions revealed that suitable sites might occur in four general areas: the Lake Bonneville area; the Lake Agassiz area; the Great Lakes area; and the lower Mississippi Valley area. Acquisition and analyses of pertinent data on these areas indicated a need for field reconnaissances except in the case of the Great Lakes area which was eliminated from further consideration because of heterogeneous soil deposits. A reconnaissance of the Lake Bonneville area indicated the presence of apparently favorable test site conditions in a portion of the Dugway Proving Ground, Utah, while a reconnaissance of the Lake Agassiz area of North Dakota and Minnesota revealed generally unfavorable soil conditions. In regard to the lower Mississippi Valley area, three possible site areas were visited. Three borings were made at the Dugway Proving Ground site and two borings at the Brickeys (lower Mississippi Valley) site to investigate the depth and homogeneity of the clay deposits. Natural water contents and unconfined compressive strengths were determined on selected undisturbed samples from both sites. Considering the soil conditions together with such factors as land ownership, proximity of cultural features, and probability of surface flooding, it was concluded that the Dugway Proving Ground site is more suitable for the project than any other site considered. (123 references.) (P.C.H.)

Techniques and Equipment

Refer also to abstract 20798.

20896 (AD-623592) A BASIC STUDY OF ELASTIC WAVE PROPAGATION. Final Report, June 28, 1963-December 31, 1964. Dorman, James (Columbia Univ., Palisades, N. Y. Lamont Geological Observatory). Contract DA31-124AROD136. 8p. (AROD-4120:2). CFSTI $1.00 cy, $0.50 mn.

Abstracts are given of the following publications: Relative excitation of surface waves by earthquakes and underground explosions in the California-Nevada region; Surface wave radiation patterns for underground nuclear explosions and small magnitude earthquakes; Use of surface wave rejection filters to record mantle waves of low order; Travel times, body waves, and dispersion in the earth; Travel times, body waves, and normal modes of the earth. (TAB)

20897 (AD-623679) ACOUSTIC PHASED ARRAYS FOR THE DETECTION OF NUCLEAR BURSTS IN THE ATMOSPHERE. Burke, T. F. (RAND Corp., Santa Monica, Calif.). Oct. 1965. Contract SD-79. 30p. (RM-4722-ARPA). CFSTI $2.00 cy, $0.50 mn.

An acoustic phased array serves to improve both the signal-to-turbulent-noise ratio and the signal-to-acoustic-noise ratio. The improvement in acoustic signal-to-noise ratio is, for isotropic noise, the array gain-which is calculable and is discussed. The improvement in the turbulent signal-to-noise ratio cannot be calculated, in view of the unknown correlation of noise in single sensors. However, it is thought likely that this improvement will be at least as much as the acoustic improvement-especially at the higher frequencies of greatest interest for small yields. An included discussion considers, for simple unshaded square plane arrays, the dependence of array gain upon frequency, azimuth, size of array, number of sensors in the array, and uncertainty in the local velocity of sound. It is shown that an array of 16 sensors at the lattice points of a $\frac{1}{2} \times \frac{1}{2}$ mile square offers a frequency-dependent gain which rises to nearly 10 db at 0.5 cps for any azimuth and for any sound speed in the range of 1000 to 1200 ft/sec. Such an array appears to be suitable for the detection of acoustic signals from atmospheric nuclear blasts. (auth)

20898 (AD-624016) SEISMIC SIGNALS FROM NUCLEAR EXPLOSIONS IN OVERDRIVEN CAVITIES. Lewis, H. W.; Treiman, S. B. (Institute for Defense Analyses, Arlington, Va. Jason Div.). June 28, 1965. Contract SD-50. 26p. CFSTI $2.00 cy, $0.50 mn.

A static treatment is given of the seismic signal from nuclear explosions in overdriven cavities, with particular attention to the role of incipient tension. When the elastic limits are exceeded, the seismic signal is larger than a purely elastic treatment would imply. This enhancement, however, grows relatively slowly with overdrive under certain circumstances. (auth)

20899 (AD-626777) LARGE APERTURE SEISMIC ARRAY FINAL SPECIFICATIONS REPORT. Final Report, October 1. 1964-June 30, 1965. Rackets, Hubert M. (Texas Instruments Inc., Dallas). Aug. 1965. Contract AF33(657)-13899. 160p. CFSTI $5.00 cy, $1.00 mn.

The installation of Angela and Hysham subarrays of the Large Aperture Seismic Array (LASA) is described. Each subarray consists of 24 peripheral instruments located on six radials. At each location within the subarrays a borehole was drilled approximately 200 ft deep, cased and cemented. A Hall-Sears HS-10 seismometer was then lowered into each borehole. Data from the seismometers are amplified at the wellhead of each borehole and transmitted to a central gathering point by buried cable. Lightning protectors were installed. Data from the two subarrays was used in carrying out two studies. First, the subarray systems were evaluated from an engineering viewpoint in order to determine those elements and characteristics which would affect the desired performance of the array. Second, characteristics of the seismic information field (signal and noise) were determined within a single subarray and between the two subarrays. Summarizing the results from the engineering study, the system noise with the seismometer replaced by its equivalent resistance is about 30 to 35 db below the ambient seismic noise at 1.0 cps. This is an improvement of 8 to 12 db of separation over previous array systems at CPO, UBO and BMO. (auth)

20900 (AD-627039) BRONZE. Long Range Seismic Measurements. Clark, Don M. (UED Earth Sciences Div., Teledyne, Inc., Alexandria, Va.). Dec. 3, 1965. Contract AF33(657)-12447. 34p. CFSTI $2.00 cy, $0.50 mn.

An analysis of seismological data from an underground nuclear explosion as a continuing study to provide information to aid in distinguishing between earthquakes and explosions. A table of travel-times and amplitudes of P, Pg, Lg, and surface waves are included along with other unidentified phases. (auth)

20901 (AD-627040) KLICKITAT. Long Range Seismic Measurements. Clark, Don M. (UED Earth Sciences Div., Teledyne, Inc., Alexandria, Va.). Nov. 24, 1965. Contract AF33(657)-12447. 34p. CFSTI $2.00 cy, $0.50 mn.

20902 (AD-627051) TURF. Long Range Seismic Measurements. Clark, Don M. (UED Earth Sciences Div., Teledyne, Inc., Alexandria, Va.). Nov. 12, 1965. Contract AF33(657)-12447. 33p. CFSTI $2.00 cy, $0.50 mn.

20903 (AEET-Radiochem.-45) TOTAL COUNT METHOD FOR OPEN CHANNEL FLOW MEASUREMENT. Eapen, A. C.; Rao, S. M. (Atomic Energy Establishment, Trombay (India)). 1964. 26p. Dep. mn.

The following radioisotope trace experiments were performed to determine flow rates: one in the Mutha River at Poona; two in the recirculating canal at the Central Water and Power Research Station, Kadakvasla, Poona; two at the Love Groove Sewage Purification Plant, Worli, Bombay; and 21 in the Tapi River near Surat. These experiments and their results are described. (M.O.W.)

20904 (STI-REP-101) THE APPLICATION OF RADIOISOTOPES TO THE STUDY OF BED LOAD MOVEMENT AND TRANSPORT IN RIVERS. Report on a Meeting of Experts, August 16-18, 1964. (International Atomic Energy Agency, Vienna (Austria)). Feb. 1966. 27p. (CONF-640816). Dep. mn. IAEA $4.00 cy, $0.50 mn.

The use of radioactive tracers for studying bed-load movement and transport in rivers and canals in various countries is discussed, along with choice of tracer, and health considerations. (P.C.H.)

20905 ^{14}C DATING. I. Hsu, Yuin-Chi; Huang, Chia-Yi; Hsu, Yi-Chuann (National Taiwan Univ., Taipei, Taiwan). Chin. J. Phys. (Taiwan), 3: 120-2(Oct. 1965).

This data list covers many of the datings made by using a 1000-ml carbon dioxide-filled proportional counter with a multiple-anode anticoincidence ring counter. (auth)

20906 UNDERGROUND TESTS: THE NEXT STEP. Gaskell, Tom. Discovery, 24: 10-11(Sept. 1963).

Problems in detecting underground nuclear explosions are discussed with reference to systems developed in the United Kingdom of distinguishing these explosions from earthquakes. Oil company mass geophone arrays were adapted to produce improved discrimination between signal and noise. For long-distance recording of either earthquakes or explosions the seismic waves travel deep, so that it is necessary that instruments be set on a solid core of rock, which connects directly to the earth's mantle. In this manner scientists were able to detect even the small French nuclear weapon detonations at a distance of 5000 miles. Another development makes use of the fact that explosions produce almost pure compressional waves (like sound waves in air), while earthquakes, because of their grinding as opposed to explosive action, give, in addition, transverse waves (which can only be transmitted through solids and which cause the ground to vibrate at right angles to the direction of the wave). Transverse waves give rise to compressional waves when they encounter a rock boundary, and they travel more slowly than compressional waves. An explosion, then, gives a record that consists of the faster compressional waves and a small tail consisting of waves traveling by different paths, together with other waves formed by reflections at different rock boundaries. An earthquake gives the same compressional wave start, but it has a powerful tail composed of transverse waves that are converted to compressional waves at rock boundaries. The AWRE technique is used to compare results from two lines of recording instruments set at right angles to each other. The other waves from the explosion arrive at the instruments out of step and so disappear in the analysis of the signals recorded at each seismometer. But the tail from the earthquake, which consists of the compressional waves formed from the slower-travelling transverse waves, shows up clearly because the waves arrive at the instruments in step. (BBB)

20907 TRAVEL TIMES FOR PACIFIC EXPLOSIONS. Jeffreys, Harold. Geophys. J., 7: 212-19(1962).

An analysis is provided of previous data of seismic pulses from Pacific thermonuclear explosions. No significant variation of times of P with azimuth is found, and none according to whether the observing station is on an island or a continent. Up to 18.6° the time appears to be a linear function of the distance with the same gradient as in European shocks, but the constant term is +4.1 sec instead of +7.7 sec. The difference is less at intermediate distances but approaches 2 sec at 95°; its behavior does not appear reconcilable with any modification of structure near the surface. The smaller times in the Pacific at small distances, as compared with Europe can be attributed to smaller depth of the Mohorovic discontinuity. But the difference has practically disappeared at 40° and remains near −1 sec to 90°. Since the nearer observations are on oceanic islands and the more distant ones on continents, the difference might be expected to be halved, but it would be increased again by a factor of about 1.4 for nearly vertical transmission. Therefore, the Pacific times at the greater distances might be less by about 3 sec. (BBB)

20908 ON THE EFFECT OF SEA SURFACE STRUCTURE UPON SPATIAL CHARACTERISTICS OF SCATTERED RADIATION. Kalmykov, A. I.; Ostrovskii, I. E.; Rosenberg, A. D.; Fuks, I. M. (Inst. of Radiophysics and Electronics, Academy of Sciences, Ukrainian SSR). Izv. Vyssh. Ucheb. Zaved., Radiofiz., 8: 1117-27(1965). (In Russian).

By means of a radar correlometer with a great range resolution measurements were carried out on the spatial correlation radius of radiation scattered by a disturbed sea surface. The relation between the values of spatial correlation radius of the scattered radio signals and sea wavelength was ascertained. The results are shown to be in a good agreement with calculations carried out under the assumption that small scale scatters are imposed on large irregularities. (auth)

20909 THE CONCEPT OF A LARGE APERTURE SEISMIC ARRAY. Frosch, R. A.; Green, P. E. Jr. Proc. Roy. Soc. (London), Ser. A, 290: 368-84(Mar. 1, 1966).

Both British work at A.W.R.E. and American work in the A.R.P.A. Vela Uniform Program have demonstrated that arrays of seismometers may be used to enhance the signal/noise ratio of distant seismic events over the single instrument signal/noise ratio. In addition, arrays may have the virtue of suppressing signal-generated noise arising in the crust below the receiver. Other Vela research has demonstrated that buried instruments frequently have a lower noise environment than surface instruments. Borehole emplacement may be particularly effective against wind-generated seismic noise. In an attempt to exploit these possible improvements to the maximum extent a large aperture seismological array of buried seismometers is being constructed. This instrument will consist of over 500 seismometers distributed in 21 clusters over a 200 km aperture. It will exploit modern array signal-processing techniques. If it performs as expected it will have major implications for worldwide seismological detection systems. The status of and plans for the experimental array are described along with some of the world-wide system possibilities. (auth)

20910 INTERPRETING ARRAY RECORDS: EXPLOSION AND EARTHQUAKE P WAVETRAINS WHICH HAVE TRAVERSED THE DEEP MANTLE. Thirlaway, H. I. S. Proc. Roy. Soc. (London), Ser. A, 290: 385-95(Mar. 1, 1966).

Before 1946 four explosions with yields of a kiloton or more were recorded by seismographs up to ranges of 10°.

After the first motion, the seismograms were not obviously different from those of earthquakes at similar distances. In 1946 Bikini Baker was recorded out to distances of 80° with amplitudes equivalent to an earthquake of magnitude m5½. Since then numerous explosions were recorded at teleseismic ranges along nine different transmission paths with signal/noise ratios large enough to enable details of the P wavetrain to be analyzed. Between 30 and 90° these explosion seismograms are characterized by a large, relatively simple onset pulse followed by 20 to 30 s of low amplitude oscillations. Variations of waveform across a large array of seismometers are shown to be due to signal-generated noise. The time-shifted and array-sum records of a given explosion are almost identical. Differences between explosion seismograms are a function of focal depth and local geology. A good working hypothesis is that the deep mantle is very homogeneous. Waveforms of the majority of shallow earthquakes recorded under these experimental conditions are dependent upon azimuth and range. Signals related to focal depth may account for only a small proportion of the observed P energy. The conversion of SV waves qualitatively explains the seismograms. The observations are consistent enough to make it worth while taking stock of the capacity of the international network to study earthquake mechanism. (auth)

20911 A QUANTITATIVE EVALUATION OF TELESEISMIC EXPLOSION RECORDS. **Carpenter, E. W. (United Kingdom Atomic Energy Authority, Blacknest, Eng.). Proc. Roy. Soc. (London), Ser. A, 290: 396-407(Mar. 1, 1966).**

The examination of array records from underground nuclear explosions has produced the qualitative picture of the generation of simple signals which are transmitted to teleseismic distances along paths which exert comparatively little effect. At the recording sites, complications in the recorded signal are caused by crustal inhomogeneities local to the site. By using records from exceptionally good sites, or those where processing techniques eliminate the complications in the records, the combined effects of source signal and transmission path can be studied. To a first approximation, explosion source functions have been quantitatively defined and therefore quantitative data about the transmission path can be deduced. Specifically, data on the non-elastic properties of the mantle have been obtained. With the source and transmission paths defined, the character of the record complication at the poorer sites can be examined with the hope of producing deconvolution operators largely to eliminate the effects of crustal inhomogeneities. Conversely where the recording site characteristics are known, then records from earthquakes at teleseismic distances can be examined with a view to determining the source function. Preliminary work on the quantitative evaluation of earthquake source functions is described. (auth)

20912 CALCULATION OF SEISMIC SOURCE MECHANISMS. **Holzer, F. (Univ. of California, Livermore). Proc. Roy. Soc. (London), Ser. A, 290: 408-29(Mar. 1, 1966).**

A method was developed which allows computation, in the inelastic region and near the inelastic–elastic boundary, of the earth motions resulting from an underground nuclear detonation. It utilizes a one-dimensional digital computer code in which the conservation equations are transformed to difference equations in Lagrangian form. Changes of state from gas to liquid to solid are handled by switching to different equations of state as the internal energy drops below the enthalpy of vaporization and fusion, respectively. Within the solid region, inelastic processes such as plastic yielding, crushing, or cracking are handled by changing the stress deviator equations. Throughout the calculation, the time and space dependence of the shock wave parameters as well as the rate of energy deposition and material behavior behind the shock front is tied to experimentally determined properties of materials including among others the Hugoniot equations of state. Experimental confirmation of this method is most convincing in the region above 10 kbar, where peak radial stresses measured on detonations in granite, dolomite, and salt agree, within 20%, with predicted values, and those for detonations in tuff and alluvium agree within 30%. Measured shock position curves from explosions in granite, tuff, and alluvium are in excellent agreement with calculations. In the lower stress region the calculation is more difficult and not quite as successful. However, there is substantial agreement between calculated and experimental stress history data from detonations in granite, alluvium, tuff, dolomite, and salt. Also the reduced displacement potential was computed both from calculated and measured displacements at 300 m from the Salmon explosion and find agreement to within 25% in peak values–about the same as the amount of disagreement that exists between different measurements. This result is encouraging since it opens the possibility of calculating seismic amplitudes from essentially first principles. A two-dimensional computer code with capabilities similar to the one-dimensional one mentioned above also was devised and is about to become operational. When it does, it will be able to handle two-dimensional sources as well as surface wave propagation problems. (auth)

20913 BRITISH SEISMOMETER ARRAY RECORDING SYSTEMS. **Keen, C. G.; Montgomery, J.; Mowat, W. M. H.; Mullard, J. E.; Platt, D. C. (Atomic Weapons Research Establishment, Aldermaston, Eng.). Radio Electron. Eng., 30: 297-306(Nov. 1965).**

Seismic systems developed primarily for research in the detection and identification of distant underground nuclear explosions are discussed. Means by which the signal/ambient seismic noise ratio may be improved were examined, and the requirements for a seismic recording system are stated for sites with a noise level of the order of 1 mμm displacement at a frequency of 1 cps. Two methods developed for the transmission of the electrical outputs from seismometers distributed over a large array to a recording center in the field are described. The first method involves direct transmission of the amplified signals, and the second uses amplitude modulated tones. The methods used for remotely calibrating the seismometers and associated field amplifiers are described. Problems of lightning and animal damage to cables are discussed. An outline of the instrumentation used in the recording center is given. The signals are recorded on a primary 24-track magnetic tape. The system also includes a secondary tape deck, and an eight-channel pen recorder, controlled by an on-line correlator. Details are given of the timing system, including the pulse code adopted, and the method of measuring and correcting errors relative to G.M.T. Digital recording is still being considered for future systems. (BBB)

20914 MULTIDIRECTIONAL PEAK PRESSURE GAUGE FOR STRONG SHOCK WAVES. **Power, Dean V.; Lombard, David B. (Univ. of California, Livermore). Rev. Sci. Instrum., 37: 480-5(Apr. 1966). (UCRL-14324).**

A gauge using a spherical Lucite shell as the active element was developed to measure peak pressures in strong shock waves. The instrument is insensitive to orientation, simple in design, and relatively easy to construct. The gage tested is useful in the ranges of 46 to 110 and 180 to 220 kbar. Theory and characteristics of operation are discussed and calibration results are presented. The gage was designed to measure shocks from an underground nuclear explosion, but the principle has wider applications. Methods for extending the usable pressure range of the gage by impedance mismatching techniques are discussed briefly. (auth)

20915 MEASURING SURFACE SOIL MOISTURE WITH THE NEUTRON DEPTH PROBE AND A SURFACE SHIELD. **Pierpoint, Geoffrey (Ontario Dept. of Lands and Forests, Can.). Soil Sci., 101: 189-92(Mar. 1966).**

The normal use of the neutron depth probe for soil moisture determination at the 6 inches depth resulted in substantial errors in count rate in moderately dry soils. The use of a separate hydrogeneous surface shield minimized the loss of fast neutrons to the atmosphere and allowed reasonably accurate count rates to be obtained. For most studies and even in soils with as low a moisture content as

7.5 per cent by volume, count rates with-shield should provide satisfactory determinations of moisture content or moisture use. For readings with the neutron probe at depths less than 6 inches, an approach is suggested whereby the per cent difference between with-shield and without-shield readings could be related to the true moisute content or merely used as an indication of relative moisture level. (auth)

20916 DETERMINATION OF COLUMBIA RIVER FLOW TIMES DOWNSTREAM FROM PASCO, WASHINGTON, USING RADIOACTIVE TRACERS INTRODUCED BY THE HANFORD REACTORS. Nelson, Jack L. (Battelle Memorial Inst., Richland, Wash.); Perkins, R. W.; Haushild, W. L. Water Resour. Res., 2: 31-9(1966). (BNWL-SA-176).

To measure flow times of the Columbia River downstream from Pasco, Washington, as far as Astoria, Oregon, the use of two tracer methods was investigated. One method used the decay of a steady release of ^{24}Na (15-hr half life) to determine flow times to various downstream locations, and flow times were also determined from the time required for peak concentration of instantaneous releases of ^{131}I (8-day half life) to reach these locations. Flow times determined from the simultaneous use of the two methods agreed closely. The measured flow times for the 224 mi from Pasco to Vancouver, Washington, ranged from 14.6 to 3.6 days, respectively, for discharges of 108,000 and 630,000 ft^3/sec at Vancouver, Washington. A graphic relation for estimating flow times at discharges other than those measured and for several locations between Pasco and Vancouver was prepared from the data of tests made at four river discharges. Some limited data are also presented on the characteristics of dispersion of ^{131}I in the Columbia River. These measurements would be of great value in the event of an accident at Hanford that released undesirable amounts of activity to the river. (TCO)

20917 TECHNIQUES OF METHANE PRODUCTION FOR ^{14}C DATING. Long, Austin (Smithsonian Institution, Washington, D. C.). 4p. (CONF-650652-14). ORINS. Gmelin, AED-CONF-65-158-21.

From International ^{14}C and ^{3}H Dating Conference, Pullman, Wash.

A modified commercial methane system with two flow type ruthenium catalyst reactors for radiocarbon dating is described. Tritium contamination may be introduced through the catalyst and the hydrogen, but can be avoided by proper selection of hydrogen and pretreatment of catalyst. Radon contamination in the methane results from certain types of samples, but can be removed on activated charcoal at −40°C. Isotopic fractionation in the various steps was checked, and could become significant if reaction yield is less than 90%. (auth)

Thorium and Uranium Minerals

20918 PITCHBLENDE AND SELENIDES OF HYDROTHERMAL URANIUM DEPOSITS. Boitsov, V. E. At. Energ. (USSR), 20: 46-50(Jan. 1966). (In Russian).

The association of pitchblende and selenides was shown, the sequence for the formation of the minerals was established, and the basic paragenesis of the association was determined. The interchange of the mineral composition of the paragenetic association made it possible to draw some conclusions on the geochemical conditions for the formation of the uranium series and the selenides. (tr-auth)

HEALTH AND SAFETY

See also BIOLOGY AND MEDICINE — Radiation Hazards and Protection
GEOLOGY, METEOROLOGY, AND MINERALOGY — Natural Radioactivity and Fallout

Refer also to abstracts 20398, 20889, 21062, 22404, 22514, and 22515.

20919 (ABCC-64-65) ATOMIC BOMB CASUALTY COMMISSION ANNUAL REPORT, JULY 1, 1964–JUNE 30, 1965. (Atomic Bomb Casualty Commission, Hiroshima (Japan)). Contract AT-49-1-GEN-72. 130p. (In English and Japanese). Dep. mn. CFSTI $4.00 cy, $1.00 mn.

Summaries are presented of results of research studies conducted during the period from July 1964 to July 1965 on the effects of radiation from the atomic explosions at Hiroshima and Nagasaki in 1945 on the life span of exposed individuals as a function of age at the time of exposure; the incidence of leukemia and malignant tumors in exposed individuals; field studies on the health status of survivors; an analysis of growth patterns of individuals exposed as children; the life span of children born to survivors; a mortality study of children exposed in utero; and pathological studies on the remains of individuals exposed to radiation at various distances from the bomb hypocenters. A list is included of 19 technical reports and 49 journal publications during the period. (C.H.)

20920 (AD-621377) THERMAL TRANSIENT RESPONSE OF UNDERGROUND SHELTERS. Sampsell, D. F. (Naval Civil Engineering Lab., Port Hueneme, Calif.). Aug. 18, 1965. 68p. CFSTI $3.00 cy, $0.75 mn.

To gain insight into the transient response of underground shelters, a series of tests using a scale model shelter was conducted. Model-prototype considerations resulted in several model temperature distortions which could be accounted for by analytical techniques. The corrected model results agreed well with results from an analog computer study which considered the same prototype shelter. The model results also indicated that shelter shape does not significantly affect its transient response. Another phase of this study was the development of a noncomputer design procedure for determining the environmental control system capacity required for a given set of climatic and soil conditions. The design procedure was applied to a number of shelter locations and climatic conditions to test its performance. As expected, the solutions indicated that ventilation rate and air-conditioning capacity depend heavily on climate, initial soil temperature, and shelter area per person. A record of the analytical and experimental methods evolved under the task to date is presented. All analytical and experimental techniques are described in detail, and numerical examples for a typical model run and design procedure solution are given. (TAB)

20921 (AD-621998) VENTILATION OF FALLOUT SHELTERS BY INDUCED DRAFT. [Period Covered], July 1, 1964–June 30, 1965. Whitehill, C. F.; Mullikin, H. F.; Kubal, O. A. (Montana State Univ., Bozeman. Dept. of Mechanical Engineering). Contract OCD-PS64-211. 148p. CFSTI $4.00 cy, $1.00 mn.

It is demonstrated that a minimum air rate can be obtained in home shelters by inducing draft in the exhaust stack by means of a flame from a kerosene burner which can simultaneously provide illumination. The ventilation test procedure included inducing air to flow through the shelter, determining the actual cubic feet per minute of air flowing, measuring air temperatures at inlet, room, and stack, measuring the pressure drop or restriction to air flow at the shelter inlet, and finding the effects of various stack sizes and configurations upon air flow rates. Data were also taken to determine the effects of various stack sizes and configurations on the fuel consumption of the heating devices. Ventilation of family-type shelters by the induced draft method is effective and reliable if the following conditions are observed: wind velocities around the stack-outlet are kept to a minimum or a good ventilator stack cap is used; filters are not used at the shelter inlet (air taken from body of house); and the intake area of shelter is much larger than the cross-sectional area of the stack. (TAB)

20922 (AD-624704) SENSITIVITY ANALYSIS OF CIVIL DEFENSE SYSTEMS AND COMPONENTS. INTRODUCTION AND SUMMARY. Final Report. Neblett, John H.; Guess, Floyd M.; Sink, H. Rodney; Willis, K. E. (Research Triangle Inst., Durham, N. C. Operations Research Economics Div.). Oct. 1, 1965. Contract OCD-PS-64-56. 26p. (R-OU-157(Summ.)). CFSTI $2.00 cy, $0.50 mn.

A three part study concerning sensitivity analysis of CD systems and components in a fallout environment is summarized. A cost/effectiveness computer program was developed for optimum allocation of fallout shelter system development funds under uniform or variable risk assumptions. This program, intended for use in OCD planning studies, is programmed for the CDC-3600. It is applied in example studies using data on OCD Region 6. A sensitivity analysis was made of selected parameters based on 8 SMSA's. It employs the transportation algorithm in a study of movement of people to fallout shelters. The results show how estimated casualties vary as movement-to-shelter patterns vary from restriction to a standard location up to free movement within the SMSA. They also indicate that detailed planning for shelter utilization can be very effective in reducing expected fallout casualties when the number of shelter spaces exceeds the population of an SMSA. A generalized sensitivity analysis was made of the parameters used in fallout vulnerability analysis models that determine total dose and equivalent residual dose. (auth)

20923 (AD-626727) STUDIES OF DECONTAMINATION EFFECTIVENESS. Ryan, Joseph T.; Douglass, J. D. Jr. (Research Triangle Inst., Durham, N. C.). Aug. 5, 1964. Contract OCD-OS-64-56. 95p. (RM-156-11). CFSTI $3.00 cy, $0.75 mn.

Examination was made by theory and by analysis of real structures, on the reductions in intensity inside and outside NFSS buildings that can be brought about by decontaminating the accessible surfaces on and around the buildings. Specifically the theory was applied to nine different NFSS buildings in order to determine: intensity reductions that can be achieved by decontamination methods applied to practical situations involving real physical structures; intensity reductions that can be achieved when the detector is located inside a structure and when the detector is located outside the structure; decontamination costs (equipment, water expended, radiation dose received by the decontamination crews) in achieving the intensity reductions; sensitivity of the achieved intensity reduction to the cleaning efficiency of the decontamination operation (and, therefore, to the type of decontamination method); and the relative importance of the various surfaces (roofs, paved roads, parking lots, etc.) that can be decontaminated to the intensity reduction that can be achieved. (auth)

20924 (AEET-232) AEROSOL GENERATOR TO PRODUCE RADIOACTIVE AEROSOLS. Kotrappa, P.; Jauhri, G. S.; Dua, S. K. (Atomic Energy Establishment, Trombay (India). Health Physics Div.). 1965. 16p. Dep. mn.

An aerosol generator (modified version of Lauterbach

type) was built to produce heterogeneous aerosols of about 0.2 micron MMD of activated sodium chloride (Na-24) and activated sodium dihydrogen phosphate (P-32). The unit is compact and being on wheels makes it versatile. It was tested for steady output over extended periods of operation. It was also found that mass median diameter of aerosols created did not vary much with concentration of NaCl in the range of 1 to 10%. However, the output increased five fold when concentration was increased from 1 to 10%. Size analyses of the aerosol were made using an electron microscope. The use of this generator in filter evaluation studies, calibrating air monitors, and other applied health physics work was demonstrated. (auth)

20925 (ANL–7055, pp 177-212) REACTOR SAFETY. Baker, L. Jr.; Tevebaugh, A. D. (Argonne National Lab., Ill.).

Results of studies concerning metal-water reactions are reported along with results of investigations relating to fast reactor safety. Information is included on Al–steam reactions, laser-induced metal-water reactions, radio-induced metal-water reactions, metal-water reactions in TREAT and reaction calculations. Information is also included on reactions of liquid Na with reactor materials, heat transfer, and Na–air reactions. (J.R.D.)

20926 (ARCRL–14) ANNUAL REPORT, 1964–65. (Agricultural Research Council, Wantage (England). Radiobiological Lab.). Sept. 1965. 90p. Dep. BIS $1.70. HMSO 8s. 6d.

Data are presented on the radioactivity due to fallout in the human diet in Great Britain in 1964 and 1965. Emphasis is placed on the content of ^{137}Cs and ^{90}Sr in representative foods and total diet. Results are included from studies on the behavior of ions in soil and the physiology of their absorption and distribution in plants, with emphasis on the movement of ^{137}Cs and ^{90}Sr in soil and the effect of their uptake by plants on their content in milk. (C.H.)

20927 (BNWL–217) SUBISOKINETIC SAMPLING OF PARTICLES IN AN AIR STREAM. Sehmel, G. A. (Battelle-Northwest, Richland, Wash. Pacific Northwest Lab.). Mar. 1, 1966. Contract AT(45-1)-1830. 66p. Dep. mn. CFSTI $3.00 cy, $0.75 mn.

The errors associated with subisokinetic sampling of aerosols from an air stream were determined for one filter holder geometry with a 41-mm diameter filter area exposed. Sampling velocities ranged from 0.008 of isokinetic to isokinetic for airspeeds from 2.7 to 30 mph. Zinc sulfide aerosol particles with diameters 3 to 25 microns were studied. Microscopic techniques were used to evaluate the number of particles on the filters. In order to determine sampling errors as a function of particle size, least squares techniques were used to determine truncated particle size distributions. To correlate the data the collection efficiencies were approximated by an expression which includes the impaction efficiency as a function of particle size for each windspeed. From these, overall sampling errors were calculated for several particle size distributions of principal use with the filter geometry. Overall sampling error correction factors were as high as 58. (auth)

20928 (CEX–59.4.17) AERORADIOACTIVITY SURVEY AND AREAL GEOLOGY OF THE DISTRICT OF COLUMBIA AND PARTS OF MARYLAND, VIRGINIA, AND WEST VIRGINIA (ARMS-I). Neuschel, Sherman K. (Geological Survey, Washington, D. C. Division of Biology and Medicine (AEC), Washington, D. C.). May 1963. 48p. Dep. mn. CFSTI $1.00 cy, $0.50 mn.

An aeroradioactivity survey of approximately 8000 square miles near Washington, D. C., was conducted. Radioactivity profiles were obtained using scintillation-detection equipment along parallel, mile-spaced, east-west flight lines approximately 500 ft above the ground. A map of aeroradioactivity units compiled from the profiles shows a wide range of radioactivity and a generally excellent correlation of radioactivity to areal geology. Parts of four physiographic provinces were covered: the Coastal Plain, Piedmont, Blue Ridge, and Appalachian Valley of the Ridge and Valley province. Radioactivity units for each province have characteristic values and a pattern that reflects the geologic structure. The Coastal Plain has predominantly low radioactivity levels, 100 to 400 cps (counts per second). Higher radioactivity (400 to 650 cps) is associated with glauconitic sand of the marine Upper Cretaceous or with detrital material that was derived from the nearby Piedmont. The Piedmont and Blue Ridge provinces have a wide range of radioactivity (100 to 1500 cps) because of the great variety of rocks. In general, low values (100 to 300 cps) are found over sandstone, quartzite, and mafic rocks. Areas underlain by shale, limestone, phyllite, schist, and gneiss have intermediate values of 400 to 600 cps. Highest radioactivity (more than 600 cps) is associated with granite and gneiss. In the Appalachian Valley radioactivity is moderate to high (400 to 850 cps), and the units distinctly parallel the regional strike. The higher radioactivity is associated with shale and lower values with calcareous rocks. (auth)

20929 (CEX–61.6.2) ALBUQUERQUE–LOS ALAMOS AREA (ARMS-II). Guillou, R. B. (Edgerton, Germeshausen and Grier, Inc., Santa Barbara, Calif.). Apr. 1964. 51p. Dep. mn. CFSTI $1.00 cy, $0.50 mn.

The decontamination facility was constructed at BNL in 1962 as an addition to the Decontamination Building. It has been used successfully since that time and is the only large facility of this type in operation at any of the U. S. Atomic Energy sites. The safety design features having to do with the environment of the operator and the surrounding area are described. Particular aspects include: air cleaning facilities (bags, bags with added fibers and absolute filters); air cleaning efficiencies of the various types of filters; air flow studies (in the environment of the operator, in the ducts and in the building to which the facility is attached); instrumentation for checking flow rates and flow patterns; air sampling equipment (automatic and manual); air requirements for special suits (monitoring, purification and volume required); special decontamination of the abrasive metal shot to enable its reuse; operating experience, including radiation exposures due to the environment in the room surrounding the operator and effluent studies from the exhaust; efficiency of the air cleaning devices; and economics of such a facility. (TCO)

20930 (HI–518-RR(Vol.1)) ENVIRONMENTAL EFFECTS OF NUCLEAR WEAPONS. Ayres, Robert U. (Hudson Inst., Inc., Harmon-on-Hudson, N. Y.). Dec. 1, 1965. Contract OCD-OS-62-218. 392p.

Discussion is presented on: primary radiological effects, including radiation damage mechanisms, fallout, plants, insects, vertebrates; primary thermal effects, including ignition and fire spread and conflagrations and firestorms; atmospheric effects; and secondary damage mechanisms, including epidemics of humans, pest outbreaks, ecosystems, erosion and flooding, and balance of nature. (145 references). (P.C.H.)

20931 (HI–518-RR(Vol.2)) ENVIRONMENTAL EFFECTS OF NUCLEAR WEAPONS. Ayres, Robert U. (Hudson Inst., Inc., Harmon-on-Hudson, N. Y.). Dec. 1, 1965. Contract OCD-OS-62-218. 85p.

Interactions of radiological, thermal, meteorological, and secondary effects from nuclear weapons with post-attack problems are discussed, particularly in connection with agriculture. The potential conflicts between short-term and long-term objectives are stressed. A number of specific countermeasures are listed and discussed. (P.C.H.)

20932 (HI–518-RR(Vol.3)) ENVIRONMENTAL EFFECTS OF NUCLEAR WEAPONS. Summary. Ayres, Robert U. (Hudson Inst., Inc., Harmon-on-Hudson, N. Y.). Dec. 1, 1965. Contract OCD-OS-62-218. 28p.

The four major classes of weapons effects capable of covering large areas are discussed. These include: radiological; thermal; meteorological; and secondary. Environmental-economic factors and countermeasures are also considered. (P.C.H.)

20933 (IDO-12045) CRITERIA FOR HIGH EFFICIENCY FILTER INSTALLATIONS AT THE NATIONAL REACTOR TESTING STATION. Collins, John T. Jr. (Idaho Operations Office (AEC), Idaho Falls. Health and Safety Div.). Dec. 15, 1965. 59p. Dep. mn. CFSTI $3.00 cy, $0.75 mn.

General criteria for determining the need for high efficiency filters, design of filter enclosures, and specifications for fire resistive filters are given. Procedures for handling, inspecting, and storage of high efficiency filters together with procedures for installation, maintenance, and in-place testing of high efficiency filters and filter systems are outlined. The basic criteria for design of new facilities and modifications as outlined in the ID Engineering Standards are supplemented by elaborating on specifications for high efficiency filters and filter installations. (auth)

20934 (JAERI-1098) CONSTRUCTION AND OPERATION OF RADIOLOGICAL MONITORING STATION. Ishihara, Toyohide; Sasaki, Satoshi; Katagiri, Hiroshi; Tsunokawa, Masayoshi (Japan Atomic Energy Research Inst., Tokyo). July 1965. 32p. (In Japanese). Dep. mn.

Construction progress, equipment, and the radiological monitoring program at JAERI are described. The eight monitoring stations in the system coordinated data on alpha, beta, and gamma activities in the atmosphere, dusts, and from other environmental parameters. Communication between the components and a central receiving station is discussed, and efficiency of the system is evaluated. (H.G.D.)

20935 (K-1657) SOME OBSERVATIONS ON FILM BADGE CALIBRATION TECHNIQUES. Becher, A. F.; Schultz, N. B.; Sipe, L. H. (Oak Ridge Gaseous Diffusion Plant, Tenn.). Apr. 22, 1966. Contract W-7405-eng-26. 13p. Dep. mn. CFSTI $1.00 cy, $0.50 mn.

A mobile gamma radiation calibration unit utilizing a multi-Curie cobalt-60 source for the interpretation of radiation dose as determined from dosimeter film measurements is described. The radiocobalt source is encapsulated in an airfoil capsule which is raised and lowered by an enclosed, recycle air stream, permitting rapid and precise positioning of the source. A wide range of dose rates can be obtained by varying either or both the distance from the source and the exposure time. Doses ranging from 50 mrad to 2,000 rad can be obtained with only two exposure cycles. The results of tests to validate the accuracy of the film calibrations by use of a calibrated standard are presented. (auth)

20936 (K-1661) FISSILE-MATERIAL CONTAINER AND PACKAGING DEVELOPMENT AND TESTING PROGRAM. Mallett, A. J.; Wheatley, S. J. (Oak Ridge Gaseous Diffusion Plant, Tenn.). Apr. 1, 1966. Contract W-7405-eng-26. 45p. Dep. mn. CFSTI $2.00 cy, $0.50 mn.

A program designed to improve protective packaging and to test the structural integrity of fissile material containers in the 5 to 30-in.-diameter range resulted in: determination of hydrostatic rupture test limits; favorable drop test assessments of existing cylinders; fabrication of a carrier tie-down unit; and development of container enclosures incorporating a foam plastic lining with excellent heat insulation, cushioning, fire resistance, and neutron attenuation properties. (auth)

20937 (NAA-SR-11761) RADIOLOGICAL ASPECTS OF REENTRY BURNUP OF SNAP REACTORS. Willis, C. A. (Atomics International, Canoga Park, Calif.). Mar. 25, 1966. Contract AT(11-1)-Gen-8. 36p. Dep. mn. CFSTI $2.00 cy, $0.50 mn.

Reentry burnup of SNAP reactors may produce low levels of worldwide fallout. The International Commission on Radiological Protection has recommended a population dose limit of 2 rem in 30 yr. The factors affecting the choice of a population dose criterion are reviewed in this report. These factors include radiological safety history and tradition, radiobiological knowledge, other radiation criteria, and the biological significance of criteria doses. No safety justification is found for reduction of the ICRP limit. This 2-rem in 30-yr dose is well within the range of variation of natural background radiation. Population safety requirements are satisfied if the dose is less than the ICRP criterion. Many possible sources of artificial, nonmedical radiation could contribute to the population dose. For planning purposes, it is recommended that one-eighth the population dose, 0.25 rem/30 yr, be taken as the allowable dose from SNAP reactor applications. (118 references.) (auth)

20938 (NP-15921) DATA FROM RADIATION PROTECTION PROGRAMS. Volume 4, Number 1. (Department of National Health and Welfare, Ottawa (Ontario). Radiation Protection Div.). Jan. 1966. 47p. Dep. mn.

Ion exchange column and fuming nitric acid precipitation procedures for the separation of Sr from Ca in liquid milk were compared. It was concluded that ^{90}Sr can be determined by either procedure with comparable precision. Data are presented on radioactivity due to fallout in samples of air particulates, precipitation, milk, water, soil, wheat, and human bone collected in Canada in Dec. 1964. Data are included on the environmental radioactivity in the environs of Canadian reactors during Dec. 1965. (C.H.)

20939 (NVO-1163-70) POSSIBILITIES OF SECONDARY EXPLOSIONS AND POST-SHOT THERMAL EFFECTS IN CAVITIES IN TUFF. Smith, Sherwood B. (Beers (Roland F.), Inc., Alexandria, Va.). Apr. 15, 1966. Contract AT(29-2)-1163. 35p. Dep. mn. CFSTI $2.00 cy, $0.50 mn.

Using the Rainier event as a model, early post-shot analyses were made to evaluate the effect of possible entry of water into a cavity and to determine the effect of thermal implosion of surface material from the cavity walls. Analyses indicate that entry of water into a cavity in tuff could cause only a relatively small increase in cavity steam pressure and would not constitute a hazard. The thermal implosion of wall surface material into the cavity would result in rapid cooling of contained steam and a decrease in pressure (except for a relatively small initial increase). In Antler, it appears that venting was caused by entry of heated explosion products into the access tunnel in combination with entry of water into the access drift at about the same time. The water was converted to steam at sufficient pressure to produce stemming failure and venting. However, provision of adequate stemming should reduce this hazard to a minimum. (P.C.H.)

20940 (ORNL-3915) NUCLEAR SAFETY PROGRAM SEMIANNUAL PROGRESS REPORT FOR PERIOD ENDING DECEMBER 31, 1965. (Oak Ridge National Lab., Tenn.). Mar. 1966. Contract W-7405-eng-26. 154p. Dep. mn. CFSTI $5.00 cy, $1.00 mn.

Results of in-pile and out-of-pile investigations of the behavior and characteristics of fission products released under accident conditions are reported. Information is included on release and transport of fission products from in-pile destruction of reactor fuels, release and transport of fission products in containment systems, filtration and adsorption under accident conditions, and behavior of accident-released fission products. Developments in data processing are discussed along with nuclear safety information. (J.R.D.)

20941 (ORNL-TM-1432) ANIMAL SPECIES ASSOCIATED WITH PIG CARRION. Payne, Jerry A.; Crossley, D. A. Jr. (Oak Ridge National Lab., Tenn.). Apr. 1966. Contract W-7405-eng-26. 67p. Dep. mn. CFSTI $3.00 cy, $0.75 mn.

Following a nuclear attack, carrion remains of domestic animals could pose difficulties for human survival because of public health and sanitation problems associated with carrion. Insects influence the course and rate of decomposition, and radiation effects on insect populations could alter the normal decomposition pattern. A study was made of the animal community in pig carrion, preliminary to experimental research on the influence of radiation and

other factors on succession in carrion. A total of 522 animal species representing 3 phyla, 9 classes, 31 orders, 151 families, and 359 genera were found associated with various decomposition stages. A systematic list of all species, their abundance, microhabitat, and food relationships is given. (auth)

20942 (ORNL-TM-1459) ENGINEERING DESIGN PRACTICES AT ORNL FOR FACILITIES CONTAINING RADIOACTIVE MATERIALS. Beckers, R. M.; Denkins, R. F.; Glen, H. M.; Golson, T. J.; Kahn, J. E.; Renfro, G. W.; Steed, J. A. (Oak Ridge National Lab., Tenn.). Apr. 1966. Contract W-7405-eng-26. 90p. Dep. mn. CFSTI $3.00 cy, $0.75 mn.

Seven papers that were presented by members of the General Engineering and Construction Division Design Department of ORNL as part of the Applied Health Physics course for state health department personnel are presented. These papers call attention to problems peculiar to design for laboratories and other facilities that handle radioactive materials. The topics discussed include the following; remote handling and maintenance for nuclear applications, viewing devices for remote operations, electrical components for nuclear laboratory facilities, a general-purpose hot laboratory for alpha and gamma radiating materials, structures for containing nuclear laboratory facilities, air handling in nuclear facilities, and fluid systems for nuclear laboratories. (M.O.W.)

20943 (RFP-453) ROCKY FLATS METHODS OF TREATING ACUTE PLUTONIUM CASES. Guzak, Steven V. (Rocky Flats Div., Dow Chemical Co., Golden, Colo.). Oct. 15, 1964. Contract AT(29-1)-1106. 8p. (CONF-798-2). Dep. mn. CFSTI $1.00 cy, $0.50 mn.

From Annual AEC and Contractor Health Protection Meeting, Los Angeles, Calif., Oct. 1964.

The treatment of plutonium contamination on the skin and in the respiratory and gastrointestinal tracts in man is discussed. Treatment used in the event of a major accident in which all three modes entry are involved is also described. (P.C.H.)

20944 (STI-PUB-110) NUCLEAR MATERIALS MANAGEMENT. Proceedings Series. Proceedings of the Symposium, held in Vienna, August 30–September 3, 1965. (International Atomic Energy Agency, Vienna (Austria)). Feb. 1966. 902p. (CONF-650803). IAEA: $18.00; S378,-; £5.8.0; F Fr 72,-; DM 63,-.

Fifty-eight articles are included; separate abstracts were prepared for 18. For the remaining 40 articles on: materials control systems; recording, reporting, and generation of quantitative data; nuclear safety and criticality control in measurement methods; economic considerations; chemical and isotopic analysis; and burnup and production that were previously abstracted in NSA, see CONF-650803 in Report Number Index. (P.C.H.)

For abstracts of individual papers see: 20964–20979, 21308, and 22517.

20945 (TRG-Report-1073) THE SAFE TRANSPORT OF RADIOACTIVE MATERIALS. A Key to the 1964 Revision of the International Atomic Energy Agency's Regulations. Shaw, A. E. (Reactor Group, United Kingdom Atomic Energy Authority, Dounreay (Scotland)). July 28, 1965. 22p. Dep. BIS $0.70, HMSO 3s. 6d.

A key is presented to the 1964 revision of the International Atomic Energy Agency Regulations for the Safe Transport of Radioactive Materials. The key was developed to help users of the regulations find the correct procedure for each operation quickly. (C.H.)

20946 STUDY ON THE BEHAVIOR OF GAMMA RADIATION IN AIR. Tisljar, Maria (Reaktorzentrum, Seibersdorf, Austria). Acta Phys. Austr., 21: 198-203 (1966). (In German).

For air protection purposes it is necessary to know the effect at the measurement site of very remote strong γ sources such as would occur after nuclear explosions. Since in such cases it is a question of the distances which are a multiple of the mean free path of γ radiation of 0.5 to 0.7 Mev, scattering effects in the air play a very important role. This effect was considered for two limiting cases: for a point γ source E_0 = 550 kev and for a homogeneous semi-infinite air space filled with specific activity. In the first case in the finite homogeneous air space the increment factor at a distance of approximately 1.4 km is $B(\mu_0\gamma,E_0)$ = 155, which corresponds to 15 mean free paths. For the second case a factor of 1.7 was calculated for the effect of the scattering. (tr-auth)

20947 MEDICAL EXPERIENCES AFTER THE FIRST RADIATION PROTECTION LAW. Rahm, G. Atomwirtschaft, 11: 124-6(Mar. 1966). (In German).

In the first radiation protection ordinance, physical examinations and monitoring were required for personnel exposed to radiation in processing radioactive materials. The results obtained with personnel dose measurements, source tightness testing, unsealed radiation sources, radioisotope incorporation, and radiation damage are reported. The conclusions to be drawn from the experiences are summarized. (J.S.R.)

20948 ADAPTATION OF THE BRITISH ATOMIC LIABILITY LAW TO INTERNATIONAL CONVENTIONS. THE NUCLEAR INSTALLATIONS ACT. Highton, C. J. (United Kingdom Atomic Energy Authority, London). Atomwirtschaft, 11: 129-32(Mar. 1966). (In German).

The principal amendments made to the British Atomic Energy Law in order to bring it into agreement with international agreements are summarized. These include the liability of the operator of nuclear installations, liability of foreign countries, liabilities for damages in foreign countries, exceptions to liability, and the limitations of liability. (J.S.R.)

20949 RADIOACTIVITY CONTROL OF THE KEURINGSDIENST VAN WAREN, AMSTERDAM. Haken, J. W.; Hardon, H. J. (Keuringsdienst van Waren, Amsterdam). Deut. Lebensm.-Rundsch., 60: 205-7(July 1964). (In German).

Analyses of ^{89}Sr, ^{90}Sr, ^{137}Cs, and ^{131}I in various foodstuffs analyzed in Amsterdam from 1960 to 1963 are reported. Chemical preparation of the samples is outlined. An anticoincidence apparatus was employed for counting. In milk, ^{90}Sr values ranged between 5 and 15 pC/kg; ^{89}Sr ranged from 80 to 120 pC/kg; iodine-131 averaged 120 pC/kg in November 1961; and ^{137}Cs values averaged about 90 pC/kg for 1962. Strontium-89, ^{90}Sr, and ^{137}Cs were also measured in: bread, cabbage, carrots, legumes, and potatoes. Determinations were made for ^{90}Sr in meats and water, and for ^{137}Cs in water. (TCO)

20950 ON THE PRESENCE OF A NEW RADIONUCLIDE CONTAMINATING COW'S MILK: ^{22}Na. Orlando, Giorgio (Univ. of Genoa). Giorn. Ig. Med. Prevent., 5: 305-12 (Oct.-Dec. 1964). (In Italian).

Samples of fresh milk at Genoa, Italy, were prepared by evaporation and analyzed by γ spectrometry. When background and the peaks due to ^{40}K and ^{137}Cs were subtracted, peaks at 1270 and 1790 kev were identified as ^{22}Na. Quantitative determinations for the five days following gave values of 24.3 to 30.6 pC/l for the ^{22}Na activity and 182 to 326 pC/l for ^{137}Cs. Implications for health are reviewed in terms of: daily turnover; per cent of Na in the bone; and mean value for exchangeable Na in respect to age. Radiocesium and radiopotassium values are compared to those obtained from other sections of the country. (H.G.D.)

20951 SELF-ABSORPTION OF X RAYS BY PLUTONIUM PARTICLES WITH SPECIAL REFERENCE TO PLUTONIUM IN WOUND MONITORING. Tyler, G. R. (United Kingdom Atomic Energy Authority, Thurso, Scotland). Health Phys., 12: 509-19(Apr. 1966). (TRG-Report-896).

The possible error in measurement of the plutonium-239 content of contaminated wounds by an x-ray sensitive probe owing to self absorption was investigated theoretically. Graphs of the theoretical relationship between activity as measured by x-ray probe and the actual activity, if the plutonium or plutonium compound is present as a single spher-

ical particle, are presented. The effect of self absorption on the alpha particle emission from an active sphere was also theoretically investigated, and further graphs are presented showing the theoretical relationship between the activity of a single spherical particle and the percentage of the initial alpha particle energy which escapes from the active sphere. The significance of the self absorption on hazard evaluation is briefly discussed. (auth)

20952 SPECTROMETRIC METHOD FOR MEASUREMENT OF LOW-LEVEL GAMMA EXPOSURE DOSE. Moriuchi, Shigeru; Miyanaga, Ichiro (Japan Atomic Energy Research Institute, Tokyo). Health Phys., 12: 541-51(Apr. 1966).

A spectrometric method for the exposure dose estimation of low level γ radiation with the use of a NaI(Tl) crystal spectrometer was presented. A function G(E) which is applied to a given γ spectrum and can eliminate the energy dependence of the crystal for the estimation of the exposure dose, was introduced. The paper describes the principle of the method and the determination of the G(E) function, and presents the results obtained for γ radiations from ^{137}Cs and Ra sources, and for environmental γ radiations in different locations in the Tokai Area. The exposure doses obtained were compared with those measured by an ionization chamber and the agreement was good. Discussions are given on the angular response of the 5 × 4-in. crystal for incoming photons, particularly in connection with the measurement of environmental radiation. The method provides a simple procedure to estimate the exposure dose of γ radiations, independent of their energy and energy distribution without a tedious procedure of spectral analysis. If it is desired, a fractional dose contribution, including that of scattered radiation, can be estimated with the aid of the spectral analysis technique. (auth)

20953 MASS OF THE TRACHEOBRONCHIAL LYMPH GLANDS. Pochin, E. E. (University College Hospital, London). Health Phys., 12: 563-4(Apr. 1966).

The mass of the tracheobronchial lymph glands was determined in order to provide an estimate of the absorbed dose of radiation that might be received by the glands following inhalation of radioactive particulates. Dissections were made at autopsy on 10 subjects who had died suddenly following short illnesses. (H.G.D.)

20954 RADIOLOGICAL PREDICTION AND MONITORING OF TESTS AT THE NUCLEAR ROCKET DEVELOPMENT STATION. Griffiths, P.; Erickson, P. B. (Space Nuclear Propulsion Office, Nevada). IEEE (Inst. Elec. Electron. Eng.), Trans. Nucl. Sci., NS-13: No. 1, 6-13(Feb. 1966).

The procedure and formula used in the radiological analysis of reactor testing at the Nuclear Rocket Development Station are described. Monitoring methods are discussed, and a comparison is made between measured dose levels and guide values. (auth)

20955 PHYSICAL EXAMINATIONS AND MEDICAL RECORDS REQUIRED IN NUCLEAR INDUSTRY. Faes, M. H. (Centre d'Etudes de l'Energie Nucleaire, Mol-Donk, Belgium). Ind. Med. Surg., 35: 195-9(Mar. 1966).

Diagnostic techniques and analyses recommended for personnel in nuclear industries are discussed, and a form for collecting and recording the required data is presented. (H.G.D.)

20956 DENTAL RADIOLOGICAL HEALTH PROGRAM. Jacobson, Gerald; Van Farowe, Donald E. (Michigan Dept. of Health, East Lansing). J. Mich. State Dent. Ass., 46: 14-15(Jan. 1964).

To help reduce total exposure from dental x rays in Michigan, a radiological health program was carried out by the Michigan Dept. of Health in cooperation with the Michigan State Dental Association, the U.S. Public Health Service, and the Detroit Dept. of Health. The primary objective of the program was to protect the health of Michigan people by assuring the most efficient, safest use of x rays in dental offices, consistent with satisfactory diagnostic results. The program was carried out primarily by means of a survey packet (surpak) mailed to every dentist in the state. As a result of the surpak program, filters and collimators were added to 1100 x-ray machines and filtration alone to an additional 535. A conservative estimate of the reduction in the air-dose to the skin of the patient's face would be 0.5 R per film, after correction of the machines. Based on this estimate, the population total facial-skin air dose was reduced by well over a million and one-half R/yr. Equally significant has been the reduction in the calculated area of facial primary beam exposure by over seven million $in.^2/hr$. (TCO)

20957 DECONTAMINATION OF NUCLEAR REACTOR SYSTEMS. Ayres, J. A. (Battelle-Northwest, Richland, Wash.). Mater. Protect., 5: 11-15(Jan. 1966).

Chemical cleaning and decontamination problems of nuclear reactor systems are discussed, with emphasis on cleaning of a reactor's primary system. Chemical cleaning of a reactor is usually done to reduce radiation levels rather than to remove thick scale or deposits. Cleaning in most cases is unsatisfactory unless the entire film is removed. Consequently, more corrosion reagents than those normally used in a chemical cleaning operation may be required. So far, decontamination has been used sparingly and many operators consider it only as a last resort. Case histories of reactor cleaning and decontamination are cited. The first full-scale reactor to be decontaminated was the Plutonium Recycle Test Reactor at Hanford. In spite of various complications, decontamination was planned, scheduled, and completed with minimum delays and difficulties. Over 90% of the contamination was removed; the residual activity levels varied from 10 to 100 mR/hr, lower than during normal operation. This decontamination demonstrated that if a reactor does become contaminated, it can be chemically cleaned effectively, efficiently, and safely. (BBB)

20958 RADIATION HYGIENE CONDITIONS DURING THE DIAGNOSTIC USE OF RADIOACTIVE KRYPTON. Rozanov, M. S. (Central Medical Inst. for Graduate Work, USSR). Med. Radiol., 10: No. 11, 60-4(Nov. 1965). (In Russian).

The results of studies of labor conditions from the viewpoint of radiation safety during the clinical employment of ^{85}Kr for diagnostic purposes are presented. Data are given relevant to dosimetry of external gamma-irradiation of the personnel at different stages of work and chronometry of individual manipulations. The investigation demonstrates that the degree of total irradiation of the personnel for a week does not exceed the permissible value. However, local irradiation of hands during certain manipulations may be very significant, reaching 40 μR/hour. (auth)

20959 MEASUREMENT OF THE RADON CONCENTRATION IN WATER BY GAMMA RADIATION. Spirin, V. D.; Belle, Yu. S.; Chimina, V. F. (Inst. for Research in Radiation Protection, Leningrad). Med. Radiol., 10: No. 12, 11-13(Dec. 1965). (In Russian).

A method of measuring the radon concentration in water by means of gamma-radiation is described. (auth)

20960 INVESTIGATION OF DETERGENTS FOR DECONTAMINATION OF SAMPLING VIALS FOR A LIQUID SCINTILLATION SPECTROMETER. Hattori, Toshie; Aoki, Hiroko (Tokyo Univ.). Radioisotopes (Tokyo), 14: 148-51(Mar. 1965). (In Japanese).

The cleaning powers of 13 detergents, including commercial ones, were compared in the decontamination of sampling vials for a liquid scintillation spectrometer. The detergents and their concentrations in solution, which were tested, were the following: anionic surfactants, sodium alkylbenzene-sulfonate (0.1%), sodium laurylsulfonate (0.1%), a mixture of sodium alkylbenzenesulfonate and potassium dichloroisocyanurate (0.25%), Lipon F (0.3%), Haemo-sol (0.8%), and Plus Z (0.3%); cationic surfactants, benzalconium chloride (0.1%); nonionic surfactants polyoxyethylene nonylphenol ether $\bar{p} = 10$ (0.1%) and

Sallat (0.2%); amphoteric surfactants, Anon BF (0.1%), Tego 51 (0.1%), Lipomin COH (0.1%), and Lipomin LA (0.1%). The radioactive samples used were nucleic acids, proteins, mixtures of nucleic acids and proteins, ^{3}H-toluene, etc., labeled with ^{3}H or ^{14}C, and the levels of radioactivity were $0.1 - 35 \times 10^{4}$ c/m, with the same level being used for duplicate experiments. After the radioactive material in the vials was discarded, it was rinsed 2–3 times with water and then kept in the detergent solution for 16 hours at 24–25°C. Then the vial was rubbed with a brush in the detergent solution, thoroughly rinsed with distilled water, and dried. The radioactivity remaining on the vial was measured with a liquid scintillation spectrometer. Fifty or twenty vials were used in the experiment with each detergent, and the average value and the standard deviation were calculated with correction for the background. There was no remarkable difference among the 13 detergents, but a mixture of sodium alkylbenzenesulfonate and potassium dichlorocyanurate was slightly inferior to others and Haemo-sol was most effective. For the ^{3}H contamination, almost all the vials were decontaminated to below the background plus 20 c/m. The decontamination of the vials contaminated by ^{14}C was relatively incomplete compared with the ^{3}H contamination. (tr-auth)

20961 MEASUREMENT OF RADIOACTIVITY IN AIR, WATER, AND FOOD. Maushart, R. (Kernforschungszentrum, Karlsruhe, Ger.). Radiologe, 4: 364-7 (Nov. 1964). (In German).

The purpose of radioactivity measurements in the biosphere and methods for measuring radioactivity are discussed. It is recommended that the biologically important radionuclides ^{90}Sr, ^{131}I, and ^{137}Cs be measured by trained personnel in well-equipped laboratories established at a relatively few centralized locations. (H.G.D.)

20962 RADIOMETRIC MEASUREMENTS FOLLOWING NUCLEAR INCIDENTS. Giuliani, Pietro. Riv. Ing. Nucl., 3: 715-20 (Jan.-Apr. 1965). (In Italian).

Monitoring problems connected with an incident at a nuclear installation and the relative monitoring techniques are discussed. The radiotoxic characteristics of iodine, tellurium, cesium, and the rare gases krypton and xenon are described. An evaluation was made of the dose received from the rare gases. The monitoring techniques used are indicated. (tr-auth)

20963 CONTRIBUTION TO THE PROBLEM OF STUDYING THE RADIOACTIVITY OF INLAND WATERS. Samburenko, I. Z. Soviet Hydrol., No. 5, 499-510 (1964).

Studies of the radioactivity of inland waters and of the methods of concentrating radioactive matter from aqueous solutions are reviewed. Under natural conditions, in the absence of sources of contamination by artificial radioisotopes, the radioactivity in inland water bodies originated chiefly from that washed from the earth's crust. As a result of the great dispersion and the low content of radioactive elements in the upper layers of the earth's crust, very small amounts of them enter inland water bodies. The normal radioactivity of natural water is caused by the presence of numerous representatives of the families of uranium, thorium, and actinium. The radioactivity level of ^{40}K in river water amounts to around 10^{-12} C/l. Methods by which contamination of the inland water by radioactive matter can occur are discussed. The degree of radioactive contamination of water is usually estimated on the basis of measurements for the total β radioactivity. Methods of separating and assaying low levels of radionuclides in natural water samples are outlined, and some data collected from various bodies of water, particularly in the USSR, are presented. (TCO)

20964 CONTROL OF MATERIALS IN ITALIAN NUCLEAR POWER STATIONS AND RESEARCH INSTITUTIONS. Santarelli, F. (Comitato Nazionale per l'Energia Nucleare, Rome). pp 3-18 of STI-PUB-110. (In French).

The management of nuclear materials at a facility with a gas-graphite power reactor using natural uranium, at another with a boiling-water reactor using enriched uranium, at an industrial installation with a research reactor, and at a nuclear research laboratory is reported. For each of these installations the control of radioactive materials during fabrication and transport operations, while the materials are being used in reactors or in laboratories, and at the time when the receiver takes delivery of the materials is discussed. The recording operations and the methods employed for the internal auditing of data on losses, production, and transfer of nuclear materials are discussed from the management point of view. The shortcomings of the systems at present used in Italy and the problems of official materials management and control services, insofar as they affect safety are also given. (auth)

20965 IMPROVEMENT OF AUDITING DATA CENTRALIZATION, IN PARTICULAR BY USING ELECTRONIC COMPUTERS. Ronteix, F. (Commissariat a l'Energie Atomique, Fontenay-aux-Roses, France). pp 19-30 of STI-PUB-110. (In French).

A brief account is given of the French system of nuclear materials management and of the problems of auditing data centralization as it arises in this system. The main difficulty in recent years has been the time required for the monthly closing and centralization of accounts for all the installations. The steps taken to cope with these difficulties are described. The main method adopted, namely, the use of office machinery for centralization of data, preparation of balances, and publication of a number of periodical documents is given. The coding system employed, document circuits, and the time involved are described. Mention is also made of the modifications which had to be made to the existing auditing system to meet the requirements imposed by the office machinery. Various conclusions, resulting from the introduction of machine accounting, in respect of the cost in manpower and money of this centralization of auditing data and, more generally, the cost of nuclear materials management are given. Reasons are given for considering the use of office machines as advantageous. (P.C.H.)

20966 CRITERIA FOR SPECIAL NUCLEAR MATERIALS INVENTORY AND CONTROL PROCEDURES. Kinderman, E. M.; Tarrice, R. R. (Stanford Research Inst., Menlo Park, Calif.). pp 31-41 of STI-PUB-110.

The criteria established for materials control specifically considers the appropriateness of various techniques of inventory control ranging from annual balancing of book records of receipts and shipments through detailed daily physical inventory in the light of the specific value and the total inventory of these special nuclear materials. A matrix of solutions to the management and inventory control of special nuclear materials is presented. The multiplicity and relative effectiveness of varied techniques at key stages of the materials supply, utilization, and recovery are assessed. (P.C.H.)

20967 ORGANIZATION OF BASIC MATERIALS AUDITING IN A FUEL-ELEMENT FABRICATION PLANT. Nadal, J. (Societe Industrielle des Combustibles Nucleaires, Saclay, France); Pinochet, J. pp 51-64 of STI-PUB-110. (In French).

Description is given of the organization of auditing at the Annecy plant of the Société industrielle des combustibles nucléaires which produces, principally from natural uranium provided by the CEA, fuel elements for reactors of the graphite-gas type (in particular, G1, G2, G3, EDF1, EDF2, EDF3). The plant may be schematically divided into five large sections: the melting shop and its annexes; machine shop; turnings recovery shop; cladding shop; and warehouse. The auditing records used at Annecy may be classified into three categories: the follow-through slips, the stock slips; and the despatch notes. The balance sheet established each month for uranium consists of two parts: one part showing stocks existing at the beginning and end of the month and internal and external movements during the month, and a recapitulation balance, which is so to say an account of the use of uranium, showing in parallel the amounts of uranium used and the production.

The debit balance of this account corresponds to real or apparent losses. (auth)

20968 PROFESSIONAL NUCLEAR MATERIALS MANAGEMENT. Forcella, A. A.; O'Leary, W. J. (Allis-Chalmers Mfg. Co., Bethesda, Md.). pp 153-65 of STI-PUB-110.

The scope of nuclear materials management for a typical power reactor in the United States is described. Since this power reactor is financed by private capital, one of the principal obligations of the reactor operator is to ensure that the investment is protected and will furnish an adequate financial return. The nuclear materials manager must therefore provide in advance against the following contingencies and maintain constant control or liaison against deviations from planning during: pre-reactor acquisition of fuel and fuel elements; in-reactor utilization of the fuel elements; and post-reactor recovery of fuel values. During pre-reactor planning and operations, it is important that the fuel element be designed for economy in manufacture, handling, shipping, and replaceability. The time schedule for manufacturing operations must minimize losses of revenue from unproductive dead storage of high cost materials. For in-reactor operations, the maximum achievable burnup of the fissionable material must be obtained by means of appropriate fuel rearrangement schemes. In the post-reactor period, when the fuel has reached a predetermined depletion of fissionable material, the nuclear materials manager must provide for the most economical reprocessing and recovery of fissionable values and by-products. (P.C.H.)

20969 NUCLEAR MATERIALS MANAGEMENT IN THE URANOTHORIANITE PROCESSING UNIT OF THE BOUCHET PLANT. Lorrain, C. (Commissariat a l'Energie Atomique, Ballancourt-sur-Essonne, France). pp 177-88 of STI-PUB-110. (In French).

The uranothorianite processing unit of the Bouchet plant supplies thorium and uranium salts of nuclear purity, obtained from ore concentrates by a process consisting mainly of the following operations: grinding of the ore, dissolution in nitric acid, successive solvent purification with uranyl nitrate and thorium nitrate, concentration by evaporation and crystallization of the thorium nitrate, and decontamination of the effluents. To maintain a continuous check on the uranium and thorium, material balances are drawn up daily for each chemical operation and monthly for the plant as a whole. This means that each management unit must determine as accurately as possible the amounts of incoming and outgoing material and the amounts involved in conversion. While uranyl nitrate and thorium nitrate of nuclear purity can be determined with an accuracy of the order of 0.1%, numerous causes of uncertainty must be eliminated in determining other uranium- and thorium-bearing products. These originate mainly with inaccurately defined volumes or weights, or with heterogeneous and impure solutions or solids which are difficult to sample and analyze. Due to progress in systematically reducing the incidence of these causes of uncertainty in the balances it has become possible during the last few years of operation to maintain quasi-continuous control of nuclear materials. This has proved particularly satisfactory in the case of uranium. (auth)

20970 A METHOD OF IDENTIFICATION AND INSPECTION FOR INVENTORY CONTROL OF IRRADIATED FUEL ELEMENTS. Kinderman, E. M.; Mills, J. S. (Stanford Research Inst., Menlo Park, Calif.). pp 275-92 of STI-PUB-110.

In an attempt to provide a system for positive identification of reactor discharged fuel, a compact and convenient optical examination system utilizing a fixed examination station, a periscope, a telescope, and camera was developed. This system was tested in a cobalt irradiation pool by examination of test coupons which were marked in various ways, and then treated in a hot, circulating water loop. In the test system, a water-filled periscope, 11-ft long, a catadioptric telescope placed 16 ft from the periscope, and a 35-mm camera for recording the observations were used. The telescope, camera, and mountings are all readily portable since they weigh in total less than 22 lb and have maximum dimensions of 29 in. Photographic observations of test resolution charts in air 20 ft away from the object lens of the telescope demonstrated that the system can resolve markings 22 μm in width. This corresponds to a resolution of 0.8 second of arc. Tests performed on the water system showed that resolution in this system is better than 50 μm at 20 ft. This corresponds to a resolution of about 1 second of arc. It is clear that the resolution can never be better than the air path system. The present system used in an actual fuel inventory should adequately reproduce any inventory markings. (P.C.H.)

20971 INVENTORY METHODS IN A CONVERSION PLANT. Billy, G. (Commissariat a l'Energie Atomique, Paris). pp 315-23 of STI-PUB-110. (In French).

The main purposes of the inventories are: to safeguard the interests of the Commissariat, to evaluate losses, and to check the measures taken for waste storage. The stock-taking operations, preceded by a preparatory meeting to determine the methods to be applied, are carried out in two stages: the weight inventory check and the physical auditing check. Some questions arising in connection with the inventory are disputes between consignors and consignees regarding weight and content; choice of weighing equipment, waste, and evaluation of losses. It appears desirable to stress the difficulties that arise during operation and to consider joint ways of surmounting them. (P.C.H.)

20972 PLANT MEASUREMENT, SAMPLING AND ANALYSIS FOR ACCOUNTANCY PURPOSES WITH PARTICULAR REFERENCE TO SEPARATION PLANTS AT WINDSCALE. Davidson, A. S.; Elliott, F.; Powell, R.; Swinburn, K. A. (United Kingdom Atomic Energy Authority, Windscale, Eng.). pp 325-40 of STI-PUB-110.

All figures for special materials accountancy purposes contain one or more of three parameters, namely plant measurement, sampling, and analysis. For plant measurements it is best to use weighings wherever possible, e.g., the plutonium in the feed to the New Separation Plant is based on the weight of uranium rods fed. Methods used for measuring volumes are discussed, and accuracies and precisions of each method are given. Sampling of solutions in a batch process is done by using evacuated tubes after thorough homogenization of the solution. For flowing streams, where high accuracy is required, a continuous sampler was devised and is used on the feed to the New Separation Plant. Drilling of metal ingots in the normal sampling method at Windscale, whereas for other solids the method is to homogenize as far as possible (e.g., a Y cone blender is used for plutonium oxide) and then sample. For chemical analysis, the precision required of the method depends on the number of determinations in each accounting period. Thus a large number of analyses are required for an accurate but imprecise method. It may be more economical to use fewer determinations with a more precise method. Methods discussed for determining plutonium are: radiochemistry; colorimetrically using thoronol; plutonium separation, complexing with EDTA and back titration of the excess EDTA; titrimetry; isotope dilution followed by mass spectrometry; and differential spectrometry. Methods outlined for determining uranium are: gravimetry as U_3O_8; ether extraction followed by gravimetry or colorimetry; titrimetry; isotope dilution followed by mass spectrometry; and enrichment determination by mass spectrometry or line shift emission spectrography. With all accounting methods standards are used to give quality control and to show any inaccuracy which requires to be corrected for. Precisions of all the methods are given and the methods actually used for the New Separation Plant are indicated. (auth)

20973 SAMPLING OPERATIONS INVOLVING SUPPLIERS AND CUSTOMERS. Artaud, J.; Bodu, R.; Lorrain, C.

(Commissariat a l'Energie Atomique, Paris). pp 353-74 of STI-PUB-110. (In French).

It is suggested that by careful study of the problem, it should be possible to classify the materials subject to specification on the basis of various requirements (considerations of neutron physics, corrosion, process, accessibility after irradiation, etc.). Studies should permit simplification of acceptance analyses and even of fabrication controls, thereby reducing the cost of analysis and no doubt also favorably affecting the price of the materials. In the assessment of materials the idea of sampling is closely linked with methods of analysis, and the interdependence of these two factors and the difficulty of treating them separately is emphasized. Each sampling study is thus a special case depending on the nature of the material and the problems of analysis involved. A subsidiary aspect of the controls connected with sampling, and one which is sometimes of considerable importance, is the problem of the containment of the products. The choice of packaging materials is a basic factor in avoiding contamination or deterioration of the product and in ensuring that samples taken at any time will be as representative as possible. In the light of these considerations, numerous examples are cited as illustrations of the solutions adopted for a number of materials in the French nuclear industry. These examples relate to the sampling of uranium ores, uraniferous concentrates, the calcium used in reduction, uranium metal, and various salts of nuclear elements. (P.C.H.)

20974 NUCLEAR MATERIALS MANAGEMENT IN RELATION TO SAFETY AND CRITICALITY CONTROL; A STUDY OF NON-INHERENTLY SAFE SYSTEMS. Fruchard, Y. (Commissariat a l'Energie Atomique, Marcoule, France). pp 481-90 of STI-PUB-110. (In French).

The relation between management and nuclear safety in the special case of a plant for the aqueous processing of irradiated fuels (the fuels are based on natural uranium) is considered. From the point of view of criticality control such a plant comprises, broadly speaking, three sections. In the first section, where fairly dilute solutions are treated, the type of control required is that over concentration. This control (based on analysis and the use of neutron counters) is easy to carry out but it is difficult to ensure that no deposits are formed. Although experience has shown that there is no particular reason for fearing such deposits, the existence of a deficit in the material balance gives rise to apprehension in respect of criticality. In this section, materials management, still imperfectly carried out, is of prime importance for safety. The second section is where concentrated solutions and wet precipitates are treated. This is the realm of safe geometry. Materials management is of less direct interest here but is still an important factor as far as safety is concerned (where special action, cleaning of equipment, etc. is necessary). In the third section, for the treatment of dry products, control by mass is required and materials management presents no particular difficulty. An additional field which, although less obvious, is nevertheless of paramount importance from the point of view of safety is that of recycling and waste processing. A look at the list of criticality accidents in the U. S. of America is sufficient to show that five out of six accidents were connected more or less directly with waste processing. In most cases one of the contributory causes to a criticality accident was faulty management of fissionable materials. The over-all importance of the relation between safety and nuclear materials management should also be stressed. Although this management may not always form the basis of primary criticality control, it is still indispensable throughout any process since what is done in this respect in one section of a plant is of significance with regard to the safety of neighboring sections, especially that concerned with waste processing. (P.C.H.)

20975 NUCLEAR SAFETY IN WORKING WITH FISSIONABLE MATERIALS. Kamaev, A. V.; Kuznetsov, F. M.; Vladykov, G. M.; Dubovskii, B. G. (Gosudarstvennyi Komitet po Ispol'zovaniyu Atomnoi Energii SSSR, Obninsk). pp 515-23 of STI-PUB-110. (In Russian).

The ensuring of nuclear safety in working with uranium whose concentration is unknown and with a large amount of uranium solutions, using neutron absorbers is discussed. The minimum critical dimensions of systems containing uranium-235 together with the safe distances between tanks containing salts or uranium solutions are considered. Data are given relating to the study of absorbers in the form of rods, rod lattices, and cylindrical baffles. The results given can be used in solving problems of nuclear safety arising in work with uranium solutions. (auth)

20976 METHODS OF ANALYSING PLUTONIUM. Regnaud, F. (Centre d'Etudes Nucleaires, Fontenay-aux-Roses, France). pp 629-38 of STI-PUB-110. (In French).

The methods involved in plutonium analysis are reviewed and their advantages and disadvantages are discussed. As an example of nuclear materials control, a recent transaction between the United Kingdom Atomic Energy Authority and the Commissariat à l'énergie atomique in connection with Rapsodie is described. This operation involved the delivery of 45 kg of plutonium as the oxide under a contract including a number of specifications that had to be checked by analysts of the two countries. (P.C.H.)

20977 ANALYTICAL METHODS FOR URANIUM CONCENTRATION MEASUREMENTS. Highfill, J. P.; Rodden, C. J. (New Brunswick Lab. (AEC), N. J.). pp 639-56 of STI-PUB-110.

A survey of analytical procedures for the determination of uranium, as performed for nuclear materials management in the United States, is presented. Methods are outlined for the measurement of the element in a variety of materials, i.e., ores, concentrates, uranium metal, alloys, ceramics, compounds of uranium, scrap processing solutions, residues, and waste stream products. It is not intended as a complete resumé dealing with the subject, but it does offer measurement methods believed to give precise and accurate results of a high order. The use of gravimetric methods are reviewed pertaining to product materials, which are generally defined as uranium metal, or compounds of the metal, such as oxides, halides, or nitrates. A pyrohydrolysis technique is included under this heading. Non-volatile metallic impurities are determined spectroscopically, and the gravimetric results are corrected accordingly. Volumetric procedures, the work horse methods for determining uranium, are thoroughly explored. Due to the valence states of uranium, reduction-oxidation schemes are particularly attractive. Dissolution problems, separation of interfering elements, reduction steps, and oxidation titrations of reduced uranium are discussed. The application of certain spectrophotometric and fluorometric procedures for analyzing low-grade materials are included. Various separation steps incorporated in the procedures before the determination of uranium are reviewed. Along these lines the utilization of differential colorimetry was examined for determining uranium in impure material. Development of measurement methods in the fields of coulometry, gamma absorptiometry, and x-ray analysis are discussed, with emphasis placed on the limits and applicability of these techniques. Finally, the subject of standard reference materials is dealt with along with information regarding analytical evaluation programs conducted in the United States for the purpose of obtaining better analytical data. (auth)

20978 METHODS USED FOR ISOTOPIC ANALYSIS OF URANIUM AND PLUTONIUM. Bir, R.; Chenouard, J.; Lucas, Monique (Commissariat a l'Energie Atomique, Saclay, France). pp 707-18 of STI-PUB-110. (In French).

Isotopic analysis is commonly done by mass spectrometry. Use is made of two methods differing technically according to the kind of ion source used in the measuring equipment. The operational techniques and the manner in which the results are calculated in the two methods are described. The precautions necessary for accurate analysis of uranium-234 and uranium-236 are given. Surface-ionization sources can be used for working with small quantities of material: samples of the order of a milligram.

Uranium analysis requires no complex chemical preparation and the measurements are absolute. Accuracy is limited; 1% accuracy is easily obtained for uranium-235 but not so easily for uranium-234 and uranium-236. Gaseous sources are supplied with uranium hexafluoride. An accuracy of $\pm 5 \times 10^{-4}$ can be reached in relative measurements. With this technique a higher analysis rate can be obtained than with the surface-ionization method, but quantities of the order of 1 gram are required and chemical treatment necessary to convert the product into UF_6. A given apparatus can operate only in a particular range of concentrations. Isotopic analysis of plutonium is generally done only by the surface-ionization method because it is desirable to handle only very small quantities of radioactive products (hundredths of a microgram). Solutions of plutonium containing uranium require chemical separation. The accuracy of analysis is of the order of 1%. Measurement of small quantities of heavy isotopes is generally done when the abundance exceeds 0.01%. (auth)

20979 INVESTIGATION OF METHODS OF CALCULATING HEAVY-ISOTOPE CONTENT OF OPERATING FUEL ELEMENTS. Valerino, M. F.; Rosztoczy, Z. R. (Combustion Engineering, Inc., Windsor, Conn.). pp 775-96 of STI-PUB-110.

A review is given of the calculational techniques used for predicting heavy-isotope content of fuel elements. The practical capabilities and limitations of the particular methods used are discussed. In particular, attention is directed to those calculations performed for purposes of fuel accountability. Calculation of heavy-isotope content for fuel accounting represents a simpler problem than for predicting reactor characteristics at later stages of core life. Several factors are responsible, namely that, for the purpose of fuel accounting: control-rod positions and fuel-management procedures actually used are known, detailed spatial variations of heavy-isotope concentrations do not have to be explicitly defined but, instead, only average values for a fuel assembly or a group of assemblies are required; and other input data may be available, as for example the results of in-core flux-wire measurements and/or of fuel-assembly activity measurements. As a result, much larger mesh spacings can be employed in the geometrical representations of the 3-dimensional spatial variations. An assessment was made of the accuracy associated with the use of such simplifications in various geometrical representations of several power reactor types. In-core instrumentation and/or fuel-assembly gamma scans used in several operating power reactors have proved susceptible to reasonably accurate interpretation in terms of the relative elementwise power output. This suggests that relatively simple methods of computing burnup and production can be evolved based on such measurement results; the possibilities of this approach were explored. (auth)

20980 UBUNGSMOEGLICHKEITEN ZUM SCHUTZ VOR MASSENVERNICHTUNGSMITTELN. (Drill Possibilities in Protection Against Mass Destruction Agents). Langhans, Kurt; Haase, Erich. Berlin, Deutscher Militaerverlag, 1965. 360p.

Military drill possibilities in training for protection against nuclear warfare and chemical warfare are reported with emphasis on nuclear warfare. Drills with and without the use of radioactive materials are given. Methods and devices for the field measurement of radioactive sources are discussed. Drills in radiation control and deactivation are considered. (J.S.R.)

20981 THE MAINTENANCE OF A HABITABLE ATMOSPHERE. Carhart, Homer W. (Naval Research Lab., Washington, D. C.). New York, American Society of Mechanical Engineers, 1965, Preprint No. 65-UNT-5, 9p., $1.00. (CONF-650550-3). ORINS.

From American Society of Mechanical Engineers, Underwater Technology Conference, New London, Conn.

A habitable atmosphere can be maintained and methods for supplying oxygen and removing carbon dioxide, hydrogen, carbon monoxide, and certain other contaminants are at least partially solved. Continuing research on oxygen sources, removal of contaminants, and methods of analysis show advantages and disadvantages that might be expected for alternate potential methods. Selection of a method for a given mission, however, also depends on engineering studies for reliability and for evaluation of tradeoffs that must be made depending on availability of power, space, and weight limitations and length of mission. In general, chemical (one-shot) systems are considered better for short missions and regenerative ones for longer missions. (auth)

20982 ADVANCES IN WATER POLLUTION RESEARCH. Proceedings of the International Conference held in London, September 1962. Volumes 1, 2, and 3. Southgate, B. A. (ed. Vol.1); Eckenfelder, W. W. (ed. Vol. 2): Pearson, E. A. (ed. Vol.3). New York, Pergamon Press, 1964. 1402p. $45.00. (CONF-620911-(Vols.1, 2,3)).

Proceedings of the First International Water Pollution Research Conference are presented in three volumes. Self-purification, organic compounds in water, purification by biological means, absorption of impurities, processing radioactive wastes, marine waste discharge, and other methods of purifying wastes are discussed with special regard for efficiency and economics. The pollution effect of waste or contaminated water on natural waters, estuaries, and coastal areas is considered. Two papers were abstracted previously for NSA and appeared as 16: 32523 and 32622. (M.C.G.)

INSTRUMENTATION

General

Refer also to abstracts 21213, 21458, 21581, 21582, 21632, 22211, and 22231.

20983 (AERE-R-4966) A DISPLAY UNIT FOR COMPLEX DATA. Best, G. C. (Atomic Energy Research Establishment, Harwell (England)). Jan. 1966. 16p. Dep. BIS $1.20. HMSO 6s. 0d.

The problems presented in designing a display unit for complex data are discussed with reference to specific equipment, the Most Active Zone Encoder. Methods are described for a range of display operations and techniques discussed which extend the monitoring facility into a direct data control. (auth)

20984 (EUR-2710.f) UN CRYOSTAT EN PHASE GAZEUSE. (Cryostat in the Gaseous Phase). Debeir, R.; Grin, M. (European Atomic Energy Community, Ispra (Italy). Joint Nuclear Research Center). June 23, 1965. 12p. Dep. mn.

A cryostat working in the gaseous phase is described. The thermostatic fluid is nitrogen which is vaporized in the measuring chamber. The apparatus is characterized by a very manageable operation and can be used at every temperature between room temperature (20°C) and the temperature of liquid nitrogen (−196°) and can be adapted to various physical measurements (resistivity, tension tests at low temperature). (auth)

20985 (N-65-29669) PLASMA COUPLING MEDIUM FOR A TRAVELING-WAVE TUBE AMPLIFIER. Gilson, Verle A.; Johnson, Curtis C. (Utah Univ., Salt Lake City. Microwave Device and Physical Electronics Lab.). July 1965. 162p.

The effects of a plasma medium in an axial d-c magnetic field on Pierce's beam coupling impedance of a traveling-wave tube are investigated. This study treats the plasma electron cyclotron frequency as a primary variable and the plasma frequency as a parameter. A disc-loaded waveguide with the plasma filling the hole region was selected for the slow-wave circuit. Theoretical calculations for the configuration show that the beam coupling can be greatly enhanced when the cyclotron frequency is near but greater than the applied frequency. The amount of increased coupling is dependent upon the relative size of the plasma frequency with respect to the applied frequency but substantial amounts are predicted when the plasma frequency is significantly less than the applied frequency. Experimental results are included. (auth)

20986 (N-65-29823) DEVELOPMENT OF ELECTRICAL SWITCHGEAR FOR SPACE NUCLEAR ELECTRICAL SYSTEMS. Quarterly Progress Report No. 2, March 4-June 4, 1965. Powell, A. H. (ed.) (General Electric Co., Cincinnati, Ohio. Space Power and Propulsion Section). Contract NAS3-6467. 133p. (NASA-CR-54447). CFSTI $4.00 cy, $1.00 mn.

Work to develop and design ground prototype a-c circuit breakers and d-c engine contactors suitable for, and tested under, expected launch and space requirements is described. The breakers will be rated 1000 volts, 600 amperes, 2000 cps, while the d-c contactors will have a rating of 10,000 volts 10 amperes. During this period, firming of the design for the actuator mechanism, the selecting of interrupter enclosure materials, and determining basic concepts for the interrupter unit was accomplished. A sketch of the overall breaker in accordance with the design concepts at the close of the period is included. (STAR)

20987 (RFP-690) CONDUCTANCE DEVICE FOR MONITORING THIN FILM GROWTH. Hart, G. E.; Martinez, J. L.; Beno, R. L. (Rocky Flats Div., Dow Chemical Co., Golden, Colo.). Mar. 11, 1966. Contract AT(29-1)-1106. 12p. Dep. mn. CFSTI $1.00 cy, $0.50 mn.

A device that can be used to measure the very low resistances (0.02 to 10,000 ohms) of evaporated metal films is described. This will be of use in coating processes where the thickness of the metal being deposited must be controlled while the substrate is in the vacuum chamber. Accuracies in the range of ±2 percent were obtained on aluminum in the 200 to 3000 Å thickness range. (auth)

20988 (UCRL-13202) FLOW CALIBRATION OF THE LONG JOHN MANIFOLDED ORIFICE ASSEMBLY WITH AIR. Final Report. Lerich, Joel (Colorado Univ., Boulder. Engineering Research Center). Feb. 1966. Contract W-7405-eng-48. 162p. Dep. mn. CFSTI $5.00 cy, $1.00 mn.

The repeatability and calibration potential of available gas flowmeters were investigated. The critical nozzle was chosen as a transfer standard based on its simplicity, inherent repeatability, and ease of usage. An investigation into the performance of various orifice tap configurations was performed. The corner tap was decided to be best suited for use in the Long John Orifice assembly because of its stability of signal. A primary calibration device was designed and fabricated to calibrate the transfer standard. A set of critical nozzles was obtained and calibrated with the primary calibration device. Additional tests provided cross-comparisons with other flowmeters. These auxiliary data were useful in the analysis of the primary data on the transfer standards. Approximately three thousand calibration points were obtained on the Long John Orifice assembly using air as a test media at flow rates ranging from 0.0004 to 6.4 lbs/sec. (M.O.W.)

20989 (Y-1506) POSITION MONITORING DEVICES. Whitten, L. G. (Union Carbide Corp., Oak Ridge, Tenn. Y-12 Plant). Apr. 20, 1966. Contract W-7405-eng-26. 32p. Dep. mn. CFSTI $2.00 cy, $0.50 mn.

Devices which monitor position over ranges of a few inches to several feet are discussed. Mechanical, optical and electrical concepts are covered. Clearly defined advantages and disadvantages are pointed out; however, no attempt is made to evaluate any one system with respect to another. (auth)

20990 (AERE-Trans-1048) REPORT OF AN INVESTIGATION OF THE PRESENT UTILISATION OF RADIOISOTOPE DEVICES. Translated by J. B. Sykes (Atomic Energy Research Establishment, Harwell, Eng.), from Radioisotopes (Tokyo), 14: 255-67(1965). 30p. Dep. mn. BIS $0.90. HMSO 4s. 6d.

A survey was made on the use or otherwise of radioisotope devices; where used, the type and number of machines, and the occurrence of breakdowns; where not used and the reason. Thickness meters and level gages were found to account for about ⅓ each of the total, the remaining third being made up of all other types. The most widely used of these were found to be vacuum meters. (P.C.H.)

20991 A NEW MAGNETLESS DYNAMIC MASS SPECTROMETER. Higatsberger, M. J.; Ruedenauer, F.; Viehboeck, F. (Reaktorzentrum, Seibersdorf, Austria). Acta Phys. Austr., 21: 32-42(1966). (In German).

A new type of mass spectrometer is described in which the energy selection is made by means of parabolic particle orbits. A review of the mathematical treatment of such a system and details of the construction of the prototype are given. The results of the first measurement gave satisfactory agreement with theory. (tr-auth)

20992 COMPENSATION OF THERMIC EFFECTS IN SEMICONDUCTOR JUNCTIONS USED FOR MEASURES IN LOGARITHMIC SCALE. Marini, R.; Fiorido, M. (CAMEN, Pisa, Italy). Energ. Nucl. (Milan), 13: 197-202(Apr. 1966).

The semiconductor junctions of diodes and transistors,

used to obtain a logarithmic conversion, are strongly affected by temperature. A method of compensation of the thermic effects, deduced mathematically, using a particular differential circuit and field effect transistors are described. The experimental results, with a transistor as logarithmic element, show that for a logarithmic scale of six decades and with variations of the ambient temperature from 25 to 75°C, the indications of the output meter change by less than 6% of the section of scale representing one decade. (auth)

20993 AUTOMATIC DEVICE FOR COLLECTING DUST-FREE PRECIPITATION. Oakes, D.; Serino, A. (Dept. of Health, Education, and Welfare, Winchester, Mass.). Health Phys., 12: 574-6(Apr. 1966).

An automatic device was designed for collecting dust-free precipitation. Design features and performance are emphasized. (H.G.D.)

20994 COMPUTATION OF ION TRAJECTORIES IN THE MONOPOLE MASS SPECTROMETER BY NUMERICAL INTEGRATION OF MATHIEU'S EQUATION. Lever, R. F. (IBM Watson Research Center, Yorktown Heights, N. Y.). IBM J. Res. Develop., 10: 26-40(Jan. 1966).

Use of magnetic and radiofrequency analyzers in mass spectroscopy is discussed. Radiofrequency analyzers of the quadrupole type have advantages in that they do not require a magnet and are equally convenient for high or low masses; furthermore, the quadrupole does not require a well-defined ion-injection velocity. An extensive compilation of trajectories derived for the monopole instrument through computer solutions to the differential equations that obtain is given. A high speed digital computer used with an off-line curve plotter enabled ion trajectories to be readily obtained in terms of the initial conditions and the parameters appearing in the differential equation of motion (Mathieu's equation). A study of these trajectories has led to the conclusion that ions should not be injected parallel to the axis of the instrument, as is done at present, but through the axis and at an angle to it. A simple empirical expression enables the variation of position of ion focus with mass and operating parameters to be predicted. Very high resolution can be attained. The main limitation is probably the amplitude stability of the alternating potential. Small deviations from perfect geometry do not greatly affect the quality of focus. (BBB)

20995 A MASTER CONTROL SYSTEM FOR NUCLEAR PHYSICS INSTRUMENT SYSTEMS. Phillips, C. Vincent; Otte, Victor A.; Sullivan, Russell P. (Ohio State Univ., Columbus). IEEE (Inst. Elec. Electron. Eng.), Trans. Nucl. Sci., NS-13: No. 1, 170-3(Feb. 1966).

A control system that was designed to act as an interface between the control functions of a nuclear physics instrumentation system and an on-line computer or a data handling system is described. (D.C.W.)

20996 ZSA-ZSA: A SELF-POLICED DATA HANDLING FACILITY FOR MULTIPLE DETECTOR EXPERIMENTS. Marquardt, R.; Simanton, J. (Argonne National Lab., Ill.). IEEE (Inst. Elec. Electron. Eng.), Trans. Nucl. Sci., NS-13: No. 1, 174-81(Feb. 1966).

A data handling facility that checks the experimental arrangement and performs spatial analysis of data from the detectors is described. (D.C.W.)

20997 A MODULAR SET OF ANALOG MICROCIRCUITS INTENDED FOR SATELLITE EXPERIMENTS. Curran, F. E.; Hayashi, I.; Medford, L. V.; Miller, G. L. (Bell Telephone Labs., Inc., Murray Hill, N. J.). IEEE (Inst. Elec. Electron. Eng.), Trans. Nucl. Sci., NS-13: No. 1, 326-35(Feb. 1966).

An amplifier, a zero-crossing discriminator, a linear gate, and a pulse shaper that were developed for use in a variety of satellite experiments are described. (D.C.W.)

20998 INTEGRATED CIRCUITS—THEIR CHARACTERIZATION AND USE IN EXPERIMENTAL PHYSICS. Zimmermann, K. A. (General Atomic Div., General Dynamics Corp., San Diego, Calif.). IEEE (Inst. Elec. Electron. Eng.), Trans. Nucl. Sci., NS-13: No. 1, 336-41 (Feb. 1966).

The implications of using integrated circuits in equipment for physics experiments are discussed. The economy and reliability of operation of a series of instruments using integrated circuits are considered. (D.C.W.)

20999 A TEMPERATURE-COMPENSATED MULTI-ELEMENT LOGARITHMIC CONVERTER MICROCIRCUIT. Gri, Norman J.; Warble, Keith V. (AVCO Corp., Tulsa, Okla.). IEEE (Inst. Elec. Electron. Eng.), Trans. Nucl. Sci., NS: No. 1, 342-5(Feb. 1966).

An eight-channel logarithmic pulse-rate measuring circuit was designed for use with a tissue equivalent gas proportional counter system is described. The use of thermal feedback in monolithic silicon microcircuitry is described together with its application to the temperature-stabilized logarithmic pulse counting circuits. With this form of temperature compensation, each channel exhibits a logarithmic characteristic which is absolutely accurate to within 50% over 3 decades for the temperature range from 0 to 60°C. (auth)

21000 ANALYSIS AND DESCRIPTION OF A HIGH-STABILITY NUCLEAR PULSE AMPLIFIER. Hatch, Kenneth F. (Univ. of California, Livermore). IEEE (Inst. Elec. Electron. Eng.), Trans. Nucl. Sci., NS-13: No. 1, 351-70(Feb. 1966). (UCRL-14284-T(Rev.1)).

A solid-state pulse amplifier that was designed with particular attention to temperature stability and linearity is described, and the response of the amplifier is analyzed. (D.C.W.)

21001 THE LOGICAL DESIGN OF A DIGITAL PSEUDORANDOM NOISE GENERATOR. Smith, K. D.; Hamilton, J. C. (Philips Petroleum Co., Idaho Falls, Idaho). IEEE (Inst. Elec. Electron. Eng.), Trans. Nucl. Sci., NS-13: No. 1, 371-81(Feb. 1966).

A digital pseudorandom noise generator is described and analyzed. Two examples of the use of the generator are discussed. (D.C.W.)

21002 FAST TIMING CIRCUITS USING STORAGE DIODES. Grunberg, J.; Tepper, L. (Soreq Nuclear Research Center, Yavne, Israel). IEEE (Inst. Elec. Electron. Eng.), Trans. Nucl. Sci., NS-13: No. 1, 389-93 (Feb. 1966).

A constant-charge pulse shaper was used as the basic element in two fast timing circuits using photomultipliers. The shaper is based on storage diodes (snap-off diodes) and delivers an approximately constant charge at the output, almost independent of the input current pulse amplitude. These constant-charge pulses are delivered to a tunnel diode, which in the sub-nanosecond range is a charge-sensitive device. A coincidence circuit and a time-to-amplitude converter were built and operated with a ^{60}Co source, two plastic scintillators used with 56 AVP tubes, and a slow coincidence discriminator. With a range of 20 to 200 mamp, the coincidence slope was 0.4 nsec for half-amplitude, while the time-to-amplitude converter showed a full-width-at-half-maximum of 0.8 nsec on a multichannel analyzer. (auth)

21003 NUCLEAR INSTRUMENTATION FOR LUNAR SURFACE AND SUBSURFACE MEASUREMENTS. Ebeoglu, D. B. (Bendix Systems Div., Ann Arbor, Mich.). IEEE (Inst. Elec. Electron. Eng.), Trans. Nucl. Sci., NS-13: No. 1, 562-8(Feb. 1966).

An instrumentation package that will perform natural gamma, spectral gamma, gamma-gamma, neutron-gamma, and neutron-neutron measurements is described. (D.C.W.)

21004 PULSE SHAPING BY TRIPLE DIFFERENTIATION IN NUCLEAR PULSE AMPLIFIERS. Fairstein, Edward (Tennelec Instrument Co., Inc., Oak Ridge, Tenn.). IEEE (Inst. Elec. Electron. Eng.), Trans. Nucl. Sci., NS-13: No. 1, 596-601(Feb. 1966).

Pulse shaping by triple differentiation is described as a technique for reducing the recovery time following heavily overloading signals in nuclear pulse amplifiers.

Tests performed on a low-noise pulse amplifer containing triple RC differentiation show recovery to the amplifier noise level in two nonoverloaded pulse widths following a 4,000× pulse amplitude overload. Experimental data are presented to show that the noise level when compared with single RC operation is worse by 1.6× to 3×, depending on the number of low-pass filter sections used in the shaping networks and the type of noise being observed. (auth)

21005 CHARACTERISTICS OF THE MOELLENSTEDT ELECTRON VELOCITY ANALYZER. Metherell, A. J. F.; Whelan, M. J. (Cambridge Univ., Eng.). J. Appl. Phys., 37: 1737-41(Mar. 15, 1966).

The performance of the Möllenstedt electron velocity analyzer was investigated by numerical trajectory tracing by digital computer. Two methods of calculating a field distribution were employed, namely (a) relaxation for an actual case of interest with cylindrical electrodes, and (b) an analytical solution for a system of two line charges between earthed plates. Suitable equipotential surfaces for this system can be chosen to simulate the cylindrical electrodes of a practical analyzer. The latter system is a reasonable approximation to the actual case, and in practice is much simpler to use in numerical calculations than (a). Using (a) one electrode system was studied in detail; using (b) several geometries were investigated. The dispersion of the instrument and the effects of slit width and angular divergence on resolution were investigated for various electrode geometries. A simple rule for slit width resolution is given. (auth)

21006 AN INSTRUMENT FOR MEASURING THE INDEX OF D-C MAGNETIC FIELDS. Sipek, L. (Inst. of Plasma Physics, Czechoslovak Academy of Sciences, Prague). J. Sci. Instrum., 42: 892-3(Dec. 1965).

A description is presented of an instrument for measuring the field index of d-c magnetic fields, particularly of those of circular accelerators. The method is based on the use of two identical vibrating measuring coils whose axes are skew and generally not parallel to the direction of the field being measured. The method is suitable for rotationally symmetric and plane fields. An instrument designed on the above principle measures the field index with an absolute accuracy to about 1.5% and a relative accuracy to 0.5% in fields greater than 100 Oe. (auth)

21007 THE DESIGN OF A VELOCITY SELECTOR FOR LONG-WAVELENGTH NEUTRONS. Clark, C. D.; Mitchell, E. W. J.; Palmer, D. W.; Wilson, I. H. (Univ., Reading, Eng.). J. Sci. Instrum., 43: 1-5(Jan. 1966).

The theory and design of a neutron velocity selector for use in the wavelength range 7–15 Å are discussed. The selector takes the form of seven thin circular disks rigidly mounted on a rotating shaft. Each disk is opaque to neutrons and has 80 slots machined at regular intervals about its circumference. In order to simplify construction the positions of the disks were determined so that the slots can be machined parallel to the axis of rotation. The theoretical resolution which can be expected of the device is discussed. (auth)

21008 NUCLEAR PULSE AMPLIFIERS—FUNDAMENTALS AND DESIGN PRACTICE. V. Fairstein, E. (Tennelec Instrument Co., Inc., Oak Ridge, Tenn.); Hahn, J. Nucleonics, 24: 68-70(Mar. 1966).

Amplifier speed and timing accuracy for nuclear pulse amplifiers are discussed. Also ground loop noise is considered. An amplifier system for canceling gain or rise-time variations without the use of feedback is shown in a diagram, and a diagram of a differential amplifier input stage and twin axial cable is shown for ground loop noise reduction. (J.F.P.)

21009 ULTRACENTRIFUGE ROTOR TEMPERATURE MEASUREMENTS AND CONTROL. Fabricant, Steve J.; Windsor, Alfred A.; Lindgren, Frank T. (Univ. of California, Berkeley). Rev. Sci. Instrum., 37: 495-6(Apr. 1966). (UCRL-16490).

A radio telemetry system for use with analytic or preparative ultracentrifuge rotors is described. Capable of sustained high speed operation, this modulated FM system simultaneously transmits with precision both rotor speed and rotor temperature. (auth)

21010 NANOSECOND PULSE STRETCHER. Larsen, Robert N. (Argonne National Lab., Ill.). Rev. Sci. Instrum., 37: 514-15(Apr. 1966).

A nanosecond pulse stretcher using current switching is described which was developed for use in a pulse-shape discrimination system. The system measures the relative specific ionization in a proportional counter by computing the ratio of the charge collected in the first 20 to 50 nsec to the total charge. The circuit diagram of the pulse stretcher is shown and its principle of operation is discussed. The rise time of the output pulse in response to a step function is approximately 5 nsec; and the differential linearity of the output is 1 to 2% over an output range of 50 mv to 10 v. (L.B.S.)

21011 A 45 DEG REMISSION PHOTOMETER FOR MEASUREMENT OF RADIATION ERYTHEMAS. Schulz, Hans-Juergen; Bohndorf, Werner (Univ., Wuerzburg, Ger.). Strahlentherapie, 129: 308-18(Feb. 1966). (In German).

A sensitive remission photometer for determining the radiation reaction of the skin is described. Changes in deeper located skin layers can be determined by a suitable optical device that can also be used easily for serial skin measurements where a great number of measurements must be done in short time intervals. The stability of the supply voltages, achieved by electronic control, reduces considerably the instrumental error of the measurement values below the biologically induced daily variations. (auth)

21012 SWITCHING CHARACTERISTICS OF SMALL-GEOMETRY THIN-FILM SUPERCONDUCTORS. Slay, B. G.; Pritchard, J. P. Jr.; Pierce, J. T. (Texas Instruments Inc., Dallas). Trans. Met. Soc. AIME, 236: 356-9 (Mar. 1966).

A short discussion is given of the cryotron as a superconducting switch. The parameters of interest such as gain, critical gate current, critical control current, and critical surface current density are described. The photomask-photoresist process makes possible the study of much narrower dimensioned cryotrons than previously possible using mask stencils. Data is given for the above parameters as a function of width, thickness, temperature, and crossing ratio. Photographs of the various circuits used are shown. The techniques involved in making connection to the circuits and the precautions taken to avoid side effects in the measurements are discussed. In particular data is given for critical currents of superconducting lines down to 2×10^{-4} in. A rise in critical surface current density is observed for the smaller lines in both lead and tin. A discussion of the impact of these measurements in the design of future cryotron circuitry is given. In addition to the improvement in device density achieved by simple scale reduction, additional gains in density may result through improved device form factor. (auth)

21013 PARAMETRIC OSCILLATING AMPLIFIER—A NEW SOLID-STATE ELECTROMETER AND ITS APPLICATION TO β THICKNESS GAGES. Katagiri, Michio; Yamasaki, Hiro (Yokohama Electric Works, Ltd., Japan). Trans. Soc. Instrum. Contr. Eng. (Tokyo), 1: 75-83 (Mar. 1965). (In Japanese).

Beta-ray thickness gage requires a pre-amplifier of high input impedance for amplification of small input current of 10^{-11}–10^{-12} amp generated in the ionization chamber. A solid-state circuit which is considered ideal to be used in automation instruments, is realized by using the technique of parametric oscillating amplifier incorporating a "Pico-diode," a variable capacitance diode with very low leakage current. This amplifier is entirely reliable and perfect for industrial instruments. The β-ray thickness gage with the solid-state electrometer (pico-diode electrometer) requires no warm-up time. Since it needs only small amounts of radio isotope for its high sensitivity and stability, radia-

tion safety is improved, too. The features of this β-ray thickness gage, principle and characteristics of the solid-state electrometer, analysis of transfer characteristics of the oscillating amplifier, and some of their applications are given in this paper. (auth)

21014 CONDITIONS FOR OBTAINING ELECTRON BUNCHES OF MINIMUM LENGTH FROM A KLYSTRON-TYPE BUNCHER WITH THE INFLUENCE OF SPACE-CHARGE TAKEN INTO ACCOUNT. Galkov, V. A.; Snedkov, B. A. (Moscow Power Engineering Inst.). Zh. Tekh. Fiz., 35: 1767-70(1965). (In Russian).

The operating conditions of a klystron buncher under which the bunches have minimum length, maximum electron content, and minimum energy scatter are discussed with space charge effects taken into account. The requirements on the bunches are to some extent contradictory, and trading must be undertaken. Phase diagrams for the electron energy and other parameters were calculated for a number of specific conditions; these are presented and discussed. The phase diagrams calculated for the energy distribution at the end of the drift space for different values of the bunching parameter are in good agreement with similar curves. The optimum bunching parameter was found to be 2.0 for bunches that are not very short and contain more than 40% of the injected particles. This is in agreement with the values 1.9 to 2.19 found experimentally. By performing calculations similar to those described here for a wide range of beam currents and energy scatter, one can calculate the modulation amplitude and bunching parameter required for obtaining bunches of minimum length containing a maximum number of particles. (ATD)

21015 VISCOMETER /Q-2235/ (Engineering Materials). (Oak Ridge National Lab., Tenn.). (CAPE-1292). 1 drawing.

The torsional-pendulum viscometer eliminates the use of sensitive photographic film and attendant lightproof housing. By utilizing simple optics, it produces a direct readout record of sufficient size that magnification and projection are not required. The viscometer is used in the precise measurement of the viscosity of molten salts. A condensing lens focuses the light from a high-intensity light source providing strong monochromatic ultraviolet light on a mirror mounted on a torsional-suspension wire. The light is reflected to a rotating drum receptor. The drum is fitted with a strip of ultraviolet-sensitive paper, which is sensitive to high levels of ultraviolet light but is insensitive to light of longer wavelengths. As the drum rotates, the traveling beam from the oscillating mirror is recorded on the paper. Exposure to low-intensity ultraviolet light from fluorescent light in the laboratory develops the trace. All of the experiments may be conducted in room light. (For details, see TID-4100.) (M.C.G.)

21016 THERMO-ELECTRIC DEVICES. Moores, Harry (to English Electric Co., Ltd.). British Patent 1,020,574. Feb. 23, 1966. Filed June 20, 1961.

A thermoelectric device is patented that is suitable for use in measuring temperature in a nuclear reactor. The device includes a thermo-junction positioned within and in good thermal relationship with a first container and a second container that has its wall spaced from and enclosing a portion of the first container adjacent to the thermo-junction. A quantity of material that undergoes a phase change at a known temperature, e.g., bismuth, is disposed in the space between the first and second container. When the temperature of the media surrounding the device rises from a value below the known temperature to a value above it, the temperature of the thermo-junction remains constant while the phase change is taking place; thus, the thermo-junction may be calibrated. The space not filled with the material is filled with an inert gas. (B.L.M.)

21017 ELECTRIC ALARM APPARATUS INCORPORATING IONISATION CHAMBERS. (to Danske Securitas A/S). British Patent 1,020,771. Feb. 23, 1966. Priority date Dec. 30, 1961, Denmark.

An electric alarm apparatus is provided for detecting the presence in a room of a gas containing solids or liquids in suspension. The apparatus includes two adjacent ionization chambers separated by an electrically insulating diaphragm with an elongated radioactive radiating member projecting through the diaphragm into both the chambers. One of the chambers is closed and one is opened for communication with the room to be monitored. A source of voltage has two poles respectively connected to the two chambers; and a voltage sensitive indicating means is connected to the two chambers and to a metallic grid that surrounds the radioactive radiating member over at least a part of its length, in such a manner that the voltage sensitive means can be caused to operate by the presence in the other chamber of the gas containing the solid or liquid in suspension. (B.L.M.)

21018 NUCLEAR REACTORS. Trussler, Geoffrey Arnold (to English Electric Co., Ltd.). British Patent 1,021,084. Feb. 23, 1966. Filed Aug. 28, 1962.

A cutting device for an electric lead is patented for incorporation into a string of fuel elements in a nuclear reactor of which at least one element is provided with an electric lead having one end secured on the fuel element and forming part of a temperature-sensitive equipment. The string of fuel elements is arranged for insertion in the reactor with the electric leads passing along the string of fuel elements to one end for connection to other parts of the temperature-sensitive equipment. The cutting device includes a cutting edge that is out of contact with a slack loop of the lead when in position in the reactor; but withdrawal of the lead away from the fuel element tightens the loop, and the lead engages the cutting edge. (B.L.M.)

21019 RADIOACTIVE APPARATUS FOR MEASURING TEMPERATURE. Schultz, Warner W.; Briggs, Harvey D. (to Geneal Electric Co.). U. S. Patent 3,234,388. Feb. 18, 1966. Filed June 22, 1962.

A temperature measuring apparatus includes an evacuated enclosure positioned in a relatively inaccessible region where the temperature is to be measured and containing a radioactive gas within the upper portion and a liquid in the lower portion of the enclosure and a radiation detector positioned in a more accessible region with the radiation detected by the detector being a measure of the temperature in the inaccessible region. A radiation shield is positioned between the enclosure and the detector so that radiation from the top part of the enclosure is detected. Increasing temperature causes the gas to be compressed by expansion of the liquid in the lower portion of the enclosure. The gas has a predetermined increase in density in response to a predetermined temperature rise in the inaccessible region. Alternatively, the shield can have an aperture positioned in such a manner that the detector senses an abrupt change in the radiation through the aperture at the specific temperature, and the abrupt change is effected by the demarcation line between the liquid and the radioactive gas passing across the region of the aperture. (B.L.M.)

Radiation Detection

Refer also to abstracts 20745, 20846, 21540, 21541, 21556, 21607, 21608, 21612, 22010, 22020, and 22438.

21020 (AD-621069) USE OF IMAGE INTENSIFIERS WITH STREAMER CHAMBERS. Jones, Lawrence W.; Loo, Billy W. (Michigan Univ., Ann Arbor. Dept. of Physics). Sept. 1965. Contract Nonr-122423. 22p. (TR-20-03106-20-T). CFSTI $1.00 cy, $0.50 mn.

A very simple Marx generator and a streamer chamber were used. Streamers of any length down to less than one mm. may be obtained by adjusting the firing delay of a spark gap which shunts the chamber. With the aid of a three stage image intensifier, cosmic ray tracks were successfully recorded on 35 mm. Kodak Tri-X film. Streamers of 5 mm. were recorded comfortably with a front lens opening of f/16 while the much fainter 1 mm

streamers require an opening of f/4.5 or less. A coincidence pulse from the counters located above and below the chamber initiates the triggering functions of the avalanch transistor, the EFP60, and the 5D21 tube which delivers a 7 kv pulse to the trigger electrode of the first stage of the Marx generator. The 101 mm. Wollensak lens images onto the first cathode of the tube the direct view of the streamers normal to the electric field together with the end view, which is parallel to the field and is reflected to the lens by means of a mirror. A pair of 76 mm. f/0.87 Super Farron lenses couples the output of the image intensifier to the film with unity magnification, while the demagnification of the entire system is about 10:1. (TAB)

21021 (AD–622629) NUCLEAR TIME BASE-FEASIBILITY STUDY. Voeller, Duane E. (Harry Diamond Labs., Washington, D. C.). Aug. 12, 1965. 50p. CFSTI $2.00 cy, $0.50 mn.

An investigation was made to determine the feasibility of using random disintegration events of a radioactive isotope in conjunction with a nuclear particle detector as a low-frequency, high-accuracy time base for an electronic timer. The objectives were directed toward a time base suited for various ordnance applications. The various types of detection devices and radioisotopes that were considered are reviewed. Test data are included from the time base that was subsequently developed. The time base evolving from this study consists of an alpha particle source, a semiconductor nuclear particle detector, and a preamplifier with voltage discriminator. A timing error of <0.1 percent was obtained with this system within a −55 to +75C range. Using integrated electronics, the system could be packaged within 1 cu in. and consume <25 mw. Based on this investigation, the use of random disintegration events of a radioisotope in conjunction with a nuclear particle detector was determined feasible but impractical at present, because of the long calibration time and relatively expensive associated electronics. (auth)

21022 (AD–624230) ANOTHER FACTOR TO BE CONSIDERED IN ENVIRONMENTAL TESTING: X RADIATION. (New York Univ., N. Y. School of Engineering and Science). Jan. 1963. Contract NOBsr-89288. 18p. CFSTI $1.00 cy, $0.50 mn.

The accurate detection and measurement of the x radiation produced by high voltage Pulsed r-f tubes involves problems of dosimetry different from the detection of similar radiation from conventional x-ray tubes or from radioactive materials. One cause of this difficulty is that the x radiation is the by-product which is produced simultaneously with the r-f energies. Radiofrequency energy may produce strong potential gradients within the x-ray detector and its associated circuitry, resulting in an erroneous indication of the x-radiation intensity. Unless the x-ray detector has an inherently low sensitivity to r-f energies, the r-f shielding required may greatly attenuate the low energy levels of x radiation before it reaches the detector, making the detecting instrument quite insensitive to the lower energy x radiation. Any shielding based on these readings will be insufficient and provide a false sense of protection. Since the x-radiation produced by these high voltage r-f tubes is generated in very short pulses, the average x radiation may be relatively low. Most of the detectors described measure the average x-radiation intensity, therefore, the reading may be off as much as 1/duty cycle. (auth)

21023 (AD–624231) SURVEY OF DEVICES FOR MONITORING X RADIATION. (New York Univ., N. Y. School of Engineering and Science). Mar. 1963. 23p. CFSTI $1.00 cy, $0.50 mn.

The existing methods of monitoring x radiation are surveyed. Their operation and limitations are described. Those portable devices capable of detecting and measuring x radiation are listed. (TAB)

21024 (AD–630693) PHOTON, NEUTRON, AND CHARGED PARTICLE ABSORBED DOSE MEASUREMENTS WITH A PORTABLE MICROCALORIMETER. Goldstein, N.; Schleiger, E. R.; Tochilin, E. (Naval Radiological Defense Lab., San Francisco, Calif.). Jan. 28, 1966. 30p. (USNRDL-TR-976).

Two compact, portable microcalorimeters were built and used to measure absorbed dose. A thermal shield near liquid nitrogen temperature provides the necessary isothermal environment for the absorber. Temperature increase of the absorber during irradiation is measured with a thermistor. Tissue equivalent plastic and beryllium absorbers were calibrated for absorbed energy as a function of temperature change by exposure to standard ^{60}Co and ^{137}Cs gamma sources. The beryllium absorber detected gamma-ray doses as low as 0.17 rads (17 ergs/g) with a standard error of 6 percent. Microcalorimetric measurements of absorbed dose from continuous and pulsed x rays, reactor neutrons, and charged particles were compared to measurements with other dosimeter systems. (auth)

21025 (AERE-R–5122) ROUTINE USE OF THE SILVER–COBALT ACTIVITY RATIO METHOD TO DETERMINE EPITHERMAL INDICES FOR LARGE NEUTRON DOSE IRRADIATIONS. Cabell, M. J.; Wilkins, M. (Atomic Energy Research Establishment, Harwell (England)). Feb. 1966. 28p. Dep. BIS $0.90. HMSO 4s. 6d.

A new determination of WESTCOTT's s_o for the reaction $^{109}Ag(n,\gamma)^{110m}Ag$ is described. The result is that $s_{o,Ag} = 18.53 \pm 0.16$, relative to $s_o = 17.02$ for gold; this corresponds to an absolute value of $s_{o,Ag} = 18.53 \pm 0.69$. The activity ratio normalization factor P is determined for silver-aluminum alloy (0.25 atom per cent silver, 0.025 in. diameter) and cobalt-aluminum alloy (0.10 atom per cent cobalt, 0.050 in. diameter) monitor wires. Using the counting equipment described, P is 0.2588 ± 0.0004. The results obtained above are used in comparing measurements of $x = r\sqrt{T/T_0}$ by the silver-cobalt activity ratio method, with similar measurements by the gadolinium ratio method. For neutron doses ($i = (nv_0)t$) of the order 4×10^{17} n/cm^2, the two sets of results are in good agreement. A measurement of x for an irradiation of 183 days duration in the lattice of PLUTO is also described. It is concluded from these experiments that the silver-cobalt activity ratio method is capable of giving x with an accuracy of better than ±5 per cent when $0.1 < x > 0.008$ and $i < 10^{20}$ n/cm^2; outside these ranges the error can be larger. SILCO, a computer program written in FORTRAN for the S2 compiler on the IBM 7030 (Stretch) computer is described. By its use x and i can be obtained directly from the raw experimental data. (auth)

21026 (BNL–948, pp 704-17) TECHNICAL DEVELOPMENTS [IN HARDWARE]. Donovan, Paul F. (Bell Telephone Labs., [Murray Hill, N. J.]).

Some advances in semiconductor detectors are discussed together with some problems with these detectors. A particle identification system and servo-stabilized analog-to-digital converters are also briefly considered as well as the use of computers in experiments in low-energy nuclear physics. (D.C.W.)

21027 (CERN–65-32, pp 41-4) REACTOR NEUTRINO EXPERIMENT. Jenkins, T. L.; Reines, F. (Case Institute of Tech., Cleveland, Ohio).

A large liquid scintillator for the purpose of measuring the cross section for the reactions $\bar{\nu}_e + p \rightarrow n + \beta^+$ and $\bar{\nu}_e + D \rightarrow 2n + \beta^+$ in the energy range 2 Mev ≤ E_ν ≤ 10 Mev is discussed. Experimental results are also presented. (B.G.D.)

21028 (CERN–65-32, pp 65-70) THE PRODUCTION OF MUONS. Cowan, C. (Catholic Univ. of America, Washington, D. C.).

An investigation into the background produced in large detectors by neutrals from cosmic rays is presented. An experimental technique using a solid state plastic scintillator detector was developed to investigate the rate and mechanism of the muons produced by these neutrals. (B.G.D.)

21029 (CERN-65-32, pp 71-2) COSMIC-RAY INDUCED 'μ-e' EVENTS. Novey, T. B. (Argonne National Lab., Ill.).

A large liquid scintillator with an anticoincidence shield for investigating cosmic ray induced μ-e events is discussed. The event rate experimentally derived is compared to the events expected from the known cosmic muon spectrum. Experimental procedures and results for determining if the pions produced in the detector lead to μ-e decay are discussed. (B.G.D.)

21030 (CERN-65-32, pp 223-4) THE UTAH NEUTRINO DETECTOR. Keuffel, J. W. (Utah Univ., Salt Lake City. Dept. of Physics).

The development of a neutrino detector consisting of a cylindrical spark counter and water Cherenkov counters is discussed. A new method for obtaining the light from a Cherenkov counter is presented. (B.G.D.)

21031 (CERN-65-32, pp 231-40) PROPOSAL TO DETECT COSMIC-RAY NEUTRINOS THROUGH THE CERENKOV LIGHT OF PRODUCED MUONS. Ueberall, H.; Cowan, C. L. (Catholic Univ. of America, Washington, D. C.).

A proposal is presented for detection of cosmic ray neutrinos by suspending counters deep in the ocean and in large water-filled excavations in moderately deep mines. Brief descriptions of counter arrangements as well as figures for expected counting rates are presented. (B.G.D.)

21032 (CERN-65-32, pp 259-62) A LARGE HYDROGEN BUBBLE CHAMBER. Derrick, M. (Argonne National Lab., Ill.).

A description of the proposed 12 ft hydrogen bubble chamber at ANL is presented. This bubble chamber with the incorporation of the ZGS can be used for neutrino experiments with accelerator beam intensities and energies up to about 2 Bev. (B.G.D.)

21033 (CERN-65-32, pp 263-8) THE "GARGAMELLE" PROJECT. Lagarrigue, A. (Ecole Polytechnique, Paris (France)).

A description of the physical characteristics of a proposed large propane chamber is presented. The advantages of such a chamber are discussed as to the additional information provided by each event and the number of events largely increased. A brief summary of the types of experiments that can be carried out by this chamber and its technical aspects are presented. (B.G.D.)

21034 (EUR-2712,e) DESIGN CONSIDERATIONS AND CALCULATIONS FOR A ^{6}Li SEMICONDUCTOR SANDWICH FAST NEUTRON SPECTROMETER EXPERIMENT. Rydin, R. A. (European Atomic Energy Community, Ispra (Italy). Joint Nuclear Research Center). 1966. 24p. Dep. mn.

A semiconductor sandwich fast neutron spectrometer, using ^{6}Li as the sensitive material, is considered for use in a fission neutron type spectrum having a thermal neutron component. Calculations were made of the true coincidence background spectrum produced by reactions in the silicon of the diodes for various conditions of depletion depth and low level discriminator settings. Calculations were also made of the detection efficiency of the spectrometer for a low level discriminator bias set to discriminate against all thermal neutron caused events. (auth)

21035 (FEI-21) ANALIZ I OBOBSHCHENIE KORRELYATSIONNOGO METODA IZMERENIYA RASPREDELENIYA VREMENI ZHIZNI CHASTITS V FIZICHESKOI SISTEME. (Analysis and Generalization of Correlation Method for Measurement of Particle-Lifetime Distribution in Physical Systems). Zolotukhin, V. G.; Kutuzov, A. A.; Broder, D. L.; Kham'yanov, L. P.; Efimenko, B. A.; Zhilkin, A. S. (Gosudarstvennyi Komitet po Ispol'zovaniyu Atomnoi Energii SSSR, Obninsk. Fiziko-Energeticheskii Institut). 1965. 12p. Dep. mn.

A complete statistical analysis was given of the correlation method for the measurement of the distribution of particle lifetimes in linear physical systems. It was shown that the correlation method has significant advantages with respect to the current method of periodic pulse excitation in cases where the measurement is accompanied by high background. A new type of pseudo-random modulation of the particle source was suggested. (tr-auth)

21036 (JINR-P-2573) OSNOVNYE KHARAKTERISTIKI MAGNITNOGO SPEKTROMETRA S VARIATSIEI POLYA. (Basic Characteristics of a Magnetic Spectrometer With a Field Variation). Tarantin, N. I. (Joint Inst. for Nuclear Research, Dubna (USSR). Lab. of Nuclear Reactions). 1966. 17p. Dep. mn.

The basic ion-optical characteristics (dispersion and angular aberrations of the second order) of a possible spectrometer with a field variation are investigated for different types of spectrometers. (auth)

21037 (JINR-P-2594) ELEKTROFOTOGRAFICHESKAYA USTANOVKA DLYA OPREDELENIYA KOORDINAT TREKOV CHASTITS V ISKROVOI KAMERE. (An Electrophotographic Device for Evaluating Particle Track Coordinates in a Spark Chamber). Biryukov, V. A.; Promova, I. I.; Pisarev, A. F. (Joint Inst. for Nuclear Research, Dubna (USSR). Lab. of Nuclear Problems). 1966. 10p. Dep. mn.

A possibility is investigated of developing a device for filmless extraction of information from the spark chambers. The device involves a metallic drum whose external surface is covered with a layer of electrophotographic material. The spark projection leaves a potential well on this layer which is read off by a static transducer. It is shown experimentally that selenium and selenium-tellurium electrophotographic materials can be successfully used to construct this device. (auth)

21038 (K-1656) A DETECTOR FOR ALPHA RADIOACTIVITY IN FLOWING WATER. Seaborn, G. B. (Oak Ridge Gaseous Diffusion Plant, Tenn.). Apr. 19, 1966. Contract W-7405-eng-26. 16p. Dep. mn. CFSTI $1.00 cy, $0.50 mn.

A detector was developed for monitoring continuously the alpha radioactivity in flowing water. The instrument is capable of detecting alpha levels down to 1 percent of the maximum permissible concentration allowed for human consumption. The required maintenance is minimal, and it is suitable for location in a remote area. The design and test results are described. (auth)

21039 (KAPL-3122) FURTHER DEVELOPMENT OF A HIGH-SPEED ELECTRON-MULTIPLIER DISCRIMINATOR FOR MASS-SPECTROMETER ION DETECTION. Hance, A. B.; Hanrahan, L. R. (Knolls Atomic Power Lab., Schenectady, N. Y.). Feb. 21, 1966. Contract W-31-109-eng-52. 10p. Dep. mn. CFSTI $1.00 cy, $0.50 mn.

A solid-state high-speed discriminator-amplifier was designed to detect negative output pulses from a high-gain electron multiplier. The input threshold sensitivity is 2 to 4 mv, and the output circuit develops ~ -2.8 volts when loaded into 50 ohms. A continuous distribution of random amplitude pulses above the input threshold produces output pulses that have <1% amplitude modulation. When used in a mass-spectrometer ion-detection system, count rates up to several megahertz can be detected. The dead time for random-pulse detection is 12 nanosec or less. (auth)

21040 (ORNL-P-1218) MONITORING OF LEACHED FUEL ELEMENTS WITH A NEUTRON GENERATOR. Ross, W. J., Landry, J. W.; Strain, J. E. (Oak Ridge National Lab., Tenn.). [1962]. Contract W-7405-eng-26. 10p. Dep. mn. CFSTI $1.00 cy, $0.50 mn.

An apparatus was designed and constructed to detect milligram amounts of ^{235}U. The apparatus is used to monitor the removal of nuclear reactor fuel from spent fuel elements as part of a proposed process that involves segmentation of the metal cladding and dissolution of the fuel by acid leaches and aqueous rinses. The prototype can be readily adapted for remote controlled operation by elimination of the remaining manual operations. The same ap-

paratus can also be used to detect fissionable material in solutions. (P.C.H.)

21041 (PPAD-585E) CURRENT STATUS OF THE PRINCETON PATTERN RECOGNITION PROGRAM. Bazin, M. J.; Benoit, J. W. (Princeton-Pennsylvania Accelerator, Princeton, N. J.). Oct. 29, 1965. Contract AT(20-1)-2137. 21p. (CONF-651044-12). Dep. mn. CFSTI $1.00 cy, $0.50 mn.

From Conference on Programming for Flying Spot Devices, New York.

The general philosophy of the pattern recognition program at Princeton is discussed. A brief outline of specific methods used and some results obtained is presented. (M.O.W.)

21042 (SGAE-E-6/1966) A NEW METHOD FOR LOW-LEVEL SCINTILLATION-COUNTING. Patzelt, R.; Halling, H. (Oesterreichische Studiengesellschaft fuer Atomenergie G.m.b.H., Siebersdorf. Elektronikinstitut). Jan. 1966. 5p. Dep. mn.

A new method is suggested that makes pulse-shape discrimination between noise and scintillation pulses possible at reasonable high efficiency. This method combines the advantages of the two-multiplier-coincidence method with the simplicity of the methods using one multiplier. (M.O.W.)

21043 (UCRL-13199) STUDY OF PROBLEMS WITH ROSSI SWEEP APPLICATIONS. Final Report. Seibel, Robert C. (Montana State Univ., Bozeman. Electronics Research Lab.). Jan. 1966. Contract W-7405-eng-48. 79p. Dep. mn. CFSTI $3.00 cy, $0.50 mn.

For Univ. of California, Lawrence Radiation Lab., Livermore.

The two types of Rossi signal feed systems presently in use by LRL were analyzed and compared. The methods presently used by LRL for Rossi Signal coupling were studied. The maximum allowable Rossi oscillator signal distortion which the various Rossi mixing systems can tolerate was determined. The feasibility of transistorizing the Rossi oscillator circuits was investigated. The feasibility of a phase-locked Rossi oscillator system and an oscillator unit integral with each oscilloscope was investigated. An experimental Rossi mixer unit is presented which was found to possess extremely high distortion toleration capabilities. (M.O.W.)

21044 (ANL-Trans-285) DEVELOPMENT OF GLASSES FOR LOW BACKGROUND MEASUREMENTS—CHARACTERISTICS OF GLASSES. Sakurai, Junji; Shibata, Sinkichi; Yamagoshi, Kazuo. (Institute for Nuclear Study, Tokyo Univ. (Japan)). Translated for Argonne National Lab., Ill., from report INS-TCA-20. 18p. Dep. mn. JCL $1.60 fs, $0.80 mf.

The development of glasses for low background measurements, especially for liquid scintillation countings, is reported. Potassium oxide contents and reproducibility, Ra contents, transparency for blue-violet lights and refractive index, phosphorescence output from glasses, aging effect due to alkalis, and other applications of glasses are discussed. (P.C.H.)

21045 AUTOMATIC-READING ELECTRONIC EQUIPMENT FOR MULTIPLE MEASUREMENTS OF RADIOACTIVITY. Izquierdo, Jesus Sanchez; Tanarro, Agustin (Junta de Energia Nuclear, Madrid). An. Real Soc. Espan. Fis. Quim. (Madrid), Ser. A, 61: 281-92(Sept.-Oct. 1965). (In Spanish).

Transistorized equipment for automatically controlling and reading out a set of up to 15 decimal scalers is described. Results are given in punched tape including signals for controlling punched tape-punched card converter for a digital computer, as well as a direct-reading electric typewriter. (auth)

21046 STUDY OF THE RADIOLUMINESCENT EFFECT OF SOME LIQUID SCINTILLATORS IN MIXTURE WITH ALCOHOL. Tibu, Margareta. An. Stiint. Univ. A. I. Cuza, Iasi, Sect. I, 11: 73-6(1965). (In Rumanian).

The scintillation characteristics of diphenyloxazole in different solvents, the effect of added alcohol, and the geometric conditions were studied. (tr-auth)

21047 THE MEASUREMENT OF GAMMA EMITTERS IN PIPE LINES. Plesch, Rolf (Siemens and Halske AG, Karlsruhe, Ger.). Atomkernenergie, 11: 141-8(Mar.-Apr. 1966). (In German).

With regard to the monitoring of gamma emitters in reactor pipe lines approximations are given for the estimation of pulse rates near the pipe. The considerations contain the influence of the wall-absorption and the selfabsorption and are further applicable to straight and circular curved pipe lines with homogeneously distributed gamma activities. The purpose is to enable the effective planning of measuring equipments. Since GM-counters are in most cases too insensitive and large scintillation counters too expensive, only the scintillation crystal with 1'' diameter and 1'' height is considered. But the equations are given in such a general manner that also larger crystals are principally applicable. The use of the approximations is illustrated by the calculation of examples. (auth)

21048 A COMPARISON OF SPARK CHAMBER PROPERTIES FOR TWO DIFFERENT TRIGGERING MODES. Allkofer, O. C.; Kraft, E. (Univ., Kiel). Atomkernenergie, 11: 149-54(Mar.-Apr. 1966). (In German).

Data are given on the efficiency and accuracy of track localization in spark chambers filled with a mixture of argon and acetone vapor and triggered by two different methods. When the spark chamber is triggered with primary ionization, the mean displacement of the spark from the particle track in the chamber is $\sigma = 0.52$ mm and by triggering in the avalanche $\sigma = 0.30$ mm. The relation between the accuracy of track location and the track angle was examined and it was found that the accuracy decreases with increasing track angle for both cases of the triggering modes. When the triggering pulse was delayed, the value of σ increases in primary ionization, where it is constant in the avalanche. The efficiency of the spark chamber increases rapidly with the voltage across the chamber and reaches a value of 95% for both triggering modes. When the high voltage pulse is delayed, the efficiency decreases more rapidly in the primary ionization than in avalanche. (auth)

21049 LITHIUM BORATE SINGLE CRYSTALS AS NEUTRON DETECTORS. Seidl, E.; Schwertfuehrer, W. (Oesterreichische Hochschule, Vienna). Atomkernenergie, 11: 155-62(Mar.-Apr. 1966). (In German).

Single crystals of the structure $Li_2O \cdot B_2O_3$ and $Li_2O \cdot 2B_2O_3$ were investigated with respect to their use as neutron detectors. The neutrons were detected through a change in the electric conductivity as irradiated in the core of the reactor TRIGA Mark II. It was possible to grow large single crystals. After preparation the crystals were put in a specific container for irradiation. Because of the irradiation within the core it was necessary to examine very carefully the effects of the high gamma-flux. Neutron-irradiation caused both a change of the electric conductivity and change of the sensitivity of the detectors. Especially in single crystals of lithium-metaborate ($Li_2O \cdot B_2O_3$) there were changes of the electric properties of the crystals, which were of good use for practical applications. The thermal neutron flux was measured between 10^8 to 2×10^{12} n/cm^{2}sec with a very good linear dependence. The upper limit was given through the maximum of reactor power. The contribution of the gamma rays to the measurement was only about 1%. The electric effects of irradiation are discussed with the help of the energy gap model. (auth)

21050 COMPARISON OF BURNUP DETERMINATIONS BY MEANS OF MONITOR-ACTIVATION AND GAMMA SPECTROSCOPY FOR AN MTR ELEMENT. Buba, L.; Hick, H.; Rumpold, K. (Oesterreichische Studiengesellschaft fuer Atomenergie GmbH, Vienna). Atomkernenergie, 11: 167-72(Mar.-Apr. 1966). (In German).

A semiconductor Compton spectrometer was developed

which allows nondestructive burnup determination of fuel elements. To test the reliability of such a measurement a partial fuel element of the ASTRA-reactor was prepared with monitor wires and irradiated. After irradiation the monitor wires were removed remotely and their activity measured. By neutron-physical evaluation the fuel-element burnup could be calculated. Then the burnup of the fuel element was determined by means of a Compton spectrometer too. The two results of 37.6 mg and 36.1 mg for the amount of ^{235}U consumed agree very well. The error of a burnup determination with the semiconductor Compton spectrometer should therefore be $\sigma \leqq 15\%$. (auth)

21051 CONSTRUCTION OF A THIN-LENS TYPE BETA-RAY SPECTROMETER. Tanabe, Tetsumi; Kokame, Jun; Ishiwari, Ryutaro. Bull. Inst. Chem. Res., Kyoto Univ., 43: 315-22(Sept. 1965).

A thin-lens-type beta spectrometer was designed and constructed. Two designs were developed, in which the focal length of the magnetic lens was 15 and 30 cm, respectively. The parameters and the properties of this spectrometer are given. (auth)

21052 TIME RESOLUTION OF A TRANSISTORIZED TIME-OF-FLIGHT SYSTEM. Matsuki, Seishi; Yamashita, Sukeaki; Miyake, Kozo. Bull. Inst. Chem. Res., Kyoto Univ., 43: 330-8(Sept. 1965).

Construction and performance of a transistorized time-of-flight system are described. Timing signals are obtained from a discriminator in which a fast tunnel diode is used, and the time intervals between two signals are converted to pulse heights by a time-to-pulse height converter of Culligan and Lipman type. The time resolution obtained with pulses from a standard mercury pulser is less than 10^{-10} sec in full width at half maximum. The full width at half maximum of a ^{60}Co γ-γ coincidence curve was 1.48×10^{-9} sec, using two photomultipliers coupled with thick plastic scintillators 65 mm in dia, 60 mm thick and 50 mm in dia, 60 mm thick, respectively. A comparison with theoretical estimations of the time resolution was made, and several causes of the finite time resolution are discussed. (auth)

21053 MEASUREMENT OF THE THERMAL NEUTRON FLUX AND ESTIMATION OF THE EPITHERMAL NEUTRON FLUX BY RADIOACTIVATION OF ^{197}Au. Peetermans, A. (Univ., Liege). Bull. Soc. Roy. Sci. Liege, 34: 726-35 (1965). (In French).

Gold is a very interesting detector for the measurement of thermal and epithermal neutron fluxes. In effect, the natural abundance of ^{197}Au is 100%, its activation cross section is relatively large, and the period of the isotope ^{198}Au formed by the reaction $^{197}Au(n,\gamma)$ is not too long. Moreover the decay scheme of the isotope ^{198}Au is very simple and convenient for the measurement of the induced activity by β-γ coincidence counting. The different correction factors which intervene in the β-γ coincidence counting are small or can be made small if the surface density of the gold windows is less than 50 mg/cm^2. The absolute activities, determined by β-γ coincidence counting, makes it possible to calculate the counting efficiency of a β detector with low background and using very low thermal neutron densities. The thermal neutron flux of a 2 C source of Pu–Be, surrounded by 10 cm polyethylene was measured and the epithermal flux was estimated. The measurements showed that the sum of the thermal and epithermal flux is approximately 40% of the total neutron flux. (tr-auth)

21054 A dE/dx-E CHARGED-PARTICLE SPECTROMETER FOR STUDYING NEUTRON-INDUCED REACTIONS. Wang, Wei-Noon (Tsing Hua Univ., Hsinchu, Taiwan). Chin. J. Phys. (Taiwan), 3: 75-89(Oct. 1965).

A dE/dx-E counter telescope with a silicon surface-barrier detector was constructed for measuring energies and angular distributions of the charged particles produced in reaction with 14-Mev neutrons. The detecting efficiency, particle discrimination, angular definition, counting rate and background were considered and discussed. Actually performance of the counter is presented. (auth)

21055 AUTOMATIC ELECTRONIC EQUIPMENT FOR THE MULTIPLE MEASUREMENTS OF RADIOACTIVITY. Sanchez Izquierdo, Jesus; Tanarro Sanz, Agustin (Junta de Energia Nuclear, Madrid). Energ. Nucl. (Madrid), 9: 421-36(Nov.-Dec. 1965). (In Spanish).

In many nuclear physics experiments it is necessary to measure with relative precision a large number of radiation samples or probes. For such studies detection equipment for β activities was constructed with multiple detectors capable of making a large number of measurements automatically and of presenting the results in a form usable by a digital computer. The apparatus consists of an electromechanical device in conjunction with radiation detectors and of an electronic auxiliary, which counts and records the proportional pulses in each case for the different detectors and records the data on perforated tape. Its basic characteristics and the principle of operation are given. The operation and efficiency of the electronic device are discussed. (J.S.R.)

21056 INVESTIGATION OF ATOMIC ENERGY COUNTERMEASURES. II. MEASUREMENT OF COLLIMATED RADIATIONS BY A GM COUNTER AND A SCINTILLATION COUNTER, AND THEIR COUNTING EFFICIENCIES. Yuhara, Jiro. Giho (Res. Devel. Headquart., Jap. Def. Agency), 3: 21-70(Nov. 1965). (In Japanese).

The results of experiments performed to determine the optimum entry point for radiation being measured by a GM counter or a scintillation counter are presented. For gamma rays entering the side rather than the end of the counter, higher counting efficiency was noted. If collimated gamma rays are measured by a scintillation counter, that part of the counter where the radiation enters should receive the radiation at right angles to the beam axis. (TCO)

21057 THERMAL ANNEALING EFFECTS ON THE THERMOLUMINESCENCE OF LiF. Zimmerman, D. W.; Rhyner, C. R.; Cameron, J. R. (Univ. of Wisconsin, Madison). Contract 11-1105. Health Phys., 12: 525-31 (Apr. 1966).

Isothermal annealing before or after irradiation is found to have a definite effect upon the thermoluminescent glow curve of LiF (TLD-100). Post-irradiation annealing, by thermally releasing electrons from their traps, reduces the size of each peak in the glow curve. The two main dosimetry peaks each have a simple exponential decay consistent with the model of Randall and Wilkins, indicating trap depths of 1.19 and 1.25 ev respectively with frequency factors between 10^{11} and 10^{12}sec^{-1}. Pre-irradiation annealing at 80°C for 24 hr reduces the area of the low temperature peaks by a factor of 10, while annealing at 125°C, 145°C or 175°C for 3 hr reduces the area of the main dosimetry peaks by a factor of 2 to 5 and increases the height of one of the low temperature peaks by a factor of 1½ to 3. The rate of cooling from temperatures greater than about 150°C affects the glow curve also. Rapid cooling in times of the order of seconds increases the heights of the low temperature peaks up to a factor of 4 compared to cooling in several minutes or more. (auth)

21058 TECHNIQUE FOR RECOIL FISSION-FRAGMENT RANGE MEASUREMENTS. Anderson, Donald Gene (U. S. Atomic Energy Commission, Albuquerque, N. Mex.). Health Phys., 12: 557-61(Apr. 1966).

A method was devised for the rapid analysis of gamma activities from the recoil fission fragments of fissile materials. The gamma spectra and range of the recoils are important in the detection of reactor fuel element rupture and in fuel element design. (auth)

21059 NEUTRON AND GAMMA SENSITIVITIES OF DYNAMIC DETECTORS. Martin, J. A.; Shatzkes, M.; Kloepper, R. M. IEEE (Inst. Elec. Electron. Eng.), Trans. Nucl. Sci., NS-12: 101-11(Oct. 1965).

The neutron and gamma sensitivities of nine detectors were studied in experiments performed at the Sandia Pulsed Reactor (SPR). Six of the detectors tested are predominantly gamma detectors at the SPR and three produce a significant fraction of their total current due

to the neutron flux during a normal SPR burst. None of the detectors studied were found to be predominantly sensitive to the neutron flux during a normal SPR burst. Tests performed at pure gamma sources on a pin diode detector are also described. The neutron induced current in the silicon detectors is treated theoretically. The pin response characteristics, and the relative neutron and gamma sensitivity of the radiation detectors are considered. (J.F.P.)

21060 THE CORPUSCULAR PHOTOGRAPHY AND SPATIAL IONOGRAPHY GROUP OF THE STRASBOURG NUCLEAR RESEARCH CENTER. Schmitt, R. (Univ. of Lyon). Ind. At., 10: 55-62(1966). (In French).

The research carried out by the group for corpuscular photography and spatial ionography of the Department of Corpuscular Physics in the Strasbourg Center of Nuclear Research is basically concentrated on three activities: the study and the perfecting of corpuscular photography, in particular by the use of the electronic microscope for the observation of traces; the use of other solid detectors such as monocrystals of silver chloride, micas and plastics and, lastly the study of primary cosmic radiation, especially in the case of the very heavy primary ions. (auth)

21061 PROBLEMS OF READER DESIGN AND MEASUREMENT ERROR IN LITHIUM FLUORIDE THERMOLUMINESCENT DOSIMETRY. Karzmark, C. J. (Stanford Univ., Palo Alto, Calif.); Fowler, J. F.; White, J. T. Int. J. Appl. Radiat. Isotop., 17: 161-73(Mar. 1966).

Lithium fluoride thermoluminescent dosimetry is undergoing rapid development in instrumentation, application, and fundamental investigations. A number of reader design and operation problems and their relevancy to measurement error are discussed. These include: effects relating to the precision of dispensing the powder, a geometrical analysis pertinent to the positioning of powder in the readout tray, infrared and tribothermoluminescence contributions and their relation to heating and readout cycle termination, powder reuse, photomultiplier fatigue and related considerations, some cautions to observe in using light standards for sensitivity checks and the presence of significant fading in certain LiF phosphors if readout is delayed more than a day or two after exposure. Operational problems in using readers are best resolved with the aid of glow curves. Systems that permit simultaneous recording of the glow curve, its integral, and the temperature are more amenable to the analytical solution of readout problems than those that do not provide this facility. (auth)

21062 APPLICATION OF THE X-RAY GAMMA-RAY DOSIMETER VA-J-15 IN RADIOLOGICAL PROTECTION. Schubert, G. (VEB Vakutronik, Dresden). Isotopenpraxis, 1: 129-30(Dec. 1965). (In German).

The characteristics of the Va-J-15 x-γ dosimeter are tabulated. The areas of applicability of this dosimeter are indicated. (J.S.R.)

21063 A TRIGGERED CLOUD CHAMBER FOR THE INVESTIGATION OF LOW ENERGY NUCLEAR REACTIONS INDUCED BY CHARGED PARTICLES. MacLeod, A. M.; Reid, J. M. (Univ., Glasgow). J. Sci. Instrum., 42: 856-61(Dec. 1965).

A cloud chamber system triggered by a combination of proportional and scintillation counters is described in detail. Triggering is designed to take place when one incident particle fails to emerge from the chamber. The performance of the system when used with a beam of protons from the $^3He(d,p)^4He$ reaction to investigate nuclear disintegrations in nitrogen is described and discussed. (auth)

21064 THE DESIGN AND APPLICATION OF LITHIUM-DRIFT SILICON DIODES AS NUCLEAR RADIATION DETECTORS. Gibbons, P. E.; Blamires, N. G. (Atomic Energy Research Establishment, Harwell, Eng.). J. Sci. Instrum., 42: 862-4(Dec. 1965). (AERE-R-4948).

A range of lithium-drifted silicon radiation detectors is described. Areas up to 8 cm^2 and thicknesses up to 0.6 cm were achieved. At $-20°C$, a resolution of 8 kev full width half maximum was obtained on 661 kev beta particles using a 1 cm^2 detector 0.1 cm thick. The performance of the detectors is discussed in relation to other device parameters. (auth)

21065 COUNTING OF TRITIUM WITH A THIN-WINDOWED GEIGER-MUELLER COUNTER TUBE. Seimiya, T.; Sekine, K.; Sasaki, T. (Tokyo Metropolitan Univ.). J. Sci. Instrum., 42: 906-7(Dec. 1965).

A thin film (10–40 $\mu g\ cm^{-2}$) of polycarbonate treated with polyvinyl alcohol was prepared and used as a Geiger-Müller tube window. The counting efficiency of this tube for a tritium sample was 6 to 15% of that for the same source obtained by using the windowless 2π counter. A Geiger-Müller tube of 17 $\mu g\ cm^{-2}$ window thickness proved satisfactory for tritium counting. (auth)

21066 A LOW-BACKGROUND IONIZER FOR MOLECULAR BEAM DETECTION. Pendlebury, J. M.; Smith, K. F. (Univ., Sussex, Eng.). J. Sci. Instrum., 43: 6-10 (Jan. 1966).

An electron bombardment ionizer for detecting molecular beams is described. It is used in conjunction with a 90° magnetic focusing mass spectrometer and an electron multiplier and counting system. A fairly simple electrode arrangement is used but the method of construction is such that the output of residual ions is very small. For many types of beams a minimum input of 10^5 neutrals per sec can be detected when the integration time is 100 sec. The overall efficiency calculated from a variety of measurements is about one count for every 3×10^4 neutrals. Some discussion of the nature and origin of the residual ions is included. (auth)

21067 A TRANSISTORIZED RADON MEASURING EQUIPMENT. Roberts, P. B.; Davies, B. L. (Radiological Protection Service, Sutton, Eng.). J. Sci. Instrum., 43: 32-5(Jan. 1966).

An apparatus is described for the simultaneous measurement of three samples of radon at activities ranging from 5×10^{-14} to 3×10^{-8} curie. The method used is electrostatic collection of the radon decay products followed by alpha scintillation counting. The equipment is transistorized and constructed in small circuit modules, making it compact, readily transportable and easy to maintain. (auth)

21068 AN ISOTHERMAL MICROCALORIMETER OPERATED IN A WATER TRIPLE-POINT CELL AND DESIGNED FOR RADIOACTIVITY MEASUREMENTS. Lowenthal, G. C.; Hicks, R. M. (Australian Atomic Energy Commission, Lucas Heights, New South Wales, Australia). J. Sci. Instrum., 43: 36-8(Jan. 1966).

The construction and operation of an isothermal microcalorimeter are described. The instrument relies on the triple point of water for the maintenance of the constant temperature envelope. This ensures a temperature stability to ±0.0001°C. Thermistor thermometry is used and the smallest detectable temperature change in the calorimeter is 0.00012°C corresponding to a power change of 0.5 μw. The microcalorimeter was employed for the measurement of alpha and beta emitting radioactivities; for example, an activity of about 4 Ci of tritiated water was measured with an estimated accuracy to ±2.5%. (auth)

21069 A SIMPLE TANDEM MOESSBAUER SPECTROMETER USING PULSE-HEIGHT ANALYSIS. Cooper, J. D.; Greenwood, N. N. (Univ., Newcastle upon Tyne, Eng.). J. Sci. Instrum., 43: 71-3(Jan. 1966).

A system is described whereby, using a multichannel analyzer in pulse height analysis mode, two Mössbauer spectra may be obtained simultaneously in about 200 channels each, with a baseline constant to ±0.2%. (auth)

21070 NUMERICAL PHOTOMETER FOR FILM DOSIMETRY. Hekrdle, Jan (Inst. of Nuclear Research, Czechoslovak Academy of Sciences, Rez). Jad. Energ., 11: 452-5(Dec. 1965). (In Czech).

An instrument was developed for use in film dosimetry by a differential method. The essential feature is two photoelectric cells on which light from an electric bulb falls, in one case passing through the film whose blacken-

which allows nondestructive burnup determination of fuel elements. To test the reliability of such a measurement a partial fuel element of the ASTRA-reactor was prepared with monitor wires and irradiated. After irradiation the monitor wires were removed remotely and their activity measured. By neutron-physical evaluation the fuel-element burnup could be calculated. Then the burnup of the fuel element was determined by means of a Compton spectrometer too. The two results of 37.6 mg and 36.1 mg for the amount of ^{235}U consumed agree very well. The error of a burnup determination with the semiconductor Compton spectrometer should therefore be $\sigma \leqq 15\%$. (auth)

21051 CONSTRUCTION OF A THIN-LENS TYPE BETA-RAY SPECTROMETER. Tanabe, Tetsumi; Kokame, Jun; Ishiwari, Ryutaro. Bull. Inst. Chem. Res., Kyoto Univ., 43: 315-22(Sept. 1965).

A thin-lens-type beta spectrometer was designed and constructed. Two designs were developed, in which the focal length of the magnetic lens was 15 and 30 cm, respectively. The parameters and the properties of this spectrometer are given. (auth)

21052 TIME RESOLUTION OF A TRANSISTORIZED TIME-OF-FLIGHT SYSTEM. Matsuki, Seishi; Yamashita, Sukeaki; Miyake, Kozo. Bull. Inst. Chem. Res., Kyoto Univ., 43: 330-8(Sept. 1965).

Construction and performance of a transistorized time-of-flight system are described. Timing signals are obtained from a discriminator in which a fast tunnel diode is used, and the time intervals between two signals are converted to pulse heights by a time-to-pulse height converter of Culligan and Lipman type. The time resolution obtained with pulses from a standard mercury pulser is less than 10^{-10} sec in full width at half maximum. The full width at half maximum of a ^{60}Co γ-γ coincidence curve was 1.48×10^{-9} sec, using two photomultipliers coupled with thick plastic scintillators 65 mm in dia, 60 mm thick and 50 mm in dia, 60 mm thick, respectively. A comparison with theoretical estimations of the time resolution was made, and several causes of the finite time resolution are discussed. (auth)

21053 MEASUREMENT OF THE THERMAL NEUTRON FLUX AND ESTIMATION OF THE EPITHERMAL NEUTRON FLUX BY RADIOACTIVATION OF ^{197}Au. Peetermans, A. (Univ., Liege). Bull. Soc. Roy. Sci. Liege, 34: 726-35 (1965). (In French).

Gold is a very interesting detector for the measurement of thermal and epithermal neutron fluxes. In effect, the natural abundance of ^{197}Au is 100%, its activation cross section is relatively large, and the period of the isotope ^{198}Au formed by the reaction $^{197}Au(n,\gamma)$ is not too long. Moreover the decay scheme of the isotope ^{198}Au is very simple and convenient for the measurement of the induced activity by β-γ coincidence counting. The different correction factors which intervene in the β-γ coincidence counting are small or can be made small if the surface density of the gold windows is less than 50 mg/cm^2. The absolute activities, determined by β-γ coincidence counting, makes it possible to calculate the counting efficiency of a β detector with low background and using very low thermal neutron densities. The thermal neutron flux of a 2 C source of Pu–Be, surrounded by 10 cm polyethylene was measured and the epithermal flux was estimated. The measurements showed that the sum of the thermal and epithermal flux is approximately 40% of the total neutron flux. (tr-auth)

21054 A dE/dx-E CHARGED-PARTICLE SPECTROMETER FOR STUDYING NEUTRON-INDUCED REACTIONS. Wang, Wei-Noon (Tsing Hua Univ., Hsinchu, Taiwan). Chin. J. Phys. (Taiwan), 3: 75-89(Oct. 1965).

A dE/dx-E counter telescope with a silicon surface-barrier detector was constructed for measuring energies and angular distributions of the charged particles produced in reaction with 14-Mev neutrons. The detecting efficiency, particle discrimination, angular definition, counting rate and background were considered and discussed. Actually performance of the counter is presented. (auth)

21055 AUTOMATIC ELECTRONIC EQUIPMENT FOR THE MULTIPLE MEASUREMENTS OF RADIOACTIVITY. Sanchez Izquierdo, Jesus; Tanarro Sanz, Agustin (Junta de Energia Nuclear, Madrid). Energ. Nucl. (Madrid), 9: 421-36(Nov.-Dec. 1965). (In Spanish).

In many nuclear physics experiments it is necessary to measure with relative precision a large number of radiation samples or probes. For such studies detection equipment for β activities was constructed with multiple detectors capable of making a large number of measurements automatically and of presenting the results in a form usable by a digital computer. The apparatus consists of an electromechanical device in conjunction with radiation detectors and of an electronic auxiliary, which counts and records the proportional pulses in each case for the different detectors and records the data on perforated tape. Its basic characteristics and the principle of operation are given. The operation and efficiency of the electronic device are discussed. (J.S.R.)

21056 INVESTIGATION OF ATOMIC ENERGY COUNTERMEASURES. II. MEASUREMENT OF COLLIMATED RADIATIONS BY A GM COUNTER AND A SCINTILLATION COUNTER, AND THEIR COUNTING EFFICIENCIES. Yuhara, Jiro. Giho (Res. Devel. Headquart., Jap. Def. Agency), 3: 21-70(Nov. 1965). (In Japanese).

The results of experiments performed to determine the optimum entry point for radiation being measured by a GM counter or a scintillation counter are presented. For gamma rays entering the side rather than the end of the counter, higher counting efficiency was noted. If collimated gamma rays are measured by a scintillation counter, that part of the counter where the radiation enters should receive the radiation at right angles to the beam axis. (TCO)

21057 THERMAL ANNEALING EFFECTS ON THE THERMOLUMINESCENCE OF LiF. Zimmerman, D. W.; Rhyner, C. R.; Cameron, J. R. (Univ. of Wisconsin, Madison). Contract 11-1105. Health Phys., 12: 525-31 (Apr. 1966).

Isothermal annealing before or after irradiation is found to have a definite effect upon the thermoluminescent glow curve of LiF (TLD-100). Post-irradiation annealing, by thermally releasing electrons from their traps, reduces the size of each peak in the glow curve. The two main dosimetry peaks each have a simple exponential decay consistent with the model of Randall and Wilkins, indicating trap depths of 1.19 and 1.25 ev respectively with frequency factors between 10^{11} and 10^{12}sec^{-1}. Pre-irradiation annealing at 80°C for 24 hr reduces the area of the low temperature peaks by a factor of 10, while annealing at 125°C, 145°C or 175°C for 3 hr reduces the area of the main dosimetry peaks by a factor of 2 to 5 and increases the height of one of the low temperature peaks by a factor of 1½ to 3. The rate of cooling from temperatures greater than about 150°C affects the glow curve also. Rapid cooling in times of the order of seconds increases the heights of the low temperature peaks up to a factor of 4 compared to cooling in several minutes or more. (auth)

21058 TECHNIQUE FOR RECOIL FISSION-FRAGMENT RANGE MEASUREMENTS. Anderson, Donald Gene (U. S. Atomic Energy Commission, Albuquerque, N. Mex.). Health Phys., 12: 557-61(Apr. 1966).

A method was devised for the rapid analysis of gamma activities from the recoil fission fragments of fissile materials. The gamma spectra and range of the recoils are important in the detection of reactor fuel element rupture and in fuel element design. (auth)

21059 NEUTRON AND GAMMA SENSITIVITIES OF DYNAMIC DETECTORS. Martin, J. A.; Shatzkes, M.; Kloepper, R. M. IEEE (Inst. Elec. Electron. Eng.), Trans. Nucl. Sci., NS-12: 101-11(Oct. 1965).

The neutron and gamma sensitivities of nine detectors were studied in experiments performed at the Sandia Pulsed Reactor (SPR). Six of the detectors tested are predominantly gamma detectors at the SPR and three produce a significant fraction of their total current due

to the neutron flux during a normal SPR burst. None of the detectors studied were found to be predominantly sensitive to the neutron flux during a normal SPR burst. Tests performed at pure gamma sources on a pin diode detector are also described. The neutron induced current in the silicon detectors is treated theoretically. The pin response characteristics, and the relative neutron and gamma sensitivity of the radiation detectors are considered. (J.F.P.)

21060 THE CORPUSCULAR PHOTOGRAPHY AND SPATIAL IONOGRAPHY GROUP OF THE STRASBOURG NUCLEAR RESEARCH CENTER. Schmitt, R. (Univ. of Lyon). Ind. At., 10: 55-62(1966). (In French).

The research carried out by the group for corpuscular photography and spatial ionography of the Department of Corpuscular Physics in the Strasbourg Center of Nuclear Research is basically concentrated on three activities: the study and the perfecting of corpuscular photography, in particular by the use of the electronic microscope for the observation of traces; the use of other solid detectors such as monocrystals of silver chloride, micas and plastics and, lastly the study of primary cosmic radiation, especially in the case of the very heavy primary ions. (auth)

21061 PROBLEMS OF READER DESIGN AND MEASUREMENT ERROR IN LITHIUM FLUORIDE THERMOLUMINESCENT DOSIMETRY. Karzmark, C. J. (Stanford Univ., Palo Alto, Calif.); Fowler, J. F.; White, J. T. Int. J. Appl. Radiat. Isotop., 17: 161-73(Mar. 1966).

Lithium fluoride thermoluminescent dosimetry is undergoing rapid development in instrumentation, application, and fundamental investigations. A number of reader design and operation problems and their relevancy to measurement error are discussed. These include: effects relating to the precision of dispensing the powder, a geometrical analysis pertinent to the positioning of powder in the readout tray, infrared and tribothermoluminescence contributions and their relation to heating and readout cycle termination, powder reuse, photomultiplier fatigue and related considerations, some cautions to observe in using light standards for sensitivity checks and the presence of significant fading in certain LiF phosphors if readout is delayed more than a day or two after exposure. Operational problems in using readers are best resolved with the aid of glow curves. Systems that permit simultaneous recording of the glow curve, its integral, and the temperature are more amenable to the analytical solution of readout problems than those that do not provide this facility. (auth)

21062 APPLICATION OF THE X-RAY GAMMA-RAY DOSIMETER VA-J-15 IN RADIOLOGICAL PROTECTION. Schubert, G. (VEB Vakutronik, Dresden). Isotopenpraxis, 1: 129-30(Dec. 1965). (In German).

The characteristics of the Va-J-15 x-γ dosimeter are tabulated. The areas of applicability of this dosimeter are indicated. (J.S.R.)

21063 A TRIGGERED CLOUD CHAMBER FOR THE INVESTIGATION OF LOW ENERGY NUCLEAR REACTIONS INDUCED BY CHARGED PARTICLES. MacLeod, A. M.; Reid, J. M. (Univ., Glasgow). J. Sci. Instrum., 42: 856-61(Dec. 1965).

A cloud chamber system triggered by a combination of proportional and scintillation counters is described in detail. Triggering is designed to take place when one incident particle fails to emerge from the chamber. The performance of the system when used with a beam of protons from the $^3He(d,p)^4He$ reaction to investigate nuclear disintegrations in nitrogen is described and discussed. (auth)

21064 THE DESIGN AND APPLICATION OF LITHIUM-DRIFT SILICON DIODES AS NUCLEAR RADIATION DETECTORS. Gibbons, P. E.; Blamires, N. G. (Atomic Energy Research Establishment, Harwell, Eng.). J. Sci. Instrum., 42: 862-4(Dec. 1965). (AERE-R-4948).

A range of lithium-drifted silicon radiation detectors is described. Areas up to 8 cm^2 and thicknesses up to 0.6 cm were achieved. At −20°C, a resolution of 8 kev full width half maximum was obtained on 661 kev beta particles using a 1 cm^2 detector 0.1 cm thick. The performance of the detectors is discussed in relation to other device parameters. (auth)

21065 COUNTING OF TRITIUM WITH A THIN-WINDOWED GEIGER-MUELLER COUNTER TUBE. Seimiya, T.; Sekine, K.; Sasaki, T. (Tokyo Metropolitan Univ.). J. Sci. Instrum., 42: 906-7(Dec. 1965).

A thin film (10−40 μg cm^{-2}) of polycarbonate treated with polyvinyl alcohol was prepared and used as a Geiger-Müller tube window. The counting efficiency of this tube for a tritium sample was 6 to 15% of that for the same source obtained by using the windowless 2π counter. A Geiger-Müller tube of 17 μg cm^{-2} window thickness proved satisfactory for tritium counting. (auth)

21066 A LOW-BACKGROUND IONIZER FOR MOLECULAR BEAM DETECTION. Pendlebury, J. M.; Smith, K. F. (Univ., Sussex, Eng.). J. Sci. Instrum., 43: 6-10 (Jan. 1966).

An electron bombardment ionizer for detecting molecular beams is described. It is used in conjunction with a 90° magnetic focusing mass spectrometer and an electron multiplier and counting system. A fairly simple electrode arrangement is used but the method of construction is such that the output of residual ions is very small. For many types of beams a minimum input of 10^5 neutrals per sec can be detected when the integration time is 100 sec. The overall efficiency calculated from a variety of measurements is about one count for every 3×10^4 neutrals. Some discussion of the nature and origin of the residual ions is included. (auth)

21067 A TRANSISTORIZED RADON MEASURING EQUIPMENT. Roberts, P. B.; Davies, B. L. (Radiological Protection Service, Sutton, Eng.). J. Sci. Instrum., 43: 32-5(Jan. 1966).

An apparatus is described for the simultaneous measurement of three samples of radon at activities ranging from 5×10^{-14} to 3×10^{-8} curie. The method used is electrostatic collection of the radon decay products followed by alpha scintillation counting. The equipment is transistorized and constructed in small circuit modules, making it compact, readily transportable and easy to maintain. (auth)

21068 AN ISOTHERMAL MICROCALORIMETER OPERATED IN A WATER TRIPLE-POINT CELL AND DESIGNED FOR RADIOACTIVITY MEASUREMENTS. Lowenthal, G. C.; Hicks, R. M. (Australian Atomic Energy Commission, Lucas Heights, New South Wales, Australia). J. Sci. Instrum., 43: 36-8(Jan. 1966).

The construction and operation of an isothermal microcalorimeter are described. The instrument relies on the triple point of water for the maintenance of the constant temperature envelope. This ensures a temperature stability to ±0.0001°C. Thermistor thermometry is used and the smallest detectable temperature change in the calorimeter is 0.00012°C corresponding to a power change of 0.5 μw. The microcalorimeter was employed for the measurement of alpha and beta emitting radioactivities; for example, an activity of about 4 Ci of tritiated water was measured with an estimated accuracy to ±2.5%. (auth)

21069 A SIMPLE TANDEM MOESSBAUER SPECTROMETER USING PULSE-HEIGHT ANALYSIS. Cooper, J. D.; Greenwood, N. N. (Univ., Newcastle upon Tyne, Eng.). J. Sci. Instrum., 43: 71-3(Jan. 1966).

A system is described whereby, using a multichannel analyzer in pulse height analysis mode, two Mössbauer spectra may be obtained simultaneously in about 200 channels each, with a baseline constant to ±0.2%. (auth)

21070 NUMERICAL PHOTOMETER FOR FILM DOSIMETRY. Hekrdle, Jan (Inst. of Nuclear Research, Czechoslovak Academy of Sciences, Rez). Jad. Energ., 11: 452-5(Dec. 1965). (In Czech).

An instrument was developed for use in film dosimetry by a differential method. The essential feature is two photoelectric cells on which light from an electric bulb falls, in one case passing through the film whose blacken-

ing is to be measured. The two currents generated are compared to give a quantitative measurement of the film density; variations in the voltage to the light source thus have no effect on the determination of current. Photographs of the equipment and block and circuit diagrams are shown. The apparatus was operated for one year and has been shown to be sturdy and reliable. The reproducibility of the film density (D = log I_0/I) measurements were shown experimentally to be ±0.0025D for densities in the range 0.00 to 1.00, and for the highest levels of D measured (D = 3) to be no greater than ±0.01D. (TTT)

21071 HIGH-EFFICIENCY GAS CHERENKOV COUNTER. **Kifune, Tadashi; Kimura, Yoshitaka; Suzuki, Toshio (Tokyo Univ.). Jap. J. Appl. Phys., 5: 218-22(Mar. 1966).**

A threshold type gas Cherenkov counter using CO_2 and freon 12 (CCl_2F_2) is constructed. The counting efficiency was measured for electrons of momentum 300 Mev/c as a function of gas pressure. The pressure was varied from vacuum to 6 kg/cm^2 with freon 12 and to 15 kg/cm^2 with CO_2. The maximum efficiency obtained is 99.3 ± 0.5%. The velocity resolution $\delta\beta$ is estimated to be better than 3×10^{-3}, which suffices to discriminate electrons from muons and pions produced by a 1.3 Bev electron synchrotron. (auth)

21072 A TRANSISTORIZED LOW-NOISE PREAMPLIFIER FOR SOLID-STATE RADIATION DETECTOR. **Yoshimura, Atsushi; Sonoda, Masateru (Kyushu Univ., Japan). Kyushu Daigaku Kogaku Shuho, 38: 38-44(Mar. 1965). (In Japanese).**

Since the capacity of a solid state detector (SSD) changes with the applied bias voltage, the preamplifier must be charge-sensitive and must have a low-noise to prevent the pulses from becoming broad due to the noise fluctuation of the preamplifier. Several low-noise charge-sensitive preamplifiers were prepared in trial for the fission fragment measurement. The operating principles of the semiconductor detector and the design considerations for the charge-sensitive amplifier are discussed. If the total voltage gain is sufficiently large, the output voltage V_0 of the charge-sensitive amplifier can be given approximately by $V_0 = Q/C_f$, where Q is the total charge deposited on the SSD and C_f is the feedback capacitor. Consequently, the output voltage is approximately proportional to the inverse of C_f. In the transistorized model, 4 silicon transistors, 2SC32, with a good S/N ratio were used. The value of C_f should be determined according to the energy of radiation to be measured. With C_f = 5pF, the amplifier exhibited good linearity up to 60-Mev equivalent pulses; and with C_f = 10pF, it could be used up to 90 Mev with the output voltage reduced somewhat. The overall energy resolution of this low-noise charge-sensitive preamplifier is about 4.1% for 6.05 and 8.78 Mev alpha particles emitted from Th C, C′ source. The use of a field effect transistor may reduce the noise considerably. (TCO)

21073 AEROSOL ACTIVITY METER. **Meszaros, Istvan; Kovacs, Gyula; Kiss, Elemer. Magyar Tud. Akad. Kozp. Fiz. Kut. Int. Kozlem., 13: 399-405(1965). (In Hungarian).**

Methods for the determination of aerosol activities concentrated in air are discussed and the measuring assembly developed comprising two meters for the two-step determination of aerosol activity concentration, are described. (auth)

21074 A DEVICE FOR THE MEASUREMENT OF AVERAGE NEUTRON ENERGIES. **Makra, Zsigmond. Magyar Tud. Akad. Kozp. Fiz. Kut. Int. Kozlem., 14: 49-61(1966). (In Hungarian).**

A device for the determination of the average energies of relatively low-neutron fluxes is described. Its principle of operation is based on that for a flux of fast- or intermediate-energy neutrons incident on a moderator, the space distribution of thermalized neutrons is dependent on the incident neutron energy. The space distribution is measured by using a boron-lined thermal-neutron counter and polyethylene discs of various thicknesses. The asymptotic behavior of the space distribution is described by the "first collision method." In this way the main characteristics of the instrument can be determined. Theoretical calculations are in good agreement with experimental results. The energy range covered by the instrument is from 10 kev to 15 Mev, its sensitivity is of the order of $10^{-1} - 10^{-2}$ count per unit fluence. (auth)

21075 THE MAYO CLINIC WHOLE-BODY COUNTER. **Tauxe, W. Newlon; Orvis, Alan L. (Mayo Clinic, Rochester, Minn.). Mayo Clin. Proc., 41: 18-23(Jan. 1965).**

The construction, characteristics, performance, and applications of the Mayo whole-body counter are described. The principal immediate aims in the use of this unit are: to estimate endogenous potassium; to perform metabolic turnover studies of exogenous isotopes for long-term turnover or for short-term turnover studies of those radionuclides with short physical half lives; and to identify and determine body burdens of unintentionally ingested or injected radionuclides. The low-background counting room is shielded by 6-in.-thick steel lined with ⅛-in.-thick lead. Plastic detectors are arranged in such a way as to minimize the dependence of counter sensitivity on the size of the patient and on the presence of any inhomogeneity in distribution of the radioisotope in the body. Preamplifiers, amplifiers, pulse-height analyzers and scalers are used, and a fast coincidence module is available for special studies. (TCO)

21076 A SIMPLE γ-RAY DOSE THRESHOLD DETECTOR USING A DYESTUFF. **Asada, Tsunesaburo; Kikuchi, Riichi (Osaka Univ.). Mem. Inst. Sci. Ind. Res. Osaka Univ., No. 22, 95-6(Mar. 1965).**

A γ-dose threshold detector is described for the detection of 2.5×10^6 R, the optimum dose for the sterilization of medical equipment by gamma irradiation. The detector is made as follows: polyvinyl chloride (PVC) powder is mixed with paraffin as the base in equal proportions; 0.1 wt % Congo red is added; all are mixed together at about 70°C; and the mixture is made into a film about 0.6 mm thick. This film, placed in an air-tight envelope of polyethylene or PVC film, changes in color from red to blue-violet when irradiated to 3×10^4 R. If 2.5 mg NaOH per gram of PVC is added to the mixture, the color change in the film is effected by irradiation of 2×10^6 R. Thus controlling the alkali content, it is possible to prepare a film whose color changes at a desired dose. The films are stable for several months against light, heat, and moisture. (TCO)

21077 SEMICONDUCTOR NUCLEAR PARTICLE DETECTORS. II. **Fujibayashi, Keiji; Miyashita, Kyoichi (Mitsubishi Electric Manufacturing Co., Ltd., Japan). Mitsubishi Denki Giho, 39: 1221-7(Oct. 1965). (In Japanese).**

Semiconductor nuclear particle detectors have been developed. They are oxide passivated silicon p-n junction detectors and lithium-drifted silicon p-i-n detectors. Also, low noise charge sensitive amplifiers for use with semiconductor detectors have been developed. The oxide-passivated detectors are 7 mm^2 and 20 mm^2 in area respectively. The energy resolution is 27 kev for 5.3 Mev alpha particles. The oxide-passivation enables the detectors to be of very low leakage currents and very stable even in high humidity. Lithium-drifted detectors are 4×5 mm^2 in area, their intrinsic region ranges from 0.5 to 2 mm, and their energy resolution is 22 kev for 625 kev beta particles. The charge sensitive amplifiers are fully transistorized, and the resolution broadening due to amplifier noise is reduced to 10–12 kev (FWHM) by newly developed circuits. (auth)

21078 INTEGRATING DOSE-RATE METER EMPLOYING IONIZATION CHAMBERS. **Tanaka, Osamu; Ikeda, Hiroshi (Mitsubishi Electric Manufacturing Co. Ltd., Japan). Mitsubishi Denki Giho, 39: 1388-90(Nov. 1965). (In Japanese).**

An instrument has been developed to measure the x-ray or gamma intensity in Roentgens per unit time and to indicate the total dose simultaneously. It is also possible with

this instrument to preset the total dose on a revolution counter. When the preset value is exceeded, the buzzer sounds, and, if desired it will shut down the x-ray apparatus or close the shield of the gamma source. It can also be connected to a recorder indicating the intensity rate. The energy range of the detector in 40 kev ~ 1300 kev, and the dose rate ranges from 1 mγ/min to 1000 γ/min. The kind of probe containing the ionization chamber can be altered according to the energy and intensity of the radiation to be measured. (auth)

21079 FEEDBACK IN ELECTROMECHANICAL DRIVE SYSTEMS. Kankeleit, E. (California Inst. of Tech., Pasadena). Contract AT(04-3)-63. pp 47-66 of Moessbauer Effect Methodology. Vol. 1. Gruverman, Irwin J. (ed.). New York, Plenum Press, 1965.

A feedback system for use in a velocity spectrometer for Mössbauer experiments is described. An amplifier in the feedback circuit drives the coil of the transducer, which moves the source and a pickup coil. A signal produced by the pickup coil proportional to the velocity is subtracted from a reference signal, and the difference passes through the circuitry and re-enters the amplifier. Velocities of the drive system can thus be controlled in the range from 10^{-5} to 10^{2} cm/sec. The system is, to a great extent, insensitive to vibrations and able to operate under unusual conditions. Possible improvements on the system and details of calibration of the transducer and corrections for nonlinearity are discussed in an appendix. (A.G.W.)

21080 CAM-DRIVEN, CONSTANT-ACCELERATION MOESSBAUER SPECTROMETER. Bearden, Alan J.; Hauser, M. G.; Mattern, P. L. (Cornell Univ., Ithaca, N. Y.). pp 67-74 of Moessbauer Effect Methodology. Vol. 1. Gruverman, Irwin J. (ed.). New York, Plenum Press, 1965.

The drive system for a constant-acceleration Mössbauer spectrometer is essentially a simple offset cam system coupled to a 600-rpm motor. The general plan of the spectrometer is to provide a timing mark to begin the channel advance of a multichannel scaler, then advance the channel with an independent pulse train and terminate the pulse train by the overflow pulse from the multichannel scaler after either 100, 200, or 400 channels. The motion of the cam follower is transferred to either the source or absorber, and the number of counts accumulated over a run in each channel then provides the primary data. Cryogenic temperatures can be established by use of liquid helium or liquid nitrogen. The spectrometer is capable of high resolution and allows data collection to ±0.2% statistical uncertainty in a period of 20 hr. Except for maintenance of cryogenic-liquid levels, it is completely automatic. (A.G.W.)

21081 CONSTANT-VELOCITY MOESSBAUER DRIVE SYSTEMS. Flinn, P. (Carnegie Inst. of Tech., Pittsburgh). pp 75-85 of Moessbauer Effect Methodology. Vol. 1. Gruverman, Irwin J. (ed.). New York, Plenum Press, 1965. (TID-22368).

Advantages of constant-velocity type Mössbauer effect apparatus over constant-acceleration type are pointed out. Suitable types of drive systems and methods of velocity measurement are discussed. Figures show a pendulum-type drive system and a moiré fringe attachment for velocity measurement. A block diagram of the electronic system for cyclic operation of the apparatus is shown. It is concluded that the operation of constant-velocity Mössbauer apparatus in the cyclic mode provides the convenience of constant-acceleration systems while retaining the advantages of constant-velocity operation. (A.G.W.)

21082 SPARK CHAMBERS IN NUCLEAR MEDICINE. Lansiart, A. J. (Centre d'Etudes Nucleaires, Saclay, France); Kellershohn, C. Nucleonics, 24: 56-60 (Mar. 1966).

A system using a spark chamber was developed for the stationary camera used in nuclear medicine. In the system gamma rays pass through a lead collimator into the spark chamber where a spark discharge is triggered. These sparks are photographed by a camera giving the distribution of the gamma-emitting isotopes. This system eliminates the crystal and photomultiplier tube required in other cameras, and is thus simpler. The design of the spark chamber is described, and photographed images showing radioisotope concentration in organs are shown. (J.F.P.)

21083 APPLICATION OF THE 256-CHANNEL TIME-OF-FLIGHT ANALYZER FOR MEASUREMENT OF AMPLITUDE SPECTRA. Hoffman, Zbigniew; Komor, Zenon; Nadachowski, Michal; Rydzewski, Tadeusz (Instytut Badan Jadrowych, Swierk, Poland). Nukleonika, 10: 535-40(1965). (In Polish).

A 256-channel time-of-flight analyzer developed in the period 1960–1962 has since undergone considerable modification, including its adaptation for analyzing pulse-height spectra. This modification was made possible by the addition of an analog-digital converter which transforms pulse height into a series of pulses ½ microsecond apart, the number of pulses being equal to 256 for a 100 volt input signal. The analyzer can store a spectrum in 256 channels, or in either half (128 channels) of its memory. The analyzer dead time is (18 + 0.5N) microseconds where N is the number of "channels" of pulse height (128 or 256 maximum). A maximum of 2^{16}-1 (65535) counts per channel can be stored, at which point the analyzer is automatically turned off to avoid overflow. The integral linearity is about 0.2% for 256 channels and 0.35% for 128 channels, the differential linearity is within ±2% over most of the range, and the stability was found to be within 0.1% over a 7 hour test period. The spectrum can be seen during analysis, in that each count produces a "light spot" during storage of the pulse height information. (TTT)

21084 LINEAR RELATIONSHIP FOR HEAVY-ION PULSE HEIGHTS IN ALKALI HALIDES. Womack, E. A.; Lazarus, A. J.; Liu, S. W. W. (Massachusetts Inst. of Tech., Cambridge). Contract AT(30-1)-2098. Phys. Rev., 144: 231-2(Apr. 8, 1966). (MIT-2098-196).

It was found that the total scintillation light from alkali halides produced by stopping energetic ions with $2 < Z < 20$ can be described by a single linear function of $E_0^{\frac{5}{3}}/A^{\frac{1}{3}}Z^{\frac{5}{3}}$, where E_0 is the initial energy, and A and Z are the mass number and charge of the incident particle, respectively. Measurements in CsI(Tl) and NaI(Tl) are shown and a brief discussion of the implications of this observation is given. (auth)

21085 THE VA-M-30 THERMOLUMINESCENCE MEASURING ASSEMBLY—A NEW DEVELOPMENT OF VEB VAKUTRONIK. Lehnert, K. (VEB Vakutronik WIB, Dresden). Radiobiol.-Radiotherap., 7: 111-14(1966). (In German).

A system for thermoluminescence dosimetry is reported which was especially developed for dose measurements in radiation therapy and radiobiology. This system consists of the dosimeters, plastic containers filled with prepared LiF, and of the evaluating device digitally indicating the measured dose value and making it possible to print this value. The small volume of the dosimeters and the possibility of adapting the shape of the dosimeters to the respective measuring problem enable the user to perform measurements in which the conventional methods of measurement are failing in the dose range of 1 to 10^4 R. (auth)

21086 TWO SIMPLE CIRCUITS FOR INERTIALESS SUPPRESSION OF PULSE RATES SELECTED AS ONE LIKES IN SCINTIGRAPHY. Potschwadek, B. (Univ., Rostock, Ger.). Radiobiol.-Radiotherap., 7: 115-21(1966). (In German).

Two circuits for the suppression of selected pulse rates are described. In the first circuit a controllable recurrent pulse train is subtracted from the pulses counted by the detector in a memory device. The second circuit operates according to the principle of pulse-time-discriminator. (auth)

21087 VOLTAGE MEASUREMENT IN X-RAY TUBES ESPECIALLY DURING FLASHES OF X RAYS. Pychlau,

P. Radiobiol.-Radiotherap., 7: 123-31(1966). (In German).

A procedure is described that enables the determination of high voltage which is really effective in an x-ray tube during flashes of x-ray. A circuit with two ionization chambers is used, with the chambers arranged one after another in the ray, a filter being inserted between them. Kilovoltage is determined from the radiation attenuation factor after the self-filter of the tube has been obtained with the same instrument. (auth)

21088 ELECTROSTATIC RELAY FOR RADIATION MEASUREMENT AND OTHER HIGH RESISTANCE PROBLEMS. Radiography, 31: 231(Oct. 1965).

It is necessary to employ electrostatic methods in connection with measurement of ionization currents for the measurement of radiation. These currents are of the order of 10^{-12} to 10^{-15} amps, and special care has to be taken in the measuring circuits to avoid poor insulation and drift. Poor insulation in this context may still be 1000 times better than conventional good insulation in other electrotechnical problems. There are many tasks where an ordinary relay has to be triggered at a preset voltage which can only be measured electrostatically. These include alarm circuits for radiation levels and radiation quantities, and end-point determination in high impedance counting, in mass spectrometry. The P.T.W. Electrostatic Relay described was developed for radiation dosimetry and for alarm circuits and was incorporated in a well-known x-ray dosimeter. This relay is characterized by small size and weight (less than 2 in. cube and 50 g), independence of position and vibration, an input resistance greater than 10^{17} Ω and an input capacity of about 2 pF. The operating voltage can be pre-adjusted between 200 and 400 v and the output contacts will switch 50 ma at 24 v or 200 ma at 6 v. The max switching rate is three per sec. The temperature range is from −40° to +60°C. (BBB)

21089 FIELD IONIZATION DETECTORS FOR MOLECULAR BEAMS. Johnston, Wilbur D. Jr.; King, John G. (Massachusetts Inst. of Tech., Cambridge). Contract DA36-039-AMC-03200(E). Rev. Sci. Instrum., 37: 475-6 (Apr. 1966).

The operating principles of the field ionization microscope were applied to the development of molecular beam detectors characterized by high geometrical resolving power, rapid time response, and unit detection efficiency for any beam substance. The detector described here has been in use for 10 months with beams of helium, argon, and nitrogen. (auth)

21090 ELECTROLUMINESCENT PANELS AS PULSED FIDUCIAL MARKS IN SPARK CHAMBER EXPERIMENT. Barna, Arpad (Stanford Univ., Calif.); Kreisler, Michael N.; Longo, Michael J. Rev. Sci. Instrum., 37: 521-2(Apr. 1966).

The main advantages of using pulsed electroluminescent panels over the usual system employing reticles illuminated by flash tubes are pointed out. The results of life tests performed using panels of 0.8 mm in thickness with 0.8-mm copper leads along two edges, and a 3-mm unlighted perimeter are reported. A photograph of a typical event from a recent spark chamber experiment is shown. (L.B.S.)

21091 SIMPLE DETECTORS FOR NEUTRONS OR HEAVY COSMIC RAY NUCLEI. Fleischer, R. L.; Price, P. B.; Walker, R. M. (General Electric Co., Schenectady, N. Y.). Rev. Sci. Instrum., 37: 525-7(Apr. 1966).

An amplification scheme is described for making visible the paths of heavily ionizing particles in thin sheets of certain dielectric solids. The technique makes it possible to measure a thermal dose as low as 1 neutron 1 cm^2 (±10%), to locate the paths of a small number of heavy particles per square meter of detector, and to produce high contrast alpha or fission autoradiographs of samples with a low activity. (L.B.S.)

21092 THE GM COUNTER, M2311. Endo, Kenji; Saito, Torao (Tokyo Shibaura Electric Co., Ltd.). Toshiba Rev., 20: 947-51(Oct. 1965). (In Japanese).

While small GM counters have long been manufactured for the diagnosis of cancer of the esophagus or the stomach, the progress of portable apparatus due to the utilization of transistors has also accelerated the miniaturization of GM counters. The miniaturized GM counter M2311, using most of the characteristics of halogen-quenched GM counter, has a performance as good as larger counter. Such small-sized counters should be in ever increasing demand with the progress of atomic industry. The M2311 counter may be considered as constituting the foundation for the realization of still smaller ones for medical purposes. (TCO)

21093 LINEARLY CONTROLLABLE LOW-FREQUENCY OSCILLATOR FOR A PROTON RESONANCE SPECTROMETER WITH INTERNAL NUCLEAR RESONANCE STABILIZATION. Rauterberg, U.; Kummer, J. (Univ., Frankfurt am Main). Z. Angew. Phys., 20: 284-9(1966). (In German).

Among the different possibilities of proton stabilization of a high resolution NMR spectrometer the internal reference scheme using dual-magnetic-field modulation is well suited, especially if an older spectrometer is to be modernized. This system makes use of an audio frequency oscillator for magnetic field modulation with frequency linearly dependent on time. After discussing the requirements one special type of this oscillator is described. It is a phase-shift generator in whose RC networks voltage-dependent resistors are used. Its frequency is proportional to the input voltage and is controlled independently of amplitude instabilities. The frequency is constant to within 10^{-4} per hour. Deviations from linearity are smaller than ±0.25%. This and the amplitude stability make the oscillator a suitable scanning device for a high resolution NMR spectrometer with internal proton stabilization. (auth)

21094 ON RECORDING OF SEVERAL PARTICLES WITH AN ACOUSTIC SPARK CHAMBER. Gorodinskii, G. M.; Damaskinskii, E. A.; Romanov, A. M. (Ioffe Physico-Technical Inst., Leningrad). Zh. Tekh. Fiz., 35: 1910-11(1965). (In Russian).

It is shown that one can uniquely determine the position of a point in a plane provided one knows the distance of the point from each of three fixed points in the plane and, that if the distances are subject to small experimental errors, the probability of mislocation can be reduced by employing more fixed points. The contemplated application is to the location of a spark in a spark chamber from measurements of the time of occurrence of the spark and the times of arrival of the resulting shock wave at several microphones. The confusion that can arise when several sparks occur simultaneously or nearly so is not discussed. References are given to descriptions of several microphones which are believed to be suitable for the contemplated application. (ATD)

21095 THE SEMICONDUCTOR FAST-NEUTRON DOSIMETER—ITS CHARACTERISTICS AND APPLICATIONS. Kramer, Gordon (Battelle Memorial Inst., Columbus, Ohio). 19p. (CONF-651001-19). ORAU. Gmelin, AED-CONF-65-293-8.

From IEEE Nuclear Science Symposium, San Francisco.

The characteristics and most recent results with a semiconductor fast-neutron dosimeter are described. This device is a wide-base Si n^+-p-p^+ junction by which it is possible to measure integrated fast-neutron flux by monitoring the decrease of carrier lifetime in its base region caused by the incident neutrons. A sensitivity range from 10^{10} nvt to $>10^{14}$ nvt is presently attainable. Accuracy of readout ranges from ±50% at 10^{10} nvt to ±5% at 10^{11} nvt and continues to improve at higher fluxes. The effect of base width, forward current level, material properties, and processing parameters on the sensitivity and uniformity of device characteristics are discussed. The current-voltage behavior of

the device is shown to correspond to a model by Rose for diffusion-dominated double injection in semiconductors. The small size and ruggedness of the dosimeter and the simplicity of readout make it particularly suited for radiation-effect experimentation, accident dosimetry, and biological dosimetry. (auth)

21096 SURFACE POTENTIAL MEASUREMENTS OF LITHIUM DRIFTED GERMANIUM DIODES. Davies, D. E.; Webb, P. P. 15p. (CONF-651001-25). ORAU. Gmelin, AED-CONF-65-293-28.

From IEEE Nuclear Science Symposium, San Francisco.

A potential probe was built to measure the distribution of potential on the etched surfaces of lithium-drifted Ge diodes. A vibrating condenser probe was used. Initial measurements with the probe confirmed a theoretical model proposed by McIntyre to explain previously observed unusual behavior of some lithium-drifted diodes. The probe was also used to determine the effect of various surface treatments designed to produce Ge diodes having high breakdown voltages and low leakage currents. It was found that a two-stage etch was frequently very useful in achieving a low-leakage diode at 77°K. For surfaces exhibiting strong n-type characteristics, dipping in H_2O_2 and washing in warm distilled water had the effect of moving the potential drop toward the front surface, but neither process was controllable. Efforts to obtain reproducible results were hampered by lack of uniformity of the crystal supplied by the manufacturer. (A.G.W.)

21097 12th ANNUAL NUCLEAR SCIENCE SYMPOSIUM, SAN FRANCISCO, CALIFORNIA, OCTOBER 18–20, 1965. IEEE (Inst. Elec. Electron. Eng.), Trans. Nucl. Sci., NS-13: No. 1, 1-766(Feb 1966). (CONF-651001).

Separate abstracts were prepared for 81 of the 109 papers included. Twenty-six of the remaining papers can be found under CONF-651001 in the report number index. One other paper appeared in NSA as 19: 46754. The remaining paper deals with the development of nuclear power. (D.C.W.)

For abstracts of individual papers see: 20844, 20954, 20995–21004, 21098–21139, 21225, 21448, 22031, 22032, 22317, 22318, 22358, 22359, 22389, 22434–22439, 22474–22484, and 22503.

21098 JUNCTION COUNTERS PRODUCED BY IRRADIATION OF SILICON WITH DOPANT IONS. Martin, F. W.; Harrison, S.; King, W. J. (Ion Physics Corp., Burlington, Mass.). IEEE (Inst. Elec. Electron. Eng.), Trans. Nucl. Sci., NS-13: No. 1, 22-9(Feb. 1966).

The fabrication of Si junctions by implantation of B ions and P ions through a previously applied layer of sputtered quartz is described, and the characteristics of the counters are summarized. The production of ten counters on a single slice for use in the focal plane of a magnetic spectrograph is also discussed, and the parameters of the 10-element counter are given. (D.C.W.)

21099 THE CHARACTERISTICS OF VERY SHALLOW SILICON JUNCTIONS. Wolfgang, L. G. (ITT Industrial Labs., Fort Wayne, Ind.); Abraham, J. M.; Inskeep, C. N. IEEE (Inst. Elec. Electron. Eng.), Trans. Nucl. Sci., NS-13: No. 1, 30-5(Feb. 1966).

The results of a series of investigations that was undertaken to optimize the properties of detector junctions are summarized-junctions ranging in depth from 0.75 micron to several angstroms were studied, particularly the diffusion of B and P into Si. The details of junction structure were determined by electron-beam scanning. (D.C.W.)

21100 RECENT RESULTS OBTAINED WITH HIGH-FIELD, INTERNALLY AMPLIFYING SEMICONDUCTOR RADIATION DETECTORS. Huth, Gerald C. (General Electric Co., Valley Forge, Pa.). IEEE (Inst. Elec. Electron. Eng.), Trans. Nucl. Sci., NS-13: No. 1, 36-42(Feb. 1966).

Gallium-diffused junctions were prepared by diffusion to a depth of 75 microns with subsequent removal of the heavily acceptor-doped, first 25-micron region. With no external bias, the window for alpha particles was found to be of the order of 1–2 microns. The window is approximately 2% of the junction depth. The response of the detectors to near infrared radiation and soft x rays was investigated. (D.C.W.)

21101 RESPONSE OF SOLID-STATE DETECTORS TO FISSION FRAGMENTS. Klema, E. D. (Northwestern Univ., Evanston, Ill.); Pleasonton, Frances; Schmitt, H. W.; Unik, J. IEEE (Inst. Elec. Electron. Eng.), Trans. Nucl. Sci., NS-13: No. 1, 43-7(Feb. 1966).

Pulse-amplitude spectra for fission fragments from the spontaneous fission of ^{252}Cf were studied for more than 50 silicon surface-barrier detectors. Silicon resistivities ranged from 100 to 2000 ohm-cm; spectra were obtained for several bias voltages for each detector. A search for correlations among shape parameters associated with ^{252}Cf fragment pulse-amplitude spectra was carried out. Such correlations were, in fact, observed and were shown to be related to the pulse-height response characteristics of surface-barrier detectors for fission fragments some guide lines by which the quality of a fission-fragment detector may be determined from the spectrum parameters are given. (auth)

21102 TEMPERATURE DEPENDENCE OF AVERAGE ENERGY PER PAIR IN SEMICONDUCTOR DETECTORS. Emery, F. E.; Rabson, T. A. (Rice Univ., Houston, Tex.). IEEE (Inst. Elec. Electron. Eng.), Trans. Nucl. Sci., NS-13: No. 1, 48-52(Feb. 1966).

A simple model for the value of ϵ, the average energy per electron-hole pair, was proposed by Shockley in 1960. This model was extended to predict temperature effects upon ϵ. Si and Ge Li-drifted counters were designed and built for detecting 1-Mev electrons and/or 5.5-Mev alpha particles over a temperature range of 4°K to 300°K. Techniques and equipment to measure the charged produced from a single incident ionizing particle within 0.4% were developed. Data were taken for Si and Ge detectors at temperatures ranging from 20 to 300°K. These data only qualitatively agree with the simple model. The evidence points to an additional effect over the ones invoked by Shockley. The room temperature values of ϵ for the Si Li-drifted counters observed agree with those for Si surface-barrier detectors which were recently published. (auth)

21103 OPERATING CHARACTERISTICS OF LITHIUM DRIFT DETECTORS. Williams, R. L.; Wilburn, C. D.; Harvey, N. P. (Simtec Ltd., Montreal). IEEE (Inst. Elec. Electron. Eng.), Trans. Nucl. Sci., NS-13: No. 1, 53-61(Feb. 1966).

A study of the operating characteristics of diffused-window Li-drifted Si detectors revealed that the level of compensation is independent of depth. The compensation corresponds to a net impurity concentration of 5×10^{10} impurities/cm^3 and is approximately three orders of magnitude poorer than that set by current flow through a diode. Using time-stability studies, it is possible to differentiate between stability of compensation in the bulk or main body of the detector and in the window (diffused type) area of the diode. By appropriate biasing, a Li distribution can be obtained in the window area which has good time stability. The stability of the compensation in the bulk of the diode is sufficiently high that the diffused-window detector will provide many years of operation, even when the detector is left largely unbiased. (auth)

21104 LARGE-VOLUME COAXIAL GERMANIUM GAMMA-RAY SPECTROMETERS. Malm, H. L.; Fowler, I. L. (Atomic Energy of Canada Ltd., Chalk River, Ont.). IEEE (Inst. Elec. Electron. Eng.), Trans. Nucl. Sci., NS-13: No. 1, 62-71(Feb. 1966).

Lithium-drifted germanium p-i-n diodes with sensitive volumes in the range of 16 to 54 cm^3 were fabricated using the coaxial method of drift. The performance of the diodes as gamma spectrometers was investigated. With a gamma energy of 122 kev, resolutions of 3.0 and 4.4 kev (full width at half maximum) were obtained using diodes with

sensitive volumes of 23 and 54 cm^3, respectively. The coaxial diodes also had high efficiencies. (D.C.W.)

21105 RADIATION DOSIMETERS DEVELOPED FOR SNAP-10A FLIGHT TEST. Kruse, W. G. (Lockheed Missiles and Space Co., Sunnyvale, Calif.). IEEE (Inst. Elec. Electron. Eng.), Trans. Nucl. Sci., NS-13: No. 1, 230-5(Feb. 1966).

The dosimeters that were developed to measure the reactor leakage radiations throughout the SNAPSHOT-Agena orbital vehicle are described, and the results of measurements of the gamma-dose and neutron-flux distributions are summarized. (D.C.W.)

21106 A METHOD FOR ANALYTICALLY REMOVING PULSE PILE-UP EFFECTS. Lilley, J. R. (Douglas Aircraft Co., Inc., Santa Monica, Calif.). IEEE (Inst. Elec. Electron. Eng.), Trans. Nucl. Sci., NS-13: No. 1, 281-6(Feb. 1966).

A method for analytically removing the effects of pulse pile-up is described. The theory of pile-up distortion of gamma spectra, the least squares fitting procedure, and experience with the experimental computer program SPADE are also covered, along with the effects of normal counting statistics on the unpiling procedure. (auth)

21107 TECHNIQUE AND APPARATUS FOR DETERMINING THE RESPONSE OF SCINTILLATORS AND SEMICONDUCTORS TO LOW-ENERGY X-RAY EXCITATION. Aitken, D. W.; Marcum, A. L; Zulliger, H. R. (Stanford Univ., Calif.). IEEE (Inst. Elec. Electron. Eng.), Trans. Nucl. Sci., NS-13: No. 1, 287-96(Feb. 1966).

Some apparatus and techniques that are being developed in order to investigate the response of scintillators and semiconductors to x-ray excitation are described. Examples of the signal-averaging technique are shown using the highly attenuated output of a precision pulse generator as the signal source. A discussion of the intended applications of the apparatus is presented. (auth)

21108 A BINARY-CODED DIGITIZED HODOSCOPE. Beall, E. F. (Univ. of Maryland, College Park). IEEE (Inst. Elec. Electron. Eng.), Trans. Nucl. Sci., NS-13: No. 1, 297-300(Feb. 1966).

A device that consists of 2^n-1 strips of plastic scintillator coupled by light pipes to n photomultiplier tubes in such a way that the combination of tubes which count at a given time gives directly the binary representation of the coordinate of the strip traversed by a high-energy particle is discussed. A device with n = 4 is described. (D.C.W.)

21109 ABSOLUTE COUNTING USING THE ZERO PROBABILITY ANALYSIS. Coats, G. I. (Public Health Service, Winchester, Mass.). IEEE (Inst. Elec. Electron. Eng.), Trans. Nucl. Sci., NS-13: No. 1, 301-4(Feb. 1966).

A method of automatically correcting for the dead-time losses in a $4\pi\ \beta$ and $4\pi\ \beta$-γ coincidence calibration facility is described, together with a three-channel instrument that measures the probability ($P_0 = e^{-\nu T}$) of observing exactly zero counts in an interval in which the average number of counts is νT. (D.C.W.)

21110 A NANOSECOND NEUTRON TIME-OF-FLIGHT SPECTROMETER USING AVALANCHE TRANSISTORS. Gibbons, F. L. (General Dynamics, Fort Worth, Tex.). IEEE (Inst. Elec. Electron. Eng.), Trans. Nucl. Sci., NS-13: No. 1, 305-10(Feb. 1966).

A neutron time-of-flight spectrometer that was developed for use in an investigation of the inelastic scattering of 14.6-Mev neutrons by ^{56}Fe and ^{7}Li is described. (D.C.W.)

21111 SUBMICROSECOND SYNCHRONIZATION OF MULTIPLE CHOPPER SYSTEMS. Haumann, J.; Ostrowski, G.; Connor, D. (Argonne National Lab., Ill.). IEEE (Inst. Elec. Electron. Eng.), Trans. Nucl. Sci., NS-13: No. 1, 311-14(Feb. 1966).

The degree of synchronization which may be achieved with choppers using commercially available hysteresis-synchronous motors was investigated. (D.C.W.)

21112 INTEGRATED-CIRCUIT CHARGE-SENSITIVE PREAMPLIFIER. Warble, Keith V.; Gri, Norman J. (AVCO Corp., Tulsa, Okla.). IEEE (Inst. Elec. Electron. Eng.), Trans. Nucl. Sci., NS-13: No. 1, 346-50(Feb. 1966).

An integrated-circuit charge-sensitive preamplifier that was developed for use with gas-filled proportional counters and/or silicon detectors is described. (D.C.W.)

21113 MINIMUM CHARGE DETECTION USING SELECTED TUNNEL DIODES AND CHARGE MULTIPLYING SEMICONDUCTORS. Locker, Robert J. (General Electric Co., Philadelphia). IEEE (Inst. Elec. Electron. Eng.), Trans. Nucl. Sci., NS-13: No. 1, 382-8(Feb. 1966).

The use of a charge-multiplying semiconductor detector in a circuit containing a tunnel diode biased for charge detection is discussed, and an instrument that was developed to detect 5.6-kev x rays from ^{55}Fe is described. The characteristics of the instrument are summarized. (D.C.W.)

21114 TRUE ZERO-CROSSING FAST DISCRIMINATOR. Shoffner, B. M.; Shrader, E. F. (Case Inst. of Tech., Cleveland). IEEE (Inst. Elec. Electron. Eng.), Trans. Nucl. Sci., NS-13: No. 1, 394-8(Feb. 1966). (COO-720-059).

A discriminator that incorporates both a pulse-height threshold and a true zero-crossing time detector is described. A negative doubly-differentiated signal is applied both to the base of an avalanche transistor and to a tunnel-diode pulse-height selector. The transistor is normally biased off; but if the leading edge of the signal trips the tunnel diode, a pedestal is applied to the emitter of the transistor allowing it to avalanche when the input signal crosses zero. By driving the discriminator directly from the anode of a proton-recoil scintillation detector, a total time shift of less than one nanosecond can be obtained for pulses ranging from 1.1 to 30 times threshold. (auth)

21115 A ZERO-CROSSING DISCRIMINATOR WITH PICOSECOND TIME SLEWING. Whittaker, J. K. (National Bureau of Standards, Washington, D. C.). IEEE (Inst. Elec. Electron. Eng.), Trans. Nucl. Sci., NS-13: No. 1, 399-405(Feb. 1966).

A zero-crossing type of discriminator with a very wide dynamic range and a short dead-time is described. When used with a 56 AVP photomultiplier with a linear dynode resistor chain, a light-amplitude variation of at least 125:1 may be accommodated. The relative time shift of the output discriminator pulse is then only 200 picoseconds. (auth)

21116 AN ELECTRON SPECTROMETER FOR PROJECT GEMINI. Marbach, James R. (Manned Spacecraft Center, Houston, Tex.). IEEE (Inst. Elec. Electron. Eng.), Trans. Nucl. Sci., NS-13: No. 1, 464-7(Feb. 1966).

A spectrometer that is designed to measure the energy and flux of electrons at Gemini orbital altitudes is described. A thick Li-drifted Si detector, coupled with a 50-micron dE/dx Si wafer and a plastic scintillator, is used to detect electrons with energies of $0.25 \leq E \leq 4.0$ Mev. Data pulses from a pulse-height analyzer using tunnel-diode discrimination feed a fully digital data processor. (D.C.W.)

21117 A DIRECTIONAL NEUTRON DETECTOR FOR SPACE RESEARCH USE. Chupp, E. L.; Forrest, D. J. (Univ. of New Hampshire, Durham). IEEE (Inst. Elec. Electron. Eng.), Trans. Nucl. Sci., NS-13: No. 1, 468-77 (Feb. 1966).

A proton-recoil detector with directional properties for neutrons with energies greater than 10 Mev is described in which plastic scintillating filaments are embedded in a non-scintillating potting compound. The axial efficiency of the detector is 2% for 14-Mev neutrons. An experiment using the detector to search for solar neutrons is described in detail. (D.C.W.)

21118 TWO SATELLITE-BORNE COSMIC-RADIATION DETECTORS. Bingham, R. G.; Erickson, W. C.; Howard, R. L.; Lezniak, J.; Sawyer, D.; Webber, W. R. (Univ. of Minnesota, Minneapolis). IEEE (Inst. Elec. Electron. Eng.), Trans. Nucl. Sci., NS-13: No. 1, 478-85(Feb. 1966).

Two telescopes that were developed for use on the Polar Orbiting Geophysical Laboratories, POGO C and D, and on the Pioneer Deep Space Probes C and D to measure the differential energy spectra of protons, helium nuclei, and heavy nuclei up to Z = 14 are described. The POGO telescope uses a combination of Cherenkov and scintillation counters together with a semiconductor detector. A Geiger tube, four Li-drifted Si detectors, and a Cherenkov counter comprise the Pioneer telescope. (D.C.W.)

21119 VIDICON SPARK CHAMBER DETECTOR FOR GAMMA-RAY ASTRONOMY. Helmken, H. F.; Fazio, G. G. (Harvard Coll. Observatory, Cambridge, Mass.). IEEE (Inst. Elec. Electron. Eng.), Trans. Nucl. Sci., NS-13: No. 1, 486-92(Feb. 1966).

A small spark chamber with vidicon readout, which was developed for high-energy gamma astronomy, is described. (D.C.W.)

21120 A SPARK CHAMBER SPECTROMETER FOR SPACE PROTONS. Madey, Richard (Clarkson Coll. of Tech., Potsdam, N. Y.); Churchill, R. J.; Aggson, Thomas. IEEE (Inst. Elec. Electron. Eng.), Trans. Nucl. Sci., NS-13: No. 1, 493-502(Feb. 1966).

A spectrometer that was designed to measure unidirectional proton spectra in six energy intervals between 21 and 210 Mev is described. The system consists of a six-channel spark chamber of ceramic and metallic construction, and associated miniaturized circuits for coincidence triggering, high-voltage pulse generation, and data readout. (D.C.W.)

21121 A DIGITIZED SPARK CHAMBER FOR GAMMA-RAY ASTRONOMY. Ehrmann, Charles H. (Goddard Space Flight Center, Greenbelt, Md.). IEEE (Inst. Elec. Electron. Eng.), Trans. Nucl. Sci., NS-13: No. 1, 503-7 (Feb. 1966).

A digitized spark chamber that was developed for gamma astronomy is described including the associated data acquisition and handling systems. Magnetic cores and magnetic tape are used for buffer storage and data logging, respectively. (D.C.W.)

21122 A PHOTOGRAPHIC SPARK CHAMBER FOR MANNED SATELLITES. Frye, G. M. Jr.; Smith. L. H. (Case Inst. of Tech., Cleveland). IEEE (Inst. Elec. Electron. Eng.), Trans. Nucl. Sci., NS-13: No. 1, 508-10(Feb. 1966).

A spark with photographic recording for use on balloons and satellites is described. The system can detect a point source of gamma rays with an intensity of 10^{-7} photons cm^{-2} sec^{-1} and can be used to determine the power-law dependence of the energy spectrum of a 10^{-6} source. The gamma energy can be measured from 2.5×10^7 to 5.0×10^9 ev. (D.C.W.)

21123 PLASMA ELECTRON DETECTOR USING AN OPEN ELECTRON MULTIPLIER. Lind, D. L.; McIlwraith, N. (Goddard Space Flight Center, Greenbelt, Md.). IEEE (Inst. Elec. Electron. Eng.), Trans. Nucl. Sci., NS-13: No. 1, 511-14(Feb. 1966).

An electron spectrometer that was developed for flight on the Orbiting Geophysical Observatory E to study the low-energy electrons in the solar wind, in the magnetospheric tail, and in the shock front at the interface of these two domains is described. The spectrometer measures energy and flux distributions of electrons with energies of 0 to 10 kev. The results of gain stability tests on two channel multipliers are presented. (D.C.W.)

21124 AN ELECTRON AND PROTON SPECTROMETER DETECTOR SYSTEM FOR AN OGO-E SATELLITE EXPERIMENT. McQuaid, James H. (Univ. of California, Livermore). IEEE (Inst. Elec. Electron. Eng.), Trans. Nucl. Sci., NS-13: No. 1, 515-22(Feb. 1966). (UCRL-14262-T).

A detector system for use with a magnetic electron spectrometer and a proton telescope on the Orbiting Geophysical Observatory E is described. Each of the seven differential energy channels of the electron spectrometer consists of an electron-plus-background detector and a background detector. A method of handling information from both detectors with the same amplifier system is discussed. The four-element proton telescope uses solid-state detectors directly in line with the collimator. A tunnel-diode discriminator and two charge-sensitive preamplifiers are also discussed. (D.C.W.)

21125 A THREE PARAMETER PULSE HEIGHT ANALYZER AND COINCIDENCE SYSTEM FOR SATELLITE COSMIC RAY STUDIES. Way, S.; Stilwell, D.; Jones, S. L. (Goddard Space Flight Center, Greenbelt, Md.). IEEE (Inst. Elec. Electron. Eng.), Trans. Nucl. Sci., NS-13: No. 1, 523-32(Feb. 1966).

A cosmic-ray experiment that is to be flown on an Orbiting Geophysical Observatory consists of Cherenkov, scintillation, and solid-state detector telescopes together with the associated electronic equipment. The 256-channel pulse-height analyzer and coincidence system electronics are described. The three-parameter system used for the scintillation telescope is emphasized. (D.C.W.)

21126 HIGH-RESOLUTION PULSE-HEIGHT ANALYZER FOR SATELLITE USE. Ely, John T. A. (Air Force Cambridge Research Labs., Bedford, Mass.). IEEE (Inst. Elec. Electron. Eng.), Trans. Nucl. Sci., NS-13: No. 1, 533-6(Feb. 1966).

A transistorized 1500-channel pulse-height analyzer that was developed for use on satellites is described. (D.C.W.)

21127 A LOW COST-LOW POWER MULTICHANNEL PULSE-HEIGHT ANALYZER FOR UNIVERSITY BALLOON AND ROCKET EXPERIMENTS. Ewald, C. J.; Sarkady, A. A. (Univ. of New Hampshire, Durham). IEEE (Inst. Elec. Electron. Eng.), Trans. Nucl. Sci., NS-13: No. 1, 537-53(Feb. 1966).

A simple multichannel pulse-height analyzer with a total average power consumption of approximately 330 Mw is described. The analyzer was designed for use in a balloon experiment with a directional neutron detector to search for solar neutrons with energies greater than 10 Mev. (D.C.W.)

21128 A NONDISPERSIVE X-RAY SPECTROMETER FOR LUNAR AND PLANETARY GEOCHEMICAL ANALYSIS. Metzger, Albert E. (California Inst. of Tech., Pasadena); Parker, Richard E.; Trombka, Jacob I. IEEE (Inst. Elec. Electron. Eng.), Trans. Nucl. Sci., NS-13: No. 1, 554-61(Feb. 1966).

A nondispersive x-ray spectrometer is described, and the results of some tests with a prototype instrument are presented. The use of nondispersive x-ray spectroscopy in the remote analysis of lunar and planetary surfaces is discussed. (D.C.W.)

21129 ROCKET GAMMA SCANNING OF NUCLEAR BURSTS. Emerling, R. A.; Mullins, J. H.; Van Putten, J.; Maloy, J. O.; Bartholomew, H. G. (Electro-Optical Systems, Inc., Pasadena, Calif.). IEEE (Inst. Elec. Electron. Eng.), Trans. Nucl. Sci., NS-13: No. 1, 569-79(Feb. 1966).

An instrument designed to locate and map the cloud of gamma-emitting debris produced by a high-altitude nuclear explosion is described. The instrument contains two scintillation detectors assembled into a directional uranium shield. (D.C.W.)

21130 DESIGN FOR A VERSATILE CHARGE-SENSITIVE PREAMPLIFIER FOR NUCLEAR RADIATION DETECTORS. Bradley, Arne E. (Univ. of California, Livermore). IEEE (Inst. Elec. Electron. Eng.), Trans. Nucl. Sci., NS-13: No. 1, 611-22(Feb. 1966).

A transistorized charge-sensitive preamplifier with a maximum gain of about 650 v/picocoulomb is described. A brief analysis of the charge-loop performance in terms of circuit parameters is included. (D.C.W.)

21131 FAST NEUTRON TRANSIENT DETECTION HODOSCOPE FOR REACTOR FUEL MELTDOWN STUDIES. De Volpi, A.; Freese, C. H. (Argonne National Lab., Tenn.). IEEE (Inst. Elec. Electron. Eng.), Trans. Nucl. Sci., NS-13: No. 1, 623-9(Feb. 1966).

A hodoscope that was developed for fuel meltdown studies in TREAT is described. (D.C.W.)

21132 IMPROVED PERFORMANCE OF BF_3 NEUTRON COUNTERS IN HIGH GAMMA FLUXES. Stokes, Arthur J.; Meal, Thomas J.; Myers, John E. Jr. (Reuter-Stokes Electronic Components, Inc., Cleveland). IEEE (Inst. Elec. Electron. Eng.), Trans. Nucl. Sci., NS-13: No. 1, 630-5(Feb. 1966).

A method is described for maintaining good operating characteristics of BF_3 counters operating in gamma fluxes of 1000 R/hr or more. Loss of good counting ability, due to accumulation of chemical dissociation products of ionization, is counteracted by placing within the counter an absorbing agent capable of removing the impurities from the gas phase. Data are presented showing pulse-height resolution of several counters exposed to various levels of gamma flux. Standard counters are compared to those containing an absorbing agent. A marked improvement in neutron counting ability in gamma fluxes is shown. (auth)

21133 A PORTABLE DOSE-RATE METER USING A SILICON p-n JUNCTION AS A DETECTOR. Jones, A. R. (Atomic Energy of Canada Ltd., Chalk River, Ont.). IEEE (Inst. Elec. Electron. Eng.), Trans. Nucl. Sci., NS-13: No. 1, 652-7(Feb. 1966).

A dose-rate meter that comprises a small-area p-n counter, charge and linear pulse amplifiers, a discriminator, and a three-decade logarithmic count-rate circuit is described. The meter is designed to measure tissue dose rates from beta particles in the range of 0.1 to 100 Rad/hr as well as dose rates from gamma rays in the same range. (D.C.W.)

21134 A STUDY OF THE SCINTILLATION PROPERTIES OF VARIOUS HYDROGENOUS AND NON-HYDROGENOUS SOLUTES DISSOLVED IN HEXAFLUOROBENZENE. Jupiter, C. P.; Parez, J. (General Atomic Div., General Dynamics Corp., San Diego, Calif.). IEEE (Inst. Elec. Electron. Eng.), Trans. Nucl. Sci., NS-13: No. 1, 692-703 (Feb. 1966).

To enhance the gamma sensitivity relative to that of fast neutrons, hexafluorobenzene (C_6F_6) was substituted for the primary solvent in a standard hydrogenous scintillator solution. The solutes used included p-terphenyl, α-NPO, PPO, POPOP, DM-POPOP and decafluorobiphenyl. Optical absorption and emission spectra were measured. The sensitivity relative to NE-211 was determined for ^{60}Co radiation, 14-Mev neutrons and 2.6-Mev neutrons as a function of solute concentration ranging between 0.03 and 3.0 g/liter. Sensitivity measurements were carried out by measuring the total integrated light output from the scintillators. For all samples studied, the relative sensitivity to ^{60}Co gamma radiation was greater than that for fast neutrons by factors ranging between 5 and 15. (auth)

21135 CALCIUM FLUORIDE AS AN X-RAY AND CHARGED PARTICLE DETECTOR. Menefee, J.; Swinehart, C. F.; O'Dell, E. W. (Harshaw Chemical Co., Cleveland). IEEE (Inst. Elec. Electron. Eng.), Trans. Nucl. Sci., NS-13: No. 1, 720-4(Feb. 1966).

The properties of europium-activated calcium fluoride crystals for use in the detection of charged particles, gamma radiation and x radiation are summarized. The results of some studies of the scintillation of europium-activated single crystals are presented. (D.C.W.)

21136 HIGH REFLECTANCE COATINGS. Dubs, Charles W. (Air Force Cambridge Research Labs., Bedford, Mass.). IEEE (Inst. Elec. Electron. Eng.), Trans. Nucl. Sci., NS-13: No. 1, 729-34(Feb. 1966).

To help maximize the photon statistical accuracy and uniformity of pulse-height measurements from a Cherenkov detector, coatings of high reflectance were made and procured. A number of various combinations of pigments and binders were tried. The reflectances of these coatings and various ready-made coatings were measured as a function of wavelength. From the results, an effective absorptance was calculated assuming an S-11 response and a Cherenkov spectrum for each coating. (D.C.W.)

21137 EXPERIMENTAL RESULTS ON THE INFORMATION AVAILABLE FROM THE RISE TIME OF PULSES SUPPLIED BY SEMICONDUCTOR PARTICLE DETECTORS. Alberigi-Quaranta, A.; Martini, M.; Ottaviani, G.; Zanarini, G. (Istituto Nazionale di Fisica Nucleare, Bologna). IEEE (Inst. Elec. Electron. Eng.), Trans. Nucl. Sci., NS-13: No. 1, 752-6(Feb. 1966).

Experimental results are presented showing that, in several cases, useful information about the impact angle or the mass of charged particles can be obtained from the rise time of the pulses supplied by semiconductor detectors. A method of correcting experimental results to permit a comparison with theoretical values is outlined, together with a method of digitizing the information. (D.C.W.)

21138 LOW-ENERGY MOSAIC ELECTRON SENSOR. Reinitz, Karl (Westinghouse Defense and Space Center, Baltimore). IEEE (Inst. Elec. Electron. Eng.), Trans. Nucl. Sci., NS-13: No. 1, 762-4(Feb. 1966).

A composite surface-barrier diode for the detection of low-energy electrons is described. The device is fabricated on a Si wafer with a diameter of approximately 1 in. and has a sensitive window (0.5 in. × 0.5 in.) on the active side of the unit. The back side of the unit has two perpendicular sets of parallel evaporated conductors that are used for readout. The location of an incident particle is determined by the particular channels through which the readout is accomplished. (D.C.W.)

21139 THE DETECTION OF SINGLE ELECTRONS AND IONS IN A RADIATION ENVIRONMENT. Krause, D. E.; White, F. A. (Rensselaer Polytechnic Inst., Troy, N. Y.). IEEE (Inst. Elec. Electron. Eng.), Trans. Nucl. Sci., NS-13: No. 1, 765-6(Feb. 1966).

A coincidence method for the detection of charged particles, even if the arrival rate of the particles is substantially below the dark current of conventional electron multiplier tubes, is described. (D.C.W.)

21140 FAST AND SLOW NEUTRON COUNTER. (to Eberline Instrument Corp.). British Patent 1,019,590. Feb. 9, 1966. Filed Jan. 1, 1965.

A neutron counter for detecting and measuring both fast and slow neutrons consists of a hand probe comprising a slow neutron counter removably mounted inside an assembly that is in turn mounted inside a housing. When the probe is positioned inside the assembly, it measures only fast neutrons; but when it is removed to the outside of the housing, it serves to measure slow neutrons. A large space surrounds the assembly as it is mounted in the housing, and a fast neutron moderator fills the space. (B.L.M.)

21141 IONIZATION CHAMBER RADIATION DOSIMETER. Kowalski, Emil (to Landis and Gyr A.G.). German Patent 1,205,630. Nov. 25, 1965. Priority date May 19, 1961, Switzerland.

The dosimeter is provided with a condenser divided into two separate capacities of which one is for the integration of the ionization current and the other is for supplying the ionization chamber voltage. The two capacities of the condenser which is wrapped around the ionization chamber are interwoven in a known manner. (Gmelin Inst.)

21142 APPARATUS RELATING TO THE DETECTION AND MEASUREMENT OF RADIOACTIVITY IN RELATIVELY LARGE BODIES. Packard, Lyle E. U. S. Patent 3,233,102. Feb. 1, 1966. Filed July 27, 1962.

An enclosed tank-like detector module is patented for use in a modular whole-body radiation counter of the type used for counting radioactivity emanating from a body disposed along an axis. The detector module is provided with opposed walls adapted to be disposed normal to the axis of the counter and selectively abutted against the corresponding end walls of adjacent modules. A liquid scintillation medium substantially fills the module for reducing light flashes upon detection of a radioactive emission. Light transducer means are mounted in a single plane parallel to and interposed between the end walls for producing an electrical signal substantially proportional in amplitude to the energy of the corresponding light flashes. These tank-like detector modules

can be assembled by the user into a counting chamber having a geometric configuration and size most suitable for the particular needs of the user. In a whole body counter made up of a number of these modules, contamination of one tank or breakage of one photomultiplier will not result in the loss of all or most of the scintillation material. (B.L.M.)

21143 NEUTRON ENERGY SPECTROMETERS. Aoki, Ryozo (to Hitachi Ltd.). U. S. Patent 3,233,103. Feb. 1, 1966. Filed Dec. 31, 1962.

A neutron energy spectrometer includes two scintillators, the first containing liquid ^3He, and the second surrounding the first. A light pipe connects the first scintillator to a photoelectric transducer element adapted to translate light rays into electrical pulses. A number of photomultiplier devices are in communication with the second scintillator. The two scintillators are arranged so that neutrons may be applied from the outside to the first scintillator and may not reach the second scintillator directly but may pass from the first to the second. An anti-coincidence gate circuit is connected to the output of the photoelectric transducer and to the combined outputs of the photomultiplier devices. (B.L.M.)

21144 HIGH ENERGY RADIOGRAPHIC APPARATUS USING A BUBBLE CHAMBER DETECTOR. Heffan, Howard. U. S. Patent 3,233,104. Feb. 1, 1966. Filed Oct. 15, 1962.

In a high energy radiographic system, an especially constructed bubble chamber rather than the usual fluorescent screen or photographic film is used to provide an image corresponding to the transmission characteristics of the subject. The bubble chamber display apparatus comprises a first planar window element transparent to the high-intensity radiation and a second planar optically transparent window element disposed in a uniform closely spaced relation to the first window element. The window elements are supported by a flexural joint means, and the elements define a chamber having a thin thickness dimension between them and filled with a bubble forming medium. Pressure can be applied to and released from the bubble medium to provide supercooled conditions in the medium. (B.L.M.)

21145 GAMMA RAY MEASURING SYSTEM UTILIZING PLURAL DETECTORS. Scherbatskoy, Serge A. U. S. Patent 3,234,382. Feb. 8, 1966. Filed Dec. 24, 1962.

A radiation detecting means is patented that is suitable for use in well logging operations where either gamma rays scattered by the formation adjacent to a gamma source or gamma rays resulting from the capture of neutrons by formations adjacent to a neutron source are detected. The usual shield between the source and detector can be completely eliminated, because the detector employed is a proportional counter that is adapted to produce impulses that are proportional to the energy of the intercepted radiation particles or quanta. Across the output terminals of the proportional counter a pulse height counter is provided that selectively transmits only the impulses within an energy range corresponding to radiation scattered or induced in the formation and attenuates the impulses within an energy range corresponding to the radiation that is directly transmitted from the source to the detector. (B.L.M.)

21146 FAST RESPONSE GAMMA-RAY IMAGE CONVERTER. Niklas, Wilfrid F. (to Rauland Corp.). U. S. Patent 3,235,737. Feb. 15, 1966. Filed Aug. 1, 1961.

A gamma image converter having a substantially increased speed of response (microseconds) over prior devices comprises, within an evacuated envelope, a composite pick-up screen comprising a heavy metal target element responsive to incident gamma rays for developing free electrons at a predetermined energy level. A secondary emission multiplying element of a material having a secondary multiplication factor greater than unity within a range of incident electron energy levels below the predetermined energy level is in juxtaposition with the target element for developing secondary electrons in response to the transmission of incident electrons through it. Means including a metal moderating element are provided for translating the free electrons developed by the target element to the multiplying layer as incident electrons at an energy level within the predetermined range. Means are further provided for utilizing the secondary electrons to produce image on a fluorescent viewing screen. (B.L.M.)

Radiation Effects

21147 (AD–621049) RADIATION DAMAGE IN SEMICONDUCTORS. Annual Summary Report No. 4. Baruch, P. (Paris Univ. (France). Laboratoire de Physique). July 20, 1965. Contract AF61(052)-543. 36p. (AFCRL–65–588). CFSTI $2.00 cy, $0.50 mn.

The effect of radiation-induced point defects on impurity diffusion in silicon is investigated using proton and electron irradiation. The active defects have a diffusion length near 3 μ in pulled silicon and dislocations are found to act as defect sinks, but are not dominant for dislocation densities less than $10^7/cm^2$. Defect precipitation is shown to occur at high defect concentrations, leading to enhanced annealing of point defects and formation of stress centers stable against annealing to 1000°C. A model is proposed by which impurities diffuse by a vacancy mechanism and vacancy diffusion is limited by complex formation with oxygen atoms. (auth)

21148 (AD–630835) EFFECT OF TRANSISTOR DESIGN PARAMETERS ON RADIATION RESPONSE (POWER TRANSISTORS). First Quarterly Report, July 1, 1965–September 30, 1965. Honnold, V. R.; Thomas, G. D.; Mazenko, J. J. (Hughes Aircraft Co., Fullerton, Calif.). Mar. 1966. Contract DA28-043-AMC-01541(E). 22p. (ECOM–01541-1; ER–66-17-105). CFSTI $1.00 cy, $0.50 mn.

An investigation was made to determine particular design characteristics and fabrication techniques for a silicon planar power transistor that will minimize the effects of ionization and lattice displacement caused by high energy radiation. The program consists of both an experimental and theoretical phase. The experimental phase uses specially designed transistors in which various design variations were included. Radiation testing of these transistors is in accordance with factorial design principles. The data are analyzed using the techniques of the analysis of variance. The theoretical effort is based on transistor physical design theory and is used to correlate and verify the results of experiment. During this quarter, the initial physical design theory was developed with injection level effects included at the outset. For the experimental phase the statistical design of the experiment begins with the proper sequencing of the steps for device fabrication. This is necessary to exclude the possibility that a given processing method, unrelated to the design parameter under consideration, will affect the experimental results. Further accomplishments during this quarter include the design and initiation of construction of the radiation test instrumentation and of transistor fabrication. (auth)

21149 (AD–630836) EFFECT OF TRANSISTOR DESIGN PARAMETERS ON RADIATION RESPONSE (POWER TRANSISTORS). Second Quarterly Report, October 1, 1965–December 31, 1965. Honnold, V. R.; Thomas, G. D.; Mazenko, J. J. (Hughes Aircraft Co., Fullerton, Calif.). Apr. 1966. Contract DA28-043-AMC-01541(E). 28p. (ECOM–01541-2; FR–66-17-106). CFSTI $2.00 cy, $0.50 mn.

An investigation was made to determine those design characteristics and fabrication techniques for a silicon planar power transistor that will minimize the deleterious effects of high energy ionizing and displacement producing radiation. The method being utilized is statistical and consists of a factorially designed experiment together with analysis of variance techniques applied to a selection of specially fabricated transistors. During this quarter the major effort was spent in working out the details of the

experimental design, and in developing the method of data analysis, which will use digital techniques. In addition, a preliminary irradiation of six representative planar power devices was carried out. A deviation from linearity was noted in a plot of common base current gain as a function of fluence. The transistors to be irradiated in the first factorial experiment were fabricated and delivered for testing. (auth)

21150 (HMI-B-45) ZUR AENDERUNG DER ELEKTRISCHEN EIGENSCHAFTEN VON SILIZIUM- UND GERMANIUM-DIODEN BEI NEUTRONEN-BESTRAHLUNG. (Contribution to the Change of the Electrical Properties of Silicon and Germanium Diodes by Neutron Irradiation). Reinicke, B.; Zander, K. (Hahn-Meitner-Institut fuer Kernforschung, Berlin (West Germany)). Dec. 1965. 62p. Dep. mn.

The influence of neutron-irradiation on the switching times of Si- and Ge-diodes is investigated. Characterising the switching behavior, the switching time constant is determined and its shortening during irradiation is measured. The behavior of a Si step recovery diode under the influence of irradiation is described. Furthermore, changes of the minority carrier lifetime in the base of unsymmetrically doped diodes during irradiation in a reactor are reported. The influence of irradiation on the breakdown of p-n junctions in Si-Zener-diodes is discussed by means of the temperature coefficient of the breakdown voltage. (auth)

21151 (IBM-66-825-1944) REACTOR AND LINEAR ACCELERATOR INDUCED EFFECTS IN DIELECTRICS. Frankovsky, F. A.; Shatzkes, M. (IBM Federal Systems Div., Owego, N. Y.). Mar. 1966. 39p.

The currents induced by nuclear radiation from a pulsed reactor on several commercial capacitors were compared with those induced by the electron beam of a linear accelerator (LINAC) source. Dependence of the radioinduced current on applied voltage, geometry, dose, and dose-rate was contrasted for Mylar, polystyrene, mica, tantalum, glass, and ceramic capacitors. The effects were analyzed in terms of models appropriate for the various capacitors, and values of parameters defining these relations are given. The relative effectiveness of neutron and gamma radiation in producing induced currents in these capacitive elements at the reactor environment was also obtained. (auth)

21152 (N-65-22353) EFFECTS OF NUCLEAR RADIATION, CRYOGENIC TEMPERATURE, AND VACUUM ON THE ELECTRICAL PROPERTIES OF DIELECTRIC MATERIALS. Gause, R. L.; McKannan, E. C. (National Aeronautics and Space Administration, Huntsville, Ala. George C. Marshall Space Flight Center). Mar. 30, 1965. 34p. (NASA-TM-X-53230). CFSTI $2.00 cy, $0.50 mn.

Commonly used dielectric materials were evaluated to determine their response to environmental parameters such as neutron and gamma radiation to 1.7×10^{10} ergs-gm^{-1} (C), cryogenic temperatures to −160°C, and low pressures to 2×10^{-7} mm Hg, simultaneously. The data which were obtained included capacitance (k), dissipation factor (tan σ), and mechanical properties. The dissipation factor data are not discussed because no significant changes were measured. The electrical measuring techniques employed for obtaining valid and reproducible information from combined environmental tests are discussed, and the test equipment is described. A preliminary evaluation is made of four dielectric materials: fluorocarbon, polyurethane, epoxy, and silicone. The results indicate that low pressure alone has little or no effect on k where the polymers are thermally stable, radiation alone increase k, and temperature in the range +70°C to −160°C has little or no effect on k of the silicone and fluorocarbon, but it has a direct and significant effect on the epoxy and polyurethane. The mechanical strength of the four polymers is reasonably stable when they are irradiated in vacuum at cryogenic temperatures. (auth)

21153 (N-65-25593) DEFECT ANNEALING IN IRRADIATED SEMICONDUCTORS. Progress Report No. 2, October 1, 1964–March 31, 1965. Pritchard, W. Maurice (Old Dominion Coll., Norfolk, Va. Dept. of Physics). Apr. 1, 1965. 13p. (NASA-CR-63253). CFSTI $1.00 cy, $0.50 mn.

Developments in a research program on defect annealing in irradiated semiconductors are presented. The annealing model was extended to include an arbitrarily large number of secondary defect complexes. Series solutions were made for the isothermal annealing equations with any number of secondary defect complexes. Computer calculations and data analysis were made to evaluate the behavior of the kinetic annealing model with one secondary defect complex. (STAR)

21154 (N-65-23290) [IRRADIATION DAMAGE IN N-TYPE SILICON CRYSTALS]. Monthly Progress Report, February 1–March 1, 1965. Downing, R. G. (Space Technology Labs., Inc., Redondo Beach, Calif.). Mar. 24, 1965. Contract NAS5-3805. 3p. (NASA-CR-62636; STL-4161-6011-SU-000). CFSTI $1.00 cy, $0.50 mn.

Specimens of n-type silicon with resistivities of 1 and 100 ohm-cm, and p-type silicon with resistivities of 150, 75, and 15 ohm-cm were irradiated to obtain valid and meaningful information on the defect introduction rates in the range from 1 to 3 Mev. Initial measurements of the irradiated 15 and 75 ohm-cm p-type silicon indicate a steeper energy dependence than that obtained for 150 ohm-cm p-type specimens. Irradiation of additional specimens of all three p-type crystals at 11.5 Mev appears to substantiate the trend to energy dependences similar to the degradation of minority carrier lifetime in p-type silicon. This defect level at ev + 0.29 ev has been referred to as a divacancy. The irradiated n-type specimens exhibited data in good agreement with those previously reported. (STAR)

21155 MODIFICATION OF THE LOGARITHMIC DAMPING DECREMENTS OF QUARTZ OSCILLATORS BY X IRRADIATION. Tilgner, Heribert (Univ., Vienna). Acta Phys. Austr., 21: 188-97(1966). (In German).

In the irradiation of a quartz oscillator by x rays, the logarithmic damping decrement is significantly increased. The measured value is 1.88×10^{-5} before and 2.33×10^{-5} after 18-hr x irradiation, which is an increase of approximately 24%. The mean relative error of the logarithmic damping decrement is 2%. A regular dependence of the logarithmic damping decrement on the length of the x irradiation could not be established. Expanded work on the effect of α and neutron collisions on quartz oscillators is necessary. The measured values of the logarithmic damping increment before the x irradiation agree well with previous values. The deviations of the logarithmic damping decrements from each other can be traced to the various types of supports for the crystals. (TCO)

21156 STUDY OF BEHAVIOR OF SEMICONDUCTOR DEVICES SUBJECTED TO IRRADIATION. Glotin, Ph. (CEN, Grenoble, France). Bull. Inform. Sci. Tech. (Paris), No. 98, 69-80(Nov. 1965). (In French).

The present knowledge on radiation effects on electronic devices is reviewed. The fundamental phenomena controlling the parameter variations (carrier lifetime and mobility evolution) are indicated and behavior of diodes (reverse and direct-biased characteristics), transistors (gain variation), field-effect transistors, and metal oxide semiconductor transistors are described. Formulas are presented for a first approximation calculation of the quantitative evolution of the parameters. The orders of magnitude of the flux present in nature and the radiation equivalence problem are considered. Several figures give an easy way for calculating transistor degradation. Polarization and surface effects are also discussed. (auth)

21157 EFFECT OF IRRADIATION BY NUCLEAR PARTICLES ON SWITCHING TIMES OF FAST DIODES. Bielle, Jean (Faculte des Sciences, Toulouse); Cambou, Francis; de Lafond, Yann Gervais; Mirat, Paul; Pichoff, Yves. Compt. Rend., Ser. B, 262: 425-8(Feb. 7, 1966). (In French).

The effect of neutron irradiation on the proportionality coefficient between the current and the charge and the

storage time were studied for two types of commercial diodes. The results are tabulated and show that an irradiation of 10^{15} fast neutrons/cm^2 reduces the storage time by a factor of 2.2 to 3.7. An irradiation with a flux of 10^{16} fast neutrons/cm^2 causes the recovery phase to disappear almost completely while maintaining the rectifying properties of the diode. The stability of the faults created was investigated by annealing the diodes after irradiation. Three stages of recovery were detected. (J.S.R.)

21158 INVESTIGATION OF ATOMIC ENERGY COUNTERMEASURES. STUDY OF HIGH POLYMER INSULATING MATERIALS FOR USE IN POCKET DOSIMETERS. Urai, Tatsuo. Giho (Res. Develop. Headquart., Jap. Def. Agency), 4: 71-9(Feb. 1965). (In Japanese).

The variation with temperature of electric conductivities (specific resistances) of various high polymer materials was studied. The resistance was measured by a vibrating reed potentiometer. For polycarbonate, the activation energy was 1.25 ev in the high temperature region, 0.57 ev in the low temperature region, and continuously varied in the region between. For polytetrafluoroethylene, it was 1.04 ev in the high temperature region above 38°C and 0.79 ev in the low temperature region below 25°C. It was observed that the values, 1.25 and 1.04 ev, were approximately the same as those of other organic materials measured. (tr-auth)

21159 γ-RAY IRRADIATION ON MOS FIELD EFFECT TRANSISTOR. Edagawa, Hiroshi (Kobe Kogyo (Industries) Corp., Kobe, Japan); Morita, Yoshinori; Maekawa, Shun-ichi; Inuishi, Yoshio. Jap. J. Appl. Phys., 5: 256-8 (Mar. 1966).

Gamma ray irradiation annealing effects of an MOS FET depletion-type transistor are described. Phosphorus diffusion into p-type silicon having a (111) surface was carried out to form an n^+ region. The irradiation led to a spurious enhancement operation mode after exposure to a 4 $(10)^7$ Roentgen dose. The donor surface state density is shown, and the activation energy of annealing is estimated to be about 1.06 ev. (J.F.P.)

21160 EFFECTS OF NUCLEAR RADIATIONS ON THE PROPERTIES OF SEMICONDUCTORS. Varicak, Milena (Inst. Ruder Boskovic, Zagreb). Nukl. Energ., No. 5-6, 15-20(1965). (In Slovak).

Studies of the effects of nuclear radiation on the properties of semiconductors offer possibilities for the investigation of the structure of materials and allow investigations of the use of semiconductor elements in the operation of nuclear machines and satellites. The main characteristics of semiconductors and the defects induced by irradiation in the solid state are reviewed. Results obtained in recent decades in this field are discussed. (auth)

21161 SOME EFFECTS OF ELECTRON IRRADIATION AND TEMPERATURE ON SOLAR CELL PERFORMANCE. Martin, J. H. (Johns-Hopkins Univ., Baltimore); Teener, J. W.; Ralph, E. L. pp 15-19 of Proceedings, 17th Annual Power Sources Conference. Red Bank, N. J.; PSC Publications Committee, 1963.

A theoretical analysis of radiation effects on the performance of solar cells is summarized, and the results of an experimental investigation of the effects of electrons on several n-p and p-n solar cells at five temperatures ranging from 10 to 90°C are presented. (D.C.W.)

21162 NUCLEAR RADIATION RESISTANT BATTERIES. Ho, Jack W. (Lockheed Missiles and Space Co., Palo Alto, Calif.). pp 68-71 of Proceedings 18th Annual Power Sources Conference. Red Bank, N. J.; PSC Publications Committee, 1964.

The design and testing of batteries for use in space vehicles are discussed using three batteries (AgO-Cd-KOH, AgO-Zn-KOH, and NiO-Cd-KOH) as examples. (D.C.W.)

21163 STUDIES ON X-AGENT. XLVI. TWO MUTUALLY ANTAGONISTIC ACTIONS OF X-AGENT ON PHOTOELECTRIC CELLS. Moriyama, Hideo (Shonan Hygiene Inst., Kamakura, Japan). Yokohama Med. Bull., 16: 255-66(Dec. 1965).

New properties are reported for this alleged cosmic radiation. It was found that the transparency or the transmittance of a small glass vessel (an absorption cell used with a Leitz photometer) sometimes changed if the glass vessel had been placed near a water bottle or a pile of lead blocks. The changes appeared to be due to a change in the sensitivity of the photoelectric cell in the photometer. The sensitivity was apparently affected by the light which had been altered by X agent by passing through the glass vessel; activation by a secondary X agent emitted from the substance occurred. That is, the glass vessel was activated by the secondary X agent emitted from lead or water, and the vessel thus activated converted the light into X agent; the light thus changed into X agent could in turn affect the sensitivity of the photo electric cell. The effect of light on the photoelectric cell depended on the nature of the glass surface through which the light passed. When the light passed through the frosted glass surface of the vessel, the sensitivity of the cell was usually increased, whereas when it entered the transparent glass surface, sensitivity was almost always decreased. Thus, the mutually antagonistic functions which are characteristic of X agent were demonstrated in the light which had passed through a glass vessel previously affected by X agent. Light which had passed through a glass vessel that was previously affected by the X agent was regarded as typical X agent. Light passing through a red filter had sensitivity-decreasing action on the photoelectric cell as the light passing through the transparent surface of the vessel which had previously been activated by X agent. However, the red light never exhibited the two mutually antagonistic actions, in contrast to the X agent. In this respect, red light could not be regarded as the X agent. (BBB)

21164 SELECTED PAPERS FROM THE 1965 CONFERENCE ON NUCLEAR AND SPACE RADIATION EFFECTS, ANN ARBOR, MICHIGAN, JULY 12-15, 1965. IEEE (Inst. Elec. Electron. Eng.), Trans. Nucl. Sci., NS-12: 1-155(Oct. 1965). (CONF-650707).

Fourteen selected papers from the conference were included. Eight of these appeared previously in NSA as 19: 32778, 40936, 41091, and 42771 and 20: 11182, 13133, 15232, and 15993. Separate abstracts were prepared for 6 papers. (J.F.P.)

For abstracts of individual papers see: 21059, and 21165–21169.

21165 SPACE RADIATION EFFECTS IN SILICON DEVICES. Rosenzweig, W. (Bell Telephone Labs., Murray Hill, N. J.). IEEE (Inst. Elec. Electron. Eng.), Trans. Nucl. Sci., NS-12: 18-29(Oct. 1965).

It was shown how the bulk-damage effectiveness of the space radiation environment is modified by shielding. The criterion used for bulk damage in silicon was the low-excess-carrier density diffusion length, and the damage effectiveness was expressed in equivalent 1 Mev electron flux. Shielding evaluations of ionization dose were also presented. These can be used in determining space radiation effects on silicon transistors and MOS structures as well as on chemical systems. The Telstar I and II solar cell power plant degradation curves were used to illustrate the degree of consistency which exists between observed and expected bulk damage in the space environment. They were also used to illustrate the phenomenon of time variation of radiation exposure due to apsidal precession. (J.F.P.)

21166 SIMPLIFIED TECHNIQUES FOR PREDICTING TREE RESPONSES. Carr, E. A. (Hughes Aircraft Co., Fullerton, Calif.). IEEE (Inst. Elec. Electron. Eng.), Trans. Nucl. Sci., NS-12: 30-9(Oct. 1965).

Improved engineering techniques are developed for predicting equilibrium primary photocurrents from transistor electric parameters. A radiation storage time parameter is defined and theoretical and empirical equations for radiation storage time are developed. A radiation storage

time transistor model and nomograph are presented to simplify pulsed radiation response predictions by circuit designers. The techniques are unique in predicting radiation responses entirely from measured pre-irradiation transistor electric parameters. (J.F.P.)

21167 GENERALIZED MODEL ANALYSIS OF IONIZING RADIATION EFFECTS IN SEMICONDUCTOR DEVICES. Raymond, J. P.; Willis, J. IEEE (Inst. Elec. Electron. Eng.), Trans. Nucl. Sci., NS-12: 55-68(Oct. 1965).

Work done on the applicability of the Linville lumped model in a generalized model analysis for complex semiconductor device behavior in the radiation environment is presented. It is shown that the lumped model analysis provides an effective technique for analyzing simple as well as complex devices in a pulsed ionizing radiation environment. Included is the representation of a simple p-n junction diode, a grown-junction transistor, and a planar diffused transistor with its monolithic-clip substrate and isolation junction. The transistor response is investigated as a function of quiescent emitter current and external base resistance. The effect of the substrate junction in the monolithic-chip transistor is qualitatively presented as a function of the transistor parameters and the substrate proximity. (J.F.P.)

21168 RADIATION INDUCED REGENERATION THROUGH THE P-N JUNCTION ISOLATION IN MONOLITHIC I/C's. Kinoshita, G.; Kleiner, C. T.; Johnson, E. D. (Autonetics, Anaheim, Calif.). IEEE (Inst. Elec. Electron. Eng.), Trans. Nucl. Sci., NS-12: 83-90(Oct. 1965).

Experimental and analytic methods which were used to determine the susceptibility of a specific type monolithic integrated circuit to regenerative operation are described. The analytic methods predicting the form of the regenerative transient effect rely heavily on the use of an automated digital computer code termed Transient Radiation Analysis by Computer (TRAC) which mechanizes the complex nonlinear equations that simulate the semiconductor behavior. A possible mechanism for the observed radiation-triggered regenerative effects in p-n junction isolated integrated circuits is discussed, and the results of computer simulation of the derived model are presented. It is concluded that the regenerative action can be viewed as a circuit response phenomenon in which the intended circuit element interaction with the parasitics is considerably more complex than the simple substrate photocurrent generation or parallel transistor concepts. (J.F.P.)

21169 EFFECT OF OPERATING CONDITIONS AND TRANSISTOR PARAMETERS ON GAIN DEGRADATION. Frank, Max; Larin, Frank (Bendix Corp., Southfield, Michigan). IEEE (Inst. Elec. Electron. Eng.), Trans. Nucl. Sci., NS-12: 126-33(Oct. 1965).

A general study is made to obtain an accurate prediction of changes in performance parameters of semiconductor devices in neutron radiation environments, from electric measurements of the device. The bulk displacement damage effect on transistor gain is covered. Data for predicting transistor gain degradation in a neutron environment were obtained from experimental studies of the variation of the radiation damage constant as a function of temperature and current during both measurement and irradiation. The resulting relative dispersions of the damage constant for minority carrier densities of $10^{15}/cm^3$ and $10^{16}/cm^3$ were typically 15 to 20 percent. These dispersions indicate that electric measurements of transistor physical parameters can provide reasonably accurate predictions of the gain degradation for a wide variety of transistors without additional radiation testing of specific transistor types. (J.F.P.)

21170 EFFECT OF HIGH-ENERGY RADIATION ON ELECTRIC CONDUCTION OF VARIOUS COPOLYMERS CONTAINING POLYETHYLENE. Ieda, M.; Yamada, Y.; Shinohara, U. (Nagoya Univ., Japan). 8p. (CONF-651028-2). ORAU. Gmelin, AED-CONF-65-310-1.

From Conference on Electrical Insulation, Buck Hill Falls, Pa.

Specimens of copolymers consisting of polyethylene and various amounts of polyvinyl acetate polymer, polypropylene polymer, or polymethylmethacrylate polymer were irradiated with gamma rays of 5 megarad from ^{60}Co at room temperature in air with a dose rate of 17×10^4 rad/hr to study the effect of high energy radiation on the electric conduction of these mixtures. The value of ρ, volume resistivity for the irradiated mixtures is compared with unirradiated polymers and mixtures of polymers. (B.L.M.)

21171 TRANSIENT EFFECT OF NUCLEAR RADIATION ON THE DIELECTRIC PROPERTIES OF CERAMICS AND PLASTICS AT MICROWAVE FREQUENCIES. Edelson, D.; Jaeger, R. E.; Williams, J. C. (Bell Telephone Labs., Inc., Murray Hill, N. J.). 12p. (CONF-651028-4). ORAU. Gmelin, AED-CONF-65-310-2.

From Conference on Electrical Insulation, Buck Hill Falls, Pa.

Several plastic and ceramic materials including polyethylene, polytetrafluoroethylene, polystyrene, alumina, magnesia, silica, and beryllia were exposed to radiation at three different frequencies in the 1–10 Gc range, corresponding to the L, S, and X bands to investigate the effect of the radiation on the dielectric properties of the materials. A resonant cavity method was chosen for the dielectric measurements, and the materials were irradiated in a General Atomics TRIGA pulsed reactor of the swimming pool type. No change in dielectric measurement was noted due to the constant radiation. (B.L.M.)

21172 SILICON SURFACE DAMAGE DUE TO GAMMA RADIATION. Littlejohn, M. A.; Lade, R. W. (North Carolina State Univ., Raleigh). 6p. (CONF-651061-1). ORAU. Gmelin, AED-CONF-65-326-6.

From 21st National Electronics Conference and Exhibition, Chicago.

A study of the results of the influence of low energy gamma radiation on the surface recombination velocity in silicon is reported. A review of some of the present models for surface recombination is given. Irradiation conditions are described in detail for rectangular Si filaments. Their lifetime was measured by the method of photoconductive decay. Lifetime of the filament was found to decrease drastically upon initial irradiation and then continued to decrease slowly with additional irradiation. The surface recombination velocity was found to decrease with initial irradiation and then increase with additional irradiation. (B.L.M.)

21173 MODELLING OF RADIATION EFFECTS IN SEMICONDUCTOR DEVICES AND CIRCUITS. Compton, J. B. (Motorola Inc., Scottsdale, Ariz.); Happ, W. W. 21p. (CONF-650655-3). ORINS. Gmelin, AED-CONF-65-159-2.

From Aerospace Technical Conference and Exhibit, Houston, Tex.

Radiation effects on semiconductor devices and circuits are modeled using flowgraph techniques. Developments in modeling techniques include: the lumped-parameter semiconductor diffusion-controlled model; the systematic formulation of equivalent circuits with independent and controlled sources; the development of the closed system approach to study variations in terms of conductivity; and the utilization of a computer routine, which provides circuit response to given excitations or given parameter changes. The model proposed by Linvill was modified to include effects of both neutron and pulse radiation sources. Examples of circuit applications illustrate the use of the lumped model with radioinduced generators of carriers. A technique was developed for evaluating sensitivity of circuit response to parameter changes. (M.C.G.)

ISOTOPE TECHNOLOGY

General

21174 (SAN-575-12) APPLICATION OF RADIOISOTOPES TO MANNED SPACECRAFT LIFE-SUPPORT SYSTEMS. SUMMARY REPORT: VOLUME I. TECHNICAL. VOLUME II. APPENDIXES. (Garrett Corp., Los Angeles, Calif. AiResearch Mfg. Div.). July 1965. Contract AT(04-3)-575. 438p. Dep. mn. CFSTI $7.38 cy, $2.00 mn.

The results of a study on the potential applications of radioisotopes to the operation of spacecraft life-support systems are reported. Planned spacecraft missions and the life-support system processes they require are discussed. The integration of radioisotope thermal sources into the specific process functions was analyzed, and weight comparisons were made between isotope energy systems and systems operated by fuel cells and solar cells. Studies were made of radioisotope selection and design considerations, and tradeoffs were made between single source and multiple source systems. Detailed studies are presented on the applications of isotopes to the processes of carbon dioxide removal, refrigeration, water and oxygen recovery, spacecraft heating, contaminant control, biological systems, and lunar material processing. It was determined that isotope heating shows considerable promise in extended spacecraft missions for processing of water, regeneration of the spacecraft atmosphere, vehicle heating, and decomposition of solid wastes. Radioisotopes are shown to be potentially suitable for providing refrigeration and for the processing of lunar materials, but the proof of these applications awaits prototype construction and testing. (auth)

21175 THE EQUIVALENT RADIOISOTOPE FACTOR. Ben-Porath, M. (Hadassah Univ. Hospital, Jerusalem). Israel J. Med. Sci., 1: 254-6 (Mar. 1965).

A simple formula is derived that permits calculation of the quantity of isotope B of an element X necessary to obtain the same count rate, under identical conditions, as obtained from isotope A. This relation is defined as the equivalent radioisotope factor (ERF). To derive the formula it was necessary to consider the number of detectable signals/atom-disintegration, the absorption of the photons in the critical organ, and the absorption of the photons in the detecting crystal. A geometric factor (g) was applied, that is a function of the size and shape of the critical organ. The derivation of the ERF formula is given. Its final form is: $ERF = (SR \times R \times g/1\Delta\mu_a)(1 - e^{-1\Delta\mu_a})$. Applications of the formula are discussed. (H.G.D.)

Industrial Applications

Refer also to abstracts 20726 and 20727.

21176 (AD-621440) APPLICATIONS OF RADIOISOTOPES FOR NAVAL FIELD ESTABLISHMENTS. Final Report. Gardner, Leonard B.; Hanna, Alfred E.; Stanton, Henry E. (Naval Civil Engineering Lab., Port Hueneme, Calif.). Sept. 8, 1965. 11p. (TN-N-726). CFSTI $1.00 cy, $0.50 mn.

Techniques employing radioisotopes were investigated in order to determine their usefulness to Public Works Departments of the Naval Shore Establishment. These techniques include: absorption, detection of location, and backscattering. The last mentioned seemed to be the most promising and offered several applications for waterfront maintenance. Several Naval Field Establishments were visited during the course of the work to ascertain problem areas. (auth)

21177 (ORNL-IIC-7) PROCEEDINGS OF INFORMATION MEETING ON IRRADIATED WOOD-PLASTIC MATERIALS HELD AT CONRAD HILTON HOTEL, CHICAGO, ILLINOIS, SEPTEMBER 15, 1965. Green, Ralph E.; Baker, Philip S. (eds.) (Oak Ridge National Lab., Tenn.). Apr. 1966. Contract W-7405-eng-26. 123p. (CONF-650960). Dep. mn. CFSTI $2.00 cy, $0.75 mn.

Sixteen articles are included; separate abstracts were prepared for each. (P.C.H.)

For abstracts of individual papers see: 21178–21191, 21348, and 21349.

21178 (ORNL-IIC-7, pp 1-5) THE ATOMIC ENERGY COMMISSION'S PROGRAM IN WOOD-PLASTIC MATERIALS. Bloom, Justin L. (Division of Isotopes Development (AEC), Washington, D. C.).

The four areas that constitute the program are: research on the fundamentals of the process and properties of the materials produced; market surveys and commercialization studies; consolidation of technical and economic information available and preparing conceptual plant design; and cooperative agreements with a representative cross section of wood-products industries to provide consulting services to industry for specific products to be converted to wood-plastic combinations for evaluation purposes. The mission of the Division of Isotopes Development, i.e., expansion of the use of radiation and radioisotopes in applications which are in the national interest, is also briefly described. (auth)

21179 (ORNL-IIC-7, pp 6-14) BASIC RESEARCH ON IRRADIATED WOOD-PLASTIC COMBINATIONS. Kent, James A. (West Virginia Univ., Morgantown).

The basic steps—evacuation, impregnation, and irradiation—for the preparation of samples of wood-plastic combinations (WPC) for physical testing are briefly described. These tests have shown WPC to have general improvements in toughness, bending and compression strength, hardness, moisture resistance, abrasion resistance, shear strength, insect and rot resistance, workability, and other properties. In a comparison of methods to induce polymerization of monomers within wood, irradiation was found to have several advantages over heat: absence of a catalyst within the monomer, which prevents danger of premature polymerization and loss of valuable monomer; enhanced safety of operation; and better control of the rate of polymerization. (auth)

21180 (ORNL-IIC-7, pp 15-21) POLYMERIZATION AND POLYMER PROPERTIES AS RELATED TO WOOD-PLASTIC COMBINATIONS. Klein, Richard M. (Rohm and Haas Co., Philadelphia, Pa. Special Products Dept.).

The basic mechanism of polymerization of a monomer is briefly described. There are four advantages of using radiation rather than chemical catalysts to induce this polymerization reaction in wood: pot life of the monomer is longer; radiation can overcome effects of resins in the wood that act as inhibitors for chemical catalysts; elevated temperatures and long curing times are not required with irradiation; and no chemical catalyst residue remains in the wood. Three types of polymerization reactions are discussed: graft polymerization between polymer and cellulose; cross-linking of polymers; and copolymers formed from two or more different monomers. The glass transition temperature, a useful parameter for qualitatively estimating mechanical properties of homopolymers and copolymers, together with its application to copolymer systems, is explained. (auth)

21181 (ORNL-IIC-7, pp 32-48) A PROGRESS REPORT ON A FEASIBILITY AND CONCEPTUAL DESIGN STUDY OF THE WOOD-PLASTIC COMBINATIONS PROCESS. Frankfort, J. H. (Vitro Engineering Co., New York).

A feasibility and conceptual design study of the wood-plastic combinations (WPC) process was made. The study

indicated that sufficient data have been generated for the design of a pilot plant facility with a 200 lb/hr production rate; recommended a pilot plant that would provide capabilities for development work on other monomer systems — work essential for design of a production facility using these materials; considered the economic factors related to a 3000 lb/hr WPC production plant; and concluded that the market potential for furniture, flooring, and specialty items is excellent. Design features for monomer handling, impregnation, and irradiation equipment as well as research functions for the pilot plant are described. Recommendations and conclusions are presented. (auth)

21182 (ORNL-IIC-7, pp 49-58) RADIATION AND ITS COMMERCIAL FUTURE. Tremmel, Ernest B. (Division of Industrial Participation (AEC), Washington, D. C.).

The responsibilities of the Division of Industrial Participation of the USAEC are described, including the functioning as a focal point for industrial inquiries for civilian applications of nuclear energy. With respect to radioinduced wood-plastic combinations (WPC), three suggestions are presented: WPC should be thought of as new products rather than replacements for existing products; much greater effort in product imagination and in development of new markets needs to be applied; and industry should accept greater responsibility in finding methods of getting these materials into new products and into use. The timely transfer of government-developed nuclear technology into the private sector of our economy is stressed. (P.C.H.)

21183 (ORNL-IIC-7, pp 59-63) SUMMARY REPORT OF RADIATION PROCESSED WOOD-PLASTIC MATERIALS. Stein, Martin H. (Division of Isotopes Development (AEC), Washington, D. C.).

The development, properties, and commercial future of wood-plastic products are discussed. Preliminary reports indicate that a production plant with a 3000 lb/hr — 8000 hr/year capacity could produce wood-plastic blanks at a reasonable cost. The Atomic Energy Commission's program for development and testing of wood-plastic combinations is also described. (P.C.H.)

21184 (ORNL-IIC-7, pp 64-75) POTENTIAL APPLICATIONS OF IRRADIATED WOOD-PLASTIC MATERIALS. Ruhl, Buford B. (Southern Interstate Nuclear Board, Atlanta, Ga.).

The objectives of the Southern Interstate Nuclear Board — (SINB) Wood-Plastic Combinations (WPC) project are described. It was concluded that further study of WPC is required before commercialization. Three specific actions were proposed to provide additional data and technology; establishment of an AEC research laboratory for WPC; continued direct support to private industry and universities for development contributions to the WPC process; and invitation for specialized conferences to provide companies with information on how to get into the business of WPC production. (P.C.H.)

21185 (ORNL-IIC-7, pp 76-80) IRRADIATED WOOD-PLASTIC MATERIALS—COMMERCIAL POSSIBILITIES IN THE PACIFIC NORTHWEST (AND THE GREAT LAKES REGION). Rohrmann, C. A. (Battelle-Northwest, Richland, Wash. Pacific Northwest Lab.). (BNWL-SA-310).

An investigation was made of the commercial possibilities of irradiated wood plastics in the Pacific Northwest and Great Lakes regions. Many wood processors were contacted and made aware of properties, production methods, and cost of wood-plastic combinations (WPC). The potential applications of interest include flooring of many types, furniture, veneers, and plywood shapes. The properties of WPC are well suited to these uses and many of the processors showed genuine interest in the new product and its manufacture. As a result of a recent price reduction announced by the USAEC, the use of ^{137}Cs as the radioactive source is suggested for consideration in the design of future WPC irradiation facilities. (auth)

21186 (ORNL-IIC-7, pp 81-8) THE INVESTIGATION OF COMMERCIAL POTENTIAL OF WOOD-PLASTIC COMBINATIONS IN THE NORTHEAST. Egan, Douglas M. (State Univ. of New York, Buffalo).

In a study of the commercialization of wood-plastic combinations (WPC), the Western New York Nuclear Research Center chose to explore only the requirements for commercialization and excluded studies of market potential and profitability. Identification of products and firms for which WPC seemed to offer promising applications, determination of interest in WPC expressed by firms, and recommendations of promising locations for WPC processing facilities were the major responsibilities of the investigation. Among the more promising applications for WPC considered in the evaluation were flooring, furniture, industrial patterns, and shapings and turnings. Cost considerations and plant siting were also considered in the evaluation. It was concluded that additional information on WPC properties and production is needed before definite results can be obtained. (auth)

21187 (ORNL-IIC-7, pp 89-94) COMMERCIAL PRODUCTION OF WOOD-PLASTIC COMBINATIONS. Barrett, Lawrence G. (American Novawood Corp., Lynchburg, Va.).

The American Novawood Corporation was incorporated in August 1964 and was the first concern to produce wood-plastic combinations (WPC) commercially. In addition to sample preparation, company-sponsored research and development, and supplying materials and consulting services, the company is heavily involved with the construction of a commercial-scale pilot-plant facility. A strong criticism of the continued support of the USAEC development program for wood-plastic combinations is presented: the AEC has adequately demonstrated the value of WPC and should therefore discontinue support and permit private industry to take both the natural business risks and the rewards of their efforts. (auth)

21188 (ORNL-IIC-7, pp 95-8) DEVELOPMENT-PRODUCTION PROGRAM FOR LOCKWOOD. Kalember, G. M. (Lockheed-Georgia Co., Marietta).

Lockheed's development program for their wood-plastic combinations — trade name Lockwood — has included expanded effort on both the process itself and commercial applications. Two problems of expanded commercialization are choosing methods of marketing and defining the types of products and customers for Lockwood. Investigation of thermoplastic monomer systems, impregnation techniques, effects of dose and dose rates on polymerization, physical and engineering properties, and testing and dyeing methods are included in the technical development program. Lockheed now produces 6000 board feet of Lockwood per month on a development-production basis. (auth)

21189 (ORNL-IIC-7, pp 99-105) THE OPPORTUNITY FOR COMMERCIAL USE OF IRRADIATED WOOD-PLASTIC MATERIALS IN THE FURNITURE INDUSTRY. Rumbaugh, Paul E. (Kroehler Mfg. Co., Louisville, Ky.).

The Kroehler Manufacturing Company has prepared an occasional-table sample with half of the top of conventionally lacquered oak and the other half of wood-plastic combination. Dealer response to a demonstration of finish resistance to cigarettes and some common household liquids was good. A large sample of hard maple impregnated with dyed methyl methacrylate had little uniformity of color; however, a cocktail table of this material was beautiful, although lighter and more varied in color than several of this firm's Early American styles. The wood worked well with conventional tools and machined cleaner and better than conventional maple. Predrilled holes were required for screws to prevent splitting. The maple WPC glued well with polyvinyl adhesive, moderately well with urea resins, and excellently with fortified urea resins. Early results with WPC veneers were, in general, disappointing but not necessarily pessimistic. The use of WPC for solid-wood furniture may be prohibited by cost except for some specific applications. The greatest possibilities for WPC in furniture appear to be in veneer applications, but further research work is required in their fabrication and finishing techniques. (auth)

21190 (ORNL-IIC-7, pp 106-11) POTENTIAL OF WOOD-PLASTIC COMBINATIONS IN THE SPORTING-GOODS INDUSTRY. Harris, Thomas R. Jr. (Hillerich and Bradsby Co., Louisville, Ky.).

Wood-plastic combinations (WPC) were used to prepare test samples of both baseball bats and golf-club heads. Improved impact strength, moisture resistance, and hardness were observed on these test samples; in addition, golf-club heads had good gluing properties with epoxy adhesives. The increased weight on WPC can easily be compensated for in golf-club heads by using fewer lead weights; however, weight addition is of concern in baseball bats. Durability and appearance of bats are good because the finish literally goes all the way through the wood. With golf-club heads, the use of dyed monomers to eliminate finishing materials and operations would be desirable. (auth)

21191 (ORNL-IIC-7, pp 112-18) POTENTIAL COMMERCIAL MANUFACTURE AND USE OF HARDWOOD PLYWOOD PLASTIC COMBINATIONS. McDonald, Clark E. (Hardwood Plywood Manufactures Association, Arlington, Va.).

The market for U. S. hardwood plywood for 1964, exclusive of captive production, was 3.667×10^9 ft^2 and was valued at $\$441 \times 10^6$. The largest portion of this market was for wall paneling, both prefinished and unfinished, followed by furniture, flush doors, mobile homes, and flooring. For these applications, wood-plastic combinations (WPC) of hardwood plywood would have many advantages — ease of cleaning, ease of repair, better appearance, resistance to staining and marring, etc. Probably the greatest potential for WPC would be for external applications — siding, doors, park benches, etc. — where conventionally treated woods cannot resist weather damage. (auth)

21192 (PB-181506, pp 19-26) THE UNITED STATES PROGRAM ON RADIATION PRESERVATION OF FOODS. Siu, Ralph G. H. (Army Materiel Command, Washington, D. C.).

Progress in research on food irradiation in the United States is reviewed. Institutions involved in the research are listed. (P.C.H.)

21193 (PB-181506, pp 29-38) FOOD IRRADIATION RESEARCH IN WESTERN GERMANY. Kuprianoff, J. (Bundesforschungsanstalt fuer Lebensmittelfrischhaltung, Karlsruhe (West Germany)).

Developments in food irradiation research in western Germany are described. These include: radiation sources; dosimetry of radiation sources; microbicidal effect in radiopreservation of fish; chemical effects in irradiated foodstuffs; processing techniques; and wholesomeness studies. (P.C.H.)

21194 (PB-181506, pp 155-67) RADIATION PRESERVATION OF FOODS—TWO DECADES OF RESEARCH AND DEVELOPMENT. Goldblith, Samuel A. (Massachusetts Inst. of Tech., Cambridge).

Problems needing solution in the radiopreservation of foods are examined by breaking them down into their component parts, and the overall problem of preservation by ionizing energy is discussed. These problems include: undesirable side reactions in radiopreservation; concurrent-radiation distillation; wholesomeness; radiation sources; and dosimetry. (P.C.H.)

21195 (TID-22509) EFFECTS OF LOW-LEVEL IRRADIATION UPON THE PRESERVATION OF FOOD PRODUCTS. Annual Report. Dennison, R. A.; Merkley, M. S.; Ahmed, E. M.; Kuhn, G. D. (Florida Univ., Gainesville. Dept. of Food Technology and Nutrition). Apr. 1965. Contract AT(40-1)-3097. 89p. Dep. mn. CFSTI $3.00 cy, $0.75 mn.

Gamma radiations at a level of 200 Krad controlled brown rot (Monolinia fructicola) infection of peaches. The radiations caused an intensification of color in the peel. Some variaties showed slight changes in flavor as a result of irradiation while flavor changes were easily detected in other varieties. The development of anthracnose on the peel of the Kent and Palmer mango varieties was controlled by 100 Krad irradiation. The flavor and texture of the fruit was very acceptable following exposure to the 100 Krad level. When the irradiation level was increased to 200 Krad there was retardation in the ripening of the fruit and flavor and texture were not acceptable. Lychees (Litchi chinensis) receiving 300 Krad irradiation were stored for three weeks with only a 14% spoilage loss while there was a 63% spoilage loss with untreated fruits stored under the same conditions and period of time. Irradiated (150 and 300 Krad) tangelo fruits had less acceptable flavor than unirradiated fruits immediately after treatment. After four weeks storage at 50°F flavor differences were not detected. Tangerines and limes developed unacceptable flavor following irradiation. There was also damage observed in the peel of the fruits. The determination of ascorbic acid in tomatoes, oranges, and tangerines did not show any major changes in this component with irradiation. In general there was some loss in the reduced form of the acid after irradiation, while the oxidized form increased in some cases and decreased in others. Measurements of pectinesterase activity in tomatoes, grapefruit, oranges, and tangerines indicated that irradiation did not effect the enzyme response uniformly. Physiological condition and stage of maturity of the fruit were probably important factors controlling the enzyme response. (auth)

21196 RECENT PROGRESS IN APPLYING HIGH DOSES OF IONIZING RADIATIONS TO ACHIEVE SHELF-STABLE FOODS. Josephson, Edward S. Activ. Rep., 17: 95-102(Fall 1965).

The high-dose food irradiation program has progressed to the point where industrial action on pilot facilities for producing irradiated meats is needed. Military objectives and current status of the Army's food irradiation program are discussed. (H.G.D.)

21197 RADIATION SOURCES FOR USE IN RADIATION PRESERVATION OF FOODS. Dietz, George R. Activ. Rep., 17: 103-10(Fall 1965).

Food irradiation facilities are surveyed. Presently ^{60}Co sources continue to offer significant advantages over other radiation sources. Uses and performance of the Research Irradiator, Mobile Gamma Irradiator, Grain Products Irradiator, Marine Products Development Irradiator, On-Board Ship Irradiator, Hawaiian Development Irradiator, and Meat Sterilization Facility are reviewed. (H.G.D.)

21198 THE WHOLESOMENESS OF IRRADIATED FOODS. Raica, Nicholas Jr. Activ. Rep., 17: 111-13 (Fall 1965).

Wholesomeness of irradiated foods is one of the most vital phases of the U. S. Army Food Irradiation Program. Data on wholesomeness are summarized for: long term animal feeding studies, carcinogenicity studies, human feeding studies, and supporting studies such as investigations of radioactivity, nutrient stability and adequacy, tissue enzyme activities in test animals, digestibility, vitamin K nutrition, and chemical changes. It is concluded that food irradiated with ionizing radiations to 5.6 Mrads with energies of up to 10 Mev are as wholesome as food processed by conventional methods. (H.G.D.)

21199 ACCEPTANCE OF IRRADIATED FOODS. Heiligman, F.; Phillips, C. E. Activ. Rep., 17: 114-19 (Fall 1965).

Acceptability tests on irradiated foods are reviewed. Testing was done at Ft. Lee and followed conventional approaches using the 9-point hedonic rating scale as a basic criterion. It was concluded that radiation processed foods such as sterilized meats and poultry, and pasteurized shrimp, oranges, and fish items are acceptable and can be adapted for use in military feeding situations. (H.G.D.)

21200 RADIOPASTEURIZATION OF FISHERY PRODUCTS. Slavin, Joseph W.; Ronsivalli, Louis J.; Kaylor, John D. Activ. Rep., 17: 120-32(Fall 1965).

Accomplishments in radiopasteurization of fishery products are summarized and recent progress in food technol-

ogy is reviewed. Variables affecting the response to irradiation and subsequent storage life of the treated product are: dose levels; inherent biological makeup of the product, particularly the lipid composition; temperature and product environment during treatment and storage; and quality of the the raw material. It has been established that the microflora of radiopasteurized fish changes as a result of irradiation. These changes must be evaluated in terms of product safety. The use of gas chromatography and mass spectrophotometry to separate and identify carbonyl compounds and sulfides in fish fillets and clams is considered. Steps leading to commercialization of radiopasteurized fish are discussed. (H.G.D.)

21201 SOME THOUGHTS ON MICROBIOLOGY OF RADIATION PRESERVATION OF FOODS. Goldblith, S. A.; Nickerson, J. T. R.; Licciardello, J. J. (Massachusetts Inst. of Tech., Cambridge). Activ. Rep., 17: 133-9(Fall 1965).

Arguments against regulation of dose requirements for radiation processed foods by the Food and Drug Administration are discussed. (H.G.D.)

21202 PERIMETERS OF THE COMMERCIALIZATION OF IRRADIATED FOODS. Ketchum, Harry W. Activ. Rep., 17: 140-4(Fall 1965).

Factors that should determine the direction and extent of commercialization of irradiated food are discussed. Such considerations include: magnitude and characteristics of the food industry; economic significance of the types of benefits possible; cost-benefit relationships; consumer acceptability; and industrial participation. (H.G.D.)

21203 EFFECT OF γ IRRADIATION ON THE MICROFLORA OF FRESHWATER FISH. I. MICROBIAL LOAD, LAG PERIOD, AND RATE OF GROWTH ON YELLOW PERCH (PERCA FLAVESCENS) FILLETS. Kazanas, N.; Emerson, J. A.; Seagran, H. L.; Kempe, L. L. (Bureau of Commercial Fisheries Technological Lab., Ann Arbor, Mich.). Appl. Microbiol., 14: 261-6(Mar. 1966).

Microbial flora were compared in irradiated and nonirradiated yellow perch fillets. These studies included effects of irradiation on the total microbial population, the lag phase, and rate of growth in this freshwater fishery product. The work was conducted concurrently with sensory and chemical evaluation, and constituted part of an investigation designed to evaluate the effect of substerilization doses (0.3 and 0.6 Mrad) of ^{60}Co γ rays on the storage life of yellow perch fillets at 1.0 or 6.0°C. In five storage tests, total plate counts prior to irradiation did not exceed 8.7×10^5 per gram of sample; this count was reduced nearly 100% by irradiation with either 0.3 or 0.6 Mrad. Progressively lower maximal bacterial populations and lengthened lag phases were obtained as more radiation was used. The growth rate of the population did not appear to decrease significantly. Microbial data obtained in these studies confirmed the sensory and chemical studies, by indicating that irradiation can significantly extend the refrigerated shelf life of freshwater fish. (auth)

21204 RADIOMETRIC INVESTIGATIONS IN PREPARATION OF ASBESTOS CEMENT PRODUCTS. Duftschmid, K. E. (Reaktorzentrum, Seibersdorf, Austria). Atomwirtschaft, 11: 118-20(Mar. 1966). (In German).

In the production of asbestos cement plates or tubes the maintenance of optimum mixing conditions is necessary in order to obtain a standard quality. By direct neutron irradiation of an asbestos component in the reactor, the radioisotope ^{24}Na, suitable for use as an indicator, can be produced. Therefore a simple method is available for accurate analysis of the asbestos distribution and its filament structure in the manufactured product. A constant monitoring of operation in the mixing installation is also possible. Studies on the applicability of this method were made with activation measurements and autoradiography. (tr-auth)

21205 ON THE ACCURACY OBTAINABLE IN MEASUREMENT OF GROSS WEIGHTS WITH GAMMA RADIATIONS. Menkhoff, H. Bauingenieur, 40: 274-7(July 1965). (In German).

The estimation of the gross weight of construction materials by ^{60}Co or ^{137}Cs γ irradiation varies considerably in accuracy. Two methods are used. One is direct, with the mass interposed between a γ source and a detector. The second method is indirect with the source and detector side by side. The gross error in measurement can be kept to a maximum of ±2% if the error from nonhomogeneity of the absorber is negligibly small, provided that operating personnel are adequately trained and that the equipment is suitable for the measurement conditions. If the error from nonhomogeneity of the absorber amounts to ±1%, the total error may amount to ±3%, but if the absorber error is greater than ±1% another measurement procedure should be used. In order to reduce error from nonhomogeneity of the absorber, the source to counter distance should not be less than 50 cm for direct measurements, and not less than 30 cm for indirect measurements. If the measurements are carried out at a rate of at least 10,000 cpm, the confidence limits of the measurement will be at the 95% level. Usually the greatest time that can be expended for a single measurement is 5 min. (BBB)

21206 FOOD PRESERVATION BY IRRADIATION: PRESENT STATUS. Schultz, H. W.; Lee, Jong S. (Oregon State Univ., Corvallis). Food Technol., 20: 38-43(Feb. 1966).

The known effects of irradiation on various foods and their acceptability to consumers and probable technological feasibility are reviewed. Except for large-scale feeding tests in the U. S. military services and a few relatively large consumer-panel studies, general acceptability has been judged on the basis of lab findings. Alterations of visual properties, of physical properties, and of nutrients are well defined, but in many instances the significance of such judgments needs to be confirmed by consumer groups by usual market testing. Changes in odor and flavors during irradiation were given the greatest attention and significance, yet not subjected to consumer market tests. Sterilized bacon, disinfested grain, sprout-inhibited potatoes, and pasteurized fish appear to hold most promise for commercial development. Radiopasteurized red meats have good potential technologically and commercially, but their acceptability is doubtful because of alteration of texture and color. Radiopasteurized milk, even at low levels of irradiation, now appears unacceptable and unfeasible. Results on studies with vegetables are encouraging enough with some kinds to justify further study, particularly with low-level doses. Pasteurized poultry and fruit are both still questionable as far as acceptability is concerned, but appear to be quite feasible otherwise. (TCO)

21207 THE WHOLESOMENESS OF IRRADIATED FOODS: PAST HISTORY, PRESENT STATUS, INTERNATIONAL ASPECTS, AND FUTURE OUTLOOK. Goldblith, Samuel A. (Massachusetts Inst. of Tech., Cambridge). Food Technol., 20: 93-8(Feb. 1966).

The following four factors involved in the wholesomeness aspect of food irradiation are evaluated: effect of irradiation on nutrients in food, possible induction of toxic substances, of carcinogenic materials, and of radioactive nuclides in foods. An examination of the international aspects of food irradiation was made, and the microbiological aspects of the substerilization (preservation or pasteurization) of marine products were considered. The irradiated foods and processes that have been cleared by the U. S. Food and Drug Administration, and regulations permitting their use, are summarized. In general, irradiated foods are as nutritious as foods that have been thermally processed in the conventional manner. The effects on the macronutrients are very slight. The destruction rate of vitamins under irradiation corresponds analogously to their response to heat. Even under the most stringent tests known, toxicologists have concurred in stating that foods treated with a sterilizing dose of 5.58 Mrad do not contain toxic substances induced by exposure to ionizing energy. In no study was there evidence of carcinogenicity induced by irradiation of foods. The radioactivity induced in foods by electron bombardment at en-

ergy levels up to 24 Mev is probably relatively small, and no measurable radioactivity is induced by electrons at energy levels up to 10 Mev. It was concluded that, foods sterilized by doses of ionizing energy are safe and wholesome. The process of substerilization is still being evaluated; however, it is believed that this process will also prove to be safe. (BBB)

21208 MEASUREMENT OF LIQUID VOLUME BY ACTIVATION ANALYSIS. Miyakoshi, Junichi; Tanaka, Kohei (Hitachi Shipbuilding and Engineering Co., Ltd., Japan.). Hitachi Zosen Tech. Rev., 26: 63-6(Nov. 1965). (In Japanese).

An activation analysis method is described for the determination of the volume of the cooling medium (water solution of $CaCl_2$) in a large-scale refrigeration system without interruption of the system's operation. A known amount of ^{60}Co in the form of $CoCl_2 \cdot 6H_2O$ is added to the system as a tracer, and the cooling medium is circulated for several hours. A sample is taken from the cooling medium; and from the concentration of the tracer in the sample and the dilution ratio, the volume of the cooling system is deduced. (TCO)

21209 DETERMINATION OF ASH CONTENT OF COALS BY GAMMA-RAY TRANSMISSION METHOD. Nagy, M.; Varga, K. (Csepel Iron and Metal Works, Budapest). Vienna, International Atomic Energy Agency, 1965, Preprint No. SM-68/23, 13p. (CONF-651023-11). ORINS.

From Symposium on Radioisotope Instruments in Industry and Geophysics, Warsaw.

A radiological method was developed for analysis of coals. A few thousand samples were examined for development of the measuring method and apparatus. Results of comparative examinations are discussed. Correlation calculations were used to determine the function between the data on coals, which were measured by the coal analyzer laboratories and which were determined by radiological method. The effects of grain size, moisture content, and differences in density are discussed, and the minimalization of these effects considered. The radiological method for determination of the ash content of coals was tried for a period of three months under industrial conditions at a Hungarian power station. It was concluded, by comparing the radiological and nonradiological methods, that the accuracy, frequency of sampling, possibilities of continuous measuring, and prompt supply of data obtainable with the radiological method can produce more information from the total amounts of used coal than the nonradiological method. (auth)

Power Application

See also ENGINEERING — Space Propulsion

21210 (SC-RR-65-609) POODLE THRUSTER AERODYNAMIC DROP TEST. Dalby, W. D. (Sandia Corp., Albuquerque, N. Mex.). Apr. 1966. Contract AT(29-1)-789. 152p. Dep. mn. CFSTI $5.00 cy, $1.00 mn.

Ten TRW Systems Poodle Thrusters were dropped at Tonopah Test Range to obtain aerodynamic data. The information obtained will be directly applicable to the safety analyses of the Poodle System. The Poodle Thruster models dropped were all 16.5 inches long and had a body diameter of 2.85 inches. Five had a fin span of 13.720 inches and weighed approximately 61.5 pounds; five had a span of 5.750 inches and weighed approximately 32.5 pounds. All aerodynamic data were obtained by optical coverage. Roll rates observed were 835 to 2940 rpm and 1450 to 1925 rpm for the larger span and smaller spans, respectively. Corresponding tumble rates were 0 to 1165 rpm and 15 to 580 rpm. Maximum velocities of 230 and 290 fps were noted for the larger and smaller span models, respectively. The corresponding values for C_DS were 1.44 to 1.80 and 0.450 to 0.510 square feet. (auth)

21211 (TID-22350) HIGH-TEMPERATURE RADIOISOTOPE THERMOELECTRIC GENERATOR FOR SPACE APPLICATIONS. (Radio Corp. of America, Princeton, N. J. Astro-Electronics Div.). Dec. 31, 1964. Contract AT(40-1)-3221. 134p. (AED-R-2621). Dep. mn. CFSTI $4.00 cy, $1.00 mn.

A 26.6-pound laboratory model of a radioisotope thermoelectric generator (RTG), resembling a flight unit in its salient parts, was built and successfully tested for two months without apparent degradation in performance. The fuel used in the RTG was five pellets of strontium-90 isotope, in the form of strontium titanate, doubly encapsulated in 2 nested cylinders of molybdenum and Hastelloy X. This capsule produced 526 watts of thermal power. The use of a very efficient multifoil insulation results in a heat loss of less than 15 percent; the remaining heat is channeled through the thermoelectric array. Of the 66 silicon-germanium thermocouples called for in the design, only 32 were installed; thermal dummies were used for the remainder. Operating between average temperatures of 800°C and 250°C, the thermoelectric array produced 12.6 watts of electrical power. If the full complement of thermocouples had been used, in conjunction with 660 thermal watts of strontium 90, the electrical output would have been 28.6 watts. The laboratory model, which included certain auxiliary components for experimental expediency, weighed 26.6 pounds. It is felt that a prototype flight generator can be built which weighs 21 pounds. This would demonstrate the achievement of 1.36 watts per pound with the high-temperature techniques which were employed. Performance could be improved to give a figure of 2.0 watts per pound using the denser strontium oxide or strontium fluoride now under development. (auth)

Separation and Production

See also CHEMISTRY — Separation Processes and Procedures

Refer also to abstracts 22153 and 22405.

21212 (CONF-660305-19) PRODUCTION OF RADIOISOTOPES IN PRODUCTION REACTORS. Overbeck, W. P. (Du Pont de Nemours (E. I.) and Co., Aiken, S. C. Savannah River Lab.). Apr. 26, 1966. Contract AT(07-2)-1. 25p. Dep. mn. CFSTI $1.00 cy, $0.50 mn.

From American Nuclear Society Topical Meeting, Augusta, Ga.

The production of radioisotopes in terms of need, production facilities and schedules, process development is discussed. Special attention is given to the production of ^{60}Co, ^{238}Pu, ^{244}Cm, ^{210}Po, and ^{252}Cf. The practical aspects of production and economics are also discussed. (P.C.H.)

21213 (IAE-974) ISSLEDOVANIE IZVLECHENIYA I FORMIROVANIYA IONNYKH PUCHKOV V PLAZMENNYKH ISTOCHNIKAKH. (Investigation of Extraction and Formation of Ion Beams in Plasma Sources). Raiko, V. I. (Institut Atomnoi Energii, Gosudarstvennyi Komitet po Ispol'zovaniyu Atomnoi Energii SSSR, Moscow). 1965. 20p. Dep. mn.

Some results of the investigation of ion-optical systems as a source for electromagnetic separation installation were reported. The examination of the decompensation mechanism of the space charge of the ion beams showed that by means of the selection of the geometry of the ion-optical system and of the appropriate optimum regime the output of the source can be significantly increased. (tr-auth)

21214 (ORNL-IIC-8) REACTOR YIELD CALCULATIONS FOR 81 RADIOISOTOPES PRODUCED BY (n,γ) REACTIONS AT FLUXES OF 10^7 TO 10^{16} n/cm^2 · sec FOR IRRADIATION TIMES OF 30 MINUTES TO ONE YEAR. Whitson, T. C.; Friend, C. W. (Oak Ridge National Lab., Tenn.). Apr. 1966. Contract W-7405-eng-26. 87p. Dep. mn. CFSTI $3.00 cy, $0.75 mn.

Calculations of reactor yields in curies per gram of target material are listed in tables for 81 radioisotopes at 21 flux values, from 10^7 to 10^{16} n/cm^2 · sec, and irradia-

tion times from 0.5 hour to 1 year. The reaction and decay scheme used in the calculations for each radioisotope is given, and the method of calculation using the computer program ISOTOPES is outlined. (auth)

21215 HOT CHAMBER FOR THE PRODUCTION OF ^{131}I. Csoke, Antal; Feit, Pal; Sipos, Tamas; Szanto, Borisz; Vizdos, Geza. Magyar Tud. Akad. Kozp. Fiz. Kut. Int. Kozlem., 13: 387-98(1965). (In Hungarian).

Some problems which had to be faced in choosing the location and in designing and building of a set of hot cells for the production of ^{131}I under adequately safe conditions ensuring the proper sterility prescribed for medical purposes are discussed. (auth)

21216 MASS-SPECTROMETRIC ISOTOPIC ANALYSIS OF URANIUM USING THERMIONIC EMISSION. Opauszky, Istvan; Matus, Lajos. Magyar Tud. Akad. Kozp. Fiz. Kut. Int. Kozlem., 14: 39-48(1966).

Experiments were performed to determine the isotopic composition of uranium mass-spectrometrically. For the production of ions thermionic emission from tungsten filament was used either in a form sintered with powdered tungsten or coated with graphite powder applied in aqueous suspension. The measurements were carried out for the former with MI-1305, for the latter with CSF-500 model mass spectrometer, each being a single-focusing type with an ion-beam radius of 20 cm and dc amplifier for ion detection. Both mass spectrometers were found to be adequate for the isotopic analysis of uranium under appropriately chosen experimental conditions. The suspension method proved to be particularly useful because of its simplicity and the fairly stable and high thermionic ion intensity obtained for quite a long time from relatively small amounts of uranium. (auth)

21217 ^{132}I-GENERATOR, TYPE JG 01/59. Feher, Istvan; Nagy, G. Agnes. Magyar Tud. Akad. Kozp. Fiz. Kut. Int. Kozlem., 14: 107-12(1966). (In Hungarian).

The iodine generator (Type JG 01/59) eluted with distilled water or isotonic sodium chloride solution yields in addition to the specified I^- ion form, IO_3^- in quantities varying from generator to generator. The IO_3^- content of eluates obtained at different periods was found to increase by a factor of about 2 over 10 days of observation. The ^{132}I eluate can be easily converted to I^- with the use of 5 mg/ml ascorbic acid. It seems from the experimental evidence that the value of the ratio I^-/IO_3^- is determined rather by processes occurring in the ion exchange resin than by those in the solution. (auth)

21218 TRITIUM ENRICHMENT BY GAS CHROMATOGRAPHY. Perschke, Helmut (International Atomic Energy Agency, Niederoesterreich, Austria). Nature, 209: 1021-2(Mar. 5, 1966).

Gas chromatographic systems are considered for the tritium enrichment of large samples of hydrogen. Two types are discussed, one of low volume, requiring high concentration factors, and the other of relatively large volume, where a lower factor can be tolerated. The results for the low-volume system in which three columns were used are shown for various combinations of column lengths. For the case of large-volume counters, a two-column system is found satisfactory. By increasing the length of the retention column to 4 m, 20 liters of hydrogen were processed yielding a final fraction of 2 liters containing 96% tritium. (J.F.P.)

21219 STUDIES OF THE INTERACTIONS OF MEDIUM-ENERGY IONS WITH MATERIALS IN THE ELECTROMAGNETIC ISOTOPE SEPARATORS. Zuk, Wlodzimiers (Cathedral of Experimental Physics, Lublin). Postepy Fiz., 16: 681-99(1965). (In Polish).

Medium-capacity electromagnetic separators are discussed in terms of their application to scientific research. The applications include isotopic separations to determine reaction yields and half life of radioisotopes, to obtain samples for beta and gamma spectroscopy, and for monoisotopic targets in nuclear reactions and cross section measurements. The interaction of the ion beam with materials in the arc, and with structural materials and neutral ions in the vicinity of the ion beam is also discussed. The effects of single scattering on the isotopic purity of the separator, and the containment of ions in metallic targets are also discussed. (TTT)

21220 OUTLINE OF RADIOISOTOPE PRODUCTION AT JAERI. PRODUCTION AND DISTRIBUTION, AND THE PRODUCTION FACILITIES. Mochizuki, Tsutomu (Japan Atomic Energy Research Inst., Tokyo). Radioisotopes (Tokyo), 14: 116-25(Mar. 1965). (In Japanese).

With the start of operation of the JRR-2 and the completion of its production facilities, the radioisotope production in the JAERI has become more active. Using JRR-1 and JRR-2, the following radioisotopes have been produced: ^{24}Na, ^{42}K, ^{64}Cu, ^{82}Br, ^{198}Au, ^{32}P, ^{56}Mn, ^{72}Ga, ^{76}As, ^{90}Y, etc. The users of these radioisotopes have been medical departments of the universities, and national and public research institutes account for the use of more than half of the total isotope production. In the JRR-3, intended mainly for radioisotope production, the test production of radioisotopes will shortly be started. For the radioisotopes of long half-life, the test production of ^{51}Cr, ^{45}Ca, ^{86}Rb, etc., will be started in the near future. For the special isotopes, preparations are now in progress for the production of ^{32}P, ^{51}Cr, ^{64}Cu, etc., of high specific activity, with some already being produced in small amounts. In March 1961, an experimental radioisotope-production plant was completed; and on the basis of the experience and knowledge gained in this plant, the large scale radioisotope-production plant was completed in March 1964. The purpose of the latter is to carry out research and development on the radioisotope production and to satisfy the radioisotope demands of Japan. (tr-auth)

MATHEMATICS AND COMPUTERS

Refer also to abstracts 20965, 22031, 22032, and 22341.

21221 (ANL–7121) A CATHODE-RAY-TUBE PLOTTING SYSTEM FOR THE CONTROL DATA 3600 COMPUTER. Robinson, G. A.; Krupp, R. F. (Argonne National Lab., Ill.). Dec. 1965. Contract W-31-109-eng-38. 21p. Dep. mn. CFSTI $1.00 cy, $0.50 mn.

The Cathode Ray Tube (CRT) Display System used on ANL's CDC 3600, including the programming systems developed for CRT plotting, is described. The CRT equipment is attached to the 3600 through a 3606 Data Channel. The data transmitted from the computer are plotted on the CRT in the form of points, lines, or binary-coded decimal characters and are photographed by a 35-mm camera. (M.O.W.)

21222 (EIR–89) ALGAN-I. SUPPLEMENTARY USERS' MANUAL OF NEW DEVELOPMENTS AND FACILITIES. Alpiar, Ronald (Eidgenoessisches Institut fuer Reaktorforschung, Wuerenlingen (Switzerland)). Mar. 1966. 57p. Dep. mn.

Five new driver routines are described, which may be used as alternatives to the "standard" ALGAN driver, and which solve special problems algebraically. The new problems solved concern the solution of differential equations by the Lie-Groebner method, the examination of sets of linear simultaneous equations for linear independence, the expansion of arbitrary functions in Taylor series, the conversion of ordinary linear equations to matrix form, and ray tracing through a system of optical surfaces. The input routines of the program were broadened, to allow the use of compound identifiers, and a number of extra subroutines available for non-standard program use are described. (auth)

21223 (JINR–P–2564) K TEORII ASIMPTOTICHESKOGO PREDSTAVLENIYA SFERPODAL'NYKH FUNKTSII. (On the Theory of the Asymptotic Representation of Spheroidal Functions). Ponomarev, L. I. (Joint Inst. for Nuclear Research, Dubna (USSR). Lab. of Theoretical Physics). 1966. 7p. Dep. mn.

Using the WKB-method a transcendental equation is obtained which allows one to approximately calculate the eigenvalues of the boundary value problem for the spheroidal functions. (auth)

21224 (ORNL–3919) MATHEMATICS DIVISION ANNUAL PROGRESS REPORT FOR PERIOD ENDING DECEMBER 31, 1965. (Oak Ridge National Lab., Tenn.). Apr. 1966. Contract W-7405-eng-26. 119p. Dep. mn. CFSTI $4.00 cy, $0.75 mn.

Brief discussions of computing services carried out on the following are presented: AEC Weather Department, analytical chemistry, biology, budget and programs planning, chemical technology, chemistry, health physics, instrumentation and controls, isotopes, metals and ceramics, neutron physics, physics, reactors, reactor chemistry, reactor operations, solid state, and thermonuclear research. Statistical research, programming, and applications are discussed. (M.O.W.)

21225 MODULAR HARDWARE FOR ON-LINE HANDLING OF NUCLEAR DATA. Broberg, J. B. (National Bureau of Standards, Washington, D. C.). IEEE (Inst. Elec. Electron. Eng.), Trans. Nucl. Sci., NS-13: No. 1, 192-8(Feb. 1966).

The modular hardware that was developed for use in the on-line data-handling system at the National Bureau of Standards linear accelerator is described. (D.C.W.)

21226 TALMI TRANSFORMATION FOR UNEQUAL-MASS PARTICLES AND RELATED FORMULAS. Kumar, Kailash (Australian National Univ., Canberra). J. Math. Phys. (N. Y.), 7: 671-8(Apr. 1966).

Three-dimensional polynomials that occur as coefficients of the exponential in the wavefunctions of the harmonic oscillator are used in nuclear physics and kinetic theory of gases. A generating function for these polynomials is used to simplify the calculation of several integrals. These include the integrals involving products of two and three polynomials and the coefficients of the Talmi transformation. Explicit formula in terms of recoupling coefficients of angular momentum theory are obtained. (auth)

21227 THEOREM ON THE CONTRACTION OF GROUPS. Sankaranarayanan, A. (Ames Lab., Ames, Iowa). Nuovo Cimento (10), 42A: 416-18(Mar. 21, 1966). (IS–1314).

A theorem is stated and proved to the effect that an inhomogeneous proper rotation group can be constructed from a homogeneous Lorentz group of higher dimensions. Some comments on the theorem are briefly outlined. (L.B.S.)

METALS, CERAMICS, AND OTHER MATERIALS

General

Refer also to abstract 22411.

21228 (AE–221) SWEDISH WORK ON BRITTLE-FRACTURE PROBLEMS IN NUCLEAR REACTOR PRESSURE VESSELS. Grounes, M. (Aktiebolaget Atomenergi, Stockholm (Sweden)). Mar. 1966. 50p. Dep. mn.

The mechanical properties of new types of pressure vessel steels with high strength, low transition temperature and good corrosion resistance are given. These steels are of the martensitic austenitic type Bofors 2RMO (13% Cr, 6% Ni, 1.5% Mo) and of the ferritic martensitic austenitic type Avesta 248 SV (16% Cr, 5% Ni, 1% Mo). A method for estimating the brittle-fracture tendency of pressure vessels is described. As a criterion of this tendency the crack-propagation transition temperature, e.g., as measured by the Robertson isothermal crack-arrest test is used. An estimate of this transition temperature at the end of the reactor's lifetime must take increases due to fabrication, welding, geometry ageing, and irradiation into account. The transition temperature vs stress curve moves toward higher temperatures during the reactor's lifetime. As long as this curve does not cross the reactor vessel stress vs temperature curve the vessel is considered safe. The magnitude of the different factors influencing the final transition temperature are discussed and data for the Marviken reactor's pressure vessel are presented. At the end of the reactor's lifetime the estimated transition temperature is 115°C, which is below the maximum permissible value. A program for the study of strain ageing was initiated owing to the uncertainty as to the extent of strain ageing at low strains. Results from irradiation tests on the Swedish carbon–manganese steels 2103/R3, SIS 142103 and SIS 142102, the low-alloy steels Degerfors DE-631A, Bofors NO 345, and Fortiweld, the new steels mentioned above, and the U. S. steels ASTM A212B and ASTM A302B, are given. Results from a series of irradiations at temperatures between 60 and 300°C to doses between 2×10^{18} and 3×10^{19} n/cm^2 (>1 Mev) show that a saturation effect is obtained at higher temperatures in some, but not all, steels. This means that, after some irradiation, further irradiation causes no further change in the properties. The experiments show that similar steels, and even different heats of the same steel, may behave in an entirely different manner as a result of irradiation. Experiments showing the effects of differences in neutron flux and neutron spectrum are described. Calculations show that the effect of differences in neutron spectra between materials testing reactors and pressure vessels may be considerable. (auth)

21229 (AEET-229) PHYSICS ASPECTS OF LARGE THORIUM-FUELLED FAST REACTORS. Singh, R. Shankar (Atomic Energy Establishment, Trombay (India)). 1965. 12p. Dep. mn.

The feasibility of using ^{233}U-Th as a fuel in a large fast breeder reactor was studied from the point of view of the Doppler and sodium void coefficients. The composition and temperature dependent cross sections for thorium were evaluated using the latest resonance parameters available. The parametric studies over a range of compositions and sizes of core for metal and oxide fuels indicate that the reactivity coefficients due to sodium loss and Doppler effects are negative even in a core volume as large as 15,000 liters. Based on these encouraging results, a performance characteristics study of a 15,000-liter, thorium-^{233}U-fueled, sodium-cooled fast reactor of the type considered for desalination of sea water was made. The parameters like critical mass, breeding ratio and reactivity coefficients were evaluated for the "clean" core as well as for the core with equilibrium composition using metallic and carbide fuels. The effect of interference interaction between the resonances of ^{239}Pu and ^{232}Th on the Doppler effect calculations and the sodium void coefficients in Th-^{239}Pu fueled fast reactors was investigated. The temperature dependent effective cross sections for ^{239}Pu and ^{232}Th were evaluated taking into account both types of interference interactions namely, the overlap of neighboring resonances in one isotope and the interaction between the resonances of the two isotopes. (auth)

21230 (AEET–233) SELF DIFFUSION IN METALS. Murarka, S. P.; Agarwala, R. P. (Atomic Energy Establishment, Trombay (India). Chemistry Div.). 1965. 8p. Dep. mn.

A survey of experimental data and various physical and thermodynamic properties of metals revealed the relation: $Q = n(S\,T_m + L_f)$, between the atomic heats (S) of metals, their latent heats of fusion (L_f), and the activation energy for self-diffusion (Q). The assumptions were made that the act of diffusion requires a local melting of n atoms to allow one atom to diffuse from one position to another. Using experimental values of the melting temperature (T_m) and Q, S, and L_f in a few cases, n was found to be approximately equal to 4. Values for the activation energy calculated from the equation were in good agreement with the experimentally obtained ones for bcc and fcc metals. (W.L.G.)

21231 (BM-RI–6713) VAPOR DEPOSITION OF COBALT–TUNGSTEN ALLOYS. Donaldson, James G. (Bureau of Mines, Rolla, Mo. Rolla Metallurgy Research Center). June 1965. 15p. Bureau of Mines Free.

Co–W binary deposits were formed by H_2 reduction of the anhydrous mixed vapors of $CoCl_2$ and WCl_6. The materials were sublimed in separately heated zones of a reaction tube and were transported in a stream of purified He into the deposition section of the tube where the chloride gases were reduced to metal by a countercurrent flow of H_2. Heat treating of the near stoichiometric binary metallic deposits converted nearly all to the intermetallic compound Co_3W; however, small quantities of both Co and W remained. Mechanical tests showed that the tensile strength of heat-treated Co–25 % W deposits was twice as high as that of similarly treated deposits of Co. (auth)

21232 (BMI–1763) THE DIFFUSION OF FISSION PRODUCTS IN FUEL-ELEMENT CLADDING MATERIALS AND RELATED ALLOYS. Howes, James E. Jr.; Morrison, David L.; Jablonowski, Edward J.; Sunderman, Duane N. (Battelle Memorial Inst., Columbus, Ohio). Feb. 21, 1966. Contract W-7405-eng-92. 49p. (EURAEC–1604). Dep. mn. CFSTI $2.00 cy, $0.50 mn.

Work Performed under United States–Euratom Joint Research and Development Program.

Fission-product diffusion in several metal systems was studied during irradiation and in postirradiation experiments over the temperature range of 600 to 1200°C. At 600°C, nonvolume diffusion processes were evident in all of the systems examined. Above this temperature, the activation energies (Q) and frequency factors (D_0) for diffusion were considerably below those expected for normal vacancy-diffusion processes in the fcc alloys, iron-29 wt % nickel-13 wt % chromium, iron-20 wt % nickel, and iron-18 wt % chromium-8 wt % nickel, and in hexagonal-close-packed zirconium and Zircaloy-4. In the body-centered-cubic metals and alloys, beta zirconium, beta Zircaloy-4, and iron-20 wt % chromium, the fission-product diffusion occurred at nearly the same rate as self-diffusion in the same material. An apparent reduction in fission-product mobility was noted for fission-product migration in Type 304 stainless steel and Incoloy 800. Irradiation appeared to have little effect on fission-product diffusion in the 600 to 800°C temperature range within the limits of concentra-

tion studied, about 5×10^{17} fission-product recoils per cm^3. (auth)

21233 (BNWL-188) A BRIGHT-FIELD, GRAIN STRUCTURE ETCH FOR DELTA PHASE STABILIZED PLUTONIUM. Hays, D. D. (Battelle-Northwest, Richland, Wash. Pacific Northwest Lab.). Feb. 1966. Contract AT(45-1)-1830. 8p. Dep. mn. CFSTI $1.00 cy, $0.50 mn.

An oxide-free surface delineating grain boundaries was produced in delta-phase, stabilized Pu alloys having a variety of metallurgical treatments. Zr-stabilized alloys were etched with solutions based on orthophosphoric, tetraphosphoric or citric acid. Delta-phase Pu stabilized with Al or Ga could only be etched with 200 ml ethanol, 116 g citric acid, and 10 ml of a solution of either potassium or sodium nitrate in 100 ml of water. (auth)

21234 (DP-1021) ELECTROWINNING PLUTONIUM METAL. Porter, J. A.; Symonds, A. E. Jr. (Du Pont de Nemours (E. I.) and Co., Aiken, S. C. Savannah River Lab.). Feb. 1966. Contract AT(07-2)-1. 22p. Dep. mn. CFSTI $2.00 cy, $0.50 mn.

Plutonium metal was produced by electrolysis of PuO_2 in molten $LiF-BaF_2-PuF_3$ salt systems. Conditions favoring efficient cell operation were determined, and a sequence of probable cell reactions was developed. (auth)

21235 (IS-1287) NUCLEATION AND CRYSTAL GROWTH FROM CERAMIC MELTS. Selected Bibliography, 1947-1964. Burlingame, J. E.; Berard, M. F. (Ames Lab., Iowa State Univ. of Science and Tech.). Sept. 1965. Contract W-7405-eng-42. 86p. Dep. mn. CFSTI $3.00 cy, $0.75 mn.

One-hundred-twenty-eight abstracts are given of papers published from 1947 to 1964 that are concerned mainly with mathematical and theoretical treatments of the subjects and not with crystal growth in specific systems nor with devitrification in glasses. The references are arranged alphabetically by authors' last name in each subdivision of the nucleation and crystal growth sections. Author and keyword indexes are included. (W.L.G.)

21236 (N-65-23835) STUDY OF GROWTH PARAMETERS FOR REFRACTORY CARBIDE SINGLE CRYSTALS. Quarterly Status Report No. 4, December 1, 1964-March 1, 1965. Halden, F. A.; Nelson, W. E. (Stanford Research Inst., Menlo Park, Calif.). Apr. 26, 1965. Contract NASr-49. 19p. (NASA-CR-62727). CFSTI $1.00 cy, $0.50 mn.

Several new techniques and procedures for the growth of single crystals of tantalum carbide, hafnium carbide, and solid solutions of the two, investigation by x-ray lattice measurements, and examination of polished sections of arc-melted, high purity tantalum carbide boules are reported. The studies confirm that a single phase can be maintained during melting and that the stoichiometry can be varied by control of the gaseous environment. On the basis of these studies, the final arc-melting furnace was designed and is now being constructed. Also, very small crystals of tantalum carbide were grown in aluminum and iron alloys. (STAR)

21237 (N-65-29395) NASA DEVELOPMENTS IN COBALT-BASE SUPERALLOYS. Freche, John C.; Ashbrook, Richard L.; Sandrock, Gary D. (National Aeronautics and Space Administration, Cleveland, Ohio. Lewis Research Center). Oct. 5, 1964. 17p. (NASA-TM-X-54737). CFSTI $1.00 cy, $0.50 mn.

Cobalt-base superalloys, in which low-volatility elements are the primary alloying constituents and the use of chromium is minimized, were investigated. A ternary alloy, Co-25W-1Ti, was selected as the basis for systematic alloying studies that initially utilized only low-volatility additives. Subsequent work utilized the addition of small amounts of chromium (up to 3%). All alloys were induction-melted under an argon gas cover. Melts weighed approximately 3 pounds. Stress rupture tests showed that the two strongest chromium-free alloys developed were Co-24W-1Ti-0.4C and Co-25W-1Ti-1Zr-0.4C. The alloys have good ductility and their tensile properties are summarized. The two strongest low-chromium-content alloys developed were Co-25W-1Ti-1Zr-3Cr-0.4C and Co-25W-1Ti-1Zr-3Cr-2Re-0.4C. The as-cast stress rupture properties and tensile properties of these alloys are illustrated. Potential aerospace applications, in which low-chromium alloys might be used, are discussed. (STAR)

21238 (NP-15928) DESCALING AND DECONTAMINATION STUDIES. D'Muhala, T. F. (General Dynamics, Chicago, Ill. Liquid Carbonic Div.). June 8, 1965. 178p.

Descaling tests were performed on laboratory test coupons which had been presoiled under varying conditions. A proprietary neutral descaling formulation designated RD16 was used in comparison with existing descaling agents for all tests conducted. Initial tests were performed on test coupons. The excellent results obtained led to subsequent testing on test loops and scrap components. Formula modifications extended the utility and effectiveness of RD16 without grossly affecting desirable characteristics of neutrality, low metal loss, and stability. Practical application test programs evolved acceptable descaling techniques which have become standard practice in several facilities. Decontamination experiments were performed on metal coupons which had been precontaminated and RD16 surpassed the requirements for a radioactive soil decontaminant. Tests were also conducted on actual reactor system components. Comparative tests were performed simultaneously with existing, approved, methods of decontamination. When used in a multi-step process, RD16 appeared to be as effective as a decontaminant as other processes tested. Further evaluation established the safety associated with RD16 for materials of construction and personnel. (P.C.H.)

21239 (RL-SEP-824) CERAMIC CELLS AND ACCESSORIES FOR ELECTROWINNING AND ELECTROREFINING OF PLUTONIUM METAL. Rosenfels, R. S. (General Electric Co., Richland, Wash. Hanford Atomic Products Operation). Dec. 17, 1965. Contract AT(45-1)-1350. 33p. Dep. mn. CFSTI $2.00 cy, $0.50 mn.

The design, method of fabrication, properties, and operating behavior are given for four continuous electrowinning and two batch electrorefining cells made of a ceramic body composed of 6 mole % Mg_2TiO_4 and 94 mole % MgO. A stirrer, made of the same material and required for batch refining cells, is also described. The ceramic components developed have proven satisfactory in complete, operating, equipment assemblies found effective in the winning and refining of plutonium metal by electrolytic deposition in molten salt. (auth)

21240 (WANL-PR-(Q)-006) DEVELOPMENT OF DISPERSION-STRENGTHENED TANTALUM-BASE ALLOY. Quarterly Report No. 5, November 20, 1964-February 19, 1965. Buckman, R. W. Jr. (Westinghouse Electric Corp., Pittsburgh, Pa. Astronuclear Lab.). Contract NAS3-2542. 35p. (NASA-CR-54462; N-65-30166). CFSTI $2.00 cy, $0.50 mn.

Development of dispersion strengthened tantalum base alloys for use in advanced space power systems continued with selection of the sheet and tubing alloy composition Ta-8W-1Re-0.7 Hf-0.025C for detailed evaluation. Scale-up of this composition to a four-inch diameter ingot was initiated. Selection of seven additional compositions in the Ta-Mo-Re-W-Hf-Zr-C-N system were made to further optimize the Ta-5.7W-1.56 Re-0.7 Mo-0.25 Hf-0.13 Zr-0.015C-0.015N alloy. Response to heat treatment investigation continued and carbides and nitrides were shown to be stable in the tantalum alloy matrix at temperatures up to 1250°C and at pressures of 10^{-10} torr for 500 hours. (auth)

21241 (LA-tr-66-15) DISSOCIATION OF NIOBIUM PENTACHLORIDE ON NIOBIUM AND CARBIDE SURFACES. Eliutin, V. P.; Pepekin G. I.; Lysov, B. S. Translated by Helen J. Dahlby (Los Alamos Scientific Lab., Univ. of California, N. Mex.), from Izv. Vyssh.

Ucheb. Zaved. Tsvetn. Met., 8: No. 4, 90-6(1965). 11p. Dep. mn. CFSTI $1.00 cy, $0.50 mn; JCL $1.60 fs, $0.80 mf.

Studies on the kinetic principles of the process of niobium pentachloride dissociation on a niobium surface with the formation of the metal were used to determine the mechanism of niobium carbide formation. The deposition of Nb and NbC from the pentachloride was carried out in a helium stream. Niobium carbide deposition on a graphite base was fulfilled at low concentrations of $NbCl_5$ in the vapor gas phase (less than 6×10^{-2} atm) and the comparatively low temperatures of 1500–1800°K, near the temperature for the onset of the formation of NbC. The dependence of the rate of $NbCl_5$ decomposition to Nb and NbC on the partial pressure of $NbCl_5$ in the vapor gas phase is described by the empirical equations, respectively, $W = KP^{0.7}$ and $W = K_2P^{0.8}$. It was concluded that during the decomposition of $NbCl_5$ in the presence of C even under conditions thermodynamically unfavorable for the deposition of Nb, the functions of C consists only of the carbiding of the Nb metal being formed in the process of the thermal dissociation of $NbCl_5$. (P.C.H.)

21242 NEW PHASE IN THE COBALT–URANIUM–OXYGEN SYSTEM. Bobo, Jean-Claude (Faculte des Sciences, Paris). Compt. Rend., Ser. C, 262: 553-4 (Feb. 14, 1966). (In French).

A crystalline phase, $CoUO_3$, was obtained either by pyrolysis under vacuum of the $CoUO_4$ or by a solid state reaction between UO_2 and CoO. The crystalline phase was identified by Debye-Scherrer powder patterns. (tr-auth)

21243 RESOURCES OF FISSIONABLE NUCLEAR MATERIALS. Bourdel, Jean Genie Civil, 142: 261-3 (June 15, 1965). (In French).

The extent and nature of resources of fissionable elements in France and the world are discussed. The rarity of uranium, despite its presence in the earth's surface at the rate of 3 to 4 mg/T, or 2 ppM, is emphasized. Sea water may be considered as a possible source when others are exhausted, but it would produce only 2 ppB U, or 0.01% of the lowest present rate of production, and the present cost would be $20/lb, as compared with $5 to $10 for other methods. The combined uranium resources of France and her African territories are estimated at 50,000 tons. Production of natural uranium increased in 1963 to 1565 tons (875 tons by the Commissariat à l'Énergie Atomique and 690 tons by private enterprise in France, Gabon, and Madagascar). Total mineral production for fissionable materials in 1963 in France was 734,800 tons at Crouzille, Forez, and Vendée, mines owned by the CEA. Uranium-thorium ore beds in Madagascar furnished 248 tons of Th in 1963 and another 227 tons in the form of the nitrate was produced at the Bonchet extraction plant in France. Plutonium production at the Marcoule center in southern France is also discussed. (BBB)

21244 PREPARATION OF RARE EARTH NITRIDES BY REACTIVE ARC MELTING. Gambino, R. J.; Cuomo, J. J. (International Business Machines Corp., Yorktown Heights, N. Y.). J. Electrochem. Soc., 113: 401-3(Apr. 1966).

The process for preparing rare earth nitrides of high purity, free of oxygen, and in an unreactive, consolidated form by reactive arc melting is described and compared with previous methods. The rare earth metal is arc melted in a high-purity nitrogen atmosphere. A steep temperature gradient in the melt caused the nitride to precipitate to the bottom of the melt. The dissociation of nitrogen gas in the arc plasma and the rapid stirring of the melt by the arc current probably contributed to the high reaction rate. The product is in the form of a dense ingot suitable for fabricating specimens for physical property measurements and is more resistant to reaction than fine powder obtained by other methods. (F.J.H.)

21245 NUCLEATION OF CLEAVAGE CRACKS IN TUNGSTEN AND MOLYBDENUM BY SPARK-MACHINING. Beardmore, P.; Hull, D. (Univ. of Liverpool). Contract AF 61(052)-689. J. Inst. Metals., 94: 14-18(Jan. 1966).

A method of producing cleavage cracks on the surface of single crystals of tungsten and molybdenum, based on the spark-machining process, is described. It is possible to vary the crack length and the crack distribution by controlling the spark intensity and the shape of the sparking tool. The introduction of cleavage cracks by this technique resulted in brittle fracture of crystals that were normally ductile. Metallographic and x-ray examination showed that the cleavage cracks were confined to {001} planes; the cracks were semi-elliptical in shape. It is suggested that this method of introducing cracks may be used to study crack propagation in brittle materials. (auth)

21246 DETERMINATION OF GOLD COATING THICKNESSES BY PROTON SCATTERING. Peisach, M.; Poole, D. O. (Southern Univ. Nuclear Inst., Faure, South Africa). J. S. Afr. Chem. Inst., 28: 61-70(Oct. 1965).

The limited penetration of charged particles with energies of a few Mev makes them suitable for the investigation of surface layers. A method using semiconductor surface barrier detectors for nondestructively measuring the thickness of surface films of gold in the range 0 to 10 $\mu g/cm^2$ on aluminum, mica, steel, and tin plate by elastic proton scattering is described. The precision of the method is ± 0.2 $\mu g/cm^2$ and its sensitivity is better than 5×10^{-10}g gold at the point of incidence of the proton beam. Proton beams of energies 1.0, 1.5, 2.0, 2.5, and 3.0 Mev were obtained from the Van de Graaff accelerator. Preliminary tests showed that with proton energies above 3 Mev, inelastic scattering effects became marked. Thus, incident proton energy of 2.5 Mev was chosen. The scattering angle was selected by taking measurements at 45, 90, 105, 120, and 135°C. Typical spectra obtained for increasing thicknesses of gold film on aluminium plates are shown. Similar families of curves were obtained for gold films on backings of mica, steel, and tin plate. The results confirm that gold can readily be resolved from light or moderately light elements, but when the mass number of the backing is about 100 or more, resolution of gold becomes difficult. The number of proton counts, as given by the area under the gold peak, was found to be proportional to the gold film thickness, as measured with radiotracers and by radioactivation analysis. (BBB)

21247 MANUFACTURE OF MOLYBDENUM AND CHROMIUM GERMANIDES AND INVESTIGATION OF SOME OF THEIR PROPERTIES. Bondarev, V. N. Porosh. Met., Akad. Nauk Ukr. SSR, No. 1, 35-40(Jan. 1966). (In Russian).

An investigation was conducted on the conditions of obtaining compact samples of molybdenum and chromium germanides of the Me_5Ge-type by the method of hot pressing. It was established that with a rise in temperature and in duration of pressing, a decrease in the coarseness of the pressed powder increases the compactness of the pressed germanide samples. The optimal conditions were determined for hot pressing to obtain samples with maximum compactness. The microhardness and resistivity of hot-pressed samples of compounds Mo_5Ge and Cr_5Ge were investigated and the picnometric density was measured. (auth)

21248 GAS GENERATION FROM TUNGSTEN AT 2500 DEG C. Burtsev, V. T.; Vasyukov, G. Kh.; Kashin, V. I.; Samarin, A. M. (Baikov Inst. of Metallurgy, USSR). Porosh. Met., Akad. Nauk Ukr. SSR, No. 1, 50-4(Jan. 1966). (In Russian).

Equipment is described that makes it possible on heating metal in a suspended state to investigate the composition of the generated gases by means of a mass spectrometer. Fusing tungsten powder in arc vacuums and electron-ray furnaces affects the gas generation on heating to 2500°C. A technology is proposed for preliminary manufacture of tungsten bars for the purpose of a further decrease in the gas content. (auth)

21249 GROWTH OF SINGLE-CRYSTAL SILICON ON BERYLLIUM OXIDE. Manasevit, H. M. (Autonetics,

Anaheim, Calif.); Forbes, D. H.; Cadoff, I. B. Trans. Met. Soc. AIME, 236: 275-9(Mar. 1966).

Single-crystal silicon films were obtained on several natural crystal faces of BeO using the thermal decomposition of silane and the hydrogen reduction of silicon tetrachloride. From an analysis of x-ray diffraction data it was determined that the following film-substrate orientation relations exist: (111) Si ||(0001) BeO, (111) Si ||(10$\bar{1}$1) BeO, (100) Si ||(10$\bar{1}$0) BeO, and (110) Si ||(10$\bar{1}$0) BeO. An analysis of the crystallographic relations between the film and substrate indicates that a match occurs between the silicon atoms in the film and the beryllium ion sites in the substrate. (auth)

21250 THERMAL-MECHANICAL PROCESSING OF A PRECIPITATION HARDENABLE-DISPERSION HARDENED COLUMBIUM ALLOY. Hoffmanner, A. L. (Thompson Ramo Wooldridge Inc., Cleveland). 26p. (CONF-651025-10). ORAU. Gmelin, AED-CONF-65-275-12.

From Symposium on Physical Metallurgy of Refractory Metals, French Lick, Ind.

An optimum thermal-mechanical process is described for obtaining the best combination of room-temperature and elevated-temperature mechanical properties for the precipitation-hardenable, dispersion-hardened niobium alloy, Cb-132, composed of Nb-20 Ta, 15 W, 5 Mo, and modified with various Zr and C additions. It was found that a critical time-temperature-deformation parameter must exist for the thermal-mechanical process, which separates the conditions under which strain induced precipitation and complete overaging or accelerated spheroidization would predominate. Small changes in the Zr concentration (and probably the C) can have a marked effect on the microstructural constituents existing during any stage of the process. (B.L.M.)

21251 BORON. VOLUME 2. PREPARATION, PROPERTIES, AND APPLICATIONS. Based on Papers Presented at the 1964 Paris International Symposium on Boron. Gaule, Gerhart K. (ed.). New York, Plenum Press, 1965. 356p. $12.50. (CONF-640713(Vol. 2)).

Twenty-five papers based on reports at the 1964 Paris International Conference on Boron are presented. Topics covered include: synthesis of red, α-rhombohedral boron; purity of boron produced by decomposition of diborane and subsequent zone-melting; ultrapure boron from halide intermediates; crystallization of pure boron; preparation and characterization of single-crystal boron; carbon determination in hyperpure elemental boron using gas chromatography; the β-rhombohedral structure; tetragonal boron and borides with similar structures; band structure calculation of rhombohedral boron by the K·p method; conductivity, Hall effect, optical absorption, and band gap of very pure boron; thermal and optical band gaps of monocrystalline β-rhombohedral boron; optical and electrical constants of β-rhombohedral boron; semiconductor properties of boron; trap-dominated electrical and optical effects in crystalline boron; EPR, electric conductivity, and impurity diffusion in doped boron; magnetoresistance in elemental boron; recombination radiation of boron; birefringence of simple rhombohedral boron; vacuum-deposited amorphous boron films; low temperature thermal conductivity of boron; mechanical behavior of bulk polycrystalline boron; effects of chemical polishing of the strength and fracture characteristics of amorphous boron filaments; boron semiconductor devices; and $^{10}B/^{11}B$ thermistor pairs and their application. (M.C.G.)

21252 METALLURGY SESSION M. BOOK FIVE [OF PREPRINTS OF] FIFTH RARE EARTH RESEARCH CONFERENCE, AUGUST 30-SEPTEMBER 1, 1965. 128p. (CONF-650804(Bk.5)). ORAU.

Eleven papers were presented, separate abstracts were prepared for eight. Three papers were previously abstracted in NSA; see CONF-650804 in the Report No. Index. (W.L.G.)

For abstracts of individual papers see: 21253, 21254, and 21398-21403.

21253 SOLID-STATE ELECTROLYSIS OF GADOLINIUM. Graham, C. D. Jr. (General Electric Research Lab., Schenectady, N. Y.). pp 89-99 of Metallurgy Session M. Book Five [of Preprints of] Fifth Rare Earth Research Conference, Aug. 30-Sept. 1, 1965.

Experiments have shown that the oxygen content of gadolinium can be reduced by solid-state electrolysis. In this method a d-c current is passed through a solid rod of gadolinium at a temperature near the melting point. Oxygen moves toward the electrically positive end of the sample. The apparatus used in the experiments is described, and metallographic evidence of the effectiveness of the process is presented. A metallographic technique for gadolinium and other rare earths is described. (auth)

21254 ELECTROTRANSPORT OF INTERSTITIAL ATOMS IN YTTRIUM. Carlson, O. N.; Schmidt, F. A.; Peterson, D. T. (Ames Lab., Ames, Iowa). pp 101-18 of Metallurgy Session M. Book Five [of Preprints of] Fifth Rare Earth Research Conference, Aug. 30-Sept. 1, 1965.

The electrotransport velocities of carbon, oxygen and nitrogen in yttrium were determined in the temperature range of 1235 to 1460°C. Diffusion coefficients and effective charges were calculated for these elements for the same temperatures. Yttrium metal purified by the electrotransport method showed a decrease in oxygen content from 780 to 90 ppM and an increase in the resistance ratio from 12 to 45. (auth)

21255 PRODUCTION OF THORIUM-URANIUM OXIDES. (to Comitato Nazionale per l'Energia Nucleaire). British Patent 1,020,287. Feb. 16, 1966. Priority date Dec. 5, 1961, Italy.

A process for the production of a ceramic grade Th-U mixed oxide from a $Th(NO_3)_4-UO_2(NO_3)_2$ solution containing less than 1.2 moles per liter of free HNO_3 consists of reducing the $UO_2(NO_3)_2$ to U(IV) nitrate with gaseous H_2 in the presence of a catalyst made of a metal of a member of the Pt-group that is finely divided or carried on a high surface area inert carrier, precipitating the mixed oxalates by the addition of excess oxalic acid, and firing the filtered mixed precipitate at a temperature higher than 400°C. (B.L.M.)

21256 PROCESS FOR THE PRODUCTION OF URANIUM METAL. (to Comitato Nazionale per l'Energia Nucleare). British Patent 1,021,043. Feb. 23, 1966. Priority date Dec. 5, 1961, Italy.

A process is described for the production of U metal from an aqueous uranyl nitrate solution containing at least 0.5 mole of free acid/mole of U. The uranyl nitrate is reduced to U(IV) nitrate with gaseous H_2 in the presence of a catalyst made of a metal of the Pt group, which may be finely divided or carried on a high surface area inert carrier. The double fluoride of U and an alkali metal is precipitated by the addition of hydrofluoric acid and an alkali metal salt, and the double fluoride is dried and blended with Mg powder in excess of the stoichiometric amount. After the blend is formed into a generally cylindrical pellet by pressing at a high pressure, the pellet is thermally reduced inside an induction coil within a container made of a thermoelectric material, not pressure tight, and filled with a refractory powder. (B.L.M.)

Corrosion

21257 (AD-621546) PROTECTIVE COATING SYSTEMS FOR NIOBIUM IN THE RANGE 1800 TO 2500 F. Lyle, R. G. (Prevention of Deterioration Center, National Academy of Sciences-National Research Council, Washington, D. C.). Jan. 1964. 23p. (PDL-50205). CFSTI $1.00 cy, $0.50 mn.

The bibliography gives pertinent references on long-time high reliability coatings for 1800 to 2500°F niobium applications. In addition to oxidation protection above 1800°F, information is given concerning ductility, flexibility, thickness, diffusional stability, and resistance of

coating systems to thermal shock and cycling, impact abrasion, and vibration. (TAB)

21258 (AGN-TM-413) ARMY GAS-COOLED REACTOR SYSTEMS PROGRAM. ISOTHERMAL OXIDATION OF HASTELLOY X AT 1750 AND 1850 DEG F IN AIR. Baciarelli, R. M. (Aerojet-General Nucleonics, San Ramon, Calif.). Dec. 1965. Contract AT(10-1)-880. 41p. Dep. mn. CFSTI $2.00 cy, $0.50 mn.

The oxidation properties of Hastelloy X when exposed in air at 1750 and 1850°F were studied using a continuous weight change recording apparatus. Samples of 1.9 and 0.07 wt % Co Hastelloy X tubing were exposed simultaneously for 5456 hr at 1750°F and similar samples were exposed simultaneously at 1850°F for 4000 hr. It was found that the low-cobalt Hastelloy X had a higher scaling rate but behaved more consistently than the high-cobalt alloy when thermal cycled from 1850°F. In this temperature range, the oxidation penetrations in the low-cobalt alloy were less severe than those observed in the high-cobalt alloy. Oxidation penetration in the high-cobalt material occurred, predominantly, in an intergranular manner and an M_6C band depleted in carbides was observed which was not present in low-cobalt alloy. The oxidation penetration of both alloys increased by about 80% when the temperature was raised from 1750 to 1850°F and a general softening occurred. This was more pronounced in the high-cobalt alloy. Two oxides, Mn_3O_4 and Cr_2O_3, were formed as spallation products and a greater amount of Mn_3O_4 was formed in the latter stages of oxidation than in the early stages. The experimental data indicate that the activation energy (Q) is not temperature dependent but is dependent upon the alloy composition and that the oxidation rate constant (k) is temperature dependent. The oxidation curves developed from the data have an exponential temperature dependency and a cubic time dependency, indicating that the oxidation is occurring at a rate less than that predicted by diffusion theory, probably as a result of the diffusion of more than one component. (auth)

21259 (AGN-TM-414) ARMY GAS-COOLED REACTOR SYSTEMS PROGRAM. STUDIES OF HASTELLOY X CORROSION IN AIR AT 1900 AND 2000 DEG F. Brunhouse, J. S. (Aerojet-General Nucleonics, San Ramon, Calif.). Dec. 1965. Contract AT(10-1)-880. 31p. Dep. mn. CFSTI $2.00 cy, $0.50 mn.

An evaluation of the corrosion resistance of Hastelloy X sheet and tubing materials at 1900 and 2000°F in air was undertaken to establish limiting oxidation rates and physical metallurgical changes in an effort to define the limiting lifetime/temperature characteristics of this material. Test specimens were to be exposed in air for 100, 1000, 2500, 5000, 7500, and 10,000 hr durations or until the time limitations were established. It appears that Hastelloy X would probably be useful as a fuel cladding for reasonably long periods of time in 1900°F air although specific limiting criteria need to be developed. At 2000°F, however, rapid oxidation and strength decreases would probably limit the service life of the material to a few thousand hours. (W.L.G.)

21260 (ANL-6985) A CONVECTIVE-DIFFUSION STUDY OF THE DISSOLUTION KINETICS OF 304 STAINLESS STEEL IN THE BISMUTH–TIN EUTECTIC ALLOY. Kassner, T. F. (Argonne National Lab., Ill.). Nov. 1965. Contract W 31-109-eng-38. 39p. Dep. mn. CFSTI $2.00 cy, $0.50 mn.

The kinetics of dissolution of type 304 stainless steel in the Bi–42 wt % Sn eutectic alloy were investigated under the well-defined hydrodynamic conditions produced by the rotating-disc sample geometry. The experiments were carried out in the temperature interval of 200 to 1100°C at rotational speeds between 2 and 150 rpm. A convective-diffusion model was used to interpret the experimental data. The dissolution process was found to be liquid-diffusion controlled under specific conditions of temperature and Reynolds number. (auth)

21261 (LA-3476) CORROSION TESTS OF HASTELLOY N, INCONEL 600, AND HYMU-80 EXPOSED TO UCl_3–KCl AT 900 DEG C. Thamer, B. J. (Los Alamos Scientific Lab., Univ. of California, N. Mex.). Feb. 4, 1966. Contract W-7405-eng-36. 14p. Dep. mn. CFSTI $1.00 cy, $0.50 mn.

Static, isothermal tests up to 84 days in length were performed in the UCl_3–KCl eutectic of the highest uranium concentration at 900°C. The maximum penetration in any case was approximately 2 mils. The corrosion was impeded by a metallic reaction layer, the composition of which was principally uranium and nickel. (auth)

21262 (N-65-25266) VAPORIZATION OF THERMIONIC REFRACTORY MATERIALS. Status Report No. 14, December 1, 1964–February 28, 1965. Plante, E. R. (National Bureau of Standards, Washington, D. C.). 5p. (NASA-CR-63188; NBS-8670). CFSTI $1.00 cy, $0.50 mn.

Measurements on the rate of sublimation of rhenium in the microbalance apparatus showed differences in the window and prism correction factors of somewhat less than $5.7 \times 10^{-6}°K^{-1}$ corresponding to differences in temperature of about 42° at 2700°K. An attempt to identify the source of contamination was made but yielded unsatisfactory results. Examination of the residuals from the least squares treatment of the series II and III data established that there was some change in the window and prism correction factor during the vapor pressure measurements. A series of measurements at about 2650°K for seven experiments of 20 minutes duration each, with a total weight loss of 1900 micrograms, did not produce any change in the window calibration and no change was predicted by the data obtained. The tentative second and third law heats were calculated. (STAR)

21263 (NASA-CR-54911) ADVANCED REFRACTORY ALLOY CORROSION LOOP PROGRAM. Quarterly Progress Report No. 3, October 15, 1965–January 15, 1966. Harrison, R. W. (ed.) (General Electric Co., Cincinnati, Ohio. Space Power and Propulsion Section). Feb. 3, 1966. Contract NAS3-6474. 36p.

Difficulties were encountered in fabricating the advanced refractory alloys. Many of the difficulties are associated with the materials vendors' deviations from established processing procedures. All of the lithium purification system drawing revisions were completed. Assembly of the argon-vacuum manifold for the lithium purification system was begun and fabrication of the hot trap was completed. Minor design changes were made and specifications are being written to assure quality fabrication and performance of the corrosion loop. (W.L.G.)

21264 (RFP-491) THE OXIDATION AND IGNITION OF PLUTONIUM. Thompson, M. A. (Rocky Flats Div., Dow Chemical Co., Golden, Colo.). Mar. 21, 1966. Contract AT(29-1)-1106. 17p. Dep. mn. CFSTI $1.00 cy, $0.50 mn.

The oxidation rates of plutonium metal at temperatures between 25 and 450°C were measured in air having a dew-point of about 8°C. A change in slope of the rate curve was noted at the alpha to beta phase transformation. A decrease in the rate above 350°C, with a minimum at 400°C was confirmed. This is thought to be associated with properties of the resulting oxide. Plutonium was found to ignite in air at temperatures between 310 and 505°C. Exotherms were observed in the heating curve at 200 and 400°C. Metallographic results suggest accelerated oxidation at the exotherm temperatures. This initial accelerated oxidation may produce a more protective oxide causing a long-term rate decrease. Decreases in the oxidation rates were observed at temperatures above the exotherm temperatures. It is thought that the oxides formed at these temperatures are more protective and thus decrease the corrosion rate. The reaction rate of plutonium with water vapor showed a more definite plateau at 100 and 200°C than the rate in air. Differences in oxide properties as influenced by the moisture content of the oxidizing atmosphere were again suggested. A positive correlation was made between the particle size and formation temperature. (auth)

21265 (RPI-2714-8) OXIDATION CHARACTERISTICS OF THE LANTHANIDE METALS. Greene, N. D.; Hodge, F. G. (Rensselaer Polytechnic Inst., Troy, N. Y. Dept. of Materials Engineering). Mar. 1966. Contract AT(30-1)-2714. 33p. Dep. mn. CFSTI $2.00 cy, $0.50 mn.

The oxidation rates and rate equations of 15 lanthanide metals including La and Y and excluding Pm, were determined in dry and moist air in the temperature range 100-800°C by precision weight gain measurements. Oxide structures were examined by both metallographic and x-ray analyses. The observed oxidation characteristics were found to be related to oxide structures and the physicochemical properties of the rare earth metals. (auth)

21266 A THERMO-SIPHON WATER FLOW IRRADIATION RIG FOR REACTOR MATERIAL TESTING. Fischer, E.; Froehner, K. R. (Institut fuer Reaktorphysik der GKSS, Geesthacht, Ger.). Atomkernenergie, 11: 127-30(Mar.-Apr., 1966). (In German).

An instrumented irradiation rig was designed which provides the conditions encountered in water reactors during operation: water flow at temperatures up to 280°C and pressures up to 65 kp/cm^2 (1000 psi); thus the rig can be used for corrosion research on cladding and structure materials used in water reactors. The water-filled rig is pressurized by an inert gas (He) and mainly heated by nuclear radiation absorption. The radial temperature distribution is influenced by additional electrical heating inside the rig and by water cooling of the pressure vessel surface. The thermo-siphon action thus produced within the rig leads to flow velocities up to 23 cm/s as is extrapolated from laboratory experiments and shown by computer calculation. (auth)

21267 OXIDATION OF URANIUM MONOCARBIDE WITH OXYGEN BETWEEN 800 AND 1000 DEG C. Moreau, Claude; Philippot, Joseph (Centre d'Etudes Nucleaires, Grenoble, France). Compt. Rend., Ser. C, 262: 560-3(Feb. 14, 1966). (In French).

The reaction of pure oxygen on a uranium carbide with the formula $UC_{1.05}$ fused by electron bombardment was studied by micrography between 800 and 1000°C. The thickness e of the carbide consumed, the thickness e' of the oxide formed (in which the expansion factor apparently depends on the temperature) increases according to a parabolic law: the corresponding velocity constants k and k′ are related to the oxygen pressure by the expressions $k = Ap/(1 + Bp)$ and $k' = A'p/(1 + B'p)$. The activation energy of the reaction is 25 kcal/mol. (tr-auth)

21268 EFFECTS OF CONTAMINATION ON OXIDATION OF Zr IN STEAM. Demant, J. T.; Wanklyn, J. N. (Atomic Energy Research Establishment, Harwell, Eng.). Corrosion, 22: 60-7(Mar. 1966). (AERE-R-4788).

Initial oxidation of zirconium in steam at 500°C and one atm pressure is considerably accelerated by contamination deposited on the metal surface during vacuum annealing in silica capsules. Radioactivation analysis shows that copper is transferred from silica to the zirconium. The layer of affected metal is less than 10 μ thick, and may be removed by electropolishing. A clean surface with a low initial oxidation rate is produced by electropolishing, followed by rinsing in methanol. Accelerated oxidation results when electropolished surfaces are dipped in aqueous solutions of several cations, including copper, or when they are given the normal HNO_3/HF pickle followed by tap water rinsing. Simple immersion in tap or redistilled waters also can accelerate oxidation, probably due to the calcium present; but exposure to HF solution with rigorous exclusion of calcium, appears to have no effect. Implications of these results for oxidation studies and corrosion testing are discussed. (auth)

21269 ORIENTED GROWTH OF THE OXIDE FILM ON BERYLLIUM. Kolomiets, L. D.; Khorenko, V. K. Fiz. Metal. Metalloved., 20: 860-3(Dec. 1965). (In Russian).

Oxide films formed during oxidation of vacuum condensates and solid polycrystalline samples were investigated using the electron diffraction method in the temperature range from 400 to 800°C. The type of predominant orientation in the oxide films, their relation to the original composition of the sample, and their dependence on temperature were established. (tr-auth)

21270 REACTIONS OF METALLIC NIOBIUM WITH CARBON MONOXIDE. Shveikin, G. P.; Perelyaev, V. A. Izv. Akad. Nauk SSSR, Metal., No. 3, 164-9(May-June 1965). (In Russian).

Samples of Nb powder (2-3g) were weighed into a graphite crucible and heated in a graphite resistance furnace for a period of two hours under a definite CO pressure at temperatures of 1300, 1500, and 1700°C. The samples were reweighed and analyzed chemically and by x rays. The results indicated that the process depended on the temperature. At 1000°C and lower the reaction was $Nb + 2CO = NbO_2 + 2C$. At 1000 to 1700°C the reaction proceeded in two stages. First, $yNb + xCo = yNbO_2 + NbC_x$ (y = 0.35 to 0.4, and x = 0.7 to 0.8). Then, NbO_2 reacted with niobium carbide to form the oxycarbide compound: $yNbO_2 + NbC_x = NbC_xO_y$. Thermodynamic calculations showed that the formation of a mixture of lower oxides and carbides ($3NB + CO = NbO + Nb_2C$ or $1.5\ Nb + CO = \frac{1}{2}\ NbO_2 + NbC$) was more probable than the formation of an oxide and free carbon ($0.4\ Nb + CO = \frac{1}{5}\ Nb_2O_5 + C$ or $Nb + CO = NbO + C$). The reaction of compact Nb with CO at 1300 to 1500°C went very slowly due to formation of a stable oxycarbide film. (TTT)

21271 PASSIVATION OF IRON IN THE PRESENCE OF PERTECHNETATE AND CHROMATE IONS. Cartledge, G. H. (Oak Ridge National Lab., Tenn.). J. Electrochem. Soc., 113: 328-33(Apr. 1966). (ORNL-P-1683).

Experiments were carried out to determine whether reducible inorganic inhibitors passivate iron solely by their own cathodic reduction or have some additional role in the passivation process. Passivation was effected potentiostatically in pertechnetate and chromate solutions at potentials noble to the calculated reversible potential of the inhibitor couple under the conditions prevailing. It was found that the inhibitors reduce greatly both the critical current density and charge required for anodic passivation when they are not themselves reduced. It is also shown that neither of the inhibitors is capable of supplying more than a very small fraction of the current density required for passivation in the absence of the additional effect that arises, presumably, through adsorption of the inhibiting anions. The results show the inadequacy of the hypothesis that the oxidation-reduction properties of the inhibitor alone are sufficient to account for its passivating action. (auth)

21272 CRACKING AND CARBON PICKUP IN THE OXIDE FORMED ON URANIUM IN CARBON DIOXIDE AT 650 DEG C. Stobbs, J. J. (Central Electricity Generating Board, Berkeley, Eng.). J. Less-Common Metals, 10: 362-5(May 1966).

The experiments were performed at 650°C and the extent of cracking of the oxide was assessed by surface area measurements in a conventional BET apparatus. The increase in surface area with time was nearly linear with the weight gain, indicating the dependence of oxidation on cracking; however, ionic diffusion through the uncracked oxide next to the metal is the rate controlling reaction. Electron microscope examinations of oxide flakes reveal that fracture of the oxide occurred via a devious path between the small particles (270 ± 100 Å in size) and this accounts for the large surface areas observed. Evidence was found for the existence of a balance between the deposition of carbon in narrow propagating cracks and the removal of carbon by oxidation in carbon dioxide that was able to diffuse into the enlarged cracks near the oxide-gas interface. (W.L.G.)

21273 INCREASE IN ZIRCONIUM DIBORIDE GRAINS DURING SINTERING. Kuzenkova, M. A.; Kislyi, P. S. (Inst. of Problems in Metallography, Academy of Sciences, Ukrainian SSR). Porosh. Met., Akad. Nauk Ukr. SSR, No. 1, 12-16(Jan. 1966). (In Russian).

The results of an investigation of increase in zirconium diboride grains during sintering are presented. It is as-

sumed that during the initial period of sintering grain growth is conditioned by the mechanism of translocation of the grains under the effect of surface tension forces, when union of grains occurs on polygonized borders. With a sintering time of over 30 minutes grain growth is due to the diffusion mechanism. The activation energy of grain growth equals 120 ± 40 kJ/mole. (auth)

21274 OXIDATION OF THIN EVAPORATED RHENIUM FILMS. Gimpl, M. L.; Fuschillo, N.; McMaster, A. D. (Melpar, Inc., Falls Church, Va.). Trans. Met. Soc. AIME, 236: 331-5(Mar. 1966).

Rhenium films protected from the atmosphere by an evaporated layer of silicon monoxide show excellent electrical stability. Unprotected films, however, are subjected to aging effects, notably the increase in electrical resistivity as a function of time. This phenomenon can be understood as primarily one of oxidation of the thin films. The oxidation and crystallization behavior of such unprotected films was studied. It was found that the oxidation rates are a function of the substrate temperatures used during the deposition of the metal films. The structures observed in the films are correlated with the film resistivities and some data are presented to establish the existence of the various types of oxides of rhenium. (auth)

21275 CORROSION AND ELECTROCHEMICAL BEHAVIOR OF RHENIUM. Tomashov, N. D.; Matveeva, T. V. (Inst. of Physical Chemistry, Academy of Sciences, USSR). Zashchita Metal., 2: 57-62(Jan.-Feb. 1966). (In Russian).

Rhenium was tested in the form of compacts obtained from electrolytic rhenium containing the following impurities (in %): K, 0.0075; Na, 0.0009; C, 0.004; Fe, 0.001; Cu, 0.00002; Ni, 0.0006; Al, 0.00015; and Mo, 0.0007. The compacts were forged (with intermediate annealing at 2000° in a vacuum) into rods from which cylinders were cut. Corrosion tests were made by complete submergence of the specimens in mild solutions in the presence of air. The relation of the solution volume to the specimen surface amounted to 40 ml/cm^2. Three parallel tests were arranged. Corrosion was determined by weight losses. For electrochemical measurements the cylindrical specimens with a wire welded onto one end were coated with epoxy resin or Teflon. Only the face side of the specimen served as the working surface in this case. The rate of corrosion of rhenium was determined in solutions of sulfuric, hydrochloric, phosphoric and nitric acids, sodium chloride, potassium hydroxide, hydrogen peroxide of varying concentrations, and distilled water at 25 and 100°C. In inorganic acids in the presence of air at 25°C the rate of rhenium corrosion was insignificant (less than 0.0001 g/m^2-hr). At 100°C, in these media, rhenium was corroded at a slow rate (not more than 0.016 q/m^2-hr). In distilled water in the presence of air at 25°C the corrosion rate of rhenium was quite small (less than 0.0001 g/m^2-hr), however, at 100°C it exceeded the rate of its dissolution in nonoxidizing acids and was the same as in solutions of sodium chloride (0.05 g/m^2-hr). Bases more actively affected rhenium than nonoxidizing acids. Even at 25°C the rate of dissolution in 3% and 10% solutions of potassium chloride amounted to 0.015 g/m^2 hr. Rhenium had a low hydrogen overvoltage in nonoxidizing acids. In 40% solution of sulfuric acid at a current density of 1 ma/cm^2 at 25°C hydrogen over-voltage was equal to 0.1 v. In nonoxidizing acids, at potentials close to stationary (up to +0.85 v), rhenium was passivated (anode current was less than 0.001 ma/cm^2). In this region of potential (0.4 to 0.8 v) a certain degree of passivity of rhenium was observed both in solutions of sodium chloride and potassium chloride, and at much larger current density values (on the order of 1 ma/cm^2). In nonoxidizing media (solutions of hydrogen peroxide at concentrations above 0.05%, nitric acid at concentrations over 10%) rhenium was completely unstable. In a 40% or greater solution of nitric acid the corrosion rate of rhenium was on the order of 200 g/m^2-hr. The stationary potential of rhenium in such solutions was very positive (up to +1 v). The corrosion of rhenium in the solutions studied had an electrochemical nature and the characteristics of its corrosion behavior were totally determined by the kinetics of the anodic and cathodic processes under the conditions examined. (CFSTI)

21276 2ND INTERNATIONAL CONGRESS ON METALLIC CORROSION, NEW YORK, MARCH 11-15, 1963. Houston, Texas, National Association of Corrosion Engineers, 1966. 985p. $50.75. (CONF-630304).

One-hundred-twenty papers are presented in the volume, eight are of particular interest to nuclear science. Three of the eight papers were previously abstracted in NSA; see: 17: 32516, 34356, and 37478. The other papers were presented in symposia on stress corrosion cracking, pitting and crevice corrosion, cathodic protection and anodic corrosion, evaluation tests for stainless steels, passivity, inhibitors, protective coatings, salt water, oxidation, electrochemical processes and general topics. (W.L.G.)

For abstracts of individual papers see: 21277–21281.

21277 RELATIONSHIP OF HEAT TREATMENT AND MICROSTRUCTURE TO CORROSION RESISTANCE IN WROUGHT Ni–Cr–Mo ALLOYS. Streicher, M. A. (E. I. du Pont de Nemours and Co., Inc., Wilmington, Del.). pp 502-16 of 2nd International Congress on Metallic Corrosion. Houston, Texas, National Association of Corrosion Engineers, 1966.

In an investigation of the effect of heat treatment on microstructure and corrosion resistance, seven heats of wrought Ni–Cr–Mo alloy were heated in the range of 800 to 2375°F. Corrosion was studied in reducing and in oxidizing acids. Oxalic acid etch structures produced by various precipitates were classified and correlated with corrosion rates. Two maxima in corrosion rates were found: one on specimens heated near 1400°F and the other on specimens heated near 1900°F. In hydrochloric acid, only the maximum at 1400°F is revealed, while in chromic acid, only the maximum at 1900°F is detected. Both maxima are revealed by exposure to nitric acid, pure sulfuric acid and ferric sulfate–sulfuric acid solution. Studies of the microstructures and analysis of residues from dissolution in bromine–methanol solution show that sigma phase, in microscopic or submicroscopic form, is mainly responsible for changes in corrosion resistance produced by heat treatments. Carbides of the M_6C type containing molybdenum and tungsten as major elements are also present but have a minor effect on corrosion. No chromium carbide, $Cr_{23}C_6$, was found. Incompletely dissolved precipitates in the form of submicroscopic phases have a deleterious influence on corrosion. Multiple solution-annealing treatments at 2250°F, rather than length of time at temperature, were found most effective in completely dissolving this phase. Corrosion in reducing acids is under cathodic control. Intergranular attack and the corrosion potentials are functions of the anions of the acid. In oxidizing solutions, corrosion is governed by anodic polarization. The cathodic process consists of reduction of metallic cations. Both grain face and grain boundary zones are passive. Anodic polarization is governed by the presence of such cations as ferric ions and hexavalent chromium ions. On the basis of data presented, a simple, rapid method for evaluating Ni–Cr–Mo alloys for susceptibility to intergranular attack is proposed. It consists of electrolytic etching in oxalic acid to detect the presence of incipient fusion resulting from overheating during annealing, and a 24-hour test in boiling solution of ferric sulfate–50% sulfuric acid. Material free of all kinds of damaging precipitates has a low rate of corrosion in this test. (auth)

21278 THE OXIDATION AND PROTECTION OF URANIUM AT TEMPERATURES NEAR AMBIENT. Owen, L. W.; Alderton, J. R. (Atomic Weapons Research Establishment, Aldermaston, Eng.). pp 865-71 of 2nd International Congress on Metallic Corrosion. Houston, Texas, National Association of Corrosion Engineers, 1966.

The oxidation of uranium in air was followed over a long period by weight increase measurements in the temperature range 40–100°C at both high and low humidity. The investigation includes assessment of the effect of material purity, source, metallurgical history, and surface preparation. The protective quality of a number of metal-

lic coatings on uranium applied at low thickness by several techniques was studied. Linear rates were found generally to prevail especially at the lower range of conditions explored and with few exceptions wide variations in rates according to source, preparation, etc., were not found. Depletion of oxygen results in accelerated attack under humid conditions. The protective quality of thin metallic coatings often seemed good from visual observation, but weight gain data indicated that the majority of coatings were only mildly protective at dry conditions and offered little or no protection at humid conditions. Over an initial period rates of weight increase in humid air were often higher than subsequent rates and in some instances were considerably in excess of the value for the unprotected metal; in certain instances an ability to occlude moisture was apparent. (auth)

21279 INTERACTION OF CARBON DIOXIDE AT LOW PRESSURES WITH TANTALUM AND ZIRCONIUM. Quinn, C. M.; Roberts, M. W. (Queen's Univ., Belfast). pp 880-4 of 2nd International Congress on Metallic Corrosion. Houston, Texas, National Association of Corrosion Engineers, 1966.

The interactions of CO_2 with clean ribbons of Ta and Zr at a pressure of about 10^{-1} mm Hg and temperatures in the range of 590 to 730°C were studied to determine the mechanisms of the initial reactions. (W.L.G.)

21280 THE OXIDATION OF PLUTONIUM. PART II. Raynor, J. B. (Univ. of Leicester, Eng.). pp 885-6 of 2nd International Congress on Metallic Corrosion. Houston, Texas, National Association of Corrosion Engineers, 1966.

Pu specimens of widely differing metallurgical histories were oxidized in air in the temperature range of 30 to 100°C and 0 to 95% relative humidity. The results indicate that: the disintegration and sharpness of breakaway are related to the purity of the metal; the oxidation is under anodic control; moisture and/or CO_2 are strongly combined with the corrosion products; and, the variation in oxidation rates for specimens of different metallurgical histories is only apparent in the presence of moisture. (W.L.G.)

21281 SOME CHARACTERISTICS OF PROTECTIVE OXIDE FILMS. Leach, J. S. Llewelyn (Imperial Coll. of Science and Technology, London). pp 859-64 of 2nd International Congress on Metallic Corrosion. Houston, Texas, National Association of Corrosion Engineers, 1966.

Theories and the supplemental experimental evidences of the mechanisms responsible for the corrosion protection properties of oxide films and the processes by which corrosion occurs in their presence are summarized. (47 references). (W.L.G.)

21282 THE PROPERTIES OF OXIDE FILMS ON ZIRCONIUM ALLOYS AND THEIR RELEVANCE TO CORROSION AND HYDROGEN UPTAKE. Wanklyn, J. N. (Atomic Energy Research Establishment, Harwell, Eng.). 29p. (CONF-651017-9). ORAU. Gmelin, AED-CONF-65-289-12.

From Electrochemical Society Meeting, Buffalo.

A discussion of reported work on the properties of oxide films on Zr alloys is presented with 74 references being cited. The relation of the various properties to corrosion phenomena is discussed, and four topics which appear profitable for further study are summarized. (B.L.M.)

21283 THE DIFFUSIONAL LIMITATION IN HIGH-TEMPERATURE PROTECTIVE OXIDE COATINGS. Brett, Jack; Seigle, Leslie L. (General Telephone and Electronics Labs. Inc., Bayside, N. Y.). 30p. (CONF-651025-9). ORAU. Gmelin, AED-CONF-65-275-17.

From Symposium on Physical Metallurgy of Refractory Metals, French Lick, Ind.

Analytical and experimental studies of several simple and complex solid oxides were carried out to identify systems of materials which might be used in the protection of W at temperatures above 2000°C. The materials must survive the diffusion of anions and/or cations through the oxide scale coating at these temperatures as well as not evaporate or break down. With the exception of alumina, whose low melting point is a serious deficiency, no presently known simple oxide was found whose measured diffusion properties admit its use as a protective coating material above 2000°C. The complex oxides, of which $MgCr_2O_4$ seems to be marginally promising, offers the greatest promise as oxidation protective materials useful at very high temperatures. (B.L.M.)

21284 NEW COMPONENTS FOR REFRACTORY METAL–ALKALI METAL CORROSION TEST SYSTEMS. Hoffman, E. E.; Holowach, J. (General Electric Corp., Cincinnati). 75p. (CONF-650411-7). ORINS.

From Joint NASA-AEC Liquid Metals Corrosion Meeting, Gatlinburg, Tenn.

Refractory metal-alkali metals systems designed to operate at maximum temperature in the range from 1800 to 2400°F are discussed. Three principal areas are discussed: vacuum test chamber components, reflux capsule corrosion test components, and components of forced-circulation, two-fluid corrosion test loop systems. The test loop systems consist of liquid metal pumps, flow control and isolation valves, resistance heaters, reflective insulation, vapor bubble nucleators, boiler, turbine simulator, condenser and subcooler, temperature measurement, and alkali metal pressure measuring devices. Other components useful in corrosion testing are also considered. (F.J.H.)

21285 PERTURBING EFFECTS OF WATER VAPOUR ON THE MECHANISM OF GRAPHITE OXIDATION IN THE PRESENCE OF OXYGEN (500 TO 650 deg C). Lang, F. M.; Magnier, P.; Gilles, P.; Pollet, R.; Brie, M. 15p. (CONF-650632-10). ORINS. Gmelin, AED-CONF-65-149-1.

From 7th Biennial Conference on Carbon, Cleveland.

The effects of traces of moisture in the oxidizing gases on graphite oxidation at 510 to 650°C are discussed. Methods of analysis and curves of oxidation as a function of weight loss are given. The effects of dry oxygen and wet oxygen on the BET surface and texture of oxidized graphite are outlined. (F.J.H.)

Fabrication

Refer also to abstracts 20964 and 20967.

21286 (AD-621920) OCCLUSION OF VARIOUS REFRACTORY MATERIALS IN CHROMIUM PLATE ON STEEL SUBSTRATES. Hassion, Francis X.; Szanto, Joseph (Springfield Armory, Mass.). Aug. 16, 1965. 43p. (SA-TR-18-1091). CFSTI $2.00 cy, $0.50 mn.

Falex test pins plated at moderate current densities from standard chromium baths containing dispersoids of diamond dust, zirconia, or thoria at volume concentrations of about 1% do not exhibit unusual wear characteristics. Falex test pins plated under similar conditions at high current densities show higher hardness and correspondingly improved wear resistance. The particle weights occluded in chromium plate deposited at high current densities amount to about 1%, an order of magnitude improvement over that achieved at conventional current densities and bath concentrations of dispersoid amounting to approximately 1%. Photomicrographs of both dispersed thoria and zirconia particles are included. The procedure is described and results are discussed. (auth)

21287 (AE-217) ELECTRODEPOSITION OF ACTINIDE AND LANTHANIDE ELEMENTS. Baerring, N. E. (Aktiebolaget Atomenergi, Stockholm (Sweden)). Feb. 1966. 22p. Dep. mn.

Deposition parameters for the quantitative electrode position of hydrolysis products of plutonium were qualitatively studied at trace concentrations of plutonium. The hydrogen ion concentration, current, and electrolysis time proved to be the determining factors in the quantitative

electrolytic precipitation of plutonium, while other factors such as cathode material, pretreatment of the cathode surface, nature of the electrolytic anion, and oxidation state of plutonium in the starting solution were found to be of less importance. The conditions selected for quantitative electrodeposition of plutonium from slightly acid nitrate solutions on a stainless steel cathode were successfully tried also with uranium, neptunium, americium, cerium, and thulium. Details of a procedure used for plating milligram amounts of plutonium and neptunium on small stainless steel cylinders are also given. (auth)

21288 (BMI–1761) DEVELOPMENT OF THORIUM–^{233}U IRRADIATION SPECIMENS. Nelson, Sidney G.; Foster, Ellis L. Jr. (Battelle Memorial Inst., Columbus, Ohio). Feb. 10, 1966. Contract W-7405-eng-92. 24p. Dep. mn. CFSTI $0.50 cy, $0.50 mn.

Fabrication techniques were developed and employed in the preparation of irradiation and calibration samples to be used in a program designed to obtain equilibrium values of ^{233}U buildup in thorium in both fast and slow neutron-flux spectra. Twenty-two standard-calibration and 60 irradiation samples consisting principally of cores of thorium or thorium with additions of ^{233}U, gold, or boron surrounded by reactor-grade zirconium cladding metallurgically bonded to the core were prepared. All specimens were evaluated after their preparation. The results of fabrication, ultrasonic and autoclave (corrosion) testing of samples, and metallographic examination of core materials are discussed. (auth)

21289 (BNWL–194) STRESSES IN ZIRCALOY-2 CLADDING DURING VIBRATORY FUEL LOADING. Gibby, R. L.; Lobsinger, R. J. (Battelle-Northwest, Richland, Wash. Pacific Northwest Lab.). Feb. 1966. Contract AT(45-1)-1830. 16p. Dep. mn. CFSTI $1.00 cy, $0.50 mn.

Longitudinal vibration of EBWR tubes during fuel loading excites transverse vibrational modes in the tube. These stresses are great enough to cause fatiguing of the Zircaloy-2 during the final stages of fuel powder loading. With a standard clamp, the end-cap crevice acts as a stress raiser and fatigue failure can occur at lower stress values. A modified tapered end clamp with nylon insert is very effective in reducing fatigue failures by relocating major stresses to the heavier cladding. Reinforcement of the resonance plate is undesirable because it increases the integrated fatigue stress level. (W.L.G.)

21290 (GA–1052) A PROGRAM OF RESEARCH ON MECHANICAL METALLURGY AS RELATED TO FUEL-ELEMENT FABRICATION. A Summary Report of Work Through September 1959. Trozera, T.; Chambers, R.; White, J. (General Atomic, San Diego, Calif. John Jay Hopkins Lab. for Pure and Applied Science). Nov. 10, 1959. Contract AT(04-3)-167. 72p. Dep. mn. CFSTI $3.00 cy, $0.75 mn.

The research program is described and the status of the equipment development is reported. Three approaches are being used to study the mechanical metallurgy problems related to the fabrication processes: the deformation and fabrication characteristics of reactor materials; the stored energy of cold work; and, the relation of formability to imperfection structure. (W.L.G.)

21291 (NP–15944) ACTIVATION SINTERING OF TUNGSTEN AND ITS EFFECT ON SOME MECHANICAL PROPERTIES [Thesis]. Toth, I. J. (Battersea Coll. of Tech., London (England)). Nov. 1965. Contract N-62558-3591. 233p.

Submitted to London Univ. (England).

Two methods of activation sintering were studied, halogen activation and metallic activation. An example of the first is the use of hydrogen and bromine as sintering atmosphere. No significant increase in densification was noted, except for a moderate improvement at temperatures around 1400°C. However, some beneficial effects were observed, notably in the rounded shape of the pores and in lowering the oxygen content. This led to an improvement in mechanical properties. Metallic activation, mainly provided by nickel and palladium salts, led to high densities at a sintering temperature of 1100°C but was accompanied by increased brittleness. This undesirable feature could be in part offset by controlling the amount of metallic activator and by some suitable subsequent heat-treatment. The two types of processes were discussed separately and some appropriate mechanisms proposed to explain the results observed, and the theoretical implications are considered. (auth)

21292 (ORNL–3932) THE MANUFACTURE OF THE CONTROL RODS FOR THE EXPERIMENTAL GAS-COOLED REACTOR. Tolson, G. M. (Oak Ridge National Lab., Tenn.). Apr. 1966. Contract W-7405-eng-26. 23p. Dep. mn. CFSTI $2.00 cy, $0.50 mn.

The Experimental Gas-Cooled Reactor, now under construction at Oak Ridge, Tennessee, is a nuclear reactor designed to provide both power demonstration and experimental testing. The control rod consists of four segments held together by a spring-loaded central rod. The lower three segments contain B_4C bushings in an annulus between two concentric tubes. The rods are sufficiently flexible to allow movement should the channel in which they travel become distorted. Type 304 stainless steel is used to encase the B_4C, and type 347 stainless steel is used for structural members. To prevent reaction with the B_4C, all of the stainless steel in contact with B_4C was copperplated. Manufacturing methods, inspection, and assembly of the components are described. Thus far 25 control rods have been successfully produced. (auth)

21293 (R–66SD3007) POTASSIUM CORROSION TEST LOOP DEVELOPMENT. TOPICAL REPORT NO. 2. MATERIAL AND PROCESS SPECIFICATIONS FOR REFRACTORY ALLOY AND ALKALI METALS. Frank, R. G.; Miketta, D. N.; Kearns, W. H.; Young, W. R.; Hand, R. B. (General Electric Co., Cincinnati, Ohio. Space Power and Propulsion Section). Dec. 13, 1965. Contract NAS3-2547. 426p.

The preparation of material and process specifications for the procurement, cleaning, and joining of refractory alloys and for the procurement, purification, and handling of the alkali metals to be used in the fabrication and evaluation of the test loops is reported. The alloys include Nb–Zr, Mo–Ti–Zr, Ta–W–Hf, and Nb–W–Zr–C, and the alkali metals include Na and K. (P.C.H.)

21294 (TID–22221) PURIFICATION AND CRYSTALLIZATION OF AMORPHOUS BORON POWDER BY ZONE REFINING. PRE-PURIFICATION OF BORON BEFORE ZONING. Period Covered: January 21–July 20, 1965. Musgrave, John R.; Starks, Ralph J.; Erwin, Harold E.; Grayson, Paul E.; Stone, Louis E. (Eagle-Picher Co., Miami, Okla. Research Labs.). Feb. 1966. Contract AT(40-1)-3327. 48p. Dep. mn. CFSTI $2.00 cy, $0.50 mn.

Studies were made on the conversion of enriched boron, which was produced in electrolytic cells, to crystalline boron of higher purity. Amorphous boron-10 powder was prepared for processing by several methods; isostatic compaction appeared to be the most desirable method. Sintering of isostatic compacts at 1700 to 1800°C improved the purity and gave good crystallinity. Multiple float zone passes further improved the purity. Horizontal zoning, employing a water-cooled boat showed considerable promise but required additional study to evaluate its potential. Simple melting, Czochralski zoning, and gradient freezings did not appear to offer as much promise. (auth)

21295 (WANL–PR–(EE)-002) EVALUATION OF REFRACTORY/AUSTENITIC BIMETAL COMBINATIONS. Quarterly Progress Report No. 2, September 22, 1965–December 22, 1965. Buckman, R. W. Jr.; Godshall, J. L. (Westinghouse Electric Corp., Pittsburgh, Pa. Astronuclear Lab.). Contract NAS 3-7634. 26p. (NASA-CR-54913).

Evaluation of the bond integrity of as-explosive bonded

refractory/austenitic bimetal composites continued using tensile tests, hardness traverses, cold rolling, and metallographic analysis. Nine combinations were selected for complete evaluation of thermal stability. Assembly of ultrahigh diffusion annealing systems for the isothermal exposures was completed and the diffusion annealing and thermal exposure runs were initiated. (auth)

21296 (Y-1510) POWDER METALLURGY OF URANIUM MONOCARBIDE. Schmitt, C. R. (Union Carbide Corp., Oak Ridge, Tenn. Y-12 Plant). Apr. 13, 1966. Contract W-7405-eng-26. 33p. Dep. mn. CFSTI $2.00 cy, $0.50 mn.

Several studies were conducted to determine ways of producing satisfactory pellets of uranium monocarbide. It was found that densification by cold pressing is dependent upon the powder particle size, oxygen content, sintering temperature and atmosphere, and the lubricant used in pressing. Certain sintering promoters were investigated. The addition of approximately 0.5% nickel was found to enhance densification, and an average density of 97% of theoretical was obtained when 2 wt % uranium disilicide was used under the proper conditions. (auth)

21297 (NP-tr-1371) IMPROVEMENTS TO NUCLEAR FUELS. Translated by R. A. Slingo (U.K.A.E.A. Atomic Energy Research Establishment, Harwell, Eng.), from French Patent No. 1,212,233. Sept. 22, 1958. 8p. Dep. mn. JCL $1.10 fs, $0.80 mf.

A fabrication method for an improved nuclear fuel is described. It includes uranium dioxide containing a fissile isotope, this uranium dioxide being in the form of particles distributed within a matrix made of a different refractory material which has a relatively high thermal conductivity, a high melting point, a low neutron capture cross section, and is mainly composed of 25 to 40% volume of the said refractory material (BeO or SiC), the remainder being uranium dioxide containing at least one fissile isotope. (M.O.W.)

21298 FABRICATION OF AN ULTRA-FINE Cb–Cu COMPOSITE BY DRAWING. **Cline, H. E.; Strauss, B. P.; Rose, R. M.; Wulff, J. (Massachusetts Inst. of Tech., Cambridge). Amer. Soc. Metals, Trans. Quart., 59: 132-6(Mar. 1966).**

Cu tubing was swaged onto a Nb rod and the ensemble then drawn to 0.0345-in. dia wire. The wire was cut into 56 pieces, placed into a Cu tube, and the ensemble drawn down again to 0.0345-in. dia wire. The procedure was repeated four times. On the final sequence the composite wire was drawn down to 0.006-in. dia. This wire contained about 10^7 Nb filaments with a dia of 100 Å each. (W.L.G.)

21299 STUDY AND OBSERVATION OF SINTERING OF OXIDES OF URANIUM AND THORIUM. Bassi, A. (CISE, Milan); Brutto, E.; Perona, G.; Screm, G.; Sesini, R. Energ. Nucl. (Milan), 13: 122-32(Mar. 1966). (In Italian).

Mixed urania and thoria are of interest for use in reactors. The same methods as those used for UO_2 pellets were considered to be fitted to the fabrication of composed pellets, starting from suitably mixed powders of the two oxides. Some sintered pellets were prepared at high temperature and with different times. The sintered materials were submitted to metallographic observation and thermal shock tests in order to control their mechanical properties. Mixtures with a high content of either components give rise to good quality homogeneous materials. Two different phases seem to be present in the intermediate composition mixtures; sintered oxides present a marked porosity, nevertheless the thermal shock resistance is so high that uses of these materials can also be foreseen. Microfractography by means of direct carbon replicas was used and a new technique for transmission observation in electron microscope was developed in order to clarify the morphology of this material. (auth)

21300 TECHNOLOGICAL AND ECONOMICAL IMPROVEMENTS IN THE FABRICATION OF UO_2 CERAMIC FUEL. Gabaglio, M.; Liscia, A. (CNEN, Saluggia, Italy). Energ. Nucl. (Milan), 13: 133-8(Mar. 1966). (In Italian).

The process commonly employed to fabricate sintered UO_2 pellets is considered with regard to the technical and economical point of view. The evaluation of the process permits one to individualize which operations may be susceptible to improvements or simplifications. Powder pressing operations and scraps recovery are taken into consideration. Experiments carried out with the "without binder" pressing technique and the oxidation-reduction process recovery technique are described. The results indicate that the tried modifications give tangible advantages with regard to the quality of product and the economy of the process. (auth)

21301 FABRICATION OF ThO_2–UO_2 CERAMIC FUEL. Gabaglio, M.; Liscia, A. (CNEN, Saluggia, Italy). Energ. Nucl. (Milan), 13: 173-81(Apr. 1966). (In Italian).

Research and development on sintered ThO_2-UO_2 fuels to support the program for the Thorium and Uranium Oxide Fuel Reprocessing and Fabrication Plant of CNEN are reviewed. Experiments carried out to investigate the best conditions of sintering a mixed thorium–uranium oxide containing 4% in uranium are described. Methods of preparation of starting coprecipitate, calcination, and sintering conditions were determined. Experiments in order to obtain on pilot-scale, ceramic compounds with density 95% of theoretical together with two different length-diameter ratios are described. The ratios between 1 and 2 are for pellets obtained employing the pressing technique; the ratio of about 10 was obtained by extrusion. The results indicated that the extrusion method is more convenient. (auth)

21302 UO_2–ZrO_2–CaO CERAMIC NUCLEAR FUELS. Amato, I.; Colombo, R. L.; Protti, A. M. (FIAT, Turin). Energ. Nucl. (Milan), 13: 189-93(Apr. 1966). (In Italian).

The use of sintered ternary mixtures UO_2-ZrO_2-CaO as fuel elements in some nuclear reactors with high specific power or designed to operate at high temperatures is to be preferred in comparison with other solutions as this material presents the crystalline structure of fluorite that is very resistant to radiation damage. Sintered materials having good characteristics were obtained by heating some compacts of ZrO_2, $CaCO_3$, and U_3O_8 to commercial powders in hydrogen atmosphere at 1600 to 1800°C. A problem still to be solved is bound to the presence of a grey phase, fusible at the sintering temperature that was observed in micrographs of finished products and should belong to the Ca–Zr–O system. (auth)

21303 FABRICATION OF THIN PLATES FROM REFRACTORY CARBIDES. Ignatiev, B. G.; Nejevenko, L. B.; Poltoratskii, N. J.; Fomin, G. S.; Yakutovich, M. V. (Atomic Energy State Committee, USSR). Int. J. Powder Met., 2: 33-9(Jan. 1966).

Two methods for the fabrication of thin plates of zirconium carbide materials were investigated: unidirectional pressure compacting and powder rolling, both with subsequent sintering. Data for the preparation of powders are given and a correlation is made between particle characteristics (specific surface area) and the compacted and sintered densities. Tests indicated that the powder rolling process results in a material of considerably higher density. (auth)

21304 FURNACE FOR UO_2 SINTERING. Muzsnay, Laszlo; Bencze, Istvan; Probald, Vilmos. Magyar Tud. Akad. Kozp. Fiz. Kut. Int. Kozlem., 13: 413-30(1965). (In Hungarian).

The furnace described was designed for sintering uranium dioxide in hydrogen flow at maximum 1800°C temperature. The combustion volume, 40 mm in diameter and 120 mm long, lends itself for the sintering of other substances in vacuum or in hydrogen or some neutral gas flow. The principles of design and some experimental results obtained during the development of the laboratory furnaces are discussed. (auth)

21305 MANUFACTURE OF ZIRCONIUM, TITANIUM, AND HAFNIUM SPONGES. Aubert, J. Met. Ital., 58: 48-52(Feb. 1966). (In Italian).

The characteristics of zirconium and the utilization of

this metal and its alloys in nuclear and nonnuclear technology are discussed. The production of zirconium and the procedures used industrially in different phases of production in order to obtain a sponge, which corresponds to the requested standards, are described. The common characteristics of this production with those of hafnium and titanium are given. (auth)

21306 GRAPHITE-CARBIDE MATERIALS PREPARED BY HOT-WORKING WITH THE CARBIDE PHASE IN THE LIQUID STATE. White, J. L.; Pontelandolfo, J. M. (General Atomic Div., General Dynamics Corp., San Diego, Calif.). Nature, 209: 1018-19(Mar. 5, 1966).

A new process is described wherein graphite bodies containing dispersed carbide particles are hot worked at temperatures such that the carbide phase is in the liquid state. Two carbides were used, zirconium carbide and molybdenum carbide, with carbide-graphite eutectic temperature at 2850 and 2584°C respectively. Photomicrographs of graphite bodies containing carbide particles are shown, and some results for the compressive strengths are given. The results show large increases in strength parallel to the direction of hot working and modest increases in the perpendicular direction. These effects are in sharp contrast to the results for a similar graphite matrix hot worked without the carbide additives. (J.F.P.)

21307 PREPARATION OF URANIUM CARBIDES STARTING WITH THE DIOXIDE, MELTING IN ARC FURNACE, AND CASTING. Porneuf, Alexandre (Univ. de Paris, Orsay, France). Rev. Hautes Temp. Refract., 2: 333-65(Oct.-Dec. 1965). (In French).

An industrial technique for the preparation of uranium carbide bars from the dioxide was investigated. The preparation of the uranium carbide by carbon reduction of the dioxide is described. Methods for the preparation of the uranium carbide bars by fusing and casting in an arc furnace are discussed. The results show that it is possible to develop, on an industrial scale, a method of carbothermy applicable to uranium oxides of different origins and characteristics and leading to a high reaction rate of the oxide with the carbon. The technique used for the preparation of the uranium carbide bars can be applied on an industrial scale. (J.S.R.)

21308 DOUBLE-SAMPLING METHOD FOR CARRYING OUT QUALITY CONTROL OF A FABRICATION PROCESS. Cerrolaza, J. A.; Lago, A.; Montojo, Rosa M. (Junta de Energia Nuclear, Madrid). pp 413-31 of STI-PUB-110. (In Spanish).

In fabricating components for use in reactors, two basic factors are of decisive importance, namely the need for very high quality, which allows for only a very small percentage of defective parts, and the very high cost of each of the components. A method has been developed in which the size of the samples and the limits of control are established as a function of the errors of first and second kind. This method, although applicable, is not really practicable for the inspection of reactor components since the samples required are too large. Therefore, a method similar to the other but which relies on double sampling and thus considerably reduces the average size of the sample is presented. (P.C.H.)

21309 WELDING OF MOLYBDENUM AND NIOBIUM WITH STAINLESS STEEL. D'yachenko, V. V.; Sivov, E. N.; Morozov, B. P. Svarochn. Proizv., No. 1, 2-4(Jan. 1966). (In Russian).

The possibility of producing direct junctions of Mo and Nb with stainless steel by welding and by the fusion of the steel without fusion of the refractory metal was investigated and the results are reported. (tr-auth)

21310 FUSION WELDING OF SOME HETEROGENEOUS METALS. Strizhevskaya, L. G.; Starova, L. L. Svarochn. Proizv., No. 1, 4-7(Jan. 1966). (In Russian).

The joining of heterogeneous metals (Fe, Ni, Pd, Cu, Ti, V, Nb, and Ta) by the use of argon-arc and electron-beam welds was investigated. (tr-auth)

21311 WELD INTERFACE POROSITY IN TANTALUM. Bradt, R. C.; Curcio, R. M. (Fansteel Metallurgical Corp., North Chicago). Weld. J. (N.Y.), 45: 124s-6s(Mar. 1966).

Porosity at the weld fusion zone-base material interface was investigated in both gas tungsten-arc and electron beam welds of sintered-powder metallurgy, vacuum-arc cast, and electron beam melted tantalum. At commercial purity levels, this type of porosity is independent of the mean interstitial concentration, but not of the consolidation process. Fusion-cast tantalum does not appear to be susceptible to this type of weld defect. The characteristic features of this porosity suggest that the formation mechanism is one of heterogeneous bubble nucleation of a hydrogen-base gas on an unidentified nucleant. This nucleant is apparently soluble or decomposable in sufficiently superheated molten tantalum, as is the case in both vacuum-arc casting and electron beam melting. (auth)

21312 DEVELOPMENT OF CHROMIUM-VANADIUM ALLOYS FOR BRAZING TUNGSTEN TO MOLYBDENUM. Smith, J. T. (Avco Corp., Wilmington, Mass.). Weld. J. (N. Y.), 45: 135s-8s(Mar. 1966).

Several metals and alloys were evaluated as brazing materials for joining Mo to W. For service times of several hundred hours at temperatures to 1800°F, Fe was a satisfactory brazing metal. For temperatures up to 2700°F and for extended operating times, a Cr–25 wt.% V alloy was selected. (W.L.G.)

21313 NUCLEAR MATERIALS MANAGEMENT AT THE JAPAN ATOMIC ENERGY RESEARCH INSTITUTE. Machida, Chuji; Hiramatsu, Ichiro (Japan Atomic Energy Research Inst., Tokyo). Vienna, International Atomic Energy Agency, 1965, Preprint No. SM-67/4, 17p. (CONF-650803-28). ORINS.

From IAEA Symposium on Nuclear Materials Management, Vienna.

The procedures for nuclear material control are reviewed, based on the experiences at Japan Atomic Energy Research Institute. Nuclear materials discussed include: both natural and enriched uranium for research; imported enriched nuclear fuel elements for JRR-2; JRR-4, JPDR, and the critical assemblies for JMTR and the propulsion reactor; domestically fabricated natural uranium fuel elements for JRR-3; domestically fabricated fuels for the critical assemblies manufactured from imported enriched uranium oxides; and domestically fabricated enriched fuel elements for JPDR and for the propulsion reactor manufactured from imported enriched uranium hexafluoride. The entire administrative pattern for nuclear material control is presented. Emphasis is placed on the domestic fabrication of enriched fuel elements from imported enriched uranium, and the details of the control procedures during and after the fabrication process are discussed. The control procedures include chemical analysis for purity check, isotopic assay by mass spectrometry, physical and mechanical tests of fabricated products, and the careful prevention of diversion of nuclear materials. Administrative problems attributed to the Japanese domestic situation are presented: for example, the segregation, collection and efficient recovery and practical uses of residual uranium from the fabrication process. Methods for keeping records on the storage and uses of nuclear materials are also discussed. (auth)

21314 BONDING OF REFRACTORY MATERIALS BY MEANS OF CERIUM OXIDE–CERIUM SULFIDE MIXTURES AND PRODUCT. Bush, Harry D. (to Union Carbide Corp.). U. S. Patent 3,232,822. Feb. 1, 1966. Filed Apr. 19, 1962.

A process is patented for bonding refractory materials so that a strong joint with a relatively low electrical resistance is produced. The process consists of applying a layer of a finely divided mixture of CeO_2 and either Ce_2S_3 or Ce_3S_4 to at least one of the refractory materials to be bonded, pressing the refractory materials into tight engagement with the mixture between them, increasing the temperature of the materials and the refractory surfaces

to between 1650°C and the melting point of the refractory materials, and maintaining the temperature until the desired degree of bonding is effected. The same refractory materials or two different refractory materials may be bonded in this manner, and the articles so bonded are particularly useful in thermoelectric devices. (B.L.M.)

21315 PROCESS FOR THE DENSIFICATION OF CARBONACEOUS BODIES. Blanchard, Rene; Blum, Pierre; Bochirol, Louis; Philippot, Joseph; Moreau, Claude (to Commissariat a l'Energie Atomique). Canadian Patent 722,560. Nov. 30, 1965. Priority date May 22, 1962, France.

Conventional sources of graphite such as coke may have their densities increased by treatment with thermally cracked hydrocarbons. Powdered forms of carbon are pressed into convenient solid shapes with the aid of a binder and then exposed to a stream of natural gas or other gaseous hydrocarbon in a furnace. The effect is to fill the undesirably large pores and increase the density to 1.75–1.90 g/cm^3. In some applications the gas stream must be purified, in others natural gas may be used. The resulting graphite has a minimal anisotropic property and is suitable for nuclear applications. (F.S.A.)

21316 NUCLEAR FUEL PELLETS OF SPECIAL PROFILES AND METHOD OF THEIR PREPARATION. Hauser, Raymond; Rambourg, Roger; Giubert, Bertrand (to Commissariat a l'Energie Atomique). Canadian Patent 725,277. Jan. 4, 1966. Priority date June 12, 1961, France.

Fuel pellets of uranium oxide, carbide, nitride, or silicide are fabricated from powder by pressing and sintering, then loaded into fuel tubes. Each pellet has a projection and/or recess on either end in the form of a truncated cone. In use, the projection on one pellet fits into the recess in its neighbor in the tube, thus preventing lateral movement so that a column of pellets acts like a rigid rod. The manufacturing process claims to produce uniform density in all parts of each pellet. (F.S.A.)

21317 METHOD OF MANUFACTURING CONTROL RODS FOR NUCLEAR REACTORS. Mills, Brian E. (to Allmanna Svenska Elektriska Aktiebolaget). Canadian Patent 725,771. Jan. 11, 1966.

Nuclear reactor control rods made of an alloy of cadmium, indium, and silver, clad with stainless steel have good mechanical properties and are corrosion resistant. To secure a good bond between the rod and the cladding, it is necessary to coat the inside of the cladding with a thin layer of copper and then a thin layer of nickel. Dies and other details of manufacture are described as well as the heat treatment necessary for secure bonding. (AECL)

21318 POWDER ROLLING OF TUNGSTEN AND ITS ALLOYS. Ready, Thomas J.; Lewis, H. D.; Hockett, J. E. (to U. S. Atomic Energy Commission). U. S. Patent 3,245,114. Apr. 12, 1966.

This patent relates to apparatus for rolling powders of tungsten or its alloys wherein a constant head of powder is maintained in the hopper by means of a baffle. One of the lips of the hopper is vibrated by a controllable electronic driver and each of the rollers are constantly roughened by an abrasive while rotating. (AEC)

Properties and Structure

See also CHEMISTRY — Inorganic and Physical Chemistry

PHYSICS — Solid State Physics

Refer also to abstracts 21044, 21458, and 22422.

21319 (AD–621064) TEST RESULTS ON FALEX PINS COATED BY THE PLASMA-ARC PROCESS. Hassion, Francis X. (Springfield Armory, Mass.). July 30, 1965. 28p. (SA-TR–18-1096). CFSTI $2.00 cy, $0.50 mn.

Coatings of nickel–alumina, molybdenum, tungsten, alumina, tungsten carbide–cobalt, stainless steel, and zirconia applied to Falex pins by the plasma-arc process were tested for wear resistance. The tungsten carbide–cobalt, the tungsten, and the molybdenum coatings showed unusually good wear characteristics comparable to dispersions of diamond, zirconia, and thoria in chromium electroplate formed at high current densities. The coefficients of friction appeared to be somewhat higher in the plasma-arc coatings. This may be due, however, to the initial roughness of the surfaces tested. The other plasma-arc coatings, i.e., nickel–alumina, alumina, stainless steel, and zirconia either flaked, wore off, or galled under test. Procedures are described and results are discussed. (auth)

21320 (AD–625475) POINT DEFECTS AND MECHANICAL PROPERTIES OF COLUMBIUM. Final Report, February 15, 1962–November 30, 1965. Coll, Jorge A.; Di Primio, Juan C.; Bisogni, Edgardo (Comision Nacional de Energia Atomica, Buenos Aires (Argentina). Departmento de Metallurgia). Nov. 1965. Contracts DA-ARO-49-092-63-G20; DA-ARO-49-092-64-G44. 39p. CFSTI $2.00 cy, $0.50 mn.

Results of R vs T for Nb show agreement with others up to 1000°C. Because of quenching some kind of defects can be retained in Nb containing certain amount of interstitial impurities. A minimum dose of 1.10 to the 17th power neutrons/cm^2 is necessary to produce a measurable increase in the hardness of polycrystalline Nb. (TAB)

21321 (AERE-Bib–143) BIBLIOGRAPHIC REVIEW OF SELF-DIFFUSION IN METAL OXIDES. Cumming, P. A.; Harrop, P. J. (Atomic Energy Research Establishment, Harwell (England)). Oct. 1965. 22p. Dep. BIS $0.80, HMSO 4s. 0d.

References (117) on the determination of self-diffusion coefficients in simple metallic oxides are given to journals and reports published from 1946 through 1965. A table is presented of useful diffusion data, and an author index is included. (P.C.H.)

21322 (AMRA-TR–65-25) EVALUATION OF REFRACTORY SHEET METALS. PART II. Gazza, George E.; Desisto, Thomas S. (Army Materials Research Agency, Watertown, Mass. Materials Engineering Div.). Oct. 1965. 16p.

Four tantalum base alloys, one molybdenum base alloy, and one tungsten base alloy were evaluated. Mechanical properties were obtained by tensile testing at temperatures to 3500°F, stress-rupture testing to 3000°F, and bend testing to –320°F. (auth)

21323 (ANL–6894) STUDIES OF STOICHIOMETRIC AND HYPERSTOICHIOMETRIC SOLID SOLUTIONS IN THE THORIA–URANIA SYSTEM. Lynch, E. D. (Argonne National Lab., Ill.). Dec. 1965. Contract W-31-109-eng-38. 40p. Dep. mn. CFSTI $2.00 cy, $0.50 mn.

Studies were made of the single-phase, solid-solution region of the thoria–urania system, including both stoichiometric and hyperstoichiometric materials. The temperature range for formation of hyperstoichiometric solid solutions was determined and related to the decomposition of U_3O_8 through oxygen loss. The degree of nonstoichiometry was shown to be reproducible for any given composition and heat treatment. Changes in x-ray lattice parameters, due to stoichiometry, were determined. The stability of thoria–urania solid solutions was investigated by study of the oxidation characteristics and thermal-expansion analysis. The reduction of hyperstoichiometric materials to stoichiometry was accompanied by permanent dimensional changes that are related to oxygen loss. (auth)

21324 (ANL–7055, pp 163-6) HIGH TEMPERATURE REACTOR MATERIALS DEVELOPMENT. Edwards, R. K.; Feder, H. M. (Argonne National Lab., Ill.).

Research devoted to determining the phase diagram of uranium–uranium oxide condensed states is reported.

Work on equilibria between vapor and condensed phases of this system is discussed. (J.R.D.)

21325 (AWRE-O-36/66) IMPACT TENSILE TESTING OF URANIUM. Tilbury, P. D. (Atomic Weapons Research Establishment, Aldermaston (England)). Mar. 1966. 14p. Dep. mn. BIS $0.50. HMSO 2s. 6d.

Results of slow (0.005 in./in./sec) and impact (150 in./in./sec) tensile tests at temperatures ranging from 125 to 250°C are reported and discussed. The ductile to brittle transition in α-uranium was raised from 25 to 120°C by the increase in strain rate. Anomalous behavior after vacuum annealing of rod and cross-rolled plate was found. This is discussed. The Stroh equation was applied and leads to a value of 1.09 ev for U. (auth)

21326 (BNWL-203) TRANSFORMATION RATES OF PLASTICALLY DEFORMED PLUTONIUM. Nelson, R. D. (Battelle-Northwest, Richland, Wash. Pacific Northwest Lab.). Feb. 1966. Contract AT(45-1)-1830. 14p. Dep. mn. CFSTI $1.00 cy, $0.50 mn.

Plastic deformation of the stable β-phase in Pu retards the $\beta \rightarrow \alpha$ transformation. This is consistent with known martensitic transformations. There are insufficient dislocations in plastically deformed α-phase Pu to retard the $\alpha \rightarrow \beta$ transformation, but sufficient dislocations are present to accelerate it. Deformed α-phase Pu can be annealed at 105°C. (auth)

21327 (CONF-660505-1) SOLID-STATE EQUILIBRIA IN THE SYSTEMS LITHIUM–CARBON AND LITHIUM–BORON. Secrist, D. R. (Knolls Atomic Power Lab., Schenectady, N. Y.). [1965]. Contract W-31-109-eng-52). 7p. Dep. mn. CFSTI $1.00 cy, $0.50 mn.

From American Ceramic Society, Washington, D. C.

A partial study of the phase relations existing in the systems lithium–carbon and lithium–boron was conducted at 2–4 atm pressure. Phases present in the 3 to 50 at. % lithium region of the system lithium–carbon to 700°C consisted of carbon and stoichiometric Li_2C_2. A single crystal of Li_2C_2 was examined by the Weissenberg x-ray method; the unit cell was identified as primitive monoclinic. A lithium boride phase corresponding to LiB_{12} was synthesized in the 9 to 50 at. % lithium region of the system lithium–boron. The reaction of lithium with $B_{4.0}$ C was also considered. (auth)

21328 (CU-2660-25) A THERMODYNAMIC STUDY OF POTASSIUM AMALGAMS [Thesis]. LaMantia, Charles Robert (Columbia Univ., New York. School of Engineering and Applied Science). 1965. Contract AT(30-1)-2660. 260p. Dep. mn. CFSTI $6.00 cy, $1.25 mn.

Experimental measurements were made of the total vapor pressure of potassium amalgams and the emf of potassium amalgam concentration cells, both as functions of temperature and of amalgam composition. Vapor pressure measurements were made at twenty compositions, including pure mercury, at pressures up to 10 atm. These data were represented by a linear relation between log P and 1/T, with composition as a parameter, and with an average standard deviation of 2.5% of the vapor pressure. Emf data were obtained for six compositions between mercury mole fractions of 0.10 and 0.55 at temperatures up to 500°C. The emf for each composition was found to be a linear function of temperature. From the above data, the pure component vapor pressure and P-V-T data, and a model for the interaction of the gas species, the following thermodynamic properties were calculated as functions of composition along the saturation curves at pressures of $\frac{1}{2}$, 1, and 2 atmospheres: mercury and potassium activities in the liquid amalgams; differential heat of vaporization; liquid heat of mixing; composition of the vapor in equilibrium with the amalgam; and equilibrium vapor compressibility factor. Isobaric thermodynamic consistency checks were performed at each pressure level. Each set of data was found to check to within 1%. In the concentration range where the equilibrium vapor is substantially pure mercury, heats of mixing were found to check precisely with those calculated from the heat of vaporization of pure mercury and its heat of vaporization from the amalgam. The experimental data checked well with literature data, which were available in the low end of the temperature range covered in this research. (auth)

21329 (DRI-1092-229) STUDIES OF THE EFFECT OF INTERSTITIAL ADDITION ON THE PHASE EQUILIBRIA OF THE NIOBIUM-RICH REGION OF THE NIOBIUM-TUNGSTEN-HAFNIUM AND NIOBIUM-TUNGSTEN-ZIRCONIUM ALLOY SYSTEMS. Quarterly Progress Report No. 6. Yamamoto, Albert S. (Denver Research Inst., Univ. of Denver, Colo.). Mar. 1966. Contract AT(11-1)-1092. 11p. Dep. mn. CFSTI $1.00 cy, $0.50 mn.

The effects of small carbon and oxygen additions on the phase equilibria of the niobium-rich region of the niobium–tungsten–hafnium and niobium–tungsten–zirconium alloy systems was investigated. Metallographic examination of the alloys annealed at 1600 and 1300°C (2912 and 2372°F) revealed that small oxygen additions to the niobium–tungsten–hafnium alloys resulted in formation of precipitates which were identified to be HfO_2 by the x-ray method. In the niobium–tungsten–zirconium alloys containing more than 10 wt % Zr and small quantity of oxygen, the presence of α-Zr was found by the x-ray diffraction method. The precipitates observed in the alloys that were high in tungsten and low in zirconium, however, were not identified. The powder x-ray data for a series of the selected oxygen-containing niobium–tungsten–hafnium and niobium–tungsten–zirconium alloys are tabulated. (auth)

21330 (EUR-2621.f) MECANISMES DE DEFORMATION DES METAUX A STRUCTURE HEXAGONALE COMPACTE. (Deformation Mechanisms in Hexagonal Compact Metals). Guyot, P. (European Atomic Energy Community, Ispra (Italy). Joint Nuclear Research Center). 1965. 34p. Dep. mn.

A review is presented on the deformation mechanisms in the hcp metals. Only the basal glide, controlled by cutting the forest of dislocations c, is well understood; the prismatic glide seems to be determined by the cross slip of basal screw dislocations. The increase of dislocations as well as twinning the basal easy glide are also considered. (79 references.) (auth)

21331 (EURAEC-1569) STUDY OF THE BASE METAL INTENDED FOR RESEARCH ON THE BRITTLE FRACTURE OF LARGE WELDMENTS. Quarterly Report No. 7, October 1–December 31, 1965. (Institut de Recherches de la Siderurgie, St. Germaine-en-Laye (France)). Jan. 1966. Contract 031-64-5-TEEF. 22p. (EUR-2805). Dep. mn. CFSTI $1.00 cy, $0.50 mn.

Work Performed under United States–Euratom Joint Research and Development Program.

The effects of the heating rates on the Ac_1 and Ac_3 transformation temperatures in Super Elso steel were found to be small. Tensile, impact strength, Robertson, and Pellini tests on the surface layers and core of Acier AMMO steel plates consistently gave different values for the three sections, the core having the lower values. (W.L.G.)

21332 (EURAEC-1573) DIFFUSION OF RARE GASES IN SOLIDS. Quarterly Report No. 22, October–December 1965. (Hahn-Meitner-Institut fuer Kernforschung, Berlin (West Germany)). Jan. 1966. 5p. (EUR-2806). Dep. mn. CFSTI $1.00 cy, $0.50 mn.

Work Performed Under United States–Euratom Joint Research and Development Program.

The diffusion of ^{88}Kr was measured in UO_2 and UC single crystals at irradiation doses of 5×10^{13} nvt. In the case of UO_2, no difference was observed in comparison with ^{133}Xe measurements at $2\text{-}10 \times 10^{16}$ nvt. UC showed slightly higher D values. In U-doped CaF_2, values were found for the diffusion of Ar, Kr, and Xe in the 900–1200°C range. (auth)

21333 (IITRI-B6042-4) VANADIUM ALLOY STUDIES. Quarterly Report No. 4, December 1, 1965–February 28, 1966. Holtz, F. C. (IIT Research Inst., Chicago, Ill.). Mar. 21, 1966. Contract NOw-65-0427-f. 19p.

Tensile data for alloys based on V–20 Nb–10Ti and V–Nb–Ta are reported. In the rolled and aged condition, the V–Nb–Ti alloys containing small Si and C additives had density-corrected strengths in the 1,210,000 to 1,300,000-in. range at –320°F; elongations ranged from 12 to 14%. These alloys, as well as the rolled and aged high-Ta compositions, had density-corrected strengths in the 800,000 to 900,000-in. range at room temperature. At 2000°F, fully annealed Ta-containing alloys were approximately twice as strong as the high-V materials on a density-corrected basis (269,000-in. vs. 123,000-in.). (auth)

21334 (IS–1325) DETERMINATION OF LIQUID METAL DIFFUSION COEFFICIENTS BY MOLECULAR DISTILLATION. Buell, C. H.; Shuck, F. O. (Ames Lab., Iowa State Univ. of Science and Tech.). Feb. 1966. Contract W-7405-eng-42. 34p. Dep. mn. CFSTI $2.00 cy, $0.50 mn.

A study was made on the feasibility of measuring liquid metal diffusion coefficients during molecular distillation. Although no other data for the zinc–indium system are available, a comparison with similar systems at this temperature (450°C) indicated that the value measured (1.69×10^{-4} cm²/sec) is high by a factor of two to five. The major error in the measurements appears to be caused by the fact that the non-volatile indium is more dense than the volatile zinc. (auth)

21335 (IS-T–76) THERMODYNAMIC PROPERTIES OF CALCIUM–ZINC ALLOYS [Thesis]. Hecht, Ralph Julius (Ames Lab., Iowa State Univ. of Science and Tech.). Feb. 1966. Contract W-7405-eng-82. 65p. Dep. mn. CFSTI $3.00 cy, $0.75 mn.

The dewpoint and Knudsen effusion methods were used to determine the equilibrium vapor pressure of zinc over solid and liquid calcium–zinc alloys. For each alloy these data were fitted to a linear equation giving the logarithm of pressure as a function of temperature. The vapor pressure data for the liquid alloys were combined with the vapor pressure of pure zinc to determine expressions for the relative excess partial molal free energy, enthalpy, and entropy for both components. The integral free energy, enthalpy, and entropy of solution for the calcium–zinc alloys were calculated from these expressions. Vapor pressure data of zinc over the solid alloys were used to calculate expressions for the standard free energy of formation of the calcium–zinc compounds for the temperature range 298 to 1123°K. (auth)

21336 (IS-T–79) LANTHANUM–LANTHANUM HYDRIDE PHASE SYSTEM [Thesis]. Straatmann, John Alphonse (Ames Lab., Iowa State Univ. of Science and Tech.). Feb. 1966. Contract W-7405-eng-82. 36p. Dep. mn. CFSTI $2.00 cy, $0.50 mn.

The phase relations between La and LaH_2 were determined. The melting point of La increased with the addition of H_2. The addition of H_2 also decreased the fcc to bcc transformation temperature of La to a eutectoid at 773°C and 23.5 at.% H_2. The solubility of LaH_2 in fcc La ranged from 2.83 at.% at 375°C to 21.3 at.% H_2 at 773°C. The enthalpy of solution was calculated to be 5.76 ± 0.17 kcal. Above 773°C the solubility of LaH_2 in bcc La increases rapidly and complete solubility occurs at temperatures above 960°C. LaH_2 has no appreciable effect on the low temperature transformation from hcp to fcc La. (auth)

21337 (JINR–P–2598) NEKOTORYE REZUL'TATY ISSLEDOVANIYA DREIFA IONOV LITIYA V KREMNIEVYKH MONOKRISTALLAKH p-TIPA. (Some Results of a Study of Lithium-Ion Drift in Silicon p-Type Monocrystals). Antonov, A. S.; Yuskeselieva, L. G. (Joint Inst. for Nuclear Research, Dubna (USSR). Lab. of Nuclear Problems). 1966. 14p. Dep. mn.

The results are reported of experimental study of p-i-n structure in the p-type silicon which is formed by lithium-ion drift in the electric field of the p-n junction. Changes (during the drift) in the boundary location between the n-i and p-regions as well as in the width of the negative space charge in the p-n junction are studied. Some regularities in the lithium-ion drift are established. The results obtained are compared with the existing theory. (auth)

21338 (JPL-TR–32-842) TENSILE AND STRUCTURAL PROPERTIES OF GLASSY CARBON. Kotlensky, W. V.; Fischbach, D. B. (Jet Propulsion Lab., Calif. Inst. of Tech., Pasadena). Nov. 15, 1965. Contract NAS-7-100. 15p.

Tensile properties of two different grades of glassy carbon (called GC-20 and GC-30 by the manufacturer) were measured from room temperature to 2900°C. The test specimens had a gauge section 0.08 in. in width by 0.10 in. in thickness with a 0.75-in. gauge length. Tests were made in a helium atmosphere, and heating was accomplished by means of an external graphite heater. Tensile strengths at room temperature for both grades were approximately 6000 psi. Both grades showed an increase in strength with increasing test temperature, reaching a maximum within the 20,000 to 25,000 psi range at 2500°C. At 2900°C, strengths of about 12,000 psi for GC-20 and 16,000 psi for GC-30 were measured. Differences in the deformation of the two grades were evident from their ductility. At 2700°C, maximum elongations of 33% for GC-20 and 5.4% for GC-30 were measured. Density, unit cell dimension, hardness, and diamagnetic susceptibility measurements were used to investigate the structural changes accompanying deformation and heat treatment. Electron micrographs revealed a difference in fracture mode for GC-20 and GC-30. The tensile and structural behavior of glassy carbon was compared with that of conventional carbon-base materials. It is suggested that cross-link bonding is responsible for the high strength of glassy carbon; however, the small crystallite size and the small pore size may also be contributing factors. (auth)

21339 (LA-DC–7095) THE PLUTONIUM–AMERICIUM SYSTEM. Ellinger, F. H.; Johnson, K. A.; Struebing, V. O. (Los Alamos Scientific Lab., Univ. of California, N. Mex.). [1964]. Contract W-7405-eng-36. 14p. Dep. mn. CFSTI $1.00 cy, $0.50 mn.

The plutonium–americium phase diagram was determined by micrographic and x-ray diffraction methods. δ-Plutonium and β-americium form a continuous series of solid solutions, which is stable at room temperature in the composition range from about 6 to 80 at. % americium. No intermediate phases were found. (auth)

21340 (LA-DC–7626) THE STRESS DEPENDENCE OF THE CREEP RATE OF TWO COMMERCIAL GRAPHITES. Green, W. V.; Zukas, E. G. (Los Alamos Scientific Lab., Univ. of California, N. Mex.). [nd]. Contract W-7405-eng-36. 19p. (CONF-660515–1). ORAU.

From Electrochemical Society Meeting, Cleveland.

The stress dependence of the creep rate of two commercial graphites was measured by a changing-stress method at 2300 and 2500°C. In this way, the structural differences that normally complicate the analysis of results from several different samples were eliminated. The creep rate was found to be proportional to the five and one-half power of stress. From this, it was concluded that stress-directed diffusion creep was not the rate-controlling process, but a dislocation mechanism was more probable. (auth)

21341 (MAB–205-M) EVALUATION TEST METHODS FOR BERYLLIUM. (Materials Advisory Board, National Academy of Sciences–National Research Council, Washington, D. C.). Mar. 1966. Contract SD-118. 52p. CFSTI $3.00 cy, $0.50 mn.

Standardized methods and procedures for conducting mechanical property tests on beryllium are discussed. Such methods are required in view of the characteristics of beryllium, which make conventional test procedures difficult to apply. The data presented are restricted to information which is well established and accepted, but

areas of testing controversy, and current technical needs in the testing area are highlighted. Attempts were made to document recommended methods, based on a review of the procedures used in a number of organizations. To permit reliable inter-comparisons between laboratories, standardized methods are needed; and it is hoped that for this reason these methods will be adopted. Recommended procedures for tensile, 3-point bend, 4-point bend, and precision elastic limit tests are described. (auth)

21342 (MLM-1301) REACTOR FUELS AND MATERIALS DEVELOPMENT. PLUTONIUM RESEARCH: JULY-SEPTEMBER 1965. Wittenberg, L. J.; Grove, G. R. (Mound Lab., Miamisburg, Ohio). Mar. 11, 1966. Contract AT-33-1-GEN-53. 22p. Dep. mn. CFSTI $2.00 cy, $0.50 mn.

Continued study of the Ce–Fe binary system showed the existence of the compound $CeFe_7$ instead of the compound identified in the literature as $CeFe_5$. The Pu–Ce–Fe ternary phase diagram was modified to show this change. An extensive terminal solid solution of Pu in Ce_5Ni_2 was shown to extend to 45 at. % Pu. The solid solution has no significant homogeneity range with regard to Ni content. The viscosities of liquid Sn, Pb, and U were determined with the liquids contained in zirconia crucibles to prevent corrosion of the viscosity capsules. Viscosity measurements on liquid U indicated 7.6 centipoise at the melting point, 1133°C, and 6.2 centipoise at 1223°C. Microscopic examination of an arc-melted pellet of PuO_2 showed the formation of the eutectoid structure of PuO_{2-x} and alpha Pu_2O_3. In several noneutectoid phase areas large acicular crystals of alpha Pu_2O_3 had formed in a matrix of PuO_{2-x}. (W.L.G.)

21343 (N-65-23013) CHARACTERISTICS OF THE HIGH-TEMPERATURE MECHANISMS OF CREEP AND RECOVERY IN GRAPHITE. Final Technical Report No. 1, August 1, 1963–July 31, 1964. (College of Aeronautics, Cranfield (England). Dept. of Materials). Feb. 1964. Contract DA-91-591-EUC-2880. 18p. (CoA-NOTE-MAT-1, Pt. IV).

Work on the torsional creep and recovery properties of graphites in the temperature range 2000 to 3000°C continued. Differences in the steady-state creep behavior were noted between extruded and pressed grades, in the latter no steady-state component being observed. In creep tests on ungraphitized extruded material after given soaking times above 2000°C, it was shown that the time at temperature influenced the initial elongation but had relatively little effect on the creep rate. Rates and amounts of recovery were, however, both reduced by increasing heat-treatment time. (auth)

21344 (N-65-26653) HIGH-TEMPERATURE CREEP BEHAVIOR OF A COLUMBIUM ALLOY, FS-85. Titran, Robert H.; Hall, Robert W. (National Aeronautics and Space Administration, Cleveland, Ohio. Lewis Research Center). June 1965. 23p. (NASA-TN-D-2885). CFSTI $1.00 cy, $0.50 mn.

Creep tests of 1000 hours' duration and greater were conducted in the temperature range 2000 to 2200°F on a commercially available niobium alloy (FS-85) in vacuum units designed and built to achieve ultimate pressures of 10^{-9} torr. At a stress level of 10,000 psi, FS-85 exhibited moderate creep resistance at 2000°F, 1% strain being achieved in 775 hours. At 2100 and 2200°F and the same stress level, the alloy was much weaker, 1% strain being achieved in 355 and 50 hours, respectively. The Manson-Haferd linear time-temperature parameter proved moderately successful in predicting the long-time creep lives from relatively short-time creep data, the maximum error between predicted and experimental lives being a factor of 1.7 and the average error being a factor of 1.3. The agreement is considered good in view of the large scatter generally observed in long-time high-temperature creep tests. In all cases, however, the observed experimental life was shorter than the predicted life. The nonconservative nature of these predictions may be due in part to the fact that the predictions were based on data obtained at a pressure level of approximately 10^{-6} to 10^{-7} torr, but the long-time tests to which the predictions are compared were made at a lower pressure level, 10^{-8} to 10^{-9} torr. Creep tests conducted in the conventional-vacuum units (10^{-6} torr) and the ultrahigh-vacuum units under the same conditions of temperature and stress yielded creep curves that are virtually identical for the first few hundred hours but that deviate with increasing test time. The conventional-vacuum tests then showed a reduced creep rate compared with that of the ultrahigh-vacuum tests. (auth)

21345 (N-65-26656) THERMODYNAMIC PROPERTIES OF CESIUM UP TO 1500 DEG K. Heimel, Sheldon (National Aeronautics and Space Administration, Cleveland, Ohio. Lewis Research Center). July 1965. 31p. (NASA-TN-D-2906). CFSTI $2.00 cy, $0.50 mn.

Tables of thermodynamic properties of elemental Cs are compiled for both the pure species and the equilibrium vapor on the saturation line using selected values of 10,500 cal/mole for the heat of dissociation of the dimer and −18,920 cal/mole for the heat of condensation of the monomer. The equilibrium vapor properties of the condensed Cs are given to 1500°K, and the properties of gaseous monomer and dimer are given to 2500°K. The following thermodynamic functions of mixture properties on the saturation line are given: temperature, total vapor pressure, weight fraction of dimer in vapor phase, molecular weight, specific volume, density, enthalpy of condensed phase, enthalpy of vaporization, enthalpy of vapor phase, entropy of condensed phase, entropy of vaporization, entropy of vapor phase, and the heat capacities. Assigned enthalpies are relative to enthalpy of the crystal at 298.15°K, which is taken as zero. (STAR)

21346 (NASA-CR-54895) GENERATION OF LONG TIME CREEP DATA OF REFRACTORY ALLOYS AT ELEVATED TEMPERATURES. Quarterly Report No. 10, September 26, 1965–December 26, 1965. Sawyer, J. C.; Steigerwald, E. A. (TRW Equipment Labs., Thompson Ramo Wooldridge Inc., Cleveland, Ohio). Jan. 8, 1965. Contract NAS 3-2545. 80p.

Studies were made on long-term creep effects on selected refractory alloys that have potential use in advanced power systems. Emphasis was made on testing sheet alloys that can be used for cladding or tubing applications and on forgeable, high-strength turbine alloys. Creep data obtained on arc-cast and vapor-deposited W, Mo base alloys TZM and TZC, and the Ta base alloys T-111 and T-222. Residual gas analyses of the vacuum environment are given for several test systems after extended test periods. (P.C.H.)

21347 (NASA-CR-54916) DETERMINATION OF ELEVATED-TEMPERATURE FATIGUE DATA ON REFRACTORY ALLOYS IN ULTRA-HIGH VACUUM. Quarterly Report No. 6, October 1, 1965–January 1, 1966. Honeycutt, C. R.; Sawyer, J. C. (TRW Equipment Labs., Thompson Ramo Wooldridge Inc., Cleveland, Ohio). Jan. 15, 1966. Contract NAS 3-6010. 35p.

Fatigue tests were conducted on notched specimens (K_T = 1.75) of TZM at 1800°F and TZC at 2000°F. Additional notched fatigue tests were also conducted at 2000°F on TZC alloy from a second heat of material. The fatigue curve was extremely sensitive to applied stress and a decrease in peak dynamic stress values from 20.1 ksi ($1.38 \times 10^8 N/cm^2$) to 15.6 ksi ($1.07 \times 10^8 N/m^2$) produced a variation in failure time for 0.6 hr (4.1×10^7 cycles) to greater than 143 hr ($>9.86 \times 10^9$ cycles). Tests conducted on smooth specimens of TZC bar stock defined the resonant wave length at 2000°F, however, no failure occurred in this material at a peak dynamic stress of 23.9 ksi ($1.65 \times 10^8 N/m^2$) after 500 hr (3.6×10^{10} cycles). (P.C.H.)

21348 (ORNL-IIC-7, pp 22-5) A TESTING PROGRAM TO INVESTIGATE CERTAIN PHYSICAL AND MECHANICAL PROPERTIES OF SELECTED WOOD-PLASTIC COMBINATIONS. Gilmore, Robert C. (North Carolina State Univ., Raleigh).

A testing program to evaluate physical and mechanical properties of wood-plastic combinations (WPC) will be conducted. The objective of the program is to assess the changes in certain physical and mechanical properties of WPC as functions of monomer and monomer loading. Four monomers at four nominal loadings, 0, 33, 66, and 100%, will be used. The program will include static bending, hardness, toughness, abrasion, rate of dimensional change relative to humidity, compression, tension, and vibration tests. (auth)

21349 (ORNL-IIC-7, pp 26-31) WOOD-PLASTIC EVALUATION PROGRAM. Burford, A. O. (Lockheed-Georgia Co., Marietta).

A program for the wood-products industry to evaluate production samples of radioproduced wood-plastic combinations (WPC) for commercial use is described. Under contract with the USAEC, the Lockheed-Georgia Company will provide impregnation and irradiation services for 78 participating wood-product producers. Evaluation criteria that were used for selection of the 78 of 181 competing companies were based on the product wood species, market potential, dimensions, increased cost, etc. A breakdown of the various types of products and the bases for evaluation of their applicability for commercial use are also included. (auth)

21350 (ORNL-TM-1426) DESIGN AND EVALUATION OF SPECIAL PURPOSE HIGH-VACUUM HIGH-TEMPERATURE EQUIPMENT FOR REFRACTORY-METAL RESEARCH. Bourgette, D. T. (Oak Ridge National Lab., Tenn.). Apr. 1966. Contract W-7405-eng-26. 21p. Dep. mn. CFSTI $1.00 cy, $0.50 mn.

Three pieces of special purpose equipment capable of 2000°C and at least 10^{-9} torr at room temperature were designed, fabricated, and evaluated for their use in metallurgical studies on refractory alloys. This equipment included a quenching apparatus, continuous duty tantalum resistance furnace, and an apparatus in which creep studies could be conducted in tension or cantilever bending. The design features, temperature-pressure evaluations, and cost data are discussed. (auth)

21351 (SRIA-425-8) SORPTION OF GASES ON METAL SURFACES IN ULTRAHIGH VACUUM. Annual Report, February 15, 1965–February 14, 1966. Bergsnov-Hansen, B.; Endow, N.; Evans, B.; Pasternak, R. A. (Stanford Research Inst., Menlo Park, Calif.). Mar. 23, 1966. Contract AT (04-3)-425. 78p. Dep. mn. CFSTI $3.00 cy, $0.75 mn.

Systematic investigation of the adsorption mechanisms of different gases on Mo films was continued. The study of nitrogen adsorption was completed. The adsorption kinetics of inert gases Xe and Kr on Mo films and Pyrex glass suggest that the adsorbate has high surface mobility. The isotherms indicate that the interaction forces between an inert gas and a surface depend only little on the physical and chemical characteristics of the adsorbent. In deuterium adsorption on Mo, the saturation amounts increased with decreasing temperature, by a factor of about 1.5 from 25 to −196°C, and increased slightly with pressure. The rate law for adsorption was also found to change with temperature. Both the saturation coverages and the kinetics can be explained by a coverage dependent heat of adsorption of deuterium. Final results are given for hydrogen-deuterium exchange reaction at steady state. In the investigation of interaction of N and O with Nb ribbons at room temperature, only adsorption occurred, diffusion into the bulk being slow, and the kinetics were similar to that observed for Mo. In an intermediate range, a complex mechanism, probably involving both formation of surface layers and diffusion was found. Detailed quantitative mechanisms for the sorption processes were formulated. (P.C.H.)

21352 (TID-21745) INTERMETALLIC COMPOUNDS WITH THE $CeCu_2$-TYPE STRUCTURE. Ryba, Earle; Michel, David (Pennsylvania State Univ., University Park. Dept. of Metallurgy). [1964]. Contract AT(30-1)-2581. 10p. Dep. mn. CFSTI $1.00 cy, $0.50 mn.

Complete structural analyses were made on intermetallic compounds of Zn and Cu with Ce, Y, La, Yb, Ca, and Sr. It was found that the positional parameters change considerably from compound to compound. Data are tabulated. (P.C.H.)

21353 (TID-22828) DIFFUSION RATE AND ACTIVATION ENERGY OF HELIUM THROUGH SINGLE CRYSTAL AND POLYCRYSTALLINE ALUMINA [Thesis]. Campbell, William Buford Jr. (Georgia Inst. of Tech., Atlanta). May 1960. Contract AT(40-1)-2420. 72p. Dep. mn. CFSTI $3.00 cy, $0.75 mn.

An investigation was made on the diffusion mechanism by which an inert gas, helium, passes through single crystal and polycrystalline alumina, Al_2O_3, at 25 to 900°C. The diffusion coefficient and activation energy for helium passing through single and polycrystalline Al_2O_3 were determined. The experimental set-up used is described. The results indicated that the coefficients of diffusion of helium migration in single crystal and polycrystalline Al_2O_3 can be experimentally determined at room temperature and above by means of a mass spectrometer. The equation for the coefficient of diffusion of helium through single crystal Al_2O_3, along the c-axis direction, in the temperature range 200 to 700°C, was determined to be: $D = 6.2 \times 10^{-6} e^{-0.32 ev/kT}$. The most probable basic mechanism for diffusion in single crystal Al_2O_3 as indicated by the experimentally determined activation energy value, 0.32 ev, was an atom-vacancy interchange type occurring along edge dislocations. It was found that the magnitude of the coefficient of diffusion for polycrystalline Al_2O_3 varies as a function of density and decreases with repeated heating. The experimentally determined activation energy, 0.13 ev, indicated the most probable basic mechanism for diffusion through polycrystalline Al_2O_3 to be an atom-vacancy interchange type occurring mainly along grain boundaries. (P.C.H.)

21354 (TRG-Report-1160) SYSTEM C.I.D. (Computerised Interpretation of Data). AN ILLUSTRATION OF THE USE OF A DIGITAL COMPUTER IN THE STORAGE, INTERPRETATION AND RECOVERY OF MATERIALS DATA. Raraty, L. E.; Gittus, J. H. (Reactor Group, United Kingdom Atomic Energy Authority, Springfields (England)). Jan. 4, 1966. 14p. Dep. BIS $0.50, HMSO 2s. 6d.

System C.I.D. (Computerised Interpretation of Data) was used to store, interpret, and extrapolate the creep properties of certain magnesium–manganese alloys. An economical, partial factorial experiment involving creep tests at four participating laboratories was used to obtain the creep data. The data were then used to define the thirty-eight constants in a physically reasonable creep equation, by multiple regression analysis in an IBM 7090 computer. The computer was programmed to use the resultant creep equation to answer (by extrapolation if necessary) designers' questions about the likely performance of the alloys in specific applications. (auth)

21355 (TRG-Report-1168) THE STRUCTURE OF 20Cr–25Ni–Nb STEEL AFTER AGEING FOR UP TO 2000 HOURS IN THE TEMPERATURE RANGE 600–800 DEG C. Sumerling, R.; Pearce, J. H.; Freeman, S.; Dobing, E. (Reactor Group, United Kingdom Atomic Energy Authority, Sellafield (England)). 1966. 24p. Dep. BIS $1.00. HMSO 5s. 0d.

Pieces of unirradiated 20 Cr–25 Ni–Nb stainless steel containing 0.01 and 0.03% carbon, respectively, were aged for 500 and 2000 hr in the range 600–800°C, in a CO_2–CO atmosphere. Structures were examined using electron microscopy of replicas, electron diffraction, and x-ray analysis of extracted residues. Sigma-FeCr was formed during ageing as isolated particles at grain boundaries, the degree of sigma formation being greatest for an ageing temperature of about 700°C. M_6C-type precipitates formed in all specimens, mainly at grain boundaries, together with intragranular NbC. The Laves phase Fe_2Nb was detected in one low carbon specimen. Specimens aged at 600 and 650°C showed selective etching at grain boundaries, but there was no susceptibility to intergranular corrosion.

Electron-probe microanalysis of extracted M_6C precipitates in a specimen aged at 750°C showed that the particles were Ni-rich and also contained some Fe. (auth)

21356 (UCRL-14724) PHYSICAL AND MECHANICAL PROPERTIES OF U-7.5 w/o Nb-2.5 w/o Zr ALLOY. Peterson, C. A. W.; Elkington, W. E. (Lawrence Radiation Lab., Univ. of California, Livermore). Feb. 17, 1966. Contract W-7405-eng-48. 12p. Dep. mn. CFSTI $1.00 cy, $0.50 mn.

The physical and mechanical properties of a uranium-7.5 wt/% Nb-2.5 wt/% Zr alloy aged in the temperature range 150-350°C are reported. The mechanical strength of the alloy increased with aging temperature and time within this range. More reproducible mechanical properties were obtained from the heat treatments than previously reported. The tensile yield strength was typically 92,000 psi after a 1-hr, 150°C heat treatment; 215,000 psi after 4-hr, 350°C heat treatment. Elongations for these strength levels were 20 and 3.5%, respectively. Electron-diffraction data show that an ordered structure was developed during aging at 150°C for 10^4 minutes. It is believed that the increase in strength which results at this aging temperature is partly due to this ordering of the alloy. (auth)

21357 (UCRL-16299) THE MAGNETIC AND ELECTRICAL PROPERTIES OF SOME METALS AT HIGH PRESSURES [Thesis]. Phillips, David B. (Lawrence Radiation Lab., Univ. of California, Berkeley). Aug. 1965. Contract W-7405-eng-48. 58p. Dep. mn. CFSTI $3.00 cy, $0.50 mn.

A device for measuring low field magnetization of high permeability materials as a function of temperature and pressure in Bridgman anvils was developed. This device was used to measure the Curie point (T_c) of Gd to 20 kbars pressure and the Neel point (T_n) of Tb to 15 kbars pressure. For Gd dT_c/dP was found to be -1.9 ± 0.2°K/kbar, and dT_n/dP for Tb was measured as -1.4 ± 0.2°K/kbar. The decrease in low field magnetization with pressure was quite marked in both cases and this limited the maximum pressures obtainable. The decrease in magnetization is shown to be a result of elastic stresses and plastic deformation caused by compression. The basic system should be capable of pressures to 100 kbars and a temperature range of 65-600°K. Suggestions for reaching these conditions and extending the measurements to higher pressures for Gd and Tb are discussed. In an attempt to determine the effect of alloying on the high pressure Fe phase transition, the ^{57}Fe Mössbauer spectra in two types of stainless steel were studied at high pressures. No evidence for any sharp phase transitions was found. In both samples a broad absorption superposed on the single central line was noted at high pressures. This behavior was reversible with pressure in one sample and irreversible in the second sample. Annealing restored the original spectrum of the second sample. These changes are discussed as a transition from a paramagnetic to a partially ferromagnetic structure under pressure. The electrical resistance of Bi was carefully investigated in the pressure region between 30 and 90 kbars in an attempt to locate the transitions noted as volume discontinuities by Bridgman. No discontinuities were found in the electrical resistance in this region. This does not necessarily mean that the phase changes reported by Bridgman at 45 and 64 kbar do not exist. (auth)

21358 (UCRL-16552) MECHANICAL PROPERTIES OF CONTINUOUS-MATRIX, DISPERSED-PHASE CERAMIC SYSTEMS [Thesis]. Hasselman, D. P. H. (Lawrence Radiation Lab., Univ. of California, Berkeley). Dec. 27, 1965. Contract W-7405-eng-48. 85p. Dep. mn. CFSTI $3.00 cy, $0.75 mn.

The mechanical properties of brittle continuous-matrix, dispersed-phase multicomponent ceramic systems were investigated. The effect of dispersed phases of crushed sapphire, spherical tungsten particles, and spherical pores on the elastic behavior of a sodium borosilicate glass was determined. Good agreement with theory was obtained. The effect of cylindrical porosity on Young's modulus of a brittle matrix was calculated, and good agreement was obtained with the experimental effect of porosity on elastic properties of polycrystalline ceramics. A fracture theory was developed for a dispersion-strengthened glass matrix based on the criterion that the dispersions within the glass matrix limit the size of the Griffith flaws responsible for failure. Experimental evidence is presented which substantiates the proposed theory. The effect of stress concentrations on strength was investigated by loading suitable specimens to failure under conditions of uniaxial and biaxial tensile stress. Specimens consisted of the sodium borosilicate glass containing spherical particles of alumina and of the same glass containing spherical pores. Results could be interpreted in terms of the maximum value of the stress concentrations and in terms of the volume of material over which the stress concentration acts. Results also indicate that for multicomponent systems any differences in strength under different stress states can be attributed at least in part to microstructure. A hypothesis is presented that suggests that the effect of stress concentrations on strength is governed by the relative size of the Griffith flaw and the size or volume of material over which the stress concentrations act. On this basis a theory is presented for the effect of porosity on strength in terms of flaw size to pore size. An approximate derivation is presented which suggests that once the effect of stress concentration on strength has occurred, further relative changes in uniaxial tensile stress are governed by the relative changes in Young's modulus with porosity. A porosity-clustering factor is introduced to take into account nonuniform distribution of the porosity throughout the ceramic body. (auth)

21359 (WAPD-T-1581) A METALLOGRAPHIC AND X-RAY STUDY OF THE $MgO.Al_2O_3$-UO_2 SYSTEM [Thesis]. Rubin, Bernard Friedman (Pittsburgh Univ., Pa.). 1966. Contract AT(11-1)-Gen-14. 56p. Dep. mn. CFSTI $3.00 cy, $0.50 mn.

An investigation on the $MgO \cdot Al_2O_3$ system showed that the phase diagram is a eutectic type with limited terminal solubility. The eutectic temperature is about 2000°C while the eutectic composition is about $MgO \cdot Al_2O_3$-40 mole % UO_2. Below 1675°C, UO_2 and spinel are present in proportions related to their concentrations. Above this temperature range, certainly at 1750°F, alumina is precipitated from spinel, with UO_2, $MgO \cdot Al_2O_3$ appearing concurrently. UO_2 apparently catalyzes the vaporization of MgO, depleting the spinel in this component and thereby reducing its ability to retain Al_2O_3 in solution at 1750°F. The limited solubility of spinel for Al_2O_3, after MgO dissociation, is in keeping with published diagrams of the $MgO-Al_2O_3$ binary system. The critical temperature for MgO vaporization is within the limits of 1675-1750°C. The structural instability of this mixture at high temperature precludes its use in power reactors operating above this temperature. (auth)

21360 (WCAP-2098) MECHANISM AND KINETICS OF NITROGEN RELEASE FROM UO_2 AT ELEVATED TEMPERATURES. Ferrari, Harry M. (Westinghouse Electric Corp., Pittsburgh, Pa. Atomic Power Div.). [1961]. 52p. Dep. mn.

The mechanism and kinetics of nitrogen release from high nitrogen UO_2 pellets were investigated at elevated temperatures. A combination of metallographic and x-ray analyses showed that nitrogen impurities present in the UO_2 exist as a second phase in the form of uranium nitrides. The kinetics of nitrogen release were measured at temperatures of 1000, 1200, 1400, and 1600°C and the mechanism of release was determined to be controlled by the diffusion of nitrogen through the UO_2 lattice. The diffusion coefficient for nitrogen in UO_2 is represented by the expression: $D = 2.25 \times 10^{-9} \exp(-33{,}400/RT)\ cm^2/sec$. The variation in nitrogen pressure upon heating a UO_2 fuel element to elevated temperatures was studied. The data showed that a reversible equilibrium pressure-temperature relation did not exist between the nitrides in the UO_2 and the nitrogen gas above it as occurs with pure uranium nitrides. Thus, suf-

ficient nitrogen if present initially in high quantities may be released during reactor operation so as to impair the operation of a fuel element. On the other hand, not all of the nitrogen will be released in a fuel element as previously assumed, and the current limitation of 75ppM on nitrogen content of UO_2 for Yankee fuel elements can be relaxed. Only part of the nitrogen will actually be liberated based on the kinetics of diffusion of nitrogen through the UO_2 lattice. (auth)

21361 (WCAP-2923) IN-PILE MEASUREMENT OF UO_2 THERMAL CONDUCTIVITY. Final Report. Balfour, M. G.; Christensen, J. A.; Ferrari, H. M. (Westinghouse Electric Corp., Pittsburgh, Pa. Atomic Power Div.). Mar. 1, 1966. Contract NAS 3-4589-PB. 48p. (NASA-CR-54740).

In-pile effects of stoichiometry and grain growth on UO_2 thermal conductivity were studied in instrumented fuel capsules. Results show that columnar grain growth has no significant effect on heat transfer in UO_2 fuels. Migration of lenticular voids during irradiation was found to have an important effect on fission product redistribution. Irradiation of a $UO_{1.94}$ capsule showed a mean thermal conductivity nearly 20% higher than in a $UO_{2.00}$ capsule under similar conditions. (auth)

21362 (SC-T-66-0723) INVESTIGATION OF SOLUBILITIES OF CHROMIUM, MOLYBDENUM, AND TUNGSTEN IN ALUMINUM BY THE MICROHARDNESS METHOD. Vigdorovich, V. N.; Glazov, V. M.; Glagoleva, N. N. Translated by Marcel I. Weinreich (Sandia Corp., Albuquerque, N. Mex.), from Izv. Vyssh. Ucheb. Zaved. Tsvetn. Met., No. 2, 143-6(1960). 7p. Dep. mn. CFSTI $1.00 cy, $0.50 mn. JCL $1.10 fs, $0.80 mf.

The solubility of chromium, molybdenum, and tungsten in aluminum, throughout a temperature range from 660 to 400°C, was studied by means of the microhardness method. It was established that the solubility diminishes, while the hardening action exerted on the solid solution increases in the order of chromium–molybdenum–tungsten. (auth)

21363 (UCRL-Trans-1299(L)) CONTRIBUTION TO THE STUDY OF THE PRESSURE-TEMPERATURE DIAGRAM OF PURE BERYLLIUM. Francois; Contre. Translated by B. Harocopos (Univ. of California Lawrence Radiation Lab., Livermore), from Paper Presented at Conference Internationale sur la Metallurgie du Beryllium, Grenoble, May 16–20, 1965. 31p. (CONF-650508-3). Dep. mn. JCL $3.60 fs, $1.13 mf.

Below the $\alpha \rightarrow \beta$ transformation of beryllium, a plateau is observed in the curve of resistivity as a function of temperature. This is attributed to the recrystallization of the specimen following the severe deformation brought about by applying pressure to it in the solid state. The first experimental results obtained enable the plotting of a provisional pressure-temperature diagram for beryllium. From this diagram, the enthalpy of the $\alpha \rightarrow \beta$ transformation, at atmospheric pressure, is established at about 1.8 kcal/mole, while the increase in volume on melting is about 10%. (auth)

21364 STRUCTURE AND MECHANICAL PROPERTIES OF Ta-Mo ALLOY SINGLE CRYSTALS. Van Torne, L. I.; Thomas, G. (Univ. of California, Berkeley). Acta Met., 14: 621-35(May 1966). (UCRL-16107).

High-purity single crystals of the Ta–Mo alloy series were grown near 10 at. % increments by electron-beam zone refining. The methods of investigation of the prepared crystals included: specific resistivity at 273, 77, and 4.2°K, critical resolved shear stress for plastic flow or cleavage at 273°K, lattice parameter determinations, transmission electron microscopy, and diffraction and quantitative x-ray diffracted intensity measurements of {200} and {220} reflections. It was found that alloys of compositions between Mo–19 Ta and Mo–58 Ta cleaved on the {100} planes. Lattice parameter measurements and electron microscopy showed that the alloy series is bcc with no long-range order, coherent over dimensions greater than 300 Å, nor intermediate phases. Kikuchi electron diffraction proved that there exist deviations from random solid solution in the brittle crystals. This result was confirmed by x-ray intensity measurements of 200 and 220 lines. The ratio of constituent atoms on {100} and {110} differed from the ratio of atoms corresponding to the total composition of the crystal in such a way as to generate quasi-cubic domains for {100} and quasi-dodecahedral domains for {110} deviations. It is suggested that the increase in critical resolved shear stress for plastic flow with alloy composition results from a corresponding increase in the Peierls-Nabarro friction of dislocations produced by alloying, composition deviations, and concomitant changes in the elastic coefficients in a local region of the crystal. Both Mo and Ta are anisotropic and have very different elastic constants. Alloying and the existence of composition deviations change the elastic coefficients, in the range of alloys which cleave, to values that marginally fulfill the strain energy restrictions. The presence of a critical density of dislocations in a local region can change the values of the elastic coefficients such that the crystal is locally energetically unstable. The crystal then cleaves on a {100} plane, which relieves the maximum strain energy. By analogy, other solid solutions are expected to become brittle when the components have widely differing and anisotropic elastic constants. Marked changes in the slope of ($\rho_{273°K}$ minus $\rho_{4.2°K}$) versus alloy composition at Mo–20 Ta, Mo–50 Ta and Ta–12 Mo indicated that a relatively large change occurs in the density of states in the d and s bands and/or marked changes in the elastic coefficients at these compositions. (auth)

21365 INFLUENCE OF CRYSTAL STRUCTURE ON FRICTION CHARACTERISTICS OF RARE-EARTH AND RELATED METALS IN VACUUM TO 10^{-10} mm of MERCURY. Buckley, Donald H.; Johnson, Robert L. (NASA-Lewis Research Center, Cleveland). ASLE (Amer. Soc. Lub. Eng.) Trans., 8: 123-32(1965).

Friction, wear, and metal-transfer characteristics were determined for rare earth and related metals in vacuum to 10^{-10} mm of mercury. The metals studied were lanthanum, neodymium, praseodymium, cerium, holmium, erbium, gadolinium, dysprosium, samarium, yttrium, and thallium. Friction and wear experiments were conducted with the rare earth or related metals generally sliding against 440-C stainless steel. The results of the investigation indicated that crystal structure considerations and polymorphism can explain the friction, wear, and metal-transfer characteristics of the rare earth and related metals in vacuum. Close-packed hexagonal crystal forms of the rare earths and thallium had much lower friction, wear, and metal-transfer characteristics than face-centered or body-centered cubic structures. (auth)

21366 FRICTION AND CLEAVAGE OF LAMELLAR SOLIDS IN ULTRAHIGH VACUUM. Flom, D. G.; Haltner, A. J.; Gaulin, C. A. (General Electric Co., Philadelphia). ASLE (Amer. Soc. Lub. Eng.) Trans., 8: 133-45(1965).

Measurements were made of sliding friction on copper surfaces at 10^{-6} to 10^{-9} torr for five lamellar solids, molybdenum sulfide, tungsten sulfide, cadmium iodide, bismuth iodide, and phthalocyanine. There was no evidence that the sliding behavior of any of these materials was improved by the presence of gas or vapors. Each evolved considerable quantities of gas during sliding. Molybdenite and surface-nucleated pyrolytic graphite were cleaved in an ultrahigh vacuum apparatus built for this purpose. The graphite specimens were in both as-deposited and annealed forms. The predominant gas given off for all three materials was methane. (auth)

21367 DIFFUSION OF ^{63}Ni IN COPPER AT LOW TEMPERATURES. Bonzel, Hans Paul (Univ., Goettingen, Ger.). Ber. Bunsenges. Physik. Chem., 70: 73-81(1966). (In German).

The diffusion of ^{63}Ni in copper at low temperatures (250 to 520°C) was investigated by the method of decrease in surface activity. The influence of surface structure and pretreatment of the copper samples on the diffusion was measured. For specimens of electrolytic copper (99.995%

pure) the surfaces which were smoothed by abrasive paper, grade 6/0, the following expression was obtained for the variation of the diffusion coefficient with temperature: $D_1 = 7.8 \times 10^{-6}$ exp (−28,000/RT cal mole^{-1})cm^2/sec. The corresponding expression for mechanically polished samples was $D_2 = 1.0 \times 10^{-5}$ exp (−32,200/RT cal mole^{-1}) cm^2/sec. For electropolished specimens an increase of the apparent activation energy and of the preexponential factor was observed: $D_3 = 6.4 \times 10^{-2}$ exp (−45,300/RT cal mole^{-1}) cm^2/sec. The electrolytic copper was extremely fine-grained. Diffusion in ultrapure (99.9999%) coarse-grained copper was also investigated. The individual grains of this specimen showed a typical hexagonal substructure after etching. Diffusion in electropolished specimens of ultra-pure copper can be described by the expression: $D_4 = 4.2 \times 10^{-2}$ exp (−46,800/RT cal mole^{-1}) cm^2/sec. The influence of dislocations on diffusion was investigated but appeared to be of secondary importance in this case. The method for measuring diffusion is suitable for the detection of a radiation effect on diffusion. (auth)

21368 THE EFFECT OF PRIOR BETA GRAIN SIZE ON THE DUCTILITY OF ZIRCONIUM–2.5 WEIGHT PER-CENT NIOBIUM ALLOY. Bell, L. G.; Dicks, T. S. (Hawker Siddeley Canada Ltd., Toronto). Contract CR11D21473. Can. Met. Quart., 4: 259-68(Oct.-Dec. 1966).

Data were collected establishing a time-temperature-beta grain size relation for the alloy zirconium-2.5 weight per cent niobium. The effect of multiple heat treatments on the beta grain size was also investigated to some extent. Tests were done to determine the effect of the prior beta grain size on the room temperature tensile properties of the alloy. It was found that the ultimate tensile strength and the offset yield strength were not significantly changed with increasing prior beta grain size. There was, however, a change in ductility; over the mean grain diameter range of 0.002 inch to 0.10 inch, the elongation decreased from 20 per cent to 8 per cent and the reduction in area from 63 per cent to 12 per cent. (auth)

21369 METHOD FOR THE DETERMINATION OF THE THEORETICAL PARTITION COEFFICIENTS. APPLICATION TO THE ALUMINUM–YTTRIUM SYSTEM. Kuchar, Lumir (Ecole des Mines et de Metallurgie, Ostrava, Czechoslovakia. Centre d'Etudes de Chimie Metallurgique, Vitry-sur-Seine, France). Compt. Rend., Ser. C, 262: 393-6(Jan. 31, 1966). (In French).

A mathematical method is proposed for the analytical determination of an approximate function representing the solidus and liquidus curves in the aluminum–yttrium binary equilibrium diagram. The diagram is traced in a region of very low concentrations following new semilogarithmic and bilogarithmic representations. The theoretical partition coefficient of yttrium in aluminum was determined as $\underline{k}_0 = 0.02$ for very dilute alloys. (tr-auth)

21370 ELECTRIC CONDUCTIVITY IN THE HAFNIUM OXIDE–YTTRIUM OXIDE SYSTEM AT HIGH TEMPERATURE. Besson, Jean; Deportes, Charles; Robert, Guy (Ecole Nationale Superieure d'Electrochimie et d'Electrometallurgie, Grenoble, France). Compt. Rend., Ser. C, 262: 527-30(Feb. 14, 1966). (In French).

The addition of Y_2O_3 to monoclinic HfO_2 causes the appearance of a cubic phase of the fluorite-type structure, which extends from 8 to about 40 mol% Y_2O_3. The study of the electric conductivity as a function of the composition between 900 and 1600°C showed a maximum of the total conductivity and a minimum for the conduction activation energy at 8 mol% Y_2O_3. Whereas the conductivity of the monoclinic phase appears partially electronic in the region of oxygen partial pressures from 1 to 10^{-5} atm., the cubic phase has a preponderant ionic conduction. The electronic conduction part is inappreciable up to very low oxygen partial pressures. (tr-auth)

21371 COMPRESSION OF MONOCRYSTALS OF BERYLLIUM PARALLEL TO THE C AXIS. Le Hazif, Roger; Dupouy, Jean-Michel (Centre d'Etudes Nucleaires de Saclay, Gif-sur-Yvette, France). Compt. Rend., Ser. C, 262: 538-40(Feb. 14, 1966). (In French).

Monocrystals of beryllium were compressed parallel to the c-axis between room temperature and 600°C. No pyramidal slip having a direction outside the base plane was observed. The deformation observed above 400°C is explained by slip on $\{10\bar{1}x\}$ planes in $\langle 11\bar{2}0\rangle$ directions. (tr-auth)

21372 METALLURGICAL STUDIES OF SOME URANIUM ALLOYS. Fizzotti, C.; Masperoni, A. (CNEN, Rome). Energ. Nucl. (Milan), 13: 139-48(Mar. 1966). (In Italian).

Different heat treatments such as continuous cooling, quenching and annealing, step cooling and step quenching, etc., were performed on a few uranium binary alloys and the structures obtained are described. After the heat treatments the alloys underwent thermal stability, ageing tests, and thermal cycling. Corrosion and mechanical tests were also performed. The phase-diagrams of some binary systems were studied with particular regard to the uranium-rich alloys. (auth)

21373 STUDYING CREEP IN CONCRETE THAT IS HOT. Engineering, 200: 122-3(July 23, 1965).

Results of tests on creep and shrinkage of concrete at 105 and 110°C are reported. The studies were conducted to provide data on the design of reinforced concrete pressure vessels for nuclear power plants. In all tests, the direct tension method of applying the stress was used. A framework of rolled steel channel sections standing on separate foundations formed the reaction beams and supports for loading the specimen. Three ovens within this framework were fed from a 440-v three-phase supply, one phase per oven. Heat was provided by an arrangement of continuously running and thermostatically controlled heaters. Blended ordinary Portland cement and Thames Valley aggregate were used. All mixes had an aggregate : cement ratio by weight of 6.1 and a water : cement ratio of 0.55. The fresh concrete had a slump of ¼ in. and a compacting factor of 0.88. The specimens were cured under wet sacking for one day and under water at 17 ± 2°C for 27 days. They were then immediately transferred to the ovens where they were allowed to dry in air temperature of 30°C for 24 hr. It was estimated that the specimens took about 5½ hr to heat up to 105°C and a further half-hour was required for the frame and enclosure to come to a state of temperature equilibrium. At this point the load which was to be held constant on the specimen throughout the creep period was applied. The approximate tensile stress of the 4 creep specimens was 455 lb/in^2. The unloaded specimens at the end of the high temperature work were found to be still shrinking. (BBB)

21374 INVESTIGATION OF EXTRUDED TUNGSTEN COMPOSITES CONTAINING FIBERED OR REACTED ADDITIVES. Quatinetz, Max; Weeton, John W.; Herbell, Thomas P. (Lewis Research Center, Cleveland). Int. J. Powder Met., 2: 21-8(Jan. 1966).

Sintered tungsten and tungsten-plus-additive billets were prepared in order to evaluate the feasibility of producing fiber-bearing composites by elongation of materials in situ (in a tungsten matrix) during extrusion, and to study reactions between the additives and the matrix, with the objective of producing high-strength materials. Composites with less than 10 vol % additive exhibited improvement in stress-rupture strength. Composites with highly elongated additives ranged from 4 to 18 times better in stress-rupture life at 3000°F than the unreinforced pure tungsten matrix. The stress-rupture lives of several composites with more reactive additives and only moderate fibering increased to 25 to 50 times that of tungsten at 3000°F. The strengthening was presumed to be caused by reactions between the additives and the matrix. (auth)

21375 DUCTILE-BRITTLE TRANSITION IN TANTALUM CARBIDE. Johansen, H. A.; Cleary, J. G. (Westinghouse Electric Corp., Pittsburgh). J. Electrochem. Soc., 113: 378-81(Apr. 1966).

Tantalum carbide was prepared in the composition range from $TaC_{0.73}$ to $TaC_{1.26}$ and consolidated by hot pressing. Compositions at ends of the range were two phase. A modified cantilever-beam test method was used to determine the ductile-brittle transition temperature (T_{db}) at a given strain rate and for this geometry as a function of carbon content. The T_{db} range from $TaC_{0.98}$ was 1825 to 1925°C, and the median nominal bend stress in this range was 23,000 psi (1617 kg/cm²). At $TaC_{0.90}$ the median nominal bend stress was at a minimum of 14,000 psi (984 kg/cm²) for the T_{db} range from 1750 to 1850°C. T_{db} increased approximately 150°C with increasing x across the single-phase cubic region of TaC_x. (auth)

21376 ELECTRICAL AND THERMAL CONDUCTIVITY OF METALLIC POTASSIUM, OVER ITS ENTIRE LIQUID RANGE, i.e., FROM THE MELTING POINT (336.4 DEG K) TO THE CRITICAL POINT (2450 DEG K). Grosse, A. V. (Temple Univ., Philadelphia). Contract AT(30-1)-2082. J. Inorg. Nucl. Chem., 28: 795-802(Mar. 1966).

The thermal and electric conductivities of metallic potassium are presented, both as a liquid and as saturated vapor, over its entire liquid temperature range, i.e., from the melting point (336.4°K) to the critical point (2450°K). Experimental data are now available up to ≃1450°K. The kinetic theory of dense gases permits estimation of the critical thermal conductivity and from this estimate and the Weidemann-Franz law (or the experimental Lorenz number) the electric conductivity at the critical point can be derived. Using these two values as anchor points, coupled with the knowledge from the free-electron theory of metals that the critical values of both properties should be practically zero at the critical point, both the thermal and electric conductivities are interpolated from the end of the experimental range to the critical point. Both λ_{therm} vs T and κ vs T formed smooth, slightly concave curves from the melting point to the critical point. (auth)

21377 AN EMPIRICAL RELATIONSHIP BETWEEN THE ELECTRICAL CONDUCTIVITY OF MERCURY AND TEMPERATURE, OVER ITS ENTIRE LIQUID RANGE, ALSO ITS THERMAL CONDUCTIVITY AND THE LATTER'S REGULAR BEHAVIOR. Grosse, A. V. (Temple Univ., Philadelphia). Contract AT(30-1)-208. J. Inorg. Nucl. Chem., 28: 803-11(Mar. 1966).

The electric and thermal conductivities of mercury were determined, over its entire liquid range, from 234.28 to 1733°K. The abnormal and normal behavior of mercury over the entire liquid range is discussed. The curve plotted for electric conductivity vs T formed an equilateral hyperbola. The curve for the thermal conductivity vs T is also given. The electric and thermal conductivities of mercury were compared with those of other elements. (F.J.H.)

21378 LOW-TEMPERATURE INTERNAL-FRICTION PEAKS IN COLD-WORKED NIOBIUM. Stanley, M. W.; Szkopiak, Z. C. (Battersea Coll. of Tech., London). J. Inst. Metals., 94: 79-80(Feb. 1966).

The results of a preliminary investigation of the effects of restraining on the internal friction peaks developed in the 220°K region of Nb after tensile strain are given. (W.L.G.)

21379 SUBOXIDES OF TANTALUM. Niebuhr, J. (Max-Planck-Institut fuer Metallforschung, Stuttgart). J. Less-Common Metals, 10: 312-22(May 1966). (In German).

The literature of the suboxides of tantalum is critically evaluated. The conditions for the formation of TaO_x, TaO_y, TaO_z, TaO_u, TaO, and TaO_2 are described, as well as their stability, structure and properties. The suboxides form only by oxidation of tantalum or tantalum compounds. TaO_x (Ta_6O) forms at ~300°C, TaO_y (Ta_4O) below 500°C, TaO_z (Ta_2O) between 350 and 1200°C, and TaO_u above 1500°C. Platelets of TaO_y or TaO_z show epitaxy with tantalum. According to x-ray diffraction of polycrystalline samples, TaO_x is tetragonal with $a = 3.36_3$ Å and $c/a = 0.97$, TaO_y orthorhombic with $a = 3.61$ Å, $b = 3.27_1$ Å, $c = 3.20_1$ Å, TaO_z tetragonal with $a = 6.68$ Å, $c/a = 0.71$. After electron diffraction of thin monocrystalline samples, the suboxides have superlattices: TaO_x is tetragonal with $a = 4a_{Ta}$ and $c/a = 0.97$, TaO_y is cubic with $a = 4a_{Ta} = 13.4$ Å, and TaO_z is cubic with $a = 2a_{Ta} = 6.68$ Å. TaO and TaO_2 form during oxidation of tantalum to Ta_2O_5 as layers between the metal and the Ta_2O_5. The structure of the TaO corresponds to the NaCl-type, that of the TaO_2 to the rutile-type. On evaporating tantalum oxide or degassing tantalum metal, TaO and TaO_2 molecules are found in the vapor. (auth)

21380 FRACTOGRAPHIC STUDY OF TUNGSTEN AND DILUTE TUNGSTEN-RHENIUM ALLOYS. Gilbert, A. (Battelle Memorial Inst., Columbus, Ohio). J. Less-Common Metals, 10: 328-43(May 1966).

Fractographic examinations, using optical and electron-replica microscopy were made on recrystallized tungsten, W–3Re, and W–5Re alloys. No evidence was found that rhenium changes the nature of the grain-boundary precipitates, but the rhenium alloys showed a greater tendency towards cleavage failure then did the tungsten—possibly as a result of rhenium-induced grain refinement. The wrought alloys were more resistant to cleavage than the recrystallized as a result of failure occurring in part by delamination, thus effectively arresting potential failure by cleavage. It is again concluded that in wrought alloys, rhenium is effective in promoting ductility primarily through its effect on grain size. (auth)

21381 MAGNETIC SUSCEPTIBILITY OF SCANDIUM. Kobayashi, Hanako (Kyoto Univ.). J. Phys. Soc. Jap., 21: 201-2(Jan. 1966).

The magnetic susceptibility of Sc metal (99.97% purity) was measured in the temperature region of 1.5 ~ 4.2°K and 14 ~ 20°K by the a-c bridge method and the McGuire's balance methods. The results are shown along with previously published data. A curve of the density of states as a function of temperature is also shown. (L.B.S.)

21382 ALUMINUM AND MAGNESIUM IN NUCLEAR METALLURGY. Herenguel, J.; Scheidecker, M.; Lelong, P.; Biais, R.; Boghen, J.; Whitwhan, D. Met. Ital., 58: 41-7(Feb. 1966). (In Italian).

Properties of aluminum and magnesium and their alloys for use in nuclear technology are discussed. (M.C.G.)

21383 A.E.R.E. HARWELL: ATOMIC ENERGY MATERIALS. Metal Treat., 32: 284-90(Aug. 1965).

The research and development program of the U. K. Atomic Energy Research Establishment at Harwell is surveyed, with attention to projects involving stainless steel cladding of reactor fuel, effects of radiation on properties of austenitic steels, oxidation behavior of canning materials, testing radioactive reactor elements, and development of carbide and cermet fuels and improved graphites. By combining special heat treatments with planetary swaging, stainless steel cladding tubes were obtained, which possess higher ductilities at elevated temperatures than those produced by other combinations of working and heat treatments. For wire-wrapped tube for fuel element canning, a wire-wrapping and brazing technique was developed in which the wire is precoated with the brazing alloy then wound on the tube and brazed using either furnace heating or by passing the tube through an r-f coil in vacuum. This method produces integral finning without contaminating the fuel can with surplus brazing alloy, which may affect its corrosion resistance. It is also more economic than the conventional brazing method. A 20% Cr : 25% Ni : Nb stabilized austenitic stainless steel is being used as the fuel element cladding material in the Windscale advanced gas-cooled reactor. The effects of neutron irradiation on the high-temperature properties of this austenitic stainless steel were studied and the results are described. The results of experiments in which the natural ratio of ^{10}B: ^{11}B in austenitic steels was varied showed that the neutron-induced reductions in high-temperature ductility are related to the concentrations of helium or lithium introduced by the reaction. Helium was shown to have the more adverse effect. Work is also described on attempts to find materials with sufficient oxidation re-

sistance to be used for classing in advanced carbon dioxide-cooled reactors at temperatures in the region of 1000°C. Possible materials include ferritic stainless steels and pure nickel (or oxide dispersion strengthened nickel). Work is also being devoted to an accurate determination of the equilibrium conditions and to the kinetics of oxidation of pure nickel in carbon dioxide/carbon monoxide mixtures containing less than the critical concentration of carbon monoxide. An important material recently developed at Harwell is a family of graphites known as HX30, intended specifically for the fabrication of fuel tubes for the Dragon high-temperature helium-cooled reactor at Winfrith. The nuclear fuel in this reactor is clad in graphite tubes, the interior of which is purged by a small bypass of helium to carry away any released fission gases. Results showed how much more suitable HX30 is for the Dragon reactor in comparison with many other graphites. (BBB)

21384 VAPOR PRESSURE MEASUREMENTS ON AMALGAMS OF YTTRIUM AND SAMARIUM. Kirchmayr, H. R.; Jangg, G. (Technische Hochschule, Vienna). Monatsh. Chem., 96: 1147-53(1965). (In German).

Amalgams of Y and Sm were examined by vapor pressure measurements using a modified isoteniscope. Thermodynamic data were derived for the compounds YHg_3, YHg_2, YHg, $SmHg_3$, $SmHg_2$, and SmHg. Within the temperature range studied for each compound (between 276 and 505°C) the following heats and entropies of formation were found, respectively: YHg_3, -18.2 ± 1.0 kcal/mol, -7.7 ± 1.5 eu/mol; YHg_2, -19.1 ± 1.0, -12.5 ± 1.5; YHg, -12.8 ± 1.0, -8.7 ± 1.5; $SmHg_3$, -10.8 ± 2.0; -1.6 ± 2.0; $SmHg_2$, -12.0 ± 2.0, -5.6 ± 2.0; and SmHg, -10.9 ± 2.0, -8.0 ± 2.0. The vapor pressure isotherms are presented; from these it was concluded that no other compounds between Y and Hg or Sm and Hg exist in the temperature range from 270 to 430°C. Vapor pressure measurements on samples containing free Hg indicated that Hg dissolves about 0.5% Y or Sm. No extended homogeneous range could be detected for the existing compounds. (BBB)

21385 NEW PHASES IN THE SYSTEMS Nb_2O_5–WO_3 AND Ta_2O_5–WO_3. Gruehn, R. (Univ., Muenster, Ger.). Monatsh. Chem., 96: 1789-92(1965). (In German).

Several new phases were found in studies of the WO_3-poor regions of the systems $Nb_2O_5-WO_3$ and $Ta_2O_5-WO_3$ up to the mole ratio $M_2O_5-WO_3 = 1:2$. These include a phase extending from $40Nb_2O_5 \cdot WO_3$ to $20Nb_2O_5 \cdot WO_3$, $13Nb_2O_5 \cdot 4WO_3$, a low-temperature phase of composition $9Nb_2O_5 \cdot 8WO_3$, $9Ta_2O_5 \cdot 8WO_3$, and a mixed phase of $Ta-Ta_2O_5$ extending to the composition $13Ta_2O_5 \cdot 4WO_3$ at 1300°C. Other phases were observed in the system $Nb_2O_5-WO_3$ corresponding to the molar ratios $8Nb_2O_5 \cdot WO_3-6Nb_2O_5 \cdot WO_3$, $7Nb_2O_5 \cdot 3WO_3$, $8Nb_2O_5 \cdot 5WO_3$, and $9Nb_2O_5 \cdot 8WO_3$ (high-temperature phase). Samples were prepared by heating in air and then in quartz ampoules at 1200–1400°C. Data from x-ray examination of various samples and structural determination results are tabulated. It was found necessary to prepare samples under the proper pressure of O_2 to avoid reduction; several samples improperly prepared showed bluish colors and indicated formation of $W(Nb_{14}W_2O_{44})$ from Nb_2O_5, NbO_2, and WO_3. The O/M ratio was determined as part of the structural study as a check on this observation. (BBB)

21386 INSTRUMENTED IMPACT TESTING OF ZIRCALOY. Fearnehough, G. D. (United Kingdom Atomic Energy Authority, Culcheth, Eng.). Nature, 209: 392-3 (Jan. 22, 1966).

The modes of brittle and ductile behavior of Zircaloy-2 are identified. Load/time relations during fracture are found using the Charpy machine. Such curves were obtained on hydrogen-free and hydrided specimens throughout the transition range. These curves and the crack speeds versus temperature are shown. It is concluded that the wide transition in unhydrided Zircaloy is due to a gradual decrease in ductility which facilitates easier ductile crack propagation. The intervention of rapid self-propagating fractures in the hydrided material results in a much narrower temperature range. (J.F.P.)

21387 THE ADSORPTION OF KRYPTON AND XENON ON EVAPORATED METAL FILMS. Brennan, D.; Graham, M. J. (Univ. of Liverpool). Phil. Trans. Roy. Soc. London, Ser. A, 258: 325-45(Nov. 11, 1965).

The relative effective areas of krypton and xenon atoms adsorbed on iron, cobalt, nickel, titanium, zirconium, molybdenum, tungsten, tantalum, and platinum were examined by determination of the 77°K isotherm for each gas adsorbed successively on the clean surface of the same evaporated film. Point A, point B, and the Brunauer-Emmett-Teller equation were used to assess the monolayer value, with the general result that the number of atoms required to complete the monolayer is the same for xenon as for krypton, despite the larger atomic size of xenon. This result is interpreted to mean that both kinds of atoms occupy the same sites and that their effective area is determined by the site area. Various configurations of adatoms were examined with the object of finding the densest occupation of available sites. For this purpose, interatomic energies were calculated using the Lennard-Jones 6:9 and 6:12 potentials and the Buckingham exp:6 potential. In several instances, clear decisions can be reached, and the general conclusion was that equal numbers of krypton and xenon atoms are required to form the monolayer, in keeping with the experimental results. (BBB)

21388 THE ADSORPTION OF CARBON MONOXIDE ON EVAPORATED METAL FILMS. Brennan, D.; Hayes, F. H. (Univ. of Liverpool). Phil. Trans. Roy. Soc. London, Ser. A, 258: 347-73(Nov. 11, 1965).

Calorimetric measurements at 0°C were made of the heats of adsorption of carbon monoxide on evaporated films of Fe, Co, Ni, Mn, Ti, Mo, W, Ta, Nb, Zr, Pt, Pd, and Rh. The variation of the heat of adsorption with coverage was considered in terms of a precursor state whose energy determines the form of the variation. For adsorption on tungsten, the results and heat values calculated from data derived from flash filament desorption studies showed similarities, but comparison with results from field emission microscopy was disappointing. Saturation coverages of carbon monoxide and monolayer values for krypton before and after chemisorption are reported. In an attempt to interpret these values, possible configurations of adsorbed carbon monoxide were considered for all the metals. Simple restrictions relating to: the form of bonding, namely linear or bridge; the M-C bond length and the M-C-M bond angle; the number of bonds in which any one metal atom can participate; the form of the potential energy of interaction energy between neighbors; and the krypton monolayer concentrations were applied in arriving at maximum coverages for the various regular arrangements of admolecules which are conceivable. For titanium and zirconium, the experimental coverages were readily accounted for by these means with the conclusion that carbon monoxide is held by a bridge bond with each metal surface atom able to participate in only one bridge. For the fcc metals, similar conclusions were compatible with the experimental results, although they were not as well founded as for the hexagonal, close-packed metals. The difficulties of applying the discussion to the bcc metals were also considered. Arguments are presented that cast doubt on the view that the reduction in the adsorption of krypton after chemisorption is the result of sintering of the metal film owing to the liberation of the heat of adsorption. An alternative explanation in terms of a redistribution of sites for the adsorption of krypton due to the presence of the chemisorbed layer was examined and found to be inadequate in the simple form used. (BBB)

21389 THE ADSORPTION OF CARBON DIOXIDE ON EVAPORATED METAL FILMS. Brennan, D.; Hayward, D. O. (Univ. of Liverpool). Phil. Trans. Roy. Soc. London, Ser. A, 258: 375-86(Nov. 11, 1965).

Calorimetric measurements at room temperature were made of the heats of adsorption of carbon dioxide on evaporated films of Fe, Co, Ni, Ti, Mo, W, Ta, and Nb. These new data, considered along with similar data obtained previously for oxygen and carbon monoxide, provide strong evidence for dissociative adsorption of carbon

dioxide into CO and O, except possibly on iron, cobalt, and nickel. The saturation coverages for the adsorption of carbon dioxide on all the metals were small. Despite this, the adsorptive capacity for hydrogen of surfaces saturated with carbon dioxide was very small, except for nickel and to a lesser degree for iron. These observations were also accounted for in terms of dissociative adsorption of carbon dioxide and the concentrations of krypton atoms in the monolayer deduced previously. For nickel and cobalt (and to some extent iron), adsorption of carbon dioxide in an undissociated form is a possibility, but a clear conclusion could not be reached. The linear dependence of heat of adsorption on metallic radius is discussed. (BBB)

21390 LOCALIZED IMPURITY STATES IN METALS: DILUTE ALLOYS OF Ni IN Be. Klein, A. P.; Heeger, A. J. (Univ. of Pennsylvania, Philadelphia). Phys. Rev., 144: 458-68(Apr. 15, 1966).

The results of an experimental study of the residual resistivity, specific heat, and magnetic susceptibility of dilute solid solutions of nickel in beryllium are presented. The addition of small amounts of Ni to the Be host metal gives rise to large changes in all three quantities. The residual resistivity due to the impurities is found to be 10 $\mu\Omega$ cm per at.% Ni, and each Ni atom contributes 1.15 states per ev to the total density of states at the Fermi level as measured by the linear term in the low-temperature specific heat. Susceptibility measurements indicate that there is no localized moment on the Ni, but the addition of Ni gives rise to a large change in the temperature-independent susceptibility. Comparison of the susceptibility and specific heat results indicates that the added susceptibility is enhanced relative to the added state density arising from the Ni impurities. The Anderson theory of localized transition-atom impurity states is developed for the case of five-fold orbitally degenerate d states, and the equivalence of the Anderson approach and the scattering approach is demonstrated from the theory of resonance scattering. It is shown in this manner that the Anderson theory can be made consistent with the Friedel sum rule. Using the Anderson model the residual resistivity, specific heat, and d-state contribution to the susceptibility are calculated for dilute alloys where the host-metal density of states is a function of energy. The experimental results are found to be consistent with theoretical expectations and are used to determine magnitudes for the parameters of the theory. It is found that there are between 8 and 9 d electrons on each nickel atom, in agreement with the Friedel sum rule. The virtual level width is determined to be 0.4 ev, and the Coulomb-exchange quantity (U + 4J) is evaluated as 7 ev. Analysis of similar data on Cu : Ni alloys yields values for these quantities which are fully consistent with the results obtained from the Be : Ni data. (auth)

21391 LATTICE PARAMETERS, THERMAL EXPANSIONS, AND GRUENEISEN COEFFICIENTS OF ZIRCONIUM, 4.2 TO 1130 DEG K. Goldak, J. (Univ. of Chicago); Lloyd, L. T.; Barrett, C. S. Phys. Rev., 144: 478-84(Apr. 15, 1966).

The lattice parameters, atomic volume, nearest-neighbor interatomic distance, axial ratio, and coefficients of thermal expansion of zirconium are reported over the temperature range 4.2 to 1130°K. The data were obtained from single crystals, using a precision x-ray diffraction technique in the range 4.2 to 300°K and an interferometric dilatometer in the range 300 to 1130°K. Polynomial expressions, based on least-squares fitting of the data, are presented. Some of the parameters in Å are: at 4.2°K, a = 3.2294, c = 5.1414 (c/a = 1.5921); at 300°K, a = 3.2331, c = 5.1491 (c/a = 1.5926); at 1125°K, a = 3.2468, c = 5.1964 (c/a = 1.6004). Expansion coefficients $\times 10^6$ are: at 300°K, $\alpha_a = 4.99$, $\alpha_c = 7.36$, $\beta = 17.35$; at 1125°K, $\alpha_a = 4.91$, $\alpha_c = 15.14$, $\beta = 24.94$. The Grüneisen coefficient is found to be essentially constant from 100 to 1130°K; the directional Grüneisen coefficients are also computed. (auth)

21392 ANNEALING OF ^{60}Co-GAMMA-IRRADIATED GERMANIUM. Saito, H.; Pigg, J. C.; Crawford, J. H. Jr. (Oak Ridge National Lab., Tenn.). Phys. Rev., 144: 725-33(Apr. 15, 1966). (ORNL-P-1821).

Annealing of changes in reciprocal mobility and carrier concentration induced by ^{60}Co gamma irradiation at 77°K in germanium doped with either arsenic or antimony was investigated by an isochronal annealing technique for materials whose initial carrier concentration ranged from 5×10^{13} to 5×10^{15} cm^{-3}. Four annealing stages were observed. The annealing of one stage in the room-temperature range was found to be dependent on the concentration and type of impurity. The data are discussed in terms of a speculative model based upon an analogy with defect behavior observed in silicon. (auth)

21393 EFFECT OF THE TIME OF EXPOSURE AT ELEVATED TEMPERATURE ON THE EMBRITTLEMENT OF THE WELDED JOINTS OF HT60 STEEL FOR NUCLEAR PRESSURE VESSELS. Inagaki, Michio (National Research Inst. of Metals, Tokyo); Suzuki, Haruyoshi. Rep. Nat. Res. Inst. Met. (Tokyo), 8: 42-53(Feb. 1965). (In Japanese).

A study was made on the effects of exposure at 550°C up to 5000 hr on the notch ductility and the microstructure change of the welded joints of Ni–Cr–Mo HT60 tempered steel. The test steel, 100 mm thick, was produced experimentally for nuclear pressure vessels, and the welded joints were made by the electroslag welding and the CO_2 arc welding. The results of the study showed that the base metal, the weld metal, and the heat-affected zone (HAZ) of the base metal tended to embrittle, due to the grain growth of ferrite and the cohering of carbide toward the grain boundaries. The process of the change in the microstructure may be divided into the following three stages, with different combinations of the three stages occurring according to the structure before exposure: tempering of martensite and spheroidizing of carbide, formation of fine ferrite, grain growth of ferrite and, cohering and coarsening of carbide toward the grain boundaries. The change in the microstructure for the base metal is due only to stage III; the HAZ with the electroslag welding stage II and III; and the HAZ with the CO_2 arc welding stage I, II, and III. (auth)

21394 RESISTIVITY AND STRUCTURE OF SPUTTERED MOLYBDENUM FILMS. d'Heurle, F. M. (International Business Machines Corp., Yorktown Heights, N. Y.). Trans. Met. Soc. AIME, 236: 321-6(Mar. 1966).

Films of molybdenum were prepared by sputtering onto oxidized silicon substrates. The resistivity, lattice parameter, orientation, and grain size were studied as a function of substrate temperature and substrate bias. Under normal sputtering conditions, the resistivity of the films was found to be quite high (600×10^{-6} ohm-cm). However, with the use of the negative substrate bias of 100 v and a substrate temperature of 350°C, films were produced with a resistivity of about twice that of bulk molybdenum. The lattice parameters measured in a direction normal to the surface of the films were found to be greater than the bulk value. This was interpreted as being at least partly due to the presence of compressive stresses. The effects of annealing in an Ar–H atmosphere were studied in terms of diffraction line width, lattice parameter, and resistivity. (auth)

21395 ELEVATED TEMPERATURE MECHANICAL PROPERTIES OF WELDS IN A Ni–Mo–Cr–Fe ALLOY. Gilliland, R. G.; Venard, J. T. (Oak Ridge National Lab., Tenn.). Weld. J. (N.Y.), 45: 103s-10s(Mar. 1966). (ORNL-TM-1341).

A non-age hardenable, high-strength alloy was developed for use as the primary containment material for the Molten Salt Reactor Experiment (MSRE). The alloy was tailored to give good strength, ductility, and corrosion resistance to molten fluoride salts in the 1100 to 1500°F temperature range. The elevated-temperature mechanical properties of welds made in this alloy, known as INOR-8, as represented by several heats of MSRE-grade material are reported. Tensile tests on transverse weld samples in the as-welded and annealed conditions show a good combination of strength and ductility at temperatures ranging from 70 to

1800°F. Tensile properties of these weld samples compare favorably with those of the base metal. Stress relieving at 1600°F for 2 hr results in a lowering of the tensile yield strength. Creep-rupture tests at 1100, 1300, and 1500°F on these same type specimens show significant improvement in strength and ductility at 1300°F following a hydrogen atmosphere stress relief. Both as-welded and stress-relieved creep-rupture behavior was as good as the base metal behavior. The nil-ductility temperature, as determined by simulated heat-affected zone thermal cycle tests, was found to be 2300°F. Reasonable recovery of mechanical properties follows a simulated welding cycle with a 2300°F maximum temperature. (auth)

21396 CAUSE OF BRITTLE FRACTURE IN TUNGSTEN WIRE. Havel, Vladimir; Cochnar, Zdenek (Forschungsabteilung Tesla-Holesovice, Prague. Forschungsinstitut fuer Eisenhuettenwesen, Prague). Z. Metallk., 57: 225-7 (Mar. 1966). (In German).

In brittle tungsten specimens Fe_3W_3C and α-W_2C carbides are ordinarily present, while specimens embrittled artificially by grease contained α-W_2C carbide only. These inclusions influence the grain growth and cause brittle fracture during recrystallization. (auth)

21397 THERMIONIC EMISSION FROM CeC_2. Paderno, Yu. B.; Fomenko, V. S.; Podchernyayeva, I. A.; Makarenko, G. N. (Inst. for Study of Problems of Materials, Kiev). Zh. Tekh. Fiz., 35: 1860-2(1965). (In Russian).

The thermal emission properties of CeC_2, whose electronic structure resembles that of ThC_2 (which is known to be a good emitter) were investigated in the temperature range of 1200–1770°K, in view of the possible use of the material for the production of efficient cathodes. The methods and instrumental setup used for the experiments were described previously. Suspended in absolute alcohol, the carbide was deposited onto a tantalum substrate upon which it formed a 0.2 to 0.3-mm-thick layer. To prevent oxidation, the deposition did not last more than three minutes. The measurements of the work function taken during the activation process showed a minimum of 2.49 ev at 1380°K, which value remained unchanged until 1520°K, when an insignificant increase could be observed. At any given fixed temperature, the stationary value of the work function was attained rapidly when the cathode temperature was high. The good emission properties of CeC_2 are indicated by its fast activation, with the work function changing from 3.20 to 2.49 ev in the temperature range of 1220 to 1380°K. The maximum current density actually measured was 3 amp/cm^2 at a cathode temperature of 1700°K, but a rough extrapolation leads to a value of 17 amp/cm^2 at 2300°K. (ATD)

21398 ELECTRONIC STATES OF RARE-EARTH METALS IN ALLOYS. Raynor, G. V. (Univ. of Birmingham, Eng.). pp 1-12 of Metallurgy Session M. Book Five [of Preprints of] Fifth Rare Earth Research Conference, Aug. 30-Sept. 1, 1965.

Results of experimental work, mainly lattice spacing determinations, on solid solutions of certain rare-earth metals with Th, Zr, and Y, and with each other, are briefly discussed. It is suggested that solute metals with complex electronic configurations (rare-earth, transition, and transuranic elements) are capable of changing this configuration on alloying according to environment. In particular, Ce, when subjected to compressive strain energy of solution, tends to contract by ionization of the 4f electron. In other circumstances a tendency to change its effective valency towards that of the solvent is observed. Similar tendencies are found in intermediate phases. The Laves phases of the cubic (C15) type are of particular interest, since both electronic and atomic size relations between the components may be widely varied. Recent results are briefly discussed. (auth)

21399 CRYSTAL STRUCTURE OF COMPOUNDS OF THE RARE EARTHS WITH Cu, Ag, Au AND Ga. Dwight, A. E.; Conner, R. A. Jr.; Downey, J. W. (Argonne National Lab., Ill.). pp 35-44 of Metallurgy Session M. Book Five [of Preprints of] Fifth Rare Earth Research Conference, Aug. 30-Sept. 1, 1965.

Equiatomic compounds were prepared, in which the A element was a rare-earth metal and the B element was Cu, Ag, Au, or Ga. The alloys were made by arc-melting and were water-quenched after annealing at an elevated temperature. Crystal structures and lattice parameters were determined by x-ray powder diffraction methods. The CsCl and FeB structure types were found in the compounds of a rare-earth metal with Cu, Ag, or Au. The CrB structure type was found in the compounds of a rare-earth metal with Ga. No experimental work was done on Eu and Yb alloys. There is a systematic variation of lattice parameters with the atomic volume. (auth)

21400 THE CRYSTAL STRUCTURES OF $CeFe_7$, $PrFe_7$, $NdFe_7$, AND $SmFe_7$. Ray, Alden E. (Univ. of Dayton, Ohio). pp 45-56 of Metallurgy Session M. Book Five [of Preprints of] Fifth Rare Earth Research Conference, Aug. 30-Sept. 1, 1965.

The isostructural phases $CeFe_7$, $PrFe_7$, $NdFe_7$, and $SmFe_7$ are rhombohedral, the probable space group is $R\bar{3}m$. The lattice constants for the triply primitive hexagonal unit cells are reported. The hexagonal unit cells contain seven rare-earth and forty-nine Fe atoms. The atomic arrangements are intermediate between those of the $D2_d$–$CaCu_5$ and Th_2Zn_{17} structural types. One rare-earth and four Fe atoms statistically occupy a set of positions that are occupied by three A atoms in AB_5 structures and by six B atoms in A_2B_{17} structures. (auth)

21401 THE CRYSTAL CHEMISTRY OF THE INTERMEDIATE PHASES IN THE YTTERBIUM – ANTIMONY SYSTEM. Bodnar, Raymond E.; Steinfink, Hugo (Univ. of Texas, Austin). pp 57-66 of Metallurgy Session M. Book Five [of Preprints of] Fifth Rare Earth Research Conference, Aug. 30-Sept. 1, 1965.

Seven intermediate phases were synthesized in the Sb–Yb system and their crystal chemistry and physical properties investigated. A partially completed phase diagram is presented. The compound richest in Sb has the stoichiometry $YbSb_2$. It is orthorhombic, a = 4.54 Å, b = 4.26 Å, c = 16.63 Å, space group Bmmb. It crystallizes in a tabular habit and shows pronounced cleavage, but its crystal structure was not determined. The compound melts congruently at 945°C. The phase YbSb has the NaCl structure, a = 6.082 Å, and melts congruently at 900°C. Another phase with the probable composition Yb_5Sb_4 is orthorhombic, a = 8.10 Å, b = 15.97 Å, c = 24.30 Å, space group Pnma. It melts incongruently at 1350°C. Yb_4Sb_3 has the inverted Th_3P_4 structure, a = 9.30 Å, space group $I\bar{4}3d$, and displays no solid solubility. It melts congruently at 1540°C. The intermediate phase Yb_5Sb_3 is formed during high temperature reactions and appears to have a narrow temperature range of stability. It is hexagonal, a = 8.97 Å, c = 6.91 Å, space group $P\frac{6}{m}cm$ and is isostructural with Mn_5Si_3. It melts incongruently at 1520°C. The compound with the probable composition Yb_2Sb appears to undergo a phase transformation around 700°C. Above this temperature, it is orthorhombic a = 12.32 Å, b = 9.60 Å, c = 8.31 Å, space group Pnma. It melts incongruently at about 1400°C. Below 700°C, the compound is body-centered tetragonal, a = 4.66 Å, c = 16.33 Å, space group $I\frac{4}{m}mm$. Another phase may exist above 900°C in the approximate 2:3 stoichiometry, but it has not been verified as yet. (auth)

21402 THE YTTRIUM–COBALT ALLOY SYSTEM. Strnat, K. J.; Ostertag, W.; Adams, N. J.; Olson, J. C. (Wright-Patterson Air Force Base, Ohio). pp 67-76 of Metallurgy Session M. Book Five [of Preprints of] Fifth Rare Earth Research Conference, Aug. 30-Sept. 1, 1965.

The Co–Y system was investigated by thermal analysis, x-ray diffraction, and metallography. There are eight intermetallic compounds present corresponding to the ideal compositions Y_3Co, Y_3Co_2, Y_2Co_3, YCo_2, YCo_3, Y_2Co_7, YCo_5, and Y_2Co_{17}. Of these, Y_2Co_{17} appears to melt congruently, the others decompose peritectically. There is a eutectic between Y_3Co and Y_3Co_2 at approximately 37 at.%

Co, which melts at 715°C. A second eutectic with a melting point of 1330°C occurs between Y_2Co_{17} and Co, near 92 at.% Co. A phase diagram is proposed and the experimental evidence discussed in some detail. Crystallographic data, based on powder diffraction patterns, are presented for most of the intermediate phases. (auth)

21403 PREPARATION OF RE-Mn ALLOYS BY THE "AMALGAM PROCESS" X-RAY-, DIFFERENTIAL THERMAL AND THERMOMAGNETIC ANALYSES. Kirchmayr, Hans R. (Technische Hochschule, Vienna). Contract 61(052)-609. pp 77-88 of Metallurgy Session M. Book Five [of Preprints of] Fifth Rare Earth Research Conference, Aug. 30-Sept. 1, 1965.

A special method for preparation of RE-alloys, the modified amalgam process, is described and its application to RE-Mn alloys discussed. It consists of the preparation of RE-Mn-Hg alloys, which after heating, yield Hg-free RE-Mn alloys at temperatures below the liquidus state (900-1100°C). The alloys are powdery or slightly sintered and can be of single phase. During a study of the systems (Y, Sm, Gd, Dy, Ho, Er)-Mn, the phases $REMn_2$, $REMn_5$ and $REMn_{12}$ were detected. The schematic phase diagrams of Gd-Mn, Dy-Mn and Ho-Mn were established by DTA. The magnetic properties of the respective $REMn_5$ phases were measured between 80 and 1400°K. These compounds are ferrimagnetic with the exception of YMn_5, which is ferromagnetic. (auth)

21404 EFFECT OF CARBIDE DISPERSION IN TANTALUM-BASE ALLOYS. Chang, W. H. (General Electric Co., Evendale, Ohio). 27p. (CONF-651025-3). ORAU. Gmelin, AED-CONF-65-275-4.

From Symposium on Physical Metallurgy of Refractory Metals, French Lick, Ind.

In studying the effect of carbide dispersion in the refractory metals, the microstructures and strength/ductility properties of two Ta-base alloys containing moderate amounts of W, Re, and Hf have been studied. Both the alloys contained small amounts of oxygen, nitrogen and carbon; but the carbon-content was sufficiently different to result in significant difference in carbide dispersion. The alloys showed high strength to 3500°F and excellent low-temperature ductility. Both the recrystallization temperature and especially the high-temperature strength are further improved by carbide dispersion as a result of increasing the carbon content to about 0.05%. The alloys do not display age-hardening behavior; and when annealed at high temperatures, both alloys maintain their room-temperature ductility but suffer hot shortness as a result of strain induced precipitation and grain coarsening. (B.L.M.)

21405 STRENGTH, WELDABILITY, AND HEAT TREATMENT OF Ta-W-Hf AND Ta-W-Zr ALLOYS. Douglass, Richard W.; Torti, M. L. (National Research Corp., Newton, Mass.). 27p. (CONF-651025-4). ORAU. Gmelin, AED-CONF-65-275-6.

From Symposium on Physical Metallurgy of Refractory Metals, French Lick, Ind.

The results of a survey program designed to identify certain Ta-W-Hf and Ta-W-Zr alloys suitable for further study in an attempt to develop a Ta-base alloy with an optimum combination of 3500°F tensile strength, weldability, and fabricability is reported. Small amounts of Yt were added to several of the alloys in an attempt to restrict the grain growth at high temperatures. Zirconium appeared to be a more effective hot strengthener than Hf, but the strengthening must be balanced against the reduction of fabricability that probably will result when Zr is substituted for Hf. Those alloys containing sufficient quantities of Zr or Hf showed improvements in hot strength resulting from heat treatment. The addition of C in the range 400 to 1500 ppM was found to have little or no effect on the 3500°F strength of the different alloys. Tabulations show comparisons of various properties of different composition alloys. (B.L.M.)

21406 THE HIGH TEMPERATURE TENSILE PROPERTIES OF TUNGSTEN AND TUNGSTEN RHENIUM ALLOYS CONTAINING A DISPERSED SECOND PHASE. King, G. W.; Morcom, W. R.; Sell, H. G. (Westinghouse Electric Co., Bloomfield, N. J.). 22p. (CONF-651025-5). ORAU. Gmelin, AED-CONF-65-275-5.

From Symposium on Physical Metallurgy of Refractory Metals, French Lick, Ind.

The influence of 25 wt % Re on the tensile properties of pure W up to 2400°C has been investigated. Also the effect of two stable dispersed phases, 1 wt % ThO_2 and 1 wt % HfN, on the properties of this alloy was investigated. The results are compared with the tensile properties of pure W, with W-1 wt % ThO_2 and W-2 wt % ThO_2. (B.L.M.)

21407 W-5Re-2.2ThO_2, A DUCTILE TUNGSTEN SHEET ALLOY. Maykuth, D. J.; Ogden, H. R.; Jaffee, R. I. (Battelle Memorial Inst., Columbus, Ohio). 29p. (CONF-651025-6). ORAU. Gmelin, AED-CONF-65-275-8.

From Symposium on Physical Metallurgy of Refractory Metals, French Lick, Ind.

A series of bars of tungsten with 5 wt % Re and 1.1 to 4.4 wt % ThO_2 were prepared and compared as to low temperature ductility and hot strength at 1600°C. The alloy having a composition of 5 wt % Re, 2.2 wt % ThO_2 and the balance W was found to be near optimum in terms of combination of these properties and was selected for further process studies in rolling and annealing. Through the use of alkali-silicate doped base and gas pressure bonding in the formation, dense sheet bars having an extremely fine grain size was achieved for the alloy. Grain growth in the sheet bars is minimized during fabrication at 1600°C by the presence of these dopants and fine initial thoria particle size. The addition of thoria as an aqueous solution of $Th(NO_3)_4$ resulted in a significant finer grain size in the final sheet product than where the thoria was added as a sol. The alloy was found also to maintain excellent tensile ductility at low temperatures in the recrystallized condition. (B.L.M.)

21408 PERMEABILITY RELATIONSHIPS USING DARCY PERMEABILITY, VACUUM DECAY, PRESSURE DECAY, AND PORE SIZE DISTRIBUTION METHODS ON GRAPHITIC MATERIALS. Anderson, W. A. (Great Lakes Carbon Corp., Niagara Falls, N. Y.). 30p. (CONF-650632-4). ORINS. Gmelin, AED-CONF-65-149-14.

From 7th Biennial Conference on Carbon, Cleveland.

The relations between different methods of permeability measurement on graphitic materials were explored. Linear relations were confirmed to exist in the laminar flow region between the Darcy permeability value and the vacuum decay permeability value, the viscous flow coefficient term from the pressure decay method, as well as the slip flow term from the pressure decay method, when considering results from various grades of graphite having markedly different pore size distribution spectra. It was also confirmed that the cumulative pore size distribution spectra may be analyzed to calculate an equivalent Darcy permeability value. The pore distribution analysis included molded and extruded samples, two of which had a permeability value twofold greater than any tested by Wiggs. An agreement in permeability values was obtained using the various methods of measurement. An analysis of the relations was made in an attempt to evaluate these data using theoretical concepts as applied to the flow of gas through a porous media. (auth)

21409 MAGNETIC TRANSFORMATION IN HEAVY RARE-EARTH ALLOYS WITH EACH OTHER. Bozorth, R. M.; Gambino, R. J. (International Business Machines Corp., Yorktown Heights, N. Y.). 29p. (CONF-650804-11). ORINS. Gmelin, AED-CONF-65-208-15.

From 5th Rare Earth Research Conference, Ames, Iowa.

The Curie (T_C) and Néel (T_N) points of the binary rare earth alloys Gd-Lu, Dy-Ho, Dy-Tm, Er-Tm, and Tm-Lu, in addition to those previously reported (Atlantic City, Nottingham) were measured. There were maxima in the Curie point vs composition curves for Ho-Er, Ho-

Tm, and Er–Tm and minima for Dy–Tm and Ho–Tm, when the average concentration of 4f electrons was near 10.5. The Tm–Lu alloys were ferromagnetic when Tm-rich, and distilled Tm had a Curie point, Néel point, and intermediate transformation point. The Lu-rich alloys were all nonferromagnetic in low fields and some became ferromagnetic at a critical field, when they had sharply increased susceptibility with onset of hysteresis. Representative data for various alloy systems are shown to deviate only slightly from a straight line when plotted against the $^2/_3$ power of the average de Gennes factor, as discussed by Koehler. (auth)

21410 THE BEND AND TENSILE DUCTILITY OF A Cb–Ti–Zr MOLYBDENUM ALLOY WITH PARTICULAR REFERENCE TO LAMINATING TENDENCY. Brentnall, W. D.; Rostoker, W. (Illinois Inst. of Tech., Chicago). 24p. (CONF-651025–8). ORAU. Gmelin, AED-CONF-65-275-16.

From Symposium on Physical Metallurgy of Refractory Metals, French Lick, Ind.

Molybdenum alloys having a nominal composition of 1.5 wt.% Nb, 0.5 wt.% Ti, and 0.3 wt.% Zr and three C levels, 0.03, 0.07, and 0.10 wt.%, were processed to 0.050 in sheets utilizing different rolling and annealing schedules. During initial hot breakdown involving extrusion and forging, cracking tendencies were observed that suggest that decarburization is a probable source of trouble. The bend transition temperatures were determined both as a function of rolling practice and final annealing temperature. Generally a single interstage recrystallization anneal at the sheet bar stage followed by cross and long rolling to finished gage produced the lowest transition temperature. The lowest carbon content with the optimum fabrication practice produced the lowest transition temperature, but the temperature span between limits of carbon content was not large. The difference in transition temperature between the unrecrystallized and recrystallized condition was nil or small. The laminating tendency disappears at or above some partial state of recrystallization, and this disappearance coincides with a sharp optimum in bend-rebend capacity. This same behavior holds over the whole carbon content range studied. The tensile transition temperatures for the alloys are all much lower than the bend transitions and at all carbon levels are below room temperatures. Both tensile and bend transition temperatures are sensitive to surface removal, which in turn appears to relate to contamination during processing and final annealing. (auth)

21411 PROPERTIES OF COLUMBIUM ALLOY Cb-753. Schussler, M. (Union Carbide Corp., Kokomo, Ind.). 22p. (CONF-651025–7). ORAU. Gmelin, AED-CONF-65-275-3.

From Symposium on Physical Metallurgy of Refractory Metals, French Lick, Ind.

The characteristics, properties, and fabrication of a niobium alloy, Haynes alloy Cb-753, containing 5 wt.% V and 1.25 wt.% Zr are described. The alloy is applicable to high temperature structural needs requiring good fabricability and weldability. (B.L.M.)

21412 TUNGSTEN-BASE ALLOY DEVELOPMENT. Semchyshen, M.; Kalns, Eric (Climax Molybdenum Co. of Michigan, Ann Arbor). 35p. (CONF-651025–11). ORAU. Gmelin, AED-CONF-65-275-9.

From Symposium on Physical Metallurgy of Refractory Metals, French Lick, Ind.

The consolidation of W-base alloys containing relatively large additions of C in conjunction with Nb, Hf, and/or Zr was achieved by vacuum-arc-melting procedures. These alloys, when encapsulated in Mo, may be successively worked by extrusion, yielding generally good recoveries in sound stock. The maximum recrystallization temperatures of the extruded billets ranged from 3400 to 4800°F. Strengths in the order of 3 to 5 times those of unalloyed W were developed by swaging the alloy bars. The highest strengths in the strain-hardened condition were demonstrated by the alloys, W–0.48% Zr–0.48% C and W–1.42% Nb-0.005% C where all compositions are expressed in weight percentages. Tests of recrystallized specimens indicated that the alloy W-1.18% Hf-0.086% C was stronger over the 3500 to 5000°F temperature range than the former alloy mentioned above. (B.L.M.)

21413 TERBIUM, ERBIUM AND YTTERBIUM GRAPHITE INTERCALATION COMPOUNDS. Ostertag, W. (Air Force Materials Lab., Wright-Patterson AFB, Ohio); Craven, W. E. 15p. (CONF-650632–7). ORINS. Gmelin, AED-CONF-65-149-9.

From 7th Biennial Conference on Carbon, Cleveland.

Graphite compounds of terbium, erbium, and ytterbium were prepared by reaction of graphite with rare earth solutions in liquid ammonia. Ytterbium dissolved in liquid ammonia whereas terbium and erbium solutions had to be obtained by electrolysis using ammonium iodide as an electrolyte, a platinum cathode, and an anode made of rare earth metal. Analyses performed on rare earth graphite samples showed that ammonia is introduced in the graphite along with the rare earth elements. Terbium and erbium graphite also contain small amounts of iodide. The compounds were found to be of hexagonal crystal structure. The magnetic susceptibilities of all the compounds were determined. The x-ray data and the results of the magnetic measurements are discussed. (auth)

21414 HIGH PRESSURE POLYMORPHISM AND MAGNETIC ORDERING IN SOME Sm-TYPE RARE EARTH ALLOYS AND SAMARIUM. Jayaraman, A.; Sherwood, R. C.; Corenzwit, E. (Bell Telephone Labs., Inc., Murray Hill, N. J.). 15p. (CONF-650804–13). ORINS. Gmelin, AED-CONF-65-208-10.

From 5th Rare Earth Research Conference, Ames, Iowa.

The rare earth alloys LaY, PrY, NdY, NdTm, and $LaGd_3$, all of which crystallize in the Sm-type structure, undergo a pressure-induced phase change to the double hexagonal close-packed structure (La-type); the high-pressure phase is metastably retained at atmospheric pressure. However, under similar pressure and temperature treatment CeY decomposed to the elements. Magnetic data are presented for the normal and high-pressure phases of NdTm, $LaGd_3$, and Sm; in the latter case the data are from earlier measurements. The significance of the breakdown of CeY and the anomalies in the low-temperature magnetization data of $LaGd_3$, NdTm, and Sm are discussed. (auth)

21415 SYSTEMATIC ARRANGEMENT OF THE BINARY RARE-EARTH ALUMINIUM SYSTEMS. Buschow, K. H. J.; van Vucht, J. H. N. (Philips' Gloeilampenfabrieken, N. V., Eindhoven, Netherlands). 11p. (CONF-650804–17). ORINS. Gmelin, AED-CONF-65-208-6.

From 5th Rare Earth Research Conference, Ames, Iowa.

A number of binary rare earth aluminum systems were investigated by x-ray diffraction and thermoanalytical methods. It is shown that both the stability and composition of the intermetallic compounds found in these systems are strongly influenced by the atomic size of the rare earth metals (R). If these binary systems were arranged in order of decreasing radius it appeared that a compound R_3Al exists only for rare earth metals with relatively large radius. With decreasing radius, a compound R_2Al was also observed. It became gradually more stable, while R_3Al disappeared. For still smaller radii a compound R_3Al_2 was found in addition to R_2Al. The compounds RAl and RAl_2 exist for all rare earth metals investigated. Some interesting relations exist between the decreasing radius and the crystal structures of the compounds. Between RAl_2 and aluminum the compounds RAl_3 and RAl_4 were found. RAl_3 was relatively more stable for small radii and RAl_4 for large radii. The compound RAl_3 was observed for all rare earth metals investigated except for europium; its crystal structure showed a remarkable dependence on the radius of the rare earth metal. (auth)

21416 PLASTIC BEHAVIOR OF METALS AT CRYOGENIC TEMPERATURES. Kula, Eric B.; DeSisto, Thomas S. (Army Materials Research Agency, Water-

town, Mass.). 43p. (CONF-650646-3). ORINS. Gmelin, AED-CONF-65-148-1.

From American Society for Testing and Materials, 68th Annual Meeting, Lafayette, Ind.

The low-temperature plastic behavior of metals is reviewed. The effect of temperature on stress-strain curves is shown for metals of various crystal structures. The variation of yield stress and ductility with temperature for pure metals and for commercial alloys is shown to depend primarily on crystal structure. This is discussed in terms of dislocation behavior and thermally activated deformation. Special emphasis is placed on the serrated yielding, which occurs in many metals tested at −269°C. This is caused by adiabatic heating, and can occur independently of the deformation mechanism. It was demonstrated that serrated yielding can be explained in terms of the general condition for maximum load and necking. (auth)

21417 IMPROVEMENTS RELATING TO LOW ALLOY STEELS. Nichols, Roy Woodward (to United Kingdom Atomic Energy Authority); Pearson, Thomas Felix; Haynes, Alan George. British Patent 1,020,572. Feb. 23, 1966. Filed May 30, 1961.

A low alloy steel is patented that has the following composition: less than 0.15 wt.% C, from 1.0 to 1.2 wt.% Mn, from 1.4 to 1.7 wt.% Ni, from 0.24 to 0.35 wt.% Mo, from 0.25 to 0.55 wt.% Cr, and from 0.08 to 0.20 wt.% V, the balance being Fe. The steel is primarily applicable in the form of rolled normalized plate to the fabrication of massive pressure vessels. (B.L.M.)

Radiation Effects

See also CHEMISTRY — Radiation Chemistry

21418 (AD-627049) THE EFFECT OF RADIATION ON THE ELECTRICAL RESISTIVITY AND BULK COMPRESSIBILITY OF POLYEPOXIDES. Summary Report. Warfield, R. W.; Kincaid, C. V. (Naval Ordnance Lab., White Oak, Md.). Dec. 13, 1965. 30p. (NOLTR-65-125). CFSTI $2.00 cy, $0.50 mn.

Three polyepoxides were exposed to varying doses of mixed neutron and gamma radiation. However, before irradiation, the electrical volume resistivity and the bulk compressibility of each of the polymers were determined as a function of temperature. The changes produced in these two parameters by radiation doses up to 25 Mrads were progressively followed by measurements after each radiation cycle. The results indicate that radiation of this type and intensity will degrade crosslinked polyepoxides and that this can be shown by electrical resistivity measurements and by changes in the bulk compressibility. (auth)

21419 (BNWL-191) EFFECT OF NEUTRON IRRADIATION ON UHTREX GRAPHITE AND CARBON. Helm, J. W. (Battelle-Northwest, Richland, Wash. Pacific Northwest Lab.). Feb. 1966. Contract AT(45-1)-1830. 17p. Dep. mn. CFSTI $1.00 cy, $0.50 mn.

The dimensional stability of the graphite and carbon materials used in UHTREX was determined to neutron exposures equal to expected lifetime exposures, and the behavior of these materials was compared with a conventional nuclear graphite. Irradiations were conducted to maximum neutron exposures of 7×10^{20} nvt, E > 0.18 Mev at sample temperatures between 900 and 1800°C. At irradiation temperatures of 1000 and 1800°C, CGL graphite behaves about the same as CSF, and the length changes are less than −0.06% in both orientations at the maximum exposures. The isotropic behavior of CGL is expected because the preirradiation CTE ratio of 1.02 indicates a very isotropic material. At 1300 to 1400°C, the amount of contraction has increased sharply to about −1%. The increase in contraction over CSF at these conditions is probably due to the impregnation treatment that CGL received. In all cases the carbons contract more than the CGL, and the more dense impregnated carbon contracts the most. CGM shows very large length changes, probably because of the impregnant material added during manufacture. However, at the maximum expected lifetime conditions (2.5×10^{20} nvt at 2000°F). the maximum contraction is only 1.3%. At the conditions studied, the CGN carbon contracted a maximum of 0.4%. Length changes in the porous carbon were about the same as in CGM. (W.L.G.)

21420 (BNWL-215) IRRADIATION-INDUCED CONTRACTION OF GRAPHITES AT HIGH TEMPERATURE FOLLOWING COLD PREIRRADIATION AND INTERMITTENT THERMAL ANNEALS. Cox, J. H.; Woodruff, E. M. (Battelle-Northwest, Richland, Wash. Pacific Northwest Lab.). Jan. 1966. Contract AT(45-1)-1830. 17p. Dep. mn. CFSTI $1.00 cy, $0.50 mn.

Defects were nucleated in KC, CSF, and TSGBF reactor-grade graphites by irradiation at 30°C to exposures of 2.9×10^{20} nvt (E > 0.18 Mev). The samples were thermally annealed to 750°C and irradiated again at 550 to 700°C to exposures of 11.1×10^{20} nvt. This treatment increased the contraction rate of the graphites by a factor of 3.2 ± 1.0. The contraction rate was independent of orientation. Samples of TSX graphite were irradiated at different temperatures and exposures to 3.0×10^{21} nvt; after each irradiation the samples were annealed to approximately the graphitization temperature. In each case, the contraction upon subsequent irradiation was less in the annealed samples. (W.L.G.)

21421 (GA-6888) EFFECT OF FAST NEUTRON IRRADIATION FROM 495 DEG TO 1035 DEG C ON NUCLEAR GRAPHITES. Engle, G. B. (General Atomic, San Diego, Calif. John Jay Hopkins Lab. for Pure and Applied Science). Feb. 11, 1966. Contract AT(04-3)-167. 43p. Dep. mn. CFSTI $2.00 cy, $0.50 mn.

Anisotropic and isotropic graphites of relatively high strength and density were irradiated between 495 and 1035°C to fast neutron exposures of 1.2 to 2.5×10^{21} nvt (E > 0.18 Mev). Changes in linear dimensions, physical and mechanical properties, and structural parameters were measured. The isotropic graphite contracted less by a factor of two in the parallel direction than anisotropic graphite in either direction at 495 to 615°C. However, the parallel contraction was about the same as that of the anisotropic graphite at 840 to 1035°C. Material prepared with needle-coke graphite contracted less in the parallel direction than conventional petroleum-coke filler graphite above 800°C but not below 800°C. There was an increase in the rate of parallel contraction between 800 and 900°C and little change in rate between 850 and 1200°C. Apparent crystallite sizes in the c-direction were reduced and showed the same relation with irradiation temperatures as parallel dimensional contraction while lattice parameters and physical properties showed much less change; electrical resistivity was an exception and increased by a factor of two or more; its change was not related to irradiation temperature. Dimensional changes of the isotropic graphite in the parallel direction, which were calculated using crystallite changes derived from anisotropic material, were in fair agreement with measured values. (auth)

21422 (GEAP-5100D) HIGH-PERFORMANCE UO_2 PROGRAM. IRRADIATION OF 0.5-INCH DIAMETER, HOLLOW PELLET UO_2 FUEL RODS UP TO 1.1×10^6 BTU/H-FT^2 PEAK HEAT FLUX EPT-COM ASSEMBLY. Lyons, M. F.; Nelson, R. C.; Pashos, T. J.; Wilson, C. R.; Weidenbaum, B. (General Electric Co., San Jose, Calif. Atomic Power Equipment Dept.). Dec. 1965. Contract AT(04-3)-1583. 102p. (EURAEC-1583). Dep. mn. CFSTI $4.00 cy, $0.75 mn.

Work Performed Under United States–Euratom Joint Research and Development Program.

The fabrication data, irradiation history, and the complete, correlated postirradiation examination results are described for a four-rod fuel assembly (designated EPT-COMposite) that operated in the GETR-PWL with significant central melting to a burnup of 1725 Mwd/tonns. The fuel rods were unsegmented, reactor-length rods containing 95% dense, hollow, sintered UO_2 pellets in free-standing Zircaloy-2 cladding. This fuel assembly was the fourth of a

series irradiated to investigate the feasibility and limitations in UO_2 fuel rod operation with central melting. The irradiation and subsequent postirradiation examination of this assembly provided the first experimental demonstration that the use of hollow fuel pellets (equal to about 3% internal free volume) would significantly reduce clad swelling resulting from the UO_2 phase change volume expansion during melting. The preceding, solid pellet fuel assembly exhibited severe clad swelling after operation at the same or slightly lower thermal performance. This change in fuel design proved a significant step towards satisfactory operation with central melting in high density fuel. (auth)

21423 (N–65–23015) PROBLEMS OF FISSION PRODUCT DIFFUSION IN GRAPHITE FUEL ELEMENTS. Cesoni, G.; Chinaglia, B.; Walther, H. (Societa Ricerche Impianti Nucleari, Saluggia (Italy). Centro Ricerche Nucleari). 1963. 25p. (SORIN–15).

Studies on diffusion problems of fission products in graphite are reported, and preliminary results concerning numerical calculations of some peculiar diffusion problems; measurements of diffusion coefficients in pyrographite, and of the fission fragment ranges in pyrographite caused by the recoil effect; and nondestructive determination of the uranium masses in coated particles, are presented. General conclusions drawn from these preliminary studies are these: Numerical methods for diffusion calculations were proven which are reliable in diffusion problems where analytical solutions do not exist. A method to measure the distribution of fission products in a plane thin pyrographite sample was developed and checked. Diffusion coefficients in pyrographite were measured. A fast migration rate for ^{140}Ba was observed, confirming that pyrographite is not a very effective diffusion barrier for Ba. Nondestructive methods to determine uranium traces were developed using activation analysis techniques. These methods were applied to measure the mass distribution of coated particles. (STAR)

21424 (N–65–23332) SURFACE EFFECTS IN ALKALI-HALIDE CRYSTALS RESULTING FROM IRRADIATION BY X RAYS. Bernstein, J. B.; Kirk, D. D.; Stierwalt, D. L. (Naval Ordnance Lab., Corona, Calif.). Dec. 1964. 10p. (NASA-CR–62617; TM–43–19). CFSTI $1.00 cy, $0.50 mn.

Results of exposing a series of alkali-halides to x-irradiation and measuring a resulting change in the absorptance spectra of the crystals are presented. The technique employed to examine the crystals is the measurement of their spectral emittance before and after their exposure to x-irradiation. The theory, techniques and experimental apparatus used in acquiring the spectral emittance (spectral absorptance) of a transparent solid, in the infrared region of the spectrum, were previously discussed. The spectral emittance measurement technique represents a direct measure of absorptance. A transmittance measurement would need a supplementary reflectance measurement to determine the spectral absorptance. The crystals measured are KCl (t = 2.10 mm), RbBr (t = 5.31 mm), NaCl (t = 6.56 mm) and KBr (t = 4.65 mm). (auth)

21425 (N–65–24491) EFFECTS OF RADIATION ON NICKEL–CADMIUM BATTERY ELECTRODES. [PART] I. Final Report, June 1963–Apr. 1965. Argue, G. R.; Recht, H. L.; McCollum, W. A.; McKenzie, D. E. (Atomics International, Canoga Park, Calif.). Apr. 15, 1965. Contracts NAS7-100; JPL-950514. 70p. (NASA-CR–62796; AI–65–66). CFSTI $3.00 cy, $0.75 mn.

For Jet Propulsion Lab., Calif. Inst. of Tech., Pasadena.

The effects of radiation on nickel–cadmium electrodes and their magnitude are studied. It was observed that voltage-current relations of nickel–cadmium batteries are not affected by gamma radiation in the short run. Radiation causes the cadmium electrodes to lose capacity, when undergoing charge-discharge cycling. Material is dislodged from the irradiated electrodes, with the most being lost at 100% of charge. This phenomenon may not be of great importance in commercial cells as their closely packed configuration appears to oppose this effect. Only 2 to 2½ psi were the highest observed pressures attained by cells in radiation fields. This effect is of little consequence, since cells are designed to retain gases up to 100 psig. (STAR)

21426 (N–65–24714) [TOJNINGSUTMATTNING, EN LITTERATURGRANSKNING AVSEENDE FENOMENETS NATUR OCH TEORI SAMT TILLAMPNING PA MATERIAL FOR OVERHETTARKAPSLING]. (Low-Cycle Strain Fatigue—A Literature Review Covering Natural Phenomena and Theory of Results on Material for Superheat Fuel Cladding). Ericsson, Torsten (Kungliga Tekniska Hogskolan, Stockholm (Sweden)). 1964. 109p.

A literature study on results from isothermal low cycle strain fatigue experiments using austenitic stainless steel and nickel alloys, as well as other materials, was conducted. Low cycle fatigue after less than 10^5 cycles is expressed in the equation: $\Delta e_p N_F^m = C$ where N_F is the fracture value and the plastic strain range is Δe_p. The constant C is mostly a little higher than half the fracture ductility e_F of a simple tensile test. Tests performed with constant stress and constant strain amplitude contribute differently to the cycles to fracture. Grain size and the orientation of a specimen in relation to the rolling direction had little influence on the fracture value. Neutron irradiation on stainless steel simultaneously with cycling diminishes the fracture value. A compilation and comparison of low cycle strain fatigue tests of various materials are presented in tables. (STAR)

21427 (NASA-CR–54904) EFFECT OF NUCLEAR RADIATION ON MATERIALS AT CRYOGENIC TEMPERATURES, Quarterly Report No. 2, October 21, 1965–January 21, 1966. Schwanbeck, C. A. (Lockheed Nuclear Products, Marietta, Ga.). Feb. 1966. Contract NAS 3-7985. 87p. (LACER–8372).

Developments in preparation and modifications of existing equipment, completed tensile test results from Titanium 55A, and partial tensile test results from Aluminum 1099 are reported. The refrigeration system and other test equipment have performed very well, resulting in unusually efficient use of available neutron flux. The flux mapping required by a new beam port gamma shield is complete. There is no significant change in neutron flux level due to the shield change. Temperature correlations and development of annealing temperature control methods are complete. The test loop alignment problem does not appear as serious with the loop to be modified for fatigue testing as it was with the prototype loop. Strengthening of the structural member of this loop is not required. (P.C.H.)

21428 (NP–15942) CINETIQUE DE L'ECHAPPEMENT DE L'HELIUM HORS DE FRITTES D'OXYDE DE BERYLLIUM PENDANT L'IRRADIATION. (Kinetics of Escape of Helium from Beryllium Oxide Frits During Irradiation). Carteret, Y.; Bareau, J. (Commissariat a l'Energie Atomique, Saclay (France). Centre d'Etudes Nucleaires). Aug. 1965. 22p. (DM–1477). Dep. mn.

The irradiation of beryllium oxide by neutrons causes the formation of helium by the (n,2n) and (n,α) reactions. Kinetics of the escape of helium was studied during the irradiation under a flux varying from 1.5×10^{13} to 4.15×10^{13} n_r/cm^2 and at temperatures from 1020 to 1350°C. Studies on the evolution of the ratio R/B (R is the quantity of the helium released per unit time and B is the quantity of helium formed) showed that after an induction period of the order of 24 hrs R/B decreased regularly and reached a constant value between 0.12 and 0.19. The results are interpreted by the capture of helium atoms by holes created during irradiation. (tr-auth)

21429 (RHEL/R–105) THE INFLUENCE OF STRUCTURE ON THE POST-IRRADIATION PHYSICAL PROPERTIES OF EPOXY RESINS. Price, M. J.; Sheldon, R. (National Inst. for Research in Nuclear Science, Chilton (England). Rutherford High Energy Lab.). Nov. 1965. 20p. Dep. mn.

Differences in radiation stability exhibited by various

epoxy structures were studied. The presence of a chain nitrogen appears to have a profound effect upon stability, and it is postulated that a different mode of breakdown occurs with the chain-nitrogen-containing material. (auth)

21430 (WADC-TR-55-58(Pt.8)) NUCLEAR RADIATION RESISTANT POLYMERS AND POLYMERIC COMPOUNDS. Annual Report. Born, John W. (comp.) (Goodrich (B. F.) Co. Research Center, Brecksville, Ohio). Mar. 1963. Contract AF33(616)-7491. 134p.

Progress is reported on studies of radiation damage in high polymers; the selection, design, synthesis, and polymerization of new monomers to produce new radioresistant thermally stable polymers; evaluation of the radiation and heat stabilities of the resulting new polymers; studies of the effects of gamma irradiation in air at room temperature on the compression set of various rubber vulcanizates; research to develop satisfactory curing systems for new, radiation-stable elastomers; and planning for radiation testing of new radiation-stable electrical insulation. (J.R.D.)

21431 (WADC-TR-55-58(Pt.9)) NUCLEAR RADIATION RESISTANT POLYMERS AND POLYMERIC COMPOUNDS. Annual Report. Born, John W. (comp.) (Goodrich (B. F.) Co. Research Center, Brecksville, Ohio). Apr. 1963. Contract AF33(616)-7491. 148p.

Research directed toward synthesis of radioresistant thermally stable elastomers and thermoplastics is described. Information is included on preparation and evaluation of 22 aromatic homopolymers, 15 aromatic elastomers, 17 new aromatic rubber compounds, 73 conventional rubber compounds, and six new aromatic thermoplastics. (J.R.D.)

21432 (WAPD-301) THE HOMOGENIZATION AND DENSIFICATION OF $ZrO_2 + UO_2$ FUELS UNDER IRRADIATION. Berman, R. M. (Bettis Atomic Power Lab., Pittsburgh, Pa.). Jan. 1966. Contract AT(11-1)-Gen-14. 63p. Dep. mn. CFSTI $3.00 cy, $0.75 mn.

Plates of ZrO_2 + 36.8 wt/% UO_2 and ZrO_2 + 46 wt/% UO_2, initially 90, 80, and 70% theoretical density (T.D.), were clad in Zircaloy and irradiated to various burnups from 1 to 6×10^{20} fissions/cm^3 in a pressurized loop in the MTR. Post-irradiation examination showed that the porosity collapsed under the loop pressure during irradiation. In ZrO_2 + 46 wt/% UO_2, large, elongated pores became strings of small spherical pores; in ZrO_2 + 36.8 wt/% UO_2, they became zones of microporosity. The plates reached a minimum thickness at about 4×10^{20} fissions/cm^3 for ZrO_2 + 46 wt/% UO_2 and at a somewhat higher exposure for ZrO_2 + 36.8 wt/% UO_2. Thereafter, they began to expand as fission gases accumulated. X-ray diffraction showed that the two phases initially present in ZrO_2 + 46 wt/% UO_2 had homogenized by 5×10^{20} fissions/cm^3. The process of homogenization can be satisfactorily defined by a diffusion equation, if a value for the diffusion constant $D = 3.32 \times 10^{-14}$ cm^2/sec is used. This D value indicates that a single fission homogenizes a volume containing 1.66×10^7 atoms. This number is two orders of magnitude too large to be explained by Brinkman's displacement spike hypothesis. Calculations based on Konobeevsky's hypothesis of a thermal pulse show that the liberation of 23 Mev of thermal energy at the center of such a volume is sufficient to cause homogenization. This seems well within the capabilities of a fission event. (auth)

21433 (UCRL-Trans-10012) X-RAY DIFFRACTION STUDY OF NEUTRON-IRRADIATED BERYLLIA. Belbeoch, B.; Rodot, J.; Roulliay, M. (Commissariat a l'Energie Atomique, Paris (France)). Translated for Univ. of California, Livermore, from report DM-1402. June 1965. 84p. Dep. mn. JCL $8.10 fs, $2.72 mf.

X-ray diagrams obtained from sintered samples of neutron-irradiated BeO (E > 1 Mev) were classified into three types, which depend on the values of the c/a ratio, whatever the characteristics of the sinter (compressed or natural sinter, varying density and grain size, and pure BeO or with additives). The observed anisotropic expansion of the BeO lattice due to irradiation depends not only on the received dose but also on the state of the intergranular stresses in the samples; thus, the sinters that stand up best to irradiation are high-density fine-grain sinters for which the c/a ratio varies very little with the irradiation dose. Single-crystal diagrams showed the same classification as sinters in terms of the c/a ratio. In addition, x-ray scattering was observed, apart from Bragg reflections. When this scattering appears, the distribution of defects is no longer isotropic; the scattering observed when $1.625 < c/a < 1.645$ is mainly described. (auth)

21434 COMMENTS ON THE EFFECT OF FAST NEUTRON DAMAGE ON THE DEFORMATION OF COPPER-TIN ALLOYS. Koppenaal, T. J. (Argonne National Lab., Ill.). Acta Met., 14: 681-2(May 1966).

The flow stress of neutron-irradiated Cu–Sn polycrystalline alloys reported by Russel (Acta Met., 13: 999(1965)) is discussed. Use of polycrystalline samples to measure the stress that opposes dislocation motion, the neutron dose dependence of the flow stress, and the force-distance behavior assumed for interaction of a dislocation and an irradiation-produced obstacle are considered. Difficulties that can arise in examining an alloy crystal while it is strengthened by both solid solution and neutron irradiation are described. (M.C.G.)

21435 STUDY BY ELECTRON PARAMAGNETIC RESONANCE OF ANNEAL EFFECTS IN IRRADIATED GRAPHITE. Kester, Tilo; Servoz-Gavin, Pierre (Centre d'Etudes Nucleaires, Grenoble, France). Compt. Rend., Ser. B, 262: 439-42(Feb. 7, 1966). (In French).

During the electron paramagnetic resonance study of the anneal of a sample of P 33 graphitized carbon black irradiated with neutrons at 77°K, anneal peaks were detected on the susceptibility x, the length of the ray ΔH, and the g factor. An anti-anneal peak was found for g and ΔH. (tr-auth)

21436 BEHAVIOR UNDER IRRADIATION OF LOW-ALLOYED URANIUM. Colabianchi, G.; Fizzotti, C. (CNEN, Rome). Energ. Nucl. (Milan), 13: 182-8(Apr. 1966). (In Italian).

The results obtained in an irradiation program for uranium alloys are described. Particular emphasis was given to some phenomena that occurred during the irradiation of the specimens, especially those occurring in adjusted uranium and U-rich alloys containing molybdenum. (auth)

21437 PHOTOVOLTAIC THEORY FOR A HOMOGENEOUSLY IRRADIATED SEMICONDUCTOR. Gold, Louis (Stevens Inst. of Tech., Hoboken, N. J.). Int. J. Electron., 19: 143-8(Aug. 1965).

An extension is made of an earlier consideration of simple model where the quanta were strongly absorbed in a surface layer small compared to the Debye length; the remaining bulk semiconductor was then treated as essentially in thermodynamic equilibrium. Another limiting case of tractable nature is developed for the circumstances where thermodynamic equilibrium no longer prevails. The concept of quasi-Fermi levels is employed with separate values for the holes and electrons, which complicates the mathematical analysis. A soluble model entails the restriction of constancy of the Fermi levels (weak dependency on charge concentration), which may be aided by having the bulk semiconductor uniformly bathed with quanta but relies upon cessation of current flow. Physically, the system considered is one where the weak absorption and/or extremely intense radiation permeates the material. The steady-state zero-current photovoltaic effect for a semiconductor subjected to strong illumination, which is only weakly attenuated, turns out to be mathematically tractable. Spatial variation of the electrostatic potential and the associated hole-electron densities, corresponding to a surface potential established by surface states and traps, is derived from a reduced Poisson-Boltzmann equation. The intrinsic or compensated semiconductor proves soluble in closed-form whereas the extrinsic case can be handled by recently

developed power series methods; the convergence of the latter is more or less assured in the region of physical interest, becoming questionable in the overly perturbed region where large shifts in the Fermi levels for the holes and electrons occur. (BBB)

21438 DEPTHS OF LOW-ENERGY ION BOMBARDMENT DAMAGE IN GERMANIUM. MacDonald, R. J.; Haneman, D. (Univ. of New South Wales, Sydney). J. Appl. Phys., 37: 1609-13(Mar. 15, 1966).

The depth of the damage induced in thin films ($\approx 10\mu$) of germanium by bombardment with low-energy ($\leq$1000 ev) argon ions was measured by a new technique. The method is based on the differences in sputtering yield for a given energy, between material previously damaged by a higher-energy bombardment and material previously undamaged. The change in yield when the previously damaged material is eroded away marks the depth of this region. The sputtering yield was obtained from changes in the resonant frequency of a piezoelectric quartz crystal on which the thin germanium films were deposited and annealed. The detector was sensitive to mass changes of 4×10^{-10} g/cm^2. The depth of the damaged region was found to be eight atomic layers when the damaging ions were of 400-ev energy increasing up to 25 atomic layers for damage induced by 1-kev argon ions. The extent of the damage induced by 1-kev argon ions was measured as a function of damaging ion dosage and found to saturate at doses of 1×10^{17} ions/cm^2 and greater. Analysis indicates the damage could be accounted for in part by embedded argon atoms. The depth of the damage was found also to depend on the film thickness in the case of very thin films. Effects of annealing treatments during film deposition are described. (auth)

21439 RECOMBINATION CENTERS IN GAMMA-IRRADIATED SILICON. Hirata, M.; Hirata, M.; Saito, H. (Osaka Univ.). J. Appl. Phys., 37: 1867-72(Mar. 15, 1966).

The minority carrier lifetime in gamma-irradiated silicon crystals was studied. The doping impurity was phosphorus, arsenic, or boron, and the crystals were either float-zoned or pulled from the melt. The silicon E center was found to be the dominant recombination center in float-zoned, n-type crystals after irradiation. The capture cross section of the center for holes was measured to be 1.1×10^{-13} cm^2 in phosphorus-doped silicon. The activation energy for annealing of an E center has been reported to be 0.94 ev, and the corresponding activation energy for the annealing in arsenic-doped crystals was found to be 1.5 ev. After annealing at 160°C, where the E center is known to anneal, the existence of some other energy level at about 0.4 ev below the conduction band was detected. In crystals other than float-zoned n-type, the A center governed the recombination. The cross section of this center was found to be 1.5×10^{-14} cm^2 for holes and 2×10^{-16} cm^2 for electrons. The introduction rate of the A center was found to be the same for a variety of samples. The value was 1.3×10^{-3} defects/cm^3 per photons/cm^2. (auth)

21440 DISCHARGE FIGURES IN DIELECTRICS BY ELECTRON IRRADIATION. Furuta, Junichiro; Hiraoka, Eiichi; Okamoto, Shinichi (Radiation Center of Osaka Prefecture). J. Appl. Phys., 37: 1873-8(Mar. 15, 1966).

The electrical breakage of glass shielding windows by intense gamma irradiation presents a severe problem for hot caves. To understand this phenomenon a study was made of the discharge conditions, their natures, and the decay of the accumulated electric charge by electron irradiation. The samples used were lead glass F62-R, nonbrowning lead glass F36-N, nonbrowning glass C-N, common window glass, polymethylmethacrylate (PMMA) and polyvinylchloride (PVC). Their specific gravities were 6.2, 3.6, 2.7, 2.5, 1.2, and 1.4 respectively. The samples were discharged by a steel needle pricking the surface prior to, or after, irradiation. The 2-Mev Van de Graaff generator and 15-Mev Linac were used in these experiments. The relation between irradiation doses and the largeness of discharge pattern in the samples and the decay of the discharge pattern after irradiation are described. The times in which the initial stored charge became its half-value were 30 min for PMMA, 70 h for PVC, 8 h for C-N and 90 h for F36-N. (auth)

21441 RECOIL GOLD ATOMS FROM FAST-NEUTRON BOMBARDMENT. Keller, Keaton; Lee, R. V. Jr. (Univ. of Arizona, Tucson). J. Appl. Phys., 37: 1890-2(Mar. 15, 1966).

Gold foils were irradiated with fast neutrons from a Pu-Be neutron source and the gold atoms knocked out of these foils were collected on aluminum foils. Sets of Au-Al foils were placed at various angles around the Pu-Be source. Some foil sets had the gold foil nearer the neutron source; some had the aluminum foil nearer. In this way, both the ejection of gold atoms from open-ended displacement spikes and the sputtering of gold atoms by fast neutrons could be studied. As was expected, no ^{198}Au was detected on the Al foils because of the small (n,γ) cross section of ^{197}Au. After neutron activation in a nuclear reactor, all the Al foils emitted the 0.412-Mev gamma ray of ^{198}Au. Calculations showed that each Al foil had approximately 10^{12} ^{197}Au atoms on it. Since the Pu-Be neutron source strength was known, the number of gold atoms ejected per open-ended displacement spike was calculated and found to be of the order of magnitude of 10^6. Focusing collisions may account for the large number of Au atoms per open-ended displacement spike. The sputtering ratio was found to be about 0.5 gold atoms sputtered per incident neutron. (auth)

21442 FISSION-FRAGMENT DAMAGE IN EPITAXIAL FILM OF URANIUM DIOXIDE. Nasu, Shoichi; Shiozawa, Ken-ichi; Kikuchi, Takeo (Japan Atomic Energy Research Inst., Tokyo). Jap. J. Appl. Phys., 5: 248(Mar. 1966).

Electron microscope observations of irradiated epitaxial uranium dioxide films were made in order to examine the effects of factors such as the crystallography or film thickness on fission fragment track registration. A transmission electron micrograph of an epitaxial film after irradiation is shown. The mosaic or island structure of the epitaxial film is considered significant in the registration of the fission fragment tracks. (J.F.P.)

21443 CHANGES IN ELECTRICAL POLARIZATION OF HIGH POLYMERS THROUGH THE ACTION OF IONIZING IRRADIATION. PART I. TRANSIENT CHANGES DURING IRRADIATION. Heyne, L.; Hauser, O. (Zentralinstitut fuer Kernforschung, Dresden). Kolloid-Z., 205: 39-46(Sept. 1965). (In German).

Dielectric properties of some polymers, as affected by ionizing irradiation, are considered, and some data on radioinduced changes in polytetrafluoroethylene, polyethylene, polytrifluorochloroethylene, and polystyrene are presented and compared with those relating to ceramics. The paraelectric susceptibility markedly increased when ionizing radiation acted on high polymers. The radioinduced polarization processes were interpreted on the basis of the formula of Schweidler with nearly all of the examined materials. The increase in the effective electrical conductivity of high polymers during irradiation was caused to a considerable degree by the induced paraelectric polarization processes which produced an increased conductivity of the so-called second kind. Also, the radioinduced change of the true conductivity contributed to the increase of the effective conductivity. The induced paraelectric susceptibility exerted an influence on the permittivity, its magnitude, and its dependence on time. The dielectric susceptibility (due to polarization by deformation) was changed only slightly as a consequence of irradiation. (BBB)

21444 RELEVANCE OF BOMBARDMENT-INDUCED MOESSBAUER EFFECTS IN IRON TO RADIATION DAMAGE THEORIES. Goldberg, D. A.; Lee, Y. K.; Ritter, E. T.; Stevens, R. R. Jr.; Walker, J. C. (Johns Hopkins Univ., Baltimore). Phys. Lett., 20: 571-3(Apr. 1, 1966).

Recent experimental work studying bombardment-induced Mössbauer effects in various targets can be related to

many-body calculations of radiation damage phenomena by Vineyard and collaborators. Such dynamical models appear more relevant to this work than macroscopic or thermal ones. (auth)

21445 RESISTIVITY RECOVERY OF DILUTE ALLOYS OF SILVER, COPPER, AND GOLD, PROTON-IRRADIATED AT 80 DEG K. Grenning, D. A.; Koehler, J. S. (Univ. of Illinois, Urbana). Contract AT(11-1)-1198. Phys. Rev., 144: 439-57(Apr. 15, 1966). (COO-1198-307).

Ag-Be, Ag-Li, Cu-Be, Au-Mg, and Au-Al were irradiated by 12-Mev protons at 80°K. High-resolution isochronals were then obtained from -130 to 90°C and activation energies were determined every 10°C using the change-of-slope method. The order associated with the reaction kinetics was determined at temperatures appropriate for the various annealing peaks by fitting 240-min isothermal anneals to first or second order. The recovery of the silver and copper alloys showed remarkable similarity to pure silver and copper, but the gold-alloy recovery was markedly altered as compared with pure gold. Activation energies for the stage-III defect in silver copper, and gold alloys were found to be 0.64, 0.71, and 0.70 ev, respectively. The copper and silver alloys had a small first-order recovery stage near the low-temperature side of the main stage-III annealing peak. The main stage-III peak obeyed second-order kinetics in all cases. In the gold alloys the stage-III recovery was composed of a main second-order annealing peak with a small second-order annealing peak on each side of the main peak. These annealing results were fitted to the various models for the recovery of damage, and some conclusions are drawn. (auth)

21446 EFFECTS OF RADIATION ON TRANSMITTANCE OF GLASSES AND ADHESIVES. Campbell, F. J. (Naval Research Lab., Washington, D. C.). pp 19-22 of Proceedings, 17th Annual Power Sources Conference. Red Bank, N. J.; PSC Publications Committee, 1963.

The effects of 1.0-Mev electrons, 4.6-Mev protons, and mercury-arc u-v radiation on the spectral transmittance of several adhesives and glasses were investigated. The effect of a decrease in spectral admittance on the conversion efficiency of a solar-cell assembly was also evaluated. (D.C.W.)

21447 DEFECT PRODUCTION IN COPPER, NICKEL, AND GOLD BY 5-Mev α BOMBARDMENT IN THE TEMPERATURE REGION 90 TO 194 DEG K. Lueck, G.; Sizmann, R. (Univ., Munich). Z. Angew. Phys., 20: 289-94 (1966). (In German).

The recombination volume α_0 of a Frenkel pair can be determined by the irradiation of metals with fast charged particles at low temperatures. α_0 means the number of lattice sites around a vacancy on which an interstitial recombines spontaneously with this vacancy. Results are presented from the irradiation of annealed copper, gold, and nickel, and of strongly cold-worked copper, at temperatures between 90 and 194°K (stage II) using 5.3-Mev α particles. For copper α_0 was found to increase by ~70% with increasing temperature. The primary production rate of Frenkel defects J_0 (which is not identical with the initial production rate) however, decreases by ~70% with rising temperature. (auth)

PHYSICS

General

Refer also to abstract 21726.

21448 MEASUREMENT OF THE STATISTICS OF SECONDARY ELECTRON EMISSION. Delaney, C. F. G.; Walton, P. W. (Univ. of Dublin). IEEE (Inst. Elec. Electron. Eng.), Trans. Nucl. Sci., NS-13: No. 1, 742-6 (Feb. 1966).

An apparatus for the direct measurement of the statistics of secondary electron emission (the frequency distribution in the number of secondaries produced by individual primary particles) is described. The secondary electrons are accelerated to about 50 kev and are focused onto a cooled silicon semiconductor detector. Unless a correction is made for the adverse effect of backscattering of electrons from the detector (up to 37%), the resolution of the system does not reach the expected value. A method by which these scattered electrons are returned to the detector by a magnetic field is described. The resolution of the system is then sufficient to distinguish clearly between the groups even when they contain as many as 15 electrons. Experimental results are compared with theory for secondary electrons produced by an alpha particle emerging from an aluminum foil. Preliminary results obtained with an image intensifier transmission dynode are also shown. (auth)

21449 CHARGE DENSITY WAVES IN A RADIAL ELECTRON FLUX. Korotun, L. I. (Inst. of Radiophysics and Electronics, Academy of Sciences, Ukrainian SSR). Izv. Vyssh. Ucheb. Zaved., Radiofiz., 9: 126-34(1966). (In Russian).

With regard for the hydrodynamic pressure the waves are being considered of the charge density in an electron flux with radial divergence of particles, possessing constant as well as variable velocity. The spatial variation character was studied of the main wave parameters. The onset of the instability is shown to be possible at the definite variation law of the nonperturbated flux velocity. Increments and phase velocities of growing waves are shown to be dependent on temperature under sufficiently high temperatures. (auth)

21450 EXPERIMENTAL INVESTIGATION OF TROCHOIDAL BUNCHING WITH HIGH SPACE CHARGE, IN CROSSED ELECTRIC AND MAGNETIC FIELDS. Mel'nichenko, A. A.; Flyagin, V. A. (Gor'kii State Univ., USSR). Izv. Vyssh. Ucheb. Zaved., Radiofiz., 9: 135-45 (1966). (In Russian).

The results are given of an experimental investigation of the trochoidal large preveance beams, formed in crossed electric and magnetic fields. By means of a sounding-ribbon electron beam, inserted into the system along the magnetic field, the external beam characteristics and the voltage distribution of an electric field were determined, in dependence of the current value of the beam. (auth)

21451 INVESTIGATION OF INSTABILITY (DIOCOTRON AMPLIFICATION) OF SMALL ELECTRON FLUXES IN CROSSED FIELDS. Gurzo, V. V.; Kulikov, M. N.; Stal'makhov, V. S. Izv. Vyssh. Ucheb. Zaved., Radiofiz., 9: 146-54(1966). (In Russian).

The results are presented of an experimental investigation of the diocotron amplification in the fine electron fluxes, moving in crossed fields. The amplification factor is compared with the form of an electron flux. A comparison was carried out of the experimental data with theoretical results and the boundaries for the linear operating conditions were determined. The investigation was made of the main characteristics of an electron wave M-type amplifier with the fine beam. (auth)

21452 DECAY OF SPACE-CHARGE WAVES ON ELECTRON BEAMS. Gunshor, R. L. (Rensselaer Polytechnic Inst., Troy, N. Y.). J. Appl. Phys., 37: 1904-11(Mar. 15, 1966).

The decay of space-charge waves with distance is observed in an electron beam with a velocity spread. This effect has previously been attributed to spatial Landau damping. Landau's theory is extended to include finite diameter electron beams and to calculate the steady-state damping of the fast and slow space-charge waves using measured axial velocity distributions. For a density modulated beam injected from a shielded cathode, it is found that the fast wave does not exhibit Landau damping, while the slow wave is damped of the order of 0.1 dB per plasma wavelength. It is concluded that the large initial damping observed by Mihran is due to a ballistic or free-streaming process, and is not primarily due to Landau damping as calculated for the steady-state regime. (auth)

21453 PERTURBATION METHOD FOR THE CLASSICAL TIME-DEPENDENT PAIR CORRELATION FUNCTION. Aronson, Raphael (New York Univ., New York). J. Math. Phys. (N. Y.), 7: 589-602(Apr. 1966).

A perturbation technique useful for computing many-time thermal averages of classical quantities is developed. The canonical distribution function for the system is shown to evolve isothermally from that for a free-particle system as the interaction is switched on slowly. This permits convenient use of an interaction picture in which to perform thermal averaging. The technique is applied to the calculation of the time-dependent pair correlation function in position for a uniform gas. The correlation function is shown to be a sum of two components, one the solution of a kinetic equation and essentially a generalization of the autocorrelation in equilibrium, the other a generalization of the mutual correlation function in equilibrium. The equations arise as sums over diagrams. The equations resulting from the random phase approximation, valid for the short-time behavior, are solved exactly. It is shown directly that the generalized dielectric function given in terms of the correlation function is identical with that found by solution of the kinetic equation in the random phase approximation for all frequencies. (auth)

21454 ON THE MOTION OF A CHARGED PARTICLE IN A MAGNETIC FIELD. Sen Gupta, N. D. (Tata Inst. of Fundamental Research, Bombay). Nuovo Cimento (10), 42B: 121-49(Mar. 11, 1966).

A discussion is given of some general properties of the motion of a charged particle in a steady magnetic field by considering the Hamilton-Jacobi characteristic function. An attempt is made to derive all the admissible adiabatic invariants directly from the characteristic function. It is established that the orbit is a geodesic on the integral surface, which is orthogonal to the equipotential surfaces. Next the connections between orbits lying close to each other are investigated; the relation between the flux intercepted by the particle and its time of flight in some special cases has been studied. The nature of motion and that of the orbit in a slowly varying field, e.g., $B_i(x) = B_i^0 + b_{ik}x_k$ in general and with special geometry, namely when the direction of projection of the particle is one of the principal axes of the field gradient tensor, are examined in detail. This is supplemented with the study of motion in the neighborhood of a neutral point. (auth)

21455 SMALL SIGNAL ENERGY CONSERVATION THEOREM FOR MULTIVELOCITY ELECTRON BEAMS. Bobroff, D. L. (Raytheon Co., Waltham, Mass.). Phys. Fluids, 9: 809-12(Apr. 1966).

The small signal energy conservation theorems for one-dimensional multivelocity electron beams are obtained for both the Boltzmann and the multistream descriptions. The relation between the theorems in the two descriptions is discussed. (auth)

21456 PULSE EXCITATION OF A MAGNETIC FIELD WITHIN A CYLINDRICAL SHIELD. Vitkov, M. G. Zh. Tekh. Fiz., 35: 1786-90(1965). (In Russian).

The magnetic field induced by a constant azimuthal current of sudden onset on the surface of a cylinder of radius a in the presence of a coaxial cylindrical shield of inner radius b and thickness d of material with given conductivity and permeability is calculated. The case of a < b is discussed. The problem is treated with the aid of the Laplace transformation, and the field is assumed to be propagated. At the initial instant it is the v-h-f components that are significant and the magnetic field within the inner cylinder is reduced from the value it would have in the absence of the shield by the factor $1 - (a/b)^2$. The subsequent development of the field in time is expressed as an infinite series. Approximate expressions are obtained in closed form for the magnetic field at times close to the initial instant when the current is switched on for the two limiting cases of a magnetically thin and a magnetically thick shield, and solutions for a number of other cases are presented graphically. (ATD)

21457 MASS SPECTROMETRIC INVESTIGATION OF A SOURCE OF POSITIVE IONS OPERATING AT A LOW GAS PRESSURE. Ekhichev, O. I.; Zinchenko, G. N.; Zinchenko, N. S.; Karnaukhov, I. M.; Slabospitskii, R. P. Zh. Tekh. Fiz., 35: 1897-1901(1965). (In Russian).

Tests of an ion source which operates at gas pressures from 10^{-4} to 10^{-6} mm Hg are reported. The ion source employs an electron gun using a flat tungsten-barium cathode with a 2-mm diameter emitting surface, a focusing electrode, and a plane-accelerating electrode located 0.5 cm from the cathode and having a 2-mm diameter opening through which the electrons enter the ionizing region. The electron beam is caught on a flat collector located 6 cm from the gun. A negative potential is applied to the collector so that ions formed in the region between the gun and the collector are attracted toward the collector and enter the accelerating tube through a 5-mm-diameter opening in the electrode. In the accelerating tube the ions were accelerated to 40 kev and focused on a point 150 cm distant. The focusing problem was somewhat complicated by the fact that the ions entered the accelerating tube with a rather wide range of energies, owing to the design of the ion source. Two different focusing systems were designed and tested, one employing an immersion lens and one employing two successive accelerating gaps. The design of these systems, which was accomplished with the aid of conventional design equations, is discussed at some length. Both performed satisfactorily. It was anticipated that owing to the low pressure in the ionizing region the production of multiply charged ions by successive ionization would be negligible. In order to test this the currents of singly and doubly charged ^3He ions were measured with a mass spectrometer as functions of the pressure of ^3He in the ion source. Both currents increased linearly with the pressure, and at the same rate, for pressures up to 10^{-4} mm Hg. The ratio of the He^{++} to the He^+ current was 5×10^{-3}; this is in good agreement with the known ratio of the corresponding cross sections for ^4He. The maximum He^{++} current obtained was 0.02 μamp; this current was obtained with an electron beam current of 10 mamp and a ^3He pressure of 10^{-4} mm Hg. The H^+ and H_2^+ ion currents were also measured when the ion source contained H_2. Both currents increased linearly with pressure for pressures up to 5×10^{-5} mm Hg, but deviations from linearity were observed at higher pressures. (ATD)

21458 PROCEEDINGS OF THE CONFERENCE ON PHOTOGRAPHIC AND SPECTROSCOPIC OPTICS, TOKYO AND KYOTO 1964. Jap. J. Appl. Phys., 4: Suppl. 1, 1-669(1965). (CONF-665).

Papers (111) are included dealing with aberration theory, lens design and testing, optical transfer functions, image formation, optical materials, far infrared instrumentation and spectroscopy, interference spectroscopy, vacuum u-v instrumentation and spectroscopy, infrared materials, optical gratings, solid-state spectroscopy, and laser spectroscopy. (D.C.W.)

Accelerators

Refer also to abstracts 21588 and 21948.

21459 (AD-623509) MEASUREMENTS AT HIGH FIELD STRENGTHS ON SUPERCONDUCTING ACCELERATOR CAVITIES. Schwettman, H. A.; Wilson, P. B.; Churilov, G. Y. (Stanford Univ., Calif. High-Energy Physics Lab.). June 1965. Contract Nonr-22567. 11p. (HEPL-392). CFSTI $1.00 cy, $0.50 mn.

High electric field strengths were produced in two superconducting r-f cavities with electroplated lead surfaces. The cavities operate near 2856 MHz in modes which are useful for particle acceleration. In a cylindrical cavity operating in the TM010 mode a Q of 2.5×10^8 was obtained at 2K. At a power input into the cavity of 2.5 watts a maximum electric field strength on the axis of about 100,000 volts/cm was produced. Also tested was a resonant section of disk-loaded accelerator structure three periods in length operating in the $2\pi/3$ mode. In this cavity a maximum electric field of 150,000 volts/cm was obtained. In both cavities the electric field strength appeared to be limited by electron loading due to field emission. Radiation, which at times exceeded 100 mR/hr, was measured in the vicinity of the cavities. The radiation provides indirect evidence of strong accelerating fields. (auth)

21460 (AD-623659) SUPERCONDUCTING RACE-TRACK MICROTRON. Wiik, B. H.; Schwettman, H. A.; Wilson, P. B. (Stanford Univ., Calif. High-Energy Physics Lab.). Sept. 1965. Contract Nonr-22567. 15p. (HEPL-396). CFSTI $1.00 cy, $0.50 mn.

A race-track microtron is proposed consisting of two 180 degree magnets spaced 2.5 meters apart with a superconducting linac section between. The magnets are two meters in diameter with a homogeneous field of 8 kilogauss. The linac section will operate at 1.2 kmc and provide an energy gain of 10 Mev per turn. The electrons are injected into the microtron at about 12 Mev from a second superconducting accelerator section. The spacing between orbits is 8 cm. Thus vertical and radial focusing can be provided on any orbit by quadrupoles placed in the field-free region between the magnets. The phase error due to the fringing fields of the magnets was calculated and can be compensated. An energy resolution of 0.001 is expected. Using superconducting linac sections, a beam current of 100 microamps at unity duty cycle is feasible. It is also possible to build the microtron using conventional linac sections. For such a machine a duty cycle greater than one percent is reasonable. (auth)

21461 (AD-624038) ELECTRON ENERGY MEASUREMENTS OF THE RACETRACK MICROTRON BEAM. Sells, V.; Froelich, H.; Brannen, E. (Racetrack Microtron Group, Univ. of Western Ontario, London). Jan. 1965. Contract AF-AFOSR-297-63. 65p. (AFOSR-65-1627). CFSTI $3.00 cy, $0.75 mn.

The momentum spread in the beam of a racetrack microtron was measured using a high resolution beta ray spectrometer. The design of the semicircular double focusing magnetic spectrometer is described. A method of continuous magnetic field measurement in the spectrometer is discussed. The object and image positions relative to the entrance and exit planes of the spectrometer were calculated. The momentum spread in the electron beam of the accelerator as taken directly from the spectrometer was 0.41% at the half width position (full width at half intensity); 0.62% at half current; 1.28% at 90% current and 1.86% at 100% current. These values may be corrected for the natural line width of the spectrometer whose theoretical base spread was 0.16%. With these corrections the upper limit of the energy spread in the 6.0-Mev beam is 22 kev at half width; 34 kev at half integrated current; 73 kev at 90% current and 110 kev at 100% current level. (auth)

21462 (BNL-948) PROCEEDINGS OF THE SUMMER STUDY GROUP ON THE PHYSICS OF THE EMPEROR TANDEM VAN DE GRAAFF REGION, JUNE 21-JULY 16, 1965. VOLUMES I, II, AND III. (Brookhaven National

Lab., Upton, N. Y.). Contract AT-30-2-GEN-16. 1270p. Dep. mn. CFSTI $16.14 cy, $5.00 mn.

Issued in three volumes, but cataloged as a unit.

Separate abstracts were prepared for 25 sections of the proceedings, which are in three volumes. (D.C.W.)

For abstracts of individual sections see: 21026, 21463, 21464, and 21971–21992.

21463 (BNL–948, pp 685-91) THE BNL LOW-ENERGY NUCLEAR ACCELERATOR PROGRAM. Alburger, David E. (Brookhaven National Lab., Upton, N. Y.).

The small Van de Graaff accelerator is briefly discussed, and the research program in low-energy nuclear physics is outlined. The background of the proposal for a Double Emperor Tandem Van de Graaff facility is summarized. (D.C.W.)

21464 (BNL–948, pp 692-703) THE BNL DOUBLE EMPEROR TANDEM FACILITY. Wegner, Harvey E. (Brookhaven National Lab., Upton, N. Y.).

The cyclotron and tandem facilities at Brookhaven National Laboratory are discussed. A brief description is given of the 60-in. cyclotron which is now being modified to a spiral-ridge variable-energy form and of the Double Emperor Tandem Van de Graaff Accelerator which is to be constructed. (D.C.W.)

21465 (CERN–65-32, pp 31-4) THE NEUTRINO EXPERIMENT AT THE ZGS. Novey, T. B. (Argonne National Lab., Ill.).

Diagrams representing the status of the experimental arrangement for neutrino experiments at the ZGS are presented. (B.G.D.)

21466 (CERN–65-32, pp 127-30) OUTLINE OF AIMS OF PROGRAMMES TO RAISE BEAM INTENSITY OF ACCELERATORS. (European Organization for Nuclear Research, Geneva (Switzerland)).

An outline of aims of programs to raise beam intensity of accelerators at Brookhaven, Argonne, Serpukhov, and at CERN is presented. (B.G.D.)

21467 (CERN–66-8) SERVO CORRECTION OF PHASE CHANGES BETWEEN DEFLECTORS IN THE R.F. SEPARATOR. Bramham, P. (European Organization for Nuclear Research, Geneva (Switzerland)). Feb. 17, 1966. 34p. Dep. mn.

Operation of a r-f particle separator requires a stability of r-f phase between deflecting cavities to two or three degrees. Most of the phase changes which occur are sufficiently slow to be corrected by a servo system involving a motor-driven waveguide phase shifter. Information to turn the motor is supplied by a phase comparison bridge connected to the cavities. The various component units of the system are described, and an analysis was made of its performance. (auth)

21468 (CERN–66-10) COLLIMATORS FOR THE RF SEPARATED BEAM. Fortune, R. D. (European Organization for Nuclear Research, Geneva (Switzerland)). Feb. 23, 1966. 15p. Dep. mn.

The design of a collimator incorporating the following features is described; remote control and direct digital indication of jaw position to a precision of ±0.1 mm, independent jaw movement allowing eccentric beam setting, monitoring of beam position by means of scintillation counters attached to the jaws, automatic closure, and especially designed microswitches of negligible degassing rate for use as limit switches inside the collimator vacuum box. (M.O.W.)

21469 (LNF–66/10) A PROPOSAL FOR THE ADMINISTRATION OF RADIATIVE CORRECTIONS. Note No. 310. Etim, Etim; Touschek, B. (Laboratori Nazionali di Frascati, Comitato Nazionale per l'Energia Nucleare (Italy)). Mar. 2, 1966. 12p. Dep. mn.

Applying the ideas of Lomon to the problem of administering the radiative corrections for the work with Adone, the adoption of the following procedure is discussed. (1) The theoretical effort should be concentrated on the determination of the first order radiative corrections for a standard experiment in which photons of energy less than $K \simeq 0.1E$ are considered unobservable. The omission of higher terms in the determination of this cross section involves an error of less than 1.5%. (2) The completion of the determination of radiative corrections in which detailed account is taken of the special arrangement of every experiment is left to the experimenter, who by the time the first experiments go into the machine should find at his disposal a computer program, ready to digest any experimental situation expressed in terms of a single function ∂ (P) of a 4-momentum variable P. The error which accrues from the second part of the program is due to the inaccuracy of the Bloch Nordsieck method and can be estimated to be $K\beta/E \lesssim 0.7\%$, so that the total error committed by applying the proposed procedure should be less than 2%. (auth)

21470 (PB–181506, pp 116-29) THREE-DIMENSIONAL DOSE DISTRIBUTION IN SAMPLES IRRADIATED BY ELECTRON BEAMS. Brynjolfsson, Ari (Danish Atomic Energy Commission, Risoe, Research Establishment).

A ^{60}Co irradiation facility with a maximum output of 5 kw and maximum electron energy of 15 Mev is described. Beam parameters and dose distribution for the accelerator are given. Experimental arrangements for dose distribution measurements in water, aluminum, wood, lucite, copper, and iron with improvements in dose uniformity and efficiency are illustrated. (P.C.H.)

21471 (PPAD–577D) LONGITUDINAL INSTABILITY THRESHOLDS IN WEAK-FOCUSING PROTON SYNCHROTRONS. Pease, Robert L. (Princeton-Pennsylvania Accelerator, Princeton, N. J.). Dec. 28, 1965. Contract AT(30-1)-2137. 27p. Dep. mn. CFSTI $2.00 cy, $0.50 mn.

The dispersion equation of Neil and Sessler is used as a starting point. There is first shown the mathematically correct but physically ridiculous result that, by an extremely slight variation in particle density distribution across the vacuum chamber, the resistive instability can be changed from incurable to absent, i.e., its threshold from zero particles to an infinite number of particles. A more thorough analysis is then made using Nyquist and modified Nyquist diagrams. The preceding argument is demolished, and it is found in general that, if the density distribution corresponds to somewhere near the most stable operation, the thresholds and optima for negative mass and for resistive instabilities are essentially the same. (auth)

21472 (RHEL/R–113) COMPUTER PROGRAMS USED FOR DESIGN CALCULATIONS ON THE HARWELL VARIABLE ENERGY CYCLOTRON. Mayhook, A. R. (National Inst. for Research in Nuclear Science, Chilton (England), Rutherford High Energy Lab.). Nov. 1965. 56p. Dep. mn.

A system of computer programs was written for doing calculations involved in the design and operation of the Harwell Variable Energy Cyclotron. The programs process field measurements from the magnetic field survey and use the results to predict the magnetic fields in the cyclotron and to compute particle trajectories in these fields. A description of the programs, including underlying theory and a brief outline of the structure of each routine, and also all information required to run the programs are included. (auth)

21473 (UCOL–535–554) STATUS REPORT FOR THE UNIVERSITY OF COLORADO ISOCHRONOUS CYCLOTRON, FEBRUARY 1966. Lind, D. A. (Colorado Univ., Boulder. Nuclear Physics Lab.). Contract AT(11-1)-535. 12p. Dep. mn. CFSTI $1.00 cy, $0.50 mn.

Operation of the Colorado Isochronous Cyclotron is discussed in terms of the following; performance, magnets and power supplies, r-f system, ion source, deflector-septum magnetic channel and external beam system, cyclotron modifications being conducted, and the external beam system and optics. (M.O.W.)

21474 (UCRL–16553) BEVATRON OPERATION AND DEVELOPMENT. 46. APRIL–JUNE 1965. Crebbin, Kenneth C. (Lawrence Radiation Lab., Univ. of California, Berkeley). Feb. 16, 1966. Contract W-7405-eng-48. 12p. Dep. mn. CFSTI $1.00 cy, $0.50 mn.

The Bevatron provided beam for physics research 85% of the scheduled operating time. The first extraction magnet in the external proton beam system was replaced because of a short to ground. Two primary experiments were ended this quarter, one primary experiment was continued through this quarter, and one new primary experiment was started. (auth)

21475 (SLAC-Trans-38) NUMERICAL CALCULATIONS ON THE SPACE-CHARGE EFFECTS IN A STORAGE RING FOR ELECTRONS AND POSITRONS. Bassetti, M. (Laboratori Nazionali di Frascati, Comitato Nazionale per l'Energia Nucleare (Italy)). Translated by S. Immirzi (Stanford Linear Accelerator Center, Stanford Univ., Calif.), from report LNF-62/35. 1962. 44p. Dep. mn. JCL $4.60 fs, $1.52 mf.

The space-charge effects were examined only in relation to the vertical betatron oscillations. The following approximations were used; the calculations are carried out per unit of radial length as if the beam were infinitely wide and radially uniform, and the dimensions of the beams along the curvilinear abscissa of the machine are small in comparison with the wavelength of the vertical betatron oscillations. This is the so-called thin lens approximation. (M.O.W.)

21476 RADIAL EXPANSION OF A BEAM IN A ELECTRON LINEAR ACCELERATOR INDUCED BY ASYMMETRIC WAVE. Voskresenskii, G. V.; Koroza, V. I.; Serebryakov, Yu. N. At. Energ. (USSR), 20: 3-8(Jan. 1966). (In Russian).

The mechanism of the radial oscillations of an electron beam in linear accelerators with large currents was investigated. The calculation was based on the examination of the properties of the hybrid asymmetric waves in the retarding structure of the accelerator and the examination of the excitation of these waves with electron beams. The electron dynamics in the field of asymmetrical waves, excited by particle beams, were investigated. It was shown that the amplitude of the radial displacement from the axis increases as a function of the injection time almost exponentially if the attenuation of the field in the retarding structure is neglected. The effect of the displacement on the dynamics of the radial motion of the particles was evaluated. (tr-auth)

21477 RADIOGRAPHY WITH THE ELECTRON LINEAR ACCELERATOR. Kimura, Hiroshi; Kuroda, Kunishige (Hitachi Ltd., Japan). J. N.D.I. (Jap.), 14: 239-44(June 1965). (In Japanese).

An electron linear accelerator known as the Mark I linac has been tested to determine its capabilities for industrial radiography of steel over 30 cm in thickness. The linac is driven by a magnetron RK7529 (S-band, peak RF output power of 4 mw) and has the following specifications: maximum energy 8 Mev, peak current 150 mamp, beam pulse width 1.7 μs, maximum repetition 360 pps, and x-ray intensity 1500 r/min at 1 m. The penetrameter sensitivity is less than 1% for 10 to 40 cm thick steel; the half intensity angle of x-ray distribution is 10.5–13.5°; the half value layer for steel is 2.7 cm; and exposure time is 28 min for 40 cm thick steel. The electron beam diameter, which is measured by scanning Faraday-cup is 9–10 mm ϕ at the end of the tube and focused to 3 mm ϕ at the end of the extension tube with the Q-magnet system. For the radiography of more than 20 cm thick steel, the scattered radiation must be shielded. The accelerator was used successfully for the radiography of the bucket runners for the 14,000 Kw Pelton wheel. (TCO)

21478 ON SOME OPERATING FEATURES OF PLASMA EXPANSION ION SOURCE. Tawara, Hiroyuki (Hitachi Ltd., Tokyo). Jap. J. Appl. Phys., 5: 208-14(Mar. 1966).

In order to produce a well-focused high-intensity ion beam, tests were made on a plasma-expansion ion source, in which the ion beam is extracted from the expanded plasma boundary formed in the plasma expansion electrode which is attached to the anode plate of the Duoplasmatron ion source. The effect of the plasma-expansion electrode length on the ion-beam focusing was investigated. It is shown that the use of longer plasma expansion electrode results in obtaining a well-focused high-intensity ion beam. In such a plasma expansion ion source, a 250 mamp pulsed hydrogen ion beam with a half-angle divergence of 180 mrad was obtained at an extraction voltage of 25 kv. (auth)

21479 TRANSPORTABLE VACUUM APPARATUS. Szalok, Mihaly; Peter, Istvan. Magyar Tud. Akad. Kozp. Fiz. Kut. Int. Kozlem., 13: 355-61(1965). (In Hungarian).

A vacuum car developed for evacuating the target space in particle accelerators is described. At the inlet of the vacuum pump pressures down to 10^{-6} Torr can be achieved, the pumping speed is 60 l/sec. The car can be operated both directly and by remote control from the control desk of the accelerator. The individual units of the car, like the diffusion pump, cold trap, valve-block are described in detail, and the operational experiences are discussed. (auth)

21480 ENGINEERING OF THE EG-2 ION-ACCELERATOR CHANNEL. Horvath, Bela. Magyar Tud. Akad. Kozp. Fiz. Kut. Int. Kozlem., 13: 377-86(1965). (In Hungarian).

Design and principle of the built-in mechanical devices for the engineering of the 2-Mev Van de Graaff-type ion accelerator channel are described. (auth)

21481 THE INFLUENCE OF THE MAGNETIC FIELD GRADIENT ON THE POSITION AND THE POLARIZATION OF A POLARIZED PARTICLE IN CIRCULAR MOTION. Lu, P. (Arizona State Univ., Tempe). Nuovo Cimento (10), 42B: 150-7(Mar. 11, 1966).

An estimate is given of the classical motion for a charged spin-$\frac{1}{2}$ particle with an anomalous magnetic moment moving in a magnetic field by including the effect of the first-order field gradient. (auth)

21482 THE LIFETIME OF ELECTRON TRAJECTORIES IN FOCUSSED MAGNETIC FIELDS. [PART] II. Bundke, W. (Univ., Frankfurt am Main). Z. Angew. Phys., 20: 282-4(1966). (In German).

A simple formula was given previously for the strength of focusing during motion of a charged particle in a magnetic guiding field. The number of particles, which can be drawn out of the potential mould by a determined voltage was represented by a diagram. The lifetime of motion of electrons is measured, and the effect of pressure in the vacuum chamber on lifetime is measured in the same way and given by diagrams. (auth)

21483 ASYMPTOTIC SOLUTION OF A DIFFUSION PROBLEM AND ITS APPLICATION TO THE THEORY OF CYCLIC PARTICLE-STORAGE DEVICES. Bakai, A. S.; Lyubarskii, G. Ya.; Rozhkov, V. V. Zh. Tekh. Fiz., 35: 1525-31(1965). (In Russian).

It is shown largely by verbal arguments that if a system has an asymptotically stable orbit and is destroyed when its representative point crosses a certain closed surface in phase space, then under certain conditions its mean lifetime when it is subjected to stochastic forces can be calculated by finding the smallest eigenvalue and the corresponding eigenfunction of the Fokker-Planck-Kolmogorov operator that describes its motion. This method is employed to calculate the mean lifetime of a charged particle in a storage ring when it is subjected to stochastic forces arising from collisions with residual gas molecules and from the quantum nature of the radiation process. The equations for the radial and the phase oscillations are assumed to linear and the stochastic forces to be uncorrelated. The corresponding Fokker-Planck-Kolmogorov operator is derived and it is shown that the eigenvalue problem allows separation of variables. The smallest eigenvalue and its eigenfunction are calculated by a perturbation method that depends on the damping constants in the equations of motion being large. Formulas are presented for the distribution of the accumulated particles and for the mean lifetime of a particle. (ATD)

21484 ABERRATION AND DISPLACEMENT OF A BEAM BY A MAGNETIC PRISM FRINGE FIELD THAT DOES NOT VARY TRANSVERSELY. Malov, A. F. Zh. Tekh. Fiz., 35: 1617-20(1965). (In Russian).

The effect of a fringe field on charged particle trajectories is calculated. The magnetic field is assumed to be everywhere parallel to the z-axis of a Cartesian coordinate system xyz and its strength is assumed to be a known function of x only. The portion of the field in the region $x > 0$ is regarded as the fringe field. The effect of the fringe field on the trajectory of a particle which moves in the x-y plane, leaves the main field (i.e., crosses the y-z plane) at the point $(0, y_0, 0)$, and in the absence of the fringe field would cross the x-axis at a distance a from the origin is calculated. The slope y_0/a of the unperturbed trajectory, which is also the slope of the perturbed trajectory where it crosses the y-z plane, is denoted by y'_0. In this calculation it is assumed that the integral from x = 0 of dx/R is small, where R is the radius of curvature of the trajectory in the fringe field. An expression involving a single integration is derived for the ordinate y(a) of the point at which the perturbed trajectory crosses the x = a plane. The quantity y(a) is called the displacement of the beam. A similar expression is derived for $dy(a)/dy'_0$. The quantity $(dy(a)/dy'_0)dy'_0$ is called the aberration. (ATD)

21485 ON THE MOTION OF A CHARGED PARTICLE IN THE FIELD OF A RETARDED PLANE ELECTROMAGNETIC WAVE. Bonch-Osmolovskii, A. G. Zh. Tekh. Fiz., 35: 1757-61(1965). (In Russian).

The acceleration of an electron in a longitudinal magnetic field by a plane electromagnetic wave propagating in a medium whose refractive index varies in such a way that the phase velocity of the wave remains everywhere equal to the velocity of the electron is discussed. The refractive index gradient is assumed to be small compared with the reciprocal wavelength. It is shown that under these conditions the electron will not be accelerated by the field of a plane or circularly polarized wave but that acceleration would occur in a quasi-azimuthally polarized field. It is suggested that a field of the requisite type might be achieved with the aid of a number of suitably polarized laser beams propagating along generators of the cylinder on which the electron executes its helical motion in the longitudinal magnetic field. Even when the field is such as to accelerate the electron there is no constant asymptotic phase such as there is in the usual traveling-wave linear accelerator; the electron energy will therefore remain limited unless the refractive index continues to vary over the full length of the device. The motion is said to be stable, but this is not proved. (ATD)

21486 NONLINEAR RESONANCES $\nu_r = (Nn/q) + \Delta$ IN AN ISOCHRONOUS CYCLOTRON. Belov, V. P. Zh. Tekh. Fiz., 35: 1791-8(1965). (In Russian).

The radial betatron resonances Nn/q of an N-element isochronous cyclotron (n and q are integers) are discussed for arbitrary structure of the magnetic field. The differential equation for the orbit in the median plane is written in a form involving the Taylor series expansion coefficients of the axial magnetic field and is solved for the equilibrium orbit in the second approximation in the Fourier coefficients describing the azimuthal variation of the magnetic field. The differential equation for the deviation from the equilibrium orbit is written, and from it the so-called contracted Bogolyubov-Krylov equations are derived by the averaging technique. A first integral of these equations is obtained in the low-amplitude approximation. The stationary amplitudes and phases of the betatron oscillations are derived, their stability is discussed, and the width of the resonance is calculated. The invariant is derived for the special case of a steep-spiral cyclotron. (ATD)

21487 FOCUSING OF AN INTENSE ELECTRON BEAM IN AN ACCELERATOR TUBE. Meshkov, I. N.; Chirikov, B. V. Zh. Tekh. Fiz., 35: 2202-11(Dec. 1965). (In Russian).

The spreading of a laminar beam of relativistic electrons under the influence of its own space charge and a longitudinal accelerating field is discussed. The beam is assumed to be sharply bounded and the trajectory of the limiting electron is calculated for the case of an axially symmetric beam and for that of a flat beam. The longitudinal component of the field due to space charge is neglected. The trajectory is first calculated for the case of zero accelerating field, and then for that of a uniform accelerating field. For the second calculation the differential equation of the trajectory is "linearized", i.e., it is assumed that the lateral displacement of the electron is small and terms of the second and higher order in this displacement are dropped from the differential equation. The results of these calculations are presented graphically in terms of dimensionless variables. The case of a spatially periodic (sinusoidal) accelerating field superimposed on a much stronger constant field is then discussed. It is assumed that the period of the periodic component is short, and the solution is effected by separating the dependent variable (the lateral displacement of the trajectory) into slowly-varying and rapidly-varying components. The focusing effect of the periodic field is discussed and it is shown that in the nonrelativistic limit the results are in agreement with those of A. M. Clogston and H. Heffner (J. Appl. Phys., 25: 436(1954)) and Ping King Tien (J. Appl. Phys., 25: 1281(1954)). The behavior of the beam in a spatially periodic accelerating field, which is alternately zero and twice its average value, is discussed. (ATD)

21488 ANALOG COMPUTER REPRESENTATION OF THE RING MAGNET POWER SUPPLY SYSTEM OF THE ZERO-GRADIENT SYNCHROTRON. Hedin, R. A. (Allis-Chalmers Mfg. Co., Milwaukee); Krause, P. C. 6p. (CONF-651061-2). ORAU. Gmelin, AED-CONF-65-326-2.

From 21st National Electronics Conference and Exhibition, Chicago.

A method of simulating a power supply system consisting essentially of an induction motor, synchronous generator, and a 12-phase rectifier combination is described. Computer recordings are compared with tests made when the facility became operational. In general, the correlation between variables of the actual system and the corresponding variables of the simulated system was quite satisfactory. The only important difference between the performances of the actual and simulated systems existed in the response time of the voltage regulator system. (A.G.W.)

Astrophysics and Cosmology

Refer also to abstracts 20406 and 21684.

21489 (AD-623803) MIXING LENGTH DAMPING AND SUNSPOTS. Lykoudis, Paul S. (RAND Corp., Santa Monica, Calif.). Nov. 1965. 18p. (P-3249(RAND)). CFSTI $1.00 cy, $0.50 mn.

An evaluation is made of the sunspot problem from the point of view of small magnetic Reynolds numbers allowing for slippage between the flow and the magnetic field. The evaluation is based on recently available laboratory experiments with liquid metal, which are predictable with a theory allowing for the damping of the turbulence, and therefore of the mixing length as a function of the magnetic field. (auth)

21490 RESULTS OF AN X-RAY SCANNING OF THE SKY IN THE 20 TO 200 kev ENERGY RANGE. Brini, D.; Cattani, D.; Ciriegi, U.; Fuligni, F.; Galli, M.; Gandolfi, A.; Moretti, E.; Sacchi, C. (Univ., Bologna). Ann. Astrophys., 28: 1034-8(Nov.-Dec. 1965).

To extend the present knowledge of the energy region above 20 kev, a scan of the sky for x-ray sources, already identified at lower energies, was performed by a balloon-borne x-ray telescope. The flight was carried out at Aire sur l'Adour (France), on 13 April 1965, at a geomagnetic latitude of 45°. In the 210–270° azimuthal interval an increase in the counting rate occurred with respect to the general average. A slight rise in count rate appearing at about 15 and 315° seemed questionable. In the region 210–270° there are x-ray sources already known, such as Cyg XR–1 and XR–2. An evaluation of the flux from this zone in the entire energy range 20–200 kev gave a value of about 0.15 cm^{-2} sec^{-1} which is considered as an upper limit, owing to the choice of the background level. The correspond-

ing energy flux is about 10^{-8} erg/cm^2 sec. The spectrum indicated could be explained by either the synchrotron or inverse Compton mechanisms. However, in both cases exceptional local conditions would be required, such as very high magnetic field intensity and/or exceptional spectrum and density of the particle fluxes. (BBB)

21491 THE 3α REACTION IN A PULSING STAR. Perdang, J. (Univ., Liege). Bull. Soc. Roy. Sci. Liege, 34: 736-49(1965). (In French).

Expressions of the effective temperature and density exponents, ν_e and μ_e, for the 3-α process were derived. These expressions differ from those for the usual thermonuclear reactions by imaginary parts that may become important at low temperatures and densities. (auth)

21492 THE APPROACH TO NUCLEAR STATISTICAL EQUILIBRIUM. Truran, J. W. (Yale Univ., New Haven); Cameron, A. G. W.; Gilbert, A. Can. J. Phys., 44: 563-92(Mar. 1966).

The transformation of a region composed initially of ^{28}Si to nuclei in the vicinity of the iron peak, which is thought to take place in the late stages of evolution of some stars, is considered in detail. In order to follow these nuclear transformations, a nuclear reaction network is established providing suitable reaction links connecting neighboring nuclei. A method of solution of the network equations is outlined. Thermonuclear reaction rates for all neutron, proton, and alpha-particle reactions involving the nuclei in this network were determined from a consideration of the statistical properties of nuclei. The evolution of this silicon region was followed in time for two cases: $T = 3 \times 10^9$ °K, $\rho = 10^6$ g cm^{-3} and $T = 5 \times 10^9$ °K, $\rho = 10^7$ g cm^{-3}. While both the observed solar and meteoritic abundances display a broad peak in the vicinity of iron, centered on ^{56}Fe, in these calculations ^{54}Fe is found to be the most abundant isotope in this mass range. Beta decays required to change the peak to ^{56}Fe are very slow. As the transformation $2\ ^{28}\text{Si} \rightarrow {}^{54}\text{Fe} + 2p$ is endothermic by ~1.3 Mev, these results suggest that the silicon-to-iron conversion may not comprise an exothermic nuclear burning stage of stellar evolution. (auth)

21493 SOLAR EVOLUTION WITH VARYING G. Ezer, D.; Cameron, A. G. W. (National Aeronautics and Space Administration, New York). Can. J. Phys., 44: 593-615 (Mar. 1966).

The model-sequence calculations for early solar evolution were extended to the case of a varying-G cosmology. In the varying-G sun there is less lithium depletion than in a constant-G sun, and the time required to burn out central hydrogen is decreased by less than the ratio of luminosities, owing to the much greater total helium production in the varying-G sun. At the present time the varying-G model has four times the ^{8}B neutrino flux of the constant-G model, a prediction that can be subjected to an experimental check. (auth)

21494 COSMIC RAY ASTRONOMY. Reber, Grote (Univ. of Tasmania, Australia). J. Franklin Inst., 281: 1-8(Jan. 1966).

The data described were obtained with two zenith pointed muon telescopes which have been operated for seven years in an abandoned railway tunnel at latitude 43° south at 110 m altitude. The collected data are analyzed for components of 24h00m, 23h56m, 23h52m, 24h04m, and 24h08m mean solar time. Repeatable daily time-count profiles are obtained for the first two periods. Their count amplitudes are, respectively, 0.187 and 0.098%. Suggestions are outlined for future development. It is recommended that the harmonic dial representation be abandoned in favor of true celestial surveying. A suggested geometrical configuration of three square apertures is shown, as is the space diagram. Directivity is secured by particle coincidence between each aperture and base. This apparatus could easily resolve the two sources near 0430 and 0900 right ascension. The looked for effects are repeatable with periods of 24h00m and 23h56m mean solar time. If the mean solar day is divided into 366 parts, these two periods may be locked to respectively 366 and 365 parts. Simplified versions of commercially available time-averaging computers may be used to raise automatically the desired phenomena out of randomness. (BBB)

21495 EFFECT OF THE INTERPLANETARY MAGNETIC FIELD ON SOLAR NEUTRON-DECAY PROTONS. Roelof, E. C. (Boeing Co., Seattle). J. Geophys. Res., 71: 1305-17(Mar. 1, 1966).

Upper bounds are placed on both steady-state and pulse (flare) outflow of neutrons above 1 Mev from the sun. The bounds are obtained by assuming that the neutron-decay protons diffuse in the interplanetary magnetic field, in order to calculate the resultant proton fluxes from simple diffusion theory, and then comparing the theoretical fluxes with recent proton observations. Using the Imp 1 proton spectrum (20–75 Mev) it is shown that there could have been no significant contribution to the inner-belt proton population in that energy range by steady neutron outflow in the first half of 1964, and perhaps as far back as 1961. For the same period and energy range it is concluded that there could have been no higher steady outflow from the sun than ~10^{22} neutrons sec^{-1} Mev^{-1}. As opposed to the meaningful upper bounds obtained for steady neutron outflow, it is found that neutron-decay protons are insensitive indicators of the presence of neutrons in solar flares. For instance, on the order of 10% of flare particles at energies 1 to 100 Mev could be neutrons and yet their decay protons would cause only marginally observable modifications of the primary proton flux during the times of diffusion behavior at 1 AU. The same is true at 0.5 and 1.5 AU. (auth)

21496 OBSERVATIONS OF THE SOLAR WIND DURING THE FLIGHT OF IMP 1. Wolfe, John H.; Silva, Richard W.; Myers, Marilyn A. (Ames Research Center, Moffett Field, Calif.). J. Geophys. Res., 71: 1319-40(Mar. 1, 1966).

Some of the principal results of an experiment designed to investigate the properties of the solar wind and its interaction with the geomagnetic field are discussed. The main objective of the experiment was to measure the energy per unit charge and gross flow characteristics of the positive ion component of the incident plasma as a function of radial distance from the earth. This experiment was carried out on the Imp 1 (Explorer 18) spacecraft using a curved plate electrostatic analyzer. Plasma observations indicate that three distinct regions of space were traversed by the satellite. The first was the geomagnetic cavity where no plasma was observed within the dynamic range of the instrument. The second was the region of turbulent plasma flow associated with the interaction between the solar wind and the geomagnetic field. The third was interplanetary space where the free streaming solar wind was observed. The results presented cover the first 2½ months of satellite life. The plasma data obtained in interplanetary space revealed that the solar wind density rarely exceeded 3 ions cm^{-3}. The free-stream velocity exhibited values from less than 300 km/sec during quiet times to more than 700 km/sec at the time of geomagnetic disturbances. Observations in the transition region consistently showed a large increase in the disorder of the plasma as compared to interplanetary space. Careful examination of the change in the plasma characteristics as the spacecraft passed through this region has allowed the extremities of the transition region boundaries to be extensively mapped. The data revealed that toward the subsolar point the outer boundary of the transition region was located some 4 to 5 earth radii upstream from the magnetospheric boundary and showed increasing standoff distance with increasing angle from the earth-sun line. The geomagnetic cavity was seen to flare out from the subsolar point running approximately parallel to the earth-sun line for angles greater than about 130 to 140° from the subsolar point. No indication of closure of the tail of the magnetosphere was observed. The transition region observations are discussed in light of present theory. (auth)

21497 SUPERNOVA PHENOMENA IN OB ASSOCIATIONS AND COSMIC X-RAY SOURCES. Braes, L. L. E.;

Hovenier, J. W. (Univ. of Leiden). Nature, 209: 360-1 (Jan. 22, 1966).

It is pointed out that most of the observed cosmic x-ray sources are located close to OB associations and that three of them are situated between associations and run-away stars which originated from them. The distribution of x-ray sources is explained by a relation with supernovas in associations within about 2kpc. It is shown that the observational data on their number, spectra, and angular diameters may also be consistent with this relation. (J.F.P.)

21498 HIGH-ENERGY ASTROPHYSICS AND A POSSIBLE SUB-NUCLEAR ENERGY SOURCE. Pacini, Franco (Institut d'Astrophysique, Paris). Nature, 209: 389-90 (Jan. 22, 1966).

Energy sources for the energy release in some extragalactic phenomena, such as radiogalaxies and quasistellar sources are considered. A suggested source for this energy is a subnuclear process based on the idea of a compound structure of the elementary particles. The quarks model of hadrons in the SU(3) and SU(6) theory of strong interactions is assumed. It is noted, however, that this process is probably not the general cosmological process, since if all matter were created in this way the universe would be extremely hot and there would be a large diffuse flux of x rays. The burning of quarks is suggested as an energy source for high energy particles. (J.F.P.)

21499 EARLY RADIATION FIELD AND HIGH-ENERGY ELECTRONS IN SUPERNOVAE. Manley, Oscar P. (American Science and Engineering, Inc., Cambridge, Mass.). Nature, 209: 901-2(Feb. 26, 1966).

It is suggested that if Woltjer's hypothesis that the observed x-ray emission from the Crab Nebula is due to synchrotron radiation is correct, a critical part is played by the intensity of the early post-explosion radiation field. This field, by the inverse Compton effect, limits the energy of the electrons in the supernova. It is estimated that no extreme relativistic electrons ($E > 10^{12}$ ev) can survive the first few weeks after the explosion. It is shown that if the early radiation field in a supernova is characterized by an equivalent black-body temperature, electrons with initial energies less than about 4×10^{17} ev decrease in energy to 2×10^{12} ev during the first 10 days. But electrons accelerated after some further dilution of the radiation field has occurred may survive with energies sufficiently large to participate in the x-ray emission. It is postulated that the absence of sufficiently high-energy electrons, and hence of observable x rays from some Type I supernovae, may be due to unfavorable relative phasing of the dilution of the radiation field, the growth of the acceleration mechanism, and the prevailing magnetic field. (M.C.G.)

21500 PRE-ABSORPTION EVENTS AT 230 Mc/s. Aller, H. D.; Jensen, C. J.; Malville, J. M. (Univ. of Michigan, Ann Arbor). Nature, 209: 1014(Mar. 5, 1966).

Four radio bursts at 230 Mc which were preceded by brief decreases in the background intensity are described. The decreases are interpreted as absorption of type-IV continuum. Three of the pre-absorption events are shown and their characteristics given. The events exhibit considerable symmetry, the total energy absorbed is comparable with that emitted. It is suggested that true absorption, storage, and re-emission of the radiofrequency energy occurred during the events. (J.F.P.)

21501 LIMITS ON THE SIZE OF VISIBLE QUASARS. Boccaletti, D. (Istituto Nazionale di Fisica Nucleare, Bologna); De Sabbata, V.; Gualdi, C. Nuovo Cimento (10), 42B: 175-7(Mar. 11, 1966).

It is pointed out that in the case of Kuchowicy's simplifying assumptions (Acta Astronomica (Warsyawa), 15: 297, 1965), some limits may exist on the mass and radius of the quasars. (L.B.S.)

21502 LABORATORY SIMULATION OF MAGNETIC FIELDS PRODUCED IN THE MOON BY THE TRAPPED FIELD OF THE SOLAR PLASMA STREAM. Brown, I. G.; (Univ. of Sydney); Watson-Munro, C. N.; Gold, T. Phys. Lett., 20: 631-2(Apr. 1, 1966).

In a laboratory experiment with an artificial moon, it was found that the measured magnetic field supports the argument that the moon's magnetic pressure will be governed by the stagnation pressure of the solar plasma wind. (auth)

21503 SOME KINEMATICAL MODELS FOR SMALL-SCALE SOLAR MAGNETIC FIELDS. Clark, Alfred Jr. (Univ. of Rochester, N. Y.). Phys. Fluids, 9: 485-92 (Mar. 1966).

Kinematical hydromagnetic theory is used to study the magnetic fields produced by the action of two prescribed, steady two-dimensional velocity fields on initially weak, large-scale magnetic fields. In both flows, the magnetic field becomes concentrated along certain vertical planes. In an effort to approximate one aspect of solar photospheric flows, it was assumed that the fluid motions occupy only a lower half-space, so that a horizontal plane of zero mass flux separates a lower region in motion from an upper one at rest. The magnetic field lines cross this boundary, so that the concentration of the field by the flow is opposed by the tendency of the field above the flow to spread. The other factor opposing the field concentration is the diffusive effect of finite conductivity. Both the time-dependent and eventual steady state magnetic fields are considered for various (large) values of the magnetic Reynolds number. (auth)

21504 STELLAR CHROMOSPHERES. Wilson, O. C. (Carnegie Institution, Washington, D. C. California Inst. of Tech., Pasadena). Science, 151: 1487-98(Mar. 25, 1966).

Studies on the chromospheres of normal, nonvariable stars are reviewed. Precise knowledge of chromospheric mechanisms and processes must be derived from solar observation since the sun is the only star whose surface features and activity can be studied in detail. Just above the visible surface of the sun, the photosphere, and not separated from it by any distinct boundary, is the chromosphere. Still higher and fading out gradually is the corona. It is concluded that the chromosphere and corona consist of material impelled upward from below and that they are dynamic rather than static structures. The only known source of mechanical energy necessary to maintain the chromosphere and corona is in the hydrogen convection zone. In general, it is shown that chromospheres of the kind such as the sun's are found in just those stars where effective hydrogen convection zones are expected. There is shown to be a relation between magnetic fields and chromospheric heating. The emission features (H_2 and K_2) at the center of the two broad, deep, absorption lines (H and K), due to ionized calcium in the solar spectrum, were found to originate in the chromosphere. Quantitative measures of line structure, intensities of H_2, K_2 lines, and applications of stellar chromospheres to studying other stellar properties are discussed. (M.C.G.)

21505 IRON METEORITES WITH LOW COSMIC-RAY EXPOSURE AGES. Cobb, James C. Brookhaven National Lab., Upton, N. Y.). Science, 151: 1524(Mar. 25, 1966). (BNL-9756).

Analysis of ^{38}Ar and ^{39}Ar produced by cosmic rays in four iron meteorites gave normal amounts of the radioactive product ^{39}Ar and abnormally low amounts of stable ^{38}Ar. This indicated that these meteorites were exposed to cosmic rays for unusually short periods of time. These exposure times were one or two orders of magnitude shorter than those for the average iron meteorite, and they overlapped the periods found for chondrites. It is suggested that perhaps 20% of the iron meteorites have similarly short exposure periods. (auth)

21506 ON SOME CHARACTERISTICS OF THE SOURCES OF RADIO EMISSION CONNECTED WITH ACTIVE REGIONS IN THE SUN. Abbasov, A. R. Vestn. Leningr. Univ., No. 19, Ser. Mat., Mekhan. Astron., No. 4, 140-2(1965). (In Russian).

From observations of IHH and Nagoy stations it is concluded that the decrease of radiation flux (S-component) is observed before sharp bursts, but the flux increases after the bursts, the sources connected with sunspots being directional. (auth)

21507 MOON AS PARENT BODY OF BRONZITE CHONDRITES. **Waenke, H. (Max-Planck-Institut fuer Chemie, Mainz). Z. Naturforsch., 21a: 93-110(Jan.-Feb. 1966). (In German).**

Knowing the cosmic ray exposure ages of a sufficiently large number of meteorites and using the earth as analyzer with special assumptions, criteria can be found to distinguish between a lunar or asteroidal origin of meteorites. Several arguments are presented, which are based on new and unpublished results of rare gas measurements by Hintenberger, Schultz and Wänke. (L.B.S.)

21508 THE PRODUCTION RATES OF ^{36}Cl AND ^{39}Ar IN METAL AND STONE PHASES OF THE LEEDEY CHONDRITE. **Begemann, F.; Vilcsek, E.; Waenke, H. (Max-Planck-Institut fuer Chemie, Mainz). Z. Naturforsch., 21a: 110-15(Jan.-Feb. 1966). (In German).**

The production rates of ^{36}Cl and ^{39}Ar by the cosmic radiation on Fe and Ca + K were determined in the chondrite Leedey. The values of 19.4 atoms/min · kg $\leqq P_{Fe}(^{36}Cl) \leqq$ 26.6 atoms/min · kg and $P_{Fe}(^{39}Ar) = (23.6 \pm 1.8)$ atoms/min · kg are in good agreement with those found in iron meteorites of comparable size. A large contribution of Ca + K to the production of both isotopes is indicated by the ratios $9.2 \leqq P_{Ca+K}(^{36}Cl)/P_{Fe}(^{36}Cl) \leqq 13.6$ and $P_{Ca+K}(^{39}Ar)/P_{Fe}(^{39}Ar) = 12.1 \pm 1.6$. The bearing of these results on the interpretation of ^{39}Ar-data obtained on other chondrites is being discussed. (auth)

21509 THE ISOTOPIC COMPOSITION OF ATMOSPHERIC NEON. **Walton, J. R.; Cameron, A. E. (Oak Ridge National Lab., Tenn.). Z. Naturforsch., 21a: 115-19(Jan.-Feb. 1966).**

Absolute values for the isotopic abundance ratios of atmospheric neon were determined by mass spectrometry. Calibration standards were prepared by mixing of nearly pure separated nuclides of neon. The percentage abundance of the three nuclides of neon are: $^{20}Ne = 90.514 \pm 0.031$, $^{21}Ne = 0.266 \pm 0.005$, $^{22}Ne = 9.220 \pm 0.029$. The calculated atomic weight of neon on the unified physical and chemical atomic weight scale ($^{12}C = 12$) is 20.1794 ± 0.0030. (auth)

21510 INFLUENCE OF THE TERRESTRIAL ENVIRONMENT ON THE TEMPORAL AND STATISTICAL CHARACTERISTICS OF JOVIAN DECAMETRIC RADIATION. **Smith, Alex G.; Block, W. F.; Morton, W. A.; Lebo, G. R.; Carr, T. D. (Univ. of Florida, Gainesville). 4p. (CONF-651059-1). ORAU. Gmelin, AED-CONF-65-311-1.**

From 2nd Symposium on Radio Astronomical and Atmosphere, Boston.

The pulse structure of Jovian radio signals was compared with scintillation phenomena known to be ionospheric in origin—signals from radio stars and from the S-66 or BE-B beacon satellite. The Jovian pulse character seemed to be independent of altitude (elevation angle), whereas the satellite and radio star scintillation indices increased as the altitude decreased. The Jovian data lacked the strong diurnal variation displayed by the satellite and radio scintillation. In general the comparisons suggested that the Jovian pulse character is not determined by the same factors that control the scintillation of satellite and radio star signals. The local ionosphere assumed more importance in a study of the gross statistics of the received radiation. Both the probability of receiving signals and the mean flux density showed a marked dependence on local time and on the hour angle of the planet. (A.G.W.)

21511 PROCEEDINGS OF THE ELEVENTH GENERAL ASSEMBLY, BERKELEY, 1961. TRANSACTIONS OF THE INTERNATIONAL ASTRONOMICAL UNION, VOL. XIB-PROCEEDINGS. **Sadler, D. H. (ed.). London, Academic Press, 1962. 543p. £4; $11.50. (CONF-610802).**

Separate abstracts were prepared for the three invited papers. The rest of the volume contains the reports of meetings of commissions and of scientific meetings as well as administrative decisions and reports. Joint discussions of stellar dynamics and motion; solar magnetic fields, celestial mechanics, and problems requiring radioastronomical observations of high resolution and sensitivity are also included. (D.C.W.)

For abstracts of individual papers see: 21512, 21513, and 21837.

21512 STELLAR EVOLUTION. **Schwarzschild, M. (Princeton Univ., N. J.). pp 137-43 of Proceedings of the Eleventh General Assembly, Berkeley, 1961. London, Academic Press, 1962.**

The phases of stellar evolution are discussed in terms of evolution by dynamical, nuclear, and thermal processes. Three areas of difficulty in the theory of evolution are outlined. (D.C.W.)

21513 PROBLEMS OF EXTRA-GALACTIC RESEARCH. **Ambartsumian, V. A. (Academy of Sciences, Erevan, Burakan Observatory, USSR). pp 145-60 of Proceedings of the Eleventh General Assembly, Berkeley, 1961. London, Academic Press, 1962.**

A number of problems that seem to constitute the most essential points in the further exploration of the outer galaxies are formulated. (G.O.Y.)

Atomic Physics

21514 (INR-598/VI/PH) CASCADE CURVES FOR XENON. **Jablonski, Zdzislaw (Institute of Nuclear Research, Warsaw (Poland)). Jan. 1965. 44p. Dep. mn.**

The calculations of the number of electrons $N_p(E_0, E^0, t)$ of the electron-photon cascade with energies greater than E^0 at the depth of t cascade units initiated by a single electron or a single photon with the energy E_0 were performed. In the calculations the moment method was used. Values of the energy E_0 were assumed in the interval 5.76×10^7 ev to 2×10^{10} ev. (auth)

21515 (JINR-P-2615) O FLYUKTUATSIYAKH IONIZATSIONNYKH POTER. (On Fluctuations of Ionization Losses). **Golovin, B. M.; Kulyukina, L. A.; Medved, S. V.; Pavlovich, P.; Shulek, P. (Joint Inst. for Nuclear Research, Dubna (USSR)). 1966. 7p. Dep. mn.**

The formula for the ionization loss distribution in thin layers obtained earlier by P. V. Vavilov is made more accurate by taking into account the charged particle collisions with electrons bound in the atoms of the stopping materials. (auth)

21516 (UCRL-14403) THEORETICAL DIFFERENTIAL SCATTERING CROSS SECTIONS OF X RAYS FOR H, He, Li, Li^+, Be, B, C, AND C IN THE VALENCE STATE. **Stinner, R. J.; McMaster, W. H.; Del Grande, N. Kerr (Lawrence Radiation Lab., Univ. of California, Livermore). Sept. 23, 1965. (Contract W-7405-eng-48. 147p. Dep. mn. CFSTI $4.00 cy, $1.00 mn.**

Theoretical differential scattering cross sections of x rays were calculated for the following light elements: H, He, Li, Li^+, Be, B, C, and C in the valence state. These cross sections are given from 1 to 50 kev in kev steps and at scattering angle intervals of 15° over a 180° range; the cross sections are presented in both graphic and tabular form. Cross section calculations were made with the Thomson and Klein-Nishina cross section equations modified to account for electron binding. (auth)

21517 APPLICATION OF A MODIFIED EFFECTIVE-RANGE THEORY TO THE ELASTIC SCATTERING OF LOW-ENERGY ELECTRONS FROM HELIUM. **Orient, O. J. (Polytechnical Univ., Budapest). Acta Phys. Acad. Sci. Hung., 20: 293-7(1966).**

Modified effective-range theory is applied to the scattering of low-energy electrons from helium. The method of partial waves is used, giving better agreement with measurement data for the differential and total scattering cross sections in the range 0 to 14 ev than that of previous theoretical results. (J.F.P.)

21518 EXPERIMENTAL INVESTIGATIONS OF OPTICAL TRANSITION RADIATION FROM 6- TO 23-kev ELECTRONS ENTERING NORMAL TO METAL SURFACES. **Michalak, S.; Rutkowski, J. (Univ. of Lodz, Poland). Acta Phys. Pol., 29: 65-70(Jan. 1966).**

Results of experimental studies of transition radiation originating on the surfaces of metal targets (Ag, Al, Au,

Cd, Cr, Cu, Ni, Pt, and Sn) bombarded with electrons of the 6 to 23 kev energy are presented. The characteristics of transition radiation were measured and the results compared with the Frank–Ginsburg theory. Good agreement with the theory was found. (auth)

21519 PRESSURE BROADENING AS A MANY-BODY PROBLEM. Ross, David W. (Univ. of Illinois, Urbana). Contract DA-31-124-ARO(D)-114. Ann. Phys. (N. Y.), 36: 458-85(Feb. 18, 1966).

The correlation functions of the many-body system are introduced to describe pressure broadening of spectral lines in a gas. The line shape is determined from the imaginary part of the frequency- and wave vector-dependent dielectric susceptibility. A T-matrix expansion is used to rederive Baranger's impact approximation, which is shown to be exact in the low density limit, provided that either the mass of the foreign particles is very different from that of the radiating atoms, or the scattering is predominantly in the forward direction. The T-matrix equations contain the full kinematics of the interacting atoms, permitting the treatment of scattering of particles of arbitrary mass at arbitrary angles. The line shape contains all the effects of the velocity distribution of the atoms, including Doppler broadening. The application to resonant self-broadening is mentioned briefly, and some terms of higher order in the density are discussed. (auth)

21520 MOBILITY OF ELECTRONS IN POTASSIUM AND CESIUM VAPOR. Shioda, Susumu (Tokyo Shibaura Electric Co., Ltd.). Bull. Inst. Space Aeron. Sci., Univ. Tokyo, 1: A1-A5(Oct. 1965). (In Japanese).

Electron mobilities in K and Cs were measured at low electron temperature (3 to 8×10^3°K). The measurements were carried out in d-c glow discharge of K or Cs by the probe technique method. The discharge tube was put in an oven, the temperature of which determined the saturated vapor pressure of each species. Number densities of K and Cs were $3.2-6.7 \times 10^{16}$cm^{-3} and $1.1-8.7 \times 10^{15}$cm^{-3}, respectively. The temperatures and number density of the electron were measured from double probe characteristics. Current densities were calculated from the discharge current, the radial distribution of which was assumed to be O-th order Bessel function. The electric field was measured from a potential difference between two probes, which were axially situated. As the oven temperature increased, the electron temperature decreased. For Cs the number density was 1 to 8×10^{15} cm^{-3}, while the electron temperature was 8 to 4×10^3°K. Calculations from measured mobilities indicate that the graphs of momentum cross sections of electron with K and Cs versus electron temperature have concave parts like those of some inert gas atoms. For K, the concave part is at about 5,500°K with its value of 7×10^{-15}cm^2, while for Cs it is below 4,000°K. These data are in satisfactory agreement above 0.8 ev and with Flavin & Meyerand, Chen & Raether and Harris's at lower energy range. (auth)

21521 DECLINE OF LUMINESCENCE OF RARE GAS ATOMS EXCITED BY α PARTICLES IN PRESENCE OF AN ELECTRIC FIELD. Teyssier, Jean-Louis; Blanc, Daniel; Cance, Michel (Faculte des Sciences, Toulouse). Compt. Rend., Ser. B, 262: 417-18(Feb. 7, 1966). (In French).

The modifications made to the decline of the luminescence of xenon and argon by the presence of electric fields with constant intensity were studied. According to the intensity of the field the photomultiplier pulses have one or two supplementary components. These two components have the same form. (tr-auth)

21522 INDUCED RADIATION FOR LARGE DENSITIES OF PHOTONS. Bondarev, B. I. Izv. Vyssh. Ucheb. Zaved., Radiofiz., 8: 1155-9(1965). (In Russian).

The induced electron radiation in the third order of the perturbation theory was considered. It was noted that as the growth of the photon number increases the expansion of the perturbation theory becomes more incorrect. For a gas laser the third term of the perturbation theory is shown to be comparable with the first one, the photon density being about 10^{10} cm^{-3}. (auth)

21523 X-RAY PHOTOEFFECT CROSS SECTIONS IN LOW- AND MEDIUM-Z ABSORBERS FOR THE ENERGY RANGE 852 ev TO 40 kev. Bearden, Alan J. (Johns Hopkins Univ., Baltimore. Cornell Univ., Ithaca, N. Y.). J. Appl. Phys., 37: 1681-92(Mar. 15, 1966).

Experimental determinations of the mass-attenuation coefficient (μ_m) using both a two-crystal (quartz) and single-crystal (beryl) monochromator for Be, C, N, O, Ne, Al, Ar, Cu, and Sn at selected photon energies between 852 and 40 kev are presented. The experimental precautions necessary to ensure freedom from effects such as small angle scattering, x-ray fluorescence, and the Borrmann effect guarantee that the measured values of μ_m are characteristic of atomic absorbers. Values of the photoelectric cross section (σ_{pe}) for these elements are determined by subtraction of the contribution of coherent (Thomson) and incoherent (Compton) scattering to enable direct comparison with calculated values of σ_{pe} based on modified Coulomb wavefunctions (Stobbe theory). Modification of inner screening constants gives calculated values of σ_{pe} in fair agreement with experiment, whereas fully screened calculations or calculations made with no screening underestimate or overestimate, respectively, the cross section. The use of nonrelativistic sum rules and the precaution necessary when using Hartree–Fock wavefunctions for the determination of σ_{pe} are discussed. (auth)

21524 MEASUREMENT OF THE TRANSMISSION SPECTRA OF 1-Mev ELECTRONS WITH NORMAL INCIDENCE ON ALUMINUM SLABS. Rester, David H.; Rainwater, Walter J. Jr. (Ling-Temco-Vought, Inc., Dallas). Contract NASw-948. J. Appl. Phys., 37: 1793-7(Mar. 15, 1966).

Measurements of transmission energy spectra of 1-Mev electrons with normal incidence on aluminum slabs were made as a function of transmission angle. Slabs of thicknesses 0.11, 0.22, and 0.33 g/cm^2, equivalent to 0.2, 0.4, and 0.6, the range of 1-Mev electrons in aluminum, were used. The electron spectra were obtained with lithium-ion-drift silicon detectors. The experimental results were compared to calculated results obtained by use of Monte Carlo techniques. These data were found to agree except at the transmission angles less than 30 deg for the 0.11-g/cm^2 slab. (auth)

21525 NUCLEAR SPIN-LATTICE RELAXATION IN LIQUID HYDROGEN. Lipsicas, M.; Hartland, A. (Rutgers Univ., New Brunswick, N. J.). J. Chem. Phys., 44: 2839-43(Apr. 15, 1966).

Measurements are reported of the nuclear spin-lattice relaxation time T_1 in pressurized samples of liquid hydrogen. T_1 was measured as a function of density, temperature, and orthohydrogen concentration in the temperature range 20.7 to 31.2°K. The data are compared with some theoretical calculations of Deutch, based on the Bloom-Oppenheim theory of nuclear spin-lattice relaxation. The density dependence of (T_1) ortho-para is found to be opposite to that of (T_1) ortho-ortho at constant temperature. This inverted density dependence is discussed and compared with an inverted "temperature" dependence reported by other workers. (auth)

21526 NUCLEAR SPIN RELAXATION IN GASES AND LIQUIDS. V. LIQUID HYDROGEN. Deutch, J. M.; Oppenheim, I. (Massachusetts Inst. of Tech., Cambridge). J. Chem. Phys., 44: 2843-9(Apr. 15, 1966).

The theory of nuclear spin relaxation in gases and liquids developed by Bloom and Oppenheim is applied to the liquid-hydrogen system. An explicit expression for T_1 in terms of correlation functions of the anisotropic intermolecular potential is obtained. Two terms contribute to T_1. The first term is independent of the ortho concentration and arises from the anisotropic potential that exists between an ortho molecule and a para molecule or the spherically symmetric part of another ortho molecule. It is suggested that three-particle correlations must be explicitly considered if one is to understand the magnitude and the temperature and density dependence of this term. The second contribution

is linear in the ortho concentration and arises from the anisotropic potential between the asymmetric part of two ortho molecules (quadrupole–quadrupole interaction). Theoretical calculation of this term agrees remarkably well with experiment. It is found that a dynamical model of the molecular motions (CAA) is more satisfactory than a diffusion model (DCAA) in the calculation of the quadrupole–quadrupole interaction effects. (auth)

21527 FINITE NUCLEAR MASS AND RELATIVISTIC EFFECTS ON THE ROTATIONAL CONSTANT OF MOLECULAR HYDROGEN. Tipping, R.; Herman, R. M. (Pennsylvania State Univ., University Park). J. Chem. Phys., 44: 3112-14(Apr. 15, 1966).

Corrections to the rotational constant of molecular hydrogen associated with finite nuclear mass and relativistic effects are calculated. They are significantly smaller in magnitude than are the corresponding corrections previously employed. After these refinements are made, the values 60.8566 ± 0.004, 45.6548 ± 0.003, and 30.4527 ± 0.002 cm^{-1} are obtained for the Dunham B_e values of H_2, HD, and D_2. The present theoretical results show reasonably good agreement with Stoicheff's measurements on H_2, HD, and D_2, and with recent measurements on H_2 by Fink, Wiggins, and Rank, while showing less good agreement with the measurements of Herzberg and Howe. The present agreement represents decided improvement over the results of previous analysis. (auth)

21528 SPECTROSCOPIC EVIDENCE FOR ROTATION-TRANSLATION COUPLING IN THE LIQUID STATE: INFRARED ABSORPTION OF HD IN LIQUID ARGON. Holleman, Gerald W.; Ewing, George E. (Indiana Univ., Bloomington). J. Chem. Phys., 44: 3121-6(Apr. 15, 1966).

The fundamental vibrational spectrum of HD in liquid argon was studied. Features were observed which correspond approximately to vibration-rotation transitions of an isolated gas-phase molecule, indicating that HD rotates in this system. Other features in the spectrum were assigned to vibration-translation combination bands, providing evidence for the existence of quantized translational energy levels for HD in its solvent cavity. The spectrum is unusual in that the rotational selection rules are relaxed and transitions corresponding to $\Delta J = 0, \pm1, +2, +3$, and +4 are present. Furthermore all the vibration-rotation absorption features are broad and their maxima are shifted from the gas-phase frequencies in an irregular pattern. Because of its asymmetrical mass distribution, rotational motion of HD is accompanied by a translation of the molecule in its solvent cavity. This rotation-translation interaction was given quantitative form by a perturbation treatment by H. Friedmann and S. Kimel, and these results are consistent with the observed selection rules, frequency shifts, and linewidths in the spectrum of HD in liquid argon. (auth)

21529 THE EFFECTS OF ION BOMBARDMENT ON MOLYBDENITE. Mihama, Kazuhiro (Nagoya Univ., Japan). Jap. J. Appl. Phys., 5: 202-7(Mar. 1966).

The effects of ion bombardment on MoS_2 are studied by means of transmission electron microscope. The bombardment is carried out by air or argon ions of 7 kv. In order to compare the bombarded and non-bombarded regions in one electron-micrograph, a technique of putting MgO smoke crystallites on the specimen is used extensively to make the shadow to the ion beam. In the stage of heavy ion damage, imbricated patterns are obtained as the results of the selective etching. In the stage of light ion damage, broadenings of extinction contours and of dislocation lines are observed. They can be interpreted as the creation of point defects due to the bombardment. In the latter stage, the pair images also appeared due to the bombardment. (auth)

21530 OBSERVATION OF A "FORBIDDEN" LEVEL CROSSING IN THE n = 2 STATE OF ATOMIC HYDROGEN. Leventhal, M. (Yale Univ., New Haven). Phys. Lett., 20: 625-7(Apr. 1, 1966).

The hyperfine interaction permits weak electric dipole coupling between the Zeeman levels $\alpha(2^2S_{1/2}, m_J = +1/2)$ and $d(2^2P_{3/2}, m_J = -3/2)$ of atomic hydrogen. This coupling is employed to detect the αd crossing and thereby to measure a fine structure interval. A method for producing polarized protons is also discussed. (auth)

21531 A NOTE ON THE INTERPRETATION OF ISOTOPE SHIFTS. Stacey, D. N. (Clarendon Lab., Oxford). Phys. Lett., 20: 644-5(Apr. 1, 1966).

It is pointed out that in tin observed irregular changes in the mean square radius of the nuclear charge distribution cannot be reconciled with the common assumption that such irregular charges are due solely to the effects of nuclear deformation. (auth)

21532 INVESTIGATION ON THE FINE STRUCTURE OF SIX LINES OF THE BALMER SERIES OF DEUTERIUM. Csillag, L. (Central Research Inst. for Physics, Budapest). Phys. Lett., 20: 645-6(Apr. 1, 1966).

The wavelengths of the apparent doublet components of six Balmer lines of deuterium were measured. The value of the Rydberg constant resulting from our measurement is in good agreement with that accepted up to now. (auth)

21533 COHERENCE AND TWO-PHOTON ABSORPTION. Lambropoulos, P. (Bendix Corp., Southfield, Mich.); Kikuchi, C.; Osborn, R. K. Phys. Rev., 144: 1081-6(Apr. 29, 1966).

A kinetic theory of the two-photon absorption from a single mode of the radiation field is presented. It is found that, in general, the rate of two-photon absorption depends on certain correlation functions, and hence on the coherence properties of the field. The results are applied to the case of a pure coherent state and the case of a chaotic field. (auth)

21534 PI-MESONIC ATOMS. Jenkins, David A.; Crowe, Kenneth M. (Univ. of California, Berkeley). Phys. Rev. Lett., 16: 637-9(Apr. 11, 1966). (UCRL-16725).

Measurements were made of mesons (π) x-ray energies for 70 elements by using a lithium-drifted germanium detector, and for aluminum by using a bent-crystal spectrometer. Differences were observed between some x-ray energies and the energies predicted by the Klein-Gordon equation. These differences were interpreted as being due to vacuum polarization and the presence of the nucleus. (B.G.D.)

21535 A MEASUREMENT OF THE CROSS SECTION FOR PRODUCTION OF $He^+(2S)$ IONS BY ELECTRON IMPACT EXCITATION OF GROUND STATE HELIUM IONS. Dance, D. F.; Harrison, M. F. A.; Smith, A. C. H. (Culham Lab., Abingdon, Eng.). Proc. Roy. Soc. (London), Ser. A, 290: 74-93(Feb. 8, 1966).

A crossed beams method was used to measure the cross section for the production of $He^+(2S)$ by electrons incident upon $He^+(1S)$ in the energy range from threshold to 750 ev. The cross section was measured in arbitrary units with an accuracy of ±5% and at the higher energies its energy dependence is in close agreement with that calculated by means of the plane-wave Born approximation. Consequently the cross section was normalized to the plane-wave Born cross section at energies between 435 and 750 ev to obtain the absolute magnitude. An independent estimate of the absolute magnitude was made to within ±30% using only the experimental parameters, and the absolute cross sections given by the two methods agree within the experimental uncertainties. The normalized cross section is compared with cross sections given by the close-coupling approximation and various Coulomb–Born approximations. At the lower energies the normalized cross section is considerably smaller than any of the theoretical values, but the measurements are consistent with the existence of a finite cross section at threshold if the energy spread of the electron beam is taken into account. (auth)

21536 ENERGY FILTERING OF SCATTERED IONS. Forst, G. (Fachschule fuer Optik und Phototechnik, Berlin). Z. Angew. Phys., 20: 265-7(1966). (In German).

Scattering experiments so far done with Li_2^+-ions on rare gas atoms showed characteristic maxima in the intensity-angle distribution. To examine, whether these maxima were caused by inelastic energy losses, the intensity-angle dis-

tribution of 30 kev Li_7^+-ions scattered by A-atoms was imaged by an electrostatic filter lens. In energy-filtering up to 4.9 ev there was no altering of the intensity-angle distribution. As the first inelastic energy loss is observed at 11.5 ev it is evident that the maxima are not connected with inelastic energy-losses of the Li_7^+-ion interacting with the A-atom. (auth)

21537 THE PRESENT KEY IMPORTANCE OF THE FINE STRUCTURE CONSTANT, α, TO A BETTER KNOWLEDGE OF ALL THE FUNDAMENTAL PHYSICAL CONSTANTS. DuMond, Jesse W. M. (California Inst. of Tech., Pasadena). Z. Naturforsch., 21a: 70-9(Jan.-Feb. 1966).

The dilemma is described that exists at the present time between the two present best sources of information as to the numerical value of the Sommerfeld fine structure constant, α. These two sources are the fine structure splitting in deuterium, determined in 1953 by Triebwasser, Dayhoff and Lamb, and the hyperfine structure splitting in hydrogen, measured more recently using the Ramsey hydrogen maser. The theoretical connection between the fine structure measurements and α is subject to little question but the experimental difficulties to obtain a precision of few ppm are considerable. The relative precision obtained with the hydrogen maser on the other hand, is phenomenal (of order 10^{-11}) but the theoretical connection between the hyperfine splitting and α is subject to a controversial correction for the internal field structure of the proton. Assuming this correction term to be correct at its present value, the hf splitting in H implies a value of α 26 ppm higher than the fs splitting in D. Present existing sources of evidence, some favorable to the lower and some to the higher value of α, are presented and discussed and the key importance of a better knowledge of this fundamental constant is stressed. (auth)

21538 INFLUENCE OF VELOCITY OF RARE GAS IONS ON EMISSION OF SECONDARY ELECTRONS. Boerboom, A. J. H.; Schram, B. L.; Kleine, W.; Kistemaker, J. (FOM-Lab., Amsterdam). Z. Naturforsch., 21a: 127-9(Jan.-Feb. 1966). (In German).

By direct comparison of the signals of a particle multiplier and a Faraday cage at the collector end of a mass spectrometer, the secondary emission coefficients of a copper-beryllium alloy were determined for single and multiply charged noble gas ions. The ions involved were He^+ and He^{2+}, $^{20}Ne^+$ up to $^{20}Ne^{3+}$, $^{22}Ne^+$, Ar^+ up to Ar^{5+}, Kr^+ up to Kr^{7+} and Xe^+ up to Xe^{9+}. The energy of the ions varied between 3 and 90 kev. The secondary emission factors show an almost exact linear dependence on the velocity of the ions, with a threshold at 5.5×10^6 cm/s. The slopes are proportional to the square roots of the ion masses. (auth)

21539 STOPPING CROSS SECTIONS IN BORON OF LOW ATOMIC NUMBER ATOMS WITH ENERGIES FROM 15 TO 140 kev. Macdonald, James R.; Ormrod, John H.; Duckworth, Henry E. (McMaster Univ., Hamilton, Ont., Can.). Z. Naturforsch., 21a: 130-4(Jan.-Feb. 1966).

The electronic stopping cross sections in boron for atomic projectiles with $Z \leq 11$ were determined in the energy interval 15 to 140 kev. Reasonable agreement is found with theory, however the previously observed periodic dependence of S_ϵ on the atomic number of the projectile is also evident. Results for the relative straggling in energy loss are reported for hydrogen projectiles in boron, carbon, and aluminium targets and for helium projectiles in boron and carbon. Theoretical straggling estimates agree reasonably well with the experimental results. (auth)

Cosmic Radiation

See also Elementary Particles and Radiations
Nuclear Properties and Reactions

Refer also to abstracts 21494 and 21999.

21540 (CERN-65-32, pp 49-56) THE K.G.F. NEUTRINO PROJECT. Sreekantan, B. V. (Tata Inst. of Fundamental Research, Bombay (India)).

Details of a large area scintillation counter telescope designed for detection of the muons produced by neutrinos in cosmic rays, which is to be set up at a depth of 7500 feet at the Kolgar Gold Fields in South India, are discussed. Expected counting rates depending on the flux of neutrinos and the behavior of the neutrino interaction cross section with energy are presented. (B.G.D.)

21541 (CERN-65-32, pp 57-60) THE USE OF NEON FLASH TUBES IN COSMIC-RAY NEUTRINO EXPERIMENTS. Wolfendale, A. W. (Durham Univ. (England)).

Measurements on the angular distribution of muons underground at the Kolar Gold Mines, with objectives of searching for anomalies which might indicate the presence of neutrino induced events, using a system of Geiger counters, scintillators, and neon flash tubes are discussed. A detailed description of neon flash tubes used in cosmic-ray neutrino experiments is presented. (B.G.D.)

21542 (CERN-65-32, pp 73-8) THE ENERGY SPECTRA OF COSMIC-RAY NEUTRINOS. Osborne, J. L. (Durham Univ. (England)).

A description of the energy spectrum of cosmic neutrinos at sea level and its variations with zenith angle is presented. The uncertainty in the intensity due to uncertainty in the parameters of cosmic ray propagation in the atmosphere is indicated. Rough estimates are made of the fluxes of muons produced by their interactions in the earth. (B.G.D.)

21543 (MIT-2098-227) PREPRINTS OF PAPERS PRESENTED AT THE NINTH INTERNATIONAL CONFERENCE ON COSMIC RAYS PERTAINING TO THE BOLIVIAN AIR SHOWER JOINT EXPERIMENT, LONDON, SEPTEMBER 1965. (Massachusetts Inst. of Tech., Cambridge). Mar. 4, 1966. Contract AT(30-1)-2098. 75p. Dep. mn. CFSTI $3.00 cy, $0.75 mn.

Separate abstracts were prepared for the 4 included papers. (M.O.W.)

For abstracts of individual papers see: 21544–21547.

21544 (MIT-2098-227, Paper EAS-8) HIGH-ENERGY NUCLEAR-ACTIVE PARTICLES IN EXTENSIVE AIR SHOWERS AT 5,200 m ALTITUDE. ANALYSIS OF BOLIVIAN AIR SHOWER JOINT EXPERIMENT. Hasegawa, H.; Noma, M. (Gakushuin Univ., Tokyo (Japan). Dept. of Physics); Suga, K. (Institute for Nuclear Study, Tokyo Univ. (Japan)); Toyoda, Y. (Kobe Univ. (Japan). Dept. of Physics)). 18p. (CONF-650948-3).

From 9th International Conference on Cosmic Rays, London.

The bursts recorded by $60 m^2$ shielded scintillation detectors of Bolivian Air Shower Joint Experiment, (BASJE) yielded information on the high energy nuclear-active particles in extensive air showers, not only near the shower axis but also at large distance up to 100m for the axis. The conclusions are: (1) The energy flow of nuclear-active particles fluctuates very widely from shower to shower. Below 10^{15} ev, there exists an interaction where the main part of the energy of the primary particle is transferred into the electromagnetic component, and the proportion of this interaction is about 3% at 2×10^{14} ev to 1×10^{15} ev. (2) The distribution of the transverse momentum of nuclear-active particles obtained from the bursts at large distance is consistent with $f(p_t) = \exp[-p_t/p_0]\, p_t/p_0^2$ up to 1 Bev/c. However, there is evidence for the possible existence of large transverse momenta of more than 2 Bev/c. (auth)

21545 (MIT-2098-227, Paper EAS-11) A MONTE CARLO SIMULATION OF THE NUCLEAR ACTIVE CASCADE IN EAS. ANALYSIS OF BOLIVIAN AIR SHOWER JOINT EXPERIMENT. Bradt, H.; La Pointe, M.; Rappaport, S. (Massachusetts Inst. of Tech., Cambridge, Mass. Lab. for Nuclear Science). 20p. (CONF-650948-4).

From 9th International Conference on Cosmic Rays, London.

A three dimensional Monte Carlo simulation of the nuclear cascade of extensive air showers of energy 1.8×10^{14} ev was carried out and the spatial and energy distribution of the nuclear active particles (n.a.p.) at the atmospheric depth of Mt. Chacaltaya (530 g/cm^2) were studied with the

following results: (1) The total energy deposited by the n.a.p. of a single shower fluctuates much less from shower to shower in the case of Fe primaries than for proton primaries. The model of nuclear interaction, two center or isobar, does not significantly affect the distribution. (2) The radial distribution of n.a.p. within 8 m in the core is presented for the case of a distribution of transverse momentum, $f(p_t) \propto p_t\, e^{-p_t^2/p_0^2}$; $\langle p_t \rangle_{av} = 350$ Mev/c; $(p_t)_{max} = 1000$ Mev/c. (3) A large proportion of the highest energy n.a.p. in a cascade are nucleons if the primary particle is a complex nucleus. Finally, the artificial burst patterns were used to simulate the burst patterns in the 60 m^2 mosaic of fifteen shielded detectors on Mt. Chacaltaya with the following results: (1) The burst patterns undergo extreme fluctuations which render remote the possibility of consistently identifying the primary particles of individual cascades. However an occasional pattern can be so identified. (2) The spatial and energy distribution of the burst pattern is presented and, on the average, the burst patterns for Fe primaries exhibit a predominance of large bursts within 4 m of the core relative to cascades arising from proton primaries. (auth)

21546 (MIT-2098-227, Paper EAS-29) LOW-mu SHOWERS. Toyoda, Y. (Kobe Univ. (Japan). Dept. of Physics); Suga, K. (Institute for Nuclear Study, Tokyo Univ. (Japan)); Murakami, K. (and others) (Institute of Physical and Chemical Research, Tokyo (Japan)). 20p. (CONF-650948-5).

From 9th International Conference on Cosmic Rays, London.

The accumulation of extensive air showers with extremely few penetrating particles (low μ showers) was continued. The low proportion of penetrating particles in these showers is consistent with that expected for nearly pure electromagnetic showers generated by primary gamma rays. The distribution in right ascension of the arrival directions of low mu showers of energy 10^{14} to 10^{16} ev shows a peak between 200 and 220°. Among about 10,000 showers in the energy range from 10^{16} to 10^{17} ev none were observed which have sufficiently few penetrating particles to be classed as of possible gamma ray origin. This result places a significant upper limit on the rate of production of high energy gamma rays in intergalactic space in collisions between cosmic rays above 2×10^{17} ev and thermal photons. With the assumption of an intergalactic thermal photon flux characterized by a 5800°K black body spectrum and an energy density of 0.1 ev cm^{-3}, this upper limit implies that the average intensity of cosmic rays above 2×10^{17} ev in intergalactic space is less than 6.5×10^{-2} times their intensity near the earth. In showers above 10^{17} ev, the distributions of number of muons at mountain altitudes and at sea level suggest that most of the primary cosmic rays above 10^{17} ev are protons. (auth)

21547 (MIT-2098-227, Paper EAS-31) THE PRIMARY ENERGY SPECTRUM FROM 8×10^{14} ev-4×10^{17} ev. Bradt, H.; Clark, G.; La Pointe, M. (Massachusetts Inst. of Tech., Cambridge. Lab. for Nuclear Science); Domingo, V.; Escobar, I.; Kamata, K. (Universidad Mayor de "San Andres," La Paz (Bolivia). Laboratorio de Fisica Cosmica de Chacaltaya); Murakami, K. (Institute of Physical and Chemical Research, Tokyo (Japan)); Suga, K. (Institute for Nuclear Study, Tokyo Univ. (Japan)); Toyoda, Y. (Kobe Univ. (Japan). Dept. of Physics). 15p. (CONF-650948-6).

From 9th International Conference on Cosmic Rays, London.

The number of extensive air showers obtained with the Bolivian Air Shower Joint Experiment on Mt. Chacaltaya in Bolivia has increased more than ten fold since the Jaipur meeting. The detector array has recently been enlarged to allow measurements on showers of up to 10^8 particles in size. With this new data, size spectra were derived at Chacaltaya at various zenith angles and from them the energy spectrum was deduced. The spectrum is substantially the same as that reported at Jaipur except that the best estimate of the logarithmic slope is now -2.2 ± 0.15. (auth)

21548 DEPOLARIZATION IN COSMIC RADIATION DUE TO DISPERSION OF FARADAY ROTATION OF POLARIZATION PLANES. Razin, V. A.; Khrulev, V. V. (Gor'kii State Univ., USSR). Izv. Vyssh. Ucheb. Zaved., Radiofiz., 8: 1063-8(1965). (In Russian).

Depolarization in cosmic radiation is considered caused by the dispersion of Faraday rotation of radio-wave polarization planes and finite bandwidth of the receiver. The general expressions were obtained, relating the position angle and the polarization degree with frequency characteristic of the receiver. For a number of known circuits the calculation results of polarization degree are given in formulas and graphs. While the degree of polarization has a considerable value ($\geq$0.05), the position angle varies only by some degrees by changing the transmission bandwidth of the receiver of about 1–2% to the resonant frequency. (auth)

21549 MEASUREMENT METHODS FOR LINEAR POLARIZATION OF THE DISTRIBUTED COSMIC RADIO EMISSION. Pupysheva, L. V.; Razin, V. A. (Gor'kii State Univ., USSR). Izv. Vyssh. Ucheb. Zaved., Radiofiz., 9: 7-10(1966). (In Russian).

The measurement methods of the linear polarization of the distributed cosmic radio emission is considered, using the black disk; the latter permitting the shielding of the antenna's beam. These methods are shown to be able to secure the sufficiently high accuracy of the polarization parameters measurements of the cosmic radio emission. (auth)

21550 COSMIC RAY AND SOLAR PROTON ALBEDO NEUTRON DECAY INJECTION. Dragt, Alex J.; Austin, Michael M.; White, R. Stephen (Aerospace Corp., El Segundo, Calif.). J. Geophys. Res., 71: 1293-1304(Mar. 1, 1966).

Probabilities for injecting protons into the radiation belts for large regions of B-L space by cosmic ray albedo neutron decay, Crand, and by solar proton albedo neutron decay, Spand, are computed. A computer program simulates the ejection of neutrons from the atmosphere of the earth. The computations are compared with both directional and omnidirectional experimental data. The trapped radiation belt protons with energies $\gtrsim$20 Mev can be explained by Crand injection and atmospheric losses only if the correct ratios of the albedo neutron fluxes to the mean atmospheric densities encountered by trapped protons are a factor of 50 larger than the values used in this paper. The trapped proton flux from Spand injection is evaluated using the currently estimated solar proton flux and found to be small compared with Crand injection. Below 20 Mev, in many regions of space, there are too many protons to be accounted for by either Crand or Spand injection, and some other source is required. (auth)

21551 RESPONSE OF A STANDARD IGY NEUTRON MONITOR. Hughes, E. B.; Marsden, P. L. (Univ. of Leeds, Eng.). J. Geophys. Res., 71: 1435-44(Mar. 1, 1966).

On the basis of experimental results on neutron production by protons and muons, the total counting rate and the detected multiplicity spectrum normally recorded by a standard IGY neutron monitor are analyzed in terms of the components of the cosmic radiation at sea level. It is shown that approximately 93% of the detected neutrons are caused by neutron and proton interactions and that a definite relation exists between the detected multiplicity spectrum and the energy spectrum of nucleons at sea level. It is expected that time variations in the rates of the detected multiplicities will reflect the behavior of the primary energy spectrum of the cosmic radiation at energies up to the order of 200 Bev, and that this will be useful in the study of the various time-dependent phenomena of the cosmic radiation. (auth)

21552 PRODUCTION SPECTRUM OF HIGH-ENERGY ELECTRONS FROM HIGH-ENERGY COSMIC-RAY COLLISIONS. Spergel, M. S.; Scanlon, J. H. (Grumman Aircraft Engineering Corp., Bethpage, N. Y.). Nuovo Cimento (10), 42A: 228-40(Mar. 21, 1966).

The distribution of charged pions from proton-proton

collisions is combined with the cosmic-ray flux and the distribution of electrons from π-μ-e decay to give the production spectrum of electrons from cosmic-ray collisions. The proton-proton collisions are described by the Landau hydrodynamical model. Calculations are performed for electron energies between 20 and 10^8 Bev. The electron production spectrum is seen to exhibit approximately an $E_e^{-3.3}$ behavior, where E_e is the electron energy. (auth)

21553 PION PRODUCTION IN HIGH-ENERGY COSMIC-RAY COLLISIONS. Spergel, M. S.; Lieber, M.; Milford, S. N. (Grumman Aircraft Engineering Corp., Bethpage, N. Y.). Nuovo Cimento (10), 42A: 251-68 (Mar. 21, 1966).

The Landau–Milekhin hydrodynamic model of very-high energy nucleon interactions is extended to calculate the pion energy and angular distributions in the center-of-mass system (c.m.s.) and laboratory frames. Consideration of the physical limitations on the average energy of the pions produced in the decomposition of the nucleonic fluids leads to truncation of the pion distribution and a rather slow energy dependence of the average c.m.s. pion energy on the incident proton energy. When a power law dependence is chosen for incident primary cosmic-ray protons, the pion production spectrum found in the laboratory frame has a steeper energy spectrum than those found using simpler models of nucleon interactions. (auth)

21554 AGE OF COSMIC RAY NUCLEI AND THEIR PROPAGATION IN SPACE. Daniel, R. R.; Durgaprasad, N. (Tata Inst. of Fundamental Research, Bombay). Progr. Theoret. Phys. (Kyoto), 35: 36-43(Jan. 1966).

Information on the origin, age and propagation of cosmic ray nuclei can be obtained from a detailed study of the intensities of Li, Be, and B nuclei in the primary radiation observed in the vicinity of the earth. While at any given energy, the absolute total flux of these nuclei, (Li + Be + B), at the top of the atmosphere will depend almost exclusively on the amount of matter traversed by the radiation, their relative intensities will depend on the extent to which the long lived ^{10}Be isotopes, produced in spallation reactions in space, have decayed during the life time (or age T) of the cosmic rays. The dependence of the ratio of the flux of Be nuclei to that of B nuclei on the age of the cosmic rays is used to set a reasonable lower limit to the age of the cosmic ray nuclei; from an experiment performed with nuclei having a geomagnetic cutoff rigidity corresponding to 7.5 Bev/n it is found that $T \gtrsim 5 \times 10^7$ years. This result is then used together with the total amount of matter traversed by cosmic ray nuclei (2.5 g/cm^2), obtained from other experiments, to deduce the average gas density of regions traversed by the cosmic rays as $\lesssim 0.03$ hydrogen atoms/cm^3. This very low value of the average density suggests that cosmic ray nuclei are not confined to the disc or spiral arm arms of our galaxy but reside for the major fraction of their life time in regions of much lower density such as the intergalactic space and the halo of our galaxy, if it exists. (auth)

21555 OBSERVATION OF HIGH ENERGY JETS WITH EMULSION CHAMBERS. GAMMA-RAYS ON MT. NORIKURA. Akashi, Makoto (Hirosaki Univ., Japan); Watanabe, Zenjiro; Misaki, Akeo; (and others). Progr. Theoret. Phys. (Kyoto), Suppl., No. 32, 1-71(1964).

Observations of high energy jets by means of emulsion chambers carried out since 1958 at Mt. Norikura Observatory at 2770 m above sea level are reported. The design of the emulsion chamber, experimental procedure, the energy spectrum of gamma rays, air cascades and their relation to the gamma-ray spectrum, comparison with other experiments, and an analysis of atmospheric interaction are considered. (J.F.P.)

21556 CALCULATION OF CASCADE FUNCTIONS FOR THE EMULSION CHAMBER PROJECT. Nishimura, Jun (Tokyo Univ.). Progr. Theoret. Phys. (Kyoto), Suppl. No. 32, 72-81(1964).

Transition curves and lateral distributions of cascade showers in the emulsion chamber are calculated for the energy measurement of electron showers observed in these chambers at balloon altitudes and mountain laboratories. The calculation is based on an analytic solution of the three-dimensional shower theory. Numerical calculations are made for electron-pair-primary cascade showers rather than for gamma-ray initiated showers, since effects from the fluctuation of the location of the first materialization process of the gamma ray in the chamber are thus eliminated. Several correction factors are estimated for the application of these results to the energy determination of the observed shower. (J.F.P.)

21557 MEAN SQUARE ANGULAR AND LATERAL SPREADS OF ELECTRONS AND PHOTONS IN A CASCADE SHOWER. Misaki, Akeo (Kohnan Univ., Kobe, Japan). Progr. Theoret. Phys. (Kyoto), Suppl., No. 32, 82-103 (1964).

Mean square angular and lateral spreads of electrons and photons in a cascade shower initiated by a photon are calculated over wide ranges of energy ratio and observational depth under Approximation A with Landau approximation according to Nishimura and Kamata's theory. Corresponding quantities weighted with energy of the shower particle are also obtained. The results are presented in the form of graphs and tables. The results are compared with those of Chartres and Messel, and their results for lateral spreads seem to be not reliable. The results are also compared with those of Monte Carlo calculations given by Adachi and others, and the agreement between those results is quite good. (auth)

21558 HIGH ENERGY GAMMA-RAYS IN THE ATMOSPHERE AND MUONS UNDERGROUND AND UNDERWATER. Hayakawa, Satio (Nagoya Univ., Japan); Nishimura, Jun; Yamamoto, Yoshiaki. Progr. Theoret. Phys. (Kyoto), Suppl. No. 32, 104-53(1964).

The behavior of high energy nuclear active particles, γ-rays, muons, and neutrinos in the atmosphere and underground is analyzed under the light of recent experimental results. Through the analysis the following conclusions are obtained. The attenuation length of the N-component of energies above a few Tev is about 110 g cm^{-2}, as derived from the altitude variations of the γ-ray flux and the nuclear interaction frequency. The break in the γ-ray spectrum can be attributed to that in the primary spectrum, implying that the features of nuclear interactions do not appreciably change as energy increases as high as 100 Tev. The intensity-depth relation of the muon flux is found to be consistent with the γ-ray spectrum by taking proper account of the range fluctuations of muons. The ratio of kaons to pions at high energies is consistent with that observed in jet showers. A summary of experimental data, the method of dealing with cascade showers, the mathematical treatment of the range fluctuations and the neutrino fluxes expected is presented. (auth)

21559 A MONTE CARLO ANALYSIS OF ELECTROMAGNETIC CASCADE SHOWERS. Adachi, Atsuko (Inst. of Physical and Chemical Research, Tokyo); Fujimoto, Yoichi; Ogita, Naofumi; Takagi, Shuji; Ueda, Akira. Progr. Theoret. Phys. (Kyoto), Suppl. No. 32, 154-92(1964).

The characteristic features of electromagnetic cascade showers initiated by high-energy γ-rays are examined in detail with the Monte Carlo method under the approximation A. The treatment is made three-dimensionally, in which a device is introduced for taking into account the deviations of shower particles from the shower axes. The various kinds of quantities, some of which can not, in principle, be derived with the analytical method, are computed and some of them are compared with those derived by the latter method. From the comparison of the Nishimura-Kamata function with the empirical lateral distribution function of electrons which is derived by the least square fitting to the computed data, it is shown that the Nishimura-Kamata function evaluated for infinite primary energy may not be applicable unconditionally. Some other distribution functions are also given. Special attention is devoted to the fluctuation problem of various quantities. Their variances and their coefficients of variation are presented and discussions on their interrelations are given.

These results mentioned are fully used to get a useful clue to the estimation of the energies of primary γ-rays and their production heights. Some basic arguments for this problem are given, which will be useful for applications. (auth)

Direct Energy Conversion

Refer also to abstract 22485.

21560 (AD–621276) NON-EQUILIBRIUM IONIZATION USING ELECTROSTATIC PROBING TECHNIQUES. Final Report, March 1, 1963–February 28, 1965. Report No. D-920072-6. Bullis, R. H. (United Aircraft Corp., East Hartford, Conn. Research Labs.). Apr. 26, 1965. Contract AF49(638)-1221. 41p. CFSTI $2.00 cy, $0.50 mn.

Research was conducted to determine the electron energy distribution in the cesium plasma in an arc-mode thermionic converter and to determine the changes in this distribution produced by the presence of a highly inert gas background pressure. Electrostatic probes were used to measure various plasma properties, such as electron energy distribution, electron number density, and plasma potential. Calculations were made of the plasma production and loss rates. A bibliography of the publications resulting from this work and reprints of the most recent papers covering portions of the research are included. (auth)

21561 (AD–623096) MEASUREMENT OF FLUID PROPERTIES FOR MAGNETOPLASMADYNAMIC POWER GENERATORS. Quarterly Technical Summary Report No. 9, May 1–August 31, 1965. Schneider, R. T.; Myers, F. G. (Allison Div., General Motors Corp., Indianapolis, Ind.). Sept. 13, 1965. Contract Nonr-410400. 52p. (EDR–4400). CFSTI $3.00 cy, $0.75 mn.

A closed loop MPD power generation device was designed, constructed, and operated. Two modes of operation were observed — saturating and nonsaturating. The saturating mode is associated with low seeding ratios while the nonsaturating mode is associated with high seeding ratios and high leakage resistances. During operation, leakage resistances varied between 0.1 and 1.0 megohms. Of the two modes observed, only the saturating mode was investigated thoroughly. The observations were made under the following conditions: Pressure — slightly above atmospheric, Magnetic field — up to 21,500 gauss, Velocities — up to 250 m/sec at the channel entrance, Temperatures (static) — up to 1500K. For the saturating mode at these conditions, no nonequilibrium ionization was observed. Theoretical considerations indicate that to observe nonequilibrium ionization, runs should be made at lower pressures and higher velocities and temperatures than those stated previously. (auth)

21562 (AD–623142) BASIC RESEARCH IN THERMIONIC ENERGY CONVERSION. Technical Summary Report, November 1, 1964–July 31, 1965. Warner, C.; Hansen, L. K. (Atomics International, Canoga Park, Calif.). Oct. 1965. Contract Nonr-319200. 107p. (AI-65-191). CFSTI $4.00 cy, $0.75 mn.

Basic processes in thermionic energy conversion are discussed. It is primarily based on papers that were given at various thermionic conferences. The subjects discussed are: transport implications of spectroscopic diode measurements, review of thermionic converter plasma physics, theory of the ignited mode with spatial temperature variation, and a theory of the ignited mode assuming uniform temperatures. (auth)

21563 (AD–623591) HIGH-TEMPERATURE THERMOELECTRIC GENERATOR. Final Report, June 14, 1963–September 14, 1964. Hicks, W. T. (Du Pont de Nemours (E. I.) and Co., Wilmington, Del. Pigments Dept.). Dec. 7, 1964. Contract NObs-88639. 97p. CFSTI $3.00 cy, $0.75 mn.

Design, construction, and operation of a high temperature thermoelectric generator are reported. A commercial, gas-fired heat source was used. The generator elements comprise encapsulated segments of Ta-doped WSe2 and Na-doped PbTe as p-type materials. No appropriate n-type semiconductor was found; however, a Au–Ni alloy was discovered and developed for use in the generator as negative legs. Total power output and efficiency were less than those calculated. Suggestions for improving generator performance and for further materials research are included. (auth)

21564 (AD–627037) PERFORMANCE OF A SELF-EXCITED MHD GENERATOR. Mattsson, Arne C. J.; Ducharme, Edward L.; Govoni, Edward M.; Morrow, Irving B. Jr.; Brogan, Thomas R. (Avco-Everett Research Lab., Everett, Mass.). Oct. 1965. Contract AF33(615)-1862. 37p. (RR–238). CFSTI $2.00 cy, $0.50 mn.

A rocket-driven self-excited MHD generator designed for a net power output of 20,000 kilowatts was successfully operated. The generator was designed to demonstrate the feasibility of using an MHD device to provide power for limited duration at very high levels with relatively simple equipment. A general description of the generator and the experimental results of a testing program performed to study the characteristics of self-excitation and the combined operation of self-excitation and power output are included. (TAB)

21565 (AD–628049) DIRECT ENERGY CONVERSION LITERATURE ABSTRACTS. (Naval Research Lab., Washington, D. C.). Dec. 1965. 154p. CFSTI $5.00 cy, $1.00 mn.

Subject coverage includes energy conversion, thermoelectricity, thermionics, photovoltaic, MHD, EHD, electrochemical, nuclear, and energy storage. Approximately 800 abstracts are included. (M.O.W.)

21566 (ANL–7055, pp 213-29) ENERGY CONVERSION. Crouthamel, C. E.; Hesson, J. C.; Tevebaugh, A. D. (Argonne National Lab., Ill.).

Research directed toward development of closed-cycle regenerative emf cells for operation in conjunction with reactor heat sources is summarized. Information is included on LiH cells, intermetallic cells, equilibria in Bi–Na cells, properties of electrolytes and bimetallic mixtures, Na-cathode thermal regenerators, and liquid metal corrosive properties. (J.R.D.)

21567 (FEI–15) RABOTA TSEZIEVOGO DIODA S PRIMES'YU INERTNOGO GAZA. (Operation of a Cesium Diode With an Admixture of an Inert Gas). Bekmukhambetov, E. S.; Gus'kov, Yu. K.; Kasikov, I. I.; Lebedev, S. Ya.; Rodin, A. V.; Stakhanov, I. P. (Gosudarstvennyi Komitet po Ispol'zovaniyu Atomnoi Energii SSSR, Obninsk. Fiziko-Energeticheskii Institut). 1965. 19p. Dep. mn.

Experiments showed that in the gap of inert gases the saturation current decreased significantly in comparison to pure cesium. A comparison of the experimental and theoretical values of the saturation current showed that the corrected experimental values were 2 to 4 times lower than the theoretical values. This can be explained, in part, by the thermodiffusion separation of the components of the cesium mixture with the inert gases. The addition of krypton reduces the saturation current more than the addition of xenon. On the supposition of the presence of thermodiffusion this can explain the very strong separation of cesium–krypton admixtures because of the large difference in the atomic mass. Using the hypothesis of the presence of thermodiffusion, the thermodiffusion ratio K_t for Cs–Kr and Cs–Xe mixtures was calculated for the case of small Cs concentrations. The values for the interaction cross section of Cs with Kr and Xe were $\sigma_{Kr} = 8 \times 10^{-14}$ cm^2 and $\sigma_{Xe} = 1.05 \times 10^{-13}$ cm^2. Additional experiments are necessary to determine the presence of thermodiffusion in Cs and inert gas mixtures. (tr-auth)

21568 (FEI–16) VLIYANIE VELICHINY MEKHELEKTRODNOGO ZAZOPA NA RABOTU TSEZIEVOGO TERMOPREOBRAZOVATELYA. (Effect of the Size of the Inter-Electrode Spacing on the Operation of a Cesium Thermal Converter). Volkov, N. V.; Gus'kov, Yu. K.; Zyukov, V. I.; Pashchenko, V. P. (Gosudarstvennyi Komitet po Ispol'zo-

vaniyu Atomnoi Energii SSSR, Obninsk. Fiziko-Energeticheskii Institut). 1965. 11p. Dep. mn.

The dependencies of the short circuit current, the discharge ignition voltage, the voltage yield, and the power of thermal emission conversion to arc regime were obtained for constant cesium pressures. The experimental and theoretical results in the equilibrium regime were compared with arbitrary number of percussions in the gap. The conditions for the optimization for discharge parameters of the converter were formulated. (tr-auth)

21569 (IPP-3/29) UEBER DIE MOEGLICHKEIT, M.H.D.-GENERATOREN MIT REINEM EDELGAS ALS ARBEITSMITTEL ZU BETREIBEN. (On the Possibility of Using a Pure Inert Gas as Working Fluid in M.H.D.-Generators). Ohlendorf, W. (Institut fuer Plasmaphysik, G.m.b.H., Garching (West Germany)). Dec. 1965. 29p. Dep. mn.

A theory is developed for a nonequilibrium MHD-generator using a pure inert gas as working fluid. Relaxation-times for the electron-drift-velocity, the electron-temperature and the recombination were calculated. (auth)

21570 (N-65-29785) PROGRAM OF ANALYTICAL AND EXPERIMENTAL STUDY OF POROUS METAL IONIZERS. Summary Report. Cho, A. Y.; Hall, D. F.; Shelton, H. (TRW Systems, Redondo Beach, Calif. Physical Electronics Lab.). July 15, 1965. Contract NAS3-5254. 163p. (NASA-CR-54325; TRW-4148-6013-SU-000). CFSTI $5.00 cy, $1.00 mn.

Twenty-three different porous tungsten materials were tested to determine their cesium ion emitting characteristics at a j^+ up to 25 mamp/cm^2. Improved performance with a low neutral fraction and low critical temperature at high j^+ was noted as the surface pore density was increased by use of small, graded, spherical W powder. Effects on porous W of carbiding, O, Cr, Be, Ta, Ti, and Zr were studied. Evaporative lifetimes of Cu, Cr, Be, Ni, Fe, and Ti on W vs temperature, coverage, and oxygenation are presented. (auth)

21571 EFFECT OF ELECTRODE SIZE IN MHD GENERATORS WITH SEGMENTED ELECTRODES. Celinski, Zdzislaw N.; Fischer, Fred W. (Institut fuer Plasmaphysik, Garching, Ger.). AIAA (Amer. Inst. Aeron. Astronaut.) J., 4: 421-8(Mar. 1966).

The effect of finite-size electrodes on the distribution of electrical parameters in MHD generators was determined for any generator geometry and for a wide range of Hall parameters. The analysis was limited to generators with a separate electrical circuit for each pair of electrodes. Numerical analysis was used, and calculations were made on an IBM 7090. From this distribution a correction factor λ was calculated, the use of which makes it possible to correct one-dimensional theory equations for two-dimensional effects. This analysis was made assuming constant gas-dynamical parameters and constant channel cross section. The influence of finite-size electrodes on electrical parameters in MHD generators is generally large. Optimum electrode sizes were determined. Ohmic losses have a steep gradient across the channel, and, therefore, the distribution of these losses must be taken into account when considering electron heating. A comparison with previous work is shown. (auth)

21572 HALL-CURRENT GENERATOR CHARACTERISTICS AT CONSTANT ELECTRON TEMPERATURE. Brandmaier, H. E. (Curtiss-Wright Corp., Los Angeles, Calif.). AIAA (Amer. Inst. Aeron. Astronaut.) J., 4: 563-5(Mar. 1966).

The development of a simple one-dimensional model for the constant-area rectangular and coaxial Hall-current generator geometries from which the significant MHD characteristics could be estimated for a nonequilibrium plasma is presented. The specific case of radial magnetic field and axial electric field for the coaxial geometry are considered. (B.G.D.)

21573 NONEQUILIBRIUM IONIZATION OF THE WORKING GASES FOR MHD GENERATORS. Hiramoto, Tatumi (Japan Atomic Energy Research Inst., Tokyo). Bull. Inst. Space Aeron. Sci., Univ. Tokyo, 1: A16-A23(Oct. 1965). (In Japanese).

This paper deals theoretically with nonequilibrium ionization of MHD gases in magnetically induced or applied electric fields in MHD devices. It is shown that electron energy in the gases is in a Maxwell distribution with the electron temperature T_e, even in nonequilibrium states. However, the degree of nonequilibrium ionization is much lower than that from the Saha equation based on T_e at low electron temperatures. The enhancements in the electron density n_e, i.e., the electrical conductivity σ and T_e in electric fields can be calculated from an electron energy balance equation containing radiative energy loss terms. In the device used for these experiments, the flow region is divided into two sections. One is a transient section about 1 cm in length and located near the inlet of the device. The other is a steady or generator section, where n_e can be assumed to be locally in equilibrium with T_e, since the relaxation times of T_e and n_e are very short compared with those of heavy species. The current density-electric field characteristics theoretically obtained in K-seeded Ar and Na-seeded Ar are in good agreement with those experimentally obtained. In these experiments, the nonequilibrium conductivity of an order of 100 mhos/m was obtained. Hence, it is concluded from the results of these experiments that the enhancements in the electrical conductivity of MHD gases in induced or applied fields in MHD devices can be expected if the decrease in the fields, e.g., by short circuit in Hall currents near the surfaces of insulators, does not occur. The optimum seeding ratio should be smaller than that in equilibrium states, since the radiation loss increases with the seeding ratio. (auth)

21574 THE COMBINED INFLUENCE OF HALL EFFECT, ION SLIP AND VISCOSITY ON MHD DEVICES. Yamanishi, Tetsuo (Government Mechanical Lab., Tokyo). J. Mech. Lab. Jap., 9: 19-24(1963).

The combined influence of the Hall effect, ion slip, and ion viscosity on the incompressible flow of viscous and weakly ionized gases under a transverse magnetic field was investigated. The method of complex representation is demonstrated for deriving the tensor conductivity solutions for simple flow cases from the corresponding scalar conductivity solutions. Since the scalar conductivity and the Hall coefficients for electrons are reduced according to a given ratio in the presence of ion slip, the ion mobility effect tends to reduce the MHD distortion of the flow patterns. This complex representation method is applicable also to the magnetoplasmadynamics proposed by Gubanov and Lunkin in which not only the anisotropic conductivity but also the anisotropic viscosity must be taken into account. (TCO)

21575 CONDUCTIVITY OF A GAS WITH SUSPENSION. Honma, Takuya; Fushimi, Kozo (Electrotechnical Lab., Tokyo). Jap. J. Appl. Phys., 5: 238-47(Mar. 1966).

The possibility for giving a required conductivity to the working fluid of an MHD-power generator using the thermionic emission from suspended powder is discussed. Particular attention is given to the examination of the electric conductivity under the conditions of an optimum concentration of solid particles. The numerical conclusions do not destroy the feasibility of a gas with suspension as a working fluid in the MHD generator. Some phenomena, such as energy transfer, current behavior, and so on, of possible importance in the generator, are also discussed. (auth)

21576 FISSION-FRAGMENT TRANSPORT EFFECTS AS RELATED TO FISSION-ELECTRIC-CELL EFFICIENCIES. Miley, George H. Nucl. Sci. Eng., 24: 322-31(1966).

An analysis of a parallel-plate UO_2-fueled fission electric cell is developed that includes a detailed treatment of the fission-fragment initial-energy spectrum, energy-charge loss during slowing, and energy dependence of the total range. The treatment of fragment transport is based, as much as possible, on correlations of experimental data. However, available data are skimpy,

and several discrepancies, e.g., between available differential and integral energy-loss data, are noted. The importance of an accurate fragment transport model is demonstrated by the differences in efficiencies obtained from this detailed treatment, as opposed to earlier calculations that used simpler models, e.g., relative differences between models of as much as 15 and 80% are attributed to the treatment of the fragment charge and energy loss, respectively. The calculations are also shown to be fairly sensitive to the total-range-mass correlation, but only weakly dependent on the choice of the initial fragment charge. While efficiencies for the parallel-plate cell with reasonable fuel-layer thickness are found to range from 2 to 10%, efficiencies for cylindrical or spherical geometry may be 5 to 6 times this, and the concept may be competitive for certain specialized applications. (auth)

21577 THE START-UP TRANSIENT BEHAVIOR OF THERMOELECTRIC GENERATORS WITH TEMPERATURE-DEPENDENT PHYSICAL PARAMETERS. Shaw, David Tai-Ko. Nucl. Sci. Eng., 24: 227-38(Mar. 1966).

The study is intended to introduce an analytical approach to the transient problem of the nonlinear thermoelectric systems. The problem of predicting the output current as a function of time and that of predicting the temperature distributions in the thermoelectric elements as a function of both time and distance are determined with a given heat-input function. The analysis of the system is complicated by the following facts: 1) There exist several singularities in the system, and these singularities make the ordinary power expansions converge very slowly. 2) The boundary conditions of the initial transient and of the transient as the system approaches steady state yield two highly nonlinear differential equations of which the approximate solutions are very hard to obtain. The first problem is solved by using logarithmic and other transformations to remove the singularities. The second problem is overcome by applying the technique of the special expansion of Jacobi. (auth)

21578 ON THE THEORY OF LOW-VOLTAGE ARC IN CESIUM. II. Moizhes, B. Ya.; Baksht, F. G.; Melikiya, M. G. Zh. Tekh. Fiz., 35: 1621-33(1965). (In Russian).

The assumption is made that the concentration and temperature of electrons are sufficiently large to make possible an energy exchange between fast and slow electrons. Under such conditions, when the starting energies are below the excitation threshold, the electron distribution function is close to the Maxwellian. The expression for ion generation and recombination is derived along with formulas for electron-electron collisions and step excitations of atoms due to electron impact. By approximating the unknown functions by polynomials, the solution of the system of differential equations reduces to a system of transcendental equations, the solution of which can be facilitated by neglecting the effect of generation. The formulas derived are used to calculate the volt-ampere characteristics of a low-voltage arc-mode energy converter. (ATD)

21579 INFLUENCE OF KRYPTON ON THE OPERATION OF A THERMIONIC CONVERTER. Bekmukhambetov, E. S.; Gus'kov, Yu. K.; Lebedev, S. Ya. Zh. Tekh. Fiz., 35: 1707-9(1965). (In Russian).

The short-circuit currents and volt-ampere characteristics of a thermionic converter were determined in the presence of pure cesium at pressures of 0.31–235 mm Hg and then with various additions of krypton. The molybdenum emitter was kept at temperatures below 600°C, and its distance from the niobium collector was about 0.15 mm. The measurements showed a parallel shift of current-temperature curves toward lower currents when krypton pressures were increased. The volt-ampere characteristics indicated that small admixtures of krypton bring about a small increase of the voltage; when krypton pressure is increased, the converter's output drops. A comparison of the experimentally obtained values for current with those calculated by the use of the diffusion theory showed the former to be 2–3 times lower than the latter. This can be attributed to insufficiently accurate values of the electron scattering cross sections of krypton atoms, or to a thermodiffusion process involving the elimination of Cs from the interelectrode gap. (ATD)

21580 OPERATION OF A CESIUM THERMIONIC CONVERTER IN THE PRESENCE OF XENON. Bekmukhambetov, E. S.; Gus'kov, Yu. K.; Lebedev, S. Ya. Zh. Tekh. Fiz., 35: 1709-11(1965). (In Russian).

The temperature dependence of short-circuit currents of a thermionic converter was measured, first in pure cesium atmospheres in the range of pressures from 2.75×10^{-2}–2 mm Hg, and then with admixtures of xenon at pressures ranging from 0.27–69 mm Hg. Generally, the experiments showed a parallel shift of the curves toward smaller currents. However, at a xenon pressure of 69 mm Hg a change in the curve's angle was observed. The lack of a plateau in the volt-ampere characteristics is explained by volume recombination. When at cesium pressure of about 2 mm Hg the cathode temperature reaches 1300 K, a small admixture of xenon at 0.27 mm Hg brings about an increase of the current and voltage of the converter due to its passing to the arc mode. A further increase of xenon pressure reduces the converter's output. (ATD)

21581 PROCEEDINGS, 19th ANNUAL POWER SOURCES CONFERENCE; 18–20 MAY 1965. Red Bank, N. J., PSC Publications Committee, 1965. 199p. (CONF-650574).

Papers (53) are included dealing with fuel cells, batteries, inverters, converters, solar cells, thermionic converters, and thermoelectric converters. (D.C.W.)

21582 PROCEEDINGS, 18TH ANNUAL POWER SOURCES CONFERENCE, 19–21 MAY 1964. Red Bank, N. J., PSC Publications Committee, [1964]. 192p. (CONF-673).

A separate abstract was prepared for one of the fifty papers included. One other paper was previously abstracted for NSA (18-44278). The remaining papers deal with fuel cells, batteries, power supplies, voltage converters, thermoelectric converters, thermionic converters, and solar cells. (D.C.W.)

For an abstract of the individual paper see: 21162.

21583 PROCEEDINGS, 17TH ANNUAL POWER SOURCES CONFERENCE, 21–23 MAY 1963. Red Bank, N. J.; PSC Publications Committee, [1963]. 194p. (CONF-630507).

Separate abstracts were prepared for 3 of the 58 papers included. The remaining papers deal with batteries, fuel cells, voltage converters, solar cells, thermionic converters, and thermoelectric converters. (D.C.W.)

For abstracts of individual papers see: 21161, 21446, and 22485.

21584 ELECTRON AND ION EMISSION FROM CESIATED REFRACTORY COMPOUND SURFACES. Wilson, R. G. (Hughes Research Labs., Malibu, Calif.). 5p. (CONF-651049-10). ORAU. Gmelin, AED-CONF-65-324-8.

From IEEE Thermionic Conversion Specialist Conference, San Diego, Calif.

The electron and ion emission characteristics were measured for cesiated polycrystalline surfaces of zirconium carbide, molybdenum carbide, molybdenum silicide, tantalum silicide, tungsten silicide, and tantalum boride. Only the carbides were found to be stoichiometrically stable at 1500°C. Only zirconium carbide has a work function below the ionization potential of Cs; it is not low enough to greatly inhibit Cs surface ionization. The maxima in the electron emission S curves are of about the same magnitude for the five high-work-function materials, while that for ZrC is much lower. The five high-work-function materials exhibit full Cs ionization with well defined critical temperatures, while for ZrC low Cs ionization efficiency was observed and no sharp critical temperatures occur. (A.G.W.)

21585 EXPERIMENTAL CORRELATION OF ELECTRON EMISSION COOLING AND OPTIMUM COLLECTOR TEMPERATURE. Kitrilakis, S.; Brosens, P. (Thermo Electron Engineering Corp., Waltham, Mass.). 9p. (CONF-651049-5). ORAU. Gmelin, AED-CONF-65-324-1.

From IEEE Thermionic Conversion Specialist Conference, San Diego, Calif.

A flat-plate-electrode variable-spacing converter equipped with an active collector guard ring was used for measurements of collector heating. Measurements were confined to the region of the knee of the volt-ampere curve. When results are plotted as collector heating vs. current density, the collector heating appears constant with output current. Numerical correlations indicate that a good approximation to the electron emission cooling may be obtained, within the ranges specified, by assuming it to be constant and equal to 2.68 ev per electron. Families of volt-ampere curves with collector tempertures as the variable parameter were generated to define the dependence of optimum collector temperature on converter parameters. A correlation was found to exist between the ratio of optimum collector temperature to reservoir temperature and the output current. (A.G.W.)

21586 PERFORMANCE OF TUNGSTEN-EMITTER THERMIONIC CONVERTER IN THE PRESENCE OF CESIUM FLUORIDE ADDITIVE. Lieb, D. (Thermo Electron Engineering Corp., Waltham, Mass.). 8p. (CONF-651049-9). ORAU. Gmelin, AED-CONF-65-324-6.

From IEEE Thermionic Conversion Specialist Conference, San Diego, Calif.

Cesium fluoride was used in a parametric converter with an active guard ring incorporating a tungsten emitter opposite a molybdenum collector. Experiments were made initially to compare the bare surface work function with that in the presence of the additive only. Parametric performance was then evaluated with both cesium and cesium fluoride present in the test cell. The most significant change produced was the lowering of the cesium pressure corresponding to a given emitter temperature. The lower-pressure device must operate at wider spacings, thereby relaxing mechanical construction of many practical devices. In the devices tested, however, the effects were not stable. (A.G.W.)

Elementary Particles and Radiations

See also Field Theory, Scattering Theory, and Symmetries

Refer also to abstracts 21027–21029, 21465, 21498, 21540, 21541, 22021, 22033, and 22152.

21587 (AD-623564) SCATTERING OF LIGHT BY PROTONS. Revised Edition. Karzas, W. J.; Watson, W. K. R.; Zachariasen, F. (RAND Corp., Santa Monica, Calif.). Nov. 11, 1957. 33p. (P-1126(RAND)). CFSTI $2.00 cy, $0.50 mn.

Within the framework of the Chew-Low-Wick development an analysis of the scattering of photons from a nucleon is carried out. It is shown that an exact relationship exists between the Compton effect amplitude and the experimental meson-nucleon scattering phase shifts for all multipoles except magnetic dipole and electric quadrupole provided that effects arising from currents inside the nucleon source are slowly varying functions of photon energy. That part of the magnetic dipole scattering which can be described in terms of the isotopic vector part of the anomalous magnetic moments of the nucleon is also treated exactly. The cross section for the Compton process is evaluated on the basis of the electric and magnetic dipole contributions only, since a non-recoil theory is clearly expected to be poor for photon energies greater than 300 Mev. Fairly good agreement with experiment is achieved. (auth)

21588 (AD-623658) WIDE-ANGLE ELECTRON-ELECTRON SCATTERING ON THE PRINCETON-STANFORD STORAGE RINGS. Barber, W. C.; Gittelman, B.; O'Neill, G. K.; Richter, B. (Stanford Univ., Calif. High-Energy Physics Lab.). Sept. 1965. Contracts Nonr-22567; Nonr-185839. 20p. (HEPL-405). CFSTI $1.00 cy, $0.50 mn.

The angular distribution of 416 electron-electron scattering events occurring when beams of 300-Mev electrons collide was measured. The experimental angular distribution was compared with that predicted by the Moller formula with a cut-off on the photon propagator. The best fit occurs for $1/K$ = about 0.18 Fermi. The value $1/K = 0$ (no breakdown of quantum electrodynamics) is only one standard deviation from the best fit. (auth)

21589 (AD-626683) POSITIVE PION PRODUCTION ASYMMETRY WITH POLARIZED BREMSSTRAHLUNG NEAR SECOND RESONANCE. Liu, F. F.; Vitale, S. (Stanford Univ., Calif. High-Energy Physics Lab.). Nov. 1965. Contract Nonr-225(67). 31p. (HEPL-393). CFSTI $2.00 cy, $0.50 mn.

The azimuthal asymmetry in meson (π^+) photoproduction by linearly polarized bremsstrahlung was measured at photon energies from 475 to 750 Mev at 90 and 135 degrees in the center of mass system. The experimental results show that even in this energy region pions are predominantly produced in the plane of the magnetic vector. This is interpreted to mean that S and P wave amplitudes are predominating over the D wave amplitude. (auth)

21590 (CERN-66-2) MESURE DES PARAMETRES DE POLARISATION ET DE CORRELATION DE SPIN DANS LA DIFFUSION PROTON-PROTON A 600 Mev A L'AIDE D'UNE CIBLE DE PROTONS POLARISES. (Measurement of Polarization Parameters and Spin Correlation in Proton-Proton Scattering at 600 Mev by Means of a Target of Polarized Protons). Coignet, G. (European Organization for Nuclear Research, Geneva (Switzerland)). Jan. 19, 1966. 65p. Dep. mn.

The general formalism of proton-proton scattering and its relation to different experiments is reviewed. The experiments are also compared to those made without a polarized target. The beam, the polarized proton target, and the experimental detection installation used are described. A beam of protons capable of easily being transformed into a polarized beam with intensity and polarization sufficient for experimentation was constructed. The beam made it possible to evaluate the analysis capacity of carbon at 575 Mev at 4 angles. By the use of this beam with a target of polarized protons the angular distribution of the parameters of polarization P^0 and of correlation C_{NN} was measured in proton-proton scattering at 600 Mev. (J.S.R.)

21591 (CERN-65-24(Vol.1)) PROCEEDINGS OF THE 1965 EASTER SCHOOL FOR PHYSICISTS USING THE CERN PROTON SYNCHROTRON AND SYNCHRO-CYCLOTRON, BAD KREUZNACH, APRIL 1–15, 1965. (European Organization for Nuclear Research, Geneva (Switzerland)). June 16, 1965. 90p. Dep. mn.

Separate abstracts were prepared for the three included papers. (M.O.W.)

For abstracts of individual papers see: 21592, 21593, and 21705.

21592 (CERN-65-24(Vol.1), pp 1-44) PERIPHERAL COLLISIONS. Schmitz, N. (Max-Planck-Institut fuer Physik und Astrophysik, Munich (West Germany)).

The peripheral model for strong interactions is briefly discussed. Various discussions are presented on the following: experimental separation of the reactions a + b → c + d from the background, quantum numbers for the excited particle, decay angular distributions, general properties of the density matrix of the produced resonance, predictions of the OME model on the density matrix elements, experimental methods of determining the density matrix elements, Δ^2 distributions, the absorptive model, and some experimental results are compared with theory. (M.O.W.)

21593 (CERN-65-24(Vol.1), pp 65-80) HIGH-ENERGY ELASTIC SCATTERING. Wetherell, A. M. (European Organization for Nuclear Research, Geneva (Switzerland)).

A general picture of established experimental results, current problems, and possible directions of future research in the field of elementary particle elastic interactions up to energies of 30 Bev is given. In particular, discussions are presented on the following; experimental results on the diffraction peak and large-angle scattering, scattering experiments at very small angles, polarization experiments, and proton-nuclear scattering at high energies. (M.O.W.)

21594 (CERN-65-32) INFORMAL CONFERENCE ON EXPERIMENTAL NEUTRINO PHYSICS HELD AT CERN 20-22 JANUARY, 1965. PROCEEDINGS. Franzinetti, C. (ed.). (European Organization for Nuclear Research, Geneva (Switzerland)). Dec. 1965. 290p. (CONF-650111). Dep. mn.

Forty-three papers were presented. Separate abstracts were prepared for thirty-four. The remaining nine papers were previously abstracted in NSA as 18: 34561, 19: 20738, 20915, 30877, 32908, 36803, and 20: 992, 4523, 4561. (B.G.D.)

For abstracts of individual papers see: 21027–21033, 21465, 21466, 21540–21542, 21595–21614, 21995, and 22306.

21595 (CERN-65-32, pp 1-10) NEUTRINO EXPERIMENTS AT BROOKHAVEN NATIONAL LABORATORY. Lederman, L. (Columbia Univ., New York. Brookhaven National Lab., Upton, N. Y.).

A discussion of results in the search for intermediate bosons in high-energy neutrino interactions is presented. A description of the neutrino arrangement based on an external proton beam at the AGS and the spark chamber is included. (B.G.D.)

21596 (CERN-65-32, pp 11-24) LOWER LIMIT FOR THE MASS OF THE INTERMEDIATE BOSON. Gaillard, J. M.; Hahn, B. (European Organization for Nuclear Research, Geneva (Switzerland)).

Results of a study of the spark chamber and the bubble chamber data in determining the lower limit for the mass of the intermediate boson with the branching ratio as a free parameter are outlined. (B.G.D.)

21597 (CERN-65-32, pp 25-30) FURTHER ANALYSIS OF THE NEUTRINO INTERACTIONS IN THE CERN HEAVY LIQUID BUBBLE CHAMBER. Burmeister, H.; Cundy, D. C.; Eiben, B.; (and others) (European Organization for Nuclear Research, Geneva (Switzerland)).

Analysis of elastic neutrino interactions giving rise to single pion events by momentum analysis of events which have small four momentum transfer and by Monte Carlo calculations is presented. To obtain the cross section for the elastic process and to estimate the axial vector form factor only those events with visible energy greater than 1 Bev were analyzed. Strange particle production in neutrino interactions is also discussed. (B.G.D.)

21598 (CERN-65-32, pp 79-82) THEORETICAL ASPECTS OF NEUTRINO PHYSICS. Veltman, M. (European Organization for Nuclear Research, Geneva (Switzerland)).

A general discussion of the theoretical aspects of neutrino reactions in relation to elastic quasielastic and inelastic processes is presented. General tests for the study of $\nu,\bar{\nu}$ reactions on complicated systems (nuclei) such as the Adler test for CVC and Goldberger-Treiman relations and the test for time reversal invariance are considered. (B.G.D.)

21599 (CERN-65-32, pp 89-96) N* PRODUCTION BY NEUTRINOS. Albright, C. H.; Liu, L. S. (Northwestern Univ., Evanston, Ill.).

The N* production cross section based on the SU(6) relation is calculated and compared to the results obtained with the CERN heavy liquid bubble chamber experiment. (B.G.D.)

21600 (CERN-65-32, pp 97-108) DETERMINATION OF NEUTRINO FLUX. Burns, R.; Goulianos, K.; Hyman, E.; (and others) (Columbia Univ., New York).

A summary of available data for the determination of the neutrino spectrum on a detector is presented. The spectra of secondary particles (pions and kaons) which subsequently decay into neutrinos and their associated leptons in the form of beam survey data are discussed. The differential muon flux which leads to the parent pion flux from which the pion neutrino yield may be calculated is presented in greater detail since the kaon contribution is relatively small. Uncertainties in the neutrino spectra are also discussed. (B.G.D.)

21601 (CERN-65-32, pp 109-10) $\pi^{\pm}$ AND $K^{\pm}$ PRODUCTION CROSS-SECTIONS FOR 12.5 Gev PROTONS ON BERYLLIUM. Lundy, R. A.; Novey, T. B.; Yovanovitch, D. D. (Argonne National Lab., Ill.); Telegdi, V. L. (Chicago Univ., Ill.).

A beam survey with the ZGS external beam operating in a parasitic mode to obtain pion and kaon yields from a beryllium target for a momentum range of 1 to 10 Bev/c and for production angles from 0 to 16° is presented. (B.G.D.)

21602 (CERN-65-32, pp 111-14) FLUXES OF NEUTRINOS AND ANTINEUTRINOS PRODUCED AT CERN (PRELIMINARY RESULTS). Orkin-Lecourtois, A. (Laboratoire de l'Accelerateur Lineaire, Univ. de Paris, Orsay (France)); Franzinetti, F.; Pedersen, T. I.; Yoshiki, H. (European Organization for Nuclear Research, Geneva (Switzerland)).

Preliminary results of an experiment for the production of neutrino and antineutrino fluxes at CERN are discussed. Analysis of the tracks produced by exposing a neutrino copper target to a proton beam inside a heavy liquid bubble chamber is presented. (B.G.D.)

21603 (CERN-65-32, pp 115-20) EXPERIMENTAL DETERMINATION OF THE NEUTRINO SPECTRUM. Holder, M. (European Organization for Nuclear Research, Geneva (Switzerland)).

An experimental determination of the neutrino flux using the elastic reaction $\nu + n \rightarrow \bar{\mu} + p$ is discussed. In the limit of zero momentum transfer ($q^2 \approx 0$) the cross section for the free nucleon is a constant, independent of assumptions about form factors. The observed event rate of low q^2 is then a direct measure of the mean neutrino flux. (B.G.D.)

21604 (CERN-65-32, pp 121-6) THE DETERMINATION OF THE SPECTRA OF HIGH-ENERGY NEUTRINO PARENTS. Plass, G.; Vahlbruch, K. M.; Wachsmuth, H. W. (European Organization for Nuclear Research, Geneva (Switzerland)).

Two methods that yield the ν spectrum without assumptions on the K/Π ratio and on weak interaction theory are discussed. These are: analysis of the ν parent production in an actual horn target in a heavy liquid bubble chamber, and a counter experiment with slowly ejected proton beams using a steering magnet and a Cherenkov spectrometer. (B.G.D.)

21605 (CERN-65-32, pp 153-6) CHAIRMAN'S SUMMARY OF THE SESSION ON NEUTRINO FACILITIES. Ramm, C. A. (European Organization for Nuclear Research, Geneva (Switzerland)).

A brief summary of the session on neutrino facilities at the congress is presented. (B.G.D.)

21606 (CERN-65-32, pp 157-60) FUTURE NEUTRINO EXPERIMENTS WITH THE CERN HEAVY LIQUID BUBBLE CHAMBER. Cundy, D. C. (European Organization for Nuclear Research, Geneva (Switzerland)).

Future neutrino experiments with the CERN heavy liquid bubble chamber using heavy freon (CF_3Br) for the ν runs can be used to study such questions as hyperon production, N* production, elastic production, and form factors. Future experiments with free nucleon targets such as hydrogen and hydrocarbons, the availability of which can lead to the study of elastic form factors, are discussed. (B.G.D.)

21607 (CERN–65-32, pp 161-8) A POSSIBLE SPARK-CHAMBER EXPERIMENT WITH ANTINEUTRINOS. Bienlein, J. K.; von Dardel, G.; Gerber, H.-J.; Reinharz, M. (European Organization for Nuclear Research, Geneva (Switzerland)).

A discussion of present problems which can be investigated by spark-chamber experiments in the near future is presented. These problems are the measurement of the transverse component of the muon polarization, the high q^2 production of Λ^0 in processes where only a Λ^0 and a μ^+ are observed, and the production of positrons in processes where only one electron shower is observed. (B.G.D.)

21608 (CERN-65-32, pp 169-74) NEUTRINO PHYSICS WITH 80-in. AND 14-ft BUBBLE CHAMBERS AT BROOKHAVEN NATIONAL LABORATORY. Samios, N. P. (Brookhaven National Lab., Upton, N. Y.).

Calculations estimating the yield of neutrino events that can be obtained by the magnetic finger as a focusing device and large bubble chambers are presented, including the basis from which these calculations are made. Future explorations in neutrino physics due to the advent of the focusing device and large bubble chambers are summarized. (B.G.D.)

21609 (CERN–65-32, pp 175-80) POSSIBLE NEUTRINO EXPERIMENTS IN EMULSIONS. Duff, B. G. (London Univ. (England). University Coll.).

An experiment to identify definitely a few high-energy ν interactions in nuclear emulsions is discussed. The technique employs a spark chamber in conjunction with the emulsion. The advantages of this method over a heavy liquid bubble chamber, with respect to resolution, are presented. (B.G.D.)

21610 (CERN–65-32, pp 181-94) STUDY OF THE FEASIBILITY OF AN EXPERIMENT TO OBSERVE THE W PRODUCED IN STRONG INTERACTIONS. Good, R. H.; Mehlhop, W. A. W.; Piccioni, O.; Swanson, R. (California Univ., La Jolla, San Diego).

A feasibility study using the AGS to investigate the existence of an intermediate W boson to about 6 Bev mass value is presented. The reaction $p + p \rightarrow d + W$ followed by $W \rightarrow \mu + \nu$ is considered. The expected production cross section of the reaction is summarized along with the apparatus proposed for this study. (B.G.D.)

21611 (CERN–65-32, pp 195-200) REPORT ON PHOTOPRODUCTION OF SINGLE W BOSONS. Ueberall, H. (Catholic Univ. of America, Washington, D. C.).

A discussion on the photoproduction of single W bosons in the process $\gamma + p \rightarrow n + W^+$ is presented. (B.G.D.)

21612 (CERN–65-32, pp 225-30) PROJECT FOR AN UNDERGROUND LABORATORY IN THE MOUNT BLANC TUNNEL FOR EXPERIMENTS ON NEUTRINO AND COSMIC RADIATION. Castagnoli, C.; De Marco, A.; Pengo, P. (Turin Univ. (Italy). Istituto di Fisica).

The establishment of an underground laboratory in the Mount Blanc tunnel for the investigation of neutrinos of atmospheric, cosmic, and solar origin is discussed. (B.G.D.)

21613 (CERN–65-32, pp 269-74) SUMMARY OF THE CONFERENCE AND CLOSING REMARKS. Goldhaber, M. (Brookhaven National Lab., Upton, N. Y.).

A summary is presented on the topics discussed at the conference. These topics are sources of neutrinos, detection techniques, cosmic neutrinos, solar neutrinos, and the future of neutrino experiments. (B.G.D.)

21614 (CERN–65-32, pp 275-84) NEUTRINO PHYSICS. Lee, T. D. (Columbia Univ., New York).

A review of the main problems in leptonic weak interactions is presented. Topics discussed are the effective lagrangian of weak interactions, intermediate boson, local leptonic current hypothesis, measurement of form factors, tests of symmetry properties and selection rules, and elastic scattering of neutrinos. (B.G.D.)

21615 (COO-1195-52) A STUDY OF THE $K^- + p \rightarrow \bar{K} + N + \pi$ REACTIONS AT 1.33 Bev/c [Thesis]. Ficenec, John Robert (Illinois Univ., Urbana. Dept. of Physics). Feb. 1966. Contract AT(11-1)-1195. 131p. Dep. mn. CFSTI $4.00 cy, $1.00 mn.

An experiment was performed on meson (K^-)-proton interactions using the 72″ Alvarez liquid hydrogen bubble chamber. As part of that experiment the University of Illinois group investigated the following topologies: 2-prong, 2-prong with 1 kink, and 0-prong with an associated vee. In particular, the reactions $K^- + p \rightarrow \bar{K} + N + \pi$ are reported. A sample of 30,000 frames containing 11,111 2-prong events was used, with measurements being done on SMP's. These reactions are found to be dominated by $\bar{K}^*(890)N$ production. Some evidence is also found for $N^*(1236)\bar{K}$ and $Y_1^*(1520)\pi^0$ production, and slight amounts of $Y_1^*(1660)\pi$ and $Y_1^*(1765)\pi$ are seen. A backward peaking is seen to exist in the production angular distribution of the $\bar{K}^{*-}(\bar{K}^0\pi^-)$. No evidence for this backward peaking is found in the other $\bar{K}N\pi$ final states. The production and decay angular distributions of the $\bar{K}^*(890)$ indicate that the $\bar{K}^{*0}n$ final state is produced predominantly by an exchange of a pseudoscalar meson of small mass, probably the pion. The $\bar{K}^{*-}p$ final states show less marked evidence for peripheral production than does the $\bar{K}^{*0}n$ final state. If the one-particle exchange model is hypothesized as a contributing mechanism, the $\bar{K}^{*-}p$ final states appear to have a large amount of T = 0 vector meson exchange contributing to their production. This could be either the ω or φ meson. (auth)

21616 (JINR–P-2429) NEITRINNYE PROTSESSY. (Neutrino Processes). Vasilevskii, I. M.; Lapidus, L. I. (Joint Inst. for Nuclear Research, Dubna (USSR). Lab. of Nuclear Problems). 1965. 123p. Dep. mn.

An exposition of a course of lectures concerned with leptonic and semi-leptonic decays as well as with neutrino-induced processes is presented. The major part is devoted to theoretical and experimental works performed at high energy particle accelerators. A brief review is given of the modern theory of weak interactions of strange and nonstrange particles. Results and techniques of neutrino experiments done at Brookhaven and CERN are presented. Future investigations with neutrinos are discussed. A possibility is discussed of checking basic features of current × current scheme of weak interaction in investigating the conserved vector current at high values of energies and momentum transfers. (auth)

21617 (JINR–P-2546) OB ODNOM PRIBLIZHENNOM METODE V ZADACHE DVUKH NUKLONOV. (On an Approximate Method in a Two-Nucleon Problem). Efimov, V. N. (Joint Inst. for Nuclear Research, Dubna (USSR). Lab. of Neutron Physics). 1966. 17p. Dep. mn.

The application of the well-known Bubnov-Galerkin's method to solving integral equations is considered. Use is made of orthogonal polynomials with weight determined by the radial dependence of the potential. An approximate factorized expression was obtained for the t-matrix off the energy surface. The Yukawa potential is considered as an example. (auth)

21618 (JINR-P-2566) ZNAK RAZHOSTI REAL'NYKH CHASTEI AMPLITUD UPRUGOGO $\pi^{\pm}$-p RASSEAYNIYA V OBLASTI OCHEN VYSOKIKH ENERGII. (A Difference Sign of Real Parts of Elastic π -p Scattering Amplitudes at Very High Energies). Barashenkov, V. S.; Truskova, N. F. (Joint Inst. for Nuclear Research, Dubna (USSR). Lab. of Theoretical Physics). 1966. 7p. Dep. mn.

It is shown that by using dispersion relations it is not possible to fit the experimental data on the zero-angle $\pi^{\pm}p$ charge exchange cross section and the energy dependence of the total $\pi^{\pm}p$ interaction cross sections at $T \approx 5$ to 20 Bev, on the one hand, and the results of measurements of the real parts of the elastic $\pi^{\pm}p$ scattering amplitudes, on the other. (auth)

21619 (JINR–P-2567) ODIN METOD RESHENIYA ZADACHI NUKLON-FONONNOGO VZAIMODEISTVIYA. (A Method for Solving the Nucleon-Phonon Interaction Problem). Mikhailov, I. N.; Dzholos, R. V. (Joint Inst. for Nuclear Research, Dubna (USSR). Lab. of Theoretical Physics). 1966. 18p. Dep. mn.

A method to solve the Schroedinger equation for fermions interacting with phonons in a system with sufficiently small number of fermion states is suggested. The method is described by an example of a problem with a scalar phonon coupling the orbitals of two degenerate fermion energy levels. The solution of the Schroedinger equation is achieved by finding the integrals given by entire functions of the two coupled differential equations. (auth)

21620 (JINR–P-2577) OB OPREDELENII SPINA BOZONOV, RASPADAYUSHCHIKHSYA NA TRI BESSPINOVYE CHASTITSY. (On Spin Test for Bosons Decaying into Three Spinless Particles). Ryndin, R. M. (Joint Inst. for Nuclear Research, Dubna (USSR). Lab. of Theoretical Physics). 1966. 6p. Dep. mn.

A possible method is suggested to determine the spin of bosons produced in the reactions of the type $0 + 0 \rightarrow S + 0$ and decaying into three spinless particles. It is shown that the coefficient for the highest Legendre polynomial in the angular correlation between the normals to the production and decay planes cannot vanish and is restricted by the absolute magnitude. (auth)

21621 (JINR–P-2584) OPREDELENIE PARAMETROV ODNOBOZONNOI OBMENNOI MODELI PO FAZOVYM SDVIGAM UPRUGOGO NUKLON-NUKLONNOGO RASSEYANIYA. (Determination of One-Boson Exchange Model Parameters by Elastic Nucleon-Nucleon Scattering Phase Shifts). Azhgirei, L. S.; Chizhikov, V. I. (Joint Inst. for Nuclear Research, Dubna (USSR). Lab. of Nuclear Problems). 1966. 20p. Dep. mn.

The least squares method is used to determine one-boson exchange model parameters from the nucleon-nucleon phase shifts in the energy range of 25 to 310 Mev. Different methods for the explicit unitarization of the Born partial-wave amplitudes are compared. The K-matrix unitarization is shown to give the best fit to the pp-phase shifts. For an exchange of a scalar meson (σ), a pseudoscalar meson (π), and two vector mesons (ω and ρ) a best fit to the NN-scattering was obtained with the following parameters: $g_\sigma^2 = 2.9 \pm 0.4$; $m_\sigma = 373 \pm 13$ Mev; $g_\pi^2 = 13.1 \pm 0.2$; $g_\omega^2 = 2.1 \pm 0.5$; $f_\omega/g_\omega = 0.5 \pm 0.1$; $m_\omega = 422 \pm 18$ Mev; $g_\rho^2 = 0.1 \pm 0.3$; $f_\rho/g_\rho = -5.4 \pm 7.0$; $m_\rho = 800 \pm 120$ Mev. The energy dependencies calculated by the above parameters are compared with the results of phase shift analyses at 435 and 657 Mev. (auth)

21622 (JINR–P-2585) FAZOVYI ANALIZ UPRUGOGO pp-RASSEYANIYA PRI 657 Mev S UCHETOM ODNOBOZONNOGO OBMENA I RELYATIVISTSKIKH KULONOVSKIKH EFFEKTOV. (Elastic pp-Scattering Phase Shift at 657 Mev With Account of One-Boson Exchange and the Relativistic Coulomb Effects). Azhgirei, L. S. (Joint Inst. for Nuclear Research, Dubna (USSR). Lab. of Nuclear Problems). 1966. 7p. Dep. mn.

The phase shift analysis of the data on elastic pp-scattering was performed in the neighborhood of 660 Mev taking into consideration relativistic corrections in the Coulomb scattering. In calculating the phase shifts of higher states of pp-system account was also taken, besides the one-pion exchange, of the scalar and two vector bosons. The one-boson exchange turns out to be essential for describing data on small-angle proton polarization. (auth)

21623 (JINR–P-2602) VKLAD VIRTUAL'NOGO KOMPTON-EFFEKTA V SECHENIE OBRAZOVANIYA ELEKTRON-POZITRONNYKH PAR. (Contribution of Virtual Compton Effect to the Cross Section for Electron-Positron Pair Production). Zhuravlev, V. I.; Solov'ev, L. D. (Joint Inst. for Nuclear Research, Dubna (USSR). Lab. of Theoretical Physics). 1966. 9p. Dep. mn.

Using the data on ρ^0 meson photoproduction the contribution of strong interactions to the cross section for the leptonic pair photoproduction is estimated. This contribution is due to the virtual Compton effect in the energy range from 5 up to 20 Bev. (auth)

21624 (JINR–P-2606) MASSOVYE FORMULY V NEODNORODNOI GRUPPE SU(6,6). (Mass Formula in the Inhomogeneous SU(6,6) Group). Nikolov, A. V.; Todorov, I. T. (Joint Inst. for Nuclear Research, Dubna (USSR). Lab. of Theoretical Physics). 1966. 17p. Dep. mn.

A symmetry breaking for the inhomogeneous SU(6,6) group is introduced in the following way: it is required that the commutators of the 143-momentum P with isospin and hypercharge give zero when acting on physical states. Using this and the invariance of TrP^2, quadratic mass formulas are obtained both for mesons and baryons. For the mesons the obtained relations are satisfied within an accuracy greater than 1%. The agreement of the mass formulas for baryons with experiment is not so good. (auth)

21625 (JINR–P-2619) PRAVILA SUMM DLYA POGLOSHCHENIYA FOTONOV NUKLONAMI I RAZMERY NUKLONA V MODELI KVARKOV. (Sum Rules for Photon Absorption by Nucleons and Nucleon Dimensions in the Quark Model). Gerasimov, S. B. (Joint Inst. for Nuclear Research, Dubna (USSR). Lab. of Theoretical Physics). 1966. 7p. Dep. mn.

The relation was obtained between the sum rules for electric dipole and quadrupole absorption with the charge distribution parameters of the proton. A strong difference of the quadrupole sum rule from experiment indicates that the quarks have their own electromagnetic structure. (auth)

21626 (LNF-66/4) PHOTODISINTEGRATION OF THE DEUTERON BY POLARIZED γ RAYS. Note No. 305. Barbiellini, G.; Bernardini, C.; Felicetti, F.; Murtas, G. P. (Laboratori Nazionali di Frascati, Comitato Nazionale per l'Energia Nucleare (Italy)). Feb. 4, 1966. 12p. Dep. mn.

A brief review of experimental and theoretical work on photodisintegration of deuterons is presented. An experiment was performed using a polarized gamma beam from the Frascati electron synchrotron. The photoproduction processes for pions are discussed. The photoproduction asymmetry functions are described. (M.O.W.)

21627 (LNF-66/9) DETERMINATION OF THE BRANCHING RATIOS AMONG THE NEUTRAL DECAY MODES OF THE η PARTICLE. Note No. 309. Di Giugno, G.; Giorgi, M.; Querzoli, R.; Schiavon, P.; Silvestrini, V.; Troise, G. (Laboratori Nazionali di Frascati, Comitato Nazionale per l'Energia Nucleare (Italy)). Mar. 1, 1966. 8p. Dep. mn.

The branching ratios among the neutral decay modes of the η particle were measured using a counter technique. Strong evidence for the presence of the mode $\eta \rightarrow \pi^0\gamma\gamma$ is obtained. The accuracy of the results is discussed. (M.O.W.)

21628 (TID–22822) A STUDY OF NEUTRAL HYPERON AND NEUTRAL KAON PRODUCTION IN K^- + p INTERACTIONS NEAR THE Y*(1765) RESONANCE [Thesis]. Technical Report No. 545. Uhlig, Ronald Paul (Maryland Univ., College Park. Dept. of Physics and Astronomy). Feb. 1966. Contract AT(40-1)-2504. 159p. Dep. mn. CFSTI $5.00 cy, $1.50 mn.

The following K^- meson interactions in hydrogen were studied: $K^- + p \rightarrow \Lambda + \pi^0$, $K^- + p \rightarrow \Lambda + \pi^+ + \pi^-$, $K^- + p \rightarrow Y_1^{*\pm}(1385) + \pi^\mp$, $K^- + p \rightarrow \Lambda + \pi^+ + \pi^- + \pi^0$, $K^- + p \rightarrow Y_0^*(1520) + \pi^0$, $K^- + p \rightarrow \Lambda + \eta$, $K^- + p \rightarrow \overline{K}^0 + n$, and $K^- + p \rightarrow \overline{K}^0 + p + \pi^-$ for incident K^- momenta between 900 and 990 Mev/c. Cross sections and angular distributions are presented and analyzed as a function of momentum. Results are interpreted in terms of the properties of the Y*(1765) resonance. Results are consistent with the existence of Y*(1765) with isotopic spin 1 and spin and parity $\frac{5}{2}^-$. Evidence is presented which shows that $\Lambda + \pi^0$, $Y_1^*(1385) + \pi$, $Y_0^*(1520) + \pi^0$, and $\overline{K}^0 + n$ are all possible decay modes of the Y*(1765). (auth)

21629 (UCRL–16332) K^+p INTERACTIONS AT 4.6 Bev/c. Goldhaber, S.; Brown, J. L.; Butterworth, I.; Goldhaber, G.; Shen, B. C.; Fu, C. M.; Trilling, G. H. (Lawrence Radiation Lab., Univ. of California, Berkeley). Feb. 28, 1966. Contract W-7405-eng-48. 18p. (CONF-650945–6). Dep. mn. CFSTI $1.00 cy, $0.50 mn.

From International Conference on Elementary Particles, Oxford.

In a preliminary analysis of 50,000 photographs of the

80-inch BNL hydrogen bubble chamber exposed to a 4.6-Bev/c K^+ meson beam, the reactions were studied; $K^+ + p \rightarrow K^0\pi^+p$, $K^+p \rightarrow K^0\pi^+\pi^0p$, and $K^+ + p \rightarrow K^+\pi^-\pi^+p$. In all these reactions $K^*(1400)$ production is observed. The distribution of the $K\pi$ scattering angle for $K^*(1400)$ shows characteristic features expected for an aligned 2^+ meson on a one-pion-exchange model. The $K^*(890)\pi$ enhancement at 1320 Mev, reported by Almeida et al., is observed in reactions (2) and (3). A definite mass enhancement was for observed reations (2) and (3) in the $K^*\pi$ mass spectrum at 1320 Mev with a width at about 80 Mev. This corresponds to the results reported by Almeida et al. The data were considered both as a bona fide resonance and a kinematical enhancement via the Deck mechanism. (auth)

21630 (UCRL-16469) A MEASUREMENT OF THE ANOMALOUS GYROMAGNETIC RATIO OF THE MUON. Schrank, G.; Henry, G. R.; Swanson, R. (Lawrence Radiation Lab., Univ. of California, Berkeley). Oct. 28, 1965. Contract W-7405-eng-48. 126p. Dep. mn. CFSTI $6.00 cy, $0.75 mn.

A measurement of (g-2) for the free, positive muon was made. The value obtained was $(g-2)_\mu = 2(0.00106 \pm 0.000067)$ and is to be compared with the theoretical value of 2(0.0011654). The technique consisted of trapping polarized muons, one at a time, in an essentially homogeneous, 28-kG magnetic field for about eight muon lifetimes. While in this field, the muon undergoes cyclotron motion (ω_c) and its magnetic dipole moment also precesses (ω_p) about the magnetic field vector. The difference frequency ($\omega_c - \omega_p$) was measured and this quantity, in appropriate units, is $(g-2)_\mu$. (auth)

21631 ELECTROMAGNETIC MASS OF THE CLASSICAL ELECTRON. Zink, J. W. (Univ. of California, Livermore). Amer. J. Phys., 34: 211-15(Mar. 1966).

The difference between the electrostatic mass of the classical electron m_0, and the electrodynamic mass $(4/3)m_0$, has caused a considerable amount of confusion because the theory of relativity seems to predict that, in the limit of small velocities, the two masses should be the same. It is shown that within the structure of relativity the two masses should not necessarily be the same. The nature of each of the two masses is brought out. (auth)

21632 INTENSITY OF ELECTRON BEAMS. Helmer, J. C. (Varian Associates, Palo Alto, Calif.). Amer. J. Phys., 34: 222-7(Mar. 1966).

The theories of D. Langmuir and J. R. Pierce on the thermal limitations of electron-beam current density have a simple interpretation through geometrical optics and the low of photometric brightness. The brightness law together with Abbe's sine law are sufficient for the design of most electron beams for laboratory experiments. Application of the theory is illustrated for the design of low voltage, high-intensity beams as used in low-energy electron-diffraction experiments. (auth)

21633 CHERENKOV RADIATION. More, Richard M. (Univ. of California, San Diego, La Jolla). Amer. J. Phys., 34: 243-5(Mar. 1966).

A simplified method for computing the energy yield in Cherenkov radiation by a fast-moving particle is described. The formalism is applied to the Cherenkov radiation of an electron-positron pair. (auth)

21634 CONTRIBUTIONS TO THE STUDY OF THE STRUCTURE OF PARTICLES USING THE GENERALIZED RELATIVITY THEORY. Gottlieb, I.; Gorbanescu, Gh.; Tereja, E. An. Stiint. Univ. A. I. Cuza, Iasi, Sect. I, 11: 21-7(1965). (In Rumanian).

On the basis of a method proposed by Vescan, the mathematical formalism of generalized relativity is used in the study of the distribution of mass ρ and of charge ρ_e of a particle with spherical symmetry in the static case. The dependence of these distributions is shown. The equations derived show that a neutral particle possesses a uniform mass distribution but a charged particle has a mass distribution decreasing from the center. The expressions for the mass distribution when it is of the Roch type and of the exponential form were derived. (tr-auth)

21635 BOUNDS FOR THE CORRECTION TO THE BORN TERM AND APPLICATIONS TO p-p SCATTERING FOR A GENERALIZED DISPERSION MODEL. Binstock, Judith (Univ. of California, Berkeley). Ann. Phys. (N. Y.), 36: 435-57(Feb. 18, 1966). (UCRL-16174).

The unitarizing corrections to the Born term, as given by the Chew-Arndt, MacGregor-Arndt (j_0 even), and Scotti-Wong models, are shown to be bounded above and below. The bounds follow from the mathematical forms of the models, to all of which forms a theorem (proved in this paper) applies. The correction bounds are given for several p-p amplitudes for the range 0 to 300 Mev. The results are shown to explain why the apparently different models mentioned above give similar Born terms after subtraction of the correction from the experimentally determined (p-p) amplitude. A generalization of these models for the unitarizing correction is proposed, which has properties leading to partial-wave dispersion relations, and which has a specified relationship between the asymptotic behavior and the fluctuation of the sign of the left-hand discontinuity. Upper and lower bounds are found for the correction term prescribed by this generalized model (which is not restricted, in its application, to nucleon-nucleon scattering). (auth)

21636 EXPERIMENTAL LIMIT OF THE MEAN LIFE OF NUCLEONS. Briatore, Luigi; Castagnoli, Carlo; De Marco, Angelo. Atti Accad. Naz. Lincei, Rend., Cl. Sci. Fis., Mat. Natur., 39: 189-95(Sept. Oct. 1965). (In Italian).

The mean life of nucleons was measured using a directional method and the time-of-flight technique. The experiment consisted of the measurement of the final particle flux emerging from the energy background greater than 50 Mev activating two telescopes consisting of two plastic scintillators placed 2.5 m apart. The experimental results made it possible to give a lower limit to the mean life of the nucleon. This value was $\geq 0.9 \times 10^{27}$ yields. (J.S.R.)

21637 ON A CERTAIN NONLOCAL POTENTIAL. De La Cruz, V.; Orman, B. A.; Razavy, M. (Univ. of Alberta, Edmonton, Canada). Can. J. Phys., 44: 629-36 (Mar. 1966).

A solvable example of a class of nonlocal potentials, whose kernels are related to Green's functions of second-order differential equations, is examined. This solvable example is applied to a few standard problems and, in particular, acceptable numerical results are obtained for p-p scattering in the ^1S state. (auth)

21638 INTERPRETATION OF ASYMMETRIES IN THE NEUTRINO PRODUCTION OF PIONS. Karpman, Gilbert (Institut de Physique Nucleaire, Orsay, France). Compt. Rend., Ser. B, 262: 383-4(Feb. 7, 1966). (In French).

It is shown that with the general hypothesis the eventual effects of violation of time reversal can be distinguished from the effects of the interaction of the final state. (J.S.R.)

21639 THE ELASTIC SCATTERING OF PROTONS ON PROTONS AT AN ENERGY OF 8 Gev. Rob, L. (Czech Technical Univ., Prague). Czech. J. Phys., 16: 249-54 (1966).

The measurement of the differential cross section for pp scattering at an energy of 8 Bev is described. The results agree well with the assumption that there exists a real part of the scattering amplitude that is 33% of the imaginary part. (auth)

21640 COUPLING CONSTANT SUM RULES FOR THE DECAY OF THE $J^P = 2^+$ NONET IN BROKEN SU(3). Gautam, V. P.; Ghose, P. (Indian Association for the Cultivation of Science, Calcutta). Indian J. Phys., 39: 451-2(Sept. 1965).

Coupling constant sum rules are given for the decay of the $J^P = 2^+$ mesons $K^{**}(1430)$, $A_2(1320)$, f'(1500), and f(1250) into a pair of pseudoscalar mesons and into a vector and pseudoscalar meson. The violation of unitary symmetry is assumed to transform like the eighth component of a unitary octet and the mixing angles are kept arbitrary. (L.B.S.)

21641 INVARIANT IMBEDDING AND TRANSPORT PROBLEMS WITH INTERNAL SOURCES. Wing, G. Milton

(Univ. of Colorado, Boulder). J. Math. Anal. Appl., 13: 361-9(Feb. 1966).

It is shown how a perturbation method is used to obtain invariant imbedding equations for transport problems involving internal sources. Previous formulas for the escape probability for several different physical situations were obtained by particle counting. These formulas are rederived using perturbation analysis. (J.F.P.)

21642 USE OF DISCRETE-ORDINATES METHODS FOR SOLUTION OF PHOTON PROBLEMS. Lathrop, K. D. Nucl. Sci. Eng., 24: 381-8(1966).

To permit numerical solution of photon transport problems by the method of discrete ordinates, an anisotropic scattering approximation and a multigroup cross-section preparation method are selected. The incorporation of the anisotropic scattering approximation in a discrete-ordinates transport-theory code is described. Results of discrete-ordinates calculations are compared to Monte Carlo and moments-methods computations in three test problems. Flux values and leakage percentages in the different methods of solution are found to be in excellent agreement, even when a relatively low-order (four or six terms of a Legendre polynomial expansion) anisotropic scattering approximation is used in the discrete-ordinates method. In the test problems considered, the discrete-ordinates method is (computationally) nearly an order of magnitude faster than the other methods. (auth)

21643 Ω^- DECAY IN A COMPOSITE-PARTICLE MODEL. Harte, J. (Univ. of Wisconsin, Madison). Contract AT(11-1)-30. Nuovo Cimento (10), 42A: 316-22 (Mar. 21, 1966). (COO-30-103).

A quasi-relativistic composite-particle model is presented which is suited for the study of the long-range behavior of the strongly bound composite system. Arguments are given to justify a particular form for the Bethe–Salpeter wave-function with emphasis placed on the treatment of the relative-energy dependence. As an application of the model, the weak decay rates of the Ω^- are calculated. Only one free parameter, an effective cut-off to which our results are insensitive, remains in the calculated decay amplitudes after a normalization condition on the Bethe–Salpeter wave-function is imposed. (auth)

21644 THE ABSORPTION MODEL AND PRODUCTION OF 2^+ MESONS. Hoegaasen, H.; Hoegaasen, J.; Keyser, R.; Svensson, B. E. Y. (CERN, Geneva). Nuovo Cimento (10), 42A: 323-50(Mar. 21, 1966).

The absorption model for high-energy peripheral production of resonances is applied to the production of spin-parity 2^+ mesons in pion-nucleon interaction with the twofold purpose of testing the model against the experimental data and of discussing some approximations made within the model. By a detailed numerical investigation of the partial-wave expansion it is shown how the impact parameter approximation, often used in the application of the model, may significantly affect both the predicted cross section and the decay distribution. Moreover, the cross section, but not so much the decay distribution, is sensitive to the detailed way in which each partial wave in the model is modified by the absorption. We trace these features back to the fact that the low partial waves, although strongly suppressed as compared to the unmodified Born approximation, still play a major role. The comparison with experiment for production of f_0 (pion exchange) shows that the slope of the cross section is correctly predicted but that the absolute magnitude is too big by a factor of around two. For A_2 (1310) production (rho exchange) the slope of the cross section can be made to agree with experiment only after the introduction of a fairly strong form factor; the absolute magnitude and the energy dependence of the cross section are wrong. These results strengthen the conclusion that the absorption model is unable to reproduce the experimental data for production of high-spin resonances, especially if vector meson exchange has to be assumed. The spin-2 formalism, including decay widths and decay distributions, is presented in the Appendices. (auth)

21645 EXPONENTIAL ASYMPTOTIC BEHAVIOR AND LOW-ENERGY PION-PION SCATTERING. Burkhardt, H. (CERN, Geneva). Nuovo Cimento (10), 42A: 351-64 (Mar. 21, 1966).

A new approach to low-energy π-π scattering is described in which it is assumed that, because of the very short range of the important forces in this problem, the distant singularity structure is relatively important. It is remarked that the exponential decrease of the amplitude at fixed angle observed experimentally, which also corresponds to the maximum rate of decrease allowed theoretically in a reasonable S-matrix theory, gives information about this structure. The high-energy and low-energy phenomena are connected by using the fixed-angle method to calculate the partial-wave amplitudes at low energy. A representation is conjectured that contains the correct asymptotic behavior as well as the nearby part of the left-hand cut, which is known from crossing symmetry. A formal solution, analogous to the full determinantal N/D method, is presented. In a simple, but fairly realistic model an additional attractive potential is produced by the asymptotic left-hand cut; it is suggested that this may be responsible for the missing attraction in the ρ bootstrap mechanism. (auth)

21646 SHADOW EFFECT IN HIGH-ENERGY SCATTERING FROM DEUTERONS. Abers, E. S.; Burkhardt, H.; Teplitz, V. L.; Wilkin, C. (CERN, Geneva). Nuovo Cimento (10), 42A: 365-89(Mar. 21, 1966).

Most of the experimental information on high-energy scattering from neutrons has been obtained by comparing cross sections from protons and deuterons. The extraction of neutron cross sections from such data is nontrivial; the most widely used model is the semiclassical ray formula of Glauber, which gives, in addition to the impulse approximation terms, a shadow correction due to the mutual eclipsing of the nucleons in the deuteron. It is shown that, if the nucleon-nucleon scattering amplitudes near the forward direction can be represented as a sum of Regge poles, the shadow term that Glauber includes vanishes rapidly at high energies but that other terms remain which provide a somewhat smaller shadow effect. A diagrammatic derivation of the Glauber formula is given and it is shown that his shadow term, which comes from the diagram where both nucleons interact with the incident fast particle, does not in fact have the Regge cut necessary for its persistence at high energies. It is then shown that certain diagrams with inelastic virtual states between the two interactions do have such cuts and their contribution is expressed in terms of a partial inelastic cross section and a statistical factor. An experimental clarification can only be achieved by accurate experiments with high-energy neutron beams. (auth)

21647 HIGH-ENERGY ρ-EXCHANGE PERIPHERAL MODEL WITH ABSORPTION AND INSTABILITY. Lassila, K. E. (Univ. of Helsinki). Nuovo Cimento (10), 42A: 403-6(Mar. 21, 1966).

The results are presented of an application of the ρ-exchange peripheral model to pion-nucleon charge-exchange scattering. An improvement in the data fit for π-p differential cross section at 5.9 and 10 Bev/c was obtained by inclusion of a new instability effect along with absorption effects in the calculations. (L.B.S.)

21648 S-WAVE $\pi\pi$-$K\bar{K}$ CROSS SECTION IN THE T = 0 STATE. Nath, R. (Moscow State Univ.). Nuovo Cimento (10), 42A: 407-9(Mar. 21, 1966).

The S-wave $\pi\pi$-$K\bar{K}$ cross section in the T = 0 state was calculated by the multichannel approach developed by Lichtenberg and Williams and by the N/D matrix method of Zachariasen and Zemach, taking into account the absorption effects due to the presence of the other open channels. The results are plotted against the total cm energy of the system. (L.B.S.)

21649 COULOMB SCATTERING OF MUONS AND ELECTRONS FROM FLUORINE AND CHLORINE. Sawicki, J. (Laboratoire Joliot-Curie de Physique Nucleaire,

Orsay, France); Yoshiki, H. Nuovo Cimento (10), 42A: 410-12(Mar. 21, 1966).

Corrections to a previous calculation of the nuclear form factor for ^{19}F in an investigation of muon and pion scattering in freon are noted. New results are presented for the nucleus ^{35}Cl. In addition, useful expressions are presented for calculating the nuclear form factor for the general case of a spherical nucleus whose ground state is given by a simple Slater determinant of j-j coupling wave functions. (L.B.S.)

21650 CURRENT COMMUTATION RULES AND THE $\Delta T = \frac{1}{2}$ RULE IN K-MESON DECAYS. Alles, W. (Istituto Nazionale di Fisica Nucleare, Bologna); Jengo, R. Nuovo Cimento (10), 42A: 419-20(Mar. 21, 1966).

It is shown that for a small-mass K meson decaying into zero-mass pions, the $\Delta T = \frac{1}{2}$ rule is just a consequence of the K meson isospin being $\frac{1}{2}$. An isospin $-\frac{3}{2}$ K meson would, in the approximation used, decay with a $\Delta T = \frac{3}{2}$ rule, while an isospin $-\frac{5}{2}$ or larger K meson would not decay. (L.B.S.)

21651 ELECTROMAGNETIC AND WEAK FORM FACTORS OF THE NUCLEON. Cocho, G. (International Atomic Energy Agency, Trieste, Italy). Nuovo Cimento (10), 42A: 421-5(Mar. 21, 1966).

It is shown that the electromagnetic and weak nucleon form factors may be fitted well to experimental data for high-momentum transfer reactions with one-pion exchange if a cut-off function is included and the masses of the ω, φ, and ρ resonances and coefficients given by $U_6 \otimes U_6$ are used. (L.B.S.)

21652 TESTS OF SU_{6w} FROM PREDICTIONS ON SPIN ALIGNMENTS. Doncel, M. G. (Ecole Polytechnique, Paris); De Rafael, E. Nuovo Cimento (10), 42A: 426-30 (Mar. 21, 1966).

Several tests of SU_{6w} invariance are proposed for single reaction processes of the types $P + B \rightarrow V + B$ and $P + B \rightarrow V + B^*$, where P and V indicate pseudoscalar and vector mesons and B and B^* correspond to the octet of $\frac{1}{2}^+$ baryons and the decuplet of $\frac{3}{2}^+$ baryon resonances. Forward-scattering amplitudes are evaluated for the different reactions and are tabulated along with the values of the predicted spin alignments. (L.B.S.)

21653 POLARIZATION IN HIGH-ENERGY π-p SCATTERING AND THE BYERS-YANG MODEL. Le Bellac, M. (Faculte des Sciences, Orsay, France). Nuovo Cimento (10), 42A: 443-7(Mar. 21, 1966).

It is shown that more precise predictions can be made about the polarization in elastic and charge-exchange π-p scattering from the recently proposed coherent-droplet model of Byers and Yang, by using an additional assumption that there exist asymptotic expansions in powers of s for the pion-nucleon scattering amplitude a_ℓ fixed t. (L.B.S.)

21654 CALCULATION OF DECAY WIDTHS AND CURRENT ALGEBRAS. Bar-Nir, I. M. (Tel-Aviv Univ., Israel). Nuovo Cimento (10), 42A: 448-50(Mar. 21, 1966).

The decay widths of the f_0-meson going into two pions, and the K* (1405) going into K + π, are calculated on the basis of the following assumptions. The space integrals of the time components of the vector and axial-vector currents generate at equal times the algebra $SU_3 \otimes SU_3$, and obey its commutation relations. The axial currents are partially conserved. (L.B.S.)

21655 EVALUATION OF THE $N^*_{33}N$ WEAK COUPLING CONSTANTS BY MEANS OF CURRENT ALGEBRA. Furlan, G. (Univ., Trieste, Italy); Jengo, R.; Remiddi, E. Phys. Lett., 20: 679-82(Apr. 1, 1966).

The form factors of the $N^*_{33}N$ weak axial vertex are expressed in terms of the form factors of the nucleon. A relation between $N^*_{33}N\pi$ and $NN\pi$ coupling constants and an estimate of the mass of a 1^+ meson are obtained. (auth)

21656 ANOMALOUS MAGNETIC MOMENT OF THE MUON. Eiend, H. H. (Univ., Freiburg i. B.). Phys. Lett., 20: 682-4(Apr. 1, 1966).

An exact calculation of the anomalous magnetic moment of the muon to second order in the fine structure constant is given. The uncertainties that limit the possible precision in testing quantum electrodynamics with this effect are also discussed. (auth)

21657 PION-NUCLEON SCATTERING AND CONSERVATION LAWS. Hamilton, J. (Nordita, Copenhagen). Phys. Lett., 20: 687-9(Apr. 1, 1966).

Most of the difficulty about explaining the high energy real parts for $\pi^+p \rightarrow \pi^+p$ can be removed, but charge independence should be further examined. (auth)

21658 AN EXPERIMENTAL INVESTIGATION OF THE K_{e3} DECAY. Bellotti, E.; Fiorini, E.; Pullia, A. (Univ., Milan). Phys. Lett., 20: 690-2(Apr. 1, 1966).

This experimental study of the K_{e3} decay shows no strong asymmetry between neutrino and positron and confirms the vector character of the coupling. The structure of the form factor is studied on the basis of the $K - \pi$ interaction. (auth)

21659 PION ELECTROMAGNETIC FORM FACTOR FROM MEASUREMENTS OF $\pi^\pm$-α ELASTIC SCATTERING. Nordberg, M. E., Jr.; Kinsey, K. F. (Univ. of Rochester, N. Y.). Phys. Lett., 20: 692-5(Apr. 1, 1966). (UR-875-122)

A complex phase shift fit to the differential cross section of $\pi^\pm$-α particle elastic scattering at 24 Mev was performed. Introducing the radius of the pion as a parameter $\gamma_\pi = 1.8 \pm 0.8$ fm was obtained. (auth)

21660 POSITIVE-PION PRODUCTION ASYMMETRY WITH POLARIZED BREMSSTRAHLUNG NEAR SECOND RESONANCE. Liu, F. F.; Vitale, S. (Stanford Univ., Calif.). Contract Nonr 225(67). Phys. Rev., 144: 1093-1100(Apr. 29, 1966).

The azimuthal asymmetry $\Sigma = (\sigma_\perp - \sigma_{||})/(\sigma_\perp + \sigma_{||})$ in π^+ photoproduction by linearly polarized bremsstrahlung was measured at photon energies from 475 to 750 Mev at 90° and 135° in the center-of-mass system. The experimental results show that even in this energy region, π^+ are produced predominantly in the plane of the magnetic vector. (auth)

21661 STRUCTURE IN THE PION-PROTON TOTAL CROSS SECTION BETWEEN 2 AND 7 Gev/c. Citron, A.; Galbraith, W.; Kycia, T. F.; Leontic, B. A.; Phillips, R. H.; Rousset, A.; Sharp, P. H. (Brookhaven National Lab., Upton, N. Y.). Contract AT(30-2)-Gen-16. Phys. Rev., 144: 1101-14(Apr. 29, 1966). (BNL-9566).

The total cross sections of $\pi^\pm$ on protons in the momentum interval 2 to 7 Bev/c were measured with high precision. The error fluctuations from point to point vary between 10 and 25 μb. Two new pion-nucleon resonances, one in each of the two isotopic states, were found at the following mass values: $M_{\frac{1}{2}} = 2.65 \pm 0.01$ Bev and $M_{\frac{3}{2}} = 2.85 \pm 0.01$ Bev. A search for other resonances at higher momenta is discussed. (auth)

21662 π^+-p SCATTERING AT 250 Mev: EXPERIMENT AND ANALYSIS. Troka, Wladyslaw; Betz, Fred; Chamberlain, Owen; Dieterle, Byron; Dost, Helmut; Schultz, Claude; Shapiro, Gilbert (Univ. of California, Berkeley). Contract W-7405-eng-48. Phys. Rev., 144: 1115-22(Apr. 29, 1966). (UCRL-11537(Rev.)).

The differential cross section for elastic scattering of positive pions on protons was measured at a nominal incident-meson kinetic energy of 250 Mev. The angular range covered in the center of mass by the 13 data was 14.9 to 160°. The fractional rms errors were typically 1.5%. A liquid-hydrogen target was bombarded by a beam of 2.5×10^6 mesons/sec. The scattered pions were detected by a counter telescope. Recoil protons were eliminated by means of a Čerenkov counter. A phase-shift analysis was performed combining the above-mentioned data with the recoil-proton polarization measurements taken recently with the help of a polarized proton target. Only one acceptable SPD Fermi-type phase-shift set was found. When F waves were included, a total of three possible phase-shift solutions emerged from the analysis. However, arguments based on the data could still be made to eliminate all but one phase-shift set. On the other hand, the remaining phase-shift set, similar in type to the SPD solution, suf-

fers from the disadvantage of large rms errors assigned to its small phase shifts. (auth)

21663 PERIPHERAL PRODUCTION AND DECAY PARAMETERS OF $N^{*++}(1238)$ IN $pp \rightarrow nN^{*++}(1238)$ AT 5.5 Gev/c. Alexander, G. (Weizmann Inst., Rehovoth, Israel); Haber, B.; Shapira, A.; Yekutieli, G.; Gotsman, E. Phys. Rev., 144: 1122-6(Apr. 29, 1966).

Experimental differential cross sections and N*(1238) decay parameters for the reaction $pp \rightarrow nN^{*++}(1238)$ at 5.5 Bev/c are presented. The differential cross sections are well described by an absorptive one-pion-exchange model with equal pp and nN*(1238) elastic cross sections. A better agreement is achieved using a steeper nN* differential cross section than that for the pp one, or with a sharp cutoff model corresponding to an absorption radius of about 0.9–1.0 F. The N*(1238) decay parameters are also found to be in good agreement with the absorption model. (auth)

21664 PAIR PRODUCTION BY 5-Gev PHOTONS IN CARBON. Walker, J. K. (Harvard Univ., Cambridge, Mass.); Wong, M.; Fessel, R.; Little, R.; Winick, H. Contract AT(30-1)-2752. Phys. Rev., 144: 1126-31 (Apr. 29, 1966). (CEAL-1024).

The production of wide-angle electron pairs by high-energy photons in the field of the carbon atom has recently been studied at the Cambridge Electron Accelerator. An apparent systematic deviation from the predictions of quantum electrodynamics was observed. Therefore the total cross section for photon absorption at high energies was rechecked and previous experimental results were reanalyzed. Theoretical cross sections were also calculated in detail and comparison of the experimental data was made with several atomic screening calculations. It was found that within about 2%, which is the present experimental and theoretical uncertainty, there is reasonable agreement between experiment and theory. (auth)

21665 MEASUREMENT OF THE LIFETIME OF THE POSITIVE PION. Kinsey, K. F.; Lobkowicz, F.; Nordberg, M. E. Jr. (Univ. of Rochester, N. Y.). Contract AT(30-1)-875. Phys. Rev., 144: 1132-7(Apr. 29, 1966). (UR-875-112).

Using fast electronic techniques, the $\pi\mu e$ decay sequence for about 10^8 stopped positive π-mesons was observed. The exponential decay of the π can be followed for 8 mean lives, and yields a value of $\tau_\pi^+ = 26.40 \pm 0.08$ nsec. This value disagrees with previously reported values. (auth)

21666 PARTIALLY CONSERVED AXIAL-VECTOR CURRENT AND THE NONLEPTONIC K-MESON DECAYS. Suzuki, Mahiko (California Inst. of Tech., Pasadena). Contract AT(11-1)-68. Phys. Rev., 144: 1154-7(Apr. 29, 1966).

Current commutation relations and a partially conserved axial-vector current hypothesis (PCAC) are applied to the nonleptonic K decays. On the assumption that the effective weak interactions should have the transformation property suggested by Gell-Mann in the quark model of the chiral symmetry, and that the axial-vector isospin charges to which the pions are related through PCAC should be generators of $U(2) \times U(2)$, the $K_{2\pi}$ and the $K_{3\pi}$ decay amplitudes, in which the four-momenta of all the final pions are continued to zero, are proved to obey the $\Delta I = \frac{1}{2}$ rule. In the approximation of neglecting the continuation, the decay rate of the $K_{3\pi}$ is related to that of the $K_{2\pi}$. The ratio of the decay rates is estimated and a reasonable agreement with experiment is obtained. Only the charge independence is assumed for the strong interactions. (auth)

21667 THRESHOLD FACTORS IN PARTIAL-WAVE DISPERSION RELATIONS. Simmons, L. M. Jr. (Cornell Univ., Ithaca, N. Y. Univ. of Minnesota, Minneapolis). Phys. Rev., 144: 1157-62(Apr. 29, 1966).

If the solution of an approximate partial-wave dispersion relation is required to satisfy unitarity and possess the threshold behavior, additional poles (representing effective forces) are introduced into the amplitude. These poles are explicitly exhibited. To enforce l-wave threshold conditions, approximately l arbitrary parameters appear (the precise number depending upon the properties of the amplitude considered). This difficulty is in principle independent of the method of solution. Using the nucleon exchange force as input, the $J = \frac{3}{2}$ amplitudes for π-N scattering are obtained by numerical solution of the N/D equations. The solutions are extremely sensitive to the arbitrary parameters. It appears that, in the present formulation, partial-wave dispersion relations do not provide a reliable means of calculating detailed properties of the amplitudes. (auth)

21668 CAN NEARBY INTERACTION SINGULARITIES GENERATE OBSERVED RESONANCES? Cook, L. F.; Jones, C. E. (Princeton Univ., N. J.). Phys. Rev., 144: 1165-70(Apr. 29, 1966).

The question of whether simple nearby singularities together with unitarity are generally capable of reproducing the masses and widths of observed low-energy resonances is studied. As a specific case, the ρ meson is studied. The left-hand cut is replaced by one or two nearby poles and it is asked if the interaction-pole parameters can be adjusted to give the known mass and width of the ρ. If elastic unitarity is assumed, the answer is no. Calculations with inelastic unitarity are also made, and the observed ρ can be reproduced if the inelastic amplitude provides an important contribution. These conclusions are reached without a detailed identification between known exchanged systems and the interaction pole parameters. (auth)

21669 ELECTROMAGNETIC FORM FACTOR OF THE NEUTRINO. Goldberg, Irwin (Clarkson Coll. of Technology, Potsdam, N. Y.); Haller, Kurt; Landovitz, Leon F. Phys. Rev., 144: 1171-6(Apr. 29, 1966).

The electromagnetic form factors of the electron and muon neutrinos are evaluated using an intermediate-vector-boson theory. The vector bosons are treated by a Feynman-propagator theory in which all divergent integrals are renormalizable by conventional means. Implications of the renormalization of the weak by the electromagnetic interactions are discussed; it is pointed out that the usual procedure of treating such a theory by using regulators might not be consistent with its conservation laws. (auth)

21670 DYNAMICS OF THE Y_1^* BRANCHING RATIO. Kayser, Boris (Univ. of California, Berkeley); Bloom, Elliott. Phys. Rev., 144: 1176-81(Apr. 29, 1966).

The $\pi\Sigma/\pi\Lambda$ branching ratio of the $Y_1^*(1385)$ is significantly smaller than the phase space estimate. The fact that in the $\frac{3}{2}^+$, $I = 1$ $\pi\Sigma$ state the force is repulsive, while in the corresponding $\pi\Lambda$ state it is attractive, is shown to be important in bringing this about. A general analysis of n-channel diagonalizable systems, and a number of specific diagonalizable and nondiagonalizable models, are presented to establish that this importance is not model-dependent. (auth)

21671 SHOULD SU(3) MASS FORMULAS FOR MESONS USE THE MASSES OF THE MESONS OR THEIR SQUARES? Macfarlane, A. J.; Socolow, R. H. (Latin American School of Physics, Mexico City). Phys. Rev., 144: 1194-9(Apr. 29, 1966).

The practice of using squares of masses in mass formulas for SU_3 meson multiplets, which arose originally in order to bring the Gell-Mann–Okubo mass formula for the 0^- meson octet more nearly into agreement with experiment, is criticized. The basis of the criticism is that X^0–η mixing can make the Gell-Mann–Okubo formula compatible with the observed 0^- meson spectrum not only when one applies it to the squares of the masses, but also when one applies it to the masses themselves. Of course, the degree of the mixing is different in the two cases and this affects the prediction of decay rates. Accordingly, the decays of 2^+ mesons into two 0^- mesons are discussed in considerable detail as an example of a situation where experimental measurements may discriminate between the values of the mixing angle corresponding to linear and quadratic mass formulas. (auth)

21672 OFF-SHELL PION-NUCLEON SCATTERING. Thiebaux, M. L. Jr. (Univ. of Massachusetts, Amherst). Phys. Rev., 144: 1224-31(Apr. 29, 1966).

The problem of off-shell pion-nucleon scattering is investigated under the assumption that the self-supporting

dynamical system made up of the nucleon and N*(1238) continues to exist when one of the pions is virtual. Partial-wave amplitudes satisfying off-shell elastic unitarity are constructed from the off-shell $P_{3,3}$ nucleon exchange and $P_{1,1}$ N*(1238) exchange Born terms, although ambiguities arise in handling the high-energy behavior of the amplitudes. The reciprocal bootstrap requirement then leads to explicit expressions for the off-shell pionic form factors of the πNN and πNN* vertexes. (auth)

21673 PROTON-NEUTRON MASS DIFFERENCE. Pagels, Heinz (Univ. of North Carolina, Chapel Hill). Contract AFOSR-153-64. Phys. Rev., 144: 1261-9 (Apr. 29, 1966).

The electromagnetic contributions to the masses of the nucleons are examined in terms of the graviton-nucleon vertex. Using the methods of sidewise dispersion relations this vertex is considered as a function of the mass of one of the external nucleons, which enables the contributions to $\delta M = M_p - M_n$ to be expressed in terms of integrals over scattering amplitudes. Applying the hypothesis of threshold dominance, it is found that a simple explanation for the observed mass difference $\delta M = -1.3$ Mev emerges. In the low-energy region, the only contributing states are the intermediate Nγ and Nπ states. For the photon contributions the usual unsuccessful result $\delta M^{\gamma} \sim +0.5$ Mev is found as a consequence of the dominance of the Coulomb over the magnetic energy in the threshold region. However, in calculating the contribution of the nucleon mass shift back on itself from the Nπ states of energy W, there is a term under the dispersion integral proportional to the difference of nucleon pole terms $(W^2 - M_n)^{-1} - (W^2 - M_p^2)^{-1} \simeq -2M\delta M (W^2 - M^2)^{-2}$, implying a large contribution due to the enhancement at threshold $W^2 \to M^2$. Including this contribution it is found that $\delta M = +0.5$ Mev $+ 1.3\,\delta M$ or $\delta M \simeq -1.7$ Mev, which suggests how the nucleon mass difference emerges in spite of the sign of the photon contribution. (auth)

21674 DYNAMICS OF $J = \frac{3}{2}^+$ $\bar{K}\Xi$ AND KN SYSTEMS IN THE 27-FOLD REPRESENTATION; SOME REMARKS ON A TYPICAL FEATURE OF THE BALAZS-TYPE PROCEDURE. Pati, Jogesh C. (Univ. of Maryland, College Park); Vasavada, Kashyap V. Contract AFOSR 500-64. Phys. Rev., 144: 1270-5(Apr. 29, 1966).

The dynamics of the $I = 1$, $J = \frac{3}{2}^+$ $\bar{K}\Xi$ and KN systems was studied by the Balázs-type N/D method and a typical feature of this procedure was observed for treating the far left-hand singularities. The dynamical singularities of the partial-wave amplitude are assumed to arise mainly from the nearby cut (due to Σ and Λ exchange in the crossed channel) and the far left-hand cut ($-\infty < s \leq 0$). The contribution of the former is evaluated explicitly in terms of the relevant Yukawa coupling constants, and that of the latter by the method of Balázs, through the introduction of effective-range pole terms. For a wide range of choice of the relevant Yukawa coupling constants, there exist self-consistent bound-state (or resonant) solutions for both $I = 1$ $\bar{K}\Xi$ and $I = 1$ KN systems. The self-consistent solution for the position in the case of the former is found to lie in the range 1650–1870 Mev, and for the latter in the range 1300–1600 Mev. The overall conclusion is found to be rather insensitive to the choice of the relevant Yukawa coupling constants. On considering the general case of arbitrary baryon-meson systems, it is found that at least in the Balázs-type procedure, one would obtain self-consistent bound-state or low-lying resonant solutions in almost any $J = \frac{3}{2}^+$ baryon-meson system, unless the Born terms are very strongly repulsive. Experimental confirmation of the existence or nonexistence of such systems would thus have strong implications for the dynamical methods such as, for example, those adopted in the present note. As one consequence of the present work, it appears that the qualitative features of any further Balázs-type calculations, especially in the $J = \frac{3}{2}^+$ baryon-meson system, could essentially be anticipated. (auth)

21675 NORMAL SCALAR NONET; $K_1 \to 2\pi$ DECAY AND K_1-K_2 MASS DIFFERENCE. Loebbaka, D.; Oneda, S.; Pati, J. C. (Univ. of Maryland, College Park). Contract NSF GP 3221. Phys. Rev., 144: 1280-8(Apr. 29, 1966).

The existence of a scalar nonet [the physical particles are designated by (κ^+,κ^0); $(\bar{\kappa}^0,\kappa^-)$, $(\epsilon^+,\epsilon^0,\epsilon^-)$, ξ^0, and σ^0] is assumed and the dynamics of $K_1 \to 2\pi$ decay, $K^0 \rightleftharpoons \bar{K}^0$ transition, and S-wave ππ scattering is considered. It is stressed that the scalar mesons, if they exist, will play a dominant role in the dynamics of each of the above three processes. It is assumed that all the parity-violating $|\Delta Y| = 1$ nonleptonic transitions are dominated by the K_1 tadpole, even though the latter is forbidden in the limit of SU(3). In order to obtain a consistent theoretical picture (in the single-particle intermediate-state approximation) for the observed sign ($m_{K_2} > m_{K_1}$) and magnitude of the K_1-K_2 mass difference as well as the observed rate of the $K_1 \to 2\pi$ decay, it appears necessary that there should exist scalar mesons lying above the mass of the K meson, especially $I = Y = 0$ scalar meson (called σ) lying close to the K meson but above it (510 Mev $< m_\sigma <$ 550 Mev, say). The width of the σ meson can be small [$\Gamma(\sigma \to 2\pi) \approx 10 \sim 30$ Mev, for example] and could lead to a small relative production cross section of the σ meson in pion-nucleon processes. (auth)

21676 APPLICATION OF THE CURRENT COMMUTATION RELATIONS TO THE N*** PHOTOPRODUCTION. Bietti, A. (California Inst. of Tech., Pasadena). Contract AT(11-1)-68. Phys. Rev., 144: 1289-93(Apr. 29, 1966). (CALT-68-57).

Three sum rules are derived by taking the expectation values between proton states at rest of three commutation relations of electric quadrupole and magnetic octupole operators. If it is assumed that the sum rules are saturated by only one intermediate state, the $I = \frac{1}{2}$, $J = \frac{5}{2}^+$ pion-nucleon resonance N*** (1688), a consistency relation is obtained, which appears to be satisfied by experimental numbers. The ratio of the E_{3-} and M_{3-} amplitudes in single-pion photoproduction is then derived and a result in good agreement with experiment is obtained. (auth)

21677 INVARIANCE PRINCIPLES AND THE K^0-$\bar{K}^0$ PROPAGATOR MATRIX. Lipshutz, Nelson R. (Univ. of Chicago, Ill.). Contract AT(11-1)-264. Phys. Rev., 144: 1300-4(Apr. 29, 1966). (COO-264-291; EFINS-65-100).

The symmetry properties of the mass and lifetime matrices for the neutral K-meson system are derived without recourse to perturbation theory for a large class of field theories. Lorentz invariance is not assumed. First, a spectral representation in the energy variable is developed for the K-meson propagator matrix. Reality conditions and the consequences for this matrix of invariance under C, P, T and all their combinations are derived. Purely formal considerations are then used to obtain an unambiguous identification of the mass and lifetime matrices as the dispersive and absorptive parts, respectively, of a related matrix of spectral integrals, whose symmetry properties are also exhibited. The consequences of the assumption of relativistic covariance are discussed in a final section. In particular, it is shown that the equality of the diagonal elements of the complex mass matrix is required by Lorentz invariance alone. Therefore, in the context of local field theory, a comparison of these matrix elements is a direct test of Lorentz invariance rather than of the CPT theorem. (auth)

21678 SPONTANEOUS SYMMETRY BREAKDOWN WITHOUT MASS SPLITTING. Acharya, R.; Narayanaswamy, P. (Tata Inst. of Fundamental Research, Bombay). Phys. Rev., 144: 1305-8(Apr. 29, 1966).

The question whether spontaneous symmetry breakdown can cause n-p and μ-e mass differences is examined, employing a nonperturbative approximation scheme to solve the Dyson-Schwinger equation for the one-particle Green's function. In both cases, mass degeneracy persists in the presence of a nontrivial symmetry-breaking solution. This result is discussed with special reference to a recent theorem of Streater. (auth)

21679 HIGH-ENERGY LIMIT OF $\pi^+\pi^0$ TOTAL CROSS SECTION. Meiere, F. T.; Sugawara, Masao (Purdue Univ., Lafayette, Ind.). Phys. Rev., 144: 1308-15(Apr. 29, 1966).

The high-energy limit of the $\pi^+\pi^0$ total cross section $\sigma(\infty)$ is estimated upon the assumption that the $\pi^+\pi^0$ forward scattering amplitude is dominated by the S wave below the ρ

resonance and becomes purely imaginary fairly rapidly above the ρ resonance. The underlying assumption is that the $\pi^+\pi^0$ forward amplitude satisfies the usual analyticity assumption. Using the experimental values of the mass and the width of the ρ resonance and also assuming an effective-range expansion for the S wave, $\sigma(\infty)$ is estimated as a function of the scattering length and the effective range in the channel of total isospin 2. It is found that, for negative scattering length (corresponding to a repulsive interaction), $\sigma(\infty)$ rises fairly steeply as the scattering length increases its magnitude for all the effective ranges. In the case of positive scattering length (corresponding to an attractive interaction), however, $\sigma(\infty)$ is much less dependent on the scattering length up to 0.8 μ^{-1} especially when the effective range lies between μ^{-1} and 2 μ^{-1} (μ^{-1} being the pion Compton wavelength). In particular, $\sigma(\infty)$ hardly decreases below 20 mb as long as the effective range is not too much greater than 2 μ^{-1}. It is argued that various corrections to be considered can quite likely increase the above estimate of $\sigma(\infty)$ 10 to 20% in the case of a weakly attractive S-wave interaction, but hardly can decrease it. It is therefore felt that the present analysis excludes the possibility of a repulsive S-wave interaction and also implies that the high-energy limit of the $\pi^+\pi^0$ total cross section is about the same as that for the pion-nucleon total cross section. (auth)

21680 APPLICATIONS OF A COULOMB-MODIFIED s-WAVE DISPERSION RELATION. Heller, Leon; Rich, Marvin (Univ. of California, Los Alamos, N. Mex.). Contract W-7405-eng-36. Phys. Rev., 144: 1324-38 (Apr. 29, 1966). (LA-DC-7565).

Low-energy proton-proton and neutron-neutron scattering is compared through the use of a Coulomb-modified dispersion relation. Basing the analysis upon a Jost-Bargmann potential, for which the s-wave amplitude in the uncharged case contains a single interaction pole at q = $\frac{1}{2}$ iμ, it is shown that the corresponding amplitude in the charged case contains a sequence of branch points at q = $\frac{1}{2}$ n iμ. However, a small region near the highly singular n = 1 point still dominates the dispersion relation. The low-energy phase shifts obtained from the solution of the dispersion relation are in excellent agreement with those obtained directly from the Schroedinger equation both for the charged and uncharged cases. In a similar analysis based upon a Yukawa potential, the convergence of the method is much slower as higher Born-approximation singularities are fed in. A technique is presented for extracting the singular parts of individual Born terms arising from superpositions of Yukawa potentials, and, serves as the basis for computing the input to the dispersion relation. This procedure does not require explicit integration of the terms of the Born series. It is also shown that the integral equation used, which was originally derived by Wong and Noyes by studying the analytic properties of the effective-range function, is identical to the D equation in the N/D method. (auth)

21681 Σ^--NEUTRON INTERACTION AND STRANGE-PARTICLE PRODUCTION. Dante, W. M.; Henley, E. M. (Univ. of Washington, Seattle). Contract AT(45-1)-1388B. Phys. Rev., 144: 1343-50(Apr. 29, 1966). (RLO-1388B-4).

A theoretical analysis of the reaction $\pi^- + d \rightarrow \Sigma^- + n + K^+$ near threshold is carried out to determine its sensitivity to the Σ-nucleon force in the isospin-$\frac{3}{2}$ channel. Since the triplet-spin-state interaction appears to be weak, attention is focused on the singlet S-state force. An impulse approximation is used to analyze the reaction, with the Σ^--n interaction treated as a final-state effect. To obtain a relative $^1S_0$ state of the Σ^--n requires a spin-flip amplitude in the $\pi^- + p \rightarrow \Sigma^- + K^+$ reaction. A peripheral model, with absorption, is employed to study this process. The exchanges of both Λ^0 and Σ^0 are taken into account. The relevant coupling constants are obtained from SU(3) symmetry. A good fit to the experimental differential cross section at 1.17 Bev/c is obtained. The computed cross section and spin-flip probability are then used to estimate the effect of various-strength attractive Σ^--n forces on the K-meson spectra obtained from deuteron targets. The possibility of a bound Σ^--n state is included. For 1-Bev incident pions, it is found that spectra observed at laboratory angles larger than approximately 40° are most likely to yield significant information on the $^1S_0$ interaction. (auth)

21682 COUPLING CONSTANTS OF SPIN-2 MESONS WITH TWO PSEUDOSCALAR MESONS. Vasavada, Kashyap V. (National Aeronautics and Space Administration, Greenbelt, Md.). Phys. Rev., 144: 1351-5(Apr. 29, 1966).

Recently discovered spin-2 mesons f, A_2, $f'(1500)$, and K**(1405) are considered as resonances in various systems containing two pseudoscalar mesons with appropriate quantum numbers. Making the single-channel approximation, exact N/D calculations are done by solving the integral equations with the help of the matrix inversion method. The input forces due to exchanges of vector and spin-2 mesons are taken into account. The input coupling constants given by experiments or SU(3) symmetry are used. By adjusting the straight cutoffs on the integrals, resonances are produced in each of these systems at the experimentally observed positions, and the output coupling constants are obtained. As expected in such calculations, the output coupling constants come out to be larger than the input ones. However, an interesting feature is found: that the hierarchy of the coupling constants given by experiments or SU(3) symmetry is maintained. (auth)

21683 DISPERSION-THEORETIC PERTURBATION SERIES IN SOME MODELS. Abarbanel, Henry D. I. (Princeton Univ., N. J.); Gilman, Frederick J. Phys. Rev., 144: 1355-62(Apr. 29, 1966).

The perturbation series of Dashen and Frautschi is derived via a "D-matrix" approach to all orders in the perturbation. Explicit formulas are given for the first and second orders, and their equivalence to the Rayleigh-Schroedinger perturbation series in potential theory is shown. A method is then given to carry out the evaluation of the series to any order. The first-order formula is examined in three models; the four-point interaction, two-particle scattering with a left-hand cut given by a single pole, and an augmented Lee model. The exact results of these models are shown to agree in each case with the theory of Dashen and Frautschi. Finally, differences between the Lee-model calculation presented here and Dashen's calculation of the neutron-proton mass difference are discussed. (auth)

21684 ANNIHILATION OF NUCLEON-ANTINUCLEON AS THE SOURCE OF ENERGY FOR CERTAIN RADIOASTRONOMICAL OBJECTS. Ekspong, A. G. (Stockholm Univ.); Yamdagni, N. K.; Bonnevier, B. Phys. Rev. Lett., 16: 664-7(Apr. 11, 1966).

Results of detailed calculations are presented regarding the shapes of the expected radio frequency spectra emitted from an ambiplasma. The nuclear processes in the ambiplasma are annihilations of nucleons and antinucleons leading to mesons, mostly pions, which through their well known decays quickly give rise to gamma rays, neutrinos, and electrons. (B.G.D.)

21685 T = 0, S-WAVE, $\pi\pi$ PHASE SHIFT. Jacobs, Laurance D.; Selove, W. (Univ. of California, Berkeley). Phys. Rev. Lett., 16: 669-71(Apr. 11, 1966). (UCRL-16616(Rev.)).

The persistent forward asymmetry in the $\pi^-\pi^+$ scattering-angle distribution for peripheral (low momentum transfer) events in the ρ mass region for the reaction $\pi^- + p \rightarrow \pi^- + \pi^+ + n$, considered together with the more symmetrical behavior for the $\pi^\pm\pi^0$ system in the reaction $\pi^\pm + p \rightarrow \pi^\pm + \pi^0 + p$ has led to the suggestion that T = 0, S-wave phase shift δ_0^0 is near 90° in this mass region. Experimental results are presented that at values of $M_{\pi\pi}$ well below the ρ mass; δ_0^0 is positive. (B.G.D.)

21686 DYNAMICAL APPROACH TO NONLEPTONIC DECAYS OF HYPERONS. Kanazawa, Akira; Sakuma, Tetsuro; Terazawa, Osamu (Hokkaido Univ., Sapporo). Progr. Theoret. Phys. (Kyoto), 35: 74-9(Jan. 1966).

The pionic decays of hyperons are analyzed under the dynamical self-consistency requirement and the assumption that the nonleptonic decay processes are originated in

driving weak interactions of the current-current type. The hadron currents are assumed to be transformed like an octet component of SU(3). It is shown that the octet enhancement of decay amplitudes can be attributed to the strong interactions. In particular, the qualitatively satisfactory numerical results can be obtained in a model where the s-wave amplitude is enhanced by two levels while the p-wave is by a single level. (auth)

21687 POSSIBLE SCHEME FOR THE NONLEPTONIC DECAYS OF HYPERONS. Hayashi, Takemi; Kaneko, Takao; Maki, Ziro (Nagoya Univ., Japan. Meijo Univ., Nagoya, Japan). Progr. Theoret. Phys. (Kyoto), 35: 80-9(Jan. 1966).

Nonleptonic decays of hyperons are discussed in the unitary symmetrical $[\chi\bar{\theta}]$ composite model for baryons, where χ and θ are triplet spinor and scalar (or pseudoscalar) fields respectively. The decays are assumed to occur through two different mechanisms $\bar{\theta} \to \bar{\theta} + \pi$, $\chi \to \chi$ and $\bar{\theta} \to \bar{\theta}$, $\chi \to \chi + \pi$. Several relations among the decay amplitudes, including the well-known Sugawara-Lee relation for the parity violating part and a new sum rule $2P(\Xi^-) - P(\Lambda^0) = -(1/\sqrt{3})P(\Sigma^+_0)$ for the parity conserving part, are derived. The Σ decays can be explained quite well by our model, but there remains a difficulty in explaining the asymmetry factors of Λ and Ξ decay simultaneously. (auth)

21688 POLE MODEL OF NON-LEPTONIC DECAY CONSISTENT WITH DECAY PARAMETERS AND SUM RULES. Kawasaki, Shoichiro (Chiba Univ., Japan); Imoto, Mitsuo; Furui, Shin-ya. Progr. Theoret. Phys. (Kyoto), 35: 90-103(Jan. 1966).

Considering the difficulties to get decay parameters and sum rules consistently and the ill forbiddeness of $K^0_1 \to 2\pi$ in SU(3) limit, the prejudice that the non leptonic decay can be expressed with trilinear interaction is rejected, and instead the pole model is adopted with all two-body type weak interactions that are CP invariant, λ_6-like and constructed from baryon octet, pseudoscalar meson octet and vector meson nonet with actual mass splittings. It follows, then, that i) $\Sigma^+ \to n + \pi^+$ is uniquely determined to be pure P-wave process consistent with both of the recent experiments and result on SU_6 theory; ii) experimental values of six α's and γ's are consistently reproduced by means of four parameters including weak and strong F/D ratios whose fittest values are F/D = 2/3 (the value suggested by the SU_6 theory) consistent with experimental values $\sim(1/\sqrt{3})$; iii) with the fixed parameters there hold exactly or approximately six sum rules for each of S and P waves. These sum rules include relations obtained on the SU_6 theory and two new ones for the P wave. It is also shown that $K^0_1 \to 2\pi$ is allowed with right order owing to our assumptions, contrasting with its forbiddeness with trilinear interaction at the SU_3-symmetry limit. (auth)

21689 GENERAL EFFECTIVE-RANGE FORMULA AND THE COMPOSITENESS OF THE DEUTERON. Ida, Masakuni (Tokyo Univ.). Progr. Theoret. Phys. (Kyoto), 35: 104-16(Jan. 1966).

In order to discuss the compositeness of the deuteron, experimental data on the low-energy n-p scattering in the $^3S_1$ state are summarized into two features by the use of a general effective-range formula introduced in a previous work. If expressed conventionally, they are: (i) $a/R - 1 = 0.25$, (ii) the effective range approximation is valid in the low-energy region. Conditions under which (ii) is true are investigated. Weinberg's argument is found to be insufficient to exclude the possibility that the deuteron is elementary. It is shown by general considerations and by an analysis in terms of a one-pole model that the features, (i) and (ii), strongly favor the deuteron to be composite. (auth)

21690 SYSTEMATICS AND PHENOMENOLOGY OF BOSON MASS LEVELS. I. Iizuka, Jugoro (Kanazawa Univ., Japan). Progr. Theoret. Phys. (Kyoto), 35: 117-25(Jan. 1966).

Systematics and phenomenology of boson mass levels are presented assuming certain characteristics of the ur-baryon dynamics. Considering that the constructive forces that bind the ur-baryon pair in the 0^-- and 1^--nonets play a dominant role for the ur-baryon pair system with $L \neq 0$ (but fairly small L), we are generally led to expect, as the next low lying excited system, the existence of 0^+-, 1^+- and 2^+-nonets (^3P_J) and $1^{+\prime}$-nonets ($^1P_1$), where the latter is the so-called abnormal axial vector. Comparisons between the present experimental situation and our results will be made in detail. It is further shown that the lower bound of the average ur-baryon mass is ~4.5 Bev. Finally applicability of our results to various ur-baryon models will be mentioned. (auth)

21691 THE ELEMENTARY PARTICLES. Wilkinson, D. H. (Oxford Univ.). Sci. J., 2: 31-40(Mar. 1966).

Elementary particles are reviewed. This review includes symmetry schemes and multiplets. The properties and decays of these particles are given, and also their spins and parities are noted. Quarks are mentioned. It is suggested that there may be an approach to an empirical ordering of particles analogous to that of atoms in the periodic table. (J.F.P.)

21692 RECENT DEVELOPMENT IN THE EXPERIMENTAL STUDY OF ELEMENTARY PARTICLES. Chang, W. Y. (Academia Sinica, Peking). Wu Li Hsueh Pao, 21: 1831-72(Nov. 1965). (In Chinese).

A comprehensive survey of the development in the experimental study of "elementary particles" during the last four or five years is given. However, the strongly interacting particles are mainly considered with only a few problems concerning the weak interaction included. It is in the area of the strongly interacting particles that there has been in these years a rapid and large accumulation of the resonant states of particles, quickly bringing the total number of particles from about 30 to about 100; moreover, in the corresponding theoretical aspect, there is also a more or less successful development in the SU(3) classification scheme as proposed from the symmetry of strong interaction. Because of these new developments it is now more than ever certain that the so-called elementary particles are not elementary but composite, i.e., having internal structure (at least as far as the strongly interacting particles are concerned). This point is discussed in some detail. Then a summary and discussion of seven groups of experiments which have been performed in the last four or five years and are considered as more important in the field of "elementary particles," four groups being concerned with the strong interaction while three groups with the weak interaction are given. After this, the discussion concentrates on the recent development of the strongly interacting particles, on the status of statistics before and after 1960, and on the physical meaning of the particle classification, etc. Finally, in discussing the two classification schemes, particularly the SU(3) scheme, effort is made to explain with as much clarity as possible the physical background and the assumption made, the mathematical basis, the theoretical results, and comparison with experiment. (auth)

21693 CONTINUATION OF THE INVESTIGATION OF INELASTIC INTERACTIONS OF π^- MESONS WITH NUCLEONS AT 6.8 Gev. Wang, Shu-wei; Wang, Tsu-tsing; Jeng, Tseing-ju; Lo, Chung-hsien; Cheng, Pu-in; Lang, Peng-fei; Huang, Te-chiang. Wu Li Hsueh Pao, 21: 1873-81(Nov. 1965). (In Chinese).

The inelastic interactions of mesons (π) with nucleons were investigated at 6.8 Bev. A peak appeared close to the 1.5 Bev mark that departs from the limit predicted by theory for the one-pion-exchange region. The distribution coefficient of inelastic protons in a mirror-system was compared with the one-pion-exchange theory. The number of protons among unidentified particles was evaluated with the help of the known meson ($\pi^\pm$) spectrum. (G.O.Y.)

21694 ON THE π-π RESONANCE STATES. Ke, Molin; Tuan, I-shih. Wu Li Hsueh Pao, 21: 1903-12(Nov. 1965). (In Chinese).

From the requirements of analyticity and unitarity, the resonance behaviors of the partial wave amplitudes for π-π scattering are discussed in general. The theory involves a function $F^I_{(l)}(\nu)$, which indicates deviation from the Breit-Wigner type resonance formula. When $F^I_{(l)}(\nu)$ =

1, the amplitude has exactly the Breit-Wigner form. Further investigation shows that the function $F^{I}_{(l)}(\nu)$ in general deviates from 1. By use of the ND^{-1} method, the crossing symmetry and the ρ- and f^0-bootstrap approximation, by comparing with the integral expression of the partial wave amplitude for the interval $-9 < \nu < 0$, the P- and D-waves self-consistent solution, i.e., the resonance solutions for ρ and f^0 are calculated. The method takes into account both the contributions of the inelastic process and the dispersion integral of the negative interval. The calculation gives $\nu_{R_1} = 6.4$, $\Gamma_1 = 0.12$ for the J = 1, I = 1 state and $\nu_{R_2} = 20$, $\Gamma_2 = 0.016$ for the J = 2, I = 0 state. These results correspond to a mass of 762 Mev and a half width of about 45 Mev for the ρ meson, and a mass of 1283 Mev for the f^0 meson. They are in good agreement with recent experimental data. (auth)

21695 THE FUNDAMENTAL PARTICLES. Swartz, Clifford E. Addison-Wesley Series in Physics. Reading, Mass., Addison-Wesley Publishing Company, Inc., 1965. 159p. $3.75 (Hardbound); $1.95 (Paperbound).

Some classification schemes which correlate facts about the matter of which the universe is composed are considered. The topics discussed include the Bohr atom, the electron, particles stable against decay through nuclear forces, interactions, conservation laws, particles stable against rapid decay through strong nuclear forces, and the resonances and short-lived particles. (J.F.P.)

21696 HIGH ENERGY PHYSICS. Lectures Delivered at Les Houches During the 1965 Session of the Summer School of Theoretical Physics, Univ. of Grenoble, France. DeWitt, C.; Jacob, M. (eds.). New York, Gordon and Breach Science Publishers, 1965. 519p.

Separate abstracts were prepared for the eight chapters of the book. (D.C.W.)

For abstracts of individual chapters see: 21697–21700, and 21771–21774.

21697 QUARK MODELS FOR THE ELEMENTARY PARTICLES. Dalitz, R. H. (Oxford Univ.). pp 251-323 of High Energy Physics. New York, Gordon and Breach Science Publishers, 1965.

The properties of the strongly interacting elementary particles are discussed in terms of a quark model. Resonances are considered in detail. (D.C.W.)

21698 PARTICLE AND POLARIZATION ANGULAR DISTRIBUTIONS FOR TWO AND THREE BODY DECAYS. Jackson, J. D. (Univ. of Illinois, Urbana). pp 325-65 of High Energy Physics. New York, Gordon and Breach Science Publishers, 1965.

A unified discussion of the angular distributions of particles and particle polarizations from the two and three body decay of resonances of well defined angular momentum is presented and it is shown how these distributions are used for a spin-parity analysis. Both mesonic and baryonic resonances are discussed. The helicity formalism and the Wigner D-functions are used. (G.O.Y.)

21699 PERIPHERAL INTERACTIONS. Jackson, J. D. (Univ. of Illinois, Urbana). pp 367-99 of High Energy Physics. New York, Gordon and Breach Science Publishers, 1965.

A brief review of the development and applications of the peripheral model is presented. The predictions of the model are compared with experimental observations, and some of the approaches to taking into account the effects of competing channels are outlined. (D.C.W.)

21700 THEORY OF WEAK INTERACTIONS. Bell, J. S. (CERN, Geneva). pp 401-502 of High Energy Physics. New York, Gordon and Breach Science Publishers, 1965.

Some recent developments in the theory of weak interactions are outlined. The invariance properties in the decay of mesons(K^0) are studied in detail. (D.C.W.)

21701 PHENOMENOLOGICAL DESCRIPTION OF K DECAY. Yang, C. N. 12p. (CONF-651043-8). ORAU. Gmelin, AED-CONF-65-320-7.

From Weak Interactions Conference, Argonne, Ill.

A general description of $K\text{-}\bar{K}$ decay is followed by discussions of 2π decays, leptonic modes, and 3π modes. Quantities of immediate experimental interest are pointed out, and experiments by which these quantities may be measured are discussed briefly. The CPT theorem and C, P, and T invariance for strong and electromagnetic interactions are assumed. (A.G.W.)

Field Theory, Scattering Theory, and Symmetries

See also Elementary Particles and Radiations

Refer also to abstract 21696.

21702 (AD-621385) FORMAL SCATTERING THEORY AND THE COULOMB PROBLEM. Hostler, Levere (Pittsburgh Univ., Pa.). 1965. Contract Nonr-62416. 55p. CFSTI $3.00 cy, $0.50 mn.

It is attempted to salvage the usual apparatus of formal scattering theory in the case when there is a Coulomb field present. For this purpose, the time dependent approach to formal scattering theory is presented without the use of adiabatic switching. Asymptotic limits are investigated with the help of the Riemann–Lebesgue lemma. For scattering by a regular potential, the usual golden rule and the Lippmann–Schwinger equation are obtained. The same formalism is applied to the case of the Coulomb potential, and is found to by-pass the ambiguities and "wrong" factors which were encountered by a number of authors, and which are due to the anomalous behavior of the Coulomb T-matrix on the energy shell. Other mathematical pathologies still remain in the Coulomb case, but these now take the form of infinite phase factors, and are presumbably fairly innocuous. (auth)

21703 (AD-622258) THE ELEMENTARY PARTICLE SPECTRUM. Corben, H. C. (TRW Systems, Redondo Beach, Calif. Quantum Physics Lab.). Oct. 1965. Contract Nonr-376900. 23p. CFSTI $1.00 cy, $0.50 mn.

The relativistic quantum theory of the symmetric top implies that the spin J of a particle state can be represented as the sum of four commuting spin operators of lengths given by the positive integers or half-integers n, n′, l, l′. If (l + l′) is identified with the isospin, 2 (n′ − n) with the strangeness, and, where applicable, (−1) to the (n + n′) power with the G parity, the simplest choices of n, n′, l, l′ lead to a correct description of J, I, S, G for every known strongly interacting meson or baryon state. (TAB)

21704 (AD-622517) PROPOSED MEASURE FOR THE INFORMATION CONTENT IN QUANTUM FIELDS. Schutzer, Daniel (Syracuse Univ., Research Inst., N. Y.). Aug. 17, 1965. Contract Nonr-66910. 104p. (SURI-EE-494-658-T-8). CFSTI $4.00 cy, $0.75 mn.

Under the present formulation of quantum mechanics, there exists a vacuum energy. The function describing an elementary particle, the field function, has random fluctuations superimposed upon it. An existence information measure is proposed to describe the information contained in a particle field. Existence information is the uncertainty in making the decision that a particle field exists, in light of the vacuum fluctuation effect. Relationships between the existence information and basic intuitive ideas of information theory are brought out. Connections are shown between Shannon's formulation of information theory, Wigner's skew information measure, and the proposed, existence information. Plausibility arguments for the appropriateness of existence information as the representation of field information are presented. Interactions between particles, and the self-interference of a particle are discussed and related to distinguishability, choice, correlation and existence information. Electromagnetic scattering is discussed and is associated with the coherence between the two particles vacuum fluctuations. Existence information is calculated and studied as a function of measurements and interactions. The total existence information content of an isolated sys-

tem (possibly interacting internally) is found to be independent of time. (auth)

21705 (CERN-65-24(Vol.1), pp 45-63) THE PERIPHERAL MODEL. Pilkuhn, H. (European Organization for Nuclear Research, Geneva (Switzerland)).

The mathematical formulation of the various versions of the peripheral model is discussed. The discussion concerns reactions of the type a + b → c + d, where the outgoing particles c and d are either stable or else resonances with definite spin, parity, and isospin quantum numbers. (M.O.W.)

21706 (CONF-640509(Pt.2)) COLLOQUE INTERNATIONAL DE PHYSIQUE THEORIQUE, MAI 28–JUIN 2, 1964. 2E PARTIE. (International Conference on Theoretical Physics, May 28–June 2, 1964. Part 2). (Bordeaux Univ. (France). Laboratoire de Physique Theorique). 93p. Dep. mn.

Separate abstracts were prepared for the 3 included papers. (M.O.W.)

For abstracts of individual papers see: 21707–21709.

21707 (CONF-640509(Pt.2), Paper 1) SYMETRIE UNITAIRE. (Unitary Symmetry). Gourdin, M. (Paris Univ., Orsay (France). Laboratoire de Physique Theorique et Hautes Energies). 21p.

The fundamentals of the mathematical formalism of unitary symmetry and the principle characteristics of the models constructed on the symmetry (the octet model. Sakata model, and quark model) are reviewed. The violations of unitary symmetry are formulated. (J.S.R.)

21708 (CONF-640509(Pt.2), Paper 2) SYMETRIE UNITAIRE ET INTERACTIONS FAIBLES. (Unitary Symmetry and Weak Interactions). Gourdin, M. (Paris Univ., Orsay (France). Laboratoire de Physique Theorique et Hautes Energies). 25p.

The mathematical formalism of currents, lepton processes, and nonleptonic processes in unitary symmetry and weak interactions is derived. In leptonic processes the leptonic decay of pseudoscalar mesons and reactions with high energy neutrinos are considered. Under nonleptonic processes, the decay of kaons into pions, the decay of non-leptons in baryons and weak radiative decay of baryons are considered. (J.S.R.)

21709 (CONF-640509(Pt.2), Paper 6) CONSEQUENCES DE LA SYMETRIE UNITAIRE. (Consequences of Unitary Symmetry). Prentki, J. (European Organization for Nuclear Research, Geneva (Switzerland)). 41p.

The physical consequences of the theory of groups, in particular of the octet model are developed. The study by Gourdin in this conference was used to determine different irreducible representations and their content in isotopic spin and hypercharge. The problems connected to the classification of problems and the model predictions with respect to the different processes of strong and weak interactions are considered in detail. (J.S.R.)

21710 (JINR-P-2554) RASSEYANIE POTOKA CHASTITS NA SISTEME ZAKREPLENNYKH TSENTROV. (Scattering of Particles by a System of Fixed Centers). Amirkhanov, I.; Demin, V. F.; Zakhar'ev, B. N.; Kuz'min, I. I. (Joint Inst. for Nuclear Research, Dubna (USSR). Lab. of Theoretical Physics). 1966. 10p. Dep. mn.

Scattering of particles by a system of fixed centers is considered. Domains of interaction of these centers with incident particles do not intersect with each other. It is shown that the problem is reduced to solving a system of N algebraic equations ($N = n_1 \cdot n_2$; n_1 is the number of centers, n_2 is the number of the considered one-particle partial amplitudes). The scattering amplitude is expressed in terms of the partial scattering amplitudes on a single center. The formalism of multiple scattering is generalized to the case where the scattered particles are complex (can be excited). (auth)

21711 (JINR–P–2559) VOS'MIRICHNYI FORMALIZM V SU(3) I 10- I 27-PLETY. (Eightfold Formalism in SU(3) and 10- and 27-Plets). Ogievetskii, V. I.; Polubarinov, I. V. (Joint Inst. for Nuclear Research, Dubna (USSR). Lab. of Theoretical Physics). 1966. 21p. Dep. mn.

A vector (eightfold) formalism in SU(3) is developed in which the octets are represented in terms of a one-index quantity, whereas the 10- and 27-plets are represented by two-index tensors. A complete set of 8 × 8 matrices is constructed and a number of relations characterizing the algebra of these matrices was obtained. (auth)

21712 (JINR–P–2562) O SIMMETRIYAKH LEPTONOV I ADRONOV V SLABYKH VZAIMODEISTVIYAKH. I. LEPTONY. (On Symmetries of Leptons and Hadrons in Weak Interactions. I. Leptons). Kadyshevskii, V. G. (Joint Inst. for Nuclear Research, Dubna (USSR). Lab. of Theoretical Physics). 1966. 26p. Dep. mn.

A classification of leptons is suggested on the basis of the group 0(5). Operators of electromagnetic and weak currents and the interaction lagrangians are constructed. (auth)

21713 (JINR–P–2568) UNITARNAYA SIMMETRIYA I SHIRINY REZONANSOV. (Unitary Symmetry and Resonance Widths). Nguyen Van Hieu, Tikhonin, F. F. (Joint Inst. for Nuclear Research, Dubna (USSR). Lab. of Theoretical Physics). 1966. 15p. Dep. mn.

Under the assumption of exact unitary symmetry two-particle decays of baryon and meson resonances are treated. The ratios of resonance decay probabilities are given using relations between the coupling constants of particles obtained from SU(3) invariance and taking into account phase volumes. A comparison is made of the results obtained with the available experimental data. (auth)

21714 (JINR–P–2578) MODEL SLABYKH VZAIMODEISTVII BARIONOV I LEPTONOV. (A Model of Weak Interactions of Baryons and Leptons). Arbuzov, B. A.; Filippov, A. T. (Joint Inst. for Nuclear Research, Dubna (USSR). Lab. of Theoretical Physics). 1966. 20p. Dep. mn.

The model is considered, in which weak interactions of the two fundamental fields describing baryons and leptons are due to the change of space-time structure at small distances. The universality of weak interactions in the Cabibbo form, the selection rule $|\Delta S| \leq 1$ for all decays and the rule $\Delta S = \Delta Q$ for leptonic decays of hadrons follow from the main assumptions of the model. (auth)

21715 (JINR-P-2576) O PRIMENENII METODA "MAKSIMAL'NOI SLOZHNOSTI" DLYA OPREDELENIYA SPINOV I CHETNOSTEI V REAKTSIYAKH S POLYARIZOVANNYMI CHASTITSAMI. (On an Application of the "Maximum Complexity" Method for Determining Spins and Parities in Reactions With Polarized Particles.). Bilen'kii, S. M.; Ryndin, R. M. (Joint Inst. for Nuclear Research, Dubna (USSR). Lab. of Theoretical Physics). 1966. 14p. Dep. mn.

A possible method is suggested to determine spins and intrinsic parities of particles produced in the reactions $0 + \frac{1}{2} \rightarrow J + S(J \rightarrow 0 + 0, S \rightarrow \frac{1}{2} + 0)$ and $\gamma + 0 \rightarrow j + 0(j \rightarrow 0 + 0)$ with polarized initial particles. The method is based on the requirement of invariance under reflections in the reaction plane (Bohr symmetry). The parity conservation in decays is not assumed. (auth)

21716 (JINR–P–2603) RESHENIE ZADACHI O RASSEYANII DVUKH PLOSKIKH VOLN V NELINEINOI SKALYARNOI TEORII POLYA TIPA BORNA-INFEL'DA. (Solving the Problem of Two-Plane Wave Scattering in the Non-Linear Scalar Field Theory of Born-Infeld Type). Barbashov, B. M.; Chernikov, N. A. (Joint Inst. for Nuclear Research, Dubna (USSR). Lab. of Theoretical Physics). 1966. 16p. Dep. mn.

The scattering problem of two plane waves is formulated and solved in the classical nonlinear mesodynamics of the Born-Infeld type. The shape and direction of the plane waves after scattering turn out not to change. Only the arguments $x - t$ and $x + t$ are shifted by magnitudes determined by the momenta of these waves. The solution was obtained on the basis of the Cauchy problem for this equation. (auth)

21717 (JINR–P–2620) SOKHRANENIE IZOSPINA I POLYARIZATSIONNYE EFFEKTY. (Isospin Conserva-

tion and Polarization Effects). Bilen'kii, S. M.; Lapidus, L. I.; Ryndin, R. M.; Shekhter, L. Sh. (Joint Inst. for Nuclear Research, Dubna (USSR)). 1966. 9p. Dep. mn.

The reactions $a + a' \rightarrow b + b'$ are treated in which the particles a and a' (or b and b') belong to the same isotopic multiplet. As to the total isotopic spin of finite (or initial) particles, it may take only one value. Relations were obtained between polarization characteristics of such reactions at the angles θ and $\pi - \theta$ (θ is the c.m.s. angle). These relations are based only on isotopic invariance and invariance under rotations and reflections. Their experimental verification would be a detailed test of isotopic invariance of strong interactions. (auth)

21718 LEHMANN–SYMANZIK–ZIMMERMANN FORMALISM IN THE ONE-BOSON LEE MODEL. Scarfone, Leonard M. (Univ. of Vermont, Burlington). Amer. J. Phys., 34: 254-9(Mar. 1966).

The one-boson Lee model of a solvable field theory with nontrivial charge and mass renormalization provides an elementary example of the Lehmann-Symanzik-Zimmermann formalism. The basic quantities of interest in this method of calculation are the vacuum expectation values of time-ordered Heisenberg operators and by studying the analytic properties of the Fourier transforms of these functions, the first nontrivial subspace of the model is solved without resorting to eigenvalue equations. The full Lee model was recently analyzed with this technique and it seems pedagogically appropriate to carry out an analogous calculation in an even more elementary context. (auth)

21719 G_2 SYMMETRY AND LEPTONIC DECAYS. Galindo, A.; Morales, A.; Nunez-Lagos, R.; Soler, M. (Junta de Energia Nuclear, Madrid). An. Real Soc. Espan. Fis. Quim. (Madrid), Ser. A, 61: 275-9(Sept.-Oct. 1965).

The vector and axial hadronic weak currents, are constructed within the framework of the G_2 group. Angular parameters are introduced in much the same way as for SU(3), and their actual value computed from experimental data. Application to the leptonic decay of hyperons and comparison with the predictions of the SU(3) model is accomplished. (auth)

21720 ON SOME CLASSICAL SPACE-TIME GROUPS AND THEIR SU_6 GENERALIZATIONS. Bacry, H. (CERN, Geneva). Ann. Inst. Henri Poincare, Sect, A, 2: 327-53 (1965).

The Lorentz group, Poincaré group, de Sitter groups are defined as subgroups of the conformal group. The four-dimensional representation of the conformal group is investigated with the aid of the γ-Dirac algebra. This leads to a new interpretation of the γ_5 operator as the generator of the scale transformation of the Minkowski space. The usual currents $\bar{\psi}\gamma_\mu(1 + \gamma_5)\psi$ for massless particles are shown to belong to the adjoint representation of the Poincaré group (it is not the case for the $\bar{\psi}\gamma_\mu(1 - \gamma_5)\psi$ components). Natural "SU_6-generalizations" of all these groups are readily derived and some of their properties are discussed. (auth)

21721 A NEW NONRELATIVISTIC LIMIT TO THE POINCARE GROUP. Levy-Leblond, Jean-Marc (Laboratoire de Physique Theorique, Orsay, France). Ann. Inst. Henri Poincare, Sect. A, 3: 1-12(1965). (In French).

It is shown that, for the Galilean approximation to the Poincaré group to be valid, not only must pure Lorentz transformation with low velocities be considered, but also great time-like intervals. Under the same conditions, the transformation properties of great space-like intervals are described by a group which is a new non-relativistic limit of the Poincaré group. This group is distinct from the Galilei group but is also obtained from the Poincaré group by a contraction. The structure of this group and its Lie algebra are studied; and their irreducible unitary representations are constructed. In a world whose invariance group would be this new group, there would be practically no causality. The name "Carroll group" is suggested for this degenerate cousin of the Poincaré group. The meaning and importance of a hitherto implicit condition for the validity of the Galilean approximation are emphasized. (auth)

21722 ON THE UNITARY REPRESENTATIONS OF SU(1,1) AND SU(2,1). Biedenharn, L. C.; Nuyts, J.; Straumann, N. (CERN, Geneva). Ann. Inst. Henri Poincare, Sect. A, 3: 13-39(1965).

The explicit construction of all unitary representations of the two-noncompact groups SU(1,1) and SU(2,1) as ancillary to the study of the family of groups SU(p,q) is considered. Lie algebra is used, and global properties are invoked only when essential. The basis for the method is the fact that the Lie algebras of SU(p + q) and SU(p,q) have the same complex extension. A principal advantage of this procedure is that it leads to explicit results for the matrix elements of the generators and to all irreducible representations for both SU(p,q) and its covering group. The possible extensions to the general case are also discussed. (J.F.P.)

21723 NONLINEAR WAVE EQUATIONS OF A SPIN 0-SPIN $2\hbar$ SYSTEM AND THE QUANTUM THEORY OF ASSOCIATED FIELDS. Petiau, Gerard (Institut Henri Poincare, Paris). Ann. Inst. Henri Poincare, Sect. A, 3: 127-59(1965). (In French).

A nonlinear extension of the formalism for a particle of total maximum spin $2\hbar$ is described in quantum theory. A scalar or pseudoscalar particle of spin 0 is associated with a spin-$2\hbar$ field having the tensor properties of the particle's gravitational field. It is shown how the mass of this particle is constructed from invariants associated with the spin-$2\hbar$ field and takes values defined by quantization of the field. The quantum theory of fields, which it is proposed to associate with this model, leads to a simultaneous quantization of the dynamic mass amplitudes. (J.F.P.)

21724 ORIGIN OF CERTAIN RESONANCES FOR THREE PARTICLES. Dennery, Ph. (Laboratoire de Physique Theorique et Hautes Energies, Orsay, France). Ann. Inst. Henri Poincare, Sect. A, 3: 175-81(1965). (In French).

A formalism is suggested which describes the interaction between a stable and an unstable particle which can lead to a resonant state of three particles. (auth)

21725 CHARGE CONJUGATION IN UNITARY SYMMETRY GROUPS. Okubo, S. (Univ. of Rochester, N. Y.); Mukunda, N. Ann. Phys. (N. Y.), 36: 311-22(Feb. 18, 1966). (UR-875-95).

A charge conjugation transformation law for infinitesimal generations of unitary symmetry groups like SU(2), SU(3) (or more generally SU(n)) and U(12) was derived from requirements that the charge conjugation is an automorphism of the group and furthermore that it changes signs of ordinary charge and hypercharges. (auth)

21726 RUDIMENTARY GEOMETRIC PARTICLE THEORY. Loos, Hendricus G. (Giannini Foundation, Indio, Calif. Univ. of California, Riverside). Contract NASw-967. Ann. Phys. (N. Y.), 36: 486-98(Feb. 18, 1966).

A particle theory is sketched on the classical level, in which all the additive particle labels are defined in terms of geometry already present in a Yang-Mills type gauge theory and general relativity, without an action principle and without using particle fields. The internal particle labels are constructed from conserved currents determined by the internal curvature, i.e., the gauge fields. The step from local to integral conservation laws is considered with care, casting some doubt on the conventional procedure and indicating an apparent possibility for geometric breaking of conservation laws. The concept of holonomy groups has been used freely; one of the remaining questions concerns the asymptotic behavior of internal holonomy groups at large distances from a physical system. Part of the dynamics is proposed to be carried by a postulate linking event space with internal space, and defining a map between the holonomy groups for these spaces. Several candidates for such a postulate have group theoretical implications similar to higher symmetry schemes. The translation group is absent here however, since the energy-momentum vector is constructed from the Einstein tensor in Riemannian event space. Spin angular momentum has been tentatively identified with a geometric construct as well. (auth)

21727 ON THE SPONTANEOUS BREAKDOWN OF γ_5 INVARIANCE AND PARITY NONCONSERVING INTERACTIONS. Stern, J.; Vancura, A. (Czech Technical Univ., Prague). Czech. J. Phys., 16: 180-5(1966).

It is shown that in γ_5-invariant theories, including those with an unsymmetrical vacuum, a nonzero mass of a spinor particle cannot arise, provided parity is conserved. (auth)

21728 DIAGRAM TECHNIQUE IN THE CASE OF MANY-PARTICLE INTERACTIONS. Aganovic, Ibrahim. Glas. Mat.-Fiz. Astron., Ser. II, 20: 137-44(1965).

A systematic diagram technique was developed for one-particle Green functions of a relativistic Fermi system of equal particles in the case when many-particle as well as two-particle interactions exist. The usual notations of field theory are used in the interaction representation. (J.F.P.)

21729 ASYMPTOTIC RENORMALIZABILITY CONDITIONS ON FIELD PROPAGATORS. Boyce, J. F. (International Center for Theoretical Physics, Trieste, Italy). J. Math. Phys. (N. Y.), 7: 603-7(Apr. 1966).

High-energy boundary conditions upon the basic Green's function, which limit the types of divergence arising in any approximational method of solution of a field theory, are derived and shown to be related to the recently defined stability criterion. (auth)

21730 SYMMETRY PROPERTIES OF THE 3j-SYMBOLS FOR AN ARBITRARY GROUP. Derome, Jean-Robert (Univ. of Toronto). J. Math. Phys. (N. Y.), 7: 612-15(Apr. 1966).

The symmetry properties of the 3j-symbols are studied for an arbitrary compact group. It is shown that when the three j's are all inequivalent it is possible to choose 3j-symbols which are invariant under any permutation of the j's and of the corresponding m's (generalized magnetic quantum numbers). When two of the three j's are equivalent, the 3j-symbols can be chosen in such a way that at most a minus sign appears when the j's and m's are permuted. It is also shown that when the three j's are equivalent it is in general not possible to choose the 3j-symbol such that its absolute value is invariant under every permutation of the m's. (auth)

21731 LIMITING FORMS OF THE SCREENED COULOMB T MATRIX. Ford, William F. (Lewis Research Center, Cleveland). J. Math. Phys. (N. Y.), 7: 626-33 (Apr. 1966).

In the complex energy plane, the pure Coulomb T matrix possesses branch points which would not appear if the force were properly defined. This is demonstrated by a study of the screened Coulomb T matrix in the limit as the screening radius R tends to infinity. No branch points develop if the proper order of limiting processes is observed and the results agree with previous calculations; however, the T matrix is discontinuous in the limit. A formula for the screened Coulomb T matrix is given which is valid to order 1/R for all energies. (auth)

21732 LEADING LANDAU CURVES OF A CLASS OF FEYNMAN DIAGRAMS. Islam, Jamal N. (Univ. of Maryland, College Park). J. Math. Phys. (N. Y.), 7: 652-60 (Apr. 1966).

It was shown previously that the leading Landau curves of some Feynman diagrams do not give singularities on the physical sheet if some of the internal and external masses satisfy certain simple inequalities. It is shown that a similar property is satisfied by a class of Feynman diagrams. The inequalities involve a fixed number of masses for the whole class. (auth)

21733 ANALYTICITY PROPERTIES OF THE SCATTERING AMPLITUDE. Minguzzi, A. (Univ., Bologna. Istituto Nazionale di Fisica Nucleare, Bologna). J. Math. Phys. (N. Y.), 7: 679-81(Apr. 1966).

Analyticity properties in three variables, energy, momentum transfer, and "squared mass" are deduced from single-variable dispersion relations. (auth)

21734 GELFAND STATES AND THE IRREDUCIBLE REPRESENTATIONS OF THE SYMMETRIC GROUP. Moshinsky, M. (Univ. Mexico, Mexico City). J. Math. Phys. (N. Y.), 7: 691-8(Apr. 1966).

The set of Gelfand states corresponding to a given partition $[h_1 \ldots h_n]$ form a basis for an irreducible representation of the unitary group U_n. The special Gelfand states are defined as those for which $[h_1 \ldots h_n]$ is a partition of n and the weight is restricted to $(11 \ldots 1)$. It is shown that the special Gelfand states constitute basis for the irreducible representations of the symmetric group S_n, and this property is used to construct explicitly states in configuration and spin-isospin space with definite permutational symmetry. (auth)

21735 POLES OF THE PROPER VERTEX FUNCTION IN THE BETHE-SALPETER FORMALISM. Nakanishi, Noboru (Brookhaven National Lab., Upton, N. Y.). J. Math. Phys. (N. Y.), 7: 698-701(Apr. 1966). (BNL-9078).

A formal general proof of the statement of Goebel and Sakita is presented on the basis of the Bethe-Salpeter formalism; namely, it is shown that the poles of a proper vertex function cannot appear in the corresponding scattering amplitude. Some related conjectures are also verified. An exactly solvable example is presented and discussed in this connection. (auth)

21736 ANALYSIS OF INTENSE, UNDRIVEN ELECTRON BEAMS WITH SIGNIFICANT SELF-FIELD FORCES. Roberts, A. S. Jr. (North Carolina State Univ., Raleigh). Plasma Phys.-Accel. Thermonucl. Res., J. Nucl. Energy: Pt. C, 8: 53-61(Jan.-Feb. 1966).

Intense, stationary electron beams are treated in paraxial analysis. The differential equation for beam envelope trajectories is obtained and includes self-magnetic effects as well as the influence of finite emittance and variable space charge. A numerical example is selected to demonstrate non-accelerated beam flow. Space charge divergent results are obtained in the absence of ion trapping. However, when space charge forces are neutralized the beam envelope trajectory described spatially periodic behavior under the influence of self-magnetic effects. (auth)

21737 EVALUATION OF THE TRACE OF THE ν-TH POWER OF A MATRIX. Toth, Kalman. Magyar Tud. Akad. Kozp. Fiz. Kut. Int. Kozlem., 14: 73-6(1966). (In Hungarian).

It is shown, that the trace S_ν of the ν-th power of any matrix A having n rows and n columns equals $x_1^\nu + x_2^\nu + \ldots + x_n^\nu$ where $x_1, x_2, \ldots, x_n$ are the roots of the characteristic equation for A. If the characteristic equation is written in the form $x^n + \alpha_1 x^{n-1} + \ldots + \alpha_n = 0$ the evaluation of S_ν can be performed with the use of the recursion relations: $S_\nu + \alpha_1 S_{\nu-1} + \ldots + \nu\alpha_\nu = 0$ if $\nu \leq n$; $S_\nu + \alpha_1 S_{\nu-1} + \ldots + \alpha_n S_{\nu-n} = 0$ if $\nu > n$. These relations are useful for the study of internal symmetry groups of elementary particles. (auth)

21738 MODEL FOR FINAL-STATE INTERACTIONS. Taha, M. O. (Univ. of Cambridge, Eng.). Nuovo Cimento (10), 42A: 201-19(Mar. 21, 1966).

A final-state interaction decay model, suggested by Landshoff and Olive, is investigated. It is found to give results somewhat similar to dispersion-theoretic treatments. S and P waves are considered, with only iterative solutions indicated. The neighborhood of the threshold is discussed and the existence and uniqueness of solutions are proved under stated conditions. (auth)

21739 MASS FORMULAE FOR BARYONS IN $S\tilde{U}_3$. Bisiacchi, G.; Fronsdal, C. (International Atomic Energy Agency, Trieste, Italy). Nuovo Cimento (10), 42A: 220-7 (Mar. 21, 1966).

It has been suggested that $S\tilde{U}_3$, a noncompact version of SU_3, might retain many of the predictions of the latter. Here we investigate the mass spectrum of baryons assigned to an infinite unitary representation, and find that many results, including the Gell-Mann-Okubo formula can be derived. The masses of some of the newly predicted particles were calculated. (auth)

21740 A PLAUSIBLE LOWER BOUND ON THE SPECTRAL FUNCTIONS OF A SPINOR PROPAGATOR AND ITS IMPLICATIONS FOR NONLOCALITY. Hadjioannou,

F. T. (Univ., Bonn). Nuovo Cimento (10), 42A: 241-50 (Mar. 21, 1966).

The spectral functions of a spinor propagator are calculated using unitarity and dispersion relation techniques. The model is a nonrenormalizable field theory, a spinor field coupled to a neutral weak vector boson. The calculation is done in the ladder approximation. The spectral functions are found to increase in a rapid, essentially exponential way. Implications of this very rapid increase are discussed. (auth)

21741 DIVERGENCE OF RENORMALIZED VS CONVERGENCE OF REGULARIZED PERTURBATIVE EXPANSIONS IN A FIELD-THEORETICAL MODEL. Guerra, F.; Marinaro, M. (Univ., Naples. GNSM, Naples). Contract AF 61(052)-826. Nuovo Cimento (10), 42A: 285-305 (Mar. 21, 1966).

The model is scalar electrodynamics with boson propagators taken to be constant in configuration space. The finite-part integration technique is applied to find the equations of the renormalization group. After renormalization, the perturbative expansions of the propagators are divergent, as the latter turn out from exact computation to be nonanalytical functions of the expansion parameter. On the other hand, the same expansions, regularized with cut-offs and finite-integration volumes, have a radius of convergence which is at least finite: this supports strongly Dyson's conjecture on perturbative expansions. (auth)

21742 REMOVAL OF POINT-LOOP AMBIGUITIES THROUGH FINITE-PART RENORMALIZATION. Guerra, F.; Marinaro, M. (Univ., Naples. GNSM, Naples). Contract AF 61(052)-826. Nuovo Cimento (10), 42A: 306-15(Mar. 21, 1966).

The definition of contracted products of field operators at coincident points is analyzed by relating it to the renormalization of ultraviolet divergences. The ambiguity contained in the definition of these products is completely incorporated in the divergent parts, as these contracted products acquire well-defined values once the prescription for finite-part integrals is fixed; finite-part integrations commute then with mass derivatives. (auth)

21743 STRUCTURE OF WEAK CURRENTS. Csikor, F.; Pocsik, G. (Roland Eoetvoes Univ., Budapest). Nuovo Cimento (10), 42A: 413-15(Mar. 21, 1966).

The general properties of a set of not necessarily conserved currents with massive vector fields were previously investigated, and certain restrictions, which are contradicted by the nonconventional nonconserved fermion currents, for the vacuum expectation values of the currents were found on the basis of the usual axioms of field theory including also the TCP invariance. The current-current type conditions are first treated without using the existence of vector mesons. It is then shown how the weak currents can be completed in order to satisfy all prescriptions. (L.B.S.)

21744 ON THE MASSES OF NONSTRANGE PSEUDOSCALAR MESONS AND THE GENERALIZED KLEIN-GORDON EQUATION. Flato, M. (Institut Henri Poincare, Paris); Sternheimer, D.; Sternheimer, J.; Vigier, J. P.; Wataghin, G. Nuovo Cimento (10), 42A: 431-4(Mar. 21, 1966).

It is shown that the degeneracy between nonstrange pseudoscalar mesons can be removed by assuming the Laplace–Beltrami eigenvalue problem to represent the Klein–Gordon equation in curved manifold. (L.B.S.)

21745 DIFFERENCE BETWEEN SOURCES AND CHARGES. Krolikowski, W. (Middle East Technical Univ., Ankara). Nuovo Cimento (10), 42A: 435-9(Mar. 21, 1966).

It is argued that in the case of a broken symmetry the concepts of sources and charges are entirely different, and cannot refer to the same physical objects. Moreover, there is no smooth transition between them, when the broken symmetry tends more and more to a strict symmetry. (L.B.S.)

21746 MIXING OF SPIN-ZERO MESONS. Pocsik, G. (Roland Eoetvoes Univ., Budapest). Nuovo Cimento (10), 42A: 440-2(Mar. 21, 1966).

A simple field-theoretical pole approximation is applied for the meson propagator taking into account the $\chi-\eta$ mixing. The departure from the Gell-Mann-Okubo mass formula is explained by choosing the $\chi-\eta$ mixing angle as $\pm 10°$. The treatment can also be extended to the scalar nonet. (L.B.S.)

21747 THRESHOLD BEHAVIOR OF 3-BODY PARTIAL-WAVE AMPLITUDES. Halliday, I. G. (Princeton Univ., N. J.). Nuovo Cimento (10), 42B: 38-50(Mar. 11, 1966).

The threshold behavior of 3-body scattering amplitudes is investigated in potential theory. For a bound state plus free-particle system the conventional J, M, l, S type of angular decomposition is used. For 3-free particle J, M, and M′ is used, the latter being the component of J along a body-fixed axis. It is then shown that the T-matrices for bound-state elastic and rearrangement collisions behave like $(p_i)^{l_i}(p_f)^{l_f}$, where p_i, p_f refer to initial and final momenta. The break-up collision T-matrices behave like $(p_i)^{l_i}$· constant. The nonrescattering part of the 3-free → 3-free amplitude behaves like a constant while the rescattering part behaves like $1/p^2$. It is emphasized that all these terms are independent of J. (auth)

21748 SATURATION PROBLEM IN THE NONRELATIVISTIC QUARK MODEL OF ELEMENTARY PARTICLES. Morpurgo, G. (Univ., Genoa). Phys. Lett., 20: 684-6(Apr. 1, 1966).

It is shown how a situation in which a three quark system is strongly bound to form a proton, while a four or more quark system is unbound or has a binding energy much smaller than expected at first sight may produce itself in the quark model of "elementary" particles. (auth)

21749 REMARKS ON THE SATURATION OF EQUAL-TIME COMMUTATORS AND PHYSICAL SUM RULES. Alessandrini, V. A.; Beg, M. A. B.; Brown, L. S. (Univ. of California, Berkeley). Contract W-7405-eng-48. Phys. Rev., 144: 1137-41(Apr. 29, 1966). (UCRL–16367).

Identities relating continuations of physical amplitudes to equal-time commutators are considered. These identities, combined with fairly innocuous and justifiable approximations on the physical amplitudes, are shown to yield useful results. Some of these results look as if they emerged from a higher symmetry. (auth)

21750 SINGLE-PARTICLE REPRESENTATIONS OF CURRENT ALGEBRAS. Gerstein, I. S.; Lee, B. W. (Univ. of Pennsylvania, Philadelphia). Phys. Rev., 144: 1142-4(Apr. 29, 1966).

The requirement that matrix elements of current commutators are saturated by single-particle intermediate states leads to kinematical restrictions on the allowed momenta of these states. For the SU(6) algebra the momentum must be zero, while for the chiral SU(3) ⊗ SU(3) algebra it must be infinite. In this single-particle limit it is shown that the chiral algebra is equivalent to the collinear SU(3) ⊗ SU(3) sub-algebra of SU(6), and so a relation between the SU(6) and chiral algebras is established. (auth)

21751 RADIATIVE NONLEPTONIC WEAK DECAYS OF BARYONS. Tripathy, K. C.; Biswas, S. N.; Saxena, R. P. (Univ. of Delhi). Phys. Rev., 144: 1163-4(Apr. 29, 1966).

Sum rules for strangeness-changing radiative nonleptonic weak decay of baryons were obtained within the framework of the U(12) symmetry scheme, incorporating the octet-dominance hypothesis of the weak hamiltonian and also CP and gauge invariance. (auth)

21752 PSEUDOSCALAR-MESON UNIVERSALITY PRINCIPLE. Capps, Richard H. (Northwestern Univ., Evanston, Ill.). Phys. Rev., 144: 1182-8(Apr. 29, 1966).

It is pointed out the P-wave interactions of the pseudoscalar-octet (P_8) mesons provide a practical method of grouping hadrons together in supermultiplets. The hypothesis that P_8-meson-meson and P_8-baryon-baryon interactions in the limit of small momentum transfer are proportional to appropriate matrix elements of the axial-vector-octet generators of SU(6) is found to agree fairly well with experiment. The P_8 universality principle provides a simple measure of the ω-φ mixing angle, and is

useful also for identifying members of SU(6) resonance multiplets. Identification of the Σ_γ(1660 Mev) and the Λ'(1405 Mev) with states of the 70-fold representation of SU(6) leads to a predicted partial width of 14–19 Mev for the $\Sigma_\gamma \rightarrow \Lambda' + \pi$ decay. The application of various universality principles suggested by SU(6) symmetry to meson-meson-meson interactions is investigated. (auth)

21753 VECTOR-MESON MIXING AND SUM RULES IN BROKEN SU(3). Gupta, K. C.; Biswas, S. N. (Univ. of Delhi). Phys. Rev., 144: 1189-93(Apr. 29, 1966).

The vector-meson mixing model for the SU(3)-symmetry-breaking mechanism was considered in order to obtain the various broken-symmetry SU(3) coupling-constant sum rules. In addition to all the previous SU(3) results a new sum rule is found that is contained in the broken SU(6) symmetry. The method was also extended to derive the baryon-magnetic-moment sum rules to all orders of electromagnetic and to first order of strong symmetry-breaking interactions. Okubo's results were rederived. Using the Goldberger-Treiman relations and the new $\bar{B}BP$ coupling-constant sum rules obtained here, Cabibbo's assumptions of the axial weak interactions for the leptonic decay modes of the baryons are re-examined. (auth)

21754 ASYMPTOTIC FORM OF THE S MATRIX FOR LARGE ANGULAR MOMENTUM IN THE LEFT HALF-PLANE. Cheng, Hung; Wu, Tai Tsun (Harvard Univ., Cambridge, Mass.). Contract AF 49(638)-1380. Phys. Rev., 144: 1232-6(Apr. 29, 1966).

Starting with the Schroedinger equation, it is proved that for all energies, $S(\lambda,s)$ approaches $e^{2i\lambda\pi}$ as $|\lambda|$ becomes large in the direction $\frac{1}{2}\pi < \arg\lambda < \frac{3}{2}\pi$, for a class of potentials. These include the square-well potential, the cut-off Coulomb potential, a single Yukawa potential, and a superposition of Yukawa potentials of the form $\int_\mu^\infty (e^{-\mu' r}/r)\, e^{-\mu'}\, d\mu'$. The asymptotic forms of the Regge-pole parameters α_n and β_n are derived. It is found that $\arg\lambda_n$ approaches $\frac{1}{2}\pi$ or $\frac{3}{2}\pi$ as $n \rightarrow \infty$, and β_n is proportional to $1 + e^{2\pi i\alpha_n}$, which grows exponentially for the Regge poles in the lower half plane. The asymptotic forms for the Jost functions and the Y function are also given. A general proof for the asymptotic formula $S(\lambda,s) \rightarrow e^{2\pi i\lambda}$ as $|\lambda| \rightarrow \infty$, $\frac{1}{2}\pi < \arg\lambda < \frac{3}{2}\pi$, is also outlined. (auth)

21755 REPRESENTATION OF THE S MATRIX BY REGGE PARAMETERS. Cheng, Hung (Harvard Univ., Cambridge, Mass.). Contract AF 49(638)-589. Phys. Rev., 144: 1237-9(Apr. 29, 1966).

The S matrix of complex angular momentum and positive energy is expressed by Regge poles, proving that a knowledge of the Regge poles enables one to determine the S matrix uniquely. The background integral in the Mandelstam-Sommerfeld-Watson transform cannot be made to vanish by closing the contour to the left. Furthermore, one cannot express the scattering amplitude by an infinite-series sum of Regge-pole terms where each term is given by the Khuri representation. (auth)

21756 SOME CONSEQUENCES OF OFF-SHELL UNITARITY. Kowalski, K. L. (Case Inst. of Tech., Cleveland). Phys. Rev., 144: 1239-40(Apr. 29, 1966).

The implications of off-shell unitarity on the structure of the off-shell, nonrelativistic, two-particle partial-wave amplitudes are investigated. It is found that the unitarity conditions along with time-reversal invariance imply certain useful factorization properties of the off-shell amplitudes. (auth)

21757 MASS DIFFERENCES, CHARGES, AND MAGNETIC MOMENTS IN SU(3) BOOTSTRAP THEORY. Hara, Yasuo (Inst. for Advanced Study, Princeton, N. J.). Phys. Rev., 144: 1241-9(Apr. 29, 1966).

Bootstrap theory is applied to the mass differences, the charges, and the magnetic moments of baryons on the following assumptions: (1) that the baryon octet and the baryon decuplet are bound states of the baryon octet and the pseudoscalar meson octet, (2) the tadpole model of mass differences and the vector-meson dominance model of electromagnetic form factors, and (3) the static approximation. The mass differences and the charges and the magnetic moments of the baryons are expressed as functions of the mass differences and the charges of the pseudoscalar mesons. The results for the octet-type mass differences of baryons show excellent agreement with experimental results, but those for the 27-plet type mass differences show poor agreement with experiments. The $B_8B_8V_8$ charge coupling is found to be of F type and is also found to have the same magnitude as the $P_8P_8V_8$ coupling. The magnitudes of the magnetic moments of B_8 by our method are small compared with experimental values. (auth)

21758 ENERGY-MOMENTUM STRUCTURE FORM FACTORS OF PARTICLES. Pagels, Heinz (Univ. of North Carolina, Chapel Hill). Contract AFOSR-153-64. Phys. Rev., 144: 1250-60(Apr. 29, 1966).

An analogy between mass and charge as sources of fields, led to the investigation of the mechanical structure of a particle in terms of the matrix elements $\langle p'|\theta_{\alpha\beta}(0)|p\rangle$, where $\theta_{\alpha\beta}(x)$ is the total energy-momentum tensor, just as the matrix elements $\langle p'|j_\alpha(0)|p\rangle$ of the current operator $j_\alpha(x)$ define its electromagnetic structure. Although the off-diagonal matrix elements $\langle p'|\theta_{\alpha\beta}(0)|p\rangle$ are not accessible to direct experimental observation, the diagonal element $\langle p|\theta_{\alpha\beta}(0)|p\rangle$ is just proportional to the total mass. Consequently, the contributions to the total mass in terms of vertex functions instead of propagators can be studied and, using the techniques of dispersion theory, the contribution to the total mass can be related to integrals over physical scattering processes. Electrodynamics and the pion-nucleon interaction in perturbation theory are examined and it is shown how the mass divergences emerge as a consequence of high-energy behavior of the Coulomb amplitude and the nucleon-nucleon scattering amplitude. Finally, using elastic unitarity, mass splittings in a multiplet can be related to integrals over the differences in S-wave phase shifts. (auth)

21759 LIE GROUP OF THE STRONG-COUPLING THEORY. I. CALCULATION OF THE COUPLING-CONSTANT RATIOS AND MAGNETIC MOMENTS FOR SYMMETRIC PSEUDOSCALAR-MESON THEORY. Singh, Virendra (Tata Inst. of Fundamental Research, Bombay). Phys. Rev., 144: 1275-9(Apr. 29, 1966).

All the isobar-pion coupling constants are calculated using the Lie algebra $[SU(2) \otimes SU(2)] \times T_9$ of the strong-coupling theory. The $N^* \rightarrow N\pi$ reduced width comes out to be in agreement with experiment. Isobar magnetic moments are also calculated in terms of proton and neutron magnetic moments. The results obtained are also compared with SU(6) and reciprocal-bootstrap predictions. (auth)

21760 SATURATION OF SU(3)-SYMMETRIC HADRON FORCES. Capps, Richard H. (Northwestern Univ., Evanston, Ill.). Phys. Rev., 144: 1293-9(Apr. 29, 1966).

It is pointed out that the problem of saturation exists not only for nuclear forces, but also for other forces among hadrons. It is shown that the coupling of the vector-meson octet to the eight currents of SU(3) provides a mechanism that can help produce saturation in states of many hadrons. Two theorems are proved within the context of a simple model of an arbitrary number of mutually interacting mesons and either zero or one baryon. The first theorem shows that very few multimeson bound states may exist, and that nearly every possible baryon bound state corresponds to a representation smaller than that of the fundamental baryon. The second theorem shows that a saturation mechanism provides some justification for neglecting states of more than two particles in composite models. In the course of the investigation, a simple formula is developed for listing the representations contained in the direct product of an irreducible representation of SU(n) and an arbitrary number of regular representations. (auth)

21761 SPACE-TIME PROPERTIES OF A SCATTERING INTERACTION. McClure, J. A. (Tufts Univ., Medford, Mass.). Phys. Rev., 144: 1316-23(Apr. 29, 1966).

The scattering of a particle wave packet by a static potential of finite range is considered. In such an interaction, the incident packet enters the potential region, is scattered, and departs, changed in a way which depends on

the nature and strength of the interaction. Intuitively there is a region of space and an interval of time in which the interaction occurs. With the aid of the Schroedinger equation, this situation is discussed, and a function is derived which can be interpreted as describing the distribution of the interaction in space and time. The properties of the function are investigated, and arguments are given which support this interpretation. With the distribution, the space-time properties of the interaction are explored. Finally, it is suggested that the distribution function, appropriately extended, may be a useful tool in studying other aspects of particle interactions. (auth)

21762 WEAK CURRENTS IN BROKEN U(3) ⊗ U(3). Schechter, J. (Univ. of Chicago); Ueda, Y. Phys. Rev., 144: 1338-42(Apr. 29, 1966).

A generalization of the Ademollo-Gatto theorem is derived in the U(3) ⊗ U(3) symmetry scheme. It is found that both the vector and axial-vector weak currents remain pure octets to first order in the SU(3)-breaking interaction. A brief discussion of the range of validity of the result is given. (auth)

21763 THREE-PARTICLE FINAL STATES AND UNITARY SYMMETRY. Bar-Nir, I. M. (Tel-Aviv Univ., Israel); Harari, H. Phys. Rev., 144: 1363-73(Apr. 29, 1966).

A large number of new predictions of SU(3) are obtained for processes with three outgoing particles. All reactions involved in these relations are scattering of charged particles on protons with no more than one neutral particle in the final state. They can all be measured by the present experimental techniques. A detailed comparison between the available data and the predictions is presented, whenever possible. In a few cases, disagreement is found; but symmetry-breaking contributions are allowed within the matrix elements which describe the processes, the data are always consistent with the predictions. The general problem of comparing the predictions of a broken symmetry with scattering data is discussed, and various possibilities for performing such comparisons are suggested. (auth)

21764 POSITIVITY CONDITIONS FOR THE DENSITY MATRIX OF SPIN-ONE PARTICLES. Minnaert, Pierre (Ecole Polytechnique, Paris). Phys. Rev. Lett., 16: 672-4(Apr. 11, 1966).

A discussion is presented to show that besides the well known condition $\mathrm{Tr}\rho^2 \leq 1$, the spin-one density matrix has to satisfy also the condition $2\mathrm{Tr}\rho^3 - 3\mathrm{Tr}\rho^2 + 1 \leq 0$ which is more restrictive than the first one. This second condition, just as the first one, is shown to be easily expressed in terms of conditions on the multipole parameters. (B.G.D.)

21765 THE IRREDUCIBLE REPRESENTATIONS OF $\tilde{U}(12)$. Charap, J. M.; Matthews, P. T.; Streater, R. F. (Imperial Coll. of Science and Tech., London). Proc. Roy. Soc. (London), Ser. A, 290: 24-43(Feb. 8, 1966).

The unitary irreducible representations of inhomogeneous $\tilde{U}(12)$ are constructed and a group theoretic basis established for the generalized Bargmann–Wigner equations, introduced by Salam, Delbourgo & Strathdee. All the complications of the problem are concerned with the spacetime transformations which require the generalization of the Poincaré group to inhomogeneous $\tilde{U}(4)$. The covariant specification of the 'little group' in terms of the Pauli–Lubanski pseudovector is generalized to $\tilde{U}(4)$, and then to $\tilde{U}(12)$, to give expressions for the infinitesimal generators of the little group which are valid for any physical representation and in any frame of reference. (auth)

21766 INTERACTION BETWEEN BASIC PARTICLES. Tati, Takao (Univ. of Kanazawa, Japan). Progr. Theoret. Phys. (Kyoto), 35: 126-8(Jan. 1966).

A new spin of magnitude one is assigned to the basic particles (quarks) in the SU_3 theory and it is assumed that, between quarks (or between antiquarks), a two-body force depending on this spin which is attractive for triplet and repulsive for singlet and quintet states. This force leads to the saturation in the three quarks (or three antiquarks) system and, when the S state is assumed for baryons, it gives the values of their (ordinary) spins i.e., $\frac{3}{2}$ for decuplet baryons and $\frac{1}{2}$ for octet baryons. In this case, the singlet baryon cannot exist in the S state. It is considered that mesons are composed of baryons by another kind of force, which is weaker than the above mentioned one and attractive only between a quark and an antiquark. (auth)

21767 SOLUTIONS FOR A FEYNMAN–GELL-MANN PARTICLE IN A COULOMB FIELD. Aldrovandi, R.; Ferreira, P. Leal (Instituto de Fisica Teorica, Sao Paulo, Brazil). Rev. Mex. Fis., 14: 261-9(1965).

Solutions of the Feynman–Gell-Mann equation in the case of a Coulomb field are given both for bound and continuum states. It turns out that the eigenfunctions are mixtures consisting mainly of the state they are assigned in Dirac's theory together with small percentages of states of opposite parity. (auth)

21768 THE APPLICATION OF LAPLACE TRANSFORMATION TO THE THEORY OF RADIATION. Fock, V. A.; Tulub, A. V. Vestn. Leningr. Univ., No. 16, Ser. Fiz. Khim., No. 3, 7-20(1965). (In Russian).

The system of atomic amplitude equations of the quantum field theory of radiation is transformed into a single integro-differential equation the solution of which may be obtained by using the Laplace transformation. The method developed is applied to the calculation of the natural line width, resonance fluorescence and to the external field problems. (auth)

21769 MOTION OF POLES IN THE LEE MODEL. Chang, T. S. (Academia Sinica, Peking). Wu Li Hsueh Pao, 21: 1882-8(Nov. 1965). (In Chinese).

The motion of the poles in the first and the second sheets of the scattering amplitude in the Lee model as the coupling constant g^2 changes is studied. It is proved that, with or without the left hand cut, with or without the inelastic cut, the theory does not permit the occurrence of poles in the second sheet representing resonances unless the CDD poles are introduced for the inverse amplitude. When the left hand cut is present and the CDD poles are introduced, a pole representing resonance may slip across the normal cut (near the right threshold) into the first sheet as the coupling constant g^2 increases. But before this occurs, another pole slips into the first sheet across the left hand cut (near the left threshold). Motion of poles in the two sheets is plotted for one such special case. When the left hand cut is absent and the CDD poles are not yet introduced, it is pointed out that no passage of poles of one sheet into another sheet is possible so long as $g^2 > 0$. When the CDD poles are introduced, such passage becomes possible. It is shown that if a pole in the second sheet slips across the normal cut on increasing g^2 beyond a certain value $g_1^2 > 0$, then before g^2 reaches this value, another pole enters the first sheet at $-\infty$. Needless to say, poles entering from the left usually provide ghosts. These general features are believed to hold for field-theoretical models in general. (auth)

21770 LECTURES ON UNITARY SYMMETRY AND ELEMENTARY PARTICLES. Lichtenberg, D. B. Lincoln, Nebraska, Univ. of Nebraska, 1965. 110p.

The lectures included preliminary concepts, basis functions and Young diagrams, Young diagrams and generators of SU(n), unitary multiplets, and SU(3) and higher symmetries. (B.G.D.)

21771 GROUP THEORY. INVARIANCE PRINCIPLES. SYMMETRIES. Wick, G. C. (Brookhaven National Lab., Upton, N. Y. Columbia Univ., New York). pp 1-52 of High Energy Physics. New York, Gordon and Breach Science Publishers, 1965.

Geometric invariance properties are discussed first including applications to some specific examples. Internal symmetries are then discussed. The Poincaré group, discrete operations, isotopic spin, and SU(3) symmetry are considered in some detail. (D.C.W.)

21772 GROUP COMBINING INTERNAL SYMMETRIES AND SPIN. Guersey, F. (Middle East Technical Univ., Ankara). pp 53-87 of High Energy Physics. New York, Gordon and Breach Science Publishers, 1965.

Wigner's group SU_4, which combines spin and isospin in a non-trivial manner, and the generalization to particle physics, SU_6, which combines spin and unitary spin SU_3, are discussed in detail. (G.O.Y.)

21773 INTRODUCTION TO STRONG INTERACTION PHYSICS. Froissart, M. (CEN, Saclay, France); Omnes, R. pp 89-186 of High Energy Physics. New York, Gordon and Breach Science Publishers, 1965.

A detailed account is given of the mathematical techniques that are used in treating strong interactions. The analytic properties of scattering amplitudes are studied in detail within the framework of potential scattering theory and with the aid of simple graphs. A treatment of Lorentz invariance and a study of particles with arbitrary spin are also included, and the three-body problem is introduced. (D.C.W.)

21774 THE ANALYTIC S-MATRIX: A THEORY FOR STRONG INTERACTIONS. Chew, Geoffrey (Univ. of California, Berkeley). pp 187-250 of High Energy Physics. New York, Gordon and Breach Science Publishers, 1965.

An S-matrix theory of strong interactions is formulated on the basis of a generalization of analytic properties that were previously studied in the framework of specific models. 80 references. (D.C.W.)

Fluid Physics and Thermodynamics

See also Plasma Physics and Thermonuclear Processes

Refer also to abstracts 20854, 20855, 21525, and 21526.

21775 (AD-620835) RADIATION SMOOTHING OF SHOCKS. Kivelson, M. G.; Welch, J. A. Jr. (RAND Corp., Santa Monica, Calif.). Aug. 1965. Contract AF49(638)-700. 43p. (RM-4683-PR). CFSTI $2.00 cy, $0.50 mn.

The structure of a steady-state shock temperature profile in a fully-ionized ideal gas in the presence of a magnetic field is examined. It is pointed out that many of the important qualitative features of the temperature profile can be obtained in a simple way from a nomogram whose use is described. The customary introduction of a simplifying assumption (such as the Milne–Eddington approximation) relating the radiation pressure to the radiation energy flux is postponed to indicate which predictions are clearly independent of the approximation and which features may be a consequence of it. The thermal equilibrium of the electrons with the ions in the plasma is considered, and a parameter which measures the importance of the deviation from equilibrium is given. (auth)

21776 (AD-621429) PRANDTL-MEYER FLOW WITH A TRANSVERSE MAGNETIC FIELD [Thesis]. Zollner, Ronald Alfred (Air Force Inst. of Tech., Wright-Patterson AFB, Ohio. School of Engineering). June 1965. 70p. (GAM-65B-AE-65-8). CFSTI $3.00 cy, $0.75 mn.

A solution is presented to the classical Prandtl–Meyer flow problem under the influence of a transverse magnetic field. Maxwell's equations, the continuity equation, the momentum equation, and the constitutive equations were used in the analytical solution along with geometrical relations. Steady, inviscid, two dimensional, compressible flow was assumed. The plasma was considered to have an infinite electrical conductivity and a constant ratio of specific heats. Solutions were obtained relating the turning angle with the magnetic Mach number and the Karman number. These properties, the magnetic Mach angle, and the gasdynamic Mach number were tabulated in an appendix. It was found that the maximum turning angle decreased as the strength of the magnetic field increased; ranging from 130.5 degrees with no magnetic field to 65.88 degrees for an infinite field. (auth)

21777 (AD-621442) A STUDY OF ONE-DIMENSIONAL MAGNETOGASDYNAMICS [Thesis]. Tracy, Peter Wayne (Air Force Inst. of Tech., Wright-Patterson AFB, Ohio. School of Engineering). May 1964. 153p. (GAM-AE-64-3). CFSTI $5.00 cy, $1.00 mn.

Five flows in steady one-dimensional magnetogasdynamics were studied. These five flows are: Fanno flow; Rayleigh flow; Isentropic flow with area change; Flow with combined heat transfer, wall friction and area change; and Magnetogasdynamic normal shock. The flow variables exhibit a discontinuity where the magnetic Mach number (M_m) is equal to one. An entropy maximum occurs at this point. The Karman number K is used to define the flow regions in one-dimensional magnetogasdynamics just as Mach number defines the flow regions in gasdynamics. The Karman number K^* at $M_m = 1$ is the critical Karman number for the magnetogasdynamic flow. In one-dimensional magnetogasdynamic Fanno flow the pressure and temperature exhibit maxima in the subcritical region ($K < K^*$). The Mach number has a minimum in the subcritical region. This behavior does not occur in gasdynamic Fanno flow. In one-dimensional magnetogasdynamic Rayleigh flow, Mach number has a minimum, pressure a maximum and temperature a maximum in the subcritical region. Gasdynamic Rayleigh flow exhibits a temperature maximum for $M < 1$ that is similar to the magnetogasdynamic temperature maximum. The analysis of isentropic flow with area change is found to involve the integration of a first order differential equation known as the Darboux equation. This integration was not accomplished. It is seen that the magnetogasdynamic flow with area change, heat transfer and wall friction can be formulated. The magnetogasdynamic equations for this combined flow reduce identically to the gasdynamic equations as the magnetic field goes to zero. (auth)

21778 (AD-621943) NONLINEAR TERMS IN THE GENERALIZED OHM'S LAW: A SCALE ANALYSIS. Physical Sciences Research Papers. Stone, Noel (Air Force Cambridge Research Labs., L. G. Hanscom Field, Mass.). Aug. 1965. 53p. (AFCRL-65-571; PSRP-126). CFSTI $3.00 cy, $0.50 mn.

It is shown that a spatial gradient in the steady flow of an ionized gas introduces terms into the generalized Ohm's law that represent an exchange of momentum between the electrons and the gas flow. Depending upon the flow geometry and gas compressibility this electrokinetic exchange can behave like a generator, a Hall current, or a resistive current. The scale of the phenomenon is L = +/V, where V is fluid velocity, + is electron-positive charge collision time. Electrokinetic conditions apply largely at boundaries. In a resistive medium with a static B-field, the principal condition for electron-flow interchange is that magnetic pressure dominate dynamic pressure. At the boundary of a plasma jet the scale over which EK terms are important is of the order of 1 mm. Only geometry and scale considerations are used in the momentum equation. The electrokinetic generation of surface currents is as fundamental for describing moving media as spacecharge effects are in the static case. (auth)

21779 (AD-621990) IONIZING SHOCK STUDIES IN AN ELECTROMAGNETICALLY DRIVEN SHOCK TUBE. Report No. 19. Miller, Bennett (Columbia Univ., New York. Plasma Lab.). June 1965. Contract AF49(638)-1254. 140p. CFSTI $4.00 cy, $1.00 mn.

A coaxial electromagnetic shock tube was used to study ionizing shocks propagating through hydrogen. An experiment is described which produced plane switch-on ionizing shocks. Studies were conducted covering the sub-Alfvenic, trans-Alfvenic and super-Alfvenic regimes. Data are presented that verify the existence of switch-on fronts in all these regimes, and demonstrate the significant effect of the initial electric field on the shock jump conditions. The results substantiate the theory of normal ionizing shocks developed by Taussig. A simple physical criterion is employed to choose from among the several theoretically

predicted ionizing waves propagating at a given speed. This criterion has strong intuitive support and results in a consistent picture of ionizing shock propagation that is in general agreement without experimental observations. The existence of a small homogeneous plasma sample, behind the ionizing shock wave and before the expansion fan, is demonstrated. Previous failures to find large homogeneous plasma samples are shown to be consistent with the theory of ionizing shock waves. (auth)

21780 (AD-622036) VARIABLE CONDUCTIVITY FULLY DEVELOPED MHD CHANNEL FLOW [Thesis]. Kieffer, Paul Clement (Air Force Inst. of Tech., Wright-Patterson AFB, Ohio. School of Engineering). June 1965. 101p. (GAM-65B-ME-65-4). CFSTI $4.00 cy, $0.75 mn.

Fully developed MHD channel flow was studied for several conductivity profiles to determine the effect of nonuniform conductivity on the flow variables. The velocity profiles, volume rate of flow, and shear at the wall were investigated. If the conductivity only varies near the wall, the flow is moderately affected. If the conductivity in the central portion of the channel varies, significant changes (as much as 300% error based on uniform conductivity results) can occur. Variable conductivity has its greatest effect when the conductivity increases from the centerline to the walls. Inflection points can occur in the velocity profiles when the conductivity decreases from the centerline to the walls. (auth)

21781 (AD-622568) TWO-DIMENSIONAL STEADY AND ONE-DIMENSIONAL UNSTEADY MGD FLOWS OF SMALL MAGNETIC REYNOLDS NUMBER. Lackner, K. (Innsbruck Univ. (Austria). Institut fuer Theoretische Physik). Feb. 3, 1965. Contract AF61(052)-675. 9p. (AFOSR-65-1320). CFSTI $1.00 cy, $0.50 mn.

The applicability of the method of characteristics to the investigation of two-dimensional steady and one-dimensional unsteady MGD flows of small magnetic Reynolds number is studied. Preliminary results are shown to be promising. (auth)

21782 (AD-623812) MAGNETOGASDYNAMIC FLOWS OF SMALL MAGNETIC REYNOLDS NUMBER. PART I. Lackner, Karl (Innsbruck Univ. (Austria). Institut fuer Theoretische Physik). June 29, 1965. Contract AF61 (052)-675. 54p. (AFOSR-65-1621). CFSTI $3.00 cy, $0.75 mn.

The two-dimensional steady case is investigated for magnetogasdynamic flows of small Reynolds number. A new method is developed for a numerical treatment of the equations for the four real characteristic directions involved. The method is described by illustrating its use in the example of the MGD flow in a steady crossed field accelerator. Results are presented of calculations carried out on a Zuse Z 23 V computer. (auth)

21783 (AECL-2530) SUBROUTINES FOR DIGITAL SIMULATIONS. Kendall, J. D. (Atomic Energy of Canada Ltd., Chalk River (Ontario)). Dec. 1965. 44p. Dep. mn. AECL $1.50.

The G-20, APEX-IV subroutines DYNA, GRAPH, BOWAT, TEMP, VSF, VSG, HF, HG, SF, SG, DVSFDP, DVSGDP, DHFDP, DHGDP, PRES and INTERP are described. These are for use in preparing digital simulations of dynamic systems, in particular, thermodynamic systems. DYNA performs the input and output and integration functions. Data cards are used to set up output formats and integration data. The programmer must prepare little more than the mathematical model and a set of data cards. GRAPH outputs data in a graphical form. BOWAT is similar to DYNA except provision is made to input thermodynamic tables. The other subroutines compute the thermodynamic properties from these tables. (auth)

21784 (LA-3450) THE TWO-DIMENSIONAL HYDRODYNAMIC HOT SPOT. VOLUME III. Mader, Charles L. (Los Alamos Scientific Lab., Univ. of California, N. Mex.). Jan. 5, 1966. Contract W-7405-eng-36. 37p. Dep. mn. CFSTI $2.00 cy, $0.50 mn.

The shock interactions formed in nitromethane by corners of Plexiglas, aluminum, and gold; the resulting formation of a hot spot; and the buildup to propagating detonation are computed using a high-resolution, Lagrangian, two-dimensional, numerical hydrodynamic code with an Arrhenius rate law and accurate equations of state. Excellent agreement is obtained with the corresponding experimental results. (auth)

21785 (ORNL-TM-1330(Rev.)) PARAMETERS OF ISOTHERMAL FISSION-PRODUCT DEPOSITION [Thesis]. Kress, Tommy Sylvester (Oak Ridge National Lab., Tenn.). Apr. 1966. Contract W-7405-eng-26. 95p. Dep. mn. CFSTI $3.00 cy, $0.75 mn.

Studies were made to better define the wall interaction and to place the theory of fission product deposition on a less heuristic basis. A specific objective was to provide a method for coupling standard gradient transport equations with a logical form for the surface interaction. An analytical model was developed and given experimental verification using stable iodine tagged with ^{131}I dissociated from a PdI_2 source. The deposition surfaces were stainless steel and mild steel held essentially at 500°F in a turbulently flowing helium stream. Distribution of the deposited iodine was determined by counting the surface activity with a NaI crystal connected to a single channel scintillation counter. The measurements were calibrated by radiochemical analyses of the surfaces and further checked by neutron activation of solutions leached from the surfaces. (P.C.H.)

21786 (ORNL-TM-1387) CONFINED VORTEX FLOW NEAR A STATIONARY DISK. THEORY AND EXPERIMENT [Thesis]. Kidd, G. J. Jr. (Oak Ridge National Lab., Tenn.). Apr. 1966. Contract W-7405-eng-26. 149p. Dep. mn. CFSTI $4.00 cy, $1.00 mn.

Submitted to Univ. of Tennessee, Knoxville.

In the theoretical portion, the complete axisymmetric steady-state Navier-Stokes equations were reduced to a set of total differential equations by means of a similarity transformation. That is, the Navier-Stokes equations were transformed into a set of equations involving dimensionless velocities in terms of a single dimensionless distance variable which included both the axial and radial variables. For the boundary conditions, it was assumed that all velocities went to zero at the end wall and approached the condition that the radial velocity was zero and the tangential velocity was inversely proportional to the radius far from the wall (i.e., the flow far from the wall was a potential vortex). The transformed equations, however, had stable solutions only for very low circulations (nominal tangential Reynolds numbers less than ~5). The experimental phase consisted of three parts: (1) A study of the flow far from the wall to see if a flow approximating a potential vortex could be generated in a real (viscous) fluid. (2) A study of the similarity properties of the flow near the wall in order to have a comparison with the theoretical results. (3) Measurement of local velocities near the wall. (M.O.W.)

21787 STATIONARY SOLUTIONS OF THE SYSTEM OF EQUATIONS OF MAGNETOHYDRODYNAMICS. Ignat, Margareta. An. Stiint. Univ. A. I. Cuza, Iasa, Sect. I, 11: 29-37(1965). (In Rumanian).

The systems of equations of magnetohydrodynamics, particularized for the case of stationary movements are studied. Two cases for $\underline{k}$ = konst. and $\underline{k} = f(r)$ were analyzed by considering the quasirigid movements. (tr-auth)

21788 SHOCK WAVES WITH RADIATION IN MAGNETODYNAMICS. [PART] I. Cristea, Maria. An. Stiint. Univ. A. I. Cuza, Iasa, Sect. I, 11: 39-48(1965). (In Rumanian).

The case of the one-dimensional motion of the plane shock wave in the presence of a magnetic field perpendicular to the direction of motion was studied with consideration of the flux of radiative energy. The magnetodynamic approximation was used. The results obtained agree with those reported in the literature for the absence of the magnetic field. An effect of the magnetic field, principally on the temperature of the medium, was established. The integral equation for the velocity was deduced and the possibility

for its transformation into a differential equation was discussed briefly. (tr-auth)

21789 MAGNETOHYDRODYNAMIC CIRCULATION OF A LIQUID OF FINITE CONDUCTIVITY IN AN ANNULUS. Moynihan, D. C. Jr.; Bankoff, S. G. (Northwestern Univ., Evanston, Ill.). Appl. Sci. Res., Sect. B, 12: 165-202 (1965).

Unsteady circulation of an incompressible fluid of finite conductivity between two infinite concentric cylinders under the influence of a radial magnetic field is considered. Three cases are treated: an external axial electric field is imposed, while the walls remain stationary; and no external electric field is imposed, but the walls either rotate at constant angular velocities, or oscillate sinusoidally. It is shown that none of the variables are dependent upon axial or angular position, and that the radial magnetic field component is independent of the fluid motion. These circumstances result in a coupled linear system of equations for the fluid velocity and the tangential magnetic field component. They are uncoupled by assuming the induced electric field to be space independent at every instant. This is exact for steady flows. Zero and first-order approximate solutions may then be obtained either by neglecting the induced electric field, or by satisfying conservation of charge requirements. It is shown that neglect of the induced electric field is permissible only at small Hartmann numbers. An interesting feature of the solution is that the orthogonal expansion is in terms of Bessel functions whose order depends upon the Hartmann number, and hence may be arbitrarily large. Finally, it is thought that the first flow may find application in a novel viscometer for monitoring physical property variations in remote, hazardous, or highly reactive fluid systems. Some numerical examples are presented in support of the feasibility of such a device. (auth)

21790 THE VARIATIONS OF THE MAGNETIC FIELD IN A CONDUCTING FLUID IN MOTION. Primicerio, Mario (Univ., Florence). Atti Seminar. Mat. Fis. Univ. Modena, 14: 30-46(1965). (In Italian).

The law governing the space-time evolution of the magnetic field of conducting fluids in motion is examined, and a rigid analogy with the problem of the heat conduction in the presence of the double mechanism after fusion and convection is shown. On this basis a study is then made, correlated with some numerical results, of a problem of "compression" of the lines of force of the magnetic field in a conducting fluid. (tr-auth)

21791 PARTICULAR CYLINDRICAL SOLUTIONS IN MAGNETOHYDRODYNAMICS. Levoni, Sergio (Univ., Modena, Italy). Atti Seminar. Mat. Fis. Univ. Modena, 14: 98-107(1965). (In Italian).

The equations of magnetohydrodynamics, in cylindrical coordinates, of a viscous and incompressible conducting fluid are examined under the assumption that the magnetic field, the velocity, and the pressure depend on the time and on the distance r from the axis of the coordinates, whereas the potential of the non-electromagnetic external force depends only on r. Solutions for the axial components of the magnetic field and of the velocity are given for the case of an ideal and perfectly conducting fluid. This leads to a radial wave propagation with evident analogies with the Alfvén plane wave. The only difference is in the propagation velocity which originates from the radial part of the velocity. In the absence of radial velocity there are given solutions with variables separated by the transverse components of the magnetic field and of the velocity. Some marginal results relative to a viscous fluid with infinite electric conductivity are reported under the hypothesis of equality of the coefficients of kinematic viscosity and magnetic diffusivity. (tr-auth)

21792 FORCE-FREE FIELD OF MAGNETOHYDROSTATICS. Ferrari, Italo (Univ., Modena, Italy). Atti Seminar. Mat. Fis. Univ. Modena, 14: 133-45(1965). (In Italian).

The equations for the general case are derived. Plane solutions and solutions with two variables are determined. Examples illustrate the various procedures. (J.S.R.)

21793 UNIQUENESS THEOREM FOR THE EQUATIONS OF MAGNETOTHERMOELASTICITY. Levoni, Sergio (Univ., Modena, Italy). Atti Seminar. Mat. Fis. Univ. Modena, 14: 146-56(1965). (In Italian).

A theorem of uniqueness is given for the solutions of the equations of magnetothermoelasticity for homogeneous and isotropic bodies and for small elastic oscillations, neglecting the displacement current and the effects of space charge. The solutions are considered in the class of regular functions and the initial conditions are the usual ones in problems of electromagnetism, linear elasticity, and heat propagation. (tr-auth)

21794 RELATIVISTIC HYDRODYNAMICS WITH IRREVERSIBLE THERMODYNAMICS WITHOUT THE PARADOX OF INFINITE VELOCITY OF HEAT CONDUCTION. Kranys, M. (Inst. of Plasma Physics, Prague). Nuovo Cimento (10), 42B: 51-70(Mar. 11, 1966).

The special relativistic hydrothermodynamics (i.e., dynamics of mechanico-thermal processes) is presented in covariant form for a simple viscous fluid, free of the paradox of infinite velocity of heat conduction. The theory was developed by correcting Eckart's theory admitting also infinitely fast heat propagation which is incompatible with Einstein's principle of relativity. The paradox was eliminated in part by replacing the relation between heat flow and temperature—the so-called Fourier's phenomenological transport equation—by a more exact equation due to Cattaneo and Vernotte, and in part by changing in a corresponding manner the energy-momentum tensor. The new energy-momentum tensor contains all terms appearing in Eckart's tensor, as well as terms having in coefficient factors $1/V^2$ where V is the greatest heat velocity in the medium. Finally it is shown that also for diffusion processes the paradox of instantaneous propagation of diffusion flux can be eliminated from the equations describing relativistic diffusion phenomena. (auth)

21795 MICROWAVE DETERMINATION OF THE DISTRIBUTION FUNCTIONS OF ELECTRONS IN LOW CURRENT DISCHARGES. Bocchieri, P. (Univ., Pavia, Italy. Istituto Nazionale di Fisica Nucleare, Pavia, Italy); Crosignani, E.; Siragusa, G. Nuovo Cimento (10), 42B: 93-9 (Mar. 11, 1966).

The distribution function and the radiation temperature of the electrons in a discharge tube in a static magnetic field are determined for the d-c densities of the order of those of a subnormal glow discharge. The measurements are performed in argon, neon and helium. It is found that in the case of argon and neon the distribution function is non-Maxwellian and consequently the radiation temperature is peaked at the electron cyclotron frequency. In the case of helium the results are compatible only with a Maxwellian distribution of the electrons. The results are discussed in relation with those found by Fields, Bekefi and Brown in the case of the glow discharge for average electron energy in the range (5 to 10) ev. (auth)

21796 NORMAL IONIZING SHOCK WAVES WITH EQUILIBRIUM CHEMISTRY IN HYDROGEN. Taussig, Robert T. (Columbia Univ., New York). Phys. Fluids, 9: 421-30(Mar. 1966).

The steady-state jump equations for normal ionizing shock waves in hydrogen are solved numerically assuming the upstream and downstream states are at chemical equilibrium. Accurate thermodynamic functions are used to include changes due to dissociation and ionization of the gas. The results show that the solutions with chemistry are qualitatively like the ideal gas normal ionizing shock wave solutions, the number and type of possible downstream states being the same. The analysis for the switch-on shock with chemistry is presented here for the first time. Inclusion of chemical effects can extend the switch-on shock velocity range above the classical limit for an ideal gas. The problem of a steady, current-driven shock traveling in an electromagnetic shock tube is solved. The results agree well with recent experimental evidence and confirm the analytic approximations made by Kunkel and Gross. (auth)

21797 SHOCK-TUBE MEASUREMENT OF VIBRATIONAL RELAXATION TIMES IN DEUTERIUM. Moreno, James B. (Cornell Univ., Ithaca, N. Y.). Phys. Fluids, 9: 431-5(Mar. 1966).

The vibrational relaxation times of deuterium in argon and in krypton were determined at temperatures between 1200 and 2300°K. The relaxations were initiated by shock-heating the gas mixtures in a shock tube. The relaxation times were inferred from recordings of the density profiles behind the shock waves, as measured by the schlieren-photomultiplier technique. The results are fitted by the relations $p\bar{\tau}_{D_2-D_2} = 0.79 \times 10^{-10} \exp(125/\bar{T}^{1/3})$ atm-sec, $p\bar{\tau}_{D_2-Ar} = 3.8 \times 10^{-10} \exp(125/\bar{T}^{1/3})$ atm-sec, $p\bar{\tau}_{D_2-Kr} = 1.3 \times 10^{-9} \exp(125/\bar{T}^{1/3})$ atm-sec. The density change measured in the relaxation region was 57% ± 19% of the change calculated to arise from vibrational equilibration. This was taken to indicate that the measured relaxation was that of ortho-deuterium and that para-deuterium relaxed considerably faster. (auth)

21798 BLAST WAVES FROM AN INVERSE PINCH MACHINE. Vlases, George C.; Jones, Donald L. (Inst. for Telecommunication Sciences and Aeronomy, Boulder, Colo.). Phys. Fluids, 9: 478-85(Mar. 1966).

Cylindrical blast waves are produced in an inverse pinch machine operating in the mode where the energy deposition time is short compared to the time required for the wave to traverse the chamber. Advantages of this method over conventional explosive and exploding wire methods are discussed. A simple formula is developed which predicts the shock trajectory over the entire range of strong shocks to the weak shock limit. (auth)

21799 TWO-DIMENSIONAL LOW-PRESSURE DISCHARGE THEORY. Kino, G. S.; Shaw, E. K. (Stanford Univ., Calif.). Phys. Fluids, 9: 587-93(Mar. 1966).

It is shown that a pressure theory, modified to take into account ion generation, can be used to describe the steady-state collisionless discharge. Both planar and cylindrical geometry one-dimensional cases are solved for various types of ion generation using this fluid-type of approach. The parameters found by this approximate technique are shown to be in good agreement with the values obtained from the more exact formulation developed by Langmuir. The analysis leads to partial differential equations which are easily generalized to describe two-dimensional problems. For the particular case of ion generation proportional to electron density, the discharge parameters of a two-dimensional rectangular box and a finite-length cylinder are obtained. (auth)

21800 ON THE EQUIVALENCE OF VORTICES AND CURRENT FILAMENTS. Fetter, A. L. (Stanford Univ., Calif.); Donnelly, R. J. Phys. Fluids, 9: 619-20(Mar. 1966).

The analogy between vortices and current filaments is discussed for the case of vortices in a rotating container. It is shown that care must be taken to avoid errors in applying the analogy in certain situations. (auth)

21801 MAGNETOHYDRODYNAMIC FLOW IN THE INLET REGION OF A STRAIGHT CHANNEL. Brandt, A.; Gillis, J. (Weizmann Inst. of Science, Rehovoth, Israel). Phys. Fluids, 9: 690-9(Apr. 1966).

The flow is considered of an incompressible conducting viscous fluid in the inlet region of a straight channel in the presence of a transverse magnetic field. The complete equations are solved numerically without any approximating assumptions. Various characteristics of the flow and their dependence on the physical parameters are deduced. Values of Reynolds number up to 500 are considered. Velocity profiles near the inlet are found to have points of inflection. The distance to the terminal regime is studied, and the results, in the limiting case of large Reynolds number, compared with those of other workers. The boundary layer thickness is found to be proportional to x^{α} (for a small range of x) where $\alpha \approx 1.2$ at zero Reynolds number and decreases to 0.5 as the Reynolds number increases. The exact pressure distribution is also obtained. (auth)

21802 SLANTING OF A MAGNETICALLY STABILIZED ELECTRIC ARC IN TRANSVERSE SUPERSONIC FLOW. Bond, Charles E. (Univ. of Michigan, Ann Arbor. Univ. of Illinois, Urbana). Phys. Fluids, 9: 705-10(Apr. 1966).

Experimental observations are presented which indicate the existence of a convective interaction mechanism affecting the direction and stability of electric current in a flowing gas. The observations were made of an electric arc confined in transverse supersonic flow by means of a nonuniform magnetic field mutually orthogonal with the free-stream velocity field and the applied electric field. The positive column exhibits remarkable stability when allowed to slant across the applied electric field, approximately parallel to the free-stream Mach line. The direction of slant is the Hall direction, cathode root downstream, but the magnitude of the slant angle does not appear to vary with the Hall parameter $\omega_e\tau_e$. At the Mach numbers investigated, 2.0, 2.5, and 3.5, the inclination of the stable arc to the free-stream is near the Mach angle, which is near the angle corresponding to a maximum in the discharge parameter $E_{||}/P_s$, the ratio of parallel component of electric field to pressure at the upstream boundary of the arc. Under conditions where the column could not assume its characteristic slant angle, a highly unstable discharge was observed. (auth)

21803 PRESSURE WAVE GENERATION IN A FISSIONING GAS. III: AMPLIFICATION OF THE PRESSURE PULSE WITH ^{3}He AS DRIVER. Busch, C. W.; Oppenheim, A. K.; Smith, H. P. Jr. (Univ. of California, Berkeley). Phys. Fluids, 9: 813-14(Apr. 1966).

Use of ^{3}He is associated with highest specific energy released in gaseous fission, but the amplitude of the resulting pressure wave is small. This can be ameliorated by use of heavier gases in driven section, yielding interesting means for amplification of pressure pulse. (auth)

21804 STABILITY OF A TANGENTIAL DISCONTINUITY IN AN INCOMPRESSIBLE CONDUCTING FLUID. Todd, Leonard (Massachusetts Inst. of Tech., Cambridge). Phys. Fluids, 9: 814-15(Apr. 1966).

A simple physical prescription is given for the stability criterion on the tangential discontinuity in an incompressible conducting fluid. (auth)

21805 STABILITY OF THE DENSE ELECTRON GAS. Amusia, M. Ya. (Ioffe Physical-Technical Inst., Leningrad). Phys. Lett., 20: 596-8(Apr. 1, 1966).

The stability of the paramagnetic ground state of a dense electron gas is considered, taking into account the screening of the Coulomb interaction. (auth)

21806 ELECTROMAGNETIC PHENOMENA AT THE INTERIOR OF THE WEAK MAGNETOHYDRODYNAMIC SHOCK WAVE FRONT. Deutsch, R. V.; Blindu, L.; Cristea, M. Stud. Univ. Babes-Bolyai, Ser. Math.-Phys., 10: No. 2, 93-9(1965). (In Rumanian).

Shock waves are of particular importance in experimental physics in the study of plasma properties. For this reason a theoretical study was made of the phenomena occurring at the interior of the shock wave front. The existence of a double electric layer and of a longitudinal electric field at the interior of the shock wave front is shown for the case where the wave is propagated in electroneutral media. The deformation of the magnetic field at the interior of the shock wave front was also studied. (tr-auth)

21807 EXPERIMENTAL INVESTIGATION OF THE INITIAL PORTION OF A MAGNETOHYDRODYNAMIC CHANNEL OF SQUARE CROSS SECTION WITH THE LONGITUDINAL INHOMOGENEITY OF THE TRANSVERSE MAGNETIC FIELD TAKEN INTO ACCOUNT. Khozhainov, A. I. Zh. Tekh. Fiz., 35: 1568-76(1965). (In Russian).

The flow of mercury in an 8 × 8 mm cross section, 1 m long plastic-walled channel in the 3.5 cm gap between the 29.2 × 10 cm pole pieces of a current-regulated electromagnet was investigated giving particular attention to tran-

sition effects in the fringe field as the fluid passes from the field free region to the region of essentially uniform field. The flow was investigated at Reynolds numbers from 2100 to 10,000 and at Hartmann numbers from 5 to 18.7. The flow rate was measured with a Venturi tube and with an electrodynamic flow meter; the pressure was measured at nine points along the channel. Information concerning the velocity profile in the channel was obtained by measuring the potential difference between two 0.6-mm-diameter amalgamated copper electrodes located diametrically opposite each other in the channel wall. Sixteen pairs of such electrodes were provided. A theoretical discussion of such potential difference measurements is given from which it is concluded that they can provide useful velocity profile information. The experimental data are presented as plots of the ratio $F = VB_0/V_0B$ against position for different Reynolds and Hartmann numbers; here V is the potential difference between the two electrodes of a pair, B is the magnetic induction, and the subscript 0 refers to a position near the center of the channel where the magnetic field is uniform. The quantity F varied by some 1 to 7% in passing from the field free region to the center of the channel, depending on the flow conditions. The length L of the transition region was found to be given by $L^2 = a^2R/M^2$, where a is the width (and depth) of the channel, R is the Reynolds number, and M is the Hartmann number. (ATD)

21808 STUDY OF A HIGH-FREQUENCY DISCHARGE IN A NEON-HELIUM LASER. Krindach, N. I.; Silin-Bekchurin, I. A.; Tunitskii, L. N.; Cherkasov, E. M. (Lebedev Inst. of Physics, Moscow). Zh. Tekh. Fiz., 35: 1678-84(1965). (In Russian).

A new method is proposed for determining the current and voltage distribution along a high-frequency discharge and a study is made of the effect on laser operation of inhomogeneties along such a discharge. The method is based on the assumption that the voltage and current at any cross section of a discharge tube can be determined by the distance of that section from the end of the glowing portion of discharge. This assumption holds for any stationary discharge at any cross section of which electron rise due to ionization is a unity. The experiments were carried out by means of a gas laser (λ = 6328 Å) which incorporated a fused-quartz discharge tube 1.7 cm long and 8 mm in diameter (internal) filled with a neon–helium mixture at a 10:1 ratio at a pressure of 0.8 mm Hg. Two plane-parallel quartz plates 0_1 and 0_2 were placed at the tube ends at Brewster's angle. The equivalent circuit of the discharge tube is shown in Fig. 2. The tube was placed between the two confocal dielectric mirrors M with a 2-m radius of curvature and an ~1% transmission around 6328 Å. The mirrors were adjusted by means of an AKT-400 collimator. The discharge tube was fed by a 30-Mc frequency from an h-f oscillator, whose voltage was supplied to 8-cm electrodes E_1 and E_2, while electrodes E_3, E_4, and E_5 (2.5 cm each) were grounded. The oscillator was L-coupled to the discharge tube and the currents I_1 and I_2 and voltages V_1 and V_2 were measured by T-22 hot-wire ammeters and S-95 electrostatic voltmeters (4-pf input capacitance) respectively. The output energy was measured by means of a calibrated thermopile. The capacity of the discharge tube, varied by a movable ground rod R placed above the tube, was determined by its distance from R. In the experiments a discharge with a maximum length of 35 cm was studied. The experimental method and results are discussed in detail and indicate good agreement with computed data. (ATD)

21809 ON THE THEORY OF THE CURRENT-VOLTAGE CHARACTERISTIC OF THE COLUMN OF A HIGH-PRESSURE NONSTATIONARY ARC DISCHARGE. Krizhanskii, S. M. (Lenin All-Union Electrotechnical Inst., Leningrad). Zh. Tekh. Fiz., 35: 1882-8(1965). (In Russian).

A useful approximation for the dynamic current-voltage characteristic of a nonstationary high-pressure alternating current arc is derived. The calculations are based on the heat-balance equation with the assumptions of axial symmetry, constant pressure, and fixed temperature on the boundary. The temperature integral S of the heat conductivity and the temperature integral N of the heat capacity are introduced as new variables. Approximate analytic expressions are introduced for the electric conductivity of the plasma, the radiation loss, and the quantity N as functions of S. Different expressions are possible and the merits of several are briefly discussed. A solution for S is assumed in the form of a product of an unknown function of time by a Bessel function of the radius. This solution is substituted into the heat balance equation and the equation is averaged over the radius. The results an approximate equation for the unknown function of time from which the dynamic current-voltage characteristic is derived. The behavior of the arc can be calculated by solving the dynamic current-voltage characteristic simultaneously with the equation for the external circuit. An expression is also derived for the thermal time constant of the arc as a function of the current. The approximation introduced by separating the variables and averaging the heat balance equation over the radius can be improved by assuming a solution in the form of a sum of several terms, in each of which the variables are separated and the radial dependence is specified, and then averaging over a corresponding number of separate radial regions. This procedure is discussed as a method of successive approximation, although the calculation of the nth approximation does not depend on the previous calculation of the lower order approximations. (ATD)

21810 CHARACTERISTICS OF A LOW-PRESSURE DISCHARGE IN A TRANSVERSE MAGNETIC FIELD. Kervalishvili, N. A.; Zharinov, A. V. Zh. Tekh. Fiz., 35: 2194-2201(Dec. 1965). (In Russian).

An investigation was made of 1 to 10 kv discharges in argon at pressures down to 5×10^{-5} mm Hg in transverse magnetic fields up to 1.3 kOe in order to elucidate the phenomena taking place in the region of negative space charge that is known to form near the anode. The anode was a 7 cm long, 1.8 cm diameter water-cooled metallic cylinder. Three cathodes were simultaneously employed: a 10 cm diameter cylinder coaxial with the anode, and two 8 cm diameter circular disks mounted normal to the axis of the cylindrical electrodes, and 7.4 cm apart. One of the disk cathodes was of nickel wire mesh, and behind it was a 1 mm^2 probe with which the radial distribution of the axial electron and ion currents could be measured. The electron and ion currents to the central portion of the cylindrical cathode were also measured with the aid of a screened opening in the electrode and a probe. The magnetic field was parallel to the axis of the cylindrical electrodes. At pressures below 10^{-3} mm Hg, there was clearly visible a luminous region around the anode; at higher pressures the discharge current increased sharply and the luminosity filled the entire chamber. The ion current measured by the probe behind the disk cathode was negligible compared with the electron current. The radial distribution of the electron current to this probe was independent of pressure and was maximum at a radius corresponding roughly to that of the luminous region. The discharge current increased approximately linearly with increasing discharge potential and increased but with approach to saturation with increasing magnetic field strength. The form of the energy spectrum of the ions reaching the center of the cylindrical cathode was independent of pressure and nearly independent of magnetic field strength. The average energy of the ions corresponded to about one-third the applied discharge potential. A simple theory of the discharge is developed on the assumptions that electrons move parallel to an infinite plane anode and ionize the atoms of a stationary gas. This theory accounts qualitatively for most of the observed phenomena except the tendency of the discharge current to saturate with increasing magnetic field strength. It is hypothesized that this saturation is due to irregularities of the anode surface. This hypothesis was verified by further calculations and experiments in which the anode was first carefully adjusted until it was parallel to the magnetic lines of force and then provided with an artificial protuberance consisting of a 0.5 cm long ring of thickness from 0.03 to 0.6 cm. (ATD)

Geophysics

Refer also to abstract 21935.

21811 (AD-620952) DETERMINATION OF THE D LAYER AIR CHEMISTRY FROM A DAYTIME, HIGH-ALTITUDE NUCLEAR EXPLOSION. LeLevier, R. E. (RAND Corp., Santa Monica, Calif.). Sept. 1965. 12p. CFSTI $1.00 cy, $0.50 mn.

Measurements of the magnitude and time dependence of x-ray induced absorption over Midway during the July 9, 1962, high-altitude nuclear explosion allows one to infer bounds on the dissociative recombination coefficient alpha of the D-layer of the ionosphere. It is shown that a day-time experiment would allow a unique determination of alpha. It is found that a low-yield explosion (a few KT) is adequate for the purpose of the experiment. (auth)

21812 (AD-622223) PLASMA WAVES IN THE FREQUENCY RANGE 0.00110 CPS IN THE EARTH'S MAGNETOSPHERE AND IONOSPHERE: A SURVEY. Final Report. Hultqvist, Bengt (Kungliga Vetenskapsakademien, Kiruna (Sweden). Geofysiska Observatoriet). June 1965. Contract AF61(052)-2619. 138p. (AFCRL-65-683). CFSTI $4.00 cy, $1.00 mn.

The plasma model for the magnetosphere and ionosphere is first discussed. A review of some parts of the theory for a warm collisionless plasma of interest in the magnetosphere in connection with waves of periods between 0.1 and 1000 seconds is given. The theory for magnetohydrodynamic waves in a slightly ionized gas is then summarized. The available observational data about magnetospheric and ionospheric phenomena, which may be interpreted in terms of waves with periods between 0.1 and 1000 seconds, are briefly surveyed and some theoretical applications to the ionosphere and magnetosphere are finally discussed. The theory of shock phenomena and transients in the magnetosphere is not included. (auth)

21813 (N-65-29816) CALCULATIONS OF LONGITUDE DEPENDENCE OF GEOMAGNETICALLY TRAPPED ELECTRON FLUXES. PART I. THE GENERAL FOKKER-PLANCK EQUATION FOR ELECTRON DIFFUSION. Roederer, J. G.; Welch, J. A. (National Aeronautics and Space Administration, Greenbelt, Md. Goddard Space Flight Center). Apr. 1965. 38p. (NASA-TM-X-55250; X-640-65-149). CFSTI $2.00 cy, $0.50 mn.

A general Fokker-Planck equation is deduced, which describes the distribution of geomagnetically trapped electrons as a function of longitude, time, energy, and mirror point field intensity. A special variable for the longitudinal position of a particle is introduced. It is found that the usual procedure of averaging over longitude in order to obtain a longitude-independent equation, is not valid for the description of electrons mirroring at low altitudes. In that case, the longitude dependence cannot be averaged out, and a four-dimensional equation must be used. The coefficients representing longitudinal drift, ionization loss and multiple. screened Coulomb scattering in the general Fokker-Planck equation are deduced. (auth)

21814 THE STRUCTURE OF THE ARCTIC AURORAL ZONE IN A PERIOD OF MINIMUM SOLAR ACTIVITY. Weill, G.; Fafiotte, M.; Huille, S.; Delannoy, J. (Institut d'Astrophysique, Paris). Ann. Geophys., 21: 469-74 (July-Sept. 1965). (In French).

Fourteen flights into the interior of the auroral zone were made between December 1963 and December 1964, all of them in early winter. These flights were between Creil, Keflavik, Sondrestrom, Frobisher, and Thule between 1700 and 0700 local solar time. Observations were made with a rotating photometer; a total of 89 hr recording time was available. Photometric registration was used to retrace a projection of auroral phenomena on the earth's surface; total of the arc segments so constructed are illustrated. Below Iceland no phenomena were observed; arcs or bands are observed strongly at higher latitudes. The invariant latitude at which the aurora is observed is a function of hour of observation, geomagnetic agitation, and solar activity; in 1963 and 1964 the external arc was observed at 68°. Other regions of activity include the southeast coast of Greenland and the western coast to the vicinity of the Straits of Davis. An intensity profile vs invariant latitude shows ten distinct bands of which that at lowest latitude is the most intense (5 kilorayleighs); the center bands are less intense, and the northernmost bands are somewhat more intense again. (BBB)

21815 STUDIES OF THE EARTH'S OUTER RADIATION ZONE. Williams, Donald J. (Johns Hopkins Univ., Silver Spring, Md.). APL Tech. Digest, 4: 10-17(July-Aug. 1965).

Data from the APL satellite 1963 38C which have provided information concerning the earth's radiation belts are reported. Results of studies concerning trapped electrons include: characteristics and the decay of the artificial radiation belt created by the high altitude nuclear detonation of July 9, 1962; the finding of a direct correlation of trapped electron intensities in the outer zone with magnetic activity and with the solar rotation period of ~27 days. These findings are indicative of the intimate connection, through the solar wind-magnetospheric interaction, between the near-earth environment and solar processes. These studies have also yielded trapping lifetimes and response times to magnetic disturbances, both as a function of electron energy and position within the magnetosphere, as well as the measurement of a significant diurnal variation of the radiation cavity and its temporal behavior. Analysis of this effect suggested that it may be explained by magnetospheric distortions caused by the incident solar wind. Observation of trapped electrons being lost in the atmosphere as they drift into the South Atlantic anomaly, and the subsequent replenishment of electrons to these trapping regions at longitudes well removed from the anomaly, may represent a slow but steady leak for the entire radiation cavity. It was found that high-energy electrons behave in a manner consistent with their motion through a distorted magnetosphere under the conservation of the adiabatic invariants, μ and J, and energy, E. It was possible to obtain a nightside configuration for the earth's magnetic field by requiring that such a field fit the observed asymmetries in the radiation cavity. (BBB)

21816 THE ELECTRON CONTENT OF THE IONOSPHERE AND ITS FLUCTUATIONS. Harnischmacher, E.; Hess, H. A.; Kraft, R.; Muenther, Ch.; Rawer, K. (Ionosphaeren-Institut, Breisach/Rhein, Ger.). Arch. Elek. Uebertr., 19: 589-601(Sept. 1965). (In German).

Multifrequency beacons in satellites allow the electron content to be determined by the differential Faraday effect. The uncertainty found in previous determinations may thus be eliminated. A method is described for calculation of moment of the Faraday null position in the electron content. Variation of electron content with the subionospheric angle in western Europe, with the time of day at 48° in western Europe, and variation from day to day over a 3-month period in early 1965 is determined with data from Explorer 22. The Faraday effect at high frequency is discussed. Simultaneous observations of the differential Doppler effect (20-40 Mc) also gave similar values for the electron content, with a dispersion of ~5% to 16%; illustrations of this method are also given. A discussion of the Doppler effect in satellites with strongly elliptical orbits is given. Observations of the Faraday rotation at high frequency from a geostationary satellite permit study of the electron content at a fixed point. (BBB)

21817 LIFETIMES OF LOW-ENERGY ELECTRONS ($\epsilon \sim 40$ kev) IN THE OUTER RADIATION ZONE AT MAGNETICALLY QUIET TIMES. McDiarmid, I. B.; Burrows, J. R. (National Research Council of Canada, Ottawa). Can. J. Phys., 44: 669-73(Mar. 1966). (NRC-8845).

While the lifetime of electrons that are mirrored near the equatorial plane ($L \sim 6$) is a few days, the lifetime of electrons that are mirrored farther down the field line may be much shorter. It is shown that the average lifetime of an electron ($E \sim 40$ kev) mirroring at a radial distance of less than three earth radii on an $L = 6$ field line is probably less than the drift period of the particle. (AECL)

21818 NIGHT-TIME DISTURBANCE FLUCTUATIONS IN GEOMAGNETIC FIELD AT EQUATORIAL STATIONS. Rastogi, R. G.; Kaushika, N. D.; Trivedi, N. B. (Physical Research Lab., Ahmedabad, India). J. Atmos. Terrest. Phys., 28: 303-10(Mar. 1966).

The fluctuations in horizontal geomagnetic field H, during the nighttime magnetic storms at stations within the equatorial electrojet are studied. The mean ratio of the amplitudes of corresponding fluctuations in H at Huancayo (dip 2°N) to that at San Juan (dip 52°N) is about 8.0 for the midday hours and about 1.7 for the midnight hours. A close similarity in the nighttime fluctuations of ΔH is noticed at all equatorial stations in Peru, the mean amplitude having a maximum over the magnetic equator; within a distance of 6° latitude from the magnetic equator the amplitude is reduced to 0.6 times its equatorial value. It is concluded that the fluctuations in ΔH during the nighttime hours are significantly enhanced over the magnetic equator for the American zone where the daytime equatorial electrojet currents are strongest, and are due to the remnant equatorial current system flowing during the nighttime hours. (auth)

21819 THE EFFECT OF IRREGULARITIES IN COLLISION FREQUENCY ON THE AMPLITUDE OF WEAK PARTIAL REFLECTIONS. Piggott, W. R.; Thrane, E. V. (Radio and Space Research Station, Bucks, Eng.). J. Atmos. Terrest. Phys., 28: 311-14(Mar. 1966).

The electron distribution in the D-region has sometimes been deduced from a knowledge of the amplitudes of weak partially reflected waves. It is pointed out that the deductions differ accordingly as the reflections are supposed to be caused by irregularities of collision frequency or of electron concentration. (auth)

21820 SLOW FLUCTUATIONS BETWEEN CONJUGATE POINTS IN THE AURORAL ABSORPTION OF COSMIC NOISE. Chivers, H. J. A.; Hargreaves, J. K. (National Bureau of Standards, Boulder, Colo.). J. Atmos. Terrest. Phys., 28: 337-42(Mar. 1966).

The auroral absorption of cosmic radio noise is not identical at magnetically conjugate points, but often exhibits a relative fluctuation with a period of about an hour. Sometimes the absorption is seen to alternate between conjugate points. Some statistical properties of the fluctuations are given. (auth)

21821 ON THE EXISTENCE OF A SECOND STANDING SHOCK WAVE ATTACHED TO THE MAGNETOSPHERE. Walters, G. K. (Rice Univ., Houston, Tex.). J. Geophys. Res., 71: 1341-4(Mar. 1, 1966).

It is shown that, except in the nose region, plasma flow in the magnetosheath is supersonic. The bulging out of the magnetopause just behind the neutral points in the noon meridional plane, and behind demarcation lines defined by the locus of points of character similar to the neutral points in other meridional planes, presents a new obstacle to the supersonically flowing plasma. Therefore, a standing shock wave is expected to exist within the magnetosheath slightly upstream of the demarcation-line bulge. (auth)

21822 MIDLATITUDE TROUGH IN THE NIGHT IONOSPHERE. Sharp, G. W. (Lockheed Palo Alto Research Labs., Calif.). J. Geophys. Res., 71: 1345-56(Mar. 1, 1966).

The October–November 1963 flight of an ion trap on a polar-orbiting oriented satellite has revealed the presence of a well defined trough in the F-region ionization that persists over the nearly four and one-half days during which data were obtained. The trough is geomagnetically oriented along the intersection of the vehicle orbit and the L = 3.5 shell, located on the equator side of the polar auroral zone, and it is found in both the northern and southern hemispheres. Rather sharp gradients in the ion concentration are found to be associated with this trough, particularly on the polar side of the trough. The trough shape does not remain fixed, but changes rather dramatically throughout this flight, and its width seems to be inversely correlated with the intensity of electrons precipitated in the polar auroral zones. (auth)

21823 ELECTRON DENSITY DISTRIBUTIONS IN THE DAYTIME F_2 LAYER AND THEIR DEPENDENCE ON NEUTRAL GAS, ION, AND ELECTRON TEMPERATURES. Thomas, Lance (Inst. for Telecommunication Sciences and Aeronomy Environmental Science Services Administration, Boulder, Colo.). J. Geophys. Res., 71: 1357-66 (Mar. 1, 1966).

Results are given of calculations of the electron-density distribution in the F region of the ionosphere when thermal nonequilibrium exists between the neutral gas, electrons, and ions. A digital computer was used to solve an equation including photoionization, loss, and diffusion of ionization for a model in which the neutral gas and electron temperatures are independent of height and the ion temperature increases from that of the neutral gas at low heights and approaches that of the electrons at great heights. It is assumed that the rate coefficient for the electron loss process is independent of the neutral gas, electron, and ion temperatures. The investigation indicates how the height distribution of ionization for steady-state conditions is determined by the neutral gas and electron temperatures and by the height variation of the ion temperature. It is shown that an increase in the neutral gas temperature causes little change in the maximum electron density but increases the height of this maximum. An increase in electron temperature causes a decrease in the maximum electron density and a small change in the height of this maximum, both effects being dependent on the height variation of ion temperature. The solutions obtained are used to discuss the shape of the F layer and the effects on the electron distribution of increases in neutral gas, electron, and ion temperatures expected during magnetic disturbances. (auth)

21824 MORPHOLOGY OF VLF HISS ZONES AND THEIR CORRELATION WITH PARTICLE PRECIPITATION EVENTS. Joergensen, T. Stockflet (Technical Univ. of Denmark, Lyngby). J. Geophys. Res., 71: 1367-75 (Mar. 1, 1966).

Observations of wide-band hiss in the frequency range 4–9 kc made at 13 stations in both hemispheres since last sunspot maximum show that hiss is generated in certain zones. Apparently these zones are the same as the zones of auroral precipitation and so are approximately circular, with their centers close to the magnetic midnight meridian some few degrees from the geomagnetic poles. Hiss is not observed equally often everywhere in these zones; there is a maximum of the occurrence at about 70° magnetic latitude shortly before magnetic midnight. Hiss seems to be a rare phenomenon at the very highest latitudes close to the geomagnetic poles. Observations by the Alouette 1 satellite of very intense electron fluxes at latitudes higher than the boundary of the outer radiation belt show that these fluxes are very well correlated to ground-based hiss observations both in space and in time. It is therefore suggested that these very intense electron fluxes are responsible for, or at least closely connected with, the generation of hiss. Owing to the positive correlation between hiss activity and high-latitude electron fluxes, which again are correlated with the intensity variations in the outer radiation belt, it would appear to be possible to monitor, from the ground, high-intensity electron fluxes in the polar regions and intensity variations in the outer radiation belt. (auth)

21825 CYCLOTRON INSTABILITIES IN THE MAGNETOSPHERE. Hruska, A. (Geophysical Inst., Prague). J. Geophys. Res., 71: 1377-84(Mar. 1, 1966).

An exchange of energy between a beam of charged particles and a small-amplitude electromagnetic perturbation is discussed. The beams usually deliver the energy to the perturbations at a considerable rate in thin sheets localized in the magnetosphere around surfaces of maximum energy exchange. The distances of the sheets from the earth are higher than 5 earth radii for perturbations with frequencies ω in the micropulsations range and become much smaller for ω corresponding to vlf emissions. The rate of the total energy input to the oscillations of the magnetosphere is estimated. The typical time during which the total energy of oscillation increases by an order of magnitude is pro-

portional to ω^{-1} and may be as short as a few tens of seconds for $\omega \sim 10^{-1}$ sec^{-1}. (auth)

21826 ROCKET-BORNE MEASUREMENTS OF PARTICLE FLUXES AND AURORAL LIGHT. Cummings, W. D. (Rice Univ., Houston, Tex.); LaQuey, R. E.; O'Brien, Brian J.; Walt, Martin. J. Geophys. Res., 71: 1399-1407 (Mar. 1, 1966).

Auroral photometers and particle detectors were flown on three Nike-Apache rockets to altitudes of ~140 km at Fort Churchill, Canada, in March 1964. The relative intensity of atomic oxygen (5577 A) and N_2^+ (3914 A) in auroras was measured as (2 ± 1) to 1, and this ratio was essentially independent of altitude and auroral intensity. Changes in the precipitated flux of electrons with energy $E_e \geq 40$ kev occurred as a rocket moved by only about a cyclotron radius transversely to the magnetic field vector B, and these changes are therefore judged to be temporal. In a flight at dawn into at region where no aurora was visible the energy spectrum of precipitated electrons was much harder than that in two midnight flights into visible auroras. The flux of backscattered electrons was measured simultaneously with the precipitated flux. Comparison is made of observed and predicted ratios of the two fluxes, and it is seen that in the dawn flight there was an apparent and unexplained dependence of the ratio on the magnitude of the precipitated flux. A qualitatively similar effect was seen on the one midnight flight where the high-energy flux was sufficient to yield statistically significant ratios. It is found that the magnetic perturbations of the pitch-angle distributions by local ionospheric current systems can be large, remarkable, and significant. (auth)

21827 ON THE RELATIONSHIP OF THE AURORA TO NON-GREAT-CIRCLE HIGH-FREQUENCY PROPAGATION. Bates, H. F.; Albee, P. R.; Hunsucker, R. D. (Univ. of Alaska, College). J. Geophys. Res., 71: 1413-20(Mar. 1, 1966).

Non-great-circle propagation was frequently noted in the year's hf forward oblique soundings recorded at College from various sites during 1963 and 1964. No direction-finding equipment was available, so a statistical analysis was made to determine the type of sidescatter involved. The number of occurrences during several periods was a maximum at night. The excess propagation time on the Palo Alto to College path varied inversely with magnetic activity. A comparison of simultaneous College backscatter and Palo Alto to College off-path data showed that the locus of off-path sidescatter extended north of the ionospheric backscattering belts. Previous work has shown the backscatter and auroral belts to be closely related, so these results are interpreted as showing that the deviated modes were produced by sidescatter from the auroral belt. (auth)

21828 PLASMA IN THE GEOMAGNETIC TAIL. Dessler, A. J.; Michel, F. C. (Rice Univ., Houston, Tex.). J. Geophys. Res., 71: 1421-6(Mar. 1, 1966).

The geomagnetic field is deformed by the solar wind so that field lines from the polar caps extend away from the earth in the antisolar direction to form a magnetic tail. The ionosphere over the polar caps is sufficiently hot that plasma (mainly ionized hydrogen) can escape from the two polar ionospheres and flow along the magnetic field lines into the tail. It is argued that the resulting flow of protons and electrons out of the ionosphere acts to limit the thermal plasma number density to the order of 10^2/cm^3 immediately above the polar ionosphere, decreasing ultimately to very small values (10^{-1}/cm^3) at large distances down the tail (30 R_E). The plasma that flows into the tail must be replaced, presumably by ionization of the neutral atmosphere over the polar caps. It is proposed that this ionization is caused by solar wind particles diffusing into the geomagnetic tail and thence down the field lines to the polar caps. Recent measurements of total cislunar electron content have been interpreted as indicating an electron number density of about 2×10^2/cm^3 in the quadrant opposite the sun. It seems difficult to account for such high densities either by transporting ionospheric plasma into the tail or by compressing solar plasma. It is concluded that either the tail is filled principally with solar plasma with a number density no greater than about 10/cm^3 or else some important physical process capable of condensing plasma in the tail to a high density was overlooked. (auth)

21829 ANALYSIS OF GEOMAGNETIC MICROPULSATIONS DUE TO HIGH-ALTITUDE NUCLEAR EXPLOSIONS. Kovach, Robert L. (Stanford Univ., Calif.); Ben-Menahem, Ari. J. Geophys. Res., 71: 1427-33(Mar. 1, 1966).

Spectra of the magnetic disturbances from the high-altitude nuclear explosion of July 9, 1962, computed from flux-rate variograph recordings obtained in Peru, Sweden, Iceland, and Canada are compared with those computed for several natural sudden commencements. The sudden commencement data show a lack of distinct spectral peaks compared with the spectra of the nuclear explosion. The Alfvén velocity-altitude profile indicates that MHD waves can be trapped in a waveguide in the altitude range from 300 to 3000 km, thus producing resonant oscillations in the waveguide. The line nature of the explosion spectra suggests that a resonance mechanism is appropriate. A review of the theory for a simple MHD resonance model is presented, and computed eigenfrequencies are compared with the observed data. The observed data are in fair agreement with theoretical predictions. An interesting feature of the present study is the evaluation of the dimensionless dissipation parameter Q, which is of the order of 1 to 10 for MHD waves, suggesting that simplifying assumptions neglecting energy dissipation mechanisms must be dropped. (auth)

21830 GEOMAGNETIC AND SOLAR DATA. Lincoln, J. Virginia (ed.) (Inst. for Telecommunication Sciences and Aeronomy Environmental Science Services Administration, Boulder, Colo.). J. Geophys. Res., 71: 1477-9 (Mar. 1, 1966).

Preliminary data on sudden commencements followed by a magnetic storm or a period of storminess and solar flare effects in the second quarter of 1965 are presented. Tables show data on principal magnetic storms (storm time, sudden commencement, activity) during July, August, and September 1965 and geomagnetic and solar data (3-hr range indices, magnetic character figures, average amplitudes, provisional sunspot numbers) for selected days in October 1965. (A.G.W.)

21831 ON THE TRANSPORT OF TRAPPED PARTICLES IN THE OUTER MAGNETOSPHERE. Faelthammar, C.-G. (Royal Inst. of Tech., Stockholm). J. Geophys. Res., 71: 1487-91(Mar. 1, 1966).

The transport terms in the one-dimensional Fokker–Planck equation generally used in computing particle distributions contain two coefficients one of which is the mean radial displacement of a particle per unit time and the other is the mean square radial displacement per unit time. It is shown that the properties of the particle motion require the two coefficients to be related, and an explicit expression for the relation is found. Previously given formulas are then applied to consideration of the transport caused by magnetic impulses. It is shown that the transport coefficients are in general different (and vary differently with the radius) for particles with different magnetic moments. (A.G.W.)

21832 INTRA- AND INTERHEMISPHERE DIFFERENCES IN OCCURRENCE TIMES OF HYDROMAGNETIC EMISSIONS. Wentworth, R. C. (Lockheed Missiles and Space Co., Palo Alto, Calif.); Tepley, Lee; Amundsen, K. D.; Heacock, R. R. J. Geophys. Res., 71: 1492-8(Mar. 1, 1966).

Preliminary results of a laboratory program designed to precisely determine occurrence times of hydromagnetic (hm) emissions recorded at widely separated latitudes in both hemispheres are presented. It was found that the regularly spaced fine-structured elements, which constitute most hm emissions, are

consistently received earlier at higher latitudes. Within an accuracy of ±0.8 sec the average time delay between College, Alaska, and Kauai, Hawaii, was found to be 5.8 sec, and between Palo Alto, California, and Kauai, 3.2 sec. This leads to an average projected propagation velocity at sea level of about 900 km/sec toward the equator—on the order of the hydromagnetic wave velocity in the F region of the ionosphere. (A.G.W.)

21833 WAVEGUIDE THEORY FOR IONOSPHERIC PROPAGATION OF HYDROMAGNETIC EMISSIONS. Tepley, Lee; Landshoff, R. K. (Lockheed Missiles and Space Co., Palo Alto, Calif.). J. Geophys. Res., 71: 1499-1504 (Mar. 1, 1966).

Previous work has suggested that hydromagnetic (hm) emissions are generated by a plasma instability at 4-8 earth radii in the vicinity of the equatorial plane. The emissions then propagate in the Alfvén mode along high-latitude geomagnetic field lines toward the earth. It is suggested here that part of the signal energy penetrates the ionosphere in or near the auroral zones, is transformed into the isotropic hm wave mode and then propagates horizontally in an ionospheric waveguide around the Alfvén velocity minimum near the F_2 peak. Spatial and temporal variations in the Alfvén velocity profile may be at least partly responsible for the spread in the apparent hm emission horizontal propagation velocity noted by other investigators. A derivation of the theory is presented. The theory is not applicable to daytime propagation conditions or to latitudes where the geomagnetic field tilts significantly from the vertical direction. (A.G.W.)

21834 X-RAY EXCITATION OF THE SECOND POSITIVE AND FIRST NEGATIVE BANDS OF NITROGEN. Low, W. (Hebrew Univ., Jerusalem. Massachusetts Inst. of Tech., Cambridge). J. Geophys. Res., 71: 1505-7 (Mar. 1, 1966).

Experiments are reported, which show that x rays can produce emission of light in air and can excite, in particular, the second positive and first negative bands of nitrogen. Experiments on nitrogen and air were made using a beam of x rays from a conventional x-ray tube. The characteristic feature of the spectra obtained is that most of the bands fall in the region from 3000 to 4500 Å. It is suggested that, in part, x rays presumably resulting from bremsstrahlung from the auroral electrons account for the excitation of the characteristic nitrogen spectra in the aurora, particularly in the lower region of the aurora where the primary electron density is small. (A.G.W.)

21835 HIGH FREQUENCY AURORAL NOISE. Hower, G. L.; Dunlap, F. C. (Washington State Univ., Pullman). J. Geophys. Res., 71: 1512-14(Mar. 1, 1966).

Over 40 cases of 18-Mc noise from the north were identified in the records from the IGY backscatter sounder operated at Washington State Univ. between Sept. 1963 and Mar. 1964. A plot of the occurrence of the noise relative to the days of geomagnetic sudden commencements shows an apparent tendency for the noise to occur before the sudden commencement is seen. A similar relation between noise occurrences and days on which the magnetic indices undergo a sudden increase is seen. A definite association between the 18-Mc noise and the occurrence of echoes from field-aligned irregularities in ionization at F-region heights was also readily apparent in the data. Plots of diurnal variation in occurrence of noise events and field-aligned echoes show little similarity between the curves. (A.G.W.)

21836 AURORAL EFFECTS AND EXCESS-ENERGY ELECTRONS. Hirsch, E. H. (Weapons Research Establishment, Salisbury, South Australia). Nature, 209: 390-1 (Jan. 22, 1966).

Similarities between auroral effects and laboratory observations of electron leakage from a magnetic mirror accompanied by electron acceleration are pointed out, and it is suggested that the same basic mechanism may exist in both cases. The experiments extend previous observations on the abnormally high energy acquisition by electrons confined in a Penning-type structure through space-charge oscillations and the diffusion of such electrons across magnetic lines of force to electron confinement in a magnetic mirror. The experimental effects resemble those encountered in auroral phenomena, and it is suggested that the arrival of comparatively slow electrons from a solar flare in the radiation belt raises the charge density within the belt beyond the threshold level required for the appearance of excess-energy electrons, and that these high-energy electrons leak out into the auroral zone. (J.F.P.)

21837 DYNAMICS, COMPOSITION AND ORIGIN OF THE GEOMAGNETICALLY-TRAPPED CORPUSCULAR RADIATION. Van Allen, James A. (Univ. of Iowa, Iowa City). pp 99-136 of Proceedings of the Eleventh General Assembly, Berkeley, 1961. London, Academic Press, 1962.

Some experimental and theoretical observations on the composition, dynamics, and origin of geomagnetically trapped particles are summarized. 94 references. (D.C.W.)

21838 MEASUREMENTS OF HIGH ENERGETIC AURORAL RADIATIONS WITH BALLOON-BORNE DETECTORS IN 1962 AND 1963. PART A TO C. TEXT. PART D. FIGURES AND DIAGRAMS. Pfotzer, G.; Ehmert, A. (comps.). Mitteilungen aus dem Mzx-Planck-Institut fuer Aeronomie, No. 18, 1965. Berlin; Heidelberg; New York; Springer-Verlag, 1965. 141p. DM 18.--.

The investigation of high-energy auroral radiations with detectors on balloon flights is considered. The discussion includes the balloons, instrumentation, and absolute values of the photon fluxes, also the representation of data for solar terrestrial relations, periods of individual flights, and data which are characteristic of the launching sites. The discussion of balloon flights in the auroral zone in 1962 considers the flight schedule, launching sites, indications for launchings, the general situation during flights in 1962, individual flights at Kabdalis, flights from Kiruma and Andenes during the solar rotation 1767, and atomic bomb debris. Also the assumptions, the ϕ_β/ϕ_γ ratio, and an estimation of activities are considered. The discussion of balloon flights at Kiruna in 1963 includes the launching site, indications for launchings, data representation, solar activity and flights and a presumably special type of x-ray events. Figures and diagrams are included. (J.F.P.)

Gravitation, Quantum Mechanics, and Relativity Theory

Refer also to abstract 22146.

21839 (AD-627067) CRITERIA FOR THE BEST BOGOLIUBOV QUASI PARTICLE. Scientific Report No. 39. Kobe, H. (Uppsala Univ. (Sweden)). Mar. 1, 1965. Contract AF61(052)-701. 8p. (ARL-65-265). CFSTI $1.00 cy, $0.50 mn.

The principle of compensation of dangerous diagrams has previously been the only general criterion for determining the coefficients in the Bogoliubov canonical transformation to quasiparticles. It is shown that the criterion of maximum overlap of the true ground state with the BCS ground state gives the same condition for determining the coefficients. The criterion of diagonalizing the quadratic part of the reaction operator, which is a generalization of the Brillouin-Brueckner condition, is also equivalent to the above criteria. Finally these criteria are evaluated from the standpoint of "least labor for the most accuracy." (auth)

21840 THE HYDRODYNAMICAL MODEL OF WAVE MECHANICS. III. ELECTRON SPIN. Janossy, L.; Ziegler-Naray, Maria (Central Research Inst. of Physics, Budapest). Acta Phys. Acad. Sci. Hung., 20: 233-51(1966).

The hydrodynamical model is extended to the problem of the electron as described by the Pauli equation. It appears that the Pauli equation can be transformed into a set of equations which have the form of the classical equations of motion describing an elastic medium which is inhomogeneously magnetized. (auth)

21841 THEORY OF CONGRUENCE IN GRAVITATIONAL FIELDS. III. SPACE INVERSION AND GRAVITA-

TION. Sueveges, Mate (Research Group for Theoretical Physics, Budapest). Acta Phys. Acad. Sci. Hung., 20: 273-84(1966).

The inversion part of the holonomy group, which is a good physical symmetry group locally, is investigated. It is shown that the existence of inversion depends on the topological properties of the gravitational field (supposed to be a Riemannian manifold M_n). Therefore M_n is defined to be a differentiable manifold and the theorem on parallelism is extended to this case. It is shown that if M_n is orientable then Ψ is a subgroup of SO(n) and if M_n is non-orientable then Ψ is a subgroup of O(n). More precisely there exists a homomorphism $h: \pi_1(M_n) \rightarrow O(n)/SO(n)$, where $\pi_1(M_n)$ is the first homotopy group of M_n and the topologically invariant classification of gravitational fields according to factor groups of $\pi_1(M_n)$ is physically meaningful. Besides some simple examples space forms of zero and constant positive local curvature are classified. For example, there exists an infinity of 3-dimensional forms of positive curvature but local space inversion is not a good operation in either of them. It is also pointed out that physical space is not simply a Riemannian manifold M_n but a fiber bundle over M_n. Therefore the theory of fiber bundles with structure group over a differentiable manifold is used. (auth)

21842 GEOMETRIZATION OF GRAVITATIONAL AND ELECTROMAGNETIC FIELDS. Guy, Roland (Univ., Montreal). Ann. Inst. Henri Poincare, Sect. A, 2: 307-25 (1965). (In French).

It is shown that it is possible to derive the Maxwell-Einstein equations and those of gravitation with the help of geometrically significant magnitudes. In this way a geometrization of electromagnetism and gravitation is obtained. An attempt is made to show the idea of variety of affine connections in as intuitive a manner as possible using elementary geometry. (J.F.P.)

21843 DISPLACEMENT OF SPECTRAL LINES IN GENERAL RELATIVITY. Papapetrou, A. (Institut Henri Poincare, Paris). Ann. Inst. Henri Poincare, Sect. A, 2: 355-68(1965). (In French).

A new method is proposed for calculating the spectral shifts in an arbitrary gravitational field. The main feature of the method is the use of the equation of motion of the photon considered as a test particle. The method is applied to some spherically symmetric gravitational fields. It is found that an expansion of the sources of the field leads to an additional (very small) violet shift; this changes into a red shift in the case of contraction. (auth)

21844 THE RAINICH PROBLEM FOR A NONLINEAR ELECTROMAGNETIC SCHEME. Poletti, Pierre (Institut Henri Poincare, Paris). Ann. Inst. Henri Poincare, Sect. A, 3: 111-26(1965). (In French).

The resolution of the Rainich problem in the case of the nonlinear electrodynamics of Born-Infeld is considered, and the necessary and sufficient conditions for a symmetric tensor of rank two to be the energy-momentum tensor of the Born-Infeld theory is given. (auth)

21845 ON THE RAYSKI FORMULATION OF THE LAWS OF CONSERVATION IN GENERAL RELATIVITY. Horsky, J. (Univ., Brno). Czech. J. Phys., 16: 175-9 (1966).

The Rayski method is used to calculate the energy of a static and spherically symmetrical gravitational system. (auth)

21846 QUANTUM THEORY IN THE ELECTRICAL ENGINEERING CURRICULUM. Grimes, D. M. (Univ. of Michigan, Ann Arbor). IEEE (Inst. elec. Electron. Eng.), Trans. Educ., E-8: 50-6(June-Sept. 1965).

An approach to quantum theory designed for students whose backgrounds include relative strength in classical electromagnetic field theory but less in classical mechanics is described. Rather than building quantum theory by following the historical steps, as is often done, the technique is to approach the subject directly from a background knowledge of electromagnetic field theory. The approach uses the postulates that the Maxwell equations are always valid for point charges, that a form of steady-state cosmology is correct, and that the superposition principle is applicable to statistical processes. The model permits a direct transition from electromagnetic field theory to quantum theory. It is self-consistent and based upon currently acceptable physical postulates. It meets the epistemological objections against the orthodox interpretation that Einstein raised and that have never been adequately answered. It does not fall into the class of proposed interpretations that Wigner showed to be inconsistent with the wave theory. (BBB)

21847 ON A NEW TRANSFORMATION SCHEME RELATED TO A 4-DIMENSIONAL LORENTZ TRANSFORMATION. Ghosh, N. N. (Indian Association for the Cultivation of Science, Calcutta). Indian J. Phys., 39: 434-42 (Sept. 1965).

In a four-space R_4 a new real transformation scheme was so framed that a new representation of a four-dimensional Lorentz transformation is obtained showing the connection between the respective transformation coefficients. The method is a modification of that used previously where the representation of a five-dimensional Lorentz transformation was considered. It is to be noted that under this new transformation scheme a system of Dirac equations can be constructed. (auth)

21848 ON THE ESSENTIAL SPECTRUM OF AN ARBITRARY OPERATOR. [PART] I. Schechter, Martin (New York Univ., New York). Contract AT(30-1)-1480. J. Math. Anal. Appl., 13: 205-15(Feb. 1966).

Sufficient conditions for the invariance for each of the various definitions of the sets for the essential spectrum of a self-adjoint operator are given. A spectral singularity is said to be in such an essential spectrum if it is not an isolated eigenvalue of finite multiplicity. It is found that in each case the compactness assumption of the perturbation can be weakened. (J.F.P.)

21849 EMPTY SPACE-TIMES OF EMBEDDING CLASS TWO. Collinson, C. D. (Univ. of Hull, Eng.). J. Math. Phys. (N. Y.), 7: 608-11(Apr. 1966).

The null tetrad notation of Newman and Penrose is used to investigate empty space-times of embedding class two. Necessary conditions are found for algebraically special empty space-times to have this property. (auth)

21850 CONTINUOUS REPRESENTATION OF AN INDEFINITE METRIC SPACE. Gundzik, M. G. (Syracuse Univ., N. Y.). J. Math. Phys. (N. Y.), 7: 641-51(Apr. 1966). (NYO-3399-28).

An overcomplete family of states (OFS) is constructed for a countably infinite linear vector space with an indefinite metric for the case that the metric is diagonal with eigenvalues $(-1)^n$, where n is an integer. A continuous representation is indicated and the properties of a semiclassical description of a quantum mechanical system (the pseudo oscillator whose creation and destruction operators $\bar{a}$ and $\bar{a}^+$ satisfy $[\bar{a},\bar{a}^+] = -1$) defined in this vector space are studied. It is found that a consistent OFS $|z>$ can be constructed if the operator G(z) which generates the state $|z>$ from the vacuum is unitary. Furthermore, with the statistical state of this system specified by a bounded pseudo-Hermitian density matrix $\bar{\rho}$, the related semiclassical complex function $\rho_A(z)$ for antinormal ordering of operators in the indefinite metric space is found to be bounded, with $\rho_A(z)$ and $|\rho_A(z)|^2$ integrable, continuous, and a boundary value of an entire analytic function of two complex variables. The semiclassical function $\rho_N(z)$ for normal ordering is associated with a sequence of functions $\rho_{N(\nu)}(z)$ whose square is integrable and related to a sequence of tempered distributions $\rho_{N(\nu)}$ such that the corresponding sequence of density matrices $\bar{\rho}_{(\nu)}$ converges to $\bar{\rho}$ in the norm. (auth)

21851 CONTINUITY OF BOUND AND UNBOUND STATES IN A FERMI GAS: A SOLUBLE EXAMPLE. Majumdar, Chanchal K. (Carnegie Inst. of Tech., Pittsburgh). J. Math. Phys. (N. Y.), 7: 682-90(Apr. 1966).

Considering a gas of independent fermions in the presence of an attractive localized potential, it can be shown that the

properties of the system as a whole are smooth (analytic) functions of the strength parameter of the potential, even at those values where new single-particle bound states appear. Thus for the system as a whole, the transition from "unbound" to "bound" states is continuous and the concept of a bound state cannot be made precise. This is illustrated for a simple mathematically soluble model–noninteracting spinless fermions moving in the presence of a delta-function potential in one dimension. Some related physical ideas are also presented. (auth)

21852 SOLUTION OF SCHROEDINGER EQUATION INVOLVING TIME. Sasakawa, Tatuya (Washington Univ., St. Louis). J. Math. Phys. (N. Y.), 7: 721-41(Apr. 1966).

The general solution of the Schrödinger equation involving the time-dependent perturbation is presented in a compact and manageable form both for periodic and aperiodic perturbations. The method includes as a special case the solution of the Schrödinger equation involving the time-independent perturbation. Formulas ready for practical uses are explicitly described. The essential part of the procedure is the determinantal method in the Laplace-transformed space. The solution is applicable to strong perturbations as well as weak perturbations. (auth)

21853 PROPAGATION OF GRAVITATIONAL FIELDS IN MATTER. Szekeres, Peter (Cornell Univ., Ithaca, N. Y.). J. Math. Phys. (N. Y.), 7: 751-61(Apr. 1966).

A purely covariant treatment is made of those solutions of the Einstein field equations which represent pure gravitational radiation propagating in fluid and electromagnetic media. The analysis involves a discussion of the full Bianchi identities in carefully selected tetrad frames. In this way the interaction between the gravitational field and the medium is transferred to a coupling between a preferred frame for the gravitational field and one for the matter field. The gravitational radiation no longer propagates along shear-free null geodesics, as it does in vacuum, and the shear and ray curvature of the propagation vector are shown to depend directly on the properties of the medium. Some new solutions of the field equations, representing transverse gravitational waves propagating in an electromagnetic field, are exhibited and discussed in some detail. It is shown that no such solutions exist, at least in simple cases, for perfect fluids. Finally, the treatment presented here is compared with the more usual electromagnetic treatment, and it is shown why the theories require basically different approaches. (auth)

21854 ASYMPTOTIC CORRELATIONS OF THE HAMILTONIAN MATRIX ELEMENTS. Ullah, Nazakat (Tata Inst. of Fundamental Research, Bombay). J. Math. Phys. (N.Y.) 7: 762-?(Apr. 1966).

The statistical correlations of the matrix elements of real symmetric hamiltonians are studied using the assumption of representation invariance and the limit of large dimension N. The diagonal–diagonal correlation coefficient is expressed in terms of a parameter, which gives the ratio of the dispersion of off-diagonal element to that of the diagonal element. It is shown that for a certain class of real-symmetric Hamiltonian ensembles in the limit $N \to \infty$, the diagonal–diagonal correlation coefficient goes as λN^{-1}, where λ is some positive constant independent of N and the correlation coefficient of two different eigenvalues is the same as the one obtained using the weak assumption of independent probabilities. (auth)

21855 DETERMINATION OF THE COMMON EIGENVECTOR SYSTEM OF OPERATORS COMMUTING IN PAIRS. Lee, Anna. Magyar Tud. Akad. Kozp. Fiz. Kut. Int. Kozlem., 14: 63-71(1966). (In Hungarian).

A method is given for determining the common eigenvector system of operators (or matrices) of simple structure which are commutable in pairs. A spectrum of each operator (or matrix) is assumed to be known. The method leads to solutions of systems of linear homogeneous equations. The procedure is illustrated by a numerical example. (auth)

21856 STUDY OF INFRARED DIVERGENT TERMS IN THE BOUND-STATE PICTURE. Verbeure, A. (Louvain Univ., Belg.). Nuovo Cimenot (10), 42A: 269-84(Mar. 21, 1966).

The infrared divergent terms of the vertex function and the self-energy function within the renormalization program are studied in the way they depend upon the external potential. The structural dependence on the potential is treated in some detail. The observable photon mass due to the presence of the potential is explicitly calculated in two-dimensional quantum electrodynamics. (auth)

21857 GRAVITATION AND QUANTUM MECHANICS OF MACROSCOPIC OBJECTS. Karolyhazy, F. (Univ. of North Carolina, Chapel Hill). Contract 153-63. Nuovo Cimento (10), 42A: 390-402(Mar. 21, 1966).

The problem of the reduction of the wave function in quantum theory is treated from a new standpoint. First, by combining Heisenberg's uncertainty relations with gravitation, quantitative limitations on the sharpness of the structure of space-time are derived. Second, the resulting uncertainty in space-time structure is incorporated into the equations for the propagation of the quantum-mechanical wave amplitudes. In the resulting theory an initially pure wave function generally develops in time into a mixture. A single pure wave function survives only as long as it corresponds to a sufficiently small spread in the position of any massive part of the system under investigation. Quantitative relations between the mass and the maximum coherent spread in the center-of-mass wave function of a single body are obtained. (auth)

21858 A THEORY OF GRAVITATION. Rastall, P. (Univ. of British Columbia, Vancouver). Nuovo Cimento (10), 42B: 13-37(Mar. 11, 1966).

A theory of gravitation is developed which is a natural generalization of the Newtonian theory and of special relativity. Space-time is Riemannian, but its metric is determined by a scalar function Φ, the analog of the Newtonian potential. The functional dependence of the metric tensor on Φ is deduced, apart from two constant parameters, from the hypothesis that no measurement in an isolated region of space-time can determine whether the potential in that region is Φ or $\Phi + K$, where K is any constant. Test particles are assumed to travel along geodesics, and one of the unknown parameters in the metric tensor is fixed by requiring that the motions of test particles should have the correct classical limit. The usual expression for the gravitational red-shift then follows. The action of a system of gravitationally interacting particles is found. A field equation is obtained for Φ, and an energy-momentum tensor for the whole system. The remaining undetermined parameter in the metric tensor is fixed by requiring that in the static case Φ depend linearly on the energy density of the sources. New units of mass, length, and time are introduced, in terms of which many equations of the theory become identical in form with the corresponding special relativistic equations. Conservation laws for energy and momentum hold when these quantities are expressed in the new units. The principle of equivalence is discussed. (auth)

21859 ON THREE-DIMENSIONAL ASPECTS OF GENERALLY COVARIANT EXPRESSIONS. Massa, E. (Univ., Genoa). Nuovo Cimento (10), 42B: 178-81(Mar. 11, 1966).

The physical three-dimensional system of reference S associated with a given set of coordinates $(x^1x^2x^3x^4)$ in the space-time continuum V is studied. It is shown that it is possible, in a very simple way, to develop a general procedure to extract three-dimensional laws (i.e., laws expressed by means of three-vectors and tensors) from the usual four-dimensional ones. The problem is treated in a contravariant form, which points directly to the tensorial character of the results. (L.B.S.)

21860 ON THE ERROR OF APPROXIMATIONS IN QUANTUM MECHANICS. I. GENERAL THEORY. Hoffmann, T. A. (Central Research Inst. for Physics, Budapest). Phil. Trans. Roy. Soc. London, Ser. A, 257: 309-26 (Mar. 18, 1965).

A basic difficulty has existed in almost all calculations in the application of quantum mechanics to electronic systems. Namely, if the calculated wave function was not an

exact solution of the problem, but only some approximation, then there was, in general, no measure for estimating the error of the approximation. There were, in general, no means to estimate the error expected before the full calculation was performed and the results compared to some other calculations or to experimental values. General formulas for estimating the errors in quantum-mechanical calculations are given in the formalism of density matrices. Some properties of the traces of matrices are used to simplify the estimations and to indicate a way of obtaining a better approximation. It is shown that the simultaneous correction of all the equations to be fulfilled leads in most cases to a faster convergence than the exact fulfillment of some of the equations and approximating stepwise to some of the others. The corrective formulas contain only direct operations of the matrices occurring and are advantageous in computer applications. A subjective error definition is given and, by taking into account the weight of the errors of the several equations, a faster convergence and a single error quantity is obtained. (BBB)

21861 ON THE ERROR OF APPROXIMATIONS IN QUANTUM MECHANICS. II. SOME PARTICULAR APPLICATIONS. **Hoffmann, T. A. (Central Research Inst. for Physics, Budapest). Phil. Trans. Roy. Soc. London, Ser. A, 257: 327-49(Mar. 18, 1965).**

The estimation of the error in a quantum-mechanical calculation was previously developed. The method, based on the properties of the common trace-forming procedure in matrix calculus, allowed the determination of the next approximating steps in a steepest descent process. The results of applying the method to some cases frequently considered in quantum-mechanical and quantum-chemical calculations are presented. Means of obtaining an explicit form for the hamiltonian include the following cases: independent one-electron eigenfunctions, independent one-electron eigenfunctions taking into account spin and the Pauli principles, one-electron eigenfunctions with spin, one-electron eigenfunctions with interaction taking into account spin and the Pauli principle, and linear combination of atomic orbitals. In the latter approximation each electron is characterized around an atom by a prescribed normalized atomic wave function and a coefficient which determines the weight of the atomic wave function in question. In this representation the subdivision of the space of an electron is made roughly into the same number of parts as there are atoms present in the system. (BBB)

21862 CONFORMAL INVARIANCE AND THE GEOMETRIZATION OF THE HOYLE-NARLIKAR MASS FIELD. **Peters, P. C. (Univ. of Washington, Seattle). Phys. Lett., 20: 641-2(Apr. , 1966).**

The Hoyle-Narlikar mass field in the "smooth fluid approximation" is geometrized in the spirit of the Rainich-Misner-Wheeler geometrization of electromagnetism. The geometric equations are derived from an action which is uniquely specified once conformal invariance is imposed. (auth)

21863 CONFIGURATION-SPACE PHOTON NUMBER OPERATORS IN QUANTUM OPTICS. **Mandel, L. (Univ. of Rochester, N. Y.). Phys. Rev., 144: 1071-7(Apr. 29, 1966).**

Some properties of the operator $\hat{n}_{V,t}$ representing the number of photons localized in a finite volume V at time t are investigated. To some extent these properties reflect the well-known difficulty of localizing photons in space-time. However, it is shown that, when the linear dimensions of V are large compared with the wavelength of any occupied mode of the field, the $\hat{n}_{V,t}$ operator acquires some simple properties. The commutator of $\hat{n}_{V,t}$ and the detection operator $\hat{A}(x,t)$ is expressible in an interesting form. The commutator and relations derived from it become particularly simple for certain space-time regions which are labeled conjoint and disjoint. An orthogonal set of eigenstates of $\hat{n}_{V,t}$ is found, together with the corresponding eigenvalues, and it is shown that an arbitrary state is expressible in terms of these eigenstates. Some Nth-order correlations of the $\hat{n}_{V,t}$ operators are evaluated, and the results are used to calculate the probability distribution of eigenvalues of $\hat{n}_{V,t}$ for an arbitrary state of the field. (auth)

21864 HAMILTON-JACOBI AND SCHROEDINGER THEORY IN THEORIES WITH FIRST-CLASS HAMILTONIAN CONSTRAINTS. **Bergmann, P. G. (Syracuse Univ., N. Y.). Phys. Rev., 144: 1078-80(Apr. 29, 1966).**

Brief proofs are given, applying in the case of classical Hamilton-Jacobi theory to the action S, and in a Schroedinger-type quantum theory to the state vector Ψ, (1) that these quantities are independent of the time t, and (2) that they as well as the equations obeyed by them are form-invariant under the invariance group of transformations, provided the invariance transformations are generated by constraints and provided these constraints include the hamiltonian. In Dirac's version the equations of general relativity have all these properties. (auth)

21865 MAGNETIC CHARGE AND QUANTUM FIELD THEORY. **Schwinger, Julian (Harvard Univ., Cambridge, Mass.). Contract AF49(638)-1380. Phys. Rev., 144: 1087-93(Apr. 29, 1966).**

A quantum field theory of magnetic and electric charge is constructed. It is verified to be relativistically invariant in consequence of the charge quantization condition $eg/\hbar c = n$, an integer. This is more restrictive than Dirac's condition, which would also allow half-integral values. (auth)

21866 RELATIVISTIC CORRECTIONS FOR TERRESTRIAL CLOCK SYNCHRONIZATION. **Cocke, W. J. (Aerospace Corp., El Segundo, Calif.). Contract AF 04(695)-669. Phys. Rev. Lett., 16: 662-4(Apr. 11, 1966).**

A discussion is presented of the relativistic effects on atomic maser clocks, which are used in accurate synchronization of time standards over the earth's surface. The emphasis of this discussion is with clocks rotating with the earth, and the aim is to derive a formula for the relative drifts of clocks at widely separated localities. (B.G.D.)

21867 SIMULTANEOUSLY LORENTZ- AND GALILEAN-INVARIANT PARTICLE DYNAMICS. **Kerner, Edward H. (Univ. of Delware, Newark). Phys. Rev. Lett., 16: 667-9(Apr. 11, 1966).**

Simple examples are presented contrary to the belief that Newtonian-type particle dynamics (direct interparticle interaction, or instantaneous action at a distance) is relativistically untenable; moreover, that the nesting of non-relativity into the tiny corner located by the limit $C \to \infty$ (as with Coulomb interactions of slowly moving charges) represents as much overlap of the two as could be looked for. Newtonian-order equations of motion for a pair of particles in one dimension which are at once Lorentz invariant and Galilean invariant are discussed. This coextensiveness of Newtonian and Einsteinian relativity is characterized by laws of motion that are devoid of the constant C and that admit super-light velocities without hindrance. (B.G.D.)

21868 GRAVITATIONAL FIELD OF A RADIATING SPHEROID. **Vaidya, P. C. (Washington State Univ., Pullman); Pandya, I. M. Progr. Theoret. Phys. (Kyoto), 35: 129-40(Jan. 1966).**

Wave solutions with axial symmetry that describe the flow of gravitational and the null electromagnetic radiation are considered in the scheme of the general theory of relativity. The coordinates are chosen such that the wave pattern is given by 3-surface x^4 = constant. It is found that the solutions split themselves into two types, i.e., (i) solutions with open wave fronts (ii) solutions with closed wave fronts. The first case has been already worked out and solutions of the second type, for which the wave patterns are the surfaces of revolution, are discussed. In particular a solution with oblate spheroidal wave fronts is derived. The deflection of a light ray which grazes the sun's limb is considered and it is found that the observed deflection of light does not allow any appreciable eccentricity in the shape of the sun. (auth)

21869 PLANE WAVES IN THE UNIFIED FIELD OF GRAVITATION AND ELECTROMAGNETISM. EXACT

PLANE WAVE SOLUTIONS IN BONDI SPACE TIME. Johari, Vinod B. (Gorakhpur Univ., India). Progr. Theoret. Phys. (Kyoto), 35: 141-6(Jan. 1966).

Bondi, Pirani and Robinson have given an invariant definition of the plane gravitational waves, based on the symmetry properties of the plane electromagnetic waves; but this definition is applicable to empty regions only. The (z-t) property of the waves is used to extend the results of Bondi, Pirani and Robinson to the unified field of gravitation and electromagnetism. The exact plane wave solutions of the field equations in general relativity is obtained in Bondi space time, the electromagnetic field considered being null in the sense of Synge. (auth)

21870 STOCHASTIC PROCESSES IN MICROPHYSICS IN CONNECTION WITH RELATIVITY. Aron, J. C. (Institut Henri Poincare, Paris). Progr. Theoret. Phys. (Kyoto), 35; 147-71(Jan. 1966).

The difficulties of extending to relativity the results obtained in a preceding paper are set forth; in particular the relativistic behavior of the time and length minimal constants brings us to a well-known problem. The proposed views attempt to deal with these questions. They give a relativistic generalization of the classical diffusion theory, from which the Klein-Gordon equation is deduced. Consistent results are obtained by a relativistic survey of Dirac's fluid model. Subsequent investigations were carried out concerning the character of relativity and the limitation of its validity in microphysics. (auth)

21871 ON THE PROBLEM OF REGGE POLE BEHAVIOR OF SCATTERING AMPLITUDE IN QUANTUM ELECTRODYNAMICS WITH HEAVY PHOTON. Serbo, V. G.; Frolov, G. V. Vestn. Leningr. Univ., No. 16, Ser. Fiz. Khim., No. 3, 36-40(1965). (In Russian).

The agreement between the Regge pole behavior and the perturbation theory is verified in detail for $s \gg u \gg m^2$ for the sixth order terms of the amplitude. The expected cancellation of the $\ln^3 s$ terms is proved for arbitrary value of u. It is shown that the sum of the Chisholm's basic terms for ladder diagrams is found to be exponential. (auth)

Low Temperature Physics

21872 (AD-627189) ON THE ORIGIN OF PHASE TRANSITIONS IN VARIOUS MODELS. Emch, Gerard G. (Maryland Univ., College Park. Inst. for Fluid Dynamics and Applied Mathematics). Jan. 1966. Contract Nonr-595(22). 20p. (BN-433). CFSTI $1.00 cy, $0.50 mn.

A formal analogy is pointed out between the Bardeen-Cooper-Schrieffer model for superconductivity and several variations of the model suggested by Kac for the exact study of phase transitions. It is shown that similar techniques (due to Haag) can be used in all these cases, and some conclusions are drawn on the origin of both equilibrium and nonequilibrium singularities. (auth)

21873 (NP-15936) LOW-TEMPERATURE RESISTIVITY, MAGNETIC SUSCEPTIBILITY, AND SUPERCONDUCTING TRANSITION TEMPERATURE IN LANTHANUM CONTAINING RARE-EARTH IMPURITIES. Technical Report, Ser. A, No. 181. Sugawara, Tadashi; Eguchi, Hiroko (Tokyo Univ. (Japan). Inst. for Solid State Physics). Dec. 1965. 35p. Dep. mn.

The resistivities and the magnetic susceptibilities of La containing small amounts of other rare-earth metals were measured at low temperatures. Resistance minima were found at about 6.4°K in fcc La-Ce alloys and at about 5.8°K in hcp La-Ce alloys. The temperature at which the resistance minimum occurs is independent of the concentration of Ce. No minimum was observed in the other alloys. The observed resistivity of all the alloys contains a term proportional to log T in accordance with the recent theories on the s-d or s-*f* resistivity. The magnetic susceptibilities of La-Ce, La-Pr, and La-Nd alloys are not inconsistent with the resistive behaviors of these alloys. The effective s-*f* exchange integrals for various rare-earth solutes were calculated from the resistivity data and compared with those calculated from the change of the superconducting transition temperature of La due to added rare-earth metals. The agreement between the two is not good for heavy rare-earth solutes. The increment of the residual resistivity of La due to the solute seems to be explained mostly by the magnetic scattering. (auth)

21874 (TT-62-23147) SUPERCONDUCTIVITY. II. MICROSCOPIC THEORY. Ginzburg, V. L. Translated from Usp. Fiz. Nauk, 48: No. 1, pp 25-118(1952). 48p. CFSTI $2.00 cy, $0.50 mn.

The inconsistency of the "spontaneous currents hypothesis" (the assumption that certain spontaneous currents always, even in the absence of an external magnetic field, flow in a metal in the superconducting state) is pointed out. Attempts to construct a superconductivity theory on the basis of the "diamagnetic hypothesis," according to which superconducting currents are compared to currents due to the diamagnetism of atoms and molecules placed in a magnetic field, are discussed. The question is discussed of the necessity of taking into account the electron-lattice interactions. The quasi-microscopic approach to the explanation of superconductivity is discussed and compared to the approach used successfully by Landau in the case of the superfluidity of helium II. (M.O.W.)

21875 ASPECTS ON THE SUPERCONDUCTING STATE AND THE λ-TRANSITION. Borelius, G. (Royal Inst. of Tech., Stockholm). Ark. Fys., 28: 285-96(1965).

Two theories were previously developed from the study of the superconducting state and λ transition. One of these determined the transition from the superconducting to the normal state by a relation between the energy difference between these states, W, the electron specific heat constant, γ, the critical temperature, T_c, and a dimensionless constant, n. The other theory involved W, γ, T_c, and a parameter, Δ, representing half the energy threshold values. The relation between n and Δ is investigated. The previous method of analysis is summarized, and values of W, γ, T_c, n, and Δ for eleven superconductors are compiled from available data. Descriptions of the λ transition are compared by using n and Δ respectively. The number, n, is introduced in the formalism of the BCS theory, and the question of whether the consideration of n requires an extension or modification of the foundations of the theory is discussed. (J.F.P.)

21876 A 45-KGAUSS SUPERCONDUCTOR MAGNET FOR CORPUSCULAR IONOGRAPHY USED AT THE CERN. Donadieu, L.; Royet, J. (Compagnie Generale d'Electricite, Marcoussis, France). Ind. At., 10: 63-8(1966). (In French).

The design and construction of a magnetic superconductor with which charge reversal of mesons (π) with energies of 70 Mev can be studied is presented. This magnet is connected with a cryostat which allows the use of the magnetic field at ambient temperatures. The test results are discussed, especially those for the effective functioning with the CERN synchrocyclotron. A diagram of the magnet, and photographs of the superconducting magnet and cryostat system are shown. (J.F.P.)

21877 HIGH-FIELD SUPERCONDUCTIVITY AND ITS APPLICATIONS. Catterall, J. A. (National Physical Lab., Teddington, Eng.). J. Inst. Metals., 94: 25-46 (Feb. 1966).

A review of the phenomenon of superconductivity is presented. The topics covered include: ideal superconductors, the effects of alloying on superconductivity, theory of superconductivity, high-field superconductivity, applications of high-field superconductors, metallurgy of high-field superconductors, and future developments. Two-hundred-twenty-eight references are included. (W.L.G.)

21878 SUPERCONDUCTING COILS USING COMPOSITE STRANDED CABLES. Cornish, D. N. (United Kingdom Atomic Energy Authority, Abingdon, Eng.). J. Sci. Instrum., 43: 16-20(Jan. 1966). (CLM-P-83).

The performance of coils wound with cables consisting of strands of superconductor and copper can be predicted from a knowledge of the minimum current at which propagation of a normal region in the superconductor can occur.

Experiments are described in which the property was measured on a variety of cable designs, and the performance of a large coil was successfully predicted from short specimen measurements. The design can be varied to optimize either the overall current density or the cost, and it is possible to take advantage of the improved "short sample" critical current of heat-treated superconductors. Current sharing between the superconductor and the copper after transition can take the form of total or partial transfer of current to the copper, depending on the proportion of copper present in the composite conductor. (auth)

21879 AN S-MATRIX APPROACH TO SUPERCONDUCTIVITY. **Mathur, V. S.; Panchapakesan, N.; Saxena, R. P. (Univ. of Delhi). Nuovo Cimento (10), 42B: 1-7 (Mar. 11, 1966).**

The problem of superconductivity is studied within the framework of partial-wave dispersion relations in the N/D form. The BCS results are obtained at zero as well as finite temperatures. An attempt is made to interpret the instability of the vacuum in terms of the energy gap. (auth)

21880 ON THE GAP EQUATION AND CURRENT DENSITY FOR LOCAL SUPERCONDUCTORS IN A MAGNETIC FIELD. **Menyhard, N. (Central Research Inst. for Physics, Budapest). Nuovo Cimento (10), 42B: 170-4 (Mar. 11, 1966).**

The Ginzburg-Landau equations and their generalizations are investigated by taking into account the more realistic effective electron-electron interactions. The case of a general nonlocal two-particle interaction is studied, which can lead to the dependence of the gap function on the relative momentum of the pair. The anisotropy of the one-particle spectrum is also taken into account. The equations obtained for the gap function and the current density are given for $T \lesssim Tc$ in which case they are generalizations of Gorkov and Melik-Barkhudarov's results and reduce to modified Ginzburg's equations. (L.B.S.)

21881 GROUND-STATE SPLITTING AND ZEEMAN EFFECT IN ERBIUM ETHYLSULFATE AT 1.6 DEG K. **Wheeler, R. G.; Hill, J. C. (Yale Univ., New Haven). Phys. Lett., 20: 496-8(Mar. 15, 1966).**

Transitions were observed between the Zeeman split Stark components of the ground J-manifold in erbium ethylsulfate at 1.6°K. The transitions appear to be primarily magnetic dipole in character. (auth)

21882 MICROWAVE-INDUCED d-c VOLTAGES ACROSS JOSEPHSON JUNCTIONS. **Langenberg, D. N.; Scalapino, D. J.; Taylor, B. N.; Eck, R. E. (Univ. of Pennsylvania, Philadelphia). Phys. Lett., 20: 563-5 (Apr. 1, 1966).**

Microwave radiation is observed to induce d-c voltages across Josephson-type superconducting tunnel junctions. Both discretely quantized and continuously varying voltages have been observed. (auth)

21883 ANOMALOUS SPECIFIC HEAT OF SUPERCONDUCTING LANTHANUM AND YTTRIUM COMPOUNDS. **Satoh, T.; Ohtsuka, T. (Tokyo Univ.). Phys. Lett., 20: 565-6(Apr. 1, 1966).**

Results and discussions are presented of the anomalously small specific heat jump at the superconducting transition observed in the silicides and germanides of yttrium and lanthanum. (auth)

21884 JOULEAN HEATING IN A HARD SUPERCONDUCTING TUBE. **Wischmeyer, C. R. (Rice Univ., Houston, Tex.). Phys. Lett., 20: 578-9(Apr. 1, 1966).**

Dissipation in homogeneous material in a changing magnetic field is computed as a function of radius and applied field. The field dependence of greatest dissipation supports our contention of the relation of flux creep and flux jumps to Joule heating. (auth)

21885 OBSERVATION OF ENERGY GAPS IN β-TUNGSTENS AND OTHER SUPERCONDUCTORS USING A SIMPLIFIED TUNNELING TECHNIQUE. **Levinstein, H. J.; Kunzler, J. E. (Bell Telephone Labs., Inc., Murray Hill, N. J.). Phys. Lett., 20: 581-3(Apr. 1, 1966).**

Superconducting energy gaps of β-tungstens from tunneling measurements are reported. They were obtained using a simple configuration consisting of a sharp anodized point placed in mechanical contact with the sample after cooling to liquid helium temperatures. (auth)

21886 CONTRIBUTION OF SURFACE CURRENTS TO MAGNETIC HYSTERESIS IN THE MIXED STATE OF A TYPE II SUPERCONDUCTOR. **Barnes, L. J.; Fink, H. J. (Atomics International, Canoga Park, Calif.). Phys. Lett., 20: 583-4(Apr. 1, 1966).**

Evidence is presented that indicates that in the mixed state of well annealed low κ type II superconducting Pb–Tl cylinders in axial fields the d-c magnetic hysteresis results from induced critical surface currents. (auth)

21887 SUPERCONDUCTING STATE OF AN ELECTRON GAS IN A HOMOGENEOUS MAGNETIC FIELD. **Rajagopal, A. K. (Univ. of California, Riverside); Vasudevan, R. Phys. Lett., 20: 585-7(Apr. 1, 1966).**

The superconducting instability of an electron gas in a homogeneous magnetic field is here investigated taking full account of quantization effects using a variational method. A Ginsburg-Landau type equation with anisotropic field dependent effective masses is derived for the gap near the transition. (auth)

21888 SURFACE NUCLEATION IN A SUPERCONDUCTOR COATED WITH A NORMAL METAL. **Hurault, J.-P. (Faculte des Sciences, Orsay, France). Phys. Lett., 20: 587-8(Apr. 1, 1966).**

It is shown that the surface sheath usually present in a type II superconductor S under high fields is completely destroyed ($H_{||} = H_{c2}$ exactly) when a normal metal N is deposited on top of S, provided that: (1) the electrical contact between N and S is good; (2) the conductivity σ_N of N is larger than the normal state conductivity σ_S of S. For the opposite case $\sigma_N < \sigma_S$, $H_{c2} < H_{||} < 1.69\ H_{c2}$ is formed. (auth)

21889 POSSIBLE HIGH-CURRENT SUPERCONDUCTIVITY IN IONIC SEMICONDUCTORS. **Eagles, D. M. (Post Office Research Station, London). Phys. Lett., 20: 591-2(Apr. 1, 1966).**

The possibility of the occurrence of superconductivity at high carrier drift velocities in ionic semiconductors is discussed. (auth)

21890 TIME-DEPENDENT GINSBURG-LANDAU THEORY. **Jakeman, E.; Pike, E. R. (Royal Radar Establishment, Malvern, Eng.). Phys. Lett., 20: 593-4 (Apr. 1, 1966).**

The results of a microscopic-theory calculation of the electrodynamic response of a local superconductor to slowly varying fields, are presented. (auth)

21891 INCREASE OF CRITICAL TEMPERATURE IN SUPERCONDUCTING FILMS. **Tavger, B. A.; Kresin, W. S. (Gor'kii State Univ., USSR). Phys. Lett., 20: 595-6(Apr. 1, 1966).**

The effect of increase of critical temperature in metal films with decreasing thickness is explained on the basis of finite transverse motion of electrons. (L.B.S.)

21892 SUPERCONDUCTING TRANSITION TEMPERATURES IN ϵ-PHASE Pb-Bi ALLOYS. **King, H. W. (Imperial Coll. of Science and Tech., London); Russell. C. M.; Hulbert, J. A. Phys. Lett., 20: 600-1(Apr. 1, 1966).**

Superconducting transition temperatures across the ϵ-phase in Pb-Bi show an accelerated rise near $e/a = 4.28$. This change in dT_c/dc is attributed to a {10.2} Brillouin zone overlap, the presence of which is confirmed by an increase in the axial ratio of the hexagonal cell. (auth)

21893 REMANENT INDUCTION IN A HARD SUPERCONDUCTOR. **Echarri, A. (Univ., Libre, Brussels). Phys. Lett., 20: 619-21(Apr. 1, 1966).**

Remanent induction was measured for a superconducting sample of Zr–26% wt. V. The results agree qualitatively with Bean's model for weak fields. (auth)

21894 OBSERVATION OF LOW-FREQUENCY MIXED-STATE RESONANCES IN PURE NIOBIUM. **Maxfield, B. W.; Johnson, E. F. (Cornell Univ., Ithaca, N. Y.).**

Phys. Rev. Lett., 16: 652-4(Apr. 11, 1966). (NYO-2150-10).

Recent observations of low frequency resonances in the mixed state of pure niobium are presented. These low-Q resonances have a line shape similar to low Q helicon resonances in a normal metal and resemble the resonances observed in the intermediate state of a pure type I superconductor although there are significant differences. (B.G.D.)

21895 VARIABLE TRANSFER RATES IN SUPERFLUID HELIUM FILMS. **Allen, J. F.; Matheson, C. C. (St. Andrews Univ., Scotland). Proc. Roy. Soc. (London), Ser. A, 290: 1-13(Feb. 8, 1966).**

From an experimental investigation of superfluid film transfer in narrow beakers in helium II it is concluded that there are probably two kinds of film. A "normal" film is formed by superfluid creep over a dry substrate. A "thick" film remains when liquid has drained from a substrate that has previously been immersed in the liquid helium bath. A comparison was made of the superfluid flow between the two types of film. Scatter of values of transfer rate associated with a normal film is attributed to third sound generated by bath waves impinging on the meniscus at the base of the film. The thick film shows an enhanced rate of transfer which can persist for long periods of time in quiet conditions, but which can be abruptly diminished by disturbances such as bath surface agitation. There is a maximum stable length for a thick film exhibiting the full enhanced rate. The enhanced rate can be as much as 60% greater than the normal rate at 1°K, but the difference between the two rates of transfer disappears above 1.8°K. No enhanced rate of transfer at any temperature is observed in beakers as large as 8-mm diameter. (auth)

21896 THICK NON-EQUILIBRIUM HELIUM II FILMS. **Tilley, J.; Kuper, C. G. (Univ. of St. Andrews, Scotland). Proc. Roy. Soc. (London), Ser. A, 290: 14-23(Feb. 8, 1966).**

Experiments by Allen & Matheson on the variability of superfluid helium film transfer are analyzed in terms of the phenomenological two-fluid model. When bulk helium II drains from a solid wall, its flow is controlled by the viscosity of the normal component. It is shown that the drainage, although initially rapid, can slow down to give a quasi-stationary film thickness, appreciably thicker than the true equilibrium film; the difference is greatest at low temperatures. Predicted flow rates for thick films are in good accord with the temperature-dependent "enhanced" rates of Allen & Matheson. The non-equilibrium character of thick films suggests that they are readily destroyed by waves of third sound, and hence accounts for the observed sensitivity of enhanced rates to vibration. (auth)

21897 SUPERCONDUCTING ALLOY IN THE Nb-Ga SYSTEM. **Gutsa, Z. A.; Krivko, N. I.; Morozova, V. K.; Sidorova, T. A.; Fogel', A. A. (Ioffe Physico-Technical Inst., Leningrad). Zh. Tekh. Fiz., 35: 1675-7(1965). (In Russian).**

Results of measurements of the superconducting properties of alloys in a Nb-Ga system at a temperature of 4.2°K and magnetic fields up to 28 kOe are presented. The alloys were prepared by means of special equipment. The starting materials consisted of vacuum-refined niobium and metallic gallium. The latter was additionally degassed at 800-1000C in vacuum at $10^{-4}-2\cdot10^{-5}$ mm Hg for a period of 2-3 min. The transition from the superconducting state to the normal state was recorded by a change in the inductance of a coil prepared from the given alloy. Mechanical experiments showed the highest plasticity in alloys with 7-12% Ga (by weight). Their hardness did not exceed 350 kg/mm^2, whereas the hardness of alloys with 12-32% Ga was 450-850 kg/mm^2. Alloys containing 7-12% Ga are apparently the most suitable for wires. (ATD)

21898 MEASUREMENT OF THE MAGNETIC FIELD AT THE SURFACE OF A Nb-Zr SUPERCONDUCTOR BY MEANS OF ELECTRON PARAMAGNETIC RESONANCE. **Krivko, N. I. (Ioffe Physico-Technical Inst., Leningrad). Zh. Tekh. Fiz., 35: 1906-7(1965). (In Russian).**

Experiments performed to prove the feasibility of using electron paramagnetic resonance (EPR) to measure the magnetic field strength at the surface of a superconductor are reported. A circular disc (dimensions not given) of Nb-Zr alloy formed the floor of a rectangular resonator. To the center of this disc there was fastened a 4×10^{-3} mm^3 chip of diphenyl picryl hydrazyl to produce the EPR signal. The 9300-Mc microwaves were modulated at 630 kc and the EPR signal was displayed on the screen of an oscilloscope synchronized with the 50 cps sweep of the magnetic field. The applied magnetic field (approximately 3 kOe) was parallel to the surface of the superconductor and was measured with a proton resonance device. The EPR line was observed at 4.2°K both with and without the superconductor present. The superconductor was cooled before the field was applied. The presence of the superconductor shifted the EPR line (altered the magnetic field strength) by 188.6 Oe and increased its width from 3.0 to 11.4 Oe. The shift of the line is ascribed to a local field at the surface of the superconductor and the increase of the line width to the inhomogeneity of the local field. The described technique for measuring the magnetic field at the surface of a superconductor is satisfactory; its advantages are high sensitivity, the small size of the detector, and the absence of leads, and its disadvantage is the small range of magnetic field strengths that can be measured. This disadvantage might be overcome by employing EPR lines from a number of different materials. (ATD)

21899 CONFERENCE ON THE PHYSICS OF TYPE II SUPERCONDUCTIVITY, CLEVELAND, OHIO, AUGUST 28 AND 29, 1964. VOLUMES 1, 2, AND 3. **Cleveland, Western Research University [1965]. 530p. (CONF-640803(Vols. 1, 2, and 3)).**

Separate abstracts are prepared for 33 of the 48 papers presented in the three volumes. Six papers were previously included in NSA as 18: 34724; 19: 6618, 10194, 16804, 19062, and 39130. Nine papers were in summary form and were not abstracted for NSA. (B.G.D.)

For abstracts of individual papers see: 21900-21932.

21900 ON THE PARAMAGNETIC EFFECT AND THE LANDAU-GINZBURG EQUATIONS. **Sarma, G.; Saint-James, D. (Centre d'Etudes Nucleaires, Saclay, France). pp I.1-14 of Conference on the Physics of Type II Superconductivity. Vol. I. Cleveland, Western Reserve University [1965].**

An extension of the Landau-Ginzburg equations in order to take into account the influence of paramagnetic effects on superconducting properties is discussed. Particular emphasis is placed on the possibility of depairing situations and also changes in critical field values. (B.G.D.)

21901 SOME THERMODYNAMIC RELATIONSHIPS FOR THE IDEAL BULK TYPE II SUPERCONDUCTOR. **Hake, R. R. (Atomics International Div., North American Aviation, Inc., Canoga Park, Calif.). pp I.15-29 of Conference on the Physics of Type II Superconductivity. Vol. I. Cleveland, Western Reserve University [1965].**

Some thermodynamic relations which include volume and pressure effects are presented for the case of the ideal bulk Type II superconductor. Comparison of the Rutgers and Ehrenfest expressions for the superconducting transition specific heat discontinuity discloses an apparent difficulty near T_c with Abrikosov expression for the limiting slope of the magnetization vs applied field curve at the upper critical field. (auth)

21902 SOLUTION OF THE GINZBURG-LANDAU EQUATIONS FOR THE ABRIKOSOV MIXED STATE NEAR THE SECOND CRITICAL FIELD. **Lasher, Gordon (IBM Watson Research Center, New York). pp I.30-3 of Conference on the Physics of Type II Superconductivity. Vol. I. Cleveland, Western Reserve University [1965].**

A systematic approximation procedure to the bulk periodic solutions of the Ginzburg-Landau equations is presented for applied fields and flux densities which are less than the second critical field by a small but finite amount. (B.G.D.)

21903 THE GENERALIZED GINZBURG-LANDAU-GOR'KOV EQUATIONS FOR A PURE SUPERCONDUCTOR.

Tewordt, L. (Univ., Hamburg). pp I.34-42 of Conference on the Physics of Type II Superconductivity. Vol. I. Cleveland, Western Reserve University [1965].

Calculations of the complete set of terms of the fourth order in ∇ and A of the gap equation and also the corresponding free energy functional are presented. These terms are then combined in such a way that the gauge invariance can be recognized. The most important aim of this calculation is to determine in a precise way the range of gap and temperature values for which the generalized Ginzburg-Landau-Gorkov (GLG) theory is valid. Moreover, the fourth order terms are of great practical interest since they can be used as correction terms to the second order terms when the GLG theory is extended from temperatures just below T_c to lower temperatures. (B.G.D.)

21904 A KRONIG-PENNEY MODEL FOR EXCITATIONS IN TYPE II SUPERCONDUCTORS. Markowitz, David; Schwartz, Brian B. (Rutgers Univ., New Brunswick, N. J.). pp I.51-64 of Conference on the Physics of Type II Superconductivity. Vol. I. Cleveland, Western Reserve University [1965].

A discussion is presented on the excitations that exist in a pure type II superconductor as a result of the periodicity of the Abrikosov vortex structure. Derivation of the excitation spectrum is proposed by a two dimensional Kronig-Penney model solution of the coupled single particle wave function. (B.G.D.)

21905 NONLOCAL EXTENSION OF THE GINZBURG-LANDAU THEORY. Toxen, Arnold M. (IBM Watson Research Center, New York). pp I.65-79 of Conference on the Physics of Type II Superconductivity. Vol. I. Cleveland, Western Reserve University [1965].

Results are presented of machine calculations showing the detailed variations with thickness, mean free path, and temperature of two of the parameters of the Ginzburg-Landau theory, the nonlinear coupling constant and the range of order parameter. These calculations were carried out for a nonlocal nonlinear model. A review is presented on the model with which the critical fields of superconducting films could be related to the parameters of any of the nonlocal theories of superconductivity. (B.G.D.)

21906 ABRIKOSOV'S STRUCTURES IN SUPERCONDUCTING ALLOYS. Maki, Kazumi (Kyoto Univ.). pp I.80-6 of Conference on the Physics of Type II Superconductivity. Vol. I. Cleveland, Western Reserve University [1965].

The application of Abrikosov's theory for superconducting alloys at temperatures below the transition temperature is discussed. Emphasis is placed on the behavior of superconductors in the field close to the upper critical field. (B.G.D.)

21907 SPECIFIC HEAT OF TYPE II SUPERCONDUCTORS IN A MAGNETIC FIELD. McConville, T.; Serin, B. (Rutgers Univ., New Brunswick, N. J.). pp II.3-12 of Conference on the Physics of Type II Superconductivity. Vol. I. Cleveland, Western Reserve University [1965].

Measurements are presented of heat capacity as a function of temperature in specimens of Nb and In + 1.9 at. % Bi. These measurements are made in both a constant magnetic field and in a zero field. Magnetic field values were chosen so that a given value corresponded to both the lower critical field and the upper critical field of the specimen as it was warmed from low to high temperatures. Results of these measurements show that for specimens cooled in zero field, and subsequently heated in a constant magnetic field, the heat capacity exhibits a very large peak at low temperatures followed by a discontinuous drop at higher temperatures. The heat capacity in the neighborhood of the peak is irreversible, but seems reversible near the discontinuity. Despite the reversibility, the magnitudes of the observed specific heat discontinuities in niobium do not agree with the predictions of the Abrikosov theory. (B.G.D.)

21908 THE PENETRATION OF A MAGNETIC FIELD INTO Nb_3Sn, V_3Si AND Nb_3Al AT LOW FIELDS. Meyer, G. (Univ. of Giessen, Ger.). pp II.25-31 of Conference on the Physics of Type II Superconductivity. Vol. I. Cleveland, Western Reserve University [1965].

A method is discussed for measuring the temperature variation of the initial magnetic susceptibility taking bulk sintered and diffusion samples, as well as finely ground sintered and melted samples of Nb_3Sn, V_3Si, and Nb_3Al. The measurements show that penetration effects must be accounted for if the interior of the sample is not completely shielded by current loops, that the depth of penetration depends on temperature, and the transition temperature obtained by susceptibility measurements is lowered with decreasing grain size. (B.G.D.)

21909 QUANTIZED FLUX PINNING IN SUPERCONDUCTING NIOBIUM. Zimmerman, J. E.; Mercereau, J. E. (Ford Motor Co., Dearborn, Mich.). pp II.32-40 of Conference on the Physics of Type II Superconductivity. Vol. I. Cleveland, Western Reserve University [1965].

Positive evidence for flux pinning in superconducting niobium in individual bundles is obtained by the experimental concept of utilization of quantum interference effects in superconductors as a flux detector. A two-contact superconducting quantum interferometer is used to measure the flux pinned in a .05 mm niobium wire passing through the interferometer. (B.G.D.)

21910 THE MOTION OF ABRIKOSOV VORTICES IN A TYPE II SUPERCONDUCTOR. Borcherds, P. H.; Gough, C. E.; Vinen, W. F.; Warren, A. C. (Univ. of Birmingham, Eng.). pp II.49-56 of Conference on the Physics of Type II Superconductivity. Vol. I. Cleveland, Western Reserve University [1965].

Experimental results on flux movement in a type II superconductor when the magnetization curve is reversible are discussed on the basis of the view that the penetration of flux into the superconductor takes place through the presence of quantized Abrikosov vortices in the superconducting electron fluid. An assumption is made that in an ideal type II superconductor an isolated vortex is free to move except for a frictional drag acting on its core. (B.G.D.)

21911 SOME SUPERCONDUCTING PROPERTIES OF SEVERAL CARBIDES AND NITRIDES OF THE TRANSITION METALS. Toth, L. E.; Johnston, J.; Wells, M.; Zackay, V. F.; Parker, E. R. (Univ. of California, Berkeley). pp II.57-81 of Conference on the Physics of Type II Superconductivity. Vol. I. Cleveland, Western Reserve University [1965].

A definite correlation has been found between the critical temperature of the carbides and nitrides of the transition metals and the total number of valence electrons. The critical temperature increases as the total number of valence electrons increases from eight to ten. This variation in T_c is discussed in terms of band models proposed by Bilz and Dempsey. A number of experiments were undertaken on MoC and TaN to substantiate the correlation. The superconducting properties of cubic MoC were determined. The cubic structure was obtained by preventing the cubic to hexagonal martensitic transformation from occurring. The critical temperature was determined to be 13.0°K. (auth)

21912 DISCONTINUOUS VARIATION OF THE MODULUS IN TYPE II SUPERCONDUCTORS. Alers, G. A.; Karbon, J. A. (Ford Motor Co., Dearborn, Mich.). pp II.82-7 of Conference on the Physics of Type II Superconductivity. Vol. I. Cleveland, Western Reserve University [1965].

For type II superconductors the elastic moduli deviate from their superconducting values at very low fields and then increase linearly with field up to the very high critical field, at which electric resistance is restored. This linear dependence of the elastic moduli in the magnetic field is investigated by preparing a series of Pb–Tl alloy single crystals covering the composition range over which the transition from type I to type II behavior occurs. (B.G.D.)

21913 RESISTANCE TRANSITIONS OF SUPERCONDUCTING LEAD–INDIUM ALLOYS. Druyvesteyn, W. F.; Volger, J. (Philips Research Labs., Eindhoven, Nether-

lands). pp II.88-119 of Conference on the Physics of Type II Superconductivity. Vol. I. Cleveland, Western Reserve University [1965].

Experiments are reported on the resistance transitions in a magnetic field, with the angle between field and current as a parameter for a series of single phase lead-indium alloys. Experimental results are compared with various theories. (B.G.D.)

21914 THERMAL CONDUCTIVITY IN THE MIXED STATE. Dubeck, L.; Lindenfeld, P.; Lynton, E. A. (Rutgers Univ., New Brunswick, N. J.). pp II.120-9 of Conference on the Physics of Type II Superconductivity. Vol. I. Cleveland, Western Reserve University [1965].

Measurements of the thermal conductivity of type II superconductors as a function of magnetic field are discussed. The specimens used in these measurements were indium alloys with 1.8 and 4.0 at. % bismuth and pure niobium. From these measurements further information about the scattering process in the mixed state is obtained. (B.G.D.)

21915 CRITICAL FIELDS OF SUPERCONDUCTING VANADIUM FILMS. Hammond, R. H.; Meyer, C. H. Jr.; Rump, B. S. (General Atomic Div., General Dynamics, San Diego, Calif.). pp III.1-14 of Conference on the Physics of Type II Superconductivity. Vol. II. Cleveland, Western Reserve University [1965].

Measurements of the critical fields of thin films of superconducting vanadium are discussed. Measurements of the resistive transitions are made in parallel and normal fields and their temperature dependences studied. The dependence of the critical field on the angle between the field and the plane of the film is discussed. The validity of the Ginzburg-Landau, Tinkham, and Abrikosov theories with regards to films of vanadium is discussed. (B.G.D.)

21916 MICROWAVE STUDIES OF THE SUPERCONDUCTING MIXED STATE. Rosenblum, Bruce; Cardona, Manuel (RCA Labs., Princeton, N. J.). pp III.15-22 of Conference on the Physics of Type II Superconductivity. Vol. II. Cleveland, Western Reserve University [1965].

Experiments on microwave surface resistance of type II superconductors are discussed. Results show that the surface resistance is largely structure-insensitive and independent of the particular material, and is therefore characteristic only of the mixed state. The model of the mixed state that is used in the explanation of these microwave experiments is an array of Abrikosov flux tubes with essentially normal core of a diameter approximately equal to the coherence length. (B.G.D.)

21917 ANGULAR DEPENDENCE OF THE CRITICAL FIELD OF SUPERCONDUCTING FILMS AND SURFACES. Tinkham, M. (Univ. of California, Berkeley). pp III.24-8 of Conference on the Physics of Type II Superconductivity. Vol. II. Cleveland, Western Reserve University [1965].

Variational calculations using the linearized Ginzburg-Landau equation are presented in an attempt to provide a more complete and reliable theoretical treatment of the angular dependence of the critical field of superconducting films and surfaces. (B.G.D.)

21918 EFFECT OF SURFACE CONDITIONS ON a-c FIELD TRANSITIONS IN TYPE II SUPERCONDUCTORS. Rollins, R. W.; Silcox, J. (Cornell Univ., Ithaca, N. Y.). pp III.32-44 of Conference on the Physics of Type II Superconductivity. Vol. II. Cleveland, Western Reserve University [1965].

The behavior of type II superconductors when subjected to a low frequency alternating magnetic field superimposed on a d-c magnetic field with differing surface conditions is discussed. Results obtained on single crystal Nb and a Pb–8% In alloy with a range of amplitudes of the a-c field from approximately 25 to 0.05 Oe at a frequency of 200 cps are presented. (B.G.D.)

21919 MEASUREMENTS OF THE CURRENT-DEPENDENT REACTANCE OF SUPERCONDUCTORS HAVING VERY SMALL COHERENCE DISTANCE. Gittleman, J. I.; Rosenblum, B.; Seidel, T.; Wicklund, A. (RCA Labs., Princeton, N. J.). pp III.47-60 of Conference on the Physics of Type II Superconductivity. Vol. II. Cleveland, Western Reserve University [1965].

The dependence of the imaginary part of the conductivity (σ_2) on current was measured at various temperatures for films of tin, indium, and tin-indium alloys. The reactance of the samples was measured with a small 23 kMc signal in a microwave bridge while direct current in the film was varied from zero to the critical value. The samples were thin, narrow films so that both the d-c and microwave currents were spatially uniform. At reduced temperatures above 0.6 both the magnitude and the temperature dependence of the nonlinearity were in remarkably good agreement with both the microscopic theory of Parmenter and the phenomenological Ginzburg-Landau theory. The only adjustable parameter was the penetration depth for each sample. The values chosen for the penetration depth were in excellent agreement with values computed from the residual resistance ratios. There is also evidence that boundary scattering in indium films is highly specular; whereas in the tin film it appears to be diffuse. (B.G.D.)

21920 DEPENDENCE OF CURRENT DEGRADATION IN SUPERCONDUCTING SOLENOIDS ON FLUX PINNING ENERGY AND TEMPERATURE. Meyerhoff, R. W.; Heise, B. H. (Union Carbide Corp., Tonawanda, N. Y.). pp IV.1-13 of Conference on the Physics of Type II Superconductivity. Vol. II. Cleveland, Western Reserve University [1965].

A discussion of the current degradation of superconducting solenoids is presented. Flux pinning energies and straight wire critical currents of Nb–Zr wire are measured as a function of magnetic field, and solenoid critical currents are reported as a function of temperature. These measurements indicate that high pinning energy causes flux jumping which causes solenoid degradation. These measurements also indicate that pinning energy can be weakened by increasing the temperature; therefore, flux jumping and coil degradation can be suppressed by increasing temperature. (auth)

21921 CRITICAL CURRENTS IN Nb_3Sn. III. Cody, G. D.; Cullen, G. W. (RCA Labs., Princeton, N. J.). pp IV.14-37 of Conference on the Physics of Type II Superconductivity. Vol. II. Cleveland, Western Reserve University [1965].

Critical currents have been measured as a function of the angle between the current axis and the external magnetic field from zero field to 103.6 kG for several specimens of vapor deposited Nb_3Sn. The results indicate excellent agreement with the Lorentz force model for the field and angular variation of the critical current. For all samples there is sharp rise in the critical current density at low longitudinal fields which is associated with an inhomogeneous current distribution at low fields. The value of the longitudinal current can be related to the self field produced by the current itself. The present results indicate that for homogeneous specimens the longitudinal current can be constant from about 10 kG to 100 kG. (auth)

21922 CRITICAL CURRENTS OF Nb_3Sn AND V_3Ga IN TRANSVERSE MAGNETIC FIELDS UP TO 150,000 OERSTEDS. Babiskin, J.; Siebenmann, P. G.; Otto, G.; Saur, E. pp IV.38-45 of Conference on the Physics of Type II Superconductivity. Vol. II. Cleveland, Western Reserve University [1965].

Critical currents were measured for new types of high field superconductors using a base of Nb_3Sn or V_3Ga up to a maximum field of 150 k Oe. These experiments were performed at 4.2°K by fixing the magnetic field at predetermined values and then increasing the current continuously until superconductivity was destroyed. (B.G.D.)

21923 EFFECTS OF HELIUM TEMPERATURE STRAIN ON THE SUPERCONDUCTING TRANSITION OF Pb–In ALLOYS. Schenck, J. F.; Willis, J. S.; Shaw, R. W. (Rensselaer Polytechnic Inst., Troy, N. Y.). pp IV.46-52 of Conference on the Physics of Type II Superconductivity. Vol. II. Cleveland, Western Reserve University [1965].

Experiments were performed on plastically deformed Pb–In alloy wires under tension at helium temperatures.

The resistive transition was measured in both longitudinal and transverse magnetic fields for various amounts of deformation. Results of these experiments indicate that in transverse fields the resistance minimum in niobium and transition metal alloys is induced and intensified by deformation and that the current carrying capability of the sample above H_{c2} is increased by deformation. (B.G.D.)

21924 EXPERIENCE WITH SUPERCONDUCTING COILS FED BY FLUX PUMPS. van Beelen, H.; Arnold, A. J. P. T.; Sypkens, H. A.; van Braam Houckgeest, J. P.; Beenakker, J. J. M.; de Bruyn Ouboter, R.; Taconis, K. W. (Kamerlingh Onnes Lab., Leiden). pp IV.53-64 of Conference on the Physics of Type II Superconductivity. Vol. II. Cleveland, Western Reserve University [1965].

The principle of the flux pump for high magnetic fields in superconducting coils is presented. To fulfill the requirement of reasonable pumping time to attain high magnetic fields, two types of flux pumps, a translating and a rotating type, were developed. In special cases, with high inductance coils, pumping speeds were increased by pumping over a stack of foils which were connected in series. The pumping speed increased proportional to the number of sheets used. Experiments were performed on superconducting coils using foil solenoids and many strand cable. (B.G.D.)

21925 THE NON-IDEAL SUPERCONDUCTING BEHAVIOR OF TIN ALLOYS. Joiner, W. C. H. (Westinghouse Electric Corp., Baltimore). pp IV.75-97 of Conference on the Physics of Type II Superconductivity. Vol. II. Cleveland, Western Reserve University [1965].

A discussion of nonideal properties of inhomogeneous superconductors is presented. These properties include rounding of the magnetization curve near the lower critical field H_{c2} delayed penetration to fields above H_{c1}, irregularities in the magnetization curve such as flux jumping, hysteresis, and trapped flux. A preliminary report on an investigation of nonideal properties in type I and type II superconducting tin alloys is also presented. (B.G.D.)

21926 FLUX TRAPPING THRESHOLD IN Nb_3Sn. Hecht, Richard (RCA Labs., Princeton, N. J.). pp IV.98-105 of Conference on the Physics of Type II Superconductivity. Vol. II. Cleveland, Western Reserve University [1965].

In high current materials such as Nb_3Sn a drop in magnetization is completely suppressed by metastable screening currents, or in an equivalent description, by pinning of Abrikosov vortices, therefore the lower critical field H_{c1} of type II superconductor cannot be easily identifiable. However, the corollary ability of high-current materials to trap flux can be used to identify H_{c1}, which being the threshold field for flux penetration, should also be the threshold field for flux trapping. An investigation of the flux trapping threshold in Nb_3Sn is discussed. (B.G.D.)

21927 ANNIHILATION INSTABILITY IN HARD SUPERCONDUCTORS. Beasley, M. R.; Fietz, W. A.; Rollins, R. W.; Silcox, J.; Webb, W. W. (Cornell Univ., Ithaca, N. Y.). pp IV.106-20 of Conference on the Physics of Type II Superconductivity. Vol. II. Cleveland, Western Reserve University [1965].

A mechanism that leads to particularly virulent instabilities that occur in low magnetic fields is described. A discussion of the characteristics of the mechanism, the region of occurrence of the instability, and observations of the phenomena in the archetypal hard superconductor, cold worked niobium-25% zirconium alloy, is presented. (B.G.D.)

21928 MAGNETIZATION OF "NONIDEAL" TYPE II SUPERCONDUCTORS. Blaugher, R. D. (Westinghouse Electric Corp., Baltimore). pp IV.121-9 of Conference on the Physics of Type II Superconductivity. Vol. II. Cleveland, Western Reserve University [1965].

A report on magnetization and resistivity measurements of bulk body centered cubic Ti–V alloys across the entire composition range is presented. Nonideal behavior as indicated by a nonreversible magnetization and a large frozen-in moment was observed for each alloy. (B.G.D.)

21929 NOTES ON THE PHENOMENOLOGICAL THEORY OF TYPE II SUPERCONDUCTORS. Marcus, Paul M. (IBM Watson Research Center, New York). pp 1-30 of Conference on the Physics of Type II Superconductivity. Vol. III. Cleveland, Western Reserve University [1965].

A discussion is presented on the magnetic behavior of the ideal type II superconductor, defined as one which satisfies the Ginzburg–Landau (GL) equations. Results of a systematic study of the exact solutions of these equations in various simple geometries are discussed. Topics included are free energy and the GL equations, application of the GL equations to slabs in tangential fields, circular cylinders in axial fields, various properties of the mixed state in bulk cylinders, surface states, and generalization and phenomenological extension of the GL theory. (B.G.D.)

21930 RECENT DEVELOPMENTS IN THE MICROSCOPIC THEORY OF TYPE II SUPERCONDUCTIVITY. Werthamer, N. R. (Bell Telephone Labs., Murray Hill, N. J.). pp 31-55 of Conference on the Physics of Type II Superconductivity. Vol. III. Cleveland, Western Reserve University [1965].

An attempt is made to relate microscopic theory to the phenomenological theory when the order parameter is a function of position using the formalism of the Gorkov Green's function equations. The underlying assumptions of the equations are listed. Topics discussed are analysis at or below the upper and lower critical fields, slope of the magnetization near to and at H_{c2}, and motion of the vortices in the presence of a transport current and associated resistance. (B.G.D.)

21931 THE BULK PROPERTIES OF PERFECT TYPE II SUPERCONDUCTORS. Goodman, B. B. (CNRS, Grenoble, France). pp 56-66 of Conference on the Physics of Type II Superconductivity. Vol. III. Cleveland, Western Reserve University [1965].

A short summary is presented on recent work in the field of bulk properties of perfect type II superconductors. Topics included are occurrence of type II superconductors, thermodynamic relations, comparison between theory and macroscopic properties, structure of the mixed state, and dynamic effects. (B.G.D.)

21932 MAGNETIC HYSTERESIS AND CRITICAL CURRENTS IN THE MIXED STATE. Livingston, J. D. (General Electric Research Lab., Schenectady, N. Y.). pp 83-104 of Conference on the Physics of Type II Superconductivity. Vol. III. Cleveland, Western Reserve University [1965].

Specimen inhomogeneities can interact strongly with the internal magnetic structure (specifically, with the flux threads) of a type II superconductor in the mixed state. Flux pinning produces nonequilibrium behavior, which can be described with the phenomenological "critical state" model developed by Bean. The major departure of some real materials from this model is caused by the phenomenon of flux jumping, which is caused by a local thermal instability. A brief review of the irreversible properties of type II superconductors is presented. (B.G.D.)

Neutron Physics

See also REACTOR TECHNOLOGY — Criticality Studies

Refer also to abstract 21035.

21933 (AD-621119) THERMAL NEUTRON SPECTRUM IN A FINITE MASS MEDIUM [Thesis]. Sims, Ernest Park (Air Force Inst. of Tech., Wright-Patterson AFB, Ohio. School of Engineering). Aug. 1965. 132p. (GNE-Phys-65-18). CFSTI $4.00 cy, $1.00 mn.

The distribution of neutrons at thermal energies in a monatomic Maxwellian gas is determined. Spectra are found in various mass media and for varying amounts of absorption by numerically solving Corngold's higher-order gas equation; a result that is new. From the spectra ob-

tained the average neutron velocity is found and the thermal diffusion length squared is calculated. Using this method and a neutron age from a moments method calculation, the migration area in selected real nuclides is determined. The deviations from Maxwellian of the thermal neutron spectra are used to determine the energy at which a neutron becomes thermal. This effective thermal transition energy, E*, is found for media of various mass with varying amounts of absorption. The neutron thermal spectrum is found to be generally non-Maxwellian for values of the absorption parameter greater than 0.01. (TAB)

21934 (AD–621473) CALCULATION OF THE ENERGY-ANGULAR RELATIONSHIP FOR NEUTRONS FROM A NEUTRON GENERATOR. Huddleston, Charles M.; Shoemaker, Nathan F. (Naval Civil Engineering Lab., Port Hueneme, Calif.). Sept. 2, 1965. 13p. (TN-N–763). CFSTI $1.00 cy, $0.50 mn.

A relativistic calculation is made to determine the energy of neutrons emitted from the NCEL neutron generator as a function of the angle of emission. Both the tritium reaction, T (d,n) ^{4}He, with a neutron energy of approximately 14 Mev, and the deuterium reaction, D (d,n) ^{3}He, with a neutron energy of approximately 2.5 Mev, are considered. Values of neutron energy as a function of angle are tabulated and plotted. (auth)

21935 (AD–624041) TIME-DEPENDENT NEUTRON TRANSPORT FROM A POINT ISOTROPIC SOURCE AT AN ALTITUDE OF 100,000 FEET. Ausman, George A. Jr.; Wimenitz, Francis N. (Harry Diamond Labs., Washington, D. C.). Sept. 10, 1965. 309p. (TR–1305). CFSTI $7.00 cy, $1.50 mn.

Results of a Monte Carlo calculation of the neutron fluence and flux density in the vicinity of a point isotropic source at an altitude of 100,000 ft (30.48 km) are presented. The fluence and flux density were obtained at 20 detector locations as functions of time and energy for 12 monoenergetic neutron sources. The variation of atmospheric density with altitude is considered in these calculations. A brief discussion of the dependence of the results on detector location is given. (auth)

21936 (AE–216) MEASUREMENT OF THE TIME DEPENDENCE OF NEUTRON SLOWING-DOWN AND THERMALIZATION IN HEAVY WATER. Moeller, E. (Aktiebolaget Atomenergi, Stockholm (Sweden)). Mar. 1966. 34p. Dep. mn.

The behavior of neutrons during their slowing down and thermalization in heavy water was followed on the time scale by measurements of the time-dependent rate of reaction between the flux and the three spectrum indicators indium, cadmium, and gadolinium. The space dependence of the reaction rate curves was also studied. The time-dependent density at 1.46 ev is well reproduced by a function, given by von Dardel, and a time for the maximum density of 7.1 ± 0.3 μs was obtained for this energy in deuterium gas in agreement with the theoretical value of 7.2 μs. The spatial variation of this time is in accord with the calculations by Claesson. The slowing-down time to 0.2 ev was found to be 16.3 ± 2.4 μs. The approach to the equilibrium spectrum takes place with a time constant of 33 ± 4 μs, and the equilibrium was established after about 200 μs. Comparison of the measured curves for cadmium and gadolinium with multigroup calculations of the time-dependent flux and reaction rate show the superiority of the scattering models for heavy water of Butler and of Brown and St. John over the mass 2 gas model. The experiment was supplemented with Monte Carlo calculations of the slowing-down time. (auth)

21937 (AEET–210) S4B PROGRAM FOR SOLVING MULTI-GROUP TRANSPORT EQUATIONS WITH CARLSON'S S_4 APPROXIMATION. Bhide, M. G. (Atomic Energy Establishment, Trombay (India)). 1965. 28p. Dep. mn.

S4B program can solve multi-group Boltzmann equations in Carlson's S4 approximation and it is a modified version of SNG code written for IBM-704 at Los Alamos by Carlson. It has additional options and special mathematical routines to accelerate its convergence making it 3 times faster than diffusion theory codes like RE-101 of ANL, U.S.A. It can handle critical and noncritical systems (with or without multiplication of neutrons by fission process) in infinite plane slab, infinite cylinder and sphere geometries. Finite slabs and cylinders can also be considered by correcting transport cross sections with transverse bucklings varying with different regions and different energy groups. The second version (S4B II) has more options like reflective boundary condition on the outside (useful for making reactor lattice calculations, etc.), and unsymmetric plane slab geometry. This code will help to derive many reactor parameters (e.g., lattice calculations) on a theoretical basis rather than on empirical basis which is a common practice at present. (auth)

21938 (BNWL–193, pp 16-20) CORRESPONDENCE BETWEEN CALCULATED AND MEASURED THERMAL UTILIZATIONS. (Battelle-Northwest, Richland, Wash. Pacific Northwest Lab.).

An expression is derived that relates the calculated and measured thermal utilization factors. A brief discussion of this relation is presented. (M.O.W.)

21939 (GA–6930) INTEGRAL NEUTRON THERMALIZATION. Quarterly Progress Report for the Period Ending December 31, 1965. Beyster, J. R.; Carriveau, G.; Crosbie, K. (and others) (General Atomic, San Diego, Calif. John Jay Hopkins Lab. for Pure and Applied Science). Jan. 24, 1966. Contract AT(04-3)-167. 132p. Dep. mn. CFSTI $4.00 cy, $1.00 mn.

During this reporting period, studies were made of the sensitivity of reactor calculations to the variations in the thermal neutron spectra. The subject is strongly related to this integral neutron thermalization program due to the sensitivity of the thermal neutron spectra to the scattering model used for the moderator. The universal scattering law code GASKET has received only minor changes during this quarter. This code is designed to calculate $S(\alpha,\beta)$ for a variety of moderators. To aid in the intercomparison of thermal reactor design methods, further effort was expended into compiling spectral data into the General Atomic spectrum book and to the conversion of these data to the format of the more general EACRP compilation. Considerable effort has been expended to obtain a force model for beryllium oxide which could be used to calculate a scattering law for that moderator. To support this theoretical work, some fresh spectral measurements in BeO were made at different poison concentrations than in previous studies. During this quarter new angular scattering studies were performed on H_2O, D_2O, and $ZrH_{1.87}$. In general, these studies were made to pin down certain anomalies in the multiple scattering correction procedure. In addition, it was demonstrated that the angular scattering detection equipment is capable of measuring diffraction patterns with improved resolution over existing measurements. An attempt was made to set up a data reduction procedure for use in the angular scattering studies. Finally a preliminary comparison of the measured and calculated leakage spectra from a fast ^{235}U metal ball reactor was obtained. Much work remains to be done before the comparison is finalized, and extended below 1.5-Mev neutron energy. Also included as three appendices are related studies with report numbers GA-6847, 6861, and 6901. (M.O.W.)

21940 (GAMD–6908) PSEUDO—A CODE FOR THE CONSTRUCTION OF STATISTICAL RESONANCES IN THE UNRESOLVED RESONANCE REGION. Dyos, M. W. (General Atomic, San Diego, Calif. John Jay Hopkins Lab. for Pure and Applied Science). Jan. 18, 1966. Contract AT (04-3)-167. 6p. Dep. mn. CFSTI $1.00 cy, $0.50 mn.

The PSEUDO code was written to sample randomly from the distribution functions for the statistical distribution of neutron widths and level spacings. The code has the flexibility to give some statistical information on the nature of the ladder (or ladders) of resonances generated. The code is written in FORTRAN IV. (M.O.W.)

21941 (IAE–977) IZUCHENIE NESTATSIONARNYKH SPEKTROV NEITRONOV V GIDRIDE TSIRKONIYA. (Study

of Transient Neutron Spectra in Zirconium Hydride). Ishmaev, S. N.; Mostovoi, V. I.; Nozik, V. Z.; Sadikov, I. P.; Chernyshov, A. A.; Yudkevich, M. S. (Institut Atomnoi Energii, Gosudarstvennyi Komitet po Ispol'zovaniyu Atomnoi Energii SSSR, Moscow). 1965. 16p. Dep. mn.

The results of the experimental and theoretical study of the transient thermal neutron processes in zirconium hydride $ZrH_{1.88}$ were reported. The time dependent neutron spectra were measured in $ZrH_{1.88}$ prisms with resolutions of 3.5 μsec according to the delay time. In the time delay range studied (T > 30 μsec) the mean energy of the neutrons had a lower energy of the first optical level of the zirconium hydride (0.13 ev) and there was energy exchange between the neutron gases and the medium caused by the excitation of the acoustical oscillation of the $ZrH_{1.88}$ lattice. The time necessary for the establishment of the equilibrium spectra in the "big" system ($B^2 = 3.8 \times 10^{-2}$ cm^{-2}) appeared to be of the order of 400 μsec. In the $ZrH_{1.88}$ system of "small" dimensions (B^2 = 0.2 cm^{-2}) a strong effect of the diffusing of the spectrum was observed and the time necessary for the establishment of the equilibrium energy distribution increased with decreased dimensions of the system. The results of the calculation of the non-stationary neutron spectrum in the P-1 approximation were reported. The two fold differential cross sections of $ZrH_{1.88}$ necessary for these calculations were obtained by use of the spectrum of the normal oscillations of hydrogen atoms in the Zr lattice. The best agreement of measured neutron spectrum with the calculations was obtained if it was assumed that the amplitude of the acoustical and optical oscillations in $ZrH_{1.88}$ had the ratio 1/360. (tr-auth)

21942 (KFK-tr-188) EXPERIMENTELLE UNTERSUCHUNG DES ZEITVERLAUFS DER NEUTRONENTHERMALISIERUNG IN GRAPHIT UND BERYLLIUM. (Experimental Study of the Neutron Thermalization Process in Time in Graphite and Beryllium). Mostovoi, V. I.; Sadikov, I. P.; Chernyshov, A. A.; Ishmaev, S. N.; Yudkevich, M. S.; Nozik, V. Z. (Institut Atomnoi Energii, Gosudarstvennyi Komitet po Ispol'zovaniyu Atomnoi Energii SSSR, Moscow). Translated into German by Liselotte Neander (Kernforschungszentrum, Karlsruhe, West Ger.), from report IAE-850. 1965. 25p. Dep. mn. JCL $2.60 fs, $0.95 mf.

Also appeared in NSA from STI/PUB-104(Vol.1), pp 623-41.

A research installation for the study of standardization of the equilibrium energy spectrum of neutrons in various medium was described. With a high flux electron linear accelerator short pulses of fast neutrons were produced in the moderators investigated. The neutron spectra in the beam emitted by the moderator were measured at various times after the fast neutron pulse with a mechanical chopper working in synchronous operation with the accelerator. The best resolution in the spectral measurement is 2.5 μsec/m and the minimum uncertainty in the slowing-down time is 3.5 μsec. The measurement results of the nonstationary spectra in graphite ($B^2 = 8.9 \times 10^{-3}$ cm^{-2}) and in beryllium ($B^2 = 9.7 \times 10^{-3}$, 24×10^{-3}, and 43×10^{-3} cm^{-2}) was given for slowing down times from 30 μsec up to 2500 μsec. The measurement results in beryllium were compared with calculated nonstationary spectra obtained from double differential cross sections after these had been calculated from the experimental values for the energy spectrum of the lattice oscillations of beryllium. The chemical compound and the thermal motion of the atoms of the moderator exert even at times of approximately 30 μsec a remarkable effect on the velocity of the approach of the neutron spectrum to the equilibrium spectrum. This corresponds to a mean spectrum energy of approximately 1 ev for graphite and approximately 0.2 ev for beryllium. The total time necessary for the attainment of the equilibrium spectrum of the neutrons is approximately 2000 μsec in graphite and approximately 1000 μsec in beryllium. The formation of neutron spectra in small beryllium blocks was determined to a great degree by the coherent scattering which leads to the formation of the so called neutron drop, which delays the process of the attainment of the equilibrium spectra. (tr-auth)

21943 INELASTIC SCATTERING OF SLOW NEUTRONS BY POLYETHYLENE. Ivanitskii, P. G.; Krotenko, V. T. At. Energ. (USSR), 20: 30-5(Jan. 1966). (In Russian).

The inelastic scattering of slow neutrons by polyethylene was investigated on one of the horizontal channels of the VVR-M reactor of the Institute of Physics of the Academy of Sciences of the USSR using the time-of-flight method. The energy spectra of the neutrons, scattered on the polyethylene at angles of 15, 30, 90, 120°, were investigated for incident neutron energies of 15.4, 25.5, 49.4, 98.8, 136.1, 193.2, and 317 Mev. The differential scattering cross section of neutrons on polyethylene was determined, the scattering law S (α,β) was found, and the frequency spectrum P(β) was generalized for polyethylene. The neutralized characteristics for the scattering of neutrons on polyethylene (mean energy break and logarithmic loss) were calculated. (tr-auth)

21944 AN EXTENSION OF THE DIFFUSION COEFFICIENT BY HIGHER TERMS DERIVED FROM NEUTRON TRANSPORT THEORY. Kuttner, P. Atomkernenergie, 11: 97-105(Mar.-Apr. 1966). (In German).

A term for the diffusion coefficient can be derived from the neutron transport theory. This term is independent of geometry. To determine the diffusion coefficient the neutron flux in plane geometry is expanded here in spherical harmonics up to terms of fifth order. (auth)

21945 ON A METHOD TO STUDY STATIONARY NEUTRON TRANSPORT PROBLEMS IN TWO-DIMENSIONAL LAMINATED MATERIAL ARRANGEMENT. Mueller, A. (Institut fuer Reaktorphysik der GKSS, Geesthacht, Ger.). Atomkernenergie, 11: 106-8(Mar.-Apr. 1966). (In German).

A method for the analytical solution of the one-dimensional stationary neutron transport equation with piecewise position-independent material constants is given. This method basing on the theory of distributions and generalized Fourier transformation, shows mathematical simplicity and leads directly to formulas which seem to be valuable for computational purposes. (auth)

21946 FAST NEUTRON FLUX PATTERN FOR A 14-Mev NEUTRON GENERATOR. Kenna, B. T.; Conrad, F. J. (Sandia Corp., Albuquerque, N. Mex.). Health Phys., 12: 564-6(Apr. 1966).

Radiographic and counting methods were employed to obtain results concerning the uniformity of the fast neutron flux of the Kaman Nuclear A-1000 accelerator as a function of distance from the neutron-generator target, both parallel to the target and in a horizontal circle around the target with the target as the center. Results indicated that the fast neutron flux is uniform from side to side and from top to bottom of the target in the area where samples were irradiated. When copper foils were placed parallel to the target at 1.25 cm distance, the flux from one side of the target to the other varied as much as 30%. However at 47 cm distance, the difference was 1%. In the study using copper foils around the target, the isotropic nature of the source was found to be marred by a low flux area in the 90° region. This phenomenon was attributed to absorption and scattering of neutrons by the target. (H.G.D.)

21947 GENERALIZED INVARIANT IMBEDDING OF TRANSPORT THEORY. Devooght, J. (Univ., Brussels). J. Math. Anal. Appl., 13: 216-44(Feb. 1966).

A generalized invariant imbedding of the Boltzmann transport equation is presented starting from an identity. The argument is analytical and does not depend on any ad hoc postulate of invariance. Different kinds of imbedding can be used, such as geometrical imbedding and albedo imbedding. Classical invariant imbedding equations are generalized to arbitrary geometry, with no restriction to stratifiable media or to reflection and transmission functions, and anisotropic scattering. (J.F.P.)

21948 TRITIUM GAS TARGET FOR T(d,n)^{4}He REACTION. Nishi, Masato; Takiyama, Masashi; Ryu, Norio (Hiroshima Univ.). Jap. J. Appl. Phys., 5: 215-17(Mar. 1966).

A tritium gas target filled up to 6.5 atmospheres which

was used for the production of neutrons by the $T(d,n)^4He$ reaction is reported. Tritium gas is supplied from a uraniumtriteride (UT_3) oven. Discussions are given of gas handling procedure and temperature dependence of decomposition pressure. This target tolerates a 1 μamp beam of 18 Mev deuterons from I.N.S. (Tokyo) 160-cm cyclotron without foil damage and gas leakage for several days. (auth)

21949 PRODUCTION OF MONOCHROMATIC COLD NEUTRON BEAM WITH THE USE OF MONOCRYSTALS. Gordon, Janos. Magyar Tud. Akad. Kozp. Fiz. Kut. Int. Kozlem., 14: 25-8(1966). (In Hungarian).

Intensity and wavelength resolution measurements of a monochromatic neutron beam reflected from magnetite, germanium monocrystals, and mica sheets are reported. Monocrystalline magnetite proved to be particularly useful for the production of a cold neutron beam with wavelength resolution $\delta\lambda/\lambda \sim 2\%$. (auth)

21950 A METHOD FOR CALCULATING THE FLUX EVOLUTION IN A FAST-NEUTRON MULTIPLYING MEDIUM AS A FUNCTION OF TIME, SPACE, AND ENERGY. Storrer, F.; Govaerts, P.; Hammer, P.; Elbersoldt, F. Nucl. Sci. Eng., 24: 344-8(1966).

A unified formalism is presented, which is applicable to a wide class of problems related to fast-neutron multiplying systems. Such problems are the search for asymptotic and transient space-energy modes in fast reactors and exponential or wave experiments and the analysis of pulsed or modulated bare systems. This formulation is based on the use of a Laplace transformation with respect to time and of a Fourier transformation with respect to space. It is greatly simplified, if it is assumed that the fission spectrum is independent of the energy of the incident neutron and of the nuclide that underwent fission. This assumption, which does not affect the results appreciably, makes it possible to describe the whole neutronic process in terms of a single scalar variable, the fission neutron source, (instead of the energy-dependent flux) without any loss of information. Futhermore, the solution can be found by convolutions over the neutronic processes between successive generations of fissions, which involve only simple slowing-down kernels. (auth)

21951 A RIGOROUS EXPRESSION FOR SHAPE OF A DOPPLER-BROADENED RESONANCE. Ishiguro, Yukio. Nucl. Sci. Eng., 24: 375-80(1966).

A rigorous expression is derived for the shape of a Doppler-broadened absorption cross section. When $\Gamma(E)$ is assumed to be constant, the expression, which is rigorous for a Maxwellian gas of resonance-absorber atoms, is written as the difference for the two ψ-functions. The results obtained by the present method are compared with those of the ψ-function approximation, which is in general use, and the accuracy of the latter approximation is discussed. Comparisons are also made of the low-lying resonances of ^{235}U, ^{239}Pu, ^{167}Er, and ^{155}Gd by numerical computations. For the low-lying resonances, it is shown that the Doppler-broadened absorption cross section is easily computed by the well-known asymptotic expansion of the ψ-function. (auth)

21952 SCATTERING OF NEUTRONS BY POLYETHYLENE. Whittemore, W. L. Nucl. Sci. Eng., 24: 394-409 (1966). (GA-6456).

A neutron velocity selector was used in conjunction with an electron linac to produce monoenergetic neutrons in the range 0.167 to 0.499 ev. The scattering of neutrons at various angles between 30 and 150° by a thin specimen of crystalline polyethylene was measured, and precise scattering cross sections $\sigma(E_0, E, \theta)$ were determined. The experimental results are compared in detail with the theoretical work of Goldman, Parks, Koppel and Young, and McMurry. The detailed comparisons indicate that a more-or-less continuous realistic frequency distribution, or an appropriate collection of isolated oscillator levels, can be used as the basis of computing a reasonably satisfactory scattering cross section for polyethylene. It appears that the models of Goldman, Parks, and Koppel and Young all overemphasize energy transfers at ≈0.089 ev, and tend to underemphasize the largest transfers at ≈0.35 ev. The extrapolation technique of Egelstaff applied to the scattering law gives a frequency distribution that is similar in broad outline to that used by Parks. However, small significance can be attributed to this agreement because of the probable and large contributions of the multiphonon terms. (auth)

21953 ON THE MAXIMUM ABSORPTION THEOREM. Corngold, Noel (Brookhaven National Lab., Upton, N. Y.). Nucl. Sci. Eng., 24: 410-12(1966). (BNL-9457).

A proof of the maximum absorption theorem is given for the case in which $\Sigma_{min}(\equiv\Sigma^+)$ is independent of the concentration of absorber and the absorption behaves as $1/\nu$ when ν is large. The proof is also valid when the absorption behaves as $1/\nu^2$. (L.B.S.)

21954 NEUTRON FLUCTUATIONS IN A MULTIPLYING MEDIUM. Otsuka, Masuhiko; Saito, Keiichi (Japan Atomic Energy Research Inst., Tokyo). Nucl. Sci. Eng., 24: 412-14(1966).

The connections between the various approaches to the theory of neutron fluctuations in a multiplying medium are investigated. The Pál-Bell equation is first solved and the result is shown to be exactly the same as that obtained through the other approaches. (L.B.S.)

21955 VARIATION OF THE TRANSPORT MEAN FREE PATH IN GRAPHITE WITH TEMPERATURE. De Juren, J. A. (Atomics International, Canoga Park, Calif.). Nucl. Sci. Eng., 24: 417-18(1966).

A beam transmission measurement of the neutron scattering cross section for graphite was performed in order to separate the variation of the transport mean free path caused by the temperature of the spectrum from the effect caused by the thermal vibrations of the scattering atoms. The temperature of a 2-cm-thick disk of graphite and the exit temperature of a neutron beam from a thermal column were varied independently. It is concluded that, within experimental error, the variation of the transport mean free path may be ascribed entirely to the temperature change of the moderator atoms and is independent of spectrum temperature. (L.B.S.)

21956 NOTE ON THE USE OF GENERALIZED FUNCTIONS AND THE POINCARE-BERTRAND FORMULA IN NEUTRON TRANSPORT THEORY. Kaper, H. G. (Groningen Univ., Netherlands). Nucl. Sci. Eng., 24: 423-5(1966).

An attempt is made to demonstrate that the angular Green's functions do not require any prescription that is in conflict with the usual Cauchy principle value integration procedure, as was previously stated, nor does the Poincafe-Bertrand formula admit any ambiguity in its interpretation. The proper use of the concept of a generalized function and of a direct product of two generalized functions is stressed. (L.B.S.)

21957 A NUMERICAL STUDY OF THE METHOD OF WEIGHTED RESIDUALS. Pomraning, G. C. Nucl. Sci. Eng., 24: 291-301(Mar. 1966).

The variational method and region-balance method, both special cases of the more general method of weighted residuals, are each used as the formalism to develop a spatial expansion of the diffusion equation for two problems. These are (1) a spatially dependent spectrum problem for the purpose of computing the self-shielding in the ^{240}Pu resonance and (2) a simple one-dimensional eigenvalue problem. In both instances numerical results indicate that the variational method is more accurate than the region-balance method. Of particular interest is the variational spatial-expansion approach to the eigenvalue problem. This may be a useful method for deriving a set of difference equations for the multigroup diffusion equation in that it should lead to an accurate representation of the flux with a relatively small number of mesh points. (auth)

21958 PROPERTIES OF THE P_L AND DOUBLE-P_L RELAXATION LENGTHS IN THE PRESENCE OF ANISOTROPIC SCATTERING. Gelbard, E. M. (Westinghouse Electric Corp., West Mifflin, Penna.). Nucl. Sci. Eng., 24: 306-7(Mar. 1966).

It is shown that the assumptions usually made in solving the P_L equations that the decay constants K_{il} are all real and distinct and that they occur in positive and negative pairs are valid so long as the differential scattering cross section $\Sigma_5(\mu_0)$ is finite and positive for all μ_0. Other properties of the decay constants are also discussed. (L.B.S.)

21959 TIME-DEPENDENT GREEN'S FUNCTION. Papmehl, Nikolai (EURATOM, Ispra, Italy). Nucl. Sci. Eng., 24: 307-8(Mar. 1966).

The one-velocity neutron transport equation is solved to obtain the time-dependent Green's function for an isotropic plane source. The Green's function is then used to find an asymptotic expression for the neutron flux at a time far enough from the initial pulse at t = 0. (L.B.S.)

Nuclear Properties and Reactions

Refer also to abstracts 20653, 20995, 21063, 21219, 21462, 21531, 21593, 21601, 21695, 21957, 22383, and 22384.

21960 (AD-621023) PREDICTION OF THE TIME-DEPENDENT BETA SPECTRUM FROM A NUCLEAR WEAPON DETONATION [Thesis]. Dieckhoner, James E. (Air Force Inst. of Tech., Wright-Patterson AFB, Ohio. School of Engineering). Aug. 1965. 187p. (GNE-Phys-65-3). CFSTI $5.00 cy, $1.00 mn.

A method is developed by which the time dependent beta spectrum from four different types of nuclear and thermonuclear fission can be predicted. From the mass chain yield and the Equal Charge Displacement theory, the initial isotopic concentrations are predicted. The time dependent relations within each mass chain are solved exactly. The shape of the beta decay spectra for each isotope is predicted by use of the Fermi theory. An estimation technique is used to predict the spectra from isotopes with unknown decay schemes. Attempts are made to predict the percent of the total available decay energy which is accounted for by beta decay, for those isotopes with unknown decay schemes. These procedures are combined in a set of computer programs written for the IBM 7044. The spectra predicted using the programs are compared with West's experimental results and agree within a factor of 1.4. (auth)

21961 (AD-624028) PHENOMENOLOGICAL AND MICROSCOPIC ANALYSIS OF PROPERTIES OF EVEN-EVEN NUCLEI. PART B. COLLECTIVE BEHAVIOUR FROM PARTICLE DYNAMICS. Interim Report, March 15, 1965-March 15, 1966. Bosch, Horacio E.; Abecasis, S. M.; Heras, C. A. (Instituto de Investigacione Aeronautica y Espacial, Buenos Aires (Argentina)). Contract DA-ARO-49-092-65-G78. 77p. CFSTI $3.00 cy, $0.75 mn.

A widening of the applicability of phenomenological models is accompanied by an increase in the number of parameters needed. More fundamental models are then required in order to explain the growing wealth of experimental data. Such models might be classified as semi-phenomenological to distinguish them from more rigorous ones. In addition some attempts to obtain collective coordinates from the particle ones will be briefly described. The aim of these attempts is to provide a foundation both to phenomenological and semiphenomenological models. The large quadrupole moments observed in nuclei with many nucleons outside closed shells have long been associated with nonspherical mass distributions. Since the common field in which the nucleons move in an independent particle model is built self-consistently from a short-range nucleon-nucleon interaction, a non-spherical mass distribution would imply a non-spherical single-particle potential. In actual calculations a common potential of prescribed form is used, generally a harmonic oscillator one. (TAB)

21962 (AD-624214) SHELL MODEL CALCULATION OF THE ODD TIN ISOTOPES. Baranger, Michel; Kuo, T. T. S.; Baranger, E. U. (Carnegie Inst. of Tech., Pittsburgh, Pa.). Sept. 1965. Contract Nonr-760(15). 76p. CFSTI $3.00 cy, $0.75 mn.

A shell-model hamiltonian with a residual two-nucleon interaction of Gaussian form is used to calculate the states of the odd tin isotopes. The Bogoliubov-Valatin quasi-particle transformation is made and the residual interaction is diagonalized in a one- and threequasi-particle space. The spurious states must be projected out. Various approximations to this procedure, such as perturbation theory and a phonon approximation, are studied. Perturbation theory is adequate for low states. The phonon approximation is correct qualitatively, but not quantitatively. The parameters of the residual interaction and the single-particle energies are determined by requiring good agreement with the experimental energies. Magnetic moments, electromagnetic transition rates, and spectroscopic factors are calculated and agree well with the experimental values. (auth)

21963 (AD-626656) ELASTIC SCATTERING OF 45-Mev PROTONS. Willmes, Henry (California Univ., Los Angeles. Dept. of Physics). Oct. 1965. Contract Nonr-233(44). 70p. CFSTI $3.00 cy, $0.75 mn.

Measurements of the differential elastic scattering cross section were carried out using the "negative ion" beam of the UCLA cyclotron, as part of a program of optical model studies. The methods of data taking and of the reduction of the raw data are discussed in detail. Brief outlines of the history of the optical model of its mathematics formulation are included. Results of the cross section measurements are given for beryllium-9, carbon-12, nickel-58, and nickel-60 for a series of angles ranging from 15 to 150 degrees. (auth)

21964 (AD-626684) ^{32}S AND ^{31}P EXCITATION BY 180 DEG ELECTRON SCATTERING. Kossanyi-Demay, P.; Vanpraet, G. J. (Stanford Univ., Calif. High-Energy Physics Lab.). Dec. 1965. Contract Nonr-225(67). 23p. (HEPL-394). CFSTI $1.00 cy, $0.50 mn.

The differential cross sections were measured for inelastic scattering of 50-Mev electrons at 180 degrees by ^{31}P and ^{32}S nuclei. Using the long wave length approximation, lower limits for radiation widths were derived for the levels. For ^{32}S the giant dipole resonance was investigated, and the results are compared with a recent calculation of B. M. Spicer. (auth)

21965 (AD-626776) A FORTRAN PROGRAM FOR THE REDUCTION OF DIFFERENTIAL CROSS SECTION DATA. Willmes, Henry (California Univ., Los Angeles. Dept. of Physics). Nov. 1965. Contract Nonr-233(44). 26p. CFSTI $2.00 cy, $0.50 mn.

A computer program in FORTRAN IV language is given for the reduction of differential cross section data for proton-induced reactions of the type A(p,x)B. Given the raw data, the program determines the cross section in the laboratory and center-of-mass coordinate systems, with options of applying a number of corrections. For elastic proton scattering, the ratio of the center-of-mass to the Rutherford cross section can also be obtained. (auth)

21966 (AE-222) TOTAL CROSS-SECTIONS OF U, UO_2 AND ThO_2 FOR THERMAL AND SUBTHERMAL NEUTRONS. Beshai, Samir F. (Aktiebolaget Atomenergi, Stockholm (Sweden)). Mar. 1966. 14p. Dep. mn.

The total neutron cross-sections of U, UO_2, and ThO_2 were measured from 0.0045 to 0.028 ev, using the time-of-flight technique. The samples were measured at 20°C. ThO_2 was also measured at 750°C. The neutron source was the reactor R1, Stockholm. The experimental results, presented as graphs, show in detail the influence of Bragg scattering. The results further show that the increase of the temperature for the ThO_2 sample gives an increase in the cross section. The work also contains some calculations of the position in energy of Bragg edges for the three materials. These calculations show a very good agreement with the experiments. For uranium metal some calculations were carried out also for the height ($\sigma^{\pm}_{hkl}$) of the edges. The agreement with the experiments is reasonable. (auth)

21967 (AEET-234) REVIEW OF NUCLEAR DATA RELATED TO THORIUM FUEL CYCLE. Singh, R. Shankar (Atomic Energy Establishment, Trombay (India)). 1965. 10p. Dep. mn.

A knowledge of accurate and reliable nuclear data for the materials in any fuel cycle is essential in assessing its technical feasibility and economic potential. The nuclear parameters, in which a reactor physicist is usually interested, are discussed for the heavy elements associated with the thorium cycle, such as ^{232}Th, ^{233}U, ^{233}Pa, and ^{234}U and the fission products. The existing data for these materials and the gaps that have to be filled up are described. Temperature dependent effective group capture cross sections for thorium, which were evaluated with the available resonance parameters, are also tabulated. (auth)

21968 (AEET–235) EMISSION OF LONG RANGE ALPHA PARTICLES IN FISSION. Methasiri, T. (Atomic Energy Establishment, Trombay (India). Nuclear Physics Div.). 1965. 30p. Dep. mn.

A survey of experimental and theoretical work on the emission of long range alpha particles in fission was made. Conclusions from this survey are presented. (M.O.W.)

21969 (ANL–7055, pp 230-3) NUCLEAR CONSTANTS. Stupegia, D. C.; Tevebaugh, A. D. (Argonne National Lab., Ill.).

Research is reported on radiative capture in Pr and Re, capture-to-fission ratios in EBR-II, and neutron inelastic scattering. (J.R.D.)

21970 (ANL–7144) THE EFFECT OF INTERFERENCE INTERACTION BETWEEN THE RESONANCES OF ^{239}Pu AND ^{232}Th ON ^{239}Pu FISSION AND CAPTURE CROSS SECTIONS AND ^{232}Th CAPTURE CROSS SECTIONS. Singh, R. S. (Argonne National Lab., Ill.). Jan. 1966. Contract W-31-109-eng-38. 15p. Dep. mn. CFSTI $1.00 cy, $0.50 mn.

The effect of interference interaction between the resonances of ^{239}Pu and ^{232}Th on Doppler-effect calculations and sodium-void coefficients was investigated. The temperature-dependent effective cross sections for ^{239}Pu and ^{232}Th were evaluated, taking into account both types of interference interactions, namely, the overlap of neighboring resonances in one isotope and the interaction between resonances of the two isotopes. A simplified method developed by R. N. Hwang was used to calculate these cross sections over a range of σ_p, the potential-scattering cross section per absorber atom for the two isotopes. (auth)

21971 (BNL–948, pp 1-65) SINGLE NUCLEON TRANSFER REACTIONS. French, J. Bruce (Rochester Univ., N. Y.); Macfarlane, Malcolm (Argonne National Lab., Ill.); Morinaga, H. (Max-Planck-Institut [fuer Kernphysik], Heidelberg (West Germany)).

Single-nucleon-transfer reactions are discussed using the methods of energy-weighted multipole sum rules. Nucleon transfer on strongly deformed nuclei and isobaric-analog resonance experiments are also discussed. It is pointed out that for heavy nuclei the isospin selection rules have some very characteristic consequences. (G.O.Y.)

21972 (BNL–948, pp 66-174) TWO AND MORE NUCLEON TRANSFER REACTIONS. Bayman, Benjamin (Minnesota Univ., Minneapolis); Bromley, D. Allan (Yale Univ., New Haven, Conn.); Hintz, Norton M. (Minnesota Univ., Minneapolis); Cohen, Bernard (Pittsburgh Univ., Pa.).

Various multi-particle transfer reactions are discussed using the DWBA method. A particular type of nucleon-transfer reaction, that involving a correlated neutron-proton pair, is discussed in detail; and a review of experimental data on this reaction is given. 74 references. (G.O.Y.)

21973 (BNL–948, pp 175-221) INELASTIC SCATTERING. McManus, Hugh (Michigan State Univ., East Lansing); Hintz, Norton M. (Minnesota Univ., Minneapolis); Tobocman, William (Case Inst. of Tech., Cleveland, Ohio).

Inelastic scattering is discussed in terms of the effective interaction using the DWBA approximation. β_L values extracted from 40-Mev (p,p′) measurements are compared with values obtained from electron inelastic scattering, coulomb excitation, and direct lifetime measurements. The results of an analysis of the ^{58}Ni$(\alpha,\alpha')^{58}$*N reaction are also presented. (G.O.Y.)

21974 (BNL–948, pp 222-68) LIGHT SPHERICAL NUCLEI. Kurath, Dieter (Argonne National Lab., Ill.); Bayman, Benjamin (Minnesota Univ., Minneapolis).

The information that can be obtained by studying the basic configurations of light spherical nuclei is discussed, together with ways of taking into account deformation effects in calculations. (D.C.W.)

21975 (BNL–948, pp 269-336) HEAVY SPHERICAL NUCLEI. Cohen, Bernard (Pittsburgh Univ., Pa.); Gove, Harry E. (Rochester Univ., N. Y.).

Some applications of stripping reactions to studies of spherical heavy nuclei are discussed. The structure of ^{63}Cu is discussed in detail. (G.O.Y.)

21976 (BNL–948, pp 337-79) LIGHT STRONGLY DEFORMED NUCLEI. Gove, Harry E.; French, J. Bruce (Rochester Univ., N. Y.).

Some investigations of the structure of light strongly deformed nuclei are summarized. The experimental techniques are discussed in some detail. Some calculations for even nickel isotopes are also discussed; the calculations were made to assess the validity of various approximations that are made for vibrational nuclei and to examine the two-phonon states. (D.C.W.)

21977 (BNL–948, pp 380-453) HEAVY STRONGLY DEFORMED NUCLEI. Moszkowski, Steven (California Univ., Los Angeles); Goldhaber, G. Scharff- (Brookhaven National Lab., Upton, N. Y.); Morinaga, H. (Max-Planck-Institut [fuer Kernphysik], Heidelberg (West Germany)).

The energy levels of strongly deformed nuclei, particularly even-even nuclei, are discussed. An analysis of the moments of inertia of odd-odd nuclei is also summarized, and a method for obtaining high-spin rotational states or collective states is discussed. The results of some studies of rotational states by this method are presented. (D.C.W.)

21978 (BNL–948, pp 454-524) OPTICAL MODEL, DWBA. Schiffer, John P. (Argonne National Lab., Ill.).

The application of the distorted-wave Born approximation and the optical model to nuclear reactions and scattering is discussed. Some of the difficulties that are encountered in this approach are emphasized. (D.C.W.)

21979 (BNL–948, pp 525-60) STRONG COUPLING, EXCHANGE, TARGET EXCITATION AND OTHER CORRECTIONS TO DWBA. Austern, Norman (Pittsburgh Univ., Pa.); Moldauer, Peter (Argonne National Lab., Ill.); de-Shalit, Amos (Weizmann Inst. of Science, Rehovoth (Israel)).

The relation between strong coupling and DWB approximations and the possible improved deuteron-nucleon wave functions of the three-body type are discussed. The importance in stripping of the so-called target-excitation terms, as well as exchange effects, knock-on, and heavy particle stripping are also discussed. (G.O.Y.)

21980 (BNL–948, pp 561-609) DIFFRACTION MODEL CALCULATIONS. Henley, Ernest (Washington Univ., Seattle); Greider, Kenneth (Pittsburgh Univ., Pa.); de-Shalit, Amos (Weizmann Inst. of Science, Rehovoth (Israel)).

A survey of the diffraction approach to the treatment of nuclear reactions is presented. The development of the diffraction model in both configuration space and angular-momentum space is outlined. A rigorous derivation of the ring-locus is presented, and it is shown that cross sections fall off much more rapidly than those obtained from previous theories. The limitations and reliability of the diffraction model are discussed. (D.C.W.)

21981 (BNL–948, pp 610-84) MULTI-BODY EXIT CHANNELS. Zupancic, Crt (Bell Telephone Labs., [Murray Hill, N. J.]); Bromley, D. Allan (Yale Univ., New Haven, Conn.); Phillips, Gerald (William Marsh Rice Univ., Houston, Tex.); Henley, Ernest (Washington Univ., Seattle).

Reactions with multi-body exit channels are discussed with emphasis on three-body exit channels. Some calculations for the reaction d$(\alpha$,pn$)\alpha$ are outlined, together with

some experiments on three-body reactions. The reaction $d + {}^3He \rightarrow (pp) + {}^3H$ is also discussed. (D.C.W.)

21982 (BNL–948, pp 718-40) COMPUTERS IN EXPERIMENTAL PHYSICS. Spinrad, Robert J. (Brookhaven National Lab., Upton, N. Y.); Donovan, Paul (Bell Telephone Labs., [Murray Hill, N. J.]).

A system that was developed to control a number of neutron spectrometers at the Brookhaven Beam Research Reactor and to process the data obtained is described, together with the use of computers to conserve memory in experiments that involve many dimensions or channels and to stimulate data. A specific example of the latter application (Publication Amplification by Simulated Experimental Results) is outlined. (D.C.W.)

21983 (BNL–948, pp 741-50) SPIN ASSIGNMENTS BY PARTICLE-GAMMA CORRELATIONS FROM ALIGNED NUCLEI. Warburton, Ernest K. (Brookhaven National Lab., Upton, N. Y.).

A method of determining the spins of levels connected by gamma transitions, the most highly excited level of which was excited by a charged-particle reaction, is discussed. The theoretical bases of the method are outlined, and a study of the gamma decay of the 1.70-Mev level of ^{18}F is summarized. The method also yields gamma mixing ratios. (D.C.W.)

21984 (BNL–948, pp 751-6) SPIN ASSIGNMENTS BY GAMMA-GAMMA CORRELATIONS FROM ALIGNED NUCLEI. Gove, Harry E. (Rochester Univ., N. Y.).

A method of determining the spins of aligned excited states from measurements of gamma-gamma correlations in the subsequent decay of the states is discussed. Some observations on the 3.58- and 4.97-Mev levels of ^{26}Mg and ^{20}Ne, respectively, are summarized, and some of the limitations of the method are indicated. (D.C.W.)

21985 (BNL–948, pp 757-62) GAMMA-RAY MULTIPOLARITIES FROM INTERNAL PAIR CORRELATION MEASUREMENTS. Alburger, David E. (Brookhaven National Lab., Upton, N. Y.).

An intermediate-image magnetic pair spectrometer is briefly described together with a method of determining the multipolarities of gamma transitions from measurements of internal pair correlations. (D.C.W.)

21986 (BNL–948, pp 763-825) CAPTURE REACTIONS. Hanna, Stanley S. (Stanford Univ., Calif.).

Some investigations of nuclear structure by capture reactions are discussed with emphasis on studies in which proton capture was used. Both experimental and theoretical considerations are covered. (D.C.W.)

21987 (BNL–948, pp 826-75) REACTIONS WITH FLUCTUATING CROSS-SECTIONS. Moldauer, Peter (Argonne National Lab., Ill.).

The statistical description of fluctuating cross sections is discussed. Some statistical models of the reaction amplitude are considered as well as average cross sections, including giant and intermediate resonance cross sections, and cross-section fluctuations about the average. (D.C.W.)

21988 (BNL–948, pp 876-904) INTERMEDIATE STRUCTURE. Lemmer, Richard (Massachusetts Inst. of Tech., Cambridge).

Some experimental evidence for the existence of intermediate structure is summarized, and an interpretation of intermediate structure is outlined. Resonance reactions in regions in which the actual compound states of the nucleus do not overlap are emphasized. (D.C.W.)

21989 (BNL–948, pp 905-27) BOUNDARY CONDITION CONSTRAINT METHOD. Tobocman, William (Case Inst. of Tech., Cleveland, Ohio).

A method of relating the shell-model representation of the nuclear interior to a realistic picture of the nuclear surface is described. The shell model is used only for the inside region, and the channel expansion is assumed to be valid in the outside region. The two representations are then forced to be mutually consistent by using the channel-expansion wave function to give boundary conditions which are imposed as constraints on the shell-model wave function used in the inside region. (D.C.W.)

21990 (BNL–948, pp 928-1004) UNCOMMON STATES OF NUCLEAR MATTER. Wilets, Lawrence; Halpern, Isaac (Washington Univ., Seattle).

The nuclidic masses off the stability line are discussed as well as the extension of the isotope chart, some experiments on the various stages of fission, and the excitation of highly excited states by direct interactions. (D.C.W.)

21991 (BNL–948, pp 1005-44) COULOMB EXCITATION WITH HEAVY IONS. Stelson, Paul H. (Oak Ridge National Lab., Tenn.).

Some expressions from the semi-classical theory of coulomb excitation are reviewed, and the possibility of performing coulomb excitation experiments with the larger tandem accelerators is discussed. The possibility of direct coulomb excitation experiments, second-order perturbation effects, and multiple coulomb excitation are considered. (D.C.W.)

21992 (BNL–948, pp 1045-1134) HEAVY ION INTERACTIONS. Bromley, D. Allan (Yale Univ., New Haven, Conn.).

A review of the use of heavy-ion reactions and scattering in the investigation of reaction mechanisms and nuclear structure is presented. The analysis of the experimental data is discussed in some detail. (D.C.W.)

21993 (BNL–9168) PRODUCTION OF ^{52}Fe. Greene, M. W.; Hillman, Manny (Brookhaven National Lab., Upton, N. Y.). May 3, 1965. Contract AT(30-2)-Gen-16. 10p. Dep. mn. CFSTI $1.00 cy, $0.50 mn.

Millicurie quantities of ^{52}Fe were produced by the $^{50}Cr(\alpha,2n)^{52}Fe$ reaction using enriched ^{50}Cr as Cr_2O_3, which was recovered for re-use. (auth)

21994 (BNL–10094) NUMERICAL ANALYSES OF NEUTRON RESONANCES BY USE OF COMPUTER PROGRAMS. Bhat, M. R.; Chrien, R. E.; Cole, I. W. (Brookhaven National Lab., Upton, N. Y.). Mar. 1966. Contract AT-30-2-GEN-16. 16p. (CONF-660303-12). Dep. mn. CFSTI $1.00 cy, $0.50 mn.

From American Physical Society, Conference of Neutron Cross Section Technology, Washington, D. C.

The use of computer-oriented, automated techniques in the analysis of slow neutron cross sections is described, with special emphasis on the measurement of neutron resonance parameters. The application of these techniques is illustrated at each stage of the data reduction process. A description of the determination of the resolution function for the BNL chopper time-of-flight system is given. The results of resonance analysis with a non-Gaussian resolution function are presented. (auth)

21995 (CERN-65-32, pp 35-40) SEARCH FOR DOUBLE β DECAY IN ^{48}Ca. der Mateosian, E.; Goldhaber, M. (Brookhaven National Lab., Upton, N. Y.).

The status of the search for double β decay in ^{48}Ca is discussed. (B.G.D.)

21996 (FTI–142/T-016) DVUKHNUKLONNYE KORRELYATSII V YADRAKH. (Two-Nucleon Correlations in Nuclei). Sitenko, A. G.; Simenog, I. V. (Akademiya Nauk Ukrainskoi SSR, Kharkov. Fiziko-Tekhnicheskii Institut). 1965. 31p. Dep. mn.

The inelastic scattering of fast electrons on nuclei and the two-particle correlations in the nuclei were shown. The general relation between the inelastic scattering cross section and the two-particle correlation functions was established for nucleons in the nucleus. The spectral distributions of the two-particle correlation functions were calculated on the basis of the shell model. The two-fold magic nuclei ^4He, ^{16}O, and ^{40}Ca were examined as examples. The sum rule for correlation functions was established. The effect of the motion of inertia centers on the correlation functions was established using ^4He as an example. (tr-auth)

21997 (INSJ–96) TABLE OF SINGULARITIES IN NUCLEAR DIRECT INTERACTION AMPLITUDE: p-SHELL NUCLEI—WITH SEVERAL REMARKS ON DIRECT INTERACTION MECHANISMS. Ui, Haruo (Institute for Nuclear Study, Tokyo Univ. (Japan)). Mar. 1, 1966. 60p. Dep. mn.

In order to see relative importance among different direct interaction mechanisms, locations of the leading singularities of the direct interaction amplitudes in q^2-as well as cos θ-planes are tabulated for the transfer (stripping or pick-up), knock-on, and heavy-particle-stripping reactions. The tables include the following twenty types of nuclear reactions, the (p,d), (p,t), (p,^{3}He), (p,α), (d,p), (d,t), (d,^{3}He), (d,α), (t,p), (t,d), (t,^{3}He), (t,α), (^{3}He,p), (^{3}He,d), (^{3}He,t), (^{3}He,α), (α,p), (α,d), (α,t) and (α,^{3}He) reactions, each from the ground states of O-p shell target nuclei of ^{6}Li, ^{7}Li, ^{9}Be, ^{10}B, ^{11}B, ^{12}C, ^{14}N, ^{15}N, and ^{16}O. By examining both qualitative and quantitative behaviors of the singularities, several remarks are added concerning the direct interaction mechanisms. In particular, it is pointed out that the heavy-particle-stripping mechanism will play the most important role in several cases such as the ^{9}Be(p,α)^{6}Li reaction at lower energy. (auth)

21998 (JINR–E–2579) CALCULATIONS OF PROPERTIES OF COLLECTIVE STATES IN DEFORMED NUCLEI IN THE REGION $176 \leq A \leq 190$. Kalpazhiu, M. K.; Vogel, P. (Joint Inst. for Nuclear Research, Dubna (USSR). Lab. of Theoretical Physics). 1966. 12p. Dep. mn.

Energies and other characteristics of collective states of nuclei in the given region were obtained in the pairing + multipole – multipole interaction model. An account is given for the strong lowering of the $K\pi = 2+$ state energies with the increasing number of neutrons and protons. It is also shown that in even-even nuclei of the given region there are no low-lying (below 1 Mev) β-vibrational or octupole states. The problem of collective states in the odd-A nuclei is investigated. (auth)

21999 (JINR–P–2552) NEUPRUGIE VZAIMODEISTVIYA KOSMICHESKIKH CHASTITS S ATOMNYMI YADRAMI PRI OCHENY VYSOKIKH ENERGIYAKH. (Inelastic Interactions of Cosmic-Ray Particles With Atomic Nuclei at Very High Energies). Artykov, I. Z.; Barashenkov, V. S.; Eliseev, S. M. (Joint Inst. for Nuclear Research, Dubna (USSR). Lab. of Theoretical Physics). 1966. 26p. Dep. mn.

It is shown that the generally accepted model of intranuclear cascades is not in agreement with experiment at $T \gg 10$ Bev, if in the calculations account is taken of the role of the leading particle carrying away 70% of the primary energy. To bring experiment and theory into agreement it is necessary to take into account many-particle interactions inside the nucleus. (auth)

22000 (JINR–P–2553) ISSLEDOVANIE α-SPEKTRA IZOTOPOV Bi. (Investigation of the α Spectrum of Bi Isotopes). Makhunka, I.; Tron, L.; Fenesh, T.; Khalkin, V. A. (Joint Inst. for Nuclear Research, Dubna (USSR). Lab. of Nuclear Problems). 1966. 8p. Dep. mn.

The α spectra of Bi isotopes formed by bombarding a lead target with 140-Mev protons were studied. Measurements were made using an α spectrometer with a semiconductor detector. The obtained half lives (T) and the α-particle energies were found. (auth)

22001 (JINR–P–2555) IZUCHENIE REAKTSII PODKHVATA NEITRONA PRI OBLUCHENII IZOTOPOV ^{181}Ta, ^{197}Au, ^{232}Th, ^{238}U IONAMI ^{15}N. (Study of Neutron Pickup in Bombardment of ^{181}Ta, ^{197}Au, ^{238}U Isotopes With ^{15}N Ions). Artyukh, A. G.; Volkov, V. V.; Kvetsinska, T. (Joint Inst. for Nuclear Research, Dubna (USSR). Lab. of Nuclear Reactions). 1966. 29p. Dep. mn.

The neutron pickup in the bombardment of ^{181}Ta, ^{197}Au, ^{232}Th, and ^{238}U with ^{15}N ions of 102-Mev energy was studied. The data on the angular distribution, effective reaction cross section and the energy spectrum of ^{16}N were obtained. It follows that the neutron transfer does not result in an appreciable excitation of the nucleus-target and that the deformation of the nucleus does not noticeably affect the neutron transfer. (auth)

22002 (JINR–P–2570) O TSEPOCHKE RASPADA ^{138}Nd → ^{138}Pr → ^{138}Ce. (On the Decay Chain of ^{138}Nd → ^{138}Pr → ^{138}Ce). Gromov, K.; Demeter, I.; Zhelev, Zh. (and others) (Joint Inst. for Nuclear Research, Dubna (USSR). Lab. of Nuclear Problems). 1966. 16p. Dep. mn.

The more exact value of the ^{138}Nd isotope half life ($T_{½}$ = 5.2 ± 0.1h) was measured. The half life of the main state of ^{138}Pr(1$^+$) ($T_{½}$ = 1.5 ± 0.15 min) and the mass difference of the nuclides ^{138}Pr(1$^+$) and ^{138}Ce (Q = 4460 ± 40 kev) were found. The energy difference of the isomeric state of ^{138}Pr ($T_{½}$ = 2.1h) and the main one (ΔE = 330 + 60 kev) were determined. The values of lg ft for beta-transfer to the lower levels of ^{138}Ce from the ^{138}Pr(1$^+$) decay were calculated. The nature of the ^{138}Ce nucleus is discussed. (auth)

22003 (JINR–P–2581) ISSLEDOVANIE ISLUCHENIYA ^{145}Eu. (Investigation of ^{145}Eu Irradiation). Adam, I.; Vil'skii, K.; Zhelev, Zh.; Iorgensen, M.; Krivopustov, M.; Kuznetsov, V.; Nil'sen, O. B.; Finger, M. (Joint Inst. for Nuclear Research, Dubna (USSR). Lab. of Nuclear Problems). 1966. 19p. Dep. mn.

Conversion electron spectra, γ spectrum, $\beta^+\gamma$ spectra and that of e–γ coincidences were studied. The gamma-spectra was investigated by using the germanium semiconductor detector with a 1024-channel pulse height analyzer. A decay scheme ^{145}Eu → ^{145}Sm is suggested. Assumptions are made about the multipolarity of transitions, the level populations by electron capture are determined, and the values lg ft are calculated. (auth)

22004 (JINR–P–2593) ISSLEDOVANIE NEITRONNYKH REZONANSOV ^{165}Ho. (Investigation of Neutron Resonances of ^{165}Ho). Karzhavina, E. N.; Popov, A. B.; Yazitskii, Yu. S.; Efimov, V. N.; Shirikova, N. Yu. (Joint Inst. for Nuclear Research, Dubna (USSR). Lab. of Neutron Physics). 1966. 21p. Dep. mn.

The data are reported on the parameters of ^{165}Ho resonances obtained on a neutron spectrometer. An application of the shape analysis on a computer M-20 to obtain the resonance parameters is described. The parameters Γ and $g\Gamma_n$ were obtained for 17 levels in the range up to 110 ev, as well as the values of $g\Gamma_n$ for 50 levels in the region 110 to 500 ev. The found parameters are used to determine the strength functions $S_0 = (1.9 \pm 0.3).10^{-4}$ and $\overline{\Gamma}_\gamma = 73 \pm 3$ Mev. (auth)

22005 (JINR–P–2596) O RAVNOVESNYKH DEFORMATSIYAKH VOZBUZHDENNYKH SOSTOYANII TYAZHELYKH YADER. (On the Equilibrium Deformations of the Excited States of Heavy Nuclei). Solov'ev, V. G. (Joint Inst. for Nuclear Research, Dubna (USSR). Lab. of Theoretical Physics). 1966. 5p. Dep. mn.

It is investigated whether there exist excited states the equilibrium deformation of which differs from that of the ground state of the corresponding even nuclei. Some examples of such states in nuclei lying outside the transition region are given. (auth)

22006 (KFKI–600) CIRCULAR POLARIZATION OF γ RADIATION FOLLOWING A DEUTERON STRIPPING REACTION. Zimanyi, J. (Magyar Tudomanyos Akademia Kozponti Fizikai Kutato Intezete, Budapest). 1960. 10p. Dep. mn.

It is suggested that if one can determine the circular polarization of the gammas following a deuteron stripping reaction, then one can determine the polarization parameters of the nucleon. A calculation made in the j,j representation is presented. (M.O.W.)

22007 (LNF–66/1) A LIQUID ^{3}He TARGET FOR HIGH-ENERGY NUCLEAR EXPERIMENTS. Note No. 302. Modena, I.; Montelatici, V.; Scaramuzzi, F. (Laboratori Nazionali di Frascati, Comitato Nazionale per l'Energia Nucleare (Italy)). Jan. 21, 1966. 8p. Dep. mn.

A liquid ^{3}He target was constructed for experiments on ^{3}He photodisintegration using the γ-beam of the Frascati 1.1-Bev electron synchrotron. The design and performance of the target cell and its associated equipment are discussed. (M.O.W.)

22008 (MLM–1337J) NUCLEAR LEVELS IN ^{223}Ra POPULATED BY THE DECAY OF ^{227}Th AND ^{223}Fr. Lange, R. C.; Hagee, G. R. (Mound Lab., Miamisburg, Ohio); McCarthy, J. T. (Cincinnati Univ., Ohio). Mar. 1966. Contract AT-31-1-GEN-53. 13p. (CONF-660303–11). Dep. mn. CFSTI $1.00 cy, $0.50 mn.

From American Physical Society, Conference of Neutron Cross Section Technology, Washington, D. C.

The levels in ^{223}Ra were studied by observing the gamma rays from the decay of ^{223}Fr and ^{227}Th, and by gamma-gamma and alpha-gamma coincidence studies from the alpha decay of ^{227}Th. (M.O.W.)

22009 (NBS-MON-81) TABLES OF ELECTRON RADIAL FUNCTIONS AND TANGENTS OF PHASE SHIFTS FOR LIGHT NUCLEI (Z = 1 THROUGH 10). Bhalla, C. P. (National Bureau of Standards, Washington, D. C.). Aug. 6, 1964. 404p. GPO $3.25.

To facilitate the theoretical analyses of beta-decay experiments in light nuclei electronic radial wave functions, evaluated at the nuclear radius, and tangents of phase-shifts are tabulated for total angular momentum equal to $\frac{1}{2}$ and $\frac{3}{2}$. Separate tables for electrons and positrons are given for ten values of Z, starting from Z equal to one, in steps of unity and for beta momentum values from 0.1 mc to 42.0 mc in steps of 0.1 mc. The nucleus is represented as a sphere with uniform charge distribution. The nuclear radius, ρ, is taken to be $1.2A^{\frac{1}{3}}10^{-13}$ cm in the major body of these tables. However, additional tables for Z = 6 and Z = 7 are given for $\rho = 1.1A^{\frac{1}{3}}10^{-13}$ cm and $\rho = 1.3A^{\frac{1}{3}}10^{-13}$ cm. (auth)

22010 (NYO–72–28) PEGRAM NUCLEAR PHYSICS LABORATORIES. Progress Report, January 1964–January 1965. (Columbia Univ., New York. Dept. of Physics). Feb. 1966. Contract AT(30-1)-Gen-72. 164p. Dep. mn. CFSTI $5.00 cy, $1.00 mn.

Various experimental and theoretical studies were made in the areas of neutron physics, nuclear reactions with charged particles, beta and gamma spectroscopy and application to nuclear structure, neutron interactions with condensed matter, macroscopic neutron physics, and instrument development. (M.O.W.)

22011 (TID–22771) NUCLEAR THEORY INDEX FOR 1964. Martin, M. J.; Ogata, H.; Bower, Georgia C. (eds.) (Oak Ridge National Lab., Tenn.). Contract W-7405-eng-26. 97p. CFSTI $2.50 cy, $0.75 mn.

A bibliography of nuclear theory papers published during 1964 is presented. Generally, only articles dealing with the low-energy aspects of nuclear theory are included. Papers concerned with meson effects are not included except as they relate specifically to nuclear properties usually associated with low-energy phenomena. The subject areas covered are nuclear structure, nuclear reactions, electromagnetic radiation, and beta decay and parity. (M.O.W.)

22012 (UCRL–14606) THE EPITHERMAL FISSION CROSS SECTION OF ^{235}U. Bowman, C. D.; Auchampaugh, G. F.; Fultz, S. C.; Moore, M. S.; Simpson, F. B. (Lawrence Radiation Lab., Univ. of California, Livermore). Mar. 8, 1966. Contract W-7405-eng-48. 15p. (CONF-660303–10). Dep. mn. CFSTI $1.00 cy, $0.50 mn.

From American Physical Society, Conference of Neutron Cross Section Technology, Washington, D. C.

The neutron-induced fission cross section of ^{235}U was remeasured over the energy range from 0.02 to 80 ev with the Livermore linear electron accelerator as the pulsed neutron source for a time-of-flight experiment. The fission events were detected in an ionization chamber containing a total of $\frac{3}{4}$ g of ^{235}U; the flux was monitored with a BF_3 tube placed in the same flight path. The cross section was normalized at thermal energy. The results are compared with earlier Livermore work and with other recent measurements. (auth)

22013 (ANL-Trans-296) PRIMARY CHARGE DISTRIBUTION AT THE LOW-ENERGY FISSION OF HEAVY (gg)-NUCLEI . Noerenberg, Wolfgang (Technische Hochschule, Munich (West Germany)). Translated by Elmar K. Wilip (Argonne National Lab., Ill.), from Thesis. Jan. 11, 1966. 54p. Dep. mn. JCL $5.60 fs, $1.82 mf.

A model was introduced for the description of the charge distribution at the low energy fission of heavy (gg)-nuclei, in which the fissioning nucleus is described before the splitting by two interacting fragments. This molecular model was treated within the framework of adiabatic concepts. Angular correlation measurements confirmed this assumption for the low energy fission in (gg)-nuclei. The ground state of the system is described by a BCS-wave function which considers the superfluidity properties of the (gg)-nuclei. The one-particle functions of the BCS-wave function are expanded over the eigenfunctions of the undisturbed spherical fragments. The determination of the ground state is carried out by a minimization of the total energy under the secondary conditions of constant fragment masses, total proton and neutron numbers and centers of gravity of fragments. Coupled equation systems of the Hartree-Fock and of the BCS-type were obtained which were simplified by means of additional assumptions. For this purpose axially symmetrically deformed one-particle potentials were introduced for the fragments within the framework of a generalized Nilsson model. Numerical results are reported for the charge distribution in the fission of ^{236}U. One obtains for plausible fragment distances ($\gtrsim$14 fm) in the region of the most probable fission for the heavy (light) fragments on the average 0.6 protons less (more) than for the case of equal charge densities of fragments. In the vicinity of magic numbers (Z = 50, N = 82) deviations were observed from the mean values, which indicate the effect of closed shells of fragments upon the nucleon distribution. The charge distribution is determined essentially by the state densities of fragments in the vicinity of the Fermi level, by the energy of asymmetry of fragments and by the Coulomb interaction between the fragments. (auth)

22014 (KFK-tr–185) DIE DICKE DES POTENTIAL-WALLES FUER DIE SPONTANSPALTUNG BEI gg-KERNEN. (The Width of Potential Barrier for Spontaneous Fission by gg-Nuclei). Feng, Hsi-chang. Translated into German by Peter Buriks (Kernforschungszentrum, Karlsruhe, West Ger.), from Wu Li Hsueh Pao, 20: 938-9(1964). 5p. Dep. mn. JCL $1.00 fs, $0.50 mf.

With the help of available experimental data on the spontaneous fission of gg-nuclei, calculations were made on the thickness of the potential wall for the isotopes ^{232}Th, ^{234}U, ^{236}U, ^{238}U, and ^{240}U. The results are tabulated and show that the width of the potential barrier decreases with increasing A. (J.S.R.)

22015 PERTURBED ANGULAR CORRELATION OF A TRIPLE GAMMA CASCADE. Bencze, Gy.; Zimanyi, J. (Central Research Inst. for Physics, Budapest). Acta Phys. Acad. Sci. Hung., 20: 209–15(1966).

The angular correlation function is derived for a triple gamma cascade perturbed by extranuclear field. Special cases are investigated for non-observed intermediate radiation and for static external magnetic field. (auth)

22016 ϵ/β^+ ELECTRON CAPTURE TO POSITRON EMISSION RATIO IN THE DECAY OF ^{56}Co TO THE SECOND EXCITED LEVEL OF ^{56}Fe. Vatai, E. Acta Phys. Acad. Sci. Hung., 20: 217-25(1966). (In Russian).

Using the $4\pi\beta^+ - \gamma$ coincidence method the probability of positron emission was determined in the 1-forbidden transition from the ground state of ^{56}Co (4+) to the second excited state of ^{56}Fe (4+). The result $P_{\beta^+} = 0.899 \pm 0.142$ is in good agreement with the previous measurements. The weighted average of the capture-to-positron emission ratio of the given results is $\epsilon/\beta^+ = 0.117 \pm 0.089$. These are in agreement with the theoretical calculations for the allowed transition. The detection efficiency of proportional counter for positrons was determined from the annihilation peak intensity in the single, coincidence, and total spectra of the same source. (auth)

22017 EXPERIMENTAL INVESTIGATION OF THE PROBABILITY OF (n,αn') REACTION IN NATURAL URANIUM. Adam, A.; Palla, Gabriella; Quittner, P. (Central

Research Inst. of Physics, Budapest). Acta Phys. Acad. Sci. Hung., 20: 227-31(1966).

Experiments were undertaken to investigate whether the $(n,\alpha n')$ reaction is responsible for the anomaly observed in the small-angle elastic scattering of 14-Mev neutrons by ^{238}U. The results show the probability of this reaction, if it occurs at all, to be so low that its contribution cannot explain the anomaly in question. An estimate of the reaction cross section gives a value of 0.5 mb in the upper limit. (auth)

22018 DIRECT PROCESSES ON RADIOACTIVE NUCLEI. Hrasko, P.; Koevesy, Zs. (Central Research Inst. for Physics, Budapest). Acta Phys. Acad. Sci. Hung., 20: 285-8(1966).

For a previously developed theory of nuclear reactions, the derivation of formulas for the reaction amplitudes is based on the assumption that because of the causality requirements the amplitudes are analytic functions of the energy everywhere on the physical sheet except on the real axes, where the location of the singularities (poles and branch points) is determined by the unitarity condition. An approximation for the amplitude is obtained by considering virtual states of a certain type only in the unitarity condition. (J.F.P.)

22019 ISOBARIC SPIN WITHOUT CHARGE SPACE. Bayman, B. F. (Univ. of Minnesota, Minneapolis). Amer. J. Phys., 34: 216-22(Mar. 1966). (COO-1371-13).

The familiar consequences of charge independence of a nuclear hamiltonian are derived without introducing the concept of charge space and the extended Pauli principle. Ordinary wave functions, separately antisymmetric in their protons and neutrons, are used throughout. This has the pedagogical advantage of emphasizing that the physical regularities associated with isobaric spin are consequences of charge independence alone, and do not depend upon the charge-space formalism. (auth)

22020 IMPROVED METHODS FOR MULTIPLE COINCIDENCE GAMMA SPECTROMETRY. Kantele, J.; Pakkanen, A. (Univ., Helsinki). Ann. Acad. Sci. Fenn., Ser. A VI, 1-32(1965).

The ordinary gamma-gamma coincidence, the sum-coincidence and the sum-peak coincidence methods were extended to systems containing several scintillation detectors arranged for the study of coincidences between three or four gamma rays. In particular, spectrometers of high detection efficiency were developed by optimizing both the geometry and the logic circuitry, yet avoiding high cost and complexity. The efficiency of the constructed spectrometers for three-fold gamma cascades is comparable to, or better than, that of a typical ordinary two-crystal coincidence spectrometer for two-gamma cascades. The treatment of random coincidences was considered and simple methods for their elimination are presented. The performance of the various triple-coincidence spectrometers and their combinations is demonstrated, whereby some new results on the decay of ThC'' (^{208}Tl) are obtained. An example of the detection of a four-fold cascade with four detectors is given. The applicability of the various multiple coincidence arrangements is discussed and some possibilities for further development are suggested. (auth)

22021 OPTICAL PROPERTIES OF LOW-ENERGY PIONS IN NUCLEI. Ericson, M. (Institut de Physique Nucleaire, Lyon); Ericson, T. E. O. Ann. Phys. (N. Y.), 36: 323-62(Feb. 18, 1966).

A simple nonlocal potential for low-energy pions in finite nuclei is calculated from the amplitudes for πN scattering and for π production in NN collisions. The potential includes absorption and has no free parameters. The appropriate multiple scattering equations are derived in the coordinate representation with nuclear pair correlations included. Owing to the large mass of the scatterers the pion field behaves nearly classically. It is shown that short-range pair correlations are important in the multiple scattering owing to the dominant dipole component in the πN scattering. To a good approximation this produces a Lorentz-Lorenz effect analogous to the one occurring in the scattering of electromagnetic waves in dense media. The contributions of Fermi motion to the potential are shown to be small. The isospin part of the potential is derived and is shown to have a tensor component in addition to the ordinary vector one. The former gives rise to direct double charge exchange of pions; its strength becomes important for high momentum pions. The potential is further found to have a term which gives a small but possibly observable hyperfine coupling. A comparison is made between predictions of the potential and experimental data on level shifts and widths for π mesic atoms. Satisfactory agreement is found within experimental uncertainties which is quantitative evidence for nuclear pair-absorption of pions. There is also some indication of short range anticorrelations between nucleons. (auth)

22022 NUCLEON-NUCLEON BOUNDARY CONDITION METHODS FOR NUCLEAR MATTER. Hoenig, M. M.; Lomon, E. L. (Massachusetts Inst. of Tech., Cambridge). Contract AT(30-1)-2098. Ann. Phys. (N. Y.), 36: 363-434(Feb. 18, 1966). (MIT-2098-169).

It is shown that, as a consequence of the energy independence of the boundary condition f on the radial Schroedinger wave function u at r_0, $u = 0$ for $r < r_0$, and that the boundary condition is equivalent to replacing Vu, in the equation for u in $r < r_0$, by an expression linear in $u(r_0 + \epsilon)$ and $u'(r_0 + \epsilon)$. The Bethe-Goldstone wave function u^N is determined by the same replacement in its integral equation. But $u^N \neq 0$ in $r < r_0$, so that u^N depends on an extra parameter b, the boundary condition at $r_0 - \epsilon$. Pseudopotentials at r_0 which give the boundary condition exactly are presented. The self-consistent single particle potential energy in nuclear matter is investigated with a simple S state boundary condition, without a potential tail. The effective mass approximation is found inadequate. For the same interaction, the effect of summing the hole-hole contributions is found to be important for the two-body correlations, and small but significant for the saturation and binding energy. A calculation is made with a more realistic model with a potential tail. A modified Moszkowski-Scott type expansion, separated at r_0, is used. Convergence is poor and binding is not obtained. More recent nucleon-nucleon boundary condition models may give convergence and binding. (auth)

22023 SCATTERING OF MEDIUM-ENERGY NEUTRONS. Korzh, I. A.; Pasechnik, M. V.; Totskii, I. A. At. Energ. (USSR), 20: 8-17(Jan. 1966). (In Russian).

A brief review is given of the work done with the electrostatic generator. The results of the investigation of the inelastic scattering of neutrons at energies of 0.8, 2.5, 3.3, 3.6, and 4.1 Mev on the nuclei C, Na, Mg, Al, P, S, Cl, Ca, Cr, Fe, Co, Ni, Cu, Zn, Se, Zr, Mo, Ag, Cd, Sn, Sb, Te, I, Ba, W, Hg, Pb, Bi, and U were reported. This study showed the possibility of establishing the effect of the nuclear shell during the inelastic scattering of neutrons. The angular distributions of elastically scattered neutrons at 0.3, 0.5, 0.65, and 0.8 Mev were studied on C, Na, Mg, Al, Si, K, Cr, Fe, Ni, Cu, Zn, Se, Zr, Mo, Ag, Cd, Sn, Sb, Te, Ba, W, Hg, Pb, Bi, and U. The results of the measurements of the angular distributions were analyzed on the basis of the optical model. (tr-auth)

22024 THE MATHEMATICAL TREATMENT OF NUCLEAR TRANSFORMATION. Bach, A. (Kernforschungszentrum, Karlsruhe, Ger.). Atomkernenergie, 11: 115-19 (Mar.-Apr. 1966). (In German).

A formula which describes the time-dependance of radioactive decay and nuclear transformation processes in constant fluxes is presented. The use of the coefficient matrix of the formula for practical calculation is shown in an example. (auth)

22025 DETERMINATION OF MAGNETIC MOMENTS OF EXCITED NUCLEAR LEVELS FROM THE γ-γ ANGULAR CORRELATION DISTURBED IN A MAGNETIC FIELD. Heuser, H.; Schneider, H. (Justus Liebig-Univ., Giessen, Ger.). Atomkernenergie, 11: 137-40(Mar.-Apr. 1966). (In German).

A survey is given of measuring methods for determination of magnetic dipole moments of short-lived excited nuclear

levels. Measurements were performed on 82 kev-level of ^{133}Cs and on 0.569 Mev-level of ^{207}Pb. (auth)

22026 THE IEC METHOD AND CONVERSION COEFFICIENTS OF THE 605-kev TRANSITION IN ^{134}Ba. Zganjar, E. F.; Hamilton, J. H. (Vanderbilt Univ., Nashville). Can. J. Phys., 44: 549-62(Mar. 1966).

Tests of the internal-external method of measuring conversion coefficients in the Vanderbilt double-focusing spectrometer were made in search of possible errors arising from scattering of photoelectrons in the converter for a photon energy of 605 kev. This scattering may affect the factor, f, which corrects for the anisotropic distribution of the photoelectrons. The 605-kev transition in ^{134}Ba populated by the beta decay of ^{134}Cs was used. An accurate determination of the K, L, and M conversion coefficients of the 2+ to 0+, 605-kev, E2 transition in ^{134}Ba was made. Three uranium converters 1.12, 2.19, and 3.71 mg/cm^2 thick were used. The results are compared with the new theoretical calculations of f which depend on the converter thickness and consequently consider the effect of scattering. For photons of energy 605 kev or greater, the IEC method used in the Vanderbilt double-focusing spectrometers is insensitive (<5%) to scattering in uranium converters <4 mg/cm^2 thick. The K, L, and M conversion coefficients were determined to be $(5.03 \pm 0.20) \times 10^{-3}$, $(7.07 \pm 0.50) \times 10^{-4}$, and $(1.64 \pm 0.18) \times 10^{-4}$, respectively. The respective theoretical values of Rose are 5.08×10^{-3}, 6.92×10^{-4}, and 2.77×10^{-4}. Sliv and Band give a value of 5.10×10^{-3} for the K conversion coefficient. (auth)

22027 NATURE OF THE 686-kev NUCLEAR LEVEL OF ^{187}Re. Widemann, Francois (CNRS, Orsay, France). Compt. Rend., Ser. B, 262: 447-9(Feb. 7, 1966). (In French).

A recent measurement of the mean life of the 686-kev level and the precise determination of the multipolarity of the 479-kev transition by measurement of the conversion ratios $L_I/L_{II}/L_{III}$ argue in favor of the interpretation of this level as γ vibrational on the Nilsson level $(^9/_2)^-$ at 206 kev. The objections presented are discussed. (tr-auth)

22028 AN ANALYTICAL EXPRESSION OF THE AMPLITUDE OF STRIPPING REACTION IN THE COULOMB APPROXIMATION. Cejpek, J. (Univ., Brno). Czech. J. Phys.,16: 186-93(1966).

A method is derived for calculating the matrix element of stripping reaction (d,p) in the so-called distorted-wave Born approximation; only Coulomb scattering of incident and outgoing particles is taken into consideration. Coulomb wave functions are expressed by means of integral representation permitting integration over angular variables and, when the radial wave function of the trapped neutron is specially chosen, also calculation of the radial integral for non-zero orbital momentum of the trapped neutron. Relations are given for calculating the differential cross section of the reaction and the polarization of products. The special case, when the orbital momentum of the captured neutron is equal to one or two, is discussed in detail. (auth)

22029 RECENT RESULTS ON ELECTRON CAPTURE. Berenyi, Denes (Atomic Research Inst., Debrecen, Hungary). Fiz. Szemle, 16: 21-4(Jan. 1966) (In Hungarian).

Electron capture is a β-decay phenomenon, discovered relatively late, in 1937. It represents a little-clarified area of radioactive decay, especially as far as forbidden transitions are concerned. Solution of the problems is of great interest for the ambitious program initiated at CERN, aimed at the doubling of the number of known isotopes. The theory of electron capture is of interest also for a deeper understanding of the transitional matrix elements and of the nuclear structure itself. Experiments in this field are in progress at the Institute in Debrecen on the transition between the ground state of ^{51}Cr$_\gamma$ and the 645-kev excited state of ^{51}V. The problem has also been attacked by means of bremsstrahlung studies. Electron capture and positron emission phenomena have also been examined at the Institute, determining the ϵ/β^+ ratio for the ^{36}Cl–^{36}S transition; similar experiments have been carried out independently at Glasgow. Results of measurements on transition from the 4+ ground state of ^{56}Co to the 2080-kev excited state of ^{56}Fe agreed with theoretical predictions. Other studies included comparison of the form factor diagram of the bremsstrahlung spectrum of ^{55}Fe and ^{36}Cl. (TTT)

22030 NUCLEAR REACTION ON ^{13}C AT THE PROTON ENERGY OF 54.9 Mev. Taketani, Hiroshi (Kyoto Univ.); Muto, Jiro. Genshikaku-Kenkyu, 10: 506-26 (Dec. 1965). (In Japanese).

A number of differential cross sections of (p,d) and (p,t) reactions on ^{13}C at the proton energy of 54.9 Mev are presented. Momentum analysis of the reaction products was performed with a magnetic analyzer, which was operated with energy resolution of about 0.6%. For (p,d) reactions, angular distributions were obtained for seven prominent deuteron groups corresponding to the excitation energies of 0 (ground, $l \simeq 1$), 4.43, 7.66 ($l = 1$), 9.64 ($l = 4$), 12.71 ($l = 1$), 15.11 ($l = 1$), and 16.11 Mev in ^{12}C. Assigned l-values obtained by fitting the Butler curves to the experimental angular distributions indicated in the ground, 4.43, 12.71, 15.11 (T = 1), and 16.11 Mev (T = 1) states are particularly large. Implications of these phenomena are discussed. For (p,t) reactions, angular distributions, some of these groups corresponding to the ground ($l \simeq 2$), first (1.99 Mev, e = 0), second (4.38 Mev), and third (4.82 Mev $l \simeq 2$) excited states in ^{11}C are presented. These angular distributions are tentatively fitted to the Butler curves and the plausible l-values are indicated in the parentheses. These results are discussed in comparison with ^{12}C (p,d) ^{11}C reaction leading to the same excited state in the residual nucleus ^{11}C. (auth)

22031 EXPERIENCE WITH AN ON-LINE COMPUTING SYSTEM IN LOW-ENERGY NUCLEAR PHYSICS EXPERIMENTS. Gemmell, D. S. (Argonne National Lab., Ill.). IEEE (Inst. Elec. Electron. Eng.), Trans. Nucl. Sci., NS-13: No. 1, 158-60(Feb. 1966).

An on-line computing system that was developed for use in nuclear physics experiments at the 4.5- and 12-Mev Van de Graaff accelerators is briefly described, together with the various uses of the system. (D.C.W.)

22032 MODULAR SOFTWARE FOR ON-LINE HANDLING OF NUCLEAR DATA. Wyckoff, J. M. (National Bureau of Standards, Washington, D. C.). IEEE (Inst. Elec. Electron. Eng.), Trans. Nucl. Sci., NS-13: No. 1, 199-205(Feb. 1966).

A set of programs that was developed for the modular on-line data handling system at the National Bureau of Standards linear accelerator is described. (D.C.W.)

22033 THE HIGH-ENERGY GROUP OF THE STRASBOURG NUCLEAR RESEARCH CENTER. Braun, H. (Nuclear Research Center, Strasbourg). Ind. At., 10: 44-54(1966). (In French).

The work done in the field of high energy physics is discussed. The guiding aim of the work of the group is to study the modes of emission of privileged baryon beams (fragments, hyperfragments) coming from nuclei bombarded by the various high energy particles, and thus to add to the knowledge of nuclear structure and of little known particles or beams of particles. (auth)

22034 THE ABSOLUTE STANDARDIZATION OF ^{57}Co. Troughton, M. E. C. (Radiochemical Centre, Amersham, Eng.). Int. J. Appl. Radiat. Isotop., 17: 145-50(Mar. 1966). (RCC-R-186).

A method (similar to the $4\pi\beta-\gamma$ coincidence technique) for measuring the disintegration rate of ^{57}Co, which decays by electron capture is described. A thin source is used so that, in addition to the K x rays, some Auger and internal conversion electrons emerge and are detected in the proportional counter. The average efficiency of detection of a disintegration in the proportional counter is reasonably high (~75). Corrections for the complex decay scheme were evolved and shown to be small. The accuracy of the method is such that the maximum systematic error is less than ±2%. This is several per cent better than can be obtained by two other 4π coincidence methods, in which electrons

are absorbed and mainly K x rays are counted. The improved accuracy is a direct result of the high efficiency of detection of the disintegrations in the proportional counter. (auth)

22035 MONTE CARLO CALCULATIONS OF RADIONUCLIDE PRODUCTION IN IRON TARGETS BOMBARDED WITH 400-Mev PROTONS. Ebeoglu, D. B.; Wainio, K. M.; More, K.; Tiffany, O. L. (Bendix Systems Div., Ann Arbor, Mich.). J. Geophys. Res., 71: 1445-51(Mar. 1, 1966).

The effective production rate of a number of radionuclides was calculated in iron targets bombarded with a monoenergetic, collimated beam of 400-Mev protons. The purpose of the calculations was to study the cosmic-ray interaction in meteorites and to follow nuclear cascades in multielement, multilayer targets due to primary and secondary protons and neutrons. The buildup of low-energy products, ^{56}Co, ^{54}Mn, ^{51}Cr, ^{52}Mn, and ^{48}V, was followed in an ^{56}Fe target, and the results were compared with those of experimental proton irradiations of identical targets reported by Shedlovsky and Rayudu. The results show good agreement for the integral production rates of nuclides and predict the same maximums as a function of depth. The calculations also give the proton and neutron fluxes at various depths along the iron target and predict the radial spread of particles and radionuclides. The computations were carried out to a depth of 50 cm and a radial spread of 30 cm to compare with the experimental data available. (auth)

22036 HALF LIFE AND SPECIFIC ACTIVITY OF ^{99}Tc. Goldstein, G. (Oak Ridge National Lab., Tenn.); Dean, J. A. J. Inorg. Nucl. Chem., 28: 285-6(Feb. 1966). (ORNL-P-1175).

The half life and specific activity of ^{99}Tc were redetermined by measuring the activity of a known weight (determined coulometrically) of ^{99}Tc by a liquid scintillation method and found to be $2.14(\pm 0.05) \times 10^5$ years and 3.75 $(\pm 0.11) \times 10^4$ disintegration/min per μg, respectively. These results are in excellent agreement with previous values. (auth)

22037 INFLUENCE OF RECOIL STOPPING TIME ON THE MOESSBAUER EFFECT FOLLOWING ALPHA DECAY. Kaplan, M. (Yale Univ., New Haven). J. Inorg. Nucl. Chem., 28: 331-4(Feb. 1966). (NYO-3219-5).

The stopping theory of high-velocity heavy ions was applied to the problem of nuclear recoil from alpha decay, and straightforward ideas were used to derive the stopping time. The case of ^{237}Np stopping in NpO_2 was worked out in detail, and is discussed in light of experiments on the Mössbauer effect following α decay of ^{241}Am. The computed range of 93-kev ^{237}Np recoil nuclei is 2.36×10^{-6} cm, and the stopping time is approximately 3.9×10^{-13} sec. Since these results are relatively insensitive to the particular system studied, it was concluded that recoil stopping times following α decay are extremely short in comparison to lifetimes of nuclear states likely to emit Mössbauer γ rays. Hence the relaxation processes, which occur at the end of the recoil track, set the influential time scale in Mössbauer experiments. (auth)

22038 THE HALF LIFE OF THE 0.305-Mev LEVEL IN ^{75}As. Lange, R. C.; Hagee, G. R.; McCarthy, J. T. (Mound Lab., Miamisburg, Ohio. Univ. of Cincinnati). J. Inorg. Nucl. Chem., 28: 651-4(Feb. 1966). (MLM-1282J).

An experiment was performed to determine the half life of the 0.305-Mev level in ^{75}As. Data collected after a total of 1,122,159 sweeps using a scintillation counter are shown. The counts per channel were plotted on a log scale vs time. The computed value for the half life, 15.64 ± 0.92 msec, is also shown. A comparison of the theoretical and experimental transition probability values for decay of the 0.305-Mev level in ^{75}As is given. The theoretical transition probability (T_{sp}) values for decay of the 0.305-Mev level in ^{75}As were computed from Moszkowski's formulas. The 0.025- and 0.305-Mev transitions were assumed to be M2 ($\Delta I = 2$) and E3 ($\Delta I = 3$). (F.J.H.)

22039 ACTIVATION CROSS SECTIONS FOR THE REACTIONS OF 14.8-Mev NEUTRONS WITH ^{99}Tc. Goldstein, G. (Oak Ridge National Lab., Tenn.). J. Inorg. Nucl. Chem., 28: 676-8(Feb. 1966). (ORNL-P-1283).

The cross sections for the reactions of 14-Mev neutrons with ^{99}Tc were determined by activation methods. Technetium metal was irradiated and the activity of the reaction determined by gamma spectrometry. The experimental results on cross sections are shown. It was concluded that 14.8-Mev neutron activation is not a useful analytical method for ^{99}Tc. The (n,p) and (n,α) cross sections are small, while measurement of the products of the (n,n′) reaction, ^{99m}Tc, is complicated by bremsstrahlung from ^{99}Tc decay. (F.J.H.)

22040 650-Mev PHOTOFISSION YIELDS FOR URANIUM. Sakamtoto, K. (Tokyo Univ.); Kuroda, P. K. J. Inorg. Nucl. Chem., 28: 679-81(Feb. 1966).

A sample of uranyl acetate (200 g) was irradiated ~1 hr with 650-Mev bremsstrahlung. The irradiated sample was dissolved in 1 liter of 3N HNO_3. Aliquots were taken from the stock solution at various time intervals, and the fission yields of barium bromine, iodine, molybdenum, silver, and strontium isotopes were measured. The peak-to-valley yield ratio for the 650-Mev photofission of uranium, taken to be equal to the ^{99}Mo/^{111}Ag ratio, is 3.7 ± 0.8. This value is in line with the general trend of the decreasing peak-to-valley ratio previously reported by investigators: >300 at 7 Mev, 200 at 10 Mev, 38 at 16 Mev, 23 at 21 Mev, 11 at 48 Mev, 8 at 100 Mev, and 4 at 300 Mev. (F.J.H.)

22041 TWO γ RAYS IN THE DECAY OF 3.0-MIN ^{85}Br. Williams, E. T.; Coryell, C. D. (Massachusetts Inst. of Tech., Cambridge). Contract AT(30-1)-905. J. Inorg. Nucl. Chem., 28: 681-2(Feb. 1966). (MIT-905-44).

The decay of 3.0-min ^{85}Br was previously reported to proceed solely by a β transition to the ground state of ^{85}Kr. In a previous study of short-lived bromine fission products 54-sec ^{86}Br and 55-sec ^{87}Br, gamma rays of 0.81 and 0.92 Mev were observed to decay with a half life of ~3 min. It is shown that these two gamma rays, at 0.81 and 0.92 Mev, arise in the decay of ^{85}Br. The β spectrum was measured and the maximum endpoint energy was found to be 2.5 ± 0.5 Mev. Experiments showed that the two gamma rays were in coincidence with each other. (F.J.H.)

22042 NUCLEAR SYSTEMATICS OF THE HEAVY ELEMENTS. I. ENERGETICS AND MASSES. Viola, V. E. Jr. (Argonne National Lab., Ill.); Seaborg, G. T. J. Inorg. Nucl. Chem., 28: 697-739(Mar. 1966).

From examination of nuclear decay energy systematics, the mass-energy surface of the heavy elements was extended to experimentally unknown isotopes. The mass predictions are made by empirical extrapolation of α- and β-decay energies, which fit together to form closed cycles. Experimental masses and energies are based on the most recent work of Wapstra et. al. The following quantities were tabulated for nuclei with $54 \leq Z \leq 108$ and $139 \leq A \leq 277$: nuclidic mass, α- and β-decay energies, and neutron and proton binding energies. In addition the systematic behavior of the kinetic energy release in fission was examined. (auth)

22043 NUCLEAR SYSTEMATICS OF THE HEAVY ELEMENTS. II. LIFETIMES FOR ALPHA, BETA, AND SPONTANEOUS FISSION DECAY. Viola, V. E. Jr. (Argonne National Lab., Ill.); Seaborg, G. T. J. Inorg. Nucl. Chem., 28: 741-61(Mar. 1966).

The experimental half lives for alpha, beta, and spontaneous fission decay were analyzed for the heavy elements ($A \geq 140$). From the systematic behavior of these data, semi-empirical relations were derived for use in the prediction of lifetimes for undiscovered nuclides. Alpha-decay predictions are based on a square well nuclear model; β decay is approximately treated in terms of average log (ft) values, and spontaneous fission is considered from the point of view of the liquid drop model. Particular emphasis is given to nucleosynthesis problems involving the trans-ferium nuclei. It was estimated that a number of relatively stable nuclei with mass number A ~ 270 to 290 exist. For nuclei having 184 neutrons, or slightly

less, special stability was expected because of the closed neutron shell at N = 184. Nuclei with N > 184 should have extremely short alpha and spontaneous fission decay lifetimes. The implications of these predictions for various problems relating to chemistry and cosmology are briefly discussed. (auth)

22044 FRACTIONAL CHAIN YIELD OF ^{126}Sb IN THERMAL-NEUTRON FISSION OF ^{235}U. Aras, N. K. (Oak Ridge National Lab., Tenn.); Gordon, G. E. Contract AT(30-1)-905. J. Inorg. Nucl. Chem., 28: 763-70(Mar. 1966). (MIT-905-41).

The fractional chain yield of 12.5-day ^{126g}Sb in thermal-neutron fission of ^{235}U was measured by following the β decay of antimony samples separated several weeks after an irradiation. The observed ^{126g}Sb is the sum of contributions from ^{126g}Sb produced in fission and that resulting from 19% min ^{126m}Sb, which decays 15% by isomeric transition. The ^{126m}Sb was not observed, but its independent yield relative to that of ^{126g}Sb was estimated on the basis of theoretical calculations, which took into account the spins, 5+ and 8−, of the upper and lower isomers, respectively. The sum of the fractional chain yields of the ^{126}Sb isomers was determined as $4.5 \pm 0.6 \times 10^{-2}$, leading to a value of most probable charge, Z_p, for A = 126 of 49.45 ± 0.05. By γ spectrometry on the samples, the yield of 60.9-day ^{124g}Sb was determined relative to that of 2.78-year ^{125}Sb. The resulting fractional chain yield for ^{124}Sb $\leq 2.6 \times 10^{-3}$, gave Z_p of $\leq$ 48.75 for A = 124. (auth)

22045 FISSION AND SPALLATION YIELDS IN THE IODINE REGION. Rudstam, G.; Soerensen, G. (CERN, Geneva). J. Inorg. Nucl. Chem., 28: 771-94(Mar. 1966).

Cross-section measurements of many iodine isotopes (ranging from ^{118}I to ^{135}I) produced in various target elements by the interaction of high energy protons are reported. The experimental technique makes extensive use of electromagnetic isotope separation followed by activity measurements of the samples obtained. The results demonstrated the variation of the yield distribution of the iodine isotopes with target element and irradiation energy (590 Mev and 18 Bev). For uranium bombarded with 18-Bev protons, it was found that the isotopic distribution could be be built up by a superposition of a spallation part and a fission part. (auth)

22046 UPPER LIMIT OF THE HALF-LIFE OF ^{199m}Au ISOMER. Gopinathan, K. P. (Tata Inst. of Fundamental Research, Bombay). J. Inorg. Nucl. Chem., 28: 911-13 (Mar. 1966).

Determination of the upper limit of the half life of ^{199m}Au isomer fraction extracted from irradiated Pt is described. Pure Pt metal (99.9%) was irradiated in a flux of $\sim 10^{12}$ n/cm^2 sec in the reactor. The irradiated Pt foil was dissolved and 5 mg of Au carrier was added as gold chloride solution. Red $HAuBr_4$ was extracted with isopropyl ether. The gamma spectrum of the washed ether layer was taken in a gamma spectrometer at successive intervals of 30 sec. The 475-kev gamma was not observed in the gamma spectrum of the milked extract. It showed peaks of x-ray, 158-, and 208-kev gamma rays of ^{199}Au, and a gamma ray at 279 kev. The spectrum taken 30 sec afterwards showed all the gamma rays, except at 279 kev. The intensity of the 279-kev gamma ray, corrected for chemical yield, was plotted as a function of the milking time. The upper limit of the half life of ^{199m}Au was calculated to be 1 sec. (F.J.H.)

22047 ELASTIC AND INELASTIC SCATTERING OF 28.4-Mev ALPHA PARTICLES BY Sn, Cd, Ag, Cu, AND Ti. Kumabe, Isao; Ogata, Hiroshi; Tomita, Shigeharu; Inoue, Makoto; Okuma, Yasuhiko (Kyoto Univ.). J. Phys. Soc. Jap., 21: 413-20(Mar. 1966).

The angular distributions of alpha particles elastically and inelastically scattered by Sn, Cd, Ag, Cu, and Ti were measured at 28.4 Mev. For Sn, Cd, and Ag, the angular distributions of the prominent groups corresponding to the quadrupole and octupole excitations were fitted by calculations based on Blair model in a preliminary step. The angular distributions of the groups near 1.22 Mev in Cd and near 0.90 Mev in Ag were found to have an intermediate phase between the corresponding elastic distribution and the distribution for the quadrupole excitation. The angular distributions for the inelastic scattering leading to various states of Cu and Ti were also obtained. Discussions are also presented based on the results of the DWBA analysis. (auth)

22048 ENERGY AND ANGULAR DISTRIBUTIONS OF PROTONS FROM ^{64}Zn BOMBARDED BY 14 Mev NEUTRONS. Fujita, Iwao (Kyushu Univ., Japan). Kyushu Daigaku Kogaku Shuho, 37: 294-9(Jan. 1965). (In Japanese).

Cross sections, energy spectra, and angular distributions of the protons were measured for the ^{64}Zn(n,p)^{64}Cu and ^{64}Zn(n,np)^{63}Cu reactions using photographic emulsion as the detectors. The results were compared with those calculated by the statistical theory of nuclear reactions. The backward emission of the protons can be described by the statistical model. The cross sections for the reactions, which take place through the compound nucleus, are 159 ± 27 and 22 ± 48 mb, respectively. The nuclear temperatures of the residual nuclei for the ^{64}Zn(n,p)^{64}Cu and ^{64}Zn(n,np)^{63}Cu reactions are 1.16 ± 0.08 and 0.44 ± 0.02 Mev, respectively. The contribution to the reaction from the direct processes is about 51 mb. Using the formula $\rho(U) = \text{const.} \exp[2\sqrt{aU}]$ for the level density, the level density parameter, a = 8.47 ± 0.76 Mev^{-1}, was obtained, which agrees well with other data. The anisotropy of the angular distributions increases with the energy of the emitted protons. This does not agree with the Allen's theory that the large anisotropy is attributable to the second proton emissions. (auth)

22049 OPTICAL MODEL CALCULATION OF TRANSMISSION COEFFICIENTS AND TOTAL CROSS SECTIONS OF HEAVY NUCLEI FOR PROTONS. Wakuta, Yoshihisa; Sonoda, Masateru (Kyushu Univ., Japan). Kyushu Daigaku Kogaku Shuho, 38: 18-27(Mar. 1965). (In Japanese).

Transmission coefficients and total nuclear reaction cross sections were calculated for the heavy nuclei, U-238, Th-232, Bi-209, Pb-208, and Au-197, using the optical model for nuclei. The incident proton energies used were from 30 to 90 Mev at 10 Mev intervals. Calculations were done with the ELIESE-1 code programmed by the Sigma Committee. The optical model potential was taken as $v_C(r) = v_{CR}(r) + iv_{CI}(r)$, where $v_{CR}(r)$ and $v_{CI}(r)$ are the central, real, and imaginary potentials, respectively, with the form factors for each potential being the Woods−Saxon and the derivative Woods−Saxon type. The potential depths of the real and imaginary parts of the optical model were extrapolated from the data already published. The spin-orbit coupling term was neglected in the calculation because of its small effect on the result. The typical optical model parameters used in the calculations are tabulated. The transmission coefficient $T_e(E)$ and the total reaction cross section σ_R are shown as a function of the incident proton energy and also the angular distribution for the elastic proton scattering for the nuclei. The distribution of the angular momentum of the incident proton was obtained and compared with the classical approximation. The agreement between them was found to be good in the energy region above 50 Mev. (TCO)

22050 MECHANICAL DRIVING UNIT FOR MOESSBAUER EXPERIMENTS. Kiss, Elemer. Magyar Tud. Akad. Kozp. Fiz. Kut. Int. Kozlem., 13: 431-8(1965). (In Hungarian).

The drum-controlled mechanical driving unit for Mössbauer effect measurements is described. The problems encountered in designing and building the mechanical unit are discussed in detail. Special care was taken of the damping of mechanical vibrations. (auth)

22051 SIMPLE METHOD FOR THE EVALUATION OF THE PARAMETERS OF EXPONENTIAL DECAY CURVES. Varga, Laszlo. Magyar Tud. Akad. Kozp. Fiz. Kut. Int. Kozlem., 14: 21-4(1966). (In Hungarian).

Expansion in exponential terms by the so-called Prony method is considered from the statistical aspect in the most simple case when the parameters of the decay curve with a single exponential term are evaluated. (auth)

22052 MEASUREMENT OF THE ISOMERIC CROSS-SECTION RATIO ON NEUTRON ACTIVATED ^{85,85m}Sr, ^{122,122m}Sb, AND ^{188,188m}Re. Kardon, Bela; Kiss, Dezso. Magyar Tud. Akad. Kozp. Fiz. Kut. Int. Kozlem., 14: 85-92(1966). (In Hungarian).

Isomeric cross-section ratios were measured on the nuclei ^{85}Sr, ^{85m}Sr, ^{122}Sb, ^{122m}Sb and ^{188}Re, ^{188m}Re activated by thermal neutron from the VVRS reactor, the values of σ_m/σ_g found to be 2.12 ± 0.08; /8.3 ± 0.9/0.10^{-3}; /8.5 ± 2.5/0.10^{-2}, respectively. (auth)

22053 LEVEL SCHEMES OF $^{67+68+70}$Ga. Rester, D. H.; Durham, F. E.; Class, C. M. (Rice Univ., Houston, Tex.). Nucl. Phys., 80: 1-13(1966). (TID-22347).

The internal conversion electron and gamma-ray spectra due to proton-induced reactions with separated zinc isotopes 67, 68 and 70 were measured at various incident beam energies between 1.5 and 5.0 Mev. Many lines seen in the spectra are attributed to transitions in the gallium isotopes produced by the Zn(p,n)Ga reaction. The transition energies together with other available data have been used to assign energy levels in ^{67}Ga at 0.166, 0.356, 0.820, 0.910, 1.25, and 1.55 Mev; in ^{68}Ga at 0.174, 0.316, 0.373, 0.510, 0.573, 0.828, 0.879 and 1.10 Mev; and in ^{70}Ga at 0.188, 0.448, 1.03 and 1.66 Mev. Threshold measurements confirmed the existence of levels at 0.174, 0.316, 0.373, and 0.510 Mev in ^{68}Ga. (auth)

22054 ANALYSIS OF FLUCTUATIONS IN SYNTHETIC EXCITATION FUNCTIONS. Van Der Woude, A. (Oak Ridge National Lab., Tenn.). Nucl. Phys., 80: 14-32(1966).

The results of the analysis of a set of synthetic excitation functions, computed according to the statistical model for nuclear reactions, are presented. The emphasis lies on the effect of experimental circumstances on the autocorrelation function, the number of maxima per unit interval and on the distribution function. Curves are presented showing the effect of finite intervals on the relative standard deviation of the coherence length Γ. It turns out that the reliability of Γ determined with the method of counting maxima is higher than in case it is determined from the autocorrelation function. It also turns out that the number of maxima per unit interval is nearly independent of the number of channels participating in the reaction and of the amount of direct interaction involved. Moreover this number is not biased for the interval length, while the Γ found from the autocorrelation function is biased for interval length. None of the techniques discussed is very useful for determining the number of independent channels and the amount of direct interaction involved. Only under very special circumstances are these methods found to give reliable information. (auth)

22055 GYROMAGNETIC RATIOS ON THE FIRST EXCITED 2^+ STATES IN EVEN Os ISOTOPES. Goldring, G.; Kalish, R.; Spehl, H. (Weizmann Inst. of Science, Rehovoth, Israel). Nucl. Phys., 80: 33-45(1966).

Integral precession measurements are reported for the 2^+ states in ^{188}Os, ^{190}Os, and ^{192}Os. The levels were Coulomb excited with high-energy oxygen ions, and gamma rays were observed in coincidence with backscattered ions. A suitable environment of low perturbation was provided by letting the excited nuclei recoil into copper. The measured g factors are g(^{188}Os) = 0.270 ± 0.018, g(^{190}Os) = 0.323 ± 0.044, g(^{192}Os) = 0.337 ± 0.045. (auth)

22056 SCATTERING OF FAST NEUTRONS BY ^{238}U. Barnard, E.; Ferguson, A. T. G.; McMurray, W. R.; Van Heerden, I. J. (Atomic Energy Research Establishment, Harwell, Eng.). Nucl. Phys., 80: 46-64(1966).

Elastic and inelastic scattering of fast neutrons by ^{238}U were studied in the energy range 75−1620 kev using time-of-flight techniques. The differential cross sections for inelastic scattering to the 45 and 149 kev levels were measured with good resolution up to an incident neutron energy of 750 kev. Excitation functions of differential scattering cross sections were obtained at 90° for 13 levels in ^{238}U up to 1190 kev. All these cross sections were determined in an absolute manner. Levels at 939 and 968 kev not previously observed by Coulomb excitation are strongly excited and are most probably intrinsic states of ^{238}U. The differential cross sections at 90° for an incident neutron energy of 1620 kev were also determined for eight ^{238}U levels between 1210 and 1470 kev. The results were analyzed using the optical model and the theory of Hauser-Feshbach corrected for level with fluctuations within the compound nucleus. (auth)

22057 DETERMINATION OF CONVERSION RATIOS OF 191-kev TRANSITIONS IN ^{197}Au. Gasser, M.; Huber, O.; Schellenberg, L. (Univ., Freiburg i. B.). Nucl. Phys., 80: 65-73(1966). (In German).

The following conversion ratios of the 191 kev transition in ^{197}Au were measured with a double focusing β spectrometer: K/L = 5.9 ± 0.2 L_I/L_{II} = 10.7 ± 0.5, L_I/L_{III} = 74 ± 15. The L_I/L_{II} value is consistent with a practically pure M1 transition (EO(L_I)/M1 ≦ 0.9% or E2/M1 ≦ 0.6%), which leads to a calculated α_K = 1.01 ± 0.03. The L_I/L_{III} value corresponds to a mixture E2/M1 = $(0.9^{+0.7}_{-0.5})$% giving α_K = 0.983 ± 0.005. The two derived α_K agree with each other. Their values exclude reported α_K which give strong EO admixtures and spin $\frac{1}{2}^+$ of the 269 kev level. Some other α_K measurements and the theoretical value (core-particle model) are in good agreement with this result and give a strong preference for spin $\frac{3}{2}^+$ of the ^{197}Au 269 kev level. (auth)

22058 NANOSECOND LIFETIME MEASUREMENTS IN THE DECAY OF ^{155}Eu, ^{157}Eu, AND ^{157}Dy. Meiling, W.; Stary, F. (Bereich Kernphysik, Dresden). Nucl. Phys., 80: 74-80(1966). (In German).

The lifetime of the 87 kev state of ^{155}Gd was measured using the delayed coincidence method. The result was $T_{½}$ = 6.65 ± 0.2 ns in agreement with measurements on the ^{155}Tb decay. The half-life of the 105 kev level in ^{155}Gd was found to be $T_{½}$ = 1.11 ± 0.06 ns. From the exponential tail of the coincidence curves upper limits of the lifetime were estimated for ^{157}Gd, $T_{½}$ (437; 477 kev) < 0.1 ns; $T_{½}$ (684 kev) < 0.3 ns; ^{157}Tb, $T_{½}$ (326 kev) < 0.25 ns. Measured E1 transition probabilities are compared with Nilsson calculations including the influence of pairing correlations. (auth)

22059 ANGULAR CORRELATIONS IN INELASTIC PROTON SCATTERING ON ^{20}Ne AND ^{32}S. Hulubei, H.; Martalogu, N.; Neamu, I.; Scintei, N.; Berinde, A. (Inst. for Atomic Physics, Bucharest). Nucl. Phys., 80: 81-92 (1966).

The mechanism of scattering of 8.5 Mev protons to the first excited states of ^{20}Ne and ^{32}S was studied by proton-gamma angular correlation measurements. The ^{20}Ne(p,$p_1\gamma$), Q = −1.63 Mev, reaction proceeds predominantly by direct interaction; the ^{32}S(p,$p_1\gamma$), Q = −2.24 Mev reaction by the statistical compound nucleus mechanism, with possibly a small contribution of the direct mechanism. (auth)

22060 MEASUREMENT OF Z DEPENDENCE OF ELASTIC SCATTERING CROSS SECTION OF GAMMA RAYS. II. Anand, S.; Singh, M.; Sood, B. S. (Punjabi Univ., Patiala, India). Nucl. Phys., 80: 93-8(1966).

Previous measurements of Z-dependence of large-angle elastic scattering cross section of gamma rays were extended to scattering angles 4° < θ < 20°. The experimental results were found to agree with the theoretical calculations of Nelms and Oppenheim and earlier measurements of various workers, wherever available. (auth)

22061 PHENOMENOLOGICAL α-α POTENTIALS. Ali, S. (The Univ., Manchester, Eng.); Bodmer, A. R. Nucl. Phys., 80: 99-112(1966).

Phenomenological l-dependent α-α potentials are obtained for l = 0, 2 and 4 from fitting the relevant phase shifts for c.m. energies ≲12 Mev. For the nuclear part of the potentials, a superposition of repulsive and attractive Gaussian shapes was used. Following theoretical indications, an attempt was made to obtain fits with an l-independent attractive part having a longer range than the repulsive parts, and to obtain, at first, the attractive

part from just the l = 4 phase shift in view of the effect of the large l = 4 centrifugal barrier in masking the inner repulsive part. It is, in fact, found possible to obtain acceptable potentials with a common attractive part. These potentials are, however, strongly l-dependent through the repulsive part which becomes weaker as l increases. For l = 4, only a quite weak repulsive part is found to be permissible. The potentials are in good agreement with those recently obtained by Darriulat et al. The possible importance of the attractive tail of the α-α potential as a selective probe into just the central, spin-independent, isospin-independent part of the nuclear force is pointed out and discussed. (auth)

22062 SURFACE REACTIONS OF STRONGLY ABSORBED NUCLEAR PARTICLES IN THE ADIABATIC APPROXIMATION. **Hahne, F. J. W. (Univ. of Cape Town). Nucl. Phys., 80: 113-24(1966).**

Nuclear surface reactions are treated in the spin-independent, zero-range, distorted-wave Born approximation formalism. It is shown that the angular distribution can be expressed essentially in terms of Fourier transforms of the radial integrals. For inelastic scattering in the adiabatic limit simple expressions are obtained. The Blair phase rule is derived. Coulomb and real nuclear phase shifts effects are included. (auth)

22063 ELASTIC ELECTRON SCATTERING BY ^{6}Li. **Lodhi, M. A. K. (Texas Technological Coll., Lubbock). Nucl. Phys., 80: 125-30(1966).**

It is possible to fit the elastic electron scattering data with a single oscillator parameter as in other 1p shell nuclei even for large momentum transfer if the residual two-body interaction in the single-particle shell model is taken into account. The residual interaction causes configuration mixing from the states higher than the lowest one including the core excitation. (auth)

22064 STUDY OF THE ^{55}Mn(n,γ)^{56}Mn REACTION. **Hughes, L. B.; Kennett, T. J.; Prestwich, W. V. (McMaster Univ., Hamilton, Can.). Nucl. Phys., 80: 131-44 (1966).**

The gamma radiation from the ^{55}Mn(n,γ)^{56}Mn reaction was studied using a Ge(Li) spectrometer and also a Ge(Li)-NaI coincidence spectrometer. A total of 130 gamma rays were observed and their intensity and energy determined. The neutron separation energy was found to be 7272 ± 3 kev. The level structure for the first 4000 kev is in excellent agreement with the (d,p) results. The decay modes of several of the low-energy states were deduced from coincidence and energy information. A calculation of the correlation between the gamma-ray reduced widths and the (d,p) strength yields a coefficient of +0.84. (auth)

22065 DEFORMATION ENERGIES AND COLLECTIVE MOTION OF HEAVY NUCLEI. **Adams, J. L.; Kuemmel, H. G. (Oklahoma State Univ., Stillwater). Nucl. Phys., 80: 145-53(1966).**

Using deformation energies from a semiphenomenological description of nuclear binding energies, the consistency of collective models was checked and β oscillation energies were predicted. (auth)

22066 INTERNAL CONVERSION STUDY OF ^{113}Cd(n,γ)^{114}Cd. **Baecklin, A.; Holmberg, N. E.; Baeckstroem, G. (Univ. of Uppsala). Nucl. Phys., 80: 154-76(1966).**

The internal conversion spectrum from ^{113}Cd(n,γ)^{114}Cd was measured with a resolution of 0.2%. Conversion lines were found for 45 transitions, and the corresponding multipolarities were obtained with the aid of gamma ray intensities from earlier crystal diffraction measurements. In addition to the known EO transitions from the 1134 and 1305 kev levels to the ground state, a line corresponding to an EO transition between these levels was found. The conversion coefficients of four transitions between levels of equal spin and parity were found to be anomalously large, which can be ascribed to EO admixture. Above 400 kev, the energy values were found to deviate in a systematic way from those obtained in the crystal diffraction measurements. The decay scheme was constructed by using a computer program based on energy relationships. The possibility of obtaining accidental relationships was taken into account. Seven levels were established above 1.4 Mev. (auth)

22067 A FORMALISM FOR DIRECT INELASTIC SCATTERING AND CHARGE EXCHANGE. **Madsen, V. A. (Oregon State Univ., Corvallis). Nucl. Phys., 80: 177-97 (1966). (TID-22636).**

A general formulation of the direct inelastic scattering problem is presented. It is applicable to collisions between a nuclear projectile having mass number A ≦ 4 and any target nucleus for which a shell model description can be given. The interaction is taken to be the sum over nucleon pairs of a central potential with arbitrary spin-isospin mixture. Expressions for the differential cross section are given in terms of spectroscopic amplitudes, which contain all detailed information about the structure of both projectile and target nucleus. Explicit expressions for the spectroscopic amplitudes are given in terms of the nuclear wave functions. (auth)

22068 AN INTERPRETATION OF TIME-DEPENDENT HARTREE-FOCK THEORY. **Rowe, D. J. (Atomic Energy Research Establishment, Harwell, Eng.). Nucl. Phys., 80: 209-22(1966).**

The eigenvalue equation of the random phase approximation (RPA) has been applied successfully to nuclear vibrations, but it is difficult to justify the approximation in physical terms. The equations have been derived from time-dependent Hartree-Fock (TDHF) theory, on the grounds that it is more physical. It is pointed out that this claim is dubious. The meaning of TDHF theory, especially of the wave function, is not nearly as apparent as might appear at first sight. The TDHF and RPA methods are studied, and it is shown that the approximations involved in the two approaches are in fact equivalent. In particular it is demonstrated that the TDHF method is not an adiabatic approximation and neither is it a classical or semi-classical treatment. A new interpretation of TDHF theory is developed; this gives insight into the mechanism of nuclear vibrational motion, and exhibits its relationship with other methods. (auth)

22069 GAMMA-RAY SPECTRA FROM INELASTIC NEUTRON SCATTERING. **Bergqvist, I. (Research Inst. of National Defence, Stockholm); Lundberg, B.; Nilsson, L.; Starfelt, N. Nucl. Phys., 80: 198-208(1966).**

The γ-ray spectra emitted after inelastic scattering of 5.8 and 7.5 Mev neutrons in Fe, Ni, Cu, Zr, Ag, I, Ta, W, Au, Hg, Pb and Bi were studied. The measured spectra were compared with γ-ray spectra emitted in the capture of 0.1 Mev neutrons. This comparison strongly indicates that a large fraction of the high-energy γ-rays observed in neutron capture is due to a direct or semi-direct capture mechanism. (auth)

22070 EVIDENCE FOR THE INFLUENCE OF SHELL STRUCTURE ON LEVEL DENSITIES IN THE CONTINUUM. **Blann, Marshall (Univ. of Rochester, N. Y.). Nucl. Phys., 80: 223-6(1966).**

Excitation functions for the production of nuclides around the $1f_{\frac{7}{2}}$ shell closure (at excitations of 22 to 65 Mev) are compared with statistical theory calculations in which four different level density models are used in order to assess the importance of shell structure on level densities in the continuum. The Weisskopf-Ewing evaporation formula was used with appropriate computer programs for these calculations. The level densities employed are Fermi gas level densities with constant level spacing parameter, with level spacing parameter varying with shell occupation according to Newton's model, with a shift in ground state energies with shell occupation according to Rosenzweig's model and a hybrid model in which the level spacing parameter is selected to give the qualitative energy variation of Newton's model with the qualitative shell occupation variation of Rosenzweig's model. A pairing correction is applied to all four level density models. Reactions producing nuclides away from the $f_{\frac{7}{2}}$ shell closure are analyzed using a Fermi gas level density. Analyses are performed both with optical model

and continuum theory inverse cross sections. It is concluded that the Fermi gas level density with constant (a = A/8.5) level spacing parameter is satisfactory away from shell closures, but inadequate for reactions producing nuclides near the $f_{\frac{7}{2}}$ shell closure. Newton's model gives neither the correct shell-occupation variation nor energy variation for level densities near closed shells, while Rosenzweig's model appears to reproduce both features adequately. The conclusions are independent of choice of inverse reaction cross sections and pairing energy. (auth)

22071 AN INVESTIGATION OF THE $^{10}B(n,\alpha)^7Li^*$, ^7Li REACTION BRANCHING RATIO. Toney, William M.; Waltner, Arthur W. (North Carolina State Univ., Raleigh). Nucl. Phys., 80: 237-40(1966).

The branching ratio of the $^{10}B(n,\alpha)^7Li^*$, ^7Li reaction was measured at thermal neutron energies by irradiating a ^{10}B film and measuring the relative number of α-particles in the peaks associated with the ground state and the first excited level. Detection was by a silicon surface barrier detector. The percent of reactions going to the ground state was found to be 6.43 ± 0.11. (auth)

22072 ROTATIONAL BANDS ON TWO-PARTICLE CONFIGURATIONS WITH $K_n = K_p = \frac{1}{2}$. Ryde, H.; Symons, G. D.; Szymanski, Z. (California Inst. of Tech., Pasadena). Nucl. Phys., 80: 241-58 (1966).

Low-lying energy levels in the odd deformed nucleus ^{170}Tm are studied by means of Coulomb excitation with heavy ions and by the $^{169}Tm(d,p)^{170}Tm$ reaction. The results are analysed in terms of the rotational model with the assumption of two rotational K = 1 and K = 0 bands coupled by Coriolis interaction. The 150 kev splitting between the two bands is found to be predominantly due to the neutron-proton residual force. The sequence of levels in the ground state K = 1 rotational band is proposed. As a part of this experiment, the Coulomb excitation of ^{170}Yb was also studied. The following members of the ground state rotational band are seen: $84(2^+)$, $278(4^+)$ and 567 kev (6^+). The intrinsic quadrupole moment, Q_0 (^{170}Yb), obtained from this measurement is 7.40 ± 0.40 b. The Q-value for the $^{169}Tm(d,p)$ ^{170}Tm reaction is measured to be 4420 ± 20 kev. (auth)

22073 LEVELS OF ^{42}Sc FROM $^{40}Ca(^3He,p)^{42}Sc$ AND ^{40}Ca $(^3He,p\gamma)^{42}Sc$. Zurmuehle, R. W. (Univ. of Pennsylvania, Philadelphia); Fou, C. M.; Swenson, L. W. Nucl. Phys., 80: 259-72(1966).

Levels of ^{42}Sc at 0.62, 1.51, 1.59, 1.88, 2.22, 2.28, 2.40, 2.50, 2.64, 2.82, 3.09, 3.25, 3.33, 3.39 and 3.47 Mev were studied by means of the $^{40}Ca(^3He,p)^{42}Sc$ reaction at 10, 12 and 15 Mev incident energies. Angular distributions were measured, which are consistent with spin assignments of J = 0, 1, 3 and 0 for the ground state, 0.62, 1.51 and 1.88 Mev excited states of ^{42}Sc, respectively. Spin assignments were made on the basis of a DWBA analysis of the 12 Mev angular distributions. The assignments are supported by observations of the gamma decays of the 0.62, 1.51 and 2.82 Mev states in coincidence with protons from the ^{40}Ca $(^3He,p\gamma)^{42}Sc$ reaction at 10 Mev incident energy. (auth)

22074 ANGULAR DISTRIBUTIONS AND CROSS SECTION RATIOS FOR THE REACTIONS $^2H(d,n)^3He$ AND $^2H(d,p)^3H$ BELOW 500 kev. Theus, R. B.; McGarry, W. I.; Beach, L. A. (Naval Research Lab., Washington, D. C.). Nucl. Phys., 80: 273-88(1966).

The competing reactions $^2H(d,n)^3He$ and $^2H(d,p)^3H$ were remeasured over the bombarding energy range of 20 kev to 350 kev with a magnetically analyzed beam incident on a gas target. The angular distributions of the charged reactions products were observed with surface barrier detectors at 10° intervals from 20° to 160° in the laboratory system. Energy dependent asymmetry coefficients from the expansion of the centre-of-mass angular distributions in terms of even powers of cos Θ and Legendre polynomials are obtained showing greater asymmetry in the neutron producing reaction. Branching ratios between the two reaction modes monotonically increase over this energy range with the neutron reaction favored above a bombarding energy of 30 kev. A theoretical analysis of these branching ratios and asymmetry coefficients indicate the mass radius of the ^3H nucleus is at least 8.5% smaller than that of the ^3He nucleus. (auth)

22075 PAIRING VIBRATIONS. Bes, D. R. (NORDITA, Copenhagen); Broglia, R. A. Nucl. Phys., 80: 289-313 (1966).

The properties of the collective states (pairing vibrations) which are associated with fields changing the numbers of particles are studied. In particular, the processes that may be enhanced by the coherence in the pairing-vibration state are discussed. (auth)

22076 CONVERSION ELECTRON-GAMMA DIRECTIONAL CORRELATION IN ^{133}Cs. Avignone III, Frank T.; Braden, C. H.; Patronis, E. T. Jr.; Wyly, L. D. (Georgia Inst. of Tech., Atlanta). Nucl. Phys., 80: 314-20(1966).

The directional correlations between the 355 kev gamma and the 81 kev gamma and the conversion electron from the 355 kev transition and the 81 kev gamma in the decay of ^{133}Cs were measured. For the gamma-gamma correlation the coefficient A_2 was found to be 0.040 ± 0.006, in reasonable agreement with prior results. For the conversion electron-gamma correlation the anisotropy was found to be 0.12 ± 0.02. These results are consistent with a spin of $\frac{1}{2}$ for the 436 kev level in ^{133}Cs and a mixing ratio $\delta = -0.16 \pm 0.02$, which is consistent with prior assignments based on the gamma-gamma correlation. A spin assignment of $\frac{3}{2}$ to the 436 kev level is consistent only with an almost pure E2 multipolarity for the 355 kev transition. (auth)

22077 INVESTIGATION OF THE $^{32}S(n,\gamma)^{33}S$ REACTION. Van Middelkoop, G.; Gruppelaar, H. (Rijksuniversiteit, Utrecht). Nucl. Phys., 80: 321-34(1966).

The γ radiation following thermal neutron capture in ^{32}S was investigated with scintillation spectrometers. From γ-γ coincidence and angular correlation measurements the following spin assignments in ^{33}S were derived: $J(1.97) \geqq \frac{3}{2}$, $J(2.31) = \frac{3}{2}$, $J(4.21) = \frac{3}{2}$, $J(4.92) = (\frac{1}{2}, \frac{3}{2})$, $J(5.71) = \frac{1}{2}$, $J(5.89) = \frac{3}{2}$, $J(7.19) = \frac{3}{2}$ and $J(7.41) = (\frac{1}{2}, \frac{3}{2})$. New transitions in the γ-ray decay were found, a few of which are of M1 character competing favorably with E1 radiation. (auth)

22078 EXCITATION FUNCTIONS FOR THE REACTIONS INDUCED BY PROTONS ON Cd UP TO 37 Mev. Otozai, K. (Osaka Univ.); Kume, S.; Mito, A.; Okamura, H.; Tsujino, R.; Kanchiku, Y.; Katoh, T.; Gotoh, H. Nucl. Phys., 80: 335-48(1966).

The excitation functions for the reactions induced by protons on ^{110}Cd and ^{111}Cd, and on ^{112}Cd were measured radiochemically in the proton energy range from 5 to 37 Mev. In order to study the effects of angular momenta of compound nuclei, the excitation functions for the ^{110}Cd + p and ^{112}Cd + p reactions were compared with those for the ^{107}Ag + α and ^{109}Ag + α reactions, which may proceed through the same compound nuclei ^{111}In and ^{113}In, respectively. The effects were recognized in the isomeric cross section ratios but were not found on the patterns of neutron evaporations from the compound nuclei. On the basis of these results, some theoretical aspects of angular momentum effects upon the excitation functions are discussed. The total reaction cross sections agree with the calculated values based on the diffuse-surface optical model. (auth)

22079 THE CLASSIFICATION OF THE OSCILLATOR SHELL MODEL WAVE FUNCTIONS ACCORDING TO THE U_3 GROUP. Wadia, Wahby (Atomic Energy Establishment, Cairo). Nucl. Phys., 80: 349-52(1966).

The application of the concept of group theory and results of plethysm to the classification of the oscillator functions according to the U_2 group is explained and illustrated. (auth)

22080 ON THE PARITY MIXING IN SINGLE-NUCLEON ORBITALS. Amiet, J.-P. (Univ., Heidelberg); Huguenin, P. Nucl. Phys., 80: 353-66(1966).

A mixture of parity in single-particle orbitals leads to specific properties of the nuclear wave function. These properties are reviewed. The wave function is obtained by projecting out a part of definite parity from a product function. Formulas are given for some quantities, such

as the magnetic dipole moment, the magnetic dipole transitions, etc., which appreciably deviate from the values predicted by the usual shell model. It is shown why a parity mixing is not incompatible with the fact that definite l-values are measured in stripping reactions. The influence of this parity mixing on nuclear spectra is studied. In the case of odd nuclei, it is similar to that of the spin-orbit coupling if the spectrum of the preceding even nucleus satisfies a simple condition. (auth)

22081 GENERATOR COORDINATE METHOD APPLIED TO NUCLEI IN THE TRANSITION REGION. Onishi, Naoki; Yoshida, Shiro (Osaka Univ.). Nucl. Phys., 80: 367-76 (1966).

The generator coordinate method is applied to the transition region nuclei. Using the deformation parameter as a generator coordinate, the trial wave function is constructed by superposing shell-model wave functions with various values of the deformation parameter. For simplicity the deformation is restricted to be axially symmetric, and the pairing correlation is taken into account by using a BCS type shell-model wave function. The generator wave function which serves as a weight function may be obtained by solving an integral equation derived through the variational principle. In the integral equation there appear overlap and energy kernels, which are matrix elements between shell-model wave functions with different values of the deformation parameter. In calculating the kernels a new method is presented. The BCS type wave function is expressed in a more suitable form to practical calculations and the matrix elements are obtained in a simple and compact form without any approximation. (auth)

22082 NEUTRON-GAMMA CORRELATIONS FOR STATES IN ^{20}Ne AT 10.33 Mev AND 11.03 Mev. Ritter, Rogers C. (Univ. of Virginia, Charlottesville). Nucl. Phys., 80: 377-84(1966).

Time-of-flight measurements by the associated particle method (n,γ) were used to study two neutron groups corresponding to levels in ^{20}Ne. The decay scheme differs from that found in a previous experiment, as does the angular distribution for the 10.33 Mev level. A spin of 2^- is inferred for this level from present results. (auth)

22083 BETA DECAY AND CORE EXCITATION IN A = 111 NUCLEI. Delabaye, M.; Deutsch, J. P.; Lipnik, P. (Univ. of Louvain, Belg.). Nucl. Phys., 80: 385-93(1966).

Beta circularly polarized gamma angular correlation measurements were performed on the ^{111}Ag($\frac{1}{2}^-$)(β) ^{111}Cd* ($\frac{3}{2}^+$)(γ) ^{111}Cd($\frac{1}{2}^+$) cascade. All relevant results of the beta-decay measurements were used to obtain information on the structure of the involved nuclear states. The extreme single-particle and the core-excitation models yield the same prediction for the beta-decay measurements that were considered. (auth)

22084 THE STATISTICAL CHARACTER OF THE REACTION ^{37}Cl(p,α)^{34}S AT 21–22 Mev EXCITATION ENERGY OF THE COMPOUND NUCLEUS. Von Witsch, W.; Von Brentano, P.; Mayer-Kuckuk, T.; Richter, A. (Max Planck Institut fuer Kernphysik, Heidelberg). Nucl. Phys., 80: 394-416(1966).

For the reaction ^{37}Cl(p,α)^{34}S excitation functions and angular distributions were measured in steps of 8 kev in the energy range between 11 and 11.952 Mev. The transitions to the ground state and to the first and second excited states of ^{34}S were analysed. The cross section as a function of energy as well as angle shows strong fluctuations. For the analysis, correlation functions and probability distributions were calculated according to the statistical theory of Ericson and of Brink and Stephen. The results are in good agreement with the predictions of the theory. The average coherence energy Γ of 18 kev corresponds to a lifetime of 3.7×10^{-20} sec for the compound nucleus ^{38}Ar excited at 21 Mev. Estimations of the number of effective channels and the amount of direct interaction are given. The level spacing D_0 in the compound nucleus has been estimated to lie between 0.53 kev and 0.90 kev. (auth)

22085 MAGNETIC PROPERTIES OF EVEN NUCLEI. Greiner, Walter (Univ., Frankfurt am Main). Nucl. Phys., 80: 417-33(1966).

A relation between the well known lowering of the rotational g_R-factors and the magnetic dipole transitions is established. The basic idea of the proposed model is the assumption that the proton distribution in nuclei is somewhat less deformed than the neutron distribution because the pairing force acting between protons is larger than that acting between the neutrons. For this reason the g_R-factors differ from Z|A and further they are not simple numbers but tensors. As a consequence of this, magnetic dipole transitions can take place between the various collective states. The theory is developed for both deformed and spherical nuclei. No parameter except the known strength of the pairing forces for protons, G_p and neutrons, G_N, enters the calculation. The various experimental data (g_R-factors and, especially, the M1 – E2 mixing parameters) are explained semi-quantitatively. (auth)

22086 STRONG ABSORPTION MODEL FOR INELASTIC NUCLEAR SCATTERING. Potgieter, J. M.; Frahn, W. E. (Univ. of Cape Town). Nucl. Phys., 80: 434-48 (1966).

The connection between inelastic and elastic nuclear scattering of strongly absorbed particles in the adiabatic approximation has recently been established by Austern and Blair. This relation is made more explicit by employing the strong absorption model assumption of Frahn and Venter for the elastic scattering coefficients η_l. By means of suitable approximations simple closed expressions for the inelastic scattering cross section are obtained which are analogous to the strong absorption model formulas for elastic scattering. The results demonstrate the effects on the inelastic angular distribution of (i) the multipolarity of the excited nuclear state, (ii) the smooth transition of η_l in l-space, (iii) the Coulomb interaction, and (iv) the imaginary part of η_l. It is shown that the Blair phase rule is generally valid for single excitation of collective nuclear states in the adiabatic approximation. The approximate expressions are compared with typical experimental data for alpha particle scattering, and satisfactory simultaneous fits of the inelastic and elastic angular distributions are obtained. (auth)

22087 ^{12}C(d,pγ)^{13}C ANGULAR DISTRIBUTIONS AND CORRELATIONS NEAR THRESHOLD. Katman, T. S.; Fletcher, N. R.; Tilley, D. R.; Williamson, R. M. (Duke Univ., Durham, N. C.). Nucl. Phys., 80: 449-64(1966).

Proton-gamma angular correlations from the ^{12}C(d,pγ)^{13}C reaction through the 3.68 and 3.85 Mev states of ^{13}C were measured at bombarding energies from 2 to 3 Mev and at a strong E_d = 2.50 Mev resonance. Yield curves and proton angular distributions for these groups and for protons leaving ^{13}C in the 3.09 Mev state were also measured. These reactions satisfy the condition $E_d \approx -2Q$ for which distortions of plane wave stripping theory might be expected to be small. The correlation anisotropies are maximum and the symmetry axis shifts and azimuthal anisotropies are almost zero both at the minimum bombarding energy and at the 2.50 Mev resonance. Highly distorted correlations and distributions are seen at only 2.62 Mev. The ^{12}C(d,p)$^{13}C_{3.85}$ angular correlation at E_d = 2.50 Mev involves single-particle resonances both in ^{14}N and in ^{13}C and is an interesting example of a resonant direct reaction. The reduced widths derived from plane wave stripping theory are too low by factors of 3 to 10 and are energy dependent. Thus, while distortions clearly affect reduced widths, the detailed angular properties of the reactions are very close to the predictions of plane wave theory. (auth)

22088 EXCITATION OF THE SPIN-ISOSPIN GIANT RESONANCE BY 180 DEG INELASTIC ELECTRON SCATTERING. Lewis, Francis H. Jr. (Univ. of Washington, Seattle). Nucl. Phys., 80: 465-70(1966).

A very simple Goldhaber-Teller type of collective model is formulated to describe the "spin-isospin" giant resonance in nuclear matter. The model is used to calculate 180° electron scattering form factors and the results are compared with experiment for ^{12}C and ^{16}O. These results account qualitatively for the observed behavior of the giant resonance form factors as functions of q, although quan-

titative agreement with experiment is not completely obtained. Some consequences of these results are discussed. (auth)

22089 GAMMA-GAMMA DIRECTIONAL CORRELATION IN ^{123}Te. Gupta, S. L.; Bajaj, M. M.; Saha, N. K. (Univ. of Delhi). Nucl. Phys., 80: 471-5(1966).

The gamma-gamma directional correlation of the 89–159 kev cascade in ^{123}Te was investigated. The value of $A_2 = -0.088 \pm 0.025$ is obtained leading to a mixing ratio (E2/M1) = 0.011 ± 0.008 and to an E2 enhancement about 7 for the 159 kev transition. The results seem to support those obtained from the L-subshell ratios and are consistent with the recent theoretical ideas. (auth)

22090 PERTURBATION OF THE ANGULAR CORRELATION ON THE 1.35 Mev–0.198 Mev γ-γ CASCADE IN ^{19}F. Roepke, H. (Univ., Freiburg i.B.). Nucl. Phys., 80: 476-80(1966).

The electric and magnetic fields acting on ^{19}F nuclei, which were accelerated into several metallic media (Cu, Sn, Pb, W, Fe, Ni) by the recoil of the nuclear reaction ^{19}F(p,p')^{19}F*, were studied. Conclusions about the fields were obtained from a measurement of the perturbation of the angular correlation of the 1.35 Mev–0.198 Mev cascade of ^{19}F. For Cu, Sn, W, Pb the perturbation is explained by quadrupole interaction of the ^{19}F nuclei, the quadrupole frequencies $\nu_0 = \omega_0/2\pi$ being about 1 MHz. The perturbations in Ni and Fe are due to magnetic dipole interaction. The magnetic field at the site of the ^{19}F nuclei is 120 kG ± 10% in the case of Ni. (auth)

22091 GAMMA-RAY BRANCHING RATIOS FOR ^{116}In, ^{147}Nd AND ^{141}Ce. Eldridge, James S.; Crowther, Peter; Lyon, William S. (Oak Ridge National Lab., Tenn.). Nucleonics, 24: 62-4(Mar. 1966). (ORNL-P-1975).

Gamma branching ratios were determined for indium-116, neodymium-147, and cerium-141. The method of determination is outlined, and the branching ratios are given. The absolute disintegration rates were found using $4\pi\beta$–γ coincidence-counting techniques. The gamma spectra of indium-116 and neodymium-147 are shown. (J.F.P.)

22092 THREE-BODY FORCES IN P-SHELL CONFIGURATIONS. Nash, G. F. Nuovo Cimento (10), 42B: 8-12(Mar. 11, 1966).

A method is given for determining the number of three-nucleon clusters in a p-shell configuration, and a formula is derived for the contribution to the interaction energy from three-body forces. (auth)

22093 SOME FORMAL PROPERTIES OF THE GROUND-STATE WAVE FUNCTION FOR EVEN-EVEN NUCLEI. Formisano, V. (Univ., Rome); Violini, G.; Salusti, E. Nuovo Cimento (10), 42B: 71-8(Mar. 11, 1966).

Some formal properties of the α-cluster wave function and of the n particles component of the quasi-particle vacuum are examined. Exact methods of calculation are also proposed. As a test the Sn isotopes are studied. (auth)

22094 PHOTONEUTRON PRODUCTION FROM C, Al, AND S BY BREMSSTRAHLUNG UP TO 200 Mev. Bishop, G. (Univ. of Glasgow); Costa, S.; Ferroni, S.; Malvano, R.; Ricco, G. Nuovo Cimento (10), 42B: 158-69(Mar. 11, 1966).

By means of a special type of moderated neutron counter for which the energy response is nearly constant up to at least 50 Mev, a study of the total photoneutron cross section below 200 Mev was undertaken at the Orsay electron linear accelerator. The investigated nuclides were C, Al, and S. It was found that the cross sections well above the giant resonance are relatively important, and that their integrated values up to meson threshold are 5 to 6 times the giant resonance contribution. Besides it was possible, by taking into account the energy response of two different parts of the neutron counter, to separate the photoneutron cross sections for neutrons below and above 15 Mev energy respectively. The fast neutron contribution is particularly important in C and S, and less so in Al. Moreover above 140 Mev there is a gradual increase of the cross sections, probably related to an effect of neutron multiplicity. (auth)

22095 ISOTOPE SHIFT IN COULOMB DISPLACEMENT ENERGY. Sherr, R. (Princeton Univ., N. J.); Blair, A. G.; Armstrong, D. D. Phys. Lett., 20: 392-5(Mar. 1, 1966). (LA-DC-7673).

Isotope shifts are obtained by measuring the energies of isobaric analog states in the relevant isotopes. These shifts are small for protons in the $f_{7/2}$ shell, indicating no significant change in spatial wave functions of the protons as neutrons are added to the shell. Shifts for the Co and Cu isotopes indicate increases in nuclear size. (auth)

22096 SHELL MODEL CALCULATIONS IN THE CALCIUM ISOTOPES. Engeland, T.; Osnes, E. (Univ. of Oslo). Phys. Lett., 20: 424-8(Mar. 1, 1966).

The Ca-isotopes ^{42}Ca through ^{47}Ca were studied by a model assuming an inert ^{40}Ca core with an effective interaction in the neutron $f_{\frac{5}{2}}^n$ and $f_{\frac{5}{2}}^{n-1}p_{\frac{1}{2}}$ configurations. Good agreement with the experiments is obtained, particularly in the odd isotopes. (auth)

22097 NUCLEAR ORIENTATION OF ^{54}Mn NUCLEI IN NOBLE METAL HOSTS. Cameron, J. A.; Campbell, I. A.; Compton, J. P.; Lines, R. A. G.; Wilson, G. V. H. (Clarendon Lab., Oxford). Phys. Lett., 20: 569-71 (Apr. 1, 1966).

Measurements are reported of the anisotropy of γ-radiation from ^{54}Mn nuclei polarized in copper, silver, and gold hosts at low temperatures. Values for the hyperfine fields on the ^{54}Mn nuclei were determined. The effect of interionic interactions is discussed. (auth)

22098 NILSSON MODEL FOR ^{57}Fe. Sood, P. C. (Univ. of Alberta, Edmonton, Can.). Phys. Lett., 20: 647-8(Apr. 1, 1966).

The low lying levels in ^{57}Fe are interpreted in terms of the Nilsson model. The energy scale is chosen to correspond to the single particle level separations in the spherical limit. Good agreement for energy levels is obtained for the deformation parameter $\eta = 3$ which corresponds to the eccentricity parameter $\delta = 0.25$ in agreement with the value derived from the B(E2) and quadrupole moment for the first excited state. (auth)

22099 EVIDENCE FOR THE PROLATE DEFORMATION OF ^{27}Mg. Lacambra, J. M.; Tilley, D. R.; Roberson, N. R. (Duke Univ., Durham, N. C.). Phys. Lett., 20: 649-51(Apr. 1, 1966).

^{26}Mg(d,pγ)^{27}Mg angular correlation measurements yield spin assignments of $J = 3/2^+$, $5/2^+$, $(5/2)$, $3/2^-$, and $(3/2)$ for the excited states of ^{27}Mg at 0.984, 1.69, 1.94, 3.56, and 3.76–3.78 Mev, respectively. Data analysis, using the extreme single-particle collective model, suggests that ^{27}Mg is a prolate spheroid with a nuclear deformation of $\eta \approx 2$. (auth)

22100 EXCITATION OF OCTUPOLE VIBRATIONAL STATES IN HEAVY DEFORMED NUCLEI BY INELASTIC PROTON SCATTERING. Shelton, W. N. (Florida State Univ., Tallahassee). Contract AT-(40-1)-2434; Contract AF AFOSR-62-423. Phys. Lett., 20: 651-3(Apr. 1, 1966).

Inelastic proton scattering is investigated by magnetic analysis, at $E_p = 12$ Mev, $\Theta = 133°$. Known states up to $E_x = 1.2$ to 1.5 Mev, are excited in ^{158}Gd, ^{160}Dy, and ^{164}Dy. By analogy, J^π assignments are given to new states in ^{160}Gd. (auth)

22101 INELASTIC SCATTERING OF 40 Mev PROTONS BY ^{208}Pb. Scott, A.; Fricke, M. P. (Univ. of Minnesota, Minneapolis). Phys. Lett., 20: 654-6(Apr. 1, 1966).

Proton groups were observed at excitation energies of 2.62, 3.20, 4.15 and 4.37 Mev in the inelastic scattering of 40-Mev protons by ^{208}Pb. Cross sections were measured and compared with theoretical predictions obtained by the distorted-waves method and using the best-fit optical-model parameters for ^{208}Pb. The results reveal a 2^+ state at 4.15 Mev and a 5^- state at 4.37 Mev. (L.B.S.)

22102 ENERGY SPECTRA OF 1p-SHELL NUCLEI CALCULATED WITH THE HAMADA-JOHNSTON POTENTIAL. Halbert, E. C. (Oak Ridge National Lab., Tenn.); Kim, Y. E.; Kuo, T. T. S. Phys. Lett., 20: 657-61(Apr. 1, 1966). (ORNL-P-2059).

An effective interaction obtained from the Hamada-Johnston potential is used to calculate shell-model spectra for the 1p-shell nuclei. Two parameters are varied with A: the harmonic-oscillator size-parameter, and the single-particle $p_{\frac{1}{2}}$-$p_{\frac{3}{2}}$ energy splitting. (auth)

22103 CORRECTIONS TO THE BCS EXPRESSIONS FOR NUCLEAR MATRIX ELEMENTS DUE TO PARTICLE NUMBER FLUCTUATIONS. Krumlinde, J.; Nilsson, S. G. (Lund Inst. of Tech., Sweden). Phys. Lett., 20: 661-4(Apr. 1, 1966).

The effect of particle-number fluctuations on matrix elements based on the BCS wave function is investigated by the employment of a saddle-point projection method. In particular, in the case of a uniform model containing 32 levels it is found that the correction is relatively small and in most cases of interest fairly well reproduced by the method discussed. (auth)

22104 DEUTERON OPTICAL POTENTIALS AND THE $^{16}O(d,p)^{17}O$ REACTION. Alty, J. L.; Green, L. L.; Huby, R.; Jones, G. D.; Mines, J. R.; Sharpey-Schafer, J. F. (Univ. of Liverpool). Phys. Lett., 20: 664-6 (Apr. 1, 1966).

Experimental results and distorted wave predictions for $^{16}O(d,p)^{17}O$ reaction are compared. (auth)

22105 EXCITATION OF NEW ELECTROMAGNETIC TRANSITIONS IN ^{9}Be INELASTIC ELECTRON SCATTERING. Clerc, H. G.; Wetzel, K. J.; Spamer, E. (Technische Hochschule, Darmstadt, Ger.). Phys. Lett., 20: 667-9(Apr. 1, 1966).

Transitions in ^{9}Be corresponding to excitation energies of 14.38, 15.99, 16.65, 16.97 and 17.50 Mev were excited. The levels at 14.38 and 16.97 Mev have negative parity, those at 16.65 and 17.50 Mev have positive parity. Probable multipolarities, ground state transition strengths and transition radii are given. (auth)

22106 STUDY OF THE REACTION $^{180}Hf(d,p)^{181}Hf$. Gastebois, J.; Barloutaud, M.; Laget, J. M.; Quidort, J. (Centre d'Etude Nucleaires, Saclay, France). Phys. Lett., 20: 669-71(Apr. 1, 1966). (In French).

Results are presented of an experimental study of the first excited states of ^{181}Hf (excitation energy, effective cross section, and angular distributions). Preliminary calculations of the cross sections show that the effect of the Coriolis force must be taken into account. (tr-auth)

22107 ON THE 3^- STATE IN ^{28}Si AND ^{24}Mg. Kokame, J. (Tokyo Univ.); Fukunaga, K.; Nakamura, H. Phys. Lett., 20: 672-3(Apr. 1, 1966).

By DWBA analysis of α-particle inelastic scattering on ^{28}Si at E_α = 28.4 Mev, the collective enhancement of the 3^- level at 6.88 Mev is determined as $B(E3)/B(E3)_{s.p.} = 6.1$. In ^{24}Mg, a 3^- level is located at 8.4 Mev with an enhancement factor of 2.9. (auth)

22108 COLLECTIVE STATES OF ^{209}Bi. Hinds, S. (Atomic Weapons Research Establishment, Aldermaston, Eng.); Marchant, H.; Bjerregaard, J. H.; Nathan, O. Phys. Lett., 20: 674-6(Apr. 1, 1966).

Energy levels of ^{209}Bi were measured from inelastic deuteron scattering. The four states observed near 2.6 Mev excitation are very likely members of the septet predicted by the weak coupling model. (auth)

22109 THE (d,n) REACTIONS ON THE ISOTOPES $^{58,60,62,64}Ni$. Okorokov, V. V.; Serezin, V. M.; Smotryaev, V. A.; Tolchenkov, D. L.; Trostin, I. S.; Cheblukov, Y. N. (Inst. of Theoretical and Experimental Physics, Moscow). Phys. Lett., 20: 676-8(Apr. 1, 1966).

The neutron spectra and the angular distributions in the (d,n) reactions on the isotopes ^{58}Ni, ^{60}Ni, ^{62}Ni, ^{64}Ni were investigated with the cyclotron of ITEP with deuteron energy 11.7 Mev. The measurements were done using a multichannel time-of-flight spectrometer with energy resolution 2% for the neutron energy 10 Mev. (auth)

22110 TOTAL NEUTRON YIELD FROM THE REACTION $^{14}C(\alpha,n)^{17}O$. Bair, J. K.; Ford, J. L. C. Jr.; Jones, C. M. (Oak Ridge National Lab., Tenn.). Phys. Rev., 144: 799-801(Apr. 22, 1966). (ORNL-P-1826).

The total neutron yield of the reaction $^{14}C(\alpha,n)^{17}O$ was measured in the alpha-particle bombarding-energy range of 2.5 to 5.1 Mev. Six new anomalies were observed in the yield curve at alpha-particle energies of 4.030 ± 0.015, 4.07 ± 0.04, 4.17 ± 0.04, 4.434 ± 0.010, 4.70 ± 0.04, and 5.004 ± 0.010 Mev. These would correspond to excitation energies in the ^{18}O compound nucleus of 9.361, 9.39, 9.47, 9.675, 9.88, and 10.119 Mev. The experimental widths vary from 21 to 200 kev. An approximate value of the average alpha-particle strength function was obtained. (auth)

22111 EXCITATION ENERGIES OF BOUND STATES OF ^{17}O AND ^{12}B. Williams, H. H.; Warburton, E. K.; Jones, K. W.; Olness, J. W. (Brookhaven National Lab., Upton, N. Y.). Phys. Rev., 144: 801-3(Apr. 22, 1966). (BNL-9759).

The energy of the ^{17}O 0.871-Mev gamma ray was measured with a lithium-drifted germanium detector using the $^{16}O(d,p)^{17}O$ reaction to populate the first excited state of ^{17}O. A result of 870.81 ± 0.22 kev was obtained using various radioactive sources for energy calibration. Using this line and various others for energy calibration, the energies of gamma rays from transitions in ^{12}B were measured and excitation energies of 953.14 ± 0.60 and 1673.65 ± 0.60 kev were deduced for the first two excited states of ^{12}B. Strong but nonconclusive evidence is presented for an excitation energy of 2618.5 ± 3.5 kev for the third excited state of ^{12}B. (auth)

22112 ENERGY GAP IN FINITE NUCLEAR SYSTEMS. Kennedy, Roger C. (Australian National Univ., Canberra). Phys. Rev., 144: 804-11(Apr. 22, 1966).

Slabs of nuclear matter are studied to assess the finite-nucleus effects on the energy gap, using realistic nucleon-nucleon interactions. The slabs are defined by square wells in one dimension only. The energy gap is found by solving numerically an approximation to the BCS integral equation, and solutions are displayed as functions of the effective mass and the size of the finite system. Empirical estimates of the gap in real nuclei are examined taking into account nuclear "blocking" and particle-number fluctuation. By identifying structures of the same surface-to-volume ratio, calculated values of the gap can be compared directly with the empirical estimates. It is found that the general trend of the magnitude of the gap as a function of the nucleon number can be reproduced with not too unreasonable values of the effective mass. (auth)

22113 NUCLEON SINGLE-PARTICLE LEVELS IN A DIFFUSE NONLOCAL POTENTIAL WELL. Koshel, R. D. (Ohio Univ., Athens). Phys. Rev., 144: 811-14(Apr. 22, 1966).

Calculations were made of the nucleon single-particle levels in ^{91}Zr using a diffuse nuclear potential. The results of both local and nonlocal calculations are presented. The nonlocal calculations were made using the equivalent local-potential model formulated by Perey and Buck. It is shown that the nonlocal model provides good shell-model ordering of the states, gives parameters which are in good agreement with those found in scattering, yields results which are in good agreement with the experimentally determined levels, and gives a value of 3.07 Mev for the binding energy per nucleon. The value of the binding energy per nucleon found in the local calculations was 0.91 Mev. (auth)

22114 CONTINUUM RESONANCES IN $^{4}He(p,p')^{4}He$. Williams, Lawrence E. (Univ. of Minnesota, Minneapolis). Phys. Rev., 144: 815-22(Apr. 22, 1966).

Two resonances are seen in the spectrum of inelastic protons from ^{4}He with 40-Mev protons incident upon a NTP helium gas target. Resonance I lies at an ^{4}He excitation energy $E^* = 20.46 \pm 0.14$ Mev and has a c.m. full width $\Gamma_{c.m.} = 340 \pm 40$ kev, while II is at $E^* = 22.00 \pm 0.14$ Mev with $\Gamma_{c.m.} = 2.4 \pm 0.5$ Mev. Data were taken over the range $19 \leq E^* \leq 24$ Mev at 11 lab angles, $15° \leq$

$\theta \leq 90°$, with a 32-detector array of solid-state passing counters mounted in the focal plane of a double-focusing 180° magnetic spectrometer. Angular distributions for the two inelastic groups were obtained through a subtraction of tentative phase space and/or experimental backgrounds. Kinematic limitations prevented following a third broad resonance which appeared at $26 \leq E^* \leq 28$ Mev. (auth)

22115 1.7-Mev ANOMALY IN THE $^{12}C(p,p)^{12}C$ REACTION. Armstrong, J. C.; Baggett, M. J.; Harris, W. R.; Latorre, V. A. (Univ. of Maryland, College Park). Phys. Rev., 144: 823-8(Apr. 22, 1966).

The $^{12}C(p,p)^{12}C$ reaction cross section was measured for laboratory proton energies from 1.48 to 2.02 Mev at center-of-mass scattering angles of 25, 35, 45, 54.7, 70, 80, 90, and 125.2°. Thin self-supporting carbon films were used as targets and the scattering protons were analyzed with a double-focusing magnetic spectrometer. The data were fitted with a theoretical one-level formula. Resonances included in the theoretical expression were the $J^\pi = 1/2^+$, $E_p = 0.461$-Mev resonance (unobserved in this experiment) and the $J^\pi = 3/2^-$ and $5/2^+$ resonances associated with the 1.7-Mev anomaly. Parameters for the $J^\pi = 1/2^+$ resonance were taken from previous experiments, and parameters for the $J^\pi = 3/2^-$ and $5/2^+$ resonances were varied to obtain a best fit to the data. The final parameter values are: $E_p = 1686 \pm 6$ kev, $\gamma^2 = (0.515 \pm 0.02) \times 10^{-13}$ Mev cm for the $J^\pi = 3/2^-$ level, and $E_p = 1734 \pm 6$ kev, $\gamma^2 = (3.55 \pm 0.18) \times 10^{-13}$ Mev cm for the $J^\pi = 5/2^+$ level. These reduced-width values are approximately 20% larger than those previously measured. Although the error in the absolute energy measurements is 6 kev, the errors in energy differences are smaller and the measured difference E_p values for the $3/2^-$ and $5/2^+$ levels is 48 ± 2 kev. (auth)

22116 PROTON POLARIZATION AND THE SPIN-ORBIT POTENTIAL. Goldfarb, L. J. B. (Univ. of Manchester, Eng.); Greenlees, G. W.; Hooper, M. B. Phys. Rev., 144: 829-33(Apr. 22, 1966).

A treatment of proton elastic scattering, valid to first order in the strength of the spin-orbit optical-model potential, shows that this quantity merely serves as a scaling factor for the polarization of the outgoing protons. The angular dependence of the polarization is then determined by the form factor of this potential together with the parameters of the central potential. At small scattering angles, however, only the spin-orbit form factor is important, aside from the well-known Coulomb interaction. Calculations of the proton polarization at various energies from 10 to 20 Mev support these conclusions and indicate that for medium-weight nuclei, the radius parameter of the spin-orbit potential $r_{so} \approx 1.1$ F instead of 1.3 F, the corresponding value used for the central potential. (auth)

22117 THREE-BODY PHOTODISINTEGRATION OF ^{3}He. Gerstenberg, H. M.; O'Connell, J. S. (National Bureau of Standards, Washington, D. C.). Phys. Rev., 144: 834-8 (Apr. 22, 1966).

The $^3He(\gamma,n)2p$ cross section was measured in 1-Mev steps from threshold to 30 Mev using the National Bureau of Standards betatron and a ^{4}He cryostat to produce a 40-cm^3 liquid-^{3}He target. The measured cross section shows a broad peak between 14 and 20 Mev with a maximum cross section at about 0.90 mb. The cross section and bremsstrahlung-weighted cross section integrated up to 28 Mev give $12.1 \pm 10\%$ Mev mb and $0.68 \pm 10\%$ mb, respectively. Theoretical calculations of the three-body photodisintegration cross section overestimate the experimental cross section by factors of 3 to 10. (auth)

22118 INELASTIC SCATTERING BASED ON A MICROSCOPIC DESCRIPTION OF NUCLEI. Glendenning, Norman K.; Veneroni, Marcel (Univ. of California, Berkeley). Phys. Rev., 144: 839-53(Apr. 22, 1966). (UCRL-16428).

The inelastic scattering of nucleons and light nuclides from nuclei is formulated in terms of a general central two-body interaction between the scattered particle and the nucleons of the nucleus, whose motions are described by detailed shell-model wave functions. Form factors based on this microscopic description are obtained as closed expressions. The theory is applied to proton scattering from the even nickel isotopes. The constructive coherence in the transition to the collective 2^+ state leads to a form factor having the general shape of that used in the macroscopic description of collective motion. Unenhanced transitions, in contrast, are characterized by a variety not present in the macroscopic description. Nucleon scattering as here calculated is sensitive to the details constituting this variety, and therefore provides a means of subjecting microscopic descriptions of nuclei to detailed tests. (auth)

22119 ELASTIC NEUTRON SCATTERING FROM B, C, K, AND Ca AT 14.0 Mev. Frasca, A. J.; Finlay, Roger W.; Koshel, R. D.; Cassola, R. L. (Ohio Univ., Athens). Phys. Rev., 144: 854-9(Apr. 22, 1966).

Differential cross sections of 14.0-Mev neutrons scattered elastically from B, C, K, and Ca were measured with a time-of-flight spectrometer. The associated-particle technique was used. A time resolution of 1.3 nsec was sufficient to guarantee discrimination against inelastic events at a flight path of 1.68 m. The data were corrected for finite geometry and double scattering. An automatic six-parameter search routine was used to calculate an optical-model fit to the data. Improved fits were obtained for the B, C, and Ca distributions. Results for the previously unmeasured K differential cross section are presented. (auth)

22120 ELASTIC ELECTRON SCATTERING FROM THE MAGNETIC MULTIPOLE DISTRIBUTIONS OF ^{6}Li, ^{7}Li, ^{9}Be, ^{10}B, ^{11}B, AND ^{14}N. Rand, R. E.; Frosch, R.; Yearian, M. R. (Stanford Univ., Calif.). Contract Nonr 225(67). Phys. Rev., 144: 859-73(Apr. 22, 1966).

The magnetic form factors of the 1p-shell nuclei ^{6}Li, ^{7}Li, ^{9}Be, ^{10}B, ^{11}B, ^{14}N, were measured by high-energy electron scattering at an angle of 180°. Incident electron energies up to 230 Mev ($q^2 \simeq 5.2$ F^{-2}) were used. The incident- and scattered-electron paths were separated by use of a uniform magnetic field. Background due to charge scattering was subtracted by varying the scattering angle around 180°. At the higher momentum transfers the scattering from those nuclei having spin $\geq 3/2$, was dominated by the octupole moment distributions. Results are interpreted in terms of harmonic-oscillator and finite-square-well shell models. Parameters dependent only on the coupling of the angular momenta in the 1p shell may be obtained from the data. They show a general trend from L-S coupling to j-j coupling as the mass number increases in agreement with calculations of magnetic dipole moments and energy-level schemes. The outstanding exception is ^{7}Li, whose form factor is accurately described by the extreme independent-particle model. (L-S coupling is quite incompatible with the data.) The ^{6}Li results may also be interpreted in terms of an "alpha plus deuteron" model. Numerical results for the harmonic-well strengths are obtained and compare favorably with electron-charge-scattering values. It is also possible to estimate magnetic octupole moments, where applicable, with fair accuracy, although these estimations are to a certain extent model-dependent. (auth)

22121 EIGENSTATES OF THE J = 0, T = 1, CHARGE-INDEPENDENT PAIRING HAMILTONIAN. I. SENIORITY-ZERO STATES. Richardson, R. W. (New York Univ., New York). Phys. Rev., 144: 873-83(Apr. 22, 1966).

Exact equations for the seniority-zero states of 2N nucleons in an arbitrary external potential well and interacting through a J = 0, T = 1, charge-independent pairing interaction are derived. Exact solutions of these equations are exhibited for the ground states and some excited states of these systems. These states are characterized by having wave functions that are totally symmetric functions of the isospins of the pairs of particles and have total isospin T = 0,2,..., N for N even and T = 1,3,..., N,

for N odd. The ground states are included in the sets of states with T = 0 or 1 and the states of the pairing hamiltonian with a single type of nucleon belong to the charge multiplet with T = N. The calculation of the energies and wave functions of these states is reduced to the solution of N coupled, nonlinear, algebraic equations in N unknowns. An explicit expression is given for the occupation probabilities of the levels of the single-particle well in these states. (auth)

22122 EFFECTIVE INTERACTION FOR NUCLEAR MATTER. Chiang, C. C.; Razavy, M. (Univ. of Alberta, Edmonton). Phys. Rev., 144: 883-90(Apr. 22, 1966).

The effective interaction in nuclear matter is defined as the long-range part of the two-body potential, which, in the Born approximation, gives the single-particle potential energy for the average momentum in the Fermi sea. For the Brueckner-Gammel-Thaler potential the effective interaction was calculated, first for the free-particle propagator and then for the nuclear spectrum. The result shows that in the first case the separation distance ξ_0 is constant over a wide range of densities and does not lead to saturation. The nuclear separation distance $\xi(k_F)$ changes quite rapidly with the Fermi momentum k_F; for low densities it is very close to ξ_0, while for higher densities it becomes very much larger. At the density corresponding to k_F = 1.5 F^{-1}, the long-range potential starts at ξ = 1.16 F, and the rate of change of ξ with k_F is $(d\xi/dk_F)$ = 0.8 F^2. The minimum of the total energy per particle occurs at k_F = 1.35 F^{-1} and is about −9 Mev. For k_F = 1.5 F^{-1} the contributions of different partial waves are also calculated by a variational technique, and the results were compared with previous calculations. (auth)

22123 ^{14}N LEVELS FROM ELASTIC SCATTERING OF PROTONS BY ^{13}C. Latorre, V. A.; Armstrong, J. C. (Univ. of Maryland, College Park). Phys. Rev., 144: 891-901(Apr. 22, 1966).

The differential cross section for elastic scattering of protons from ^{13}C was measured to an accuracy of 7% for proton energies from 1.0 to 2.6 Mev at center-of-mass scattering angles of 39.2°, 54.7°, 90.0°, and 125.3°. Thin targets were prepared from methyl iodide enriched to 62% in ^{13}C and the scattered protons were analyzed using a double-focusing magnetic spectrometer. Proton groups corresponding to ^{12}C and ^{13}C were cleanly separated except for energies below 1.8 Mev at 39.2° and 54.7°. A theoretical curve calculated from a two-level formula was fitted to the data over the entire energy range. Seven resonances, all previously observed, were necessary to fit the data. The laboratory resonance energies (Mev), center-of-mass reduced widths (Mev cm $\times 10^{-13}$) and J^π values assigned in this analysis are as follows: 1.150 ± 0.002, 0.19, 0^+; 1.366 ± 0.050, 3.60, 0^-; 1.461 ± 0.003, 1.76, 3^-, 1.540 ± 0.003, 0.09, 2^+; 1.980 ± 0.003, 0.45, $3^-(2^-)$; 2.110 ± 0.003, 1.66, 2^-; 2.319 ± 0.005, 0.09, 1^+. These resonance energies and reduced widths are in fair agreement with previous measurements. The spin and parity assignments for all levels, except those at E_p = 1.540 Mev and 1.980 Mev, confirm previous experiments. The 1.540-Mev resonance had previously been assumed to have $J^\pi = 1^+$ and the 1.980-Mev resonance had been assigned $J^\pi = 1^-$. Comparison of experiment and theory suggests the possibility of a broad resonance having $J \leq 1$ in the vicinity of E_p = 2.8 Mev. (auth)

22124 ELECTRON SCATTERING FROM AN ALIGNED DEFORMED NUCLEUS. Greenstein, H. B. (Stanford, Univ., Calif.). Contract AF 49(638)-1389. Phys. Rev., 144: 902-17(Apr. 22, 1966).

The problem of scattering high-energy electrons from a deformed nucleus which has been aligned in a magnetic field is considered from the point of view of the Schiff approximation for high-energy potential scattering. Integrals for the scattering amplitude are evaluated in the asymptotic limit of large β ($\beta \equiv QR$) assuming a model for the charge-density distribution which is equivalent to a uniformly charged ellipsoid of revolution. It is found that terms bilinear in the quadrupole strength must be retained. The formalism is extended to take account of nuclear spin-state transitions. Low-lying rotational levels are summed over, using the Bohr-Mottelson model in the strong-coupling limit. Application is made to the case of the holmium nucleus. (auth)

22125 EXCITATION FUNCTIONS FOR SIMPLE NUCLEAR REACTIONS OF π^- MESONS WITH ^{40}Ar. Hower, Charles O.; Kaufman, Sheldon (Princeton Univ., N. J.). Phys. Rev., 144: 917-22(Apr. 22, 1966). (PPAD-573E).

Cross sections were measured for the reactions ^{40}Ar(π^-, π^-p)^{39}Cl and ^{40}Ar(π^-, π^-pn)^{38}Cl in the energy range 500–1100 Mev. The excitation function of the former reaction has peaks at about 600 and 900 Mev pion kinetic energy, corresponding to known resonances in the π^--p scattering cross section. This implies that a quasifree pion-proton collision occurs as the initial step of this simple reaction. The (π^-, π^-pn) excitation function, in contrast, is essentially independent of energy in this energy range, indicating a mechanism or combination of mechanisms sufficiently complex to average out the structure in the π^--p and π^--n cross sections. The effect of the proton momentum distribution on the π^--p resonances is calculated, and by comparison with the (π^-, π^-p) cross section a momentum distribution is deduced which is in agreement with the results of (p,2p) quasifree scattering experiments. Cross sections for the reactions ^{40}Ar(π^-, π^-2p)^{38}S, ^{40}Ar(p, 2p)^{39}Cl, and ^{40}Ar(p, 2pn)^{38}Cl at a single energy were also measured. (auth)

22126 MEASUREMENT OF THE SPINS OF SOME STATES IN ^{55}Fe. Gemmell, D. S.; Lee, L. L. Jr.; Marinov, A.; Schiffer, J. P. (Argonne National Lab., Ill.). Phys. Rev., 144: 923-7(Apr. 22, 1966).

The p-γ angular correlations in the reaction ^{54}Fe(d,pγ)^{55}Fe* were measured for several proton groups. The groups chosen correspond to states for which the proton angular distribution shows formation by l = 1 neutron capture. These states must therefore have spins $\frac{1}{2}^-$ or $\frac{3}{2}^-$. A state with spin $\frac{1}{2}^-$ must exhibit an isotropic angular correlation while a state of spin $\frac{3}{2}^-$ will ordinarily show some anisotropy. The results indicate spin $\frac{1}{2}^-$ for the first excited state of ^{55}Fe at 413 kev, and spin $\frac{3}{2}^-$ for states at 2.490-, 3.556-, and 3.800-Mev excitation. The conclusions are compared with previous results and with theoretical predictions. (auth)

22127 ^{60}Ni(^{3}He,α)^{59}Ni REACTION AT 15 Mev. Fou, C. M. (Univ. of Pennsylvania, Philadelphia); Zurmuehle, R. W.; Swenson, L. W. Phys. Rev., 144: 927-32(Apr. 22, 1966).

Measurements were made of the angular distributions of alpha particles from the ^{60}Ni(^{3}He,α)^{59}Ni reaction leading to the ground state and the 0.34-, 0.47-, 0.89-, 1.32-, 1.97-, 2.70-, 3.15-, 3.74-, and 7.33-Mev excited states of ^{59}Ni. Distorted-wave Born-approximation analysis of the angular distributions was carried out and spectroscopic factors extracted. The spectroscopic factors were compared with the occupation-number predictions of pairing theory. The isobaric analog of the ^{59}Co ground state was observed at an excitation of 7.33 Mev in ^{59}Ni. (auth)

22128 POLARIZATION OF 45-Mev PROTONS BY COMPLEX NUCLEI. Cahill, T. A.; Richardson, J. Reginald; Haddock, R. P. (Univ. of California, Los Angeles). Contract Nonr 233-(44). Phys. Rev., 144: 932-40(Apr. 22, 1966).

The asymmetry produced by a beam of 45-Mev protons incident upon targets of beryllium, carbon, aluminum, vanadium, and rhodium was measured utilizing the polarized proton beam of the U.C.L.A. sector-focused cyclotron. The development of the polarized beam is discussed, with emphasis upon the provision for an independent calibration of the polarization of the beam. The techniques used in the polarization measurements are given in detail, and the data are compared with previous results at similar energies. (auth)

22129 HOLE STATES OF ^{43}Ca AND ^{47}Ca. Conlon, T. W.; Bayman, B. F.; Kashy, E. (Princeton Univ., N. J.). Phys. Rev., 144: 941-5(Apr. 22, 1966).

Levels in ^{43}Ca and ^{47}Ca, which can be interpreted as

neutron hole states in the $1d_{\frac{3}{2}}$ and $2s_{\frac{1}{2}}$ shells, were observed through the (p,d) reaction. For ^{43}Ca, the $1d_{\frac{3}{2}}$ hole state ($T = \frac{3}{2}$) lies at 0.993 Mev, while for ^{47}Ca, the indications are that the $2s_{\frac{1}{2}}$ and the $1d_{\frac{3}{2}}$ levels lie very close to 2.60 Mev. Small amounts of p-wave admixtures are found in ^{44}Ca and to a much smaller degree in ^{48}Ca. (auth)

22130 DECAY OF 54-SEC ^{86}Br AND 55-SEC ^{87}Br. Williams, Evan T.; Coryell, Charles D. (Massachusetts Inst. of Tech., Cambridge). Contract AT(30-1)-905. Phys. Rev., 144: 945-51(Apr. 22, 1966). (MIT-905-46).

The decay of ^{86}Br and ^{87}Br, produced by fission of ^{235}U, was studied with β- and γ-ray scintillation spectrometers in singles and coincidence operation. Rapid chemical techniques taking advantage of the difference in half lives of the selenium precursors were used to produce samples having different proportions of ^{86}Br and ^{87}Br, and the radiations following the decay of these two isotopes were resolved in this way. A decay scheme is proposed for ^{86}Br, with $Q_\beta = 7.5 \pm 0.5$ Mev. (auth)

22131 $f_{\frac{7}{2}}$ MODEL OF ^{46}V, ^{47}V, ^{49}Cr, AND ^{50}Mn. Ginocchio, J. N. (Rutgers State Univ., New Brunswick, N. J.). Phys. Rev., 144: 952-5(Apr. 22, 1966).

Using a pure $f_{\frac{7}{2}}$ configuration and an effective two-nucleon interaction, the energy spectra, magnetic moments, and beta decays of ^{46,47}V, ^{49}Cr, and ^{50}Mn are calculated. The empirical data available for comparison are sparse, but an attempt is made at comparison to point out both what would be of interest to look for experimentally and the deficiencies of the model. The spectacular features are predicted by the model, namely, the inversion of the lowest $T = 0$ and $T = 1$ levels of the self-mirror nucleus ^{46}V, the isomeric $J = 5$ level in ^{50}Mn, and the "anomalous" $J = \frac{5}{2}$ ground-state spin of ^{47}V and ^{49}Cr. It is more difficult to make judgments about the excited levels since the data are scarce; however, it is clear that the first excited ($J = 5$) level for ^{46}V predicted by the model is pushed up above other excited levels. (auth)

22132 (^{3}He,n) REACTIONS WITH 19- TO 25-Mev ^{3}He IONS. Manley, J. H.; Stein, W. E. (Los Alamos Scientific Lab., N. Mex.). Phys. Rev., 144: 956-61(Apr. 22, 1966). (LA-DC-7567).

Three threshold detectors with thresholds at 1, 4.5, and 12 Mev were used to investigate neutron emission from 10 targets (Be, C, N, O, Al, Fe, Ni, Cu, Mo, Ag) when bombarded by 19-, 22-, and 25-Mev ^{3}He ions. Laboratory angular distributions and production cross sections were measured. The results are compared with an evaporation spectrum and it is concluded that a direct-interaction mechanism operates in the production of neutrons with energies greater than 12 Mev. (auth)

22133 (p,xn) AND (p,pxn) REACTIONS OF ^{89}Y WITH 5- TO 85-Mev PROTONS. Saha, G. B. (McGill Univ., Montreal. Purdue Univ., Lafayette, Ind.); Porile, N. T.; Yaffe, L. Phys. Rev., 144: 962-71(Apr. 22, 1966). (COO-1505-4).

Excitation functions for the (p,xn) ($x = 1-4$) and (p,pxn) ($x = 1-5$) reactions of ^{89}Y with 5-85 Mev protons were determined. Isomer ratios were measured for the (p,p2n), (p,p3n), and (p,p4n) reactions. The cross sections were compared with the results of a cascade-evaporation calculation based on the recent code by Chen et al. This calculation predicts close to 100% compound-nucleus formation up to bombarding energies of about 35 Mev, and the excellent agreement with experiment attests to the validity of this prediction. A number of discrepancies between experiment and calculation are noted at higher energies. These are due to the fact that the calculation by Chen et al. appears to overestimate the amount of compound-nucleus formation in the energy range of 45-85 Mev. (auth)

22134 OPTICAL-MODEL AND DISTORTED-WAVE ANALYSES OF SOME 18-Mev ALPHA-PARTICLE SCATTERING CROSS SECTIONS FOR ^{40}Ar, ^{32}S, ^{31}P, ^{23}Na, AND ^{20}Ne. Lucas, B. T.; Cosper, S. W.; Johnson, O. E. (Purdue Univ., Lafayette, Ind.). Phys. Rev., 144: 972-9 (Apr. 22, 1966). (COO-1420-119).

The 18-Mev elastic and inelastic alpha-particle cross sections for some states of ^{20}Ne (Gnd., 1.632 Mev), ^{23}Na (Gnd., 0.439, 2.080 Mev), ^{31}P (Gnd., 1.265, 2.232 Mev), ^{32}S (Gnd.), and ^{40}Ar (Gnd., 1.462 Mev) were analyzed in terms of the nuclear optical model and the distorted-wave theory. Although good qualitative agreement between the empirical and optical-model cross sections is found, particularly at forward angles, the quantitative agreement is significantly poorer than that found for heavier target nuclei at higher incident energies. Further intercomparison of the results of the present and previous studies strongly suggests that for the prevailing experimental and physical circumstances ($E_\alpha \approx 18$ Mev and $A < 40$) of the present investigation the applicability of the optical model is marginal. The distorted-wave predictions are in fair agreement with the experimental data at the more forward angles ($\theta \lesssim 80°$) in that they generally reproduce the positions and relative amplitudes of two or more of the maxima. For larger angles ($\theta > 80°$) the quality of the fits deteriorates insofar as detail is concerned; however, the calculated curves do follow the general trend of the data. For the inelastic angular distributions the quality of the fits is poorer and the angular range over which the fits are acceptable is smaller than for the corresponding elastic cross sections. (auth)

22135 SYMMETRY OF NEUTRON-INDUCED ^{239}Pu FISSION AT INDIVIDUAL RESONANCES. Cowan, G. A.; Bayhurst, B. P.; Prestwood, R. J.; Gilmore, J. S.; Knobeloch, G. W. (Los Alamos Scientific Lab., N. Mex.). Phys. Rev., 144: 979-83(Apr. 22, 1966).

Neutrons resolved in energy by time-of-flight from an underground nuclear explosion ("Petrel," 11 June 1965) were used to produce resonance fissions in ^{239}Pu in sufficient numbers to permit radiochemical measurements of the symmetry of fission at individual levels in the energy region 15 to 82 ev. About two-thirds of the levels examined are characterized by fission less symmetric than thermal-neutron fission. At these resonances the modal yield of the nearly symmetric fission product ^{115}Cd is approximately $\frac{1}{3}$ the thermal yield. For the remainder of levels, fission is more symmetric; modal yield of ^{115}Cd is approximately $\frac{1}{2}$ the thermal yield. There is correspondence between groupings by enhanced or decreased fission symmetry, level widths ("broad" or "narrow"), and some recently measured J values. Based on relative fission symmetry, spin assignments are proposed for 22 levels. It is suggested that those levels for which the ^{115}Cd yield is low represent 1+ states; the higher ^{115}Cd yields presumably occur at levels which represent 0+ states. The 0+ levels are broad compared to the more readily recognized and categorized 1+ levels. The proposed assignments are: for the J = 1 group, resonances at 17.7, 22.3, 26.3, 41.5, 44.6, 47.7, 50.2, 52.7, 55.8, 59.4, 66.0, 75.2, and, with less confidence, 15.4 ev; for the J = 0 group, resonances at 49.8, 57.6-58, 61.1, 66.8, 81.7, and, with less confidence, 32.4 ev. In addition, from other published data, it is suggested that J = 1 for the 0.3-ev level and J = 0 for the first negative-energy level. (auth)

22136 NUCLEAR-CHARGE DISTRIBUTION OF FISSION-PRODUCT CHAINS OF MASS NUMBERS 131-133. Strom, P. O.; Love, D. L.; Greendale, A. E.; Delucchi, A. A.; Sam, D.; Ballou, N. E. (Naval Radiological Defense Lab., San Francisco). Phys. Rev., 144: 984-93(Apr. 22, 1966).

New information on the nature of the nuclear charge distribution in thermal-neutron fission of ^{235}U was obtained from measurements of fission yields of the principal constituents in each of three adjacent mass chains. A regular variation in the width of the charge-distribution curves with mass number was shown, and values of the most probable nuclear charge (Z_p) were determined. No effects attributable to the 50-proton or 82-neutron closed shells were observed in the charge-distribution curves examined. Independent and cumulative fission yield values were determined for the principal constituents in each of the three mass chains 131, 132, and 133. Values measured are: ^{131}Sn, (1.28 ± 0.21)% cumulative; ^{131}Sb, (1.66 ± 0.40)%

independent; ^{132}Sn, (0.59 ± 0.17)% cumulative; ^{132}Sb, (2.76 ± 0.35)% independent; ^{132}Te, (0.86 ± 0.10)% independent; ^{133}Sn, <0.015% cumulative; ^{133}Sb, (3.05 < 0.39)% independent; ^{133m}Te, (2.19 ± 0.33)% independent; ^{133g}Te, (2.07 ± 0.31)% independent; and ^{133}I, (0.17 ± 0.06)% independent. The charge distribution curve for each mass chain was established from the fission yield data. The data were fitted to the Gaussian relationship, $P(Z) = A \exp -(Z-Z_p)^2/c$. The widths of the curves as given by values of c for mass chains 131, 132, and 133 are, respectively: 1.10 ± 0.05, 0.74 ± 0.08, and 0.57 ± 0.05. The data show a monotonic decrease in the width of the charge distribution curves with increasing fission-product mass number. Implications of this observation are discussed in respect to previous assumptions of a single charge distribution curve for all fission-product masses in low-energy fission. Values of Z_p as given by the Gaussian curves for mass chains 131, 132, and 133 are, respectively: 50.72 ± 0.07, 51.07 ± 0.06, and 51.59 ± 0.04. These values are compared with published values derived from assumptions of a single charge distribution curve for all mass chains. Predicted effects of nuclear shells on charge distribution have been examined in the light of the present data. No effect was detected in mass chains 131, 132, and 133. New half-life values determined are: ^{131}Sn, 1.32 ± 0.23 min; ^{132}Sn, 1.00 ± 0.17 min; ^{132}Sb, 3.13 ± 0.33 min; and ^{133}Sb, 2.67 ± 0.33 min. The half life of ^{133}Sn was estimated to be 55 sec. (auth)

22137 NUCLEAR MOMENTS OF ^{241}Am AND 16-h ^{242}Am AND ANALYSIS OF THE HYPERFINE FIELDS. Armstrong, Lloyd Jr.; Marrus, Richard (Univ. of California, Berkeley). Phys. Rev., 144: 994-8(Apr. 22, 1966). (UCRL-16494).

The nuclear moments of ^{241}Am and 16-h ^{242}Am were directly measured by the method of triple resonance in an atomic beam. They are $\mu_I(^{241}Am) = +1.58(3)$ nm and $\mu_I(^{242}Am) = +0.3808(15)$ nm, including a correction for diamagnetic shielding. On the collective model $\mu_I(^{242}Am)$ is a direct measure of the gyromagnetic ratio of the core (g_R), and the measured value of μ_I is in excellent agreement with the value $g_R = Z/A$. From these values for the magnetic moments and previous measurements of the hyperfine constants, values are deduced for the magnetic fields at the nucleus. It is shown that breakdown of Russell-Saunders coupling including relativistic effects gives contributions of the wrong sign to the magnetic field. Arguments are given which show that the residual effect is most probably due to core polarization. (auth)

22138 NUCLEAR-STRUCTURE STUDIES OF ^{88}Sr AND ^{89}Y BY INELASTIC ALPHA-PARTICLE SCATTERING. Alster, J.; Shreve, D. C.; Peterson, R. J. (Univ. of Washington, Seattle). Phys. Rev., 144: 999-1012(Apr. 22, 1966).

The inelastic scattering of 42-Mev alpha particles from ^{88}Sr and ^{89}Y, was studied in order to test the validity of the weak-coupling core-excitation model for these nuclei and to obtain an angular distribution for the excitation of the $g_{9/2}$ single-particle state at 0.906 Mev in ^{89}Y. Angular distributions were obtained for scattering to the ground state and the 1.84-Mev (2^+), 2.74-Mev (3^-), and 3.21-Mev (2^+) states in ^{88}Sr; and to the ground state and the 0.906-Mev ($^9/_2^+$), 1.51-Mev ($^3/_2^-$), 1.75-Mev ($^5/_2^-$), 2.22-Mev ($^5/_2^+$), 2.53-Mev ($^1/_2^+$), 2.84-Mev, and 3.1-Mev states in ^{89}Y. The phase rule was used to obtain parities for additional levels in ^{89}Y at 3.70, 3.98, and 4.17 Mev. A parametrized phase-shift analysis was used to fit the elastic-scattering data, and the Austern-Blair model with the same parameters was used to extract values of $\beta_I R$ from the inelastic angular distributions. It is shown that the weak-coupling model is not a good description for the excited states of ^{89}Y. A shell-model calculation correlating the differential cross sections to the 2^+ states in ^{88}Sr and the 1.51- and 1.75-Mev states in ^{89}Y is made, and the results are found to be in slightly better agreement with experiment. The differential cross section to the 0.906-Mev ($g_{9/2}$) single-particle state is in agreement with the Austern-Blair model for an I = 5 transition. (auth)

22139 THEORETICAL INVESTIGATION OF THE NUCLEAR PROPERTIES OF ^{143}Pr IN THE UNIFIED MODEL. Choudhury, D. C.; Kujawski, E. (Polytechnic Inst. of Brooklyn). Phys. Rev., 144: 1013-19(Apr. 22, 1966).

Experimental data on the low-energy nuclear properties of ^{143}Pr are analyzed by using the intermediate-coupling approach in the unified nuclear model. For this purpose it is assumed that the last odd proton, having available the $1g_{7/2}$ and $2d_{5/2}$ states, is coupled to the quadrupole vibrations of the surface of the even-even core of the nucleus. The resulting hamiltonian of the coupled system is diagonalized including all states with up to three phonons in the space of the basic eigenvectors of the uncoupled system. With reasonable values for the coupling strength and for the "effective" spacing in energy between $g_{7/2}$ and $d_{5/2}$ states, the calculated energy levels for the low-lying levels of ^{143}Pr and their spins and parities are in fairly good agreement with the experimental data. Further, the wave functions obtained from the model are used to calculate the electric and magnetic transition probabilities, and these results are also found to be in good agreement with the experimentally observed values. Finally, discussions are given of the validity of the approximations used in the present analysis and also of the circumstances in which more extensive experimental investigations are needed. (auth)

22140 NUCLEAR SPIN AND MAGNETIC DIPOLE MOMENT OF 39-MIN ^{190}Au. Chan, Yau Wa; Ehlers, Vernon J.; Nierenberg, William A. (Univ. of California, Berkeley). Phys. Rev., 144: 1020-1(Apr. 22, 1966). (UCRL-16248).

Some of the nuclear properties of 39-min ^{190}Au were investigated with the atomic-beam magnetic-resonance method. The result I = 1 was obtained for the nuclear spin and $|\Delta\nu| = 3105 \pm 425$ Mc/sec for the hyperfine-structure separation. Substitution of this $\Delta\nu$ and the known values of $\Delta\nu$ and μ for ^{197}Au into the Fermi-Segrè formula yields a calculated magnetic dipole moment of $|\mu_I| = 0.065$ nm. (auth)

22141 RECOIL-FREE ABSORPTION HYPERFINE SPECTRA OF THE 90-kev MIXED TRANSITION IN ^{99}Ru. Kistner, O. C. (Brookhaven National Lab., Upton, N. Y.). Phys. Rev., 144: 1022-30(Apr. 22, 1966). (BNL-9766).

The Mössbauer effect was employed to measure hyperfine splittings of the 90-kev transition in ^{99}Ru. A fully resolved magnetic hyperfine pattern was obtained with an absorber consisting of a solid solution of 2.3 at.% enriched Ru in metallic Fe. Partially resolved quadrupole hyperfine spectra were obtained with absorbers of $Ru(C_5H_5)_2$ and RuO_2. A single line source of ^{99}Rh in metallic Ru was used for these measurements. From these spectra the following information was deduced. The ratio of the magnetic g factors of the 90-kev level to that of the ground state, $g_1/g_0 = 0.759 \pm 0.016$. The 90-kev transition is a mixture of dipole and quadrupole (M1 and E2) radiation with a mixing ratio $E2/M1 = \delta^2 = 2.7 \pm 0.6$. By using the known spin and magnetic moment of the ground state, it is inferred that the spin of the 90-kev level is $^5/_2$, that $g_1 = 0.19 \pm 0.05$, and that the field at the nucleus of the ruthenium atom in the iron environment is 500 kG. The ratio of the quadrupole moment of the excited state to that of the ground state, $|Q_1/Q_0| \geq 3$, and $|Q_1| \geq 0.15$ b. With the use of a 30-kG superconducting solenoid the relative sign of the magnetic field at the Ru nucleus in the Fe absorber was shown to be negative and an absolute measurement of the nuclear g factors was made with the result that $g_1 = 0.20 \pm 0.02$. A measurement of the absorption spectrum of ferromagnetic $GdRu_2$ gave the result that the magnetic field at the nucleus in this compound is <10 kG. Hyperfine measurements were made with the Ru-Fe absorber magnetically polarized both parallel and perpendicular to the direction of the resonant radiation. Under these conditions it was possible to observe, for the first time, the interference between two multipole components for the individual hyperfine components of a radiative transition. From these measurements the sign of the conventional mixing param-

eter δ was determined to be negative, and an upper limit of 30% could be placed on the time-reversal-odd component of the gamma-decay matrix element. The properties of the 90-kev level, which are not compatible with a simple shell-model description, are compared with the predictions of a core-excitation description. If the latter description is correct, then these results give evidence that the magnitude of the time-average quadrupole moment associated with the 2+ core is ≥0.29 b. (auth)

22142 DECAY SCHEME OF ^{254}Es. McHarris, William; Stephens, F. S.; Asaro, F.; Perlman, I. (Univ. of California, Berkeley). Phys. Rev., 144: 1031-45(Apr. 22, 1966). (UCRL-11676).

The alpha decay of ~280-day ^{254}Es to ^{250}Bk was studied, and the following alpha groups were observed: 6.486 Mev, 0.27%; 6.437, 93%; 6.424, 1.7%; 6.392, 0.13%; 6.367, 2.9%; 6.355, 0.74%; 6.331, 0.05%; 6.284, 0.16%; 6.276, 0.22%, 6.200, ~0.05%; 6.193, ~0.05%; 6.113, 0.33%; and 6.056, 0.16%. In addition, from conversion electron and gamma-ray (Ge and NaI) spectra, some 20 gamma-ray transitions were observed. Most of this information has been used in characterizing rather unambiguously four low-lying rotational bands in ^{250}Bk. The properties of these bands were compared rather carefully with those predicted by considering the odd neutron and odd proton to move independently of each other. The predicted and observed properties are in surprisingly good agreement. (auth)

22143 FISSION OF ^{238}U AND ^{240}Pu NUCLEI EXCITED BY INELASTIC ALPHA-PARTICLE SCATTERING. Britt, H. C.; Plasil, F. (Univ. of California, Berkeley). Phys. Rev., 144: 1046-59(Apr. 22, 1966).

Angular correlations were measured for fission fragments emitted from nuclei excited by an (α,α') reaction. The angular correlations were measured as a function of the excitation energy of the fissioning nucleus. From an analysis of the results an attempt is made to identify the vibrational bands that are present in the transition-state spectrum below the energy necessary for two quasiparticle excitations. The transition-state spectrum, which is obtained from the analysis, is found to be consistent with previous ^{232}Pu(d,pf) results. (auth)

22144 EMISSION OF ALPHA PARTICLES IN THE FISSION OF ^{238}U BY 11- TO 21-Mev PROTONS. Thomas, T. D.; Whetstone, S. L. Jr. (Los Alamos Scientific Lab., N. Mex.). Phys. Rev., 144: 1060-?(Apr. 22, 1966). (LA-DC-7597).

The rate of emission of alpha particles in coincidence with fission was measured for ^{238}U bombarded with protons of energies 11, 12, 13, 14, 15, 17, and 21 Mev. The results of these measurements may be summarized by the formula $Y_\alpha = (1.53 \pm 0.18) + (0.044 \pm 0.010)E_p$, where Y_α is the number of alpha particles per thousand fissions and E_p is the incident proton energy in Mev. For spontaneous fission of ^{252}Cf, Y_α is now known to include (2 ± 1)% of ^{6}He and possibly much smaller amounts of slightly heavier particles. Y_α increases by about 2.2% per Mev from 11 to 21 Mev, with no evidence for a minimum in this range. The angular correlations between alpha particles and fission fragments were measured at 11-, 15-, 17-, and 21-Mev proton energy and for the spontaneous fission of ^{252}Cf. When corrected for the angular resolution of the detectors, the distributions are found to be approximately Gaussian with means and standard deviations 94 ± 0.3° (center-of-mass) and 14.7 ± 0.4° (nearly independent of incident proton energy) for the induced fission, and 93 ± 0.6° and 12.0 ± 0.4° for ^{252}Cf. Absolute values of Y_α were obtained relative to the absolute rate of emission of alpha particles from the spontaneous fission of ^{252}Cf as given in the literature and by an independent measurement. (auth)

22145 APPLICATION OF NUCLEAR COHERENCE PROPERTIES TO ELEMENTARY-PARTICLE REACTIONS. Stodolsky, Leo (Univ. of Michigan, Ann Arbor). Phys. Rev., 144: 1145-53(Apr. 29, 1966).

The use of nuclei as targets in low-momentum-transfer elementary-particle reactions is considered. At low momentum transfer the nucleus acts coherently and may be used to enhance or suppress various exchange mechanisms for the elementary particles. The impulse approximation and optical-model wave-functions representing the absorption of the particles passing through the nucleus are used. For production reactions in which π exchange on hydrogen is dominant, coherent nuclear reactions may be used to eliminate π exchange and enhance ω-φ-type exchanges, thus allowing study of the behavior of these exchanges. Calculations are given for production on ^{4}He, giving a crude estimate of 35 μb for $\pi + {}^4\text{He} \rightarrow \rho + {}^4\text{He}$. The general properties of coherent production reactions are also considered, including the A dependence of coherent reactions, the suppression of incoherent mechanisms at low momentum transfer, and the competition with production in the Coulomb field. Semicoherent reactions in which the nucleus is excited to special states are considered as a means of isolating particular components of the two-body scattering matrix. (auth)

22146 WIDE-ANGLE ELECTRON-PAIR PRODUCTION. Blumenthal, R. B.; Ehn, D. C.; Faissler, W. L.; Joseph, P. M.; Lanzerotti, L. J.; Pipkin, F. M.; Stairs, D. G. (Harvard Univ., Cambridge, Mass.). Contract AT(30-1)-2752. Phys. Rev., 144: 1199-1223(Apr. 29, 1966).

An experiment testing quantum electrodynamics at high energies and small distances is described. The photoproduction from carbon of electron-positron pairs was measured at laboratory angles of 4.60°, 6.23°, and 7.46°. Symmetrical electron-positron pairs in the energy range from 1 to 5 Bev were detected with a magnet-counter system that consisted of two mirror-image arms. Extensive internal checks of the apparatus were made and the results were reproducible. The theoretical values for the electron-pair yield were calculated by integrating the differential pair-production cross section over the acceptance of the apparatus using a Monte Carlo technique. The ratio R = (experimental yield)/(theoretical yield) was not 1.0. R was approximately given by $R = 0.62\{(1.00 \pm 0.05) + k^2/(4.31 \pm 0.17)^2\}$, where k is the energy in Bev of the photon which produced the pair, and by $R = 0.67\{(1.00 \pm 0.04) - Q_f^2/(313 \pm 13)^2\}$, where Q_f^2 is the four-momentum of the virtual fermion in (Mev)^2. The apparatus studies and a comparison of the measured single-electron yields with the theoretical yields suggest than an error exists in the absolute normalization of the results. There are no indications that the observed variation of the electron-pair yields with momentum or the large excess of wide-angle electron pairs at high energies is due to any systematic error. The experimental results do not agree with the predictions of quantum electrodynamics; they indicate a breakdown of the theory or the presence of other processes. (auth)

22147 QUASIPARTICLE RANDOM-PHASE APPROXIMATION IN ODD-ODD NUCLEI AND THE NEUTRON-PROTON INTERACTION. Kisslinger, L. S.; Rote, D. M. (Western Reserve Univ., Cleveland). Phys. Rev. Lett., 16: 659-62(Apr. 11, 1966).

A discussion is presented to point out that a consistent theory for many odd-odd nuclei can be obtained and that new knowledge about two-body interaction can be derived from this theory. It is suggested that the quasiparticle random-phase approximation might be accurate in at least some of the odd-odd nuclei. Numerical calculations are presented for several nuclei using various exchange mixtures and ranges. (B.G.D.)

22148 BLOCKING EFFECT AND CORIOLIS ANTI-PAIRING EFFECT ON DEFORMED ODD NUCLEI. Sugawara, Kazuko (Univ. of Osaka). Progr. Theoret. Phys. (Kyoto), 35: 44-64(Jan. 1966).

Effects of rotational motion on the pairing correlation in odd-mass nuclei and their various nuclear properties are investigated. The rotational motion weakens the pairing interactions (Coriolis anti-pairing effect), and further in odd-mass nuclei the odd nucleon also reduces the effect of the pairing interaction by blocking the scattering of the nucleon pairs into the orbit occupied by the

odd nucleon (blocking effect). The blocking effect is also affected by the rotational motion and weakened by dispersing the odd nucleon into other orbits by configuration mixing. The Hartree-Bogoliubov equation is solved assuming the pairing and quadrupole interactions in consideration of the rotational motion. The second order perturbation approximations are used and the self-consistent calculations are carried out in obtaining the energy-gap parameter and chemical potential. The moments of inertia and the gyromagnetic ratio are numerically calculated and compared with experimental data. Agreements are generally good. (auth)

22149 DECAYS OF LIGHT DOUBLE HYPERNUCLEI AND THE FOUR-BARYON WEAK INTERACTIONS. Kohmura, Toshitake (Tokyo Univ.). Progr. Theoret. Phys. (Kyoto), 35: 65-73(Jan. 1966).

The decay rates for light double hypernuclei are estimated and it is noted that the nonmesic decays are of interest. The characteristic decay modes, i.e., Λ-n, Σ^--p and Σ^0-n decays, give valuable information on the weak interaction. The relations between the coupling constants of the four-baryon weak interactions are derived from the data for the one-lambda hypernuclei in the framework of the SU(3) symmetry model, and the cancellation of the coupling constants for I = 0 pointed out by Block and Dalitz is compatible with the model. (auth)

22150 ASSIGNMENT OF NEUTRON CAPTURE ANGULAR MOMENTA IN ANGULAR DISTRIBUTIONS OF THE ^{23}Na(d,p)^{24}Na REACTION. Lopez, M. E. Ortiz de; Carrillo, Lila (Univ. Nacional de Mexico, Mexico City). Rev. Mex. Fis., 14: 225-39(1965). (In Spanish).

The ground state and sixteen excited levels of ^{24}Na were analyzed through (d,p) reactions in ^{23}Na with a 1.5 Mev Van de Graaff accelerator and the aid of a double broad-range magnetic spectrograph technique. As most cases show typical stripping patterns, Butler and DWBA computations were undertaken. Neutron capture angular momenta $l_n = 0$ could be assigned to levels 3, 4, 5, 7, 8, 12, and 13; $l_n = 1$ to levels 6, 9, and 15; and $l_n = 2$ to the ground, 1, 10, 11, and 14 excited states. Neutron-capture angular momenta of higher excited states may be assigned using simple Butler theory, in contrast to DWBA computations, in which the maxima show larger shifts as their Q values diminish. (auth)

22151 ANGULAR DISTRIBUTIONS OF ^{6}Li(d,p)^{7}Li AT ENERGY OF 1.5 Mev. Rickards, J. (Univ. Nacional de Mexico, Mexico City). Rev. Mex. Fis., 14: 241-60(1965). (In Spanish).

The second excited state of ^{7}Li at 4.63 Mev excitation, whose spin and parity have not yet been determined experimentally is considered. The expected similarity between mirror nuclei, on one hand, and on the other calculations based on the shell model, the cluster model, and the collective model, suggest the assignment $^7/_2^-$. In order to obtain more information, the angular distributions of ^{6}Li(d,p)^{7}Li(0), (1) and (2) were carried out at an incident energy of 1.5 Mev. For level (2), with a low Q value and low E_d, Wilkinson's argument pertaining to the use of Butler curves for stripping reactions is expected to be valid. An anisotropy that seems to indicate $l_n = 1$ was observed, suggesting that the spin of the level be $\leq^5/_2$. (auth)

22152 PROBABILITY OF THE $\mu^- + {}^3\mathrm{He} \rightarrow {}^3\mathrm{H} + \nu$ PROCESS AND NUCLEAR WAVE FUNCTIONS. Chen, Hao-chin (Peking Univ.). Wu Li Hsueh Pao, 21: 1897-1902(Nov. 1965). (In Chinese).

The probability of the $\mu^- + {}^3\mathrm{He} \rightarrow {}^3\mathrm{H} + \nu$ process was obtained using three essentially different nuclear wave functions. The results were compared with those of other authors. (G.O.Y.)

22153 PRECISE ATOMIC MASS DIFFERENCES INVOLVING ISOTOPES OF Nd, Sm, Cd, AND Pb. Macdougall, John D.; McLathie, William; Whineray, Scott; Duckworth, Henry (McMaster Univ., Ontario, Can.). Z. Naturforsch., 21a: 63-8(Jan.-Feb. 1966).

During the past year, certain of our experimental techniques have been re-evaluated and modified. In the course of these investigations, two atomic mass differences involving isotopes of cadmium and one involving isotopes of lead were redetermined. The new values are consistent with reaction data and with our older measurements. Thirteen mass differences involving isotopes of neodymium and samarium were also determined, several for the first time. These new results are consistent with reaction data and with other recent mass spectroscopic data, but indicate that our previously-reported mass differences in the neodymium-samarium region are systematically too large by small but real amounts. An unusually concordant situation now exists in this region of the mass table. (auth)

22154 A CORRECTION TO THE 1964 MASS TABLE. Wapstra, A. H. (Instituut voor Kernphysisch Onderzoek, Amsterdam). Z. Naturforsch., 21a: 68-9(Jan.-Feb. 1966).

It is pointed out that, very probably, the masses of all nuclides decaying by an α-β decay chain into ^{213}Bi are low by about 150 kev. (auth)

22155 A NOTE ON THE THEORY OF DECAYING SYSTEMS AND THE COMPUTATION OF DECAY RATES. Kuemmel, H. (Research Inst. for Theoretical Physics, Helsinki). Z. Naturforsch., 21a: 79-83(Jan.-Feb. 1966).

The theory of decaying systems of Franz—which seems finally to settle the basic questions left open so far—was reformulated assuming a slightly altered initial situation. The currently used formulas for the decay rates were derived as an approximation to this practically rigorous theory. (auth)

22156 MOESSBAUER EFFECT METHODOLOGY. Volume 1. Proceedings of the First Symposium, New York City, January 26, 1965. Gruverman, Irwin J. (ed.). New York, Plenum Press, 1965. 208p. $12.50. (CONF-650101(Vol.1).

Fifteen papers are included. Separate abstracts were prepared for nine papers. Six papers were previously abstracted for NSA as 19: 14507, 40306, 40922, 41845, 41848, and 46748. (A.G.W.)

For abstracts of individual papers see: 20684, 20850, 21079—21081, 22157—22159, and 22327.

22157 f MEASUREMENTS WITH BLACK ABSORBERS. Dash, J. G. (Univ. of Washington, Seattle). pp 107-14 of Moessbauer Effect Methodology. Vol. 1. Gruverman, Irwin J. (ed.). New York, Plenum Press, 1965.

The theory involved in the use of opaque absorbers in the measurement of the Mössbauer fraction of emitted or absorbed gamma radiation is considered. The requirement for an opaque absorber is that the resonant cross section should be large in a region that is wide relative to a natural line width but very narrow in comparison to the recoil radiation. The resonance absorption can then be turned off by a large Doppler shift. A good approximation to such an absorber was developed for the 14-kev ^{57}Fe line by combining compounds having a wide distribution of isomer shifts and quadrupole splittings. The compounds are lithium and ammonium fluoroferrates in which the elements other than iron all have low atomic numbers. Advantages and applications of wide absorbers are discussed briefly. (A.G.W.)

22158 STANDARDIZATION OF THE DIFFERENTIAL CHEMICAL SHIFT FOR ^{57}Fe. Spijkerman, J. J.; Ruegg, F. C.; DeVoe, J. R. (National Bureau of Standards, Washington, D. C.). pp 115-20 of Moessbauer Effect Methodology. Vol. 1. Gruverman, Irwin J. (ed.). New York, Plenum Press, 1965.

Among materials considered as standard reference absorbers for ^{57}Fe Mössbauer studies, sodium nitroprusside appears most promising. Its use and properties are discussed briefly. No suitable standard for ^{119}Sn Mössbauer studies has yet been found. (A.G.W.)

22159 COMPUTATION OF MOESSBAUER SPECTRA. Gabriel, J. R. (Argonne National Lab., Ill.). pp 121-32 of Moessbauer Effect Methodology. Vol. 1. Gruverman, Irwin J. (ed.). New York, Plenum Press, 1965.

Three new computer programs written at Argonne National Lab. for computing Mössbauer spectra are described. The three versions, UNIXTL, LVSPHS, and PDRHXT, apply respectively to experiments using single-crystal samples, magnetic powders in the absence of external magnetic fields, and powder samples in external fields. They are written almost entirely within the constraints of the FORTRAN II computer language. Basically, Hamiltonian matrices are constructed for the ground and excited nuclear states, their eigenvalues and eigenvectors found, and these are used to calculate the transition probabilities for absorption or emission of photons. The physics systems that can be simulated by the program, the mathematics used, the problems to be expected in using computers other than that for which the program was originally written, and preparation of input data cards are discussed. (A.G.W.)

22160 $^{16}O(d,\alpha)^{14}N$ DIFFERENTIAL CROSS SECTIONS AND FLUCTUATION STUDIES. Jobst, Joel. 10p. (CONF-651015-5). ORAU. Gmelin, AED-CONF-65-312-20.

From American Physical Society, Chicago.

Alpha-particle cross sections from the $^{16}O(d,\alpha)^{14}N$ reaction were measured at six angles with the deuteron energy varied in 10- to 20-kev steps from 5 to 9 Mev. An energy level diagram of the final state ^{14}N is shown. Detailed cross sections for the α_3 and α_4 groups at cms angles of 30, 45, 90, 135, 150, and 168° are presented. Previous data on the i-spin forbidden α_1 group and the α_0 and α_2 groups are included in a study of cross correlations between each pair of groups and self correlations for all five groups. (A.G.W.)

22161 THE LAMBDA-HYPERON BINDING ENERGY IN NUCLEAR MATTER. Prowse, D. J. (Univ. of California, Los Angeles. Univ. of Wyoming, Laramie); Lou, Alice. 12p. (CONF-651015-8). ORAU. Gmelin, AED-CONF-65-312-19.

From American Physical Society, Chicago.

The spallation model in which a K^- beam incident on a nuclear emulsion is assumed to impart a forward momentum to the nucleus and generate a cascade of particles is used in an attempt to determine the Λ hyperon binding energy in matter. The range and mass spectra of the short-range hyperfragments produced by the spallation process were obtained by following the history of both the cascade process and the evaporating nucleus with a Monte Carlo procedure. From this Monte Carlo calculation a distribution of the binding energy of the last proton in the residual nucleus was also obtained. It is concluded that the binding energy of a Λ hyperon in nuclear matter will be 40.0 Mev if the hyperfragment mass A is ≈40 and 33 Mev if A ≈ 105 depending on the radius and shape of the well chosen. (A.G.W.)

Plasma Physics and Thermonuclear Processes

See also Fluid Physics and Thermodynamics

Refer also to abstracts 21478, 21491, 21560, 21569, and 21836.

22162 (AD-621020) NON-ADIABATIC PARTICLE MOTION IN COMPLEX MAGNETIC FIELDS [Thesis]. Oss, John P. (Air Force Inst. of Tech., Wright-Patterson AFB, Ohio. School of Engineering). 1965. 87p. (GNE-PH-65-15). CFSTI $3.00 cy, $0.75 mn.

The motion of particles in a four bar Ioffe bottle was studied. A set of normalized equations was used to follow the motion of the guiding center of particles in the Ioffee bottle. The nonrelativistic equations of motion assumed conservation of energy but did not assume an adiabatic motion. The motion tended to be an oscillation from one quadrant of the system to another with a simultaneous motion along the longitudinal axis. The majority of the reflections occurred due to the longitudinal bars of the container rather than to the end mirrors. The magnetic moment of a particular particle was calculated at equally spaced steps in time. The moment varied in magnitude by twenty percent of the average value. The variation tended to fall within an envelope which could be correlated to reflections which the particle experienced. (auth)

22163 (AD-621034) BOUND WAVES IN COMPRESSIBLE PLASMA GAPS. Tamir, T. (Polytechnic Inst. of Brooklyn, N. Y. Microwave Research Inst.). July 1965. Contract AF19(628)-2357. 36p. (AFCRL-65-534). CFSTI $2.00 cy, $0.50 mn.

It is shown that a planar gap in a plasma medium is an appropriate idealized model for studying electromagnetic and plasma waves in a variety of situations, including plasma sheaths and ionospheric layers. A uniform, isotropic, lossless, warm plasma gap is investigated and is found to support both surface and interface waves which consist of an electromagnetic mode coupled to a plasma pressure mode. The surface waves are fast and they occur primarily at frequencies below the plasma frequency, whereas, the interface waves are slow and are present at all frequencies; in both cases, the waves may be either of the forward- or backward traveling variety. In addition, the presence of leaky waves of the spectral type is demonstrated at frequencies above the plasma frequency. Dispersion curves are calculated for a large range of the parameters involved and the results are compared to those for surface waves along a dielectric slab which, in certain respects, represents a configuration analogous to the plasma if pressure effects are neglected. (auth)

22164 (AD-621213) AN EXPERIMENTAL DETERMINATION OF THE THERMAL AND ELECTRICAL CONDUCTIVITY OF ATMOSPHERIC ARGON PLASMA. Knopp, Carl F. (Northwestern Univ., Evanston, Ill. Gas Dynamics Lab.). Jan. 1965. Contract AF49(638)-879. 212p. (AFOSR-65-1338). CFSTI $6.00 cy, $1.25 mn.

A wall stabilized arc was used to produce an equilibrium, cylindrically symmetric, argon plasma column. It was demonstrated that axial temperature gradients are negligible over a significant length of the plasma column, thus verifying the assumption that, at low flow rates, convective heat losses are not important for this type of device. The radial temperature distribution within the arc column was ascertained by spectroscopic analysis for arc currents of 30 to 60 amperes. Temperatures obtained from absolute line and absolute continuum radiation were in excellent agreement. An empirical expression, based upon the Kramers–Unsold theoretical model, was obtained for the radiated power, as a function of temperature, of argon plasma. The electrical conductivity of argon was calculated using Spitzer's electron-electron collision correction. A technique was developed to determine the electrical conductivity from the arc currents, voltage gradients and the measured temperature profiles. Using this technique, the electrical conductivity of argon plasma as a function of temperature was determined for the temperature range of 8,500 K to 12,000 K. The experimental electrical conductivity showed good agreement with the calculated electrical conductivity. Using the measured temperature profiles, calculated radiated power, and experimentally verified electrical conductivity, the thermal conductivity of argon was determined for the same temperature range as the electrical conductivity. The data were in good agreement with theoretically predicted results. (auth)

22165 (AD-621457) WAVE PROPAGATION IN INHOMOGENEOUS ISOTROPIC HOT PLASMAS. Unz, H. (RAND Corp., Santa Monica, Calif.). Sept. 1965. 28p. CFSTI $2.00 cy, $0.50 mn.

The three dimensional wave equations for waves propagating in inhomogeneous, isotropic, hot compressible plasmas are derived from the macroscopic, linearized electro-magneto-plasma-gas-dynamics equations. Particular cases are discussed and compared with previous results. (auth)

22166 (AD-621913) THE DEPENDENCE OF LONGITUDINAL PLASMA WAVE DAMPING AND GROWTH ON THE SHAPE OF THE VELOCITY DISTRIBUTION FUNCTION. Mioduszewski, Daniel P. (Pennsylvania State

Univ., University Park. Ionosphere Research Lab.). Nov. 15, 1965. Contract AF19(628)-4014. 76p. (AFCRL-65-638). CFSTI $3.00 cy, $0.75 mn.

The transform and perturbation theory approach is used for the problem of longitudinal plasma oscillations. The plasma dispersion relation is shown to be a natural consequence of both the initial value problem and the problem of forced oscillations. Distribution functions of the form $F_0(v) = A_n\, 1/(V-U)^{2n} + \Sigma^{2n}$ where $n = \int$ are investigated for both the single and double hump case. For the forced oscillations problem wave growth is obtained in space when the driving frequency is less than the plasma frequency. Wave growth is also described for the double hump distribution. (auth)

22167 (AD-622391) RESEARCH ON RADIATION FROM ARC-HEATED PLASMA. Final Technical Report, March 1, 1964-April 1, 1965. Morris, J. C.; Krey, R. U.; Liebermann, R. W. (Research and Advanced Development Div., Avco Corp., Wilmington, Mass.). July 9, 1965. Contract AF33(616)-8390. 113p. (ARL-65-164). CFSTI $4.00 cy, $0.75 mn.

Spectral continuum intensity measurements from 2500 Å to 20,000 Å and total radiation measurements were made for oxygen and nitrogen plasmas for a temperature range of 9000 K to 13,000 K using a mechanically constricted d-c arc as a radiation source. The spectral data were treated analytically to separate the radiation from electron neutral atom and electron positive ion collisions. The electron neutral data were further reduced to radiative cross sections which are in turn compared with the results of other experimental investigations and with theoretical predictions. The spectral continuum data were integrated to find the total continuum for $\lambda > 2000$ A. These data were subtracted from the total radiation measurements $\lambda > 2000$ A to obtain the contribution from line radiation. These data are compared with analytical predictions for atomic line radiation and found to be in good agreement. Radiation tables were generated, based upon these experimental data, for the total continuum plus atomic line radiation for wavelengths greater than 2000 A and for the total continuum plus total atomic line radiation for all wavelengths for temperatures ranging from 9000 K to 18,000 K and for pressures from 0.1 to 10.0 atmospheres. These data are also presented in terms of flight velocity. These data are compared with reported values gathered from shock tube and ballistic range work. (auth)

22168 (AD-622569) PLASMA DENSITY AHEAD OF PRESSURE DRIVEN SHOCK WAVES [Thesis]. Holmes, Lawrence Bruce (Rochester Univ., N. Y. Dept. of Mechanical and Aerospace Sciences). May 1965. Contract AF-AFOSR-478-65. 200p. (AFOSR-65-0974). CFSTI $5.00 cy, $1.25 mn.

A review of the literature on electrical precursors associated with strong shock waves is presented. Negative well-type electrostatic precursor signals are obtained from the potential probe experiments. Potential probe experiments in conjunction with a solenoidal magnetic field show that the electrostatic precursor signal is due in part to radial diffusion of electrons to the wall of the shock tube. A theory is presented for the diffusion of the electrons and ions to the grid of the probe and for the motion of the charged particles inside the probe. This theory relates the collected currents to the plasma density in the shock tube. The evidence of the existence of a neutral plasma and the high velocity of propagation of the precursor strongly suggests that the gas ahead of the shock wave is photoionized. It was established that multiple step photoionization produces the plasma. (TAB)

22169 (AD-622684) STUDY OF COLLISION PROCESSES IN GASEOUS PLASMAS. Status Report No. 7, July 1-October 1, 1965. Oskam, H. J. (Minnesota Univ., Minneapolis. Physical Electronics Research Lab.). Contract Nonr-71037. 5p. CFSTI $1.00 cy, $0.50 mn.

Studies related to collision processes in gaseous plasmas are summarized for the period July 1, 1965 to October 1, 1965. The main results obtained are related to recombination mechanisms in helium and neon, and to the mobility of positive ions in helium. (auth)

22170 (AD-622701) BASIC STUDIES IN MAGNETOHYDRODYNAMICS. Final Report. Patrick, Richard M. (Avco-Everett Research Lab., Everett, Mass.). Nov. 1964. Contract AF49(638)-1129. 14p. (AFOSR-65-1207). CFSTI $1.00 cy, $0.50 mn.

A magnetic annular shock tube (MAST) is developed and used to study plasma phenomena important for collision free plasmas. Studies are carried out to bring the MAST to a state of development where it will become an established research tool. It is found that for a given shock velocity the shock tube must have a minimum length and that the plasma must be contained away from the walls of the tube, this being done by the use of magnetic fields. The annulus ratio and ablation are also important considerations in successful MAST operation. The plasma produced by the shock wave is collisionless in that the mean free path for ordinary collisions is large compared to the shock thickness. However, the importance of collisions in the shock front itself is not clear. (auth)

22171 (AD-622811) DETERMINATION OF ELECTRON DENSITIES USING A RADIAL TRANSMISSION LINE. Mullen, J. H.; Medgyesi-Mitschang, L. N. (McDonnell Aircraft Corp., St. Louis, Mo. Research Div.). May 1965. Contract AF19(628)-2764. 36p. (AFCRL-65-553). CFSTI $2.00 cy, $0.50 mn.

A new method for measuring the electron density and collision frequency of plasmas is described. This diagnostic technique which is applicable to low as well as high density plasmas, minimizes the usual field problems associated with microwave plasma diagnostic schemes. The effect of plasma nonuniformity on this technique was calculated. Spectrographic measurements and thermodynamic partition function calculations were found to be consistent with the plasma parameters measured with the present technique. (auth)

22172 (AD-623718) RESEARCH ON ELECTROMAGNETICS FOR PROJECT DEFENDER. Semiannual Technical Summary Report for September 30, 1965. Weber, Ernst (Polytechnic Inst. of Brooklyn, N. Y. Microwave Research Inst.). Contract Nonr-839(38). 198p. CFSTI $5.00 cy, $1.25 mn.

Progress is reported on a fairly large number of projects dealing generally with electromagnetic phenomena in plasmas and plasma-like media, such as the properties of antennas, excitation of electromagnetic waves in plasmas, coupling of acoustic and electromagnetic waves, propagation through time-varying random media, electron densities in shock waves, basic kinetic theory of ionized media, instabilities in plasmas, and properties of laboratory type plasmas. A smaller group of projects deals with characteristics of transmitters and receivers for communication through randomly time-varying media and with the problem of pattern recognition. (auth)

22173 (AD-623788) ELECTROPHORETIC POWER GENERATION IN THERMALLY IONIZED PLASMAS. Physical Sciences Research Papers. Leiby, C. C. Jr.; Fields, J. C. (Air Force Cambridge Research Labs., L. G. Hanscom Field, Mass.). Oct. 1965. 38p. (AFCRL-65-73). CFSTI $2.00 cy, $0.50 mn.

Druyvesteyn's solutions for electrophoretically induced gas flows in electrical discharges in gases were extended over a larger pressure range and corrected for the influence of Debye shielding effects. The effects of molecular or "slip" flow were also taken into account. These more accurate and general solutions were applied to the reverse phenomenon of space charge field generation arising from the flow of a thermally ionized cesium plasma through a tube. Under such flow conditions, a nonlinear differential equation for the axial pressure distribution was obtained but not solved. However, it was possible to obtain estimates of the ranges of cesium pressure, temperature and tube radii which would be required for sensible levels of electric power generation. Anaphoretic flow power levels of the order of 0.1 to 10 watts, in tubes of laboratory dimensions (radii of 10 cm or less), appear feasible at temperatures from 1700 to 2400K. Sensible power generation levels at lower temperature require

very large diameter tubes, and therefore are not feasible. (auth)

22174 (AD-623789) WAVE PHENOMENA IN IONIZED GASES. Physical Sciences Research Papers. Haskell, Richard E.; Papa, Robert J. (Air Force Cambridge Research Labs., L. G. Hanscom Field, Mass.). Aug. 1965. 53p. (AFCRL-65-64). CFSTI $3.00 cy, $0.50 mn.

The propagation of waves in uniform, unbounded magnetoplasmas is reviewed. Emphasis is placed on describing the various approaches and plasma models which may be used. The results and limitations of the different methods are discussed and compared. Dispersion curves for each model are presented in the form of omega-k plots. (auth)

22175 (AD-624081) PROBING OF THE DYNAMICAL RESPONSE OF A PLASMA. Friedman, Herbert (Polytechnic Inst. of Brooklyn, N. Y. Microwave Research Inst.). June 1963. Contract AF30(602)-2149. 49p. CFSTI $2.00 cy, $0.50 mn.

The dynamical response of a gaseous plasma to the self-induced magnetic fields in a toroid switch tube was experimentally investigated using a magnetic field probe and a set of excitation current measurements. The magnetic field, experimentally measured, is compared with the representation of the plasma current distribution as an ideal current sheet. The excitation current measurements reveal oscillations in the plasma whose detailed nature, unexplainable by the current sheet model may yield information on the thermal pressure within the plasma. (auth)

22176 (AD-624165) HALL EFFECT IN A COLLISION-DOMINATED GASEOUS PLASMA. Chen, C. L. (Westinghouse Research Labs., Pittsburgh, Pa.). 1965. Contract Nonr-4725(00). 29p. CFSTI $2.00 cy, $0.50 mn.

A theoretical treatment of the Hall voltage developed in a gaseous plasma immersed in a uniform magnetic field is presented. The plasma considered is collision dominated and is confined by parallel planes with insulating walls. The Hall voltage is found to depend on electron-ion volume recombination and on the tensor character of the electron mobility. The cases to be discussed are: (i) negligible diffusion, (ii) negligible electron-ion volume recombination, and (iii) diffusion with small but not negligible volume recombination. (auth)

22177 (CLM-Bib-6) PLASMA SHEATH. A Bibliography. Francis, L. S. (Culham Lab., United Kingdom Atomic Energy Authority, Abingdon (England)). Jan. 1966. 17p. Dep. mn. BIS $0.60. HMSO 3s. 0d.

Abstracts of current 1960-1964 papers on plasma sheath theory are presented. (M.O.W.)

22178 (FEI-17) K RASCHETU VOL'T-AMPERNYKH KHARAKTERISTIK TEPA V DUGOVOM REZHIME. (Calculation of the Volt-Ampere Characteristics of the TEP (Thermoelectron Potential) in an Arc). Stakhanov, I. P.; Kasikov, I. I. (Gosudarstvennyi Komitet po Ispol'zovaniyu Atomnoi Energii SSSR, Obninsk. Fiziko-Energeticheskii Institut). 1965. 23p. Dep. mn.

The transport equations in the diffusion approximation were formulated for gas discharge plasma. The ionization mechanism in the space was assumed to be thermal. The charge recombination was disregarded. The equations were solved for constant temperature of the ions (T_i) and electrons (T_e). Under this assumption it was shown that the ionization coefficient does not depend on the magnitude of the current. This result was obtained by means of exact solution of the equation on an electronic computer. (tr-auth)

22179 (FTI-080/P-032) RABOTA KOAKSIAL'NOGO PLAZMENNOGO ISTOCHNIKA V PRODOL'NOM MAGNITNOM POLE. (Performance of a Coaxial Plasma Source in a Longitudinal Magnetic Field). Zolototubov, I. M.; Kiselev, V. A.; Novikov, Yu. M.; Tolok, V. T. (Akademiya Nauk Ukrainskoi SSR, Kharkov. Fiziko-Tekhnicheskii Institut). 1964. 9p. Dep. mn.

During installation of a coaxial plasma gun in a longitudinal magnetic field, rotation of the plasma in the azimuthal direction was observed. This was caused by its drift in crossed electric and magnetic fields. This leads on the one hand to an increase of an ionization degree and of the dimensions of the transverse component of the particle energy in the pulse and on the other hand to significant decrease to the quantity of impurities because of the symmetrization of the discharge with respect to the azimuth and decrease of the current density on the gun electrode. (tr-auth)

22180 (IAE-960) K MAGNITOGIDRODINAMICHESKOI TEORII PINCH-EFFEKTA V VYSOKOTEMPERATURNOI PLOTNOI PLAZME. (A Magnetohydrodynamic Theory of the Pinch Effect in a High-Temperature, Dense Plasma). Imshennik, V. S.; D'yachenko, V. F. (Institut Atomnoi Energii, Gosudarstvennyi Komitet po Ispol'zovaniyu Atomnoi Energii SSSR, Moscow). 1965. 66p. Dep. mn.

The magnetohydrodynamic problem of the pinch effect in deuterium was investigated. The one-dimensional cylindrical symmetrical equations were solved numerically using different physical hypotheses. The role of dissipation processes, essential in the case of ionized plasmas, was investigated. Emphasis was given to the process of accumulation of shock waves. The relation of the structure of the preaxial range and the structure of the convergent collision waves was established. The thermonuclear yield of neutrons and the soft x-ray radiation were calculated. The results of the calculation were compared with experimental data and the possibility of determining the plasma temperature (approximately 1 kev) and the ejection of the gas mass from the plasma (approximately 90%) using the measured velocity of the current sheath near the axis (approximately 2.5×10^7 cm/sec) was shown. (tr-auth)

22181 (IPP-1/45) BERECHNUNGEN ZUM THETA-PINCH-EXPERIMENT MIT UEBERLAGERTEM HEXAPOL. (Calculation of Forces and Inductances for the Hexapole Experiment). Finkelmeyer, H.; Lotz, W. (Institut fuer Plasmaphysik, G.m.b.H., Garching (West Germany)). Feb. 1966. 17p. Dep. mn.

For the experiment "Spinne" (toroidal theta-pinch with superimposed hexapole) current forces and inductances are being calculated. The calculations are easily applicable to other experiments with different parameters. The capacitor banks for the theta-pinch main discharge and for the hexapole have each an energy of approximately 50 kJ. In each "wire" of the hexapole there flows a current of approximately 100 kA, the magnetic field on the surface of the "wire" is about 50 kG and the force radially inward is about 100 kp/cm (at current maximum). (auth)

22182 (IPP-3/35) MIKROWELLENINTERFEROMETRIE AN ELEKTROMAGNETISCH ERZEUGTEN STOSSWELLEN. (Microwave Interferometry in Electromagnetically Produced Shock Waves). Makios, W. (Institut fuer Plasmaphysik, G.m.b.H., Garching (West Germany)). Feb. 1966. 62p. Dep. mn.

Microwave measurements were made of the electron density and the electron collision frequency in the plasma between the shock front and the discharge plasma of electromagnetically produced shock waves. These investigations were carried out in argon and hydrogen at $p_0 = 2$ mm Hg initial pressure and velocities ranging from $M = 5$ to $M = 20$. At higher velocities the discharge plasma advances right into the shock front. In this range of Mach numbers, the expected electron density is so low that optical interferometers cease to be of interest as diagnostic tools. Four mm-microwave interferometers were therefore used. With a reflection interferometer the velocities of the various plasma zones could be measured by utilizing the Doppler effect. Next, transmission measurements were made with an interferometer of the standard type with horns and lenses. However, its spatial resolution was insufficient even though the limits of the technically and physically possible were reached. Finally, a system of Lecher wires in the measuring arm of the interferometer provided a spatial resolution of approximately half a wavelength and proved successful in measuring the electron density distribution between the shock front and the

following discharge plasma. In the case of hydrogen the rise of the electron density in the shock front is caused by compression of the precursor electrons. In argon, on the other hand, most of the electrons are produced behind the shock front. A typical relaxation of the electron density towards equilibrium was measured. It was also possible to measure the electron collision frequency in argon as a function of time (and hence of the distance from the shock front). (auth)

22183 (LRP-21-66) PRESSURE BAR AND PHOTOGRAPHIC MEASUREMENTS ON A HIGH FREQUENCY THETA-DISCHARGE. Jones, Ieuan R. (Laboratoire de Recherches sur la Physique des Plasmas, Lausanne (Switzerland)). Feb. 1966. 32p. Dep. mn.

A hydrogen plasma is produced by means of a θ-coil which is fed by a high frequency (4.8 Mc) generator of 12 Mw maximum power. Pressure measurements of the plasma are made by means of the pressure bar technique and a photographic investigation is made with an image converter camera. A tentative description of the gross physical behavior of the discharge is given. (auth)

22184 (LRP-22-66) ON THE DESIGN OF A ROTATING FIELD PINCHED DISCHARGE. Weibel, E. S.; Keller, R. (Laboratoire de Recherches sur la Physique des Plasmas, Lausanne (Switzerland)). Feb. 1966. 25p. Dep. mn.

The dynamics of a rotating field pinch is described in terms of the macroscopic quantities temperature, pressure, plasma radius and magnetic field strength. The amplitude program necessary for maintaining the pinch is established and heating rates are given. The energy transfer between generator and plasma is examined and the condition for maximum efficiency is derived. (auth)

22185 (LRP-23-66) TEMPERATURE IONIQUE DANS UN CONFINEMENT HF MESUREE AVEC UN SELECTEUR ELECTROSTATIQUE. (Ionic Temperature in an h-f Confinement Measured with an Electrostatic Selector). Keller, R. (Laboratoire de Recherches sur la Physique des Plasmas, Lausanne (Switzerland)). Mar. 1966. 25p. Dep. mn.

A hydrogen plasma is confined and heated by means of a θ-coil which is fed by a high-frequency generator of 13 megawatt maximum power. The energy distribution of the axially emitted ions is measured by means of an electrostatic analyzer which is designed for large currents. The possibility of ion heating arising from the oscillation of the boundary layer of the discharge is discussed. (auth)

22186 (MATT-358) BALLOONING INTERCHANGE INSTABILITIES OF MAGNETIZED PLASMAS UNDER GRAVITATIONAL FIELDS. Yoshikawa, S. (Princeton Univ., N. J. Plasma Physics Lab.). Sept. 1965. Contract AT(30-1)-1238. 21p. Dep. mn. CFSTI $2.00 cy, $0.50 mn.

The relation between the resistive ballooning mode and the "universal" type instability with gravitational field (simulating the magnetic field curvature) is discussed. It is shown that under appropriate assumptions, the instability of the "universal" type is an extension of the resistive ballooning mode if one replaces the collision frequency in the resistive ballooning mode by the effective kinetic collision frequency $k_z v_c$. The relative importance of these ballooning instabilities to toroidal plasmas is discussed. (auth)

22187 (MATT-424) RESISTIVE INSTABILITIES IN TOROIDAL HYDROMAGNETIC SYSTEMS. Kulsrud, R. M. (Princeton Univ., N. J. Plasma Physics Lab.). Jan. 1966. Contract AT(30-1)-1238. 16p. (CONF-651056-2). Dep. mn. CFSTI $1.00 cy, $0.50 mn.

From Symposium on the Dynamics of Plasmas and Fluids, College Park, Md.

A situation is discussed in which the inclusion of even a small resistance of a plasma makes a drastic change in its stability from that of a zero resistance plasma. The situation considered is basically the so-called min-B system in a torus. The instability in question is the interchange instability. (M.O.W.)

22188 (N-65-22776) PARTICLE INJECTION TECHNIQUES FOR VELOCITY MEASUREMENT IN ARC PLASMAS. Seymour, Errol V. (Harvard Univ., Cambridge, Mass. Engineering Sciences Lab.). Dec. 1964. 62p. (TR-12).

An investigation of a technique for measuring velocity profiles in an ionized gas flowing through a tube is summarized. Small particles are injected into the plasma under known conditions, and the motion of the particles is related to the plasma velocity. The general equations for particle drag and heat transfer are presented. It is shown that the effects of slip flow are negligibly small and that the effects of thermal radiation on heat transfer are less than 4.5%. (D.C.W.)

22189 (TID-22809) PLASMA RADIATIONS. Final Report, June 1, 1964-August 31, 1965. Kursunoglu, Behram (Center for Theoretical Studies, Univ. of Miami, Coral Gables, Fla.). Dec. 1965. Contract AT(40-1)-2761. 135p. (CST-PA-65-1). Dep. mn. CFSTI $4.00 cy, $1.00 mn.

Separate detailed theoretical discussions are presented on the following: diffusion as a problem of statistical path, nonrelativistic theory of plasma oscillations, plasma diffusion across a magnetic field, relativistic plasma in the absence of a magnetic field, relativistic plasma in a magnetic field, and conservation laws of a relativistic plasma. (M.O.W.)

22190 (TID-22821) PLASMA INSTABILITIES AND WAVES EXCITED BY AN ANISOTROPIC VELOCITY DISTRIBUTION PRODUCED BY ELECTRON CYCLOTRON RESONANCE. Annual Report, June 1, 1965-February 28, 1966. Shohet, J. L. (Johns Hopkins Univ., Baltimore, Md. Dept. of Electrical Engineering). Mar. 1966. Contract AT(30-1)-3565. 25p. Dep. mn. CFSTI $1.00 cy, $0.50 mn.

Research during this period was spent in designing, building, testing, and initially operating an electron cyclotron resonance plasma device. The experimental apparatus consists of a cylindrical vacuum chamber placed inside an air-core solenoid. The electron cyclotron resonance radiation is supplied from a pulsed magnetron at a wavelength of 3 cm. The essential parts of the development of the experiment are described. Some initial measurements made on the plasma are reported. (M.O.W.)

22191 (UCRL-14697) MEASUREMENTS OF THE PROFILE OF THE ELECTRON BEAM FROM THE ASTRON ACCELERATOR. Barnes, William S.; Swain, James E. (Lawrence Radiation Lab., Univ. of California, Livermore). Mar. 3, 1966. Contract W-7405-eng-48. 12p. Dep. mn. CFSTI $1.00 cy, $0.50 mn.

An experiment was performed to investigate the electron density profile of a 4-Mev electron beam from the Astron accelerator in air at various distances from the beam port. The results of this experiment and a technique by which such measurements may be made are included. Some knowledge of this profile is required in order to more accurately assess the results of measurements of the conductivity of air and other gases under bombardment with the Astron beam. (auth)

22192 THEORY OF ELECTROSTATIC DOUBLE PROBE COMPRISED OF TWO PARALLEL PLATES. Chung, Paul M.; Blankenship, Victor D. (Aerospace Corp., San Bernardino, Calif.). AIAA (Amer. Inst. Aeron. Astronaut.) J., 4: 442-50 (Mar. 1966).

The difficulties with continuum single probes in plasma diagnostics may arise from the uncertainties surrounding the other electrode (ground), which usually does not assume the plasma potential at the point of interest, and from the fact that the probe disturbs the plasma to a much greater extent than that predicted by classical theories. In order to circumvent these difficulties, an analysis of the double probes comprised of two parallel plates is presented. Because of the simple geometry, the complete flow region between the two electrodes, comprised of two boundary layers and an inviscid layer, can be analyzed in detail. The governing equations for the electric and flow properties of

the continuum, weakly ionized plasma are solved. The cases of electron temperature in frozen state, with respect to the neutral gas temperature, and in equilibrium are considered. From the solution, simple equations are derived which can be used to translate the potential-current characteristics of the probe into the electron temperature and number density of the freestream plasma. The analysis also shows the detailed mechanism by which electricity is conducted between two plates across a flowing plasma. (auth)

22193 LANGMUIR PROBE DIAGNOSIS OF TURBULENT PLASMAS. **Demetriades, Anthony; Doughman, Ernest L. (Philco Corp., Newport Beach, Calif.).** AIAA (Amer. Inst. Aeron. Astronaut.) J., 4: 451-9(Mar. 1966).

The response of Langmuir probes to periodic or random fluctuations in plasmas is analyzed with the specific aim of developing methods for measuring statistical properties of unsteady or turbulent electron-rich gases. Beginning with the classical theory of Langmuir and Mott-Smith for the probe steady-state characteristics, the waveform-independent effect of fluctuations in the electron density and temperature and the plasma potential is found on the response of plane, cylindrical, and spherical probes operating with positive or negative bias. Relations are derived showing the effect of fluctuations on the average current, as well as formulas connecting the fluctuations and the rms probe current. It is found that the average current of the positive cylindrical probe is independent of fluctuations of any magnitude and that the electron density fluctuations can be easily measured with this probe. Experiments were performed in a low-density flowing argon plasma with fine cylindrical tungsten wires during which both the average and rms probe current were measured. Relevant features of the theory were verified, and fluctuations were measured quantitatively. (auth)

22194 ELECTRON TEMPERATURES IN SEVERAL rf-GENERATED PLASMAS. **Clarkson, M. H.; Field, R. E. Jr.; Keefer, D. R. (Univ. of Florida, Gainesville).** AIAA (Amer. Inst. Aeron. Astronaut.) J., 4: 546-7(Mar. 1966).

A discussion is given of experiments which present an insight into r-f discharges as plasma sources using air as the working gas, with power, pressure and coil configuration as the main variables. Electron temperature data obtained by using the floating double-probe technique are plotted against chamber pressure for each of two coil configurations. (B.G.D.)

22195 ELECTRON-ION RECOMBINATION PROCESSES IN A NONEQUILIBRIUM PLASMA. **Sakao, Fujihiko (Tokyo Univ.).** Bull. Inst. Space Aeron. Sci., Univ. Tokyo, 1: A6-A15(Oct. 1965). (In Japanese).

Published results of research on nonequilibrium electric conduction in gases are reviewed. Various processes concerning energy exchange between electrons and heavier particles are considered. It is concluded that under typical conditions in a nonequilibrium MHD generator the following assumptions, which are commonly made are valid: electrons and heavier particles are, respectively, in thermal equilibrium at their own temperatures; fraction of ionization can be obtained by inserting electron temperature into Saha's equation; and the most important losses of energy from electrons are loss by elastic collision against heavier particles and loss by radiation. However, close examination shows that these assumptions may be invalid when electron density is low, even in a MHD generator, and at low temperature-low current density regions, the validity of those assumptions is doubtful. (auth)

22196 ELECTROMAGNETIC RADIATION FROM AN ACOUSTIC POINT SOURCE WITHIN A COMPRESSIBLE PLASMA BUBBLE. **Wait, James R. (Inst. for Telecommunication Sciences, Boulder, Colo.).** Can. J. Phys., 44: 467-75(Mar. 1966).

A solution is presented for the boundary-value problem of an acoustic point-source antenna within a homogeneous compressible plasma region with an assumed rigid boundary. The small signal theory of plasma electrodynamics is employed and all damping mechanisms are neglected. It is shown that a fraction of the original acoustic power is converted into electromagnetic waves in the external free-space region. (auth)

22197 ELECTRON CYCLOTRON INSTABILITY. **Jungwirth, K.; Preinhaelter, J. (Inst. for Plasma Physics, Prague).** Czech. J. Phys., 16: 228-33(1966).

A study of the dependence of initiation and development of instability on the cyclotron frequency of electrons in a homogeneous plasma with cold ions and electrons forming two beams which move in the direction of, and opposite to, that of a constant magnetic field is presented. It is demonstrated that for $v_{\parallel}^2 \ll v_{\perp}^2$, the instability can already arise at $\omega_{pe}^2 \ll \omega_{ce}^2$, and a brief comparison with the experimental results is carried out. (auth)

22198 COMPLEX DOPPLER EFFECT IN PLASMA. **Bazhanova, A. E.** Izv. Vyssh. Ucheb. Zaved., Radiofiz., 8: 1110-16(1965). (In Russian).

A complex Doppler effect is considered in a rather dense, cold, magnetized plasma. On the basis of numerical calculations it is shown that radiation of an electron, moving in the plasma takes place mainly near two frequencies corresponding to cyclotron and plasma resonances. The radiation intensity in the first region is commensurable with that in vacuum and exceeds it by several orders in the second one. (auth)

22199 PECULIARITIES OF ELECTROMAGNETIC WAVE RADIATION IN ANISOTROPIC DISPERSIVE MEDIA. **Aleksin, V. F.; Pakhomov, V. I.; Stepanov, K. N. (Inst. of Physics and Tech., Academy of Sciences, Ukrainian SSR).** Izv. Vyssh. Ucheb. Zaved., Radiofiz., 8: 1135-47(1965). (In Russian).

The behavior of an electromagnetic field in a fare zone produced by an external source in a homogeneous anisotropic dispersive medium (magneto-active plasma) is considered. For some specific directions coinciding with magnetic field direction or with boundary of radiation cone (the boundary of transparence region), the radiation field greatly increases. Similar growth of a correlation in fluctuating electromagnetic fields in magnetoactive plasma is considered. (auth)

22200 ELECTROMAGNETIC WAVE SELF-FOCUSING IN PLASMA IN STRONG MAGNETIC FIELD. **Litvak, A. G. (Gor'kii State Univ.).** Izv. Vyssh. Ucheb. Zaved., Radiofiz., 8: 1148-54(1965). (In Russian).

The longitudinal electromagnetic wave propagation in a nonlinear plasma in a strong magnetic field is studied. The electromagnetic wave self-focusing accompanied by plasma displacement from the axis and waveguide channel formed is shown to be possible in a boundless plasma. The effect of nonlinearity on wave propagation in a cylindrical plasma waveguide is taken into account. By using the perturbation method, nonlinear corrections are found for the field distribution and phase velocity of a wave. (auth)

22201 PLASMA FLUX INSTABILITY IN INHOMOGENEOUS MEDIA. **Eidman, V. Ya. (Gor'kii State Univ., USSR).** Izv. Vyssh. Ucheb. Zaved., Radiofiz., 9: 11-15 (1966). (In Russian).

The convective instability with respect to the longitudinal perturbations is shown to take place in a plasma flux, piercing the slightly nonuniform medium. (auth)

22202 RESONANCES OF FLUCTUATING EMISSION OF A PLASMA CYLINDER. **Yakimenko, I. P. (Kharkov State Univ.).** Izv. Vyssh. Ucheb. Zaved., Radiofiz., 9: 33-8 (1966). (In Russian).

The thermal radiation resonances were determined of a fine uniform plasma cylinder in a longitudinal magnetic field. (auth)

22203 THE TENSOR OF AN EFFECTIVE PERMITTIVITY OF A STRONG NONUNIFORM ANISOTROPIC MEDIUM. **Ryzhov, Yu. A. (Gor'kii State Univ., USSR).** Izv. Vyssh. Ucheb. Zaved., Radiofiz., 9: 39-49(1966). (In Russian).

An expression was obtained for the tensor of an effective permittivity and Green function of an anisotropic strong

nonuniform infinite medium. The general relations are analyzed in the example of a magnetoactive plasma with isotropic fluctuations of the electron density. The case of small (in comparison with the wavelength) scale inhomogeneities was investigated. (auth)

22204 ELECTROMAGNETIC WAVES IN AN ISOTROPIC STRATIFIED PLASMA WAVEGUIDE. Shevchenko, V. V. (Inst. of Radiotechniques and Electronics, USSR). Izv. Vyssh. Ucheb. Zaved., Radiofiz., 9: 110-25(1966). (In Russian).

Orthogonal waveguide eigenwaves in isotropic stratified nonhomogeneous plasma were investigated. The waveguide has a mixed (discrete and continuous) frequency spectrum. A discrete part of the spectrum corresponds to waves localized near waveguide and a continuous one to the radiation field. The problem of stratified plasma waveguide excitation was solved in a general form. (auth)

22205 RELAXATION OF THE VELOCITY DISTRIBUTION OF IONS IN A PLASMA. APPLICATION OF THE UNIFIED THEORY. Hatori, Tadatsugu; Itikawa, Yukikazu (Tokyo Univ.). J. Phys. Soc. Jap., 21: 515-23(Mar. 1966).

A relaxation equation for the velocity distribution of the ions in a plasma is derived from the convergent kinetic equation taking account of both the short-range and collective interactions. The equation is solved by expanding the distortion of the distribution from equilibrium into a series of orthogonal polynomials. The rate of relaxation of each mode is obtained exactly without any cut-off procedure. The Coulomb logarithms in the rates of each mode are different from each other. (auth)

22206 OBSERVATION ON A NON-LINEAR EFFECT IN BEAM-PLASMA INTERACTION. Yamamoto, Takayoshi; Ohniwa, Kohji; Akimune, Hideo; Suita, Tokuo (Osaka Univ.). J. Phys. Soc. Jap., 21: 550(Mar. 1966).

Experimental results are shown in which nonlinear effects in electron plasmas which cause the incoherent interaction responsible for the breakdown of organized large-scale motion into disorganized small-scale motion in plasmas seem to be important in the system composed of an electron beam and a plasma. The gain versus the frequency characteristics is shown for various beam densities with constant plasma density and beam velocity. The maximum gain of each curve seems to be related to the amplitude of the excited plasma oscillations. The amplitude starts to grow with the beam density and reaches a maximum at a certain critical value above which it starts to decrease, while the half width of the frequency spectrum increases monotonically with the beam density. It is suggested that the wave-breaking process contributes to these phenomena. (J.F.P.)

22207 INJECTION TRAPPING OF HIGH-ENERGY MOLECULAR IONS INTO THE MIRROR FIELD WITH THE R-F ELECTRIC FIELD. [PART] II. Akimune, Hideo; Fujita, Yoshihiro; Miyake, Shoji; Suita, Tokuo (Osaka Univ.). J. Phys. Soc. Jap., 21: 556-7(Mar. 1966).

Preliminary experimental results on molecular ion injection performed in the HX apparatus in order to study the function of the r-f electric field are described. Axial density distributions both with and without the r-f field are shown. The latter distribution shows that of atomic ions from dissociations during a single turn of H_2^+ ions. The variation of the detector signal and slow ion current with the r-f amplitude is also shown. This variation indicated that the r-f field served to build up atomic ions in a small volume and to ionize the background ions. (J.F.P.)

22208 ANOMALOUS BREMSSTRAHLUNG AND ANOMALOUS CYCLOTRON EMISSION FROM PARTIALLY IONIZED GASES. Tanaka, S.; Honzawa, T. (Nagoya Univ., Japan). Kakuyugo-Kenkyu, 14: 162-80(Feb. 1965).

The radiowave emissions from the partially ionized plasma in a magnetic field in the frequency range from 20 to 1000 Mc/sec were investigated experimentally. Two kinds of anomalous emission, the anomalous cyclotron emission and anomalous bremsstrahlung appeared. The former appeared above the critical frequency ω_{crit}, and the latter below ω_{crit} for the weaker magnetic field strengths. These anomalous emissions are pulsive and are associated with the low frequency oscillation in the plasma. They appear only at a definite phase of the LF oscillation. The emission intensities are enormously large and are also sensitive to the state of plasma. These are observed in the Xe, Kr, and Ar plasmas but cannot be observed in the Ne or He plasmas. The theoretical treatment, based on the negative absorption due to the Ramsauer effect in the rare gases, explains qualitatively the experimental results. (tr-auth)

22209 MICROWAVE ABSORPTION OF MAGNETO-PLASMA WITH BOUNDARIES. Minami, Kazuo; Takeda, Susumu (Nagoya Univ., Japan). Kakuyugo-Kenkyu, 15: 306-39(Oct. 1965). (In Japanese).

The absorption, reflection, and transmission of microwaves by plasma slabs with magnetic fields are calculated for the assumption that the collision damping is only the power dissipating mechanism. The solution of Maxwell equations for electromagnetic wave propagation is derived as a boundary value problem and numerically computed for various plasma parameters, magnetic fields, and the slab thickness. The maximum absorptions appear not only in the vicinity of the hybrid resonance but of the cut off points for uniform plasma slabs thicker than a wave length in free space, and the conditions of maximum absorption somewhat deviate from the resonance or cut off. Such maximum absorptions cannot be easily expected from an Allis diagram, which is valid only for an infinite collisionless plasma. Such an absorption pattern is also useful for estimating the electron temperature from the microwave power emitted from the plasmas, since the absorptivity is related to the emissivity. An example of a plasma slab with nonuniformly distributed electrons is also computed by directly solving wave equations. (auth)

22210 SPECTROSCOPIC MEASUREMENT OF ELECTRON TEMPERATURE IN HELIUM ARC PLASMA. Ando, Kozo (Inst. of Physics and Chemistry Research, Tokyo); Yabe, Eiji. Kakuyugo-Kenkyu, 15: 340-51(Oct. 1965). (In Japanese).

The intensities of the neutral helium spectral lines emitted from helium plasma produced by the energetic arc have been measured, and the population densities of the energy levels of neutral helium have been calculated. Electron temperature can be deduced from them, since the distribution of the measured population densities above the fifth principal quantum number was Maxwellian. Discharge conditions of the helium arc were helium pressure 10^{-2} torr; currents of 100, 150, and 240 amp, and magnetic field strength of 3540 G. For these conditions, electron temperatures of 0.19, 0.34, and 0.34 ev, respectively, were obtained. From consideration of the radial intensity distribution of neutral helium lines, the measured electron temperatures were taken to be the values around the arc column. (auth)

22211 POSSIBILITY OF THE NEGATIVE ABSORPTION OF A PLASMA-CAVITY SYSTEM. Idehara, Toshitaka; Terumichi, Yasushi (Kyoto Univ.). Kakuyugo-Kenkyu, 15: 352-84(Oct. 1965). (In Japanese).

A discussion is presented on the amplification of an incident wave by a reflection-type cylindrical cavity coaxial with a plasma column along a static magnetic field. The Q-value contributed by the plasma (Q_p) is calculated under the following conditions: the plasma is so tenuous that the perturbation theory is applicable, the velocity distribution function of plasma electrons is described by the function $f^0(v) \alpha v^q \exp.(-bv^s)$, the effective collision frequency for momentum transfer is dominantly due to the collision of electron with neutral particles and varies with the speed v as $\nu_c(v) \propto v^h$, and the radius of the plasma is sufficiently smaller than the radius of the cavity. In the case of $Q_p > 0$, the incident wave is always attenuated by the plasma-cavity system. However, when $Q_p < 0$, the plasma-cavity system has a possibility of amplification or oscillation. This characteristic of the plasma-cavity system is dependent upon the velocity distribution function of plasma electrons. (auth)

22212 STUDY ON THE MAGNETIC INTERRUPTION OF THE LARGE CURRENTS THROUGH A LINEAR DISCHARGE PLASMA STABILIZED BY ALTERNATING MAGNETIC FIELDS. Enjoji, Hiroshi (Inst. of Physics and Chemistry Research, Tokyo). Kakuyugo-Kenkyu, 15: 385-412(Oct. 1965). (In Japanese).

A hot plasma produced by a large capacity condenser bank with a capacity and working voltage of 1.1×10^4 μ F and 500 v, respectively, has been stabilized by strong alternating magnetic fields produced by condenser discharge through the external coil. The linear discharge current is interrupted steeply at the wave tail near the transition point between the first and the second half cycle of the magnetic field. The rate of decay of the currents at the interrupted point is of the order of 10^7 to 10^8 amp/sec. This interruption is caused by the magnetic fields of cusp geometry, which are composed of the external magnetic field and those produced by the induced eddy currents in the electrodes. This mechanism of interruption of large currents is considered to be of importance to a kind of controlling switches for high temperature plasma devices, as well as to the fast recovery of insulation of vacuum switches. (auth)

22213 ION TEMPERATURE MEASUREMENT IN A STREAMING PLASMA BY THE LANGMUIR DOUBLE PROBE. Kawashima, Nobuki (Japan Atomic Energy Research Inst., Tokyo). Kakuyugo-Kenkyu, 15: 413-19 (Oct. 1965). (In Japanese).

Double probe characteristics in a streaming plasma from a plasma gun were investigated experimentally. When the probe is set parallel to the plasma stream, the plasma density around the leeward electrode is diminished in the shade of the windward electrode, and the double probe characteristic is asymmetric. The decrease of the ion saturation current for the leeward electrode is determined by the ion temperature in the plasma stream, when the plasma stream is collision-free. This method can also be applied to the ion temperature determination in the ionosphere or upper spaces by space probes. (auth)

22214 DIRECT DISPLAY SYSTEM OF PLASMA PARAMETERS BY MEANS OF A NON-FLOATING TRIPLE-PROBE. Chen, Sin-Li (Musashi Inst. of Tech., Japan). Kakuyugo-Kenkyu, 15: 436-50(Oct. 1965). (In Japanese).

The case of the direct display system of plasma parameters utilizing a non-floating triple probe is discussed. The probe current, as well as the voltage difference between the probes, was measured for the determination of electron temperature T_e and electron density N_e that are calculated as the function of R (resistance), for stationary cases. Thus, it is possible to determine T_e and N_e even when $R \neq \infty$. The percentage errors of T_e and N_e measured by means of the usual direct display system, in which the condition $R \neq \infty$ is assumed, are also discussed for various kinds of plasmas to be measured under conditions of changing R. (TCO)

22215 STABILIZATION OF THE PLASMA IN P.I.G. DISCHARGE. Kuroda, Tsutomu; Nagao, Shiego (Nagoya Univ., Japan). Kakuyugo-Kenkyu, 15: 523-41(Nov. 1965). (In Japanese).

The stabilization of the plasma in PIG discharge has been studied in various magnetic field configurations, a cusp, a mirror, and Heliotron. The frequency spectrum, the amplitude of the anode voltage fluctuations, and plasma density were measured. A stable and optimum discharge condition, as a plasma source, is obtained in a Heliotron field. In such a field, the plasma noise is reduced to $1/_{50}$ that in a uniform field, and the plasma density becomes much greater than in other field configurations. (auth)

22216 INTERACTION BETWEEN A PLASMA AND A MICROWAVE FIELD IN A MIRROR-TYPE MAGNETIC FIELD. I. Honzawa, Tadao; Tanaka, Shigetoshi (Nagoya Univ., Japan). Kakuyugo-Kenkyu, 15: 575-97(Nov. 1965). (In Japanese).

The results of experiments to determine the interaction between a plasma, in particular, its electron component and a microwave in some types of magnetic field are described. A static magnetic field was externally produced by a pair of air core coil blocks consisting of some separated coils, and a cylindrical cavity was set between the coil blocks. A plasma beam was stationarily injected into the cavity on and along its axis. Microwave power was pulsively fed into it from a magnetron oscillator. The interaction of interest was investigated by measuring the flux and energy of soft x rays emitted from the plasma with an x-ray detector and by analyzing pulses of current diffusing across magnetic lines of force accepted by a probe. The emission of soft x-ray was observed only when the magnetic field was of mirror geometry and was found to depend strongly upon the position of electron cyclotron resonance zone in a mirror field. Furthermore, the observation of pressure dependence of the emission showed that, if any gas was used, secondary electrons produced by fast ones in the trapping region could gain much energy from the microwave and become energetic particles, under an appropriate condition. From the decaying slope of probe current, pulses were obtained indicative of the mean lifetime of trapped particles. Some informations about the accelerating rate for trapped electrons could be obtained from the decay slopes, as well as from the x-ray energy. Interpretations of the results mentioned also are made from the standpoint of the single particle model. (auth)

22217 SKIN EFFECT IN ANISOTROPIC PLASMAS AND RESONANCE EXCITATION OF ELECTRON-CYCLOTRON WAVES. I. THEORY. Pfeiffer, B. (Eidgenoessisches Technische Hochschule, Zurich). J. Appl. Phys., 37: 1624-7(Mar. 15, 1966).

The complete electromagnetic field was calculated within a homogeneous infinite two-dimensional plasma sheath with a perpendicularly applied static magnetic field. The plasma is produced by a high-frequency electromagnetic field at the surface. When the electron-cyclotron frequency is greater than the frequency of the applied high-frequency electromagnetic field at the surface, the refractive index of the medium becomes real for the right-hand polarized wave and one has an increased penetration of high-frequency energy into the interior of the plasma. It is also possible for the refractive index to reach a value such that the thickness of the plasma sheath is half a wavelength. In this case, resonance effects should be expected for the electron-cyclotron wave which propagates in the plasma. (auth)

22218 SKIN EFFECT IN ANISOTROPIC PLASMAS AND RESONANCE EXCITATION OF ELECTRON-CYCLOTRON WAVES. II. EXPERIMENTS. Pfeiffer, B. (Eidgnoessisches Technische Hochschule, Zurich). J. Appl. Phys., 37: 1628-33(Mar. 15, 1966).

The high-frequency magnetic fields within a homogeneous plasma sheath were measured as a function of the plasma parameters and a perpendicularly superimposed static magnetic field. These fields are compared with those calculated taking collision into account. A theoretically predicted resonance of the electron cyclotron wave is observed. Investigations on an electrodeless ring discharge with a superimposed static magnetic field perpendicular to the axis of the discharge also exhibit a similar resonance behavior which in the literature was first reported in 1948. However a valid physical explanation has not been previously established thus far. The phenomenon is widely used to optimize the carrier production in inductively coupled high-frequency ion sources. (auth)

22219 HIGH-FREQUENCY DIELECTRIC RESONANCE PROBE FOR THE MEASUREMENT OF PLASMA DENSITIES. Messiaen, A. M.; Vandenplas, P. E. (Ecole Royale Militaire, Brussels). J. Appl. Phys., 37: 1718-24(Mar. 15, 1966).

Recent theory and experiments show that the resonance value of the high-frequency signal of a metallic probe can only be used to measure the plasma density accurately if the detailed structure of the sheath is known. A new reso-

nance probe described, which makes use of the fact that a system consisting of a vacuum cylinder embedded in an infinite plasma has an eigenfrequency equal to $\omega_e/\sqrt{2}$ and independent of the radius of the cylinder. It is shown that the resonance frequency of the probe—and thus the plasma density found—depends only slightly on the sheath. There is very good agreement between theory and experiments when the density obtained by this method is compared to the values measured by the electron and ion characteristics of the Langmuir probe. Plasma densities can be measured over a wide range by this method. General considerations on the difference between the resonant (or antiresonant) behavior of a metallic probe and that of a dielectric structure are given. (auth)

22220 WAVE PROPAGATION ALONG WARM PLASMA COLUMNS. Diament, Paul (Columbia Univ., New York); Granatstein, Victor L.; Schlesinger, S. Perry. J. Appl. Phys., 37: 1771-8(Mar. 15, 1966).

Dispersion relations for waves propagating along homogeneous, isotropic, warm plasma columns surrounded by a dielectric medium are obtained. A steady-state linearized model with temperature introduced through a scalar pressure is analyzed both quasistatically and more rigorously from Maxwell's equations. The results show effects of temperature on the cold plasma surface wave and predict a new series of propagating modes above the plasma frequency related to the Tonks-Dattner scattering resonances near cutoff and to the Bohm-Gross longitudinal plasma waves for large wave numbers. Warm and cold plasmas, large and small columns, and quasistatic and rigorous predictions are contrasted. Regions of the Brillouin diagram corresponding to different bound and radiating wave types are delineated and related to their physical properties. (auth)

22221 ELECTROSTATIC AND MAGNETIC PINCH EFFECTS IN BEAM-GENERATED PLASMAS. Halsted, A. S.; Dunn, D. A. (Stanford Univ., Calif.). Contract DA36-039-AMC-00094(E). J. Appl. Phys., 37: 1810-20 (Mar. 15, 1966).

A kilovolt electron beam of a few mm diameter passing through a gas at pressures of 10^{-2} torr or lower is not significantly scattered by collisions with neutrals in distances of many beam diameters. The beam will ionize the gas and generate a plasma that has a potential distribution that will cause the beam to be pinched toward its axis. This electrostatic pinch effect is compared with the magnetic pinch and the electrostatic pinch is found to be the dominant effect at low voltages and currents. Experimental results confirming the results of early experiments at a few hundred volts demonstrate that the electrostatic pinch exists at higher voltages and can be more important than the magnetic pinch at voltages up to the order of 100 kv for typical plasma electron temperatures and beam currents. Computer studies of beam trajectories in a simulated beam-generated plasma provide an explanation for the detailed structure of the beam profiles that have been observed. (auth)

22222 AN INVERSE BRUSH CATHODE FOR THE NEGATIVE-GLOW PLASMA SOURCE. Musal, Henry M. Jr. (General Motors Corp., Santa Barbara, Calif.). J. Appl. Phys., 37: 1935-7(Mar. 15, 1966).

An inverse-brush cathode design is described for producing an extended negative-glow plasma, which is easy to construct and has several advantages over the brush cathode design. Typical voltage-current characteristics of the inverse brush cathode, compared to a flat cathode and Persson's brush cathode, are shown for operation in helium. (L.B.S.)

22223 STATISTICAL MECHANICS OF HIGH-TEMPERATURE QUANTUM PLASMAS BEYOND THE RING APPROXIMATION. DeWitt, Hugh E. (Univ. of California, Livermore). Contract W-7405-eng-48. J. Math. Phys. (N. Y.), 7: 616-26(Apr. 1966). (UCRL-14102).

A quantum mechanical perturbation expansion of the partition function is used to evaluate the free energy of the electron gas and multicomponent plasmas to logarithmic accuracy in the particle number density, thus including the next important contribution beyond the ring approximation. The quantum generalization of Abe's work on the classical electron gas is given for the ladder interactions with the dynamic screened Coulomb potential, and each ladder is shown to be separately finite because of the finite size of the wave packets describing point electrons [of the order of the thermal de Broglie wavelength $\lambda = \hbar(\beta/2m)^{\frac{1}{2}}$]. The results show that quantum effects due to the uncertainty principle persist at high temperature, and that when kT > Ryd plasmas are quantum systems, rather than classical, because λ is greater than the average distance of closest approach, βe^2. Results are also obtained for the Wigner–Kirkwood wave mechanical diffraction corrections to the classical electron-gas free energy which are valid for low temperature (kT < Ryd). The connection between the high- and low-temperature formula is discussed, and it is shown how the logarithmic divergence in the free energy that is cut off at βe^2 in the low-temperature electron gas in the Abe theory is cut off at λ in the high-temperature case. Also it is shown that the quantum diffraction effects contained in the Montroll–Ward ring sum formula are valid only for kT > Ryd, even though the quantum ring sum formula contains the classical Debye–Hückel result. (auth)

22224 THE ENTRY OF A TENUOUS PLASMA INTO AN AXIAL MAGNETIC FIELD. Ashby, D. E. T. F.; Avis, B. E. (Culham Lab., Abingdon, Eng.). Plasma Phys.-Accel. Thermonucl. Res., J. Nucl. Energy: Pt. C, 8: 1-9 (Jan.-Feb. 1966).

A coaxial gun is used to inject a burst of energetic, low-density hydrogen plasma along the axis of the magnetic field produced by a long solenoid. The portion of this plasma that penetrates the magnetic field has a density of 10^{11}–10^{12} electrons/cm^3 and a mean directed energy of 10–20 kev. The properties of the plasma were studied as it moved along the magnetic field. The mean ion velocity perpendicular to the magnetic field was measured with Faraday cups and the transverse energy of the plasma was deduced from its diamagnetism. These measurements show that the transverse energy of the plasma resides predominantly in the ions, which have considerable angular momentum. It is shown that this momentum is produced by electrons flowing from the vicinity of the vacuum chamber walls as the plasma enters the cusp-shaped field at the end of the solenoid. (auth)

22225 PERFORMANCE OF A COAXIAL PLASMA GUN. Little, P. F.; Avis, B. E. (Culham Lab., Abingdon, Eng.). Plasma Phys.-Accel. Thermonucl. Res., J. Nucl. Energy: Pt. C, 8: 11-20(Jan.-Feb. 1966).

Coaxial plasma guns operating with about 20 kv applied at a peak current of approximately 80 kamp are shown to produce a fast burst of clean plasma containing no other ions than H^+. Densities of about 10^{11} cm^{-3} are measured at distances of 100 cm from the gun for ions of energy between 5 and 20 kev; peak ion energies of about 70 kev are observed. In the slow plasma following the fast burst the impurity ions are mainly copper. The ion density depends on the amount of gas admitted before firing the gun, but does not vary much with gun voltage. The measured ion velocity perpendicular to the guide field is within a factor two of the predictions of a simple theory. Discrepancies are expected because the ions do not appear in a field-free region, as the theory assumes. (auth)

22226 TRANSMISSION CHARACTERISTICS OF CYCLOTRON HARMONIC WAVES IN PLASMA. Crawford, F. W.; Weiss, H. H. (Stanford Univ., Calif.). Plasma Phys.-Accel. Thermonucl. Res., J. Nucl. Energy: Pt. C, 8: 21-9(Jan.-Feb. 1966).

In recent years the importance of cyclotron harmonic waves has become apparent in many branches of plasma physics. For example, it has been demonstrated that they are involved in the anomalously high noise radiation near the electron cyclotron harmonic frequencies that has been observed from thermonuclear fusion study devices, and that they can explain the cyclotron harmonic resonances observed in satellite studies of the ionosphere. Experiments on propagation perpendicular to a magnetic field in a low-pressure mercury-vapor discharge are described.

This mode is particularly important since it is not subject to Landau damping. The relevant dispersion curves are compared with results of the experimental study and show evidence of such transmission across the plasma between two parallel cylindrical probes. Cyclotron resonance phenomena have many potential applications to plasma diagnostics, the theory of extraterrestrial noise excitation, and to microwave oscillators and amplifiers. Some of these are discussed briefly. (auth)

22227 CESIUM PLASMA TRANSPORT PROPERTIES. Eastlund, B. J. (Columbia Univ., New York). Plasma Phys.-Accel. Thermonucl. Res., J. Nucl. Energy: Pt. C, 8: 31-41(Jan.-Feb. 1966).

The transport properties of a cesium gas are computed for the temperature range of 350-10,000°K and for pressures of 1 atm to 10^{-6} mm Hg. Values of electrical, thermal, and viscosity transport coefficients are determined. The thermoelectric coefficients are also determined. The extensively developed theory for gas mixture transport properties, which solves the Boltzmann equation with the assumption of binary collisions, is employed. The Debye length is used as the cut-off in the coulomb collision integrals and convergence of the solution for each transport property as a function of the degree of approximation is determined for all degrees of ionization. Experimental data for cesium are used to find values for the collision integrals for ion-atom and atom-atom interactions. Theoretical expressions are used for electron-atom and charged particle interactions. Results of the calculations indicate that at low pressure and small ionization and thermoelectric coefficient α exhibits a maximum. In the slightly ionized region the value of the zero current thermal conductivity K' is found to be dependent on ion-atom interactions as well as electron-atom interactions. The thermal conductivity K is found to differ from K' at degrees of ionization as low as 10^{-4}. Ion-atom interactions influence the viscosity in the partially ionized region. Electron-atom interactions dominate the electrical conductivity in the partially ionized region. (auth)

22228 COLLISIONAL EFFECTS IN THE REGION OF THE ELECTRON CYCLOTRON FREQUENCY ON ELECTROMAGNETIC WAVE PROPAGATION IN PLASMAS. Bachynski, M. P.; Gibbs, B. W. (RCA Victor Research Labs., Montreal). Plasma Phys.-Accel. Thermonucl. Res., J. Nucl. Energy: Pt. C, 8: 43-51(Jan.-Feb. 1966).

Electromagnetic wave propagation in plasmas in the region of the electron cyclotron frequency was investigated at a frequency of 9.2 Gc in a helium afterglow plasma. The behavior of the wave is characterized by small phase changes and high attenuation rates for the right-hand circularly polarized wave while there is no significant variation in the left-hand wave as the frequency passes through the electron cyclotron frequency. Measurements show a reversal in phase of the wave passing through the plasma as the electron density is increased. This phenomenon occurs only for the right-hand circularly polarized wave at frequencies very near but just above the electron cyclotron frequency. Collisional effects based on cold-plasma theory can account for this behavior, which may be a very sensitive way of measuring certain plasma parameters. At frequencies just below the electron cyclotron frequency extremely small electron densities (as low as 0.002 of the critical density) affect the right-hand wave and can be detected. The attenuation of e-m waves in the region about the electron cyclotron frequency agrees well with cold-plasma theory for low electron densities. (auth)

22229 CONFINEMENT OF CHARGED PARTICLES IN MAGNETIC MIRROR SYSTEMS. Lacina, J. (Czechoslovakian Academy of Sciences, Prague). Plasma Phys.-Accel. Thermonucl. Res., J. Nucl. Energy: Pt. C, 8: 63-77(Jan.-Feb. 1966).

By means of the perturbation method, a complete set of integrals describing the motion of particles is an axially symmetric stationary electromagnetic field (magnetic field of mirror systems with an electric field), not restricted by the condition of adiabaticity, is derived. The integrals are used to derive the boundaries of particles' motion and to determine the regions of values of the integrals within which the particles are permanently trapped by the given magnetic system, regions within which the particles are trapped transiently (i.e., the particles execute a definite number of longitudinal oscillations between the mirrors and thereafter escape from the system), regions of particles traversing the system without being reflected, and regions of particles found only outside the system. A study of the resonance with cyclotron oscillations is also presented. (auth)

22230 MICROWAVE TRANSMISSION THROUGH TURBULENT PLASMA. Wort, D. J. H. (Culham Lab., Abingdon, Eng.). Plasma Phys.-Accel. Thermonucl. Res., J. Nucl. Energy: Pt. C, 8: 79-93(Jan.-Feb. 1966).

Ray-optic theory is applied to a collisionless strongly deviating turbulent plasma to determine the microwave power transmitted through the plasma. The transmission coefficient is calculated for two cases: (1) the "Fraunhofer" region, in which the receiving aerial is at a quasiinfinite distance, and (2) the "Fresnel" region, in which both aerials are close to the plasma boundaries. The Fresnel region results apply to most experimental installations, and an example of their application to zeta measurements is given. The main feature of the transmission coefficient is its strong dependence on the turbulence parameters, but subsidiary directional effects may be of practical interest. The deduction of the mean square ray deflection from the turbulence parameters is made possible by a reduction of the parameters followed by an application of a previous ray-theory work. (auth)

22231 ON THE INTERPRETATION OF MULTIPLE REFLECTIONS IN MICROWAVE INTERFEROMETERS USED IN PLASMA DIAGNOSTICS. Lonngren, K. E. (Univ. of Iowa, Iowa City). Jap. J. Appl. Phys., 5: 223-4(Mar. 1966).

The problem of the multiple reflections occurring when the two horns are present in the use of microwave interferometers for plasma diagnostics is analyzed. and it is shown that the interpretation of the density must be modified to include this effect. (auth)

22232 SCATTERING OF ELECTROMAGNETIC WAVES BY ELECTRO-ACOUSTIC PLASMA WAVES. Little, P. F.; Hamberger, S. M. (Culham Lab., Abingdon, Eng.). Nature, 209: 972-4(Mar. 5, 1966). (CLM-P95).

Some preliminary measurements of the scattering of an incident beam of microwaves by self-excited plasma waves in a mercury arc column are reported. From the results an experimental dispersion curve for the plasma waves is derived and compared with a dispersion curve measured directly with Langmuir probes in the column. In this way the waves responsible for the scattering are identified as propagating electro-acoustic waves. which are known to be present in the positive column of low-density arcs. A spectrum of the scattered radiation as a function of the frequency shift, the variation of 50-kc components of mixer output with observation angle, the measured values for electro-acoustic waves excited in the same plasma are given. (J.F.P.)

22233 ELECTROSTATIC DAMPING ON THE MOTION OF A CHARGED PARTICLE IN A PLASMA. Tam, Christopher K. W. (California Inst. of Tech., Pasadena). Phys. Fluids, 9: 493-8(Mar. 1966).

The electrohydrodynamic phenomena associated with the motion of a charged particle in a plasma are investigated. It is shown that the type of disturbance produced in the plasma depends significantly on the speed of the particle. i.e., whether it is subsonic, transonic, or supersonic. In the subsonic case, the electrohydrodynamic drag experienced by the particle is caused by an unsymmetric wake formed by the screening electrons. In the supersonic case. electron screening is confined to the Mach cone. Ahead of the Mach cone, the plasma behaves as if it were an incompressible fluid. The electrohydrodynamic drag in this case has a logarithmic nature. (auth)

22234 VELOCITY GRADIENT INSTABILITY. Grad, Harold (New York Univ., N. Y.). Phys. Fluids, 9: 498-513(Mar. 1966).

A recently formulated variational definition of stability for a guiding center plasma confined by mirrors was found to yield as a necessary condition for stability that the equilibrium distribution function $f^0(\epsilon,\mu,\alpha,\beta)$ be monotone in energy on each magnetic line, $\partial f^0/\partial\epsilon \leq 0$. It is now shown conversely that if $\partial f^0/\partial\epsilon$ has too large a negative value, the plasma is always unstable. A quantitative formulation of this condition yields two inequalities that are necessary for stability of an arbitrary contained plasma. The same inequalities are sufficient for stability against all localized disturbances. Thus any remaining instabilities can only involve large scale disturbances of the plasma (e.g., interchanges). The localized (small wavelength) instabilities are found to be micro-instabilites even though the latter are usually thought to be missing in a theory with zero Debye radius. These micro-stability criteria are related to conditions for the stability of an infinite homogeneous plasma, and they serve to correct and generalize certain estimates of the maximum pressure that can be stably contained in a magnetic well. (auth)

22235 STABILITY CRITERIA AND THE INITIAL VALUE PROBLEM FOR COLLISIONLESS GUIDING CENTER PLASMA. **Kadish, Abraham (New York Univ., N. Y.). Phys. Fluids, 9: 514-19(Mar. 1966).**

Necessary conditions for the stability of collisionless, guiding center plasma are derived. These are compared with those obtained by others using assumptions different than those employed here. The derived conditions are shown to be necessary and sufficient for the stability of equilibrium configurations whose distribution functions are bell shaped in the component of velocity parallel to the magnetic field. (auth)

22236 PROPAGATION IN PLASMAS ALONG THE MAGNETIC FIELD. I. CIRCULAR POLARIZATION. **Bachynski, M. P.; Gibbs, B. W. (RCA Victor Research Labs., Montreal). Phys. Fluids, 9: 520-31(Mar. 1966).**

A carefully designed experiment was conducted in which the propagation of circularly polarized plane waves through a helium plasma along the direction of a static magnetic field was quantitatively investigated. Determination of electron densities from independent measurements using the left-hand and right-hand circularly polarized wave modes show excellent agreement with each other and with theory over all ranges of magnetic fields. Attenuation measurements also agree well with theory, except when the cyclotron frequency exceeds the radio frequency for the right-hand mode, the dependence of the collisional effects on electron velocity should be included in the analysis. The regions of the parameters where boundary effects are important can also be ascertained from the measurements. (auth)

22237 PROPAGATION IN PLASMAS ALONG THE MAGNETIC FIELD. II. LINEAR POLARIZATION. **Bachynski, M. P.; Gibbs, B. W. (RCA Victor Research Labs., Montreal). Phys. Fluids, 9: 532-8(Mar. 1966).**

The propagation of incident linearly polarized plane electromagnetic waves through a helium afterglow plasma along the direction of a static magnetic field was experimentally investigated. Measurements of the phase and intensity of the components of the electric field transmitted through the plasma in the same orientation as the incident polarization and cross-polarized to the incident polarization were made. Comparison with theory, which includes the losses due to the plasma, show relatively good agreement. (auth)

22238 QUANTUM KINETIC EQUATIONS FOR UNSTABLE PLASMAS. **Matsudaira, Noboru (Univ. of British Columbia, Vancouver, Can. National Research Council, Ottawa). Phys. Fluids, 9: 539-48(Mar. 1966).**

A treatment of the transport equation for a classical unstable electron plasma by K. Nishikawa and Y. Osaka [Progr. Theoret. Phys. (Kyoto) 33, 402 (1965)] is extended to the quantum-mechanical multicomponent case. The quantum Bogoliubov – Born – Green – Kirkwood – Yvon hierarchy of equations is truncated at the second stage, and the technique due to Dupree is employed. In the limit of weak instability, the kinetic equation, that proves to be the direct extension of the classical case, can be rewritten in the form of a set of simultaneous equations, the form of which agrees completely with the equations proposed by Pines and Schrieffer. (auth)

22239 HARMONICS OF THE ELECTRON GYROFREQUENCY IN PLASMAS. **Canobbio, E.; Croci, R. (Institut fuer Plasmaphysik, Munich). Phys. Fluids, 9: 549-60(Mar. 1966).**

Intense radiation emitted by plasmas at harmonics of the electron gyrofrequency is discussed. The nonrelativistic dispersion relation for propagation vectors nearly perpendicular to the external magnetic field is studied for an unperturbed Maxwellian distribution function. The real and complex wavenumbers of ordinary and extraordinary waves are given when Landau and collisional damping are negligible. Their behavior near the harmonics, the upper hybrid frequency, and cutoffs is considered in detail. When damping is present, the wave propagation undergoes a deep change. In typical experimental conditions no ordinary and no transverse extraordinary waves exist in the very neighborhood of the harmonics with a large index of refraction, while there are sets of short quasi-electrostatic waves which are of interest in explaining the experiments. Near the hybrid frequency the relatively fast quasi-electrostatic waves are substituted for elliptically polarized waves (still predominantly longitudinal) which originate from the coupling between the cold-plasma and the electrostatic modes. The equation for the electrostatic waves is also discussed in plasmas with electron streams and temperature anisotropies. (auth)

22240 DIELECTRIC TENSOR IN VLASOV PLASMAS NEAR CYCLOTRON HARMONICS. **Shkarofsky, I. P. (RCA Victor Co., Ltd., Montreal). Phys. Fluids, 9: 561-70(Mar. 1966).**

The relativistic expression for the dielectric tensor obtained by Trubnikov is simplified in the very weakly relativistic limit at and near electron cyclotron harmonics. Wavenumbers parallel to magnetic field are included, leading to relativistic damping when this wavenumber is minute and to cyclotron damping when it is sufficiently large. The transition to the nonrelativistic Z function is shown and the regions of validity of the various functions are indicated. Collisional damping is neglected. The dielectric elements given are also applicable to cases of complex ω and real k. An example of such a situation arises in Alouette cyclotron harmonic reception when one is concerned with an initial time value problem. For this application the analytic continuation of a complicated function is provided, and the tracks where it is real for complex ω are investigated. (auth)

22241 DISPERSION OF WAVES IN CYCLOTRON HARMONIC RESONANCE REGIONS IN PLASMAS. **Shkarofsky, I. P. (RCA Victor Co., Ltd., Montreal). Phys. Fluids, 9: 570-80(Mar. 1966).**

The dispersion of waves near electron cyclotron harmonics is investigated including to first order wavenumbers parallel to the magnetic field. The proper relativistic form for the dielectric tensor elements is applied. The relativistic formulation is compared with the nonrelativistic one applicable for larger wavenumbers parallel to magnetic field and the differences are noted. In either analysis, different behaviors result depending on whether the wavenumber or frequency is taken to be complex. In the former case, the waves near the Appleton – Hartree values are localized and a gap exists between them and the higher-order cyclotron harmonic plasma waves. In the latter case, this gap does not occur but the relativistic analysis shows a rapid rise in frequency above the harmonic and one tends to zero wavenumber perpendicular to magnetic field. It is also shown that the large argument expansion in terms of inverse argument of the nonrelativistic Z function produces incorrect dispersion results in certain regions. (auth)

22242 SPATIAL VARIATIONS OF PLASMA ELECTRON TEMPERATURE IN A STANDING WAVE AT MICRO-

WAVE FREQUENCIES. Cronson, H. M. (Polytechnic Inst. of Brooklyn). Phys. Fluids, 9: 581-6(Mar. 1966).

Spatial variations in electron temperature produced in a steady state, room temperature plasma by an electromagnetic standing wave are considered both theoretically and experimentally. The field amplitudes treated are strong enough to raise the electron temperature considerably, but are still too weak to cause inelastic collision. The electron temperature balance equation for a steady state, spatially varying plasma is derived from a two-term expansion of Boltzmann's equation. In the weakly ionized case, the theoretical equations yield a temperature relaxation distance, which determines the spatial dependence of the electron temperature in response to the standing wave. This spatial variation in electron temperature was then measured experimentally in an afterglow plasma, and the observed degree of variation agreed with theoretical predictions. (auth)

22243 DIFFUSION MEASUREMENTS IN A FULLY IONIZED CESIUM PLASMA. Eastlund, Bernard J. (Columbia Univ., New York). Phys. Fluids, 9: 594-602 (Mar. 1966).

Diffusion coefficients both parallel ($D_{||}$) and perpendicular ($D_{\perp}$) to a magnetic field were measured in a fully ionized plasma. Pulses of potassium plasma were launched at one end of a steady state, fully ionized cesium plasma column and $D_{||}$ and $D_{\perp}$, along with the macroscopic drift velocity of the column, were found from the change of pulse shape. Experimental values for $D_{||}$ agree very well with theory. However, values for $D_{\perp}$ do not agree with present theoretical predictions. It is observed that $D_{\perp}$ is inversely proportional to the number density, while theory predicts direct proportionality. (auth)

22244 NONLINEAR SUM AND DIFFERENCE FREQUENCY GENERATION IN AN INHOMOGENEOUS PLASMA Sodha, Mahendra Singh; Kaw, Predhiman Krishan (Indian Inst. of Tech., New Delhi). Phys. Fluids, 9: 603-14(Mar. 1966).

An analytical study is made of the nonlinear generation of the sum and difference frequency components in the current density in a plasma due to two alternating electric fields, an electron density gradient and a temperature gradient. The results of this study were used in investigating the nonlinear growth of sum and difference frequency waves in a plasma when two electromagnetic waves of different frequencies are propagating along the same direction in it and, also, the magnitude of these frequency components in the reflected wave from a plasma free space interface when the two electromagnetic waves are incident normally on the interface. (auth)

22245 LASER-GENERATED IMPLOSIONS. Daiber, J. W.; Hertzberg, A.; Wittliff, C.E. (Cornell Aeronautical Lab., Inc., Buffalo). Phys. Fluids, 9: 617-19(Mar. 1966).

By using a weak spherical blast wave to shape the initial density distribution, the laser energy can be preferentially coupled to the periphery of this sphere. This energy addition to the shell of high density gas then produces an imploding plasma. (auth)

22246 EQUIVALENCE BETWEEN TWO FORMALISMS OF PLASMA FLUCTUATIONS. Weinstock, Jerome (Environmental Science Services Administration, Boulder Colo.). Phys. Fluids, 9: 621-2(Mar. 1966).

The expression for auto-correlation functions given in terms of the two-time distribution function is related by a trivial identity to the expression for auto-correlation functions, which is given in terms of the usual distribution function. (auth)

22247 EXCITATION OF THE m = 2 MODE BY THE HELICAL INSTABILITY. Holter, Oeivin (Univ. of Oslo); Johnson, Roy R. Phys. Fluids, 9: 622-4(Mar. 1966).

The conditions whereby the helical instability can excite higher modes in the plasma column are investigated. The wavelengths and frequencies of the helical and m = 2 modes are calculated at the onset of the m = 2 mode for the case of helium. (auth)

22248 EXTENSION OF THE PENROSE CONDITION. Weitzner, Harold (New York Univ., N. Y.). Phys. Fluids, 9: 624-6(Mar. 1966).

It is shown that the Penrose condition for the existence of plane wave modes that grow exponentially in time in a plasma described by the linearized Vlasov equation and Poisson's equation is necessary and sufficient for the existence of any modes that grow in time in such a plasma. (auth)

22249 MEASUREMENT OF AN ANOMALOUS DIFFUSION COEFFICIENT. Thomassen, K. I. (Stanford Univ., Calif.). Phys. Fluids, 9: 626-8(Mar. 1966).

A diffusion coefficient is calculated for the fluctuations due to a flute instability in a low pressure Penning discharge using the measured correlation times and flute amplitudes, eliminating the very difficult task of having to calculate the spectra due to the instability. (auth)

22250 COMMENTS ON DEVIATIONS FROM IONIZATION EQUILIBRIUM IN PLASMAS GENERATED BY ELECTRIC SHOCK TUBES. Griem, H. R. (Univ. of Maryland, College Park); Kolb, A. C.; McLean, E. A. Phys. Fluids, 9: 628-30(Mar. 1966).

It was previously concluded by Isler and Kerr (Phys. Fluids 8: 1176(1965)) from observations of absolute continuum and line intensities from a predominantly helium plasma that the density of doubly ionized helium is as much as five orders of magnitude higher than that corresponding to thermal local equilibrium. It is argued that their interpretation for the large deviations from thermal ionization in terms of recombination relaxation is invalid, because too many photons escape on the Stark-broadened wings. (L.B.S.)

22251 EXPERIMENTS ON THE PLASMA FLOW PAST BODIES IN A MAGNETIC FIELD. Kawashima, Nobuki; Mori, Sigeru (Japan Atomic Energy Research Inst., Ibaraki). Phys. Fluids, 9: 700-4(Apr. 1966).

Plasma flows past bodies in a magnetic field are investigated experimentally by the use of a plasma from a plasma gun. The downstream wake of an ordinary hydrodynamic shock wave is observed for a collision-dominant plasma flow. The structure of the shock is investigated in detail for a wedge-shaped conductor. The plasma flow is divided into four regions by three characteristic lines: (1) the shock front, (2) the expansion wave from the tail of the wedge, and (3) the magnetic line of force passing through the tail of the wedge. When a wake of the shock wave interacts with the other wake, they join into one along the magnetic lines of force. Plasma flows past a wave-shaped wall are also investigated. As the plasma flow becomes collision-free, this downstream wake gradually disappears and no collision-free shock wave is observable. When the plasma flow is sub-Alfvénic, a disturbance propagating upstream along the magnetic lines of force is observed. (auth)

22252 FLUTE INSTABILITY AT LOW DENSITY. Simon, Albert; Rosenbluth, Marshall N. (General Atomic Div., General Dynamics Corp., San Diego, Calif.). Phys. Fluids, 9: 726-9(Apr. 1966). (GA-6784).

Some of the results of a previous paper (M. N. Rosenbluth and A. Simon, Phys. Fluids, 8: 1300(1965)) are extended to low plasma densities. The proper macroscopic equations for use with a weakly unstable plasma are listed, and the differential equation for stability analysis is derived. In the moderate density regime, this leads to a variational principle and a sufficiency condition. In a special case, this becomes a minimization principle analogous to the δW one. At very low densities, the effect of a nonuniform electric field on a marginally stable system is considered, and it is shown that stabilization depends only on the second spatial derivative of E, a result which has a simple drift interpretation, and which may have some relevance to observations in "OGRA" and "Phoenix." (auth)

22253 ELECTROSTATIC INSTABILITIES IN FINITE MIRROR-CONFINED PLASMAS. Post, R. F. (Univ. of California, Livermore); Rosenbluth, M. N. Phys. Fluids, 9: 730-49(Apr. 1966). (UCRL-14388(Rev.1)).

Three classes of electrostatic instabilities deemed likely

to be encountered in magnetic mirror-confined plasmas are examined theoretically: (A) a convective type, maser-like in nature, with waves propagating essentially parallel to the field lines; (B) a nonconvective (absolute) instability, arising in the presence of radial density gradients; and (C) a limiting case of (B), not requiring radial density gradients for its stimulation. All three instabilities, which owe their origin to the loss-cone nature of the particle distributions, exhibit critical conditions for onset or growth that are sensitively dependent on the shape of the distribution functions. These conditions are least restrictive for plasmas that have reached a state of collisional equilibrium in confining fields of high mirror ratio. In this limit (C) disappears and the critical conditions imposed by (A) and (B) are not unduly restrictive. In particular, at high plasma densities it is required: (1) for adequate stability against (A), the length of the plasma between the mirrors must not be greater than about 300 to 500 ion-orbit radii, and (2) to satisfy conditions (on the radial density gradient) imposed by (B), the plasma dimensions transverse to the field must also be of the same order; i.e., the plasma must be roughly spherical. Examples are also given that show that the confinement of highly peaked distributions leads to required conditions of orders of magnitude more restrictive than those found for well-randomized distributions. (auth)

22254 HIGH-VELOCITY PLASMA INJECTION INTO A CUSPED MAGNETIC FIELD. Karr, H. J.; Osher, J. E. (Univ. of California, Los Alamos, N. Mex.). Phys. Fluids, 9: 750-60(Apr. 1966). (LA-DC-7397).

The injection and subsequent behavior of a dense ($\sim 3 \times 10^{13}$/cm^3) fast ($\bar{V} \sim 10^8$ cm/sec) deuterium plasma jet fired from a coaxial plasma gun into a simple biconical cusped magnetic field was studied. The experiment shows that for sufficiently high cusp fields up to 90% the plasma jet penetrates the entrance cusp and is lost through the ring without being trapped. In the process of injection a part of the ion energy in the plasma jet is found to be transferred to a group of electrons. X rays of up to 220-kev energy are observed from these energetic electrons with a characteristic decay time of up to 1 msec for cusp fields of 8.5 kG. These long duration energetic electrons are found to be accompanied by a variety of slow high momenta impurity ions (e.g., Fe, O, Si, etc.) in transit through the field and lower energy ions trapped for times in essential agreement with theoretical values for a low-β plasma in a simple cusped field. Observations on the plasma potential are also described. (auth)

22255 BOUNDS ON FLUCTUATIONS IN A HOMOGENEOUS PLASMA. Chen, Robert L. W. (Emory Univ., Atlanta). Phys. Fluids, 9: 761-7(Apr. 1966).

A homogeneous collisionless plasma is considered whose velocity distribution is initially unstable. Making use of the constraints inherent in the Maxwell-Vlasov equations — along the lines of C. S. Gardner and of T. K. Fowler — it is shown that the nonlinear fluctuations grown out of the instability are subject to the following bounds: $[(\overline{\Delta\rho})^2/(\overline{\rho})^2] \lessapprox 0.4\,(\epsilon_G/\epsilon_{total} - \epsilon_G)$, $\sum_{k \leqq k_0} (E^2(k)/8\pi) \lessapprox [\epsilon_G/1 + 1.2(hk_0)^2]$, where ρ and $\Delta\rho$ are density and its fluctuation, ϵ_G the available energy in the plasma in the sense of Gardner's, E(k) the Fourier component of the electrostatic oscillations, and h the Debye length. The variation of the density function f(r,v) is considered from an originally homogeneous and Maxwellian density $f_0(v)$ under the constraint of Liouville invariance. The total kinetic energy is then minimized under the further constraint that a given level of density perturbation $\Delta\rho$ is maintained. Solutions to this variational problem yield minimum energies associated with density fluctuations and lead to results which, in their approximate forms, are given in the above inequalities. (auth)

22256 EFFECTS OF A VELOCITY-DEPENDENT COLLISION FREQUENCY ON WAVE-PLASMA INTERACTIONS. Whitmer, R. F.; Herrmann, G. F. (Lockheed Missiles and Space Co., Palo Alto, Calif.). Phys. Fluids, 9: 768-73(Apr. 1966).

Two parameters, an effective collision frequency and an effective plasma frequency, are introduced to describe the effects of the velocity dependence of the collision frequency on wave-plasma interactions. Although mathematically related to other parameters previously used, this particular choice has the decided advantage of providing physical insight into the effect of the collision frequency variation. These parameters are calculated from actual cross section data for He, Ne, A, and N_2. A discussion is also given of the effect of the velocity dependence of the collision frequency on the electron cyclotron line shape in magnetoplasmas. The introduction of these effective parameters provides a means for understanding the non-Lorentzian line shapes obtained from exact calculations of the absorption coefficients. (auth)

22257 IONIZATION PROCESS OF A PLASMA. Lehnert, B. (Royal Inst. of Tech., Stockholm). Phys. Fluids, 9: 774-9(Apr. 1966).

The ionization due to thermal electrons is discussed. Earlier theories on the voltage characteristics of a partially ionized homopolar cell are reconsidered. It is found that the results obtained from the theory on thermal ionization do not agree with experiments within the range of neutral gas densities studied so far, but a better agreement is expected at higher densities. In several cases the ionization rates estimated from experiments suggest that there exists a more powerful ionization mechanism than that provided by thermal electrons. Such a mechanism is probably associated with a highly nonthermal distribution of electron velocities within considerable parts of the plasma volume. (auth)

22258 RECOMBINATION, IONIZATION, AND NONEQUILIBRIUM ELECTRICAL CONDUCTIVITY IN SEEDED PLASMAS. Cool, Terrill A.; Zukoski, Edward E. (California Inst. of Tech., Pasadena). Phys. Fluids, 9: 780-96(Apr. 1966).

New data are presented which provide direct experimental confirmation of the validity of a physical model which has been widely employed to predict the electrical conductivity of dense, two-temperature, seeded plasmas. Experimental measurements of electron temperature, and ionization and recombination rates are presented for partially ionized plasmas of potassium-seeded argon. Experimental conditions were chosen to cover those ranges of interest in connection with proposed magnetohydrodynamic energy conversion devices for which nonequilibrium electrical conductivity measurements have been previously reported, e.g., translational atom temperatures of about 2000°K, total atom densities near 10^{18}/cm^3, potassium densities of about 10^{16}/cm^3, electron densities from 10^{13}/cm^3 to 10^{15}/cm^3, and electron temperatures from 2200 to 3500°K. Measured values of electron–electron–ion recombination coefficients for potassium show good agreement with theoretical values based upon the Gryzinski classical inelastic-collision cross-section expressions. Observed ionization rates and relaxation characteristics appear to be adequately explained by a similar formulation for the ionization process. (auth)

22259 ELECTRON PROBE CURRENT IN A MAGNETIZED PLASMA. Sugawara, Minoru (Central Research Inst. of Electric Power Industry, Tokyo). Phys. Fluids, 9: 797-800(Apr. 1966).

An experimental study is presented of the electron saturation current arriving at a plane probe situated in a magnetized plasma. Using a simplified Bohm's model, the equations of electron probe current in a magnetized plasma are derived and compared with the experimental results. The equations show that the electron temperature is determined for a sufficiently large range of negative probe potentials and an apparent space potential is lowered by the presence of the magnetic field. (auth)

22260 EXPERIMENTALLY DETERMINED PLASMA PERTURBATION BY A PROBE. Little, Roger G.; Waymouth, John F. (Massachusetts Inst. of Tech., Cambridge. Sylvania Electric Products, Danvers, Mass.). Phys. Fluids, 9: 801-8(Apr. 1966).

The perturbation of a plasma by a probe with radius large in comparison to a mean free path is examined with a small movable probe. Electron density, electron temperature, and plasma potential are determined as a func-

tion of distance from the large probe. The experimental conditions corresponded well to those assumed by Waymouth; Waymouth's theory applied to the large-probe electron current characteristic yields a value for electron density in the unperturbed plasma that is correct within a few percent. The electron temperature so determined is too low by 19%. A fundamental assumption of all theories, that electron temperature in the perturbed volume of plasma is independent of position, is found to be incorrect, at least in a plasma containing drift currents. (auth)

22261 COUPLING OF TRANSVERSE AND LONGITUDINAL WAVES AT THE UPPER HYBRID FREQUENCY. Horton, C. W. Jr. (Univ. of California, San Diego, La Jolla). Phys. Fluids, 9: 815-16(Apr. 1966).

Propagation of an electromagnetic wave into an increasingly dense plasma perpendicularly to a constant magnetic field is considered. The reflection coefficient is calculated in the limit of small electron Larmor radius and high frequency. (auth)

22262 FINITE LARMOR RADIUS EQUATIONS FOR A PLASMA. Ware, A. A. (United Kingdom Atomic Energy Authority, Abingdon, Eng.). Phys. Fluids, 9: 816-18 (Apr. 1966).

The approximate moment equations for a low β plasma obtained by Rosenbluth and Simon are shown to be special cases of the more general equations of Herdan and Liley. The pressure tensor modification is found to arise from an ion heat conduction contribution. (auth)

22263 RELATION BETWEEN THE KELVIN-HELMHOLTZ INSTABILITY AND THE RESISTIVE DRIFT INSTABILITIES. Von Goeler, S. (Princeton Univ., N. J.). Phys. Fluids, 9: 818-20(Apr. 1966). (MATT-406).

The Kelvin-Helmholtz instability and the resistive drift instabilities both lie on the same branch of the dispersion relation, the Kelvin-Helmholtz instability traveling at a somewhat smaller angle with respect to the magnetic field. (auth)

22264 STABILIZATION OF HOT ELECTRON PLASMA BY A COLD BACKGROUND. Krall, Nicholas A. (General Atomic Div., General Dynamics Corp., San Diego, Calif.). Phys. Fluids, 9: 820-1(Apr. 1966).

A stabilizing effect of cold plasma, distinct from line tying, is described, and its influence on the flute stability of a hot-electron plasma is evaluated. (auth)

22265 HOT-ELECTRON PLASMA STABILITY IN MIRROR AND MINIMUM-B CONTAINMENT SYSTEMS. Hartman, Charles W. (Univ. of California, Livermore). Phys. Fluids, 9: 821-4(Apr. 1966). (UCRL-14310(Rev.1)).

For all "saddle in B" fields, independent of shear, a dominant cross-field loss is observed, which can be suppressed by a cold-plasma background. In minimum-B fields, cross-field loss is suppressed independent of the cold plasma. (auth)

22266 NONLINEAR DIFFUSION WITH RECOMBINATION IN AN ELECTRON BEAM EXCITED PLASMA. Mosburg, Earl R. Jr. (National Bureau of Standards, Boulder, Colo.). Phys. Fluids, 9: 824-6(Apr. 1966).

The radial distributions of electron density and light intensity are calculated from the nonlinear diffusion equations with a recombination term added. Two-body and three-body recombination mechanisms are considered in addition to the intermediate case of collisional-radiative recombination. (auth)

22267 EQUIVALENCE OF ELECTRON AND EXCITATION TEMPERATURES IN AN ARGON PLASMA. McGregor, W. K.; Brewer, L. E. (ARO, Inc., Arnold Air Force Station, Tenn.). Phys. Fluids, 9: 826-7(Apr. 1966).

The excitation temperature, measured spectroscopically in a low density, flowing, argon plasma using relative line intensities, was found to agree very well with the electron temperature, measured using a conventional Langmuir probe, across a diameter of the plasma stream. (auth)

22268 HIGH DENSITY CORRECTIONS TO THE SCATTERING CROSS SECTION OF A PLASMA. Theimer, O. (Institut fuer Plasmaphysik GmbH, Garching, Munich). Phys. Lett., 20: 639-40(Apr. 1, 1966).

It is shown that corrections to the Debye-Hückel approximation affect plasma scattering, particularly the intensity ratio of ion and electron line, significantly if the number of electrons in the Debye sphere drops below 0.5. (auth)

22269 SPECTROSCOPIC ANALYSIS OF A HELIUM PLASMA PRODUCED BY A CONICAL ϑ-PINCH DISCHARGE. Costa, Sergio; Tondello, Giuseppe (Univ., Padua. CNR, Padua). Ric. Sci. Rend., Sez. A, 8: 949-71 (Sept.-Oct. 1965).

Shock waves, produced by a device of the annular discharge type with a conical coil outside the tube, were analyzed. Measurements of temperature and electron density with various methods of photographic and spectroscopic investigations in the visible range were obtained. The reliability of a recent method of temperature measurement through the ratio of the intensity of He II λ 4686 Å line to its corresponding continuum was examined. The essential agreement of the results obtained by different spectroscopic methods was confirmed. The disagreement between spectroscopic temperature measurements and those obtained using the Rankine-Hugoniot equations was also confirmed. (auth)

22270 KINETIC THEORY OF ELECTROMAGNETIC WAVES IN A PLASMA LAYER. Kondratenko, A. N. Zh. Tekh. Fiz., 35: 1546-51(1965). (In Russian).

The propagation of electromagnetic waves in a plasma layer of thickness 2a is discussed on the basis of the kinetic equation with self-consistent field but no collision terms. In this problem the frequency $f_0 = a/v_0$ is important (v_0 is the electron thermal velocity). For the boundary condition on the distribution function, it is assumed that the fraction p of the plasma particles that strike the plasma surface are specularly reflected and the rest escape from the plasma into the surrounding vacuum. The dispersion equation for E-waves (electromagnetic waves with a nonvanishing longitudinal electric field component) is derived by an approximate method that may be valid only when p is less than unity. The resulting dispersion equation is very different from the dispersion equation previously derived with different boundary conditions. It is found that E-waves can propagate only when the frequency is less than $f_0 m/M$, where m and M are the electron and ion masses, respectively. The dispersion equation for H-waves in a cold plasma layer is derived by an approximation method which, it is postulated, is capable of giving only qualitative results. It is found that high frequency H-waves propagate with a phase velocity greater than the velocity of light. When thermal motions are taken into account, however, it is found that these waves are damped out with a damping constant proportional to the cube of the thermal velocity. (ATD)

22271 FREQUENCY DOUBLING ON REFLECTION OF A WAVE AT A PLASMA BOUNDARY. Alanakyan, Yu. R. (Lebedev Inst. of Physics, Moscow). Zh. Tekh. Fiz., 35: 1552-7(1965). (In Russian).

Reflection of electromagnetic waves at the plane boundary of a semi-infinite plasma with lowest order nonlinear effects taken into account is discussed. Conditions of low-space dispersion (electron thermal velocity small compared with wave phase velocity) are assumed. The calculations are based on the kinetic equation for the electron distribution with self-consistent field but no collision term. The distribution function is expanded in powers of the electric field strength, and from the second order term there are derived the volume and surface currents excited by the simultaneous presence of two electromagnetic waves. These currents are employed to calculate the amplitudes and directions of the second harmonic waves that are produced in the reflection of a plane electromagnetic wave obliquely incident on the surface from within the plasma or from free space. The excitation and behavior of surface waves are also discussed. Langmuir waves are produced when the second harmonic frequency is close to the Langmuir frequency; this case is discussed

separately. A surface wave whose frequency is close to half the Langmuir frequency gradually transforms into a Langmuir wave and disappears into the depths of the plasma; the rate at which this occurs is calculated. (ATD)

22272 POSITIVE COLUMN IN THE INVERSE HOMOPOLAR DEVICE. **Drobyshevskii, E. M.; Chekmarev, I. B. (Ioffe Physico-Technical Inst., Leningrad). Zh. Tekh. Fiz., 35: 1558-67(1965). (In Russian).**

The "direct" homopolar device consists of two coaxial cylindrical electrodes with a radial electric field and an axial magnetic field in the plasma-filled annular space between them. The "inverse" homopolar device discussed has cylindrical dielectric walls, a radial magnetic field, and an axial electric field. The plasma is assumed to be weakly ionized, so that collision of electrons and ions are almost entirely with neutral atoms. The magnetic field strength is assumed to be such that the electron Larmor frequency is much higher than the electron collision frequency and the ion Larmor frequency is much lower than the ion collision frequency. The plasma is treated in the hydrodynamic approximation. The equations were solved on a computer for the case of a hydrogen plasma, and the results are presented graphically. At high magnetic field strengths the ion temperature can exceed the electron temperature. When this occurs the discharge becomes unstable and the electric field strength required to maintain the discharge increases. This theoretically derived instability is employed to explain the instability of the homopolar device observed experimentally. (ATD)

22273 POLARIZATION INTERACTION OF OPPOSED PLASMA STREAMS IN A COMPOSITE MAGNETIC FIELD TRAP. **Zykov, V. G.; Stepanenko, I. A.; Tolok, V. T. Zh. Tekh. Fiz., 35: 1585-9(1965). (In Russian).**

The behavior of plasma bursts colliding within a magnetic mirror system provided with an auxiliary quadrupole or octupole magnetic field was investigated. The magnetic mirror system was produced in a 30 cm diameter stainless steel chamber by discharge of a 2700 microfarad capacitor through suitable windings. The maximum magnetic field at the center of the system was 2800 Oe and the mirror ratio was 2.16. The auxiliary field was provided by currents in eight copper rods parallel to the main field and disposed at equal intervals on the surface of a 10.6 cm diameter cylinder. The rods could be connected variously in series or series-parallel, but the rod system was always connected in series with the main windings so that the ratio of the auxiliary to the main field remained constant during the discharge. At the surface of the 1-cm-diameter rods this ratio was 0.87. Plasma bursts from four conical plasma guns disposed symmetrically in the equatorial plane of the mirror system were injected transversely to the main magnetic field. The velocity of the leading edge of a plasma jet was 2×10^6 cm/sec and the ion density was of the order of 10^{13} cm^{-3}. In the presence of the auxiliary magnetic field the turbulent plasma "protuberances" observed earlier did not occur, and there was no difficulty in assuring head on collision between oppositely directed jets. It was established with the aid of probes that the oppositely polarized colliding jets interacted strongly. The maximum plasma density in the center of the system was much greater when the auxiliary field was present than when it was not, but the confinement time was the same in both cases. (ATD)

22274 INTERMINGLING OF PARTICLES IN A COMPOSITE MAGNETIC FIELD TRAP. **Volkov, B. I.; Glasko, V. B.; Sveshnikov, A. G.; Semashko, N. N. (Moscow State Univ.). Zh. Tekh. Fiz., 35: 1590-3(1965). (In Russian).**

Trajectories of charged particles in a magnetic mirror system with an auxiliary transverse magnetic field were calculated with the aid of a computer. The auxiliary field was that produced by six current-carrying rods parallel to the axis of the system and symmetrically disposed about it. The calculations were undertaken to determine whether the complex magnetic field would cause sufficient intermingling of particles with different velocities significantly to reduce the anisotropy of the ion velocity distribution of a plasma injected into the system. This question is important because the anisotropic velocity distribution of plasmas in magnetic mirror systems gives rise to cyclotron instability and greatly reduces the confinement time. The charged particles were assumed to be produced within the field by ionization of atoms of a monoenergetic beam moving in the median plane through the center of the system. The ions were accordingly injected at different radii and with different longitudinal velocities. The positions of the successive intersections of the ion trajectories with the median plane and with two other planes normal to the axis were calculated. It was found that ions injected at small radii move in nonintersecting regions, and that intermingling of such ions, therefore, does not occur. Ions injected at large radii, however, penetrate into regions of smaller radius, so that on the whole there is intermingling. It was also found that this intermingling would significantly reduce the anisotropy of the velocity distribution of a rarefied injected plasma. (ATD)

22275 INVESTIGATION OF THE POLARIZATION OF A PLASMA MOVING IN A HELICAL MAGNETIC FIELD. **Il'enko, B. P.; Lats'ko, E. M.; Zalkind, V. M.; Zykov, V. G.; Tolok, V. T. Zh. Tekh. Fiz., 35: 1594-7(1965). (In Russian).**

The effect of an additional triple helical magnetic field on the polarization of plasmas moving in a toroidal magnetic field was investigated. The longitudinal magnetic field (up to 200 kamp/m) was produced in a 4 cm radius U-shaped copper-drift tube by suitable windings powered with d-c generators. The large radius of the toroidal section of the drift tube was 42 cm and the straight legs were 80 cm long. The helical field was produced by a 134-cm reciprocal-pitch 5.4-cm radius triple-helical winding carrying currents up to 3 kamp. Plasmas with ion densities exceeding 10^{13} cm^{-3} were injected at one end by a conical plasma gun. The electric (polarization) field in the plasma was measured with a plane probe at the exit from the toroidal section; this probe could be rotated in azimuth in order accurately to determine the direction of the polarization. In the absence of the helical field, the polarization vector rotated through an angle of $\pi/2$ when the longitudinal field was reversed; this behavior is in agreement with theory. Application of the helical field did not decrease the polarization but rotated its direction through an angle corresponding to the rotation of the lines of force; this rotation was $\pi/3$ radians when the longitudinal field strength was 160 kamp/m and the current in the helical winding was 3 kamp. The density of the plasmas at the exit from the toroidal section was measured with a screened probe. In the absence of the helical field the plasma density was approximately 8×10^{10} cm^{-3} when the longitudinal field strength was 40 kamp/m and 6×10^{11} cm^{-3} when the longitudinal field strength was 200 kamp/m. Application of the helical field (when the longitudinal field was 56 kA/m) increased the plasma density at the exit from the toroidal section by as much as a factor 10. This increase was greater for the slower components of the plasma burst than for the faster components. (ATD)

22276 INVESTIGATION OF THE POLARIZATION OF A PLASMA MOVING IN A TOROIDAL MAGNETIC FIELD. **Il'enko, B. P.; Lats'ko, E. M.; Zalkind, V. M.; Zykov, V. G.; Tolok, V. T. Zh. Tekh. Fiz., 35: 1598-1601(1965). (In Russian).**

The polarization of plasmas moving in a toroidal magnetic field was measured. The magnetic field (up to 200 kamp/m) was produced in a U-shaped copper-drift tube (diameter not given). The large radius of the toroidal section of the drift tube was 42 cm and the straight legs were 60 cm long. Plasmas with ion densities exceeding 10^{13} cm^{-3} were injected at one end of the drift tube with a conical plasma gun powered by the 8-12 kV 6.5 μ sec discharge of a 3 μfd capacitor. The charged particle density of the injected plasmas was not less than 10^{13} cm^{-3}. The electric field polarization in the plasma was measured with probes at the exit from the toroidal section. The polarization field had components in the direction of the large radius of the torus and in the direction of the axis

of the torus. The axial component changed signs when the direction of the longitudinal field was reversed, and the component did not. The distribution of the polarization field across the section of the drift tube and the variation of the polarization field with the longitudinal magnetic field strength were measured and are presented graphically. By comparing the time of maximum polarization with that at which a 3-cm wave crossing the drift tube was cut off by the plasma, it was established that the polarization was confined almost entirely to the more rapid, less dense leading portion of the plasma burst. (ATD)

22277 INVESTIGATION OF THE POLARIZATION OF PLASMAS MOVING IN MAGNETIC FIELDS OF OPPOSITE CURVATURES. **Il'enko, B. P.; Lats'ko, E. M.; Zalkind, V. M.; Zykov, V. G.; Tolok, V. T. Zh. Tekh. Fiz., 35: 1602-5(1965). (In Russian).**

The polarization of plasmas moving in a toroidal magnetic field was measured using the apparatus described previously and, in addition, a 7.4-cm diameter S-shaped copper-drift tube consisting of two half-tori of 35 cm large radius joined by a 20 cm long straight section. A longitudinal magnetic field of 200 kamp/m was maintained in both drift tubes. Plasmas could be injected at either or both ends of both drift tubes by means of conical plasma guns. The polarization of the plasmas was measured with probes located at the center of the toroidal section of the U-shaped drift tube and in the straight section joining the two half-tori of the S-shaped drift tube. The polarization is analyzed in terms of three components V_z, V_R, and V_r: V_z is parallel to the axis of the torus, V_R is in the direction of the large radius of the torus, and V_r is in the plane of V_z and V_R and is directed away from the axis of the drift tube (along the small radius of the torus). It was found that V_z changes sign when the direction of the magnetic field is reversed but not when the direction of motion of the plasma through the U-shaped drift tube is reversed without reversing the field. When the direction of motion of the plasma through the S-shaped drift tube was reversed, however, the V_z component of the polarization measured in the straight section joining the two half-tori changes sign. When two oppositely moving plasmas collided in the center of the U-shaped drift tube the value of V_z was approximately the same as when only one plasma was present. When two oppositely moving plasmas collided in the straight section joining the two half-tori of the S-shaped drift tube, the V_z polarization components of the two plasmas canceled each other and only V_r was measured. The distributions of V_z and V_r across the drift tube are presented graphically. It was found that V_z and V_r are of comparable magnitude in the fast leading edge of the plasma burst, but that V_z predominates in the tail. (ATD)

22278 CONCERNING PECULIARITIES OF THE RADIATION OF POINT DIPOLES MOVING IN NARROW CAVITIES IN MAGNETOACTIVE MEDIA. **Barsukov, K. A.; Kadantsev, V. N. (Lebedev Inst. of Physics, Moscow). Zh. Tekh. Fiz., 35: 1606-9(1965). (In Russian).**

The Cherenkov radiation of an electric or magnetic dipole moving in a narrow linear or plane cavity in an active medium characterized either by a hermitian dielectric tensor similar to that of a magnetized plasma or by a hermitian magnetic permeability tensor similar to that of a magnetized ferrite is calculated. It is shown that if the axis of the dipole is parallel to that of the linear cavity or to the walls of the plane cavity, the presence of the narrow cavity has no effect. If the axis of the dipole is perpendicular to its direction of motion, however, the presence of the infinitely narrow cavity has a finite effect. This effect is calculated for both linear and plane cavities for the case in which the cavity is cut in a normal (scalar) medium and filled with an active medium and for the case in which the cavity is cut in an active medium and is filled with a normal medium. If one assumes that the active medium is a magnetized plasma, one finds that the expression obtained for the power radiated from the plane cavity is singular at the two frequencies that limit the pass band of a plasma waveguide. This singularity is only apparent and is due to neglecting higher powers of af/c, where a is the thickness of the cavity, f is the frequency, and c is the velocity of light. (ATD)

22279 OPERATION OF A GAS-FILLED DIODE WHEN THE ELECTRON DISTRIBUTION IS NOT MAXWELLIAN. **Nagaev, E. L. Zh. Tekh. Fiz., 35: 1634-41(1965). (In Russian).**

The theory of a plane hot-cathode plasma diode operating under such conditions that the Maxwell distribution of electron velocities is not established. The theory is applicable to the case in which the electrode spacing is large compared with the mean free path of an electron for collision with atoms, for although electrons readily exchange momentum in collisions with atoms, the energy exchanged in such collisions is very slight owing to the large mass difference. The case in which there is a single potential maximum between the electrodes is considered. The calculations are based on the kinetic equation including the collision integral for electron-atom collisions. The potential is assumed to be a linear function of distance from the cathode except at the two electrodes themselves, where it is discontinuous. The kinetic equation is solved by methods that were discussed previously in more detail. The stability of the solution is discussed in the diffusion approximation with electron-electron collisions taken into account, and stability conditions are derived. The ion distribution is discussed and a procedure is devised whereby one can calculate the current-voltage characteristic of the diode. The beam instability of the plasma was neglected. Although this effect provides the predominant mechanism for the establishment of a Maxwell electron velocity distribution when the cathode potential drop is very great, it appears to be of secondary importance in cesium diodes. (ATD)

22280 DETERMINATION OF THE CONDUCTIVITY IN A HIGH-FREQUENCY INDUCTION DISCHARGE IN ARGON BY CALORIMETRIC AND SPECTROMETRIC METHODS. **Dresvin, S. V.; Donskoi, A. V.; Gol'dfarb, V. M. (Polytechnic Inst., Leningrad). Zh. Tekh. Fiz., 35: 1646-51 (1965). (In Russian).**

The conductivity of a high-frequency-discharge argon plasma by calorimetric and optical methods in order to compare the two techniques. The plasma was produced in a 3-cm diameter quartz tube with water-cooled walls containing flowing argon at atmospheric pressure and located on the axis of a 4.6-cm diameter 4-turn coil connected to a 26-Mc 10-kw oscillator. The conductivity of the plasma is calculated from the current and voltage in the exciting coil and the heat evolved, with the aid of theory, the previous derivation of which contains some errors that are corrected. The absolute intensity of the radiation from the arc between 4400 and 4700 Å was determined by photographing the arc through suitable filters, and the absolute intensity of Ar I 4510, the Doppler broadening of H_β, and the intensity of the recombination continuum near 4500 Å were determined with a type ISP-51 spectrometer. With the optical measurements it was possible to estimate the temperature, electron density, and conductivity in different parts of the plasma. The conductivities measured optically were some 800% greater than those measured calorimetrically. This discrepancy is ascribed to the variation of the conductivity between different parts of the plasma. The conductivity distribution determined optically is discussed at some length, and an "effective" conductivity that one should expect to measure calorimetrically is calculated from the optical measurements. This optically determined effective conductivity is only some 275% greater than the calorimetrically measured value. The calorimetric method for measuring plasma conductivities is subject to large absolute errors (associated largely with complex and unknown features of the discharge geometry) which can easily exceed 100%, but it is capable of good accuracy (5%) in relative measurements. (ATD)

22281 BOLOMETRIC MEASUREMENTS OF THE RADIATION OF AN IONIZED SHOCK WAVE IN ARGON. **Redkoborodyi, Yu. N.; Fedulov, V. I. Zh. Tekh. Fiz., 35: 1652-7(1965). (In Russian).**

The radiation from reflected shock waves with Mach numbers between 7 and 11 in argon at 10 mm Hg was measured. The shock waves were produced in an electric-discharge shock tube which was provided with a lithium fluoride glass window at the far end. A bolometer mounted outside this window recorded on an oscilloscope the radiation from the reflected shock wave. The bolometer was similar to the instrument described by L. L. Gorelik (ZhTF, 34, 496, 1964); it had a resolving time of 10 microsec and an equilibration time of 0.1 sec. The surface of the bolometer was blackened by depositing aluminum on it in a nitrogen atmosphere at 1 mm Hg; this increased the sensitivity by a factor 7. The radiation intensity of the shock wave plasma was calculated from the bolometer readings recorded during approximately the first 100 microsec after the reflection; preliminary calculations indicated that the layer of plasma involved would be optically thin, and this was confirmed by the measurements. The measured radiation intensities were compared with values calculated with the theory of F. H. Mies (J. Chem. Phys., 37: No. 5, (1963)). Only recombination radiation was taken into account in the calculations, preliminary estimates having indicated that the bremsstrahlung and line spectrum intensities would be negligible. When the logarithms of the measured intensities were plotted against the reciprocals of the corresponding temperatures, the points fell near a straight line that was parallel to but somewhat below the theoretical curve. This discrepancy is ascribed to incorrect temperature determination; the velocity of the shock wave was measured at some distance from the window and its decrease with increasing age of the wave was neglected. Comparison of the measured radiation intensities with enthalpies of argon indicate that in the theory of argon shock waves radiative energy losses can be neglected at temperatures up to 10,000°K but must be taken into account at higher temperatures. (ATD)

22282 ON PLASMA DRIFT WAVES PROPAGATING TRANSVERSELY TO AN EXTERNAL MAGNETIC FIELD. Kostomarov, D. P. (Moscow State Univ.). Zh. Tekh. Fiz., 35: 1713-19(1965). (In Russian).

The stability of plasma drift waves propagating transversely to an external magnetic field in an inhomogeneous plasma is discussed on the basis of the linearized equation of Vlasov for the distribution function perturbation. The plasma is assumed to be dense (ion Langmuir frequency much higher than the ion Larmor frequency) and to be inhomogeneous in only one dimension. The magnetic field is assumed to be perpendicular to the direction of the inhomogeneity and the waves are assumed to propagate transversely to both. The length D characterizing the plasma inhomogeneity is assumed to be much greater than the electron and ion Larmor radii. A differential equation for the electric potential is derived and reduced with the aid of different simplifying assumptions to different equations of the Sturm-Liouville type, the eigenvalues of which are approximated and discussed. The parameter $P = (f_i D/c)(1 + (T_e/T_i))^{\frac{1}{2}}$ plays a significant role in the simplification of the differential equation for the potential. Here f_i is the ion Langmuir frequency and T_e and T_i are the electron and ion temperatures. It is shown that the plasma drift oscillations are stable when $P \gg 1$ and are unstable when $P \ll 1$. (ATD)

22283 ELECTROSTATIC SEPARATION OF CHARGE IN A PLASMA IN THERMODYNAMIC EQUILIBRIUM. Samokhin, M. V. Zh. Tekh. Fiz., 35: 1720-9(1965). (In Russian).

The Debye-Hückel problem for a completely ionized isothermal plasma above an infinite charged plane is treated without the usual linearization of Poisson's equation. For the case of a plasma with singly charged ions the solution is obtained in terms of elementary transcendental functions. Such a solution appears not to be possible for the case of multiply charged ions, and the solution for this case is given as an infinite series. The analogous problem of a plasma between two inifinite parallel planes at different potentials is also treated, both for the case of a neutral plasma and for that of a plasma with an excess of electrons or ions. Numerical solutions were computed for a number of special cases and these are presented in graphical and tabular form. Simple formulas are derived which facilitate the expansion in a power series of a function of the form F(f(x)) when the power series expansions of the functions F and f are known. (ATD)

22284 ON THE LONGITUDINAL OSCILLATIONS OF A NONUNIFORM PLASMA. Eidman, V. Ya. Zh. Tekh. Fiz., 35: 1730-5(1965). (In Russian).

Longitudinal oscillations of a nonuniform plasma are treated on the basis of a linearized kinetic equation in which the static force responsible for the nonuniformity is retained. The treatment differs from other, earlier treatments in retaining this static force factor. It is assumed that the length characterizing the plasma nonuniformity is much greater than the wavelength, and the solution of the kinetic equation is sought in the approximation of geometric optics. The zeroth approximation is derived in detail and it is shown how the higher order approximations can be calculated if necessary. It is found that retaining the static force leads to a lower estimate of the Landau damping due to charged plasma particles with velocities close to the phase velocity of the waves. An integral that occurs in the expression for the current density, for which an asymptotic expression was derived is evaluated in terms of the error function. Replacing the error function in this integral by its asymptotic expansion, however, leads to a less useful expression for the current density than that derived in the text. (ATD)

22285 ON THE NONLINEAR OSCILLATIONS OF THE PLASMA BEHIND A FRONT ON WHICH CHARGED PARTICLES ARE PRODUCED. Kolesnikov, P. M.; Khizhnyak, N. A. (Kharkow Aviation Inst.). Zh. Tekh. Fiz., 35: 1736-42(1965). (In Russian).

The behavior of the completely ionized plasma behind an "ionization front" propagating in an unionized gas and ionizing it is discussed. The treatment is based on the inhomogeneous kinetic equations for the electron and ion distribution functions and Poisson's equation for the self-consistent electric potential describing the Coulomb interactions. The collision integrals are not included in the kinetic equations. These equations are solved by Cauchy's method of characteristics and the resulting general solution is specialized for the case of an infinitely thin ionization front and for delta-function and Maxwell distributions of the velocities of the nascent ions and electrons. It is shown that under certain conditions (which are derived) longitudinal traveling waves develop in the plasma with a frequency close to the Langmuir frequency. For the case of a Maxwell distribution of the velocities of the nascent ions and electrons, a first integral of Poisson's equation is derived; this relates the amplitude of the oscillations to the electron and ion temperatures and to other parameters and plays a role analogous to that of a dispersion equation. The effect of an ionization front of finite thickness is discussed briefly. When the amplitude of the oscillations is small the finite thickness of the front reduces the amplitude but leaves the frequency unchanged. For high amplitude oscillations the thickness of the front also influences the frequency. (ATD)

22286 INTERACTION OF A CHARGED PARTICLE BEAM WITH A CONFINED PLASMA. Giorgadze, N. P.; Lominadze, D. G. Zh. Tekh. Fiz., 35: 1743-5(1965). (In Russian).

The excitation of waves in a cold plasma within a perfectly conducting cylindrical tube by a charged particle beam propagating parallel to the axis of the tube in the presence of an external magnetic field is discussed. The calculations are based on the hydrodynamic approximation. The dispersion equation is written without derivation or reference and is simplified by considering only frequencies that are small compared with the electron Larmor frequency and retaining only lowest order terms in the ratio of the electron to the ion mass. Under these conditions the dispersion equation breaks up into two factors, of which one has been previously derived. Expressions are given for the

logarithmic increments of the different types of waves that can be excited by the charged particle beam. These waves include the ordinary and extraordinary waves near the ion cyclotron resonance incident to the anomalous Doppler effect and waves with phase velocity near the particle velocity of the beam (Cherenkov excitation). The conditions for propagation of the different waves are discussed very briefly. (ATD)

22287 ON THE SELF-CONSISTENT HYDRODYNAMIC PROBLEM OF THE MOTION OF RELATIVISTIC ELECTRONS IN A UNIFORM MAGNETIC FIELD. Rubin, S. B. Zh. Tekh. Fiz., 35: 1746-8(1965). (In Russian).

The relativistic motion of a cylindrical shell of electrons in a uniform magnetic field is treated in the self-consistent hydrodynamic approximation. The calculations were undertaken because of the application of cylindrical shells of relativistic electrons in the "Astron" thermonuclear device. A general solution in cylindrical coordinates r, θ, z is obtained for which the r- and z-components of the electron velocity vanish and the electron density and velocity depend only on r. Conditions are sought that this solution may obtain for $b < r < a$ with vanishing electron density for $r < b$ and $a < r$, and it is shown that this is possible only in the presence of an external field. Conditions are found that the required external electric field vanish; in this case the external field reduces to a uniform magnetic field. The final solution depends on three parameters, of which one determines the outer radius of the cylindrical shell of electrons, a second fixes the minimum electron velocity, and the third is associated with the total number of electrons per unit length of the shell; the thickness of the electron shell and the strength of the external magnetic field depend on all three parameters. (ATD)

22288 ENTRAINMENT OF A PLASMA BY A ROTATING ELECTROMAGNETIC FIELD. Sidorov, V. P.; Soldatenkov, T. R. Zh. Tekh. Fiz., 35: 1749-54(1965). (In Russian).

The entrainment of a plasma cylinder in a uniform magnetic field by a rotating electromagnetic field is discussed in the magnetohydrodynamic approximation. The calculations were undertaken because rotation of a plasma cylinder can be useful in prolonging its life, in suppressing flute instability, and possibly in heating it. The rotating electromagnetic field discussed is that due to currents proportional to $\exp i(ft + m\theta)$ in the z direction on a cylindrical surface coaxial with the plasma cylinder. Here r, θ, z are cylindrical coordinates, f is the frequency, and m is an integer. The magnetohydrodynamic equations are solved by a successive approximation method based on expansion in powers of the ratio of the strength of the alternating magnetic field to that of the uniform axial magnetic field. In the zeroth approximation the plasma is assumed to be at rest. The first approximation describes the distribution of the high frequency fields in the plasma, but the plasma motion appears only in the second approximation. In order to obtain the second approximation it is assumed that the entrainment time is long compared with the period of the high frequency field, and all quantities are separated into slowly varying and high-frequency parts. In the second approximation there appear radial and azimuthal motions of the plasma, a radial electric field, and an azimuthal current. The second approximation describes only the initial stages of the plasma entrainment because the reaction of the plasma motion on the field appears only in higher order approximations, which are not calculated in general form. The entrainment time is estimated under further restrictive assumptions. The effect on the entrainment process of the finite plasma lifetime and the possibility of instabilities due to the rotational velocity gradients and the azimuthal currents must be further investigated. (ATD)

22289 PLASMA ACCELERATION IN A CONSTANT ELECTRIC FIELD COMBINED WITH HIGH-FREQUENCY FIELD. Kononov, B. P. Zh. Tekh. Fiz., 35: 1755-6 (1965). (In Russian).

A theoretical discussion is presented of plasma acceleration by various methods in which only electrons in a homogeneous plasma are affected by the forces applied. The difficulty here is that the acceleration of electrons results in an electric current, while the plasma as a whole remains unaffected. The situation can be corrected by application of a longitudinal electric field capable of compensating for electron acceleration. It is demonstrated analytically that the addition of such a field causes electrons and ions to move with equal velocities and thus brings about an acceleration of the plasma as a whole. At the same time, the electric current in the direction of acceleration will be reduced to zero; the applied field, therefore, is used exclusively for the redistribution of acting forces. The method is of interest in cyclic acceleration of plasma, particularly in toroidal arrangements where parasitic electric current is generated. Here, application of a supplementary electric field or an electromagnetic wave in a doughnut accelerator would correct the situation. The constant electric field can also be used for directed energy exchange between electrons and ions. This occurs, for instance, with ions and electrons with differing velocities when their beam enters an area of constant electric field. With a proper concentration ratio of both components the current will be zero, and the field will do no work but will result in energy transfer between ions and electrons. (ATD)

22290 ON THE THEORY OF THE CHERENKOV RADIATION OF A CHARGE IN A COLD PLASMA. Kurdyumov, V. N. Zh. Tekh. Fiz., 35: 1771-81(1965). (In Russian).

The Cherenkov radiation of a point charge moving parallel to an applied magnetic field through an infinite cold plasma is calculated. The calculations were undertaken because of recent interest in possible practical applications of the effect and because of errors in previous calculations which led to an overestimate of the energy radiated in the ordinary wave when two Cherenkov cones are simultaneously present. It is shown that when two Cherenkov cones are present, only one corresponds to radiation of energy, and the other corresponds to absorption. In the present calculations, collisions among the plasma particles and the motions of the ions are neglected. Conditions are derived for radiation of the ordinary and extraordinary waves and the spectral density of the radiation is presented graphically for certain values of the parameters. Formulas are given for the total energy radiated in the ordinary and in the extraordinary wave as functions of the particle velocity and the magnetic field strength. (ATD)

22291 INVESTIGATION OF ELECTRODE EROSION IN THE BRIDGE STAGE WHEN BREAKING 1 TO 5 kA CURRENTS IN VACUUM. Potokin, V. S.; Rakhovskii, V. I.; Tikhonov, V. N. (Lenin All-Union Electrotechnical Inst., USSR). Zh. Tekh. Fiz., 35: 1848-52(1965). (In Russian).

Earlier investigations of a heavy-current-vacuum circuit breaker, with particular reference to the stage in which a bridge of molten metal forms between the separating electrodes, were extended to higher currents (up to 5 kamp). The experimental technique was similar to that previously employed: cylindrical tungsten electrodes were rapidly separated, the voltage across the gap was observed with an oscilloscope, and the loss of electrode material was estimated by weighing tantalum foils that had been mounted near the gap. It was not possible to interrupt the discharge at any desired stage. It was found, however, that the loss of electrode material was always proportional to the duration of the arc stage of the discharge. From this it is concluded that in breaking currents up to 5 kamp the loss of electrode material due to formation of a liquid bridge is negligible compared with the total electrode erosion. The voltage drop during the bridge stage rose considerably when the current was increased beyond about 3 kamp. As a result of the increased Joule heat the bridge material presumably became very hot (temperatures up to 14,800°K are estimated), and a mass of highly ionized plasma was formed. This highly ionized plasma joining the electrodes is called the "anomalous bridge." Spontaneous explosive

formation of an anomalous bridge with consequent spontaneous separation of the electrodes was sometimes observed. There is a brief theoretical discussion of the formation and vaporization of the bridge. It is concluded that in breaking currents of 2 to 5 kamp there is formed between tungsten electrodes a mass of highly ionized plasma, that the mass of material eroded from the electrodes during the bridge stage exerts no appreciable influence on the duration of the subsequent vacuum arc, and that in designing high-current vacuum circuit breakers one must take measures to avoid spontaneous separation of the electrodes. Such measures might be to increase the contact pressure or to employ softer electrode materials. (ATD)

22292 INVESTIGATION OF THE CATHODE SPOTS OF A PULSED DISCHARGE BETWEEN PARALLEL ELECTRODES. **Basharov, R.; Gavrilovskaya, E. N.; Malkin, O. A.; Trekhov, E. S. (Moscow Engineering Physics Inst.). Zh. Tekh. Fiz., 35: 1853-9(1965). (In Russian).**

The 3 kv discharge of a 36 μfd capacitor between plane-parallel copper electrodes in 9×10^{-3} mm Hg of air was investigated in order to obtain information concerning the processes taking place near the electrodes in a plasma gun. Ordinary and streak photographs of the electrodes were recorded during the discharge and the damaged electrode was subsequently examined under optical and electron microscopes. The streak photographs showed that while the discharge moved along the cathode at velocities up to 5×10^6 cm/sec there were bright regions that did not move. The presence of these stationary glowing regions was confirmed by the ordinary photographs, and small damaged regions were found by microscopic examination. These stationary glowing regions did not appear on the anode, and they are identified as cathode spots. The cathode spots showed a complex microstructure (including microfractures observable only with the electron microscope), which is described in some detail. It is concluded that the cathode spots of a pulsed discharge moving rapidly along a plane electrode in a rarefied gas arise and exist independently of each other and remain stationary during their whole life. It is also concluded that one must take account of the fine structure of the cathode spot when attempting to estimate the current density; estimates based on the gross structure alone will necessarily be too small. (ATD)

22293 ON THE BREMSSTRAHLUNG FROM A SOLID TARGET IN A PLASMA. **Aleksin, V. F.; Suprunenko, V. A. Zh. Tekh. Fiz., 35: 1902-5(1965). (In Russian).**

The plasma diagnostic technique which consists of observing the intensities of x rays passing through different absorbers after having been produced by plasma electrons striking a solid target is considered. The energy flux of x rays behind the absorber is expressed as a sum, the terms of which relate to the different absorption edges of the absorber. Suitable formulas for these terms are given for a number of special cases. In calculating these formulas it was assumed that the angular distribution of the bremsstrahlung is either isotropic or is that given for a thick target of light elements by Sommerfeld (Proc. Nat. Acad. Sci. USA, 15, 393, 1929), that the plasma electron velocity distribution is either Maxwellian or is velocity independent over a finite range, and that the x-ray intensity is observed either normally to the target and the absorber or throughout the full hemisphere behind them. For a Maxwell distribution of the plasma electrons each term in the expression for the x-ray intensity depends on a single parameter which involves the thickness and absorption coefficient of the absorber and the temperature of the electrons. For the case of hemispheric observation and Maxwell distribution this dependence is presented graphically. (ATD)

22294 ON THE RADIAL DEPENDENCE OF THE ELECTRON VELOCITY DISTRIBUTION IN THE POSITIVE COLUMN OF A DISCHARGE. **Kagan, Yu. M.; Milenin, V. M. (Leningrad State Univ.). Zh. Tekh. Fiz., 35: 1907-9 (1965). (In Russian).**

The electron velocity distribution functions were measured on and off the axes of the 2.5-cm diameter positive columns of 150 to 500 mamp discharges in Ne at 0.25 to 1.5 mm Hg and 100 mamp discharges in He at 0.2 to 1.2 mm Hg. Four 6-mm long 0.06-mm diameter probes were employed, two being mounted 50 mm apart on the axis of the column and two at corresponding positions 9 mm off the axis. The longitudinal electric-field strength measured with these probes was the same on and off the axis. The electron velocity distributions on and off the axis were derived from the second derivatives of the corresponding probe characteristics. At the lowest pressures the distributions were nearly Maxwellian and were the same on and off the axis. At higher pressures there were relatively more low energy electrons and fewer high energy electrons off the axis. The difference between the on and off axis distribution functions increased with increasing pressure. Measurements could not be obtained at higher pressures because of increasing noise. The difference between the average electron energy on and off the axis was not great and almost did not exceed the experimental error. The observed difference between the electron distributions on and off the axis is in agreement with a theory previously proposed. (ATD)

22295 PLASMA DIAGNOSTICS BY SCATTERING OF LIGHT ON ELECTRONS. **Malyshev, G. M. (Ioffe Inst. of Physics and Tech., Leningrad). Zh. Tekh. Fiz., 35: 2129-42(Dec. 1965). (In Russian).**

The theory of light scattering is reviewed and the limits of applicability of the laser-beam method for plasma diagnosis are discussed. The conclusions are summarized in a figure, which shows the limiting electron concentrations n_e that can be measured at different electron temperatures T_e with laser beams of different intensities. Advantages of the method include the high space and time resolutions that can be achieved by using narrow beams and short pulses, and the lack of interference with the plasma. A number of experimental investigations are reviewed in some detail. The experimental results confirm the theoretical predictions, and it is concluded that the usefulness of light scattering as a diagnostic tool has been confirmed. (35 references.) (L.B.S.)

22296 INSTABILITY OF ELECTRONIC WAVES IN NONUNIFORM PLASMA STREAMS. **Mikhailovskii, A. B.; Rukhadze, A. A. (Lebedev Inst. of Physics, Moscow). Zh. Tekh. Fiz., 35: 2143-9(Dec. 1965). (In Russian).**

The effect of convective drift of charged particles on the high-frequency slipping instability of a nonuniform plasma carrying a current in an external magnetic field is calculated. The equation for small potential oscillations in a cold nonuniform current-carrying plasma in which the current is parallel and the gradients are perpendicular to an external magnetic field is quoted from previous work and a dispersion equation is derived from it in the geometric optics approximation. The stability condition is derived and an approximate expression is obtained for the logarithmic increment of the oscillations. It was found that the plasma is unstable over a much wider range of velocity gradient than was concluded by Harrison and Stinger, who neglected drift. The solution is obtained and discussed in detail for the case in which the plasma density is constant for $|x| < a$ and zero for $|x| > a$, and the z-component of the velocity is a linear function of x (x, y, z are rectangular Cartesian coordinates with the z-axis parallel to the uniform magnetic field). Experiments on inductive acceleration of plasma in a toroidal chamber are discussed. (L.B.S.)

22297 KINETIC THEORY OF THE PASSAGE OF ELECTROMAGNETIC WAVES THROUGH A PLASMA LAYER. [PART] I. **Kondratenko, A. N.; Miroshnichenko, V. I. Zh. Tekh. Fiz., 35: 2154-9(Dec. 1965). (In Russian).**

The reflection, transmission, and absorption of plane electromagnetic waves incident at an arbitrary angle on an infinite plane layer of plasma of finite thickness were calculated, the incident waves being polarized with the electric vector normal to the plane of incidence. The calculations are based on Maxwell's equations and the kinetic

equation for the deviation from Maxwellian form of the distribution function for the plasma electrons. Ion motions are neglected. There are imposed on the distribution function boundary conditions, which correspond to the assumption of a fixed probability p for specular reflection of a plasma electron arriving at the plasma–vacuum boundary. The fate of the fraction 1–p of the electrons that are not reflected is not discussed. With the aid of these boundary conditions an expression is derived for the current in the plasma, and a system of coupled equations is derived for the spatial Fourier components of the electric field within the plasma. These equations are solved for the two limiting cases when the distance traversed by a plasma electron during a period of the wave owing to the thermal velocity is very large or very small compared with the thickness of the plasma layer, and expressions are obtained for the reflection, transmission, and absorption coefficients of the electromagnetic waves. These coefficients depend significantly on the electron reflection probability p. For the case when the plasma layer is thin (or the electron thermal velocity is high) and the electron reflection probability p is not too close to unity, the reflection and transmission coefficients of the incident wave are derived directly from the expression for the current. The results derived in this case can be obtained phenomenologically in the hydrodynamic approximation by employing an electron collision frequency equal to the ratio of the electron thermal velocity to the thickness of the plasma layer. (ATD)

22298 INVESTIGATION OF THE STRUCTURE OF MAGNETIC SURFACES IN A STELLARATOR WITH A DOUBLE HELICAL FIELD. Berezhetskii, M. S.; Grebenshchikov, S. E.; Popyradukhin, A. P.; Shpigel', I. S. (Lebedev Inst. of Physics, Moscow). Zh. Tekh. Fiz., 35: 2167-75(Dec. 1965). (In Russian).

The magnetic surfaces of the stellarator field in the L-1 toroidal magnetic trap were explored with electron beams, using three different techniques. (1) A beam of 60–100 ev electrons was directed along a line of force at a selected point in the chamber and was collected after a single revolution on an electrode that filled the entire cross section of the chamber. By varying the position of the gun the area was mapped out from which substantially all the injected electrons reached the collector. (2) A pulse of 20 ev electrons was injected along a line of force and the lifetime of the electrons in the chamber was determined with an electrostatic induction probe. Lifetimes of 200–300 μsec, corresponding to 150–200 revolutions, were usual. (3) An electron pulse was injected and the corresponding magnetic surface was mapped out with a small movable electrostatic induction probe. By measuring the time between injection and detection of the pulse, the number of revolutions (up to about 20) corresponding to a given point on the magnetic surface could be determined. The presence of closed magnetic surfaces was established for values of the h/H ratio of the fundamental harmonic of the helical field h to the longitudinal field H less than 0.6. The magnetic surfaces were highly distorted or destroyed when h/H was increased beyond 0.6; the reason for this is not understood. Low order resonant perturbations were detected. These were evinced by a sharp decrease in the lifetime of the injected electron pulse at the resonant values of h/H and by break-up of the magnetic surface into two or three pieces, depending on the order of the resonance. The resonances were observed at the predicted values of h/H. The effect of a transverse magnetic field on the magnetic surfaces was investigated. This was found to shift the positions of the magnetic surfaces without significantly distorting them, in accord with theoretical calculations. (ATD)

22299 TOROIDAL MACHINE FOR ADIABATIC COMPRESSION OF PLASMA. Golant, V. E.; Kaganskii, M. G.; Ovsyannikov, V. A.; Piliya, A. D. (Ioffe Inst. of Physics and Tech., Leningrad). Zh. Tekh. Fiz., 35: 2176-84(Dec. 1965). (In Russian).

A brief description is given of a new machine, the "Tuman," for ohmic heating and subsequent adiabatic compression of plasma. The chamber is in the form of a racetrack with 60 cm long straightaways and 20 cm radius semicircular ends. In order to meet the conflicting requirements for stable, efficient ohmic heating and high adiabatic compression ratio, the quasistationary longitudinal magnetic field (half-period 3 millisec) was made strong (up to 50 kOe) in the semicircular end regions and weak (1.5–3 kOe) in the straightaways. The radius of the chamber in the semicircular end regions is 2 cm, and the plasma is stabilized by a 5 mm thick copper liner, which is slotted to permit penetration of the magnetic field. The radius of the chamber in the straightaways is 8.5 cm and the walls are of glass, there being no metallic liners that might reduce the rate of rise of the compressing magnetic field. The quasistationary magnetic field is produced by discharge of two 6 μ F5 kv capacitors through suitable windings. Preliminary ionization is effected by a 30 μ sec r-f pulse. Ohmic heating is accomplished with the aid of a 0.2 v sec demountable transformer powered by a 25 μ F10 kv capacitor bank and having a gap in the core of not more than 0.5 mm. Duration of ohmic heating is ordinarily 300 μ sec. The magnetic field in the straightaways can be raised from a few kOe or less to as high as 30 kOe in from 20 to 240 μ sec by discharge of an adjustable capacitor bank (possible values are 600 μ F and 20 kv) through special windings. These windings are similar to those described by Bartels (Naturwissenschaften, 50: 396(1963)); they were made in two layers of four turns each with the turns in the two layers inclined oppositely to the axis of the chamber in order to minimize the transverse component of the field. The machine was designed to compress 15 liters of plasma to a volume of 1 liter. The inhomogeneous quasistationary magnetic field was mapped out by means of probes with the windings excited at 400 Hz; the results are presented graphically and discussed briefly. In an appendix there is a brief theoretical discussion of the stability of the plasma. (ATD)

22300 PRODUCTION OF A DENSE PLASMA IN A METAL CHAMBER BY A HIGH-FREQUENCY METHOD. Shvets, O. M.; Ovchinnikov, S. S.; Tarasenko, V. F.; Pavlichenko, O. S.; Tolok, V. T. Zh. Tekh. Fiz., 35: 2185-8(Dec. 1965). (In Russian).

Dense (up to 2×10^{14} cm^{-3}) plasmas were produced in a 12.5 cm diameter, 2 m long cylindrical copper chamber of 2.5 mm wall thickness with glass ends by exciting two 5 cm diameter, 7 cm long aluminum electrodes located 1 m apart on the axis of the chamber at 1.82 MHz with a 100 kw oscillator. A longitudinal magnetic field up to 2.5 kOe was provided by a suitable winding. The experiments are preliminary to a projected investigation of plasma heating by ion cyclotron waves. The plasma densities were determined from the Stark broadening of H_β, observed with a 1.3 m focal length spectrometer, and from reflection of 3 cm and 0.8 cm wavelength microwaves. Electron temperatures were determined from the intensity ratio of triplet to singlet helium lines. Plasma densities were also determined from the intensity of H_β on the assumption that excitation is entirely by electron impact; the densities so determined were in agreement with the values obtained from microwave reflection. Owing to the rectifying action of the plasma, the electrodes became negatively charged to a potential of several kilovolts; this gave rise to an oscillatory motion of the electrons near the axis of the chamber between the electrodes, as a result of which the dense plasmas were produced. The dense plasma was confined to a 2 cm diameter region about the axis; at 3 cm from the axis the plasma density was less by an order of magnitude. The plasma density did not depend strongly on the magnetic field strength. The maximum observed plasma density was 2×10^{14} cm^{-3} at a gas pressure of 3×10^{-3} mm Hg. The plasma density remained above 10^{13} cm^{-3} for 3.6 millisec, and above 10^{12} cm^{-3} for 17 millisec. Electron temperatures of 40 to 50 ev were observed. Advantages of the described technique are the low impedance, which eliminated difficulties associated with high-voltage r-f systems, and the good coupling between the electrodes and the plasma. (ATD)

22301 RADIAL CHARGED PARTICLE FLUX IN A DISCHARGE EXCITED BY HIGH-FREQUENCY TRAVELING

H WAVES. Kossyi, I. A. Zh. Tekh. Fiz., 35: 2189-93 (Dec. 1965). (In Russian).

In connection with the proposal of S. M. Osovets to confine a hot plasma by means of the field of a high-frequency traveling electromagnetic wave, the diffusion equations were solved to determine the radial flux and density distribution of charged particles in a weakly ionized plasma in the presence of traveling H waves. It was assumed that the frequency of the waves exceeds the ion Larmor frequency (so that the effect of the high-frequency field on the ion motions can be neglected), that the wavelength is much longer than the radius of the plasma filament, that the only radial force on the plasma due to the traveling wave is that arising from the radial gradient of the average magnetic pressure, and that the electron temperature is much higher than the ion temperature. Numerical solutions are presented graphically for a hydrogen plasma with an electron temperature of 10 ev and traveling wave field strengths from 70 to 200 Oe. These solutions are in agreement with experimental data of R. A. Demirkhanov et al. (Zh. Tekh. Fiz., 32: 1248(1962)). At a gas pressure of 0.1 mm Hg the radial flux of charged particles to the wall of a 2 cm radius chamber increases with increasing strength of the high frequency field up to a field strength of 200 Oe and decreases with further increase of the field strength. Contraction of the plasma can be expected in traveling H waves with field strengths exceeding 500 Oe. The presented solutions of the diffusion equations together with results obtained by R. A. Demirkhanov et al. (Zh. Tekh. Fiz., 35: 43(1965)) can be employed to estimate the effectiveness of traveling H waves as a means for confining hot plasmas. (ATD)

22302 FUSION RESEARCH. Hurwitz, H. Jr. (General Electric Co., Schenectady, N. Y.). New York, Inst. of Electrical and Electronics Engineers, 1965, Preprint No. 31 CP 65-775, 20P., $1.00. (CONF-650970-2). ORAU.

From National Power Conference, Albany.

A brief history of studies concerning exothermic reactions in the past thirty years is followed by a review of the general status of present investigations. Problems considered include the production of suitably strong magnetic fields, plasma production and heating, instabilities in plasma, and other problems pertaining to plasma confinement. Engineering and economic aspects of fusion power production are discussed briefly. (A.G.W.)

22303 CONDENSER DISCHARGING DEVICE. Seki, Yoshinaga (to Mitsubishi Electric Mfg. Co., Ltd.). Japanese Patent 1964-4585. Mar. 11, 1965. Filed Jan. 18, 1963.

An improved discharge circuit of high voltage condensers is proposed for supplying an electric current of large vertical steepness and of long duration to the load of inductive reactance in a pyroplasma generator, a large electric current generator, etc. In the proposed device adequately divided voltage is given to a series of electric valves with no leakage of the condenser load, and a short circuit of the load is formed when the discharge current of the condenser circuit, and its discharging circuit passes the peak. The condenser discharging circuit includes a plural number of condensers in series, inductive loads in series with the condensers through the making switchgear, a short-circuit switchgear parallel with the condensers or inductive loads a power source to charge these condensers, and a device to control the switching time of the two switchgears. Each of the condensers is charged corresponding to the impressed voltage of the above switchgears, and the corresponding parts of the switchgears are impressed by the charged voltage. (NSA of Japan)

Shielding

Refer also to abstracts 20838 and 20840.

22304 (AD-612031) UTILIZATION INSTRUCTIONS FOR GENERAL APPLICATION OF THE L05 MONTE CARLO PROCEDURE. Collins, D. G. (Radiation Research Associates, Inc., Fort Worth, Tex.). Nov. 1965. Contract DA-49-146-XZ-254. 32p. (AFRRI-CR-65-1).

Instructions for the utilization of L05, a Monte Carlo procedure for performing neutron and gamma ray penetration and scattering calculations on the IBM-7090, were rewritten to clarify and add detail to the previous instructions. The revised utilization instructions apply to the original L05 Code as well as to the RRA version of L05 which was modified to enhance its applicability to general shielding calculations. A description of the principal mathematical relations used by the code in the solution of neutron and gamma ray transport problems is included. Detailed definitions and formats for the input data which comprise problem deck and the energy and element library decks are given. In addition, peculiarities in the input data requirements discovered in extensive use of the code are discussed. General operational information for running the code on the IBM-7090 are also given. (auth)

22305 (AD-621441) MONTE CARLO CALCULATIONS OF GAMMA-RAY ALBEDO. Huddleston, Charles M.; Shoemaker, Nathan F. (Naval Civil Engineering Lab., Port Hueneme, Calif.). Sept. 7, 1965. 10p. (TN-N-764). CFSTI $1.00 cy, $0.50 mn.

A Monte Carlo computer program was used to generate values for the differential dose albedo of gamma rays on concrete. The values were fit to a semiempirical formula containing two adjustable parameters. Values for the parameters are reported as a function of gamma-ray energy. (auth)

22306 (CERN-65-32, pp 147-52) MUON FLUX MEASUREMENT IN THE NEUTRINO SHIELDING. Plass, G.; Wachsmuth, H. W. (European Organization for Nuclear Research, Geneva (Switzerland)).

Two groups of measurements of the flux of muons in the neutrino shielding are presented in order to assess the effectiveness of present shielding and to obtain a basis for any new shielding design. One set of measurements is taken at one depth for various momenta (21 Bev/c to 25.5 Bev/c) of the proton incident on the target. The other measurements are taken with the proton momenta being constant at three shielding depths. (B.G.D.)

22307 (DC-61-3-69) DATA REPORT OF RADIATION LEVEL MEASUREMENTS WITHIN AND BEHIND BERYLLIUM. Schreiber, P. W.; Kodras, F. D. (General Electric Co., Cincinnati, Ohio. Aircraft Nuclear Propulsion Dept.). Feb. 14, 1961. Contract AT(11-1)-171. 74p. Dep. mn. CFSTI $3.00 cy, $0.75 mn.

The data obtained from extensive shielding measurements, using beryllium slabs in the GE-ANPD Source Plate Facility at Battelle Memorial Institute, are reported. The measurements include fast neutron dose rates, thermal fluxes, gamma dose rates, resonance foil activations and threshold foil activations. Dose rate measurements and thermal flux measurements were made within a 32½-inch slab array of beryllium and in water behind various thicknesses of beryllium. Resonance foil measurements were made to a penetration of 16 inches of beryllium, and threshold foil measurements were made to a penetration of 12 inches of beryllium. (auth)

22308 (HASL-167) AN EXPERIMENTAL DETERMINATION OF DIFFERENTIAL ENERGY AND ANGLE SPECTRA FOR ^{137}Cs γ-RAYS IN SAND. Alberg, M.; O'Brien, K.; McLaughlin, J.; Lazanoff, A. (Health and Safety Lab., New York Operations Office (AEC), N. Y.). Feb. 1966. 35p. Dep. mn. CFSTI $2.00 cy, $0.50 mn.

Differential energy and angle spectra from a point isotropic ^{137}Cs source in an effectively infinite medium of sand were determined for γ-ray penetrations of 1, 2, and 3 mean free paths. The spectra were obtained from scintillation spectrometer measurements by an analytic method based on the Scofield iteration scheme. An integration of the results over all angles yielded differential energy spectra which are consistent with interpolated values of Goldstein and Wilkins' moments method calculations for aluminum. (auth)

22309 (ORNL-3041) SDC—A SHIELDING-DESIGN CALCULATION CODE FOR FUEL-HANDLING FACILITIES. Arnold, E. D.; Maskewitz, B. F. (Oak Ridge Na-

tional Lab., Tenn.). Mar. 1966. Contract W-7405-eng-26. 73p. Dep. mn. CFSTI $3.00 cy, $0.75 mn.

A simplified computer code, SDC, is presented for calculating the gamma-shielding requirements for chemical processing, fabrication, or fuel-handling facilities. It is a FORTRAN code designed for the IBM 7090 computer. SDC was designed to handle 13 source geometries (point, line, disk, plane, slab, cylinder with shield at side, cylinder with shield at end, sphere, ring, rod cluster, skew line, annular cylinder with shield at side, and annular cylinder with shield at end) either unshielded or shielded by slab shields. Materials of construction for shield, cladding, or source volume may be selected from a list of 17. As many as 12 gamma-energy groups, covering an energy range of 0.10 to 10 Mev, with corresponding source strengths, may be used to describe the gamma spectrum. Integration of the basic exponential attenuation-point kernel over the various geometries was the method chosen for calculating the uncollided gamma flux. Biological dose rate was obtained by multiplying this uncollided flux by the product of a flux-weighted buildup factor and a dose-conversion factor. (M.O.W.)

22310 (ORNL-RSIC-13) ABSTRACTS OF DIGITAL COMPUTER CODE PACKAGES ASSEMBLED BY THE RADIATION SHIELDING INFORMATION CENTER. Maskewitz, Betty F. (Oak Ridge National Lab., Tenn.). [nd]. Contract W-7405-eng-26. 212p. ORNL Free.

Abstracts on computer programs for calculating various shielding parameters are included. (M.O.W.)

Solid State Physics

See also CHEMISTRY — Inorganic and Physical Chemistry
METALS, CERAMICS, AND OTHER MATERIALS — Properties and Structure

Refer also to abstract 21135.

22311 (AD-622068) PROPERTIES OF RARE EARTH AND TRANSITION GROUP IONS. Final Report, April 1, 1963–June 30, 1965. Bleaney, B. (Clarendon Lab., Oxford Univ. (England)). July 10, 1965. Contract AF61(052)-677. 131p. (AFCRL-65-687). CFSTI $4.00 cy, $1.00 mn.

Results of research in the following areas are reported: growth and analysis of single crystals of rare-earth gallium and rare-earth aluminum garnets, lanthanum aluminate, thorium dioxide, calcium oxide, magnesium oxide, and various fluorides; optical absorption spectra of rare-earth ions in magnetic materials; specific heat and magnetic susceptibility of dysprosium and holmium trichlorides; nuclear magnetic resonance in manganese rubidium fluoride, manganese potassium fluoride, Tb, Dy, and Ho; ENDOR of Tb (4+) and Gd (3+) in thoria; EPR pair spectra of Tb, Ho, and Dy ethyl sulfates; magneto-optic effects in semiconducting diamond; ESR of silver chloride with Fe (2+) impurities and of U2 centers in KCl : H crystals; absorption spectra of H (–) and D (–) in calcium fluoride; and ENDOR of the ground state of Tm-169 (2+) in calcium fluoride. (TAB)

22312 (AD-622796) GROWTH AND CHARACTERIZATION OF SINGLE CRYSTALS OF RARE EARTH COMPOUNDS. Quarterly Technical Report No. 9. (Westinghouse Electric Corp., Pittsburgh, Pa.). 1965. Contract AF49(638)-1245. 8p. CFSTI $1.00 cy, $0.50 mn.

The electrical resistivities of the intra-rare-earth alloys of dysprosium were determined at 4.2, 77, and 296°K for a continued study of the impurity scattering of the conduction electrons. The resistivity data revealed that substitution of La, Ce, Pr, Nd, and Sm in Dy led to considerable increases in the residual resistivity Dy at low temperatures, but the increases disappeared at 296°K. The impurity-induced resistivities were predominantly due to the exchange scattering of the electrons via the Ruderman-Kittel type exchange interaction between the 4f and conduction electrons. The exchange scattering was found to depend only on the difference between the atomic spins of the solvent and solute ions, with the spin-orbit coupling playing an insignificant role. Neutron diffraction studies of the CrTe–CrSb solid solutions revealed the formation of a canted spin structure in the pseudo-binary system with cosine of the cant angle varying as a linear function of the composition. Work was continued on the electrical properties of EuS single crystals, Si-doped $CrBr_3$, and dilute alloys of Pd and Al containing Gd. A magnetic study was initiated of Mn_3ZnC. (TAB)

22313 (AD-624719) RARE EARTH–IRON EXCHANGE INTERACTION IN THE GARNETS. II. EXCHANGE POTENTIAL FOR YTTERBIUM. Levy, Peter M. (Pennsylvania Univ., Philadelphia. Dept. of Physics). Sept. 1965. Contract Nonr-551(36). 41p. (TR-26). CFSTI $2.00 cy, $0.50 mn.

To determine the magnitude of the anisotropy of the ytterbium–iron (Yb–Fe) exchange interaction, the exchange splittings of the lowest 2F (5/2) and 2F (7/2) doublets of ytterbium (Yb^{3+}) in ytterbium iron garnet were evaluated. By using the wave functions of Yb^{3+} in yttrium gallium garnet (those for YbIG are not known) these splittings are expressed in terms of ten parameters which characterize the anisotropy of the exchange interaction. As there are only six experimental splittings it is necessary to reduce the number of unknowns by assuming: that the rare earth-iron (RE–Fe) exchange interaction takes place through the neighboring eight oxygen ions, and (somewhat more uncertainly) that the rare earth–oxygen (RE–O) exchange interaction is axial about the Re–O axis. This leads to expressing the exchange splittings in two sets of four exchange constants. A good four parameter fit of the experimental exchange splittings was found by adopting essentially zero values for the rare earth-ferric ion exchange interactions that take place through the nearest neighbor oxygen ions (at 2.37 A). (auth)

22314 (AD-626865) GROWTH AND CHARACTERIZATION OF SINGLE CRYSTALS OF RARE EARTH COMPOUNDS. Quarterly Technical Report No. 10. (Westinghouse Research Labs., Pittsburgh, Pa.). 1964. Contract AF49(638)-1245. 6p. CFSTI $1.00 cy, $0.50 mn.

Magnetization measurements were made on the GdNd alloys to ascertain the mode of the spin coupling between a heavy and a light rare earth atom. The magnetic data substantiated the ferromagnetic spin coupling assumed in the Dekker theory of electrical resistivity of the rare earth alloys. It has been disclosed that the Dekker theory is inapplicable to approximately half of the possible intra-rare earth alloys. Its failure reflects a lack of understanding of the light rare earth ions. A remedy of the theory necessitates a major change of the analysis basing on the actual energy-level structure of these ions, which is not known at the present time. Low-temperature resistivities were determined of several Pd alloys containing solute atoms of Gd, Rh, and Fe. The electrical data reconfirmed the absence of the abnormally large spin-polarization effect of the localized moments of the Fe atoms in Pd. Experimental efforts were made to explore the possible occurrence of resistance minimum in the Pd–Gd alloys. The effects of local modes at the impurity centers were examined upon the scattering of electrons in aluminum between 4.2 and 300°K. (auth)

22315 (IS-1337) INTERPLANAR ANGLES AND PLANAR SPACINGS OF FIFTEEN TYPES OF PLANES FOR HCP YTTRIUM. Koepke, B. G.; Scott, T. E. (Ames Lab., Iowa State Univ. of Science and Tech.). Mar. 1966. Contract W-7405-eng-82. 70p. Dep. mn. CFSTI $3.00 cy, $0.75 mn.

A computer program in Fortran II language for the crystallographic angles in hcp yttrium was processed and the data tabulated. The data include 15 types of planes and all their equivalent planes, or a total of 109 sets of Miller-Bravais indices. Relevant d-spacings and an (0001) standard projection are also included. (auth)

22316 (JINR-P-2081) MATERIALY RABOCHEGO SOVESHCHANIYA PO NEUPRUGOMU RASSEYANNYU MEDLENNYKH NEITRONOV V KRISTALLAKH I ZHIDKOSTYAKH. (Proceedings of the Working Conference on Inelastic Scattering of Slow Neutrons in Crystals and Liquids, June 12–16, 1964, Dubna). (Joint Inst. for Nuclear Research, Dubna (USSR). Lab. of Neutron Physics). 1965. 68p. (CONF-640631). Dep. mn.

Eighteen of the 35 papers presented at the conference on inelastic scattering of slow neutrons are compiled. Some of the papers are in abstract form only. Neutron scattering by molecules, magnetic scattering of neutrons, experimental methods, and the utilization of slow neutrons for the investigation of the dynamics of crystals and liquids were discussed. (J.S.R.)

22317 QUANTUM STATISTICAL TREATMENT OF RELATIVE LIGHT INTENSITY OF NaI (PURE) CRYSTAL AS A FUNCTION OF ABSOLUTE TEMPERATURE. Hsu, Joseph; Kaiser, William C. (Argonne National Lab., Ill.). IEEE (Inst. Elec. Electron. Eng.), Trans. Nucl. Sci., NS-13: No. 1, 704-15(Feb. 1966).

An equation for the quantitative analysis of the relative light intensity of an excited diatomic cubic crystal as a function of absolute temperature is derived using the quantum statistical approach. (D.C.W.)

22318 RESPONSE OF CsI(Tl) CRYSTALS TO LOW-ENERGY HEAVY IONS. Lockwood, Grant J.; Cano, Gilbert L. (Sandia Lab., Albuquerque, N. Mex.). IEEE (Inst. Elec. Electron. Eng.), Trans. Nucl. Sci., NS-13: No. 1, 716-19(Feb. 1966).

The relative light output of thallium-activated cesium iodide was measured as a function of incident ion energy for ions of H, He, C, N, O, Ne, Ar, Kr, Xe, and Hg. Pulse height versus energy curves were obtained. In all cases studied, the relation of the pulse height to the incident ion energy is linear; the slope decreases as the mass is increased. The resolution (ratio of full width of the peak at half-maximum intensity to the peak central value) is approximately proportional to the inverse of the square root of the energy. (auth)

22319 LOW-ENERGY ELECTRON-DIFFRACTION STUDY OF MOLYBDENUM (110) SURFACES. Haas, T. W. (Aerospace Research Labs., Wright-Patterson AFB, Ohio); Jackson, A. G. J. Chem. Phys., 44: 2921-5(Apr. 15, 1966).

A study of the clean and oxygen-covered molybdenum (110) surface was carried out using low-energy electron-diffraction techniques. The clean surface is found to be the same as an ideal (110) plane in the bulk. Oxygen structures corresponding to $\frac{1}{4}$, $\frac{1}{2}$, and $\frac{3}{4}$ monolayer were found. These structures are very similar to those found for the tungsten (110) surface. Experiments on nitrogen and hydrogen adsorption are inconclusive due to interference from other residual gases (primarily carbon monoxide). (auth)

22320 SCATTERING OF SLOW NEUTRONS BY CRYSTALS CONTAINING MASS DEFECTS. Parlinski, Krzystof (Inst. of Nuclear Physics, Krakow). Postepy Fiz., 16: 667-79(1965). (In Polish).

Two types of experiments are feasible for neutron inelastic scattering by crystals with small concentrations of impurity atoms. They are the determination of the local frequency of oscillation (polycrystal), or the location of resonances (single crystal). These investigations are especially interesting in metals, where other methods do not give such detailed information. The physical fundamentals are reviewed for the case of low concentrations of impurity atoms, and some experimental results are discussed. (TTT)

22321 HARDENING OF SILVER-DOPED POTASSIUM CHLORIDE BY LOW-TEMPERATURE X-RAY IRRADIATION. Nadeau, John S. (General Electric Co., Schenectady, N. Y.). J. Appl. Phys., 37: 1602-8(Mar. 15, 1966).

Silver-doped KCl was much more susceptible than pure KCl to radiation hardening at low temperature. Pulse-annealing experiments showed that a large fraction of the hardening was caused by self-trapped holes, Cl_2^-. The silver ion that substitutes for the potassium ion in the structure performs the function of electron trap, thus stabilizing large numbers of isolated holes. The silver is relatively ineffective as a hardening agent in any of its several ionization states. This indicates that electric interactions between dislocations and point defects are not an important source of hardening in ionic crystals. Just as with metals, the strongest hardening effects are caused by elastic interactions. (auth)

22322 FORMATION AND BLEACHING PROPERTIES OF THE T BANDS IN KCl. Ring, James G.; Grossweiner, L. I. (Illinois Inst. of Tech., Chicago). Contract AT(11-1)-1052. J. Appl. Phys., 37: 1852-7(Mar. 15, 1966). (TID-22683).

Optical bleaching of additively colored or ^{60}Co irradiated KCl with "F light" and/or red light at 100°C produces three new absorption bands at 839 mμ (T_1), 894 mμ (T_2), and 992 mμ (T_3), which have been designated as "T bands." The most prominent T band is T_2, with a thermal stability exceeding the R and N bands and less than the M and F bands. Illumination of a crystal containing T bands at −195°C causes a temporary interconversion between the T_2 and T_3 bands, the direction depending on the spectral intensity of the ambient light. The transformation kinetics were investigated with 20-μsec pulse and steady bleaching techniques and were found to be of first order. The rate constants are linear functions of the light absorption rates in the T_2 and T_3 bands with significant dark contributions. The analysis indicates that the temporarily bleached T_2 and T_3 centers maintain a constant concentration ratio. The available information indicates that the T bands are due to distinct F-aggregate color centers, possibly isomers of F_5, and that the T_2 and T_3 centers are closely related in structure. (auth)

22323 ANNEALING OF E CENTER IN IRRADIATED SILICON. Hirata, Mitsuji; Hirata, Masako; Saito, Haruo (Osaka Univ.). Jap. J. Appl. Phys., 5: 252(Mar. 1966).

Isothermal annealing studies of irradiated crystals containing As, Sb, or Bi were made by the measurements of minority-carrier lifetime and resistivity. A typical annealing curve is shown from the results of the isothermal annealings of arsenic-doped crystals. The activation energy for the annealing of the Si−E center was found to increase with increased tetrahedral covalent radius of the impurity atom, and the relation between the covalent radii and activation energies was expressed as a linear function. (J.F.P.)

22324 DIELECTRIC PROPERTIES OF THIN FILMS OF PRASEODYMIUM, CERIUM, AND NEODYMIUM FLUORIDES. Bertulis, K. P.; Tolutis, V. B. (Inst. of Physics and Mathematics, Academy of Sciences, Lithuanian SSR). Lietuvos Fiz. Rinkinys, Lietuvos TSR Mokslu Akad., Lietuvos TSR Aukstosios Mokyklos, 5: 387-93(1965). (In Russian).

Some results of investigation of both effective dielectric constant (ϵ_{ef}) and dielectric losses of thin films of praseodymium (PrF_3), cerium (CeF_3) and neodymium (NdF_3) fluorides are presented. It was shown that the large values of ϵ_{ef} and the dependence of dielectrical losses vs temperature and frequency may be explained by the presence of the barrier layers under the electrodes. The effective impurity activation energies were determined to be: for PrF_3 0.5–0.6 ev, for NdF_3 and CeF_3 0.8–1.1 ev. The value of forbidden band of CeF_3, determined from the absorption measurements, is 4.85 ev, while the values for PrF_3 and NdF_3 seem to be close to the ones in the gap of 5.9–6.4 ev. The process of aging of ϵ_{ef} was investigated and the dependence of the breakdown field was determined according to the thickness of the films. (auth)

22325 ANGULAR RESOLUTION OF CRITICAL SCATTERING EXPERIMENTS. Gordon, Janos; Solyom, Jeno. Magyar Tud. Akad. Kozp. Fiz. Kut. Int. Kozlem., 14: 29-32 (1966). (In Hungarian).

Scattering of cold and thermal neutrons is a useful tool for investigating the behavior of magnetic materials in the vicinity of their Curie temperature. It is shown that the

angular distribution of the intensity approximates the cross section formula, if the vertical and horizontal angular divergence of the collimators applied is small as compared with the scattering angle. The correction is smaller than $(\epsilon_1/\theta)^2$, if $\epsilon_2 = 2\epsilon_1$, where ϵ_1 and ϵ_2 are the horizontal and vertical divergencies, respectively, and θ is the scattering angle. (auth)

22326 TEMPERATURE DEPENDENCE OF INTERNAL MAGNETIC FIELD. Dezsi, Istvan; Keszthelyi, Lajos; Kiss, Adam; Pocs, Lajos. Magyar Tud. Akad. Kozp. Fiz. Kut. Int. Kozlem., 14: 77-83(1966). (In Hungarian).

The temperature dependence of the internal magnetic field of ^{194}Pt produced by beta decay from ^{194}Ir in ferromagnetic 1% Fe–Ir alloy was investigated by perturbed gamma-gamma singular correlation experiments. Measurements were performed at three values of temperature, namely 24, 70, 737°C. The results were compared with the magnetization-versus-temperature curve of the alloy and the temperature dependence of the internal field was found to be essentially of the same shape as that of the magnetization. (auth)

22327 REVIEW OF ADVANCES IN PHYSICS. Ruby, S. L. (Argonne National Lab., Ill.). pp 13-20 of Moessbauer Effect Methodology. Vol. 1. Gruverman, Irwin J. (ed.). New York, Plenum Press, 1965.

Progress in use of the Mössbauer effect in the fields of magnetism, lattice dynamics, chemical structure, and nuclear physics is reviewed. It is concluded that much of the anticipated accomplishment with the Mössbauer effect still remains to be done and that, in general, the theorists are behind the experimentalists. (A.G.W.)

22328 NEW STRUCTURE IN THE ELECTRON SPIN RESONANCE SPECTRUM OF γ-IRRADIATED SINGLE CRYSTALS OF ICE. Dibdin, G. H. (Chelsea Coll. of Science and Tech., Eng.). Nature, 209: 394-5(Jan. 22, 1966).

Electron spin resonance spectra were obtained for single crystals of ice gamma irradiated and measured at 77°K. These spectra show structure for the resonance near g = 2, which is generally assumed to be due to OH radicals. Single crystals from both ordinary and heavy water were used in the experiments. Three examples of second-derivative and electronically integrated spectra, and the bond symmetry for each orientation are shown. The results suggest that the various orientations have a symmetry very similar to that of the hydrogen bonding of the lattice. (J.F.P.)

22329 HEAT TRANSPORT BY RADIATION IN SOLIDS. Engelmann, F.; Schmidt, H. E. Nucl. Sci. Eng., 24: 317-22(1966).

An expression for the effective thermal conductivity λ_{eff} of solids is derived, taking into account conduction by phonons and radiation, which displays the fact that λ_{eff} depends, generally in an involved manner, on temperature, temperature gradient, and the geometry of the experimental device. Explicit results are obtained in the limit of small temperature gradients, yielding a correction to the well-known radiation term proportional to T^3, which is frequently employed to explain the observed rise of the thermal conductivity of certain semiconductors and insulators at elevated temperatures. (auth)

22330 FREE ION HYPERFINE FIELDS IN INTERMETALLIC COMPOUNDS OF DYSPROSIUM. Nowik, I.; Ofer, S.; Wernick, J. H. (Bell Telephone Labs., Inc., Murray Hill, N. J.). Phys. Lett., 20: 232-3(Feb. 15, 1966).

Recoilless absorption spectra of the 26-kev γ-rays of ^{161m}Dy show that for all intermetallic compounds of Dy, except those containing Co or Fe, the value of H_{eff} acting on the Dy nuclei does not differ by more than 2% from the free-ion value. (auth)

22331 R CENTER LUMINESCENCE IN LiF. Baumann, G.; von der Osten, W.; Waidelich, W. (Technische Hochschule, Darmstadt, Ger.). Phys. Lett., 20: 579-81 (Apr. 1, 1966).

The 530 nm luminescence band and the luminescence zero phonon line at 487.5 nm in subtractively colored LiF are ascribed to an R center transition. The transition takes place between an energy level lower than the R_2 level and the ground state. (auth)

22332 PRESSURE-INDUCED CHANGES OF THE SPIN STRUCTURE IN EuSe. Busch, G.; Schwob, P.; Vogt, O. (Laboratorium fuer Festkoerperphysik, Zurich). Phys. Lett., 20: 602-3(Apr. 1, 1966).

A pressure of about 4 kbar is sufficient to suppress the intermediate spin structure of EuSe. Ferromagnetic exchange, as well as antiferromagnetic exchange or anisotropy forces seem to be enhanced by pressure. (auth)

22333 MAGNETORESISTIVITY OF METALS AT LOW TEMPERATURES. Seeger, A. (Max-Planck-Institut fuer Metallforschung, Stuttgart. Technische Hochschule, Stuttgart). Phys. Lett., 20: 608-9(Apr. 1, 1966).

A general expression for the low-temperature magnetoresistivity of metals is derived without assuming the existence of a relaxation time. The result allows fully for the anisotropy of both the Fermi surface and of the scattering mechanism. (auth)

22334 LUMINESCENCE OF FERROMAGNETIC EuSe. Busch, G.; Wachter, P. (Laboratorium fuer Festkoerperphysik, Zurich). Phys. Lett., 20: 617-19(Apr. 1, 1966).

When excited with green light EuSe shows a dark red luminescence at low temperatures. Near the Curie temperature and below the emission shifts to longer wavelengths and the intensity decreases. An applied magnetic field enhances the effect. (auth)

22335 THE NEGATIVE HYPERFINE FIELD IN HEXAGONAL COBALT METAL. A SPECIFIC HEAT METHOD FOR DETERMINING THE SIGN OF THE HYPERFINE FIELD IN A FERROMAGNET. Proctor, W.; Scurlock, R. G.; Wray, E. M. (Univ. of Southampton, Eng.). Phys. Lett., 20: 621-2(Apr. 1, 1966).

The $1/T^2$ nuclear contribution to the specific heat of hexagonal cobalt metal between 0.7° and 2.5°K was observed to decrease in magnetic fields up to 29.5 kOe. The sign of the hyperfine field is therefore negative in h.c.p. cobalt. (auth)

22336 MOESSBAUER STUDIES ON IRON IN THE PEROVSKITES $La_{1-x}Sr_xFeO_3$ ($0 \leq x \leq 1$). Shimony, Uri; Knudsen, Jens M. (Massachusetts Inst. of Tech., Cambridge). Phys. Rev., 144: 361-6(Apr. 8, 1966).

Mössbauer spectra of the perovskite series $La_{1-x}Sr_xFeO_3$ ($0.0 \leq x \leq 1.0$; $y \simeq 3$) with ^{57}Fe as the photon-emitting and -absorbing nucleus were analyzed. The Néel temperature of antiferromagnetic $LaFeO_3$ decreases with increasing Sr concentration. Characteristic Fe^{4+} lines for high x have isomer shifts between +0.10 and +0.20 mm/sec relative to a source of ^{57}Co in stainless steel. However, for intermediate x a $Fe^{3+ \leftrightarrow 4+}$ mixed state seems to exist. Increasing x causes a significant discontinuity in the total isomer shift (transition from magnetic order to disorder). Linewidths vary around 0.40 mm/sec and show broadening in a sample fired briefly. (auth)

22337 EMPIRICAL FERMI-SURFACE PARAMETERS FOR W AND Mo. Sparlin, D. M.; Marcus, J. A. (Northwestern Univ., Evanston, Ill.). Phys. Rev., 144: 484-94(Apr. 15, 1966).

Torsion measurements were made of the de Haas-van Alphen effect in tungsten and molybdenum. The results of these measurements are extremal cross-section areas of the Fermi surface and their corresponding cyclotron effective masses. These data are shown to be qualitatively interpretable in terms of orbits assigned to the various sheets of a Fermi-surface topology proposed by Lomer. A semiquantitative Fermi-surface model based on the Lomer topology is constructed and is shown to be compatible with the compensation of carriers, the connectivity of surfaces, the total surface area, the extremal dimensions, and the cyclotron effective masses reported by other investigators. (auth)

22338 FERMI SURFACE AND POSITRON ANNIHILATION IN YTTRIUM. Loucks, T. L. (Ames Lab., Ames, Iowa). Phys. Rev., 144: 504-11(Apr. 15, 1966). (IS-1264).

The electronic structure of yttrium was calculated at the equivalent of 6000 general points in the primitive Brillouin zone using the augmented-plane-wave method. The density of states and the Fermi surface are presented. The topology of the Fermi surface is discussed, and experimental results for de Haas-van Alphen measurements are predicted. Wave functions were also calculated for each of the occupied eigenvalues, and these were used to study the angular distribution of radiation resulting from positron annihilation in the metal. Few experimental results are currently available for comparison with this work. (auth)

22339 TRANSPORT PROPERTIES OF LaF_3. Sher, A.; Solomon, R.; Lee, K.; Muller, M. W. (Varian Associates, Palo Alto, Calif.). Phys. Rev., 144: 593-604(Apr. 15, 1966).

Measurements are reported of the lattice and bulk thermal expansion, fluorine nuclear magnetic resonance, and electric conductivity of single-crystal LaF_3 in the temperature range 300–1000°K. In the lower portion of this temperature range, the measurements yield activation energies for the formation of Schottky defects of ~0.07 ev and for fluorine ion diffusion of ~0.45 ev. The activation energy for diffusion appears to decrease at higher temperatures. A model is proposed for the crystal with low activation energy for the formation of neutral defects, and a higher energy for defect dissociation and diffusion. The apparent changes of activation energy are ascribed to the excitation of lattice vibrations near the Debye temperature. (auth)

22340 ON THE DISAPPEARANCE OF QUADRUPOLE SPLITTING IN THE MOESSBAUER SPECTRA OF ^{57}Co-CONTAINING AgCl AT 300 DEG K. Hennig, K. (Institut fuer Kristallphysik, Deutsche Akademie der Wissenschaften, Berlin); Meisel, W.; Schnorr, H. Phys. Status Solidi, 13: K9-14(Jan. 1, 1966). (In German).

The Moessbauer emission spectra of ^{57}Co-doped AgCl was measured at 80 and 300°K. The results are presented graphically and showed that the association $Fe_k \cdot G'_k$ between divalent iron at the cation site Fe_k and a cation gap G'_k is responsible for the quadrupole splitting observed in the spectrum. At 300°K $Fe_k \cdot G'_k$ is also present in detectable concentrations in addition to $Fe_k \cdot G'_k$. The previously known temperature dependence of the quadrupole splitting does not affect the disappearance of the splitting at 400°K. An explanation of this behavior can be based theoretically and followed experimentally by sufficiently fast motion of the cation gap around Fe_k. (J.S.R.)

22341 ATOMIC COLLISIONS IN CRYSTALS. Chadderton, Lewis T.; Torrens, Ian McC. (Cavendish Lab., Cambridge, Eng.). Sci. J., 2: 60-7(Mar. 1966).

The effects of radiation on atomic movement in a crystal lattice are considered. Computers are used to simulate this motion, and the effects are shown for various crystals. Channeling and focusing effects are considered. (J.F.P.)

22342 A PROPOSAL FOR THE AMPLIFICATION OF SOLID-STATE PLASMA WAVES WITH MASS ANISOTROPY. Hoefflinger, B. (Siemens and Halske A.G., Munich). Solid-State Electron., 8: 907-12(Dec. 1965). (In German).

Mathematical expressions are derived for the dispersion and amplification of transverse waves in drifting solid-state plasmas. The system is represented by the superposition of a wave in the hole plasma and an electron helix. It is found that a left circular-polarized wave near cyclotron resonance of the holes is amplified if both electron and hole cyclotron frequencies are large compared with their collision frequencies, and if the electron drift mobility is much higher than that of the holes. These conditions are fulfilled in a solid with special anisotropy of the effective electron and hole masses, e.g., in the trigonal direction of a bismuth single crystal. However the local theory presented here is only qualitatively applicable in this case since the electron Fermi velocity is much higher than the calculated drift velocity. (BBB)

22343 SOME MAGNETIC AND STRUCTURAL PROPERTIES OF GADOLINIUM–CERIUM ALLOYS. Pop, Iuliu. Stud. Univ. Babes-Bolyai, Ser. Math.-Phys., 10: No. 2, 101-4(1965). (In Rumanian).

The magnetic properties of Gd–Ce alloys were studied as a function of temperature and magnetic field. A linear relation was established between the magnetic properties and the crystalline structure data of the alloy systems in the sense that the diversity of the crystalline lattice types, proper to the Gd–Ce alloy system, determines an anomalous dependence very different from the isotherms of magnetization intensity as a function of the magnetic field. The existence of critical values H_c of the magnetic field was established. Because of the critical values of the magnetic field the magnetization intensity has discontinuities which are attributed to a spin structure, helicoidal or even more complicated in the alloys studied. (tr-auth)

22344 SPACE CHARGE IN PLASTICS BY LOW ENERGY ELECTRONS (REVISED). Caldecourt, V. J. 24p. (CONF-651028-3). ORAU. Gmelin, AED-CONF-65-310-4.

From Conference on Electrical Insulation, Buck Hill Falls, Pa.

An apparatus was devised for introducing a space charge into a polystyrene film, and various measurements were made in an attempt to explain the space charge phenomena. Net charge measurements show that polystyrene traps electrons. The gradual buildup of polarization of the film when subject to voltage suggests the gradual orientation of dipoles. Conductivity data and electric field decay curves indicate that the process changes abruptly at about 500 v. The resistivity decreases rapidly with increasing temperature. The Arrhenius plot shows a discontinuity between 40 and 60°C for data taken on biaxially oriented polystyrene film, correlating with the reported secondary phase transition at 50°C. The activation energies differ for the temperature ranges above and below the transition region. Polystyrene film subjected to a high voltage gradient appears to have trapped electrons near one surface and trapped holes near the other surface. Emission of electrons takes place at voltage gradients as low as 135 v/mil. (A.G.W.)

22345 DYNAMIC POLARIZATION OF PROTONS IN RADIATION-DAMAGED POLYETHYLENE. Hill, D. A.; Hwang, C. F. (Northwestern Univ., Evanston, Ill.). 11p. (CONF-651015-4). ORAU. Gmelin, AED-CONF-65-312-16.

From American Physical Society, Chicago.

Measurements of dynamic polarization of protons in radiation-damaged polyethylene were extended from 12.5 to 25 kG. A maximum polarization of 10% was found at 25 kG, 1.2°K, and an estimated radiation dose of 1.2×10^{17} n/cm^2. The following characteristics of polyethylene disks irradiated by the fast neutron flux of Argonne reactor facilities for periods ranging up to 10 days were also measured as a function of radiation dose: the EPR spectrum, the concentration of radiation-damage centers, and the electron longitudinal relaxation time. It is concluded that the main limitations on proton polarization are the phonon bottlenecking of the electron relaxation time and the inability of the irradiation techniques employed to produce larger center concentrations without oxidation damage to the polyethylene. (A.G.W.)

22346 RADIATION DAMAGE STUDIES IN DEGENERATE Si, IRRADIATED AT LOW TEMPERATURES. Sivo, L. L.; Klontz, E. E. 12p. (CONF-651015-2). ORAU. Gmelin, AED-CONF-65-312-2.

From American Physical Society, Chicago.

The results of low temperature radiation damage studies for the following types of degenerate Si are reported: pulled or Czochralski n-type with oxygen content of about 10^{18}/cc, floating zone n-type with oxygen content of about 10^{16}/cc, pulled p-type, and floating zone p-type. The samples were irradiated with 1 mev electrons at temperatures ranging from 7°–110°K and changes in dc σ and R_H measurements were observed. The samples were chosen with highly different oxygen content to show the influence of the σ on the defect formations, if any. The n-type degenerate samples were considerably less affected by the low temperature irradiation than the p-type ones. The defect type structure for the samples have not been identified, but apparently oxygen plays no direct role in it. (B.L.M.)

REACTOR TECHNOLOGY

General

Refer also to abstracts 20957, 21097, 21224, 21785, 21786, and 22466.

22347 (ANL–7138) CATALOG OF NUCLEAR REACTOR CONCEPTS. PART I. HOMOGENEOUS AND QUASI-HOMOGENEOUS REACTORS. SECTION IV. REACTORS FUELED WITH LIQUID METALS. Teeter, Charles E.; Lecky, James A.; Martens, John H. (Argonne National Lab., Ill.). Jan. 1966. Contract W-31-109-eng-38. 86p. Dep. mn. CFSTI $3.00 cy, $0.75 mn.

Data sheets are presented which give brief descriptions of liquid metal fueled reactors. (M.O.W.)

22348 SHOCK FRONT CONDITIONS IN TWO-PHASE FLOW INCLUDING THE CASE OF DESUPERHEAT. Fischer, M.; Haefele, W. (Kernforschungszentrum, Karlsruhe, Ger.). 35p. (CONF-651009–10). ORAU. Gmelin, AED-CONF-65-307-5.

From Conference on Safety, Fuels and Core Design in Large Fast Power Reactors, Argonne, Ill.

The time characteristic for the expulsion of coolant from the channels of a large fast sodium-cooled reactor during a power excursion is considered theoretically. The appearance of shock front phenomena brings the expulsion process to a time scale dictated by the velocity of sound, because after having passed a shock front the velocity of the medium is subsonic. Therefore, calculations of both the velocity of sound in the medium and shock front conditions are undertaken. The effects of changes of phase in shocks and of superheating and desuperheating are also considered. It is concluded that an overall effective expulsion velocity could be in the order of at least 4 m/sec and at most 60 m/sec. (A.G.W.)

22349 LOSS-OF-COOLANT ACCIDENTS IN A LARGE SODIUM-COOLED FAST REACTOR. Judd, A. M. (United Kingdom Atomic Energy Authority, Winfrith, Eng.). 33p. (CONF-651009–16). ORAU. Gmelin, AED-CONF-65-307-14.

From Conference on Safety, Fuels, and Core Design in Large Fast Power Reactors, Argonne, Ill.

In an analysis of accidents in a typical oxide-fueled, sodium-cooled fast reactor, some mechanisms important for several of the accidents are first considered in detail. These include behavior of the coolant as it boils, the release of fission-product gas from a burst fuel can, and coolant and fuel reactivity worth. These results are then used in following specific accidents initiated by faults affecting either a single subassembly or the whole core. Initial faults in a single subassembly considered are restriction of coolant flow, sudden complete failure of coolant flow, and local coolant blockage affecting a small amount of fuel. Also considered are whole-core accidents initiated by coolant circulating pump failure and sudden complete coolant flow failure occurring while the reactor is operating at power. It is concluded that particularly important problems in reactor safety include the possibility of a single subassembly accident spreading to the whole core and the time available for a trip mechanism to operate. (A.G.W.)

22350 COOLANT EJECTION STUDIES WITH ANALOGY EXPERIMENTS. Griz, G. (EURATOM-CCR, Ispra, Italy). 12p. (CONF-651009–11). ORAU. Gmelin, AED-CONF-65-307-7.

From Conference on Safety, Fuels, and Core Design in Large Fast Power Reactors, Argonne, Ill.

The ejection of primary stagnant coolant from a single vertical reactor channel as a consequence of a sudden depressurization was studied in an analogy experiment using water as the test liquid. A liquid column closed at the top by a thin plastic diaphragm was pressurized up to 4 atm. The diaphragm was ruptured and the process was observed by taking high-speed movies. A qualitative picture of the ejection process was obtained from the film, and the medium velocity of the acceleration front formed was measured. Calculations based on various theoretical assumptions are compared with the experimental observations. (A.G.W.)

Auxiliaries and Components

Refer also to abstracts 20792 and 21047.

22351 (AD–623020) TRANSPIRATION COOLING WITH LIQUID METALS. PART II. THEORETICAL DETERMINATION OF OPTIMUM COOLING PARAMETERS NEAR STAGNATION REGIONS. Thielbahr, William H. (Naval Ordnance Test Station, China Lake, Calif.). Aug. 1965. 68p. (NAVWEPS–8732-P2). CFSTI $3.00 cy, $0.75 mn.

Three cooling mechanisms associated with liquid metal transpiration near stagnation regions were investigated theoretically. The cooling mechanisms considered were boundary layer shielding, heat absorption by vaporization, and heat absorption within the matrix as coolant travels under the action of some pressure force to the hot surface. Optimum coolant flow rate necessary for complete vaporization of liquid coolant at the hot wall was derived from knowledge of these mechanisms. Lithium, tin, and copper were the metal coolants investigated, with gaseous helium being included for comparative purposes. Tungsten was the matrix material for all coolants. Results of this analysis demonstrate that each coolant's effectiveness depends on the magnitude of the heat flux. In general, low melting point is the desirable coolant property at low and intermediate heat fluxes, while low molecular weight and high heat of vaporization become the important properties at high heat fluxes. (auth)

22352 (AEET-ED-SG/25) RESULTS OF TEST OF CONNECTORS USED IN SEMICONDUCTOR LOGIC MODULES. Krzycki, Andrzej (Atomic Energy Establishment, Trombay (India)). Dec. 10, 1964. 8p. Dep. mn.

The semiconductor safety and interlock system for Apsara reactor uses plug-in type logic modules. Because of the possibility of frequent plugging and unplugging of the connectors it was decided to perform a test which would give the average number of successful operations of a pair of connectors. In addition, a test of long-time operation (plug inserted into receptacle) was performed. The results of the tests are described. (M.O.W.)

22353 (CEA-R–2829) COMPORTEMENT D'UN CAISSON EN BETON PRECONTRAINT SOUMIS A UN GRADIENT DE TEMPERATURE ELEVE. (Behavior of a Pre-Stressed Concrete Pressure Vessel Subjected to a High-Temperature Gradient). Dubois, Frederic; Bonvalet, Charles; Dawance, Guy; Marechal, Jean-Claude (Commissariat a l'Energie Atomique, Saclay (France). Centre d'Etudes Nucleaires). Dec. 1965. 97p. Dep. mn.

After a review of the problems presented by pressure-vessels for atomic reactors (shape of the vessel, openings, foundations, etc.) the advantages of prestressed concrete vessels with respect to steel ones are given. The use of prestressed concrete vessels, however, presents many difficulties connected with the properties of concrete. Thus, because of the absence of an exact knowledge of the material, it is necessary to place a sealed layer of steel against the concrete, to have a thermal insulator or a cooling circuit for limiting the deformations and stresses, etc. It follows that the study of the behavior of prestressed concrete and of the vessel subjected to a high temperature gradient can yield useful information. A one-tenth scale model of a prestressed concrete cylindrical vessel without any side openings and without a base was built. Theoretical

aspects concerning scale model-actual structure similitude conditions and the calculation of the thermal and mechanical effects are discussed. The prestressed concrete model was heated internally by a pyrotenax element and cooled externally by a very strong air current. The concrete was prestressed using horizontal and vertical cables held at 80 kg/cm^2; the thermal gradient was 160°C. During the various tests, measurements were made of the overall and local deformations, the changes in water content, the elasticity modulus, the stress and creep of the cables and the depths of the cracks. The overall deformations observed are in line with thermal deformation theories and the creep of the cables attained 20 to 30% according to their position relative to the internal surface. The dynamic elasticity modulus decreased by half but the concrete retained its good mechanical properties. Finally, cracks 8 to 12 cm deep and 2 to 3 mm wide appeared in that part of the concrete which was not prestressed. The results obtained make it possible both to draw up a program for future tests and to propose a calculation model for prestressed concrete pressure-vessels. (auth)

22354 (CEND–3336-260) DEVELOPMENT AND TESTING OF A TEMPERATURE TRANSIENT METHOD FOR PERFORMING IN-PILE THERMAL CONDUCTANCE TESTING. Final Summary Report, March 1, 1964–November 30, 1965. Burdg, C. E.; Parrette, J. R.; Brockett, R. I.; Chernock, W. P. (Combustion Engineering, Inc., Windsor, Conn. Nuclear Div.). Jan. 1966. Contract AT(30-1)-3336. 98p. (EURAEC–1567). Dep. mn. CFSTI $3.00 cy, $0.75 mn.

Work Performed under United States–Euratom Joint Research and Development Program.

The objective of the program was to develop a method of measuring the effective thermal conductivity of an operating nuclear fuel element, by analysis of the transient temperature response at the surface of the cladding following a change in the power level. The two-phase study was designed to first conduct out-of-pile experiments to demonstrate feasibility of the methods, followed by in-pile confirmation. Concurrent mathematical analyses of the thermal models provided the bases for data interpretation as well as guides for the design of the experiments. The various experiments performed and their results are discussed. (M.O.W.)

22355 (LA–3470) FISSION COUPLES APPLIED TOWARD REACTOR DIAGNOSTICS AND SAFETY. Morrison, R. G.; Stillman, D. B. (Los Alamos Scientific Lab., Univ. of California, N. Mex.). Jan. 15, 1966. Contract W-7405-eng-36. 31p. Dep. mn. CFSTI $2.00 cy, $0.50 mn.

A technique was developed for the Kiwi Transient Nuclear Test which used fissile material as a sensing element for reactor transient measurements and detailed fuel studies. This was done by welding very small thermocouple leads to the actual fuel material and forming an "intrinsic" junction. The response of this sensor has given accurate measurements of the reactor periods as short as 15 μsec. A hypothesis is discussed that the heat produced by fission fragments in the fissile material can be monitored with sufficient accuracy to form a direct measurement of reactor power. (auth)

22356 (ORNL–3929) PARALLEL-PLATE MULTISECTION IONIZATION CHAMBERS FOR HIGH-PERFORMANCE REACTORS. Roux, D. P. (Oak Ridge National Lab., Tenn.). Apr. 1966. Contract W-7405-eng-26. 19p. Dep. mn. CFSTI $2.00 cy, $0.50 mn.

A new model of parallel-plate multisection ionization chambers was developed for reactor control applications in high-performance reactors. This chamber model has several improved performance features required by such reactors, and, in addition, the arrangement of the chamber allows the combination of diffcrent active sections in a single reactor penetration. Each active section is comprised of parallel-plate electrodes, each 1.8 in. in diameter and 0.005 in. thick. The electrodes are coated with ^{10}B for use as neutron-sensitive chambers, with ^{235}U for use as fission chambers, or left uncoated for use as gamma-sensitive chambers. Also, a gamma-compensated neutron-sensitive chamber can be made by using boron-coated and uncoated electrodes (appropriately coated and connected). A new electrode configuration is used to achieve an electrically adjustable gamma compensation. This compensation technique has the advantage over methods previously used, in that both the neutron- and gamma-section currents are well saturated at all polarizing voltages ordinarily used, and thus, electrical compensation is not obtained at the expense of saturation. Experimental results show the insensitivity of the gamma compensation to wide variations in intensity, energy, and geometry of the gamma background. (auth)

22357 (RT-FI–(65)50) SUL PROBLEMA DELLA OMOGENEIZZAZIONE DELLE BARRE DI CONTROLLO CRUCIFORMI IN UN REATTORE MODERATO AD ACQUA. (On the Problem of Homogenization of Cruciform Control Rods in a Water Moderated Reactor). Marchesi, F. (Comitato Nazionale per l'Energia Nucleare, Rome (Italy)). Nov. 1965. 12p. Dep. mn.

The area absorption method was used in some reactors in order to check the validity range. In some cases the results were not satisfactory both for the equivalent quantity of homogeneous poison and the macroscopic peak factor. (auth)

22358 SOME ASPECTS OF REACTOR SAFETY SYSTEMS. Wenzinger, Edward C. (Bureau of Yards and Docks, Washington, D. C.); Scholl, Raymond F.; Fort, Robert E. IEEE (Inst. Elec. Electron. Eng.), Trans. Nucl. Sci., NS-13: No. 1, 426-37 (Feb. 1966).

The importance of system engineering and of establishing the levels of safety and availability required for reactor installations are discussed. Safety system logic schemes, operator confidence in the equipment, and protection against the effects of chance failures in safety circuits are considered. (auth)

22359 A TRANSISTORIZED a-c CARRIER-TYPE SHUTDOWN AMPLIFIER AS A PROTECTIVE DEVICE IN NUCLEAR POWER STATIONS. Ahmed, Muhammad I. (Rank Research Labs., London). IEEE (Inst. Elec. Electron. Eng.), Trans. Nucl. Sci., NS-13: No. 1, 589-95 (Feb. 1966).

A description of the shutdown amplifier and its operation is presented. The design requirements on shutdown amplifiers are outlined. (D.C.W.)

22360 A COMPARISON OF SOLID STATE AND RELAY REACTOR SAFETY SYSTEMS. O'Sullivan, George A. (Nuclear Utility Services, Inc., Washington, D. C.). 16p. (CONF-651001–20). ORAU. Gmelin, AED-CONF-65-293-10.

From IEEE Nuclear Science Symposium, San Francisco.

The merits of both relay logic safety systems and solid state logic systems are discussed. Both individual and mixed logic systems are considered. Circuit diagrams are shown for each type of system. Each of the four logic systems are evaluated on the basis of nine criteria: perform when required with any single fault, independence of redundant channels, freedom from false scrams, speed of response, ease of testing, ease of maintenance, ease of annunciation, simplicity, and cost. Each criterion can be weighed according to the particular application for which a system is being chosen. (A.G.W.)

22361 FLOW RESTRICTOR. Pendleton, Joseph Raymond; Beard, John (to United Kingdom Atomic Energy Authority). British Patent 1,020,668. Feb. 23, 1966. Filed Feb. 24, 1964.

A flow restrictor designed to restrict the flow of coolant through a nuclear reactor comprises a tubular coolant duct and a pair of concentric, tubular bellows within the duct that are sealed together at each end to define an open central coolant flow channel and an expansible fluid-filled interspace between the bellows. An anchorage is provided between one end of the pair of bellows and the coolant duct. A throttle is carried by the coolant duct to regulate the

flow of coolant through the duct, and a link provided between the throttle and the end of the bellows remote from the anchorage renders the throttle aperture responsive to the bellows movement and thus responsive to coolant temperature changes. (B.L.M.)

22362 IMPROVEMENTS IN OR RELATING TO NUCLEAR REACTOR CORE STRUCTURES. Blake, Gordon (to United Kingdom Atomic Energy Authority). British Patent 1,021,034. Feb. 23, 1966. Filed Nov. 1, 1963.

A nuclear reactor core comprises first and second support plates with fuel assemblies in parallel array mounted substantially perpendicular to both support plates. Each fuel assembly has one end located in the first core support plate and at the other end a spindle extends through the second support plate. A resilient armed latch member is slidable on the spindle between a latched position within the second core support plate and an unlatched position. The resilient means is retained on the spindle and tends to drive the latch member toward the fuel assembly; so that, with the latch in the latched position, the fuel assembly is retained against the second support plate by the force exerted by the resilient means on the latch member. (B.L.M.)

22363 COUPLING FOR FUEL AND/OR MODERATOR ELEMENTS OF A NUCLEAR REACTOR. Zimmermann, Heinrich (to Interatom Internationale Atomreaktorbau GmbH). German Patent 1,206,097. Dec. 2, 1965. Filed July 24, 1962.

The coupling comprises at least three radially directed and movable levers pivotally fastened to an axially movable tubular actuating element located in the axis of moderator element. The levers are provided with spherical heads which are arranged to engage with corresponding recesses in the upper head of the fuel element. (Gmelin Inst.)

22364 ARRANGEMENT FOR THE TRANSLATION OF A SHORT PATH LENGTH INTO A LONG ONE FOR THE CONTROL OF THROTTLE VALVES IN THE COOLANT FLOW OF NUCLEAR REACTORS. Arndt, Horst (to VEB Atomkraftwerk Rheinsberg mit Betriebsteil). German Patent 1,206,100. Dec. 2, 1965. Filed Apr. 13, 1960.

The arrangement given comprises a ring element located within the coolant channel which is provided with a roller on a bearing block attached to the ring element, and a cam plate attached to the throttle valve which is in engagement with the roller. Twisting of the ring element effects the inclination of the throttle valve. (Gmelin Inst.)

22365 DEVICE FOR THE CONTROL OF NUCLEAR REACTORS BY MEANS OF NEUTRON-ABSORBING LIQUIDS. Knecht, Othmar (to Interatom Internationale Atomreaktorbau GmbH). German Patent 1,206,101. Dec. 2, 1965. Filed Oct. 12, 1960.

The device comprises a plurality of upright tubes extending into the core and communicating with a container exterior to and above the core, a body of liquid, neutron absorbing metals, and pumps for varying the height of the liquid metal in the tubes. (Gmelin Inst.)

22366 NUCLEAR REACTOR CONTROL ROD DRIVE MECHANISM. Fortescue, Peter; Bell, Francis R.; Harris, Arthur M. (to General Dynamics Corp.). U. S. Patent 3,232,841. Feb. 1, 1966. Filed May 6, 1963.

An apparatus is patented for use with a nuclear reactor having a vertically movable control rod that during an emergency is inserted to its full length or to a sufficient depth so as to stop the reaction until the emergency can be corrected. The control rod is suspended by a cable to which a flywheel is geared, and a motor is connected to the cable by means that include a clutch for adjusting the height of the rod. In case of an emergency, the clutch disengages the control rod. The patented device disengages such a clutch and then uses a percentage of the potential energy of the falling rod to effect rotary movement of the fly wheel. This percentage of the energy is automatically increased during the fall of the rod by the automatic increasing of the effective inertia of the wheel itself during the fall. The gearing is disconnected at about the time when the rod reaches its bottom position in the reactor so as to permit the wheel to coast free from the rod and to remove from the rod system the kinetic energy absorbed by the flywheel. (B.L.M.)

22367 FILM BOILING INDICATOR. Ogle, Hugh M. (to General Electric Co.). U. S. Patent 3,234,100. Feb. 8, 1966. Filed May 8, 1961.

A film boiling indicator for a liquid cooled reactor is based on the change in type of radiation from the fuel elements when boiling occurs. During normal operation, the fuel elements emit radiation in the visible region of the spectrum; however, when film boiling occurs, the elements emit red radiation made up of more visible radiation in the red region of the spectrum and infrared radiation. Detectors sensitive to this red radiation are positioned to view the fuel elements in the reactor and upon detection of the red radiation indicating the approach of some fuel elements to an unsafe operating condition may actuate an audio alarm or may automatically reduce the power level of the reactor to a safe level. (B.L.M.)

22368 NUCLEAR REACTOR CONTROL ROD HAVING PARTICULATE CORE. Gale, Richard H.; Burdg, Charles E. (to Combustion Engineering, Inc.). U. S. Patent 3,234,104. Feb. 8, 1966. Filed Dec. 30, 1963.

A blade type control rod for a nuclear reactor includes a number of blade members extending radially outward from a common axis. Each blade is formed of sheet metal members that are maintained in accurately spaced relation by indentions formed on one of the members extending toward and engaging the other, with the members bonded together at these points of contact. A loose particulate material containing a neutron poison is dispersed in the volume between the plates and compacted to a density of about 75% of theoretical. (B.L.M.)

22369 FUEL ELEMENT HOLD-DOWN ARRANGEMENT FOR NUCLEAR REACTORS. McDaniel, Weymouth N.; Amorosi, Alfred (to Atomic Power Development Associates, Inc.). U. S. Patent 3,235,465. Feb. 15, 1966. Filed May 16, 1961.

A fuel element hold-down arrangement is patented for a reactor in which the reactor vessel has a lower inlet and an upper outlet for circulation of a liquid coolant upward through the vessel and in which a support plate spans the reactor vessel and divides it into lower and upper plenums communicating with the inlet and outlet, respectively. A series of tube-encased fuel element subassemblies are removably supported in upstanding relation on the plate. The tubes have tapered lower ends of downwardly and progressively decreasing section projecting through apertures of the plate into the lower plenum. The lower end of the tube seats on a fixedly mounted plug to coact to form a converging–diverging inner tubular wall opening into the lower plenum. The tube and the plug are separable at the throat of the inner tubular wall. (B.L.M.)

Criticality Studies

22370 (AD–621021) MULTI-GROUP DISCRETE SN TRANSPORT CALCULATION FOR CYLINDRICAL GEOMETRY [Thesis]. Saqui, Ronald M. (Air Force Inst. of Tech., Wright-Patterson AFB, Ohio. School of Engineering). May 1965. 115p. (GNE-Phys-65-17). CFSTI $4.00 cy, $0.75 mn.

A computer code is presented for neutron transport calculations on a cylindrical geometry, gaseous core, nuclear rocket. The code is applied to a simplified reactor system model consisting of a two region right cylindrical cavity core with an effective temperature of 3980K. The calculations are performed using a five energy group, discrete S4 approximation of the Boltzmann equation. The cylindrical form of the Boltzmann equation is developed in detail. Application of the discrete Sn approximation to obtain the finite difference equations and the boundary conditions is shown. An iterative procedure having the total fission source production as the eigenvalue is used by the computer code to solve these equations numerically. This

code is written in Fortran IV language for the IBM 7094 coupled system. The atom density results of the two systems tested are within 2.5% and 0.6% agreement with those of another code written by T. F. Plunckett of Douglas Aircraft. Although these results are good, variations in the multiplication factor and the inability to significantly effect this factor by small changes in system parameters leads to the conclusion that further tests of the code are required before it may be used in the analysis of the propulsion device. (auth)

22371 (AD-621026) DETERMINATION OF THE THERMAL NEUTRON FLUX DISTRIBUTION IN A HEXAGONAL LATTICE CELL [Thesis]. Fleming, Paul Byron (Air Force Inst. of Tech., Wright-Patterson AFB, Ohio. School of Engineering). Aug. 1965. 157p. (GNE-Phys-65-6). CFSTI $5.00 cy, $1.00 mn.

Thermal neutron flux distributions were obtained in hexagonal and square lattice cells by a finite difference approximation to the diffusion equation. The grid network used to approximate the lattice cells was created from a combination of cylindrical and cartesian coordinate systems to facilitate the handling of the normal boundary conditions at the rod surface. Square lattice cell flux distributions for nonabsorbing media compare favorably to those predicted in an analytic solution by Cohen. Marked deviations in this result occur as absorption is increased. Hexagonal and square cell flux distributions agreed within 1.5 per cent to the results predicted by the cylindricalization technique at interior points in the cell for all cases of absorption studied. Large deviations in flux distributions along the cell boundaries indicate that errors may arise in calculations of the thermal utilization based upon the cylindricalization assumption. Deviations in all results near the rod surface are attributed to truncation error or normalization technique. (auth)

22372 (AFRRI-TN-65-1) A DETAILED DERIVATION OF THE COURANT-WALLACE EXPRESSIONS FOR THE SECOND MOMENTS OF THE NEUTRON PROBABILITY DISTRIBUTION AND FOR THE VARIANCE/MEAN RATIO. Schow II, Horace (Armed Forces Radiobiology Research Inst., Bethesda, Md.). Oct. 1965. 34p.

A detailed mathematical derivation and verification of the three Courant-Wallace expressions, which have the three second moments of the neutron probability distribution in a pile as the three unknowns, are given. The solution of these equations for a steady pile with one equivalent delayed neutron group for the variance/mean ratio is verified. Minor corrections to the original Courant-Wallace text are noted. (auth)

22373 (BNWL-193) PHYSICS RESEARCH QUARTERLY REPORT, JULY, AUGUST, SEPTEMBER 1965. (Battelle-Northwest, Richland, Wash. Pacific Northwest Lab.). Oct. 15, 1965. Contract AT(45-1)-1830. 65p. Dep. mn. CFSTI $3.00 cy, $0.75 mn.

Separate abstracts were prepared for the 6 included sections. (M.O.W.)

For abstracts of individual sections see: 20840, 21938, 22374, 22375, 22493, and 22494.

22374 (BNWL-193, pp 5-15) MODIFICATIONS TO THE COMPUTER CODE, THERMOS, AND COMPARATIVE STUDIES ON SCATTERING KERNELS. Worden, J. R.; Purcell, W. L.; Liikala, R. C. (Battelle-Northwest, Richland, Wash. Pacific Northwest Lab.).

The options available at Battelle-Northwest for calculations using THERMOS are described. The modifications have proven useful and are summarized since similar changes may be of use at other laboratories. The method by which cross section data are obtained and prepared for THERMOS and an extended version of THERMOS available for use on the Univac 1107 are described. Finally, scattering kernels in use for the common moderating materials are described along with a summary of the results of some comparative studies on the effect of the choice of scattering model on calculated reactor parameters. (M.O.W.)

22375 (BNWL-193, pp 45-56) MEASUREMENTS OF MATERIAL BUCKLINGS FOR 1.002, 1.25, AND 1.95 WT PERCENT ^{235}U ENRICHED URANIUM TUBE LATTICES IN LIGHT WATER. Brown, C. L.; Lloyd, R. C. (Battelle-Northwest, Richland, Wash. Pacific Northwest Lab.).

Material bucklings and extrapolation distances were measured for light water lattices of 1.002, 1.25, and 1.95 wt % ^{235}U enriched uranium tubes, and 1.002 wt %/1.002 wt % and 1.25 wt %/0.95 wt % ^{235}U enriched uranium tube-in-tube assemblies. Detailed results are presented. (M.O.W.)

22376 (GA-6901) THE ROLE OF THERMAL SPECTRUM MEASUREMENTS IN REACTOR DESIGN. Neill, J. M.; Young, J. C. (General Atomic, San Diego, Calif. John Jay Hopkins Lab. for Pure and Applied Science). Jan. 14, 1966. Contract AT(04-3)-167. 28p. Dep. mn. CFSTI $2.00 cy, $0.50 mn.

It was shown that thermal spectral measurements are extremely useful in checking the data and methods used in thermal reactor calculations. It is clear that numerical errors play a large part in the uncertainties in the thermal scattering kernels. These errors are in addition to the approximations in the scattering models and they can be detected many times in spectral data. A degree of sensitivity of reactor parameters to the choice of scattering model for graphite and beryllium was demonstrated. For the most part this choice has consisted of the free gas model and just one bound model. It is suspected that reactor calculations may not be sensitive to refinements in the scattering model, but remain sensitive to numerical errors in generating the scattering kernel, to cross section data, and to the certain other items. Therefore, the thermal spectral measurements play a useful part as a reactor design aid. (auth)

22377 (GA-6930, App. B) THE INFLUENCE OF THERMALIZATION MODELS ON THE REACTIVITY AND TEMPERATURE COEFFICIENT OF ZIRCONIUM HYDRIDE REACTORS. West, G. B. (General Atomic, San Diego, Calif. John Jay Hopkins Lab. for Pure and Applied Science). 29p. (GA-6847).

Three different thermalization models for hydrogen as bound in zirconium hydride, H(ZrH), are investigated with regard to their influence on the reactivity and temperature coefficient of two different reactor systems: a TRIGA Mark III, where neutrons are moderated both by zirconium hydride and water, and an all-hydride system characteristic of the SNAP reactors. The thermalization models used are a free gas model and two versions of the Einstein oscillator model; one of the Einstein models uses a discrete value for energy exchange, and the other, newer model, incorporates a frequency distribution. Results show variations of up to ~2% in reactivity for an infinite medium TRIGA-type lattice, which would also be reflected in any k_{eff} calculations. Infinite medium SNAP-type cores, with their much harder thermal neutron spectrum, show variations in k_∞ with model of ~.3% while the reflected cores give differences of up to ~1% in k_{eff} depending on the reflector material. Temperature coefficients showed variations of up to ~50% in both systems. (auth)

22378 (KFK-367) THEORIE DER DOPPLERKOEFFIZIENTEN SCHNELLER REAKTOREN UNTER BERUECKSICHTIGUNG DER GEGENSEITIGEN ABSCHIRMUNG DER RESONANZEN. (Theory of Doppler Coefficients of Fast Reactors with Consideration of Self Shielding of Resonances). Froelich, Reinhard (Kernforschungszentrum, Karlsruhe (West Germany)). Nov. 1965. 81p. Dep. mn.

The formulas for the calculation of the Doppler coefficients of fast reactors with consideration of the mutual shielding of resonances are derived. General considerations on the calculation of the Doppler coefficients of fast reactors are given. The neutron effective cross section and the resonance parameters are derived. The basic formulas of reactor physics are given. The use of statistical specification for the calculation of the reactor rate behavior and its temperature derivatives is discussed. The reactivity rate ratios in the energy range determinative for Doppler coefficients were discussed. The mean values necessary for the calculation of the Doppler coefficients were described by nuclear physical data. The re-

sults are given and compared with earlier works. The accuracy of the calculations is discussed. (J.S.R.)

22379 (LA-DC-7800) CRITICALITY DEPENDENCE ON NEUTRON CROSS SECTIONS ABOVE 100 kev. Hansen, Gordon E. (Los Alamos Scientific Lab., Univ. of California, N. Mex.). [1962]. Contract W-7405-eng-36. 5p. (CONF-660303-26). ORAU.

From American Physical Society, Conference of Neutron Cross Section Technology, Washington, D. C.

The influence of fast-neutron cross sections on criticality is sketched in a qualitative manner and with little reference to specific reactor concepts. First, infinite media are considered and the energy range limited to above the ^{238}U fission threshold where well-defined removal cross sections exist from which one can portion out the probabilities of various fast capture or fission reactions. Second, the energy range is extended downward towards 100 kev where the usefulness of removal cross sections diminish and details of neutron energy-reduction processes become more important. Finally, the one-group diffusion approximation for critical dimension is introduced as a basis for inferring criticality dependence on flux-weighted cross sections. (auth)

22380 (ORNL-TM-1246) 05R MONTE CARLO ANALYSIS ROUTINES FOR CALCULATING VARIOUS MEAN TIMES IN REACTOR PROBLEMS. Irving, D. C.; Morrison, G. W.; Mihalczo, J. T. (Oak Ridge National Lab., Tenn.). Feb. 15, 1966. Contract W-7405-eng-26. 27p. Dep. mn. CFSTI $1.00 cy, $0.50 mn.

Routines are described which analyze the neutron history tapes produced by the 05R Monte Carlo neutron transport code and calculate the mean time for various events in the lifetime of neutrons produced by fission. The times calculated are the mean time from birth to loss by absorption or leakage, from birth to production of another fission, the mean time to loss minus the time from final collision to escape, and the mean time spent in crossing internal voids. (auth)

22381 (RT-FI-(65)49) DETERMINAZIONE DEI PARAMETRI CINETICI DI UN REATTORE DA UN'ANALISI STATISTICA DELLA DISTRIBUZIONE DEI NEUTRONI PRONTI. (Determination of Reactor Kinetic Parameters by Statistical Analysis of Prompt Neutron Distribution). Pacilio, N. (Comitato Nazionale per l'Energia Nucleare, Rome (Italy)). Dec. 1965. 40p. Dep. mn.

The distribution of neutrons from a detector placed inside a steady state operating reactor is considered. Under some assumptions, the probability distribution of this process may be approximated by the negative binomial model. This circumstance suggests useful methods to determine reactor kinetic parameters; so the direct method, the d.b.n. method and the zero probability method are studied in order to be applied in experimental techniques. (auth)

22382 (RT-FI-(65)57) TECHNICHE DI MISURA DELLO SPETTRO DEI NEUTRONI INTERMEDI. (Technique for Measuring the Spectrum of Intermediate Neutrons). Pauli, G. (Comitato Nazionale per l'Energia Nucleare, Rome (Italy)). Dec. 1965. 19p. Dep. mn.

Some methods for determining the slowing-down spectra in a reactor from the activation of resonance detectors are examined and a few examples are reported. (auth)

22383 (AEC-tr-6693) CALCULATIONS OF CRITICAL EXPERIMENTS ON ASSEMBLIES IN ZPR-3 WITH THE AID OF THE SYSTEM OF CONSTANTS FEI. Bazazyants, N. O.; Zaritskii, S. N.; Troyanov, M. F. Translated for Argonne National Lab., Ill., from Byull. Inform. Tsentra Yadern. Dannym, 2: 247-80(1965). 39p. Dep. mn. CFSTI $2.00 cy, $0.50 mn. JCL $3.60 fs, $1.37 mf.

Critical experiments were made in 11 assemblies in ZPR-3, simulating metallic, oxide, carbide, and ceramic cores of fast reactors of various volumes with uranium fuel. The following characteristics of spherical assemblies were measured and calculated; critical mass (effective coefficient of multiplication k_{eff}), fission cross section indices σ_f^p/σ_f^a and reactivity introduced by various samples, R_i, in the center of the assembly and lifetime of prompt neutrons l. (M.O.W.)

22384 CONSIDERATION OF THE HETEROGENEOUS RESONANCE EFFECT IN CALCULATIONS OF MULTIGROUP CONSTANTS FOR THERMAL REACTORS. Shikhov, S. B. At. Energ. (USSR), 20: 17-21(Jan. 1966). (In Russian).

A method for the calculation of multigroup cross sections with consideration of the effective resonance integral was proposed. Concrete formulas for cases where the resonance can be considered narrow were reported. The corrections of V. V. Orlov to the formulas were given when the criteria of narrow resonances were not achieved. (tr-auth)

22385 A MODIFIED RITZ METHOD FOR THE DIFFUSION-THEORETICAL CALCULATION OF NONSEPARABLE REACTOR GEOMETRIES. Schaeffler, H. (Technische Hochschule, Stuttgart). Atomkernenergie, 11: 109-14 (Mar.-Apr. 1966). (In German).

The modified Ritz method allows, without too much computational effort, a rather exact calculation of nonseparable reactor geometries, as they result for example from different black control elements (rods, plates, crosses), inserted in the reactor. Contrary to the modified Kantorowitsch method one obtains instead of a transcendental equation for the eigenvalue an algebraical equation, from which the eigenvalue can be calculated iteratively. Compared to the usual Ritz method this procedure has the advantage of reducing the double sum for the flux approximation to a single sum. The method is demonstrated by means of a bare cylindrical reactor with a black partially inserted central control rod. (auth)

22386 AIR SCATTERED RADIATION IN THE ENVIRONMENT OF A CRITICAL FACILITY. Fiebig, R.; Janssen, U. Atomkernenergie, 11: 119-25(Mar.-Apr. 1966). (In German).

Measurements of the radiation doses in the environment of the critical facility at the Reactor Station Geesthacht before final replacement of the concrete shielding on the roof of the reactor hall showed a strong contribution of air scattered neutrons and gammas to dose rates in accessible areas. The neutron dose rates show a well defined maximum at 10 to 20 m distance from the wall of the critical facility. Far from the critical facility for calculational purposes on upper boundary to the measurements is given by assuming a point isotropic source normalized to the measured dose rates on the roof of the hall. No reduction has to be made to the total source intensity in accord with the angle of aperture. At shorter distances (<100 m) calculation of once scattered radiation neglecting attenuation in air gives a good resemblance of the slopes, but in absolute values a disagreement of by a factor of 2 to 3 lower theoretical results compared to measurements occurs after normalization to roof dose rates. γ-dose rates in this region results from leakage through the wall and behave in the manner expected. The methods of calculation thus show reliable by a common factor of 3 for use in a case of skyshine from a critical facility. (auth)

22387 VARIATIONAL ITERATIVE METHODS FOR ELLIPTICAL PROBLEMS IN THE THEORY OF NUCLEAR REACTORS. Albertoni, S.; Lunelli, M.; Maggioni, G. (Univ., Milan). Atti Seminar. Mat. Fis. Univ. Modena, 14: 169-201(1965). (In Italian).

A variational iterative method is derived for the solution of elliptical problems in nuclear reactor theory. The variational bases for the resolution of transmission problems are given. The iterative-variational technique used for the numerical solution is examined. Numerical examples are then given. (J.S.R.)

22388 THE ZR-2 CRITICAL ASSEMBLY. Muzsnay, Laszlo; Zobor, Ervin; Bencze, Istvan; Bollok, Lajos; Haber, Gyula; Kovacs, Gyula; Probald, Vilmos; Szamosi, Gyoergy. Magyar Tud. Akad. Kozp. Fiz. Kut. Int. Kozlem., 13: 363-76 (1965). (In Hungarian).

The design and construction of the ZR-2 critical assembly

developed, built and operated at the Institute are described, and some of the important safety and operational features are discussed. (auth)

22389 ON-LINE COMPUTERS IN OPTIMAL REACTOR SHUTDOWN. **Roberts, John J.; Smith, Harold P. Jr. (Univ. of California, Berkeley). IEEE (Inst. Elec. Electron. Eng.), Trans. Nucl. Sci., NS-13: No. 1, 448-53(Feb. 1966).**

The solution associated with a minimum-time optimality criterion is reviewed. The effect of spatial variations in power, xenon, and iodine are shown to affect greatly the optimal power trajectories. Numerical comparisons between point and one-dimensional models are presented for a bare sphere reactor. The role of a digital computer in analyzing and controlling the shutdown procedure is discussed. (auth)

22390 BOUNDARY CONDITIONS IN GAP GEOMETRY. **Rothenstein, W.; Helholtz, J. Nucl. Sci. Eng., 24: 362-74(1966).**

It is shown that the most suitable boundary conditions connecting the moments of the angular flux at the two faces of an annular void surrounding the fuel in a reactor lattice cell are obtained from the consistent use of the transport-theory P_N approximation in the void as well as in the other media, when N is not restricted to very low values. A different procedure, which is particularly appropriate in diffusion theory, had been used previously by Newmarch and extended to N = 3 and N = 5 by Tait and Clendenin. However, the algebraic difficulties are considerable, and, although their method is preferable to the systematic use of the P_N approximation in all media for the lowest values of N, it is not capable of generalization to higher N. Comparisons of the different approaches are given for the lowest-order approximations; the method based on applying the P_N approximation to all regions is given in a form suitable for any odd value of N, and numerical results are presented up to N = 11 to show that it converges rapidly. (auth)

22391 THE EFFECT OF RANDOMNESS ON GROUP CROSS SECTIONS. **Kelber, Charles N.; Kier, Philip H. Nucl. Sci. Eng., 24: 389-93(1966).**

As suggested by Brissenden, it is possible to analyze the reaction rate in the unresolved resonance region by generating sets of random resonance parameters that have the correct statistical properties. Since each set of parameters is itself a random variable, an estimate of the probable error in an average-group cross section or reaction rate can be made by averaging over many random sets. This was done for a mixture representative of fast breeder reactors and for the energy range 700 to 900 ev. This region is a typical one for studying the Doppler effect. If we make the assumption (a great oversimplification) that the response in this small energy band is typical, not only for the mean but also for the variance, then we would conclude that, if all fine groups (of width 200 ev) have the same weight, the probable error in the fissile component of the Doppler coefficient is about equal to its mean value. For the fine group itself, the probable error in the difference in the relative changes of the fission and the absorption rates is about ten times the mean value. (auth)

22392 SUBCRITICAL DETERMINATION OF RELATIVE NATURAL-NEUTRON-SOURCE STRENGTHS. **Rohr, R. C.; Storm, M. L. (Knolls Atomic Power Lab., Schnectady, N. Y.). Nucl. Sci. Eng., 24: 414-17(1966). (KAPL-P-3132).**

An experiment is described in which the relative source strengths due to (α,n) reactions in boron-bearing fuel (S_B) and the combined effects of spontaneous fission and (α,n) reactions on impurities in fuel containing no boron (S_F) are determined. Experimental data were obtained in cores of identical geometry, for U-Zr alloy (93.2 wt.% ^{235}U) containing no boron, the alloy fuel containing 0.15 wt.% boron, and a core containing 70.5 g of natural boron with a total fuel load of 8.50 kg ^{235}U. Measurements were made of the fundamental-mode prompt decay constant, in addition to counter data, to permit the determination of the multiplication factor of each configuration. From an analysis of the combined data, obtained from the pulsed-neutron and counter measurements, the relative natural-neutron source strength S_B/S_F for 0.15 wt.% boron-bearing fuel was determined to be 38.0 ± 0.6. (L.B.S.)

22393 THE SPACE DEPENDENCE OF REACTOR NOISE. I. THEORY. **Sheff, James R.; Albrecht, Robert W. Nucl. Sci. Eng., 24: 246-59(Mar. 1966).**

The theory of space-dependent stochastic fluctuations is developed in sufficient generality that any specialization can be made to a particular reactor model by finding the appropriate Green's function for the mean-neutron-density equation of the system in question. The approach used is the Langevin technique which, as developed here, yields the cross-correlation function as a double convolution over two Green's functions and the correlation function of equivalent "noise sources" present within the system. The character of these noise sources is examined in considerable detail to gain the basic physical understanding necessary to arrive at a calculational procedure and specific formulas. It is shown that when delayed-neutron effects are included, the input noise sources are not white. That is, their spectral-density functions are not constant. A clear distinction is made between fluctuations in the neutron density and the fluctuations observed with a detector. The density fluctuations include contributions from a neutron correlated with itself and direct progeny, whereas the mechanism of detection (invariably removing a neutron) eliminates this correlation. (auth)

22394 CRITICAL CALCULATIONS OF THE SLAB REACTORS. **Kowalska, Krystyna. Nucl. Sci. Eng., 24: 260-71(Mar. 1966).**

The problem of critical dimensions of an infinite-slab multi-layer multiplying system can be solved by a general procedure due to K. M. Case. The angular neutron distribution and the critical core size can then be found by solving the Fredholm type integral equation with an additional critical condition. Numerical calculations were done for the case of a multiplying slab surrounded by an infinite reflector, assuming one-energy group and isotropic scattering of neutrons, the mean number of secondary neutrons per collision in a medium-c being a variable parameter. Various approximations of the exact solution were compared and the asymptotic theory was found applicable in a wide range of c values in both media. (auth)

22395 CALCULATION OF REACTIVITY WORTH OF ROD-CLUSTER CONTROL ELEMENTS AND CORRELATION OF THEORY WITH EXPERIMENT. **Eich, W. J.; Williams, H. T. Jr.; Aisu, H.; Minton, G. H. Nucl. Sci. Eng., 24: 272-83(Mar. 1966).**

Analytical procedures for the representation of rod-cluster control elements in nuclear design calculations are developed and evaluated by application to a variety of critical experiments. Methods suitable for use in few-group diffusion theory studies are utilized in predicting critical water heights and integral "worth" measurements for reactors containing arrays of cylindrical absorbers. Results indicate that worth can be calculated to within ±3% for a wide range of configurations involving clad and unclad absorbers of 0.260, 0.330, and 0.403-in. diam. (auth)

22396 THE CALCULATION OF NEUTRON SPECTRA IN REFLECTED CORES AND REFLECTOR REGIONS. **Perkins, S. T. Nucl. Sci. Eng., 24: 284-90(Mar. 1966).**

The neutron spectrum equations are investigated for regions in which the neutron source includes both volume and surface components. The results are thereby applicable to reflected cores and reflector regions. The spectrum is analyzed in the volume-integrated P_1 approximation. The difference from the corresponding bare-core relations is an additional source, plus the redefinition of the leakage parameter. It is shown, with the approximation of diffusion theory, that the leakage parameter is always nonpositive. Several simplified forms are also developed for this term. A numerical calculation is pre-

sented to show the details of the procedure, and the results are compared to a multiregion analysis. (auth)

22397 MONTE CARLO INVESTIGATION OF THE HETEROGENEITY OF FAST REACTOR CORES. Shaviv, G.; Yiftah, S. (Israel Atomic Energy Commission, Yavne. Technion-Israel Inst. of Tech., Haifa, Israel). Nucl. Sci. Eng., 24: 302-4(Mar. 1966).

Monte Carlo calculations were carried out for a two-region lattice with an inner region of radius between 0.18 and 0.25 cm containing ^{238}U of density 18.75 g/cm^3. The outer region contained Na, and its volume was taken to be equal to twice the volume of the uranium. The difference between the integrated flux over 400-ev interval in the two regions of the cell was found negligible. It is shown that the effect of the ^{23}Na resonance on the effective cross section of ^{238}U for absorption is small and is limited to a narrow energy region in which there is a strong flux depression. Histograms of the relative absorption rate in equal-volume subdivisions of the inner zone, as a function of radial distance, show that the effect decreases rapidly with decrease in radius. The results confirm the fact that the core heterogeneity has only a slight influence of the effective group cross sections in fast reactors. (L.B.S.)

22398 ON THE DIFFUSION OF NEUTRONS IN A REACTOR LATTICE. Stewart, J. D. (Atomic Energy of Canada Ltd., Chalk River). Nucl. Sci. Eng., 24: 304-6 (Mar. 1966).

Two main points that must be considered in defining thermal diffusion parameters for a lattice are presented and proved, assuming a simplified parallel-plate lattice and considering only diffusion perpendicular to the plates. The first is that the lattice has a material buckling B^2 irrespective of any simplifying assumptions that may be made in practice for the purpose of calculation. The second is that a source $s(\gamma) = s_0 \exp(i K \cdot \gamma)$ gives rise to a flux proportional to it. (L.B.S.)

22399 VARIATION PRINCIPLES FOR THE CRITICAL FLUX CURVES OF REFLECTED REACTORS. Breitenhuber, L. (Technische Hochschule, Graz). Z. Angew. Phys., 20: 267-71(1966). (In German).

New minimum principles and stationary expressions are given and discussed for the boundary conditions $\Phi = 0$ and $\partial\Phi/\partial n + (1/d)\,\Phi = 0$ for the equation $\Delta\Phi + B^2\Phi = 0$. It is suggested to fulfill conditions at boundaries and interfaces only in the form of natural boundary conditions. Thus, the use of discontinuous trial functions is encouraged, yielding greater flexibility and better numerical approximations in the mean. Boundary conditions are, nevertheless, satisfied in the limit. (auth)

22400 ITERATIVE SOLUTION OF ELLIPTIC SYSTEMS AND APPLICATIONS TO THE NEUTRON DIFFUSION EQUATIONS OF REACTOR PHYSICS. Wachspress, Eugene L. Prentice-Hall International Series in Applied Mathematics. Englewood Cliffs, N. J., Prentice-Hall, Inc., 1966. 310p.

A description of practical techniques for the solution of elliptic systems with high-speed digital computers is presented. The three predominant iterative methods—successive overrelaxation, polynomial extrapolation, and alternating-direction-implicit iteration—are described in detail. The relative merits of each method are discussed and are substantiated with numerical studies. (G.O.Y.)

22401 AN ANALYSIS OF FAST REACTOR TRANSIENT RESPONSE AND SAFETY IN SELECTED ACCIDENTS. Sherer, D. B. (General Electric Co., San Jose, Calif.). 26p. (CONF-651009-12). ORAU. Gmelin, AED-CONF-65-307-21.

From Conference on Safety, Fuels, and Core Design in Large Fast Power Reactors, Argonne, Ill.

Accidents analyzed were nonterminating ramp reactivity insertions at twenty cents per second and two dollars per second and loss of pumping power with resultant flow coastdown. The FORE computer program was used to calculate the course of these accidents in typical large fast reactor cores under a variety of assumptions. The analysis consists in large part of identifying the failure mechanism in each transient, the time elapsed before failure, and its location in the core. Parameters important to safety, such as the Doppler and sodium reactivity coefficients, are discussed. (A.G.W.)

Design and Feasibility

22402 NUCLEAR REACTOR MODERATOR STRUCTURE. Tollet, Louis H. J. (to Societe Anglo-Belge Vulcain Societe Anonyme). Canadian Patent 725,773. Jan. 11, 1966.

The moderator flows in through a central tube enclosed by a larger tube closed at one end and having insulated walls. The overflow from the shorter central tube is then collected and recycled. Several sets of such concentric tubes are used. The disposition and type of fuel and coolant are not stated but moderator and coolant do not come into contact with each other. Advantages claimed are reduced leakage because of fewer entries into the reactor vessel and free thermal expansion. (AECL)

22403 BOILING STATE OF AN OPERATING HOMOGENEOUS NUCLEAR REACTOR. Grenon, Michel; Berthod, Louis; de Lara, Georges Cohen; Delachanal, Michel; Halbronn, Georges (to Commissariat a l'Energie Atomique). German Patent 1,203,887. Oct. 28, 1965. Priority date May 10, 1957, France.

The reactor comprises means which, by injection of fluid from at least one fluid injector in a tangential direction in relation to the envelope of the reactor, are adapted to produce a turbulent flow in a stationary core in such a manner as to effect the separation of the vapor so that it is gathered into a funnel located substantially along the axis of revolution, from which funnel the said vapor is discharged. (Gmelin Inst.)

Fuels

Refer also to abstracts 20970 and 20979.

22404 (USNRDL-TR-987) BETA ENERGY EMISSION RATE FROM NEUTRON-IRRADIATED, ^{235}U CARBIDE PARTICLES. Pestaner, J. F.; Yahiku, R. (Naval Radiological Defense Lab., San Francisco, Calif.). Jan. 11, 1966. Contract AT(49)-2505. 12p. Dep. mn. CFSTI $1.00 cy, $0.50 mn.

The beta energy emission rate from neutron-irradiated, uranium-235–carbide particles was measured by chemical dosimetry. The particles were suspended by vigorous stirring in ferrous sulfate solutions. The oxidation of ferrous to ferric ion was the chemical change measured, this change being related to the energy absorbed by the solution. Good agreement was obtained between the existing calculated and the experimental values of beta energy emission rate. From these data simplified equations were derived for calculating beta energy emission rate as a function of particle size and time after fission, and they are presented. (auth)

22405 RESULTS WITH A MULTIPURPOSE ISOTOPE SEPARATOR. Viehboeck, F. P. (Oesterreichische Studiengesellschaft fuer Atomenergie GmbH, Seibersdorf, Austria). Atomkernenergie, 11: 131-6(Mar.-Apr. 1966). (In German).

Mass spectrometric burnup determinations of irradiated nuclear fuel were carried out by means of a surface ionization source and a Faraday collector. An ion source was developed by which the chemical preparation of the sample can be carried out in the source itself for analysis of high temperature fuel particles. Single crystal foils were bombarded by 40-kev Ta^+ ions at currents of 10^{-9}–10^{-7} A for solid state physics investigations. Isotopic pure radioactive targets were produced for nuclear spectroscopic measurements. Also the intensity distribution of the separated isotopes was determined by means of radioactive tracers. Stable isotopes of rare earth elements were separated for measurements of thermal nuclear cross sections and

enrichment factors of >2000 were achieved at a collector current of 5 mamp. Essential constructional details are described. (auth)

22406 THE THERMIONIC CONVERTER AND ITS USE IN A REACTOR. Bohdansky, Josef (EURATOM, Ispra, Italy). Euratom Bull., 5: 24-30(Mar. 1966).

The development of thermionic converters and their method of operation are discussed. The theoretical efficiency of the converter is considered, along with methods of achieving optimum efficiency. The cesium converter and its use in connection with a reactor are described. (M.C.G.)

22407 AN ANALYSIS OF CONTINUOUS REACTOR REFUELING. Yasukawa, Sigeru. Nucl. Sci. Eng., 24: 239-45(Mar. 1966).

An analytical method for continuous refuelings is developed. The starting point is the first-order nonlinear differential equation, and the technique for solving this is a use of an elliptic function theory. The nature of the neutron-flux distribution, eigenvalue, and critical velocity are investigated for the in-out and the out-in continuous refueling. Numerical results for neutron-flux distribution are given. (auth)

Power and Power-Breeder Reactors

Refer also to abstracts 20968 and 21967.

22408 (BMI-1764) EXAMINATION OF THE 1B STEAM GENERATOR FROM THE SHIPPINGPORT ATOMIC POWER STATION (PWR). Berry, Warren E.; Stiegelmeyer, William N.; Boyd, Walter K. (Battelle Memorial Inst., Columbus, Ohio). Feb. 24, 1966. Contract AT(11-1)-Gen-14; Subcontract 73-14-1219. 113p. Dep. mn. CFSTI $4.00 cy, $0.75 mn.

For Bettis Atomic Power Lab., Pittsburgh, Pa.

An examination was made of selected components from the 1B steam generator after more than 5 years of operation in the Shippingport Atomic Power Station. Cracking and pitting were found and are discussed. (M.O.W.)

22409 (EUR-2735.d) TECHNISCHER UND WIRTSCHAFTLICHER VERGLEICH EINES 237 MWe ZWEIKREIS- UND EINES EINKREIS-SIEDEWASSERKERNKRAFTWERKES. Abschluss-Bericht. (Technical and Economic Comparison of a 237 MWe Double-Cycle and a Single-Cycle Boiling-Water Nuclear Power Plant. Final Report). (Kernenergieanlagen, Allgemeine Elektricitaets-Gesellschaft, Frankfurt am Main (West Germany). Societe Alsthom, Paris (France)). Mar. 1966. 92p. Dep. mn.

In the technical part of this study, the KRB plant (double cycle) was compared with a single-cycle BWR plant designed by AEG. In the economic part, this latter plant was compared with a double-cycle plant supplied, unlike the KRB, exclusively by AEG. After this, studies were carried out, first, of the kinetic behavior of the single cycle BWR reactor and, secondly, of the parameters of the single-cycle BWR plant. The results of the studies can be summarized as follows: the single-cycle plant is cheaper than the double-cycle by about DM 7.500.000 or 5%; similarly, the cost per kWh generated by the former is DM 0,14 or 3,7%, lower than the double-cycle kWh, the single-cycle BWR is less stable than the double-cycle, from the kinetic standpoint, and the optimum feed-water heating temperature of the single-cycle BWR is about 155°C, which is some 30°C lower than the temperature specified for the KRB plant. (auth)

22410 (GA-5238) EXPERIMENTAL BERYLLIUM OXIDE REACTOR PROGRAM. Quarterly Progress Report for the Period Ending March 31, 1964. (General Atomic, San Diego, Calif. John Jay Hopkins Lab. for Pure and Applied Science). Apr. 30, 1964. Contract AT(04-3)-187. 48p. Dep. mn. CFSTI $2.00 cy, $0.50 mn.

During the quarter, the test apparatus for measuring the thermal characteristics of the tipping-reflector thermal fuse was assembled, and a series of test runs was conducted. Test data, for steady-state and transient conditions in helium and in nitrogen, are in the process of being evaluated. A nonbrazing alloy of aluminum–germanium–silicon that melts at temperatures between 800 and 1100°F (depending on the composition) is being evaluated as a candidate fuse material. An automatic test-cycle control system was installed in the fuel-pin test rig, and checkout runs were satisfactorily performed. The test autoclave is being modified to accommodate a fuel-pin array that is more representative of the design fuel element than previous specimens. The modification and control automation will improve the testing time and provide better representation of the design element. Beryllia thermal stresses were recomputed for various core components as part of the preparation of the final safety analysis report for EBOR. Revised material properties data and recent heat-generation values were used in the computation, and steady-state thermal stress levels at the start and end of life were obtained. Fabrication of fuel pellets in excess of the full core inventory requirement was completed. A total of 793 fuel pins were loaded with pellets, and all pins were end sealed, leak tested, and creep shrunk. The fuel pellets contain two sizes of fuel particles, but the different sizes are not mixed in any given pin. Assembly of the fuel elements is scheduled to begin after assembly of the stationary and tipping-reflector elements is complete, at which time all subcomponents will be on hand. Assembly of six stationary reflector elements was completed with almost trouble-free effort. Installation of core instrumentation, including fuel- and reflector-element components, progressed during the quarter. Sixteen reflector-element shipping containers were assembled, and the others are well along in the assembly operation. Six assembled stationary reflector elements were stored in the finished containers to await shipment to the Idaho site. Fabrication and delivery of the four cruciform control elements were completed during the quarter. The first phase of the fatigue analysis of the pressure vessel was completed and the data are being evaluated. In the pressure-vessel fabrication effort, the pressure-vessel shell was stress relieved and sent to a subcontractor for machining of the shell flange and support rings. Preliminary scram testing of the prototype control-rod-drive mechanism was terminated after a combination of settings of system parameters was obtained. (M.O.W.)

22411 (GA-6113) TARGET—A PROGRAM FOR A 1000-Mw(e) HIGH-TEMPERATURE GAS-COOLED REACTOR. Quarterly Progress Report for the Period Ending February 28, 1965. (General Atomic, San Diego, Calif. John Jay Hopkins Lab. for Pure and Applied Science). Mar. 31, 1965. Contract AT(04-3)-167. 127p. Dep. mn. CFSTI $4.00 cy, $0.75 mn.

Further developments in the steam generator and the reactor core are reported. The fuel element development is discussed in terms of various studies on the mechanical design, thermal design, fission product transport, materials, and chemistry. The performance of the GAIL loop operation is discussed. Further developments in the nuclear analysis of the reactor core are reported. Developments in the prestressed concrete reactor structure are discussed. (M.O.W.)

22412 (GA-6622) GARGOYLE—AN INFINITE MEDIUM FUEL CYCLE ANALYSIS CODE WITH FUEL AND POISON SEARCHES. Todt, F. W. (General Atomic, San Diego, Calif. John Jay Hopkins Lab. for Pure and Applied Science). Feb. 12, 1966. Contract AT(04-3)-167. 156p. Dep. mn. CFSTI $5.00 cy, $1.00 mn.

GARGOYLE employs a flexible nuclide scheme (specified by input) and depletes up to 12 fuel regions (fuel types or stages of irradiation) by subjecting them all to the same average flux. A control poison search may be performed at each time step. Feed material searches may be performed at the end of each burnup cycle before refueling. Any nuclide or combination of nuclides may be included

in the feed search. Any nuclide or combination of nuclides may be completely or partially recycled in accordance with input specifications. Concentration-dependent self-shielding factors may be applied to any nuclide. The current restrictions of the program are: 12 energy groups, 3 nuclides with thermal transfer matrix (moderators), 12 fuel types or regions, 40 nuclides per region, and 25 heavy nuclides (producing fission products). (M.O.W.)

22413 (GA–6929) EXPERIMENTAL BERYLLIUM OXIDE REACTOR PROGRAM. Quarterly Progress Report for the Period Ending December 31, 1965. (General Atomic, San Diego, Calif. John Jay Hopkins Lab. for Pure and Applied Science). Jan. 31, 1966. Contract AT(04-3)-187. 24p. Dep. mn. CFSTI $1.00 cy, $0.50 mn.

A critical review of the control rod drive mechanism was made to pinpoint causes of difficulties encountered during testing. The principal difficulty was found to be tooth interference in the positioning motor speed reducing gears. A two-phase program is being carried out to provide interim units for initial loading and testing, to be followed by drives of final design for use during high power. System Operation (SO) Tests were completed for all systems except Nos. 9, 11, and 16. EBOR systems, for the most part, are operational. Some modifications were made, with routine maintenance continuing. (M.O.W.)

22414 (GEAP–4961) DEVELOPMENT OF PULSED NEUTRON APPLICATION TO POWER REACTOR START-UP PROCEDURES. Quarterly Progress Report No. 14, July 1–October 30, 1965. Garelis, E.; Meyer, P.; Del Cotto, J. (General Electric Co., San Jose, Calif. Atomic Power Equipment Dept.). Nov. 9, 1965. Contract AT(04-3)-189. 18p. Dep. mn. CFSTI $1.00 cy, $0.50 mn.

An investigation was made to apply pseudo-random impulse techniques to the measurement of reactivity. The experimental equipment necessary for the impulse measurements was built and a description of the individual components is given. The experiments are briefly discussed. Results of an experiment demonstrating the measured ($k\beta/l$) dependence on the neutron pulse width are reported. (M.O.W.)

22415 (RPI–321-4) GLASS-CLAD URANIUM GLASS FIBERS FOR POWER REACTORS. PART II. REACTOR PHYSICS ASPECTS. Valente, Frank A. (Rensselaer Polytechnic Inst., Troy, N. Y.). [nd]. Contract AT(30-1)-2159. 60p. Dep. mn. CFSTI $3.00 cy, $0.75 mn.

A preliminary study of the nuclear power-reactor potential of glass fiber fuel elements indicates that the use of light-water and diphenyl moderation will result in critical systems under appropriate conditions of fuel-moderator concentrations, meat radii, fuel-enrichments, and temperatures. Under the same conditions of comparison, diphenyl moderation appears to require larger amounts of critical masses than light water; for example, at 350°C, the critical masses are approximately 10.4 Kg to 8.8 Kg for a meat radius of 100 μ and a concentration of 96/4. On the other hand, above roughly 200°C, the critical mass requirements appear to drop faster with temperature with light water than with diphenyl; therefore, although both moderators are potentially "cold accident" prone, water appears to be more hazardous in this respect. As expected, the use of reflectors of the same material as the moderator leads to critical volume savings of substantial amounts, lying in a very rough range of 15–40%. (auth)

22416 (TID–22736) PM-3A CONTROL ROD DRIVE MECHANISM AND CABLE REPAIR. Summary Report. (Martin Co., Baltimore, Md.). Mar. 8, 1965. Contract AT(30-1)-3512. 73p. Dep. mn. CFSTI $3.00 cy, $0.75 mn.

Malfunctions in the control rod drive mechanism of the PM-3A reactor are reported. It was noted that one of the difficulties with the actuator system was moisture in the actuator coil assembly feed cables. New cable assemblies were designed and are presented. (M.O.W.)

22417 (TID–22759) DESIGN PROPOSAL FOR A RATE-OF-CHANGE-OF-PRESSURE SCRAM SAFETY CHANNEL FOR THE EGCR. Munns, J. M. Jr. (Tennessee Valley Authority, Oak Ridge). Apr. 9, 1965. Contract AT(40-1)-2742. 10p. Dep. mn. CFSTI $1.00 cy, $0.50 mn.

A design proposal for a two-out-of-three rate-of-change-of-pressure scram system for use during nitrogen pressurization of the EGCR core is presented. The dp/dt scram instrumentation, in conjunction with the proposed period scram, should limit the consequences of reactivity accidents during the EGCR Phase IVa physics tests to acceptable levels. (M.O.W.)

22418 STATISTICAL BASIS FOR DYNAMIC MODEL OF STATIONARY ZERO POWER REACTOR. Kozik, Ben'yamin. At. Energ. (USSR), 20: 21-6(Jan. 1966). (In Russian).

On the basis of the statistical theory of the processes of neutron multiplication, a precise expression was derived for the spectral density of the noise for power and stationary reactors. It has the form of the product of the square of the modulus of the transmission function of the reactor at some multiple, slightly dependent on the frequency. (tr-auth)

22419 RECYCLING OF PLUTONIUM IN HEAVY WATER POWER REACTORS. Khristenko, P. I. At. Energ. (USSR), 20: 26-9(Jan. 1966). (In Russian).

The operation of heavy water ^{238}U reactors with equal-weight concentrations of ^{234}U, ^{240}Pu, ^{241}Pu, and small additions of ^{235}U was shown during supplementary fueling of the reactor with natural and depleted uranium. One fraction of the exposed fuel unloaded from the reactor was purified and returned to the reactor. Another smaller fraction was removed from the cycle after the extraction of the plutonium and was substituted by natural uranium. (tr-auth)

22420 THERMAL EFFICIENCY AND CONDENSER OUTPUT IN THE STEAM-COOLED REACTOR. Deubel, K. L. (Kernforschungszentrum, Karlsruhe, Ger.). Atomwirtschaft, 11: 139-43(Mar. 1966). (In German).

With water vapor as a reactor coolant the direct circuit can be used even in large power units. In fast reactors moderation of the neutron spectra is lower and there is a larger breeding factor than in cooling with the liquid H_2O phase. The thermal efficiency, condenser output, and rotation time were calculated for a steam power process with a steam-cooled reactor and external evaporation. It is shown that at higher system pressures efficiencies can be obtained that deviate only slightly from that of modern conventional power installations. (tr-auth)

22421 COMPETITIVE REACTORS BECOME NECESSARY. Zihlmann, Eduard (Direktionspraesident der Centralschweizerische Kraftwerke, Lucerne, Switzerland). Bull. Schweiz. Elektrotech. Ver., 56: 854-6(Sept. 18, 1965). (In German).

The electric power companies of Switzerland have recently published investigation of the adoption of the first atomic power plant into the Swiss economy. This would be possible in 1970–1971. The question of development by the Swiss of their own reactors is discussed. (TCO)

22422 PARTICULAR ASPECTS OF THE UTILIZATION OF URANIUM DIOXIDE AS FUEL IN A POWER REACTOR. Chenebault, P.; Francois, B. (CEN, Grenoble, France). Bull. Soc. Franc. Ceram., No. 66, 81-102(Jan.-Mar. 1965). (In French).

The physical properties of UO_2 of interest to the problem are first listed, with several reactors using UO_2 as fuel, in tabular form. A review of flow methods for fuel enrichment is given with photomicrographs of product prepared by various methods. The problem of temperature distribution is reviewed; thermal conductivity of UO_2 for several operating piles is graphed. The variation of conductivity with method of preparation is recounted; techniques of temperature measurement are outlined. Behavior of gases produced by fission is outlined; techniques for studying associated phenomena are listed: variation of gas production with time, with temperature, with the coefficient of diffusion through UO_2, and with radiation yield are mentioned. Experimentation in the pile is outlined, with the

experimental arrangements for such studies illustrated; similar types of information gained from postirradiation experiments are also discussed. (BBB)

22423 POSITIONING OF THE CHARGE-DISCHARGE MACHINE OF THE EXPERIMENTAL NUCLEAR POWER PLANT AT LUCENS. Sommer, H.; Schopfer, B. (SECA, Geneva). Energ. Nucl., 8: 3-8(Jan.-Feb. 1966). (In French).

The problem of locating the charge machine is discussed in the context of the power plant and reactor; its three phases are described. The locating facilities and their manipulating device are expiained with the help of block diagrams and sketches. Electromagnetic principles were combined to allow safe location with a precision of ±0.20 mm. (auth)

22424 DESIGN OF THE 500 MW CPVR TYPE MAGNOX REACTOR. STUDY OF THE CONSTRUCTION OF THE CONCRETE PRESSURE VESSEL. FAPIG (Tokyo), No. 35, 302-7(Jan. 1965). (In Japanese).

A study was made by the FAPIG sub-committee on the design and construction of the 500 Mw CPVR type magnox reactor with special emphasis on the design procedure and anti-earthquake structure of the reactor core and boiler. The design studies were carried out on a cylindrical pressure vessel, and it was concluded that unreasonable stresses will be avoided by having an equilibrium between the gases inside and the prestresses by means of cables. There are still problems in connection with thermal stresses, which must be resolved in the actual design. Both the reactor core system used in the reactor at the Tokai Power Station and the radial key system were considered for their anti-earthquake advantages. It was concluded that by either approach it is possible to design a reactor core with sufficient strength for the necessary earthquake resistance with no significant sacrifice in economy. (TCO)

22425 CONSTRUCTION OF THE REACTOR CORE OF THE TOKAI POWER STATION. Ando, Tetsuya (Fuji Electric Mfg. Co., Ltd., Japan). FAPIG (Tokyo), No. 35, 309-11;316(Jan. 1965). (In Japanese).

After the pressure test of the reactor pressure vessel for the Calder Hall type reactor, for the Tokai Power Station, construction was started on the reactor core in February 1964 and was finished in August. Although much of the construction was carried out on the basis of experience and knowledge gained in England, unique methods were developed and utilized for the construction of that part of the core in which anti-earthquake considerations were necessary. The entire work of construction was completed satisfactorily in a shorter period of time than in similar power stations in England. The report on the construction of the reactor core is described in the following sections: structure of the reactor core; carrying in of the components and other equipment (metal parts or components and graphite blocks); procedures of the construction (plates for supporting the core, eccentric units, piling up of the graphite blocks, and charge-pots); preliminary experiments and rehearsal (rehearsal for the core construction, welding tests in general, and welding tests for the reflector coverplate); supervision and control of the process of construction; and nuclear clarity (division of the construction area, control of the clothing, tools, and the components to be constructed, and air conditioning). (tr-auth)

22426 MAGNOX REACTORS PROPOSED FOR THE DOMESTIC PRODUCTION OF POWER REACTORS. FAPIG (Tokyo), No. 36, 5-26(Apr. 1965). (In Japanese).

Three aspects concerning magnox reactors proposed for domestic power production are discussed. In the proposals for the natural uranium-graphite reactor section of the report, the natural uranium-graphite reactor is compared, especially with reference to costs, with the light water reactor. The natural uranium reactor has the advantages of stabilized supply of nuclear fuel, stock piling of ^{238}U for the future, economizing in foreign currencies, and the shortest course to the domestic power production. A conceptual design made on the basis of information gained from the Tokai Power Station is described for the 500 Mw CVP reactor. A prestressed pressure vessel was substituted for a steel vessel to permit increased pressure of the coolant gas. As a result of the conceptual design, it was found that the overall construction costs, power costs, nuclear safety, etc. may be considerably improved over those of the Tokai reactor. The initial capital cost would be about the same as that for a light water reactor with the power cost being reduced. The future of the gas cooled natural uranium-graphite reactor is discussed, and the indication is that this reactor is rapidly approaching economical power reactors. (TCO)

22427 EQUIPMENT FOR DETECTING RUPTURED FUEL ELEMENTS AT THE TOKAI POWER STATION. Takahashi, Masazumi (Fuji Electric Mfg. Co., Ltd., Japan). FAPIG (Tokyo), No. 36, 28-32(Apr. 1965). (In Japanese).

The tubings and their welding method for the purpose of detecting ruptured fuel elements are described. Only tubes made of 2052 stainless steel are used to carry the sample gas from the fuel elements to the detectors. These tubes measure 13.5 mm OD and 1.6 mm in wall thickness. The total length of the tubings is 80 Km, and a total of 22,000 welding joints are used in the reactor fuel system. The inert gas arc welding was employed. An automatic welder was constructed with the optimum operating conditions being determined. (TCO)

22428 CHEMICAL SHIM CONTROL IN THE CONCEPTUAL DESIGN OF A DOMESTIC POWER REACTOR. Horibe, Osamu; Shirahane, Mutsuhiro. FAPIG (Tokyo), No. 36, 49-53(Apr. 1965). (In Japanese).

Chemical shim control for a D_2O moderated, gas cooled reactor employing a soluble neutron absorber (natural boron) is discussed. The control is brought about by the introduction and removal of the soluble poison in a manner similar to the conventional control by control rods. Initiation of introduction and of withdrawal and stoppage of withdrawal of boron are delayed appropriately by detecting the position of a fine regulating rod. In each case, introduction and removal are done automatically, corresponding to the position of a fine regulating rod. This chemical shim control is evaluated quantitatively under the ideal condition of reactor operation. (TCO)

22429 CONCEPTUAL DESIGN OF MAGNOX REACTOR PLANT. Ishigami, Hitoshi (Fuji Electric Manufacturing Co., Ltd., Japan). Fuji Elec. J., 38: 801-11(Dec. 1965). (In Japanese).

An analysis and evaluation of reactor performance for magnox type reactor has been completed. The conceptual design of 500 Mw magnox type reactor, as a part of the study, is described. The prestressed concrete pressure vessel and bore supported fuel elements make this design unique. (auth)

22430 DESIGN OF A HEAVY-WATER MODERATED, BOILING LIGHT-WATER TYPE POWER REACTOR. Haneda, Mikio (Nippon Atomic Industrial Group Co., Ltd., Japan). Genshiryoku Hatsuden, 8: 28-39(Sept. 1964). (In Japanese).

A conceptual design was made of a heavy-water moderated, boiling light-water power reactor. The reactor employs natural uranium oxide and depleted uranium oxide as the fuel with boiling light water as the coolant. Light water is boiled in 516 pressure tubes in the reactor core, and the steam produced directly drives a dynamo turbine. The pressure tubes made of Zircaloy-2 with an inside diameter 113.6 mm and a length 950 mm can withstand a pressure of 60 kg/cm^2 at an operating temperature of 253.4°C. The main features of the power plant using the reactor are as follows: heat output, 1000 Mw; turbine power output, 320 Mw; dynamo power output, 376 kva; steam flow rate 2145 t/hr; and turbine inlet steam pressure, 63 kg/cm^2 abs. (tr-auth)

22431 ATOMIC POWER STATION, USING A HEAVY-WATER MODERATED BOILING LIGHT-WATER REACTOR. Oki, Arahiko (Hitachi Ltd., Japan). Genshiryoku Hatsuden, 8: 40-50(Sept. 1964). (In Japanese).

In the domestic power reactor development program of Japan, the heavy-water moderated type reactor was selected by the Atomic Energy Commission as the first candidate. In order to choose the most suitable coolant system, five conceptual designs were made for five different coolants. The conceptual design of the heavy-water moderated boiling light-water reactor is described, and the description is concerned with the features, characteristics, and problems of the reactor. Some statistics of the reactor are outlined briefly as follows: total heat output 964 Mw; net electrical output 300 Mw; average fast neutron flux 11×10^{13} n/cm^2/sec; average thermal neutron flux 16×10^{13} n/cm^2/sec; coolant pressure at reactor entrance, 93 Kg/cm^2 abs; coolant temperatures at entrance 286.2°C and at exit 297.9°C; coolant amount 14.2 t/h; reactor core diameter 3700 × 4722 mm; reflector, D_2O, 500 mm radial and 300 mm axial; fuel 48.2 t UO_2 (1.0, 0.9, 0.8% enrichment); cladding, Zircaloy-2; 37 fuel elements, 538.5 mm length; control rods, booster and B_2O_3 poison in the moderator; and moderator D_2O, 100 m^3. (TCO)

22432 DESIGN STUDY OF THE CO_2 GAS-COOLED POWER REACTOR. Fujita, Mototsugu (Fuji Electric Mfg. Co., Ltd., Japan). Genshiryoku Hatsuden, 8: 62-71 (Sept. 1964). (In Japanese).

One conceptual design made by the atomic power groups of Japan for the D_2O moderated type reactor for domestic power production used CO_2 as a coolant. The design study for the reactor is described under the following headings: characteristics of the D_2O-moderated CO_2 gas-cooled reactor, basic considerations in the design, main parameters, and outline of the conceptual design (fuel elements, reactor, primary coolant system, and fuel-handling facilities). Some statistics for the reactor are total heat output 1078.5 Mw; overall thermal efficiency 31.3%; bus-bar electrical output 322 Mw; reactor core diameter 500 × 607 cm; reflector D_2O; fuel, 1% enriched uranium, 32 t, 1.2% enriched uranium 32 t; control rods, booster rods and natural boron in the moderator; 19 fuel-rod clusters, UO_2 pellets; cladding, stainless steel; average thermal neutron flux 8.32×10^{13} n/cm^2/sec; moderator D_2O, 245 m^3; and coolant, CO_2 gas. (TCO)

22433 DESIGN STUDY OF A HEAVY-WATER MODERATED, ORGANIC COOLED POWER REACTOR. Nagashima, Kikusaburo (Sumitomo Atomic Energy Industries, Ltd., Japan). Genshiryoku Hatsuden, 8: 72-9(Sept. 1964). (In Japanese).

In order to compare the coolants for a heavy water moderated power reactor, the conceptual design of an organic cooled power reactor was undertaken. The design study of this reactor is described. The reactor uses natural-uranium oxide and 0.6% depleted uranium oxide as fuel, and Santowax OM at 400°C is employed as the primary coolant. Light water serves as the secondary coolant in the heat exchanger, and the steam produced is used to drive a dynamo-turbine. The main feature of a power plant using the reactor are as follows: heat output, 1094 Mw; turbine power output, 323 kw; dynamo power output, 380 kva; steam flow rate, 1528 t/hr; steam temperature, 389°C; turbine inlet steam pressure, 41 kg/cm^2 G; reactor core Santowax pressure, 15 kg/cm^2 abs.; inlet Santowax temperature, 337°C; and Santowax flow rate, 24450 t/hr. (tr-auth)

22434 PUBLIC SAFETY ASPECTS OF NUCLEAR POWER PLANT LICENSING. Doan, R. L. (Atomic Energy Commission, Washington, D. C.). IEEE (Inst. Elec. Electron. Eng.), Trans. Nucl. Sci., NS-13: No. 1, 120-5 (Feb. 1966).

Various aspects of the siting, design, construction and operation of nuclear power plants to which the AEC gives attention in its licensing activities are discussed, together with the reasons why they are considered important to public safety. This includes the measures taken to assure the integrity of the nuclear fuel and primary coolant system under all operating conditions; to provide adequate means of coping with emergency situations; and to limit the consequences of accidents to levels which do not endanger the health and safety of the public. (auth)

22435 A REVIEW OF RESULTS OF REACTOR SAFETY RESEARCH. Nyer, W. E.; Schroeder, F.; Wilson, T. R. (Phillips Petroleum Co., Idaho Falls, Idaho). IEEE (Inst. Elec. Electron. Eng.), Trans. Nucl. Sci., NS-13: No. 1, 126-32(Feb. 1966).

A survey of research on reactor safety is presented. The relation between the results of research and practical applications is stressed. (D.C.W.)

22436 SAFETY ASPECTS OF NUCLEAR POWER PLANTS—A UTILITY CONSULTANT'S VIEW. Witzig, Warren F. (Nuclear Utility Services, Inc., Washington, D. C.). IEEE (Inst. Elec. Electron. Eng.), Trans. Nucl. Sci., NS-13: No. 1, 133-7(Feb. 1966).

Projections of installed nuclear power plant capacity are provided as a background for the scope of activities with which utilities will be concerned for safety purposes. A description of the types of safety analyses is presented as well as the assumptions basic to such analyses. Finally, the "layers of conservatism" in present methods of analysis are illustrated and suggestions are made to attach quantitative values to these layers. (auth)

22437 SAFETY AND THE NUCLEAR PLANT ENGINEER. Bernsen, S. A.; Griffin, R. F. (Bechtel Corp., San Francisco, Calif.). IEEE (Inst. Elec. Electron. Eng.), Trans. Nucl. Sci., NS-13: No. 1, 138-43(Feb. 1966).

The safety of nuclear power plants is discussed in terms of the engineering conventions and problems. (D.C.W.)

22438 APPLICATION OF IN-CORE DETECTORS TO THE STARTUP OF LARGE BOILING WATER REACTORS. DuBridge, R. A.; Neissel, J. P.; Boyd, L. R. (General Electric Co., San Jose, Calif.). IEEE (Inst. Elec. Electron. Eng.), Trans. Nucl. Sci., NS-13: No. 1, 438-42(Feb. 1966).

An in-pile system that uses fission counters and fission chambers to cover neutron fluxes in the range of 10^5 to 5×10^{12} nv in a gamma field of 2.5×10^7 R/hr at 550°F is described. (D.C.W.)

22439 DESIGN OF THE INFORMATION PROCESSING UNIT OF THE FERD (FUEL ELEMENT RUPTURE DETECTOR) SYSTEM OF EBR-II. Porges, K. G.; McGinnis, Gerald (Argonne National Lab., Ill.). IEEE (Inst. Elec. Electron. Eng.), Trans. Nucl. Sci., NS-13: No. 1, 454-6 (Feb. 1966).

A system that was developed to record excursions in the count rate delivered by a bank of neutron detectors located on a coolant bypass loop of the EBR-II is described. (D.C.W.)

22440 CONTROL TECHNIQUE CONCEPTS FOR NUCLEAR POWER REACTORS. Profos, P. (Technische Hochschule, Zurich). Neue Tech., 8: 1-8(1966). (In German).

From the dynamics of the fission procedure used now in atomic power plants, a survey of the control characteristics of power reactors and their dependence upon the retrospective effects from the thermal installation parts is given. The correlations between the control of the neutron flux and that of the output of the plant are shown and some possibilities of adaptation are discussed. A view of the concepts of the output control of atomic power plants as they are used today is given with the aid of some examples. (auth)

22441 POWER FROM PLUTONIUM. Penney, William New Sci., 29: 484-6(Feb. 24, 1966).

The use of plutonium as a fuel for fast reactors is discussed. The Dounreay Fast Reactor Experiment is mentioned as having a part in the development of the use of plutonium fuel. The Prototype Fast Reactor is considered. Its design is shown and discussed. This reactor continues the development of more economical reactor systems from the Dounreay reactor experiment to future larger fast power reactors. (J.F.P.)

22442 EVOLUTION AND PROMISE OF ORGANIC-COOLED REACTORS. Campbell, K. H. Nucl. Eng., 11: 102-5(Feb. 1966).

The development of organic-cooled reactors is considered. A brief history is given of this development. The

organic-cooled heavy-water moderated reactor, an engineering comparison of converter systems, cladding and fuel material, and coolant tubes are discussed. (J.F.P.)

22443 EFFECT OF DELAYED NEUTRONS ON THE STABILITY OF A NUCLEAR POWER REACTOR. Baran, Viktor; Meyer, Kenneth. Nucl. Sci. Eng., 24: 356-61(1966).

An example is given to show that stability without delayed neutrons does not imply stability with delayed neutrons. A new criterion for stability in the large is derived. An example is given that shows that the new criterion predicts stability in some cases when the older criterion fails. (auth)

22444 OPERATING EXPERIENCE AND FUEL PERFORMANCE IN POWER REACTORS. FIRST ANNUAL SURVEY. Nucleonics, 24: 39-54(Mar. 1966).

Nuclear electricity generation throughout the world in 1965 is summarized. Operating experience from the Yankee water reactor is discussed, and the British Magnox stations are considered. Fuel performance data are also presented. (J.F.P.)

22445 PM-3A: FIRST NUCLEAR POWER PLANT IN ANTARCTICA. Fegley, C. E.; Zobel, W. M. Power Eng., 69: 46-8(Dec. 1965).

The operation, design, and specifications of this reactor, which has been in operation for 18 months, are outlined. The PM-3A, designed as an air-transportable nuclear power plant, was built and shipped in 18 basic portable units. For shipping, no single unit was larger than 8 × 8 × 30 ft or weighed more than 30,000 lb. The design criteria were based on the payload of a C-130 Hercules aircraft. The entire primary system, in four vertical containers, is set in an excavation of solid bedrock and backfilled with crushed rock for shielding. Leak-tested annually, the containment must have a measured leakage rate of less than 1.5% of the total volume (3300 ft^3) per day at 30 psig. The reactor and spent-core storage tank are filled with water for radiation shielding. The secondary steam plant is relatively conventional in design. The main generator rated output is 1800 kw at 0.8 power factor. Generated voltage is 4160 v. About 300 kw of the plant's output is used for station service load. In addition to electric output, the plant is designed to furnish 650,000 BTU/hr in the form of building space heating steam, plant auxiliary steam, and steam to run a salt-water distillation plant. (TCO)

22446 DOWN COME NUCLEAR FUEL COSTS. Power Eng., 70: 30-7(Dec. 1965).

Economic aspects of use of nuclear energy for power generation are discussed, with particular reference to changes in fuel costs. Reactor operating experience of the Dresden, Yankee, Indian Point, and other pioneer plants of utility systems is considered. Operation at the Yankee plant yields the most important experience based on a pressurized water reactor (PWR) power producer. Here, since the initial core, average power density in the fuel has increased by 50% and fuel burnup has been doubled. These improvements have reduced the cost of power in the Yankee plant by several mill/kw-hr. High burnup has been the most significant factor in reducing fuel costs. In Yankee burnup tests, an average burnup of 31,000 Mwd/t has been achieved on a standard fuel assembly irradiated in the first two Yankee cores. A peak burnup of close to 41,000 Mwd/t is expected. Current PWR proposals capitalize on higher burnups and advanced fuel management methods, with extended periods between refuelings, shorter (two to three weeks) downtime for refueling, and reduced costs made possible by smaller fuel inventories required. The optimum combination of burnup and power density (power produced in reactor core, divided by core volume) for future PWR is determined primarily by economics. Behavior of fuel or cladding does not appear to be a limiting factor. Additional burnup could be achieved by reducing the fuel density, providing sufficient volume for fuel swelling. Theoretical fuel lifetime can be increased by starting with a larger concentration of fissionable atoms within a fuel element. However, possible savings in fuel fabrication and recovery costs would be offset by poorer neutron economy and higher fuel inventory changes. Spent-fuel shipping problems are also considered, as well as nuclear fuel reprocessing expenses. (BBB)

22447 FROM WATTS TO MEGAWATTS WITH PACKAGED NUCLEAR POWER. Cohn, Paul D. (Battelle-Northwest, Richland, Wash.). Power Eng., 70: 50-3(Feb. 1966).

The development of a portable nuclear plant which may eventually compete with diesel-electric generation is considered. Packaged transportable nuclear power potentially is one of the most versatile and easily used electrical energy sources available. At present only one plant appears available for packaged power. The ML-1, built by Aerojet-General, is a mobile nuclear power plant generating 300-500 kw(e). One promising route is to use the standard technology of boiling water reactors (BWR), while retaining desired compactness. The competitive nuclear plant should have the following general characteristics: ease of installation and relocation; small operating crew and minimum maintenance needs; 20-yr plant life; and one-yr min between fuel changes. The cost characteristics of a 5- to 10-Mw(e) nuclear plant which would be competitive in many parts of the world, including the U. S. and Canada where diesel fuel costs in excess of 12 cents/gal, are tabulated and compared with estimated present costs. (BBB)

22448 THE INFLUENCE OF TECHNICAL AND ECONOMIC INDICATORS ON THE OPTIMUM TEMPERATURE OF THE FEED WATER AND ON THE OPTIMUM NUMBER OF REGENERATIVE PREHEATERS IN THE NUCLEAR STAGE OF ATOMIC ELECTRIC POWER PLANTS COMBINED WITH PRESSURIZED WATER REACTORS. Haiduc, C. Stud. Cercet. Energ. Electroteh., 15: 163-75(1965). (In Rumanian).

In view of the lack of economic data concerning the nuclear engineering portion of atomic power plants, the relative variations of electric energy generating costs were used as reference criteria in calculations aimed at the determination of specific conditions leading to minimum specific power costs. After examining the effect of the feed water temperature of a pressurized water reactor on the efficiency of the overall operation, equations were derived for determining the changes in the net yield of the nuclear stage of the plant, considering also the influence of the feed water temperature on the internal power consumption of the system. The factors examined included specific steam consumption at various temperatures, flow rate of the steam in the condenser, pressure losses in the condenser and power requirements of the primary circuit's pumps. Data from the following operating atomic power plants were used in the calculations: Novo-Voronezh, (USSR), Rheinsberg (West Germany), Shippingport, Indian Point, and Dresden (USA) and Punta Fiume (Italy). The lower optimum temperature at Indian Point where fossile fuels are used for the superheat is due to the fact that the steam pressure was 26 atm. rather than 35 atm. used in this study. The higher temperature at the Dresden plant is caused by the use of a cycle with 2 pressures. The following parameters were used in the calculation: initial steam pressure—35 atm; temperature—435°C. (TTT)

22449 CHARACTERISTICS OF THE HEAT CALCULATIONS OF BOILING WATER REACTORS WITH NUCLEAR SUPERHEATING OF THE STEAM. Haiduc, C. (Inst. of Atomic Energy, Bucharest). Stud. Cercet. Energ. Electroteh., 15: 327-41(1965). (In Rumanian).

Recent studies on heat transfer in reactors under conditions of boiling and superheating indicated that high heat fluxes may be obtained in a direct thermodynamic cycle. The improved heat transfer, especially when combined with supercritical steam parameters resulted in the elimination of the steam generator, a marked increase of the initial cycle parameters and an overall increase of the yield of the plant. In the design examined, the boiling region surrounded the zone of superheating. The thermal and physical parameters considered in the calculation included the lat-

tice parameters, multiplication coefficients, dimensions of the reflector, fuel element characteristics, control, safety and regulating rods, reactor period, etc. A 200-Mw boiling water reactor was examined; the steam at the outlet of the nuclear superheat was $P_0 = 90$ atm and $t_0 = 535°C$. The UO_2 fuel was enriched to 1.5%. Relations were obtained for determining the distribution of nonuniformity coefficients of the heat generation as a function of the height and radius of the core and for the temperature distribution of the cooling agent, together with the gradient within the walls of the fuel elements. The method derived may be extended for other reactor types. (TTT)

22450 A MAJOR CONTRIBUTION TO THE BRITISH NUCLEAR POWER PROGRAMME. Whetstone, Eng., English Electric Co. Ltd., [1964]. 22p.

The design, development, and performance of the Magnox reactors are described. The Hinkley Point, Sizewell, and Wylfa reactors are described and compared and performance data for these stations are presented. Research programs and future development are also considered. (J.F.P.)

22451 SAFETY AND COST ANALYSIS OF A 1000 MWe SODIUM COOLED FAST POWER REACTOR. Smidt, D.; Frisch, W.; Giordano, P.; Heusener, G.; Kessler, G.; Krewer, K. H.; Merk, W.; Malmberg, T.; Schoenfeld, E. (Kernforschungszentrum, Karlsruhe, Ger.). 39p. (CONF-651009-18). ORAU. Gmelin, AED-CONF-65-307-15.

From Conference on Safety, Fuels, and Core Design in Large Fast Power Reactors, Argonne, Ill.

Three general safety criteria for a fast reactor are considered: the time between the beginning of an infinite reactivity ramp input and the starting of melting of the hottest fuel, the maximum rate of the reactivity ramp that can be counteracted by the safety system without starting fuel melting, and the maximum hypothetical accident. The effects of systematic small displacements of important design parameters on safety and costs were calculated. The results are tabulated. In general it is concluded that the 1000-Mw(e) reactor proposed by the Karlsruhe group is very safe. Parametric studies show advantages in cost and safety in the direction of lower coolant fractions, larger coolant temperature rise, and a not too compact carbide core. (A.G.W.)

22452 COMPARISON OF He, CO_2, AND STEAM AS COOLANTS OF A 1000 MWe FAST REACTOR. Dalle Donne, M. (Kernforschungszentrum, Karlsruhe, Ger.). 60p. (CONF-651009-25). ORAU. Gmelin, AED-CONF-65-307-35.

From Conference on Safety, Fuels, and Core Design in Large Fast Power Reactors, Argonne, Ill.

A comparison of steam, helium, and carbon dioxide as coolants for a 1000-Mw(e) fast breeder reactor core indicates that steam is by far the best coolant from a thermal point of view, followed by helium. Carbon-dioxide-cooled reactors are the best breeders, and steam-cooled reactors have the smallest breeding ratios. If the available Doppler minus the total coolant void reactivity is taken as a criterion indicative for safety, then helium is the safest coolant and steam the most dangerous with the difference between helium and carbon dioxide being very small. These conclusions are not considered definitive because too many assumptions are made. General heat transfer and neutron calculations and results of calculations for particular reactors are included in appendixes. (A.G.W.)

22453 THE KARLSRUHE REFERENCE DESIGN OF A 1000 MWe SODIUM COOLED FAST BREEDER REACTOR. Haefele, W.; Smidt, D.; Wirtz, K. (Kernforschungszentrum, Karlsruhe, Ger.). 51p. (CONF-651009-15). ORAU. Gmelin, AED-CONF-65-307-17.

From Conference on Safety, Fuels, and Core Design in Large Fast Power Reactors, Argonne, Ill.

The design of the 1000-Mw(e) fast breeder reactor presently being studied by the Karlsruhe Fast Breeder Project is described. The reactor uses UO_2/PuO_2 fuel clad with austenitic stainless steel in the form of conventional pins in a hexagonal assembly. Sodium coolant is used in a loop-type primary circuit. The safety features of the reactor are discussed with respect to incidents, the maximum hypothetical accident, and the design basis accident. It is concluded that the proposed reactor is feasible and that no major safety problems are involved. The expected fuel cycle cost is 0.7 mil/kwh and capital costs are $100/kwh. It is anticipated that further study will lead to improvements in both safety and economy. (A.G.W.)

22454 A RE-EXAMINATION OF DESIGN FACTORS FOR A 1000 Mwe FAST BREEDER REACTOR. Farmer, William S.; Strawson, David G. (Allis-Chalmers Mfg. Co., Milwaukee). 16p. (CONF-651009-14). ORAU. Gmelin, AED-CONF-65-307-1.

From Conference on Safety, Fuels, and Core Design in Large Fast Power Reactors, Argonne, Ill.

Designs for large fast breeder reactors proposed independently by Allis-Chalmers Mfg. Co., Combustion Engineering, General Electric Co., and Westinghouse Electric Corp. are compared. It is concluded that a single core capable of producing 1000 Mw(e) with fuel cycle costs under 1 mil/kwh is generally feasible. Comparison of the safety characteristics of cores using oxide and carbide fuel indicates that, at present, neither fuel appears to offer a significant safety advantage. Core geometries are compared with respect to plutonium inventory and outside core diameter. Neither annular, pancake, or modular designs appear to have any significant advantage. (A.G.W.)

22455 THE SEPARATELY FIRED SUPERHEATER—A NUCLEAR APPLICATION AT INDIAN POINT. McCormick, D. J. (Indian Point Consolidated Edison Co., Buchanan, N. Y.); Gorzegno, W. P. New York, The American Society of Mechanical Engineers, 1965, Preprint No. 65-PWR-14, 16p., $1.00. (CONF-650970-4). ORAU.

From National Power Conference, Albany.

The separately fired superheaters in the flow cycle are described, and the economics and design criteria involved are discussed. The design of the superheaters is outlined with respect to circuitry and equipment arrangement. A brief summary of operating history and a description of initial difficulties with the superheaters is included. The nature of corrective work to the superheaters is outlined, together with the analytic methods used to evaluate functional requirements. Some aspects of control during startup and startup procedures are covered. (auth)

22456 PREPARING FOR OPERATIONS AT PEACH BOTTOM ATOMIC POWER STATION. Boyer, Vincent S. (Philadelphia Electric Co.). 11p. (CONF-650970-1). ORAU.

From National Power Conference, Albany.

A brief description of basic plant systems is followed by a report on personnel organization and training. The training program was initiated in the fall of 1960, and the entire plant operating organization has been at the site since Nov. 1963. Activities since 1963 included writing of normal and emergency operating procedures for the entire plant, on-site training of operators, and testing of equipment as it was installed. Problems encountered in equipment testing and resultant modifications are considered briefly. (A.G.W.)

22457 OPERATING EXPERIENCE OF YANKEE—UPDATED. Reed, Glenn A.; Howard, J. Edward (Yankee Atomic Electric Co., Boston). New York, Inst. of Electrical and Electronics Engineers, 1965, Preprint No. 31 CP 65-784, 32p., $1.00. (CONF-650970-3). ORAU.

From National Power Conference, Albany.

The Yankee plant has been in operation since 1960 and in that time the power level was increased in three steps from about 125 to 185 Mw(e). The reactor was refuelled three times with reduction each time in length of time required. The present fuel assembly and annealed 348 stainless steel cladding has given superior performance, but Zircaloy cladding is being tested for economic reasons. Problems associated with personnel, fuel and refueling, chemistry, reactor physics, and waste disposal and shipping are discussed. Tables of operating statistics are included. (A.G.W.)

22458 IMPROVEMENTS IN AND RELATING TO NUCLEAR POWER PLANTS. Lawrence, Arthur Charles (to Foster Wheeler Ltd.). British Patent 1,019,622. Feb. 9, 1966. Filed May 15, 1961.

In a nuclear power plant two independent circulation circuits are provided for the primary coolant through the heat exchange elements so that if one should fail the other will prevent excessive overheating until the reactor can be closed down. Both the coolant circuits are included in the same steam generator shell that is anchored at a single point in its periphery as is the shell of the reactor. The two points of anchorage are close to each other if not coincident with each other. (B.L.M.)

Process Heat Reactors

22459 (66-1-RE) ENGINEERING FEASIBILITY AND ECONOMIC STUDY FOR DUAL-PURPOSE ELECTRIC POWER-WATER DESALTING PLANT FOR ISRAEL. (Kaiser Engineers, Oakland, Calif. Catalytic Construction Co., Philadelphia, Pa.). Jan. 1966. 302p. Dep. mn. CFSTI $2.00 cy, $1.50 mn.

For United States–Israel Joint Board.

The study was conducted in two phases. The first phase was directed toward determining the feasibility of a dual-purpose electric power-water desalting plant ready for commercial operation in Israel by mid-1972 and included; (1) comparisons of various dual-purpose nuclear power and desalting plants using the multi-stage flash evaporation process and selection of one of these plants (hereinafter referred to as the reference plant) for detailed evaluation, (2) comparison of this selected plant with a comparable fossil-fuel dual-purpose plant, and (3) a recommended development program to confirm certain desalting plant components and design criteria. The second phase was directed toward preparing a detailed evaluation of the reference plant and to develop information for use in preparing an application to funding agencies. During Phase II the conceptual design was refined and new estimates of the capital cost, annual cost, and the unit cost of water were prepared. In addition, several plant alternatives and factors important in the determination of the total annual cost were examined such as; (1) differences in the desalting plant design and in the cost of water resulting from the selection of either a boiling-water or pressurized-water reactor for the nuclear steam supply, (2) differences in the cost of water resulting from the selection of a concrete instead of a steel reactor containment building, (3) differences in the cost of water resulting from the selection of concrete instead of steel evaporator chambers, (4) review of the plant operating factor, (5) determination of the effect of seasonal seawater temperature on the capital cost and the unit cost of water, and (6) determination of the change in the cost of water which would result if potential decreases in the nuclear fuel cycle costs materialize. Included are the results of the Phase I work and the results of the above Phase II studies including the estimates of capital cost, annual cost, and the unit cost of water. (M.O.W.)

22460 (IC-66/28) ARE QUARKS FRACTIONALLY OR INTEGRALLY CHARGED? Khanna, M. P.; Okubo. S. (International Centre for Theoretical Physics, Trieste (Italy)). Mar. 31, 1966. 9p. Dep. mn.

On the basis of algebra of currents, the decay rate $\pi^0 \rightarrow 2\gamma$ and the axial vector renormalization constant g_A were calculated. These numbers are model dependent. and it was found that the fractionally charged quark model gives more satisfactory results than the integrally charged quark model. (auth)

22461 COST DETERMINATION AND COMPARISON OF NUCLEAR AND FOSSIL FUELED DUAL-PURPOSE POWER AND DESALINATION PLANTS. Fruth, Hans. 19p. (CONF-651005–4). ORAU. Gmelin, AED-CONF-65-276-8.

From 1st International Symposium on Water Desalination, Washington, D. C.

The general conditions and reasons for which lower fresh water costs may be expected with the nuclear-dual purpose plants than fossil fueled plants are presented. A determination method is developed by means of the exergy concept to allow the accomplishment of an equitable cost breakdown in a dual-purpose plant based on the design data of the plant itself, independent of cost comparisons with reference plants or market conditions. The economics of nuclear–fueled single-purpose desalting plants is discussed. (B.L.M.)

22462 APPLICATION OF THE VENTED FUEL CONCEPT TO A SODIUM COOLED POWER BREEDER WITH 1000 MWe. Smidt, D.; Sommer, W. (Kernforschungszentrum, Karlsruhe, Ger.). 16p. (CONF-651009–19). ORAU. Gmelin, AED-CONF-65-307-16.

From Conference on Safety, Fuels, and Core Design in Large Fast Power Reactors, Argonne, Ill.

The advantages and disadvantages of venting the fission gas from a 1000-Mw(e) sodium-cooled power breeder reactor to the coolant are listed. Principal design specifications are given for the gas purification plant required, amounts of fission gases produced are calculated, and costs are evaluated. It is concluded that the venting of fission gases to the sodium coolant allows for savings in the order of 2% of the total plant cost compared to the reference reactor. The main savings are from lower costs for core and radial blanket resulting from the elimination of the fission gas plenum and the reduction of cladding thickness. The most important advantage is considered to be the gain in safety. (A.G.W.)

Production Reactors

22463 (DP–1028) PERFORMANCE OF ACTIVATED CARBON BEDS IN SRP REACTOR CONFINEMENT FACILITIES. Progress Report, September 1962–September 1965. Durant, William S. (Du Pont de Nemours (E. I.) and Co., Aiken, S. C. Savannah River Lab.). Jan. 1966. Contract AT(07-2)-1. 27p. Dep. mn. CFSTI $2.00 cy, $0.50 mn.

The efficiency of activated C beds for removal of elemental iodine remains greater than the design efficiency of 99.9% after ~2 years of continuous exposure to exhaust ventilation air from Savannah River Plant reactor buildings. Because of corrosion of both the Cd-plated and the painted mild steel frames that contain the C, replacement units are being fabricated of Type 304L stainless steel. (auth)

22464 (IC–66/29) COMPLETENESS, UNITARITY, AND DISPERSION RELATIONS IN POTENTIAL SCATTERING. Saavedra, I. (International Centre for Theoretical Physics, Trieste (Italy)). Apr. 5, 1966. 10p. Dep. mn.

It is shown that the assumption of completeness of the set of scattering states implies the unitarity condition for the total scattering amplitude and dispersion relations for the S-matrix for each value of the angular momentum. (auth)

22465 NUCLEAR REACTOR. Sankovich, Melvin F. (to Babcock and Wilcox Co.). U. S. Patent 3,235,463. Feb. 15, 1966. Filed Oct. 9, 1961.

A nuclear reactor includes a subcritical mass of fuel containing a mixture of fertile and fissionable material disposed as a number of elongated and longitudinally contiguous fuel element assemblies of heterogeneous form geometrically arranged in the core to undergo a controlled chain reaction. The element assemblies are contained in an elongated pressure vessel, and an upper and lower grid arrangement serves to support the fuel element assemblies. The assemblies are separate, replaceable, and individually removable and have end portions that are arranged to be fitted into the grid plates. The upper grid plate is arranged to hold the assemblies in position irrespective of thermal expansion changes, and the lower grid is provided with orifices to adjustably control the flow of cooling fluid through it. The controls for the reactor are bottom mounted and arranged to pass through the pressure vessel. Thermal shields are arranged concentrically about the core within the vessel, and a light water filled neutron shield tank is arranged exteriorly about the pressure ves-

sel. The control rods are located in the center of the fuel element assemblies surrounded by the fuel elements. (B.L.M.)

Propulsion and Space

See also ENGINEERING — Space Propulsion

Refer also to abstracts 20870, 20871, 20937, and 20954.

22466 (ANL–7180) CATALOG OF NUCLEAR REACTOR CONCEPTS. PART I. HOMOGENEOUS AND QUASI-HOMOGENEOUS REACTORS. SECTION V. REACTORS FUELED WITH URANIUM HEXAFLUORIDE, GASES, OR PLASMAS. Teeter, Charles E.; Lecky, James A.; Martens, John H. (Argonne National Lab., Ill.). Mar. 1966. Contract W-31-109-eng-38. 50p. Dep. mn. CFSTI $3.00 cy, $0.50 mn.

Brief descriptions of reactors fueled with uranium hexafluoride, either as a gas or a liquid, and those fueled with other gases (such as vaporized fissile metals) or with plasmas are presented in data sheet form. (M.O.W.)

22467 (IDO–17077) STEP PROJECT. Quarterly Technical Report, July 1964–September 1964; October 1964–December 1964. Dietz, K. A.; Mellow, E. W.; Pace, N. E. (Phillips Petroleum Co., Idaho Falls, Idaho. Atomic Energy Div.). Mar. 1966. Contract AT(10-1)-205. 219p. Dep. mn. CFSTI $6.00 cy, $1.25 mn.

During this period, the test program of the SNAPTRAN 2/10A-1 reactor consisted primarily of the nondamage, step-reactivity-insertion, transient tests. The preliminary modifications and nuclear operations are briefly discussed as are the power calibration and drum calibration. The experimental measurements and instrumentation used in the transient tests are described in detail. A series of eighteen transient tests was performed (using step-reactivity insertions) to evaluate the reactivity feedback effects as related to average core fuel temperature in the range of ambient to 700°F. The tests were initiated from ambient temperatures of less than 100°F. The test procedure consisted of inserting successively higher step reactivities to obtain successively higher energy releases and, correspondingly, successively higher fuel temperatures. The power and energy response of the SNAPTRAN 2/10A-1 reactor during an impulse reactivity insertion was investigated by means of digital computer calculations. The impulse test predictions resulting from this investigation are presented. A study of the proposed SNAPTRAN 2/10A-2 destructive test was undertaken to provide an estimate of the energy release and to predict the behavior of the reactor. A discussion of the calculations used in the study and an evaluation of the results obtained are given. The Loss-of-Fluid Test (LOFT) was originally proposed for a stainless steel clad core; however, since emphasis was recently placed on the use of zirconium-clad fuels, preliminary studies were undertaken to investigate the effect that the use of zirconium cladding would have on the design of the LOFT reactor and facility. Since metal-water-reaction energy releases can be significant if zirconium cladding is used, the extent and rate of the reactions were studied to evaluate the effect of the energy on the reactor containment pressure and temperature response and on the fission product release. The results of these studies are reported for the zirconium-clad core. Also reported are thermal and hyraulic studies and studies to indicate the axial position at which the temperature of the stainless steel cladding reaches the melting point. These studies are reported only for the stainless-steel-clad core; whereas, nuclear studies are reported for both the stainless-steel-clad and zirconium-clad cores. During this period, the fission product sampling systems were designed; sampling system activity studies were performed; the radiological computer code (RSAC) was completed for the cloud gamma calculation; and a series of cases involving the release of fission products to the atmosphere was studied. Containment coating materials were exposed to conditions simulating those expected during the loss-of-coolant test. The coating materials were evaluated to determine their resistance to humidity, temperature, radiation, and decontamination solutions. The results of the studies are summarized, and illustrations are given showing the physical effects of the environments to which the coating materials were exposed. (auth)

22468 (LA–3395) RADIATION MEASUREMENTS OF THE EFFLUENT FROM THE KIWI TNT EXPERIMENT. Henderson, R. W.; Fultyn, R. V. (Los Alamos Scientific Lab., Univ. of California, N. Mex.). Oct. 1965. Contract W-7405-eng-36. 42p. Dep. mn. CFSTI $2.00 cy, $0.50 mn.

Included is a compilation of data resulting from the collection of samples of, and direct measurements of, the effluent cloud from the Kiwi Transient Nuclear Test experiment. Data are presented concerning the magnitude and isotopic composition of the airborne and ground deposited material at distances from 4,000 feet to 50 miles from the test point. Data from samples collected by cascade type impactors are given. Film dosimetry radiation measurements taken at the various stations are presented. A brief description of equipment and techniques used in the reduction is included. An appendix gives the true distance and azimuth of each sampling station with regard to the TNT test point. (auth)

22469 (N–65–29479) APPLICATIONS OF LOW-POWER NUCLEAR ROCKETS. Rom, Frank E. (National Aeronautics and Space Administration, Cleveland, Ohio. Lewis Research Center). [1964]. 17p. (NASA-TM-X-52048). CFSTI $1.00 cy, $0.50 mn.

Large velocity increments necessary to achieve scientific missions of interest require the use of lightweight nuclear power plants since all chemical systems cannot accomplish many missions which the nuclear systems can. The velocity requirements of low-power missions are pointed out. The performance that would be attainable with the use of these low-power missions on booster systems that are currently developed or being developed is discussed. (STAR)

22470 (N–65–29480) FAST AND MODERATED LOW-POWER, LIGHTWEIGHT REACTORS FOR NUCLEAR ROCKET PROPULSION. Rom, Frank E. (National Aeronautics and Space Administration, Cleveland, Ohio. Lewis Research Center). 1964. 75p. (NASA-TM-X-52047). CFSTI $3.00 cy, $0.75 mn.

Fundamental reactor types are described, the properties of high temperature materials available for nuclear rocket reactor applications are examined, and various reactor concepts suitable for low power lightweight nuclear rocket powerplants are presented. The study showed that it is possible to conceive of lightweight nuclear rocket powerplants suitable for low power applications. In examining the basic properties of the refractory materials such as melting point, vaporization rate, thermal stress resistance, and strength, tungsten was found to offer the greatest potential for both fast and thermal reactors. (STAR)

22471 (NAA-SR–11814) SNAP-10A FSM—4-SYSTEM TEST. Soske, Paul L. (Atomics International, Canoga Park, Calif.). Mar. 25, 1966. Contract AT-11-1-GEN-8. 80p. Dep. mn. CFSTI $3.00 cy, $0.75 mn.

FSM-4 is a non-nuclear test system designed to provide preflight qualifications for SNAP 10A. The FSM-4 test system duplicated in every detail the SNAP 10A unit except for the nuclear heat source, which was simulated in the FSM-4 tests by electric heating. Before the flight system could be launched, FSM-4 was required to demonstrate successful performance in surviving the startup temperature transient. The FSM-4 testing had four objectives: (1) shock and vibration testing of a NaK-loaded system; (2) simulated orbital operation before startup; (3) simulated orbital startup sequence with emphasis on the thermal transient; and (4) thermal reference endurance testing. The FSM-4 tests demonstrated that the flight system would produce rated power after being subjected to launch and orbital environment. The endurance testing indicated problem areas where additional inspection and modification on the flight system were required. (auth)

22472 (SC-CR-66-2017) ROVER DESTRUCT TEST THREE, ABERDEEN PROVING GROUND. Final Report. Castonguay, T. T.; Anderson, T. B.; Bower, R. C. (New Mexico Univ., Albuquerque). Dec. 1965. Contracts AT(29-1)-789; 48-2512. 15p. Dep. mn. CFSTI $1.00 cy, $0.50 mn.

For Sandia Corp., Albuquerque, N. Mex.

Particle collection and sizing are reported from the ROVER destruct test. These data are expected to provide a few of the inputs to a computer program designed to analyze particle distribution from a space destruct of the ROVER/NERVA propulsion engine. These data were obtained from polystyrene blocks containing graphite particles, which were dissolved in trichloroethylene. The graphite particles were collected, cleaned and sized through a series of Tyler sieves. Graphite particles embedded in rotating polystyrene plastic were also recovered and sized, but prior to dissolving, the angle of entry and depth of penetration were tabulated. (auth)

22473 BINARY DIFFUSION IN A CONFINED VORTEX. Lewellen, W. S.; Ross, D. H.; Rosenzweig, M. L. (Aerospace Corp., El Segundo, Calif.). AIAA (Amer. Inst. Aeron. Astronaut.) J., 4: 396-405(Mar. 1966).

Pressure diffusion of a binary mixture in confined vortices (of a type considered for possible hydrodynamic containment in a gas-core nuclear rocket) is investigated theoretically and experimentally. An approximate integral solution is presented for the species distribution resulting from the combined actions of convection, and concentration and pressure diffusion. The flow model includes secondary flows induced by boundary-layer interaction on the end walls of the vortex chamber. The qualitative effect of varying the degree of boundary-layer interaction is demonstrated by a flow-visualization experiment using dye in a water vortex. Quantitative data are obtained from an experiment in which iodine vapor and heated helium are premixed and injected tangentially into a vortex chamber, forming a low-density, high-velocity flowfield. The resulting radial distribution of iodine concentration is determined optically. Peak density ratios of iodine to helium within the vortex are found to be as much as three times the density ratio of the mixture flowing into the chamber. The experimental data agree favorably with the theoretical predictions and demonstrate that a gas of high molecular weight can be substantially retained in a vortex comprised of a gas of low molecular weight. (auth)

22474 DEVELOPMENT OF THE CONTROL SYSTEM FOR SNAP REACTORS. Steele III, O. P.; Kellogg, L. G.; Dewart, W. G. (Atomics International, Canoga Park, Calif.). IEEE (Inst. Elec. Electron. Eng.), Trans. Nucl. Sci., NS-13: No. 1, 206-23(Feb. 1966).

The development of the various components of the control systems of the SNAP-2, SNAP-8, and SNAP-10A reactors is discussed. The electromechanical actuators, bearings, and gears are considered in detail. (D.C.W.)

22475 SNAP ENVIRONMENT SIMULATION PROBLEMS. Long, W. G.; Davies, N. F.; Warren, M. (Atomics International, Canoga Park, Calif.). IEEE (Inst. Elec. Electron. Eng.), Trans. Nucl. Sci., NS-13: No. 1, 224-9 (Feb. 1966).

The engineering problems that were encountered in the course of the SNAP reactor component irradiation program are described along with the test facilities. The environmental tests of two SNAP-10A control drum actuators coupled to two drum position sensors are summarized. (D.C.W.)

22476 SNAP-10A INSTRUMENTATION AND CONTROL DEVELOPMENT AND TESTING. Smith, A. K.; Zerbel, D. (Atomics International, Canoga Park, Calif.). IEEE (Inst. Elec. Electron. Eng.), Trans. Nucl. Sci., NS-13: No. 1, 236-43(Feb. 1966).

The SNAP-10A instrumentation and control subsystems are described, and the testing of the components and systems is summarized. (D.C.W.)

22477 GROUND TESTING OF THE SNAP-10A/AGENA SPACE SYSTEM. Pohlman, John F. (Lockheed Missiles and Space Co., Sunnyvale, Calif.). IEEE (Inst. Elec. Electron. Eng.), Trans. Nucl. Sci., NS-13: No. 1, 244-53 (Feb. 1966).

The SNAP-10A/Agena power system is briefly described, and the ground test program is summarized. (D.C.W.)

22478 SNAPSHOT LAUNCH OPERATIONS. Ureda, B. F. (Atomics International, Canoga Park, Calif.). IEEE (Inst. Elec. Electron. Eng.), Trans. Nucl. Sci., NS-13: No. 1, 254-63(Feb. 1966).

The activities leading up to the launching of the SNAP-10A/Agena are summarized including the testing, shipment, and inspection of the SNAP-10A system as well as the safety analysis that was performed. (D.C.W.)

22479 SNAP-8 REACTOR TEST PROGRAM. Johnson, C. E.; Roecker, J. H. (Atomics International, Canoga Park, Calif.). IEEE (Inst. Elec. Electron. Eng.), Trans. Nucl. Sci., NS-13: No. 1, 264-9(Feb. 1966).

A summary of the SNAP-8 reactor test program is presented. The experimental reactors and mockup are briefly described, and the tests that have been performed are summarized. Other tests are also outlined. (D.C.W.)

22480 FLOW SYSTEM STARTUP OF A FULL-SCALE SIMULATED NUCLEAR ROCKET ENGINE. Colmery, Benjamin H.; Powers, Albert G. (National Aeronautics and Space Administration, Cleveland). IEEE (Inst. Elec. Electron. Eng.), Trans. Nucl. Sci., NS-13: No. 1, 658-62 (Feb. 1966).

The performance of the liquid hydrogen flow system during the startup transient of a nuclear rocket was measured in a full-scale simulated engine system. In-flight exhaust conditions were approximated by maintaining a nozzle outlet pressure of 1 psia. Data and general conclusions on overall system performance are presented for nonnuclear operation. The ability of the rocket system to bootstrap (i.e., to build up appreciable hydrogen flow and pressure in the nuclear reactor without extra-system assistance) was clearly demonstrated by using only the energy from hydrogen tank pressure and latent heat of engine components. The severity (small) and characteristics of two-phase flow oscillations during windmill were determined. No significant operating problems were encountered. (auth)

22481 RADIATION ENVIRONMENT ABOUT THE NERVA REACTORS. Brooks, E. H.; Woodsum, H. C.; Capo, M. A. (Westinghouse Electric Corp., Pittsburgh). IEEE (Inst. Elec. Electron. Eng.), Trans. Nucl. Sci., NS-13: No. 1, 663-9(Feb. 1966).

Some measurements of gamma dose rates and neutron-flux distributions that were made during the testing of the NRX-A2 and NRX-A3 reactors are summarized. The experimental results are compared with theoretical predictions. (D.C.W.)

22482 NEW CONTROL TECHNIQUES FOR NERVA REACTORS. Kirschbaum, H. S.; Morris, W.R.; Hohmann, G. L. (Westinghouse Electric Corp., Pittsburgh). IEEE (Inst. Elec. Electron. Eng.), Trans. Nucl. Sci., NS-13: No. 1, 670-5(Feb. 1966).

The control systems that were used to test the early KIWI and NRX reactors are briefly discussed, together with improvements in the control systems. (D.C.W.)

22483 DYNAMICS OF CLUSTERED NUCLEAR ENGINES. Woyski, Jan. S. (Douglas Aircraft Co., Santa Monica, Calif.). IEEE (Inst. Elec. Electron. Eng.), Trans. Nucl. Sci., NS-13: No. 1, 676-84(Feb. 1966).

A method of evaluating reactivity coupling between clustered rocket reactors was developed, and an analog model of a clustered nuclear propulsion system was used for the simulation of the complete operating cycle of such a system. (D.C.W.)

22484 NERVA NUCLEAR REACTOR INSTRUMENTATION. Malick, F. S.; Ramp, R. L.; Gilmour, G. A. (Westinghouse Electric Corp., Pittsburgh). IEEE (Inst. Elec. Electron. Eng.), Trans. Nucl. Sci., NS-13: No. 1, 685-91(Feb. 1966).

The instrumentation problems associated with the de-

velopment of the reactor are discussed, together with the extent of the solution of the problems. Vibration, displacement, and pressure transducers; strain gages; high-temperature thermocouples; neutron detectors; and calorimeters are discussed. (D.C.W.)

22485 NUCLEAR LIQUID METAL CELL FOR SPACE POWER. Agruss, B. (General Motors Corp., Indianapolis). pp 100-3 of Proceedings, 17th Annual Power Sources Conference. Red Bank, N. J., PSC Publications Committee, 1963.

The results are presented of an investigation of the characteristics and performance of a thermally regenerative system in which Hg and K are reacted electrochemically in a cell to produce power and the mercury is distilled away from the resulting amalgam for re-use. (D.C.W.)

22486 MEANS AND METHODS OF ASSEMBLY OF A NUCLEAR AIRCRAFT ENGINE. Newcomb, Philip P. U. S. Patent 3,235,205. Feb. 15, 1966. Filed Oct. 2, 1957.

A nuclear gas-turbine engine-driven aircraft is so designed that the major mounts supporting the engine on the airframe are located on the radiator section with any component parts that may need to be removed for periodic inspection mounted in such a way that they may be easily removed. The easily demountable parts may include the engine turbine section, the engine compressor section, the engine shaft, and the engine bearings. The radiator with its fluid connections to the reactor is a relatively permanent part of the aircraft structure. (B.L.M.)

Research and Test Reactors

Refer also to abstracts 20721, 21050, and 22410.

22487 (AD-621118) FUEL BURNUP STUDIES OF THE AIR FORCE NUCLEAR ENGINEERING TEST FACILITY [Thesis]. Thompson, Max Forest Jr. (Air Force Inst. of Tech., Wright-Patterson AFB, Ohio. School of Engineering). June 1965. 185p. (GNE-Phys-65-19). CFSTI $5.00 cy, $1.00 mn.

To study the effect of fuel burnup on the AFNETF a new code, called Twenty Grand Burnup, was developed. Included is a discussion of the theory and the code as well as the results of the calculations of fuel burnup. (auth)

22488 (AD-621121) A TRANSPORT CALCULATION OF THE FLUX IN THE NUCLEAR ENGINEERING TEST REACTOR TEST CELLS [Thesis]. Livingston, Lee Haltom (Air Force Inst. of Tech., Wright-Patterson AFB, Ohio. School of Engineering). June 1965. 78p. (GNE-Phys-65-10). CFSTI $3.00 cy, $0.75 mn.

A calculation of the neutron flux in the test cells using the discrete S_n approximation to the transport equation in xy-geometry is described. The calculation was done by writing a computer program, S4C40, for the IBM 7094 using three energy groups and 1600 mesh points. Fast cross sections were generated with the General Atomics code GAM-1, and thermal cross sections were calculated by hand assuming a Maxwell-Boltzmann distribution. The results, which were compared with the multigroup, two-dimensional diffusion theory code PDQ, show a significantly higher thermal flux over the entire reactor and a more slowly decreasing flux for all groups in the test cell. (auth)

22489 (AD-621123) THE CONSTRUCTION AND INSTRUMENTATION OF A CRYOSTAT FOR THE AIR FORCE NUCLEAR ENGINEERING TEST FACILITY [Thesis]. McAllister, Karl D. (Air Force Inst. of Tech., Wright-Patterson AFB, Ohio. School of Engineering). Aug. 1965. 93p. (GNE-Phys-65-4-A). CFSTI $3.00 cy, $0.75 mn.

The cryostat and associated helium supply systems were constructed. Instruments were designed to measure the various parameters of the experiments to be conducted with the cryostat. Instruments to measure temperature and liquid level were constructed and tested. Biological shielding for use with the cryostat, in the reactor, was designed. Some changes in the design were incorporated because of available fabrication techniques. (auth)

22490 (AD-621124) A KINETIC ANALYSIS OF THE AIR FORCE NUCLEAR ENGINEERING TEST REACTOR [Thesis]. Palmer, John Arnold (Air Force Inst. of Tech., Wright-Patterson AFB, Ohio. School of Engineering). Aug. 1965. 205p. (GNE-65-16). CFSTI $6.00 cy, $1.25 mn.

A series of parametric relationships are derived which predict the kinetic behavior of the Air Force Nuclear Engineering Test Reactor. These parametric relations are based both on the reactor's physical design and its calculated nuclear constants. The analytical model chosen was based heavily on experimental and theoretical results from the SPERT I and IV test series. Neutron kinetics was designed using the space independent kinetics equations with six delayed groups. Thermal kinetics was obtained by breaking the reactor cooling system into a series of blocks and writing a heat balance equation for each. Reactivity feedback was based on an effective void volume due to moderator density change, core expansion, and steam formation. A digital computer code was constructed to solve the resulting set of differential equations. The theory was checked by inserting nuclear and physical characteristics of the SPERT IV reactor facility into the code. Time-dependent plots of power, temperature and reactivity which compared favorably with experiment resulted. A series of parametric power and temperature curves were then obtained for the NETR by varying void coefficient, delayed fraction, generation time, and metal–water ratio, for various step inputs of reactivity. (auth)

22491 (AD-621269) NEUTRON TRANSPORT CALCULATIONS OF THE AIR FORCE NUCLEAR ENGINEERING TEST FACILITY CORE [Thesis]. Norman, Donald Lloyd (Air Force Inst. of Tech., Wright-Patterson AFB, Ohio. School of Engineering). Aug. 1965. 61p. (GNE-Phys-65-14). CFSTI $3.00 cy, $0.75 mn.

The neutron flux in segments of the core of the Air Force Nuclear Engineering Test Reactor was investigated using transport theory. Two portions of the core were treated; the fuel plates and the control rods. These regions were represented as a one-dimensional array of thin slabs. A matrix collapsing technique for the solution of many-region, slab-geometry problems using the P-3 approximation was developed and a computer code to make the calculations was written. It was determined that no flux weighting was necessary in calculating homogeneous cross sections for the fuel regions. A technique was developed to compute a simplified control rod model, but computing difficulty prevented its being tested. (auth)

22492 (AD-626861) PRE-STARTUP HYDRAULIC TESTS AT THE AIR FORCE NUCLEAR ENGINEERING TEST FACILITY. Final Report, 1961–1965. Buoni, Frederick B.; Hary, Laszlo B.; Lewisand, Valta G.; Vallish, Edward J. (Air Force Flight Dynamics Lab., Wright-Patterson AFB, Ohio). Oct. 1965. 50p. (AFFDL-TR-65-131). CFSTI $2.00 cy, $0.50 mn.

Hydraulic measurements were performed in the reactor to determine coolant distribution in the core. This study consisted of three parts: the flow through each of the four control rod fuel followers; the coolant velocity through flow channels of representative core positions; and, pressure differentials between coolant channels within several core positions. Flow velocity through the shimrod assemblies was of prime interest. This was obtained with a pitot-static tube inserted in the poison section of the dummy assembly, which was then placed in a test loop and calibrated against a previously calibrated Potter turbine flowmeter. The assembly was then inserted into the core and leads were brought out, and was eventually run in each shim-rod position under varying flow conditions. Results were reproducible and verified design values. Flow velocities in the fuel element channels were directly measured using the salt-velocity method. Thirty of the 41 core stationary element positions were tested, and the results, while generally verifying calculated values, did exhibit

variation with position. The final phase of the program consisted of instrumenting a dummy fuel element with eleven static pressure probes and to insert this element into the core in various positions to study the absolute and differential pressure between fuel plates, end plates, and side plates of the element in various positions, and to verify the design pressure drop across the core. (auth)

22493 (BNWL–193, pp 21-9) PCTR OPERATIONAL TECHNIQUES—ESTIMATION OF EXPECTED EXPERIMENTAL PRECISION. Lanning, D. D.; Heineman, R. E. (Battelle-Northwest, Richland, Wash. Pacific Northwest Lab.).

By utilizing the previous experience of k_∞ measurements with the PCTR it is possible to make a good preliminary estimate of the experimental uncertainty and thus determine an important required quantity for the decision of whether a given experiment is worth the effort. A procedure for making the desired estimate is presented. Results from a reactivity worth calculation for a control rod is presented. (M.O.W.)

22494 (BNWL–193, pp 30-44) NUCLEAR CRITICALITY SAFETY STUDY OF FFTF FUEL. Brown, C. L. (Battelle-Northwest, Richland, Wash. Pacific Northwest Lab.).

Critical parameters were calculated for moderated and unmoderated FTR driver fuel to provide criticality safety guidance for the conceptual design of FFTF examination and storage facilities. Measurements are given for the SS-clad PuO_2 fuel pins in both air and water. (M.O.W.)

22495 (GEAP–4742) SOUTHWEST EXPERIMENTAL FAST OXIDE REACTOR DEVELOPMENT PROGRAM. Quarterly Report No. 2, July–September 1964. Horst, K. M. (ed.) (General Electric Co., San Jose, Calif. Atomic Power Equipment Dept.). Oct. 1964. Contract AT(04-3)-540. 73p. Dep. mn. CFSTI $3.00 cy, $0.75 mn.

Developments during this quarter are reported for the following: planning the experimental program, experimental program in ZPR-III, fuel development, special instrumentation, steady-state and transient characteristics of the core assembly, reactivity controls required for experimentation, fuel handling, and core design. (M.O.W.)

22496 (GEAP–4864) SOUTHWEST EXPERIMENTAL FAST OXIDE REACTOR DEVELOPMENT PROGRAM. Quarterly Report No. 4, February–April 1965. Horst, K. M. (ed.) (General Electric Co., San Jose, Calif. Advanced Products Operation). May 1965. Contract AT(04-3)-540. 142p. Dep. mn. CFSTI $4.00 cy, $1.00 mn.

Developments during this period are reported for the following; planning the experimental program, experimental program in ZPR-III, fuel development, special instrumentation, steady-state and transient characteristics of the core assembly, reactivity controls required for experimentation, fuel handling, and core design. (M.O.W.)

22497 (IAE–992) REKONSTRUKTSIYA REAKTORA IRT V IAE IM. I. V. KURCHATOVA. (Reconstruction of Research Reactor IRT at the Atomic Energy Institute). Goncharov, V. V.; Chernilin, Yu. F.; Shavrov, P. I.; Chernyshevich, V. N.; Egorenkov, P. M.; Zhigachev, V. M.; Larin, I. I.; Korneev, V. T.; Yashin, A. F. (Institut Atomnoi Energii, Gosudarstvennyi Komitet po Ispol'zovaniyu Atomnoi Energii SSSR, Moscow). 1965. 27p. Dep. mn.

The reconstruction of the IRT and the IAE reactors, based on the use of a new heat exchange installation and a new design for the cooling of the active zones was described. As a result of the reconstruction, the reactor power was increased and their experimental facilities were expanded. The maximum thermal neutron flux was 5×10^{13} n/cm^{2}sec. The schedule of the disassembly and assembly work in the reactor vessel in the presence of induced radioactivity in the structure adjacent to the active zone and in the steel cladding of the thermal screen of the biological shield was described. The experimental facility of the reconstructed IRT-M reactor, a horizontal channel as a cold neutron source and trap for thermal neutrons, was described. (tr-auth)

22498 (IAE–993) O POVYSHENII MOSHCHNOSTI REAKTOROV VVR-S. (On Increase of Power of VVR-S Reactors). Ambartsumyan, R. S.; Goncharov, V. V.; Plukhov, A. M.; Egoroenkov, P. M.; Smirnova, R. F.; Shavrov, P. I. (Institut Atomnoi Energii, Gosudarstvennyi Komitet po Ispol'zovaniyu Atomnoi Energii SSSR, Moscow). 1965. 18p. Dep. mn.

The possibility of increasing the power of VVR-S reactors by the use of some altered heat release elements of the MR reactors was investigated. The modification of the heat exchange elements does not require essential modification in the active zone of the VVR-S reactors. The power of the reactors can be increased from 8 to 11 Mw by increase of the maximum neutron flux on the uranium up to approximately 9×10^{13} neutrons/cm^{2}sec. (tr-auth)

22499 (IDO–17150) A PHYSICAL COMPARISON OF THE ATR AND ATRC CORES. Henscheid, J. W.; Gregory, W. D. (Phillips Petroleum Co., Idaho Falls, Idaho. Atomic Energy Div.). Mar. 1966. Contract AT(10-1)-205. 46p. Dep. mn. CFSTI $2.00 cy, $0.50 mn.

How well the ATRC can fulfill its role of providing technical support for the ATR depends largely on how well the ATRC core simulates the ATR core. Differences between the two reactors are generally believed to be inconsequential, the most notable being (1) the coolant slots in the neck shim housing, (2) the neck shim hafnium sections, and (3) the hafnium plates and coolant hole pattern on the outer shim cylinders. Dimensional and material comparisons between components in the ATR and ATRC cores are pointed out by using simplified cross-sectional diagrams. Engineering drawings of all core components are referenced for those interested in obtaining greater detail. (auth)

22500 (NAA-SR–11175) STARTUP AND OPERATION OF THE ONE-MEGAWATT SHIELD TEST AND IRRADIATION REACTOR. Randen, K. G.; Golliher, K. G. (Atomics International, Canoga Park, Calif.). Mar. 25, 1966. Contract AT(11-1)-Gen-8. 38p. Dep. mn. CFSTI $2.00 cy, $0.50 mn.

Experiments performed in connection with the startup of the 1-Mw core and operating experience gained during its first six months of operation are described. The reactor was first made critical on December 7, 1964, and was taken to full power for the first time on January 6, 1965. Some of the experiments described were completed subsequent to the first full power run. (M.O.W.)

22501 (EURFNR–49F) FIRST EXPERIMENTAL RESULTS ON THE ENGINEERING MODEL OF RAPSODIE. Chalot, A.; Ginier, R.; Sauvage, M. (Commissariat a l'Energie Atomique, Cadarache (France). Centre d'Etudes Nucleaires). Translation of report CEA-R–2557. 109p. Dep. mn. CFSTI $4.00 cy, $0.75 mn.

Work Performed under United States–Euratom Fast Reactor Exchange Program.

The first series of experiments carried out on the engineering model of Rapsodie and on an associated sodium facility set in a laboratory hall of Cadarache are described. In particular, described are: the difficulties encountered during the erection and assembly of the engineering model and a compilation of the results of the first series of experiments and tests carried out on this installation (loading of the subassemblies, preheating, thermal shocks ...), and the experiments and tests carried out on the two prototypes control rod drive mechanisms which brought to the choice for the design of the definitive drive mechanism. As a whole, the results proved the validity of the general design principles adopted for Rapsodie. (auth)

22502 NEUTRON PHYSICS AT THE TRIGA MARK II REACTOR IN THE ATOMIC INSTITUTE OF THE AUSTRIAN HOCHSCHULE. Ortner, Gustav; Rauch, Helmut (Oesterreichische Hochschule, Vienna). Acta Phys. Austr., 21: 75-98(1966). (In German).

The results obtained in the measurement of the neutron properties of the TRIGA Mark II reactor are reported. The neutron flux at the external end of the radiation tube, the spectra of thermal neutrons, the cold neutron flux, polarized neutrons, and the reactor pulse are discussed. The measurements made with the double crystal spectrometer and coarse structure studies with neutrons are indicated. (J.S.R.)

22503 ACCELERATOR PULSED FAST ASSEMBLY. **Crosbie, K. L.; Russell, J. L. Jr.; Beyster, J. R. (General Atomic Div., General Dynamics Corp. San Diego, Calif.). IEEE (Inst. Elec. Electron. Eng.), Trans. Nucl. Sci., NS-13: No. 1, 457-63(Feb. 1966).**

An accelerator-pulsed fast assembly is described in which a 20-Mev L-band electron accelerator drives a supercritical ^{235}U metal reactor. The peak power and the pulse width can be varied independently by adjusting various accelerator and reactor parameters. Some improvements in accelerator-pulsed assemblies are discussed. (D.C.W.)

22504 DIDO HIGH-PRESSURE WATER LOOP. **Everson, I. (Atomic Energy Research Establishment, Harwell, Eng.). Nucl. Eng., 11: 110-15(Feb. 1966).**

The design of the DIDO high-pressure water loop is described. This provides a facility for irradiation experiments to be carried out in support of water power reactors. This loop can carry separate experiments simultaneously and is suitable for irradiating both fissile and nonfissile materials. Loop water samples can be taken from selected points for additional experimental data. The design, chemical control for sample analysis, instrumentation, leakage minimization, in-pile vessels, and operational problems are discussed. (J.F.P.)

22505 SPENT-FUEL STORAGE POOL FOR JRR-2. **Sawai, Sadamu (Japan Atomic Energy Research Inst., Tokyo). Nucl. Eng. (Tokyo), 11: 49-55(June 1965). (In Japanese).**

The spent-fuel storage pool now in use with the JRR-2 reactor in Japan is described in detail. Certain problems, improvements, and modifications that have occurred during the past three years are described also. (TCO)

22506 MULTIGROUP CALCULATIONS OF THE FAST SPECTRUM AND FAST FISSION EFFECT. **Helhotz, J.; Rothenstein, W. Nucl. Sci. Eng., 24: 349-55(1966).**

A multigroup procedure for the calculation of the fast fission phenomena in thermal uranium–water reactors was developed. The method essentially consists of applying the single-flight collision concept in a manner analogous to the calculation of resonance capture in thermal reactor lattices. The collision and escape probabilities are calculated by numerical integration over the actual neutron paths encountered in a reactor lattice. The multigroup equations are solved by an iterative procedure which converges rapidly. The fast-neutron spectrum, δ_{28}, and ϵ can be obtained. Results of calculations are presented in which the value of δ_{28} for homogeneous uranium–water mixtures and for slightly enriched uranium–water lattices are compared with Monte Carlo calculations and experiment. Very satisfactory agreement has been obtained. Fast-neutron spectra in the core of a pool type reactor and in the fuel and moderator regions of a uranium–water lattice, calculated by the present method, are also shown. (auth)

WASTE DISPOSAL AND PROCESSING

See also BIOLOGY AND MEDICINE — Ecology
CHEMISTRY — Radiochemistry
CHEMISTRY — Separation Processes and Procedures
HEALTH AND SAFETY

Refer also to abstracts 20875 and 20982.

22507 (AD–622372) EVALUATION PROGRAM FOR A RADIOACTIVE WASTE TREATMENT FACILITY. Thieme, Allen A.; Bloore, Ernest W.; Crisco, Carl (Army Nuclear Defense Lab., Edgewood Arsenal, Md.). Oct. 1961. 21p. (NDL-TM–4). CFSTI $1.00 cy, $0.50 mn.

A facility for the concentration of low level radioactive liquid waste was designed and fabricated. Prior to releasing this facility for routine operations, an evaluation program was conducted. The objectives of the evaluation were to determine: optimum operating conditions of the radioactive liquid waste treatment facility; capabilities and limitations of the facility; and the effects of the operating variables on the decontamination factor (DF) and concentration factor (CF). (TAB)

22508 (AEET–220) THE USE OF INCINERATORS FOR TREATMENT OF COMBUSTIBLE WASTES. Amalraj, R. V.; Khan, A. A. (Atomic Energy Establishment, Trombay (India)). 1965. 12p. Dep. mn.

The use of incinerators for waste disposal is discussed, and use of incinerators in India for various wastes is reported. (P.C.H.)

22509 (BNL–10109) BROOKHAVEN NATIONAL LABORATORY PROCESS FOR THE CONTINUOUS CONVERSION OF HIGH-LEVEL RADIOACTIVE WASTE TO PHOSPHATE GLASS. Tuthill, E. J.; Weth, G. G.; Emma, L. C.; Strickland, G.; Hatch, L. P. (Brookhaven National Lab., Upton, N. Y.). [1965]. Contract AT(30-2)-Gen-16. 36p. (CONF-660208–16). Dep. mn. CFSTI $2.00 cy, $0.50 mn.

From Symposium on Solidification and Long-Term Storage of Highly Radioactive Wastes, Richland, Wash.

The results of an investigation at Brookhaven on the development of the phosphate glass process are reported with emphasis on the performance characteristics of the individual process units. The process was tested on a pilot plant scale for some 3000 hr using simulated Purex waste most of the time. In the Brookhaven process, phosphoric acid is added to the aqueous waste and the solution converted to phosphate glass in a continuous operation upon raising the temperature in two steps to 1100–1200°C. (P.C.H.)

22510 (BNWL-SA–564) FIXATION OF HIGH-LEVEL RADIOACTIVE WASTES IN PHOSPHATE GLASS. Upson, U. L.; Weth, G. C. (Battelle-Northwest, Richland, Wash. Pacific Northwest Lab.). Feb. 1, 1965. Contract AT (45-1)-1830. 22p. (CONF-660208–14). Dep. mn. CFSTI $1.00 cy, $0.50 mn.

From Symposium on Solidification and Long-Term Storage of Highly Radioactive Wastes, Richland, Wash.

The Brookhaven process for converting high-level aqueous fuel reprocessing waste directly to a phosphate glass, without an intermediate drying step, was demonstrated with actual Purex 1WW waste. A small-scale pilot plant was remotely installed in a hot cell containing the equipment from a preceding study on waste calcination. Technical feasibility of the process was tested, operating characteristics were observed, and the off-gas decontamination problem evaluated. Samples of glass were produced for observation and evaluation of stability and chemical durability. (auth)

22511 (IDO–14666) A FLOW DIVERTER-VALVE FOR GRANULAR SOLIDS. Petrie, J. C.; Cooper, E. D. (Phillips Petroleum Co., Idaho Falls, Idaho. Atomic Energy Div.). Mar. 1966. Contract AT(10-1)-205. 17p. Dep. mn. CFSTI $1.00 cy, $0.50 mn.

The design and operating characteristics of a nonmechanical, pneumatically operated, solids flow diverter-valve are described. The device is useful in diverting the flow of granular solids from a common supply header to any one of several terminals. The absence of moving parts makes the device attractive for use where minimum maintenance is important. (auth)

22512 (K–1651) REMOVAL OF LOW-LEVEL RADIOACTIVE WASTES BY A SANITARY WATER TREATMENT PROCESS. Schultz, N. B. (Oak Ridge Gaseous Diffusion Plant, Tenn.). Apr. 12, 1966. Contract W-7405-eng-26. 13p. Dep. mn. CFSTI $1.00 cy, $0.50 mn.

The cleanup factors that were obtained across a potable water treatment plant using normal treatment methods are reported; the average gross beta radioactivity was reduced by 15% and the strontium beta concentrations by 6%. A summary and evaluation of six months data obtained from daily field samples of the raw water supply, as well as the finished water product, is included. Sample analysis included determinations for gross beta radioactivity and radiostrontium. The raw water radioactivity concentrations were less than 25% of the maximum permissible concentrations in water recommended by the National Committee on Radiation Protection. (auth)

22513 (NYO–10447) OPERATIONS RESEARCH IN DISPOSAL OF LIQUID RADIOACTIVE WASTES IN STREAMS. Final Report. Thomas, Harold A. Jr. (Harvard Univ., Cambridge, Mass.). Dec. 1965. Contracts AT(30-1)-966; AT(30-1)-3068. 202p. Dep. mn. CFSTI $6.00 cy, $1.25 mn.

A review and summary of the general principles of disposal of low-level radioactive wastes in streams is presented. A classification of physical and economic factors that are important in radioactive waste disposal in streams is included. From this, a classification of rivers and other fresh water bodies into four basic types was developed. A descriptive mathematical model is presented to show the logical structure of the scheme and to indicate the wide variety of waste disposal environments that obtain in different streams. In some types of streams a potential exists for storage and sporadic release of activity from benthal deposits and biomasses that may constitute a public health hazard. Various mechanisms of release are discussed. Three different models are also presented for economic and engineering analysis of stream disposal systems for radioactive wastes. Test results of model laboratory streams that were operated to supply information about the interaction of stream and radiocontaminant compounds and processes that could not readily be obtained from field studies on prototype streams are described. (P.C.H.)

22514 (ORNL–P–2021) EVALUATION OF RADIATION DOSE TO MAN FROM RADIONUCLIDES RELEASED TO THE CLINCH RIVER. Cowser, K. E.; Snyder, W. S.; McCammon, C. P.; Straub, C. P.; Kochtitzky, O. W.; Hervin, R. L.; Struxness, E. G.; Morton, R. J. (Oak Ridge National Lab., Tenn.). [1965]. Contract W-7405-eng-26. 35p. (SM–72/41; CONF-660507–4). Dep. mn. CFSTI $2.00 cy, $0.50 mn.

From Symposium for the Disposal of Radioactive Wastes into Sea, Oceans, and Surface Waters, Vienna.

Low-level contaminated waste water, generated by the operations at Oak Ridge National Laboratory, has been released to the Clinch River near Oak Ridge for the past 20 years under controls consistent with the recommenda-

tions of ICRP and NCRP. Results are reported from an evaluation of radiation dose equivalents to populations downstream, made on the basis of long-term monitoring data and the identification of critical exposure pathways and critical population groups. A study of water utilization downstream indicated that the important avenues of exposure resulting from discharge of radioactive fluids to the Clinch River include the consumption of contaminated water and fish, the consumption of agricultural produce that may be irrigated with river water, exposure to contaminated water and bottom sediments during recreational and industrial use of the water, and exposure to build-up of radionuclides in sludge and deposits in water systems utilizing river water. The major sources of exposure were due to the ingestion of contaminated water and fish. Mathematical models were developed for internal dose calculations which include the differences in intake and size of the critical organ as a function of the individual's age. (26 references.) (C.H.)

22515 (ORNL-tr-965) PROPOSAL FOR THE CONSTRUCTION OF A SEWER FOR THE DISCHARGE OF INDUSTRIAL WASTE WATER CONTAINING RADIOACTIVE SUBSTANCES INTO THE ESCAUT RIVER. (Ministere de la Sante Publique et de la Famille, Brussels (Belgium). Administration de l'Hygiene Publique). Translated for Oak Ridge National Lab., Tenn., from manuscript dated Aug. 1964. 30p. Dep. mn. JCL $2.60 fs, $0.83 mf.

The construction of a sewer along the Albert Canel is proposed to move industrial waste water to the Escaut River downstream from Antwerp from already established industries or from those to be established in the region traversed by this waterway as well as the construction of a side-sewer along the canal from Herentals to Bocholt, discharging into the former at Herentals and intended to collect the industrial waste from plants established in Mol, Dessel, and Olen. Control of radioactivity of Escaut water before and after disposal is discussed, and data on various radioisotopes present in the water are tabulated. (P.C.H.)

22516 DECONTAMINATION OF RADIOACTIVE EFFLUENTS. Brodsky, Michel; Moneton, Jean-Louis; Pagny, Pierre. Energ. Nucl., 8: 9-22(Jan.-Feb. 1966). (In French).

Following a description of methods used for the decontamination of radioactive effluents and the operation of the evaporation installations, the technical and financial results obtained on these installations are compared according to their treatment capacity. Thus, capital investments and the cost per unit for an effluent treatment in a single-acting evaporator (with or without mechanical recompression of stream) are included in the financial study of the chemical treatment. With the results obtained from this study, a choice can be made, for a future project, of the type of treatment to be used according to the characteristics of the effluents and certain local requirements. (auth)

22517 COMPARISON OF THE ECONOMIC ASPECTS OF THE TREATMENT AND STORAGE OF FISSION PRODUCTS FROM INSTALLATIONS PROCESSING IRRADIATED NATURAL URANIUM. Thiriet, L. (Commissariat a l'Energie Atomique, Paris); Lesur, P.; Giraud, R.; Wanlin, J. pp 571-83 of STI-PUB-110. (In French).

Policies adopted for the management of fission product effluents are summarized, and the essential technical features of the stainless steel storage installations (in acid medium) used in France are described, with breakdown of the cost involved. The dependence of these costs on the activity of the solutions stored and on their heat release is shown. The cost of storage in terms of feasible tank size is also discussed. The optimum size for such tanks and the rate at which they are placed in service were determined in relation to the characteristics of the fission products to be stored and to the respective capacities of the installations for processing irradiated natural uranium. It is shown that although storage costs depend on the assumptions made regarding the useful life of installations, rates of interest, and operating costs, optimum policy decisions (as to size and rate of entry into service) are independent of these assumptions, being determined solely by the variation in the cost of tanks, according to size. These are the factors that enter into the optimized cost of storing these effluents indefinitely. This method of indefinite storage was compared with other possibilities of fission product management, e.g., vitrification and separation of Cs and Sr. Economics of the various methods are discussed, and some possible long-term solutions are summarized. (auth)

GENERAL AND MISCELLANEOUS

22518 (ANL–7055) CHEMICAL ENGINEERING DIVISION SEMIANNUAL REPORT, JANUARY–JUNE 1965. (Argonne National Lab., Ill.). Oct. 1965. Contract W-31-109-eng-38. 234p. Dep. mn. CFSTI $6.00 cy, $1.25 mn.

Research progress is reported in seven sections. Separate abstracts were prepared for each section. (J.R.D.)

For abstracts of individual sections see: 20650, 20802, 20803, 20925, 21324, 21566, and 21969.

22519 (DP–929(Suppl.2)). PUBLICATIONS, 1965. Hilborn, H. S. (comp.) (Du Pont de Nemours (E. I.) and Co., Aiken, S. C. Savannah River Lab.). Mar. 1966. Contract AT(07-2)-1. 26p. Dep. mn. CFSTI $2.00 cy, $0.50 mn.

References (182) are given to research and development reports, journals, books, and computer programs published in 1965 by Du Pont. Subject and author indexes are included. (P.C.H.)

22520 (NAA-SR–11805) AEC UNCLASSIFIED PROGRAMS. Quarterly Technical Progress Report, October–December 1965. (Atomics International, Canoga Park, Calif.). Feb. 15, 1966. Contract AT(11-1)-Gen-8. 147p. Dep. mn. CFSTI $5.00 cy, $1.00 mn.

Progress is reported on boiling studies for Na reactor safety, effects of high-temperatures and fast neutrons on cladding and structural materials, operation of SRE, sodium components test installation operation, high-temperature strain measurements, reactions of high-temperature Na, PNPF fuel studies, SAP-clad UC fuel development, design of PNPF Core-II, PNPF coolant make-up studies, diffusion of neutrons in graphite, development and production of nuclear data, fast-spectrum Doppler measurements, reactor theory improvement, refractory cermet development, refractory moderator development, effects of fission in metal fuels, studies of ternary zirconium hydrides, preparation and analysis of pure Na, Doppler coefficient studies, studies of Na fires, studies on high-temperature chemistry, radiation chemistry studies, electronic structure studies of metals, and radiation damage in crystalline solids. (J.R.D.)

22521 (RFP–516A(Suppl.1)) UNCLASSIFIED PUBLICATIONS, 1965. (Rocky Flats Div., Dow Chemical Co., Golden, Colo.). Mar. 28, 1966. Contract AT(29-1)-1106. 22p. Dep. mn. CFSTI $2.00 cy, $0.50 mn.

References (111) of unclassified publications of the scientific and technical personnel of the DOW Chemical Co. are given for the year 1965. References are categorized according to patents, engineering drawings, reports, journals, and speeches. An author index is included. (P.C.H.)

22522 (TID–3734) BIBLIOGRAPHIES OF ATOMIC ENERGY LITERATURE. Issued or in Progress During the Period, February–March 1966. (Division of Technical Information Extension (AEC), Oak Ridge, Tenn.). 15p. Dep. DTI Extension Free.

References (85) are given to bibliographies on atomic energy that were issued or in preparation from Feb. to March 1966. Report number, author, and subject indexes are included. (P.C.H.)

22523 (UCRL–14602) DETECTION AND DIAGNOSIS OF MALFUNCTIONS IN STRAIN GAGE SYSTEMS. Osborne, Robert L. (Lawrence Radiation Lab., Univ. of California, Livermore). Dec. 14, 1965. Contract W-7405-eng-48. 14p. Dep. mn. CFSTI $1.00 cy, $0.50 mn.

A method is presented for detecting, in a strain gage system, all short or open circuit conditions in either the strain gage bridge or in the cables connecting the bridge to the power supply and voltage-sensing equipment. The method necessitates the sensing of supply current and the addition of resistors to the balancing circuit. In the case of a bridge with a single active leg, no modification of the normal system is necessary for detection of malfunctions. (auth)

22524 KEAGE LABORATORY OF NUCLEAR SCIENCE. DECENNIAL REPORT 1955–1965. Kimura, Kiichi. Bull. Inst. Chem. Res., Kyoto Univ., 43: 499-568(Dec. 1965).

Work carried out in various fields using the Kyoto University Cyclotron from 1955 to 1965 is reviewed. Topics covered include: the site and building, facilities and technique development, research in nuclear physics, and research in radiation biology and related problems. (66 references) (M.C.G.)

22525 NUCLEAR TECHNIQUES AND THE DEVELOPING COUNTRIES. Van Hoeck, Fernand (EURATOM, Brussels). Euratom Bull., 5: 2-7(Mar. 1966).

The value of nuclear techniques to developing countries is discussed and some examples are given. Dual-purpose reactors, medical uses of radioisotopes, radiopreservation of food, and the uses of radiation in agriculture are considered. (M.C.G.)

22526 ATOMIC INDUSTRY OF JAPAN, ITS GROWTH, CAPABILITIES AND PROSPECTS, 1964. Tokyo, Japan Atomic Industrial Forum, Inc., 1964. 106p.

The present status of Japan's nuclear industry is discussed with special emphasis on manufacturing. Power reactors, research reactors, nuclear equipment, fuels and materials, radiation equipment, and accelerators are discussed. A list of companies is presented and major products of Japanese industries are discussed. (M.C.G.)

22527 THE UNITED STATES ATOMIC ENERGY COMMISSION PROGRAM OF NUCLEAR MATERIALS MANAGEMENT. George D. E. (Atomic Energy Commission, Washington, D. C.). Vienna, International Atomic Energy Agency, 1965, Preprint No. SM-67/59, 16p. (CONF-650803–21). ORINS.

From IAEA Symposium on Nuclear Materials Management, Vienna.

Nuclear materials management as conceived by the USAEC is defined and its development traced from 1943 to the present time. The general program is outlined and its principal features discussed. Emphasis is placed on administration of those portions of the USAEC program that pertain to the development and maintenance of quantity data, the establishment of internal controls, and the evaluation of performance. The techniques whereby transfer data are recorded and processed within the AEC are discussed, as are the techniques for presentation of material balance reports, which periodically summarize the transactions and the results of operations. Also, the techniques used by the AEC to ascertain the effectiveness of the nuclear materials management programs of its operating contractors are discussed. In addition to material being held by contractors, which operate AEC-owned plants and laboratories, there are large quantities of special nuclear material held under a wide variety of financial and administrative arrangements, e.g., under lease, private ownership, under contract with the AEC where the user is financially liable for losses, as well as those where the risk of losses is taken by the AEC. This divergence of circumstances causes variation in the emphasis and approach used by the AEC and this variation is noted. Unresolved problem areas are also reviewed. (auth)

22528 ADMINISTRATIVE CO-ORDINATION OF FISSILE MATERIAL MANAGEMENT AND ACCOUNTING IN THE U.K.A.E.A. Hood, St. C. C. (United Kingdom Atomic Energy Authority, London). Vienna, International Atomic Energy Agency, 1965, Preprint No. SM-67/55, 20p. (CONF-650803–24). ORINS.

From IAEA Symposium on Nuclear Materials Management, Vienna.

The UKAEA is engaged as a supplier in fissile material production, distribution, recycle, and reprocessing. As a consumer, the Authority requires fissile material for power reactors, a variety of prototypes, MTRs, zero-energy facilities and fuel development projects; and for other experimental and research purposes in laboratory quantities. Executive responsibility for these activities lies with four Groups through which the Authority discharges these functions. It was found useful to keep these activities under review in specialized inter-Group Committees, with a common secretariat. These committees study all projects or proposals for work involving significant quantities of fissile material (plutonium and enriched uranium, other than natural U or U depleted in ^{235}U) in the light of expected supplies over a number of years from all sources, including new production, scrap recovery, and imports; and all uses including burnup, losses, and exports. They also recommend the optimum allocation of specific amounts for approved purposes in relation to other calls upon available supplies and with regard to the economic issues involved. They record and progress all approved allocations, and examine the nature, amount, and purpose of all existing stockholdings in relation to current policies and objectives. The committees record and study all losses of fissile material during fabrication or other processing and the measures taken to reduce them and assist in developing procedures and incentives to ensure that the material is used economically and returned promptly. A simplified flowsheet of the main flows of fissile material within the Authority for civil purposes during the year ending March 31, 1965, is presented. (auth)

22529 CASE STUDY IN INTERNAL AUDIT OF NUCLEAR MATERIAL. Kops, S. (Chicago Operations Office, AEC, Argonne, Ill.). Vienna, International Atomic Energy Agency, 1965, Preprint No. SM-67/27, 10p. (CONF-650803-27). ORINS.

From IAEA Symposium on Nuclear Materials Management, Vienna.

The general need for the internal audit function and the basic principles of management underlying this need are discussed. The size, complexity and degree of centralization, or decentralization, are usually the main factors in determining the need for a conventional internal audit. The more specialized needs and characteristics of an internal audit peculiar to an organization handling source or special fissionable material (nuclear material) are discussed and contrasted with an audit of the standard type. The necessity of a special audit, because of the high monetary and strategic value, is demonstrated. Planning the internal audit within a production plant, is discussed in detail. A qualified statistical plan in choosing the items to be tested is discussed. The application of the plans in the actual performance of the internal audit are described. Possible variances from a recognized norm and possible approaches to audit resolution are discussed. Although in many other manufacturing situations there are variations in the methods of verifying inventories without physically doing so, the necessity for physically testing inventories of nuclear material is demonstrated. The various means of reporting the results of the internal audit are presented. The needs of individual groups within the organization are considered in determining the format of the report, as well as the basic content. Distribution of the report and its variations are discussed. (auth)

CORPORATE AUTHOR INDEX

This index contains entries for this period for all report literature and, in addition, for certain published literature items for which it is felt that a corporate approach is especially desirable, e.g., symposia, conference proceedings, and meetings.

Each entry under a corporate author is a shortened version of the title of the publication, followed by the *NSA* volume and abstract number. Report numbers are given in parentheses.

The phrase "Progress report" is abbreviated as "Prog. rpt.," permitting a more rapid and complete alphabetical arrangement of the titles without changing the location of the progress report titles in relation to the other titles.

A

AEROJET-GENERAL NUCLEONICS, SAN RAMON, CALIF.
Hastelloy X corrosion in air at 1900 and 2000°F, 20: 21259 (AGN-TM-414)
Isothermal oxidation of Hastelloy X at 1750 and 1850°F in air, 20: 21258 (AGN-TM-413)

AGRICULTURAL RESEARCH COUNCIL, WANTAGE (ENGLAND). RADIOBIOLOGICAL LAB.
Prog. rpt., annual, 1964–65, 20: 20926 (ARCRL-14)

AIR FORCE CAMBRIDGE RESEARCH LABS., L. G. HANSCOM FIELD, MASS.
Electrophoretic power generation in thermally ionized plasmas, 20: 22173 (AD-623788)
Nonlinear terms in the generalized Ohm's law: a scale analysis, 20: 21778 (AD-621943)
Wave phenomena in ionized gases, 20: 22174 (AD-623789)

AIR FORCE FLIGHT DYNAMICS LAB., WRIGHT-PATTERSON AFB, OHIO.
Prog. rpt. on pre-startup hydraulic tests on AF-NETF, final, 1961–65, 20: 22492 (AD-626861)

AIR FORCE INST. OF TECH., WRIGHT-PATTERSON AFB, OHIO. SCHOOL OF ENGINEERING.
Construction and instrumentation of cryostat for AF-NETF, 20: 22489 (AD-621123)
Determination of thermal neutron flux distribution in a hexagonal lattice cell, 20: 22371 (AD-621026)
Fuel burnup studies of Air Force Nuclear Engineering Test Facility, 20: 22487 (AD-621118)
Intercalation of rare earth elements into graphite and dichalcogenides, 20: 20648 (AD-621029)
Kinetic analysis of AF-NETF, 20: 22490 (AD-621124)
Multi-group discrete SN transport calculation for cylindrical geometry, 20: 22370 (AD-621021)
Neutron activation analysis service, 20: 20554 (AD-621017)
Neutron transport calculations of AF-NETF core, 20: 22491 (AD-621269)
Non-adiabatic particle motion in complex magnetic fields, 20: 22162 (AD-621020)
One-dimensional magnetogasdynamics, 20: 21777 (AD-621442)
Prandtl-Meyer flow with transverse magnetic field, 20: 21776 (AD-621429)
Prediction of time-dependent β spectrum from nuclear weapon detonation, 20: 21960 (AD-621023)
Radiolysis of solid ethyl iodide, 20: 20716 (AD-621022)
Thermal neutron spectrum in a finite mass medium, 20: 21933 (AD-621119)
Transport calculation of flux in Nuclear Engineering Test Reactor test cells, 20: 22488 (AD-621121)
Variable conductivity fully developed MHD channel flow, 20: 21780 (AD-622036)

AKADEMIYA NAUK UKRAINSKOI SSR, KHARKOV. FIZIKO-TEKHNICHESKII INSTITUT.
Performance of coaxial plasma source in longitudinal magnetic field, 20: 22179 (FTI-080/P-032)
Two-nucleon correlations in nuclei, 20: 21996 (FTI-142/T-016)

AKRON UNIV., OHIO. INST. OF RUBBER RESEARCH.
Prog. rpt. on low-temperature polymerization, 7–9/65, 20: 20718 (AD-623307)

AKTIEBOLAGET ATOMENERGI, STOCKHOLM (SWEDEN).
Brittle-fracture problems in reactor pressure vessels, 20: 21228 (AE-221)
Electrodeposition of actinide and lanthanide elements, 20: 21287 (AE-217)
Time dependence of neutron slowing-down and thermalization of H_2O, 20: 21936 (AE-216)
Total cross-sections of U, UO_2 and ThO_2 for thermal and subthermal neutrons, 20: 21966 (AE-222)

ALLISON DIV., GENERAL MOTORS CORP., INDIANAPOLIS, IND.
Prog. rpt. on fluid properties for MPD power generators, 5–8/65, 20: 21561 (AD-623096)

AMERICAN NOVAWOOD CORP., LYNCHBURG, VA.
Commercial production of wood-plastic combinations, 20: 21187 (ORNL-IIC-7, pp 89-94)

AMERICAN OIL CO., WHITING, IND.
Prog. rpt. on radiation chemistry of acetylenic compounds, final, 12/61–5/65, 20: 20717 (AD-621719)

AMES LAB., IOWA STATE UNIV. OF SCIENCE AND TECH.
Bibliography on nucleation and crystal growth from ceramic melts, 20: 21235 (IS-1287)
Determination of liquid metal diffusion coefficients by molecular distillation, 20: 21334 (IS-1325)
Flash desorption and isotopic mixing of simple diatomic gases on W, Ir, and Rh, 20: 20652 (IS-T-67)
Interplanar angles and planar spacings of fifteen types of planes for HCP yttrium, 20: 22315 (IS-1337)
Lanthanum–lanthanum hydride phase system, 20: 21336 (IS-T-79)
Separation of Cd from the Pb–Bi eutectic by high-vacuum single-stage distillation, 20: 20805 (IS-1329)
Thermodynamic properties of Ca–Zn alloys, 20: 21335 (IS-T-76)

ARGONNE NATIONAL LAB., ILL.
Calculations of critical experiments on assemblies in ZPR-3, 20: 22383 (AEC-tr-6693)
Calorimetry, 20: 20650 (ANL-7055, pp 167-76)
Catalog of nuclear reactor concepts, Pt. I, Sec. IV, 20: 22347 (ANL-7138)
Catalog of nuclear reactor concepts, Pt. I, Sec. V, 20: 22466 (ANL-7180)
Compact pyrochemical processes, 20: 20802 (ANL-7055, pp 21-98)
Convective-diffusion study of dissolution kinetics of stainless steel in Bi–Sn alloy, 20: 21260 (ANL-6985)
Cosmic-ray induced μ-e events, 20: 21029 (CERN-65-32, pp 71-2)
Effect of interference interaction between resonances of ^{239}Pu and ^{232}Th on ^{239}Pu fission and capture cross sections and ^{232}Th capture cross sections, 20: 21970 (ANL-7144)
Energy conversion, 20: 21566 (ANL-7055, pp 213-29)
Engineering development of fluid-bed fluoride volatility processes. II., 20: 20801 (ANL-6830)
Fuel cycle applications of volatility and fluidization techniques, 20: 20803 (ANL-7055, pp 99-162)
High-temperature reactor materials development, 20: 21324 (ANL-7055, pp 163-6)
Large hydrogen bubble chamber, 20: 21032 (CERN-65-32, pp 259-62)
Light spherical nuclei, 20: 21974 (BNL-948, pp 222-68)
Neutrino experiment at the ZGS, 20: 21465 (CERN-65-32, pp 31-4)
Nuclear constants, 20: 21969 (ANL-7055, pp 230-3)
Optical model, DWBA, 20: 21978 (BNL-948, pp 454-524)

$\pi^{\pm}$ and $K^{\pm}$ production cross sections for 12.5-Bev protons on Be, 20: 21601 (CERN-65-32, pp 109-10)
Plotting system for Control Data 3600 computer, 20: 21221 (ANL-7121)
Prog. rpt. on chemical engineering, semiannual, 1–6/65, 20: 22518 (ANL-7055)
Reactions with fluctuating cross sections, 20: 21987 (BNL-948, pp 826-75)
Reactor safety, 20: 20925 (ANL-7055, pp 177-212)
Single-nucleon transfer reactions, 20: 21971 (BNL-948, pp 1-65)
Stoichiometric and hyperstoichiometric solid solutions in ThO_2–UO_2 system, 20: 21323 (ANL-6894)
Strong coupling, exchange, target excitation, and other corrections to DWBA, 20: 21979 (BNL-948, pp 525-60)

ARMED FORCES RADIOBIOLOGY RESEARCH INST., BETHESDA, MD.
Courant-Wallace expressions for second moments of neutron probability distribution and for variance/mean ratio, 20: 22372 (AFRRI-TN-65-1)

ARMY ENGINEER WATERWAYS EXPERIMENT STATION, VICKSBURG, MISS.
Engineering properties of nuclear craters. I., 20: 20895 (AD-626899)

ARMY MATERIALS RESEARCH AGENCY, WATERTOWN, MASS. MATERIALS ENGINEERING DIV.
Evaluation of refractory sheet metals. II., 20: 21322 (AMRA-TR-65-25)

ARMY MATERIEL COMMAND, WASHINGTON, D. C.
Conference on radiation research, U. S. Army Natick Labs., Mass., 1/63, 20: 20726 (PB-181506)
Food irradiation research in West Germany, 20: 21193 (PB-181506, pp 29-38)
Mechanism of ultraviolet and high-energy radiation damage, 20: 20731 (PB-181506, pp 133-42)
Radiation chemistry in the solid state as studied with electron paramagnetic resonance, 20: 20729 (PB-181506, pp 85-103)
Radiation in biological systems, 20: 20443 (PB-181506, pp 143-54)
Radiation preservation of foods—two decades of research and development, 20: 21194 (PB-181506, pp 155-67)
Radiation research in Japan, 20: 20727 (PB-181506, pp 9-18)
Radiochemistry in France, 20: 20730 (PB-181506, pp 104-15)
Some aspects of the radiation chemistry of organic compounds, 20: 20728 (PB-181506, pp 49-58)
Three-dimensional dose distribution in samples irradiated by electron beams, 20: 21470 (PB-181506, pp 116-29)
United States program on radiation preservation of foods, 20: 21192 (PB-181506, pp 19-26)

ARMY NATICK LABS., MASS.
Conference on radiation research, U. S. Army Natick Labs., Mass., 1/63, 20: 20726 (PB-181506)
Food irradiation research in West Germany, 20: 21193 (PB-181506, pp 29-38)
Mechanism of ultraviolet and high-energy radiation damage, 20: 20731 (PB-181506, pp 133-42)
Radiation chemistry in the solid state as studied with electron paramagnetic resonance, 20: 20729 (PB-181506, pp 85-103)
Radiation in biological systems, 20: 20443 (PB-181506, pp 143-54)
Radiation preservation of foods—two decades of research and development, 20: 21194 (PB-181506, pp 155-67)
Radiation research in Japan, 20: 20727 (PB-181506, pp 9-18)
Radiochemistry in France, 20: 20730 (PB-181506, pp 104-15)
Some aspects of the radiation chemistry of organic compounds, 20: 20728 (PB-181506, pp 49-58)
Three-dimensional dose distribution in samples irradiated by electron beams, 20: 21470 (PB-181506, pp 116-29)
United States program on radiation preservation of foods, 20: 21192 (PB-181506, pp 19-26)

ARMY NUCLEAR DEFENSE LAB., EDGEWOOD ARSENAL, MD.
Evaluation program for radioactive waste treatment facility, 20: 22507 (AD-622372)

ATOMIC BOMB CASUALTY COMMISSION, HIROSHIMA (JAPAN).
Prog. rpt. on Atomic Bomb Casualty Commission, annual 7/64–6/65, 20: 20919 (ABCC-64-65)

ATOMIC ENERGY ESTABLISHMENT, TROMBAY (INDIA).
Physics aspects of large Th-fueled fast reactors, 20: 21229 (AEET-229)
Review of nuclear data related to Th fuel cycle, 20: 21967 (AEET-234)
Role of substrate symmetry in gas-solid reactions. II and II., 20: 20649 (AEET-CD-24)
Stabilities and allied properties of organic coolants, 20: 20708 (AEET-213)
S4B program for solving multi-group transport equations with Carlson's S_4 approximation, 20: 21937 (AEET-210)
Test of connectors used in semiconductor logic modules, 20: 22352 (AEET-ED-SG/25)
Total count method for open channel flow measurement, 20: 20903 (AEET-Radiochem.-45)
Use of incinerators for treatment of combustible wastes, 20: 22508 (AEET-220)

ATOMIC ENERGY ESTABLISHMENT, TROMBAY (INDIA). CHEMISTRY DIV.
Self diffusion in metals, 20: 21230 (AEET-233)

ATOMIC ENERGY ESTABLISHMENT, TROMBAY (INDIA). ELECTRONICS DIV.
Force reflecting servos in electrical master slave manipulators, 20: 20839 (AEET-ED-SG/14)

ATOMIC ENERGY ESTABLISHMENT, TROMBAY (INDIA). HEALTH PHYSICS DIV.
Aerosol generator to produce radioactive aerosols, 20: 20924 (AEET-232)

ATOMIC ENERGY ESTABLISHMENT, TROMBAY (INDIA). NUCLEAR PHYSICS DIV.
Emission of long-range α particles in fission, 20: 21968 (AEET-235)

ATOMIC ENERGY OF CANADA LTD., CHALK RIVER (ONTARIO).
Subroutines for digital simulations, 20: 21783 (AECL-2530)

ATOMIC ENERGY RESEARCH ESTABLISHMENT, HARWELL (ENGLAND).
Analysis of uranium silicides, 20: 20557 (AERE-R-5129)
Bibliographic review of self-diffusion in metal oxides, 20: 21321 (AERE-Bib-143)
Display unit for complex data, 20: 20983 (AERE-R-4966)
Use of the Ag–Co activity ratio method to determine epithermal indices for large neutron dose irradiations, 20: 21025 (AERE-R-5122)

ATOMIC WEAPONS RESEARCH ESTABLISHMENT, ALDERMASTON (ENGLAND).
Impact tensile testing of U, 20: 21325 (AWRE-O-36/66)

ATOMICS INTERNATIONAL, CANOGA PARK, CALIF.
Prog. rpt. on AEC unclassified programs, 10–12/65, 20: 22520 (NAA-SR-11805)
Prog. rpt. on radiation effects on Ni–Cd electrodes, final, 6/63–4/65. I., 20: 21425 (N-65-24491)
Prog. rpt. on thermionic energy conversion, 11/64–7/65, 20: 21562 (AD-623142)
Radiological aspects of reentry burnup of SNAP reactors, 20: 20937 (NAA-SR-11761)
SNAP-10A FSM—4-system test, 20: 22471 (NAA-SR-11814)
Startup and operation of 1-Mw shield test and irradiation reactor, 20: 22500 (NAA-SR-11175)

AVCO-EVERETT RESEARCH LAB., EVERETT, MASS.
Basic studies in magnetohydrodynamics, 20: 22170 (AD-622701)
Performance of self-excited MHD generator, 20: 21564 (AD-627037)

AZTEC INSTRUMENTS, INC., WESTPORT, CONN.
Bibliography on atomic absorption, 20: 20563 (NP-15918)

B

BALLISTIC RESEARCH LABS., ABERDEEN PROVING GROUND, MD.
Study of the fast neutron-induced gelation of triethylene glycol dimethacrylate using 14-Mev neutrons, 20: 20720 (AD-630891)

BATTELLE MEMORIAL INST., COLUMBUS, OHIO.
Development of Th–^{233}U irradiation specimens, 20: 21288 (BMI-1761)
Diffusion of fission products in fuel-element cladding materials and related alloys, 20: 21232 (BMI-1763)
Examination of 1B steam generator from Shippingport Atomic Power Station, 20: 22408 (BMI-1764)

BATTELLE-NORTHWEST, RICHLAND, WASH. PACIFIC NORTHWEST LAB.
Accumulation and transport of radionuclides by Columbia River biota, 20: 20382 (BNWL-SA-623)
Accumulation of ^{137}Cs in litter and understory plants of forest stands from various climatic zones of Washington, 20: 20879 (BNWL-SA-530)
Bright-field, grain structure etch for delta phase stabilized Pu, 20: 21233 (BNWL-188)
Correspondence between calculated and measured thermal utilizations, 20: 21938 (BNWL-193, pp 16-20)
Effect of neutron irradiation on UHTREX graphite and C, 20: 21419 (BNWL-191)
Fixation of high-level radioactive wastes in phosphate glass, 20: 22510 (BNWL-SA-564)
Irradiated wood-plastic materials—commercial possibilities in Pacific Northwest, 20: 21185 (ORNL-IIC-7, pp 76-80)
Irradiation-induced contraction of graphites at high temperature, 20: 21420 (BNWL-215)
Material bucklings for ^{235}U-enriched U tube lattices in light water, 20: 22375 (BNWL-193, pp 45-56)
Modifications to computer code, THERMOS, 20: 22374 (BNWL-193, pp 5-15)
Neutron interaction between multiplying media separated by various materials, 20: 20840 (BNWL-193, pp 57-67)
Nuclear criticality safety study of FFTF fuel, 20: 22494 (BNWL-193, pp 30-44)
PCTR operational techniques, 20: 22493 (BNWL-193, pp 21-9)
Prog. rpt. on physics research, 7–9/65, 20: 22373 (BNWL-193)

Stresses in Zy-2 cladding during vibratory fuel loading, 20: 21289 (BNWL-194)
Subisokinetic sampling of particles in an air stream, 20: 20927 (BNWL-217)
Transformation rates of plastically deformed plutonium, 20: 21326 (BNWL-203)
BATTERSEA COLL. OF TECH., LONDON (ENGLAND).
Activation sintering of W and effect on mechanical properties, 20: 21291 (NP-15944)
BEERS (ROLAND F.), INC., ALEXANDRIA, VA.
Possibilities of secondary explosions and post-shot thermal effects in cavities in tuff, 20: 20939 (NVO-1163-70)
BELL TELEPHONE LABS., MURRAY HILL, N. J.
Computers in experimental physics, 20: 21982 (BNL-948, pp 718-40)
Multi-body exit channels, 20: 21981 (BNL-948, pp 610-84)
Technical developments in hardware, 20: 21026 (BNL-948, pp 704-17)
BETTIS ATOMIC POWER LAB., PITTSBURGH, PA.
DUZ-1—program for solving axisymmetric and plane elasticity problems on Philco-2000, 20: 20862 (WAPD-TM-555)
Examination of 1B steam generator from Shippingport Atomic Power Station, 20: 22408 (BMI-1764)
Homogenization and densification of $ZrO_2 + UO_2$ fuels under irradiation, 20: 21432 (WAPD-301)
BORDEAUX UNIV. (FRANCE). LABORATOIRE DE PHYSIQUE THEORIQUE.
Conference on Theoretical physics, Bordeaux, France, 5/28–6/2/64. II., 20: 21706 (CONF-640509(Pt.2))
Consequences of unitary symmetry, 20: 21709 (CONF-640509(Pt.2), (Paper 6)
Unitary symmetry, 20: 21707 (CONF-640509(Pt.2), Paper 1)
Unitary symmetry and weak interactions, 20: 21708 (CONF-640509 (Pt.2), Paper 2)
BRITISH COLUMBIA UNIV., VANCOUVER.
Mechanism of ultraviolet and high-energy radiation damage, 20: 20731 (PB-181506, pp 133-42)
BROOKHAVEN NATIONAL LAB., UPTON, N. Y.
BNL double Emperor tandem facility, 20: 21464 (BNL-948, pp 692-703)
BNL low-energy nuclear accelerator program, 20: 21463 (BNL-948, pp 685-91)
Boundary condition constraint method, 20: 21989 (BNL-948, pp 905-27)
Capture reactions, 20: 21986 (BNL-948, pp 763-825)
Computers in experimental physics, 20: 21982 (BNL-948, pp 718-40)
Conversion of high-level radioactive waste to phosphate glass, 20: 22509 (BNL-10109)
Coulomb excitation with heavy ions, 20: 21991 (BNL-948, pp 1005-44)
Diffraction model calculations, 20: 21980 (BNL-948, pp 561-609)
Gamma-ray multipolarities from internal pair correlation measurements, 20: 21985 (BNL-948, pp 757-62)
Heavy ion interactions, 20: 21992 (BNL-948, pp 1045-1134)
Heavy spherical nuclei, 20: 21975 (BNL-948, pp 269-336)
Heavy strongly deformed nuclei, 20: 21977 (BNL-948, pp 380-453)
Inelastic scattering, 20: 21973 (BNL-948, pp 175-221)
Intermediate structure, 20: 21988 (BNL-948, pp 876-904)
Light spherical nuclei, 20: 21974 (BNL-948, pp 222-68)
Light strongly deformed nuclei, 20: 21976 (BNL-948, pp 337-79)
Multi-body exit channels, 20: 21981 (BNL-948, pp 610-84)
Neutrino experiments at BNL, 20: 21595 (CERN-65-32, pp 1-10)
Neutrino physics with 80-in. and 14-ft. bubble chambers at BNL, 20: 21608 (CERN-65-32, pp 169-74)
Numerical analyses of neutron resonances by use of computer programs, 20: 21994 (BNL-10094)
Optical model, DWBA, 20: 21978 (BNL-948, pp 454-524)
Proceedings of summer study group on physics of the Emperor Tandem Van de Graaff region, Brookhaven National Lab., 6/21–7/16/65. I-III., 20: 21462 (BNL-948)
Production of ^{52}Fe, 20: 21993 (BNL-9168)
Reactions with fluctuating cross sections, 20: 21987 (BNL-948, pp 826-75)
Search for double-β decay in ^{48}Ca, 20: 21995 (CERN-65-32, pp 35-40)
Single-nucleon transfer reactions, 20: 21971 (BNL-948, pp 1-65)
Spin assignments by particle-γ correlations from aligned nuclei, 20: 21983 (BNL-948, pp 741-50)
Spin assignments by γ-γ correlations from aligned nuclei, 20: 21984 (BNL-948, pp 751-6)
Strong coupling, exchange, target excitation, and other corrections to DWBA, 20: 21979 (BNL-948, pp 525-60)
Summary of neutrino physics conference and closing remarks, 20: 21613 (CERN-65-32, pp 269-74)
Technical developments in hardware, 20: 21026 (BNL-948, pp 704-17)
Two and more nucleon transfer reactions, 20: 21972 (BNL-948, pp 66-174)
Uncommon states of nuclear matter, 20: 21990 (BNL-948, pp 928-1004)
BUNDESFORSCHUNGSANSTALT FUER LEBENSMITTELFRISCHHALTUNG, KARLSRUHE (WEST GERMANY).
Food irradiation research in West Germany, 20: 21193 (PB-181506, pp 29-38)
BUREAU OF MINES, ROLLA, MO. ROLLA METALLURGY RESEARCH CENTER.
Vapor deposition of cobalt–tungsten alloys, 20: 21231 (BM-RI-6713)

C

CALIFORNIA UNIV., DAVIS.
Environmental and biological factors affecting accumulation of ^{90}Sr and ^{137}Cs in deer and sheep, 20: 20388 (SAN-34-2)
CALIFORNIA UNIV., LA JOLLA, SAN DIEGO.
Feasibility of experiment to observe the W produced in strong interactions, 20: 21610 (CERN-65-32, pp 181-94)
CALIFORNIA UNIV., LOS ANGELES.
Heavy strongly deformed nuclei, 20: 21977 (BNL-948, pp 380-453)
CALIFORNIA UNIV., LOS ANGELES. DEPT. OF PHYSICS.
Elastic scattering of 45-Mev protons, 20: 21963 (AD-626656)
FORTRAN program for reduction of differential cross section data, 20: 21965 (AD-626776)
CARNEGIE INST. OF TECH., PITTSBURGH, PA.
Shell model calculation of the odd tin isotopes, 20: 21962 (AD-624214)
CASE INST. OF TECH., CLEVELAND, OHIO.
Boundary condition constraint method, 20: 21989 (BNL-948, pp 905-27)
Inelastic scattering, 20: 21973 (BNL-948, pp 175-221)
Reactor neutrino experiment, 20: 21027 (CERN-65-32, pp 41-4)
Thermal stability of completely confined fluids including MHD effects, 20: 20854 (AD-621523)
CATALYTIC CONSTRUCTION CO., PHILADELPHIA, PA.
Feasibility for dual-purpose electric power–water desalting plant for Israel, 20: 22459 (66-1-RE)
CATHOLIC UNIV. OF AMERICA, WASHINGTON, D. C.
Photoproduction of single W bosons, 20: 21611 (CERN-65-32, pp 195-200)
Production of muons, 20: 21028 (CERN-65-32, pp 65-70)
Proposal to detect cosmic-ray neutrinos through the Cherenkov light of produced muons, 20: 21031 (CERN-65-32, pp 231-40)
CENTER FOR THEORETICAL STUDIES, UNIV. OF MIAMI, CORAL GABLES, FLA.
Prog. rpt. on plasma physics, final, 6/64–8/65, 20: 22189 (TID-22809)
CENTRE D'ETUDE DE L'ENERGIE NUCLEAIRE, BRUSSELS (BELGIUM).
Design problems of pilot plants for volatilization recycling, 20: 20810 (ANL-Trans-250)
CENTRE D'ETUDE DE L'ENERGIE NUCLEAIRE, MOL (BELGIUM).
Migration of radio elements in soil, 20: 20875 (EUR-2481.f)
CHICAGO UNIV., ILL.
$\pi^{\pm}$ and $K^{\pm}$ production cross sections for 12.5-Bev protons on Be, 20: 21601 (CERN-65-32, pp 109-10)
CHICAGO UNIV., ILL. DEPT. OF PHARMACOLOGY.
Distribution of and discrimination against naturally occurring ^{226}Ra in swine, 20: 20385 (COO-1184-3)
CINCINNATI UNIV., OHIO.
Nuclear levels in ^{223}Ra populated by decay of ^{227}Th and ^{223}Fr, 20: 22008 (MLM-1337J)
CLARENDON LAB., OXFORD UNIV. (ENGLAND).
Prog. rpt. on properties of rare earth and transition group ions, final, 4/63–6/65, 20: 22311 (AD-622068)
COLLEGE OF AERONAUTICS, CRANFIELD (ENGLAND). DEPT. OF MATERIALS.
Prog. rpt. on creep and recovery in graphite, final, 8/63–7/64, 20: 21343 (N-65-23013)
COLORADO STATE UNIV., FORT COLLINS. DEPT. OF RADIOLOGY AND RADIATION BIOLOGY.
Concentration patterns of ^{90}Sr, ^{137}Cs, ^{131}I in a wild deer population and environment, 20: 20384 (COO-1156-13)
COLORADO UNIV., BOULDER.
Radioecology of the Colorado Front Range, 20: 20379 (COO-1191-10)
COLORADO UNIV., BOULDER. ENGINEERING RESEARCH CENTER.
Flow calibration of the Long John manifolded orifice assembly with air, 20: 20988 (UCRL-13202)
COLORADO UNIV., BOULDER. NUCLEAR PHYSICS LAB.
Prog. rpt. on isochronous cyclotron, 2/66, 20: 21473 (UCOL-535-554)
COLUMBIA UNIV., NEW YORK.
Determination of neutrino flux, 20: 21600 (CERN-65-32, pp 97-108)
Neutrino experiments at BNL, 20: 21595 (CERN-65-32, pp 1-10)
Neutrino physics, 20: 21614 (CERN-65-32, pp 275-84)
COLUMBIA UNIV., NEW YORK. DEPT. OF CHEMICAL ENGINEERING.
Prog. rpt. on high-temperature thermal properties of gases and vapors, 1965/66, 20: 20651 (CU-2660-26)
COLUMBIA UNIV., NEW YORK. DEPT. OF PHYSICS.
Prog. rpt. on nuclear physics, annual, 1964–65, 20: 22010 (NYO-72-28)
COLUMBIA UNIV., NEW YORK. PLASMA LAB.

Ionizing shock studies in an electromagnetically driven shock tube, 20: 21779 (AD-621990)

COLUMBIA UNIV., NEW YORK. SCHOOL OF ENGINEERING AND APPLIED SCIENCE.
Thermodynamic study of K amalgams, 20: 21328 (CU-2660-25)

COLUMBIA UNIV., PALISADES, N. Y. LAMONT GEOLOGICAL OBSERVATORY.
Final rpt. on elastic wave propagation, 20: 20896 (AD-623592)
Microbiological assays of seawater using radioisotopes, 20: 20368 (CONF-640309-1)

COMBUSTION ENGINEERING, INC., WINDSOR, CONN. NUCLEAR DIV.
Prog. rpt. on temperature transient method for performing in-pile thermal conductance testing, final, 3/64–11/65, 20: 22354 (CEND-3336-260)

COMISION NACIONAL DE ENERGIA ATOMICA, BUENOS AIRES (ARGENTINA).
Hepatic scintigram, 20: 20522 (CNEA-167)
Insulin labeling with ^{131}I, 20: 20383 (CNEA-185)
Labeling lipids with ^{131}I, 20: 20789 (CNEA-182)

COMISION NACIONAL DE ENERGIA ATOMICA, BUENOS AIRES (ARGENTINA). DEPARTMENTO DE METALLURGIA.
Prog. rpt. on point defects and mechanical properties of Nb, final, 2/15/62–11/30/65, 20: 21320 (AD-625475)

COMITATO NAZIONALE PER L'ENERGIA NUCLEARE, ROME (ITALY).
Determination of reactor kinetic parameters, 20: 22381 (RT-FI-(65)49)
Flux of neutrons and gamma rays in paraffin moderator, 20: 20524 (RT-PROT-(65)32)
Homogenization of cruciform control rods in water-moderated reactor, 20: 22357 (RT-FI-(65)50)
Measuring spectrum of intermediate neutrons, 20: 22382 (RT-FI(65)57)
Radioluminescent watches: international trends of radioprotection, 20: 20518 (RT-PROT-(65)41)

COMMISSARIAT A L'ENERGIE ATOMIQUE, CADARACHE (FRANCE). CENTRE D'ETUDES NUCLEAIRES.
Experimental results on engineering model of Rapsodie, 20: 22501 (EURFNR-49F)

COMMISSARIAT A L'ENERGIE ATOMIQUE, FONTENAY-AUX-ROSES (FRANCE). CENTRE D'ETUDES NUCLEAIRES.
Physical methods of analysis of UF_6, 20: 20558 (CEA-R-2863)

COMMISSARIAT A L'ENERGIE ATOMIQUE, GRENOBLE (FRANCE). CENTRE D'ETUDES NUCLEAIRES.
Determination of inception of nucleate boiling in terphenyl OM2 in conditions of forced convection, 20: 20709 (EUR-2442.f)
Technological study of polyphenyls. I., II., III., 20: 20721 (EUR-2295.f)

COMMISSARIAT A L'ENERGIE ATOMIQUE, PARIS (FRANCE).
X-ray diffraction study of neutron-irradiated beryllia, 20: 21433 (UCRL-Trans-10012)

COMMISSARIAT A L'ENERGIE ATOMIQUE, SACLAY (FRANCE). CENTRE D'ETUDES NUCLEAIRES.
Behavior of concrete pressure vessel subjected to high temperature gradient, 20: 22353 (CEA-R-2829)
Kinetics of escape of He from BeO frits during irradiation, 20: 21428 (NP-15942)
Radiochemistry in France, 20: 20730 (PB-181506, pp 104-15)
Recovery of ^{90}Sr and ^{144}Ce from concentrated fission-product solutions, 20: 20804 (EUR-2754.f)
Technological study of polyphenyls. I., II., III., 20: 20721 (EUR-2295.f)
Technological study on polyphenyls, 20: 20722 (EUR-2401.f)

CONSOLIDATION COAL CO., LIBRARY, PA. RESEARCH DIV.
Prog. rpt. on radiation-induced telomerization of methanol, final, 11/64–4/65, 20: 20724 (NYO-2978-44)

CULHAM LAB., UNITED KINGDOM ATOMIC ENERGY AUTHORITY, ABINGDON (ENGLAND).
Bibliography on plasma sheath, 20: 22177 (CLM-Bib-6)
Monte Carlo computer program for analysis of molecular gas flow, 20: 20855 (CLM-R-54)

D

DANISH ATOMIC ENERGY COMMISSION, RISOE. RESEARCH ESTABLISHMENT.
Three-dimensional dose distribution in samples irradiated by electron beams, 20: 21470 (PB-181506, pp 116-29)

DENVER RESEARCH INST., UNIV. OF DENVER, COLO.
Prog. rpt. on effect of interstitial addition on phase equilibria on Nb-rich region of Nb–W–Hf and Nb–W–Zr alloy systems, 3/66, 20: 21329 (DRI-1092-229)

DEPARTMENT OF NATIONAL HEALTH AND WELFARE, OTTAWA (ONTARIO). RADIATION PROTECTION DIV.
Data from Radiation Protection Programs, Vol. 2, No. 12, 20: 20883 (NP-15914)
Data from Radiation Protection Programs, Vol. 4, No. 1, 20: 20938 (NP-15921)

DIVISION OF BIOLOGY AND MEDICINE (AEC), WASHINGTON, D. C.
Aeroradioactivity survey and geology of District of Columbia area, 20: 20928 (CEX-59.4.17)

DIVISION OF INDUSTRIAL PARTICIPATION (AEC), WASHINGTON, D. C.
Radiation and its commercial future, 20: 21182 (ORNL-IIC-7, pp 49-58)

DIVISION OF ISOTOPES DEVELOPMENT (AEC), WASHINGTON, D. C.
Atomic Energy Commission's program in wood-plastic materials, 20: 21178 (ORNL-IIC-7, pp 1-5)
Conference on pure and applied chemistry, 20th International, Moscow, 7/65, 20: 20552 (CONF-650723(Abstr.))
Radiation processed wood-plastic materials, 20: 21183 (ORNL-IIC-7, pp 59-63)

DIVISION OF TECHNICAL INFORMATION EXTENSION, (AEC), OAK RIDGE, TENN.
Bibliographies of atomic energy literature, 20: 22522 (TID-3734)

DU PONT DE NEMOURS (E. I.) & CO., AIKEN, S. C. SAVANNAH RIVER LAB.
Electrowinning plutonium metal, 20: 21234 (DP-1021)
Production of radioisotopes in production reactors, 20: 21212 (CONF-660305-19)
Prog. rpt. on performance of activated carbon beds in SRP reactor confinement facilities, 9/62–9/65, 20: 22463 (DP-1028)
Publications, 1965, 20: 22519 (DP-929(Suppl.2))

DU PONT DE NEMOURS (E. I.) AND CO., WILMINGTON, DEL. PIGMENTS DEPT.
Prog. rpt. on high-temperature thermoelectric generator, final, 6/14/63–6/14/64, 20: 21563 (AD-623591)

DUKE UNIV., DURHAM, N. C.
Radiation chemistry in the solid state as studied with electron paramagnetic resonance, 20: 20729 (PB-181506, pp 85-103)

DURHAM UNIV. (ENGLAND).
Energy spectra of cosmic-ray neutrinos, 20: 21542 (CERN-65-32, pp 73-8)
Use of neon flash tubes in cosmic-ray neutrino experiments, 20: 21541 (CERN-65-32, pp 57-60)

E

EAGLE-PICHER CO., MIAMI, OKLA. RESEARCH LABS.
Purification and crystallization of B, 20: 21294 (TID-22221)

ECOLE POLYTECHNIQUE, PARIS (FRANCE).
"Gargamelle" project, 20: 21033 (CERN-65-32, pp 263-8)

EDGERTON, GERMESHAUSEN AND GRIER, INC., SANTA BARBARA, CALIF.
Albuquerque–Los Alamos area (ARMS-II), 20: 20929 (CEX-61.6.2)
Cincinnati area (ARMS-II), 20: 20880 (CEX-62.6.5)
Development of airborne surveillance instrumentation, 20: 20881 (DASA-1704)

EIDGENOESSISCHES INSTITUT FUER REAKTORFORSCHUNG, WUERENLINGEN (SWITZERLAND).
ALGAN-I. Supplementary users' manual of new developments and facilities, 20: 21222 (EIR-89)

EUROPEAN ATOMIC ENERGY COMMUNITY.
Cryostat in the gaseous phase, 20: 20984 (EUR-2710.f)
Deformation mechanisms in hexagonal compact metals, 20: 21330 (EUR-2621.f)
Design and calculations for a ^6Li semiconductor sandwich fast neutron spectrometer experiment, 20: 21034 (EUR-2712.e)
Effect of radiations on the detoxication of α-methylnaphthalene, 20: 20439 (EUR-2628.i)
Effects of micro-irradiation of chromosome segments, 20: 20438 (EUR-2518.f)
Mechanical radiography techniques for quality control of thin walled SAP tubes, 20: 20861 (EUR-2443.f)
Method of analyzing activity profile of radiochromatograph, 20: 20559 (EUR-2626.f)
Migration of radio elements in soil, 20: 20875 (EUR-2481.f)
Neutron activation determination of impurities in some materials strongly activated upon irradiation, 20: 20560 (EUR-2753.f)
Prog. rpt. on effects of radiation on embryo and its organs, 10/64–9/65, 20: 20440 (EUR-2643.f)
Recovery of ^{90}Sr and ^{144}Ce from concentrated fission-product solutions, 20: 20804 (EUR-2754.f)
Technical and economic comparison of double-cycle and single-cycle boiling-water nuclear power plant, 20: 22409 (EUR-2735.d)
Technological study of polyphenyls. I., II., III., 20: 20721 (EUR-2295.f)
Technological study on polyphenyls, 20: 20722 (EUR-2401.f)

EUROPEAN ATOMIC ENERGY COMMUNITY, ISPRA (ITALY). JOINT NUCLEAR RESEARCH CENTER.
Cryostat in the gaseous phase, 20: 20984 (EUR-2710.f)
Deformation mechanisms in hexagonal compact metals, 20: 21330 (EUR-2621.f)

Design and calculations for a ^{6}Li semiconductor sandwich fast neutron spectrometer experiment, 20: 21034 (EUR-2712.e)
Effect of radiations on the detoxication of α-methylnaphthalene, 20: 20439 (EUR-2628.i)
Mechanical radiography techniques for quality control of thin walled SAP tubes, 20: 20861 (EUR-2443.f)
Neutron activation determination of impurities in some materials strongly activated upon irradiation, 20: 20560 (EUR-2753.f)

EUROPEAN ORGANIZATION FOR NUCLEAR RESEARCH, GENEVA (SWITZERLAND).
Chairman's summary of the session on neutrino facilities, 20: 21605 (CERN-65-32, pp 153-6)
Collimators for r-f separated beam, 20: 21468 (CERN-66-10)
Conference on experimental neutrino physics, CERN, 1/65, 20: 21594 (CERN-65-32)
Consequences of unitary symmetry, 20: 21709 (CONF-640509(Pt.2), Paper 6)
Cosmic-ray induced μ-e events, 20: 21029 (CERN-65-32, pp 71-2)
Determination of neutrino flux, 20: 21600 (CERN-65-32, pp 97-108)
Determination of spectra of high-energy neutrino parents, 20: 21604 (CERN-65-32, pp 121-6)
Energy spectra of cosmic-ray neutrinos, 20: 21542 (CERN-65-32, pp 78-8)
Experimental determination of the neutrino spectrum, 20: 21603 (CERN-65-32, pp 115-20)
Feasibility of experiment to observe the W produced in strong interactions, 20: 21610 (CERN-65-32, pp 181-94)
Fluxes of neutrinos and antineutrinos produced at CERN, 20: 21602 (CERN-65-32, pp 111-14)
Further analysis of neutrino interactions in the CERN heavy liquid bubble chamber, 20: 21597 (CERN-65-32, pp 25-30)
Future neutrino experiments with the CERN heavy liquid bubble chamber, 20: 21606 (CERN-65-32, pp 157-60)
"Gargamelle" project, 20: 21033 (CERN-65-32, pp 263-8)
High-energy elastic scattering, 20: 21593 (CERN-65-24(Vol.1), pp 65-80)
K.G.F. neutrino project, 20: 21540 (CERN-65-32, pp 49-56)
Large hydrogen bubble chamber, 20: 21032 (CERN-65-32, pp 259-62)
Lower limit for mass of the intermediate boson, 20: 21596 (CERN-65-32, pp 11-24)
Measurement of polarization parameters and spin correlation in proton-proton scattering at 600 Mev, 20: 21590 (CERN-66-2)
Muon flux measurement in neutrino shielding, 20: 22306 (CERN-65-32, pp 147-52)
N* production by neutrinos, 20: 21599 (CERN-65-32, pp 89-96)
Neutrino experiment at the ZGS, 20: 21465 (CERN-65-32, pp 31-4)
Neutrino experiments at BNL, 20: 21595 (CERN-65-32, pp 1-10)
Neutrino physics with 80-in. and 14-ft. bubble chambers at BNL, 20: 21608 (CERN-65-32, pp 169-74)
Neutrino physics, 20: 21614 (CERN-65-32, pp 275-84)
Outline of programs to raise beam intensity of accelerators, 20: 21466 (CERN-65-32, pp 127-30)
Peripheral collisions, 20: 21592 (CERN-65-24(Vol.1), pp 1-44)
Photoproduction of single W bosons, 20: 21611 (CERN-65-32, pp 195-200)
$\pi^\pm$ and $K^\pm$ production cross sections for 12.5-Bev protons on Be, 20: 21601 (CERN-65-32, pp 109-10)
Possible neutrino experiments in emulsions, 20: 21609 (CERN-65-32, pp 175-80)
Possible spark chamber experiment with antineutrinos, 20: 21607 (CERN-65-32, pp 161-8)
Proceedings of 1965 Easter School for physicists, Bad Kreuznach, Germany, 4/65, 20: 21591 (CERN-65-24(Vol.1))
Production of muons, 20: 21028 (CERN-65-32, pp 65-70)
Project for underground laboratory in the Mont Blanc tunnel for experiments on neutrino and cosmic radiation, 20: 21612 (CERN-65-32, pp 235-30)
Proposal to detect cosmic-ray neutrinos through the Cherenkov light of produced muons, 20: 21031 (CERN-65-32, pp 231-40)
Reactor neutrino experiment, 20: 21027 (CERN-65-32, pp 41-4)
Search for double-β decay in ^{48}Ca, 20: 21995 (CERN-65-32, pp 35-40)
Servo correction of phase changes between deflectors in the r-f separator, 20: 21467 (CERN-66-8)
Summary of neutrino physics conference and closing remarks, 20: 21613 (CERN-65-32, pp 269-74)
The peripheral model, 20: 21705 (CERN-65-24(Vol.1), pp 45-63)
Theoretical aspects of neutrino physics, 20: 21598 (CERN-65-32, pp 79-82)
Utah neutrino detector, 20: 21030 (CERN-65-32, pp 223-4)

F

FLORIDA UNIV., GAINESVILLE. DEPT. OF FOOD TECHNOLOGY AND NUTRITION.
Prog. rpt. on effects of low-level irradiation upon preservation of food products, annual, 4/65, 20: 21195 (TID-22509)

G

GAKUSHUIN UNIV., TOKYO (JAPAN). DEPT. OF PHYSICS.
High-energy nuclear-active particles in extensive air showers at 5,200 m altitude, 20: 21544 (MIT-2098-227, Paper EAS-8)

GARRETT CORP., LOS ANGELES, CALIF. AIRESEARCH MFG. DIV.
Application of radioisotopes to manned spacecraft life-support systems. I and II., 20: 21174 (SAN-575-12)

GENERAL ATOMIC, SAN DIEGO, CALIF. JOHN JAY HOPKINS LAB. FOR PURE AND APPLIED SCIENCE.
Effect of fast neutron irradiation from 495 to 1035°C on nuclear graphites, 20: 21421 (GA-6888)
GARGOYLE—infinite medium fuel cycle analysis code with fuel and poison searches, 20: 22412 (GA-6622)
Influence of thermalization models on reactivity and temperature coefficient of zirconium hydride reactors, 20: 22377 (GA-6930, App. B)
Prog. rpt. on EBOR program, 3/31/64, 20: 22410 (GA-5238)
Prog. rpt. on EBOR program, 10–12/65, 20: 22413 (GA-6929)
Prog. rpt. on integral neutron thermalization, 10–12/65, 20: 21939 (GA-6930)
Prog. rpt. on metallurgy as related to fuel element fabrication, 9/59, 20: 21290 (GA-1052)
Prog. rpt. on TARGET, 12/64–2/65, 20: 22411 (GA-6113)
PSEUDO—code for construction of statistical resonances in unresolved resonance region, 20: 21940 (GAMD-6908)
Role of thermal spectrum measurements in reactor design, 20: 22376 (GA-6901)

GENERAL DYNAMICS, CHICAGO, ILL. LIQUID CARBONIC DIV.
Descaling and decontamination studies, 20: 21238 (NP-15928)

GENERAL DYNAMICS/CONVAIR, SAN DIEGO, CALIF.
Prog. rpt. on switchgear for space nuclear electric systems, 3–5/65, 20: 20986 (N-65-29823)

GENERAL ELECTRIC CO., CINCINNATI, OHIO. AIRCRAFT NUCLEAR PROPULSION DEPT.
Radiation level measurements within and behind Be, 20: 22307 (DC-61-3-69)

GENERAL ELECTRIC CO., CINCINNATI, OHIO. SPACE POWER AND PROPULSION SECTION.
Material and process specifications for refractory alloy and alkali metals, 20: 21293 (R-66SD3007)
Prog. rpt. on advanced refractory alloy corrosion loop program, 10/65–1/66, 20: 21263 (NASA-CR-54911)

GENERAL ELECTRIC CO., RICHLAND, WASH. HANFORD ATOMIC PRODUCTS OPERATION.
Ceramic cells for electrowinning and electrorefining of Pu metal, 20: 21239 (RL-SEP-824)

GENERAL ELECTRIC CO., SAN JOSE, CALIF. ADVANCED PRODUCTS OPERATION.
Prog. rpt. on SEFOR, 2–4/65, 20: 22496 (GEAP-4864)

GENERAL ELECTRIC CO., SAN JOSE, CALIF. ATOMIC POWER EQUIPMENT DEPT.
Irradiation of 0.5-inch diameter, hollow-pellet UO_2 fuel rods, 20: 21422 (GEAP-5100D)
Prog. rpt. on pulsed neutron application to power reactor startup, 7–10/65, 20: 22414 (GEAP-4961)
Prog. rpt. on SEFOR, 7–9/64, 20: 22495 (GEAP-4742)
Turbulent flow in an annulus, 20: 20856 (GEAP-4976)

GEOLOGICAL SURVEY, WASHINGTON, D. C.
Aeroradioactivity survey and geology of District of Columbia area, 20: 20928 (CEX-59.4.17)

GEORGIA INST. OF TECH., ATLANTA.
Diffusion rate and activation energy of He through single crystal and polycrystalline Al_2O_3, 20: 21353 (TID-22828)

GOODRICH (B. F.) CO. RESEARCH CENTER, BRECKSVILLE, OHIO.
Prog. rpt. on nuclear radiation-resistant polymers and polymeric compounds, annual, 6/61–5/62, 20: 21430 (WADC-TR-55-58(Pt.8))
Prog. rpt. on nuclear radiation-resistant polymers and polymeric compounds, annual, 6/62–3/63, 20: 21431 (WADC-TR-55-58(Pt.9))

GOSUDARSTVENNYI KOMITET PO ISPOL'ZOVANIYU ATOMNOI ENERGII SSSR, OBNINSK. FIZIKO-ENERGETICHESKII INSTITUT.
Analysis and generalization of correlation method for measurement of particle-lifetime distribution in physical systems, 20: 21035 (FEI-21)
Effect of size of the inter-electrode spacing on operation of a cesium thermal converter, 20: 21568 (FEI-16)
Operation of a cesium diode with an admixture of an inert gas, 20: 21567 (FEI-15)
Volt-ampere characteristics of the TEP (thermoelectron potential) in an arc, 20: 22178 (FEI-17)

H

HAHN-MEITNER-INSTITUT FUER KERNFORSCHUNG, BERLIN (WEST GERMANY).
Change of electrical properties of Si and Ge diodes by neutron irradiation, 20: 21150 (HMI-B-45)
Prog. rpt. on diffusion of rare gases in solids, 10–12/65, 20: 21332 (EURAEC-1573)
HARDWOOD PLYWOOD MANUFACTURERS ASSOCIATION, ARLINGTON, VA.
Potential commercial manufacture and use of hardwood plywood plastic combinations, 20: 21191 (ORNL-IIC-7, pp 112-18)
HARRY DIAMOND LABS., WASHINGTON, D. C.
Nuclear time base-feasibility study, 20: 21021 (AD-622629)
Time-dependent neutron transport from point isotropic source at an altitude of 100,000 feet, 20: 21935 (AD-624041)
HARVARD UNIV., CAMBRIDGE, MASS.
Operations research in disposal of liquid radioactive wastes in streams, 20: 22513 (NYO-10447)
HARVARD UNIV., CAMBRIDGE, MASS. ENGINEERING SCIENCES LAB.
Particle injection techniques for velocity measurement in arc plasmas, 20: 22188 (N-65-22776)
HEALTH AND SAFETY LAB., NEW YORK OPERATIONS OFFICE (AEC), N. Y.
Differential energy and angle spectra for ^{137}Cs rays in sand, 20: 22308 (HASL-167)
Prog. rpt. on fallout program, 12/65–3/66, 20: 20882 (HASL-171)
HILLERICH AND BRADSBY CO., LOUISVILLE, KY.
Potential of wood-plastic combinations in the sporting-goods industry, 20: 21190 (ORNL-IIC-7, pp 106-11)
HUDSON INST., INC., HARMON-ON-HUDSON, N. Y.
Environmental effects of nuclear weapons, 20: 20930 (HI-518-RR(Vol.1))
Environmental effects of nuclear weapons, 20: 20931 (HI-518-RR(Vol.2))
Environmental effects of nuclear weapons, 20: 20932 (HI-518-RR(Vol.3))
HUGHES AIRCRAFT CO., FULLERTON, CALIF.
Prog. rpt. on effect of transistor design parameters on radiation response, 7–9/65, 20: 21148 (AD-630835)
Prog. rpt. on effect of transistor design parameters on radiation response, 10–12/65, 20: 21149 (AD-630836)

I

IBM FEDERAL SYSTEMS DIV., OWEGO, N. Y.
Reactor and linear accelerator induced effects in dielectrics, 20: 21151 (IBM-66-825-1944)
IDAHO OPERATIONS OFFICE (AEC), IDAHO FALLS. HEALTH AND SAFETY DIV.
Criteria for high-efficiency filter installations, 20: 20933 (IDO-12045)
IIT RESEARCH INST., CHICAGO, ILL.
Prog. rpt. on V alloy studies, 12/65–2/66, 20: 21333 (IITRI-B6042-4)
ILLINOIS UNIV., URBANA. DEPT. OF PHYSICS.
$K^- + p \rightarrow \bar{K} + N + \pi$ reactions at 1.33 Bev/c, 20: 21615 (COO-1195-52)
IMPERIAL COLL. OF SCIENCE AND TECH., LONDON (ENGLAND).
Some aspects of the radiation chemistry of organic compounds, 20: 20728 (PB-181506, pp 49-58)
INNSBRUCK UNIV. (AUSTRIA). INSTITUT FUER THEORETISCHE PHYSIK.
Magnetogasdynamic flows of small magnetic Reynolds number. I., 20: 21782 (AD-623812)
Two-dimensional steady and one-dimensional unsteady MGD flows of small magnetic Reynolds number, 20: 21781 (AD-622568)
INSTITUT ATOMNOI ENERGII, GOSUDARSTVENNYI KOMITET PO ISPOL'ZOVANIYU ATOMNOI ENERGII SSSR, MOSCOW.
A magnetohydrodynamic theory of the pinch effect in a high-temperature, dense plasma, 20: 22180 (IAE-960)
Increase of power of VVR-S reactors, 20: 22498 (IAE-993)
Investigation of extraction and formation of ion beams in plasma sources, 20: 21213 (IAE-974)
Neutron thermalization process in time in graphite and Be, 20: 21942 (KFK-tr-188)
Reconstruction of IRT research reactor, 20: 22497 (IAE-992)
Transient neutron spectra in zirconium hydride, 20: 21941 (IAE-977)
INSTITUT DE RECHERCHES DE LA SIDERUGRIE, ST. GERMAINE-EN-LAYE (FRANCE).
Prog. rpt. on study of base metal intended for research on brittle fracture of large weldments, 10–12/65, 20: 21331 (EURAEC-1569)
INSTITUT D'EMBRYOLOGIE EXPERIMENTALE, NOGENT-SUR-MARNE (FRANCE).
Prog. rpt. on effects of radiation on embryo and its organs, 10/64–9/65, 20: 20440 (EUR-2643.f)
INSTITUT FUER PLASMAPHYSIK, G.M.B.H. GARCHING (WEST GERMANY).
Calculation of forces and inductances for the hexapole experiment, 20: 22181 (IPP-1/45)
Microwave interferometry in electromagnetically produced shock waves, 20: 22182 (IPP-3/35)
Possibility of using pure inert gas as working fluid in MHD generators, 20: 21569 (IPP-3/29)
INSTITUT "RUDJER BOSKOVIC," ZAGREB (YUGOSLAVIA).
Prog. rpt. on marine radiobiology, 7/64–6/65, 20: 20386 (NP-15916)
INSTITUTE FOR DEFENSE ANALYSES, ARLINGTON, VA. JASON DIV.
Seismic signals from nuclear explosions in overdriven cavities, 20: 20898 (AD-624016)
INSTITUTE FOR NUCLEAR STUDY, TOKYO UNIV. (JAPAN).
Development of glasses for low-background measurements—characteristics of glasses, 20: 21044 (ANL-Trans-285)
High-energy nuclear-active particles in extensive air showers at 5,200 m altitude, 20: 21544 (MIT-2098-227, Paper EAS-8)
Low-mu showers, 20: 21546 (MIT-2098-227, Paper EAS-29)
Primary energy spectrum from 8×10^{14} to 4×10^{17} ev, 20: 21547 (MIT-2098-227, Paper EAS-31)
Table of singularities in nuclear direct interaction amplitude, 20: 21997 (INSJ-96)
INSTITUTE OF NUCLEAR RESEARCH, WARSAW (POLAND).
Cascade curves for Xe, 20: 21514 (INR-598/VI/PH)
INSTITUTE OF PHYSICAL AND CHEMICAL RESEARCH, TOKYO (JAPAN).
Low-mu showers, 20: 21546 (MIT-2098-227, Paper EAS-29)
Primary energy spectrum from 8×10^{14} to 4×10^{17} ev, 20: 21547 (MIT-2098-227, Paper EAS-31)
Radiation research in Japan, 20: 20727 (PB-181506, pp 9-18)
INSTITUTO DE INVESTIGACIONE AERONAUTICA Y ESPACIAL, BUENOS AIRES (ARGENTINA).
Phenomenological and microscopic analysis of properties of even-even nuclei. B., 20: 21961 (AD-624028)
INTERNATIONAL ATOMIC ENERGY AGENCY, VIENNA (AUSTRIA).
Conference on application of radioisotopes to study of bed load movement and transport in rivers, Vienna, 8/64, 20: 20904 (STI-REP-101)
Conference on nuclear materials management, Vienna, 8/30–9/3/65, 20: 20944 (STI-PUB-110)
Radioactivity of Thorotrast and its in-vitro distribution between the various physical phases, 20: 20790 (CONF-651069-1)
Symposium on isotopes and radiation in soil-plant nutrition studies, Ankara, 6/65, 20: 20389 (STI-PUB-108)
INTERNATIONAL CENTRE FOR THEORETICAL PHYSICS, TRIESTE (ITALY).
Are quarks fractionally or integrally charged? 20: 22460 (IC-66/28)
Completeness, unitarity, and dispersion relations in potential scattering, 20: 22464 (IC-66/29)

J

JAPAN ATOMIC ENERGY RESEARCH INST., TOKYO.
Construction and operation of radiological monitoring station, 20: 20934 (JAERI-1098)
Radiochemical studies of Np, 20: 20561 (JAERI-1099)
JET PROPULSION LAB., CALIF. INST. OF TECH., PASADENA.
Prog. rpt. on radiation effects on Ni–Cd electrodes, final, 6/63–4/65. I., 20: 21425 (N-65-24491)
Tensile and structural properties of glassy carbon, 20: 21338 (JPL-TR-32-842)
JOHNS HOPKINS UNIV., BALTIMORE, MD. DEPT. OF ELECTRICAL ENGINEERING.
Prog. rpt. on plasma waves and instabilities, 6/65–2/66, 20: 22190 (TID-22821)
JOINT INST. FOR NUCLEAR RESEARCH, DUBNA (USSR).
Application of nuclear reaction in chemical research, 20: 20653 (JINR-P-2558)
Fluctuations of ionization losses, 20: 21515 (JINR-P-2615)
Isospin conservation and polarization effects, 20: 21717 (JINR-P-2620)
JOINT INST. FOR NUCLEAR RESEARCH, DUBNA (USSR). LAB. OF NEUTRON PHYSICS.
Approximate method in two-nucleon problem, 20: 21617 (JINR-P-2546)
Conference on inelastic scattering of slow neutrons in crystals and liquids, 6/64, 20: 22316 (JINR-P-2081)
Investigation of neutron resonances of ^{165}Ho, 20: 22004 (JINR-P-2593)
JOINT INST. FOR NUCLEAR RESEARCH, DUBNA (USSR). LAB OF NUCLEAR PROBLEMS.
Decay chain of $^{138}Nd \rightarrow {}^{138}Pr \rightarrow {}^{138}Ce$, 20: 22002 (JINR-P-2570)
Determination of one-boson exchange parameters by nucleon-nucleon phase shifts, 20: 21621 (JINR-P-2584)
Elastic p-p scattering phase shift at 657 Mev, 20: 21622 (JINR-P-2585)
Electrophotographic device for evaluating particle track coordinates in spark chamber, 20: 21037 (JINR-P-2594)
Investigation of the α spectrum of Bi isotopes, 20: 22000 (JINR-P-2553)

Investigation of ^{145}Eu irradiation, 20: 22003 (JINR-P-2581)
Lithium-ion drift in silicon p-type monocrystals, 20: 21337 (JINR-P-2598)
Neutrino processes, 20: 21616 (JINR-P-2429)
JOINT INST. FOR NUCLEAR RESEARCH, DUBNA (USSR). LAB OF NUCLEAR REACTIONS.
Magnetic spectrometer with field variation, 20: 21036 (JINR-P-2573)
Neutron pickup in bombardment of ^{181}Ta, ^{197}Au, ^{232}Th, ^{238}U isotopes with ^{15}N ions, 20: 22001 (JINR-P-2555)
JOINT INST. FOR NUCLEAR RESEARCH, DUBNA (USSR). LAB OF THEORETICAL PHYSICS.
Application of "maximum complexity" method for determining spins and parities in reactions with polarized particles, 20: 21715 (JINR-P-2576)
Calculations of properties of collective states in deformed nuclei, 20: 21998 (JINR-E-2579)
Contribution of virtual Compton effect to cross section for electron-positron pair production, 20: 21623 (JINR-P-2602)
Difference sign of real parts of elastic $\pi^{\pm}$-p scattering amplitudes at high energies, 20: 21618 (JINR-P-2566)
Eightfold formalism in SU(3) and 10- and 27-plets, 20: 21711 (JINR-P-2559)
Equilibrium deformations of excited states of heavy nuclei, 20: 22005 (JINR-P-2596)
Inelastic interactions of cosmic-ray particles with atomic nuclei at very high energies, 20: 21999 (JINR-P-2552)
Mass formula in inhomogeneous SU(6,6) group, 20: 21624 (JINR-P-2606)
Model of weak interactions of baryons and leptons, 20: 21714 (JINR-P-2578)
Nucleon-phonon interaction problem, 20: 21619 (JINR-P-2567)
Photon absorption by nucleons and nucleon dimensions in quark model, 20: 21625 (JINR-P-2619)
Scattering of particles by system of fixed centers, 20: 21710 (JINR-P-2554)
Spin test for bosons decaying into three spinless particles, 20: 21620 (JINR-P-2577)
Symmetries of leptons and hadrons in weak interactions. I., 20: 21712 (JINR-P-2562)
Theory of asymptotic representation of spheroidal functions, 20: 21223 (JINR-P-2564)
Two-plane wave scattering in nonlinear scalar field theory of Born-Infeld type, 20: 21716 (JINR-P-2603)
Unitary symmetry and resonance widths, 20: 21713 (JINR-P-2568)

K

KAISER ENGINEERS, OAKLAND, CALIF.
Feasibility for dual-purpose electric power-water desalting plant for Israel, 20: 22459 (66-1-RE)
KERNENERGIEANLAGEN, ALLGEMEINE ELEKTRICITAETS-GESELLSCHAFT, FRANKFURT AM MAIN (WEST GERMANY).
Technical and economic comparison of double-cycle and single-cycle boiling-water nuclear power plant, 20: 22409 (EUR-2735.d)
KERNFORSCHUNGSZENTRUM, KARLSRUHE (WEST GERMANY).
Theory of Doppler coefficients of fast reactors with consideration of mutual shielding of resonances, 20: 22378 (KFK-367)
KNOLLS ATOMIC POWER LAB., SCHENECTADY, N. Y.
High-speed electron-multiplier discriminator for mass-spectrometer ion detection, 20: 21039 (KAPL-3122)
Solid-state equilibria in systems Li–C and Li–B, 20: 21327 (CONF-660505-1)
KOBE UNIV. (JAPAN). DEPT. OF PHYSICS.
High-energy nuclear-active particles in extensive air showers at 5,200 m altitude, 20: 21544 (MIT-2098-227, Paper EAS-8)
Low-mu showers, 20: 21546 (MIT-2098-227, Paper EAS-29)
Primary energy spectrum from 8×10^{14} to 4×10^{17} ev, 20: 21547 (MIT-2098-227, Paper EAS-31)
KROEHLER MFG. CO., LOUISVILLE, KY.
Commercial use of irradiated wood-plastic materials in furniture industry, 20: 21189 (ORNL-IIC-7, pp 99-105)
KUNGLIGA TEKNISKA HOGSKOLAN, STOCKHOLM (SWEDEN).
Low-cycle strain fatigue—a literature review, 20: 21426 (N-65-24714)
KUNGLIGA VETENSKAPSAKADEMIEN, KIRUNA (SWEDEN). GEOFYSISKA OBSERVATORIET.
Plasma waves in frequency range 0.00110 c/s in earth's magnetosphere and ionosphere: a survey, 20: 21812 (AD-622223)

L

LABORATOIRE DE L'ACCELERATEUR LINEAIRE, UNIV. DE PARIS, ORSAY (FRANCE).
Fluxes of neutrinos and antineutrinos produced at CERN, 20: 21602 (CERN-65-32, pp 111-14)
LABORATOIRE DE RECHERCHES SUR LA PHYSIQUE DES PLASMAS, LAUSANNE (SWITZERLAND).
Design of rotating-field pinched discharge, 20: 22184 (LRP-22-66)
Ionic temperature in an h-f confinement measured with an electrostatic selector, 20: 22185 (LRP-23-66)
Pressure bar and photographic measurements on h-f theta discharge, 20: 22183 (LRP-21-66)
LABORATORI NAZIONALI DI FRASCATI, COMITATO NAZIONALE PER L'ENERGIA NUCLEARE (ITALY).
Determination of branching ratios among neutral decay modes of the η particle, 20: 21627 (LNF-66/9)
Liquid ^3He target for high-energy nuclear experiments, 20: 22007 (LNF-66/1)
Numerical calculations on the space-charge effects in storage ring for electrons and positrons, 20: 21475 (SLAC-Trans-38)
Photodisintegration of the deuteron by polarized γ rays, 20: 21626 (LNF-66/4)
Proposal for administration of radiative corrections, 20: 21469 (LNF-66-10)
LAWRENCE RADIATION LAB., UNIV. OF CALIFORNIA, BERKELEY.
Heat capacity of liquid metals, 20: 20657 (UCRL-11931)
K^+ p interactions at 4.6 Bev/c, 20: 21629 (UCRL-16332)
Magnetic and electrical properties of some metals at high pressures, 20: 21357 (UCRL-16299)
Measurement of anomalous gyromagnetic ratio of the muon, 20: 21630 (UCRL-16469)
Mechanical properties of continuous-matrix, dispersed-phase ceramic systems, 20: 21358 (UCRL-16552)
Prog. rpt. on Bevatron operation and development, 4–6/65, 20: 21474 (UCRL-16553)
Viscosity of liquid metals, 20: 20656 (UCRL-11930)
LAWRENCE RADIATION LAB., UNIV. OF CALIFORNIA, LIVERMORE.
Effectiveness NTU relations for one-, two-, and three-pass cross counterflow heat exchangers to NTU of 40, 20: 20858 (UCRL-14620)
Epithermal fission cross section of ^{235}U, 20: 22012 (UCRL-14606)
Ischemic heart disease, atherosclerosis, and longevity, 20: 20370 (UCRL-14658)
Malfunctions in strain gage systems, 20: 22523 (UCRL-14602)
Physical and mechanical properties of U–Nb–Zr alloy, 20: 21356 (UCRL-14724)
Problems with Rossi sweep applications, 20: 21043 (UCRL-13199)
Profile of electron beam from Astron accelerator, 20: 22191 (UCRL-14697)
Theoretical differential scattering cross sections of x rays, 20: 21516 (UCRL-14403)
LOCKHEED–GEORGIA CO., MARIETTA.
Development-production program for Lockwood, 20: 21188 (ORNL-IIC-7, pp 95-8)
Wood-plastic evaluation program, 20: 21349 (ORNL-IIC-7, pp 26-31)
LOCKHEED NUCLEAR PRODUCTS, MARIETTA, GA.
Prog. rpt. on effect of radiation on materials at cryogenic temperatures, 10/21/65–1/21/66, 20: 21427 (NASA-CR-54904)
LONDON UNIV. (ENGLAND). UNIVERSITY COLL.
Activation sintering of W and effect on mechanical properties, 20: 21291 (NP-15944)
Possible neutrino experiments in emulsions, 20: 21609 (CERN-65-32, pp 175-80)
LOS ALAMOS SCIENTIFIC LAB., UNIV. OF CALIFORNIA, N. MEX.
Advanced concepts for nuclear propulsion and related problems in high-temperature chemistry, 20: 20870 (LA-DC-7703)
Corrosion tests of Hastelloy N, Inconel 600, and Hymu-80 exposed to UCl_3–KCl at 900°C, 20: 21261 (LA-3476)
Criticality dependence on neutron cross sections above 100 kev, 20: 22379 (LA-DC-7800)
Fission couples applied toward reactor diagnostics and safety, 20: 22355 (LA-3470)
High-temperature chemistry of non-fissionable ceramics, 20: 20654 (LA-DC-7784)
Plutonium–americium system, 20: 21339 (LA-DC-7095)
Prog. rpt. on study of base metal intended for research on brittle fracture of large weldments, 10–12/65, 20: 21331 (EURAEC-1569)
Radiation measurements of effluent from Kiwi–TNT experiment, 20: 22468 (LA-3395)
Stress dependence of creep rate of two commercial graphites, 20: 21340 (LA-DC-7626)
Two-dimensional hydrodynamic hot spot. III., 20: 21784 (LA-3450)
LOUISIANA STATE UNIV., BATON ROUGE.
Prog. rpt. on γ spectra by stepwise statistical method, 9/64–1/65, 20: 20555 (AD-622200)
LOUISVILLE UNIV., KY. DEPT. OF BIOLOGY.
Prog. rpt. on radioecological study of biota, final, 5/59–10/64, 20: 20884 (TID-22815)
LOUVAIN UNIV. (BELGIUM). LABORATOIRE DE CYTOGENETIQUE.
Effects of micro-irradiation of chromosome segments, 20: 20438 (EUR-

2518.f)

LYON UNIV. (FRANCE). INSTITUT DE PHYSIQUE NUCLEAIRE.
Activation analysis of a mixture of rare earths, 20: 20562 (LYCEN-6538)

M

MCDONNEL AIRCRAFT CORP., ST. LOUIS, MO. RESEARCH DIV.
Determination of electron densities using a radial transmission line, 20: 22171 (AD-622811)

MAGYAR TUDOMANYOS AKADEMIA KOZPONTI FIZIKAI KUTATO INTEZETE, BUDAPEST.
Circular polarization of γ radiation following deuteron stripping reaction, 20: 22006 (KFKI-600)

MARTIN CO., BALTIMORE, MD.
PM-3A control rod drive mechanism and cable repair, 20: 22416 (TID-22736)

MARYLAND UNIV., COLLEGE PARK. DEPT. OF PHYSICS AND ASTRONOMY.
Neutral hyperon and neutral kaon production in $K^- + p$ interactions near the Y^* (1765) resonance, 20: 21628 (TID-22822)

MARYLAND UNIV., COLLEGE PARK. INST. FOR FLUID DYNAMICS AND APPLIED MATHEMATICS.
Origin of phase transitions in various models, 20: 21872 (AD-627189)

MASSACHUSETTS INST. OF TECH., CAMBRIDGE.
High-energy nuclear-active particles in extensive air showers at 5,200 m altitude, 20: 21544 (MIT-2098-227, Paper EAS-8)
Intermediate structure, 20: 21988 (BNL-948, pp 876-904)
Low-mu showers, 20: 21546 (MIT-2098-227, Paper EAS-29)
Monte Carlo simulation of nuclear active cascade in EAS, 20: 21545 (MIT-2098-227)
Preprints of papers presented at the ninth international conference on cosmic rays, London, September 1965, 20: 21543 (MIT-2098-227)
Primary energy spectrum from 8×10^{14} to 4×10^{17} ev, 20: 21547 (MIT-2098-227, Paper EAS-31)
Prog. rpt. on autoradiographic investigation of brain metabolism, annual, 6/65–3/66, 20: 20391 (TID-22825)
Radiation preservation of foods—two decades of research and development, 20: 21194 (PB-181506, pp 155-67)

MASSACHUSETTS INST. OF TECH., CAMBRIDGE. DEPT. OF NUCLEAR ENGINEERING.
Friction factor and heat transfer correlation for irradiated organic coolants, 20: 20710 (MIT-334-23)
Prog. rpt. on in-pile loop irradiation studies of organic coolant materials, 1–9/65, 20: 20723 (MIT-334-33)

MASSACHUSETTS INST. OF TECH., CAMBRIDGE. LAB. FOR NUCLEAR SCIENCE.
Monte Carlo simulation of nuclear active cascade in EAS, 20: 21545 (MIT-2098-227)
Primary energy spectrum from 8×10^{14} to 4×10^{17} ev, 20: 21547 (MIT-2098-227, Paper EAS-31)

MATERIALS ADVISORY BOARD, NATIONAL ACADEMY OF SCIENCES–NATIONAL RESEARCH COUNCIL, WASHINGTON, D. C.
Evaluation test methods for Be, 20: 21341 (MAB-205-M)

MAX-PLANCK-INSTITUT FUER KERNPHYSIK, HEIDELBERG (WEST GERMANY).
Heavy strongly deformed nuclei, 20: 21977 (BNL-948, pp 380-453)
Single-nucleon transfer reactions, 20: 21971 (BNL-948, pp 1-65)

MAX-PLANCK-INSTITUT FUER PHYSIK UND ASTROPHYSIK, MUNICH (WEST GERMANY).
Peripheral collisions, 20: 21592 (CERN-65-24(Vol.1), pp 1-44)

MECHANICAL TECHNOLOGY INC., LATHAM, N. Y.
Prog. rpt. on gas-bearing Brayton cycle turbocompressor, 12/65–2/66, 20: 20841 (NYO-3237-5)

MICHIGAN STATE UNIV., EAST LANSING.
Inelastic scattering, 20: 21973 (BNL-948, pp 175-221)

MICHIGAN UNIV., ANN ARBOR. DEPT. OF PHYSICS.
Use of image intensifiers with streamer chambers, 20: 21020 (AD-621069)

MINISTERE DE LA SANTE PUBLIQUE ET DE LA FAMILLE, BRUSSELS (BELGIUM). ADMINISTRATION DE L'HYGIENE PUBLIQUE.
Construction of sewer for discharge of industrial waste water containing radioactive substances, 20: 22515 (ORNL-tr-965)

MINNESOTA UNIV., MINNEAPOLIS.
Inelastic scattering, 20: 21973 (BNL-948, pp 175-221)
Light spherical nuclei, 20: 21974 (BNL-948, pp 222-68)
Two and more nucleon transfer reactions, 20: 21972 (BNL-948, pp 66-174)

MINNESOTA UNIV., MINNEAPOLIS. PHYSICAL ELECTRONICS RESEARCH LAB.
Prog. rpt. on collision processes in gaseous plasmas, 7–10/65, 20: 22169 (AD-622684)

MONTANA STATE UNIV., BOZEMAN. DEPT. OF MECHANICAL ENGINEERING.
Prog. rpt. on ventilation of fallout shelters, 7/64–6/65, 20: 20921 (AD-621998)

MONTANA STATE UNIV., BOZEMAN. ELECTRONICS RESEARCH LAB.
Problems with Rossi sweep applications, 20: 21043 (UCRL-13199)

MOUND LAB., MIAMISBURG, OHIO.
Nuclear levels in ^{223}Ra populated by decay of ^{227}Th and ^{223}Fr, 20: 22008 (MLM-1337J)
Prog. rpt. on Pu research, 7–9/65, 20: 21342 (MLM-1301)
Prog. rpt., 10/28/62, 20: 20553 (MLM-1142)
Prog. rpt., 7/65, 20: 20806 (MLM-1274)
Prog. rpt., 8/65, 20: 20807 (MLM-1287)

N

NATIONAL ACADEMY OF SCIENCES–NATIONAL RESEARCH COUNCIL, WASHINGTON, D. C. ADVISORY BOARD ON MILITARY PERSONNEL SUPPLIES.
Conference on radiation research, U. S. Army Natick Labs., Mass., 1/63, 20: 20726 (PB-181506)
Food irradiation research in West Germany, 20: 21193 (PB-181506, pp 29-38)
Mechanism of ultraviolet and high-energy radiation damage, 20: 20731 (PB-181506, pp 133-42)
Radiation chemistry in the solid state as studied with electron paramagnetic resonance, 20: 20729 (PB-181506, pp 85-103)
Radiation in biological systems, 20: 20443 (PB-181506, pp 143-54)
Radiation preservation of foods—two decades of research and development, 20: 21194 (PB-181506, pp 155-67)
Radiation research in Japan, 20: 20727 (PB-181506, pp 9-18)
Radiochemistry in France, 20: 20730 (PB-181506, pp 104-15)
Some aspects of the radiation chemistry of organic compounds, 20: 20728 (PB-181506, pp 49-58)
Three-dimensional dose distribution in samples irradiated by electron beams, 20: 21470 (PB-181506, pp 116-29)
United States program on radiation preservation of foods, 20: 21192 (PB-181506, pp 19-26)

NATIONAL AERONAUTICS AND SPACE ADMINISTRATION, CLEVELAND, OHIO. LEWIS RESEARCH CENTER.
Applications of low-power nuclear rockets, 20: 22469 (N-65-29479)
Fast and moderated low-power, lightweight reactors for nuclear rocket propulsion, 20: 22470 (N-65-29480)
High-temperature creep behavior of Nb alloy, FS-85, 20: 21344 (N-65-26653)
NASA developments in Co-base superalloys, 20: 21237 (N-65-29395)
Non-chemical propulsion, 20: 20871 (N-65-29443)
Thermodynamic properties of Cs up to 1500°K, 20: 21345 (N-65-26656)

NATIONAL AERONAUTICS AND SPACE ADMINISTRATION, GREENBELT, MD. GODDARD SPACE FLIGHT CENTER.
Longitude dependence of geomagnetically trapped electron fluxes. I., 20: 21813 (N-65-29816)

NATIONAL AERONAUTICS AND SPACE ADMINISTRATION, HUNTSVILLE, ALA. GEORGE C. MARSHALL SPACE FLIGHT CENTER.
Effects of nuclear radiation dielectric materials, 20: 21152 (N-65-22353)

NATIONAL AERONAUTICS AND SPACE ADMINISTRATION, WASHINGTON, D. C. SCIENTIFIC AND TECHNICAL INFORMATION DIV.
Bibliography on aerospace medicine and biology, 20: 20369 (NASA-SP-7011(22))

NATIONAL BUREAU OF STANDARDS, WASHINGTON, D. C.
Prog. rpt. on vaporization of refractories, 12/64–2/65, 20: 21262 (N-65-25266)
Tables of electron radial functions and tangents of phase shifts for light nuclei (Z = 1 through 10), 20: 22009 (NBS-MON-81)

NATIONAL INST. FOR RESEARCH IN NUCLEAR SCIENCE, CHILTON (ENGLAND). RUTHERFORD HIGH ENERGY LAB.
Influence of structure on post-irradiation physical properties of epoxy resins, 20: 21429 (RHEL/R-105)
Programs for design calculations on Harwell Variable Energy Cyclotron, 20: 21472 (RHEL/R-113)

NAVAL CIVIL ENGINEERING LAB., PORT HUENEME, CALIF.
Applications of radioisotopes for Naval field establishments, 20: 21176 (AD-621440)
Calculation of energy-angular relationship for neutrons from a neutron generator, 20: 21934 (AD-621473)
Monte Carlo calculations of gamma-ray albedo, 20: 22305 (AD-621441)
Thermal transient response of underground shelters, 20: 20920 (AD-621377)

NAVAL ORDNANCE LAB., CORONA, CALIF.
Surface effects in alkali-halide crystals from irradiation, 20: 21424 (N-65-23332)

NAVAL ORDNANCE LAB., WHITE OAK, MD.
Effect of radiation on electric resistivity and bulk compressibility of

polyepoxides, 20: 21418 (AD-627049)
NAVAL ORDNANCE TEST STATION, CHINA LAKE, CALIF.
Transpiration cooling with liquid metals. II., 20: 22351 (AD-623020)
NAVAL RADIOLOGICAL DEFENSE LAB., SAN FRANCISCO, CALIF.
Beta energy emission rate from neutron-irradiated, ^{235}U carbide, 20: 22404 (USNRDL-TR-987)
Comparison of dose patterns in a dog exposed to neutrons and to x rays, 20: 20432 (AD-630332)
Effect in stomach of ionizing radiation on acid secretion, potential, ATP, and phosphocreatine in comparison to spleen, 20: 20433 (AD-630390)
Photon, neutrons, and charged particle absorbed dose measurements with a portable microcalorimeter, 20: 21024 (AD-630693)
Responses of single neurons in olfactory bulbs, 20: 20431 (AD-630323)
Ultrastructural study of the development of radiation injury in the lung, 20: 20434 (AD-630870)
NAVAL RESEARCH LAB., WASHINGTON, D. C.
Bibliography on direct energy conversion, 20: 21565 (AD-628049)
NEW ENGLAND MEDICAL CENTER HOSPITALS, BOSTON, MASS.
Prog. rpt. on small in vivo β-ray detectors and their diagnostic applications, annual, 5/65–5/66, 20: 20523 (NYO-1726-15)
NEW JERSEY STATE DEPT. OF HEALTH, WEST ORANGE. RADIUM RESEARCH PROJECT.
Epidemiological follow-up of the New Jersey radium cases, 9/65, 20: 20387 (NYO-2181-3)
NEW MEXICO UNIV., ALBUQUERQUE.
Rover destruct Test Three, 20: 22472 (SC-CR-66-2017)
NEW YORK OPERATIONS OFFICE (AEC), N. Y.
Gamma spectrometric measurement of ^{235}U in 24-in. × 24-in. × 12-in. absolute air filters and associated economics of uranium recovery, 20: 20564 (NYO-10740)
NEW YORK UNIV., N. Y. SCHOOL OF ENGINEERING AND SCIENCE.
Another factor to be considered in environmental testing: x radiation, 20: 21022 (AD-624230)
Survey of devices for monitoring x radiation, 20: 21023 (AD-624231)
NORTH CAROLINA STATE UNIV., RALEIGH.
Physical and mechanical properties of selected wood-plastic combinations, 20: 21348 (ORNL-IIC-7, pp 22-5)
NORTH CAROLINA UNIV., CHAPEL HILL. DEPT. OF BOTANY.
Development of a ^{137}Cs facility for ecological research, 20: 20380 (TID-22499)
NORTH TEXAS STATE UNIV., DENTON. DEPT. OF BIOLOGY.
Changes in 5-OH tryptamine content in rat brain tissues x-irradiated in vitro, 20: 20437 (CONF-650560-18)
Oxygen uptake in rat brain tissues x-irradiated in vitro, 20: 20436 (CONF-650560-17)
NORTHWESTERN UNIV., EVANSTON, ILL.
N^* production by neutrinos, 20: 21599 (CERN-65-32, pp 89-96)
NORTHWESTERN UNIV., EVANSTON, ILL. GAS DYNAMICS LAB.
Determination of thermal and electrical conductivity of atmospheric Ar plasma, 20: 22164 (AD-621213)
NUCLEAR METALS, WEST CONCORD, MASS.
Analytical techniques for C and N in Be, 20: 20556 (AD-626987)
NUCLEAR SCIENCE AND ENGINEERING CORP., PITTSBURGH, PA.
Role of radioactivity and hydrothermal processes in protobiochemistry, 20: 20406 (N-65-27062)

O

OAK RIDGE GASEOUS DIFFUSION PLANT, TENN.
Detector for alpha radioactivity in flowing water, 20: 21038 (K-1656)
Fissile-material container and packaging development and testing program, 20: 20936 (K-1661)
Removal of radioactive wastes by sanitary water treatment process, 20: 22512 (K-1651)
Some observations on film badge calibration techniques, 20: 20935 (K-1657)
OAK RIDGE NATIONAL LAB., TENN.
Abstracts of digital computer code packages assembled by RSIC, 20: 22310 (ORNL-RSIC-13)
Animal species associated with pig carrion, 20: 20941 (ORNL-TM-1432)
Atomic Energy Commission's program in wood-plastic materials, 20: 21178 (ORNL-IIC-7, pp 1-5)
Basic research on irradiated wood-plastic combinations, 20: 21179 (ORNL-IIC-7, pp 6-14)
Change in partition of total-body N in radiation chimeras, 20: 20407 (ORNL-P-1118)
Commercial potential of wood plastic combinations in northern U. S., 20: 21186 (ORNL-IIC-7, pp 81-8)
Commercial production of wood-plastic combinations, 20: 21187 (ORNL-IIC-7, pp 89-94)
Commercial use of irradiated wood-plastic materials in furniture industry, 20: 21189 (ORNL-IIC-7, pp 99-105)
Comparative observation on radiation carcinogenesis in man and animals, 20: 20442 (ORNL-P-2053)
Conference on irradiated wood-plastic materials, Chicago, 9/65, 20: 21177 (ORNL-IIC-7)
Confined vortex flow near a stationary disk, theory and experiment, 20: 21786 (ORNL-TM-1387)
Coulomb excitation with heavy ions, 20: 21991 (BNL-948, pp 1005-44)
Critical-path method for scheduling the transuranium processing plant: an appraisal, 20: 20809 (ORNL-3925)
Decomposition rates of ceria in vacuum between 1100 and 1700°C, 20: 20655 (ORNL-P-1260)
Design of high-temperature furnace (3,000°C), 20: 20842 (ORNL-TM-1410)
Development-production program for Lockwood, 20: 21188 (ORNL-IIC-7, pp 95-8)
Engineering design practices for facilities containing radioactive materials, 20: 20942 (ORNL-TM-1459)
Evaluation of radiation dose to man from radionuclides released to Clinch River, 20: 22514 (ORNL-P-2021)
Feasibility and conceptual design study of wood-plastic combinations process, 20: 21181 (ORNL-IIC-7, pp 32-48)
Hydrous zirconium oxide/nitric acid system for use in a ^{99}Mo–^{99m}Tc generator, 20: 20566 (ORNL-TM-1468)
Irradiated wood-plastic materials—commercial possibilities in Pacific Northwest, 20: 21185 (ORNL-IIC-7, pp 76-80)
Late somatic effects of radiation exposure in mice, 20: 20441 (ORNL-P-1173)
Manufacture of control rods for EGCR, 20: 21292 (ORNL-3932)
Monitoring of leached fuel elements with a neutron generator, 20: 21040 (ORNL-P-1218)
Monte Carlo analysis routines for calculating various mean times in reactor problems, 20: 22380 (ORNL-TM-1246)
Nuclear theory index for 1964, 20: 22011 (TID-22771)
Parallel-plate multisection ionization chambers for reactors, 20: 22356 (ORNL-3929)
Parameters of isothermal fission-product deposition, 20: 21785 (ORNL-TM-1330(Rev.))
Physical and mechanical properties of selected wood-plastic combinations, 20: 21348 (ORNL-IIC-7, pp 22-5)
Polymerization and polymer properties as related to wood-plastic combinations, 20: 21180 (ORNL-IIC-7, pp 15-21)
Potential applications of irradiated wood-plastic materials, 20: 21184 (ORNL-IIC-7, pp 64-75)
Potential commercial manufacture and use of hardwood plywood plastic combinations, 20: 21191 (ORNL-IIC-7, pp 112-18)
Potential of wood-plastic combinations in the sporting-goods industry, 20: 21190 (ORNL-IIC-7, pp 106-11)
Prog. rpt. on chemical technology, 7–9/65, 20: 20808 (ORNL-3916)
Prog. rpt. on mathematics and computing, annual, 12/31/65, 20: 21224 (ORNL-3919)
Prog. rpt. on nuclear safety, semiannual, 12/65, 20: 20940 (ORNL-3915)
Radiation and its commercial future, 20: 21182 (ORNL-IIC-7, pp 49-58)
Radiation processed wood-plastic materials, 20: 21183 (ORNL-IIC-7, pp 59-63)
Reactor yield calculations for 81 radioisotopes produced by (n,γ) reactions, 20: 21214 (ORNL-IIC-8)
SDC—shielding-design calculation code for fuel-handling facilities, 20: 22309 (ORNL-3041)
Special purpose high-vacuum high-temperature equipment for refractory-metal research, 20: 21350 (ORNL-TM-1426)
Wood-plastic evaluation program, 20: 21349 (ORNL-IIC-7, pp 26-31)
^3He activation analysis, 20: 20565 (ORNL-P-1216)
OESTERREICHISCHE STUDIENGESELLSCHAFT FUER ATOMENERGIE G.M.B.H., SIEBERSDORF. ELEKTRONIKINSTITUT.
Method for low-level scintillation counting, 20: 21042 (SGAE-E-6/1966)
OESTERREICHISCHE STUDIENGESELLSCHAFT FUER ATOMENERGIE G.M.B.H., SEIBERSDORF. INSTITUT FUER CHEMIE.
Cobalt-60 γ-induced carboxylation of methylamine, 20: 20732 (SGAE-CH-21/1965)
OHIO STATE UNIV., COLUMBUS.
Mechanism of the tritium beta-ray induced exchange reactions of deuterium with methane and ethane in the gas phase, 20: 20719 (AD-624657)
OLD DOMINION COLL., NORFOLK, VA. DEPT. OF PHYSICS.
Prog. rpt. on defect annealing in irradiated semiconductors, 10/64–3/65, 20: 21153 (N-65-25593)

P

PARIS UNIV. (FRANCE).
Physical methods of analysis of UF_6, 20: 20558 (CEA-R-2863)
PARIS UNIV. (FRANCE). LABORATOIRE CURIE.
Method of analyzing activity profile of radiochromatograph, 20: 20559

(EUR-2626.f)
PARIS UNIV. (FRANCE). LABORATOIRE DE PHYSIQUE.
Prog. rpt. on radiation damage in semiconductors, annual, 7/20/65, 20: 21147 (AD-621049)
PARIS UNIV., ORSAY (FRANCE).
Unitary symmetry and weak interactions, 20: 21708 (CONF-640509 (Pt.2), Paper 2)
PARIS UNIV., ORSAY (FRANCE). LABORATOIRE DE PHYSIQUE THEORIQUE ET HAUTES ENERGIES.
Unitary symmetry, 20: 21707 (CONF-640509(Pt.2), Paper 1)
PENNSYLVANIA STATE UNIV., UNIVERSITY PARK.
Radiation in biological systems, 20: 20443 (PB-181506, pp 143-54)
PENNSYLVANIA STATE UNIV., UNIVERSITY PARK. DEPT. OF CHEMISTRY.
Prog. rpt. on radiation chemistry of silane, annual, 4/66, 20: 20725 (NYO-3570-2)
PENNSYLVANIA STATE UNIV., UNIVERSITY PARK. DEPT. OF METALLURGY.
Intermetallic compounds with the $CeCu_2$-type structure, 20: 21352 (TID-21745)
PENNSYLVANIA STATE UNIV., UNIVERSITY PARK. IONOSPHERE RESEARCH LAB.
Dependence of longitudinal plasma wave damping and growth on the shape of the velocity distribution function, 20: 22166 (AD-621913)
PENNSYLVANIA UNIV., PHILADELPHIA. DEPT. OF PHYSICS.
Rare earth–Fe exchange interaction. II., 20: 22313 (AD-624719)
PHILLIPS PETROLEUM CO. IDAHO FALLS, IDAHO., ATOMIC ENERGY DIV.
Flow-diverter valve for granular solids, 20: 22511 (IDO-14666)
Physical comparison of ATR and ATRC cores, 20: 22499 (IDO-17150)
Prog. rpt. on STEP project, 7–12/64, 20: 22467 (IDO-17077)
PHYSICS INTERNATIONAL CO., SAN LEANDRO, CALIF.
Pulsed x-ray prompt gamma simulator, 20: 20838 (AD-624019)
PITTSBURGH UNIV., PA.
Diffraction model calculations, 20: 21980 (BNL-948, pp 561-609)
Formal scattering theory and the Coulomb problem, 20: 21702 (AD-621385)
Heavy spherical nuclei, 20: 21975 (BNL-948, pp 269-336)
Metallographic and x-ray study of $MgO–Al_2O_3–UO_2$ system, 20: 21359 (WAPD-T-1581)
Strong coupling, exchange, target excitation, and other corrections to DWBA, 20: 21979 (BNL-948, pp 525-60)
Two and more nucleon transfer reactions, 20: 21972 (BNL-948, pp 66-174)
POLYTECHNIC INST. OF BROOKLYN, N. Y. MICROWAVE RESEARCH INST.
Bound waves in compressible plasma gaps, 20: 22163 (AD-621034)
Probing of the dynamical response of a plasma, 20: 22175 (AD-624081)
Prog. rpt. on electromagnetics for Project Defender, semiannual, 9/65, 20: 22172 (AD-623718)
PREVENTION OF DETERIORATION CENTER, NATIONAL ACADEMY OF SCIENCES–NATIONAL RESEARCH COUNCIL, WASHINGTON, D. C.
Protective coating systems for Nb in range 1800 to 2500°F, 20: 21257 (AD-621546)
PRINCETON–PENNSYLVANIA ACCELERATOR, PRINCETON, N. J.
Longitudinal instability thresholds in weak-focusing proton synchrotrons, 20: 21471 (PPAD-577D)
Status of Princeton pattern recognition program, 20: 21041 (PPAD-585E)
PRINCETON UNIV., N. J.
Radiolysis of lithium nitrate, 20: 20733 (TID-22796)
PRINCETON UNIV., N. J. PLASMA PHYSICS LAB.
Ballooning interchange instabilities of magnetized plasmas under gravitational fields, 20: 22186 (MATT-358)
Resistive instabilities in toroidal hydromagnetic systems, 20: 22187 (MATT-424)

R

RACETRACK MICROTRON GROUP, UNIV. OF WESTERN ONTARIO, LONDON.
Electron energy measurements of the race-track microtron beam, 20: 21461 (AD-624038)
RADIATION RESEARCH ASSOCIATES, INC., FORT WORTH, TEX.
Gamma energy and angular distributions above infinite fallout field, 20: 20878 (AD-612030)
Instructions for application of LO5 Monte Carlo procedure, 20: 22304 (AD-612031)
RADIO CORP. OF AMERICA, PRINCETON, N. J. ASTRO-ELECTRONICS DIV.
High-temperature radioisotope thermoelectric generator for space applications, 20: 21211 (TID-22350)
RAND CORP., SANTA MONICA, CALIF.
Acoustic phased arrays for the detection of nuclear bursts in the atmosphere, 20: 20897 (AD-623679)
Determination of D layer air chemistry from high-altitude nuclear explosion, 20: 21811 (AD-620952)
Mixing length damping and sunspots, 20: 21489 (AD-623803)
Radiation smoothing of shocks, 20: 21775 (AD-620835)
Scattering of light by protons, 20: 21587 (AD-623564)
Wave propagation in inhomogeneous isotropic hot plasmas, 20: 22165 (AD-621457)
REACTOR GROUP, UNITED KINGDOM ATOMIC ENERGY AUTHORITY, DOUNREAY (SCOTLAND).
Safe transport of radioactive materials, 20: 20945 (TRG-Report-1073)
REACTOR GROUP, UNITED KINGDOM ATOMIC ENERGY AUTHORITY, SELLAFIELD (ENGLAND).
Structure of 20Cr–25Ni–Nb steel after ageing in temperature range 600 to 800°C, 20: 21355 (TRG-Report-1168)
REACTOR GROUP, UNITED KINGDOM ATOMIC ENERGY AUTHORITY, SPRINGFIELDS (ENGLAND).
System C.I.D. Illustration of use of digital computer in storage, interpretation and recovery of materials data, 20: 21354 (TRG-Report-1160)
RENSSELAER POLYTECHNIC INST., TROY, N. Y.
Glass-clad U glass fibers for power reactors. II., 20: 22415 (RPI-321-4)
RENSSELAER POLYTECHNIC INST., TROY, N. Y. DEPT. OF MATERIALS ENGINEERING.
Oxidation characteristics of lanthanide metals, 20: 21265 (RPI-2714-8)
RESEARCH AND ADVANCED DEVELOPMENT DIV., AVCO CORP., WILMINGTON, MASS.
Prog. rpt. on radiation from arc-heated plasma, final, 3/64–4/65, 20: 22167 (AD-622391)
RESEARCH TRIANGLE INST., DURHAM, N. C.
Decontamination effectiveness, 20: 20923 (AD-626727)
RESEARCH TRIANGLE INST., DURHAM, N. C. OPERATIONS RESEARCH ECONOMICS DIV.
Sensitivity analysis of civil defense systems and components summary, 20: 20922 (AD-624704)
RHODES AND BLOXSOM, CANOGA PARK, CALIF.
Heat transfer and flow visualization on cylinders in laminar hypersonic flow, 20: 20857 (SC-DC-65-1907)
ROCHESTER UNIV., N. Y.
Heavy spherical nuclei, 20: 21975 (BNL-948, pp 269-336)
Light strongly deformed nuclei, 20: 21976 (BNL-948, pp 337-79)
Single-nucleon transfer reactions, 20: 21971 (BNL-948, pp 1-65)
Spin assignments by γ-γ correlations from aligned nuclei, 20: 21984 (BNL-943, pp 751-6)
ROCHESTER UNIV., N. Y. DEPT. OF MECHANICAL AND AEROSPACE SCIENCES.
Plasma density ahead of pressure driven shock waves, 20: 22168 (AD-622569)
ROCHESTER UNIV., N. Y. DEPT. OF RADIATION BIOLOGY.
Biochemical aspects of radiation injury and recovery, 20: 20435 (CONF-650560-15)
ROCKY FLATS DIV., DOW CHEMICAL CO., GOLDEN, COLO.
Conductance device for monitoring thin film growth, 20: 20987 (RFP-690)
Oxidation and ignition of Pu, 20: 21264 (RFP-491)
Treating acute Pu cases, 20: 20943 (RFP-453)
Unclassified publications, 1965, 20: 22521 (RFP-516A(Suppl.1))
ROHM AND HAAS CO., PHILADELPHIA, PA. SPECIAL PRODUCTS DEPT.
Polymerization and polymer properties as related to wood-plastic combinations, 20: 21180 (ORNL-IIC-7, pp 15-21)

S

SANDIA CORP., ALBUQUERQUE, N. MEX.
Heat transfer and flow visualization on cylinders in laminar hypersonic flow, 20: 20857 (SC-DC-65-1907)
POODLE thruster aerodynamic drop test, 20: 21210 (SC-RR-65-609)
Rover destruct Test Three, 20: 22472 (SC-CR-66-2017)
Solubilities of Cr, Mo, and W in Al, 20: 21362 (SC-T-66-0723)
SAVANNAH RIVER ECOLOGY LAB., AIKEN, S. C.
Development of a ^{137}Cs facility for ecological research, 20: 20380 (TID-22499)
SOCIETA RICHERCHE IMPIANTI NUCLEARI, SALUGGIA (ITALY).
Problems of fission product diffusion in graphite fuel elements, 20: 21423 (N-65-23015)
SOCIETE ALSTHOM, PARIS (FRANCE).
Technical and economic comparison of double-cycle and single-cycle boiling-water nuclear power plant, 20: 22409 (EUR-2735.d)
SOUTHERN INTERSTATE NUCLEAR BOARD, ATLANTA, GA.
Potential applications of irradiated wood-plastic materials, 20: 21184 (ORNL-IIC-7, pp 64-75)
SPACE TECHNOLOGY LABS., INC., REDONDO BEACH, CALIF.
Prog. rpt. on radiation damage in Si, 2/65, 20: 21154 (N-65-23290)
SPRINGFIELD ARMORY, MASS.

Falex pins coated by plasma-arc process, 20: 21319 (AD-621064)
Occlusion of various refractory materials in chromium plate on steel substrates, 20: 21286 (AD-621920)
STANFORD RESEARCH INST., MENLO PARK, CALIF.
Prog. rpt. on growth parameters for refractory carbide single crystals, 12/64–3/65, 20: 21236 (N-65-23835)
Prog. rpt. on sorption of gases on metal surfaces, annual, 2/15/65–2/14/66, 20: 21351 (SRIA-425-8)
STANFORD UNIV., CALIF.
Capture reactions, 20: 21986 (BNL-948, pp 763-825)
STANFORD UNIV., CALIF. HIGH-ENERGY PHYSICS LAB.
Measurements at high field strengths on superconducting accelerator cavities, 20: 21459 (AD-623509)
Positive pion production asymmetry with polarized bremsstrahlung near second resonance, 20: 21589 (AD-626683)
Superconducting race-track microtron, 20: 21460 (AD-623659)
Wide-angle electron-electron scattering on the Princeton-Stanford storage rings, 20: 21588 (AD-623658)
^{32}S and ^{31}P excitation by 180° electron scattering, 20: 21964 (AD-626684)
STATE UNIV. OF NEW YORK, BUFFALO.
Commercial potential of wood-plastic combinations in northeastern U. S., 20: 21186 (ORNL-IIC-7, pp 81-8)
SYRACUSE UNIV. RESEARCH INST., N. Y.
Proposed measure for the information content in quantum fields, 20: 21704 (AD-622517)

T

TATA INST. OF FUNDAMENTAL RESEARCH, BOMBAY (INDIA).
K.G.F. neutrino project, 20: 21540 (CERN-65-32, pp 49-56)
TECHNISCHE HOCHSCHULE, MUNICH (WEST GERMANY).
Primary charge distribution at low-energy fission of heavy (gg)-nuclei, 20: 22013 (ANL-Trans-296)
TENNESSEE UNIV., KNOXVILLE.
Confined vortex flow near a stationary disk, theory and experiment, 20: 21786 (ORNL-TM-1387)
Design of high-temperature furnace (3,000°C), 20: 20842 (ORNL-TM-1410)
TENNESSEE VALLEY AUTHORITY, OAK RIDGE.
Design proposal for rate-of-change-of-pressure scram safety channel for the EGCR, 20: 22417 (TID-22759)
TEXAS INSTRUMENTS INC., DALLAS.
Prog. rpt. on large-aperture seismic array, final, 10/64–6/65, 20: 20899 (AD-626777)
TEXAS TECHNOLOGICAL COLL., LUBBOCK.
Prog. rpt. on effects of radiation on natural populations of lizards, 6/60–12/65, 20: 20444 (TID-22820)
TOKYO UNIV. (JAPAN). INST. FOR SOLID STATE PHYSICS.
Low-temperature resistivity, magnetic susceptibility, and superconducting transition temperature in La containing rare-earth impurities, 20: 21873 (NP-15936)
TRW EQUIPMENT LABS., THOMPSON RAMO WOOLDRIDGE INC., CLEVELAND, OHIO.
Prog. rpt. on creep data on refractory alloys, 9/26–12/26/65, 20: 21346 (NASA-CR-54895)
Prog. rpt. on determination of elevated-temperature fatigue data on refractory alloys, 10/65–1/66, 20: 21347 (NASA-CR-54916)
TRW SYSTEMS, REDONDO BEACH, CALIF. PHYSICAL ELECTRONICS LAB.
Study of porous metal ionizers, 20: 21570 (N-65-29785)
TRW SYSTEMS, REDONDO BEACH, CALIF. QUANTUM PHYSICS LAB.
Elementary particle spectrum, 20: 21703 (AD-622258)
TULANE UNIV., NEW ORLEANS, LA. DEPT. OF CIVIL ENGINEERING.
School designs to resist integrated nuclear weapons effects, 20: 20868 (AD-626770)
TURIN UNIV. (ITALY). ISTITUTO DI FISICA.
Project for underground laboratory in the Mont Blanc tunnel for experiments on neutrino and cosmic radiation, 20: 21612 (CERN-65-32, pp 225-30)

U

UED EARTH SCIENCES DIV., TELEDYNE, INC., ALEXANDRIA, VA.
Long-range seismic measurements on YUBA, 20: 20876 (NP-15949)
Long-range seismic measurements on Bronze, 20: 20900 (AD-627039)
Long-range seismic measurements on Klickitat, 20: 20901 (AD-627040)
Long-range seismic measurements on Turf, 20: 20902 (AD-627051)
UNION CARBIDE CORP., OAK RIDGE, TENN. Y-12 PLANT.
Position monitoring devices, 20: 20989 (Y-1506)
Powder metallurgy of UC, 20: 21296 (Y-1510)
UNITED AIRCRAFT CORP., EAST HARTFORD, CONN. RESEARCH LABS.
Prog. rpt. on non-equilibrium ionization using electrostatic probing techniques, final, 3/63–2/65, 20: 21560 (AD-621276)
UNITED STATES–EURATOM FAST REACTOR EXCHANGE PROGRAM.
Experimental results on engineering model of Rapsodie, 20: 22501 (EURFNR-49F)
UNITED STATES–EURATOM JOINT RESEARCH AND DEVELOPMENT PROGRAM.
Diffusion of fission products in fuel-element cladding materials and related alloys, 20: 21232 (BMI-1763)
Irradiation of 0.5-inch diameter, hollow-pellet UO_2 fuel rods, 20: 21422 (GEAP-5100D)
Prog. rpt. on diffusion of rare gases in solids, 10–12/65, 20: 21332 (EURAEC-1573)
Prog. rpt. on temperature transient method for performing in-pile thermal conductance testing, final, 3/64–11/65, 20: 22354 (CEND-3336-260)
UNIVERSIDAD MAYOR DE "SAN ANDRES," LA PAZ (BOLIVIA). LABORATORIO DE FISICA COSMICA DE CHACALTAYA.
Primary energy spectrum from 8×10^{14} to 4×10^{17} ev, 20: 21547 (MIT-2098-227, Paper EAS-31)
UPPSALA UNIV. (SWEDEN).
Criteria for best Bogoliubov quasi particle, 20: 21839 (AD-627067)
USAF RADIATION LAB., UNIV. OF CHICAGO, ILL.
Effect of x-radiation on the hexobarbital metabolizing system of liver microsomes, 20: 20429 (AD-629311, pp 15-25)
Effects of various drugs on the ATP activity of the hematopoietic tissues of rats exposed repeatedly to ^{60}Co γ radiation, 20: 20503 (AD-629311, pp 1-14)
Hypobaric oxygen exposure and acute radiation lethality in mice, 20: 20430 (AD-629311, pp 26-32)
Prog. rpt., 1/15/66, 20: 20516 (AD-629311)
USTAV JADERNEHO VYZKUMU, CESKOSLOVENSKA AKADEMIE VED, REZ.
Extraction radiometric titrations, 20: 20567 (UJV-1418/65)
Influence of electric fields on heat transfer to partially ionized CO_2, 20: 20859 (UJV-1421/65)
UTAH UNIV., SALT LAKE CITY. DEPT. OF PHYSICS.
Utah neutrino detector, 20: 21030 (CERN-65-32, pp 223-4)
UTAH UNIV., SALT LAKE CITY. MICROWAVE DEVICE AND PHYSICAL ELECTRONICS LAB.
Plasma-coupling medium for traveling-wave tube amplifier, 20: 20985 (N-65-29669)

V

VITRO ENGINEERING CO., NEW YORK.
Feasibility and conceptual design study of wood-plastic combinations process, 20: 21181 (ORNL-IIC-7, pp 32-48)

W

WALTER REED ARMY INST. OF RESEARCH, WASHINGTON, D. C. DEPT. OF RADIOBIOLOGY.
Biochemical aspects of radiation injury and recovery, 20: 20435 (CONF-650560-15)
WASHINGTON UNIV., SEATTLE.
Diffraction model calculations, 20: 21980 (BNL-948, pp 561-609)
Multi-body exit channels, 20: 21981 (BNL-948, pp 610-84)
Uncommon states of nuclear matter, 20: 21990 (BNL-948, pp 928-1004)
WAYNE STATE UNIV., DETROIT, MICH. DEPT. OF RADIOLOGY.
Prog. rpt. on pre- and post-natal sequellae of intrauterine administration of ^{131}I in rat, final, 6/63–2/65, 20: 20390 (TID-22767)
WEIZMANN INST. OF SCIENCE, REHOVOTH (ISRAEL).
Diffraction model calculations, 20: 21980 (BNL-948, pp 561-609)
Strong coupling, exchange, target excitation, and other corrections to DWBA, 20: 21979 (BNL-948, pp 525-60)
WEST VIRGINIA UNIV., MORGANTOWN.
Basic research on irradiated wood-plastic combinations, 20: 21179 (ORNL-IIC-7, pp 6-14)
WESTINGHOUSE ELECTRIC CORP., PITTSBURGH, PA.
Prog. rpt. on growth of single crystals of rare earth compounds, 20: 22312 (AD-622796)
WESTINGHOUSE ELECTRIC CORP., PITTSBURGH, PA. ASTRO-NUCLEAR LAB.
Prog. rpt. on dispersion-strengthened Ta alloys, 11/20/64–2/19/65, 20: 21240 (WANL-PR-(Q)-006)
Prog. rpt. on evaluation of refractory/austenitic bimetal combinations, 9/22–12/22/65, 20: 21295 (WANL-PR-(EE)-002)
WESTINGHOUSE ELECTRIC CORP., PITTSBURGH, PA. ATOMIC POWER DIV.
In-pile measurement of UO_2 thermal conductivity, 20: 21361 (WCAP-2923)
Mechanism and kinetics of nitrogen release from UO_2 at elevated tem-

peratures, 20: 21360 (WCAP-2098)
WESTINGHOUSE RESEARCH LABS., PITTSBURGH, PA.
Hall effect in a collision-dominated gaseous plasma, 20: 22176 (AD-624165)
Prog. rpt. on growth of single crystals of rare earth compounds, 20: 22314 (AD-626865)
WILLIAM MARSH RICE UNIV., HOUSTON, TEX.
Multi-body exit channels, 20: 21981 (BNL-948, pp 610-84)

Y

YALE UNIV., NEW HAVEN, CONN.
Heavy ion interactions, 20: 21992 (BNL-948, pp 1045-1134)
Multi-body exit channels, 20: 21981 (BNL-948, pp 610-84)
Two and more nucleon transfer reactions, 20: 21972 (BNL-948, pp 66-174)

PERSONAL AUTHOR INDEX

Each entry after an author's name is a shortened version of the title of the report or article, followed by the *NSA* volume and abstract number. Report numbers are given in parentheses.

The phrase "Progress report" is abbreviated as "Prog. rpt.," permitting a more rapid and complete alphabetical arrangement of the titles without changing the location of the progress report titles in relation to the other titles.

Because of problems involving the mechanical preparation of this index, all accent marks are omitted. The following changes in spelling have been introduced to reduce some of the confusion which might result from omitting the accents:

ä	becomes	ae
ö		oe
ø		oe
ü		ue (except in transliterated Chinese names)

A

ABARBANEL, Henry D. I., Dispersion-theoretic perturbation series in some models, 20: 21683

ABBASOV, A. R., Characteristics of sources of radio emission connected with active regions in the sun, 20: 21506

ABECASIS, S. M., Phenomenological and microscopic analysis of properties of even-even nuclei. B., 20: 21961 (AD-624028)

ABERS, E. S., Shadow effect in high-energy scattering from deuterons, 20: 21646

ABHYANKAR, S. S., Force reflecting servos in electrical master slave manipulators, 20: 20839 (AEET-ED-SG/14)

ABRAHAM, J. M., Characteristics of very shallow silicon junctions, 20: 21099

ACHARYA, R., Spontaneous symmetry breakdown without mass splitting, 20: 21678

ACHEY, Phillip M., Action of ionizing radiation on postirradiation synthesis and degradation of DNA in E. coli, 20: 20421

ADACHI, Atsuko, Monte Carlo analysis of electromagnetic cascade showers, 20: 21559

ADAM, A., Probability of $(n,\alpha n')$ reaction in natural uranium, 20: 22017

ADAM, I., Investigation of ^{148}Eu irradiation, 20: 22003 (JINR-P-2581)

ADAMS, J. L., Deformation energies and collective motion of heavy nuclei, 20: 22065

ADAMS, M. J., Yttrium--cobalt alloy system, 20: 21402

ADOLPHE, M., Radioprotective power of some organophosphorus compounds, 20: 20515

AFANAS'EV, Yu. A., Chromatographic separation of UX_1 and U_1, 20: 20828

AGANOVIC, Ibrahim, Diagram technique in case of many-particle interactions, 20: 21728

AGARWALA, R. P., Self-diffusion in metals, 20: 21230 (AEET-233)

AGGSON, Thomas, Spark chamber spectrometer for space protons, 20: 21120

AGRUSS, B., Nuclear liquid metal cell for space power, 20: 22485

AHLUWALIA, S. S., Separation of uranium by combined ion exchange and solvent extraction, 20: 20811

AHMED, E. M., Prog. rpt. on effects of low-level irradiation upon preservation of food products, annual, 4/65, 20: 21195 (TID-22509)

AHMED, Mohammad I., Transistorized a-c carrier-type shutdown amplifier as protective device in nuclear power stations, 20: 22359

AINSWORTH, E. J., Acute mortality and recovery studies in sheep irradiated with ^{60}Co γ rays or 1-Mvp x rays, 20: 20487

AINSWORTH, E. J., Comparison of dose patterns in a dog exposed to neutrons and to x rays, 20: 20432 (AD-630332)

AISU, H., Reactivity worth of rod-cluster control elements, 20: 22395

AITKEN, D. W., Response of scintillators and semiconductors to low-energy x-ray excitation, 20: 21107

AKASHI, Makoto, Observation of high-energy jets with emulsion chambers, 20: 21555

AKATSU, Eiko, Radiochemical studies of Np, 20: 20561 (JAERI-1099)

AKERMAN, M., Diagnosis of space-occupying processes in the skull with a combination of γ encephalography and echo encephalography, 20: 20529

AKIMUNE, Hideo, Injection trapping of high-energy molecular ions into the mirror field with the r-f electric field. II., 20: 22207

AKIMUNE, Hideo, Nonlinear effect in beam-plasma interaction, 20: 22206

ALANAKYAN, Yu. R., Frequency doubling on reflection of a wave at a plasma boundary, 20: 22271

ALBAREDE, P., Analysis of the spatial distribution of radioactive iodine in the thyroid by the method of level diagrams, 20: 20528

ALBEE, P. R., Relationship of the aurora to non-great-circle high-frequency propagation, 20: 21827

ALBERG, M., Differential energy and angle spectra for ^{137}Cs γ rays in sand, 20: 22308 (HASL-167)

ALBERIGI-QUARANTA, A., Experimental results on the information available from the rise time of pulses supplied by semiconductor particle detectors, 20: 21137

ALBERTONI, S., Variational iterative methods for elliptical problems in theory of nuclear reactors, 20: 22387

ALBRECHT, Robert W., Space dependence of reactor noise. I., 20: 22393

ALBRIGHT, C. H., N^* production by neutrinos, 20: 21599 (CERN-65-32, pp 89-96)

ALBURGER, David E., BNL low-energy nuclear accelerator program, 20: 21463 (BNL-948, pp 685-91)

ALBURGER, David E., Gamma-ray multipolarities from internal pair correlation measurements, 20: 21985 (BNL-948, pp 757-62)

ALCANTARA, Raul, Photochemistry of thymine in aqueous solution, 20: 20771

ALDERTON, J. R., Oxidation and protection of uranium at temperatures near ambient, 20: 21278

ALDROVANDI, R., Solutions for a Feynman-Gell-Mann particle in a Coulomb field, 20: 21767

ALEKSEENKO, V. A., Ion exchange separation of uranium and rare earth elements, 20: 20813

ALEKSIN, V. F., Bremsstrahlung from a solid target in a plasma, 20: 22293

ALEKSIN, V. F., Peculiarities of electromagnetic wave radiation in anisotropic dispersive media, 20: 22199

ALERS, G. A., Discontinuous variation of the bulk modulus in type II superconductors, 20: 21912

ALESSANDRINI, V. A., Remarks on saturation of equal-time commutators and physical sum rules, 20: 21749

ALEXANDER, G., Peripheral production and decay parameters of $N^{*++}(1238)$ in $pp \rightarrow pN^{*++}(1238)$ at 5.5 Bev/c, 20: 21663

ALI, S., Phenomenological α-α potentials, 20: 22061

ALIEV, B. M., Experimental data on dose assessment during remote-control γ therapy, 20: 20541

ALLEN, J. F., Variable transfer rates in superfluid helium films, 20: 21895

ALLER, H. D., Pre-absorption events at 230 Mc/s, 20: 21500

ALLES, W., Current commutation rules and the $\Delta T = \frac{1}{2}$ rule in K-meson decays, 20: 21650

ALLKOFER, O. C., Comparison of spark chamber properties for two different triggering modes, 20: 21048

ALPEN, E. L., Acute mortality and recovery studies in sheep irradiated with ^{60}Co γ rays or 1-Mvp x rays, 20: 20487

ALPIAR, Ronald, ALGAN-I. Supplementary users' manual of new develop-

ments and facilities, 20: 21222 (EIR-89)
ALSINA, J., Detection of La with hydroquinone, 20: 20591
ALSTER, J., Nuclear-structure studies of ^{89}Sr and ^{89}Y by inelastic α-particle scattering, 20: 22138
ALTMAN, Joseph, Prog. rpt. on autoradiographic investigation of brain metabolism, annual, 6/65–3/66, 20: 20391 (TID-22825)
ALTY, J. L., Deuteron optical potentials and the $^{16}O(d,p)^{17}O$ reaction, 20: 22104
AMALRAJ, R. V., Use of incinerators for treatment of combustible wastes, 20: 22508 (AEET-220)
AMALRIC, R., Results of post-operative irradiation of patients with tumors of the brain, 20: 20530
AMATO, I., UO_2–ZrO_2–CaO ceramic nuclear fuels, 20: 21302
AMBARTSUMIAN, V. A., Problems of extra-galactic research, 20: 21513
AMBARTSUMYAN, R. S., Increase of power of VVR-S reactors, 20: 22498 (IAE-993)
AMIET, J.-P., Parity mixing in single-nucleon orbitals, 20: 22080
AMIRKHANOV, I., Scattering of particles by system of fixed centers, 20: 21710 (JINR-P-2554)
AMOROSI, Alfred, Fuel element hold-down arrangement for nuclear reactors, 20: 22369
AMUNDSEN, K. D., Intra- and interhemisphere differences in occurrence times of hydromagnetic emissions, 20: 21832
AMUSIA, M. Ya., Stability of the dense electron gas, 20: 21805
ANAND, S., Measurement of Z dependence of elastic scattering cross section of γ rays. II., 20: 22060
ANDERSON, Donald Gene, Technique for recoil fission-fragment range measurements, 20: 21058
ANDERSON, T. B., Rover destruct Test Three, 20: 22472 (SC-CR-66-2017)
ANDERSON, W. A., Permeability relationships of graphitic materials, 20: 21408
ANDO, Kozo, Spectroscopic measurement of electron temperature in helium arc plasma, 20: 22210
ANDO, Tetsuya, Construction of reactor core of the Tokai power station, 20: 22425
ANGEL, Charles R., Biochemical aspects of radiation injury and recovery, 20: 20435 (CONF-650560-15)
ANTONOV, A. S., Lithium-ion drift in silicon p-type monocrystals, 20: 21337 (JINR-P-2598)
AOKI, Hiroko, Detergents for decontamination of sampling vials for liquid scintillation spectrometer, 20: 20960
AOKI, Ryozo, Neutron energy spectrometers, 20: 21143
APELGOT, S., Method of analyzing activity profile of radiochromatograph, 20: 20559 (EUR-2626.f)
ARAKI, Chiroro, Effect of γ radiation on α, β, γ, ∂-tetraphenylporphine, 20: 20774
ARAS, N. K., Fractional chain yield of ^{128}Sb in thermal-neutron fission of ^{235}U, 20: 22044
ARBUZOV, B. A., Model of weak interactions of baryons and leptons, 20: 21714 (JINR-P-2578)
ARGUE, G. R., Prog. rpt. on radiation effects on Ni–Cd electrodes, final, 6/63–4/65. L., 20: 21425 (N-65-24491)
ARMSTRONG, D. D., Isotope shift in Coulomb displacement energy, 20: 22095
ARMSTRONG, G. A., Application of radiography to the inspection of fuel pins, 20: 20864
ARMSTRONG, J. C., 1.7-Mev anomaly in the $^{12}C(p,p)^{12}C$ reaction, 20: 22115
ARMSTRONG, J. C., ^{14}N levels from elastic scattering of protons by ^{13}C, 20: 22123
ARMSTRONG, Lloyd Jr., Nuclear moments of ^{241}Am and 16-h ^{242}Am and analysis of the hyperfine fields, 20: 22137
ARNDT, Horst, Control of throttle valves in the coolant flow of nuclear reactors, 20: 22364
ARNOLD, A. J. P. T., Experience with superconducting coils fed by flux pumps, 20: 21924
ARNOLD, E. D., SDC—shielding-design calculation code for fuel-handling facilities, 20: 22309 (ORNL-3041)
ARON, J. C., Stochastic processes in microphysics in connection with relativity, 20: 21870
ARONIN, L. R., Analytical techniques for C and N in Be, 20: 20556 (AD-626987)
ARONSON, James L., Reconnaissance rubidium–strontium geochronology of New Zealand plutonic and metamorphic rocks, 20: 20888
ARONSON, Raphael, Perturbation method for classical time-dependent pair correlation function, 20: 21453
ARTAUD, J., Sampling operations involving suppliers and customers, 20: 20973
ARTYKOV, I. Z., Inelastic interactions of cosmic-ray particles with atomic nuclei at very high energies, 20: 21999 (JINR-P-2552)
ARTYUKH, A. G., Neutron pickup in bombardment of ^{181}Ta, ^{197}Au, ^{232}Th, ^{238}U isotopes with ^{15}N ions, 20: 22001 (JINR-P-2555)
ASADA, Tsuneoburo, Simple γ dose threshold detector using a dyestuff, 20: 21076
ASARO, R., Decay scheme of ^{254}Es, 20: 22142
ASHBROOK, Richard L., NASA developments in Co-base superalloys, 20: 21237 (N-65-29395)
ASHBY, D. E. T. F., Entry of tenuous plasma into an axial magnetic field, 20: 22224
ASUNDI, R. K., Absorption and fluorescence spectra of praseodymium-doped KCl single crystal, 20: 20663
ATKINSON, C. H., Project Gasbuggy—a nuclear fracturing experiment, 20: 20837
AUBERT, J., Manufacture of zirconium, titanium, and hafnium sponges, 20: 21305
AUCHAMPAUGH, G. F., Epithermal fission cross section of ^{235}U, 20: 22012 (UCRL-14606)
AUER-WELSBACH, Helga, Dissolution of rare earth metals in methanolic solutions of ammonium acetate, 20: 20686
AUER-WELSBACH, Helga, Spectrophotometric determination of Nd in presence of Pr, 20: 20568
AUSLOOS, P., Ion-molecule reactions in liquid- and solid-phase radiolysis of hydrocarbon mixtures, 20: 20752
AUSMAN, George A. Jr., Time-dependent neutron transport from point isotropic source at an altitude of 100,000 feet, 20: 21935 (AD-624041)
AUSTERN, Norman, Strong coupling, exchange, target excitation, and other corrections to DWBA, 20: 21979 (BNL-948, pp 525-60)
AUSTIN, Michael M., Cosmic-ray and solar proton albedo neutron decay injection, 20: 21550
AVIGNONE III, Frank T., Conversion electron-γ directional correlation in ^{133}Cs, 20: 22076
AVIS, B. E., Entry of tenuous plasma into an axial magnetic field, 20: 22224
AVIS, B. E., Performance of coaxial plasma gun, 20: 22225
AYRES, J. A., Decontamination of nuclear reactor systems, 20: 20957
AYRES, Robert U., Environmental effects of nuclear weapons, 20: 20930 (HI-518-RR(Vol.1))
AYRES, Robert U., Environmental effects of nuclear weapons, 20: 20932 (HI-518-RR(Vol.3))
AYRES, Robert U., Environmental effects of nuclear weapons, 20: 20931 (HI-518-RR(Vol.2))
AZHGIREI, L. S., Determination of one-boson exchange parameters by nucleon-nucleon phase shifts, 20: 21621 (JINR-P-2584)
AZHGIREI, L. S., Elastic p-p scattering phase shift at 657 Mev, 20: 21622 (JINR-P-2585)

B

BABA, Kozi, Temporal observations on peripheral hemograms of atomic bomb casualties as company employees. III., 20: 20481
BABISKIN, J., Critical currents of Nb_3Sn and V_3Ga in transverse magnetic fields up to 150 kOe, 20: 21922
BACCAREDDA, Mario, Effects of nuclear radiations on structure and molecular motions in crystalline stereoregular polymers, 20: 20753
BACH, A., Mathematical treatment of nuclear transformation, 20: 22024
BACHYNSKI, M. P., Collisional effects in electromagnetic wave propagation in plasmas, 20: 22228
BACHYNSKI, M. P., Propagation in plasmas along the magnetic field. I., 20: 22236
BACHYNSKI, M. P., Propagation in plasmas along the magnetic field. II., 20: 22237
BACIARELLI, R. M., Isothermal oxidation of Hastelloy X at 1750 and 1850°F in air, 20: 21258 (AGN-TM-413)
BACRY, H., On some classical space-time groups and their SU_6 generalizations, 20: 21720
BAECKLIN, A., Internal conversion study of $^{113}Cd(n,\gamma)^{114}Cd$, 20: 22066
BAECKSTROEM, G., Internal conversion study of $^{113}Cd(n,\gamma)^{114}Cd$, 20: 22066
BAERNIGHAUSEN, H., Lattice constants and space groups of $Eu(OH)_2 \cdot H_2O$, $Sr(OH)_2 \cdot H_2O$, and $Ba(OH)_2 \cdot H_2O$, 20: 20694
BAERRING, N. E., Electrodeposition of actinide and lanthanide elements, 20: 21287 (AE-217)
BAESSLER, R., Experimental inflammation and fibrosis of lung stroma by ionizing radiation. Light- and electron-microscopic investigations, 20: 20459
BAETSLE, L., Migration of radio elements in soil, 20: 20875 (EUR-2481.f)
BAGGETT, M. J., 1.7-Mev anomaly in the $^{12}C(p,p)^{12}C$ reaction, 20: 22115
BAGSHAW, M. A., Radiation necrosis of the cervical spinal cord imitating metastases of carcinoma, 20: 20545
BAINBRIDGE, A. E., Peak in tritium content of atmospheric hydrogen following accident at Windscale, 20: 20889
BAIR, J. K., Total neutron yield from the reaction $^{14}C(\alpha,n)^{17}O$, 20: 22110
BAJAJ, M. M., Gamma-gamma directional correlation in ^{123}Te, 20: 22089
BAKAI, A. S., Asymptotic solution of diffusion problem and its application to the theory of cyclic particle-storage devices, 20: 21483

BAKER, L. Jr., Reactor safety, 20: 20925 (ANL-7055, pp 177-212)
BAKER, Philip S., Conference on irradiated wood-plastic materials, Chicago, 9/65, 20: 21177 (ORNL-IIC-7)
BAKSHT, F. G., Theory of low-voltage arcs in cesium. II., 20: 21578
BALASHOV, V. L., Calcium and strontium partition by exchange in amalgam-solution system, 20: 20829
BALDUCCI, D. D., Cytopathic effects of tumor viruses in human diploid cells, 20: 20377
BALFOUR, M. G., In-pile measurement of UO_2 thermal conductivity, 20: 21361 (WCAP-2923)
BALLONI, W., Influence of irradiated nitrogen on the nitrogen-fixing activity of blue-green algae, 20: 20408
BALLOU, N. E., Nuclear-charge distribution of fission-product chains of mass numbers 131-133, 20: 22136
BANDO, Shoji, Determination of copper content in o-diphenol oxidase by neutron activation analysis, 20: 20569
BANKOFF, S. G., Magnetohydrodynamic circulation of liquid of finite conductivity in an annulus, 20: 21789
BANKS, D. C., Engineering properties of nuclear craters. I., 20: 20895 (AD-626899)
BANNISTER, Edward R., Mechanism by which hadacidin potentiates the damaging action of ionizing irradiation on bacteria, 20: 20456
BARAKAT, M. F., Gas-liquid chromatography for determining specific activity and survival of mother compounds labeled with recoil atoms, 20: 20783
BARAN, Viktor, Effect of delayed neutrons on stability of a nuclear power reactor, 20: 22443
BARANGER, E. U., Shell model calculation of the odd tin isotopes, 20: 21962 (AD-624214)
BARANGER, Michel, Shell model calculation of the odd tin isotopes, 20: 21962 (AD-624214)
BARANOVA, N. M., Radiation carbonylation of paraffinic hydrocarbons with carbon monoxide, 20: 20770
BARASHENKOV, V. S., Difference sign of real parts of elastic πp scattering amplitudes at high energies, 20: 21618 (JINR-P-2566)
BARASHENKOV, V. S., Inelastic interactions of cosmic-ray particles with atomic nuclei at very high energies, 20: 21999 (JINR-P-2552)
BARBANO, P. G., Solvent extraction separation of Pa from elements of the IVa and Va groups, 20: 20816
BARBASHOV, B. M., Two-plane wave scattering in nonlinear scalar field theory of Born-Infeld type, 20: 21716 (JINR-P-2603)
BARBER, W. C., Wide-angle electron-electron scattering on the Princeton-Stanford storage rings, 20: 21588 (AD-623658)
BARBIELLINI, G., Photodisintegration of the deuteron by polarized γ rays, 20: 21626 (LNF-66/4)
BARDENSHTEIN, S. B., Structure of polypropylene chlorinated by radiation and sulfochlorinated, 20: 20779
BAREAU, J., Kinetics of escape of He from BeO frits during irradiation, 20: 21428 (NP-15942)
BARKER, S. A., Effect of γ radiation. X., 20: 20759
BARLOUTAUD, M., Reaction $^{180}Hf(d,p)^{181}Hf$, 20: 22106
BARNA, Arpad, Electroluminescent panels as pulsed fiducial marks in spark chamber experiment, 20: 21090
BARNARD, E., Scattering of fast neutrons by ^{238}U, 20: 22056
BARNES, L. J., Contribution of surface currents to magnetic hysteresis in mixed state of a type II superconductor, 20: 21886
BARNES, William S., Profile of electron beam from Astron accelerator, 20: 22191 (UCRL-14697)
BAR-NIR, I. M., Calculation of decay widths and current algebras, 20: 21654
BAR-NIR, I. M., Three-particle final states and unitary symmetry, 20: 21763
BARRETT, C. S., Lattice parameters, thermal expansions, and Grueneisen coefficients of Zr at 4.2 to 1130°K, 20: 21391
BARRETT, Lawrence G., Commercial production of wood-plastic combinations, 20: 21187 (ORNL-IIC-7, pp 89-94)
BARRICELLI, Nils Aall, DNA strands injected by a virus into its host and hereditary information transmission, 20: 20426
BARRICELLI, Nils Aall, Evidence that only one of the two DNA strands injected by phage T4 transmits genetic information, 20: 20427
BARSUKOV, K. A., Peculiarities of radiation of point dipoles moving in narrow cavities in magnetoactive media, 20: 22278
BARTHOLOMEW, H. G., Rocket gamma scanning of nuclear bursts, 20: 21129
BARUCH, P., Prog. rpt. on radiation damage in semiconductors, annual, 7/20/65, 20: 21147 (AD-621049)
BASHAROV, R., Cathode spots of pulsed discharge between parallel electrodes, 20: 22292
BASKIN, Y., Melting point of uranium monophosphide, 20: 20687
BASSETTI, M., Numerical calculations on the space-charge effects in storage ring for electrons and positrons, 20: 21475 (SLAC-Trans-38)
BASSI, A., Sintering of oxides of uranium and thorium, 20: 21299
BATES, H. F., Relationship of the aurora to non-great-circle high-frequency propagation, 20: 21827
BATTIG, F., Stereo-specific hydrogen exchange accompanying catalytic hydrogenation of methyl β, β-dimethylacrylate, 20: 20715
BATTISTONE, Gino C., Fluorine microdetermination by neutron activation analysis, 20: 20594
BAUMAN, F. A., Analytical techniques for C and N in Be, 20: 20556 (AD-626987)
BAUMANN, G., R center luminescence in LiF, 20: 22331
BAYANOV, A. P., Analysis of zinc and lead for rare earth metals, 20: 20607
BAYHURST, B. P., Symmetry of neutron-induced ^{239}Pu fission at individual resonances, 20: 22135
BAYMAN, B. F., Hole states of ^{43}Ca and ^{47}Ca, 20: 22129
BAYMAN, B. F., Isobaric spin without charge space, 20: 22019
BAYMAN, Benjamin, Light spherical nuclei, 20: 21974 (BNL-948, pp 222-68)
BAYMAN, Benjamin, Two and more nucleon transfer reactions, 20: 21972 (BNL-948, pp 66-174)
BAZAZYANTS, N. O., Calculations of critical experiments on assemblies in ZPR-3, 20: 22383 (AEC-tr-6693)
BAZHANOVA, A. E., Complex Doppler effect in plasma, 20: 22198
BAZIN, M. J., Status of Princeton pattern recognition program, 20: 21041 (PPAD-585E)
BEACH, L. A., Angular distributions and cross section ratios for the reactions $^2H(d,n)^3He$ and $^2H(d,p)^3H$ below 500 kev, 20: 22074
BEALL, E. F., Binary-coded digitized hodoscope, 20: 21108
BEARD, John, Flow restrictor, 20: 22361
BEARDEN, Alan J., Cam-driven, constant-acceleration Moessbauer spectrometer, 20: 21080
BEARDEN, Alan J., X-ray photoeffect cross sections in low- and medium-Z absorbers at 852 ev to 40 kev, 20: 21523
BEARDMORE, P., Nucleation of cleavage cracks in tungsten and molybdenum by spark-machining, 20: 21245
BEASLEY, M. R., Annihilation instability in hard superconductors, 20: 21927
BEATTY, Alvin V., Assay for ATP in x-irradiated Tradescantia anthers, 20: 20418
BEATTY, Jeanne W., Assay for ATP in x-irradiated Tradescantia anthers, 20: 20418
BECHER, A. F., Some observations on film badge calibration techniques, 20: 20935 (K-1657)
BECKER, Sam W. Jr., Patterns of cutaneous pigmentation following sunlight irradiation, 20: 20458
BECKERS, R. M., Engineering design practices for facilities containing radioactive materials, 20: 20942 (ORNL-TM-1459)
BEENAKKER, J. J. M., Experience with superconducting coils fed by flux pumps, 20: 21924
BEG, M. A. B., Remarks on saturation of equal-time commutators and physical sum rules, 20: 21749
BEGEMANN, F., Production rates of ^{36}Cl and ^{39}Ar in Leedey chondrite, 20: 21508
BEHL, W. K., Molar free energy of formation of UC_2 and U_2C_3, 20: 20672
BEK, V., Nonmalignant new growth in irradiated growing bones, 20: 20460
BEKMUKHAMBETOV, E. S., Influence of krypton on operation of a thermionic converter, 20: 21579
BEKMUKHAMBETOV, E. S., Operation of a cesium diode with an admixture of an inert gas, 20: 21567 (FEI-15)
BEKMUKHAMBETOV, E. S., Operation of cesium thermionic converter in presence of xenon, 20: 21580
BELBEOCH, B., X-ray diffraction study of neutron-irradiated beryllia, 20: 21433 (UCRL-Trans-10012)
BELL, Francis R., Nuclear reactor control rod drive mechanism, 20: 22366
BELL, J. S., Theory of weak interactions, 20: 21700
BELL, L. G., Effect of prior beta grain size on ductility of zirconium–2.5 wt.% niobium alloy, 20: 21368
BELLE, Yu. S., Measurement of the radon concentration in water by γ radiation, 20: 20959
BELLOTTI, E., Experimental investigation of the $K_{\ell 3}$ decay, 20: 21658
BELOV, V. P., Nonlinear resonances $\nu_r = Nn/q + \Delta$ in an isochronous cyclotron, 20: 21486
BENCZE, Gy., Perturbed angular correlation of a triple gamma cascade, 20: 22015
BENCZE, Istvan, Furnace for UO_2 sintering, 20: 21304
BENCZE, Istvan, ZR-2 critical assembly, 20: 22388
BENESOVSKY, F., New borides with the $Cr_{23}C_6$ structure, 20: 20685
BENJAMIN, B. M., Recombination of hydrogen and oxygen in the presence of water vapor under the influence of radiation, 20: 20749
BEN-MENAHEM, Ari., Analysis of geomagnetic micropulsations due to high-altitude nuclear explosions, 20: 21829
BENNER, J. A. Jr., Changes in uv absorbency of cultured cells during interphase as estimated by flying-spot microscopy, 20: 20473
BENO, M., Metabolism of carrier-free $^{106}RuCl_3$ after intratracheal application, 20: 20396

BENO, R. L., Conductance device for monitoring thin film growth, 20: 20987 (RFP-690)
BENOIT, J. W., Status of Princeton pattern recognition program, 20: 21041 (PPAD-S85E)
BEN-PORATH, M., Comparison of ^{125}I and ^{131}I in diagnosis of thyroid disease. I., 20: 20533
BEN-PORATH, M., Comparison of ^{125}I and ^{131}I in diagnosis of thyroid disease. II., 20: 20534
BEN-PORATH, M., Equivalent radioisotope factor, 20: 21175
BENTZ, L. L., Simple technique for rapid analysis of radioactive gases by liquid scintillation counting, 20: 20582
BERARD, M. F., Bibliography on nucleation and crystal growth from ceramic melts, 20: 21235 (IS-1287)
BERENYI, Denes, Recent results on electron capture, 20: 22029
BERESS, M., Neutron activation analysis for investigation of manganesian rocks, 20: 20646
BEREZHETSKII, M. S., Structure of magnetic surfaces in stellarator with with double helical field, 20: 22298
BERGER, Fr., Influence of electric fields on heat transfer to partially ionized CO_2, 20: 20859 (UJV-1421/65)
BERGMANN, P. G., Hamilton-Jacobi and Schroedinger theory in theories with first-class Hamiltonian constraints, 20: 21864
BERGQVIST, I., Gamma spectra from inelastic neutron scattering, 20: 22069
BERGSNOV-HANSEN, B., Prog. rpt. on sorption of gases on metal surfaces, annual, 2/15/65–2/14/66, 20: 21351 (SRIA-425-8)
BERINDE, A., Angular correlations in inelastic proton scattering on ^{20}Ne and ^{32}S, 20: 22059
BERMAN, R. M., Homogenization and densification of $ZrO_2 + UO_2$ fuels under irradiation, 20: 21432 (WAPD-301)
BERMAN, S. S., Extraction and spectrophotometric determination of thorium with 8-quinolinol, 20: 20576
BERNARDINI, C., Photodisintegration of the deuteron by polarized γ rays, 20: 21626 (LNF-66/4)
BERNSEN, S. A., Safety and the nuclear plant engineer, 20: 22437
BERNSTEIN, Bernard, Pulsed x-ray prompt gamma simulator, 20: 20838 (AD-624019)
BERNSTEIN, J. B., Surface effects in alkali-halide crystals from irradiation, 20: 21424 (N-65-23332)
BERRY, Warren E., Examination of 1B steam generator from Shippingport Atomic Power Station, 20: 22408 (BMI-1764)
BERSON, Solomon A., Iodoinsulin used to determine specific activity of ^{131}I, 20: 20604
BERTHOD, Louis, Boiling state of operating homogeneous reactor, 20: 22403
BERTULIS, K. P., Dielectric properties of thin films of Pr, Ce, and Nd fluorides, 20: 22324
BES, D. R., Pairing vibrations, 20: 22075
BESHAI, Samir F., Total cross-sections of U, UO_2 and ThO_2 for thermal and subthermal neutrons, 20: 21966 (AE-222)
BESSON, Jean, Electric conductivity in HfO_2–Y_2O_3 at high temperature, 20: 21370
BEST, G. C., Display unit for complex data, 20: 20983 (AERE-R-4966)
BETZ, Fred, π^+-p Scattering at 250 Mev: experiment and analysis, 20: 21662
BEYSTER, J. R., Accelerator pulsed fast assembly, 20: 22503
BEYSTER, J. R., Prog. rpt. on integral neutron thermalization, 10–12/65, 20: 21939 (GA-6930)
BHALLA, C. P., Tables of electron radial functions and tangents of phase shifts for light nuclei (Z = 1 through 10), 20: 22009 (NBS-MON-81)
BHAT, M. R., Numerical analyses of neutron resonances by use of computer programs, 20: 21994 (BNL-10094)
BHIDE, K. N., Stabilities and allied properties of organic coolants, 20: 20708 (AEET-213)
BHIDE, M. G., S4B program for solving multi-group transport equations with Carlson's S_4 approximation, 20: 21937 (AEET-210)
BIAIS, R., Aluminum and magnesium in nuclear metallurgy, 20: 21382
BIEDENHARN, L. C., Unitary representations of SU(1,1) and SU(2,1), 20: 21722
BIELLE, Jean, Effect of irradiation by nuclear particles on switching times of fast diodes, 20: 21157
BIENLEIN, J. K., Possible spark chamber experiment with antineutrinos, 20: 21607 (CERN-65-32, pp 161-8)
BIERY, John C., Reaction of tantalum with molten cerium–cobalt alloys, 20: 20671
BIETTI, A., Application of current commutation relations to N*** photoproduction, 20: 21676
BILEN'KII, S. M., Application of "maximum complexity" method for determining spins and parities in reactions with polarized particles, 20: 21715 (JINR-P-2576)
BILEN'KII, S. M., Isospin conservation and polarization effects, 20: 21717 (JINR-P-2620)
BILLY, G., Inventory methods in a conversion plant, 20: 20971
BINGHAM, R. G., Two satellite-borne cosmic-radiation detectors, 20: 21118
BINGHAM, William G. Jr., Low activation materials for nuclear test vault construction, 20: 20869
BINSTOCK, Judith, Bounds for correction to the Born term and applications to p-p scattering for generalized dispersion model, 20: 21635
BIR, R., Isotopic analysis of U and Pu, 20: 20978
BIRYUKOV, V. A., Electrophotographic device for evaluating particle track coordinates in spark chamber, 20: 21037 (JINR-P-2594)
BISHOP, G., Photoneutron production from C, Al, and S by bremsstrahlung up to 200 Mev, 20: 22094
BISIACCHI, G., Mass formulae for baryons in SU_3, 20: 21739
BISOGNI, Edgardo, Prog. rpt. on point defects and mechanical properties of Nb, final, 2/15/62–11/30/65, 20: 21320 (AD-625475)
BISWAS, S. N., Radiative nonleptonic weak decays of baryons, 20: 21751
BISWAS, S. N., Vector-meson mixing and sum rules in broken SU(3), 20: 21753
BJERREGAARD, J. H., Collective states of ^{209}Bi, 20: 22108
BLAIR, A. G., Isotope shift in Coulomb displacement energy, 20: 22095
BLAKE, Gordon, Improvements in or relating to nuclear reactor core structures, 20: 22362
BLAMIRES, N. G., Design and application of lithium-drift silicon diodes as nuclear radiation detectors, 20: 21064
BLANC, Daniel, Decline of luminescence of rare gas atoms excited by α particles in presence of electric field, 20: 21521
BLANCHARD, Rene, Process for the densification of carbonaceous bodies, 20: 21315
BLANCHARD, Richard L., Rapid method for determining ^{210}Pb and ^{210}Po in environmental samples, 20: 20643
BLANKENSHIP, Victor D., Theory of electrostatic double probe comprised of two parallel plates, 20: 22192
BLANN, Marshall, Evidence for influence of shell structure on level densities in the continuum, 20: 22070
BLAUGHER, R. D., Magnetization of "nonideal" type II superconductors, 20: 21928
BLEANEY, B., Prog. rpt. on properties of rare earth and transition group ions, final, 4/63–6/65, 20: 22311 (AD-622068)
BLINDU, L., Electromagnetic phenomena at interior of the weak MHD shock wave front, 20: 21806
BLOCK, W. F., Temporal and statistical characteristics of Jupiter decametric radiation, 20: 21510
BLOOM, Elliott, Dynamics of the Y_1^* branching ratio, 20: 21670
BLOOM, Justin L., Atomic Energy Commission's program in wood-plastic materials, 20: 21178 (ORNL-IIC-7, pp 1-5)
BLOORE, Ernest W., Evaluation program for radioactive waste treatment facility, 20: 22507 (AD-622372)
BLUM, Pierre, Process for the densification of carbonaceous bodies, 20: 21315
BLUMENTHAL, R. B., Wide-angle electron-pair production, 20: 22146
BOBO, Jean-Claude, New phase in cobalt–uranium–oxygen system, 20: 21242
BOBROFF, D. L., Small signal energy conservation theorem for multi-velocity electron beams, 20: 21455
BOCCALETTI, D., Limits on size of visible quasars, 20: 21501
BOCCHIERI, P., Microwave determination of distribution functions of electrons in low current discharges, 20: 21795
BOCHIROL, Louis, Process for the densification of carbonaceous bodies, 20: 21315
BODMER, A. R., Phenomenological α-α potentials, 20: 22061
BODNAR, Raymond E., Crystal chemistry of intermediate phases in the ytterbium–antimony system, 20: 21401
BODU, R., Sampling operations involving suppliers and customers, 20: 20973
BOERBOOM, A. J. H., Influence of velocity of rare gas ions on emission of secondary electrons, 20: 21538
BOGHEN, J., Aluminum and magnesium in nuclear metallurgy, 20: 21382
BOGNER, R. L., Role of radioactivity and hydrothermal processes in protobiochemistry, 20: 20406 (N-65-27062)
BOHDANSKY, Josef, Thermionic converter and use in a reactor, 20: 22406
BOHNDORF, Werner, 45° Remission photometer for measurement of radiation erythemas, 20: 21011
BOITSOV, Y. E., Pitchblende and selenides of hydrothermal uranium deposits, 20: 20918
BOLLOK, Lajos, ZR-2 critical assembly, 20: 22388
BONCH-OSMOLOVSKII, A. G., Motion of charged particle in field of retarded plane electromagnetic wave, 20: 21485
BOND, Charles E., Slanting of a magnetically stabilized electric arc in transverse supersonic flow, 20: 21802
BONDAREV, B. I., Induced radiation for large densities of photons, 20: 21522
BONDAREV, V. N., Manufacture of molybdenum and chromium germanides and investigation of some of their properties, 20: 21247
BONILLA, Charles F., Prog. rpt. on high-temperature thermal properties of gases and vapors, 1965/66, 20: 20651(R) (CU-2660-26)

BONNET, P., Mechanical radiography techniques for quality control of thin-walled SAP tubes, 20: 20861 (EUR-2443.f)
BONNEVIER, B., Nucleon-antinucleon annihilation as source of energy for certain radioastronomical objects, 20: 21684
BONVALET, Charles, Behavior of concrete pressure vessel subjected to high temperature gradient, 20: 22353 (CEA-R-2829)
BONZEL, Hans Paul, Diffusion of ^{63}Ni in copper at low temperatures, 20: 21367
BORCHERDS, P. H., Motion of Abrikosov vortices in a type II superconductor, 20: 21910
BORELIUS, G., Superconducting state and the λ transition, 20: 21875
BORGERS, Marcel, Cytomorphologic and cytochemical study of cytolysomes of duodenal crypts of x-irradiated mice, 20: 20413
BORN, John W., Prog. rpt. on nuclear radiation-resistant polymers and polymeric compounds, annual, 6/61–5/62, 20: 21430 (WADC-TR-55-58(Pt.8))
BORN, John W., Prog. rpt. on nuclear radiation-resistant polymers and polymeric compounds, annual, 6/62–3/63, 20: 21431 (WADC-TR-55-58(Pt.9))
BOSCH, Horacio E., Phenomenological and microscopic analysis of properties of even-even nuclei. B., 20: 21961 (AD-624028)
BOSCO, G., Utilization of sodium sulfate–^{35}S by hepatic tissue of the normal and irradiated rat, 20: 20410
BOURDEL, Jean, Resources of fissionable nuclear materials, 20: 21243
BOURG, Antoinette, Thin layers of lanthanum fluoride studied by electron microscopy, 20: 20681
BOURGETTE, D. T., Special purpose high-vacuum high-temperature equipment for refractory-metal research, 20: 21350 (ORNL-TM-1426)
BOWER, Georgia C., Nuclear theory index for 1964, 20: 22011 (TID-22771)
BOWER, R. C., Rover destruct Test Three, 20: 22472 (SC-CR-66-2017)
BOWMAN, C. D., Epithermal fission cross section of ^{238}U, 20: 22012 (UCRL-14606)
BOWMAN, Melvin G., Advanced concepts for nuclear propulsion and related problems in high-temperature chemistry, 20: 20870 (LA-DC-7703)
BOWMAN, Melvin G., High-temperature chemistry of non-fissionable ceramics, 20: 20654 (LA-DC-7784)
BOYCE, I. S., Rapid analysis of Cu alloys and steels, 20: 20642
BOYCE, J. F., Asymptotic renormalizability conditions on field propagators, 20: 21729
BOYD, L. R., Application of in-core detectors to startup of large boiling water reactors, 20: 22438
BOYD, Walter K., Examination of 1B steam generator from Shippingport Atomic Power Station, 20: 22408 (BMI-1764)
BOYER, Vincent S., Preparing for operations at Peach Bottom, 20: 22456
BOZORTH, R. M., Magnetic transformation in heavy rare-earth alloys with each other, 20: 21409
BOZZO, S. R., Strontium and calcium skeletal discrimination determined by compartmental analysis, 20: 20400
BRAAMS, Reinier, Rate constants of hydrated electron reactions with amino acids, 20: 20403
BRADEN, C. H., Conversion electron-γ directional correlation in ^{133}Cs, 20: 22076
BRADLEY, Arne E., Design for a versatile charge-sensitive preamplifier for nuclear radiation detectors, 20: 21130
BRADT, H., Monte Carlo simulation of nuclear active cascade in EAS, 20: 21545 (MIT-2098-227, Paper EAS-11)
BRADT, H., Primary energy spectrum from 8×10^{14} to 4×10^{17} ev, 20: 21547 (MIT-2098-227, Paper EAS-31)
BRADT, R. C., Weld interface porosity in tantalum, 20: 21311
BRAES, L. L. E., Supernova phenomena in OB associations and cosmic x-ray sources, 20: 21497
BRAMHAM, P., Servo correction of phase changes between deflectors in the r-f separator, 20: 21467 (CERN-66-8)
BRANCH, James E., School designs to resist integrated nuclear weapons effects, 20: 20868 (AD-626770)
BRANDMAIER, H. E., Hall-current generator characteristics at constant electron temperature, 20: 21572
BRANDON, George W. Jr., Heat-shield ablation and sublimation determinations through radioisotope techniques, 20: 20860
BRANDT, A., Magnetohydrodynamic flow in inlet region of a straight channel, 20: 21801
BRANNEN, E., Electron energy measurements of the race-track microtron beam, 20: 21461 (AD-624038)
BRAUMAN, John I., Least squares analysis and simplification of multi-isotope mass spectra, 20: 20580
BRAUN, H., High-energy group of the Strasbourg Nuclear Research Center, 20: 22033
BRAY, Bruce G., Economics of contained nuclear explosions applied to petroleum reservoir stimulation, 20: 20836
BRECHER, G., Influence of extracorporeal irradiation of the blood and lymph on skin homograft rejection, 20: 20485
BRECHER, George, Effects of bacterial endotoxin on the occurrence of spleen colonies in irradiated mice, 20: 20512
BREITENHUBER, L., Variation principles for critical flux curves of reflected reactors, 20: 22399
BRENNAN, D., Adsorption of Kr and Xe on evaporated metal films, 20: 21387
BRENNAN, D., Adsorption of carbon monoxide on evaporated metal films, 20: 21388
BRENNAN, D., Adsorption of carbon dioxide on evaporated metal films, 20: 21389
BRENTNALL, W. D., Bend and tensile ductility of Cb–Ti–Zr molybdenum alloy, 20: 21410
BRETT, Jack, Diffusional limitation in high-temperature protective oxide coatings, 20: 21283
BREUKINK, C. J., Reactions of hydrocarbons as foams under the influence of gas discharges. IV., 20: 20740
BREWER, L. E., Equivalence of electron and excitation temperatures in an argon plasma, 20: 22267
BRIATORE, Luigi, Experimental limit of the mean life of nucleons, 20: 21636
BRIE, M., Perturbing effects of water vapor on mechanism of graphite oxidation in presence of oxygen (500 to 650°C), 20: 21285
BRIGGS, Harvey D., Radioactive apparatus for measuring temperature, 20: 21019
BRIMACOMBE, J. S., Effect of γ radiation. X., 20: 20759
BRINI, D., X-ray scanning of sky in 20- to 200-kev range, 20: 21490
BRITT, H. C., Fission of ^{238}U and ^{240}Pu nuclei excited by inelastic α-particle scattering, 20: 22143
BROBERG, J. B., Modular hardware for on-line handling of nuclear data, 20: 21225
BROCKETT, R. I., Prog. rpt. on temperature transient method for performing in-pile thermal conductance testing, final, 3/64–11/65, 20: 22354 (CEND-3336-260)
BRODER, D. L., Analysis and generalization of correlation method for measurement of particle-lifetime distribution in physical systems, 20: 21035 (FEI-21)
BRODSKY, Michel, Decontamination of radioactive effluents, 20: 22516
BROGAN, Thomas R., Performance of self-excited MHD generator, 20: 21564 (AD-627037)
BROGLIA, R. A., Pairing vibrations, 20: 22075
BROHEE, H., Recovery of ^{90}Sr and ^{144}Ce from concentrated fission-product solutions, 20: 20804 (EUR-2754.f)
BROMLEY, D. Allan, Heavy ion interactions, 20: 21992 (BNL-948, pp 1045-1134)
BROMLEY, D. Allan, Multi-body exit channels, 20: 21981 (BNL-948, pp 610-84)
BROMLEY, D. Allan, Two and more nucleon transfer reactions, 20: 21972 (BNL-948, pp 66-174)
BROOKS, E. H., Radiation environment about NERVA reactors, 20: 22481
BROSENS, P., Correlation of electron emission cooling and optimum collector temperature, 20: 21585
BROWN, C. L., Material bucklings for ^{235}U-enriched U tube lattices in light water, 20: 22375 (BNWL-193, pp 45-56)
BROWN, C. L., Nuclear criticality safety study of FFTF fuel, 20: 22494 (BNWL-193, pp 30-44)
BROWN, I. G., Simulation of magnetic fields produced in the moon by trapped field of solar plasma stream, 20: 21502
BROWN, J. L., K+p interactions at 4.6 Bev/c, 20: 21629 (UCRL-16332)
BROWN, L. S., Remarks on saturation of equal-time commutators and physical sum rules, 20: 21749
BRUCE, Robert N. Jr., School designs to resist integrated nuclear weapons effects, 20: 20868 (AD-626770)
BRUNFELT, Arild O., Distribution patterns of rare earth elements in terrestrial rocks, 20: 20877
BRUNHOUSE, J. S., Hastelloy X corrosion in air at 1900 and 2000°F, 20: 21259 (AGN-TM-414)
BRUSTAD, Tor, Effects of radical scavengers on radiosensitivity of lysozyme, 20: 20423
BRUTTO, E., Sintering of oxides of uranium and thorium, 20: 21299
BRYNJOLFSSON, Ari, Three-dimensional dose distribution in samples irradiated by electron beams, 20: 21470 (PB-181506, pp 116-29)
BUBA, L., Comparison of burnup determinations by means of monitor-activation and γ spectroscopy for an MTR element, 20: 21050
BUCHWALD, W., Experimental inflammation and fibrosis of lung stroma by ionizing radiation. Light- and electron-microscopic investigations, 20: 20459
BUCKLEY, Donald H., Friction characteristics of rare-earth and related metals in vacuum, 20: 21365
BUCKMAN, R. W. Jr., Prog. rpt. on dispersion-strengthened Ta alloys, 11/20/64–2/19/65, 20: 21240 (WANL-PR-(Q)-006)
BUCKMAN, R. W. Jr., Prog. rpt. on evaluation of refractory/austenitic bimetal combinations, 9/22–12/22/65, 20: 21295 (WANL-PR-(EE)-002)
BUDD, Roger A., Effects of bacterial endotoxin on the occurrence of spleen colonies in irradiated mice, 20: 20512
BUDD, Roger A., Estimation of radiation dose-reduction factor for β-

mercaptoethylamine by endogenous spleen colony counts, 20: 20511
BUELL, C. H., Determination of liquid metal diffusion coefficients by molecular distillation, 20: 21334 (IS-1325)
BULLIS, R. H., Prog. rpt. on non-equilibrium ionization using electrostatic probing techniques, final, 3/63–2/65, 20: 21560(R) (AD-621276)
BUNDKE, W., Lifetime of electron trajectories in focussed magnetic fields. II., 20: 21482
BUONI, Frederick B., Prog. rpt. on pre-startup hydraulic tests on AFNETF, final, 1961–65, 20: 22492 (AD-626861)
BURCH, W. D., Critical-path method for scheduling the transuranium processing plant: an appraisal, 20: 20809 (ORNL-3925)
BURDG, C. E., Prog. rpt. on temperature transient method for performing in-pile thermal conductance testing, final, 3/64–11/65, 20: 22354 (CEND-3336-260)
BURDG, Charles E., Nuclear reactor control rod having particulate core, 20: 22368
BURFORD, A. O., Wood-plastic evaluation program, 20: 21349 (ORNL-IIC-7, pp 26-31)
BURIKS, Peter, Width of potential barrier for spontaneous fission by gg nuclei, 20: 22014 (KFK-tr-185)
BURKE, T. F., Acoustic phased arrays for the detection of nuclear bursts in the atmosphere, 20: 20897 (AD-623679)
BURKHARDT, H., Exponential asymptotic behavior and low-energy pion-pion scattering, 20: 21645
BURKHARDT, H., Shadow effect in high-energy scattering from deuterons, 20: 21646
BURLAKOVA, E. B., Relation between radioprotective and antineoplastic effects of antioxidant-inhibitors, 20: 20506
BURLINGAME, J. E., Bibliography on nucleation and crystal growth from ceramic melts, 20: 21235 (IS-1287)
BURMEISTER, H., Further analysis of neutrino interactions in the CERN heavy liquid bubble chamber, 20: 21597 (CERN-65-32, pp 25-30)
BURNET, George, Separation of Cd from the Pb–Bi eutectic by high-vacuum single-stage distillation, 20: 20805 (IS-1329)
BURNS, R., Determination of neutrino flux, 20: 21600 (CERN-65-32, pp 97-108)
BURNS, Richard S., Neutron activation analysis service, 20: 20554 (AD-621017)
BURROWS, J. R., Lifetimes of low-energy electrons in outer radiation zone at magnetically quiet times, 20: 21817
BURTSEV, V. T., Gas generation from tungsten at 2500°C, 20: 21248
BUSCARONS, F., Detection of La with hydroquinone, 20: 20591
BUSCH, C. W., Pressure wave generation in a fissioning gas. III., 20: 21803
BUSCH, G., Luminescence of ferromagnetic EuSe, 20: 22334
BUSCH, G., Pressure-induced changes of spin structure in EuSe, 20: 22332
BUSCHOW, K. H. J., Systematic arrangement of binary rare earth–aluminum systems, 20: 21415
BUSH, Harry D., Bonding of refractory materials by cerium oxide–cerium sulfide mixtures, 20: 21314
BUSULINI, Loris, Effect of intense radiation fields on electrode processes, 20: 20791
BUTTA, Enzo, Effects of nuclear radiations on structure and molecular motions in crystalline stereoregular polymers, 20: 20753
BUTTERWORTH, I., K+p interactions at 4.6 Bev/c, 20: 21629 (UCRL-16332)

C

CABELL, M. J., Use of the Ag–Co activity ratio method to determine epithermal indices for large neutron dose irradiation, 20: 21025 (AERE-R-5122)
CADOFF, I. B., Growth of single-crystal silicon on beryllium oxide, 20: 21249
CAGNETTI, P., Radioluminescent watches: international trends of radioprotection, 20: 20518 (RT-PROT-(65)41)
CAHILL, Daniel F., Determination of ^{90}Sr in urine by anion exchange, 20: 20583
CAHILL, T. A., Polarization of 45-Mev protons by complex nuclei, 20: 22128
CALDECOURT, V. J., Space charge in plastics by low-energy electrons, 20: 22344
CALLEBAUT, Marc, Incorporation of tritiated thymidine by the germinal cells of the embryonic ovary of the chicken cultivated in vitro, 20: 20395
CALLERI, G., Eurex plant, 20: 20815
CAMBOU, Francis, Effect of irradiation by nuclear particles on switching times of fast diodes, 20: 21157
CAMERON, A. E., Isotopic composition of atmospheric neon, 20: 21509
CAMERON, A. G. W., Approach to nuclear statistical equilibrium, 20: 21492
CAMERON, A. G. W., Solar evolution with varying G, 20: 21493
CAMERON, J. A., Nuclear orientation of ^{54}Mn nuclei in noble metal hosts, 20: 22097
CAMERON, J. R., Thermal annealing effects on thermoluminescence of LiF, 20: 21057
CAMPBELL, F. J., Radiation effects on transmittance of glasses and adhesives, 20: 21446
CAMPBELL, I. A., Nuclear orientation of ^{54}Mn nuclei in noble metal hosts, 20: 22097
CAMPBELL, K. H., Evolution and promise of organic-cooled reactors, 20: 22442
CAMPBELL, William Buford Jr., Diffusion rate and activation energy of He through single crystal and polycrystalline Al_2O_3, 20: 21353 (TID-22828)
CANCE, Michel, Decline of luminescence of rare gas atoms excited by α particles in presence of electric field, 20: 21521
CANO, Gilbert L., Response of CsI(Tl) crystals to low-energy heavy ions, 20: 22318
CANOBBIO, E., Harmonics of the electron gyrofrequency in plasmas, 20: 22239
CAPALNA, S., Radioprotective effect of glycine during x irradiation. II., 20: 20517 (NP-15925)
CAPO, M. A., Radiation environment about NERVA reactors, 20: 22481
CAPPS, Richard H., Pseudoscalar-meson universality principle, 20: 21752
CAPPS, Richard H., Saturation of SU(3)-symmetric hadron forces, 20: 21760
CARDONA, Manuel, Microwave studies of the superconducting mixed state, 20: 21916
CARHART, Homer W., Maintenance of a habitable atmosphere, 20: 20981
CARLSON, O. N., Electrotransport of interstitial atoms in yttrium, 20: 21254
CARMAN, Charles J., X ray fluorescent determination of major constituents in multi-element matrices, 20: 20644
CARMON, J. L., Effect of γ and neutron irradiation on litter size in the mouse, 20: 20453
CARPENTER, E. W., Quantitative evaluation of teleseismic explosion records, 20: 20911
CARR, E. A., Simplified techniques for predicting TREE responses, 20: 21166
CARR, T. D., Temporal and statistical characteristics of Jupiter decametric radiation, 20: 21510
CARRILLO, Lile, Assignment of neutron capture angular momenta in angular distributions of $^{23}Na(d,p)^{24}Na$ reaction, 20: 22150
CARRIVEAU, G., Prog. rpt. on integral neutron thermalization, 10–12/65, 20: 21939 (GA-6930)
CARTERET, Y., Kinetics of escape of He from BeO frits during irradiation, 20: 21428 (NP-15942)
CARTLEDGE, G. H., Passivation of iron in presence of pertechnetate and chromate ions, 20: 21271
CASAZINA, Sireh, Temporal observations on peripheral hemograms of atomic bomb casualties as company employees. III., 20: 20481
CASSOLA, R. L., Elastic neutron scattering from B, C, K, and Ca at 14.0 Mev, 20: 22119
CASTAGNOLI, C., Project for underground laboratory in the Mont Blanc tunnel for experiments on neutrino and cosmic radiation, 20: 21612 (CERN-65-32, pp 225-30)
CASTAGNOLI, Carlo, Experimental limit of the mean life of nucleons, 20: 21636
CASTONGUAY, T. T., Effect of γ radiation on dynamic mechanical properties of styrene–butadiene rubbers, 20: 20754
CASTONGUAY, T. T., Rover destruct Test Three, 20: 22472 (SC-CR-66-2017)
CATER, E. David, Uranium monosulfide. III., 20: 20669
CATTANI, D., X-ray scanning of sky in 20- to 200-kev range, 20: 21490
CATTERALL, J. A., High-field superconductivity and its applications, 20: 21877
CEJPEK, J., Analytical expression of amplitude of stripping reaction in the Coulomb approximation, 20: 22028
CELINSKI, Zdzislaw N., Effect of electrode size in MHD generators with segmented electrodes, 20: 21571
CERROLAZA, J. A., Double-sampling method for carrying out quality control of a fabrication process, 20: 21308
CESCON, Paolo, Effect of intense radiation fields on electrode processes, 20: 20791
CESONI, G., Problems of fission product diffusion in graphite fuel elements, 20: 21423 (N-65-23015)
CHABRIER, P., Radioprotective power of some organophosphorus compounds, 20: 20515
CHADDERTON, Lewis T., Atomic collisions in crystals, 20: 22341
CHAIKOFF, I. L., Induction of benign and malignant thyroid neoplasms in the rat, 20: 20448
CHALOT, A., Experimental results on engineering model of Rapsodie, 20: 22501 (EURFNR-49F)
CHAMBERLAIN, Owen, π^+-p Scattering at 250 Mev: experiment and analysis, 20: 21662
CHAMBERS, R., Prog. rpt. on metallurgy as related to fuel-element fabrication, 9/59, 20: 21290 (GA-1052)

CHAN, Yau Wo, Nuclear spin and magnetic dipole moment of 39-min ^{190}Au, 20: 22140
CHANANA, A. D., Influence of extracorporeal irradiation of the blood and lymph on skin homograft rejection, 20: 20485
CHANG, Shuh-Ming, Hydrolysis of salicyl phosphate and effect of radiation energy, 20: 20744
CHANG, Shu-sen, Study of the water content in UF_4 by gas volumetric method with calcium hydride, 20: 20609
CHANG, T. S., Motion of poles in the Lee model, 20: 21769
CHANG, W. H., Effect of carbide dispersion in tantalum-base alloys, 20: 21404
CHANG, W. Y., Recent development in experimental study of elementary particles, 20: 21692
CHAPMAN, Thomas W., Heat capacity of liquid metals, 20: 20657 (UCRL-11931)
CHAPMAN, Thomas W., Viscosity of liquid metals, 20: 20656 (UCRL-11930)
CHARAP, J. M., Irreducible representations of U(12), 20: 21765
CHATEL, J.-L., Detecting leaks by sniffing, 20: 20845
CHEBLUKOV, Y. N., Reactions (d,n) on isotopes ^{58,60,62,64}Ni, 20: 22109
CHEKMAREV, I. B., Positive column in the inverse homopolar device, 20: 22272
CHEN, C. L., Hall effect in a collision-dominated gaseous plasma, 20: 22176 (AD-624165)
CHEN, Hao-chin, Probability of the $\mu^- + {}^3He \rightarrow {}^3H + \nu$ process and nuclear wave functions, 20: 22152
CHEN, Robert L. W., Bounds on fluctuations in a homogeneous plasma, 20: 22255
CHEN, Sin-Li, Direct display system of plasma parameters by means of a non-floating triple probe, 20: 22214
CH'EN, Yu-te, Study of the water content in UF_4 by gas volumetric method with calcium hydride, 20: 20609
CHENEBAULT, P., Particular aspects of utilization of UO_2 as fuel in power reactor, 20: 22422
CHENG, Hung, Asymptotic form of the S matrix for large angular momentum in the left half-plane, 20: 21754
CHENG, Hung, Representation of the S matrix by Regge parameters, 20: 21755
CHENG, Pu-in, Inelastic interactions of π^- mesons with nucleons at 6.8 Bev, 20: 21693
CHENION, J., Study of compounds formed at temperatures above 600°C by action of carbon dioxide on graphite, 20: 20702
CHENOUARD, J., Isotopic analysis of U and Pu, 20: 20978
CHERDYNTSEV, V. V., Non-equilibrium uranium in carbonate deposits and their age determination, 20: 20887
CHERKASOV, E. M., High-frequency discharge in a neon–helium laser, 20: 21808
CHERNIK, T. P., Induction of mutations by uv radiation and nitrous acid in extracellular phage ϕX174, 20: 20463
CHERNIKOV, N. A., Two-plane wave scattering in nonlinear scalar field theory of Born-Infeld type, 20: 21716 (JINR-P-2603)
CHERNILIN, Yu. F., Reconstruction of IRT research reactor, 20: 22497 (IAE-992)
CHERNOCK, W. P., Prog. rpt. on temperature transient method for performing in-pile thermal conductance testing, final, 3/64–11/65, 20: 22354 (CEND-3336-260)
CHERNYSHEVICH, V. N., Reconstruction of IRT research reactor, 20: 22497 (IAE-992)
CHERNYSHOV, A. A., Neutron thermalization process in time in graphite and Be, 20: 21942 (KFK-tr-188)
CHERNYSHOV, A. A., Transient neutron spectra in zirconium hydride, 20: 21941 (IAE-977)
CHERRY, Cora P., Ten-year results of individualized treatment of carcinoma of the cervix based on the analysis of serial biopsies, 20: 20536
CHEW, Geoffrey, Analytic S matrix: theory for strong interactions, 20: 21774
CHEYMOL, J., Radioprotective power of some organophosphorus compounds, 20: 20515
CHIANG, C. C., Effective interaction for nuclear matter, 20: 22122
CHIMINA, V. F., Measurement of the radon concentration in water by γ radiation, 20: 20959
CHINAGLIA, B., Problems of fission product diffusion in graphite fuel elements, 20: 21423 (N-65-23015)
CHIRIKOV, B. V., Focusing of intense electron beam in an accelerator tube, 20: 21487
CHIVERS, H. J. A., Slow fluctuations between conjugate points in auroral absorption of cosmic noise, 20: 21820
CHIZHIKOV, V. I., Determination of one-boson exchange parameters by nucleon-nucleon phase shifts, 20: 21621 (JINR-P-2584)
CHO, A. Y., Study of porous metal ionizers, 20: 21570 (N-65-29785)
CHOLIN, V. V., Peculiarities due to age in acute radiation sickness in mice, 20: 20494
CHOUDHURY, D. C., Investigation of nuclear properties of ^{143}Pr in the unified model, 20: 22139
CHOWDHURY, Jayasree Roy, Uptake of ^{32}P in nucleic acids of developing chick embryo, 20: 20399
CHRIEN, R. E., Numerical analyses of neutron resonances by use of computer programs, 20: 21994 (BNL-10094)
CHRISTENSEN, Gerald M., Sodium and potassium binding in x-irradiated nuclei, 20: 20422
CHRISTENSEN, Hilbert C., Radiolysis of aqueous benzene solutions in the presence of inorganic oxides, 20: 20768
CHRISTENSEN, J. A., In-pile measurement of UO_2 thermal conductivity, 20: 21361 (WCAP-2923)
CHRUSCEV, V. G., Behavior of living organisms in radiation fields, 20: 20495
CHUBB, J. N., Monte Carlo computer program for analysis of molecular gas flow, 20: 20855 (CLM-R-54)
CHUBUKOVA, T. M., Polarographic determination of U in nitric acid media containing TBP. I., 20: 20630
CHUBUKOVA, T. M., Polarographic determination of U in nitric acid media containing TBP. II., 20: 20631
CHUNG, Paul M., Theory of electrostatic double probe comprised of two parallel plates, 20: 22192
CHUPP, E. L., Directional neutron detector for space research use, 20: 21117
CHURCHILL, R. J., Spark chamber spectrometer for space protons, 20: 21120
CHURILOV, G. Y., Measurements at high field strengths on superconducting accelerator cavities, 20: 21459 (AD-623509)
CHWOJNIK, Abraham, Hepatic scintigram, 20: 20522 (CNEA-167)
CIRIEGI, U., X-ray scanning of sky in 20- to 200-kev range, 20: 21490
CITRON, A., Structure in the pion-proton total cross section between 2 and 7 Bev/c, 20: 21661
CITTADINI, Giorgio, Morphine, codeine, nalorphine and survival test of the pan-irradiated mouse, 20: 20513
CLARK, Alfred Jr., Kinematical models for small-scale solar magnetic fields, 20: 21503
CLARK, C. D., Design of a velocity selector for long-wavelength neutrons, 20: 21007
CLARK, Don M., Long-range seismic measurements on Bronze, 20: 20900 (AD-627039)
CLARK, Don M., Long-range seismic measurements on Turf, 20: 20902 (AD-627051)
CLARK, Don M., Long-range seismic measurements on Klickitat, 20: 20901 (AD-627040)
CLARK, G., Primary energy spectrum from 8×10^{14} to 4×10^{17} ev, 20: 21547 (MIT-2098-227, Paper EAS-31)
CLARKSON, M. H., Electron temperatures in several r-f plasmas, 20: 22194
CLASS, C. M., Level schemes of ^{67,68,70}Ga, 20: 22053
CLEARY, J. G., Ductile-brittle transition in tantalum carbide, 20: 21375
CLERC, H. G., Excitation of new electromagnetic transitions in ^{9}Be inelastic electron scattering, 20: 22105
CLINE, H. E., Fabrication of an ultra-fine Nb–Cu composite by drawing, 20: 21298
COATS, G. I., Absolute counting using zero probability analysis, 20: 21109
COBB, James C., Iron meteorites with low cosmic-ray exposure ages, 20: 21505
COCHNAR, Zdenek, Cause of brittle fracture in tungsten wire, 20: 21396
COCHO, G., Electromagnetic and weak form factors of the nucleon, 20: 21651
COCKE, W. J., Relativistic corrections for terrestrial clock synchronization, 20: 21866
COCKETT, A. T. K., Effect of whole-body irradiation (300 R) on experimental bladder calculus formation in rats, 20: 20467
CODY, G. D., Critical currents in Nb_3Sn. III., 20: 21921
COHEN, Bernard, Heavy spherical nuclei, 20: 21975 (BNL-948, pp 269-336)
COHEN, Bernard, Two and more nucleon transfer reactions, 20: 21972 (BNL-948, pp 66-174)
COHEN, Bernice H., Radiation exposure in parents of children with mongolism, 20: 20454
COHEN, Ira, Gamma spectrometric measurement of ^{235}U in 24-in. × 24-in. × 12-in. absolute air filters and associated economics of uranium recovery, 20: 20564 (NYO-10740)
COHN, Paul D., From watts to megawatts with packaged nuclear power, 20: 22447
COHN, S. H., Strontium and calcium skeletal discrimination determined by compartmental analysis, 20: 20400
COIGNET, G., Measurement of polarization parameters and spin correlation in proton-proton scattering at 600 Mev, 20: 21590 (CERN-66-2)
COLABIANCHI, G., Behavior under irradiation of low-alloyed uranium, 20: 21436
COLE, I. W., Numerical analyses of neutron resonances by use of computer programs, 20: 21994 (BNL-10094)
COLLIN, Robert L., Precipitate formation in strontium–phosphate system,

20: 20690
COLLINS, D. G., Instructions for application of LO5 Monte Carlo procedure, 20: 22304 (AD-612031)
COLLINS, John T. Jr., Criteria for high-efficiency filter installations, 20: 20933 (IDO-12045)
COLLINSON, C. D., Empty space-times of embedding class two, 20: 21849
COLMERY, Benjamin H., Flow system startup of full-scale simulated nuclear rocket engine, 20: 22480
COLOMBO, R. L., UO_2–ZrO_2–CaO ceramic nuclear fuels, 20: 21302
COMPTON, J. B., Modeling of radiation effects in semiconductor devices and circuits, 20: 21173
COMPTON, J. P., Nuclear orientation of ^{54}Mn nuclei in noble metal hosts, 20: 22097
CONEN, Patrick E., Chromosome studies on a radiographer and her family, 20: 20447
CONGDON, C. C., Change in partition of total-body N in radiation chimeras, 20: 20407 (ORNL-P-1118)
CONLON, T. W., Hole states of ^{43}Ca and ^{47}Ca, 20: 22129
CONNER, R. A. Jr., Crystal structure of compounds of rare earths with Cu, Ag, Au, and Ga, 20: 21399
CONNOR, D., Submicrosecond synchronization of multiple chopper systems, 20: 21111
CONRAD, F. J., Fast neutron flux pattern for 14-Mev neutron generator, 20: 21946
CONSTANTINIDES, C., Strontium and calcium skeletal discrimination determined by compartmental analysis, 20: 20400
CONWAY, W. D., Simplification of oxygen-flask combustion procedure for preparation of samples for liquid scintillation counting, 20: 20570
COOK, L. F., Can nearby interaction singularities generate observed resonances?, 20: 21668
COOL, Terrill A., Recombination, ionization, and nonequilibrium electrical conductivity in seeded plasmas, 20: 22258
COOPER, E. D., Flow-diverter valve for granular solids, 20: 22511 (IDO-14666)
COOPER, G. P., Responses of single neurons in olfactory bulbs, 20: 20431 (AD-630323)
COOPER, J. D., Simple tandem Moessbauer spectrometer using pulse-height analysis, 20: 21069
CORBEN, H. C., Elementary particle spectrum, 20: 21703 (AD-622258)
CORENZWIT, E., High-pressure polymorphism and magnetic ordering in some Sm-type rare earth alloys and samarium, 20: 21414
CORNFIELD, Jerome, Estimation of radiation dose-reduction factor for β-mercaptoethylamine by endogenous spleen colony counts, 20: 20511
CORNGOLD, Noel, Maximum absorption theorem, 20: 21953
CORNISH, D. N., Superconducting coils using composite stranded cables, 20: 21878
CORNWELL, Roy S., Effectiveness NTU relations for one-, two-, and three-pass cross counterflow heat exchangers to NTU of 40, 20: 20858 (UCRL-14620)
CORYELL, C. D., Two γ rays in decay of 3.0-min ^{85}Br, 20: 22041
CORYELL, Charles D., Decay of 54-sec ^{86}Br and 55-sec ^{87}Br, 20: 22130
COSANDEY, M., Comparison of different procedures to measure simultaneously ^{32}P and ^{45}Ca in inorganic salts by liquid scintillation counting, 20: 20584
COSGROVE, G. E., Late somatic effects of radiation exposure in mice, 20: 20441 (ORNL-P-1173)
COSPER, S. W., Analyses of 18-Mev α-particle scattering cross sections for ^{40}Ar, ^{32}S, ^{31}P, ^{23}Na, and ^{20}Ne, 20: 22134
COSTA, S., Photoneutron production from C, Al, and S by bremsstrahlung up to 200 Mev, 20: 22094
COSTA, Sergio, Spectroscopic analysis of helium plasma produced by a conical θ-pinch discharge, 20: 22269
COULON, M., Mass spectrometer for isotopic analysis of UF_6, 20: 20588
COWAN, C., Production of muons, 20: 21028 (CERN-65-32, pp 65-70)
COWAN, C. L., Proposal to detect cosmic-ray neutrinos through the Cherenkov light of produced muons, 20: 21031 (CERN-65-32, pp 231-40)
COWAN, G. A., Symmetry of neutron-induced ^{239}Pu fission at individual resonances, 20: 22135
COWSER, K. E., Evaluation of radiation dose to man from radionuclides released to Clinch River, 20: 22514 (ORNL-P-2021)
COX, J. H., Irradiation-induced contraction of graphites at high temperature, 20: 21420 (BNWL-215)
CRAVEN, W. E., Terbium, erbium, and ytterbium graphite intercalation compounds, 20: 21413
CRAVEN, William Ernest, Intercalation of rare earth elements into graphite and dichalcogenides, 20: 20648 (AD-621029)
CRAWFORD, F. W., Transmission characteristics of cyclotron harmonic waves in plasma, 20: 22226
CRAWFORD, J. H. Jr., Annealing of ^{60}Co-γ-irradiated germanium, 20: 21392
CREBBIN, Kenneth C., Prog. rpt. on Bevatron operation and development, 4–6/65, 20: 21474 (UCRL-16553)
CREUZBURG, M., Formation of alkali metals from alkali halides by irradiation with 50-kev electrons, 20: 20781
CRISCO, Carl, Evaluation program for radioactive waste treatment facility, 20: 22507 (AD-622372)
CRISTEA, M., Electromagnetic phenomena at interior of the weak MHD shock wave front, 20: 21806
CRISTEA, Maria, Shock waves with radiation in magnetodynamics. I., 20: 21788
CROCI, R., Harmonics of the electron gyrofrequency in plasmas, 20: 22239
CRONKITE, E. P., Influence of extracorporeal irradiation of the blood and lymph on skin homograft rejection, 20: 20485
CRONSON, H. M., Spatial variations of plasma electron temperature in standing wave at microwave frequencies, 20: 22242
CROSBIE, K., Prog. rpt. on integral neutron thermalization, 10–12/65, 20: 21939 (GA-6930)
CROSBIE, K. L., Accelerator pulsed fast assembly, 20: 22503
CROSIGNANI, E., Microwave determination of distribution functions of electrons in low current discharges, 20: 21795
CROSSLEY, D. A. Jr., Animal species associated with pig carrion, 20: 20941 (ORNL-TM-1432)
CROUTHAMEL, C. E., Energy conversion, 20: 21566 (ANL-7055, pp 213-29)
CROWE, Kenneth M., Pi-mesonic atoms, 20: 21534
CROWTHER, Peter, Gamma-ray branching ratios for ^{116}In, ^{147}Nd, and ^{141}Ce, 20: 22091
CSIKOR, F., Structure of weak currents, 20: 21743
CSILLAG, L., Fine structure of six lines of Balmer series of deuterium, 20: 21532
CSOKE, Antal, Hot chamber for production of ^{131}I, 20: 21215
CSOKE, Antal, Manipulator with ball and socket joint, 20: 20848
CULLEN, G. W., Critical currents in Nb_3Sn. III., 20: 21921
CULTRERA, G., Utilization of sodium sulfate–^{35}S by hepatic tissue of the normal and irradiated rat, 20: 20410
CUMINGE, Danielle, Effects of a radiomimetic substance, nitrogenous yperite, on morphology and oxygen consumption of an embryonic organ cultivated in vitro, 20: 20372
CUMMING, P. A., Bibliographic review of self-diffusion in metal oxides, 20: 21321 (AERE-Bib-143)
CUMMINGS, W. D., Rocket-borne measurements of particle fluxes and auroral light, 20: 21826
CUMMINS, J. T., Effect in stomach of ionizing radiation on acid secretion, potential, ATP, and phosphocreatine in comparison to spleen, 20: 20433 (AD-630390)
CUNDY, D. C., Further analysis of neutrino interactions in the CERN heavy liquid bubble chamber, 20: 21597 (CERN-65-32, pp 25-30)
CUNDY, D. C., Future neutrino experiments with the CERN heavy liquid bubble chamber, 20: 21606 (CERN-65-32, pp 157-60)
CUOMO, J. J., Preparation of rare earth nitrides by reactive arc melting, 20: 21244
CURCIO, R. M., Weld interface porosity in tantalum, 20: 21311
CURRAN, F. E., Modular set of analog microcircuits intended for satellite experiments, 20: 20997
CURTIS, Mary L., Simple technique for rapid analysis of radioactive gases by liquid scintillation counting, 20: 20582
CURWEN, P. W., Prog. rpt. on gas-bearing Brayton cycle turbocompressor, 12/65–2/66, 20: 20841 (NYO-3237-5)
CUSHING, C. E., Accumulation and transport of radionuclides by Columbia River biota, 20: 20382 (BNWL-SA-623)
CUTSHALL, Norman, ^{51}Cr in sea water: chemistry, 20: 20603
CZERNIEWSKI, Michal, Bone tissue sterilization using reactor fuel γ radiation, 20: 20482
CZIHARZ, H., Effects of radiation on $NADH_2$ oxidation in preparation of mitochondria, 20: 20496

D

DAHANUKAR, S. M., Heavy concrete used for construction of pilot plutonium plant at Trombay, 20: 20819
DAHL, A. H., Concentration patterns of ^{90}Sr, ^{137}Cs, and ^{131}I in a wild deer population and environment, 20: 20384 (COO-1156-13)
DAHLBY, Helen J., Dissociation of $NbCl_5$ on Nb and carbide surfaces, 20: 21241 (LA-tr-66-15)
DAIBER, J. W., Laser-generated implosions, 20: 22245
DALBY, W. D., POODLE thruster aerodynamic drop test, 20: 21210 (SC-RR-65-609)
DALITZ, R. H., Quark models for the elementary particles, 20: 21697
DALLE, Donne M., Comparison of He, CO_2, and steam as coolants of 1000-Mw(e) fast reactor, 20: 22452
DALLMANN, Wayne E., Determination of O in Th and Y metals, 20: 20572
DAMANI, V. D., Role of substrate symmetry in gas-solid reactions. I and II., 20: 20649 (AEET-CD-24)
DAMASKINSKII, E. A., Recording of several particles with an acoustic spark chamber, 20: 21094
DANCE, D. F., Cross section for production of $He^+(2S)$ ions by electron

impact excitation of ground state helium ions, 20: 21535
DANCEWICZ, Antoni M., Biochemical lesions induced in subcellular structures by ionizing radiation. III., 20: 20417
DANIEL, R. R., Age of cosmic-ray nuclei and their propagation in space, 20: 21554
DANKERT, Mercelo A., Labeling lipids with ^{131}I, 20: 20789 (CNEA-182)
DANTE, W. M., Σ^--neutron interaction and strange-particle production, 20: 21681
DARENSKAJA, N. G., Behavior of living organisms in radiation fields, 20: 20495
DARNLEY, A. G., Analysis of Sn and Cu ores, 20: 20640
DASH, J. G., Measurements with black absorbers, 20: 22157
DAVIDSON, A. S., Plant measurement, sampling, and analysis for accountancy purposes, 20: 20830
DAVIDSON, A. S., Plant measurement, sampling and analysis for accountancy purposes with particular reference to separation plants at Windscale, 20: 20972
DAVIES, B. L., Transistorized radon measuring equipment, 20: 21067
DAVIES, D. E., Surface potential measurements of lithium-drifted germanium diodes, 20: 21096
DAVIES, N. F., SNAP environment simulation problems, 20: 22475
DAVIS, Thomas P., Hybrid radioisotope scanner, 20: 20535
DAVIS, William G., Heat-shield ablation and sublimation determinations through radioisotope techniques, 20: 20860
DAWANCE, Guy, Behavior of concrete pressure vessel subjected to high temperature gradient, 20: 22353 (CEA-R-2829)
DAWSON, K. B., Autoradiographic differentiation of tritium and another β emitter by a combined color-coupling and double stripping-film technique, 20: 20605
DAYAL, S. K., Stabilities and allied properties of organic coolants, 20: 20708 (AEET-213)
DEAN, J. A., Half life and specific activity of ^{99}Tc, 20: 22036
DEBEIR, R., Cryostat in the gaseous phase, 20: 20984 (EUR-2710.f)
DE BRUYN OUBOTER, R., Experience with superconducting coils fed by flux pumps, 20: 21924
DE FABRITIIS, Adriano, Cytopathic effects of tumor viruses in human diploid cells, 20: 20377
DEGROSSI, Osvaldo, Hepatic scintigram, 20: 20522 (CNEA-167)
DE JUREN, J. A., Variation of transport mean free path in graphite with temperature, 20: 21955
DELABAYE, M., Beta decay and core excitation in A = 111 nuclei, 20: 22083
DELACHANAL, Michel, Boiling state of operating homogeneous reactor, 20: 22403
DE LA CRUZ, V., On a certain nonlocal potential, 20: 21637
DE LAFOND, Yvon Gervais, Effect of irradiation by nuclear particles on switching times of fast diodes, 20: 21157
DELANEY, C. F. G., Measurement of statistics of secondary electron emission, 20: 21448
DELANNOY, J., Structure of Arctic auroral zone in period of minimum solar activity, 20: 21814
DE LA PAZ, L. R., Cobalt-60 γ-induced carboxylation of methylamine, 20: 20732 (SGAE-CH-21/1965)
DE LARA, Georges Cohen, Boiling state of operating homogeneous reactors, 20: 22403
DEL COTTO, J., Prog. rpt. on pulsed neutron application to power reactor startup, 7–10/65, 20: 22414 (GEAP-4961)
DEL GRANDE, N. Kerr, Theoretical differential scattering cross sections of x rays, 20: 21516 (UCRL-14403)
DELLA ROSA, R. J., Environmental and biological factors affecting accumulation of ^{90}Sr and ^{137}Cs in deer and sheep, 20: 20388 (SAN-34-2)
DELUCCHI, A. A., Nuclear-charge distribution of fission-product chains of mass numbers 131-133, 20: 22136
DEMANT, J. T., Effects of contamination on oxidation of Zr in steam, 20: 21268
DE MARCO, A., Project for underground laboratory in the Mont Blanc tunnel for experiments on neutrino and cosmic radiation, 20: 21612 (CERN-65-32, pp 225-30)
DE MARCO, Angelo, Experimental limit of the mean life of nucleons, 20: 21636
DEMETER, I., Decay chain of $^{138}Nd \rightarrow {}^{138}Pr \rightarrow {}^{138}Ce$, 20: 22002 (JINR-P-2570)
DEMETRIADES, Anthony, Langmuir probe diagnosis of turbulent plasmas, 20: 22193
DEMIN, V. F., Scattering of particles by system of fixed centers, 20: 21710 (JINR-P-2554)
DENKINS, R. F., Engineering design practices for facilities containing radioactive materials, 20: 20942 (ORNL-TM-1459)
DENNERY, Ph., Origin of certain resonances for three particles, 20: 21724
DENNISON, R. A., Prog. rpt. on effects of low-level irradiation upon preservation of food products, annual, 4/65, 20: 21195 (TID-22509)
DE NOBLET, M., Study of compounds formed at temperatures above 600°C by action of carbon dioxide on graphite, 20: 20702
DEPORTES, Charles, Electric conductivity in HfO_2–Y_2O_3 at high temperature, 20: 21370
DE RAFAEL, E., Tests of SU_{6W} from predictions on spin alignments, 20: 21652
DEREPPE, Jean Marie, Nuclear quadrupole resonance and its applications in chemistry, 20: 20699
DERIAN, L., Influence of electric fields on heat transfer to partially ionized CO_2, 20: 20859 (UJV-1421/65)
DER MATEOSIAN, E., Search for double β decay in ^{48}Ca, 20: 21995 (CERN-65-32, pp 35-40)
DEROME, Jean-Robert, Symmetry properties of 3j-symbols for an arbitrary group, 20: 21730
DERRICK, M., Large hydrogen bubble chamber, 20: 21032 (CERN-65-32, pp 259-62)
DE SABBATA, V., Limits on size of visible quasars, 20: 21501
DE-SHALIT, Amos, Diffraction model calculations, 20: 21980 (BNL-948, pp 561-609)
DE-SHALIT, Amos, Strong coupling, exchange, target excitation, and other corrections to DWBA, 20: 21979 (BNL-948, pp 525-60)
DESISTO, Thomas S., Evaluation of refractory sheet metals. II., 20: 21322 (AMRA-TR-65-25)
DE SISTO, Thomas S., Plastic behavior of metals at cryogenic temperatures, 20: 21416
DESSLER, A. J., Plasma in the geomagnetic tail, 20: 21828
DEUBEL, K. L., Thermal efficiency and condenser output in the steam-cooled reactor, 20: 22420
DEUTCH, J. M., Nuclear spin relaxation in gases and liquids. V., 20: 21526
DEUTSCH, J. P., Beta decay and core excitation in A = 111 nuclei, 20: 22083
DEUTSCH, R. V., Electromagnetic phenomena at interior of the weak MHD shock wave front, 20: 21806
DEVANI, M., Dephosphorylation of some coferments with thorium and zirconium ions, 20: 20375
DEVANNEY, John A., Fast neutron-induced gelation of triethylene glycol dimethacrylate using 14-Mev neutrons, 20: 20720 (AD-630891)
DEVI, K. Shyamala, Conductometric study on quantitative estimation of thorium as tungstate, 20: 20592
DE VILLIERS, P. D., Natulan (procarbazine) combined with radiotherapy in management of inoperable malignant melanoma, 20: 20504
DE VOE, J. R., Standardization of differential chemical shift for ^{57}Fe, 20: 22158
DE VOLPI, A., Fast neutron transient detection hodoscope for reactor fuel meltdown studies, 20: 21131
DEVOOGHT, J., Generalized invariant imbedding of transport theory, 20: 21947
DEW, John N., Economics of contained nuclear explosions applied to petroleum reservoir stimulation, 20: 20836
DE WAARD, R. H., Mechanisms of necrosis and preparation of cells damaged by ionizing radiation, 20: 20416
DEWART, W. G., Development of control system for SNAP reactors, 20: 22474
DE WITT, C., Lectures on high-energy physics, 20: 21696
DE WITT, Hugh E., Statistical mechanics of high-temperature quantum plasmas beyond the ring approximation, 20: 22223
DEYSSON, G., Radioprotective power of some organophosphorus compounds, 20: 20515
DEZSI, Istvan, Temperature dependence of internal magnetic field, 20: 22326
D'HEURLE, F. M., Resistivity and structure of sputtered molybdenum films, 20: 21394
DIAMENT, Paul, Wave propagation along warm plasma columns, 20: 22220
DIBDIN, G. H., New structure in ESR spectrum of γ-irradiated single crystals of ice, 20: 22328
DICKS, T. S., Effect of prior beta grain size on ductility of zirconium–2.5 wt.% niobium alloy, 20: 21368
DIECKHONER, James E., Prediction of time-dependent β spectrum from nuclear weapon detonation, 20: 21960 (AD-621023)
DIENSTBIER, Z., Influence of polyols on course of experimental radiation disease, 20: 20520
DIETERLE, Byron, π^+-p Scattering at 250 Mev: experiment and analysis, 20: 21662
DIETZ, George R., Radiation sources for use in radiation preservation of foods, 20: 21197
DIETZ, K. A., Prog. rpt. on STEP project, 7–12/64, 20: 22467 (IDO-17077)
DI GIUGNO, G., Determination of branching ratios among neutral decay modes of the η particle, 20: 21627 (LNF-66/9)
DIMMOCK, T. H., Significance of nonequilibrium conductivity on plasma engine performance, 20: 20873
DI PAOLA, M., Analysis of the spatial distribution of radioactive iodine in the thyroid by the method of level diagrams, 20: 20528
DI PAOLA, R., Analysis of the spatial distribution of radioactive iodine in the thyroid by the method of level diagrams, 20: 20528

DI PRIMIO, Jean C., Prog. rpt. on point defects and mechanical properties of Nb, final, 2/15/62–11/30/65, 20: 21320 (AD-625475)
D'MUHALA, T. F., Descaling and decontamination studies, 20: 21238 (NP-15928)
DOAN, R. L., Public safety aspects of nuclear power plant licensing, 20: 22434
DOBING, E., Structure of 20Cr–25Ni–Nb steel after aging in temperature range 600 to 800°C, 20: 21355 (TRG-Report-1168)
DOLLINGER, Melin R., Myocardial infarction due to postirradiation fibrosis of the coronary arteries, 20: 20468
DOLPHIN, G. W., Estimation of internal radiation dose from metabolic and urinary excretion, 20: 20398
DOMINGO, V., Primary energy spectrum from 8×10^{14} to 4×10^{17} ev, 20: 21547 (MIT-2098-227, Paper EAS-31)
DONADIEU, L., Superconductor magnet for corpuscular ionography used at CERN, 20: 21876
DONALDSON, James G., Vapor deposition of cobalt–tungsten alloys, 20: 21231 (BM-RI-6713)
DONCEL, M. G., Tests of SU_{6W} from predictions on spin alignments, 20: 21652
DONNELLY, R. J., Equivalence of vortices and current filaments, 20: 21800
DONOVAN, Paul, Computers in experimental physics, 20: 21982 (BNL-948, pp 718-40)
DONOVAN, Paul F., Technical developments in hardware, 20: 21026 (BNL-948, pp 704-17)
DONSKOI, A. V., Conductivity in h-f induction discharge in argon, 20: 22280
DORMAN, E., Concentration broadening and oscillator strengths in $Pr:LaCl_3$, 20: 20667
DORMAN, James, Final rpt. on elastic wave propagation, 20: 20896 (AD-623592)
DOST, Helmut, π^+-p Scattering at 250 Mev: experiment and analysis, 20: 21662
DOUGHMAN, Ernest L., Langmuir probe diagnosis of turbulent plasmas, 20: 22193
DOUGLAS, R. Gordon, Treatment of carcinoma of the cervix with combined radiation and extensive surgery, 20: 20526
DOUGLASS, J. D. Jr., Decontamination effectiveness, 20: 20923 (AD-626727)
DOUGLASS, Richard W., Strength, weldability, and heat treatment of Ta–W–Hf and Ta–W–Zr alloys, 20: 21405
DOULL, J., Hypobaric oxygen exposure and acute radiation lethality in mice, 20: 20430 (AD-629311, pp 26-32)
DOWNEY, J. W., Crystal structure of compounds of rare earths with Cu, Ag, Au, and Ga, 20: 21399
DOWNING, R. G., Prog. rpt. on radiation damage in Si, 2/65, 20: 21154 (N-65-23290)
DRAGO, Russell S., Nuclear quadrupole resonance, 20: 20578
DRAGT, Alex J., Cosmic-ray and solar proton albedo neutron decay injection, 20: 21550
DRESVIN, S. V., Conductivity in h-f induction discharge in argon, 20: 22280
DROBYSHEVSKII, E. M., Positive column in the inverse homopolar device, 20: 22272
DRUYVESTEYN, W. F., Resistance transitions of superconducting lead–indium alloys, 20: 21913
DUA, S. K., Aerosol generator to produce radioactive aerosols, 20: 20924 (AEET-232)
DUBECK, L., Thermal conductivity in the mixed state, 20: 21914
DUBOIS, Frederic, Behavior of concrete pressure vessel subjected to high temperature gradient, 20: 22353 (CEA-R-2829)
DU BOIS, Kenneth P., Effect of x radiation on the hexobarbital metabolizing system of liver microsomes, 20: 20429 (AD-629311, pp 15-25)
DU BOIS, Kenneth P., Effects of various drugs on the ATP activity of the hematopoietic tissues of rats exposed repeatedly to ^{60}Co γ radiation, 20: 20503 (AD-629311, pp 1-14)
DUBOIS, Regis, Incorporation of tritiated thymidine by the germinal cells of the embryonic ovary of the chicken cultivated in vitro, 20: 20395
DUBOVSKII, B. G., Nuclear safety in working with fissionable materials, 20: 20975
DU BRIDGE, R. A., Application of in-core detectors to startup of large boiling water reactors, 20: 22438
DUBS, Charles W., High reflectance coatings, 20: 21136
DUCHARME, Edward L., Performance of self-excited MHD generator, 20: 21564 (AD-627037)
DUCKSBURY, N. A., Polarographic determination of uranium in binary chromium–uranium alloys, 20: 20595
DUCKWORTH, Henry, Atomic mass differences involving isotopes of Nd, Sm, Cd, and Pb, 20: 22153
DUCKWORTH, Henry E., Stopping cross sections in B of atoms with energies 15 to 140 kev, 20: 21539
DUFF, B. G., Possible neutrino experiments in emulsions, 20: 21609 (CERN-65-32, pp 175-80)
DUFTSCHMID, K. E., Radiometric investigations in preparation of asbestos cement products, 20: 21204
DUMAS, J., Effect of uv rays on gastric transit in the rat, 20: 20414
DU MOND, Jesse W. M., Present key importance of fine structure constant, α, 20: 21537
DUMONT, Jacques E., Nuclear medicine in the service of Africa, 20: 20373
DUNLAP, F. C., High-frequency auroral noise, 20: 21835
DUNN, D. A., Electrostatic and magnetic pinch effects in beam-generated plasmas, 20: 22221
DUPOUY, Jean-Michel, Compression of monocrystals of Be parallel to C axis, 20: 21371
DUQUESNE, M., Method of analyzing activity profile of radiochromatograph, 20: 20559 (EUR-2626.f)
DURANT, William S., Prog. rpt. on performance of activated carbon beds in SRP reactor confinement facilities, 9/62–9/65, 20: 22463 (DP-1028)
DURGAPRASAD, N., Age of cosmic-ray nuclei and their propagation in space, 20: 21554
DURHAM, F. E., Level schemes of $^{67,68,70}Ga$, 20: 22053
DURKAN, Frances K., Gamma spectrometric measurement of ^{235}U in 24-in × 24-in. × 12-in. absolute air filters and associated economics of uranium recovery, 20: 20564 (NYO-10740)
DUTT, Yog, Complex formation of metal ions with tropolones. II., 20: 20673
DUYCKAERTS, G., Separation of lanthanides and actinides by hydroxyethylenediaminetriacetic acid. I., 20: 20822
DWIGHT, A. E., Crystal structure of compounds of rare earths with Cu, Ag, Au, and Ga, 20: 21399
D'YACHENKO, V. F., A magnetohydrodynamic theory of the pinch effect in a high-temperature, dense plasma, 20: 22180 (IAE-960)
D'YACHENKO, V. V., Welding of molybdenum and niobium with stainless steel, 20: 21309
DYER, F. F., ^{3}He activation analysis, 20: 20565 (ORNL-P-1216)
DYOS, M. W., PSEUDO—code for construction of statistical resonances in unresolved resonance region, 20: 21940 (GAMD-6908)
DZANTIEV, B. G., Methods for hot synthesis of ^{35}S-labeled biologically active substances. I., 20: 20785
DZANTIEV, B. G., Methods for hot synthesis of ^{35}S labeled biologically active substances. II., 20: 20786
DZANTIEV, B. G., Reactions of hot S atoms. I., 20: 20784
DZHAGATSPANYAN, R. V., Structure of polypropylene chlorinated by radiation and sulfochlorinated, 20: 20779
DZHOLOS, R. V., Nucleon-phonon interaction problem, 20: 21619 (JINR-P-2567)

E

EACHUS, Alan C., Procedure for eliminating temperature-sensitive impurities in toluene-methyl-^{3}H used for hydrogen abstraction reactions, 20: 20711
EAGLES, D. M., Possible high-current superconductivity in ionic semiconductors, 20: 21889
EAPEN, A. C., Total count method for open channel flow measurement, 20: 20903 (AEET-Radiochem.-45)
EASTLUND, B. J., Cesium plasma transport properties, 20: 22227
EASTLUND, Bernard J., Diffusion measurements in fully ionized cesium plasma, 20: 22243
EBEOGLU, D. B., Monte Carlo calculations of radionuclide production in iron targets bombarded with 400-Mev protons, 20: 22035
EBEOGLU, D. B., Nuclear instrumentation for lunar surface and subsurface measurements, 20: 21003
ECHARRI, A., Remanent induction in a hard superconductor, 20: 21893
ECK, R. E., Microwave-induced d-c voltages across Josephson junctions, 20: 21882
ECKENFELDER, W. W., Conference on water pollution research, London, 9/62, 20: 20982
EDAGAWA, Hiroshi, Gamma irradiation on MOS field effect transistor, 20: 21159
EDELSON, D., Transient effect of nuclear radiation on the dielectric properties of ceramics and plastics at microwave frequencies, 20: 21171
EDWARDS, R. K., High-temperature reactor materials development, 20: 21324 (ANL-7055, pp 163-6)
EFIMENKO, B. A., Analysis and generalization of correlation method for measurement of particle-lifetime distribution in physical systems, 20: 21035 (FEI-21)
EFIMOV, Y. N., Approximate method in two-nucleon problem, 20: 21617 (JINR-P-2546)
EFIMOV, V. N., Investigation of neutron resonances of ^{165}Ho, 20: 22004 (JINR-P-2593)
EGAN, Douglas M., Commercial potential of wood-plastic combinations in northeastern U. S., 20: 21186 (ORNL-IIC-7, pp 81-8)
EGAN, J. J., Molar free energy of formation of UC_2 and U_2C_3, 20: 20672

nuclear rocket development station, 20: 20954
ERICKSON, W. C., Two satellite-borne cosmic-radiation detectors, 20: 21118
ERICSON, M., Optical properties of low-energy pions in nuclei, 20: 22021
ERICSON, T. E. O., Optical properties of low-energy pions in nuclei, 20: 22021
ERICSSON, Torsten, Low-cycle strain fatigue—a literature review, 20: 21426 (N-65-24714)
ERKMAN, Bayzar, Chromosome studies on a radiographer and her family, 20: 20447
ERMANS, Andre M., Nuclear medicine in the service of Africa, 20: 20373
ERWIN, Harold E., Purification and crystallization of B, 20: 21294 (TID-22221)
ESCH, Harold E., Dose-dependent gamma irradiation effects on the resting potential of Nitella flexilis, 20: 20419
ESCOBAR, I., Primary energy spectrum from 8×10^{14} to 4×10^{17} ev, 20: 21547 (MIT-2098-227, Paper EAS-31)
ETIM, Etim, Proposal for administration of radiative corrections, 20: 21469 (LNF-66/10)
EVANS, B., Prog. rpt. on sorption of gases on metal surfaces, annual, 2/15/65–2/14/66, 20: 21351 (SRIA-425-8)
EVANS, Charles Charlton, Improvements in or relating to luminous compositions, 20: 20787
EVANS, Robley D., Determination of silver in minerals and ores by neutron activation analysis, 20: 20574
EVVARD, John C., Non-chemical propulsion, 20: 20871 (N-65-29443)
EWALD, C. J., Multichannel pulse-height analyzer for university balloon and rocket experiments, 20: 21127
EWING, George E., Infrared absorption of HD in liquid Ar, 20: 21528
EYRING, LeRoy, Conference on rare earth research, Phoenix, Ariz., 4/64, 20: 20704
EZER, D., Solar evolution with varying G, 20: 21493

F

FABRICANT, Steve J., Ultracentrifuge rotor temperature measurements and control, 20: 21009
FAELTHAMMAR, C.-G., Transport of trapped particles in the outer magnetosphere, 20: 21831
FAES, M. H., Physical examinations and medical records required in nuclear industry, 20: 20955
FAFIOTTE, M., Structure of Arctic auroral zone in period of minimum solar activity, 20: 21814
FAIRSTEIN, E., Nuclear pulse amplifiers—fundamentals and design practice. V., 20: 21008
FAIRSTEIN, Edward, Pulse shaping by triple differentiation in nuclear pulse amplifiers, 20: 21004
FAISSLER, W. L., Wide-angle electron-pair production, 20: 22146
FALK, C. D., Isotopic exchange reactions of trans-hydridochlorobis(triethylphosphine) platinum(II), 20: 20701
FALKSON, Geoffrey, Natulan (procarbazine) combined with radiotherapy in management of inoperable malignant melanoma, 20: 20504
FALKSON, H. C., Natulan (procarbazine) combined with radiotherapy in management of inoperable malignant melanoma, 20: 20504
FARMER, William S., Re-examination of design factors for 1000-Mw(e) fast breeder, 20: 22454
FARRIS, G. C., Concentration patterns of ^{90}Sr, ^{137}Cs, and ^{131}I in a wild deer population and environment, 20: 20384 (COO-1156-13)
FASSEL, Velmer A., Determination of O in Th and Y metals, 20: 20572
FAULKIN, Leslie John Jr., Changes in the mammary gland of the BALB/c mouse, 20: 20502
FAZIO, G. G., Vidicon spark chamber detector for γ astronomy, 20: 21119
FEARNEHOUGH, G. D., Instrumented impact testing of Zircaloy, 20: 21386
FEDER, H. M., Calorimetry, 20: 20650 (ANL-7055, pp 167-76)
FEDER, H. M., High-temperature reactor materials development, 20: 21324 (ANL-7055, pp 163-6)
FEDOROV, B. A., Spermatogenesis in irradiated rats during the prophylactic administration of β-mercaptoethylamine, 20: 20509
FEDULOV, V. I., Bolometric measurements of radiation of ionized shock wave in argon, 20: 22281
FEGLEY, C. E., PM-3A: First nuclear power plant in Antarctica, 20: 22445
FEHER, Istvan, 132I generator, type JG 01/59, 20: 21217
FEINER, R. R., Effect of dark repair on uv sensitivity of bacteriophage-infected bacteria, 20: 20471
FEIT, Pal, Hot chamber for production of ^{131}I, 20: 21215
FELDMAN, Milton H., Fluorine microdetermination by neutron activation analysis, 20: 20594
FELICETTI, F., Photodisintegration of the deuteron by polarized γ rays, 20: 21626 (LNF-66/4)
FENESH, T., Investigation of the α spectrum of Bi isotopes, 20: 22000

EGORENKOV, P. M., Reconstruction of IRT research reactor, 20: 22497 (IAE-992)
EGOROENKOV, P. M., Increase of power of VVR-S reactors, 20: 22498 (IAE-993)
EGUCHI, Hiroko, Low-temperature resistivity, magnetic susceptibility, and superconducting transition temperature in La containing rare-earth impurities, 20: 21873 (NP-15936)
EHHALT, D. H., Peak in tritium content of atmospheric hydrogen following accident at Windscale, 20: 20889
EHLERS, Vernon J., Nuclear spin and magnetic dipole moment of 39-min ^{190}Au, 20: 22140
EHMERT, A., Measurements of high energetic auroral radiations with balloon-borne detectors in 1962 and 1963, 20: 21838
EHN, D. C., Wide-angle electron-pair production, 20: 22146
EHRMANN, Charles H., Digitized spark chamber for γ astronomy, 20: 21121
EIBEN, B., Further analysis of neutrino interactions in the CERN heavy liquid bubble chamber, 20: 21597 (CERN-65-32, pp 25-30)
EICH, W. J., Reactivity worth of rod-cluster control elements, 20: 22395
EICHELBERGER, J. F., Prog. rpt., 7/65, 20: 20806 (MLM-1274)
EICHELBERGER, J. F., Prog. rpt., 8/65, 20: 20807 (MLM-1287)
EICHELBERGER, J. F., Prog. rpt., 10/62, 20: 20553 (MLM-1142)
EICK, Harry A., Vaporization behavior of europium dicarbide, 20: 20666
EIDMAN, V. Ya., Longitudinal oscillations of a nonuniform plasma, 20: 22284
EIDMAN, V. Ya., Plasma flux instability in inhomogeneous media, 20: 22201
EIKERT, B., Effects of γ rays on polyriboadenylic and polyribouridylic acids, 20: 20411
EIKHICHEV, O. I., Mass spectrometric investigation of source of positive ions operating at low gas pressure, 20: 21457
EKSPONG, A. G., Nucleon-antinucleon annihilation as source of energy for certain radioastronomical objects, 20: 21684
ELBERSOLDT, F., Method for calculating flux evolution in a fast-neutron multiplying medium as function of time, space, and energy, 20: 21950
ELDRIDGE, James S., Gamma-ray branching ratios for ^{116}In, ^{147}Nd, and ^{141}Ce, 20: 22091
ELEND, H. H., Anomalous magnetic moment of the muon, 20: 21656
ELISEEV, S. M., Inelastic interactions of cosmic-ray particles with atomic nuclei at very high energies, 20: 21999 (JINR-P-2552)
ELIUTIN, V. P., Dissociation of $NbCl_5$ on Nb and carbide surfaces, 20: 21241 (LA-tr-66-15)
ELKINGTON, W. E., Physical and mechanical properties of U–Nb–Zr alloy, 20: 21356 (UCRL-14724)
ELLINGER, F. H., Plutonium–americium system, 20: 21339 (LA-DC-7095)
ELLIOTT, F., Plant measurement, sampling, and analysis for accountancy purposes, 20: 20830
ELLIOTT, F., Plant measurement, sampling and analysis for accountancy purposes with particular reference to separation plants at Windscale, 20: 20972
ELLIOTT, J. P., Sample holder for ESR studies on x-irradiated fibers, 20: 20846
ELY, John T. A., High-resolution pulse-height analyzer for satellite use, 20: 21126
EMANUEL', N. M., Relation between radioprotective and antineoplastic effects of antioxidant-inhibitors, 20: 20506
EMCH, Gerard G., Origin of phase transitions in various models, 20: 21872 (AD-627189)
EMELEUS, H. J., Advances in inorganic chemistry and radiochemistry. VII., 20: 20658
EMERY, F. E., Temperature dependence of average energy per pair in semiconductor detectors, 20: 21102
EMERLING, R. A., Rocket gamma scanning of nuclear bursts, 20: 21129
EMERSON, J. A., Effect of γ irradiation on microflora of fresh water fish. I., 20: 21203
EMMA, L. C., Conversion of high-level radioactive waste to phosphate glass, 20: 22509 (BNL-10109)
ENDO, Kenji, GM counter, M2311, 20: 21092
ENDOW, N., Prog. rpt. on sorption of gases on metal surfaces, annual, 2/15/65–2/14/66, 20: 21351 (SRIA-425-8)
ENGELAND, T., Shell model calculations in the calcium isotopes, 20: 22096
ENGELMANN, F., Heat transport by radiation in solids, 20: 22329
ENGLE, G. B., Effect of fast neutron irradiation from 495 to 1035°C on nuclear graphites, 20: 21421 (GA-6888)
ENJOJI, Hiroshi, Magnetic interruption of large currents through a linear discharge plasma, 20: 22212
EPSTEIN, H. T., Chloroplast development in Euglena. XIII., 20: 20450
EPSTEIN, Samuel, Oxygen isotope fractionation in the system dolomite calcite-carbon dioxide, 20: 20691
ERENRICH, Eric H., Tritiated alumina as a reagent for self-labeling chromatographic analyses, 20: 20575
ERICKSON, Duane G., Anemia in mice infected with γ-irradiated or non-irradiated Schistosoma mansoni, 20: 20446
ERICKSON, P. B., Radiological prediction and monitoring of tests at the

(JINR-P-2553)
FENG, Hsi-chang, Width of potential barrier for spontaneous fission by gg nuclei, 20: 22014 (KFK-tr-185)
FERGUSON, A. T. G., Scattering of fast neutrons by ^{238}U, 20: 22056
FERNANDEZ, H. G., Low activation materials for nuclear test vault construction, 20: 20869
FERRARI, H. M., In-pile measurement of UO_2 thermal conductivity, 20: 21361 (WCAP-2923)
FERRARI, Henry M., Mechanism and kinetics of nitrogen release from UO_2 at elevated temperatures, 20: 21360 (WCAP-2098)
FERRARI, Italo, Force-free field of magnetohydrostatics, 20: 21792
FERRARI, R. A., Photochemical synthesis of norepinephrine from tyramine, 20: 20409
FERREIRA, P. Leal, Solutions for a Feynman-Gell-Mann particle in a Coulomb field, 20: 21767
FERRONI, S., Photoneutron production from C, Al, and S by bremsstrahlung up to 200 Mev, 20: 22094
FESSEL, R., Pair production by 5-Bev photons in carbon, 20: 21664
FETIZON, Marcel, Reduction of α,β-ethylenic ketones with lithium and deuterated propylamine, 20: 20799
FETTER, A. L., Equivalence of vortices and current filaments, 20: 21800
FICENEC, John Robert, $K^- + p \rightarrow \bar{K} + N + \pi$ reactions at 1.33 Bev/c, 20: 21615 (COO-1195-52)
FICHARDT, T., Natulan (procarbazine) combined with radiotherapy in management of inoperable malignant melanoma, 20: 20504
FIEBIG, R., Air-scattered radiation in environment of critical facility, 20: 22386
FIELD, E. O., Autoradiographic differentiation of tritium and another β emitter by a combined color-coupling and double stripping-film technique, 20: 20605
FIELD, R. E. Jr., Electron temperatures in several r-f plasmas, 20: 22194
FIELDS, J. C., Electrophoretic power generation in thermally ionized plasmas, 20: 22173 (AD-623788)
FIETZ, W. A., Annihilation instability in hard superconductors, 20: 21927
FILIPPOV, A. T., Model of weak interactions of baryons and leptons, 20: 21714 (JINR-P-2578)
FINGER, M., Investigation of ^{148}Eu irradiation, 20: 22003 (JINR-P-2581)
FINGERHUT, A. G., Effect of whole-body irradiation (300 R) on experimental bladder calculus formation in rats, 20: 20467
FINK, H. J., Contribution of surface currents to magnetic hysteresis in mixed state of a type II superconductor, 20: 21886
FINKELMEYER, H., Calculation of forces and inductances for the hexapole experiment, 20: 22181 (IPP-1/45)
FINLAY, Roger W., Elastic neutron scattering from B, C, K, and Ca at 14.0 Mev, 20: 22119
FIORE, A., Determination of inception of nucleate boiling in terphenyl OM2 in conditions of forced convection, 20: 20709 (EUR-2442.f)
FIORELLI, M., Eurex plant, 20: 20815
FIORIDO, M., Compensation of thermic effects in semiconductor junctions used for measures in logarithmic scale, 20: 20992
FIORINI, E., Experimental investigation of the K_{e3} decay, 20: 21658
FIRSOVA, L. P., Gas-liquid chromatography for determining specific activity and survival of mother compounds labeled with recoil atoms, 20: 20783
FISCHBACH, D. B., Tensile and structural properties of glassy carbon, 20: 21338 (JPL-TR-32-842)
FISCHER, E., Thermo-siphon water flow irradiation rig for reactor material testing, 20: 21266
FISCHER, Fred W., Effect of electrode size in MHD generators with segmented electrodes, 20: 21571
FISCHER, H., Radiation-induced reaction in polyethylene oxide, 20: 20766
FISCHER, M., Shock front conditions in two-phase flow including the case of desuperheat, 20: 22348
FISHER, Frank R., Conference on radiation research, U. S. Army Natick Labs., Mass., 1/63, 20: 20726 (PB-181506)
FISHMAN, Alan M., Gamma spectrometric measurement of ^{235}U in 24-in. × 24-in. × 12-in. absolute air filters and associated economics of uranium recovery, 20: 20564 (NYO-10740)
FITTING, W., Determination of inorganic iodine in human serum, 20: 20401
FITZSIMMONS, B. W., Supposed complexes of uranium(VI) and uranium(IV) with triphenylphosphine, 20: 20679
FIZZOTTI, C., Behavior under irradiation of low-alloyed uranium, 20: 21436
FIZZOTTI, C., Metallurgical studies of some uranium alloys, 20: 21372
FLATO, M., Masses of nonstrange pseudoscalar mesons and the generalized Klein-Gordon equation, 20: 21744
FLEISCHER, R. L., Simple detectors for neutrons or heavy cosmic ray nuclei, 20: 21091
FLEMING, Paul Byron, Determination of thermal neutron flux distribution in a hexagonal lattice cell, 20: 22371 (AD-621026)
FLETCHER, N. R., $^{12}C(d,p\gamma)^{13}C$ angular distributions and correlations near threshold, 20: 22087
FLINN, P., Constant-velocity Moessbauer drive systems, 20: 21081
FLOM, D. G., Friction and cleavage of lamellar solids in ultrahigh vacuum, 20: 21366
FLORENZANO, G., Influence of irradiated nitrogen on the nitrogen-fixing activity of blue-green algae, 20: 20408
FLYAGIN, V. A., Trochoidal bunching with high space charge, in crossed electric and magnetic fields, 20: 21450
FOCK, V. A., Application of Laplace transformation to the theory of radiation, 20: 21768
FOGEL', A. A., Superconducting alloy in the Nb–Ga systems, 20: 21897
FOMENKO, V. S., Thermionic emission from CeC_2, 20: 21397
FOMIN, G. S., Fabrication of thin plates from refractory carbides, 20: 21303
FORBES, D. H., Growth of single-crystal silicon on beryllium oxide, 20: 21249
FORCELLA, A. A., Professional nuclear materials management, 20: 20968
FORD, Franklin C., Pulsed x-ray prompt gamma simulator, 20: 20838 (AD-624019)
FORD, J. L. C. Jr., Total neutron yield from the reaction $^{14}C(\alpha,n)^{17}O$, 20: 22110
FORD, William F., Limiting forms of the screened Coulomb T matrix, 20: 21731
FORMISANO, V., Formal properties of the ground-state wave function for even-even nuclei, 20: 22093
FORREST, D. J., Directional neutron detector for space research use, 20: 21117
FORST, G., Energy filtering of scattered ions, 20: 21536
FORT, Robert E., Some aspects of reactor safety systems, 20: 22358
FORTESCUE, Peter, Nuclear reactor control rod drive mechanism, 20: 22356
FORTUNE, R. D., Collimators for r-f separated beam, 20: 21468 (CERN-66-10)
FOSTER, Ellis L. Jr., Development of Th–^{233}U irradiation specimens, 20: 21288 (BMI-1761)
FOU, C. M., Levels of ^{42}Sc from $^{40}Ca(^3He,p)^{42}Sc$ and $^{40}Ca(^3He,p\gamma)^{42}Sc$, 20: 22073
FOU, C. M., Reaction $^{60}Ni(^3He,\alpha)^{59}Ni$ at 15 Mev, 20: 22127
FOWLER, I. I. L., Large-volume coaxial germanium γ spectrometers, 20: 21104
FOWLER, J. F., Problems of reader design and measurement error in LiF thermoluminescent dosimetry, 20: 21061
FOYE, Lawrence V. Jr., Myocardial infarction due to postirradiation fibrosis of the coronary arteries, 20: 20468
FRAHN, W. E., Strong absorption model for inelastic nuclear scattering, 20: 22086
FRANCIS, L. S., Bibliography on plasma sheath, 20: 22177 (CLM-Bib-6)
FRANCOIS, B., Particular aspects of utilization of UO_2 as fuel in power reactor, 20: 22422
FRANCOIS, Centre, Pressure-temperature diagram of pure beryllium, 20: 21363 (UCRL-Trans-1299(L))
FRANK, Max, Effect of operating conditions and transistor parameters on gain degradation, 20: 21169
FRANK, R. G., Material and process specifications for refractory alloy and alkali metals, 20: 21293 (R-66SD3007)
FRANKFORT, J. H., Feasibility and conceptual design study of wood-plastic combinations process, 20: 21181 (ORNL-IIC-7, pp 32-48)
FRANKLIN, J. B., Dangers of radiation in cephalometric radiography, 20: 20543
FRANKOVSKY, F. A., Reactor and linear accelerator induced effects in dielectrics, 20: 21151 (IBM-66-825-1944)
FRANZINETTI, C., Conference on experimental neutrino physics, CERN, 1/65, 20: 21594 (CERN-65-32)
FRANZINETTI, F., Fluxes of neutrinos and antineutrinos produced at CERN, 20: 21602 (CERN-65-32, pp 111-14)
FRASCA, A. J., Elastic neutron scattering from B, C, K, and Ca at 14.0 Mev, 20: 22119
FRECHE, John C., NASA developments in Co-base superalloys, 20: 21237 (N-65-29395)
FRED, Sallie, Effects of bacterial endotoxin on the occurrence of spleen colonies in irradiated mice, 20: 20512
FREED, J. J., Changes in uv absorbency of cultured cells during interphase as estimated by flying-spot microscopy, 20: 20473
FREEMAN, Robert G., Patterns of cutaneous pigmentation following sunlight irradiation, 20: 20458
FREEMAN, S., Structure of 20Cr–25Ni–Nb steel after aging in temperature range 600 to 800°C, 20: 21355 (TRG-Report-1168)
FREESE, C. H., Fast neutron transient detection hodoscope for reactor fuel meltdown studies, 20: 21131
FRENCH, J. Bruce, Light strongly deformed nuclei, 20: 21976 (BNL-948, pp 337-79)
FRENCH, J. Bruce, Single-nucleon transfer reactions, 20: 21971 (BNL-948, pp 1-65)
FRENCH, R. L., Gamma energy and angular distributions above infinite fallout field, 20: 20878 (AD-612030)

FRENZEL, W., Control of source and special nuclear material at Eurochemic, 20: 20831
FRICKE, M. P., Inelastic scattering of 40-Mev protons by ^{208}Pb, 20: 22101
FRIEDMAN, Herbert, Probing of the dynamical response of a plasma, 20: 22175 (AD-624081)
FRIEND, C. W., Reactor yield calculations for 81 radioisotopes produced by (n,γ) reactions, 20: 21214 (ORNL-IIC-8)
FRISCH, W., Safety and cost analysis of 1000-Mw(e) sodium-cooled fast power reactor, 20: 22451
FROEHNER, K. R., Thermo-siphon water flow irradiation rig for reactor material testing, 20: 21266
FROELICH, H., Electron energy measurements of the race-track microtron beam, 20: 21461 (AD-624038)
FROELICH, Reinhard, Theory of Doppler coefficients of fast reactors with consideration of mutual shielding of resonances, 20: 22378 (KFK-367)
FROISSART, M., Introduction to strong interaction physics, 20: 21773
FROLOV, G. V., Regge pole behavior of scattering amplitude in quantum electrodynamics, 20: 21871
FRONSDAL, C., Mass formulae for baryons in SU_3, 20: 21739
FROSCH, R., Elastic electron scattering from magnetic multipole distributions of ^{6}Li, ^{7}Li, ^{9}Be, ^{10}B, ^{11}B, and ^{14}N, 20: 22120
FROSCH, R. A., Concept of a large-aperture seismic array, 20: 20909
FROSINI, Vittorio, Effects of nuclear radiations on structure and molecular motions in crystalline stereoregular polymers, 20: 20753
FRUCHARD, Y., Nuclear materials management in relation to safety and criticality control, 20: 20974
FRUTH, Hans, Cost determination and comparison of nuclear and fossil-fueled dual-purpose power and desalination plants, 20: 22461
FRYE, G. M. Jr., Photographic spark chamber for manned satellites, 20: 21122
FU, C. M., K+p interactions at 4.6 Bev/c, 20: 21629 (UCRL-16332)
FUERST, W., Oxidation products of ergosterol. I., 20: 20738
FUHS, G. Wolfgang, Action of uranyl salts on the structure of the bacterial nucleoid. I., 20: 20392
FUJIBAYASHI, Keiji, Semiconductor nuclear particle detectors. II., 20: 21077
FUJIMOTO, Yasuo, Selective ^{2}H- and ^{3}H-labeling reaction of c-terminal amino acids through oxazolone, 20: 20714
FUJIMOTO, Yoichi, Monte Carlo analysis of electromagnetic cascade showers, 20: 21559
FUJITA, Iwao, Energy and angular distributions of protons from ^{64}Zn bombarded by 14-Mev neutrons, 20: 22048
FUJITA, Mototsugu, Design study of CO_2 gas-cooled power reactor, 20: 22432
FUJITA, Yoshihiro, Injection trapping of high-energy molecular ions into the mirror field with the r-f electric field. II., 20: 22207
FUKS, I. M., Effect of sea surface structure upon spatial characteristics of scattered radiation, 20: 20908
FUKUNAGA, K., 3- State in ^{28}Si and ^{24}Mg, 20: 22107
FULIGNI, F., X-ray scanning of sky in 20- to 200-kev range, 20: 21490
FULTYN, R. V., Radiation measurements of effluent from Kiwi-TNT experiment, 20: 22458 (LA-3395)
FULTZ, S. C., Epithermal fission cross section of ^{235}U, 20: 22012 (UCRL-14606)
FURLAN, G., Evaluation of $N^{*}_{\Delta}N$ weak coupling constants, 20: 21655
FURUI, Shin-ya, Pole model of nonleptonic decay consistent with decay parameters and sum rules, 20: 21688
FURUTA, Junichiro, Discharge figures in dielectrics by electron irradiation, 20: 21440
FUSCHILLO, N., Oxidation of thin evaporated rhenium films, 20: 21274
FUSHIMI, Kozo, Conductivity of a gas with suspension, 20: 21575
FUZIMOTO, Ukio, Results of physical examination of atomic bomb casualties, 20: 20480
FUZINAGA, Utaka, Results of physical examination of atomic bomb casualties, 20: 20480

G

GABAGLIO, M., Fabrication of ThO_2–UO_2 ceramic fuel, 20: 21301
GABAGLIO, M., Technological and economical improvements in fabrication of UO_2 ceramic fuel, 20: 21300
GABRIEL, J. R., Computation of Moessbauer spectra, 20: 22159
GAILLARD, J. M., Lower limit for mass of the intermediate boson, 20: 21596 (CERN-65-32, pp 11-24)
GAINTSEVA, V. D., Relation between radioprotective and antineoplastic effects of antioxidant-inhibitors, 20: 20506
GALBRAITH, W., Structure in the pion-proton total cross section between 2 and 7 Bev/c, 20: 21661
GALE, Richard H., Nuclear reactor control rod having particulate core, 20: 22368
GALINDO, A., G_2 symmetry and leptonic decays, 20: 21719
GALKOV, V. A., Obtaining electron bunches of minimum length from klystron-type buncher, 20: 21014
GALLI, M., X-ray scanning of sky in 20- to 200-kev range, 20: 21490
GAMBINO, R. J., Magnetic transformation in heavy rare-earth alloys with each other, 20: 21409
GAMBINO, R. J., Preparation of rare earth nitrides by reactive arc melting, 20: 21244
GANDOLFI, A., X-ray scanning of sky in 20- to 200-kev range, 20: 21490
GANGE, Jean-Marie, Standardization of recorded spectra using Fabry-Perot photoelectric spectrometer, 20: 20662
GANGLBERGER, E., New borides with the $Cr_{23}C_6$ structure, 20: 20685
GANS, P., Supposed complexes of uranium(VI) and uranium(IV) with triphenylphosphine, 20: 20679
GARDNER, Leonard B., Applications of radioisotopes for naval field establishments, 20: 21176 (AD-621440)
GARELIS, E., Prog. rpt. on pulsed neutron application to power reactor startup, 7–10/65, 20: 22414 (GEAP-4961)
GASKELL, Tom, Underground tests: the next step, 20: 20906
GASS, Arthur E., Substrate protection of enzymes against ionizing radiation, 20: 20514
GASSER, M., Determination of conversion ratios of 191-kev transitions in ^{197}Au, 20: 22057
GASTEBOIS, J., Reaction $^{180}Hf(d,p)^{181}Hf$, 20: 22106
GAT, Joel R., Determination of characteristics of water bodies with aid of bomb-produced tritium pulses, 20: 20894
GAULE, Gerhart K., Symposium on Boron, Paris, 7/64. II., 20: 21251
GAULIN, C. A., Friction and cleavage of lamellar solids in ultrahigh vacuum, 20: 21366
GAUSE, R. L., Effects of nuclear radiation dielectric materials, 20: 21152 (N-65-22353)
GAUTAM, V. P., Coupling constant sum rules for decay of $J^{\pi} = 2^{+}$ nonet in broken SU(3), 20: 21640
GAVRILOVSKAYA, E. N., Cathode spots of pulsed discharge between parallel electrodes, 20: 22292
GAZZA, George E., Evaluation of refractory sheet metals. II., 20: 21322 (AMRA-TR-65-25)
GEBELT, Robert E., Vaporization behavior of europium dicarbide, 20: 20666
GEDEONOV, L. I., Determination of small quantities of radioactive substances in surrounding media, 20: 20616
GEDEONOV, L. I., ^{137}Cs behavior during the analysis of atmospheric precipitation specimens, 20: 20625
GELBARD, E. M., Properties of P_L and double P_L relaxation lengths in presence of anisotropic scattering, 20: 21958
GEMMELL, D. S., Experience with an on-line computing system in low-energy nuclear physics experiments, 20: 22031
GEMMELL, D. S., Measurement of spins of some states in ^{56}Fe, 20: 22126
GEORGE, D. E., AEC program of nuclear materials management, 20: 22527
GERASIMOV, S. B., Photon absorption by nucleons and nucleon dimensions in quark model, 20: 21625 (JINR-P-2619)
GERBAULET, K., Effect of radiations on the detoxification of α-methylnaphthalene, 20: 20439 (EUR-2628.i)
GERBER, H.-J., Possible spark chamber experiment with antineutrinos, 20: 21607 (CERN-65-32, pp 161-8)
GERSHENSON, S. M., Mutability in the wasp Mormoniella vitripennis, 20: 20464
GERSTEIN, I. S., Single-particle representations of current algebras, 20: 21750
GERSTENBERG, H. M., Three-body photodisintegration of ^{3}He, 20: 22117
GETOFF, N., Cobalt-60 γ-induced carboxylation of methylamine, 20: 20732 (SGAE-CH-21/1965)
GHIZARI, Eugenia, Radioprotective effect of glycine during x irradiation. II., 20: 20517 (NP-15925)
GHOSE, P., Coupling constant sum rules for decay of $J^{\pi} = 2^{+}$ nonet in broken SU(3), 20: 21640
GHOSH, N. N., Scheme related to 4-dimensional Lorentz transformation, 20: 21847
GIBBONS, F. L., Nanosecond neutron time-of-flight spectrometer using avalanche transistors, 20: 21110
GIBBONS, P. E., Design and application of lithium-drift silicon diodes as nuclear radiation detectors, 20: 21064
GIBBS, B. W., Collisional effects in electromagnetic wave propagation in plasmas, 20: 22228
GIBBS, B. W., Propagation in plasmas along the magnetic field. I., 20: 22236
GIBBS, B. W., Propagation in plasmas along the magnetic field. II., 20: 22237
GIBBS, Hugh Harper, Fluorination with uranium hexafluoride, 20: 20717
GIBBS, J. E., Autoradiographic differentiation of tritium and another β emitter by a combined color-coupling and double stripping-film technique, 20: 20605
GIBBY, R. L., Stresses in Zy-2 cladding during vibratory fuel loading, 20: 21289 (BNWL-194)
GILBERT, A., Approach to nuclear statistical equilibrium, 20: 21492

GILBERT, A., Fractographic study of tungsten and dilute tungsten–rhenium alloys, 20: 21380
GILLES, P., Perturbing effects of water vapor on mechansim of graphite oxidation in presence of oxygen (500 to 650°C), 20: 21285
GILLILAND, R. G., Elevated temperature mechanical properties of welds in a Ni–Mo–Cr–Fe alloy, 20: 21395
GILLIS, J., Magnetohydrodynamic flow in inlet region of straight channel, 20: 21801
GILMORE, J. S., Symmetry of neutron-induced ^{239}Pu fission at individual resonances, 20: 22135
GILMORE, Robert C., Physical and mechanical properties of selected wood-plastic combinations, 20: 21348 (ORNL-IIC-7, pp 22-5)
GILMOUR, G. A., NERVA reactor instrumentation, 20: 22484
GILSON, Verle A., Plasma-coupling medium for a traveling-wave tube amplifier, 20: 20985 (N-65-29669)
GIMPL, M. L., Oxidation of thin evaporated rhenium films, 20: 21274
GINDIN, L. G., Kinetics of DNA denaturation under ultraviolet radiation, 20: 20412
GINIER, R., Experimental results on engineering model of Rapsodie, 20: 22501 (EURFNR-49F)
GINOCCHIO, J. N., $f_{7/2}$ model of ^{46}V, ^{47}V, ^{49}Cr, and ^{50}Mn, 20: 22131
GINZBURG, V. L., Superconductivity. II., 20: 21874 (TT-62-23147)
GIORDANO, P., Safety and cost analysis of 1000-Mw(e) sodium-cooled fast power reactor, 20: 22451
GIORGADZE, N. P., Interaction of a charged particle beam with a confined plasma, 20: 22286
GIORGI, M., Determination of branching ratios among neutral decay modes of the η particle, 20: 21627 (LNF-66/9)
GIRAUD, R., Comparison of economic aspects of treatment of fission products from installations processing irradiated natural uranium, 20: 22517
GIRAUD-HERAUD, Francois, Microanalysis by X-ray emission in an electron microscope, 20: 20593
GITTELMAN, B., Wide-angle electron-electron scattering on the Princeton-Stanford storage rings, 20: 21588 (AD-623658)
GITTLEMAN, J. I., Measurements of current-dependent reactance of superconductors having very small coherence distance, 20: 21919
GITTUS, J. H., System C.I.D. Illustration of use of digital computer in storage, interpretation and recovery of materials data, 20: 21354 (TRG-Report-1160)
GIUBERT, Bertrand, Nuclear fuel pellets of special profiles and method of their preparation, 20: 21316
GIULIANI, Pietro, Radiometric measurements following nuclear incidents, 20: 20962
GLAGOLEVA, N. N., Solubilities of Cr, Mo, and W in Al, 20: 21362 (SC-T-66-0723)
GLASKO, V. B., Intermingling of particles in a composite magnetic field trap, 20: 22274
GLAZOV, V. M., Radiochemical analysis using two γ-radioactive isotopes, 20: 20637
GLAZOV, V. M., Solubilities of Cr, Mo, and W in Al, 20: 21362 (SC-T-66-0723)
GLAZOV, V. M., Use of several γ-radioactive isotopes in radiochemical analysis, 20: 20638
GLEN, H. M., Engineering design practices for facilities containing radioactive materials, 20: 20942 (ORNL-TM-1459)
GLENDENNING, Norman K., Inelastic scattering based on a microscopic description of nuclei, 20: 22118
GLOERSEN, P., Energy efficiency trends in a coaxial gun plasma engine system, 20: 20872
GLOTIN, Ph., Behavior of semiconductor devices subjected to irradiation, 20: 21156
GLUCKSMANN, Alfred, Ten-year results of individualized treatment of carcinoma of the cervix based on the analysis of serial biopsies, 20: 20536
GOBILLON, Yves, Nuclear quadrupole resonance and its applications in chemistry, 20: 20699
GODEK, Jerzy, Determination of ^{90}Sr by Y method, 20: 20586
GODSHALL, J. L., Prog. rpt. on evaluation of refractory/austenitic bimetal combinations, 9/22–12/22/65, 20: 21295 (WANL-PR-(EE)-002)
GOENVEC, H., Study of compounds formed at temperatures above 600°C by action of carbon dioxide on graphite, 20: 20702
GOFMAN, John W., Ischemic heart disease, atherosclerosis, and longevity, 20: 20370 (UCRL-14658)
GOLANT, V. E., Toroidal machine for adiabatic compression of plasma, 20: 22299
GOLD, Kenneth, Microbiological assays of seawater using radioisotopes, 20: 20368 (CONF-640309-1)
GOLD, Louis, Photovoltaic theory for homogeneously irradiated semiconductor, 20: 21437
GOLD, T., Simulation of magnetic fields produced in the moon by trapped field of solar plasma stream, 20: 21502
GOLDAK, J., Lattice parameters, thermal expansions, and Grueneisen coefficients of Zr at 4.2 to 1130°K, 20: 21391
GOLDBERG, D. A., Relevance of bombardment-induced Moessbauer effects in iron to radiation damage theories, 20: 21444
GOLDBERG, Irwin, Electromagnetic form factor of the neutrino, 20: 21669
GOLDBLITH, S. A., Microbiology of radiation preservation of foods, 20: 21201
GOLDBLITH, Samuel A., Radiation preservation of foods—two decades of research and development, 20: 21194 (PB-181506, pp 155-67)
GOLDBLITH, Samuel A., Wholesomeness of irradiated foods, 20: 21207
GOLDFARB, L. J. B., Proton polarization and the spin-orbit potential, 20: 22116
GOL'DFARB, V. M., Conductivity in h-f induction discharge in argon, 20: 22280
GOLDHABDR, M., Search for double β decay in ^{48}Ca, 20: 21995 (CERN-65-32, pp 35-40)
GOLDHABER, G., K+p interactions at 4.6 Bev/c, 20: 21629 (UCRL-16332)
GOLDHABER, G. Scharff, Heavy strongly deformed nuclei, 20: 21977 (BNL-948, pp 380-453)
GOLDHABER, M., Summary of neutrino physics conference and closing remarks, 20: 21613 (CERN-65-32, pp 269-74)
GOLDHABER, S., K+p interactions at 4.6 Bev/c, 20: 21629 (UCRL-16332)
GOLDMAN, M., Environmental and biological factors affecting accumulation of ^{90}Sr and ^{137}Cs in deer and sheep, 20: 20388 (SAN-34-2)
GOLDRING, G., Gyromagnetic ratios on first excited 2^+ states in even Os isotopes, 20: 22055
GOLDSTEIN, G., Activation cross sections for reactions of 14.8-Mev neutrons with ^{99}Tc, 20: 22039
GOLDSTEIN, G., Half life and specific activity of ^{99}Tc, 20: 22036
GOLDSTEIN, N., Photon, neutron, and charged particle absorbed dose measurements with a portable microcalorimeter, 20: 21024 (AD-630693)
GOLICHENKOV, V. A., Pathogenesis of iodacetate cataract and its similarity to radiation cataract, 20: 20507
GOLLEY, Frank B., Development of a ^{137}Cs facility for ecological research, 20: 20380 (TID-22499)
GOLLIHER, K. G., Startup and operation of 1-Mw shield test and irradiation reactor, 20: 22500 (NAA-SR-11175)
GOLOVIN, B. M., Fluctuations of ionization losses, 20: 21515 (JINR-P-2515)
GOLSON, T. J., Design of high-temperature furnace (3,000°C), 20: 20842 (ORNL-TM-1410)
GOLSON, T. J., Engineering design practices for facilities containing radioactive materials, 20: 20942 (ORNL-TM-1459)
GONCHAROV, V. V., Increase of power of VVR-S reactors, 20: 22498 (IAE-993)
GONCHAROV, V. V., Reconstruction of IRT research reactor, 20: 22497 (IAE-992)
GOOD, R. H., Feasibility of experiment to observe the W produced in strong interactions, 20: 21610 (CERN-65-32, pp 181-94)
GOODMAN, B. B., Bulk properties of perfect type II superconductors, 20: 21931
GOPINATHAN, K. P., Upper limit of the half life of the ^{199m}Au isomer, 20: 22046
GORBANESCU, Gh., Structure of particles using the generalized relativity theory, 20: 21634
GORDON, G. E., Fractional chain yield of ^{126}Sb in thermal-neutron fission of ^{235}U, 20: 22044
GORDON, James, Angular resolution of critical scattering experiments, 20: 22325
GORDON, James, Production of monochromatic cold neutron beam with the use of monocrystals, 20: 21949
GORDY, Walter, Radiation chemistry in the solid state as studied with electron paramagnetic resonance, 20: 20729 (PB-181506, pp 85-103)
GORE, Jacques, Reduction of α,β-ethylenic ketones with lithium and deuterated propylamine, 20: 20799
GORELOV, P. N., Radiometric method of determining sulfur in naphthalene, 20: 20615
GORIN, E., Prog. rpt. on radiation-induced telomerization of methanol, final, 11/64–4/65, 20: 20724 (NYO-2978-44)
GORODINSKII, G. M., Recording of several particles with an acoustic spark chamber, 20: 21094
GOROWITZ, B., Energy efficiency trends in a coaxial gun plasma engine system, 20: 20872
GORZEGNO, W. P., Separately fired superheater—nuclear application at Indian Point, 20: 22455
GOTO, Katsumi, Extraction and spectrophotometric determination of thorium with 8-quinolinol, 20: 20576
GOTOH, H., Excitation functions for reactions induced by protons on Cd up to 37 Mev, 20: 22078
GOTSMAN, E., Peripheral production and decay parameters of $N^{*++}(1238)$ in $pp \to nN^{*++}(1238)$ at 5.5 Bev/c, 20: 21663
GOTTLIEB, I., Structure of particles using the generalized relativity theory, 20: 21634
GOUGH, C. E., Motion of Abrikosov vortices in a type II superconductor, 20: 21910

GOULIANOS, K., Determination of neutrino flux, 20: 21600 (CERN-65-32, pp 97-108)
GOURDIN, M., Unitary symmetry, 20: 21707 (CONF-640509(Pt.2), Paper 1)
GOURDIN, M., Unitary symmetry and weak interactions, 20: 21708 (CONF-640509(Pt.2), Paper 2)
GOVAERTS, P., Method for calculating flux evolution in a fast-neutron multiplying medium as function of time, space, and energy, 20: 21950
GOVE, Harry E., Heavy spherical nuclei, 20: 21975 (BNL-948, pp 269-336)
GOVE, Harry E., Light strongly deformed nuclei, 20: 21976 (BNL-948, pp 337-79)
GOVE, Harry E., Spin assignments by γ-γ correlations from aligned nuclei, 20: 21984 (BNL-948, pp 751-6)
GOVONI, Edward M., Performance of self-excited MHD generator, 20: 21564 (AD-627037)
GRACE, A. J., Simplification of oxygen-flask combustion procedure for preparation of samples for liquid scintillation counting, 20: 20570
GRACHEV, S. A., Measurement of activity of components in organic mixtures containing ^{14}C, 20: 20639
GRAD, Harold, Velocity gradient instability, 20: 22234
GRAHAM, C. D. Jr., Solid-state electrolysis of gadolinium, 20: 21253
GRAHAM, M. J., Adsorption of Kr and Xe on evaporated metal films, 20: 21387
GRANATSTEIN, Victor L., Wave propagation along warm plasma columns, 20: 22220
GRASHCHENKO, S. M., Extraction-radiometric determination of microgram amounts of lead by isotopic dilution method, 20: 20620
GRAY, Peter, Arrhenius parameters for elementary combustion reactions: H-atom abstraction from N-H bonds, 20: 20713
GRAYSON, Paul E., Purification and crystallization of B, 20: 21294 (TID-22221)
GREBENSHCHIKOV, S. E., Structure of magnetic surfaces in stellarator with double helical field, 20: 22298
GREEN, D. H., Excess radiogenic argon in pyroxenes and isotopic ages on minerals from Norwegian eclogites, 20: 20891
GREEN, L. L., Deuteron optical potentials and the $^{16}O(d,p)^{17}O$ reaction, 20: 22104
GREEN, P. E. Jr., Concept of a large-aperture seismic array, 20: 20909
GREEN, Ralph E., Conference on irradiated wood-plastic materials, Chicago, 9/65, 20: 21177 (ORNL-IIC-7)
GREEN, W. V., Stress dependence of creep rate of two commercial graphites, 20: 21340 (LA-DC-7626)
GREENBERG, A., Lung scanning following radioaerosol inhalation, 20: 20532
GREENDALE, A. E., Nuclear-charge distribution of fission-product chains of mass numbers 131-133, 20: 22136
GREENE, M. W., Production of ^{52}Fe, 20: 21993 (BNL-9168)
GREENE, N. D., Oxidation characteristics of lanthanide metals, 20: 21265 (RPI-2714-8)
GREENLEES, G. W., Proton polarization and the spin-orbit potential, 20: 22116
GREENSTEIN, H. B., Electron scattering from an aligned deformed nucleus, 20: 22124
GREENWOOD, N. N., Simple tandem Moessbauer spectrometer using pulse-height analysis, 20: 21069
GREGORY, W. D., Physical comparison of ATR and ATRC cores, 20: 22499 (IDO-17150)
GREIDER, Kenneth, Diffraction model calculations, 20: 21980 (BNL-948, pp 561-609)
GREINER, Walter, Magnetic properties of even nuclei, 20: 22085
GRENNING, D. A., Resistivity recovery of dilute alloys of silver, copper, and gold, proton-irradiated at 80°K, 20: 21445
GRENON, Michel, Boiling state of operating homogeneous reactor, 20: 22403
GRI, Norman J., Integrated-circuit charge-sensitive preamplifier, 20: 21112
GRI, Norman J., Temperature-compensated multielement logarithmic converter microcircuit, 20: 20999
GRIEM, H. R., Deviations from ionization equilibrium in plasmas generated by electric shock tubes, 20: 22250
GRIFFIN, D. S., DUZ-1—program for solving axisymmetric and plane elasticity problems on Philco-2000, 20: 20862 (WAPD-TM-555)
GRIFFIN, R. F., Safety and the nuclear plant engineer, 20: 22437
GRIFFITHS, P., Radiological prediction and monitoring of tests at the nuclear rocket development station, 20: 20954
GRIGOR'EV, V. A., Determination of the amounts of trace components captured by a macrocomponent precipitate, 20: 20619
GRIMES, D. M., Quantum theory in the electrical engineering curriculum, 20: 21846
GRIN, M., Cryostat in the gaseous phase, 20: 20984 (EUR-2710.f)
GRITCHENKO, Z. G., ^{137}Cs behavior during the analysis of atmospheric precipitation specimens, 20: 20625
GRIZ, G., Coolant ejection studies with analogy experiments, 20: 22350
GROMOV, K., Decay chain of $^{138}Nd \rightarrow {}^{138}Pr \rightarrow {}^{138}Ce$, 20: 22002 (JINR-P-2570)
GRONBECK, Marion P., School designs to resist integrated nuclear weapons effects, 20: 20868 (AD-626770)
GROSS, J., Comparison of ^{125}I and ^{131}I in diagnosis of thyroid disease. I., 20: 20533
GROSS, J., Comparison of ^{125}I and ^{131}I in diagnosis of thyroid disease. II., 20: 20534
GROSSE, A. V., Electrical and thermal conductivity of metallic K, 20: 21376
GROSSE, A. V., Empirical relationship between electric conductivity of Hg and temperature, 20: 21377
GROSSWEINER, L. I., Formation and bleaching properties of T bands in KCl, 20: 22322
GROUNES, M., Brittle-fracture problems in reactor pressure vessels, 20: 21228 (AE-221)
GROVE, G. R., Prog. rpt., 7/65, 20: 20806 (MLM-1274)
GROVE, G. R., Prog. rpt., 8/65, 20: 20807 (MLM-1287)
GROVE, G. R., Prog. rpt. on Pu research, 7-9/65, 20: 21342 (MLM-1301)
GROVE, G. R., Prog. rpt., 10/62, 20: 20553 (MLM-1142)
GROZ, P., Preparation of XeF_2, 20: 20678
GRUEHN, R., New phases in systems Nb_2O_5–WO_3 and Ta_2O_5–WO_3, 20: 21385
GRUNBERG, J., Fast timing circuits using storage diodes, 20: 21002
GRUPPELAAR, H., Reaction $^{32}S(n,\gamma)^{33}S$, 20: 22077
GRUVERMAN, Irwin J., Cam-driven, constant-acceleration Moessbauer spectrometer, 20: 21080
GRUVERMAN, Irwin J., Computation of Moessbauer spectra, 20: 22159
GRUVERMAN, Irwin J., Constant-velocity Moessbauer drive systems, 20: 21081
GRUVERMAN, Irwin J., Feedback in electromechanical drive systems, 20: 21079
GRUVERMAN, Irwin J., Measurements with black absorbers, 20: 22157
GRUVERMAN, Irwin J., Review of advances in physics, 20: 22327
GRUVERMAN, Irwin J., Standardization of differential chemical shift for ^{57}Fe, 20: 22158
GRUVERMAN, Irwin J., Symposium on Moessbauer effect methodology, New York City, 1/65. I., 20: 22156
GUALDI, C., Limits on size of visible quasars, 20: 21501
GUERIN, Marie-Therese, Binding of radio-calcium ^{47}Ca and radio-strontium ^{85}Sr with the plasma proteins in disease, 20: 20404
GUERRA, F., Divergence of renormalized VS convergence of regularized perturbative expansions in field-theoretical model, 20: 21741
GUERRA, F., Removal of point-loop ambiguities through finite-part renormalization, 20: 21742
GUERSEY, F., Group combining internal symmetries and spin, 20: 21772
GUESS, Floyd M., Sensitivity analysis of civil defense systems and components, 20: 20922 (AD-624704)
GUILBOT, A., Action of ionizing radiations on starch, 20: 20737
GUILLEM MONZONIS, Claudio D., Chemistry of the noble gases, 20: 20659
GUILLOU, R. B., Albuquerque–Los Alamos area (ARMS-II), 20: 20929 (CEX-61.6.2)
GUILLOU, R. B., Cincinnati Area (ARMS-II), 20: 20880 (CEX-62.6.5)
GUIOT, G., Diagnosis of space-occupying processes in the skull with a combination of γ encephalography and echo encephalography, 20: 20529
GULLBRING, Bengt, Action of x rays on blood typing sera, 20: 20425
GUNDZIK, M. G., Continuous representation of an indefinite metric space, 20: 21850
GUNSHOR, R. L., Decay of space-charge waves on electron beams, 20: 21452
GUPTA, B. P., Thorium and molybdenum complexes with myricetin, 20: 20674
GUPTA, K. C., Vector-meson mixing and sum rules in broken SU(3), 20: 21753
GUPTA, S. L., Gamma-gamma directional correlation in ^{123}Te, 20: 22089
GUPTA, S. S., Formation of complex compounds between rare earth nitrate and uranyl nitrate, 20: 20682
GURZO, V. V., Instability of small electron fluxes in crossed fields, 20: 21451
GUSEV, N. I., Polarographic determination of U in nitric acid media containing TBP. I., 20: 20630
GUSEV, N. I., Polarographic determination of U in nitric acid media containing TBP. II., 20: 20631
GUSEV, Yu. K., Measurement of activity of components in organic mixtures containing ^{14}C, 20: 20639
GUS'KOV, Yu. K., Effect of size of the inter-electrode spacing on operation of a cesium thermal converter, 20: 21568 (FEI-16)
GUS'KOV, Yu. K., Influence of krypton on operation of a thermionic converter, 20: 21579
GUS'KOV, Yu. K., Operation of a cesium diode with an admixture of an inert gas, 20: 21567 (FEI-15)
GUS'KOV, Yu. K., Operation of cesium thermionic converter in presence of xenon, 20: 21580
GUSMANO, E. A., Strontium and calcium skeletal discrimination determined

by compartmental analysis, 20: 20400
GUTS, Z. A., Superconducting alloy in the Nb–Ga system, 20: 21897
GUY, Roland, Geometrization of gravitational and electromagnetic fields, 20: 21842
GUYOT, P., Deformation mechanisms in hexagonal compact metals, 20: 21330 (EUR-2621.f)
GUZAK, Steven V., Treating acute Pu cases, 20: 20943 (RFP-453)

H

HAAS, P. A., Prog. rpt. on chemical technology, 7–9/65, 20: 20808 (ORNL-3916)
HAAS, T. W., Low-energy electron-diffraction study of molybdenum (110) surfaces, 20: 22319
HAASE, Erich, Drill possibilities in protection against mass destruction agents, 20: 20980
HABASHI, Fathi, Radioactivity in phosphate rock, 20: 20886
HABER, B., Peripheral production and decay parameters of $N^{*++}(1238)$ in $pp \rightarrow nN^{*++}(1238)$ at 5.5 Bev/c, 20: 21663
HABER, Gyula, ZR-2 critical assembly, 20: 22388
HADDOCK, R. P., Polarization of 45-Mev protons by complex nuclei, 20: 22128
HADJIOANNOU, F. T., Plausible lower bound on spectral functions of spinor propagator, 20: 21740
HAEFELE, W., Karlsruhe reference design of 1000-Mw(e) sodium-cooled fast breeder, 20: 22453
HAEFELE, W., Shock front conditions in two-phase flow including the case of desuperheat, 20: 22348
HAESELER, G., Production and properties of cerium and lanthanum oxychlorides, 20: 20680
HAGEE, G. R., Half life of 0.305-Mev level in ^{75}As, 20: 22038
HAGEE, G. R., Nuclear levels in ^{223}Ra populated by decay of ^{227}Th and ^{223}Fr, 20: 22008 (MLM-1337J)
HAHN, B., Lower limit for mass of the intermediate boson, 20: 21596 (CERN-65-32, pp 11-24)
HAHN, J., Nuclear pulse amplifiers—fundamentals and design practice. V., 20: 21008
HAHN, R. L., ^{3}He activation analysis, 20: 20565 (ORNL-P-1216)
HAHNE, F. J. W., Surface reactions of strongly absorbed nuclear particles in the adiabatic approximation, 20: 22062
HAIDUC, C., Heat calculations of boiling water reactors with nuclear superheating of the steam, 20: 22449
HAIDUC, C., Optimum temperature of feed water and optimum number of regenerative preheaters in atomic electric power plants, 20: 22448
HAJDUKOVIC, Srdjan, Amount of catecholamines in auricles of irradiated rabbits and their response to quinidine, 20: 20451
HAJDUKOVIC, Srdjan, Proliferative activity of bone marrow cells in mice bled immediately after irradiation with 600 R, 20: 20452
HAKE, R. R., Thermodynamic relationships for the ideal bulk type II superconductor, 20: 21901
HAKEN, J. W., Radioactivity control of the Keuringsdienst Van Waren, Amsterdam, 20: 20949
HAKKILA, E. A., Three-wavelength x-ray absorption edge method for determination of plutonium in nitrate media, 20: 20573
HALBERT, E. C., Energy spectra of 1p-shell nuclei calculated with the Hamada-Johnston potential, 20: 22102
HALBRONN, Georges, Boiling state of operating homogeneous reactor, 20: 22403
HALDEN, F. A., Prog. rpt. on growth parameters for refractory carbide single crystals, 12/64–3/65, 20: 21236 (N-65-23835)
HALL, D. F., Study of porous metal ionizers, 20: 21570 (N-65-29785)
HALL, P. L., Sulfur dioxide elimination in radiolytic decomposition of solid diaryl sulfonates, 20: 20760
HALL, Robert W., High-temperature creep behavior of Nb alloy, FS-85, 20: 21344 (N-65-26653)
HALLER, Kurt, Electromagnetic form factor of the neutrino, 20: 21669
HALLIDAY, I. G., Threshold behavior of 3-body partial-wave amplitudes, 20: 21747
HALLING, H., Method for low-level scintillation counting, 20: 21042 (SGAE-E-6/1966)
HALPERN, Isaac, Uncommon states of nuclear matter, 20: 21990 (BNL-948, pp 928-1004)
HALPERN, J., Isotopic exchange reactions of trans-hydridochlorobis(triethylphosphine) platinum(II), 20: 20701
HALSTED, A. S., Electrostatic and magnetic pinch effects in beam-generated plasmas, 20: 22221
HALTNER, A. J., Friction and cleavage of lamellar solids in ultrahigh vacuum, 20: 21366
HAMADA, Hakuo, Radiation-induced polymerization of isocyanic acid, 20: 20747
HAMBERGER, S. M., Scattering of electromagnetic waves by electro-acoustic plasma waves, 20: 22232
HAMILL, William H., Trapped electrons in γ-irradiated 3-methylpentane at −196°, 20: 20755
HAMILTON, J., Pion-nucleon scattering and conservation laws, 20: 21657
HAMILTON, J. C., Logical design of a digital pseudorandom noise generator, 20: 21001
HAMILTON, J. H., IEC method and conversion coefficients of 605-kev transition in ^{134}Ba, 20: 22026
HAMMER, P., Method for calculating flux evolution in a fast-neutron multiplying medium as function of time, space, and energy, 20: 21950
HAMMOND, R. H., Critical fields of superconducting vanadium films, 20: 21915
HANCE, A. B., High-speed electron-multiplier discriminator for mass-spectrometer ion detection, 20: 21039 (KAPL-3122)
HAND, J. E., Development of airborne surveillance instrumentation, 20: 20881 (DASA-1704)
HAND, R. B., Material and process specifications for refractory alloy and alkali metals, 20: 21293 (R-66SD3007)
HANEDA, Mikio, Design of heavy-water-moderated, boiling light-water type power reactor, 20: 22430
HANEMAN, D., Depths of low-energy ion bombardment damage in germanium, 20: 21438
HANKS, G. E., Acute mortality and recovery studies in sheep irradiated with ^{60}Co γ rays or 1-Mvp x rays, 20: 20487
HANLE, W., Suitability of electron postemission of $CaSO_4$ for dosimetry, 20: 20769
HANLEY, John T., School designs to resist integrated nuclear weapons effects, 20: 20868 (AD-626770)
HANNA, Alfred E., Applications of radioisotopes for naval field establishments, 20: 21176 (AD-621440)
HANNA, Stanley S., Capture reactions, 20: 21986 (BNL-948, pp 763-825)
HANRAHAN, L. R., High-speed electron-multiplier discriminator for mass-spectrometer ion detection, 20: 21039 (KAPL-3122)
HANSEN, Gordon E., Criticality dependence on neutron cross sections above 100 kev, 20: 22379 (LA-DC-7800)
HANSEN, L. K., Prog. rpt. on thermionic energy conversion, 11/64–7/65, 20: 21562 (AD-623142)
HARA, Yasuo, Mass differences, charges, and magnetic moments in SU(3) bootstrap theory, 20: 21757
HARARI, H., Three-particle final states and unitary symmetry, 20: 21763
HARDON, H. J., Radioactivity control of the Keuringsdienst Van Waren, Amsterdam, 20: 20949
HARDY, Edward P. Jr., Prog. rpt. on fallout program, 12/65–3/66, 20: 20882 (HASL-171)
HARDY, Gyula, Radiation-induced solid-state polymerization. XII., 20: 20763
HARGREAVES, J. K., Slow fluctuations between conjugate points in auroral absorption of cosmic noise, 20: 21820
HARNISCHMACHER, E., Electron content of the ionosphere and its fluctuations, 20: 21816
HAROCOPOS, B., Pressure-temperature diagram of pure beryllium, 20: 21363 (UCRL-Trans-1299(L))
HARPER, P. V., ^{103}Pd as a therapeutic radiation source, 20: 20542
HARRIS, Arthur M., Nuclear reactor control rod drive mechanism, 20: 22366
HARRIS, Thomas R. Jr., Potential of wood-plastic combinations in the sporting-goods industry, 20: 21190 (ORNL-IIC-7, pp 106-11)
HARRIS, W. R., 1.7-Mev anomaly in the $^{12}C(p,p)^{12}C$ reaction, 20: 22115
HARRISON, M. F. A., Cross section for production of He^{+} (2S) ions by electron impact excitation of ground state helium ions, 20: 21535
HARRISON, R. W., Prog. rpt. on advanced refractory alloy corrosion loop program, 10/65–1/66, 20: 21263 (NASA-CR-54911)
HARRISON, S., Junction counters produced by irradiation of silicon with dopant ions, 20: 21098
HARROP, P. J., Bibliographic review of self-diffusion in metal oxides, 20: 21321 (AERE-Bib-143)
HART, G. E., Conductance device for monitoring thin film growth, 20: 20987 (RFP-690)
HART, H. E., Analysis of tracer experiments. V., 20: 20393
HART, H. E., Analysis of tracer experiments. VI., 20: 20394
HARTE, J., Ω⁻ decay in a composite-particle model, 20: 21643
HARTLAND, A., Nuclear spin-lattice relaxation in liquid hydrogen, 20: 21525
HARTMAN, Charles W., Hot-electron plasma stability in mirror and minimum-B containment systems, 20: 22265
HARVEY, N. P., Operating characteristics of lithium-drift detectors, 20: 21103
HARY, Laszlo B., Prog. rpt. on pre-startup hydraulic tests on AF-NETF, final, 1961–65, 20: 22492 (AD-626861)
HASEGAWA, H., High-energy nuclear-active particles in extensive air showers at 5,200 m altitude, 20: 21544 (MIT-2098-227, Paper EAS-8)
HASHITANI, Hiroshi, Determination of traces of fluorine in uranium oxides by pyrolysis-alizarin complexone photometric method, 20: 20597
HASKELL, Richard E., Wave phenomena in ionized gases, 20: 22174 (AD-623789)
HASSELMAN, D. P. H., Mechanical properties of continuous-matrix,

dispersed-phase ceramic systems, 20: 21358 (UCRL-16552)
HASSION, Francis X., Falex pins coated by plasma-arc process, 20: 21319 (AD-621064)
HASSION, Francis X., Occlusion of various refractory materials in chromium plate on steel substrates, 20: 21286 (AD-621920)
HASTERLIK, Robert J., Consequences of ingestion by man of real and simulated fallout, 20: 20466
HATCH, Kenneth F., Analysis and description of a high-stability nuclear pulse amplifier, 20: 21000
HATCH, L. P., Conversion of high-level radioactive waste to phosphate glass, 20: 22509 (BNL-10109)
HATORI, Tadatsugu, Relaxation of velocity distribution of ions in a plasma, 20: 22205
HATTORI, Tadao, Present state of the analysis of nuclear fuels and reactor materials, 20: 20589
HATTORI, Toshio, Detergents for decontamination of sampling vials for liquid scintillation spectrometer, 20: 20960
HAUMANN, J., Submicrosecond synchronization of multiple chopper systems, 20: 21111
HAUSER, M. G., Cam-driven, constant-acceleration Moessbauer spectrometer, 20: 21080
HAUSER, O., Changes in electrical polarization of high polymers through action of ionizing radiation. I., 20: 21443
HAUSER, Raymond, Nuclear fuel pellets of special profiles and method of their preparation, 20: 21316
HAUSHILD, W. L., Determination of Columbia River flow times downstream from Pasco, 20: 20916
HAVEL, Vladimir, Cause of brittle fracture in tungsten wire, 20: 21396
HAYAKAWA, Satio, High-energy γ rays in the atmosphere and muons underground and underwater, 20: 21558
HAYASHI, I., Modular set of analog microcircuits intended for satellite experiments, 20: 20997
HAYASHI, Koichiro, Radiation-induced polymerization of isocyanic acid, 20: 20747
HAYASHI, Takemi, Possible scheme for nonleptonic decays of hyperons, 20: 21687
HAYES, F. H., Adsorption of carbon monoxide on evaporated metal films, 20: 21388
HAYNES, Alan George, Improvements relating to low alloy steels, 20: 21417
HAYNES, C. Vance Jr., Radiocarbon samples: chemical removal of plant contaminants, 20: 20798
HAYS, D. D., Bright-field grain structure etch for delta phase stablized Pu, 20: 21233 (BNWL-188)
HAYTON, B., Supposed complexes of uranium(VI) and uranium(IV) with triphenylphosphine, 20: 20679
HAYWARD, D. O., Adsorption of carbon dioxide on evaporated metal films, 20: 21389
HAZEN, E. E., Electron paramagnetic resonance study of solutions of europium in liquid ammonia, 20: 20668
HEACOCK, R. R., Intra- and interhemisphere differences in occurrence times of hydromagnetic emissions, 20: 21832
HECHT, Ralph Julius, Thermodynamic properties of Ca–Zn alloys, 20: 21335 (IS-T-76)
HECHT, Richard, Flux trapping threshold in Nb_3Sn, 20: 21926
HEDIN, R. A., Analog computer representation of the ring magnet power supply system of the ZGS, 20: 21488
HEEGER, A. J., Localized impurity states in metals: dilute alloys of Ni in Be, 20: 21390
HEFFAN, Howard, High-energy radiographic apparatus using a bubble chamber detector, 20: 21144
HEGEMAN, G. D., Synthesis of enzymes of mandelate pathway by Pseudomonas putida. III., 20: 20376
HEGEMAN, G. D., Synthesis of enzymes of mandelate pathway by Pseudomonas putida. II., 20: 20470
HEILIGMAN, F., Acceptance of irradiated foods, 20: 21199
HEIMEL, Sheldon, Thermodynamic properties of Cs up to 1500°K, 20: 21345 (N-65-26656)
HEINEMAN, R. E., PCTR operational techniques, 20: 22493 (BNWL-193, pp 21-9)
HEISE, B. H., Dependence of current degradation in superconducting solenoids on flux pinning energy and temperature, 20: 21920
HEITZ, F., Radioprotective power of some organophosphorus compounds, 20: 20515
HEKRDLE, Jan, Numerical photometer for film dosimetry, 20: 21070
HELHOLTZ, J., Boundary conditions in gap geometry, 20: 22390
HELHOTZ, J., Multigroup calculations of fast spectrum and fast fission effect, 20: 22506
HELLER, Leon, Applications of Coulomb-modified s-wave dispersion relation, 20: 21680
HELLWEGE, K.-H., Radiation-induced reaction in polyethylene oxide, 20: 20766
HELMER, J. C., Intensity of electron beams, 20: 21632
HELM, J. W., Effect of neutron irradiation on UHTREX graphite and C, 20: 21419 (BNWL-191)
HELMKEN, H. F., Vidicon spark chamber detector for γ astronomy, 20: 21119
HENDERSON, R. W., Radiation measurements of effluent from Kiwi–TNT experiment, 20: 22468 (LA-3395)
HENGLEIN, A., Reaction of white phosphorus with free radicals from γ-radiolyzed organic liquids, 20: 20736
HENGLEIN, A., Studies of chemical reactions by pulse radiolysis: free electrons and free radicals in aqueous solution, 20: 20735
HENLEY, E. M., Σ^--neutron interaction and strange-particle production, 20: 21681
HENLEY, Ernest, Diffraction model calculations, 20: 21980 (BNL-948, pp 561-609)
HENLEY, Ernest, Multi-body exit channels, 20: 21981 (BNL-948, pp 610-84)
HENNIG, K., Disappearance of quadrupole splitting in Moessbauer spectra of ^{57}Co-containing AgCl at 300°K, 20: 22340
HENRY, G. R., Measurement of anomalous gyromagnetic ratio of the muon, 20: 21630 (UCRL-16469)
HENSCHEID, J. W., Physical comparison of ATR and ATRC cores, 20: 22499 (IDO-17150)
HERAK, M. J., Determination of ion adsorption by radioactive tracer technique, 20: 20683
HERAS, C. A., Phenomenological and microscopic analysis of properties of even-even nuclei. B., 20: 21961 (AD-624028)
HERBELL, Thomas P., Investigation of extruded tungsten composites containing fibered or reacted additives, 20: 21374
HERBER, Rolfe H., Moessbauer spectroscopy: some recent applications to chemical problems, 20: 20684
HEREMANS, R., Design problems of pilot plants for volatilization recycling, 20: 20810 (ANL-Trans-250)
HERENGUEL, J., Aluminium and magnesium in nuclear metallurgy, 20: 21382
HERMAN, R. M., Finite nuclear mass and relativistic effects on the rotational constant of molecular hydrogen, 20: 21527
HERMANN, Gordon L., Radiolysis of solid ethyl iodide, 20: 20716 (AD-621022)
HERRMANN, Friedbert, Radioactivity and fossil content at the core of new red sandstone southwest of Braunschweig, 20: 20890
HERRMANN, G. F., Effects of velocity-dependent collision frequency on wave-plasma interactions, 20: 22256
HERTZBERG, A., Laser-generated implosions, 20: 22245
HERVIN, R. L., Evaluation of radiation dose to man from radionuclides released to Clinch River, 20: 22514 (ORNL-P-2021)
HERZMANN, A., Technique of labeling human serum albumin with ^{99m}Tc, 20: 20712
HERZMANN, H., Technique of labeling human serum albumin with ^{99m}Tc, 20: 20712
HESS, G. G., Prog. rpt. on radiation chemistry of silane, annual, 4/66, 20: 20725 (NYO-3570-2)
HESS, H. A., Electron content of the ionosphere and its fluctuations, 20: 21816
HESSON, J. C., Energy conversion, 20: 21566 (ANL-7055, pp 213-29)
HEUSENER, G., Safety and cost analysis of 1000-Mw(e) sodium-cooled fast power reactor, 20: 22451
HEUSER, H., Determination of magnetic moments of excited nuclear levels from the γ-γ angular correlation disturbed in magnetic field, 20: 22025
HEYNE, L., Changes in electrical polarization of high polymers through action of ionizing radiation. I., 20: 21443
HICK, H., Comparison of burnup determinations by means of monitor-activation and γ spectroscopy for an MTR element, 20: 21050
HICKS, R. M., Isothermal microcalorimeter operated in a water triple-point cell and designed for radioactivity measurements, 20: 21068
HICKS, W. T., Prog. rpt. on high-temperature thermoelectric generator, final, 6/14/63–6/14/64, 20: 21563 (AD-623591)
HIDGON, John P., Substrate protection of enzymes against ionizing radiation, 20: 20514
HIGATSBERGER, M. J., Magnetless dynamic mass spectrometer, 20: 20991
HIGHFILL, J. P., Analytical methods for U concentration measurements, 20: 20977
HIGHTON, C. J., Adaptation of the British Atomic Liability Law to international conventions, 20: 20948
HILBORN, H. S., Publications, 1965, 20: 22519 (DP-929(Suppl.2))
HILL, C. Clifton, Determination of O in Th and Y metals, 20: 20572
HILL, D. A., Dynamic polarization of protons in radiation-damaged polyethylene, 20: 22345
HILL, Helen Z., Chloroplast development in Euglena. XIII., 20: 20450
HILL, J. C., Ground-state splitting and Zeeman effect in erbium ethylsulfate at 1.6°K, 20: 21881
HILL, R. F., Effect of dark repair on uv sensitivity of bacteriophage-

infected bacteria, 20: 20471
HILLMAN, Manny, Production of ^{52}Fe, 20: 21993 (BNL-9168)
HINDS, S., Collective states of ^{209}Bi, 20: 22108
HINES, John F., Changes in 5-OH tryptamine content in rat brain tissues x-irradiated in vitro, 20: 20437 (CONF-650560-18)
HINES, John F., Oxygen uptake in rat brain tissues x-irradiated in vitro, 20: 20436 (CONF-650560-17)
HINTZ, Norton M., Inelastic scattering, 20: 21973 (BNL-948, pp 175-221)
HINTZ, Norton M., Two and more nucleon transfer reactions, 20: 21972 (BNL-948, pp 66-174)
HIPPE, Zdzislew, Gamma-radiation-induced chemical changes in polyvinyl butyral, 20: 20775
HIRAMATSU, Ichiro, Nuclear materials management at JAERI, 20: 21313
HIRAMOTO, Tetsuo, Nonequilibrium ionization of working gases for MHD generators, 20: 21573
HIRAOKA, Eiichi, Discharge figures in dielectrics by electron irradiation, 20: 21440
HIRATA, M., Recombination centers in γ-irradiated silicon, 20: 21439
HIRATA, Masako, Annealing of E center in irradiated silicon, 20: 22323
HIRATA, Mitsuji, Annealing of E center in irradiated silicon, 20: 22323
HIROTA, Kozo, Radiolysis of methylal and ethylene glycol dimethyl ether, 20: 20758
HIRSCH, E. H., Auroral effects and excess-energy electrons, 20: 21836
HO, Jack W., Nuclear radiation-resistant batteries, 20: 21162
HOCHMAN, A., Comparison of ^{125}I and ^{131}I in diagnosis of thyroid disease. I., 20: 20533
HOCHMAN, A., Comparison of ^{125}I and ^{131}I in diagnosis of thyroid disease. II., 20: 20534
HOCKETT, J. E., Powder rolling of tungsten and its alloys, 20: 21318
HODGE, F. G., Oxidation characteristics of lanthanide metals, 20: 21265 (RPI-2714-8)
HOEFFLINGER, B., Proposal for amplification of solid-state plasma waves with mass anisotropy, 20: 22342
HOEGAASEN, H., Absorption model and production of 2^+ mesons, 20: 21644
HOEGAASEN, J., Absorption model and production of 2^+ mesons, 20: 21644
HOENIG, M. M., Nucleon-nucleon boundary condition methods for nuclear matter, 20: 22022
HOFFMAN, E. E., New components for refractory metal–alkali metal corrosion test systems, 20: 21284
HOFFMAN, Zbigniew, Application of the 256-channel time-of-flight analyzer for measurement of amplitude spectra, 20: 21083
HOFFMANN, T. A., Error of approximations in quantum mechanics. I., 20: 21860
HOFFMANN, T. A., Error of approximations in quantum mechanics. II., 20: 21861
HOFFMANNER, A. L., Thermal-mechanical processing of precipitation-hardenable dispersion-hardened Nb alloy, 20: 21250
HOHMANN, G. L., New control techniques for NERVA reactors, 20: 22482
HOLDER, M., Experimental determination of the neutrino spectrum, 20: 21603 (CERN-65-32, pp 115-20)
HOLLEMAN, Gerald W., Infrared absorption of HD in liquid Ar, 20: 21528
HOLMBERG, N. E., Internal conversion study of $^{113}Cd(n,\gamma)^{114}Cd$, 20: 22066
HOLMES, Lawrence Bruce, Plasma density ahead of pressure driven shock waves, 20: 22168 (AD-622569)
HOLOWACH, J., New components for refractory metal–alkali metal corrosion test systems, 20: 21284
HOLTER, Oeivin, Excitation of the m = 2 mode by the helical instability, 20: 22247
HOLTZ, F. C., Prog. rpt. on V alloy studies, 12/65–2/66, 20: 21333 (IITRI-B6042-4)
HOLZAPFEL, H., Extraction of rare earths with TBP. I., 20: 20824
HOLZER, F., Calculation of seismic source mechanisms, 20: 20912
HONAZAWA, T., Anomalous bremsstrahlung and anomalous cyclotron emission from partially ionized gases, 20: 22208
HONEYCUTT, C. R., Prog. rpt. on determination of elevated-temperature fatigue data on refractory alloys, 10/65–1/66, 20: 21347 (NASA-CR-54916)
HONMA, Takuya, Conductivity of a gas with suspension, 20: 21575
HONNOLD, V. R., Prog. rpt. on effect of transistor design parameters on radiation response, 7–9/65, 20: 21148 (AD-630835)
HONNOLD, V. R., Prog. rpt. on effect of transistor design parameters on radiation response, 10–12/65, 20: 21149 (AD-630836)
HONZAWA, Todao, Interaction between plasma and microwave field in mirror-type magnetic field. I., 20: 22216
HOOD, S. L., Role of radioactivity and hydrothermal processes in protobiochemistry, 20: 20406 (N-65-27062)
HOOD, St. C. C., Administrative coordination of fissile material management and accounting in UKAEA, 20: 22528
HOOPER, M. B., Proton polarization and the spin-orbit potential, 20: 22116
HOPPER, Arthur F., Effect of low-protein diet on ability of adult rat to recover from sublethal dose of irradiation, 20: 20508
HORIBE, Osamu, Chemical shim control in conceptual design of a domestic power reactor, 20: 22428
HORSKY, J., Rayski formulation of laws of conservation in general relativity, 20: 21845
HORST, K. M., Prog. rpt. on SEFOR, 7–9/64, 20: 22495 (GEAP-4742)
HORST, K. M., Prog. rpt. on SEFOR, 2–4/65, 20: 22496 (GEAP-4864)
HORTON, C. W. Jr., Coupling of transverse and longitudinal waves at the upper hybrid frequency, 20: 22261
HORTON, R. W., Prog. rpt. on chemical technology, 7–9/65, 20: 20808 (ORNL-3916)
HORVATH, Bela, Engineering of EG-2 ion-accelerator channel, 20: 21480
HOSTLER, Lewrence, Formal scattering theory and the Coulomb problem, 20: 21702 (AD-621385)
HOUILLIER, A., Technological study on polyphenyls, 20: 20722 (EUR-2401.f)
HOVENIER, J. W., Supernova phenomena in OB associations and cosmic x-ray sources, 20: 21497
HOWARD, J. Edward, Operating experience of Yankee—updated, 20: 22457
HOWARD, R. L., Two satellite-borne cosmic-radiation detectors, 20: 21118
HOWER, Charles O., Excitation functions for simple nuclear reactions of π^- mesons with ^{40}Ar, 20: 22125
HOWER, G. L., High-frequency auroral noise, 20: 21835
HOWES, James E. Jr., Diffusion of fission products in fuel-element cladding materials and related alloys, 20: 21232 (BMI-1763)
HOWLAND, Joe W., Biochemical aspects of radiation injury and recovery, 20: 20435 (CONF-650560-15)
HRASKO, P., Direct processes on radioactive nuclei, 20: 22018
HRUSKA, A., Cyclotron instabilities in the magnetosphere, 20: 21825
HSU, Joseph, Relative light intensity of NaI crystal as function of absolute temperature, 20: 22317
HSU, Yi-Chuana, ^{14}C dating. I., 20: 20905
HSU, Yuin-Chi, ^{14}C dating. I., 20: 20905
HUANG, Chia-Yi, ^{14}C dating. I., 20: 20905
HUANG, Te-chiang, Inelastic interactions of π^- mesons with nucleons at 6.8 Bev, 20: 21693
HUBBARD, W. N., Calorimetry, 20: 20650 (ANL-7055, pp 167-76)
HUBER, O., Determination of conversion ratios of 191-kev transitions in ^{197}Au, 20: 22057
HUBY, R., Deuteron optical potentials and the $^{16}O(d,p)^{17}O$ reaction, 20: 22104
HUDDLESTON, Charles M., Calculation of energy-angular relationship for neutrons from a neutron generator, 20: 21934 (AD-621473)
HUDDLESTON, Charles M., Monte Carlo calculations of gamma-ray albedo, 20: 22305 (AD-621441)
HUENER, H., Importance of nonspecific resistance and its increase in the etiology of acute hematogenic osteomyelitis, 20: 20371
HUGHES, E. B., Response of standard IGY neutron monitor, 20: 21551
HUGHES, L. B., Reaction $^{55}Mn(n,\gamma)^{56}Mn$, 20: 22064
HUGON, Jean, Cytomorphologic and cytochemical study of cytolysomes of duodenal crypts of x-irradiated mice, 20: 20413
HUGUENIN, P., Parity mixing in single-nucleon orbitals, 20: 22080
HUILLE, S., Structure of Arctic auroral zone in period of minimum solar activity, 20: 21814
HULBERT, J. A., Superconducting transition temperatures in ε-phase Pb–Bi alloys, 20: 21892
HULL, D., Nucleation of cleavage cracks in tungsten and molybdenum by spark-machining, 20: 21245
HULTQVIST, Bengt, Plasma waves in frequency range 0.00110 c/s in earth's magnetosphere and ionosphere: a survey, 20: 21812 (AD-622223)
HULUBEI, H., Angular correlations in inelastic proton scattering on ^{20}Ne and ^{32}S, 20: 22059
HUNG, Tsu-Chang, Aqueous terephthalic acid as sensitive dosimeter for ionizing radiations, 20: 20745
HUNG, Tsu-Chang, Radiolysis of ethanol in liquid phase, 20: 20746
HUNSUCKER, R. D., Relationship of the aurora to non-great-circle high-frequency propagation, 20: 21827
HURAULT, J. P., Surface nucleation in a superconductor coated with a normal metal, 20: 21888
HURLEY, R. G., Three-wavelength x-ray absorption edge method for determination of plutonium in nitrate media, 20: 20573
HURWITZ, H. Jr., Fusion research, 20: 22302
HUTH, Gerald C., Recent results obtained with high-field, internally amplifying semiconductor radiation detectors, 20: 21100
HWANG, C. F., Dynamic polarization of protons in radiation-damaged polyethylene, 20: 22345
HYMAN, E., Determination of neutrino flux, 20: 21600 (CERN-65-32, pp 97-108)
HYODO, Hiroshi, Determination of copper content in o-diphenol oxidase by neutron activation analysis, 20: 20569

I

ICHIKAWA, Takahisa, ESR of γ-irradiated single crystal of H_2O_2–urea addition compound at 77°K, 20: 20756

IDA, Masakuni, General effective-range formula and compositeness of the deuteron, 20: 21689

IDEHARA, Toshitaka, Possibility of negative absorption of a plasma-cavity system, 20: 22211

IDOHARA, Mitsuru, Spectrographic analysis of high-purity tantalum by the d-c arc method, 20: 20608

IEDA, M., Effect of high-energy radiation on electric conduction of various copolymers containing polyethylene, 20: 21170

IGNAT, Margareta, Stationary solutions of system of equations of magneto-dynamics, 20: 21787

IGNATIEV, B. G., Fabrication of thin plates from refractory carbides, 20: 21303

IIZUKA, Jugoro, Systematics and phenomenology of boson mass levels. I., 20: 21690

IKADA, Yoshito, Degradation of polymers in solution under the influence of of ^{60}Co γ radiation, 20: 20765

IKEDA, Hiroshi, Integrating dose-rate meter employing ionization chambers, 20: 21078

IKEDA, Yasuaki, Temporal observations on peripheral hemograms of atomic bomb casualties as company employees. III., 20: 20481

IL'ENKO, B. P., Polarization of plasma moving in helical magnetic field, 20: 22275

IL'ENKO, B. P., Polarization of plasma moving in toroidal magnetic field, 20: 22276

IL'ENKO, B. P., Polarization of plasmas moving in magnetic fields of opposite curvatures, 20: 22277

IMOTO, Mitsuo, Pole model of nonleptonic decay consistent with decay parameters and sum rules, 20: 21688

IMSHENNIK, V. S., A magnetohydrodynamic theory of the pinch effect in a high-temperature, dense plasma, 20: 22180 (IAE-960)

INAGAKI, Michio, Embrittlement of welded joints of HT60 steel for nuclear pressure vessels, 20: 21393

INGALLS, R., High-pressure techniques, 20: 20850

INOUE, Makoto, Elastic and inelastic scattering of 28.4-Mev α particles by Sn, Cd, Ag, Cu, and Ti, 20: 22047

INOUE, Yasushi, Hot atom chemistry of ^{76}As using zirconium benzene-arsonate as target, 20: 20797

INOUYE, Henry, Decomposition rates of ceria in vacuum between 1100 and 1700°C, 20: 20655 (ORNL-P-1260)

INOUYE, Tamon, Image analysis of thermal neutron radiograph, 20: 20866

INSKEEP, C. N., Characteristics of very shallow silicon junctions, 20: 21099

INUISHI, Yoshio, Gamma irradiation on MOS field effect transistor, 20: 21159

INUKAI, Kan, Radiation-induced addition reaction of dialkyl phosphonates to fluorine-containing olefins, 20: 20772

INUKAI, Kan, Radiation-induced addition reaction of ethers to 1,2-dichloro-tetrafluorocyclobutene and 1,2-dichlorohexafluorocyclopentene, 20: 20773

IORGENSEN, M., Investigation of ^{145}Eu irradiation, 20: 22003 (JINR-P-2581)

IRVING, D. C., 05R Monte Carlo analysis routines for calculating various mean times in reactor problems, 20: 22380 (ORNL-TM-1246)

ISBIN, H. S., Recombination of hydrogen and oxygen in the presence of water vapor under the influence of radiation, 20: 20749

ISHIDA, Koji, Separation of scandium by cation exchange in acid ammonium sulfate media, 20: 20821

ISHIGAMI, Hitoshi, Conceptual design of Magnox reactor plant, 20: 22429

ISHIGURO, Yukio, Rigorous expression for shape of a Doppler-broadened resonance, 20: 21951

ISHIHARA, Toyohide, Construction and operation of radiological monitoring station, 20: 20934 (JAERI-1098)

ISHIWARI, Ryutaro, Construction of thin-lens-type β spectrometer, 20: 21051

ISHMAEV, S. N., Neutron thermalization process in time in graphite and Be, 20: 21942 (KFK-tr-188)

ISHMAEV, S. N., Transient neutron spectra in zirconium hydride, 20: 21941 (IAE-977)

ISIDA, Kitamu, Results of physical examination of atomic bomb casualties, 20: 20480

ISLAM, Jamal N., Leading Landau curves of a class of Feynman diagrams, 20: 21732

ISOARDI PONS, A., Effects of radiations on immunologic phenomena in Ehrlich's ascites tumor, 20: 20479

ITIKAWA, Yukikazu, Relaxation of velocity distribution of ions in a plasma, 20: 22205

IVANITSKII, P. G., Inelastic scattering of slow neutrons by polyethylene, 20: 21943

IVANOV, V. N., Action of ^{90}Sr–^{90}Y on developing khamsa spawn, 20: 20445 (TRG-Inf. Ser.-166)

IWASAKI, Machio, ESR of γ-irradiated single crystal of H_2O_2–urea addition compound at 77°K, 20: 20756

IYER, Meena, Stabilities and allied properties of organic coolants, 20: 20708 (AEET-213)

IYER, R. Mahadeva, Stabilities and allied properties of organic coolants, 20: 20708 (AEET-213)

IZQUIERDO, Jesus Sanchez, Automatic electronic equipment for multiple measurements of radioactivity, 20: 21055

IZQUIERDO, Jesus Sanchez, Automatic-reading electronic equipment for multiple measurements of radioactivity, 20: 21045

J

JABLONOWSKI, Edward J., Diffusion of fission products in fuel-element cladding materials and related alloys, 20: 21232 (BMI-1763)

JABLONSKI, Zdzislaw, Cascade curves for Xe, 20: 21514 (INR-598/VI/PH)

JACHYM, B., Ion mobility in higher saturated hydrocarbons, 20: 20734

JACKSON, A. G., Low-energy electron-diffraction study of molybdenum (110) surfaces, 20: 22319

JACKSON, J. D., Particle and polarization angular distributions for two- and three-body decays, 20: 21698

JACKSON, J. D., Peripheral interactions, 20: 21699

JACKSON, Kenneth L., Sodium and potassium binding in x-irradiated nuclei, 20: 20422

JACKSON, S., Estimation of internal radiation dose from metabolic and urinary excretion, 20: 20398

JACOB, M., Lectures on high-energy physics, 20: 21696

JACOBI, G., Influence of x radiation on the Hill reaction and photosynthesis phosphorylation for chloroplasts, 20: 20428

JACOBS, J. J., Separation of Cs from fission-product wastes, 20: 20818

JACOBS, Laurance D., T = 0, S-wave, $\pi\pi$ phase shift, 20: 21685

JACOBSON, Gerald, Dental radiological health program, 20: 20956

JAEGER, R. E., Transient effect of nuclear radiation on the dielectric properties of ceramics and plastics at microwave frequencies, 20: 21171

JAFFEE, R. I., Ductile tungsten sheet alloy, W–5Re–2.2ThO_2, 20: 21407

JAKEMAN, E., Time-dependent Ginsburg-Landau theory, 20: 21890

JANGG, G., Vapor pressure measurements on amalgams of yttrium and samarium, 20: 21384

JANOSSY, L., Hydrodynamical model of wave mechanics. III., 20: 21840

JANSEN, J., Mechanical radiography techniques for quality control of thin-walled SAP tubes, 20: 20861 (EUR-2443.f)

JANSSEN, U., Air-scattered radiation in environment of critical facility, 20: 22386

JASELSKIS, Bruno, Titrimetric determination of primary and secondary alcohols by xenon trioxide oxidation, 20: 20579

JAUHRI, G. S., Aerosol generator to produce radioactive aerosols, 20: 20924 (AEET-232)

JAYARAMAN, A., High-pressure polymorphism and magnetic ordering in some Sm-type rare earth alloys and samarium, 20: 21414

JEDLINSKI, Zbigniew, Gamma-radiation-induced chemical changes in polyvinyl butyral, 20: 20775

JEFFREYS, Harold, Travel times for Pacific explosions, 20: 20907

JENG, Tseing-ju, Inelastic interactions of π^- mesons with nucleons at 6.8 Bev, 20: 21693

JENGO, R., Current commutation rules and the $\Delta T = \frac{1}{2}$ rule in K-meson decays, 20: 21650

JENGO, R., Evaluation of $N^*_{33}N$ weak coupling constants, 20: 21655

JENKINS, David A., Pi-mesonic atoms, 20: 21534

JENKINS, T. L., Reactor neutrino experiment, 20: 21027 (CERN-65-32, pp 41-4)

JENSEN, Brenda B., Distribution patterns of rare earth elements in terrestrial rocks, 20: 20877

JENSEN, C. J., Pre-absorption events at 230 Mc/s, 20: 21500

JESSEPH, J. E., Strontium and calcium skeletal discrimination determined by compartmental analysis, 20: 20400

JIANG, Zuo-yi, Composition of lanthanum carbonate and cerium carbonate, 20: 20664

JIMENEZ, Rosa, Inactivation of vaccinia virus by γ radiation, 20: 20500

JOBST, Joel, $^{16}O(d,\alpha)^{14}N$ differential cross sections and fluctuation studies, 20: 22160

JOEKES, A. M., Radioactive renography in diagnosis and treatment of acute obstructive renal failure, 20: 20538

JOEL, D., Influence of extracorporeal irradiation of the blood and lymph on skin homograft rejection, 20: 20485

JOERGENSEN, T. Stockflet, Morphology of vlf hiss zones and their correlation with particle precipitation events, 20: 21824

JOHANSEN, H. A., Ductile-brittle transition in tantalum carbide, 20: 21375

JOHARI, Vinod B., Plane waves in the unified field of gravitation and electromagnetism, 20: 21869

JOHNSEN, Edwin G., Telesensors, teleoperators, and telecontrols for remote operations, 20: 20844

JOHNSEN, U., Radiation-induced reaction in polyethylene oxide, 20: 20766
JOHNSON, C. E., SNAP-8 reactor test program, 20: 22479
JOHNSON, Curtis C., Plasma-coupling medium for a traveling-wave tube amplifier, 20: 20985 (N-65-29669)
JOHNSON, E. D., Radiation-induced regeneration through p-n junction isolation in monolithic I/C's, 20: 21168
JOHNSON, E. F., Observation of low-frequency mixed-state resonances in pure niobium, 20: 21894
JOHNSON, Elwanda P., Mechanism by which hadacidin potentiates the damaging action of ionizing irradiation on bacteria, 20: 20456
JOHNSON, K. A., Plutonium–americium system, 20: 21339 (LA-DC-7095)
JOHNSON, O. E., Analyses of 18-Mev α-particle scattering cross sections for ^{40}Ar, ^{32}S, ^{31}P, ^{23}Na, and ^{20}Ne, 20: 22134
JOHNSON, Robert L., Friction characteristics of rare-earth and related metals in vacuum, 20: 21365
JOHNSON, Roy R., Excitation of the m = 2 mode by the helical instability, 20: 22247
JOHNSON, Vernon, ^{51}Cr in sea water: chemistry, 20: 20603
JOHNSTON, J., Some superconducting properties of several carbides and nitrides of the transition metals, 20: 21911
JOHNSTON, Wilbur D. Jr., Field ionization detectors for molecular beams, 20: 21089
JOINER, W. C. H., Non-ideal superconducting behavior of tin alloys, 20: 21925
JONES, A. R., Portable dose-rate meter using a silicon p-n junction as a detector, 20: 21133
JONES, C. E., Can nearby interaction singularities generate observed resonances?, 20: 21668
JONES, C. M., Total neutron yield from the reaction ^{14}C(α,n)^{17}O, 20: 22110
JONES, Donald L., Blast waves from an inverse pinch machine, 20: 21798
JONES, G. D., Deuteron optical potentials and the ^{16}O(d,p)^{17}O reaction, 20: 22104
JONES, Iowan R., Pressure bar and photographic measurements on h-f theta discharge, 20: 22183 (LRP-21-66)
JONES, K. W., Excitation energies of bound states of ^{17}O and ^{12}B, 20: 22111
JONES, L. V., Prog. rpt., 7/65, 20: 20806 (MLM-1274)
JONES, L. V., Prog. rpt., 8/65, 20: 20807 (MLM-1287)
JONES, L. V., Prog. rpt., 10/62, 20: 20553 (MLM-1142)
JONES, Lawrence W., Use of image intensifiers with streamer chambers, 20: 21020 (AD-621069)
JONES, S. L., Three-parameter pulse-height analyzer and coincidence system for satellite cosmic-ray studies, 20: 21125
JONKE, A. A., Engineering development of fluid-bed fluoride volatility processes. II., 20: 20801 (ANL-6830)
JONKE, A. A., Fuel cycle applications of volatility and fluidization techniques, 20: 20803 (ANL-7055, pp 99-162)
JORDAN, P., Stereo-specific hydrogen exchange accompanying catalytic hydrogenation of methyl β, β-dimethylacrylate, 20: 20715
JORGE, A., Prog. rpt. on point defects and mechanical properties of Nb, final, 2/15/62–11/30/65, 20: 21320 (AD-625475)
JOSEPH, P. M., Wide-angle electron-pair production, 20: 22146
JOSEPHSON, Edward S., Recent progress in applying high doses of ionizing radiations to achieve shelf-stable foods, 20: 21196
JOZUKA, Kenji, Calcium uptake by teleost fishes. I., 20: 20405
JUDD, A. M., Loss-of-coolant accidents in large sodium-cooled fast reactor, 20: 22349
JULIANI, G., Effects of radiations on immunologic phenomena in Ehrlich's ascites tumor, 20: 20479
JUNGWIRTH, K., Electron cyclotron instability, 20: 22197
JUPITER, C. P., Scintillation properties of various hydrogenous and non-hydrogenous solutes dissolved in hexafluorobenzene, 20: 21134

K

KADANTSEV, V. N., Peculiarities of radiation of point dipoles moving in narrow cavities in magnetoactive media, 20: 22278
KADISH, Abraham, Stability criteria and initial value problem for collisionless guiding center plasma, 20: 22235
KADYSHEVSKII, V. G., Symmetries of leptons and hadrons in weak interactions. I., 20: 21712 (JINR-P-2562)
KAGAN, Yu. M., Radial dependence of electron velocity distribution in positive column of discharge, 20: 22294
KAGANSKII, M. G., Toroidal machine for adiabatic compression of plasma, 20: 22299
KAHN, J. E., Engineering design practices for facilities containing radioactive materials, 20: 20942 (ORNL-TM-1459)
KAISER, E. T., Sulfur dioxide elimination in radiolytic decomposition of solid diaryl sulfones, 20: 20760
KAISER, William C., Relative light intensity of NaI crystal as function of absolute temperature, 20: 22317
KALEMBER, G. M., Development-production program for Lockwood, 20: 21188 (ORNL-IIC-7, pp 95-8)
KALININ, A. E., Radioactivation analysis of SiO_2 using ion exchange chromatography. II., 20: 20633
KALININ, A. I., Radioactivation analysis of SiO_2 using ion exchange chromatography. I., 20: 20632
KALININ, A. I., Radioactivation analysis of SiO_2 using ion exchange chromatography. III., 20: 20634
KALININ, A. I., Radioactivation analysis of SiO_2 using ion exchange chromatography. IV., 20: 20635
KALININ, A. I., Radioactivation analysis of SiO_2 using ion exchange chromatography. V., 20: 20636
KALISH, R., Gyromagnetic ratios on first excited 2$^+$ states in even Os isotopes, 20: 22055
KALMYKOV, A. I., Effect of sea surface structure upon spatial characteristics of scattered radiation, 20: 20908
KALNS, Eric, Tungsten-base alloy development, 20: 21412
KALPAZHIU, M. K., Calculations of properties of collective states in deformed nuclei, 20: 21998 (JINR-E-2579)
KALYAZIN, E. P., Radiation carbonylation of paraffinic hydrocarbons with carbon monoxide, 20: 20770
KAMAEV, A. V., Nuclear safety in working with fissionable materials, 20: 20975
KAMATA, K., Primary energy spectrum from 8×10^{14} to 4×10^{17} ev, 20: 21547 (MIT-2098-227, Paper EAS-31)
KAMEMOTO, Yoichiro, Determination of polonium in neutron-irradiated bismuth, 20: 20585
KANAZAWA, Akira, Dynamical approach to nonleptonic decays of hyperons, 20: 21686
KANCHIKU, Y., Excitation functions for reactions induced by protons on Cd up to 37 Mev, 20: 22078
KANEKO, Takao, Possible scheme for nonleptonic decays of hyperons, 20: 21687
KANKELEIT, E., Feedback in electromechanical drive systems, 20: 21079
KANTELE, J., Improved methods for multiple coincidence gamma spectrometry, 20: 22020
KAO, Li, Study of the water content in UF_4 by gas volumetric method with calcium hydride, 20: 20609
KAPER, H. G., Use of generalized functions and the Poincare-Bertrand formula in neutron transport theory, 20: 21956
KAPLAN, M., Influence of recoil stopping time on the Moessbauer effect following α decay, 20: 22037
KARANOVIC, Dobrila, Proliferative activity of bone marrow cells in mice bled immediately after irradiation with 600 R, 20: 20452
KARANOVIC, Jovo, Proliferative activity of bone marrow cells in mice bled immediately after irradiation with 600 R, 20: 20452
KARBON, J. A., Discontinuous variation of the bulk modulus in type II superconductors, 20: 21912
KARDON, Bela, Measurement of isomeric cross-section ratio on neutron-activated ^{85,85m}Sr, ^{122,122m}Sb, and ^{188,188m}Re, 20: 22052
KARKHANAVALA, M. D., Role of substrate symmetry in gas-solid reactions. 20: 20649 (AEET-CD-24)
KARNAUKHOV, I. M., Mass spectrometric investigation of source of positive ions operating at low gas pressure, 20: 21457
KAROLYHAZY, F., Gravitation and quantum mechanics of macroscopic objects, 20: 21857
KARPMAN, Gilbert, Interpretation of asymmetries in the neutrino production pions, 20: 21638
KARR, H. J., High-velocity plasma injection into cusped magnetic field, 20: 22254
KARZAS, W. J., Scattering of light by protons, 20: 21587 (AD-623564)
KARZHAVINA, E. N., Investigation of neutron resonances of ^{165}Ho, 20: 22004 (JINR-P-2593)
KARZMARK, C. J., Problems of reader design and measurement error in thermoluminescent dosimetry, 20: 21061
KASHIN, V. I., Gas generation from tungsten at 2500°C, 20: 21248
KASHY, E., Hole states of ^{43}Ca and ^{47}Ca, 20: 22129
KASIKOV, I. I., Operation of a cesium diode with an admixture of an inert gas, 20: 21567 (FEI-15)
KASIKOV, I. I., Volt-ampere characteristics of the TEP (thermoelectron potential) in an arc, 20: 22178 (FEI-17)
KASSNER, T. F., Convective-diffusion study of dissolution kinetics of stainless steel in Bi–Sn alloy, 20: 21260 (ANL-6985)
KATAGIRI, Hiroshi, Construction and operation of radiological monitoring station, 20: 20934 (JAERI-1098)
KATAGIRI, Michio, Parametric oscillating amplifier, 20: 21013
KATMAN, T. S., ^{12}C(d,py)^{13}C angular distributions and correlations near threshold, 20: 22087
KATOH, T., Excitation functions for reactions induced by protons on Cd up to 37 Mev, 20: 22078
KATYAL, Mohan, Thorium and molybdenum complexes with myricetin, 20: 20674
KAUFMAN, Sheldon, Excitation functions for simple nuclear reactions of π^- mesons with ^{40}Ar, 20: 22125

KAUSHIKA, N. D., Night-time disturbance fluctuations in geomagnetic field at equatorial stations, 20: 21818
KAVESHNIKOVA, S. V., Experimental data on dose assessment during remote-control γ therapy, 20: 20541
KAW, Predhiman Krishen, Nonlinear sum and difference frequency generation in an inhomogeneous plasma, 20: 22244
KAWASAKI, Shoichiro, Pole model of nonleptonic decay consistent with decay parameters and sum rules, 20: 21688
KAWASE, Akira, Determination of trace zinc in thorium, 20: 20601
KAWASHIMA, Nobuki, Ion temperature measurement in a streaming plasma by the Langmuir double probe, 20: 22213
KAWASHIMA, Nobuki, Plasma flow past bodies in a magnetic field, 20: 22251
KAYLOR, John D., Radiopasteurization of fishery products, 20: 21200
KAYSER, Boris, Dynamics of the Y_1^* branching ratio, 20: 21670
KAZACHEVSKII, I. V., Non-equilibrium uranium in carbonate deposits and their age determination, 20: 20887
KAZANAS, N., Effect of γ irradiation on microflora of fresh water fish. I., 20: 21203
KAZANKIN, Yu. N., Clathrate compounds of p-cresol with rare gases. I., 20: 20688
KAZANTSEV, E. I., Separation of Th from ions of certain metals on anion exchanger AV-17 from nitric acid solutions, 20: 20624
KE, Mo-lin, On the π-π resonance states, 20: 21694
KEARNS, W. H., Material and process specifications for refractory alloy and alkali metals, 20: 21293 (R-66SD3007)
KEEFER, D. R., Electron temperatures in several r-f plasmas, 20: 22194
KEEN, C. G., British seismometer array recording systems, 20: 20913
KELBER, Charles N., Effect of randomness on group cross sections, 20: 22391
KELLER, Keston, Recoil gold atoms from fast-neutron bombardment, 20: 21441
KELLER, R., Design of rotating-field pinched discharge, 20: 22184 (LRP-22-66)
KELLER, R., Ionic temperature in an h-f confinement measured with an electrostatic selector, 20: 22185 (LRP-23-66)
KELLERSHOHN, C., Spark chambers in nuclear medicine, 20: 21082
KELLOGG, L. G., Development of control system for SNAP reactors, 20: 22474
KELLOGG, R. B., DUZ-1—program for solving axisymmetric and plane elasticity problems on Philco-2000, 20: 20862 (WAPD-TM-555)
KEMPE, L. L., Effect of γ irradiation on microflora of fresh water fish. I., 20: 21203
KENDALL, J. D., Subroutines for digital simulations, 20: 21783 (AECL-2530)
KENNA, B. T., Fast neutron flux pattern for 14-Mev neutron generator, 20: 21946
KENNEDY, Roger C., Energy gap in finite nuclear systems, 20: 22112
KENNETT, T. J., Reaction $^{55}Mn(n,\gamma)^{56}Mn$, 20: 22064
KENNEY, J. T., Energy efficiency trends in a coaxial gun plasma engine system, 20: 20872
KENT, James A., Basic research on irradiated wood-plastic combinations, 20: 21179 (ORNL-IIC-7, pp 6-14)
KERNER, Edward H., Simultaneously Lorentz- and Galilean-invariant particle dynamics, 20: 21867
KERVALISHVILI, N. A., Characteristics of a low-pressure discharge in a transverse magnetic field, 20: 21810
KESSLER, G., Safety and cost analysis of 1000-Mw(e) sodium-cooled fast power reactor, 20: 22451
KESTER, Tilo, EPR study of annealed effects in irradiated graphite, 20: 21435
KESZTHELYI, Lajos, Temperature dependence of internal magnetic field, 20: 22326
KETCHUM, Harry W., Perimeters of the commercialization of irradiated foods, 20: 21202
KEUFFEL, J. W., Utah neutrino detector, 20: 21030 (CERN-65-32, pp 223-4)
KEVAN, Larry, Sulfur dioxide elimination in radiolytic decomposition of solid diaryl sulfones, 20: 20760
KEYSER, R., Absorption model and production of 2+ mesons, 20: 21644
KHALKIN, V. A., Investigation of the α spectrum of Bi isotopes, 20: 22000 (JINR-P-2553)
KHAM'YANOV, L. P., Analysis and generalization of correlation method for measurement of particle-lifetime distribution in physical systems, 20: 21035 (FEI-21)
KHAN, A. A., Use of incinerators for treatment of combustible wastes, 20: 22508 (AEET-220)
KHANNA, M. P., Are quarks fractionally or integrally charged? 20: 22460 (IC-66/28)
KHIZHNYAK, N. A., Nonlinear oscillations of plasma behind a front on which charged particles are produced, 20: 22285
KHORENKO, V. K., Oriented growth of oxide film on beryllium, 20: 21269
KHOZHAINOV, A. I., Initial portion of MHD channel with longitudinal inhomogeneity of transverse magnetic field taken into account, 20: 21807
KHRAPOVA, N. G., Relation between radioprotective and antineoplastic effects of antioxidant-inhibitors, 20: 20506
KHRISTENKO, P. I., Recycling of Pu in heavy water power reactors, 20: 22419
KHRULEV, V. V., Depolarization in cosmic radiation due to dispersion of Faraday rotation of polarization planes, 20: 21548
KIDD, G. J. Jr., Confined vortex flow near a stationary disk. Theory and experiment, 20: 21786 (ORNL-TM-1387)
KIEFFER, Paul Clement, Variable conductivity fully developed MHD channel flow, 20: 21780 (AD-622036)
KIER, Philip H., Effect of randomness on group cross sections, 20: 22391
KIFUNE, Tadashi, High-efficiency gas Cherenkov counter, 20: 21071
KIKUCHI, C., Coherence and two-photon absorption, 20: 21533
KIKUCHI, Riichi, Simple γ dose threshold detector using a dyestuff, 20: 21076
KIKUCHI, Tokeo, Fission-fragment damage in epitaxial film of UO_2, 20: 21442
KIM, Stephen M., Electrodeposition method for counting alpha and beta emitters, 20: 20795
KIM, Y. E., Energy spectra of 1p-shell nuclei calculated with the Hamada-Johnston potential, 20: 22102
KIMELDORF, D. J., Responses of single neurons in olfactory bulbs, 20: 20431 (AD-630323)
KIMELDORF, Donald J., Age and dose dependence of bone growth retardation induced by x irradiation, 20: 20486
KIMURA, Hiroshi, Radiography with the electron linear accelerator, 20: 21477
KIMURA, Kiichi, Keage Laboratory of Nuclear Science report, 1955–1965, 20: 22524
KIMURA, Yoshitoka, High-efficiency gas Cherenkov counter, 20: 21071
KINCAID, C. V., Effect of radiation on electric resistivity and bulk compressibility of polyepoxides, 20: 21418 (AD-627049)
KIND, N. V., Non-equilibrium uranium in carbonate deposits and their age determination, 20: 20887
KINDERMAN, E. M., Criteria for special nuclear materials inventory and control procedures, 20: 20966
KINDERMAN, E. M., Identification and inspection for inventory control of irradiated fuel elements, 20: 20970
KING, G. W., Properties of W and W–Re alloys, 20: 21406
KING, H. W., Superconducting transition temperatures in ε-phase Pb–Bi alloys, 20: 21892
KING, John G., Field ionization detectors for molecular beams, 20: 21089
KING, W. J., Junction counters produced by irradiation of silicon with dopant ions, 20: 21098
KINO, G. S., Two-dimensional low-pressure discharge theory, 20: 21799
KINOSHITA, G., Radiation-induced regeneration through p-n junction isolation in monolithic I/C's, 20: 21168
KINOSHITA, Hideo, Study on U refining, 20: 20817
KINSEY, K. F., Measurement of lifetime of the positive pion, 20: 21665
KINSEY, K. F., Pion electromagnetic form factor from measurements of $\pi^{\pm}$-α elastic scattering, 20: 21659
KIRCHMANN, R., ^{90}Sr contamination of cultivated plants, 20: 20381
KIRCHMAYR, H. R., Vapor pressure measurements on amalgams of yttrium and samarium, 20: 21384
KIRCHMAYR, Hans R., Preparation of rare earth–manganese alloys, 20: 21403
KIRIN, I. S., Measurement of activity of components in organic mixtures containing ^{14}C, 20: 20639
KIRK, D. D., Surface effects in alkali-halide crystals from irradiation, 20: 21424 (N-65-23332)
KIRRMANN, Jean-Michel, Effects of a radiomimetic substance, nitrogenous yperite, on morphology and oxygen consumption of an embryonic organ cultivated in vitro, 20: 20372
KIRSCHBAUM, H. S., New control techniques for NERVA reactors, 20: 22482
KISELEV, V. A., Performance of coaxial plasma source in longitudinal magnetic field, 20: 22179 (FTI-080/P-032)
KISH, I., Radiochemical stability of high-boiling hydrocarbons in reactor, 20: 20792
KISLITSINA, G. I., Non-equilibrium uranium in carbonate deposits and their age determination, 20: 20887
KISLYI, P. S., Increase in ZrB_2 grains during sintering, 20: 21273
KISS, Adam, Temperature dependence of internal magnetic field, 20: 22326
KISS, Dezso, Measurement of isomeric cross-section ratio on neutron-activated $^{85,85m}Sr$, $^{122,122m}Sb$, and $^{188,188m}Re$, 20: 22052
KISS, Elemer, Aerosol activity meter, 20: 21073
KISS, Elemer, Mechanical driving unit for Moessbauer experiments, 20: 22050
KISS, I., Preparation of XeF_2, 20: 20678
KISSLINGER, L. S., Quasiparticle random-phase approximation in odd-odd nuclei and the neutron-proton interaction, 20: 22147
KISTEMAKER, J., Influence of velocity of rare gas ions on emission of

secondary electrons, 20: 21538
KISTNER, O. C., Recoil-free absorption hyperfine spectra of the 90-kev mixed transition in ^{99}Ru, 20: 22141
KITRILAKIS, S., Correlation of electron emission cooling and optimum collector temperature, 20: 21585
KIVELSON, M. G., Radiation smoothing of shocks, 20: 21775 (AD-620835)
KLEIN, A. P., Localized impurity states in metals: dilute alloys of Ni in Be, 20: 21390
KLEIN, Gerhart P., Electronic conductivity of defective anodic tantalum oxide films, 20: 20670
KLEIN, Peter D., Tritiated alumina as a reagent for self-labeling chromatographic analyses, 20: 20575
KLEIN, Richard M., Polymerization and polymer properties as related to wood-plastic combinations, 20: 21180 (ORNL-IIC-7, pp 15-21)
KLEINE, W., Influence of velocity of rare gas ions on emission of secondary electrons, 20: 21538
KLEINER, C. T., Radiation-induced regeneration through p-n junction isolation in monolithic I/C's, 20: 21168
KLEMA, E. D., Response of solid-state detectors to fission fragments, 20: 21101
KLEMM, A., Mobility of lithium isotopes in molten $^{6}LiCl$ and $^{7}LiCl$, 20: 20695
KLEMM, Th., Separation of air from isotopic noble-gas mixtures, 20: 20820
KLOEPPER, R. M., Neutron and γ sensitivities of dynamic detectors, 20: 21059
KLONTZ, E. E., Radiation damage studies in degenerate Si, irradiated at low temperatures, 20: 22346
KLOSE, A., Recovery of ^{90}Sr and ^{144}Ce from concentrated fission-product solutions, 20: 20804 (EUR-2754.f)
KNECHT, Othmar, Device for control of reactors by means of neutron-absorbing liquids, 20: 22365
KNOBELOCH, G. W., Symmetry of neutron-induced ^{239}Pu fission at individual resonances, 20: 22135
KNOPP, Carl F., Determination of thermal and electrical conductivity of atmospheric Ar plasma, 20: 22164 (AD-621213)
KNOX, John M., Patterns of cutaneous pigmentation following sunlight irradiation, 20: 20458
KNUDSEN, Jens M., Moessbauer studies on iron in perovskites $La_{1-x}Sr_xFeO_3 (0 \leq x \leq 1)$, 20: 22336
KNUTSON, Carroll F., Economics of contained nuclear explosions applied to petroleum reservoir stimulation, 20: 20836
KOBAYASHI, Hanako, Magnetic susceptibility of scandium, 20: 21381
KOBAYASHI, K., Irradiation changes in organic polymers at various accelerating voltages, 20: 20762
KOBE, H., Criteria for best Bogoliubov quasi particle, 20: 21839 (AD-627067)
KOCHTITZKY, O. W., Evaluation of radiation dose to man from radionuclides released to Clinch River, 20: 22514 (ORNL-P-2021)
KOEHLER, J. S., Resistivity recovery of dilute alloys of silver, copper, and gold, proton-irradiated at 80°K, 20: 21445
KOEPKE, B. G., Interplanar angles and planar spacings of fifteen types of planes for HCP yttrium, 20: 22315 (IS-1337)
KOEVESY, Zs., Direct processes on radioactive nuclei, 20: 22018
KOHL, H. H., Effect in stomach of ionizing radiation on acid secretion, potential, ATP, and phosphocreatine in comparison to spleen, 20: 20433 (AD-630390)
KOHMURA, Toshitake, Decays of light double hypernuclei and the four-baryon weak interactions, 20: 22149
KOKAME, J., 3⁻ State in ^{28}Si and ^{24}Mg, 20: 22107
KOKAME, Jun, Construction of thin-lens-type β spectrometer, 20: 21051
KOKES, Antonin, Fraction collector for microchromatography of radioactive substances, 20: 20587
KOKOTOV, Yu. A., Measurements of amounts of radioactive trace element adsorption from solutions, 20: 20617
KOKOTOV, Yu. A., Radiochromatographic determination of microquantities of ^{137}Cs sorption by soil, clay, and mica, 20: 20696
KOKOTOV, Yu. A., Successive desorption method in studies of ion adsorption from solutions, 20: 20618
KOLAR, J., Nonmalignant new growth in irradiated growing bones, 20: 20460
KOLB, A. C., Deviations from ionization equilibrium in plasmas generated by electric shock tubes, 20: 22250
KOLBASOV, V. I., Structure of polypropylene chlorinated by radiation and sulfochlorinated, 20: 20779
KOLESNIKOV, P. M., Nonlinear oscillations of plasma behind a front on which charged particles are produced, 20: 22285
KOLLMANN, George, Mechanism of action of AET. VI., 20: 20424
KOLOMIETS, L. D., Oriented growth of oxide film on beryllium, 20: 21269
KOMAI, Kenichiro, Electron irradiation apparatus, 20: 20853
KOMOR, Zenon, Application of the 256-channel time-of-flight analyzer for measurement of amplitude spectra, 20: 21083
KONDRAS, F. D., Radiation level measurements within and behind Be, 20: 22307 (DC-61-3-69)
KONDRATENKO, A. N., Kinetic theory of electromagnetic waves in a plasma layer, 20: 22270
KONDRATENKO, A. N., Kinetic theory of passage of electromagnetic waves through a plasma layer. I., 20: 22297
KONONOV, B. P., Plasma acceleration in constant electric field combined with high-frequency field, 20: 22289
KOPPENAAL, T. J., Effect of fast neutron damage on deformation of Cu–Sn alloys, 20: 21434
KOPS, S., Case study in internal audit of nuclear material, 20: 22529
KORGAONKAR, K. S., Evaluation of acridine orange fluorescence test in viability studies on E. coli, 20: 20457
KORKISCH, Johann, Separation of uranium by combined ion exchange and solvent extraction, 20: 20811
KORNEEV, V. T., Reconstruction of IRT research reactor, 20: 22497 (IAE-992)
KORNHAUSER, Andrija, Isotope effects in photochemical transformation of tritium-labeled uracil, 20: 20782
KOROBEINIKOV, V. L., Separation of Th from ions of certain metals on anion exchanger AV-17 from nitric acid solutions, 20: 20624
KOROLEV, B. M., Structure of polypropylene chlorinated by radiation and sulfochlorinated, 20: 20779
KOROTUN, L. I., Charge density waves in radial electron flux, 20: 21449
KOROZA, V. I., Radial expansion of a beam in an electron linear accelerator induced by asymmetric wave, 20: 21476
KORZH, I. A., Scattering of medium-energy neutrons, 20: 22023
KOSHA-SHAMODI, I., Radiochemical stability of high-boiling hydrocarbons in reactor, 20: 20792
KOSHEL, R. D., Elastic neutron scattering from B, C, K, and Ca at 14.0 Mev, 20: 22119
KOSHEL, R. D., Nucleon single-particle levels in diffuse nonlocal potential well, 20: 22113
KOSSANYI-DEMAY, P., ^{32}S and ^{31}P excitation by 180° electron scattering, 20: 21964 (AD-626684)
KOSSYI, I. A., Radial charged particle flux in discharge excited by h-f traveling H waves, 20: 22301
KOSTOMAROV, D. P., Plasma drift waves propagating transversely to an external magnetic field, 20: 22282
KOTLENSKY, W. V., Tensile and structural properties of glassy carbon, 20: 21338 (JPL-TR-32-842)
KOTRAPPA, P., Aerosol generator to produce radioactive aerosols, 20: 20924 (AEET-232)
KOURILSKY, Raoul, Recording respiratory function by x rays, 20: 20546
KOVACH, Robert L., Analysis of geomagnetic micropulsations due to high-altitude nuclear explosions, 20: 21929
KOVACS, Gyula, Aerosol activity meter, 20: 21073
KOVACS, Gyula, ZR-2 critical assembly, 20: 22388
KOWALSKA, Krystyna, Critical calculations of slab reactors, 20: 22394
KOWALSKI, Emil, Ionization chamber radiation dosimeter, 20: 21141
KOWALSKI, K. L., Consequences of off-shell unitarity, 20: 21756
KOYAMA, Shinji, Deoxidation and desulfurization of liquid iron by uranium, 20: 20692
KOZIK, Ben'yamin, Statistical basis for dynamic model of stationary zero power reactor, 20: 22418
KRAFT, E., Comparison of spark chamber properties for two different triggering modes, 20: 21048
KRAFT, R., Electron content of the ionosphere and its fluctuations, 20: 21816
KRALL, Nicholas A., Stabilization of hot electron plasma by a cold background, 20: 22264
KRAMER, Gordon, Semiconductor fast-neutron dosimeter—its characteristics and applications, 20: 21095
KRANYS, M., Relativistic hydrodynamics with irreversible thermodynamics, 20: 21794
KRAUSE, D. E., Detection of single electrons and ions in a radiation environment, 20: 21139
KRAUSE, P. C., Analog computer representation of the ring magnet power supply system of the ZGS, 20: 21488
KREISLER, Michael N., Electroluminescent panels as pulsed fiducial marks in spark chamber experiment, 20: 21090
KRESIN, W. S., Increase of critical temperature in superconducting films, 20: 21891
KRESS, Tommy Sylvester, Parameters of isothermal fission-product deposition, 20: 21785 (ORNL-TM-1330(Rev.))
KRETCHMAR, A. L., Change in partition of total-body N in radiation chimeras, 20: 20407 (ORNL-P-1118)
KREWER, K. H., Safety and cost analysis of 1000-Mw(e) sodium-cooled fast power reactor, 20: 22451
KREY, R. U., Prog. rpt. on radiation from arc-heated plasma, final, 3/64–4/65, 20: 22167 (AD-622391)
KRINDACH, N. I., High-frequency discharge in a neon–helium laser, 20: 21808

KRISYUK, E. M., Peculiar features in radiation sickness induced by soft x rays, 20: 20475
KRIVANEK, M., Contribution to the extraction radiometric titrations, 20: 20567 (UJV-1418/65)
KRIVITSKII, A. S., Induction of mutations by uv radiation and nitrous acid in extracellular phage ϕX174, 20: 20463
KRIVKO, N. I., Measurement of magnetic field at surface of Nb–Zr superconductor by means of EPR, 20: 21898
KRIVKO, N. I., Superconducting alloy in the Nb–Ga system, 20: 21897
KRIVOPUSTOV, M., Investigation of ^{145}Eu irradiation, 20: 22003 (JINR-P-2581)
KRIZHANSKII, S. M., Current-voltage characteristic of column of high-pressure arc discharge, 20: 21809
KROH, J., EPR studies of γ-irradiated ethanol–benzene system at –196°C, 20: 20742
KROH, J., Influence of cyrstal size on yield of n-vinylcarbazole polymerization, 20: 20743
KROH, J., Radiolysis of ethanol-benzene systems under the influence of ^{60}Co γ radiation, 20: 20741
KROH, Jerzy, Achievements of Polish radiation chemistry, 20: 20780
KROLIKOWSKI, W., Difference between sources and charges, 20: 21745
KROTENKO, V. T., Inelastic scattering of slow neutrons by polyethylene, 20: 21943
KRUGER, O. L., Preparation of sulfides and phosphides of plutonium, 20: 20676
KRUGLYAKOVA, K. E., Kinetics of DNA denaturation under ultraviolet radiation, 20: 20412
KRUMHOLZ, Louis A., Prog. rpt. on radioecological study of biota, final, 5/59–10/64, 20: 20884 (TID-22815)
KRUMLINDE, J., Corrections to BCS expressions for nuclear matrix elements, 20: 22103
KRUPP, R. F., Plotting system for Control Data 3600 computer, 20: 21221 (ANL-7121)
KRUSE, W. G., Radiation dosimeters developed for SNAP-10A flight test, 20: 21105
KRZYCKI, Andrzej, Test of connectors used in semiconductor logic modules, 20: 22352 (AEET-ED-SG/25)
KUBAL, O. A., Prog. rpt. on ventilation of fallout shelters, 7/64–6/65, 20: 20921 (AD-621998)
KUCHAR, Lumir, Partition coefficients of Al–Y system, 20: 21369
KUDUSOV, V. A., Separation of Th from ions of certain metals on anion exchanger AV-17 from nitric acid solutions, 20: 20624
KUEMMEL, H., Theory of decaying systems, 20: 22155
KUEMMEL, H. G., Deformation energies and collective motion of heavy nuclei, 20: 22065
KUHN, G. D., Prog. rpt. on effects of low-level irradiation upon preservation of food products, annual, 4/65, 20: 21195 (TID-22509)
KUJAWSKI, E., Investigation of nuclear properties of ^{143}Pr in the unified model, 20: 22139
KUKULA, F., Contribution to the extraction radiometric titrations, 20: 20567 (UJV-1418/65)
KULA, Eric B., Plastic behavior of metals at cryogenic temperatures, 20: 21416
KULESH, I., Radiochemical stability of high-boiling hydrocarbons in reactor, 20: 20792
KULIKOV, M. N., Instability of small electron fluxes in crossed fields, 20: 21451
KULSRUD, R. M., Resistive instabilities in toroidal hydromagnetic systems, 20: 22187 (MATT-424)
KULYUKINA, L. A., Fluctuations of ionization losses, 20: 21515 (JINR-P-2615)
KUMABE, Isao, Elastic and inelastic scattering of 28.4-Mev α particles by Sn, Cd, Ag, Cu, and Ti, 20: 22047
KUMAR, Keilash, Talmi transformation for unequal-mass particles and related formulas, 20: 21226
KUME, S., Excitation functions for reactions induced by protons on Cd up to 37 Mev, 20: 22078
KUMMER, J., Linearly controllable low-frequency oscillator for a proton resonance spectrometer with internal nuclear resonance stabilization, 20: 21093
KUNDEL, Harold L., Effect of gamma irradiation on cardiovascular system of the rhesus monkey, 20: 20488
KUNDSIN, Ruth B., Characterization of Mycoplasma aerosols, 20: 20469
KUNZLER, J. E., Energy gaps in β tungstens and other superconductors, 20: 21885
KUO, T. T. S., Endrgy spectra of 1p-shell nuclei calculated with the Hamada-Johnston potential, 20: 22102
KUO, T. T. S., Shell model calculation of the odd tin isotopes, 20: 21962 (AD-624214)
KUPER, C. G., Thick non-equilibrium helium II films, 20: 21896
KUPRIANOFF, J., Food irradiation research in West Germany, 20: 21193 (PB-181506, pp 29-38)
KURAMOTO, Kiyoshi, Results of physical examination of atomic bomb casualties, 20: 20480
KURATA, N., Biological effects of x irradiation on the heart, 20: 20474
KURATH, Dieter, Light spherical nuclei, 20: 21974 (BNL-948, pp 222-68)
KURDYUMOV, V. N., Theory of Cherenkov radiation of a charge in a cold plasma, 20: 22290
KURODA, Kenichige, Radiography with the electron linear accelerator, 20: 21477
KURODA, P. K., 650-Mev photofission yields for uranium, 20: 22040
KURODA, Rokuro, Separation of scandium by cation exchange in acid ammonium sulfate media, 20: 20821
KURODA, Tsutomu, Stabilization of plasma in P.I.G. discharge, 20: 22215
KURSUNOGLU, Behram, Prog. rpt. on plasma physics, final, 6/64–8/65, 20: 22189 (TID-22809)
KURZ, Ernst, X rays, radiation injury, and radiation protection, 20: 20544
KUTTNER, P., An extension of the diffusion coefficient by higher terms derived from neutron transport theory, 20: 21944
KUTUZOV, A. A., Analysis and generalization of correlation method for measurement of particle-lifetime distribution in physical systems, 20: 21035 (FEI-21)
KUWATA, Keiji, ESR of γ-irradiated single crystal of H_2O_2–Urea addition compound at 77°K, 20: 20756
KUZENKOVA, M. A., Increase in ZrB_2 grains during sintering, 20: 21273
KUZHETSOV, R. A., Radioactivation analysis of SiO_2 using ion exchange chromatography. I., 20: 20632
KUZ'MIN, I. I., Scattering of particles by system of fixed centers, 20: 21710 (JINR-P-2554)
KUZ'MINA, E. A., Non-equilibrium uranium in carbonate deposits and their age determination, 20: 20887
KUZNETSOV, F. M., Nuclear safety in working with fissionable materials, 20: 20975
KUZNETSOV, R. A., Radioactivation analysis of SiO_2 using ion exchange chromatography. II., 20: 20633
KUZNETSOV, R. A., Radioactivation analysis of SiO_2 using ion exchange chromatography. III., 20: 20634
KUZNETSOV, R. A., Radioactivation analysis of SiO_2 using ion exchange chromatography. IV., 20: 20635
KUZNETSOV, R. A., Radioactivation analysis of SiO_2 using ion exchange chromatography. V., 20: 20636
KUZNETSOV, V., Investigation of ^{145}Eu irradiation, 20: 22003 (JINR-P-2581)
KUZNETSOV, V. I., Zirconium and Y cupferronates and a method for separating ^{89}Zr from irradiated carrier-free Y, 20: 20626
KUZNETSOVA, A. K., Determination of the amounts of trace components captured by a macrocomponent precipitate, 20: 20619
KVETSINSKA, T., Neutron pickup in bombardment of ^{181}Ta, ^{197}Au, ^{232}Th, ^{238}U isotopes with ^{15}N ions, 20: 22001 (JINR-P-2555)
KYCIA, T. F., Structure in the pion-proton total cross section between 2 and 7 Bev/c, 20: 21661

L

LACAMBRA, J. M., Evidence for the prolate deformation of ^{27}Mg, 20: 22099
LACINA, J., Confinement of charged particles in magnetic mirror systems, 20: 22229
LACKNER, K., Two-dimensional steady and one-dimensional unsteady MGD flows of small magnetic Reynolds number, 20: 21781 (AD-622568)
LACKNER, Karl, Magnetogasdynamic flows of small magnetic Reynolds number. I., 20: 21782 (AD-623812)
LADE, R. W., Silicon surface damage due to γ radiation, 20: 21172
LAGARRIGUE, A., "Gargamelle" project, 20: 21033 (CERN-65-32, pp 263-8)
LAGET, J. M., Reaction ^{180}Hf(d,p)^{181}Hf, 20: 22106
LAGO, A., Double-sampling method for carrying out quality control of a fabrication process, 20: 21308
LAI, Tsai-Teh, Polarography of uranyl-semicarbazide hydrochloride complexes, 20: 20677
LA MANTIA, Charles Robert, Thermodynamic study of K amalgams, 20: 21328 (CU-2660-25)
LA MASTER, C. H., Critical-path method for scheduling the transuranium processing plant: an appraisal, 20: 20809 (ORNL-3925)
LAMBROPOULOS, P., Coherence and two-photon absorption, 20: 21533
LAMONDS, H. A., Development of airborne surveillance instrumentation, 20: 20881 (DASA-1704)
LAMPE, F. W., Prog. rpt. on radiation chemistry of silane, annual, 4/66, 20: 20725 (NYO-3570-2)
LANDOVITZ, Leon F., Electromagnetic form factor of the neutrino, 20: 21669
LANDRY, J. W., Monitoring of leached fuel elements with a neutron generator, 20: 21040 (ORNL-P-1218)
LANDSHOFF, R. K., Waveguide theory for ionospheric propagation of hydromagnetic emissions, 20: 21833
LANG, F. M., Perturbing effects of water vapor on mechanism of graphite

oxidation in presence of oxygen (500 to 650°C), 20: 21285
LANG, F. M., Study of compounds formed at temperatures above 600°C by action of carbon dioxide on graphite, 20: 20702
LANG, Peng-fei, Inelastic interactions of π^- mesons with nucleons at 6.8 Bev, 20: 21693
LANGBEIN, W., Radiation-induced reactions in polyethylene oxide, 20: 20766
LANGE, R. C., Half life of 0.305-Mev level in ^{75}As, 20: 22038
LANGE, R. C., Nuclear levels in ^{223}Ra populated by decay of ^{227}Th and ^{223}Fr, 20: 22008 (MLM-1337J)
LANGENBERG, D. N., Microwave-induced d-c voltages across Josephson junctions, 20: 21882
LANGHANS, Kurt, Drill possibilities in protection against mass destruction agents, 20: 20980
LANNING, D. D., PCTR operational techniques, 20: 22493 (BNWL-193, pp 21-9)
LANSIART, A. J., Spark chambers in nuclear medicine, 20: 21082
LANZEROTTI, L. J., Wide-angle electron-pair production, 20: 22146
LAPADU-HARGUES, Philippe, Equipment of research laboratories, 20: 20851
LAPIDUS, L. I., Isospin conservation and polarization effects, 20: 21717 (JINR-P-2620)
LAPIDUS, L. I., Neutrino processes, 20: 21616 (JINR-P-2429)
LA POINTE, M., Monte Carlo simulation of nuclear active cascade in EAS, 20: 21545 (MIT-2098-227, Paper EAS-11)
LA POINTE, M., Primary energy spectrum from 8×10^{14} to 4×10^{17} ev, 20: 21547 (MIT-2098-227, Paper EAS-31)
LA QUEY, R. E., Rocket-borne measurements of particle fluxes and auroral light, 20: 21826
LARIN, Frank, Effect of operating conditions and transistor parameters on gain degradation, 20: 21169
LARIN, I. I., Reconstruction of IRT research reactor, 20: 22497 (IAE-992)
LARSEN, Robert N., Nanosecond pulse stretcher, 20: 21010
LASHER, Gordon, Solution of Ginzburg-Landau equations for the Abrikosov mixed state near the second critical field, 20: 21902
LASKI, Bernard, Chromosome studies on a radiographer and her family, 20: 20447
LASKORIN, B. N., Uranyl ion-exchange behavior in hydrochloric acid media, 20: 20827
LASSILA, K. E., High-energy ρ-exchange peripheral model with absorption and instability, 20: 21647
LATHROP, K. D., Use of discrete-ordinates methods for solution of photon problems, 20: 21642
LATHROP, Katherine, ^{103}Pd as a therapeutic radiation source, 20: 20542
LATORRE, V. A., 1.7-Mev anomaly in the $^{12}C(p,p)^{12}C$ reaction, 20: 22115
LATORRE, V. A., ^{14}N levels from elastic scattering of protons by ^{13}C, 20: 22123
LATS'KO, E. M., Polarization of plasma moving in helical magnetic field, 20: 22275
LATS'KO, E. M., Polarization of plasma moving in toroidal magnetic field, 20: 22276
LATS'KO, E. M., Polarization of plasmas moving in magnetic fields of opposite curvatures, 20: 22277
LAVINE, Daniel M., Myocardial infarction due to postirradiation fibrosis of the coronary arteries, 20: 20468
LAWRENCE, Arthur Charles, Improvements in and relating to nuclear power plants, 20: 22458
LAWRENCE, Robert Henry Jr., Tritium beta-ray induced exchange reactions of deuterium with methane and ethane in the gas phase, 20: 20719 (AD-624657)
LAZANOFF, A., Differential energy and angle spectra for ^{137}Cs γ rays in sand, 20: 22308 (HASL-167)
LAZARUS, A. J., Linear relationship for heavy-ion pulse heights in alkali halides, 20: 21084
LEACH, S. Llewelyn, Characteristics of protective oxide films, 20: 21281
LEAMY, C. C., Analysis of Sn and Cu ores, 20: 20640
LEBEDEV, S. Ya., Influence of krypton on operation of a thermionic converter, 20: 21579
LEBEDEV, S. Ya., Operation of a cesium diode with an admixture of an inert gas, 20: 21567 (FEI-15)
LEBEDEV, S. Ya., Operation of cesium thermionic converter in presence of xenon, 20: 21580
LE BELLAC, M., Polarization in high-energy π-ρ scattering and the Byers-Yang model, 20: 21653
LEBO, G. R., Temporal and statistical characteristics of Jupiter decametric radiation, 20: 21510
LECKY, James A., Catalog of nuclear reactor concepts, Pt. I, Sec. IV, 20: 22347 (ANL-7138)
LECKY, James A., Catalog of nuclear reactor concepts, Pt. I, Sec. V, 20: 22466 (ANL-7180)
LEDERER, M., Adsorption of metal ions on exchangers with phosphoric groups from perchloric acid solutions, 20: 20823
LEDERMAN, L., Neutrino experiments at BNL, 20: 21595 (CERN-65-32, pp 1-10)
LEE, Anna, Determination of the common eigenvector system of operators commuting in pairs, 20: 21855
LEE, B. W., Single-particle representations of current algebras, 20: 21750
LEE, Jong S., Food preservation by irradiation, 20: 21206
LEE, K., Transport properties of LaF_3, 20: 22339
LEE, L. L. Jr., Measurement of spins of some states in ^{55}Fe, 20: 22126
LEE, R. V. Jr., Recoil gold atoms from fast-neutron bombardment, 20: 21441
LEE, T. D., Neutrino physics, 20: 21614 (CERN-65-32, pp 275-84)
LEE, Y. K., Relevance of bombardment-induced Moessbauer effects in iron to radiation damage theories, 20: 21444
LEGRE, J., Results of post-operative irradiation of patients with tumors of the brain, 20: 20530
LE HAZIF, Roger, Compression of monocrystals of Be parallel to C axis, 20: 21371
LEHNERT, B., Ionization process of a plasma, 20: 22257
LEHNERT, K., VA-M-30 thermoluminescence measuring assembly, 20: 21085
LEIBY, C. C. Jr., Electrophoretic power generation in thermally ionized plasmas, 20: 22173 (AD-623788)
LE LEVIER, R. E., Determination of D layer air chemistry from high-altitude nuclear explosion, 20: 21811 (AD-620952)
LELONG, P., Aluminium and magnesium in nuclear metallurgy, 20: 21382
LEMMER, Richard, Intermediate structure, 20: 21988 (BNL-948, pp 876-904)
LENKE, R., Mobility of lithium isotopes in molten ^6LiCl and ^7LiCl, 20: 20695
LEONG, G. F., Acute mortality and recovery studies in sheep irradiated with ^{60}Co γ rays or 1-Mvp x rays, 20: 20487
LEONOV, V. V., Measurement of activity of components in organic mixtures containing ^{14}C, 20: 20639
LEONTIC, B. A., Structure in the pion-proton total cross section between 2 and 7 Bev/c, 20: 21661
LERCH, P., Comparison of different procedures to measure simultaneously ^{32}P and ^{45}Ca in inorganic salts by liquid scintillation counting, 20: 20584
LERICH, Joel, Flow calibration of the Long John manifolded orifice assembly with air, 20: 20988 (UCRL-13202)
LE ROY, George V., Consequences of ingestion by man of real and simulated fallout, 20: 20466
LESUR, P., Comparison of economic aspects of treatment of fission products from installations processing irradiated natural uranium, 20: 22517
LEVENTHAL, M., "Forbidden" level crossing in n = 2 state of atomic hydrogen, 20: 21530
LEVEQUE, Pierre, Radiochemistry in France, 20: 20730 (PB-181506, pp 104-15)
LEVER, R. F., Computation of ion trajectories in the monopole mass spectrometer by numerical integration of Mathieu's equation, 20: 20994
LEVINSTEIN, H. J., Energy gaps in β tungstens and other superconductors, 20: 21885
LEVITZ, N. M., Engineering development of fluid-bed fluoride volatility processes. II., 20: 20801 (ANL-6830)
LEVONI, Sergio, Particular cylindrical solutions in magnetohydrodynamics, 20: 21791
LEVONI, Sergio, Uniqueness theorem for equations of magnetothermo-elasticity, 20: 21793
LEVOY, M. M., Significance of nonequilibrium conductivity on plasma engine performance, 20: 20873
LEVY, Peter M., Rare earth–Fe exchange interaction. II., 20: 22313 (AD-624719)
LEVY, S., Turbulent flow in an annulus, 20: 20856 (GEAP-4976)
LEVY-LEBLOND, Jean-Marc, New nonrelativistic limit to the Poincare group, 20: 21721
LEWELLEN, W. S., Binary diffusion in a confined vortex, 20: 22473
LEWIS, B. S., Materials control system for enriched U chemical processing facility, 20: 20832
LEWIS, Francis H. Jr., Excitation of spin-isospin giant resonance by 180° inelastic electron scattering, 20: 22088
LEWIS, H. D., Powder rolling of tungsten and its alloys, 20: 21318
LEWIS, H. W., Seismic signals from nuclear explosions in overdriven cavities, 20: 20898 (AD-624016)
LEWISAND, Volta G., Prog. rpt. on pre-startup hydraulic tests on AFNETF, final, 1961–65, 20: 22492 (AD-626861)
LEZNIAK, J., Two satellite-borne cosmic-radiation detectors, 20: 21118
LIAS, S. G., Ion-molecule reactions in liquid- and solid-phase radiolysis, 20: 20752
LIBERMAN, A. N., Peculiar features in radiation sickness induced by soft x rays, 20: 20475
LICCIARDELLO, J. J., Microbiology of radiation preservation of foods, 20: 21201
LICHTENBERG, D. B., Lectures on unitary symmetry and elementary particles, 20: 21770

LIEB, D., Performance of tungsten-emitter thermionic converter in presence of CsF additive, 20: 21586
LIEBER, M., Pion production in high-energy cosmic-ray collisions, 20: 21553
LIEBERMANN, R. W., Prog. rpt. on radiation from arc-heated plasma, final, 3/64-4/65, 20: 22167 (AD-622391)
LIIKALA, R. C., Modifications to computer code, THERMOS, 20: 22374 (BNWL-193, pp 5-15)
LILLEY, J. R., Method for analytically removing pulse pile-up effects, 20: 21106
LILLIENFELD, Abraham M., Radiation exposure in parents of children with mongolism, 20: 20454
LIN, Chen-Chong, Radiation-induced effects on water-soluble polymers in aqueous solutions. III., 20: 20748
LINCOLN, J. Virginia, Geomagnetic and solar data, 20: 21830
LIND, D. A., Prog. rpt. on isochronous cyclotron, 2/66, 20: 21473 (UCOL-535-554)
LIND, D. L., Plasma electron detector using an open electron multiplier, 20: 21123
LINDENFELD, P., Thermal conductivity in the mixed state, 20: 21914
LINDGREN, Frank T., Ultracentrifuge rotor temperature measurements and control, 20: 21009
LINDSAY, Stuart, Induction of benign and malignant thyroid neoplasms in the rat, 20: 20448
LINDSEY, Georgia I., Determination of ^{90}Sr in urine by anion exchange, 20: 20583
LINES, R. A. G., Nuclear orientation of ^{54}Mn nuclei in noble metal hosts, 20: 22097
LIPNIK, P., Beta decay and core excitation in A = 111 nuclei, 20: 22083
LIPSHUTZ, Nelson R., Invariance principles and the K^0- $\bar{K}^0$ propagator matrix, 20: 21677
LIPSICAS, M., Nuclear spin-lattice relaxation in liquid hydrogen, 20: 21525
LISCIA, A., Fabrication of ThO_2–UO_2 ceramic fuel, 20: 21301
LISCIA, A., Technological and economical improvements in fabrication of UO_2 ceramic fuel, 20: 21300
LITTLE, P. F., Performance of coaxial plasma gun, 20: 22225
LITTLE, P. F., Scattering of electromagnetic waves by electro-acoustic plasma waves, 20: 22232
LITTLE, R., Pair production by 5-Bev photons in carbon, 20: 21664
LITTLE, Roger G., Experimentally determined plasma perturbation by a probe, 20: 22260
LITTLEJOHN, M. A., Silicon surface damage due to γ radiation, 20: 21172
LITTON, Felix B., Reaction of tantalum with molten cerium–cobalt alloys, 20: 20671
LITVAK, A. G., Electromagnetic wave self-focusing in plasma in strong magnetic field, 20: 22200
LIU, F. F., Positive pion production asymmetry with polarized bremsstrahlung near second resonance, 20: 21589 (AD-626683)
LIU, F. F., Positive-pion production asymmetry with polarized bremsstrahlung near second resonance, 20: 21660
LIU, L. S., Production by neutrinos, 20: 21599 (CERN-65-32, pp 89-96)
LIU, S. W. W., Linear relationship for heavy-ion pulse heights in alkali halides, 20: 21084
LIVINGSTON, J. D., Magnetic hysteresis and critical currents in the mixed state, 20: 21932
LIVINGSTON, Lee Holton, Transport calculation of flux in Nuclear Engineering Test Reactor test cells, 20: 22488 (AD-621121)
LLOYD, L. T., Lattice parameters, thermal expansions, and Grueneisen coefficients of Zr at 4.2 to 1130°K, 20: 21391
LLOYD, R. C., Material bucklings for ^{235}U-enriched U tube lattices in light water, 20: 22375 (BNWL-193, pp 45-56)
LO, Chung-hsien, Inelastic interactions of π^- mesons with nucleons at 6.8 Bev, 20: 21693
LOBKOWICZ, F., Measurement of lifetime of the positive pion, 20: 21665
LOBO, Pedro W., Nuclear quadrupole resonance and its applications in chemistry, 20: 20699
LOBSINGER, R. J., Stresses in Zy-2 cladding during vibratory fuel loading, 20: 21289 (BNWL-194)
LOCKER, Robert J., Minimum charge detection using selected tunnel diodes and charge multiplying semiconductors, 20: 21113
LOCKWOOD, Grant J., Response of CsI(Tl) crystals to low-energy heavy ions, 20: 22318
LODHI, M. A. K., Elastic electron scattering by ^6Li, 20: 22063
LOEBBAKA, D., Normal scalar nonet; $K_1 \rightarrow 2\pi$ decay and K_1-K_2 mass difference, 20: 21675
LOEWDIN, Per-Olov, Advances in quantum chemistry. II., 20: 20698
LOMBARD, D. G., Recovering oil from shale with nuclear explosives, 20: 20835
LOMBARD, David B., Multidirectional peak pressure gauge for strong shock waves, 20: 20914
LOMINADZE, D. G., Interaction of charged particle beam with a confined plasma, 20: 22286
LOMON, E. L., Nucleon-nucleon boundary condition methods for nuclear matter, 20: 22022
LONG, Austin, Techniques of methane production for ^{14}C dating, 20: 20917
LONG, W. G., SNAP environment simulation problems, 20: 22475
LONGHURST, W. M., Environmental and biological factors affecting accumulation of ^{90}Sr and ^{137}Cs in deer and sheep, 20: 20388 (SAN-34-2)
LONGO, Michael J., Electroluminescent panels as pulsed fiducial marks in spark chamber experiment, 20: 21090
LONNGREN, K. E., Interpretation of multiple reflections in microwave interferometers used in plasma diagnostics, 20: 22231
LOO, Billy W., Use of image intensifiers with streamer chambers, 20: 21020 (AD-621069)
LOOS, Hendricus G., Rudimentary geometric particle theory, 20: 21726
LOPEZ, M. E. Ortiz de, Assignment of neutron capture angular momenta in angular distributions of $^{23}Na(d,p)^{24}Na$ reaction, 20: 22150
LORD, L. H., Progressive myelopathy in a dog caused by ThO_2, 20: 20455
LORRAIN, C., Nuclear materials management in uranothorianite processing, 20: 20969
LORRAIN, C., Sampling operations involving suppliers and customers, 20: 20973
LOTT, James R., Changes in 5-OH tryptamine content in rat brain tissues x-irradiated in vitro, 20: 20437 (CONF-650560-18)
LOTT, James R., Oxygen uptake in rat brain tissues x-irradiated in vitro, 20: 20436 (CONF-650560-17)
LOTZ, W., Calculation of forces and inductances for the hexapole experiment, 20: 22181 (IPP-1/45)
LOU, Alice, Lambda-hyperon binding energy in nuclear matter, 20: 22161
LOUCKS, T. L., Fermi surface and positron annihilation in yttrium, 20: 22338
LOVE, D. L., Nuclear-charge distribution of fission-product chains of mass numbers 131-133, 20: 22136
LOW, W., X-ray excitation of second positive and first negative bands of nitrogen, 20: 21834
LOWENTHAL, G. C., Isothermal microcalorimeter operated in a water triple-point cell and designed for radioactivity measurements, 20: 21068
LU, P., Position and the polarization of a polarized particle in circular motion, 20: 21481
LUCAS, B. T., Analyses of 18-Mev α-particle scattering cross sections for ^{40}Ar, ^{32}S, ^{31}P, ^{23}Na, and ^{20}Ne, 20: 22134
LUCAS, Monique, Isotopic analysis of U and Pu, 20: 20978
LUDUENA, F. P., Photochemical synthesis of norepinephrine from tyramine, 20: 20409
LUECK, G., Defect production in copper, nickel, and gold by 5-Mev α bombardment in region 90 to 194°K, 20: 21447
LUNDBERG, B., Gamma spectra from inelastic neutron scattering, 20: 22069
LUNDY, R. A., $\pi^\pm$ and $K^\pm$ production cross sections for 12.5-Bev protons on Be, 20: 21601 (CERN-65-32, pp 109-10)
LUNELLI, M., Variational iterative methods for elliptical problems in theory of nuclear reactors, 20: 22387
LUYSTERBORG, J., Rapid and quantitative method for the detection of plutonium in urine, 20: 20590
LYASHENKO, V. A., Separation of Th from ions of certain metals on anion exchanger AV-17 from nitric acid solutions, 20: 20624
LYKOUDIS, Paul S., Mixing length damping and sunspots, 20: 21489 (AD-623803)
LYLE, R. G., Protective coating systems for Nb in range 1800 to 2500°F, 20: 21257 (AD-621546)
LYNCH, E. D., Stoichiometric and hyperstoichiometric solid solutions in ThO_2–UO_2 system, 20: 21323 (ANL-6894)
LYNTON, E. A., Thermal conductivity in the mixed state, 20: 21914
LYON, Mary F., Mutation rates at a new set of specific loci in the mouse, 20: 20461
LYON, William S., Gamma-ray branching ratios for ^{116}In, ^{147}Nd, and ^{141}Ce, 20: 22091
LYONS, M. F., Irradiation of 0.5-inch diameter, hollow-pellet UO_2 fuel rods, 20: 21422 (GEAP-5100D)
LYSOV, B. S., Dissociation of $NbCl_5$ on Nb and carbide surfaces, 20: 21241 (LA-tr-66-15)
LYUBARSKII, G. Ya., Asymptotic solution of diffusion problem and its application to the theory of cyclic particle-storage devices, 20: 21483

M

MAAS, Eugene V., Selective inhibition of cation absorption by uranyl, 20: 20402
MACDONALD, James R., Stopping cross sections in B of atoms with energies 15 to 140 kev, 20: 21539
MAC DONALD, R. J., Depths of low-energy ion bombardment damage in germanium, 20: 21438
MAC DOUGALL, John D., Atomic mass differences involving isotopes of Nd, Sm, Cd, and Pb, 20: 22153
MACFARLANE, A. J., Should SU(3) mass formulas for mesons use the

masses of the mesons or their squares? 20: 21671
MACFARLANE, Malcolm, Single-nucleon transfer reactions, 20: 21971 (BNL-948, pp 1-65)
MACHIDA, Chuji, Nuclear materials management at JAERI, 20: 21313
MAC LEOD, A. M., Triggered cloud chamber for low-energy nuclear reactions, 20: 21063
MADER, Charles L., Two-dimensional hydrodynamic hot spot. III., 20: 21784 (LA-3450)
MADEY, Richard, Spark chamber spectrometer for space protons, 20: 21120
MADSEN, V. A., Formalism for direct inelastic scattering and charge exchange, 20: 22067
MAEKAWA, Shun-ichi, Gamma irradiation on MOS field effect transistor, 20: 21159
MAES, W. F., Migration of radio elements in soil, 20: 20875 (EUR-2481.f)
MAGDON, E., Effects of radiation on $NADH_2$ oxidation in preparation of mitochondria, 20: 20496
MAGGIONI, G., Variational iterative methods for elliptical problems in theory of nuclear reactors, 20: 22387
MAGNIER, P., Perturbing effects of water vapor on mechanism of graphite oxidation in presence of oxygen (500 to 650°C), 20: 21285
MAJUMDAR, Chanchal K., Continuity of bound and unbound states in a Fermi gas, 20: 21851
MAKARENKO, G. N., Thermionic emission from CeC_2, 20: 21397
MAKHUNKA, I., Investigation of the α spectrum of Bi isotopes, 20: 22000 (JINR-P-2553)
MAKI, Kazuni, Abrikosov's structures in superconducting alloys, 20: 21906
MAKI, Ziro, Possible scheme for nonleptonic decays of hyperons, 20: 21687
MAKIOS, W., Microwave interferometry in electromagnetically produced shock waves, 20: 22182 (IPP-3/35)
MAKLAKOV, V. N., Radiometric method of determining sulfur in naphthalene, 20: 20615
MAKRA, Zsigmond, Device for the measurement of average neutron energies, 20: 21074
MALICK, F. S., NERVA reactor instrumentation, 20: 22484
MALKIN, O. A., Cathode spots of pulsed discharge between parallel electrodes, 20: 22292
MALLARD, J. R., Medical radioisotope visualization, 20: 20531
MALLETT, A. J., Fissile-material container and packaging development and testing program, 20: 20936 (K-1661)
MALM, H. L., Large-volume coaxial germanium γ spectrometers, 20: 21104
MALM, John G., Preparation and thermal properties of pure XeF_6, 20: 20665
MALMBERG, T., Safety and cost analysis of 1000-Mw(e) sodium-cooled fast power reactor, 20: 22451
MALOV, A. F., Aberration and displacement of beam by a magnetic prism fringe field that does not vary transversely, 20: 21484
MALOY, J. O., Rocket gamma scanning of nuclear bursts, 20: 21129
MALVANO, R., Photoneutron production from C, Al, and S by bremsstrahlung up to 200 Mev, 20: 22094
MALVILLE, J. M., Pre-absorption events at 230 Mc/s, 20: 21500
MALYSHEV, G. M., Plasma diagnostics by scattering of light on electrons, 20: 22295
MANABE, Katsumi, Nondestructive testing of nuclear fuel elements. I., 20: 20865
MANASEVIT, H. M., Growth of single-crystal silicon on beryllium oxide, 20: 21249
MANDEL, L., Configuration-space photon number operators in quantum optics, 20: 21863
MANLEY, J. H., Reactions (^{3}He,n) with 19- to 25-Mev ^{3}He ions, 20: 22132
MANLEY, Oscar P., Early radiation field and high-energy electrons in supernovae, 20: 21499
MARBACH, James R., Electron spectrometer for project Gemini, 20: 21116
MARCHAL, Marie-Therese, Recording respiratory function by x rays, 20: 20546
MARCHAL, Maurice, Recording respiratory function by x rays, 20: 20546
MARCHANT, H., Collective states of ^{209}Bi, 20: 22108
MARCHESI, F., Homogenization of cruciform control rods in water-moderated reactor, 20: 22357 (RT-FI-(65)50)
MARCUM, A. I., Response of scintillators and semiconductors to low-energy x-ray excitation, 20: 21107
MARCUS, J. A., Empirical Fermi-surface parameters for W and Mo, 20: 22337
MARCUS, Paul M., Phenomenological theory of type II superconductors, 20: 21929
MARECHAL, Jean-Claude, Behavior of concrete pressure vessel subjected to high temperature gradient, 20: 22353 (CEA-R-2829)
MARINARO, M., Divergence of renormalized VS convergence of regularized perturbative expansions in field-theoretical model, 20: 21741
MARINARO, M., Removal of point-loop ambiguities through finite-part renormalization, 20: 21742
MARINI, R., Compensation of thermic effects in semiconductor junctions used for measures in logarithmic scale, 20: 20992
MARINOV, A., Measurement of spins of some states in ^{55}Fe, 20: 22126
MARKOWITZ, David, Kronig-Penney model for excitations in type II superconductors, 20: 21904
MARQUARDT, R., ZSA-ZSA: a self-policed data handling facility for multiple detector experiments, 20: 20996
MARRUS, Richard, Nuclear moments of ^{241}Am and 16-h ^{242}Am and analysis of the hyperfine fields, 20: 22137
MARSDEN, P. L., Response of standard IGY neutron monitor, 20: 21551
MARTALOGU, N., Angular correlations in inelastic proton scattering on ^{20}Ne and ^{32}S, 20: 22059
MARTENS, John H., Catalog of nuclear reactor concepts, Pt. I, Sec. IV, 20: 22347
MARTENS, John H., Catalog of nuclear reactor concepts, Pt. I, Sec. V, 20: 22466 (ANL-7180)
MARTIN, Donald, Pulsed x-ray prompt gamma simulator, 20: 20838 (AD-624019)
MARTIN, F. W., Junction counters produced by irradiation of silicon with dopant ions, 20: 21098
MARTIN, J. A., Neutron and γ sensitivities of dynamic detectors, 20: 21059
MARTIN, J. H., Effects of electron irradiation and temperature on solar cell performance, 20: 21161
MARTIN, M. J., Nuclear theory index for 1964, 20: 22011 (TID-22771)
MARTINEZ, J. L., Conductance device for monitoring thin film growth, 20: 20987 (RFP-690)
MARTINI, M., Experimental results on the information available from the rise time of pulses supplied by semiconductor particle detectors, 20: 21137
MARTONE, Ronald J., Hybrid radioisotope scanner, 20: 20535
MARWAH, S. D., Formation of complex compounds between rare earth nitrate and uranyl nitrate, 20: 20682
MASHIKO, Kikuya, Calcium uptake by teleost fishes. I., 20: 20405
MASKEWITZ, B. F., SDC—shielding-design calculation code for fuel-handling facilities, 20: 22309 (ORNL-3041)
MASKEWITZ, Betty F., Abstracts of digital computer code packages assembled by RSIC, 20: 22310 (ORNL-RSIC-13)
MASON, Benjamin J., Selective inhibition of cation absorption by uranyl, 20: 20402
MASON, E. A., Friction factor and heat transfer correlation for irradiated organic coolants, 20: 20710 (MIT-334-23)
MASPERONI, A., Metallurgical studies of some uranium alloys, 20: 21372
MASSA, E., Three-dimensional aspects of generally covariant expressions, 20: 21859
MATERASSI, R., Influence of irradiated nitrogen on the nitrogen-fixing activity of blue-green algae, 20: 20408
MATHESON, C. C., Variable transfer rates in superfluid helium films, 20: 21895
MATHUR, V. S., S-matrix approach to superconductivity, 20: 21879
MATSUDAIRA, Noboru, Quantum kinetic equations for unstable plasmas, 20: 22238
MATSUKI, Seishi, Time resolution of transistorized time-of-flight system, 20: 21052
MATSUMURA, Seiji, Radiation-induced variegations in Einkorn wheat and their inheritance, 20: 20497
MATSUO, Hisayuki, Selective ^{2}H- and ^{3}H-labeling reaction of c-terminal amino acids through oxazolone, 20: 20714
MATTERN, P. L., Cam-driven, constant-acceleration Moessbauer spectrometer, 20: 21080
MATTHES, F., Production and properties of cerium and lanthanum oxychlorides, 20: 20680
MATTHEWS, P. T., Irreducible representations of U(12), 20: 21765
MATTSSON, Arne C. J., Performance of self-excited MHD generator, 20: 21564 (AD-627037)
MATUS, Lajos, Mass-spectrometric isotopic analysis of uranium using thermionic emission, 20: 21216
MATVEEVA, T. V., Corrosion and electrochemical behavior of rhenium, 20: 21275
MAUSHART, R., Measurement of radioactivity in air, water, and food, 20: 20961
MAXFIELD, B. W., Observation of low-frequency mixed-state resonances in pure niobium, 20: 21894
MAY, S., Study of compounds formed at temperatures above 600°C by action of carbon dioxide on graphite, 20: 20702
MAYER, J., EPR studies of γ-irradiated ethanol—benzene system at −196°C, 20: 20742
MAYER, J., Radiolysis of ethanol-benzene systems under the influence of ^{60}Co γ radiation, 20: 20741
MAYER-KUCKUK, T., Statistical character of reaction ^{37}Cl(p,α)^{34}S at 21- to 22-Mev excitation energy of the compound nucleus, 20: 22084
MAYHOOK, A. R., Programs for design calculations on Harwell Variable Energy Cyclotron, 20: 21472 (RHEL/R-113)
MAYKUTH, D. J., Ductile tungsten sheet alloy, W–5Re–2.2ThO_2, 20: 21407
MAYNARD, John Charles, Improvements in or relating to luminous compositions, 20: 20787

MAZANOWSKA, Anna, Biochemical lesions induced in subcellular structures by ionizing radiation. III., 20: 20417

MAZENKO, J. J., Prog. rpt. on effect of transistor design parameters on radiation response, 7–9/65, 20: 21148 (AD-630835)

MAZENKO, J. J., Prog. rpt. on effect of transistor design parameters on radiation response, 10–12/65, 20: 21149 (AD-630836)

MAZZOCCO, N. J., Prog. rpt. on radiation-induced telomerization of methanol, final, 11/64–4/65, 20: 20724 (NYO-2978-44)

MC ALLISTER, Karl D., Construction and instrumentation of cryostat for AF-NETF, 20: 22489 (AD-621123)

MC ARTHUR, W. H., Change in partition of total-body N in radiation chimeras, 20: 20407 (ORNL-P-1118)

MC CAHILL, Dennis F., School designs to resist integrated nuclear weapons effects, 20: 20868 (AD-626770)

MC CAMMON, C. P., Evaluation of radiation dose to man from radionuclides released to Clinch River, 20: 22514 (ORNL-P-2021)

MC CARTHY, J. T., Half life of 0.305-Mev level in ^{75}As, 20: 22038

MC CARTHY, J. T., Nuclear levels in ^{223}Ra populated by decay of ^{227}Th and ^{223}Fr, 20: 22008 (MLM-1337J)

MC CLURE, J. A., Space-time properties of a scattering interaction, 20: 21761

MC COLLUM, W. A., Prog. rpt. on radiation effects on Ni–Cd electrodes, final, 6/63–4/65. I., 20: 21425 (N-65-24491)

MC CONVILLE, T., Specific heat of type II superconductors in a magnetic field, 20: 21907

MC CORMICK, D. J., Separately fired superheater—nuclear application at Indian Point, 20: 22455

MC CORMICK, J. Frank, Development of a ^{137}Cs facility for ecological research, 20: 20380 (TID-22499)

MC DANIEL, Weymouth N., Fuel element hold-down arrangement for nuclear reactors, 20: 22369

MC DIARMID, I. B., Lifetimes of low-energy electrons in outer radiation zone at magnetically quiet times, 20: 21817

MC DONALD, Clark E., Potential commercial manufacture and use of hardwood plywood plastic combinations, 20: 21191 (ORNL-IIC-7, pp 112-18)

MC GARRY, W. I., Angular distributions and cross section ratios for the reactions $^{2}H(d,n)^{3}He$ and $^{2}H(d,p)^{3}H$ below 500 kev, 20: 22074

MC GINNIS, Gerald, Information processing unit of fuel element rupture detector system of EBR-II, 20: 22439

MC GOUGALL, Ian, Excess radiogenic argon in pyroxenes and isotopic ages on minerals from Norwegian eclogites, 20: 20891

MC GREGOR, W. K., Equivalence of electron and excitation temperatures in an argon plasma, 20: 22267

MC HARRIS, William, Decay scheme of ^{254}Es, 20: 22142

MC ILWRAITH, N., Plasma electron detector using an open electron multiplier, 20: 21123

MC KANNAN, E. C., Effects of nuclear radiation dielectric materials, 20: 21152 (N-65-22353)

MC KENZIE, D. E., Prog. rpt. on radiation effects on Ni–Cd electrodes, final, 6/63–4/65. I., 20: 21425 (N-65-24491)

MC LATHIE, William, Atomic mass differences involving isotopes of Nd, Sm, Cd, and Pb, 20: 22153

MC LAUGHLIN, J., Differential energy and angle spectra for ^{137}Cs γ rays in sand, 20: 22308 (HASL-167)

MC LEAN, E. A., Deviations from ionization equilibrium in plasmas generated by electric shock tubes, 20: 22250

MC MANUS, Hugh, Inelastic scattering, 20: 21973 (BNL-948, pp 175-221)

MC MASTER, A. D., Oxidation of thin evaporated rhenium films, 20: 21274

MC MASTER, W. H., Theoretical differential scattering cross sections of x rays, 20: 21516 (UCRL-14403)

MC MURRAY, W. R., Scattering of fast neutrons by ^{238}U, 20: 22056

MC QUAID, James H., Electron and proton spectrometer detector system for an OGO-E satellite experiment, 20: 21124

MEABURN, Malcolm, Effect of hydrogen atom and electron scavengers on the radiolysis of methanol vapor, 20: 20776

MEAL, Thomas J., Improved performance of BF_3 neutron counters in high gamma fluxes, 20: 21132

MEDFORD, L. V., Modular set of analog microcircuits intended for satellite experiments, 20: 20997

MEDGYESI-MITSCHANG, L. N., Determination of electron densities using a radial transmission line, 20: 22171 (AD-622811)

MEDVED, S. V., Fluctuations of ionization losses, 20: 21515 (JINR-P-2615)

MEHLHOP, W. A. W., Feasibility of experiment to observe the W produced in strong interactions, 20: 21610 (CERN-65-32, pp 181-94)

MEIERE, F. T., High-energy limit of $\pi^{+}n^{0}$ total cross section, 20: 21679

MEILING, W., Nanosecond lifetime measurements in decay of ^{155}Eu, ^{157}Eu, and ^{157}Dy, 20: 22058

MEISEL, W., Disappearance of quadrupole splitting in Moessbauer spectra of ^{57}Co-containing AgCl at 300°K, 20: 22340

MELENCHUK, I. P., Assessment of method of recording radiophosphorus bremsstrahlung for diagnosis of milk-duct carcinoma, 20: 20540

MELIKIYA, M. G., Theory of low-voltage arcs in cesium. II., 20: 21578

MELLOW, E. W., Prog. rpt. on STEP project, 7–12/64, 20: 22467 (IDO-17077)

MELLOWS, Frank W., Effect of hydrogen atom and electron scavengers on the radiolysis of methanol vapor, 20: 20776

MEL'NICHENKO, A. A., Trochoidal bunching with high space charge, in crossed electric and magnetic fields, 20: 21450

MENEFEE, J., Calcium fluoride as x-ray and charged particle detector, 20: 21135

MENKES, C. K., Acute mortality and recovery studies in sheep irradiated with ^{60}Co γ rays or 1-Mvp x rays, 20: 20487

MENKHOFF, H., Accuracy obtainable in measurement of gross weights with γ radiation, 20: 21205

MENYHARD, N., Gap equation and current density for local superconductors in a magnetic field, 20: 21880

MERCEREAU, J. E., Quantized flux pinning in superconducting niobium, 20: 21909

MERCINY, E., Separation of lanthanides and actinides by hydroxyethylenediaminetriacetic acid. I., 20: 20822

MERK, W., Safety and cost analysis of 1000-Mw(e) sodium-cooled fast power reactor, 20: 22451

MERKLEY, M. S., Prog. rpt. on effects of low-level irradiation upon preservation of food products, annual, 4/65, 20: 21195 (TID-22509)

MESHKOV, I. N., Focusing of intense electron beam in an accelerator tube, 20: 21487

MESSIAEN, A. M., High-frequency dielectric resonance probe for measurement of plasma densities, 20: 22219

MESZAROS, Istvan, Aerosol activity meter, 20: 21073

METHASIRI, T., Emission of long-range α particles in fission, 20: 21968 (AEET-235)

METHERELL, A. J. F., Characteristics of the Moellenstedt electron velocity analyzer, 20: 21005

METZGER, Albert E., Nondispersive x-ray spectrometer for lunar and planetary geochemical analysis, 20: 21128

MEYER, C. H. Jr., Critical fields of superconducting vanadium films, 20: 21915

MEYER, G., Penetration of a magnetic field into Nb_3Sn, V_3Si and Nb_3Al at low fields, 20: 21908

MEYER, J. A., Procedure for eliminating temperature-sensitive impurities in toluene-methyl-^{3}H used for hydrogen abstraction reactions, 20: 20711

MEYER, Kenneth, Effect of delayed neutrons on stability of a nuclear power reactor, 20: 22443

MEYER, P., Prog. rpt. on pulsed neutron application to power reactor startup, 7–10/65, 20: 22414 (GEAP-4961)

MEYER, Rudolf X., Plasma generator and propulsion exhaust system, 20: 20874

MEYERHOFF, R. W., Dependence of current degradation in superconducting solenoids on flux pinning energy and temperature, 20: 21920

MICHAELSON, Sol M., Biochemical aspects of radiation injury and recovery, 20: 20435 (CONF-650560-15)

MICHALAK, S., Optical transition radiation from 6- to 23-kev electrons entering normal to metal surfaces, 20: 21518

MICHEL, Dovid, Intermetallic compounds with the $CeCu_2$-type structure, 20: 21352 (TID-21745)

MICHEL, F. C., Plasma in the geomagnetic tail, 20: 21828

MIHAMA, Kazuhiro, Effects of ion bombardment on molybdenite, 20: 21529

MIKETTA, D. N., Material and process specifications for refractory alloy and alkali metals, 20: 21293 (R-66SD3007)

MIKHAILOV, I. N., Nucleon-phonon interaction problem, 20: 21619 (JINR-P-2567)

MIKHAILOVSKII, A. B., Instability of electronic waves in nonuniform plasma streams, 20: 22296

MIKLER, J., Dissolution of rare earth metals in methanolic solutions of ammonium acetate, 20: 20686

MILENIN, V. M., Radial dependence of electron velocity distribution in positive column of discharge, 20: 22294

MILEY, George H., Fission-fragment transport effects as related to fission-electric-cell efficiencies, 20: 21576

MILFORD, S. N., Pion production in high-energy cosmic-ray collisions, 20: 21553

MILHALCZO, J. T., 05R Monte Carlo analysis routines for calculating various mean times in reactor problems, 20: 22380 (ORNL-TM-1246)

MILLER, Bennett, Ionizing shock studies in an electromagnetically driven shock tube, 20: 21779 (AD-621990)

MILLER, G. L., Modular set of analog microcircuits intended for satellite experiments, 20: 20997

MILLER, W. W., Electrodeposition method for counting alpha and beta emitters, 20: 20795

MILLS, Brian E., Method of manufacturing control rods for nuclear reactors, 20: 21317

MILLS, J. S., Identification and inspection for inventory control of irradiated fuel elements, 20: 20970

MILMAN, Miriam, Isotopic and phase effects in neutron-irradiated ethyl

bromide, 20: 20751
MILNER, D. J., Effect of γ radiation. X., 20: 20759
MILNER, G. W. C., Analysis of uranium silicides, 20: 20557 (AERE-R-5129)
MIMEAULT, Victor Joseph, Flash desorption and isotopic mixing of simple diatomic gases on, 20: 20652 (IS-T-67)
MINAMI, Kozo, Microwave absorption of magnetoplasma with boundaries, 20: 22209
MINES, J. R., Deuteron optical potentials and the $^{16}O(d,p)^{17}O$ reaction, 20: 22104
MINGUZZI, A., Analyticity properties of the scattering amplitude, 20: 21733
MINNAERT, Pierre, Positivity conditions for the density matrix of spin-one particles, 20: 21764
MINTON, G. H., Reactivity worth of rod-cluster control elements, 20: 22395
MIODUSZEWSKI, Daniel P., Dependence of longitudinal plasma wave damping and growth on the shape of the velocity distribution function, 20: 22166 (AD-621913)
MIRAT, Paul, Effect of irradiation by nuclear particles on switching times of fast diodes, 20: 21157
MIRNIK, M., Determination of ion adsorption by radioactive tracer technique, 20: 20683
MIROSHNICHENKO, V. I., Kinetic theory of passage of electromagnetic waves through a plasma layer. I., 20: 22297
MISAKI, Akeo, Mean square angular and lateral spreads of electrons and photons in a cascade shower, 20: 21557
MISAKI, Akeo, Observation of high-energy jets with emulsion chambers, 20: 21555
MISHINA, Akira, Properties of γ-irradiated starch and graft copolymers as adhesives and dyeing mordants, 20: 20767
MISYUNAS, I. I., Experimental data on dose assessment during remote-control γ therapy, 20: 20541
MITCHELL, E. W. J., Design of a velocity selector for long-wavelength neutrons, 20: 21007
MITO, A., Excitation functions for reactions induced by protons on Cd up to 37 Mev, 20: 22078
MITTA, Aldo E., Labeling lipids with ^{131}I, 20: 20789 (CNEA-182)
MITTA, Aldo E. A., Insulin labeling with ^{131}I, 20: 20383 (CNEA-185)
MIYAKE, Kozo, Time resolution of transistorized time-of-flight system, 20: 21052
MIYAKE, Shoji, Injection trapping of high-energy molecular ions into the mirror field with the r-f electric field. II., 20: 22207
MIYAKE, Takeo, Effect of uv or γ radiation on luminol, 20: 20777
MIYAKOSHI, Junichi, Measurement of liquid volume by activation analysis, 20: 21208
MIYANAGA, Ichiro, Spectrometric method for measurement of low-level γ exposure dose, 20: 20952
MIYASHITA, Kyoichi, Semiconductor nuclear particle detectors. II., 20: 21077
MIYAZAWA, Kiyoshi, Hitachi power manipulator, 20: 20843
MOCHIZUKI, Tsutomu, Outline of the radioisotope production at JAERI, 20: 21220
MODENA, I., Liquid ^3He target for high-energy nuclear experiments, 20: 22007 (LNF-66/1)
MOELLER, E., Time dependence of neutron slowing-down and thermalization in H_2O, 20: 21936 (AE-216)
MOISEEV, V. V., Radioactivation analysis of SiO_2 using ion exchange chromatography. I., 20: 20632
MOISEEV, V. V., Radioactivation analysis of SiO_2 using ion exchange chromatography. II., 20: 20633
MOISEEV, V. V., Radioactivation analysis of SiO_2 using ion exchange chromatography. III., 20: 20634
MOISEEV, V. V., Radioactivation analysis of SiO_2 using ion exchange chromatography. IV., 20: 20635
MOISEEV, V. V., Radioactivation analysis of SiO_2 using ion chromatography. V., 20: 20636
MOIZHES, B. Ye., Theory of low-voltage arcs in cesium. II., 20: 21578
MOLDAUER, Peter, Reactions with fluctuating cross sections, 20: 21987 (BNL-948, pp 826-75)
MOLDAUER, Peter, Strong coupling, exchange, target excitation, and other corrections to DWBA, 20: 21979 (BNL-948, pp 525-60)
MONETON, Jean-Louis, Decontamination of radioactive effluents, 20: 22516
MONTELATICI, V., Liquid ^3He target for high-energy nuclear experiments, 20: 22007 (LNF-66/1)
MONTGOMERY, J., British seismometer array recording systems, 20: 20913
MONTOJO, Rosa M., Double-sampling method for carrying out quality control of a fabrication process, 20: 21308
MOORE, David P., Selective inhibition of cation absorption by uranyl, 20: 20402
MOORE, F. L., Improved extraction method for isolation of trivalent actinide–lanthanide elements from nitrate solutions, 20: 20812
MOORE, M. S., Epithermal fission cross section of ^{235}U, 20: 22012 (UCRL-14606)
MOORES, Harry, Thermoelectric devices, 20: 21016
MORALES, A., G_2 symmetry and leptonic decays, 20: 21719
MORCOM, W. R., Properties of W and W–Re alloys, 20: 21406
MORE, K., Monte Carlo calculations of radionuclide production in iron targets bombarded with 400-Mev protons, 20: 22035
MORE, Richard M., Cherenkov radiation, 20: 21633
MOREAU, Claude, Oxidation of UC with oxygen between 800 and 1000°C, 20: 21267
MOREAU, Claude, Process for the densification of carbonaceous bodies, 20: 21315
MORENO, James B., Shock-tube measurement of vibrational relaxation times in deuterium, 20: 21797
MORETTI, E., X-ray scanning of sky in 20- to 200-kev range, 20: 21490
MORGAN, D. T., Prog. rpt. on in-pile loop irradiation studies of organic coolant materials, 1–9/65, 20: 20723 (MIT-334-33)
MORI, Sigeru, Plasma flow past bodies in a magnetic field, 20: 22251
MORINAGA, H., Heavy strongly deformed nuclei, 20: 21977 (BNL-948, pp 380-453)
MORINAGA, H., Single-nucleon transfer reactions, 20: 21971 (BNL-948, pp 1-65)
MORITA, Yoshinori, Gamma irradiation on MOS field effect transistor, 20: 21159
MORIUCHI, Shigeru, Spectrometric method for measurement of low-level γ exposure dose, 20: 20952
MORIYAMA, Hideo, Studies on X agent. XLVI., 20: 21163
MOROZOV, B. P., Welding of molybdenum and niobium with stainless steel, 20: 21309
MOROZOVA, V. K., Superconducting alloy in the Nb–Ga system, 20: 21897
MORPURGO, G., Saturation problem in nonrelativistic quark model of elementary particles, 20: 21748
MORRIS, J. C., Prog. rpt. on radiation from arc-heated plasma, final, 3/64–4/65, 20: 22167 (AD-622391)
MORRIS, T., Mutation rates at a new set of specific loci in the mouse, 20: 20461
MORRIS, W. R., New control techniques for NERVA reactors, 20: 22482
MORRISON, David L., Diffusion of fission products in fuel-element cladding materials and related alloys, 20: 21232 (BMI-1763)
MORRISON, G. W., 05R Monte Carlo analysis routines for calculating various mean times in reactor problems, 20: 22380 (ORNL-TM-1246)
MORRISON, R. G., Fission couples applied toward reactor diagnostics and safety, 20: 22355 (LA-3470)
MORROW, Irving B. Jr., Performance of self-excited MHD generator, 20: 21564 (AD-627037)
MORTON, Maurice, Prog. rpt. on low-temperature polymerization, 7–9/65, 20: 20718 (AD-623307)
MORTON, R. J., Evaluation of radiation dose to man from radionuclides released to Clinch River, 20: 22514 (ORNL-P-2021)
MORTON, W. A., Temporal and statistical characteristics of Jupiter decametric radiation, 20: 21510
MOSBURG, Earl R. Jr., Nonlinear diffusion with recombination in an electron-beam-excited plasma, 20: 22266
MOSER, J. B., Preparation of sulfides and phosphides of plutonium, 20: 20676
MOSHINSKY, M., Gelfand states and the irreducible representations of the symmetric group, 20: 21734
MOSKVIN, L. N., Partition chromatography on polytetrafluoroethylene. I., 20: 20621
MOSKVIN, L. N., Partition chromatography on polytetrafluoroethylene. II., 20: 20622
MOSKVIN, L. N., Partition chromatography on polytetrafluoroethylene. III., 20: 20623
MOSTOVOI, V. I., Neutron thermalization process in time in graphite and Be, 20: 21942 (KFK-tr-188)
MOSTOVOI, V. I., Transient neutron spectra in zirconium hydride, 20: 21941 (IAE-977)
MOSZKOWSKI, Steven, Heavy strongly deformed nuclei, 20: 21977 (BNL-948, pp 380-453)
MOTT, W. E., Hydrogen analysis by slow neutron transmission, 20: 20641
MOWAT, W. M. H., British seismometer array recording systems, 20: 20913
MOYNIHAN, D. C. Jr., Magnetohydrodynamic circulation of liquid of finite conductivity in an annulus, 20: 21789
MUELLER, A., Method to study stationary neutron transport problems in two-dimensional laminated material arrangement, 20: 21945
MUENTHER, Ch., Electron content of the ionosphere and its fluctuations, 20: 21816
MUKUNDA, N., Charge conjugation in unitary symmetry groups, 20: 21725
MULLARD, J. E., British seismometer array recording systems, 20: 20913
MULLEN, J. H., Determination of electron densities using a radial transmission line, 20: 22171 (AD-622811)
MULLER, M. W., Transport properties of LaF_3, 20: 22339
MULLIKIN, H. F., Prog. rpt. on ventilation of fallout shelters, 7/64–6/65, 20: 20921 (AD-621998)

MULLINS, J. N., Rocket gamma scanning of nuclear bursts, 20: 21129
MUNNS, J. M. Jr., Design proposal for rate-of-change-of-pressure scram safety channel for the EGCR, 20: 22417 (TID-22759)
MURAKAMI, K., Low-μ showers, 20: 21546 (MIT-2098-227, Paper EAS-29)
MURAKAMI, K., Primary energy spectrum from 8×10^{14} to 4×10^{17} ev, 20: 21547 (MIT-2098-227, Paper EAS-31)
MURAMATSU, Hiroshige, Radiation-induced addition reaction of ethers to 1,2-dichlorotetrafluorocyclobutene and 1,2-dichlorohexafluorocyclopentene, 20: 20773
MURARKA, S. P., Self-diffusion in metals, 20: 21230 (AEET-233)
MURDOCH, Lawrence B., Separation of Cd from the Pb–Bi eutectic by high-vacuum single-stage distillation, 20: 20805 (IS-1329)
MURTAS, G. P., Photodisintegration of the deuteron by polarized γ rays, 20: 21626 (LNF-66/4)
MUSAL, Henry M. Jr., Inverse brush cathode for negative-glow plasma source, 20: 22222
MUSGRAVE, John R., Purification and crystallization of B, 20: 21294 (TID-22221)
MUTO, Hiroshi, Determination of traces of fluorine in uranium oxides by pyrolysis-alizarin complexone photometric method, 20: 20597
MUTO, Jiro, Nuclear reaction on ^{13}C at the proton energy of 54.9 Mev, 20: 22030
MUZSNAY, Laszlo, Furnace for UO_2 sintering, 20: 21304
MUZSNAY, Laszlo, ZR-2 critical assembly, 20: 22388
MUZZARELLI, R. A. A., Automatic scanning of chromatoplates by multi-scaling using a γ spectrometer, 20: 20606
MYERS, F. G., Prog. rpt. on fluid properties for MPD power generators, 5–8/65, 20: 21561 (AD-623096)
MYERS, John E. Jr., Improved performance of BF_3 neutron counters in high gamma fluxes, 20: 21132
MYERS, Marilyn A., Observations of solar wind during flight of Imp 1, 20: 21496

N

NADACHOWSKI, Michel, Application of the 256-channel time-of-flight analyzer for measurement of amplitude spectra, 20: 21083
NADAL, J., Organization of basic materials auditing in a fuel-element fabrication plant, 20: 20967
NADEAU, John S., Hardening of silver-doped KCl by low-temperature x irradiation, 20: 22321
NAGAEV, E. L., Operation of gas-filled diode when electron distribution is not Maxwellian, 20: 22279
NAGAI, Hideo, Separation of binary mixtures of some lanthanoids, 20: 20814
NAGAO, Shiego, Stabilization of plasma in P.I.G. discharge, 20: 22215
NAGASHIMA, Kikusaburo, Design study of a heavy-water moderated, organic-cooled power reactor, 20: 22433
NAGY, G. Agnes, Analysis of radioactive iodine in isotopic tracers by paper electrophoresis, 20: 20599
NAGY, G. Agnes, ^{132}I generator, type JG 01/59, 20: 21217
NAGY, Lajos, Radiation-induced solid-state polymerization. XII., 20: 20763
NAGY, M., Determination of ash content of coals by γ transmission method, 20: 21209
NAIK, R. C., Absorption and fluorescence spectra of praseodymium-doped KCl single crystal, 20: 20663
NAKAGOMI, Yoshihito, Separation of scandium by cation exchange in acid ammonium sulfate media, 20: 20821
NAKAMURA, H., 3$^-$ State in ^{28}Si and ^{24}Mg, 20: 22107
NAKAMURA, R. M., Effect of whole-body irradiation (300 R) on experimental bladder calculus formation in rats, 20: 20467
NAKANISHI, Nobuo, Poles of the proper vertex function in the Bethe-Salpeter formalism, 20: 21735
NARAYANASWAMY, P., Spontaneous symmetry breakdown without mass splitting, 20: 21678
NARITA, Kiichi, Deoxidation and desulfurization of liquid iron by uranium, 20: 20692
NASH, G. F., Three-body forces in p-shell configurations, 20: 22092
NASU, Shoichi, Fission-fragment damage in epitaxial film of UO_2, 20: 21442
NATH, R., S-wave m-KK cross section in the T = 0 state, 20: 21648
NATHAN, O., Collective states of ^{209}Bi, 20: 22108
NEAMU, I., Angular correlations in inelastic proton scattering on ^{20}Ne and ^{32}S, 20: 22059
NEBLETT, John H., Sensitivity analysis of civil defense systems and components, 20: 20922 (AD-624704)
NEILL, J. M., Role of thermal spectrum measurements in reactor design, 20: 22376 (GA-6901)
NEISSEL, J. P., Application of in-core detectors to startup of large boiling water reactors, 20: 22438
NEJEVENKO, L. B., Fabrication of thin plates from refractory carbides, 20: 21303
NELSON, Jack L., Determination of Columbia River flow times downstream from Pasco, 20: 20916
NELSON, Neal S., Distribution of and discrimination against naturally occurring ^{226}Ra in swine, 20: 20385 (COO-1184-3)
NELSON, R. C., Irradiation of 0.5-inch diameter, hollow-pellet UO_2 fuel rods, 20: 21422 (GEAP-5100D)
NELSON, R. D., Transformation rates of plastically deformed plutonium, 20: 21326 (BNWL-203)
NELSON, Sidney G., Development of Th–^{233}U irradiation specimens, 20: 21288 (BMI-1761)
NELSON, W. E., Prog. rpt. on growth parameters for refractory carbide single crystals, 12/64–3/65, 20: 21236 (N-65-23835)
NEOGY, Rajat Kumar, Uptake of ^{32}P in nucleic acids of developing chick embryo, 20: 20399
NESS, Sandra L., Simple technique for rapid analysis of radioactive gases by liquid scintillation counting, 20: 20582
NEUSCHEL, Sherman K., Aeroradioactivity survey and geology of District of Columbia area, 20: 20928 (CEX-59.4.17)
NEWCOMB, Philip P., Assembly of nuclear aircraft engine, 20: 22486
NGUYEN VAN HIEU, Unitary symmetry and resonance widths, 20: 21713 (JINR-P-2568)
NICHOLS, C. W. Jr., Induction of benign and malignant thyroid neoplasms in the rat, 20: 20448
NICHOLS, Roy Woodward, Improvements relating to low alloy steels, 20: 21417
NICKERSON, J. T. R., Microbiology of radiation preservation of foods, 20: 21201
NIEBUHR, J., Suboxides of tantalum, 20: 21379
NIERENBERG, William A., Nuclear spin and magnetic dipole moment of 39-min ^{190}Au, 20: 22140
NIKASHINA, V. A., Ion exchange separation of uranium and rare earth elements, 20: 20813
NIKITINA, N. G., Ion-exchange concentration and separate isolation of cesium, strontium, and cerium from fresh water, 20: 20627
NIKLAS, Wilfrid F., Fast response gamma-ray image converter, 20: 21146
NIKOLAEV, A. V., Determination of the amounts of trace components captured by a macrocomponent precipitate, 20: 20619
NIKOLOV, A. V., Mass formula in inhomogeneous SU(6,6) group, 20: 21624 (JINR-P-2606)
NIKUNI, Zire, Properties of γ-irradiated starch and graft copolymers as adhesives and dyeing mordants, 20: 20767
NIL'SEN, O. B., Investigation of ^{145}Eu irradiation, 20: 22003 (JINR-P-2581)
NILSSON, L., Gamma spectra from inelastic neutron scattering, 20: 22069
NILSSON, S. G., Corrections to BCS expressions for nuclear matrix elements, 20: 22103
NISHI, Masato, Tritium gas target for T(d,n)^{4}He reaction, 20: 21948
NISHIKAWA, Kazuyuki, Study on U refining, 20: 20817
NISHIMURA, Jun, Calculation of cascade functions for the emulsion chamber project, 20: 21556
NISHIMURA, Jun, High-energy γ rays in the atmosphere and muons underground and underwater, 20: 21558
NOAKES, John E., Electrodeposition method for counting alpha and beta emitters, 20: 20795
NOERENBERG, Wolfgang, Primary charge distribution at low-energy fission of heavy (gg)-nuclei, 20: 22013 (ANL-Trans-296)
NOMA, M., High-energy nuclear-active particles in extensive air showers at 5,200 m altitude, 20: 21544 (MIT-2098-227, Paper EAS-8)
NORDBERG, M. E. Jr., Measurement of lifetime of the positive pion, 20: 21665
NORDBERG, M. E. Jr., Pion electromagnetic form factor from measurements of $\pi^\pm$-α elastic scattering, 20: 21659
NORMAN, Donald Lloyd, Neutron transport calculations of AF-NETF core, 20: 22491 (AD-621269)
NOVEY, T. B., Cosmic-ray induced μ-e events, 20: 21029 (CERN-65-32, pp 71-2)
NOVEY, T. B., Neutrino experiment at the ZGS, 20: 21465 (CERN-65-32, pp 31-4)
NOVEY, T. B., $\pi^\pm$ and $K^\pm$ production cross sections for 12.5-Bev protons on Be, 20: 21601 (CERN-65-32, pp 109-10)
NOVIKOV, V. T., Partition chromatography on polytetrafluoroethylene. III., 20: 20623
NOVIKOV, Yu. M., Performance of coaxial plasma source in longitudinal magnetic field, 20: 22179 (FTI-080/P-032)
NOWIK, I., Free ion hyperfine fields in Dy intermetallic compounds, 20: 22330
NOWOTNY, H., New borides with the $Cr_{23}C_6$ structure, 20: 20685
NOZIK, V. Z., Neutron thermalization process in time in graphite and Be, 20: 21942 (KFK-tr-188)
NOZIK, V. Z., Transient neutron spectra in zirconium hydride, 20: 21941 (IAE-977)
NUNEZ-LAGOS, R., G_2 symmetry and leptonic decays, 20: 21719
NUYTS, J., Unitary representations of SU(1,1) and SU(2,1), 20: 21722

NYER, W. E., Review of results of reactor safety research, 20: 22435

O

OAKES, D., Automatic device for collecting dust-free precipitation, 20: 20993
O'BRIEN, Brian J., Rocket-borne measurements of particle fluxes and auroral light, 20: 21826
O'BRIEN, K., Differential energy and angle spectra for ^{137}Cs γ rays in sand, 20: 22308 (HASL-167)
O'CONNELL, J. S., Three-body photodisintegration of ^{3}He, 20: 22117
ODA, Nakaaki, Spectrographic analysis of high-purity tantalum by the d-c arc method, 20: 20608
O'DELL, E. W., Calcium fluoride as x-ray and charged particle detector, 20: 21135
OFER, S., Free ion hyperfine fields in Dy intermetallic compounds, 20: 22330
OGATA, H., Nuclear theory index for 1964, 20: 22011 (TID-22771)
OGATA, Hiroshi, Elastic and inelastic scattering of 28.4-Mev α particles by Sn, Cd, Ag, Cu, and Ti, 20: 22047
OGAWA, Kazuyuki, Image analysis of thermal neutron radiograph, 20: 20866
OGDEN, H. R., Ductile tungsten sheet alloy, W–5Re–2.2ThO_2, 20: 21407
OGIEVETSKII, V. I., Eightfold formalism in SU(3) and 10- and 27-plets, 20: 21711 (JINR-P-2559)
OGITA, Naofumi, Monte Carlo analysis of electromagnetic cascade showers, 20: 21559
OGLE, Hugh M., Film boiling indicator, 20: 22367
OHLBAUM, Adele, Inactivation of vaccinia virus by γ radiation, 20: 20500
OHLENDORF, W., Possibility of using pure inert gas as working fluid in MHD generators, 20: 21589 (IPP-3/29)
OHNIWA, Kohji, Nonlinear effect in beam-plasma interaction, 20: 22206
OHTSUKA, T., Anomalous specific heat of superconducting lanthanum and yttrium compounds, 20: 21883
OKAMOTO, Shinichi, Discharge figures in dielectrics by electron irradiation, 20: 21440
OKAMURA, H., Excitation functions for reactions induced by protons on Cd up to 37 Mev, 20: 22078
OKI, Arahiko, Atomic power station, using a heavy-water moderated boiling light-water reactor, 20: 22431
OKOROKOV, V. V., Reactions (d,n) on isotopes $^{58,60,62,64}Ni$, 20: 22109
OKUBO, S., Are quarks fractionally or integrally charged? 20: 22460 (IC-66/28)
OKUBO, S., Charge conjugation in unitary symmetry groups, 20: 21725
OKUMA, Yasuhiko, Elastic and inelastic scattering of 28.4-Mev α particles by Sn, Cd, Ag, Cu, and Ti, 20: 22047
O'LEARY, W. J., Professional nuclear materials management, 20: 20968
OLIVARI, America, Hepatic scintigram, 20: 20522 (CNEA-167)
OLNESS, J. W., Excitation energies of bound states of ^{17}O and ^{12}B, 20: 22111
OLSON, J. C., Yttrium–cobalt alloy system, 20: 21402
OMNES, R., Introduction to strong interaction physics, 20: 21773
OMOKI, Yosinoki, Temporal observations on peripheral hemograms of atomic bomb casualties as company employees. III., 20: 20481
ONEDA, S., Normal scalar nonet; $K_1 \rightarrow 2\pi$ decay and K_1-K_2 mass difference, 20: 21675
O'NEIL, James R., Oxygen isotope fractionation in the system dolomite calcite-carbon dioxide, 20: 20691
O'NEILL, G. K., Wide-angle electron-electron scattering on the Princeton-Stanford storage rings, 20: 21588 (AD-623658)
ONISHI, Hiroshi, Separation of uranium from thorium by tri-iso-octylamine extraction and photometric determination of uranium with Arsenazo III, 20: 20598
ONISHI, Naoki, Generator coordinate method applied to nuclei in transition region, 20: 22081
OPAUSZKY, Istvan, Mass-spectrometric isotopic analysis of uranium using thermionic emission, 20: 21216
OPPENHEIM, A. K., Pressure wave generation in a fissioning gas. III., 20: 21803
OPPENHEIM, I., Nuclear spin relaxation in gases and liquids. V., 20: 21526
ORIENT, O. J., Elastic scattering of low-energy electrons from He, 20: 21517
ORKIN-LECOURTOIS, A., Fluxes of neutrinos and antineutrinos produced at CERN, 20: 21602 (CERN-65-32, pp 111-14)
ORLANDO, Giorgio, Presence of a new radionuclide contaminating cow's milk: ^{22}Na, 20: 20950
ORMAN, B. A., On a certain nonlocal potential, 20: 21637
ORMROD, John H., Stopping cross sections in B of atoms with energies 15 to 140 kev, 20: 21539
Ortiz de Lopez, M. E.
see Lopez, M. E. Ortiz de
ORTNER, Gustav, Neutron physics at the TRIGA Mark II reactor, 20: 22502
ORVIS, Alan L., Mayo Clinic whole-body counter, 20: 21075
OSBORN, R. K., Coherence and two-photon absorption, 20: 21533
OSBORNE, Darrell W., Preparation and thermal properties of pure XeF_6, 20: 20665
OSBORNE, J. L., Energy spectra of cosmic-ray neutrinos, 20: 21542
OSBORNE, Robert L., Malfunctions in strain gage systems, 20: 22523 (UCRL-14602)
OSBURN, W. S. Jr., Radioecology of the Color Front Range, 20: 20379 (COO-1191-10)
OSHER, J. E., High-velocity plasma injection into cusped magnetic field, 20: 22254
OSKAM, H. J., Prog. rpt. on collision processes in gaseous plasmas, 7–10/65, 20: 22169 (AD-622684)
OSNES, E., Shell model calculations in the calcium isotopes, 20: 22096
OSS, John P., Non-adiabatic particle motion in complex magnetic fields, 20: 22162 (AD-621020)
OSSICINI, L., Adsorption of metal ions on exchangers with phosphoric groups from perchloric acid solutions, 20: 20823
OSTERBERG, Charles, ^{51}Cr in sea water: chemistry, 20: 20603
OSTERTAG, W., Terbium, erbium, and ytterbium graphite intercalation compounds, 20: 21413
OSTERTAG, W., Yttrium–cobalt alloy system, 20: 21402
OSTRACH, Simon, Thermal stability of completely confined fluids including MHD effects, 20: 20854 (AD-621523)
OSTROVSKII, I. E., Effect of sea surface structure upon spatial characteristics of scattered radiation, 20: 20908
OSTROWSKI, G., Submicrosecond synchronization of multiple chopper systems, 20: 21111
O'SULLIVAN, George A., Comparison of solid-state and relay reactor safety systems, 20: 22360
OTOZAI, K., Excitation functions for reactions induced by protons on Cd up to 37 Mev, 20: 22078
OTSUKA, Masuhiko, Neutron fluctuations in a multiplying medium, 20: 21954
OTTAVIANI, G., Experimental results on the information available from the rise time of pulses supplied by semiconductor particle detectors, 20: 21137
OTTE, Victor A., Master control system for nuclear physics instrument systems, 20: 20995
OTTENDORFER, Lambert J., Evaluation of autoradiograms on basis of linear relation between activity and blackening, 20: 20611
OTTO, G., Critical currents of Nb_3Sn and V_3Ga in transverse magnetic fields up to 150 kOe, 20: 21922
OU, Li-Tse, Radiolysis of ethanol in liquid phase, 20: 20746
OVCHINNIKOV, S. S., Production of dense plasma in a metal chamber by a high-frequency method, 20: 22300
OVERBECK, W. P., Production of radioisotopes in production reactors, 20: 21212 (CONF-660305-19)
OVSYANNIKOV, V. A., Toroidal machine for adiabatic compression of plasma, 20: 22299
OWEN, L. W., Oxidation and protection of uranium at temperatures near ambient, 20: 21278
OYA, Shinzo, Polymerization of n-butyraldehyde by ionizing radiation, 20: 20788

P

PACE, N. E., Prog. rpt. on STEP project, 7–12/64, 20: 22467 (IDO-17077)
PACILIO, N., Determination of reactor kinetic parameters, 20: 22381 (RT-FI-(65)49)
PACINI, Franco, High-energy astrophysics and a possible sub-nuclear energy source, 20: 21498
PACKARD, Lyle E., Apparatus relating to the detection and measurement of radioactivity in relatively large bodies, 20: 21142
PACKER, T. W., Rapid analysis of Cu alloys and steels, 20: 20642
PADERNO, Yu. B., Thermionic emission from CeC_2, 20: 21397
PAGE, N. P., Acute mortality and recovery studies in sheep irradiated with ^{60}Co γ rays or 1-Mvp x rays, 20: 20487
PAGE, N. P., Comparison of dose patterns in a dog exposed to neutrons and to x rays, 20: 20432 (AD-630332)
PAGELS, Heinz, Energy-momentum structure form factors of particles, 20: 21758
PAGELS, Heinz, Proton-neutron mass difference, 20: 21673
PAGNY, Pierre, Decontamination of radioactive effluents, 20: 22516
PAKHOMOV, V. I., Peculiarities of electromagnetic wave radiation in anisotropic dispersive media, 20: 22199
PAKKANEN, A., Improved methods for multiple coincidence gamma spectrometry, 20: 22020
PALEI, P. N., Polarographic determination of U in nitric acid media containing TBP. II., 20: 20631
PALLA, Gabriella, Probability of (n,cn') reaction in natural uranium, 20: 22017
PALMER, D. W., Design of a velocity selector for long-wavelength

neutrons, 20: 21007
PALMER, John Arnold, Kinetic analysis of AF-NETF, 20: 22490 (AD-621124)
PANAJKAR, M. S., Stabilities and allied properties of organic coolants, 20: 20708 (AEET-213)
PANCHAPAKESAN, N., S-matrix approach to superconductivity, 20: 21879
PANDYA, I. M., Gravitational field of a radiating spheroid, 20: 21868
PANFIL, Barbara, Biochemical lesions induced in subcellular structures by ionizing radiation. III., 20: 20417
PANGARO, Juan Cerioni, Hepatic scintigram, 20: 20522 (CNEA-167)
PANTA, Przemyslaw, Bone tissue sterilization using reactor fuel γ radiation, 20: 20482
PAPA, Robert J., Wave phenomena in ionized gases, 20: 22174 (AD-623789)
PAPAPETROU, A., Displacement of spectral lines in general relativity, 20: 21843
PAPMEHL, Nikolai, Time-dependent Green's function, 20: 21959
PAPPAS, W. S., Continuous moisture analyzer for gases containing hydrogen fluoride, 20: 20581
PAREZ, J., Scintillation properties of various hydrogenous and non-hydrogenous solutes dissolved in hexafluorobenzene, 20: 21134
PARKER, E. R., Some superconducting properties of several carbides and nitrides of the transition metals, 20: 21911
PARKER, Richard E., Nondispersive x-ray spectrometer for lunar and planetary geochemical analysis, 20: 21128
PARLINSKI, Krzystof, Scattering of slow neutrons by crystals containing mass defects, 20: 22320
PARR, Robert M., Radioactivity of Thorotrast and its in vitro distribution between the various physical phases, 20: 20790 (CONF-651069-1)
PARRETTE, J. R., Prog. rpt. on temperature transient method for performing in-pile thermal conductance testing, final, 3/64–11/65, 20: 22354 (CEND-3336-260)
PASECHNIK, M. V., Scattering of medium-energy neutrons, 20: 22023
PASHCHENKO, V. P., Effect of size of the inter-electrode spacing on operation of a cesium thermal converter, 20: 21568 (FEI-16)
PASHOS, T. J., Irradiation of 0.5-inch diameter, hollow-pellet UO_2 fuel rods, 20: 21422 (GEAP-5100D)
PASMAN, H. J., Reactions of hydrocarbons as foams under the influence of gas discharges. IV., 20: 20740
PASTERNAK, R. A., Prog. rpt. on sorption of gases on metal surfaces, annual, 2/15/65–2/14/66, 20: 21351 (SRIA-425-8)
PATI, J. C., Normal scalar nonet; $K_1 \to 2\pi$ decay and K_1-K_2 mass difference, 20: 21675
PATI, Jogesh C., Dynamics of $J = {}^3/_2{}^+$ $\bar{K}\Xi$ and KN systems in the 27-fold representation, 20: 21674
PATRICK, Richard M., Basic studies in magnetohydrodynamics, 20: 22170 (AD-622701)
PATRONIS, E. T. Jr., Conversion electron-γ directional correlation in ^{133}Cs, 20: 22076
PATZELT, R., Method for low-level scintillation counting, 20: 21042 (SGAE-E-6/1966)
PAULI, G., Measuring spectrum of intermediate neutrons, 20: 22382 (RT-FI-(65)57)
PAULY, J., Neutron activation determination of impurities in some materials strongly activated upon irradiation, 20: 20560 (EUR-2753.f)
PAVLICHENKO, O. S., Production of dense plasma in a metal chamber by a high-frequency method, 20: 22300
PAVLOVICH, P., Fluctuations of ionization losses, 20: 21515 (JINR-P-2615)
PAYNE, B. R., Distribution of tritium in precipitation over continents and its significance to ground-water dating, 20: 20892
PAYNE, Jerry A., Animal species associated with pig carrion, 20: 20941 (ORNL-TM-1432)
PEACOCK, R. D., Chemistry of technetium and rhenium, 20: 20697
PEARCE, J. H., Structure of 20Cr–25Ni–Nb steel after aging in temperature range 600 to 800°C, 20: 21355 (TRG-Report-1168)
PEARSON, E. A., Conference on water pollution research, London, 9/62, 20: 20982
PEARSON, Thomas Felix, Improvements relating to low alloy steels, 20: 21417
PEASE, Robert L., Longitudinal instability thresholds in weak-focusing proton synchrotrons, 20: 21471 (PPAD-577D)
PECORINI, Victorio, Hepatic scintigram, 20: 20522
PEDERSEN, T. I., Fluxes of neutrinos and antineutrinos produced at CERN, 20: 21602 (CERN-65-32, pp 111-14)
PEETERMANS, A., Measurement of thermal neutron flux and estimation of epithermal neutron flux by radioactivation of ^{197}Au, 20: 21053
PEISACH, M., Determination of gold coating thicknesses by proton scattering, 20: 21246
PEISACH, M., Preparation of potassium hexacyanocobaltate(III) labeled with ^{58}Co and ^{60}Co for hydrological studies, 20: 20794
PEKALA, W., Influence of crystal size on yield of n-vinylcarbazole polymerization, 20: 20743
PELLEGRINI-SCOSSIROLI, S., Radiation applied to seeds to induce new genetic variation for quantitative traits in durum wheat, 20: 20501
PENALVA, Hernan Juarez, Insulin labeling with ^{131}I, 20: 20383 (CNEA-185)
PENDLEBURY, J. M., Low-background ionizer for molecular beam detection, 20: 21066
PENDLETON, Joseph Raymond, Flow restrictor, 20: 22361
PENENGO, P., Project for underground laboratory in the Mont Blanc tunnel for experiments on neutrino and cosmic radiation, 20: 21612 (CERN-65-32, pp 225-30)
PENNEY, William, Power from plutonium, 20: 22441
PEPEKIN, G. I., Dissociation of $NbCl_5$ on Nb and carbide surfaces, 20: 21241 (LA-tr-66-15)
PERDANG, J., The 3α reaction in a pulsing star, 20: 21491
PERDIJON, J., Rapid determination of oxygen in metals by radioactivation, 20: 20602
PERELYAEV, V. A., Reactions of metallic Nb with CO, 20: 21270
PERES, G., Effect of uv rays on gastric transit in the rat, 20: 20414
PERKINS, R. W., Determination of Columbia River flow times downstream from Pasco, 20: 20916
PERKINS, S. T., Calculation of neutron spectra in reflected cores and reflector regions, 20: 22396
PERLMAN, I., Decay scheme of ^{254}Es, 20: 22142
PERNER, E., Influence of x radiation on the Hill reaction and photosynthesis phosphorylation for chloroplasts, 20: 20428
PERONA, G., Sintering of oxides of uranium and thorium, 20: 21299
PERSCHKE, Helmut, Tritium enrichment by gas chromatography, 20: 21218
PESTANER, J. F., Beta energy emission rate from neutron-irradiated, ^{235}U carbide particles, 20: 22404 (USNRDL-TR-987)
PETER, Istvan, Transportable vacuum apparatus, 20: 21479
PETERS, P. C., Conformal invariance and the geometrization of the Hoyle-Narlikar mass field, 20: 21862
PETERSON, C. A. W., Physical and mechanical properties of U–Nb–Zr alloy, 20: 21356 (UCRL-14724)
PETERSON, D. T., Electrotransport of interstitial atoms in yttrium, 20: 21254
PETERSON, R. J., Nuclear-structure studies of ^{89}Sr and ^{89}Y by inelastic α-particle scattering, 20: 22138
PETERSON, W. D., DUZ-1—program for solving axisymmetric and plane elasticity problems on Philco-2000, 20: 20862 (WAPD-TM-555)
PETIAU, Gerard, Nonlinear wave equations of spin 0-spin 2$\hbar$ system and quantum theory of associated fields, 20: 21723
PETRIE, J. C., Flow-diverter valve for granular solids, 20: 22511 (IDO-14666)
PETRUKHIN, V. I., Application of nuclear reaction in chemical research, 20: 20653 (JINR-P-2558)
PFEIFFER, B., Skin effect in anisotropic plasmas and resonance excitation of electron-cyclotron waves. I., 20: 22217
PFEIFFER, B., Skin effect in anisotropic plasmas and resonance excitation of electron-cyclotron waves. II., 20: 22218
PFOTZER, G., Measurements of high energetic auroral radiations with balloon-borne detectors in 1962 and 1963, 20: 21838
PFREPPER, G., Interference coefficient for characterization of interfering reactions in activation analysis, 20: 20612
PHILIPPOT, Joseph, Oxidation of UC with oxygen between 800 and 1000°C, 20: 21267
PHILIPPOT, Joseph, Process for the densification of carbonaceous bodies, 20: 21315
PHILLIPS, C. E., Acceptance of irradiated foods, 20: 21199
PHILLIPS, C. Vincent, Master control system for nuclear physics instrument systems, 20: 20995
PHILLIPS, David B., Magnetic and electrical properties of some metals at high pressures, 20: 21357 (UCRL-16299)
PHILLIPS, G., Analysis of uranium silicides, 20: 20557 (AERE-R-5129)
PHILLIPS, Gerald, Multi-body exit channels, 20: 21981 (BNL-948, pp 610-84)
PHILLIPS, R. H., Structure in the pion-proton total cross section between 2 and 7 Bev/c, 20: 21661
PHILLIPS, Richard D., Age and dose dependence of bone growth retardation induced by x irradiation, 20: 20486
PHILLIPS, T. L., Ultrastructural study of the development of radiation injury in the lung, 20: 20434 (AD-630870)
PICCIONI, O., Feasibility of experiment to observe the W produced in strong interactions, 20: 21610 (CERN-65-32, pp 181-94)
PICCOTTI, F., Effects of radiations on immunologic phenomena in Ehrlich's ascites tumor, 20: 20479
PICHOFF, Yves, Effect of irradiation by nuclear particles on switching times of fast diodes, 20: 21157
PIERCE, J. T., Switching characteristics of small-geometry thin-film superconductors, 20: 21012
PIERINI, G., Design problems of pilot plants for volatilization recycling, 20: 20810 (ANL-Trans-250)
PIERPOINT, Geoffrey, Measuring surface soil moisture with the neutron

depth probe and a surface shield, 20: 20915
PIETRA, R., Neutron activation determination of impurities in some materials strongly activated upon irradiation, 20: 20560 (EUR-2753.f)
PIGG, J. C., Annealing of ^{60}Co-γ-irradiated germanium, 20: 21392
PIGGOTT, W. R., Effect of irregularities in collision frequency on the amplitude of weak partial reflections, 20: 21819
PIKE, E. R., Time-dependent Ginsburg-Landau theory, 20: 21890
PILIYA, A. D., Toroidal machine for adiabatic compression of plasma, 20: 22299
PILKUHN, H., The peripheral model, 20: 21705 (CERN-65-24(Vol.1), pp 45-63)
PINAJIAN, J. J., Hydrous zirconium oxide-nitric acid system for use in a ^{99}Mo–^{99m}Tc generator, 20: 20566 (ORNL-TM-1468)
PINOCHET, J., Organization of basic materials auditing in a fuel-element fabrication plant, 20: 20967
PIPKIN, F. M., Wide-angle electron-pair production, 20: 22146
PIRATONI, A., Results of post-operative irradiation of patients with tumors of the brain, 20: 20530
PISAREV, A. F., Electrophotographic device for evaluating particle track coordinates in spark chamber, 20: 21037 (JINR-P-2594)
PITTILLO, Robert F., Mechanism by which hadacidin potentiates the damaging action of ionizing irradiation on bacteria, 20: 20456
PLANTE, E. R., Prog. rpt. on vaporization of refractories, 12/64–2/65, 20: 21262 (N-65-25266)
PLASIL, F., Fission of ^{238}U and ^{240}Pu nuclei excited by inelastic α-particle scattering, 20: 22143
PLASS, G., Determination of spectra of high-energy neutrino parents, 20: 21604 (CERN-65-32, pp 121-6)
PLASS, G., Muon flux measurement in neutrino shielding, 20: 22306 (CERN-65-32, pp 147-52)
PLATT, D. C., British seismometer array recording systems, 20: 20913
PLEASONTON, Frances, Response of solid-state detectors to fission fragments, 20: 21101
PLESCH, Rolf, Measurement of γ emitters in pipe lines, 20: 21047
PLESKOVA, A., Metabolism of carrier-free $^{106}RuCl_3$ after intratracheal application, 20: 20396
PLUKHOV, A. M., Increase of power of VVR-S reactors, 20: 22498 (IAE-993)
PLZAK, V., Hypobaric oxygen exposure and acute radiation lethality in mice, 20: 20430 (AD-629311, pp 26-32)
POCHIN, E. E., Mass of the tracheobronchial lymph glands, 20: 20953
POCS, Lajos, Temperature dependence of internal magnetic field, 20: 22326
POCSIK, G., Mixing of spin-zero mesons, 20: 21746
POCSIK, G., Structure of weak currents, 20: 21743
PODCHERNYAYEVA, I. A., Thermionic emission from CeC_2, 20: 21397
POE, N. D., Lung scanning following radioaerosol inhalation, 20: 20532
POESCHL, R., Production and properties of cerium and lanthanum oxychlorides, 20: 20680
POHLMAN, John F., Ground testing of SNAP-10A/Agena space system, 20: 22477
POLETTI, Pierre, Rainich problem for nonlinear electromagnetic scheme, 20: 21844
POLIKARPOV, G. G., Action of ^{90}Sr–^{90}Y on developing khamsa spawn, 20: 20445 (TRG-Inf. Ser.-166)
POLLARD, Ernest C., Action of ionizing radiation on postirradiation synthesis and degradation of DNA in E. coli, 20: 20421
POLLARD, Ernest C., Radiation in biological systems, 20: 20443 (PB-181506, pp 143-54)
POLLET, R., Perturbing effects of water vapor on mechanism of graphite oxidation in presence of oxygen (500 to 650°C), 20: 21285
POLTORATSKII, N. J., Fabrication of thin plates from refractory carbides, 20: 21303
POLUBARINOV, I. V., Eightfold formalism in SU(3) and 10- and 27-plets, 20: 21711 (JINR-P-2559)
POLYSHCHUK, Yu. N., Radiation-induced methylmethacrylate and styrene polymerization in presence of mineral filters, 20: 20778
POMRANING, G. C., Numerical study of method of weighted residuals, 20: 21957
PONOMAREV, J. T., Influence of y and x rays on coagulability of blood and qualitative changes of fibrinogens in animals, 20: 20490
PONOMAREV, J. T., Pathogenesis of predisposition for bleeding in acute radiation sickness, 20: 20491
PONOMAREV, L. I., Application of nuclear reaction in chemical research, 20: 20653 (JINR-P-2558)
PONOMAREV, L. I., Theory of asymptotic representation of spheroidal functions, 20: 21223 (JINR-P-2564)
PONTELANDOLFO, J. M., Graphite–carbide materials preparation, 20: 21306
POOLE, D. O., Determination of gold coating thicknesses by proton scattering, 20: 21246
POP, Iuliu, Magnetic and structural properties of gadolinium–cerium alloys, 20: 22343
POPOV, A. B., Investigation of neutron resonances of ^{165}Ho, 20: 22004 (JINR-P-2593)
POPOV, V. V., Pathogenesis of iodacetate cataract and its similarity to radiation cataract, 20: 20507
POPOVA, R. F., Radiochromatographic determination of microquantities of ^{137}Cs sorption by soil, clay, and mica, 20: 20696
POPOVA, R. F., Successive desorption method in studies of ion adsorption from solutions, 20: 20618
POPYRADUKHIN, A. P., Structure of magnetic surfaces in stellarator with double helical field, 20: 22298
PORGES, K. G., Information processing unit of fuel element rupture detector system of EBR-II., 20: 22439
PORILE, N. T., Reactions (p,xn) and (p,pxn) of ^{89}Y with 5- to 85-Mev protons, 20: 22133
PORNEUF, Alexandre, Preparation of uranium carbides starting with the dioxide, melting in arc furnace, and casting, 20: 21307
PORTER, J. A., Electrowinning plutonium metal, 20: 21234 (DP-1021)
POSPISIL, J., Influence of polyols on course of experimental radiation disease, 20: 20520
POST, R. F., Electrostatic instabilities in finite mirror-confined plasmas, 20: 22253
POTGIETER, J. M., Strong absorption model for inelastic nuclear scattering, 20: 22086
POTOKIN, V. S., Electrode erosion in bridge stage when breaking 1 to 5kA currents in vacuum, 20: 22291
POTSCHWADEK, B., Circuits for inertialess suppression of pulse rates in scintigraphy, 20: 21086
POWELL, A. H., Prog. rpt. on switchgear for space nuclear electric systems, 3–5/65, 20: 20986 (N-65-29823)
POWELL, R., Plant measurement, sampling, and analysis for accountancy purposes, 20: 20830
POWELL, R., Plant measurement, sampling and analysis for accountancy purposes with particular reference to separation plants at Windscale, 20: 20972
POWER, Dean V., Multidirectional peak pressure gauge for strong shock waves, 20: 20914
POWERS, Albert G., Flow system startup of full-scale simulated nuclear rocket engine, 20: 22480
POZDNYAKOV, A. A., Chromatographic separation of technetium and rhenium, 20: 20629
PRASAD, Sarju, Conductometric study on quantitative estimation of thorium as tungstate, 20: 20592
PRAVDINA, G. M., Behavior of living organisms in radiation fields, 20: 20495
PRAVDINA, G. M., Problem of seasonal fluctuations in radiosensitivity of rabbits, 20: 20493
PREINHAELTER, J., Electron cyclotron instability, 20: 22197
PRENTKI, J., Consequences of unitary symmetry, 20: 21709 (CONF-640509(Pt.2), Paper 6)
PREOBRAZHENSKII, B. K., Partition chromatography on polytetrafluoroethylene. I., 20: 20621
PRESTWICH, W. V., Reaction $^{55}Mn(a,\gamma)^{56}Mn$, 20: 22064
PRESTWOOD, R. J., Symmetry of neutron-induced ^{239}Pu fission at individual resonances, 20: 22135
PRICE, M. J., Influence of structure on post-irradiation physical properties of epoxy resins, 20: 21429 (RHEL/R-105)
PRICE, P. B., Simple detectors for neutrons or heavy cosmic ray nuclei, 20: 21091
PRIMICERIO, Mario, Variations of the magnetic field in a conducting fluid in motion, 20: 21790
PRITCHARD, J. P. Jr., Switching characteristics of small-geometry thin-film superconductors, 20: 21012
PRITCHARD, W. Maurice, Prog. rpt. on defect annealing in irradiated semiconductors, 10/64–3/65, 20: 21153 (N-65-25593)
PRITZKOW, J., Extraction of rare earths with TBP. I., 20: 20824
PROBALD, Vilmos, Furnace for UO_2 sintering, 20: 21304
PROBALD, Vilmos, ZR-2 critical assembly, 20: 22388
PROCTOR, W., Negative hyperfine field in hexagonal cobalt metal, 20: 22335
PROFOS, P., Control technique concepts for nuclear power reactors, 20: 22440
PROKOSHKIN, Yu. D., Application of nuclear reaction in chemical research, 20: 20653 (JINR-P-2558)
PROKSCH, E., Pile radiolysis of terphenyls, 20: 20739
PROMOVA, I. I., Electrophotographic device for evaluating particle track coordinates in spark chamber, 20: 21037 (JINR-P-2594)
PROTTI, A. M., UO_2–ZrO_2–CaO ceramic nuclear fuels, 20: 21302
PROWSE, D. J., Lambda-hyperon binding energy in nuclear matter, 20: 22161
PUIG, J. R., Industrial application of radiochemistry, 20: 20793
PUIG, J. R., Technological study on polyphenyls, 20: 20722 (EUR-2401.f)
PULLIA, A., Experimental investigation of the K_{e3} decay, 20: 21658
PUPYSHEVA, L. V., Linear polarization fo distributed cosmic radio emission, 20: 21549

PURCELL, W. L., Modifications to computer code, THERMOS, 20: 22374 (BNWL-193, pp 5-15)
PUSHKAREV, V. V., Concentration of radioactive isotopes with colloidal MnO_2 by foaming, 20: 20628
PYCHLAU, P., Voltage measurement in x-ray tubes especially during flashes of x rays, 20: 21087

Q

QUATINETZ, Max, Investigation of extruded tungsten composites containing fibered or reacted additives, 20: 21374
QUERZOLI, R., Determination of branching ratios among neutral decay modes of the η particle, 20: 21627 (LNF-66/9)
QUIDORT, J., Reaction $^{180}Hf(d,p)^{181}Hf$, 20: 22106
QUINN, C. M., Interaction of carbon dioxide at low pressures with tantalum and zirconium, 20: 21279
QUITTNER, P., Probability of (a,α') reaction in natural uranium, 20: 22017

R

RABSON, T. A., Temperature dependence of average energy per pair in semiconductor detectors, 20: 21102
RACKETS, Hubert M., Prog. rpt. on large aperture seismic array, final, 10/64–6/65, 20: 20899 (AD-626777)
RAFTER, T. A., Problems in establishment of a ^{14}C and tritium laboratory, 20: 20893
RAGAINI, Richard C., Determination of silver in minerals and ores by neutron activation analysis, 20: 20574
RAGHUNATH, V. M., Physiological norms in Indian adults. Statistical analyses of data on organ weights, 20: 20374
RAHM, G., Medical experiences after the first radiation protection law, 20: 20947
RAICA, Nicholas Jr., Wholesomeness of irradiated foods, 20: 21198
RAIKO, V. I., Extraction and formation of ion beams in plasma sources, 20: 21213 (IAE-974)
RAINWATER, Walter J. Jr., Measurement of transmission spectra of 1-Mev electrons with normal incidence on Al slabs, 20: 21524
RAJAGOPAL, A. K., Superconducting state of electron gas in homogeneous magnetic field, 20: 21887
RAKHOVSKII, V. I., Electrode erosion in bridge stage when breaking 1 to 5 kA currents in vacuum, 20: 22291
RALPH, E. L., Effects of electron irradiation and temperature on solar cell performance, 20: 21161
RAMASWAMI, D., Engineering development of fluid-bed fluoride volatility processes. II., 20: 20801 (ANL-6830)
RAMBOURG, Roger, Nuclear fuel pellets of special profiles and method of their preparation, 20: 21316
RAMM, C. A., Chairman's summary of the session on neutrino facilities, 20: 21605 (CERN-65-32, pp 153-6)
RAMP, R. L., NERVA reactor instrumentation, 20: 22484
RAMADE, S. S., Evaluation of acridine orange fluorescence test in viability studies on E. coli, 20: 20457
RAND, R. E., Elastic electron scattering from magnetic multipole distributions of ^6Li, ^7Li, ^9Be, ^{10}B, ^{11}B, and ^{14}N, 20: 22120
RANDEN, K. G., Startup and operation of 1-Mw shield test and irradiation reactor, 20: 22500 (NAA-SR-11175)
RAO, K. Narayana, Stabilities and allied properties of organic coolants, 20: 20708 (AEET-213)
RAO, K. V. S. Rama, Stabilities and allied properties of organic coolants, 20: 20708 (AEET-213)
RAO, S. M., Total count method for open channel flow measurement, 20: 20903 (AEET-Radiochem.-45)
RAPPAPORT, S., Monte Carlo simulation of nuclear active cascade in EAS, 20: 21545 (MIT-2098-227, Paper EAS-11)
RARATY, L. E., System C.I.D. Illustration of use of digital computer in storage, interpretation and recovery of materials data, 20: 21354 (TRG-Report-1160)
RASKIND, R., Radiation necrosis of the cervical spinal cord imitating metastases of carcinoma, 20: 20545
RASTALL, P., Theory of gravitation, 20: 21858
RASTOGI, R. G., Night-time disturbance fluctuations in geomagnetic field at equatorial stations, 20: 21818
RAUCH, Helmut, Neutron physics at the TRIGA Mark II reactor, 20: 22502
RAUH, E. G., Uranium monosulfide. III., 20: 20669
RAUSCHER, H. E., Determination of sodium, arsenic, copper, and gallium in tin oxide by neutron activation, 20: 20577
RAUTERBERG, U., Linearly controllable low-frequency oscillator for a proton resonance spectrometer with internal nuclear resonance stabilization, 20: 21093
RAWER, K., Electron content of the ionosphere and its fluctuations, 20: 21816
RAY, Alden E., Crystal structures of $CeFe_7$, $PrFe_7$, $NdFe_7$, and $SmFe_7$, 20: 21400
RAYMOND, J. P., Generalized model analysis of ionizing radiation effects in semiconductor devices, 20: 21167
RAYNOR, G. V., Electronic states of rare-earth metals in alloys, 20: 21398
RAYNOR, J. B., Oxidation of plutonium. II., 20: 21280
RAZAVY, M., Effective interaction for nuclear matter, 20: 22122
RAZAVY, M., On a certain nonlocal potential, 20: 21637
RAZIN, V. A., Depolarization in cosmic radiation due to disperaion of Faraday rotation of polarization planes, 20: 21548
RAZIN, V. A., Linear polarization of distributed cosmic radio emission, 20: 21549
READY, Thomas J., Powder rolling of tungsten and its alloys, 20: 21318
REBER, Grote, Cosmic ray astronomy, 20: 21494
RECHT, H. L., Prog. rpt. on radiation effects on Ni–Cd electrodes, final, 6/63–4/65. I., 20: 21425 (N-65-24491)
REDKOBORODYI, Yu. N., Bolometric measurements of radiation of ionized shock wave in argon, 20: 22281
REED, Glenn A., Operating experience of Yankee—updated, 20: 22457
REEVES, Lane, Modified method of radioisotopic placental localization, 20: 20527
REGNAUD, F., Methods of analyzing Pu, 20: 20976
REID, Cyril, Mechanism of ultraviolet and high-energy radiation damage, 20: 20731 (PB-181506, pp 133-42)
REID, J. M., Triggered cloud chamber for low-energy nuclear reactions, 20: 21063
REINES, F., Reactor neutrino experiment, 20: 21027 (CERN-65-32, pp 41-4)
REINHARZ, M., Possible spark chamber experiment with antineutrinos, 20: 21607 (CERN-65-32, pp 161-8)
REINICKE, B., Change of electrical properties of Si and Ge diodes by neutron irradiation, 20: 21150 (HMI-B-45)
REINITZ, Karl, Low-energy mosaic electron sensor, 20: 21138
REINKHARDT, M., Gas-liquid chromatography for determining specific activity and survival of mother compounds labeled with recoil atoms, 20: 20783
RELLAN, D. R., Radioactive renography in diagnosis and treatment of acute obstructive renal failure, 20: 20538
REMBOLD, E. A., Prog. rpt., 10/62, 20: 20553 (MLM-1142)
REMIDDI, E., Evaluation of $N^*_{\frac{1}{2}}N$ weak coupling constants, 20: 21655
RENFRO, G. W., Engineering design practices for facilities containing radioactive materials, 20: 20942 (ORNL-TM-1459)
RESTER, D. H., Level schemes of $^{67,68,70}Ga$, 20: 22053
RESTER, David H., Measurement of transmission spectra of 1-Mev electrons with normal incidence on Al slabs, 20: 21524
REUSCHL, H., Action of ionizing radiations on starch, 20: 20737
REVESZ, A., Preparation of XeF_2, 20: 20678
RHODES, D. F., Hydrogen analysis by slow neutron transmission, 20: 20641
RHODES, J. R., Rapid analysis of Cu alloys and steels, 20: 20642
RHYNER, C. R., Thermal annealing effects on thermoluminescence of LiF, 20: 21057
RICCI, E., ^3He activation analysis, 20: 20565 (ORNL-P-1216)
RICCO, G., Photoneutron production from C, Al, and S by bremsstrahlung up to 200 Mev, 20: 22094
RICH, Marvin, Applications of Coulomb-modified s-wave dispersion relation, 20: 21680
RICHARDSON, J. Reginald, Polarization of 45-Mev protons by complex nuclei, 20: 22128
RICHARDSON, R. W., Eigenstates of the J = 0, T = 1, charge-independent pairing Hamiltonian. I., 20: 22121
RICHEY, C. R., Neutron interaction between multiplying media separated by various materials, 20: 20840 (BNWL-193, pp 57-67)
RICHTER, A., Statistical character of reaction $^{37}Cl(p,\alpha)^{34}S$ at 21- to 22-Mev excitation energy of the compound nucleus, 20: 22084
RICHTER, B., Wide-angle electron-electron scattering on the Princeton-Stanford storage rings, 20: 21588 (AD-623658)
RICKARD, W. H., Accumulation of ^{137}Cs in litter and understory plants of forest stands from various climatic zones of Washington, 20: 20879 (BNWL-SA-530)
RICKARDS, J., Angular distributions of $^6Li(d,p)^7Li$ at energy of 1.5 Mev, 20: 22151
RICQUE, R., Determination of inception of nucleate boiling in terphenyl OM2 in conditions of forced convection, 20: 20709 (EUR-2442.f)
RIEDEL, Oswald, Intensity calculations of isotopic peaks in mass spectrograms, 20: 20610
RIGALI, L., Solvent extraction separation of Pa from elements of the IVa and Va groups, 20: 20816
RING, James G., Formation and bleaching properties of T bands in KCl, 20: 22322
RITTER, E. T., Relevance of bombardment-induced Moessbauer effects in iron to radiation damage theories, 20: 21444
RITTER, Rogers C., Neutron-gamma correlations for states in ^{20}Ne at

10.33 and 11.03 Mev, 20: 22082
RIVERA, Joseph, Prog. rpt. on fallout program, 12/65–3/66, 20: 20882 (HASL-171)
ROB, L., Elastic scattering of protons on protons at 8 Bev, 20: 21639
ROBERSON, N. R., Evidence for the prolate deformation of ^{27}Mg, 20: 22099
ROBERT, Guy, Electric conductivity in HfO_2–Y_2O_3 at high temperature, 20: 21370
ROBERTS, A. P., Effect of whole-body irradiation (300 R) on experimental bladder calculus formation in rats, 20: 20467
ROBERTS, A. S. Jr., Analysis of intense, undriven electron beams with significant self-field forces, 20: 21736
ROBERTS, John J., On-line computers in optimal reactor shutdown, 20: 22389
ROBERTS, M. W., Interactions of carbon dioxide at low pressures with tantalum and zirconium, 20: 21279
ROBERTS, P. B., Transistorized radon measuring equipment, 20: 21067
ROBERTSON, J. S., Strontium and calcium skeletal discrimination determined by compartmental analysis, 20: 20400
ROBINSON, G. A., Plotting system for Control Data 3600 computer, 20: 21221 (ANL-7121)
ROBINSON, G. A., Progressive myelopathy in a dog caused by ThO_2, 20: 20455
RODDEN, C. J., Analytical methods for U concentration measurements, 20: 20977
RODER, M., Radiochemical stability of high-boiling hydrocarbons in reactor, 20: 20792
RODIN, A. V., Operation of a cesium diode with an admixture of an inert gas, 20: 21567 (FEI-15)
RODOT, J., X-ray diffraction study of neutron-irradiated beryllia, 20: 21433 (UCRL-Trans-10012)
RODRIQUEZ, Dominguez, Artificial elements, 20: 20796
ROE, E. M. F., Effects of uv and visible radiation on mouse ascites tumor cells, 20: 20484
ROE, E. M. F., Method of assaying in vivo the survival of uv irradiated tumor cells, 20: 20483
ROECKER, J. H., SNAP-8 reactor test program, 20: 22479
ROEDERER, J. G., Longitude dependence of geomagnetically trapped electron fluxes. I., 20: 21813 (N-65-29816)
ROELOF, E. C., Effect of interplanetary magnetic field on solar neutron-decay protons, 20: 21495
ROEPKE, H., Perturbation of angular correlation on the 1.35 to 0.198 Mev γ-γ cascade in ^{19}F, 20: 22090
ROGERS, Frank, Improvements in or relating to irradiation apparatus, 20: 20852
ROGERS, J. E., Simplification of oxygen-flask combustion procedure for preparation of samples for liquid scintillation counting, 20: 20570
ROGOVOI, A. G., Radiometric method of determining sulfur in naphthalene, 20: 20615
ROHR, R. C., Subcritical determination of relative natural-neutron-source strengths, 20: 22392
ROHRMANN, C. A., Irradiated wood-plastic materials—commercial possibilities in Pacific Northwest, 20: 21185 (ORNL-IIC-7, pp 76-80)
ROLANDI, G., Eurex plant, 20: 20815
ROLLINS, R. W., Annihilation instability in hard superconductors, 20: 21927
ROLLINS, R. W., Effect of surface conditions on a-c field transitions in type II superconductors, 20: 21918
ROM, Frank E., Applications of low-power nuclear rockets, 20: 22469 (N-65-29479)
ROM, Frank E., Fast and moderated low-power, lightweight reactors for nuclear rocket propulsion, 20: 22470 (N-65-29480)
ROMANO, F., Technological study on polyphenyls, 20: 20722 (EUR-2401.f)
ROMANOV, A. M., Recording of several particles with an acoustic spark chamber, 20: 21094
RONDEAU, R. E., Prog. rpt. on radiation chemistry of acetylenic compounds, final, 12/61–5/65, 20: 20717 (AD-621719)
RONSIVALLI, Louis J., Radiopasteurization of fishery products, 20: 21200
RONTEIX, F., Improvement of auditing data centralization, 20: 20965
ROONEY, J., Application of radiography to the inspection of fuel pins, 20: 20864
ROSE, Florence C., Role of normal epidermis in recovery of regenerative ability in x-rayed limbs of triturus, 20: 20465
ROSE, R. M., Fabrication of an ultrafine Nb–Cu composite by drawing, 20: 21298
ROSE, S. Meryl, Role of normal epidermis in recovery of regenerative ability in x-rayed limbs of triturus, 20: 20465
ROSENBERG, A. D., Effect of sea surface structure upon spatial characteristics of scattered radiation, 20: 20908
ROSENBLUM, B., Measurements of current-dependent reactance of superconductors having very small coherence distance, 20: 21919
ROSENBLUM, Bruce, Microwave studies of the superconducting mixed state, 20: 21916
ROSENBLUTH, M. N., Electrostatic instabilities in finite mirror-confined plasmas, 20: 22253
ROSENBLUTH, Marshall N., Flute instability at low density, 20: 22252
ROSENFELS, R. S., Ceramic cells for electrowinning and electrorefining of Pu metal, 20: 21239 (RL-SEP-824)
ROSENZWEIG, M. L., Binary diffusion in a confined vortex, 20: 22473
ROSENZWEIG, W., Space radiation effects in silicon devices, 20: 21165
ROSIER, D., Technological study on polyphenyls, 20: 20722 (EUR-2401.f)
ROSOFF, Betty, Effect of chelating agents on the removal of ^{65}Zn in man, 20: 20397
ROSS, D. H., Binary diffusion in a confined vortex, 20: 22473
ROSS, David W., Pressure broadening as many-body problem, 20: 21519
ROSS, Harley H., New concept in precision photometric analysis using a radioisotopic light source, 20: 20571
ROSS, W. J., Monitoring of leached fuel elements with a neutron generator, 20: 21040 (ORNL-P-1218)
ROSTOKER, W., Bend and tensile ductility of Nb–Ti–Zr molybdenum alloy, 20: 21410
ROSZTOCZY, Z. R., Calculating heavy-isotope content of operating fuel elements, 20: 20979
ROTE, D. M., Quasiparticle random-phase approximation in odd-odd nuclei and the neutron-proton interaction, 20: 22147
ROTHENSTEIN, W., Boundary conditions in gap geometry, 20: 22390
ROTHENSTEIN, W., Multigroup calculations of fast spectrum and fast fission effect, 20: 22506
ROULLIAY, M., X-ray diffraction study of neutron-irradiated beryllia, 20: 21433 (UCRL-Trans-10012)
ROUSSET, A., Structure in the pion-proton total cross section between 2 and 7 Bev/c, 20: 21661
ROUX, D. P., Parallel-plate multisection ionization chambers for reactors, 20: 22356 (ORNL-3929)
ROWE, D. H., Analysis of uranium silicides, 20: 20557 (AERE-R-5129)
ROWE, D. J., Interpretation of time-dependent Hartree-Fock theory, 20: 22068
ROYET, J., Superconductor magnet for corpuscular ionography used at CERN, 20: 21876
ROZANOV, M. S., Radiation hygiene conditions during the diagnostic use of radioactive krypton, 20: 20958
ROZHKOV, V. V., Asymptotic solution of diffusion problem and its application to the theory of cyclic particle-storage devices, 20: 21483
RUBIN, Bernard Friedman, Metallographic and x-ray study of MgO–Al_2O_3–UO_2 system, 20: 21359 (WAPD-T-1581)
RUBIN, S. B., Self-consistent hydrodynamic problem of motion of relativistic electrons in a uniform magnetic field, 20: 22287
RUBY, S. L., Review of advances in physics, 20: 22327
RUDENKO, N. P., Zirconium and Y cupferronates and a method for separating ^{89}Zr from irradiated carrier-free Y, 20: 20626
RUDSTAM, G., Fission and spallation yields in the iodine region, 20: 22045
RUEDENAUER, F., Magnetless dynamic mass spectrometer, 20: 20991
RUEGG, F. C., Standardization of differential chemical shift for ^{57}Fe, 20: 22158
RUHL, Buford B., Potential applications of irradiated wood-plastic materials, 20: 21184 (ORNL-IIC-7, pp 64-75)
RUKHADZE, A. A., Instability of electronic waves in nonuniform plasma streams, 20: 22296
RUMBAUGH, Paul E., Commercial use of irradiated wood-plastic materials in furniture industry, 20: 21189 (ORNL-IIC-7, pp 99-105)
RUMP, B. S., Critical fields of superconducting vanadium films, 20: 21915
RUMPOLD, K., Comparison of burnup determinations by means of monitor-activation and γ spectroscopy for an MTR element, 20: 21050
RUSSELL, C. M., Superconducting transition temperatures in ϵ-phase Pb–Bi alloys, 20: 21892
RUSSELL, D. S., Extraction and spectrophotometric determination of thorium with 8-quinolinol, 20: 20576
RUSSELL, J. L. Jr., Accelerator pulsed fast assembly, 20: 22503
RUST, John H., Consequences of ingestion by man of real and simulated fallout, 20: 20466
RUST, John H., Distribution of and discrimination against naturally occurring ^{226}Ra in swine, 20: 20385 (COO-1184-3)
RUTKOWSKI, J., Optical transition radiation from 6- to 23-kev electrons entering normal to metal surfaces, 20: 21518
RYABCHIKOV, D. I., Chromatographic separation of technetium and rhenium, 20: 20629
RYABININ, A. I., Chromatographic separation of UX_1 and U_1, 20: 20828
RYAN, Joseph T., Decontamination effectiveness, 20: 20923 (AD-626727)
RYBA, Earle, Intermetallic compounds with the $CeCu_2$-type structure, 20: 21352 (TID-21745)
RYDE, H., Rotational bands on two-particle configurations with $K_n = K_p = ½$, 20: 22072
RYDIN, R. A., Design and calculations for a ^6Li semiconductor sandwich fast neutron spectrometer experiment, 20: 21034 (EUR-2712.e)
RYDZEWSKI, Tadeusz, Application of the 256-channel time-of-flight analyzer

for measurement of amplitude spectra, 20: 21083
RYNDIN, R. M., Application of "maximum complexity" method for determining spins and parities in reactions with polarized particles, 20: 21715 (JINR-P-2576)
RYNDIN, R. M., Isospin conservation and polarization effects, 20: 21717 (JINR-P-2620)
RYNDIN, R. M., Spin test for bosons decaying into three spinless particles, 20: 21620 (JINR-P-2577)
RYON, A. D., Prog. rpt. on chemical technology, 7–9/65, 20: 20808 (ORNL-3916)
RYU, Norio, Tritium gas target for T(d,n)^{4}He reaction, 20: 21948
RYZHOV, Yu. A., Tensor of an effective permittivity of strong nonuniform anisotropic medium, 20: 22203

S

SAAVEDRA, I., Completeness, unitarity, and dispersion relations in potential scattering, 20: 22464 (IC-66/29)
SABBIONI, S., Neutron activation determination of impurities in some materials strongly activated upon irradiation, 20: 20560 (EUR-2753.f)
SACCHI, C., X-ray scanning of sky in 20- to 200-kev range, 20: 21490
SADIKOV, I. P., Neutron thermalization process in time in graphite and Be, 20: 21942 (KFK-tr-188)
SADIKOV, I. P., Transient neutron spectra in zirconium hydride, 20: 21941 (IAE-977)
SADLER, D. H., Transactions of the International Astronomical Union, Berkeley, 8/61, XIB, 20: 21511
SAHA, G. B., Reactions (p,xn) and (p,pxn) of ^{89}Y with 5- to 85-Mev protons, 20: 22133
SAHA, N. K., Gamma-gamma directional correlation in ^{123}Te, 20: 22089
SAINT-JAMES, D., Paramagnetic effect and the Landau-Ginzburg equations, 20: 21900
SAITO, H., Annealing of ^{60}Co-γ-irradiated germanium, 20: 21392
SAITO, H., Recombination centers in γ-irradiated silicon, 20: 21439
SAITO, Haruo, Annealing of E center in irradiated silicon, 20: 22323
SAITO, Kolichi, Neutron fluctuations in a multiplying medium, 20: 21954
SAITO, Makoto, Hot atom chemistry of ^{76}As using zirconium benzenearsonate as target, 20: 20797
SAITO, Osamu, Production of polymer gel with least radiation dose, 20: 20761
SAITO, Torao, GM counter, M2311, 20: 21092
SAKAMTOTO, K., 650-Mev photofission yields for uranium, 20: 22040
SAKAO, Fujihiko, Electron-ion recombination processes in a nonequilibrium plasma, 20: 22195
SAKAOKU, K., Irradiation changes in organic polymers at various accelerating voltages, 20: 20762
SAKUMA, Sadayuki, Beam focus radiography for taking radiogram of the axial transverse cross section of treated region in high density of dose, 20: 20547
SAKUMA, Sadayuki, Beam focus and its image on beam focus radiogram, 20: 20549
SAKUMA, Sadayuki, Cassette and interspacer in beam focus radiography, 20: 20548
SAKUMA, Tetsuro, Dynamical approach to nonleptonic decays of hyperons, 20: 21686
SAKURAI, Junji, Development of glasses for low background measurements—characteristics of glasses, 20: 21044 (ANL-Trans-285)
SALUSTI, E., Formal properties of the ground-state wave function for even-even nuclei, 20: 22093
SAM, D., Nuclear-charge distribution of fission-product chains of mass numbers 131-133, 20: 22136
SAMARIN, A. M., Gas generation from tungsten at 2500°C, 20: 21248
SAMBURENKO, I. Z., Studying the radioactivity of inland waters, 20: 20963
SAMIOS, N. P., Neutrino physics with 80-in. and 14-ft bubble chambers at BNL, 20: 21608 (CERN-65-32, pp 169-74)
SAMOKHIN, M. V., Electrostatic separation of charge in a plasma in thermodynamic equilibrium, 20: 22283
SAMPSELL, D. F., Thermal transient response of underground shelters, 20: 20920 (AD-621377)
SANDROCK, Gary D., NASA developments in Co-base superalloys, 20: 21237 (N-65-29395)
SANKARANARAYANAN, A., Theorem on contraction of groups, 20: 21227
SANKOVICH, Melvin F., Nuclear reactor, 20: 22465
SANTAGATI, G., Utilization of sodium sulfate–^{35}S by hepatic tissue of the normal and irradiated rat, 20: 20410
SANTARELLI, F., Control of materials in Italian nuclear power stations and research institutions, 20: 20964
SANTHANAM, K., Physiological norms in Indian adults. Statistical analyses of data on organ weights, 20: 20374
SAQUI, Ronald M., Multi-group discrete SN transport calculation for cylindrical geometry, 20: 22370 (AD-621021)
SARKADY, A. A., Multichannel pulse-height analyzer for university balloon and rocket experiments, 20: 21127
SARMA, G., Paramagnetic effect and the Landau-Ginzburg equations, 20: 21900
SASAKAWA, Tatuya, Solution of Schroedinger equation involving time, 20: 21852
SASAKI, Satoshi, Construction and operation of radiological monitoring station, 20: 20934 (JAERI-1098)
SASAKI, T., Counting of tritium with thin-windowed G-M counter tube, 20: 21065
SATOH, T., Anomalous specific heat of superconducting lanthanum and yttrium compounds, 20: 21883
SAUCIER, R. T., Engineering properties of nuclear craters. I., 20: 20895 (AD-626899)
SAULNIER, Adrien, Microanalysis by x-ray emission in an electron microscope, 20: 20593
SAUR, E., Critical currents of Nb_3Sn and V_3Ga in transverse magnetic fields up to 150 kOe, 20: 21922
SAUTIN, Andre, Activation analysis of a mixture of rare earths, 20: 20562 (LYCEN-6538)
SAUVAGE, M., Experimental results on engineering model of Rapsodie, 20: 22501 (EURFNR-49F)
SAWAI, Sadamu, Spent-fuel storage pool for JRR-2, 20: 22505
SAWICKI, J., Coulomb scattering of muons and electrons from fluorine and chlorine, 20: 21649
SAWYER, D., Two satellite-borne cosmic-radiation detectors, 20: 21118
SAWYER, J. C., Prog. rpt. on creep data on refractory alloys, 9/26–12/26/65, 20: 21346 (NASA-CR-54895)
SAWYER, J. C., Prog. rpt. on determination of elevated-temperature fatigue data on refractory alloys, 10/65–1/66, 20: 21347 (NASA-CR-54916)
SAXENA, R. P., Radiative nonleptonic weak decays of baryons, 20: 21751
SAXENA, R. P., S-matrix approach to superconductivity, 20: 21879
SCAIFE, J. F., Enzymatic evaluation of thiol radioprotectors, 20: 20505
SCALA, A. A., Ion-molecule reactions in liquid- and solid-phase radiolysis, 20: 20742
SCALAPINO, D. J., Microwave-induced d-c voltages across Josephson junctions, 20: 21882
SCANLON, J. H., Production spectrum of high-energy electrons from high-energy cosmic-ray collisions, 20: 21552
SCARAMUZZI, F., Liquid ^{3}He target for high-energy nuclear experiments, 20: 22007 (LNF-66/1)
SCARFONE, Leonard M., Lehmann-Symanzik-Zimmermann formalism in the one-boson Lee model, 20: 21718
SCHAEFER, Klaus, Inhibited energy exchange between platinum and adsorbed ortho-deuterium and para-deuterium, 20: 20661
SCHAEFFER, H., Formation equilibrium of ammonias and trideuteroammonias, 20: 20660
SCHAEFFLER, H., Modified Ritz method for diffusion-theoretical calculation of nonseparable reactor geometries, 20: 22385
SCHARMANN, A., Suitability of electron postemission of $CaSO_4$ for dosimetry, 20: 20769
SCHECHTER, J., Weak currents in broken U(3) ⊗ U(3), 20: 21762
SCHECHTER, Martin, Essential spectrum of an arbitrary operator. I., 20: 21848
SCHEIDECKER, M., Aluminum and magnesium in nuclear metallurgy, 20: 21382
SCHELLENBERG, L., Determination of conversion ratios of 191-kev transitions in ^{197}Au, 20: 22057
SCHENCK, J. F., Effects of helium temperature strain on superconducting transition of Pb–In alloys, 20: 21923
SCHERBATSKOY, Serge A., Gamma-ray measuring system utilizing plural detectors, 20: 21145
SCHIAVON, P., Determination of branching ratios among neutral decay modes of the η particle, 20: 21627 (LNF-66/9)
SCHIFF, Jerome A., Chloroplast development in Euglena. XIII., 20: 20450
SCHIFFER, J. P., Measurement of spins of some states in ^{55}Fe, 20: 22126
SCHIFFER, John P., Optical model, DWBA, 20: 21978 (BNL-948, pp 454-524)
SCHILDT, Evert E. son, Action of x rays on blood typing sera, 20: 20425
SCHLEIGER, E. R., Photon, neutron, and charged particle absorbed dose measurements with a portable microcalorimeter, 20: 21024 (AD-630693)
SCHLESINGER, S. Perry, Wave propagation along warm plasma columns, 20: 22220
SCHMETS, J., Design problems of pilot plants for volatilization recycling, 20: 20810 (ANL-Trans-250)
SCHMIDT, F. A., Electrotransport of interstitial atoms in yttrium, 20: 21254
SCHMIDT, G. B., Isotopic ligand exchange of some six coordinated inorganic complexes with halide ions, 20: 20706
SCHMIDT, H. E., Heat transport by radiation in solids, 20: 22329
SCHMIDT, J. F., Radiation chemistry studies of silane, annual, 4/66, 20: 20725 (NYO-3570-2)
SCHMIDT, R., Influencing radiation-induced cerebellar defects of the domestic mouse by chemical radioprotective agents, 20: 20521

SCHMITT, C. R., Powder metallurgy of UC, 20: 21296 (Y-1510)
SCHMITT, H. W., Response of solid-state detectors to fission fragments, 20: 21101
SCHMITT, R., Corpuscular photography and spatial ionography group of the Strasbourg Nuclear Research Center, 20: 21060
SCHMITZ, N., Peripheral collisions, 20: 21592 (CERN-65-24(Vol.1), pp 1-44)
SCHNABEL, Wolfram, Degradation of polymers in solution under the influence of ^{60}Co γ radiation, 20: 20765
SCHNABEL, Wolfram, Radiation reaction of polyvinylchloride, polydimethylsiloxane, and polymethacrylic acid methyl esters in solution, 20: 20764
SCHNAPPAUF, Hp., Influence of extracorporeal irradiation of the blood and lymph on skin homograft rejection, 20: 20485
SCHNEIDER, H., Determination of magnetic moments of excited nuclear levels from the γ-γ angular correlation disturbed in magnetic field, 20: 22025
SCHNEIDER, R. T., Prog. rpt. on fluid properties for MPD power generators, 5-8/65, 20: 21561 (AD-623096)
SCHNORR, H., Disappearance of quadrupole splitting in Moessbauer spectra of ^{57}Co-containing AgCl at 300°K, 20: 22340
SCHOBER, M., Chemistry of U(IV). I., 20: 20675
SCHOENFELD, E., Safety and cost analysis of 1000-Mw(e) sodium-cooled fast power reactor, 20: 22451
SCHOLL, Raymond F., Some aspects of reactor safety systems, 20: 22358
SCHOPFER, B., Positioning of charge-discharge machine of experimental nuclear power plant at Lucens, 20: 22423
SCHOW II, Horace, Courant-Wallace expressions for second moments of neutron probability distribution and for variance/mean ratio, 20: 22372 (AFRRI-TN-65-1)
SCHRAM, B. L., Influence of velocity of rare gas ions on emission of secondary electrons, 20: 21538
SCHRANK, G., Measurement of anomalous gyromagnetic ratio of the muon, 20: 21630 (UCRL-16469)
SCHREIBER, P. W., Radiation level measurements within and behind Be, 20: 22307 (DC-61-3-69)
SCHREINER, Felix, Preparation and thermal properties of pure XeF_6, 20: 20665
SCHREINER, H. R., Biological effects of the noble gases, 20: 20378
SCHROEDER, F., Review of results of reactor safety research, 20: 22435
SCHROEDER, Gerold L., Determination of silver in minerals and ores by neutron activation analysis, 20: 20574
SCHUBERT, G., Application of the x-ray γ dosimeter VA-J-15 in radiological protection, 20: 21062
SCHUELLER, W., Control of source and special nuclear material at Eurochemic, 20: 20831
SCHULLER, Dieter, Inhibited energy exchange between platinum and adsorbed ortho-deuterium and para-deuterium, 20: 20661
SCHULTZ, Claude, π^+-p Scattering at 250 Mev: experiment and analysis, 20: 21662
SCHULTZ, H. W., Food preservation by irradiation, 20: 21206
SCHULTZ, N. B., Removal of radioactive wastes by sanitary water treatment process, 20: 22512 (K-1651)
SCHULTZ, N. B., Some observations on film badge calibration techniques, 20: 20935 (K-1657)
SCHULTZ, Werner W., Radioactive apparatus for measuring temperature, 20: 21029
SCHULZ, G., Formation equilibrium of ammonias and trideuteroammonias, 20: 20660
SCHULZ, Hans-Juergen, 45° Remission photometer for measurement of radiation erythemas, 20: 21011
SCHUSSLER, M., Properties of niobium alloy Cb-753, 20: 21411
SCHUTZER, Daniel, Proposed measure for the information content in quantum fields, 20: 21704 (AD-622517)
SCHWANBECK, C. A., Prog. rpt. on effect of radiation on materials at cryogenic temperatures, 10/21/65-1/21/66, 20: 21427 (NASA-CR-54904)
SCHWARTZ, Brian B., Kronig-Penney model for excitations in type II superconductors, 20: 21904
SCHWARZ, E., Determination of uranium and thorium in sedimentary carboniferous deposits, 20: 20613
SCHWARZSCHILD, M., Stellar evolution, 20: 21512
SCHWERTFUEHRER, W., Lithium borate single crystals as neutron detectors, 20: 21049
SCHWETTMAN, H. A., Measurements at high field strengths on superconducting accelerator cavities, 20: 21459 (AD-623509)
SCHWETTMAN, H. A., Superconducting race-track microtron, 20: 21460 (AD-623659)
SCHWINGER, Julian, Magnetic charge and quantum field theory, 20: 21865
SCHWOB, P., Pressure-induced changes of spin structure in EuSe, 20: 22332
SCINTEI, N., Angular correlations inelastic proton scattering on ^{20}Ne and ^{32}S, 20: 22059
SCOPPA, P., Effect of radiations on the detoxification of α-methylnaphthalene, 20: 20439 (EUR-2628.i)
SCOSSIROLI, R. E., Radiation applied to seeds to induce new genetic variation for quantitative traits in durum wheat, 20: 20501
SCOTT, A., Inelastic scattering of 40-Mev protons by ^{208}Pb, 20: 22101
SCOTT, T. E., Interplanar angles and planar spacings of fifteen types of planes for HCP yttrium, 20: 22315 (IS-1337)
SCREM, G., Sintering of oxides of uranium and thorium, 20: 21299
SCURLOCK, R. G., Negative hyperfine field in hexagonal cobalt metal, 20: 22335
SEABORG, G. T., Nuclear systematics of the heavy elements. I., 20: 22042
SEABORG, G. T., Nuclear systematics of the heavy elements. II., 20: 22043
SEABORN, G. B., Detector for alpha radioactivity in flowing water, 20: 21038 (K-1656)
SEAGRAN, H. L., Effect of γ irradiation on microflora of fresh water fish. I., 20: 21203
SECRIST, D. R., Solid-state equilibria in systems Li-C and Li-B, 20: 21327 (CONF-660505-1)
SEDLACEK, Martin, Grain size distribution of natural radioactive aerosols, 20: 20885
SEEBER, Jose Martinez, Hepatic scintigram, 20: 20522 (CNEA-167)
SEEGER, A., Magnetoresistivity of metals at low temperatures, 20: 22333
SEHMEL, G. A., Subisokinetic sampling of particles in an air stream, 20: 20927 (BNWL-217)
SEIBEL, Robert C., Problems with Rossi sweep applications, 20: 21043 (UCRL-13199)
SEIBERT, G., Suitability of electron postemission of $CaSO_4$ for dosimetry, 20: 20769
SEIBERT, J., Suitability of electron postemission of $CaSO_4$ for dosimetry, 20: 20769
SEIBL, J., Stereo-specific hydrogen exchange accompanying catalytic hydrogenation of methyl β, β-dimethylacrylate, 20: 20715
SEIDEL, T., Measurements of current-dependent reactance of superconductors having very small coherence distance, 20: 21919
SEIDL, E., Lithium borate single crystals as neutron detectors, 20: 21049
SEIGLE, Leslie L., Diffusional limitation in high-temperature protective oxide coatings, 20: 21283
SEIMIYA, T., Counting of tritium with thin-windowed G-M counter tube, 20: 21065
SEKI, Yoshinobu, Condenser discharging device, 20: 22303
SEKINE, K., Counting of tritium with thin-windowed G-M counter tube, 20: 21065
SELBIN, J., Chemistry of U(IV). I., 20: 20675
SELL, H. G., Properties of W and W-Re alloys, 20: 21406
SELLS, V., Electron energy measurements of the race-track microtron beam, 20: 21461 (AD-624038)
SELOVE, W., T = 0, S-wave, $\pi\pi$ phase shift, 20: 21685
SELVERSTONE, Bertram, Prog. rpt. on small in vivo β-ray detectors and their diagnostic applications, annual, 5/65-5/66, 20: 20523 (NYO-1726-15)
SEMAGIN, V. N., Dynamics of conditioned reflexes in stereotype during the whole life in rats after repeated prenatal irradiation with small doses, 20: 20492
SEMASHKO, N. N., Intermingling of particles in a composite magnetic field trap, 20: 22274
SEMCHYSHEN, M., Tungsten-base alloy development, 20: 21412
SEMENIKHINA, L. A., Uranyl ion-exchange behavior in hydrochloric acid media, 20: 20827
SENETT, William P., Coherent gamma radiation, 20: 20800
SEN GUPTA, N. D., Motion of charged particle in a magnetic field, 20: 21454
SENYAVIN, M. M., Ion exchange separation of uranium and rare earth elements, 20: 20813
SENYAVIN, M. M., Ion-exchange concentration and separate isolation of cesium, strontium, and cerium from fresh water, 20: 20627
SERBO, V. G., Regge pole behavior of scattering amplitude in quantum electrodynamics, 20: 21871
SERDAREVIC, B., Stereo-specific hydrogen exchange accompanying catalytic hydrogenation of methyl β, β-dimethylacrylate, 20: 20715
SEREBRENNIKOV, V. V., Analysis of zinc and lead for rare earth metals, 20: 20607
SEREBRYAKOV, Yu. N., Radial expansion of a beam in an electron linear accelerator induced by asymmetric wave, 20: 21476
SEREZIN, V. M., Reactions (d,n) on isotopes ^{58,60,62,64}Ni, 20: 22109
SERIN, B., Specific heat of type II superconductors in a magnetic field, 20: 21907
SERINO, A., Automatic device for collecting dust-free precipitation, 20: 20993
SERVOZ-GAVIN, Pierre, EPR study of anneal effects in irradiated graphite, 20: 21435
SESINI, R., Sintering of oxides of uranium and thorium, 20: 21299
SEYMOUR, Errol V., Particle injection techniques for velocity measurement in arc plasmas, 20: 22188 (N-65-22776)

SHAPIRA, A., Peripheral production and decay parameters of $N^{*++}(1238)$ in $pp \to pN^{*++}(1238)$ at 5.5 Bev/c, 20: 21663
SHAPIRO, Bernard, Mechanism of action of AET. VI., 20: 20424
SHAPIRO, Gilbert, π^+-p Scattering at 250 Mev: experiment and analysis, 20: 21662
SHARP, G. W., Midlatitude trough in the night ionosphere, 20: 21822
SHARP, P. H., Structure in the pion-proton total cross section between 2 and 7 Bev/c, 20: 21661
SHARPE, A. G., Advances in inorganic chemistry and radiochemistry. VII., 20: 20658
SHARPEY-SCHAFER, J. F., Deuteron optical potentials and the $^{16}O(d,p)^{17}O$ reaction, 20: 22104
SHATZKES, M., Neutron and γ sensitivities of dynamic detectors, 20: 21059
SHATZKES, M., Reactor and linear accelerator induced effects in dielectrics, 20: 21151 (IBM-66-825-1944)
SHAVIV, G., Monte Carlo investigation of heterogeneity of fast reactor cores, 20: 22397
SHAVROV, P. I., Increase of power of VVR-S reactors, 20: 22498 (IAE-993)
SHAVROV, P. I., Reconstruction of IRT research reactor, 20: 22497 (IAE-992)
SHAW, A. E., Safe transport of radioactive materials, 20: 20945 (TRG-Report-1073)
SHAW, David Tai-Ko, Startup transient behavior of thermoelectric generators with temperature-dependent physical parameters, 20: 21577
SHAW, E. K., Two-dimensional low-pressure discharge theory, 20: 21799
SHAW, R. W., Effects of helium temperature strain on superconducting transition of Pb–In alloys, 20: 21923
SHEFF, James R., Space dependence of reactor noise. I., 20: 22393
SHEKHTER, L. Sh., Isospin conservation and polarization effects, 20: 21717 (JINR-P-2620)
SHELDON, R., Influence of structure on post-irradiation physical properties of epoxy resins, 20: 21429 (RHEL/R-105)
SHELTON, H., Study of porous metal ionizers, 20: 21570 (N-65-29785)
SHELTON, W. N., Excitation of octupole vibrational states in heavy deformed nuclei by inelastic proton scattering, 20: 22100
SHEN, B. C., K+p interactions at 4.6 Bev/c, 20: 21629 (UCRL-16332)
SHER, A., Transport properties of LaF_3, 20: 22339
SHERER, D. B., Analysis of fast reactor transient response and safety in selected accidents, 20: 22401
SHERMAN, Michael, Thermal stability of completely confined fluids including MHD effects, 20: 20854 (AD-621523)
SHERMAN, Warren V., Reactivity of electrons produced in the γ radiolysis of aliphatic alcohols, 20: 20750
SHERR, R., Isotope shift in Coulomb displacement energy, 20: 22095
SHERWOOD, R. C., High-pressure polymorphism and magnetic ordering in some Sm-type rare earth alloys and samarium, 20: 21414
SHEVCHENKO, V. V., Electromagnetic waves in an isotropic stratified plasma waveguide, 20: 22204
SHIBATA, Sinkichi, Development of glasses for low background measurements—characteristics of glasses, 20: 21044 (ANL-Trans-285)
SHIKATA, Sanji, Multi-curie ^{60}Co irradiation unit, 20: 20849
SHIKHOV, S. B., Consideration of heterogeneous resonance effect in calculations of multigroup constants for thermal reactors, 20: 22384
SHILLER, R., Radiochemical stability of high-boiling hydrocarbons in reactor, 20: 20792
SHIMANKO, I. I., Influence of ionizing radiation on outcome of auto- and homovenous plastic repair of arteries, 20: 20478
SHIMONY, Uri, Moessbauer studies on iron in perovskites $La_{1-x}Sr_xFeO_3 (0 \leq x \leq 1)$, 20: 22336
SHINOHARA, Kenichi, Radiation research in Japan, 20: 20727 (PB-181506, pp 9-18)
SHINOHARA, U., Effect of high-energy radiation on electric conduction of various copolymers containing polyethylene, 20: 21170
SHIODA, Susumu, Mobility of electrons in potassium and cesium vapor, 20: 21520
SHIOZAWA, Ken-ichi, Fission-fragment damage in epitaxial film of UO_2, 20: 21442
SHIRAHANE, Mutsuhiro, Chemical shim control in conceptual design of a domestic power reactor, 20: 22428
SHIRIKOVA, N. Yu., Investigation of neutron resonances of ^{165}Ho, 20: 22004 (JINR-P-2593)
SHISHKOV, A. V., Methods for hot synthesis of ^{35}S-labeled biologically active substances. I., 20: 20785
SHISHKOV, A. V., Methods for hot synthesis of ^{35}S labeled biologically active substances. II., 20: 20786
SHITIKOVA, A. S., Influence of mucopolysaccharide preparation on hematopoiesis and survival of animals after irradiation, 20: 20510
SHKAROFSKY, I. P., Dielectric tensor in Vlasov plasmas near cyclotron harmonics, 20: 22240
SHKAROFSKY, I. P., Dispersion of waves in cyclotron harmonic resonance regions in plasmas, 20: 22241
SHOEMAKER, Nathan F., Calculation of energy-angular relationship for neutrons from a neutron generator, 20: 21934 (AD-621473)
SHOEMAKER, Nathan F., Monte Carlo calculations of gamma-ray albedo, 20: 22305 (AD-621441)
SHOFFNER, B. M., True zero-crossing fast discriminator, 20: 21114
SHOHET, J. L., Prog. rpt. on plasma waves and instabilities, 6/65–2/66, 20: 22190 (TID-22821)
SHPIGEL', I. S., Structure of magnetic surfaces in stellarator with double helical field, 20: 22298
SHRADER, E. F., True zero-crossing fast discriminator, 20: 21114
SHREVE, D. C., Nuclear-structure studies of ^{89}Sr and ^{89}Y by inelastic α-particle scattering, 20: 22138
SHUCK, F. O., Determination of liquid metal diffusion coefficients by molecular distillation, 20: 21334 (IS-1325)
SHULEK, P., Fluctuations of ionization losses, 20: 21515 (JINR-P-2615)
SHVEDCHIKOV, A. P., Reactions of hot S atoms. I., 20: 20784
SHVEDOV, V. P., ^{137}Cs behavior during the analysis of atmospheric precipitation specimens, 20: 20625
SHVEIKIN, G. P., Reactions of metallic Nb with CO, 20: 21270
SHVETS, O. M., Production of dense plasma in a metal chamber by a high-frequency method, 20: 22300
SIDOROV, V. P., Entrainment of plasma by a rotating electromagnetic field, 20: 22288
SIDOROVA, T. A., Superconducting alloy in the Nb–Ga system, 20: 21897
SIEBENMANN, P. G., Critical currents of Nb_3Sn and V_3Ga in transverse magnetic fields up to 150 kOe, 20: 21922
SIEMENS, H., Determination of uranium and thorium in sedimentary carboniferous deposits, 20: 20613
SIFFERLEN, Raymond, Microanalysis by x-ray emission in an electron microscope, 20: 20593
SIGLER, Arnold T., Radiation exposure in parents of children with mongolism, 20: 20454
SIKOV, Melvin R., Prog. rpt. on pre- and post-natal sequellae of intrauterine administration of ^{131}I in rat, final, 6/63–2/65, 20: 20390 (TID-22767)
SILCOX, J., Annihilation instability in hard superconductors, 20: 21927
SILCOX, J., Effect of surface conditions on a-c field transitions in type II superconductors, 20: 21918
SILIN-BEKCHURIN, I. A., High-frequency discharge in a neon–helium laser, 20: 21808
SILVA, Richard W., Observations of solar wind during flight of Imp 1, 20: 21496
SILVESTRINI, V., Determination of branching ratios among neutral decay modes of the η particle, 20: 21627 (LNF-66/9)
SIMANTON, J., ZSA-ZSA: a self-policed data handling facility for multiple detector experiments, 20: 20996
SIMENOG, I. V., Two-nucleon correlations in nuclei, 20: 21996 (FTI-142/T-016)
SIMMONS, L. M. Jr., Threshold factors in partial-wave dispersion relations, 20: 21667
SIMON, Albert, Flute instability at low density, 20: 22252
SIMPSON, F. B., Epithermal fission cross section of ^{235}U, 20: 22012 (UCRL-14606)
SIMS, Ernest Park, Thermal neutron spectrum in a finite mass medium, 20: 21933 (AD-621119)
SINGH, M., Measurement of Z dependence of elastic scattering cross section of γ rays. II., 20: 22060
SINGH, R. P., Complex formation of metal ions with tropolones. II., 20: 20673
SINGH, R. P., Thorium and molybdenum complexes with myricetin, 20: 20674
SINGH, R. S., Effect of interference interaction between resonances of ^{239}Pu and ^{232}Th on ^{239}Pu fission and capture cross sections and ^{232}Th capture cross sections, 20: 21970 (ANL-7144)
SINGH, R. Shanker, Physics aspects of large Th-fueled fast reactors, 20: 21229 (AEET-229)
SINGH, R. Shanker, Review of nuclear data related to Th fuel cycle, 20: 21967 (AEET-234)
SINGH, Virendra, Lie group of the strong-coupling theory. I., 20: 21759
SINGHAL, Narayan S., Prog. rpt. on gamma spectra by stepwise statistical method, 9/64–1/65, 20: 20555 (AD-622200)
SINHA, S. P., 2,2'-dipyridyl complexes of rare earths. III., 20: 20703
SINK, H. Rodney, Sensitivity analysis of civil defense systems and components, 20: 20922 (AD-624704)
SIPE, L. H., Some observations on film badge calibration techniques, 20: 20935 (K-1657)
SIPEK, L., Instrument for measuring the index of d-c magnetic fields, 20: 21006
SIPOS, T., Preparation of XeF_2, 20: 20678
SIPOS, Tamas, Hot chamber for production of ^{131}I, 20: 21215
SIRAGUSA, G., Microwave determination of distribution functions of electrons in low current discharges, 20: 21795
SITENKO, A. G., Two-nucleon correlations in nuclei, 20: 21996 (FTI-142/T-016)
SIU, Ralph G. H., United States program on radiation preservation of foods,

20: 21192 (PB-181506, pp 19-26)
SIVO, L. L., Radiation damage studies in degenerate Si, irradiated at low temperatures, 20: 22346
SIVOV, E. N., Welding of molybdenum and niobium with stainless steel, 20: 21309
SIZMANN, R., Defect production in copper, nickel, and gold by 5-Mev α bombardment in region 90 to 194°K, 20: 21447
SIZOV, P. P., Experimental data on dose assessment during remote-control γ therapy, 20: 20541
SJOBLOM, J. J., Acetylacetonates of transition metals and rare earth metals, 20: 20700
SKELLY, David W., Trapped electrons in γ-irradiated 2-methylpentane at −196°, 20: 20755
SKLYARENKO, I. S., Polarographic determination of U in nitric acid media containing TBP. II., 20: 20631
SKLYARENKO, I. S., Polarographic determination of U in nitric acid media containing TBP. I., 20: 20630
SLABOSPITSKII, R. P., Mass spectrometric investigation of source of positive ions operating at low gas pressure, 20: 21457
SLAVIERO, G. E., Utilization of sodium sulfate—^{35}S by hepatic tissue of the normal and irradiated rat, 20: 20410
SLAVIN, Joseph W., Radiopasteurization of fishery products, 20: 21200
SLAY, B. G., Switching characteristics of small-geometry thin-film superconductors, 20: 21012
SLEPUKHINA, L. B., Relation between radioprotective and antineoplastic effects of antioxidant-inhibitors, 20: 20506
SLESAREVA, D. D., Uranyl ion-exchange behavior in hydrochloric acid media, 20: 20827
SLINGO, R. A., Improvements to nuclear fuels, 20: 21297 (NP-tr-1371)
SMIDT, D., Application of vented fuel concept to a sodium-cooled power breeder with 1000 Mw(e), 20: 22462
SMIDT, D., Karlsruhe reference design of 1000-Mw(e) sodium-cooled fast breeder, 20: 22453
SMIDT, D., Safety and cost analysis of 1000-Mw(e) sodium-cooled fast power reactor, 20: 22451
SMIRNOVA, R. F., Increase of power of VVR-S reactors, 20: 22498 (IAE-993)
SMIT, J. Van R., Separation of Cs from fission-product wastes, 20: 20818
SMITH, A. C. H., Cross section for production of $He^+(2S)$ ions by electron impact excitation of ground state helium ions, 20: 21535
SMITH, A. K., SNAP-10A instrumentation and control development and testing, 20: 22476
SMITH, Alex G., Temporal and statistical characteristics of Jupiter decametric radiation, 20: 21510
SMITH, B. C., Supposed complexes of uranium(VI) and uranium(IV) with triphenylphosphine, 20: 20679
SMITH, H. P. Jr., Pressure wave generation in a fissioning gas. III., 20: 21803
SMITH, Harold P. Jr., On-line computers in optimal reactor shutdown, 20: 22389
SMITH, J. T., Development of chromium–vanadium alloys for brazing tungsten to molybdenum, 20: 21312
SMITH, K. D., Logical design of a digital pseudorandom noise generator, 20: 21001
SMITH, K. F., Low-background ionizer for molecular beam detection, 20: 21066
SMITH, L. H., Photographic spark chamber for manned satellites, 20: 21122
SMITH, Sherwood B., Possibilities of secondary explosions and post-shot thermal effects in cavities in tuff, 20: 20939 (NVO-1163-70)
SMITH, Tennyson, Mechanism of reduction of adsorbed oxygen on zirconium dioxide with hydrogen, 20: 20705
SMITH, Willie W., Effects of bacterial endotoxin on the occurrence of spleen colonies in irradiated mice, 20: 20512
SMITH, Willie W., Estimation of radiation dose-reduction factor for β-mercaptoethylamine by endogenous spleen colony counts, 20: 20511
SMOTRYAEV, V. A., Reactions (d,n) on isotopes $^{58,60,62,64}Ni$, 20: 22109
SNEDKOV, B. A., Obtaining electron bunches of minimum length from klystron-type buncher, 20: 21014
SNYDER, Fred, Triglyceride biosynthesis in irradiated bone marrow, 20: 20420
SNYDER, W. S., Evaluation of radiation dose to man from radionuclides released to Clinch River, 20: 22514 (ORNL-P-2021)
SOBKOWSKI, Jerzy, Oxidation of U(IV) ions with molecular O, 20: 20689
SOBOTOVICH, E. V., Extraction-radiometric determination of microgram amounts of lead by isotopic dilution method, 20: 20620
SOCOLOW, R. H., Should SU(3) mass formulas for mesons use the masses of the mesons or their squares? 20: 21671
SODHA, Mahendra Singh, Nonlinear sum and difference frequency generation in an inhomogeneous plasma, 20: 22244
SOERENSEN, G., Fission and spallation yields in the iodine region, 20: 22045
SOKOLOVA, M. N., Radioactivation analysis of SiO_2 using ion exchange chromatography. V., 20: 20636
SOLDATENKOV, T. R., Entrainment of plasma by a rotating electromagnetic field, 20: 22288
SOLER, M., G_2 symmetry and leptonic decays, 20: 21719
SOLOMKO, V. P., Radiation-induced methylmethacrylate and styrene polymerization in presence of mineral filters, 20: 20778
SOLOMON, R., Transport properties of LaF_3, 20: 22339
SOLOV'EV, L. D., Contribution of virtual Compton effect to cross section for electron-positron pair production, 20: 21623 (JINR-P-2602)
SOLOV'EV, V. G., Equilibrium deformations of excited states of heavy nuclei, 20: 22005 (JINR-P-2596)
SOLYOM, Jeno, Angular resolution of critical scattering experiments, 20: 22325
SOMANI, S., Role of radioactivity and hydrothermal processes in protobiochemistry, 20: 20406 (N-65-27062)
SOMASUNDARAM, S., Physiological norms in Indian adults. Statistical analyses of data on organ weights, 20: 20374
SOMMER, H., Positioning of charge-discharge machine of experimental nuclear power plant at Lucens, 20: 22423
SOMMER, W., Application of vented fuel concept to a sodium-cooled power breeder with 1000 Mw(e), 20: 22462
SONKA, J., Influence of polyols on course of experimental radiation disease, 20: 20520
SONODA, Masateru, Cobalt-60 γ irradiation laboratory. II., 20: 20847
SONODA, Masateru, Total cross sections of heavy nuclei for protons, 20: 22049
SONODA, Masateru, Transistorized low-noise preamplifier for solid-state radiation detector, 20: 21072
SOOD, B. S., Measurement of Z dependence of elastic scattering cross section of γ rays. II., 20: 22060
SOOD, P. C., Nilsson model for ^{57}Fe, 20: 22098
SOROCHAN, A. M., Ion exchange separation of uranium and rare earth elements, 20: 20813
SOSKE, Paul L., SNAP-10A FASM—4-system test, 20: 22471 (NAA-SR-11814)
SOUFFRIAU, J., Migration of radio elements in soil, 20: 20875 (EUR-2481.f)
SOUTHGATE, B. A., Conference on water pollution research, London, 9/62, 20: 20982
SPAMER, R., Excitation of new electromagnetic transitions in ^9Be inelastic electron scattering, 20: 22105
SPARLIN, D. M., Empirical Fermi-surface parameters for W and Mo, 20: 22337
SPEHL, H., Gyromagnetic ratios on first excited 2^+ states in even Os isotopes, 20: 22055
SPENCER, Herta, Effect of chelating agents on the removal of ^{65}Zn in man, 20: 20397
SPERGEL, M. S., Pion production in high-energy cosmic-ray collisions, 20: 21553
SPERGEL, M. S., Production spectrum of high-energy electrons from high-energy cosmic-ray collisions, 20: 21552
SPIJKERMAN, J. J., Standardization of differential chemical shift for ^{57}Fe, 20: 22158
SPINRAD, Robert J., Computers in experimental physics, 20: 21982 (BNL-948, pp 718-40)
SPIRA, Jacob, Photon activation analysis of cesium, 20: 20645
SPIRIN, V. D., Measurement of the radon concentration in water by γ radiation, 20: 20959
SREEKANTAN, B. V., K.G.F. neutrino project, 20: 21540 (CERN-65-32, pp 49-56)
STACEY, D. N., Interpretation of isotope shifts, 20: 21531
STADLER, David R., Glutamic dehydrogenase in revertants of AM mutants in neurospora, 20: 20462
STAIRS, D. G., Wide-angle electron-pair production, 20: 22146
STAKHANOV, I. P., Operation of a cesium diode with an admixture of an inert gas, 20: 21567 (FEI-15)
STAKHANOV, I. P., Volt-ampere characteristics of the TEP (thermoelectron potential) in an arc, 20: 22178 (FEI-17)
STAL'MAKHOV, V. S., Instability of small electron fluxes in crossed fields, 20: 21451
STANER, P. I., Migration of radio elements in soil, 20: 20875 (EUR-2481.f)
STANLEY, M. W., Low-temperature internal-friction peaks in cold-worked niobium, 20: 21378
STANTON, Henry E., Applications of radioisotopes for naval field establishments, 20: 21176 (AD-621440)
STARFELT, N., Gamma spectra from inelastic neutron scattering, 20: 22069
STARKS, Ralph J., Purification and crystallization of B, 20: 21294 (TID-22221)
STAROVA, L. L., Fusion welding of some heterogeneous metals, 20: 21310
STARY, F., Nanosecond lifetime measurements in decay of ^{155}Eu, ^{157}Eu, and ^{157}Dy, 20: 22058

STEED, J. A., Engineering design practices for facilities containing radioactive materials, 20: 20942 (ORNL-TM-1459)
STEELE III, O. P., Development of control system for SNAP reactors, 20: 22474
STEFAN, Maria, Radioprotective effect of glycine during x irradiation. II., 20: 20517 (NP-15925)
STEIGERWALD, E. A., Prog. rpt. on creep data on refractory alloys, 9/26–12/26/65, 20: 21346 (NASA-CR-54895)
STEIN, Martin H., Radiation processed wood-plastic materials, 20: 21183 (ORNL-IIC-7, pp 59-63)
STEIN, W. E., Reactions (^{3}He,n) with 19- to 25-Mev ^{3}He ions, 20: 22132
STEINFINK, Hugo, Crystal chemistry of intermediate phases in the ytterbium–antimony system, 20: 21401
STELSON, Paul H., Coulomb excitation with heavy ions, 20: 21991 (BNL-948, pp 1005-44)
STEPANENKO, I. A., Polarization interaction of opposed plasma streams in composite magnetic field trap, 20: 22273
STEPANOV, K. N., Peculiarities of electromagnetic wave radiation in anisotropic dispersive media, 20: 22199
STEPANOVIC, Stepan, Amount of catecholamines in auricles of irradiated rabbits and their response to quinidine, 20: 20451
STEPHENS, F. S., Decay scheme of ^{254}Es, 20: 22142
STERN, J., On the spontaneous breakdown of γ_5 invariance and parity nonconserving interactions, 20: 21727
STERNHEIMER, D., Masses of nonstrange pseudoscalar mesons and the generalized Klein-Gordon equation, 20: 21744
STERNHEIMER, J., Masses of nonstrange pseudoscalar mesons and the generalized Klein-Gordon equation, 20: 21744
STEVENS, Edward M., Modified method of radioisotopic placental localization, 20: 20527
STEVENS, G. H., Effects of uv and visible radiation on mouse ascites tumor cells, 20: 20484
STEVENS, G. H., Method of assaying in vivo the survival of uv irradiated tumor cells, 20: 20483
STEVENS, R. R. Jr., Relevance of bombardment-induced Moessbauer effects in iron to radiation damage theories, 20: 21444
STEWART, J. D., Diffusion of neutrons in a reactor lattice, 20: 22398
STIEGELMEYER, William N., Examination of 1B steam generator from Shippingport Atomic Power Station, 20: 22408 (BMI-1764)
STIERWALT, D. L., Surface effects in alkali-halide crystals from irradiation, 20: 21424 (N-65-23332)
STILLMAN, D. B., Fission couples applied toward reactor diagnostics and safety, 20: 22355 (LA-3470)
STILWELL, D., Three-parameter pulse-height analyzer and coincidence system for satellite cosmic-ray studies, 20: 21125
STINNER, R. J., Theoretical differential scattering cross sections of x rays, 20: 21516 (UCRL-14403)
STOBBS, J. J., Cracking and carbon pickup in the oxide formed on uranium CO_2 at 650°C, 20: 21272
STODOLSKY, Leo, Application of nuclear coherence properties to elementary-particle reactions, 20: 22145
STOKES, Arthur J., Improved performance of BF_3 neutron counters in high gamma fluxes, 20: 21132
STONE, Louis E., Purification and crystallization of B, 20: 21294 (TID-22221)
STONE, Noel, Nonlinear terms in the generalized Ohm's law: a scale analysis, 20: 21778 (AD-621943)
STORM, M. L., Subcritical determination of relative natural-neutron-source strengths, 20: 22392
STORRER, F., Method for calculating flux evolution in a fast-neutron multiplying medium as function of time, space, and energy, 20: 21950
STOUGHTON, R. W., Spectrophotometry of aqueous homogeneous fuel solutions, 20: 20600
STRAATMANN, John Alphonse, Lanthanum–lanthanum hydride phase system, 20: 21336 (IS-T-79)
STRAIN, J. E., Monitoring of leached fuel elements with a neutron generator, 20: 21040 (ORNL-P-1218)
STRAIN, J. E., ^{3}He activation analysis, 20: 20565 (ORNL-P-1216)
STRATUMANN, N., Unitary representations of SU(1,1) and SU(2,1), 20: 21722
STRAUB, C. P., Evaluation of radiation dose to man from radionuclides released to Clinch River, 20: 22514 (ORNL-P-2021)
STRAUSS, B. P., Fabrication of an ultra-fine Nb–Cu composite by drawing, 20: 21298
STRAWSON, David G., Re-examination of design factors for 1000-Mw(e) fast breeder, 20: 22454
STREATER, R. F., Irreducible representations of U(12), 20: 21765
STREICHER, M. A., Corrosion resistance in wrought Ni–Cr–Mo alloys, 20: 21277
STRICKLAND, G., Conversion of high-level radioactive waste to phosphate glass, 20: 22509 (BNL-10109)
STRIZHEVSKAYA, L. G., Fusion welding of some heterogeneous metals, 20: 21310
STRNAT, K. J., Yttrium–cobalt alloy system, 20: 21402
STROM, P. O., Nuclear-charge distribution of fission-product chains of mass numbers 131-133, 20: 22136
STRUEBING, V. O., Plutonium–americium system, 20: 21339 (LA-DC-7095)
STRUXNESS, E. G., Evaluation of radiation dose to man from radionuclides released to Clinch River, 20: 22514 (ORNL-P-2021)
STUART, Carlo, Morphine, codeine, nalorphine and survival test of the pan-irradiated mouse, 20: 20513
STUKAN, R. A., Reactions of hot S atoms. I., 20: 20784
STUPEGIA, D. C., Nuclear constants, 20: 21969 (ANL-7055, pp 230-3)
SUCHAN, W. W., Chelates of β-diketone derivatives. II., 20: 20693
SUDDATH, J. C., Prog. rpt. on chemical technology, 7–9/65, 20: 20808 (ORNL-3916)
SUEVEGES, Mate, Theory of congruence in gravitational fields. III., 20: 21841
SUGA, K., High-energy nuclear-active particles in extensive air showers at 5,200 m altitude, 20: 21544 (MIT-2098-227, Paper EAS-8)
SUGA, K., Low-μ showers, 20: 21546 (MIT-2098-227, Paper EAS-29)
SUGA, K., Primary energy spectrum from 8×10^{14} to 4×10^{17} ev, 20: 21547 (MIT-2098-227, Paper EAS-31)
SUGAWARA, Kazuko, Blocking effect and coriolis anti-pairing effect on deformed odd nuclei, 20: 22148
SUGAWARA, Masao, High-energy limit of $\pi^+\pi^0$ total cross section, 20: 21679
SUGAWARA, Minoru, Electron probe current in a magnetized plasma, 20: 22259
SUGAWARA, Tadashi, Low-temperature resistivity, magnetic susceptibility, and superconducting transition temperature in La containing rare-earth impurities, 20: 21873 (NP-15936)
SUGIER, Henryk, Achievements of Polish radiation chemistry, 20: 20780
SUITA, Tokuo, Injection trapping of high-energy molecular ions into the mirror field with the r-f electric field. II., 20: 22207
SUITA, Tokuo, Nonlinear effect in beam-plasma interaction, 20: 22206
SULLIVAN, Russell P., Master control system for nuclear physics instrument systems, 20: 20995
SUMERLING, R., Structure of 20Cr–25Ni–Nb steel after aging in temperature range 600 to 800°C, 20: 21355 (TRG-Report-1168)
SUMNER, A. E. Jr., DUZ-1—program for solving axisymmetric and plane elasticity problems on Philco-2000, 20: 20862 (WAPD-TM-555)
SUNDERMAN, Donne N., Diffusion of fission products in fuel-element cladding materials and related alloys, 20: 21232 (BMI-1763)
SUPRUNENKO, V. A., Bremsstrahlung from a solid target in a plasma, 20: 22293
SUZUKI, Haruyoshi, Embrittlement of welded joints of HT60 steel for nuclear pressure vessels, 20: 21393
SUZUKI, Mahiko, Partially conserved axial-vector current and the nonleptonic K-meson decays, 20: 21666
SUZUKI, Shin, Hot atom chemistry of ^{76}As using zirconium benzenearsonate as target, 20: 20797
SUZUKI, Toshio, High-efficiency gas Cherenkov counter, 20: 21071
SVECENSKI, Nadezda, Amount of catecholamines in auricles of irradiated rabbits and their response to quinidine, 20: 20451
SVENSSON, B. E. Y., Absorption model and production of 2$^+$ mesons, 20: 21644
SVESHNIKOV, A. G., Intermingling of particles in a composite magnetic field trap, 20: 22274
SVIDERSKAYA, T. A., Utilization of certain biochemical indices for assessing effects of ionizing radiation on the organism, 20: 20415
SWAIN, James E., Profile of electron beam from Astron accelerator, 20: 22191 (UCRL-14697)
SWALLOW, A. J., Aspects of radiation chemistry of organic compounds, 20: 20728 (PB-181506, pp 49-58)
SWAN, A. H., Friction factor and heat transfer correlation for irradiated organic coolants, 20: 20710 (MIT-334-23)
SWANSON, R., Feasibility of experiment to observe the W produced in strong interactions, 20: 21610 (CERN-65-32, pp 181-94)
SWANSON, R., Measurement of anomalous gyromagnetic ratio of the muon, 20: 21630 (UCRL-16469)
SWARTZ, Clifford E., Fundamental particles, 20: 21695
SWEENEY III, William J., Treatment of carcinoma of the cervix with combined radiation and extensive surgery, 20: 20526
SWENSON, L. W., Levels of ^{42}Sc from ^{40}Ca(^{3}He,p)^{42}Sc and ^{40}Ca(^{3}He,py)^{42}Sc, 20: 22073
SWENSON, L. W., Reaction ^{60}Ni(^{3}He,α)^{59}Ni at 15 Mev, 20: 22127
SWINBURN, K. A., Plant measurement, sampling, and analysis for accountancy purposes, 20: 20830
SWINBURN, K. A., Plant measurement, sampling and analysis for accountancy purposes with particular reference to separation plants at Windscale, 20: 20972
SWINEHART, C. F., Calcium fluoride as x-ray and charged particle detector, 20: 21135
SYKES, J. B., Utilization of radioisotope devices, 20: 20990 (AERE-

Trans-1048)
SYMONDS, A. E. Jr., Electrowinning plutonium metal, 20: 21234 (DP-1021)
SYMONS, G. D., Rotational bands on two-particle configurations with $K_n = K_p = ½$, 20: 22072
SYPKENS, H. A., Experience with superconducting coils fed by flux pumps, 20: 21924
SYROMYATNIKOV, N. G., Determination of uranium, thorium, and zirconium by Arsenazo III without chemical separation, 20: 20614
SZALOK, Mihely, Transportable vacuum apparatus, 20: 21479
SZAMOSI, Gyoergy, ZR-2 critical assembly, 20: 22388
SZANTO, Borisz, Hot chamber for production of ^{131}I, 20: 21215
SZANTO, Joseph, Occlusion of various refractory materials in chromium plate on steel substrates, 20: 21286 (AD-621920)
SZEKERES, Peter, Propagation of gravitational fields in matter, 20: 21853
SZKOPIAK, Z. C., Low-temperature internal-friction peaks in cold-worked niobium, 20: 21378
SZYMANSKI, Z., Rotational bands on two-particle configurations with $K_n = K_p = ½$, 20: 22072

T

TACONIS, K. W., Experience with superconducting coils fed by flux pumps, 20: 21924
TAHA, M. O., Model for final-state interactions, 20: 21738
TAKAGI, Shuji, Monte Carlo analysis of electromagnetic cascade showers, 20: 21559
TAKAHASHI, Masazumi, Detecting ruptured fuel elements at the Tokai power station, 20: 22427
TAKAHASHI, Shinji, Beam focus radiography for taking radiogram of the axial transverse cross section of treated region in high density of dose, 20: 20547
TAKAHASHI, Tsuneto, Production of polymer gel with least radiation dose, 20: 20761
TAKAYANAGI, M., Cobalt-60 γ irradiation laboratory. II., 20: 20847
TAKEDA, Susumu, Microwave absorption of magnetoplasma with boundaries, 20: 22209
TAKEHISA, Masaaki, Reaction of ethylene with methylene chloride induced by γ-radiation, 20: 20757
TAKETANI, Hiroshi, Nuclear reaction on ^{13}C at the proton energy of 54.9 Mev, 20: 22030
TAKEZAKI, Junichi, Radiolysis of methylal and ethylene glycol dimethyl ether, 20: 20758
TAKIYAMA, Masashi, Tritium gas target for $T(d,n)^4He$ reaction, 20: 21948
TAM, Christopher K. W., Electrostatic damping on motion of charged particle in a plasma, 20: 22233
TAMIR, T., Bound waves in compressible plasma gaps, 20: 22163 (AD-621034)
TANABE, Tetsumi, Construction of thin-lens-type β spectrometer, 20: 21051
TANAKA, Kohei, Measurement of liquid volume by activation analysis, 20: 21208
TANAKA, Osamu, Integrating dose-rate meter employing ionization chambers, 20: 21078
TANAKA, S., Anomalous bremsstrahlung and anomalous cyclotron emission from partially ionized gases, 20: 22208
TANAKA, Shigetoshi, Interaction between plasma and microwave field in mirror-type magnetic field. I., 20: 22216
TANARRO, Agustin, Automatic-reading electronic equipment for multiple measurements of radioactivity, 20: 21045
TANARRO SANZ, Agustin, Automatic electronic equipment for multiple measurements of radioactivity, 20: 21055
TANDY, Robert, Ischemic heart disease, atherosclerosis, and longevity, 20: 20370 (UCRL-14658)
TANIFUJI, Takeaki, Determination of polonium in neutron-irradiated bismuth, 20: 20585
TAPLIN, G. V., Lung scanning following radioaerosol inhalation, 20: 20532
TARANTIN, N. I., Magnetic spectrometer with field variation, 20: 21036 (JINR-P-2573)
TARASENKO, V. F., Production of dense plasma in a metal chamber by a high-frequency method, 20: 22300
TARDIFF, Robert G., Effects of various drugs on the ATP activity of the hematopoietic tissues of rats exposed repeatedly to ^{60}Co γ radiation, 20: 20503 (AD-629311, pp 1-14)
TARRICE, R. R., Criteria for special nuclear materials inventory and control procedures, 20: 20966
TATI, Takao, Interaction between basic particles, 20: 21766
TATSIEVSKII, V. A., Assessment of method of recording radiophosphorus bremsstrahlung for diagnosis of milk-duct carcinoma, 20: 20540
TATSUNO, Takeshi, Selective ^2H- and ^3H-labeling reaction of c-terminal amino acids through oxazolone, 20: 20714
TAUSSIG, Robert T., Normal ionizing shock waves with equilibrium chemistry in hydrogen, 20: 21796
TAUTZ, M., Problem of fetal radiation burden in isotopic placentography using human serum albumin labeled with ^{131}I or ^{132}I, 20: 20537
TAUXE, W. NEWLON, Mayo Clinic whole-body counter, 20: 21075
TAVGER, B. A., Increase of critical temperature in superconducting films, 20: 21891
TAWARA, Hiroyuki, Operating features of plasma expansion ion source, 20: 21478
TAYLOR, B. N., Microwave-induced d-c voltages across Josephson junctions, 20: 21882
TAYLOR, G. R., Action of ^{90}Sr–^{90}Y on developing khamsa spawn, 20: 20445 (TRG-Inf. Ser.-166)
TEENER, J. W., Effects of electron irradiation and temperature on solar cell performance, 20: 21161
TEETER, Charles E., Catalog of nuclear reactor concepts, Pt. I, Sec. IV, 20: 22347 (ANL-7138)
TEETER, Charles E., Catalog of nuclear reactor concepts, Pt. I, Sec. V, 20: 22466 (ANL-7180)
TEPLEY, Lee, Intra- and interhemisphere differences in occurrence times of hydromagnetic emissions, 20: 21832
TEPLEY, Lee, Waveguide theory for ionospheric propagation of hydromagnetic emissions, 20: 21833
TEPLITZ, V. L., Shadow effect in high-energy scattering from deuterons, 20: 21646
TEPPER, L., Fast timing circuits using storage diodes, 20: 21002
TERAZAWA, Osamu, Dynamical approach to nonleptonic decays of hyperons, 20: 21686
TEREJA, E., Structure of particles using the generalized relativity theory, 20: 21634
TERTYKH, L. I., Radiation-induced methylmethacrylate and styrene polymerization in presence of mineral filters, 20: 20778
TERUMICHI, Yasushi, Possibility of negative absorption of a plasma-cavity system, 20: 22211
TEVEBAUGH, A. D., Energy conversion, 20: 21566 (ANL-7055, pp 213-29)
TEVEBAUGH, A. D., Nuclear constants, 20: 21969 (ANL-7055, pp 230-3)
TEVEBAUGH, A. D., Reactor safety, 20: 20925 (ANL-7055, pp 177-212)
TEWORDT, L., Generalized Ginzburg-Landau-Gor'kov equations for a pure superconductor, 20: 21903
TEYSSIER, Jean-Louis, Decline of luminescence of rare gas atoms excited by α particles in presence of electric field, 20: 21521
THAMER, B. J., Corrosion tests of Hastelloy N, Inconel 600, and Hymu-80 exposed to UC_3–KCl at 900°C, 20: 21261 (LA-3476)
THATCHER, L. L., Distribution of tritium in precipitation over continents and its significance to ground-water dating, 20: 20892
THEIMER, O., High density corrections to the scattering cross section of a plasma, 20: 22268
THEUS, R. B., Angular distributions and cross section ratios for the reactions $^2H(d,n)^3He$ and $^2H(d,p)^3H$ below 500 kev, 20: 22074
THIEBAUX, M. L. Jr., Off-shell pion-nucleon scattering, 20: 21672
THIELBAHR, William H., Transpiration cooling with liquid metals. II., 20: 22351 (AD-623020)
THIEME, Allen A., Evaluation program for radioactive waste treatment facility, 20: 22507 (AD-622372)
THIRIET, L., Comparison of economic aspects of treatment of fission products from installations processing irradiated natural uranium, 20: 22517
THIRLAWAY, H. I. S., Interpreting array records: explosion and earthquake P wavetrains which have traversed the deep mantle, 20: 20910
THOMAS, G., Structure and mechanical properties of Ta–Mo alloy single crystals, 20: 21364
THOMAS, G. D., Prog. rpt. on effect of transistor design parameters on radiation response, 7–9/65, 20: 21148 (AD-630835)
THOMAS, G. D., Prog. rpt. on effect of transistor design parameters on radiation response, 10–12/65, 20: 21149 (AD-620836)
THOMAS, Harold A. Jr., Operations research in disposal of liquid radioactive wastes in streams, 20: 22513 (NYO-10447)
THOMAS, Lance, Electron density distributions in the daytime F_2 layer, 20: 21823
THOMAS, T. D., Emission of α-particles in fission of ^{238}U by 11- to 21-Mev protons, 20: 22144
THOMASSEN, K. I., Measurement of anomalous diffusion coefficient, 20: 22249
THOMPSON, D. S., Electron paramagnetic resonance study of solutions of europium in liquid ammonia, 20: 20668
THOMPSON, M. A., Oxidation and ignition of Pu, 20: 21264 (RFP-491)
THOMPSON, Max Forest Jr., Fuel burnup studies of Air Force Nuclear Engineering Test Facility, 20: 22487 (AD-621118)
THORN, R. J., Uranium monosulfide. III., 20: 20669
THRANE, E. V., Effect of irregularities in collision frequency on the amplitude of weak partial reflections, 20: 21819
THYNNE, J. C. J., Arrhenius parameters for elementary combustion reactions: H-atom abstraction from N-H bonds, 20: 20713
TIBU, Margareta, Radioluminescent effect of some liquid scintillators in mixture with alcohol, 20: 21046

TIFFANY, O. L., Monte Carlo calculations of radionuclide production in iron targets bombarded with 400-Mev protons, 20: 22035
TIKHOMIROVA, M. D., Peculiar features in radiation sickness induced by soft x rays, 20: 20475
TIKHONIN, F. F., Unitary symmetry and resonance widths, 20: 21713 (JINR-P-2568)
TIKHONOV, V. N., Electode erosion in bridge stage when breaking 1 to 5kA currents in vacuum, 20: 22291
TILBURY, P. D., Impact tensile testing of U, 20: 21325 (AWRE-O-36/66)
TILGNER, Horibert, Modification of the logarithmic damping decrements of quartz oscillators by x irradiation, 20: 21155
TILLEY, D. R., Evidence for the prolate deformation of ^{27}Mg, 20: 22099
TILLEY, D. R., $^{12}C(d,p\gamma)^{13}C$ angular distributions and correlations near threshold, 20: 22087
TILLEY, J., Thick non-equilibrium helium II films, 20: 21896
TINGEY, F. H., Economic considerations in the measurement of nuclear materials, 20: 20647
TINGEY, F. H., Materials control system for enriched U chemical processing facility, 20: 20832
TINKHAM, M., Angular dependence of the critical field of superconducting films and surfaces, 20: 21917
TINKLE, Donald W., Prog. rpt. on effects of radiation on natural populations of lizards, 6/60–12/65, 20: 20444 (TID-22820)
TIPPING, R., Finite nuclear mass and relativistic effects on the rotational constant of molecular hydrogen, 20: 21527
TISLJAR, Mario, Behavior of γ radiation in air, 20: 20946
TISLJAR-LENTULIS, Georg M., Investigation of negative π mesons with reference to their applicability in radiotherapy, 20: 20525
TISNE, M. R., Effects of γ rays on polyriboadenylic and polyribouridylic acids, 20: 20411
TITRAN, Robert H., High-temperature creep behavior of Nb alloy, FS-85, 20: 21344 (N-65-26653)
TOBOCMAN, William, Boundary condition constraint method, 20: 21989 (BNL-948, pp 905-27)
TOBOCMAN, William, Inelastic scattering, 20: 21973 (BNL-948, pp 175-221)
TOCHILIN, E., Photon, neutron, and charged particle absorbed dose measurements with a portable microcalorimeter, 20: 21024 (AD-630693)
TODD, Leonard, Stability of tangential discontinuity in an incompressible conducting fluid, 20: 21804
TODOROV, I. T., Mass formula in inhomogeneous SU(6,6) group, 20: 21624 (JINR-P-2606)
TOOT, F. W., GARGOYLE—infinite medium fuel cycle analysis code with fuel and poison searches, 20: 22412 (GA-6622)
TOITA, Yukio, Separation of uranium from thorium by tri-iso-octylamine extraction and photometric determination of uranium with Arsenazo III, 20: 20598
TOLCHENKOV, D. L., Reactions (d,n) on isotopes $^{58,60,62,64}Ni$, 20: 22109
TOLLET, Louis H. J., Nuclear reactor moderator structure, 20: 22402
TOLOK, V. T., Performance of coaxial plasma source in longitudinal magnetic field, 20: 22179 (FTI-080/P-032)
TOLOK, V. T., Polarization interaction of opposed plasma streams in composite magnetic field trap, 20: 22273
TOLOK, V. T., Polarization of plasma moving in helical magnetic field, 20: 22275
TOLOK, V. T., Polarization of plasma moving in toroidal magnetic field, 20: 22276
TOLOK, V. T., Polarization of plasmas moving in magnetic fields of opposite curvatures, 20: 22277
TOLOK, V. T., Production of dense plasma in a metal chamber by a high-frequency method, 20: 22300
TOLSON, G. M., Manufacture of control rods for EGCR, 20: 21292 (ORNL-3932)
TOLUTIS, V. B., Dielectric properties of thin films of Pr, Ce, and Nd fluorides, 20: 22324
TOMASHOV, N. D., Corrosion and electrochemical behavior of rhenium, 20: 21275
TOMILOV, S. B., Partition chromatography on polytetrafluoroethylene. II., 20: 20622
TOMITA, Shigeharu, Elastic and inelastic scattering of 28.4-Mev α particles by Sn, Cd, Ag, Cu, and Ti, 20: 22047
TONDELLO, Giuseppe, Spectroscopic analysis of helium plasma produced by a conical θ-pinch discharge, 20: 22269
TONEY, William M., Investigation of the $^{10}B(n,\alpha)^{7}Li^{*}$, ^{7}Li reaction branching ratio, 20: 22071
TONOMURA, Shizo, Effect of γ radiation on α, β, γ, δ-tetraphenylporphine, 20: 20774
TORIYAMA, Hideshi, Progress of radiation nondestructive testing equipment, 20: 20867
TORRENS, Ian McC., Atomic collisions in crystals, 20: 22341
TORTI, M. L., Strength, weldability, and heat treatment of Ta–W–Hf and Ta–W–Zr alloys, 20: 21405
TOTH, I. J., Activation sintering of W and effect on mechanical properties, 20: 21291 (NP-15944)
TOTH, Kalman, Evaluation of the trace of the ν-th power of a matrix, 20: 21737
TOTH, L. E., Some superconducting properties of several carbides and nitrides of the transition metals, 20: 21911
TOTSKII, I. A., Scattering of medium-energy neutrons, 20: 22023
TOUSCHEK, B., Proposal for administration of radiative corrections, 20: 21469 (LNF-66/10)
TOXEN, Arnold M., Nonlocal extension of the Ginzburg-Landau theory, 20: 21905
TOYODA, Y., High-energy nuclear-active particles in extensive air showers at 5,200 m altitude, 20: 21544 (MIT-2098-227, Paper EAS-8)
TOYODA, Y., Low-μ showers, 20: 21546 (MIT-2098-227, Paper EAS-29)
TOYODA, Y., Primary energy spectrum from 8×10^{14} to 4×10^{17} ev, 20: 21547 (MIT-2098-227, Paper EAS-31)
TRACY, Peter Wayne, One-dimensional magnetogasdynamics, 20: 21777 (AD-621442)
TRAEGER, Lothar, Isotope effects in photochemical transformation of tritium-labeled uracil, 20: 20782
TRAEGER, R. K., Effect of γ radiation on dynamic mechanical properties of styrene–butadiene rubbers, 20: 20754
TRAPMANN, H., Dephosphorylation of some coferments with thorium and zirconium ions, 20: 20375
TREIMAN, S. B., Seismic signals from nuclear explosions in overdriven cavities, 20: 20898 (AD-624016)
TREKHOV, E. S., Cathode spots of pulsed discharge between parallel electrodes, 20: 22292
TREMMEL, Ernest B., Radiation and its commercial future, 20: 21182 (ORNL-IIC-7)
TRILLING, G. H., $K^{+}p$ interactions at 4.6 Bev/c, 20: 21629 (UCRL-16332)
TRIPATHY, K. C., Radiative nonleptonic weak decays of baryons, 20: 21751
TRIVEDI, N. B., Night-time disturbance fluctuations in geomagnetic field at equatorial stations, 20: 21818
TRNOVEC, T., Metabolism of carrier-free $^{106}RuCl_3$ after intratracheal application, 20: 20396
TROCHEV, T., Flux of neutrons and γ rays in paraffin moderator, 20: 20524 (RT-PROT-(65)32)
TROFIMOV, A. M., Clathrate compounds of p-cresol with rare gases. I., 20: 20688
TROFIMOVA, L. A., Determination of uranium, thorium, and zirconium by Arsenazo III without chemical separation, 20: 20614
TROISE, G., Determination of branching ratios among neutral decay modes of the η particle, 20: 21627 (LNF-66/9)
TROKA, Wladyslaw, π^{+}-p Scattering at 250 Mev: experiment and analysis, 20: 21662
TROMBKA, Jacob I., Nondispersive x-ray spectrometer for lunar and planetary geochemical analysis, 20: 21128
TRON, L., Investigation of the α spectrum of Bi isotopes, 20: 22000 (JINR-P-2553)
TROSTIN, I. S., Reactions (d,n) on isotopes $^{58,60,62,64}Ni$, 20: 22109
TROUGHTON, M. E. C., Absolute standardization of ^{57}Co, 20: 22034
TROYANOV, M. F., Calculations of critical experiments on assemblies in ZPR-3, 20: 22383 (AEC-tr-6693)
TROZERA, T., Prog. rpt. on metallurgy as related to fuel-element fabrication, 9/59, 20: 21290 (GA-1052)
TRURAN, J. W., Approach to nuclear statistical equilibrium, 20: 21492
TRUSKOVA, N. F., Difference sign of real parts of elastic $\pi^{\pm}p$ scattering amplitudes at high energies, 20: 21618 (JINR-P-2566)
TRUSSLER, Geoffrey Arnold, Nuclear reactors, 20: 21018
TSEPURNEK, V. E., Radioactivation analysis of SiO_2 using ion exchange chromatography. I., 20: 20632
TSUDA, Eiichi, Multi-curie ^{60}Co irradiation unit, 20: 20849
TSUJI, Haruo, Radioactivation analysis of N and P with 14-Mev neutrons, 20: 20596
TSUJINO, R., Excitation functions for reactions induced by protons on Cd up to 37 Mev, 20: 22078
TSUNOKAWA, Masayoshi, Construction and operation of radiological monitoring station, 20: 20934 (JAERI-1098)
TUAN, I-shih, On the π-π resonance states, 20: 21694
TUBIANA, M., Analysis of the spatial distribution of radioactive iodine in the thyroid by the method of level diagrams, 20: 20528
TULUB, A. V., Application of Laplace transformation to the theory of radiation, 20: 21768
TUNITSKII, L. N., High-frequency discharge in a neon–helium laser, 20: 21808
TURGUNOV, M. B., Influence of urethan on changes in the skin of mice caused by x irradiation, 20: 20478
TUTHILL, E. J., Conversion of high-level radioactive waste to phosphate glass, 20: 22509 (BNL-10109)
TYLER, G. R., Self-absorption of x rays by plutonium particles with special reference to plutonium in wound monitoring, 20: 20951

U

UEBERALL, H., Photoproduction of single W bosons, 20: 21611 (CERN-65-32, pp 195-200)

UEBERALL, H., Proposal to detect cosmic-ray neutrinos through the Cherenkov light of produced muons, 20: 21031 (CERN-65-32, pp 231-40)

UEDA, Akira, Monte Carlo analysis of electromagnetic cascade showers, 20: 21559

UEDA, Teruo, Radiation-induced addition reaction of dialkyl phosphonates to fluorine-containing, 20: 20772

UHLEMANN, E., Chelates of β-diketone derivatives. II., 20: 20693

UHLIG, Ronald Paul, Neutral hyperon and neutral kaon production in $K^- + p$ interactions near the $Y^*(1765)$ resonance, 20: 21628 (TID-22822)

UI, Haruo, Table of singularities in nuclear direct interaction amplitude, 20: 21997 (INSJ-96)

ULANOV, B. P., Kinetics of DNA denaturation under ultraviolet radiation, 20: 20412

ULLAH, Nazakat, Asymptotic correlations of the Hamiltonian matrix elements, 20: 21854

UNIK, J., Response of solid-state detectors to fission fragments, 20: 21101

UNZ, H., Wave propagation in inhomogeneous isotropic hot plasmas, 20: 22165 (AD-621457)

UPSON, U. L., Fixation of high-level radioactive wastes in phosphate glass, 20: 22510 (BNWL-SA-564)

UPTON, Arthur C., Comparative observations on radiation carcinogenesis in man and animals, 20: 20442 (ORNL-P-2053)

URAI, Tetsuo, Study of high polymer insulating materials for use in pocket dosimeters, 20: 21158

UREDA, B. F., SNAPSHOT launch operations, 20: 22478

USKOV, I. A., Radiation-induced methylmethacrylate and styrene polymerization in presence of mineral filters, 20: 20778

V

VAHLBRUCH, K. M., Determination of spectra of high-energy neutrino parents, 20: 21604 (CERN-65-32, pp 121-6)

VAIDYA, P. C., Gravitational field of a radiating spheroid, 20: 21868

VAINSHTEIN, P. R., Peculiar features in radiation sickness induced by soft x rays, 20: 20475

VALENTE, Frank A., Glass-clad U glass fibers for power reactors. II., 20: 22415 (RPI-321-4)

VALENTIN, N., Rapid and quantitative method for the detection of plutonium in urine, 20: 20590

VALERINO, M. F., Calculating heavy-isotope content of operating fuel elements, 20: 20979

VALLISH, Edward J., Prog. rpt. on pre-startup hydraulic tests on AF-NETF, final, 1961–65, 20: 22491 (AD-626861)

VAN ALLEN, James A., Dynamics, composition, and origin of geomagnetically trapped corpuscular radiation, 20: 21837

VAN BEELEN, H., Experience with superconducting coils fed by flux pumps, 20: 21924

VAN BRAAM HOUCKGEEST, J. P., Experience with superconducting coils fed by flux pumps, 20: 21924

VANCURA, A., On the spontaneous breakdown of γ_5 invariance and parity nonconserving interactions, 20: 21727

VANDENBUSSCHE, Gerard, Physical methods of analysis of UF_6, 20: 20558 (CEA-R-2863)

VANDENPLAS, P. E., High-frequency dielectric resonance probe for measurement of plasma densities, 20: 22219

VAN DER WOUDE, A., Analysis of fluctuations in synthetic excitation functions, 20: 22054

VAN FAROWE, Donald E., Dental radiological health program, 20: 20956

VAN HEERDEN, I. J., Scattering of fast neutrons by ^{238}U, 20: 22056

VAN HOECK, Fernand, Nuclear techniques and the developing countries, 20: 22525

VAN LINT, J., Economic management of a center for processing radioactive residues, 20: 20833

VAN MIDDELKOOP, G., Reaction $^{32}S(\pi,\gamma)^{32}S$, 20: 22077

VANPRAET, G. J., ^{32}S and ^{31}P excitation by 180° electron scattering, 20: 21964 (AD-626684)

VAN PUTTEN, J., Rocket gamma scanning of nuclear bursts, 20: 21129

VAN TORNE, L. I., Structure and mechanical properties of Ta–Mo alloy single crystals, 20: 21364

VAN VUCHT, J. H. N., Systematic arrangement of binary rare earth–aluminum systems, 20: 21415

VARAGIC, Vladislav, Amount of catecholamines in auricles of irradiated rabbits and their response to quinidine, 20: 20451

VARGA, K., Determination of ash content of coals by γ transmission method, 20: 21209

VARGA, Laszlo, Method for evaluation of parameters of exponential decay curves, 20: 22051

VARICAK, Milena, Effects of nuclear radiations on properties of semiconductors, 20: 21160

VASAVADA, Kashyap V., Coupling constants of spin-2 mesons with two pseudoscalar mesons, 20: 21682

VASAVADA, Kashyap V., Dynamics of $J = 3/2^+$ $\bar{K}\Xi$ and KN systems in the 27-fold representation, 20: 21674

VASILEVSKII, I. M., Neutrino processes, 20: 21616 (JINR-P-2429)

VASTEL, J., Mass spectrometer for isotopic analysis of UF_6, 20: 20588

VASUDEVAN, R., Superconducting state of electron gas in homogeneous magnetic field, 20: 21887

VASYUKOV, G. Kh., Gas generation from tungsten at 2500°C, 20: 21248

VATAI, E., ϵ/β^+ Electron capture to positron emission ratio in decay of ^{56}Co to second excited level of ^{56}Fe, 20: 22016

VAUGHAN, B. E., Effect in stomach of ionizing radiation on acid secretion, potential, ATP, and phosphocreatine in comparison to spleen, 20: 20433 (AD-630390)

VELTMAN, M., Theoretical aspects of neutrino physics, 20: 21598 (CERN-65-32, pp 79-82)

VENARD, J. T., Elevated temperature mechanical properties of welds in a Ni–Mo–Cr–Fe alloy, 20: 21395

VENERONI, Marcel, Inelastic scattering based on a microscopic description of nuclei, 20: 22118

VENKATARAMAN, K., Physiological norms in Indian adults. Statistical analyses of data on organ weights, 20: 20374

VERBEURE, A., Infrared divergent terms in the bound-state picture, 20: 21856

VIEHBOECK, F., Magnetless dynamic mass spectrometer, 20: 20991

VIEHBOECK, F. P., Results with multipurpose isotope separator, 20: 22405

VIGDOROVICH, V. N., Solubilities of Cr, Mo, and W in Al, 20: 21362 (SC-T-66-0723)

VIGIER, J. P., Masses of nonstrange pseudoscalar mesons and the generalized Klein-Gordon equation, 20: 21744

VILCSEK, E., Production rates of ^{36}Cl and ^{39}Ar in Leedey chondrite, 20: 21508

VIL'SKII, K., Investigation of ^{148}Eu irradiation, 20: 22003 (JINR-P-2581)

VINEN, W. F., Motion of Abrikosov vortices in a type II superconductor, 20: 21910

VIOLA, V. E. Jr., Nuclear systematics of the heavy elements. I., 20: 22042

VIOLA, V. E. Jr., Nuclear systematics of the heavy elements. II., 20: 22043

VIOLINI, G., Formal properties of the ground-state wave function for even-even nuclei, 20: 22093

VIS, Henri L., Nuclear medicine in the service of Africa, 20: 20373

VITALE, S., Positive pion production asymmetry with polarized bremsstrahlung near second resonance, 20: 21589 (AD-626683)

VITALE, S., Positive-pion production asymmetry with polarized bremsstrahlung near second resonance, 20: 21660

VITKOV, M. G., Pulse excitation of magnetic field within a cylindrical shield, 20: 21456

VIZDOS, Geza, Hot chamber for production of ^{131}I, 20: 21215

VLADYKOV, G. M., Nuclear safety in working with fissionable materials, 20: 20975

VLASES, George C., Blast waves from an inverse pinch machine, 20: 21798

VLUGTER, J. C., Reactions of hydrocarbons as foams under the influence of gas discharges. IV., 20: 20740

VOELLER, Duane E., Nuclear time base-feasibility study, 20: 21021 (AD-622629)

VOGEL, P., Calculations of properties of collective states in deformed nuclei, 20: 21998 (JINR-E-2579)

VOGT, O., Pressure-induced changes of spin structure in EuSe, 20: 22332

VOLGER, J., Resistance transitions of superconducting lead–indium alloys, 20: 21913

VOLKOV, A. A., Toxicity and pyrogenicity of colloidal preparations of ^{198}Au and $Cr^{32}PO_4$ in neuro-oncological practice, 20: 20539

VOLKOV, B. I., Intermingling of particles in a composite magnetic field trap, 20: 22274

VOLKOV, N. V., Effect of size of the inter-electrode spacing on operation of a cesium thermal converter, 20: 21568 (FEI-16)

VOLKOV, V. V., Neutron pickup in bombardment of ^{181}Ta, ^{197}Au, ^{232}Th, ^{238}U isotopes with ^{15}N ions, 20: 22001 (JINR-P-2555)

VON BRENTANO, P., Statistical character of reaction $^{37}Cl(p,\alpha)^{34}S$ at 21- to 22-Mev excitation energy of the compound nucleus, 20: 22084

VON DARDEL, G., Possible spark chamber experiment with antineutrinos, 20: 21607 (CERN-65-32, pp 161-8)

VON DER OSTEN, W., R center luminescence in LiF, 20: 22331

VON FALCK, S., Influence of x radiation on the Hill reaction and photosynthesis phosphorylation for chloroplasts, 20: 20428

VON GOELER, S., Relation between Kelvin-Helmholtz instability and resistive drift instabilities, 20: 22263

VON WITSCH, W., Statistical character of reaction $^{37}Cl(p,\alpha)^{34}S$ at 21- to 22-Mev excitation energy of the compound nucleus, 20: 22084

VOS, O., Mortality of radiation chimeras in relation to the number of transplanted bone marrow and lymph node cells, 20: 20472

VOSKRESENSKII, G. V., Radial expansion of a beam in an electron linear accelerator induced by asymmetric wave, 20: 21476
VSEVOLODOV, E. B., Pathogenesis of iodacetate cataract and its similarity to radiation cataract, 20: 20507

W

WACHSMUTH, H. W., Determination of spectra of high-energy neutrino parents, 20: 21604 (CERN-65-32, pp 121-6)
WACHSMUTH, H. W., Muon flux measurement in neutrino shielding, 20: 22306 (CERN-65-32, pp 147-52)
WACHSPRESS, Eugene L., Iterative solution of elliptic systems for neutron diffusion equations, 20: 22400
WACHTER, P., Luminescence of ferromagnetic EuSe, 20: 22334
WACKER, Adolf, Isotope effects in photochemical transformation of tritium-labeled uracil, 20: 20782
WADIA, Wahby, Classification of oscillator shell model wave functions according to the U(3) group, 20: 22079
WAENKE, H., Moon as parent body of bronzite chondrites, 20: 21507
WAENKE, H., Production rates of ^{36}Cl and ^{38}Ar in Leedey chondrite, 20: 21508
WAGGENER, W. C., Spectrophotometry of aqueous homogeneous reactor fuel solutions, 20: 20600
WAHL, Harry A., Economics of contained nuclear explosions applied to petroleum reservoir stimulation, 20: 20836
WAI, Ngonshou, Aqueous terephthalic acid as sensitive dosimeter for ionizing radiations, 20: 20745
WAI, Ngonshou, Hydrolysis of salicyl phosphate and effect of radiation energy, 20: 20744
WAIDELICH, W., R center luminescence in LiF, 20: 22331
WAINIO, K. M., Monte Carlo calculations of radionuclide production in iron targets bombarded with 400-Mev protons, 20: 22035
WAIT, James R., Electromagnetic radiation from an acoustic point source within a compressible plasma bubble, 20: 22196
WAKUTA, Yoshihisa, Total cross sections of heavy nuclei for protons, 20: 22049
WALKER, J. C., Relevance of bombardment-induced Moessbauer effects in iron to radiation damage theories, 20: 21444
WALKER, J. K., Pair production by 5-Bev photons in carbon, 20: 21664
WALKER, R. M., Simple detectors for neutrons or heavy cosmic ray nuclei, 20: 21091
WALT, Martin, Rocket-borne measurements of particle fluxes and auroral light, 20: 21826
WALTERS, G. K., Existence of second standing shock wave attached to the magnetosphere, 20: 21821
WALTHER, H., Problems of fission product diffusion in graphite fuel elements, 20: 21423 (N-65-23015)
WALTNER, Arthur W., Investigation of the $^{10}B(n,\alpha)^{7}Li^{*}$, ^{7}Li reaction branching ratio, 20: 22071
WALTON, J. R., Isotopic composition of atmospheric neon, 20: 21509
WALTON, P. W., Measurement of statistics of secondary electron emission, 20: 21448
WANG, Shih Yi, Photochemistry of thymine in aqueous solution, 20: 20771
WANG, Shu-wei, Inelastic interactions of π^- mesons with nucleons at 6.8 Bev, 20: 21693
WANG, Tsu-tsing, Inelastic interactions of π^- mesons with nucleons at 6.8 Bev, 20: 21693
WANG, Wei-Neen, Charged-particle spectrometer for studying neutron-induced reactions, 20: 21054
WANKLYN, J. N., Effects of contamination on oxidation of Zr in steam, 20: 21268
WANKLYN, J. N., Properties of oxide films on zirconium alloys and their relevance to corrosion and hydrogen uptake, 20: 21282
WANLIN, J., Comparison of economic aspects of treatment of fission products from installations processing irradiated natural uranium, 20: 22517
WANNEMACHER, Robert W. Jr., Effect of low-protein diet on ability of adult rat to recover from sublethal dose of irradiation, 20: 20508
WAPSTRA, A. H., Correction to 1964 mass table, 20: 22154
WARBLE, Keith V., Integrated-circuit charge-sensitive preamplifier, 20: 21112
WARBLE, Keith V., Temperature-compensated multielement logarithmic converter microcircuit, 20: 20999
WARBURTON, E. K., Excitation energies of bound states of ^{17}O and ^{12}B, 20: 22111
WARBURTON, Ernest K., Spin assignments by particle-γ correlations from aligned nuclei, 20: 21983 (BNL-948, pp 741-50)
WARD, D. C., Project Gasbuggy—a nuclear fracturing experiment, 20: 20837
WARD, Thomas G. Jr., Radiolysis of lithium nitrate, 20: 20733 (TID-22796)
WARE, A. A., Finite Larmor radius equations for a plasma, 20: 22262
WARFIELD, R. W., Effect of radiation on electric resistivity and bulk compressibility of polyepoxides, 20: 21418 (AD-627049)
WARNER, C., Prog. rpt. on thermionic energy conversion, 11/64–7/65, 20: 21562 (AD-623142)
WARREN, A. C., Motion of Abrikosov vortices in a type II superconductor, 20: 21910
WARREN, M., SNAP environment simulation problems, 20: 22475
WARRINER, J. P., Titrimetric determination of primary and secondary alcohols by xenon trioxide oxidation, 20: 20579
WASE, Keizo, Hitachi power manipulator, 20: 20843
WATAGHIN, G., Masses of nonstrange pseudoscalar mesons and the generalized Klein-Gordon equation, 20: 21744
WATANABE, Zenjiro, Observation of high-energy jets with emulsion chambers, 20: 21555
WATERBURY, G. R., Three-wavelength x-ray absorption edge method for determination of plutonium in nitrate media, 20: 20573
WATKINS, J. W., Project Gasbuggy—a nuclear fracturing experiment, 20: 20837
WATSON, C. D., Prog. rpt. on chemical technology, 7–9/65, 20: 20808 (ORNL-3916)
WATSON, D. G., Accumulation and transport of radionuclides by Columbia River biota, 20: 20382
WATSON, W. K. R., Scattering of light by protons, 20: 21587 (AD-623564)
WATSON-MUNRO, C. N., Simulation of magnetic fields produced in the moon by trapped field of solar plasma stream, 20: 21502
WAUGH, J. S., Electron paramagnetic resonance study of solutions of europium in liquid ammonia, 20: 20668
WAY, S., Three-parameter pulse-height analyzer and coincidence system for satellite cosmic-ray studies, 20: 21125
WAY, Stanley, Ten-year results of individualized treatment of carcinoma of the cervix based on the analysis of serial biopsies, 20: 20536
WAYMOUTH, John F., Experimentally determined plasma perturbation by a probe, 20: 22260
WEBB, P. P., Surface potential measurements of lithium-drifted germanium diodes, 20: 21096
WEBB, W. W., Annihilation instability in hard superconductors, 20: 21927
WEBBER, W. R., Two satellite-borne cosmic-radiation detectors, 20: 21118
WEBER, Ernst, Prog. rpt. on electromagnetics for Project Defender, semi-annual, 9/65, 20: 22172 (AD-623718)
WEETON, John W., Investigation of extruded tungsten composites containing fibered or reacted additives, 20: 21374
WEGNER, Harvey E., BNL double Emperor tandem facility, 20: 21464 (BNL-948, pp 692-703)
WEIBEL, E. S., Design of rotating-field pinched discharge, 20: 22184 (LRP-22-66)
WEIDENBAUM, B., Irradiation of 0.5-inch diameter, hollow-pellet UO_2 fuel rods, 20: 21422 (GEAP-5100D)
WEILL, G., Structure of Arctic auroral zone in period of minimum solar activity, 20: 21814
WEINBERGER, A. J., Spectrophotometry of aqueous homogeneous reactor fuel solutions, 20: 20600
WEINREICH, Marcel I., Solubilities of Cr, Mo, and W in Al, 20: 21362 (SC-T-66-0723)
WEINSTOCK, Jerome, Equivalence between two formalisms of plasma fluctuations, 20: 22246
WEISS, H. H., Transmission characteristics of cyclotron harmonic waves in plasma, 20: 22226
WEITZNER, Harold, Extension of the Penrose condition, 20: 22248
WELCH, J. A., Longitude dependence of geomagnetically trapped electron fluxes. I., 20: 21813 (N-65-29816)
WELCH, J. A. Jr., Radiation smoothing of shocks, 20: 21775 (AD-620835)
WELLS, M., Some superconducting properties of several carbides and nitrides of the transition metals, 20: 21911
WENTWORTH, R. C., Intra- and interhemisphere differences in occurrence times of hydromagnetic emissions, 20: 21832
WENZINGER, Edward C., Some aspects of reactor safety systems, 20: 22358
WERNER, G., Extraction of rare earths with TBP. I., 20: 20824
WERNER, G., Separation of the rare earths by liquid ion exchange. II., 20: 20825
WERNICK, J. H., Free ion hyperfine fields in Dy intermetallic compounds, 20: 22330
WERTHAMER, N. R., Recent developments in microscopic theory of type II superconductivity, 20: 21930
WEST, G. B., Influence of thermalization models on reactivity and temperature coefficient of zirconium hydride reactors, 20: 22377 (GA-6930, App. B)
WESTLAKE, Jeannette E., Radiation exposure in parents of children with mongolism, 20: 20454
WETH, G. C., Fixation of high-level radioactive wastes in phosphate glass, 20: 22510 (BNWL-SA-564)
WETH, G. G., Conversion of high-level radioactive waste to phosphate glass, 20: 22509 (BNL-10109)
WETHERELL, A. M., High-energy elastic scattering, 20: 21593 (CERN-65-24(Vol.1), pp 65-80)

WETZEL, K. J., Excitation of new electromagnetic transitions in ^{9}Be inelastic electron scattering, 20: 22105
WEYERS, C., Rapid and quantitative method for the detection of plutonium in urine, 20: 20590
WHATLEY, M. E., Prog. rpt. on chemical technology, 7–9/65, 20: 20808 (ORNL-3916)
WHEATLEY, S. J., Fissile-material container and packaging development and testing program, 20: 20936 (K-1661)
WHEELER, Paul C., Modified method of radioisotopic placental localization, 20: 20527
WHEELER, R. G., Ground-state splitting and Zeeman effect in erbium ethylsulfate at 1.6°K, 20: 21881
WHELAN, M. J., Characteristics of the Moellenstedt electron velocity analyzer, 20: 21005
WHETSTONE, S. L. Jr., Emission of α-particles in fission of ^{238}U by 11- to 21-Mev protons, 20: 22144
WHICKER, F. W., Concentration patterns of ^{90}Sr, ^{137}Cs, and ^{131}I in a wild deer population and environment, 20: 20384 (COO-1156-13)
WHINERAY, Scott, Atomic mass differences involving isotopes of Nd, Sm, Cd, and Pb, 20: 22153
WHITE, E. R., Role of radioactivity and hydrothermal processes in protobiochemistry, 20: 20406 (N-65-27062)
WHITE, F. A., Detection of single electrons and ions in a radiation environment, 20: 21139
WHITE, J., Prog. rpt. on metallurgy as related to fuel-element fabrication, 9/59, 20: 21290 (GA-1052)
WHITE, J. D., Neutron interaction between multiplying media separated by various materials, 20: 20840 (BNWL-193, pp 57-67)
WHITE, J. L., Graphite–carbide materials preparation, 20: 21306
WHITE, J. T., Problems of reader design and measurement error in LiF thermoluminescent dosimetry, 20: 21061
WHITE, R. Stephen, Cosmic-ray and solar proton albedo neutron decay injection, 20: 21550
WHITEHILL, C. F., Prog. rpt. on ventilation of fallout shelters, 7/64–6/65, 20: 20921 (AD-621998)
WHITMER, R. F., Effects of velocity-dependent collision frequency on wave-plasma interactions, 20: 22256
WHITSON, T. C., Reactor yield calculations for 81 radioisotopes produced by (n,γ) reactions, 20: 21214 (ORNL-IIC-8)
WHITTAKER, J. K., Zero-crossing discriminator with picosecond time slewing, 20: 21115
WHITTEMORE, W. L., Scattering of neutrons by polyethylene, 20: 21952
WHITTEN, L. G., Position monitoring devices, 20: 20989 (Y-1506)
WHITWHAM, D., Aluminum and magnesium in nuclear metallurgy, 20: 21382
WICK, G. C., Group theory. Invariance principles. Symmetries, 20: 21771
WICKLUND, A., Measurements of current-dependent reactance of superconductors having very small coherence distance, 20: 21919
WIDEMANN, Francois, Nature of the 686-kev nuclear level of ^{187}Re, 20: 22027
WIDMAIER, R., Influence of x radiation on postnatal testicular development and germ cell maturation in the mouse, 20: 20499
WIIK, B. H., Superconducting race-track microtron, 20: 21460 (AD-623659)
WILBURN, C. D., Operating characteristics of lithium-drift detectors, 20: 21103
WILDNER, O., Extraction of rare earths with TBP. I., 20: 20824
WILETS, Lawrence, Uncommon states of nuclear matter, 20: 21990 (BNL-948, pp 928-1004)
WILIP, Elmer K., Primary charge distribution at low-energy fission of heavy (gg)-nuclei, 20: 22013 (ANL-Trans-296)
WILKIN, C., Shadow effect in high-energy scattering from deuterons, 20: 21646
WILKINS, M., Use of the Ag–Co activity ratio method to determine epithermal indices for large neutron dose irradiations, 20: 21025 (AERE-R-5122)
WILKINSON, D. H., Elementary particles, 20: 21691
WILLIAMS, Donald J., Earth's outer radiation zone, 20: 21815
WILLIAMS, E. T., Two γ rays in decay of 3.0-min ^{88}Br, 20: 22041
WILLIAMS, Evan T., Decay of 54-sec ^{86}Br and 55-sec ^{87}Br, 20: 22130
WILLIAMS, H. H., Excitation energies of bound states of ^{17}O and ^{12}B, 20: 22111
WILLIAMS, H. T. Jr., Reactivity worth of rod-cluster control elements, 20: 22395
WILLIAMS, J. C., Transient effect of nuclear radiation on the dielectric properties of ceramics and plastics at microwave frequencies, 20: 21171
WILLIAMS, Lawrence E., Continuum resonances in $^{4}He(p,p')^{4}He$, 20: 22114
WILLIAMS, R. G., Effect of γ and neutron irradiation on litter size in the mouse, 20: 20453
WILLIAMS, R. L., Operating characteristics of lithium-drift detectors, 20: 21103
WILLIAMSON, R. M., $^{12}C(d,p\gamma)^{13}C$ angular distributions and correlations near threshold, 20: 22087
WILLIS, C. A., Radiological aspects of reentry burnup of SNAP reactors, 20: 20937 (NAA-SR-11761)
WILLIS, J., Generalized model analysis of ionizing radiation effects in semiconductor devices, 20: 21167
WILLIS, J. S., Effects of helium temperature strain on superconducting transition of Pb–In alloys, 20: 21923
WILLIS, K. E., Sensitivity analysis of civil defense systems and components, 20: 20922 (AD-624704)
WILLMES, Henry, Elastic scattering of 45-Mev protons, 20: 21963 (AD-626656)
WILLMES, Henry, FORTRAN program for reduction of differential cross section data, 20: 21965 (AD-626776)
WILSON, C. R., Irradiation of 0.5-inch diameter, hollow-pellet UO_2 fuel rods, 20: 21422 (GEAP-5100D)
WILSON, G. V. N., Nuclear orientation of ^{54}Mn nuclei in noble metal hosts, 20: 22097
WILSON, I. H., Design of a velocity selector for long-wavelength neutrons, 20: 21007
WILSON, L., Polarographic determination of uranium in binary chromium–uranium alloys, 20: 20595
WILSON, O. C., Stellar chromospheres, 20: 21504
WILSON, P. B., Measurements at high field strengths on superconducting accelerator cavities, 20: 21459 (AD-623509)
WILSON, P. B., Superconducting race-track microtron, 20: 21460 (AD-623659)
WILSON, R. G., Electron and ion emission from cesiated refractory compound surfaces, 20: 21584
WILSON, T. R., Review of results of reactor safety research, 20: 22435
WIMENITZ, Francis N., Time-dependent neutron transport from point isotropic source at an altitude of 100,000 feet, 20: 21935 (AD-624041)
WINDSOR, Alfred A., Ultracentrifuge rotor temperature measurements and control, 20: 21009
WING, G. Milton, Invariant imbedding and transport problems with internal sources, 20: 21641
WINGATE, C. L., Comparison of dose patterns in a dog exposed to neutrons and to x rays, 20: 20432 (AD-630332)
WINICK, H., Pair production by 5-Bev photons in carbon, 20: 21664
WINSTEAD, Jack A., Substrate protection of enzymes against ionizing radiation, 20: 20514
WIRTZ, K., Karlsruhe reference design of 1000-Mw(e) sodium-cooled fast breeder, 20: 22453
WISCHMEYER, C. R., Joulean heating in a hard superconducting tube, 20: 21884
WISE, L. K., Color radiography—photographic considerations, 20: 20863
WITTENBERG, L. J., Prog. rpt. on Pu research, 7–9/65, 20: 21342 (MLM-1301)
WITTLIFF, C. E., Laser-generated implosions, 20: 22245
WITZIG, Warren F., Safety aspects of nuclear power plants—a utility consultant's view, 20: 22436
WOLFE, John H., Observations of solar wind during flight of Imp 1, 20: 21496
WOLFENDALE, A. W., Use of neon flash tubes in cosmic-ray neutrino experiments, 20: 21541 (CERN-65-32, pp 57-60)
WOLFF, A. K., Analytical techniques for C and N in Be, 20: 20556 (AD-626987)
WOLFGANG, L. G., Characteristics of very shallow silicon junctions, 20: 21099
WOMACK, E. A., Linear relationship for heavy-ion pulse heights in alkali halides, 20: 21084
WOMACK, Frances, DNA strands injected by a virus into its host and hereditary information transmission, 20: 20426
WOMACK, Frances, Evidence that only one of the two DNA strands injected by phage T4 transmits genetic information, 20: 20427
WONG, M., Pair production by 5-Bev photons in carbon, 20: 21664
WOODRUFF, E. M., Irradiation-induced contraction of graphites at high temperature, 20: 21420 (BNWL-215)
WOODSUM, H. C., Radiation environment about NERVA reactors, 20: 22481
WOODWARD, Kent T., Biochemical aspects of radiation injury and recovery, 20: 20435 (CONF-650560-15)
WORDEN, J. R., Modifications to computer code, THERMOS, 20: 22374 (BNWL-193, pp 5-15)
WORT, D. J. H., Microwave transmission through turbulent plasma, 20: 22230
WOYSKI, Jon. S., Dynamics of clustered nuclear engines, 20: 22483
WRAY, E. M., Negative hyperfine field in hexagonal cobalt metal, 20: 22335
WU, Che-Kuang, Polarography of uranyl-semicarbazide hydrochloride complexes, 20: 20677
WU, Tai Tsun, Asymptotic form of the S matrix for large angular momentum in the left half-plane, 20: 21754
WULFF, J., Fabrication of an ultra-fine Nb–Cu composite by drawing, 20: 21298
WYCKOFF, J. M., Modular software for on-line handling of nuclear data, 20: 22032

VYKOFF, M. H., Effects of neutron irradiation on the blood-cerebral spinal fluid barrier of the sheep and burro, 20: 20489
VYLY, L. D., Conversion electron-γ directional correlation in ^{133}Cs, 20: 22076

X

XIE, Gong-hua, Composition of lanthanum carbonate and cerium carbonate, 20: 20664

Y

YABE, Eiji, Spectroscopic measurement of electron temperature in helium arc plasma, 20: 22210
YAFFE, L., Reactions (p,xn) and (p,pxn) of ^{89}Y with 5- to 85-Mev protons, 20: 22133
YAHIKU, R., Beta energy emission rate from neutron-irradiated, ^{238}U carbide particles, 20: 22404 (USNRDL-TR-987)
YAKIMENKO, I. P., Resonances of fluctuating emission of a plasma cylinder, 20: 22202
YAKUTOVICH, M. V., Fabrication of thin plates from refractory carbides, 20: 21303
YALOW, Rosalyn S., Iodoinsulin used to determine specific activity of ^{131}I, 20: 20604
YAM, Koi-ming, Effect of x radiation on the hexobarbital metabolizing system of liver microsomes, 20: 20429 (AD-629311, pp 15-25)
YAMADA, Y., Effect of high-energy radiation on electric conduction of various copolymers, 20: 21170
YAMAGOSHI, Kazuo, Development of glasses for low background measurements—characteristics of glasses, 20: 21044 (ANL-Trans-285)
YAMAMOTO, Albert S., Prog. rpt. on effect of interstitial addition on phase equilibria on Nb-rich region of Nb–W–Hf and Nb–W–Zr alloy systems, 3/66, 20: 21329 (DRI-1092-229)
YAMAMOTO, Kiyoko, Effect of γ radiation on α, β, γ, ∂-tetraphenylporphine, 20: 20774
YAMAMOTO, Takeyoshi, Nonlinear effect in beam-plasma interaction, 20: 22206
YAMAMOTO, Yoshiaki, High-energy γ rays in the atmosphere and muons underground and underwater, 20: 21558
YAMANISHI, Tetsuo, Combined influence of Hall effect, ion slip, and viscosity on MHD devices, 20: 21574
YAMASAKI, Hiro, Parametric oscillating amplifier, 20: 21013
YAMASHITA, Sukeaki, Time resolution of transistorized time-of-flight system, 20: 21052
YAMDAGNI, N. K., Nucleon-antinucleon annihilation as the source of energy for certain radioastronomical objects, 20: 21684
YANG, C. N., Phenomenological description of K decay, 20: 21701
YANG, Chi-Chuen, Radiolysis of ethanol in liquid phase, 20: 20746
YASHIN, A. F., Reconstruction of IRT research reactor, 20: 22497 (IAE-992)
YASUKAWA, Sigeru, Analysis of continuous reactor refueling, 20: 22407
YASUMOTO, Masahiko, Reaction of ethylene with methylene chloride induced by γ-radiation, 20: 20757
YATVIN, Milton B., Effect of low-protein diet on ability of adult rat to recover from sublethal dose of irradiation, 20: 20508
YAVORSKY, P. M., Prog. rpt. on radiation-induced telomerization of methanol, 11/64–4/65, 20: 20724 (NYO-2978-44)
YAZITSKII, Yu. S., Investigation of neutron resonances of ^{165}Ho, 20: 22004 (JINR-P-2593)
YEARIAN, M. R., Elastic electron scattering from magnetic multipole distributions of ^{6}Li, ^{7}Li, ^{9}Be, ^{10}B, ^{11}B, and ^{14}N, 20: 22120
YEKUTIELI, G., Peripheral production and decay parameters of N*••(1238) in pp → nN*••(1238) at 5.5 Bev/c, 20: 21663
YIFTAH, S., Monte Carlo investigation of heterogeneity of fast reactor cores, 20: 22397
YOSHIDA, Shiro, Generator coordinate method applied to nuclei in transition region, 20: 22081
YOSHIKAWA, S., Ballooning interchange instabilities of magnetized plasmas under gravitational fields, 20: 22186 (MATT-358)
YOSHIKI, H., Coulomb scattering of muons and electrons from fluorine and chlorine, 20: 21649
YOSHIKI, H., Fluxes of neutrinos and antineutrinos produced at CERN, 20: 21602 (CERN-65-32, pp 111-14)
YOSHIMOTO, Yukiko, Properties of γ-irradiated starch and graft copolymers as adhesives and dyeing mordants, 20: 20767
YOSHIMURA, Atsushi, Transistorized low-noise preamplifier for solid-state radiation detector, 20: 21072
YOUNG, J. C., Role of thermal spectrum measurements in reactor design, 20: 22375 (GA-6901)
YOUNG, Myron H., Prog. rpt. on gamma spectra by stepwide statistical method, 9/64–1/65, 20: 20555 (AD-622200)
YOUNG, W. R., Material and process specifications for refractory alloy and alkali metals, 20: 21293 (R-66SD3007)
YOUNG, Wei, Ischemic heart disease, atherosclerosis, and longevity, 20: 20370 (UCRL-14658)
YOVANOVITCH, D. D., $\pi^{\pm}$ and $K^{\pm}$ production cross sections for 12.5-Bev protons on Be, 20: 21601 (CERN-65-32, pp 109-10)
YUDKEVICH, M. S., Neutron thermalization process in time in graphite and Be, 20: 21942 (KFK-tr-188)
YUDKEVICH, M. S., Transient neutron spectra in zirconium hydride, 20: 21941 (IAE-977)
YUHARA, Jiro, Investigation of atomic energy countermeasures. II., 20: 21056
YUSKESELIEVA, L. G., Lithium-ion drift in silicon p-type monocrystals, 20: 21337 (JINR-P-2598)

Z

ZACHARIASEN, F., Scattering of light by protons, 20: 21587 (AD-623564)
ZACKAY, V. F., Some superconducting properties of several carbides and nitrides of the transition metals, 20: 21911
ZAGORSKAJA, I. B., Problem of seasonal fluctuations in radiosensitivity of rabbits, 20: 20493
ZAITSEVA, N. G., Rapid separation methods for radioactive elements (review), 20: 20826
ZAK, Wieslaw, Bone tissue sterilization using reactor fuel γ radiation, 20: 20482
ZAKHAR'EV, B. N., Scattering of particles by system of fixed centers, 20: 21710 (JINR-P-2554)
ZALKIND, V. M., Polarization of plasma moving in helical magnetic field, 20: 22275
ZALKIND, V. M., Polarization of plasma moving in toroidal magnetic field, 20: 22276
ZALKIND, V. M., Polarization of plasmas moving in magnetic fields of opposite curvatures, 20: 22277
ZALYALYUTDINOVA, S. Z., Comparative assessment of growth of skin grafts in radiation-burn injury of maxillary region, 20: 20477
ZANARINI, G., Experimental results on the information available from the rise time of pulses supplied by semiconductor particle detectors, 20: 21137
ZANDER, K., Change of electrical properties of Si and Ge diodes by neutron irradiation, 20: 21150 (HMI-B-45)
ZARITSKII, S. N., Calculations of critical experiments on assemblies in ZPR-3, 20: 22383 (AEC-tr-6693)
ZARNOWIECKI, Krzysztof, Bone tissue sterilization using reactor fuel γ radiation, 20: 20482
ZASUKHIN, E. N., Radioactivation analysis of SiO_2 using ion exchange chromatography. II., 20: 20633
ZBOROVSKII, A. G., Radiometric method of determining sulfur in naphthalene, 20: 20615
ZEMAN, Wolfgang, Radiation injuries of the nervous system, 20: 20449
ZERBEL, D., SNAP-10A instrumentation and control development and testing, 20: 22476
ZGANJAR, E. F., IEC method and conversion coefficients of 605-kev transition in ^{134}Ba, 20: 22026
ZHARINOV, A. V., Characteristics of a low-pressure discharge in a transverse magnetic field, 20: 21810
ZHELEV, Zh., Decay chain of ^{138}Nd → ^{138}Pr → ^{138}Ce, 20: 22002 (JINR-P-2570)
ZHELEV, Zh., Investigation of ^{148}Eu irradiation, 20: 22003 (JINR-P-2581)
ZHIGACHEV, V. M., Reconstruction of IRT research reactor, 20: 22497 (IAE-992)
ZHILKIN, A. S., Analysis and generalization of correlation method for measurement of particle-lifetime distribution in physical systems, 20: 21035 (FEI-21)
ZHILKINA, M. I., ^{137}Cs behavior during the analysis of atmospheric precipitation specimens, 20: 20625
ZHIL'TSOVA, V. M., Kinetics of DNA denaturation under ultraviolet radiation, 20: 20412
ZHURAVLEV, V. I., Contribution of virtual Compton effect to cross section for electron-positron pair production, 20: 21623 (JINR-P-2602)
ZIEGLER-NARAY, Maria, Hydrodynamical model of wave mechanics. III., 20: 21840
ZIELCZYNSKI, Mieczyslaw, Bone tissue sterilization using reactor fuel γ radiation, 20: 20482
ZIHLMANN, Eduard, Competitive reactors become necessary, 20: 22421
ZIMANYI, J., Circular polarization of γ radiation following deuteron stripping reaction, 20: 22006 (KFKI-600)
ZIMANYI, J., Perturbed angular correlation of a triple gamma cascade, 20: 22015
ZIMMERMAN, D. W., Thermal annealing effects on thermoluminescence of LiF, 20: 21057
ZIMMERMAN, J. E., Quantized flux pinning in superconducting niobium, 20: 21909
ZIMMERMANN, Heinrich, Coupling for fuel and/or moderator elements

of a reactor, 20: 22363
ZIMMERMANN, K. A., Integrated circuits—their characterization and use in experimental physics, 20: 20998
ZINCHENKO, G. N., Mass spectrometric investigation of source of positive ions operating at low gas pressure, 20: 21457
ZINCHENKO, N. S., Mass spectrometric investigation of source of positive ions operating at low gas pressure, 20: 21457
ZINK, J. W., Electromagnetic mass of the classical electron, 20: 21631
ZLOTNIKOV, S. A., Action of radium emanation on the ear, 20: 20498
ZOBEL, W. M., PM-3A: First nuclear power plant in Antarctica, 20: 22445
ZOBOR, Ervin, ZR-2 critical assembly, 20: 22388
ZOLLNER, Ronald Alfred, Prandtl-Meyer flow with transverse magnetic field, 20: 21776 (AD-621429)
ZOLOTOTUBOV, I. M., Performance of coaxial plasma source in longitudinal magnetic field, 20: 22179 (FTI-080/P-032)
ZOLOTUKHIN, V. G., Analysis and generalization of correlation method for measurement of particle-lifetime distribution in physical systems, 20: 21035 (FEI-21)
ZUK, Wlodzimiers, Interactions of medium-energy ions with materials in isotope separators, 20: 21219
ZUKAS, E. G., Stress dependence of creep rate of two commercial graphites, 20: 21340 (LA-DC-7626)
ZUKOSKI, Edward E., Recombination, ionization, and nonequilibrium electrical conductivity in seeded plasmas, 20: 22258
ZULLIGER, H. R., Response of scintillators and semiconductors to low-energy x-ray excitation, 20: 21107
ZUM WINKEL, Karl, Kidney diagnosis with radioisotopes, 20: 20550
ZUPANCIC, Crt, Multi-body exit channels, 20: 21981 (BNL-948, pp 610-84)
ZURMUEHLE, R. W., Levels of ^{42}Sc from ^{40}Ca(^{3}He,p)^{42}Sc and ^{40}Ca(^{3}He,py)^{42}Sc, 20: 22073
ZURMUEHLE, R. W., Reaction ^{60}Ni(^{3}He,α)^{59}Ni at 15 Mev, 20: 22127
ZYKOV, V. G., Polarization interaction of opposed plasma streams in composite magnetic field trap, 20: 22273
ZYKOV, V. G., Polarization of plasma moving in helical magnetic field, 20: 22275
ZYKOV, V. G., Polarization of plasma moving in toroidal magnetic field, 20: 22276
ZYKOV, V. G., Polarization of plasmas moving in magnetic fields of opposite curvatures, 20: 22277
ZYUKOV, V. I., Effect of size of the inter-electrode spacing on operation of a cesium thermal converter, 20: 21568 (FEI-16)

SUBJECT INDEX

Main entries in this index are generally specific materials, things, and processes. These are followed by modifiers that describe the properties of, and processes applied to, the main entries.

The number preceding the colon is the *NSA* volume number, and the number following is the abstract number. The designation (R) following the abstract number indicates that the abstract is of a progress report; (P) indicates a patent; and (T) indicates a translation. Abstracts for reports other than progress reports carry no letter designation. References to report numbers, where appropriate, are included after the abstract number of the citation. Published literature (journal article or book) is identifiable by the absence of a report number.

The user should bear in mind that the ideas presented in the original literature, rather than key words, have been indexed. The indexers have tried to select what seemed the most probable and logical place to look for typical information. Since it is not possible to anticipate where a user would look for information, numerous cross references are included in cumulative indexes to assist him in his search.

Experience in using an index of this type will be the best guide in obtaining the desired information, and a consideration of synonymous or closely related terms will prove valuable.

Information must be so indexed as to be of the greatest use to the greatest number of users. This requires that a topic be indexed to headings that most specifically describe it and not ordinarily to the headings that describe its ultimate use, nor to the general class headings that include the specific headings. For example, information on the treatment of thyroid disease with I-131 would be indexed under Thyroid Gland and under Iodine Isotopes I-131, but not necessarily under Radiotherapy. A study of the effects of x radiation on hair would be indexed under both X Radiation and Hair. However, the information would not be indexed under the experimental animal, e.g., Rats, unless the report discusses the effects on rat hair as compared with the effect on the hair of other animals.

The broad, general class headings are used only for general information or for comprehensive reports or articles.

Subject Heading Styles

Generally, the direct form of subject entry is used rather than inverted headings, e.g., Amino Acids rather than Acids, Amino; Helium Isotopes He-4 rather than Helium—isotopes He-4 or Helium—He-4 isotopes. Note, however, that in some cases parenthetic modifying terms or inverted headings of the form Neutrons, Fast are used in preference to a direct entry that would result in the scattering of information. Organic compounds are usually entered in the index in the inverted form so that substituted compounds can be listed near the parent compound; e.g., Benzene, Bromo- rather than Bromobenzene. In general, the style of nomenclature used is that of Chemical Abstracts, except that some items listed in that publication as subheadings are elevated to form part of the main heading; e.g., Butyric Acid, Methyl Ester rather than Butyric Acid—methyl ester.

Alphabetization

Main headings are alphabetized word-by-word. A parenthetic qualifier following a main heading is disregarded in alphabetizing unless there are two or more headings identical except for the parenthetic qualifier, in which case the qualifier determines the order. Headings involving Greek letters are arranged as if the names of the letters were spelled out.

Examples:

M-Capture
  see Electron Capture
Magnesium
Magnesium Alloys
Manganese Fluorides
Manganese(II) Fluorides
Mesons
Mesons (π)
Mesons (ρ)
3-Pentanol, 2,4-Dimethyl-
2-Pentanol, 2-Methyl-
2-Pentanol, 4-Methyl-

Nomenclature of Inorganic Compounds

Inorganic compounds are indexed in the direct form, listing cations in the order of increasing valence in the case of polycationic salts of varying valence and in alphabetic order for polycationic salts in which all cations have the same valence; e.g., Sodium Aluminum Silicates and Potassium Sodium Sulfates.

Multicomponent Alloys and Other Systems

Multicomponent alloys, except well-known trade names, are indexed under a main heading in the form "element alloy" for each element in the alloy. The modifier begins with element symbols for each component arranged alphabetically as if the English name for the element were spelled out.

Example: Copper-Gold Alloy is indexed
  Copper Alloys
    Cu-Au...
  Gold Alloys
    Cu-Au...

Well-known alloys such as Zircaloy-2 are indexed directly to the trade name; cross references referring from each component of the alloy to the entry for the trade name appear in cumulative indexes.

Multicomponent systems of non-metallic elements are indexed in a manner similar to alloys except the main heading used contains the word "Systems" in place of "Alloys."

Example: Silicon–Tungsten Systems are indexed
  Silicon Systems
    Si-W...
  Tungsten Systems
    Si-W...

Multicompound systems and mixtures of compounds are indexed under the main heading for each component com-

pound; the modifiers begin with an alphabetical listing of compound formulas.

Example: Lead Titanate–Lead Zirconate is indexed
Lead Titanates
$PbTiO_3$-$PbZrO_3$...
Lead Zirconates
$PbTiO_3$-$PbZrO_3$...

A mixed system of compounds and elements is indexed using a combined form of the above conventions, e.g., a dispersion of copper and alumina would be indexed

Aluminum Oxides
Al_2O_3-Cu...
Copper Systems
Al_2O_3-Cu..

Physical States and Configurations of Materials

Specification of the physical state, if other than normal, or geometric configuration of the material is included in the modifying phrase, i.e., liquid metals would be indexed to the metal with "liquid" in the modifier, and carbon crucibles would be indexed to Carbon with "crucibles" appropriately placed in the modifier and also to Crucibles if appropriate.

Modifying Phrases

The modifiers appearing under a main heading are written specifically to describe the relation of the item being indexed to that main heading. The modifier, therefore, will generally contain more useful information about that relation than will a title or a phrase written to be used under every main heading assigned to the item. Effort is exerted to begin the modifier with the word judged to be of greatest use to the greatest number of users; this, however, does not obviate the need to consider all modifiers under the main heading(s) of interest.

Modifiers are usually intended to form a meaningful phrase when combined with the main heading. Some are intended to be read following the main heading, e.g., the entry Hydrogen—sorption by charcoal is read "hydrogen sorption by charcoal"; however, as a result of placing the important word first, many modifiers must be arranged for smooth reading, e.g., Formaldehyde—yields in radiolysis of ethyl ether, effects of deuterium on is read "effects of deuterium on formaldehyde yields in radiolysis of ethyl ether" and Uranium—crystal structure of, effect of cooling rate on allotropic transformations in is read "effect of cooling rate on allotropic transformations in crystal structure of uranium." Prepositions are sometimes omitted if no ambiguity results.

Special characters are added to modifiers in the field of physics; if the modifier does not establish the experimental or theoretical character of a reference, a symbol (E), (T), or (E/T) is placed immediately after the modifying phrase and before the journal reference number. The value of this identification has been established by the American Institute of Physics.

A

ABSTRACTS
of computer programs for radiation shielding parameters, 20: 22310 (ORNL-RSIC-13)
of papers presented at 20th International Congress of Pure and Applied Chemistry, Moscow, July 12–18, 1965, 20: 20552 (CONF-650723 (Absts.))
on aerospace medicine and biology, 20: 20369 (NASA-SP-7011(22))
on direct energy conversion, 20: 21565 (AD-628049)
on elastic wave propagation, 20: 20896 (AD-623592)
on plasma sheath theory, 20: 22177 (CLM-Bib-6)
ACCELERATOR TUBES
electron beam focusing in, (T), 20: 21487
ACCELERATORS
beam density profile of Astron, (E), 20: 22191 (UCRL-14697)
beam instability thresholds in weak-focusing cyclic proton, longitudinal, (T), 20: 21471 (PPAD-577D)
beam polarization in, effects of field gradients on, (T), 20: 21481
cavity resonators for, electric field measurements in superconducting, 20: 21459 (AD-623509)
neutron flux patterns from, 14-mev, 20: 21946
storage rings for cyclic, space-charge effects in, (T), 20: 21475(T) (SLAC-Trans-38)
storage rings for, radiative corrections for Adone, 20: 21469 (LNF-66/10)
storage rings for, particle lifetimes in, (T), 20: 21483
target-space evacuation for, vacuum pump for, 20: 21479
ACCIDENTS
analysis of coolant-loss, in sodium cooled fast reactors, 20: 22349
analysis of, in large fast reactors, 20: 22401
coolant ejection in reactor, shock front conditions in, 20: 22348
coolant ejection in reactor, 20: 22350
fission product behavior in reactor, scale-up of experiments on, 20: 20940(R) (ORNL-3915)
materials management relation to, 20: 20974
radiation monitoring following, 20: 20962
tritium release in Windscale, October 1957, 20: 20889
ACETALDEHYDE
yields from gamma radiolysis of benzene–ethanol mixture, 20: 20741
yields from gamma radiolysis of ethanol, 20: 20746
ACETIC ACID
effects on polarographic determination of hexavalent uranium in TBP solutions, 20: 20631
ACETIC ACID, [(CARBOXYMETHYLIMINO)BIS(ETHYLENENITRILO)]TETRA-
effects on zinc-65 excretion in man, 20: 20397
ACETIC ACID, [1,2-DIMETHYLETHYLENE)DINITRILO]TETRA-
effects on ruthenium chloride metabolism in rats, 20: 20396
ACETIC ACID, (ETHYLENEDIAMINE)TETRA-
determination in decontaminating solution, method for, 20: 21238 (NP-15928)
effects on zinc-65 excretion in man, 20: 20397
ACETIC ACID, (ETHYLENEDIAMINE)TETRA- COMPLEXES
with neptunium, thorium, and zirconium, solvent extraction studies on formation of, 20: 20561 (JAERI-1099)
ACETIC ACID, (ETHYLENEDIIMINO)BIS(*o*-HYDROXYPHENYL)-
effects on zinc-65 excretion in man, 20: 20397
ACETIC ACID, (*N*-HYDROXYETHYLETHYLENEDIAMINE)TRI-
solvent properties for actinides and lanthanides, 20: 20822
ACETIC ACID, IODO-
sodium salts, effects on rabbit eyes, 20: 20507(T)
ACETIC ACID, [OXYBIS(ETHYLENENITRILO)]TETRA-
effects on zinc-65 excretion in man, 20: 20397
ACETIC ACID, VINYL ESTER POLYMERS
radiation effects on, light-scattering and viscosity measurements of gamma, 20: 20765
ACETONITRILE
radiolysis of liquid, mechanism and yields in, 20: 20717(R) (AD-621719)
ACETYLENE
production by gas discharge and radioinduced cracking of butane, 20: 20740
radioinduced polymerization of, 20: 20727 (PB-181506, pp 9-18)
ACOUSTIC WAVES
detection of atmospheric nuclear burst, pulsed arrays for, 20: 20897 (AD-623679)
ACRIDINES
radiosensitivity effects on rats, 20: 20503(R) (AD-629311, pp 1-14)
ACRYLAMIDE
radioinduced solid-state polymerization with acrylic acid, 20: 20763
acrylamide–amyloses, radiation effects on polymers of, as adhesive and dyeing mordant, 20: 20767
ACRYLAMIDE POLYMERS
properties and radiation effects on, 20: 21431(R) (WADC-TR-55-58 (Pt.9))
ACRYLIC ACID
radioinduced solid-state polymerization with acrylamide, gamma, 20: 20763
ACRYLIC ACID, ESTERS
preparation of, for polyphenyl acrylate production studies, 20: 21430(R) (WADC-TR-55-58(Pt.8))
preparation of, for polyphenyl acrylate production, 20: 21431(R) (WADC-TR-55-58(Pt.9))
ACRYLIC ACID POLYMERS
properties and radiation effects on, 20: 21431(R) (WADC-TR-55-58 (Pt.9))
ACRYLONITRILES
radioinduced polymerization of, 20: 20727 (PB-181506, pp 9-18)
radioinduced polymerization with isocyanic acid at low temperatures, 20: 20747
ACTINIDES
separation by ion exchange chromatography, tracer studies on, 20: 20822
separation from nitrate solutions by solvent extraction using tricarpylmethylammonium nitrate, 20: 20812
ACTIVATION ANALYSIS
equipment for lunar surface, 20: 21003
errors in, interference coefficient for characterization of side-reaction, 20: 20612
product separation in, ion exchange chromatographic, 20: 20632
spectra in, instrumentation for gamma scintillation, 20: 20554 (AD-621017)
use of helium-3 ions in, 20: 20565 (ORNL-P-1216)
ACTIVATION DETECTORS
performance of gold, for epithermal and thermal neutron detection, 20: 21053
performance of implanted-sulfur, for neutron dosimetry, 20: 20432 (AD-630332)
use for neutron slowing-down spectra in reactors, 20: 22382 (RT-FI (65)57)
use of aluminum–cobalt and aluminum–silver alloy wire, for neutrons, 20: 21025 (AERE-R-5122)
ADDITION COMPOUNDS
production of xenon–*p*-cresol, 20: 20688
ADENINE
radiosensitivity effects on hadacidin-treated *E. coli*, 20: 20456
ADENOSINEPHOSPHORIC ACIDS
content in rat tissues, effects of AET on, 20: 20505
radiation effects on content in Tradescantia anthers, x, 20: 20418
radiosensitivity effects on hadacidin-treated *E. coli*, 20: 20456
ADHESIVES
radiation effects on optical properties of, 20: 21446
shrinkage of Eastman 910, 20: 20807(R) (MLM-1287)
testing Adiprene and Oxiron, at high and low temperatures, 20: 20553(R) (MLM-1142)
ADRENAL GLANDS
weight norms for human, use in establishing standards for radiation dosimetry, 20: 20374
ADRIATIC SEA
ecology and hydrology of Bay of Venice, 20: 20386(R) (NP-15916)
ADVANCED TEST REACTOR
design, 20: 22499 (IDO-17150)
AERIAL SURVEYING
gamma activity data from Cincinnati area, 20: 20880 (CEX-62.6.5)
of radioactivity in Maryland, Virginia, Washington, D. C., and West Virginia, 20: 20928 (CEX-59.4.17)
AEROSOL GENERATORS
design, operation, and performance, for producing radioactive aerosols, 20: 20924 (AEET-232)
AEROSOLS
activities in air, meter for monitoring, 20: 21073
analysis of radioactive, using fibrous filter analyzer, 20: 20940(R) (ORNL-3915)
composition of containment mockup facility, after clad urania meltdown, 20: 20940(R) (ORNL-3915)
deposition of inhaled labeled, in lungs, 20: 20532
electric conductivity of MHD cells, 20: 21575
grain size distributions of natural radioactive, 20: 20885
production of radioactive, design and performance of generator for, 20: 20924 (AEET-232)
radiation effects on mycoplasma, lethal uv, 20: 20469
sampling in air stream, errors in subisokinetic, 20: 20927 (BNWL-217)
AGE
effects on fertility in gamma- and neutron-irradiated male mice, 20: 20453
effects on organ weight in man, 20: 20374
radiosensitivity effects in mice, 20: 20494

radiosensitivity effect on spermatogenesis and testicular development in mice, x, 20: 20499

AGE ESTIMATION
carbon-14 method of, review of New Zealand research on, 20: 20893
carbon-14 method of, production of methane for, 20: 20917
data list from carbon-14, 20: 20905
methods of, for carbonate deposits according to nonequilibrium uranium, in Russia, 20: 20887
potassium–argon method of, for minerals of Norwegian eclogites, 20: 20891
rubidium–strontium method of, for minerals of Norwegian eclogites, 20: 20891
rubidium-strontium method of, for New Zealand plutonic and metamorphic rocks, 20: 20888
separation processes for radiocarbon dating, 20: 20798

AGING
radioinduced in Hiroshima nuclear-explosion survivors, 20: 20480

AGRICULTURE
effects of nuclear weapons on, environmental, 20: 20931 (HI-518-RR (Vol.2))
radioisotopes in, in developing countries, 20: 22525

AIR
aerosol activity concentration in, meter for monitoring, 20: 21073
aerosol sampling in stream of, errors in subisokinetic, 20: 20927 (BNWL-217)
analysis for beryllium, spectroscopic, 20: 20807(R) (MLM-1287)
cleaning and monitoring at BNL decontamination facility, 20: 20929 (CEX-61.6.2)
corrosive effects on Hastelloy X at 1750 and 1850°F, effects of cobalt content on, 20: 21258 (AGN-TM-413)
corrosive effects on Hastelloy X at 1900 and 2000°F, 20: 21259 (AGN-TM-414)
corrosive effects on plutonium at 30 to 100°C, effects of humidity and metallurgical history on, 20: 21280
gamma propagation in, from strong remote sources, (T), 20: 20946
pollution control in, on nuclear-powered submarines, 20: 20981
reactions with sodium, calculations on, 20: 20925(R) (ANL-7055, pp 177-212)
reactions with uranium at 40 to 100°C, effects of sample preparation and humidity on, 20: 21278
separation from iodine and methyl iodide by activated charcoal filters, 20: 20940(R) (ORNL-3915)
separation from plutonium hexafluoride by hydrolysis, 20: 20803(R) (ANL-7055, pp 99-162)
separation from rare gases, equipment for, 20: 20820
sputtering of ions of, on molybdenite crystals, 20: 21529

AIR FORCE ENGINEERING TEST REACTOR
coolant flow distribution in, analysis of, 20: 22492(R) (AD-626861)
fuel burnup calculations for, computer program for, 20: 22487 (AD-621118)
instrumentation for, design of cryostat, 20: 22489 (AD-621123)
neutron flux determination in, using transport theory, 20: 22491 (AD-621269)
neutron flux in, computer program for, 20: 22488 (AD-621121)
neutron kinetics in, determination of, 20: 22490 (AD-621124)

ALANINE
yields in radioinduced carboxylation of methylamine, 20: 20732 (SGAE-CH-21/1965)

ALARM SYSTEMS
design for monitoring gases for suspended solids or liquids, 20: 21017(P)
relay for, electrostatic, 20: 21088

ALBUMINS
labeling with technetium-99m, 20: 20712
use of iodine-131- or iodine-132-labeled human serum, in isotopic placentography, radiation doses to fetuses from, 20: 20537

ALCOHOLS
determination by xenon trioxide oxidation, titrimetric, 20: 20579
effects on oxidation and reduction of iron at radioactive electrodes, 20: 20791
polyhydroxyl, radiosensitivity effects in mice, 20: 20520
yields in beta radioinduced telomerization of ethanol and methanol with ethylene, 20: 20724(R) (NYO-2978-44)

ALGAE
nitrogen fixation in blue-green, effects of uv-irradiated nitrogen on, 20: 20408
radioisotope uptake by Columbia River, factors affecting phosphorus-32 and zinc-65, 20: 20382 (BNWL-SA-623)
use of *Cyclotella nana*, and carbon-14 for measuring vitamin B_{12} in seawater, 20: 20368 (CONF-640309-1)

ALKALI METAL HALIDES
entropies and heat capacities of molten, 20: 22520(R) (NAA-SR-11805)

ALKALI METALS
critical point and liquid and vapor phase densities of, equipment and method for measuring, 20: 20651(R) (CU-2660-26)
effects of liquid, on refractory metals, test loop systems for studying, 20: 21284

ALKENES
fluoro-, radioinduced addition reactions with dialkyl phosphonates, 20: 20772

ALLOYS
decontamination and descaling of, development of solution for, 20: 21238 (NP-15928)
mechanical properties of, use of computer for storage, interpretation, and recovery of data on, 20: 21354 (TRG-Report-1160)

ALPHA DECAY
lifetimes of heavy-element, (T), 20: 22043
rates of, equations for, 20: 22155
theory of, time-dependent equations in, 20: 22024

ALPHA PARTICLES
detection in flowing water, monitor for, 20: 21038 (K-1656)
detection of, oxide-passivated silicon p-n junction detector for, 20: 21077
detection using lithium-drifted germanium and silicon detectors, 20: 21102
effects on annealed copper, gold, and nickel, Frenkel pair recombination volume from, (E), 20: 21447
effects on argon and xenon luminescence, electric field effects on decline of, (E), 20: 21521
effects on chromosomes in Tradescantia pollen grains, morphological, 20: 20438 (EUR-2518.f)
effects on electron postemission of calcium sulfate, 20: 20769
effects on poly(vinylchloride), poly(dimethylsiloxane), and poly(methyl methacrylate), 20: 20764
emission in fission, review of long-range, 20: 21968 (AEET-235)
emission in proton fission of uranium-238 at 11 to 21 Mev, (E), 20: 22144
emission in spontaneous fission of californium-252, (E), 20: 22144
interactions with mesons ($\pi^{\pm}$) at 24 Mev, meson (π) electromagnetic form factor from elastic, (E), 20: 21659
interactions with alpha particles, l-dependent potentials for, (T), 20: 22061
reactions ($\alpha,\alpha'f$) with plutonium-240 and uranium-238, fragment angular correlations from, (E), 20: 22143
reactions (α,n) with carbon-14 at 2.5 to 5.1 Mev, neutron yields from, (E), 20: 22110
reactions (α,pn) with deuterium, (T), 20: 21981 (BNL-948, pp 610-84)
reactions (α,2n) with chromium-50, iron-52 production in, (E), 20: 21993 (BNL-9168)
reactions in pulsing stars, effective density and temperature exponents for thermonuclear, (T), 20: 21491
reactions with nuclei, amplitude singularities in knockon and stripping, (T), 20: 21997 (INSJ-96)
scattering by magnesium-24 and silicon-28 at 28.4 Mev, collective enhancement of 3⁻ state by inelastic, (T), 20: 22107
scattering by nickel-58, DWBA analysis of inelastic, 20: 21973 (BNL-948, pp 175-221)
scattering by nickel-58 at 64.3 Mev, strong absorption model for inelastic, 20: 22086
scattering by nuclei at 28.4 Mev, angular distributions from, (E), 20: 22047
scattering by strontium-88 at yttrium-89 at 42 Mev, level structures from inelastic, (E), 20: 22138

ALPHA SOURCES
content in Escaut River, Belgium, 20: 22515(T) (ORNL-tr-965)
use with semiconductor detectors as timing devices, 20: 21021 (AD-622629)

ALUMINUM
bremsstrahlung reactions (γ,n) at threshold to 200 Mev, cross sections for, (E), 20: 22094
coating thickness of gold on, use of proton beam scattering for measuring, 20: 21246
determination in high-purity tantalum by spectrography using d-c arc method, 20: 20608
determination in rocks, activation, 20: 20646
dose distribution in, from electron beam irradiation, three dimensional, 20: 21470 (PB-181506, pp 116-29)
ductility of, at −269°C, 20: 21416
electron reactions at 6 to 23 kev, optical transition radiation from, 20: 21518
electron scattering at 4.2 to 300°K in, effects of impurity centers on, 20: 22314(R) (AD-626865)
electron transmission at 1 Mev in slabs of, energy spectra from, 20: 21524
enthalpy of formation of AlF_3, 20: 20650(R) (ANL-7055, pp 167-76)
fission product deposition on, from air–steam mixtures, 20: 20940(R) (ORNL-3915)
gamma elastic scattering at 280 and 662 kev, Z dependence of cross section for, (E), 20: 22060

helium-3 reactions (He-3,n) at 19 to 25 Mev, angular distributions and cross sections for, (E), 20: 22132
neutron cross sections and shielding coefficients for, 20: 22383(T) (AEC-tr-6693)
neutron flux and spectrum measurements on foils of, 20: 21427(R) (NASA-CR-54904)
photoelectric effect at 852 ev to 40 kev in, cross sections for, (E), 20: 21523
properties for use in nuclear reactors, 20: 21382
proton reactions with, straggling effects in energy loss from, (E/T), 20: 21539
proton scattering at 45 Mev, polarization in, (E), 20: 22128
radiation effects on, electron, 20: 22520(R) (NAA-SR-11805)
radiation effects on tensile properties of, at cryogenic temperatures, 20: 21427(R) (NASA-CR-54904)
reactions with steam at high pressures and temperatures, 20: 20925(R) (ANL-7055, pp 177-212)
reactions with water, laser-induced, 20: 20925(R) (ANL-7055, pp 177-212)
separation from perchloric acid solutions by ion exchange materials, 20: 20823
separation from scandium by ion exchange chromatography, 20: 20821
separation from thorium by ion exchange in nitric acid solution, 20: 20624
separation from uranium by combined ion exchange-solvent extraction using nitric acid–tetrahydrofuran solutions, 20: 20811
solvent properties for chromium, molybdenum, and tungsten at 400 to 660°C, microhardness studies on, 20: 21362(T) (SC-T-66-0723)
superconducting properties of, effects of λ transition on, 20: 21875
thickness measurements on films of, conductance device for, 20: 20987 (RFP-690)
viscosity of liquid, based on atomic parameters, 20: 20656 (UCRL-11930)
yttrium distribution coefficient in, mathematical determination of, 20: 21369

ALUMINUM ALLOYS
effects of decontaminating and descaling solution on metal loss on, 20: 21238 (NP-15928)
properties for use in nuclear reactors, 20: 21382
properties of, for use in space nuclear power plant testing vault, 20: 20869
Al–Ag, use for neutron dosimetry, 20: 21025 (AERE-R-5122)
Al–Au, radiation effects at 80°K on, resistivity recovery from proton, 20: 21445
Al–Ce, crystal structure and stability of intermetallic compounds in, 20: 21415
Al–Co, use for neutron dosimetry, 20: 21025 (AERE-R-5122)
Al–Dy, crystal structure and stability of intermetallic compounds in, 20: 21415
Al–Dy, dysprosium hyperfine magnetic field in intermetallic compounds of, (E), 20: 22330
Al–Er, crystal structure and stability of intermetallic compounds in, 20: 21415
Al–Gd, crystal structure and stability of intermetallic compounds in, 20: 21415
Al–Gd–Pd, electric properties of, 20: 22312(R) (AD-622796)
Al–Ho, crystal structure and stability of intermetallic compounds in, 20: 21415
Al–In–Sn, superconducting properties of, nonideal, 20: 21925
Al–La, crystal structure and stability of intermetallic compounds in, 20: 21415
Al–Mg, solvent properties of liquid, for praseodymium, 20: 20802(R) (ANL-7055, pp 21-98)
Al–Nb, magnetic field penetration into superconducting intermetallic compounds of, (E), 20: 21908
Al–Nd, crystal structure and stability of intermetallic compounds in, 20: 21415
Al–Ni–U, reactions with water during Kiwi-TNT transients, 20: 20925(R) (ANL-7055, pp 177-212)
Al–Pr, crystal structure and stability of intermetallic compounds in, 20: 21415
Al–Pu, etching of delta-phase, bright-field grain structure, 20: 21233 (BNWL-188)
Al–rare earths, crystal structure and stability of intermetallic compounds in, 20: 21415
Al–Sm, crystal structure and stability of intermetallic compounds in, 20: 21415
Al–Sn, superconducting properties of, nonideal, 20: 21925
Al–Tb, crystal structure and stability of intermetallic compounds in, 20: 21415
Al–U, processing for uranium recovery by fluoride volatility, 20: 20803(R) (ANL-7055, pp 99-162)
Al–U, processing by fluid-bed fluoride volatility, 20: 20801 (ANL-6830)
Al–Y, crystal structure and stability of intermetallic compounds in, 20: 21415
Al–Y, phase diagram of, mathematical determination of, 20: 21369

ALUMINUM COMPLEXES
with 2,4-pentanedione, preparation and crystal structure of, 20: 20700

ALUMINUM COMPOUNDS
growth and properties of rare earth garnets of, 20: 22311(R) (AD-622068)

ALUMINUM ISOTOPES Al-27
energy levels of, Doppler shift measurements of lifetimes of, (E), 20: 22010(R) (NYO-72-28)
neutron reactions (n,α) at 8.6 Mev, cross section and threshold energy for, 20: 21427(R) (NASA-CR-54904)

ALUMINUM OXIDES
diffusion of helium in poly- and single-crystal, activation energy and rate of, 20: 21353 (TID-22828)
labeling with tritium, for use in self-labeling chromatographic analysis, 20: 20575
reactions with bromine pentafluoride, 20: 20803(R) (ANL-7055, pp 99-162)
reactions with gaseous uranium trioxide, effects of substrate symmetry in, 20: 20649 (AEET-CD-24)
removal from aluminum by dissolution, descaling solution for, 20: 21238 (NP-15928)
wear properties of plasma-arc-deposited coatings of, 20: 21319 (AD-621064)
Al_2O_3–MgO–UO_2, phase studies, properties, and structures of, 20: 21359 (WAPD-T-1581)
Al_2O_3–Ni, wear properties of plasma-arc-deposited coatings of, 20: 21319 (AD-621064)

AMERICIUM
deposition on metals, conditions for electrolytic, 20: 21287 (AE-217)
production of, review of methods for, 20: 20796
separation from nitrate solutions by solvent extraction using tricaprylmethylammonium nitrate, 20: 20812

AMERICIUM ALLOYS
Am–Pu, phase diagram, 20: 21339 (LA-DC-7095)

AMERICIUM ISOTOPES Am-241
alpha decay of, effects of recoil stopping time on Mössbauer effects following, 20: 22037
nuclear magnetic moments and hyperfine structure of, 20: 22137

AMERICIUM ISOTOPES Am-242
nuclear magnetic moments and hyperfine structure of, 20: 22137

AMIDE POLYMERS
radiation effects on, of electrons at 300 to 500 kv, 20: 20762

AMIDES
N-acryl-, preparation of, for acrylamide polymer production, 20: 21431(R) (WADC-TR-55-58(Pt.9))

AMINO ACIDS
labeling with deuterium or tritium by isotopic exchange with water-d_2 or water-t_2, 20: 20714
metabolism in nerve cells, effects of behavioral activation on, 20: 20391(R) (TID-22825)
radiation effects on synthesis of, by rat liver, x, 20: 20410
radiation effects on aqueous solutions of, review on, 20: 20728 (PB-181506, pp 49-58)
reactions with hydrated electrons, 20: 20403

AMMONIA
effects on solubility of rare earth oxides in alcohols, 20: 20686
europium ion EPR in solutions of, 20: 20668
hydrogen abstraction by methyl radicals from, isotope effects on, 20: 20713
labeling with deuterium at 386 to 461°C, equilibrium constant for, 20: 20660
labeling with tritium, equilibrium constant for, 20: 20660
preparation of, at 294 to 400°C, equilibrium constant for, 20: 20660

AMMONIUM COMPOUNDS, QUATERNARY
solvent properties of tricarpylmethylammonium nitrate for trivalent actinide-lanthanide elements, 20: 20812
solvent properties for hafnium, niobium, protactinium, titanium, uranium, and zirconium, 20: 20816

AMMONIUM FLUOFERRATES
properties as absorber in Mössbauer measurements using iron-57, 20: 22157

AMMONIUM PHOSPHOMOLYBDATES
properties as ion exchange material for cesium, 20: 20818

AMMONIUM URANIUM FLUORIDES
thermal decomposition to UF_4, 20: 20817

AMPHIBIANS
radiosensitivity of, 20: 20440(R) (EUR-2643.f)
tissue regeneration in, effects of radiomimetic substances on, 20: 20440(R) (EUR-2643.f)

AMPLIFIERS
design and performance of low-noise charge-sensitive transistorized pre-, for semiconductor detectors, 20: 21072
design for photomultiplier, 20: 22010(R) (NYO-72-28)
design of charge-sensitive pre-, 20: 21124

design of charge-sensitive transistorized pre-, for radiation detectors, 20: 21130
design of integrated-circuit charge-sensitive pre-, 20: 21112
design of modular solid-state, 20: 20997
design of nuclear pulse, ground-loop noise and timing accuracy in, 20: 21008
design of solid-state, for photomultipliers, 20: 21039 (KAPL-3122)
design of solid-state pulse, 20: 21000
properties of plasma wave, (T), 20: 22211
pulse shaping in, by triple differentiation, 20: 21004
use of a-c, with ionization chamber in reactor shutdown system, 20: 22359

AMYLOSES
radiation effects on, in aqueous solutions, x, 20: 20748
acrylamide–amyloses, radiation effects on polymers of, as adhesive and dyeing mordant, 20: 20767

ANALYSIS
methods of, for trace impurities in reactor fuels and materials, 20: 20589
nuclear quadrupole resonance uses in, 20: 20578

ANEMIA
induced in mice by gamma-irradiated schistosomes, 20: 20446

ANILINE, *N,N*-DIMETHYL-*p*-PHENYLAZO-
effects on radioinduced oxidation of ergosterol, 20: 20738

ANIMAL CELLS
infection with tumor viruses of human diploid, in culture, 20: 20377
radiation absorption by Chinese hamster, use of flying-spot microscopy for detecting uv, 20: 20473
radiation effects on, mechanism for, 20: 20416
radiation effects on potassium and sodium content in nuclei of, x, 20: 20422
radiation effects on chicken germ cells, physiological x, 20: 20440(R) (EUR-2643.f)
radiation effects on ascites tumor, transplanted into x-irradiated mice, uv, 20: 20484

ANIMAL RESPIRATION
analysis of, using x radiation, 20: 20546

ANIMALS
effects of nuclear weapons on, environmental, 20: 20930 (HI-518-RR (Vol.1))
effects of nuclear weapons on, environmental, 20: 20931 (HI-518-RR (Vol.2))
effects of scavenger, on decomposition of swine carrion, 20: 20941 (ORNL-TM-1432)
radiation effects on survival of ascites tumor, transplanted into x-irradiated animals, uv, 20: 20483
radioactivity due to fallout in Doe Run, Meade County, Ky., 1959 to 1965, 20: 20884(R) (TID-22815)
radioinduced carcinogenesis in, review, 20: 20442 (ORNL-P-2053)
radioinduced hematogenic osteomyelitis in, mechanism for x, 20: 20371

ANION EXCHANGE MATERIALS
sorptive properties for uranyl ions in hydrochloric acid media, 20: 20827

ANNEALING
effects of thermal, on luminescence in lithium fluorides, 20: 21057

ANOXIA
radiosensitivity effect in mice, 20: 20430(R) (AD-629311, pp 26-32)

ANTENNAS
electromagnetic radiation from acoustic point-source, in compressible plasma bubble, (T), 20: 22196

ANTHRANILIC ACID
radiosensitivity effects on hadacidin-treated *E. coli*, 20: 20456

ANTIBODIES
radiation effects on hemagglutinin, x, 20: 20425

ANTIMONY
determination in silicon dioxide, activation, 20: 20635
separation from molybdenum, tantalum, and tin by ion exchange chromatography on chloride form resin, 20: 20635

ANTIMONY ALLOYS
Sb–Ga, radiation effects on semiconductor, electron, 20: 22520(R) (NAA-SR-11805)
Sb–Yb, phase studies, 20: 21401

ANTIMONY ISOTOPES Sb-121
neutron capture by, isomeric cross section ratios for, (E), 20: 22052

ANTIMONY ISOTOPES Sb-122
production of isomeric and ground-state, from antimony-121 neutron capture, (E), 20: 22052

ANTIMONY ISOTOPES Sb-124
yields from thermal-neutron fission of uranium-235, 20: 22044

ANTIMONY ISOTOPES Sb-125
yields from thermal-neutron fission of uranium-235, 20: 22044

ANTIMONY ISOTOPES Sb-126
yields from thermal-neutron fission of uranium-235, (E), 20: 22044

ANTIMONY SYSTEMS
Sb–Cr–Te, neutron diffraction studies on solid solutions of, 20: 22312(R) (AD-622796)

ANTINEUTRINOS
interactions with nucleons, spark chamber experiments on, 20: 21607 (CERN-65-32, pp 161-8)
production of CERN experiment on, 20: 21602 (CERN-65-32, pp 111-14)

ANTIPROTONS
interaction with protons in ambiplasma, energy distribution from annihilation, (T), 20: 21684

ANTLER OPERATION
secondary explosion in, effects of water entry on, 20: 20939 (NVO-1163-70)

ARGON
detection of molecular beams of, field-ionization detector for, 20: 21089
deuterium hydride infrared absorption spectra in liquid, rotational-translational coupling from, (E), 20: 21528
deuterium vibrational relaxation times in, shock-tube measurement of, 20: 21797
diagnostics of plasma of, Langmuir probe for, (E/T), 20: 22193
diffusion in uranium-doped calcium fluoride single crystals at 900 to 1200°C, 20: 21332(R) (EURAEC-1573)
effects on growth rates in Neurospora, 20: 20378
electric conductivity of atmospheric, determination of, (E), 20: 22164 (AD-621213)
electric conductivity, ionization, and recombination in potassium-seeded plasma of, (E), 20: 22258
electric conductivity of h-f discharge plasma of, calorimetric- and optical-methods for measuring, (E), 20: 22280
electric discharges in, electron distribution function for, (E), 20: 21795
electric discharges in, in transverse magnetic fields, (E), 20: 21810
electron and excitation temperatures in plasma of, (E), 20: 22267
lithium-7 scattering at 30 kev, intensity angular distributions from, (E), 20: 21536
performance in plasma engines, effects of nonequilibrium conductivity on, 20: 20873
photoelectric effect at 852 ev to 40 kev in, cross sections for, (E), 20: 21523
radioinduced luminescence of, electric field effects on decline of alpha, (E), 20: 21521
separation from air, equipment for, 20: 20820
separation from nitrogen by titanium gettering, 20: 20802(R) (ANL-7055, pp 21-98)
shock propagation in plasma of, microwave interferometry of, (E), 20: 22182 (IPP-3/35)
shock propagation in plasma of, radiation intensity from, (E/T), 20: 22281
solubility in potassium nitrate, 20: 22520(R) (NAA-SR-11805)
thermal conductivity at 750°C, 20: 20651(R) (CU-2660-26)
thermal conductivity of atmospheric, determination of, (E), 20: 22164 (AD-621213)

ARGON IONS
reactions with beryllium–copper alloys at 3 to 90 kev, secondary electron emission from, (E), 20: 21538
reactions with thin films of germanium at low energy, depth of induced damage from, 20: 21438
sputtering on molybdenite crystals, 20: 21529

ARGON ISOTOPES Ar-38
concentration in gaseous argon by thermal diffusion, 20: 20806(R) (MLM-1274)
concentration in gaseous argon by thermal diffusion, 20: 20807(R) (MLM-1287)
content in iron meteorites, 20: 21505
energy levels from chlorine-37 (p,α) reactions, lifetime and spacing of, (E), 20: 22084

ARGON ISOTOPES Ar-39
content in iron meteorites, 20: 21505
production by cosmic-ray reactions with iron, calcium, and potassium in Leedey chondrites, 20: 21508

ARGON ISOTOPES Ar-40
alpha scattering at 18 Mev, cross sections for, (T), 20: 22134
meson (π^-) reactions (π^-,π^-2p) with, cross sections for, (E), 20: 22125
meson (π^-) reactions (π^-,π^-p) and (π^-,π^-pn) at 500 to 1100 Mev, excitation functions for, (E), 20: 22125
proton reactions (p,2p) and (p,2pn) with, cross sections for, (E), 20: 22125

ARGON SYSTEMS
Ar–N, corrosive effects on structural alloys and metals at 900°C, 20: 20802(R) (ANL-7055, pp 21-98)

ARGONNE SYNCHROTRON
beam intensity of, program for increasing, 20: 21466 (CERN-65-32, pp 127-30)
experimental facilities for neutrino studies, development status of, 20: 21465 (CERN-65-32, pp 31-4)

magnet power supply for, analog computer representation of, 20: 21488
ARKANSAS
site selection for wet medium cratering experiments in Lee Co., 20: 20895 (AD-626899)
ARMY REACTORS (PM-3)
control rod drive mechanism of 3A, cable repair for, 20: 22416 (TID-22736)
design and performance of 3A, in Antarctica, 20: 22445
ARSENAZO III
uses in determination of thorium, uranium, and zirconium, 20: 20614
ARSENIC
determination in silicon dioxide, activation, 20: 20635
determination in tin oxide, activation, 20: 20577
separation from phosphorus and tungsten by ion exchange chromatography on fluoride resin, 20: 20635
ARSENIC ISOTOPES As-75
energy level lifetimes, 0.305-Mev, (E), 20: 22038
ARSENIC ISOTOPES As-76
concentration by recoil reactions from neutron irradiation of zirconium benzenearsonate, 20: 20797
ASBESTOS
fabrication of plates or tubes of, radiometric control of, 20: 21204
ASCORBIC ACID
radiosterilization effects on content of, in citrus fruits and tomatoes, 20: 21195(R) (TID-22509)
ASTRONOMY
conference, 20: 21511
development of cosmic-ray, 20: 21494
ASTROPHYSICS
conference, 20: 21511
energy release in extragalactic phenomena, energy source for very high, (T), 20: 21498
ATHEROSCLEROSIS
etiology of, relation of serum lipid and lipoprotein content to, 20: 20370 (UCRL-14658)
ATMOSPHERE
neon isotope abundance ratios in, (E), 20: 21509
neutron transport at altitude 10^5 feet in, flux density calculations for, 20: 21935 (AD-624041)
radiation monitoring of Japanese, alpha, beta, and gamma, 20: 20934 (JAERI-1098)
radioactivity due to fallout in Canadian, 1964, 20: 20938 (NP-15921)
radioactivity due to fallout in Canadian, 1965, 20: 20883 (NP-15914)
radioactivity due to fallout, 1965, 20: 20882(R) (HASL-171)
radioactivity in, importance of measuring, 20: 20961
tritium content of, at Hamburg, Germany, following Windscale accident, 20: 20889
ATOMIC CLOUDS
analysis of, development of airborne instrumentation for, 20: 20881 (DASA-1704)
ATOMIC ENERGY
bibliography of bibliographies on, Feb.-March 1966, 20: 22522 (TID-3734)
development in Japan, review of industrial, 20: 22526
ATOMIC ENERGY COMMISSION
nuclear materials management program of, review of, 20: 22527
peaceful uses of, in industry, 20: 21182 (ORNL-IIC-7, pp 49-58)
program on plastic–wood materials, 20: 21178 (ORNL-IIC-7, pp 1-5)
support of program on plastic–wood combinations, 20: 21187 (ORNL-IIC-7, pp 89-94)
ATOMIC ENERGY, LEGAL ASPECTS
British Atomic Liability Law, amendments to, 20: 20948
for dental radiology, 20: 20519
for radiation processing of foods, 20: 21201
radiation protection law, medical experiences following, 20: 20947
ATOMIC EXPLOSIONS
acoustic waves from, pulsed arrays for detecting, 20: 20897 (AD-623679)
beta spectra from, time-dependent, (T), 20: 21960 (AD-621023)
crater production by high-energy, site selection for, 20: 20895 (AD-626899)
debris identification from, detector design and performance for, 20: 20881 (DASA-1704)
effects on human aging, 20: 20480
effects on human blood picture, 20: 20481
effects on populations of Hiroshima and Nagasaki, 20: 20919(R) (ABCC-64-65)
gamma radiation from, pulsed x-ray simulator for, 20: 20838 (AD-624019)
gamma radiation from debris of high-altitude, instrument for detection and measurement of, 20: 21129
seismic waves from, in overdriven cavities, 20: 20898 (AD-624016)
seismic wavetrain propagation from, interpretations of, 20: 20910
ATOMS
photon absorption by, kinetic theory of two-body, 20: 21533
radiation effects on motion in crystals, computer simulation of, 20: 22341
AUDITORY ORGANS
radiation effects on rabbit, gamma, 20: 20498
AURORAL STORMS
effects on off-great-circle high-frequency propagation, 20: 21827
intensity during solar activity minimum, 20: 21814
light intensity and particle fluxes in, 20: 21826
noise from, high-frequency, 20: 21835
spectral bands of nitrogen in, excitation by x radiation, 20: 21834
AUTORADIOGRAPHY
method for determining carbon-14 and tritium alone or simultaneously, 20: 20605
uses for determination of long-lived beta-gamma activities, 20: 20611
AZOBENZENE
effects on radioinduced decomposition of Santowax-OM1, 20: 20708 (AEET-213)

B

BACTERIA
enzyme synthesis in Pseudomonas mutants, 20: 20376
enzyme synthesis in Pseudomonas mutants, 20: 20470
nuclear structure in, effects of uranyl ions on, 20: 20392
radiation effects on mycoplasma aerosols, lethal uv, 20: 20469
radioinduced mutations of Pseudomonas, uv, 20: 20470
BACTERIOPHAGES
radiation effects on T4D, uv, 20: 20427
radioinduced inactivation and mutagenesis in ϕX174, uv, 20: 20463
radiosensitivity of *Escherichia coli* complexes with, uv, 20: 20471
BARIUM
determination in irradiated silica, activation, 20: 20636
diffusion in graphite fuel elements, 20: 21423 (N-65-23015)
separation from irradiated silica and sodium by chromatography, 20: 20636
separation from perchloric acid solutions by ion exchange materials, 20: 20823
BARIUM CARBONATES
properties for buffering emission spectrograph samples, 20: 20553(R) (MLM-1142)
BARIUM HYDROXIDES
crystal structure of hydrates of, 20: 20694
BARIUM ISOTOPES Ba-133
decay of, cesium-133 level multipolarity and spins from, (E), 20: 22076
BARIUM ISOTOPES Ba-134
energy level transitions from cesium-134 decay, conversion coefficients for 605-kev, (E), 20: 22026
BARIUM ISOTOPES Ba-140
diffusion in irradiated fuel element cladding alloys and materials at 600 to 1200°C, 20: 21232 (BMI-1763)
yields from photofission of uranium by 650-Mev bremsstrahlung, 20: 22040
BARLEY
cation uptake by roots of, uranyl effects on selective inhibition in, 20: 20402
BARYONS
charge, magnetic moments, and mass differences for, SU(3) bootstrap theory for, 20: 21757
decay of, axial weak interactions in leptonic, (T), 20: 21753
decay of, sum rules for radiative nonleptonic, 20: 21751
decay of, unitary symmetry for, 20: 21708 (CONF-640509(Pt.2), Paper 2)
interactions with leptons, model for weak, (T), 20: 21714 (JINR-P-2578)
interactions with mesons, parity and spin of particles in polarized, (T), 20: 21715 (JINR-P-2576)
mass formula for, using SU(6,6) group, 20: 21624 (JINR-P-2606)
mass formulas in SU(3) for, 20: 21739
symmetry for, vector-meson mixing model for sum rules in broken SU(3), 20: 21753
BARYONS, RESONANCE
coupling constants for $N^*_{\frac{3}{2}}N\pi$ and $NN\pi$, weak, 20: 21655
decay of N*** (1238), (E), 20: 21663
decay of Y^*_1, dynamics of branching ratio for, (T), 20: 21670
decay of, particle and polarization angular distributions in two- and three-body, (T), 20: 21698
decay of, resonance widths in, (T), 20: 21713 (JINR-P-2568)
magnetic moments of isobar, (T), 20: 21759
models for, quark, (T), 20: 21697
photoproduction of N***(1688) current commutation relations for, 20: 21676
production, (E/T), 20: 21592 (CERN-65-24(Vol.1), pp 1-44)
production in meson (K⁻)-proton interactions at 1.33 Bev/c, (E), 20: 21615 (COO-1195-52)
production of (2650) and (2850), in meson (π)-proton interactions at 2 to 7 Bev/c, (E), 20: 21661
production of N* and N** in neutrino interactions, methods for,

20: 21606 (CERN-65-32, pp 157-60)
production of N*++(1238) in proton interactions with protons at 5.5 Bev/c, (E), 20: 21663
production of N* in neutrino-neutron interactions, cross sections for, (T), 20: 21599 (CERN-65-32, pp 89-96)
production of Y* (1765), in meson (K−)-proton interactions at 900 to 990 Mev/c, (E), 20: 21628 (TID-22832)

BATTERIES
conference, 20: 21581
conference, 20: 21582
conference, 20: 21583
radiation effects on, hardening against, 20: 21162

BEACHES
maintenance of waterfront, evaluation of tracer techniques for, 20: 21176 (AD-621440)

BEANS
radiosensitivity of roots of, partial pressures of inert gases for halving oxygen-dependent, 20: 20378

BEARINGS
performance testing of gas-lubricated, for Brayton-cycle turbocompressors, 20: 20841(R) (NYO-3237-5)
testing refractory metal, in liquid sodium, 20: 22520(R) (NAA-SR-11805)

BEHAVIOR
activation of nucleic acid metabolism in brain cells by, tracer study, 20: 20391(R) (TID-22825)
radiation effects on animal, γ, 20: 20495
radioinduced mongoloid, effects of parental exposure on, in children, 20: 20454

BENZALDEHYDE
yields from gamma radiolysis of DL-mandelic acid in oxygenated solutions, 20: 20759

BENZANTHRACENE
dimethyl-, effects on mouse mammary glands, neoplastic, 20: 20502

BENZENE
radiolysis of aqueous solutions of, effects of oxides on gamma, 20: 20768
benzene–ethanol, radiolysis of, at 20 and −196°C, yields from gamma, 20: 20741
benzene–ethanol, radiolysis of, at −196°C, EPR spectra of ethyl radicals from gamma, 20: 20742

BENZENE, HEXAFLUORO-
effects on scintillation response of liquid phosphors, 20: 21134

BENZENEARSONIC ACID
complexes with neptunium, thorium, and zirconium, solvent extraction studies on formation of, 20: 20561 (JAERI-1099)

BENZENEARSONIC ACID, ZIRCONIUM SALTS
arsenic-76 enrichment in, by recoil reactions in neutron irradiation, 20: 20797

BENZENESULFONIC ACID, DODECYL-
solvent properties for neptunium, 20: 20561 (JAERI-1099)

BENZYL ALCOHOLS
α-(aminomethyl)-3,4-dihydroxy-, yields from photolysis of tyramine, 20: 20409

BERKELIUM
production of, review of methods for, 20: 20796
separation from nitrate solutions by solvent extraction using tricaprylmethylammonium nitrate, 20: 20812

BERKELIUM ISOTOPES Bk-250
energy levels from einsteinium-254 decay, (E), 20: 22142

BERYLLIUM
analysis for carbon and nitrogen, modified combustion-conductometric, 20: 20556 (AD-626987)
determination by activation using helium-3 ions, 20: 20565 (ORNL-P-1216)
determination in air, spectroscopic, 20: 20807(R) (MLM-1287)
evaporation from porous tungsten ionizers, 20: 21570 (N-65-29785)
gamma dosimetry in and behind, tabulations for, 20: 22307 (DC-61-3-69)
helium-3 reactions (He-3,n) at 19 to 25 Mev, angular distributions and cross sections from, (E), 20: 22132
mechanical properties of, evaluation and standardization of methods for testing, 20: 21341 (MAB-205-M)
neutron dosimetry in and behind, tabulations for, 20: 22307 (DC-61-3-69)
neutron spectra in, reactor design considerations from thermal, 20: 22376 (GA-6901)
neutron thermalization in, (E), 20: 21942(T) (KFK-tr-188)
oxidation of, orientation in film growth in, 20: 21269
phase diagram of, pressure-temperature, 20: 21363(T) (UCRL-Trans-1299(L))
photoelectric effect at 852 ev to 40 kev in, cross sections for, (E), 20: 21523
proton reactions at 12.5 Bev, meson (K) and (π) production cross sections for, (E), 20: 21601 (CERN-65-32, pp 109-10)
proton scattering at 45 Mev, polarization in, (E), 20: 22128
separation from scandium by ion exchange chromatography, 20: 20821
slip in single-crystal, compressed parallel to c-axis, 20: 21371
sorption from perchloric acid solutions by ion exchange materials, 20: 20823
x-ray scattering cross sections at 1 to 150 kev, (T), 20: 21516 (UCRL-14403)

BERYLLIUM ALLOYS
Be–Ag, radiation effects at 80°K on, resistivity recovery from proton, 20: 21445
Be–Cu, ductility of, at −269°C, 20: 21416
Be–Cu, radiation effects at 80°K on, resistivity recovery from proton, 20: 21445
Be–Cu, rare-gas ion reactions at 3 to 90 kev, secondary electron emission from, (E), 20: 21538
Be–Ni, properties of localized impurity states in, 20: 21390

BERYLLIUM COMPLEXES
with thiodibenzoylmethane, stability of, 20: 20693

BERYLLIUM ISOTOPES Be-7
energy levels of, use of Hamada-Johnston potential for, (T), 20: 22102

BERYLLIUM ISOTOPES Be-8
energy levels of, use of Hamada-Johnston potential for, (T), 20: 22102

BERYLLIUM ISOTOPES Be-9
charged-particle reactions with, amplitude singularities in knockon and stripping, (T), 20: 21997 (INSJ-96)
electron elastic scattering to 230 Mev, magnetic form factors from, (E), 20: 22120
electron inelastic scattering by, excitation of electromagnetic transitions in, (E), 20: 22105
energy levels of, use of Hamada-Johnston potential for, (T), 20: 22102
proton elastic scattering at 45 Mev, differential cross sections for, (T), 20: 21963 (AD-626656)

BERYLLIUM OXIDE REACTOR EXPERIMENT
control rod drive mechanism performance, 20: 22410(R) (GA-5238)
development, Jan.-Mar. 1964, 20: 22410(R) (GA-5238)
development, Oct.-Dec. 1965, 20: 22413(R) (GA-6929)
fuel fabrication for, uranium dioxide, 20: 22410(R) (GA-5238)
pressure vessel fatigue analysis, 20: 22410(R) (GA-5238)

BERYLLIUM OXIDES
coating with single-crystal silicon, 20: 21249
crystal structure, 20: 22520(R) (NAA-SR-11805)
formation of films of, on beryllium, 20: 21269
neutron spectra in, thermal, 20: 21939(R) (GA-6930)
properties for skull reclamation crucibles, 20: 20802(R) (ANL-7055, pp 21-98)
radiation effects on structure of sintered, x-ray diffraction studies of neutron, 20: 21433(T) (UCRL-Trans-10012)
radiation effects on crystalline, 20: 22520(R) (NAA-SR-11805)
radiation effects on helium diffusion from, kinetics of neutron, 20: 21428 (NP-15942)
BeO–UO_2, fabrication of fuel particles of, 20: 21297(T) (NP-tr-1371)

BETA DECAY
bibliography on, 20: 22011 (TID-22771)
electron radial function and tangents of phase shifts for nuclei ($1 \leq Z \leq 10$), 20: 22009 (NBS-MON-81)
lifetimes of heavy-element, (T), 20: 22043
theory of, time-dependent equations in, 20: 22024

BETA PARTICLES
detection and measurement of, automatic equipment for multiple, 20: 21055
detection and measurement of, performance of lithium-drifted silicon diodes for, 20: 21064
detection of, lithium-drifted silicon p-i-n detector for, 20: 21077
dosimetry of iodine-131, in rat fetuses, 20: 20390(R) (TID-22767)
dosimetry using silicon p-n junctions, instrument for, 20: 21133
effects on development of fish spawn in sea water, 20: 20445(T) (TRG-Inf. Ser.-166)
effects on electron postemission of calcium sulfate, 20: 20769
effects on fetuses in isotopic placentography using human serum albumin labeled with iodine-131 or iodine-132, 20: 20537
effects on rat thyroid, carcinogenic, 20: 20448
effects on telomerization of ethanol and methanol with ethylene, yields from, 20: 20724(R) (NYO-2978-44)
effects on variegation in Einkorn wheat, mutagenic, 20: 20497
effects on viability of *E. coli*, 20: 20457
emission in uranium carbide fission, energy measurements for, 20: 22404 (USNRDL-TR-987)

BETA SOURCES
content in biota of Doe Run, Ky., 1959 to 1965, 20: 20884(R) (TID-22815)
content in Escaut River, Belgium, 20: 22515(T) (ORNL-tr-965)

BETA SPECTRA
determination for nuclear explosions, time-dependent, (T), 20: 21960 (AD-621023)

BETA SPECTROMETERS

design and construction of thin-lens, 20: 21051
design for Orbiting Geophysical Observatory, 20: 21124
design for use in Gemini Project, 20: 21116
design using open electron multiplier for Orbiting Geophysical Observatory, 20: 21123

BETATRONS
storage rings for, space-charge effects in, (T), 20: 21475(T) (SLAC-Trans-38)

BEVATRON
development and operation, Apr.–June 1965, 20: 21474(R) (UCRL-16553)

BIBLIOGRAPHIES
of bibliographies on atomic energy literature, Feb.-March 1966, 20: 22522 (TID-3734)
of du Pont publications, 1965, 20: 22519 (DP-929(Suppl.2))
on aerospace medicine and biology, 20: 20369 (NASA-SP-7011(22))
on analysis of uranium hexafluoride, 20: 20558 (CEA-R-2863)
on analytic S-matrix theory of strong interactions, 20: 21774
on atomic absorption determination of elements, 20: 20563 (NP-15918)
on chemical applications of Mössbauer effect, 20: 20684
on corrosion inhibition properties of oxide films, 20: 21281
on corrosion protection coatings for niobium, 20: 21257 (AD-621546)
on deformation mechanisms in hexagonal compact metals, 20: 21330 (EUR-2621.f)
on direct energy conversion, 20: 21565 (AD-628049)
on environmental effects of nuclear weapons, 20: 20930 (HI-518-RR (Vol.I))
on fallout, · 20: 20882(R) (HASL-171)
on geomagnetically trapped particles, 20: 21837
on heavy-ion reactions and scattering, 20: 21992 (BNL-948, pp 1045-1134)
on nuclear theory, 20: 22011 (TID-22771)
on nucleation and crystal growth in ceramic melts, 20: 21235 (IS-1287)
on plasma sheath theory, 20: 22177 (CLM-Bib-6)
on quark models for strongly interacting particles, 20: 21697
on radiation chemistry and radiochemistry research in France, 20: 20730 (PB-181505, pp 104-15)
on radiochemical studies on neptunium, 20: 20561 (JAERI-1099)
on radioisotopes and radiation in soil-plant nutrition studies, 20: 20389 (STI-PUB-108)
on radiolysis of lithium nitrate, · 20: 20733 (TID-22796)
on self-diffusion in metal oxides, 20: 21321 (AERE-Bib-143)
on site selection for wet medium cratering experiments, 20: 20895 (AD-626899)
on superconductivity, 20: 21877
on two-nucelon-transfer reactions, 20: 21972 (BNL-948, pp 86-174)
on unclassified publications of Dow Chemical Co., 20: 22521 (RFP-516A(Suppl.1))

BIOCHEMISTRY
radiation effects in, from central nervous system exposure, 20: 20449
research programs on, using Kyoto University cyclotron, 20: 22524

BIOLOGICAL MATERIALS
analysis for carbon-14 and tritium, combustion procedure in liquid scintillation counting for, 20: 20570
analysis for carbon-14 and tritium, autoradiographic method for, 20: 20605
analysis for fluorine, activation, 20: 20594
effects of rare gases on, mechanism, 20: 20378
radiation effects on molecular, mechanism of high-energy and uv, 20: 20731 (PB-181505, pp 133-42)
radioactivity in, importance of measuring, 20: 20961

BIOLOGICAL STRESS
radioinduced, effects on physiological functions in dogs, · 20: 20435 (CONF-650560-15)

BIOLOGICAL SYSTEMS
radiation effects on, mechanism of, 20: 20443 (PB-181506, pp 143-54)
radiosterilization of, use of radioisotopes in space vehicles for, 20: 21174 (SAN-575-12)
tracer studies in, data analysis for, 20: 20393
tracer studies in, data analysis, 20: 20394

BIOLOGY
research programs on, using Kyoto University cyclotron, 20: 22524

BIOMETRY
data analysis for biological tracer studies, 20: 20394
data analysis for biological tracer studies, 20: 20393

BIPHENYL
alkyl-, heat transfer properties and radiation stability of reactor coolants of, 20: 20792
biphenyl–diphenyl methane, heat transfer properties and radiation stability of, for use in reactor loops, 20: 20792

BIPYRIDINES
complexes with rare earths, fluorescence of, effects of ligand substitution on, 20: 20703

BISMUTH
corrosive effects on molybdenum alloys at 1000°C, (E), 20: 21566(R) (ANL-7055, pp 213-29)
electric conductivity at 301°K, effects of pressure at 30 to 90 kbars on, 20: 21357 (UCRL-16299)
heat of fusion, · 20: 20553(R) (MLM-1142)
neutron inelastic scattering at 5.8 and 7.5 Mev, gamma spectra from thermal, (E), · 20: 22069
neutron reactions with, production of polonium-210 in, 20: 20585
proton reactions, production of polonium by, · 20: 20553(R) (MLM-1142)
separation from thorium by ion exchange in nitric acid solution, 20: 20624
separation from uranium by combined ion exchange-solvent extraction using nitric acid–tetrahydrofuran solutions, 20: 20811
separation of polonium from ... by deposition on silver plate, 20: 20585
sorption from perchloric acid solutions by ion exchange materials, 20: 20823

BISMUTH ALLOYS
Bi–In, microwave surface resistance in superconducting, (E), 20: 21916
Bi–In, thermal capacity of superconducting, (E), 20: 21907
Bi–In, thermal conductivity of superconducting, (E), 20: 21914
Bi–Na, equilibria in regenerative cells, liquid-vapor, (E), 20: 21566(R) (ANL-7055, pp 213-29)
Bi–Na, solubility in sodium halide mixtures, (E), 20: 21566(R) (ANL-7055, pp 213-29)
Bi–Pb, separation of cadmium from, by vacuum distillation, · 20: 20805 (IS-1329)
Bi–Pb, superconducting transition temperatures in epsilon-phase, (E), 20: 21892
Bi–Pb, superconducting critical currents and fields in flux-pump fed coils of, (E), 20: 21924
Bi–Sn, corrosive effects on type 304 stainless steel at 200 to 1100°C, kinetics of hydrodynamic, 20: 21260 (ANL-6985)

BISMUTH BROMIDES
Bi–$BiBr_3$, diffusion in liquid, thermal, 20: 22520(R) (NAA-SR-11805)

BISMUTH IODIDES
electric conductivity and phase studies of, 20: 22520(R) (NAA-SR-11805)
friction on copper surfaces in ultrahigh vacuum, 20: 21366

BISMUTH ISOTOPES Bi-199
alpha spectra, (E), · 20: 22000 (JINR-P-2553)

BISMUTH ISOTOPES Bi-201
alpha spectra, (E), · 20: 22000 (JINR-P-2553)

BISMUTH ISOTOPES Bi-209
deuteron inelastic scattering by, collective levels from, (E), · 20: 22108
proton capture cross sections and transmission coefficients for, optical model calculation of, · 20: 22049

BISMUTH ISOTOPES Bi-210
determination in environmental samples by deposition on nickel and counting, 20: 20643

BISMUTH ISOTOPES Bi-214
occurrence in phosphate rocks, 20: 20886

BISMUTH SYSTEMS
Bi–$BiBr_3$, diffusion in liquid, thermal, 20: 22520(R) (NAA-SR-11805)

BLADDER
radiation effects on experimental calculus formation in rat, x, 20: 20467

BLOOD
radiation effects on sulfhydryl content, γ and x, 20: 20415
radiation effects on alkaline phosphatase activity in, γ and x, 20: 20415
radiation effects on immune properties of circulating, in calves, extracorporeal γ, 20: 20485

BLOOD COAGULATION
radiation effects on, in dogs and rats, γ and x, 20: 20490
radiation effects on, in dogs, 20: 20491

BLOOD FORMATION
radiation effects on mouse and rabbit, x, 20: 20510

BLOOD PICTURE
radiation effects on human, gamma and neutron, 20: 20481

BLOOD PLASMA
calcium-47 binding with, in patients with bone metastases, 20: 20404
radiation effects on chemical composition of, in burros and sheep, neutron, 20: 20489
strontium-85 binding with, in patients with bone metastases, 20: 20404

BLOOD PRESSURE
radiation effects on, in monkeys, γ, 20: 20488

BLOOD SERUM
analysis for iodine, methods for, 20: 20401
insulin binding by proteins of, tracer study, 20: 20383 (CNEA-185)
lipid and lipoprotein content of, relation to atherosclerosis and ischemic heart disease, 20: 20370 (UCRL-14658)

BLOOD VESSELS
radiation effects of dog arterial, auto- and homovenous repair of x, 20: 20478
radioinduced coronary fibrosis in human, following radiotherapy of Hodgkin's disease, 20: 20468

BODY FLUIDS
radiation effects on chemical composition of, in burros and sheep, neutron, 20: 20489
BOILING
detector for film, in liquid-cooled reactors, 20: 22367(P)
nucleate, in terphenyl OM2 in forced convection, (E/T), 20: 20709 (EUR-2442.f)
BOILING REACTORS
design of light water-cooled, heavy water-moderated, for power production, 20: 22431
design of light-water cooled, heavy-water moderated, pressure-tube, 20: 22430
design with coolant vapor separation system, 20: 22403(P)
design with steam superheating, 20: 22449
economics of double- and single-cycle, comparison of, 20: 22409 (EUR-2735.d)
heat transfer in 200-Mw, (T), 20: 22449
kinetics of double- and single-cycle, comparison of, 20: 22409 (EUR-2735.d)
neutron flux monitoring during startup, in-pile system for, 20: 22438
BONE MARROW
effects on nitrogen distribution in x-irradiated mice, 20: 20407 (ORNL-P-1118)
radiation effects on triglyceride synthesis in separated cells of rat, γ, 20: 20420
radiation effects on immune reactions to injected, in mice, x, 20: 20472
radiation effects on proliferation activity of mouse, effects of bleeding on x, 20: 20452
BONE TUMORS
radioinduced in children, 20: 20460
BONES
etiology of acute hematogenic osteomyelitis in, 20: 20371
radiation effects from radium dial paint on human, epidemiology of New Jersey cases of, 20: 20387(R) (NYO-2181-3)
radiation effects on growth of rat, x, 20: 20486
radioactivity of Canadian, collected in 1964, 20: 20938 (NP-15921)
radioactivity of Canadian, collected in 1965, 20: 20883 (NP-15914)
radiosterilization of grafts of human, method for gamma, 20: 20482
strontium discrimination in, compartmental analysis, 20: 20400
BORIDES
properties for containment of molten uranium alloys, 20: 20802(R) (ANL-7055, pp 21-98)
BORON
book: *Boron.* Vol. 2. *Preparation, Properties, and Applications,* 20: 21251
crystallization and purification of amorphous powdered boron-10-enriched, methods for, 20: 21294 (TID-22221)
ion reactions at 15 to 140 kev, stopping cross sections for $Z \leq 11$, (E/T), 20: 21539
ion reactions with, straggling effects in energy loss from helium and hydrogen, (E/T), 20: 21539
neutron elastic scattering at 14.0 Mev, cross sections for, (E), 20: 22119
reactions with fluorine, thermodynamics of, 20: 20650(R) (ANL-7055, pp 167-76)
x-ray scattering cross sections at 1 to 150 kev, (T), 20: 21516 (UCRL-14403)
BORON CARBIDES
fabrication for use in EGCR control rods, 20: 21292 (ORNL-3932)
reactions with lithium, 20: 21327 (CONF-560505-1)
BORON ISOTOPES B-10
charged-particle reactions with, amplitude singularities in knockon and stripping, (T), 20: 21997 (INSJ-96)
electron elastic scattering to 230 Mev, magnetic form factors from, (E), 20: 22120
energy levels of, use of Hamada-Johnston potential for, (T), 20: 22102
neutron reactions (n,*α*) with, branching ratio for thermal, (E), 20: 22071
BORON ISOTOPES B-11
charged-particle reactions with, amplitude singularities in knockon and stripping, (T), 20: 21997 (INSJ-96)
electron elastic scattering to 230 Mev, magnetic form factors from, (E), 20: 22120
energy levels of, use of Hamada-Johnston potential for, (T), 20: 22102
BORON ISOTOPES B-12
energy levels in, transitions and excitation energies of bound, 20: 22111
BORON STEEL
B–Mo, radiation effects on pressure vessels of, fast-neutron, 20: 21228 (AE-221)
BORON SYSTEMS
B–Co–Hf, crystal structure, 20: 20685
B–Co–Ti, crystal structure, 20: 20685
B–Co–U, crystal structure, 20: 20685
B–Co–V, crystal structure, 20: 20685
B–Co–Zr, crystal structure, 20: 20685
B–Hf–Ni, crystal structure, 20: 20685
B–Li, phase studies, 20: 21327 (CONF-560505-1)
B–Ni–Ti, crystal structure, 20: 20685
B–Ni–U, crystal structure, 20: 20685
B–Ni–V, crystal structure, 20: 20685
B–Ni–Zr, crystal structure, 20: 20685
B–polyethylene, performance for separating fissile materials, 20: 20840(R) (BNWL-193, pp 57-67)
B–Th, fabrication and corrosion testing of radiation targets of, 20: 21288 (BMI-1761)
B–U–Zr, neutron multiplication factor of, (E), 20: 22392
BOROSILICATE GLASS
elastic properties of, effects of dispersed phases on, 20: 21358 (UCRL-16552)
BOSONS
decay into three spin-zero particles, spin test for, (T), 20: 21620 (JINR-P-2577)
exchange model parameters for, using elastic nucleon-nucleon phase shifts, (T), 20: 21621 (JINR-P-2584)
interactions with fermions, Lee model for, 20: 21718
mass levels of, systematics and phenomenology of, 20: 21690
mass of intermediate, lower limit for, (E/T), 20: 21596 (CERN-65-32, pp 11-24)
mass of intermediate, lower limit for, 20: 21597 (CERN-65-32, pp 25-30)
photoproduction of intermediate W, on protons, 20: 21611 (CERN-65-32, pp 195-200)
production in spin-zero particle interactions, spin test for, (T), 20: 21620 (JINR-P-2577)
production of intermediate, in proton-proton interactions, 20: 21610 (CERN-65-32, pp 181-94)
production of intermediate, in high energy neutrino interactions, (E), 20: 21595 (CERN-65-32, pp 1-10)
weight norms for human, use in establishing standards for radiation dosimetry, 20: 20374
BRAIN
radiation effects on oxygen uptake by tissues of rat, x, 20: 20436 (CONF-650560-17)
radiation effects on tryptamine content of tissues of rat, x, 20: 20437 (CONF-650560-18)
radiosensitivity of mouse, effects of AET and potassium cyanide, 20: 20521
BRAIN TUMORS
localization using proportional probe and phosphorus-32, 20: 20523(R) (NYO-1726-15)
radiodiagnosis using iodine-131 and external scanning, 20: 20529
radiodiagnosis using iodine-131 and external scanning, 20: 20535
radiotherapy after surgical procedures for, γ and x, 20: 20530
radiotherapy of, using gold-198 and phosphorus-32-labeled chromium phosphate, 20: 20539
BRASS
analysis for copper and zinc by x-ray fluorescence methods, 20: 20642
Cu–Ni, effects of decontaminating and descaling solution on metal loss on, 20: 21238 (NP-15928)
BREASTS
radioinduced tumors in mouse, incidence of x, 20: 20441 (ORNL-P-1173)
BREEDER REACTORS
design of, with elongated fuel assemblies in cylindrical core, 20: 22465
fuel analysis of sodium-cooled, thorium, 20: 21229 (AEET-229)
neutron group cross sections in fast, effect of randomness on, 20: 22391
BREMSSTRAHLUNG
emission by partially ionized plasma, 20: 22208
emission from plasma electron reactions with solid target, diagnostics from, (E), 20: 22293
interactions with nucleons at 475 to 750 Mev, meson (π^+) production from polarized, (E), 20: 21660
interactions with protons at 475 to 750 Mev, asymmetry of meson (π^+) production in, (E/T), 20: 21589 (AD-626683)
production in paraffin by radiophosphorus, diagnostic use in mammary cancer, 20: 20540
reactions (γ,n) with aluminum, carbon, and sulfur at threshold to 200 Mev, cross sections for, (E), 20: 22094
reactions (γ,n) with helium-3 at threshold to 30 Mev, cross sections for, (E), 20: 22117
reactions with carbon at 1 to 5 Bev, cross sections for electron pair production in, (E/T), 20: 22146
reactions with carbon at 5 Bev, electron pair production in, (E), 20: 21664
reactions with uranium at 650 Mev, yields from fission, 20: 22040
BRITISH REACTORS
design of plutonium-fueled prototype fast reactor, 20: 22441
BROMIDES
bromine-82 exchange with iridium and rhodium pentammine bromo

complexes, 20: 20706
BROMINE
determination in potassium halogenides, activation, 20: 20560 (EUR-2753.f)
effects on sintering of tungsten, 20: 21291 (NP-15944)
BROMINE FLUORIDES
reactions with uranium fluorides, research on selectivity of, 20: 20803(R) (ANL-7055, pp 99-162)
waste disposal methods for, 20: 20803(R) (ANL-7055, pp 99-162)
BROMINE ISOTOPES Br-82
beta decay, (E), 20: 22010(R) (NYO-72-28)
exchange between rhodium or iridium complexes and bromide ions in solutions and crystals, 20: 20706
BROMINE ISOTOPES Br-83
yields from photofission of uranium by 650-Mev bremsstrahlung, 20: 22040
BROMINE ISOTOPES Br-85
decay of 3.0-min, gamma rays from, 20: 22041
BROMINE ISOTOPES Br-86
decay scheme, (E), 20: 22130
BROMINE ISOTOPES Br-87
decay scheme, (E), 20: 22130
BRONZE
Cu–Ni, effects of decontaminating and descaling solution on metal loss on, 20: 21238 (NP-15928)
BROOKHAVEN ALTERNATING-GRADIENT SYNCHROTRON
beam intensity of, program for increasing, 20: 21466 (CERN-65-32, pp 127-30)
BROOKHAVEN BEAM RESEARCH REACTOR
experimental facilities for neutron spectroscopy, data analysis and control system for, 20: 21982 (BNL-948, pp 718-40)
BROOKHAVEN NATIONAL LAB., UPTON, N. Y.
health physics program for decontamination facility at, 20: 20929 (CEX-61.6.2)
BROOKHAVEN SYNCHROTRON
beam intensity of, program for increasing, 20: 21466 (CERN-65-32, pp 127-30)
BUBBLE CHAMBERS
data analysis from CERN neutrino experiments, 20: 21597 (CERN-65-32, pp 25-30)
design for high-energy radiographic apparatus, 20: 21144(P)
design of large propane, 20: 21033 (CERN-65-32, pp 263-8)
design of 12 ft hydrogen, at A.N.L., 20: 21032 (CERN-65-32, pp 259-62)
neutrino experiments in 80 in. and 14 ft., at BNL, 20: 21608 (CERN-65-32, pp 169-74)
particle track analysis in, research on pattern recognition for, 20: 21041 (PPAD-585E)
use in determining lower limit for intermediate boson, mass, 20: 21596 (CERN-65-32, pp 11-24)
BUILDING MATERIALS
development of, for space nuclear power plant testing vault, 20: 20869
weight measurements on, by gamma absorption, 20: 21205
BURROS
radiation effects on blood–brain barrier permeability in, neutron, 20: 20489
BUTADIENE
radioinduced polymerization with isocyanic acid at low temperatures, 20: 20747
BUTADIENE POLYMERS
radiation effects on molecular motion and structure of isotactic, gamma and neutron, 20: 20753
with styrene, radiation effects on mechanical properties of, gamma, 20: 20754
BUTANE
decomposition of, by gas discharge and radiation, comparison of, 20: 20740
BUTANE, 2-METHYL-
carbon tetrachloride–cyclopropane–2-methylbutane, radiolysis of, at 77 to 193°K, tracer studies of mechanisms in, 20: 20752
carbon tetrachloride–ethylene–2-methylbutane, radiolysis of, tracer studies of mechanisms in, 20: 20752
BUTYL PHOSPHATES
effects on analytical procedures involving uranyl ions, 20: 20630
effects on polarographic determination of hexavalent uranium in nitric acid media, 20: 20631
solvent properties for rare earths in nitric acid solutions containing calcium phosphate, 20: 20824
solvent properties for neptunium, 20: 20561 (JAERI-1099)
1-BUTYNE
radiolysis of gaseous and liquid, mechanism and yields in, 20: 20717(R) (AD-621719)
2-BUTYNE
radiolysis of liquid, mechanism and yields in, 20: 20717(R) (AD-621719)
BUTYRALDEHYDE
radioinduced polymerization of, 20: 20788(P)
vinyl polymers of, radiation effects on, gamma, 20: 20775
BUTYRIC ACID, 2-AMINO-
yields in radioinduced carboxylation of methylamine, 20: 20732 (SGAE-CH-21/1965)
BUTYRIC ACID, 4-AMINO-
yields in radioinduced carboxylation of methylamine, 20: 20732 (SGAE-CH-21/1965)

C

CADARACHE REACTORS (RAPSODIE)
design and performance testing of, model for, 20: 22501(T) (EURFNR-49F)
CADMIUM
alpha scattering at 28.4 Mev, angular distributions from, (E), 20: 22047
determination in silicon dioxide, activation, 20: 20634
electron reactions at 6 to 23 kev, optical transition radiation from, 20: 21518
heat of fusion, 20: 20553(R) (MLM-1142)
performance for separating fissile materials, 20: 20840(R) (BNWL-193, pp 57-67)
radiation effects on battery electrodes of, gamma, 20: 21425(R) (N-65-24491)
separation from bismuth–lead eutectic by vacuum distillation, chamber design for, 20: 20805 (IS-1329)
separation from gallium, indium, and transition elements by ion exchange chromatography, 20: 20634
separation from perchloric acid solutions by ion exchange materials, 20: 20823
separation from scandium by ion exchange chromatography, 20: 20821
separation from thorium by ion exchange in nitric acid solution, 20: 20624
separation from uranium by combined ion exchange-solvent extraction using nitric acid–tetrahydrofuran solutions, 20: 20811
viscosity of liquid, based on atomic parameters, 20: 20656 (UCRL-11930)
CADMIUM ALLOYS
Cd–In–Ag, fabrication of reactor control rods of, 20: 21317(P)
Cd–Mg–U–Zn, corrosive effects in fused chloride mixtures, on stainless steel, 20: 20802(R) (ANL-7055, pp 21-98)
Cd–rare earths, thermodynamic properties of intermetallic compounds in, 20: 20802(R) (ANL-7055, pp 21-98)
CADMIUM COMPLEXES
with thiodibenzoylmethane, stability of, 20: 20693
CADMIUM IODIDES
friction on copper surfaces in ultrahigh vacuum, 20: 21366
CADMIUM ISOTOPES
mass differences of, (E), 20: 22153
CADMIUM ISOTOPES Cd-110
proton reactions (p,n), (p,2n) and (p,pn) at 5 to 37 Mev, excitation functions for, (E), 20: 22078
CADMIUM ISOTOPES Cd-111
energy levels from silver-111 decay, (E), 20: 22083
energy levels of, g-factors for, (E), 20: 22010(R) (NYO-72-28)
proton reactions (p,n) and (p,2n) at 5 to 37 Mev, excitation functions for, (E), 20: 22078
CADMIUM ISOTOPES Cd-112
proton reactions (p,n) and (p,3n) at 5 to 37 Mev, excitation functions for, (E), 20: 22078
CADMIUM ISOTOPES Cd-113
neutron reactions (n,γ) with, internal conversion spectra from thermal, (E), 20: 22066
CADMIUM ISOTOPES Cd-114
energy levels from thermal neutron reactions (n,γ) with cadmium-113, (E), 20: 22066
CADMIUM ISOTOPES Cd-115
yields from neutron resonance fission of plutonium-238 at 15 to 82 ev, (E), 20: 22135
CADMIUM OXIDES
reactions with gaseous uranium trioxide, effects of substrate symmetry in, 20: 20649 (AEET-CD-24)
CALCITES
carbon-13 exchange between, and carbon dioxide, 20: 20691
oxygen-18 exchange between, and carbon dioxide, 20: 20691
CALCIUM
determination in high-purity tantalum by spectrography using d-c arc method, 20: 20608
determination in irradiated silica, activation, 20: 20636
effects on calcium-45 uptake by fish, 20: 20405
metabolism in bones, compartmental analysis, 20: 20400
neutron elastic scattering at 14.0 Mev, cross sections for, (E), 20: 22119
radiation effects on plasma content of, in rats affected with experimental

bladder calculus, x, 20: 20467
separation from irradiated silica and sodium by chromatography, 20: 20636
separation from perchloric acid solutions by ion exchange materials, 20: 20823
separation from scandium by ion exchange chromatography, 20: 20821
separation from strontium in milk, 20: 20938 (NP-15921)
separation from strontium by exchange in amalgam–solution system, 20: 20829
separation from thorium by ion exchange in nitric acid solution, 20: 20624
separation from uranium by combined ion exchange-solvent extraction using nitric acid–tetrahydrofuran solutions, 20: 20811
viscosity of liquid, based on atomic parameters, · 20: 20656 (UCRL-11930)

CALCIUM ALLOYS
Ca–Zn, intermetallic compound with $CeCu_2$-type structure in, 20: 21352 (TID-21745)
Ca–Zn, thermodynamic properties, 20: 21335 (IS-T-76)

CALCIUM FLUORIDES
deuterium and hydrogen spectra in, absorption, 20: 22311(R) (AD-622068)
diffusion of argon, krypton, and xenon in uranium-doped single-crystal, at 900 to 1200°C, 20: 21332(R) (EURAEC-1573)
thulium-169 ground state ENDOR spectra in, 20: 22311(R) (AD-622068)
use of europium-activated single crystals of, in detection of charged particles, gamma radiation and x radiation, 20: 21135

CALCIUM ISOTOPES Ca-40
electron inelastic scattering by, two-nucleon correlation functions from cross sections for, (T), · 20: 21996 (FTI-142/T-016)
energy levels of, double gamma emission from, (E/T), 20: 22010(R) (NYO-72-28)
helium-3 reactions (He-3,p) and (He-3,pγ) at 10, 12, and 15 Mev, · scandium-42 levels from, (E), 20: 22073

CALCIUM ISOTOPES Ca-42
energy levels of, shell model calculations of, · 20: 22096

CALCIUM ISOTOPES Ca-43
energy levels from proton reactions (p,d) with calcium-44 at 17.5 Mev, neutron-hole, (E), · 20: 22129
energy levels of, shell model calculations of, 20: 22096

CALCIUM ISOTOPES Ca-44
energy levels of, shell model calculations of, · 20: 22096
proton reactions (p,d) at 17.5 Mev, calcium-43 neutron-hole states from, (E), · 20: 22129

CALCIUM ISOTOPES Ca-45
determination simultaneously with phosphorus-32 in inorganic salts by liquid scintillation counting, 20: 20584
energy levels of, shell model calculations of, · 20: 22096
metabolism in crucian carp, effects of stable calcium on, 20: 20405

CALCIUM ISOTOPES Ca-46
energy levels of, shell model calculations of, · 20: 22096

CALCIUM ISOTOPES Ca-47
binding with plasma proteins in patients with bone metastases, 20: 20404
energy levels from proton reactions (p,d) with calcium-48 at 17.5 Mev, · neutron-hole, (E), 20: 22129
energy levels of, shell model calculations of, · 20: 22096
metabolism in bones, compartmental analysis, 20: 20400

CALCIUM ISOTOPES Ca-48
beta decay of, instrumentation for detecting double, 20: 22010(R) (NYO-72-28)
beta decay of, lepton nonconservation in double, (E/T), · 20: 21995 (CERN-65-32, pp 35-40)
proton reactions (p,d) at 17.5 Mev, calcium-47 neutron-hole states from, (E), · 20: 22129

CALCIUM OXIDES
growth and properties of crystals of, 20: 22311(R) (AD-622068)
reactions with gaseous uranium trioxide, effects of substrate symmetry in, 20: 20649 (AEET-CD-24)
CaO–UO_2–ZrO_2, preparation and properties of, for ceramic nuclear fuels, 20: 21302

CALCIUM PHOSPHATES
analysis for calcium-45 and phosphorus-32 by liquid scintillation counting, 20: 20584
effects on solvent extraction of rare earths from nitric acid solutions using TBP, 20: 20824
solubility in descaling solution for alloys and metals, 20: 21238 (NP-15928)

CALCIUM SULFATES
radiation effects on electron postemission from, 20: 20769
uses for radiation dosimetry, 20: 20769

CALDER HALL REACTORS
design and performance, 20: 22450
performance, 20: 22444

CALIFORNIUM
production of, review of methods for, 20: 20796
separation from nitrate solutions by solvent extraction using tricaprylmethylammonium nitrate, 20: 20812

CALIFORNIUM ISOTOPES Cf-252
fission of, alpha emission in spontaneous, (E), · 20: 22144

CALORIMETERS
design and performance of isothermal micro-, for radioactivity measurements, 20: 21068
design and performance of portable micro-, 20: 21024 (AD-630693)
design for high temperatures, · 20: 20650(R) (ANL-7055, pp 167-76)
design of micro-, for in-pile dosimetry, 20: 20721 (EUR-2295.f)
development, · 20: 20553(R) (MLM-1142)
development of, for dosimetry of mixed radiations, 20: 20722 (EUR-2401.f)

CAMS
use in drive system for Mössbauer spectrometers, 20: 21080

CANADA
fallout monitoring, 1965, 20: 20883 (NP-15914)
fallout monitoring, 1964, 20: 20938 (NP-15921)

CANADIAN REACTORS
environs monitoring, 1965, 20: 20938 (NP-15921)
environs monitoring, 1965, 20: 20883 (NP-15914)

CAPTURE-TO-FISSION RATIOS
measurement of plutonium and uranium, plans for EBR-II use in, 20: 21969(R) (ANL-7055, pp 230-3)

CARBAMIC ACID, ETHYL ESTER
radiosensitivity effects on skin of mice, x, 20: 20476

CARBAZOLE, VINYL- POLYMERS
radioinduced formation of, effects of monomer crystal size on, 20: 20743

CARBIDES
effects of dispersed, on properties of tantalum-base alloys, 20: 21404
properties at high temperatures, chemical, · 20: 20654 (LA-DC-7784)
properties for containment of molten uranium alloys, · 20: 20802(R) (ANL-7055, pp 21-98)

CARBON
bremsstrahlung reactions (γ,n) at threshold to 200 Mev, cross sections for, (E), 20: 22094
bremsstrahlung reactions at 1 to 5 Bev, cross section for electron pair production in, (E/T), · 20: 22146
bremsstrahlung reactions at 5 Bev, electron pair production in, (E), 20: 21664
corrosion by liquid magnesium–uranium–zinc alloys with fused chlorides, 20: 20802(R) (ANL-7055, pp 21-98)
densification of, process for, 20: 21315(P)
determination by activation using helium-3 ions, · 20: 20565 (ORNL-P-1216)
determination in beryllium by modified combustion-conductometric method, 20: 20556 (AD-626987)
determination in coal by gamma transmission method, 20: 21209
determination in cesium by photon activation methods, 20: 20645
diffusion in yttrium at 1235 to 1460°C, coefficient for, 20: 21254
effects on efficiency of porous tungsten ionizers, 20: 21570 (N-65-29785)
effects on phase equilibria in hafnium or zirconium alloys with niobium and tungsten, 20: 21329(R) (DRI-1092-229)
effects on tensile properties of vanadium-base alloys, 20: 21333(R) (IITRI-B6042-4)
helium-3 reactions (He-3,n) at 19 to 25 Mev, angular distributions and cross sections for, (E), · 20: 22132
ion reactions with, straggling effects in energy loss from helium and hydrogen, (E/T), 20: 21539
neutron cross sections and shielding coefficients for, 20: 22383(T) (AEC-tr-6693)
neutron elastic scattering at 14.0 Mev, cross sections for, (E), · 20: 22119
photoelectric effect at 852 ev to 40 kev in, cross sections for, (E), 20: 21523
preparation of purified elemental, from carbon dioxide, · 20: 20806(R) (MLM-1274)
properties of glassy, at room temperature to 2900°C, structural and tensile, 20: 21338 (JPL-TR-32-842)
radiation effects on dimensional stability of, at 900 to 1800°C, fast-neutron, 20: 21419 (BNWL-191)
radiation effects on fuel particle coatings of pyrolytic, 20: 22411(R) (GA-6113)
reactions with sodium, effects on metal corrosion, · 20: 20802(R) (ANL-7055, pp 21-98)
reactions with uranium dioxide to prepare uranium carbide, 20: 21307
x-ray scattering cross sections at 1 to 150 kev, (T), 20: 21516 (UCRL-14403)

CARBON (ACTIVATED)
performance for iodine sorption at Savannah Production Reactors, 20: 22463(R) (DP-1028)
sorptive properties for iodine and methyl iodide, 20: 20940(R) (ORNL-3915)

CARBON BLACK
radiation effects in graphitized, EPR determination of anneal effects from neutron, 20: 21435
CARBON DIOXIDES
carbon-13 exchange between, and calcites or dolomites, 20: 20691
dissociation into carbon monoxide and oxygen on metallic films, 20: 21389
heat of adsorption by metallic films at room temperature, calorimetric measurements of, 20: 21389
heat transfer in ionized, electric field effects on, 20: 20859 (UJV-1421/65)
oxygen-18 exchange between, and calcites or dolomites, 20: 20691
performance as coolant for 1000-Mw(e) fast breeder reactor, 20: 22452
reactions with graphite above 600°C, tracer studies of, 20: 20702
reactions with tantalum and zirconium at 590 to 730°C at low pressures, 20: 21279
reactions with uranium at 650°C, carbon pickup and oxide cracking during, 20: 21272
use in gas Cherenkov counter, 20: 21071
yields from gamma radiolysis of DL-mandelic acid in oxygenated solutions, 20: 20759
CO_2–CO, reactions with nickel and stainless steel, 20: 21383
CARBON ISOTOPES C-11
energy levels from proton reactions on carbon-13, (E), 20: 22030
CARBON ISOTOPES C-12
charged-particle reactions with, amplitude singularities in knockon and stripping, (T), 20: 21997 (INSJ-96)
concentration in deuterated methane by thermal diffusion, 20: 20807(R) (MLM-1287)
deuteron elastic scattering at 2.0 to 3.2 Mev, cross sections for, (E), 20: 22087
deuteron reactions (d,pγ) at 2 to 3.2 Mev, angular correlations from, (E), 20: 22087
electron inelastic scattering by, excitation of spin-isospin giant resonance by, (T), 20: 22088
energy levels of, use of Hamada-Johnston potential for, (T), 20: 22102
neutron elastic scattering by, resonance parameters for, (T), 20: 22010(R) (NYO-72-28)
proton elastic scattering at 45 Mev, differential cross sections for, (T), 20: 21963 (AD-626656)
proton inelastic scattering by, 3α decay of excited nucleus from, 20: 22033
proton scattering at 1.48 to 2.02 Mev, cross sections and resonances from, (E), 20: 22115
CARBON ISOTOPES C-13
concentration in deuterated methane by thermal diffusion, 20: 20807(R) (MLM-1287)
concentration in methane by thermal diffusion, 20: 20806(R) (MLM-1274)
energy levels from carbon-12 (d,pγ) reactions, (E), 20: 22087
exchange between carbon dioxide and calcite or dolomite, 20: 20691
proton elastic scattering at 1.0 to 2.6 Mev, nitrogen-14 levels from, (E), 20: 22123
proton reactions (p,d) and (p,t) at 54.9 Mev, differential cross sections and product momentum and angular distributions for, (E), 20: 22030
separation from other isotopes by thermal diffusion in carbon monoxide and methane, 20: 20553(R) (MLM-1142)
separation from other isotopes by carbamate–carbon dioxide exchange, 20: 20806(R) (MLM-1274)
CARBON ISOTOPES C-14
alpha reactions (α,n) at 2.5 to 5.1 Mev, neutron yields from, (E), 20: 22110
content in volcanic ash in New Zealand, 20: 20893
determination in biological materials, combustion procedure for sample preparation for liquid scintillation counting for, 20: 20570
determination with tritium in biological materials, autoradiographic method for, 20: 20605
incorporation in organic mixtures, separation using gas chromatography, 20: 20639
use as tracer for measuring algal nutrients in seawater, 20: 20368 (CONF-640309-1)
use in age estimation, data list from, 20: 20905
CARBON MONOXIDES
carbon-13 enrichment in, by thermal diffusion, 20: 20553(R) (MLM-1142)
desorption from iridium, rhodium, and tungsten, flash, 20: 20652 (IS-T-67)
heat of adsorption by metallic films at 0°C, calorimetric measurements of, 20: 21388
radioinduced reactions with hydrocarbons, gamma, 20: 20770(T)
reactions with niobium at 1300 to 1700°C, 20: 21270
CO_2–CO, reactions with nickel and stainless steel, 20: 21383
CARBON STEEL
cesium deposition on, 20: 22411(R) (GA-6113)
fission product deposition on, from air–steam mixtures, 20: 20940(R) (ORNL-3915)
radiation effects on pressure vessels of, fast-neutron, 20: 21228 (AE-221)
CARBON SYSTEMS
C–Co–Ti–W, development and tensile properties of cobalt-base, 20: 21237 (N-65-29395)
C–Co–Ti–W–Zr, development and tensile properties of cobalt-base, 20: 21237 (N-65-29395)
C–Cr–Co–Re–Ti–W–Zr, development and tensile and stress-rupture properties of cobalt-base, 20: 21237 (N-65-29395)
C–Cr–Co–Ti–W–Zr, development and tensile and stress-rupture properties of cobalt-base, 20: 21237 (N-65-29395)
C–Hf–Mo–N–Re–Ta–W–Zr, development of dispersion-strengthened tantalum-base, 20: 21240(R) (WANL-PR-(Q)-006)
C–Hf–Nb–W, properties at very high temperatures, 20: 21412
C–Hf–Re–Ta–W, development of dispersion-strengthened tantalum-base T-333, 20: 21240(R) (WANL-PR-(Q)-006)
C–Hf–Ta–W, bonding of T-222, to Inconel 600 and stainless steels, process development for explosive, 20: 21295(R) (WANL-PR-(EE)-002)
C–Li, phase studies, 20: 21327 (CONF-560505-1)
C–Mn–Zn, magnetic properties of Mn_3ZnC in, 20: 22312(R) (AD-622796)
C–Mo–Nb–Ta–W–Zr, extrusion parameters for Cb-132M, 20: 21263(R) (NASA-CR-54911)
C–Mo–Nb–Ta–Zr, thermal-mechanical processing of a precipitation-hardenable, dispersion-hardened, 20: 21250
C–Mo–Nb–Ti–Zr, bend and tensile ductility properties of, 20: 21410
C–Mo–Ti–Zr, extrusion parameters for TZC, 20: 21263 (NASA-CR-54911)
C–Nb–W–Zr, properties at very high temperatures, 20: 21412
C–Nb–W–Zr, specifications of D-43, for use in corrosion test loop fabrication, 20: 21293 (R-66SD3007)
CARBON TETRACHLORIDE
effects on yields from radiolysis of methanol vapor, 20: 20776
reactions with cyclohexane, production of labeled polymers in, 20: 20784
carbon tetrachloride–cyclopropane–pentane, radiolysis of, at 77 to 193°K, tracer studies of mechanisms in, 20: 20752
carbon tetrachloride–cyclopropane–2-methylbutane, radiolysis of, at 77 to 193°K, tracer studies of mechanisms in, 20: 20752
carbon tetrachloride–cyclopropane–hexane, radiolysis of, at 77 to 193°K, tracer studies of mechanisms in, 20: 20752
carbon tetrachloride–ethylene–2-methylbutane, radiolysis of, tracer studies of mechanisms in, 20: 20752
carbon tetrachloride–pentane–propene, radiolysis of, tracer studies of mechanisms in, 20: 20752
CCl_4–P, radiolysis of, mechanisms in gamma, 20: 20736
CARBONATES
age estimation of, from isotopic abundance of thorium and uranium, 20: 20887
CARBONYLS
radioinduced formation of, from hydrocarbons and carbon monoxide, 20: 20770(T)
radioinduced in fish fillets, determination and separation, 20: 21200
CARCINOGENESIS
radioinduced in animals, review, 20: 20442 (ORNL-P-2053)
CARCINOGENS
effects on mouse mammary glands, comparison of x-radiation effects and, 20: 20502
CARCINOMAS
radiation effects on cervical, combined with surgery, γ, 20: 20536
radiotherapy of cervical, effectiveness of combined surgery and x-ray, 20: 20526
CARDIOGRAPHY
radiation effects on human, x, 20: 20474
CASCADE SHOWERS
calculation of electron- and photon-induced, in xenon, (T), 20: 21514 (INR-598/VI/PH)
electron and photon mean-square angular and lateral spreads in photon-initiated, (T), 20: 21557
CATALASES
radiolysis of, reactions of hydroxyl ions in pulse, 20: 20735
CATARACTS
induced by iodoacetate in rabbits, 20: 20507(T)
radioinduced in mice, x, 20: 20441 (ORNL-P-1173)
CATHODE-RAY TUBES
use with CDC 3600 for data plotting, 20: 21221 (ANL-7121)
CATHODES
design and performance of inverse brush, for negative-glow plasma source, 20: 22222
electric discharge effects on, in parallel-electrode plasma gun, 20: 22292
CATION EXCHANGE MATERIALS
performance of KU-2, for separation of rare earths and uranium, 20: 20813
CATS

radiation effects on electrical activity of olfactory neurons in, x, 20: 20431 (AD-630323)
CATTLE
radiation effects on potassium and sodium content of thymus cell nuclei, x, 20: 20422
CAVES
atmosphere control in argon-filled, · 20: 20802(R) (ANL-7055, pp 21-98)
design for bench-scale testing of fluid-bed fluoride volatility unit, · 20: 20803(R) (ANL-7055, pp 99-162)
development of hot chamber, for iodine-131 production, 20: 21215
CAVITY RESONATORS
electric field measurements in superconducting, 20: 21459 (AD-623509)
CENTRIFUGES
rotor control for, radio telemetry system for, 20: 21009
CERAMIC BONDING
process for, using cerium oxide–cerium sulfide, 20: 21314(P)
CERAMIC MATERIALS
mechanical properties of continuous-matrix, dispersed-phase, 20: 21358 (UCRL-16552)
mechanical properties of, use of computer for storage, interpretation, and recovery of data on, 20: 21354 (TRG-Report-1160)
nucleation and crystal growth in melts of, bibliography on, 20: 21235 (IS-1287)
radiation effects on current induction in capacitor of, electron beam, fast neutron, and gamma, 20: 21151 (IBM-66-825-1944)
radiation effects on dielectric properties of, 20: 21171
CERIUM
deposition on metals, conditions for electrolytic, 20: 21287 (AE-217)
determination in rare earth mixtures, activation, 20: 20562 (LYCEN-6538)
friction and wear properties of, in vacuum, effects of crystal structure on, 20: 21365
oxidation in dry and moist air at 100 to 800°C, rate of, 20: 21265 (RPI-2714-8)
reactions with powdered graphite, preparation of intercalation compounds by, 20: 20648 (AD-621029)
separation from lanthanum by partition chromatography on polytetrafluoroethylene, 20: 20623
separation from other rare earths by paper precipitation chromatography using 8 quinolinol. 20: 20814
separation from perchloric acid solutions by ion exchange materials, 20: 20823
separation from praseodymium by fused salt extraction, · 20: 20802(R) (ANL-7055, pp 21-98)
separation from rare earths by reversed-phase partition chromatography on polytetrafluoroethylene, 20: 20621
separation from thorium by ion exchange in nitric acid solution, 20: 20624
separatica from uranium by combined ion exchange-solvent extraction using nitric acid–tetrahydrofuran solutions, 20: 20811
sorption and diffusion by graphite, 20: 22411(R) (GA-6113)
CERIUM ACETATES
preparation by oxide solubility in alcohols containing ammonia, 20: 20686
CERIUM ALLOYS
Al–Ce, crystal structure and stability of intermetallic compounds in, 20: 21415
Ce–Co, reactions of molten, with tantalum, 20: 20671
Ce–Cu, intermetallic compound with $CeCu_2$-type structure in, 20: 21352 (TID-21745)
Ce–Cu–Pu, phase diagrams, · 20: 20553(R) (MLM-1142)
Ce–Dy, electric conductivity at 4.2, 77, and 296°K, 20: 22312(R) (AD-22312(R) (AD-622796)
Ce–Fe, crystal structure of $CeFe_7$, 20: 21400
Ce–Fe–Pu, phase studies, 20: 21342 (MLM-1301)
Ce–Gd, crystal structure and magnetic properties, 20: 22343
Ce–La, electric conductivity, magnetic susceptibility, and superconductivity at low temperatures, 20: 21873 (NP-15936)
Ce–Ni–Pu, phase studies, 20: 21342(R) (MLM-1301)
Ce–Y, magnetic properties and phase transformations in, 20: 21414
CERIUM CARBIDES
thermionic emission from, 20: 21397
CERIUM FLUORIDES
dielectric properties of thin films of, 20: 22324
CERIUM IONS
effects on dephosphorylation of cocarboxylase, riboflavin-5-phosphate, and pyridoxal phosphate, 20: 20375
CERIUM ISOTOPES Ce-138
energy levels from praseodymium-138 decay, (E), · 20: 22002 (JINR-P-2570)
CERIUM ISOTOPES Ce-141
decay of, gamma branching ratios for, (E), 20: 22091
diffusion in irradiated fuel element cladding alloys and materials at 600 to 1200°C, 20: 21232 (BMI-1763)
CERIUM ISOTOPES Ce-144
determination of microquantities of, precipitated with zinc tetrathiocyanatomercurate(II), 20: 20619
separation from fission product solutions by oxalic acid precipitation, 20: 20804 (EUR-2754.f)
separation from fresh water by ion exchange chromatography, 20: 20627
CERIUM NITRATES
$Ce(NO_3)_3$–K_2CO_3–H_2O, composition of, effects of reactant concentration on, 20: 20664
$Ce(NO_3)_3$–$UO_2(NO_3)_2$–H_2O, compound formation in, 20: 20682
CERIUM NITRIDES
preparation by reactive arc melting, 20: 21244
CERIUM OXIDES
solubility in ethyl, isopropyl, methyl, and propyl alcohols in presence of ammonia, 20: 20686
thermal decomposition at 1100 to 1700°C, rates of, · 20: 20655 (ORNL-P-1260)
CeO_2–Ce_3S_4, bonding refractory materials with, 20: 21314(P)
CeO_2–Ce_2S_3, bonding refractory materials with, 20: 21314(P)
CERIUM OXYCHLORIDES
preparation and properties, 20: 20680
CERIUM SULFIDES
CeO_2–Ce_3S_4, bonding refractory materials with, 20: 21314(P)
CeO_2–Ce_2S_3, bonding refractory materials with, 20: 21314(P)
CERMETS
processing stainless steel–urania by fluorination, · 20: 20803(R) (ANL-7055, pp 99-162)
CESIUM
analysis for carbon, nitrogen, and oxygen by photon activation methods, 20: 20645
density and thermodynamic properties of, · 20: 20802(R) (ANL-7055, pp 21-98)
deposition on carbon and stainless steels, 20: 22411(R) (GA-6113)
determination in silicon dioxide, activation, 20: 20633
diffusion of potassium ions in fully ionized plasma of, (E), 20: 22243
effects on performance of tungsten-emitter thermionic converter, 20: 21586
electric discharge in, ampere-voltage characteristics for, (T), 20: 21578
electron distribution in thermionic cell plasma of, electrostatic probe measurements of, 20: 21560(R) (AD-621276)
electron mobility in vapors of, at low energies, (E), 20: 21520
excretion and metabolism of, use in dosimetry, 20: 20398
flow in tubes, electrophoretic properties of ionized, (T), 20: 22173 (AD-623788)
ionization on surfaces of refractory compounds, (E), 20: 21584
kinetics of plasma of, in hot-cathode diode, (T), 20: 22279
performance in thermionic cells, krypton effects on, 20: 21579
performance in thermionic cells, xenon effects on, 20: 21580
separation from fission-product waste solutions by ion exchange on ammonium molybdophosphate, 20: 20818
separation from nitrate solutions by solvent extraction using tricaprylmethylammonium nitrate, 20: 20812
sorption and diffusion by graphite, 20: 22411(R) (GA-6113)
thermal properties of vaporous, at high temperatures, · 20: 20651(R) (CU-2660-26)
thermodynamic properties to 1500°K, 20: 21345 (N-65-26656)
transport properties of plasma of, computation of, 20: 22227
uptake by man, 20: 20466
viscosity of liquid, based on atomic parameters, · 20: 20656 (UCRL-11930)
viscosity of vaporous, at atmospheric pressure, · 20: 20651(R) (CU-2660-26)
CESIUM CHLORIDES
spectra of, effects of tellurides on, (E), 20: 21566(R) (ANL-7055, pp 213-29)
uptake by man, 20: 20466
CESIUM FLUORIDES
effects on performance of tungsten-emitter thermionic converter, 20: 21586
CESIUM IODIDES
scintillation response of thallium-activated crystals of, to low-energy heavy ions, 20: 22318
scintillation yields for $2 < Z < 20$ ions, linear relation for, 20: 21084
CESIUM IONS
emission from tungsten ionizers, 20: 21570 (N-65-29785)
CESIUM ISOTOPES
gamma spectra in sand, (E), 20: 22308 (HASL-167)
CESIUM ISOTOPES Cs-133
energy levels from barium-133 decay, multipolarity and spins of, (E), 20: 22076
energy levels of, magnetic dipole moment of 82-kev, (E), · 20: 22025
CESIUM ISOTOPES Cs-134
beta decay of, conversion coefficients for 605-kev transition in, (E),

20: 22026
dispersion and movement in soils, mechanism of, 20: 20875 (EUR-2481.f)
CESIUM ISOTOPES Cs-137
content in biota of Doe Run, Ky., 1959 to 1965, 20: 20884(R) (TID-22815)
content in Colorado deer, 20: 20384 (COO-1156-13)
content in food in Amsterdam, 1960 to 1963, 20: 20949
content in foods and soil in Great Britain, 1964 and 1965, 20: 20926(R) (ARCRL-14)
content in Italian milk, 20: 20950
content in litter and plants of Washington state forests, 20: 20879 (BNWL-SA-530)
content in silt in Escaut River, Belgium, control of, 20: 22515(T) (ORNL-tr-965)
determination in atmospheric precipitates during reduction, 20: 20625
determination of microquantities of, precipitated with zinc tetrathiocyanatomercurate(II), 20: 20619
diffusion in irradiated Zircaloy-4 at 800°C, 20: 21232 (BMI-1763)
distribution in forest ecosystems, effects of climatic zones on, 20: 20879 (BNWL-SA-530)
dosimetry of, spectrometric method for, 20: 20952
radiation hazards from, following nuclear incidents, 20: 20962
separation from fresh water by ion exchange chromatography, 20: 20627
separation from radioisotopes in aqueous solutions by foam chromatography using colloidal manganese dioxide, 20: 20628
sorption by clays, mica, and soils, 20: 20696
sorption by clays, mica, soils, and zeolites, successive desorption method for calculating, 20: 20618
transport in soil and plants, 20: 20926(R) (ARCRL-14)
uptake by deer and sheep, effects of biological and environmental factors on, 20: 20388 (SAN-34-2)
use as radiation source in irradiation facilities for plastic–wood combinations, 20: 21185 (ORNL-IIC-7, pp 76-80)
use in ecological studies, 20: 20380 (TID-22499)
CESIUM ISOTOPES Cs-144
separation from radioisotopes in aqueous solutions by foam chromatography using colloidal manganese dioxide, 20: 20628
CESIUM NITRATES
proton reactions at 590 Mev and 18 Bev, yields of iodine isotopes from, (E), 20: 22045
CESIUM SYSTEMS
Cs–Xe, thermal diffusion in, 20: 21567 (FEI-15)
CESIUM TELLURIDES
effects on cesium chloride spectra, (E), 20: 21566(R) (ANL-7055, pp 213-29)
CHARCOAL
ignition by fission product heat, research on, 20: 20940(R) (ORNL-3915)
separation from contaminants for radiocarbon dating, 20: 20798
CHARGED PARTICLE BEAMS
collimators for r-f separated, design of, 20: 21468 (CERN-66-10)
motion in prism-fringe magnetic field, aberration and displacement in, (T), 20: 21484
propagation in cold plasma in external magnetic field, wave excitation from, (T), 20: 22286
CHARGED PARTICLES
charge and mass distributions of spherically symmetric, in static case in general relativity, 20: 21634
containment in magnetic mirror systems, (T), 20: 22229
detection and measurement using semiconductor detectors, 20: 21026 (BNL-948, pp 704-17)
detection and measurement using semiconductor detectors, pulse rise times in, 20: 21137
detection in radiation background, coincidence method for, 20: 21139
detection of, emulsion and solid-state detectors for, 20: 21060
detection using europium-activated single crystals of calcium fluorides, 20: 21135
dosimetry of, portable microcalorimeter for, 20: 21024 (AD-630693)
flux distribution in hydrogen plasma, effect of h-f traveling electromagnetic waves on radial, (T), 20: 22301
interactions in plasma, effects on electromagnetic wave propagation, (E/T), 20: 22228
interactions with electromagnetic perturbations in magnetosphere, 20: 21825
lifetime in storage rings, asymptotic diffusion-problem solutions for, 20: 21483
motion in magnetic fields, (T), 20: 21454
motion in magnetic field, effect of field gradient on polarization of spin-½, (T), 20: 21481
motion in plasma, electrostatic damping of, (T), 20: 22233
production in neutron-induced reactions, design and performance of telescope counter for, 20: 21054
scattering by thin layers, ionization losses in, (T), 20: 21515 (JINR-P-2615)
trajectories in composite magnetic mirrors, intermingling in, (T), 20: 22274
transport of trapped, in outer magnetosphere, 20: 28131
trapping by geomagnetic fields, (E/T), 20: 21837
CHELATES
effects on zinc-65 excretion in man, 20: 20397
CHEMICAL ANALYSIS
abstracts of papers on, 20: 20552 (CONF-650723(Absts.))
CHEMICAL RADIATION DETECTORS
design for gamma threshold dosimetry, 20: 21076
CHEMICALS AND REAGENTS
effects of impregnating, on charcoal retention of methyl iodide, 20: 20940(R) (ORNL-3915)
radiation effects on blood typing, x, 20: 20425
CHEMISTRY
abstracts of papers on pure and applied, 20: 20552 (CONF-650723 (Absts.))
book: *Advances in Inorganic Chemistry and Radiochemistry*, Vol. 7, 20: 20658
book: *Advances in Quantum Chemistry, Vol. 2*, 20: 20698
nuclear quadrupole resonance uses in, 20: 20699
CHERENKOV DETECTORS
photon reflection coatings for, preparation and properties of, 20: 21136
CHERENKOV RADIATION
design and counting efficiency of threshold-type gas, for electrons, 20: 21071
detection of meson (μ), from cosmic neutrino events, 20: 21031 (CERN-65-32, pp 231-40)
emission from dipole moving in plasma, narrow- and plane-cavity effects on, (T), 20: 22278
emission from electron pairs, energy yield for, (T), 20: 21633
emission from point-charge motion in cold plasma, (T), 20: 22290
use in neutrino detection, 20: 21030 (CERN-65-32, pp 223-4)
CHICKENS
morphology and oxygen consumption of embryonic intestine of, cultivated *in vitro*, effects of nitrogen mustard on, 20: 20372
phosphorus-32 metabolism in developing embryos of, 20: 20399
radiation effects on physiology of germ cells of, x, 20: 20440(R) (EUR-2643.f)
radiation effects on physiology and respiration in embryos of, x, 20: 20440(R) (EUR-2643.f)
CHIMERAS
radiation mouse, lethal effects of injected bone marrow and lymph cells in, 20: 20472
CHLORIDES
radiation effects on chlorine-36 exchange with rhodium pentammine chloro complexes, 20: 20706
CHLORINE
determination in potassium halogenides, activation, 20: 20560 (EUR-2753.f)
CHLORINE ISOTOPES Cl-35
electron Coulomb scattering by, (T), 20: 21649
meson (μ) Coulomb scattering by, (T), 20: 21649
CHLORINE ISOTOPES Cl-36
decay of, ϵ/β^+ ratio for, (E), 20: 22029
exchange between osmium or rhodium complexes and chloride ions in solutions and crystals, 20: 20706
production by cosmic-ray reactions with iron, calcium, and potassium in Leedey chondrites, 20: 21508
CHLORINE ISOTOPES Cl-37
proton reactions (p,α) at 11.0 to 11.952 Mev, angular distributions and excitation functions for, (E), 20: 22084
CHLOROHYDROCARBONS
production of sulfur-35 labeled polymers of, 20: 20784
CHLOROPHYLLS
radiation effects on algal, solar, 20: 20382 (BNWL-SA-623)
CHLOROPLASTS
radiation effects on Hill activity and phosphorylation of, x, 20: 20428
radioinduced inactivation of Euglena, uv, 20: 20450
CHOLANTHRENE, 3-METHYL-
effects on mouse mammary glands, neoplastic, 20: 20502
CHROMATE IONS
effects on passivation of iron, 20: 21271
CHROMATOGRAPHIC SEPARATIONS
procedures for ion exchange, for use in activation analysis, 20: 20632
CHROMATOGRAPHY
activity profile of radiochromatograph, method for analyzing, 20: 20559 (EUR-2626.f)
analysis by, tritiated alumina as reagent for self-labeling, 20: 20575
radioactive tracer location on papers or thin layers in, use of gamma spectrometers for, 20: 20606
use of gas, for separation of carbon-14-labeled organic mixtures, 20: 20639
CHROMIC ACID

corrosive effects on nickel–chromium–molybdenum alloys at 800 to 2375°F, 20: 21277
CHROMIUM
deposition on steel of, containing ceramic dispersions, electrolytic, 20: 21286 (AD-621920)
determination in high-purity tantalum by spectrography using d-c arc method, 20: 20608
determination in silicon dioxide, activation, 20: 20634
distribution in products of fluidized-bed fluorination of spent fuel mixtures, 20: 20803(R) (ANL-7055, pp 99-162)
electron reactions at 6 to 23 kev, optical transition radiation from, 20: 21518
evaporation from porous tungsten ionizers, 20: 21570 (N-65-29785)
neutron cross sections and shielding coefficients for, 20: 22383(T) (AEC-tr-6693)
separation from manganese, nickel, rare earths, and silver by ion exchange chromatography, 20: 20634
separation from scandium by ion exchange chromatography, 20: 20821
separation from thorium by ion exchange in nitric acid solution, 20: 20624
separation from uranium by combined ion exchange-solvent extraction using nitric acid–tetrahydrofuran solutions, 20: 20811
solubility in aluminum, microhardness studies on, 20: 21362(T) (SC-T-66-0723)
wear properties of electrolytic plating of, containing ceramic dispersions, 20: 21286 (AD-621920)
CHROMIUM ALLOYS
Cr–Co–Mo–Ni–W, testing for bearing parts in liquid sodium, 20: 22520(R) (NAA-SR-11805)
Cr–Fe, fission product diffusion in irradiated, at 600 to 1200°C, 20: 21232 (BMI-1763)
Cr–Fe–Mo–Ni, corrosion of Hymu-80 by potassium chloride–uranium trichloride eutectic at 900°C, 20: 21261 (LA-3476)
Cr–Fe–Ni, fission product diffusion in irradiated, at 600 to 1200°C, 20: 21232 (BMI-1763)
Cr–Ge, production of Cr_3Ge by hot-pressing, 20: 21247
Cr–Mo–Ni, corrosion by acids at 800 to 2375°F, effects of heat treatments and microstructure on, 20: 21277
Cr–U, analysis for uranium by polarographic methods, 20: 20595
Cr–V, brazing material for joining molybdenum to tungsten for use to 2700°F, 20: 21312
CHROMIUM BROMIDES
electric properties of silicon-activated, 20: 22312(R) (AD-622796)
CHROMIUM COMPLEXES
with 2,4-pentanedione, preparation and crystal structure of, 20: 20700
CHROMIUM FLUORIDES
separation from molten salt fuels by sodium fluoride sorption, 20: 20808(R) (ORNL-3916)
CHROMIUM ISOTOPES Cr-49
beta decay, energy spectra, and magnetic moment of, $f_{7/2}$ model for, 20: 22131
energy levels of, model for, 20: 22121
CHROMIUM ISOTOPES Cr-50
alpha reactions (α,2n), iron-52 production in, (E), 20: 21993 (BNL-9165)
helium-3 reactions (He-3,t) at 22 Mev, Coulomb displacement-energy from, (E), 20: 22095
CHROMIUM ISOTOPES Cr-51
abundance in Pacific Ocean, 20: 20603
content in Columbia River invertebrates, 1964 and 1965, 20: 20382 (BNWL-SA-623)
decay of, vanadium-51 645-kev state from electron-capture, (E), 20: 22029
determination in sea water by precipitation with iron hydroxide and gamma spectroscopy, 20: 20603
production in proton reactions with iron at 400 Mev, Monte Carlo calculation of, 20: 22035
CHROMIUM ISOTOPES Cr-52
helium-3 reactions (He-3,t) at 22 Mev, Coulomb displacement-energy from, (E), 20: 22095
CHROMIUM ISOTOPES Cr-54
helium-3 reactions (He-3,t) at 22 Mev, Coulomb displacement-energy from, (E), 20: 22095
CHROMIUM OXIDES
effects of colloidal and solid, on radiolysis of benzene in aqueous solutions, 20: 20768
CHROMIUM PHOSPHATES
use of phosphorus-32-labeled, in brain tumor radiotherapy, pyrogenic and toxic effects from, 20: 20539
CHROMIUM STEEL
Cr–Mo–Ni, transformation temperatures in Super Elso, effects of heating rate on, 20: 21331(R) (EURAEC-1569)
Cr–Mo–Ni, weld embrittlement in joints in, effects of time at high temperatures on, 20: 21393
Cr–Ni–Nb, effects of aging at 600 to 800°C on microstructure of, 20: 21355 (TRG-Report-1168)
CHROMIUM SYSTEMS
C–Cr–Co–Re–Ti–W–Zr, development and tensile and stress-rupture properties of cobalt-base, 20: 21237 (N-65-29395)
C–Cr–Co–Ti–W–Zr, development and tensile and stress-rupture properties of cobalt-base, 20: 21237 (N-65-29395)
Sb–Cr–Te, neutron diffraction studies on solid solutions of, 20: 22312(R) (AD-622796)
CHROMOSOMES
radiation effects on, in radiographic personnel and their families, x, 20: 20447
radioinduced aberrations in Tradescantia pollen grain, 20: 20438 (EUR-2518.f)
CIRCUITS
design of analog modular micro-, 20: 20997
design of temperature-compensated logarithmic converter, 20: 20999
development for suppression of pulse rates in scintigraphy, 20: 21086
radiation effects on semiconductor, modeling of, 20: 21173
use of individual and mixed logic, in reactor safety systems, 20: 22360
use of integrated, in equipment for physics experiments, 20: 20998
CIRCULATORY DISEASES
radiation effects on, in monkeys, γ, 20: 20488
CIVILIAN DEFENSE
effects of nuclear weapons on, environmental, 20: 20930 (HI-518-RR (Vol.1))
effects of nuclear weapons on agriculture, environmental, 20: 20931 (HI-518-RR(Vol.2))
effects of nuclear weapons on, environmental, 20: 20932 (HI-518-RR (Vol.3))
sensitivity analysis of components and systems of, in fall environment, 20: 10922 (AD-624704)
shelter design for protection against nuclear weapons effects in schools, evaluation of, 20: 20868 (AD-626770)
thermal transient response in underground shelters, scale model tests on, 20: 20920 (AD-621377)
ventilation of fallout shelters by induced draft, method for, 20: 20921(R) (AD-621998)
CLAYS
cesium-137 sorption by, successive desorption method for calculating, 20: 20618
radioactivity of, Braunschweig, Germany, 20: 20890
sorptive properties for cesium-137, 20: 20696
CLINCH RIVER
waste disposal in, radiation dose to man from, 20: 22514 (ORNL-P-2021)
CLOUD CHAMBERS
performance of triggered, for analyzing proton reactions with nitrogen, (E), 20: 21063
COAL
analysis for ash and carbon contents by gamma transmission method, 20: 21209
COATINGS
effects of decontaminating and descaling solution on, 20: 21238 (NP-15928)
fission product deposition on, from air–steam mixtures, 20: 20940(R) (ORNL-3915)
preparation and properties for surfaces of Cherenkov detectors and scintillation detectors, 20: 21136
radionuclide retentive properties, tables on, 20: 20808(R) (ORNL-3916)
symposia on corrosion-protection, New York, March 11–15, 1963, 20: 21276
COBALT
determination in silicon dioxide, activation, 20: 20634
effects on Hastelloy X oxidation by air at 1750 and 1850°F, 20: 21258 (AGN-TM-413)
magnetic hyperfine field in hexagonal, specific heat method for determination of negative, 20: 22335
performance as liquid-phase sintering promoter for uranium monocarbide, 20: 21296 (Y-1510)
separation from gallium, indium, and transition elements by ion exchange chromatography, 20: 20634
separation from scandium by ion exchange chromatography, 20: 20821
separation from thorium by ion exchange in nitric acid solution, 20: 20624
separation from uranium by combined ion exchange–solvent extraction using nitric acid–tetrahydrofuran solutions, 20: 20811
sorption from perchloric acid solutions by ion exchange materials, 20: 20823
sorptive properties of evaporated films of, for krypton and xenon, 20: 21387
sorptive properties of evaporated films of, for carbon dioxide at room temperature, 20: 21389
viscosity of liquid, based on atomic parameters, 20: 20656 (UCRL-11930)
COBALT ALLOYS

development for aerospace applications, 20: 21237 (N-65-29395)
Al–Co, use for neutron dosimetry, 20: 21025 (AERE-R-5122)
Ce–Co, reactions of molten, with tantalum, 20: 20671
Co–Dy, dysprosium hyperfine magnetic field in intermetallic compounds of, (E), 20: 22330
Co–W, deposition of, by hydrogen reduction of mixed chloride vapors, 20: 21231 (BM-RI-6713)
Co–Y, phase studies, 20: 21402
Cr–Co–Mo–Ni–W, testing for bearing parts in liquid sodium, 20: 22520(R) (NAA-SR-11805)
COBALT(II) CHLORIDES
$CoCl_2$–WCl_6, deposition of cobalt–tungsten from vaporous, by hydrogen reduction, 20: 21231 (BM-RI-6713)
COBALT COMPLEXES
with tetraphenylporphine, radiolysis of, kinetics of gamma, 20: 20774
COBALT IONS
sorption by silver iodide, tracer studies on, 20: 20683
COBALT ISOTOPES
uptake by crustacea, mollusks, and plankton in Bay of Venice, 20: 20386(R) (NP-15916)
COBALT ISOTOPES Co-54
energy levels of, isotope shifts of isobaric-analog, (E), 20: 22095
COBALT ISOTOPES Co-56
decay of, electron capture-to-positron emission ratio in l-forbidden, (E), 20: 22016
decay of, iron-56 2080-kev level from, (E), 20: 22029
energy levels of, isotope shifts of isobaric analog, (E), 20: 22095
production in proton reactions with iron at 400 Mev, Monte Carlo calculation of, 20: 22035
COBALT ISOTOPES Co-57
Mössbauer emission spectra in silver chloride crystals, quadrupole splitting in, (E), 20: 22340
standardization of, absolute, 20: 22034
COBALT ISOTOPES Co-58
energy levels of, isotope shifts of isobaric analog, (E), 20: 22095
incorporation in potassium hexacyanocobaltate(III) for hydrological studies, 20: 20794
production by neutron irradiation of nickel carbonate targets, 20: 20794
COBALT ISOTOPES Co-59
use in measurements of liquid volume in closed systems, 20: 21208
COBALT ISOTOPES Co-60
dispersion and movement in soils, mechanism of, 20: 20875 (EUR-2481.f)
incorporation in potassium hexacyanocobaltate(III) for hydrological studies, 20: 20794
production by neutron irradiation of cobalt chloride targets, 20: 20794
use as gamma source, beam focus imaging for, 20: 20547
use as gamma source, dose distribution for, 20: 20549
use in irradiation unit at Takasaki Laboratory in Japan, 20: 20849
COBALT OXIDES
CoO–UO_2, preparation and x-ray diffraction pattern of $CoUO_3$, 20: 21242
COBALT SYSTEMS
B–Co–Hf, crystal structure, 20: 20685
B–Co–Ti, crystal structure, 20: 20685
B–Co–U, crystal structure, 20: 20685
B–Co–V, crystal structure, 20: 20685
B–Co–Zr, crystal structure, 20: 20685
C–Co–Ti–W, development and tensile properties of cobalt-base, 20: 21237 (N-65-29395)
C–Co–Ti–W–Zr, development and tensile properties of cobalt-base, 20: 21237 (N-65-29395)
C–Cr–Co–Re–Ti–W–Zr, development and tensile and stress-rupture properties of cobalt-base, 20: 21237 (N-65-29395)
C–Cr–Co–Ti–W–Zr, development and tensile and stress-rupture properties of cobalt-base, 20: 21237 (N-65-29395)
Co–WC, wear properties of plasma-arc-deposited coatings of, 20: 21319 (AD-621064)
CODEINE
radiosensitivity effects on mice, x, 20: 20513
COILS
performance of superconducting, using composite stranded cables, 20: 21878
COINCIDENCE CIRCUITS
design of fast, using storage diodes, 20: 21002
COINCIDENCE COUNTERS
dead-time corrections for 4π β-γ, 20: 21109
design and performance of telescope, for neutron-induced reactions, 20: 21054
design for detection of charged particles in radiation background, 20: 21139
design for fast-neutron detection in TREAT fuel meltdown studies, 20: 21131
design of binary-coded digitized scintillation hodoscope, 20: 21108
design of proton telescope for Orbiting Geophysical Observatory, 20: 21124
design of scintillation telescope for cosmic radiation, 20: 21125
design of scintillation counter telescope for underground detection of cosmic mesons (μ), 20: 21540 (CERN-65-32, pp 49-56)
design of telescopes for detection and measurement of cosmic nuclei, 20: 21118
COINCIDENCE MEASUREMENTS
data handling facility for, using multiple detectors, 20: 20996
COLLIMATORS
design for r-f separated charged-particle beams, 20: 21468 (CERN-66-10)
COLLOIDS
production of polymer-gel, radioinduced, 20: 20761
COLORADO
fallout content of wild deer populations in, 20: 20384 (COO-1156-13)
fallout monitoring in Boulder County, 1962 and 1963, 20: 20379 (COO-1191-10)
COLORADO (BOULDER CO.)
ecology of Boulder City watershed, 20: 20379 (COO-1191-10)
radioactivity of ground surface of Boulder City watershed, 20: 20379 (COO-1191-10)
COLUMBIA RIVER
flow time measurements in, using tracer techniques, 20: 20916
radionuclides in, transport and uptake by organisms, 20: 20382 (BNWL-SA-623)
COMPRESSORS
performance testing of Brayton-cycle gas-bearing turbo-, 20: 20841(R) (NYO-3237-5)
COMPUTER PROGRAMS
ALGAN-I, for solving mathematical equations, 20: 21222 (EIR-89)
development for space-dependent neutron fluxes, 20: 22520(R) (NAA-SR-11805)
DUZ-1, for axisymmetric and plane elasticity problems, for Philco 2000, 20: 20862 (WAPD-TM-555)
for allocation of fallout shelter system development funds, for CDC-3600, 20: 20922 (AD-624704)
for calculating effectiveness for 1-, 2-, and 3-pass cross counterflow heat exchangers, FORTRAN for CDC-3600, 20: 20858 (UCRL-14620)
for crystallographic angles in hcp yttrium, FORTRAN II for IBM 7074, 20: 22315 (IS-1337)
for design and operation of Harwell Variable Energy Cyclotron, 20: 21472 (RHEL/R-113)
for digital simulation of dynamic systems, APEX IV for G-20, 20: 21783 (AECL-2530)
for molecular collisions in gases, 20: 20806(R) (MLM-1274)
for molecular gas flows, FORTRAN for IBM 7030, 20: 20855 (CLM-R-54)
for Mössbauer spectra computations, FORTRAN II, 20: 22159
for neutron transport in gaseous core reactors, FORTRAN IV for IBM 7094, 20: 22370 (AD-621021)
for proton differential cross sections, FORTRAN IV, 20: 21965 (AD-626776)
for shielding parameters, abstracts on, 20: 22310 (ORNL-RSIC-13)
GARGOYLE, for reactor fuel cycle analysis, FORTRAN IV for IBM 7044, 20: 22412 (GA-6622)
PSEUDO, for statistical resonances in unresolved resonance region, FORTRAN IV, 20: 21940 (GAMD-6908)
SDC, for gamma shielding design, FORTRAN for IBM 7090, 20: 22309 (ORNL-3041)
SILCO, for neutron dosimetry, FORTRAN for IBM 7030, 20: 21025 (AERE-R-5122)
S4B, for neutron transport equations, for CDC 3600, 20: 21937 (AEET-210)
S4C40, for neutron flux in reactors, 20: 22488 (AD-621121)
THERMOS, for neutron thermalization in reactors, 20: 22374(R) (BNWL-193, pp 5-15)
05R, subroutines for mean times in reactor problem, 20: 22380 (ORNL-TM-1246)
COMPUTERS
data handling system for experiments using multiple detectors, 20: 20996
data handling system for on-line use with linear accelerator, modular, 20: 21225
data handling system for on-line use with linear accelerator, modular programming for, 20: 22032
data plotting system for CDC 3600, cathode-ray tube, 20: 21221 (ANL-7121)
LO5, for gamma and neutron transport, FORTRAN for IBM 7090, 20: 22304 (AD-612031)
use for auditing data centralization in nuclear materials management program, 20: 20965
use for neutron resonance analysis, 20: 21994 (BNL-10094)
use for simulation of atomic collisions in crystals, 20: 22341
use in analysis and simplification of multi-isotope mass spectra,

20: 20580
use in calculation of electron density distributions in ionosphere, 20: 21823
use in experimental physics, 20: 21981 (BNL-948, pp 718-40)
use in experiments in low-energy nuclear physics, 20: 21026 (BNL-948, pp 704-17)
use in simulating neutron injection from earth's atmosphere, 20: 21550
use in storage, interpretation, and recovery of materials data, 20: 21354 (TRG-Report-1160)
use of analog, for magnet power supply representation, 20: 21488
use of on-line in control of xenon buildup in reactors after shutdown, 20: 22389
use on-line in low-energy nuclear physics experiments, 20: 22031
uses in research, 20: 21224(R) (ORNL-3919)

CONCRETES
creep and shrinkage of heated, measurement of, 20: 21373
gamma dose albedos for, Monte Carlo calculation of, 20: 22305 (AD-621441)
performance for separating fissile materials, 20: 20840(R) (BNWL-193, pp 57-67)
performance of borated, for separating fissile materials, 20: 20840(R) (BNWL-193, pp 57-67)
preparation of iron ore-containing, for pilot plutonium plant, 20: 20819
properties of prestressed, as reactor pressure vessels, 20: 22353 (CEA-R-2829)
properties of, for use in space nuclear power plant testing vault, 20: 20869

CONFERENCES
see also introduction to Report Number Index
Photographic and Spectroscopic Optics, Kyoto and Tokyo, Sept. 1–8, 1964, 20: 21458
Physics of Emperor Tandem Van de Graaff Region, Upton, N. Y., June 21–July 16, 1965, 20: 21462 (BNL-948)
Rare Earth Research, Proceedings of Fourth, Phoenix, Arizona, April 22 to 25, 1964, 20: 20704

CONGO REPUBLIC (LEOPOLDVILLE)
nuclear medicine in, 20: 20373

CONNECTORS (ELECTRIC)
performance testing for use in semiconductor logic modules, 20: 22352 (AEET-ED-SG/25)

CONVECTION
properties in confined fluids, 20: 20854 (AD-621523)

CONVECTION (FORCED)
boiling in terphenyl OM2 in, inception of nucleate, (E/T), 20: 20709 (EUR-2442.f)

COPPER
alpha scattering at 28.4 Mev, angular distributions from, (E), 20: 22047
determination in brass by x-ray fluorescence methods, 20: 20642
determination in high-purity tantalum by spectrography using d-c arc method, 20: 20608
determination in o-diphenol oxidase by neutron activation analysis, 20: 20569
determination in ore by radioisotope x-ray fluorescence method, 20: 20640
determination in silicon dioxide, activation, 20: 20634
determination in tin oxide, activation, 20: 20577
diffusion of nickel-63 in, at 250 to 520° C, 20: 21367
dose distribution in, from electron beam irradiation, three-dimensional, 20: 21470 (PB-181506, pp 116-29)
ductility of, at −269°C, 20: 21416
effects of decontaminating and descaling solution on metal loss on, 20: 21238 (NP-15928)
electron reactions at 6 to 23 kev, optical transition radiation from, 20: 21518
evaporation from porous tungsten ionizers, 20: 21570 (N-65-29785)
gamma elastic scattering at 280 and 662 kev, Z dependence of cross section for, (E), 20: 22060
helium-3 reactions (He-3,n) at 19 to 25 Mev, angular distributions and cross sections for, (E), 20: 22132
manganese-54 orientation in, gamma-ray anisotropy from, (E), 20: 22097
neutron inelastic scattering at 5.8 and 7.5 Mev, gamma spectra from thermal, (E), 20: 22069
performance as liquid-phase sintering promoter for uranium monocarbide, 20: 21296 (Y-1510)
performance of molten, as reactor coolant, (T), 20: 22351 (AD-623020)
photoelectric effect at 852 ev to 40 kev in, cross sections for, (E), 20: 21523
proton reactions at 19 Bev/c, meson (K) and (π) yields from, (E), 20: 21602 (CERN-65-32, pp 111-14)
radioinduced defects in annealed, Frenkel pair recombination volume from alpha, 20: 21447
separation from gallium, indium, and transition elements by ion exchange chromatography, 20: 20634
separation from perchloric acid solutions by ion exchange materials, 20: 20823
separation from scandium by ion exchange chromatography, 20: 20821
separation from thorium by ion exchange in nitric acid solution, 20: 20624
viscosity of liquid, based on atomic parameters, 20: 20656 (UCRL-11930)
welding of, argon-arc and electron-beam methods of, 20: 21310

COPPER ALLOYS
analysis of, using radioisotope portable analyzer, 20: 20642
Be–Cu, ductility of, at −269°C, 20: 21416
Be–Cu, radiation effects at 80°K on, resistivity recovery from proton, 20: 21445
Be–Cu, rare-gas ion reactions at 3 to 90 kev, secondary electron emission from, (E), 20: 21538
Ce–Cu, intermetallic compound with $CeCu_2$-type structure in, 20: 21352 (TID-21745)
Ce–Cu–Pu, phase diagrams, 20: 20553(R) (MLM-1142)
Cu–Dy, dysprosium hyperfine magnetic field in intermetallic compounds of, (E), 20: 22330
Cu–Mg, solvent properties of liquid, for plutonium, praseodymium, and uranium, 20: 20802(R) (ANL-7055, pp 21-98)
Cu–Mn–Zr, analysis for bonding and inclusions in, by x-ray emission in electron microscopy, 20: 20593
Cu–Ni, effects of decontaminating and descaling solution on metal loss on, 20: 21238 (NP-15928)
Cu–rare earth, crystal structure of equiatomic intermetallic compounds of, 20: 21399
Cu–Sn, radiation effects on deformation of, fast-neutron, 20: 21434
Cu–Y, intermetallic compound with $CeCu_2$-type structure in, 20: 21352 (TID-21745)

COPPER CHLORIDES
electric conductivity, 20: 22520(R) (NAA-SR-11805)

COPPER COMPLEXES
with tetraphenylporphine, radiolysis of, kinetics of gamma, 20: 20774

COPPER COUPLES
Cu/Nb, fabrication of composite wires of, by drawing, 20: 21298

COPPER ISOTOPES
determination in radiation sources, extraction radiometric titration method for, 20: 20567 (UJV-1418/65)

COPPER ISOTOPES Cu-58
energy levels of, isotope shifts of isobaric analog, (E), 20: 22095

COPPER ISOTOPES Cu-60
energy levels of, isotope shifts of isobaric analog, (E), 20: 22095

COPPER ISOTOPES Cu-62
energy levels of, isotope shifts of isobaric analog, (E), 20: 22095

COPPER ISOTOPES Cu-63
nuclear structure, 20: 21975 (BNL-948, pp 269-336)

COPPER ISOTOPES Cu-64
energy levels of, isotope shifts of isobaric analog, (E), 20: 22095

COPPER OXIDES
effects on radiolysis of benzene in aqueous solutions, 20: 20768
removal from copper by dissolution, descaling solution for, 20: 21238 (NP-15928)

COPPER SULFATES
$CuSO_4$–D_2SO_4–UO_2SO_4–H_2O–D_2O, spectrophotometry of reactor fuel solutions of, 20: 20600

CORROSION
conference on metallic, New York, March 11–15, 1963, 20: 21276

CORROSION FILMS
corrosion inhibition properties of oxide, mechanisms of, 20: 21281

CORROSION LOOPS
design for testing reactor materials, 20: 21266
development of lithium, 20: 21263(R) (NASA-CR-54911)
development of, for liquid metal tests, 20: 21566(R) (ANL-7055, pp 213-29)
development of, for refractory metal–alkali metal studies, 20: 21284
materials procurement and specifications for fabrication of, 20: 21293 (R-66SD3007)

CORROSION-RESISTANT ALLOYS
testing for fluoride volatility process construction, 20: 20803(R) (ANL-7055, pp 99-162)

COSMIC ELECTRONS
detection and measurement using Orbiting Geophysical Observatory, spectrometer for, 20: 21123
production spectra of high-energy, from cosmic-ray interactions, 20: 21552

COSMIC MESONS (μ)
angular distribution underground, measurement of, 20: 21541 (CERN-65-32, pp 57-60)
attenuation underground and underwater, intensity-depth relations for, 20: 21558
detection of, plastic scintillation detector for, 20: 21028 (CERN-65-32, pp 65-70)

detection underground using scintillation counter telescope, 20: 21540 (CERN-65-32, pp 49-56)
flux of, diurnal variation of, (E), 20: 21494
properties of high-energy, review of, 20: 21558
reactions with lead in IGY neutron monitor, neutron multiplicities from, 20: 21551
COSMIC MESONS (π)
production in high-energy cosmic nucleon interactions, 20: 21553
reactions with lead in IGY neutron monitor, neutron multiplicities from, 20: 21551
COSMIC NEUTRINOS
detection underground using neon flash tubes, 20: 21541 (CERN-65-32, pp 57-60)
detection underwater, methods for, 20: 21031 (CERN-65-32, pp 231-40)
energy spectra at sea level, (E), 20: 21542 (CERN-65-32, pp 73-8)
interactions deep underground, meson (μ) production in, 20: 21540 (CERN-65-32, pp 49-56)
properties of high-energy, review of, 20: 21558
reactions underground, meson (μ) production in, (E/T), 20: 21542 (CERN-65-32, pp 73-8)
COSMIC NEUTRONS
decay of albedo, proton injection into radiation belts by, 20: 21550
detection and measurement of, directional scintillation detector for, 20: 21117
reactions with lead in IGY neutron monitor, neutron multiplicities from, 20: 21551
COSMIC NUCLEONS
interactions of high energies, meson (π) production in, (T), 20: 21553
COSMIC PARTICLES
detection and measurement of, performance of dielectric track detectors for, 20: 21091
detection and measurement of nuclei, counter telescopes for, 20: 21118
lifetime and propagation of light nuclei, (T), 20: 21554
reactions with nuclei above 10 Bev, model for inelastic, (T), 20: 21999 (JINR-P-2552)
COSMIC PHOTONS
properties of high-energy, determination using emulsion chambers, 20: 21555
properties of high-energy, review of, 20: 21558
COSMIC PROTONS
detection and measurement of nuclei, counter telescopes for, 20: 21118
detection and measurement using spark chambers, spectrometer for, 20: 21120
interactions with protons, production spectra of secondary high-energy electrons from, 20: 21552
reactions with lead in IGY neutron monitor, neutron multiplicities from, 20: 21551
reactions with meteorites, Monte Carlo calculation of radionuclide production in, 20: 22035
COSMIC RADIATION
absorption of cosmic noise at magnetically conjugate points, fluctuations in auroral, (E), 20: 21820
detection and measurement of gamma, spark chamber with vidicon readout for, 20: 21119
detection and measurement of gamma, digitized spark chamber for, 20: 21121
detection and measurement of gamma, spark chamber with photographic recording for, 20: 21122
detection and measurement using Orbiting Geophysical Observatory, coincidence system for, 20: 21125
effects on hydrolysis of salicyl phosphate, 20: 20744
flux of, diurnal variation of, (E), 20: 21494
lifetime and propagation of nuclear components of, beryllium–boron intensity ratios for, (T), 20: 21554
polarization in, Faraday rotation effects on, (T), 20: 21548
polarization of r-f, measurement methods for linear, 20: 21549
reactions in Leedey chondrites, chlorine-36 and argon-39 production rates from, 20: 21508
reactions in liquid scintillators, meson (μ) production in, (E), 20: 21029 (CERN-65-32, pp 71-2)
reactions in nuclear emulsions, cascade showers from, 20: 21556
COSMIC SHOWERS
analysis of electromagnetic, three-dimensional Monte Carlo, 20: 21559
analysis of, review of, 20: 21558
energy of cosmic-ray initiated, in emulsions, 20: 21556
energy spectra from 8×10^{14} to 4×10^{17} ev, primary, (E), 20: 21547 (MIT-2098-227, Paper EAS-31)
particle cascades in, Monte Carlo simulation of, 20: 21545 (MIT-2098-227)
particle energy and interactions in EAS, (E), 20: 21544 (MIT-2098-227, Paper EAS-8)
properties of low meson (μ), 20: 21546 (MIT-2098-227, Paper EAS-29)
properties of, determination using emulsion chambers, 20: 21555
reactions with lead in IGY neutron monitor, neutron multiplicities from, 20: 21551
COSMOLOGY
galactic kinetics and properties, 20: 21513
stellar evolution, (T), 20: 21512
CRATERS
production by high-energy detonations, site selection for, 20: 20895 (AD-626899)
***p*-CRESOL**
reactions with xenon, heat of formation of clathrate compounds formed in, 20: 20688
***o*-CRESOL, 2,6-Di-*tert*-BUTYL-**
radiosensitivity effects in mice, 20: 20506
CRITICAL ASSEMBLIES
criticality studies in ZPR-III uranium-fueled, 20: 22383(T) (AEC-tr-6693)
design and construction of ZR-2, 20: 22388
design of accelerator-pulsed fast, 20: 22503
radiation dose rates in environment of, air-scattered gamma and neutron, 20: 22386
CRITICALITY STUDIES
for shipping and storage container materials evaluation, 20: 20840(R) (BNWL-193, pp 57-67)
for uranium-fueled ZPR-III assemblies, 20: 22383(T) (AEC-tr-6693)
of uranium tube lattices in water, (E), 20: 22375(R) (BNWL-193, pp 45-56)
CROTONIC ACID, 3-METHYL-, METHYL ESTERS
deuterium exchange with, in catalytic hydrogenation, 20: 20715
CRUCIBLES
performance of beryllia, for halide slagging of fuel alloys, 20: 20802(R) (ANL-7055, pp 21-98)
testing beryllia and tungsten, for skull reclamation processes, 20: 20802(R) (ANL-7055, pp 21-98)
CRUSTACEA
isotope uptake by Bay of Venice, cobalt, manganese-54, ruthenium-106, and zinc-65, 20: 20386(R) (NP-15916)
CRYOGENICS
equipment for use with irradiation studies on alloys and metals, 20: 21427(R) (NASA-CR-54904)
CRYOSTATS
design and operation of nitrogen gas, 20: 20984 (EUR-2710.f)
design for AFNETF, 20: 22489 (AD-621123)
CRYSTAL STRUCTURE
lattice dynamics in, review of Mössbauer studies of, 20: 22327
CRYSTALS
neutron inelastic scattering by, research on slow, 20: 22316 (JINR-P-2081)
radiation effects on atomic motion in, computer simulation of, 20: 22341
CUPFERRON
solvent properties for zirconium-89, 20: 20626
CURIUM
production of, review of methods for, 20: 20796
separation from nitrate solutions by solvent extraction using tricaprylmethylammonium nitrate, 20: 20812
CUTTING TOOLS
design for incorporation in instrumented reactor fuel elements, 20: 21018(P)
1-CYCLOBUTENE, 1,2-DICHLORO-3,3,4,4-TETRAFLUORO-
radioinduced reactions with tetrahydrofuran, dioxane, and diethyl ether, 20: 20773
CYCLOHEXANE
radiolysis of, yields in, 20: 20727 (PB-181506, pp 9-18)
reactions with carbon tetrachloride, production of labeled polymers in, 20: 20784
cyclohexane–P, radiolysis of, mechanisms in gamma, 20: 20736
CYCLOPENTENE, 1,2-DICHLOROHEXAFLUORO-
radioinduced reactions with tetrahydrofuran, dioxane, and diethyl ether, 20: 20773
CYCLOPROPANE
carbon tetrachloride–cyclopropane–pentane, radiolysis of, at 77 to 193°K, tracer studies of mechanisms in, 20: 20752
carbon tetrachloride–cyclopropane–2-methylbutane, radiolysis of, at 77 to 193°K, tracer studies of mechanisms in, 20: 20752
carbon tetrachloride–cyclopropane–hexane, radiolysis of, at 77 to 193°K, tracer studies of mechanisms in, 20: 20752
CYCLOTRON RADIATION
emission by partially ionized plasma, 20: 22208
emission from electrons in plasma, complex Doppler effect on, (T), 20: 22198
production in plasma, equipment for, 20: 22190(R) (TID-22821)
propagation in plasma, (E), 20: 22226
CYCLOTRONS
beam energy measurements from race-track microtrons, (E), 20: 21461

(AD-624038)
betatron resonances in isochronous, nonlinear, (T), 20: 21486
description of variable-energy spiral-ridge, 20: 21464 (BNL-948, pp 692-703)
design of superconducting race-track microtron, 20: 21460 (AD-623659)
operation of Colorado Isochronous, 20: 21473(R) (UCOL-535-554)
research programs with Kyoto University, review of, 20: 22524
CYLINDERS
heating rates in laminar hypersonic flow, · 20: 20857 (SC-DC-65-1907)
magnetic field excitation in, by electric pulse, (T), 20: 24156
CYSTEINE
radiation effects on aqueous solutions of, review on, 20: 20728 (PB-181506, pp 49-58)
radiosensitivity effects on DNA, uv, 20: 20412
CYTOCHROME OXIDASE
radiation effects on activity of, in rat liver, 20: 20417
CYTOLOGY
effects of tumor viruses in human diploid cells, 20: 20377
radiation effects on intracellular organelles in mouse, x, 20: 20413
radiation effects in, from central nervous system exposure, 20: 20449
radiation effects in, mechanism of, 20: 20443 (PB-181506, pp 143-54)

D

DATA RECORDING SYSTEMS
design and performance of automatic, for multiple radioactivity measurements, 20: 21045
development, · 20: 20553(R) (MLM-1142)
development for use with seismometer, 20: 20913
development of medical, for nuclear industrial hygiene, 20: 20955
DATA TABULATIONS
ages of archeological specimens, carbon-14, 20: 20905
electron radial function and tangents of phase shifts for nuclei ($1 \leq Z \leq 10$), · 20: 22009 (NBS-MON-81)
geomagnetic activity parameters, 20: 21830
of radioisotope yields in reactors, 20: 21214 (ORNL-IIC-8)
on radioresistant paints, · 20: 20808(R) (ORNL-3916)
radiation levels within and behind beryllium, 20: 22307 (DC-61-3-69)
reactor fuel performance, 20: 22444
solar activity parameters, 20: 21830
DECAY SCHEMES
equations for decay rates for, 20: 22155
DECAY SERIES
mass corrections to $\alpha-\beta$, leading to bismuth-213, 20: 22154
DECONTAMINATING SOLUTIONS
development and effectiveness of, for alloys and metals, 20: 21238 (NP-15928)
DECONTAMINATION
effectiveness of, inside and outside buildings, 20: 20923 (AD-626727)
efficiency of detergent for, of glass vials, 20: 20960
of reactors, efficiency of, 20: 20957
sanitary water-treatment process for, of water supplies, 20: 22512 (K-1651)
DEER
fallout content of Colorado, cesium-137, iodine-131, and strontium-90, · 20: 20384 (COO-1156-13)
fallout uptake by, effects of biological and environmental factors on cesium-137 and strontium-90, · 20: 20388 (SAN-34-2)
DEHYDROGENASES
radioinduced production of, in Neurospora, uv, 20: 20462
radiosensitivity of lactic, effects of nicotinamide adenine dinucleotide on, 20: 20514
DENSITOMETERS
development of, for measuring near-critical saturated liquid and vapor phase densities for alkali metals, · 20: 20651(R) (CU-2660-26)
use of radiometric, survey on, 20: 20990(T) (AERE-Trans-1048)
DETERGENTS
properties in glass vial, 20: 20960
DEUTERIUM
alpha reactions (α,pn) with exit channel calculations for, 20: 21981 (BNL-948, pp 610-84)
deuteron reactions (d,n) with, neutron angular and energy distributions from, (T), 20: 21934 (AD-621473)
deuteron reactions (d,n) and (d,p) at 20 to 350 kev, angular distributions and cross sections for, (E), · 20: 22074
effects on hydrogen abstraction from ammonia, hydrazine, and methylamine, 20: 20713
exchange between constituents in catalytic hydrogenation of methyl β,β-dimethylacrylate, 20: 20715
exchange between *trans*-hydridochlorobis(triethylphosphine)-platinum(II) and heavy water, 20: 20701
exchange between water-d_2 and amino acids or peptides, 20: 20714
exchange with hydrogen on molybdenum film, steady-state, 20: 21351(R) (SRIA-425-8)
fine structure constant for, 20: 21537
incorporation in amino acids or peptides by isotopic exchange, 20: 20714
incorporation in ammonia at 386 to 461°C, equilibrium constant for, 20: 20660
incorporation in ketosteroids, 20: 20799
incorporation in ketosteroids, 20: 20799
pinch effect in plasma of, MHD theory for, 20: 22180 (IAE-960)
radioinduced exchange reactions with gaseous ethane and methane, mechanism of tritium, 20: 20719 (AD-624657)
reactions on molybdenum film surface, kinetics of, 20: 21351(R) (SRIA-425-8)
rotational constant of molecular, finite nuclear mass and relativistic effects on, 20: 21527
sorption by molybdenum films in ultrahigh vacuum, kinetics of, 20: 21351(R) (SRIA-425-8)
sorption of ortho- and para-, by platinum, energy exchange in, 20: 20661
spectra in calcium fluoride crystals, absorption, 20: 22311(R) (AD-622068)
spectra of, fine structure of Balmer series lines in, (E), 20: 21532
vibrational relaxation times in argon and krypton, shock-tube measurement of, 20: 21797
DEUTERIUM HYDRIDES
rotational constant of molecular, finite nuclear mass and relativistic effects on, 20: 21527
spectra in liquid argon, rotational-translational coupling from infrared absorption, (E), 20: 21528
DEUTERIUM SYSTEMS
D–H, sorption by iridium, rhodium, and tungsten, isotopic mixing during, 20: 20652 (IS-T-67)
DEUTERONS
exchange in nuclear reactions, (T), 20: 21972 (BNL-948, pp 86-174)
interactions with polarized gamma rays, meson (π) production in, (E), 20: 21626 (LNF-66/4)
interactions with elementary particles at high energies, shadow effect in, (T), 20: 21646
interactions with mesons (π^-), hyperon (Σ^-)-neutron production and final-state interaction in, (T), 20: 21681
model of, effect-range formula for composite, 20: 21689
reactions (d,α) with oxygen-16 at 5–9 Mev, differential cross sections for, (E), 20: 22160
reactions (d,Ny) with nuclei, gamma polarization from, (T), · 20: 22006 (KFKI-600)
reactions (d,nγ) with fluorine-19 at 1 Mev, neon-20 levels from, (E), 20: 22082
reactions (d,n) and (d,p) with deuterium at 20 to 350 kev, angular distributions and cross sections for, (E), · 20: 22074
reactions (d,n) with nickel-58, -60, -62, and -64 at 11.7 Mev, neutron spectra and angular distributions from, (E), · 20: 22109
reactions (d,n) with deuterium and tritium, neutron angular and energy distributions from, (T), · 20: 21934 (AD-621473)
reactions (d,p γ) with magnesium-26 at 3.0 to 4.8 Mev, magnesium-27 level spins and deformation parameter from, (E), · 20: 22099
reactions (d,pγ) with iron-54 at 7 Mev, iron-55 level spins from, (E), 20: 22126
reactions (d,pγ) with carbon-12 at 2 to 3.2 Mev, angular correlations from, (E), · 20: 22087
reactions (d,p) with oxygen-16, optical potentials for, (E/T), · 20: 22104
reactions (d,p) with hafnium-180, hafnium-181 levels from, (E), 20: 22106
reactions (d,p) with oxygen-16, oxygen-17 excitation energies and level transitions from, (E), · 20: 22111
reactions (d,p) with sodium-23 at 1.5 Mev, neutron-capture angular momenta for levels from, (E), 20: 22150
reactions (d,p) with lithium-6 at 1.5 Mev, angular distributions, (E), 20: 22151
reactions (d,p) with nuclei, amplitude in Coulomb approximation, 20: 22028
reactions (d,2p) with hydrogen at 10.5 Mev, exit channels for, (E), 20: 21981 (BNL-948, pp 610-84)
reactions with nuclei, amplitude singularities in knockon and stripping, (T), · 20: 21997 (INSJ-96)
scattering by bismuth-209, collective levels from inelastic, (E), 20: 22108
scattering by carbon-12 at 2.0 to 3.2 Mev, cross sections for elastic, (E), 20: 22087
DIABETES
effects on insulin metabolism, tracer study, 20: 20383 (CNEA-185)
DIAMONDS
deposition on steel of chromium plating containing dispersions of, electrolytic, 20: 21286 (AD-621920)
magneto-optic effects in semiconducting, 20: 22311(R) (AD-622068)

DIBENZOTHIOPHENE, 5,5-DIOXIDE
radiolysis of, sulfur dioxide yields from gamma, 20: 20760
DIDO REACTORS
experimental facilities for, design of high-pressure water-loop, 20: 22504
neutron dosimetry in PLUTO, cobalt-silver activity method for, 20: 21025 (AERE-R-5122)
DIELECTRICS
radiation effects on current induction in commercial capacitors, electron beam, fast neutron, and gamma, 20: 21151 (IBM-66-825-1944)
radiation effects on, 20: 21171
DIET
effects of low-protein, on rat recovery from gamma irradiation, 20: 20508
effects on uptake of cesium-137 and strontium-90 by deer and sheep, 20: 20388 (SAN-34-2)
radioactivity due to fallout, 1965, 20: 20882(R) (HASL-171)
radioactivity in, Great Britain, 1964 and 1965, 20: 20926(R) (ARCRL-14)
DIFFERENTIAL EQUATIONS
book: *Iterative Solution of Elliptic Systems and Applications to the Neutron Diffusion Equations of Reactor Physics*, 20: 22400
solution of, computer program for, 20: 21222 (EIR-89)
DIFFUSION
measurement of coefficients for liquid metal, during molecular distillation, 20: 21334 (IS-1325)
theory for self-, in bcc and fcc metals, 20: 21230 (AEET-233)
DIODES
operation of plane hot-cathode cesium-plasma, with single potential maximum between electrodes, (T), 20: 22279
radiation effects on switching times of fast, neutron, 20: 21157
surface potential of lithium-drifted germanium, 20: 21096
thermal effects in, compensation of, 20: 20992
use of storage, in fast timing circuits, 20: 21002
use of tunnel, with charge-multiplying semiconductor detectors, 20: 21113
DIOXANE
radioinduced addition to 1,2-dichlorohexafluorocyclopentene and 1,2-dichlorotetrafluorocyclobutene, 20: 20773
DIRECT ENERGY CONVERSION DEVICES
bibliography, 20: 21565 (AD-628049)
conference, 20: 21581
conference, 20: 21582
conference, 20: 21583
DISCONNECTS
design for reactor fuel or moderator elements, 20: 22363(P)
DISEASES
radiotherapy of Hodgkin's, myocardial infarction induced by, 20: 20468
DISTILLATION APPARATUS
design of, for measuring diffusion coefficients of liquid metals, 20: 21334 (IS-1325)
design of, for separation of cadmium from bismuth–lead eutectic, 20: 20805 (IS-1329)
DISTRICT OF COLUMBIA
areal geology and aeroradioactivity surveying of, 20: 20928 (CEX-59.4.17)
tritium content of rain water in, 20: 20892
DISULFIDES
effects on α-ketoglutarate oxidation by rat-liver homogenates, 20: 20505
DODECANE
radiolysis of, ion mobility in x, 20: 20734
DOGS
radiation dose measurements in, γ, neutron, and x, 20: 20432 (AD-630332)
radiation effects on, physiological x, 20: 20435 (CONF-650560-15)
radiation effects on electrical activity of olfactory neurons in, x, 20: 20431 (AD-630323)
radiation effects on arteries in, auto- and homovenous repair of x, 20: 20478
radiation effects on blood coagulation in, γ and x, 20: 20490
radioinduced myelopathy in, Thorotrast, 20: 20455
DOLOMITES
carbon-13 exchange between, and carbon dioxide, 20: 20691
oxygen-18 exchange between, and carbon dioxide, 20: 20691
DOSIMETERS
design and performance of portable microcalorimetric, 20: 21024 (AD-630693)
design and uses of gamma-x, 20: 21062
design for beta particles and gamma radiation using silicon p-n junctions, 20: 21133
design of gamma, using ionization chambers, 20: 21078
design of ionization-chamber, 20: 21141(P)
development for flight test of SNAP-10A, 20: 21105
development for x radiation from pulsed r-f tubes, 20: 21022 (AD-624230)
development of thermoluminescent, with print-out device, 20: 21085
performance for depth dose radiation measurements in dogs and phantoms, 20: 20432 (AD-630332)
performance of calcium sulfate, 20: 20769
performance of semiconductor fast-neutron, 20: 21095
performance of, using terephthalic acid, 20: 20745
reader design and measurement errors in lithium fluoride thermoluminescent, 20: 21061
readout system for film, numerical photometer, 20: 21070
relay for, electrostatic, 20: 21088
DUSTS
radiation monitoring of Japanese, alpha, beta, and gamma, 20: 20934 (JAERI-1098)
DYES
effects of Sudan Red on radioinduced oxidation of ergosterol, 20: 20738
properties of acridine orange in viability tests on *E. coli*, 20: 20457
DYSPROSIUM
determination in rare earth mixtures, activation, 20: 20562 (LYCEN-6538)
electric conductivity at 4.2, 77, and 296°K, 20: 22312(R) (AD-622796)
friction and wear properties of, in vacuum, effects of crystal structure on, 20: 21365
magnetic hyperfine field in intermetallic compounds of, (E), 20: 22330
nuclear magnetic resonance spectra in, 20: 22311(R) (AD-622068)
oxidation in dry and moist air at 100 to 800°C, rate of, 20: 21265 (RPI-2714-8)
reactions with powdered graphite, preparation of intercalation compounds by, 20: 20648 (AD-621029)
separation from perchloric acid solutions by ion exchange materials, 20: 20823
separation from uranium by combined ion exchange-solvent extraction using nitric acid–tetrahydrofuran solutions, 20: 20811
DYSPROSIUM ALLOYS
Al–Dy, crystal structure and stability of intermetallic compounds in, 20: 21415
Al–Dy, dysprosium hyperfine magnetic field in intermetallic compounds of, (E), 20: 22330
Co–Dy, electric conductivity at 4.2, 77, and 296°K, 20: 22312(R) (AD-622796)
Co–Dy, dysprosium hyperfine magnetic field in intermetallic compounds of, (E), 20: 22330
Cu–Dy, dysprosium hyperfine magnetic field in intermetallic compounds of, (E), 20: 22330
Dy–Fe, dysprosium hyperfine magnetic field in intermetallic compounds of, (E), 20: 22330
Dy–Ga, dysprosium hyperfine magnetic field in intermetallic compounds of, (E), 20: 22330
Dy–Gd, magnetic transformations in, 20: 21409
Dy–Ho, magnetic transformations in, 20: 21409
Dy–Ir, dysprosium hyperfine magnetic field in intermetallic compounds of, (E), 20: 22330
Dy–La, electric conductivity at 4.2, 77, and 296°K, 20: 22312(R) (AD-622796)
Dy–Mn, crystal structures of intermetallic compounds of, 20: 21403
Dy–Mn, dysprosium hyperfine magnetic field in intermetallic compounds of, (E), 20: 22330
Dy–Mn, phase diagram, 20: 21403
Dy–Nd, electric conductivity at 4.2, 77, and 296°K, 20: 22312(R) (AD-622796)
Dy–Ni, dysprosium hyperfine magnetic field in intermetallic compounds of, (E), 20: 22330
Dy–Pr, electric conductivity at 4.2, 77, and 296°K, 20: 22312(R) (AD-622796)
Dy–Pt, dysprosium hyperfine magnetic field in intermetallic compounds of, (E), 20: 22330
Dy–Rh, dysprosium hyperfine magnetic field in intermetallic compounds of, (E), 20: 22330
Dy–Ru, dysprosium hyperfine magnetic field in intermetallic compounds of, (E), 20: 22330
Dy–Sn, electric conductivity at 4.2, 77, and 296°K, 20: 22312(R) (AD-622796)
Dy–Tb, magnetic transformations in, 20: 21409
Dy–Tm, magnetic transformations in, 20: 21409
DYSPROSIUM CHLORIDES
magnetic properties of, 20: 22311(R) (AD-622068)
DYSPROSIUM COMPLEXES
with 2,4-pentanedione, preparation and crystal structure of, 20: 20700
DYSPROSIUM ETHYL SULFATES
dysprosium EPR pair spectra in, 20: 22311(R) (AD-622068)
DYSPROSIUM IONS
electron paramagnetic resonance pair spectra in dysprosium ethyl sulfate, 20: 22311(R) (AD-622068)
DYSPROSIUM ISOTOPES Dy-157
beta decay of, terbium-157 level lifetimes from, (E), 20: 22058

DYSPROSIUM ISOTOPES Dy-160
proton inelastic scattering at 12 Mev, excitation of octupole vibrational states by, (E), 20: 22100
DYSPROSIUM ISOTOPES Dy-161
Mössbauer effect in dysprosium intermetallic compounds, hyperfine magnetic field from, (E), 20: 22330
DYSPROSIUM ISOTOPES Dy-164
proton inelastic scattering at 12 Mev, excitation of octupole vibrational states by, (E), 20: 22100
DYSPROSIUM NITRIDES
preparation by reactive arc melting, 20: 21244
DYSPROSIUM OXIDES
solubility in ethyl, isopropyl, methyl, and propyl alcohols in the presence of ammonia, 20: 20686

E

EARTHQUAKES
seismic data from, for comparison with underground explosions, 20: 20900 (AD-627039)
seismic data from, for comparison with underground explosions, 20: 20901 (AD-627040)
seismic data from, for comparison with underground explosions, 20: 20902 (AD-627051)
seismic wavetrain propagation from, interpretations of, 20: 20910
ECOLOGY
effects of climatic zones on forest, 20: 20879 (BNWL-SA-530)
effects of dietary habits on, of deer and sheep, 20: 20388 (SAN-34-2)
effects of nuclear weapons on, environmental, 20: 20930 (HI-518-RR (Vol.1))
effects of nuclear weapons on, environmental, 20: 20931 (HI-518-RR (Vol.2))
of Doe Run, Meade County, Ky., 20: 20884(R) (TID-22815)
radiation effects in, design of portable γ source for studies of, 20: 20380 (TID-22499)
EINSTEINIUM
production of, review of methods for, 20: 20796
EINSTEINIUM ISOTOPES E_{s}-254
alpha decay of, berkelium-250 levels from, (E), 20: 22142
ELASTICITY
calculation of axisymmetric and plane, computer program for general, 20: 20862 (WAPD-TM-555)
oscillations in magnetothermo-, uniqueness theorem for homogeneous isotropic bodies, 20: 21793
ELECTRIC ARCS
current-voltage characteristics of high-pressure nonstationary a-c, (T), 20: 21809
stability of magnetically confined, in transverse supersonic gaseous flow, 20: 21802
ELECTRIC CELLS
efficiency of fission-, fragment transport effects on, 20: 21576
ELECTRIC CHARGES
motion in cold plasma, Cherenkov radiation from, (T), 20: 22290
quantum field theory of, 20: 21865
ELECTRIC CONDENSERS
discharge circuit for, 20: 22303(P)
radiation effects on current induction in commercial capacitors, electron beam, fast neutron, and gamma, 20: 21151 (IBM-66-825-1944)
ELECTRIC CONDUCTIVITY
effects on MHD channel flow, (T), 20: 21780 (AD-622036)
ELECTRIC CURRENTS
magnetic field excitation by pulsed, in cylinder with coaxial shield, (T) 20: 21456
ELECTRIC DISCHARGE
current-voltage characteristics in arc, (T), 20: 22178 (FEI-17)
diffusion coefficient for low-pressure Penning, for flute instability, (E), 20: 22249
effects of pulsed, on cathodes in parallel-electrode plasma gun, 20: 22292
effects on cracking of butane and isobutane foams, 20: 20740
electron distribution in argon, helium, and neon, (E), 20: 21795
plasma production from, in heavy-current-vacuum circuit breaker, 20: 22291
theory of two-dimensional low-pressure, for ion generation, 20: 21799
ELECTRIC FIELDS
effects on argon and xenon alpha-induced luminescence decline, (E), 20: 21521
effects on heat transfer from reactor fuel elements to ionized carbon dioxide, 20: 20859 (UJV-1421/65)
effects on molecular hydrogen ion injection in HX apparatus, (E), 20: 22207
measurement in superconducting accelerator cavities, 20: 21459 (AD-623509)
plasma acceleration in constant and high-frequency, (T), 20: 22289
ELECTRIC INSULATORS
testing polymeric, 20: 21431(R) (WADC-TR-55-58(Pt.9))
thermal conductivity of, effect of heat transport by radiation on, 20: 22329
use of polymeric, in pocket dosimeters, 20: 21158
ELECTRIC POWER
production by fusion, review of research on, 20: 22302
ELECTRIC PROBES
current collected in magnetized plasma, electron temperature from, 20: 22259
design and performance of high-frequency dielectric resonance, for plasma density measurements, 20: 22219
performance for diagnostics of perturbed plasma, (E), 20: 22260
performance of electrostatic parallel-plate, for plasma diagnostics, (T), 20: 22192
performance of Langmuir, for plasma diagnostics, (E/T), 20: 22193
properties of double Langmuir, for plasma ion temperature measurement, 20: 22213
ELECTRIC PROPERTIES
measurement at high pressures, device for, 20: 21357 (UCRL-16299)
radiation effects on, of plant cells, γ, 20: 20419
ELECTRICITY
production by power reactors, 20: 22444
ELECTROCHEMICAL CORROSION
symposia on, New York, March 11–15, 1963, 20: 21276
ELECTRODES
design for Moellenstedt electron velocity analyzer, 20: 21005
erosion in vacuum discharges, 20: 22291
radiation effects on processes at polonium-210, 20: 20791
thermionic emission from cesiated surfaces of refractory, (E), 20: 21584
ELECTRODYNAMICS
Rainich problem in nonlinear, Born-Infeld theory for, 20: 21844
ELECTROLYTIC CELLS
design for winning plutonium from plutonia in molten fluoride salts, 20: 21234 (DP-1021)
design of ceramic, for winning and refining of plutonium, 20: 21239 (RL-SEP-824)
ELECTROLYTIC SEPARATION PROCESSES
description of, for short-lived isotopes, review of, 20: 20826
ELECTROMAGNETIC FIELDS
gravitational field propagation in, 20: 21853
Maxwell-Einstein equations for, geometrization of, 20: 21842
plasma cylinder containment in uniform magnetic field by rotating, (T), 20: 22288
properties in magneto-active plasma, (T), 20: 22199
ELECTROMAGNETIC SEPARATION
ion source for, extraction and formation in plasma, 20: 21213 (IAE-974)
ELECTROMAGNETIC WAVES
absorption, reflection, and transmission through plasma layers, 20: 22297
amplification in plasma columns, (T), 20: 22211
effect of h-f traveling, on radial charged-particle flux in hydrogen plasma, (T), 20: 22301
electron acceleration by, in longitudinal magnetic field, (T), 20: 21485
emission from acoustic point-source antenna, in compressible plasma bubble, (T), 20: 22196
interactions with charged particles in magnetosphere, 20: 21825
interactions with plasma, effects of velocity-dependent collision frequency on, (T), 20: 22256
propagation at sum and difference frequencies in plasma, nonlinear, (T), 20: 22244
propagation from rotating spheroid field equations for, 20: 21868
propagation in boundless nonlinear plasma in strong magnetic field, self-focusing effects in, (T), 20: 22200
propagation in compressible plasma gaps, properties of, 20: 22163 (AD-621034)
propagation in inhomogeneous isotropic hot plasmas, (T), 20: 22165 (AD-621457)
propagation in isotropic stratified plasma waveguide, 20: 22204
propagation in magnetoplasma, models for, (T), 20: 22174 (AD-623789)
propagation in plasma, research on, 20: 22172(R) (AD-623718)
propagation in plasma, collisional effects near electron cyclotron frequency on, (E/T), 20: 22228
propagation in plasma across magnetic field, reflection at upper hybrid frequency of, (T), 20: 22261
propagation in plasma layer, kinetic theory for, 20: 22270
propagation of circularly polarized plane, in helium plasma along magnetic field, (E), 20: 22236
propagation of linearly polarized, in helium plasma along magnetic field, (E), 20: 22237
scattering by electro-acoustic waves in mercury plasma arc column, (E), 20: 22232

scattering from plane boundary of semi-infinite plasma, frequency doubling in, (T), 20: 22271

ELECTROMAGNETISM

oscillations in thermoelastic, uniqueness theorem for homogeneous isotropic bodies, 20: 21793

ELECTROMETERS

design of solid-state, for beta-ray thickness gages, 20: 21013

ELECTRON BEAMS

bunching in crossed electric and magnetic fields, trochoidal, (E), 20: 21450

current density of, thermal limitations of, 20: 21632

effects on current induction in commercial capacitors, 20: 21151 (IBM-66-825-1944)

effects on defect introduction rate in n-type silicon, energy dependence of, 20: 21154(R) (N-65-23290)

effects on degenerate silicon at low temperatures, 20: 22346

effects on electric discharge figures in dielectrics, 20: 21440

effects on impurity diffusion in silicon semiconductors, 20: 21147(R) (AD-621049)

effects on OM_2 terphenyl at 250 to 450°C, 20: 20721 (EUR-2295.f)

effects on polyethylene oxides at 14°C, 20: 20766

energy conservation theorem for multivelocity, small-signal, 20: 24155

focusing in accelerator tubes, (T), 20: 21487

interactions in plasma, nonlinear effects from, (E), 20: 22206

interactions with electron beams at 300 Mev, angular distributions for, (E), 20: 21588 (AD-623658)

interactions with plasma, nonlinear diffusion with recombination in, (T), 20: 22266

oscillations in linear accelerators with large currents, asymmetric wave effects on radial-expansion, 20: 21476

reactions with gases, electrostatic and magnetic pinch effects in plasma from, 20: 22221

reactions with metals at 6 to 23 kev, optical transition radiation from, 20: 21518

reactions with polystyrene films at low energies, space charge buildup from, 20: 22344

space-charge waves in, decay of, (T), 20: 21452

stability in crossed fields, diocotron amplification in, (E/T), 20: 21451

trajectory of intense nonaccelerated, with self-field forces, (T), 20: 21736

transmission through aluminum slabs at 1 Mev, energy spectra from, 20: 21524

velocity analyzer for, characteristics of Moellenstedt, 20: 21005

ELECTRON MICROSCOPY

radiation effects on organic polymers in, 20: 20762

ELECTRON PAIRS

Cherenkov radiation from, energy yield for, (T), 20: 21633

photoproduction of, virtual Compton effect on cross sections for, (T), 20: 21623 (JINR-P-2602)

photoproduction on carbon at 1 to 5 Bev, cross sections for, (E/T), 20: 22146

production in bremsstrahlung reactions with carbon at 5 Bev, (E), 20: 21664

ELECTRON SOURCES

design of low-voltage, high-intensity, for electron diffraction experiments, 20: 21632

ELECTRON TUBES

performance of klystron-buncher, with space-charge effects, 20: 21014

plasma coupling media for traveling wave, properties of, 20: 20985 (N-65-29669)

x-ray emission from high-voltage pulsed, dosimetry of, 20: 21022 (AD-624230)

ELECTRONIC EQUIPMENT

circuits in, for physics experiments, properties of integrated, 20: 20998

design for multiple measurements of radioactivity, 20: 21055

radiation effects on, pulsed x-ray facility for studying, 20: 20838 (AD-624019)

radiation effects on, review of, 20: 21156

ELECTRONS

acceleration in longitudinal magnetic field, by plane electromagnetic wave propagation, (T), 20: 21485

charge-density waves in radial flux of, 20: 21449

content in ionosphere, differential Doppler and Faraday effects for determining fluctuations in, (E/T), 20: 21816

density distribution in daytime F2 layer, 20: 21823

density distribution in ionospheric D region, weak partially reflected wave amplitudes for determining, (T), 20: 21819

density fluctuations in plasma, Langmuir probe technique for measuring, (E/T), 20: 22193

density in plasma in geomagnetic tail, 20: 21828

density in plasma, nonfloating triple probe technique for measuring, 20: 22214

density in plasma, determination using radial transmission line, 20: 22171 (AD-622811)

detection and measurement in space, system for, 20: 21116

detection and measurement of low-energy, semiconductor device for, 20: 21138

detection of, gas Cherenkov counter for, 20: 21071

detection using lithium-drifted germanium and silicon detectors, 20: 21102

distribution in argon, helium, and neon discharges, (E), 20: 21795

distribution in magnetosphere, general Fokker-Planck equation for, 20: 21813 (N-65-29816)

effects of pulsed, on aqueous solutions of catalase, hydrogen sulfide, nitromethane, and tetranitromethane, 20: 20735

effects on aluminum and platinum, 20: 22520(R) (NAA-SR-11805)

effects on antimony–gallium semiconductors, 20: 22520(R) (NAA-SR-11805)

effects on doped silicon crystals, annealing of E centers from, (E), 20: 22323

effects on lithium fluoride, R-center luminescence from, (E), 20: 22331

effects on optical properties of adhesives and glass, 20: 21446

effects on organic polymers, at 300 to 500 kv, 20: 20762

effects on performance of solar cells at 10 to 90°C, 20: 21161

effects on silicon devices in space, 20: 21165

effects on sodium chloride at 50 kev, 20: 20781

emission from cesiated surfaces of refractory compounds, 20: 21584

emission from rare-gas ion reactions with beryllium–copper alloys at 3 to 90 kev, secondary, (E), 20: 21538

emission of secondary, statistics of, 20: 21448

energy and flux in auroral ionosphere, 20: 21826

energy and lifetime in outer radiation belt, (E), 20: 21815

energy distributions in cesium thermionic cells, electrostatic probe measurement of, 20: 21560(R) (AD-621276)

energy losses in supernovae, 20: 21499

flux at latitudes beyond outer radiation belt, correlation with v-l-f hiss, 20: 21824

interactions in plasma, high-density corrections to cross sections for, (T), 20: 22268

lifetime of low-energy, in outer radiation belt at magnetically quiet times, (T), 20: 21817

mass of, relativity theory for electromagnetic, 20: 21631

mass relative to mesons (μ) from spontaneous symmetry breakdown, 20: 21678

mobility in cesium and potassium vapor at low energies, (E), 20: 21520

motion in cold, dense, magnetized plasma, complex Doppler effect on radiation from, (T), 20: 22198

motion in plasma, electrostatic damping of, (T), 20: 22233

motion in uniform magnetic field, self-consistent hydrodynamic approximation for relativistic, 20: 22287

motion of, hydrodynamic model for, 20: 21840

precipitation in auroral-zone ionosphere, correlations with leakage from magnetic mirrors, (E), 20: 21836

production in photon-initiated showers, mean square angular and lateral spreads for, (T), 20: 21557

radiosensitivity effects of hydrated, in aqueous lysozyme solutions, 20: 20423

reactions of hydrated, with amino acids, 20: 20403

reactions of hydrated, with hydrogen sulfide, nitromethane, and tetranitromethane in pulse radiolysis, 20: 20735

reactions with ground-state helium ion beams at threshold to 750 ev, helium ion (2S) production from, (E), 20: 21535

reactions with ions in nonequilibrium plasma, 20: 22195

reactions with solid targets in plasma, bremsstrahlung from, (E), 20: 22293

reactions with xenon, electron cascade curves for, (T), 20: 21514 (INR-598/VI/PH)

scattering by aligned deformed nuclei, amplitudes of high-energy, 20: 22124

scattering by beryllium 9, excitation of electromagnetic transitions by inelastic, (E), 20: 22105

scattering by carbon-12 and oxygen-16, excitation of spin-isospin giant resonance by, (T), 20: 22088

scattering by chlorine-35 and fluorine-19, Coulomb, (T), 20: 21649

scattering by helium at 0 to 14 ev, modified effective-range theory for, 20: 21517

scattering by holmium at high energies, analysis of, (T), 20: 22124

scattering by light nuclei to 230 Mev, magnetic form factors from elastic, (E), 20: 22120

scattering by lithium-6, single harmonic-oscillator parameter for inelastic, (T), 20: 22063

scattering by nuclei, two-nucleon correlation functions from cross sections for inelastic, (T), 20: 21996 (FTI-142/T-016)

scattering by phosphorus-31 and sulfur-32 at 50 Mev, differential cross sections for inelastic, (T), 20: 21964 (AD-626684)

scattering in aluminum at 4.2 to 300°K, effects of impurity centers on,

20: 22314(R) (AD-626865)
stability of paramagnetic ground state of dense gas of, (T), 20: 21805
stability of plasma of hot, effect of cold background on, (T), 20: 22264
superconductivity of gas of, in homogeneous magnetic field, (T), 20: 21887
temperature fluctuations in plasma, Langmuir probe technique for measuring, (E/T), 20: 22193
temperature in afterglow plasma, spatial variations of, (E/T), 20: 22242
temperature in argon plasma, equivalence of excitation temperature and, (E), 20: 22267
temperature in ionosphere, effects on density distribution, 20: 21823
temperature in magnetized plasma from electron-probe current, 20: 22259
temperature in plasma, nonfloating triple probe technique for measuring, 20: 22214
temperature in plasma, double probe method for determining, 20: 22192
temperature in r-f generated plasma, method for measuring, (E), 20: 22194
temperatures in helium plasma, spectroscopic measurement of, 20: 22210
temperatures of, in gases of MHD cells, (T), 20: 21573
trajectories in focused magnetic fields, pressure effects on lifetime of, (E/T), 20: 21482

ELECTROSTATIC PRECIPITATORS
development for radon decay products, 20: 21067

ELEMENT ONE HUNDRED AND THREE
production of, review of methods for, 20: 20796

ELEMENTARY PARTICLES
book: *High Energy Physics*, 20: 21696
book: *The Fundamental Particles*, 20: 21695
charge and mass distributions of spherically symmetric, in static case in general relativity, 20: 21634
charge of quarks, 20: 22460 (IC-66/28)
decay of, pole model for nonleptonic, 20: 21688
decay of, unitary symmetry for, 20: 21708 (CONF-640509(Pt.2), Paper 2)
density matrix of spin-one, positivity conditions for, (T), 20: 21764
electromagnetic structure of quarks, 20: 21625 (JINR-P-2619)
energy levels of, Feynman–Gell-Mann equation solutions for Coulomb field for bound and continuum, 20: 21767
field theory of, quantum, (T), 20: 21704 (AD-622517)
form factors of, energy-momentum structure, 20: 21758
interactions at high energies, review of elastic, 20: 21593 (CERN-65-24(Vol.1), pp 65-80)
interactions in stars, energy release mechanism from, (T), 20: 21498
interactions of quarks in SU(3) theory, 20: 21766
interactions of quarks as stellar energy release mechanism, (T), 20: 21498
interactions of stable with unstable, three-body resonance system from, (T), 20: 21724
interactions of, analytic S-matrix theory of strong, 20: 21774
interactions of, diagram technique for many-body, (T), 20: 21728
interactions of, γ_5 invariance spontaneous breakdown in parity-nonconserving, (T), 20: 21727
interactions of, isospin conservation and polarization effects in, (T), 20: 21717 (JINR-P-2620)
interactions of, inelastic, (E/T), 20: 21592 (CERN-65-24(Vol.1), pp 1-44)
interactions of, model for final-state, 20: 21738
interactions of, motion of poles in Lee model for, 20: 21769
interactions of, peripheral model for, 20: 21699
interactions of, peripheral model for, 20: 21705 (CERN-65-24(Vol.1), pp 45-63)
interactions of, poles of proper vertex function in, 20: 21735
interactions of, structure of weak currents for, 20: 21743
interactions of, saturation of SU(3)-symmetric hadron forces in, 20: 21760
interactions of, SU(3) symmetry for three-particle final states in, 20: 21763
interactions of, theory of weak, 20: 21700
interactions of, threshold behavior of p-wave amplitudes for three-body, 20: 21747
interactions of, theory of strong, 20: 21773
interactions of, unitary symmetry for weak, 20: 21708 (CONF-640509 (Pt.2), Paper 2)
interactions of, weak currents in broken U(3) ⊗ U(3) for, 20: 21762
interactions with deuterons, at high energies, shadow effect in, (T), 20: 21646
kinetics of, simultaneous Lorentz and Galilean invariant, 20: 21867
mass of 0-spin 2h system of, nonlinear wave equations in quantum field theory for, 20: 21723
masses of, dispersion-theoretical perturbation series in particle models for, 20: 21683
model of, saturation problem in nonrelativistic quark, 20: 21748
models for strongly interacting, quark, (T), 20: 21697
properties of, review of, 20: 21691
reactions with nuclei, coherence properties for low-momentum transfer, 20: 22145
research on, survey of experimental, 20: 21692
scattering by system of fixed centers, amplitudes for, 20: 21710 (JINR-P-2554)
symmetries for, trace if ν-th power of matrix using recursion relations for internal groups in, 20: 21737
symmetries of, lectures on, (T), 20: 21771
symmetry for, axial and vector weak currents in G_2 group, 20: 21719
symmetry for, concepts of sources and charges in broken, 20: 21745
symmetry for, consequences of unitary, 20: 21709 (CONF-640509(Pt.2), Paper 6)
symmetry for, de Sitter, Lorentz, and Poincare group generalizations in, 20: 21720
symmetry for, eightfold formalism in SU(3), 20: 21711 (JINR-P-2559)
symmetry for, irreducible representation of $\bar{U}(12)$, 20: 21765
symmetry for, lectures on unitary, 20: 21770
symmetry for, nonrelativistic limit for Poincare group in, 20: 21721
symmetry for, review of unitary, 20: 21707 (CONF-640509(Pt.2), Paper 1)
symmetry for, single-particle representations of current algebras in, 20: 21750
symmetry for, unitary representations of SU(1,1) and SU(2,1), 20: 21722
symmetry group combining spin and isospin, (T), 20: 21772
symmetry groups for, charge conjugation in unitary, 20: 21725
theory for, quantum, 20: 21703 (AD-622258)
theory of, rudimentary geometric, 20: 21726

ELEMENTS
decay of heavy, lifetime for, (T), 20: 22043
determination by atomic absorption, bibliography on, 20: 20563 (NP-15918)
synthesis in stars, statistical equilibrium in, (T), 20: 21492

EMBRYONIC TISSUES
morphology and oxygen consumption of, effects of nitrogen mustard on, 20: 20372

EMBRYOS
phosphorus-32 metabolism in developing chick, 20: 20399
radiation effects on physiology and respiration of chick, x, 20: 20440(R) (EUR-2643.f)
thymidine incorporation in ovaries of chicken, *in vitro*, 20: 20395

ENZYMES
radiation effects on synthesis in rat liver, x, 20: 20429(R) (AD-629311, pp 15-25)
radiation effects on activity in chick embryos, x, 20: 20440(R) (EUR-2643.f)
radiosensitivity of enolase, effects of nicotinamide adenine dinucleotide and 2-phosphoglyceric acid on, 20: 20514
radiosterilization effects on activity of, in citrus fruits and tomatoes, 20: 21195(R) (TID-22509)
synthesis of mandelate pathway, in Pseudomonas mutants, 20: 20376
synthesis of mandelate pathway, in Pseudomonas mutants, 20: 20470

EOSIN
effects on radioinduced oxidation of ergosterol, 20: 20738

EPIDEMIOLOGY
of New Jersey radium cases, 20: 20387(R) (NYO-2181-3)

EPITHELIUM
radiation effects on rabbit skin, 20: 20477

EQUIPMENT AND PROCEDURES
for analysis of lunar surface, 20: 21003
for EBR-II fuel cycle facility operations, 20: 20802(R) (ANL-7055, pp 21-98)

ERBIUM
determination in rare earth mixtures, activation, 20: 20562 (LYCEN-6538)
friction and wear properties of, in vacuum, effects of crystal structure on, 20: 21365
oxidation in dry and moist air at 100 to 800°C, rate of, 20: 21265 (RPI-2714-8)
reactions with powdered graphite, preparation of intercalation compounds by, 20: 20648 (AD-621029)
separation from perchloric acid solutions by ion exchange materials, 20: 20823
separation from uranium by combined ion exchange-solvent extraction using nitric acid–tetrahydrofuran solutions, 20: 20811

ERBIUM ACETATES
preparation by oxide solubility in alcohols containing ammonia, 20: 20686

ERBIUM ALLOYS
Al–Er, crystal structure and stability of intermetallic compounds in, 20: 21415
Er–Gd, magnetic transformations in, 20: 21409
Er–Ho, magnetic transformations in, 20: 21409
Er–Mn, crystal structures of intermetallic compounds of, 20: 21403
Er–Tb, magnetic transformations in, 20: 21409

Er–Tm, magnetic transformations in, 20: 21409
ERBIUM ETHYL SULFATES
Zeeman effect at 1.6°K, M1 transitions from, (E), 20: 21881
ERBIUM ISOTOPES Er-167
neutron resonance absorption by, cross sections for Doppler-broadened, (T), 20: 21951
ERBIUM NITRIDES
preparation by reactive arc melting, 20: 21244
ERBIUM OXIDES
solubility in ethyl, isopropyl, methyl, and propyl alcohols in presence of ammonia, 20: 20686
ERBIUM SYSTEMS
Er–graphite, preparation and magnetic susceptibility of, 20: 21413
ERGOSTEROL
radioinduced oxidation of, chromatographic method for separating products in, 20: 20738
ESCHERICHIA COLI
nuclear structure in, effects of uranyl ions on, 20: 20392
radiation effects on DNA metabolism in, γ, 20: 20421
radiation effects on, mechanism for hadacidin potentiation of, 20: 20456
radiation effects on viability of, evaluation of acridine orange fluorescence test for, 20: 20457
radiosensitivity of bacteriophage complexes of, uv, 20: 20471
ETHANE
production by gas discharge and radioinduced cracking of butane, 20: 20740
radioinduced deuterium exchange reactions in gaseous, mechanism of tritium, 20: 20719 (AD-624657)
ETHANE, BROMO-
radiation effects on, isotopic and phase effects in neutron, 20: 20751
ETHANE, DIETHOXY-
solvent properties for neptunium, 20: 20561 (JAERI-1099)
ETHANE, DIMETHOXY-
radiolysis, 20: 20758
ETHANE, IODO-
radiolysis of frozen, in glass and polycrystalline states, 20: 20716 (AD-621022)
ETHANETHIOL, 2-AMINO-
radiosensitivity effects in chick embryo tissue cultures, 20: 20440(R) (EUR-2643.f)
radiosensitivity effects in rats, x, 20: 20509
radiosensitivity effects on mouse spleen, 20: 20511
ETHANOL
determination by xenon trioxide oxidation, titrimetric, 20: 20579
radioinduced telomerization with ethylene, yields from beta, 20: 20724(R) (NYO-2978-44)
radiolysis of, yields from gamma, 20: 20746
solvent properties for rare earth oxides in the presence of ammonia, 20: 20686
benzene–ethanol, radiolysis of, at 20 and –196°C, yields from gamma, 20: 20741
benzene–ethanol, radiolysis of, at –196°C, EPR spectra of ethyl radicals from gamma, 20: 20742
ETHERS
radiation effects on bulk compressibility and electric conductivity of cyclic, 20: 21418 (AD-627049)
ETHYL ETHER
radioinduced addition to 1,2-dichlorohexafluorocyclopentene and 1,2-dichlorotetrafluorocyclobutene, 20: 20773
ETHYL RADICALS
electron paramagnetic resonance spectra of, in gamma-irradiated benzene–ethanol mixtures, 20: 20742
ETHYLENE
production by gas discharge and radioinduced cracking of butane, 20: 20740
radioinduced polymerization with isocyanic acid at low temperatures, 20: 20747
radioinduced reactions with dichloromethane, gamma, 20: 20757
radioinduced telomerization with ethanol and methanol, yields in beta, 20: 20724(R) (NYO-2978-44)
carbon tetrachloride–ethylene–2-methylbutane, radiolysis of, tracer studies of mechanisms in, 20: 20752
ETHYLENE, CHLORO- POLYMERS
effects of decontaminating and descaling solution on coating of, 20: 21238 (NP-15928)
radiation effects on, role of LET in gamma and helium-4/lithium-7, 20: 20764
radioinduced electric discharge figures in, electron, 20: 21440
paraffin–polyvinyl chloride, properties as gamma dosimeter, 20: 21076
ETHYLENE, CHLOROTRIFLUORO- POLYMERS
radiation effects on dielectric properties of, 20: 21443
ETHYLENE, FLUORO-
radioinduced polymerization of, at low temperatures, 20: 20718(R) (AD-623307)
ETHYLENE OXIDE POLYMERS
radiation effects on, of electrons at 300 to 500 kv, 20: 20762
radiolysis of, kinetic measurements on electron beam, 20: 20766
ETHYLENE POLYMERS
energy absorption from meson (π^-) and proton beams, 20: 20525
neutron inelastic scattering at 0.0154 to 0.317 mev, (E), 20: 21943
neutron scattering at 0.167 to 0.499 ev, cross sections for, (E), 20: 21952
performance for separating fissile materials, 20: 20840(R) (BNWL-193, pp 57-67)
radiation effects on electric conductivity of, γ, 20: 21170
radiation effects on, of electrons at 300 to 500 kv, 20: 20762
radiation effects on dielectric properties of, 20: 21443
radioinduced polymerization of, ESR spectral studies on, 20: 20727 (PB-181506, pp 9-18)
radioinduced proton polarization in, neutron, (E), 20: 22345
B–polyethylene, performance for separating fissile materials, 20: 20840(R) (BNWL-193, pp 57-67)
ETHYLENE, TETRAFLUORO- POLYMERS
analytical use for reversed-phase partition chromatography separation of rare earths, 20: 20621
analytical use for partition chromatography separation of europium from irradiated terbium oxide, 20: 20622
analytical use for chromatographic separation of cerium from lanthanum, 20: 20623
radiation effects on dielectric properties of, 20: 21443
ETHYLENE, TETRAPHENYL-
effects on radioinduced decomposition of Santowax-OM1, 20: 20708 (AEET-213)
EUGLENA
radioinduced inactivation of green colony-forming ability in, uv, 20: 20450
EUROPIUM
determination in rare earth mixtures, activation, 20: 20562 (LYCEN-6538)
oxidation in dry and moist air at 100 to 800°C, rate of, 20: 21265 (RPI-2714-8)
separation from irradiated terbium oxide by partition chromatography on polytetrafluoroethylene, 20: 20622
separation from nitrate solutions by solvent extraction using tricapryl-methylammonium nitrate, 20: 20812
separation from perchloric acid solutions by ion exchange materials, 20: 20823
separation from rare earths by reversed-phase partition chromatography on polytetrafluoroethylene, 20: 20621
separation from uranium by combined ion exchange-solvent extraction using nitric acid–tetrahydrofuran solutions, 20: 20811
EUROPIUM CARBIDES
vaporization behavior of $EuC_{1.87}$, 20: 20666
EUROPIUM COMPLEXES
with bipyridines, fluorescence of, effects of methyl substitution on, 20: 20703
with 2,4-pentanedione, preparation and crystal structure of, 20: 20700
EUROPIUM HYDROXIDES
crystal structure of hydrates of, 20: 20694
EUROPIUM IONS
electron paramagnetic resonance of, in liquid ammonia solutions, 20: 20668
sorption by silver iodide, tracer studies on, 20: 20683
EUROPIUM ISOTOPES Eu-145
decay of, coincidence spectra from, (E), 20: 22003 (JINR-P-2581)
EUROPIUM ISOTOPES Eu-155
beta decay of, gadolinium-155 level lifetimes from, (E), 20: 22058
EUROPIUM ISOTOPES Eu-157
beta decay of, gadolinium-157 level lifetimes from, (E), 20: 22058
EUROPIUM OXIDES
solubility in ethyl, isopropyl, methyl, and propyl alcohols in presence of ammonia, 20: 20686
EUROPIUM SELENIDES
luminescence of ferromagnetic, 20: 22334
magnetic structure in, pressure-induced changes in, (E), 20: 22332
EUROPIUM SULFIDES
electric properties of single crystals of, 20: 22312(R) (AD-622796)
EXPERIMENTAL BOILING WATER REACTOR
loading of fuel elements for, stresses in Zircaloy-2 cladding during vibratory, 20: 21289 (BNWL-194)
EXPERIMENTAL BREEDER REACTOR-II
fuel element failure detection system of, data processing unit of, 20: 22439
fuel processing, development and testing equipment and facilities for, 20: 20802(R) (ANL-7055, pp 21-98)
EXPERIMENTAL GAS COOLED REACTOR

control rods for, fabrication of, 20: 21292 (ORNL-3932)
shutdown system for, design of rate-of-change-of-pressure, 20: 22417 (TID-22759)

EXTRACTION APPARATUS
performance of stacked-clone, using Amsco, hexone, and mineral oil, 20: 20808(R) (ORNL-3916)

EYE LESIONS
effects of iodoacetate on rabbit, 20: 20507(T)

F

FALLOUT
bibliography on, 20: 20882(R) (HASL-171)
distribution in alpine watershed, 20: 20379 (COO-1191-10)
dose criteria for, from reentry burnup of SNAP reactors, 20: 20937 (NAA-SR-11761)
gamma angular distributions and energy above infinite field, Monte Carlo calculations of, 20: 20878 (AD-612030)
monitoring in biota of Doe Run, Meade County, Ky., 1959 to 1965, 20: 20884(R) (TID-22815)
monitoring in Boulder County, Colo., 1962 and 1963, 20: 20379 (COO-1191-10)
monitoring in Canada, 1964, 20: 20938 (NP-15921)
monitoring in Canada, 1965, 20: 20883 (NP-15914)
monitoring in Colorado, 20: 20384 (COO-1156-13)
monitoring in Great Britain, 1964 and 1965, 20: 20926(R) (ARCRL-14)
monitoring in New Zealand, 1965, 20: 20882(R) (HASL-171)
monitoring in U.S., 1965, 20: 20882(R) (HASL-171)
shelters against, sensitivity analysis of components and systems of, 20: 20922 (AD-624704)
tritium content of, in southern hemisphere, uses of strontium-90 for estimating, 20: 20892
uptake of real and simulated, by man, 20: 20466

FAST FLUX TEST FACILITY
fuel critical mass calculations for, 20: 22494(R) (BNWL-193, pp 30-44)

FAST REACTORS
coolant ejection from, in accidents, shock front conditions in, 20: 22348
coolant-loss accidents in sodium-cooled, analysis of, 20: 22349
coolants for, comparison of carbon dioxide, helium, and steam as, 20: 22452
cost analysis of 1000-Mw(e) sodium-cooled power, 20: 22451
design of prototype, using plutonium fuel, 20: 22441
design of sodium-cooled power breeder, vented fuel concept applied to, 20: 22462
design of 1000-Mw(e) sodium-cooled breeder, 20: 22453
design of 1000-Mw(e) sodium-cooled breeder, 20: 22454
fuels for, methods of preparation of, 20: 20802(R) (ANL-7055, pp 21-98)
neutron Doppler coefficients for, (T), 20: 22378 (KFK-367)
neutron flux in two-region, Monte Carlo calculations for heterogeneity of, 20: 22397
neutron group cross sections in, effects of randomness on, 20: 22391
safety analysis of large, 20: 22401
safety analysis of 1000-Mw(e) sodium-cooled power, 20: 22451

FEEDBACK SYSTEMS
design and performance of, for drive system control in Mössbauer spectrometers, 20: 21079

FERMIONS
interactions with phonons, Schroedinger equation solution for, (T), 20: 21619 (JINR-P-2567)
interactions with bosons, Lee model for, 20: 21718
motion in single delta-function potential, one-dimensional, 20: 21851

FERMIUM
production of, review of methods for, 20: 20796

FERTILIZERS
metabolism by plants, tracer study, 20: 20389 (STI-PUB-108)

FETUSES
iodine-131 metabolism in rat, 20: 20390(R) (TID-22767)
radiation dose to rat, from prenatally administered iodine-131, 20: 20390(R) (TID-22767)
radiation doses to, in isotopic placentography using human serum albumin labeled with iodine-131 or iodine-132, 20: 20537
radiation effects on nervous system in rat, x, 20: 20492

FIBRIN
radiation effects on structure of, γ and x, 20: 20490

FIBRINOGEN
radiation effects on properties of, γ and x, 20: 20490
radiation effects on properties of, x, 20: 20491

FIELD THEORY
boson propagators in, perturbative expansions of, 20: 21741
commutators and physical sum rules in, saturation of equal-time, 20: 21749
field operators in, renormalization of ultraviolet divergences for, 20: 21742
Green functions for field propagators in, high-energy boundary conditions on, 20: 21729
Lee model in, LSZ formalism for one-boson, 20: 21718
quantum, existence of elementary particles in, (T), 20: 21704 (AD-622517)
scattering in nonlinear scalar, two-plane wave, 20: 21716 (JINR-P-2603)
spinor propagator in, spectral functions of, 20: 21740
symmetry breakdown in, concepts of sources and charges on, 20: 21745

FILMS
charged-particle ionization losses in, fluctuations of, (T), 20: 21515 (JINR-P-2615)
flow on flat surface, velocity in recirculating gravity, 20: 20651 (CU-2660-26)
thickness measurements on thin, conductance device for, 20: 20987 (RFP-690)

FILTERS
analysis for uranium-235 in air, non-destructive gamma spectrometric, 20: 20564 (NYO-10740)
design criteria and specifications of, for installation at National Reactor Testing Station, 20: 20933 (IDO-12045)
holder geometry for subisokinetic aerosol sampling in air stream, 20: 20927 (BNWL-217)
performance of activated carbon, for iodine sorption, 20: 22463(R) (DP-1028)
performance of charcoal, under HFIR and LOFT accident conditions, 20: 20940(R) (ORNL-3915)
performance of diffusion-tube and May pack, for separation of radioiodine from steam, 20: 20940(R) (ORNL-3915)
testing in nuclear safety pilot plant, 20: 20940(R) (ORNL-3915)

FIRES
fission-product release in sodium reactor coolant, 20: 22520(R) (NAA-SR-11805)

FISH
calcium-45 uptake by crucian carp, effects of stable calcium on, 20: 20405
radiation effects on development of spawn of marine, beta, 20: 20445(T) (TRG-Inf. Ser.-166)
radiation processing of perch, effects on microflora, 20: 21203
radioactivity in Clinch River, effects of ORNL wastes on, 20: 22514 (ORNL-P-2021)
radiopasteurization of, factors affecting, 20: 21200
radiopreservation of, acceptance tests for, 20: 21199
zinc-65 content in Columbia River white-, 20: 20382 (BNWL-SA-623)

FISSION
alpha particle emission in, review of long-range, 20: 21968 (AEET-235)
beta spectra from, time-dependent, (T), 20: 21960 (AD-621023)
charge distribution in low-energy, (T), 20: 22013(T) (ANL-Trans-296)
effects on metallic fuels, 20: 22520(R) (NAA-SR-11805)
kinetics, (E/T), 20: 21990 (BNL-948, pp 928-1004)

FISSION-COUNTING ANALYSIS
equipment and method for, of leached fuel elements, 20: 21040 (ORNL-P-1218)

FISSION FRAGMENTS
angular correlations from fission of excited uranium-238 and plutonium-240, 20: 22143
charge distribution, (T), 20: 22013(T) (ANL-Trans-296)
detection and measurement using silicon surface-barrier detectors, 20: 21101
gamma activity of recoil, analysis in fissile materials, 20: 21058
track registration in epitaxial uranium dioxide films, 20: 21442
transport effects on fission-electric-cell efficiency, 20: 21576

FISSION PRODUCTS
decay heat from, charcoal ignition by, 20: 20940(R) (ORNL-3915)
deposition from carrier stream, model for isothermal, (E/T), 20: 21785 (ORNL-TM-1330(Rev.))
deposition on reactor materials in air–steam, 20: 20940(R) (ORNL-3915)
diffusion in graphite fuel elements, 20: 21423 (N-65-23015)
diffusion in irradiated fuel element cladding alloys and materials at 600 to 1200°C, 20: 21232 (BMI-1763)
diffusion of, from irradiated clad urania in air–steam meltdown, 20: 20940(R) (ORNL-3915)
distribution in clad fuel meltdown residues in TREAT, 20: 20940(R) (ORNL-3915)
distribution in products of fluidized-bed fluorination of spent fuel mixtures, 20: 20803(R) (ANL-7055, pp 99-162)
management of, relation of waste solution storage to economics of, 20: 22517
production of gaseous, in sodium-cooled power breeder reactors, 20: 22462
reactions of oxidized, with bromine pentafluoride, 20: 20803(R) (ANL-7055, pp 99-162)
release in burnup of pyrolytic carbon-coated uranium dioxide fuel

particles, 20: 22411(R) (GA-6113)
release in sodium coolant fires, · 20: 22520(R) (NAA-SR-11805)
separation from reactor fuels by fluoride volatility processes, decontamination of uranium by, · 20: 20803(R) (ANL-7055, pp 99-162)
separation of cerium-144 and strontium-90 from, by oxalic acid precipitation, 20: 20804 (EUR-2754.f)
separation of cesium from waste solutions of, by ion exchange on ammonium molybdophosphate, 20: 20818
sorption and diffusion in graphite, 20: 22411(R) (GA-6113)
transport in nuclear safety pilot plant tests, 20: 20940(R) (ORNL-3915)
venting of gaseous, to coolant in sodium-cooled power breeder reactors, 20: 22462
yields from thermal neutron induced fission of uranium-235, charge distribution of $131 \leq A \leq 133$, (E), · 20: 22136

FISSIONABLE MATERIAL
fission fragments from, gamma activities of recoil, 20: 21058
handling of, safety in, 20: 20975
management of, relation of criticality control and safety to, 20: 20974
production in France, 20: 21243
production of, internal audit in plant for, 20: 22529
shipping container for, development and testing of, 20: 20936 (K-1661)
shipping of, container development for, · 20: 20840(R) (BNWL-193, pp 57-67)
storage of, container development for, · 20: 20840(R) (BNWL-193, pp 57-67)

FLAVONOIDS
complexes with molybdenum, composition and stability of, 20: 20674
complexes with thorium, composition and stability of, 20: 20674

FLOWMETERS
calibration of Long John, using air, 20: 20988 (UCRL-13202)

FLUID FLOW
control of, in channels or ducts, device for, 20: 22361
heat transfer in viscous, theory of, 20: 21794
magnetohydrodynamic, thermal stability of, 20: 20854 (AD-621523)
magnetohydrodynamic, variable conductivity effects on, (T), 20: 21780 (AD-622036)
magnetohydrodynamic, field variations in conducting, 20: 21790
magnetohydrodynamic, in inlet region of straight channel, (T), 20: 21801
magnetohydrodynamic, transverse magnetic field in Prandtl-Meyer, (T), 20: 21776 (AD-621429)
shock front conditions and sound velocity in two-phase, 20: 22348
two-phase, model for transient, 20: 22520(R) (NAA-SR-11805)
velocity of film, on flat surface, 20: 20651(R) (CU-2660-26)

FLUID FLOW (TURBULENT)
equations for annular, · 20: 20856 (GEAP-4976)

FLUID FUEL REACTORS
description of liquid-metal, survey of, 20: 22347 (ANL-7138)

FLUID PROPELLANTS
flow during startup transient of nuclear rocket motors, 20: 22480

FLUIDIZATION
of fine plutonia–uranium oxide particles, basic studies on, 20: 20803(R) (ANL-7055, pp 99-162)

FLUIDS
pressure waves in incompressible conducting, stability of tangential discontinuity of, (T), 20: 21804

FLUORAL
radioinduced polymerization of, in methylene chloride at low temperatures, 20: 20718(R) (AD-623307)

FLUORIDE VOLATILITY PROCESSES
development of fluid-bed, for aluminum–uranium and stainless steel–cermet fuels, · 20: 20801 (ANL-6830)
development of fluid-bed, for recovery of plutonium and uranium, 20: 20803(R) (ANL-7055, pp 99-162)
use for irradiated fuels, problems in design of pilot plants for, 20: 20810(T) (ANL-Trans-250)

FLUORIDES
growth and properties of crystals of, 20: 22311(R) (AD-622068)

FLUORINE
determination by activation using helium-3 ions, · 20: 20565 (ORNL-P-1216)
determination in uranium oxides by pyrolysis and alizarin complexone photometric method, 20: 20597
determination of, activation, 20: 20594
reactions with aluminum, gadolinium, holmium, and yttrium, enthalpies of, 20: 20650(R) (ANL-7055, pp 167-76)
reactions with boron and silicon carbide, thermodynamics of, 20: 20650(R) (ANL-7055, pp 167-76)
reactions with selenium, sulfur, and tellurium, enthalpies of, 20: 20650(R) (ANL-7055, pp 167-76)

FLUORINE ISOTOPES F-18
energy level transitions in, (T), 20: 21983 (BNL-948, pp 741-50)

FLUORINE ISOTOPES F-19
deuteron reactions (d,$\alpha\gamma$) at 1 Mev, neon-20 levels from, (E), 20: 22082
electron Coulomb scattering by, (T), 20: 21649
meson (μ) Coulomb scattering by, (T), 20: 21649
proton reactions (p,pγ) at 4.3 Mev in metallic media, perturbation of angular correlations from, 20: 22090

FLUOROCARBONS
radiation effects on dielectric and mechanical properties of, combined effects of low-temperature, vacuum, and gamma and neutron, 20: 21152 (N-65-22353)

FLUOROHYDROCARBONS
preparation in hydrocarbon–uranium hexafluoride reactions, 20: 20707(P)

FONTENAY-AUX-ROSES REACTORS (TRITON)
dosimetry of, design of microcalorimeter for, 20: 20721 (EUR-2295.f)

FOOD
effects of nuclear weapons on, environmental, 20: 20931 (HI-518-RR (Vol.2))
radiation processing of, wholesomeness tests after, 20: 21198
radiation processing of, legal aspects, 20: 21201
radioactivity in, Great Britain, 1964 and 1965, 20: 20926(R) (ARCRL-14)
radioactivity in, importance of measuring, 20: 20961
radionuclide content in Amsterdam, 1960 to 1963, 20: 20949
radiopreservation of, in developing countries, 20: 22525
radiopreservation of, research in Western Germany on, 20: 21193 (PB-181506, pp 29-38)
radiopreservation of, developments in research on, 20: 21194 (PB-181506, pp 155-67)
radiopreservation of, acceptance tests for, 20: 21199
radiopreservation of, review on, 20: 21206
radiopreservation of, research in U.S.A. on, 20: 21192 (PB-181506, pp 19-26)
radiopreservation of, in Japan, 20: 20727 (PB-181506, pp 9-18)
radiosterilization of, status, 20: 21196
radiosterilization of, feasibility of commercializing, 20: 21202
radiosterilization of, review on effects of, on wholesomeness, 20: 21207

FOOD IRRADIATION FACILITIES
performance and use, survey, 20: 21197

FORESTS
cesium-137 content of litter and plants of Washington state, · 20: 20879 (BNWL-SA-530)

FORMALDEHYDE
radioinduced polymerization with isocyanic acid at low temperatures, 20: 20747
yields from gamma radiolysis of ethanol, 20: 20746

FORMAMIDE, *N,N*-DIMETHYL-
effects on radioinduced polymerization of fluoral, at low temperatures, 20: 20718(R) (AD-623307)

FOSSILS
occurrence in clays and sandstone, Braunschweig, Germany, 20: 20890

FRANCE
fissionable nuclear material resources of, 20: 21243
research laboratories in, equipment design for, 20: 20851

FRANCIUM ISOTOPES Fr-223
beta decay, (E), 20: 22008 (MLM-1337J)

FREE RADICALS
radioinduced in solids, ESR studies on, 20: 20729 (PB-181506, pp 85-103)
radiosensitivity effects in aqueous lysozyme solutions, 20: 20423

FREONS
use in heavy liquid bubble chamber at CERN, 20: 21606 (CERN-65-32, pp 157-60)

FRUITS
radiopreservation of, acceptance tests for, 20: 21199
radiosterilization effects on, low-level gamma, 20: 21195(R) (TID-22509)

FUEL CELLS
conference, 20: 21581
conference, 20: 21582
conference, 20: 21583

FURAN, TETRAHYDRO-
radioinduced addition to 1,2-dichlorohexafluorocyclopentene and 1,2-dichlorotetrafluorocyclobutene, 20: 20773

HNO_3–tetrahydrofuran, solvent properties for uranium, 20: 20811

FURNACES
design and performance of, for uranium dioxide sintering in hydrogen flow, 20: 21304
design for thermal analysis of plutonium hexafluoride–uranium hexafluoride, 20: 20803(R) (ANL-7055, pp 99-162)
design of 3000°C, 20: 20842 (ORNL-TM-1410)

FUSED SALTS
corrosive effects with magnesium–uranium–zinc alloys on carbon and zirconium boride, 20: 20802(R) (ANL-7055, pp 21-98)
solvent properties for plutonium and uranium, · 20: 20802(R) (ANL-7055, pp 21-98)
viscosity of, engineering drawings of instrument for measuring, 20: 21015

G

GADOLINIUM
- determination in rare earth mixtures, activation, 20: 20562 (LYCEN-6538)
- electric and magnetic properties at high pressures, 20: 21357 (UCRL-16299)
- enthalpy of formation of GdF_3, 20: 20650(R) (ANL-7055, pp 167-76)
- friction and wear properties of, in vacuum, effects of crystal structure on, 20: 21365
- neutron scattering at 0.01 to 0.4 ev, cross sections for, (E), 20: 22010 (NYO-72-28)
- oxidation in dry and moist air at 100 to 800°C, rate of, 20: 21265 (RPI-2714-8)
- reactions with powdered graphite, preparation of intercalation compounds by, 20: 20648 (AD-621029)
- refining by solid-state electrolysis, 20: 21253
- sample preparation of, metallographic, 20: 21253
- separation from perchloric acid solutions by ion exchange materials, 20: 20823
- separation from uranium by combined ion exchange-solvent extraction using nitric acid–tetrahydrofuran solutions, 20: 20811

GADOLINIUM ACETATES
- preparation by oxide solubility in alcohols containing ammonia, 20: 20686

GADOLINIUM ALLOYS
- Al–Gd, crystal structure and stability of intermetallic compounds in, 20: 21415
- Al–Gd–Pd, electric properties of, 20: 22312(R) (AD-622796)
- Ce–Gd, crystal structure and magnetic properties, 20: 22343
- Dy–Gd, magnetic transformations in, 20: 21409
- Er–Gd, magnetic transformations in, 20: 21409
- Gd–La, magnetic properties and phase transformations in, 20: 21414
- Gd–Lu, magnetic transformations in, 20: 21409
- Gd–Mn, crystal structure and magnetic properties of intermetallic compounds of, 20: 21403
- Gd–Mn, phase diagram, 20: 21403
- Gd–Nd, ferromagnetic spin coupling in, 20: 22314(R) (AD-626865)
- Gd–Pd, electric conductivity at low temperatures, 20: 22314(R) (AD-626865)

GADOLINIUM IONS
- electron nuclear double resonance spectra in thoria, 20: 22311(R) (AD-622068)

GADOLINIUM ISOTOPES Gd-155
- energy levels from gadolinium-155 decay, lifetime of, (E), 20: 22058
- neutron resonance absorption by, cross sections for Doppler-broadened, (T), 20: 21951

GADOLINIUM ISOTOPES Gd-157
- energy levels from gadolinium-157 decay, lifetime of, (E), 20: 22058

GADOLINIUM ISOTOPES Gd-158
- proton inelastic scattering at 12 Mev, excitation of octupole vibrational states by, (E), 20: 22100

GADOLINIUM ISOTOPES Gd-160
- energy levels in, spin and parity for, (E), 20: 22100

GADOLINIUM NITRIDES
- preparation by reactive arc melting, 20: 21244

GADOLINIUM OXIDES
- solubility in ethyl, isopropyl, methyl, and propyl alcohols in presence of ammonia, 20: 20686

GALAXIES
- energy sources for radio-, subnuclear processes as, (T), 20: 21498
- kinetics and properties of, 20: 21513

GALLIC ACID, PROPYL ESTER
- radiosensitivity effects on DNA, uv, 20: 20412

GALLIUM
- determination in silicon dioxide, activation, 20: 20634
- determination in tin oxide, activation, 20: 20577
- separation from indium and transition elements by ion exchange, 20: 20634
- separation from scandium by ion exchange chromatography, 20: 20821
- superconducting properties of, effects of λ transition on, 20: 21875

GALLIUM ALLOYS
- Dy–Ga, dysprosium hyperfine magnetic field in intermetallic compounds of, (E), 20: 22330
- Ga–Nb, superconducting properties, (E), 20: 21897
- Ga–Pu, etching of delta-phase, bright-field grain structure, 20: 21233 (BNWL-188)
- Ga–rare earth, crystal structure of equiatomic intermetallic compounds of, 20: 21399
- Ga–Va, superconducting critical currents in intermetallic compounds of, in high fields, (E), 20: 21922
- Sb–Ga, radiation effects on semiconductor, electron, 20: 22520(R) (NAA-SR-11805)

GALLIUM COMPOUNDS
- growth and properties of rare earth garnets of, 20: 22311(R) (AD-622068)

GALLIUM ISOTOPES Ga-67
- energy levels from proton reactions (p,n) with zinc-67 at 1.5 to 5 Mev, (E), 20: 22053

GALLIUM ISOTOPES Ga-68
- energy levels from proton reactions (p,n) with zinc-68 at 1.5 to 5 Mev, (E), 20: 22053

GALLIUM ISOTOPES Ga-70
- energy levels from proton reactions (p,n) with zinc-70 at 1.5 to 5 Mev, (E), 20: 22053

GAMMA CAMERAS
- image converters for, fast response, 20: 21146(P)
- use in radiodiagnosis, spark chambers for, 20: 21082

GAMMA RADIATION
- absorption of, materials evaluation for Mössbauer studies, 20: 22157
- angular correlations from proton reactions (p,p γ) with fluorine-19 in metallic media, perturbation, 20: 22090
- angular correlations with protons from deuteron reactions (d,pγ) with carbon-12 at 2 to 3.2 Mev, (E), 20: 22087
- angular distributions and energy above infinite fallout field, Monte Carlo calculations of, 20: 20878 (AD-612030)
- detection and measurement of cosmic, digitized spark chamber for, 20: 21121
- detection and measurement of cosmic, spark chamber with photographic recording for, 20: 21122
- detection and measurement from debris of high-altitude atomic explosions, instrument for, 20: 21129
- detection of, semiconductor sensitivity for, 20: 21059
- detection using europium-activated single crystals of calcium fluorides, 20: 21135
- dosage determinations for sheep, lethal, 20: 20487
- dose albedos for concrete, Monte Carlo calculation of, 20: 22305 (AD-621441)
- dose-rates in critical assembly environment, air-scattered, 20: 22386
- dosimeter for, chemical threshold, 20: 21076
- dosimetry during diagnostic use of krypton-85, 20: 20958
- dosimetry in and behind beryllium slabs, tabulations for, 20: 22307 (DC-61-3-69)
- dosimetry in dogs and phantoms, 20: 20432 (AD-630332)
- dosimetry near reactor tubes using scintillation counters, 20: 21047
- dosimetry of, design of integrating dose-rate meter using ionization chamber for, 20: 21078
- dosimetry of, equipment for, 20: 21062
- dosimetry of, spectrometric method for, 20: 20952
- dosimetry using silicon p-n junctions, instrument for, 20: 21133
- effect on 3-aminophthalhydrazine, 20: 20777
- effects of extracorporeal exposure of blood and lymph to, on rejection of skin homografts in calves, 20: 20485
- effects of, combined with surgery on cervical carcinomas, 20: 20536
- effects of, combined with procarbazine on tumors, 20: 20504
- effects of, with neutrons on size of litters produced by male mice, 20: 20453
- effects on adenosine triphosphatase activity of rat spleen, 20: 20503(R) (AD-629311, pp 1-14)
- effects on aging in Japanese nuclear-explosion survivors, 20: 20480
- effects on aliphatic alcohols, 20: 20750
- effects on alkaline phosphatase activity in blood, 20: 20415
- effects on aqueous solutions of benzene in presence of oxides, 20: 20768
- effects on ascorbic acid content and enzyme activity in citrus fruits and tomatoes, 20: 21195(R) (TID-22509)
- effects on batteries, hardening against, 20: 21162
- effects on behavior of animals, 20: 20495
- effects on benzene–ethanol mixture at 20 and –196°C, 20: 20741
- effects on benzene–ethanol mixture at –196°C, EPR studies of, 20: 20742
- effects on blood coagulation in dogs and rats, 20: 20490
- effects on bulk compressibility and electric conductivity of polyepoxides, 20: 21418 (AD-627049)
- effects on cadmium and nickel battery electrodes, 20: 21425(R) (N-65-24491)
- effects on canine spinal cord, 20: 20455
- effects on carbonylation of hydrocarbons with carbon monoxide, 20: 20770(T)
- effects on carboxylation of methylamine, products formed by, 20: 20732 (SGAE-CH-21/1965)
- effects on cardiovascular system in monkeys, 20: 20488
- effects on chlorination and sulfochlorination of polypropylene, 20: 20779
- effects on current induction in commercial capacitors, 20: 21151 (IBM-66-825-1944)
- effects on decomposition of terphenyls at 350°C, 20: 20722 (EUR-

2401.f)
effects on degradation of polymers in solution, light scattering and viscosity measurements of, 20: 20765
effects on dielectric and mechanical properties of dielectrics, combined effects of low-temperature, vacuum, and, 20: 21152 (N-65-22353)
effects on DL-mandelic acid in oxygenated solutions, 20: 20759
effects on doped germanium, annealing of, 20: 21392
effects on doped silicon crystals, annealing of E centers from, (E), 20: 22323
effects on dynamic mechanical properties of butadiene–styrene rubbers, 20: 20754
effects on elastomers, polymers, and rubber, 20: 21430(R) (WADC-TR-55-58(Pt.8))
effects on electric potential in plant cells, 20: 20419
effects on electric conductivity of ethylene-base copolymers, 20: 21170
effects on ESR spectra of hydrogen peroxide·urea single crystals, 20: 20756
effects on ethanol at 29°C, 20: 20746
effects on frozen ethyl iodide in glass and polycrystalline states, products formed in, 20: 20716 (AD-621022)
effects on hematopoietic system and spleen of mice, pathological, 20: 20512
effects on human blood picture in Nagasaki, 20: 20481
effects on ice crystals, ESR spectra from, 20: 22328
effects on immune reactions in transplanted mouse tumors, 20: 20479
effects on isomeric terphenyl, decomposition, 20: 20739
effects on lithium fluoride, R-center luminescence from, (E), 20: 22331
effects on metabolism of DNA in *Escherichia coli*, 20: 20421
effects on methanol vapor, 20: 20776
effects on microflora on perch fillets, 20: 21203
effects on molecular motions and structure of crystalline stereoregular polymers, 20: 20753
effects on molten lithium nitrate at 270°C, mechanism of, 20: 20733 (TID-22796)
effects on MOS FET transistors, annealing of, 20: 21159
effects on mouse spleen, pathological, 20: 20511
effects on paints, tables on, 20: 20808(R) (ORNL-3916)
effects on physical properties of epoxy resins, effects of resin structure on, 20: 21429 (RHEL/R-105)
effects on poly(vinylchloride), poly(dimethylsiloxane), and poly(methyl methacrylate), 20: 20764
effects on polymerization of fluoral and vinyl fluoride at low temperature, 20: 20718(R) (AD-623307)
effects on polymers and rubber, 20: 21431(R) (WADC-TR-55-58(Pt.9))
effects on polymerization of methyl methacrylate and styrene in presence of mineral fillers, 20: 20778
effects on polyvinyl butyral films, 20: 20775
effects on potassium chloride crystals, T bands from, (E), 20: 22322
effects on potato starch, 20: 20737
effects on properties of starch and amylose–acrylamide copolymers as adhesives and dyeing mordants, 20: 20767
effects on rabbit auditory organs, 20: 20498
effects on rabbits, seasonal variations in lethal, 20: 20493
effects on rats, effects of low-protein diet on recovery from, 20: 20508
effects on recombination rates of hydrogen and oxygen in presence of water vapor, 20: 20749
effects on recombination centers in silicon, 20: 21439
effects on Schistosoma infectivity in mice, 20: 20446
effects on silicon surfaces, 20: 21172
effects on size of litters produced by male mice, 20: 20453
effects on solid diaryl sulfones, 20: 20760
effects on solid-state polymerization of *N*-vinylcarbazole, 20: 20743
effects on solid-state polymerization of acrylamide and acrylic acid, 20: 20763
effects on structure of polyriboadenylic and polyribouridylic acids, 20: 20411
effects on sulfhydryl content of blood, 20: 20415
effects on systems of white phosphorus with carbon tetrachloride, cyclohexane, or styrene, 20: 20736
effects on terephthalic acid, 20: 20745
effects on triglyceride synthesis in rat bone marrow cells, 20: 20420
effects on *Vaccinia virus*, 20: 20500
effects on variegation in Einkorn wheat, mutagenic, 20: 20497
effects on viability of *E. coli*, 20: 20457
effects on 3-methylpentane, yield of solvent-trapped electrons from, 20: 20755
emission by 3.0-min bromine-85, 20: 22041
emission from nuclei, perturbed angular correlation of triple cascades of, (T), 20: 22015
emission of polarized, in deuteron stripping reactions, (T), 20: 22006 (KFKI-600)
flux distribution in in-pile loop (BLO 3), 20: 20722 (EUR-2401.f)
flux moderation in paraffin, 20: 20524 (RT-PROT-(65)32)
interactions with deuterons, meson (π) production in polarized, (E), 20: 21626 (LNF-66/4)
measurement of collimated, efficiencies of G-M and scintillation counters for, 20: 21056
monitoring in Cincinnati area, aerial, 20: 20880 (CEX-62.6.5)
propagation in air, from strong remote sources, (T), 20: 20946
properties of, bibliography on, (T), 20: 22011 (TID-22771)
scattering by nuclei at 280 and 662 kev, Z-dependence of cross sections for elastic, (E), 20: 22060
transport of, computer program for, 20: 22304 (AD-612031)
use for post-operative, therapy of brain tumors, 20: 20530
use for sterilization of human bone grafts, 20: 20482
use in measuring radon content in water, 20: 20959
uses in measurement of gross weight of construction materials, 20: 21205

GAMMA SHIELDING
design for fuel handling facilities, computer program for, 20: 22309 (ORNL-3041)

GAMMA SOURCES
avoidance of, by guinea pigs, mice, monkeys, and rats, 20: 20495
beam focus for cobalt-60 rotating unit, cassette and interspacer for, 20: 20548
beam focus of cobalt-60 rotation unit, imaging for, 20: 20547
design of coherent, 20: 20800(P)
design of portable cesium-137, for ecological studies, 20: 20380 (TID-22499)
dose distribution from beam of cobalt-60, correlations of, with beam-focus densitometry, 20: 20549
dosimetry of, design of microcalorimeter for, 20: 20721 (EUR-2295.f)
use of cobalt-60, for calibration of film badges, 20: 20935 (K-1657)
uses for measuring gross weight of building materials, 20: 21205

GAMMA SPECTRA
determination from multiple radioisotopes, stepwise statistical analysis for, 20: 20555(R) (AD-622200)
measurement from cesium-137 in sand, (E), 20: 22308 (HASL-167)
measurement using photomultipliers and scintillators, pulse pile-up effects in, 20: 21106

GAMMA SPECTROMETERS
description of magnetic pair, 20: 21985 (BNL-948, pp 757-62)
design of Mössbauer tandem, using pulse-height analysis, 20: 21069
drive mechanism for Mössbauer, 20: 21080
drive system for Mössbauer, 20: 21079
drive system for Mössbauer, 20: 21081
performance of semiconductor Compton, for nondestructive burnup determination of fuel elements, 20: 21050
performance of triple-coincidence, 20: 22020
performance using large-volume lithium-drifted germanium detectors, 20: 21104
use in activation analysis, 20: 20554 (AD-621017)
use in low-level dosimetry, 20: 20952
uses for locating radioactive tracers on chromatographic thin layers or papers, 20: 20606

GAMMA SPECTROSCOPY
use in measuring radionuclides in milk, 20: 20950

GARNETS
growth and properties of rare earth aluminum and gallium, 20: 22311(R) (AD-622068)

GAS COOLED REACTORS
coolant performance in, comparison of carbon dioxide, helium, and steam, 20: 22452
design of heavy-water moderated, for power production, 20: 22432
design of natural uranium-fueled, graphite-moderated, power production, 20: 22426
design of 500-Mw magnox, 20: 22424
design of 500-Mw magnox, 20: 22429

GAS FLOW
analysis of molecular, computer program for, 20: 20855 (CLM-R-54)
electric arcs in transverse supersonic, stability of magnetically confined, 20: 21802
in gaseous core reactor, diffusion in vortex, (E/T), 20: 22473
magnetohydrodynamic, properties of small Reynolds number, 20: 21782 (AD-623812)
magnetohydrodynamic, one-dimensional, (T), 20: 21777 (AD-621442)
magnetohydrodynamic, Ohm's law for, 20: 21778 (AD-621943)

GASEOUS FUEL REACTORS
description of, survey of, 20: 22466 (ANL-7180)
fuel containment in vortex-flow, (E/T), 20: 22473
fuel vortex flow in, (E/T), 20: 21786 (ORNL-TM-1337)
neutron transport in, computer program for, 20: 22370 (AD-621021)

GASES
analysis of hydrogen fluoride-containing, for moisture, equipment for continuous, 20: 20581
collision integrals in, theory of molecular, 20: 20807(R) (MLM-1287)

electron beam reactions with, electrostatic and magnetic pinch effects in plasma from, 20: 22221
flow in MHD cells, effects of Hall effect, ion slip, and viscosity on, (T), 20: 21574
flow of molecular, computer program for analysis of, 20: 20855 (CLM-R-54)
ionization nonequilibrium in MHD cells, (T), 20: 21573
kinetic theory of, use of Talmi transformation and related formulas in, 20: 21226
kinetics of, perturbation method for classical time-dependent pair correlation function for, 20: 21453
monitoring for suspended solids or liquids, alarm apparatus for, 20: 21017(P)
neutron spectra in Maxwellian, properties of thermal, 20: 21933 (AD-621119)
pressure-wave generation in fissioning, use of helium-3 as driver for, (T), 20: 21803
purification of reactor cover, plant for, 20: 22462
shock propagation in, ionization front of, (T), 20: 22285
sorption by metals, method for measuring, 20: 21351(R) (SRIA-425-8)
stability of paramagnetic ground state of electron, (T), 20: 21805
statistical mechanics of high-temperature electron, beyond ring approximation, 20: 22223
temperature of ionospheric neutral, effects on electron density distribution, 20: 21823

GASTRIC JUICE
radiation effects on secretion in rats, x, 20: 20433 (AD-630390)

GASTROINTESTINAL TRACT
contamination by plutonium, method for treatment of, 20: 20943 (RFP-453)

GATING SYSTEMS
design of modular linear gate, 20: 20997

GEIGER-MUELLER TUBES
efficiency for collimated gamma rays, 20: 21056
performance of thin-window, for tritium counting, 20: 21065

GENETICS
mechanism for transmittal by viral DNA, uv-method for determining, 20: 20426
radiation effects in, from central nervous system exposure, 20: 20449
radiation hazards to human, from radioluminescent watches, 20: 20518 (RT-PROT-(65)41)
transmittal in phage, role of DNA in, 20: 20427

GEOLOGY
aeroradioactivity surveying of rocks in Maryland, Virginia, Washington, D. C., and West Virginia, 20: 20928 (CEX-59.4.17)

GEOMAGNETIC FIELDS
charged-particle trapping by, (E), 20: 21837
disturbances by high-altitude nuclear explosions, analysis of, 20: 21829
electron diffusion in, general Fokker-Planck equation for, 20: 21813 (N-65-29816)
fluctuations in horizontal, during night-time geomagnetic storms in equatorial electrojet, (E), 20: 21818

GEOMAGNETIC STORMS
commencement of, correlation with occurrence of high-frequency auroral noise, 20: 21835
data for April–Oct. 1965, 20: 21830
geomagnetic field horizontal fluctuations during, in night-time equatorial electrojet, (E), 20: 21818

GERMAN REACTORS
design of 1000-Mw(e) gas-cooled fast, Karlsruhe project for, 20: 22452
design of 1000-Mw(e) sodium-cooled fast breeder, Karlsruhe project for, 20: 22453
design of 1000-Mw(e) sodium-cooled breeder, Karlsruhe project for, 20: 22462

GERMANIUM
analysis for phosphorus, activation, 20: 20560 (EUR-2753.f)
argon ion reactions with thin-film, depth of induced damage from low-energy, 20: 21438
fabrication of lithium-drifted detectors of, 20: 22010(R) (NYO-72-28)
performance as cold neutron monochromator, 20: 21949
radiation effects on electric properties of, neutron, 20: 21150 (HMI-B-45)
radiation effects on doped, annealing of gamma, 20: 21392
surface potential of lithium-drifted diodes of, 20: 21096

GERMANIUM ALLOYS
Cr–Ge, production of Cr_3Ge by hot-pressing, 20: 21247
Ge–Mo, production of Mo_3Ge by hot-pressing, 20: 21247

GERMANY
radioactivity and fossil content of clays and sandstone, Braunschweig, 20: 20890
tritium content in atmosphere at Hamburg, following Windscale accident, 20: 20889

GLASS
decontamination of vials of, using detergents, 20: 20960
development and properties of, for liquid scintillation counting, 20: 21044(T) (ANL-Trans-285)
fracture of dispersion-strengthened, theory for, 20: 21358 (UCRL-16552)
radiation effects on current induction in capacitor of, electron beam, fast neutron, and gamma, 20: 21151 (IBM-66-825-1944)
radiation effects on optical properties of, 20: 21446
radioinduced electric discharge figures in, electron, 20: 21440

GLASS TEXTILES
performance of uranium containing, as reactor fuel elements, 20: 22415 (RPI-321-4)

GLOBULIN
calcium-45 binding with, in patients with bone metastases, 20: 20404

GLUCOSE
radiation effects on gastric transit of, in laparotomized and vagotomized rats, uv, 20: 20414
radiation effects on, in aqueous solutions, x, 20: 20748

GLUCURONIDES
radiation effects on excretion by rats, x, 20: 20439 (EUR-2628.f)

GLUTARIC ACID, 2-OXO-
oxidation by rat-liver homogenates, effects of disulfides and thiols on, 20: 20505

GLUTATHIONE
radiosensitivity effects on DNA, uv, 20: 20412

GLYCERIC ACID
phospho-, effects on radiosensitivity of enzymes, 20: 20514

GLYCERIDES
radiation effects on synthesis in rat bone marrow cells, γ, 20: 20420

GLYCINE
radiosensitivity effects on phosphatase activity in rats, 20: 20517 (NP-15925)
yields in radioinduced carboxylation of methylamine, 20: 20732 (SGAE-CH-21/1965)

GLYOXYLIC ACID, PHENYL-
yields from gamma radiolysis of DL-mandelic acid in oxygenated solutions, 20: 20759

GOITER
radiodiagnosis of, in Congo, 20: 20373

GOLD
analysis for impurities, spectroscopic, 20: 20807(R) (MLM-1287)
coating thickness of, proton scattering measurements on, 20: 21246
electron reactions at 6 to 23 kev, optical transition radiation from, 20: 21518
manganese-54 orientation in, gamma-ray anisotropy from, (E), 20: 22097
neutron Doppler effect in, 20: 22520(R) (NAA-SR-11805)
neutron inelastic scattering at 5.8 and 7.5 Mev, gamma spectra from thermal, (E), 20: 22069
performance as epithermal and thermal neutron activation detector, 20: 21053
proton reactions at 590 Mev and 18 Bev, yields of iodine isotopes from, (E), 20: 22045
radioinduced defects in annealed, Frenkel pair recombination volume from alpha, 20: 21447
sputtering by fast neutrons, 20: 21441
viscosity of liquid, based on atomic parameters, 20: 20656 (UCRL-11930)

GOLD ALLOYS
Al–Au, radiation effects at 80°K on, resistivity recovery from proton, 20: 21445
Au–Mg, radiation effects at 80°K on, resistivity recovery from proton, 20: 21445
Au–rare earth, crystal structure of equiatomic intermetallic compounds of, 20: 21399
Au–Th–U, fabrication and corrosion testing of radiation targets of, 20: 21288 (BMI-1761)

GOLD ISOTOPES Au-190
nuclear magnetic dipole moment and spin of, (E), 20: 22140

GOLD ISOTOPES Au-197
energy level transitions from platinum 197 decay, conversion ratios of 191-kev, 20: 22057
nitrogen-15 reactions at 102 Mev, neutron pickup in, (E), 20: 22001 (JINR-P-2555)
proton capture cross sections and transmission coefficients for, optical model calculation of, 20: 22049

GOLD ISOTOPES Au-198
use in radiotherapy of brain tumors, pyrogenic and toxic effects from, 20: 20539

GOLD ISOTOPES Au-199
half life of isomeric, (E), 20: 22046

GONADS
radiation effects on mouse testicular, effects of age at irradiation on x, 20: 20499
radiation effects on male rat, protective effects of MEA against x,

20: 20509
radioinduced tumors in mouse, incidence of x, 20: 20441 (ORNL-P-1173)
thymidine incorporation in embryonic chicken ovaries *in vitro*, tracer studies on, 20: 20395
weight norms for human, use in establishing standards for radiation dosimetry, 20: 20374
GRANITES
analysis for lead, extraction-radiometric method of isotopic dilution for, 20: 20620
GRAPHITE
analysis for uranium in fuel particle coatings of, nondestructive method for, 20: 21423 (N-65-23015)
creep properties at 2000 to 3000°C, 20: 21343(R) (N-65-23013)
creep rate of commercial, stress dependence of, 20: 21340 (LA-DC-7626)
crystal cleavage of, in ultrahigh vacuum, 20: 21366
densification of, process for, 20: 21315(P)
development for use as fuel tubes for Dragon, 20: 21383
dissociation of niobium pentachloride on surface of, mechanism of niobium carbide formation by, 20: 21241(T) (LA-tr-66-15)
fabrication for TARGET reactor, 20: 22411(R) (GA-6113)
fission product diffusion in fuel elements of, 20: 21423 (N-65-23015)
fission product sorption and diffusion in, 20: 22411(R) (GA-6113)
neutron diffusion lengths in, 20: 22520(R) (NAA-SR-11805)
neutron spectra in, reactor design considerations from thermal, 20: 22376 (GA-6901)
neutron thermalization in, (E), 20: 21942(T) (KFK-tr-188)
neutron transport in, temperature-dependent variation of mean free path of, (E), 20: 21955
oxidation by oxygen at 510 to 650°C, effects of water vapor on, 20: 21285
permeability of, evaluation of methods for measuring, 20: 21408
radiation effects on dimensional stability of, at 900 to 1800°C, fast-neutron, 20: 21419 (BNWL-191)
radiation effects on, at 495 to 1035°C, fast-neutron, 20: 21421 (GA-6888)
radioinduced contraction in, fast-neutron, 20: 21420 (BNWL-215)
reactions with carbon dioxide above 600°C, tracer studies of, 20: 20702
reactions with rare earths, preparation of intercalation compounds by, 20: 20648 (AD-621029)
GRAPHITE MODERATED REACTORS
design of natural uranium-fueled, gas-cooled, for power production, 20: 22426
design of 500-Mw magnox, 20: 22424
design of 500-Mw magnox, 20: 22429
GRAPHITE SYSTEMS
Er–graphite, preparation and magnetic susceptibility of, 20: 21413
graphite–ZrC, fabrication of dispersions of, by hot-working, 20: 21306
graphite–MoC, fabrication of dispersions of, by hot-working, 20: 21306
graphite–Tb, preparation and magnetic susceptibility of, 20: 21413
graphite–Yb, preparation and magnetic susceptibility of, 20: 21413
GRASS
strontium-90 uptake by rye, effects of applications of stable strontium to soils on, 20: 20381
GRAVITATION
effects on plasma interchange instability in magnetic fields, (T), 20: 22186 (MATT-358)
effects on wave functions for macroscopic objects in quantum mechanics, 20: 21857
energy of systems of, general relativity conservation laws for static spherically symmetric, 20: 21845
field equations for radiating spheroid in general relativity theory, 20: 21868
field equations in general relativity for, plane-wave solution to, 20: 21869
field propagation in electromagnetic media and fluids, 20: 21853
spectral shift in spherically symmetric fields of, 20: 21843
theory for fields of, congruence in, 20: 21841
theory for fields of, geometrization of, 20: 21842
theory of, in Riemannian geometry, 20: 21858
GREAT BRITAIN
atomic energy liability laws in, amendments to, 20: 20948
fallout monitoring, 1964 and 1965, 20: 20926(R) (ARCRL-14)
GRENOBLE REACTORS (MELUSINE)
core development for, 20: 20721 (EUR-2295.f)
operation and performance for in-pile radiolysis of terphenyls, 20: 20721 (EUR-2295.f)
GROUND WATERS
age estimation of, effects of tritium content of rain on, 20: 20892
analysis for radioactivity, methods for, 20: 20963
book: *Advances in Water Pollution Research*, Vol. 1, 2, and 3, 20: 20982
tritium content of, in New Zealand, 20: 20893
velocity in soils, device for measuring, 20: 20875 (EUR-2481.f)
GUANIDINE, 1,1'-(DITHIODIETHYLENE)DI-
radiosensitivity effects on protein solutions, 20: 20424
GUINEA PIGS
radiation source avoidance by, y, 20: 20495

H

HADACIDIN
radiosensitivity effects on *E. coli*, 20: 20456
HAFNIUM
production of sponges of, 20: 21305
separation from hydrochloric acid solutions by solvent extraction using quaternary ammonium chlorides, 20: 20816
separation from protactinium by solvent extraction using quaternary ammonium chlorides, 20: 20816
HAFNIUM ALLOYS
Hf–Nb–W, effects of carbon and oxygen on phase equilibria in niobium-rich region of, 20: 21329(R) (DRI-1092-229)
Hf–Re–Ta–W, properties of, effect of carbide dispersion on microstructures and strength/ductility, 20: 21404
Hf–Ta–W, creep tests on T-111 and T-222 at high temperatures, 20: 21346(R) (NASA-CR-54895)
Hf–Ta–W, extrusion parameters for T-111, 20: 21263(R) (NASA-CR-54911)
Hf–Ta–W, mechanical properties at 25 to 3500°F, 20: 21322 (AMRA-TR-65-25)
Hf–Ta–W, specifications of T-111, for use in corrosion test loop fabrication, 20: 21293 (R-66SD3007)
Hf–Ta–W, strength, weldability, and heat treatment of, 20: 21405
Hf–W, mechanical properties at 25 to 3500°F, 20: 21322 (AMRA-TR-65-25)
HAFNIUM BORIDES
effects on mechanical properties of sintered and extruded tungsten, 20: 21374
HAFNIUM CARBIDES
effects on mechanical properties of sintered and extruded tungsten, 20: 21374
production of single crystals of, 20: 21236(R) (N-65-23835)
HfC–TaC, production of single crystals of, 20: 21236(R) (N-65-23835)
HAFNIUM ISOTOPES Hf-180
deuteron reactions (d,p) with, hafnium-181 levels from, (E), 20: 22106
HAFNIUM ISOTOPES Hf-181
energy levels from deuteron reactions (d,p) with hafnium-180, (E), 20: 22106
HAFNIUM NITRIDES
effects on mechanical properties of sintered and extruded tungsten, 20: 21374
HfN–Re–W, tensile properties at high temperatures, 20: 21406
HfN–W, tensile properties at high temperatures, 20: 21406
HAFNIUM OXIDES
effects on mechanical properties of sintered and extruded tungsten, 20: 21374
reactions with gaseous uranium trioxide, effects of substrate symmetry in, 20: 20649 (AEET-CD-24)
HfO_2–Y_2O_3, electric conductivity at 900 to 1600°C, effects of composition on, 20: 21370
HAFNIUM SYSTEMS
B–Co–Hf, crystal structure, 20: 20685
B–Hf–Ni, crystal structure, 20: 20685
C–Hf–Mo–N–Re–Ta–W–Zr, development of dispersion-strengthened tantalum-base, 20: 21240(R) (WANL-PR-(Q)-006)
C–Hf–Nb–W, properties at very high temperatures, 20: 21412
C–Hf–Re–Ta–W, development of dispersion-strengthened tantalum-base T-333, 20: 21240(R) (WANL-PR-(Q)-006)
C–Hf–Ta–W, bonding of T-222, to Inconel 600 and stainless steels, process development for explosive, 20: 21295(R) (WANL-PR-(EE)-002)
HAIR
radiation effects on pigmentation in mouse, x, 20: 20441 (ORNL-P-1173)
HALL EFFECT
determination in collision-dominated plasma, (T), 20: 22176 (AD-624165)
HANFORD PRODUCTION REACTORS
radioisotope production in, 20: 21212 (CONF-660305-19)
HARWELL VARIABLE ENERGY CYCLOTRON
design and operation of, computer programs for, 20: 21472 (RHEL/R-113)
HASTELLOY C
corrosion by acids at 800 to 2375°F, effects of heat treatments and microstructure on, 20: 21277
corrosion by argon–nitrogen mixtures at 900°C, 20: 20802(R) (ANL-7055, pp 21-98)
testing for bearing parts in sodium, 20: 22520(R) (NAA-SR-11805)
HASTELLOY X
corrosion by air at 1900 and 2000°F, 20: 21259 (AGN-TM-414)
corrosion by argon–nitrogen mixtures at 900°C, 20: 20802(R) (ANL-7055, pp 21-98)
oxidation by air at 1750 and 1850°F, effects of cobalt content on,

20: 21258 (AGN-TM-413)
HEAD
radiography of, safety hazards from, 20: 20543
HEALTH PHYSICS
program for BNL decontamination facility, 20: 20929 (CEX-61.6.2)
HEART
etiology of ischemic diseases of, relation of serum lipid and lipoprotein content to, 20: 20370 (UCRL-14658)
radiation effects on auricles in rabbit, 20: 20451
radiation effects on human, following radiotherapy, x, 20: 20474
radioinduced myocardial infarction in human, following radiotherapy of Hodgkin's disease, 20: 20468
weight norms for human, use in establishing standards for radiation dosimetry, 20: 20374
HEAT
use of radioisotope, in operation of spacecraft life-support systems, 20: 21174 (SAN-575-12)
HEAT EXCHANGERS
cleaning of, descaling solution for, 20: 21238 (NP-15928)
efficiency of 1-, 2-, and 3-pass cross counterflow, computer program for, 20: 20858 (UCRL-14620)
HEAT-RESISTING ALLOYS
research on, design of high-temperature high-vacuum equipment for, 20: 21350 (ORNL-TM-1426)
HEAT TRANSFER
from nickel spheres to water, 20: 20925(R) (ANL-7055, pp 177-212)
from reactor fuel element to ionized carbon dioxide, electric field effects on, 20: 20859 (UJV-1421/65)
in boiling water reactors, (T), 20: 22449
of irradiated organic coolants, correlation of friction factor and, 20: 20710 (MIT-324-23)
oscillations in magnetoelastic, uniqueness theorem for homogeneous isotropic bodies, 20: 21793
HEATERS
design and development of, for two-phase sodium loops, 20: 22520(R) (NAA-SR-11805)
design for use in MIT organic loop, 20: 20710 (MIT-324-23)
HEAVY WATER REACTORS
design of boiling light water-cooled, for power production, 20: 22431
design of gas-cooled, for power production, 20: 22432
design of light-water cooled pressure-tube, 20: 22430
design of organic-cooled, 20: 22433
development of organic-cooled, 20: 22442
fuel recycling in power, plutonium, 20: 22419
HELIUM
analysis for tritium by liquid scintillation counting, 20: 20582
detection of molecular beams of, field-ionization detector for, 20: 21089
diffusion in poly- and single-crystal alumina at 25 to 900°C, activation energy and rate of, 20: 21353 (TID-22828)
effects on growth rates in Neurospora, 20: 20378
electric discharges in, electron distribution function for, (E), 20: 21795
electromagnetic wave propagation along magnetic field in plasma of, circularly polarized plane, (E), 20: 22236
electromagnetic wave propagation along magnetic field in plasma of, linearly polarized, (E), 20: 22237
electron elastic scattering at 0 to 14 ev, modified effective-range theory for, 20: 21517
electron temperature in plasmas of, spectroscopic measurement of, 20: 22210
electron velocity distribution in positive column of discharge plasma of, radial dependence of, (E), 20: 22294
film transfer in liquid II, two-fluid model for thick nonequilibrium, (T), 20: 21896
film transfer rates in liquid II, variable, (E), 20: 21895
ion mobility and recombination in plasma of, 20: 22169(R) (AD-622684)
ionization equilibrium in shock-generated plasma of, 20: 22250
performance as coolant for 1000-Mw(e) fast breeder reactor, 20: 22452
performance in plasma engines, effects of nonequilibrium conductivity on, 20: 20873
production of negative glow plasma of, design and performance of inverse brush cathode for, 20: 22222
radiation effects on diffusion from beryllium oxide, kinetics of neutron, 20: 21428 (NP-15942)
solubility in potassium nitrate, 20: 22520(R) (NAA-SR-11805)
spectra of theta-pinch plasma of, 20: 22269
stability in plasma of, excitation of m = 2 mode by helical, 20: 22247
thermal conductivity at 750°C, 20: 20651(R) (CU-2660-26)
transport properties at low temperatures, calculations of, 20: 20806(R) (MLM-1274)
trapping in fast reactor materials, 20: 22520(R) (NAA-SR-11805)
use in leak detection, 20: 20845
x-ray scattering cross sections at 1 to 150 kev, (T), 20: 21516 (UCRL-14403)
HELIUM IONS
electron reactions at threshold to 750 ev, helium ion (2S) production from crossed beam, (E), 20: 21535
production of (2S) excited, from helium ground-state ion crossed beam reactions with electrons, (E), 20: 21535
reactions with beryllium–copper alloys at 3 to 90 kev, secondary electron emission from, (E), 20: 21538
reactions with boron and carbon, straggling effects in energy loss from, (E/T), 20: 21539
HELIUM ISOTOPES He-3
bremsstrahlung reactions (γ,n) at threshold to 30 Mev, cross sections for, (E), 20: 22117
mesons (μ^-) reactions with, probability of neutrino yield in, (T), 20: 22152
neutron reactions (n,p) with gaseous, pressure-wave generation in, (T), 20: 21803
reactions (He-3,α) with nickel-60 at 15 Mev, angular distributions from, (E), 20: 22127
reactions (He-3,n) with nuclei at 19 to 25 Mev, angular distributions and cross sections for, (E), 20: 22132
reactions (He-3,p) and (He-3,$p\gamma$) with calcium-40 at 10, 12, and 15 Mev, scandium-42 levels from, (E), 20: 22073
reactions (He-3,t) with nuclei at 22 Mev, isotope shift in Coulomb displacement-energy from, (E), 20: 22095
reactions with nuclei, use of, in activation analysis, 20: 20565 (ORNL-P-1216)
reactions with nuclei, amplitude singularities in knockon and stripping, (T), 20: 21997 (INSJ-96)
separation from helium-4 by low-temperature distillation, 20: 20807(R) (MLM-1287)
separation from tritium by charcoal trapping, 20: 20807(R) (MLM-1287)
HELIUM ISOTOPES He-4
electron inelastic scattering by, two-nucleon correlation functions from cross sections for, (T), 20: 21996 (FTI-142/T-016)
mesons (π) reactions with, meson (ρ) production in coherent, (T), 20: 22145
proton inelastic scattering at 40 Mev, continuum resonances from, (E), 20: 22114
separation from helium-3 by low-temperature distillation, 20: 20807(R) (MLM-1287)
HELIUM SYSTEMS
He–I, diffusion in confined vortex flow of, (E/T), 20: 22473
He–Ne, electric discharge in lasers of, current-voltage characteristics of h-f, (E), 20: 21808
HEMATITES
uses in concrete for construction of pilot plutonium plant, 20: 20819
HEMATO-ENCEPHALIC BARRIER
radiation effects on permeability of, in burros and sheep, neutron, 20: 20489
HEMATOPOIETIC SYSTEM
radiosensitivity of rat, effects of dose rate on, 20: 20503(R) (AD-629311, pp 1-14)
radiosensitivity of mouse, effects of bacterial toxins on, 20: 20512
HEPTANE
radioinduced reactions with carbon monoxide, gamma, 20: 20770(T)
HEXADECANE
radiolysis of, ion mobility in x, 20: 20734
HEXANE
radioinduced reactions with carbon monoxide, gamma, 20: 20770(T)
carbon tetrachloride–cyclopropane–hexane, radiolysis of, at 77 to 193°K, tracer studies of mechanisms in, 20: 20752
3-HEXYNE
radiolysis of liquid, mechanism and yields in, 20: 20717(R) (AD-621719)
HIGH-ALTITUDE EXPLOSIONS
gamma radiation from debris of atomic, instrument for detection and measurement of, 20: 21129
geomagnetic disturbances from July 9, 1962, 20: 21829
use for determining D layer air chemistry, 20: 21811 (AD-620952)
HIGH ENERGY INJECTION DEVICES
beam density profile for Astron, (E), 20: 22191 (UCRL-14697)
ion injection in HX apparatus, r-f electric field effects on molecular hydrogen, (E), 20: 22207
HIGH-PRESSURE SYSTEMS
design for Mössbauer effect experiments, 20: 20850
HIGH TEMPERATURE GAS COOLED REACTOR EXPERIMENT
fuel tube development for, graphite, 20: 21383
HIGH-TEMPERATURE REACTIONS
problems of, in methods for nuclear propulsion, 20: 20870 (LA-DC-7703)
HIGH TEMPERATURE SEPARATION PROCESSES
equipment and flowsheets for skull reclamation, 20: 20802(R) (ANL-7055, pp 21-98)
HIPPURIC ACID, *o*-IODO-, SODIUM SALTS

use of iodine-131-labeled, in renograms, 20: 20538
HIROSHIMA
radiation effects on population exposed in 1945, summary of 1965 findings on, 20: 20919(R) (ABCC-64-65)
radioinduced human aging in, 20: 20480
HOISTS
operation of EBR-II fuel cycle facility, 20: 20802(R) (ANL-7055, pp 21-98)
HOLMIUM
determination in rare earth mixtures, activation, 20: 20562 (LYCEN-6538)
electron scattering at high energies, analysis of, (T), 20: 22124
enthalpy of formation of HoF_3, 20: 20650(R) (ANL-7055, pp 167-76)
friction and wear properties of, in vacuum, effects of crystal structure on, 20: 21365
nuclear magnetic resonance spectra in, 20: 22311(R) (AD-622068)
oxidation in dry and moist air at 100 to 800°C, rate of, 20: 21265 (RPI-2714-8)
reactions with powdered graphite, preparation of intercalation compounds by, 20: 20648 (AD-621029)
separation from perchloric acid solutions by ion exchange materials, 20: 20823
separation from uranium by combined ion exchange-solvent extraction using nitric acid–tetrahydrofuran solutions, 20: 20811
HOLMIUM ALLOYS
Al–Ho, crystal structure and stability of intermetallic compounds in, 20: 21415
Dy–Ho, magnetic transformations in, 20: 21409
Er–Ho, magnetic transformations in, 20: 21409
Ho–Mn, crystal structure and magnetic properties of intermetallic compounds of, 20: 21403
Ho–Mn, phase diagram, 20: 21403
Ho–Tb, magnetic transformations in, 20: 21409
Ho–Tm, magnetic transformations in, 20: 21409
HOLMIUM CHLORIDES
magnetic properties of, 20: 22311(R) (AD-622068)
HOLMIUM ETHYL SULFATES
holmium EPR pair spectra of, 20: 22311(R) (AD-622068)
HOLMIUM IONS
electron paramagnetic resonance pair spectra in holmium ethyl sulfate, 20: 22311(R) (AD-622068)
HOLMIUM ISOTOPES Ho-165
energy levels of, half life of, (E), 20: 22004 (JINR-P-2503)
neutron resonance parameters for, (E), 20: 22004 (JINR-P-2593)
HOLMIUM NITRIDES
preparation by reactive arc melting, 20: 21244
HOLMIUM OXIDES
solubility in ethyl, isopropyl, methyl, and propyl alcohols in the presence of ammonia, 20: 20686
HOMOGENEOUS REACTORS
description of liquid-metal fueled, survey of, 20: 22347 (ANL-7138)
design of boiling, with vapor separation system, 20: 22403(P)
HORMONES
radiosensitivity effects on rats, 20: 20503(R) (AD-629311, pp 1-14)
HYDRAZINE
hydrogen abstraction by methyl radicals from, isotope effects on, 20: 20713
HYDRIODIC ACID
iodine-131 exchange with osmium iodide complexes, 20: 20706
HYDROCARBONS
analysis for hydrogen using slow-neutron transmission methods, 20: 20641
radioinduced reactions with carbon monoxide, gamma, 20: 20770(T)
radiolysis of saturated, yields of hydrogen from, 20: 22520(R) (NAA-SR-11805)
reactions with uranium hexafluoride, fluorohydrocarbon preparation in, 20: 20707(P)
HYDROCHLORIC ACID
chlorine-36 exchange with osmium chloride complexes, 20: 20706
corrosive effects on nickel–chromium–molybdenum alloys at 800 to 2375°F, 20: 21277
effects on corrosion of rhenium at 25 and 100°C, 20: 21275
effects on radioinduced oxidation of vitamins, 20: 20738
effects on uranyl ion adsorption by ion exchangers, 20: 20827
HYDRODYNAMICS
of viscous fluid, relativistic, 20: 21794
shock interactions in nitromethane-filled corners, (E/T), 20: 21784 (LA-3450)
vortices in rotating cylinders in, analogy with current filaments, (T), 20: 21800
HYDROFLUORIC ACID
HF–O, solvent properties for stainless steel, 20: 20808(R) (ORNL-3916)
HYDROGEN
abstraction by methyl radicals from ammonia, hydrazine, and methylamine, isotope effects on, 20: 20713
abstraction from hydrocarbons by methyl radicals in tritiated toluene, 20: 20711
desorption from iridium, rhodium, and tungsten, flash, 20: 20652 (IS-T-67)
determination in hydrocarbons by slow-neutron transmission methods, 20: 20641
determination in metals, equipment and method for activation, 20: 20602
deuteron reactions (d,2p) at 10.5 Mev, exit channels for, (E), 20: 21981 (BNL-948, pp 610-84)
effects on mechanical properties of Zircaloy-2, (E), 20: 21386
energy-level crossing in, forbidden Zeeman, (E), 20: 21530
evolution of, during use of decontaminating and descaling solution, 20: 21238 (NP-15928)
exchange with hydrogen on molybdenum film, steady-state, 20: 21351(R) (SRIA-425-8)
fine structure constant for, 20: 21537
injection of molecular ions of, in HX apparatus, (E), 20: 22207
ion heating in theta-pinch plasma of, (E), 20: 22185 (LRP-23-66)
meson (π^-) charge exchange on, distinction of bonding by, 20: 20653 (JINR-P-2558)
nuclear spin relaxation in liquid, (T), 20: 21526
nuclear spin-lattice relaxation in liquid, (E), 20: 21525
performance in plasma engines, effects of nonequilibrium conductivity on, 20: 20873
pinch effect in, structure of theta, (E), 20: 22183 (LRP-21-66)
production of plasma of, performance of coaxial gun for, 20: 22225
radiation effects on recombination rates of, with oxygen in presence of water vapor, gamma, 20: 20749
radiosensitivity effects in aqueous lysozyme solutions, 20: 20423
reactions on molybdenum film surface, kinetics of, 20: 21351(R) (SRIA-425-8)
reactions with oxygen adsorbed on zirconium oxide, mechanisms of reduction, 20: 20705
rotational constant of molecular, finite nuclear mass and relativistic effects on, 20: 21527
shock propagation in plasma of, microwave interferometry of, (E), 20: 22182 (IPP-3/35)
shock propagation in, properties of electromagnetically driven, (T), 20: 21779 (AD-621990)
shock propagation in, equilibrium chemistry of ionizing, (T), 20: 21796
solubility in Santowax-OMI, 20: 20708 (AEET-213)
sorption by zirconium alloys, effects of oxide films on, 20: 21282
sorption of, by metallic film surfaces saturated with carbon dioxide, 20: 21389
spectra in calcium fluoride crystals, absorption, 20: 22311(R) (AD-622068)
stability of plasma of, in inverse homopolar device, (T), 20: 22272
tritium concentration in, by gas chromatography, 20: 21218
x-ray scattering cross sections at 1 to 150 kev, (T), 20: 21516 (UCRL-14403)
yields from gamma radiolysis of benzene–ethanol mixture, 20: 20741
yields from radiolysis of saturated hydrocarbons, 20: 22520(R) (NAA-SR-11805)
yields from radiolysis of methanol vapor, effects of scavengers on, 20: 20776
yields in gamma radiolysis of silane, 20: 20725(R) (NYO-3570-2)
HYDROGEN ION CONCENTRATION
radiosensitivity effects in aqueous lysozyme solutions, 20: 20423
HYDROGEN PEROXIDES
compounds with urea ($H_2O_2 \cdot$ urea), ESR in γ-irradiated single crystals of, 20: 20756
effects on corrosion of rhenium at 25 and 100°C, 20: 21275
yields from gamma radiolysis of ethanol, 20: 20746
HYDROGEN SULFIDES
radiolysis of, reactions of hydrated electrons in pulse, 20: 20735
reactions with plutonium hydride at 400 to 600°C, 20: 20676
HYDROGEN SYSTEMS
D–H, sorption by iridium, rhodium, and tungsten, isotopic mixing during, 20: 20652 (IS-T-67)
HYDROLOGY
radioisotope preparation for tracer studies in, 20: 20794
HYDROMAGNETIC WAVES
propagation from Starfish burst, model for resonant oscillations in, 20: 21829
propagation in ionosphere, waveguide theory for, 20: 21833
propagation in MHD ideal perfectly conducting liquid, particular cylindrical solutions for, 20: 21791
propagation velocity at sea level, 20: 21832
HYDROQUINONE
analytical use for colorimetric determination of lanthanum in oxalate precipitates, 20: 20591
radiosensitivity effects on DNA, uv, 20: 20412

HYDROXYL IONS
reactions with catalase in pulse radiolysis, 20: 20735
HYDROXYL RADICAL
radiosensitivity effects in aqueous lysozyme solutions, 20: 20423
HYPERFRAGMENTS
decay of light double, coupling constants for four-baryon weak interactions from, 20: 22149
production in meson (K-) reactions with emulsion nuclei, (E), 20: 22161
research, 20: 22033
HYPERONS
decay of, dynamical approach to nonleptonic, 20: 21686
decay of, G_2 symmetry for leptonic, 20: 21719
decay of, sum rules for radiative nonleptonic, 20: 21751
decay of, unitary symmetrical composite model for nonleptonic, 20: 21687
production in neutrino interactions, methods for, 20: 21606 (CERN-65-32, pp 157-60)
HYPERONS (Λ)
binding energy in nuclear matter, (E), 20: 22161
HYPERONS (Ω^-)
decay of, composite-particle model for, 20: 21643
HYPERONS (Σ^-)
interactions with neutrons from meson (π^-) interactions with deuterons, final-state, (T), 20: 21681
HYPERONS (Σ^+)
decay of, pole model for nonleptonic, 20: 21688
HYPERONS (Ξ)
interactions with mesons ($\bar{K}$) in 27-fold representation, dynamics of, 20: 21674
HYPERTHYROIDISM
radiodiagnosis of, in Congo, 20: 20373
radiodaignosis using iodine-131, 20: 20528
HYPOTHYROIDISM
radiodiagnosis using iodine-131, 20: 20528

I

ICE
radiation effects on, ESR spectra from gamma, 20: 22328
ICE-d_2
radiation effects on, ESR spectra from gamma, 20: 22328
IGNEOUS ROCKS
rare earth distribution in, 20: 20877
IMAGE BRIGHTNESS INTENSIFIERS
design and performance for streamer chambers, 20: 21020 (AD-621069)
IMMUNE REACTIONS
radiation effects on mouse, to uv-irradiated transplants of ascites tumor cells, x, 20: 20484
radiation effects on, to skin homografts in calves, y, 20: 20485
role in etiology of acute hematogenic osteomyelitis, 20: 20371
IMMUNITY
radiation effects on mouse, to transplanted tumors, 20: 20479
INCINERATORS
use for waste disposal, review on, 20: 22508 (AEET-220)
INCOLOY
properties of type 800, 20: 22520(R) (NAA-SR-11805)
INCONEL
bonding of type 600, to refractory metals and alloys, process development for explosive, 20: 21295(R) (WANL-PR-(EE)-002)
corrosion of types 600 and 800, by argon–nitrogen mixtures at 900°C, 20: 20802(R) (ANL-7055, pp 21-98)
corrosion of 600, by potassium chloride–uranium trichloride eutectic at 900°C, 20: 21261 (LA-3476)
INDIAN POINT POWER REACTOR
superheaters at, design and operation of separately fired, 20: 22455
INDIUM
determination in silicon dioxide, activation, 20: 20634
electric conductivity of superconducting, current dependence of imaginary part of, (E/T), 20: 21919
electron tunneling from, boundary and resonance effects in, 20: 22520(R) (NAA-SR-11805)
neutron flux and spectrum measurements on foils of, 20: 21427(R) (NASA-CR-54904)
separation from gallium and transition elements by ion exchange, 20: 20634
separation from scandium by ion exchange chromatography, 20: 20821
separation from uranium by combined ion exchange-solvent extraction using nitric acid–tetrahydrofuran solutions, 20: 20811
superconducting properties of, effects of λ transition on, 20: 21875
thermal capacity of liquid, corresponding states correlation of configurational, 20: 20657 (UCRL-11931)
viscosity of liquid, based on atomic parameters, 20: 20656 (UCRL-11930)
INDIUM ALLOYS
Al–In–Sn, superconducting properties of, nonideal, 20: 21925
Bi–In, microwave surface resistance in superconducting, (E), 20: 21916
Bi–In, thermal capacity of superconducting, (E), 20: 21907
Bi–In, thermal conductivity of superconducting, (E), 20: 21914
Cd–In–Ag, fabrication of reactor control rods of, 20: 21317(P)
In–Pb, magnetic field transitions in superconducting, surface effects on a-c, 20: 21918
In–Pb, microwave surface resistance in superconducting, (E), 20: 21916
In–Pb, superconducting transitions in, (E/T), 20: 21913
In–Pb, superconducting transitions in, effects of strain on, (E), 20: 21923
In–Sn, electric conductivity of superconducting, current dependence of imaginary part of, (E/T), 20: 21919
In–Sn, superconducting properties of, nonideal, (E/T), 20: 21925
In–Zn, diffusion coefficient measurements on liquid, during molecular distillation, 20: 21334 (IS-1325)
INDIUM ISOTOPES In-115
neutron reactions (n,n′) at 0.45 Mev, cross section and threshold energy for, 20: 21427(R) (NASA-CR-54904)
INDIUM ISOTOPES In-116
decay of, gamma branching ratios for, (E), 20: 22091
INDOLE,3-(2-AMINOETHYL)-
radiation effects on content in rat brain tissues, x, 20: 20437 (CONF-650560-18)
INDUSTRIAL HYGIENE
data recording system for nuclear, 20: 20955
INDUSTRIAL MANAGEMENT
critical-path method for scheduling construction of Transuranium Processing Plant at ORNL, 20: 20809 (ORNL-3925)
INFORMATION CENTERS
operation of ORNL nuclear safety, 20: 20940(R) (ORNL-3915)
INFRARED RADIATION
detection using internally amplifying gallium-diffused junctions, 20: 21100
INFRARED SPECTROSCOPY
conference on photographic and spectroscopic optics, 20: 21458
INOR-8
corrosion by potassium chloride–uranium trichloride eutectic at 900°C, 20: 21261 (LA-3476)
mechanical properties of welds in, 20: 21395
INSECTS
effects on decomposition of swine carrion, 20: 20941 (ORNL-TM-1432)
INSTRUMENTATION
conference on nuclear, 20: 21097
control system for nuclear physics experiments, 20: 20995
development for SNAP-10A, 20: 22476
position monitoring devices for, 20: 20989 (Y-1506)
INSTRUMENTS
design and performance of Moellenstedt electron velocity analyzer, 20: 21005
use of radiometric, survey on, 20: 20990(T) (AERE-Trans-1048)
INSULIN
binding by blood serum proteins, tracer study, 20: 20383 (CNEA-185)
labeling with iodine-131, 20: 20383 (CNEA-185)
metabolism in diabetic and normal man, tracer study, 20: 20383 (CNEA-185)
INTERFEROMETERS
performance for plasma diagnostics, multiple-reflection effects in, 20: 22231
INVERTEBRATES
gamma activity of Columbia River, 1964 and 1965, 20: 20382 (BNWL-SA-623)
IODINE
determination in human serum, methods for, 20: 20401
dissociation of molecular, effects of pressure and temperature on, 20: 20940(R) (ORNL-3915)
neutron inelastic scattering at 5.8 and 7.5 Mev, gamma spectra from thermal, (E), 20: 22069
reactions with Zircaloy-2 in helium–steam mixtures, 20: 20940(R) (ORNL-3915)
separation from air by activated charcoal filters, 20: 20940(R) (ORNL-3915)
sorption of gaseous, by activated carbon, 20: 22463(R) (DP-1028)
IODINE COMPOUNDS
activity of iodine-131-labeled, method for determining specific, 20: 20604
IODINE ISOTOPES
detection and measurement of radioactive, using diffusion tubes and May packs, 20: 20940(R) (ORNL-3915)
determination of chemical forms of carrier-free, paper-electrophoresis method for, 20: 20599
determination of radioactive, by gas chromatography, 20: 20940(R) (ORNL-3915)

IODINE ISOTOPES I-118
production in target elements by high-energy protons, cross sections for, (E), 20: 22045

IODINE ISOTOPES I-119
production in target elements by high-energy protons, cross sections for, (E), 20: 22045

IODINE ISOTOPES I-120
production in target elements by high-energy protons, cross sections for, (E), 20: 22045

IODINE ISOTOPES I-121
production in target elements by high-energy protons, cross sections for, (E), 20: 22045

IODINE ISOTOPES I-122
production in target elements by high-energy protons, cross sections for, (E), 20: 22045

IODINE ISOTOPES I-123
production in target elements by high-energy protons, cross sections for, (E), 20: 22045

IODINE ISOTOPES I-124
production in target elements by high-energy protons, cross sections for, (E), 20: 22045

IODINE ISOTOPES I-125
production in target elements by high-energy protons, cross sections for, (E), 20: 22045
use for diagnosis of thyroid diseases, 20: 20533
use for diagnosis of thyroid diseases, 20: 20534

IODINE ISOTOPES I-126
production in target elements by high-energy protons, cross sections for, (E), 20: 22045

IODINE ISOTOPES I-127
production in target elements by high-energy protons, cross sections for, (E), 20: 22045

IODINE ISOTOPES I-128
production in target elements by high-energy protons, cross sections for, (E), 20: 22045

IODINE ISOTOPES I-129
production in target elements by high-energy protons, cross sections for, (E), 20: 22045

IODINE ISOTOPES I-130
production in target elements by high-energy protons, cross sections for, (E), 20: 22045

IODINE ISOTOPES I-131
abundance in iodine solutions, use of autoradiography and iodoinsulin to determine, 20: 20604
content in colorado deer, 20: 20384 (COO-1156-13)
content in food in Amsterdam, 1960 to 1963, 20: 20949
deposition and transport on mild and stainless steels, model for, (E/T), 20: 21785 (ORNL-TM-1330(Rev.))
determination in human serum, methods for, 20: 20401
diffusion in irradiated fuel element cladding alloys and materials at 600 to 1200°C, 20: 21232 (BMI-1763)
dispersion and movement in soils, mechanism of, 20: 20875 (EUR-2481.f)
effects of dietary, on rats, carcinogenic, 20: 20448
effects on variegation in Einkorn wheat, mutagenic, 20: 20497
exchange between hydriodic acid and osmium complexes, 20: 20706
incorporation in insulin, 20: 20383 (CNEA-185)
incorporation in lipids, 20: 20789 (CNEA-182)
metabolism of prenatally administered, in rats, 20: 20390(R) (TID-22767)
production of, hot chamber for, 20: 21215
radiation hazards from, following nuclear incidents, 20: 20962
use as tracer for measuring Columbia River flow times, 20: 20916
use for diagnosis of thyroid diseases, 20: 20533
use for diagnosis of thyroid diseases, 20: 20534
use for placenta localization by dual-probe scintillation counting, 20: 20527
use for radiodiagnosis, 20: 20535
use for thyroid disease diagnosis, 20: 20528
use in diagnosis of kidney tumors, 20: 20522 (CNEA-167)
use in diagnosis of brain tumors, 20: 20529
use of Hippuran-incorporated, in renograms, 20: 20538
yields from photofission of uranium by 650-Mev bremsstrahlung, 20: 22040

IODINE ISOTOPES I-132
production in target elements by high-energy protons, cross sections for, (E), 20: 22045
production of, generator for, (E), 20: 21217
radiation hazards from, following nuclear incidents, 20: 20962
yields from photofission of uranium by 650-Mev bremsstrahlung, 20: 22040

IODINE ISOTOPES I-133
production in target elements by high-energy protons, cross sections for, (E), 20: 22045
radiation hazards from, following nuclear incidents, 20: 20962
yields from photofission of uranium by 650-Mev bremsstrahlung, 20: 22040

IODINE ISOTOPES I-134
production in target elements by high-energy protons, cross sections for, (E), 20: 22045
radiation hazards from, following nuclear incidents, 20: 20962
yields from photofission of uranium by 650-Mev bremsstrahlung, 20: 22040

IODINE ISOTOPES I-135
production in target elements by high-energy protons, cross sections for, (E), 20: 22045
radiation hazards from, following nuclear incidents, 20: 20962
yields from photofission of uranium by 650-Mev bremsstrahlung, 20: 22040

IODINE SYSTEMS
He–I, diffusion in confined vortex flow of, (E/T), 20: 22473

ION BEAMS
production and extraction from plasma sources, 20: 21213 (IAE-974)
reactions in electromagnetic isotope separators, 20: 21219

ION EXCHANGE MATERIALS
cesium-137 sorption by, successive desorption method for calculating, 20: 20618

ION EXCHANGE PROCESSES
description of, for short-lived isotopes, review of, 20: 20826

ION PUMPS
use for electron bombardment ionizer, for molecular beam detection, 20: 21066

ION SOURCES
design and performance of positive, 20: 21457
performance of plasma, for electromagnetic separation, 20: 21213 (IAE-974)
performance of plasma-expansion, 20: 21478

IONIZATION CHAMBERS
design of dosimeter, 20: 21141(P)
design of parallel-plate multisection, for reactor control, 20: 22356 (ORNL-3929)
use in integrating gamma dose-rate meter, 20: 21078
use of dual, for voltage measurements in x-ray tubes, 20: 21087

IONOSPHERE
chemistry of D layer of, determination using nuclear explosions, 20: 21811 (AD-620952)
cosmic noise absorption at magnetically conjugate points in auroral, fluctuations in, (E), 20: 21820
effects on characteristics of radio signals from Jupiter, 20: 21510
electron content in, differential Doppler and Faraday effects for determining fluctuations in, (E/T), 20: 21816
electron density distribution in daytime F2 layer of, 20: 21823
electron distribution in D region of, weak partially reflected wave amplitudes for determining, (E), 20: 21819
electron precipitation in auroral-zone, correlations with electron leakage from magnetic mirrors, (E), 20: 21836
hydromagnetic wave propagation in, waveguide theory for, 20: 21833
ion temperature in, Langmuir double probe device for measuring, 20: 22213
ionization trough in F region of night, midlatitude, 20: 21822
plasma density and flow in polar, 20: 21828
plasma waves in, survey of low frequency, 20: 21812 (AD-622223)
radiation measurements in auroral, using balloon-borne instruments, 20: 21838
radio wave propagation in, back- and sidescatter effects on, 20: 21827
structure of arctic auroral-zone, during solar activity minimum, (E), 20: 21814

IONS
distribution near midlatitude trough in night ionosphere, 20: 21822
emission from cesiated surfaces of refractory compounds, 20: 21584
motion in plasma, electrostatic damping of, (T), 20: 22233
production by low-pressure electric discharges, (T), 20: 21799
reactions of heavy, with nuclei, 20: 21992 (BNL-948, pp 1045-1134)
reactions with alkali halide crystals, linear relation for scintillation yields, 20: 21084
reactions with electrons in nonequilibrium plasma, 20: 22195
scattering by nuclei, level excitation by Coulomb, 20: 21991 (BNL-948, pp 1005-44)
scattering by nuclei, microscopic description of, (T), 20: 22118
scintillation response of thallium-activated sodium-iodide crystals to low-energy heavy, 20: 22318
sorption from solutions, successive desorption method for calculating, 20: 20618
temperature in ionosphere, effects on electron density distribution, 20: 21823
temperatures in streaming plasma, Langmuir double probe device for measurement of, 20: 22213
trajectories in monopole mass spectrometers, (T), 20: 20994

IRIDIUM
desorption of carbon monoxide, hydrogen, and nitrogen from, flash, 20: 20652 (IS-T-67)

IRIDIUM ALLOYS
Dy–Ir, dysprosium hyperfine magnetic field in intermetallic compounds

of, (E), 20: 22330
Ir–Fe, iridium-194 beta decay in, temperature dependence of platinum-194 internal magnetic field from, (E), 20: 22326
IRIDIUM BROMIDES
ammine complexes of, bromine-82 exchange with bromides, 20: 20706
IRIDIUM ISOTOPES Ir-194
beta decay in iridium–iron alloy, temperature dependence of platinum-194 internal magnetic field from, (E), 20: 22326
IRON
brazing material for joining molybdenum to tungsten for use to 1800°F, 20: 21312
detection of inclusions of, in zirconium alloys by x-ray emission in electron microscopy, 20: 20593
determination in high-purity tantalum by spectrography using d-c arc method, 20: 20608
determination in silicon dioxide, activation, 20: 20634
distribution in products of fluidized-bed fluorination of spent fuel mixtures, 20: 20803(R) (ANL-7055, pp 99-162)
dose distribution in, from electron beam irradiation, three-dimensional, 20: 21470 (PB-181506, pp 116-29)
ductility of, at –269°C, 20: 21416
evaporation from porous tungsten ionizers, 20: 21570 (N-65-29785)
fatigue tests on Armco, at high temperatures, 20: 21347(R) (NASA-CR-54916)
gamma elastic scattering at 280 and 662 kev, Z dependence of cross section for, (E), 20: 22060
helium-3 reactions (He-3,n) at 19 to 25 Mev, angular distributions and cross sections for, (E), 20: 22132
Mössbauer effects in, relevance of, to radiation damage theories of bombardment-induced, 20: 21444
neutron cross sections and shielding coefficients for, 20: 22383(T) (AEC-tr-6693)
neutron inelastic scattering at 5.8 and 7.5 Mev, gamma spectra from thermal, (E), 20: 22069
passivation of, effects of chromate and pertechnetate ions on, 20: 21271
performance as liquid-phase sintering promoter for uranium monocarbide, 20: 21296 (Y-1510)
phase transformation in, effects of alloying on high-pressure, 20: 21357 (UCRL-16299)
proton reactions at 400 Mev, Monte Carlo calculation of radionuclide production in, 20: 22035
separation from gallium, indium, and transition elements by ion exchange chromatography, 20: 20634
separation from scandium by ion exchange chromatography, 20: 20821
separation from thorium by ion exchange in nitric acid solution, 20: 20624
separation from uranium by combined ion exchange–solvent extraction using nitric acid–tetrahydrofuran solutions, 20: 20811
separation of oxygen and sulfur from, by compound formation with uranium at 1600°C, 20: 20692
sorption from perchloric acid solutions by ion exchange materials, 20: 20823
sorptive properties of evaporated films of, for krypton and xenon, 20: 21387
sorptive properties of evaporated films of, for carbon monoxide at 0°C, 20: 21388
sorptive properties of evaporated films of, for carbon dioxide at room temperature, 20: 21389
viscosity of liquid, based on atomic parameters, 20: 20656 (UCRL-11930)
welding of, argon-arc and electron-beam methods of, 20: 21310
IRON ALLOYS
Ce–Fe, crystal structure of $CeFe_7$, 20: 21400
Ce–Fe–Pu, phase studies, 20: 21342(R) (MLM-1301)
Cr–Fe, fission product diffusion in irradiated, at 600 to 1200°C, 20: 21232 (BMI-1763)
Cr–Fe–Mo–Ni, corrosion of Hymu-80 by potassium chloride–uranium trichloride eutectic at 900°C, 20: 21261 (LA-3476)
Cr–Fe–Ni, fission product diffusion in irradiated, at 600 to 1200°C, 20: 21232 (BMI-1763)
Dy–Fe, dysprosium hyperfine magnetic field in intermetallic compounds of, (E), 20: 22330
Fe–Nd, crystal structure of $NdFe_7$, 20: 21400
Fe–Ni, fission product diffusion in irradiated, at 600 to 1200°C, 20: 21232 (BMI-1763)
Fe–Pd, electric conductivity at low temperatures, 20: 22314(R) (AD-626865)
Fe–Pr, crystal structure of $PrFe_7$, 20: 21400
Fe–Sm, crystal structure of $SmFe_7$, 20: 21400
Ir–Fe, iridium-194 beta decay in, temperature dependence of platinum-194 internal magnetic field from, (E), 20: 22326
IRON CARBIDES
effects on tensile properties of tungsten wire, 20: 21396
IRON IONS
electron spin resonance in silver chloride crystals, 20: 22311(R) (AD-622068)
interactions with yttrium ions in garnets, 20: 22313 (AD-624719)
IRON ISOTOPES
determination in radiation sources, extraction radiometric titration method for, 20: 20567 (UJV-1418/65)
IRON ISOTOPES Fe-52
production in chromium-50(α,2n) reactions, (E), 20: 21993 (BNL-9168)
IRON ISOTOPES Fe-54
deuteron reactions (d,pγ) at 7 Mev, iron-55 level spins from, (E), 20: 22126
helium-3 reactions (He-3,t) at 22 Mev, Coulomb displacement-energy from, (E), 20: 22095
IRON ISOTOPES Fe-55
energy levels from deuteron reactions (d,pγ) with iron-54 at 7 Mev, spins of, (E), 20: 22126
IRON ISOTOPES Fe-56
energy levels from cobalt-56 l-forbidden decay, second excited, (E), 20: 22016
energy levels from cobalt-56 decay, 2080-kev, (E), 20: 22029
helium-3 reactions (He-3,t) at 22 Mev, Coulomb displacement-energy from, (E), 20: 22095
IRON ISOTOPES Fe-57
energy levels in, Nilsson model for, 20: 22098
Mössbauer spectra in $La_{1-x}Sr_xFeO_3$ ($0 \leq x \leq 1$) perovskites, (E), 20: 22336
Mössbauer studies using, 20: 20684
use in Mössbauer studies, opaque absorber for, 20: 22157
use in Mössbauer studies, standard reference absorber for, 20: 22158
IRON ISOTOPES Fe-58
helium-3 reactions (He-3,t) at 22 Mev, Coulomb displacement-energy from, (E), 20: 22095
IRON OXIDES
removal from iron by dissolution, descaling solution for, 20: 21238 (NP-15928)
IRON(III) SULFATES
$Fe_2(SO_4)_3$–H_2SO_4, corrosive effects on nickel–chromium–molybdenum alloys at 800 to 2375°F, 20: 21277
IRRADIATION FACILITIES
beam focus imaging for gamma, 20: 20547
description of, for producing plastic–wood combinations, 20: 21181 (ORNL-IIC-7, pp 32-48)
design of cobalt-60, of Kyushu University, 20: 20847
design of cobalt-60 pool-type, at Takasaki Laboratory in Japan, 20: 20849
design of electron, for films, 20: 20853(P)
design of gamma, for granular materials, 20: 20852(P)
equipment for gamma, beam focus cassette and interspacer, 20: 20548
sample holders for, 20: 20846
IRRADIATION TECHNIQUES
development for micro-exposure of chromosome segments, 20: 20438 (EUR-2518.f)
ISOCYANIC ACID
radioinduced polymerization and co-polymerization at low temperatures, 20: 20747
ISOTOPE EFFECTS
in neutron-irradiated ethyl bromide, 20: 20751
in photolysis of tritium-labeled uracil, 20: 20782
on hydrogen abstraction from ammonia, hydrazine, and methylamine, 20: 20713
ISOTOPE SEPARATION METHODS
electromagnetic, ion beam reactions with materials in, 20: 21219
ISOTOPES
abundance determination in compounds from mass spectrograms, 20: 20610
mass spectra of, least squares analysis and simplification of, 20: 20580
ISOTOPIC EQUILIBRATION
uses in age estimation by potassium–argon and rubidium–strontium methods, 20: 20891
ISOTOPIC EXCHANGE
between six coordinated inorganic complexes and halides in crystals and solutions, 20: 20706
between *trans*-hydridochlorobis(triethylphosphine)-platinum(II) and heavy water, 20: 20701
in catalytic hydrogenation of methyl β,β-dimethylacrylate, 20: 20715
ITALY
radionuclide detection and measurement in milk in, 20: 20950

J

JAPAN
atomic industry in, review of growth and prospects of, 20: 22526

environs monitoring at Tokai, spectrometric method for low-level gamma, 20: 20952
radiation monitoring program in, 20: 20934 (JAERI-1098)

K

KAOLINITES
sorptive properties for cesium-137, 20: 20696
KENTUCKY
fallout monitoring in biota of Doe Run, Meade County, 1959 to 1965, 20: 20884(R) (TID-22815)
KETENE
radioinduced polymerization with isocyanic acid at low temperatures, 20: 20747
KETONES
labeling with deuterium, 20: 20799
KIDNEYS
radiodiagnosis of tumors of, using iodine-131-rose bengal or colloidal albumin and external scanning, 20: 20522 (CNEA-167)
radiodiagnosis of acute obstructive failure of, using iodine-131-labeled Hippuran, 20: 20538
radioinduced glomerulosclerosis in mouse, x, 20: 20441 (ORNL-P-1173)
radioisotope function tests for, 20: 20550
ruthenium chloride metabolism in rat, 20: 20396
weight norm for human, use in establishing standards for radiation dosimetry, 20: 20374
KRYPTON
deuterium vibrational relaxation times, shock-tube measurement of, 20: 21797
diffusion in uranium and uranium monocarbide single crystals, 20: 21332(R) (EURAEC-1573)
diffusion in uranium-doped calcium fluoride single crystals at 900 to 1200°C, 20: 21332(R) (EURAEC-1573)
effects on cesium thermionic converter electric properties, 20: 21579
effects on growth rates in Neurospora, 20: 20378
effects on sporulation in Neurospora, 20: 20378
heat of absorption by molecular sieves, 20: 20806(R) (MLM-1274)
sorption by evaporated metallic films, 20: 21387
sorption by metallic film surfaces saturated with carbon monoxide, 20: 21388
sorption by molybdenum films and Pyrex glass in ultrahigh vacuum, kinetics of, 20: 21351(R) (SRIA-425-8)
KRYPTON FLUORIDES
preparation and properties of, 20: 20659
KRYPTON IONS
reactions with beryllium–copper alloys at 3 to 90 kev, secondary electron emission from, (E), 20: 21538
KRYPTON ISOTOPES Kr-82
energy level transitions from bromine-82 decay, (E), 20: 22010(R) (NYO-72-28)
KRYPTON ISOTOPES Kr-84
concentration in gaseous krypton by thermal diffusion, 20: 20807(R) (MLM-1287)
KRYPTON ISOTOPES Kr-85
determination in xenon by scintillation counting, 20: 20553(R) (MLM-1142)
determination in xenon by liquid scintillation counting, 20: 20582
radiation hazards from, following nuclear incidents, 20: 20962
use in diagnosis, personnel dosimetry during, 20: 20958
KRYPTON ISOTOPES Kr-86
concentration in gaseous krypton by thermal diffusion, cascade for, 20: 20806(R) (MLM-1274)
concentration in gaseous krypton by thermal diffusion, 20: 20807(R) (MLM-1287)
KRYPTON ISOTOPES Kr-87
radiation hazards from, following nuclear incidents, 20: 20962
KRYPTON ISOTOPES Kr-88
radiation hazards from, following nuclear incidents, 20: 20962
KRYPTON SYSTEMS
Ce–Kr, thermal diffusion in, 20: 21567 (FEI-15)

L

LABORATORIES
description of underground, for neutrino detection, 20: 21612 (CERN-65-32, pp 225-30)
design criteria for, for storing radioactive materials, 20: 20942 (ORNL-TM-1459)
design of industrial, for research in France, 20: 20851
design of, for carbon-14 and tritium (measurements,) New Zealand, 20: 20893
LABORATORY EQUIPMENT
design for industrial laboratories for research and control in France, 20: 20851
LABORATORY FURNITURE
design for research laboratories in France, 20: 20851
LAMINATES
neutron transport in, equations for, 20: 21945
LANTHANUM
determination in oxalate precipitates using hydroquinone, colorimetric, 20: 20591
determination in rare earth mixtures, activation, 20: 20562 (LYCEN-6538)
friction and wear properties of, in vacuum, effects of crystal structure on, 20: 21365
oxidation in dry and moist air at 100 to 800°C, rate of, 20: 21265 (RPI-2714-8)
proton reactions at 590 Mev and 18 Bev, yields of iodine isotopes from, (E), 20: 22045
separation from cerium by partition chromatography on polytetrafluoroethylene, 20: 20623
separation from other rare earths by paper precipitation chromatography using 8 quinolinol, 20: 20814
separation from perchloric acid solutions by ion exchange materials, 20: 20823
separation from praseodymium by fused salt extraction, 20: 20802(R) (ANL-7055, pp 21-98)
separation from rare earths by reversed-phase partition chromatography on polytetrafluoroethylene, 20: 20621
separation from scandium by ion exchange chromatography, 20: 20821
separation from thorium by ion exchange in nitric acid solution, 20: 20624
separation from uranium by combined ion exchange-solvent extraction using nitric acid–tetrahydrofuran solutions, 20: 20811
LANTHANUM ALLOYS
Al–La, crystal structure and stability of intermetallic compounds in, 20: 21415
Ce–La, electric conductivity, magnetic susceptibility, and superconductivity at low temperatures, 20: 21873 (NP-15936)
Dy–La, electric conductivity at 4.2, 77, and 296°K, 20: 22312(R) (AD-622796)
Gd–La, magnetic properties and phase transformations in, 20: 21414
La–Nd, electric conductivity, magnetic susceptibility, and superconductivity at low temperatures, 20: 21873 (NP-15936)
La–Pr, electric conductivity, magnetic susceptibility, and superconductivity at low temperatures, 20: 21873 (NP-15936)
La–rare earth, electric conductivity, magnetic susceptibility, and superconductivity at low temperatures, 20: 21873 (NP-15936)
La–Y, magnetic properties and phase transformations in, 20: 21414
La–Zn, intermetallic compound with $CeCu_2$-type structure in, 20: 21352 (TID-21745)
LANTHANUM ALUMINATES
growth and properties of crystals of, 20: 22311(R) (AD-622068)
LANTHANUM BORIDES
LaB_6–N, electric conductivity of suspensions of, in MHD cells, 20: 21575
LANTHANUM CHLORIDES
praseodymium ion absorption and fluorescence spectra in, 20: 20667
LANTHANUM FERRITES
magnetic properties of, effects of strontium substitution on, 20: 22336
LANTHANUM FLUORIDES
crystal structure, 20: 20681
precipitation with neptunium, oxidation states in, 20: 20561 (JAERI-1099)
transport properties, (E), 20: 22339
LANTHANUM HYDRIDES
La–LaH_2, phase diagram, 20: 21336 (IS-T-79)
LANTHANUM IONS
effects on dephosphorylation of cocarboxylase, riboflavin-5-phosphate, and pyridoxal phosphate, 20: 20375
LANTHANUM NITRATES
$La(NO_3)_3$–K_2CO_3–H_2O, composition of, effects of reactant concentration on, 20: 20664
LANTHANUM OXALATES
preparation and properties, 20: 20680
LANTHANUM OXIDES
preparation by oxide solubility in alcohols containing ammonia, 20: 20686
solubility in ethyl, isopropyl, methyl, and propyl alcohols in presence of ammonia, 20: 20686
LANTHANUM SILICIDES
thermal capacity of superconducting, anomalous, (E), 20: 21883
LANTHANUM SYSTEMS
La–LaH_2, phase diagram, 20: 21336 (IS-T-79)
LEAD
analysis for rare earths, 20: 20607

determination in granites, extraction-radiometric method of isotopic dilution for, 20: 20620
determination in steels by x-ray fluorescence methods, 20: 20642
electron tunneling from, boundary resonance effects in, 20: 22520(R) (NAA-SR-11805)
gamma elastic scattering at 280 and 662 kev, Z dependence of cross section for, (E), 20: 22060
microwave reactions with Josephson junctions of superconducting, induced d-c voltages from, (E), 20: 21882
neutron inelastic scattering at 5.8 and 7.5 Mev, gamma spectra from thermal, (E), 20: 22069
performance for separating fissile materials, 20: 20840(R) (BNWL-193, pp 57-67)
separation from thorium by ion exchange in nitric acid solution, 20: 20624
separation from uranium by combined ion exchange-solvent extraction using nitric acid–tetrahydrofuran solutions, 20: 20811
sorption from perchloric acid solutions by ion exchange materials, 20: 20823
superconductivity properties of, effects of λ transition on, 20: 21875
thermal capacity of liquid, corresponding states correlation of configurational, 20: 20657 (UCRL-11931)
viscosity at 335 to 1114°C, 20: 21342(R) (MLM-1301)
viscosity of liquid, based on atomic parameters, 20: 20656 (UCRL-11930)

LEAD ALLOYS
analysis for rare earths, 20: 20607
Bi–Pb, separation of cadmium from, by vacuum distillation, 20: 20805 (IS-1329)
Bi–Pb, superconducting transition temperatures in epsilon-phase, (E), 20: 21892
Bi–Pb, superconducting critical currents and fields in flux-pump fed coils of, (E), 20: 21924
Hg–Pb, superconducting critical currents and fields in flux-pump fed coils of, (E), 20: 21924
In–Pb, magnetic field transitions in superconducting, surface effects on a-c, (E), 20: 21918
In–Pb, microwave surface resistance in superconducting, (E), 20: 21916
In–Pb, superconducting transitions in, (E/T), 20: 21913
In–Pb, superconducting transitions in, effects of strain on, (E), 20: 21923
Pb–Tl, elastic modulus of superconducting, magnetic field dependence of, 20: 21912
Pb–Tl, magnetic hysteresis in mixed state of superconducting, effect of surface currents on, (E), 20: 21886
Pb–Tl, microwave surface resistance in superconducting, (E), 20: 21916

LEAD COMPLEXES
with thiodibenzoylmethane, stability of, 20: 20693

LEAD GLASS
radioinduced electric discharge figures in, electron, 20: 21440

LEAD ISOTOPES
mass differences of, (E), 20: 22153

LEAD ISOTOPES Pb-207
energy levels of, magnetic dipole moment of 569-kev, (E), 20: 22025

LEAD ISOTOPES Pb-208
energy levels from thallium-208 decay, (E), 20: 22020
proton capture cross sections and transmission coefficients for, optical model calculation of, 20: 22049
proton inelastic scattering at 40 Mev, energy levels from, (E), 20: 22101

LEAD ISOTOPES Pb-210
content in tissues of radium dial painter, 20: 20387(R) (NYO-2181-3)
determination in environmental samples by deposition on nickel and counting, 20: 20643

LEAK DETECTORS
design and performance, 20: 20845
use of radiometric, survey on, 20: 20990(T) (AERE-Trans-1048)

LEAVES
cesium-137 content in forest, in Washington state, 20: 20879 (BNWL-SA-530)

LECTURES
book: *High Energy Physics*, 20: 21696
on neutrino processes, 20: 21616 (JINR-P-2429)
on unitary symmetry and elementary particles, 20: 21770

LEPTONS
interactions at high energies, weak, (T), 20: 21614 (CERN-65-32, pp 275-84)
interactions of, symmetries for weak, 20: 21712 (JINR-P-2562)
interactions with baryons, model for weak, (T), 20: 21714 (JINR-P-2578)
properties of, lectures on, 20: 21616 (JINR-P-2429)

LEUKEMIA
incidence in populations of Hiroshima and Nagasaki exposed to atomic bomb in 1945, 20: 20919(R) (ABCC-64-65)
radioinduced in mice, incidence of x, 20: 20441 (ORNL-P-1173)

LEUKOCYTES
radiation effects on mouse, x, 20: 20475

LEVEL INDICATORS
development and testing eddy-current, for liquid metals, 20: 20802(R) (ANL-7055, pp 21-98)
use of radiometric, survey on, 20: 20990(T) (AERE-Trans-1048)

LIFE SPANS
radiation effects on, in populations of Hiroshima and Nagasaki, 20: 20919(R) (ABCC-64-65)

LIGHT
emission in air from x-ray excitation of nitrogen, 20: 21834
intensity of 3914 and 5577A, in auroral storms, 20: 21826

LIGHT SOURCES
conference on photographic and spectroscopic optics, 20: 24158

LIMBS
radiation effects on regeneration of salamander, role of normal epidermis in recovery from x, 20: 20465

LINEAR ACCELERATORS
beam radial expansion in electron, asymmetric wave effects on, 20: 21476
data handling system for on-line use with, modular, 20: 21225
data handling system for on-line use with, modular programming for, 20: 22032
dose distribution in samples irradiated by electron beams from, three-dimensional, 20: 21470 (PB-181506, pp 116-29)
use of electron, for radiography of steel plates, 20: 21477

LIPIDS
content in blood serum, relation to development of atherosclerosis and ischemic heart disease in man, 20: 20370 (UCRL-14658)
labeling with iodine-131, 20: 20789 (CNEA-182)

LIPOPROTEINS
content in blood serum, relation to development of atherosclerosis and ischemic heart disease in man, 20: 20370 (UCRL-14658)

LIQUID FLOW
magnetohydrodynamics, in annular, (T), 20: 21789
magnetohydrodynamic, in square channels, (E), 20: 21807

LIQUID METAL COOLED REACTORS
coolant ejection from, in accidents, shock front conditions in, 20: 22348
coolant-loss accidents in, analysis of, 20: 22349
cost analysis of 1000-Mw(e) fast power, 20: 22451
design of sodium-cooled power breeder, vented fuel concept applied to, 20: 22462
design of 1000-Mw(e) sodium-cooled fast, 20: 22453
design of 1000-Mw(e) sodium-cooled fast, 20: 22454
fuel analysis for fast-breeder sodium, thorium, 20: 21229 (AEET-229)
safety analysis of 1000-Mw(e) fast power, 20: 22451

LIQUIDS
hydromagnetic wave propagation in ideal perfectly conducting, particular cylindrical solutions for radial, 20: 21791
neutron inelastic scattering by, research on slow, 20: 22316 (JINR-P-2081)
volume of, tracer technique for measurement of, 20: 21208

LITHIUM
determination in silicon crystals, activation, 20: 20560 (EUR-2753.f)
performance of molten, as reactor coolant, (T), 20: 22351 (AD-623020)
reactions with boron carbide, 20: 21327 (CONF-560505-1)
thermal conductivity of vaporous, at 750°C, 20: 20651(R) (CU-2660-26)
viscosity of liquid, based on atomic parameters, 20: 20656 (UCRL-11930)
x-ray scattering cross sections at 1 to 150 kev, (T), 20: 21516 (UCRL-14403)

LITHIUM ALLOYS
Li–Ag, radiation effects at 80°K on, resistivity recovery from proton, 20: 21445

LITHIUM BORATES
performance of single crystals of, as neutron detectors, 20: 21049

LITHIUM CHLORIDES
effects on efficiency of actinide and lanthanide separations by ion exchange chromatography, 20: 20822

LITHIUM FLUOFERRATES
mobility of lithium-6 and -7 in molten, 20: 20695
properties as absorber in Mössbauer measurements using iron-57, 20: 22157

LITHIUM FLUORIDES
radioinduced R-center luminescence in, electron, gamma, and x, (E), 20: 22331
thermoluminescent properties of, effects of thermal annealing on, 20: 21057
use as thermoluminescent dosimeter, reader design and measurement error in, 20: 21061

LITHIUM HYDRIDES
properties for thermionic cells, 20: 21566(R) (ANL-7055, pp 213-29)

LITHIUM IONS
diffusion in p-type silicon, (E), 20: 21337 (JINR-P-2598)
uptake by barley roots, uranyl effects on selective inhibition in,

20: 20402
x-ray scattering cross sections at 1 to 150 kev, (T), 20: 21516 (UCRL-14403)
LITHIUM ISOTOPES Li-6
charged-particle reactions with, amplitude singularities in knockon and stripping, (T), 20: 21997 (INSJ-96)
deuteron reactions (d,p) at 1.5 Mev, angular distributions from, (E), 20: 22151
electron elastic scattering to 230 Mev, magnetic form factors from, (E), 20: 22120
electron inelastic scattering by, single harmonic-oscillator parameter for, (T), 20: 22063
energy levels of, use of Hamada-Johnston potential for, (T), 20: 22102
mobility in molten lithium fluorides, 20: 20695
recoil reactions in crystalline and molten lithium nitrate, mechanism of, 20: 20733 (TID-22796)
LITHIUM ISOTOPES Li-7
charged-particle reactions with, amplitude singularities in knockon and stripping, (T), 20: 21997 (INSJ-96)
effects of ions of, on poly(vinylchloride), poly(dimethylsiloxane), and poly(methyl methacrylate), 20: 20764
electron elastic scattering to 230 Mev, magnetic form factors from, (E), 20: 22120
energy levels from lithium-6 (d,p) reactions, parities and spins for, (E), 20: 22151
mobility in molten lithium fluorides, 20: 20695
scattering by argon at 30 kev, intensity angular distributions from, (E), 20: 21536
LITHIUM NITRATES
radiolysis of crystalline and molten, mechanism of gamma and recoil, 20: 20733 (TID-22796)
LITHIUM SYSTEMS
B–Li, phase studies, 20: 21327 (CONF-560505-1)
C–Li, phase studies, 20: 21327 (CONF-560505-1)
LITHIUM TELLURIDES
effects on cesium chloride spectra, (E), 20: 21566(R) (ANL-7055, pp 213-29)
LITTER SIZES
radiation effects on mouse, gamma and neutron, 20: 20453
LIVER
analysis of tissues from, for carbon-14, combustion procedure in liquid scintillation counting for, 20: 20570
analysis of tissues from, for tritium, combustion procedure in liquid scintillation counting for, 20: 20570
insulin metabolism in diabetic and normal, tracer study, 20: 20383 (CNEA-185)
radiation effects on sodium sulfate metabolism in rat, x, 20: 20410
radiation effects on amino acid synthesis in rat, x, 20: 20410
radiation effects on cytochrome c oxidase and glucose-6-activity in rat, whole-body x, 20: 20417
radiation effects on enzyme synthesis in rat, x, 20: 20429(R) (AD-629311, pp 15-25)
radiodiagnosis of lesions of, using iodine-131 and external scanning, 20: 20535
weight norms for human, use in establishing standards for radiation dosimetry, 20: 20374
LOOPS
design and operation of, for filter testing in nuclear safety pilot plant, 20: 20940(R) (ORNL-3915)
development of sodium, 20: 22520(R) (NAA-SR-11805)
LUBRICATION
conference on, Washington, D. C., Oct. 1964, 20: 20834
LUCENS REACTOR
loading of, positioning of charge-discharge machine for, 20: 22423
LUMINESCENT DETECTORS
performance of implanted, for γ and x radiation dosimetry in dogs and phantoms, 20: 20432 (AD-630332)
LUMINESCENT MATERIALS
preparation of, containing phosphor particles in tritiated silicone polymer, 20: 20787(P)
radiation hazards from radium dial paint, epidemiology of New Jersey cases on, 20: 20387(R) (NYO-2181-3)
radiation hazards from, on watches, 20: 20518 (RT-PROT-(65)41)
LUNGS
analysis of tissues from, for carbon-14, combustion procedure in liquid scintillation counting for, 20: 20570
analysis of, using x radiation, 20: 20546
radiation effects on rat, pathological x, 20: 20434 (AD-630870)
radioactive aerosol deposition in, 20: 20532
radioinduced fibrosis in rat, 20: 20459
ruthenium chloride metabolism in rat, 20: 20396
weight norms for human, use in establishing standards for radiation dosimetry, 20: 20374
LUTETIUM
oxidation in dry and moist air at 100 to 800°C, rate of, 20: 21265 (RPI-2714-8)
separation from perchloric acid solutions by ion exchange materials, 20: 20823
separation from scandium by ion exchange chromatography, 20: 20821
separation from uranium by combined ion exchange-solvent extraction using nitric acid–tetrahydrofuran solutions, 20: 20811
LUTETIUM ALLOYS
Gd–Lu, magnetic transformations in, 20: 21409
Lu–Tb, magnetic transformations in, 20: 21409
Lu–Tm, magnetic transformations in, 20: 21409
LYMPH
radiation effects on immune properties of circulating, in calves, extracorporeal γ, 20: 20485
LYMPH CELLS
radiation effects on immune reactions to injected, in mice, x, 20: 20472
LYMPH SYSTEM
mass of tracheobronchial, use in dosimetry of inhaled radioactive particulates, 20: 20953
radiotherapy of mammary nodes using palladium-103, 20: 20542
LYSOZYME
radioinduced inactivation of aqueous solutions of, x, 20: 20423

M

MACHINE TOOLS
position monitoring devices for, 20: 20989 (Y-1506)
MAGNESIUM
determination in high-purity tantalum by spectrography using d-c arc method, 20: 20608
neutron flux and spectrum measurements on foils of, 20: 21427(R) (NASA-CR-54904)
properties for use in nuclear reactors, 20: 21382
separation from perchloric acid solutions by ion exchange materials, 20: 20823
separation from scandium by ion exchange chromatography, 20: 20821
separation from thorium by ion exchange in nitric acid solution, 20: 20624
separation from uranium by combined ion exchange-solvent extraction using nitric acid–tetrahydrofuran solutions, 20: 20811
viscosity of liquid, based on atomic parameters, 20: 20656 (UCRL-11930)
MAGNESIUM ALLOYS
properties for use in nuclear reactors, 20: 21382
Al–Mg, solvent properties of liquid, for praseodymium, 20: 20802(R) (ANL-7055, pp 21-98)
Au–Mg, radiation effects at 80°K on, resistivity recovery from proton, 20: 21445
Cd–Mg–U–Zn, corrosive effects in fused chloride mixtures, on stainless steel, 20: 20802(R) (ANL-7055, pp 21-98)
Cu–Mg, solvent properties of liquid, for plutonium, praseodymium, and uranium, 20: 20802(R) (ANL-7055, pp 21-98)
Mg–Pu–U–Zn, corrosive effects on type 405 stainless steel, 20: 20802(R) (ANL-7055, pp 21-98)
Mg–U–Zn, corrosive effects with fused chlorides, on carbon and zirconium boride, 20: 20802(R) (ANL-7055, pp 21-98)
Mg–Zr, analysis for bonding and inclusions in, by x-ray emission in electron microscopy, 20: 20593
MAGNESIUM CHLORIDES
$MgCl_2$–KCl–NaCl, corrosive effects with cadmium alloys, on stainless steel, 20: 20802(R) (ANL-7055, pp 21-98)
$MgCl_2$–KCl–NaCl, solvent properties of liquid, for praseodymium, 20: 20802(R) (ANL-7055, pp 21-98)
MAGNESIUM IONS
uptake by barley roots, uranyl effects on selective inhibition in, 20: 20402
MAGNESIUM ISOTOPES Mg-24
alpha inelastic scattering at 28.4 Mev, collective enhancement of 3⁻ state in, (T), 20: 22107
neutron reactions (n,p) at 6.3 Mev, cross section and threshold energy for, 20: 21427(R) (NASA-CR-54904)
MAGNESIUM ISOTOPES Mg-26
deuteron reactions (d,pγ) at 3.0 to 4.8 Mev, magnesium-27 level spins and deformation parameter from, (E), 20: 22099
energy level transitions in, 20: 21984 (BNL-948, pp 751-6)
MAGNESIUM ISOTOPES Mg-27
energy levels and nuclear deformation from deuteron reactions (d,p γ) with magnesium-26, 20: 22099
MAGNESIUM OXIDES
growth and properties of crystals of, 20: 22311(R) (AD-622068)
Al_2O_3–MgO–UO_2, phase studies, properties, and structures of, 20: 21359 (WAPD-T-1581)
MgO–Mg_2TiO_4, properties as electrolytic cells for winning and refining

of plutonium, 20: 21239 (RL-SEP-824)
MAGNESIUM TITANATES
$MgO-Mg_2TiO_4$, properties as electrolytic cells for winning and refining of plutonium, 20: 21239 (RL-SEP-824)
MAGNETIC FIELDS
charged-particle beam aberration and displacement in prism fringe, (T), 20: 21484
charged-particle motion in, (T), 20: 21454
charged-particle motion in, effect of field gradient on polarization of spin-½, (T), 20: 21481
deformation in MHD shock-front interior, during propagation in electro-neutral media, (T), 20: 21806
effects of interplanetary, on solar neutron-decay protons, 20: 21495
effects of longitudinal inhomogeneity of transverse, on MHD mercury flow in square channel, (E), 20: 21807
effects of self-induced, on toroidal plasmas, (E), 20: 22175 (AD-624081)
effects on charged particle beam propagation in cold plasma, wave excitation from, (T), 20: 22286
effects on MHD shock wave propagation, radiative energy flux from, (T), 20: 21788
electron acceleration in longitudinal, by plane electromagnetic wave propagation, (T), 20: 21485
electron motion in uniform, self-consistent hydrodynamic approximation for relativistic, 20: 22287
electron trajectories in focused, pressure effects on lifetime of, (E/T), 20: 21482
excitation in cylinder with coaxial shield, by electric pulse, (T), 20: 21456
flux variations in conducting fluid flow, lines-of-force compression, 20: 21790
index of d-c, instrument for measuring, 20: 21006
measurement of residual, using galvanometers and flip coils, 20: 20806(R) (MLM-1274)
plasma cylinder containment in uniform, by rotating electromagnetic field, 20: 22288
plasma diffusion across, (T), 20: 22189(R) (TID-22809)
plasma drift wave propagation transverse to external, stability of, (T), 20: 22282
plasma entry into axial, mechanism of, (E/T), 20: 22224
plasma polarization in toroidal, triple-helical field effects on, (E), 20: 22275
plasma polarization in toroidal, (E), 20: 22276
plasma polarization in opposite-curved toroidal, (E), 20: 22277
plasma wave propagation in, cyclotron harmonic, (E), 20: 22226
production for thermonuclear research, review of, 20: 22302
properties of small-scale solar, kinematical hydromagnetic model for, 20: 21503
MAGNETIC MATERIALS
neutron scattering at Curie temperature, angular resolution for cold and thermal, 20: 22325
rare earth ion spectra in, optical absorption, 20: 22311(R) (AD-622068)
MAGNETIC MIRRORS
charged particle trajectories in composite, intermingling in, (T), 20: 22274
charged-particle containment in, (T), 20: 22229
electron leakage from, correlations with electron precipitation in auroral-zone ionosphere, (E), 20: 21836
ion injection in HX apparatus, r-f electric field effects on molecular hydrogen, (E), 20: 22207
plasma electron cyclotron instability in, (E/T), 20: 22197
plasma ion velocity in composite, (T), 20: 22274
plasma jet polarization interactions in countercurrent, (E), 20: 22273
MAGNETIC PROPERTIES
measurement at high pressures, device for, 20: 21357 (UCRL-16299)
MAGNETIC RESONANCE
use in radiation chemistry in solid state, 20: 20729 (PB-181506, pp 85-103)
MAGNETISM
Mössbauer studies of, review of advances in, 20: 22327
MAGNETITES
performance as cold neutron monochromator, 20: 21949
MAGNETOHYDRODYNAMIC CELLS
design for space propulsion power systems, 20: 20874(P)
gas flow in, effects of Hall effect, ion slip and viscosity on, (T), 20: 21574
gas suspensions for, electric conductivity enhancement by thermionic emission from, 20: 21575
ionization in, nonequilibrium, (T), 20: 21573
performance of Hall-current, at constant electron temperature, (E), 20: 21572
performance of self-excited, 20: 21564 (AD-627037)
performance of, effect of electrode size on, (T), 20: 21571
plasma diagnostics in, theory for inert, 20: 21569 (IPP-3/29)
plasma flow properties in, (E/T), 20: 21561(R) (AD-623096)
MAGNETOHYDRODYNAMICS
fields in magnetohydrostatics, equations for force-free, 20: 21792
fluid flow in open channels, variable conductivity effects on, (T), 20: 21780 (AD-622036)
fluid flow in straight channel inlet region, (T), 20: 21801
fluid flow in, thermal stability of confined, 20: 20854 (AD-621523)
fluid flow in, transverse magnetic field in Prandtl-Meyer, (T), 20: 21776 (AD-621429)
fluid flow with field variations in, 20: 21790
fluid motion in, quasirigid stationary, (T), 20: 21787
gas flow in, one-dimensional, (T), 20: 21777 (AD-621442)
gas flow in, properties of small magnetic Reynolds number, (T), 20: 21781 (AD-622568)
gas flows in, properties of small Reynolds number, (T), 20: 21782 (AD-623812)
liquid flow in annulus, radial magnetic field effects on finitely conducting, unsteady, (T), 20: 21789
liquid flow in, square-channel, (E), 20: 21807
Ohm's law for, nonlinear terms in generalized, (T), 20: 21778 (AD-621943)
shock propagation in perpendicular magnetic field, radiative energy flux from one-dimensional plane, (T), 20: 21788
shock wave propagation in electroneutral media in, magnetic field deformation and electric structure in wave-front interior, (T), 20: 21806
wave propagation in ideal perfectly conducting liquid in, particular cylindrical solutions for radial, 20: 21791
MAGNETOMETERS
design for d-c field index measurement, 20: 21006
MAGNETOSPHERE
charged-particle transport in outer, computation of trapped, 20: 21831
cyclotron instabilities in, 20: 21825
plasma density and flow in tail of, 20: 21828
plasma flow around, second standing shock wave in, 20: 21821
plasma waves in, survey of low frequency, 20: 21812 (AD-622223)
MAGNETS
design and construction of superconducting, for corpuscular ionography, 20: 21876
power supply for ZGS, analog computer representation of, 20: 21488
MAMMARY GLAND
neoplastic lesions in mouse, chemically induced, 20: 20502
radiodiagnosis of tumors of, using bremsstrahlung produced by radiophosphorus in paraffin, 20: 20540
radioinduced neoplastic lesions in mouse, x, 20: 20502
radiotherapy using palladium-103, 20: 20542
MAN
body weight norms in Indian, use in establishing standards for radiation dosimetry, 20: 20374
epidemiology of New Jersey radium cases, 20: 20387(R) (NYO-2181-3)
fallout uptake by, real and simulated, 20: 20466
heart disease incidence in, relation of serum lipid and lipoprotein content to atherosclerosis and ischemic, 20: 20370 (UCRL-14658)
insulin metabolism in diabetic and normal, tracer study, 20: 20383 (CNEA-185)
radiation dose to, from radionuclides released to Clinch River, 20: 22514 (ORNL-P-2021)
radiation effects on incidence of mongolism in children after parental exposure, 20: 20454
radiation effects on melanin patterns in, solar, 20: 20458
radiation effects on blood picture in Japanese, gamma and neutron, 20: 20481
radioinduced aging in Japanese, γ and neutron, 20: 20480
radioinduced bone tumors in, 20: 20460
zinc-65 constant in, effects of chelates on, 20: 20397
MANDELIC ACID
complexes with neptunium, thorium, and zirconium, solvent extraction studies on formation of, 20: 20561 (JAERI-1099)
metabolism in Pseudomonas mutants, 20: 20376
metabolism in Pseudomonas mutants, 20: 20470
radiolysis of oxygenated solutions of, product yields from gamma, 20: 20759
MANGANESE
determination in high-purity tantalum by spectrography using d-c arc method, 20: 20608
determination in multielement mixtures by x-ray fluorescence methods, 20: 20644
determination in rocks, activation, 20: 20646
determination in silicon dioxide, activation, 20: 20634
separation from chromium, nickel, rare earths, and silver by ion exchange chromatography, 20: 20634
separation from scandium by ion exchange chromatography, 20: 20821
separation from thorium by ion exchange in nitric acid solution, 20: 20624

separation from uranium by combined ion exchange–solvent extraction using nitric acid–tetrahydrofuran solutions, 20: 20811
sorptive properties of evaporated films of, for carbon monoxide at 0°C, 20: 21388

MANGANESE ALLOYS
Cu–Mn–Zr, analysis for bonding and inclusions in, by x-ray emission in electron microscopy, 20: 20593
Dy–Mn, crystal structures of intermetallic compounds of, 20: 21403
Dy–Mn, dysprosium hyperfine magnetic field in intermetallic compounds of, (E), 20: 22330
Dy–Mn, phase diagram, 20: 21403
Er–Mn, crystal structures of intermetallic compounds of, 20: 21403
Gd–Mn, crystal structure and magnetic properties of intermetallic compounds of, 20: 21403
Gd–Mn, phase diagram, 20: 21403
Ho–Mn, crystal structure and magnetic properties of intermetallic compounds of, 20: 21403
Ho–Mn, phase diagram, 20: 21403
Mn–rare earth, preparation by amalgam process, 20: 21403
Mn–Sm, crystal structure and magnetic properties of intermetallic compounds of, 20: 21403
Mn–Y, crystal structure and magnetic properties of intermetallic compounds of, 20: 21403

MANGANESE COMPLEXES
with thiodibenzoylmethane, stability of, 20: 20693

MANGANESE IONS
effects on dephosphorylation of cocarboxylase, riboflavin-5-phosphate, and pyridoxal phosphate, 20: 20375
uptake by barley roots, uranyl effects on selective inhibition in, 20: 20402

MANGANESE ISOTOPES Mn-50
beta decay, energy spectra, and magnetic moment of, $f_{7/2}$ model for, 20: 22131
energy levels of, isotope shifts of isobaric-analog, (E), 20: 22095
energy levels of, model for, 20: 22131

MANGANESE ISOTOPES Mn-52
energy levels of, isotope shifts of isobaric-analog, (E), 20: 22095
production in proton reactions with iron at 400 Mev, Monte Carlo calculation of, 20: 22035

MANGANESE ISOTOPES Mn-54
content in silt in Escaut River, Belgium, control of, 20: 22515(T) (ORNL-tr-965)
energy levels of, isotope shifts of isobaric-analog, (E), 20: 22095
nuclear orientation in copper, gold, and silver, gamma-ray anisotropy from, (E), 20: 22097
production in proton reactions with iron at 400 Mev, Monte Carlo calculation of, 20: 22035
uptake by crustacea, mollusks, and plankton in Bay of Venice, 20: 20386(R) (NP-15916)

MANGANESE ISOTOPES Mn-55
neutron reactions (n,γ) with, gamma spectra from thermal, (E), 20: 22064

MANGANESE ISOTOPES Mn-56
energy levels from thermal neutron reactions (n,γ) with manganese 56, (E), 20: 22064

MANGANESE OXIDES
analytical use of colloidal, in foam chromatography separation of radioisotopes in aqueous solutions, 20: 20628

MANGANESE STEEL
radiation effects on pressure vessels of, fast-neutron, 20: 21228 (AE-221)
Mn–Mo, radiation effects on pressure vessels of, fast-neutron, 20: 21228 (AE-221)

MANGANESE SYSTEMS
C–Mn–Zn, magnetic properties of Mn_3ZnC in, 20: 22312(R) (AD-622796)

MARYLAND
areal geology and aeroradioactivity surveying of, 20: 20928 (CEX-59.4.17)

MASERS
performance in time measurements, relativistic effects on, (T), 20: 21866

MASERS (OPTICAL)
beam reactions with plasma, imploding shock waves driven by, 20: 22245
conference on photographic and spectroscopic optics, 20: 21458
electric discharges in helium–neon, current-voltage characteristics of h-f, 20: 21808
radiation from gas, third order perturbation theory for, 20: 21522
use for induction of metal–water reactions, 20: 20925(R) (ANL-7055, pp 177-212)
use for plasma electron density measurements, review on, 20: 22295

MASS SPECTROGRAPHY
isotopic peak height calculations in, 20: 20610

MASS SPECTROMETERS
design and performance of magnetless dynamic, (E/T), 20: 20991
design and performance of, for reactor fuel burnup determinations, 20: 22405
design for isotopic analysis of uranium hexafluoride, 20: 20588
ion beam reactions with materials in, 20: 21219
ion detection in, amplifier design for, 20: 21039 (KAPL-3122)
ion trajectories in monopole, (T), 20: 20994

MATERIALS TESTING
color radiography for, photographic methods in, 20: 20863
design of high-temperature high-vacuum equipment for, 20: 21350 (ORNL-TM-1426)
equipment and techniques for radiometric, in Japan, 20: 20867
facility for, operation of, for sodium-cooled reactor components, 20: 22520(R) (NAA-SR-11805)
methods for reactor fuel element, nondestructive, 20: 20865

MATERIALS TESTING REACTOR
fuel burnup determination using gamma spectrometry, 20: 21050

MATHEMATICS
book: *Iterative Solution of Elliptic Systems and Applications to the Neutron Diffusion Equations of Reactor Physics*, 20: 22400
embedding class two, empty space-times of, 20: 21849
functions in, asymptotic representation of spheroidal, 20: 21223 (JINR-P-2564)
group theory in, symmetry properties of 3j-symbols in, 20: 21730
Lie groups in, theorem on contraction of, 20: 21227
research, 20: 21224(R) (ORNL-3919)
symmetry groups in, Gelfand states and irreducible representations of, 20: 21734
Talmi transformation and related formulas in, 20: 21226

MATTER
meson (π) optical properties in nuclear, low-energy, (T), 20: 22021
nucleon interaction boundary condition method for nuclear, 20: 22022
radiation reactions with, pressure broadening of spectral lines from, (T), 20: 21519

MEATS
decomposition of carrion, effects of scavenger animals on, 20: 20941 (ORNL-TM-1432)
radiopreservation of, acceptance tests for, 20: 21199

MECHANICAL DRIVES
design and operation of, for Mössbauer studies, 20: 21081
design and performance of cam-type, for Mössbauer spectrometers, 20: 21080
velocity control in Mössbauer spectrometer, feedback system for, 20: 21079

MECHANICAL ENGINEERING
conference on lubrication, Washington, D. C., Oct. 1964, 20: 20834

MECHANICS
correlation function in statistical, perturbation method for classical time-dependent pair, 20: 21453

MEDICAL PERSONNEL
chromosome studies on radiographic, and their families, 20: 20447

MEDICINE
epidemiology of New Jersey radium cases, 20: 20387(R) (NYO-2181-3)
nuclear techniques in, in Congo, 20: 20373
radiation protection measures for dental, 20: 20519
radioisotopes in, in developing countries, 20: 22525
radiology in dental, survey of hazards from, 20: 20956
role in nuclear industry hygiene, 20: 20955
safety hazards of radiological, 20: 20544
scintiscanning in, review, 20: 20531

MENDELEVIUM
production of, review of methods for, 20: 20796

MERCAPTO GROUP
effects on α-ketoglutarate oxidation by rat-liver homogenates, 20: 20505
radiation effects on blood content of, γ and x, 20: 20415

MERCURY
electric conductivity of, at 234.28 to 1733°K, 20: 21377
electromagnetic wave scattering by electro-acoustic waves in arc column of plasma of, (E), 20: 22232
magnetohydrodynamic flow of, properties of square-channel, (E), 20: 21807
neutron inelastic scattering at 5.8 and 7.5 Mev, gamma spectra from thermal, (E), 20: 22069
separation from perchloric acid solutions by ion exchange materials, 20: 20823
separation from scandium by ion exchange chromatography, 20: 20821
superconducting properties of, effects of λ transition on, 20: 21875
thermal capacity of liquid, corresponding states correlation of configurational, 20: 20657 (UCRL-11931)
viscosity of liquid, based on atomic parameters, 20: 20656 (UCRL-11930)

MERCURY ALLOYS
Hg–K, thermodynamic properties, 20: 21328 (CU-2660-25)
Hg–K, thermodynamic properties at high temperatures, 20: 20651(R) (CU-2660-26)
Hg–Pb, superconducting critical currents and fields in flux-pump fed

coils of, (E), 20: 21924
Hg–Sm, thermodynamic properties and vapor pressure measurements, 20: 21384
Hg–Y, thermodynamic properties and vapor pressure measurements, 20: 21384
MERCURY CHLORIDES
$Hg–HgCl_2$, electric conductivity, 20: 22520(R) (NAA-SR-11805)
MERCURY ISOTOPES
determination in radiation sources, extraction radiometric titration method for, 20: 20567 (UJV-1418/65)
MERCURY SYSTEMS
$Hg–HgCl_2$, electric conductivity, 20: 22520(R) (NAA-SR-11805)
MESIC ATOMS
x-ray spectra of (π), (E), 20: 21534
MESON BEAMS
energy transfer from 70-Mev(π^-), to polyethylene, 20: 20525
MESONS
coupling constants for spin-2, with two pseudoscalar mesons, 20: 21682
decay of, unitary symmetry for, 20: 21708 (CONF-640509(Pt.2), Paper 2)
density matrix of spin-one, positivity conditions for, (T), 20: 21764
interaction mixing of spin-zero, 20: 21746
interactions of pseudoscalar–octet, university principle for, 20: 21752
interactions with protons, SU(6W) predictions for spin alignment and forward amplitudes for, 20: 21652
interactions with baryons and photons, parity and spin of particles from polarized, (T), 20: 21715 (JINR-P-2576)
interactions with protons, SU(3) symmetry for three-particle final states in, 20: 21763
mass formula for, using SU(6,6) group, 20: 21624 (JINR-P-2606)
mass formulas for SU(3) multiplets of, 20: 21671
mass of nonstrange pseudoscalar, generalized Klein-Gordon equation for, 20: 21744
MESONS, RESONANCE
coupling constants for spin-2, with two pseudoscalar mesons, 20: 21682
decay of $J_p = 2^+$, coupling constant sum rules for, 20: 21640
decay of, particle and polarization angular distributions in two- and three-body, (T), 20: 21698
decay of, resonance widths in, (T), 20: 21713 (JINR-P-2568)
decay widths of K*(1405), current algebra for, 20: 21654
models for, quark, (T), 20: 21697
production, (E/T), 20: 21592 (CERN-65-24(Vol.1), pp 1-44)
production in meson (K−)-proton interactions at 1.33 Bev/c, (E), 20: 21615 (COO-1195-52)
production of K*, in meson (K+)-proton interactions at 4.6 Bev/c, (E), 20: 21629 (UCRL-16332)
production of 2^+, absorption model for, 20: 21644
MESONS (η^0)
decay of, branching ratios for, (E), 20: 21627 (LNF-66/9)
MESONS (I^0)
decay widths of, current algebra for, 20: 21654
properties from p-wave amplitudes of meson (π)-meson (π) interactions, (T), 20: 21694
MESONS (K)
decay of, current commutation rules and $\Delta T = \frac{1}{2}$ rule in, 20: 21650
decay of, partially conserved axial-vector current hypothesis for non-leptonic, 20: 21666
decay of, phenomenological description of, 20: 21701
energy spectra in CERN neutrino experiment, determination of, (E/T), 20: 21604 (CERN-65-32, pp 121-6)
interactions of mesons ($\bar{K}$) with hyperons (Σ) in 27-fold representation, dynamics of, 20: 21674
interactions with nucleons in 27-fold representation, dynamics of, 20: 21674
MESONS (K^-)
decay of, neutrino spectra from, (E), 20: 21602 (CERN-65-32, pp 111-14)
interactions with protons at 1.33 Bev/c, resonance production in, (E), 20: 21615 (COO-1195-52)
interactions with protons at 900 to 990 Mev/c, angular distributions and cross sections for, (E), 20: 21628 (TID-22822)
production in proton reactions with beryllium at 12.5 Bev, cross sections for, (E), 20: 21601 (CERN-65-32, pp 109-10)
reactions with emulsion nuclei, hyperfragments from, (E), 20: 22161
reactions with light nuclei, hyperon (Λ) and (Σ) production from, 20: 22033
MESONS (K^0)
decay of K_2^0, 2π, (T), 20: 21675
decay of, CP invariance in, (E/T), 20: 21700
decay of, pole model for nonleptonic, 20: 21688
mass and lifetime matrices for (K^0–$\bar{K}^0$), invariance principles for, 20: 21677
mass of K_1^0 and K_2^0, difference in, (T), 20: 21675
MESONS ($\bar{K}^0$)
mass and lifetime matrices for (K^0–$\bar{K}^0$), invariance principles for, 20: 21677
MESONS (K^+)
decay of, neutrino spectra from, (E), 20: 21602 (CERN-65-32, pp 111-14)
interactions with protons at 4.6 Bev/c, K* production in, (E), 20: 21629 (UCRL-16332)
production in proton reactions with beryllium at 12.5 Bev, cross sections for, (E), 20: 21601 (CERN-65-32, pp 109-10)
MESONS ($K_{\sigma 2}^+$)
decay of, form factor from, (E), 20: 21658
MESONS ($K_{\sigma 2}$)
decay of, partially conserved axial-vector current hypothesis for, 20: 21666
MESONS ($K_{\sigma 1}$)
decay of, partially conserved axial-vector current hypothesis for, 20: 21666
MESONS (μ)
Cherenkov light of cosmic neutrino produced, detection of, 20: 21031 (CERN-65-32, pp 231-40)
decay in ambiplasma, energy distribution from, (T), 20: 21684
detection of neutrino-produced, deep underground, 20: 21540 (CERN-65-32, pp 49-56)
energy spectra in CERN neutrino experiment, determination of, (E/T), 20: 21604 (CERN-65-32, pp 121-6)
flux in neutrino shielding, measurement of, 20: 22306 (CERN-65-32, pp 147-52)
magnetic moment of, anomalous, (T), 20: 21656
mass relative to electrons from spontaneous symmetry breakdown, 20: 21678
production in antiproton-proton annihilation in ambiplasma, (T), 20: 21684
production in large plastic scintillators by background neutrals, mechanism and rate of, 20: 21028 (CERN-65-32, pp 65-70)
production in liquid scintillators by cosmic rays, (E), 20: 21029 (CERN-65-32, pp 71-2)
production underground by cosmic neutrinos, (E/T), 20: 21542 (CERN-65-32, pp 73-8)
scattering by chlorine-35 and fluorine-19, Coulomb, (T), 20: 21649
MESONS (μ^-)
reactions with helium-3, probability of neutrino yield in, (T), 20: 22152
MESONS (μ^+)
gyromagnetic ratio of, measurement of anomalous, (E), 20: 21630 (UCRL-16469)
MESONS (π)
coupling constants for $N_{\frac{3}{2}}^{\frac{3}{2}}N\pi$ and $NN\pi$, weak, 20: 21655
decay in ambiplasma, energy distribution from, (T), 20: 21684
energy spectra in CERN neutrino experiment, determination of, (E/T), 20: 21604 (CERN-65-32, pp 121-6)
interactions in nuclei and nuclear matter at low energies, nonlocal potentials for, (T), 20: 22021
interactions with nucleons, absorption model for 2^+-meson production in, 20: 21644
interactions with mesons (π), exponential asymptotic behavior of amplitude for low-energy, (T), 20: 21645
interactions with mesons (π) in T = 0 state, cross sections for $K\bar{K}$ production in S-wave, 20: 21648
interactions with protons at high energies, polarization in, (T), 20: 21653
interactions with nucleons, threshold factor in p-wave dispersion relations for, 20: 21667
interactions with nucleons, p-wave amplitudes for off-shell, 20: 21672
interactions with mesons (π), resonance properties of p-wave amplitudes for, (T), 20: 21694
interactions with nucleons, mass splittings from, 20: 21758
interactions with nucleons, Lee algebra for isobar-coupling, 20: 21759
photoproduction on deuterons, asymmetry functions for polarized, (E), 20: 21626 (LNF-66/4)
production from neutrino-nucleon interactions, asymmetries in, (T), 20: 21638
production in antiproton-proton annihilation in ambiplasma, (T), 20: 21684
reactions with helium-4, meson (ρ) production in coherent, (T), 20: 22145
reactions with light nuclei, double charge exchange in, 20: 22033
MESONS (π^-)
charge exchange on hydrogen, detection of chemical bonding by, 20: 20653 (JINR-P-2558)
decay of, neutrino spectra from, (E), 20: 21602 (CERN-65-32, pp 111-14)
energy transfer from 70-Mev beams of, to polyethylene, 20: 20525
interactions with protons at 5 to 20 Bev, amplitudes for, (T), 20: 21618 (JINR-P-2566)
interactions with protons at high energies, ρ-exchange peripheral model for, 20: 21647
interactions with protons at high energies, conservation laws for, 20: 21657
interactions with alpha particles at 24 Mev, meson (π) electromagnetic form

factor from elastic, (E), 20: 21659
interactions with protons at 2 to 7 Bev/c, total cross sections for, (E), 20: 21661
interactions with protons, T = 0 S-wave $\pi\pi$ phase shift in, (E), 20: 21685
interactions with nucleons at 6.8 Bev, inelastic, (E/T), 20: 21693
interactions with deuterons, hyperon (Σ^-)-neutron production and final-state interaction in, (T), 20: 21681
production in proton reactions with beryllium at 12.5 Bev, cross sections for, (E), 20: 21601 (CERN-65-32, pp 109-10)
reactions (π^-,π^-p) and (π^-,π^-pa) with argon-40 at 500 to 1100 Mev, excitation functions for, (E), 20: 22125

MESONS (π^0)
decay of, 2γ, (T), 20: 22460 (IC-66/28)
interactions with mesons (π^+), high-energy limit of total cross section for, (T), 20: 21679

MESONS (π^+)
decay of, neutrino spectra from, (E), 20: 21602 (CERN-65-32, pp 111-14)
interactions with protons at 5 to 20 Bev, amplitudes for, (T), 20: 21618 (JINR-P-2566)
interactions with protons at high energies, conservation laws for, 20: 21657
interactions with alpha particles at 24 Mev, meson (π) electromagnetic form factor from elastic, (E), 20: 21659
interactions with protons at 2 to 7 Bev/c, total cross sections for, (E), 20: 21661
interactions with protons at 250 Mev, cross section for elastic, (E/T), 20: 21662
interactions with protons, T = 0 S-wave $\pi\pi$ phase shift in, (E), 20: 21685
interactions with mesons (π^0), high-energy limit of total cross section for, (T), 20: 21679
lifetime, (E), 20: 21665
photoproduction on nucleons by polarized bremsstrahlung at 475 to 750 Mev, (E), 20: 21660
photoproduction on protons at 475 to 750 Mev, asymmetry in polarized, (E/T), 20: 21589 (AD-626683)
production in proton reactions with beryllium at 12.5 Bev, cross sections for, (E), 20: 21601 (CERN-65-32, pp 109-10)

MESONS (ρ)
mass and width of, from interaction singularities, (T), 20: 21668
production in meson (π) coherent reactions with helium-4, (T), 20: 22145
properties from p-wave amplitudes of meson (π)-meson (π) interactions, (T), 20: 21694

METAL CRYSTALS
neutron scattering by low-impurity, oscillation frequency and resonance location from slow, (E), 20: 22320

METALS
analysis for hydrogen and oxygen, equipment and method for activation, 20: 20602
boiling and entrainment of, mechanisms of, 20: 20802(R) (ANL-7055, pp 21-98)
conference on corrosion of, New York, March 11–15, 1963, 20: 21276
corrosion by sodium, effects of carbon on, 20: 20802(R) (ANL-7055, pp 21-98)
decontamination and descaling of, development of solution for, 20: 21238 (NP-15928)
deformation in hexagonal compact, mechanisms of, 20: 21330 (EUR-2621.f)
determination in liquid, plans for ultrasonic, 20: 20802(R) (ANL-7055, pp 21-98)
diffusion in bcc and fcc, self-, 20: 21230 (AEET-233)
magnetoresistivity at low temperatures, (T), 20: 22333
mechanical properties of, use of computer for storage, interpretation, and recovery of data on, 20: 21354 (TRG-Report-1160)
sorptive properties for gases, method for measuring, 20: 21351(R) (SRIA-425-8)
sorptive properties for helium, 20: 22520(R) (NAA-SR-11805)
viscosity of liquid, equation for determining, 20: 20656 (UCRL-11930)

METASTASES
radiodiagnosis of bone, using calcium-47 or strontium-85, 20: 20404

METEORITES
argon-38 and -39 contents of iron, estimation of cosmic-ray exposure ages from, 20: 21505
cosmic proton reactions with, Monte Carlo calculation of radionuclide production in, 20: 22035
cosmic-ray reactions in, argon-39 and chlorine-36 production, 20: 21508
origin of bronzite chondrites, lunar, 20: 21507

METHACRYLIC ACID
ester (di-) with triethylene glycol, radioinduced gelation of, fast-neutron, 20: 20720 (AD-630891)
radioinduced polymerization with isocyanic acid at low temperatures, 20: 20747

METHACRYLIC ACID, METHYL ESTER
radioinduced polymerization of, effects of mineral fillers on gamma, 20: 20778

METHACRYLIC ACID, METHYL ESTER POLYMERS
dose distribution in, from electron beam irradiation, three-dimensional, 20: 21470 (PB-181506, pp 116-29)
radiation effects on, role of LET in gamma and helium-4/lithium-7, 20: 20764
radioinduced electric discharge figures in, electron, 20: 21440

METHANE
analysis for impurities by infrared spectrometry, 20: 20553(R) (MLM-1142)
carbon-13 concentration in, by thermal diffusion, 20: 20806(R) (MLM-1274)
carbon-13 enrichment in, by thermal diffusion, 20: 20553(R) (MLM-1142)
production by gas discharge and radioinduced cracking of butane, 20: 20740
production for carbon-14 dating, 20: 20917
radioinduced deuterium exchange reactions in gaseous, mechanism of tritium, 20: 20719 (AD-624657)
solubility in Santowax-OM1, 20: 20708 (AEET-213)
yields from radiolysis of methanol vapor, effects of scavengers on, 20: 20776

METHANE, BROMO-
effects on yields from radiolysis of methanol vapor, 20: 20776

METHANE, DICHLORO-
radioinduced polymerization of fluoral in, at low temperatures, 20: 20718(R) (AD-623307)
radioinduced reactions with ethylene, gamma, 20: 20757

METHANE, DICHLORODIFLUORO-
use in gas Cherenkov counter, 20: 21071

METHANE, DIPHENYL-
biphenyl–diphenyl methane, heat transfer properties and radiation stability of, for use in reactor loops, 20: 20792

METHANE, IODO-
separation from air by activated charcoal filters, 20: 20940(R) (ORNL-3915)

METHANE, NITRO-
radiolysis of, reactions of hydrated electrons in pulse, 20: 20735
shock interactions in corners filled by, hydrodynamics of, (E/T), 20: 21784 (LA-3450)

METHANE, TETRANITRO-
radiolysis of, reactions of hydrated electrons in pulse, 20: 20735

METHANOL
determination by xenon trioxide oxidation, titrimetric, 20: 20579
radioinduced telomerization with ethylene, yields from beta, 20: 20724(R) (NYO-2978-44)
radiolysis of vapors of, effects of scavengers on hydrogen yields from gamma, 20: 20776
radiolysis of, reactivity of electrons produced in gamma, 20: 20750
solvent properties for rare earth oxides in the presence of ammonia, 20: 20686

METHIONINE
radioinduced synthesis of sulfur-35-labeled, 20: 20786
radiolysis in reactors, 20: 20786

METHYL RADICALS *(Free Radicals)*
hydrogen abstraction by, from ammonia, hydrazine, and methylamine, isotope effects on, 20: 20713

METHYLAL
radiolysis, 20: 20758

METHYLAMINE
hydrogen abstraction by methyl radicals from, isotope effects on, 20: 20713
radioinduced carboxylation of, yields in, 20: 20732 (SGAE-CH-21/1965)

METHYLENE BLUE
effects on radioinduced oxidation of ergosterol, 20: 20738

MICA
age estimation of, by rubidium–strontium method, 20: 20891
cesium-137 sorption by, successive desorption method for calculating, 20: 20618
coating thickness of gold on, use of proton beam scattering for measuring, 20: 21246
performance as cold neutron monochromator, 20: 21949
radiation effects on current induction in capacitor of, electron beam, fast neutron, and gamma, 20: 21151 (IBM-66-825-1944)
sorptive properties for cesium-137, 20: 20696
use for detecting charged particles, 20: 21060

MICE
anemia in, effects of gamma-irradiated schistosome infections on, 20: 20446
neoplastic lesions in mammary glands of, chemically induced, 20: 20502
radiation effects on nitrogen distribution in bone marrow-treated, x, 20: 20407 (ORNL-P-1118)

radiation effects on, late somatic x, 20: 20441 (ORNL-P-1173)
radiation effects on intracellular organelles in, x, 20: 20413
radiation effects on litter size in, gamma and neutron, 20: 20453
radiation effects of mutation rates in, x, 20: 20461
radiation effects on immune reactions to injected bone marrow and lymph cells in, x, 20: 20472
radiation effects on, 10-kev x, 20: 20475
radiation effects on skin of urethan-tested, x, 20: 20476
radiation effects on immunity to uv-irradiated ascites tumor cells transplanted into, x, 20: 20484
radiation effects on spermatogenesis and testicular development in, effects of age at irradiation on x, 20: 20499
radiation effects on, protective effects of antioxidant inhibitors against x, 20: 20506
radiation effects on blood formation in, protective effects of mucopolysaccharides against x, 20: 20510
radiation effects on, protective effects of drugs against x, 20: 20513
radiation effects on survival of, protective effects of organophosphorus derivatives against x, 20: 20515
radiation injuries to, effects of bleeding on proliferative activity of bone marrow cells after x, 20: 20452
radiation source avoidance by, γ, 20: 20495
radioinduced neoplastic lesions in mammary glands of, x, 20: 20502
radiosensitivity of, effects of oxygen environment on, 20: 20430(R) (AD-629311, pp 26-32)
radiosensitivity of, effects of age on, 20: 20494
radiosensitivity of, effects of β-mercaptoethylamine on, 20: 20511
radiosensitivity of, effects of bacterial toxins on, 20: 20512
radiosensitivity of, effects of polyhydroxyl alcohols on, 20: 20520
radiosensitivity of brain of, effects of AET and potassium cyanide on, 20: 20521

MICHIGAN
radiology in, survey of dental, 20: 20956

MICROANALYSIS
x-ray emission in electron probe, of alloys and metals, 20: 20593

MICROORGANISMS
effects on decomposition of swine carrion, 20: 20941 (ORNL-TM-1432)
growth of, on irradiated starch and amylose–acrylamide copolymers, 20: 20767
radiation effects on, in fish, 20: 21200

MICROSCOPY
use of flying-spot, for detecting uv-absorbency of cultured cells during interphase, 20: 20473

MICROWAVES
absorption by plasma in magnetic fields, (T), 20: 22209
effects on Josephson superconducting junctions, induced d-c voltages from, (E), 20: 21882
interactions with plasma in mirror-type magnetic fields, (E), 20: 22216
propagation in compressible plasma gaps, properties of, 20: 22163 (AD-621034)
transmission by turbulent plasma, coefficient for, (T), 20: 22230
use for diagnostics of shock propagation in gases, 20: 22182 (IPP-3/35)

MILK
analysis for strontium-90, 20: 20938 (NP-15921)
fallout content in, effects of soil-plant transport on cesium-137 and strontium-90, 20: 20926(R) (ARCRL-14)
radioactivity due to fallout in Canadian, 1964, 20: 20938 (NP-15921)
radioactivity due to fallout in Canadian, 1965, 20: 20883 (NP-15914)
radioactivity due to fallout, 1965, 20: 20882(R) (HASL-171)
radionuclide content in Amsterdam, 1960 to 1963, 20: 20949
radionuclides in Italian, detection and measurement, 20: 20950
strontium-90 content in, effects of diet of cattle on, 20: 20882(R) (HASL-171)

MINERALS
age estimation of, by potassium–argon and rubidium–strontium methods in Norwegian eclogites, 20: 20891
analysis for rubidium, activation, 20: 20560 (EUR-2753.f)
analysis for silver, activation, 20: 20574
effects as fillers on radioinduced polymerization of methyl methacrylate and styrene, 20: 20778

MIT RESEARCH REACTOR
fast neutron dosimetry in, using calorimeter and threshold detectors, 20: 20723(R) (MIT-334-33)

MITOCHONDRIA
radiation effects on $NADH_2$ oxidation in suspensions of cattle heart, x, 20: 20496
respiration in rat, effects of AET on, 20: 20505

MIXER-SETTLERS
development and testing for production of thoria microspheres, 20: 20808(R) (ORNL-3916)
testing for pyrochemical fuel processing, 20: 20802(R) (ANL-7055, pp 21-98)

MOLECULAR BEAMS
detection of, electron bombardment ionizer for, 20: 21066
detection of, field-ionization detector for, 20: 21089
scattering of, measurement methods for, 20: 20807(R) (MLM-1287)

MOLECULES
flow of gases of, computer program for analysis of, 20: 20855 (CLM-R-54)

MOLLUSKS
isotope uptake by Bay of Venice, cobalt, manganese-54, ruthenium-106, and zinc-65, 20: 20386(R) (NP-15916)

MOLTEN SALT REACTOR EXPERIMENT
fuel reprocessing facility for, continuous moisture analyzer for gases containing hydrogen fluoride in, 20: 20581

MOLYBDENITES
crystal cleavage of, in ultrahigh vacuum, 20: 21366

MOLYBDENUM
cleavage cracks in single-crystal, method for producing, 20: 21245
determination in high-purity tantalum by spectrography using d-c arc method, 20: 20608
determination in multielement mixtures by x-ray fluorescence methods, 20: 20644
determination in silicon dioxide, activation, 20: 20635
determination in steels by x-ray fluorescence methods, 20: 20642
deuterium exchange with hydrogen on films of, steady-state, 20: 21351(R) (SRIA-425-8)
electric conductivity and structure of thin films of sputtered, 20: 21394
Fermi surface parameters for, (E), 20: 22337
helium-3 reactions (He-3,n) at 19 to 25 Mev, angular distributions and cross sections for, (E), 20: 22132
joining to tungsten, brazing materials for, 20: 21312
reactions with sodium at high temperatures, 20: 20925(R) (ANL-7055, pp 177-212)
separation from antimony, tantalum, and tin by ion exchange chromatography on chloride form resin, 20: 20635
separation from scandium by ion exchange chromatography, 20: 20821
solubility in aluminum, microhardness studies on, 20: 21362(T) (SC-T-66-0723)
sorptive properties for deuterium, nitrogen, and rare gases, kinetics of, 20: 21351(P) (SRIA-425-8)
sorptive properties of evaporated films of, for krypton and xenon, 20: 21387
sorptive properties of evaporated films of, for carbon monoxide at 0°C, 20: 21388
sorptive properties of evaporated films of, for carbon dioxide at room temperature, 20: 21389
superconducting properties of, effects of λ transition on, 20: 21875
surface structures of clean and oxygen-covered, low-energy electron-diffraction study of, 20: 22319
wear properties of plasma-arc-deposited coatings of, 20: 21319(AD-621064)
welding to stainless steel, 20: 21309

MOLYBDENUM ALLOYS
Cr–Co–Mo–Ni–W, testing for bearing parts in liquid sodium, 20: 22520(R) (NAA-SR-11805)
Cr–Fe–Mo–Ni, corrosion of Hymu-80 by potassium chloride–uranium trichloride eutectic at 900°C, 20: 21261 (LA-3476)
Cr–Mo–Ni, corrosion by acids at 800 to 2375°F, effects of heat treatments and microstructure on, 20: 21277
Ge–Mo, production of Mo_3Ge by hot-pressing, 20: 21247
Mo–Re, corrosion by bismuth and tin at 1000°C, (E), 20: 21566(R) (ANL-7055, pp 213-29)
Mo–Ta, crystal structure of electron-beam zone-refined, 20: 21364
Mo–Ta, mechanical properties of single-crystal, 20: 21364
Mo–Ti–Zr, creep tests on TZC and TZM at high temperatures, 20: 21346(R) (NASA-CR-54895)
Mo–Ti–Zr, fatigue tests on TZC and TZM at high temperatures, 20: 21347(R) (NASA-CR-54916)
Mo–Ti–Zr, mechanical properties at 25 to 3500°F, 20: 21322 (AMRA-TR-65-25)
Mo–Ti–Zr, specifications of TZM, for use in corrosion test loop fabrication, 20: 21293 (R-66SD3007)
Mo–U, microstructure of uranium-rich, effects of heat treatments on, 20: 21372
Mo–U, radiation effects on uranium-rich, neutron, 20: 21436
Mo–W, corrosion by argon–nitrogen mixtures at 900°C, 20: 20802(R) (ANL-7055, pp 21-98)
Mo–W, corrosion by bismuth and tin at 1000°C, (E), 20: 21566(R) (ANL-7055, pp 213-29)

MOLYBDENUM CARBIDES
superconducting critical temperature of, correlation with valence electrons, (E), 20: 21911
thermionic emission from cesiated surfaces of, (E), 20: 21584
graphite–MoC, fabrication of dispersions of, by hot-working, 20: 21306

MOLYBDENUM COMPLEXES

with myricetin, composition and stability of, 20: 20674
MOLYBDENUM FLUORIDES
MoF_6–UF_6, phase studies, 20: 20803(R) (ANL-7055, pp 99-162)
MOLYBDENUM ISOTOPES Mo-99
diffusion in irradiated fuel element cladding alloys and materials at 600 to 1200°C, 20: 21232 (BMI-1763)
separation from technetium-99m by ion exchange on hydrous zirconium oxide in nitric acid, 20: 20566 (ORNL-TM-1468)
yields from photofission of uranium by 650-Mev bremsstrahlung, 20: 22040
MOLYBDENUM SILICIDES
thermionic emission from cesiated surfaces of, (E), 20: 21584
MOLYBDENUM STEEL
B–Mo, radiation effects on pressure vessels of, fast-neutron, 20: 21228 (AE-221)
Cr–Mo–Ni, transformation temperatures in Super Elso, effects of heating rate on, 20: 21331(R) (EURAEC-1569)
Cr–Mo–Ni, weld embrittlement in joints in, effects of time at high temperatures on, 20: 21393
Mn–Mo, radiation effects on pressure vessels of, fast-neutron, 20: 21228 (AE-221)
MOLYBDENUM SULFIDES
friction on copper surfaces in ultrahigh vacuum, 20: 21366
reactions with samarium and ytterbium, preparation of intercalation compounds by, 20: 20648 (AD-621029)
sputtering by air and argon ions, (E), 20: 21529
MOLYBDENUM SYSTEMS
C–Hf–Mo–N–Re–Ta–W–Zr, development of dispersion-strengthened tantalum-base, 20: 21240(R) (WANL-PR-(Q)-006)
C–Mo–Nb–Ta–W–Zr, extrusion parameters for Cb-132M, 20: 21263(R) (NASA-CR-54911)
C–Mo–Nb–Ta–Zr, thermal-mechanical processing of a precipitation-hardenable, dispersion-hardened, 20: 21250
C–Mo–Nb–Ti–Zr, bend and tensile ductility properties of, 20: 21410
C–Mo–Ti–Zr, extrusion parameters for TZC, 20: 21263 (NASA-CR-54911)
MOMENTS
measurement of nuclear quadrupole, using Coulomb excitation, 20: 21991 (BNL-948, pp 1005-44)
MONEL
ductility of, at –269°C, 20: 21416
effects of decontaminating and descaling solution on metal loss on, 20: 21238 (NP-15928)
MONKEYS
radiation effects on cardiovascular system in *Macaca mulatta*, γ, 20: 20488
radiation source avoidance by, γ, 20: 20495
MONTE CARLO METHOD
use for cosmic particle cascades analysis, 20: 21545 (MIT-2098-227)
use in calculating radionuclide production in proton reactions with iron at 400 Mev, 20: 22035
use in hyperon (Λ) binding energy calculations, 20: 22161
MOON
magnetic field production by solar plasma wind, laboratory simulation of, 20: 21502
meteorites from, bronzite chondrite, 20: 21507
MORPHINES
radiosensitivity effects on mice, x, 20: 20513
MÖSSBAUER EFFECT
absorber for iron-57, 20: 22158
conference of methodology, 20: 22156
detection of, cam-driven constant-acceleration spectrometer for, 20: 21080
drive systems for studying, design and operation of constant-velocity, 20: 21081
equipment for studies of, electromechanical drive system for, 20: 21079
measurement of, following alpha decay, effects of recoil stopping times on, 20: 22037
measurement of, mechanical driving unit for, 20: 22050
measurement of, spectrometer for, 20: 21069
measurement of, using opaque absorbers, 20: 22157
pressure cell for studying, 20: 20850
spectra of, computer programs for, 20: 22159
standards for chemical applications of, review, 20: 20684
use in molecular structure studies, review, 20: 20684
use in physics, review of advances in, 20: 22327
MULTIPLICATION FACTOR
calculation for spherical uranium-fueled assemblies, 20: 22383(T) (AEC-tr-6693)
MUSCLES
analysis of tissues from, for tritium, combustion procedure in liquid scintillation counting for, 20: 20570
MUTATIONS
radiation effects on rate of mouse specific locus, x, 20: 20461
radioinduced in Einkorn wheat seeds, beta, fast neutron, gamma, and thermal neutron, 20: 20497
radioinduced in Mormoniella males, frequency of dominant lethal, x, 20: 20464
radioinduced in phage φX174, uv, 20: 20463
radioinduced in wheat seeds, x, 20: 20501
radioinduced reversions in Neurospora, uv, 20: 20462

N

NAGASAKI
blood picture of nuclear-explosion survivors in, survey, 20: 20481
radiation effects on population exposed in 1945, summary of 1965 findings on, 20: 20919(R) (ABCC-64-65)
NALORPHINE
radiosensitivity effects on mice, x, 20: 20513
NAPHTHALENE
analysis for sulfur by x-ray absorption methods, 20: 20615
methyl-, radiation effects on metabolism in rats, x, 20: 20439 (EUR-2628.f)
NAPHTHALENESULFONIC ACID, DINONYL-
properties as ion exchanger for separation of rare earths, scandium, and thorium, 20: 20825
NATURAL GAS
production of, Project Gasbuggy for stimulating, 20: 20837
NATURAL WATERS
separation of cerium-144, cesium-137, and strontium-90 from, by ion exchange chromatography, 20: 20627
NEODYMIUM
determination in presence of praseodymium, spectrophotometric, 20: 20568
determination in rare earth mixtures, activation, 20: 20562 (LYCEN-6538)
friction and wear properties of, in vacuum, effects of crystal structure on, 20: 21365
oxidation in dry and moist air at 100 to 800°C, rate of, 20: 21265 (RPI-2714-8)
separation from other rare earths by paper precipitation chromatography using 8 quinolinol, 20: 20814
separation from perchloric acid solutions by ion exchange materials, 20: 20823
separation from uranium by combined ion exchange-solvent extraction using nitric acid–tetrahydrofuran solutions, 20: 20811
NEODYMIUM ACETATES
preparation by oxide solubility in alcohols containing ammonia, 20: 20686
NEODYMIUM ALLOYS
Al–Nd, crystal structure and stability of intermetallic compounds in, 20: 21415
Dy–Nd, electric conductivity at 4.2, 77, and 296°K, 20: 22312(R) (AD-622796)
Fe–Nd, crystal structure of $NdFe_7$, 20: 21400
Gd–Nd, ferromagnetic spin coupling in, 20: 22314(R) (AD-626865)
La–Nd, electric conductivity, magnetic susceptibility, and superconductivity at low temperatures, 20: 21873 (NP-15936)
Nd–Tm, magnetic properties and phase transformations in, 20: 21414
Nd–Y, magnetic properties and phase transformations in, 20: 21414
NEODYMIUM FLUORIDES
dielectric properties of thin films of, 20: 22324
NEODYMIUM ISOTOPES
mass differences of, (E), 20: 22153
NEODYMIUM ISOTOPES Nd-138
beta decay of, half life for, (E), 20: 22002 (JINR-P-2570)
NEODYMIUM ISOTOPES Nd-147
decay of, gamma branching ratios for, (E), 20: 22091
NEODYMIUM NITRIDES
preparation by reactive arc melting, 20: 21244
NEODYMIUM OXIDES
proton reactions at 590 Mev and 18 Bev, yields of iodine isotopes from, (E), 20: 22045
solubility in ethyl, isopropyl, methyl, and propyl alcohols in presence of ammonia, 20: 20686
NEON
effects on growth rates in Neurospora, 20: 20378
electric discharges in, electron distribution function for, (E), 20: 21795
electron velocity distribution in positive column of discharge plasma of, radial dependence of, (E), 20: 22294
ion mobility and recombination in plasma of, 20: 22169(R) (AD-622684)
photoelectric effect at 852 ev to 40 kev in, cross sections for, (E), 20: 21523
NEON IONS
reactions with beryllium–copper alloys at 3 to 90 kev, secondary electron emission from, (E), 20: 21538

NEON ISOTOPES
abundance ratios in atmosphere, (E), 20: 21509
NEON ISOTOPES Ne-20
alpha scattering at 18 Mev, cross sections for, (T), 20: 22134
energy level transitions in, 20: 21984 (BNL-948, pp 751-6)
energy levels from deuteron reactions (d,nγ) with fluorine-19 at 1 Mev, parity and spin of, (E), 20: 22082
proton reactions (p,p′γ) at 8.5 Mev, angular correlations from, (E), 20: 22059
transport coefficients for thermal diffusion at 800°C, 20: 20806(R) (MLM-1274)
NEON ISOTOPES Ne-21
concentration in gaseous neon, equipment for, 20: 20807(R) (MLM-1287)
NEON ISOTOPES Ne-22
transport coefficients for thermal diffusion at 800°C, 20: 20806(R) (MLM-1274)
NEON SYSTEMS
He–Ne, electric discharge in lasers of, current-voltage characteristics of h-f, (E), 20: 21808
NEPTUNIUM
deposition on stainless steel, parameters for quantitative electrolytic, 20: 21287 (AE-217)
neutron flux and spectrum measurements on foils of, 20: 21427(R) (NASA-CR-54904)
precipitation with lanthanum trifluoride, oxidation states in, 20: 20561 (JAERI-1099)
production of, review of methods for, 20: 20796
separation from nuclear materials by solvent extraction, reagents for, 20: 20561 (JAERI-1099)
NEPTUNIUM COMPLEXES
with EDTA, mandelic, oxalic, and phenylarsonic acids, solvent extraction studies on formation of, 20: 20561 (JAERI-1099)
NEPTUNIUM(VI) FLUORIDES
spectra of gaseous, absorption, 20: 20803(R) (ANL-7055, pp 99-162)
NEPTUNIUM ISOTOPES Np-237
neutron reactions (n,f) at 0.75 Mev, cross section and threshold energy for, 20: 21427(R) (NASA-CR-54904)
separation from waste solutions, method for, 20: 20561 (JAERI-1099)
stopping times of recoil, in neptunium dioxide, 20: 22037
NEPTUNIUM ISOTOPES Np-238
decay, 20: 20561 (JAERI-1099)
preparation by neutron irradiation of neptunium-237, 20: 20561 (JAERI-1099)
NEPTUNIUM OXIDES
neptunium-237 recoil stopping time in, 20: 22037
NERVE CELLS
development in postnatal rats, tracer study, 20: 20391(R) (TID-22825)
nucleic acid metabolism in, effects of behavioral activation on, 20: 20391(R) (TID-22825)
radiation effects on electrical activity of olfactory, x, 20: 20431 (AD-630323)
NERVOUS SYSTEM
development in postnatal rats, tracer study, 20: 20391(R) (TID-22825)
radiation effects on, controlling metabolic activity in rats, x, 20: 20433 (AD-630390)
radiation effects on central, review, 20: 20449
radiation effects on, in burros and sheep, neutron, 20: 20489
radiation effects on conditions reflexes in rats exposed *in utero*, x, 20: 20492
NETHERLANDS
radionuclide content in food in Amsterdam, 1960 to 1963, 20: 20949
NEUROSPORA
growth rates in, effects of rare gases on, 20: 20378
radioinduced mutant reversion in, for glutamic dehydrogenase production, uv, 20: 20462
NEUTRINOS
conference on, 20: 21594 (CERN-65-32)
detection of, development of 12 ft bubble chamber for, 20: 21032 (CERN-65-32, pp 259-62)
detection of, method for, 20: 21030 (CERN-65-32, pp 223-4)
detection underground, laboratory for, 20: 21612 (CERN-65-32, pp 225-30)
flux calculation of, method for, 20: 21608 (CERN-65-32, pp 169-74)
flux of, method for determining, (E), 20: 21603 (CERN-65-32, pp 115-20)
flux of, methods for calculating, 20: 21600 (CERN-65-32, pp 97-108)
interaction with nucleons, (T), 20: 21598 (CERN-65-32, pp 79-82)
interactions at high energies, weak, (T), 20: 21614 (CERN-65-32, pp 275-84)
interactions in bubble and spark chambers at high energies, lower limit for intermediate boson mass from, (E/T), 20: 21596 (CERN-65-32, pp 11-24)
interactions in bubble chambers at high energies, intermediate boson mass from, 20: 21597 (CERN-65-32, pp 25-30)
interactions in nuclear emulsions, method for determining, 20: 21609 (CERN-65-32, pp 175-80)
interactions of, experiments on, 20: 21606 (CERN-65-32, pp 157-60)
interactions of, summary on detection and properties of, 20: 21613 (CERN-65-32, pp 269-74)
interactions with nucleons, asymmetries in meson (w) production from, (T), 20: 21638
interactions with neutrons, flux determination from, (E), 20: 21603 (CERN-65-32, pp 115-20)
production facilities for, summary of, 20: 21605 (CERN-65-32, pp 153-6)
production in mesons (μ−) reactions with helium-3 interactions, probability for, (T), 20: 22152
production of CERN experiment on, 20: 21602 (CERN-65-32, pp 111-14)
properties of, lectures on, 20: 21616 (JINR-P-2429)
NEUTRINOS (ν_e)
form factor of, intermediate vector-boson theory for electromagnetic, 20: 21669
interactions with protons, liquid scintillator for measuring cross sections for, 20: 21027 (CERN-65-32, pp 41-4)
interactions with nucleons at high energies, intermediate boson production in, (E), 20: 21595 (CERN-65-32, pp 1-10)
NEUTRINOS (ν_μ)
form factor of, intermediate vector-boson theory for electromagnetic, 20: 21669
interactions with nucleons at high energies, intermediate boson production in, (E), 20: 21595 (CERN-65-32, pp 1-10)
interactions with neutrons, cross sections for N* production in, (T), 20: 21599 (CERN-65-32, pp 89-96)
NEUTRON BEAMS
production of monochromatic cold, intensity and wavelength resolution for, 20: 21949
NEUTRON CAPTURE CROSS SECTIONS
measurement at 0.2 to 2.5 Mev for praseodymium-141, (E), 20: 21969(R) (ANL-7055, pp 230-3)
NEUTRON CROSS SECTIONS
calculations for thermal reactors, resonance effects in multigroup, 20: 22384
resonances in, numerical techniques for analysis of, 20: 21994 (BNL-10094)
tabulations for thorium fuel cycle development, 20: 21967 (AEET-234)
NEUTRON MONOCHROMATORS
design and performance of, for long-wavelength neutrons, 20: 21007
development of cold, 20: 21949
phase synchronization of multiple-chopper, 20: 21111
NEUTRON SOURCES
development of pulsed, for power reactor startup, 20: 22414(R) (GEAP-4961)
efficiency of beryllium–plutonium, effects of composition on, 20: 20553(R) (MLM-1142)
flux patterns for 14-mev, 20: 21946
intensity in subcritical cores, relative, (E), 20: 22392
neutron angular distribution-energy relationship for, calculation of, 20: 21934 (AD-621473)
properties of helium-3 cyclotron for use as, 20: 20565 (ORNL-P-1216)
tritium target for (d,n), 20: 21948
NEUTRON SPECTRA
measurement in reactors, methods for, 20: 22382 (RT-FI(65)57)
measurement of leakage, from uranium-235 spheres, 20: 21939(R) (GA-6930)
measurement of thermal, in beryllium oxide, 20: 21939 (GA-6930)
use of thermal, for reactor design, 20: 22376 (GA-6901)
NEUTRON SPECTROMETERS
choppers for, for wavelength range 7 to 15 Å, 20: 21007
data analysis and control system using digital computer, 20: 21982 (BNL-948, pp 718-40)
design and performance of lithium-6-semiconductor, for fast neutrons, 20: 21034 (EUR-2712.e)
design for fast and slow neutron, 20: 21140(P)
design of time-of-flight, using avalanche transistors, 20: 21110
design of, with two scintillators, 20: 21143(P)
performance of helium-3, extended range, 20: 22010(R) (NYO-72-28)
NEUTRON SPECTROSCOPY
use of computers in, 20: 21982 (BNL-948, pp 718-40)
NEUTRONS
absorption by holmium-165, resonance parameters for, (E), 20: 22004 (JINR-P-2593)
absorption by nuclei, Doppler-broadened resonance, 20: 21951
absorption in fast breeder reactors, effect of randomness on group cross sections for resonance, 20: 22391
absorption of, statistical resonances for unresolved region of, 20: 21940 (GAMD-6908)
absorption theorem for, maximum, 20: 21953
angular distributions and energy from deuteron reactions with deuterium and tritium, (T), 20: 21934 (AD-621473)

capture by antimony-121, rhenium-187, and strontium-84, isomeric cross section ratios for, (E), 20: 22052
decay of solar, proton flux from, 20: 21495
decay of, G_2 symmetry for, 20: 21719
detection and measurement using semiconductor detectors, 20: 21026 (BNL-948, pp 704-17)
detection and measurement of, performance of dielectric track detectors for, 20: 21091
detection of, lithium borate crystals for, 20: 21049
detection of, semiconductor sensitivity for, 20: 21059
diffusion equations for, iterative methods for solution of, 20: 22400
diffusion equation for, formalisms of method of weighted residuals for, 20: 21957
diffusion in nonseparable reactor geometries, modified Ritz method for, 20: 22385
diffusion in parallel-plate lattices, 20: 22398
diffusion lengths in graphite, 20: 22520(R) (NAA-SR-11805)
diffusion of, transport theory for extension of coefficient of, 20: 21944
dose-rates in critical assembly environment, air-scattered, 20: 22386
dosimetry in and behind beryllium slabs, tabulations for, 20: 22307 (DC-61-3-69)
dosimetry of, portable microcalorimeter for, 20: 21024 (AD-630693)
effects of, with gamma radiation on size of litters produced by male mice, 20: 20453
effects on austenitic stainless steel, 20: 21383
effects on bulk compressibility and electric conductivity of polyepoxides, 20: 21418 (AD-627049)
effects on densification and homogenization of uranium dioxide–zirconium dioxide fuels, 20: 21432 (WAPD-301)
effects on dielectric and mechanical properties of dielectrics, combined effects of low-temperature, vacuum, and, 20: 21152 (N-65-22353)
effects on electric properties of germanium and silicon, 20: 21150 (HMI-B-45)
effects on ethyl bromide, isotopic and phase effects in, 20: 20751
effects on fast diode switching times, 20: 21157
effects on gain degradation in silicon semiconductors, 20: 21169
effects on graphitized carbon black, EPR determination of anneal effects from, 20: 21435
effects on helium diffusion from beryllium oxide, kinetics of, 20: 21428 (NP-15942)
effects on mechanical properties and point defects in niobium, 20: 21320(R) (AD-625475)
effects on molecular motions and structure of crystalline stereoregular polymers, 20: 20753
effects on size of litters produced by male mice, 20: 20453
effects on stability of carbon-14-labeled heterocyclics, 20: 20783
effects on strain fatigue of austenitic stainless steels and nickel alloys, 20: 21426 (N-65-24714)
effects on structure of sintered beryllium oxide, x-ray diffraction studies on, 20: 21433(T) (UCRL-Trans-10012)
effects on uranium and uranium alloys, 20: 21436
emission by sun, upper bounds of flux of, 20: 21495
energy spectra in TRIGA Mark II, 20: 22502
flux distribution in reactors, computer program for, 20: 22488 (AD-621121)
flux distribution in uniform isotropic media, time-dependent Green function for, 20: 21959
flux distributions in reactors, Courant-Wallace expressions for, (T), 20: 22372 (AFRRI-TN-65-1)
flux in fast reactor cores, Monte Carlo calculations of heterogeneity of, 20: 22397
flux in reactors, variation principles for critical, 20: 22399
flux lifetime distribution in physical systems, analysis of correlation method for measuring, (T), 20: 21035 (FEI-21)
flux moderation in paraffin, 20: 20524 (RT-PROT-(65)32)
flux moments in gap geometry, boundary condition for, 20: 22390
flux monitoring during startup of boiling-water reactors, in-pile system for, 20: 22438
flux variations in multiplying medium, (T), 20: 21954
interactions with hyperons (Σ^-) from meson (π^-) interactions with deuterons, final-state, (T), 20: 21681
interactions with protons, deuteron compositeness from effective-range formula for, 20: 21689
interactions with protons in nuclei, quasi-particle random-phase approximation in, 20: 22147
interactions with neutrons, Coulomb-modified S-wave dispersion relation for, 20: 21680
interactions with neutrinos (ν_μ), cross sections for N* production in, (T), 20: 21599 (CERN-65-32, pp 89-96)
interactions with neutrinos, flux determination from, (E), 20: 21603 (CERN-65-32, pp 115-20)
kinetics in reactors, statistical analysis for determining, 20: 22381 (RT-FI(65)49)
kinetics in reactors, iterative variational method for elliptical problems in, 20: 22387
kinetics in reactors, statistical theory for, 20: 22418
lifetime of, lower limit for mean, (E), 20: 21636
mass relative to protons, (T), 20: 21673
mass relative to protons from spontaneous symmetry breakdown, 20: 21678
mass relative to protons, dispersion-theoretical perturbation series in particle models for, 20: 21683
photoproduction on aluminum, carbon, and sulfur at threshold to 200 Mev, cross sections for, (E), 20: 22094
production in IGY neutron monitor, counting rate and multiplicity spectrum of, 20: 21551
production in subcritical cores, relative source strengths of, (E), 20: 22392
production of, tritium gas target for, 20: 21948
reactions (n,αn′) with heavy nuclei, direct, (T), 20: 22018
reactions (n,αn′) with uranium-238 at 14.7 Mev, cross sections for, (E), 20: 22017
reactions (n,γ) with rhenium-185 at 4 kev to 2.6 Mev, cross sections for, (E), 20: 21969(R) (ANL-7055, pp 230-3)
reactions (n,γ) with rhenium-187 at 4 kev to 7.6 Mev, cross sections for, (E), 20: 21969(R) (ANL-7055, pp 230-3)
reactions (n,p) with helium-3 gas, pressure wave generation in, (T), 20: 21803
reactions in plutonium-239–thorium-232 systems, resonance interference effects on cross sections for, (T), 20: 21970 (ANL-7144)
reactions with bismuth, production of polonium-210 in, 20: 20585
reactions with heavy even-even nuclei, model of, 20: 22520(R) (NAA-SR-11805)
reactions with nuclei at 14 Mev, design and performance of counter telescope for, 20: 21054
reactions with plutonium-239 at 15 to 82 ev, cadmium-115 yields from symmetric resonance fission, (E), 20: 22135
reactions with technetium-99 at 14.8 Mev, activation cross sections for, 20: 22039
scattering by boron, calcium, carbon, and potassium at 14.0 Mev, cross sections for elastic, (E), 20: 22119
scattering by carbon-12 and oxygen-16, resonance parameters for elastic, (T), 20: 22010(R) (NYO-72-28)
scattering by crystals and liquids, research on slow inelastic, 20: 22316 (JINR-P-2081)
scattering by fused quartz at 0.00065 to 2.0 ev, cross sections for, (E), 20: 22010(R) (NYO-72-28)
scattering by gadolinium at 0.01 to 0.4 ev, cross sections for, (E), 20: 22010(R) (NYO-72-28)
scattering by hydrogenous compounds, cross sections for, 20: 22010(R) (NYO-72-28)
scattering by niobium-93, excited states from inelastic, (E), 20: 21969(R) (ANL-7055, pp 230-3)
scattering by nuclei at low energies, intermediate structure, (T), 20: 21988 (BNL-948, pp 876-904)
scattering by nuclei at 0.8 to 4.1 Mev, nuclear shell effects on inelastic, (E), 20: 22023
scattering by nuclei at 0.3 to 0.8 Mev, angular distributions from elastic, (E), 20: 22023
scattering by polyethylene at 0.0154 to 0.317 mev, (E), 20: 21943
scattering by uranium-238, (n,αn′) reaction effects on anomaly in small-angle elastic, (E), 20: 22017
scattering by yttrium-89 at 0.00064 to 8.0 ev, cross sections for, (E/T), 20: 22010(R) (NYO-72-28)
slowing down in heavy water, time dependence of, (E/T), 20: 21936 (AE-216)
spectra and yield from helium-3 reactions (He-3,n) with nuclei at 19 to 25 Mev, 20: 22132
spectra from uranium-235 spheres, leakage, 20: 21939(R) (GA-6930)
spectra in reflected cores and reflector regions, 20: 22396
spectra of space-dependent fluxes of, calculation of, 20: 22520(R) (NAA-SR-11805)
thermal utilization factors for, correlation of calculated and measured, 20: 21938(R) (BNWL-193, pp 16-20)
thermalization in reactors, computer program for, 20: 22374(R) (BNWL-193, pp 5-15)
thermalization in zirconium hydrides, models for, 20: 22377 (GA-6930, App. B)
thermalization in heavy water, time dependence of, (E/T), 20: 21936 (AE-216)
thermalization in beryllium and graphite, (E), 20: 21942(T) (KFK-tr-188)
transport equations for, computer program for solving, 20: 21937 (AEET-210)
transport from point source at altitude 10^5 feet, flux density calculations for, (T), 20: 21935 (AD-624041)
transport in gaseous core reactors, computer program for, 20: 22370

(AD-621021)
transport in graphite, temperature-dependent variation of mean free path of, (E), 20: 21955
transport in reactors, computer programs for, 20: 22380 (ORNL-TM-1246)
transport in two-dimensional laminated materials, method for solution of one-dimensional stationary equation for, 20: 21945
transport of, computer program for, 20: 22304 (AD-612031)
transport theory for, generalized invariant imbedding of, 20: 21947
transport theory of, use of generalized functions and Poincare-Bertrand formula in, 20: 21956
transport theory of, properties of P_L and double P_L relaxation lengths in, 20: 21958
yields from alpha reactions (α,n) with carbon-14 at 2.5 to 5.1 Mev, (E), 20: 22110
yields from beryllium–plutonium sources, effects of elemental ratios on, 20: 20553(R) (MLM-1142)

NEUTRONS, COLD
production of beams of, monochromators for, 20: 21949
reactions with thorium dioxide, uranium dioxide, and uranium at 0.0045 to 0.028 ev, total cross sections for, (E/T), 20: 21966 (AE-222)
scattering by magnetic materials at Curie temperature, angular resolution for, 20: 22325

NEUTRONS, DELAYED
effects on stability of power reactors, (T), 20: 22443

NEUTRONS, EPITHERMAL
dosimetry of, cobalt-silver activity ratio method for, 20: 21025 (AERE-R-5122)
flux determination using gold activation detectors, (T), 20: 21053
reactions with uranium-235 at 0.02 to 80 ev, fission cross sections for, (E), 20: 22012 (UCRL-14606)

NEUTRONS, FAST
absorption by reactor fuels, Doppler coefficients for resonance, (T), 20: 22378 (KFK-367)
detection and measurement in thermal neutron background, semiconductor detector for, 20: 21034 (EUR-2712.e)
detection and measurement of, counter for, 20: 21140(P)
dosimeter for, semiconductor, 20: 21095
dosimetry in dogs and phantoms, 20: 20432 (AD-630332)
dosimetry in MIT Reactor using calorimeter and threshold detectors, 20: 20723(R) (MIT-334-33)
effects on aging in Japanese nuclear-explosion survivors, 20: 20480
effects on blood–brain barrier permeability in burros and sheep, 20: 20489
effects on decomposition of terphenyls at 350°C, 20: 20722 (EUR-2401.f)
effects on deformation of copper–tin alloys, 20: 21434
effects on dimensional stability of carbon and graphite at 900 to 1800°C, 20: 21419 (BNWL-191)
effects on dimensions of graphite, 20: 21420 (BNWL-215)
effects on gelation of triethylene glycol dimethacrylate at 14 Mev, 20: 20720 (AD-630891)
effects on human blood picture in Nagasaki, 20: 20481
effects on isomeric terphenyl, decomposition, 20: 20739
effects on properties and structure of graphite at 495 to 1035°C, 20: 21421 (GA-6888)
effects on properties of pressure vessel steels, 20: 21228 (AE-221)
effects on proton polarization in polyethylenes, (E), 20: 22345
effects on Santowax WR, effects of temperature on, 20: 20723(R) (MIT-334-33)
effects on tensile properties of aluminum and titanium at cryogenic temperatures, 20: 21427(R) (NASA-CR-54904)
effects on variegation in Einkorn wheat, mutagenic, 20: 20497
flux distribution in in-pile loop (BLO 3), 20: 20722 (EUR-2401.f)
flux evolution in multiplying medium, energy, space, and time dependence of, (T), 20: 21950
flux measurement using metallic foils, 20: 21427(R) (NASA-CR-54904)
flux patterns from a 14-Mev generator, 20: 21946
reactions (n,np) and (n,p) with zinc-64 at 14 Mev, (E), 20: 22048
reactions with gold foils, recoil atoms from, 20: 21441
scattering by uranium-238 at 75 to 1620 kev, excitation functions and differential cross sections for, (E), 20: 22056
spectra and fast-fission effect in thermal uranium–water reactors, 20: 22506

NEUTRONS, FISSION
effects on batteries, hardening against, 20: 21162

NEUTRONS, PROMPT
lifetime in spherical assemblies, 20: 22383(T) (AEC-tr-6693)

NEUTRONS, THERMAL
detection and measurement of, counter for, 20: 21140(P)
effects on current induction in commercial capacitors, 20: 21151 (IBM-66-825-1944)
effects on variegation in Einkorn wheat, 20: 20497
flux average energy of, boron-lined counter for determining, 20: 21074
flux determination using gold activation detectors, 20: 21053
flux distribution in hexagonal lattices, determination of, (T), 20: 22371 (AD-621026)
reactions (n,α) with boron-10, branching ratio for, (E), 20: 22071
reactions (n,γ) with manganese-55, gamma spectra from, 20: 22064
reactions (n,γ) with cadmium-113, internal conversion spectra from, (E), 20: 22066
reactions (n,γ) with sulfur-32, sulfur-33 level spins from, (E), 20: 22077
reactions with thorium dioxide, uranium dioxide, and uranium at 0.0045 to 0.028 ev, total cross sections for, (E/T), 20: 21966 (AE-222)
scattering by heavy water, water, and zirconium hydride, cross sections for, (E), 20: 21939(R) (GA-6930)
scattering by low-impurity metal crystals, oscillation frequency and resonance location determination from, (E), 20: 22320
scattering by magnetic materials at Curie temperature, angular resolution for, 20: 22325
scattering by nuclei at 5.8 and 7.5 Mev, gamma spectra from inelastic, (E), 20: 22069
spectra in beryllium oxide, 20: 21939(R) (GA-6930)
spectra in finite mass media, properties of, 20: 21933 (AD-621119)
spectra in zirconium hydrides, transient properties of, (E/T), 20: 21941 (IAE-977)
use in radiographic, image analysis in, 20: 20866

NEW ZEALAND
carbon-14 content of volcanic ash in, 20: 20893
fallout monitoring, 1965, 20: 20882(R) (HASL-171)
geochronology of metamorphic and plutonic rocks in, by rubidium-strontium method, 20: 20888
tritium content in rain water in, 20: 20893

NICKEL
detection of inclusions of, in zirconium alloys by x-ray emission in electron microscopy, 20: 20593
determination in high-purity tantalum by spectrography using d-c arc method, 20: 20608
determination in silicon dioxide, activation, 20: 20634
ductility of, at −269°C, 20: 21416
electron reactions at 6 to 23 kev, optical transition radiation from, 20: 21518
evaporation from porous tungsten ionizers, 20: 21570 (N-65-29785)
heat transfer to water by, 20: 20925(R) (ANL-7055, pp 177-212)
helium-3 reactions (He-3,n) at 19 to 25 Mev, angular distributions and cross sections for, (E), 20: 22132
neutron cross sections and shielding coefficients for, 20: 22383(T) (AEC-tr-6693)
neutron flux and spectrum measurements on foils of, 20: 21427(R) (NASA-CR-54904)
neutron inelastic scattering at 5.8 and 7.5 Mev, gamma spectra from thermal, (E), 20: 22069
oxidation by carbon dioxide–carbon monoxide mixtures, 20: 21383
performance as liquid-phase sintering promoter for uranium monocarbide, 20: 21296 (Y-1510)
radiation effects on battery electrodes of, gamma, 20: 21425(R) (N-65-24491)
radioinduced defects in annealed, Frenkel pair recombination volume from alpha, 20: 21447
reactions with sodium at high temperatures, 20: 20925(R) (ANL-7055, pp 177-212)
separation from chromium, manganese, rare earths, and silver by ion exchange chromatography, 20: 20634
separation from scandium by ion exchange chromatography, 20: 20821
separation from thorium by ion exchange in nitric acid solution, 20: 20624
separation from uranium by combined ion exchange–solvent extraction using nitric acid–tetrahydrofuran solutions, 20: 20811
sorption from perchloric acid solutions by ion exchange materials, 20: 20823
sorptive properties of evaporated films of, for krypton and xenon, 20: 21387
sorptive properties of evaporated films of, for carbon monoxide at 0°C, 20: 21388
sorptive properties of evaporated films of, for carbon dioxide at room temperature, 20: 21389
viscosity of liquid, based on atomic parameters, 20: 20656 (UCRL-11930)
welding of, argon-arc and electron-beam methods of, 20: 21310

NICKEL ALLOYS
effects of decontaminating and descaling solution on metal loss on Hy-80, 20: 21238 (NP-15928)
radiation effects on strain fatigue of, neutron, 20: 21426 (N-65-24714)
Al–Ni–U, reactions with water during Kiwi-TNT transients, 20: 20925(R) (ANL-7055, pp 177-212)
Be–Ni, properties of localized impurity states in, 20: 21390
Ce–Ni–Pu, phase studies, 20: 21342(R) (MLM-1301)
Cr–Co–Mo–Ni–W, testing for bearing parts in liquid sodium,

20: 22520(R) (NAA-SR-11805)
Cr–Fe–Mo–Ni, corrosion of Hymu-80 by potassium chloride–uranium trichloride eutectic at 900°C, 20: 21261 (LA-3470)
Cr–Fe–Ni, fission product diffusion in irradiated, at 600 to 1200°C, 20: 21232 (BMI-1763)
Cr–Mo–Ni, corrosion by acids at 800 to 2375°F, effects of heat treatments and microstructure on, 20: 21277
Cu–Ni, effects of decontaminating and descaling solution on metal loss on, 20: 21238 (NP-15928)
Dy–Ni, dysprosium hyperfine magnetic field in intermetallic compounds of, (E), 20: 22330
Fe–Ni, fission product diffusion in irradiated, at 600 to 1200°C, 20: 21232 (BMI-1763)

NICKEL CHLORIDES
effects on sintering of tungsten, 20: 21291 (NP-15944)

NICKEL ISOTOPES
nuclear structure of even, (T), 20: 21976
proton inelastic scattering by even, microscopic description of, (T), 20: 22118

NICKEL ISOTOPES Ni-58
alpha inelastic scattering by, (T), 20: 21973 (BNL-948, pp 175-221)
alpha inelastic scattering at 64.3 Mev, strong absorption model for, 20: 22086
deuteron reactions (d,n) at 11.7 Mev, neutron spectra and angular distributions from, (E), 20: 22109
helium-3 reactions (He-3,t) at 22 Mev, Coulomb displacement-energy from, (E), 20: 22095
neutron reactions (n,p) at 5.0 Mev, cross section and threshold energy for, 20: 21427(R) (NASA-CR-54904)
proton elastic scattering at 45 Mev, differential cross sections for, (T), 20: 21963 (AD-626656)

NICKEL ISOTOPES Ni-59
energy levels from helium-3 reactions (He-3,α) with nickel-60 at 15 Mev, (E), 20: 22127

NICKEL ISOTOPES Ni-60
deuteron reactions (d,n) at 11.7 Mev, neutron spectra and angular and angular distributions from, (E), 20: 22109
helium-3 reactions (He-3,t) at 22 Mev, Coulomb displacement-energy from, (E), 20: 22095
helium-3 reactions (He-3,α) at 15 Mev, angular distributions from, (E), 20: 22127
proton elastic scattering at 45 Mev, differential cross sections for, (T), 20: 21963 (AD-626656)

NICKEL ISOTOPES Ni-62
deuteron reactions (d,n) at 11.7 Mev, neutron spectra and angular distributions from, (E), 20: 22109
helium-3 reactions (He-3,t) at 22 Mev, Coulomb displacement-energy from, (E), 20: 22095

NICKEL ISOTOPES Ni-63
diffusion in copper at 250 to 520°C, 20: 21367

NICKEL ISOTOPES Ni-64
deuteron reactions (d,n) at 11.7 Mev, neutron spectra and angular distributions from, (E), 20: 22109
helium-3 reactions (He-3,t) at 22 Mev, Coulomb displacement-energy from, (E), 20: 22095

NICKEL STEEL
Cr–Mo–Ni, transformation temperatures in Super Elso, effects of heating rate on, 20: 21331(R) (EURAEC-1569)
Cr–Mo–Ni, weld embrittlement in joints in, effects of time at high temperatures on, 20: 21393
Cr–Ni–Nb, effects of aging at 600 to 800°C on microstructure of, 20: 21355 (TRG-Report-1168)

NICKEL SYSTEMS
Al_2O_3–Ni, wear properties of plasma-arc-deposited coatings of, 20: 21319 (AD-621064)
B–Hf–Ni, crystal structure, 20: 20685
B–Ni–Ti, crystal structure, 20: 20685
B–Ni–U, crystal structure, 20: 20685
B–Ni–V, crystal structure, 20: 20685
B–Ni–Zr, crystal structure, 20: 20685

NIOBIUM
bonding of, to Inconel 600 and stainless steels, process development for explosive, 20: 21295(R) (WANL-PR-(EE)-002)
corrosion protection coatings for, bibliography on properties of, 20: 21257 (AD-621546)
determination in high-purity tantalum by spectrography using d-c arc method, 20: 20608
ductility of, at −269°C, 20: 21416
internal friction of coid-worked, effects of restraining on, 20: 21378
magnetic field transitions in superconducting, surface effects on a-c, (E), 20: 21918
magnetic flux pinning in superconducting, quantized, (E), 20: 21909
magnetic resonances in superconducting, low-frequency mixed-state, (E), 20: 21894
microwave surface in superconducting, (E), 20: 21916
radiation effects on mechanical properties and point defects in, neutron, 20: 21320(R) (AD-625475)
reactions with carbon monoxide at 1300 to 1700°C, 20: 21270
reactions with sodium at high temperatures, 20: 20925(R) (ANL-7055, pp 177-212)
separation from hydrochloric acid solutions by solvent extraction using quaternary ammonium chlorides, 20: 20816
separation from protactinium by solvent extraction using quaternary ammonium chlorides, 20: 20816
sorptive properties for nitrogen and oxygen, kinetics of, 20: 21351(R) (SRIA-425-8)
sorptive properties of evaporated films of, for carbon monoxide at 0°C, 20: 21388
sorptive properties of evaporated films of, for carbon dioxide at room temperature, 20: 21389
superconducting critical currents and fields in flux-pump fed coils of, (E), 20: 21924
superconducting properties of, effects of λ transition on, 20: 21875
thermal capacity of superconducting, (E), 20: 21907
thermal conductivity of superconducting, (E), 20: 21914
welding of, argon-arc and electron-beam methods of, 20: 21310
welding to stainless steel, 20: 21309

NIOBIUM ALLOYS
Al–Nb, magnetic field penetration into superconducting intermetallic compounds of, (E), 20: 21908
Ga–Nb, superconducting properties, (E), 20: 21897
Hf–Nb–W, effects of carbon and oxygen on phase equilibria in niobium-rich region of, 20: 21329(R) (DRI-1092-229)
Nb–Sn, magnetic field penetration into superconducting intermetallic compounds of, (E), 20: 21908
Nb–Sn, magnetic flux trapping threshold in superconducting Nb_3Sn, (E), 20: 21926
Nb–Sn, microwave surface resistance in superconducting, (E), 20: 21916
Nb–Sn, superconducting critical currents in intermetallic compounds of, (E), 20: 21921
Nb–Sn, superconducting critical currents and fields in flux-pump fed coils of, (E), 20: 21924
Nb–Ta, magnetic flux motion in superconducting, (E/T), 20: 21910
Nb–Ta–V, tensile properties of vanadium-base, effects of carbon and silicon additions on, 20: 21333(R) (IITRI-B6042-4)
Nb–Ta–W–Zr, bonding of FS-85, to Inconel 600 and stainless steels, process development for explosive, 20: 21295(R) (WANL-PR-(EE)-002)
Nb–Ta–W–Zr, creep of FS-85, at 2000 to 2200°F in ultrahigh vacuum, 20: 21344 (N-65-26653)
Nb–Ti–V, tensile properties of vanadium-base, effects of carbon and silicon additions on, 20: 21333(R) (IITRI-B6042-4)
Nb–U, microstructure of uranium-rich, effects of heat treatments on, 20: 21372
Nb–U, phase studies on uranium-rich, 20: 21372
Nb–U–Zr, properties of, at 150 to 350°C, mechanical and physical, 20: 21356 (UCRL-14724)
Nb–U–Zr, reactions with water during Kiwi-TNT transients, 20: 20925(R) (ANL-7055, pp 177-212)
Nb–V–Zr, properties of Cb-753, 20: 21411
Nb–W–Zr, effects of carbon and oxygen on phase equilibria in niobium-rich region of, 20: 21329(R) (DRI-1092-229)
Nb–Zr, bonding of, to Inconel 600 and stainless steels, process development for explosive, 20: 21295(R) (WANL-PR-(EE)-002)
Nb–Zr, corrosion by liquid alkali metals, test loops for studying, 20: 21284
Nb–Zr, current degradation in superconducting solenoids of, (E), 20: 21920
Nb–Zr, flux creep and jump in superconducting, effect of Joule heating on, 20: 21884
Nb–Zr, magnetic field strength at surface of superconducting, EPR measurements for, (E), 20: 21898
Nb–Zr, magnetic fluxoid annihilation instability in superconducting, (E/T), 20: 21927
Nb–Zr, mechanical properties of, effects of beta grain size on, 20: 21368
Nb–Zr, reactions with sodium at high temperatures, 20: 20925(R) (ANL-7055, pp 177-212)
Nb–Zr, specifications of, for use in corrosion test loop fabrication, 20: 21293 (R-66SD3007)
Nb–Zr, superconducting critical currents and fields in flux-pump fed coils of, (E), 20: 21924
Ni–Sn, superconducting critical currents in intermetallic compounds of, in high fields, (E), 20: 21922

NIOBIUM CARBIDES
formation by niobium pentachloride dissociation on graphite and niobium surfaces, mechanism of, 20: 21241(T) (LA-tr-66-15)

NIOBIUM CHLORIDES
dissociation of niobium pentachloride on surface of, mechanism of niobium carbide formation by, 20: 21241(T) (LA-tr-66-15)
dissociation on graphite and niobium surfaces, mechanism of niobium carbide formation by, 20: 21241(T) (LA-tr-66-15)
NIOBIUM COUPLES
Cu/Nb, fabrication of composite wires of, by drawing, 20: 21298
NIOBIUM FLUORIDES
NbF_5–UF_6, liquid–vapor equilibria in, 20: 20808(R) (ORNL-3916)
NIOBIUM ISOTOPES Nb-93
energy levels, (E), 20: 21969(R) (ANL-7055, pp 230-3)
neutron scattering by, excited states from inelastic, (E), 20: 21969(R) (ANL-7055, pp 230-3)
NIOBIUM ISOTOPES Nb-95
diffusion in irradiated fuel element cladding alloys and materials at 600 to 1200°C, 20: 21232 (BMI-1763)
separation from radioisotopes in aqueous solutions by foam chromatography using colloidal manganese dioxide, 20: 20628
NIOBIUM OXIDES
Nb_2O_5–WO_3, phase studies on, 20: 21385
NIOBIUM STEEL
Cr–Ni–Nb, effects of aging at 600 to 800°C on microstructure of, 20: 21355 (TRG-Report-1168)
NIOBIUM SYSTEMS
C–Hf–Nb–W, properties at very high temperatures, 20: 21412
C–Mo–Nb–Ta–W–Zr, extrusion parameters for Cb-132M, 20: 21263(R) (NASA-CR-54911)
C–Mo–Nb–Ta–Zr, thermal-mechanical processing of a precipitation-hardenable, dispersion-hardened, 20: 21250
C–Mo–Nb–Ti–Zr, bend and tensile ductility properties of, 20: 21410
C–Nb–W–Zr, properties at very high temperatures, 20: 21412
C–Nb–W–Zr, specifications of D-43, for use in corrosion test loop fabrication, 20: 21293 (R-66SD3007)
NITRATE IONS
yields in radiolysis of lithium nitrate, 20: 20733 (TID-22796)
NITRATES
analysis of solutions of, for plutonium, by x-ray absorption edge method, 20: 20573
NITRIC ACID
effects on analytical procedures involving uranyl ions, 20: 20630
effects on corrosion of rhenium at 25 and 100°C, 20: 21275
effects on polarographic determination of hexavalent uranium in TBP medium, 20: 20631
HNO_3–tetrahydrofuran, solvent properties for uranium, 20: 20811
NITRIDES
properties for containment of molten uranium alloys, 20: 20802(R) (ANL-7055, pp 21-98)
NITROGEN
desorption from iridium, rhodium, and tungsten, flash, 20: 20652 (IS-T-67)
detection of molecular beams of, field-ionization detector for, 20: 21089
determination by activation using helium-3 ions, 20: 20565 (ORNL-P-1216)
determination by neutron activation methods, 20: 20596
determination in beryllium by modified combustion-conductometric method, 20: 20556 (AD-626987)
determination in cesium by photon activation methods, 20: 20645
diffusion from urania pellets, kinetics and mechanisms of, 20: 21360 (WCAP-2098)
diffusion in yttrium at 1235 to 1460°C, coefficient for, 20: 21254
helium-3 reactions (He-3,n) at 19 to 25 Mev, angular distributions and cross sections for, (E), 20: 22132
light intensity from electron-excited, in auroral storms, 20: 21826
photoelectric effect at 852 ev to 40 kev in, cross sections for, (E), 20: 21523
proton reactions with, performance of triggered cloud chamber for analyzing, (E), 20: 21063
radiation effects on distribution of, in mice treated with bone marrow, x, 20: 20407 (ORNL-P-1118)
radiation effects on, effects on algal nitrogen fixation of uv, 20: 20408
separation from argon by titanium gettering, 20: 20802(R) (ANL-7055, pp 21-98)
solubility in Santowax-OM1, 20: 20708 (AEET-213)
sorption by molybdenum films in ultrahigh vacuum, kinetics of, 20: 21351(R) (SRIA-425-8)
sorption by niobium surfaces, kinetics of, 20: 21351(R) (SRIA-425-8)
spectra of arc-heated plasma of, radiation data from, (E), 20: 22167(R) (AD-622391)
spectra of, x-ray excitation of first negative and second positive bands of, 20: 21834
thermal conductivity at 750°C, 20: 20651(R) (CU-2660-26)
NITROGEN FIXATION
effects of uv-irradiated nitrogen on algal, 20: 20408
NITROGEN ISOTOPES
sorption by iridium, rhodium, and tungsten, isotopic mixing during, 20: 20652 (IS-T-67)
NITROGEN ISOTOPES N-13
energy levels of, use of Hamada-Johnston potential for, (T), 20: 22102
NITROGEN ISOTOPES N-14
charged-particle reactions with, amplitude singularities in knockon and stripping, (T), 20: 21997 (INSJ-96)
electron elastic scattering to 230 Mev, magnetic form factors from, (E), 20: 22120
energy levels from proton elastic scattering by carbon-13 at 1.0 to 2.6 Mev, 20: 22123
energy levels from oxygen-16 (d,α) reactions (E), 20: 22160
energy levels from carbon-12 (d,pγ) reactions, (E), 20: 22087
energy levels of, use of Hamada-Johnston potential for, (T), 20: 22102
proton reactions (p,dp) with, 3α decay of excited nucleus from, 20: 22033
NITROGEN ISOTOPES N-15
charged-particle reactions with, amplitude singularities in knockon and stripping, (T), 20: 21997 (INSJ-96)
reactions with heavy nuclei at 102 Mev, neutron pickup in, (E), 20: 22001 (JINR-P-2555)
NITROGEN ISOTOPES N-16
production in nitrogen-15 neutron-pickup reactions with heavy nuclei, cross sections for, (E), 20: 22001 (JINR-P-2555)
NITROGEN MUSTARDS
effects on embryonic intestine of chicken cultivated *in vitro*, 20: 20372
effects on tissue regeneration of amphibians, 20: 20440(R) (EUR-2643.f)
NITROGEN SYSTEMS
Ar–N, corrosive effects on structural alloys and metals at 900°C, 20: 20802(R) (ANL-7055, pp 21-98)
C–Hf–Mo–N–Re–Ta–W–Zr, development of dispersion-strengthened tantalum-base, 20: 21240(R) (WANL-PR-(Q)-006)
LaB_6–N, electric conductivity of suspensions of, in MHD cells, 20: 21575
NOBELIUM
production of, review of methods for, 20: 20796
NOISE
occurrence of high-frequency auroral, relation to geomagnetic disturbances, 20: 21835
NORLEUCINE
reactions with sulfur-35, formation of labeled methionine in, 20: 20786
NORVALINE
reactions with sulfur-35, formation of labeled methionine in, 20: 20786
NORWAY
age estimation of minerals in eclogites of, by potassium argon and rubidium–strontium methods, 20: 20891
NOSE
radiation effects on response of olfactory neutrons in, x, 20: 20431 (AD-630323)
NUCLEAR AIRCRAFT POWER PLANTS
maintenance of, method for, 20: 22486
NUCLEAR BATTERIES
conference, 20: 21583
NUCLEAR EMULSIONS
cascade showers in, energy of cosmic-ray initiated, 20: 21556
development for detecting charged particles, 20: 21060
meson (K$^-$) reactions in, hyperfragments from, (E), 20: 22161
neutrino interactions in, method for determining, 20: 21609 (CERN-65-32, pp 175-80)
use for cosmic shower analysis, 20: 21555
NUCLEAR MATERIALS MANAGEMENT
analysis and sampling methods for, economics of, 20: 20647
computer use for auditing data centralization in, 20: 20965
conference on, 20: 20944 (STI-PUB-110)
control and inventory in, criteria for, 20: 20966
criticality control and safety in, relation of, 20: 20974
isotopic analysis methods for, of plutonium and uranium, 20: 20978
isotopic content of operating fuel elements, methods for calculating, 20: 20979
method for identification and inspection of irradiated fuel elements, 20: 20970
methods for analysis, measurement, and sampling in separation plants at Windscale, 20: 20972
methods for fission product, relation of waste solution storage to economics of, 20: 22517
methods for inventory in conversion plant, 20: 20971
methods of, at Windscale New Separation Plant, 20: 20830
methods of, for economic processing of radioactive residues, 20: 20833
methods of, for enriched uranium chemical processing facility, 20: 20832
methods of, in Eurochemic's Mol fuel reprocessing facility, 20: 20831
methods of, in fabrication of enriched fuel elements, 20: 21313
methods of, in production, distribution, recycle, and reprocessing, UKAEA, 20: 22528
methods of, using internal audit, 20: 22529

methods used in Italian power stations and research institutions, 20: 20964
methods used in uranothorianite processing unit of Bouchet Plant, France, 20: 20969
organization of auditing in fuel element fabrication plant, 20: 20967
plutonium determination in, methods for, 20: 20976
program for, by USAEC, 20: 22527
sampling methods in French nuclear industry, 20: 20973
scope of, for typical power reactor in U. S., 20: 20968
uranium determination in, methods for, 20: 20977
NUCLEAR MODELS
bibliography on, 20: 22011 (TID-22771)
development, 20: 21961 (AD-624028)
NUCLEAR MODELS (OPTICAL)
potentials in, spin-orbit part of, (T), 20: 22116
use for proton differential elastic scattering cross sections, 20: 21963 (AD-626656)
use in nuclear analysis structure, (T), 20: 21978 (BNL-948, pp 454-524)
NUCLEAR MODELS (SHELL)
energy level calculations for odd tin isotopes, 20: 21962 (AD-624214)
wave functions in, U(3)-group classification of oscillator, 20: 22079
NUCLEAR PHYSICS
instrumentation for experiments in, control system for, 20: 20995
Mössbauer effect uses in, review of advances in, 20: 22327
research program using Van de Graaff accelerators, 20: 21463 (BNL-948, pp 685-91)
research programs on, using Kyoto University cyclotron, 20: 22524
use of on-line computers in low-energy experiments in, 20: 22031
NUCLEAR POWER
development, 20: 21097
development in Great Britain, 20: 22450
development in Switzerland, 20: 22421
NUCLEAR POWER PLANTS
design with dual cooling circuits, 20: 22458
licensing of, public safety aspects of, 20: 22434
materials management in Italian, 20: 20964
operation of PWR, conditions for minimum specific power cost in, (T), 20: 22448
safety analysis, 20: 22536
safety of, engineering aspects of, 20: 22437
safety systems for, design and evaluation of, 20: 22358
NUCLEAR QUADRUPOLE RESONANCE
development and uses in analytical chemistry, 20: 20578
uses in chemistry, 20: 20699
NUCLEAR REACTIONS
amplitude of deuteron stripping, in Coulomb approximation, 20: 22028
angular distributions in surface, adiabatic approximation for, 20: 22062
bibliography on, 20: 22011 (TID-22771)
cross sections and spectroscopic amplitudes for direct inelastic scattering and charge exchange, 20: 22067
cross sections for, statistical description of fluctuations in, (T), 20: 21987 (BNL-948, pp 826-75)
excitation functions for, statistical-model analysis of fluctuations in, 20: 22054
gamma polarization from deuteron stripping, (T), 20: 22006 (KFKI-600)
models for, diffraction, (T), 20: 21980 (BNL-948, pp 561-609)
nucleon transfer in, single, (T), 20: 21971 (BNL-948, pp 1-65)
nucleon transfer in, multi-, (T), 20: 21972 (BNL-948, pp 86-174)
theory for direct, 20: 22018
theory of intermediate structure in, 20: 21988 (BNL-947, pp 876-904)
theory of, corrections in distorted-wave, 20: 21979 (BNL-948, pp 525-60)
theory of, time-dependent equations in, 20: 22024
theory of, with multibody exit channels, 20: 21981 (BNL-948, pp 610-84)
use in distinguishing between chemically bound and free hydrogen, 20: 20653 (JINR-P-2558)
NUCLEAR STRUCTURE
alpha-alpha potentials for forces in, (T), 20: 22061
analysis using DWBA and optical model, (T), 20: 21978 (BNL-948, pp 454-524)
analysis using heavy-ion reactions and scattering, 20: 21992 (BNL-948, pp 1045-1134)
analysis using proton capture, 20: 21986 (BNL-948, pp 763-825)
calculations using shell model, boundary-condition constraint method for, 20: 21989 (BNL-948, pp 905-27)
effects of shell structure on level densities in continuum, 20: 22070
of heavy spherical nuclei, (T), 20: 21975 (BNL-948, pp 269-336)
of light spherical nuclei, 20: 21974 (BNL-948, pp 222-68)
of strongly deformed light nuclei, (E/T), 20: 21976 (BNL-948, pp 337-79)
of strongly deformed heavy nuclei, (E/T), 20: 21977 (BNL-948, pp 380-453)
NUCLEAR THEORY
energy gap in finite nuclear systems, 20: 22112
forces in p-shell configurations in, three-body, 20: 22092
isobaric spin without charge space for, 20: 22019
matrix elements and wave functions for transition-region nuclei, generator coordinate method for, 20: 22081
nuclear vibrations in, time-dependent Hartree-Fock theory for, 20: 22068
parity mixing in single-nucleon orbitals, properties of wave functions from, 20: 22080
Talmi transformation and related formulas in, 20: 21226
NUCLEI
alpha clustering potentials for, (T), 20: 22061
alpha reactions with, amplitude singularities in knockon and stripping, (T), 20: 21997 (INSJ-96)
charged-particle scattering by, ionization losses in, (T), 20: 21515 (JINR-P-2615)
collective motion and deformation energies of heavy, 20: 22065
cosmic particle reactions above 10 Bev, model for inelastic, (T), 20: 21999 (JINR-P-2552)
decay of heavy, lifetimes for alpha, beta, and spontaneous-fission, (T), 20: 22043
decay of, gamma-gamma angular correlations for, (T), 20: 22010(R) (NYO-72-28)
decay of, perturbed angular correlation of triple gamma cascades from, (T), 20: 22015
deuteron reactions with, amplitude singularities in knockon and stripping, (T), 20: 21997 (INSJ-96)
deuteron reactions (d,Ny) with, gamma polarization from, (T), 20: 22006 (KFKI-600)
deuteron reactions (d,p) with, amplitudes in Coulomb approximation for, 20: 22028
electron inelastic scattering by, two-nucleon correlation functions from cross sections for, (T), 20: 21996 (FTI-142/T-016)
electron radial functions and tangents of phase shifts for $1 \leq Z \leq 10$, 20: 22009 (NBS-MON-81)
electron scattering by aligned deformed, amplitudes for high-energy, (T), 20: 22124
elementary-particle reactions at low-momentum transfer, coherence properties for, 20: 22145
energy gap in finite systems of, 20: 22112
energy level excitation by direct interactions, 20: 21990 (BNL-948, pp 928-1004)
energy level excitation by Coulomb scattering of heavy ions, 20: 21991 (BNL-948, pp 1005-44)
energy level transitions in, determination of multipolarities from internal pair correlation measurements, 20: 21985 (BNL-948, pp 757-62)
energy level transitions in even, M1, (T), 20: 22085
energy levels in, pairing vibrations of, (T), 20: 22075
energy levels of deformed ($176 \leq A \leq 190$), collective, (T), 20: 21998 (JINR-E-2579)
energy levels of even-even, alpha-cluster wave function for ground state, 20: 22093
energy levels of even, g_R factors for, (T), 20: 22085
energy levels of transition-region, generator coordinate method for matrix elements and wave functions for, 20: 22081
energy levels of 1p-shell, use of Hamada-Johnston potential for, (T), 20: 22102
energy levels of, spin assignment using gamma-particle correlations, 20: 21983 (BNL-948, pp 741-50)
energy levels of, spin assignment using gamma-gamma correlations, 20: 21984 (BNL-948, pp 751-6)
energy levels of, quasiparticle random-phase approximation for, 20: 22147
energy levels of, equilibrium deformations in excited, (T), 20: 22005 (JINR-P-2596)
energy levels of, gamma correlation methods determining magnetic dipole moment of, 20: 22025
energy levels of, parity mixing in single-nucleon, 20: 22080
energy-level densities in, effects of shell structure on, 20: 22070
fission of, primary charge distribution in low-energy, (T), 20: 22013(T) (ANL-Trans-296)
hyperon (Λ) and proton binding energies in, (E), 20: 22161
ion reactions and scattering on, review on, 20: 21992 (BNL-948, pp 1045-1134)
ion scattering by, microscopic description of, (T), 20: 22118
isobaric spin without charge space for, 20: 22019
lifetimes of undiscovered, prediction of, 20: 22043
mass corrections to 1964 tables of alpha–beta decay chain into bismuth-213, 20: 22154
mass systematics, 20: 21990 (BNL-948, pp 928-1004)
matrix elements for, effect of particle number fluctuations on, 20: 22103
meson (K^-) reactions with light, hyperon (Λ) and (Σ) production from, 20: 22033
meson (π) optical properties in, low-energy, (T), 20: 22021

meson (π) reactions with light, double charge exchange in, 20: 22033
neutron absorption cross sections for, Doppler-broadened, (T), 20: 21951
neutron elastic scattering at 0.3 to 0.8 Mev, angular distributions from, (E), 20: 22023
neutron inelastic scattering at 0.8 to 4.1 Mev, nuclear shell effects on, (E), 20: 22023
neutron reactions at 14 Mev, design and performance of counter telescope for, 20: 21054
neutron reactions (n,αn′) with heavy, direct, (T), 20: 22018
neutron resonance absorption in unresolved region, computer program for, 20: 21940 (GAMD-6908)
neutron scattering at low energies, intermediate structure in, (T), 20: 21988 (BNL-948, pp 876-904)
nucleon inelastic scattering by, microscopic description of, (T), 20: 22118
nucleon interactions in p-shell configurations in, three-body, 20: 22092
nucleon interactions in, separation distance for effective, (T), 20: 22122
nucleon pairing correlations in odd-mass, effects of rotational motion on, 20: 22148
nucleon pairing interactions in, eigenstates for J = 0, T = 1, charge-independent, 20: 22121
particle inelastic scattering by, (T), 20: 21973 (BNL-948, pp 175-221)
particle inelastic scattering by, strong absorption model for, 20: 22086
properties of even-even, microscopic and phenomenological analysis of, 20: 21961 (AD-624028)
properties of $139 \leq A \leq 177$, $54 \leq Z \leq 108$, (T), 20: 22042
proton elastic scattering at 10 to 20 Mev by medium, spin-orbit potential for polarization from, (T), 20: 22116
proton elastic scattering at high energies, review of, 20: 21593 (CERN-65-24(Vol.1), pp 65-80)
proton reactions with, amplitude singularities in knockon and stripping, (T), 20: 21997 (INSJ-96)
reactions of heavy even-even, with neutrons, 20: 22520(R) (NAA-SR-11805)
structure of heavy spherical, (T), 20: 21975 (BNL-948, pp 269-336)
structure of light spherical, 20: 21974 (BNL-948, pp 222-68)
structure of strongly deformed light, (E/T), 20: 21976 (BNL-948, pp 337-79)
structure of strongly deformed heavy, (E/T), 20: 21977 (BNL-948, pp 380-453)
structure of, analysis using proton capture, 20: 21986 (BNL-948, pp 763-325)
triton reactions with, amplitude singularities in knockon and stripping, (T), 20: 21997 (INSJ-96)

NUCLEI (CELLS)
radiation effects on potassium and sodium content of animal, x, 20: 20422
structure of bacterial, effects of uranyl ions on, 20: 20392

NUCLEONS
exchange in nuclear reactions, (T), 20: 21972 (BNL-948, pp 86-174)
exchange of single, in nuclear reactions, (T), 20: 21971 (BNL-948, pp 1-65)
form factors of, electromagnetic and weak, (T), 20: 21651
interactions in nuclei, separation distance for effective, (T), 20: 22122
interactions of three-body systems of, in p-shell configurations, 20: 22092
interactions with antineutrinos, spark chamber experiments on, 20: 21607 (CERN-65-32, pp 161-8)
interactions with nucleons, T-matrix for, (T), 20: 21617 (JINR-P-2546)
interactions with phonons, Schroedinger equation solution for, (T), 20: 21619 (JINR-P-2567)
interactions with nucleons, one-boson exchange model parameters from, (T), 20: 21621 (JINR-P-2584)
interactions with nucleons, bounds for correction to Born term for, 20: 21635
interactions with neutrinos, asymmetries in meson (π) production from, (T), 20: 21638
interactions with mesons (π), absorption model for 2^+-meson production in, 20: 21644
interactions with polarized bremsstrahlung at 475 to 750 Mev, meson (π^+) production from, (E), 20: 21660
interactions with mesons (π), threshold factor in p-wave dispersion relations for, 20: 21667
interactions with mesons (π), p-wave amplitudes for off-shell, 20: 21672
interactions with mesons (K) in 27-fold representation, dynamics of, 20: 21674
interactions with mesons (π^-) at 6.8 Bev, inelastic, (E/T), 20: 21693
interactions with mesons (π), mass splittings from, 20: 21758
interactions with mesons (π), Lie algebra for isobar-coupling, 20: 21759
interactions with photons, analysis of, (T), 20: 21587 (AD-623564)
interactions with neutrinos at high energies, intermediate boson production in, (E), 20: 21595 (CERN-65-32, pp 1-10)
interactions with neutrinos, (T), 20: 21598 (CERN-65-32, pp 79-82)
interactions with nucleons, boundary condition methods for nuclear matter, 20: 22022
interactions with hyperons (Λ), research on, 20: 22033
pairing correlations in odd-mass, effects of rotational motion on, 20: 22148
pairing interactions in nuclei, eigenstates for J = 0, T = 1, charge-independent, 20: 22121
scattering by nuclei, microscopic description of, (T), 20: 22118

NUCLEOTIDES
nicotinamide adenine, effects on radiosensitivity of enzymes, 20: 20514
radiation effects on $NADH_2$ oxidation in suspensions of cattle heart mitochondria, 20: 20496
radiation effects on aqueous solutions of, review on, 20: 20728 (PB-181506, pp 49-58)

NUTRIENTS
content in seawater, tracer techniques for measuring, 20: 20368 (CONF-640309-1)
uptake by plants from soil, tracer study, 20: 20389 (STI-PUB-108)

O

OAK RIDGE NATIONAL LAB., TENN.
waste disposal in Clinch River by, radiation dose to man from, 20: 22514 (ORNL-P-2021)

OCTANE
radioinduced reactions with carbon monoxide, gamma, 20: 20770(T)

OHIO
radiation monitoring in area of Cincinnati, aerial, 20: 20880 (CEX-62.6.5)

OHMMETERS
design for controlling film thicknesses, 20: 20987 (RFP-690)

OIL SHALES
breaking of, use of underground nuclear explosions for, 20: 20835

OPTICAL MATERIALS
conference on photographic and spectroscopic, 20: 21458

OPTICAL SYSTEMS
conference on photographic and spectroscopic, 20: 21458

ORES
analysis for copper and tin by radioisotope x-ray fluorescence methods, 20: 20640
analysis for silver, activation, 20: 20574

ORGANIC COMPOUNDS
preparation of intermediate and monomeric, for radioresistant polymer synthesis, 20: 21430(R) (WADC-TR-55-58(Pt.8))
radiation effects on aqueous solutions of, review on, 20: 20728 (PB-181506, pp 49-58)
radiation effects on, mechanism of high-energy and uv, 20: 20731 (PB-181506, pp 133-42)
radiation effects on, of electrons at 300 to 500 kv, 20: 20762
radiation effects on free radical formation in, ESR studies on oxygen effects in, 20: 20729 (PB-181506, pp 85-103)
separation of carbon-14-labeled, gas chromatography and scintillation method for, 20: 20639
synthesis of, role of hydrothermal radiation in abiogenic, (T), 20: 20406 (N-65-27062)

ORGANIC COOLED REACTORS
boiling indicator for, design of film, 20: 22367(P)
coolant radiation and thermal stability, 20: 20792
design of heavy-water moderated, 20: 22433
development, 20: 22442

ORGANIC MODERATED REACTORS
criticality of glass-clad uranium-fueled, 20: 22415 (RPI-321-4)

ORNL RESEARCH REACTOR
coolant-loss accidents in, fission product behavior in simulated, 20: 20940(R) (ORNL-3915)

OSCILLATORS
radiation effects on logarithmic damping decrements of quartz, x, 20: 21155

OSCILLOGRAPHS
design for direct data control, 20: 20983 (AERE-R-4966)
sweep voltages for, analysis of Rossi, 20: 21043 (UCRL-13199)

OSMIUM COMPLEXES
chloride, chlorine-36 exchange with hydrochloric acid, 20: 20706
iodide, iodine-131 exchange with hydriodic acid, 20: 20706

OSMIUM ISOTOPES Os-188
oxygen 16 inelastic scattering at 35.6 Mev, gyromagnetic ratios of 2^+ states from, (E), 20: 22055

OSMIUM ISOTOPES Os-190
oxygen 16 inelastic scattering at 35.6 Mev, gyromagnetic ratios of 2^+ states from, (E), 20: 22055

OSMIUM ISOTOPES Os-192
oxygen 16 inelastic scattering at 35.6 Mev, gyromagnetic ratios of 2^+ states from, (E), 20: 22055

OXALACETIC ACID
radiosensitivity effects on hadacidin-treated *E. coli*, 20: 20456

OXALATES
analysis for lanthanum using hydroquinone, colorimetric, 20: 20591
OXALIC ACID
complexes with neptunium, thorium, and zirconium, solvent extraction studies on formation of, 20: 20561 (JAERI-1099)
effects on polarographic determination of hexavalent uranium in TBP solutions, 20: 20631
precipitation of cerium-144 and strontium-90 by, in fission product solutions, 20: 20804 (EUR-2754.f)
OXAZOLE, DIPHENYL-
radioinduced luminescence of liquid, 20: 21046
OXIDASES
o-diphenol, analysis for copper, by neutron activation methods, 20: 20569
OXIDES
corrosion inhibition by corrosion films of, mechanisms of, 20: 21281
diffusion in, bibliography on self-, 20: 21321 (AERE-Bib-143)
properties as coatings for tungsten at temperatures above 2000°C, 20: 21283
properties of films of, on zirconium alloys, 20: 21282
solubility of, in decontaminating and descaling solution, 20: 21238 (NP-15928)
OXYGEN
determination by activation using helium-3 ions, detection limits and sensitivity of, 20: 20565 (ORNL-P-1216)
determination in cesium by photon activation methods, 20: 20645
determination in metals, equipment and method for activation, 20: 20602
determination in thorium and yttrium metals, 20: 20572
diffusion in yttrium at 1235 to 1460°C, coefficient for, 20: 21254
effects on efficiency of porous tungsten ionizers, 20: 21570 (N-65-29785)
effects on gamma and fast-neutron radiolysis of isomeric terphenyl, 20: 20739
effects on phase equilibria in hafnium or zirconium alloys with niobium and tungsten, 20: 21329(R) (DRI-1092-229)
effects on yields from radiolysis of methanol vapor, 20: 20776
helium-3 reactions (He-3,n) at 19 to 25 Mev, angular distributions and cross sections for, (E), 20: 22132
light intensity from electron-excited, in auroral storms, 20: 21826
neutron cross sections and shielding coefficients for, 20: 22383(T) (AEC-tr-6693)
photoelectric effect at 852 ev to 40 kev in, cross sections for, (E), 20: 21523
radiation effects on uptake by rat brain tissues, x, 20: 20436 (CONF-650560-17)
radiation effects on recombination rates of, with hydrogen in presence of water vapor, gamma, 20: 20749
radiosensitivity effects in mice, 20: 20430(R) (AD-629311, pp 26-32)
radiosensitivity effects on free radical formation in biochemicals, ESR studies on, 20: 20729 (PB-181506, pp 85-103)
reactions of zirconium oxide-sorbed, with hydrogen, mechanisms of, 20: 20705
reactions with graphite at 510 to 650°C, effects of water vapor on, 20: 21285
reactions with tetravalent uranium, 20: 20689
reactions with uranium monocarbide at 800 to 1000°C, 20: 21267
removal from gadolinium by solid-state electrolysis, 20: 21253
separation from liquid iron and steel by compound formation with uranium, 20: 20692
sorption by niobium surfaces, kinetics of, 20: 21351(R) (SRIA-425-8)
sorption on molybdenum surfaces, low-energy electron-diffraction study of, 20: 22319
spectra of arc-heated plasma of, radiation data from, (E), 20: 22167(R) (AD-622391)
yields in radiolysis of lithium nitrate, 20: 20733 (TID-22796)
OXYGEN ISOTOPES O-16
charged-particle reactions with, amplitude singularities in knockon and stripping, (T), 20: 21997 (INSJ-96)
deuteron reactions (d,p) with, optical potentials for, (E/T), 20: 22104
deuteron reactions (d,p) with, oxygen-17 excitation energies and level transitions from, (E), 20: 22111
deuteron reactions (d,α) at 5–9 Mev, differential cross sections for, (E), 20: 22160
electron inelastic scattering by, two-nucleon correlation functions from cross sections for, (T), 20: 21996 (FTI-142/T-016)
electron inelastic scattering by, excitation of spin-isospin giant resonance by, (T), 20: 22088
neutron elastic scattering by, resonance parameters for, (T), 20: 22010(R) (NYO-72-26)
proton inelastic scattering by, 4α decay of excited nucleus from, 20: 22033
reactions (O-16,O-16y) with ytterbium 170 at 42 Mev, intrinsic quadrupole moment from, (E), 20: 22072
scattering by osmium-188, -190, and -192 at 35.6 Mev, gyromagnetic ratios of 2^+ states from, (E), 20: 22055
OXYGEN ISOTOPES O-17
excitation energies and level transitions from deuteron reactions (d,p) with oxygen-16, (E), 20: 22111
OXYGEN ISOTOPES O-18
exchange between carbon dioxide and calcite or dolomite, 20: 20691
OXYGEN SYSTEMS
F–O, solvent properties for stainless steel, 20: 20808(R) (ORNL-3916)

P

PACIFIC OCEAN
chromium-51 abundance in, 20: 20603
radioactivity due to fallout, 1965, 20: 20882(R) (HASL-171)
PACKAGE POWER REACTORS
development, 20: 22447
PACKED COLUMNS
testing for separation of uranium from cadmium using fused salts, 20: 20802(R) (ANL-7055, pp 21-98)
PAINTS
radiation hazards from radium dial, epidemiology of New Jersey cases on, 20: 20387(R) (NYO-2181-3)
testing radioresistant, by gamma exposure, 20: 20808(R) (ORNL-3916)
PALLADIUM
effects on isotopic exchange in hydrogenation of methyl β,β-dimethylacrylate, 20: 20715
sorptive properties of evaporated films of, for carbon monoxide at 0°C, 20: 21388
welding of, argon-arc and electron-beam methods of, 20: 21310
PALLADIUM ALLOYS
Al–Gd–Pd, electric properties of, 20: 22312(R) (AD-622796)
Fe–Pd, electric conductivity at low temperatures, 20: 22314(R) (AD-626865)
Gd–Pd, electric conductivity at low temperatures, 20: 22314(R) (AD-626865)
Pd–Rh, electric conductivity at low temperatures, 20: 22314(R) (AD-626865)
PALLADIUM CHLORIDES
effects on sintering of tungsten, 20: 21291 (NP-15944)
PALLADIUM ISOTOPES Pd-103
use in radiotherapy of mammary nodes or parametrium, 20: 20542
PANCREAS
weight norms for human, use in establishing standards for radiation dosimetry, 20: 20374
PARAFFIN
bremsstrahlung emission from radiophosphorus-containing, use in diagnosing mammary cancer, 20: 20540
gamma moderation by, 20: 20524 (RT-PROT-(65)32)
neutron flux moderation by, 20: 20524 (RT-PROT-(65)32)
paraffin–polyvinyl chloride, properties as gamma dosimeter, 20: 21076
PARTICLE TRACKS
amplification scheme for, 20: 21091
analysis in bubble chambers, research on pattern recognition for, 20: 21041 (PPAD-585E)
determination in spark chambers, electrophotographic device for, 20: 21037 (JINR-P-2594)
determination in spark chambers, 20: 21048
location in acoustic spark chambers, from shock wave analysis, (T), 20: 21094
registration of fission fragment, in epitaxial uranium dioxide films, 20: 21442
PARTICLES
mass field of, conformal invariance and geometrization of Hoyle-Narlikar, 20: 21862
motion in complex magnetoplasmas, nonadiabatic, (T), 20: 22162 (AD-621020)
scattering by nuclei, strong absorption model for inelastic, 20: 22086
separation from gases under reactor accident conditions, methods for, 20: 20940(R) (ORNL-3915)
size distribution in natural radioactive aerosols, 20: 20885
theory of, rudimentary geometric, 20: 21726
PEACH BOTTOM POWER REACTOR
description of basic systems of, 20: 22456
operation of, preparations for, 20: 22456
PENTANE, 3-METHYL-
radiation effects on, yield of solvent-trapped electrons in gamma, 20: 20755
2,4-PENTANEDIONE COMPLEXES
with rare earth and transition metals, preparation and crystal structure of, 20: 20700
PENTANES
carbon tetrachloride–cyclopropane–pentane, radiolysis of, at 77 to

193°K, tracer studies of mechanisms in, 20: 20752
carbon tetrachloride–pentane–propene, radiolysis of, tracer studies of mechanisms in, 20: 20752
3-PENTANONE, 2,4-DIMETHYL-
solvent properties for neptunium, 20: 20561 (JAERI-1099)
2-PENTANONE, 4-METHYL-
solvent properties for neptunium, 20: 20561 (JAERI-1099)
1-PENTYNE
radiolysis of liquid, mechanism and yields in, 20: 20717(R) (AD-621719)
2-PENTYNE
radiolysis of liquid, mechanism and yields in, 20: 20717(R) (AD-621719)
PEPTIDES
labeling with deuterium or tritium by isotopic exchange with water-d_2 or water-t_2, 20: 20714
radiation effects on polymers of, ESR studies on, 20: 20729 (PB-181506, pp 85-103)
PEROVSKITES
iron-57 Mössbauer spectra in $La_{1-x}Sr_xFeO_3$ ($0 \leq x \leq 1$), (E), 20: 22336
PERSONNEL
plutonium contamination of, treatment of, 20: 20943 (RFP-453)
radiation dose to, during diagnostic use of krypton-85, 20: 20958
radiation protection measures for BNL decontamination facility, 20: 20929 (CEX-61.6.2)
radiation protection of, in processing radioactive materials, 20: 20947
safety of, using decontaminating solution for alloys and metals, 20: 21238 (NP-15928)
training program for Peach Bottom Reactor, 20: 22456
PERTECHNETATE IONS
effects on passivation of iron, 20: 21271
PETROLEUM
production of, economics of nuclear explosion stimulation of reservoirs for, 20: 20836
PHANTOMS
radiation dose measurements in dog, γ, neutron, and x, 20: 20432 (AD-630332)
PHENOL
radiosensitivity effects on DNA, uv, 20: 20412
PHENOL, AMINO-
radiosensitivity effects on mouse tumors, 20: 20506
PHENOLS
radiosensitivity effects on mouse tumors, 20: 20506
reactions with lanthanum, 20: 20591
yields from gamma radiolysis of DL-mandelic acid in oxygenated solutions, 20: 20759
PHENYL SULFIDE
effects on radioinduced decomposition of Santowax-OM1, 20: 20708 (AEET-213)
PHENYL SULFONE
radiolysis of, sulfur dioxide yields from gamma, 20: 20760
PHONONS
interactions with fermions, Schroedinger equation solution for, (T), 20: 21619 (JINR-P-2567)
PHOSPHATASE ACTIVITY
radiation effects on glucose-6-, in rat liver, 20: 20417
PHOSPHATASES
radiation effects on activity in blood, γ and x, 20: 20415
radiation effects on activity of adenosine, in rat spleen, 20: 20503(R) (AD-629311, pp 1-14)
radiation effects on activity in rat tissues, x, 20: 20517 (NP-15925)
PHOSPHATE GLASS
waste fixation in, Brookhaven process for continuous, 20: 22509 (BNL-10109)
waste fixation in, evaluation of Purex, 20: 22510 (BNWL-SA-564)
PHOSPHATE ROCKS
radioactivity of, gamma spectrometric measurements of, 20: 20886
uranium occurrence in, 20: 20886
PHOSPHATES
separation from uranium in anion exchanger desorption, 20: 20827
PHOSPHINE
reactions with plutonium hydride at 400 to 600°C, 20: 20676
PHOSPHINE OXIDE, TRIBUTYL-
solvent properties for neptunium, 20: 20561 (JAERI-1099)
PHOSPHINE, TRIPHENYL-
complexes with uranyl compounds, preparation of, 20: 20679
PHOSPHONIC ACID, ALKYL ESTERS
radioinduced addition reactions with fluorine-containing olefins, 20: 20772
PHOSPHONIC ACID, ETHYLENEDI-
tetrabutyl ester, solvent properties for neptunium, 20: 20561 (JAERI-1099)
PHOSPHONIC ACID, METHYLENEDI-
tetrabutyl ester, solvent properties for neptunium, 20: 20561 (JAERI-1099)
PHOSPHORIC ACID
derivatives of hypo- and ortho-, radiosensitivity effects on HeLa cells and mice, x, 20: 20515
effects on corrosion of rhenium at 25 and 100°C, 20: 21275
H_3PO_4–$Sr(OH)_2$, precipitate formation in, phase transformations in, 20: 20690
PHOSPHORIC ACID, BIS(2-ETHYLHEXYL) ESTER
solvent properties for neptunium, 20: 20561 (JAERI-1099)
PHOSPHORS
light intensity from pure crystals of sodium iodide, dependence on absolute temperature, (T), 20: 22317
radioinduced luminescence of liquid diphenyloxazole, 20: 21046
scintillation response of liquid, effect of hexafluorobenzene on, 20: 21134
phosphors–tritiated silicone polymers, preparation of luminous compositions from, 20: 20787(P)
PHOSPHORUS
determination by neutron activation methods, 20: 20596
determination in germanium crystals, activation, 20: 20560 (EUR-2753.f)
determination in multielement mixtures by x-ray fluorescence methods, 20: 20644
determination in silicon dioxide, activation, 20: 20635
effects of white, on gamma radioinduced polymerization of styrene, 20: 20736
excretion and metabolism of, use in dosimetry, 20: 20398
radiation effects on plasma content of, in rats affected with experimental bladder calculus, x, 20: 20467
separation from arsenic and tungsten by ion exchange chromatography on fluoride form resin, 20: 20635
PHOSPHORUS ISOTOPES
use of paraffin-incorporated, as source in bremsstrahlung radiodiagnosis, 20: 20540
PHOSPHORUS ISOTOPES P-31
alpha scattering at 18 Mev, cross sections for, (T), 20: 22134
electron inelastic scattering at 50 Mev, differential cross sections for, (T), 20: 21964 (AD-626684)
PHOSPHORUS ISOTOPES P-32
content in Columbia River invertebrates, 1964 and 1965, 20: 20382 (BNWL-SA-623)
determination simultaneously with calcium-45 in inorganic salts by liquid scintillation counting, 20: 20584
metabolism in developing chick embryos, 20: 20399
uptake by Columbia River algae, factors affecting, 20: 20382 (BNWL-SA-623)
uptake by Columbia River plankton, 20: 20382 (BNWL-SA-623)
use for localization of brain tumors, 20: 20523(R) (NYO-1726-15)
use of chromium phosphate-incorporated, in brain tumor radiotherapy, pyrogenic and toxic effects from, 20: 20539
PHOSPHORUS SYSTEMS
CCl_4–P, radiolysis of, mechanisms in gamma, 20: 20736
cyclohexane–P, radiolysis of, mechanisms in gamma, 20: 20736
PHOTOELECTRIC CELLS
sensitivity of, effects of x agent on, 20: 21163
PHOTOGRAPHIC FILM DETECTORS
calibration of, use of cobalt-60 gamma sources for, 20: 20935 (K-1657)
readout system for dosimeter, photometer for, 20: 21070
PHOTOMETERS
design and performance of remission, for measuring radioinduced erythemas, 20: 21011
design and performance of numerical, for film dosimeter data analysis, 20: 21070
PHOTOMETRY
radioisotope light source in, 20: 20571
PHOTOMULTIPLIER TUBES
amplifiers for use with, design of, 20: 22010(R) (NYO-72-28)
amplifiers for, design of solid-state, 20: 21039 (KAPL-3122)
use with scintillation detectors for low-level counting, 20: 21042 (SGAE-E-6/1966)
PHOTONS
absorption by atoms, kinetic theory of two-body, 20: 21533
emission from gas lasers, third order perturbation theory for, 20: 21522
interactions with protons, intermediate boson production in, 20: 21611 (CERN-65-32, pp 195-200)
interactions with protons, sum rules for absorption in, (T), 20: 21625 (JINR-P-2619)
interactions with protons, N***(1688) production in, (T), 20: 21676
interactions with mesons, parity and spin of particles in polarized, (T), 20: 21715 (JINR-P-2576)
interactions with nucleons, analysis of, (T), 20: 21587 (AD-623564)
mass calculation in quantum electrodynamics, 20: 21856

production in photon-initiated showers, mean square angular and lateral spreads for, (T), 20: 21557
reactions with xenon, electron cascade curves for, (T), 20: 21514 (INR-598/VI/PH)
scattering amplitude in quantum electrodynamics for heavy, Regge pole behavior of, 20: 21871
theory for, configuration-space number operators in quantum optics, 20: 21863
transport calculations for, use of discrete–ordinates methods for, 20: 21642

1,4-PHTHALAZINEDIONES
5-amino-2,3-dihydro-, radiation effects on, γ or uv, 20: 20777

PHTHALOCYANINES
friction on copper surfaces in ultrahigh vacuum, 20: 21366

PHYSICAL CONSTANTS TESTING REACTOR
operational techniques for, error estimation for, 20: 22493(R) (BNWL-193, pp 21-9)

PHYSIOLOGY
radiation effects on reserve capacity in dogs, 20: 20435 (CONF-650560-15)

PICOLINE
radiation effects on stability of carbon-14-labeled, neutron, 20: 20783

PIGMENTS
radiation effects on patterns of human melanin, solar, 20: 20458

PINCH DEVICES
design criteria for rotating field, (T), 20: 22184 (LRP-22-66)
properties of toroidal-theta, with superimposed hexapole fields, 20: 22181 (IPP-1/45)
shock-wave production in inverse, 20: 21798

PINCH EFFECT
plasma dynamics in, MHD theory for, 20: 22180 (IAE-960)
plasma structure in theta, photographic and pressure-bar measurements for, (E), 20: 22183 (LRP-21-66)

PIPERIDINE
radiation effects on stability of carbon-14-labeled, neutron, 20: 20783

PIQUA POWER REACTOR
coolant processing system for, 20: 22520(R) (NAA-SR-11805)
design of Core-II for, 20: 22520(R) (NAA-SR-11805)

PITCHBLENDES
formation of, paragenesis with selenides in, 20: 20918

PLACENTA
localization of, using iodine-131 and dual probe scintillation counting, 20: 20527
radiography of, using human serum albumin labeled with iodine-131 or iodine-132, radiation doses to fetuses in, 20: 20537

PLANETS
chemical evolution and organic synthesis in primitive environment of, (T), 20: 20406 (N-65-27062)
radio emission from Jupiter, effects of ionosphere on characteristics of, 20: 21510

PLANKTON
ecology of, in Bay of Venice, 20: 20386(R) (NP-15916)
isotope uptake by Bay of Venice, cobalt and zinc-65, 20: 20386(R) (NP-15916)
radioisotope uptake by Columbia River, phosphorus-32 and zinc-65, 20: 20382 (BNWL-SA-623)

PLANT CELLS
radiation effects on electric potential of *Nitella flexilis*, γ, 20: 20419

PLANT METABOLISM
tracer studies of, 20: 20389 (STI-PUB-108)

PLANTS
cesium-137 content in forest, in Washington state, 20: 20879 (BNWL-SA-530)
effects of nuclear weapons on, environmental, 20: 20930 (HI-518-RR (Vol.1))
effects of nuclear weapons on, environmental, 20: 20931 (HI-518-RR (Vol.2))
effects of nuclear weapons on, environmental, 20: 20932 (HI-518-RR (Vol.3))
fallout uptake by, cesium-137 and strontium-90, 20: 20926(R) (ARCRL-14)
radioactivity due to fallout in Doe Run, Meade County, Ky., 1959 to 1965, 20: 20884(R) (TID-22815)
separation from charcoal, for radiocarbon dating, 20: 20798
strontium-90 uptake by clover, effects of applications of stable strontium to soils on, 20: 20381

PLASMA
acceleration of homogeneous, in static and h-f electric fields, (T), 20: 22289
boundary of, bibliography on, 20: 22177 (CLM-Bib-6)
charge motion in cold, Cherenkov radiation from point, (T), 20: 22290
charge separation in completely ionized isothermal, in thermodynamic equilibrium, (T), 20: 22283
charged particle beam propagation in cold, wave excitation from, (T), 20: 22286
charged-particle flux in discharge hydrogen, effect of h-f traveling electromagnetic waves on radial, (T), 20: 22301
charged-particle motion in, electrostatic damping of, (T), 20: 22233
Cherenkov radiation from dipole moving in, narrow- and plane-cavity effects on, (T), 20: 22278
compression and ohmic heating of, design of toroidal machine for, 20: 22299
containment of cylinder of, in uniform magnetic field by rotating electromagnetic field, (T), 20: 22288
current density and electromagnetic wave generation at sum and difference frequencies in, nonlinear, (T), 20: 22244
cyclotron harmonic waves in, transmission of, (E), 20: 22226
density fluctuations in homogeneous, bounds on, (T), 20: 22255
density in geomagnetic tail, 20: 21828
density measurements in, high-frequency dielectric resonance probe for, 20: 22219
density measurement in pressure-driven shock waves, (E/T), 20: 22168 (AD-622569)
diagnostics of collisionless, shock tube development for, 20: 22170 (AD-622701)
diagnostics of perturbed, using electric probes, (E), 20: 22260
diagnostics of turbulent, Langmuir probe for, (E/T), 20: 22193
diagnostics of, by bremsstrahlung emission intensity from electron reactions with solid target, (E), 20: 22293
diagnostics of, multiple-reflection effects in microwave-interferometer, 20: 22231
diagnostics of, performance of electrostatic double probe for, (T), 20: 22192
diagnostics using laser beams, review on, 20: 22295
dielectric tensor in Vlasov, near cyclotron harmonics, (T), 20: 22240
diffusion across magnetic fields, (T), 20: 22189(R) (TID-22809)
electric conductivity of atmospheric argon, determination of, (E), 20: 22164 (AD-621213)
electric conductivity of h-f discharge argon, calorimetric- and optical-methods for measuring, (E), 20: 22280
electric conductivity, ionization, and recombination in potassium-seeded argon, (E), 20: 22258
electric permittivity of anisotropic magnetoactive, (T), 20: 22203
electromagnetic field properties in magneto-active, (T), 20: 22199
electromagnetic phenomena in, research on, 20: 22172(R) (AD-623718)
electromagnetic radiation from acoustic point-source antenna in compressible bubble of, (T), 20: 22196
electromagnetic wave self-focusing in boundless, in strong magnetic field, (T), 20: 22200
electromagnetic wave propagation in stratified waveguide, 20: 22204
electromagnetic wave propagation in inhomogeneous isotropic hot, (T), 20: 22165 (AD-621457)
electromagnetic wave propagation in magneto-, models for, (T), 20: 22174 (AD-623789)
electromagnetic wave propagation in, collisional effects near electron cyclotron frequency on, (E/T), 20: 22228
electromagnetic wave scattering by electro-acoustic waves in arc column of mercury, (E), 20: 22232
electromagnetic wave propagation along magnetic field in helium, circularly polarized plane, (E), 20: 22236
electromagnetic wave propagation along magnetic field in helium, linearly polarized, (E), 20: 22237
electromagnetic wave interactions with, effects of velocity-dependent collision frequency on, (T), 20: 22256
electromagnetic wave propagation across magnetic field in, reflection at upper hybrid frequency of, (T), 20: 22261
electromagnetic wave propagation in layer of, kinetic theory for, 20: 22270
electromagnetic wave reflection from plane boundary of semi-infinite, frequency doubling in, (T), 20: 22271
electromagnetic-wave absorption, reflection and transmission through layers of, 20: 22297
electron and excitation temperatures in argon, (E), 20: 22267
electron beam interactions in, nonlinear effects from, (E), 20: 22206
electron cyclotron resonance in, equipment for generating, 20: 22190(R) (TID-22821)
electron-cyclotron waves in, skin effect and resonance excitation of, (T), 20: 22217
electron-cyclotron waves in, skin effect and resonance excitation of, (E), 20: 22218
electron density and temperature measurement in, direct display system using nonfloating triple probe for, 20: 22214
electron density determination using radial transmission line, 20: 22171 (AD-622811)
electron distribution in cesium thermionic cell, electrostatic probe measurements of, 20: 21560(R) (AD-621276)

electron motion in cold, dense, magnetized, complex Doppler effect on radiation from, (T), 20: 22198
electron probe current in magnetized, electron temperature from, 20: 22259
electron scattering by, high-density corrections to cross sections for, (T), 20: 22268
electron temperature in r-f generated, double probe method for measuring, (E), 20: 22194
electron temperature in helium, spectroscopic measurement of, 20: 22210
electron temperature in afterglow, spatial variations of, (E/T), 20: 22242
electron velocity distributions in positive column of helium and neon discharge, radial dependence of, (E), 20: 22294
electron-beam interactions in, nonlinear diffusion with recombination in, (T), 20: 22266
electrophoretic properties of thermally ionized cesium, (T), 20: 22173 (AD-623788)
flow in geomagnetic tail, 20: 21828
flow in MHD cells, effects of Hall effect, ion slip, and viscosity on, (T), 20: 21574
flow in MPD generators, properties of, (E/T), 20: 21561(R) (AD-623096)
flow past bodies in magnetic field, shock structure in, (E), 20: 22251
heating by laser-generated implosions, 20: 22245
injection into axial magnetic fields, mechanism of, (E/T), 20: 22224
injection into cusped magnetic fields at high velocity, (E), 20: 22254
interactions with microwaves in mirror-type magnetic fields, (E), 20: 22216
ion beam extraction from, 20: 21213 (IAE-974)
ion diffusion in fully ionized cesium, potassium, (E), 20: 22243
ion heating in hydrogen theta-pinch, (E), 20: 22185 (LRP-23-66)
ion Larmor radius in beta, finite, (T), 20: 22262
ion mobility and recombination in, 20: 22169(R) (AD-622684)
ion temperature of streaming, Langmuir double probe device for measuring, 20: 22213
ion velocity distribution in nonequilibrium, convergent kinetic equation for relaxation of, 20: 22205
ion velocity distribution in magnetic mirrors, (T), 20: 22274
ionization equilibrium in shock-generated helium, 20: 22250
ionization mechanism in, thermal, (T), 20: 22257
kinetic equations for unstable, quantum, 20: 22238
kinetics of cesium, in hot-cathode diode, (T), 20: 22279
kinetics of completely ionized, behind ionization front, (T), 20: 22285
kinetics of, autocorrelation functions in, (T), 20: 22246
magnetic fields in collision-dominated, determination of Hall effect in, (T), 20: 22176 (AD-624165)
microwave absorption by magnetically confined, (T), 20: 22209
microwave transmission by turbulent, coefficient for, (T), 20: 22230
oscillations in homogeneous, bounds on electrostatic, (T), 20: 22255
oscillations in nonrelativistic, (T), 20: 22189(R) (TID-22809)
oscillations in, velocity distribution function for longitudinal, (T), 20: 22166 (AD-621913)
oscillations of nonuniform, kinetic equation for longitudinal, 20: 22284
particle motion in complex magneto-, nonadiabatic, (T), 20: 22162 (AD-621020)
pinch effect in high-temperature dense, MHD theory for, 20: 22180 (IAE-960)
pinch effects in beam-generated, electrostatic and magnetic, 20: 22221
polarization in toroidal magnetic field, triple-helical magnetic field effects on, (E), 20: 22275
polarization of moving, in toroidal magnetic field, (E), 20: 22276
polarization of moving, in opposite-curved toroidal magnetic fields, (E), 20: 22277
production by electric discharges in heavy-current-vacuum circuit breaker, (E), 20: 22291
production in metal chamber by high-frequency generator, (E), 20: 22300
production of hot, molecular hydrogen ion injection in HX apparatus for, (E), 20: 22207
production of hydrogen, performance of coaxial gun for, 20: 22225
production of negative-glow helium, design and performance of inverse brush cathode for, 20: 22222
properties in ionosphere and magnetosphere, low frequency, 20: 21812 (AD-622223)
radiation emission at harmonics of electron gyrofrequency from, 20: 22239
radiations from partially ionized, anomalous bremsstrahlung and cyclotron, 20: 22208
recombination process in nonequilibrium, electron–ion, 20: 22195
research on, review of, 20: 22302
shock propagation in, microwave interferometry of, (E), 20: 22182 (IPP-3/35)
shock propagation in argon, radiation intensity from, (E/T), 20: 22281
shock temperature profile in, radiation smoothing of, 20: 21775 (AD-620835)
spectra of arc-heated oxygen and nitrogen, radiation data from, (E), 20: 22167(R) (AD-622391)
spectra of helium, produced by conical theta-pinch discharge, 20: 22269
stability criteria for collisionless guiding-center, (T), 20: 22235
stability in finite mirror-confined, electrostatic, (T), 20: 22253
stability in helium, excitation of m = 2 mode by helical, 20: 22247
stability in inhomogeneous media, convective, (T), 20: 22201
stability in low-density, flute, (T), 20: 22252
stability in low-pressure Penning discharge, diffusion coefficient for flute, (E), 20: 22249
stability in toroidal systems, interchange, (T), 20: 22187 (MATT-424)
stability of confined guiding-center, velocity gradient, (T), 20: 22234
stability of homogeneous two-stream, electron cyclotron, (E/T), 20: 22197
stability of hot electron, effect of cold background on, (T), 20: 22264
stability of hot-electron, in mirror and minimum-B confinement, 20: 22265
stability of hydrogen, in inverse homopolar device, (T), 20: 22272
stability of magneto-, in gravitational fields, (T), 20: 22186 (MATT-358)
stability of nonuniform conducting, effect of convective charged-particle drift on, (T), 20: 22296
stability of toroidal, self-induced magnetic field effects on, (E), 20: 22175 (AD-624081)
stability of, relation between Kelvin-Helmholtz and resistive drift, 20: 22263
stabilization of P.I.G. discharge, (E), 20: 22215
stabilization using alternating magnetic fields, (E), 20: 22212
statistical mechanics of high-temperature quantum, beyond ring approximation, 20: 22223
structure of hydrogen theta-pinch, (E), 20: 22183 (LRP-21-66)
thermal conductivity of atmospheric argon, determination of, (E), 20: 22164 (AD-621213)
thermal radiation resonances of cylindrical, in magnetic fields, 20: 22202
transport properties of cesium, computation of, 20: 22227
use as coupling media for traveling-wave tube, properties of, 20: 20985 (N-65-29669)
velocity profiles of arc, measurement using particle injection, (E/T), 20: 22188 (N-65-22776)
wave attenuation in, relation to Q-value, (T), 20: 22211
wave dispersion in cyclotron-harmonics resonance regions in, (T), 20: 22241
wave modes in, Penrose condition for exponential growth of, 20: 22248
wave propagation along warm cylindrical, dispersion relations for, 20: 22220
wave propagation in compressible gaps of, properties of, 20: 22163 (AD-621034)
wave propagation transverse to external magnetic field in dense inhomogeneous, stability of drift, (T), 20: 22282

PLASMA JETS

design for space propulsion, 20: 20874(P)
interactions of countercurrent, in magnetic mirrors, (E), 20: 22273
performance of coaxial, in longitudinal magnetic fields, (E), 20: 22179 (FTI-080/P-032)
performance of coaxial hydrogen, 20: 22225
performance of two-stage coaxial, 20: 20872
performance of, effects of nonequilibrium conductivity on, 20: 20873

PLASTIC-FILM DETECTORS

design for gamma threshold dosimetry, 20: 21076
particle tracks in, amplification scheme for, 20: 21091

PLASTIC FILMS

preparation of thin polycarbonate, for G-M tube windows, 20: 21065

PLASTICS

radiation effects on dielectric properties of, 20: 21171
use for detecting charged particles, 20: 21060
plastic–plywood, commercial production and use of irradiated combinations of, 20: 21191 (ORNL-IIC-7, pp 112-18)
plastic–wood, AEC program on materials of, 20: 21178 (ORNL-IIC-7, pp 1-5)
plastic–wood, commercial development and uses of, 20: 21182 (ORNL-IIC-7, pp 49-58)
plastic–wood, commercial possibilities of irradiated, in Pacific Northwest, 20: 21185 (ORNL-IIC-7, pp 76-80)
plastic–wood, commercial potential of irradiated combinations of, 20: 21186 (ORNL-IIC-7, pp 81-8)
plastic–wood, commercial production of irradiated combinations of, 20: 21187 (ORNL-IIC-7, pp 89-94)
plastic–wood, commercial use of irradiated combinations of, 20: 21189 (ORNL-IIC-7, pp 99-105)
plastic–wood, conceptual design and feasibility study of combinations of, 20: 21181 (ORNL-IIC-7, pp 32-48)
plastic–wood, development, properties, and commercial future of, 20: 21183 (ORNL-IIC-7, pp 59-63)
plastic–wood, development-production program for Lockwood, 20: 21188 (ORNL-IIC-7, pp 95-8)

plastic–wood, mechanical and physical properties of irradiated combinations of, 20: 21348 (ORNL-IIC-7, pp 22-5)
plastic–wood, radiation processing of, 20: 21177 (ORNL-IIC-7)
plastic–wood, radiation processing and testing of, method for, 20: 21179 (ORNL-IIC-7, pp 6-14)
plastic–wood, radiation processing of, commercialization aspects of, 20: 21184 (ORNL-IIC-7, pp 64-75)
plastic–wood, radiation processing of, program for evaluation of, for commercial use, 20: 21349 (ORNL-IIC-7, pp 26-31)
plastic–wood, radioinduced polymerization reactions in, 20: 21180 (ORNL-IIC-7, pp 15-21)
plastic–wood, use of irradiated combinations of, in sporting-goods industry, 20: 21190 (ORNL-IIC-7, pp 106-11)

PLATINUM
effects on isotopic exchange in hydrogenation of methyl β,β-dimethylacrylate, 20: 20715
electron reactions at 6 to 23 kev, optical transition radiation from, 20: 21518
radiation effects on, electron, 20: 22520(R) (NAA-SR-11805)
sorptive properties of evaporated films of, for krypton and xenon, 20: 21387
sorptive properties of evaporated films of, for carbon monoxide at 0°C, 20: 21388
sorptive properties for ortho- and para-deuterium, energy exchange in, 20: 20661

PLATINUM ALLOYS
Dy–Pt, dysprosium hyperfine magnetic field in intermetallic compounds of, (E), 20: 22330

PLATINUM COMPLEXES
trans-hydridochlorobis(triethylphosphine)-, deuterium exchange between, and heavy water, 20: 20701

PLATINUM ISOTOPES Pt-194
magnetic field from iridium-194 decay in iridium–iron alloy, temperature dependence of internal, (E), 20: 22326

PLATINUM ISOTOPES Pt-197
beta decay of, conversion ratios of 191-kev transitions in, (E), 20: 22057

PLUTONIUM
contamination of personnel by, treatment of, 20: 20943 (RFP-453)
corrosion by air at 30 to 100°C, effects of humidity and metallurgical history on, 20: 21280
deposition on stainless steel, parameters for quantitative electrolytic, 20: 21287 (AE-217)
determination and control of, at Eurochemic's mol fuel reprocessing facility, 20: 20831
determination during solution processing and waste recovery, methods for, 20: 20976
determination in fuel reprocessing plant for accountancy purposes at Windscale, 20: 20830
determination in nuclear materials by isotopic analysis, 20: 20978
determination in nitrate solutions by x-ray absorption edge method, 20: 20573
determination in urine, method for, 20: 20590
determination in Windscale separation plants, methods for, 20: 20972
economics of, as fuel for large fast breeder reactors, 20: 22454
excretion and metabolism of, use in dosimetry, 20: 20398
ignition in air at 310 to 505°C, 20: 21264 (RFP-491)
oxidation at 25 to 450°C, rate of, 20: 21264 (RFP-491)
phase transformations in, effects of plastic deformation on rates of, 20: 21326 (BNWL-203)
production and processing of, UKAEA accounting and control in, 20: 22528
production by electrolysis of plutonia in molten fluoride salts, 20: 21234 (DP-1021)
production in France, 20: 21243
production of, heavy concrete for hot cells for, 20: 20819
refining of, ceramic cells for electrolytic, 20: 21239 (RL-SEP-824)
separation from alumina used in fuel-processing fluidized beds, by leaching, 20: 20803(R) (ANL-7055, pp 99-162)
separation from fuel alloys by extraction using liquid copper–magnesium alloys, 20: 20802(R) (ANL-7055, pp 21-98)
separation from uranium alloys by chloride extraction, 20: 20802(R) (ANL-7055, pp 21-98)
solubility in copper–magnesium alloys, 20: 20802(R) (ANL-7055, pp 21-98)
solubility in fused salts, 20: 20802(R) (ANL-7055, pp 21-98)
transformations in, heats of, 20: 20553(R) (MLM-1142)
use as fuel in heavy water power reactors, recycling for, 20: 22419
use for reactor fuel, 20: 22441
viscosity of liquid, based on atomic parameters, 20: 20656 (UCRL-11930)
winning of, ceramic cells for electrolytic, 20: 21239 (RL-SEP-824)
x-ray sorption by particles of, 20: 20951

PLUTONIUM ALLOYS
Al–Pu, etching of delta-phase, bright-field grain structure, 20: 21233 (BNWL-188)
Am–Pu, phase diagram, 20: 21339 (LA-DC-7095)
Ce–Cu–Pu, phase diagrams, 20: 20553(R) (MLM-1142)
Ce–Fe–Pu, phase studies, 20: 21342(R) (MLM-1301)
Ce–Ni–Pu, phase studies, 20: 21342(R) (MLM-1301)
Ga–Pu, etching of delta-phase, bright-field grain structure, 20: 21233 (BNWL-188)
Mg–Pu–U–Zn, corrosive effects on type 405 stainless steel, 20: 20802(R) (ANL-7055, pp 21-98)
Pu–Th, feasibility for use in fast breeder reactors, 20: 21229 (AEET-229)
Pu–U, processing by cadmium alloy–molten salts, flowsheets for, 20: 20802(R) (ANL-7055, pp 21-98)
Pu–Zr, etching of delta-phase, bright-field grain structure, 20: 21233 (BNWL-188)

PLUTONIUM CARBIDES
PuC–UC, preparation methods, 20: 20802(R) (ANL-7055, pp 21-98)

PLUTONIUM(VI) FLUORIDES
separation from exhaust air by hydrolysis, 20: 20803(R) (ANL-7055, pp 99-162)
PuF_6–UF_6, liquid-solid equilibria in, equipment for, 20: 20803(R) (ANL-7055, pp 99-162)

PLUTONIUM HYDRIDES
reactions with hydrogen sulfide or phosphine at 400 to 600°C, 20: 20676

PLUTONIUM ISOTOPES
content in operating fuel elements, methods for calculating, 20: 20979

PLUTONIUM ISOTOPES Pu-238
production by neutron irradiation of neptunium-237, 20: 20561 (JAERI-1099)
separation from uranium-234 by ion exchange and solvent extraction, 20: 20553(R) (MLM-1142)

PLUTONIUM ISOTOPES Pu-239
content in contaminated wounds, errors in measurement of, 20: 20951
neutron fission cross sections for, 20: 22383(T) (AEC-tr-6693)
neutron resonance fission at 15 to 82 ev, cadmium-115 yields from symmetric, (E), 20: 22135
neutron resonance absorption by, cross sections for Doppler-broadened, (T), 20: 21951
Pu-239–Th-232, resonance interference effects on neutron cross sections of, (T), 20: 21970 (ANL-7144)

PLUTONIUM ISOTOPES Pu-240
alpha reactions $(\alpha,\alpha' f)$ with, fragment angular correlations from, (E), 20: 22143
neutron fission cross sections for, 20: 22383(T) (AEC-tr-6693)
neutron resonances of, self-shielding of, (T), 20: 21957

PLUTONIUM OXIDES
properties and structure of, effects of, on oxidation rate of plutonium metal, 20: 21264 (RFP-491)
shipping of, materials management in, 20: 20976

PLUTONIUM(III) OXIDES
microstructure of arc-melted pellets of, 20: 21342(R) (MLM-1301)

PLUTONIUM(IV) OXIDES
PuO_2–U_3O_8, fluorination in fluid beds, effects of fission products on, 20: 20803(R) (ANL-7055, pp 99-162)
PuO_2–UO_2, microsphere preparation by plasma-torch heating, 20: 20553(R) (MLM-1142)
PuO_2–UO_2, processing irradiated, by fluoride volatility, 20: 20803(R) (ANL-7055, pp 99-162)

PLUTONIUM PHOSPHIDES
preparation and properties of, 20: 20676

PLUTONIUM SULFIDES
preparation and properties of, 20: 20676

PLYWOOD
plastic–plywood, commercial production and use of irradiated combinations of, 20: 21191 (ORNL-IIC-7, pp 112-18)

POCKET CHAMBERS
electric insulators for, use of polymeric, 20: 21158

POLAND
radiation chemistry developments in, 20: 20780

POLLEN
radioinduced chromosome aberrations in grains of Tradescantia, 20: 20438 (EUR-3528.f)

POLONIUM
excretion and metabolism of, use in dosimetry, 20: 20398
separation from neutron-irradiated bismuth by deposition on silver plate, 20: 20585
x-ray-diffraction patterns of metallic isotopic mixtures of, 20: 20807(R) (MLM-1287)

POLONIUM ISOTOPES Po-208
preparation for chemical and physical property testing, 20: 20553(R) (MLM-1142)

POLONIUM ISOTOPES Po-209
preparation for chemical and physical property testing, 20: 20553(R)

(MLM-1142)
POLONIUM ISOTOPES Po-210
determination in environmental samples by deposition on nickel and counting, 20: 20643
production by neutron reactions with bismuth, 20: 20585
properties as electrode in oxidation-reduction processes, 20: 20791
POLYMERIZATION
radioinduced in plastic–wood combinations, 20: 21180 (ORNL-IIC-7, pp 15-21)
radioinduced, research in Japan on, 20: 20727 (PB-181506, pp 9-18)
POLYMERS
preparation and radioinduced reactions of aryl-substituted vinyl, summary on, 20: 21430(R) (WADC-TR-55-58(Pt.8))
production of gels of, radioinduced, 20: 20761
properties and radiation effects on vinyl, 20: 21431(R) (WADC-TR-55-58(Pt.9))
properties as electric insulators in pocket dosimeter, 20: 21158
radiation effects on electric conductivity of, 20: 21158
radiation effects on electric conduction of co-, containing polyethylene, γ, 20: 21170
radiation effects on, research in Japan on, 20: 20727 (PB-181506, pp 9-18)
radiation effects on organic, of electrons at 300 to 500 kv, 20: 20762
radiation effects on crosslinked and scissionable, 20: 21430(R) (WADC-TR-55-58(Pt.8))
radiation effects on, gamma, 20: 21430(R) (WADC-TR-55-58(Pt.8))
synthesis of condensation, for radiation stability testing, 20: 21430(R) (WADC-TR-55-58(Pt.8))
POLYPHENYL SYSTEMS
properties of irradiated coolants of, correlation of friction factor and heat transfer, 20: 20710 (MIT-324-23)
pyrolysis of, gas and polymer formation in, 20: 20708 (AEET-213)
POLYPHENYLS
properties and stabilities of organic coolants of, 20: 20708 (AEET-213)
radioinduced decomposition of Santowax-OM1, additive effects on, 20: 20708 (AEET-213)
solvent properties of Santowax-OM1 for hydrogen, methane, and nitrogen, 20: 20708 (AEET-213)
POLYSACCHARIDES
radiosensitivity of muco-, in mice and rabbits, 20: 20510
POODLE PROPULSION SYSTEMS
testing of, aerodynamics in drop, 20: 21210 (SC-RR-65-609)
POPULATIONS
effects of nuclear weapons on, environmental, 20: 20930 (HI-518-RR (Vol.1))
effects of nuclear weapons on, environmental, 20: 20932 (HI-518-RR (Vol.3))
radiation doses from testing of rocket reactors, 20: 20954
radiation doses to, from radioluminescent watches, 20: 20518 (RT-PROT-(65)41)
radiation effects on human, epidemiological studies of, 20: 20442 (ORNL-P-2053)
PORPHINE, $\alpha, \beta, \gamma, \delta$-TETRAPHENYL-
complexes with cobalt or copper, radiolysis of, gamma, 20: 20774
radiolysis of, kinetics of gamma, 20: 20774
POSITRONS
annihilation in yttrium, photon angular distributions from, (T), 20: 22338
POTASSIUM
density and thermodynamic properties of, 20: 20802(R) (ANL-7055, pp 21-98)
determination in sedimentary carboniferous deposits by scintillation counting, 20: 20613
determination in silicon dioxide, activation, 20: 20633
electric and thermal conductivity of, at 336.4 to 2450°K, 20: 21376
electron mobility in vapors of, at low energies, (E), 20: 21520
handling and purification of, for use in corrosion test loop, 20: 21293 (R-66SD3007)
neutron elastic scattering at 14.0 Mev, cross sections for, (E), 20: 22119
radiation effects on content in animal cell nuclei, x, 20: 20422
surface tension of, at high temperatures, 20: 20651(R) (CU-2660-26)
thermal capacity of liquid, corresponding states correlation of configurational, 20: 20657 (UCRL-11931)
thermal conductivity of vaporous, at 750°C, 20: 20651(R) (CU-2660-26)
viscosity of liquid, based on atomic parameters, 20: 20656 (UCRL-11930)
POTASSIUM ALLOYS
Hg–K, thermodynamic properties, 20: 21328 (CU-2660-25)
Hg–K, thermodynamic properties at high temperatures, 20: 20651(R) (CU-2660-26)
K–Na, thermodynamic properties, 20: 20802(R) (ANL-7055, pp 21-98)
POTASSIUM BROMIDES
fluorescence and absorption spectra of praseodymium in single crystals of, 20: 20663
radiation effects on absorption spectra of, x, 20: 21424 (N-65-23332)
POTASSIUM CARBONATES
$Ce(NO_3)_3$–K_2CO_3–H_2O, composition of, effects of reactant concentration on, 20: 20664
$La(NO_3)_3$–K_2CO_3–H_2O, composition of, effects of reactant concentration on, 20: 20664
POTASSIUM CHLORIDES
color centers in hydrogen-activated crystals of, U2, 20: 22311(R) (AD-622068)
color centers in, T bands from aggregate F, (E), 20: 22322
effects on efficiency of actinide and lanthanide separations by ion exchange chromatography, 20: 20822
fluorescence and absorption spectra of praseodymium in single crystals of, 20: 20663
radiation effects on absorption spectra of, x, 20: 21424 (N-65-23332)
radioinduced formation of T bands in, gamma, (E), 20: 22322
radioinduced hardening of silver-doped, low-temperature x, (E), 20: 22321
KCl–UCl_3, corrosive effects on Inconel 600, INOR-8, and Hymu-80 nickel-base alloys at 900°C, 20: 21261 (LA-3476)
$MgCl_2$–KCl–NaCl, corrosive effects with cadmium alloys, on stainless steel, 20: 20802(R) (ANL-7055, pp 21-98)
$MgCl_2$–KCl–NaCl, solvent properties of liquid, for praseodymium, 20: 20802(R) (ANL-7055, pp 21-98)
POTASSIUM CYANIDES
radiosensitivity effects on mouse brain, 20: 20521
POTASSIUM CYANOCOBALTATES(III)
labeling with cobalt-58 and cobalt-60 for hydrological studies, 20: 20794
POTASSIUM HALIDES
analysis for bromine, chlorine, and sodium, activation, 20: 20560 (EUR-2753.f)
POTASSIUM HYDROXIDES
effects on corrosion of rhenium at 25 and 100°C, 20: 21275
POTASSIUM IONS
diffusion in fully ionized cesium plasma, (E), 20: 22243
uptake by barley roots, uranyl effects on selective inhibition in, 20: 20402
POTASSIUM ISOTOPES K-40
content in Italian milk, 20: 20950
content in silt in Escaut River, Belgium, control of, 20: 22515(T) (ORNL-tr-965)
POTASSIUM MANGANESE FLUORIDES
nuclear magnetic resonance in, 20: 22311(R) (AD-622068)
POTASSIUM NITRATES
solvent properties for argon and helium, 20: 22520(R) (NAA-SR-11805)
POWER BREEDER REACTORS
coolants for, comparison of carbon dioxide, helium, and steam as, 20: 22452
design of plutonium-fueled prototype fast, 20: 22441
design of sodium-cooled, vented fuel concept applied to, 20: 22462
design of 1000-Mw(e) sodium-cooled fast, 20: 22453
design of 1000-Mw(e) sodium-cooled fast, 20: 22454
POWER PLANTS
performance of nuclear space, using electrochemical reaction of liquid mercury and potassium, 20: 22485
POWER REACTORS
control concepts for, characteristics of, 20: 22440
control using chemical shim, 20: 22428
cost analysis of 1000-Mw(e) sodium-cooled fast, 20: 22451
criticality of glass-clad uranium-fueled, biphenyl and water moderated, 20: 22415 (RPI-321-4)
design of gas-cooled heavy water-moderated, 20: 22432
design of heavy water-moderated boiling light water-cooled, 20: 22431
design of heavy-water moderated, boiling light-water cooled, 20: 22430
design of heavy-water moderated, organic-cooled, 20: 22433
design of magnox, 20: 22426
design of 500-Mw magnox, 20: 22424
design of 500-Mw magnox, 20: 22429
development in Switzerland, 20: 22421
economics and technical feasibility of dual-purpose, for Israel, 20: 22459 (66-1-RE)
economics of, in sea water desalination plants, 20: 22461
fuel for, review of properties of uranium dioxide, 20: 22422
fuel recycling in heavy water, plutonium, 20: 22419
licensing of, public safety aspects of, 20: 22434
materials management for, scope of, 20: 20968
neutron spectral density in, statistical theory for, 20: 22418
safety analysis of 1000-Mw(e) sodium-cooled fast, 20: 22451
safety of, engineering aspects of, 20: 22437
safety systems for, design and evaluation of, 20: 22358
shutdown system using a-c amplifier with ionization chamber, 20: 22359
stability of, effects of delayed neutrons on, (T), 20: 22443
startup using pulsed neutron sources, equipment for, 20: 22414(R) (GEAP-4961)
thermal efficiency and condenser output of steam-cooled, 20: 22420

uses of, in developing countries, 20: 22525
POWER SUPPLIES
conference, 20: 21581
conference, 20: 21582
design for ZGS magnets, analog computer representation in, 20: 21488
PRASEODYMIUM
determination in rare earth mixtures, activation, 20: 20562 (LYCEN-6538)
effects on neodymium spectrophotometric determinations, 20: 20568
fluorescence and absorption spectra of, in sodium and potassium chloride and potassium bromide single crystals, 20: 20663
friction and wear properties of, in vacuum, effects of crystal structure on, 20: 21365
oxidation in dry and moist air at 100 to 800°C, rate of, 20: 21265 (RPI-2714-8)
separation from fuel alloys by extraction using fused salts, 20: 20802(R) (ANL-7055, pp 21-98)
separation from other rare earths by paper precipitation chromatography using 8 quinolinol, 20: 20814
separation from other rare earths by extraction using aluminum–magnesium alloys, 20: 20802(R) (ANL-7055, pp 21-98)
separation from perchloric acid solutions by ion exchange materials, 20: 20823
separation from uranium by combined ion exchange-solvent extraction using nitric acid–tetrahydrofuran solutions, 20: 20811
solubility in copper–magnesium alloys, 20: 20802(R) (ANL-7055, pp 21-98)
solubility in fused salts, 20: 20802(R) (ANL-7055, pp 21-98)
viscosity at 936 to 1009°C, 20: 20553(R) (MLM-1142)
PRASEODYMIUM ACETATES
preparation by oxide solubility in alcohols containing ammonia, 20: 20686
PRASEODYMIUM ALLOYS
Al–Pr, crystal structure and stability of intermetallic compounds in, 20: 21415
Dy–Pr, electric conductivity at 4.2, 77, and 296°K, 20: 22312(R) (AD-622796)
Fe–Pr, crystal structure of $PrFe_7$, 20: 21400
La–Pr, electric conductivity, magnetic susceptibility, and superconductivity at low temperatures, 20: 21873 (NP-15936)
Pr–Y, magnetic properties and phase transformations in, 20: 21414
PRASEODYMIUM FLUORIDES
dielectric properties of thin films of, 20: 22324
PRASEODYMIUM IONS
spectra in lanthanum chlorides, absorption and fluorescence, 20: 20667
PRASEODYMIUM ISOTOPES Pr-138
beta decay of, half life for, (E), 20: 22002 (JINR-P-2570)
PRASEODYMIUM ISOTOPES Pr-141
neutron capture cross sections at 0.2 to 2.5 Mev, (E), 20: 21969(R) (ANL-7055, pp 230-3)
PRASEODYMIUM ISOTOPES Pr-143
nuclear properties of, unified model for, 20: 22139
PRASEODYMIUM ISOTOPES Pr-144
separation from radioisotopes in aqueous solutions by foam chromatography using colloidal manganese dioxide, 20: 20628
PRASEODYMIUM OXIDES
solubility in ethyl, isopropyl, methyl, and propyl alcohols in presence of ammonia, 20: 20686
PRECIPITATION, ATMOSPHERIC
analysis of dry residues of, cesium-137 behavior during, 20: 20625
collection of dust-free, automatic device for, 20: 20993
radioactivity due to fallout in Canadian, 1964, 20: 20938 (NP-15914)
radioactivity due to fallout in Canadian, 1965, 20: 20883 (NP-15914)
radioactivity in, of watershed of Boulder City, Colo., 20: 20379 (COO-1191-10)
PRESSURE GAGES
design and operation of maltidirectional peak, for shock waves, 20: 20914
PRESSURE VESSELS
brittle fracture properties of, method for estimating, 20: 21228 (AE-221)
design of concrete, for 500-Mw magnox reactor, 20: 22424
design of prestressed concrete, 20: 22429
properties of prestressed concrete, 20: 22353 (CEA-R-2829)
steel for, development of low-alloy, 20: 21417(P)
welded joints in steel, effect of time at high temperatures on embrittlement of, 20: 21393
PRESSURIZED WATER REACTORS
coolant preheating in, economic and engineering aspects of, (T), 20: 22448
PROCESS HEAT REACTORS
economics and technical feasibility of dual-purpose, for Israel, 20: 22459 (66-1-RE)
uses of, in developing countries, 20: 22525
PRODUCTION REACTORS
radioisotope production in, 20: 21212 (CONF-660305-19)
PROLINE
yields in radioinduced carboxylation of methylamine, 20: 20732 (SGAE-CH-21/1965)
PROMETHIUM
production of, review of methods for, 20: 20796
separation from nitrate solutions by solvent extraction using tricaprylmethylammonium nitrate, 20: 20812
separation from rare earths by reversed-phase partition chromatography on polytetrafluoroethylene, 20: 20621
separation from uranium by combined ion exchange-solvent extraction using nitric acid–tetrahydrofuran solutions, 20: 20811
PROPANE
production by gas discharge and radioinduced cracking of butane, 20: 20740
use in heavy liquid bubble chamber at CERN, 20: 21606 (CERN-65-32, pp 157-60)
PROPANE, 2-METHYL-
decomposition of, by gas discharge and radiation, comparison of, 20: 20740
1,3-PROPANEDIONE, 1,3-DIPHENYLTHIO-
complexes with metals, stability of, 20: 20693
1-PROPANOL
solvent properties for rare earth oxides in the presence of ammonia, 20: 20686
2-PROPANOL
determination by xenon trioxide oxidation, titrimetric, 20: 20579
radiolysis of, reactivity of electrons produced in gamma, 20: 20750
solvent properties for rare earth oxides in the presence of ammonia, 20: 20686
yields from gamma radiolysis of ethanol, 20: 20746
PROPENE
production by gas discharge and radioinduced cracking of butane, 20: 20740
carbon tetrachloride–pentane–propene, radiolysis of, tracer studies of mechanisms in, 20: 20752
PROPENE, 2-METHYL-
polymerization by gas discharge and irradiation, yields in, 20: 20740
PROPENE POLYMERS
radiation effects on molecular motion and structure of isotactic, gamma and neutron, 20: 20753
radioinduced chlorination and sulfochlorination of, infrared studies of structure changes in gamma, 20: 20779
PROPIONITRILES
radiolysis of liquid, mechanism and yields in, 20: 20717(R) (AD-621719)
PROPORTIONAL DETECTORS
amplifiers for, design of integrated-circuit charge-sensitive pre-, 20: 21112
performance of boron trifluoride, for neutron in high gamma fluxes, 20: 21132
performance of small, for localization of brain tumors after administration of phosphorus-32, 20: 20523(R) (NYO-1726-15)
PROPULSION
electric, review of, 20: 20871 (N-65-29443)
nuclear rocket, materials evaluation for lightweight, 20: 22470 (N-65-29480)
nuclear, problems of high-temperature chemistry in methods for, 20: 20870 (LA-DC-7703)
nuclear, review of, 20: 20871 (N-65-29443)
plasma engine for, effects of nonequilibrium conductivity on, 20: 20873
plasma jet, performance of two-stage coaxial, 20: 20872
PROPYNE
radiolysis of gaseous, mechanism and yields in, 20: 20717(R) (AD-621719)
PROSTATE GLAND
weight norms for human, use in establishing standards for radiation dosimetry, 20: 20374
PROTACTINIUM
deposition on platinum disks for α and β counting, electrolytic, 20: 20795
separation from hydrochloric acid solutions by solvent extraction using quaternary ammonium chlorides, 20: 20816
separation from some elements of Groups IVa and Va by solvent extraction using quaternary ammonium chlorides, 20: 20816
PROTACTINIUM ISOTOPES Pa-233
neutron cross sections for, 20: 21967 (AEET-234)
PROTEINS
effects of dietary deficiency of, on rat recovery from gamma irradiation, 20: 20508
radiation effects on aqueous solutions of, review on, 20: 20728 (PB-181506, pp 49-58)

radiosensitivity of, effects of GED on, 20: 20424
PROTON BEAMS
effects on impurity diffusion in silicon semiconductors, 20: 21147(R) (AD-621049)
energy transfer from 150-Mev, to polyethylene, 20: 20525
scattering by gold coatings on metals, thickness measurements by, 20: 21246
PROTON CAPTURE CROSS SECTIONS
calculation for heavy nuclei using optical model, 20: 22049
PROTON CROSS SECTIONS
calculation of differential, computer program for, 20: 21965 (AD-626776)
PROTON SPECTROMETERS
design using spark chambers, for cosmic protons, 20: 21120
PROTONS
angular correlations with gamma radiation from deuteron reactions (d,pγ) with carbon-12 at 2 to 3.2 Mev, (E), 20: 22087
binding energy in residual nuclei from meson (K⁻) reactions in emulsions, 20: 22161
capture by nuclei, use in analysis of nuclear structure, 20: 21986 (BNL-948, pp 763-825)
effects on dilute alloys of copper, gold, and silver at 80°K, resistivity recovery from, 20: 21445
effects on optical properties of adhesives and glass, 20: 21446
effects on silicon devices in space, 20: 21165
emission in neutron reactions with zinc-64 at 14 Mev, (E), 20: 22048
flux from solar neutron decay, 20: 21495
injection into radiation belts by cosmic ray and solar proton albedo neutron decay, 20: 21550
interaction with antiprotons in ambiplasma, energy distribution from annihilation, (T), 20: 21684
interactions with mesons (K⁻) at 900 to 990 Mev/c, angular distributions and cross sections for, (E), 20: 21628 (TID-22822)
interactions with mesons (K⁺) at 4.6 Bev/c, K* production in, (E), 20: 21629 (UCRL-16332)
interactions with mesons (K⁻) at 1.33 Bev/c, resonance production in, (E), 20: 21615 (COO-1195-52)
interactions with neutrinos (ν_e), liquid scintillator for measuring cross sections for, 20: 21027 (CERN-65-32, pp 41-4)
interactions with protons, intermediate boson production in, 20: 21610 (CERN-65-32, pp 181-94)
interactions with photons, intermediate boson production in, 20: 21611 (CERN-65-32, pp 195-200)
interactions with mesons (π^-) and (π^+) at 5 to 20 Bev, amplitudes for, (T), 20: 21618 (JINR-P-2566)
interactions with protons, one-boson exchange model parameters from, (T), 20: 21621 (JINR-P-2584)
interactions with protons at 657 Mev, phase shift analysis for elastic, (T), 20: 21622 (JINR-P-2585)
interactions with photons, sum rules for absorption in, (T), 20: 21625 (JINR-P-2619)
interactions with protons, bounds for correction to Born term in generalized dispersion model for, 20: 21635
interactions with protons in ^1S state, nonlocal potential for, (T), 20: 21637
interactions with protons at 8 Bev, differential cross sections for elastic, (E), 20: 21639
interactions with mesons (π^-) at high energies, ρ-exchange peripheral model for, 20: 21647
interactions with pseudoscalar mesons, SU(6W) predictions for spin alignment and forward scattering for, 20: 21652
interactions with mesons (π) at high energies, polarization in, (T), 20: 21653
interactions with mesons ($\pi^\pm$) at high energies, conservation laws for, 20: 21657
interactions with mesons ($\pi^\pm$) at 2 to 7 Bev/c, total cross sections for, (E), 20: 21661
interactions with mesons (π^+) at 250 Mev, cross section for elastic, (E/T), 20: 21662
interactions with protons at 5.5 Bev/c, N*↔(1238) peripheral production in, (E), 20: 21663
interactions with photons, N***(1688) production in, (T), 20: 21676
interactions with protons, Coulomb-modified S-wave dispersion relation for, 20: 21680
interactions with mesons ($\pi^\pm$), T = 0 S-wave ππ phase shift in, (E), 20: 21685
interactions with neutrons, deuteron compositeness from effective-range formula for, 20: 21689
interactions with neutrons in nuclei, quasi-particle random-phase approximation in, 20: 22147
interactions with charged mesons, SU(3) symmetry for three-particle final states in, 20: 21763
interactions with photons, analysis of, (T), 20: 21587 (AD-623564)
interactions with bremsstrahlung at 475 to 750 Mev, asymmetry of meson (π^+) production in, (E/T), 20: 21589 (AD-626683)
interactions with protons at 600 Mev, polarization parameters and spin correlations in, (E), 20: 21590 (CERN-66-2)
lifetime of, lower limit for mean, (E), 20: 21636
mass relative to neutrons, (T), 20: 21673
mass relative to neutrons from spontaneous symmetry breakdown, 20: 21678
mass relative to neutrons, dispersion-theoretical perturbation series in particle models for, 20: 21683
model of, binding energy in quark, 20: 21748
polarization in neutron-irradiated polyethylenes, (E), 20: 22345
reactions (p,α) with chlorine-37 at 11.0 to 11.952 Mev, angular distributions and excitation functions for, (E), 20: 22084
reactions (p,dp) with nitrogen-14, 3α decay of excited nucleus from, 20: 22033
reactions (p,d) and (p,t) with carbon-13 at 54.9 Mev, differential cross section and product momentum and angular distributions for, (E), 20: 22030
reactions (p,d) with calcium-44 and -47 at 17.5 Mev, calcium-43 and -48 neutron-hole states from, (E), 20: 22129
reactions (p,n) with yttrium-89 at 4.5 to 5.5 Mev, cross sections for, (E), 20: 22010(R) (NYO-72-28)
reactions (p,n) with zinc-67 at 1.5 to 5 Mev, gallium-67 levels from, (E), 20: 22053
reactions (p,n) with zinc-68 at 1.5 to 5 Mev, gallium-68 levels from, (E), 20: 22053
reactions (p,n) with zinc-70 at 1.5 to 5 Mev, gallium-70 levels from, (E), 20: 22053
reactions (p,n) with cadmium-110, -111, and -112 at 5 to 37 Mev, excitation functions for, (E), 20: 22078
reactions (p,pγ) with fluorine-19 at 4.3 Mev in metallic media, perturbation of angular correlations from, 20: 22090
reactions (p,p′γ) with neon-20 and sulfur-32 at 8.5 Mev, angular correlations from, (E), 20: 22059
reactions (p,pn) with cadmium-110 at 5 to 37 Mev, excitation functions for, (E), 20: 22078
reactions (p,xn) and (p,pxn) with yttrium 89 at 5 to 85 Mev, excitation functions for, (E), 20: 22133
reactions (p,2n) with cadmium-110 and -111 at 5 to 37 Mev, excitation functions for, (E), 20: 22078
reactions (p,2p) and (p,2pn) with argon-40, cross sections for, (E), 20: 22125
reactions (p,3n) with cadmium-112 at 5 to 37 Mev, excitation functions for, (E), 20: 22078
reactions with beryllium at 12.5 Bev, meson (K) and (π) production cross sections for, (E), 20: 21601 (CERN-65-32, pp 109-10)
reactions with bismuth, polonium production by, 20: 20553(R) (MLM-1142)
reactions with boron, carbon, and aluminum, straggling effects in energy loss from, (E/T), 20: 21539
reactions with copper at 19 Bev/c, meson (K) and (π) yields from, (E), 20: 21602 (CERN-65-32, pp 111-14)
reactions with iron at 400 Mev, Monte Carlo calculation of radionuclide production in, 20: 22035
reactions with nitrogen, performance of triggered cloud chamber for analyzing, (E), 20: 21063
reactions with nuclei, amplitude singularities in knockon and stripping, (T), 20: 21997 (INSJ-96)
reactions with nuclei at 590 Mev and 18 Bev, yields of iodine isotopes in spallation, 20: 22045
reactions with uranium-238 at 11 to 21 Mev, alpha emission in fission, (E), 20: 22144
scattering by beryllium-9, carbon-12, and nickel-58 and -60 at 45 Mev, differential cross sections for elastic, (T), 20: 21963 (AD-626656)
scattering by carbon-13 at 1.0 to 2.6 Mev, nitrogen-14 levels from, (E), 20: 22123
scattering by carbon-12 at 1.48 to 2.02 Mev, cross sections and resonances from, (E), 20: 22115
scattering by carbon-12, 3α decay of excited nucleus from inelastic, 20: 22033
scattering by complex nuclei at 45 Mev, polarization in, (E), 20: 22128
scattering by dysprosium-160 and -164, at 12 Mev, excitation of octupole vibrational states by inelastic, (E), 20: 22100
scattering by even nickel isotopes, microscopic description of inelastic, (T), 20: 22118
scattering by gadolinium-158 at 12 Mev, excitation of octupole vibrational states by inelastic, (E), 20: 22100
scattering by lead-208 at 40 Mev, energy levels from inelastic, (E), 20: 22101
scattering by medium nuclei at 10 to 20 Mev, spin-orbit potential for polarization from elastic, (T), 20: 22116
scattering by nuclei at high energies, review of elastic, 20: 21593 (CERN-65-24(Vol.1), pp 65-80)
scattering by oxygen-16, 4α decay of excited nucleus from inelastic,

20: 22033
scattering with helium-4 at 40 Mev, continuum resonances from inelastic, (E), 20: 22114
PSEUDOUREA, 2-(2-AMINOETHYL)-2-THIO-
effects on ATP content in rat tissues, 20: 20505
effects on mitochondrial respiration in rat tissues, 20: 20505
radiosensitivity effects on mouse brain, 20: 20521
PULSE ANALYZERS
converters for, servo-stabilized analog-to-digital, 20: 21026 (BNL-948, pp 704-17)
design and development of, 20: 22010(R) (NYO-72-28)
design and performance of 256-channel time-of-flight, with analog-to-digital converter, 20: 21083
design of differential discriminator using tunnel diodes, 20: 21124
design of fast zero-crossing discriminators, 20: 21114
design of multichannel, for use on balloons and rockets, 20: 21127
design of zero-crossing discriminator with picosecond time slewing, 20: 21115
design of 1500-channel transistorized, 20: 21126
design of 256-channel three-parameter, 20: 21125
pulse pile-up effects in measurement of gamma spectra using photomultipliers and scintillators, 20: 21106
PULSE GENERATORS (ELECTRONICS)
design of digital pseudorandom, 20: 21001
PULSE MODIFIERS
design of nanosecond pulse stretcher, 20: 21010
PUREX PROCESS
waste fixation in phosphate glass, Brookhaven process for continuous, 20: 22509 (BNL-10109)
waste fixation in phosphate glass, evaluation of, 20: 22510 (BNWL-SA-564)
PYRIDINE
radiation effects on stability of carbon-14-labeled, neutron, 20: 20783
PYRIDINE-1-OXIDE
radiosensitivity effects on mouse tumors, 20: 20506
3-PYRIDINOL
radiosensitivity effects on DNA, uv, 20: 20412
PYRIDOXINE
phosphate, dephosphorylation of, catalytic effects of cerium, lanthanum, manganese, thorium, and zirconium ions on, 20: 20375
PYROCATECHOL
amine derivatives of, content in auricles of irradiated rabbits, 20: 20451
PYROPHOSPHORIC ACID
derivatives of, radiosensitivity effects on HeLa cells and mice, x, 20: 20515
PYRROLE
radiation effects on stability of carbon-14-labeled, neutron, 20: 20783
PYRROLE, 2-METHYL-
radiation effects on stability of carbon-14-labeled, neutron, 20: 20783
PYRROLIDONE, VINYL- POLYMERS
radiation effects on, light-scattering and viscosity measurements of gamma, 20: 20765

Q

QUALITY CONTROL
method for, during reactor component fabrication, 20: 21308
radiographic methods for, of SAP tubes, 20: 20861 (EUR-2443.f)
radiometric methods of, in production of plates and tubes of asbestos cement, 20: 21204
QUANTUM ELECTRODYNAMICS
electric and magnetic charge in, 20: 21865
photon mass in two-dimensional, infrared divergence in, 20: 21856
radiative corrections in, 20: 21469 (LNF-66/10)
scattering amplitude for heavy photons in, Regge pole behavior of, 20: 21871
QUANTUM MECHANICS
approximations in, error of, 20: 21860
approximations in, estimation of error of, 20: 21861
Bogoliubov quasiparticles in, criteria for, 20: 21839 (AD-627067)
book: *Advances in Quantum Chemistry, Vol. 2*, 20: 20698
electron motion in, hydrodynamic model of, 20: 21840
elementary particle fields in, (T), 20: 21704 (AD-622517)
hamiltonian matrix elements in, asymptotic correlations of, 20: 21854
operators commuting in pairs in, determination of common eigenvector system of, 20: 21855
operators in, essential spectrum of arbitrary, 20: 21848
representation of indefinite metric space for semiclassical description of systems in, 20: 21850
theory in electrical engineering, 20: 21846
wave equations in, time-dependent perturbations in Schroedinger, 20: 21852
wave functions and gravitation of macroscopic objects in, 20: 21857
QUARTZ
neutron scattering at 0.00065 to 2.0 ev, cross sections for, (E), 20: 22010 (NYO-72-28)
radiation effects on logarithmic damping decrements of oscillators of, x, 20: 21155
QUATERPHENYL
radioinduced in Santowax WR, properties of, 20: 20723(R) (MIT-334-33)
QUINIDINE
effects on irradiated rabbits' response to exogenous pulses, 20: 20451
8-QUINOLINOL
uses in separation of cerium, lanthanum, neodymium, and praseodymium by paper chromatography, 20: 20814
uses in spectrophotometric determination of thorium, 20: 20576

R

RABBITS
cataracts in, effects of iodoacetate on, 20: 20507(T)
radiation effects on electrical activity of olfactory neurons in, x, 20: 20431 (AD-630323)
radiation effects on heart auricles, 20: 20451
radiation effects on skin epithelium and skin grafts, 20: 20477
radiation effects on auditory organs in, gamma, 20: 20498
radiation effects on blood formation in, protective effects of mucopolysaccharides against x, 20: 20510
radiosensitivity of, seasonal variations in γ, 20: 20493
RADIATION
detection and measurement in auroral ionosphere using balloon-borne instruments, 20: 21838
dosimetry of, from inhaled particulates, 20: 20953
dosimetry standards for, physiological norms for, 20: 20374
dosimetry using metabolism and urinary excretion data, 20: 20398
effects in abiogenic formation of organic compounds, (T), 20: 20406 (N-65-27062)
effects of, relevance of bombardment-induced Mössbauer effects in iron to theories on, 20: 21444
effects on acetylenic compounds, products formed by, 20: 20717(R) (AD-621719)
effects on animals, review of carcinogenic, 20: 20442 (ORNL-P-2053)
effects on atomic motion in crystals, computer simulation of, 20: 22341
effects on biological systems, mechanism of, 20: 20443 (PB-181506, pp 143-54)
effects on bones in children, tumorigenic, 20: 20460
effects on central nervous system, review, 20: 20449
effects on cracking gaseous and liquid butane and isobutane, 20: 20740
effects on decomposition of Santowax-OM1, additive effects on, 20: 20708 (AEET-213)
effects on dielectric properties of ethylene, styrene, tetrafluoroethylene, and trifluorochloroethylene polymers, 20: 21443
effects on food wholesomeness, 20: 21198
effects on human blood vessels and heart following radiotherapy of Hodgkin's disease, 20: 20468
effects on man, effects on mongolism incidence in children, 20: 20454
effects on man, epidemiological studies of, 20: 20442 (ORNL-P-2053)
effects on mechanical and physical properties of plastic–wood combinations, 20: 21348 (ORNL-IIC-7, pp 22-5)
effects on organic compounds in aqueous solutions, review on, 20: 20728 (PB-181506, pp 49-58)
effects on organic compounds of biological interest, mechanism of, 20: 20731 (PB-181506, pp 133-42)
effects on oxidation of ergosterol, chromatographic method for separating products formed by, 20: 20738
effects on plastic–wood combinations, commercial possibilities for, in Pacific Northwest, 20: 21185 (ORNL-IIC-7, pp 76-80)
effects on polymerization reactions in plastic–wood combinations, properties of products formed by, 20: 21180 (ORNL-IIC-7, pp 15-21)
effects on polymerization of gels, 20: 20761
effects on populations of Hiroshima and Nagasaki, pathological, 20: 20919(R) (ABCC-64-65)
effects on power transistor response, design study for, (E/T), 20: 21148(R) (AD-630835)
effects on power transistor response, design study for, (E/T), 20: 21149(R) (AD-630836)
effects on production of plastic–wood materials, 20: 21177 (ORNL-IIC-7)
effects on production of plastic–wood combinations, testing of, 20: 21179 (ORNL-IIC-7, pp 6-14)
effects on properties of dielectrics, 20: 21171
effects on rabbit skin, 20: 20477
effects on rat lungs, fibrotic, 20: 20459
effects on rates of specific locus mutations in mice, 20: 20461
effects on semiconductor devices, review of, 20: 21156
effects on semiconductors, review of, 20: 21160

effects on semiconductors, conference on, 20: 21164
effects on semiconductor devices, generalized model analysis for, (T), 20: 21167
effects on semiconductor devices and circuits, modeling of, 20: 21173
effects on silicon semiconductors, regeneration susceptibility from, 20: 21168
effects on skin transplants in rabbits, 20: 20477
effects on skin, photometer for measuring, 20: 21011
effects on transistors, prediction of transient, 20: 21166
effects on tumor cells, mechanism for, 20: 20416
emission from plasma at harmonics of electron gyrofrequency, 20: 22239
quantum field theory of, use of Laplace transformation in, 20: 21768
reactions with matter, pressure broadening of spectral lines from, (T), 20: 21519
transport theory with internal sources of, invariant imbedding of, 20: 21641
use for commercial production of plastic–wood combinations, 20: 21187 (ORNL-IIC-7, pp 89-94)
use for commercial production of plastic–wood combinations, 20: 21189 (ORNL-IIC-7, pp 99-105)
use for commercial production of plastic–plywood combinations, 20: 21191 (ORNL-IIC-7, pp 112-18)
use for plastic–wood combinations, commercial potential of, 20: 21186 (ORNL-IIC-7, pp 81-8)
use for production of plastic–wood combinations, 20: 21182 (ORNL-IIC-7, pp 49-58)
use for production of plastic–wood combinations, commercialization aspects of, 20: 21184 (ORNL-IIC-7, pp 64-75)
use for production of plastic–wood combinations for sporting-goods industry, 20: 21190 (ORNL-IIC-7, pp 106-11)
use for production of plastic–wood combinations, Lockwood program for, 20: 21188 (ORNL-IIC-7, pp 95-8)
use in development of plastic–wood materials, AEC program on, 20: 21178 (ORNL-IIC-7, pp 1-5)

RADIATION CHEMISTRY
abstracts of papers on, 20: 20552 (CONF-650723(Absts.))
book: *Advances in Inorganic Chemistry and Radiochemistry*, Vol. 7, 20: 20658
developments in Poland, review on, 20: 20780
research in, 20: 20726 (PB-181506)
research on, in France, 20: 20730 (PB-181506, pp 104-15)
research on, in Japan, 20: 20727 (PB-181506, pp 9-18)
research programs on, using Kyoto University cyclotron, 20: 22524
solid state, ESR studies on, 20: 20729 (PB-181506, pp 85-103)
uses of, review of industrial, 20: 20793

RADIATION DETECTION INSTRUMENTS
amplifiers for, design of charge-sensitive transistorized pre-, 20: 21130
conference, 20: 21097
data recording systems for, automatic, 20: 21045
design for aerosol monitoring, 20: 21073
design for detection and measurement of gamma radiation from debris of high-altitude atomic explosions, 20: 21129
design for multiple measurements, 20: 21055
operation and properties of x, review of, 20: 21023 (AD-624231)
performance of field-ionization, for molecular beams, 20: 21089

RADIATION DETECTION INSTRUMENTS (ION CURRENT TYPE)
design and performance for alpha activity in flowing water, 20: 21038 (K-1656)

RADIATION DETECTION INSTRUMENTS (PULSE TYPE)
amplifiers for, design of solid-state, 20: 21039 (KAPL-3122)
amplifiers for, design of, 20: 22010(R) (NYO-72-28)
circuit development for, 20: 21086
design and performance for whole-body facility, 20: 21075
design for whole-body counting, 20: 21142(P)
design of miniature G-M, for medical uses, 20: 21092
design using multiple detectors for gamma well logging, 20: 21145(P)
development for clinical scanning using iodine-131, 20: 20535
efficiency for collimated gamma rays, comparison of G-M and scintillation, 20: 21056
performance for low-neutron-flux average-energy determination, 20: 21074
performance for neutron lifetime measurements, correlation method for, (T), 20: 21035 (FEI-21)
time resolution of transistorized time-of-flight, 20: 21052

RADIATION DETECTORS
development for molecular beams, 20: 21066
performance of dielectric track, for neutrons and heavy cosmic nuclei, 20: 21091

RADIATION INJURIES
epidemiology of, to radium dial painters, 20: 20387(R) (NYO-2181-3)
pathology of, in rat lungs, x, 20: 20434 (AD-630870)
protection against, using liver extracts, yeast extracts, and acridine orange in rats, 20: 20503(R) (AD-629311, pp 1-14)
protection against, using β-mercaptoethylamine in mice, 20: 20511

RADIATION MONITORING
during testing of rocket reactors, 20: 20954
program at JAERI, 20: 20934 (JAERI-1098)

RADIATION PROTECTION
law for personnel, experience with, 20: 20947
measures for dental radiology in Michigan, 20: 20956
measures for medical radiology, 20: 20544
methods for, in radiological warfare, 20: 20980
regulations for, in manufacture of luminescent watches, 20: 20518 (RT-PROT-(65)41)

RADIATION SICKNESS
effects on blood coagulation in dogs and rats, 20: 20490
effects on blood coagulation in dogs, 20: 20491
effects on skin graft growth on rabbits, 20: 20477
pathology of mouse, effects of age on, 20: 20494

RADIATION SOURCES
shielding, 20: 21174 (SAN-575-12)

RADIATION TARGET CANS
design for samples for ESR studies, 20: 20846

RADIATION TARGETS
design and performance of tritium gas, for (d,n) reactions, 20: 21948
design and performance of liquid helium-3, 20: 22007 (LNF-66/1)

RADIO WAVES
emission from Jupiter, effects of ionosphere on characteristics of, 20: 21510
emission from solar flares, pre-absorption events in type-IV bursts, (E), 20: 21500
emission from sun, characteristics of, 20: 21506
emission of v-l-f hiss, from auroral zones, 20: 21824
polarization of cosmic, measurement methods for linear, 20: 21549
propagation of high-frequency, relation of aurora to off-great-circle, 20: 21827
scattering by disturbed sea surface, structure effects on spatial characteristics of, (E), 20: 20908
use in electron distribution determinations in ionospheric D region, (T), 20: 21819

RADIOACTIVE CONTAMINATION
treatment of plutonium, in man, 20: 20943 (RFP-453)

RADIOACTIVE MATERIALS
analysis of, extraction radiometric titration method for, 20: 20567 (UJV-1418/65)
control and inventory in management of, criteria for, 20: 20966
control during fabrication and transport in Italy, 20: 20964
determination by microchromatography, fraction collector for, 20: 20587
management in France, sampling methods for, 20: 20973
processing of, economic management of, 20: 20833
processing of, radiation protection of personnel in, 20: 20947
size distribution in natural aerosols, 20: 20885
transport regulations for, key to 1964 IAEA, 20: 20945 (TRG-Report-1073)

RADIOACTIVE MINERALS
inhalation of particulate, radiation dose from, 20: 20953

RADIOACTIVE WATERS
decontamination of, using sanitary water-treatment process, 20: 22512 (K-1651)

RADIOACTIVITY
aereal surveying of, in Maryland, Virginia, Washington, D. C., and West Virginia, 20: 20928 (CEX-59.4.17)
content in Escaut River, Belgium, control of, 20: 22515(T) (ORNL-tr-965)
determination in inland waters, problems in, 20: 20963
measurement of environmental, importance of, 20: 20961
measurement of, automatic equipment for multiple, 20: 21055

RADIOBIOLOGY
conference on clinical, 20: 20551
research in, 20: 20726 (PB-181506)

RADIOCHEMICAL PROCESSING PLANTS
analysis for plutonium in, methods for, 20: 20976
construction of Transuranium Processing Plant at ORNL, critical-path method for scheduling, 20: 20809 (ORNL-3925)
design and testing Alpha Facility, for plutonia–urania fuels, 20: 20803(R) (ANL-7055, pp 99-162)
design of Eurex, in Italy, for spent reactor fuels, 20: 20815
design of fluoride volatility, problems in, 20: 20810(T) (ANL-Trans-250)
development and testing equipment for EBR-II fuel cycling, 20: 20802(R) (ANL-7055, pp 21-98)
nuclear materials accounting in, at Windscale, 20: 20830

RADIOCHEMISTRY
research on, in France, 20: 20730 (PB-181506, pp 104-15)
research programs on, using Kyoto University cyclotron, 20: 22524
uses of, review of industrial, 20: 20793

RADIODIAGNOSIS

conference on x-ray, 20: 20551
developments in scintiscanning, review, 20: 20531
equipment for, spark chamber gamma camera, 20: 21082
method for placental localization, 20: 20527
methods for mammary cancer, assessment of bremsstrahlung, 20: 20540
RADIOFREQUENCY OSCILLATORS
design and performance of linearly controllable low-frequency, for NMR spectrometer, 20: 21093
RADIOFREQUENCY SPECTROMETERS
oscillator for NMR, with internal stabilization, 20: 21093
sample holders for ESR, 20: 20846
RADIOGRAPHY
effects on canine spinal cord, Thorotrast, 20: 20455
equipment for electron-beam, 20: 21477
equipment for high-energy, bubble chamber, 20: 21144(P)
image analysis in thermal neutron, 20: 20866
methods for quality control of thin walled SAP tubes, mechanical, 20: 20861 (EUR-2443.f)
personnel in, chromosome studies on families and, 20: 20447
photographic methods in color, 20: 20863
safety hazards of cephalometric, 20: 20543
techniques for, in Japan, 20: 20867
uses for fuel pin inspection, 20: 20864
RADIOISOTOPES
activity of, isothermal microcalorimeter for measuring, 20: 21068
decay of, formula for time dependence of, 20: 22024
decay of, perturbed angular correlation of triple gamma cascades from, (T), 20: 22015
decay of, Prony method for evaluation of exponential curves for, 20: 22051
decay rates for, computation of, 20: 22155
determination in radiation sources, extraction radiometric titration method for, 20: 20567 (UJV-1418/65)
determination of long-lived beta- and gamma-emitting, by autoradiography, 20: 20611
determination of precipitated microquantities of, two-indicator method for, 20: 20619
determination of small quantities of, in environment, 20: 20616
equivalence formula for, 20: 21175
gamma spectra from multiple, stepwise statistical analysis of, 20: 20555(R) (AD-622200)
production by (n,γ) reactions in reactors, yield tabulations for, 20: 21214 (ORNL-IIC-8)
production in Japan, 20: 21220
production in production reactors, 20: 21212 (CONF-660305-19)
production of, internal audit in plant for, 20: 22529
retention by protective coatings, tables of, 20: 20808(R) (ORNL-3916)
separation from aqueous solutions by foam chromatography using colloidal manganese dioxide, 20: 20628
separation methods for short-lived, review of rapid, 20: 20826
sorption of trace amounts of, from solutions onto container walls, 20: 20617
use as time base for electronic timers, feasibility for, 20: 21021 (AD-622629)
use for radiodiagnosis in Congo, 20: 20373
use for space vehicle heat shield ablation and sublimation determination, 20: 20860
use in development of plastic–wood materials, 20: 21178 (ORNL-IIC-7, pp 1-5)
use in medical scanning, review, 20: 20531
use in microbiological assays of seawater, 20: 20368 (CONF-640309-1)
use in portable x-ray fluorescence analyzer, 20: 20640
use in studies on bed-load movement and transport in canals and rivers, 20: 20904 (STI-REP-101)
use in waterfront maintenance, 20: 21176 (AD-621440)
uses in biology, chemistry, and food studies, 20: 20726 (PB-181506)
uses in manned spacecraft life-support systems, 20: 21174 (SAN-575-12)
uses of beta-emitting, in light source for precision photometric analysis, 20: 20571
RADIOLOGICAL WARFARE
protective measures against, 20: 20980
public health aspects of carrion decomposition during, 20: 20941 (ORNL-TM-1432)
RADIOLOGY
hazards from dental, survey in Michigan, 20: 20956
safety hazards from medical, protection against, 20: 20544
safety measures for dental, 20: 20519
RADIOMETERS
use of, survey on, 20: 20990(T) (AERE-Trans-1048)
RADIOMETRIC ANALYSIS
method of gamma, using two radioisotopes, 20: 20637
method of gamma, using mixture of several radioisotopes, 20: 20638
RADIOMIMETIC SUBSTANCES
iodoacetate effects, on rabbit eyes, 20: 20507(T)
RADIOPROTECTIVE COMPOUNDS
spectra of, ESR, 20: 20729 (PB-181506, pp 85-103)
RADIOSENSITIVITY
effects of age on mouse, 20: 20494
effects of oxygen environment on mouse, 20: 20430(R) (AD-629311, pp 26-32)
effects of polyhydroxyl alcohols on mouse, 20: 20520
variations in rabbit, seasonal, 20: 20493
RADIOSENSITIZERS
effects of Natulan, combined with gamma or x radiation on tumors, 20: 20504
RADIOSTERILIZATION
acceptance tests for food, 20: 21199
commercialization of fish, 20: 21200
commercialization of food, feasibility, 20: 21202
developments in research on food, 20: 21194 (PB-181506, pp 155-67)
effects on food wholesomeness, 20: 21198
effects on food, review on, 20: 21206
effects on fruits, low-level gamma, 20: 21195(R) (TID-22509)
effects on microflora on perch fillets, 20: 21203
effects on wholesomeness of foods, review on, 20: 21207
legal aspects of food, 20: 21201
method for gamma, of human bone grafts, 20: 20482
program of food, status, 20: 21196
research in, 20: 20726 (PB-181506)
research on food, in U.S.A., 20: 21192 (PB-181506, pp 19-26)
research on food, in Western Germany, 20: 21193 (PB-181506, pp 29-38)
research on food, in Japan, 20: 20727 (PB-181506, pp 9-18)
RADIOTHERAPY
beam focus imaging for gamma, 20: 20547
conference on x-ray, 20: 20551
dosimetry in, development of thermoluminescent detectors for, 20: 21085
dosimetry method for remote-controlled, 20: 20541
effects on human electrocardiographs, x, 20: 20474
energy deposition in meson (π^-), 20: 20525
equipment for gamma, beam focus cassette and interspacer, 20: 20548
gamma dose distribution of cobalt-60 unit, 20: 20549
RADIUM
dosimetry of, spectrometric method for, 20: 20952
effects of, combined with surgery on cervical carcinomas, 20: 20536
effects on rabbit auditory organs, 20: 20498
excretion and metabolism of, use in dosimetry, 20: 20398
radiation effects from, epidemiology of New Jersey cases on, 20: 20387(R) (NYO-2181-3)
RADIUM ISOTOPES Ra-223
energy levels from francium-223 and thorium-227 decay, (E), 20: 22008 (MLM-1337])
half life of, effects of actinium-227 on determination of, 20: 20553(R) (MLM-1142)
RADIUM ISOTOPES Ra-226
content in Escaut River, Belgium, 20: 22515(T) (ORNL-tr-965)
content in silt in Escaut River, Belgium, control of, 20: 22515(T) (ORNL-tr-965)
content in tissues of radium dial painter, 20: 20387(R) (NYO-2181-3)
distribution in swine tissues, 20: 20385 (COO-1184-3)
occurrence in phosphate rocks, 20: 20886
RADIUM ISOTOPES Ra-228
content in tissues of radium dial painter, 20: 20387(R) (NYO-2181-3)
RADON
detection and measurement in aerosols, equipment for, 20: 21067
measurement in water using gamma radiation, 20: 20959
RADON FLUORIDES
preparation and properties of, 20: 20659
RAIN WATER
tritium content of, Washington, D. C., 20: 20892
tritium content of, in New Zealand, 20: 20893
RARE EARTH ACETATES
preparation by oxide solubility in alcohols containing ammonia, 20: 20686
RARE EARTH ALLOYS
electric conductivity of, Dekker theory on, 20: 22314(R) (AD-626865)
Al–rare earths, crystal structure and stability of intermetallic compounds in, 20: 21415
Au–rare earth, crystal structure of equiatomic intermetallic compounds of, 20: 21399
Cd–rare earths, thermodynamic properties of intermetallic compounds in, 20: 20802(R) (ANL-7055, pp 21-98)
Cu–rare earth, crystal structure of equiatomic intermetallic compounds of, 20: 21399
Ga–rare earth, crystal structure of equiatomic intermetallic compounds of, 20: 21399
La–rare earth, electric conductivity, magnetic susceptibility, and super-

conductivity at low temperatures, 20: 21873 (NP-15936)
Mn–rare earth, preparation by amalgam process, 20: 21403
rare earth–Ag, crystal structure of equiatomic intermetallic compounds of, 20: 21399
rare earth–Th, solid solutions of, electronic states of, 20: 21398
rare earth–Y, solid solutions of, electronic states of, 20: 21398
rare earth–Zr, solid solutions of, electronic states of, 20: 21398

RARE EARTH COMPOUNDS
growth and properties of aluminum and gallium garnets of, 20: 22311(R) (AD-622068)

RARE EARTH IONS
spectra of, in magnetic materials, 20: 22311(R) (AD-622068)

RARE EARTH NITRIDES
preparation by reactive arc melting, 20: 21244

RARE EARTHS
conference on research on, Phoenix, Arizona, April 22 to 25, 1964, 20: 20704
determination in lead, lead alloys, and zinc, 20: 20607
determination in mixtures, activation, 20: 20562 (LYCEN-6538)
determination in silicon dioxide, activation, 20: 20634
distribution in terrestrial rocks, 20: 20877
friction and wear properties of, in vacuum, effects of crystal structure on, 20: 21365
metallurgy of, conference on, Ames, Iowa, Aug. 30 to Sept. 1, 1965, 20: 21252
separation by ion exchange chromatography, tracer studies on, 20: 20822
separation by microchromatography, fraction collector for, 20: 20587
separation by reversed-phase partition chromatography on polytetrafluoroethylene, 20: 20621
separation from chromium, manganese, nickel, and silver by ion exchange chromatography, 20: 20634
separation from nitrate solutions by solvent extraction using tricarpylmethylammonium nitrate, 20: 20812
separation from nitric acid solutions containing calcium phosphate by solvent extraction using TBP, 20: 20824
separation from scandium by ion exchange chromatography, 20: 20821
separation from scandium and thorium by paper chromatography, 20: 20825
separation from uranium in acid solutions using cation exchange materials, 20: 20813

RARE GAS COMPOUNDS
preparation and properties of, 20: 20659

RARE GASES
chemistry of, 20: 20659
diagnostics of MHD cell plasma of, (T), 20: 21569 (IPP-3/29)
effects on biological materials, mechanism, 20: 20378
partial pressures of, for halving oxygen-dependent radiosensitivity in bean roots, 20: 20378
separation from air, equipment for, 20: 20820

RATE METERS
design of gamma, using ionization chambers, 20: 21078

RATS
α-ketoglutarate oxidation in, effects of disulfides and thiols on, 20: 20505
etiology of thyroid tumors in, 20: 20448
iodine-131 metabolism in fetuses of, 20: 20390(R) (TID-22767)
neurogenesis in postnatal, tracer study, 20: 20391(R) (TID-22825)
radiation effects on oxygen uptake in brain tissues of, x, 20: 20436 (CONF-650560-17)
radiation effects on tryptamine content of brain tissues, x, 20: 20437 (CONF-650560-18)
radiation effects on sodium sulfate metabolism in liver of, x, 20: 20410
radiation effects on gastric transit in laparotomized and vagotomized, uv, 20: 20414
radiation effects on cytochrome c oxidase and glucose-6-phosphatase activity in liver of, whole-body x, 20: 20417
radiation effects on potassium and sodium content of spleen cell nuclei, x, 20: 20422
radiation effects on enzyme synthesis in liver of, x, 20: 20429(R) (AD-629311, pp 15-25)
radiation effects on metabolic activity in spleen and stomach of, 20: 20433 (AD-630390)
radiation effects on lungs of, x, 20: 20434 (AD-630870)
radiation effects on metabolism of methylnaphthalene in, x, 20: 20439 (EUR-2628.f)
radiation effects on experimental bladder calculus formation in, x, 20: 20467
radiation effects on blood coagulation in, γ and x, 20: 20490
radiation effects on conditioned reflexes in, exposed *in utero*, 20: 20492
radiation effects on bone growth in, x, 20: 20486
radiation effects on, effects of low-protein diet on recovery from gamma, 20: 20508
radiation effects on testes in, protective effects of MEA against x, 20: 20509
radiation effects on phosphatase activity in, effects of injected glycine on, 20: 20517 (NP-15925)
radiation injuries of, effects of liver extracts, yeast extracts, and acridine orange on, 20: 20502(R) (AD-629311, pp 1-14)
radiation source avoidance by, γ, 20: 20495
radioinduced lung fibrosis in, 20: 20459
radioinduced thyroid tumors in, effects of propylthiouracil or dessicated thyroid on iodine-131, 20: 20448
ruthenium chloride metabolism in, 20: 20396

REACTOR ATMOSPHERES
purification plant for, 20: 22462

REACTOR COMPONENTS
conference, 20: 21097
decontamination of, development of solution for, 20: 21238 (NP-15928)
fabrication of, method for quality control during, 20: 21308
instrumentation for NERVA, 20: 22484

REACTOR CONTROL RODS
design of blade type, filled with particulate poison, 20: 22368(P)
drive mechanism for, design of emergency, 20: 22366(P)
fabrication of cadmium–indium–silver alloy, 20: 21317(P)
fabrication of, for EGCR, 20: 21292 (ORNL-3932)
homogenization of cruciform, in water moderated reactors, 20: 22357 (RT-FI-(65)50)
reactivity worth of cluster-, 20: 22395

REACTOR CONTROL SYSTEMS
circuits of, performance testing of plug-in connectors for, 20: 22352 (AEET-ED-SG/25)
design of NERVA, 20: 22482
design using chemical shim, 20: 22428
design using liquid poisons, 20: 22365(P)
development of SNAP, 20: 22474
development of SNAP-10A, 20: 22476
shutdown system using a-c amplifier with ionization chamber, 20: 22359

REACTOR COOLANTS
ejection from reactor channels in accidents, shock front conditions in, 20: 22348
ejection from reactor channels in accidents, 20: 22350
flow regulation in channels, device for, 20: 22361
performance in 1000-Mw(e) fast breeder reactor, 20: 22452
performance of molten copper, lithium, and tin, (T), 20: 22351 (AD-623020)
processing of organic, by hydrocracking, 20: 22520(R) (NAA-SR-11805)
properties of irradiated organic, correlation of friction factor and heat transfer, 20: 20710 (MIT-324-23)

REACTOR COOLING SYSTEMS
design of dual, 20: 22458
valves for flow control, design of, 20: 22364(P)

REACTOR EXPERIMENTAL FACILITIES
data analysis and control system for neutron spectroscopy, design using digital computer, 20: 21982 (BNL-948, pp 718-40)

REACTOR FUEL ALLOYS
fission effects on, 20: 22520(R) (NAA-SR-11805)
processing for uranium recovery by fluoride volatility, 20: 20803(R) (ANL-7055, pp 99-162)
processing plutonium–uranium, by chloride extraction, 20: 20802(R) (ANL-7055, pp 21-98)

REACTOR FUEL ELEMENTS
analysis for uranium-235 in leached, equipment and method for, 20: 21040 (ORNL-P-1218)
burnup analysis of, semiconductor Compton spectrometer for nondestructive, 20: 21050
control of irradiated, identification and inspection method for inventory, 20: 20970
fabrication and uses of, material control in, 20: 21313
fabrication of SAP-clad uranium carbide, 20: 22520(R) (NAA-SR-11805)
fabrication of, research program on mechanical metallurgy related to, 20: 21290(R) (GA-1052)
fabrication plant for, organization of basic materials auditing in, 20: 20967
failure detection system for EBR-II, data processing unit of, 20: 22439
failure of, detection system for, 20: 22427
handling of, coupling device for, 20: 22363(P)
heat transfer to ionized carbon dioxide, electric field effects on, 20: 20859 (UJV-1421/65)
hold-down arrangement for rod type, 20: 22369
instruments in, device for cutting leads from, 20: 21018(P)
isotopic content of operating, methods for calculating, 20: 20979
materials management of power, scope of, 20: 20968
performance of glass-clad uranium, 20: 22415 (RPI-321-4)
processing cermet and clad urania, by fluorination, 20: 20803(R) (ANL-7055, pp 99-162)
processing EBR-II for uranium recovery by skull reclamation,

20: 20802(R) (ANL-7055, pp 21-98)
processing of irradiated, Eurex Pilot Plant for, 20: 20815
processing of irradiated, heavy concrete for hot cells for, 20: 20819
processing of irradiated, nuclear materials management in Eurochemic's Mol facility for, 20: 20831
processing of irradiated, materials control system for facility for, 20: 20832
processing of metal-clad, development of shear-leach method for, 20: 20808(R) (ORNL-3916)
storage pool for spent, for JRR-2 reactor, 20: 22505
temperature of, thermocouple for measuring, 20: 21016(P)
testing for Piqua Power Reactor, 20: 22520(R) (NAA-SR-11805)
testing of, nondestructive method for, 20: 20865
thermal conductivity of in-pile, temperature transient method for determining, 20: 22354(R) (CEND-3336-260)
venting to coolant in 1000-Mw(e) sodium-cooled fast breeder reactor, 20: 22462

REACTOR FUEL ELEMENTS (CERAMIC)
fabrication of thorium(IV) oxide–uranium(IV) oxide, 20: 21301
fabrication of urania, economic and technical evaluation of process for, 20: 21300
loading by vibratory compaction, stresses in Zircaloy-2 cladding during, 20: 21289 (BNWL-194)
preparation and properties of calcium oxide–uranium(IV) oxide–zirconium oxide, 20: 21302
processing stainless steel- and Zircaloy-clad by fluoride volatility, 20: 20803(R) (ANL-7055, pp 99-162)
radiation effects on hollow-core urania pellets irradiated with central melting, reactor, 20: 21422 (GEAP-5100D)

REACTOR FUEL ELEMENTS (DISPERSION)
preparation and properties, 20: 22520(R) (NAA-SR-11805)

REACTOR FUEL ELEMENTS (THERMOELECTRIC)
development of, review, 20: 22406

REACTOR FUEL PINS
fabrication by injection casting, 20: 20802(R) (ANL-7055, pp 21-98)
inspection of, uses of x-ray radiography for, 20: 20864

REACTOR FUEL SPHERES
preparation of plutonia–urania, by plasma-torch heating, 20: 20553(R) (MLM-1142)

REACTOR FUEL TUBES
brazing of wire-wrapped, 20: 21383
criticality of enriched uranium, in water, (E), 20: 22375(R) (BNWL-193, pp 45-56)

REACTOR FUELS
analysis for trace impurities, summary of methods for, 20: 20589
burnup determination using mass-spectrometric isotope separator, 20: 22405
cycle analysis of, computer program for, 20: 22412 (GA-6622)
development of, at Harwell, 20: 21383
fabrication of beryllium oxide–uranium dioxide and silicon carbide–uranium dioxide particles for, 20: 21297(T) (NP-tr-1371)
handling facilities for, computer program for shielding design of, 20: 22309 (ORNL-3041)
materials management of power, scope of, 20: 20968
meltdown studies in TREAT, fast-neutron detection system for, 20: 21131
neutron Doppler coefficients for fast, (T), 20: 22378 (KFK-367)
performance data, 20: 22444
preparation of mixed thorium oxide–uranium oxide, 20: 21255(P)
processing aluminum–uranium alloy and stainless steel–cermet, fluid-bed fluoride volatility processes for, 20: 20801 (ANL-6830)
processing by fluoride volatility, design problems in pilot plants for, 20: 20810(T) (ANL-Trans-250)
processing carbide, oxide, and metallic, flowsheets for, 20: 20802(R) (ANL-7055, pp 21-98)
processing fast breeder, pyrochemical methods for, 20: 20802(R) (ANL-7055, pp 21-98)
processing irradiated, criticality control and safety relation to materials management in plant for, 20: 20974
properties of uranium dioxide, for power reactors, 20: 22422
reactions with water in Kiwi-TNT transients, 20: 20925(R) (ANL-7055, pp 177-212)
reactions with water in TREAT, 20: 20925(R) (ANL-7055, pp 177-212)

REACTOR FUELS (FUSED SALTS)
processing for uranium recovery, chromium fluoride trapping in, 20: 20808(R) (ORNL-3916)

REACTOR MATERIALS
analysis for trace impurities, summary of methods for, 20: 20589
development of high-temperature, 20: 21324(R) (ANL-7055, pp 163-6)
fabrication of, research program on mechanical metallurgy related to, 20: 21290(R) (GA-1052)

REACTOR MATRICES
criticality calculations for slab, 20: 22394
neutron diffusion in parallel-plate, 20: 22398
neutron Doppler measurements in, 20: 22520(R) (NAA-SR-11805)
neutron flux moments in gap geometry, boundary conditions for, 20: 22390
neutron spectra in reflected, 20: 22396

REACTOR MODERATORS
neutron spectra in, reactor design considerations from thermal, 20: 22376 (GA-6901)

REACTOR REFLECTORS
neutron flux in regions of, 20: 22396

REACTOR SAFETY
accident analysis using nuclear safety pilot plant data, 20: 20940(R) (ORNL-3915)
accident analysis for large fast reactors, 20: 22401
accident analysis for 1000-Mw(e) sodium-cooled fast breeder reactor, 20: 22453
analysis for nuclear power plants, 20: 22436
coolant-loss accidents in sodium-cooled fast reactors, analysis of, 20: 22349
detection apparatus for film boiling in liquid-cooled reactors, 20: 22367(P)
effects of vented fuel concept on, in power breeder reactors, 20: 22462
research on, survey of, 20: 22435
systems for, comparison of relay and solid-state logic, 20: 22360

REACTOR SAFETY EXPERIMENTS
coolant ejection in simulated accidents, 20: 22350
design and development of Containment Research Installation, 20: 20940(R) (ORNL-3915)
design of LOFT facility with zirconium-clad fuels, 20: 22467(R) (IDO-17077)
fuel meltdown in TREAT, during transients, 20: 20940(R) (ORNL-3915)
fuel meltdown studies in TREAT, fast-neutron detection system for, 20: 21131
fuel–water reactions in TREAT, 20: 20925(R) (ANL-7055, pp 177-212)
metal–water reactions in LOFT, 20: 20925(R) (ANL-7055, pp 177-212)
operation of LOFT, effects of zirconium cladding on, 20: 22467(R) (IDO-17077)
radioactivity release from LOFT test, 20: 22467(R) (IDO-17077)

REACTOR SOLUTIONS
analysis of, spectrophotometric, 20: 20600

REACTOR TUBES
gamma dosimetry near, using scintillation counters, 20: 21047

REACTORS
containment vessels for, design of, for in-pile experiments, 20: 20940(R) (ORNL-3915)
control circuits for, performance testing of plug-in connectors of, 20: 22352 (AEET-ED-SG/25)
control of, ionization chambers for, 20: 22356 (ORNL-3929)
control of, performance of fission-couples for, 20: 22355 (LA-3470)
core support design, 20: 22362
criticality of, dependence on neutron cross sections above 100 kev, 20: 22379 (LA-DC-7800)
decontamination of, efficiency of, 20: 20957
design of, role of thermal neutron spectra measurements for, 20: 22376 (GA-6901)
design with recycled moderator, 20: 22402(P)
loading equipment for, coupling device for, 20: 22363(P)
loading of, analysis of continuous, 20: 22407
neutron critical flux curves for reflected, variation principles for, 20: 22399
neutron diffusion in nonseparable geometries of, modified Ritz method for, 20: 22385
neutron distribution in, Courant-Wallace expressions for, (T), 20: 22372 (AFRRI-TN-65-1)
neutron flux distribution in hexagonal lattices of, determination of thermal, (T), 20: 22371 (AD-621026)
neutron flux in, computer program for, 20: 22488 (AD-621121)
neutron kinetics in, statistical analysis for determining, 20: 22381 (RT-FI(65)49)
neutron kinetics in, iterative variational method for elliptical problems in, 20: 22387
neutron slowing-down spectra in, methods for measuring, 20: 22382 (RT-FI-65)57)
neutron thermalization in, computer program for, 20: 22374(R) (BNWL-193, pp 5-15)
neutron transport in, computer programs for, 20: 22380 (ORNL-TM-1246)
reactivity noise in, space-dependence of, (T), 20: 22393
testing of, evaluation of materials for vault for, 20: 20869
xenon buildup after shutdown, use of on-line computers in control of, 20: 22389

REFRACTORY COATINGS
properties of corrosion protection, for niobium, bibliography on, 20: 21257 (AD-621546)

REFRACTORY MATERIALS

bonding process for, use of cerium oxide–cerium sulfide in, 20: 21314(P)
properties at high temperatures, chemical, 20: 20654 (LA-DC-7784)

REFRIGERATION
use of radioisotope heat for, in space vehicles, 20: 21174 (SAN-575-12)

REGENERATION
radiation effects on salamander limb, role of normal epidermis in recovery from x, 20: 20465

RELATIVITY THEORY
covariant formalism of three-dimensional physical system, 20: 21859
diffusion processes in, equations for stochastic, 20: 21870
gravitational systems in general, conservation laws for energy of static spherically symmetric, 20: 21845
Hamilton-Jacobi and Schroedinger theory in general, 20: 21864
Lorentz transformation in, representation of four-dimensional, 20: 21847
particle kinetics in, simultaneous Lorentz- and Galilean-invariant, 20: 21867

RELAYS
design and performance of electrostatic, for alarm circuits and radiation dosimetry, 20: 21088
use in reactor safety systems, 20: 22360

REMOTE-CONTROL EQUIPMENT
design criteria for, 20: 20942 (ORNL-TM-1459)
design of manipulator with ball and socket joint, 20: 20848
development of electronically controlled master-slave manipulators, problems in, 20: 20839 (AEET-ED-SG/14)
manipulator design, 20: 20843
operation of EBR-II fuel cycle facility, 20: 20802(R) (ANL-7055, pp 21-98)
technology of, status of, 20: 20844

REMOTE-VIEWING EQUIPMENT
design criteria for, 20: 20942 (ORNL-TM-1459)
technology of, status of, 20: 20844

REPTILES
radiation effects on natural populations of lizards, whole-body x-ray, 20: 20444(R) (TID-22820)

RESEARCH REACTORS
fuel element storage pool for JRR-2, 20: 22505
neutron physics at Austrian TRIGA Mark II, 20: 22502
power expansion for Russian VVR-S, redesign for, 20: 22498 (IAE-993)
power expansion for IRT, redesign for, 20: 22497 (IAE-992)
reactivity and temperature coefficient of TRIGA, effects of neutron thermalization on, 20: 22377 (GA-6930, App. B)
startup and operation of STIR, 20: 22500 (NAA-SR-11175)

RESINS
radiation effects on dielectric and mechanical properties of epoxy, combined effects of low-temperature, vacuum, and gamma and neutron, 20: 21152 (N-65-22353)
radiation effects on physical properties of epoxy, effects of resin structure on gamma, 20: 21429 (RHEL/R-105)

RESPIRATORY TRACTS
contamination by plutonium, method for treatment of, 20: 20943 (RFP-453)
radiodiagnosis of obstructions of, 20: 20532
visualization by scanning after inhalation of labeled aerosols, 20: 20532

RHENIUM
book: *Chemistry of Technetium and Rhenium*, 20: 20697
corrosion by acid, base, and salt solutions at 25 and 100°C, 20: 21275
crystallization of thin films of vacuum-evaporated, 20: 21274
effects of alloying additions of, on ductility of tungsten, 20: 21380
electrochemical properties, 20: 21275
oxidation of thin films of vacuum-evaporated, effects of deposition parameters on, 20: 21274
separation from technetium by chromatography, 20: 20629
sublimation of, rate of, 20: 21262(R) (N-65-25266)

RHENIUM ALLOYS
Hf–Re–Ta–W, properties of, effect of carbide dispersion on microstructures and strength/ductility, 20: 21404
Mo–Re, corrosion by bismuth and tin at 1000°C, (E), 20: 21566(R) (ANL-7055, pp 213-29)
Re–Ta–W, mechanical properties at 25 to 3500°F, 20: 21322 (AMRA-TR-65-25)
Re–W, ductility of, effects of rhenium content on, 20: 21380
Re–W, tensile properties to 2400°C, 20: 21406

RHENIUM ISOTOPES Re-185
neutron reactions (n,γ) at 4 kev to 2.6 Mev, cross sections for, (E), 20: 21969(R) (ANL-7055, pp 230-3)

RHENIUM ISOTOPES Re-187
energy levels of, properties of 686-kev, (T), 20: 22027
neutron capture by, isomeric cross section ratios for, (E), 20: 22052
neutron reactions (n,γ) at 4 kev to 2.6 Mev, cross sections for, (E), 20: 21969(R) (ANL-7055, pp 230-3)

RHENIUM ISOTOPES Re-188
production of isomeric and ground-state, from rhenium-187 neutron capture, (E), 20: 22052

RHENIUM SYSTEMS
C–Cr–Co–Re–Ti–W–Zr, development and tensile and stress-rupture properties of cobalt-base, 20: 21237 (N-65-29395)
C–Hf–Mo–N–Re–Ta–W–Zr, development of dispersion-strengthened tantalum-base, 20: 21240(R) (WANL-PR-(Q)-006)
C–Hf–Re–Ta–W, development of dispersion-strengthened tantalum-base T-333, 20: 21240(R) (WANL-PR-(Q)-006)
HfN–Re–W, tensile properties at high temperatures, 20: 21406
Re–ThO_2–W, ductility and hot strength, 20: 21407
Re–ThO_2–W, tensile properties at high temperatures, 20: 21406

RHODAMINE B
effects on radioinduced oxidation of ergosterol, 20: 20738

RHODIUM
desorption of carbon monoxide, hydrogen, and nitrogen from, flash, 20: 20652 (IS-T-67)
proton scattering at 45 Mev, polarization in, (E), 20: 22128
sorptive properties of evaporated films of, for carbon monoxide at 0°C, 20: 21388

RHODIUM ALLOYS
Dy–Rh, dysprosium hyperfine magnetic field in intermetallic compounds of, (E), 20: 22330
Pd–Rh, electric conductivity at low temperatures, 20: 22314(R) (AD-626865)

RHODIUM BROMIDES
ammine complexes of, bromine-82 exchange with bromides, 20: 20706

RHODIUM CHLORIDES
ammine complexes of, radiation effects on chlorine-36 exchange with chlorides, 20: 20706

RHODIUM ISOTOPES Rh-106
separation from radioisotopes in aqueous solutions by foam chromatography using colloidal manganese dioxide, 20: 20628

RIBONUCLEIC ACID
phosphorus-32 uptake by, in chick embryos, 20: 20399
preparation from *E. coli*, flowsheet for, 20: 20808(R) (ORNL-3916)
radiation effects on structure of polyriboadenylic and polyribouridylic, γ, 20: 20411

RIBONUCLEIC ACID, DESOXY-
genetic transmittal by viral, uv-method for determining duplex or simplex, 20: 20426
phosphorus-32 uptake by, in chick embryos, 20: 20399
radiation effects on metabolism in *Escherichia coli*, γ, 20: 20421
radioinduced denaturation of, uv, 20: 20412
role in genetic transmittal in phages, 20: 20427

RIBONUCLEIC ACID, DESOXY- COMPLEXES
with uranyl ions, formation of bacterial, 20: 20392

ROCKET MOTORS
propellant flow during startup transient of nuclear, 20: 22480
reactivity coupling of clustered nuclear, 20: 22483

ROCKET REACTORS
control systems for NERVA, design of, 20: 22482
development of lightweight, materials evaluation for, 20: 22470 (N-65-29480)
development of, high-temperature chemistry problems in, 20: 20870 (LA-DC-7703)
instrumentation for NERVA, 20: 22484
propellant flow during startup transient, 20: 22480
radiation monitoring during testing of, 20: 20954
reactivity coupling of clustered, 20: 22483
uses of low-power lightweight, 20: 22469 (N-65-29479)

ROCKET REACTORS (KIWI)
control of, performance of fission-couples for, 20: 22355 (LA-3470)
destruct test of ROVER, graphite particle distribution and size from, 20: 22472 (SC-CR-66-2017)
radiation distributions from NRX-A2 and NRX-A3, 20: 22481
radiation measurements from TNT experiment, 20: 22468 (LA-3395)
reactivity excursion of Kiwi-TNT, metal–water reactions in, 20: 20925(R) (ANL-7055, pp 177-212)

ROCKS
aeroradioactivity surveying of, in Maryland, Virginia, Washington, D. C., and West Virginia, 20: 20928 (CEX-59.4.17)
age estimation of plutonic and metamorphic, by rubidium-strontium method in New Zealand, 20: 20888
age estimation of pyroxenes and minerals from eclogites in Norway, 20: 20891
analysis for aluminum, manganese, and silicon, activation, 20: 20646

ROOTS
cation uptake by barley, uranyl effects on selective inhibition in, 20: 20402
radiosensitivity of bean, partial pressures of inert gases for halving oxygen-dependent, 20: 20378

ROTORS

control of ultracentrifuge, radio telemetry system for, 20: 21009
RUBBER
effects of decontaminating and descaling solution on coating of, 20: 21238 (NP-15928)
preparation of heat-resisting and radioresistant, summary on, 20: 21430(R) (WADC-TR-55-58(Pt.8))
properties of, effects of cure on elastic and tensile, 20: 21431(R) (WADC-TR-55-58(Pt.9))
radiation effects on, gamma, 20: 21430(R) (WADC-TR-55-58(Pt.8))
radiation effects on elastic and tensile properties of, 20: 21431(R) (WADC-TR-55-58(Pt.9))
RUBIDIUM
density and thermodynamic properties of, 20: 20802(R) (ANL-7055, pp 21-98)
determination in minerals, activation, 20: 20560 (EUR-2753.f)
determination in silicon dioxide, activation, 20: 20633
thermal conductivity of vaporous, at 750°C, 20: 20651(R) (CU-2660-26)
viscosity of liquid, based on atomic parameters, 20: 20656 (UCRL-11930)
RUBIDIUM BROMIDES
radiation effects on absorption spectra of, x, 20: 21424 (N-65-23332)
RUBIDIUM ISOTOPES Rb-86
content in plutonic and metamorphic rocks of New Zealand, 20: 20888
RUBIDIUM ISOTOPES Rb-87
content in plutonic and metamorphic rocks of New Zealand, 20: 20888
RUBIDIUM MANGANESE FLUORIDES
nuclear magnetic resonance in, 20: 22311(R) (AD-622068)
RUTHENIUM ALLOYS
Dy–Ru, dysprosium hyperfine magnetic field in intermetallic compounds of, (E), 20: 22330
RUTHENIUM CHLORIDES
metabolism in rat tissues, 20: 20396
RUTHENIUM ISOTOPES Ru-99
energy level transitions in, Mössbauer hyperfine splitting of 90-kev, (E/T), 20: 22141
RUTHENIUM ISOTOPES Ru-103
diffusion in irradiated fuel element cladding alloys and materials at 600 to 1200°C, 20: 21232 (BMI-1763)
RUTHENIUM ISOTOPES Ru-106
content in silt in Escaut River, Belgium, control of, 20: 22515(T) (ORNL-tr-965)
separation from radioisotopes in aqueous solutions by foam chromatography using colloidal manganese dioxide, 20: 20628
uptake by crustacea, mollusks, and plankton in Bay of Venice, 20: 20386(R) (NP-15916)

S

SAFETY
in handling uranium by using neutron absorbers, 20: 20975
materials management relation to, 20: 20974
methods for handling beryllium, 20: 21341 (MAB-205-M)
problems of, in design of pilot plants for irradiated fuel processing by fluoride volatility, 20: 20810(T) (ANL-Trans-250)
SALAMANDERS
radiation effects on limb regeneration in, role of normal epidermis in recovery from x, 20: 20465
SALICYL PHOSPHATE
radiation effects on hydrolysis of, background, 20: 20744
SAMARIUM
determination in rare earth mixtures, activation, 20: 20562 (LYCEN-6538)
friction and wear properties of, in vacuum, effects of crystal structure on, 20: 21365
magnetic properties, 20: 21414
oxidation in dry and moist air at 100 to 800°C, rate of, 20: 21265 (RPI-2714-8)
reactions with dichalcogenides and powdered graphite, preparation of intercalation compounds by, 20: 20648 (AD-621029)
separation from perchloric acid solutions by ion exchange materials, 20: 20823
separation from scandium by ion exchange chromatography, 20: 20821
separation from uranium by combined ion exchange-solvent extraction using nitric acid–tetrahydrofuran solutions, 20: 20811
SAMARIUM ALLOYS
Al–Sm, crystal structure and stability of intermetallic compounds in, 20: 21415
Dy–Sm, electric conductivity at 4.2, 77, and 295°K, 20: 22312(R) (AD-622796)
Fe–Sm, crystal structure of $SmFe_7$, 20: 21400
Hg–Sm, thermodynamic properties and vapor pressure measurements, 20: 21384
Mn–Sm, crystal structure and magnetic properties of intermetallic compounds of, 20: 21403
SAMARIUM ISOTOPES
mass differences of, (E), 20: 22153
SAMARIUM ISOTOPES Sm-145
energy level transitions from europium-145 decay, (E), 20: 22003 (JINR-P-2581)
SAMARIUM ISOTOPES Sm-149
Mössbauer effect on, use of europium for studies on, 20: 20622
SAMARIUM OXIDES
proton reactions at 590 Mev and 18 Bev, yields of iodine isotopes from, (E), 20: 22045
solubility in ethyl, isopropyl, methyl, and propyl alcohols in presence of ammonia, 20: 20686
SAMPLING
equipment for reactor containment test facilities, 20: 20940(R) (ORNL-3915)
errors in subisokinetic, of aerosol particles in air stream, 20: 20927 (BNWL-217)
method for quality control, during reactor component fabrication, 20: 21308
methods used in France for nuclear materials management, 20: 20973
SANDS
cesium-137 gamma spectra in, (E), 20: 22308 (HASL-167)
SANDSTONE
radioactivity of, Braunschweig, Germany, 20: 20890
SAP (SINTERED ALUMINUM PRODUCTS)
quality control of tubes of, mechanical radiographic methods for, 20: 20861 (EUR-2443.f)
SATELLITES
radio signals from, comparison with Jupiter radio emission, 20: 21510
SAVANNAH RIVER PRODUCTION REACTORS
containment filter system for, performance of carbon-bed, 20: 22463(R) (DP-1028)
radioisotope production in, 20: 21212 (CONF-660305-19)
SCANDIUM
magnetic susceptibility at 1.5 to 4.2°K and at 14 to 20°K, (E), 20: 21381
separation from metal ions by ion exchange chromatography, 20: 20821
separation from perchloric acid solutions by ion exchange materials, 20: 20823
separation from rare earths and thorium by paper chromatography, 20: 20825
SCANDIUM ISOTOPES Sc-42
energy levels from helium-3 reactions (He-3,p) and (He-3,pγ) with calcium-40 at 10, 12, and 15 Mev, (E), 20: 22073
SCANDIUM ISOTOPES Sc-47
energy levels, (E), 20: 22010(R) (NYO-72-28)
SCATTERING
amplitudes for system of fixed centers, 20: 21710 (JINR-P-2554)
amplitudes for three-body, threshold behavior of, 20: 21747
amplitudes in, analyticity properties of, 20: 21733
amplitudes in, unitarity conditions for off-shell two-particle p-wave, 20: 21756
Feynman diagrams in, Landau curves of, 20: 21732
potential, completeness, dispersion relations, and unitarity in, 20: 22464 (IC-66/29)
potential, space-time properties for particle wave packet, 20: 21761
S-matrix for large angular momentum, asymptotic form of, 20: 21754
S-matrix in, Regge pole representation of, 20: 21755
S-matrix theory for strongly interacting particles, 20: 21774
T-matrix in, limiting forms of screened Coulomb, 20: 21731
theory for strongly interacting particles, 20: 21773
theory for two-plane wave, (T), 20: 21716 (JINR-P-2603)
theory for, Coulomb problem in, 20: 21702 (AD-621385)
SCHISTOSOMA
radiation effects on infectivity of, in mice, gamma, 20: 20446
SCINTILLATION DETECTORS
circuit development suppression of pulse rates from, 20: 21086
design and operation of transistorized, for radon monitoring, 20: 21067
design and performance for whole-body facility, 20: 21075
design and performance for nuclear debris analysis, 20: 20881 (DASA-1704)
design of directional proton-recoil, for cosmic neutrons, 20: 21117
development for clinical scanning using iodine-131, 20: 20535
development for low-level counting, 20: 21042 (SGAE-E-6/1966)
development of liquid, for measurement of neutrino-proton interaction cross sections, 20: 21027 (CERN-65-32, pp 41-4)
development of plastic, for cosmic particles, 20: 21028 (CERN-65-32, pp 65-70)
efficiency for collimated gamma rays, 20: 21056
efficiency for simultaneous determination of calcium-45 and phosphorus-32 in inorganic salts, 20: 20584
glasses for, development and properties of, 20: 21044(T) (ANL-Trans-285)
meson (μ) production in large plastic, by background neutrals, 20: 21028

(CERN-65-32, pp 65-70)
meson (μ) production in liquid, by cosmic rays, (E), 20: 21029 (CERN-65-32, pp 71-2)
performance for gamma dosimetry near reactor pipes, 20: 21047
photon reflection coatings for, preparation and properties of, 20: 21136
pulse discriminator for proton-recoil, design of fast zero-crossing, 20: 21114
pulse yield relations for heavy ions in, 20: 21084
response to low-energy x radiation, equipment and methods for studying, 20: 21107
use in medical radiodiagnosis, review, 20: 20531
use of dual-probe, for placenta localization using iodine-131, 20: 20527

SEA WATER
book: *Advances in Water Pollution Research*, Vol. 1, 2, and 3, 20: 20982
desalination of, cost of nuclear and fossil fueled plants for, 20: 22461
microbiological assays in, tracer techniques for, 20: 20368 (CONF-640309-1)
radio wave scattering by surface of disturbed, structure effects on spatial characteristics of, (E), 20: 20908
radioisotope content of, effects on development of fish spawn of strontium-90 and yttrium-90, 20: 20445(T) (TRG-Inf. Ser.-166)
uranium occurrence in, 20: 21243

SEDIMENTARY DEPOSITS
analysis for potassium, thorium, and uranium by scintillation counting and x-ray fluorescence, 20: 20613

SEED
radioinduced mutations for variegation in Einkorn wheat, beta, fast neutron, gamma, and thermal neutron, 20: 20497
radioinduced mutations in wheat, x, 20: 20501

SEISMIC WAVES
detection and comparison of, from earthquakes and underground nuclear explosions, 20: 20906
detection of, large-aperture detector array for, 20: 20909
production of, computer code for source mechanism determination for, 20: 20912
propagation from nuclear explosions in overdriven cavities, 20: 20898 (AD-624016)
propagation from thermonuclear explosions, analysis of, 20: 20907
propagation of elastic, abstracts on, 20: 20896 (AD-623592)

SEISMOLOGY
measurements for comparing earthquakes and underground explosions, 20: 20900 (AD-627039)
measurements for comparing earthquakes and underground explosions, 20: 20901 (AD-627040)
measurements for comparing earthquakes and underground explosions, 20: 20902 (AD-627051)
measurements in Vela Project, 20: 20876 (NP-15949)
seismic wave source mechanism, computer code for determining, 20: 20912
underground explosion detection in, teleseismic record evaluation for, 20: 20911

SEISMOMETERS
design and performance of large aperture, 20: 20899(R) (AD-626777)
design of large array of, for detection of distant underground nuclear explosions, 20: 20913
design of large-aperture array of, 20: 20909

SELENIDES
formation of, paragenesis with pitchblendes in, 20: 20918

SELENIUM
performance as electrophotographic material for particle track coordinates in spark chambers, 20: 21037 (JINR-P-2594)

SELENIUM FLUORIDES
enthalpy of formation of SeF_6, 20: 20650(R) (ANL-7055, pp 167-76)

SELENIUM SYSTEMS
Se–Te, performance as electrophotographic material for particle track coordinates in spark chambers, 20: 21037 (JINR-P-2594)

SEMICARBAZIDE
complexes with uranyl chlorides, polarographic behavior of, 20: 20677

SEMICONDUCTOR DETECTORS
amplifier for, design of low-noise charge-sensitive transistorized pre-, 20: 21072
amplifiers for, design of integrated-circuit charge-sensitive pre-, 20: 21112
design and performance of lithium-6-silicon, for fast neutrons, 20: 21034 (EUR-2712.e)
design and performance of lithium-drifted silicon-diode, 20: 21064
design for detection and measurement of low-energy electrons, 20: 21138
design of oxide-passivated silicon p-n junction, for alpha particles, 20: 21077
development, 20: 21026 (BNL-948, pp 704-17)
development of silicon surface barrier, for charged-particle spectrometers, 20: 21054
fabrication and performance of large-volume lithium-drifted germanium, 20: 21104
fabrication of lithium-drifted germanium, 20: 22010(R) (NYO-72-28)
fabrication of silicon junctions using ion implantation, 20: 21098
performance of Compton spectrometer, for nondestructive burnup determination of fuel elements, 20: 21050
performance of silicon, as fast-neutron dosimeter, 20: 21095
preparation and properties of shallowly diffused silicon junctions, 20: 21099
properties of internally amplifying gallium-diffused junctions, 20: 21100
pulse rise times in detection and measurement of charged particles, 20: 21137
response of lithium-drifted germanium and silicon, temperature dependence of, 20: 21102
response of silicon surface-barrier, to fission fragments, 20: 21101
response to low-energy x radiation, equipment and methods for studying, 20: 21107
sensitivity to gamma rays and neutrons, 20: 21059
surface potential of lithium-drifted germanium, 20: 21096
use of silicon p-n, in dosimeter for beta particles and gamma radiation, 20: 21133
use of tunnel diodes with charge-multiplying, 20: 21113
use with alpha sources as timing devices, 20: 21021 (AD-622629)

SEMICONDUCTORS
design of lithium-drifted silicon p-i-n, for beta particles, 20: 21077
radiation effects on electric properties of germanium and silicon, neutron, 20: 21150 (HMI-B-45)
radiation effects on, review of, 20: 21156
radiation effects on, review of, 20: 21160
radiation effects on, conference on, 20: 21164
radiation effects on, generalized model analysis of ionizing, (T), 20: 21167
radiation effects on, modeling of, 20: 21173
radiation effects on, photovoltaic theory for, 20: 21437
radioinduced damage in silicon, gain degradation from neutron, 20: 21169
radioinduced defects in, model for annealing, 20: 21153(R) (N-65-25593)
radioinduced regeneration effects in p-n junction, in isolated circuits, 20: 21168
stability of lithium-drifted silicon, 20: 21103
superconductivity of ionic, high-current, (T), 20: 21889
thermal conductivity of, effect of heat transport by radiation on, 20: 22329
thermal effects in, compensation of, 20: 20992
use in reactor safety systems, 20: 22360

SEPARATION PROCESSES
development and use of rapid radiochemical, review of, 20: 20826
development of shear-leach, for clad fuel elements, 20: 20808(R) (ORNL-3916)
materials management during, at Windscale, 20: 20972

SEPARATORS
ion beam reactions in electromagnetic isotope, 20: 21219

SERVOMECHANISMS
use for correction of phase changes between deflectors in r-f separator, 20: 21467 (CERN-66-8)

SEWAGE
conference on water pollution research, London, Sept. 1962, 20: 20982

SEWAGE SYSTEMS
construction for waste-solution discharge, into Escaut River in Belgium, proposal for, 20: 22515(T) (ORNL-tr-965)

SEX
effects on organ weight in man, 20: 20374

SF MATERIALS ACCOUNTING
methods of, at Windscale New Separation Plant, 20: 20830
methods of, review of UKAEA, 20: 22528

SHEEP
fallout uptake by, effects of biological and environmental factors on cesium-137 and strontium-90, 20: 20388 (SAN-34-2)
radiation effects on blood–brain barrier permeability in, neutron, 20: 20489
radiation lethality in, dose determinations for *y* and x, 20: 20487

SHELTERS
design for protection against nuclear weapons effects in schools, evaluation of, 20: 20868 (AD-626770)
fallout, sensitivity analysis of components and systems of, 20: 20922 (AD-624704)
thermal transient response of underground, scale model tests on, 20: 20920 (AD-621377)
ventilation of fallout, by induced draft, 20: 20921(R) (AD-621998)

SHIELDED CONTAINERS
development for shipping and storage of fissile materials, 20: 20840(R) (BNWL-193, pp 57-67)

SHIELDING
computer programs for parameters of, abstracts on, 20: 22310 (ORNL-RSIC-13)

meson (μ) flux in neutrino, measurement of, 20: 22306 (CERN-65-32, pp 147-52)
SHIPPING
container and packaging for uranium hexafluoride, development and testing of, 20: 20936 (K-1661)
regulations for radioactive materials, key to IAEA 1964, 20: 20945 (TRG-Report-1073)
SHIPPINGPORT PRESSURIZED WATER REACTOR
steam generator for, metallographic inspection of, 20: 22408 (BMI-1764)
SHOCK TUBES
development for plasma diagnostics, 20: 22170 (AD-622701)
SHOCK WAVES
effects on coolant expulsion in reactor accidents, 20: 22348
heating rates for cylinders in laminar hypersonic, 20: 20857 (SC-DC-65-1907)
interactions in nitromethane-filled corners, hydrodynamics of, (E/T), 20: 21784 (LA-3450)
interactions of laser-driven imploding, in plasma, 20: 22245
plasma density measurement in pressure-driven, (E/T), 20: 22168 (AD-622569)
pressure gages for, design and operation of multidirectional peak, 20: 20914
production in acoustic spark chambers, spark location from analysis of, (T), 20: 21094
production in inverse pinch devices, 20: 21798
propagation in argon plasma, radiation intensity from, (E/T), 20: 22281
propagation in electromagnetic shock tube, (T), 20: 21796
propagation in electroneutral media, magnetic deformation and electric structure in wave-front interior during, (T), 20: 21806
propagation in gases, ionization from, (T), 20: 22285
propagation in hydrogen, properties of electromagnetically driven, (T), 20: 21779 (AD-621990)
propagation in hydrogen, equilibrium chemistry of ionizing, (T), 20: 21796
propagation in perpendicular magnetic field, radiative energy flux from one-dimensional plane, (T), 20: 21788
propagation in plasma, microwave interferometry of, (E), 20: 22182 (IPP-3/35)
properties of second standing, in magnetosheath, 20: 21821
structure in plasma, radiation smoothing of, 20: 21775 (AD-620835)
structure in plasma flow past bodies in magnetic field, (E), 20: 22251
SILANE
ion-molecule reactions in, 20: 20725(R) (NYO-3570-2)
radiolysis of, yields in gamma, 20: 20725(R) (NYO-3570-2)
SILICON
analysis for lithium, activation, 20: 20560 (EUR-2753.f)
deposition on beryllia of single-crystal, chemical vapor, 20: 21249
determination in high-purity tantalum by spectrography using d-c arc method, 20: 20608
determination in rocks, activation, 20: 20646
determination in uranium silicides, method for, 20: 20557 (AERE-R-5129)
effects on tensile properties of vanadium-base alloys, 20: 21333(R) (IITRI-B6042-4)
fabrication of junctions of, using ion implantation, 20: 21098
lithium-ion drift in p-type monocrystals of, (E), 20: 21337 (JINR-P-2598)
performance as fast-neutron dosimeter, 20: 21095
performance of lithium-drifted diodes of, as radiation detectors, 20: 21064
preparation and properties of shallowly diffused junctions of, 20: 21099
radiation damage at low temperatures in degenerate, 20: 22346
radiation damage in space environment, electron and proton, 20: 21165
radiation effects on impurity diffusion in, electron and proton, 20: 21147(R) (AD-621049)
radiation effects on electric properties of, neutron, 20: 21150 (HMI-B-45)
radiation effects on defect introduction rate in n-type, energy dependence of electron, 20: 21154(R) (N-65-23290)
radiation effects on MOS FET transistor of, annealing of gamma, 20: 21159
radiation effects on transistors of, prediction of transient, 20: 21166
radiation effects on recombination centers in, gamma, 20: 21439
radiation response of power transistors of, effects of design on, (E/T), 20: 21148(R) (AD-630835)
radiation response of power transistors of, effects of design on, (E/T), 20: 21149(R) (AD-630836)
radioinduced damage in semiconductors of, gain degradation from, 20: 21169
radioinduced E centers in arsenic-, antimony-, and bismuth-doped, annealing of gamma and electron, (E), 20: 22323
radioinduced regeneration effects in p-n junction, in isolated circuits, 20: 21168
radioinduced surface damage in, gamma, 20: 21172
SILICON CARBIDES
reactions with fluorine, thermodynamics of, 20: 20650(R) (ANL-7055, pp 167-76)
$SiC-UO_2$, fabrication of fuel particles of, 20: 21297(T) (NP-tr-1371)
SILICON HYDRIDES
yields in gamma radiolysis of silane, 20: 20725(R) (NYO-3570-2)
SILICON ISOTOPES Si-28
alpha inelastic scattering at 28.4 Mev, collective enhancement of 3- state in, (T), 20: 22107
reactions in stars, statistical equilibrium for, 20: 21492
SILICON OXIDES
analysis for barium, calcium, and strontium in irradiated, activation, 20: 20636
analysis for impurities, activation, 20: 20632
analysis for impurities, activation, 20: 20634
analysis for impurities, activation, 20: 20635
analysis for oxygen by activation using helium-3 ions, detection limits and sensitivity of, 20: 20565 (ORNL-P-1216)
effects of colloidal, on radiolysis of benzene in aqueous solutions, 20: 20768
reactions with gaseous uranium trioxide, effects of substrate symmetry in, 20: 20649 (AEET-CD-24)
separation of barium, calcium, and strontium from irradiated, chromatographic method for, 20: 20636
SiO_2-SO_2, properties for use as adsorption refrigeration system, 20: 21174 (SAN-575-12)
SILICONE POLYMERS
radiation effects on, role of LET in gamma and helium-4/lithium-7, 20: 20764
radiation effects on, light-scattering and viscosity measurements of gamma, 20: 20765
phosphors—tritiated silicone polymers, preparation of luminous compositions from, 20: 20787(P)
SILICONES
radiation effects on dielectric and mechanical properties of, combined effects of low-temperature, vacuum, and gamma and neutron, 20: 21152 (N-65-22353)
SILTS
radioactivity in Escaut River, Belgium, control of, 20: 22515(T) (ORNL-tr-965)
rare earth distribution in, 20: 20877
SILVER
alpha scattering at 28.4 Mev, angular distributions from, (E), 20: 22047
determination in minerals and ores, activation, 20: 20574
determination in silicon dioxide, activation, 20: 20634
electron reactions at 6 to 23 kev, optical transition radiation from, 20: 21518
gamma elastic scattering at 280 and 662 kev, Z dependence of cross section for, (E), 20: 22060
helium-3 reactions (He-3,n) at 19 to 25 Mev, angular distributions and cross sections for, (E), 20: 22132
manganese-54 orientation in, gamma-ray anisotropy from, (E), 20: 22097
neutron inelastic scattering at 5.8 and 7.5 Mev, gamma spectra from thermal, (E), 20: 22069
removal of brazing flux of, from metals, descaling solution for, 20: 21238 (NP-15928)
separation from chromium, manganese, nickel, and rare earths by ion exchange chromatography, 20: 20634
separation from perchloric acid solutions by ion exchange materials, 20: 20823
viscosity of liquid, based on atomic parameters, 20: 20656 (UCRL-11930)
SILVER ALLOYS
Al–Ag, use for neutron dosimetry, 20: 21025 (AERE-R-5122)
Be–Ag, radiation effects at 80°K on, resistivity recovery from proton, 20: 21445
Cd–In–Ag, fabrication of reactor control rods of, 20: 21317(P)
Li–Ag, radiation effects at 80°K on, resistivity recovery from proton, 20: 21445
rare earth–Ag, crystal structure of equiatomic intermetallic compounds of, 20: 21399
SILVER CHLORIDES
cobalt-57 Mössbauer emission spectra in, quadrupole splitting in, (E), 20: 22340
iron ESR spectra in, 20: 22311(R) (AD-622068)
use for detecting charged particles, 20: 21060
SILVER COMPLEXES
with thiodibenzoylmethane, stability of, 20: 20693
SILVER IODIDES
sorptive properties for cobalt, europium, and sodium ions, tracer studies on, 20: 20683
SILVER ISOTOPES
determination in radiation sources, extraction radiometric titration method for, 20: 20567 (UJV-1418/65)
SILVER ISOTOPES Ag-111

beta decay of, cadmium-111 level structure from, (E), 20: 22083
yields from photofission of uranium by 650-Mev bremsstrahlung, 20: 22040
SKIN
contamination by plutonium, method for treatment of, 20: 20943 (RFP-453)
radiation effects on nitrogen content in mouse, effects of bone marrow transplants on x, 20: 20407 (ORNL-P-1118)
radiation effects on melanin patterns in human, solar, 20: 20458
radiation effects on mouse, x, 20: 20475
radiation effects on, of urethan-treated mice, x, 20: 20476
SKIN GRAFTING
effects of extracorporeal γ irradiation of blood and lymph on rejection of, in calves, 20: 20485
radiation effects on rabbit, 20: 20477
SKIN LESIONS
radioinduced in man, design and performance of remission photometer for measuring erythemic, 20: 21011
radioinduced in mice, x, 20: 20475
SODIUM
analysis for impurities, methods of, 20: 22520(R) (NAA-SR-11805)
combustion of reactor coolant, fission-product release in, 20: 22520(R) (NAA-SR-11805)
density and thermodynamic properties of, 20: 20802(R) (ANL-7055, pp 21-98)
determination in potassium halogenides, activation, 20: 20560 (EUR-2753.f)
determination in silicon dioxide, activation, 20: 20633
determination in tin oxide, activation, 20: 20577
handling and purification of, for use in corrosion test loop, 20: 21293 (R-66SD3007)
neutron cross sections and shielding coefficients for, 20: 22383(T) (AEC-tr-6693)
preparation for coolant loop studies, 20: 22520(R) (NAA-SR-11805)
preparation of purified, 20: 22520(R) (NAA-SR-11805)
radiation effects on content in animal cell nuclei, x, 20: 20422
radioinduced formation in sodium chloride by 50-kev electrons, 20: 20781
reactions with air, calculations on, 20: 20925(R) (ANL-7055, pp 177-212)
reactions with carbon, effects on metal corrosion, 20: 20802(R) (ANL-7055, pp 21-98)
reactions with metals at high temperatures, 20: 20925(R) (ANL-7055, pp 177-212)
separation of barium, calcium, and strontium from irradiated, by chromatography, 20: 20636
thermal capacity of liquid, corresponding states correlation of configurational, 20: 20657 (UCRL-11931)
thermal conductivity of vaporous, at 750°C, 20: 20651(R) (CU-2660-26)
viscosity of liquid, based on atomic parameters, 20: 20656 (UCRL-11930)
wetting of uranium nitride by liquid, use of, in preparation of pastes, 20: 20802(R) (ANL-7055, pp 21-98)
SODIUM ACID PHOSPHATES
production of phosphorus-32-labeled, aerosols of, design and performance of generator for, 20: 20924 (AEET-232)
SODIUM ALLOYS
Bi–Na, equilibria in regenerative cells, liquid-vapor, (E), 20: 21566(R) (ANL-7055, pp 213-29)
Bi–Na, solubility in sodium halide mixtures, (E), 20: 21566(R) (ANL-7055, pp 213-29)
K–Na, thermodynamic properties, 20: 20802(R) (ANL-7055, pp 21-98)
SODIUM CHLORIDES
effects on corrosion of rhenium at 25 and 100°C, 20: 21275
effects on efficiency of actinide and lanthanide separations by ion exchange chromatography, 20: 20822
fluorescence and absorption spectra of praseodymium in single crystals of, 20: 20663
production of sodium-24-labeled aerosols of, design and performance of generator for, 20: 20924 (AEET-232)
radiation effects on sodium formation in, 50-kev-electron, 20: 20781
radiation effects on absorption spectra of, x, 20: 21424 (N-65-23332)
$MgCl_2$–KCl–NaCl, corrosive effects with cadmium alloys, on stainless steel, 20: 20802(R) (ANL-7055, pp 21-98)
$MgCl_2$–KCl–NaCl, solvent properties of liquid, for praseodymium, 20: 20802(R) (ANL-7055, pp 21-98)
NaCl–NaF–NaI, density of, temperature effects on, (E), 20: 21566(R) (ANL-7055, pp 213-29)
NaCl–NaF–NaI, solvent properties for bismuth–sodium alloys, (E), 20: 21566(R) (ANL-7055, pp 213-29)
SODIUM FLUORIDES
sorptive properties for chromium fluorides, 20: 20808(R) (ORNL-3916)
NaCl–NaF–NaI, density of, temperature effects on, (E), 20: 21566(R) (ANL-7055, pp 213-29)
NaCl–NaF–NaI, solvent properties for bismuth–sodium alloys, (E), 20: 21566(R) (ANL-7055, pp 213-29)
SODIUM IODIDES
light intensity from pure crystals of, dependence on absolute temperature, (T), 20: 22317
scintillation yields for $2 < Z < 20$ ions, linear relation for, 20: 21084
NaCl–NaF–NaI, density of, temperature effects on, (E), 20: 21566(R) (ANL-7055, pp 213-29)
NaCl–NaF–NaI, solvent properties for bismuth–sodium alloys, (E), 20: 21566(R) (ANL-7055, pp 213-29)
SODIUM IONS
sorption by silver iodide, tracer studies on, 20: 20683
uptake by barley roots, uranyl effects on selective inhibition in, 20: 20402
SODIUM ISOTOPES Na-22
content in Italian milk, 20: 20950
SODIUM ISOTOPES Na-23
alpha scattering at 18 Mev, cross sections for, (T), 20: 22134
deuteron reactions (d,p) at 1.5 Mev, neutron-capture angular momenta for levels from, (E/T), 20: 22150
SODIUM ISOTOPES Na-24
energy levels from sodium-23 (d,p) reactions, neutron-capture angular momenta for, (E), 20: 22150
production in asbestos cement by neutron irradiation, quality control by, 20: 21204
use as tracer for measuring Columbia River flow times, 20: 20916
SODIUM NITROPRUSSIDE
properties as absorber in iron-57 Mössbauer studies, 20: 22158
properties as standard for iron-57 Mössbauer studies, 20: 20684
SODIUM OXIDES
analysis for cesium, potassium, rubidium, and sodium, activation, 20: 20633
SODIUM REACTOR EXPERIMENT
development and operation, 20: 22520(R) (NAA-SR-11805)
SODIUM SULFATES
radiation effects on metabolism of sulfur-35-labeled, in rat liver, x, 20: 20410
SODIUM TUNGSTATES
uses in determination of thorium by conductometric titration, 20: 20592
SOILS
cesium-137 sorption by, successive desorption method for calculating, 20: 20618
cesium-137 uptake by forest, 20: 20879 (BNWL-SA-530)
chemistry of, tracer studies, 20: 20389 (STI-PUB-108)
ground water velocity in, device for measuring, 20: 20875 (EUR-2481.f)
moisture content of, neutron probe measurement, 20: 20915
radioactivity in, of watershed of Boulder City, Colo., 20: 20379 (COO-1191-10)
radioisotope dispersion and movement in, mechanisms of, 20: 20875 (EUR-2481.f)
sorptive properties for cesium-137, 20: 20696
strontium applications to agricultural, effects on strontium-90 uptake by clover and rye grass, 20: 20381
strontium-90 content in, effects of depth on, 20: 20882(R) (HASL-171)
strontium-90 retention by, effects of chemical treatments on, 20: 20875 (EUR-2481.f)
strontium-90 separation from, 20: 20882(R) (HASL-171)
SOLAR BATTERIES
conference, 20: 21581
conference, 20: 21582
conference, 20: 21583
radiation effects at 10 to 90°C, electron, 20: 21161
SOLAR FLARES
data for second quarter 1965, 20: 21830
neutrons in, detection of protons from decay of, 20: 21495
radio emission from, pre-absorption events in bursts of type-IV, (E), 20: 21500
SOLAR RADIATION
effect of solar wind on magnetic field of moon, 20: 21502
effects of solar wind on plasma in geomagnetic tail, 20: 21828
effects on chlorophyll a and net production rates in Columbia River algae, 20: 20382 (BNWL-SA-623)
effects on gastric transit in laparotomized and vagotomized rats, 20: 20414
effects on melanin patterns in man, 20: 20458
properties of r-f, 20: 21506
properties of solar wind, 20: 21496
SOLENOIDS
current degradation in superconducting, (E), 20: 21920
magnetic fields of superconducting, measurement of, using galvanometers and flip coils, 20: 20806(R) (MLM-1274)
SOLIDS
flow-diverter valve for granular, design of, 20: 22511 (IDO-14666)
plasma waves with mass anisotropy in, amplification of, 20: 22342
radioinduced free radicals in, ESR studies on, 20: 20729 (PB-181506,

pp 85-103)
thermal conductivity of, effect of heat transport by radiation on, 20: 22329
SOLUTIONS
activity profile of radiochromatograph of radioactive, method for analyzing, 20: 20559 (EUR-2626.f)
SOLVENT EXTRACTION PROCESSES
description of, for short-lived isotopes, review of, 20: 20826
SOUND
velocity in two-phase sodium flow, 20: 22348
SOUTHWEST EXPERIMENTAL FAST OXIDE REACTOR
control systems for, development of, 20: 22496(R) (GEAP-4864)
core design for, steady-state and transient testing of, 20: 22496(R) (GEAP-4864)
development and research program, July-Sept. 1964, 20: 22495(R) (GEAP-4742)
development and research program, Feb.-Apr. 1965, 20: 22496(R) (GEAP-4864)
fuel development for, 20: 22496(R) (GEAP-4864)
instrumentation development for, 20: 22496(R) (GEAP-4864)
SOVIET UNION
age estimation of carbonate deposits in, 20: 20887
SPACE
chemical evolution and organic synthesis in primitive planetary environment, (T), 20: 20406 (N-65-27062)
electron detection and measurement in, system for, 20: 21116
radiation damage in silicon devices in, 20: 21165
radiation effects in, conference on, 20: 21164
SPACE FLIGHT
electron spectrometers for use in Gemini Project, 20: 21116
SPACE MEDICINE
bibliography on, 20: 20369 (NASA-SP-7011(22))
SPACE VEHICLES
electric circuits of, design of switchgear for, 20: 20986(R) (N-65-29823)
equipment for analysis of lunar surface, 20: 21003
power plants using electrochemical reaction of liquid mercury and potassium, nuclear, 20: 22485
power supplies for, conference on, 20: 21582
power systems for, conference on, 20: 21097
propulsion of, design of plasma engine for, 20: 20874(P)
reentry of, use of radioisotopes for measuring heat-shield ablation and sublimation in, 20: 20860
testing of SNAP-10A/Agena power system, 20: 22477
uses of radioisotopes in operation of life-support systems in, 20: 21174 (SAN-575-12)
SPARK CHAMBERS
design and performance, for gamma cameras, 20: 21082
design for detecting double beta decay of calcium-48, 20: 22010(R) (NYO-72-28)
design of digitized, for detection and measurement of cosmic gamma radiation, 20: 21121
design with photographic recording for detection and measurement of cosmic gamma radiation, 20: 21122
design with vidicon readout for detection and measurement of cosmic gamma radiation, 20: 21119
image intensifiers for, design and performance of, 20: 21020 (AD-621069)
particle track coordinates in, electrophotographic device for evaluating, 20: 21037 (JINR-P-2594)
particle-track localization efficiency of, for different triggering modes, 20: 21048
spark location in acoustic, from shock wave analysis, (T), 20: 21094
track photographs from, electroluminescent panels as pulsed fiducial marks for, 20: 21090
use in antineutrino experiments, 20: 21607 (CERN-65-32, pp 161-8)
use in determining lower limit for intermediate boson, mass, 20: 21596 (CERN-65-32, pp 11-24)
use in neutrino detection, 20: 21030 (CERN-65-32, pp 223-4)
use in spectrometer for cosmic protons, 20: 21120
SPECTRA
gravitational effects on, line displacements in, 20: 21843
lines of, pressure broadening of, (T), 20: 21519
SPECTROMETERS
conference on photographic and spectroscopic optics, 20: 21458
design modification for isotopic shift studies, 20: 20662
properties of magnetic, with field variation, 20: 21036 (JINR-P-2573)
SPECTROPHOTOMETRY
conference on photographic and spectroscopic optics, 20: 21458
SPECTROSCOPY
conference on photographic and spectroscopic optics, 20: 21458
determination of elements by atomic, bibliography on, 20: 20563 (NP-15918)
SPERMATOGENESIS
radiation effects on, in lizards, 20: 20444(R) (TID-22820)
radiation effects on mouse, effects of age at irradiation of x, 20: 20499
SPINAL CORD
radiation injury in supervoltage therapy, x, 20: 20545
radioinduced myelopathy in dog, Thorotrast, 20: 20455
SPLEEN
analysis of tissues from, for carbon-14, combustion procedure in liquid scintillation counting for, 20: 20570
radiation effects on metabolic activity in rat, x, 20: 20433 (AD-630390)
radiation effects on adenosine triphosphatase activity of rat, 20: 20503(R) (AD-629311, pp 1-14)
radiosensitivity of mouse, effects of β-mercaptoethylamine on, 20: 20511
radiosensitivity of mouse, effects of bacterial toxins on, 20: 20512
weight norms for human, use in establishing standards for radiation dosimetry, 20: 20374
SPONTANEOUS FISSION
lifetimes of heavy-element, (T), 20: 22043
STAINLESS STEEL
bonding of types 316, 321, and 347, to refractory metals and alloys, process development for explosive, 20: 21295(R) (WANL-PR-(EE)-002)
cesium deposition on, 20: 22411(R) (GA-6113)
coating by neptunium and plutonium by electrolytic deposition, 20: 21287 (AE-217)
corrosion of type 304, by bismuth–tin alloy at 200 to 1100°C, kinetics of hydrodynamic, 20: 21260 (ANL-6985)
corrosion of type 405, by cadmium alloy–fused chloride mixtures at high temperatures, 20: 20802(R) (ANL-7055, pp 21-98)
corrosion of type 405, by liquid plutonium and uranium alloys, 20: 20802(R) (ANL-7055, pp 21-98)
corrosion of types 304 and 316, by argon–nitrogen mixtures at 900°C, 20: 20802(R) (ANL-7055, pp 21-98)
diffusion of fission products in irradiated type 304, at 600 to 1200°C, 20: 21232 (BMI-1763)
ductility and rupture strength of types 304 and 316, 20: 22520(R) (NAA-SR-11805)
ductility of, at −269°C, 20: 21416
effects of decontaminating and descaling solution on metal loss on, 20: 21238 (NP-15928)
effects on reactions of bromine pentafluoride with uranium, 20: 20803(R) (ANL-7055, pp 99-162)
fabrication of control rods of, for EGCR, 20: 21292 (ORNL-3932)
fission product deposition on, from air–steam mixtures, 20: 20940(R) (ORNL-3915)
iodine-131 deposition and transport on, model for, (E/T), 20: 21785 (ORNL-TM-1330(Rev.))
mechanical properties of Swedish pressure vessel, 20: 21228 (AE-221)
oxidation by carbon dioxide–carbon monoxide mixtures, 20: 21383
properties of austenitic, 20: 22502(R) (NAA-SR-11805)
properties of, for use as fuel cladding, 20: 21383
radiation effects on austenitic, neutron, 20: 21383
radiation effects on strain fatigue of austenitic, neutron, 20: 21426 (N-65-24714)
reactions with sodium at high temperatures, 20: 20925(R) (ANL-7055, pp 177-212)
removal from fuel elements using hydrofluoric acid–oxygen solutions, 20: 20808(R) (ORNL-3916)
removal of oxides from, descaling solution for, 20: 21238 (NP-15928)
use in reactor control rod cladding, 20: 21317(P)
wear properties of plasma-arc-deposited coatings of, 20: 21319 (AD-621064)
welding to molybdenum and niobium, 20: 21309
stainless steel–UO_2, processing by fluorination for uranium recovery, 20: 20803(R) (ANL-7055, pp 99-162)
stainless steel–UO_2, processing by fluid-bed fluoride volatility, 20: 20801 (ANL-6830)
STANFORD LINEAR ACCELERATOR
beam interactions in storage ring of, angular distributions from electron, (E), 20: 21588 (AD-623658)
STARCHES
radiation effects on properties of, as adhesive and dyeing mordant, 20: 20767
radiolysis of potato, effects of water content on gamma, 20: 20737
STARS
chromospheres of, properties of, 20: 21504
detection of x-ray source, at 20 to 200 kev, (E), 20: 21490
distribution of x-ray source, supernova correlations with, 20: 21497
energy sources for quasistellar, subnuclear processes as, (T), 20: 21498
evolution, (T), 20: 21512
evolution of, silicon-28 statistical equilibrium for, 20: 21492
mass and radius of visible quasars, limits on, 20: 21501
radio emission from, comparison with Jupiter radio emission, 20: 21510
thermonuclear reactions in pulsing, effective density and temperature

exponents for 3α, (T), 20: 21491
x-ray emission from supernovae, effects of early radiation field and high-energy electrons on, 20: 21499

STATISTICS
research, 20: 21224 (ORNL-3919)

STEAM
corrosive effects on zirconium at 500°C, effects of surface contamination on, 20: 21268
performance as coolant for 1000-Mw(e) fast breeder reactor, 20: 22452
reactions with aluminum at high pressures and temperatures, 20: 20925(R) (ANL-7055, pp 177-212)

STEAM POWER PLANTS
economics of, in sea water desalination plants, 20: 22461

STEEL
analysis for lead and molybdenum by x-ray fluorescence methods, 20: 20642
analysis of, using radioisotope portable analyzer, 20: 20642
coating thickness of gold on, use of proton beam scattering for measuring, 20: 21246
coating with chromium containing ceramic dispersions, electrolytic, 20: 21286 (AD-621920)
corrosion by decontaminating solution, stress, 20: 21238 (NP-15928)
development of low-alloy, for pressure vessels, 20: 21417(P)
ductility of, at −269°C, 20: 21416
effects of decontaminating and descaling solution on metal loss on, 20: 21238 (NP-15928)
iodine-131 deposition and transport on, model for, (E/T), 20: 21785 (ORNL-TM-1330(Rev.))
mechanical properties of plates of Acier AMMO, effects of specimen location on, 20: 21331(R) (EURAEC-1569)
properties of austenitic, for use as fuel cladding, 20: 21383
radiation effects on pressure vessels of low-alloy, fast-neutron, 20: 21228 (AE-221)
radiography of thick plates of, electron linear accelerator for, 20: 21477
reactions with sodium at high temperatures, 20: 20925(R) (ANL-7055, pp 177-212)
separation of oxygen and sulfur from, by compound formation with uranium at 1600°C, 20: 20692

STELLARATORS
magnetic surfaces in L-1, with double helical field, 20: 22298

STEROIDS
deuterium incorporation in, 20: 20799

STILBENE
effects on radioinduced decomposition of Santowax-OM1, 20: 20708 (AEET-213)

STOMACH
radiation effects on glucose diffusion in rat, uv, 20: 20414
radiation effects on metabolic activity in rat, x, 20: 20433 (AD-630390)
weight norms for human, use in establishing standards for radiation dosimetry, 20: 20374

STRAIN GAGES
development and testing of high-temperature, 20: 22520(R) (NAA-SR-11805)
failures in, detection and diagnosis of, 20: 22523 (UCRL-14602)

STREPTOMYCIN
effects on viability of *E. coli*, 20: 20457

STRESS ANALYSIS
calculation of axisymmetric and plane elasticity problems for, computer program for, 20: 20862 (WAPD-TM-555)

STRESS CORROSION
symposia on, New York, March 11–15, 1963, 20: 21276

STRONTIUM
determination in irradiated silica, activation, 20: 20636
excretion and metabolism of, use in dosimetry, 20: 20398
metabolism in bones, compartmental analysis, 20: 20400
separation from calcium in milk, 20: 20938 (NP-15921)
separation from calcium by exchange in amalgam–solution system, 20: 20829
separation from irradiated silica and sodium by chromatography, 20: 20636
separation from perchloric acid solutions by ion exchange materials, 20: 20823
separation from uranium by combined ion exchange-solvent extraction using nitric acid–tetrahydrofuran solutions, 20: 20811

STRONTIUM ALLOYS
Sr–Zn, intermetallic compound with $CeCu_2$-type structure in, 20: 21352 (TID-21745)

STRONTIUM CHLORIDES
uptake by man, 20: 20466

STRONTIUM HYDROXIDES
crystal structure of hydrates of, 20: 20694
H_3PO_4–$Sr(OH)_2$, precipitate formation in, phase transformations in, 20: 20690

STRONTIUM ISOTOPES Sr-84
neutron capture by, isomeric cross section ratios for, (E), 20: 22052

STRONTIUM ISOTOPES Sr-85
binding with plasma proteins in patients with bone metastases, 20: 20404
dispersion and movement in soils, mechanism of, 20: 20875 (EUR-2481.f)
metabolism in bones, compartmental analysis, 20: 20400
production of isomeric and ground-state, from strontium-84 neutron capture, (E), 20: 22052
uptake by man, 20: 20466

STRONTIUM ISOTOPES Sr-86
content in plutonic and metamorphic rocks of New Zealand, 20: 20888

STRONTIUM ISOTOPES Sr-87
content in plutonic and metamorphic rocks of New Zealand, 20: 20888

STRONTIUM ISOTOPES Sr-88
alpha inelastic scattering at 42 Mev, level structure from, (E), 20: 22138

STRONTIUM ISOTOPES Sr-89
content in food in Amsterdam, 1960 to 1963, 20: 20949
determination of microquantities of, precipitated with zinc tetrathiocyanatomercurate(II), 20: 20619
diffusion in irradiated Zircaloy-4 at 800°C, 20: 21232 (BMI-1763)
dispersion and movement in soils, mechanism of, 20: 20875 (EUR-2481.f)
separation from radioisotopes in aqueous solutions by foam chromatography using colloidal manganese dioxide, 20: 20628
separation from water supplies, using sanitary water-treatment process, 20: 22512 (K-1651)
yields from photofission of uranium by 650-Mev bremsstrahlung, 20: 22040

STRONTIUM ISOTOPES Sr-90
content in biota of Doe Run, Ky., 1959 to 1965, 20: 20884(R) (TID-22815)
content in Colorado deer, 20: 20384 (COO-1156-13)
content in cow's milk, effects of diet on, 20: 20882(R) (HASL-171)
content in fallout, estimation of tritium fallout in southern hemisphere from, 20: 20892
content in food in Amsterdam, 1960 to 1963, 20: 20949
content in foods and soil in Great Britain, 1964 and 1965, 20: 20926(R) (ARCRL-14)
content in sea water, effects on development of fish spawn, 20: 20445(T) (TRG-Inf. Ser.-166)
content in soil, effects of depth on, 20: 20882(R) (HASL-171)
determination by yttrium-90 precipitation method, 20: 20586
determination in milk, 20: 20938 (NP-15921)
determination in urine by anion exchange and beta counting, 20: 20583
performance in high-temperature thermoelectric generator for space, 20: 21211 (TID-22350)
retention by soils, effects of chemical treatments on, 20: 20875 (EUR-2481.f)
separation from fission product solutions by oxalic acid precipitation, 20: 20804 (EUR-2754.f)
separation from fresh water by ion exchange chromatography, 20: 20627
separation from radioisotopes in aqueous solutions by foam chromatography using colloidal manganese dioxide, 20: 20628
separation from soil, method for, 20: 20882(R) (HASL-171)
separation from water supplies, using sanitary water-treatment process, 20: 22512 (K-1651)
transport in soil and plants, 20: 20926(R) (ARCRL-14)
uptake by clover and rye grass, effects of applications of stable strontium to soil on, 20: 20381
uptake by deer and sheep, effects of biological and environmental factors on, 20: 20388 (SAN-34-2)

STRONTIUM LANTHANUM FERRATES
iron-57 Mössbauer spectra in perovskite series $La_{1-x}Sr_xFeO_3$ ($0 \leq x \leq 1$), (E), 20: 22336

STRONTIUM PHOSPHATES
crystal structure, 20: 20690

STRUCTURES
decontamination of, effectiveness of inside and outside, 20: 20923 (AD-626727)

STYRENE
radioinduced polymerization of, effects of white phosphorus on gamma, 20: 20736
radioinduced polymerization with isocyanic acid at low temperatures, 20: 20747
radioinduced polymerization of, effects of mineral fillers on gamma, 20: 20778

STYRENE POLYMERS
electron beam reactions at low energies, space charge buildup from, (E), 20: 22344
radiation effects on current induction in capacitor of, electron beam, fast neutron, and gamma, 20: 21151 (IBM-66-825-1944)
radiation effects on molecular motion and structure of isotactic, gamma and neutron, 20: 20753
radiation effects on, light-scattering and viscosity measurements of gamma, 20: 20765
radiation effects on dielectric properties of, 20: 21443

with butadiene, radiation effects on mechanical properties of, gamma, 20: 20754

SUBMARINES
nuclear-powered, atmosphere control on, 20: 20981

SUCROSE
radiation effects on, in aqueous solutions, x, 20: 20748

SULFATES
separation from uranium in anion exchanger desorption, 20: 20827

SULFIDES
radioinduced in fish fillets, determination and separation, 20: 21200

SULFUR
bremsstrahlung reactions (γ,n) at threshold to 200 Mev, cross sections for, (E), 20: 22094
determination in naphthalene by x-ray absorption methods, 20: 20615
excretion and metabolism of, use in dosimetry, 20: 20398
neutron flux and spectrum measurements on foils of, 20: 21427(R) (NASA-CR-54904)
separation from liquid iron and steel by compound formation with uranium, 20: 20692

SULFUR DIOXIDES
yields from gamma radiolysis of solid diaryl sulfones, 20: 20760
SiO_2–SO_2, properties for use as adsorption refrigeration system, 20: 21174 (SAN-575-12)

SULFUR FLUORIDES
enthalpy of formation of SF_6, 20: 20650(R) (ANL-7055, pp 167-76)

SULFUR ISOTOPES S-32
alpha scattering at 18 Mev, cross sections for, (T), 20: 22134
electron inelastic scattering at 50 Mev, differential cross sections for, (T), 20: 21964 (AD-626684)
neutron reactions (n,p) at 2.9 Mev, cross section and threshold energy for, 20: 21427(R) (NASA-CR-54904)
neutron reactions (n,γ) with, sulfur-33 level spins from thermal, (E), 20: 22077
proton reactions (p,p′γ) at 8.5 Mev, angular correlations from, (E), 20: 22059

SULFUR ISOTOPES S-33
energy levels from thermal neutron reactions (n,γ) with sulfur-32, spins of, (E), 20: 22077

SULFUR ISOTOPES S-35
incorporation in methionine, 20: 20786
incorporation in polymers formed from reactions of carbon tetrachloride and cyclohexane, 20: 20784
incorporation in 4-methyl-5-thiazoleethanol, 20: 20785
radiation effects on metabolism of sodium sulfate-incorporated, in rat liver, x, 20: 20410

SULFUR ISOTOPES S-36
energy levels from chlorine-36 decay, (E), 20: 22029

SULFURIC ACID
effects on corrosion of rhenium at 25 and 100°C, 20: 21275
$CuSO_4$–D_2SO_4–UO_2SO_4–H_2O–D_2O, spectrophotometry of reactor fuel solutions of, 20: 20600
$Fe_2(SO_4)_3$–H_2SO_4, corrosive effects on nickel–chromium–molybdenum alloys at 800 to 2375°F, 20: 21277

SUN
evolution of, with varying gravitation, (T), 20: 21493
gravitational field of, equations for, 20: 21868
magnetic fields of, kinematical hydromagnetic model for small-scale, 20: 21503
neutron outflow from, upper bounds of, 20: 21495
radio emission from active regions of, characteristics of, 20: 21506
spot number for Oct. 1965, 20: 21830
spot structure on, mixing length damping for, (T), 20: 21489 (AD-623803)

SUPERCONDUCTIVITY
Bogoliubov quasiparticles in, criteria for, 20: 21839 (AD-627067)
critical temperature in films of, effects of thickness on, 20: 21891
models for, phase transitions in, 20: 21872 (AD-627189)
of electron gas in homogeneous magnetic field, (T), 20: 21887
of ionic semiconductors, high-current, (T), 20: 21889
theory for, microscopic, 20: 21874(T) (TT-62-23147)
theory of high-field, review of, 20: 21877
theory of hysteresis and low-frequency losses in, 20: 22520(R) (NAA-SR-11805)
theory of nonlocal extension of Ginzburg-Landau, 20: 21905
theory of type II, developments in microscopic, 20: 21930
theory of, S-matrix approach to, 20: 21879
theory of, time-dependent Ginzburg-Landau, 20: 21890

SUPERCONDUCTORS
conference on type II, 20: 21899
critical currents in niobium-tin alloy, (E), 20: 21921
critical currents in niobium–tin and gallium–vanadium intermetallic compound, in high fields, (E), 20: 21922
critical currents and fields in flux-pump fed coils of, (E), 20: 21924
critical currents and magnetic hysteresis in mixed state, (T), 20: 21932
critical fields of vanadium film, (E/T), 20: 21915
critical fields of films and surfaces of, angular dependence of, (T), 20: 21917
critical temperatures of carbide and nitride, correlation with valence electrons, (E), 20: 21911
current degradation in solenoids of, flux pinning energy and temperature dependence of, 20: 21920
current density and gap equation for local, in magnetic fields, 20: 21880
design and construction of magnets of, for corpuscular ionography, 20: 21876
elastic modulus in type II, discontinuous variation of, (E/T), 20: 21912
electric conductivity of, current dependence of imaginary part of, (E/T), 20: 21919
electric conductivity and magnetization of titanium–vanadium alloy, at 4.2°K, (E), 20: 21928
electrodynamic response of local, microscopic-theory calculation of, 20: 21890
electron excitation spectra in type II, Kronig-Penney model for, 20: 21904
energy gaps in, tunneling techniques for measuring, (E), 20: 21885
magnetic field penetration at low field, (E), 20: 21908
magnetic field strength at surface of niobium–zirconium alloy, EPR measurements for, (E), 20: 21898
magnetic field transitions in type II, surface effects on a-c, (E), 20: 21918
magnetic flux creep and jumps in niobium–zirconium, effect of Joule heating on, (T), 20: 21884
magnetic flux motion in type II, (E/T), 20: 21910
magnetic flux pinning in niobium, quantized, (E), 20: 21909
magnetic flux trapping threshold in niobium–tin alloy, (E), 20: 21926
magnetic fluxoid annihilation instability in hard, (E/T), 20: 21927
magnetic hysteresis in mixed state of lead–thallium, effect of surface currents on, (E), 20: 21866
magnetic induction in hard vanadium–zirconium, remanent, (E), 20: 21893
magnetic properties of Abrikosov structures in alloy, (T), 20: 21906
magnetic properties of ideal type II, (T), 20: 21929
magnetic resonances in niobium, low-frequency mixed-state, (E), 20: 21894
metallurgy and uses of high-field, 20: 21877
microwave reactions with Josephson junctions of, induced d-c voltages from, 20: 21882
microwave surface resistance in type II, (E), 20: 21916
performance of soils of, with composite stranded cables, 20: 21878
properties of Abrikosov mixed state near second critical field, Ginzburg-Landau equations for, 20: 21902
properties of ideal type II, bulk, 20: 21931
properties of pure, fourth order terms of Ginzburg–Landau–Gorkov equations for, 20: 21903
properties of tin alloys, nonideal, (E/T), 20: 21925
properties of type II, paramagnetic effects on, (T), 20: 21900
properties of, effects of λ transition on, 20: 21875
superconducting transition of indium–lead alloy, effects of strain on, (E), 20: 21923
surface nucleation in normal-metal-coated, (T), 20: 21888
switching properties of small-geometry thin-film, 20: 21012
theory of high-field, review of, 20: 21877
thermal capacity of lanthanum- and yttrium-silicide, at transition temperature, (E), 20: 21883
thermal capacity of type II, in magnetic field, (E), 20: 21907
thermal conductivity of type II, (E), 20: 21914
thermodynamic properties of ideal bulk type II, (T), 20: 21901
transition temperatures in epsilon-phase lead-bismuth alloys, (E), 20: 21892
transitions of indium–lead alloys, (E/T), 20: 21913

SUPERHEATERS
design and operation of separately fired, at Indian Point Power Station, 20: 22455

SUPERSONIC FLOW
heating rates for cylinders in laminar, 20: 20857 (SC-DC-65-1907)

SURFACE-ACTIVE AGENTS
effects on analytical procedures involving uranyl ions, 20: 20630
effects on polarographic determination of hexavalent uranium in nitric acid media, 20: 20631

SURFACE WATERS
age estimation of, by tritium abundance variations, 20: 20894
alpha detection in, monitor for, 20: 21038 (K-1656)
analysis for radioactivity, methods for, 20: 20963
book: *Advances in Water Pollution Research*, Vol. 1, 2, and 3, 20: 20982
flow rate measurements in rivers, tracer techniques for, 20: 20903 (AEET-Radiochem.-45)
radioactive waste disposal in, operations research on liquid, 20: 22513 (NYO-10447)
radioactivity due to fallout in Canadian, 1964, 20: 20938 (NP-15914)

radioactivity due to fallout in Canadian, 1965, 20: 20883 (NP-15914)
radioactivity due to fallout in Doe Run, Meade County, Ky., 1959 to 1965, 20: 20884(R) (TID-22815)
radioactivity of Escaut River, Belgium, 20: 22515(T) (ORNL-tr-965)
radon content in, measurement using gamma radiation, 20: 20959
tracer techniques for studying bed-load movement and transport in, 20: 20904 (STI-REP-101)

SURFACES
for fission product deposition, preparation of standard, 20: 20940(R) (ORNL-3915)

SURGERY
effects of, combined with x radiation on cervical carcinomas, 20: 20526
effects of, combined with γ radiation on cervical carcinomas, 20: 20536

SWINE
decomposition of carrion of, effects of scavenger animals, insects, and microorganisms on, 20: 20941 (ORNL-TM-1432)
radium-226 distribution in tissues of, 20: 20385 (COO-1184-3)

SWITCHES
design for space nuclear electric systems, 20: 20986(R) (N-65-29823)
properties of cryotron, 20: 21012

SWITZERLAND
power reactor development in, 20: 22421

SYNCHROTRONS
beam collimators for, r-f separated, 20: 21468 (CERN-66-10)
beam instability thresholds in weak-focusing proton, longitudinal, (T), 20: 21471 (PPAD-577D)
beam intensity of, program for increasing, 20: 21466 (CERN-65-32, pp 127-30)
beam separator for, servo correction of phase changes between deflectors in, 20: 21467 (CERN-66-8)

SYSTEMS FOR NUCLEAR AUXILIARY POWER
development of reactor, high-temperature chemistry problems in, 20: 20870 (LA-DC-7703)
reactivity and temperature coefficient for, effects of neutron thermalization on, 20: 22377 (GA-6930, App. B)
reentry burnup of, dose criteria for fallout from, 20: 20937 (NAA-SR-11761)
testing in simulated environment, 20: 22475

SYSTEMS FOR NUCLEAR AUXILIARY POWER (SNAP-2)
control systems for, development of, 20: 22474
energy release in SNAPTRAN 2/10A-2, destruct, 20: 22467(R) (IDO-17077)
reactivity transient testing of SNAPTRAN 2/10A-1, step, 20: 22467(R) (IDO-17077)

SYSTEMS FOR NUCLEAR AUXILIARY POWER (SNAP-8)
control systems for, development of, 20: 22474
test program for, summary of, 20: 22479

SYSTEMS FOR NUCLEAR AUXILIARY POWER (SNAP-10)
control system testing for 10A, in simulated environment, 20: 22475
control systems and instrumentation of 10A, development of, 20: 22476
control systems for, development of, 20: 22474
energy release in SNAPTRAN 2/10A-2, destruct, 20: 22467(R) (IDO-17077)
performance testing of 10A, FSM-4 mockup for, 20: 22471 (NAA-SR-11814)
radiation dosimeters for flight test of 10A, 20: 21105
reactivity transient testing of SNAPTRAN 2/10A-1, step, 20: 22467(R) (IDO-17077)
testing of SNAP-10A/Agena, 20: 22477
testing of SNAP-10A/Agena, pre-launch operations in, 20: 22478

T

TANTALUM
analysis for impurities by d-c arc method, spectrographic, 20: 20608
bonding of, to Inconel 600 and stainless steels, process development for explosive, 20: 21295(R) (WANL-PR-(EE)-002)
determination in silicon dioxide, activation, 20: 20635
ductility of, at −269°C, 20: 21416
effects on efficiency of porous tungsten ionizers, 20: 21570 (N-65-29785)
neutron inelastic scattering at 5.8 and 7.5 Mev, gamma spectra from thermal, (E), 20: 22069
proton reactions at 590 Mev and 18 Bev, yields of iodine isotopes from, (E), 20: 22045
radiation effects on current induction in capacitor of, electron beam, fast neutron, and gamma, 20: 21151 (IBM-66-825-1944)
reactions with carbon dioxide at 590 to 730°C at low pressures, 20: 21279
reactions with molten cerium–cobalt alloys, 20: 20671
reactions with sodium at high temperatures, 20: 20925(R) (ANL-7055, pp 177-212)
separation from antimony, molybdenum, and tin by ion exchange chromatography on chloride form resin, 20: 20635
sorptive properties of evaporated films of, for krypton and xenon, 20: 21387
sorptive properties of evaporated films of, for carbon monoxide at 0°C, 20: 21388
sorptive properties of evaporated films of, for carbon dioxide at room temperature, 20: 21389
superconducting properties of, effects of λ transition on, 20: 21875
weld interface porosity in, effects of consolidation process on, 20: 21311
welding of, argon-arc and electron-beam methods of, 20: 21310

TANTALUM ALLOYS
properties of, effect of carbide dispersion on microstructures and strength/ductility, 20: 21404
Hf–Re–Ta–W, properties of, effect of carbide dispersion on microstructures and strength/ductility, 20: 21404
Hf–Ta–W, creep tests on T-111 and T-222 at high temperatures, 20: 21346(R) (NASA-CR-54895)
Hf–Ta–W, extrusion parameters for T-111, 20: 21263(R) (NASA-CR-54911)
Hf–Ta–W, mechanical properties at 25 to 3500°F, 20: 21322 (AMRA-TR-65-25)
Hf–Ta–W, specifications of T-111, for use in corrosion test loop fabrication, 20: 21293 (R-66SD3007)
Hf–Ta–W, strength, weldability, and heat treatment of, 20: 21405
Mo–Ta, crystal structure of electron-beam zone-refined, 20: 21364
Mo–Ta, mechanical properties of single-crystal, 20: 21364
Nb–Ta, magnetic flux motion in superconducting, (E/T), 20: 21910
Nb–Ta–V, tensile properties of vanadium-base, effects of carbon and silicon additions on, 20: 21333(R) (IITRI-B6042-4)
Nb–Ta–W–Zr, bonding of FS-85, to Inconel 600 and stainless steels, process development for explosive, 20: 21295(R) (WANL-PR-(EE)-002)
Nb–Ta–W–Zr, creep of FS-85, at 2000 to 2200°F in ultrahigh vacuum, 20: 21344 (N-65-26653)
Re–Ta–W, mechanical properties at 25 to 3500°F, 20: 21322 (AMRA-TR-65-25)
Ta–W, ductility of, at −269°C, 20: 21416
Ta–W, mechanical properties at 25 to 3500°F, 20: 21322 (AMRA-TR-65-25)
Ta–W–Zr, strength, weldability, and heat treatment of, 20: 21405

TANTALUM BORIDES
thermionic emission from cesiated surfaces of, (E), 20: 21584

TANTALUM CARBIDES
ductility, 20: 21375
effects on mechanical properties of sintered and extruded tungsten, 20: 21374
production of single crystals of, 20: 21236(R) (N-65-23835)
HfC–TaC, production of single crystals of, 20: 21236(R) (N-65-23835)

TANTALUM ISOTOPES Ta-181
nitrogen-15 reactions at 102 Mev, neutron pickup in, (E), 20: 22001 (JINR-P-2555)

TANTALUM NITRIDES
superconducting critical temperature of, correlation with valence electrons, 20: 21911

TANTALUM OXIDES
electric conductivity of anodic films of, on taltalum, 20: 20670
formation, stability, and structures of, 20: 21379
radiation effects on current induction in commercial capacitor of, electron beam, fast neutron, and gamma, 20: 21151 (IBM-66-825-1944)
Ta_2O_5–WO_3, phase studies on, 20: 21385

TANTALUM SILICIDES
thermionic emission from cesiated surfaces of, (E), 20: 21584

TANTALUM SYSTEMS
C–Hf–Mo–N–Re–Ta–W–Zr, development of dispersion-strengthened tantalum-base, 20: 21240(R) (WANL-PR-(Q)-006)
C–Hf–Re–Ta–W, development of dispersion-strengthened tantalum-base T-333, 20: 21240(R) (WANL-PR-(Q)-006)
C–Hf–Ta–W, bonding of T-222, to Incone! 600 and stainless steels, process development for explosive, 20: 21295(R) (WANL-PR-(EE)-002)
C–Mo–Nb–Ta–W–Zr, extrusion parameters for Cb-132M, 20: 21263(R) (NASA-CR-54911)
C–Mo–Nb–Ta–Zr, thermal-mechanical processing of a precipitation-hardenable, dispersion-hardened, 20: 21250

TARGET REACTOR
development, Dec.-Feb. 1965, 20: 22411(R) (GA-6113)
fuel element design for, 20: 22411(R) (GA-6113)

TECHNETIUM
book: *Chemistry of Technetium and Rhenium*, 20: 20697
determination by neutron activation, 20: 22039
production of, review of methods for, 20: 20796
separation from rhenium by chromatography, 20: 20629

TECHNETIUM ISOTOPES Tc-99
half life and specific activity, (E), 20: 22036

incorporation of isomer of, in human serum albumin, 20: 20712
neutron reactions at 14.8 Mev, activation cross sections for, 20: 22039
separation from molybdenum-99 by ion exchange on hydrous zirconium oxide in nitric acid, 20: 20566 (ORNL-TM-1468)
TECHNICAL REPORTS
by Dow Chemical Co. personnel, for 1965, 20: 22521 (RFP-516A (Suppl.1))
TEETH
radiation effects from radium dial paint on human, epidemiology of New Jersey cases of, 20: 20387(R) (NYO-2181-3)
TELEMETERING SYSTEMS
design for ultracentrifuge rotor temperature measurements and control, 20: 21009
TELLURIUM
determination in multielement mixtures by x-ray fluorescence methods, 20: 20644
TELLURIUM FLUORIDES
enthalpy of formation of TeF_6, 20: 20650(R) (ANL-7055, pp 167-76)
TELLURIUM ISOTOPES Te-123
energy level transitions in, E2/M1 mixing ratio for, (E), 20: 22089
isomeric transitions in, $\gamma-\gamma$ directional correlations from, (E), 20: 22089
TELLURIUM ISOTOPES Te-131
radiation hazards from, following nuclear incidents, 20: 20962
TELLURIUM ISOTOPES Te-132
diffusion in irradiated fuel element cladding alloys and materials at 600 to 1200°C, 20: 21232 (BMI-1763)
radiation hazards from, following nuclear incidents, 20: 20962
TELLURIUM ISOTOPES Te-133
radiation hazards from, following nuclear incidents, 20: 20962
TELLURIUM SYSTEMS
Sb–Cr–Te, neutron diffraction studies on solid solutions of, 20: 22312(R) (AD-622796)
Se–Te, performance as electrophotographic material for particle track coordinates in spark chambers, 20: 21037 (JINR-P-2594)
TEMPERATURE
control of centrifuge rotor, radio telemetry system for, 20: 21009
effects on thermal conductivity of irradiated uranium dioxide to 2000°C, in-pile measurements on, 20: 21361 (WCAP-2923)
measurement in reactors, thermocouple for, 20: 21016(P)
measurement in remote regions, radioactive apparatus for, 20: 21019(P)
TERBIUM
determination in rare earth mixtures, activation, 20: 20562 (LYCEN-6538)
electric and magnetic properties at high pressures, 20: 21357 (UCRL-16299)
nuclear magnetic resonance spectra in, 20: 22311(R) (AD-622068)
oxidation in dry and moist air at 100 to 800°C, rate of, 20: 21265 (RPI-2714-8)
reactions with powdered graphite, preparation of intercalation compounds by, 20: 20648 (AD-621029)
separation from perchloric acid solutions by ion exchange materials, 20: 20823
separation from uranium by combined ion exchange-solvent extraction using nitric acid–tetrahydrofuran solutions, 20: 20811
with bipyridines, fluorescence of, effects of methyl substitution on, 20: 20703
TERBIUM ALLOYS
Al–Tb, crystal structure and stability of intermetallic compounds in, 20: 21415
Dy–Tb, magnetic transformations in, 20: 21409
Er–Tb, magnetic transformations in, 20: 21409
Ho–Tb, magnetic transformations in, 20: 21409
Lu–Tb, magnetic transformations in, 20: 21409
Tb–Tm, magnetic transformations in, 20: 21409
TERBIUM ETHYL SULFATES
terbium EPR pair spectra in, 20: 22311(R) (AD-622068)
TERBIUM IONS
electron nuclear double resonance spectra in thoria, 20: 22311(R) (AD-622068)
electron paramagnetic resonance pair spectra in terbium ethyl sulfate, 20: 22311(R) (AD-622068)
TERBIUM ISOTOPES Tb-157
energy levels from dysprosium-157 decay, lifetime of, (E), 20: 22058
TERBIUM ISOTOPES Tb-160
decay of, $\beta-\gamma$ angular correlations from, (E), 20: 22010(R) (NYO-72-28)
TERBIUM OXIDES
separation of europium from irradiated, by partition chromatography on polytetrafluoroethylene, 20: 20622
solubility in ethyl, isopropyl, methyl, and propyl alcohols in presence of ammonia, 20: 20686
TERBIUM SYSTEMS
graphite–Tb, preparation and magnetic susceptibility of, 20: 21413
TEREPHTHALIC ACID
properties for use in radiation dosimetry, 20: 20745
radiation effects on, gamma, 20: 20745
TEREPHTHALIC ACID, ETHYLENE POLYMER ESTERS
radiation effects on current induction in capacitor of, electron beam, fast neutron, and gamma, 20: 21151 (IBM-66-825-1944)
TERPHENYL
boiling in OM2 in forced convection, inception of nucleate, (E/T), 20: 20709 (EUR-2442.f)
decomposition of, radiolytic and thermal, 20: 20722 (EUR-2401.f)
friction factor and heat transfer studies on Santowax WR, 20: 20723(R) (MIT-334-33)
properties and stabilities of organic coolants of, 20: 20708 (AEET-213)
pyrolysis of, gas and polymer formation in, 20: 20708 (AEET-213)
radiation effects on Santowax WR, effects of temperature on fast-neutron, 20: 20723(R) (MIT-334-33)
radiolysis of isomeric, gamma and fast-neutron, 20: 20739
radiolysis of OM_2, in-pile, 20: 20721 (EUR-2295.f)
radiolysis of, in-pile, 20: 20721 (EUR-2295.f)
TETRADECANE
radiolysis of, ion mobility in x, 20: 20734
THALLIUM
friction and wear properties of, in vacuum, effects of crystal structure on, 20: 21365
sorption from perchloric acid solutions by ion exchange materials, 20: 20823
superconducting properties of, effects of λ transition on, 20: 21875
THALLIUM ALLOYS
Pb–Tl, elastic modulus of superconducting, magnetic field dependence of, 20: 21912
Pb–Tl, magnetic hysteresis in mixed state of superconducting, effect of surface currents on, (E), 20: 21886
Pb–Tl, microwave surface resistance in superconducting, (E), 20: 21916
THALLIUM COMPLEXES
with thiodibenzoylmethane, stability of, 20: 20693
THALLIUM ISOTOPES Tl-208
beta decay of, lead-208 levels from, (E), 20: 22020
THERMAL CONDUCTIVITY
measurement in in-pile fuel elements, temperature transient method for, 20: 22354(R) (CEND-3336-260)
THERMAL DIFFUSION
column design and performance for carbon-13 concentration, 20: 20806(R) (MLM-1274)
column transport measurements for determining stagnant gas barriers in, 20: 20807(R) (MLM-1287)
THERMAL REACTORS
neutron cross sections for, heterogeneous resonance effects in multigroup, (T), 20: 22384
neutron spectra and fast-fission effect in, fast, 20: 22506
THERMAL STRESSES
effects on viability of *E. coli*, 20: 20457
THERMIONIC CELLS
arc properties of low-voltage cesium, 20: 21578
electric properties of cesium, krypton effects on, 20: 21579
electric properties of cesium, xenon effects on, 20: 21580
electron distribution in cesium plasma in, electrostatic probe measurements of, 20: 21560(R) (AD-621676)
electron emission cooling and optimum collector temperature in, correlation of, (E), 20: 21585
operation of cesium diode, with admixture of inert gas, 20: 21567 (FEI-15)
operation of cesium, effect of inter-electrode spacing on, 20: 21568 (FEI-16)
performance of tungsten-emitter, effects of cesium and cesium fluoride additives on, 20: 21586
properties of, review, 20: 21562(R) (AD-623142)
regeneration of bimetallic, equipment for, 20: 21566(R) (ANL-7055, pp 213-29)
testing bismuth–sodium, 20: 21566(R) (ANL-7055, pp 213-29)
THERMOCOUPLES
design for fuel elements, 20: 21016(P)
leakage current errors in long sheathed, at high temperatures, (T), 20: 20651(R) (CU-2660-26)
performance of fission-heated, for reactor diagnostics and safety, 20: 22355 (LA-3470)
THERMODYNAMICS
calculations for, computer programs for, 20: 21783 (AECL-2530)
formalism of irreversible, for viscous fluids, 20: 21794
THERMOELECTRIC CELLS
design and operation of high-temperature, 20: 21563(R) (AD-623591)
development of lightweight isotope-fueled, for space uses, 20: 21211 (TID-22350)
development of liquid metal, 20: 21566(R) (ANL-7055, pp 213-29)
startup transient behavior of, (T), 20: 21577

THERMOLUMINESCENT DETECTORS
development for dosimetry, 20: 21085
effects of thermal annealing on, in lithium fluorides, 20: 21057
reader design and measurement errors in lithium fluoride, 20: 21061
THERMOMETRY
thermomolecular pressure of helium-3 and -4 at 77°K, 20: 20807(R) (MLM-1287)
THERMONUCLEAR EXPLOSIONS
seismic pulse propagation from, analysis of, 20: 20907
THERMONUCLEAR REACTIONS
density and temperature exponents for 3α, in pulsing stars, (T), 20: 21491
research on controlled, review of, 20: 22302
THERMONUCLEAR REACTORS
design of toroidal machine for adiabatic compression of plasma, 20: 22299
electron motion in Astron, relativistic, (T), 20: 22287
injection device for Astron, beam density profile of, (E), 20: 22191 (UCRL-14697)
plasma injection into Picket Fence II, at high velocity, (E), 20: 22254
plasma stability in positive column of inverse, hydrogen, (T), 20: 22272
5-THIAZOLEETHANOL, 4-METHYL-
radioinduced synthesis of sulfur-35-labeled, 20: 20785
THICKNESS GAGES
development for measurements on thin films by conductance, 20: 20987 (RFP-690)
electrometer design for beta, 20: 21013
use of radiometric, survey on, 20: 20990(T) (AERE-Trans-1048)
THORIUM
analysis for oxygen, 20: 20572
analysis for zinc, photometric and polarographic, 20: 20601
creep of, effects of fission on, 20: 22520(R) (NAA-SR-11805)
deposition on platinum disks for α and β counting, electrolytic, 20: 20795
determination by conductometric titration using sodium tungstate, 20: 20592
determination in presence of uranium and zirconium using Arsenazo-III, 20: 20614
determination in sedimentary carboniferous deposits, x-ray fluorescence and scintillation counting, 20: 20613
determination of, using 8-quinolinol, spectrophotometric, 20: 20576
occurrence in phosphate rocks, 20: 20886
production in France, 20: 21243
separation from di- and trivalent metallic ions in nitric acid by ion exchange, 20: 20624
separation from perchloric acid solutions by ion exchange materials, 20: 20823
separation from protactinium by solvent extraction using quaternary ammonium chlorides, 20: 20816
separation from rare earths and scandium by paper chromatography, 20: 20825
separation from scandium by ion exchange chromatography, 20: 20821
separation from uranium by combined ion exchange-solvent extraction using nitric acid–tetrahydrofuran solutions, 20: 20811
separation from uranium by extraction using triisooctylamine, 20: 20598
THORIUM ALLOYS
Au–Th–U, fabrication and corrosion testing of radiation targets of, 20: 21288 (BMI-1761)
Pu–Th, feasibility for use in fast breeder reactors, 20: 21229 (AEET-229)
rare earth–Th, solid solutions of, electronic states of, 20: 21398
Th–U, fabrication and corrosion testing of radiation targets of, 20: 21288 (BMI-1761)
Th–U, feasibility for use in fast breeder reactors, 20: 21229 (AEET-229)
THORIUM CARBIDES
thermal conductivity, 20: 22411(R) (GA-6113)
ThC_2–UC_2, thermal conductivity of, 20: 22411(R) (GA-6113)
THORIUM COMPLEXES
with EDTA, mandelic, oxalic, and phenylarsonic acids, solvent extraction studies on formation of, 20: 20561 (JAERI-1099)
with myricetin, composition and stability of, 20: 20674
THORIUM IONS
effects on dephosphorylation of cocarboxylase, riboflavin-5-phosphate, and pyridoxal phosphate, 20: 20375
THORIUM ISOTOPES Th-227
alpha decay, (E), 20: 22008 (MLM-1337J)
content in carbonate deposits in Russia, 20: 20887
THORIUM ISOTOPES Th-228
content in silt in Escaut River, Belgium, control of, 20: 22515(T) (ORNL-tr-965)
content in tissues of radium dial painter, 20: 20387(R) (NYO-2181-3)
THORIUM ISOTOPES Th-230
content in carbonate deposits in Russia, 20: 20887
THORIUM ISOTOPES Th-232
fission of, potential barrier widths for spontaneous, (T), 20: 22014(T) (KFK-tr-185)
neutron cross sections for, 20: 21967 (AEET-234)
nitrogen-15 reactions at 102 Mev, neutron pickup in, (E), 20: 22001 (JINR-P-2555)
proton capture cross sections and transmission coefficients for, optical model calculation of, 20: 22049
Pu-239–Th-232, resonance interference effects on neutron cross sections of, (T), 20: 21970 (ANL-7144)
THORIUM ISOTOPES Th-234
content in carbonate deposits in Russia, 20: 20887
separation from uranyl nitrate solutions, chromatographic, 20: 20828
separation from uranium solutions by ion exchange, 20: 20624
THORIUM NITRATES
$Th(NO_3)_4$–$UO_2(NO_3)_2$, reduction to ceramic-grade mixed thorium oxide–uranium oxide, 20: 21255(P)
THORIUM(IV) OXIDES
activity and phase distributions of Thorotrast, 20: 20790 (CONF-651069-1)
deposition on steel of chromium plating containing dispersions of, electrolytic, 20: 21286 (AD-621920)
effects on canine spinal cord, 20: 20455
effects on mechanical properties of sintered and extruded tungsten, 20: 21374
effects on radiolysis of benzene in aqueous solutions, 20: 20768
gadolinium and terbium ion electron nuclear double resonance spectra in, 20: 22311(R) (AD-622068)
growth and properties of crystals of, 20: 22311(R) (AD-622068)
neutron cross sections at 0.0045 to 0.028 ev, (E/T), 20: 21966 (AE-222)
preparation of microspheres and sols of, equipment for, 20: 20808(R) (ORNL-3916)
reactions with gaseous uranium trioxide, effects of substrate symmetry in, 20: 20649 (AEET-CD-24)
Re–ThO_2–W, ductility and hot strength, 20: 21407
Re–ThO_2–W, tensile properties at high temperatures, 20: 21406
ThO_2–UO_2, densification properties of solid solutions of, 20: 21323 (ANL-6894)
ThO_2–UO_2, fabrication of, for ceramic fuels, 20: 21301
ThO_2–UO_2, oxidation properties of solid solutions of, 20: 21323 (ANL-6894)
ThO_2–UO_2, phase studies, 20: 21323 (ANL-6894)
ThO_2–UO_2, production of ceramic-grade, 20: 21255(P)
ThO_2–UO_2, sintering and thermal shock properties of, effects of composition on, 20: 21299
ThO_2–W, tensile properties at high temperatures, 20: 21406
THORIUM SULFIDES
ThS–US, magnetic susceptibilities, 20: 20802(R) (ANL-8055, pp 21-98)
THORIUM SYSTEMS
B–Th, fabrication and corrosion testing of radiation targets of, 20: 21288 (BMI-1761)
THULIUM
deposition on metals, conditions for electrolytic, 20: 21287 (AE-217)
oxidation in dry and moist air at 100 to 800°C, rate of, 20: 21265 (RPI-2714-8)
reactions with powdered graphite, preparation of intercalation compounds by, 20: 20648 (AD-621029)
separation from nitrate solutions by solvent extraction using tricaprylmethylammonium nitrate, 20: 20812
separation from perchloric acid solutions by ion exchange materials, 20: 20823
separation from uranium by combined ion exchange-solvent extraction using nitric acid–tetrahydrofuran solutions, 20: 20811
THULIUM ALLOYS
Dy–Tm, magnetic transformations in, 20: 21409
Er–Tm, magnetic transformations in, 20: 21409
Ho–Tm, magnetic transformations in, 20: 21409
Lu–Tm, magnetic transformations in, 20: 21409
Nd–Tm, magnetic properties and phase transformations in, 20: 21414
Tb–Tm, magnetic transformations in, 20: 21409
THULIUM ISOTOPES Tm-169
deuteron reactions (d,p) at 11 and 12 Mev, thulium-170 rotational levels from, (E), 20: 22072
electron nuclear double resonance spectra in calcium fluoride, ground-state, 20: 22311(R) (AD-622068)
THULIUM ISOTOPES Tm-170
energy levels from deuteron reactions (d,p) with thulium-169 at 11 and 12 Mev, rotational, 20: 22072
THYMIDINE
incorporation in germinal cells of embryonic chicken ovaries *in vitro*, tracer studies on, 20: 20395
THYMINE

effects on viability of *E. coli*, 20: 20457
radioinduced oxidation of aqueous solutions of, mechanism of uv, 20: 20771
radiosensitivity effects on DNA, uv, 20: 20412
THYMUS GLAND
radioinduced tumors in mouse, incidence of x, 20: 20441 (ORNL-P-1173)
THYROID GLAND
effects of desiccated dietary, in rats, carcinogenic, 20: 20448
effects of prenatally administered iodine-131 on rat, physiological, 20: 20390(R) (TID-22767)
radiodiagnosis of diseases of, using iodine-125 or iodine-131 as tracer, 20: 20533
radiodiagnosis of diseases of, using iodine-125 or iodine-131 as tracer, 20: 20534
tumor etiology in rat, 20: 20448
weight norms for human, use in establishing standards for radiation dosimetry, 20: 20374
TIME MEASUREMENT
performance of atomic maser clocks for, relativistic effects on, (T), 20: 21866
TIMING CIRCUITS
design of fast, using storage diodes, 20: 21002
nuclear time base for, feasibility of, 20: 21021 (AD-622629)
TIN
coating thickness of gold on, use of proton beam scattering for measuring, 20: 21246
corrosive effects on molybdenum alloys at 1000°C, (E), 20: 21566(R) (ANL-7055, pp 213-29)
determination in ore by radioisotope x-ray fluorescence method, 20: 20640
determination in silicon dioxide, activation, 20: 20635
effects of decontaminating and descaling solution on metal loss on, 20: 21238 (NP-15928)
electric conductivity of superconducting, current dependence of imaginary part of, (E/T), 20: 21919
electron reactions at 6 to 23 kev, optical transition radiation from, 20: 21518
gamma elastic scattering at 280 and 662 kev, Z dependence of cross section for, (E), 20: 22060
microwave reactions with Josephson junctions of superconducting, induced d-c voltages from, (E), 20: 21882
performance of molten, as reactor coolant, (T), 20: 22351 (AD-623020)
photoelectric effect at 852 ev to 40 kev in, cross sections for, (E), 20: 21523
separation from antimony, molybdenum, and tantalum by ion exchange chromatography on chloride form resin, 20: 20635
superconductivity properties of, effects of λ transition on, 20: 21875
thermal capacity of liquid, corresponding states correlation of configurational, 20: 20657 (UCRL-11931)
viscosity at 231 to 1158°C, 20: 21342(R) (MLM-1301)
viscosity of liquid, based on atomic parameters, 20: 20656 (UCRL-11930)
TIN ALLOYS
Al–In–Sn, superconducting properties of, nonideal, 20: 21925
Al–Sn, superconducting properties of, nonideal, 20: 21925
Bi–Sn, corrosive effects on type 304 stainless steel at 200 to 1100°C, kinetics of hydrodynamic, 20: 21260 (ANL-6985)
Cu–Sn, radiation effects on deformation of, fast-neutron, 20: 21434
In–Sn, electric conductivity of superconducting, current dependence of imaginary part of, (E/T), 20: 21919
In–Sn, superconducting properties of, nonideal, (E/T), 20: 21925
Nb–Sn, magnetic field penetration into superconducting intermetallic compounds of, (E), 20: 21908
Nb–Sn, magnetic flux trapping threshold in superconducting Nb_3Sn, (E), 20: 21926
Nb–Sn, microwave surface resistance in superconducting, (E), 20: 21916
Nb–Sn, superconducting critical currents in intermetallic compounds of, (E), 20: 21921
Nb–Sn, superconducting critical currents and fields in flux-pump fed coils of, (E), 20: 21924
Ni–Sn, superconducting critical currents in intermetallic compounds of, in high fields, (E), 20: 21922
TIN COMPOUNDS
Mössbauer studies of organic, review, 20: 20684
TIN HYDRIDES
Mössbauer studies of, 20: 20684
TIN ISOTOPES
energy levels of even-even, alpha-cluster wave function for ground state, 20: 22093
spectra of, effects of nuclear deformation on isotope shift in, 20: 21531
TIN ISOTOPES Sn-109
energy levels of, shell model calculations of, 20: 21962 (AD-624214)
TIN ISOTOPES Sn-111
energy levels of, shell model calculations of, 20: 21962 (AD-624214)
TIN ISOTOPES Sn-113
energy levels of, shell model calculations of, 20: 21962 (AD-624214)
TIN ISOTOPES Sn-115
energy levels of, shell model calculations of, 20: 21962 (AD-624214)
TIN ISOTOPES Sn-117
energy levels of, shell model calculations of, 20: 21962 (AD-624214)
TIN ISOTOPES Sn-119
energy levels of, shell model calculations of, 20: 21962 (AD-624214)
Mössbauer studies using, 20: 20684
use in Mössbauer studies, standard reference absorber for, 20: 22158
TIN ISOTOPES Sn-121
energy levels of, shell model calculations of, 20: 21962 (AD-624214)
TIN ISOTOPES Sn-123
energy levels of, shell model calculations of, 20: 21962 (AD-624214)
TIN ISOTOPES Sn-125
energy levels of, shell model calculations of, 20: 21962 (AD-624214)
TIN ISOTOPES Sn-127
energy levels for, shell model calculations of, 20: 21962 (AD-624214)
TIN ISOTOPES Sn-129
energy levels for, shell model calculations of, 20: 21962 (AD-624214)
TIN ISOTOPES Sn-131
energy levels for, shell model calculations of, 20: 21962 (AD-624214)
TIN ISOTOPES Sn-133
energy levels for, shell model calculations of, 20: 21962 (AD-624214)
TIN OXIDES
analysis for arsenic, copper, gallium, and sodium, activation, 20: 20577
removal from tin by dissolution, descaling solution for, 20: 21238 (NP-15928)
TISSUE CULTURES
morphology and oxygen consumption of embryonic chicken intestine, effects of nitrogen mustard on, 20: 20372
radiation absorption by Chinese hamster, use of flying-spot microscopy for detecting uv, 20: 20473
radioinduced chromatin anomalies in HeLa cell, protective effects of organophosphorus derivatives against x, 20: 20515
radiosensitivity of chick embryo, effects of cysteamine on, 20: 20440(R) (EUR-2643.f)
radiosensitivity of tumor nodules in, 20: 20440(R) (EUR-2643.f)
TISSUE HOMOGENATES
radiosensitivity effects of liver, on rats, 20: 20503(R) (AD-629311, pp 1-14)
TISSUE TRANSPLANTS
use of auto- and homovenous, for repairing arterial injuries in x-irradiated dogs, 20: 20478
TISSUES
calcium-45 uptake by fish osseous, effects of stable calcium on, 20: 20405
radiation effects from radium dial paint on human, epidemiology of New Jersey cases of, 20: 20387(R) (NYO-2181-3)
radiosterilization of human bone graft, method for gamma, 20: 20482
radiotherapy of parametrium, using palladium-103, 20: 20542
role of epidermal, in recovery of regenerative capacity by x-irradiated salamander limbs, 20: 20465
TITANIUM
alpha scattering at 28.4 Mev, angular distributions from, (E), 20: 22047
determination in high-purity tantalum by spectrography using d-c arc method, 20: 20608
ductility of, at −269°C, 20: 21416
evaporation from porous tungsten ionizers, 20: 21570 (N-65-29785)
production of sponges of, 20: 21305
radiation effects on tensile properties of, at cryogenic temperatures, 20: 21427(R) (NASA-CR-54904)
separation from hydrochloric acid solutions by solvent extraction using quaternary ammonium chlorides, 20: 20816
separation from perchloric acid solutions by ion exchange materials, 20: 20823
separation from protactinium by solvent extraction using quaternary ammonium chlorides, 20: 20816
separation from scandium by ion exchange chromatography, 20: 20821
separation from uranium by combined ion exchange-solvent extraction using nitric acid–tetrahydrofuran solutions, 20: 20811
sorptive properties of evaporated films of, for krypton and xenon, 20: 21387
sorptive properties of evaporated films of, for carbon dioxide at room temperature, 20: 21389
sorptive properties of evaporated films of, for carbon monoxide at 0°C, 20: 21388
welding of, argon-arc and electron-beam methods of, 20: 21310
TITANIUM ALLOYS
Mo–Ti–Zr, creep tests on TZC and TZM at high temperatures, 20: 21346(R) (NASA-CR-54895)
Mo–Ti–Zr, fatigue tests on TZC and TZM at high temperatures, 20: 21347(R) (NASA-CR-54916)

Mo–Ti–Zr, mechanical properties at 25 to 3500°F, 20: 21322 (AMRA-TR-65-25)
Mo–Ti–Zr, specifications of TZM, for use in corrosion test loop fabrication, 20: 21293 (R-66SD3007)
Nb–Ti–V, tensile properties of vanadium-base, effects of carbon and silicon additions on, 20: 21333(R) (IITRI-B6042-4)
Ti–U, microstructure of uranium-rich, effects of heat treatments on, 20: 21372
Ti–V, electric conductivity and magnetization of superconducting, at 4.2°K, (E), 20: 21928
Ti–V, removal from reactor fuel alloys, chemical methods for, 20: 20802(R) (ANL-7055, pp 21-98)

TITANIUM ISOTOPES Ti-46
helium-3 reactions (He-3,t) at 22 Mev, Coulomb displacement-energy from, (E), 20: 22095

TITANIUM ISOTOPES Ti-48
helium-3 reactions (He-3,t) at 22 Mev, Coulomb displacement-energy from, (E), 20: 22095

TITANIUM ISOTOPES Ti-50
helium-3 reactions (He-3,t) at 22 Mev, Coulomb displacement-energy from, (E), 20: 22095

TITANIUM OXIDES
effects on radiolysis of benzene in aqueous solutions, 20: 20768

TITANIUM SYSTEMS
B–Co–Ti, crystal structure, 20: 20685
B–Ni–Ti, crystal structure, 20: 20685
C–Co–Ti–W, development and tensile properties of cobalt-base, 20: 21237 (N-65-29395)
C–Co–Ti–W–Zr, development and tensile properties of cobalt-base, 20: 21237 (N-65-29395)
C–Cr–Co–Re–Ti–W–Zr, development and tensile and stress-rupture properties of cobalt-base, 20: 21237 (N-65-29395)
C–Cr–Co–Ti–W–Zr, development and tensile and stress-rupture properties of cobalt-base, 20: 21237 (N-65-29395)
C–Mo–Nb–Ti–Zr, bend and tensile ductility properties of, 20: 21410
C–Mo–Ti–Zr, extrusion parameters for TZC, 20: 21263 (NASA-CR-54911)

TOKAI-MURA POWER REACTOR
core design and construction for, 20: 22425
fuel element rupture in, detection of, 20: 22427

***p*-TOLUAMIDE, *N*-ISOPROPYL-α-(2-METHYLHYDRAZINO)-**
radiosensitivity effects on malignant melanomas, 20: 20504

TOLUENE
labeling with tritium in methyl side chain, elimination of impurities in, 20: 20711

TOLYL SULFONE
radiolysis of, sulfur dioxide yields from gamma, 20: 20760

TOMATOES
radiosterilization effects on, low-level gamma, 20: 21195(R) (TID-22509)
radiosterilization effects on respiration in, 20: 21195(R) (TID-22509)

TOXINS
radiosensitivity effects of bacterial, in mice, 20: 20512

TRACER TECHNIQUES
for measurement of liquid volume in closed systems, 20: 21208

TRACER TECHNIQUES (AGRICULTURE)
use in plant nutrition studies, 20: 20389 (STI-PUB-108)

TRACER TECHNIQUES (BIOLOGY)
data analysis for steady-state multi-compartment systems, 20: 20393
data analysis for partitioned initial entry functions, 20: 20394
for ecological studies in Columbia River whitefish, zinc-65, 20: 20382 (BNWL-SA-623)
for microbiological assays in seawater, 20: 20368 (CONF-640309-1)

TRACER TECHNIQUES (HYDROLOGY)
development and performance for river flow rates, 20: 20903 (AEET-Radiochem.-45)
use in ground water studies, 20: 20389 (STI-PUB-108)
use in studies on bed-load movement and transport in canals and rivers, 20: 20904 (STI-REP-101)

TRACER TECHNIQUES (MEDICINE)
for diagnosis of brain tumors, 20: 20529
for diagnosis of thyroid diseases, 20: 20528
for diagnosis of thyroid diseases, 20: 20533
for diagnosis of thyroid diseases, 20: 20534
for kidney function tests, 20: 20550
for respiratory tract studies, 20: 20532

TRACER TECHNIQUES (OCEANOGRAPHY)
evaluation of, for waterfront maintenance, 20: 21176 (AD-621440)

TRADESCANTIA
radiation effects on content of ATP in anthers of, x, 20: 20418
radioinduced chromosome aberrations in pollen of, 20: 20438 (EUR-2518.f)

TRANSDUCERS
calibration of, in Mössbauer experiment systems, 20: 21079

TRANSISTORS
radiation effects on, review of, 20: 21156
radiation effects on MOS FET, annealing of gamma, 20: 21159
radiation effects on, prediction of transient, 20: 21166
radiation response of power, effect of design on, (E/T), 20: 21148(R) (AD-630835)
radiation response of power, effect of design on, (E/T), 20: 21149(R) (AD-630836)
thermal effects in, compensation of, 20: 20992
use in reactor safety systems, 20: 22360
use of avalanche, in neutron time-of-flight spectrometer, 20: 21110

TRANSURANIC ELEMENTS
production and separation of, review of, 20: 20796

TRIETHYLENE GLYCOL
dimethacrylate, radioinduced gelation of, fast-neutron, 20: 20720 (AD-630891)

TRIISOOCTYLAMINE
solvent properties for neptunium, 20: 20561 (JAERI-1099)
solvent properties for uranium in thorium or zirconium solutions, 20: 20598

TRITIUM
concentration in hydrogen by gas chromatography, systems for, 20: 21218
content in atmosphere at Hamburg, Germany, following Windscale accident, 20: 20889
content in precipitation and ground water, 20: 20892
content in rain water in New Zealand, 20: 20893
detection and measurement of, performance of thin-window G-M tubes for, 20: 21065
determination in biological materials, combustion procedure for sample preparation for liquid scintillation counting for, 20: 20570
determination in helium by liquid scintillation counting, 20: 20582
determination with carbon-14 in biological materials, autoradiographic method for, 20: 20605
deuteron reactions (d,n) with, neutron angular and energy distributions from, (T), 20: 21934 (AD-621473)
effects on induction of deuterium exchange reactions in gaseous ethane and methane, mechanism of, 20: 20719 (AD-624657)
effects on uv photolysis of uracil, 20: 20782
exchange between water-t_2 and amino acids or peptides, 20: 20714
excretion and metabolism of, use in dosimetry, 20: 20398
incorporation in amino acids or peptides by isotopic exchange, 20: 20714
incorporation in alumina for use in self-labeling chromatographic analysis, 20: 20575
incorporation in ammonia, equilibrium constant for, 20: 20660
incorporation in methyl side chain of toluene, elimination of impurities in, 20: 20711
radiation target design and performance using gas of, for (d,n) reactions, 20: 21948
separation from helium-3 by charcoal trapping, 20: 20807(R) (MLM-1287)
use for determination of characteristics of water bodies exposed to atmosphere, 20: 20894

TRITONS
reactions with nuclei, amplitude singularities in knockon and stripping, (T), 20: 21997 (INSJ-96)

TROPOLONES
complexes with uranium, stability of, 20: 20673
decomposition constants of substituted, 20: 20673

TUBES
fluid flow in annular, equations for turbulent, 20: 20856 (GEAP-4976)
quality control of SAP, mechanical radiographic methods for, 20: 20861 (EUR-2443.f)

TUMORS
effects of antioxidant inhibitors on x irradiated mouse, 20: 20506
etiology of, role of viruses in, 20: 20377
incidence in populations of Hiroshima and Nagasaki exposed to atomic bomb in 1945, 20: 20919(R) (ABCC-64-65)
radiation effects on immune reactions in transplanted mouse, γ, 20: 20479
radiation effects on cellular survival in ascites, transplanted into x-irradiated animals, uv, 20: 20483
radiation effects on cells of ascites, transplanted into x-irradiated mice, 20: 20484
radiation effects combined with procarbazine on melanomas, 20: 20504
radiodiagnosis of hepatic, using iodine-131-rose bengal or colloidal albumin and external scanning, 20: 20522 (CNEA-167)
radiodiagnosis of mammary, using bremsstrahlung produced by radiophosphorus in paraffin, 20: 20540
radioinduced in mice, incidence of x, 20: 20441 (ORNL-P-1173)
radioinduced necrosis in cells of, mechanism for, 20: 20416
radiosensitivity of tissue cultures of, 20: 20440(R) (EUR-2643.f)
radiotherapy of nasopharyngeal, delayed pathological effects on spinal cord of supervoltage x, 20: 20545
radiotherapy of, conference on megavolt, 20: 20551

Ta–W–Zr, strength, weldability, and heat treatment of, 20: 21405

TUNGSTEN CARBIDES

effects on tensile properties of tungsten wire, 20: 21396
Co–WC, wear properties of plasma-arc-deposited coatings of, 20: 21319 (AD-621064)

TUNGSTEN CHLORIDES

$CoCl_2$–WCl_6, deposition of cobalt–tungsten from vaporous, by hydrogen reduction, 20: 21231 (BM-RI-6713)

TUNGSTEN OXIDES

Nb_2O_5–WO_3, phase studies on, 20: 21385
Ta_2O_5–WO_3, phase studies on, 20: 21385

TUNGSTEN SELENIDES

reactions with samarium and ytterbium, preparation of intercalation compounds by, 20: 20648 (AD-621029)

TUNGSTEN SILICIDES

thermionic emission from cesiated surfaces of, (E), 20: 21584

TUNGSTEN SULFIDES

friction on copper surfaces in ultrahigh vacuum, 20: 21366
reactions with samarium and ytterbium, preparation of intercalation compounds by, 20: 20648 (AD-621029)

TUNGSTEN SYSTEMS

C–Co–Ti–W, development and tensile properties of cobalt-base, 20: 21237 (N-65-29395)
C–Co–Ti–W–Zr, development and tensile properties of cobalt-base, 20: 21237 (N-65-29395)
C–Cr–Co–Re–Ti–W–Zr, development and tensile and stress-rupture properties of cobalt-base, 20: 21237 (N-65-29395)
C–Cr–Co–Ti–W–Zr, development and tensile and stress-rupture properties of cobalt-base, 20: 21237 (N-65-29395)
C–Hf–Mo–N–Re–Ta–W–Zr, development of dispersion-strengthened tantalum-base, 20: 21240(R) (WANL-PR-(Q)-006)
C–Hf–Nb–W, properties at very high temperatures, 20: 21412
C–Hf–Re–Ta–W, development of dispersion-strengthened tantalum-base T-333, 20: 21240(R) (WANL-PR-(Q)-006)
C–Hf–Ta–W, bonding of T-222, to Inconel 600 and stainless steels, process development for explosive, 20: 21295(R) (WANL-PR-(EE)-002)
C–Mo–Nb–Ta–W–Zr, extrusion parameters for Cb-132M, 20: 21263(R) (NASA-CR-54911)
C–Nb–W–Zr, properties at very high temperatures, 20: 21412
C–Nb–W–Zr, specifications of D-43, for use in corrosion test loop fabrication, 20: 21293 (R-66SD3007)
HfN–Re–W, tensile properties at high temperatures, 20: 21406
HfN–W, tensile properties at high temperatures, 20: 21406
Re–ThO_2–W, ductility and hot strength, 20: 21407
Re–ThO_2–W, tensile properties at high temperatures, 20: 21406
ThO_2–W, tensile properties at high temperatures, 20: 21406

TYRAMINE

radiation effects on, tracer studies of norepinephrine synthesis in uv, 20: 20409

U

ULTRAVIOLET RADIATION

absorption by cultured cells during interphase, use of flying-spot microscopy for detecting, 20: 20473
effect on 3-aminophthalhydrazine, 20: 20777
effects on ascites tumor cells transplanted into x-irradiated mice, 20: 20484
effects on chromosomes in Tradescantia pollen grains, morphological, 20: 20438 (EUR-2518.f)
effects on cultured cells during interphase, 20: 20473
effects on DNA, kinetics of denaturation, 20: 20412
effects on *Escherichia coli*-bacteriophage complexes, 20: 20471
effects on gastric transit in laparotomized and vagotomized rats, 20: 20414
effects on glutamic dehydrogenase in Neurospora mutants, 20: 20462
effects on green colony-forming ability in Euglena, 20: 20450
effects on growth of ascites tumor cells in x-irradiated animals, 20: 20483
effects on mycoplasma aerosols, lethal, 20: 20469
effects on nitrogen, effects on algal nitrogen fixation, 20: 20408
effects on optical properties of adhesives and glass, 20: 21446
effects on organic compounds of biological interest, mechanism of, 20: 20731 (PB-181506, pp 133-42)
effects on phage ϕX174, inactivation and mutagenic, 20: 20463
effects on phage T4D, 20: 20427
effects on photooxidation of thymine in aqueous solutions, 20: 20771
effects on Pseudomonas, genetic, 20: 20470
effects on tritium-labeled uracil, 20: 20782
effects on tyramine, tracer studies of products from, 20: 20409
effects on viability of *E. coli*, 20: 20457
use in analysis of genetic transmittal by viral DNA, 20: 20426

ULTRAVIOLET SPECTROSCOPY

conference on photographic and spectroscopic optics, 20: 21458
UNDERGROUND EXPLOSIONS
detection of distant, seismometer array recording system for, 20: 20913
detection of, by seismic wave pattern, 20: 20906
detection of, teleseismic record evaluation for, 20: 20911
post-shot thermal effects and secondary explosions in cavities in tuff, hazards of water in, 20: 20939 (NVO-1163-70)
seismic data from, for comparison with earthquakes, 20: 20900 (AD-627039)
seismic data from, for comparison with earthquakes, 20: 20901 (AD-627040)
seismic data from, for comparison with earthquakes, 20: 20902 (AD-627051)
seismic measurements on, in Vela Project, 20: 20876 (NP-15949)
seismic wave propagation from, abstracts on elastic, 20: 20896 (AD-623592)
shock waves from nuclear, design and operation of multidirectional peak pressure gage for, 20: 20914
use for fracturing of natural gas reservoirs in Project Gasbuggy, 20: 20837
use for recovery of oil from oil shale, 20: 20835
uses for petroleum reservoir stimulation, economics of, 20: 20836
UNITED STATES
fallout monitoring, 1965, 20: 20882(R) (HASL-171)
URACIL
photolysis of, tritium effects on uv, 20: 20782
yields of, in uv-radioinduced oxidation of thymine in aqueous solutions, 20: 20771
URACIL, 5-FORMYL-
preparation of, new method for, 20: 20771
URACIL, 5-HYDROXYMETHYL-
yields of, in uv-radioinduced oxidation of thymine in aqueous solutions, 20: 20771
URACIL, 6-PROPYL-2-THIO-
effects of dietary, on rats, carcinogenic, 20: 20448
URANIUM
corrosion inhibition coatings on, evaluation of, 20: 21278
deformation properties of alpha-phase, at 125 to 250°C, impact, 20: 21325 (AWRE-O-36/66)
deposition on metals, conditions for electrolytic, 20: 21287 (AE-217)
deposition on platinum disks for α and β counting, electrolytic, 20: 20795
determination and control of, at Eurochemic's mol fuel reprocessing facility, 20: 20831
determination in chromium–uranium alloys, polarographic, 20: 20595
determination in fuel reprocessing plant for accountancy purposes at Windscale, 20: 20830
determination in graphite coatings on fuel particles, nondestructive method for, 20: 21423 (N-65-23015)
determination in nuclear materials by isotopic analysis, 20: 20978
determination in presence of thorium and zirconium using Arsenazo-III, 20: 20614
determination in sedimentary carboniferous deposits, x-ray fluorescence and scintillation counting, 20: 20613
determination in uranium silicides by controlled-potential coulometry, 20: 20557 (AERE-R-5129)
determination in various materials for materials management, methods for, 20: 20977
determination in Windscale separation plants, methods for, 20: 20972
determination of hexavalent, in nitric acid media, polarographic, 20: 20630
determination of hexavalent, in nitric acid media containing TBP, polarographic, 20: 20631
determination using Arsenazo III, spectrophotometric, 20: 20598
excretion and metabolism of, use in dosimetry, 20: 20398
fabrication of, material control in, 20: 21313
handling of, safety in, 20: 20975
isotopic analysis of, using thermionic emission, mass spectrometric, 20: 21216
management in France, sampling methods for, 20: 20973
neutron cross sections at 0.0045 to 0.028 ev, (E/T), 20: 21966 (AE-222)
neutron flux and spectrum measurements on foils of, 20: 21427(R) (NASA-CR-54904)
occurrence in clays and sandstone, Braunschweig, Germany, 20: 20890
occurrence in phosphate rocks, 20: 20886
occurrence in sea water, 20: 21243
oxidation by air at 40 to 100°C, effects of sample preparation and humidity on, 20: 21278
oxidation by carbon dioxide at 650°C, carbon pickup and oxide cracking during, 20: 21272
photofission at 650 Mev, yields from, 20: 22040
preparation by magnesium reduction of uranium(IV) fluoride, 20: 21256
processing of irradiated, materials control system for facility for, 20: 20832
production and processing of, UKAEA accounting and control in, 20: 22528
production in France, 20: 21243
proton reactions at 590 Mev and 18 Bev, yields of iodine isotopes from, (E), 20: 22045
radiation effects on, neutron, 20: 21436
reactions with bromine pentafluoride, effects of stainless steel and Zircaloy on, 20: 20803(R) (ANL-7055, pp 99-162)
recovery from crucible residues by skull reclamation, 20: 20802(R) (ANL-7055, pp 21-98)
recovery from EBR-II fuel processing residues by skull reclamation, 20: 20802(R) (ANL-7055, pp 21-98)
recovery from high-burnup fuels, effects of fission products and radiation on, 20: 20803(R) (ANL-7055, pp 99-162)
separation from cadmium alloys by fused chlorides in extraction columns, 20: 20802(R) (ANL-7055, pp 21-98)
separation from fuel alloys by extraction using liquid copper–magnesium alloys, 20: 20802(R) (ANL-7055, pp 21-98)
separation from hydrochloric acid solutions by solvent extraction using quaternary ammonium chlorides, 20: 20816
separation from other elements by combined ion exchange-solvent extraction, using nitric acid–tetrahydrofuran solutions, 20: 20811
separation from phosphates and sulfates in anion exchanger desorption, 20: 20827
separation from plutonium alloys by chlorination and reduction, 20: 20802(R) (ANL-7055, pp 21-98)
separation from protactinium by solvent extraction using quaternary ammonium chlorides, 20: 20816
separation from rare earths in acid solutions using cation exchange materials, 20: 20813
separation from thorium by ion exchange in nitric acid solution, 20: 20624
separation from thorium-234 by ion exchange, 20: 20624
solubility in copper–magnesium alloys, 20: 20802(R) (ANL-7055, pp 21-98)
solubility in fused salts, 20: 20802(R) (ANL-7055, pp 21-98)
spectra of, instrument for studying isotopic shift in, 20: 20662
uses for deoxidation and desulfurization of iron and steel, 20: 20692
viscosity at 1133 to 1223°C, 20: 21342(R) (MLM-1301)
URANIUM ALLOYS
Al–Ni–U, reactions with water during Kiwi-TNT transients, 20: 20925(R) (ANL-7055, pp 177-212)
Al–U, processing for uranium recovery by fluoride volatility, 20: 20803(R) (ANL-7055, pp 99-162)
Al–U, processing by fluid-bed fluoride volatility, 20: 20801 (ANL-6830)
Au–Th–U, fabrication and corrosion testing of radiation targets of, 20: 21288 (BMI-1761)
Cd–Mg–U–Zn, corrosive effects in fused chloride mixtures, on stainless steel, 20: 20802(R) (ANL-7055, pp 21-98)
Cr–U, analysis for uranium by polarographic methods, 20: 20595
Mg–Pu–U–Zn, corrosive effects on type 405 stainless steel, 20: 20802(R) (ANL-7055, pp 21-98)
Mg–U–Zn, corrosive effects with fused chlorides, on carbon and zirconium boride, 20: 20802(R) (ANL-7055, pp 21-98)
Mo–U, microstructure of uranium-rich, effects of heat treatments on, 20: 21372
Mo–U, radiation effects on uranium-rich, neutron, 20: 21436
Nb–U, microstructure of uranium-rich, effects of heat treatments on, 20: 21372
Nb–U, phase studies on uranium-rich, 20: 21372
Nb–U–Zr, properties of, at 150 to 350°C, mechanical and physical, 20: 21356 (UCRL-14724)
Nb–U–Zr, reactions with water during Kiwi-TNT transients, 20: 20925(R) (ANL-7055, pp 177-212)
Pu–U, processing by cadmium alloy–molten salts, flowsheets for, 20: 20802(R) (ANL-7055, pp 21-98)
Th–U, fabrication and corrosion testing of radiation targets of, 20: 21288 (BMI-1761)
Th–U, feasibility for use in fast breeder reactors, 20: 21229 (AEET-229)
Ti–U, microstructure of uranium-rich, effects of heat treatments on, 20: 21372
U–Zircaloy-2, processing for uranium recovery by fluoride volatility, 20: 20803(R) (ANL-7055, pp 99-162)
U–Zr, corrosion inhibition by oxide films on, mechanisms of, 20: 21281
U–Zr, microstructure of uranium-rich, effects of heat treatments on, 20: 21372
U–Zr, neutron multiplication factor of, (E), 20: 22392
U–Zr, phase studies on uranium-rich, 20: 21372
URANIUM CARBIDES
casting bars of, techniques for, 20: 21307
diffusion of krypton in single-crystal, at 1700°C, 20: 21332(R)

(EURAEC-1573)
fabrication of fuel pellets of, with special profile, 20: 21316(P)
fabrication of SAP-clad, for reactor fuel, 20: 22520(R) (NAA-SR-11805)
neutron fission of, beta emission energies in, (E/T), 20: 22404 (USNRDL-TR-987)
oxidation by oxygen at 800 to 1000°C, 20: 21267
preparation and properties of tungsten-bearing, 20: 22520(R) (NAA-SR-11805)
preparation by carbon reduction of dioxide, 20: 21307
preparation by fludized bed processes, 20: 20802(R) (ANL-7055, pp 21-98)
sintering of, performance of sintering promoters in, 20: 21296 (Y-1510)
sintering of, process variables for, 20: 21296 (Y-1510)
thermal conductivity, 20: 22411(R) (GA-6113)
thermodynamics of formation, 20: 20672
PuC–UC, preparation methods, 20: 20802(R) (ANL-7055, pp 21-98)
ThC_2–UC_2, thermal conductivity of, 20: 22411(R) (GA-6113)

URANIUM(III) CHLORIDES
reactions with plutonium at high temperatures, mechanisms of, 20: 20802(R) (ANL-7055, pp 21-98)
KCl–UCl_3, corrosive effects on Inconel 600, INOR-8, and Hymu-80 nickel-base alloys at 900°C, 20: 21261 (LA-3476)

URANIUM(IV) CHLORIDES
hydrolysis of, uranium–oxygen bonds in products from, 20: 20675

URANIUM COMPLEXES
formation in uranyl chloride solutions containing ferric, phosphate, and sulfate ions, 20: 20827
with thiodibenzoylmethane, stability of, 20: 20693
with tropolones, stability of, 20: 20673

URANIUM CONCENTRATES
management in France, sampling methods for, 20: 20973

URANIUM(IV) FLUORIDES
analysis for uranium content, pyrohydrolysis-gravimetric method for, 20: 20977
analysis for water by gas volumetric methods using calcium hydride, 20: 20609
reactions with bromine pentafluoride, effects of alumina and fission products on, 20: 20803(R) (ANL-7055, pp 99-162)
reduction to metal using magnesium, 20: 20817
reduction to metal using magnesium, 20: 21256

URANIUM(VI) FLUORIDES
analysis of, mass spectrometer for isotopic, 20: 20588
analysis of, methods for, 20: 20558 (CEA-R-2863)
reactions with hydrocarbons, fluorohydrocarbon preparation in, 20: 20707(P)
shipping of, development and testing of container and packaging for, 20: 20936 (K-1661)
MoF_6–UF_6, phase studies, 20: 20803(R) (ANL-7055, pp 99-162)
NbF_5–UF_6, liquid–vapor equilibria in, 20: 20808(R) (ORNL-3916)
PuF_6–UF_6, liquid-solid equilibria in, equipment for, 20: 20803(R) (ANL-7055, pp 99-162)

URANIUM IONS
oxidation of tetravalent, by molecular oxygen, 20: 20689

URANIUM ISOTOPES
content in operating fuel elements, methods for calculating, 20: 20979

URANIUM ISOTOPES U-233
buildup in reactors, fabrication of calibration and irradiation samples for analyzing, 20: 21288 (BMI-1761)
neutron cross sections for, 20: 21967 (AEET-234)
neutron fission cross sections for, 20: 22383(T) (AEC-tr-6693)

URANIUM ISOTOPES U-234
content in carbonate deposits in Russia, 20: 20887
fission of, potential barrier widths for spontaneous, (T), 20: 22014(T) (KFK-tr-185)
neutron cross sections for, 20: 21967 (AEET-234)
neutron fission cross sections for, 20: 22383(T) (AEC-tr-6693)
separation from plutonium-238 by ion exchange and solvent extraction, 20: 20553(R) (MLM-1142)

URANIUM ISOTOPES U-235
determination in air filters, non-destructive gamma spectrometric, 20: 20564 (NYO-10740)
determination in leached fuel elements, equipment and method for, 20: 21040 (ORNL-P-1218)
neutron cross sections and shielding coefficients for, 20: 22383(T) (AEC-tr-6693)
neutron fission cross sections at 0.02 to 80 ev, epithermal, (E), 20: 22012 (UCRL-14606)
neutron fission cross sections for, 20: 22383(T) (AEC-tr-6693)
neutron fission of, fragment charge distribution from thermal, (E), 20: 22136
neutron fission of, yields of antimony-126 from thermal, (E), 20: 22044
neutron spectra from spheres of, leakage, 20: 21939(R) (GA-6930)

URANIUM ISOTOPES U-236
fission of, potential barrier widths for spontaneous, (T), 20: 22014(T) (KFK-tr-185)
fission of, primary charge distribution in low-energy, (T), 20: 22013(T) (ANL-Trans-296)
neutron fission cross sections for, 20: 22383(T) (AEC-tr-6693)
nuclear magnetic moments, 20: 20662

URANIUM ISOTOPES U-238
alpha reactions ($\alpha,\alpha' f$) with, fragment angular correlations from, (E), 20: 22143
content in carbonate deposits in Russia, 20: 20887
fission of, potential barrier widths for spontaneous, (T), 20: 22014(T) (KFK-tr-185)
neutron cross sections and shielding coefficients for, 20: 22383(T) (AEC-tr-6693)
neutron elastic scattering by, ($n,n\alpha'$) reaction effects on anomaly in small-angle, (E), 20: 22017
neutron fission cross sections for, 20: 22383(T) (AEC-tr-6693)
neutron reactions (n,f) at 1.45 Mev, cross section and threshold energy for, 20: 21427(R) (NASA-CR-54904)
neutron reactions ($n,n\alpha'$) at 14.7 Mev, cross sections for, (E), 20: 22017
neutron resonance absorption by, cross sections for Doppler-broadened, (T), 20: 21951
neutron scattering at 75 to 1620 kev, excitation functions and differential cross sections for, (E), 20: 22056
nitrogen-15 reactions at 102 Mev, neutron pickup in, (E), 20: 22001 (JINR-P-2555)
nuclear magnetic moments, 20: 20662
proton capture cross sections and transmission coefficients for, optical model calculation of, 20: 22049
proton fission at 11 to 21 Mev, alpha emission in, (E), 20: 22144
separation from uranyl nitrate solutions, chromatographic, 20: 20828

URANIUM ISOTOPES U-240
fission of, potential barrier widths for spontaneous, (T), 20: 22014(T) (KFK-tr-185)

URANIUM NITRIDES
fabrication of fuel pellets of, with special profile, 20: 21316(P)
preparation and properties, 20: 20802(R) (ANL-7055, pp 21-98)

URANIUM ORE PROCESSING PLANTS
materials management in, inventory methods for, 20: 20971

URANIUM ORES
management in France, sampling methods for, 20: 20973
processing by bicarbonate leaching and solvent extraction, 20: 20817

URANIUM OXIDES
analysis for fluorine by pyrolysis and alizarin complexone photometric method, 20: 20597
fabrication of fuel pellets of, with special profile, 20: 21316(P)

URANIUM(IV) OXIDES
burnup of pyrolytic carbon coated fuel particles of, fission product release in, 20: 22411(R) (GA-6113)
diffusion of krypton in single-crystal, at 1400 to 1600°C, 20: 21332(R) (EURAEC-1573)
diffusion of nitrogen from pellets of, kinetics and mechanisms of, 20: 21360 (WCAP-2098)
effects on radiolysis of benzene in aqueous solutions, 20: 20768
fabrication of fuels of, economic and technical evaluation of process for, 20: 21300
fission fragment track registration in epitaxial films of, 20: 21442
fission-product diffusion from clad, in air–steam meltdown, 20: 20940(R) (ORNL-3915)
fluorination of pelletized, effects of crushing on, 20: 20803(R) (ANL-7055, pp 99-162)
meltdown in ORR, temperature history of high-burnup, 20: 20940(R) (ORNL-3915)
meltdown of stainless steel-clad and Zircaloy-clad in TREAT, 20: 20940(R) (ORNL-3915)
neutron cross sections at 0.0045 to 0.028 ev, (E/T), 20: 21966 (AE-222)
performance in fission electric cells, 20: 21576
preparation of microspheres of, equipment and procedures for, 20: 20808(R) (ORNL-3916)
processing Zircaloy-clad, by fluorination and oxidation, 20: 20803(R) (ANL-7055, pp 99-162)
radiation effects on hollow-core pellets of, irradiated with central melting, reactor, 20: 21422 (GEAP-5100D)
reactions of clad, with water during Kiwi-TNT transients, 20: 20925(R) (ANL-7055, pp 177-212)
reactions with carbon to prepare uranium carbide, 20: 21307
thermal conductivity of irradiated, inpile measurements to 2000°C on, 20: 21361 (WCAP-2923)
use as power reactor fuel, review of properties for, 20: 22422
Al_2O_3–MgO–UO_2, phase studies, properties, and structures of, 20: 21359 (WAPD-T-1581)
BeO–UO_2, fabrication of fuel particles of, 20: 21297(T) (NP-tr-1371)
CaO–UO_2–ZrO_2, preparation and properties of, for ceramic nuclear fuels,

20: 21302
$CoO–UO_2$, preparation and x-ray diffraction pattern of $CoUO_3$, 20: 21242
$PuO_2–UO_2$, microsphere preparation by plasma-torch heating, 20: 20553(R) (MLM-1142)
$PuO_2–UO_2$, processing irradiated, by fluoride volatility, 20: 20803(R) (ANL-7055, pp 99-162)
$SiC–UO_2$, fabrication of fuel particles, 20: 21297(T) (NP-tr-1371)
stainless steel–UO_2, processing by fluorination for uranium recovery, 20: 20803(R) (ANL-7055, pp 99-162)
stainless steel–UO_2, processing by fluid-bed fluoride volatility, 20: 20801 (ANL-6830)
$ThO_2–UO_2$, densification properties of solid solutions of, 20: 21323 (ANL-6894)
$ThO_2–UO_2$, fabrication of, for ceramic fuels, 20: 21301
$ThO_2–UO_2$, oxidation properties of solid solutions of, 20: 21323 (ANL-6894)
$ThO_2–UO_2$, phase studies, 20: 21323 (ANL-6894)
$ThO_2–UO_2$, production of ceramic-grade, 20: 21255(P)
$ThO_2–UO_2$, sintering and thermal shock properties of, effects of composition on, 20: 21299
$UO_2–ZrO_2$, radiation effects on densification and homogenization of, neutron, 20: 21432 (WAPD-301)
U–UO_2, phase studies of hypostoichiometric, 20: 21324(R) (ANL-7055, pp 163-6)
U–UO_2, vapor pressure of uranium over, 20: 21324(R) (ANL-7055, pp 163-6)

URANIUM(IV-VI) OXIDES
$PuO_2–U_3O_8$, fluorination in fluid beds, effects of fission products on, 20: 20803(R) (ANL-7055, pp 99-162)

URANIUM(VI) OXIDES
reactions with metallic and silicon oxides, effects of substrate symmetry in, 20: 20649 (AEET-CD-24)
sintering of, furnace for, 20: 21304

URANIUM PHOSPHIDES
melting point of stoichiometric, (E), 20: 20687

URANIUM SILICIDES
analysis for silicon and uranium, methods for, 20: 20557 (AERE-R-5129)
fabrication of fuel pellets of, with special profile, 20: 21316(P)
performance as sintering promoter for uranium monocarbide, 20: 21296 (Y-1510)

URANIUM SULFIDES
thermochemical properties of US and US_2, 20: 20669
ThS–US, magnetic susceptibilities, 20: 20802(R) (ANL-7055, pp 21-98)

URANIUM SYSTEMS
B–Co–U, crystal structure, 20: 20685
B–Ni–U, crystal structure, 20: 20685
B–U–Zr, neutron multiplication factor of, (E), 20: 22392
U–H_2O, criticality studies, (E), 20: 22375(R) (BNWL-193, pp 45-56)

URANOTHORIANITES
processing plant for, nuclear materials management in, 20: 20969

URANYL BROMIDES
complexes with triphenylphosphine, preparation of, 20: 20679

URANYL CHLORIDE COMPLEXES
with semicarbazide hydrochloride, polarographic behavior of, 20: 20677
with triphenylphosphine, preparation of, 20: 20679

URANYL FLUORIDES
reactions with bromine pentafluoride, effects of alumina and fission products on, 20: 20803(R) (ANL-7055, pp 99-162)

URANYL IODIDES
complexes with triphenylphosphine, preparation of, 20: 20679

URANYL IONS
complexes with bacterial DNA, 20: 20392
effects on cation uptake by barley roots, selective-inhibition, 20: 20402
effects on nuclear structure in bacteria, 20: 20392
reactions with TBP, effects of, on analytical procedures, 20: 20630
sorption by ion exchangers in hydrochloric acid media, 20: 20827
sorption from perchloric acid solutions by ion exchange materials, 20: 20823

URANYL NITRATE COMPLEXES
with triphenylphosphine, preparation of, 20: 20679

URANYL NITRATES
chromatography of, thorium-234 and uranium-238 separation in, 20: 20828
production by reduction of uranyl nitrate, equipment for continuous, 20: 20808(R) (ORNL-3916)
purification by combined ion exchange-solvent extraction using nitric acid–tetrahydrofuran solutions, 20: 20811
reduction to uranous nitrate, equipment for continuous, 20: 20808(R) (ORNL-3916)
$Ce(NO_3)_3–UO_2(NO_3)_2–H_2O$, compound formation in, 20: 20682
$Th(NO_3)_4–UO_2(NO_3)_2$, reduction to ceramic-grade mixed thorium oxide–uranium oxide, 20: 21255(P)

URANYL SULFATES
$CuSO_4–D_2SO_4–UO_2SO_4–H_2O–D_2O$, spectrophotometry of reactor fuel solutions of, 20: 20600

UREA
compounds with hydrogen peroxide (H_2O_2 · urea), ESR in gamma-irradiated single crystals of, 20: 20756

URETHAN POLYMERS
effects of decontaminating and descaling solution on coating of, 20: 21238 (NP-15928)
radiation effects on dielectric and mechanical properties of, combined effects of low-temperature, vacuum, and gamma and neutron, 20: 21152 (N-65-22353)

URINE
analysis for plutonium, 20: 20590
analysis for strontium-90 by anion exchange method using beta counting, 20: 20583
analysis for yttrium-90 by anion exchange method using beta counting, 20: 20583

UTAH
site selection for wet medium cratering experiments at Dugway Proving Ground, 20: 20895 (AD-626899)

UTERUS
radiotherapy of carcinomas of, effectiveness of combined surgery and x-ray, 20: 20526
radiotherapy of carcinomas of, combined with surgery, γ, 20: 20536

V

VACUUM GAGES
use of radiometric, survey on, 20: 20990(T) (AERE-Trans-1048)

VACUUM PUMPS
design and performance for evacuating target space in particle accelerators, 20: 21479

VACUUM SYSTEMS
design of high-temperature, for refractory metal research, 20: 21350 (ORNL-TM-1426)

VALVES
design for reactor cooling systems, 20: 22364(P)
design of flow-diverter, for granular solids, 20: 22511 (IDO-14666)

VAN ALLEN RADIATION BELTS
electron energy and lifetime in outer, (E), 20: 21815
electron leakage from, correlations with leakage from magnetic mirrors, (E), 20: 21836
electron lifetime in outer, at magnetically quiet times, (T), 20: 21817
properties of, review of, 20: 21837
proton flux in, from decay of solar neutrons, 20: 21495
proton injection into, by cosmic ray and solar proton albedo neutron decay, 20: 21550

VAN DE GRAAFF ACCELERATORS
conference on tandem, 20: 21462 (BNL-948)
description of double tandem, 20: 21464 (BNL-948, pp 692-703)
ion-channel for 2-Mev, development of, 20: 21480
use for research in nuclear physics, 20: 21463 (BNL-948, pp 685-91)

VANADIUM
critical fields in films of, (E/T), 20: 21915
determination in high-purity tantalum by spectrography using d-c arc method, 20: 20608
ductility of, at −269°C, 20: 21416
proton scattering at 45 Mev, polarization in, (E), 20: 22128
reactions with sodium at high temperatures, 20: 20925(R) (ANL-7055, pp 177-212)
superconductivity properties of, effects of λ transition on, 20: 21875
welding of, argon-arc and electron-beam methods of, 20: 21310

VANADIUM ALLOYS
development of fabricable high-strength, 20: 21333(R) (IITRI-B6042-4)
Cr–V, brazing material for joining molybdenum to tungsten for use to 2700°F, 20: 21312
Ga–Va, superconducting critical currents in intermetallic compounds of, in high fields, (E), 20: 21922
Nb–Ta–V, tensile properties of vanadium-base, effects of carbon and silicon additions on, 20: 21333(R) (IITRI-B6042-4)
Nb–Ti–V, tensile properties of vanadium-base, effects of carbon and silicon additions on, 20: 21333(R) (IITRI-B6042-4)
Nb–V–Zr, properties of Cb-753, 20: 21411
Ti–V, electric conductivity and magnetization of superconducting, at 4.2°K, (E), 20: 21928
Ti–V, removal from reactor fuel alloys, chemical methods for, 20: 20802(R) (ANL-7055, pp 21-98)
V–Zr, magnetic induction in hard superconducting, (E), 20: 21893

VANADIUM ISOTOPES V-46
beta decay, energy spectra, and magnetic moment of, $f_{7/2}$ model for, 20: 22131
energy levels of, isotope shifts of isobaric-analog, (E), 20: 22095
energy levels of, model for, 20: 22131

VANADIUM ISOTOPES V-47

beta decay, energy spectra, and magnetic moment of, $f_{7/2}$ model for, 20: 22131
energy levels of, model for, 20: 22121
VANADIUM ISOTOPES V-48
energy levels of, isotope shifts of isobaric-analog, (E), 20: 22095
VANADIUM ISOTOPES V-50
energy levels of, isotope shifts of isobaric-analog, (E), 20: 22095
VANADIUM ISOTOPES V-51
energy levels from chromium-51 decay, 645-kev, (E), 20: 22029
VANADIUM SILICIDES
magnetic field penetration of superconducting, (E), 20: 21908
microwave surface resistance in superconducting, (E), 20: 21916
VANADIUM SYSTEMS
B–Co–V, crystal structure, 20: 20685
B–Ni–V, crystal structure, 20: 20685
U–UO_2, phase studies of hypostoichiometric, 20: 21324(R) (ANL-7055, pp 163-6)
U–UO_2, vapor pressure of uranium over, 20: 21324(R) (ANL-7055, pp 163-6)
VELA PROJECT
seismic measurements on underground explosion in, 20: 20876 (NP-15949)
VELOCITY
control and measurement in Mössbauer apparatus, 20: 21081
VENTILATION
capacity and rate of, in underground shelters, 20: 20920 (AD-621377)
filter design criteria and specifications for, at National Reactor Testing Station, 20: 20933 (IDO-12045)
method for, of fallout shelters by induced draft, 20: 20921 (AD-621998)
VERMICULITES
sorptive properties for cesium-137, 20: 20696
VESPIDAE
radioinduced dominant lethals in males of, frequency of x, 20: 20464
VESSELS
materials testing for fissile materials storage, 20: 20840(R) (BNWL-193, pp 57-67)
VINYL COMPOUNDS
properties and radiation effects on polymeric, 20: 21431(R) (WADC-TR-55-58(Pt.9))
VIRGINIA
areal geology and aeroradioactivity surveying of, 20: 20928 (CEX-59.4.17)
VIRUSES
genetic transmittal by DNA in, uv-method for determining mechanism for, 20: 20426
infection of human diploid cells in culture by tumor, 20: 20377
radioinduced inactivation of Vaccinia, 20: 20500
VISCOMETERS
calibration of, for measurements on alkali metals at high temperatures, 20: 20651(R) (CU-2660-26)
design of torsional-pendulum, engineering drawings for, 20: 21015
VISCOSITY
equation for determining, of liquid metals, 20: 20656 (UCRL-11930)
radiation effects on DNA, uv, 20: 20412
VITAMIN B
dephosphorylation of, catalytic effects of cerium, lanthanum, manganese, thorium, and zirconium ions on, 20: 20375
VITAMIN B_2
dephosphorylation of, catalytic effects of cerium, lanthanum, manganese, thorium, and zirconium ions on, 20: 20375
radiation effects on aqueous solutions of, review on, 20: 20728 (PB-181506, pp 49-58)
VITAMIN B_{12}
content in sea water, determination using carbon-14 and *Cyclotella nana*, 20: 20368 (CONF-640309-1)
VITAMINS
radioinduced reactions with HCl, chromatographic method for separating products in, 20: 20738
VOLATILITY SEPARATION PROCESSES
description of, for short-lived isotopes, review of, 20: 20826
VOLCANOES
age estimation of ash from, by carbon-14 method, in New Zealand, 20: 20893

W

WASHINGTON
cesium-137 content in forests of, effects of climatic zones on, 20: 20879 (BNWL-SA-530)
WASTE DISPOSAL
book: *Advances in Water Pollution Research*, Vol. 1, 2, and 3, 20: 20982
in streams, operations research on liquid, 20: 22513 (NYO-10447)
incinerators for, review on, 20: 22508 (AEET-220)
Oak Ridge National Lab., effects on radioactivity in Clinch River, 20: 22514 (ORNL-P-2021)
storage of irradiated uranium, relation of fission product management to economics of, 20: 22517
WASTE PROCESSING
evaporation methods of, comparison of economics and performance of installations for, 20: 22516
fixation in phosphate glass, Brookhaven process for continuous, 20: 22509 (BNL-10109)
fixation of Purex solutions in phosphate glass, evaluation of, 20: 22510 (BNWL-SA-564)
WASTE SOLUTIONS
analysis for plutonium, methods for, 20: 20976
concentration of low-level, operation and performance of facility for, 20: 22507 (AD-622372)
discharge into Escaut River in Belgium, proposed sewer for, 20: 22515(T) (ORNL-tr-965)
flow-diverter valve for, design of, 20: 22511 (IDO-14666)
separation of cesium from fission-product, by ion exchange on ammonium molybdophosphate, 20: 20818
separation of neptunium-237 from, method for, 20: 20561 (JAERI-1099)
WATER
alpha activity in flowing, monitor for, 20: 21038 (K-1656)
analysis for chromium-51 by precipitation with iron hydroxide and gamma spectroscopy, 20: 20603
cesium-137 content in Amsterdam, 1960 to 1963, 20: 20949
content in soil, neutron probe measurement of, 20: 20915
determination in gas streams containing hydrogen fluoride, equipment for continuous, 20: 20581
determination in uranium tetrafluoride by gas volumetric methods using calcium hydride, 20: 20609
dose distribution in, from electron beam irradiation, three dimensional, 20: 21470 (PB-181506, pp 116-29)
effects on corrosion of rhenium at 25 and 100°C, 20: 21275
effects on post-shot thermal effects and secondary explosions in cavities in tuff, 20: 20939 (NVO-1163-70)
effects on radiolysis of potato starch, 20: 20737
ejection from pressurized column on depressurization, 20: 22350
neutron scattering by, differential cross sections and corrections for thermal, (E), 20: 21939(R) (GA-6930)
processing in space vehicles, use of radioisotopes for, 20: 21174 (SAN-575-12)
radioactivity in, importance of measuring, 20: 20961
reactions with aluminum, laser-induced, 20: 20925(R) (ANL-7055, pp 177-212)
yields from gamma radiolysis of ethanol, 20: 20746
$Ce(NO_3)_3$–K_2CO_3–H_2O, composition of, effects of reactant concentration on, 20: 20664
$Ce(NO_3)_3$–$UO_2(NO_3)_2$–H_2O, compound formation in, 20: 20682
$CuSO_4$–D_2SO_4–UO_2SO_4–H_2O–D_2O, spectrophotometry of reactor fuel solutions of, 20: 20600
$La(NO_3)_3$–K_2CO_3–H_2O, composition of, effects of reactant concentration on, 20: 20664
U–H_2O, criticality studies, (E), 20: 22375(R) (BNWL-193, pp 45-56)
WATER-d_2
deuterium exchange between, and *trans*-hydridochlorobis(triethylphosphine)platinum(II), 20: 20701
deuterium exchange between, and amino acids or peptides, 20: 20714
neutron scattering by, differential cross sections and corrections for thermal, (E), 20: 21939(R) (GA-6930)
neutron slowing down and thermalization in, time dependence of, (E/T), 20: 21936 (AE-216)
$CuSO_4$–D_2SO_4–UO_2SO_4–H_2O–D_2O, spectrophotometry of reactor fuel solutions of, 20: 20600
WATER-t_2
tritium exchange between, and amino acids or peptides, 20: 20714
WATER COOLED REACTORS
boiling indicator for, design of film, 20: 22367(P)
coolant-loss accidents in, metal–water reaction calculations for, 20: 20925(R) (ANL-7055, pp 177-212)
materials testing for, corrosion loop for, 20: 21266
thermal efficiency and condenser output of, 20: 22420
WATER MODERATED REACTORS
control rods for, homogenization of curciform, 20: 22357 (RT-FI-(65)50)
criticality of glass-clad uranium-fueled, 20: 22415 (RPI-321-4)
neutron spectra and fast-fission effect in, fast, 20: 22506
WATER SUPPLIES
decontamination of, using sanitary water-treatment process, 20: 22512 (K-1651)
radioactivity due to fallout, 1965, 20: 20882(R) (HASL-171)
separation of cerium-144, cesium-137, and strontium-90 from, by ion exchange chromatography, 20: 20627
WATER VAPOR
effects on gamma radioinduced recombination rate of hydrogen and

oxygen, 20: 20749
effects on graphite oxidation by oxygen at 510 to 650°C, 20: 21285
effects on plutonium corrosion by air at 30 to 100°C, 20: 21280
WEAPONS
effects of, meteorological, radiological, secondary, and thermal, 20: 20930 (HI-518-RR(Vol.1))
effects of, meteorological, radiological, secondary, and thermal, 20: 20932 (HI-518-RR(Vol.3))
effects on agriculture, environmental, 20: 20931 (HI-518-RR(Vol.2))
protection against, evaluation of school fallout shelter designs for, 20: 20868 (AD-626770)
WELDED JOINTS
embrittlement of steel, effect of time at high temperatures on, 20: 21393
WELDS
inspection of, uses of x-ray radiography for, 20: 20864
WELL LOGGING
equipment for gamma or neutron-gamma, using multiple detectors, 20: 21145(P)
equipment for soil moisture measurements, 20: 20915
WEST VIRGINIA
areal geology and aeroradioactivity surveying of, 20: 20928 (CEX-59.4.17)
WHEAT
radioactivity due to fallout in Canadian, 1964, 20: 20938 (NP-15914)
radioactivity due to fallout in Canadian, 1965, 20: 20883 (NP-15914)
radioinduced mutations for quantitative traits in Durum, x, 20: 20501
radioinduced variegation mutations in Einkorn, beta, fast neutron, gamma, and thermal neutron, 20: 20497
WINDSCALE PRODUCTION REACTORS
accident at, tritium release to atmosphere in, 20: 20889
WIRES
cutting tool for, in instrumented reactor fuel elements, 20: 21018(P)
WOOD
dose distribution in, from electron beam irradiation, three dimensional, 20: 21470 (PB-181506, pp 116-29)
plastic–wood, AEC program on materials of, 20: 21178 (ORNL-IIC-7, pp 1-5)
plastic–wood, commercial development and uses of, 20: 21182 (ORNL-IIC-7, pp 49-58)
plastic–wood, commercial possibilities of irradiated, in Pacific Northwest, 20: 21185 (ORNL-IIC-7, pp 76-80)
plastic–wood, commercial potential of irradiated combinations of, 20: 21186 (ORNL-IIC-7, pp 81-8)
plastic–wood, commercial production of irradiated combinations of, 20: 21187 (ORNL-IIC-7, pp 89-94)
plastic–wood, commercial use of irradiated combinations of, 20: 21189 (ORNL-IIC-7, pp 99-105)
plastic–wood, conceptual design and feasibility study of combinations of, 20: 21181 (ORNL-IIC-7, pp 32-48)
plastic–wood, development, properties, and commercial future of, 20: 21183 (ORNL-IIC-7, pp 59-63)
plastic–wood, development-production program for Lockwood, 20: 21188 (ORNL-IIC-7, pp 95-8)
plastic–wood, mechanical and physical properties of irradiated combinations of, 20: 21348 (ORNL-IIC-7, pp 22-5)
plastic–wood, radiation processing of, 20: 21177 (ORNL-IIC-7)
plastic–wood, radiation processing and testing of, method for, 20: 21179 (ORNL-IIC-7, pp 6-14)
plastic–wood, radiation processing of, commercialization aspects of, 20: 21184 (ORNL-IIC-7, pp 64-75)
plastic–wood, radiation processing of, program for evaluation of, for commercial use, 20: 21349 (ORNL-IIC-7, pp 26-31)
plastic–wood, radioinduced polymerization reactions in, 20: 21180 (ORNL-IIC-7, pp 15-21)
plastic–wood, use of irradiated combinations of, in sporting-goods industry, 20: 21190 (ORNL-IIC-7, pp 106-11)
WOUNDS
contamination by plutonium, method for treatment of, 20: 20943 (RFP-453)
plutonium-239 content in, errors in measurement of, 20: 20951

X

X AGENT
effects on sensitivity of photoelectric cells, 20: 21163
X RADIATION
absorption by plutonium particles, self-, 20: 20951
detection of low-energy, using scintillation detectors and semiconductor detectors, 20: 21107
detection of, survey of devices for, 20: 21023 (AD-624231)
detection using europium-activated single crystals of calcium fluorides, 20: 21135
detection using internally amplifying gallium-diffused junctions, 20: 21100
dosage determinations for sheep, lethal, 20: 20487
dosimetry in cephalometric radiography, 20: 20543
dosimetry in dogs and phantoms, 20: 20432 (AD-630332)
dosimetry of high voltage pulsed r-f tube, 20: 21022 (AD-624230)
dosimetry of, design of integrating dose-rate meter using ionization chamber for, 20: 21078
dosimetry of, equipment for, 20: 21062
dosimetry of, portable microcalorimeter for, 20: 21024 (AD-630693)
effects of therapeutic, on spinal cord, pathological, 20: 20545
effects of 10-kev, on mice, 20: 20475
effects of, combined with procarbazine on tumors, 20: 20504
effects of, combined with surgery on cervical carcinomas, 20: 20526
effects on absorption spectra of alkali halide crystals, 20: 21424 (N-65-23332)
effects on alkaline phosphatase activity in blood, 20: 20415
effects on amino acid synthesis in rat liver, 20: 20410
effects on ATP content in Tradescantia anthers, 20: 20418
effects on auricles of rabbits, 20: 20451
effects on biochemical activity and physiological functions in dogs, 20: 20435 (CONF-650560-15)
effects on blood coagulation in dogs and rats, 20: 20490
effects on blood coagulation in dogs, 20: 20491
effects on blood typing sera, 20: 20425
effects on bone growth in rats, 20: 20486
effects on bones, mechanism for osteomyelitic, 20: 20371
effects on chlorine-36 exchange between rhodium complexes and chlorides, 20: 20706
effects on chromatin anomalies in HeLa cells, protective effects of organophosphorus derivatives against, 20: 20515
effects on chromosomes in Tradescantia pollen grains, morphological, 20: 20438 (EUR-2518.f)
effects on chromosomes in radiographic personnel and their families, 20: 20447
effects on conditioned reflexes in rats exposed *in utero*, 20: 20492
effects on cytochrome c oxidase and glucose-6-phosphatase activity in rat liver, whole-body exposure, 20: 20417
effects on dog arteries, auto- and homovenous repair of, 20: 20478
effects on electron postemission of calcium sulfate, 20: 20769
effects on enzyme synthesis in rat liver, 20: 20429(R) (AD-629311, pp 15-25)
effects on enzyme activity in chick embryos, 20: 20440(R) (EUR-2643.f)
effects on experimental bladder calculus formation in rats, 20: 20467
effects on gelation of triethylene glycol dimethacrylate at 14 Mev, 20: 20720 (AD-630891)
effects on growth of uv-irradiated ascites tumor cells, 20: 20483
effects on hardening of silver-doped potassium chlorides at low temperatures, (E), 20: 22321
effects on hematopoiesis in mice and rabbits, effects of mucopolysaccarides on, 20: 20510
effects on Hill activity and phosphorylation of chloroplasts, 20: 20428
effects on human electrocardiographs, 20: 20474
effects on hydrolysis of salicyl phosphate, 20: 20744
effects on immune reactions to injected bone marrow and lymph cells in mice, 20: 20472
effects on intracellular organelles in mice, 20: 20413
effects on ion mobility in liquid dodecane, hexadecane, and tetrodecane, 20: 20734
effects on limb regeneration in salamanders, role of normal epidermis in recovery from, 20: 20465
effects on lithium fluoride, R-center luminescence from, (E), 20: 22331
effects on logarithmic damping decrements of quartz oscillators, 20: 21155
effects on lysozyme aqueous solutions, inactivating, 20: 20423
effects on metabolic activity in rat spleen and stomach, 20: 20433 (AD-630390)
effects on metabolism of methylnaphthalene in rats, 20: 20439 (EUR-2628.f)
effects on mice, biological, 20: 20430(R) (AD-629311, pp 26-32)
effects on mice, late somatic, 20: 20441 (ORNL-P-1173)
effects on mice, protective effects of antioxidant inhibitors against, 20: 20506
effects on mice, protective effects of drugs against, 20: 20513
effects on Mormoniella males, mutagenic, 20: 20464
effects on mouse bone marrow proliferative activity, 20: 20452
effects on mouse immunity to uv-irradiated transplants of ascites tumor cells, 20: 20484
effects on mouse mammary glands, comparison of effects of carcinogens and, 20: 20502
effects on mouse survival, protective effects of organophosphorus derivatives against, 20: 20515
effects on natural population of lizards, whole-body, 20: 20444(R) (TID-22820)

effects on nitrogen distribution in mice treated with bone marrow, 20: 20407 (ORNL-P-1118)
effects on nucleotide oxidation in suspensions of cattle heart mitochondria, 20: 20496
effects on oxygen uptake in rat brain tissues, 20: 20436 (CONF-650560-17)
effects on physiology of chicken germ cells, 20: 20440(R) (EUR-2643.f)
effects on physiology and respiration in chick embryos, 20: 20440(R) (EUR-2643.f)
effects on potassium and sodium content in animal cell nuclei, 20: 20422
effects on rat lungs, pathological, 20: 20434 (AD-630870)
effects on rat phosphatase systems, effects of injected glycine on, 20: 20517 (NP-15925)
effects on rat testes, protective effects of MEA against, 20: 20509
effects on response of olfactory neurons, 20: 20431 (AD-630323)
effects on skin of urethan-treated mice, 20: 20476
effects on sodium sulfate metabolism in rat liver, 20: 20410
effects on sugars in aqueous solutions, 20: 20748
effects on sulfhydryl content of blood, 20: 20415
effects on testicular development and spermatogenesis in mice, effects of age at irradiation on, 20: 20499
effects on tryptamine content in rat brain tissues, 20: 20437 (CONF-650560-18)
effects on wheat seeds, mutagenic, 20: 20501
emission by supernovae, effects of early radiation field and high-energy electrons on, 20: 21499
emission from mesic atoms, energy spectra of, (E), 20: 21534
hazards from dental, 20: 20519
production of pulsed, facility design for, 20: 20838 (AD-624019)
reactions in low- and medium-Z absorbers at 852 ev to 40 kev, photoelectric cross sections for, (E), 20: 21523
reactions with nitrogen, excitation of first negative and second positive bands by, 20: 21834
scattering by nuclei $1 \leq Z \leq 6$ at 1 to 150 kev, cross sections for, (T), 20: 21516 (UCRL-14403)
use for post-operative, therapy of brain tumors, 20: 20530
use in respiratory function studies, 20: 20546

X-RAY EQUIPMENT
voltage measurements in, 20: 21087

X-RAY FLUORESCENCE ANALYSIS
efficiency of, for determining major constituents in multi-element matrices by coherent to incoherent scattering ratios, 20: 20644

X-RAY SOURCES
development of light-weight 160-kv portable, 20: 20867

X-RAY SPECTROMETERS
design of nondispersive, for lunar and planetary geochemical analysis, 20: 21128

XENON
analysis for krypton-85 by scintillation counting, 20: 20553(R) (MLM-1142)
analysis for krypton-85 by liquid scintillation counting, 20: 20582
diffusion in uranium-doped calcium fluoride single crystals at 900 to 1200°C, 20: 21332(R) (EURAEC-1573)
effects on cesium thermionic converter short-circuit currents, 20: 21580
effects on growth rates in Neurospora, 20: 20378
effects on sporulation in Neurospora, 20: 20378
electron and photon reactions with, electron cascade curves for, (T), 20: 21514 (INR-598/VI/PH)
heat of absorption by molecular sieves, 20: 20806(R) (MLM-1274)
radioinduced luminescence of, electric field effects on decline of alpha, (E), 20: 21521
reactions with *p*-cresol, heat of formation of clathrate compounds formed in, 20: 20688
sorption by evaporated metallic films, 20: 21387
sorption by molybdenum films and Pyrex glass in ultrahigh vacuum, kinetics of, 20: 21351(R) (SRIA-425-8)

XENON FLUORIDES
preparation and properties of XeF_2, 20: 20678
preparation and properties of, 20: 20659
preparation and thermal properties of XeF_6, 20: 20665
radiolysis, 20: 20678

XENON IONS
reactions with beryllium–copper alloys at 3 to 90 kev, secondary electron emission from, (E), 20: 21538

XENON ISOTOPES Xe-124
concentration in gaseous xenon by thermal diffusion, 20: 20807(R) (MLM-1287)
separation from natural xenon by thermal diffusion, 20: 20806(R) (MLM-1274)

XENON ISOTOPES Xe-131
concentration in gaseous xenon by thermal diffusion, 20: 20806(R) (MLM-1274)

XENON ISOTOPES Xe-133
radiation hazards from, following nuclear incidents, 20: 20962

XENON ISOTOPES Xe-135
radiation hazards from, following nuclear incidents, 20: 20962

XENON OXIDES
preparation and properties of, 20: 20659
uses in titrimetric determination of primary and secondary alcohols, 20: 20579

XENON OXYFLUORIDES
preparation and properties of, 20: 20659

XENON SYSTEMS
Ce–Kr, thermal diffusion in, 20: 21567 (FEI-15)
Cs–Xe, thermal diffusion in, 20: 21567 (FEI-15)

Y

YANKEE POWER REACTOR
fuel burnup in, economics of, 20: 22446
operation experience 1960–1965, 20: 22457
performance, 20: 22444

YEASTS
radiosensitivity effects of extracts of, on rats, 20: 20503(R) (AD-629311, pp 1-14)

YTTERBIUM
oxidation in dry and moist air at 100 to 800°C, rate of, 20: 21265 (RPI-2714-8)
reactions with dichalcogenides and powdered graphite, preparation of intercalation compounds by, 20: 20648 (AD-621029)
separation from perchloric acid solutions by ion exchange materials, 20: 20823
separation from uranium by combined ion exchange-solvent extraction using nitric acid–tetrahydrofuran solutions, 20: 20811

YTTERBIUM ACETATES
preparation by oxide solubility in alcohols containing ammonia, 20: 20686

YTTERBIUM ALLOYS
Sb–Yb, phase studies, 20: 21401
Yb–Zn, intermetallic compound with $CeCu_2$-type structure in, 20: 21352 (TID-21745)

YTTERBIUM ISOTOPES Yb-170
oxygen-16 reactions (O-16,O-16γ) at 42 Mev, intrinsic quadrupole moment from, (E), 20: 22072

YTTERBIUM OXIDES
solubility in ethyl, isopropyl, methyl, and propyl alcohols in presence of ammonia, 20: 20686

YTTERBIUM SYSTEMS
graphite–Yb, preparation and magnetic susceptibility of, 20: 21413

YTTRIUM
analysis for oxygen, 20: 20572
diffusion of carbon, nitrogen, and oxygen in, at 1235 to 1460°C, 20: 21254
distribution coefficient in aluminum, mathematical determination of, 20: 21369
enthalpy of formation of YF_3, 20: 20650(R) (ANL-7055, pp 167-76)
Fermi surface, (T), 20: 22338
friction and wear properties of, in vacuum, effects of crystal structure on, 20: 21365
oxidation in dry and moist air at 100 to 800°C, rate of, 20: 21265 (RPI-2714-8)
positron annihilation in, photon angular distributions from, (T), 20: 22338
refining by electrotransport, 20: 21254
separation from nitrate solutions by solvent extraction using tricaprylmethylammonium nitrate, 20: 20812
separation from perchloric acid solutions by ion exchange materials, 20: 20823
separation from praseodymium by fused salt extraction, 20: 20802(R) (ANL-7055, pp 21-98)
separation from scandium by ion exchange chromatography, 20: 20821
separation from uranium by combined ion exchange-solvent extraction using nitric acid–tetrahydrofuran solutions, 20: 20811
separation of zirconium-89 from irradiated carrier-free, by solvent extraction using cupferron, 20: 20626

YTTRIUM ACETATES
preparation by oxide solubility in alcohols containing ammonia, 20: 20686

YTTRIUM ALLOYS
crystallographic angles in hcp, computer program for calculation of, 20: 22315 (IS-1337)
Al–Y, crystal structure and stability of intermetallic compounds in, 20: 21415
Al–Y, phase diagram of, mathematical determination of, 20: 21369
Ce–Y, magnetic properties and phase transformations in, 20: 21414
Co–Y, phase studies, 20: 21402
Cu–Y, intermetallic compound with $CeCu_2$-type structure in, 20: 21352

(TID-21745)
Hg–Y, thermodynamic properties and vapor pressure measurements, 20: 21384
La–Y, magnetic properties and phase transformations in, 20: 21414
Mn–Y, crystal structure and magnetic properties of intermetallic compounds of, 20: 21403
Nd–Y, magnetic properties and phase transformations in, 20: 21414
Pr–Y, magnetic properties and phase transformations in, 20: 21414
rare earth–Y, solid solutions of, electronic states of, 20: 21398
Y–Zn, intermetallic compound with $CeCu_2$-type structure in, 20: 21352 (TID-21745)

YTTRIUM COMPLEXES
with 2,4-pentanedione, preparation and crystal structure of, 20: 20700

YTTRIUM FERRATES(III)
ion interactions in, iron–yttrium, 20: 22313 (AD-624719)

YTTRIUM IONS
interactions with iron ions in garnets, 20: 22313 (AD-624719)

YTTRIUM ISOTOPES Y-89
alpha inelastic scattering at 42 Mev, level structure from, (E), 20: 22138
neutron scattering at 0.00064 to 8.0 ev, cross sections for, (E/T), 20: 22010(R) (NYO-72-28)
proton reactions (p,n) at 4.5 to 5.5 Mev, cross sections for, (E), 20: 22010(R) (NYO-72-28)
proton reactions (p,xn) and (p,pxn) at 5 to 85 Mev, excitation functions for, (E), 20: 22133

YTTRIUM ISOTOPES Y-90
content in sea water, effects on development of fish spawn, 20: 20445(T) (TRG-Inf. Ser.-166)
determination in urine by anion exchange and beta counting, 20: 20583
separation from radioisotopes in aqueous solutions by foam chromatography using colloidal manganese dioxide, 20: 20628

YTTRIUM ISOTOPES Y-91
diffusion in irradiated Zircaloy-4 at 800°C, 20: 21232 (BMI-1763)
separation from radioisotopes in aqueous solutions by foam chromatography using colloidal manganese dioxide, 20: 20628

YTTRIUM NITRIDES
preparation by reactive arc melting, 20: 21244

YTTRIUM OXIDES
effects on mechanical properties of sintered and extruded tungsten, 20: 21374
solubility in ethyl, isopropyl, methyl, and propyl alcohols in presence of ammonia, 20: 20686
HfO_2–Y_2O_3, electric conductivity at 900 to 1600°C, effects of composition on, 20: 21370

YTTRIUM SILICIDES
thermal capacity of superconducting, anomalous, (E), 20: 21883

Z

ZINC
analysis for rare earths, 20: 20607
determination in brass by x-ray fluorescence methods, 20: 20642
determination in silicon dioxide, activation, 20: 20634
determination in thorium, photometric and polarographic, 20: 20601
separation from gallium, indium, and transition elements by ion exchange chromatography, 20: 20634
separation from perchloric acid solutions by ion exchange materials, 20: 20823
separation from scandium by ion exchange chromatography, 20: 20821
separation from thorium by ion exchange in nitric acid solution, 20: 20624
separation from uranium by combined ion exchange-solvent extraction using nitric acid–tetrahydrofuran solutions, 20: 20811
viscosity of liquid, based on atomic parameters, 20: 20656 (UCRL-11930)
Cu–Ni, effects of decontaminating and descaling solution on metal loss on, 20: 21238 (NP-15928)

ZINC ALLOYS
Ca–Zn, intermetallic compound with $CeCu_2$-type structure in, 20: 21352 (TID-21745)
Cs–Zn, thermodynamic properties, 20: 21335 (IS-T-76)
Cd–Mg–U–Zn, corrosive effects in fused chloride mixtures, on stainless steel, 20: 20802(R) (ANL-7055, pp 21-98)
In–Zn, diffusion coefficient measurements on liquid, during molecular distillation, 20: 21334 (IS-1325)
La–Zn, intermetallic compound with $CeCu_2$-type structure in, 20: 21352 (TID-21745)
Mg–Pu–U–Zn, corrosive effects on type 405 stainless steel, 20: 20802(R) (ANL-7055, pp 21-98)
Mg–U–Zn, corrosive effects with fused chlorides, on carbon and zirconium boride, 20: 20802(R) (ANL-7055, pp 21-98)
Sr–Zn, intermetallic compound with $CeCu_2$-type structure in, 20: 21352 (TID-21745)
Yb–Zn, intermetallic compound with $CeCu_2$-type structure in, 20: 21352 (TID-21745)
Y–Zn, intermetallic compound with $CeCu_2$-type structure in, 20: 21352 (TID-21745)

ZINC CHROMATES
effects of decontaminating and descaling solution on coating of, 20: 21238 (NP-15928)

ZINC COMPLEXES
with thiodibenzoylmethane, stability of, 20: 20693

ZINC ISOTOPES Zn-64
neutron reactions (n,np) and (n,p) at 14 Mev, cross section, energy spectra, and angular distributions from, (E), 20: 22048

ZINC ISOTOPES Zn-65
content in Columbia River invertebrates, 1964 and 1965, 20: 20382 (BNWL-SA-623)
content in Columbia River whitefish, 20: 20382 (BNWL-SA-623)
excretion by man, effects of chelates on, 20: 20397
uptake by Columbia River algae, factors affecting, 20: 20382 (BNWL-SA-623)
uptake by Columbia River plankton, 20: 20382 (BNWL-SA-623)
uptake by crustaces, mollusks, and plankton in Bay of Venice, 20: 20386(R) (NP-15916)

ZINC ISOTOPES Zn-67
proton reactions (p,n) at 1.5 to 5 Mev, galloum-67 levels from, (E), 20: 22053

ZINC ISOTOPES Zn-68
proton reactions (p,n) at 1.5 to 5 Mev, gallium-68 levels from, (E), 20: 22053

ZINC ISOTOPES Zn-70
proton reactions (p,n) at 1.5 to 5 Mev, gallium-70 levels from, (E), 20: 22053

ZINC OXIDES
effects on radiolysis of benzene in aqueous solutions, 20: 20768

ZINC SULFIDES
particle sampling in air stream, errors in subisokinetic, 20: 20927 (BNWL-217)

ZINC SYSTEMS
C–Mn–Zn, magnetic properties of Mn_3ZnC in, 20: 22312(R) (AD-622796)

ZINC TETRATHIOCYANATOMERCURATE(II)
precipitation with microquantities of cerium-144, cesium-137, and strontium-89, 20: 20619

ZIRCALOY-2
effects on reactions of bromine pentafluoride with uranium, 20: 20803(R) (ANL-7055, pp 99-162)
mechanical properties of, effects of hydrogen on, (E), 20: 21386
reactions with iodine in helium–steam mixtures, 20: 20940(R) (ORNL-3915)
stresses in cladding of, during fuel powder loading by vibratory compaction, 20: 21289 (BNWL-194)
U–Zircaloy-2, processing for uranium recovery by fluoride volatility, 20: 20803(R) (ANL-7055, pp 99-162)

ZIRCALOY-4
diffusion of fission products in irradiated, at 600 to 1200°C, 20: 21232 (BMI-1763)

ZIRCONIUM
determination in presence of thorium and uranium using Arsenazo-III, 20: 20614
diffusion of fission products in irradiated, at 600 to 1200°C, 20: 21232 (BMI-1763)
effects on efficiency of porous tungsten ionizers, 20: 21570 (N-65-29785)
neutron inelastic scattering at 5.8 and 7.5 Mev, gamma spectra from thermal, (E), 20: 22069
oxidation by steam at 500°C, effects of surface contamination on, 20: 21268
production of sponges of, 20: 21305
properties at 4.2 to 1130°K, structural and thermal, 20: 21391
reactions with carbon dioxide at 590 to 730°C at low pressures, 20: 21279
reactions with sodium at high temperatures, 20: 20925(R) (ANL-7055, pp 177-212)
reactions with water during reactor coolant-loss accidents, 20: 20925(R) (ANL-7055, pp 177-212)
separation from hydrochloric acid solutions by solvent extraction using quaternary ammonium chlorides, 20: 20816
separation from perchloric acid solutions by ion exchange materials, 20: 20823
separation from protactinium by solvent extraction using quaternary ammonium chlorides, 20: 20816
separation from uranium by combined ion exchange–solvent extraction using nitric acid–tetrahydrofuran solutions, 20: 20811
separation from uranium by extraction using triisooctylamine, 20: 20598
sorptive properties of evaporated films of, for krypton and xenon, 20: 21387

sorptive properties of evaporated films of, for carbon monoxide at 0°C, 20: 21388

ZIRCONIUM ALLOYS
corrosion of, effects of oxide films on, 20: 21282
hydridation of, effects of oxide films on, 20: 21282
Cu–Mn–Zr, analysis for bonding and inclusions in, by x-ray emission in electron microscopy, 20: 20593
Mg–Zr, analysis for bonding and inclusions in, by x-ray emission in electron microscopy, 20: 20593
Mo–Ti–Zr, creep tests on TZC and TZM at high temperatures, 20: 21346(R) (NASA-CR-54895)
Mo–Ti–Zr, fatigue tests on TZC and TZM at high temperatures, 20: 21347(R) (NASA-CR-54916)
Mo–Ti–Zr, mechanical properties at 25 to 3500°F, 20: 21322 (AMRA-TR-65-25)
Mo–Ti–Zr, specifications of TZM, for use in corrosion test loop fabrication, 20: 21293 (R-66SD3007)
Nb–Ta–W–Zr, bonding of FS-85, to Inconel 600 and stainless steels, process development for explosive, 20: 21295(R) (WANL-PR-(EE)-002)
Nb–Ta–W–Zr, creep of FS-85, at 2000 to 2200°F in ultrahigh vacuum, 20: 21344 (N-65-26653)
Nb–U–Zr, properties of, at 150 to 350°C, mechanical and physical, 20: 21356 (UCRL-14724)
Nb–U–Zr, reactions with water during Kiwi-TNT transients, 20: 20925(R) (ANL-7055, pp 177-212)
Nb–V–Zr, properties of Cb-753, 20: 21411
Nb–W–Zr, effects of carbon and oxygen on phase equilibria in niobium-rich region of, 20: 21329(R) (DRI-1092-229)
Nb–Zr, bonding of, to Inconel 600 and stainless steels, process development for explosive, 20: 21295(R) (WANL-PR-(EE)-002)
Nb–Zr, corrosion by liquid alkali metals, test loops for studying, 20: 21284
Nb–Zr, current degradation in superconducting solenoids of, (E), 20: 21920
Nb–Zr, flux creep and jump in superconducting, effect of Joule heating on, 20: 21884
Nb–Zr, magnetic field strength at surface of superconducting, EPR measurements for, (E), 20: 21898
Nb–Zr, magnetic fluxoid annihilation instability in superconducting, (E/T), 20: 21927
Nb–Zr, mechanical properties of, effects of beta grain size on, 20: 21368
Nb–Zr, reactions with sodium at high temperatures, 20: 20925(R) (ANL-7055, pp 177-212)
Nb–Zr, specifications of, for use in corrosion test loop fabrication, 20: 21293 (R-66SD3007)
Nb–Zr, superconducting critical currents and fields in flux-pump fed coils of, (E), 20: 21924
Pu–Zr, etching of delta-phase, bright-field grain structure, 20: 21233 (BNWL-188)
rare earth–Zr, solid solutions of, electronic states of, 20: 21398
Ta–W–Zr, strength, weldability, and heat treatment of, 20: 21405
U–Zr, corrosion inhibition by oxide films on, mechanisms of, 20: 21281
U–Zr, microstructure of uranium-rich, effects of heat treatments on, 20: 21372
U–Zr, neutron multiplication factor of, (E), 20: 22392
U–Zr, phase studies on uranium-rich, 20: 21372
V–Zr, magnetic induction in hard superconducting, (E), 20: 21893

ZIRCONIUM BORIDES
corrosion by liquid magnesium–uranium–zinc alloys with fused chlorides, 20: 20802(R) (ANL-7055, pp 21-98)
sintering of, grain growth during, 20: 21273

ZIRCONIUM CARBIDES
fabrication into thin plates by pressure compacting or powder rolling, 20: 21303
thermionic emission from cesiated surfaces of, (E), 20: 21584
graphite–ZrC, fabrication of dispersions of, by hot-working, 20: 21306

ZIRCONIUM COMPLEXES
with EDTA, mandelic, oxalic, and phenylarsonic acids, solvent extraction studies on formation of, 20: 20561 (JAERI-1099)

ZIRCONIUM HYDRIDES
neutron scattering by, differential cross sections and corrections for thermal, (E), 20: 21939(R) (GA-6930)
neutron spectra in, transient properties of, (E/T), 20: 21941 (IAE-977)
neutron thermalization in, models for, 20: 22377 (GA-6930, App. B)
preparation and self-diffusion in, 20: 22520(R) (NAA-SR-11805)

ZIRCONIUM IONS
effects on dephosphorylation of cocarboxylase, riboflavin-5-phosphate, and pyridoxal phosphate, 20: 20375

ZIRCONIUM ISOTOPES Zr-89
energy levels of, parity and spin of, (E), 20: 22010(R) (NYO-72-28)
separation from irradiated carrier-free yttrium by solvent extraction using cupferron, 20: 20626

ZIRCONIUM ISOTOPES Zr-90
energy levels of, double gamma emission from, (E/T), 20: 22010(R) (NYO-72-28)

ZIRCONIUM ISOTOPES Zr-91
energy levels of, single-particle, (T), 20: 22113
nucleon binding energy, (T), 20: 22113

ZIRCONIUM ISOTOPES Zr-95
content in silt in Escaut River, Belgium, control of, 20: 22515(T) (ORNL-tr-965)
diffusion in irradiated fuel element cladding alloys and materials at 600 to 1200°C, 20: 21232 (BMI-1763)
separation from radioisotopes in aqueous solutions by foam chromatography using colloidal manganese dioxide, 20: 20628

ZIRCONIUM NITRIDES
preparation, 20: 22520(R) (NAA-SR-11805)

ZIRCONIUM OXIDES
analysis for oxygen by activation using helium-3 ions, detection limits and sensitivity of, 20: 20565 (ORNL-P-1216)
deposition on steel of chromium plating containing dispersions of, electrolytic, 20: 21286 (AD-621920)
effects on mechanical properties of sintered and extruded tungsten, 20: 21374
oxygen sorbed on, mechanisms for hydrogen reactions with, 20: 20705
reactions with gaseous uranium trioxide, effects of substrate symmetry in, 20: 20649 (AEET-CD-24)
sorptive properties of hydrous, for molybdenum-99 and technetium-99m in nitric acid solution, 20: 20566 (ORNL-TM-1468)
wear properties of plasma-arc-deposited coatings of, 20: 21319 (AD-621064)
$CaO–UO_2–ZrO_2$, preparation and properties of, for ceramic nuclear fuels, 20: 21302
$UO_2–ZrO_2$, radiation effects on densification and homogenization of, neutron, 20: 21432 (WAPD-301)

ZIRCONIUM SYSTEMS
B–Co–Zr, crystal structure, 20: 20685
B–Ni–Zr, crystal structure, 20: 20685
B–U–Zr, neutron multiplication factor of, (E), 20: 22392
C–Co–Ti–W–Zr, development and tensile properties of cobalt-base, 20: 21237 (N-65-29395)
C–Cr–Co–Re–Ti–W–Zr, development and tensile and stress-rupture properties of cobalt-base, 20: 21237 (N-65-29395)
C–Cr–Co–Ti–W–Zr, development and tensile and stress-rupture properties of cobalt-base, 20: 21237 (N-65-29395)
C–Hf–Mo–N–Re–Ta–W–Zr, development of dispersion-strengthened tantalum-base, 20: 21240(R) (WANL-PR-(Q)-006)
C–Mo–Nb–Ta–W–Zr, extrusion parameters for Cb-132M, 20: 21263(R) (NASA-CR-54911)
C–Mo–Nb–Ta–Zr, thermal-mechanical processing of a precipitation-hardenable, dispersion-hardened, 20: 21250
C–Mo–Nb–Ti–Zr, bend and tensile ductility properties of, 20: 21410
C–Mo–Ti–Zr, extrusion parameters for TZC, 20: 21263 (NASA-CR-54911)
C–Nb–W–Zr, properties at very high temperatures, 20: 21412
C–Nb–W–Zr, specifications of D-43, for use in corrosion test loop fabrication, 20: 21293 (R-66SD3007)

REPORT NUMBER INDEX

Reports, conference papers and proceedings, numbered translations, and patents abstracted during the period are included in this index. Each item is listed by report number; this is followed by the abstract number and a brief notation regarding public availability. The index entries show which reports are on file in the depository libraries, which reports have been published in open-literature journals (journal citation given), and which reports can be purchased (source and price). Whenever a report is identified by more than one number, cross references from secondary to primary report numbers are cited.

The report number codes apply to AEC reports unless designated otherwise. Non-AEC reports are identified by parenthetical notes after the report codes; e.g., (non-AEC), (British), (Canadian), (French). The note (Misc.) identifies those codes used for both USAEC and non-AEC reports. Patents are listed under the heading "PATENTS"; the country of origin is included in parentheses.

A comprehensive listing of both AEC and non-AEC report codes is contained in TID-85(5th Rev.), *Report Number Series Used by the Division of Technical Information in Cataloging Reports*. This information is also included in the Cumulative Report Number Index (issued annually).

Public Availability of USAEC Reports

All USAEC reports abstracted in *NSA* are available to the public through one or more of the following sources:

(1) Depository libraries in the United States, in other countries, and in international agencies. A list of these depositories appears on the inside covers of each issue of *NSA*.

(2) Scientific and technical journals or other publications.

(3) Microcard Editions, Inc., in Microcard and micronegative form. Orders and inquiries should be sent to: Accounting and Shipping Department, West Salem, Wisconsin 54669.

(4) Clearinghouse for Federal Scientific and Technical Information, U. S. Department of Commerce, Springfield, Virginia 22151.

(5) Superintendent of Documents, U. S. Government Printing Office, Washington, D. C. 20402.

Public Availability of Non-AEC Reports

U. S. Reports. Many reports of U. S. Government agencies are available to the public from the Clearinghouse for Federal Scientific and Technical Information (CFSTI). This availability is given when known. Such reports should be ordered by AD number or NASA-N number. If availability is not shown, inquiries may be directed to CFSTI. In the case of NP numbers, inquiries should be by title and author.

Non-U. S. Reports. Many reports of atomic energy establishments of other countries are deposited in the libraries listed on the inside covers of each issue of *NSA*.

Additionally, the following have made their reports available as indicated.

AUSTRALIA

Australian Atomic Energy Commission Research Establishment. Available upon request from the Library, Australian Atomic Research Establishment, Private Mail Bag, Sutherland, New South Wales, Australia.

BELGIUM

Centre d'Étude de l'Énergie Nucléaire. Available upon request to individuals and organizations, from the Centre d'Étude de l'Énergie Nucléaire (CEN), 31, Rue Belliard, Bruxelles, Belgium.

CANADA

Atomic Energy of Canada Limited. For sale by the Technical Information Officer, Atomic Energy of Canada Limited, Chalk River, Ontario, Canada. Copies are also deposited in libraries in the United Kingdom.

National Research Council of Canada. Available from the National Research Council of Canada, Ottawa 2, Ontario, Canada.

DENMARK

Atomic Energy Commission Research Establishment, Risø. Available on exchange from the Library, Danish Atomic Energy Commission, Risø, Roskilde, Denmark. Also for sale by Jul. Gjellerup, Booksellers, 87 Sölvgade, København K., Denmark.

Danatom. Available on loan from Research Establishment, Risø, Roskilde, Denmark. Copies are available from Danatom, Aurehøjvej 2, Hellerup, Denmark.

EURATOM

Reports from the Commission of the European Atomic Energy Community are available from: Presses academiques europeennes, 98, chaussee de Charleroi, Brussels 6, Belgium; and Office central de vente des publications des Communautes eurodeennes 2, place de Metz, Luxemburg.

FRANCE

Commissariat à l'Énergie Atomique. Inquiries for reports numbered 1-2199 should be addressed to Commissariat à l'Énergie Atomique, Service Central de Documentation, Centre d'Études Nucléaires de Saclay, Boite Postale No. 2, Gif-sur-Yvette (S. et O.), France. Reports numbered 2200 and above are available from La Documentation Francaise, 16 Rue Lord-Byron, Paris VIII, France.

Service Central de Protection contre les Rayonnements Ionisants. Copies are available from Ministère de la Santé Publique, Service Central de Protection contre les Rayonnements Ionisants, B. P. n° 35—LE VESINET (S. et O.), France.

GERMANY

Deutsches Elektronen-Synchrotron DESY. Copies are available from Deutsches Elektronen-Synchrotron Desy, Dokumentation, 2000 Hamburg-Gr. Flottbek 1, Notkestieg 1, Germany.

Gesellschaft für Kernforschung mbH (KFK). Copies are available from Gesellschaft für Kernforschung mbH, 75 Karlsruhe, Postfach 947, Germany. Copies are also deposited in many national nuclear centers in the world.

Kernforschungsanlage. Copies may be ordered from Zentralbibliothek der Kernforschungsanlage Jülich, Jülich, Bundesrepublik Deutschland.

Hahn-Meitner-Institute für Kernforschung. Available without charge from Hahn-Meitner-Institute für Kernforschung Berlin, Bibliothek, Glienicker Strasse 100, 1 Berlin

39, Germany. Copies are deposited in many national nuclear centers in the world.

Johann-Wolfgang-Goethe Universität, Frankfurt Am Main, Institut für Kernphysik, (IKF). Copies are available from Gmelin Institut, 40-42 Varrentrappstrasse, Frankfurt (Main), West Germany.

ISRAEL

Israel Atomic Energy Commission. Available without charge from Ministry of Defence/Atomic Energy Commission, Soreq Research Establishment, Yavne, Israel. Copies are deposited in libraries in Israel and in other countries.

ITALY

Centro Informazioni Studi Esperienze (CISE). For sale at CISE Press Office, Casella Postale 3986, Milano, Italy. Copies are deposited in libraries in Italy.

Comitato Nazionale per l'Energia Nucleare. Copies are available from Comitato Nazionale per l'Energia Nucleare, Divisione Affari Internazionali e Studi Economici, Ufficio Pubblicazioni, Via Belisario, 15, Roma, Italy.

JAPAN

Japan Atomic Energy Research Institute (JAERI). Available from the Staff Supply Cooperative of Japan Atomic Energy Research Institute (JAERI), 1-1 Tamura-Cho, Shiba, Minato-Ku, Tokyo, Japan. Copies are deposited in depositories in Tokyo, Nagoya, and Osaka.

Nagoya University. Copies are available from Research Information Center, Institute of Plasma Physics, Nagoya University, Nagoya, Japan.

University of Tokyo. Available free of charge from Institute for Nuclear Study, University of Tokyo, Tanashi-Machi, Kitatama-gun, Tokyo, Japan.

NETHERLANDS

Reactor Centrum Nederland. For sale by Reactor Centrum Nederland, 112 Scheveningseweg, 's-Gravenhage, The Netherlands. Copies are deposited in university libraries in Holland and in many national nuclear centers in the world.

NEW ZEALAND

Institute of Nuclear Sciences. Copies are available from Librarian, Institute of Nuclear Sciences, D.S.I.R., Private Bag, Lower Hutt, New Zealand. Copies are deposited in other countries.

NORWAY

Forsvarets Forskningsinstitutt. Copies available from Norwegian Defence Research Establishment, Library, P. O. Box 25, Kjeller, Norway.

Institutt for Atomenergi. "KR" reports are available on an exchange basis from the Library, Institutt for Atomenergi, Box 40, Kjeller, Norway. Other series are not generally available to the public.

Norwegian Reactor School. Copies are available from The Library, Institutt for Atomenergi, P.O. Box 40, Kjeller, Norway.

PAKISTAN

Atomic Energy Center. Copies are available from Atomic Energy Center, P. O. Box 658, Lahore, (West Pakistan).

POLAND

Reports of the Polish nuclear institutes are published by the Nuclear Energy Information Center of the Government Commissioner for Use of Nuclear Energy. Copies are available from Ośrodek Informacji o Energii Jądrowej, Warszawa, PKiN, Poland.

SPAIN

Junta de Energia Nuclear. "JEN" reports are available without charge from Servicio de Documentation, Junta de Energia Nuclear, Ciudad Universitaria, Madrid (3), Spain.

SWEDEN

Aktiebolaget Atomenergi. "AE" reports are for sale from Aktiebolaget Atomenergi, Library Section, Box 43041, Stockholm 43, Sweden. Bibliographies and literature surveys of the VDDIT- series may be obtained from Aktiebolaget Atomenergi, Information Office, Scientific and Technical Information, Box 43041, Stockholm 43, Sweden. Other series are not generally available to the public. Organizations in the atomic energy field may obtain copies from Aktiebolaget Atomenergi. Microcopy of AE reports is available from the International Documentation Centre, Tumba, Sweden.

SWITZERLAND

CERN European Organization for Nuclear Research. Available without charge from CERN European Organization for Nuclear Research, Geneva 23, Switzerland. Copies are deposited in libraries in 13 countries.

Eidgenössisches Institut für Reaktorforschung. "EIR" reports are available from Eidgenössiches Institut für Reaktorforschung, c/o Bibliothek, Würenlingen/Ag, Switzerland.

TURKEY

Turkish Atomic Energy Commission. Copies are available free of charge from T.A.E.C., Çekmece Nuclear Research Center, P. O. Box 1, Airport, Istanbul, Turkey.

UNITED KINGDOM

United Kingdom Atomic Energy Authority. Some reports are for sale in the United States by the British Information Service (BIS), 845 Third Avenue, New York, N. Y. 10022. United Kingdom reports generally may be purchased from Her Majesty's Stationery Office, London. Copies not for sale by Her Majesty's Stationery Office may be purchased in microcopy form from Micro Methods Limited, East Ardsley, Wakefield, Yorks, England. Report copies are deposited in a large number of libraries in England, depositories of the USAEC in the United States and abroad, and in most national nuclear centers throughout the world.

Conferences

Published conference proceedings as well as individual unpublished papers from conferences are included in this index. A CONF number is assigned to the conference if published proceedings are received and also if only a single paper is received. The base number used is year-month-sequence. Thus, the number CONF-650101 would indicate that the conference was held in 1965, in January, and that this was the first January 1965 conference so received. This number would be assigned to complete published proceedings, or if individual papers are received, the base number would be extended to include a paper number, i.e., CONF-650101-1. As additional papers are received, they will be assigned consecutive numbers in the series, CONF-650101-1, 2, 3, 4, etc. This numbering system ensures that all papers received from a conference will be associated with that conference in this index.

If published proceedings are received after the receipt of individual papers, the complete proceedings will be abstracted and the abstract number will appear in this index with the base CONF number.

Abbreviations Used in Availability Column

AECL	For sale by Atomic Energy of Canada Ltd., Chalk River, Ontario, Canada.
BIS	For sale by British Information Service, 845 Third Avenue, New York, N. Y. 10022
CFSTI	For sale by the Clearinghouse for Federal Scientific and Technical Information, U.S. Department of Commerce, Spring-

field, Virginia 22151. The symbol "cy" indicates that the format of the item sold may be either a printed document or a photographic reproduction (two-thirds of original size) depending upon the availability of printed stock. The indicated price is for either format. The symbol "mn" is used to indicate that copy is also available in the form of micronegatives (microfiche).

Dep. — AEC reports: Full-size copy is on deposit in the depository libraries both inside and outside the United States. These reports are also for sale by Microcard Editions, Inc., Accounting and Shipping Department, West Salem, Wisconsin 54669.

Non-AEC reports: Full-size copy on deposit in the depository libraries in the United States only.

Dep.(mc) — Same as for Dep., except copy is in Microcard form.

Dep.(mn) — Same as for Dep., except copy is in micronegative (microfiche) form.

DSIR — For sale by the National Lending Library for Science and Technology (D.S.I.R.), Boston Spa, Yorkshire, England.

DTI Extension — Available from the U. S. Atomic Energy Commission, Division of Technical Information Extension, P. O. Box 62, Oak Ridge, Tennessee 37830.

EM — Blueprints and microcopy of AEC engineering drawings are available from Clearinghouse for Federal Scientific and Technical Information, U. S. Department of Commerce, Springfield, Virginia 22151. Current prices of the CAPE- packages may be obtained from this address. TID-4100, available from the Division of Technical Information Extension, P. O. Box 62, Oak Ridge, Tennessee 37831, contains information on all the CAPE- packages for sale.

Gmelin — Available at a nominal charge and under the AED- number shown from Atomic Energy Documentation Center, Gmelin Institute, 40-42 Varrentrappstrasse Frankfurt (Main), West Germany.

GPO — For sale by the Superintendent of Documents, Government Printing Office, Washington, D. C. 20402.

HMSO — Her Majesty's Stationery Office, London.

IAEA — Available from the International Atomic Energy Agency, Vienna, Austria, and from its sales agencies in various countries throughout the world. A list of these agencies is found in each STI/DOC and STI/PUB publication.

JCL — For sale by the Special Libraries Association Translation Center, John Crerar Library, 35 West 33rd Street, Chicago, Illinois 60616.

LC — For sale by the Library of Congress, Photoduplication Service, Washington, D. C. 20540.

NAS — National Academy of Sciences, National Research Council, Washington, D. C. 20418.

NRC — For sale by the National Research Council of Canada, Ottawa, Ontario, Canada.

ORAU — Available on interlibrary loan from the Library, Oak Ridge Associated Universities, Post Office Box 117, Oak Ridge, Tennessee 37830.

ORINS — See ORAU.

UKAEA, London — Available from United Kingdom Atomic Energy Authority, 11 Charles II Street, London, S. W. 1.

UN — United Nations Bookshop, United Nations Headquarters, New York, New York.

USGS — Available free of charge from the U. S. Geological Survey, Washington, D. C. 20242.

[The symbols "ph," "mf," and "fs" are used to designate that copy is available only in photostat, microfilm, or facsimile form. The symbol "mn" is used to designate that copy is available in micronegative (microfiche) form. The symbol "cy" is used to designate full size or photographically enlarged copy (two-thirds of original size).]

Report No. NUMERIC
66-1-RE

ABCC-
64-65

AD-
612030
612031
620835
620952
621017
621020
621021
621022
621023
621026
621029
621034
621049
621064
621069
621118
621119
621121
621123
621124
621213
621269
621276
621377
621385
621429
621440
621441
621442
621457
621473
621523
621546
621719
621913
621920
621943
621990
621998
622036
622068
622200
622223
622258
622372
622391
622517
622568
622569
622629
622684
622701
622796
622811
623020
623096
623142
623307
623509
623564
623591
623592
623658
623659
623679
623718
623788
623789
623803
623812
624016
624019
624028
624038
624041
624081

Report No.	Abstract No.	Availability
NUMERICAL	**(Misc.)**	
66-1-RE	20-22459	Dep. mn. CFSTI $2.00 cy, $1.50 mn
ABCC–		
64-65	20-20919	Dep. mn. CFSTI $4.00 cy, $1.00 mn
AD–	**(Misc.)**	
612030	20-20878	CFSTI $3.00 cy, $0.73 mn
612031	20-22304	CFSTI $4.00 cy, $1.00 mn
620835	20-21775	CFSTI $2.00 cy, $0.50 mn
620952	20-21811	CFSTI $1.00 cy, $0.50 mn
621017	20-20554	CFSTI $3.00 cy, $0.75 mn
621020	20-22162	CFSTI $3.00 cy, $0.75 mn
621021	20-22370	CFSTI $4.00 cy, $0.75 mn
621022	20-20716	CFSTI $3.00 cy, $0.75 mn
621023	20-21960	CFSTI $5.00 cy, $1.00 mn
621026	20-22371	CFSTI $5.00 cy, $1.00 mn
621029	20-20648	CFSTI $3.00 cy, $0.75 mn
621034	20-22163	CFSTI $2.00 cy, $0.50 mn
621049	20-21147	CFSTI $2.00 cy, $0.50 mn
621064	20-21319	CFSTI $2.00 cy, $0.50 mn
621069	20-21020	CFSTI $1.00 cy, $0.50 mn
621118	20-22487	CFSTI $5.00 cy, $1.00 mn
621119	20-21933	CFSTI $4.00 cy, $1.00 mn
621121	20-22488	CFSTI $3.00 cy, $0.75 mn
621123	20-22489	CFSTI $3.00 cy, $0.75 mn
621124	20-22490	CFSTI $6.00 cy, $1.25 mn
621213	20-22164	CFSTI $6.00 cy, $1.25 mn
621269	20-22491	CFSTI $3.00 cy, $0.75 mn
621276	20-21560	CFSTI $2.00 cy, $0.50 mn
621377	20-20920	CFSTI $3.00 cy, $0.75 mn
621385	20-21702	CFSTI $3.00 cy, $0.50 mn
621429	20-21776	CFSTI $3.00 cy, $0.75 mn
621440	20-21176	CFSTI $1.00 cy, $0.50 mn
621441	20-22305	CFSTI $1.00 cy, $0.50 mn
621442	20-21777	CFSTI $5.00 cy, $1.00 mn
621457	20-22165	CFSTI $2.00 cy, $0.50 mn
621473	20-21934	CFSTI $1.00 cy, $0.50 mn
621523	20-20854	CFSTI $6.00 cy, $1.50 mn
621546	20-21257	CFSTI $1.00 cy, $0.50 mn
621719	20-20717	CFSTI $2.00 cy, $0.50 mn
621913	20-22166	CFSTI $3.00 cy, $0.75 mn
621920	20-21286	CFSTI $2.00 cy, $0.50 mn
621943	20-21778	CFSTI $3.00 cy, $0.50 mn
621990	20-21779	CFSTI $4.00 cy, $1.00 mn
621998	20-20921	CFSTI $4.00 cy, $1.00 mn
622036	20-21780	CFSTI $4.00 cy, $0.75 mn
622068	20-22311	CFSTI $4.00 cy, $1.00 mn
622200	20-20555	CFSTI $1.00 cy, $0.50 mn
622223	20-21812	CFSTI $4.00 cy, $1.00 mn
622258	20-21703	CFSTI $1.00 cy, $0.50 mn
622372	20-22507	CFSTI $1.00 cy, $0.50 mn
622391	20-22167	CFSTI $4.00 cy, $0.75 mn
622517	20-21704	CFSTI $4.00 cy, $0.75 mn
622568	20-21781	CFSTI $1.00 cy, $0.50 mn
622569	20-22168	CFSTI $5.00 cy, $1.25 mn
622629	20-21021	CFSTI $2.00 cy, $0.50 mn
622684	20-22169	CFSTI $1.00 cy, $0.50 mn
622701	20-22170	CFSTI $1.00 cy, $0.50 mn
622796	20-22312	CFSTI $1.00 cy, $0.50 mn
622811	20-22171	CFSTI $2.00 cy, $0.50 mn
623020	20-22351	CFSTI $3.00 cy, $0.75 mn
623096	20-21561	CFSTI $3.00 cy, $0.75 mn
623142	20-21562	CFSTI $4.00 cy, $0.75 mn
623307	20-20718	CFSTI $3.00 cy, $0.50 mn
623509	20-21459	CFSTI $1.00 cy, $0.50 mn
623564	20-21587	CFSTI $2.00 cy, $0.50 mn
623591	20-21563	CFSTI $3.00 cy, $0.75 mn
623592	20-20896	CFSTI $1.00 cy, $0.50 mn
623658	20-21588	CFSTI $1.00 cy, $0.50 mn
623659	20-21460	CFSTI $1.00 cy, $0.50 mn
623679	20-20897	CFSTI $2.00 cy, $0.50 mn
623718	20-22172	CFSTI $5.00 cy, $1.25 mn
623788	20-22173	CFSTI $2.00 cy, $0.50 mn
623789	20-22174	CFSTI $3.00 cy, $0.50 mn
623803	20-21489	CFSTI $1.00 cy, $0.50 mn
623812	20-21782	CFSTI $3.00 cy, $0.75 mn
624016	20-20898	CFSTI $2.00 cy, $0.50 mn
624019	20-20838	CFSTI $3.00 cy, $0.75 mn
624028	20-21961	CFSTI $3.00 cy, $0.75 mn
624038	20-21461	CFSTI $3.00 cy, $0.75 mn
624041	20-21935	CFSTI $7.00 cy, $1.50 mn
624081	20-22175	CFSTI $2.00 cy, $0.50 mn
624165	20-22176	CFSTI $2.00 cy, $0.50 mn
624214	20-21962	CFSTI $3.00 cy, $0.75 mn
624230	20-21022	CFSTI $1.00 cy, $0.50 mn
624231	20-21023	CFSTI $1.00 cy, $0.50 mn
624657	20-20719	CFSTI $4.00 cy, $0.75 mn
624704	20-20922	CFSTI $2.00 cy, $0.50 mn
624719	20-22313	CFSTI $2.00 cy, $0.50 mn
625475	20-21320	CFSTI $2.00 cy, $0.50 mn
626656	20-21963	CFSTI $3.00 cy, $0.75 mn
626683	20-21589	CFSTI $2.00 cy, $0.50 mn
626684	20-21964	CFSTI $1.00 cy, $0.50 mn
626727	20-20923	CFSTI $3.00 cy, $0.75 mn
626770	20-20868	CFSTI $6.00 cy, $1.25 mn
626776	20-21965	CFSTI $2.00 cy, $0.50 mn
626777	20-20899	CFSTI $5.00 cy, $1.00 mn
626861	20-22492	CFSTI $2.00 cy, $0.50 mn
626865	20-22314	CFSTI $1.00 cy, $0.50 mn
626899	20-20895	CFSTI $3.00 cy, $0.75 mn
626987	20-20556	CFSTI $2.00 cy, $0.50 mn
627037	20-21564	CFSTI $2.00 cy, $0.50 mn
627039	20-20900	CFSTI $2.00 cy, $0.50 mn
627040	20-20901	CFSTI $2.00 cy, $0.50 mn
627049	20-21418	CFSTI $2.00 cy, $0.50 mn
627051	20-20902	CFSTI $2.00 cy, $0.50 mn
627067	20-21839	CFSTI $1.00 cy, $0.50 mn
627189	20-21872	CFSTI $1.00 cy, $0.50 mn
628049	20-21565	CFSTI $5.00 cy, $1.00 mn
629311	20-20516	CFSTI $2.00 cy, $0.50 mn
630323	20-20431	CFSTI $1.00 cy, $0.50 mn
630332	20-20432	CFSTI $1.00 cy, $0.50 mn
630390	20-20433	CFSTI $1.00 cy, $0.50 mn
630693	20-21024	CFSTI $1.00 cy, $0.50 mn
630835	20-21148	CFSTI $1.00 cy, $0.50 mn
630836	20-21149	CFSTI $2.00 cy, $0.50 mn
630870	20-20434	CFSTI $1.00 cy, $0.50 mn
630891	20-20720	CFSTI $2.00 cy, $0.50 mn
AE–	**(Non-AEC)**	
216	20-21936	Dep. mn
217	20-21287	Dep. mn
221	20-21228	Dep. mn
222	20-21966	Dep. mn
AEC-tr–	**(For complete listing see TID-4025)**	
6693	20-22383	Dep. mn. CFSTI $2.00 cy, $0.50 mn. JCL $3.60 fs, $1.37 mf
AECL–	**(Canadian)**	
2530	20-21783	Dep. mn. AECL $1.50
AED-R–		
2621	20-21211	See TID-22350
AEET–	**(Indian)**	
210	20-21937	Dep. mn
213	20-20708	Dep. mn
220	20-22508	Dep. mn
229	20-21229	Dep. mn
232	20-20924	Dep. mn
233	20-21230	Dep. mn
234	20-21967	Dep. mn
235	20-21968	Dep. mn
AEET-CD–	**(Indian)**	
24	20-20649	Dep. mn
AEET-ED–	**(Indian)**	
SG/14	20-20839	Dep. mn
SG/25	20-22352	Dep. mn
AEET-Radiochem.–	**(Indian)**	
45	20-20903	Dep. mn
AERE-Bib–	**(British)**	
143	20-21321	Dep. BIS $0.80. HMSO 4s. 0d.
AERE-R–	**(British)**	
4788	20-21268	Corrosion, 22: 60-7(1966)
4948	20-21064	J. Sci. Instrum., 42: 862-4(1965)
4966	20-20983	Dep. BIS $1.20. HMSO 6s. 0d.
5122	20-21025	Dep. BIS $0.90. HMSO 4s. 6d.

Report No.	Abstract No.	Availability
5129	20-20557	Dep. BIS $0.50. HMSO 2s. 6d.
AERE-Trans–	**(British)**	
1048	20-20990	Dep. mn. BIS $0.90. HMSO 4s. 6d.
AFCRL–	**(Non-AEC)**	
65-64	20-22174	See AD-623789
65-73	20-22173	See AD-623788
65-534	20-22163	See AD-621034
65-553	20-22171	See AD-622811
65-571	20-21778	See AD-621943
65-588	20-21147	See AD-621049
65-638	20-22166	See AD-621913
65-683	20-21812	See AD-622223
65-687	20-22311	See AD-622068
AFFDL-TR–	**(Non-AEC)**	
65-131	20-22492	See AD-626861
AFML-TR–	**(Non-AEC)**	
65-195	20-20556	See AD-626987
AFOSR–	**(Misc.)**	
65-0974	20-22168	See AD-622569
65-1207	20-22170	See AD-622701
65-1320	20-21781	See AD-622568
65-1338	20-22164	See AD-621213
65-1621	20-21782	See AD-623812
65-1627	20-21461	See AD-624038
AFRRI-CR–	**(Non-AEC)**	
65-1	20-22304	See AD-612031
65-3	20-20878	See AD-612030
AFRRI-TN–	**(Non-AEC)**	
65-1	20-22372	
AGN-TM–		
413	20-21258	Dep. mn. CFSTI $2.00 cy, $0.50 mn
414	20-21259	Dep. mn. CFSTI $2.00 cy, $0.50 mn
AHSB(RP)–	**(British)**	
R-51	20-20398	Health Phys., 12: 481-500(1966)
AI–	**(Misc.)**	
65-66	20-21425	See N-65-24491
65-191	20-21562	See AD-623142
AMRA-TR–	**(Non-AEC)**	
65-25	20-21322	
ANL–		
6830	20-20801	Dep. mn. CFSTI $3.00 cy, $0.50 mn
6894	20-21323	Dep. mn. CFSTI $2.00 cy, $0.50 mn
6985	20-21260	Dep. mn. CFSTI $2.00 cy, $0.50 mn
7055	20-22518	Dep. mn. CFSTI $6.00 cy, $1.25 mn
7121	20-21221	Dep. mn. CFSTI $1.00 cy, $0.50 mn
7138	20-22347	Dep. mn. CFSTI $3.00 cy, $0.75 mn
7144	20-21970	Dep. mn. CFSTI $1.00 cy, $0.50 mn
7180	20-22466	Dep. mn. CFSTI $3.00 cy, $0.50 mn
ANL-Trans–		
250	20-20810	Dep. mn. JCL $2.60 fs, $1.01 mf
285	20-21044	Dep. mn. JCL $1.60 fs, $0.80 mf
296	20-22013	Dep. mn. JCL $5.60 fs, $1.82 mf
ARCRL–	**(British)**	
14	20-20926	Dep. BIS $1.70. HMSO 8s. 6d.
ARL–	**(Non-AEC)**	
65-164	20-22167	See AD-622391
65-265	20-21839	See AD-627067
AROD–	**(Misc.)**	
4120:2	20-20896	See AD-623592
AWRE-O–	**(British)**	
36/66	20-21325	Dep. mn. BIS $0.50. HMSO 2s. 6d.
BM-RI–	**(Misc.)**	
6713	20-21231	Bureau of Mines Free

Report No.	Abstract No.	Availability
BMI–	**(Misc.)**	
1761	20-21288	Dep. mn. CFSTI $0.50 cy, $0.50 mn
1763	20-21232	Dep. mn. CFSTI $2.00 cy, $0.50 mn
1764	20-22408	Dep. mn. CFSTI $4.00 cy, $0.75 mn
BN–	**(Misc.)**	
433	20-21872	See AD-627189
BNL–		
948	20-21462	Dep. mn. CFSTI $16.14 cy, $5.00 mn
8924	20-20525	Acta Phys. Austr., 21: 204-17(1966)
9078	20-21735	J. Math. Phys. (N. Y.), 7: 698-701(1966)
9089	20-20400	J. Appl. Physiol., 21: 67-72(1966)
9168	20-21993	Dep. mn. CFSTI $1.00 cy, $0.50 mn
9362	20-20485	Radiat. Res., 27: 330-46(1966)
9457	20-21953	Nucl. Sci. Eng., 24: 410-12(1966)
9566	20-21661	Phys. Rev., 144: 1101-14(1966)
9710	20-20672	J. Electrochem. Soc., 113: 376-8(1966)
9756	20-21505	Science, 151: 1524(1966)
9759	20-22111	Phys. Rev., 144: 801-3(1966)
9766	20-22141	Phys. Rev., 144: 1022-30(1966)
10094	20-21994	Dep. mn. CFSTI $1.00 cy, $0.50 mn
10109	20-22509	Dep. mn. CFSTI $2.00 cy, $0.50 mn
BNWL–		
188	20-21233	Dep. mn. CFSTI $1.00 cy, $0.50 mn
191	20-21419	Dep. mn. CFSTI $1.00 cy, $0.50 mn
193	20-22373	Dep. mn. CFSTI $3.00 cy, $0.75 mn
194	20-21289	Dep. mn. CFSTI $1.00 cy, $0.50 mn
203	20-21326	Dep. mn. CFSTI $1.00 cy, $0.50 mn
215	20-21420	Dep. mn. CFSTI $1.00 cy, $0.50 mn
217	20-20927	Dep. mn. CFSTI $3.00 cy, $0.75 mn
BNWL-SA–		
176	20-20916	Water Resour. Res., 2: 31-9(1966)
310	20-21185	See ORNL-IIC-7, pp 76-80
530	20-20879	Dep. mn. CFSTI $1.00 cy, $0.50 mn
564	20-22510	Dep. mn. CFSTI $1.00 cy, $0.50 mn
623	20-20382	Dep. mn. CFSTI $1.00 cy, $0.50 mn
BRL-M–	**(Misc.)**	
1686	20-20720	See AD-630891
CALT–		
68-57	20-21676	Phys. Rev., 144: 1289-93(1966)
CAPE–		
1292	20-21015	
CEA-R–	**(French)**	
2829	20-22353	Dep. mn
2863	20-20558	Dep. mn
CEAL–		
1024	20-21664	Phys. Rev., 144: 1126-31(1966)
CEND–	**(Misc.)**	
3336-260	20-22354	Dep. mn. CFSTI $3.00 cy, $0.75 mn
CERN–	**(European Organization for Nuclear Research)**	
65-24(Vol.1)	20-21591	Dep. mn
65-32	20-21594	Dep. mn
66-2	20-21590	Dep. mn
66-8	20-21467	Dep. mn
66-10	20-21468	Dep. mn
CEX–		
59.4.17	20-20928	Dep. mn. CFSTI $1.00 cy, $0.50 mn
61.6.2	20-20929	Dep. mn. CFSTI $1.00 cy, $0.50 mn
62.6.5	20-20880	Dep. mn. CFSTI $1.00 cy, $0.50 mn
CLM-Bib–	**(British)**	
6	20-22177	Dep. mn. BIS $0.60. HMSO 3s. 0d.
CLM-P–	**(British)**	
83	20-21878	J. Sci. Instrum., 43: 16-20(1966)
95	20-22232	Nature, 209: 972-4(1966)
CLM-R–	**(British)**	
54	20-20855	Dep. mn. BIS $1.20. HMSO 6s. 0d.
CNEA–	**(Argentinian)**	

Report No.	Abstract No.	Availability
167	20-20522	Dep. mn
182	20-20789	Dep. mn
185	20-20383	Dep. mn
CoA-NOTE-NAT-1, Pt.IV	(British) 20-21343	See N-65-23013
CONF-27-	20-20726	(International Conference on Radiation Research Commemorating the Operational Availability of the Radiation Laboratory for the Preservation of Food, Natick, Mass., Jan. 1963) See PB-181506
CONF-405-	20-20704	(4th Rare Earth Research Conference, Phoenix, Ariz., Apr. 1964) New York, Gordon and Breach Science Publishers, 1965.
CONF-665-	20-21458	(Conference on Photographic and Spectroscopic Optics, Tokyo and Kyoto, Sept. 1–8, 1964) Jap. J. Appl. Phys., 4: Suppl. 1, 1-669(1965)
CONF-673-	20-21582	(18th Annual Power Sources Conference, Fort Monmouth, N. J., May 1964) Red Bank, N. J., PSC Publications Committee, [1964].
CONF-798-	(Annual AEC and Contractor Health Protection Meeting, Los Angeles, Oct. 13–16, 1964)	
2	20-20943	See RFP-453
CONF-610802-	20-21511	(Transactions of the International Astronomical Union, 11th General Assembly, Berkeley, Aug. 15–24, 1961) London, Academic Press, 1962. £4; $11.50.
CONF-620911-	(International Conference on Advances in Water Pollution Research, London, Sept. 1962)	
Vols.1,2,3	20-20982	New York, Pergamon Press, 1964
CONF-630304-	20-21276	(2nd International Congress on Metallic Corrosion, New York, Mar. 11–15, 1963) Houston, Texas, National Association of Corrosion Engineers, 1966. $50.75
CONF-630507-	20-21583	(17th Annual Power Sources Conference, Fort Monmouth, N. J., May 21–23, 1963) Red Bank, N. J., PSC Publications Committee, [1963].
CONF-640309-	(Conference on Estuaries, Mar. 31–Apr. 4, 1964, Jekyll Island, Ga.)	
I	20-20368	Dep. mn. CFSTI $1.00 cy, $0.50 mn
CONF-640414-	(45th Session of the German X-Ray Society, Wiesebaden, Apr. 9–13, 1964)	
Pt.B	20-20551	Strahlentherapie, Sonderbaende, 61: 1-432(1965)
CONF-640509-	(Colloquium on Theoretical Physics, Bordeaux, May 1964)	
Pt.2	20-21706	Dep. mn
Pt.2, Paper 1	20-21707	
Pt.2, Paper 2	20-21708	
Pt.2, Paper 6	20-21709	
CONF-640631-	20-22316	(Working Conference on Inelastic Scattering of Slow Neutrons in Crystals and Liquids, Dubna, June 12–16, 1964) See JINR-P-2081
CONF-640713-	(Symposium on Boron, Paris, July 17–18, 1964)	
Vol.2	20-21251	New York, Plenum Press, 1965. $12.50
CONF-640803-	(Conference on the Physics of Type II Superconductivity, Cleveland, Aug. 28–29, 1964)	
Vols.1,2,3	20-21899	
CONF-640816-	20-20904	(Applications of Radioactive Tracers in Studying Bed Load Movement in Rivers Meeting, Vienna, Aug. 16–18, 1964) See STI-REP-101
CONF-641007-	20-20834	(American Society of Lubrication Engineers and American Society of Mechanical Engineers Lubrication Conference, Washington, D. C., Oct. 13–16, 1964) ASLE (Amer. Soc. Lub. Eng.) Trans., 8: 1-777(1965)
CONF-641126-	(1st Symposium on Nuclear Medicine, Mendoza, Argentina, Nov. 1964)	
3	20-20789	See CNEA-182
CONF-650101-	(Mössbauer Symposium, New York, Jan. 26, 1965)	
Vol.1	20-22156	New York, Plenum Press, 1965. $12.50
CONF-650111-	20-21594	(CERN Informal Neutrino Conference, Geneva, Jan., 1965) See CERN-65-32
CONF-650405-	(International Conference on Modern Trends in Activation Analysis, College Station, Tex., Apr. 19–22, 1965)	
25	20-20565	See ORNL-P-1216
CONF-650411-	(Joint NASA–AEC Liquid Metals Corrosion Meeting, Gatlinburg, Tenn., Apr. 21–23, 1965)	
7	20-21284	ORINS
CONF-650508-	(International Conference on Beryllium Metallurgy, Grenoble, France, May 20, 1965)	
3	20-21363	For translation see UCRL-Trans-1299(L)
CONF-650549-	20-18635	(International Atomic Energy Agency, Symposium on Exchange Reactions, Upton, N. Y., May 31–June 4, 1965) See STI-PUB-107
1	20-20706	ORINS
2	20-20715	ORINS
15	20-20701	ORINS
CONF-650550-	(American Society of Mechanical Engineers, Underwater Technology Conference, New London, Conn., May 5–7, 1965)	
3	20-20981	ORINS
CONF-650560-	(13th Annual Meeting of the Radiation Research Society, Philadelphia, May 23–26, 1965)	
15	20-20435	Dep. mn. CFSTI $1.00 cy, $0.50 mn
17	20-20436	Dep. mn. CFSTI $1.00 cy, $0.50 mn
18	20-20437	Dep. mn. CFSTI $1.00 cy, $0.50 mn
CONF-650574-	20-21581	(19th Annual Power Sources Conference, Fort Monmouth, N. J., May 18–20, 1965) Red Bank, N. J., PSC Publications Committee, 1965.
CONF-650614-	20-20389	(Symposium on the Use of Isotopes and Radiation in Soil-Plant Nutrition, Ankara, June 28–July 2, 1965) See STI-PUB-108
CONF-650616-	(Health Physics Society, Annual Meeting, Los Angeles, June 14–17, 1965)	
9	20-20643	ORINS. Gmelin, AED-CONF-65-153-3
CONF-650632-	(7th Biennial Conference on Carbon, Cleveland, June 21–25, 1965)	
4	20-21408	ORINS. Gmelin, AED-CONF-65-149-14
7	20-21413	ORINS. Gmelin, AED-CONF-65-149-9
8	20-20702	ORINS. Gmelin, AED-CONF-65-149-3
10	20-21285	ORINS. Gmelin, AED-CONF-65-149-1
CONF-650634-	(16th Annual Mid-America Symposium on Spectroscopy, Chicago, June 14–17, 1965)	
3	20-20644	ORINS. Gmelin, AED-CONF-65-155-1
CONF-650646-	(American Society for Testing and Materials, 68th Annual Meeting, Lafayette, Ind., June 13–18, 1965)	
3	20-21416	ORINS. Gmelin, AED-CONF-65-148-1
CONF-650652-	(6th International Conference on Radiocarbon and Tritium Dating, Pullman, Wash., June 7–11, 1965)	
7	20-20893	ORAU. Gmelin, AED-CONF-65-158-5

Report No.	Abstract No.	Availability
10	20-20892	ORAU. Gmelin, AED-CONF-65-158-10
13	20-20894	ORINS. Gmelin, AED-CONF-65-158-20
14	20-20917	ORINS. Gmelin, AED-CONF-65-158-21
CONF-650655–		(Aerospace Technical Conference and Exhibit, Houston, Tex., June 21–24, 1965)
2	20-20860	ORINS. Gmelin, AED-CONF-65-159-6
3	20-21173	ORINS. Gmelin, AED-CONF-65-159-2
CONF-650707–	20-21164	(IEEE Annual Conference on Nuclear and Space Radiation Effects, Ann Arbor, Mich., July 12–15, 1965) Trans. Nucl. Sci., NS-12: 1-155(1965)
CONF-650723–		(20th International Congress of Pure and Applied Chemistry, Moscow, U.S.S.R., July 12–18, 1965)
Absts.	20-20552	CFSTI $2.00 cy, $1.00 mn
CONF-650803–	20-20944	(IAEA Symposium on Nuclear Materials Management, Vienna, Aug. 30–Sept. 3, 1965) See STI-PUB-110
17	20-20830	ORINS
19	20-20831	ORINS
21	20-22527	ORINS
24	20-22528	ORINS
27	20-22529	ORINS
28	20-21313	ORINS
47	20-20832	ORINS
48	20-20647	ORINS
49	20-20833	ORINS
CONF-650804–		(5th Rare Earth Research Conference, Ames, Iowa, Aug. 30–Sept. 1, 1965)
Bk.5	20-21252	ORAU
11	20-21409	ORINS. Gmelin, AED-CONF-65-208-15
13	20-21414	ORINS. Gmelin, AED-CONF-65-208-10
15	20-20700	ORINS. Gmelin, AED-CONF-65-208-14
17	20-21415	ORINS. Gmelin, AED-CONF-65-208-6
18	20-20703	ORINS. Gmelin, AED-CONF-65-208-5
CONF-650945–	20-19603	(International Conference on Elementary Particles, Oxford, Sept. 19–25, 1965) Chilton, Eng., The Rutherford High Energy Laboratory, 1966.
6	20-21629	See UCRL-16332
CONF-650948–		(9th International Conference on Cosmic Rays, London, Sept. 6–17, 1965)
3	20-21544	See MIT-2098-227, Paper EAS-8
4	20-21545	See MIT-2098-227, Paper EAS-11
5	20-21546	See MIT-2098-227, Paper EAS-29
6	20-21547	See MIT-2098-227, Paper EAS-31
CONF-650960–	20-21177	(Information Meeting on Irradiated Wood Plastic Materials, Chicago, Sept. 15, 1965) See ORNL-IIC-7
CONF-650964–		(Symposium on Design and Construction Problems of Pilot Plants for Recycling Irradiated Fuels, Turin, Sept. 23–24, 1965)
1	20-20810	For translation see ANL-Trans-250
CONF-650967–		(Italian Society of Experimental Biology, 34th General Assembly, Sorrento, Italy, Sept. 30–Oct. 2, 1965)
2	20-20439	See EUR-2628.i
CONF-650970–		(National Power Conference, Albany, N. Y., Sept. 19–23, 1965)
1	20-22456	ORAU
2	20-22302	ORAU
3	20-22457	ORAU
4	20-22455	ORAU
CONF-651001–	20-21097	(IEEE Nuclear Science Symposium, San Francisco, Oct. 1965) Trans. Nucl. Sci., NS-13: No. 1, 1-766(1966)
19	20-21095	ORAU. Gmelin, AED-CONF-65-293-8
20	20-22360	ORAU. Gmelin, AED-CONF-65-293-10
25	20-21096	ORAU. Gmelin, AED-CONF-65-293-28
CONF-651004–		(9th Conference on Analytical Chemistry in Nuclear Technology, Gatlinburg, Tenn., Oct. 12, 1965)
3	20-20581	See K-L-6059
8	20-20582	See MLM-1305J
9	20-20645	ORINS
CONF-651005–		(1st International Symposium on Water Desalination, Washington, D. C., Oct. 3–9, 1965)
4	20-22461	ORAU. Gmelin, AED-CONF-65-276-8
CONF-651009–		(Conference on Safety, Fuels and Core Design in Large Fast Power Reactors, Argonne, Oct. 11–14, 1965)
10	20-22348	ORAU. Gmelin, AED-CONF-65-307-5
11	20-22350	ORAU. Gmelin, AED-CONF-65-307-7
12	20-22401	ORAU. Gmelin, AED-CONF-65-307-21
14	20-22454	ORAU. Gmelin, AED-CONF-65-307-1
15	20-22453	ORAU. Gmelin, AED-CONF-65-307-17
16	20-22349	ORAU. Gmelin, AED-CONF-65-307-14
18	20-22451	ORAU. Gmelin, AED-CONF-65-307-15
19	20-22462	ORAU. Gmelin, AED-CONF-65-307-16
25	20-22452	ORAU. Gmelin, AED-CONF-65-307-35
CONF-651015–		(American Physical Society, Chicago, Oct. 7, 1965)
2	20-22346	ORAU. Gmelin, AED-CONF-65-312-2
4	20-22345	ORAU. Gmelin, AED-CONF-65-312-16
5	20-22160	ORAU. Gmelin, AED-CONF-65-312-20
8	20-22161	ORAU. Gmelin, AED-CONF-65-312-19
CONF-651017–		(Electrochemical Society Meeting, Buffalo, Oct. 10–14, 1965)
6	20-20705	ORAU. Gmelin, AED-CONF-65-289-5
9	20-21282	ORAU. Gmelin, AED-CONF-65-289-12
CONF-651023–		(Symposium on Radioisotope Instruments in Industry and Geophysics, Warsaw, Oct. 18–22, 1965)
3	20-20646	ORINS
7	20-20640	ORINS
10	20-20641	ORINS
11	20-21209	ORINS
15	20-20642	ORINS
CONF-651025–		(Symposium on Physical Metallurgy of Refractory Metals, French Lick, Ind., Oct. 3–5, 1965)
3	20-21404	ORAU. Gmelin, AED-CONF-65-275-4
4	20-21405	ORAU. Gmelin, AED-CONF-65-275-6
5	20-21406	ORAU. Gmelin, AED-CONF-65-275-5
6	20-21407	ORAU. Gmelin, AED-CONF-65-275-8
7	20-21411	ORAU. Gmelin, AED-CONF-65-275-3
8	20-21410	ORAU. Gmelin, AED-CONF-65-275-16
9	20-21283	ORAU. Gmelin, AED-CONF-65-275-17
10	20-21250	ORAU. Gmelin, AED-CONF-65-275-12
11	20-21412	ORAU. Gmelin, AED-CONF-65-275-9
CONF-651028–		(Conference on Electrical Insulation, Buck Hill Falls, Penna., Oct. 25–27, 1965)
2	20-21170	ORAU. Gmelin, AED-CONF-65-310-1
3	20-22344	ORAU. Gmelin, AED-CONF-65-310-4
4	20-21171	ORAU. Gmelin, AED-CONF-65-310-2
CONF-651036–		(American Society of Civil Engineers, Environmental Engineering Conference and Annual Convention, Kansas City, Kan., Oct. 18–22, 1965)
3	20-20869	ORINS
CONF-651043–	20-19426	(Weak Interactions Conference, Argonne, Ill., Oct. 25–27, 1965) Dep. mn. CFSTI $4.75 cy, $2.00 mn
8	20-21701	ORAU. Gmelin, AED-CONF-65-320-7
CONF-651044–		(Conference on Programming for Flying Spot Devices, New York, Oct. 24–26, 1965)
12	20-21041	See PPAD-585E
CONF-651049–		(IEEE Thermionic Conversion Specialist Conference, San Diego, Calif., Oct. 25–27, 1965)
5	20-21585	ORAU. Gmelin, AED-CONF-65-324-1
9	20-21586	ORAU. Gmelin, AED-CONF-65-324-6
10	20-21584	ORAU. Gmelin, AED-CONF-65-324-8
CONF-651056–		(Symposium on the Dynamics of Plasmas and Fluids, College Park, Md., Oct. 6–8, 1965)
2	20-22187	See MATT-424
CONF-651059–		(2nd Symposium on Radio Astronomical and Atmospheric,

Report No.	Abstract No.	Availability
	Boston, Oct. 19–21, 1965)	
1	20-21510	ORAU. Gmelin, AED-CONF-65-311-1
CONF-651061–	(21st National Electronics Conference and Exhibition, Chicago, Oct. 25–27, 1965)	
1	20-21172	ORAU. Gmelin, AED-CONF-65-326-6
2	20-21488	ORAU. Gmelin, AED-CONF-65-326-2
CONF-651069–	(IAEA Meeting on Dosimetry and Toxicity of Thorotrast, Vienna, Oct. 4–7, 1965)	
1	20-20790	Dep. mn. CFSTI $1.00 cy, $0.50 mn
CONF-660106–	(Meeting on Current and Future Problems in High Temperature Chemistry, Houston, Jan. 26–27, 1966)	
1	20-20870	See LA-DC-7703
CONF-660208–	(Symposium on Solidification and Long-Term Storage of Highly Radioactive Wastes, Richland, Wash., Feb. 14–18, 1966)	
14	20-22510	See BNWL-SA-564
16	20-22509	See BNL-10109
CONF-660303–	(American Physical Society, Conference of Neutron Cross Section Technology, Washington, D. C., Mar. 22–24, 1966)	
2	20-21994	See BNL-10094
10	20-22012	See UCRL-14606
11	20-22008	See MLM-1337J
26	20-22379	See LA-DC-7800
CONF-660305–	(American Nuclear Society, Topical Meeting, Augusta, Ga, Mar. 21–23, 1966)	
19	20-21212	Dep. mn. CFSTI $1.00 cy, $0.50 mn
CONF-660314–	(20th Annual Symposium on Fundamental Cancer Research, Houston, Tex., Mar. 7–9, 1966)	
1	20-20442	See ORNL-P-2053
CONF-660405–	(Symposium on Radioecological Concentration Processes, Stockholm, Apr. 25–29, 1966)	
1	20-20879	See BNWL-SA-530
2	20-20384	See COO-1156-13
4	20-20388	See SAN-34-2
5	20-20385	See COO-1184-3
CONF-660505–	(American Ceramic Society, Washington, D. C., May 7–12, 1966)	
1	20-21327	Dep. mn. CFSTI $1.00 cy, $0.50 mn
2	20-20654	See LA-DC-7784
CONF-660507–	(Symposium for the Disposal of Radioactive Wastes into Sea, Oceans, and Surface Waters, Vienna, May 17, 1966)	
4	20-22514	See ORNL-P-2021
5	20-20382	See BNWL-SA-623
CONF-660515–	(Electrochemical Society Meeting, Cleveland, May 2–4, 1966)	
1	20-21340	See LA-DC-7626
COO–		
30-103	20-21643	Nuovo Cimento (10), 42A: 316-22(1966)
205-57	20-20419	Radiat. Res., 27: 355-62(1966)
264-291	20-21677	Phys. Rev., 144: 1300-4(1966)
716-0014	20-20666	J. Chem. Phys., 44: 2872-6(1966)
720-059	20-21114	IEEE (Inst. Elec. Electron. Eng.), Trans. Nucl. Sci., NS-13: No. 1, 394-8(1966)
1156-13	20-20384	Dep. mn. CFSTI $2.00 cy, $0.50 mn
1184-3	20-20385	Dep. mn. CFSTI $2.00 cy, $0.50 mn
1191-10	20-20379	Dep. mn. CFSTI $5.00 cy, $1.00 mn
1195-52	20-21615	Dep. mn. CFSTI $4.00 cy, $1.00 mn
1198-307	20-21445	Phys. Rev., 144: 439-57(1966)
1371-13	20-22019	Amer. J. Phys., 34: 216-22(1966)
1420-119	20-22134	Phys. Rev., 144: 972-9(1966)
1505-4	20-22133	Phys. Rev., 144: 962-71(1966)
CST-PA–		
65-1	20-22189	See TID-22809
CU–	(Misc.)	
2660-26	20-20651	Dep. mn. CFSTI $1.00 cy, $0.50 mn
2660-25	20-21328	Dep. mn. CFSTI $6.00 cy, $1.25 mn
DASA–	(Misc.)	
1704	20-20881	
DC–	(Misc.)	
61-3-69	20-22307	Dep. mn. CFSTI $3.00 cy, $0.75 mn
DM–	(Misc.)	
1477	20-21428	See NP-15942
DP–		
929(Suppl.2)	20-22519	Dep. mn. CFSTI $2.00 cy, $0.50 mn
1021	20-21234	Dep. mn. CFSTI $2.00 cy, $0.50 mn
1028	20-22463	Dep. mn. CFSTI $2.00 cy, $0.50 mn
DRI–	(Misc.)	
1092-229	20-21329	Dep. mn. CFSTI $1.00 cy, $0.50 mn
DUBNA REPORTS	(Russian)	
See JINR (Russian)		
ECOM–	(Non-AEC)	
01541-1	20-21148	See AD-630835
01541-2	20-21149	See AD-630836
EDR–	(Misc.)	
4400	20-21561	See AD-623096
EFINS–	(Misc.)	
65-100	20-21677	See COO-264-291
EIR–	(Swiss)	
89	20-21222	Dep. mn
ER–	(Misc.)	
66-17-105	20-21148	See AD-630835
EUR–	(European Atomic Energy Community)	
2295.f	20-20721	Dep. mn
2401.f	20-20722	Dep. mn
2442.f	20-20709	Dep. mn
2443.f	20-20861	Dep. mn
2481.f	20-20875	Dep. mn
2518.f	20-20438	Dep. mn
2621.f	20-21330	Dep. mn
2626.f	20-20559	Dep. mn
2628.i	20-20439	Dep. mn
2643.f	20-20440	Dep. mn
2710.f	20-20984	Dep. mn
2712.e	20-21034	Dep. mn
2735.d	20-22409	Dep. mn
2753.f	20-20560	Dep. mn
2754.f	20-20804	Dep. mn
2805	20-21331	See EURAEC-1569
2806	20-21332	See EURAEC-1573
EURAEC–		
1567	20-22354	See CEND-3336-260
1569	20-21331	Dep. mn. CFSTI $1.00 cy, $0.50 mn
1573	20-21332	Dep. mn. CFSTI $1.00 cy, $0.50 mn
1583	20-21422	See GEAP-5100D
1604	20-21232	See BMI-1763
EURFNR–	(Misc.)	
49F	20-22501	Dep. mn. CFSTI $4.00 cy, $0.75 mn
FDL-TR–	(Non-AEC)	
65-86	20-20555	See AD-622200
FEI–	(Russian)	
15	20-21567	Dep. mn
16	20-21568	Dep. mn
17	20-22178	Dep. mn
21	20-21035	Dep. mn
FR–	(Non-AEC)	
66-17-106	20-21149	See AD-630836
FTI–	(Non-AEC)	
080/P-032	20-22179	Dep. mn
142/T-016	20-21996	Dep. mn

Report No.	Abstract No.	Availability
GA–	**(Misc.)**	
1052	20-21290	Dep. mn. CFSTI $3.00 cy, $0.75 mn
5238	20-22410	Dep. mn. CFSTI $2.00 cy, $0.50 mn
6113	20-22411	Dep. mn. CFSTI $4.00 cy, $0.75 mn
6456	20-21952	Nucl. Sci. Eng., 24: 394-409(1966)
6622	20-22412	Dep. mn. CFSTI $5.00 cy, $1.00 mn
6784	20-22252	Phys. Fluids, 9: 726-9(1966)
6847	20-22377	See GA-6930, App. B
6888	20-21421	Dep. mn. CFSTI $2.00 cy, $0.50 mn
6901	20-22376	Dep. mn. CFSTI $2.00 cy, $0.50 mn
6929	20-22413	Dep. mn. CFSTI $1.00 cy, $0.50 mn
6930	20-21939	Dep. mn. CFSTI $4.00 cy, $1.00 mn
6930, App. B	20-22377	
GAM–	**(Non-AEC)**	
65B-AE-65-8	20-21776	See AD-621429
65B-ME-65-4	20-21780	See AD-622036
GAM-AE–	**(Non-AEC)**	
64-3	20-21777	See AD-621442
GAMD–	**(Misc.)**	
6908	20-21940	Dep. mn. CFSTI $1.00 cy, $0.50 mn
GEAP–	**(Misc.)**	
4742	20-22495	Dep. mn. CFSTI $3.00 cy, $0.75 mn
4864	20-22496	Dep. mn. CFSTI $4.00 cy, $1.00 mn
4961	20-22414	Dep. mn. CFSTI $1.00 cy, $0.50 mn
4976	20-20856	Dep. mn. CFSTI $1.00 cy, $0.50 mn
5100D	20-21422	Dep. mn. CFSTI $4.00 cy, $0.75 mn
GNE–	**(Non-AEC)**	
65-16	20-22490	See AD-621124
GNE-PH–	**(Non-AEC)**	
65-1	20-20554	See AD-621017
65-9	20-20716	See AD-621022
65-02	20-20648	See AD-621029
65-15	20-22162	See AD-621020
GNE-Phys.–	**(Non-AEC)**	
65-3	20-21960	See AD-621023
65-4-A	20-22489	See AD-621123
65-6	20-22371	See AD-621026
65-10	20-22488	See AD-621121
65-14	20-22491	See AD-621269
65-17	20-22370	See AD-621021
65-18	20-21933	See AD-621119
65-19	20-22487	See AD-621118
HASL–		
167	20-22308	Dep. mn. CFSTI $2.00 cy, $0.50 mn
171	20-20882	Dep. mn. CFSTI $7.30 cy, $2.00 mn
HEPL–	**(Misc.)**	
392	20-21459	See AD-623509
393	20-21589	See AD-626683
394	20-21964	See AD-626684
396	20-21460	See AD-623659
405	20-21588	See AD-623658
HI–	**(Non-AEC)**	
518-RR(Vol.1)	20-20930	
518-RR(Vol.2)	20-20931	
518-RR(Vol.3)	20-20932	
HMI-B–	**(German)**	
45	20-21150	Dep. mn
IAE–	**(Non-AEC)**	
960	20-22180	Dep. mn
974	20-21213	Dep. mn
977	20-21941	Dep. mn
992	20-22497	Dep. mn
993	20-22498	Dep. mn
IBJ–	**(Polish)**	
See INP		
IBM–	**(Non-AEC)**	
66-825-1944	20-21151	

Report No.	Abstract No.	Availability
IC–	**(Misc.)**	
66/28	20-22460	Dep. mn
66/29	20-22464	Dep. mn
IDO–		
12045	20-20933	Dep. mn. CFSTI $3.00 cy, $0.75 mn
14666	20-22511	Dep. mn. CFSTI $1.00 cy, $0.50 mn
17077	20-22467	Dep. mn. CFSTI $6.00 cy, $1.25 mn
17150	20-22499	Dep. mn. CFSTI $2.00 cy, $0.50 mn
IFJ–	**(Polish)**	
See INP		
IITRI–	**(Misc.)**	
B6042-4	20-21333	
INR–	**(Non-AEC)**	
598/V1/PH	20-21514	Dep. mn
INSJ–	**(Japanese)**	
96	20-21997	Dep. mn
IPP–	**(Non-AEC)**	
1/45	20-22181	Dep. mn
3/29	20-21569	Dep. mn
3/35	20-22182	Dep. mn
IS–		
1264	20-22338	Phys. Rev., 144: 504-11(1966)
1287	20-21235	Dep. mn. CFSTI $3.00 cy, $0.75 mn
1314	20-21227	Nuovo Cimento (10), 42A: 416-18(1966)
1325	20-21334	Dep. mn. CFSTI $2.00 cy, $0.50 mn
1329	20-20805	Dep. mn. CFSTI $2.00 cy, $0.50 mn
1337	20-22315	Dep. mn. CFSTI $3.00 cy, $0.75 mn
IS-T–		
67	20-20652	Dep. mn. CFSTI $6.00 cy, $1.25 mn
76	20-21335	Dep. mn. CFSTI $3.00 cy, $0.75 mn
79	20-21336	Dep. mn. CFSTI $2.00 cy, $0.50 mn
JAERI–	**(Japanese)**	
1098	20-20934	Dep. mn
1099	20-20561	Dep. mn
JINR–	**(Russian)**	
E-2579	20-21998	Dep. mn
P-2081	20-22316	Dep. mn
P-2429	20-21616	Dep. mn
P-2546	20-21617	Dep. mn
P-2552	20-21999	Dep. mn
P-2553	20-22000	Dep. mn
P-2554	20-21710	Dep. mn
P-2555	20-22001	Dep. mn
P-2558	20-20653	Dep. mn
P-2559	20-21711	Dep. mn
P-2562	20-21712	Dep. mn
P-2564	20-21223	Dep. mn
P-2566	20-21618	Dep. mn
P-2567	20-21619	Dep. mn
P-2568	20-21713	Dep. mn
P-2570	20-22002	Dep. mn
P-2573	20-21036	Dep. mn
P-2576	20-21715	Dep. mn
P-2577	20-21620	Dep. mn
P-2578	20-21714	Dep. mn
P-2581	20-22003	Dep. mn
P-2584	20-21621	Dep. mn
P-2585	20-21622	Dep. mn
P-2593	20-22004	Dep. mn
P-2594	20-21037	Dep. mn
P-2596	20-22005	Dep. mn
P-2598	20-21337	Dep. mn
P-2602	20-21623	Dep. mn
P-2603	20-21716	Dep. mn
P-2606	20-21624	Dep. mn
P-2615	20-21515	Dep. mn
P-2619	20-21625	Dep. mn
P-2620	20-21717	Dep. mn
JPL-TR–	**(Non-AEC)**	
32-842	20-21338	
K–		

Report No.
1651
1656
1657
1661

K-L–
6059

KAPL–
3122

KAPL-P–
3132

KFK–
367

KFK-tr–
185
188

KFKI–
600

LA–
3395
3450
3470
3476

LA-DC–
6431
7095
7397
7565
7567
7597
7626
7673
7703
7784
7800

LA-tr–
66-15

LAC-ER–
8372

LNF–
66/1
66/4
66/9
66/10

LRP–
21-66
22-66
23-66

LYCEN–
6538

MAB–
205-M

MATT–
358
406
424

MIT–
334-23
334-33
905-41
905-44
905-46
2098-169
2098-196
2098-227
2098-227,
Paper E

Report No.	Abstract No.	Availability
1651	20-22512	Dep. mn. CFSTI $1.00 cy, $0.50 mn
1656	20-21038	Dep. mn. CFSTI $1.00 cy, $0.50 mn
1657	20-20935	Dep. mn. CFSTI $1.00 cy, $0.50 mn
1661	20-20936	Dep. mn. CFSTI $2.00 cy, $0.50 mn
K-L–		
6059	20-20581	Anal. Chem., 38: 615-18(1966)
KAPL–		
3122	20-21039	Dep. mn. CFSTI $1.00 cy, $0.50 mn
KAPL-P–		
3132	20-22392	Nucl. Sci. Eng., 24: 414-17(1966)
KFK–	**(German)**	
367	20-22378	Dep. mn
KFK-tr–	**(German)**	
185	20-22014	Dep. mn. JCL $1.00 fs, $0.50 mf
188	20-21942	Dep. mn. JCL $2.60 fs, $0.95 mf
KFKI–	**(Hungarian)**	
600	20-22006	Dep. mn
LA–		
3395	20-22468	Dep. mn. CFSTI $2.00 cy, $0.50 mn
3450	20-21784	Dep. mn. CFSTI $2.00 cy, $0.50 mn
3470	20-22355	Dep. mn. CFSTI $2.00 cy, $0.50 mn
3476	20-21261	Dep. mn. CFSTI $1.00 cy, $0.50 mn
LA-DC–		
6431	20-20671	J. Electrochem. Soc., 113: 371-6(1966)
7095	20-21339	Dep. mn. CFSTI $1.00 cy, $0.50 mn
7397	20-22254	Phys. Fluids, 9: 750-60(1966)
7565	20-21680	Phys. Rev., 144: 1324-38(1966)
7567	20-22132	Phys. Rev., 144: 956-61(1966)
7597	20-22144	Phys. Rev., 144: 1060-?(1966)
7626	20-21340	ORAU
7673	20-22095	Phys. Lett., 20: 392-5(1966)
7703	20-20870	Dep. mn. CFSTI $1.00 cy, $0.50 mn
7784	20-20654	Dep. mn. CFSTI $1.00 cy, $0.50 mn
7800	20-22379	ORAU
LA-tr–		
66-15	20-21241	Dep. mn. CFSTI $1.00 cy, $0.50 mn; JCL $1.60 fs, $0.80 mf
LAC-ER–	**(Non-AEC)**	
8372	20-21427	See NASA-CR-54904
LNF–	**(Italian)**	
66/1	20-22007	Dep. mn
66/4	20-21626	Dep. mn
66/9	20-21627	Dep. mn
66/10	20-21469	Dep. mn
LRP–	**(Swiss)**	
21-66	20-22183	Dep. mn
22-66	20-22184	Dep. mn
23-66	20-22185	Dep. mn
LYCEN–	**(French)**	
6538	20-20562	Dep. mn
MAB–	**(Non-AEC)**	
205-M	20-21341	CFSTI $3.00 cy, $0.50 mn
MATT–		
358	20-22186	Dep. mn. CFSTI $2.00 cy, $0.50 mn
406	20-22263	Phys. Fluids, 9: 818-20(1966)
424	20-22187	Dep. mn. CFSTI $1.00 cy, $0.50 mn
MIT–	**(Misc.)**	
334-23	20-20710	Dep. mn. CFSTI $5.00 cy, $1.00 mn
334-33	20-20723	Dep. mn. CFSTI $2.00 cy, $0.50 mn
905-41	20-22044	J. Inorg. Nucl. Chem., 28: 763-70(1966)
905-44	20-22041	J. Inorg. Nucl. Chem., 28: 681-2(1966)
905-46	20-22130	Phys. Rev., 144: 945-51(1966)
2098-169	20-22022	Ann. Phys. (N. Y.), 36: 363-434(1966)
2098-196	20-21084	Phys. Rev., 144: 231-2(1966)
2098-227	20-21543	Dep. mn. CFSTI $3.00 cy, $0.75 mn
2098-227, Paper EAS-8	20-21544	
2098-227, Paper EAS-11	20-21545	
2098-227, Paper EAS-29	20-21546	
2098-227, Paper EAS-31	20-21547	
ML-TR–	**(Non-AEC)**	
65-236	20-20717	See AD-621719
MLM–		
1142	20-20553	Dep. mn. CFSTI $2.00 cy, $0.50 mn
1274	20-20806	Dep. mn. CFSTI $2.00 cy, $0.50 mn
1282J	20-22038	J. Inorg. Nucl. Chem., 28: 651-4(1966)
1287	20-20807	Dep. mn. CFSTI $2.00 cy, $0.50 mn
1301	20-21342	Dep. mn. CFSTI $2.00 cy, $0.50 mn
1305J	20-20582	Anal. Chem., 38: 636-7(1966)
1337J	20-22008	Dep. mn. CFSTI $1.00 cy, $0.50 mn
MTI–	**(Misc.)**	
66TR14	20-20841	See NYO-3237-5
N–	**(Misc.)**	
65-22353	20-21152	CFSTI $2.00 cy, $0.50 mn
65-22776	20-22188	
65-23013	20-21343	
65-23015	20-21423	
65-23290	20-21154	CFSTI $1.00 cy, $0.50 mn
65-23332	20-21424	CFSTI $1.00 cy, $0.50 mn
65-23835	20-21236	CFSTI $1.00 cy, $0.50 mn
65-24491	20-21425	CFSTI $3.00 cy, $0.75 mn
65-24714	20-21426	
65-25266	20-21262	CFSTI $1.00 cy, $0.50 mn
65-25593	20-21153	CFSTI $1.00 cy, $0.50 mn
65-26653	20-21344	CFSTI $1.00 cy, $0.50 mn
65-26656	20-21345	CFSTI $2.00 cy, $0.50 mn
65-27062	20-20406	CFSTI $3.00 cy, $0.75 mn
65-29395	20-21237	CFSTI $1.00 cy, $0.50 mn
65-29443	20-20871	CFSTI $3.00 cy, $0.75 mn
65-29479	20-22469	CFSTI $1.00 cy, $0.50 mn
65-29480	20-22470	CFSTI $3.00 cy, $0.75 mn
65-29669	20-20985	
65-29785	20-21570	CFSTI $5.00 cy, $1.00 mn
65-29816	20-21813	CFSTI $2.00 cy, $0.50 mn
65-29823	20-20986	CFSTI $4.00 cy, $1.00 mn
65-30166	20-21240	See WANL-PR-(Q)-006
NAA-SR–		
11175	20-22500	Dep. mn. CFSTI $2.00 cy, $0.50 mn
11761	20-20937	Dep. mn. CFSTI $2.00 cy, $0.50 mn
11805	20-22520	Dep. mn. CFSTI $5.00 cy, $1.00 mn
11814	20-22471	Dep. mn. CFSTI $3.00 cy, $0.75 mn
NASA-CR–	**(Misc.)**	
54325	20-21570	See N-65-29785
54447	20-20986	See N-65-29823
54462	20-21240	See WANL-PR-(Q)-006
54740	20-21361	See WCAP-2923
54895	20-21346	
54904	20-21427	
54911	20-21263	
54913	20-21295	See WANL-PR-(EE)-002
54916	20-21347	
62617	20-21424	See N-65-23332
62636	20-21154	See N-65-23290
62727	20-21236	See N-65-23835
62796	20-21425	See N-65-24491
63188	20-21262	See N-65-25266
63253	20-21153	See N-65-25593
63560	20-20406	See N-65-27062
NASA-SP–	**(Misc.)**	
7011(22)	20-20369	CFSTI $1.00 cy, $1.00 mn
NASA-TM–	**(Misc.)**	
X-31993	20-20871	See N-65-29443
X-52047	20-22470	See N-65-29480
X-52048	20-22469	See N-65-29479
X-53230	20-21152	See N-65-22353
X-54737	20-21237	See N-65-29395
X-55250	20-21813	See N-65-29816

Report No.	Abstract No.	Availability
NASA-TN–	**(Misc.)**	
D-2885	20-21344	See N-65-26653
D-2906	20-21345	See N-65-26656
NAVWEPS–	**(Non-AEC)**	
8782-P2	20-22351	See AD-623020
NBS–	**(Misc.)**	
8670	20-21262	See N-65-25266
NBS-MON–	**(Misc.)**	
81	20-22009	GPO $3.25
NDL-TM–	**(Non-AEC)**	
4	20-22507	See AD-622372
NOLTR–	**(Misc.)**	
65-125	20-21418	See AD-627049
NP–	**(AEC File No. for Non-AEC Reports)**	
15914	20-20883	Dep. mn
15916	20-20386	Dep. mn
15918	20-20563	
15921	20-20938	Dep. mn
15925	20-20517	Dep. mn
15928	20-21238	
15936	20-21873	Dep. mn
15942	20-21428	Dep. mn
15944	20-21291	
15949	20-20876	
NP-tr–	**(AEC File No. for Non-AEC Translations)**	
1371	20-21297	Dep. mn. JCL $1.10 fs, $0.80 mf
NRC–	**(Canadian)**	
8845	20-21817	Can. J. Phys., 44: 669-73(1966)
NSEC–	**(Misc.)**	
118	20-20406	See N-65-27062
NYO–		
1163-70	20-20939	Dep. mn. CFSTI $2.00 cy, $0.50 mn
NYO–		
72-28	20-22010	Dep. mn. CFSTI $5.00 cy, $1.00 mn
1726-15	20-20523	Dep. mn. CFSTI $1.00 cy, $0.50 mn
2150-10	20-21894	Phys. Rev. Lett., 16: 652-4(1966)
2181-3	20-20387	Dep. mn. CFSTI $4.00 cy, $1.00 mn
2978-44	20-20724	Dep. mn. CFSTI $3.00 cy, $0.50 mn
3219-5	20-22037	J. Inorg. Nucl. Chem., 28: 331-4(1966)
3237-5	20-20841	Dep. mn. CFSTI $3.00 cy, $0.75 mn
3399-28	20-21850	J. Math. Phys. (N. Y.), 7: 641-51(1966)
3570-2	20-20725	Dep. mn. CFSTI $1.00 cy, $0.50 mn
10447	20-22513	Dep. mn. CFSTI $6.00 cy, $1.25 mn
10740	20-20564	Dep. mn. CFSTI $2.00 cy, $0.50 mn
ORNL–		
3041	20-22309	Dep. mn. CFSTI $3.00 cy, $0.75 mn
3915	20-20940	Dep. mn. CFSTI $5.00 cy, $1.00 mn
3916	20-20808	Dep. mn. CFSTI $3.00 cy, $0.75 mn
3919	20-21224	Dep. mn. CFSTI $4.00 cy, $0.75 mn
3925	20-20809	Dep. mn. CFSTI $2.00 cy, $0.50 mn
3929	20-22356	Dep. mn. CFSTI $2.00 cy, $0.50 mn
3932	20-21292	Dep. mn. CFSTI $2.00 cy, $0.50 mn
ORNL-IIC–		
7	20-21177	Dep. mn. CFSTI $2.00 cy, $0.75 mn
8	20-21214	Dep. mn. CFSTI $3.00 cy, $0.75 mn
ORNL-P–	**(Misc.)**	
1118	20-20407	Dep. mn. CFSTI $1.00 cy, $0.50 mn
1173	20-20441	Dep. mn. CFSTI $1.00 cy, $0.50 mn
1175	20-22036	J. Inorg. Nucl. Chem., 28: 285-6(1966)
1216	20-20565	Dep. mn. CFSTI $1.00 cy, $0.50 mn
1218	20-21040	Dep. mn. CFSTI $1.00 cy, $0.50 mn
1283	20-22039	J. Inorg. Nucl. Chem., 28: 676-8(1966)
1599	20-20600	Nucl. Sci. Eng., 24: 336-43(1966)
1683	20-21271	J. Electrochem. Soc., 113: 328-33(1966)
1694	20-20571	Anal. Chem., 38: 414-20(1966)
1821	20-21392	Phys. Rev., 144: 725-33(1966)
1826	20-22110	Phys. Rev., 144: 799-801(1966)
1975	20-22091	Nucleonics, 24: 62-4(1966)
2021	20-22514	Dep. mn. CFSTI $2.00 cy, $0.50 mn
2053	20-20442	Dep. mn. CFSTI $3.00 cy, $0.75 mn
2059	20-22102	Phys. Lett., 20: 657-61(1966)
ORNL-RSIC–		
13	20-22310	ORNL Free
ORNL-TM–		
1246	20-22380	Dep. mn. CFSTI $1.00 cy, $0.50 mn
1330(Rev.)	20-21785	Dep. mn. CFSTI $3.00 cy, $0.75 mn
1341	20-21395	Weld. J. (N. Y.), 45: 103s-10s(1966)
1387	20-21786	Dep. mn. CFSTI $4.00 cy, $1.00 mn
1410	20-20842	Dep. mn. CFSTI $3.00 cy, $0.75 mn
1426	20-21350	Dep. mn. CFSTI $1.00 cy, $0.50 mn
1432	20-20941	Dep. mn. CFSTI $3.00 cy, $0.75 mn
1459	20-20942	Dep. mn. CFSTI $3.00 cy, $0.75 mn
1468	20-20566	Dep. mn. CFSTI $1.00 cy, $0.50 mn
ORNL-tr–		
965	20-22515	Dep. mn. JCL $2.60 fs, $0.83 mf
P–	**(Misc.)**	
1126(RAND)	20-21587	See AD-623564
3249(RAND)	20-21489	See AD-623803
PAN–	**(Polish)**	**(This series of reports was terminated in 1965. Subsequent reports are identified by the code INR.)**
PATENTS	**(British)**	**(4s. 6d. each, U. K. Patent Office)**
1,019,440	20-20852	
1,019,590	20-21140	
1,019,622	20-22458	
1,020,287	20-21255	
1,020,572	20-21417	
1,020,574	20-21016	
1,020,668	20-22361	
1,020,752	20-20787	
1,020,771	20-21017	
1,021,034	20-22362	
1,021,043	20-21256	
1,021,084	20-21018	
PATENTS	**(Canadian)**	
722,560	20-21315	
725,277	20-21316	
725,771	20-21317	
725,773	20-22402	
PATENTS	**(German)**	
1,203,887	20-22403	
1,205,630	20-21141	
1,206,097	20-22363	
1,206,100	20-22364	
1,206,101	20-22365	
PATENTS	**(Japanese)**	
1964-545	20-20788	
1964-4163	20-20853	
1964-4585	20-22303	
PATENTS	**(U. S.)**	**($0.50 each, U. S. Patent Office)**
3,232,046	20-20874	
3,232,822	20-21314	
3,232,841	20-22366	
3,233,102	20-21142	
3,233,103	20-21143	
3,233,104	20-21144	
3,233,107	20-20800	
3,234,100	20-22367	
3,234,104	20-22368	
3,234,382	20-21145	
3,234,388	20-21019	
3,235,205	20-22486	
3,235,463	20-22465	
3,235,465	20-22369	
3,235,608	20-20707	
3,235,737	20-21146	
3,245,114	20-21318	
PB–	**(Non-AEC)**	

Report No.	Abstract No.	Availability
181506	20-20726	CFSTI $3.00 cy, $1.00 mn
PDL–	**(Non-AEC)**	
50205	20-21257	See AD-621546
PPAD–		
573E	20-22125	Phys. Rev., 144: 917-22(1966)
577D	20-21471	Dep. mn. CFSTI $2.00 cy, $0.50 mn
585E	20-21041	Dep. mn. CFSTI $1.00 cy, $0.50 mn
PSRP–	**(Non-AEC)**	
126	20-21778	See AD-621943
R–	**(Misc.)**	
66SD3007	20-21293	
R-OU–	**(Non-AEC)**	
157(Summ.)	20-20922	See AD-624704
RCC-R–	**(British)**	
186	20-22034	Int. J. Appl. Radiat. Isotop., 17: 145-50(1966)
RFP–		
453	20-20943	Dep. mn. CFSTI $1.00 cy, $0.50 mn
491	20-21264	Dep. mn. CFSTI $1.00 cy, $0.50 mn
516A(Suppl.1)	20-22521	Dep. mn. CFSTI $2.00 cy, $0.50 mn
690	20-20987	Dep. mn. CFSTI $1.00 cy, $0.50 mn
RHEL-R–	**(British)**	
105	20-21429	Dep. mn
113	20-21472	Dep. mn
RL-SEP–		
824	20-21239	Dep. mn. CFSTI $2.00 cy, $0.50 mn
RLO–		
1388B-4	20-21681	Phys. Rev., 144: 1343-50(1966)
1750-1	20-20603	Science, 152: 202-3(1966)
RM–	**(Misc.)**	
156-11	20-20923	See AD-626727
4683-PR	20-21775	See AD-620835
4722-ARPA	20-20897	See AD-623679
RPI–	**(Misc.)**	
321-4	20-22415	Dep. mn. CFSTI $3.00 cy, $0.75 mn
2714-8	20-21265	Dep. mn. CFSTI $2.00 cy, $0.50 mn
RR–	**(Misc.)**	
238	20-21564	See AD-627037
RT-FI–	**(Italian)**	
(65)49	20-22381	Dep. mn
(65)50	20-22357	Dep. mn
(65)57	20-22382	Dep. mn
RT-PROT–	**(Italian)**	
(65)32	20-20524	Dep. mn
(65)41	20-20518	Dep. mn
SA-TR–	**(Non-AEC)**	
18-1091	20-21286	See AD-621920
18-1096	20-21319	See AD-621064
SAN–		
34-2	20-20388	Dep. mn. CFSTI $2.00 cy, $0.50 mn
575-12	20-21174	Dep. mn. CFSTI $7.38 cy, $2.00 mn
SC-CR–		
66-2017	20-22472	Dep. mn. CFSTI $1.00 cy, $0.50 mn
SC-DC–		
65-1907	20-20857	Dep. mn. CFSTI $3.00 cy, $0.50 mn
SC-RR–		
65-609	20-21210	Dep. mn. CFSTI $5.00 cy, $1.00 mn
SC-T–		
66-0723	20-21362	Dep. mn. CFSTI $1.00 cy, $0.50 mn. JCL $1.10 fs, $0.80 mf
SGAE-CH–	**(Austrian)**	
21/1965	20-20732	Dep. mn
SGAE-E–	**(Austrian)**	
6/1966	20-21042	Dep. mn
SLAC-Trans–		
38	20-21475	Dep. mn. JCL $4.60 fs, $1.52 mf
SM–	**(Misc.)**	
72/41	20-22514	See ORNL-P-2021
SORIN–	**(Italian)**	
15	20-21423	See N-65-23015
SRIA–		
425-8	20-21351	Dep. mn. CFSTI $3.00 cy, $0.75 mn
STI-PUB–	**(International Atomic Energy Agency)**	
108	20-20389	IAEA: $12.00; Sch 252,-; £3.12.0; F Fr 48,-; DM 42,-.
110	20-20944	IAEA: $18.00; S378,-; £5.8.0; F Fr 72,-; DM 63,-.
STI-REP–	**(International Atomic Energy Agency)**	
101	20-20904	Dep. mn. IAEA $4.00 cy, $0.50 mn
STL–	**(Misc.)**	
4161-6011-SU-000	20-21154	See N-65-23290
SURI-EE–	**(Non-AEC)**	
494-658-T-8	20-21704	See AD-622517
TID–		
3734	20-22522	Dep. DTI Extension Free
19077	20-20473	J. Roy. Microscop. Soc., 83: 79-82(1964)
21745	20-21352	Dep. mn. CFSTI $1.00 cy, $0.50 mn
22163	20-22072	Nucl. Phys., 80: 241-58(1966)
22221	20-21294	Dep. mn. CFSTI $2.00 cy, $0.50 mn
22347	20-22053	Nucl. Phys., 80: 1-13(1966)
22350	20-21211	Dep. mn. CFSTI $4.00 cy, $1.00 mn
22368	20-21081	pp 75-85 of Moessbauer Effect Methodology. Vol. 1. New York, Plenum Press, 1965.
22499	20-20380	Dep. mn. CFSTI $2.00 cy, $0.50 mn
22509	20-21195	Dep. mn. CFSTI $3.00 cy, $0.75 mn
22636	20-22067	Nucl. Phys., 80: 177-97(1966)
22683	20-22322	J. Appl. Phys., 37: 1852-7(1966)
22736	20-22416	Dep. mn. CFSTI $3.00 cy, $0.75 mn
22759	20-22417	Dep. mn. CFSTI $1.00 cy, $0.50 mn
22767	20-20390	Dep. mn. CFSTI $2.00 cy, $0.50 mn
22771	20-22011	CFSTI $2.50 cy, $0.75 mn
22796	20-20733	Dep. mn. CFSTI $5.00 cy, $1.00 mn
22809	20-22189	Dep. mn. CFSTI $4.00 cy, $1.00 mn
22815	20-20884	Dep. mn. CFSTI $3.00 cy, $0.75 mn
22820	20-20444	Dep. mn. CFSTI $1.00 cy, $0.50 mn
22821	20-22190	Dep. mn. CFSTI $1.00 cy, $0.50 mn
22822	20-21628	Dep. mn. CFSTI $5.00 cy, $1.50 mn
22825	20-20391	Dep. mn. CFSTI $1.00 cy, $0.50 mn
22828	20-21353	Dep. mn. CFSTI $3.00 cy, $0.75 mn
TM–	**(Misc.)**	
43-19	20-21424	See N-65-23332
TN-N–	**(Non-AEC)**	
726	20-21176	See AD-621440
763	20-21934	See AD-621473
764	20-22305	See AD-621441
TR–	**(Misc.)**	
3-699	20-20895	See AD-626899
12	20-22188	See N-65-22776
20-03106-20-T	20-21020	See AD-621069
26	20-22313	See AD-624719
100	20-20868	See AD-626770
1305	20-21935	See AD-624041
TRG-Inf.Ser.–	**(British)**	
166	20-20445	Dep. mn. BIS $0.40. HMSO 2s.
TRG-Report–	**(British)**	

Report No.	Abstract No.	Availability
896	20-20951	Health Phys., 12: 509-19(1966)
1073	20-20945	Dep. BIS $0.70. HMSO 3s. 6d.
1160	20-21354	Dep. BIS $0.50. HMSO 2s. 6d.
1168	20-21355	Dep. BIS $1.00. HMSO 5s. 0d.
TRW–	**(Non-AEC)**	
4148-6013-SU-000	20-21570	See N-65-29785
TT–	**(Canadian)**	
62-23147	20-21874	CFSTI $2.00 cy, $0.50 mn
UCOL–	**(Misc.)**	
535-554	20-21473	Dep. mn. CFSTI $1.00 cy, $0.50 mn
UCRL–		
11537(Rev.)	20-21662	Phys. Rev., 144: 1115-22(1966)
11676	20-22142	Phys. Rev., 144: 1031-45(1966)
11931	20-20657	CFSTI $1.00 cy, $0.50 mn
13199	20-21043	Dep. mn. CFSTI $3.00 cy, $0.50 mn
13202	20-20988	Dep. mn. CFSTI $5.00 cy, $1.00 mn
14102	20-22223	J. Math. Phys. (N. Y.), 7: 616-26(1966)
14262-T	20-21124	IEEE (Inst. Elec. Electron. Eng.), Trans. Nucl. Sci., NS-13: No. 1, 515-22(1966)
14284-T(Rev.1)	20-21000	IEEE (Inst. Elec. Electron. Eng.), Trans. Nucl. Sci., NS-13: No. 1, 351-70(1966)
14310(Rev.1)	20-22265	Phys. Fluids, 9: 821-4(1966)
14324	20-20914	Rev. Sci. Instrum., 37: 480-5(1966)
14388(Rev.1)	20-22253	Phys. Fluids, 9: 730-49(1966)
14403	20-21516	Dep. mn. CFSTI $4.00 cy, $1.00 mn
14602	20-22523	Dep. mn. CFSTI $1.00 cy, $0.50 mn
14606	20-22012	Dep. mn. CFSTI $1.00 cy, $0.50 mn
14620	20-20858	Dep. mn. CFSTI $1.00 cy, $0.50 mn
14658	20-20370	Dep. mn. CFSTI $2.00 cy, $0.50 mn
14697	20-22191	Dep. mn. CFSTI $1.00 cy, $0.50 mn
14724	20-21356	Dep. mn. CFSTI $1.00 cy, $0.50 mn
16107	20-21364	Acta Met., 14: 621-35(1966)
16174	20-21635	Ann. Phys. (N. Y.), 36: 435-57(1966)
16248	20-22140	Phys. Rev., 144: 1020-1(1966)
16299	20-21357	Dep. mn. CFSTI $3.00 cy, $0.50 mn
16332	20-21629	Dep. mn. CFSTI $1.00 cy, $0.50 mn
16367	20-21749	Phys. Rev., 144: 1137-41(1966)
16428	20-22118	Phys. Rev., 144: 839-53(1966)
16469	20-21630	Dep. mn. CFSTI $6.00 cy, $0.75 mn
16490	20-21009	Rev. Sci. Instrum., 37: 495-6(1966)
16494	20-22137	Phys. Rev., 144: 994-8(1966)
16552	20-21358	Dep. mn. CFSTI $3.00 cy, $0.75 mn
16553	20-21474	Dep. mn. CFSTI $1.00 cy, $0.50 mn
16616(Rev.)	20-21685	Phys. Rev. Lett., 16: 669-71(1966)
16725	20-21534	Phys. Rev. Lett., 16: 637-9(1966)
UCRL-Trans–		
1299(L)	20-21363	Dep. mn. JCL $3.60 fs, $1.13 mf
10012	20-21433	Dep. mn. JCL $8.10 fs, $2.72 mf
UJV–	**(Czechoslovakian)**	
1418/65	20-20567	Dep. mn
1421/65	20-20859	Dep. mn
UR–		
875-95	20-21725	Ann. Phys. (N. Y.), 36: 311-22(1966)
875-112	20-21665	Phys. Rev., 144: 1132-7(1966)
875-122	20-21659	Phys. Lett., 20: 692-5(1966)
USNRDL-TR–	**(Misc.)**	
969	20-20431	See AD-630323
973	20-20434	See AD-630870
974	20-20432	See AD-630332
976	20-21024	See AD-630693
980	20-20433	See AD-630390
987	20-22404	Dep. mn. CFSTI $1.00 cy, $0.50 mn
WADC-TR–	**(Non-AEC)**	
55-58(Pt.8)	20-21430	
55-58(Pt.9)	20-21431	
WANL-PR–	**(Misc.)**	
(EE)-002	20-21295	
(Q)-006	20-21240	CFSTI $2.00 cy, $0.50 mn
WAPD–	**(Misc.)**	
301	20-21432	Dep. mn. CFSTI $3.00 cy, $0.75 mn
WAPD-T–		
1581	20-21359	Dep. mn. CFSTI $3.00 cy, $0.50 mn
WAPD-TM–	**(Misc.)**	
555	20-20862	Dep. mn. CFSTI $4.00 cy, $0.75 mn
WCAP–	**(Misc.)**	
2098	20-21360	Dep. mn
2923	20-21361	
X–	**(Misc.)**	
640-65-149	20-21813	See N-65-29816
Y–		
1506	20-20989	Dep. mn. CFSTI $2.00 cy, $0.50 mn
1510	20-21296	Dep. mn. CFSTI $2.00 cy, $0.50 mn

DEPOSITORIES OF USAEC REPORTS

In Countries Other than the U.S.

ARGENTINA
Buenos Aires, Comisión Nacional de Energía Atómica
AUSTRALIA
Canberra, Australian National Library
Sutherland, New South Wales, Australian Atomic Energy Commission
AUSTRIA
Vienna, Zentral Bibliothek der Physikalischen Institute der Universität
BELGIUM
Mol-Donk, Centre d'Etude de l'Energie Nucleaire
BOLIVIA
La Paz, Comisión Nacional de Energiá Nuclear
BRAZIL
Rio de Janeiro, Instituto Brasileiro de Bibliografia e Documentacao
São Paulo, Instituto de Energia Atomica, Cidade Universitaria São Paulo
BURMA
Rangoon, Union of Burma Applied Research Institute, Atomic Energy Center Library
CANADA
Hamilton, McMaster University
Ottawa, National Research Council Library
Vancouver, University of British Columbia
CHILE
Santiago, Instituto de Fisica y Matematicas, Universidad de Chile
CHINA
Hsinchu, Taiwan, Free China, National Tsing Hua University
COLOMBIA
Bogota, Instituto De Asuntos Nucleares
COSTA RICA
San Pedro, University of Costa Rica Library
DENMARK
Risö, Danish Atomic Energy Commission
ECUADOR
Quito, Escuela Politécnica Nacional
EL SALVADOR
San Salvador, Universidad de El Salvador, Biblioteca de Energia Nuclear
FINLAND
Helsinki, Teknillisen Korkeakoulun Kirjasto
FRANCE
Gif-sur-Yvette, Centre d'Etudes Nucléaires de Saclay
Paris, Académie des Sciences
GERMANY
Berlin, Hahn-Meitner-Institut für Kernforschung Berlin
Frankfurt/Main, Gmelin-Institut
Munich, Technische Hochschule, Bibliothek
GHANA
Accra, University College of Ghana
GREECE
Athens, Nuclear Research Center "Democritus"
GUATEMALA
Guatemala, Comisión Nacional de Energía Nuclear
INDIA
Bombay, Department of Atomic Energy
IRAN
Tehran, Tehran University Nuclear Centre
IRAQ
Baghdad, Iraqi Atomic Energy Commission
IRELAND
Dublin, University College
ISRAEL
Rehovoth, Israel Atomic Energy Commission
ITALY
Rome, Centro di Studi Nucleari della Casaccia
Rome, Comitato Nazionale per l'Energia Nucleare
JAPAN
Tokyo, National Diet Library
KOREA
Seoul, Office of Atomic Energy
LEBANON
Beirut, Lebanese National Council for Scientific Research
LUXEMBOURG
Luxembourg, Ministry of Transport and Electricity
MALAYSIA
Kuala Lumpur, University of Malaysia
MEXICO
Mexico, D.F., Comisión Nacional de Energía Nuclear
NETHERLANDS
The Hague, Reactor Centrum Nederland
NEW ZEALAND
Lower Hutt, Institute of Nuclear Sciences
NIGERIA
Ibadan, University of Ibadan
NORWAY
Lillestrøm, Institutt för Atomenergi
PAKISTAN
Lahore, West Pakistan, Atomic Energy Centre
PERU
Lima, Junta de Control de Energia Atomica
PHILIPPINE REPUBLIC
Manila, Philippine Atomic Energy Commission
POLAND
Warsaw, Biura Pelnomocnika Rzadu do Spraw Wykorzystania Energii Jadrowej
PORTUGAL
Sacavem, Junta de Energía Nuclear
REPUBLIC OF SOUTH AFRICA
Pretoria, Atomic Energy Board Library
REPUBLIC OF THE CONGO
Leopoldville, Université Lovanium
SPAIN
Madrid, Junta de Energía Nuclear, Biblioteca Documentación y Publicaciones, Ciudad Universitaria
SWEDEN
Nyköping, Aktiebolaget Atomenergi
SWITZERLAND
Zürich, Eidgenössische Technische Hochschule, Bibliothek
THAILAND
Bangkok, Office of the Thai Atomic Energy Commission, Department of Science
TURKEY
Ankara, Turkish Atomic Energy Commission, Atomic Energy Library
UNITED ARAB REPUBLIC
Cairo, Atomic Energy Commission
UNITED KINGDOM
Birmingham, Central Library
Boston Spa, National Lending Library for Science and Technology
Kingston upon Hull, Central Library
Liverpool, Central Library
London, Central Library, Acton
London, National Reference Library
London, Science Museum Library, South Kensington
Manchester, Central Library
Newcastle upon Tyne, Central Library
Nottingham, Central Library
Sheffield, Central Library
URUGUAY
Montevideo, Comision Nacional de Energia Atomica
VENEZUELA
Caracas, Instituto Venezolano de Investigaciones Científicas
VIET-NAM
Saigon, Atomic Energy Office
YUGOSLAVIA
Belgrade, Federal Commission for Nuclear Energy

In International Agencies

AUSTRIA
Vienna, International Atomic Energy Agency
BELGIUM
Brussels, La Bibliotheque EURATOM
FRANCE
Paris, European Nuclear Energy Agency, O.E.C.D.
ITALY
Ispra, EURATOM Research Center
SWITZERLAND
Geneva, United Nations Library

UNITED STATES
GOVERNMENT PRINTING OFFICE
DIVISION OF PUBLIC DOCUMENTS
WASHINGTON, D.C. 20402

OFFICIAL BUSINESS

POSTAGE AND FEES PAID
U.S. GOVERNMENT PRINTING OFFICE

TECHNICAL PROGRESS REVIEWS

The Division of Technical Information, U. S. Atomic Energy Commission, also publishes the Technical Progress Reviews, a series of five quarterly journals on nuclear technology. These journals, compiled by specialists and recognized authorities, summarize, evaluate, and reference the progress of development in five important fields

Isotopes and Radiation Technology P. S. Baker, A. F. Rupp, and associates, Oak Ridge National Laboratory. Reviews AEC-sponsored projects and related significant worldwide developments in radioisotopes and radiation technology.

Nuclear Safety Wm. B. Cottrell, W. H. Jordan, and associates, Oak Ridge National Laboratory. Covers topics relevant to the analysis and control of hazards associated with nuclear reactors and with operations involving fissionable materials and the products of nuclear fission.

Power Reactor Technology Argonne National Laboratory. Reviews research, development, design practices, and operating experiences associated with power reactors, including aerospace applications.

Reactor Fuel Processing Stephen Lawroski and associates, Argonne National Laboratory. Reviews all aspects of the fuel-processing field, including aqueous and nonaqueous processing and waste disposal.

Reactor Materials R. W. Dayton, E. M. Simons, and associates, Battelle Memorial Institute. Covers the properties, behavior, and fabrication processes of materials used in nuclear reactors and associated equipment.

Availability

SUBSCRIPTION RATE: The Technical Progress Reviews may be purchased from the Superintendent of Documents, U. S. Government Printing Office, Washington, D. C. 20402, at $2.50 per year for each subscription or $0.70 per issue.

POSTAGE: Postpaid within the United States, Canada, Mexico, and all Central and South American countries except Argentina, Brazil, British and French Guiana, Surinam, and British Honduras. For these Central and South American countries and all other countries, add $0.75 per year or $0.20 per single issue.

REMITTANCE: Payment should be by check, money order, or document coupons and MUST accompany order. Remittances from foreign countries should be made by international money order or draft on an American bank payable to the Superintendent of Documents or by UNESCO book coupons.